DOC.20100412.0001

QA: QA

ANL-WIS-MD-000027 REV 00

March 2008

THIS DOCUMENT CONTAINS THE FOLLOWING, LOCATED AT THE BACK OF THE DOCUMENT:
1) ADDENDUM 001, DATED 04/06/2010

Features, Events, and Processes for the Total System Performance Assessment: Analyses

NOTICE OF OPEN CHANGE DOCUMENTS - THIS DOCUMENT IS IMPACTED BY THE LISTED CHANGE DOCUMENTS AND CANNOT BE USED WITHOUT THEM.
---
1) ACN-001, DATED 04/03/2008

THIS DOCUMENT IS IMPACTED BY THE FOLLOWING "ERROR RESOLUTION DOCUMENTS", WHICH SHOULD BE REVIEWED PRIOR TO USING THIS DOCUMENT:
---
1) ANL-WIS-MD-000027 ERD 01
2) ANL-WIS-MD-000027 ERD 02
3) ANL-WIS-MD-000027 ERD 03
4) ANL-WIS-MD-000027 ERD 04
5) ANL-WIS-MD-000027 ERD 05
6) ANL-WIS-MD-000027 ERD 06

Prepared for:
U.S. Department of Energy
Office of Civilian Radioactive Waste Management
Office of Repository Development
1551 Hillshire Drive
Las Vegas, Nevada 89134-6321

Prepared by:
Sandia National Laboratories

Under Contract Number:
DE-AC04-94AL85000

DISCLAIMER

This report was prepared as an account of work sponsored by an agency of the United States Government. Neither the United States Government nor any agency thereof, nor any of their employees, nor any of their contractors, subcontractors or their employees, makes any warranty, express or implied, or assumes any legal liability or responsibility for the accuracy, completeness, or any third party's use or the results of such use of any information, apparatus, product, or process disclosed, or represents that its use would not infringe privately owned rights. Reference herein to any specific commercial product, process, or service by trade name, trademark, manufacturer, or otherwise, does not necessarily constitute or imply its endorsement, recommendation, or favoring by the United States Government or any agency thereof or its contractors or subcontractors. The views and opinions of authors expressed herein do not necessarily state or reflect those of the United States Government or any agency thereof.

QA: QA

Features, Events, and Processes for the Total System Performance Assessment: Analyses

ANL-WIS-MD-000027 REV 00

March 2008

Scientific Analysis/Calculation Signature Page/Change History

1. Total Pages: 2042

Complete only applicable items.

2. Document Title

Features, Events, and Processes for the Total System Performance Assessment: Analyses

3. DI (Including Revision No. and Addendum No.)

ANL-WIS-MD-000027 REV 00

	Printed Name	Signature	Date
4. Originator	Thomas F. Fishburn Russell Jarek	Thos F Fish Russell Jarek	3-05-08 3-05-08
5. Checker	Daniel G. Levitt	Dan G Levitt	3-05-08
6. QA: QA or Lead CA Reviewer	Charles Beuth	Charles F. Beuth	3-5-08
7. Responsible Manager/Lead	Peter Swift	Peter Swift	3/5/08
8. Responsible Manager	Stephanie P. Kuzio	Stephanie P. Kuzio	3/6/08

9. Remarks

Minor editorial changes were made to the DIRs report on 3/6/08. SPK 3/4/08

In addition to the nine FEP screening analysis documents listed in Section 1.2, this document also supersedes Development of the Total System Performance Assessment – License Application Features, Events, and Processes (BSC 2005 [DIRS 173800]. SPK 3/7/08

Change History

10. Revision No. and Addendum No.	11. Description of Change
00	Initial issue. Addresses CRs 5600, 7452, 7523, 8408, 8655, 9518, 10383, 10765, 10899, 11323, 11357, 11633, and 11745.

INTENTIONALLY LEFT BLANK

ACKNOWLEDGEMENTS

This report is the result of an effort involving virtually every discipline and department in the Lead Laboratory organization. Its scope is reflected in the approximately 10,000 citations of over 800 separate sources of data and information.

In addition to the indispensable contributions made by the dozens of authors who developed the material presented in this report, significant contributions were made by the many checkers, reviewers, and Quality Compliance Specialists who checked and reviewed the document during its development. Significant contributions were also made by individual members of several other Lead Laboratory departments, among them the Technical Data Management System, the Document Input Reference System, Document Production, Records, and Information Technology.

INTENTIONALLY LEFT BLANK

CONTENTS

Page

ACKNOWLEDGEMENTS v
ACRONYMS AND ABBREVIATIONS xxv

1. PURPOSE 1-1
   1.1 PLANNING AND DOCUMENTATION 1-2
   1.2 SCOPE 1-2

2. QUALITY ASSURANCE 2-1

3. USE OF SOFTWARE 3-1

4. INPUTS 4-1
   4.1 DIRECT INPUTS 4-1
   4.2 CRITERIA 4-1
   4.3 CODES, STANDARDS, AND REGULATIONS 4-2

5. ASSUMPTIONS 5-1

6. SCIENTIFIC ANALYSIS DISCUSSION 6-1
   6.1 METHODS AND APPROACH 6-1
   6.2 FEATURE, EVENT, AND PROCESS SCREENING ANALYSES 6-4

7. CONCLUSIONS 7-1
   7.1 RELEVANT ACCEPTANCE CRITERIA 7-11

8. INPUTS AND REFERENCES 8-1
   8.1 DOCUMENTS CITED 8-1
   8.2 CODES, STANDARDS, REGULATIONS, AND PROCEDURES 8-63
   8.3 SOURCE DATA, LISTED BY DATA TRACKING NUMBER 8-66
   8.4 OUTPUT DATA, LISTED BY DATA TRACKING NUMBER 8-79
   8.5 SOFTWARE CODES 8-79

APPENDIX A: REPOSITORY DESIGN USE IN PERFORMANCE ASSESSMENT A-1

APPENDIX B: ANALYSIS OF ROCKFALL AND ITS IMPACT TO DRIP SHIELD DENTING B-1

APPENDIX C: BOUNDING ANALYSIS OF WATER FLOW THROUGH SCC CRACKS IN DRIP SHIELD AND WASTE PACKAGE UNDER SHEET FLOW AND IMPINGING SEEPAGE CONDITIONS C-1

APPENDIX D: SCIENTIFIC ANALYSES DISCUSSION AND SUPPORTING DOCUMENTATION FOR METEORITE IMPACT AND CRATERING PROBABILITY AND CONSEQUENCES D-1

CONTENTS (Continued)

Page

APPENDIX E: LOW CONSEQUENCE CALCULATION FOR RUPTURE OF DRIP SHIELD PLATES FROM SEISMIC-INDUCED ROCK BLOCK IMPACTS E-1

APPENDIX F: CROSS-REFERENCE OF YMP LA FEPS TO INTERNATIONAL AND OTHER FEP DATABASES F-1

APPENDIX G: CROSS-REFERENCE BETWEEN YMP LICENSE APPLICATION FEPS AND SITE RECOMMENDATION FEPS G-1

APPENDIX H: DESCRIPTION OF FEPS DATABASE H-1

APPENDIX I: ANALYSIS OF SENSITIVITY OF TRANSPORT TO CHANGES IN FRACTURE APERTURE I-1

APPENDIX J: QUALIFICATION OF DATA AND JUSTIFICATION OF EQUATIONS J-1

LISTING OF FEPS

0.1.02.00.0A 6-6
0.1.03.00.0A 6-7
0.1.09.00.0A 6-9
0.1.10.00.0A 6-12
1.1.01.01.0A 6-18
1.1.01.01.0B 6-24
1.1.02.00.0A 6-26
1.1.02.00.0B 6-29
1.1.02.01.0A 6-32
1.1.02.02.0A 6-34
1.1.02.03.0A 6-37
1.1.03.01.0A 6-39
1.1.03.01.0B 6-41
1.1.04.01.0A 6-43
1.1.05.00.0A 6-45
1.1.07.00.0A 6-47
1.1.08.00.0A 6-52
1.1.09.00.0A 6-62
1.1.10.00.0A 6-64
1.1.11.00.0A 6-66
1.1.12.01.0A 6-70
1.1.13.00.0A 6-72
1.2.01.01.0A 6-74
1.2.02.01.0A 6-81
1.2.02.02.0A 6-87
1.2.02.03.0A 6-90
1.2.03.02.0A 6-94
1.2.03.02.0B 6-99
1.2.03.02.0C 6-112
1.2.03.02.0D 6-118
1.2.03.02.0E 6-122
1.2.03.03.0A 6-126
1.2.04.02.0A 6-129
1.2.04.03.0A 6-139
1.2.04.04.0A 6-142
1.2.04.04.0B 6-147
1.2.04.05.0A 6-149
1.2.04.06.0A 6-153
1.2.04.07.0A 6-157
1.2.04.07.0B 6-163
1.2.04.07.0C 6-166
1.2.05.00.0A 6-170
1.2.06.00.0A 6-174
1.2.07.01.0A 6-182
1.2.07.02.0A 6-184

LISTING OF FEPS (Continued)

Page

1.2.08.00.0A 6-189
1.2.09.00.0A 6-194
1.2.09.01.0A 6-196
1.2.09.02.0A 6-199
1.2.10.01.0A 6-202
1.2.10.02.0A 6-209
1.3.01.00.0A 6-215
1.3.04.00.0A 6-220
1.3.05.00.0A 6-223
1.3.07.01.0A 6-226
1.3.07.02.0A 6-229
1.3.07.02.0B 6-233
1.4.01.00.0A 6-235
1.4.01.01.0A 6-237
1.4.01.02.0A 6-241
1.4.01.03.0A 6-244
1.4.01.04.0A 6-248
1.4.02.01.0A 6-250
1.4.02.02.0A 6-253
1.4.02.03.0A 6-257
1.4.02.04.0A 6-259
1.4.03.00.0A 6-263
1.4.04.00.0A 6-265
1.4.04.01.0A 6-267
1.4.05.00.0A 6-270
1.4.06.01.0A 6-272
1.4.07.01.0A 6-274
1.4.07.02.0A 6-277
1.4.07.03.0A 6-280
1.4.08.00.0A 6-285
1.4.09.00.0A 6-286
1.4.11.00.0A 6-287
1.5.01.01.0A 6-288
1.5.01.02.0A 6-292
1.5.02.00.0A 6-297
1.5.03.01.0A 6-298
1.5.03.02.0A 6-300
2.1.01.01.0A 6-302
2.1.01.02.0A 6-304
2.1.01.02.0B 6-306
2.1.01.03.0A 6-308
2.1.01.04.0A 6-310
2.1.02.01.0A 6-312
2.1.02.02.0A 6-314

LISTING OF FEPS (Continued)

Page

2.1.02.03.0A 6-316
2.1.02.04.0A 6-318
2.1.02.05.0A 6-325
2.1.02.06.0A 6-327
2.1.02.07.0A 6-329
2.1.02.08.0A 6-331
2.1.02.09.0A 6-342
2.1.02.10.0A 6-344
2.1.02.11.0A 6-346
2.1.02.12.0A 6-348
2.1.02.13.0A 6-350
2.1.02.14.0A 6-352
2.1.02.15.0A 6-354
2.1.02.16.0A 6-356
2.1.02.17.0A 6-358
2.1.02.18.0A 6-360
2.1.02.19.0A 6-362
2.1.02.20.0A 6-364
2.1.02.21.0A 6-366
2.1.02.22.0A 6-368
2.1.02.23.0A 6-370
2.1.02.24.0A 6-372
2.1.02.25.0A 6-374
2.1.02.25.0B 6-376
2.1.02.26.0A 6-377
2.1.02.27.0A 6-379
2.1.02.28.0A 6-381
2.1.02.29.0A 6-383
2.1.03.01.0A 6-386
2.1.03.01.0B 6-389
2.1.03.02.0A 6-392
2.1.03.02.0B 6-396
2.1.03.03.0A 6-400
2.1.03.03.0B 6-405
2.1.03.04.0A 6-414
2.1.03.04.0B 6-418
2.1.03.05.0A 6-422
2.1.03.05.0B 6-424
2.1.03.06.0A 6-427
2.1.03.07.0A 6-430
2.1.03.07.0B 6-444
2.1.03.08.0A 6-447
2.1.03.08.0B 6-450
2.1.03.09.0A 6-453

LISTING OF FEPS (Continued)

Page

2.1.03.10.0A 6-456
2.1.03.10.0B 6-466
2.1.03.11.0A 6-481
2.1.04.01.0A 6-484
2.1.04.02.0A 6-486
2.1.04.03.0A 6-488
2.1.04.04.0A 6-490
2.1.04.05.0A 6-492
2.1.04.09.0A 6-494
2.1.05.01.0A 6-496
2.1.05.02.0A 6-501
2.1.05.03.0A 6-502
2.1.06.01.0A 6-504
2.1.06.02.0A 6-509
2.1.06.04.0A 6-512
2.1.06.05.0A 6-515
2.1.06.05.0B 6-519
2.1.06.05.0C 6-522
2.1.06.05.0D 6-527
2.1.06.06.0A 6-530
2.1.06.06.0B 6-534
2.1.06.07.0A 6-538
2.1.06.07.0B 6-542
2.1.07.01.0A 6-547
2.1.07.02.0A 6-552
2.1.07.04.0A 6-557
2.1.07.04.0B 6-560
2.1.07.05.0A 6-563
2.1.07.05.0B 6-565
2.1.07.06.0A 6-569
2.1.08.01.0A 6-572
2.1.08.01.0B 6-574
2.1.08.02.0A 6-577
2.1.08.03.0A 6-579
2.1.08.04.0A 6-581
2.1.08.04.0B 6-584
2.1.08.05.0A 6-588
2.1.08.06.0A 6-591
2.1.08.07.0A 6-593
2.1.08.09.0A 6-596
2.1.08.11.0A 6-599
2.1.08.12.0A 6-601
2.1.08.14.0A 6-604
2.1.08.15.0A 6-612

LISTING OF FEPS (Continued)

Page

2.1.09.01.0A 6-615
2.1.09.01.0B 6-618
2.1.09.02.0A 6-620
2.1.09.03.0A 6-623
2.1.09.03.0B 6-625
2.1.09.03.0C 6-634
2.1.09.04.0A 6-636
2.1.09.05.0A 6-638
2.1.09.06.0A 6-640
2.1.09.06.0B 6-641
2.1.09.07.0A 6-643
2.1.09.07.0B 6-644
2.1.09.08.0A 6-646
2.1.09.08.0B 6-648
2.1.09.09.0A 6-650
2.1.09.10.0A 6-658
2.1.09.11.0A 6-660
2.1.09.12.0A 6-662
2.1.09.13.0A 6-664
2.1.09.15.0A 6-666
2.1.09.16.0A 6-669
2.1.09.17.0A 6-671
2.1.09.18.0A 6-673
2.1.09.19.0A 6-675
2.1.09.19.0B 6-677
2.1.09.20.0A 6-679
2.1.09.21.0A 6-681
2.1.09.21.0B 6-683
2.1.09.21.0C 6-689
2.1.09.22.0A 6-691
2.1.09.23.0A 6-693
2.1.09.24.0A 6-695
2.1.09.25.0A 6-697
2.1.09.26.0A 6-699
2.1.09.27.0A 6-701
2.1.09.28.0A 6-705
2.1.09.28.0B 6-711
2.1.10.01.0A 6-716
2.1.11.01.0A 6-719
2.1.11.02.0A 6-722
2.1.11.03.0A 6-724
2.1.11.05.0A 6-730
2.1.11.06.0A 6-732
2.1.11.06.0B 6-737

LISTING OF FEPS (Continued)

Page

2.1.11.07.0A 6-740
2.1.11.08.0A 6-743
2.1.11.09.0A 6-745
2.1.11.09.0B 6-747
2.1.11.09.0C 6-751
2.1.11.10.0A 6-753
2.1.12.01.0A 6-757
2.1.12.02.0A 6-759
2.1.12.03.0A 6-762
2.1.12.04.0A 6-765
2.1.12.06.0A 6-768
2.1.12.07.0A 6-771
2.1.12.08.0A 6-774
2.1.13.01.0A 6-776
2.1.13.02.0A 6-793
2.1.13.03.0A 6-798
2.1.14.15.0A 6-800
2.1.14.16.0A 6-810
2.1.14.17.0A 6-812
2.1.14.18.0A 6-815
2.1.14.19.0A 6-817
2.1.14.20.0A 6-833
2.1.14.21.0A 6-841
2.1.14.22.0A 6-843
2.1.14.23.0A 6-845
2.1.14.24.0A 6-848
2.1.14.25.0A 6-852
2.1.14.26.0A 6-859
2.2.01.01.0A 6-866
2.2.01.01.0B 6-868
2.2.01.02.0A 6-872
2.2.01.02.0B 6-876
2.2.01.03.0A 6-878
2.2.01.04.0A 6-881
2.2.01.05.0A 6-883
2.2.03.01.0A 6-886
2.2.03.02.0A 6-891
2.2.06.01.0A 6-897
2.2.06.02.0A 6-900
2.2.06.02.0B 6-907
2.2.06.03.0A 6-914
2.2.06.04.0A 6-916
2.2.06.05.0A 6-919
2.2.07.01.0A 6-921

LISTING OF FEPS (Continued)

Page

2.2.07.02.0A 6-923
2.2.07.03.0A 6-927
2.2.07.04.0A 6-929
2.2.07.05.0A 6-933
2.2.07.06.0A 6-937
2.2.07.06.0B 6-940
2.2.07.07.0A 6-942
2.2.07.08.0A 6-944
2.2.07.09.0A 6-948
2.2.07.10.0A 6-950
2.2.07.11.0A 6-952
2.2.07.12.0A 6-954
2.2.07.13.0A 6-956
2.2.07.14.0A 6-958
2.2.07.15.0A 6-964
2.2.07.15.0B 6-966
2.2.07.16.0A 6-967
2.2.07.17.0A 6-968
2.2.07.18.0A 6-969
2.2.07.19.0A 6-971
2.2.07.20.0A 6-973
2.2.07.21.0A 6-975
2.2.08.01.0A 6-978
2.2.08.01.0B 6-982
2.2.08.03.0A 6-985
2.2.08.03.0B 6-990
2.2.08.04.0A 6-995
2.2.08.05.0A 6-999
2.2.08.06.0A 6-1002
2.2.08.06.0B 6-1005
2.2.08.07.0A 6-1007
2.2.08.07.0B 6-1010
2.2.08.07.0C 6-1012
2.2.08.08.0A 6-1015
2.2.08.08.0B 6-1017
2.2.08.09.0A 6-1019
2.2.08.09.0B 6-1022
2.2.08.10.0A 6-1025
2.2.08.10.0B 6-1027
2.2.08.11.0A 6-1029
2.2.08.12.0A 6-1033
2.2.08.12.0B 6-1036
2.2.09.01.0A 6-1038
2.2.09.01.0B 6-1042

LISTING OF FEPS (Continued)

Page

2.2.10.01.0A 6-1046
2.2.10.02.0A 6-1050
2.2.10.03.0A 6-1056
2.2.10.03.0B 6-1058
2.2.10.04.0A 6-1060
2.2.10.04.0B 6-1063
2.2.10.05.0A 6-1065
2.2.10.06.0A 6-1069
2.2.10.07.0A 6-1073
2.2.10.08.0A 6-1079
2.2.10.09.0A 6-1083
2.2.10.10.0A 6-1086
2.2.10.11.0A 6-1088
2.2.10.12.0A 6-1092
2.2.10.13.0A 6-1094
2.2.10.14.0A 6-1097
2.2.11.01.0A 6-1103
2.2.11.02.0A 6-1106
2.2.11.03.0A 6-1108
2.2.12.00.0A 6-1111
2.2.12.00.0B 6-1114
2.2.14.09.0A 6-1116
2.2.14.10.0A 6-1119
2.2.14.11.0A 6-1127
2.2.14.12.0A 6-1130
2.3.01.00.0A 6-1137
2.3.02.01.0A 6-1139
2.3.02.02.0A 6-1141
2.3.02.03.0A 6-1144
2.3.04.01.0A 6-1147
2.3.06.00.0A 6-1149
2.3.09.01.0A 6-1151
2.3.11.01.0A 6-1154
2.3.11.02.0A 6-1158
2.3.11.03.0A 6-1160
2.3.11.04.0A 6-1163
2.3.13.01.0A 6-1164
2.3.13.02.0A 6-1167
2.3.13.03.0A 6-1169
2.3.13.04.0A 6-1174
2.4.01.00.0A 6-1175
2.4.04.01.0A 6-1177
2.4.07.00.0A 6-1179
2.4.08.00.0A 6-1181

LISTING OF FEPS (Continued)

Page

2.4.09.01.0A 6-1183
2.4.09.01.0B 6-1184
2.4.09.02.0A 6-1187
2.4.10.00.0A 6-1189
3.1.01.01.0A 6-1191
3.2.07.01.0A 6-1195
3.2.10.00.0A 6-1197
3.3.01.00.0A 6-1200
3.3.02.01.0A 6-1202
3.3.02.02.0A 6-1205
3.3.02.03.0A 6-1208
3.3.03.01.0A 6-1210
3.3.04.01.0A 6-1212
3.3.04.02.0A 6-1215
3.3.04.03.0A 6-1218
3.3.05.01.0A 6-1220
3.3.06.00.0A 6-1223
3.3.06.01.0A 6-1224
3.3.06.02.0A 6-1226
3.3.07.00.0A 6-1228
3.3.08.00.0A 6-1229

INTENTIONALLY LEFT BLANK

FIGURES

Page

6-1. Schematic Illustration of the Features, Events, and Processes Analysis Method 6-2
2.1.02.04.0A-1. Conceptual Illustration of Alpha Recoil Mechanics 6-318
2.1.03.10.0A-1. Typical Examples of (a) Transgranular SCC and (b) Intergranular SCC Cracks in Stainless Steel 6-458
2.1.03.10.0B-1. Typical Examples of (a) Transgranular SCC and (b) Intergranular SCC Cracks in Stainless Steel 6-472
2.1.06.06.0A-1. Potential Flow Pathways in the EBS 6-532
2.1.09.21.0B-1. Schematic Illustration of the Physical Situation Associated with the Forces and Velocities Calculated for Table 2.1.09.21.0B-1 6-686
2.3.13.03.0A-1. Time History of the Temperature Difference through the Top (surface) Layer (tcw12 hydrostratigraphic unit) in a Repository Thermal Model, and the Associated Heat Flux at the Repository Center (max heat flux point, node g3) 6-1172
B-1. Drift Length per Simulation B-3
B-2. Section View of Drip Shield B-6
B-3. Definition of Impact Angle and Drip Shield Block Local Coordinate System B-7
C-1. A Schematic Showing Simplified Geometry of a Through-wall Crack C-3
D-1. Waste Emplacement and Repository Target Area and Surrounding Boreholes D-4
D-2. Contours of Depth to the Top of the PTn Unit D-7
D-3. Contours of Thickness of the PTn Unit D-8
D-4. Contours of Depth to the Base of the PTn Unit D-9
D-5. Cratering Rate Distribution from Four Sources D-12
D-6. Annualized Frequency of Cratering above the Repository for the Target Area D-19
I-1. Comparison of Site Recommendation and License Application Transport Results for an Instantaneous Release of (Nonsorbing) Tracer Mass at the Repository Horizon at Time Zero under Present-Day Climate: (a) Individual Fractional Breakthrough Curves, (b) Average Fractional Breakthrough Curves I-8
I-2. Comparison of Site Recommendation and License Application Transport Results for an Instantaneous Release of (Nonsorbing) Tracer Mass at the Repository Horizon at Time Zero under Glacial-Transition Climate: (a) Individual Fractional Breakthrough Curves, (b) Average Fractional Breakthrough Curves I-9
I-3a. Plan View of the UZ Flow Model Domain for Site Recommendation Showing Nearby Faults and Boreholes I-11
I-3b. Plan View of the UZ Flow Model Domain for License Application Showing Nearby Faults and Boreholes I-12

FIGURES (Continued)

Page

I-4. Breakthrough Curves under Present-Day Infiltration When Fracture Property Changes Are Limited to the Fault Fractures I-17
I-5. Breakthrough Curves under Glacial-Transition Infiltration When Fracture Property Changes Are Limited to the Fault Fractures I-18
I-6. Breakthrough Curves under Present-Day Infiltration with Change in Fracture Properties Throughout the Entire Model Domain I-20
I-7. Breakthrough Curves under Glacial-Transition Infiltration with Change in Fracture Properties Throughout the Entire Model Domain I-21

TABLES

Page

4-1.	Direct Inputs	4-1
6-1.	Indirect Inputs	6-4
1.1.01.01.0A-1.	Deep Boreholes in or Close to the Repository Block	6-19
2.1.02.04.0A-1.	Alpha Recoil Enhanced (from α and α-Recoil Atom) Dissolution Rates Due to the Major Mass-Based Constituents of SNF and HLW to be Disposed of in the Yucca Mountain Repository	6-323
2.1.03.03.0B-1.	Comparison of Solutions from Corrosion Testing with the Expected Repository Compositions	6-410
2.1.03.11.0A-1.	Waste Package Dimensions and Design Basis Inventory	6-482
2.1.06.06.0B-1.	Results of Sensitivity Analysis for Oxygen Embrittlement of Drip Shield	6-535
2.1.09.03.0B-1.	Parameter Values Used to Calculate t_{fill}	6-630
2.1.09.21.0B-1.	Forces and Velocities Acting on a Spherical Particle Resting on a Horizontal Surface against an Asperity with Height Equal to Half the Particle Diameter (Figure 2.1.09.21.0B-1)	6-685
2.1.11.06.0A-1.	Comparison of Alloy 22 ASTM Composition Specification to Range of Compositions Studied in Alloy 22 Aging and Phase Stability Model and Recommended Alloy 22 Composition Range of Applicability	6-733
2.1.14.15.0A-1.	Undetected Errors in Waste Package Fabrication and Operational Processes	6-804
2.1.14.19.0A-1.	Probability of Seismic Vibratory Ground Motion Events Causing Damage to TAD Canister-Bearing Waste Packages	6-821
2.1.14.19.0A-2.	Probability of Seismic Vibratory Ground Motion Events Causing Damage to Codisposal Waste Packages	6-822
2.1.14.19.0A-3.	Probability of Damage for Intact Codisposal Waste Package	6-822
2.1.14.19.0A-4.	Probability of Potential Criticality from Waste Package OCB Failure from Localized Corrosion due to Drip Shield Rupture from Rockfall Loading	6-824
2.1.14.19.0A-5.	Fractional Length per Waste Package Variant	6-826
2.1.14.19.0A-6.	Expected Number of Waste Packages by Type Emplaced on Faults	6-826
2.1.14.19.0A-7.	Cumulative Number of Failed Commercial SNF Waste Packages Expected versus Annual Exceedance Frequency	6-826
2.1.14.19.0A-8.	Cumulative Number of Failed Codisposal Waste Packages Expected versus Annual Exceedance Frequency	6-827
2.1.14.19.0A-9.	Probabilities of Seismic Faulting Events with Waste Package Failure Capability	6-827
2.1.14.20.0A-1.	Summary of Seismic Scenario External Criticality Results	6-837
2.1.14.26.0A-1.	Summary of Igneous Scenario External Criticality Results	6-862
2.2.14.10.0A-1.	Summary of Seismic Scenario External Criticality Results	6-1123
2.2.14.12.0A-1.	Summary of Igneous Scenario External Criticality Results	6-1134
2.3.13.03.0A-1.	Fractional Change in Total Evapotranspiration Due to Thermally Induced Decrease in Shrub Coverage	6-1172

TABLES (Continued)

Page

7-1. Yucca Mountain Project FEP List and Screening Decisions Listed by FEP Number 7-1
A-1. Repository Design Use in Performance Assessment A-2
A-2. Indirect Inputs for Appendix A A-19
B-1. Selection of Blocks with Highest Impact Energy That Could Dent Drip Shield Crown Area B-4
B-2. Results for Edge-On Impacts B-9
B-3. Direct Inputs for Appendix B B-11
B-4. Indirect Inputs for Appendix B B-12
C-1. Yield Strength and Modulus of Elasticity of Titanium Grade 7 and Alloy 22 Used in This Analysis C-3
C-2. Direct Inputs for Appendix C C-15
C-3. Indirect Inputs for Appendix C C-18
D-1. Summary of Velocity Data from Reviewed Literature D-3
D-2. Emplacement Drift Endpoint Coordinates D-5
D-3. Annual Frequency of Cratering above Repository for TSPA-LA Emplacement Area D-18
D-4. Data Sets for Use within this Technical Product D-22
D-5. Direct Inputs for Appendix D D-28
D-6. Indirect Inputs for Appendix D D-29
E-1. Direct Inputs for Appendix E E-2
E-2. Indirect Inputs for Appendix E E-5
E-3. Comparison of Mean Annual Dose Due to Nonlithophysal Rockfall with the Dose from the Seismic Ground Motion Modeling Case E-9
F-1. Source FEP Information F-2
F-2. Cross Reference of TSPA-LA FEPs to Source FEPs F-3
F-3. Cross Reference of Source FEPs to TSPA-LA FEPs F-103
F-4. Direct Inputs for Appendix F F-213
F-5. Indirect Inputs for Appendix F F-213
G-1. Cross-Reference of TSPA-LA FEPs to TSPA-SR FEPs G-2
G-2. Cross Reference of TSPA-SR FEPs to TSPA-LA FEPs G-84
G-3. Indirect Inputs for Appendix G G-164
H-1. Indirect Inputs for Appendix H H-10
I-1. Indirect Inputs for Appendix I I-23
J-1. List of Sources by Section and FEP Number J-2
J21-1. Summary of Main Results of EQ3/6 Equilibrium Solubility Calculations J-58
J30-1. Nuclide Inventories at 1,000 years and Calculated Helium Inventory Change Due to Decay between 1,000 and 10,000 years J-83

TABLES (Continued)

Page

J-2. Data Qualification Plan for Project Data, Project and External Source Data to be Qualified for Intended Use in Document ANL-WIS-MD-000027 ..... J-126
J-3. Direct Inputs for Appendix J J-141
J-4. Indirect Inputs for Appendix J J-147

INTENTIONALLY LEFT BLANK

ACRONYMS AND ABBREVIATIONS

The following is a list of acronyms and abbreviations commonly used in this report. Types of acronyms and abbreviations not listed below would include: (1) acronyms and abbreviations that are defined and used on a limited or a case-by-case basis, (2) widely known acronyms and abbreviations (e.g., "N/A"), or (3) acronyms that appear only in source titles or descriptions, or in organization-specific designations.

Because most users of this document will likely consult individual sections of it according to specific interests or purposes, rather than reading it sequentially, acronyms are not defined in the text upon first use. Instead, they are defined on a case-by-case basis when deemed appropriate or useful. It is therefore recommended that users of this report consult the following list, in conjunction with individual report sections, when seeking the definition of a particular acronym.

Å	angstrom
AICC	adiabatic, constant volume (isochoric) complete combustion (model)
AMR	analysis/model report
ASM	American Society for Metals
ASME	American Society of Mechanical Engineers
ASTM	American Society for Testing and Materials
atm	atmosphere
ATR	advanced test reactor
BDCF	biosphere dose conversion factor
BWR	boiling water reactor
CDF	cumulative distribution function
CDSP	codisposal (waste package)
cm	centimeter
CR	condition report
CSNF	commercial spent nuclear fuel
DHLW	defense high-level waste
DIRS	Document Input Reference System
DLL	dynamic link library
DOE	U.S. Department of Energy
DSNF	DOE spent nuclear fuel
DTN	data tracking number
EBS	Engineered Barrier System
ECRB	Enhanced Characterization of the Repository Block
EDZ	excavation disturbed zone
EPA	U.S. Environmental Protection Agency
ESF	Exploratory Studies Facility
eV	electronvolt

ACRONYMS AND ABBREVIATIONS (Continued)

FAO	Food and Agriculture Organization
FAR	Fortymile Wash Ash Redistribution (model or code)
FEHM	Finite Element Heat and Mass (model or code)
FEP	feature, event, or process
FFTF	Fast Fuel Transport Facility
FIFRA	Federal Insecticide, Fungicide, and Rodenticide Act
g	gram
gmole	gram mole
GPa	gigapascal
GPS	Global Positioning System
GWd	gigawatt day
Gy	gray (equivalent to J kg^{-1})
HFM	hydrogeologic framework model
hr	hour
HLW	high-level (radioactive) waste
IDPS	in-drift precipitates/salts (model)
IOM	Institute of Medicine
IPC	in-package chemistry
J	joule
K	kelvin
kbar	kilobar
kg	kilogram
kJ	kilojoule
km	kilometer
ksi	kilopounds per square inch
kyr	kiloyear
LTCTF	Long-Term Corrosion Testing Facility
LWBR	light-water breeder reactor
m	meter
m	molal
M	molar
µCi	microcurie
MCO	multi-canister overpack
MeV	megaelectronvolt
MIC	microbially induced corrosion
mL	milliliter
mm	millimeter
µm	micrometer

ACRONYMS AND ABBREVIATIONS (Continued)

MOX	mixed-oxide
MPa	megapascal
mrem	millirem
MSTHM	multiscale thermohydrologic model
MT	metric ton
MTHM	metric tons heavy metal
MTU	metric tons uranium
mV	millivolt
Myr	million years
NAC	Nevada Administrative Code
NAE	National Academy of Engineering
NAP	National Academies Press
NAS	National Academy of Science
NEA	Nuclear Energy Agency
NFC	near-field chemistry
nm	nanometer
NRC	U.S. Nuclear Regulatory Comission
NSNFP	National Spent Nuclear Fuel Program
OCB	outer corrosion barrier
OCRWM	Office of Civilian Radioactive Waste Management
OECD	Organisation for Economic Co-operation and Development
OQA	Office of Quality Assurance
P&CE	physical and chemical environment
PGA	peak ground acceleration
PGV	peak ground velocity
PLFA	phospholipid fatty acid
ppm	parts per million
PSHA	Probabilistic Seismic Hazard Analysis
PVHA	Probabilistic Volcanic Hazard Analysis
PWR	pressurized water reactor
QA	quality assurance
QARD	*Quality Assurance Requirements and Description*
rad	radiation absorbed dose (100 rad are equal to 1 gray)
RH	relative humidity
RMEI	reasonably maximally exposed individual
RST	residual stress threshold
RTA	radionuclide transport abstraction
RTTF	residence-time transfer function

ACRONYMS AND ABBREVIATIONS (Continued)

s	second
SAR	Safety Analysis Report
SAW	simulated acidified water
SCC	stress corrosion cracking
SCW	simulated concentrated water
SDW	simulated dilute water
SEM	scanning electron microscopy
SNF	spent nuclear fuel
SR	Site Recommendation
SZ	saturated zone
TAD	transportation, aging, and disposal (canister)
TBD	to be determined
TBV	to be verified
TFM	tracers, fluids, and materials
TH	thermal-hydrologic
THC	thermal-hydrologic chemical
THM	thermal-hydrologic-mechanical
TMI	Three-Mile Island
TPSA	total system performance assessment
TSPA-LA	total system performance assessment for the license application
TWP	technical work plan
USGS	United States Geological Survey
UTM	Universal Transverse Mercator
UZ	unsaturated zone
V	volt
vol %	volume percent
WIPP	Waste Isolation Pilot Plant
WPOB	waste package outer barrier
WRIP	water–rock interaction parameter
wt %	weight percent
YMP	Yucca Mountain Project
yr	year

1. PURPOSE

The purpose of this analysis report is to document the screening decisions and technical bases for inclusion or exclusion of each FEP identified as relevant to the TSPA and the Yucca Mountain disposal system, in accordance with the regulatory screening criteria identified for the Yucca Mountain Site. The companion report, *Features, Events, and Processes for the Total System Performance Assessment: Methods* (SNL 2008 [DIRS 179476]) documents: (1) the origin, and the methods used in the development of a comprehensive list of FEPs that could potentially affect the postclosure performance of the Yucca Mountain disposal system; (2) the methodology and guidance used to screen FEPs for inclusion or exclusion from TSPA; (3) the methodology and guidance used to create scenario classes; and (4) compliance with NUREG-1804 (NRC 2003 [DIRS 163274]) acceptance criteria. The screening decision results presented in this report are reflected in the current performance assessments (or TSPA) described in *Total System Performance Assessment Model/Analysis for the License Application* (SNL 2008 [DIRS 183478]).

Performance assessment is required to demonstrate compliance with the postclosure performance objective for the DOE YMP as stated in proposed 10 CFR 63.2 (70 FR 53313 [DIRS 178394]) and in 10 CFR 63.2 [DIRS 180319]. A performance assessment is an analysis that:

1. Identifies the features, events, processes (except human intrusion), and sequences of events and processes (except human intrusion) that might affect the Yucca Mountain disposal system and their probabilities of occurring;

2. Examines the effects of those features, events, processes, and sequences of events and processes upon the performance of the Yucca Mountain disposal system; and

3. Estimates the dose incurred by the reasonably maximally exposed individual, including the associated uncertainties, as a result of releases caused by all significant features, events, processes, and sequences of events and processes, weighted by their probability of occurrence.

In addition, the performance assessment is required to "provide the technical basis for either inclusion or exclusion of specific features, events, and processes in the performance assessment" as stated in 10 CFR 63.114 [DIRS 180319]. This report describes the required technical basis for the FEPs excluded from the TSPA model, a summary of how the included FEPs are implemented in the TSPA model, and develops an electronic database that is useful to catalog and display the FEP information.

The conclusions drawn from this report include screening decisions and technical bases for each of the FEPs on the TSPA-LA FEP list, and text describing compliance of these activities with the applicable NUREG-1804 (NRC 2003 [DIRS 163274]) acceptance criteria outlined in Section 4.2.

1.1 PLANNING AND DOCUMENTATION

Documentation requirements for this analysis report are described in *Technical Work Plan for the Performance Assessment Features, Events, and Processes* (SNL 2007 [DIRS 184327]).

There is one deviation from the TWP; the title of the report has been changed from that specified in the TWP (SNL 2007 [DIRS 184327], Section 1.1) for consistency with the associated methods report (SNL 2008 [DIRS 179476]).

1.2 SCOPE

This report describes the screening decisions and technical bases for each of the 374 TSPA-LA FEPs identified in *Features, Events, and Processes for the Total System Performance Assessment: Methods* (SNL 2008 [DIRS 179476], Table 7-1). These screening analyses consider new proposed regulations, new repository design considerations, and new technical information that have been developed since the completion of the previous FEP analysis and screening report, *Development of the Total System Performance Assessment—License Application Features, Events, and Processes* (BSC 2005 [DIRS 173800]). The updated FEP screening analyses in this report supersede the following FEP screening analysis documents:

- *Evaluation of Features, Events, and Processes (FEP) for the Biosphere Model* (BSC 2005 [DIRS 174107])
- *Clad Degradation – FEPs Screening Arguments* (BSC 2004 [DIRS 170019])
- *Features, Events, and Processes: Disruptive Events* (BSC 2005 [DIRS 173981])
- *Engineered Barrier System Features, Events, and Processes* (BSC 2005 [DIRS 175014])
- *Features, Events, and Processes: System Level* (BSC 2004 [DIRS 170021])
- *Features, Events, and Processes in SZ Flow and Transport* (BSC 2005 [DIRS 174190])
- *Features, Events, and Processes in UZ Flow and Transport* (BSC 2005 [DIRS 174191])
- *Waste Form Features, Events, and Processes* (BSC 2004 [DIRS 170020])
- *Screening of Features, Events, and Processes in Drip Shield and Waste Package Degradation* (BSC 2005 [DIRS 174995]).

This report does not supersede *Screening Analysis of Criticality Features, Events, and Processes for License Application* (SNL 2008 [DIRS 173869]), but does consolidate information presented in that criticality FEP analysis.

FEP screening is an important process for YMP FEP analysis and scenario development (SNL 2008 [DIRS 179476], Section 1.2). The FEP screening analysis addresses acceptance criterion 2, as outlined in NUREG-1804 (NRC 2003 [DIRS 163274], Section 2.2.1.2.1.3). The methods and approach for FEP screening are outlined in Section 6.1. The screening decisions

and technical bases for each of the 374 FEPs are presented in Section 6.2. The key information provided in Section 6.2 for each FEP is the screening decision (included or excluded) and the associated technical basis. For excluded FEPs, the technical basis is a "screening justification," which documents the rationale for exclusion from the TSPA model. For included FEPs, the technical basis is a "TSPA disposition," which documents how the FEP is implemented in the TSPA model. Section 7 summarizes the screening decisions and describes how the FEP screening addresses the applicable acceptance criterion outlined in NUREG-1804 (NRC 2003 [DIRS 163274], Section 2.2.1.2.1.3).

Additional output from this report includes an update to the FEP electronic database as product output (DTN: MO0706SPAFEPLA.001) that is useful to catalog and display the FEP information. It is acknowledged that the FEP justifications and implementations provided in Section 6.2 may differ from those contained within the output DTN, but only at an editorial level.

The CRs associated with this report are listed below. The actions associated with each CR addressed by this report are summarized below each CR title:

- CR 5600, *Direct Inputs for FEPs AMRs*
  - Appropriate direct inputs are cited, qualified, or justified as necessary, with at least one direct input supporting each FEP excluded from TSPA.
- CR 7452, *Inadequate Justification for Use of Superseded Information in Engineered System AMR*
  - The canceled report identified is no longer used to support excluded FEP 2.1.02.08.0A (Pyrophoricity from DSNF) or excluded FEP 2.1.11.03.0A (Exothermic Reactions in the EBS).
- CR 7523, *TSPA Evaluation of Low-Consequence and Low-Probability FEPs*
  - Screening issues were considered and further FEP examination has culminated in this analysis report.
- CR 8408, *Exchanged Information Was Out of Date When Provided for Use*
  - The table indicated by this CR is outdated and no longer used.
- CR 8655, *FEP 2.1.11.09.0C in EBS FEPs Report Needs Discussion of Chemical Aspects*
  - The indicated FEP has been revised to briefly discuss the in-drift chemical effects of convection and references the excluded dust deliquescence FEP 2.1.09.28.0A (Localized Corrosion on Waste Package Outer Surface Due to Deliquescence).
- CR 9518, *Direct Input Not Included on Information Exchange Drawing*
  - Procedural requirement for design information from the information exchange drawing has since changed, current input usages are compliant.

- CR 10388, *Improper Direct Input Citations to ANL-DSD-MD-000001 for Ti Gr 24 Corrosion Rate*
  - Titanium Grade 24 is not in the current design, so no direct input usages refer to it.
- CR 10755, *EBS FEPs AMR, Section 6.2.64 Contains Citation Error*
  - Usages of "heat treatment" and "annealing" in drip shield FEPs have been clarified.
- CR 10899, *Thermal Alteration of the PTn Unit is Not Explicitly Addressed in FEP Analysis*
  - FEP 2.2.08.03.0B (Geochemical Interactions and Evolution in the UZ) justification is expanded to discuss the potential for thermal alteration of the properties within the PTn hydrogeologic unit.
- CR 11323, *Unexpected Literature Results re: Titanium Localized Corrosion*
  - FEP 2.1.03.03.0B (Localized Corrosion of Drip Shields) has been expanded to discuss the information identified by this CR.
- CR 11357, *Pallet Chemical Degradation FEP Status Change*
  - FEP 2.1.06.05.0C (Chemical Degradation of Emplacement Pallet) is now screened as *included*.
- CR 11633, *DTN Submittal Review of FEP Database is Incomplete*
  - The product output DTN of this report is updated and resubmitted with appropriate reviews completed and submitted to records.
- CR 11745, *Exclusion of Hydrothermal Activity FEPs*
  - FEP 1.2.06.00.0A (Hydrothermal Activity) identifies a recently published assessment of DOE's screening approach regarding this process.

Limitations on the use of this report are as follows:

- The screening of TSPA-LA FEPs potentially relevant to the postclosure performance of the Yucca Mountain repository is based on site-specific information, design, and regulations. Therefore, the FEP screening is specific to the regulations, repository design, and processes for the YMP available at this time.

2. QUALITY ASSURANCE

Development of this report and the supporting analyses are subject to the Office of Civilian Radioactive Waste Management quality assurance program as identified in *Technical Work Plan for the Performance Assessment Features, Events, and Processes* (SNL 2007 [DIRS 184327], Section 8.1).

Approved quality assurance procedures were used to conduct and document the activities described in this report as directed by the TWP (SNL 2007 [DIRS 184327], Section 4). Documentation was prepared in accordance with SCI-PRO-005, *Scientific Analyses and Calculations*, and related procedures and guidance documents as outlined in the TWP (SNL 2007 [DIRS 184327], Sections 2 and 4). The TWP (SNL 2007 [DIRS 184327], Section 8.4) also identifies applicable controls for compliance with IM-PRO-002, *Control of the Electronic Management of Information*, during the analysis and documentation activities.

INTENTIONALLY LEFT BLANK

3. USE OF SOFTWARE

Except as noted below, this analysis report does not directly use any qualified software. The analyses and justifications are generally based on results of analyses presented and documented in other analysis reports, and other technical literature. Software and models used in the supporting documentation may be indirectly cited for traceability and transparency purposes in Section 6.2 and in the appendices. Unqualified but controlled software, exempt from software qualification, are used and briefly described here. Only in a single instance is baseline qualified software used, and it is fully described at the end of this section.

The FEPs Viewer (STN: 611664-1.0-00 [DIRS 181089]) is a Visual BASIC for Applications program written within Microsoft Access that was used to produce portions of Sections 6.2, 7, and 8 of this report from the FEP database. This software was used strictly to generate portions of the printed document for visual display and accomplished no calculations or other mathematical processes. This analysis report is subject to check and approval (per SCI-PRO-005, *Scientific Analyses and Calculations*), and therefore in accordance with IM-PRO-003, *Software Management* (Section 2.0), the FEP Viewer software is exempt from qualification requirements.

The software EarthVision V7.5.2 (STN: 607871-7.5.2-00 [DIRS 184835]) is utilized in Appendix D. This software use was only for producing graphical representations of geologic unit depths and thicknesses (Figures D-2 to D-4). As this analysis report is subject to check and approval, it is therefore exempt from qualification requirements in accordance with IM-PRO-003 (Section 2.0).

MathCad Version 13.1 (STN: 611161-13.1-00), running under the Microsoft Windows 2000 Professional operating system, has been used to perform the calculation documented in Appendix E. The standard features of MathCad are sufficient for these calculations. No macros, codes, or software routines are required for or developed during this work. As used here, MathCad Version 13.1 is not required to be qualified or documented in accordance with IM-PRO-003. The formulas, inputs to the formulas, and outputs from the formulas in the MathCad calculation are identified in Appendix E and in the MathCad file itself.

The qualified software EQ3/6 Version 8.1 (STN: 10813-8.1-00 [DIRS 176889]) was used on a Windows 2000 computer to predict the concentration of calcium in Section J21.2. This software is used within its specified limitations of temperature, pressure, and composition range, as determined by the input thermodynamic database.

Much of this report was developed using the common commercial off-the shelf software suite of Microsoft Office. Microsoft Word 2000, Microsoft Word 2003, and Microsoft Word 2007 were used for word processing. Microsoft Excel 2000 and 2003 are used for data organization and simple calculations. Access 2003 is used for creation and manipulation of the FEPs database. All are exempt from qualification in accordance with IM-PRO-003 (Section 2.0).

INTENTIONALLY LEFT BLANK

4. INPUTS

Direct inputs are discussed in Section 4.1. Criteria relevant to FEP screening are described in Section 4.2. Applicable codes, standards, and regulations are identified in Section 4.3.

4.1 DIRECT INPUTS

The bulk of this report consists of Section 6.2, which contains the compilation of 374 FEP screening analyses. Each FEP in Section 6.2 and each appendix have their own table of direct inputs and indirect inputs. Direct inputs are appropriately selected and qualified for use in this report. Direct input from project and external data sources are qualified for their intended use in this report and are provided in Appendix J.

The direct inputs applicable to this report are listed in Table 4-1. The use of the TSPA-LA FEPs list as direct input is appropriate because it identifies the list of FEPS to be used for the screening process performed in this report.

Table 4-1. Direct Inputs

Input	Source	Description
NRC 2003 [DIRS 163274]	Section 2.2.1.2.1.3	Acceptance criteria
SNL 2008. *Features, Events, and Processes for the Total System Performance Assessment: Methods.* [DIRS 179476]	Table 7-1; Section 6.2	List of 374 TSPA-LA FEPs; methodology and criteria for screening FEPs for exclusion from or inclusion in the TSPA model

4.2 CRITERIA

The areas of review, review methods, and acceptance criteria relevant to FEP analysis and scenario development are described in NUREG-1804 (NRC 2003 [DIRS 163274], Section 2.2.1.2.1). These criteria stem from applicable regulations in 10 CFR Part 63 [DIRS 180319] and proposed 10 CFR Part 63 (70 FR 53313 [DIRS 178394]). Relevant to this FEP screening analysis report is NUREG-1804 (NRC 2003 [DIRS 163274], Section 2.2.1.2.1.3, Acceptance Criterion 2). Descriptions of other relevant criteria specific to the FEP screening analyses are presented in *Features, Events, and Processes for the Total System Performance Assessment: Methods* (SNL 2008 [DIRS 179476], Section 4.2.2).

Other NUREG-1804 criteria, related to the process models that represent the FEPs, are addressed within the specific process model reports and are not presented here.

4.3 CODES, STANDARDS, AND REGULATIONS

The following applicable regulatory requirements are most relevant to this report:

- 10 CFR Part 63 [DIRS 180319]
- Proposed 10 CFR Part 63 (70 FR 53313 [DIRS 178394])
- NUREG-1804 (NRC 2003 [DIRS 163274])

5. ASSUMPTIONS

There are no assumptions that have broad applicability to FEP screening analyses in this report. Since the FEP documentation in Section 6.2 is presented as a collection of individual FEP analyses, their relevant assumptions are documented in the FEP discussions to which they apply.

Section D1.1 contains the assumption "Zone of Fracturing is Cylindrical with Depth, Rather than Parabolic." Section E.5 contains assumptions from several supporting documents relevant to the calculations in Appendix E.

INTENTIONALLY LEFT BLANK

6. SCIENTIFIC ANALYSIS DISCUSSION

The primary focus of this report is to document the screening analyses for each of the identified 374 TSPA-LA FEPs, and to indicate the screening decision for each of them as being included in or excluded from the TSPA model (SNL 2008 [DIRS 183478]). The methods and approach for FEP screening are outlined in Section 6.1, with the complete FEP process described in detail in the methods report (SNL 2008 [DIRS 179476]). The screening decisions (whether a FEP is included or excluded) and technical bases for each of the 374 FEPs are presented in Section 6.2. For excluded FEPs, the technical basis for that decision is a "screening justification," which documents the rationale for exclusion from the TSPA model. For included FEPs, the technical basis is a "TSPA disposition" which documents how the FEP is implemented within the TSPA model. Section 7 summarizes the results with a listing of the 374 TSPA-LA FEPs and their screening decisions (Table 7-1), and describes how the relevant design criteria are addressed.

6.1 METHODS AND APPROACH

The identification and classification of a comprehensive list of FEPs potentially relevant to repository postclosure performance, based on site-specific information, design, and regulations, is described in *Features, Events, and Processes for the Total System Performance Assessment: Methods* (SNL 2008 [DIRS 179476], Section 6.1). The methodology and criteria for screening these FEPs for exclusion from or inclusion in the TSPA model were also outlined in that report (SNL 2008 [DIRS 179476], Section 6.2).

In accordance with the methodology outlined in *Features, Events, and Processes for the Total System Performance Assessment: Methods* (SNL 2008 [DIRS 179476], Section 6.2), each of the TSPA-LA FEPs is screened to determine whether it should be included or excluded from the TSPA. Criteria for exclusion are by reason of low probability, low consequence, or by regulation. These screening criteria are described elsewhere in detail along with their underlying regulatory basis (SNL 2008 [DIRS 179476], Sections 4.2.2 and 6.2), but can be summarized as follows:

- Low Probability – FEPs having less than one chance in 10,000 of occurring within 10,000 years of disposal.

- Low Consequence – FEPs whose omission would not result in significantly adverse changes in the magnitude or time of the radiological exposures to the reasonably maximally exposed individual (RMEI), or radionuclide releases to the accessible environment.

- By Regulation – FEPs that are inconsistent with the characteristics, concepts, and definitions specified in 10 CFR Part 63 [DIRS 180319] or in proposed changes to that rule (70 FR 53313 [DIRS 178394]).

A FEP need only to satisfy one of these exclusion criteria to be excluded from the TSPA model. A FEP that does not meet any of the exclusion criteria must be included (screened in) in the TSPA model. The steps of this process are illustrated in Figure 6-1.

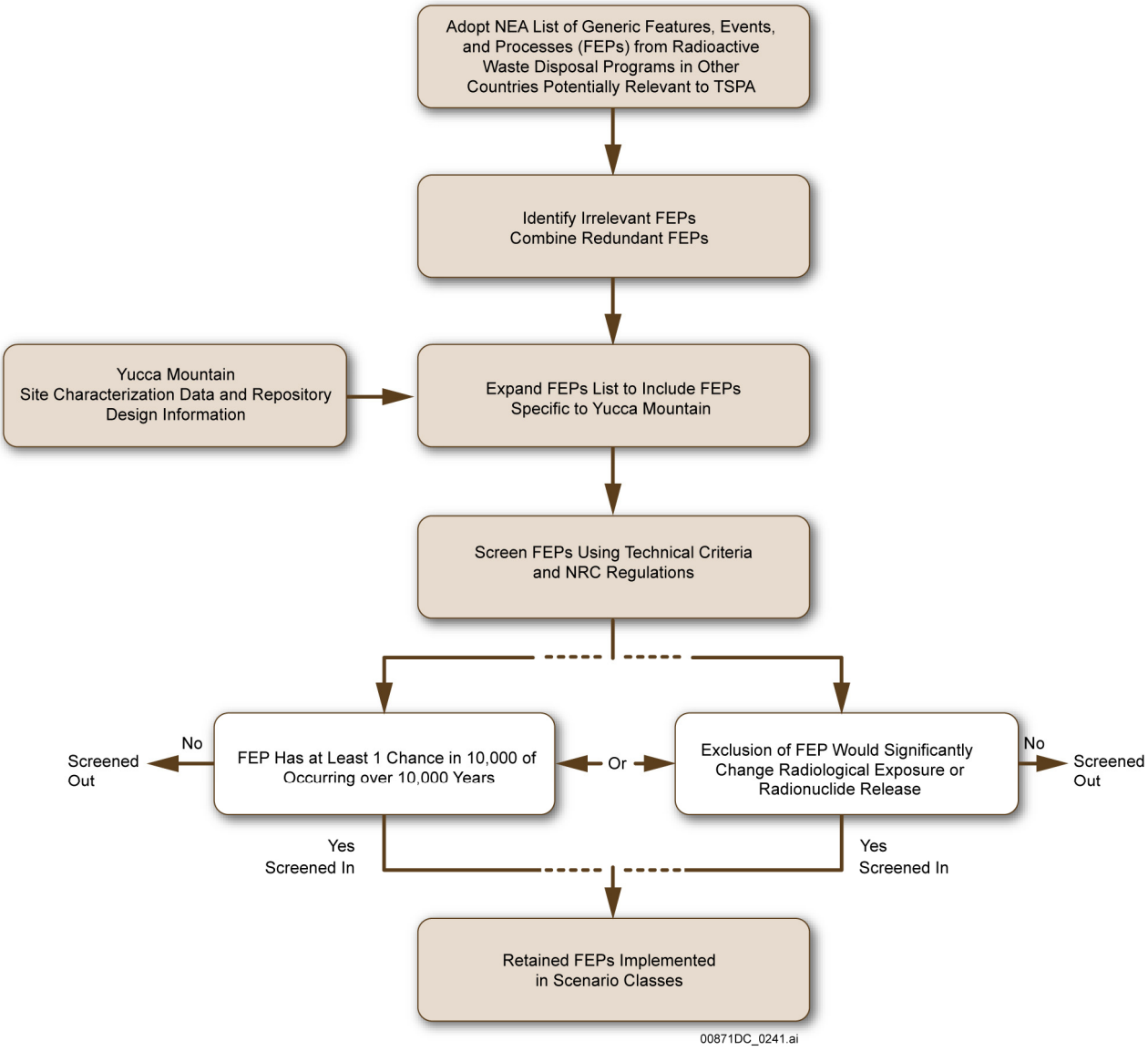

Source: SNL 2008 [DIRS 183478], Figure 6.1.1-2.

Figure 6-1. Schematic Illustration of the Features, Events, and Processes Analysis Method

Evaluation of the FEPs against the screening criteria may be done in any order. In practice, by-regulation criteria were examined first, and then either low probability or low consequence criteria were examined. FEPs that could not be excluded based on one criterion (e.g., regulatory guidance) were also considered against the other criteria (probability and consequence). Consequently, judgment regarding the order in which to apply the criteria did not affect the final decision. Choosing the most appropriate order to apply the criteria prevented needless work, such as developing quantitative probability arguments for low-consequence events or complex consequence models for low-probability events.

Exclusion of a FEP indicates exclusion with respect to each of the three different postclosure standards: Individual Protection, Individual Protection for Human Intrusion, and Groundwater

Protection (proposed 10 CFR 63.311 and 63.321 (70 FR 53313 [DIRS 178394]), and 10 CFR 63.331 [DIRS 180319], respectively). The justification for excluding a FEP may rely on more than one line of reasoning, but the primary basis for exclusion is presented as the overall basis. For example, FEP 1.5.01.01.0A (Meteorite Impact) is excluded on the basis of low probability because large, potentially consequential, impacts are shown to be very unlikely, but as discussed in detail in the screening justification, smaller impact events that may occur with an annual probability above one in 100 million are also shown to have a low consequence. An included FEP is included in the TSPA for one or more of the postclosure standards. If a FEP is included for some but not all of the standards (e.g., inadvertent human intrusion is included for Human Intrusion, excluded for the others), text in the FEP disposition statement will explicitly indicate which standards it is included for and why it is excluded from others. FEPs that are included for performance assessment for all standards are either simply described as included in the screening decision with no exclusion language in the FEP disposition or all three postclosure standards are specifically referenced.

As described in *Features, Events, and Processes for the Total System Performance Assessment: Methods* (SNL 2008 [DIRS 179476], Section 6.1.1), preliminary TSPA-LA FEP analyses were completed in 2005. Those analyses are described in *Development of the Total System Performance Assessment—License Application Features, Events, and Processes* (BSC 2005 [DIRS 173800]) and the results are contained in DTN: MO0508SEPFEPLA.002 [DIRS 175064]. Subsequent to those preliminary FEP analyses, new regulations and changes in the design of the repository and disposal packages occurred, necessitating a "reanalysis" of the FEPs.

This reanalysis involved a general reevaluation of the FEP list, integration of scope between FEPs, and a reanalysis of the FEP screening decisions and technical bases. The reanalysis included contributions from YMP subject matter experts, licensing and performance assessment team members, and external experts. The results of the current FEP screening are presented in Section 6.2 and summarized in Table 7-1.

Indirect inputs are cited to support the direct inputs and to provide background or ancillary information for the analyses. As with direct inputs, indirect inputs used in the individual FEP analyses are identified in a table for each FEP in Section 6.2. Similarly, indirect inputs used in the appendices can be found within those appendices. Indirect inputs applicable to the remainder of the report are provided in Table 6-1.

Table 6-1. Indirect Inputs

Citation	Title	DIRS
10 CFR 63	Energy: Disposal of High-Level Radioactive Wastes in a Geologic Repository at Yucca Mountain, Nevada	180319
70 FR 53313	Implementation of a Dose Standard After 10,000 Years	178394
BSC 2004	*Features, Events, and Processes: System Level*	170021
BSC 2004	*Clad Degradation – FEPs Screening Arguments*	170019
BSC 2004	*Waste-Form Features, Events, and Processes*	170020
BSC 2005	*Development of the Total System Performance Assessment-License Application Features, Events, and Processes*	173800
BSC 2005	*Engineered Barrier System Features, Events, and Processes*	175014
BSC 2005	*Evaluation of Features, Events, and Processes (FEP) for the Biosphere Model*	174107
BSC 2005	*Features, Events, and Processes in SZ Flow and Transport*	174190
BSC 2005	*Features, Events, and Processes in UZ Flow and Transport*	174191
BSC 2005	*Features, Events, and Processes: Disruptive Events*	173981
BSC 2005	*Screening of Features, Events, and Processes in Drip Shield and Waste Package Degradation*	174995
DTN: MO0508SEPFEPLA.002	LA FEP List and Screening (from 2005)	175064
SNL 2007	*Technical Work Plan for the Performance Assessment Features, Events, and Processes*	184327
SNL 2008	*Features, Events, and Processes for the Total System Performance Assessment: Methods*	179476
SNL 2008	*Screening Analysis of Criticality Features, Events, and Processes for License Application*	173869
SNL 2008	*Total System Performance Assessment Model/Analysis for the License Application*	183478

6.2 FEATURE, EVENT, AND PROCESS SCREENING ANALYSES

This section documents the individual FEP screening analyses for each of the 374 TSPA-LA FEPs. They are ordered numerically by FEP Number.

Each FEP contains the following information:

- **FEP**: The unique identification number assigned to the FEP.
- **FEP Name**: The title of the FEP.
- **FEP Description**: A detailed description of the scope of the FEP.

- **Screening Decision**: Identifies the screening decision for the FEP. Possible screening decisions are:

  - Included
  - Excluded – Low Probability
  - Excluded – Low Consequence
  - Excluded – By Regulation.

- **Screening Justification (Excluded FEPs only)**: Description of the technical basis for excluding the FEP from the TSPA.

- **TSPA Disposition (Included FEPs only)**: Description of how the FEP is included in the TSPA. If the FEP is excluded for one or more of the postclosure standards, a short justification is given for the exclusion relative to that standard.

- **Inputs**: Tables of direct and indirect inputs for the FEP.

This FEP identification and screening information, along with additional FEP source and traceability information, is cataloged in the electronic FEP database. The FEP database content is described in Appendix H. The database itself is in the YMP Technical Data Management System as technical product output (DTN: MO0706SPAFEPLA.001) and is a Microsoft Access database. The FEPs Viewer (STN: 611664-1.0-00 [DIRS 181089]) is useful, but not necessary, to utilize the database; however, it does provide a user-friendly interface for viewing data elements and their relationships.

FEP: 0.1.02.00.0A

FEP NAME:

Timescales of Concern

FEP DESCRIPTION:

This FEP addresses the timescales of concern over which the disposal system may present a significant health or environmental hazard.

SCREENING DECISION:

Included

TSPA DISPOSITION:

The timescales of concern have been set by the NRC in proposed 10 CFR Part 63 (70 FR 53313 [DIRS 178394]). Compliance with the individual protection standard after permanent closure (proposed 10 CFR 63.311 (70 FR 53313 [DIRS 178394])) and the individual protection standard for human intrusion (proposed 10 CFR 63.321 (70 FR 53313 [DIRS 178394])) must be demonstrated for the timescale of geologic stability. The period of geologic stability is defined in proposed 10 CFR 63.302 [DIRS 178394] as "the time during which the variability of geologic characteristics and their future behavior in and around the Yucca Mountain site can be bounded, that is, they can be projected within a reasonable range of possibilities. This period is defined to end at 1 million years after disposal." Compliance with the groundwater protection standard (10 CFR 63.331 [DIRS 180319]) must be demonstrated on a timescale of 10,000 years.

Proposed 10 CFR 63.303(a) (70 FR 53313 [DIRS 178394]) states that "Compliance is based upon the arithmetic mean of the projected doses from DOE's performance assessments for the period within 10,000 years after disposal" and proposed 10 CFR 63.303(b) (70 FR 53313 [DIRS 178394]) states that "Compliance is based upon the median of the projected doses from DOE's performance assessments for the period after 10,000 years of disposal and through the period of geologic stability…." This FEP is implemented at the model level in the TSPA model by simulations run for the appropriate time period and outputs were generated at the appropriate times (10,000 and 1,000,000 years, respectively).

INPUTS:

Table 0.1.02.00.0A-1. Indirect Inputs

Citation	Title	DIRS
10 CFR 63	Energy: Disposal of High-Level Radioactive Wastes in a Geologic Repository at Yucca Mountain, Nevada	180319
70 FR 53313	Implementation of a Dose Standard After 10,000 Years	178394

FEP: 0.1.03.00.0A

FEP NAME:

Spatial Domain of Concern

FEP DESCRIPTION:

This FEP addresses the spatial domain of concern over which the disposal system may present a significant health or environmental hazard.

SCREENING DECISION:

Included

TSPA DISPOSITION:

From a modeling perspective, the spatial domain of concern is a function of the scale of the analysis being performed. The extent of the spatial domain that is considered in different components of the TSPA model also depends on the phenomenon that is being considered. Individual model domains are described in the documentation of each component of the TSPA model and in individual model or analysis reports.

The spatial domain encompassed by the entire TSPA model extends vertically downwards from the land surface in the vicinity of the repository through the unsaturated zone, through the repository and into the saturated zone, and extends laterally away from the repository to the location of the RMEI.

The potential for environmental impact has been addressed in *Final Environmental Impact Statement for a Geologic Repository for the Disposal of Spent Nuclear Fuel and High-Level Radioactive Waste at Yucca Mountain, Nye County, Nevada* (DOE 2002 [DIRS 155970]) and in *TSPA Information Package for the Draft Supplemental Environmental Impact Statement* (SNL 2007 [DIRS 182846]). In the TSPA, for demonstrations of compliance with the individual protection standard after permanent closure (proposed 10 CFR 63.311 (70 FR 53313 [DIRS 178394])) and the individual protection standard for human intrusion (proposed 10 CFR 63.321 (70 FR 53313 [DIRS 178394])), the spatial domain in which there is a potential for a significant health hazard is primarily defined by the location of the RMEI. As specified in 10 CFR 63.312(a) [DIRS 180319], the RMEI:

> (a) Lives in the accessible environment above the highest concentration of radionuclides in the plume of contamination,

and according to 10 CFR 63.302 [DIRS 180319]:

> *Accessible environment* means any point outside of the controlled area,

and the controlled area is defined within 10 CFR 63.302 [DIRS 180319] as:

(1) The surface area, identified by passive institutional controls, that encompasses no more than 300 square kilometers. It must not extend farther:

(i) South than 36° 40′ 13.6661″ North latitude, in the predominant direction of ground-water flow; and

(ii) Than five kilometers from the repository footprint in any other direction; and

(2) The subsurface underlying the surface area.

The compliance location for the groundwater protection standards in 10 CFR 63.331 [DIRS 180319] is the representative volume in the accessible environment, which is defined in 10 CFR 63.332(a) [DIRS 180319].

Therefore, the spatial domain over which the disposal system may present a significant health or environmental hazard extends to approximately 18 km in the direction of groundwater flow (generally to the south) and over the whole of the controlled area (DTN: MO0712DELNPCCA.001 [DIRS 184172]) The postclosure area boundary includes a representative volume of groundwater in the accessible environment as defined in 10 CFR 63.332 (a) [DIRS 180319]. In summary, the spatial domain for the TSPA model is defined by specifying the spatial boundary conditions for the various models used in the performance assessment, and includes the region over which the disposal system may present a significant health or environmental hazard. In practical application, the spatial domain of concern in the TSPA includes the whole of the controlled area and extends to the location of the RMEI approximately 18 km south of the repository, and a representative volume of groundwater in the accessible environment.

INPUTS:

Table 0.1.03.00.0A-1. Indirect Inputs

Citation	Title	DIRS
10 CFR 63	Energy: Disposal of High-Level Radioactive Wastes in a Geologic Repository at Yucca Mountain, Nevada	180319
70 FR 53313	Implementation of a Dose Standard After 10,000 Years	178394
DOE 2002	*Final Environmental Impact Statement for a Geologic Repository for the Disposal of Spent Nuclear Fuel and High-Level Radioactive Waste at Yucca Mountain, Nye County, Nevada*	155970
DTN: MO0712DELNPCCA.001	Delineation of Postclosure Controlled Area	184172
SNL 2007	*TSPA Information Package for the Draft Supplemental Environmental Impact Statement*	182846

FEP: 0.1.09.00.0A

FEP NAME:

Regulatory Requirements and Exclusions

FEP DESCRIPTION:

This FEP addresses regulatory requirements and guidance specific to the Yucca Mountain repository.

SCREENING DECISION:

Included

TSPA DISPOSITION:

10 CFR Part 63 [DIRS 180319] and proposed 10 CFR 63 (70 FR 53313 [DIRS 178394]) are the NRC licensing regulations that provide the requirements for Yucca Mountain repository design, construction, operation, and preclosure and postclosure performance. These regulations adopt the three postclosure public health and environmental protection standards promulgated by the EPA in 40 CFR Part 197 [DIRS 155216] and proposed 40 CFR Part 197 [DIRS 105065], respectively. 10 CFR Part 63 [DIRS 180319] and proposed 10 CFR Part 63 (70 FR 53313 [DIRS 178394]) require performance assessments to demonstrate compliance with these postclosure radiation protection standards: individual protection standard of proposed 10 CFR Part 63.311 (70 FR 53313 [DIRS 178394]), the human intrusion individual protection standard (although optional in the regulations, the YMP has chosen to use a performance assessment to demonstrate compliance with the human intrusion individual radiation protection standard and groundwater protection standard) of proposed 10 CFR Part 63.321 (70 FR 53313 [DIRS 178394]), and groundwater protection standards of 10 CFR Part 63.331 [DIRS 180319]. The TSPA is the tool used to implement these performance assessments.

Current 10 CFR Part 63 [DIRS 180319] and proposed 10 CFR 63.114 and 63.342 (70 FR 53313 [DIRS 178394]) provide the criteria for the screening of FEPs to determine whether the FEP will be excluded from the TSPA model on the basis of either low probability, low consequence, or by regulation, or included in the TSPA. Included FEPs are used to construct the scenario classes that are evaluated by the TSPA.

NUREG-1804 (NRC 2003 [DIRS 163274]) provides guidance (acceptance criteria) to the NRC staff on how to assess the completeness and adequacy of the information in the DOE license application. The DOE has provided information in the license application to address the acceptance criteria. Therefore, although NUREG-1804 (NRC 2003 [DIRS 163274]) is not a regulatory requirement, the YMP has treated the acceptance criteria as important guidance for development of process models. There are other NUREGs relevant to and adopted by the YMP, including, but not limited to, for example, NUREG-1563, *Branch Technical Position on the Use of Expert Elicitation in the High-Level Radioactive Waste Program* (Kotra et al. 1996 [DIRS 100909]); NUREG-1297, *Peer Review for High-Level Nuclear Waste Repositories: Generic Technical Position* (Altman et al. 1988 [DIRS 103597]); and NUREG-1298,

Qualification of Existing Data for High-Level Nuclear Waste Repositories: Generic Technical Position (Altman et al. 1988 [DIRS 103750]).

The YMP has established regulatory guidance agreements (see BSC 2007 [DIRS 184446] and BSC 2007 [DIRS 184422]).

Management Plan for Development of the Yucca Mountain License Application (LA Management Plan) (ORD 2007 [DIRS 184800]) serves as the implementing document and governs License Application project activities necessary to achieve compliance with regulatory requirements. For example, the results of the performance assessments implemented with the TSPA will be described in the license application pursuant to *Management Plan for Development of the Yucca Mountain License Application* (ORD 2007 [DIRS 184800]).

The OCRWM Lead Laboratory for Repository Systems (Lead Lab) is responsible for postclosure science and performance assessment, including the TSPA. The Lead Lab receives its requirements from a variety of sources, including federal agency orders applicable to Sandia National Laboratories via its Prime Contract; also, via Programmatic Guidance letters from the OCRWM Contracting Officer's Representative. PI-PRO-005, *Requirements Management,* documents the requirements management process for the Lead Lab. Ongoing compliance with requirements is validated through a program of internal and external audits, surveillance, self-assessments, management assessments and/or peer reviews, as appropriate.

The current and proposed 10 CFR Part 63 ([DIRS 180319] and 70 FR 53313 [DIRS 178394]), respectively), as well as NUREG-1804 (NRC 2003 [DIRS 163274]), require a robust quality assurance program. The Lead Lab implements YMP *Quality Assurance Requirements Description* (QARD) (DOE 2007 [DIRS 182051]) and *Augmented Quality Assurance Program (AQAP)* (DOE 2006 [DIRS 177173]) through its procedures (e.g., SCI-PRO-001 *Qualification of Unqualified Data*; SCI-PRO-002, *Planning for Science Activities*; SCI-PRO-003, *Document Review*; SCI-PRO-004, *Managing Technical Product Inputs*; SCI-PRO-005, *Scientific Analyses and Calculations*; and SCI-PRO-006, *Models*).

The technical basis for the license application is based upon reports that have been produced in compliance with these and other requisite quality assurance procedures. These reports discuss the technical basis of specific areas of postclosure science, notably process models. Process models describe the expected future behavior of the repository. Parameters used in the process models reflect relevant FEPs that have been included in the process models and in the TSPA. The process models are abstracted, and the abstractions used, along with other submodels, in the TSPA model to demonstrate compliance with the radiation and groundwater protection standards of current and proposed 10 CFR Part 63 ([DIRS 180319] and 70 FR 53313 [DIRS 178394], respectively).

In conclusion, the TSPA addresses and complies with all applicable postclosure regulatory requirements and guidance.

INPUTS:

Table 0.1.09.00.0A-1. Indirect Inputs

Citation	Title	DIRS
10 CFR 63	Energy: Disposal of High-Level Radioactive Wastes in a Geologic Repository at Yucca Mountain, Nevada	180319
64 FR 46976	Environmental Radiation Protection Standards for Yucca Mountain, Nevada	105065
66 FR 32074	40 CFR Part 197, Public Health and Environmental Radiation Protection Standards for Yucca Mountain, NV; Final Rule	155216
70 FR 53313	Implementation of a Dose Standard After 10,000 Years	178394
Altman et al. 1988	*Peer Review for High-Level Nuclear Waste Repositories: Generic Technical Position*	103597
Altman et al. 1988	*Qualification of Existing Data for High-Level Nuclear Waste Repositories: Generic Technical Position*	103750
BSC 2007	*Regulatory Guidance Agreement, Agreement for NUREG/CR 5485, November, 1998, Guidelines on Modeling Common-Cause Failures in Probabilistic Risk Assessment*	184422
BSC 2007	*Regulatory Guidance Agreement, Agreement for NUREG-1297, February 1988, Peer Review for High Level Nuclear Waste Repositories - Generic Technical Position*	184446
DOE 2006	*Augmented Quality Assurance Program (AQAP)*	177173
DOE 2007	*Quality Assurance Requirements and Description*	182051
Kotra et al. 1996	*Branch Technical Position on the Use of Expert Elicitation in the High-Level Radioactive Waste Program*	100909
NRC 2003	*Yucca Mountain Review Plan, Final Report*	163274
ORD 2007	*Management Plan for Development of the Yucca Mountain License Application*	184800

FEP: 0.1.10.00.0A

FEP NAME:

Model and Data Issues

FEP DESCRIPTION:

This FEP addresses issues related to modeling of the disposal system. Model and data issues are general (i.e., methodological) issues affecting the modeling process and data usage. Model issues include the approach and assumptions associated with the selection of conceptual models, the mathematical implementation of conceptual models, model geometry and dimensionality, models of coupled processes, and boundary and initial conditions. Data issues include the derivation of data values, correlations, and dependence of parameter selection on model scale.

SCREENING DECISION:

Included

TSPA DISPOSITION:

The representation of models and data in the TSPA will be detailed in *Total System Performance Assessment Model/Analysis for the License Application* (SNL 2008 [DIRS 183478]). This document will describe the method, structure, validation or confidence building, and application of a computational model of the performance of the repository system, the TSPA model. The TSPA model draws together data from numerous sources in order to evaluate the ability of the repository to adequately isolate nuclear waste in accordance with NRC regulations set out in proposed 10 CFR 63.114(a)(1)(2) and (3) (70 FR 53313 [DIRS 178394]). These state that any performance assessment used to demonstrate compliance with 10 CFR 63.113 [DIRS 180319] must:

(1) Include data related to the geology, hydrology, and geochemistry (including disruptive processes and events) of the Yucca Mountain site, and the surrounding region to the extent necessary, and information on the design of the engineered barrier system used to define, for 10,000 years after disposal, parameters and conceptual models used in the assessment.

(2) Account for uncertainties and variabilities in parameter values, for 10,000 years after disposal, and provide for the technical basis for parameter ranges, probability distributions, or bounding values used in the performance assessment.

(3) Consider alternative conceptual models of features and processes, for 10,000 years after disposal, that are consistent with available data and current scientific understanding and evaluate the effects that alternative conceptual models have on the performance of the geologic repository.

In addition, proposed 10 CFR 63.114(a)(7) (70 FR 53313 [DIRS 178394]) states that the performance assessment must:

> (7) Provide the technical basis for models used to represent the 10,000 years after disposal in the performance assessment, such as comparisons made with outputs of detailed process-level models and/or empirical observations (e.g., laboratory testing, field investigations, and natural analogs).

The TSPA model will evaluate the performance of engineered and natural components of the Yucca Mountain repository system for the expected natural conditions prevailing at the Yucca Mountain site. The expected natural conditions (referred to as the nominal scenario class) were derived by considering FEPs potentially relevant to the long-term performance of a waste-disposal repository.

METHODOLOGY

The general performance assessment process adopted by the DOE follows the methodology developed by Cranwell et al. (1990 [DIRS 101234], Sections 2 and 3). Over time, the methodology has been enhanced, including input from the NRC, and applied to numerous projects by various international organizations involved in radioactive waste management. Previous performance assessments and related supplemental analyses of the performance of the Yucca Mountain repository were conducted to meet various regulatory milestones, following the publication of the Nuclear Waste Policy Amendments Act of 1987, Public Law No. 100-203 [DIRS 100016]. The Yucca Mountain performance assessments have been iterative, with each succeeding performance assessment building on and extending the scope and results of the previous performance assessments by incorporating both an improved understanding of the processes affecting performance and, through additional field observations and laboratory analyses, better identification and quantification of the parameters used in the TSPA models. The current TSPA model is built on the foundation of those earlier performance assessments and has been enhanced by updated analyses of the processes affecting Yucca Mountain, new proposed regulations, and the design elements of the repository, including a comprehensive consideration of the FEPs that are relevant to repository system performance (SNL 2008 [DIRS 183478]).

The foundation and first stage of the performance assessment consists of a system characterization involving assimilation of the information collected by scientists and engineers involved in site characterization and engineering design. The repository system and site characterization provides information regarding waste properties, facility design, regional geology, regional hydrology, and environmental characteristics of the Yucca Mountain site. Design TSPA data input packages (SNL 2007 [DIRS 179394], SNL 2007 [DIRS 179567], SNL 2007 [DIRS 179354], and SNL 2007 [DIRS 179466]) are used to provide EBS component parameters for conceptual models used in performance assessment. The foundation represents the more than 20-year body of knowledge, collected in the field and in the laboratory, regarding the Yucca Mountain repository system. These data were used to identify the set of possible FEPs that may be part of and affect the performance of the repository system. The second stage of the performance assessment methodology consists of the development and testing of process models that include the retained FEPs, and their outcomes regarding repository performance.

The process models consist of sets of hypotheses, assumptions, simplifications, and idealizations that, together, describe the essential aspects of a system or subsystem of the repository relative to performance. An example of such a process model is one that describes the movement of water and dissolved radionuclides by diffusive flow in rock pores or by advective flow in fracture openings in the unsaturated bedrock surrounding the repository and through the saturated zone below the repository. Because the performance assessment methodology deals with future outcomes and includes uncertainty in both descriptions of processes and parameter values, an essential element of the performance assessment methodology is to capture uncertainty in probabilistic analyses that represent expected outcomes, based on the best available values of process model parameters and the processes involved.

The third stage of the methodology involves the development of abstraction models. These abstractions are progressive representations of the detailed models of physical and chemical processes to more compact, efficient numerical models. Abstractions consist of statistical or mathematical abstractions, including look-up tables, equations representing response surfaces, probability distributions, linear transfer functions, or reductions of model dimensionality. The abstractions used to analyze the projected evolution through time of the various components of the repository system are compact but still capture the salient features of the process models, along with their associated uncertainties.

The outputs of both the process models and their abstractions are subject to confidence-building activities as part of the model development process. These confidence-building activities include comparisons of output with alternative process models or with empirical observations, such as results from laboratory testing, field investigations, and natural analogues. These comparisons strengthen confidence in the technical basis for the models used in the performance assessment.

The last stage of the performance assessment consists of the integrated total system models. The total system model is a numerical model that is used to simulate the integrated behavior of the entire Yucca Mountain repository system. The TSPA model incorporates the abstracted detailed models that describe the TSPA model components, and their submodels, from their development to their implementation, including information from the analysis and model reports. The abstractions and associated process models and submodels describing various repository attributes in a series of analysis and model reports form the technical basis for the TSPA model.

Use of the TSPA model to simulate Yucca Mountain repository behavior and project future outcomes is aided by the development of scenario classes to assist in the analysis of repository performance and provide the framework for the TSPA model analyses. The TSPA model is structured to address a specific set of scenario classes that span the range of possible FEPs for both expected conditions and disruptive events. The TSPA model scenario classes include the nominal scenario class, the early failure scenario class, two disruptive event scenario classes, the igneous scenario class and the seismic scenario class, and a human intrusion scenario.

Features, Events, and Processes Analysis

The development of the TSPA model for the Yucca Mountain repository system includes an analysis and screening of the FEPs that could affect repository performance after closure. The results of the FEPs analyses led to the development of process models and abstractions that

address the attributes necessary to allow the TSPA model to assess repository safety and determine whether or not the repository meets regulatory standards. These process models and their abstractions considered FEPs that could affect the Yucca Mountain repository system and, in turn, FEPs that could be affected by the presence of the repository.

Development of the Scenario Classes

A scenario is a well-defined, connected sequence of FEPs that describes a possible future condition of the repository system. A scenario class is a set of related scenarios that share sufficient similarities that they can usefully be aggregated for the purposes of screening or analysis. The objective of scenario development for the TSPA-LA model is to define a limited set of scenario classes that are representative of the range of future FEPs that are potentially relevant to the licensing of the facility.

The TSPA approach focuses on a set of scenario classes that are distinguished by initiating events. The nominal scenario class includes all possible future outcomes except those initiated by early failure of the drip shields or waste packages, igneous or seismic activity, and inadvertent human intrusion into the repository. The igneous scenario class includes all possible future outcomes initiated by igneous activity. The seismic scenario class includes all possible future outcomes initiated by seismic activity. In addition to the analyses of the scenario classes, the TSPA model also simulates a human intrusion scenario according to the scenario and criteria described in 10 CFR 63.322 [DIRS 180319].

Incorporation of Uncertainty

Uncertainty and variability in the expected behavior of the Yucca Mountain repository system requires that the performance assessment analyses be probabilistic in order to capture the full range of potential outcomes.

Uncertainty in the TSPA model is characterized as either epistemic or aleatory uncertainty where:

- **Epistemic Uncertainty,** also referred to as "reducible" uncertainty, concerns the state of uncertainty in knowledge about a parameter value due to limited data or alternative interpretations of the available data. Epistemic uncertainty can be reduced, in principle, using the results of experimental testing and additional data collection. However, given the complexity of nature and the variability observed over time and space in natural phenomena, there are practical limits below which many uncertainties cannot be reduced. Neither is their reduction necessary once there is a sound technical basis for finding that a proposed system is expected to be sufficiently safe to allow moving forward to the next phase of its development. Scientific work continues at a significant level until the final closure and sealing of the repository, allowing safety evaluations to be informed by new information and repeated in advance of subsequent decision-points in the repository life.

- **Aleatory Uncertainty,** also referred to as "irreducible" uncertainty, concerns whether or not there is a chance occurrence of a FEP. No amount of exploratory work will allow determining whether or not a chance event will or will not occur at any given time, but determining a range of likelihoods of occurrence for a given timeframe is generally supportable through using various formalized means for combining scientific insights from experts in the field.

The TSPA model utilizes multiple realizations to calculate future outcomes using distributions of values for uncertain parameters that may be important to performance, rather than deterministic or single-value calculations for each parameter in the repository system. The model realizations are performed using various combinations of parameter values obtained from the parameter-value distributions in the TSPA input database, where each of the combinations of parameter values is representative of a subset of the full range of potential outcomes. These probabilistic analyses thus reflect an appropriate range of process behaviors or parameter values, or both, of the inherently variable Yucca Mountain repository system, given that complete knowledge of the system is not attainable.

Alternative Conceptual Models

A conceptual model is a set of working hypotheses and assumptions that provide an acceptable description of a system for its intended purpose. Because the performance assessment process deals with future outcomes and includes uncertainty in both process descriptions and parameter values, there may be alternative conceptual models that provide reasonable descriptions of a particular system or subsystem. Considering alternative conceptual models helps build confidence that plausible changes in modeling assumptions or simplifications will not change conclusions regarding subsystem and total-system performance. The model development process includes evaluations of alternative conceptual models, where appropriate. For example, the development of the EBS physical and chemical environment process model included consideration of an alternate initial water chemistry and the potential effect of feldspar equilibrium on seepage water composition, and the potential for carbonate exchange to affect CO_2 composition in the unsaturated zone. These alternative conceptual models were considered but not incorporated in the EBS physical and chemical environment process model.

Because alternative conceptual models must be compatible with known data and established facts, their number is limited. Typically, when two or more models exist for the same phenomena and data, the more conservative one from a total-system perspective has been chosen for implementation. Another approach is to assign probabilities to each alternative conceptual model and probabilistically bring them into the calculations according to their relative frequencies, but this approach places a greater demand on knowledge and adds complexity that is avoided by the more conservative approach.

Data, analysis and model reports, as well as the TSPA, have been developed per procedures which are compliant with *Quality Assurance Requirements and Description* (DOE 2007 [DIRS 182051]). These requirements and the procedures that implement them were developed to ensure adequate treatment of models and data, including the selection of conceptual models, the mathematical implementation of conceptual models, model geometry and dimensionality,

and boundary and initial conditions, as well as data values, correlations, and dependence of parameter selection on model scale.

INPUTS:

Table 0.1.10.00.0A-1. Indirect Inputs

Citation	Title	DIRS
10 CFR 63	Energy: Disposal of High-Level Radioactive Wastes in a Geologic Repository at Yucca Mountain, Nevada	180319
70 FR 53313	Implementation of a Dose Standard After 10,000 Years	178394
Cranwell et al. 1990	*Risk Methodology for Geologic Disposal of Radioactive Waste, Scenario Selection Procedure*	101234
DOE 2007	*Quality Assurance Requirements and Description*	182051
Nuclear Waste Policy Amendments Act of 1987	Public Law No. 100-203, 101 Stat. 1330	100016
SNL 2007	*Total System Performance Assessment Data Input Package for Requirements Analysis for EBS In-Drift Configuration*	179354
SNL 2007	*Total System Performance Assessment Data Input Package for Requirements Analysis for DOE SNF/HLW and Navy SNF Waste Package Overpack Physical Attributes Basis for Performance Assessment*	179567
SNL 2007	*Total System Performance Assessment Data Input Package for Requirements Analysis for Subsurface Facilities*	179466
SNL 2007	*Total System Performance Assessment Data Input Package for Requirements Analysis for TAD Canister and Related Waste Package Overpack Physical Attributes Basis for Performance Assessment*	179394
SNL 2008	*Total System Performance Assessment Model/Analysis for the License Application*	183478

FEP: 1.1.01.01.0A

FEP NAME:

Open Site Investigation Boreholes

FEP DESCRIPTION:

Site investigation boreholes that have been left open, degraded, improperly sealed, or reopened, could modify flow and transport properties and produce enhanced pathways between the surface and the repository.

SCREENING DECISION:

Excluded – low consequence

SCREENING JUSTIFICATION:

The potential impact of site-investigation boreholes on repository performance depends on the location and depth of the boreholes and the properties of the borehole seals. Site investigation boreholes are to be backfilled and plugged according to the Nevada Administrative Code (NAC) at NAC 534.4371 [DIRS 151873]. The hydrologic and transport characteristics of backfilled and plugged boreholes may not be the same as the natural rock formation. However, due to the predominantly vertical flow patterns in the unsaturated zone (BSC 2004 [DIRS 169734], Section 7), only boreholes within or close to the repository block could potentially affect repository performance. Boreholes well outside the footprint of the repository block (more than 300 m) will not influence water movement to the waste emplacement drifts or radionuclide transport from the waste emplacement drifts to the water table. Table 1.1.01.01.0A-1 lists eight deep boreholes in the repository block and seven deep boreholes near the repository block. The locations of these boreholes relative to waste emplacement locations are referenced in *Total System Performance Assessment Data Input Package for Requirements Analysis for Subsurface Facilities* (SNL 2007 [DIRS 179466], Table 4-1, Parameter Number 01-03). A deep borehole in the repository block is a borehole that penetrates the TSw (Topopah Spring welded hydrogeologic unit). A deep borehole near the repository block is a borehole that penetrates below the elevation of waste emplacement (DTNs: MO9906GPS98410.000 [DIRS 109059] and MO0004QGFMPICK.000 [DIRS 152554]; SNL 2007 [DIRS 179466], Table 4-1, Parameter Number 01-01).

Boreholes that terminate in or above the PTn (Paintbrush Tuff nonwelded hydrogeologic unit) will have a negligible effect on percolation flux at the repository because flow through these boreholes will be homogenized by matrix flow in the underlying Paintbrush nonwelded hydrogeologic unit relative to spatial variability of infiltration (SNL 2007 [DIRS 184614], Section 6.1.2[a]).

Table 1.1.01.01.0A-1. Deep Boreholes in or Close to the Repository Block

Borehole Identifier	Surface Elevation (feet)	Lowest Stratigraphic Contact Depth (feet)[a] (except as noted)	Tptpv3[b] Depth (feet)[a] (except as noted)	Nominal Borehole Diameter (inches)[c]	Nevada State Plane Easting (feet)	Nevada State Plane Northing (feet)
UE-25 WT #18[d]	4,384	1,620	1,501	8.75[e]	564,855	771,167
USW G-1[f]	4,350	3,558	1,287	3.875[g]	561,001	770,502
USW G-4[d]	4,166	2,950	1,317	12.25[h]	563,082	765,808
USW H-1[f]	4,274	3,661	1,410	13.25[i]	562,388	770,255
USW H-5[f]	4,851	3,422	1,582	14.75[j]	558,908	766,634
USW NRG-7a[d]	4,207	1,498	1,415	5.5[k]	562,984	768,880
USW SD-7[f]	4,472	2,612	1,182	8.75[l]	561,240	758,950
USW SD-9[f]	4,273	2,016	1,358	8.5[m]	561,818	767,998
USW SD-12[f]	4,343	2,138	1,278	12.25[n]	561,606	761,957
USW UZ-1[f]	4,425	1,145	983[o]	17.5[p]	560,222	771,277
USW UZ-6[d]	4,925	1,829	1,333	17.5[q]	558,325	759,730
USW UZ-7a[d]	4,228	759[r]	632[o]	12.25[s]	562,270	760,693
USW UZ-14[f]	4,425	2,072	1,279	12.25[t]	560,142	771,310
USW WT-2[d]	4,268	1,794	1,179	8.75[u]	561,924	760,662
USW SD-6[d]	4,905[v]	2,506[w]	1,456[w]	12.25[x]	558,608[v]	762,421[v]

Source: DTN: MO9906GPS98410.000 [DIRS 109059], except where other source noted; Nevada State Plane easting and northing and elevation values have been rounded to the nearest foot.

[a] DTN: MO0004QGFMPICK.000 [DIRS 152554], designates borehole UE-25 WT#18 as USW WT#18.
[b] BSC 2004 [DIRS 169855], Table 6-5, top contact of Tptpv3, or lower contact of Tptpln; SNL 2007 [DIRS 179466], Table 4-1, Parameter Number 01-01, Tptpln is the lowest stratigraphic unit that was identified for waste emplacement. The Tptpv3 lies immediately below the Tptpln.
[c] Based on drill bit size used to create borehole in the repository host rock.
[d] Close to repository block.
[e] Fenix & Scisson 1986 [DIRS 101238], p. 63.
[f] In repository block.
[g] Fenix & Scisson 1987 [DIRS 103102], p. 3.
[h] Fenix & Scisson 1987 [DIRS 103102], p. 109.
[i] Fenix & Scisson 1987 [DIRS 126415], p. 3.
[j] Fenix & Scisson 1987 [DIRS 126415], p. 51.
[k] DTN: TMUSWNRG7A0096.002 [DIRS 166424], MOL.19971023.0323, Attachment VII.
[l] CRWMS M&O 1996 [DIRS 129957], p. 13.
[m] CRWMS M&O 1996 [DIRS 114799], p. 11.
[n] DTN: TM000000SD12RS.012 [DIRS 105627], DRC.19960926.0090, p. 14.
[o] SNL 2007 [DIRS 179466], Table 4-1, Parameter Number 01-01, nearest repository waste emplacement depth; shows USW UZ-7a is close to drift 2-19. Elevation of drift 2-19 is subtracted from the surface elevation for USW UZ-7a given above to give the depth to waste emplacement and shows that USW UZ-1 is close to drift 3-11W. Elevation of drift 3-11W from drawings 800-IED-WIS0-01701-000-00C and 800-IED-WIS0-01801-000-00C is subtracted from the surface elevation for USW UZ-1 to give the depth to waste emplacement.
[p] Fenix & Scisson 1987 [DIRS 165939], p. 3.
[q] Fenix & Scisson 1987 [DIRS 165939], p. 35.
[r] DTN: MO0010CPORGLOG.003 [DIRS 155959], Table S00148.013, maximum depth of borehole data.
[s] CRWMS M&O 1996 [DIRS 130425], p. 2.
[t] CRWMS M&O 1996 [DIRS 130429], p. 9.
[u] Fenix & Scisson 1986 [DIRS 101238], p. 75.
[v] DTN: MO9912GSC99492.000 [DIRS 165922].
[w] DTN: SNF40060298001.001 [DIRS 107372].
[x] YMP 1999 [DIRS 166080], Attachment 8.

Based on the design layout (SNL 2007 [DIRS 179466], Table 4-1, Parameter Number 01-01) and borehole locations in Table 1.1.01.01.0A-1, no waste emplacement drifts are expected to intersect existing boreholes. Water entering these boreholes would continue to flow through the boreholes to the water table, bypassing waste emplacement locations. Therefore, boreholes will not produce significant enhanced pathways for flow and transport between the surface and waste package emplacement locations.

The potential impact of boreholes on radionuclide migration between the repository and the water table may be assessed by considering the range of permeabilities for open boreholes and the fracture network. Fractures and faults represent continuous rapid-transport pathways from the repository to the water table as discussed in included FEP 2.2.07.08.0A (Fracture Flow in the UZ). Lateral flow beneath the repository eventually could encounter one of these high-permeability pathways to the water table. The principal difference between these high-permeability pathways and boreholes is that the cross-sectional area of the boreholes available to intercept lateral flow is much smaller than the area associated with fractures and faults. The 15 boreholes in Table 1.1.01.01.0A-1 with depths greater than 1,000 ft present a total cylindrical area (available to intercept lateral flow) per unit depth equal to πdN, where d is the average borehole diameter, conservatively estimated to be 1 m on the basis that the borehole diameter can exceed the size of the drill bit, and N is the number of boreholes. This gives a total borehole sidewall area of 15π m^2/m. The fractured rock between the repository and the water table has an average fracture area per unit volume of at least 0.1 m^2/m^3 (BSC 2004 [DIRS 170038], Table 6-5). Multiplying this by the 5×10^6 m^2 footprint of the repository (SNL 2007 [DIRS 179466], Table 4-1, Parameter Number 01-01) gives a minimum fracture area per unit depth of about 5×10^5 m^2/m. Therefore, the contribution of open boreholes to the flow and transport pathways between the repository and the water table would be negligible compared to that of the fracture network.

Perched water zones, which could also contain radionuclides, may flow through the boreholes. The closure requirements relative to boreholes requires that they are backfilled; however, there are no requirements to make the boreholes impermeable or barriers to flow. Therefore, perched water in contact with the boreholes may be expected to flow along these pathways, which would also carry any dissolved radionuclides contained in the perched water. Although transport may be relatively rapid to the water table through the borehole pathways, an analysis of transport times has been conducted under the assumption that the borehole pathways do not exist (SNL 2008 [DIRS 184748], Section 6.6.2.1 and Appendix D). This analysis demonstrates that transport times for radionuclides released in the northern section of the repository, where large perched water bodies are present, are generally less than 100 years, particularly for the glacial-transition climate that dominates the 10,000 years after repository closure (SNL 2008 [DIRS 184748], Figures D.1-1 through D.1-3). Furthermore, sensitivity analyses for the effects of sorption on neptunium and plutonium radionuclide transport show that changes in sorption for rock units below perched water (mainly the Calico Hills rock units) have little effect on transport, whereas changes in sorption for the Topopah Spring rock units (which comprise the rock between the repository and perched water bodies) have pronounced effects on transport behavior (SNL 2007 [DIRS 177396], Figures 6-37 and 6-44). This result indicates that transport below the perched water bodies has relatively less interaction with the rock matrix as compared with transport through the Topopah Spring rock units, hence transport from perched water levels

to the water table, dominated by transport through faults, is relatively fast compared with transport from the repository to the perched water. Any reduction in travel time associated with radionuclide transport through borehole pathways (rather than fault pathways) would have a negligible effect on performance because travel times through this part of the unsaturated zone are primarily a result of transport between the repository and perched water locations; regardless of the borehole pathways, transport times between perched water zones and the water table are relatively smaller than transport times to those zones.

The borehole closure requirement is to backfill all but the upper 10 ft of a borehole, where a 10-ft cement plug is installed per NAC 534.4371 [DIRS 151873]. If the cement plug is intact, the low permeability of the cement will limit infiltration. If the cement plug should crack, it would not be substantially different than the fractured rock or soil in which it resides, particularly given the very small amount of ground surface area represented by boreholes (on the order of 1 ft in diameter; see Table 1.1.01.01.0A-1). Therefore, boreholes should not play a significant role for infiltration.

Existing test boreholes drilled in the underground facility could provide potential water flow and radionuclide transport pathways. However, these boreholes are all relatively short (they do not penetrate multiple hydrogeologic units) and are only present in access drifts, niches, and alcoves (BSC 2004 [DIRS 170004], Sections 6.1 through 6.12), not in the waste emplacement drifts. Therefore, these boreholes will have no significant effect on radionuclide transport between the repository and the water table. The potential effects of any holes that may be drilled in the waste emplacement drifts are discussed in excluded FEP 1.1.01.01.0B (Influx through Holes Drilled in Drift Wall or Crown).

In summary, site investigation boreholes are expected to be backfilled and plugged but will not prevent water movement into or through the boreholes. However, the boreholes are not expected to produce significant enhanced pathways for flow between the ground surface and the repository or for flow and radionuclide transport between the repository and the water table. Based on the previous discussion, omission of FEP 1.1.01.01.0A (Open Site Investigation Boreholes) will not result in a significant adverse change in the magnitude or timing of either radiological exposures to the RMEI or radionuclide releases to the accessible environment. Therefore, this FEP is excluded from the performance assessments conducted to demonstrate compliance with proposed 10 CFR 63.311 and 63.321 (70 FR 53313 [DIRS 178394]), and with 10 CFR 63.331 [DIRS 180319], on the basis of low consequence.

INPUTS:

Table 1.1.01.01.0A-2. Direct Inputs

Input	Source	Description
DTN: MO9912GSC99492.000. Surveyed USW SD-6 As-Built Location. [DIRS 165922]	TDMS-GI link to *MO9912GSC99492.000.doc*	Elevation of borehole USW SD-6
DTN: MO0004QGFMPICK.000. Lithostratigraphic Contacts from MO9811MWDGFM03.000 to be Qualified Under the Data Qualification Plan, TDP-NBS-GS-000001. [DIRS 152554]	Table S00214_001	Stratigraphic information for boreholes
DTN: MO0010CPORGLOG.003. Calculated Porosity Values at Depth Derived from Qualified Geophysical Log Data from Modern Boreholes. [DIRS 155959]	Table S00148_013	Maximum depth of borehole data
DTN: SNF40060298001.001. Unsaturated Zone Lithostratigraphic Contacts in Borehole USW SD-6. [DIRS 107372]	Table S98430_001	Depth of borehole USW SD-6
SNL 2007. *Total System Performance Assessment Data Input Package for Requirements Analysis for Subsurface Facilities.* [DIRS 179466]	Table 4-1, Parameter Number 01-01	Repository footprint design layout
	Table 4-1, Parameter Number 01-03	Locations of boreholes relative to waste emplacement locations

Table 1.1.01.01.0A-3. Indirect Inputs

Citation	Title	DIRS
10 CFR 63	Energy: Disposal of High-Level Radioactive Wastes in a Geologic Repository at Yucca Mountain, Nevada	180319
70 FR 53313	Implementation of a Dose Standard After 10,000 Years	178394
BSC 2004	*Analysis of Hydrologic Properties Data*	170038
BSC 2004	*Development of Numerical Grids for UZ Flow and Transport Modeling*	169855
BSC 2004	*In Situ Field Testing of Processes*	170004
BSC 2004	*Yucca Mountain Site Description*	169734
CRWMS M&O 1996	*Forensic Evaluation of Geophysical Log Data for Borehole USW SD-7 in Support of the Yucca Mountain Site Characterization Project*	129957
CRWMS M&O 1996	*Forensic Evaluation of Geophysical Log Data for Borehole USW SD-9 in Support of the Yucca Mountain Site Characterization Project*	114799
CRWMS M&O 1996	*Forensic Evaluation of Geophysical Log Data for Borehole USW SZ-7a in Support of the Yucca Mountain Site Characterization Project*	130425
CRWMS M&O 1996	*Forensic Evaluation of Geophysical Log Data for Borehole USW UZ-14 in Support of the Yucca Mountain Site Characterization Project*	130429

Table 1.1.01.01.0A-3. Indirect Inputs (Continued)

Citation	Title	DIRS
DTN: MO9906GPS98410.000	Yucca Mountain Project (YMP) Borehole Locations	109059
DTN: TM000000SD12RS.012	USW SD-12 Composite Borehole Log (0	105627
DTN: TMUSWNRG7A0096.002	Geophysical Logs for Borehole USW NRG-7/7A	166424
Fenix & Scisson 1986	*NNWSI Hole Histories, UE-25 WT #3, UE-25 WT #4, UE-25 WT #5, UE-25 WT #6, UE-25 WT #12, UE-25 WT #13, UE-25 WT #14, UE-25 WT #15, UE-25 WT #16, UE-25 WT #17, UE-25 WT #18, USW WT-1, USW WT-2, USW WT-7, USW WT-10, USW WT-11*	101238
Fenix & Scisson 1987	*NNWSI Hole Histories, USW G-1, USW G-2, USW G-3, USW G-4, USW GA-1, USW GU-3*	103102
Fenix & Scisson 1987	*NNWSI Hole Histories, USW H-1, USW H-3, USW H-4, USW H-5, USW H-6*	126415
Fenix & Scisson 1987	*NNWSI Hole Histories, USW UZ-1, UE-25 UZ #4, UE-25 UZ #5, USW UZ-6, USW UZ-6s, USW UZ-7, USW UZ-8, USW UZ-13*	165939
NAC 534	Underground Water and Wells	151873
SNL 2007	*Radionuclide Transport Models Under Ambient Conditions*	177396
SNL 2007	*UZ Flow Models and Submodels*	184614
SNL 2008	*Particle Tracking Model and Abstraction of Transport Processes*	184748
SNL 2008	*Saturated Zone Flow and Transport Model Abstraction*	183750
YMP 1999	*Borehole USW SD-6*	166080

FEP: 1.1.01.01.0B

FEP NAME:

Influx Through Holes Drilled in Drift Wall or Crown

FEP DESCRIPTION:

Holes may be drilled through the drift walls or crown for a variety of reasons including, but not limited to, rock bolt and ground support, monitoring and testing, or construction related activities. These openings may promote flow or seepage into the drifts and onto the waste packages.

SCREENING DECISION:

Excluded – low consequence

SCREENING JUSTIFICATION:

The boreholes drilled through the walls of emplacement drifts are designed for rock bolts and ground support (SNL 2007 [DIRS 179354], Table 4-1, Parameter 01-15). Other activities such as monitoring, testing, or construction, will not require drilling through drift walls. Detailed simulations have been made using the predictive seepage model for performance assessment (BSC 2004 [DIRS 167652], Sections 6.5 and 6.6.4) to study the effect of rock bolt boreholes extending vertically upward from the drift crown. In a sensitivity analysis, several combinations of capillarity and permeability were examined, including cases representing both grouted and ungrouted boreholes. According to the simulation results (BSC 2004 [DIRS 167652], Section 6.6.4 and Table 6-4), these features were found to have only a minor effect on seepage, increasing the predicted seepage rates by less than 2% compared to seepage simulations without rock bolts. This result is understandable considering that: (1) an open borehole without grout acts as a capillary barrier to unsaturated flow, (2) the cross-sectional area of the rock bolt borehole, onto which flow may be incident, is small, and (3) water that may have seeped into the borehole can imbibe back into the rock along its length. Note that only ungrouted boreholes will be used in emplacement drifts (SNL 2007 [DIRS 179354], Table 4-1, Parameter Numbers 01-15 and 01-16). From these results, the presence of boreholes drilled in drift wall or crown is not considered to have significant impact on seepage into drifts.

Based on the above discussion, omission of FEP 1.1.01.01.0B (Influx through Holes Drilled in Drift Wall or Crown) will not result in a significant adverse change in the magnitude or time of radiological exposures to the RMEI or radionuclide releases to the accessible environment. Therefore, this FEP is excluded from the performance assessments conducted to demonstrate compliance with proposed 10 CFR 63.311 and 63.321 (70 FR 53313 [DIRS 178394]), and with 10 CFR 63.331 [DIRS 180319], on the basis of low consequence.

INPUTS:

Table 1.1.01.01.0B-1. Direct Inputs

Input	Source	Description
BSC 2004. *Seepage Model for PA Including Drift Collapse*. [DIRS 167652]	Section 6.6.4, Table 6-4	Minor effects of rockbolts on drift seepage
	Sections 6.5, 6.6.4	Effects of rock bolt holes on drift seepage

Table 1.1.01.01.0B-2. Indirect Inputs

Citation	Title	DIRS
10 CFR 63	Energy: Disposal of High-Level Radioactive Wastes in a Geologic Repository at Yucca Mountain, Nevada	180319
70 FR 53313	Implementation of a Dose Standard After 10,000 Years	178394
SNL 2007	*Total System Performance Assessment Data Input Package for Requirements Analysis for EBS In-Drift Configuration*	179354

FEP: 1.1.02.00.0A

FEP NAME:

Chemical Effects of Excavation and Construction in EBS

FEP DESCRIPTION:

Chemical effects associated with excavation and construction of the underground regions of the repository may affect the long-term behavior of the engineered and natural barriers. Excavation-related effects include chemical changes to the rock and incoming groundwater due to explosives residue. Excavation and other construction activities could also directly cause groundwater chemistry changes within the tunnel due to contaminants such as diesel exhaust or other organic contaminants. Finally, oxidizing water introduced into the repository during excavation and construction could impact repository conditions and performance.

SCREENING DECISION:

Excluded – low consequence

SCREENING JUSTIFICATION:

Use of explosives for repository excavation could introduce small amounts of chemical components to the repository. Related excavation and operational activities could also introduce other organic and inorganic substances in residual amounts, such as diesel exhaust, lubricants, coolants, battery acid, cleaning solvents, and/or oil mist from compressed air systems. These materials could conceivably have an impact on groundwater chemistry within the EBS by impacting corrosion processes and/or facilitating radionuclide transport. Other potential impacts of excavation and construction are considered in excluded FEP 2.2.01.01.0B (Chemical Effects of Excavation and Construction in the Near Field) and excluded FEP 1.1.02.00.0B (Mechanical Effects of Excavation and Construction in EBS). Excluded FEP 2.1.06.01.0A (Chemical Effects of Rock Reinforcement and Cementitious Materials in EBS) considers the effects of cement dust that may blow into emplacement drifts. Potential effects from residual organics are considered in excluded FEP 2.1.10.01.0A (Microbial Activity in EBS).

To limit undesired effects from excavation and construction (e.g., corrosion and radionuclide transport impacts), requirements have been established to identify, analyze, and control the use of any materials (including water) that will be present in the repository at closure and could adversely impact postclosure performance. The application of these controls is described in *Total System Performance Assessment Data Input Package for Requirements Analysis for Engineered Barrier System In-Drift Configuration* (SNL 2007 [DIRS 179354], Table 4-1, Parameter Number 02-03). Prior to construction of the emplacement drifts and operation and closure of the repository, administrative controls will be developed and imposed to prevent impact on waste isolation from materials used, lost, or left in the repository. These controls will be supported by technical evaluation.

The following constraints will be imposed on the administrative control of tracers, fluids, and materials, construction materials, and committed materials (SNL 2007 [DIRS 179354],

Table 4-1, Parameter Number 02-03): (1) all material not technically evaluated and determined acceptable prior to the permanent closure of the repository will be removed from subsurface facilities prior to permanent closure; (2) committed materials that are proposed to remain in the underground repository following the permanent closure period will be technically evaluated and determined acceptable prior to use; and (3) administrative controls will include accounting and inspection, as appropriate, to confirm that controls on the approved quantities and compositions of tracers, fluids, and materials are met.

The emplacement drifts will be excavated using tunnel boring machines (SNL 2007 [DIRS 179466], Table 4-1, Parameter Number 01-09). Water will be introduced by tunnel boring machines, and any such water remaining in the emplacement areas after construction will be removed by ventilation, which will operate during waste emplacement and for a minimum of 50 years after waste emplacement (SNL 2007 [DIRS 179466], Table 4-2, Parameter Number 06-01). Dryout of the repository during ventilation is discussed in *Multiscale Thermohydrologic Model* (SNL 2008 [DIRS 184433], Section 6.1.3).

Salt-bearing dust generated by construction activities could cause localized corrosion of EBS components as a result of deliquescence and subsequent formation of highly concentrated brine droplets. Screening justifications for this process are presented in excluded FEP 2.1.09.28.0A (Localized Corrosion on Waste Package Outer Surface Due to Deliquescence) and excluded FEP 2.1.09.28.0B (Localized Corrosion on Drip Shield Surfaces Due to Deliquescence).

Evaluation of effects from degradation of construction materials used for ground support (principally Stainless Steel Type 316L rock bolts and steel sheets (SNL 2007 [DIRS 179466], Table 4-1, Parameter Number 01-15)) and for construction of the invert (crushed tuff and carbon steel; SNL 2007 [DIRS 179354], Table 4-1, Parameter Number 02-08) is described for excluded FEP 2.2.01.01.0B (Chemical Effects of Excavation and Construction in the Near Field). Sensitivity analyses of the effects of ground support and invert steels on aqueous chemistry are documented in *Engineered Barrier System: Physical and Chemical Environment* (SNL 2007 [DIRS 177412], Section 6.8). When relatively large quantities of degrading Stainless Steel Type 316L (up to 1.3×10^{-1} moles per kilogram H_2O) were added to representative seepage water only slight differences were calculated in the ionic strength and dissolved inorganic carbon total molality (SNL 2007 [DIRS 177412], Section 6.8.4.1, Tables 6.8-5 and 6.8-6). Similar analysis to characterize the impact of invert steel corrosion also produced only negligible changes in water chemistry (SNL 2007 [DIRS 177412], Section 6.8.4.1, Tables 6.8-3 and 6.8-4). A bounding approach was used, so the conclusions of this analysis are not tied directly to a particular design or set of degradation rate data. Under oxidizing conditions (SNL 2007 [DIRS 177412], Section 6.7), additional steel leads to greater accumulations of corrosion-product precipitates and effectively no change in fluid chemistry (SNL 2007 [DIRS 177412], Section 6.8.4.2).

Based on the above discussion, omission of FEP 1.1.02.00.0A (Chemical Effects of Excavation and Construction in EBS) will not result in a significant adverse change in the magnitude or time of radiological exposures to the RMEI or radionuclide releases to the accessible environment. Therefore, this FEP is excluded from the performance assessments conducted to demonstrate compliance with proposed 10 CFR 63.311 and 63.321 (70 FR 53313 [DIRS 178394]), and with 10 CFR 63.331 [DIRS 180319], on the basis of low consequence.

INPUTS:

Table 1.1.02.00.0A-1. Direct Inputs

Input	Source	Description
SNL 2007. *Total System Performance Assessment Data Input Package for Requirements Analysis for EBS In-Drift Configuration*. [DIRS 179354]	Table 4-1, Parameter Number 02-03	Controls and inspection processes for undesired effects from excavation and construction
SNL 2007. *Engineered Barrier System: Physical and Chemical Environment*. [DIRS 177412]	Section 6.8.4.1; Tables 6.8-5, 6.8-6	Impact of Stainless Steel Type 316L corrosion produces negligible changes in water chemistry
	Section 6.8.4.2	There is no impact on seepage water chemistry due to corrosion of steels
	Section 6.8	Sensitivity analyses of the effects of ground support and invert steels on aqueous chemistry
	Section 6.8.4.1; Tables 6.8-3, 6.8-4	Impact of invert steel corrosion produces negligible changes in water chemistry
	Section 6.7	Oxic conditions will be maintianed in the drift
SNL 2007. *Total System Performance Assessment Data Input Package for Requirements Analysis for Subsurface Facilities*. [DIRS 179466]	Table 4-1, Parameter Number 01-15	The ground support construction materials will be Stainless Steel Type 316L
	Table 4-2, Parameter Number 06-01	50 years of ventilation
	Table 4-1, Parameter Number 01-09	Emplacement drifts will be excavated using tunnel boring machines

Table 1.1.02.00.0A-2. Indirect Inputs

Citation	Title	DIRS
10 CFR 63	Energy: Disposal of High-Level Radioactive Wastes in a Geologic Repository at Yucca Mountain, Nevada	180319
70 FR 53313	Implementation of a Dose Standard After 10,000 Years	178394
SNL 2007	*Total System Performance Assessment Data Input Package for Requirements Analysis for EBS In-Drift Configuration*	179354
SNL 2008	*Multiscale Thermohydrologic Model*	184433

FEP: 1.1.02.00.0B

FEP NAME:

Mechanical Effects of Excavation and Construction in EBS

FEP DESCRIPTION:

Mechanical effects associated with excavation and construction of the underground regions of the repository may affect the long-term behavior of the engineered and natural barriers. Excavation-related effects include changes to rock properties due to boring and blasting.

SCREENING DECISION:

Excluded – low consequence

SCREENING JUSTIFICATION:

Emplacement drifts, access mains, and exhaust mains will be excavated using tunnel boring machines (SNL 2007 [DIRS 179466], Table 4-1, Parameter Number 01-09). Tunnel boring machines use a series of rolling disc cutters mounted on a rotating face to gradually cut the rock by forming rock chips under the shearing action of the cutters, and produce the least excavation damage among available excavation methods. This is because energy is focused on the rock to be removed, so that excess energy is not dispersed into the surrounding rock, as from blasting (Craig 2001 [DIRS 171411], pp. 1, 3, and 8).

The potential effects of excavation on the mechanical response of the rock mass fall into three categories: (1) a compromised ability to excavate nominally circular tunnel profiles consistent with modeled geometry; (2) altered or degraded mechanical properties in an excavation disturbed zone (EDZ) around the periphery of the opening; and (3) altered transport properties in the EDZ that could affect the quantity or chemistry of seepage water entering the drift, or radionuclide transport processes. Changes in rock properties that could affect water flow and radionuclide transport are addressed by included FEP 2.2.01.01.0A (Mechanical Effects of Excavation and Construction in the Near Field). Accordingly, the following analysis addresses only categories (1) and (2), the geometry and rock mechanical properties resulting from excavation and construction.

The ESF and ECRB Cross-Drift tunnels were driven with tunnel boring machines, to diameters comparable to the repository emplacement drifts (Craig 2001 [DIRS 171411], p. 1; SNL 2007 [DIRS 179466], Table 4-1, Parameter Number 01-10) and provide data on the effects of excavation and construction activities in the repository host rock units. Examination of exposed rock through full-periphery geologic mapping and borehole logging has been used to define the character and extent of mechanical damage induced by tunnel boring (Craig 2001 [DIRS 171411], pp. 3 to 11, 16; BSC 2004 [DIRS 166107], Section 7.6.5.2). The observations are summarized as follows:

Circular Cross Section: Where the rock mass has relatively few natural fractures, the roughness of the tunnel walls (resulting from the action of the disc cutters) is on the order of 1 to 10 mm.

Where the rock is heavily fractured with natural jointing, the tunnel wall surface roughness is controlled by plucking of rock blocks bounded by natural fractures from the tunnel wall, resulting in a "blocky" surface appearance. Areas with abundant large (>60 cm) lithophysae produce a similar surface due to plucking along both abundant natural fractures connecting the lithophysae and along excavation-induced fractures. In all cases, the circular cross-section of the tunnel is maintained, and the variability of this cross-section introduced by surface roughness is small in comparison to the tunnel radius, and therefore the initial circular geometry used in modeling studies is reasonable.

Excavation-Induced Damage to Rock Mass: In rock with few fractures, the tunnel boring machine-induced fracturing of the tunnel periphery is confined to a depth of influence of less than 5 cm (Craig 2001 [DIRS 171411], p. 16). The depth of mechanically induced damage is therefore less than 1% of the tunnel diameter (5.5 m). In the poorest quality rock, rock containing abundant large lithophysae and/or an abundance of natural fractures, damage effects can penetrate to depths of approximately 50 cm, along the springline of the tunnel where the effects are greatest (Craig 2001 [DIRS 171411], p. 16; corroborated by BSC 2004 [DIRS 166107], Section 7.6.5.2). In either case, no significant impacts on the probability or amount of rockfall are expected to result from mechanical damage associated with tunnel boring activities.

In summary, excavation using tunnel boring machines will maintain circular tunnel geometry, and the resulting changes in the mechanical properties of the rock around the drift are insignificant for drift stability analyses. Hence, the effects of excavation damage do not need to be included in mechanical modeling studies.

Consistent with the above discussion, omission of FEP 1.1.02.00.0B (Mechanical Effects of Excavation and Construction in EBS) will not result in a significant adverse change in the magnitude or time of radiological exposures to the RMEI or radionuclide releases to the accessible environment. Therefore, this FEP 1.1.02.00.0B is excluded from the performance assessments conducted to demonstrate compliance with proposed 10 CFR 63.311 and 63.321 (70 FR 53313 [DIRS 178394]), and with 10 CFR 63.331 [DIRS 180319], on the basis of low consequence.

INPUTS:

Table 1.1.02.00.0B-1. Direct Inputs

Input	Source	Description
Craig 2001. "Transmittal of Level 5 Deliverable SPW205M5, 'Excavation-Induced Fracture Study'." [DIRS 171411]	pp. 3 to 11, 16	Examination of the tunnel walls and associated alcoves, niches, and drillholes has been used to define the character and extent of mechanical damage induced by tunnel boring
	pp. 1, 3, 8	Energy is focused on the rock to be removed, so that excess energy is not dispersed into the surrounding rock, as from blasting
	p. 16	In rock with few fractures, the tunnel boring machine-induced fracturing of the tunnel periphery is confined to a depth of influence of less than 5 cm
SNL 2007. *Total System Performance Assessment Data Input Package for Requirements Analysis for Subsurface Facilities*. [DIRS 179466]	Table 4-1, Parameter Number 01-10	Diameter of emplacement drifts
	Table 4-1, Parameter Number 01-09	The primary construction method for emplacement drifts, access mains, and exhaust mains will be tunnel boring machines

Table 1.1.02.00.0B-2. Indirect Inputs

Citation	Title	DIRS
10 CFR 63	Energy: Disposal of High-Level Radioactive Wastes in a Geologic Repository at Yucca Mountain, Nevada	180319
70 FR 53313	Implementation of a Dose Standard After 10,000 Years	178394
BSC 2004	*Drift Degradation Analysis*	166107
Craig 2001	"Transmittal of Level 5 Deliverable SPW205M5, 'Excavation-Induced Fracture Study'"	171411

FEP: 1.1.02.01.0A

FEP NAME:

Site Flooding (During Construction and Operation)

FEP DESCRIPTION:

Flooding of the site during construction and operation could introduce water into the underground tunnels, which could affect the long-term performance of the repository.

SCREENING DECISION:

Excluded – low consequence

SCREENING JUSTIFICATION:

Flooding during storm events is not unusual and leads to infiltration and runoff. Areas that would be inundated in the probable maximum flood in the vicinity of the North Portal pad were calculated in *Preliminary Hydrologic Engineering Studies for the North Portal Pad and Vicinity* (BSC 2002 [DIRS 157928], Figures 17 through 19), and presented in DTN: MO0209EBSPMFSD.029 [DIRS 161845]. The maps contained therein show that flooding is not expected to reach the main portals of the Exploratory Studies Facility or the intake and exhaust shafts. To preclude repository flooding during construction and operation, the current design requires that portal and shaft locations are outside of the probable maximum flood areas (SNL 2007 [DIRS 179466], Table 4-1, Parameter Number 01-19).

Areas that would be inundated in the maximum potential flood for the Yucca Mountain area have also been calculated in *Flood Inundation Areas in the Vicinity of Yucca Mountain* (DTN: MO0004YMP98132.004 [DIRS 149806]). Percolation flux in the UZ is predominantly vertical (BSC 2004 [DIRS 169734], Section 7), so flooding over waste emplacement areas is expected to impact long-term performance of the repository. However, very little of the flood zone overlies waste emplacement zones. A small region of the maximum potential flood zone overlies the repository footprint in the upper part of Drill Hole Wash. Boreholes USW NRG-7a, USW G-1, and USW H-1 lie near the potential flood zone within Drill Hole Wash, which overlies the repository footprint (DTN: MO0011YMP00114.000 [DIRS 171565]). To minimize the introduction of surface runoff into these boreholes prior to the final borehole plugging, each borehole casing, which is cemented into the hole, extends above the ground surface (DTN: MO9906GPS98410.000 [DIRS 109059]). This FEP is intended to address the effects of site flooding during the preclosure period only, and the casings are not relied upon for long-term performance. All boreholes within the repository area have casings that extend above the ground surface (DTNs: MO9906GPS98410.000 [DIRS 109059]; MO9912GSC99492.000 [DIRS 165922]; MO0011YMP00114.000 [DIRS 171565]). As discussed for excluded FEP 1.1.01.01.0A (Open Site Investigation Boreholes), it is not expected that open boreholes will significantly increase the amount of water that enters the waste emplacement locations. Any flooding of the subsurface repository during construction or operations will be addressed as a non-conforming condition, as consistent with excluded FEP 1.1.08.00.0A (Inadequate Quality Control and Deviations from Design) and remediated prior to repository closure.

The effects of flooding for the postclosure time period are addressed in excluded FEPs 1.1.04.01.0A (Incomplete Closure) and 2.1.05.01.0A (Flow Through Seals (Access Ramps and Ventilation Shafts)) and included FEP 2.3.11.02.0A (Surface Runoff and Evapotranspiration).

Based on the preceding discussion, omission of FEP 1.1.02.01.0A (Site Flooding (During Construction and Operation)) will not result in a significant adverse change in the magnitude or time of radiological exposures to the RMEI or radionuclide releases to the accessible environment. Therefore, this FEP is excluded from the performance assessments conducted to demonstrate compliance with proposed 10 CFR 63.311 and 63.321 (70 FR 53313 [DIRS 178394]), and with 10 CFR 63.331 [DIRS 180319], on the basis of low consequence.

INPUTS:

Table 1.1.02.01.0A-1. Direct Inputs

Input	Source	Description
DTN: LB0304RDTRNSNS.001. Supporting Files of 3D Flow and Transport Sensitivity Analyses. [DIRS 165922]	TDMS-GI link to *MO9912GSC99492.000.doc*	Borehole locations and elevations
DTN: MO0209EBSPMFSD.029. Probable Maximum Flood Study Data. [DIRS 161845]	Table S02250_001	Map of area near north portal innundated by probably maximum flood
DTN: MO9906GPS98410.000. Yucca Mountain Project (YMP) Borehole Locations. [DIRS 109059]	file: *mo9906gps98410.xls*	Borehole locations and elevations
SNL 2007. *Total System Performance Assessment Data Input Package for Requirements Analysis for Subsurface Facilities*. [DIRS 179466]	Table 4-1, Parameter Number 01-19	Design requirements

Table 1.1.02.01.0A-2. Indirect Inputs

Citation	Title	DIRS
10 CFR 63	Energy: Disposal of High-Level Radioactive Wastes in a Geologic Repository at Yucca Mountain, Nevada	180319
70 FR 53313	Implementation of a Dose Standard After 10,000 Years	178394
BSC 2002	*Preliminary Hydrologic Engineering Studies for the North Portal Pad and Vicinity*	157928
BSC 2004	*Yucca Mountain Site Description*	169734
DTN: MO0004YMP98132.004	Flood Inundation Areas in the Vicinity of Yucca Mountain	149806
DTN: MO0011YMP00114.000	Potential Repository Site	171565

FEP: 1.1.02.02.0A

FEP NAME:

Preclosure Ventilation

FEP DESCRIPTION:

The duration of preclosure ventilation acts together with waste package spacing (as per design) to control the extent of the boiling front (zone of reduced water content).

SCREENING DECISION:

Included

TSPA DISPOSITION:

As discussed in *Ventilation Model and Analysis Report* (BSC 2004 [DIRS 169862], Section 1), there are two distinct phases considered in repository operation. The first phase, or preclosure phase, which includes emplacement of the waste, is a period when heat generated from the decay of radionuclides contained in waste packages is actively removed from the repository by forced ventilation of the emplacement drifts. In the second phase, or postclosure phase, forced ventilation of the drifts is stopped and the repository is closed; natural ventilation and convective air movement through the drift continues to occur. The analysis described in *Ventilation Model and Analysis Report* (BSC 2004 [DIRS 169862]) calculates the preclosure thermal conditions in the host rock and characterizes the postclosure host rock response in terms of ventilation efficiency. The ventilation efficiency is computed as a percentage of total decay heat that is removed from the repository by the exhaust ventilation; the method of calculation is shown in *Ventilation Model and Analysis Report* (BSC 2004 [DIRS 169862], Section 6.4). The ventilation efficiency is determined through simulation of temporally and spatially dependent heat transfer processes (thermal radiation, convection, and conduction), which occur simultaneously in the drift and the surrounding rock mass during the ventilated preclosure period. The analytical ventilation model developed in *Ventilation Model and Analysis Report* (BSC 2004 [DIRS 169862], Section 6.4) was further developed in *Thermal Management Flexibility Analysis* (SNL 2007 [DIRS 179196], Section 6.3). Modifications to the original ventilation model included implementing alternative thermal loading schemes and host rock properties, expanding the ventilation duration analysis options, and correcting/updating several inputs to the calculation. The ventilation duration used for performance assessment is 50 years following final emplacement (SNL 2007 [DIRS 179466], Table 4-2, Parameter Number 06-01).

The ventilation efficiency is a direct input to *Multiscale Thermohydrologic Model* (SNL 2008 [DIRS 184433], Section 6.2.15[a]), where it is used to calculate the reduction in the heat generation rate during preclosure ventilation (the heat generation rate is multiplied by a specified fraction). The MSTHM (SNL 2008 [DIRS 184433], Section 8.3[a]) in turn provides postclosure thermal and relative humidity conditions to the TSPA. The ventilation model (BSC 2004 [DIRS 169862]) and the MSTHM (SNL 2008 [DIRS 184433]), therefore, address the effect of ventilation on the removal of waste package heat during the preclosure period.

The condensation model described in *In-Drift Natural Convection and Condensation* (SNL 2007 [DIRS 181648], Section 6.3.5.2.5) accounts for preclosure ventilation when calculating in-drift thermal conditions for use in determining condensation rates within the drift. That model uses the average annual ventilation efficiency based on a 600-m drift for the 50-year postemplacement ventilation period (SNL 2007 [DIRS 181648], Section 6.1.1[a]). The condensation model provides correlations of drift wall condensation rates and probabilities, as functions of percolation rate, to TSPA.

The impact of preclosure ventilation on the thermal load provided to the rock is explicitly simulated in *Drift-Scale Coupled Processes (DST and TH Seepage) Models* (BSC 2005 [DIRS 172232], Sections 4.1.1.3 and 6.2.1.3.3). Those results are incorporated into the seepage abstraction by using time-dependent boundary conditions for the thermal load (SNL 2007 [DIRS 181244], Section 6.4.3.1). Thus, the thermal-hydrologic (TH) modeling results from the TH seepage model directly account for the impact of preclosure ventilation and waste package spacing on two-phase flow and the TH conditions in the near-drift rock. As discussed in *Abstraction of Drift Seepage* (SNL 2007 [DIRS 181244], Section 6.5.2), the abstraction of thermal seepage utilizes these modeling results to develop an appropriate thermal seepage abstraction methodology.

For each of the three models discussed above, a single value for ventilation efficiency is used in simulations providing inputs to TSPA. In each case, the impact of uncertainty in the ventilation efficiency is evaluated using sensitivity analyses (SNL 2008 [DIRS 184433], Section 6.3.12[a]; SNL 2007 [DIRS 181648], Section 6.1.3[a]; SNL 2007 [DIRS 172232], Section 6.2.2.1.3), and is shown to be small relative to other model uncertainties that are propagated to the TSPA.

Preclosure ventilation also causes initial rock drying in the drift vicinity because of evaporation effects. The reduced relative humidity in the emplacement drifts leads to evaporation of water at the drift surfaces and development of a small zone of reduced saturation in the drift vicinity. This early dryout due to evaporation is not credited in the MSTHM (SNL 2008 [DIRS 184433], Section 7.5.2) and the TH seepage model (SNL 2007 [DIRS 181244], Section 6.5.2) because the effects are small, and seepage into ventilated drifts is not expected. The effects of preclosure ventilation on dryout of the rock are treated similarly in the thermal-hydrologic-chemical (THC) model (SNL 2007 [DIRS 177404], Section 6.5.5.2).

Ventilation efficiencies are used in *Engineered Barrier System: Physical and Chemical Environment* (SNL 2007 [DIRS 177412], Section 6.3.2.4.3) to model evolution of the thermal field through time. Results from that report (SNL 2007 [DIRS 177412], Section 8.2) are implemented in TSPA in the form of the lookup tables for the determination of seepage water chemistries.

To summarize, the dominant effect of preclosure ventilation is to reduce the thermal load provided to the drift walls, limiting the temperature rise in the rock during this period. This effect is incorporated into models supporting performance assessment. Ventilation also results in dryout of the rock proximal to the drift. This effect is not credited because it has no impact on postclosure modeling of the repository; once ventilation ceases, a dryout zone rapidly develops around the drift in any case.

INPUTS:

Table 1.1.02.02.0A-1. Indirect Inputs

Citation	Title	DIRS
BSC 2004	*Ventilation Model and Analysis Report*	169862
BSC 2005	*Drift-Scale Coupled Process (DST and TH Seepage) Models*	172232
SNL 2007	*Abstraction of Drift Seepage*	181244
SNL 2007	*Drift-Scale THC Seepage Model*	177404
SNL 2007	*Engineered Barrier System: Physical and Chemical Environment*	177412
SNL 2007	*In-Drift Natural Convection and Condensation*	181648
SNL 2007	*Thermal Management Flexibility Analysis*	179196
SNL 2007	*Total System Performance Assessment Data Input Package for Requirements Analysis for Subsurface Facilities*	179466
SNL 2008	*Multiscale Thermohydrologic Model*	184433

FEP: 1.1.02.03.0A

FEP NAME:

Undesirable Materials Left

FEP DESCRIPTION:

During construction and preclosure operation of the repository, unwanted materials might be left in the vicinity of the radioactive waste. These materials could, to some extent, affect many long-term processes in the repository from waste package corrosion to radionuclide transport mechanisms.

SCREENING DECISION:

Excluded – low consequence

SCREENING JUSTIFICATION:

Inherent in the approach to FEP evaluation is the expectation that the repository will be constructed, operated, and closed according to the design used as the basis for FEP screening and in accordance with NRC license requirements. Repository construction, operation, and closure will be subject to a quality assurance program and quality control procedures that will evaluate and disposition any deviations from the design. Of particular relevance, controls on activities and materials used during the excavation, construction, and preclosure operation phases of the repository will aim to prevent unwanted materials from being left in the repository after repository closure.

Requirements have been established to identify, analyze, and control the use of any materials that will be present in the repository at closure and could adversely impact postclosure performance. Controls on activities and materials used during the excavation, construction, and preclosure operation phases of the repository will aim to prevent unwanted materials from being left in the vicinity of radioactive waste. The application of controls on materials is described in *Total System Performance Assessment Data Input Package for Requirements Analysis for Engineered Barrier System In-Drift Configuration* (SNL 2007 [DIRS 179354], Table 4-1, Parameter Number 02-03). The following constraints will be imposed on the administrative control of tracers, fluids, and materials, construction materials, and committed materials: (1) all material technically evaluated and determined not to be acceptable prior to the permanent closure of the repository will be removed from subsurface facilities prior to permanent closure; (2) committed materials that are proposed to remain in the underground repository following the permanent closure period will be technically evaluated and determined acceptable prior to use; and (3) administrative controls will include accounting and inspection, as appropriate, to confirm that controls on the approved tracers, fluids, and materials quantities and compositions are met.

The controls on materials will be sufficient to ensure that if any materials are left in the repository, they would not significantly affect radionuclide transport pathways or radiological dose to the RMEI. These controls will be supported by technical evaluation. Therefore, the effects of undesirable materials left in the repository after closure are excluded from the

performance assessments on the basis of low consequence. The potential impacts of chemical components left in the repository as a result of excavation and construction are considered in excluded FEP 1.1.02.00.0A (Chemical Effects of Excavation and Construction in EBS) and are also excluded on the basis of low consequence. Significant quantities of unwanted materials could only be left in the repository in the event that controls on activities and the materials used during the excavation, construction, and preclosure operation phases were inadequate. Inadequate controls are discussed in excluded FEP 1.1.08.00.0A (Inadequate Quality Control and Deviations from Design).

Based on the previous discussion, omission of FEP 1.1.02.03.0A (Undesirable Materials Left) will not result in a significant adverse change in the magnitude or timing of either radiological exposures to the RMEI or radionuclide releases to the accessible environment. Therefore, this FEP is excluded from the performance assessments conducted to demonstrate compliance with proposed 10 CFR 63.311 and 63.321 (70 FR 53313 [DIRS 178394]), and with 10 CFR 63.331 [DIRS 180319], on the basis of low consequence.

INPUTS:

Table 1.1.02.03.0A-1. Direct Inputs

Input	Source	Description
SNL 2007. *Total System Performance Assessment Data Input Package for Requirements Analysis for EBS In-Drift Configuration*. [DIRS 179354]	Table 4-1, Parameter Number 02-03	Describes the application of controls on materials

Table 1.1.02.03.0A-2. Indirect Inputs

Citation	Title	DIRS
10 CFR 63	Energy: Disposal of High-Level Radioactive Wastes in a Geologic Repository at Yucca Mountain, Nevada	180319
70 FR 53313	Implementation of a Dose Standard After 10,000 Years	178394

FEP: 1.1.03.01.0A

FEP NAME:

Error in Waste Emplacement

FEP DESCRIPTION:

Deviations from the design and/or errors in waste emplacement could affect long-term performance of the repository. A specific example of such an error would be erroneously emplacing the waste packages in a saturated or wet zone of the repository. Errors of this type would impact repository performance by affecting waste package corrosion and radionuclide transport.

SCREENING DECISION:

Excluded – by regulation

SCREENING JUSTIFICATION:

Possible types of waste emplacement errors are emplacement of packages closer to each other than in the design specification, and emplacement of a package so that it straddles a known Quaternary fault with potential for significant displacement. The emplacement of waste packages in a wet zone (i.e., zones of potential seepage) is not an erroneous emplacement, and is expected, and is included in the TSPA (see included FEP 2.1.08.01.0A (Water Influx at the Repository)). Saturated conditions are not expected in the repository (see excluded FEP 2.1.08.09.0A (Saturated Flow in the EBS)).

Inherent in the approach to FEP evaluation is the expectation that the repository be constructed, operated, and closed according to the design used as the basis for FEP screening and in accordance with NRC license requirements. Repository construction, operation, and closure will be subject to a quality assurance program and quality control procedures that will evaluate and disposition any deviations from the design. Of particular relevance, control procedures imposed during the repository operation phase will aim to ensure that any errors in waste emplacement are rectified before repository closure.

Inadequate quality controls on operational issues such as these are discussed in detail in excluded FEP 1.1.08.00.0A (Inadequate Quality Control and Deviations from Design), and are excluded from the performance assessments. As a result of the rigorous quality assurance/quality control requirements governing emplacement of waste packages and inspection and approval of such emplacement, errors in emplacement location resulting in waste packages being placed substantially closer to each other than specified by design, or being placed on a known fault, are not expected. The regulatory requirements for performance confirmation and quality assurance require that any deviation from design be evaluated for potential impact, and that significant deviations which are detected during the operational period be corrected. Erroneous emplacement of waste packages is not expected because of quality controls.

In summary, FEP 1.1.03.01.0A (Error in Waste Emplacement) is excluded from the performance assessments conducted to demonstrate compliance with proposed 10 CFR 63.311 and 63.321 (70 FR 53313 [DIRS 178394]), and with 10 CFR 63.331 [DIRS 180319], on the basis of regulation.

INPUTS:

Table 1.1.03.01.0A-1. Direct Inputs

Input	Source	Description
10 CFR 63. 2007. Energy: Disposal of High-Level Radioactive Wastes in a Geologic Repository at Yucca Mountain, Nevada. [DIRS 180319]	10 CFR 63.331	Separate standards for protection of groundwater
70 FR 53313. Implementation of a Dose Standard After 10,000 Years. [DIRS 178394]	10 CFR 63.321	Individual protection standard for human intrusion
	10 CFR 63.311	Individual protection standard after permanent closure

FEP: 1.1.03.01.0B

FEP NAME:

Error in Backfill Emplacement

FEP DESCRIPTION:

Deviations from the design and/or errors in the backfill emplacement could affect long-term performance of the repository.

SCREENING DECISION:

Excluded – low consequence

SCREENING JUSTIFICATION:

Backfill is not part of the design for the waste emplacement regions of the repository. Specifically, engineered backfill shall not be present in the space between the drip shield and the drift wall, and there is no design requirement for backfill in access mains or exhausts (SNL 2007 [DIRS 179354], Parameter Number 05-04). Closure of shafts and ramps shall include backfill of the opening (SNL 2007 [DIRS 179466], Parameter Number 09-01); however, as discussed in excluded FEP 2.1.05.01.0A (Flow through Seals (Access Ramps and Ventilation Shafts)), long-term performance of the repository is not adversely affected by flow in the shafts and ramps. Hypothetical deviations from backfill design and/or errors in backfill emplacement in shafts and ramps are not relevant to the emplacement area and would have no impact on overall performance of the repository if they occurred. Omission of FEP 1.1.03.01.0B (Error in Backfill Emplacement) will not result in a significant adverse change in the magnitude or timing of either radiological exposure to the RMEI or radionuclide releases to the accessible environment. Therefore, this FEP is excluded from the performance assessments conducted to demonstrate compliance with proposed 10 CFR 63.311 and 63.321 (70 FR 53313 [DIRS 178394]), and with 10 CFR 63.331 [DIRS 180319], on the basis of low consequence.

INPUTS:

Table 1.1.03.01.0B-1. Direct Inputs

Input	Source	Description
SNL 2007. *Total System Performance Assessment Data Input Package for Requirements Analysis for EBS In-Drift Configuration*. [DIRS 179354]	Parameter Number 05-04	Design requirement for backfill
SNL 2007. *Total System Performance Assessment Data Input Package for Requirements Analysis for Subsurface Facilities*. [DIRS 179466]	Parameter Number 09-01	Closure of shafts and ramps shall include backfill of the opening

Table 1.1.03.01.0B-2. Indirect Inputs

Citation	Title	DIRS
10 CFR 63	Energy: Disposal of High-Level Radioactive Wastes in a Geologic Repository at Yucca Mountain, Nevada	180319
70 FR 53313	Implementation of a Dose Standard After 10,000 Years	178394

FEP: 1.1.04.01.0A

FEP NAME:

Incomplete Closure

FEP DESCRIPTION:

Disintegration of society could result in incomplete closure, sealing, and decommissioning of the disposal vault.

SCREENING DECISION:

Excluded – by regulation

SCREENING JUSTIFICATION:

10 CFR 63.305(a),(b), and (c) [DIRS 180319] specifies that:

(a) Features, events, and processes that describe the reference biosphere must be consistent with present knowledge of the conditions in the region surrounding the Yucca Mountain site.

(b) DOE should not project changes in society, the biosphere (other than climate), human biology, or increases or decreases of human knowledge or technology. In all analyses done to demonstrate compliance with this part, DOE must assume that all of those factors remain constant as they are at the time of submission of the license application.

(c) DOE must vary factors related to the geology, hydrology, and climate based upon cautious, but reasonable assumptions consistent with present knowledge of factors that could affect the Yucca Mountain disposal system over the next 10,000 years.

Incomplete closure due to inadequate quality control is covered by excluded FEP 1.1.08.00.0A (Inadequate Quality Control and Deviations from Design). Included FEP 0.1.09.00.0A (Regulatory Requirements and Exclusions) addresses regulatory requirements and guidance specific to the Yucca Mountain repository including postclosure activities.

Because FEP 1.1.04.01.0A (Incomplete Closure) is, by definition, predicated on an assumption of a disintegration of society (i.e., an increase or decrease of human knowledge or technology), it is therefore excluded by regulation. Incomplete closure is excluded from the performance assessments conducted to demonstrate compliance with proposed 10 CFR 63.311 and 63.321 (70 FR 53313 [DIRS 178394]), and with 10 CFR 63.331 [DIRS 180319], on the basis of regulation.

INPUTS:

Table 1.1.04.01.0A-1. Direct Inputs

Input	Source	Description
10 CFR 63. 2007. Energy: Disposal of High-Level Radioactive Wastes in a Geologic Repository at Yucca Mountain, Nevada. [DIRS 180319]	10 CFR 63.331	Separate standards for protection of groundwater
	10 CFR 63.305(a)(b)(c)	Specifies that DOE should not project changes in society
70 FR 53313. Implementation of a Dose Standard After 10,000 Years. [DIRS 178394]	10 CFR 63.321	Individual protection standard for human intrusion
	10 CFR 63.311	Individual protection standard after permanent closure

FEP: 1.1.05.00.0A

FEP NAME:

Records and Markers for the Repository

FEP DESCRIPTION:

This FEP addresses the retention of records of the contents of the repository and markers constructed to inform future humans of the location and contents of the repository. Performance assessments must consider the potential effects of human activities that might take place within the controlled area at a future time when institutional controls and/or knowledge of the presence of a repository cannot be assumed.

SCREENING DECISION:

Excluded – by regulation

SCREENING JUSTIFICATION:

The requirements for constructing monuments as repository markers, preserving and archiving records, and a program of continued oversight are listed in 10 CFR 63.51(a)(3)(i-iii), 10 CFR 63.72(a), and 10 CFR 63.72(b)(1-11) [DIRS 180319]. 10 CFR 63.72(a) states:

> DOE shall maintain records of construction of the geologic repository operations area at the Yucca Mountain site in a manner that ensures their usability for future generations.

10 CFR 63.102(k) [DIRS 180319] addresses the use of institutional controls that are expected to reduce significantly, but not eliminate, the potential for human activity that could inadvertently cause or accelerate the release of radioactive materials. The regulation requires that both passive and active institutional controls be maintained. Specifically, 10 CFR 63.302 [DIRS 180319] defines passive institutional controls as:

(1) Markers, as permanent as practicable, placed on the Earth's surface;

(2) Public records and archives;

(3) Government ownership and regulations regarding land or resource use; and

(4) Other reasonable methods of preserving knowledge about the location, design, and contents of the Yucca Mountain disposal system.

Proposed 10 CFR 63.321 (70 FR 53313 [DIRS 178394]) requires an analysis of the consequences of a stylized human intrusion taking no credit for the efficacy of records and markers. Accordingly, FEP 1.1.05.00.0A (Records and Markers for the Repository) is excluded from consideration in the TSPA by regulation. Further discussion of institutional controls is provided in excluded FEP 1.1.10.00.0A (Administrative Control of the Repository Site).

INPUTS:

Table 1.1.05.00.0A-1. Direct Inputs

Input	Source	Description
10 CFR 63. 2007. Energy: Disposal of High-Level Radioactive Wastes in a Geologic Repository at Yucca Mountain, Nevada. [DIRS 180319]	10 CFR 63.302	Definition of passive institutional records
	10 CFR 63.102(k)	Use of institutional controls
	10 CFR 63.51(a)(3)(i-iii), 10 CFR 63.72(a), 10 CFR 63.72(b)(1-11)	Requirements for constructing monuments, preserving, and archiving records, and ovesight
70 FR 53313. Implementation of a Dose Standard After 10,000 Years. [DIRS 178394]	10 CFR 63.321	Individual protection standard for human intrusion

FEP: 1.1.07.00.0A

FEP NAME:

Repository Design

FEP DESCRIPTION:

This FEP addresses the consideration of the design of the repository and the ways in which the design contributes to long-term performance. The performance assessment must account for design features, material characteristics, and the ways in which the design influences the evolution of the in-drift environment.

SCREENING DECISION:

Included

TSPA DISPOSITION:

Repository design is one of the bases for the models used for the performance assessments. Particularly relevant to this FEP are the model components for waste package and drip shield degradation, waste form degradation and mobilization, and EBS flow and transport. These model components take into account the physical dimensions, material characteristics, and evolution of the in-drift environment, all of which stem directly from design considerations. The design elements are included in the TSPA as parameters that define the physical dimensions, characteristics, and long-term behavior of the waste form, waste packages, emplacement drift, drip shields and other components of the EBS. A mapping of these parameters to FEPs evaluations and their use in performance assessment is contained in Appendix A.

Proposed 10 CFR 63.114(a) (70 FR 53313 [DIRS 178394]) states that any performance assessment prepared to demonstrate compliance with 10 CFR 63.113 [DIRS 180319] must:

> (1) Include data related to the geology, hydrology, and geochemistry (including disruptive processes and events) of the Yucca Mountain site, and the surrounding region to the extent necessary, and information on the design of the engineered barrier system used to define, for 10,000 years after disposal, parameters and conceptual models used in the assessment.

The following is a summary description of the design of the repository subsurface facility and EBS considered in the FEPs evaluation and included in the performance assessments. Descriptions of the repository subsurface facility are found in *Postclosure Modeling and Analyses Design Parameters* (BSC 2008 [DIRS 183627]); *Total System Performance Assessment Data Input Package for Requirements Analysis for Transportation Aging and Disposal Canister and Related Waste Package Physical Attributes Basis for Performance Assessment* (SNL 2007 [DIRS 179394]); *Total System Performance Assessment Data Input Package for Requirements Analysis for Engineered Barrier System In-Drift Configuration* (SNL 2007 [DIRS 179354]); and *Total System Performance Assessment Data Input Package for Requirements Analysis for Subsurface Facilities* (SNL 2007 [DIRS 179466]).

Repository Layout

The layout of the subsurface facility analyzed is generally defined by *Total System Performance Assessment Data Input Package for Requirements Analysis for Subsurface Facilities* (SNL 2007 [DIRS 179466], Table 4-1, Parameter Number 01-02). The emplacement drifts will be excavated using a tunnel boring machine to a diameter of 5.5 m, with a nominal length of 600 m (available drift lengths will range from 324 to 777 m). Emplacement drifts will be excavated in a sequence of panels, which will contain 70,000 metric tons of heavy metal waste. Emplacement drifts will be arranged with a uniform spacing of 81 m between their centerlines (SNL 2007 [DIRS 179466],Table 4-1, Parameter Number 01-13). The repository design used in the postclosure performance analyses (BSC 2005 [DIRS 174101], Section 4.1.12) calls for approximately 100 waste packages to be placed in a single emplacement drift with a nominal length of 600 m (SNL 2008 [DIRS 183478], Section ES 5.1). There is an area in the southern section of the repository that will be constructed to allow for contingencies during waste emplacement. The repository host-rock units contain lithophysal and nonlithophysal units (SNL 2007 [DIRS 179466], Table 4-1, Parameter 01-03). The lithophysal rock units are characterized by numerous cavities (lithophysae), which result in high porosities. The lithophysal rock units are highly fractured and the fractures have short trace lengths. In contrast, the nonlithophysal rock units are characterized by few cavities, lower porosities, and fractures with generally longer trace lengths. Approximately 80% to 85% of the emplacement drift area will be excavated in lithophysal units, and 15% to 20% will be excavated in nonlithophysal units of the repository host horizon (BSC 2007 [DIRS 182926], Table 1).

Features of the Engineered Barrier System

The subsurface facility system includes ground support, such as rock bolts, steel liner, cement, and wire mesh. The EBS design includes a drip shield, a two-layer waste package, a corrosion-resistant emplacement pallet (made of Alloy 22 and stainless steel) on which the waste packages will be placed, and an invert, consisting of a steel support structure and crushed, welded tuff, at the base of the emplacement drifts. The following provides a description of each of the EBS components and repository thermal loading.

Drip Shield

The drip shields will be composed of two corrosion-resistant titanium alloys. The function of the drip shields is to reduce the effect of rockfall and dripping on the waste packages. The drip shields are designed to link together, forming a single continuous barrier for the entire length of the emplacement drifts (SNL 2007 [DIRS 179354], Table 4-2, Parameter Number 07-02). The drip shields will be fabricated from Titanium Grade 7 plates, with Titanium Grade 29 for structural support (SNL 2007 [DIRS 179354], Section 4.1.2). The base plates will be composed of Alloy 22 to prevent direct contact between titanium and the steel members of the invert horizon (SNL 2007 [DIRS 179354], Table 4-2, Parameter Number 07-07).

Waste Package

Waste packages will consist of an outer corrosion barrier and an inner vessel. The outer corrosion barrier is 25-mm-thick corrosion-resistant Alloy 22. The waste packages will be

treated to minimize the possibility of SCC, and the outer closure weld will be stress mitigated. The inner vessel is 50-mm-thick stainless steel and serves three functions. First, the inner vessel provides structural strength to resist rockfall, to support the internal waste form components, to allow the waste packages to be supported by the emplacement pallets, and to facilitate handling. Second, the inner layer provides radiation shielding to reduce the exterior surface contact dose rate (SNL 2007 [DIRS 179394], Table 4-1, Parameter Numbers 03-09 and 03-10; Table 4-3). Third, because of sorption of radionuclides on corrosion products from the degradation of the inner vessel, it acts as a limited containment part of the EBS barrier for the radioactive waste inside the waste packages. The inner vessel is not considered to be a barrier to flow. To calculate radionuclide transport through the waste packages, the TSPA uses the TAD canister with 21-PWR fuel assemblies as the representative commercial SNF waste package, and the 5-DHLW/DOE Long waste package as the representative configuration for the codisposal waste packages. These commercial SNF and codisposal waste packages are planned to be the most common two types of waste packages in the repository (SNL 2007 [DIRS 177407], Section 6.3.3.1).

Emplacement Pallet

An emplacement pallet will support each waste package (SNL 2007 [DIRS 179394], Table 4-3, Parameter Numbers 03-03 and 03-04). The emplacement pallets are designed to prevent the waste packages from coming in contact with the invert of the emplacement drifts and, therefore, prevent direct exposure to invert moisture or materials that may induce accelerated corrosion of the waste packages. The material supporting the waste packages will consist of Alloy 22, providing long-term corrosion resistance and an identical material in contact with the outer surfaces of the waste packages. To reduce the possibility of SCC, the emplacement pallets will also be annealed to remove stresses from welding and fabrication.

Invert

The invert will provide support for the waste package emplacement pallets and the drip shields. The invert consists of two components: a steel invert structure and a crushed tuff fill. The granular crushed tuff will be composed of crushed welded tuff produced from the excavation of the repository underground openings with the tunnel boring machines, and will be placed in and around the steel invert structure to an elevation just below the top of the longitudinal and transverse support beams. The crushed tuff will be compacted (BSC 2007 [DIRS 182746], Report Summary) to prevent long-term settlement (SNL 2007 [DIRS 179354], Table 4-1, Parameter Number 02-08).

Waste Form

Spent nuclear fuel consists of fuel removed from nuclear reactors after its useful heat-generating capacity has been spent. The performance assessments analyze the disposal of waste packages containing commercial SNF and codisposal waste packages, containing DOE SNF (BSC 2004 [DIRS 169766]; BSC 2008 [DIRS 185102]) and HLW (BSC 2004 [DIRS 169988]). Commercial SNF consists primarily of uranium oxide, some of which has been enriched with surplus plutonium to create a MOX fuel. DOE SNF is fuel associated with DOE defense programs and research and development programs. The majority of DOE SNF consists of a

uranium-metal compound SNF with zirconium cladding, which accounts for approximately 86% of the mass of the DOE SNF inventory. However, there are 11 categories of DOE SNF representing a variety of uranium-based waste forms. Naval SNF, a category of DOE SNF, is classified material and, as such, cannot be included in the unclassified postclosure performance assessments. Naval fuel is represented as commercial SNF for modeling purposes. HLW consists of by-products of nuclear reactions, material generated during fuel preparation and reprocessing, and sludges and residues recovered from nuclear-waste storage tanks. HLW will be mixed and solidified in a high-temperature, borosilicate glass for storage in stainless-steel canisters. Codisposal waste packages typically contain five HLW canisters surrounding one DOE SNF canister.

Waste Form Cladding

Nuclear fuel generally consists of stacked pellets of uranium-based fuel encased in a metallic protective cladding. However, for the performance assessments, it is assumed that commercial SNF cladding is failed at the time the waste packages are breached. In addition, DOE SNF cladding is in poor condition and is considered to be failed upon emplacement.

Emplacement Drift

The nuclear waste will be placed in 5.5-m diameter, circular emplacement drifts excavated with tunnel boring machines (SNL 2007 [DIRS 179354], Table 4-1, Parameter Number 01-10). The drifts will serve to enhance the role of the natural barriers and the EBS due to two processes: (1) the formation of a capillary barrier at drift walls that will be active during the thermal and ambient postclosure periods, and (2) the formation of a dryout zone helping to prevent percolation from reaching the repository during the thermal period (SNL 2008 [DIRS 184433], Section 6.1.3). The effectiveness of these processes depends on the strength of the capillary pressure in the fractures close to the drift, the host rock permeability close to the drifts, the local percolation flux above the drifts, the temperature of the rock near the drift walls, and the shape of the drift openings.

Internal Waste Package Components

There are two general waste package types evaluated in the performance assessment: the CSNF waste package and the codisposal waste package. For commercial SNF waste packages, the waste package internal component is the TAD canister. Codisposed waste packages will have internal steel components consisting primarily of carbon-steel basket guides and basket tubes, and stainless steel canisters for HLW and DOE SNF (SNL 2007 [DIRS 179394], Tables A-1, A-2, and 4-2). Additionally, TAD canisters and DOE SNF canisters will contain neutron absorbers for criticality control (SNL 2007 [DIRS 179394], Table A-4). The internal steel components are expected to degrade to iron oxyhydroxides upon exposure to water and repository atmospheric conditions following waste package failure. These degradation products could potentially sorb radionuclides released from the degradation of the waste forms.

Waste Emplacement Approach

Waste packages will be placed in the emplacement drifts in a line-load configuration with a waste package-to-waste package spacing of approximately 10 cm, and a line-averaged heat load of 2.0 kW/m. No waste package will exceed 18 kW (SNL 2007 [DIRS 179354], Table 4-4, Parameter Numbers 05-02 and 05-03). Preclosure ventilation will be active for at least 50 years after final waste emplacement (SNL 2007 [DIRS 179466], Table 4-2, Parameter Number 06-01).

The performance assessment modeling of engineered systems recognizes that degradation can lead to deterioration and alteration of engineered features that are included in models of EBS performance and, therefore, can affect system performance. Related included FEPs 2.1.03.08.0A (Early Failure of Waste Packages) and 2.1.03.08.0B (Early Failure of Drip Shields) specifically include the consideration of manufacturing and welding defects within the waste package and drip shield degradation analyses. Deficiencies beyond those specifically included in these FEPs are addressed in excluded FEP 1.1.08.00.0A (Inadequate Quality Control and Deviations from Design). The incorporation of repository design elements for waste retrievability is discussed in included FEP 1.1.13.00.0A (Retrievability). In conclusion, FEP 1.1.07.00.0A (Repository Design) is included in the TSPA.

INPUTS:

Table 1.1.07.00.0A-1. Indirect Inputs

Citation	Title	DIRS
10 CFR 63	Energy: Disposal of High-Level Radioactive Wastes in a Geologic Repository at Yucca Mountain, Nevada	180319
70 FR 53313	Implementation of a Dose Standard After 10,000 Years	178394
BSC 2004	*Commercial SNF Waste Package Design Report*	169766
BSC 2005	*Mountain-Scale Coupled Processes (TH/THC/THM) Models*	174101
BSC 2007	*IED Emplacement Drift Invert*	182746
BSC 2007	*IED Subsurface Facilities Geological Data*	182926
BSC 2008	*HLW/DOE SNF Co-Disposal Waste Package Design Report*	185102
BSC 2008	*Postclosure Modeling and Analyses Design Parameters*	183627
SNL 2007	*Drift-Scale THC Seepage Model*	177404
SNL 2007	*EBS Radionuclide Transport Abstraction*	177407
SNL 2007	*Total System Performance Assessment Data Input Package for Requirements Analysis for EBS In-Drift Configuration*	179354
SNL 2007	*Total System Performance Assessment Data Input Package for Requirements Analysis for Subsurface Facilities*	179466
SNL 2007	*Total System Performance Assessment Data Input Package for Requirements Analysis for TAD Canister and Related Waste Package Overpack Physical Attributes Basis for Performance Assessment*	179394
SNL 2008	*Multiscale Thermohydrologic Model*	184433
SNL 2008	*Total System Performance Assessment Model/Analysis for the License Application*	183478

FEP: 1.1.08.00.0A

FEP NAME:

Inadequate Quality Control and Deviations from Design

FEP DESCRIPTION:

This FEP addresses issues related to inadequate quality assurance and control procedures and inadequate testing during the design, construction, and operation of the repository. It also includes inadequacy in the manufacture of the waste forms, waste packages, and engineered features. Lack of quality control could result in a poorly designed repository, unmodeled design features, deviations from design, material defects, faulty waste package fabrication, and faulty or non-design standard construction. All of these may lead to reduction in the effectiveness of the engineered barriers.

SCREENING DECISION:

Excluded – low consequence

SCREENING JUSTIFICATION:

As described below, this FEP is excluded from the performance assessments on the basis of low consequence. Implementation of sound administrative and safety controls including a quality assurance program that meets the regulatory requirements of 10 CFR 63.142 [DIRS 180319] provides the foundation for demonstrating that unanalyzed defects in quality control or deviations from design will not have a significant adverse impact on postclosure performance of the repository.

Inherent in the FEPs evaluation approach is the expectation that the repository will be constructed, operated, and closed according to the design used as the basis for the FEP screening and in accordance with NRC license requirements. The postclosure-relevant aspects of the repository design are consistent with included FEP 1.1.07.00.0A (Repository Design). The inclusion of the repository design is accomplished through analyses of individual FEPs that are either excluded or included based on that design. The structures, systems, and components of the repository design that are relevant to the features of the natural barriers and the EBS used in performance assessment are identified in *Postclosure Modeling and Analyses Design Parameters* (BSC 2008 [DIRS 183627]); *Total System Performance Assessment Data Input Package for Requirements Analysis for Transportation Aging and Disposal Canister and Related Waste Package Overpack Physical Attributes Basis for Performance Assessment* (SNL 2007 [DIRS 179394]); *Total System Performance Assessment Data Input Package for Requirements Analysis for DOE SNF/HLW and Naval SNF Waste Package Physical Attributes Basis for Performance Assessment* (SNL 2007 [DIRS 179567]); *Total System Performance Assessment Data Input Package for Requirements Analysis for Engineered Barrier System In-Drift Configuration* (SNL 2007 [DIRS 179354]); and *Total System Performance Assessment Data Input Package for Requirements Analysis for Subsurface Facilities* (SNL 2007 [DIRS 179466]).

If there are significant deviations from the design that result from inadequate quality control, it is possible to affect the analyzed conditions. In recognition of this, regulations establish requirements for the management systems for the construction and operation of the repository to include administrative and procedural safety controls as well as design verification, testing, and performance confirmation. The establishment of adequate administrative and procedural safety controls ensure construction and operations are within analyzed conditions of the postclosure safety analysis and TSPA or that any deviations are analyzed for significance. This is consistent with the approach used to establish bounds for the performance evaluation of any engineering project. It is also necessary because the determination of the degree of the deviation (due to the potential inadequacy of the quality assurance, quality control, or testing) cannot always be evaluated a priori and must ultimately be based on specific deviations on a case-by-case basis.

Adequate Quality Assurance and Quality Control Procedures

The DOE Quality Assurance Program is established by regulation. As specified by 10 CFR 63.142 [DIRS 180319], "Quality assurance criteria:"

> *(a) Introduction and Applicability*.
>
> DOE is required by § 63.21(c)(20) to include in its safety analysis report a description of the quality assurance program to be applied to all structures, systems, and components important to safety, to design and characterization of barriers important to waste isolation, and to related activities. These activities include: site characterization; acquisition, control, and analyses of samples and data; tests and experiments; scientific studies; facility and equipment design and construction; facility operation; performance confirmation; permanent closure; and decontamination and dismantling of surface facilities.

Of particular relevance is the fact that 10 CFR Part 63 [DIRS 180319] requires the DOE to implement a layered quality assurance program for DOE, major contractor, and vendor activities similar to those for the 10 CFR Part 50 [DIRS 181964] power reactor and utilization facility environment. These programs provide a layered, defense-in-depth approach to activities (control of design, materials, shipping, handling, storage, fabrication, construction, installation, inspection, testing, operations, maintenance, oversight, identification and correction of nonconformances and conditions adverse to quality, etc.) for the applicant/licensee; engineering, procurement, and construction contractors; and vendors of equipment, materials, and services. In regulating other activities and facilities, the NRC has found that these programs are sufficiently self critical and self correcting to permit a conclusion that their implementation provides a reasonable assurance of safety. Since the 10 CFR Part 63 [DIRS 180319] quality assurance requirements are drawn from those established for reactors in 10 CFR Part 50 [DIRS 181964], repository safety analyses place the same reliance on the effectiveness of the quality assurance program as is done in the case of reactors.

In addition, provisions exist to evaluate the acceptability of and uncertainty in data that were not produced in accordance with the quality assurance program. These provisions require DOE to evaluate data required to support its license application. If data related to structures, systems, and components important to safety, to design and characterization of barriers important to waste isolation, and to activities related, thereto, have not been collected in accordance with a quality

assurance program that meets these requirements, the DOE is required to show that such data have been qualified for their intended use. The NRC recognizes that some data supporting a license application for a high-level waste repository may not have been initially collected under the quality assurance program. NUREG–1298 (Altman et al. 1988 [DIRS 103750], *Qualification of Existing Data for High-Level Nuclear Waste Repositories*, provides guidance on the use and qualification of data not initially collected in accordance with the quality assurance program. This guidance has been incorporated into the quality assurance program.

Adequate Testing During Design, Construction, and Operation of the Repository

Adequate testing requirements are also established by regulation. 10 CFR 63.74 establishes testing requirements during design, construction, and operation of the repository. In particular:

> (a) DOE shall perform, or permit the Commission to perform, those tests the Commission considers appropriate or necessary for the administration of the regulations in this part. This may include tests of—
>
> (1) Radioactive waste,
> (2) The geologic repository, including portions of the geologic setting and the structures, systems, and components constructed or placed therein,
> (3) Radiation detection and monitoring instruments, and
> (4) Other equipment and devices used in connection with the receipt, handling, or storage of radioactive waste.
>
> (b) The tests required under this section must include a performance confirmation program carried out in accordance with subpart F of this part.

The performance confirmation program is being conducted to evaluate the adequacy of assumptions, data, and analyses that form the bases of the postclosure performance assessment. Key geotechnical and design parameters, including any interactions between natural and engineered systems and components, will be monitored throughout site characterization, construction, emplacement, and operation to identify any significant changes in the conditions assumed in the license application that may affect compliance with the performance objectives specified in 10 CFR 63.113(b) and (c) [DIRS 180319].

Adequacy in the manufacture and testing of waste forms, waste packages, and engineered features.

As noted, the quality assurance program is required to be applied to design and characterization of barriers important to waste isolation, and to related activities; this includes the manufacture and testing of waste forms, waste packages, and engineered features. The performance confirmation program specifies requirements for the testing and monitoring waste forms, waste packages, and engineered features in 10 CFR 63.133 and 10 CFR 63.134 [DIRS 180319]. These requirements include:

> 10 CFR 63.133, Design testing.
>
> (a) During the early or developmental stages of construction, a program for testing of engineered systems and components used in the design, such as, for

> example, borehole and shaft seals, backfill, and drip shields, as well as the thermal interaction effects of the waste packages, backfill, drip shields, rock, and unsaturated zone and saturated zone water, must be conducted.

and

> 10 CFR 63.134, Monitoring and testing waste packages.
>
> (a) A program must be established at the geologic repository operations area for monitoring the condition of the waste packages. Waste packages chosen for the program must be representative of those to be emplaced in the underground facility.
>
> (b) Consistent with safe operation at the geologic repository operations area, the environment of the waste packages selected for the waste package monitoring program must be representative of the environment in which the wastes are to be emplaced.
>
> (c) The waste package monitoring program must include laboratory experiments that focus on the internal condition of the waste packages. To the extent practical, the environment experienced by the emplaced waste packages within the underground facility during the waste package monitoring program must be duplicated in the laboratory experiments.

Errors in the manufacture and fabrication of waste packages.

The treatment of waste-package failure as a result of errors (which remain undetected) due to inadequacy in their manufacture and fabrication are addressed in included FEP 2.1.03.08.0A (Early Failure of Waste Packages). Several general types of manufacturing defects are considered as mechanisms that could possibly adversely affect waste package performance, and include weld flaws, improper weld material, improper base metal, improper heat treatment, improper low plasticity burnishing, improper weld-flux material, poor weld-joint design, surface contamination, mislocated welds, missing welds, handling or installation damage, and administrative or operational error (SNL 2007 [DIRS 178765]). These defects are considered in the development of the early waste package failure event probabilities.

The closure lid welding process could also induce stresses in the waste package outer barrier lid, which could contribute to stress corrosion cracking of the waste packages. Induced stresses from the final closure weld process are addressed in included FEP 2.1.03.02.0A (Stress Corrosion Cracking of Waste Packages). This FEP accounts not only for stresses induced by welding the lid, but also lid weld flaws. Therefore, lid weld stresses and lid weld flaws that contributed to stress corrosion cracking of the waste packages are directly accounted for in the performance assessments.

Errors in the manufacture and fabrication of waste forms and waste package internals.

The radionuclides in the waste form are generally of a form that are highly insoluble to water and are not expected to mobilize, except for a limited number of radionuclides, thus significantly

reducing the radionuclide release rate. Control parameters related to the waste form capabilities are waste form moisture removal and inerting, loading of waste forms, and handling of waste forms. Deviations from design with respect to loading waste packages is addressed in excluded FEP 2.1.14.15.0A (In-Package Criticality (Intact Configuration)) Waste form manufacture and fabrication errors related to the use of improper absorber materials or waste form misloads are addressed in the excluded criticality FEPs (see for example FEP 2.1.14.15.0A (In-Package Criticality (Intact configuration))). Excluded FEP 2.1.13.01.0A (Radiolysis) evaluates the effects of a design-specified quantity of water being left inside a waste package.

As indicated in included FEP 2.1.02.12.0A (Degradation of Cladding Prior to Disposal), cladding degradation prior to receipt at the repository can occur during reactor operation, spent fuel pool storage, dry storage, transport, and handling. The representation of all defense SNF cladding (with the exception of naval SNF cladding) and commercial SNF cladding in performance assessments assumes the cladding will be breached on emplacement in the repository and will inhibit neither groundwater contacting the fuel matrix nor the release of radionuclides after groundwater contact (SNL 2008 [DIRS 183478], Section 6.3.7.3.1). This representation bounds any errors that may have occurred during the manufacture, fabrication, and handling of cladding.

Errors in the manufacture and fabrication of engineered features (drip shields)

Evaluation of undetected errors during manufacture and installation of drip shields is addressed in included FEP 2.1.03.08.0B (Early Failure of Drip Shields). Such errors could lead to early failure of the drip shields. Several general types of manufacturing defects are considered as possible mechanisms that could adversely affect drip shield performance, including weld flaws, base metal flaws, improper weld material, improper base metal, improper heat treatment, improper low plasticity burnishing, improper weld-flux material, poor weld-joint design, surface contamination, mislocated welds, missing welds, handling or installation damage (including gaps between drip shields), and administrative or operational error.

Deviations from design and non-standard construction.

Deviations from design and non-standard construction are also addressed by regulatory requirements linked to testing and quality assurance. For example, 10 CFR 63.132 [DIRS 180319], "Confirmation of geotechnical and design parameters" requires:

> (a) During repository construction and operation, a continuing program of surveillance, measurement, testing, and geologic mapping must be conducted to ensure that geotechnical and design parameters are confirmed and to ensure that appropriate action is taken to inform the Commission of design changes needed to accommodate actual field conditions encountered.
>
> (b) Subsurface conditions must be monitored and evaluated against design assumptions.
>
> (c) Specific geotechnical and design parameters to be measured or observed, including any interactions between natural and engineered systems and components, must be identified in the performance confirmation plan.

> (d) These measurements and observations must be compared with the original design bases and assumptions. If significant differences exist between the measurements and observations and the original design bases and assumptions, the need for modifications to the design or in construction methods must be determined and these differences, their significance to repository performance, and the recommended changes reported to the Commission.
>
> (e) In situ monitoring of the thermomechanical response of the underground facility must be conducted until permanent closure, to ensure that the performance of the geologic and engineering features is within design limits.

In 10 CFR 63.73(a) [DIRS 180319], the NRC requires prompt notification if there is a significant deficiency found in: (1) the characteristics of the Yucca Mountain site, or (2) the design and construction of the geologic repository area, including significant deviations from the design criteria and design bases stated in the application. Significant deviations that are detected during the operational period will be evaluated and, as needed, corrected. Any residual defects or fabrication or construction deficiencies, therefore, will be of a minor nature and will not lead to significant effects on repository performance. Compliance with the requirements described will ensure that significant effects from undetected deviations in design are not expected.

Modifications and deviations from the design are subject to regulatory requirements and review that address deliberate changes and modifications. The manner in which the DOE must address changes, and by which the NRC is informed of the changes, is codified in 10 CFR 63.44 [DIRS 180319]. After the NRC authorizes construction of the repository, changes to the repository design or procedures as described in the SAR will be subject to the requirements of 10 CFR 63.44 [DIRS 180319], "Changes, tests, and experiments," as well as any specific license conditions imposed in accordance with 10 CFR 63.32 [DIRS 180319], "Conditions of construction authorization;" 10 CFR 63.42 [DIRS 180319], "Conditions of license;" or 10 CFR 63.43 [DIRS 180319], "License specification."

The DOE process for controlling changes under 10 CFR 63.44 [DIRS 180319] is subject to the DOE Quality Assurance Program, in accordance with the guidance in NUREG-1804 (NRC 2003 [DIRS 163274], Section 2.5.1.3, Acceptance Criteria 2(7), 2(10), and 3(21)).

The DOE Quality Assurance Program includes the following provisions for controlling design changes (DOE 2007 [DIRS 182051], Section 3.2.6):

A. Changes to final designs, field changes, and nonconforming items dispositioned "use-as-is" or "repair" shall be justified and shall be subject to design control measures commensurate with those applied to the original design.

B. Changes shall be approved by the same affected groups or organizations that approved the original design documents.

    1. If an organization that originally was responsible for approving a particular design document is no longer responsible, a new responsible organization shall be designated by the OCRWM.

2. The designated approving organization shall have demonstrated competence in the specific design area of interest and have an adequate understanding of the requirements and intent of the original design.

C. The design process and design verification methods and implementing documents shall be reviewed and modified, as necessary, when a significant design change is necessary because of an incorrect design.

D. Errors and deficiencies in approved design documents, including design methods (i.e., computer software supporting a safety or waste isolation function), that could adversely affect [structures, systems, and components] important to safety or waste isolation shall be documented and action taken to ensure all errors and deficiencies are corrected.

E. Deviations from specified quality standards shall be identified and formally documented. Procedures shall be established to ensure control of these deviations.

F. Measures shall be provided to ensure personnel are notified of design changes/modifications that may affect the performance of their duties.

G. Prior to the issuance of a design change initiated after the construction authorization, the design changes shall be evaluated pursuant to applicable regulatory requirements.

The potential impacts of excavation and construction are considered in excluded FEPs 1.1.02.03.0A (Undesirable Materials Left), 1.1.03.01.0A (Error in Waste Emplacement), 1.1.12.01.0A (Accidents and Unplanned Events during Construction and Operation), 1.1.02.00.0A (Chemical Effects of Excavation and Construction in EBS), 2.2.01.01.0B (Chemical Effects of Excavation and Construction in the Near Field), and 1.1.02.00.0B (Mechanical Effects of Excavation and Construction in EBS). Excluded FEP 2.1.06.01.0A (Chemical Effects of Rock Reinforcement and Cementitious Materials in EBS) considers the effects of cement dust that may blow into emplacement drifts. Improper placement of drip shields is addressed in included FEP 2.1.03.08.0B (Early Failure of Drip Shields). Potential effects from residual organics are considered in excluded FEP 2.1.10.01.0A (Microbial Activity in the EBS). To limit undesired effects from excavation and construction (e.g., corrosion and radionuclide transport impacts), requirements have been established to identify, analyze, and control the use of any materials (including water) that will be present in the repository at closure and could adversely impact postclosure performance. The application of these controls is described in *Total System Performance Assessment Data Input Package for Requirements Analysis for Engineered Barrier System In-Drift Configuration* (SNL 2007 [DIRS 179354], Table 4-1, Parameter Number 02-03).

The provided examples are not exhaustive because the deviation and the degree of deviation (due to the potential inadequacy of the quality assurance, quality control, or testing) cannot always be evaluated a priori and must be evaluated on a case-by-case basis. The DOE approach to demonstrating waste isolation includes a repository system that relies on multiple barriers, the use of multiple lines of evidence related to system performance, and a continuous learning approach to repository design and construction. The subsurface facilities are planned to be

constructed in phases. The development of the subsurface facility will proceed while emplacement operations are conducted in the completed drifts and will be done in a manner that safely accommodates waste package emplacement. Phased construction and operation provides an opportunity for orderly implementation of lessons learned and incorporation of new information that would improve the safety of construction and operations. The repository will implement a management system that includes the evaluation of changes, tests, and experiments. Lessons learned and new information will be evaluated against the criteria in 10 CFR 63.44 [DIRS 180319], and the lessons learned or new information will be implemented following construction authorization or license amendment if any of the criteria are met; otherwise, the proposed changes will be implemented and documented in updates to the SAR. This is consistent with the National Research Council's description of staged development that allows for proposed adaptation without unacceptable impacts on safety or waste isolation (National Research Council 1995 [DIRS 100018], Chapter 3), incorporation of new knowledge on features and processes that determine repository performance, and accommodation of significant changes in repository requirements.

Finally, 10 CFR 63.51 [DIRS 180319] requires the DOE to submit an application to amend the license before permanent closure of a geologic repository. The submission must include an update of the assessment of the performance of the geologic repository for the period after permanent closure. The updated assessment must include any performance confirmation data collected under the program required by Subpart F, and pertinent to compliance with 10 CFR 63.113 [DIRS 180319]. This ensures that effectiveness of the engineered barriers are evaluated with respect to any significant deviations from design during construction and operation of the repository.

In summary, FEP 1.1.08.00.0A (Inadequate Quality Control and Deviations from Design) is excluded from the performance assessments conducted to demonstrate compliance with proposed 10 CFR 63.311 and 63.321 (70 FR 53313 [DIRS 178394]), and with 10 CFR 63.331 [DIRS 180319], on the basis of low consequence. In addition, the regulatory requirements for performance confirmation and quality assurance require that any deviation from design during the operational period be evaluated for potential impact, and that deviations with a significant adverse impact on postclosure performance be corrected.

INPUTS:

Table 1.1.08.00.0A-1. Direct Inputs

Input	Source	Description
10 CFR 63. 2007. Energy: Disposal of High-Level Radioactive Wastes in a Geologic Repository at Yucca Mountain, Nevada [DIRS 180319]	10 CFR 63.51	Requires the DOE to submit an application to amend the license before permanent closure of a geologic repository
	10 CFR 63.43	After the NRC authorizes construction of the repository, changes to the repository design or procedures as described in the SAR will be subject to license specification

Table 1.1.08.00.0A-1. Direct Inputs (Continued)

Input	Source	Description
10 CFR 63. 2007. Energy: Disposal of High-Level Radioactive Wastes in a Geologic Repository at Yucca Mountain, Nevada [DIRS 180319] (continued)	10 CFR 63.42	After the NRC authorizes construction of the repository, changes to the repository design or procedures as described in the SAR will be subject to conditions of license
	10 CFR 63.32	After the NRC authorizes construction of the repository, changes to the repository design or procedures as described in the SAR will be subject to conditions of construction authorization
	10 CFR 63.132	Requirements of geotechnical and design parameters
	10 CFR 63.133 and 10 CFR 63.134	Performance confirmation program specifies requirements for the testing and monitoring waste forms, waste packages, and engineered features
	10 CFR 63.113(b) and (c)	Performance objectives
	10 CFR 63.142	Quality assurance criteria
	10 CFR 63.142	Foundation for demonstrating that unanalyzed defects in quality control or deviations from design will not have a significant adverse impact on postclosure performance of the repository
	10 CFR 63.331	Separate standards for protection of groundwater
	10 CFR 63 Subpart G	Requires quality assurance and quality control programs be applied to all systems, structures, and components important to safety
	10 CFR Part 63	Provides a list of requirements that have been incorporated into the performance confirmation program to provide data related to encountered subsurface conditions, functioning of the natural and engineered systems, monitoring and testing
	10 CFR 63.73(a)	NRC requires prompt notification if there is a significant deficiency found in (1) the characteristics of the Yucca Mountain site, or (2) the design and construction of the geologic repository area, including significant deviations from the design criteria
	10 CFR 63.44	List the manner in which the DOE must address changes, and by which the NRC is informed of the changes

Table 1.1.08.00.0A-2. Indirect Inputs

Citation	Title	DIRS
10 CFR 50	Energy: Domestic Licensing of Production and Utilization Facilities. Internet Accessible	181964
10 CFR 63	Energy: Disposal of High-Level Radioactive Wastes in a Geologic Repository at Yucca Mountain, Nevada	180319
70 FR 53313	Implementation of a Dose Standard After 10,000 Years	178394
Altman et al. 1988	*Qualification of Existing Data for High-Level Nuclear Waste Repositories: Generic Technical Position.* NUREG-1298.	103750
DOE 2007	*Quality Assurance Requirements and Description*	182051
National Research Council 1995	*Technical Bases for Yucca Mountain Standards*	100018
SNL 2007	*Total System Performance Assessment Data Input Package for Requirements Analysis for EBS In-Drift Configuration*	179354
SNL 2007	*Analysis of Mechanisms for Early Waste Package/Drip Shield Failure*	178765
SNL 2007	*Total System Performance Assessment Data Input Package for Requirements Analysis for DOE SNF/HLW and Navy SNF Waste Package Overpack Physical Attributes Basis for Performance Assessment*	179567
SNL 2007	*Total System Performance Assessment Data Input Package for Requirements Analysis for Subsurface Facilities*	179466
SNL 2007	*Total System Performance Assessment Data Input Package for Requirements Analysis for TAD Canister and Related Waste Package Overpack Physical Attributes Basis for Performance Assessment*	179394
SNL 2008	*Total System Performance Assessment Model/Analysis for the License Application*	183478

FEP: 1.1.09.00.0A

FEP NAME:

Schedule and Planning

FEP DESCRIPTION:

This FEP addresses the sequences of events and activities occurring during construction, operation, and closure of the repository. Deviations from the design construction or waste emplacement schedule may affect the long-term performance of the disposal system.

SCREENING DECISION:

Included

TSPA DISPOSITION:

Scheduling and planning are components of the process implemented to achieve the expected repository postclosure conditions. The subsurface facilities are planned to be constructed in phases and the development of the subsurface facilities will proceed while emplacement operations are conducted in the completed drifts. The schedule for waste emplacement and planned subsurface ventilation will affect the radionuclide inventories and thermal-hydrological conditions at the time of repository closure. In particular, conditions at closure will depend on the implementation of design requirements for subsurface facilities and their ventilation, sealing, and closure (SNL 2007 [DIRS 179466]), and for waste emplacement (SNL 2007 [DIRS 179354]).

Modifications and deviations from the design for construction, operation, and closure of the repository are subject to regulatory requirements and review that address deliberate changes and modifications. The manner in which the DOE must address changes, and by which the NRC is informed of the changes, is codified in 10 CFR 63.44 [DIRS 180319]. After the NRC authorizes construction of the repository, changes to the repository design or procedures as described in the SAR will be subject to the requirements of 10 CFR 63.44 [DIRS 180319], "Changes, tests, and experiments," as well as any specific license conditions imposed in accordance with 10 CFR 63.32, "Conditions of construction authorization," 10 CFR 63.42 [DIRS 180319], "Conditions of license," or 10 CFR 63.43 [DIRS 180319], "License specification." Deviations from design as a result of inadequate quality control during repository construction, operation, and closure is addressed in excluded FEP 1.1.08.00.0A (Inadequate Quality Control and Deviations from Design), which is excluded from the TSPA by regulation.

Phased construction and operation provides an opportunity for orderly implementation of lessons learned and incorporation of new information that would improve the safety of construction and operations. The repository will implement a management system that includes the evaluation of changes, tests and experiments. Lessons learned and new information will be evaluated against the criteria in 10 CFR 63.44 [DIRS 180319], and the lessons learned or new information will be implemented following construction authorization or license amendment if any of the criteria are met; otherwise, the proposed changes will be implemented and documented in updates to the

SAR. This is consistent with the National Research Council description of staged development (National Research Council 1995 [DIRS 100018], Chapter 3) that allows for proposed adaptation without unacceptable impacts on safety or waste isolation, incorporation of new knowledge on features and processes that determine repository performance, and accommodation of significant changes in repository requirements.

In summary, scheduling and planning are included in the TSPA model because they influence the conditions at repository closure and are components of the process implemented to achieve the expected repository postclosure conditions, both of which are inputs to the TSPA model.

INPUTS:

Table 1.1.09.00.0A-1. Indirect Inputs

Citation	Title	DIRS
10 CFR 63	Energy: Disposal of High-Level Radioactive Wastes in a Geologic Repository at Yucca Mountain, Nevada	180319
National Research Council 1995	*Technical Bases for Yucca Mountain Standards*	100018
SNL 2007	*Total System Performance Assessment Data Input Package for Requirements Analysis for EBS In-Drift Configuration*	179354
SNL 2007	*Total System Performance Assessment Data Input Package for Requirements Analysis for Subsurface Facilities*	179466

FEP: 1.1.10.00.0A

FEP NAME:

Administrative Control of the Repository Site

FEP DESCRIPTION:

Administrative control can reduce the potential for detrimental or unplanned human activities within the controlled area that could inadvertently cause or accelerate the release of radioactive material.

SCREENING DECISION:

Excluded – by regulation

SCREENING JUSTIFICATION:

Administrative controls are defined in 10 CFR 63.43(6) [DIRS 180319] as "provisions relating to organization and management, procedures, recordkeeping, review and audit, and reporting necessary to assure that activities at the facility are conducted in a safe manner and in conformity with the other license specification." This definition of administrative controls addresses preclosure operational activities that are addressed in included FEPs 0.1.09.00.0A (Regulatory Requirements and Exclusions) and 1.1.09.00.0A (Schedule and Planning), and excluded FEPs 1.1.08.00.0A (Inadequate Quality Control and Deviations from Design) and 1.1.12.01.0A (Accidents and Unplanned Events during Construction and Operation).

Administrative controls may also include the use of policies, procedures, markers, training or supervision of records to control risk. Markers and repository archives are discussed in excluded FEP 1.1.05.00.0A (Records and Markers for the Repository). The NRC recognizes that such institutional controls are expected to significantly reduce, but not eliminate, the potential for human activity that causes or accelerates the release of radioactive material. In 10 CFR 63.102(k) [DIRS 180319], the regulations address the use of institutional controls; they require that both passive and active institutional controls be maintained, but not relied upon for TSPA. The regulation states:

> Active and passive institutional controls will be maintained over the Yucca Mountain site, and are expected to reduce significantly, but not eliminate, the potential for human activity that could inadvertently cause or accelerate the release of radioactive material. However, because it is not possible to make scientifically sound forecasts of the long-term reliability of institutional controls, it is not appropriate to include consideration of human intrusion into a fully risk-based performance assessment for purposes of evaluating the ability of the geologic repository to achieve the performance objective at §63.113(b). Hence, human intrusion is addressed in a stylized manner as described in paragraph (I) of this section.

The requirements for constructing monuments, preserving and archiving records, and oversight are also of relevance to administrative controls and are listed in 10 CFR 63.51(a)(3)(i-iii), 10 CFR 63.72(a), and 10 CFR 63.72(b)(1-11) [DIRS 180319]. Land ownership and control requirements are specified in 10 CFR 63.121 [DIRS 180319]. On the basis of the quoted regulation, and the aforementioned FEPs, this FEP is excluded by regulation from consideration in performance assessments.

INPUTS:

Table 1.1.10.00.0A-1. Direct Inputs

Input	Source	Description
10 CFR 63. 2007. Energy: Disposal of High-Level Radioactive Wastes in a Geologic Repository at Yucca Mountain, Nevada. [DIRS 180319]	10 CFR 63.121	Land ownership and control requirements
	10 CFR 63.51(a)(3)(i-iii), 10 CFR 63.72(a), 10 CFR 63.72(b)(1-11)	Requirements for constructing monuments, preserving, and archiving records, and ovesight
	10 CFR 63.102(k)	It is required that both passive and active institutional controls be maintained but not relied upon for TSPA

Table 1.1.10.00.0A-2. Indirect Inputs

Citation	Title	DIRS
10 CFR 63	Energy: Disposal of High-Level Radioactive Wastes in a Geologic Repository at Yucca Mountain, Nevada	180319

FEP: 1.1.11.00.0A

FEP NAME:

Monitoring of the Repository

FEP DESCRIPTION:

Monitoring that is carried out during or after operations, for either operational safety or verification of long-term performance, has the potential to detrimentally affect long-term performance. For example, monitoring boreholes could provide enhanced pathways between the surface and the repository.

SCREENING DECISION:

Excluded – low consequence

SCREENING JUSTIFICATION:

Appropriate planning of repository activities and the effective implementation of quality control procedures will ensure that monitoring activities have an insignificant effect on long-term repository performance. The extent and, correspondingly, the impact of invasive activities for the purpose of monitoring will be insignificant compared to the scale of construction of the repository itself and will therefore be of low consequence to the long-term performance of the repository. As for all repository activities, these activities will be performed in accordance with NRC regulatory requirements during the preclosure period. Modifications to, and deviations from, the design are subject to regulatory requirements that address deliberate changes and modifications (10 CFR 63.44 [DIRS 180319]). Furthermore, 10 CFR 63.73(a) [DIRS 180319] requires that DOE "promptly notify the [NRC] of each deficiency found in the characteristics of the Yucca Mountain site, and design, and construction of the geologic repository operations area that, were it to remain uncorrected, could: (1) adversely affect safety at any future time; (2) represent a significant deviation from the design criteria and design basis stated in the design application; or (3) represent a deviation from the conditions stated in the terms of a construction authorization or the license, including license specification." As discussed below, deviations in the design, conditions of construction authorization, or license related to monitoring activities, or findings that the monitoring activities may adversely affect safety at any future time, will be evaluated and corrected, as needed.

Regulation 10 CFR Part 63, Subpart F [DIRS 180319] provides a list of requirements for a performance confirmation program to confirm design parameters and to ensure that the NRC is informed of changes needed in the design to accommodate field conditions. 10 CFR 63.131(c) [DIRS 180319] requires that "The program must include in situ monitoring, laboratory and field testing, and in situ experiments, as may be appropriate to provide the data required by paragraph (a) of this section," where paragraph (a) establishes the performance confirmation program. Consequently, the use of in situ monitoring and experimentation is anticipated. However, the regulation also states that any monitoring program must be implemented so that "It does not adversely affect the ability of the geologic and engineered elements of the geologic repository to meet the performance objectives" (10 CFR 63.131(d)(1) [DIRS 180319]). The repository

performance confirmation program for a repository at Yucca Mountain is described in *Performance Confirmation Plan* (BSC 2004 [DIRS 172452]). Appropriate planning of repository activities and the effective implementation of quality control procedures will ensure that monitoring activities have an insignificant effect on long-term repository performance as described in *Perfomance Confirmation Plan* (BSC 2004 [DIRS 172452], Section 3.3; note that the procedure governing the evaluation of site activites has been superseded by SCI-PRO-007, *Determination of Importance and Site Performance Protection Evaluations*). These topics are discussed further in excluded FEPs 1.1.09.00.0A (Schedule and Planning) and 1.1.08.00.0A (Inadequate Quality Control and Deviations from Design), although not with specific reference to monitoring.

The strategy for collection, evaluation, and presentation of monitoring data throughout site characterization, construction, and operation is an integral component of the performance confirmation plan. Preclosure monitoring activities will be diverse and will be modified as appropriate to current and ongoing repository activities. The performance confirmation activities that could have the greatest impact on repository performance are those that are, in some way, intrusive to the repository, through the use of boreholes, wells, drilling, construction of monitoring alcoves, or equipment emplacement in the drifts. These activities include seepage monitoring, subsurface water and rock testing, unsaturated zone testing, saturated zone monitoring, saturated zone alluvium testing, construction effects monitoring, seal testing, monitoring in or near thermally accelerated drifts, and saturated zone fault hydrology testing (BSC 2004 [DIRS 172452], Section 3.3).

Planned monitoring activities in the unsaturated zone, including seepage monitoring, rock and water sampling, and testing of transport properties and field sorptive properties of the host rock, are described in *Performance Confirmation Plan* (BSC 2004 [DIRS 172452], Sections 3.3.1.2, 3.3.1.3, and 3.3.1.4). Seepage monitoring is expected to have low impact because the amount of seepage that could be sampled is insignificant so as to not impact water reaching the drifts. In thermally accelerated drifts, the monitoring and testing period will be followed by closure of the test bed, which may include removing waste packages and instrumentation and sealing, as appropriate (BSC 2004 [DIRS 172452], Sections 3.3.1.2 and 3.3.1.9). Rock and water sampling is expected to have low impact because the drilling to obtain samples is very limited and occurs in a very small portion of the drift and main cross section. Since the amount of rock that may be sampled is an insignificant amount, impact to the pathway of water reaching the drifts is negligible, especially during the periods after closure (BSC 2004 [DIRS 172452], Section 3.3.1.3). Testing of transport properties and field sorptive properties of the host rock are expected to have low impact because the alcoves and drilling to obtain samples is very limited and occurs in a very small portion of the repository. The amount of rock anticipated to contain residual concentrations of tracers is negligible with respect to performance (BSC 2004 [DIRS 172452], Section 3.3.1.4). In general, further evaluations of waste isolation, test-to-test interference, and operations will be conducted during the detailed test planning. Any boreholes or alcoves used may be sealed prior to closure if modeling results indicated that they would increase seepage potential or alter the chemistry of potential water leaving the drifts. Any monitoring boreholes that unexpectedly intercept waste emplacement drifts have addtional sealing requirements (SNL 2007 [DIRS 179466], Table 4-1, Parameter Number 09-03).

Planned monitoring activities in the saturated zone, including monitoring, sampling, and analyzing saturated zone water from Nye County and site wells, hydraulic and tracer testing of fault zone hydrologic characteristics, and evaluation of transport properties of the alluvium are described in *Performance Confirmation Plan* (BSC 2004 [DIRS 172452], Sections 3.3.1.5, 3.3.1.6, and 3.3.1.7). Monitoring and sampling from Nye County and site wells are not expected to have an impact because the monitoring of existing wells, including the obtaining of samples, will remove only a very small amount of water from the groundwater reservoir. The amount of water that may be sampled is of such an insignificant amount as to not impact the saturated zone (BSC 2004 [DIRS 172452], Section 3.3.1.5). Hydraulic and tracer testing of faults is not expected to have an impact because the new wells that may be tested, including obtaining samples, remove only a very small amount of water from the fractured and nonwelded tuffs of the groundwater reservoir. The amount of water that may be sampled is of such an insignificant amount as to not impact the saturated zone. The amount of rock that could contain residual concentrations of tracers is of such an insignificant amount as to not impact the chemical environment of groundwater in the flow path (BSC 2004 [DIRS 172452], Section 3.3.1.6). The evaluation of transport properties of the alluvium is not expected to have an impact because the existing wells that will be tested, including obtaining samples, remove only a very small amount of water from the alluvial deposits of groundwater reservoir. The amount of water that may be sampled is of such an insignificant amount as to not impact the saturated zone. The amount of alluvium that will contain residual concentrations of tracers is of such an insignificant amount as to not impact the chemical environment of groundwater in the flow path (BSC 2004 [DIRS 172452], Section 3.3.1.7). In general, further evaluations of waste isolation, test-to-test interference, and operations will be conducted during the detailed test planning. Any boreholes or wells used for performance confirmation may be sealed prior to closure if modeling results indicated that they would increase the probability of vertical migration or alter the chemistry of potential water traveling through the saturated zone along radionuclide transport pathways.

Testing of borehole seals is a regulatory requirement in 10 CFR 63.133(d) [DIRS 180319], which states that "[t]ests must be conducted to evaluate the effectiveness of borehole, shaft, and ramp seals before full scale operation proceeds to seal boreholes, shafts, and ramps." Excluded FEP 2.1.05.03.0A (Degradation of Seals) evaluates the impacts of seal degradation on performance. The impacts of boreholes and monitoring wells are discussed in excluded FEP 1.1.01.01.0A (Open Site Investigation Boreholes) and excluded FEP 1.1.01.01.0B (Influx Through Holes Drilled in Drift Wall or Crown). The effects of boreholes on the transport of radionuclides were shown to be negligible in comparison to the transport pathways associated with fractures and faults. The effects of rock-bolt boreholes drilled in the drift wall or crown were analyzed (BSC 2004 [DIRS 167652], Section 6.5), and the holes were found to increase seepage by less than 2% (DTN: LB0304SMDCREV2.001 [DIRS 173235]; BSC 2004 [DIRS 167652], Table 6-4).

All other performance confirmation activities (including precipitation monitoring, subsurface mapping, seismicity monitoring, corrosion testing, waste-form/waste package testing, drift inspection, and dust buildup monitoring) involve remote monitoring, minimal instrumentation and/or analysis off-site (BSC 2004 [DIRS 172452], Section 3.3). These activities are not expected to adversely affect the ability of the repository to meet performance objectives because the instrumentation is very small and covers an insignificant portion of the rock in the repository (BSC 2004 [DIRS 172452], Section 3.3).

In general, further evaluations of waste isolation, test-to-test interference, and operations will be conducted during the detailed test planning. Any boreholes or alcoves used may be sealed prior to closure if modeling results indicated that they would increase seepage potential or alter the chemistry of potential water leaving the drifts. Any boreholes or wells used for performance confirmation may be sealed prior to closure if modeling results indicated that they would increase the probability of vertical migration or alter the chemistry of potential water traveling through the saturated zone along radionuclide transport pathways.

In summary, monitoring is required to provide data for the assessment of repository performance confirmation (10 CFR 63.131(c) [DIRS 180319]). However, monitoring must not adversely affect the ability of the geologic and engineered elements of the repository to meet the repository performance objectives (10 CFR 63.131(d)(1) [DIRS 180319]). Appropriate planning of repository activities and the effective implementation of quality control procedures will ensure that monitoring activities have an insignificant effect on long-term repository performance.

Based on the preceding discussion, omission of FEP 1.1.11.00.0A (Monitoring of the Repository) will not result in a significant adverse change in the magnitude or time of radiological exposures to the RMEI or radionuclide releases to the accessible environment. Therefore, this FEP is excluded from the performance assessments conducted to demonstrate compliance with proposed 10 CFR 63.311 and 63.321 (70 FR 53313 [DIRS 178394]), and with 10 CFR 63.331 [DIRS 180319], on the basis of low consequence.

INPUTS:

Table 1.1.11.00.0A-1. Direct Inputs

Input	Source	Description
10 CFR 63. 2007. Energy: Disposal of High-Level Radioactive Wastes in a Geologic Repository at Yucca Mountain, Nevada. [DIRS 180319]	10 CFR 63.73(a)	Requires that DOE promptly notify the NRC of each deficiency found in the characteristics of the Yucca Mountain site, and design, and construction of the geologic repository operations area
DTN: LB0304SMDCREV2.001. Seepage Modeling for Performance Assessment, Including Drift Collapse: Input/Output Files. [DIRS 173235]	Table 6-4	Rock-bolt boreholes drilled in the drift wall or crown were found to increase seepage by less than 2%

Table 1.1.11.00.0A-2. Indirect Inputs

Citation	Title	DIRS
10 CFR 63	Energy: Disposal of High-Level Radioactive Wastes in a Geologic Repository at Yucca Mountain, Nevada	180319
70 FR 53313	Implementation of a Dose Standard After 10,000 Years	178394
BSC 2004	*Performance Confirmation Plan*	172452
BSC 2004	*Seepage Model for PA Including Drift Collapse*	167652
SNL 2007	*Total System Performance Assessment Data Input Package for Requirements Analysis for Subsurface Facilities*	179466

FEP: 1.1.12.01.0A

FEP NAME:

Accidents and Unplanned Events During Construction and Operation

FEP DESCRIPTION:

The long-term performance of the disposal system might be seriously affected by unplanned or improper activities that take place during construction, operation, and closure of the repository.

SCREENING DECISION:

Excluded – by regulation

SCREENING JUSTIFICATION:

Inherent in the FEP evaluation approach used as the basis for the FEP screening is the expectation that the repository will be constructed, operated, and closed in accordance with DOE design control, DOE QA process, and NRC license requirements. In 10 CFR 63.73 [DIRS 180319], the NRC requires prompt notification if there is a significant deficiency found in the characteristics, design, and construction of the geologic repository operations area that, were it to remain uncorrected, could adversely affect safety in the future. This includes significant deviations from the design criteria and design basis stated in the application, construction authorization, or the license. Quality control procedures are designed to detect operational events, such as accidents and unplanned events, resulting in deviations from the repository design that might affect long-term performance. It is expected that significant deviations would be detected during regular audits and inspections, pursuant to 10 CFR Part 63, Subpart D [DIRS 180319], and corrected before further work in the repository would be allowed to continue.

In 10 CFR 63.73(a) [DIRS 180319], the NRC requires the DOE to "promptly notify the commission of each deficiency found in the characteristics of the Yucca Mountain site, and design, and construction of the geologic repository operations area that, were it to remain uncorrected, could: (1) adversely affect safety at any future time." Significant deviations that are detected during the operational period will be evaluated and, as needed, corrected. Undetected accidents or undetected unplanned events are expected to be inconsequential, because detected accidents and events will be analyzed and remediated (as necessary). Compliance with the requirements described will ensure that significant effects from accidents or unplanned events on design are not expected.

Further discussion of quality control procedures and regulations covering deviations from design is provided in excluded FEP 1.1.08.00.0A (Inadequate Quality Control and Deviations from Design).

In summary, regulation of accidents and unplanned events during construction and operation will prevent any effects on long-term performance of the repository and will not cause a significant adverse effect on the magnitude or timing of calculated radiological exposures to the RMEI or

radionuclide releases to the accessible environment. Therefore, FEP 1.1.12.01.0A (Accidents and Unplanned Events During Construction and Operation) is excluded from the performance assessments conducted to demonstrate compliance with proposed 10 CFR 63.311 and 63.321 (70 FR 53313 [DIRS 178394]), and with 10 CFR 63.331 (10 CFR 63 [DIRS 180319]), on the basis of regulation.

INPUTS:

Table 1.1.12.01.0A-1. Direct Inputs

Input	Source	Description
10 CFR 63. 2007. Energy: Disposal of High-Level Radioactive Wastes in a Geologic Repository at Yucca Mountain, Nevada. [DIRS 180319]	10 CFR 63.331	Separate standards for protection of groundwater
	10 CFR 63.73(a)	NRC requires prompt notification if there is a significant deficiency found in the characteristics, design, and construction of the geologic repository operations area
	10 CFR 63.73	NRC requires prompt notification if there is a significant deficiency found
	10 CFR 63, Subpart D	Any significant deviations would be detected during regulator audits and inspections
70 FR 53313. Implementation of a Dose Standard After 10,000 Years. [DIRS 178394]	10 CFR 63.321	Individual protection standard for human intrusion
	10 CFR 63.311	Individual protection standard after permanent closure

FEP: 1.1.13.00.0A

FEP NAME:

Retrievability

FEP DESCRIPTION:

This FEP addresses design, emplacement, operational, or administrative measures that might be applied or considered to enable or ease retrieval of waste. There may be a requirement to retrieve all or part of the waste stored in the repository, for example, to recover valuable fissile materials or to replace defective waste packages.

SCREENING DECISION:

Included

TSPA DISPOSITION:

Retrievability is a performance objective of the repository as specified in 10 CFR 63.111(e)(1, 2, and 3) [DIRS 180319], and features are included in the design to allow for retrievability for any reason including resource recovery. The regulation specifies that the repository be designed in such a way that it preserves "the option of waste retrieval throughout the period during which wastes are being emplaced … so that any or all of the emplaced waste could be retrieved on a reasonable schedule starting at any time up to 50 years after waste emplacement operations are initiated" (10 CFR 63.111(e)(1) [DIRS 180319]). This precludes further FEP consideration for retrieval past 50 years after the start of waste emplacement. Postclosure retrieval of wastes or other repository system components for resource recovery was addressed by the NRC in the supplementary information for 10 CFR Part 63 (66 FR 55732 [DIRS 156671], p. 55743) as follows:

> As for longer retrieval periods [>50 years]…the Commission has previously noted that its retrieval provision is not intended to facilitate recovery. Waste retrieval is intended to be an unusual event only to be undertaken to protect public health and safety.

Regardless, the repository design is part of the basis of the postclosure evaluation, and aspects of the repository design related to waste retrievability are therefore considered as part of the basis for the TSPA modeling and are included, as noted in included FEP 1.1.07.00.0A (Repository Design). The incorporation of repository design information into the framework of the various TSPA model components has been accomplished using TSPA data input packages (SNL 2007 [DIRS 179394], SNL 2007 [DIRS 179567], SNL 2007 [DIRS 179354], and SNL 2007 ([DIRS 179466]) which are cited, as needed, in the individual model or analysis reports. The drawings contain information regarding material characteristics and properties, component dimensions, and component performance properties under various specified test conditions (e.g., corrosion rates, and seismic response damage areas).

The approach to support successful retrieval operations is to develop the subsurface facility in such a manner that access to the waste is maintained throughout the preclosure period. *Concepts for Waste Retrieval and Alternate Storage of Radioactive Waste* (BSC 2007 ([DIRS 183416], Section 6.2) discusses the details of waste retrieval operations using an electrically powered rail-based vehicle. The design requirements established for the subsurface facility incorporate aspects and parameters that enable retrieval of waste. For example, a design life of 100 years (including maintenance) has been established for the ground support system in the access mains, ventilation mains, and emplacement drifts, to assure access to the emplaced waste packages (BSC 2007 [DIRS 183416], Section 4). A maintenance plan to test, inspect, and repair ground support as necessary in the future has also been planned to support this design strategy. Similarly, the subsurface communication and transportation infrastructure is designed for the preclosure operating life and supports access for maintenance or equipment replacement as needed. The repository design as described in included FEP 1.1.07.00.0A (Repository Design) is based on this approach.

INPUTS:

Table 1.1.13.00.0A-1. Indirect Inputs

Citation	Title	DIRS
10 CFR 63	Energy: Disposal of High-Level Radioactive Wastes in a Geologic Repository at Yucca Mountain, Nevada	180319
66 FR 55732	Disposal of High-Level Radioactive Wastes in a Proposed Geologic Repository at Yucca Mountain, NV, Final Rule. 10 CFR Parts 2, 19, 20, 21, 30, 40, 51, 60, 61, 63, 70, 72, 73, and 75	156671
BSC 2007	*Concepts for Waste Retrieval and Alternate Storage of Radioactive Waste*	183416
SNL 2007	*Total System Performance Assessment Data Input Package for Requirements Analysis for EBS In-Drift Configuration*	179354
SNL 2007	*Total System Performance Assessment Data Input Package for Requirements Analysis for DOE SNF/HLW and Navy SNF Waste Package Overpack Physical Attributes Basis for Performance Assessment*	179567
SNL 2007	*Total System Performance Assessment Data Input Package for Requirements Analysis for Subsurface Facilities*	179466
SNL 2007	*Total System Performance Assessment Data Input Package for Requirements Analysis for TAD Canister and Related Waste Package Overpack Physical Attributes Basis for Performance Assessment*	179394

FEP: 1.2.01.01.0A

FEP NAME:

Tectonic Activity - Large Scale

FEP DESCRIPTION:

Large-scale tectonic activity, such as regional uplift, subsidence, folding, mountain building, or other processes related to plate movements, could affect repository performance by altering the physical and thermohydrologic properties of the geosphere.

SCREENING DECISION:

Excluded – low consequence

SCREENING JUSTIFICATION:

Large-scale tectonic activity results from interactions between the lithospheric plates covering the surface of the earth. These interactions produce effects that are expressed at a regional scale such as broad uplift, subsidence, folding, faulting, and related changes in geothermal characteristics. These regional-scale effects, if they were to occur at a sufficient rate, could potentially impact flow in the unsaturated and saturated zones and transport properties, thereby affecting dose and radionuclide release to the accessible environment. However, as described below, because rates of tectonic activity in the vicinity of Yucca Mountain are low, the magnitude of any related effects would be small with consequent low impact on flow and transport of radionuclides. Thus, this FEP is excluded based on low consequence.

Site-scale effects of seismic and igneous activity at Yucca Mountain are explicitly addressed in FEPs separate from this one for large-scale tectonic activity. Site-scale effects are expressed locally and include effects such as fault displacement within the waste emplacement area and igneous intrusion of a waste emplacement drift. Seismic-related FEPs addressing local, site-scale effects are:

- 1.2.02.03.0A Fault Displacement Damages EBS Components (Included)
- 1.2.03.02.0A Seismic Ground Motion Damages EBS Components (Included)
- 1.2.03.02.0B Seismic-Induced Rockfall Damages EBS Components (Excluded)
- 1.2.03.02.0C Seismic-Induced Drift Collapse Damages EBS Components (Included)
- 1.2.03.02.0D Seismic-Induced Drift Collapse Alters In-Drift Thermohydrology (Included)

- 1.2.03.02.0E Seismic-Induced Drift Collapse Alters In-Drift Chemistry (Excluded)
- 1.2.03.03.0A Seismicity Associated With Igneous Activity (Included)
- 1.2.10.01.0A Hydrologic Response to Seismic Activity (Excluded)
- 2.2.06.01.0A Seismic Activity Changes Porosity and Permeability of Rock (Excluded)
- 2.2.06.02.0A Seismic Activity Changes Porosity and Permeability of Faults (Excluded)
- 2.2.06.02.0B Seismic Activity Changes Porosity and Permeability of Fractures (Excluded)
- 2.2.06.03.0A Seismic Activity Alters Perched Water Zones (Excluded)

Igneous-related FEPs addressing site-scale effects are:

- 1.2.04.02.0A Igneous Activity Changes Rock Properties (Excluded)
- 1.2.04.03.0A Igneous Intrusion Into Repository (Included)
- 1.2.04.04.0A Igneous Intrusion Interacts With EBS Components (Included)
- 1.2.04.04.0B Chemical Effects of Magma and Magmatic Volatiles (Included)
- 1.2.04.05.0A Magma or Pyroclastic Base Surge Transports Waste (Excluded)
- 1.2.04.06.0A Eruptive Conduit to Surface Intersects Repository (Included)
- 1.2.04.07.0A Ash Fall (Included)
- 1.2.04.07.0B Ash Redistribution in Groundwater (Excluded)
- 1.2.04.07.0C Ash Redistribution Via Soil and Sediment Transport (Included)
- 1.2.06.00.0A Hydrothermal Activity (Excluded)
- 1.2.10.02.0A Hydrologic Response to Igneous Activity (Excluded)

This approach of separately considering regional-scale and site-scale effects ensures that all aspects of tectonic activity are appropriately addressed.

Low Rates of Tectonic Activity—Yucca Mountain lies within the southern Great Basin of the Basin and Range physiographic province (BSC 2004 [DIRS 169734], Figure 2-1a) and is located on the south flank of a large Miocene caldera complex (BSC 2004 [DIRS 168030], Section 6.3.1). Yucca Mountain is also within the Walker Lane domain, an approximately 100-km-wide structural belt along the western edge of the Basin and Range province. Walker Lane is characterized by northwest- and north-to-northeast-striking strike-slip faults that accommodated much of the early extension in this region (BSC 2004 [DIRS 169734], Section 2.2.1).

On a more local scale, Yucca Mountain is within the Crater Flat structural domain as defined by Fridrich (1999 [DIRS 118942], pp. 170 through 178). The Crater Flat structural domain (also referred to as the Crater Flat structural basin) includes the Crater Flat topographic basin on the west, and Yucca Mountain, near the center of the structural basin, where Miocene ash-flow tuffs crop out. These exposed tuff units comprise Yucca Mountain and adjacent mesas. Structurally, Yucca Mountain is dominated by subparallel fault blocks that trend to the north and tilt to the east. The blocks of ash-flow tuff are bounded by typical Basin and Range style, high-angle, generally west-dipping, normal and oblique faults that formed by rapid east-west extension during the waning phases of Miocene volcanism. Secondary intrablock faults are common (BSC 2004 [DIRS 168030], Section 6.3.1; BSC 2004 [DIRS 169734], Section 3.5).

Extensional tectonics has characterized the Yucca Mountain region since Oligocene time (BSC 2004 [DIRS 169734], Section 2.4.2). During the period of peak tectonism (approximately 11.6 Ma to 12.7 Ma), the western part of Crater Flat basin subsided due to the basin extending from 18% to 40% in 1.1 million years or less (Fridrich et al. 1998 [DIRS 164051], p. 1). After 11.6 Ma, the rate of extension in the basin declined in a roughly exponential manner. The late Quaternary rate of extension is less than 1% of the initial rate (Fridrich et al. 1998 [DIRS 164051], pp. 1 and 13) and may be as low as 0.1% to 0.2% per million years (Fridrich et al. 1998 [DIRS 164051], pp. 19 and 20). The pattern of Quaternary deformation mimics the pattern of middle Miocene activity, but at substantially lower rates (Fridrich et al. 1998 [DIRS 164051], pp. 1 and 2). Even during the Quaternary, the rate of subsidence appears to have diminished consistently over the last several million years and the locus of subsidence due to extension has migrated west of Yucca Mountain (inferred from Fridrich 1999 [DIRS 118942], p. 189; Dixon et al. 1995 [DIRS 102793], p. 765).

Fridrich (1999 [DIRS 118942], p. 190) also notes that recent extension across the Crater Flat structural domain diminishes from south to north. Across the southern part of the Crater Flat basin, the northwest-southeast lengthening is approximately 0.1 m per thousand years. Across central Yucca Mountain the late Quaternary extension rate is approximately one-half as great, and across northern Yucca Mountain it is an order of magnitude lower.

Average slip rates over the past tens to hundreds of thousands of years for block bounding faults in the Crater Flat structural domain provide additional evidence of the low rate of tectonic activity (BSC 2004 [DIRS 168030], Table 6). As part of the probabilistic seismic hazard analysis for Yucca Mountain, six teams of experts assessed fault slip rates. Their interpretations of the data indicate that slip rates for active faults in the Yucca Mountain vicinity range from 0.001 to 0.05 mm/yr. Even given uncertainties in slip-rate estimation, the slip rates at Yucca Mountain are low to very low. For example, faults with slip rates of 0.01 mm/yr or less are

associated with extremely low rates of activity in a classification of active faulting developed by Slemmons and dePolo (1986 [DIRS 106815]). The slip rates observed at Yucca Mountain also fall within the moderately low to low activity fault classification in a regional scheme developed by dePolo (1994 [DIRS 104855], p. 49). This scheme uses slip rates to categorize the activity of normal faults in the Basin and Range province. The slip rates on faults at Yucca Mountain are equal to, or less than, the lowest values in a regional compilation of slip rates developed by McCalpin (1995 [DIRS 104770]) from fault studies in the entire Basin and Range province. It should be noted that paleoseismic investigations capable of providing slip rates are rarely conducted on faults with these low rates of activity.

In addition to the information on the rate of tectonism over the past tens to hundreds of thousands of years from average fault slip rates, data are also available on shorter-term deformation rates from geodetic studies. Savage et al. (1999 [DIRS 118952]; 2001 [DIRS 183366]) evaluated strain accumulation in the vicinity of Yucca Mountain for the periods 1983 to 1998 and 1993 to 1998 using Geodolite and Global Positioning System data. The measurement networks had apertures of about 35 and 50 km. They found principal strain accumulation rates of 22.8±8.8 nanostrain/year N77.6±13.5°W and −8.8±11.9 nanostrain/yr N12.5±13.5°E for the 1993 to 1998 period and 2±12 nanostrain/year N87±12°W and −22±12 nanostrain/year N03±12°E for the 1983 to 1998 period. Wernicke et al. (1998 [DIRS 103485]) interpreted Global Positioning System data for the period 1991 to 1998 to indicate a N65°W extension rate of 50±9 nanostrain/year. However, the factor of 2 greater extension rate may result from not explicitly taking into account transient post-seismic effects of the Little Skull Mountain earthquake that occurred in 1992 (Savage et al. 1999 [DIRS 118952], p. 17,627; Wernicke et al. 2004 [DIRS 175199], Section 1). For the Savage et al. (2001 [DIRS 183366]) results, only the west-northwest extension rate differs significantly from zero.

A network of continuously recording Global Positioning System stations was established in the Yucca Mountain region in 1999. Data from the first 3.75 years of operation indicate 20±2 nanostrain/year N20°W right-lateral shear (Wernicke et al. 2004 [DIRS 175199], Section 5). The source of this contemporary strain accumulation is not well resolved. Models of strain accumulation associated with regional faults suggest that the effect of just the Death Valley fault is insufficient to explain the data, implying that other faults may be contributing to the strain field (Wernicke et al. 2004 [DIRS 175199], Section 4). While questions remain as to the source and significance of contemporary strain accumulation, if any, in the Yucca Mountain region, the data suggest that strain rates are low, although perhaps currently higher than the long-term average determined from geologic observations of fault slip over the past tens to hundreds of thousands of years.

Volcanism in the Yucca Mountain vicinity also provides information on the rate of large-scale tectonic activity. The earliest volcanism in the Yucca Mountain region was dominated by a major episode of caldera-forming, silicic volcanism that occurred primarily between about 15 and 11 million years ago, forming the southwestern Nevada volcanic field (Sawyer et al. 1994 [DIRS 100075]). Silicic volcanism was approximately synchronous with a major period of extension, which occurred primarily between 13 and 9 million years ago (Sawyer et al. 1994 [DIRS 100075], Figure 4). Silicic volcanism has not occurred in the Yucca Mountain region in the last 7 or 8 million years. The commencement of basaltic volcanism occurred during the latter part of the silicic caldera-forming phase as extension rates waned. Small-volume basaltic

volcanism has continued into the Quaternary as part of a general decline in eruption volume over the past 11 million years (Perry et al. 1998 [DIRS 144335], Chapter 2).

Post-Miocene volcanism (younger than 5 million years) has occurred in six episodes in the Yucca Mountain region, at approximately 4.8, 3.7, 3.1, 1.0, 0.4, and 0.08 million years ago (Perry et al. 1998 [DIRS 144335], Table 2.B; Heizler et al. 1999 [DIRS 107255]). The total eruption volume of the post-Miocene basalts is about 6 km^3. The volume of individual episodes has decreased progressively through time, with the three Pliocene episodes having volumes of approximately 1 to 3 km^3 each and the three Quaternary episodes having a total volume of only about 0.5 km^3 (Perry et al. 1998 [DIRS 144335], Table 3.1; DTN: LA0004FP831811.002 [DIRS 149593], Table S00235_001). The Quaternary volcanoes are of small volume (about 0.1 km3 or less) and typically consist of a single main scoria cone surrounded by a small field of aa basalt flows, which commonly extend about 1 km from the scoria cone.

The decreased eruptive volume through time, together with geochemical evidence (Perry et al. 1998 [DIRS 144335], p. 4-8), indicates that the intensity of mantle melting processes that produce basaltic magma beneath the Yucca Mountain region has waned over the past 5 million years (Perry and Crowe 1992 [DIRS 106488], p. 2,359). Considered in terms of total eruption volume, frequency of eruptions, and duration of volcanism, basaltic volcanic activity in the Yucca Mountain region in the past 5 million years defines one of the least active basaltic volcanic fields in the western United States (CRWMS M&O 1998 [DIRS 105347], Figure 4-2).

Thus, geologic, geodetic, and volcanic evidence indicate that the rate of large-scale tectonic activity in the Yucca Mountain region is currently low and has been low during the recent geologic past (i.e., tens to hundreds of thousands of years). Because the rate of large-scale tectonic activity changes slowly, in response to changes in the plate tectonic setting, rates similar to those observed now and in the recent geologic past are expected to persist for the coming tens to hundreds of thousands of years. Effects related to large-scale tectonic activity (such as uplift, subsidence, folding, and mountain building) during the postclosure period, therefore, are expected to be on the order of meters. For example, if subsidence related to faulting occurred at a rate of 0.01 mm/yr, the net subsidence over ten thousand years would be 0.1 m. Even for a rate of 1 mm/yr, the total subsidence over ten thousand years would be only 10 m. Such a change is negligible relative to the current distance between the base of the repository and the saturated zone (about 300 m) and to maximum increases in water table elevation (about 115 m) during Plio-Pleistocene time when different climates were in effect at Yucca Mountain (Stuckless 1996 [DIRS 119051], pp. 98 to 99). Thus, the low rate of large-scale tectonic activity leads to small magnitude effects that have low consequence to overall repository performance. Therefore, large scale tectonic activity has been excluded from the TSPA on the basis of low consequence.

Based on the previous discussion, omission of FEP 1.2.01.01.0A (Large-Scale Tectonic Activity) will not result in a significant adverse change in the magnitude or timing of either radiological exposure to the RMEI or radionuclide releases to the accessible environment. Therefore, this FEP is excluded from the performance assessments conducted to demonstrate compliance with proposed 10 CFR 63.311 and 10 CFR 63.321 (70 FR 53313 [DIRS 178394]), and with 10 CFR 63.331 [DIRS 180319], on the basis of low consequence.

INPUTS:

Table 1.2.01.01.0A-1. Direct Inputs

Input	Source	Description
DTN: LA0004FP831811.002. Volume of Volcanic Centers in the Yucca Mountain Region. [DIRS 149593]	Table S00235_001	Volumes of volcanic centers near Yucca Mountain
Fridrich et al. 1998. *Space-Time Patterns of Late Cenozoic Extension, Vertical-Axis Rotation, and Volcanism in the Crater Flat Basin, Southwest Nevada*. [DIRS 164051]	pp. 1 and 2	The pattern of Quaternary deformation mimics the pattern of middle Miocene activity, but at substantially lower rates
	pp. 1, 13, 19, and 20	After 11.6 Ma, the rate of extension in the basin declined in a roughly exponential manner. The late Quaternary rate of extension is less than 1% of the initial rate and may be as low as 0.1% to 0.2% per million years
	p. 1	During the period of peak tectonism (approximately 11.6 Ma to 12.7 Ma), the western part of Crater Flat basin subsided due to the basin extending from 18% to 40% in 1.1 million years or less

Table 1.2.01.01.0A-2. Indirect Inputs

Citation	Title	DIRS
10 CFR 63	Energy: Disposal of High-Level Radioactive Wastes in a Geologic Repository at Yucca Mountain, Nevada	180319
70 FR 53313	Implementation of a Dose Standard After 10,000 Years	178394
BSC 2004	*Characterize Framework for Seismicity and Structural Deformation at Yucca Mountain, Nevada*	168030
BSC 2004	*Yucca Mountain Site Description*	169734
CRWMS M&O 1998	*Synthesis of Volcanism Studies for the Yucca Mountain Site Characterization Project*	105347
Dixon et al. 1995	"Constraints on Present-Day Basin and Range Deformation from Space Geodesy"	102793
Fridrich 1999	"Tectonic Evolution of the Crater Flat Basin, Yucca Mountain Region, Nevada"	118942
Savage et al. 1999	"Strain Accumulation at Yucca Mountain, Nevada, 1983-1998"	118952
Savage et al. 2001	"Strain Accumulation Near Yucca Mountain, Nevada, 1993-1998"	183366
Sawyer et al. 1994	"Episodic Caldera Volcanism in the Miocene Southwestern Nevada Volcanic Field: Revised Stratigraphic Framework, $^{40}Ar/^{39}Ar$ Geochronology, and Implications for Magmatism and Extension"	100075
Wernicke et al. 1998	"Anomalous Strain Accumulation in the Yucca Mountain Area, Nevada"	103485
Wernicke et al. 2004	"Tectonic Implications of a Dense Continuous GPS Velocity Field at Yucca Mountain, Nevada"	175199
Perry et al. 1998	*Volcanism Studies: Final Report for the Yucca Mountain Project*	144335
McCalpin 1995	*Short Notes Frequency Distribution of Geologically Determined Slip Rates for Normal Faults in the Western United States*	104770

Table 1.2.01.01.0A-2. Indirect Inputs (Continued)

Citation	Title	DIRS
de Polo 1994	"Estimating Fault Slip Rates in the Great Basin, USA"	104855
Perry and Crowe 1992	"Geochemical Evidence for Waning Magmatism and Polycyclic Volcanism at Crater Flat, Nevada"	106488
Slemmons and dePolo 1986	"Evaluation of Active Faulting and Associated Hazards"	106815
Heizler et al. 1999	"The Age of Lathrop Wells Volcanic Center: An $^{40}Ar/^{39}Ar$ Dating Investigation"	107255

FEP: 1.2.02.01.0A

FEP NAME:

Fractures

FEP DESCRIPTION:

Groundwater flow in the Yucca Mountain region and transport of any released radionuclides may take place along fractures. The rate of flow and the extent of transport in fractures are influenced by characteristics such as orientation, aperture, asperity, fracture length, connectivity, and the nature of any linings or infills.

SCREENING DECISION:

Included

TSPA DISPOSITION:

Fractures are included in process models for flow and transport in the UZ and the SZ flow and transport models. The UZ flow model is based on a dual-permeability concept with fractures and matrix each represented by a continuum in the dual permeability mesh (SNL 2007 [DIRS 184614]). The fracture continuum represents the spatially averaged flow through discrete fractures and interacts with the matrix continuum, which comprises matrix blocks separated by fractures. The SZ flow model is based on a single, effective continuum with the effects of fractures intrinsically incorporated into unit permeabilities.

Unsaturated Zone Flow Model

Fracture continuum properties include permeability, porosity, interface area per unit volume, van Genuchten α and m parameters (the saturation-capillary pressure and relative permeability factors), residual saturation, and an active fracture parameter (which accounts for preferential flow in a subset of the total fracture population). These parameters and the associated ranges of values are obtained as described in *UZ Flow Models and Submodels* (SNL 2007 [DIRS 184614], Section 6.1.5) and adjusted as described in Section 6.2.3 of that report (SNL 2007 [DIRS 184614]) for each unsaturated zone model layer (DTN: LB0205REVUZPRP.001 [DIRS 159525]).

Fracture permeability is based on field measurements that integrate discrete fracture characteristics such as orientation, aperture, asperity, fracture length, connectivity, and the nature of any linings or infills. Permeabilities and other properties are further calibrated as described in *Calibrated Unsaturated Zone Properties* (SNL 2007 [DIRS 179545], Section 6.3) and *Analysis of Hydrologic Properties Data* (BSC 2004 [DIRS 170038]). The fracture continuum properties are used as inputs to the UZ flow model and their effects are incorporated into the output flow fields developed for use in the TSPA (output flow fields are in DTNs: LB0612PDFEHMFF.001 [DIRS 179296], LB0701MOFEHMFF.001 [DIRS 179297], LB0701GTFEHMFF.001 [DIRS 179160], and LB0702PAFEM10K.002 [DIRS 179507], where each DTN represents a different climate).

The permeability of bedrock (either unfractured PTn or fractured TCw depending on location) significantly impacts rates and distributions of net infiltration (SNL 2008 [DIRS 182145], Section 6.1.2). *Simulation of Net Infiltration for Present-Day and Potential Future Climates* (SNL 2008 [DIRS 182145], Section 6.5.2.6) discusses conceptual treatment of fractures in the infiltration model and numerical values and parameters used (SNL 2008 [DIRS 182145], Sections 6.5.2.5[a] and 6.5.2.6).

The influence of fractures on radionuclide transport through the unsaturated zone is implicitly investigated using a dual-permeability model (SNL 2008 [DIRS 184748], Section 6.4.3). The influences of fracture characteristics on unsaturated zone flow are evident in the output flow fields (SNL 2008 [DIRS 184748], Section 6.5.1; DTNs: LB0612PDFEHMFF.001 [DIRS 179296]; LB0701MOFEHMFF.001 [DIRS 179297]; LB0701GTFEHMFF.001 [DIRS 179160]; LB0702PAFEM10K.002 [DIRS 179507]). Fracture aperture, porosity, and frequency (DTNs: LB0205REVUZPRP.001 [DIRS 159525] and LB0207REVUZPRP.001 [DIRS 159526]) affecting unsaturated zone radionuclide transport are summarized in *Particle Tracking Model and Abstraction of Transport Processes* (SNL 2008 [DIRS 184748], Section 6.5.7). Fracture porosity and frequency data are statistically sampled during TSPA multirealization simulations using the distributions provided in DTN: LA0701PANS02BR.003 [DIRS 180497].

Flow processes in fractures or other channels are important for seepage because the amount of seepage is controlled by the fracture diversion capacity in the drift vicinity. This process is modeled in *Seepage Model for PA Including Drift Collapse* (BSC 2004 [DIRS 167652], Section 6.3). Seepage-relevant parameters are determined in *Seepage Calibration Model and Seepage Testing Data* (BSC 2004 [DIRS 171764], Sections 6.3 and 6.5) and are based upon data related to fracture–matrix interactions developed in *In Situ Field Testing of Processes* (BSC 2004 [DIRS 170004], Sections 6.1 and 6.2). The seepage simulation results developed in *Seepage Model for PA Including Drift Collapse* (BSC 2004 [DIRS 167652]) are abstracted for use in *Abstraction of Drift Seepage* (SNL 2007 [DIRS 181244], Section 6.3.1). These flow processes are influenced by fracture characteristics such as orientation, aperture, asperity, length, connectivity, and fillings. All seepage process models that feed into the seepage abstraction explicitly simulate the flow processes in fractures using appropriate continuum properties (SNL 2007 [DIRS 181244], Section 6.4).

For ambient seepage, the relevant continuum properties are the continuum permeability and the effective fracture capillary strength in the vicinity of the drift. For the seepage abstraction, probability distributions describing the spatial variability and uncertainty of these parameters have been developed in *Abstraction of Drift Seepage* (SNL 2007 [DIRS 181244], Section 6.6) based on air-permeability measurements and liquid-release tests combined with inverse modeling (SNL 2007 [DIRS 181244], Sections 6.6 and 6.4). Ambient seepage calculations will be conducted within the TSPA by sampling from these probability distributions and interpolating seepage rates from the lookup tables given in DTNs: LB0702PASEEP01.001 [DIRS 179511] and LB0702PASEEP02.001 [DIRS 181635]. During the thermal period, the ambient seepage rates will be adjusted based on the TH modeling results from *Drift-Scale Coupled Processes (DST and TH Seepage) Models* (BSC 2005 [DIRS 172232]), which explicitly simulate thermally perturbed fracture flow conditions. Results are given in DTN: LB0301DSCPTHSM.002 [DIRS 163689]. Thermal-hydrologic-mechanical (THM) and thermal-hydrologic-chemical

(THC) effects on fracture characteristics are evaluated with process models that explicitly account for fracture flow affected by THM and THC parameter alterations (SNL 2007 [DIRS 181244], Section 6.4.4; excluded FEPs 2.1.09.12.0A (Rind (Chemically Altered Zone) Forms in the Near-Field) and 2.2.10.04.0A (Thermo-Mechanical Stresses Alter Characteristics of Fractures Near Repository)). It has been demonstrated that these potential alterations need not be addressed in TSPA because the effects on seepage quantities are expected to be small and any anticipated changes are expected to lead to less seepage (SNL 2007 [DIRS 181244], Section 6.5.1.4[a]).

Flow processes in fractures or other channels affect modeled THC coupled processes because of their strong effect on thermal-hydrologic behavior (SNL 2007 [DIRS 181244], Sections 6.4.4.1 and 6.4.4.2) and their strong effect on water and gas chemistry (SNL 2007 [DIRS 177404], Section 6.2.1). The latter effect is primarily due to volatilization of steam and CO_2 from the rock-matrix water and subsequent transport and condensation in fractures. The amount of CO_2 mobilized by steam directly affects the pH of the condensate, which in turn affects the degree of water–rock interaction and water chemistry. These THC processes are influenced by fracture characteristics such as orientation, aperture, asperity, length, connectivity, and fillings. The THC seepage model explicitly simulates the flow processes in fractures using appropriate continuum properties (SNL 2007 [DIRS 177404], Sections 6.4.3, 6.4.4, and 6.4.7).

Summary tables of concentrations through time are presented in DTNs LB0302DSCPTHCS.002 [DIRS 161976], which is output from *Drift-Scale THC Seepage Model* (SNL 2007 [DIRS 177404]), and in DTN: LB0307DSTTHCR2.002 [DIRS 165541], which is output from *Drift-Scale Coupled Processes (DST and TH Seepage) Models* (BSC 2005 [DIRS 172232]), and summary statistics through time are presented in DTN: LB0311ABSTHCR2.001 [DIRS 166714], which is output from *Abstraction of Drift Seepage* (SNL 2007 [DIRS 181244]). These data are used to feed and/or provide the technical basis for *Engineered Barrier System: Physical and Chemical Environment* (SNL 2007 [DIRS 177412]), which generates the lookup tables used in the TSPA model.

Saturated Zone Flow Model

Groundwater flow through fractures in the volcanic units is included in the SZ flow and transport model described in *Saturated Zone Flow and Transport Model Abstraction* (SNL 2008 [DIRS 183750]). Groundwater flow through the fractured volcanic units is modeled in *Saturated Zone Site-Scale Flow Model* (SNL 2007 [DIRS 177391], Sections 6.3.1.2, 6.3.1.9, and 6.3.1.10) using an effective continuum approach (SNL 2007 [DIRS 177391], Section 6.4.1). Observations at Yucca Mountain indicate that in the fractured volcanic units delineated in the hydrogeologic framework model (SNL 2007 [DIRS 174109]), flow is primarily through the fracture network instead of the matrix. Furthermore, at the scales of interest (hundreds of meters to kilometers), the fracture networks appear to be well-connected over large distances. The drawdown response to pumping at wells surrounding the C-wells complex in multiwell pump tests indicates a well-connected fracture network in the Miocene tuffaceous rocks in this area (Geldon et al. 1997 [DIRS 100397]; Geldon et al. 1998 [DIRS 129721], p. 31; SNL 2007 [DIRS 177394], Section 6.2). In addition, Finsterle (2000 [DIRS 151875]) demonstrated through a comparison of continuum and discrete-fracture models that the continuum approach is valid for predicting long-term average seepage rates. These findings support the use of a continuum approach for

simulating groundwater flow in fractured rocks in the saturated zone, which is a larger scale process than drift seepage and, thus, more accurately represented as a continuum.

Groundwater flow through the fractured rock in the saturated zone was simulated using a continuum representation of the media. Several continuum approaches are available, including single continuum, dual porosity, and dual permeability–dual porosity. Often, the single continuum approach is used to model relatively homogeneous media while the dual-permeability approach is used for heterogeneous media that contain distinct and variable permeability zones lying in the same representative elemenatary volume (e.g., a fractured porous medium). In such heterogeneous media, advective flow demonstrates distinctively different flow rates and a dual-permeability model may be better suited to predict flow and transport through this type of system.

The dual-porosity approach simulates the flow of water in a heterogeneous system where local interzonal permeabilities differ by several orders of magnitude. This method is useful for simulating flow and transport in fractured media where the permeability of the matrix is much less than fractures, as is the case for fractured tuff units in the saturated zone. Fast flow occurs in fractures, but solute transport is tempered by diffusion into the matrix. In this case, the matrix acts as a large storage reservoir for water and solutes. Steady-state flow in fractured media can be successfully simulated with a single-continuum approach; however, accurate representation of transport processes, including matrix diffusion, requires a dual-porosity, effective-continuum approach for fractured tuff in the saturated zone (SNL 2008 [DIRS 184806], Section 6.3).

As discussed in *Probability Distribution for Flowing Interval Spacing* (BSC 2004 [DIRS 170014], Section 6.3), only a subset of existing fractures is observed to transmit flow in the saturated zone. The hydrogeologic characteristics of these "flowing interval" zones vary spatially. In the SZ transport abstraction and the one-dimensional transport models (SNL 2008 [DIRS 183750], Sections 6.3.1 and 6.3.2]), variability in the groundwater specific discharge due to variability in fracture permeability and orientation is modeled by scaling the horizontal anisotropy in permeabilities (SNL 2007 [DIRS 177391], Section 6.5.2.10) with stochastically sampled scaling parameters for groundwater specific discharge and horizontal anisotropy in the volcanic units. Additionally, the characteristics of the fracture properties, such as fracture orientation, aperture size, degree of infilling, and tortuosity are modeled through probabilistically modeled parameters. The parameters are described in *Saturated Zone Flow and Transport Model Abstraction* (SNL 2008 [DIRS 183750], Sections 6.5.2.1, 6.5.2.4, 6.5.2.5, 6.5.2.8, 6.5.2.9, 6.5.2.10, 6.5.2.11, 6.5.2.12, and 6.5.2.15, Tables 6-8, and 6-7[a]).

INPUTS:

Table 1.2.02.01.0A-1. Indirect Inputs

Citation	Title	DIRS
BSC 2004	*Probability Distribution for Flowing Interval Spacing*	170014
BSC 2004	*Analysis of Hydrologic Properties Data*	170038
BSC 2004	*In Situ Field Testing of Processes*	170004
BSC 2004	*Seepage Calibration Model and Seepage Testing Data*	171764
BSC 2004	*Seepage Model for PA Including Drift Collapse*	167652
BSC 2005	*Drift-Scale Coupled Process (DST and TH Seepage) Models*	172232
DTN: LA0701PANS02BR.003	UZ Transport Parameters	180497
DTN: LB0205REVUZPRP.001	Fracture Properties for UZ Model Layers Developed from Field Data	159525
DTN: LB0207REVUZPRP.001	Revised UZ Fault Zone Fracture Properties	159526
DTN: LB0301DSCPTHSM.002	Drift-Scale Coupled Process Model for Thermohydrologic Seepage: Data Summary	163689
DTN: LB0302DSCPTHCS.002	Drift-Scale Coupled Processes (THC Seepage) Model: Data Summary	161976
DTN: LB0307DSTTHCR2.002	Drift-Scale Coupled Processes (DST Seepage) Model: Data Summary	165541
DTN: LB0311ABSTHCR2.001	Drift Scale Coupled Process Abstraction Model (for Intact-Drift Case)	166714
DTN: LB0612PDFEHMFF.001	Flow-Field Conversions from TOUGH2 to FEHM Format for Present Day 10-, 30-, 50-, and 90-Percentile Infiltration Maps	179296
DTN: LB0701GTFEHMFF.001	Flow-Field Conversions from TOUGH2 to FEHM Format for Glacial Transition Climate 10th-, 30th-, 50th-, and 90th-Percentile Infiltration Maps	179160
DTN: LB0701MOFEHMFF.001	Flow-Field Conversions from TOUGH2 to FEHM Format for Monsoon Climate 10th-, 30th-, 50th-, and 90th-Percentile Infiltration Maps	179297
DTN: LB0702PAFEM10K.002	Flow Field Conversions to FEHM Format for Post 10,000 Year Peak Dose Fluxes in the Unsaturated Zone for Four Selected Infiltration Rates	179507
DTN: LB0702PASEEP01.001	New Extended-Range Seepage Look-Up Tables for Intact and Collapsed Drifts Plus Supporting Files	179511
DTN: LB0702PASEEP02.001	Seepage Abstraction for Degraded Drifts	181635
Finsterle 2000	“Using the Continuum Approach to Model Unsaturated Flow in Fractured Rock”	151875
Geldon et al. 1997	*Results of Hydraulic and Conservative Tracer Tests in Miocene Tuffaceous Rocks at the C-Hole Complex, 1995 to 1997, Yucca Mountain, Nye County, Nevada*	100397
Geldon et al. 1998	*Analysis of a Multiple-Well Interference Test in Miocene Tuffaceous Rocks at the C-Hole Complex, May-June 1995, Yucca Mountain, Nye County, Nevada*	129721
SNL 2007	*Saturated Zone Site-Scale Flow Model*	177391
SNL 2007	*Abstraction of Drift Seepage*	181244
SNL 2007	*Calibrated Unsaturated Zone Properties*	179545
SNL 2007	*Drift-Scale THC Seepage Model*	177404

Table 1.2.02.01.0A-1. Indirect Inputs (Continued)

Citation	Title	DIRS
SNL 2007	*Engineered Barrier System: Physical and Chemical Environment*	177412
SNL 2007	*Hydrogeologic Framework Model for the Saturated Zone Site Scale Flow and Transport Model*	174109
SNL 2007	*Saturated Zone In-Situ Testing*	177394
SNL 2007	*UZ Flow Models and Submodels*	184614
SNL 2008	*Particle Tracking Model and Abstraction of Transport Processes*	184748
SNL 2008	*Simulation of Net Infiltration for Present-Day and Potential Future Climates*	182145
SNL 2008	*Saturated Zone Flow and Transport Model Abstraction*	183750
SNL 2008	*Site-Scale Saturated Zone Transport*	184806

FEP: 1.2.02.02.0A

FEP NAME:

Faults

FEP DESCRIPTION:

Numerous faults of various sizes have been noted in the Yucca Mountain region, and specifically in the repository area. Faults may represent an alteration of the rock permeability and continuity of the rock mass, an alteration or short-circuiting of the flow paths and flow distributions close to the repository, and/or unexpected pathways through the repository.

SCREENING DECISION:

Included

TSPA DISPOSITION:

Stratigraphic units or layers and fault geometries in the Yucca Mountain vicinity are defined in *Geological Framework Model (GFM2000)* (BSC 2004 [DIRS 170029]) and in DTN: MO0012MWDGFM02.002 [DIRS 153777]. These sources provide the basis for the UZ model grid as outlined in *Development of Numerical Grids for UZ Flow and Transport Modeling* (BSC 2004 [DIRS 169855]). Major displacement, dip-slip, strike-slip, and detachment faults within the model domain are discretized in the mountain-scale UZ flow and transport models described in *UZ Flow Models and Submodels* (SNL 2007 [DIRS 184614], Sections 6.1.5, 6.2.2, 6.6.2.3, and 6.7.3) and *Development of Numerical Grids for UZ Flow and Transport Modeling* (BSC 2004 [DIRS 169855], Section 6.6.1). These faults are represented in the UZ model grid developed in *Development of Numerical Grids for UZ Flow and Transport Modeling* (BSC 2004 [DIRS 169855]) as 30-m-wide vertical or inclined discrete zones that include existing displacements affecting the relative geometry of the hydrogeologic model units. Specific hydrogeologic properties are assigned to fault zones. Fault properties (matrix and fracture parameters) are found in DTN: LB0612MTSCHPFT.001 [DIRS 180296]. Calibration of these properties is described in *Calibrated Unsaturated Zone Properties* (SNL 2007 [DIRS 179545], Section 6.3.4) and *Analysis of Hydrologic Properties Data* (BSC 2004 [DIRS 170038]). The fault properties are used as inputs to the UZ flow model and their effects are incorporated into the output flow fields developed for use in TSPA (output flow fields are in DTNs: LB0612PDFEHMFF.001 [DIRS 179296]; LB0701MOFEHMFF.001 [DIRS 179297]; LB0701GTFEHMFF.001 [DIRS 179160]; and LB0702PAFEM10K.002 [DIRS 179507], where each DTN represents a different climate).

The influence of faults on TSPA dose predictions is based on the effects of faults on radionuclide transport and drift seepage abstractions. The influence of faults on radionuclide transport is included through the use of pregenerated flow fields from the UZ flow model (as described above) that include the faults in the three-dimensional model in *Particle Tracking Model and Abstraction of Transport Processes* (SNL 2008 [DIRS 184748], Section 6.5.1; DTNs: LB0612PDFEHMFF.001 [DIRS 179296]; LB0701MOFEHMFF.001 [DIRS 179297]; LB0701GTFEHMFF.001 [DIRS 179160]; and LB0702PAFEM10K.002 [DIRS 179507]), and

through the assignment of specific transport propeties of fractures within the faults (SNL 2008 [DIRS 184748], Section 6.5.7). The UZ flow model and UZ transport model compute processes on the same numerical grid, therefore, the direct representation of major faults in the UZ flow model grid is also contained in the UZ transport model abstraction (SNL 2008 [DIRS 184748], Section 6.5.1). The effects of faults on the percolation flux arriving at the waste emplacement drifts are included through the UZ flow model output of percolation flux at the PTn/TSw interface (DTNs: LB0612PDPTNTSW.001 [DIRS 179150]; LB0701MOPTNTSW.001 [DIRS 179156]; LB0701GTPTNTSW.001 [DIRS 179153]; and LB0702UZPTN10K.002 [DIRS 179332]). This flux is the boundary condition used by the seepage abstraction in TSPA (SNL 2007 [DIRS 181244], Section 6.6.5.1).

Geologic features and hydrostratigraphic units are included in *Saturated Zone Flow and Transport Model Abstraction* (SNL 2008 [DIRS 183750]), Section 6.3.1) in a configuration that accounts for the effects of existing faults based on the hydrogeologic framework model (SNL 2007 [DIRS 174109], Section 6) and mapped faults identified in DTNs: GS010608312332.001 [DIRS 155307] and GS010908314221.001 [DIRS 162874]. Important faults were represented as calibration parameters in *Saturated Zone Site-Scale Flow Model* (SNL 2007 [DIRS 177391], Section 6.3.1.10). As discussed in that report (SNL 2007 [DIRS 177391], Section 6.4.3.1), and in *Hydrogeologic Framework Model for the Saturated Zone Site-Scale Flow and Transport Model* (SNL 2007 [DIRS 174109], Sections 6.1, 6.3.1.1, 6.3.1.2, 6.4.2, and 6.4.4), the hydrogeologic framework model presents a simplified representation of faults and other hydrogeologic features (such as zones of hydrothermal alteration) that affect saturated zone flow and provide the basis upon which the saturated zone site scale flow model is developed.

The hydrogeologic properties of discrete features are developed through calibration of the saturated zone site-scale flow model (SNL 2007 [DIRS 177391], Section 6.5.1.3). Faults in the model area can dip at almost any angle, but most are high-angle faults. Given numerical flow model resolution (250 × 250 m^2 horizontal cells) and uncertainties in fault orientation, they are treated as vertical features. Hydraulic testing in the volcanic units of the saturated zone has investigated portions of the aquifer and has yielded sufficient data to estimate horizontal permeability anisotropy, which may be influenced by faults (SNL 2007 [DIRS 177394], Section 6.2.6). Faults in the saturated zone site-scale flow model domain that were considered important to groundwater flow (some of which are critical to achieve calibration like the Solitario Canyon Fault) were included in the model. Although numerous faults exist near Yucca Mountain, only some affect groundwater flow patterns by acting as either conduits or barriers (SNL 2007 [DIRS 177391], Sections 6.3.1.10 and 6.4.3.7). Additionally, faults can enhance dispersion by increasing permeability heterogeneities along saturated zone flowpaths (SNL 2008 [DIRS 184806], Sections 6.3.1.0 and 6.4.3.7, and Table 6-7).

The offsets of hydrostratigraphic units across major faults are incorporated into the model and some key faults (e.g., the Solitario Canyon, U.S. Highway 95, and Fortymile Wash Faults) are included as low- or high-permeability features (SNL 2007 [DIRS 177391], Table 6-7).

Abstraction model parameters, including the ratio of horizontal anisotropy in permeability (SNL 2008 [DIRS 183750], Section 6.5.2.10), and the groundwater specific discharge multiplier (SNL 2008 [DIRS 183750], Section 6.5.2.1[a]), include the potential impacts of faults on

groundwater flow and are modeled probabilistically to account for the uncertainty in hydrologic properties associated with faults and fractures in the volcanic units (SNL 2008 [DIRS 183750], Sections 6.5.2.1[a] and 6.5.2.10). For a more detailed description of specific faults, see *Saturated Zone Site-Scale Flow Model* (SNL 2007 [DIRS 177391], Table 6-7).

INPUTS:

Table 1.2.02.02.0A-1. Indirect Inputs

Citation	Title	DIRS
BSC 2004	*Analysis of Hydrologic Properties Data*	170038
BSC 2004	*Development of Numerical Grids for UZ Flow and Transport Modeling*	169855
BSC 2004	*Geologic Framework Model (GFM2000)*	170029
DTN: GS010608312332.001	Potentiometric-Surface Map, Assuming Perched Conditions North of Yucca Mountain, in the Saturated Site-Scale Model	155307
DTN: GS010908314221.001	Geologic Map of the Yucca Mountain Region, Nye County, Nevada	162874
DTN: LB0612MTSCHPFT.001	Calibrated UZ Fault Property Sets	180296
DTN: LB0612PDFEHMFF.001	Flow-Field Conversions from TOUGH2 to FEHM Format for Present Day 10-, 30-, 50-, and 90-Percentile Infiltration Maps	179296
DTN: LB0612PDPTNTSW.001	Vertical Flux at PTN/TSW Interface for Present-Day Climate of 10th, 30th, 50th, and 90-Percentile Infiltration Maps	179150
DTN: LB0701GTFEHMFF.001	Flow-Field Conversions from TOUGH2 to FEHM Format for Glacial Transition Climate 10th-, 30th-, 50th-, and 90th-Percentile Infiltration Maps	179160
DTN: LB0701GTPTNTSW.001	Vertical Flux at PTN/TSW Interface for Glacial Transition Climate of 10th, 30th, 50th, and 90th-Percentile Infiltration Maps	179153
DTN: LB0701MOFEHMFF.001	Flow-Field Conversions from TOUGH2 to FEHM Format for Monsoon Climate 10th-, 30th-, 50th-, and 90th-Percentile Infiltration Maps	179297
DTN: LB0701MOPTNTSW.001	Vertical Flux at PTN/TSW Interface for Monsoon Climate of 10th, 30th, 50th and 90th-Percentile Infiltration Maps	179156
DTN: LB0702PAFEM10K.002	Flow Field Conversions to FEHM Format for Post 10,000 Year Peak Dose Fluxes in the Unsaturated Zone for Four Selected Infiltration Rates	179507
DTN: LB0702UZPTN10K.002	Vertical Flux at PTN/TSW Interface for Post-10K-Year Climate Infiltration Maps	179332
DTN: MO0012MWDGFM02.002	Geologic Framework Model (GFM2000)	153777
SNL 2008	*Site-Scale Saturated Zone Transport*	184806
SNL 2007	*Saturated Zone Site-Scale Flow Model*	177391
SNL 2007	*Abstraction of Drift Seepage*	181244
SNL 2007	*Calibrated Unsaturated Zone Properties*	179545
SNL 2007	*Hydrogeologic Framework Model for the Saturated Zone Site Scale Flow and Transport Model*	174109
SNL 2007	*Saturated Zone In-Situ Testing*	177394
SNL 2007	*UZ Flow Models and Submodels*	184614
SNL 2008	*Particle Tracking Model and Abstraction of Transport Processes*	184748
SNL 2008	*Saturated Zone Flow and Transport Model Abstraction*	183750

FEP: 1.2.02.03.0A

FEP NAME:

Fault Displacement Damages EBS Components

FEP DESCRIPTION:

Movement of a fault that intersects drifts within the repository may cause the EBS components to experience related movement or displacement. Repository performance may be degraded by such occurrences as tilting of components, component-to-component contact, or drip shield separation. Fault displacement could cause a failure as significant as shearing of drip shields and waste packages by virtue of the relative offset across the fault, or as extreme as exhumation of the waste to the surface.

SCREENING DECISION:

Included

TSPA DISPOSITION:

Fault displacement is considered to be a potentially disruptive process with sudden relative rock/soil displacements across a fault surface. The effects of fault displacement are potentially relevant to the integrity of the waste packages, drip shields, and cladding, and are included in the performance assessment to demonstrate compliance with the individual protection requirements of the proposed 10 CFR 63.311 (70 FR 53313 [DIRS 178394]). The effects of fault displacement are excluded from the performance assessments to demonstrate compliance with the individual protection standard for human intrusion (proposed 10 CFR 63.321 (70 FR 53313 [DIRS 178394])) and with the groundwater protection standard (10 CFR 63.331 [DIRS 180319]). This is appropriate because damage from fault displacement occurs for seismic events with exceedance frequencies less than 2.5×10^{-7} per year (SNL 2007 [DIRS 176828], Table 6-67), which is substantially below the requirement to consider events with 1 chance in 10 over 10,000 years (10^{-5} per year) for the individual protection and groundwater protection standards, in accordance with the proposed rule in 10 CFR 63.342(b) and (c)(1) (70 FR 53313 [DIRS 178394])).

Once a waste package has failed from fault displacement, it is conservatively assumed that its associated drip shield cannot deflect seepage away from the waste package and that the waste form within the failed waste package is directly exposed to the water or air of the repository environment. The impacts of seismically induced ground motion, rockfall, and drift collapse on EBS components are addressed under separate FEPs: included FEP 1.2.03.02.0A (Seismic Ground Motion Damages EBS Components), excluded FEP 1.2.03.02.0B (Seismic-Induced Rockfall Damages EBS Components), and included FEP 1.2.03.02.0C (Seismic-Induced Drift Collapse Damages EBS Components), respectively. Floor buckling damage to the emplacement pallet and the invert in the absence of seismic events is discussed in excluded FEP 2.1.07.06.0A (Floor Buckling).

This FEP description mentions extreme conditions of fault displacements leading to waste exhumation. The depth of the repository below the surface is approximately 200 m or greater (SNL 2007 [DIRS 179466], Table 4-1, Parameter Number 01-06). The potential for exhumation due to fault movement is not considered credible given the low fault slip rates on the block-bounding faults (i.e., Solitario Canyon and Bow Ridge). Anticipated fault slip rates for these faults are at most 0.03 mm/yr, equivalent to 30 cm or less in 10,000 years (BSC 2004 [DIRS 168030], Table 6). The potential for waste exhumation from fault displacement is not considered further.

Technical Approach for Inclusion—The potential for fault displacement damage from block-bounding faults, such as the Solitario Canyon Fault, is not considered in the TSPA model, as discussed in *Seismic Consequence Abstraction* (SNL 2007 [DIRS 176828], Section 6.11.3). The Solitario Canyon Fault lies outside the emplacement area of the repository and repository design requires a minimum stand-off of 60 m between this type of fault and the emplacement drifts (SNL 2007 [DIRS 179466], Table 4-1, Parameter Number 01-05). A second named fault, the Ghost Dance Fault, runs parallel to the Solitario Canyon Fault and between the waste emplacement areas of the repository (SNL 2007 [DIRS 176828], Figure D-1). The main Ghost Dance Fault is not considered in the TSPA model because no waste packages will lie on it, although the western splay off the main Ghost Dance Fault is considered in the TSPA model (SNL 2007 [DIRS 176828], Section 6.11.3).

The potential for fault displacement damage from intra-block faults and other generic faulting features that may exist within the repository footprint is included in the TSPA model for the individual protection requirement. For a fault displacement that occurs across an emplacement drift, a sudden discontinuity in the floor and roof of the tunnel may occur. Fault displacement is assumed to be on a discrete plane, and to occur perpendicular to the tunnel axis with the displacement being purely vertical (SNL 2007 [DIRS 176828], Section 6.11.1.1). Such a displacement would result in a vertical offset of the tunnel relative to the adjacent section across the fault. The vertical offset could cause shearing of the waste package and drip shield and cladding at that location. The vertical offset could also cause separation between adjacent drip shields.

The technical basis for inclusion of this FEP involves a comparison of the potential fault displacements to the clearances between various elements of the repository design (i.e., waste package-to-drip shield spacing, waste package-to-drift wall spacing, and set-back requirements). The clearances have been analyzed for two conditions: (1) with an intact drip shield, and (2) with a failed drip shield, when the waste package is surrounded by rubble (SNL 2007 [DIRS 176828], Section 6.11.1). For the intact drip shield, the approximation is made that the emplacement pallet collapses into the invert on the elevated side of the fault. No credit is taken for the potential increase in clearances due to further shifting of the ballast in the invert or for the potential upward movement of the drip shield during the fault displacement. For a failed drip shield, the waste package is surrounded by rubble and the available clearance around the waste package during a fault displacement is estimated to be one-quarter of the waste package outer diameter. The fault displacement damage abstraction for TSPA is based on the minimum predicted clearances, which correspond to the clearances for the case with the failed drip shield.

If a waste package is damaged by fault displacement, the damaged area is sampled from a uniform distribution of 0% to 100% of the lid area of the waste package (SNL 2007 [DIRS 176828], Section 6.11.5). The uniform distribution is a simple approximation to the upper and lower damage bounds in lieu of detailed structural response calculations. The upper bound is a reasonable estimate for a severely crimped waste package that loses its lid because of cracking in the welds that hold the lid in place. The lower bound is a reasonable estimate for a waste package that is minimally damaged, either because the fault displacement slightly exceeds the available clearance or because the vertical displacement occurs toward the center of the waste package, resulting in a crimp that is far from the waste package lids.

Crimping and shear from vertical displacement are the main damage mechanisms for the waste package because the package is a robust structure that will not be damaged by tilting or minor displacements. In addition, because of the ability of the waste package to move on the pallet, it is not anticipated that a large enough bending moment or torsion can be applied to cause failure while the drip shield is intact. After the drip shield fails, the rubble surrounding the waste package acts to distribute loads over the surface of the waste package, reducing concentrated bending moments or torsion on the waste package.

The lid welds have the potential to fracture, separating the lid from the waste package and potentially exposing the entire waste form to water seepage and consequent release (SNL 2007 [DIRS 176828], Section 6.11.5). Once radionuclides are released from the EBS, flow and transport in the unsaturated zone and the saturated zone are based on the same models and algorithms as are used for nominal conditions. An exception is that changes can occur in the in-drift environment, due to seismic-induced drift collapse, as discussed in included FEP 1.2.03.02.0D (Seismic-induced Drift Collapse Alters In-drift Thermohydrology).

Damage to a drip shield from fault displacement is assumed to be 100% if it surrounds a damaged waste package or 0% if it does not. A sheared drip shield will allow all seepage to pass through it; that is, there is no flux splitting (diversion of seepage) on the drip shield. Drip shield separation is not relevant here because a sheared drip shield already allows seepage to pass through it. For example, the relative vertical displacement required to separate two adjacent drip shields is on the order of one meter (BSC 2004 [DIRS 169753], Section 5.2.1). A one meter displacement corresponds to an exceedance frequency less that 10^{-7} per year for the intrablock faults that can intersect the emplacement drifts (SNL 2007 [DIRS 176828], Table 6-61). The ground motions associated with exceedance frequencies less than 10^{-7} per year will generally result in sheared drip shields on the intrablock faults, so drip shield separation is not relevant.

The output of the fault displacement damage abstraction is the number of waste packages failed by fault displacement and the combined surface area from the waste packages that fail from fault displacement. The number of waste packages failed is based on lookup tables that relate exceedance frequencies between 2.5×10^{-7} and 10^{-8} per year with the expected number of waste package failures for two representative waste package groups (SNL 2007 [DIRS 176828], Sections 6.11.4 and 6.11.5, particularly Table 6-67). The two representative waste package groups abstracted into the TSPA model are a TAD canister group, with naval waste packages and TAD canister-bearing waste packages, and a codisposal group with all types of codisposal waste packages.

Seismic Consequence Abstraction (SNL 2007 [DIRS 176828]) provides an algorithmic description for the fault displacement damage abstraction for the EBS components (SNL 2007 [DIRS 176828], Section 6.12.2, step 21), as well as a definition of parameters for the TSPA model that specifically relate to breach of the waste packages and drip shields from fault displacement (SNL 2007 [DIRS 176828], Table 6-93).

INPUTS:

Table 1.2.02.03.0A-1. Indirect Inputs

Citation	Title	DIRS
10 CFR 63	Energy: Disposal of High-Level Radioactive Wastes in a Geologic Repository at Yucca Mountain, Nevada	180319
70 FR 53313	Implementation of a Dose Standard After 10,000 Years	178394
BSC 2004	*Mechanical Assessment of the Drip Shield Subject to Vibratory Ground Motion and Dynamic and Static Rock Loading*	169753
BSC 2004	*Characterize Framework for Seismicity and Structural Deformation at Yucca Mountain, Nevada*	168030
SNL 2007	*Seismic Consequence Abstraction*	176828
SNL 2007	*Total System Performance Assessment Data Input Package for Requirements Analysis for Subsurface Facilities*	179466

FEP: 1.2.03.02.0A

FEP NAME:

Seismic Ground Motion Damages EBS Components

FEP DESCRIPTION:

Seismic activity that causes repeated vibration of the EBS components (drip shield, waste package, pallet, and invert) could result in severe disruption of the drip shields and waste packages, through vibration damage or through contact between EBS components. Such damage mechanisms could lead to degraded performance.

SCREENING DECISION:

Included

TSPA DISPOSITION:

Ground motion associated with seismic activity has the potential to disrupt the integrity of the waste package and other EBS components, which could lead to breaching of the waste packages and radionuclide release. The EBS components are the waste package, the waste package internals, the waste form/cladding, the emplacement pallet, the drip shield, the drift invert, and the emplacement drift. Damage to the waste package and its internals from vibratory ground motion is included in TSPA. Damage to the cladding is not considered here because all fuel cladding (stainless steel and Zircaloy) for commercial SNF is considered to be breached upon emplacement in the repository, as discussed in included FEP 2.1.02.12.0A (Degradation of Cladding Prior to Disposal) and in *Cladding Degradation Summary for LA* (SNL 2007 [DIRS 180616], Table 7-2[a]). Damage to the drip shield is excluded because: (1) the presence of stress corrosion cracks on the drip shield does not compromise its ability to divert seepage away from the waste package (see excluded FEP 2.1.03.10.0B (Advection of Liquids and Solids Through Cracks in the Drip Shield)), (2) drip shield separation is not predicted to occur (SNL 2007 [DIRS 176828], Section 6.7.3), and (3) failure of the drip shield from waste package impacts is not predicted to occur (SNL 2007 [DIRS 176828], Section 6.8.5). The drift invert and the emplacement pallet could also be damaged as a result of ground motion, but these components do not contribute to the capability of the EBS barrier to prevent the release of radionuclides and, in this respect, such effects do not require further consideration.

The rockfall induced by vibratory ground motion can have a significant impact on the emplacement drifts and other EBS components. The response of EBS components to rockfall induced by vibratory ground motion is considered by several other FEPs. The response of waste packages and drip shields in a partly or completely collapsed drift in the lithophysal units of the repository is discussed in included FEP 1.2.03.02.0C (Seismic-Induced Drift Collapse Damages EBS Components). The response of the drip shield plates and waste packages to rock block impacts in nonlithophysal units is discussed in excluded FEP 1.2.03.02.0B (Seismic-Induced Rockfall Damages EBS Components).

The effects of seismic events with exceedance frequencies as low as 10^{-8} per year are included in the performance assessments to demonstrate compliance with the individual protection stardard after permanent closure (proposed 10 CFR 63.311 (70 FR 53313 [DIRS 178394])). These performance assessments are represented by the seismic scenario class (SNL 2007 [DIRS 178765], Section 6.6). The seismic scenario class is represented by two modeling cases. The first modeling case includes the response of EBS components to the vibratory ground motion associated with a seismic event. This first modeling case includes the effects of general corrosion on EBS components during the period of geologic stability, as required by proposed 10 CFR 63.342(c)(i) (70 FR 53313 [DIRS 178394]). The second modeling case includes the response of EBS components to fault displacement, and is discussed further in included FEP 1.2.02.03.0A (Fault Displacement Damages EBS Components).

The effects of unlikely seismic events (events having less than one chance in 10 of occurring in 10,000 years) are not included in performance assessments to demonstrate compliance with the groundwater protection standards (10 CFR 63.331 [DIRS 180319]) and the individual protection standard for human intrusion (proposed 10 CFR 63.321 (70 FR 53313 [DIRS 178394])), consistent with the requirements of the proposed rule in 10 CFR 63.342(b) and (c)(1) (70 FR 53313 [DIRS 178394]).

The effects of likely seismic events, with exceedance frequencies greater than or equal to 10^{-5} per year, have been considered for inclusion in the performance assessments to demonstrate compliance with the individual protection standard for human intrusion (proposed 10 CFR 63.321; proposed 10 CFR 63.342(b) and (c)(1) (70 FR 53313 [DIRS 178394])). Inclusion of the effects of likely seismic events on EBS components in the assessment of the stylized human intrusion scenario would not increase the calculated annual dose to the RMEI, as discussed in excluded FEP 1.4.02.04.0A (Seismic Event Precedes Human Intrusion). The effects of vibratory ground motion are therefore excluded from the performance assessment to demonstrate compliance with the individual protection standard for human intrusion on the basis of low consequence.

The effects of vibratory ground motion from likely seismic events are included in the performance assessments to demonstrate compliance with the groundwater protection standards, consistent with the requirements in 10 CFR 63.331 [DIRS 180319] and proposed 10 CFR 63.342(b) (70 FR 53313 [DIRS 178394]).

Failure Mechanisms in Response to Vibratory Ground Motion—Seismic-induced deformation of EBS components may result in plastic yielding or failure of EBS components. If the residual stress on a plastically deformed EBS component exceeds a threshold value, then stress corrosion cracks may initiate and propagate through-wall, resulting in transport pathways into and out of the waste packages. The area in which the residual stress threshold is exceeded is referred to as a "damaged area," and is conceptualized to result in the immediate formation of a tightly spaced network of stress corrosion cracks. Stress corrosion cracking of waste packages and drip shields is discussed further in included FEP 2.1.03.02.0A (Stress Corrosion Cracking (SCC) of Waste Packages) and in excluded FEP 2.1.03.02.0B (Stress Corrosion Cracking (SCC) of Drip Shields). The combined mechanical-corrosion failure mechanism of deformation caused by vibratory ground motion followed by potential SCC is expected to be a primary cause of damage to the waste packages and drip shields (SNL 2007 [DIRS 176828], Section 6.1.4 and 6.1.5).

Damaged areas are distinct from structural failures, which corresponding to the tearing, rupture, or buckling of an EBS component. A rupture or tear may occur if the local strain exceeds the ultimate tensile strain, and may partly or completely negate the effectiveness of the EBS component in preventing the inflow of seepage water or the outward transport of radionuclides. Buckling of an EBS component may change its structural configuration, possibly changing a component's effectiveness as part of the EBS barrier to seepage or rockfall. Rupture or puncture of the OCB of the waste package and buckling of the sidewalls of the drip shield are important failure mechanisms in the seismic damage abstractions (SNL 2007 [DIRS 176828], Section 6.1.4).

The effects of vibratory ground motion depend on the condition of the components and the in-drift environment. The thicknesses of EBS components will be continually reduced by general corrosion during the time scale of geologic stability. The in-drift environment will change as emplacement drifts fill with rubble and as drip shields fail under the combined loading of rockfall and vibratory ground motion. Damage from multiple seismic events may accumulate, leading to failure of EBS components. These responses have been incorporated into the seismic damage abstractions for the TSPA model (SNL 2007 [DIRS 176828], Section 6.1.2).

Abrasion between the waste package and pallet could also potentially reduce the thickness of the OCB. However, abrasion is not included in the seismic damage abstractions because abrasion is anticipated to be a secondary or tertiary effect on waste package response that will have low consequence for seismic response. Any effect from abrasion is encompassed by the existing seismic damage abstractions:

- The kinematic damage abstractions are based on structural response calculations with an OCB thickness of 23 mm, and the results for the 23-mm-thick OCB determine the response of the waste package for OCB thicknesses between 23 mm and 25.4 mm (SNL 2007 [DIRS 176828], Equation 6.5-1 in Section 6.5.2.2 and Equation 6.5-4 in Section 6.5.2.5). That is, the probability of damage and the damaged area are set to their values for a 23-mm-thick OCB if the OCB thickness is greater than 23 mm. As it requires several hundred thousand years after repository closure for the spatially averaged thickness of the OCB to thin from 25.4 mm to 23 mm (SNL 2007 [DIRS 176828], Section 6.5.1.2), the kinematic damage abstractions encompass any potential thickness loss from abrasion during this time period.

- The seismic damage abstractions for a waste package surrounded by rubble are based on two-dimensional structural response calculations that ignore the bending moment from the waste package lids at both ends of the package, thereby underestimating the load-bearing capacity of the waste package (SNL 2007 [DIRS 178851], Section 6.5.1.1). The two-dimensional representation is thought to encompass any potential strength reduction from abrasion of the rubble on the OCB.

Drip Shield Damage due to Vibratory Ground Motion−Vibratory ground motion associated with a seismic event may cause impacts between waste packages and drip shields that could compromise the structural stability of the drip shields or tear the interior support bulkhead beneath the crown of the drip shields (SNL 2007 [DIRS 176828], Section 6.8.5). The structural stability of the drip shields when surrounded by rubble and subjected to lateral impacts by the

waste packages has been investigated with three-dimensional finite-element calculations (BSC 2005 [DIRS 173172], Section 5.6.2 and Attachment VI). The results from these calculations demonstrate that lateral impacts would not cause catastrophic failure of the drip shields, as discussed in *Seismic Consequence Abstraction* (SNL 2007 [DIRS 176828], Section 6.8.5). Three-dimensional finite-element calculations were also performed for a waste package that "clips" a bulkhead support beam on the underside of the crown of the drip shield (SNL 2007 [DIRS 178851], Section 6.4.5). Such impacts were determined to have a low probability of occurrence in comparison to the buckling of the sidewalls of the drip shield under dynamic load (SNL 2007 [DIRS 176828], Section 6.8.5). Therefore, waste package-to-drip shield impacts are not represented in the TSPA model.

Vibratory ground motion may cause adjacent drip shields to separate if there is a large vertical displacement between adjacent drip shields or if the welds holding the drip shield connector guides tear loose from the drip shield plates during the dynamic response. However, the frictional forces between EBS components and the loads from rockfall provide a restraint on the movement of the drip shields, preventing the differential motion that could lead to separation (SNL 2007 [DIRS 176828], Section 6.7.3). Therefore, drip shield separation as a result of vibratory ground motion is excluded from the TSPA model.

Waste Package Damage due to Vibratory Ground Motion−The mechanical response of a waste package to a seismic event will depend on the configuration and structural integrity of the EBS components at the time of the seismic event (SNL 2007 [DIRS 176828], Section 6.1.2). The mechanical response of the waste packages to seismic events is defined for three configurations or states of the system: (1) an initial state in which the drip shield is intact, (2) an intermediate state in which the sidewalls of the drip shield have buckled, but the drip shield plates remain intact, and (3) a final state in which the waste packages are surrounded by rubble after the drip shield plates have failed.

These three states lead to three distinct damage "modes" for the waste packages (SNL 2007 [DIRS 176828], Section 6.1.3). In the first state, the waste packages are free to move beneath the drip shield and the "kinematic" response can cause impact-related damage. The kinematic response can also cause severe deformation of the waste package, potentially causing rupture of the OCB from multiple impacts. These impact-related mechanisms are the subject of this FEP and are discussed below. The damage that can occur in the second and third states is discussed in included FEP 1.2.03.02.0C (Seismic-Induced Drift Collapse Damages EBS Components).

In the initial state, when the drip shield is intact, waste packages can move freely beneath the drip shield and there is minimal accumulation of rockfall. The predominant mechanism for damage is seismic-induced impact between EBS components. The potential for damage from impacts between adjacent waste packages and between a waste package and its emplacement pallet are discussed below. The potential for damage to the waste package from impacts with the invert is not included in the seismic damage abstractions because the damaged areas from the side-on impact of a waste package on a flat elastic surface is zero or very small (SNL 2007 [DIRS 176828], Section 6.5.6). The potential for damage to the waste package from lateral impacts between the waste package and drip shield is not included in the seismic damage abstractions based on a similar rationale (SNL 2007 [DIRS 176828], Section 6.8.5).

Rigid body kinematic calculations have been performed for an emplacement drift containing a combination of TAD canister-bearing waste packages and codisposal waste packages. The responses of waste packages with Alloy 22 OCB thicknesses of 23 mm or 17 mm and with intact or degraded internals have been analyzed (SNL 2007 [DIRS 178851], Section 6.3.1). The 23-mm-thick OCB represents a reduction from the initial OCB thickness of 25.4 mm and provides a representation for an intact or almost intact waste package. The 17-mm-thick OCB represents a waste package that has undergone substantial corrosion at late times after repository closure. The waste package internals are assumed to degrade as a structural component after the first breach of the OCB and before the next seismic event occurs. Structural response calculations were performed for seventeen ground motion time histories (i.e., 17 three-component accelerograms) for four levels of horizontal PGV: 0.4, 1.05, 2.44, and 4.07 m/s (SNL 2007 [DIRS 178851], Section 6.3.2.1.2). Damaged areas were determined for three values of the residual stress threshold (RST): 90%, 100%, and 105% of the yield strength of Alloy 22 (SNL 2007 [DIRS 176828], Section 6.1.4). The output from the structural response calculations provide the basis for the kinematic damage abstractions for the TAD canister and codisposal waste packages in response to a seismic event (SNL 2007 [DIRS 176828], Sections 6.5 and 6.6).

Summary−As documented in *Seismic Consequence Abstraction* (SNL 2007 [DIRS 176828]), the potential for damage to a TAD canister or codisposal waste package from end-to-end impacts between adjacent waste packages and from waste package-to-pallet impacts is included in the performance assessments to demonstrate compliance with the individual protection standard (proposed 10 CFR 63.311 (70 FR 53313 [DIRS 178394)) in the seismic scenario class. Damage from waste package-to-drip shield impacts and drip shield separation as a result of vibratory ground motion are not included in these performance assessments.

INPUTS:

Table 1.2.03.02.0A-1. Indirect Inputs

Citation	Title	DIRS
10 CFR 63	Energy: Disposal of High-Level Radioactive Wastes in a Geologic Repository at Yucca Mountain, Nevada	180319
70 FR 53313	Implementation of a Dose Standard After 10,000 Years	178394
BSC 2005	*Mechanical Assessment of the Waste Package Subject to Vibratory Ground Motion*	173172
SNL 2007	*Seismic Consequence Abstraction*	176828
SNL 2007	*Cladding Degradation Summary for LA*	180616
SNL 2007	*Mechanical Assessment of Degraded Waste Packages and Drip Shields Subject to Vibratory Ground Motion*	178851
SNL 2007	*Analysis of Mechanisms for Early Waste Package/Drip Shield Failure*	178765

FEP: 1.2.03.02.0B

FEP NAME:

Seismic-Induced Rockfall Damages EBS Components

FEP DESCRIPTION:

Seismic activity could produce jointed-rock motion and/or changes in rock stress leading to enhanced rockfall that could impact drip shields, waste packages, or other EBS components.

SCREENING DECISION:

Excluded – low consequence

SCREENING JUSTIFICATION:

Introduction—Vibratory ground motion from seismic activity could cause failure of the host rock around emplacement drifts. The potential for the resulting rockfall to damage the drip shields, waste packages, and waste package internals is evaluated in this excluded FEP. The screening justification for this FEP is structured into ten sections: (1) Introduction, (2) Rock Failure Mechanisms, (3) Mechanical Failure Mechanisms, (4) Drip Shield Damage Due to Rock Block Impacts, (5) Exclusion of Damaged Areas on the Drip Shield Plates, (6) Exclusion of Tearing of the Drip Shield Plates, (7) Exclusion of Tearing of the Axial Stiffeners, (8) Exclusion of Waste Package Damage Due to Rock Block Impacts, (9) Response During the Period of Geologic Stability, and (10) Summary. Each of these sections describes an important aspect of the response of the drip shields or waste packages to rockfall generated by jointed-rock motion in the nonlithophysal units of the repository.

At Yucca Mountain, the emplacement drifts will transect both nonlithophysal and lithophysal rock types. In the nonlithophysal units, vibratory ground motion could cause jointed-rock motion that dislodges large rock blocks from the sides or crown of drifts in the nonlithophysal units. Damage to EBS components from rockfall generated by jointed-rock motion is excluded from the TSPA model based on the screening justification in this FEP. In the lithophysal units, vibratory ground motion could fracture the host rock into smaller fragments that partly or completely collapse a drift. The damage to EBS components from seismic-induced drift collapse of the lithophysal units is included in the TSPA model (see included FEP 1.2.03.02.0C (Seismic-Induced Drift Collapse Damages EBS Components)), and the resulting seismic damage abstractions (SNL 2007 [DIRS 176828], Sections 6.7.1 and 6.10.1) are applied to all the drip shields and waste packages in the repository. In other words, the damage to the drip shields and waste packages from the seismic-induced response of the host rock is based on the rockfall process in the lithophysal units (included FEP 1.2.03.02.0C (Seismic-induced Drift Collapse Damages EBS Components)), rather than on rockfall generated by jointed-rock motion in nonlithophysal units. This is a reasonable approach because of the screening justifications in this FEP and because the rockfall volume and loads from drift collapse in the lithophysal units are much greater than those from rockfall induced by jointed-rock motion in the nonlithophysal units (SNL 2007 [DIRS 176828], Section 6.7.2.1).

The emplacement pallet and invert are also features of the EBS, but do not need detailed evaluation as part of this FEP. The emplacement pallet could be damaged as a result of host rock failure induced by vibratory ground motion, but the TSPA does not take credit for the pallet's contribution to delaying or preventing the transport of radionuclides, so it does not require further consideration. The invert is filled with compacted ballast that will not be damaged by host rock failure because the ballast is made from run-of-mine rock tailings, so the invert does not require further consideration. Finally, the emplacement drift is also a feature of the EBS, and the response of the emplacement drift to rockfall is represented in the TSPA model through included FEP 1.2.03.02.0D (Seismic-induced Drift Collapse Alters In-Drift Thermohydology).

Vibratory ground motion can cause direct damage to the EBS components through rigid body motions and impacts between adjacent EBS components. These effects are addressed in included FEP 1.2.03.02.0A (Seismic Ground Motion Damages EBS Components). The direct effects of fault displacement on the EBS components are discussed in included FEP 1.2.02.03.0A (Fault Displacement Damages EBS Components).

Rock Failure Mechanisms—The type of rock failure that could occur in an emplacement drift as a result of seismic activity depends on the local strata that the drift transects. At Yucca Mountain, the nonlithophysal units encompass 15% to 20% of the repository emplacement area (SNL 2007 [DIRS 179466], Table 4-1, Parameter Number 01-03). The nonlithophysal rock is composed of strong, intact blocks of welded tuff separated by fracture planes (BSC 2004 [DIRS 166107], Section 6.4.1.1). Vibratory ground motion could cause jointed-rock motion that dislodges large rock blocks from the sides or crown of drifts in the nonlithophysal units. The potential damage to EBS components from large rock blocks in the nonlithophysal units is addressed and excluded in this FEP. Rockfall resulting from non-seismic causes is addressed in excluded FEP 2.1.07.01.0A (Rockfall).

In contrast, the lithophysal units encompass about 80% to 85% of the repository emplacement area (SNL 2007 [DIRS 179466], Table 4-1, Parameter Number 01-03). The lithophysal rock is characterized by low compressive strength due to widespread lithophysal voids interconnected by intense local fracturing. Large rock blocks are not expected in the lithophysal zone due to the presence of numerous lithophysal voids interconnected by densely spaced fractures. Individual lithophysal rock fragments are less massive than the large nonlithophysal rock blocks, and hence less damaging to EBS components. However, the total volume and resulting static load from lithophysal rubble fragments that accumulate during multiple seismic events are significantly greater than the rockfall volume and loads in the nonlithophysal zones (SNL 2007 [DIRS 176828], Section 6.7.2.1). Failure of EBS components could occur as a result of the static load from the accumulated lithophysal rubble amplified by the dynamic load during vibratory ground motion. The potential damage to EBS components from partial or complete drift collapse in lithophysal units is addressed in included FEP 1.2.03.02.0C (Seismic-Induced Drift Collapse Damages EBS Components).

Mechanical Failure Mechanisms—Impact-related dynamic loads may dent the drip shields and waste packages, resulting in residual stress from permanent structural deformation. High tensile levels of residual stress may lead to local degradation from stress corrosion cracking, potentially resulting in a network of through-going cracks that can form transport pathways for water or radionuclides. The dented area that exceeds the residual stress threshold is referred to as the

"damaged area" and is conceptualized to result in the immediate formation of a tightly spaced network of through-going stress corrosion cracks. Stress corrosion cracking of the waste packages' outer corrosion barrier and of the drip shield plates is discussed further in included FEP 2.1.03.02.0A (Stress Corrosion Cracking (SCC) of Waste Packages) and in excluded FEP 2.1.03.02.0B (Stress Corrosion Cracking (SCC) of Drip Shields). The combined failure mechanism of plastic deformation (which causes the residual stress) followed by accelerated stress corrosion cracking is hypothesized to be a primary cause of seismic-induced damage to the drip shields and waste packages (SNL 2007 [DIRS 176828], Section 6.1.4).

Damaged areas are distinct from structural failures, which correspond to the tearing or rupture of an EBS component. A rupture or tear may occur if the local strain exceeds the ultimate tensile strain, and would partly or completely negate the effectiveness of the EBS component as an impediment to the inflow of seepage water or the outward transport of radionuclides. The potential for structural failure of EBS components from a seismic event has been analyzed in detail in *Mechanical Assessment of Degraded Waste Packages and Drip Shields Subject to Vibratory Ground Motion* (SNL 2007 [DIRS 178851], Section 6.2.2) and is modeled and abstracted in *Seismic Consequence Abstraction* (SNL 2007 [DIRS 176828], Section 6.1.4).

Once stress corrosion cracks form, they could reduce the ultimate plastic load capacity of the drip shield framework in response to static rockfall loading and vibratory ground motion. However, the structural response calculations for the drip shields include several conservatisms that offset the potential reduction of plastic load capacity from a preexisting crack network: (1) stress relaxation from the creep of titanium could arrest crack growth if the local stresses drop below the residual stress threshold before the crack reaches a critical length for propagation (BSC 2005 [DIRS 174715], Section 5.5.3); (2) crack propagation will cause further deformation of the drip shields. This deformation will increase the reactive pressure from the rubble surrounding the drip shields, possibly arresting crack growth; (3) the ultimate plastic load capacity of the drip shield is based on a quasi-static approach that underestimates the plastic load capacity relative to dynamic calculations of drip shield response; and (4) the variability of the vertical component of the ground motion is overestimated by the postclosure ground motions (SNL 2007 [DIRS 178851], Section 6.4.7.3). The combined effect of these four conservatisms is expected to more than offset the potential reduction in plastic load capacity due to preexisting crack networks (SNL 2007 [DIRS 178851], Section 6.4.7.3), and the effect of a preexisting crack network on plastic load capacity of the drip shields is not included in the structural response calculations for the drip shields.

Drip Shield Damage Due to Rock Block Impacts—The computational approach for defining drip shield damage due to rock block impacts is described in detail in *Seismic Consequence Abstraction* (SNL 2007 [DIRS 176828], Sections 6.10.2, 6.10.2.1, 6.10.2.2, and 6.10.2.3). This computational approach considers the potential for general corrosion to reduce the robustness of the drip shields over the period of geologic stability. In particular, the structural response is determined for three thicknesses of the drip shield components, as noted below. These three thicknesses represent the impact of general corrosion on the structural response of the drip shields throughout the period of geologic stability, as required by the proposed 10 CFR 63.342 (70 FR 53313 [DIRS 178394]). The major features of the rockfall and structural response calculations are documented as follows:

- *Drift Degradation Analysis* (BSC 2004 [DIRS 166107], Section 6.3) provides a detailed description of the nonlithophysal rockfall calculations performed with 3DEC, a three-dimensional discontinuum computer program. The computational results define the size, velocity, and frequency of the multiple rock blocks that can be dislodged during seismic events at the 1.05, 2.44, and 5.35 m/s PGV levels.

- Structural response calculations were performed for a set of seven representative block sizes that span the range of block kinetic energies (SNL 2007 [DIRS 178851], Section 6.4.7.2.2), and for one intact and two degraded states of the drip shields. The intact state has no thickness reduction, and the degraded states have 5- and 10-mm thickness reductions for all drip shield components (SNL 2007 [DIRS 176828], Section 6.10.2.2). The results from these calculations form the basis for "catalogs" of damage areas, maximum plastic strains and maximum stiffener displacements for individual block impacts as a function of block kinetic energy and plate thickness (SNL 2007 [DIRS 176828], Table 6-51). The damaged area and maximum plastic strain from an individual block impact is calculated by interpolation within the catalog of damaged areas. The methodology of the calculations is described in detail in *Seismic Consequence Abstraction* (SNL 2007 [DIRS 176828], Sections 6.10.2.2 and 6.10.2.3).

- The rock block is represented as an edge-on impact at the center of the drip shield, with the center of mass of the block directly above the impact point (SNL 2007 [DIRS 178851], Section 6.4.7.2.2). The center impact tends to overestimate seepage onto the waste packages or damage to the drip shields for the following reasons. First, seepage through a dented or failed plate at the center of the drip shields is more liable to result in water dripping onto the waste packages than seepage through a dent or failed plate at the "shoulder" (where the crown meets the vertical side) or sidewall of the drip shields. Second, an impact to the shoulder or sidewalls of the drip shields will generally create a crease that diverts the flow of seepage water toward the side(s) of the drip shields, rather than forming a central depression that could collect seepage water. The collection of seepage is potentially important because the resulting hydrostatic head from the pooled water could facilitate advective flow through stress corrosion cracks. Third, the alignment of the block's center of mass with the impact point maximizes deformation for a given kinetic energy, providing an upper bound for the calculated damage areas.

Multiple seismic events will cause the waste packages and emplacement pallets to reposition themselves beneath the drip shields. However, the limited clearance between the outside of the emplacement pallet and the inside of the drip shield, as shown in *Total System Performance Assessment Data Input Package for Requirements Analysis for Engineered Barrier System In-Drift Configuration* (SNL 2007 [DIRS 179354], Figure 4-1), acts to position the waste packages near the centerline of the drip shields after a seismic event. In other words, the lateral movement of the waste packages relative to the drip shields is limited by the lateral clearance between the pallets and drip shields. It follows that the reasoning in the preceding paragraph is applicable to block impacts after multiple seismic events.

Exclusion of Damaged Areas on the Drip Shield Plates—Damaged areas on the drip shield plates are excluded from the TSPA model because advective flow through stress corrosion cracks in the

drip shields is excluded from the TSPA model on the basis of low consequence (see excluded FEP 2.1.03.10.0B (Advection of Liquids and Solids Through Cracks in the Drip Shield)). If advective flow is excluded, then the presence of stress corrosion cracks from seismic-induced rockfall does not compromise the ability of the drip shield to divert seepage away from the waste packages.

Exclusion of Tearing of the Drip Shield Plates—The tearing or rupture of drip shield plates from large block impacts is also excluded from the TSPA model because of low consequence. The dose that could result from rupture of the drip shield plates is estimated using the results of calculations estimating the results of early drip shield failure as discussed in Appendix E. The drip shield early failure calculations compute the dose that results from manufacturing defects or emplacement damage to drip shields. The effects of an early failure are simulated by removing a single drip shield as an impediment to seepage. If seepage occurs in a location with an early failed drip shield, the associated waste package is conservatively assumed to also have failed. Hence, the drip shield early failure calculations describe the dose that may result if a drip shield and its associated waste package fail simultaneously. The mathematical details of this calculation are documented in Appendix E.

The estimate of dose from rupture of the drip shield plates accounts for the frequency of occurrence of seismic-induced rock block impacts in the nonlithophysal units, and the extent of ruptured drip shields caused by these impacts. This estimate considers localized corrosion as the process that may fail the waste package subsequent to rupture of the drip shield plates. Sections E.6.1 and E.6.2 provide a detailed discussion of the technical approach and the mathematical formulation for the calculation. The mean annual dose due to nonlithophysal rockfall over a 10,000-year period is not significant in comparison to the mean annual dose due to seismic ground motion or in comparison to the regulatory limit of 15 mrem/yr (proposed 10 CFR 63.311(a)(1) (70 FR 53313 [DIRS 178394])), as shown in Section E.6.3. The mean annual dose due to nonlithophysal rockfall over the 10,000-year to 1,000,000-year period after closure is estimated to be less than 1% of the mean annual dose due to seismic ground motion, based on the analysis in Section E.6.3. The effects of nonlithophysal rockfall on the drip shield are therefore not included in the performance assessment on the basis of low consequence because the maximum mean dose from drip shield plate failures and seismic-induced nonlithophysal rockfall is a small fraction of the mean annual dose from seismic ground motion during the period of geologic stability.

Exclusion of Tearing of the Axial Stiffeners—Rupture of the axial stiffeners beneath the crown of the drip shields is also considered in the structural response calculations for drip shield response to rock block impacts (SNL 2007 [DIRS 178851], Section 6.4.7). The axial stiffeners rupture only for the impact of the largest of the seven representative rock blocks (SNL 2007 [DIRS 176828], block 1 in Tables 6-50 and 6-51). This statement is true for the intact drip shield and for degraded drip shields with 5-mm and 10-mm thickness reductions. Block 1 has the maximum kinetic energy (706,914 Joules) of any block from the rockfall analyses. The following observations are relevant here:

- The rock block that causes the axial stiffeners to fail occurs at the 5.35 m/s PGV level, which is beyond the maximum PGV level of 4.07 m/s on the bounded hazard curve (SNL 2007 [DIRS 176828], Section 6.4.3). In other words, the exceedance probability

for the 5.35 m/s PGV level seismic event is less than 10^{-8} per year, so this maximum block is not included in the TSPA model on the basis of low probability.

- The simplified representation of the blocks in the structural response calculation provides an upper bound on rockfall damage. For these calculations, the rock block is represented as a cubic block with an edge-on impact at the center of the drip shield, with the center of mass of the block directly above the impact point (SNL 2007 [DIRS 178851], Section 6.4.7.2.2). However, large rock blocks are expected to have a highly irregular shape, and the center of mass that will seldom be directly over the impact point. In this situation, the block will rotate upon impact, providing a larger contact surface that distributes the impact load over a larger area, thereby reducing the possibility of rupture of the axial stiffeners.

The prediction of rupture of the axial stiffeners is, therefore, not expected even for the maximum rock block. This failure mode is therefore not included in the TSPA model.

Exclusion of Waste Package Damage Due to Rock Block Impacts—Seismic-induced damage to the waste package and its internals from rock block impacts in nonlithophysal units is not included in the TSPA model on the basis of low probability.

The impact calculations show that block 1 would cause the drip shield to fail through rupture of its axial stiffeners, potentially contacting the waste packages (SNL 2007 [DIRS 176828], block 1 in Table 6-51). The maximum stiffener displacement for impact of block 1 on the drip shield is 0.204 m (20.4 cm) with a 5-mm thickness reduction (SNL 2007 [DIRS 176828], Table 6-51). For all other blocks, the maximum stiffener displacement is 0.0417 m (4.17 cm) for block 2 with the 10-mm thickness reduction (SNL 2007 [DIRS 176828], Table 6-51). When compared to the initial clearance between the drip shields and the waste packages of 14 inches (35.6 cm) to 27 inches (68.6 cm) (SNL 2007 [DIRS 179354], Figure 4-1, dimension D3), no contact between the drip shields and waste packages is predicted. However, the calculations for block 1 do not represent the complete mechanical response after rupture because the failed component (i.e., the axial stiffener) has not been removed from the calculation and because the calculation for block 1 with a 10-mm thickness reduction did not run to completion. In this situation, it is possible that the deformation of the drip shields may increase after rupture such that the drip shields contacts the waste packages. As the drip shields continue to deform, the energy of the rock block impact will be dissipated and any potential impact of the drip shields into the waste packages will be at a substantially reduced velocity. In addition, any contact between the drip shields and the waste packages as a result of a rock block impact will be spread over a large area, resulting in insignificant deformations to waste packages with intact internals, and fairly small deformations to waste packages with degraded internals (SNL 2007 [DIRS 178851], Section 6.4.7.3). It is possible to conclude that, should block 1 cause a drip shield to contact a waste package, there would be no rupture of the waste packages and any damaged areas would be insignificant (SNL 2007 [DIRS 178851], Section 6.4.7.3).

Failure of the drip shield plates from impacts by rock blocks 2 through 7 for the 0-, 5-, and 10-mm thickness reductions does not cause contact between the drip shields and the waste packages because the axial stiffeners do not tear or rupture (SNL 2007 [DIRS 176828], Table 6-51 and p. 6-185). So there is no potential for damage to the waste packages from rupture

of the drip shield plates due to impacts by rock blocks 2 through 7 because the framework of the drip shields remains structurally intact (i.e., the axial stiffeners remain intact) and is able to deflect rockfall away from the waste package and its internals (SNL 2007 [DIRS 176828], Section 6.10.2.11).

The waste packages could also be damaged by rock block impacts if the drip shields separate during vibratory ground motion. Drip shield separation is defined as an axial or vertical gap or space between two adjacent drip shields that allows in-drift seepage to flow directly onto waste packages. Separation is important because it negates the functionality of the drip shields as a barrier to seepage and rockfall for the waste packages. Drip shield separation is excluded from the TSPA model based on low probability of occurrence (SNL 2007 [DIRS 176828], Section 6.7.3).

Axial separation of adjacent drip shields is excluded from the TSPA model because: (1) ground motion amplitudes that are sufficient to cause axial separation are also large enough to partially or completely collapse drifts in the repository, (2) rockfall occurs within the first second or two of the arrival of these large amplitude ground motions, and (3) a kinematic study indicates that small static loads from rubble or frictional loads between EBS components are sufficient to eliminate axial separation of drip shields (SNL 2007 [DIRS 176828], Section 6.7.3.1). In this situation, rockfall provides restraints on the motion of the drip shields, preventing differential motion that could lead to separation. Axial separation is excluded from the TSPA model based on low probability.

Vertical separation of adjacent drip shields is excluded from the TSPA model because: (1) rockfall provides restraints on the motion of the drip shields, preventing differential motion that could lead to separation, as discussed above, and (2) the drip shield connector subassemblies provide a 320-mm-long (12.6-in-long) overlap at the joint between adjacent drip shields (SNL 2007 [DIRS 179354], Table 4-2, Parameter Number 07-01; SNL 2007 [DIRS 176828], Section 6.7.3.2). This overlap will protect the waste packages from direct seepage and direct rockfall that might result from a vertical displacement of a few inches between adjacent drip shields. Vertical separation is not included in the TSPA model on the basis of low probability.

Response During the Period of Geologic Stability—Performance assessment for seismic response must consider the damage to the drifts and failure of the waste package beyond the 10,000-year postdisposal period through the period of geologic stability subject to the probability limits in proposed 10 CFR 63.342 (70 FR 53313 [DIRS 178394]). This screening justification must, therefore, consider the response of the EBS components beyond the 10,000 year postdisposal period. Two key aspects of the long-term response in the nonlithophysal units are considered here: (1) the exclusion of tearing of the drip shield plates, and (2) the potential for general corrosion to eliminate the drip shield as a mechanical structure, allowing rock blocks to directly impact the waste package.

The estimate of dose from tearing or rupture of the drip shield plates due to nonlithophysal rock block impacts is based on the technical approach and mathematical calculations discussed in Appendix E. As discussed previously, the mean annual dose due to nonlithophysal rockfall over the 10,000-year to 1,000,000-year period after closure is estimated to be less than 1% of the mean annual dose due to seismic ground motion, based on the analysis in Section E.6.3. The

effects of tearing or rupture of the drip shield plates due to nonlithophysal rock block impacts are, therefore, not included in the performance assessment on the basis of low consequence throughout the period of geologic stability.

The response of the drip shield and drifts beyond the postdisposal period through the period of geologic stability is considered next. This discussion demonstrates that the drip shield is expected to fail from general corrosion, rather than dynamic loading of the drip shields from a seismic event, potentially exposing the waste package to direct impact of rock blocks during the period of geologic stability.

The mean time for a 10-mm thickness reduction due to general corrosion on the top and bottom sides of the drip shield plates is 195,000 years after closure (SNL 2007 [DIRS 176828], Section 6.10.2.11). Since the initial plate thickness is 15 mm, the mean time for plate failure from general corrosion is (15 mm/10 mm)(195,000 years) = 293,000 years. Using 1 inch as a typical initial thickness for the components of the drip shield framework, the time for framework failure from general corrosion is estimated to be (25.4 mm/10 mm)(195,000 years) = 495,000 years. This is an estimate because the framework is fabricated from Titanium Grade 29, which has modestly higher corrosion rates than the Titanium Grade 7 plates. However, the estimate provides a reasonable time scale for this analysis. In summary, the mean time for failure of the drip shield plates from general corrosion is on the order of 300,000 years, and the estimated time for failure of the framework is on the order of 500,000 years.

Rockfall will accumulate in the nonlithophysal zones from multiple seismic events during these time periods. However, the volume of rockfall per seismic event is much smaller in the nonlithophysal units than in the lithophysal units (SNL 2007 [DIRS 176828], Figure 6-58 and Section 6.7.2.1). For example, the mean rockfall in the nonlithophysal units is only (0.24 m^3 per meter/7.8 m^3 per meter) = 3% of the mean rockfall in the lithophysal units at the 1.05 m/s PGV level (SNL 2007 [DIRS 176828], Table 6-32). It follows that the drifts in the nonlithophysal units are not expected to fill with a significant amount of rubble during the first 500,000 years after closure, and that the drip shields are not expected to be covered with a significant amount of rubble during this time frame.

If the drip shields are not covered with a significant amount of rubble, the failure mode of the drip shield is primarily from general corrosion, rather than the dynamic amplification of the static load from rubble during a seismic event. For example, the probability of failure of the drip shield plates with 10% of the rockfall load from a fully collapsed drift is 0 for a 5-mm-thick plate and only 0.036 for a 2-mm-thick plate at the 4.07 m/s PGV level (SNL 2007 [DIRS 176828], Table 6-36). Since the limited rubble volume in the nonlithophysal units will generally come to rest along the sides of the drip shields, a seismic event will not amplify the static vertical rockfall loads, and the primary failure mechanism is general corrosion.

After the drip shields fail from general corrosion in the nonlithophysal units, the waste packages become exposed to direct impact from large rock blocks because the rubble is not expected to cover the tops of the waste packages. However, direct impact of a large rock block on a degraded waste package is not expected to rupture the package because the structural response calculations for individual impacts of a waste package with degraded internals on an

emplacement pallet (SNL 2007 [DIRS 178851], Sections 6.3.2.2, 6.3.2.2.3, and 6.3.2.2.7) provide a bounding analogue for the rock block impact on a waste package, as explained next.

The nonlithophysal rock block with the maximum kinetic energy is a 28.29 MT rock block with a velocity of 7.07 m/s and a kinetic energy of 706,914 joules (SNL 2007 [DIRS 176828], Table 6-50). This is the largest rock block from the nonlithophysal rockfall calculations at the highest unbounded PGV level, 5.35 m/s, which has a probability of less than 10^{-8} per year probability of occurring based on the bounded hazard curve. The rock block volume is 11.7 m^3 (SNL 2007 [DIRS 176828], Table 6-50), equivalent to a cube 2.27 meters on a side. In reality, this block is expected to have a highly irregular, elongated shape, but its shape is not critical to this analysis.

Fully loaded waste packages are much more massive than this maximum rock block. For example, a fully loaded TAD canister-bearing waste package weighs 162,055 lbs (SNL 2007 [DIRS 176828], Table 6-48), equivalent to 73,700 kg. A fully loaded 5-DHLW/DOE SNF-Long codisposal waste package weighs 127,870 lbs (SNL 2007 [DIRS 176828], Table 6-48), equivalent to 58,100 kg. These masses are between 2 and 2.6 times greater than the mass of the maximum rock block. The range of impact velocities for the waste package-to-pallet impacts encompass the maximum impact velocities observed in the kinematic analyses, with a typical range of 0.2 to 10 m/s (SNL 2007 [DIRS 178851], Section 6.3.2.2.3 and Table 6-11). It follows that the kinetic energies for the most energetic waste package-to-pallet impacts are more than a factor of two greater than the nonlithophysal rock block with the maximum kinetic energy. Note also that the kinetic energy for waste package-to-pallet impacts will be orders of magnitude greater than for many of the smaller rock blocks shown in *Seismic Consequence Abstraction* (SNL 2007 [DIRS 176828], Table 6-50).

Key results from the structural response calculations for waste package-to-pallet impacts are as follows:

- The structural response calculations for the TAD canister-bearing waste package with intact or degraded internals demonstrate that the strain in the outer corrosion barrier (OCB) from a single impact is always below the ultimate tensile strain for Alloy 22, and does not result in rupture (SNL 2007 [DIRS 178851], Section 6.3.4). These structural response calculations are based on spatially averaged OCB thicknesses of 23 and 17 mm, which represent the expected OCB thickness at several hundred thousand years and more than 1 million years after repository closure, respectively (SNL 2007 [DIRS 176828], Sections 6.5.1.2 and 6.5.2.2).

- The structural response calculations for the codisposal waste package with intact or degraded internals demonstrate that the strain in the OCB from a single impact is always below the ultimate tensile strain for Alloy 22, and does not result in rupture (SNL 2007 [DIRS 178851], Section 6.3.4). These structural response calculations are based on spatially averaged OCB thicknesses of 23 and 17 mm, which represent the expected OCB thickness at several hundred thousand years and more than 1 million years after repository closure, respectively (SNL 2007 [DIRS 176828], Sections 6.5.1.2 and 6.5.2.2).

These results demonstrate that an individual rock block impact will not rupture either a TAD canister-bearing or a codisposal waste package because the kinetic energy for a waste package-to-pallet impact is at least a factor of two greater than the kinetic energy for the largest rock block for the same impact velocity and because the impact process is similar, in the sense that the edge-on impact of a rock block onto the side of a waste package is functionally similar to the side-on impact of a waste package onto the vertical side of an emplacement pallet.

Although a single waste package-to-pallet impact cannot rupture the waste package, the seismic damage abstractions consider the potential for two or more severe impacts to fail a waste package (SNL 2007 [DIRS 176828], Sections 6.5.2.1 and 6.6.2.1). An initial impact with severe deformation of the OCB has the potential to weaken the OCB, potentially causing rupture if there is severe deformation from a subsequent impact. The second impact that causes severe deformation could occur during a single ground motion or during subsequent events. The accumulation of extreme deformation in the OCB is conceptualized to have the potential to rupture the OCB from multiple severe impacts.

A similar approach could be applied for rock block impacts in the nonlithophysal units. However, severe deformation will only occur for the most energetic rock blocks, which will come to rest on top of the waste package because of their large size and irregular shape (i.e., they cannot fit between the waste package and drift walls). In this situation, a large block will shield the waste package from subsequent impacts by distributing the loads over a large area and preventing severe deformation. The potential for rupture from multiple rock block impacts directly on the waste package is therefore not included in performance assessment for the period of geologic stability.

It should be noted that the rupture abstractions based on the kinematic response are applied to waste packages in all units of the repository, including those in the nonlithophysal units. Waste packages in nonlithophysal units can rupture during the period of geologic stability in the performance assessment, but not from the mechanism of rock block impact.

Summary—In summary, damage to the drip shields and waste packages as a result of seismic-induced rockfall from jointed-rock motion in nonlithophysal units is excluded from the TSPA model. The effects of rockfall on the drip shields have been quantified in terms of damaged areas and the probability of rupture of the drip shield plates. However, damaged area on the drip shields is excluded from the TSPA model because advective flow through stress corrosion cracks in the drip shields is excluded from the TSPA model (see excluded FEP 2.1.03.10.0B (Advection of Liquids and Solids Through Cracks in the Drip Shield)), and failure of the drip shield plates is excluded because it has low consequence for the TSPA. Rupture of the axial stiffeners occurs only for an impact by a 28.3 MT rock block impact and is excluded on the basis of low probability. Finally, damage to the waste packages and waste package internals from seismic-induced rockfall in jointed rock in nonlithophysal units is excluded from the TSPA model because the drip shields do not separate and because the drip shields remain intact mechanically and can deflect rockfall away from the waste packages.

Based on the previous discussion, omission of FEP 1.2.03.02.0B (Seismic-Induced Rockfall Damages EBS Components) will not result in a significant adverse change in the magnitude or timing of either radiological exposure to the RMEI or radionuclide releases to the accessible

environment. Therefore, this FEP is excluded from the performance assessments conducted to demonstrate compliance with proposed 10 CFR 63.311 and 63.321 (70 FR 53313 [DIRS 178394]), and with 10 CFR 63.331 [DIRS 180319], on the basis of low consequence.

INPUTS:

Table 1.2.03.02.0B-1. Direct Inputs

Input	Source	Description
SNL 2007. *Seismic Consequence Abstraction*. [DIRS 176828]	Section 6.7.3.2	Reasons for excluding the vertical separation of adjacent drip shields is excluded from the compliance case for the TSPA
	Section 6.7.3.1	Reasons for excluding the axial separation of adjacent drip shields from the compliance case for the TSPA
	Table 6-51 and p. 6-185	Failure of the drip shield plates from impacts by rock blocks 2 through 7 for the 0 mm, 5 mm, and 10 mm thickness reductions do not cause contact between the drip shields and the waste packages because the axial stiffeners do not tear or rupture
	Section 6.10.2.11	For impacts from blocks 2 through 7 the framework of the drip shield remains structurally intact and able to deflect rockfall away from the waste package
	Table 6-51	Catalogs of damage areas, maximum plastic strains, and maximum stiffener displacements for individual block impacts as a function of block kinetic energy and plate thickness
	Sections 6.5.1.2 and 6.5.2.2	Discusses expected OCB thickness and the potential for two or more severe impacts to fail a waste package
	Table 6-48	Characteristics of a fully loaded TAD-bearing waste package
	Section 6.7.2.1, Tables 6-32, 6-36, Figure 6-58	Rockfall volume per seismic event is much smaller in the nonlithophysal units than in the lithophysal units
	Section 6.10.2.11	The mean time for a 10-mm thickness reduction due to general corrosion on the top and bottom sides of the drip shield plates
	Section 6.7.2.1	The rockfall volume and loads from drift collapse in the lithophysal units are much greater than those from rockfall induced by jointed-rock motion in the nonlithophysal units
	Sections 6.10.2, 6.10.2.1, 6.10.2.2, 6.10.2.3	Description of the computational approach for defining drip shield damage due to rock block impacts

Table 1.2.03.02.0B-1. Direct Inputs (Continued)

Input	Source	Description
SNL 2007. *Seismic Consequence Abstraction*. [DIRS 176828] (continued)	Sections 6.10.2.2 and 6.10.2.3	Description of the methodology for calculating the damaged areas
	Tables 6-50 and 6-51	The axial stiffeners rupture only for the impact of the largest of the seven representative rock blocks
	Section 6.4.3	The rock block that causes the axial stiffeners to fail occurs at the 5.35 m/s PGV level, which is beyond the maximum PGV level of 4.07 m/s on the bounded hazard curve
	Table 6-51	The maximum stiffener displacement for impact of Block 1 on the drip shield is 0.204 m
	Table 6-51	For all other blocks the maximum stiffener displacement is 0.0417 m
	Table 6-50	Characteristics of the nonlithophysal rock block
SNL 2007. *Mechanical Assessment of Degraded Waste Packages and Drip Shields Subject to Vibratory Ground Motion*. [DIRS 178851]	Section 6.4.7.2.2	Structural response calculations were performed for a set of seven representative block sizes that span the range of block kinetic energies and for one intact and two degraded states of the drip shield
	Section 6.4.7.3	The combined effect of four conservatisms is expected to more than offset the potential reduction in plastic load capacity due to preexisting crack networks
	Section 6.4.7.2.2	The rock block is represented as an edge-on impact at the center of the drip shield, with the center of mass of the block directly above the impact point
	Section 6.4.7	Rupture of the axial stiffeners beneath the crown of the drip shield is also considered in the structural response calculations for drip shield response to rock block impacts
	Section 6.4.7.3	Contact between the drip shield and the waste package as a result of a rock block impact will be spread over a large area, resulting in insignificant deformations to waste packages with intact internals, and fairly small deformations to waste packages with degraded internals
	Section 6.4.7.3	Should Block 1 cause the drip shield to contact the waste package, there would be no rupture of the waste package and any damaged areas would be insignificant

Table 1.2.03.02.0B-1. Direct Inputs (Continued)

Input	Source	Description
SNL 2007. *Mechanical Assessment of Degraded Waste Packages and Drip Shields Subject to Vibratory Ground Motion*. [DIRS 178851] (continued)	Section 6.3.4	The strain in the OCB of the TAD-bearing or CDSP waste package from a single impact is always below the ultimate tensile strain for Alloy 22, and does not result in rupture.
	Sections 6.3.2.2, 6.3.2.2.3, 6.3.2.2.7; Table 6-11	Provides a bounding analog for the rock block impact on a waste package
SNL 2007. *Total System Performance Assessment Data Input Package for Requirements Analysis for EBS In-Drift Configuration*. [DIRS 179354]	Table 4-2, Parameter Number 07-01	The drip shield connector subassembly provides a 320-mm-long (12.6-inch-long) overlap at the joint between adjacent drip shields
	Figure 4-1, dimension D3	The initial clearance between the drip shield and the waste package is 14 inches to 27 inches
	Figure 4-1	The limited clearance between the outside of the emplacement pallet and the inside of the drip shield acts to position the waste package near the centerline of the drip shield after a seismic event
SNL 2007. *Total System Performance Assessment Data Input Package for Requirements Analysis for Subsurface Facilities*. [DIRS 179466]	Table 4-1, Parameter Number 01-03	The nonlithophysal units encompass 15% to 20% of the repository emplacement area

Table 1.2.03.02.0B-2. Indirect Inputs

Citation	Title	DIRS
10 CFR 63	Energy: Disposal of High-Level Radioactive Wastes in a Geologic Repository at Yucca Mountain, Nevada	180319
70 FR 53313	Implementation of a Dose Standard After 10,000 Years	178394
BSC 2004	*Drift Degradation Analysis*	166107
BSC 2005	*Creep Deformation of the Drip Shield*	174715
SNL 2007	*Seismic Consequence Abstraction*	176828
SNL 2007	*Mechanical Assessment of Degraded Waste Packages and Drip Shields Subject to Vibratory Ground Motion*	178851

FEP: 1.2.03.02.0C

FEP NAME:

Seismic-Induced Drift Collapse Damages EBS Components

FEP DESCRIPTION:

Seismic activity could produce jointed-rock motion and/or changes in rock stress leading to enhanced drift collapse that could impact drip shields, waste packages, or other EBS components. Possible effects include both dynamic and static loading.

SCREENING DECISION:

Included

TSPA DISPOSITION:

The effects of seismic-induced drift collapse are included in the performance assessment to demonstrate compliance with the individual protection standard of the proposed 10 CFR 63.311 (70 FR 53313 [DIRS 178394]). The effects of seismic-induced drift collapse are also included in the performance assessments to demonstrate compliance with the groundwater protection standards (10 CFR 63.331 [DIRS 180319]), although seismic events having less than 1 chance in 10 of occurring in 10,000 years are excluded from these latter performance assessments, consistent with the requirements of proposed 10 CFR 63.342(b) and (c)(1) (70 FR 53313 [DIRS 178394]). The effects of seismic-induced drift collapse are excluded from the performance assessments to demonstrate compliance with the human intrusion standard based on low consequence. As discussed in excluded FEP 1.4.02.04.0A (Seismic Event Precedes Human Intrusion), the effects of such events would be insufficient to alter the material properties of the waste packages to the extent that an intersected waste package would not be noticed by a driller during the first 10,000 years after repository closure, and inclusion of the effects of seismic events on the EBS in the assessment of dose releases due to human intrusion would not significantly affect the calculated annual dose to the reasonably maximally exposed individual.

Introduction—Vibratory ground motions associated with seismic activity could cause failure of the host rock around emplacement drifts. The resulting rockfall coupled with the dynamic loads from vibratory ground motion could cause damage to the drip shields and possibly to the outer barriers of the waste packages (if the drip shields fail) through mechanical loading. The drift invert and emplacement pallet could also be damaged as a result of host rock failure induced by vibratory ground motion, but these components are not part of the EBS barrier to the release of radionuclides and, in this respect, such impacts do not require further consideration. Vibratory ground motion can also disrupt the EBS components through rigid body motion and impacts between adjacent EBS components. The effects of these impacts are addressed in included FEP 1.2.03.02.0A (Seismic Ground Motion Damages EBS Components). The direct effects of fault displacement on the EBS components are discussed in included FEP 1.2.02.03.0A (Fault Displacement Damages EBS Components).

Rock Failure Mechanisms—The type of rock failure that could occur in an emplacement drift as a result of seismic activity depends on the local strata that the drift transects. At Yucca Mountain, the emplacement drifts will transect both nonlithophysal and lithophysal rock types. Nonlithophysal units are composed of strong, intact blocks of welded tuff that are separated by fracture planes (BSC 2004 [DIRS 166107], Section 6.4.1.1). Damage to the waste package and drip shield as a result of rock block impacts induced by vibratory ground motion is excluded from the TSPA model, as discussed in excluded FEP 1.2.03.02.0B (Seismic-Induced Rockfall Damages EBS Components). Rockfall for the nominal (nonseismic) condition is addressed in excluded FEP 2.1.07.01.0A (Rockfall).

In contrast, the rock units in lithophysal zones, which encompass about 80% to 85% of the repository emplacement area (SNL 2007 [DIRS 179466], Table 4-1, Parameter Number 01-03), are characterized by a lower compressive strength due to widespread lithophysal voids interconnected by intense fracturing. Rock failure in lithophysal zones is anticipated to generate relatively small fragmented rock particles and impact-related damage is anticipated to be less significant than in the nonlithophysal zones. However, en masse fall of rock fragments, which constitutes "drift collapse," could occur in the lithophysal zones. The volume of rock fragments generated by rock failure in lithophysal zones is significantly greater than the rockfall volume in nonlithophysal zones (SNL 2007 [DIRS 176828], Section 6.7.2.1). Failure of EBS components could occur as a result of the static load from the lithophysal rubble amplified by the dynamic load during vibratory ground motion. The dynamic response of the drip shield and waste package in partly or completely collapsed drifts in the lithophysal units is the focus of this FEP.

Lithophysal Rockfall Analyses—Rockfall analyses have been performed for emplacement drifts in lithophysal units under vibratory ground motion at horizontal PGV levels of 0.4, 1.05, and 2.44 m/s (BSC 2004 [DIRS 166107], Section 6.4). These PGV levels correspond to exceedance frequencies of 10^{-4} per year, 10^{-5} per year, and 4.5×10^{-7} per year, respectively, on the bounded hazard curve (SNL 2007 [DIRS 176828], Table 6-3). The volume of rock that must collapse to completely fill a drift is estimated to be 30 m^3 per meter to 120 m^3 per meter of drift length (SNL 2007 [DIRS 176828], Section 6.7.1.4). The uncertainty in this volume is represented in the TSPA model by a uniform distribution between 30 m^3 per meter and 120 m^3 per meter of drift length. Complete drift collapse was predicted for a single seismic event at or above the 2.44 m/s PGV level for drifts in lithophysal units (SNL 2007 [DIRS 176828], Section 6.7.1). The effect of multiple seismic events is incorporated into the TSPA model by defining the total lithophysal rockfall volume as the sum of the rockfall volumes from the individual seismic events.

Mechanical Failure Mechanisms—The rockfall loads from drift collapse may result in plastic deformation of EBS components. This plastic deformation and the associated residual stresses may lead to local degradation from stress corrosion cracking, potentially resulting in a network of through-going cracks that can form transport pathways for water or radionuclides. The area that exceeds the residual stress threshold is referred to as the "damaged area" and is conceptualized to result in the immediate formation of a tightly spaced network of through-going stress corrosion cracks. Stress corrosion cracking of the waste package outer corrosion barrier and of the drip shield plates is discussed further in included FEP 2.1.03.02.0A (Stress Corrosion Cracking (SCC) of Waste Packages), and excluded FEP 2.1.03.02.0B (Stress Corrosion Cracking (SCC) of Drip Shields). The combined mechanical-corrosion failure mechanism of plastic

deformation followed by stress corrosion cracking is expected to be a primary cause of damage to both waste packages and drip shields (SNL 2007 [DIRS 176828], Section 6.1.4).

Damaged areas are distinct from structural failures, which correspond to the tearing, rupture, or buckling of an EBS component. A rupture or tear may occur if the local strain exceeds the ultimate tensile strain, and may partly or completely negate the effectiveness of an EBS component as a barrier to the inflow of seepage water or the outward transport of radionuclides. Buckling of an EBS component may change the structural configuration and possibly compromise a component's effectiveness as a barrier to seepage or rockfall.

Drip Shield Damaged Area Due to Drift Collapse—Drip shields may accumulate damaged areas from vibratory ground motion and from lithophysal rockfall induced by vibratory ground motion until the drip shield plates fail. The damaged areas on drip shield plates have been analyzed as a function of the thickness of the plate, the rockfall load on the drip shield in a partly or completely collapsed drift, and the vertical component of peak ground acceleration for the seismic event (SNL 2007 [DIRS 176828], Section 6.10.1). However, damaged areas on the drip shield are excluded from the TSPA model because advective flow through stress corrosion cracks on the drip shield is excluded in FEP 2.1.03.10.0B (Advection of Liquids and Solids Through Cracks in the Drip Shield), so the presence of a crack network in the damaged areas does not compromise the drip shield's ability to divert seepage away from the waste package.

Drip Shield Failure Due to Drift Collapse—The accumulated rubble on the drip shield can also cause failure (rather than just damaged area) during a seismic event. The probability of failure is defined as a function of the thickness and ultimate plastic load capacity of the drip shield components, the static rockfall load on the drip shield, and the vertical component of PGA for the seismic event. The probability of failure is represented as fragility curves for two failure modes of the drip shield: (1) rupture or tearing of the drip shield plates, and (2) buckling or collapse of the sidewalls of the drip shield (SNL 2007 [DIRS 176828], Section 6.8).

Finite-difference calculations have been performed to define the ultimate plastic load bearing capacity of the curved plates on the crown of the drip shield (SNL 2007 [DIRS 178851], Section 6.4.4). These calculations define the magnitude of the uniform load that causes an area of the plate to exceed the ultimate tensile strain of Titanium Grade 7. The finite-difference calculations were performed for 100% rockfall loads on drip shield plates that are 15-mm, 10-mm, and 5-mm thick to represent one intact and two degraded states of the drip shields.

The probability of failure is evaluated for drifts that are 0%, 10%, 50% and 100% filled with lithophysal rock for seismic events at the 0.2, 0.4, 1.05, 2.44, and 4.07 m/s PGV levels (SNL 2007 [DIRS 176828], Sections 6.8.2.1 and 6.8.2.2). These PGV levels correspond to the 10^{-4} per year, 10^{-5} per year, 4.5×10^{-7} per year, and 10^{-8} per year exceedance frequencies, respectively, on the bounded hazard curve (SNL 2007 [DIRS 176828], Table 6-3). These results define the probability of failure in lookup tables that are interpolated for the PGV level of the seismic event and plate thickness at the time of the seismic event within the TSPA model.

Finite-difference calculations have also been performed to define the plastic load bearing capacity of the drip shield framework. The calculations determine the magnitude of the load on the crown that causes the sidewalls of the drip shield to buckle. The finite-difference

calculations were performed for 100% rockfall loads with 0-mm, 5-mm, and 10-mm thickness reductions of drip shield components, representing one intact and two degraded states of the drip shields. The probability of failure is evaluated for drifts that are 0%, 10%, 50% and 100% filled with lithophysal rock for seismic events at the 0.2, 0.4, 1.05, 2.44, and 4.07 m/s PGV levels (SNL 2007 [DIRS 176828], Sections 6.8.3.2 and 6.8.3.3). These results are represented as lookup tables within the TSPA model. The key parameters for the lookup tables are the PGV level of the seismic event and the frame thickness at the time of the seismic event, both of which are determined internally by the TSPA model.

Waste Package Damage and Puncture Due to Drift Collapse—The mechanical response of a waste package to a seismic event will depend on the configuration and structural integrity of the EBS components at the time of the seismic event (SNL 2007 [DIRS 176828], Section 6.1.2). The configuration of the EBS and the mechanical response of the waste packages to seismic events are defined for three states of the system: (1) an initial state in which the drip shield is intact, (2) an intermediate state in which the legs of the drip shield have buckled, but the drip shield plates remain intact, and (3) a final state in which the waste packages are surrounded by rubble after the drip shield plates have failed. The transition between these configurations is determined by the fragility curves for the drip shield framework and plates discussed above.

These three states lead to distinct damage mechanisms for waste packages (SNL 2007 [DIRS 176828], Section 6.1.3). In the first state, the waste packages are free to move beneath the drip shield and "kinematic" damage can occur. This damage mechanism is discussed in detail in included FEP 1.2.03.02.0A (Seismic Ground Motion Damages EBS Components) and is not discussed further here.

In the second state, the motion of the waste packages is restricted and the extent of damage is determined for a waste package beneath a buckled or collapsed drip shield. *Seismic Consequence Abstraction* (SNL 2007 [DIRS 176828], Section 6.8.4) provides an evaluation of the deformation and stresses in the OCB of a TAD canister-bearing waste package that is loaded by a collapsed drip shield. The entire drip shield was not explicitly represented in the model. Only the bulkhead flanges that are expected to contact the waste package after collapse of the framework were modeled, and the structural response of the OCB was calculated by moving the bulkhead flanges downward at a velocity that is sufficiently small to maintain a quasi-static response in the OCB. The response of the waste package with OCB thicknesses of 17 mm and 23 mm and intact or degraded internals provides the damaged area as a function of the effective vertical load (SNL 2007 [DIRS 176828], Section 6.8.4).

The resulting damaged areas for a waste package that is loaded by a collapsed drip shield are approximated by other damage abstractions because this intermediate state ceases to exist once the drip shield plates fail during a subsequent seismic event (SNL 2007 [DIRS 176828], Section 6.8.4). When the waste package internals are intact, the damage abstraction for a waste package surrounded by rubble (the final configuration of the EBS discussed below) provides a conservative bound for the damage to a waste package loaded by the drip shield framework. When the waste package internals are degraded, the kinematic damage abstractions for the waste package with degraded internals (see included FEP 1.2.03.02.0A (Seismic Ground Motion Damages EBS Components)) provide a conservative bound for the damage to a waste package

loaded by the drip shield framework. These abstractions approximate the response of the waste package after the drip shield framework has collapsed, but before the drip shield plates fail.

In the third and final state, the drip shield plates have failed and the waste packages are surrounded by rubble. *Seismic Consequence Abstraction* (SNL 2007 [DIRS 176828], Section 6.9) provides abstractions for the mechanical response of a waste package to a seismic event for this EBS configuration. Two future states of the waste package have been considered: a 23-mm-thick OCB with degraded internals and a 17-mm-thick OCB with degraded internals. The 23-mm-thick OCB represents a reduction from the initial thickness of 25.4 mm to take account of the potential effects of general corrosion during the first few hundred thousand years after repository closure (SNL 2007 [DIRS 178851], Sections 6.5.1.2). The 17-mm-thick OCB represents a waste package that has undergone extensive corrosion during the period of geologic stability after repository closure (SNL 2007 [DIRS 178851], Section 6.5.2.2). The abstractions are based on the TAD canister-bearing waste package. As the response of the TAD canister-bearing waste package with degraded internals is expected to be similar (but conservative) to that of a codisposal waste package with degraded internals, a single damage abstraction has been developed for both types of waste packages (SNL 2007 [DIRS 176828], Section 6.9.10).

The calculated strain in the OCB is always below the ultimate tensile strain for Alloy 22 for the full range of PGV levels (SNL 2007 [DIRS 178851], Section 6.5.1.4.1). Therefore, the waste package surrounded by rubble is not anticipated to rupture. However, a severely deformed OCB may be punctured by the sharp edges of fractured or partly degraded internal components. The OCB may be deformed or even crushed as a result of the dynamic rubble load in response to vibratory ground motion. Calculated probabilities of puncture for the 17-mm-thick OCB and 23-mm-thick OCB are provided in *Seismic Consequence Abstraction* (SNL 2007 [DIRS 176828], Section 6.9.1), based on calculations for 17 ground motions at each of the 0.4, 1.05, 2.44, and 4.07 m/s PGV levels. OCB puncture is not expected to occur on the 23-mm-thick OCB unless the PGV is at least 1.05 m/s, or on the 17-mm-thick OCB unless the PGV is at least 0.4 m/s.

When a waste package is determined to be punctured, the failed area is defined by sampling a uniform distribution with a lower bound of 0 m^2 and an upper bound of 0.10 m^2 (SNL 2007 [DIRS 176828], Section 6.9.1). This failed area is conceptualized to be located randomly on the surface of the OCB. The failed area allows flow through the punctured waste package and advective and diffusive transport of radionuclides out of the waste package.

Summary—In summary, damaged area on the waste package and failure of the waste package and drip shield as result of seismic-induced drift collapse in lithophysal zones is included in the performance assessments to demonstrate compliance with the individual protection standards after permanent closure (proposed 10 CFR 63.311 (70 FR 53313 [DIRS 178394])) and the groundwater protection standards (10 CFR 63.331 [DIRS 180319]). The effects of drift collapse on the drip shields are quantified in terms of fragility curves that are a function of the PGV value for a given seismic event and the thickness of the drip shield components at the time of the seismic event. The effects of drift collapse on waste packages surrounded by rubble are quantified in terms of damaged areas or puncture areas based on the PGV level for a given seismic event and the thickness of the waste package OCB at the time of the seismic event.

The effects of seismic-induced drift collapse are excluded from the performance assessments to demonstrate compliance with the individual protection standard for human intrusion (proposed 10 CFR 63.321 (70 FR 53313 [DIRS 178394])) based on low consequence.

INPUTS:

Table 1.2.03.02.0C-1. Indirect Inputs

Citation	Title	DIRS
10 CFR 63	Energy: Disposal of High-Level Radioactive Wastes in a Geologic Repository at Yucca Mountain, Nevada	180319
70 FR 53313	Implementation of a Dose Standard After 10,000 Years	178394
BSC 2004	*Drift Degradation Analysis*	166107
SNL 2007	*Seismic Consequence Abstraction*	176828
SNL 2007	*Mechanical Assessment of Degraded Waste Packages and Drip Shields Subject to Vibratory Ground Motion*	178851
SNL 2007	*Total System Performance Assessment Data Input Package for Requirements Analysis for Subsurface Facilities*	179466

FEP: 1.2.03.02.0D

FEP NAME:

Seismic-Induced Drift Collapse Alters In-Drift Thermohydrology

FEP DESCRIPTION:

Seismic activity could produce jointed-rock motion and/or changes in rock stress leading to enhanced drift collapse and/or rubble infill throughout part or all of the drifts. Drift collapse could impact flow pathways and condensation within the EBS, mechanisms for water contact with EBS components, and thermal properties within the EBS.

SCREENING DECISION:

Included

TSPA DISPOSITION:

Seismic-induced rockfall and seismic-induced drift collapse can alter the hydrologic and thermal environment in the drifts after a seismic event. The potential for drift collapse and its consequences are addressed in two steps. *Drift Degradation Analysis* (BSC 2004 [DIRS 166107], Sections 6.3 and 6.4) addresses rockfall and drift collapse responses to seismic ground motion. *Seismic Consequence Abstraction* (SNL 2007 [DIRS 176828]) then quantifies the response of various EBS components to drift collapse. Thermal-hydrologic changes from drift collapse are described in *Multiscale Thermohydrologic Model* (SNL 2008 [DIRS 184433], Section 6.3.17[a]).

The term "drift collapse" (in this discussion of the technical basis for inclusion of this FEP) refers to en masse fall of rock fragments that fill the drift, and only occurs in lithophysal zones. In contrast, "rockfall" is limited to relatively fewer and possibly larger blocks of rock and may constitute the full extent of seismic response for drifts in nonlithophysal rock.

Effects from rockfall and drift collapse on performance of engineered barriers such as the drip shield are addressed in excluded FEP 1.2.03.02.0B (Seismic-induced Rockfall Damages EBS Components) and included FEP 1.2.03.02.0C (Seismic-induced Drift Collapse Damages EBS Components). The direct effects from ground motion are addressed in included FEP 1.2.03.02.0A (Seismic Ground Motion Damages EBS Components). Effects from drift collapse on in-drift chemistry are addressed in excluded FEP 1.2.03.02.0E (Seismic-induced Drift Collapse Alters In-drift Chemistry).

The potential thermal-hydrologic consequences of seismic-induced drift collapse, relative to the uncollapsed case, are: (1) increased EBS temperatures and delayed cooling if collapse occurs during the thermal period; (2) lower relative humidity associated with increased temperatures; (3) changes in drift seepage caused by the increased span of collapsed openings and the irregular geometry of collapsed-opening profiles; and (4) decreased axial transport of water vapor and associated condensation effects. Each of these effects is included in performance assessments to demonstrate compliance with the individual protection standard after permanent closure

(proposed 10 CFR 63.311 (70 FR 53313 [DIRS 178394])) and the groundwater protection standards (10 CFR 63.331 [DIRS 180319]). Consistent with the requirements of proposed 10 CFR 63.342(b) (70 FR 53313 [DIRS 178394]), the effects of drift collapse associated with seismic events that are estimated to be unlikely to occur have been excluded from the groundwater protection and human intrusion performance assessments. As discussed in excluded FEP 1.4.02.04.0A (Seismic Event Precedes Human Intrusion), likely seismic events have also been excluded from the human intrusion performance assessment (proposed 10 CFR 63.321 (70 FR 53313 [DIRS 178394])).

Conditions for Drift Collapse and Rockfall—Drift collapse will occur in the lithophysal host rock units, which are characterized by lithophysal voids interconnected by close fracturing as discussed in *Drift Degradation Analysis* (BSC 2004 [DIRS 166107], Section 6.4.1.1). Postclosure ground motion in lithophysal rock could result in substantial or complete drift collapse (SNL 2007 [DIRS 176828], Section 6.7.1) affecting the hydrologic and thermal environment in the EBS. For implementation in performance assessment calculations, partial drift collapse may occur at all ground motions with a PGV greater than 0.274 m/s (exceedance frequencies of about 2.5×10^{-4} per year) in the lithophysal units (SNL 2007 [DIRS 176828], Sections 6.4.3 and 6.7.1.1). The probability of occurrence of partial drift collapse increases with increasing PGV, and reaches a value of 1.0 at 1.05 m/s (an exceedance frequency of about 1×10^{-5} per year). If rockfall is predicted to occur, then the volume of rockfall and the bulking factor (a measure of the change in the diameter of the drift opening) are calculated as a function of the PGV. A PGV level of about 2.0 m/s (an exceedance frequency of about 9×10^{-7} per year) is generally sufficient to result in complete drift collapse in the lithophysal units (SNL 2007 [DIRS 176828], Section 6.7.1.4 and Table 6-3). In the case of multiple seismic events, the cumulative amount of rockfall is tracked through time until the drift is completely filled.

Seismic-induced rockfall will accumulate to a much lesser extent in the nonlithophysal host rock units (SNL 2007 [DIRS 176828], Section 6.7.2), which are stronger and composed of intact blocks delineated by fractures. Complete drift collapse is not observed in the nonlithophysal zones for ground motion amplitudes at or below a PGV of 5.35 m/s. Using the bounded hazard curve, the PGV is expected to be less than 4.07 m/s at the repository horizon (SNL 2007 [DIRS 176828], Section 6.4.3), so complete drift collapse due to a single seismic event will not occur. Within performance assessment, complete drift collapse within the nonlithophysal units is either not implemented, or, in submodels that do not distinguish between the lithophysal and nonlithophysal units, the lithophysal model for drift damage is conservatively applied to both lithologies. In the case of multiple seismic events, the cumulative amount of rockfall from partial drift collapse is tracked through time until the drift is completely filled.

Effect on Temperature and Relative Humidity—Once the drifts are completely filled with rubble, the in-drift thermal-hydrologic conditions used by TPSA are modified for drift collapse. The influence of a collapsed drift in lithophysal rock on in-drift temperature and relative humidity is evaluated in *Multiscale Thermohydrologic Model* (SNL 2008 [DIRS 184433], Section 6.3.17[a]). The temperatures of the drip shields and waste packages as represented in the multiscale model will increase relative to uncollapsed drifts, because the drift rubble acts as an insulating blanket over the drip shield. The insulating effect increases peak temperatures and increases the duration of thermal conditions in the EBS. The effects of drift collapse are implemented in performance assessment calculations as a series of "deltas" relative to the open-

drift results for temperature and relative humidity, representing the differences between the open-drift and the rubble-filled cases (SNL 2008 [DIRS 184433], Section 6.3.17[a]). Without seepage, the rubble will dry out, then gradually rewet after hundreds to thousands of years, due to capillary condensation, with essentially zero percolation flux (SNL 2007 [DIRS 181244], Section 6.5.3). With seepage, the surface of the drip shield under collapse-rubble remains dry until the waste package surface has cooled to approximately 100°C (SNL 2008 [DIRS 184433], Sections 6.3.7.3 and Table 6.3-44). Uncertainty in the effects of drift collapse on the in-drift environment is propagated to performance assessment through use of two sets of "deltas" for the low- and high-thermal conductivity rubble, respectively, which are sampled epistemically for each realization.

Effects on Seepage—Changes in seepage behavior caused by seismically induced rockfall and drift collapse are also included in performance assessment calculations for the lithophysal host rock only. A seepage abstraction is used to represent the range from intact (uncollapsed) to fully collapsed openings (SNL 2007 [DIRS 181244], Section 6.2[a]). The approach interpolates linearly between the uncollapsed and collapsed abstractions using rockfall volume as modeled in *Seismic Consequence Abstraction* (SNL 2007 [DIRS 176828], Section 6.7.1) to define the extent of collapse; in the case of multiple seismic events, the cumulative rockfall volume is used. *Abstraction of Drift Seepage* (SNL 2007 [DIRS 181244], Section 6.4.2.4.2) and *Seepage Model for PA Including Drift Collapse* (BSC 2004 [DIRS 167652], Section 6.6.3) represent the fully collapsed opening as a circular profile with twice the intact diameter, filled with rubble. Capillary properties for the rubble are different from the host rock, forming a capillary barrier to seepage. Seepage into collapsed drifts can occur at any temperature (not constrained to temperatures less than 100°C as for intact drifts) because no "vaporization barrier effect" at the boundary of the intact rock was observed in simulations (SNL 2007 [DIRS 181244], Section 6.5.3). The "vaporization barrier effect" involves evaporation of water in the host rock above the drift opening, and condensation elsewhere, with the effect of diverting liquid flow around the drift. It acts in concert with capillary diversion of liquid flux. With doubled diameter in the collapsed-drift simulations, the intact rock was much cooler at the crown and sides of the degraded opening. In other respects, the collapsed drift abstraction is similar to that for intact drifts.

Seepage simulations conducted to evaluate parametric sensitivity for the collapsed-drift case showed that the effects from local rockfall in nonlithophysal units are small (SNL 2007 [DIRS 181244], Section 6.4.2.4.2). Therefore, no explicit change is made in the seepage abstraction to represent rockfall in nonlithophysal units. The seepage abstraction for intact drifts is already increased by 20% to account for the possibility of irregular opening geometry associated with minor drift degradation (SNL 2007 [DIRS 181244], Section 6.7.1.2).

Temperature Limit for Seepage Contact with Waste Packages in Rubble—A temperature constraint is applied to the flow conditions within the drift after drift collapse. Seepage can enter the drift and be diverted through the rubble to the invert beneath the waste package, but cannot contact the waste package surface until the waste package surface temperature drops below 100°C. This threshold temperature of 100°C is based on sensitivity studies (SNL 2008 [DIRS 184433], Section 6.3.7.3 and Table 6.3-44; SNL 2007 [DIRS 181244], Section 6.5.3) of conditions required for seepage to penetrate the rubble in a collapsed drift and contact the drip shield. The value of 100°C is a reasonable upper bound from the sensitivity studies, and

therefore an appropriate threshold to limit the seepage of liquid water to the drip shield, and, in the event of drip shield failure, to the waste package.

Drift-Wall Condensation—Condensation is expected to occur in an intact drift as discussed in included FEP 2.1.08.04.0A (Condensation Forms on Roofs of Drifts/Drift-Scale Cold Traps) and included FEP 2.1.08.04.0B (Condensation Forms at Repository Edges/Repository-Scale Cold Traps), and locally in a collapsed, rubble-filled drift. However, the presence of rubble will inhibit the long-range axial transport of water vapor along the drift axis. The presence of rubble has a strong insulating effect (SNL 2008 [DIRS 184433], Section 6.3.7.3) that increases the temperature differences between the waste package and the adjacent drift wall in comparison to an uncollapsed drift. The temperature difference under these conditions can be as high as 100°C at waste-package peak temperatures, although this diminishes with time (BSC 2005 [DIRS 172232], Figure 6.2.5-3). This steep gradient will drive water vapor toward cooler locations such as the drift wall, where it can condense locally rather than migrate for significant distances axially in the rubble-filled drift. The relatively large surface area of the cool rubble at the drift wall will rapidly absorb latent heat of vapor and promote local condensation. Because axial transport is minimized and evaporation/condensation are localized, resulting in no net change in the flux through the invert at any given location, the effects of condensation are not implemented in performance assessment calculations in the collapsed drift case.

In summary, the thermal-hydrologic effects from drift collapse (or partial drift collapse in the case of seepage) are included in the performance assessment model as: (1) increased EBS temperatures and delayed cooling; (2) lower relative humidity associated with increased temperatures; (3) changes in drift seepage caused by the increased span of collapsed openings and the irregular geometry of collapsed-opening profiles; and (4) decreased axial transport of water vapor and associated condensation effects. Seismic-induced drift collapse is possible in the lithophysal host rock, but not the nonlithophysal rock, which is limited to minor rockfall. However, in cases where these two lithologies are not distinguished, the lithophysal drift damage model is implemented.

INPUTS:

Table 1.2.03.02.0D-1. Indirect Inputs

Citation	Title	DIRS
10 CFR 63	Energy: Disposal of High-Level Radioactive Wastes in a Geologic Repository at Yucca Mountain, Nevada	180319
70 FR 53313	Implementation of a Dose Standard After 10,000 Years	178394
BSC 2004	*Drift Degradation Analysis*	166107
SNL 2007	*Seismic Consequence Abstraction*	176828
SNL 2007	*Abstraction of Drift Seepage*	181244
SNL 2008	*Multiscale Thermohydrologic Model*	184433

FEP: 1.2.03.02.0E

FEP NAME:

Seismic-Induced Drift Collapse Alters In-Drift Chemistry

FEP DESCRIPTION:

Seismic activity could produce jointed-rock motion and/or changes in rock stress leading to enhanced drift collapse and/or rubble infill throughout part or all of the drifts. Drift collapse, and the associated changes in seepage and in-drift thermohydrology could impact in-drift chemistry.

SCREENING DECISION:

Excluded – low consequence

SCREENING JUSTIFICATION:

In-drift chemistry is a function of incoming seepage water composition, the local conditions of temperature, relative humidity, and carbon dioxide activity, and water–rock interaction as described in *Engineered Barrier System: Physical and Chemical Environment* (SNL 2007 [DIRS 177412], Section 6.9). The composition of potential incoming seepage is evaluated with the near-field chemistry model (SNL 2007 [DIRS 177412], Section 6.3.2), while the effects of evaporation/dilution in the drift are estimated using the seepage dilution/evaporation abstraction (SNL 2007 [DIRS 177412], Section 6.3.3). Widespread rockfall induced by vibratory ground motion could alter the hydrologic and thermal environment in the drifts, which could affect the in-drift chemistry. The indirect effects from collapse-induced changes in temperature and relative humidity on the in-drift chemical environment are included in the TSPA through use of the seepage dilution/evaporation abstraction, and are discussed further in included FEP 1.2.03.02.0D (Seismic-Induced Drift Collapse Alters In-Drift Thermohydrology). This screening justification evaluates the effects of drift collapse on factors that directly control in-drift chemistry, including the composition of incoming seepage and the composition of dust on the waste package surface.

Although limited rockfall may occur in nonlithophysal host rock units, drift collapse is expected to occur in the lithophysal host rock units, which are characterized by lithophysal voids interconnected by intense fracturing as discussed in *Drift Degradation Analysis* (BSC 2004 [DIRS 166107], Section 6.4.1.1). Postclosure ground motion in lithophysal rock could result in substantial or complete drift collapse (SNL 2007 [DIRS 176828], Section 6.7.1) affecting the hydrologic and thermal environment in the EBS. Seepage could increase because the greater span and irregular shape of collapsed drift openings will reduce the effectiveness of the drift wall due to the capillary barrier effect (SNL 2007 [DIRS 181244], Section 6.2). The temperature of the drip shields and waste packages will increase relative to uncollapsed drifts because the drift rubble acts as an insulating blanket over the drip shield (SNL 2008 [DIRS 184433], Section 6.3.17[a]).

In the case of drift collapse, rock dust generated by comminution of host rock fragments will be deposited on waste package surfaces. This dust is expected to resemble dust samples collected

from the ESF, which consist largely of powdered rock generated during tunneling and underground activities, with very small amounts (<<1%) of relatively chloride-rich salts representing dried pore water (SNL 2007 [DIRS 181267], Section 6.1.2.4). It is compositionally distinct from dust deposited during the ventilation period, which is anticipated to have a large, nitrate-rich atmospheric dust component, and contain more than 10% soluble salts (SNL 2007 [DIRS 181267], Section 6.1.2.4). As discussed in excluded FEP 2.1.09.28.0A (Localized Corrosion on Waste Package Outer Surface Due to Deliquescence), brines formed by both tunnel dusts and atmospheric dusts are generally benign with respect to localized corrosion of Alloy 22. In addition, the smaller salt load in the rock dust will increase capillary retention of brine by the dust, minimizing contact with the waste package surface and reducing the continuity of the deliquesced liquid phase within the dust. This inhibits development of the separate anodic and cathodic zones necessary for localized corrosion (SNL 2007 [DIRS 181267], Section 6.4). Hence, the screening justification presented in excluded FEP 2.1.09.28.0A (Localized Corrosion on Waste Package Outer Surface due to Deliquescence) remains valid in the event of drift collapse. A similar justification is presented for dust deposited on the drip shield in excluded FEP 2.1.09.28.0B (Localized Corrosion on Drip Shield Surfaces Due to Deliquescence). Drip shields are emplaced after ventilation, and the predominant dust is anticipated to be powdered rock; hence, the discussion in excluded FEP 2.1.09.28.0B (Localized Corrosion on Waste Package Outer Surface due to Deliquescence) applies directly to dust deposited by drift collapse.

The presence of collapsed drift rubble in contact with the drip shield and the resulting change in in-drift thermal hydrologic conditions (included FEP 1.2.03.02.0D (Seismic-Induced Drift Collapse Alters In-drift Thermohydrology)) will not influence the representation of drip shield corrosion in TSPA. The principal corrosion mode for the drip shield is general corrosion, and the rate is independent of temperature and relative humidity. In addition, no distinction in the corrosion rate is made for humid-air versus aqueous environments; the same rate is used for both conditions in TSPA calculations (SNL 2007 [DIRS 180778], Section 8.1[a]).

The near-field chemistry model (SNL 2007 [DIRS 177412], Section 6.3.2), evaluates the composition of potential seepage water at the drift wall as a function of the interactions with minerals in the rock and the thermal evolution of the percolating water. Drift collapse has no effect on the mineralogy of the tuff and a negligible effect on the accessible mineral surface area (which is largely exposed in matrix pores). In addition, the presence of a rubble-filled, collapsed drift produces an insignificant change in the overall thermal evolution of the water as it percolates downward to the drift, effectively only changing the length of the reaction path by a few meters (SNL 2007 [DIRS 177412], Section 6.15.1). Therefore, the effects of drift collapse on potential seepage water composition are insignificant, and the near-field chemistry model can be used to represent potential seepage composition in the collapse-rubble, even though model simulations do not directly evaluate this condition. This conclusion is also applicable to conditions after drip shield failure, which is expected to occur at some time after 10,000 years.

The influence of a collapsed-drift on in-drift temperature and relative humidity and the indirect effects on in-drift chemistry are discussed in included FEP 1.2.03.02.0D (Seismic-Induced Drift Collapse Alters In-drift Thermohydrology). Thermal-hydrologic effects are considered in *Multiscale Thermohydrologic Model* (SNL 2008 [DIRS 184433], Section 6.3.17[a]), and in *Postclosure Analysis of the Range of Design Thermal Loadings* (SNL 2008 [DIRS 179962], Section 6.4.2). Without seepage, the rubble will dry out and then gradually rewet after hundreds

to thousands of years due to capillary condensation, with zero or very small liquid flux (SNL 2007 [DIRS 181244], Section 6.5.3). With seepage, the hydrologic conditions at the surface of the drip shield under collapse-rubble will remain dry until the surface has cooled to approximately 100°C (SNL 2008 [DIRS 184433], Section 6.3.7.3), after which contact with aqueous solutions is possible. In-drift chemistry is determined with the seepage dilution/evaporation abstraction (SNL 2007 [DIRS 177412], Section 6.3.3), using an in-drift temperature and relative humidity modified for the drift collapse condition.

Based on the preceding discussion, omission of FEP 1.2.03.02.0E (Seismic-Induced Drift Collapse Alters In-Drift Chemistry) will not result in a significant adverse change in the magnitude or time of radiological exposures to the RMEI or radionuclide releases to the accessible environment. Therefore, this FEP is excluded from the performance assessments conducted to demonstrate compliance with proposed 10 CFR 63.311 and 63.321 (70 FR 53313 [DIRS 178394]), and with 10 CFR 63.331 [DIRS 180319], on the basis of low consequence.

INPUTS:

Table 1.2.03.02.0E-1. Direct Inputs

Input	Source	Description
BSC 2004. *Drift Degradation Analysis*. [DIRS 166107]	Section 6.4.1.1	Drift collapse may occur in the lithophysal host rock units, which are characterized by lithophysal voids interconnected by intense fracturing
SNL 2007. *Abstraction of Drift Seepage*. [DIRS 181244]	Section 6.2	Seepage could increase because the greater span and irregular shape of collapsed drift openings will reduce the effectiveness of the drift wall as a capillary barrier
SNL 2007. *Engineered Barrier System: Physical and Chemical Environment*. [DIRS 177412]	Section 6.3.2	Near-field chemistry model predicts the composition of incoming seepage
	Section 6.15.1	The presence of rubble produces an insignificant change in the overall thermal evolution of seeping water
SNL 2007. *General Corrosion and Localized Corrosion of the Drip Shield*. [DIRS 180778]	Section 8.1[a]	The principal corrosion mode for the drip shield is general corrosion, and no distinction in the corrosion rate is made for humid-air versus aqueous environments
SNL 2007. *Seismic Consequence Abstraction*. [DIRS 176828]	Section 6.7.1	Postclosure ground motion in lithophysal rock could result in substantial or complete drift collapse

Table 1.2.03.02.0E-2. Indirect Inputs

Citation	Title	DIRS
10 CFR 63	Energy: Disposal of High-Level Radioactive Wastes in a Geologic Repository at Yucca Mountain, Nevada	180319
70 FR 53313	Implementation of a Dose Standard After 10,000 Years	178394
SNL 2007	*Abstraction of Drift Seepage*	181244
SNL 2007	*Analysis of Dust Deliquescence for FEP Screening*	181267
SNL 2007	*Engineered Barrier System: Physical and Chemical Environment*	177412
SNL 2008	*Multiscale Thermohydrologic Model*	184433
SNL 2008	*Postclosure Analysis of the Range of Design Thermal Loadings*	179962

FEP: 1.2.03.03.0A

FEP NAME:

Seismicity Associated with Igneous Activity

FEP DESCRIPTION:

Seismicity associated with future igneous activity in the Yucca Mountain region may affect repository performance.

SCREENING DECISION:

Included

TSPA DISPOSITION:

Seismicity associated with igneous activity was explicitly considered and included as part of the PSHA for Yucca Mountain (CRWMS M&O 1998 [DIRS 103731]). In that analysis, which involved a formal expert elicitation process, expert teams either defined specific seismic sources for igneous-related seismicity, specified that such seismicity was included as part of the characterization of background seismicity, or indicated that such seismicity was insignificant relative to other seismic sources in the region (BSC 2004 [DIRS 168030], Table 5). Because the effects are included in the hazard curves and derived ground motions used to evaluate seismic consequences, igneous-related seismicity is included in the TSPA.

At Yucca Mountain, earthquakes associated with igneous activity would be related to basaltic intrusion and volcanism. Volcanic eruption is commonly preceded and accompanied by swarms of earthquakes that indicate progressive rock-strength failure as magma migrates to the Earth's surface, as, for example, reported in a study by Smith et al. (1998 [DIRS 118967], p. 158). That study specifically mentions that magma intrusion into the seismogenic crust tends to supplant large tectonic earthquakes with swarms of low to moderate magnitude earthquakes. Smith et al. (1998 [DIRS 118967], Table 1) summarize published accounts of observed seismicity that is clearly associated with dike intrusion, including the maximum magnitude assocaited with each series of earthquakes. This summary indicates that dike-induced earthquakes in volcanic rift zones worldwide have a mean maximum magnitude of 3.8 with a standard deviation of 0.8, and are generally less than magnitude 5. In *Characterize Eruptive Processes at Yucca Mountain, Nevada* (SNL 2007 [DIRS 174260], Section 6.3.3.2), the dike length distribution based on analogue studies in the Yucca Mountain region is used as a proxy for surface-fault lengths to calculate maximum magnitudes of dike-induced earthquakes. Calculations indicated maximum magnitudes of 4.6, 5.4, 6.0, and 6.1 for dike lengths of 0.4 km (minimum), 2.0 km (mean), 6.0 km (95th percentile), and 8.0 km (cutoff). An analysis of the ground motion associated with earthquakes of magnitude 4.8, 5.8, and 6.2, covering the assessed range of maximum dike-induced earthquakes at Yucca Mountain, is presented in *Development of Earthquake Ground Motion Input for Preclosure Seismic Design and Postclosure Performance Assessment of a Geologic Repository at Yucca Mountain, NV* (BSC 2004 [DIRS 170027], Section 6.5).

The method used to estimate the ground motion hazard for the PSHA is described in *Characterize Framework for Seismicity and Structural Deformation at Yucca Mountain, Nevada* (BSC 2004 [DIRS 168030], Section 6.5.1). Seismicity related to volcanic processes, particularly basaltic volcanoes and dike injection, was explicitly modeled as volcanic source zones by two of the six expert teams working on the PSHA (as summarized in BSC 2004 [DIRS 168030], Table 5). The maximum magnitudes assigned by the two expert teams put greater weight on magnitudes from 5.4 and 5.8, which is consistent with the range of maximum earthquake magnitudes calculated based on dike length distributions (SNL 2007 [DIRS 174260], Section 6.3.3.2). The other PSHA expert teams concluded either that the low magnitude and frequency of igneous-related seismicity was accounted for by the areal source zone evaluation used for the PSHA or was insignificant.

Seismicity associated with igneous activity is included in the TSPA because seismicity associated with igneous activity is included in the PSHA results (through volcanic source zones or areal source zones). Consequently, all seismic inputs developed to support postclosure seismic analyses account for the igneous component of the seismic hazard.

Unlikely events (events having less than one chance in 10 of occurring in 10,000 years) are included in performance assessments to demonstrate compliance with the individual protection standard after permanent closure (proposed 10 CFR 63.311 (70 FR 53313 [DIRS 178394])), but are not included in performance assessments to demonstrate compliance with the groundwater protection standards (10 CFR 63.331 [DIRS 180319]) and the individual protection standard for human intrusion (proposed 10 CFR 63.321 (70 FR 53313 [DIRS 178394])), consistent with the requirements of proposed 10 CFR 63.342(b) and (c)(1) (70 FR 53313 [DIRS 178394]). Therefore, the effects of seismicity associated with igneous activity that are estimated to be unlikely to occur have been excluded from the groundwater protection and human intrusion performance assessments.

The effects of likely seismicity associated with igneous activity (having a probability of occurrence greater than 10^{-5} per year) have also been excluded from the human intrusion performance assessment. As discussed in excluded FEP 1.4.02.04.0A (Seismic Event Precedes Human Intrusion), the effects of such events would be insufficient to alter the material properties of the waste packages to the extent that an intersected waste package would not be noticed by a driller in 10,000 years. Further, as discussed in excluded FEP 1.4.02.04.0A (Seismic Event Precedes Human Intrusion), inclusion of the effects of seismic events on the EBS in the assessment of the stylized human intrusion scenario would not affect the calculated annual dose to the RMEI significantly. Therefore, seismic events are excluded from the assessment to demonstrate compliance with the individual protection standard for human intrusion (proposed 10 CFR 63.321 (70 FR 53313 [DIRS 178394])), based on low consequence.

Waste package damage due to an igneous intrusion into the repository is addressed separately in included FEP 1.2.04.04.0A (Igneous Intrusion Interacts with EBS Components).

INPUTS:

Table 1.2.03.03.0A-1. Indirect Inputs

Citation	Title	DIRS
10 CFR 63	Energy: Disposal of High-Level Radioactive Wastes in a Geologic Repository at Yucca Mountain, Nevada	180319
70 FR 53313	Implementation of a Dose Standard After 10,000 Years	178394
BSC 2004	*Characterize Framework for Seismicity and Structural Deformation at Yucca Mountain, Nevada*	168030
BSC 2004	*Development of Earthquake Ground Motion Input for Preclosure Seismic Design and Postclosure Performance Assessment of a Geologic Repository at Yucca Mountain, NV*	170027
CRWMS M&O 1998	*Probabilistic Seismic Hazard Analyses for Fault Displacement and Vibratory Ground Motion at Yucca Mountain, Nevada*	103731
Smith et al. 1998	"Magma Intrusion and Seismic-Hazards Assessment in the Basin and Range Province"	118967
SNL 2007	*Characterize Eruptive Processes at Yucca Mountain, Nevada*	174260

FEP: 1.2.04.02.0A

FEP NAME:

Igneous Activity Changes Rock Properties

FEP DESCRIPTION:

Igneous activity near the underground facility may cause extreme changes in rock stress and the thermal regime, and may lead to rock deformation, including activation, creation, and sealing of faults and fractures. This may cause changes in the rock hydrologic and mineralogic properties. Permeabilities of dikes and sills and the heated regions immediately around them can differ from those of country rock. Mineral alterations can also change the chemical response of the host rock to contaminants.

SCREENING DECISION:

Excluded – low consequence

SCREENING JUSTIFICATION:

This justification is based on information that shows that changes in rock properties associated with igneous activity have little effect on flow and transport in the saturated and unsaturated zones at Yucca Mountain. The technical basis for the exclusion from the TSPA of the effects of future igneous activity on rock properties relies in part on studies of analogue sites in the Yucca Mountain Region. In addition, analyses of igneous activity and analyses of the effects of fault displacement on the unsaturated zone are utilized. This FEP is concerned with post-intrusion effects on rock properties and the following paragraphs of this justification consider the zone of influence around an igneous intrusion, the effects on permeability, the effects on faults and fractures, and the effects on mineralogy. Impacts of an igneous intrusion on the repository and the EBS are addressed in included FEP 1.2.04.03.0A (Igneous Intrusion into Repository) and included FEP 1.2.04.04.0A (Igneous Intrusion Interacts with EBS Components).

Limited Zone of Influence Around Igneous Intrusions—Sills and dikes initially intrude into the country rock as molten material and then cool and solidify. In the Yucca Mountain area, the dikes typically range in width from 1 to 12 m (SNL 2007 [DIRS 174260], Table 7-1) and tend to be variably continuous along strike. Cooling joints are formed both within the intrusive body (a dike or a sill) and in the country rock adjacent to the intrusion, due to a combination of thermal and stress effects. The resulting permeabilities of these jointed rocks may be greater than, equivalent to, or less than the surrounding unaffected country rocks (see section entitled *Potential Effects on Flow in the UZ*). However, the scale of these effects and the associated changes in properties are limited to a few meters around the sill or dike (Valentine and Krogh 2006 [DIRS 177282]). Laboratory analytical data and field observations of mineral alterations around igneous intrusions at natural analogue sites show that alteration extends less than 10 m away from the intrusion-host rock contact (CRWMS M&O 1998 [DIRS 105347], pp. 5-41 to 5-71). Two appropriate analogues for understanding the components of a potential future igneous event at Yucca Mountain are the Paiute Ridge intrusive/extrusive center (Byers and Barnes 1967 [DIRS 101859]) on the northeastern margin of the Nevada Test Site and the Grants

Ridge site in western New Mexico (CRWMS M&O 1998 [DIRS 105347], p. 5-57). The Paiute Ridge center is a small-volume Miocene volcanic center comparable in volume and composition to Quaternary volcanoes near Yucca Mountain (SNL 2007 [DIRS 174260], Section 6.3.3.1). Paleomagnetic, geochronologic, and geochemical data indicate that the entire intrusive/extrusive complex formed during a brief magmatic pulse and, thus, represents a single volcanic event. The vents and associated dike system formed within a north-northwest-trending extensional graben, and exposures exist at a variety of system depths, including remnants of surface lava flows, volcanic conduits, and dikes and sills intruded into tuff country rock at depths of up to 300 m. Evidence of shallow structural control of dike emplacement exists at Paiute Ridge, including dike emplacement along fault planes (Byers and Barnes 1967 [DIRS 101859]; Valentine and Krogh 2006 [DIRS 177282]). Dike lengths at Paiute Ridge range from less than 1 km to 5 km, which is comparable to the range estimated for post-Miocene volcanism near Yucca Mountain (SNL 2007 [DIRS 174260], Table 7-1).

Valentine and Krogh (2006 [DIRS 177282], pp. 221 to 223) described the margins of the Paiute Ridge dike complex and the interaction of dikes and faults. The description is as follows (note that the dike designators PR, M, and E in the following text refer to the Paiute Ridge, Middle, and East dikes, respectively, as described by Valentine and Krogh 2006 [DIRS 177282]):

> PR dike contains ubiquitous near-vertical joints that result in a pervasive platy texture with plates parallel to the dike-host contact. Conversely, with the exception of local cooling joints in fused wall rock (extending 10-20 cm into the wall rock, perpendicular to the dike margin), joints are nowhere visible in the host rock along the length of the dike. The contact between basalt and the tuff host rock is consistently smooth and shows no brecciation. Along strike at this contact, the tuff host rock is fused or welded to varying degrees …. In places the tuff is densely welded and forms black vitrophyre that grades rapidly away from the contact, over a distance of ~20 - 100 cm, into nonwelded tuff that is apparently unaffected by the dike. In other places the tuff is only partially welded at the contact and black fiamme are flattened parallel to the contact. We infer that this "contact welding" is the combined result of heat from the dike and compressive stress exerted by the magma on the wall rocks.... Welded host rock commonly contains vesicles that are elongated vertically and parallel to the margin. In some places, welded tuff coats the basalt and displays rills or elongate smooth ridges (flutes). Most rills plunge nearly vertically, however, a sub-horizontal rill is present in the central part of the dike …. The two eastern dikes, M and E … show geometries and textures similar to those of PR, however, M dike is much shorter and does not feed a sill, and E dike feeds two sills. M dike radiates out from the neck-like body mentioned above … and visibly occupies a normal fault, oriented N25-40°W, 61°E, that displaces the Tertiary tuff. M dike varies in width between 2 and 4 m, and has an exposed length of 400 m. Its host rocks are only Tertiary tuffs that show no brecciation or jointing near the dike contact. Near the neck M dike is a single continuous dike, whereas farther from the neck it is composed of several segments. The north end of the dike veers west and narrows before terminating. Dike texture is characterized by a vertical platy fabric that parallels the dike margins.

> E dike is the eastern-most dike studied within the graben. Like M dike, it extends from the neck, and was emplaced into Tertiary tuffs. Near the neck the dike visibly occupies a NNW-trending, E-dipping normal fault that displaces bedded tuffs 3.5 m and does not cut the dike. The exposed dike length is 2020 m and the width varies from 3 m near the northern tip, to 6 m near the southern (ES) sill. A zone comprising about 30 m along strike forms a pod with about 20 m width, presumably representing localized wall rock erosion, between the neck and ES sill. E dike is less segmented than PR dike, and is composed of fewer than a dozen segments. In at least three places near the contact with the Timber Mountain Tuff…and one location near the neck, the dike locally diverges to form two segments that engulf an 8 meter wide lens of the tuff host rock. The texture of E dike is characterized by the pervasive vertical platy fabric common to M and PR dikes. Adjacent host tuffs are neither jointed nor brecciated, except for local vertical jointing of the Rainier Mesa member of the Timber Mountain Tuff (related to post-emplacement cooling of that ignimbrite) that is intruded by the dike at its shallowest level. The contact of the dike and host tuff is well exposed in places and varies from partially to densely welded in the same manner as described above for the PR dike. Where dense welding has occurred, vesicles in the host tuff are vertical and parallel the dike margin. Contact welding of the host tuffs formed oblate fiamme that parallel the dike-host contact. Visible thermal effects on the wall rocks disappear within one meter of the dike margin.

This analogue study demonstrates that zones of change in rock properties (i.e., formation of vitrophyres and/or various degrees of welding of the host rock and formation of fiamme, which are flattened glassy inclusions) are limited to a few tens of centimeters to, at most, a meter perpendicular to the dike. Also, features such as the platy texture along the dike margins and vesicles in the welded tuff are oriented parallel to the dike margins.

Another good analogue site for the various rocks in the vadose zone at Yucca Mountain is Grants Ridge, New Mexico, where a thick sequence of rhyolite ignimbrite, fallout, and reworked volcaniclastic deposits were intruded by a basaltic plug. Erosion of the Grants Ridge site has since produced a natural cross section through the scoria cone, its feeding system, and the pyroclastic host rocks. Similar to the Paiute Ridge site, the basaltic intrusion at Grants Ridge shows limited alteration of the host rock caused by hydrothermal circulation and no brecciation or other deformation related to basaltic intrusion into the vitric and zeolitized tuffs. Field and analytical evidence from the localized contact metamorphic aureoles and devitrification of the silicic tuffs adjacent to the intrusions, minimal hydrothermal alteration, and presence of low-temperature minerals close to the intrusions also suggest insignificant thermal and chemical effects of the shallow basaltic intrusions on the vitric and zeolitized tuffs (CRWMS M&O 1998 [DIRS 123201], p. 5-57).

Potential Effects on Flow in the SZ—Although uncertainty exists regarding the impacts of past basaltic intrusions on the SZ site-scale groundwater flow system, no such features have been explicitly included as having an impact on the calibration of the saturated zone site-scale flow model (SNL 2007 [DIRS 177391], Tables 6-7 and 6-9). The following discussion on the potential for a future intrusion to impact permeability includes an evaluation of the orientation of a possible future dike, because orientation could affect the consequences of an intrusion. Most

researchers conclude that when ascending dikes enter the shallow upper crust, their location and orientation are influenced by the orientation of the local stress field and the presence of faults that may locally control alignment (SNL 2007 [DIRS 174260], Section 6.3.3.1). The evidence cited for this conclusion, in addition to the interaction of faults and dikes at the Paiute Ridge center described above, includes several northeast-oriented vent alignments in the Yucca Mountain region and the association of eruptive centers with known or inferred faults (CRWMS M&O 1996 [DIRS 100116], Appendix E, p. AM-4; Connor et al. 1996 [DIRS 135969], p. A-192; SNL 2007 [DIRS 174260], p. 6-17). Mapping of dikes in Crater Flat found dike orientations between N10°W and N5°E (SNL 2007 [DIRS 174260], p. 6-18). The separate volcanic cones in Crater Flat appear to be controlled by individual dikes occupying north-south faults formed during the east-west extension of Crater Flat basin (SNL 2007 [DIRS 174260], p. 6-18). The only dike mapped at Yucca Mountain was found to be oriented along Solitario Canyon Fault to the south and along Drill Hole Wash Fault to the north (BSC 2004 [DIRS 169989], Figure 6-5; SNL 2007 [DIRS 184614], Figure 6.1-1).

In the saturated zone in the Yucca Mountain region the direction of maximum principal transmissivity is approximately N15°E (SNL 2008 [DIRS 183750], Section 6.5.2.10), which is generally consistent with the fault orientations. A north-to-northeast orientation parallels or sub-parallels the faults active in the present-day in situ stress field. Dike features that may form in the future, such as the platy texture and welded surfaces that could affect permeability, will parallel the dike orientation and are expected to be aligned in a north-to-northeast orientation. Hence, any releases of radionuclides into the saturated zone are expected to move generally toward the south (SNL 2008 [DIRS 184806], Figure 6.5-2). Within the 18-km compliance boundary, the southern region of Yucca Mountain contains faults with orientations that are approximately north to northeast (SNL 2007 [DIRS 177391], Figures 6-3 and 6-17).

The dike widths, described previously, are small relative to the width of the areally extensive saturated zone flow and transport domain (approximately 1,350 km^2) and the predicted widths of the contaminant plume flow path (in excess of hundreds of meters; SNL 2008 [DIRS 184806], as inferred from Figure 6.5-2).

The narrow widths of future dikes and their expected parallel to subparallel orientation relative to the direction of maximum principal transmissivity, combined with the expected limited affected volume of material around the dikes, indicates that, even if differing in permeability, dikes will not significantly affect groundwater flow patterns at the mountain scale. Given the scale of the SZ flow and transport model (18 km to the discharge point) and the uncertainties in the flowing interval properties and anisotropy incorporated in *Saturated Zone Flow and Transport Model Abstraction* (SNL 2008 [DIRS 183750], Table 6-8), smaller-scale effects caused by igneous activity would have negligible impacts on the saturated zone flow field.

Potential Effects on Flow in the UZ—Changes in fault and fracture properties due to igneous activity (i.e., activation, creation, and sealing of faults and fractures) might affect UZ flow processes. The UZ flow model results show that flow is principally through the fractured rock mass rather than faults in the TCw, PTn, and TSw (SNL 2007 [DIRS 184614], Tables 6.6-1 and 6.6-2). Because of these flow patterns, faults have very limited impact on flow behavior above the base of the TSw. The narrow, tabular dikes observed in the Yucca Mountain region (SNL 2007 [DIRS 174260], Section 6.3.3.1) are similar, geometrically, to faults. Furthermore,

dikes in the region are often found occupying faults (SNL 2007 [DIRS 174260], p. 6-18). Because of their geometrical similarity to faults, dikes would be expected likewise to have very little impact on vertical flow in the unsaturated zone between the ground surface and the base of the TSw. Lateral flow has been postulated to occur in the PTn as a result of capillary barriers (SNL 2007 [DIRS 184614], Section 6.2.2.1). Given the expected geometry of a dike, one with lower permeability could act as an impediment to lateral flow in the PTn. However, the UZ flow model results indicate that lateral flow above the repository is small. This conclusion is supported by the similar infiltration and percolation maps over the repository footprint (SNL 2007 [DIRS 184614], Figures 6.1-1 to 6.1-5 and 6.6-1 to 6.6-4) and by the small fraction of flux through faults at the TCw/PTn interface and at the repository (SNL 2007 [DIRS 184614], Tables 6.6-1 and 6.6-2).

Strong lateral diversion occurs where the TSw contacts zeolitic CHn; perched water bodies are observed near the same contact (SNL 2007 [DIRS 184614], Section 6.6.2.2 and Table 6.6-3). The lateral flow is diverted into sub-vertical faults resulting in substantial unsaturated zone flow in faults from the base of the TSw to the water table (SNL 2007 [DIRS 184614], Table 6.6-3). However, transport sensitivity analyses indicate that most of the delay in radionuclide movement to the water table occurs within the TSw and above the zone of strong lateral diversion (SNL 2007 [DIRS 177396], Sections 6.9.1.5 and 6.10.1.4). Hence, any changes in lateral diversion resulting from dikes would have negligible effects on radionuclide transport times.

The potential effects of changes in fracture and rock matrix hydrologic properties on unsaturated zone flow may be evaluated from sensitivity studies performed in *Parameter Sensitivity Analysis for Unsaturated Zone Flow* (BSC 2005 [DIRS 174116]). The sensitivity studies considered changes in properties for permeability and capillary strength for fractures, faults, and rock matrix. The changes were investigated as individual parameter variations (e.g., an increase in matrix permeability) that were applied globally over the unsaturated zone domain; changes in fracture properties also included changes in fault properties. The average variation in fracture and matrix permeabilities were factors of 9 and 42, respectively, and the variations in fracture and matrix capillary strength were 3 and 7, respectively (averaged from values given in BSC 2005 [DIRS 174116], Table 6.2-1). The integrated effects of these changes are most readily understood through their effects on transport from the repository to the water table because transport integrates the effects of flow over the domain. The breakthrough curves in Figures 6-25 to 6-32 in *Particle Tracking Model and Abstraction of Transport Processes* (SNL 2008 [DIRS 184748]) were computed using the flow fields generated in *Parameter Sensitivity Analysis for Unsaturated Zone Flow* (BSC 2005 [DIRS 174116]). These results demonstrate that transport behavior is relatively insensitive to changes in fracture and matrix capillary strength, only moderately sensitive to changes in fracture permeability, and most sensitive to increases in matrix permeability (with decreases in matrix permeability having little effect). The effects of infiltration uncertainty on transport behavior are found to be much larger (SNL 2007 [DIRS 184614], Figures 6.7-1 and 6.7-2). These sensitivity studies only considered changes in properties of the entire UZ model domain. In a second sensitivity study, the effect of changes in fracture aperture within fault zones was examined for the unsaturated zone (Appendix I). This sensitivity study correlated the changes in fault-fracture porosity, capillary strength, and permeability through scaling relationships for these properties with fracture aperture. Apertures were varied by a factor of 10 and 0.2, resulting in similar changes in fault-fracture porosity and capillary strength. The same variations in aperture resulted in changes in fault permeability of

factors of 1,000 and 0.008, respectively (Section I3.2.4). The results of this sensitivity study found a negligible effect on transport between the repository and the water table (Figures I-7 and I-8); changes in fault properties were excluded from further consideration in TSPA on that basis (Appendix I).

Seismicity Associated With Igneous Activity—The effects of seismicity associated with igneous activity were included in the development of the descriptions of background seismic sources used in the PSHA (CRWMS 1998 [DIRS 103731]) as described in *Characterize Framework for Seismicity and Structural Deformation at Yucca Mountain, Nevada* (BSC 2004 [DIRS 168030], Table 5) and are included implicitly in the probabilistic assessment of seismic ground motion hazards (see included FEP 1.2.03.03.0A (Seismicity Associated with Igneous Activity)). The PSHA (CRWMS 1998 [DIRS 103731]) seismic source characterization was also used as the basis for the approach to estimating probabilistic fault displacements. Thus, displacements from igneous events have been implicitly included in evaluation of probabilistic fault displacement (i.e., reactivation and creation of new faults) described in Appendix I and further consideration is unwarranted.

Potential Effects on Perched Water—The possibility of perched water forming near low-permeability intrusive bodies, and the potential for a dike to prevent or slow the rate of flow and/or cause impoundments, are addressed in *Synthesis of Volcanism Studies for the Yucca Mountain Site Characterization Project* (CRWMS M&O 1998 [DIRS 105347], p. 5-56). In the unsaturated zone, the primary direction of groundwater flow is vertically downward through the fractures (BSC 2004 [DIRS 169734], Section 7). Because the joints on a dike margin would be near vertical (e.g., SNL 2007 [DIRS 174260], Section 6.3.3.3), the formation of a significant perched water zone associated with a dike is not expected.

Perched water could also be associated with an intrusion that results in sill formation. Most sills studied at sites that are considered suitable analogues for Yucca Mountain are small and are directly connected to a parent dike (SNL 2007 [DIRS 174260], Section 6.3.3.1 and Sections F.2.1, F.2.4, and F.3). These sills are too small and their associated zones of changed rock properties are too localized to have significant effects on hydrologic properties at the scale of the UZ model. The spatially variable hydrologic properties of the UZ model are calibrated so that model predictions match perched water observations, as discussed in included FEP 2.2.07.07.0A (Perched Water Develops). Therefore, the calibrated UZ flow model output used in TSPA includes the effects of perched water.

Based on analogue information, sills with lateral extents exceeding a few tens of meters from their parent dikes are not expected to occur at Yucca Mountain (SNL 2007 [DIRS 174260], Section 6.3.3.1 and Appendix F). *Characterize Eruptive Processes at Yucca Mountain, Nevada* (SNL 2007 [DIRS 174260], Appendix F) describes analogue sites where erosion has exposed the uppermost ~250 m of intrusive bodies associated with small-volume basaltic volcanoes. One site, East Basalt Ridge, has no evidence for the presence of sills. A second site, Basalt Ridge, has one minor sill that extends about 30 m from its parent dike at a depth of about 35 m below the pre-basaltic land surface. Grants Ridge has a few minor subhorizontal intrusions that extend no more than a few meters from the main (vertically oriented) intrusive body. Only Paiute Ridge has sills that are more than 10 m thick and with lateral extents of several tens of meters to about one kilometer. However, these sills are thought to be related to the specific structural setting at

Paiute Ridge where a combination of normal faulting and rocks with highly contrasting mechanical properties, at relatively shallow depths associated with sill formation, caused localized rotation of the stress field and injection of sills (Valentine and Krogh 2006 [DIRS 177282]). This setting does not exist at shallow depths in Yucca Mountain. The most reasonable scenario for a potential future volcanic event at Yucca Mountain would consist mainly of one or a few vertical to subvertical dikes that feed an eruption. Any sills that form would have lateral extents limited to a few tens of meters from the dikes, which is not sufficient to alter water flow and transport pathways or generate significant amounts of perched water. The effects of larger sills on flow and transport pathways are not considered because such features are not expected to form. The potential impact of sill formation as a result of igneous intrusion into a repository drift is addressed in included FEP 1.2.04.03.0A (Igneous Intrusion into Repository).

In some locations, such as in Hawaii (USGS 2000 [DIRS 183277]), the presence of numerous dikes have been observed to cause the perching or impoundment of groundwater, but at Yucca Mountain, this kind of perching is not expected to occur even if an igneous event intersected the repository. For the Yucca Mountain region, dike size and orientation distributions are summarized in *Characterize Eruptive Processes at Yucca Mountain, Nevada* (SNL 2007 [DIRS 174260], Section 6.3.3.1 and Table 7-1). Dikes are expected to have a mean width of 8 m (minimum of 1 m and 95th percentile of 12 m) and a mean length of 2 km (minimum of 0.4 km, maximum of 8 km). Up to five parallel dikes, spaced up to 1,500 m apart, might occur in a future event, but the most reasonable number is one or two dikes. Dikes are expected to be vertical or subvertical (i.e., if a dike follows a preexisting steeply dipping fault) in orientation with azimuths centered on N10°E (±15°) and N20°W (±15°), reflecting both the roles of the stress field and of pre-existing faults in determining dike orientation. Comparison of characteristics of dikes and associated volcanic systems in the Yucca Mountain region with the large, long-lived Hawaiian volcanic systems shows that the numerous cross-cutting dikes, which resulted from long-lived, high-flux activity in the Hawaiian system, are not compatible with the small, monogenetic volcanoes with their associated subparallel, thin dikes found in the Yucca Mountain region. Hence, the volcanic features characteristic of the Yucca Mountain region could not produce impoundment of groundwater and local elevation of the groundwater system, similar to features observed in Hawaiian volcanic systems.

Potential Effects on Mineralogy—It is possible that the thermal and geochemical influence of igneous activity could affect the mineralogy of the host rock surrounding the igneous intrusion and thus alter the response of the host rock to contaminants. Mineral alterations around igneous intrusions at natural analogue sites are generally confined to relatively thin zones (CRWMS M&O 1998 [DIRS105347], pp. 5-41 to 5-57). In particular, natural analogue studies in similar host rocks at the Nevada Test Site show that alteration is limited to a zone less than 10 m away from the intrusion/host rock contact (CRWMS M&O 1998 [DIRS 105347], pp. 5-41 and 5-71). *Synthesis of Volcanism Studies for the Yucca Mountain Site Characterization Project* (CRWMS M&O 1998 [DIRS 105347], p. 5-42) further states, "Based on natural-analogue sites, there is no indication for extensive hydrothermal circulation and alteration, brecciation and deformation related to magmatic intrusion, and vapor phase recrystallization during the magmatic intrusion into the vitric and zeolitized tuffs." Because the alteration zone around dikes is limited to the immediate proximity of the dike, then (at the scale of the repository) the changes

in mineralogy would have negligible effects on host rock mineralogy and on the chemical response of the host rock to contaminants.

These results may be generalized to evaluate the effects of changes in mineralogy on UZ radionuclide transport. Changes in mineralogy can result in changes in sorption characteristics for radionuclides and therefore may affect radionuclide transport. For the unsaturated zone, sensitivity studies have been conducted for changes in sorption coefficients within different hydrologic units, where the sorption coefficients have been set to zero within individual hydrologic units. These sensitivity studies have found that transport behavior has low sensitivity to changes in sorption in the zeolitized and vitric CHn, although transport behavior is sensitive to sorption in the TSw (SNL 2007 [DIRS 177396], Figures 6-37 and 6-44). Because dikes are not expected to significantly impact flow in the TSw and because flow is generally dispersed in the fractured rock in this unit, radionuclides would have very limited contact with dikes or zones affected by dikes within the TSw. Greater contact could occur between dikes and radionuclides in the CHn, particularly if the dikes are present in faults where focused flow and transport occur. However, the impact of changes in sorption in this part of the unsaturated zone is negligible (SNL 2007 [DIRS 177396], Figures 6-37 and 6-44).

Similarly, the limited small volume of material around the dike affected in terms of mineral alteration compared with the volume of saturated zone transport pathways and the relatively small impact of dike flow in the saturated zone would result in the altered zones associated with dikes having a negligible effect on saturated zone transport.

Summary—In summary, each element of the FEP description has been evaluated based on site data and analyses or information from natural analogues. For saturated zone flow, the subparallel orientation of potential future dikes to transmissivity, coupled with the expected limited affected volume, indicate that dikes, even if differing in permeability, will not significantly affect groundwater flow patterns. For unsaturated zone flow, the typical vertical orientation of dikes along with the insensitivity of flow behavior to fracture and fault properties leads to the expectation that alterations in such properties by an igneous intrusion would have negligible effect on flow behavior. The effects of an igneous intrusion with respect to the formation of additional perched water bodies are expected to be negligible because of the expected extent and configuration of any dikes or sills that might form. Furthermore, natural analogue studies show that mineral alteration is limited to a zone less than 10 m away from the contact, and due to the limited extent of the alteration, such zones, even if formed, would not have adverse impacts on radionuclide transport in the saturated and unsaturated zones. Consequently, changes in rock properties due to igneous activity do not provide mechanisms to significantly affect exposure or release of radionuclides to the accessible environment. Therefore, the effects of igneous activity on rock properties are excluded from the TSPA on the basis of low consequence.

Based on the previous discussion, omission of FEP 1.2.04.02.0A (Igneous Activity Changes Rock Properties) will not result in a significant adverse change in the magnitude or timing of either radiological exposure to the RMEI or radionuclide releases to the accessible environment. Therefore, this FEP is excluded from the performance assessments conducted to demonstrate compliance with proposed 10 CFR 63.311 and 63.321 (70 FR 53313 [DIRS 178394]), and with 10 CFR 63.331 [DIRS 180319], on the basis of low consequence.

INPUTS:

Table 1.2.04.02.0A-1. Direct Inputs

Input	Source	Description
BSC 2005. *Parameter Sensitivity Analysis for Unsaturated Zone Flow*. [DIRS 174116]	Entire, Table 6.2-1	UZ flow sensitivity study and the ranges of hydrologic properties investigated in parameter sensitivity study
CRWMS M&O 1998. *Synthesis of Volcanism Studies for the Yucca Mountain Site Characterization Project*. [DIRS 105347]	pp. 5-41 to 5-57	Laboratory analytical data and field observations of mineralogic alteration around igneous intrusions in similar rocks at the Nevada Test Site and other natural analogue sites show that altertion extends less than 10 m away from the intrusion/host rock contact
SNL 2007. *Saturated Zone Site-Scale Flow Model*. [DIRS 177391]	Figures 6-3 and 6-17	The southern region of Yucca Mountain contains faults with orientations that are approximately north to northeast
	Tables 6-7 and 6-9	Impact of basaltic intrusions on the calibration of the SZ site-scale flow model
SNL 2007. *Characterize Eruptive Processes at Yucca Mountain, Nevada*. [DIRS 174260]	Table 7-1	Range of dike widths
SNL 2007. *Radionuclide Transport Models Under Ambient Conditions*. [DIRS 177396]	Figures 6-37 and 6-44	Radionulcide transport sensitivity to sorption
	Sections 6.9.1.5, 6.10.1.4	Radionuclide delay primarily in the TSw above zones of strong lateral diversion
SNL 2007. *UZ Flow Models and Submodels*. [DIRS 184614]	Tables 6.6-1, 6.6-2	Flow is principally through the fractured rock mass rather than faults in the TCw, PTn, and TSw
	Section 6.2.2.1, Figures 6.1-1 to 6.1-5 and 6.6-1 to 6.6-4, Tables 6.6-1 and 6.6-2	Lateral flow in the PTn
	Section 6.6.2.2, Table 6.6-3	Strong lateral diversion occurs where the TSw contacts zeolitic CHn
	Table 6.6-3	Lateral flow into faults below the repository
SNL 2008. *Particle Tracking Model and Abstraction of Transport Processes*. [DIRS 184748]	Figures 6-25 to 6-32	Breakthrough curves were computed using flow fields generated in Parameter Sensitivity Analysis for Unsaturated Zone Flow
SNL 2008. *Saturated Zone Flow and Transport Model Abstraction*. [DIRS 183750]	Table 6-8	Uncertainties in the flowing interval properties and anisotropy incorporated
	Section 6.5.2.10	Description of the anisotropic transmissivity observed in the saturated zone

Table 1.2.04.02.0A-2. Indirect Inputs

Citation	Title	DIRS
10 CFR 63	Energy: Disposal of High-Level Radioactive Wastes in a Geologic Repository at Yucca Mountain, Nevada	180319
70 FR 53313	Implementation of a Dose Standard After 10,000 Years	178394
BSC 2004	*Characterize Framework for Igneous Activity at Yucca Mountain, Nevada*	169989
BSC 2004	*Characterize Framework for Seismicity and Structural Deformation at Yucca Mountain, Nevada*	168030
BSC 2004	*Yucca Mountain Site Description*	169734
Byers and Barnes 1967	*Geologic Map of the Paiute Ridge Quadrangle, Nye and Lincoln Counties, Nevada*	101859
Conner et al. 1996	"Integrating Structural Models into Probabilistic Volcanic Hazard Analyses: An Example from Yucca Mountain, NV"	135969
CRWMS M&O 1996	*Probabilistic Volcanic Hazard Analysis for Yucca Mountain, Nevada*	100116
CRWMS M&O 1998	"Physical Processes of Magmatism and Effects on the Potential Repository: Synthesis of Technical Work through Fiscal Year 1995"	123201
CRWMS M&O 1998	*Probabilistic Seismic Hazard Analyses for Fault Displacement and Vibratory Ground Motion at Yucca Mountain, Nevada*	103731
CRWMS M&O 1998	*Synthesis of Volcanism Studies for the Yucca Mountain Site Characterization Project*	105347
SNL 2007	*Characterize Eruptive Processes at Yucca Mountain, Nevada*	174260
SNL 2007	*UZ Flow Models and Submodels*	184614
SNL 2008	*Site-Scale Saturated Zone Transport*	184806
USGS 2000	*Ground Water in Hawaii*	183277
Valentine and Krogh 2006	"Emplacement of Shallow Dikes and Sills Beneath a Small Basaltic Volcanic Center – The Role of Pre-Existing Structure (Paiute Ridge, Southern Nevada, USA)"	177282

FEP: 1.2.04.03.0A

FEP NAME:

Igneous Intrusion into Repository

FEP DESCRIPTION:

Magma from an igneous intrusion may flow into the drifts and extend over a large portion of the repository site, forming a sill, dike, or dike swarm, depending on the stress conditions. This intrusion could involve multiple drifts. The sill could be limited to the drifts or a continuous sill could form along the plane of the repository, bridging between adjacent drifts.

SCREENING DECISION:

Included

TSPA DISPOSITION:

The primary focus of this FEP is magmatic intrusion directly into the repository. The following discussion addresses the potential for such an intrusion and the resulting damage to EBS components. The damage potential is included in the performance assessment to demonstrate compliance with the individual protection standard after permanent closure (proposed 10 CFR 63.311 (70 FR 53313 [DIRS 178394])). Related FEPs discuss changes in hydrology (excluded FEP 1.2.10.02.0A (Hydrologic Response to Igneous Activity)) and rock properties (excluded FEP 1.2.04.02.0A (Igneous Activity Changes Rock Properties)). A volcanic eruption featuring the development of one or more eruptive conduits within the repository footprint, which might intersect one or more drifts or waste packages, is discussed in included FEP 1.2.04.06.0A (Eruptive Conduit to Surface Intersects Repository).

The technical basis for inclusion of igneous intrusion into the repository in the TSPA is founded on the results of the PVHA (CRWMS M&O 1996 [DIRS 100116]) described in *Characterize Framework for Igneous Activity at Yucca Mountain, Nevada* (BSC 2004 [DIRS 169989], Table 7-1), which indicates that the computed mean annual frequency of intersection of the repository footprint by a dike is 1.7×10^{-8}. The computed 5th and 95th percentiles of the uncertainty distribution for frequency of intersection are 7.4×10^{-10} and 5.5×10^{-8}, respectively. The PVHA presented a slightly lower annualized mean annual frequency of intersection of 1.5×10^{-8} (CRWMS M&O 1996 [DIRS 100116], p. 4-10) than the current estimate (1.7×10^{-8}/yr) (BSC 2004 [DIRS 169989], Table 7-1), but the difference is the result of using a somewhat different and smaller repository footprint.

Igneous intrusion into the repository has the potential to affect the thermal, geochemical, and hydrologic characteristics of the site (see included FEP 1.2.04.02.0A (Igneous Activity Changes Rock Properties) and excluded FEP 1.2.10.02.0A (Hydrologic Response to Igneous Activity) for discussions of rock properties and hydrologic impacts, respectively). Igneous intrusion into the repository could damage EBS components and the waste packages because of extreme changes in the in-drift environment. This damage could result in the release of radionuclides and affect the radiological exposure of the RMEI.

Because the probability of igneous intrusion is greater than the FEP screening probability threshold of 10^{-8} per year (proposed 10 CFR 63.342 (70 FR 53313 [DIRS 178394])) and because waste package damage cannot be constrained due to the thermal, mechanical, and geochemical environment associated with an intrusion into an emplacement drift, igneous intrusion into the repository is included within the performance assessment to demonstrate compliance with the individual protection standard after permanent closure (proposed 10 CFR 63.311 (70 FR 53313 [DIRS 178394]). The environmental conditions and their effect on waste packages are discussed in included FEP 1.2.04.04.0A (Igneous Intrusion Interacts with EBS Components).

However, disruptive igneous events have estimated frequencies of occurrence that are less than 10^{-5} per year, and therefore such events are not included in performance assessments to demonstrate compliance with the groundwater protection standards (10 CFR 63.331 [DIRS 180319]) and the individual protection standard for human intrusion (proposed 10 CFR 63.321 (70 FR 53313 [DIRS 178394])) based on low probability of occurrence. The exclusion of unlikely events (events having less than one chance in 10 of occurring in 10,000 years) from these assessments is consistent with the requirements of proposed 10 CFR 63.342(b) and (c)(1) (70 FR 53313 [DIRS 178394]).

Total System Performance Assessment Model/Analysis for the License Application describes the approach for considering igneous intrusion and documents the implementation of the igneous intrusion abstractions (SNL 2008 [DIRS 178871], Sections 6.5 and 8.2.3). The two types of igneous activity (with individual probabilities and consequences) modeled are:

- An igneous intrusion featuring the ascent of a basaltic dike or dike system (i.e., a set, or swarm, of multiple dikes comprising a single intrusive event) to the repository level where it intersects drifts (this FEP)

- A volcanic eruption featuring the development of one or more volcanoes within the repository footprint, each with a conduit that may intersect waste packages (included FEP 1.2.04.06.0A (Eruptive Conduit to Surface Intersects Repository)).

The overall concept represented in the TSPA is that of a dike propagating toward the surface and intersecting the repository. If the rising magma encounters the repository, it flows into and along the intersected repository drifts (this FEP). Coincident with dike intersection, one or more conduits may form within the repository footprint that have the potential to bring waste to the surface (included FEP 1.2.04.06.0A (Eruptive Conduit to Surface Intersects Repository)). The characteristics and properties of magma that are used as input to the analyses and models are identified and described in *Characterize Eruptive Processes at Yucca Mountain, Nevada* (SNL 2007 [DIRS 174260], Table 7-1). The consequences of the dike intersecting the repository drifts and magma flow into the drifts are addressed in *Number of Waste Packages Hit by Igneous Events* (SNL 2007 [DIRS 177432], Table 7-1), and damage to EBS components is described in *Dike/Drift Interactions* (SNL 2007 [DIRS 177430], Section 6.4).

Dike/Drift Interactions (SNL 2007 [DIRS 177430], Sections 6.2, 6.3, and 6.4) documents the analyses that represent potential processes included in TSPA associated with propagation of a dike migrating upward toward the surface, including the potential for sill development, intersection of the dike with repository drifts, and the environment in drifts after intrusion. The

analyses of the dike/drift interaction conceptual model provide the technical basis for assessing the potential impacts of an igneous intrusion on repository performance, including those FEPs related to dike/drift interaction (this FEP and included FEPs 1.2.04.04.0A (Igneous Intrusion Interacts with EBS Component), 1.2.04.04.0B (Chemical Effects of Magma and Magmatic Volatiles), and 1.2.04.06.0A (Eruptive Conduit to Surface Intersects Repository)).

The consequences of igneous intrusion into the repository are included in the performance assessment to demonstrate compliance with the individual protection standard after permanent closure (proposed 10 CFR 63.311 (70 FR 53313 [DIRS 178394])) for the period of geologic stability.

INPUTS:

Table 1.2.04.03.0A-1. Indirect Inputs

Citation	Title	DIRS
10 CFR 63	Energy: Disposal of High-Level Radioactive Wastes in a Geologic Repository at Yucca Mountain, Nevada	180319
70 FR 53313	Implementation of a Dose Standard After 10,000 Years	178394
BSC 2004	*Characterize Framework for Igneous Activity at Yucca Mountain, Nevada*	169989
CRWMS M&O 1996	*Probabilistic Volcanic Hazard Analysis for Yucca Mountain, Nevada*	100116
SNL 2007	*Characterize Eruptive Processes at Yucca Mountain, Nevada*	174260
SNL 2007	*Dike/Drift Interactions*	177430
SNL 2007	*Number of Waste Packages Hit by Igneous Events*	177432
SNL 2008	*Total System Performance Assessment Model/Analysis for the License Application*	178871

FEP: 1.2.04.04.0A

FEP NAME:

Igneous Intrusion Interacts with EBS Components

FEP DESCRIPTION:

An igneous intrusion in the form of a dike may occur through the repository, intersecting the repository drifts, resulting in magma, pyroclastic debris, and volcanic gases entering the drift and interacting with the EBS components (drip shields, waste packages, pallet, and invert). This could lead to accelerated drip shield and waste package failure (e.g., attack by magmatic volatiles, damage by flowing or fragmented magma, thermal effects) and dissolution or volatilization of waste.

SCREENING DECISION:

Included

TSPA DISPOSITION:

The primary focus of this FEP is interactions between the intrusion, the waste, and the waste packages. These interactions are included in the performance assessment to demonstrate compliance with the individual protection standard after permanent closure (proposed 10 CFR 63.311 (70 FR 53313 [DIRS 178394])) because magma could interact with the elements of the EBS and the waste packages could be impaired due to perturbations of the drift environment, thereby resulting in damage to the waste packages and mobilization of waste.

As discussed in included FEP 1.2.04.03.0A (Igneous Intrusion into Repository), disruptive igneous events are not included in performance assessments to demonstrate compliance with the groundwater protection standards (10 CFR 63.331 [DIRS 180319]) and the individual protection standard for human intrusion (proposed 10 CFR 63.321 (70 FR 53313 [DIRS 178394])) because they are unlikely events (events having less than one chance in 10 of occurring in 10,000 years). The exclusion of unlikely events from the groundwater protection and human intrusion performance assessments is consistent with the requirements of proposed 10 CFR 63.342(b) and (c)(1) (70 FR 53313 [DIRS 178394]).

The technical basis for including igneous intrusion into the repository (i.e., igneous activity) in the performance assessment to demonstrate compliance with the individual protection standard after permanent closure (proposed 10 CFR 63.311 (70 FR 53313 [DIRS 178394])) is that igneous intrusion would cause changes in the in-drift environment that could damage EBS components and the waste packages. Such events have the potential to affect both the geochemical and hydrologic characteristics of the site (see excluded FEPs 1.2.04.02.0A (Igneous Activity Changes Rock Properties) and 1.2.10.02.0A (Hydrologic Response to Igneous Activity) for discussions of rock properties and hydrologic impacts, respectively). This damage could result in the release of radionuclides and affect the radiological exposure of the RMEI. The environmental conditions and their effect on waste packages are discussed in this FEP. Environmental conditions affecting the waste form and subsequent dissolution and transport of

radionuclides by groundwater after seepage has been reestablished are considered under included FEP 1.2.04.04.0B (Chemical Effects of Magma and Magmatic Volatiles).

The two types of igneous event (with individual probabilities and consequences) being modeled by the TSPA are:

- An igneous intrusion featuring the ascent of a basaltic dike or dike system (i.e., a set of one or more dikes comprising a single intrusive event) to repository level where it intersects drifts

- A volcanic eruption featuring the development of one or more volcanoes within the repository footprint, each with a conduit that may intersect waste packages.

These are treated separately within TSPA for two reasons: (1) the transport pathways that might produce radiation dose to the RMEI are very different; (2) as described below, while any igneous event that intersects the repository is assumed to result in both intrusion and eruption, not all eruptions carry waste to the surface. As a consequence of igneous intrusion into the repository, waste from packages that are contacted by magma may provide a source of radionuclides when groundwater moves through the damaged packages at some time in the future (igneous intrusion). The potential consequence of the volcanic eruption is that waste packages entrained within a conduit may be breached, releasing radionuclides in an erupting ash plume where they can be dispersed downwind to the RMEI. The location of the RMEI is defined as being approximately 18-km south of the repository (10 CFR 63.312 and 63.302 [DIRS 180319]). It is assumed that any igneous event that intersects the repository will also result in an eruption. However, the conduit(s) for that eruption may or may not intersect repository drifts. A dike intersection with a drift is assumed to result in flooding of the entire repository with magma, and this is the starting point for the evaluation of the consequences of igneous intrusion. However, only a fraction of such events will also have eruptive conduits that intersect a drift and are therefore able to erupt radioactive waste onto the surface. *Total System Performance Assessment Model/Analysis for the License Application* (SNL 2008 [DIRS 178871], Section 6.5) describes the approach for considering igneous intrusion and documents the actual implementation of the igneous intrusion abstractions.

Dike/Drift Interactions (SNL 2007 [DIRS 177430], Section 6.4.8.3) provides an analysis of magma interactions with the EBS. The analysis indicates that an igneous intrusion would damage drip shields, waste packages, and cladding materials in magma-flooded drifts such that they would no longer protect the waste form. In particular, following contact by magma, the Alloy 22 and stainless steels in the waste package would lose their tensile strength and deform plastically at magmatic temperatures (up to about 1,200°C). Waste packages could fail in response to external or internal pressures and temperatures as creep strains exceed the strain limits of the end cap materials, and magma could enter the failed waste packages (SNL 2007 [DIRS 177430], Section 8.1.2). Waste packages also could be subjected to corrosive vapor, which could have a significant impact on the corrosion rates of metals embedded in the cooling magma (SNL 2007 [DIRS 177430], Sections 6.4.8.3.1 and 6.4.8.3.3). Once the drift has filled with magma, the magma is apt to stagnate. Because of this stagnation and subsequent cooling and solidification of the magma, significant flow of magma through the affected waste packages is not anticipated (SNL 2007 [DIRS 177430], Section 8.1.2). The forces generated by magma

would not be sufficient to move intact waste packages along a drift into an errupting conduit (SNL 2007 [DIRS 177430], Section 6.4.8.3.2). The evaluation of potential damage mechanisms supports the TSPA assumption that waste packages in magma-flooded drifts will provide no protection for the contained waste. Therefore, TSPA assumes that all waste packages and drip shields are failed (SNL 2007 [DIRS 177432], Table 7-1). Within the TSPA, no credit is taken for any partial protection that residual elements of the waste package shells and the encapsulating basalt might provide.

Commercial SNF, which is a ceramic composed of UO_2, will not melt or volatilize in a basalt magma (SNL 2007 [DIRS 177430], Section 6.4.8.3.3). The melting temperature of the ceramic ranges from approximately 2,600°C to 2,800°C, while the temperature of the magma is over a thousand degrees less (up to approximately 1,150°C; SNL 2007 [DIRS 177430], Section 8.1.2). However, when waste packages fail, the fuel pellets may be assimilated into cooling basalt magma (no credit is taken for cladding) (SNL 2007 [DIRS 180616], Section 6.2.1.2[a] and Table 7-2[a]).

Glass waste is contained within waste packages and would be expected to re-melt and re-solidify as the drift is intruded and then cools (SNL 2007 [DIRS 177430], Section 6.4.8.3.3). Some interaction would be expected between the exposed and partially degraded glass waste and basalt magma given the melting temperature of glass waste (melting begins at about 915°C (BSC 2004 [DIRS 169988], Section 6.5.5.3) compared to basalt magma at about 1,150°C (SNL 2007 [DIRS 177430], Section 8.1.2), and the large difference in composition between glass waste (e.g., BSC 2004 [DIRS 169988], Section 6.5.2.2) and basalt magma (SNL 2007 [DIRS 174260], Section 6.3.2). For TSPA, once intrusion occurs, all waste is assumed unprotected, instantaneously degraded, and the radionuclides are assumed immediately available for mobilization by groundwater (SNL 2008 [DIRS 178871], Section 6.5.1.1.1).

Interactions of the intrusion with repository drifts are implemented within the TSPA for intrusions occurring within the period of geologic stability. These interactions are incorporated into the TSPA as assumptions or parameters as follows:

- Assumptions underlying the consequences of igneous intrusion on the waste package and waste form
- Parameters related to resumption of seepage following cooling of the drift after the magmatic intrusion.

Within the TSPA, lookup tables are used to model magma temperature as a function of time for the center of the cooling magma body. These lookup tables determine when seepage is reestablished, exposing the encased waste form to seepage flux. The abstraction considers the temperature of the waste form for a period of 100 years following intrusion, after which the intrusion-related temperature perturbation is negligible. The decline in temperature of the waste form and magma body is related to the temperature due to waste heat alone at 25°C, 50°C, 100°C, 150°C, and 200°C (SNL 2007 [DIRS 177430], Section 6.4.7.2).

Dike/Drift Interactions (SNL 2007 [DIRS 177430], Section 6.6) contains a summary of analogue compositions of water in contact with basalt. Included FEP 1.2.04.04.0B (Chemical Effects of

Magma and Magmatic Volatiles) describes the TSPA method used to simulate basalt–seepage water reactions within the drift for the igneous intrusion model. *Atmospheric Dispersal and Deposition of Tephra from a Potential Volcanic Eruption at Yucca Mountain, Nevada* (SNL 2007 [DIRS 177431]) provides a description of a potential eruption through the repository. Included FEPs 1.2.04.06.0A (Eruptive Conduit to Surface Intersects Repository) and 1.2.04.07.0A (Ashfall) describe how eruptions are incorporated into the TSPA.

Volatilization of Waste—Volatilization of some fission products (cesium and strontium) by magmatic temperatures is identified as a process that could affect waste forms (SNL 2007 [DIRS 177430], Sections 6.4.8.3.3 and 8.1.2). Although not included in the above description, iodine could also be volatilized by magmatic temperatures. If any of these radionuclides were volatilized, it is expected that as those gas species moved away from the waste form, they would be incorporated, in part, into the magma and in part redissolved into water (e.g., matrix pore water) at its closest location to the drift perimeter because of their high solubilities. It is further expected that these volatilized radionuclides would be located preferentially, and possibly exclusively, above the emplacement drifts because the hot gases would generally rise as they move down the temperature gradient.

Waste form volatilization processes are not directly included in TSPA. Rather, when intersection of the repository occurs, magma engulfs all drip shields and waste packages in the repository and neutralizes their abilities to inhibit flow of seepage (percolation) (SNL 2008 [DIRS 178871], Section 6.5.5.1) and protect the waste. Waste forms in the engulfed waste packages are instantly degraded during the intrusion event (SNL 2008 [DIRS 178871], Section 6.5). Hence, upon intrusion, the entire waste inventory of the repository is immediately available for transport through normal mobilization processes once the magma cools below the boiling point of water and seepage returns to the basalt filled drifts (SNL 2008 [DIRS 178871], Section 6.5.1.1.1). Since the entire waste inventory is assumed to be completely degraded at the time of intrusion, any contribution to degradation that would be associated with volatilization processes is already included. Furthermore, the cooled basalt is assumed to provide no additional impediment to water flow (SNL 2008 [DIRS 178871], Section 6.5.1.3), and the percolation flux contacts all the radionuclides of the degraded waste form which are available for advective transport of radionuclides from the EBS (SNL 2008 [DIRS 178871], Section 6.5.1.3) once flow is restored to the basalt-filled drifts.

In summary, FEP 1.2.04.04.0A (Igneous Intrusion Interacts with EBS Components), which includes interactions between igneous intrusions, waste, and waste packages are included in the performance assessment to demonstrate compliance with the individual protection standard after permanent closure (proposed 10 CFR 63.311 (70 FR 53313 [DIRS 178394])). However, disruptive igneous events are not included in performance assessments to demonstrate compliance with the groundwater protection standards (10 CFR 63.331 [DIRS 180319]) and the individual protection standard for human intrusion (proposed 10 CFR 63.321 (70 FR 53313 [DIRS 178394])) because they have been determined to be unlikely events (proposed 10 CFR 63.342(b) and (c)(1) (70 FR 53313 [DIRS 178394])).

INPUTS:

Table 1.2.04.04.0A-1. Indirect Inputs

Citation	Title	DIRS
10 CFR 63	Energy: Disposal of High-Level Radioactive Wastes in a Geologic Repository at Yucca Mountain, Nevada	180319
70 FR 53313	Implementation of a Dose Standard After 10,000 Years	178394
BSC 2004	*Defense HLW Glass Degradation Model*	169988
SNL 2007	*Cladding Degradation Summary for LA*	180616
SNL 2007	*Atmospheric Dispersal and Deposition of Tephra from a Potential Volcanic Eruption at Yucca Mountain, Nevada*	177431
SNL 2007	*Characterize Eruptive Processes at Yucca Mountain, Nevada*	174260
SNL 2007	*Dike/Drift Interactions*	177430
SNL 2007	*Number of Waste Packages Hit by Igneous Events*	177432
SNL 2008	*Total System Performance Assessment Model/Analysis for the License Application*	178871

FEP: 1.2.04.04.0B

FEP NAME:

Chemical Effects of Magma and Magmatic Volatiles

FEP DESCRIPTION:

An igneous intrusion into the repository may be accompanied by the release of magmatic volatiles. The volatiles may affect in-drift chemistry (potentially leading to increased waste package corrosion), or may be absorbed by the host rock, where they could change the chemistry of the water seeping back into the drift following the intrusive event. Seepage water chemistry following magma cooling could also be affected by flowing through and interacting with the intruded basalt.

SCREENING DECISION:

Included

TSPA DISPOSITION:

This FEP is concerned with magmatic volatiles and their potential effects on in-drift chemistry and on water chemistry, and with the basaltic magma that may fill one or more repository drifts and its effect on water chemistry. The FEP is included in the performance assessment to demonstrate compliance with the individual protection standard after permanent closure (proposed 10 CFR 63.311 (70 FR 53313 [DIRS 178394])). The effects of magmatic volatiles on in-drift chemistry and specifically effects on EBS components have been analyzed (SNL 2007 [DIRS 177430], Section 6.4.8.3).

As discussed in included FEP 1.2.04.03.0A (Igneous Intrusion into Repository), disruptive igneous events are not included in performance assessments to demonstrate compliance with the groundwater protection standards (10 CFR 63.331 [DIRS 180319]) and with the individual protection standard for human intrusion (proposed 10 CFR 63.321 (70 FR 53313 [DIRS 178394])) because they are unlikely events (events having less than one chance in 10 of occurring in 10,000 years). The exclusion of unlikely events from the groundwater protection and human intrusion performance assessments is consistent with the requirements of proposed 10 CFR 63.342(b) and (c)(1) (70 FR 53313 [DIRS 178394]).

The effects of magmatic volatiles on water chemistry are not relevant because the temperatures that accompany intrusion are much greater than the boiling temperature of water, and any water present in the host rock would be displaced away from the drift perimeter by the increased temperatures and would not return until temperatures had fallen below boiling temperatures. Based on analysis results (SNL 2007 [DIRS 177430], Table 8-2), the period of time required for temperatures to return to sub-boiling depends on the pre-intrusion drift temperature, which is related to the amount of heat from emplaced waste. The results (SNL 2007 [DIRS 177430], Table 8-2) show that the amount of time needed for drift temperatures to return to sub-boiling levels varies from 2 to 3 years for drifts initially at 25°C to more than 100 years for drifts initially at 200°C. In any case, by the time water flow is reestablished near the drift perimeter,

magmatic gases would no longer be present and therefore could not alter groundwater chemistry. However, changes in water chemistry associated with interaction with cooled basalt are included in the TSPA.

As stated in included FEP 1.2.04.04.0A (Igneous Intrusion Interacts with EBS Component), if any drift in the repository is intersected by a basaltic dike, all drifts are assumed to flood with magma, and all waste packages are compromised.

Assuming that an igneous intrusion occurs and the magma subsequently cools to ambient conditions, seepage water is expected to flow through and react with the basalt in the intruded emplacement drifts. The chemical interaction of the seepage water chemistry with the basalt is included in the TSPA.

Because transport of radionuclides by groundwater is included in TSPA and since radionuclide mobility is influenced by groundwater chemistry, the analysis requires consideration of the chemistry of groundwater that has been in contact with the basalt surrounding the waste packages. For development of the pH and ionic strength abstractions that are used in TSPA, three groundwater samples from large fractured basalt reservoirs were selected for sensitivity analyses that examined pH and ionic strength of water that has reacted with cooled basalt (SNL 2007 [DIRS 180506], Section 4.1.2[a]). These sensitivity studies described in *In-Package Chemistry Abstraction* (SNL 2007 [DIRS 180506], Section 6.6.2[a]) were used to estimate solution development during reactions between basalt-equilibrated water and the in-package materials. The analyses showed that in-package chemistry is insensitive to seepage water composition and subsequent reaction with basalt. Therefore, in-package chemistry abstraction for nominal conditions is used in the TSPA to simulate the waste form chemical conditions following an igneous intrusion.

The TSPA parameters for pH and ionic strength have been described in *In-Package Chemistry Abstraction* (SNL 2007 [DIRS 180506], Section 8.2[a] and Table 6-21[a]), and the details for TSPA implementation of these abstractions are also provided (SNL 2007 [DIRS 180506], Section 6.10.9[a]). Uncertainties in the values of pH and ionic strength are quantified and propagated in TSPA as described in *In-Package Chemistry Abstraction* (SNL 2007 [DIRS 180506], Section 6.10.8[a]).

INPUTS:

Table 1.2.04.04.0B-1. Indirect Inputs

Citation	Title	DIRS
10 CFR 63	Energy: Disposal of High-Level Radioactive Wastes in a Geologic Repository at Yucca Mountain, Nevada	180319
70 FR 53313	Implementation of a Dose Standard After 10,000 Years	178394
SNL 2007	*Dike/Drift Interactions*	177430
SNL 2007	*In-Package Chemistry Abstraction*	180506

FEP: 1.2.04.05.0A

FEP NAME:

Magma or Pyroclastic Base Surge Transports Waste

FEP DESCRIPTION:

As a result of an igneous intrusion, extrusive processes may result in a pyroclastic density current (base surge), effusive lava flows, and/or development of a volcanic cone at the land surface. Some of the waste (entrained, dissolved, or volatized) could then be transported away from the repository. Of most concern is transport directly along the land surface to the RMEI.

SCREENING DECISION:

Excluded – low consequence

SCREENING JUSTIFICATION:

This FEP is focused on near-surface eruption-related phenomena and transport of entrained wastes by lava flows and base surges (also referred to as pyroclastic surges). Hydrovolcanic phenomena also are addressed in this FEP. Due to the distance to the RMEI, and the limited distance that basaltic lavas and hydrovolcanic deposits are expected to flow, hydrovolcanic phenomena are excluded based on low consequence. Transport directly to the receptor by aerial dispersal and/or subsequent reworking of the deposited ash following an eruptive event are addressed separately in included FEP 1.02.04.07.0A (Ashfall) and its companion included FEP 1.02.04.07.0C (Ash Redistribution Via Soil and Sediment Transport).

The technical basis for exclusion for this FEP begins with definition of the term RMEI, which specifies that the affected individual is located no closer to the repository than 18 km to the south (which is in the direction of groundwater flow) and over a contaminated groundwater plume (10 CFR 63.312 and 63.302 [DIRS 180319]). For flowing lava or a pyroclastic base surge (potentially containing entrained waste) to be of consequence to the accessible environment or the RMEI, it would have to travel across the land surface a distance of 18 km. In contrast to this distance, the eight Quaternary volcanoes in the vicinity of Yucca Mountain are small volume (approximately 0.1 km^3 or less) (SNL 2007 [DIRS 174260], Table 6-2), and typically consist of a single main basaltic scoria cone surrounded by one or two small lava flow fields that, in most cases, extend about 1 km from the source (SNL 2007 [DIRS 174260], Section 6.1.3.3; Valentine and Perry 2006 [DIRS 177495], Table 1). The Quaternary volcanism continues the well-documented record of waning monogenetic volcanism that began in the Miocene within the Yucca Mountain region (BSC 2004 [DIRS 169989], Section 6.2; Valentine and Perry 2006 [DIRS 177495], Table 1). Consequently, it is not credible to presume that future extruded basalts with entrained wastes would extend to the RMEI located 18 km south of the repository. Potential pyroclastic (base) surge deposits are also of limited geographic extent as described below.

Pyroclastic deposits are characterized by a wide range of materials, transport mechanisms, and depositional environments. Two main types of pyroclastic activity are recorded in Quaternary

volcanoes of the Yucca Mountain area (SNL 2007 [DIRS 174260], Section 6.3.1): (1) Strombolian eruptions in which discrete bursts eject coarse lapilli, blocks, and bombs, which accumulate within a few hundred meters of the vent; and (2) violent Strombolian eruptions that produce sustained columns of gas, ash, and lapilli that can extend to several kilometers altitude above the vent. Ash and lapilli fall out of violent Strombolian eruption columns (or plumes) as the plumes are dispersed downwind. For example, the ash deposited during the Lathrop Wells eruptions (~77,000 years ago) has been traced to distances of about 20 km from the vent (SNL 2007 [DIRS 174260], Appendix C). Pyroclastic eruptive mechanisms associated with violent Strombolian eruptions may result in transport of pyroclastic tephra (e.g., lapilli and ash) to distances sufficient to reach the RMEI. This aspect of an igneous event has been included and is addressed separately in included FEP 1.02.04.07.0A (Ashfall) and its companion included FEP 1.02.04.07.0C (Ash Redistribution via Soil and Sediment Transport); they are not discussed further in this section.

A third type of explosive eruptive phenomenon, which is recorded very rarely in deposits of Quaternary volcanoes in the Yucca Mountain region, is pyroclastic density currents or base surges (SNL 2007 [DIRS 174260] Appendix C). Base surges are mixtures of gas and pyroclasts that are denser than the atmosphere and therefore travel along the ground as density currents. They may be produced by the following mechanisms: (1) fountaining of a violent Strombolian eruption column if it is unable to buoyantly rise into the atmosphere; and (2) localized lateral flow of ash and fine lapilli and entrained air during very heavy fallout of particles from an eruption column that is otherwise buoyant, and (3) collapse of pyroclast-steam clouds that are ejected by explosive interaction of magma with ground or surface waters (hydrovolcanic eruptions).

Only two localized deposits that have indicators of lateral transport such as a base surge mechanism have been found in the eight Quaternary volcanoes of the Yucca Mountain region. Both of these deposits are found at the Lathrop Wells volcano. One of the occurrences is a thin (~40 cm maximum thickness) sequence of laminated and cross-laminated deposits near the summit of the Lathrop Wells cone. The lateral extent of this sequence is on the order of several tens of meters (SNL 2007 [DIRS 174260], Section C.6.1). The interpretation for this deposit is emplacement by weak density currents adjacent to the vent due to locally heavy ash fallout from an eruption column (second mechanism listed in preceding paragraph). The second occurrence of deposits that might have been emplaced by a base surge mechanism is found on the cone-facing side of a hill at distances of ~200 to 300 m northwest of the base of the cone (SNL 2007 [DIRS 174260]), Section C.6.2). The origin of this deposit is uncertain. It might have been produced by any of the three mechanisms listed in the preceding paragraph or it might have been produced by eolian reworking of preexisting ash deposits during a pause in explosive activity at the vent.

Given the lateral scale of the observed Quaternary deposits that might have been produced by base surges (on the order of 1 km or less from the vent), it is not credible to presume that pyroclastic surges with entrained waste particles would reach from the vent to the RMEI located 18 km south or to the controlled area boundaries at no greater than 5 km from the repository in other directions. This implies that base (pyroclastic) surges from a volcanic eruption at the Yucca Mountain site would have no consequence to the RMEI.

A related issue is whether a large steam explosion could occur, such that a large phreatic or a hydrovolcanic crater (maar) might form. Theoretically, such a process could excavate to the depth of the repository (~300 m) and disperse waste over a large area of the surrounding surface. Hydrovolcanic activity requires that rising magma encounter water in an aquifer(s) or a shallow water body at the ground surface (BSC 2004 [DIRS 174260], Section 6.1.3.2; Fisher and Schmincke 1984 [DIRS 162806], pp. 231 to 264; Wohletz and Heiken 1992 [DIRS 105544], pp. 85 to 154). The resulting steam explosion finely fragments the magma and produces large amounts of kinetic energy. If the encounter occurs below the ground surface, the host rocks are fragmented and are incorporated in the eruption products, which become elevated in lithic clast content. For such a disruptive steam explosion to occur, magma must come in rapid contact with a large volume of water at a shallow depth. Confining pressures must be sufficiently low to permit the formation of steam and to allow disruption of the surrounding rock as the steam violently expands. Crowe et al. (1986 [DIRS 101532], p. 47) suggest that a limited area of contact, such as a dike projecting through a thin (less than 10 m) perched aquifer, does not allow development of explosive instability, whereas contact with a standing body of surface water or thick (greater than 30 m) horizon of water-saturated rock permits water to vaporize at explosive rates. Additionally, magma–water mixing and explosion associated with maars, tuff rings, and tuff cones generally occur at depths less than 200 m, which corresponds to a confining pressure of 5 MPa or less. However, the distribution of potential Quaternary hydrovolcanic deposits in the Yucca Mountain region is limited to areas proximal to vents (SNL 2007 [DIRS 174260], Sections C.6.2 and E.6.1), and the extents of such deposits are insufficient to reach the RMEI. Consequently, transport by a hydrovolcanic cratering event is excluded from the TSPA based on low consequence.

Based on the previous discussion, omission of FEP 1.2.04.05.0A (Magma or Pyroclastic Base Surge Transports Waste) will not result in a significant adverse change in the magnitude or timing of either radiological exposures to the RMEI or radionuclide releases to the accessible environment. Therefore, this FEP is excluded from the performance assessments conducted to demonstrate compliance with proposed 10 CFR 63.311 and 63.321 (70 FR 53313 [DIRS 178394]), and with 10 CFR 63.331 [DIRS 180319], on the basis of low consequence.

INPUTS:

Table 1.2.04.05.0A-1. Direct Inputs

Input	Source	Description
BSC 2007. *Waste Package Fabrication*. [DIRS 180190]	Section B4.2.2	The inner vessel of the waste package is designed to withstand internal pressures of up to 140 psia at 707°F (375°C)
SNL 2007. *Characterize Eruptive Processes at Yucca Mountain, Nevada*. [DIRS 174260]	Section 6.3.1	Two main types of pyroclastic activity
	Section C.6.2	The second occurrence of deposits that might have been emplaced by a base surge mechanism is found on the cone-facing side of a hill at distances of ~200 to 300 m northwest of the base of the cone
	Table 6-2	The Quaternary volcanoes in the vicinity of Yucca Mountain are small volume
	Section C.6.1	The lateral extent of this sequence is on the order of several tens of meters
	Appendix C	The distance traveled of the ash deposited during the Lathrop Wells eruptions

Table 1.2.04.05.0A-2. Indirect Inputs

Citation	Title	DIRS
10 CFR 63	Energy: Disposal of High-Level Radioactive Wastes in a Geologic Repository at Yucca Mountain, Nevada	180319
70 FR 53313	Implementation of a Dose Standard After 10,000 Years	178394
BSC 2004	*Characterize Framework for Igneous Activity at Yucca Mountain, Nevada*	169989
Crowe et al. 1986	*Status of Volcanic Hazard Studies for the Nevada Nuclear Waste Storage Investigations*	101532
Fisher and Schmincke 1984	*Pyroclastic Rocks*	162806
SNL 2007	*Characterize Eruptive Processes at Yucca Mountain, Nevada*	174260
Valentine and Perry 2006	"Decreasing Magmatic Footprints on Individual Volcanoes in a Waning Basaltic Field"	177495
Wohletz and Heiken 1992	*Volcanology and Geothermal Energy*	105544

FEP: 1.2.04.06.0A

FEP NAME:

Eruptive Conduit to Surface Intersects Repository

FEP DESCRIPTION:

As a result of an igneous intrusion, one or more volcanic vents may form at land surface. The conduit(s) supplying the vent(s) could pass through the repository, interacting with and entraining waste.

SCREENING DECISION:

Included

TSPA DISPOSITION:

This FEP is included in the performance assessment to demonstrate compliance with the individual protection requirements of proposed 10 CFR 63.311 (70 FR 53313 [DIRS 178394]) and is addressed by the modeling of an eruption. The probability of occurrence of this event is less than 1×10^{-5} per year and is thus excluded from the performance assessments conducted to demonstrate compliance with the individual protection standard for human intrusion (proposed 10 CFR 63.321 (70 FR 53313 [DIRS 178394])) and the groundwater protection standard (10 CFR 63.331 [DIRS 180319]), consistent with the requirements in proposed 10 CFR 63.342(b) and (c)(1) (70 FR 53313 [DIRS 178394]). The consequences of an igneous intrusion through the repository and an associated eruptive event are explicitly included in TSPA through modeling of aerial dispersion followed by deposition and redistribution of potentially contaminated pyroclastic materials; the consequences are appropriately weighted by the probability of occurrence of the event.

The technical basis for inclusion of this FEP relies on the definition of an igneous event, which includes eruption at the Earth's surface (BSC 2004 [DIRS 169989], Section 5.2), and on the results described in *Number of Waste Packages Hit by Igneous Events* (SNL 2007 [DIRS 177432], Table 7-1). Those results indicate that the proportion of calculated intrusive igneous events in which eruption also occurs is 0.28 (SNL 2007 [DIRS 177432], Table 7-1), representing a mean annual probability of about 4.8×10^{-9}. Even though the estimated mean annual probability is less than the probability screening threshold in 10 CFR 63.114(d) [DIRS 180319], the consequences of volcanic eruption are evaluated because the event definition is based on the mean annual frequency of intrusion (BSC 2004 [DIRS 169989], Section 5.2) (see included FEP 1.2.04.03.0A (Igneous Intrusion into Repository) and BSC 2004 [DIRS 169989], Table 7-1).

Total System Performance Assessment Model/Analysis for the License Application describes the approach for considering igneous intrusion and documents the actual implementation of the igneous intrusion abstractions (SNL 2008 [DIRS 183478], Section 6.5). Igneous consequences modeled by the TSPA are:

- An igneous intrusion featuring the ascent of a basaltic dike or dike system (i.e., a set or swarm of multiple dikes comprising a single intrusive event) to the repository level where it intersects drifts (included FEP 1.2.04.03.0A (Igneous Intrusion into Repository))

- A volcanic eruption featuring the development of one or more eruptive conduits within the repository footprint, each of which might intersect waste packages (this FEP).

The potential consequences of the volcanic eruption are that waste packages intersected by a conduit may be breached, releasing radionuclides in an erupting ash plume followed by dispersal downwind to the RMEI, and redistribution by surface transport processes after deposition. The location of the RMEI is approximately 18-km south of the repository (10 CFR 63.312 and 10 CFR 63.302 [DIRS 180319]).

Properties and characteristics of typical basaltic eruptions are described in *Characterize Eruptive Processes at Yucca Mountain*, *Nevada* (SNL 2007 [DIRS 174260], Section 6). The eruption characteristics used in the TSPA model are based on the characteristics of preserved basaltic eruption products in the Yucca Mountain region and other observed analogous eruptions. For the volcanic eruption, a dike rises to the repository level, intersects one or more drifts in the repository, and proceeds vertically toward the surface. After magma in the dike encounters the ground surface, a fissure eruption develops, which proceeds to focus to one or more eruption sites as conduits develop from the surface downward. Conduits within the repository footprint are presumed to be located randomly along the dikes. It is presumed that where conduits intersect drifts, the waste packages in the intersected areas no longer provide any protection for the waste, which is then entrained in the erupted materials. Section 6.5.2.15 of *Atmospheric Dispersal and Deposition of Tephra from a Potential Volcanic Eruption at Yucca Mountain, Nevada* (SNL 2007 [DIRS 177431]) provides the basis for assuming that the erupted waste materials are finely divided particles amenable for airborne transport, and Section 6.5.2.22 of that report provides the basis for partitioning the contaminated eruption products among lava, cone-forming material, and aerially dispersable material.

Dike/Drift Interactions (SNL 2007 [DIRS 177430], Sections 6.4.7.1.5, 6.4.7.2.2, 6.5.1.5, and 6.5.4), provides conclusions related to various conceptual models for magma flow in drifts, including consideration of the "dog-leg scenario." That scenario involves magma flow from the point of the dike/drift intersection to the end of the drift, and development of a secondary dike that continues to the land surface at some location along the drift and away from the intersection. With regard to the secondary breakout, *Dike/Drift Interactions* (SNL 2007 [DIRS 177430], Section 6.5.2) states:

> Based on the discussion in this section, effusive magma will continue along the trajectory of the original dike after intruding the drift complex. Even if an existing joint at the drift periphery is invaded by magma, the flow will be interrupted by magma freezing long before it is able to reach the surface. Therefore, it is concluded that the dog-leg scenario is not credible for effusive magma.

The analysis of dike propagation potential, including the formation of a secondary breakout and pyroclastic flow, is extended in *Magma Dynamics at Yucca Mountain, Nevada* (BSC 2005 [DIRS 174070]) and the study by Dartevelle and Valentine (2007 [DIRS 182090]). The analyses

include potential initial and boundary conditions and the resulting effect on magma freezing (BSC 2005 [DIRS 174070], Section 6.3.2). The work also includes simulated pyroclastic magma flow into pre-existing cracks, and evaluates characteristics of a more energetic dike/drift intersection at repository depth, specifically recognizing the two-phase nature of the hawaiitic magma that could contain from 1 wt % to 5 wt % water (SNL 2007 [DIRS 174260], Section 6.3.2.2). The studies conclude the following:

- Magma attempting to open a secondary dike by intruding a preexisting crack will solidify before the crack can grow to an appreciable width, even considering elevated temperatures for the wall rock (BSC 2005 [DIRS 174070], Section 6.3.2).

- In the event a drift is intersected by a dike with two-phase (pyroclastic) magma, the simulated presence of a secondary opening down-drift from the main dike results in only minor calculated differences in the flow dynamics of the magma-drift interaction relative to a drift with no secondary opening (BSC 2005 [DIRS 174070], Section 6.4.2).

Thus, multiple analyses conclude that the main dike is the preferred pathway through which effusive or pyroclastic magma will flow into or out of an intersected drift (SNL 2007 [DIRS 177430], Section 6.5.2). Consequently, the "dog-leg" alternative conceptual model of a secondary breakout is is not further considered in the TSPA.

Atmospheric transport of the ash–waste mixture is modeled directly in TSPA using ASHPLUME, the atmospheric ash dispersal model. *Atmospheric Dispersal and Deposition of Tephra from a Potential Volcanic Eruption at Yucca Mountain, Nevada,* (SNL 2007 [DIRS 177431], Section 6.5.2) describes the technical basis for input parameters required for the ASHPLUME model. The model is based on assumed incorporation and entrainment of waste fuel particles into the ash cloud associated with a volcanic eruption through the Yucca Mountain repository, and evaluates downwind transport of contaminated tephra and deposition of radioactive waste or ash on the ground surface. The ASHPLUME model is based on a model of Suzuki (1983 [DIRS 100489]) that Jarzemba et al. (1997 [DIRS 100987]) refined to represent the entrainment of radioactive waste in the convective eruptive plumes associated with violent Strombolian eruptions. The ASHPLUME model is implemented in TSPA as a DLL, ASHPLUME_DLL_LA V2.1 [DIRS 178870]. Values for the 36 ASHPLUME input parameters are provided as constants, stochastic ranges, or tables (SNL 2007 [DIRS 177431], Section 6.5.2). The TSPA model for atmospheric dispersal and deposition of waste-containing tephra uses a parameter, magma partitioning factor, which acts as a fractional multiplier on the mass of waste available for transport. This magma partitioning factor is provided as a range (0.1 to 0.5, uniform probability (SNL 2007 [DIRS 177431], Section 6.5.2.22). In a given TSPA realization, the initial value of total waste mass available for transport is derived from sampling the number of waste packages hit (SNL 2007 [DIRS 177432], Table 7-1). The number of waste packages hit by an eruption is multiplied by the magma partitioning factor to produce a value for the input parameter *mass of waste available for transport*.

Redistribution of radionuclide-contaminated ash after an eruption intersects the repository drifts is addressed in *Redistribution of Tephra and Waste by Geomorphic Processes Following a Potential Volcanic Eruption at Yucca Mountain, Nevada* (SNL 2007 [DIRS 179347]). The tephra redistribution model is implemented in TSPA as a DLL (FAR V1.2 [DIRS 182225],

STN: 11190-1.2-00). Values for the FAR input parameters are provided as constants, stochastic ranges, or tables (SNL 2007 [DIRS 179347], Section 6.5). The FAR V1.2 code ([DIRS 182225], STN: 11190-1.2-00) redistributes contaminated ash down Fortymile Wash and its distributaries to the depositional fan where the RMEI is located. The concentration of waste particles within the redistributed ash volume at a given location is influenced by the number of waste packages impacted by intersection of the repository drifts by the ascending magmatic dike, the volume of erupted ash, the magma partitioning factor, wind direction, how the contaminated ash is distributed upon the landscape, and surface transport processes, among others. TSPA uses this information to calculate dose to the RMEI.

The consequences of an eruptive conduit intersecting the repository are included in the TSPA from the perspectives of dike intersection, ash/waste eruption to the atmosphere, deposition from an eruptive ash cloud, and redistribution by surface processes. The associated processes of ash/waste eruption to the atmosphere, deposition from an eruptive ash cloud, and redistribution by surface processes are described in included FEP 1.2.04.07.0A (Ashfall) and in excluded FEP 1.2.04.07.0B (Ash Redistribution in Groundwater).

INPUTS:

Table 1.2.04.06.0A-1. Indirect Inputs

Citation	Title	DIRS
10 CFR 63	Energy: Disposal of High-Level Radioactive Wastes in a Geologic Repository at Yucca Mountain, Nevada	180319
70 FR 53313	Implementation of a Dose Standard After 10,000 Years	178394
ASHPLUME_DLL_LA V. 2.1. 2006.	Windows 2000/XP. STN: 11117-2.1-00.	178870
BSC 2004	*Characterize Framework for Igneous Activity at Yucca Mountain, Nevada*	169989
BSC 2005	*Magma Dynamics at Yucca Mountain, Nevada*	174070
Dartevelle and Valentine 2007	*Interaction of Multiphase Magmatic Flows with Underground Openings at the Proposed Yucca Mountain Radioactive Waste Repository (Southern Nevada, USA)*	182090
FAR V 1.2	WINDOWS 2000 & WINDOWS 2003. S TN: 11190-1.2-00.	182225
Jarzemba et al. 1997	*ASHPLUME Version 1.0—A Code for Contaminated Ash Dispersal and Deposition, Technical Description and User's Guide*	100987
SNL 2007	*Atmospheric Dispersal and Deposition of Tephra from a Potential Volcanic Eruption at Yucca Mountain, Nevada*	177431
SNL 2007	*Characterize Eruptive Processes at Yucca Mountain, Nevada*	174260
SNL 2007	*Dike/Drift Interactions*	177430
SNL 2007	*Number of Waste Packages Hit by Igneous Events*	177432
SNL 2007	*Redistribution of Tephra and Waste by Geomorphic Processes Following a Potential Volcanic Eruption at Yucca Mountain, Nevada*	179347
SNL 2008	*Total System Performance Assessment Model/Analysis for the License Application*	183478
Suzuki 1983	“A Theoretical Model for Dispersion of Tephra”	100489

FEP: 1.2.04.07.0A

FEP NAME:

Ashfall

FEP DESCRIPTION:

Finely divided waste particles may be carried up a volcanic vent and deposited on the land surface from an ash cloud.

SCREENING DECISION:

Included

TSPA DISPOSITION:

Ashfall is included in the performance assessment to demonstrate compliance with the individual protection standard after permanent closure (proposed 10 CFR 63.311 (70 FR 53313 [DIRS 178394])). This FEP is addressed through the modeling of an eruption that includes airborne transport and tephra (ash) deposition. (The preferred term "tephra" refers to pyroclasts resulting from a volcanic eruption, regardless of size, in contrast to the term "ash" which refers only to pyroclasts less than 2-mm in diameter.) Consequences of the resulting tephra fall are explicitly included in the TSPA and are appropriately weighted by the probability of occurrence of the event.

The technical basis for inclusion of this FEP relies on the definition of an igneous event, which includes eruption at the Earth's surface (BSC 2004 [DIRS 169989], Section 5.2), and on the results described in *Number of Waste Packages Hit by Igneous Events* (SNL 2007 [DIRS 177432], Table 7-1). Those results indicate that the proportion of calculated intrusive igneous events in which eruption also occurs is 0.28 (SNL 2007 [DIRS 177432], Table 7-1), representing a mean annual probability of about 4.8×10^{-9}. Even though the estimated mean annual probability is less than the probability screening threshold in 10 CFR 63.114(d) [DIRS 180319], volcanic eruption is included in the TSPA because the event definition is based on the mean annual frequency of intrusion (BSC 2004 [DIRS 169989], Section 5.2) (see included FEP 1.2.04.03.0A (Igneous Intrusion into a Repository) and BSC 2004 [DIRS 169989], Table 7-1).

The lateral extent of tephra fall from such activity is sufficient to reach the location of the RMEI, so the FEP has been included in the performance assessment to demonstrate compliance with the individual protection standard after permanent closure (proposed 10 CFR 63.311 (70 FR 53313 [DIRS 178394])). Radioactive waste-containing volcanic tephra is the initial source of contamination for the volcanic scenario. However, as discussed in included FEP 1.2.04.03.0A (Igneous Intrusion into Repository), disruptive igneous events are not included in performance assessments to demonstrate compliance with the groundwater protection standards (10 CFR 63.331 [DIRS 180319]) and the individual protection standard for human intrusion (proposed 10 CFR 63.321 (70 FR 53313 [DIRS 178394])) because they are unlikely events (events having less than one chance in 10 of occurring in 10,000 years). The exclusion of this

FEP from the groundwater protection and human intrusion performance assessments is consistent with the requirements of proposed 10 CFR 63.342(b) and (c)(1) (70 FR 53313 [DIRS 178394]).

Total System Performance Assessment Model/Analysis for the License Application (SNL 2008 [DIRS 178871], Section 6.5) describes the approach for considering volcanic eruption and documents the implementation of the volcanic eruption abstractions. The two types of igneous activity (with individual probabilities and consequences) are considered:

- An igneous intrusion featuring the ascent of a basaltic dike or dike system (i.e., a set or swarm of multiple dikes comprising a single intrusive event) to the repository level where it intersects drifts (included FEP 1.2.04.03.0A (Igneous Intrusion into Repository))

- A volcanic eruption featuring the development of one or more volcanoes within the repository footprint, each with a conduit that may intersect waste packages (included FEP 1.2.04.06.0A (Eruptive Conduit to Surface Intersects Repository)).

The potential consequence of a volcanic eruption is that waste packages entrained within a conduit may be breached to form a well-mixed suspension in the rising magma and comprising a component of the tephra upon magma fragmentation at the vent. The resulting waste-containing tephra is dispersed downwind in the tephra plume and may be deposited at the RMEI location. The location of the RMEI is assumed to be approximately 18-km south of the repository (10 CFR 63.312 and 63.302 [DIRS 180319]). *Total System Performance Assessment Model/Analysis for the License Application* implements this airborne pathway and assesses its impact on the RMEI (SNL 2008 [DIRS 178871], Section 6.5.2.2). The conceptual model for the eruptive process is discussed under included FEP 1.2.04.06.0A (Eruptive Conduit to Surface Intersects Repository). The following discussion is focused on the eruption of a tephra-waste mixture into the atmosphere and subsequent transport and deposition.

Eruption parameters described in *Characterize Eruptive Processes at Yucca Mountain*, *Nevada* (SNL 2007 [DIRS 174260], Table 7-1) are based on the observed characteristics of past basaltic eruptions in the Yucca Mountain region and other analogous eruptions. This report includes the results of field investigations dealing with physical volcanology and tephra distribution and includes the conceptual models for eruptive processes. This information is used to develop parameter value distributions appropriate for analysis of the consequences of volcanic eruptions through a proposed repository at Yucca Mountain, Nevada. The parameters related to this FEP include the following (SNL 2007 [DIRS 174260], Table 7-1):

- Eruption duration for formation of an entire volcano

- Duration of a single explosive phase constituting a violent Strombolian eruptive phase

- Tephra fall or ash volume

- Standard deviation of particle size distribution for a given mean

- Clast characteristics
- Density of erupted particles
- Tephra deposit density
- Magmatic temperatures, viscosities, densities, and water contents
- Magma ascent rate below fragmentation depth
- Mean ash particle diameter
- Ash particle diameter standard deviation for particle size distribution
- Ash particle shape factor
- Ash particle density variation with particle size.

The results of the analysis in Table 7-1 of *Characterize Eruptive Processes at Yucca Mountain, Nevada* (SNL 2007 [DIRS 174260],) do not directly feed to the TSPA model; rather the results provide the technical basis for inputs to *Atmospheric Dispersal and Deposition of Tephra from a Potential Volcanic Eruption at Yucca Mountain, Nevada* (SNL 2007 [DIRS 177431], Table 6-3). Many other outputs from *Characterize Eruptive Processes at Yucca Mountain, Nevada* (SNL 2007 [DIRS 174260], Table 7-1) support analyses resulting in parameter distributions that are used in analyses that support the TSPA (e.g., conduit diameter in SNL 2007 [DIRS 177432], Table 4-1) or support the conceptual model implemented in the TSPA (e.g., magma chemistry).

Atmospheric Dispersal and Deposition of Tephra from a Potential Volcanic Eruption at Yucca Mountain, Nevada (SNL 2007 [DIRS 177431], Table 6-3) lists parameters used to implement this FEP within the TSPA. The technical bases developed within that report (SNL 2007 [DIRS 177431], Section 6.5.2) include, but are not limited to, the following parameters:

- Eruptive power and eruption duration
- Column diffusion constant, which affects the distribution of particles within the tephra column
- Waste incorporation ratio, a mathematical construct used to transport a density-corrected "combined" tephra and fuel particle
- Waste particle size (min, max, mode)
- Maximum particle diameter for transport
- Wind speed and wind direction, based on site-specific data collected over the appropriate range of tephra column height
- Initial rise velocity of plume

- Eddy diffusivity constant, with the simplification made that particle diffusion time equals particle fall time
- Magma partitioning factor
- Model grid parameters.

Atmospheric transport of the tephra–waste mixture is modeled directly in TSPA using ASHPLUME, the atmospheric tephra dispersal model. The model is based on assumed incorporation and entrainment of waste fuel particles associated with a volcanic eruption through the Yucca Mountain repository, and it evaluates downwind transport of contaminated tephra and radioactive waste and their deposition on the ground surface. The ASHPLUME model for Yucca Mountain is based on a model of Suzuki (1983 [DIRS 100489]) that Jarzemba et al. (1997 [DIRS 100987]) refined to represent the entrainment of radioactive waste in the convective eruptive plume associated with violent Strombolian eruptions. The ASHPLUME model is implemented in TSPA as a DLL, ASHPLUME_DLL_LA V2.1 (2006 [DIRS 178870], STN: 11117-2.1-00). Values for the 36 ASHPLUME input parameters are provided as constants, stochastic ranges, or tables. The TSPA model for atmospheric dispersal and deposition of waste-containing tephra uses a parameter that acts as a fractional multiplier on the mass of waste available for transport and accounts for the waste-containing magma that would form lava flows and scoria cones and would therefore not be available for atmospheric transport. This "magma partitioning factor" is provided as a range (0.1 to 0.5, uniform; see SNL 2007 [DIRS 177431], Table 8-2). In a given TSPA realization, the initial value of total waste mass available for transport derived from sampling the number of waste packages hit (SNL 2007 [DIRS 177432], Table 7-1) is multiplied by the magma partitioning factor to produce a value for the input parameter, "mass of waste available for transport."

Volcanic tephra is the source of inhalation dose during a volcanic eruption and all-pathway dose following the tephra fallout (SNL 2007 [DIRS 177399], Sections 6.3.2 and 6.15.2). The TSPA model, using ASHPLUME, estimates concentrations of radioactive waste in tephra falling at and redistributed to the location of the RMEI, based on incorporation of the waste into the volcanic tephra, the eruption of the tephra plume into the atmosphere, and the atmospheric transport and deposition of the tephra and entrained waste. Redistribution of waste-containing tephra from the Fortymile Wash watershed to the RMEI area via fluvial processes is calculated in TSPA using the FAR (Fortymile wash Ash Redistribution) V1.2 code ([DIRS 182225]) (SNL 2007 [DIRS 179347]). Radionuclides in the contaminated volcanic tephra may be inhaled, incorporated into the food chain, or may result in external radiation doses. The effects of inhalation of radioactive waste-containing volcanic tephra during a tephra fallout event are evaluated separately from the annual all-pathway doses resulting from tephra deposition and redistribution to the compliance location. The former are evaluated for inclusion in the TSPA model using the inhalation dose factors. The latter are incorporated in the TSPA through the use of volcanic ash exposure scenario BDCFs. BDCFs include inhalation exposure to resuspended tephra and contaminated soil, external exposure, and ingestion exposure, and are calculated on the annual basis, regardless of the actual eruption time and day (SNL 2007 [DIRS 177399], Section 6.5). The eruption phase is treated separately from the effects of deposition of contaminated tephra. Its consequences are evaluated as those arising from the exposure occurring during an event of a limited duration (acute or near-acute exposure), rather than from a

long-term, chronic exposure thereafter. The inhalation dose factors are used in TSPA assessments to evaluate whether the doses received by the RMEI during an eruption need to be included in calculation of the expected dose (SNL 2007 [DIRS 177399], Section 6.15.2).

Surface soil contaminated by the deposition or redistribution of radioactive waste-containing volcanic tephra is the initial source of radionuclides in the reference biosphere under the volcanic ash exposure scenario (SNL 2007 [DIRS 177399], Sections 6.1.3, 6.3.2, and 6.5). In the biosphere model, this source is represented by the quantity of radionuclide concentration in volcanic tephra deposited on the ground per unit surface area of the surface soil and per unit mass of the resuspendable layer of the surface soil. In the mathematical model, this FEP is directly addressed in the soil and air submodels (SNL 2007 [DIRS 177399], Table 6.7-1) through the use of the following model input parameters: mass loading for crops (BSC 2006 [DIRS 177101], Sections 6.2.5 and 6.3.5), soil-to-plant transfer factor (BSC 2004 [DIRS 169672], Sections 6.2.1.2 to 6.2.1.5), mass loading for receptor environments (BSC 2006 [DIRS 177101], Section 6.3), and mass loading time decay function (BSC 2006 [DIRS 177101], Section 6.4). It is also considered in developing inhalation dose factors (SNL 2007 [DIRS 177399], Section 6.15.2).

Because variations in radionuclide concentrations in the soil contaminated by the deposited and redistributed volcanic tephra are not part of the biosphere model, BDCFs are calculated based on a unit radionuclide concentration in the surface soil (SNL 2007 [DIRS 177399], Section 6.5). Initial ashfall depth is considered in development of the atmospheric mass loading parameters (BSC 2006 [DIRS 177101], Sections 6.3 and 6.4). The TSPA model calculates annual radiation dose as a product of the time-dependent source terms, the source-independent BDCF components, and the mass loading time decrease function. For the volcanic ash exposure scenario, three BDCF components are provided as inputs to the TSPA model. The first component accounts for exposure to sources external to the body, ingestion, and inhalation of radon decay products. The second and third BDCF components (the short-term and long-term inhalation components) account for inhaling airborne particulates. The short-term inhalation component is numerically equal to the inhalation exposure during the first year following a volcanic eruption. This term is used together with the time function to calculate short-term increase in inhalation exposure. This increase is due to elevated levels of airborne particulate matter after a volcanic eruption and is calculated relative to the conditions existing before and long after an eruption. With time, particulate concentration in air returns to the pre-eruption level. These conditions are described by the long-term inhalation component, which represents long-term inhalation of resuspended particulates under nominal conditions (i.e., when the mass loading is not elevated as the result of volcanic eruption) (SNL 2007 [DIRS 177399], Section 6.12.3). As noted above, FEP 1.2.04.07.0A (Ashfall) is also considered in the inhalation dose factors (SNL 2007 [DIRS 177399], Section 6.15.2), which are used to evaluate the dose contribution of inhalation of particulate matter during an ashfall for inclusion in the TSPA.

INPUTS:

Table 1.2.04.07.0A-1. Indirect Inputs

Citation	Title	DIRS
10 CFR 63	Energy: Disposal of High-Level Radioactive Wastes in a Geologic Repository at Yucca Mountain, Nevada	180319
70 FR 53313	Implementation of a Dose Standard After 10,000 Years	178394
ASHPLUME_DLL_LA V. 2.1	Windows 2000/XP. STN: 11117-2.1-00.	178870
BSC 2004	*Characterize Framework for Igneous Activity at Yucca Mountain, Nevada*	169989
BSC 2004	*Environmental Transport Input Parameters for the Biosphere Model*	169672
BSC 2006	*Inhalation Exposure Input Parameters for the Biosphere Model*	177101
FAR V 1.2	WINDOWS 2000 & WINDOWS 2003. STN: 11190-1.2-00.	182225
Jarzemba et al. 1997	*ASHPLUME Version 1.0—A Code for Contaminated Ash Dispersal and Deposition, Technical Description and User's Guide*	100987
SNL 2007	*Biosphere Model Report*	177399
SNL 2007	*Atmospheric Dispersal and Deposition of Tephra from a Potential Volcanic Eruption at Yucca Mountain, Nevada*	177431
SNL 2007	*Characterize Eruptive Processes at Yucca Mountain, Nevada*	174260
SNL 2007	*Number of Waste Packages Hit by Igneous Events*	177432
SNL 2007	*Redistribution of Tephra and Waste by Geomorphic Processes Following a Potential Volcanic Eruption at Yucca Mountain, Nevada*	179347
SNL 2008	*Total System Performance Assessment Model/Analysis for the License Application*	178871
Suzuki 1983	“A Theoretical Model for Dispersion of Tephra”	100489

FEP: 1.2.04.07.0B

FEP NAME:

Ash Redistribution in Groundwater

FEP DESCRIPTION:

Following deposition of contaminated ash on the surface, contaminants may leach out of the ash deposit and be transported through the subsurface to the compliance point.

SCREENING DECISION:

Excluded – low consequence

SCREENING JUSTIFICATION:

This FEP evaluates the effect of an eruption that intersects the repository, deposition of contaminated ash on the ground surface, leaching of the contaminants into the ground, and contamination of the groundwater. This FEP does not evaluate doses due to exposures from the contaminated ash above ground. Other FEPs related to exposure of the RMEI resulting from volcanic ash are included FEPs 1.2.04.07.0A (Ashfall), 1.2.04.07.0C (Ash Redistribution Via Soil and Sediment Transport), and 1.2.04.06.0A (Eruptive Conduit to Surface Intersects Repository) (SNL 2007 [DIRS 174260]; SNL 2007 [DIRS 177431]). The probability of the disruption of the repository by igneous activity (intersection of the repository by a basaltic dike) has a mean annual probability of 1.7×10^{-8} (BSC 2004 [DIRS 169989], Table 7.1). If igneous intrusion intersects the repository, there is an additional probability that the repository will be disrupted by an eruption as well. The probability that the repository will be disrupted by an eruption is the product of the annual probability of an igneous event intersecting the proposed repository and the probability of an eruptive conduit intersecting the repository footprint given an igneous event. The probability of an eruptive conduit being produced within the repository footprint is 0.28 (SNL 2007 [DIRS 177432], Table 7-1). This results in an annual frequency of occurrence of about 4.8×10^{-9}. This FEP is not excluded based on a probability justification because eruptive events are included in TSPA (consistency is maintained).

The modeling of igneous intrusion (SNL 2008 [DIRS 183478], Section 6.5.1) describes the consequences of magma that intrudes into repository emplacement drifts, damages waste packages in the intruded drifts, and solidifies. Because the flow characteristics of the magma could cause it to intrude into every drift within the repository, every waste package and drip shield in the repository is assumed to be incapable of protecting its contents. Conceptually, the engineered features are treated in TSPA as if they were no longer present, leaving radionuclides available for transport through normal dissolution processes when seepage re-enters the drift.

For the modeling of volcanic eruption (SNL 2008 [DIRS 183478], Section 6.5.2), the mass of waste incorporated in the tephra plume from an eruptive event depends on the waste inventory, the number of waste packages intersected, and the fraction of waste-containing magma that is erupted as a tephra plume instead of as a lava flow or deposited as a scoria cone. There is a 72% probability that no waste packages will be hit by a volcanic eruption intersecting the repository.

In the 28% of cases where one or more packages is hit, the number of waste packages hit ranges from one to seven with a median of four (SNL 2007 [DIRS 177432], Section 7.1).

The modeling of volcanic eruption (SNL 2008 [DIRS 183478], Section 6.5.2) considers the mass of waste in the waste packages that are hit, and the proportions of each kind of waste released from the repository to the erupting volcanic magma. The mass of waste hit is multiplied by the magma partitioning factor to account for the partitioning of magma into surface lava flows, scoria cone, and tephra plume. The magma partitioning factor is specified as a uniform distribution from 0.1 to 0.5 and represents the fraction of magma that is erupted into the tephra plume to be considered when modeling volcanic eruption (SNL 2007 [DIRS 177431], Table 8-2).

Because the number of packages entrained in an eruption is very small (seven or less) compared to the number of packages damaged by intrusion (all waste packages in the repository), and not every intrusive event is accompanied by an eruptive event, the TSPA simplifies the analysis and overestimates the consequences of intrusive events by not reducing the inventory released by intrusions by the amount that could be released by an associated eruption (SNL 2008 [DIRS 183478], Section 6.1.3). Thus, the consequences of any radionuclides that could leach out of the ash deposit and be transported in groundwater through the subsurface to the compliance point are bounded by the consequences of igneous intrusion, for which the radionuclide inventory from all packages (including those which might be included in an eruption) are available for transport in groundwater.

This conclusion is based on the observation that the simulated consequences of releases from any given number of waste packages (e.g., seven) should igneous intrusion occur are greater than the potential consequences of radionuclides that might enter the groundwater by leaching from the same number of packages (e.g., seven) involved in a volcanic eruption. This is reasonable given the following considerations: (1) all of the waste in the packages that would be subject to eruptive release is included in the release resulting from intrusion, but up to half of that waste would be released due to the magma partitioning factor (SNL 2007 [DIRS 177431], Section 6.5.2.9); and (2) not all of the waste that is erupted would fall on the land surface above the saturated zone flow pathways between the repository and the accessible environment. Consequently, not all of the waste would be available for leaching of radionuclides back to the water table for subsequent migration to the RMEI. Furthermore, as discussed above, the probability of eruptive events intersecting the repository is less than the probability of intrusion. The transport pathways and mechanisms for radionuclides leached from ash close to the vent, which is the large majority of the radionuclides included in the eruption (SNL 2007 [DIRS 177431], Section 6.5.2.9), are generally similar to those from the exposure to seepage following igneous intrusion, including downward migration through the unsaturated zone followed by lateral transport in the saturated zone. Thus, the probability-weighted consequences of leaching from ash would be less than the probability-weighted consequences of exposing the same number of waste packages to direct seepage.

Overall, this FEP is excluded on low consequence because the consequences associated with leaching of radionuclides from the basis of an ashfall into groundwater are small compared with the consequences of directly exposing the same inventory of radionuclides to seepage following igneous intrusion. The latter pathway is explicitly modeled in the TSPA and there could be no

additional increment to the total mean annual dose to the RMEI if the leaching pathway to groundwater from ashfall was included in the TSPA.

Based on the previous discussion, omission of FEP 1.2.04.07.0B (Ash Redistribution in Groundwater) will not result in a significant adverse change in the magnitude or timing of either radiological exposures to the RMEI or radionuclide releases to the accessible environment. Therefore, this FEP is excluded from the performance assessments conducted to demonstrate compliance with proposed 10 CFR 63.311 and 63.321 (70 FR 53313 [DIRS 178394]), and with 10 CFR 63.331 [DIRS 180319], on the basis of low consequence.

INPUTS:

Table 1.2.04.07.0B-1. Direct Inputs

Input	Source	Description
BSC 2004. *Characterize Framework for Igneous Activity at Yucca Mountain, Nevada*. [DIRS 169989]	Table 7.1	Probability of the disruption of the repository by igneous activity (intersection of the repository by a basaltic dike)
SNL 2007. *Atmospheric Dispersal and Deposition of Tephra from a Potential Volcanic Eruption at Yucca Mountain, Nevada*. [DIRS 177431]	Table 8-2	The magma partitioning factor is specified as a uniform distribution
SNL 2007. *Number of Waste Packages Hit by Igneous Events*. [DIRS 177432]	Table 7.1	There is approximately a 70% probability that no waste packages will be hit by a volcanic eruption intersecting the repository. In the approximately 30% of cases in which one or more packages are hit, the most likely number hit is four and the maximum
	Table 7.1	Probability of an eruptive conduit being produced within the repository footprint is 0.28

Table 1.2.04.07.0B-2. Indirect Inputs

Citation	Title	DIRS
10 CFR 63	Energy: Disposal of High-Level Radioactive Wastes in a Geologic Repository at Yucca Mountain, Nevada	180319
70 FR 53313	Implementation of a Dose Standard After 10,000 Years	178394
SNL 2007	*Atmospheric Dispersal and Deposition of Tephra from a Potential Volcanic Eruption at Yucca Mountain, Nevada*	177431
SNL 2007	*Characterize Eruptive Processes at Yucca Mountain, Nevada*	174260
SNL 2008	*Total System Performance Assessment Model/Analysis for the License Application*	183478

FEP: 1.2.04.07.0C

FEP NAME:

Ash Redistribution via Soil and Sediment Transport

FEP DESCRIPTION:

Following deposition of contaminated ash on the surface, ash deposits may be redistributed on the surface via aeolian and fluvial processes.

SCREENING DECISION:

Included

TSPA DISPOSITION:

Ashfall is included in the performance assessment to demonstrate compliance with the individual protection standard after permanent closure (proposed 10 CFR 63.311 (70 FR 53313 [DIRS 178394])) and is addressed through the modeling of an eruption that includes airborne transport of waste-contaminated tephra (ash) and subsequent deposition of the tephra on the land surface. (The preferred term "tephra" refers to pyroclasts resulting from a volcanic eruption, regardless of size, in contrast to the term "ash" which technically refers only to pyroclasts less than 2 mm in diameter. Both terms are used in the discussion of this FEP.) Ashfall and associated aerial dispersal of contaminated tephra is addressed in included FEP 1.2.04.07.0A (Ashfall), and ashfall characteristics are discussed in detail in *Atmospheric Dispersal and Deposition of Tephra from a Potential Volcanic Eruption at Yucca Mountain, Nevada* (SNL 2007 [DIRS 177431]). In addition to the initial ashfall, the performance assessment also includes consideration of exposure from contaminated tephra that could be redistributed to the RMEI location from other locations by sediment transport processes.

As discussed in included FEP 1.2.04.03.0A (Igneous Intrusion into Repository), disruptive igneous events are not included in performance assessments to demonstrate compliance with the groundwater protection standards (10 CFR 63.331 [DIRS 180319]) and the individual protection standard for human intrusion (proposed 10 CFR 63.321 (70 FR 53313 [DIRS 178394])) because they are unlikely events. The exclusion of this FEP from the groundwater protection and human intrusion performance assessments is consistent with the requirements of proposed 10 CFR 63.342(b) and (c)(1) (70 FR 53313 [DIRS 178394]).

The technical basis for inclusion of FEP 1.2.04.07.0C (Ash Redistribution via Soil and Sediment Transport) in the performance assessment relies on analysis results presented in *Characterize Framework for Igneous Activity at Yucca Mountain, Nevada* (BSC 2004 [DIRS 169989], Table 7-1). The volcanic hazard is the annual frequency of intersection of the repository by a volcanic dike. The annual frequency of an igneous event ranges from approximately 7.4×10^{-10} to 5.5×10^{-8} for the 5th and 95th percentiles, respectively, with a mean annual frequency of 1.7×10^{-8} (BSC 2004 [DIRS 169989], Table 7-1). Since the mean annual frequency of intersection is greater than the screening criterion value (1 in 10,000 in 10,000 years; proposed 10 CFR 63.342(a) (70 FR 53313 [DIRS 178394])) an igneous event must be included in the

performance assessment, and the consequences of such an event must be evaluated. This FEP deals with one possible consequence of such an event, transfer of contaminated tephra to the RMEI location by sediment transport processes.

Eruptions involving the intersection of an eruptive conduit with the repository could result in the atmospheric dispersal of waste-contaminated tephra and subsequent deposition on the ground surface. The quantity of waste ejected into the atmosphere in any one eruption would depend on many factors, such as the volume and power of the volcanic eruption, the distribution of waste packages in the emplacement drifts, the location, number, and size of eruptive conduits intersecting the drifts, the degree of damage to the waste packages, the amount of waste from the waste packages that is entrained into the erupting material, and the fraction of magma that is erupted into the atmosphere (SNL 2007 [DIRS 177432], Section 6.3.2.2; SNL 2007 [DIRS 177431], Table 6-3).

Waste-contaminated tephra that has been deposited on the ground surface in the Fortymile Wash drainage basin by atmospheric transport immediately following the eruption could potentially be redistributed to the RMEI location by a combination of eolian and fluvial processes.

Based on the results of analogue studies, eolian transport of contaminated tephra to the RMEI location is assumed to be negligible when compared to the potential for fluvial transport. The basis for the assumption is described in *Redistribution of Tephra and Waste by Geomorphic Processes Following a Potential Volcanic Eruption at Yucca Mountain, Nevada* (SNL 2007 [DIRS 179347], Section 5.2.2). The prevailing wind direction at the RMEI location is generally to the north toward Yucca Mountain. Significant eolian transport from Yucca Mountain to the RMEI location is therefore precluded. Other more complicated pathways are considered insignificant when compared to the potential magnitude of fluvial transport. For example, fine material may be transported as suspended load in Fortymile Wash during large floods and deposited in Franklin Lake Playa, a significant depozone for such material in this region. Following deposition in the playa, some of the fine material is remobilized by eolian processes, and examples of this process have been described. Studies show that thicknesses of eolian deposits on interchannel divides 1 to 2 km downwind (north) of Franklin Lake Playa are 0.5 to 3 cm on early Holocene to late Pleistocene surfaces. This range of thicknesses results in an estimated eolian deposition rate on the order of only 1 cm/10 kyr north of Franklin Lake Playa, and this rate is considered to be a maximum rate for deposition at the RMEI location because Franklin Lake Playa is one of the most emissive playas in the western United States, and Franklin Lake Playa is about 30 km upwind from the RMEI location. Another eolian mechanism involves contaminated tephra that is transported to the RMEI location as bedload, blown out of the channels, and deposited on the interchannel divides. Several sand streaks from this process are visible in aerial photos of the alluvial fan that represents the RMEI location. The deposition is localized to narrow margins along active channels that extend only 10 to 20 m from the active channels (SNL 2007 [DIRS 179347], Section 5.2.2). The relatively limited extent of the sand streaks indicates that their contribution to the amount of material redistributed to interchannel divides by eolian processes would not be significant.

For the other (non-eolian) components, the conceptual model for tephra redistribution includes hillslope, fluvial, and diffusion processes that address: (1) mobilization of tephra from hillslopes; (2) mixing and dilution with uncontaminated sediments during channel transport; and

(3) diffusion of radionuclides into the soil column at the RMEI location. A detailed description of the tephra redistribution conceptual model can be found in *Redistribution of Tephra and Waste by Geomorphic Processes Following a Potential Volcanic Eruption at Yucca Mountain, Nevada* (SNL 2007 [DIRS 179347], Section 6.2).

The conceptual tephra redistribution model divides the Fortymile Wash drainage area into two domains: the drainage basin and the alluvial fan (SNL 2007 [DIRS 179347], Section 6.2). The drainage basin includes the vent location and the tephra and waste deposited on the landscape following a hypothetical volcanic eruption through the repository. The RMEI location is on the Fortymile Wash alluvial fan south of the fan apex. The drainage basin and the alluvial fan are divided at the fan apex.

The tephra redistribution model uses a spatially distributed analysis of hillslopes and channels in the drainage basin upstream of the fan apex to provide an estimate of the mass of tephra and waste that could be transported from the upper drainage basin to the RMEI location by hillslope and fluvial processes (SNL 2007 [DIRS 179347], Section 6.2). The model mobilizes and transports tephra and waste deposited on steep slopes or in active channels that connect to the main Fortymile Wash channel. Before the mobilized tephra and waste are deposited at the RMEI location, they are transported through the alluvial channel system where mixing with uncontaminated channel sediments leads to dilution. Mixing occurs during flood events as sediment and tephra are entrained from the bed, mixed by turbulent flow, and redeposited on the bed. The depth to which tephra and channel sediment are mixed is the scour depth. A divergent flow-routing algorithm is used to estimate the tephra (and waste) concentration in the bedload sediments at the fan apex (SNL 2007 [DIRS 179347], Section 6.3).

The tephra and waste transported from the upper drainage basin and primary tephra and waste deposited at the RMEI location provide the initial conditions for redistribution of radionuclides within the soil column at the RMEI location (SNL 2007 [DIRS 179347], Section 6.3.3, Step 6). The tephra redistribution model represents the migration of radionuclides within the soil at the RMEI location with a one-dimensional diffusion model. The actual mechanisms that lead to vertical radionuclide migration include suspension and redeposition of fine particles by infiltration, and physical mixing of soil particles by freeze/thaw cycles and bioturbation. Studies have shown that the resulting radionuclide concentration profiles can be represented as a diffusion process in a variety of climate and soil environments. The time-dependent average concentration within a depth interval resulting from the diffusion process is used by the volcanic ash exposure submodel (SNL 2007 [DIRS 177399], Section 6.3.2) to calculate dose to the RMEI.

FEP 1.2.04.07.0C (Ash Redistribution via Soil and Sediment Transport) is implemented for performance assessment using the computer code FAR V.1.2 ([DIRS 182225], STN: 11190-1.2-00). The FAR V.1.2 code is implemented as a DLL and is incorporated directly within the TSPA computational structure. The mathematical description of the FAR V.1.2 code is provided in *Redistribution of Tephra and Waste by Geomorphic Processes Following a Potential Volcanic Eruption at Yucca Mountain, Nevada* (SNL 2007 [DIRS 179347], Section 6.3.3).

INPUTS:

Table 1.2.04.07.0C-1. Indirect Inputs

Citation	Title	DIRS
10 CFR 63	Energy: Disposal of High-Level Radioactive Wastes in a Geologic Repository at Yucca Mountain, Nevada	180319
70 FR 53313	Implementation of a Dose Standard After 10,000 Years	178394
BSC 2004	*Characterize Framework for Igneous Activity at Yucca Mountain, Nevada*	169989
FAR V 1.2.	WINDOWS 2000 & WINDOWS 2003. STN: 11190-1.2-00.	182225
SNL 2007	*Biosphere Model Report*	177399
SNL 2007	*Atmospheric Dispersal and Deposition of Tephra from a Potential Volcanic Eruption at Yucca Mountain, Nevada*	177431
SNL 2007	*Number of Waste Packages Hit by Igneous Events*	177432
SNL 2007	*Redistribution of Tephra and Waste by Geomorphic Processes Following a Potential Volcanic Eruption at Yucca Mountain, Nevada*	179347

FEP: 1.2.05.00.0A

FEP NAME:

Metamorphism

FEP DESCRIPTION:

If it occurs, metamorphism has the potential to affect the long-term performance of the repository. Metamorphism is defined as solid state changes to rock properties and geologic structures by means of recrystallization through the effects of heat and/or pressure.

SCREENING DECISION:

Excluded – low consequence

SCREENING JUSTIFICATION:

This justification will address regional and contact metamorphism. Regional metamorphism refers to the processes by which rocks are changed through the effects of heat and pressure at depths of a few kilometers beneath the surface of the earth. Metamorphism may also occur in conjunction with intrusive igneous activity (referred to as contact metamorphism). Changes in sediments and rocks at lower temperatures and pressures are referred to as diagenesis (see excluded FEP 1.2.08.00.0A (Diagenesis); see also Bates and Jackson (1984 [DIRS 128109], pp. 137 and 322; and Berry and Mason 1959 [DIRS 135236], p. 240 for additional definitions).

Conditions conducive to the onset of regional metamorphism correspond to temperatures of 150°C to 200°C and pressures of 0.5 to 1 kilobars, which occur at depths of 4 to 5 km (Ehlers and Blatt 1972 [DIRS 167802], p. 566). The geothermal gradient at convergent plate boundaries may range from less than 10°C per km to greater than 25°C per km (Ehlers and Blatt 1982 [DIRS 167802], pp. 684 and 685), while at Yucca Mountain, which lies in an extensional terrain, the geothermal gradient, as measured in 300- to 600-m-deep boreholes, is approximately 30°C/km (Sass et al. 1988 [DIRS 100644], p. 35). These measurements at Yucca Mountain are consistent with the occurrence of regional metamorphism at depths of 4 to 5 km as described by Ehlers and Blatt (1972 [DIRS 167802], p. 566). The potential for regional metamorphism at Yucca Mountain depends on regional-scale tectonic deformation and, therefore, the strain accumulation rates and slip rates. The rate of subsidence (vertical movement leading to deep burial) is controlled by movement along fault-bounded blocks. Savage et al. (1999 [DIRS 118952], p. 17,627) presented an evaluation of the strain accumulation rate at Yucca Mountain during 1983 to 1998, indicating that the strain rate in the Yucca Mountain area is low, equivalent to 2 nanostrain/yr. Savage et al. (1999 [DIRS 118952], p. 17,627) also addressed alternative interpretations indicating higher strain rates on the order of 50 nanostrain/yr (Wernicke et al. 1998 [DIRS 103485]). Regardless of which strain rate is used, the result has been cumulative fault slip rates at Bare Mountain and Yucca Mountain of 0.001 to 0.05 mm/yr (BSC 2004 [DIRS 168030], Table 6). The higher slip rate of 0.05 mm/yr would result in a vertical movement of approximately 0.5 m in 10,000 years. Such vertical movement is insufficient to result in pressure and temperature conditions at the repository depth (minimum of 200 m (SNL 2007 [DIRS 179466], Table 4-1, Parameter Number 01-06) which would be

conducive to regional metamorphism, as this is well above the necessary depth of 4 to 5 km at which metamorphism may occur (Ehlers and Blatt 1972 [DIRS 167802], p. 566). Additionally, the locus of any regional subsidence has moved to the southwest corner of the Crater Flat basin, away from Yucca Mountain (Fridrich 1999 [DIRS 118942], p. 189). Transport simulations of particles released at the repository show that transport occurs south-southeast of Yucca Mountain a few hundred meters to a kilometer (DTN: SN0704T0510106.008 [DIRS 181283], file: *sz06-1000.sptr2*) below the surface, considerably removed from the region where regional metamorphism is possible. Thus, any effects from regional metamorphism would be inconsequential on flow and transport and dose to the RMEI.

Contact metamorphism results from the thermal interaction between an intruding body of magma and the surrounding rock. Contact metamorphism is more fully addressed as part of excluded FEP 1.2.04.02.0A (Igneous Activity Changes Rock Properties), which gives a detailed justification for a low-consequence exclusion of all effects on rock properties by igneous activity, including dikes. To summarize some important points from excluded FEP 1.2.04.02.0A (Igneous Activity Changes Rock Properties), dikes at Yucca Mountain are typically 1 to 12 m in width (SNL 2007 [DIRS 174260], Section 6.3.3.1) and tend to be variably continuous along strikes, parallel or subparallel to the direction of maximum principal transmissivity. The resulting effects of dike intrusion may be to increase, decrease, or not change permeabilities as compared to the host (unaffected) rock. The scale at which permeabilities would change is limited to a few meters around the dike (Valentine and Krogh 2006 [DIRS 177282], p. 221). The dike widths and associated volume of metamorphized rock described above are small relative to the 30 km width of the saturated zone flow domain and the 1- to 5-km width and depth of the region in which radionuclide transport occurs near the repository (DTN: SN0704T0510106.008 [DIRS 181283], file: *sz06-1000.sptr2*). The predicted width over which radionuclide transport occurs is in excess of hundreds of meters (SNL 2008 [DIRS 184806, as inferred from Figure 6.5-2), and the distance downgradient over which transport occurs to the RMEI is at least 18 km. Given the small scale of the affected rock and its alignment relative to the direction of principal transmissivity, the effect of local metamorphism on flow and transport in the saturated zone is negligible.

If contact metamorphism occurs, it might affect infiltration through the unsaturated zone to the repository. Average infiltration to the repository is principally limited by surface precipitation and evapotranspiration. Computations show that the average flux flowing to the repository is within 3% of the average flux specified at the ground surface over the projected repository area (SNL 2007 [DIRS 184614], Section 6.1.4). The UZ flow model results show that flow is principally through the fractured rock mass rather than faults in the TCw, PTn, and TSw hydrologic units (SNL 2007 [DIRS 184614], Tables 6.6-1 and 6.6-2) above the repository. Flow is modeled as isothermal and steady below the highly porous nonwelded PTn unit since it is relatively unfractured. Dike penetration and contact metamorphism of this unit could change the timing and spatial distribution of infiltration pulses to the repository, but the scale of the rock affected by contact metamorphism is much smaller than the repository footprint and the average infiltration is controlled by surface processes, so the effects would not be significant.

UZ Flow Models and Submodels (SNL 2007 [DIRS 184614], Section 6.6.2.2) states that in the northern half of the Yucca Mountain domain below the repository, flow is focused significantly into major faults. Over the entire model, the percentage flow in major faults increases with depth, beginning at 12% to 32% at the repository horizon and reaching 44% to 65% at the water table

(SNL 2007 [DIRS 184614], Section 6.6.2.3). The narrow, tabular dikes observed in the Yucca Mountain region (SNL 2007 [DIRS 174260], Section 6.3.3.1) are similar, geometrically, to faults. Furthermore, dikes in the region are often found occupying faults (SNL 2007 [DIRS 174260], p. 6-18). Thus, the effects of contact metamorphism in this area would not be significant since flow and transport is already dominated by major faults. Finally, we note that the radionuclide travel time through the 300 meter zone between the repository and the water table (SNL 2008 [DIRS 184433], Section 5.1.5) is a very small component of the total travel time through the entire 18 km distance to the RMEI, so that even if contact metamorphism introduced a major change in the unsaturated zone below the repository, the effect over the entire flow and transport domain would be insignificant.

In summary, regional metamorphism requires greatly increased pressure (generally resulting from burial on the order of kilometers) and increased temperatures (greater than 150°C to 200°C). Development of these conditions on a regional scale in the rocks surrounding the repository would require many millions of years at current rates of subsidence. Regional metamorphism during the next 10,000 years will be limited to rocks far below the repository and the associated groundwater flow system. Contact metamorphism, should it occur, would introduce changes to rock parameters at a scale that is insignificant with that of the overall scale of flow and transport to the RMEI. Based on the above discussion, omission of metamorphism will not result in a significant adverse change in the magnitude or time of radiological exposures to the RMEI or radionuclide releases to the accessible environment.

Based on the previous discussion, omission of FEP 1.2.05.00.0A (Metamorphism) will not result in a significant adverse change in the magnitude or timing of either radiological exposures to the RMEI or radiological releases to the accessible environment. Therefore, this FEP is excluded from the performance assessments conducted to demonstrate compliance with proposed 10 CFR 63.311 and 63.321 (70 FR 53313 [DIRS 178394]), and 10 CFR 63.331 [DIRS 180319], on the basis of low consequence.

INPUTS:

Table 1.2.05.00.0A-1. Direct Inputs

Input	Source	Description
BSC 2004. *Characterize Framework for Seismicity and Structural Deformation at Yucca Mountain, Nevada*. [DIRS 168030]	Table 6	Local cumulative fault slip rates
DTN: SN0704T0510106.008. Flux, Head and Particle Track Output from the Qualified, Calibrated Saturated Zone (SZ) Site-Scale Flow Model. [DIRS 181283]	file: *sz06-1000.sptr2*	Shallow transport of radionuclides
Ehlers and Blatt 1982. *Petrology, Igneous, Sedimentary, and Metamorphic*. [DIRS 167802]	pp. 684 to 685	The geothermal gradient at convergent plate boundaries may range from less than 10°C per km to greater than 25°C per km
	p. 566	Conditions conducive to the onset of regional metamorphism correspond to temperature of 150°C to 200°C and pressures of 0.5 to 1 kilobars, which occur at depths of 4 to 5 km

Table 1.2.05.00.0A-1. Direct Inputs (Continued)

Input	Source	Description
SNL 2007. *UZ Flow Models and Submodels*. [DIRS 184614]	Section 6.6.2.2	In the northern half of the Yucca Mountain domain below the repository, flow is focused significantly into major faults
	Section 6.6.2.3	Over the entire model, the percentage flow in major faults increases with depth, beginning at 12% to 32% at the repository horizon and reaching 44% to 65% at the water table
	Tables 6.6-1, 6.6-2	Flow in TCw, PTn, and TSw through rock mass not faults
	Section 6.1.4	Average flux at repository 3% average flux at surface
SNL 2007. *Total System Performance Assessment Data Input Package for Requirements Analysis for Subsurface Facilities*. [DIRS 179466]	Table 4-1, Parameter Number 01-06	Repository depth
SNL 2008. *Site-Scale Saturated Zone Transport*. [DIRS 184806]	Figure 6.5-2	Plume width hundreds of meters wide
Valentine and Krogh 2006. "Emplacement of Shallow Dikes and Sills Beneath a Small Basaltic Volcanic Center – The Role of Pre-Existing Structure (Paiute Ridge, Southern Nevada, USA)." [DIRS 177282]	p. 221	The resulting effects of dike intrusion may be to increase, decrease or not change permeabilities as compared to the host (unaffected) rock. The scale at which permeabilities would change is limited to a few meters around the dike

Table 1.2.05.00.0A-2. Indirect Inputs

Citation	Title	DIRS
10 CFR 63	Energy: Disposal of High-Level Radioactive Wastes in a Geologic Repository at Yucca Mountain, Nevada	180319
70 FR 53313	Implementation of a Dose Standard After 10,000 Years	178394
Bates and Jackson 1984	*Dictionary of Geological Terms*	128109
Berry and Mason 1959	*Mineralogy: Concepts, Descriptions, Determinations*	135236
Fridrich 1999	"Tectonic Evolution of the Crater Flat Basin, Yucca Mountain Region, Nevada"	118942
Sass et al. 1988	*Temperature, Thermal Conductivity, and Heat Flow Near Yucca Mountain, Nevada: Some Tectonic and Hydrologic Implications*	100644
Savage et al. 1999	"Strain Accumulation at Yucca Mountain, Nevada, 1983-1998"	118952
SNL 2007	*Characterize Eruptive Processes at Yucca Mountain, Nevada*	174260
SNL 2008	*Multiscale Thermohydrologic Model*	184433
Wernicke et al. 1998	"Anomalous Strain Accumulation in the Yucca Mountain Area, Nevada"	103485

FEP: 1.2.06.00.0A

FEP NAME:

Hydrothermal Activity

FEP DESCRIPTION:

Naturally occurring high-temperature groundwater may induce hydrothermal alteration of minerals in the rocks through which the high-temperature groundwater flows.

SCREENING DECISION:

Excluded – low consequence

SCREENING JUSTIFICATION:

Hydrothermal activity is the circulation and release of high-temperature water by a buried source of heat. The source of heat is either an igneous intrusion or a high thermal gradient associated with thinned and extending crust (Blackwell et al. 2000 [DIRS 183582], p. 1). Hydrothermal activity can result in mineral alteration that affects flow and transport characteristics of the rock.

Non-Magmatic Hydrothermal Activity

Hydrothermal activity associated with non-magmatic heat sources are common in the Basin and Range province (Blackwell et al. 2000 [DIRS 183582], p. 1), which includes almost all of Nevada and portions of other states (DOE 2002 [DIRS 155943], Figure 1-7). These hydrothermal systems have been found to be highly correlated to regional heat flow when that flow is in excess of 80 mW/m^2 (Blackwell et al. 2000 [DIRS 183582], Section 2.3). However, heat flux values within the Topopah Spring welded unit at Yucca Mountain in boreholes NRG-7a, UZ-7a, and SD-12 are about 37, 39, and 32 mW/m^2, respectively (Rousseau et al. 1997 [DIRS 100178], Section 5.2). This gives an average of 36 mW/m^2, and a standard deviation of 3.6 mW/m^2, substantially below a heat flow of 85 mW/m^2 characteristic of the Basin and Range province (Sass et al. 1988 [DIRS 100644], p. 3).

Any change that may result in the circulation of hydrothermal fluids below Yucca Mountain would not be able to drive significant temperature changes in the repository area over 10,000 years. Hydrothermal systems have been found to circulate to depths of at least 4 km (Blackwell et al. 2000 [DIRS 183582], Section 3.5) and high heat-flow areas of the Great Basin have heat flux rates in excess of 120 mW/m^2 (Flynn et al. 1996 [DIRS 112530], p. 11). The rock mass heat capacity is approximately 1,000 J/kg-K (BSC 2004 [DIRS 170003], Table 6-9) and the bulk rock density of approximately 2,000 kg/m^3 (SNL 2008 [DIRS 184748], Table 6-6). Assume that the heat flux increases by 200 mW/m^2 as a result of new deep circulation patterns. The time required to raise the temperature 10°C along the new circulation path is computed from the heat capacity multiplied by the bulk rock density, circulation path length of 4 km, and temperature change, divided by the increase in heat flux. This gives a time in excess of 10,000 years. These results are consistent with simulations of transient geothermal systems in the Basin and Range (McKenna and Blackwell 2003 [DIRS 185042], Figure 8). Drift wall temperatures are computed

to be about 25°C to 60°C at 10,000 years as a result of waste heat (SNL 2008 [DIRS 184433], Figure 6.3-76[a]). Measured ambient temperatures at repository elevations of 1,040 to 1,100 m (BSC 2007 [DIRS 183743], Table 1-5) are approximately 20°C to 25°C (SNL 2007 [DIRS 184614], Figures 6.3-2 to 6.3-6). Therefore, a temperature rise of 10°C at the water table over the 10,000-year period is expected to have a negligible influence on the repository environment because temperatures at the drift wall are about 20°C above ambient at 10,000 years as a result of waste heat. Therefore, the effects of temperatures changes associated with any future hydrothermal activity from a nonmagmatic heat source are expected to be negligible.

Hydrothermal Activity Associated with Magmatic Activity

The earliest volcanism in the Yucca Mountain region was dominated by a major episode of caldera-forming, silicic volcanism that occurred primarily between approximately 15 and 11 million years ago (Ma), forming the southwestern Nevada volcanic field (Sawyer et al. 1994 [DIRS 100075]). Yucca Mountain is an uplifted, erosional remnant of voluminous ash-flow tuff deposits formed during the early phase of silicic volcanism (BSC 2004 [DIRS 169989], Section 6.2). Silicic volcanism was approximately coincident with a major period of extension, which occurred primarily between 13 and 9 Ma (Sawyer et al. 1994 [DIRS 100075], Figure 4). The southwestern Nevada volcanic field ceased silicic eruptive activity about 7.5 Ma (BSC 2004 [DIRS 169989], Section 6.2). Basaltic volcanism within the Yucca Mountain region commenced during the latter part of the caldera-building phase, around 9 Ma, as extension rates waned. Postcaldera basaltic igneous activity within the Yucca Mountain region has been declining since about 7 Ma. Small-volume basaltic volcanism continued into the Quaternary (BSC 2004 [DIRS 169989], Section 6.2).

Since the cessation of silicic magmatism about 11.4 Ma, basaltic igneous activity has been characteristic of the Yucca Mountain region. Silicic volcanism during the regulatory period is therefore not expected (Reamer 1999 [DIRS 119693], p. 5). Although basaltic magmatism could occur during the 10,000-year regulatory period the effects of any related hydrothermal system would be of limited scale as described in excluded FEP 1.2.04.02.0A (Igneous Activity Changes Rock Properties). Due to the limited scale of effects from basaltic intrusions, the potential effects of hydrothermal alteration are negligible. With significant thermal perturbations limited to less than 100 years and alteration limited to zones on the order of a meter around a basaltic intrusion, the effects of basaltic magmatism on unsaturated zone transport pathways, advective velocities, and sorption coefficients (K_ds) are also considered to be negligible.

The focus of igneous-related FEPs is on the potential for small-scale basaltic volcanism to occur in the future. The mean probability of a basaltic dike intersecting the repository footprint has been calculated to be 1.7×10^{-8} per year (BSC 2004 [DIRS 169989], Table 7-1). The negligible difference in the north-south dimension of the repository footprint between the design in effect in 2003 and the current design (BSC 2007 [DIRS 179640]) would have a negligible effect on the frequency of intersection. If future igneous activity within the Crater Flat basin occurs, it is expected to take the form of basaltic dike-like intrusions with average widths on the order of one meter (CRWMS M&O 1996 [DIRS 100116], Section 3.2.3). Although intruding dikes could induce alteration of the in situ mineralogy adjacent to the intruded rock (i.e., the contact zone), the alteration in this contact zone is expected to be minimal. This assumption is supported by investigations at the Grants Ridge analogue site, which indicates that basaltic intrusion produced

only localized formation of volcanic glass within the contact zone (CRWMS M&O 1998 [DIRS 105347], Section 5, p. 74). Investigations of basaltic intrusions at Paiute Ridge (Carter Krogh and Valentine 1996 [DIRS 160928], pp. 7 to 8) suggest that igneous activities altered rock properties by decreasing permeability only out to a few tens of centimeters to, at most, a meter perpendicular to an intruding dike. The time scales for significant thermal perturbations from such intrusions are on the order of 100 years as discussed in excluded FEP 1.2.04.02.0A (Igneous Activity Changes Rock Properties). Given the small length and time scales associated with basaltic igneous activity in the region, any hydrothermal activity associated with basaltic intrusions is expected to be negligible.

Evidence Concerning Hydrothermal Activity in the Unsaturated Zone

Yucca Mountain is located outside the margin of the Timber Mountain caldera complex (BSC 2004 [DIRS 169989], Figure 6-1). The Timber Mountain magmatic activity represents the last significant heating event for Yucca Mountain (Whelan et al. 2006 [DIRS 179305]). The level of heating at Yucca Mountain associated with the Timber Mountain volcanic center (and its associated hydrothermal system) was relatively minor, with peak fluid inclusion homogenization temperatures near 90°C occurring at >9 Ma (BSC 2004 [DIRS 170004], Figure 6-199; Whelan et al. 2006 [DIRS 179305], Section 5.2.2 and Table 4). This heating event at Yucca Mountain did not result in pervasive hydrothermal alteration of the tuffs.

Studies of secondary minerals at Yucca Mountain using petrography, fluid-inclusion thermometry, and uranium-lead dating indicate that temperatures have remained close to the current ambient values over the past 2 to 5 Ma (Wilson et al. 2003 [DIRS 163589], Section 8). Mineral coatings composed primarily of calcite, opal, chalcedony, and quartz provide evidence of the thermal-hydrothermal history of Yucca Mountain. The minerals were deposited under unsaturated conditions as evidenced by the fact that they are found only on fracture footwalls and lithophysal cavity bottoms (Marshall and Whelan 2000 [DIRS 154415]). Various lines of evidence, including (1) stable oxygen isotope data of calcite, which indicates the temperature of mineral precipitation; (2) homogenization temperatures of fluid inclusions, which indicate the temperature at which the inclusions were trapped; and, (3) uranium and lead isotope ratios in opal associated with the calcite (Neymark et al. 2003 [DIRS 163681]), which constrain the age of deposited minerals, altogether suggest that temperatures in the unsaturated zone decreased over time from approximately 90°C at >10 Ma to near ambient temperatures at 2 Ma. These secondary minerals were interpreted to have been deposited from downward percolating meteoric water and not the result of upwelling groundwaters (Wilson et al. 2003 [DIRS 163589], Sections 7.3 and 8; Whelan et al. 2003 [DIRS 163590]; National Research Council 1992 [DIRS 105162], p. 3).

Additional evidence of elevated paleotemperatures at Yucca Mountain may be provided by observations of thick-twinned calcite samples in discrete narrow faults (2 to 20 cm) (Gray et al. 2000 [DIRS 171202]). Thick-twinned calcite was interpreted to indicate deformation at temperature above 170°C (Ferrill et al. 2004 [DIRS 171196]), which is higher than the temperatures indicated by calcite fluid inclusions reported by Whelan et al. (2003 [DIRS 163590]) and Wilson et al. (2003 [DIRS 163589], Section 8). If the higher temperatures indicated by thick twins (which have not been confirmed by studies of fluid inclusions in the same samples) are correct, they may indicate that the twinned calcite was formed during an

early, higher-temperature event. It is expected that such temperatures would have occurred shortly after emplacement of the ash-flow tuff deposits at Yucca Mountain, when degassing and cooling of the ash-flow tuff could have resulted in devitrification, vapor-phase alteration, and development of localized meteoric-hydrothermal activity in the upper parts of ash-flow sheets (Holt 2002 [DIRS 162326]). Gray et al. (2000 [DIRS 171202]) note that the calcite mineralization observed in the narrow faults is not encountered in the intrablock and block-bounding faults, which would be good candidates for fluid flow and mineralization in the event of widespread hydrothermal alteration. The absence of pervasive hydrothermal mineralization of the Yucca Mountain tuffs is consistent with the interpretation that large-scale hydrothermal activity has not occurred in the Yucca Mountain area.

Evaluation of Unsaturated Zone Thermal History at Yucca Mountain

Whelan et al. (2006 [DIRS 179305]) present a conceptual model of heat transfer from the Timber Mountain magma chamber to explain the temperature history of Yucca Mountain that was inferred from geological evidence. The conceptual model is implemented in a computational analysis of the thermal history of Yucca Mountain (Whelan et al. 2006 [DIRS 179305], Section 6.3). This analysis expands upon a previous analysis presented by Marshall and Whelan (2001 [DIRS 171061]). The model used a 7-km thick, 30-km diameter, 5,000 km^3 magma chamber at depths of 5 or 2.5 km from the top of the magma chamber to the ground surface (shallower depth yields faster cooling of the magma). In the model, the diameter of the magma chamber is spatially restricted to the caldera margin. The magma chamber was filled at 12.8 Ma, corresponding to the Paintbrush Group eruptions, and again at 11.6 Ma, corresponding to the Timber Mountain Group eruptions. The depth of the magma chamber is highly uncertain, hence, the use of two distinct values. Heat transfer by conduction and hydrothermal convection are represented in the model; convection was limited to shallower zones between 10 Ma and 8 Ma. Predicted temperatures are generally representative of the observed thermal history given the large uncertainty in the timing of many of the observations. Certain aspects of the observations, in particular the maximum temperature at the base of borehole G-2 and deposition temperatures of early/intermediate stage secondary minerals at the top of the TSw, appear to be underestimated by the model. However, uncertainties concerning the volume and extent of the magma chamber could explain the differences in the maximum temperature at borehole G-2. Preliminary results incorporating the additional process of vapor-phase convection appears to explain the higher temperature, early/intermediate stage secondary minerals at the top of the TSw (Whelan et al. 2006 [DIRS 179305], Section 6.3). Similarly, high-temperature, secondary mineral deposition observations in the TCw, just tens of meters below the surface, appear to be consistent with shallow-rooted fumarolic systems (Whelan et al. 2006 [DIRS 179305], Section 6.2).

The spatial and temporal extents of magmatic activity of the Timber Mountain system are significant uncertainties in the model. While only minor volcanic activity is associated with Timber Mountain after 11.4 Ma, it is possible that the system received continued injections of mantle-derived mafic magmas that would have provided additional heating to the region (Farmer et al. 1991 [DIRS 153024]). Continuing silicic volcanism at the Black Mountain caldera (9.4 Ma) and Stonewall Mountain volcanic center (7.5 Ma), both located northwest of the Timber Mountain caldera, indicates that regional silicic magmatism and associated heating persisted beyond 11 Ma (Sawyer et al. 1994 [DIRS 100075]). The size of the magma chamber

may be underestimated given the uncertainties in the size of the magma chamber relative to the erupted volume. Furthermore, the lateral extent of the magma chamber relative to the Timber Mountain caldera margin may also be underestimated based on comparison with analogous spatial relationships in the Yellowstone volcanic system (Whelan et al. 2006 [DIRS 179305], Section 6.3).

Evidence Concerning Hydrothermal Activity in the Saturated Zone

Evidence of hydrothermal alteration and mineralization that followed the deposition of the Paintbrush Group is present within a few kilometers of the Yucca Mountain site in the Calico Hills, in Claim Canyon, and along the south flank of Shoshone Mountain (SNL 2007 [DIRS 177391], Section 6.3.1.11, Figures 6-13 and A6-3; BSC 2004 [DIRS 169989], Figure 6-1; Whelan et al. 1994 [DIRS 100091]). The spatial and temporal patterns of thermal alteration of clays in the Yucca Mountain region are also consistent with the evidence of magmatism and associated hydrothermal activity (Bish and Aronson 1993 [DIRS 100006]; McKee and Bergquist 1993 [DIRS 106339]). None of the three past hydrothermal areas (SNL 2007 [DIRS 177391], Figures A6-1, A6-3, and 6-13) where mineralogical changes may have occurred that could alter flow and transport are along the saturated zone flow path from the repository to the RMEI, so there is no impact on flow and transport to the RMEI. Yucca Mountain is located outside the caldera margin that encompasses Claim Canyon and Shoshone Mountain; hence, it was never within this ancient hydrothermal source (SNL 2007 [DIRS 177391], Figures A6-1, A6-3, and 6-13).

Given the lack of evidence of any past hydrothermal activity along Crater Flat (SNL 2007 [DIRS 177391], Appendix A, Figure A6-3), coupled with the relatively small widths of igneous intrusions that would intersect the saturated zone flow domain and small contact zone where the in-situ rock's mineralogy would be thermally altered, it is concluded that any associated hydrothermal activity produced from any future igneous activity would be localized and of low consequence to saturated zone flow paths.

Flow and transport processes in the saturated zone could potentially be impacted by hydrothermal activity associated with the intrusion of igneous dikes. The effects of hydrothermal activity could include mineralogical changes and changes of sorption coefficient values in response to elevated temperatures. However, as noted in the section entitled *Hydrothermal Activity Associated with Magmatic Activity*, mineralogical changes would be localized around any igneous intrusions and would not affect a significant portion of the entire volume of the tuff aquifer within the saturated zone. Furthermore, the time scale for elevated temperatures associated with basaltic intrusions is on the order of 100 years. Given the small length and time scales associated with basaltic igneous activity in the region, any hydrothermal activity associated with basaltic intrusions is expected to be negligible.

Dublyansky (2007 [DIRS 185029]) presents a review of a previous version of the screening analyses for this FEP (BSC 2004 [DIRS 170012]; BSC 2004 [DIRS 170013]). The review is critical of the screening analyses, particularly that previous thermal history modeling results (Marshall and Whelan 2001 [DIRS 171061]) do not match the inferred temperature history. The review does not recognize the fact that the primary support for exclusion of the FEP is the evidence indicating that hydrothermal waters have not risen from the saturated zone into the

unsaturated zone, where waste emplacement is contemplated (see *Evidence Concerning Hydrothermal Activity in the Unsaturated Zone*). Furthermore, the analyses presented here indicate that any significant heating of the unsaturated zone as a result of silicic or basaltic magmatism or non-magmatic mechanisms is not expected within the time frame addressed by the FEP. The more recent results from Whelan et al. (2006 [DIRS 179305]) concerning numerical modeling of the thermal history (recognizing associated uncertainties) are closer to the measurements than those reported by Marshall and Whelan (2001 [DIRS 171061]).

Conclusion

In summary, there is no evidence for large scale hydrothermal activity in the unsaturated zone at Yucca Mountain or along potential saturated zone radionuclide transport pathways since the formation of the tuff deposits between 11.6 and 13.5 Ma. Secondary minerals that are present indicate that temperatures have been close to current ambient levels for the last 2 to 5 Ma. Available evidence indicates these minerals were deposited from downward percolating meteoric water in the unsaturated zone, rather than hot, upwelling groundwater. Peak fluid temperatures of around 80°C to 90°C due to the Timber Mountain volcanic center occurred >10 Ma, but were not sufficient to cause pervasive hydrothermal alteration. There is some evidence to suggest hydrothermal activity at up to 170°C, but if this is the case, evidence indicates it (Solitario Canyon Fault and Bow Ridge Fault) to have occurred shortly after formation of the Yucca Mountain tuff deposits. Any igneous activity within the 10,000-year regulatory timeframe is expected to be basaltic and will cause only localized heating/alteration. Based on the previous discussion, exclusion of FEP 1.2.06.00.0A (Hydrothermal Activity) will not result in a significant adverse change in the magnitude or timing of either radiological exposure to the RMEI or radionuclide releases to the accessible environment. Therefore, this FEP is excluded from the performance assessments conducted to demonstrate compliance with proposed 10 CFR 63.311 and 63.321 (70 FR 53313 [DIRS 178394]), and with 10 CFR 63.331 [DIRS 180319], on the basis of low consequence.

INPUTS:

Table 1.2.06.00.0A-1. Direct Inputs

Input	Source	Description
Blackwell et al. 2000. *Geothermal Resource/Reservoir Investigations Based on Heat Flow and Thermal Gradient Data for the United States.* [DIRS 183582]	Section 3.5	Hydrothermal systems have been found to circulate at least 4 km below the surface
	Section 2.3	Hydrothermal systems have been found to be highly correlated to regional heat flow in excess of 80 mW/m^2
BSC 2004. *Characterize Framework for Igneous Activity at Yucca Mountain, Nevada*. [DIRS 169989]	Table 7-1	Part of the technical basis for inclusion of this FEP
Rousseau et al. 1997. *Results of Borehole Monitoring in the Unsaturated Zone Within the Main Drift Area of the Exploratory Studies Facility, Yucca Mountain, Nevada*. [DIRS 100178]	Section 5.2	The measured heat flux in the Yucca Mountain area at boreholes NRG-7a, UZ-7a, and SD-12 have heat fluxes within the TSw of 37, 39, and 32 mW/m^2, respectively. This gives an average of 36 mW/m^2, and a standard deviation of 3.6 mW/m^2

Table 1.2.06.00.0A-1. Direct Inputs (Continued)

Input	Source	Description
SNL 2007. *Saturated Zone Site-Scale Flow Model*. [DIRS 177391]	Section 6.3.1.11, Appendix A, Figures 6-13 and A6-3	Evidence of hydrothermal alteration and mineralization and their location
SNL 2008. *Multiscale Thermohydrologic Model.* [DIRS 184433]	Figure 6.3-76[a]	Drift wall temperatures are computed to be about 25°C to 60°C at 10,000 years as a result of waste heat
Wilson et al. 2003. "Origin, Timing, and Temperature of Secondary Calcite—Silica Mineral Formation at Yucca Mountain, Nevada." [DIRS 163589]	Sections 7.3, 8	The unsaturated-zone secondary minerals were interpreted to have been deposited from downward percolating meteoric water and not the result of upwelling groundwaters
	Section 8	Studies of secondary minerals at Yucca Mountain using petrography, fluid inclusion thermometry, and uranium-lead dating indicate that unsaturated-zone temperatures have remained close to the current ambient values over the past 2 to 5 Ma

Table 1.2.06.00.0A-2. Indirect Inputs

Citation	Title	DIRS
10 CFR 63	Energy: Disposal of High-Level Radioactive Wastes in a Geologic Repository at Yucca Mountain, Nevada	180319
70 FR 53313	Implementation of a Dose Standard After 10,000 Years	178394
Bish and Aronson 1993	"Paleogeothermal and Paleohydrologic Conditions in Silicic Tuff from Yucca Mountain, Nevada"	100006
Blackwell et al. 2000	*Geothermal Resource/Reservoir Investigations Based on Heat Flow and Thermal Gradient Data for the United States*	183582
BSC 2004	*Characterize Framework for Igneous Activity at Yucca Mountain, Nevada*	169989
BSC 2004	*Features, Events, and Processes in SZ Flow and Transport*	170013
BSC 2004	*Features, Events, and Processes in UZ Flow and Transport*	170012
BSC 2004	*Heat Capacity Analysis Report*	170003
BSC 2004	*In Situ Field Testing of Processes*	170004
BSC 2007	*Underground Layout Configuration for LA*	179640
Carter Krogh and Valentine 1996	*Structural Control on Basaltic Dike and Sill Emplacement, Paiute Ridge Mafic Intrusion Complex, Southern Nevada*	160928
CRWMS M&O 1996	*Probabilistic Volcanic Hazard Analysis for Yucca Mountain, Nevada*	100116
CRWMS M&O 1998	*Synthesis of Volcanism Studies for the Yucca Mountain Site Characterization Project*	105347
DOE 2002	*Yucca Mountain Science and Engineering Report*	155943
Dublyansky 2007	"Analysis of the Treatment, by the U.S. Department of Energy, of the FEP Hydrothermal Activity in the Yucca Mountain Performance Assessment"	185029
Farmer et al. 1991	"Nd, Sr, and O Isotopic Variations in Metaluminius Ash-Flow Tuffs and Related Volcanic Rocks at the Timber Mountain/Oasis Valley Caldera, Complex, SW Nevada: Implications for the Origin and Evolution of Large-Volume Silicic Magma Bodies"	153024

Table 1.2.06.00.0A-2. Indirect Inputs (Continued)

Citation	Title	DIRS
Ferrill et al. 2004	"Calcite Twin Morphology: A Low-Temperature Deformation Geothermometer"	171196
Flynn et al. 1996	*Geothermal Resource Assessment of the Yucca Mountain Area, Nye County, Nevada*	112530
Gray et al. 2000	"Polygenetic Secondary Calcite Mineralization in Yucca Mountain, NV"	171202
Holt 2002	"$^{18}0/^{16}0$ Evidence for an Early, Short-Lived (~10 yr), Fumarolic Event in the Topopah Spring Tuff Near the Proposed High-Level Nuclear Waste Repository Within Yucca Mountain, Nevada, USA"	162326
McKenna and Blackwell 2004	"Numerical Modeling of Transient Basin and Range Extensional Geothermal Systems"	185042
Marshal and Whelan 2001	*Simulating the Thermal History of the Unsaturated Zone at Yucca Mountain, Nevada*	171061
Marshall and Whelan 2000	"Isotope Geochemistry of Calcite Coatings and the Thermal History of the Unsaturated Zone at Yucca Mountain, Nevada"	154415
McKee and Bergquist 1993	*New Radiometric Ages Related to Alteration and Mineralization in the Vicinity of Yucca Mountain, Nye County, Nevada*	106339
Neymark et al. 2003	"Reliability of U-Th-Pb Dating of Secondary Silica at Yucca Mountain, Nevada"	163681
National Research Council. 1992	*Ground Water at Yucca Mountain, How High Can It Rise? Final Report of the Panel on Coupled Hydrologic/Tectonic/Hydrothermal Systems at Yucca Mountain*	105162
Reamer 1999	"Issue Resolution Status Report (Key Technical Issue: Igneous Activity, Revision 2)"	119693
Sass et al. 1988	*Temperature, Thermal Conductivity, and Heat Flow Near Yucca Mountain, Nevada: Some Tectonic and Hydrologic Implications*	100644
Sawyer et al. 1994	"Episodic Caldera Volcanism in the Miocene Southwestern Nevada Volcanic Field: Revised Stratigraphic Framework, 40Ar/39Ar Geochronology and Implications for Magmatism and Extension"	100075
SNL 2007	*UZ Flow Models and Submodels*	184614
SNL 2008	*Particle Tracking Model and Abstraction of Transport Processes*	184748
Whelan et al. 1994	"Paleoclimatic and Paleohydrologic Records from Secondary Calcite: Yucca Mountain, Nevada"	100091
Whelan et al. 2003	"Thermochronology of Secondary Minerals from the Yucca Mountain Unsaturated Zone"	163590
Whelan et al. 2006	*Thermal History of the Unsaturated Zone at Yucca Mountain, Nevada, USA*	179305

FEP: 1.2.07.01.0A

FEP NAME:

Erosion/Denudation

FEP DESCRIPTION:

Erosion and weathering are processes which can cause significant changes to the present day topography through denudation and are thus capable of affecting both local and regional hydrology. Weathering refers to physical and chemical processes that alter and degrade rocks and soil at and near the land surface. Erosion involves the transport of surficial material away from the site by various mechanisms including glacial, fluvial, eolian (involving wind), and chemical processes. Surficial materials, including weathering products, are also subject to gravity, and erosion can take place by mass wastage processes (e.g., landslides). The extent of denudation depends to a large extent on climate and the rate of local uplift.

SCREENING DECISION:

Excluded – low consequence

SCREENING JUSTIFICATION:

Weathering and erosion are processes that will be ongoing at Yucca Mountain. Within the terrain of Yucca Mountain, erosion and erosional processes occur in the high, steep, and relatively wet uplands, whereas deposition and depositional processes are more dominant in the low, relatively arid lowlands (BSC 2004 [DIRS 169734], p. 2-3).

The calculated maximum possible erosion rates for bedrock outcrops using a ^{10}Be cosmogenic dating technique is 0.4 to 2.7 cm/10,000 years (Stuckless and Levich 2007 [DIRS 181507], p. 83). The long-term erosion rates of stripping of unconsolidated material from Yucca Mountain hillslopes were calculated to be 0.2 to 6 cm/10,000 years using both the rock-varnish carion ratio and the in situ, ^{36}Cl cosmogenic dating methods (Stuckless and Levich 2007 [DIRS 181507], p. 84). Large-scale erosion of 6 cm is within the range of existing surface irregularities (or surface roughness) and is negligible compared to the minimum distance of 200 m from the ground surface to the repository emplacement areas (SNL 2007 [DIRS 179466], Table 4-1, Parameter Number 01-06).

Erosion of surface soils can affect local net infiltration rates because the net infiltration model (MASSIF) was found to be sensitive to soil depth in the shallow soil depth class, which ranges in thickness from 0.1 to 0.5 m (SNL 2008 [DIRS 182145], Section 6.5.2.4.1[a]). However, any increased localized net infiltration will have an insignificant effect on seepage, as a result of the damping and homogenizing of downward-moving percolation fluxes by the Paintbrush nonwelded hydrogeologic unit (SNL 2007 [DIRS 184614], Section 6.1.2).

Weathering of bedrock can lead to soil development. Increases in soil depth as a result of soil development from weathering of bedrock is expected to result in a decrease in net infiltration. This is supported by the Yucca Mountain infiltration model (MASSIF), which was found to be

sensitive to soil depth in the shallow soil depth class where infiltration decreases with increasing soil depth (SNL 2008 [DIRS 182145], Section 6.7). Increased soil depth as a result of weathering of bedrock is analogous to the process of deposition, and the deposition process (FEP 1.2.07.02.0A (Deposition)) is excluded from TSPA by low consequence.

Denudation also includes mechanisms other than erosion and weathering, in particular dissolution and glaciation. The effects of dissolution are discussed in excluded FEP 1.2.09.02.0A (Large Scale Dissolution) and the effects of glaciation are discussed in excluded FEP 1.3.05.00.0A (Glacial and Ice Sheet Effect). *Site Characterization Plan, Yucca Mountain Site, Nevada Research and Development Area, Nevada* (DOE 1988 [DIRS 100282], Section 1.1.3.3.2) indicates that mass wasting processes, such as landslides, do not play a significant role in the present erosional regime at Yucca Mountain.

Debris flows (as opposed to large-scale mass wasting processes such as landslides) are the primary mechanism for hillslope erosion of unconsolidated deposits in the Yucca Mountain region (YMP 1995 [DIRS 102215], Section 2.5.2). However, the effects of debris flows are generally restricted to channelized areas (YMP 1995 [DIRS 102215], Section 4.2) and are not an effective erosion mechanism for unweathered bedrock. Therefore, debris flows have a limited influence on the evolution of surficial materials at Yucca Mountain.

Climatic conditions exert a strong influence on geomorphic processes and, thus, are a factor in controlling depositional and erosional patterns (BSC 2004 [DIRS 169734], p. 3-5). In the present-day climate, eolian processes of sand movement and dust deposition are active around Yucca Mountain (BSC 2004 [DIRS 169734], p. 3-46). Intense local thunderstorms commonly produce flash floods, during which the flow of water and rock debris typically causes hillslope erosion and the deposition of coarse debris on alluvial fans and in stream channels (BSC 2004 [DIRS 169734], p. 3-46). This type of deposition should be more common during the monsoon climate than the present-day or glacial transition climates due to the predicted higher frequency of intense thunderstorms (BSC 2004 [DIRS 170002], p. 6-50). Although present-day deposition and erosion generally occur at very low rates and sporadically because of the arid climate, the middle to late Pleistocene depositional record (indicative of a wetter climate than present-day) indicates a highly variable and localized succession of sedimentary deposits (BSC 2004 [DIRS 169734], p. 2-15). In general, colluvial deposits that are produced during pluvial climates (wetter than present-day) dominate hillslopes. The erosion and redistribution of these deposits takes place during drier climates, when hillslopes are no longer stabilized by vegetation. Hence, most of the alluvial map units in the basins and valleys that dominate the landscape at Yucca Mountain were deposited during interpluvial (i.e., present-day climate) episodes (BSC 2004 [DIRS 169734], p. 3-45). In summary, climate conditions exert a strong influence on depositional and erosional patterns, with deposition generally occurring during wetter periods and erosion generally occurring during drier periods. The 10,000-year period after repository closure is dominated by the glacial-transition climate (8,000 years). Therefore, deposition is expected to be the dominant geomorphic process for the 10,000-year period after repository closure (excluded FEP 1.2.07.02.0A (Deposition)). The extent of denudation also depends on the rate of local uplift. However, local rates of uplift are low, generally on the order of 0.01 mm/yr (BSC 2004 [DIRS 169734], Section 3.3.7.5).

The effects of surface construction and characterization activities at the ground surface on future erosion will also be negligible because of the planned reclamation of the site ground surface. As stated in *Reclamation Implementation Plan* (YMP 2001 [DIRS 154386], Section 5.2.2.1):

> Recontouring and erosion control practices include backfilling spoil material and grading disturbed sites, so that a stable land form is created that blends with the surrounding topography. Following site decommissioning, disturbed areas will be graded such that the natural drainage pattern (predisturbance drainage) is restored. The sites will be stabilized and recontoured to blend into the natural topography of the area.

In addition, reclamation of lands disturbed by the repository is a design constraint listed in *Total System Performance Assessment Data Input Package for Requirements Analysis for Subsurface Facilities* (SNL 2007 [DIRS 179466], Table 4-1, Parameter Number 09-04).

Based on the previous discussion, omission of FEP 1.2.07.01.0A (Erosion/Denudation) will not result in a significant adverse change in the magnitude or timing of either radiological exposures to the RMEI or radionuclide releases to the accessible environment. Therefore, this FEP is excluded from the performance assessments conducted to demonstrate compliance with proposed 10 CFR 63.311 and 63.321 (70 FR 53313 [DIRS 178394]), and with 10 CFR 63.331 [DIRS 180319], on the basis of low consequence.

INPUTS:

Table 1.2.07.01.0A-1. Direct Inputs

Input	Source	Description
SNL 2007. *Total System Performance Assessment Data Input Package for Requirements Analysis for Subsurface Facilities*. [DIRS 179466]	Table 4-1, Parameter Number 01-06	Distance from the ground surface to the repository emplacement areas
Stuckless and Levich 2007. *The Geology and Climatology of Yucca Mountain and Vicinity, Southern Nevada and California*. [DIRS 181507]	p. 84	The long-term erosion rates of stripping of unconsolidated material from Yucca Mountain hillslopes were calculated to be 0.2 to 6 cm/10,000 years using both the rock-varnish carion ratio and the in situ, ^{36}Cl cosmogenic dating methods
	pp. 83, 84	The calculated maximum possible erosion rates for bedrock outcrops using a ^{10}Be cosmogenic dating technique is 0.4 to 2.7 cm/10,000 years

Table 1.2.07.01.0A-2. Indirect Inputs

Citation	Title	DIRS
10 CFR 63	Energy: Disposal of High-Level Radioactive Wastes in a Geologic Repository at Yucca Mountain, Nevada	180319
70 FR 53313	Implementation of a Dose Standard After 10,000 Years	178394
BSC 2004	*Future Climate Analysis*	170002
BSC 2004	*Yucca Mountain Site Description*	169734
DOE 1988	*Site Characterization Plan Yucca Mountain Site, Nevada Research and Development Area, Nevada*	100282
SNL 2007	*Saturated Zone Site-Scale Flow Model*	177391
SNL 2007	*Total System Performance Assessment Data Input Package for Requirements Analysis for Subsurface Facilities*	179466
SNL 2007	*UZ Flow Models and Submodels*	184614
SNL 2008	*Simulation of Net Infiltration for Present-Day and Potential Future Climates*	182145
YMP 1995	*Technical Basis Report for Surface Characteristics, Preclosure Hydrology, and Erosion*	102215
YMP 2001	*Reclamation Implementation Plan*	154386

FEP: 1.2.07.02.0A

FEP NAME:

Deposition

FEP DESCRIPTION:

Deposition is a process that causes significant changes in the present-day topography and thus affects local and regional hydrology. Deposition of surficial materials can occur by a variety of means, including fluvial, eolian, and lacustrine deposition and redistribution of soil through weathering and mass wasting processes.

SCREENING DECISION:

Excluded – low consequence

SCREENING JUSTIFICATION:

Deposition is a process that will be ongoing at Yucca Mountain. Within the terrain of Yucca Mountain, erosion and erosional processes occur in the high, steep, and relatively wet uplands, whereas deposition and depositional processes are more dominant in the low, relatively arid lowlands (BSC 2004 [DIRS 169734], p. 2-3).

Climatic conditions exert a strong influence on geomorphic processes and, thus, are an important factor in controlling depositional and erosional patterns (BSC 2004 [DIRS 169734], p. 3-5). In the present-day climate, eolian processes of sand movement and dust deposition are active around Yucca Mountain (BSC 2004 [DIRS 169734], p. 3-46). Intense local thunderstorms commonly produce flash floods, during which the flow of water and rock debris typically causes hillslope erosion and the deposition of coarse debris on alluvial fans and in stream channels (BSC 2004 [DIRS 169734], p. 3-46). This type of deposition should be more common during the monsoon climate than the present-day or glacial transition climates due to the predicted frequency of intense thunderstorms (BSC 2004 [DIRS 170002], p. 6-50). Although present-day deposition and erosion generally occur at very low rates and sporadically because of the arid climate, the middle to late Pleistocene depositional record (indicative of a wetter climate than present-day) indicates a highly variable and localized succession of sedimentary deposits (BSC 2004 [DIRS 169734], p. 2-15). In general, colluvial deposits that are produced during pluvial climates (wetter than present-day) dominate hillslopes. The erosion and redistribution of these deposits takes place during drier climates, when hillslopes are no longer stabilized by vegetation. Hence, most of the alluvial map units in the basins and valleys that dominate the landscape at Yucca Mountain were deposited during interpluvial (i.e., present-day climate) episodes (BSC 2004 [DIRS 169734], p. 3-45).

Deposition of surface soils can affect local net infiltration rates because the net infiltration model (MASSIF) was found to be most sensitive to soil depth in the shallow depth class (soil depth class 4), where net infiltration is inversely related to soil depth class 4 (SNL 2008 [DIRS 182145], Section 6.7). Therefore, in areas with shallow soils (0.25-m nominal value), deposition will result in deeper surface soils that will lead to a reduction in localized net

infiltration. In areas with intermediate (3.26-m nominal value) and moderately deep soils (16.47-m nominal value), deposition will have no significant impact on net infiltration rates based on MASSIF model sensitivity results (SNL 2008 [DIRS 182145], Section 7.1.4). Altered topography from erosion or deposition may result in slight changes to the runoff and local net infiltration, but these changes are insignificant compared with the uncertainties associated with estimating net infiltration and runoff and therefore can be considered negligible.

Deposition is believed to be a dominant process in Fortymile Wash (YMP 1993 [DIRS 100520], Section 3.4). This drainage is part of the saturated zone model domain, but the accumulation of sediment as a result of depositional processes will not affect recharge rates because calculated recharge rates for all climate states are independent of deep soil depths or depth to water table (BSC 2007 [DIRS 177391], Section 6.6.4).

The effects of igneous disruptive events and the possibility of subsequent ash deposition altering the surface topography are discussed in excluded FEP 1.2.10.02.0A (Hydrologic Response to Igneous Activity).

Based on the previous discussion, omission of FEP 1.2.07.02.0A (Deposition) will not result in a significant adverse change in the magnitude or timing of either radiological exposures to the RMEI or radionuclide releases to the accessible environment. Therefore, this FEP is excluded from the performance assessments conducted to demonstrate compliance with proposed 10 CFR 63.311 and 63.321 (70 FR 53313 [DIRS 178394]), and with 10 CFR 63.331 [DIRS 180319], on the basis of low consequence.

INPUTS:

Table 1.2.07.02.0A-1. Direct Inputs

Input	Source	Description
SNL 2008. *Simulation of Net Infiltration for Present-Day and Potential Future Climates*. [DIRS 182145]	Section 6.7	Deposition of surface soils can affect local net infiltration rates because the net infiltration model (MASSIF) was found to be most sensitive to soil depth in the shallow depth class (soil depth class 4), where net infiltration is inversely related to soil depth class 4. Therefore, in areas with shallow soils (0.25-m nominal value), deposition will result in deeper surface soils that will lead to a reduction in localized net infiltration

Table 1.2.07.02.0A-2. Indirect Inputs

Citation	Title	DIRS
10 CFR 63	Energy: Disposal of High-Level Radioactive Wastes in a Geologic Repository at Yucca Mountain, Nevada	180319
70 FR 53313	Implementation of a Dose Standard After 10,000 Years	178394
BSC 2004	*Future Climate Analysis*	170002
BSC 2004	*Yucca Mountain Site Description*	169734
SNL 2007	*Saturated Zone Site-Scale Flow Model*	177391
SNL 2008	*Simulation of Net Infiltration for Present-Day and Potential Future Climates*	182145
YMP 1993	*Evaluation of the Potentially Adverse Condition "Evidence of Extreme Erosion During the Quaternary Period" at Yucca Mountain, Nevada*	100520

FEP: 1.2.08.00.0A

FEP NAME:

Diagenesis

FEP DESCRIPTION:

This FEP addresses natural processes that alter the mineralogy or other properties of rocks after the rocks have formed under temperature and pressure conditions normal to the upper few kilometers of the earth's crust. Diagenesis includes chemical, physical, and biological processes that take place in rocks after formation but before eventual metamorphism or weathering. This FEP refers to natural diagenetic processes only.

SCREENING DECISION:

Excluded – low consequence

SCREENING JUSTIFICATION:

Diagenesis is defined as physical or chemical changes in sediment brought about by chemical, physical or biological processes after a soil has been deposited and buried under another layer of sediment or after rock formation but before metamorphism or weathering. Diagenesis could affect repository performance by changing the infiltration in the unsaturated zone above the repository or unsaturated zone flow/transport below the repository and could act on surficial material deposited above the repository from postclosure through the period of geologic stability. This FEP discusses the diagenesis of newly deposited material; the effect of compaction, cementation, bacteria, and climate change on diagenesis in shallow sediments above the repository; and diagenesis of rocks below the repository and along the flowpath to the RMEI.

Possible effects of diagenesis on newly deposited material at the surface above the repository are excluded as deposition is expected to be of low consequence (see excluded FEP 1.2.07.02.0A (Deposition)). Erosion and weathering effects on rocks are considered in excluded FEP 1.2.07.01.0A (Erosion/Denudation). Possible effects on diagenesis due to the thermal excursion induced by emplaced repository waste are addressed in excluded FEPs 2.2.10.01.0A (Repository-Induced Thermal Effects on Flow in the UZ); 2.2.10.05.0A (Thermo-Mechanical Stresses Alter Characteristics of Rocks Above and Below the Repository); 2.2.10.04.0A (Thermo-Mechanical Stresses Alter Characteristics of Fractures near Repository); 2.2.10.06.0A (Thermo-Chemical Alteration in the UZ (Solubility, Speciation, Phase Changes, Precipitation/Dissolution)); 2.2.10.09.0A (Thermo-Chemical Alteration of the Topopah Spring Basal Vitrophyre); and 2.2.10.07.0A (Thermo-Chemical Alteration of the Calico Hills Unit), all of which have been excluded on the basis of low-consequence.

Yucca Mountain is composed primarily of pyroclastic deposits with rare lava flows as well as colluvium, alluvium, and soils (BSC 2004 [DIRS 169734], Section 3.3.5), and was selected in part for its arid to semi-arid climate (BSC 2004 [DIRS 169734], Executive Summary). Diagenesis in the shallow environment (extending from the surface to the downward limit of evapotranspiration) may occur in desert environments (Lattman and Simonberg 1971

[DIRS 129306], p. 277; Krystinik 1990 [DIRS 135295], p. 8-1), especially in areas where the water table is close to the surface. The two primary stages for diagenetic changes are compaction and cementation. Compaction may reduce the porosity of eolian sediments by as much as 20% to 30% (Krystinik 1990 [DIRS 135295], p. 8-2), but after this initial stage, "compaction does not become an important factor in diagenesis until the onset of grain deformation and pressure solution during deeper burial diagenesis" (Krystinik 1990 [DIRS 135295], p. 8-3). The geologic setting of Yucca Mountain, however, is characterized by relatively shallow soils and one of low subsidence rates (as discussed in excluded FEPs 1.2.07.02.0A (Deposition) and 1.2.05.00.0A (Metamorphism), and in BSC 2004 [DIRS 169734], Section 7.1.3.3), and therefore deep burial and significant compaction of alluvial, colluvial, and/or eolian deposits is not a plausible diagenetic mechanism at Yucca Mountain during the next 10,000 years.

Cementation, however, may be of significance in shallow diagenesis. Surface materials at Yucca Mountain contain pedogenic calcite ($CaCO_3$) and opal (BSC 2004 [DIRS 169734], Section 3.3.5). The predominance of silicon dioxide (SiO_2) cements at Yucca Mountain is documented in the study by Taylor (1986 [DIRS 102864], Figure 9); which indicates that the accumulation rate of calcite, while occurring, is significantly less than that for SiO_2, as $CaCO_3$ is primarily derived from airborne dust (BSC 2004 [DIRS 169734], Sections 7.1.3.3 and 5.2.2.2.1), while the opaline SiO_2 originates from in-place weathering of the parent material (BSC 2004 [DIRS 169734], Sections 3.3.2 and 3.3.5.1). Therefore, cementation by opaline SiO_2 is common in the study area, and its accumulation in the soils is favored over that of $CaCO_3$ (Taylor 1986 [DIRS 102864], pp. 31 to 33). The more soluble $CaCO_3$ tends to translocate to the base of the wetting zone where it tends to form lenses (Taylor 1986 [DIRS 102864]). The net effects of shallow diagenesis and associated cementation on infiltration in an arid environment are to stabilize the surface environment and decrease the net vertical infiltration rate (Reeves 1976 [DIRS 104303], p. 110; BSC 2004 [DIRS 169734], Section 5.2.1.1, pp. 5-3, and 5-4).

Subsurface bacteria have the potential to influence sediments and fractured rocks. Cementation in the presence of microorganisms may be enhanced by sorption of minerals to microbial cells or through microbially mediated redox reactions that form insoluble precipitates. Alternatively, microorganisms may accelerate the transport minerals by chelation, by pH changes that increase radionuclide solubilities, or by redox reactions that generate soluble species, and by affecting colloid transport. Plate count, direct count, and phospholipid fatty-acid data indicate a low abundance of microorganisms in Yucca Mountain tuff (Kieft et al. 1997 [DIRS 100767], p. 3,130). According to the study by Kieft et al. (1997 [DIRS 100767]), "the low numbers of culturable aerobic heterotrophs in Yucca Mountain samples is consistent with previous findings for unsaturated tuff," and, "water appears to be the primary factor limiting microbial growth and activity in the unsaturated volcanic tuff." Likewise, the low levels of active bacterial and fungal biomass (0 to 16 micrograms of carbon per gram of soil; CRWMS M&O 1999 [DIRS 105031], Figure 14) in the shallow soils above Yucca Mountain are not expected to contribute appreciably to diagenesis in the next 10,000 years. Excluded FEPs 2.2.09.01.0A (Microbial Activity in the SZ) and 2.2.09.01.0B (Microbial Activity in the UZ) address the effects of microbial activity in the saturated zone and unsaturated zone. These FEPs are excluded on the basis of low consequence. In view of these findings, it may be inferred that microbial activity does not play a major role in the development of diagenesis at Yucca Mountain.

The effect of variability in rates and location of infiltration is already addressed in TSPA by varying the infiltration rates associated with varying climatic conditions. The net effect of past diagenesis in the host rocks is included implicitly in the TSPA through the assignment of models and parameters for flow and transport in the unsaturated zone and saturated zone. The potential for future climate change to affect shallow diagenesis is minimal in comparison, as discussed below. Taylor (1986 [DIRS 102864], Chapter 5) indicates that silts that formed in alluvium and eolian fines of Holocene to early Pleistocene or late Pliocene age (times associated with wetter climatic conditions) near Yucca Mountain are characterized by distinctive trends in the accumulation of secondary clay, $CaCO_3$, and opaline SiO_2 that correspond with the ages of the surficial deposits. Notwithstanding, Taylor (1986 [DIRS 102864]) states that accumulation rates of these materials during the Holocene can be attributed to several possible climatic scenarios associated with the Holocene-Pleistocene climate change, but suggests that precipitation has not been a limiting factor and that climatic change was not sufficient to greatly decrease rates of accumulation. Although Taylor (1986 [DIRS 102864]) suggests that increased precipitation in the future may transfer $CaCO_3$ accumulations to greater depths in those areas where precipitation is greater, this process over the next 10,000 years is expected to be insignificant compared to the variability that has resulted since deposition of the host rock.

The rocks within the unsaturated zone below the repository and along the saturated zone flowpath to the RMEI exhibit diagenetic features that have been established over millions of years (Whelan 2004 [DIRS 170697], Figures 3 and 5). These changes tend to transform minerals in rock to more stable forms in equilibrium with their surroundings (Press and Siever 1978 [DIRS 167965], p. 484). A principal effect of deeper diagenesis at Yucca Mountain is the infilling and coating of open fractures and lithophysal cavities by calcite and silica (Whelan 2004 [DIRS 170697], p. 3). Although these coatings may dissolve and reprecipitate, the net effect is a reduction of pore space and permeability in the rock. The effects of fracture infilling is considered in the assignment of flow parameters in TSPA modeling through in situ testing (BSC 2004 [DIRS 170014]). Faults and fractures are addressed in included FEPs 1.2.02.01.0A (Fractures), 1.2.02.02.0A (Faults), 2.2.03.02.0A (Rock Properties), and 2.2.07.08.0A (Fracture flow in the UZ).

Based on the previous discussion, omission of FEP 1.2.08.00.0A (Diagenesis) will not result in a significant adverse change in the magnitude or timing of either radiological exposures to the RMEI or radionuclide releases to the accessible environment. Therefore, this FEP is excluded from the performance assessments conducted to demonstrate compliance with proposed 10 CFR 63.311 and 63.321 (70 FR 53313 [DIRS 178394]), and with 10 CFR 63.331 [DIRS 180319], on the basis of low consequence.

INPUTS:

Table 1.2.08.00.0A-1. Direct Inputs

Input	Source	Description
Kieft et al. 1997. "Factors Limiting Microbial Growth and Activity at a Proposed High-Level Nuclear Repository, Yucca Mountain, Nevada." [DIRS 100767]	pp. 3,130	Total counts (microscopic direct and plate) ranged from below limit of detection (3.2×10^4 cells per gram) to 2.3×10^5 cells per gram; Phospholipid fatty acid concentrations were generally low, ranging from 0.1 to 3.7 pmol per gram
Krystinik 1990. "Early Diagenesis in Continental Eolian Deposits" [DIRS 135295]	pp. 8-2 to 8-3	Compaction may reduce eolian sediments by as much as 20% to 30% but after this initial stage, compaction does not become an important factor in diagenesis until the onset of grain deformation and pressure solution during deeper burial diagenesis
Reeves 1976. *Caliche: Origin, Classification, Morphology and Uses*. [DIRS 104303]	p. 110	Net effects of shallow diagenesis and associated cementation are to stabilize the surface environment and decrease the net vertical infiltration rate
Taylor 1986. *Impact of Time and Climate on Quaternary Soils in the Yucca Mountain Area of the Nevada Test Site*. [DIRS 102864]	Chapter 5	Accumulation rates are attributable to several climatic scenarios, but climate change was insufficient to significantly decrease the rate of accumulations
	Figure 9 and pp. 31 to 33	Cementation by opaline SiO_2 is common in the study area, and that opaline SiO_2 accumulation in the soils is favored over that of pedogenic calcite $CaCO_3$
	Chapter 5	SiO_2 cementation is not dependent on climatic conditions, but cementation does exhibit distinctive trends that correspond with the ages of the surficial deposits
Whelan 2004. *Secondary Mineral Deposits and Evidence of Past Seismicity and Heating of the Proposed Repository Horizon at Yucca Mountain, Nevada*. [DIRS 170697]	p. 3	Description of the process of infilling and coating of open fractures and lithophysal cavities by calcite and silica at Yucca Mountain

Table 1.2.08.00.0A-2. Indirect Inputs

Citation	Title	DIRS
10 CFR 63	Energy: Disposal of High-Level Radioactive Wastes in a Geologic Repository at Yucca Mountain, Nevada	180319
70 FR 53313	Implementation of a Dose Standard After 10,000 Years	178394
BSC 2004	*Probability Distribution for Flowing Interval Spacing*	170014
BSC 2004	*Yucca Mountain Site Description*	169734
CRWMS M&O 1999	*Final Report: Plant and Soil Related Processes Along a Natural Thermal Gradient at Yucca Mountain, Nevada*	105031
Kieft et al. 1997	"Factors Limiting Microbial Growth and Activity at a Proposed High-Level Nuclear Repository, Yucca Mountain, Nevada"	100767
Krystinik 1990	"Early Diagenesis in Continental Eolian Deposits"	135295
Lattman and Simonberg 1971	"Case-Hardening of Carbonate Alluvium and Colluvium, Spring Mountains, Nevada"	129306
Press and Siever 1978	*Earth*	167965
Taylor 1986	*Impact of Time and Climate on Quaternary Soils in the Yucca Mountain Area of the Nevada Test Site*	102864
Whelan 2004	*Secondary Mineral Deposits and Evidence of Past Seismicity and Heating of the Proposed Repository Horizon at Yucca Mountain, Nevada*	170697

FEP: 1.2.09.00.0A

FEP NAME:

Salt Diapirism and Dissolution

FEP DESCRIPTION:

This FEP addresses geologic processes that are primarily relevant to repositories located in salt deposits. Salt diapirism refers to the tendency of salt to flow under lithostatic loading when density and viscosity contrasts with surrounding strata are favorable. Such a process would modify the groundwater flow regime and affect radionuclide transport. Salt domes are the best-known example of salt diapirism. Dissolution can occur when any soluble mineral within the formation is removed by flowing water. Large scale dissolution is a potentially important process in rocks that are composed predominantly of water-soluble evaporite minerals, such as salt.

SCREENING DECISION:

Excluded – low consequence

SCREENING JUSTIFICATION:

Yucca Mountain is located in the southwestern Nevada volcanic field and consists of tilted fault blocks composed of layered sequences of ash flow, ashfall, carbonates, and bedded tuffs of Miocene age (BSC 2004 [DIRS 170029], Sections 6, 6.5, and Table 6-2; SNL 2007 [DIRS 174109], Sections 6.3, 6.4, and Table 6-2; BSC 2004 [DIRS 169734], Section 3.3.4; Day et al. 1998 [DIRS 100027]). Evaporite deposits of sufficient volume to result in significant salt diapirism and dissolution have not been reported to exist near Yucca Mountain (DTN: GS010908314221.001 [DIRS 162874], file: *i-2755_map.pdf*). Any sizable deposit would be evident in well logs or high sodium or chloride measurements in groundwater. Measured sodium levels at the saturated zone site scale flow model ranges from 46 to 130 mg/L (SNL 2007 [DIRS 177391], Section A6.3.4.9) and measured chloride ranges from 3 to 125 mg/L (SNL 2007 [DIRS 177391], Section A6.3.4.2). By comparison, at the Waste Isolation Pilot Plant site in Carlsbad, NM, sodium concentrations in the Rustler/Culebra dolomite (non-sodium) formation, range from 54 to 63,000 mg/L with most wells more then 10,000 mg/L (Siegel et al. 1991 [DIRS 183944], Figure 1-8), reflecting dissolution of the underlying Salado (halite) formation and contamination of wells throughout the area. Thus, the presence of any sizable salt formation would be noticed in well logs or high sodium or chloride concentrations in wells.

The repository is not planned to be developed in a salt dome or cavern, and the related process of lithologic flow is therefore not relevant to the geologic setting for Yucca Mountain. Any salt formations in the area would necessarily be either too small or so far away as to not be of significance to flow and transport in the repository area. Based on the above discussion, omission of FEP 1.2.09.00.0A (Salt Diapirism and Dissolution) will not result in a significant adverse change in the magnitude or time of radiological exposures to the RMEI or radionuclide releases to the accessible environment. Therefore, this FEP is excluded from the performance assessments conducted to demonstrate compliance with proposed 10 CFR 63.311 and 63.321

(70 FR 53313 [DIRS 178394]), and with 10 CFR 63.331 [DIRS 180319], on the basis of low consequence.

Large-scale dissolution of minerals other than salt is discussed in excluded FEP 1.2.09.02.0A (Large-scale Dissolution) and diapir formation in non-salt deposits is discussed in excluded FEP 1.2.09.01.0A (Diapirism).

INPUTS:

Table 1.2.09.00.0A-1. Direct Inputs

Input	Source	Description
DTN: GS010908314221.001. Geologic Map of the Yucca Mountain Region, Nye County, Nevada. [DIRS 162874]	file: *i-2755_map.pdf*	Evaporite deposits of sufficient volume to result in significant salt diapirism and dissolution have not been reported to exist near Yucca Mountain

Table 1.2.09.00.0A-2. Indirect Inputs

Citation	Title	DIRS
10 CFR 63	Energy: Disposal of High-Level Radioactive Wastes in a Geologic Repository at Yucca Mountain, Nevada	180319
70 FR 53313	Implementation of a Dose Standard After 10,000 Years	178394
BSC 2004	*Geologic Framework Model (GFM2000)*	170029
BSC 2004	*Yucca Mountain Site Description*	169734
Day et al. 1998	*Bedrock Geologic Map of the Yucca Mountain Area, Nye County, Nevada*	100027
Siegel et al. 1991	*Hydrogeochemical Studies of the Rustler Formation and Related Rocks in the Waste Isolation Pilot Plant Area, Southeastern New Mexico*	183944
SNL 2007	*Saturated Zone Site-Scale Flow Model*	177391
SNL 2007	*Hydrogeologic Framework Model for the Saturated Zone Site Scale Flow and Transport Model*	174109

FEP: 1.2.09.01.0A

FEP NAME:

Diapirism

FEP DESCRIPTION:

Diapirism is the process by which plastic, low density rocks (most commonly evaporites) may flow under lithostatic loading when density and viscosity contrasts with the surrounding strata are favorable. Such a process would modify the groundwater flow regime and affect radionuclide transport.

SCREENING DECISION:

Excuded – low consequence

SCREENING JUSTIFICATION:

In the broadest sense, diapirism encompasses "the piercing or rupturing of domed or uplifted rocks by mobile core material, by tectonic stresses as in anticlinal folds, by the effect of geostatic load in sedimentary strata as in salt domes or shale diapirs, or by igneous intrusions, forming diapiric structures such as plugs" (Bates and Jackson 1984 [DIRS 128109], p. 138). The concept of diapirism is usually applied to salt structures resulting from geostatic loading (see excluded FEP 1.2.09.00.0A (Salt Diapirism and Dissolution)) but can also be applied to the doming effects associated with igneous intrusion.

Current tectonic stresses in the region are extensional (BSC 2004 [DIRS 168030], Section 6.3.1), and such a stress regime is not conducive to the compression-related anticlinal folding and doming associated with diapirism. The geologic materials at Yucca Mountain are brittle (particularly the welded tuffs), and exhibit deformation by faulting and jointing, with the formation of breccias, rather than folding and doming. The volcanic rocks present at the site are not capable of ductile flow under the stresses and at the temperatures expected due to geostatic loading and waste emplacement. In general, ductile behavior is associated with increased temperatures and hydrostatic pressures and is only expected at deep levels of the Earth's crust and in the mantle. Yucca Mountain is located in an area of moderate heat flow in the Southern Great Basin, south of any regions of relatively high crustal heat flow that might be more conducive to diapirism (Lachenbruch and Sass 1978 [DIRS 142990], pp. 212 and 246). Thus, diapirism related to tectonic stresses and geostatic loading is precluded because the necessary geologic materials and stress environment conducive to diapirism do not occur at Yucca Mountain.

Diapirism related to igneous intrusion is relevant to the disruptive event scenario in FEP 1.2.04.03.0A (Igneous Intrusion into Repository). Because of the stress regime at Yucca Mountain, an igneous event is expected to be in the form of a dike (BSC 2004 [DIRS 169989], Section 6.1). By way of corroboration, Smith et al. (1998 [DIRS 118967], p. 155) point out that extension is generally accommodated in the upper crust by intrusion of vertical dikes perpendicular to the extension direction, with surface deformation possibly including open

fissures, monoclines, normal faults, and grabens, and with surface uplift being approximately a few meters (Smith et al. 1998 [DIRS 118967], Figure 2). Thus, dike formation would tend to be oriented parallel to the existing faults and fractures and therefore would have minimal effect on groundwater flow systems because the possible associated diapirism would be of small scale compared to the volume over which flow and transport occurs. The potential for hydrologic response to igneous intrusion is more fully evaluated in excluded FEP 1.2.10.02.0A (Hydrologic Response to Igneous Activity). In particular, for the case of a 10 km-long, 5 km-deep, and 100 m-wide disc-shaped dike initially intruded into the saturated zone, the maximum rise in the water table due to heat effects would be on the order of 25 m (Kuiper (1991 [DIRS 163417], p. 121), not a sufficiently large increase to impact flow pathways or saturate the repository horizon (see included FEP 1.3.07.02.0A (Water Table Rise Affects SZ), and included FEP 1.3.07.02.0B (Water Table Rise Affects UZ)). Furthermore, the estimated size distributions for any potential future dikes at Yucca Mountain (SNL 2007 [DIRS 174260], Table 7-1) show that the dike analyzed by Kuiper (1991 [DIRS 163417]) is much larger than those potentially relevant to the repository. Because igneous-related diapirism from such a dike would be on the same scale, igneous-related diapirism is excluded based on low consequence.

Based on the preceding discussion, omission of FEP 1.2.09.01.0A (Diapirism) will not result in a significant adverse change in the magnitude or time of radiological exposures to the RMEI or radionuclide releases to the accessible environment. Therefore, this FEP is excluded from the performance assessments conducted to demonstrate compliance with the proposed 10 CFR 63.311 and 63.321 (70 FR 53313 [DIRS 178394]), and with 10 CFR 63.331 [DIRS 180319], on the basis of low consequence.

INPUTS:

Table 1.2.09.01.0A-1. Direct Inputs

Input	Source	Description
BSC 2004. *Characterize Framework for Igneous Activity at Yucca Mountain, Nevada*. [DIRS 169989]	Section 6.1	Form of igneous intrusion will be in dikes rather than large diapirs
BSC 2004. *Characterize Framework for Seismicity and Structural Deformation at Yucca Mountain, Nevada*. [DIRS 168030]	Section 6.3.1	Regional setting of Yucca Mountain is extensional
SNL 2007. *Characterize Eruptive Processes at Yucca Mountain, Nevada*. [DIRS 174260]	Table 7-1	Estimated size distributions for any potential future dikes

Table 1.2.09.01.0A-2. Indirect Inputs

Citation	Title	DIRS
10 CFR 63	Energy: Disposal of High-Level Radioactive Wastes in a Geologic Repository at Yucca Mountain, Nevada	180319
70 FR 53313	Implementation of a Dose Standard After 10,000 Years	178394
Bates and Jackson 1984	*Dictionary of Geological Terms*	128109
Kuiper 1991	"Water-Table Rise Due to Magma Intrusion Beneath Yucca Mountain"	163417
Lachenbruch and Sass 1978	"Models of an Extending Lithosphere and Heat Flow in the Basin and Range Province"	142990
Smith et al. 1998	"Magma Intrusion and Seismic-Hazards Assessment in the Basin and Range Province"	118967

FEP: 1.2.09.02.0A

FEP NAME:

Large-Scale Dissolution

FEP DESCRIPTION:

Dissolution can occur when any soluble mineral is removed by flowing water. Large-scale dissolution is a potentially important process in rocks that are composed predominantly of water-soluble evaporite minerals, such as salt.

SCREENING DECISION:

Excluded – low consequence

SCREENING JUSTIFICATION:

Large-scale dissolution is a process principally affecting highly soluble evaporite rocks such as halite or carbonates. The unsaturated zone at Yucca Mountain has only a trace abundance of evaporitic minerals, as demonstrated by very low salt content in leachates from leaching numerous unsaturated zone rock samples (DTNs: LL030408023121.027 [DIRS 162949], GS030608312272.005 [DIRS 163745], LA0305RR831222.001 [DIRS 163422], and LA0307RR831222.002 [DIRS 164090]), and is primarily composed of high-silica minerals such as quartz, feldspar, and glass (BSC 2004 [DIRS 170031], Appendices C and E). Solubilities of these minerals are too low to produce large dissolution cavities, breccia pipes, or solution chimneys over the time scales of interest and expected water flow rates. Local dissolution processes are discussed in excluded FEP 2.2.08.03.0B (Geochemical Interaction and Evolution in the UZ).

The volcanic rocks present in the saturated zone are not readily soluble in water and their solubility is low enough that large-scale dissolution does not occur. Volcanic rocks tend to weather to clay minerals with only a relatively small amount of silica going into solution. The volcanic units in the saturated zone in the vicinity of Yucca Mountain are primarily comprised of silica (quartz and cristobalite), alkali feldspars, and zeolites (SNL 2008 [DIRS 184806], Section A2). The solubility of quartz, for example, is 12 mg/L at 1 bar pressure and pH 7 at 25°C (Freeze and Cherry 1979 [DIRS 101173], p. 106), which is relatively low compared to evaporite and carbonate solubilities. Large-scale dissolution of evaporites such as halite, with a solubility of 360,000 mg/L at 1 bar pressure and pH 7 at 25°C (Freeze and Cherry 1979 [DIRS 101173], p. 106), can be excluded from the saturated zone flow and transport models because evaporites are present in only trace amounts in any of the formations along the saturated zone transport pathways from underneath the repository to the accessible environment. This low abundance is apparent not only from the quantitative mineralogy of the rocks, but also from relatively low halide concentrations and generally low total dissolved solids concentrations in saturated zone water samples taken from the entire saturated zone flow model domain (SNL 2007 [DIRS 177391], Appendix A), which precludes a significant presence of evaporites.

Of all the hydrogeologic units in the Yucca Mountain hydrogeologic framework model (Belcher 2004 [DIRS 173179]; SNL 2007 [DIRS 174109], Figures 6-5 to 6-7), those containing carbonates are the most soluble in groundwater (solubility of 90 mg/L to 500 mg/L, depending on the pCO_2, at 1 bar pressure and pH 7 at 25°C (Freeze and Cherry 1979 [DIRS 101173], p. 106)). The permeability of these units is typically quite high, primarily due to solution channels and fractures (SNL 2007 [DIRS 177391], Section 6.3.1.1). Carbonates in the vicinity of Yucca Mountain exist only in the saturated zone at depths of 500 m or more below the water table (SNL 2007 [DIRS 174109], Figure 6-5). New extensive carbonate dissolution cavities are not expected to develop because such dissolution is not typically observed in carbonates at such depths below the water table (Freeze and Cherry 1979 [DIRS 101173], pp. 514 to 515).

Under unusually drier climatic conditions than at present, which is not expected within the next 10,000 years (BSC 2004 [DIRS 170002], Section 7.1), the water table may drop from its current potentiometric surface to lower levels. While not expected, there is mineralogical evidence to suggest that the maximum drop could be as much as 300 m (see excluded FEP 1.3.07.01.0A (Water Table Decline)). Even given this unexpected drop, the water table would still remain several hundreds of meters above the carbonate aquifer along the saturated zone transport paths (SNL 2007 [DIRS 174109], Figure 6-5), and significant dissolution of the carbonates would not occur.

Even if dissolution did occur in the carbonate aquifer, its depth below the water table, combined with the upward vertical hydraulic gradient throughout the saturated zone flow model domain (SNL 2007 [DIRS 177391], Section 6.3.1.5), preclude the possibility that radionuclides will reach the carbonate aquifer. In addition to head and borehole flow/pressure measurements that indicate an upward vertical hydraulic gradient in the saturated zone, the lack of a volcanic aquifer geochemical signature in the carbonate aquifer and vice-versa (SNL 2007 [DIRS 177391], Appendix A) suggests a lack of hydraulic communication between the two aquifers. Thus, large-scale dissolution in the carbonate aquifer can be excluded on the basis of low consequence because, even if dissolution cavities form in the carbonates, radionuclides are not expected to reach them.

Based on the previous discussion, omission of FEP 1.2.09.02.0A (Large-Scale Dissolution) will not result in a significant adverse change in the magnitude or timing of either radiological exposures to the RMEI or radionuclide releases to the accessible environment. Therefore, this FEP is excluded from the performance assessments conducted to demonstrate compliance with proposed 10 CFR 63.311 and 63.321 (70 FR 53313 [DIRS 178394]), and with 10 CFR 63.331 [DIRS 180319], on the basis of low consequence.

INPUTS:

Table 1.2.09.02.0A-1. Direct Inputs

Input	Source	Description
BSC 2004. *Future Climate Analysis*. [DIRS 170002]	Section 7.1	Drier climatic conditions than at present are not expected in the next 10,000 years
BSC 2004. *Mineralogic Model (MM3.0) Report*. [DIRS 170031]	Appendices C and E	Bulk mineral composition of Yucca Mountain tuffs in the unsaturated zone

Table 1.2.09.02.0A-1. Direct Inputs (Continued)

Input	Source	Description
DTN: LA0305RR831222.001. Chlorine-36 and Cl in Salts Leached from Rock Samples for the Chlorine-36 Validation Study. [DIRS 163745]	Table S03246_001	Low salt content of leachates from leaching unsaturated zone rock samples
DTN: LL030408023121.027. Cl Abundance and Cl Ratios of Leachates from ESF Core Samples. [DIRS 162949]	Table S03181_001	Low salt content of leachates from leaching unsaturated zone rock samples
Freeze and Cherry 1979. *Groundwater*. [DIRS 101173]	pp. 514 to 515	Extensive carbonate dissolution cavities are not expected to develop because such dissolution is not typically observed in carbonates at great depths below the water table
	p. 106	Carbonate, quartz, and halite solubilities
SNL 2007. *Hydrogeologic Framework Model for the Saturated Zone Site Scale Flow and Transport Model*. [DIRS 174109]	Figures 6-5 to 6-7	Basis for hydrogeologic units adopted in SZ flow and transport models
	Figure 6-5	Along the predicted SZ transport path the depth of carbonate aquifer is well below the current water table
SNL 2007. *Saturated Zone Site-Scale Flow Model*. [DIRS 177391]	Appendix A	Saturated zone water contain low halide concentrations and generally low total dissolved solids concentrations
	Section 6.3.1.5	Upward hydraulic gradient exists throughout the saturated zone flow model domain
	Section 6.3.1.1	Permeability of carbonates is primarily due to solution channels and fractures.
SNL 2008. *Site-Scale Saturated Zone Transport*. [DIRS 184806]	Appendix A, Section A2	The volcanic units in the vicinity of Yucca Mountain are primarily comprised of silica (quartz and cristobalite), alkali feldspars, and zeolites

Table 1.2.09.02.0A-2. Indirect Inputs

Citation	Title	DIRS
10 CFR 63	Energy: Disposal of High-Level Radioactive Wastes in a Geologic Repository at Yucca Mountain, Nevada	180319
70 FR 53313	Implementation of a Dose Standard After 10,000 Years	178394
Belcher 2004	*Death Valley Regional Ground-Water Flow System, Nevada and California - Hydrogeologic Framework and Transient Ground-Water Flow Model*	173179
DTN: LA0305RR831222.001	Chlorine-36 and Cl in Salts Leached from Rock Samples for the Chlorine-36 Validation Study	163422
DTN: LA0307RR831222.002	Chloride, Bromide, Sulfate, and Chlorine-36 Analyses of Salts Leached from ESF 36Cl Validation Drillcore Samples in FY99	164090

FEP: 1.2.10.01.0A

FEP NAME:

Hydrologic Response to Seismic Activity

FEP DESCRIPTION:

Seismic activity, associated with fault movement, may create new or enhanced flow pathways and/or connections between stratigraphic units, or it may change the stress (and therefore fluid pressure) within the rock. These responses have the potential to significantly change the surface and groundwater flow directions, water level, water chemistry, and temperature.

SCREENING DECISION:

Excluded – low consequence

SCREENING JUSTIFICATION:

The extent and significance of water table rise in response to seismic activity and changes in the large hydraulic gradient that exists to the north of the repository are assessed. The effects of seismic activity on groundwater chemistry are also considered.

Hydrologic responses to seismic activity, either modeled or measured at analogue sites are documented here. Indirect causes of such behavior due to changes in the hydrologic properties of the rock matrix, faults or fracture network are discussed in excluded FEPs 2.2.06.01.0A (Seismic Activity Changes Porosity and Permeability of Rock), 2.2.06.02.0A (Seismic Activity Changes Porosity and Permeability of Faults) and 2.2.06.02.0B (Seismic Activity Changes Porosity and Permeability of Fractures). Changes in the porosity and permeability of the regional geology (and hence, in flow and transport properties of the unsaturated zone, saturated zone, and potentially through the emplacement drifts) can be brought about by vibratory ground motion and alteration of the local stress fields (which may lead to the formation of new faults and/or fractures or in some cases the closing of existing fractures). A change in flow through the drifts has the potential to increase degradation of EBS components and waste packages, leading to radionuclide release. Aspects of flow change through the repository drift are addressed separately in included FEP 1.2.03.02.0D (Seismic-Induced Drift Collapse Alters In-Drift Thermohydrology). The effect of seismic activity on radionuclide transport is addressed in a sensitivity study that is detailed in excluded FEPs 2.2.06.02.0A (Seismic Activity Changes Porosity and Permeability of Faults) and 2.2.06.02.0B (Seismic Activity Changes Porosity and Permeability of Fractures).

A hypothesis has been proposed that long-term changes in water table elevations are associated with seismic-induced permanent changes in regional permeability (Davies and Archambeau 1997 [DIRS 103180]). A transient change in water table elevations is associated with seismically induced changes to the local stress fields, which can lead to processes such as “seismic pumping.” Seismic pumping (Szymanski 1989 [DIRS 106963], pp. 3 to 22) is defined here as the temporary increase in height of the water table caused by fault movement. This movement of the water table is caused by the opening and closing of fractures during an earthquake cycle.

Longer-term changes are not expected to result from such permanent changes in stress because the existing data do not show any relationship between the long-term state of stress and water table elevation (Stock et al. 1985 [DIRS 101027]; Stock and Healy 1988 [DIRS 101022]). Water table elevations can change from a few centimeters to several tens of meters in response to seismic activity (National Research Council 1992 [DIRS 105162], Chapter 5). The change in water table elevation can also affect: (1) saturated zone flow and pathways, if the change in water table elevations are extensive enough to change the regional potentiometric surfaces, and (2) groundwater geochemistry, as the displaced water is moved into, and interacts with, rocks composed of different mineralogy. Because seismic activity is closely associated with tectonic activity, a decline in tectonic activity coincides with a decline in the frequency and intensity of seismic activity.

Investigations of analogue sites and numerical studies indicate that hydrologic response to seismic activity at the Yucca Mountain repository will be of low consequence. A brief summary of these investigations is given below.

Earthquakes can cause changes in groundwater levels, sometimes at distances far removed from the epicenter. The hydrologic effects of three seismic events in 1992 that were observed in groundwater monitoring wells at Yucca Mountain provide estimates of water-level fluctuations occurring in response to earthquakes. A magnitude 7.5 earthquake occurred at Landers, California, on June 28, 1992, followed a few hours later by a magnitude 6.6 earthquake at Big Bear Lake, California (O'Brien 1993 [DIRS 101276], Table 1). These earthquakes were regional, located about 293 and 296 km away from Yucca Mountain, respectively. A magnitude 5.6 earthquake occurred June 29, 1992, about 23 km from Yucca Mountain at Little Skull Mountain.

The 1992 data from the groundwater monitoring wells are listed in DTN: GS930108312312.003 [DIRS 171974] and document the earthquake-induced fluctuations in water level. Based on the data in DTN: GS930108312312.003 [DIRS 171974], the three earthquakes produced mostly short-term water level fluctuations on the order of tens of centimeters. The Landers earthquake caused about a 90-cm water-level fluctuation at well USW H-5. The following Big Bear Lake earthquake caused a 20-cm water-level fluctuation. The response of well USW H-3 to the Landers earthquake involved a brief water-level spike followed by a 20-cm decrease, returning to near normal levels within several hours. The response of wells USW H-5 and USW H-6 to the magnitude 5.6 Little Skull Mountain earthquake were 40 and 20 cm, respectively. The water level decreased about 50 cm at well UE-25 P#1 over three days following the earthquake, but the recovery of the water table in this well required about six months. Many other wells showed no response or smaller fluctuations over short time periods (on the order of hours) (O'Brien 1993 [DIRS 101276], Table 1). For perspective, it is noted that the repository would be located approximately 300 m above the current water table so that future water-level fluctuations of the magnitude of those observed in 1992 would not affect the repository horizon.

Several modeling investigations have been conducted to estimate the hydrologic response (i.e., change in water table elevations) given predicted fault displacements in the Yucca Mountain region. One investigation was performed by the National Research Council (1992 [DIRS 105162], Chapter 5). This group estimated the maximum changes in water table elevations over a 10,000-year period in response to seismic activity, which presumes some

degree of fault displacement. They estimated fault displacement using two modeling approaches: (1) a dislocation approach, where zones of extension on one side of a fault are balanced by compression across the fault; and (2) the more realistic "changes in the regional stress" approach caused by normal fault slippage in regions of extension. The regional stress approach evaluated the effect of stress on pore pressure, which is dependent on the elastic properties of the bulk rock and the mineral grains. Both models resulted in a transient change in water table elevation given a seismic event in the Yucca Mountain region. However, the extent of the rise differed for both models. Adopting the dislocation model, the maximum rise in the water table is approximately 17 m (Carrigan et al. 1991 [DIRS 100967], p. 1,159) (discussed below). Results from the regional stress approach resulted in a maximum water table rise of 50 m (National Research Council 1992 [DIRS 105162], Chapter 5, p. 116). The latter approach was developed by determining a realistic parameter range for the ratio of rock to mineral compressibility and then computing a result using the extreme value from this range that produced the highest water table rise. The durations of the changes were not specifically evaluted; however, the panel concluded that the increase in water level would gradually dissipate. The panel concluded that regardless of the approach, the maximum water table rise given a seismic event would be less than 50 m. Given the National Research Council study, it is inferred that a 13-m slip along Solitario Canyon fault (the approximate mean displacement for the Solitario Canyon fault based on an annual exceedance probability of 10^{-8}), which could implicitly impose the maximum change in volume stress strain changes on pore pressure, would result in no more than a 50-m rise in the water table.

By way of corroboration, Gauthier et al. (1996 [DIRS 100447], pp. 163 to 164) analyzed the potential effects of seismic activity as a result of three different types of fault displacements (normal, listric, and strike-slip faulting) on contaminant transport in the saturated zone due to changes in water table elevation. For all three fault types, a 1-m displacement with a 30-km rupture length was considered. Their simulations for the TSPA used in the viability assessment of the timing, amplitude, and duration of water table rise indicated a maximum rise of 50 m within an hour of a simulated strike-slip seismic event, with a smaller rise for the other types of events. The simulated system returned to steady-state conditions within six months. Gauthier et al. (1996 [DIRS 100447], pp. 163 to 164) conclude that:

> In general, seismically induced water-table excursions caused by poroelastic coupling would not influence the models presently being used to determine long-term performance of a repository at Yucca Mountain; therefore, we excluded them from the total-system simulations.

Investigations focusing on the potentiometric hydrologic response, given changes in rock properties adjacent to a fault, demonstrate that the changes in water table elevation are transient and local in nature. Numerical simulations by Carrigan et al. (1991 [DIRS 100967]) of seismic pumping involving earthquakes typical of the Basin and Range province (approximately 1-m fault slip) produced 2- to 3-m excursions of a water table 500 m below the ground surface. Extrapolation to an event of about 4-m slip would result in a transient rise of 17 m near the fault (Carrigan et al. 1991 [DIRS 100967], p. 1,159). Carrigan et al. (1991 [DIRS 100967]) modeled a 100-m-wide fracture zone centered on a vertical fault, with vertical permeability increased by a factor of 1,000. Water-level excursions in the fracture zone were twice as great as in the

adjacent block. For a fault-fracture zone with 1-m slip, transient excursions of about 12 m were modeled by Carrigan et al. (1991 [DIRS 100967]).

The significance of a rise in the water table is that it reduces the contribution to the barrier capability of the unsaturated zone by shortening the flow path from the repository to the saturated zone. Regardless, data and modeling results indicate that changes in water table elevation at Yucca Mountain are not expected to exceed 50 m and are expected to be transient. It is therefore expected that the water table excursions caused by earthquakes will not cause sufficient water table level fluctuations to threaten, even temporarily, the repository horizon, which in the current design is approximately 300 m above the water table. The water table could rise by up to about 120 m in the vicinity of the repository under wetter climates expected in the future (see included FEP 1.3.07.02.0A (Water Table Rise Affects SZ)), but seismic events are still unlikely to affect hydrologic conditions at the repository horizon.

Another aspect of the water table rise issue concerns the large hydraulic gradient of up to 0.13 just to the north of the repository (SNL 2007 [DIRS 177391], Section 6.3.1.4). The water table elevation rises as one moves from south to north away from the repository. If this gradient were to migrate southward, the resulting water table below the repository could be much higher than present-day conditions.

The work of Davies and Archambeau (1997 [DIRS 103180], p. 28) presents a hypothesis that the large hydraulic gradient is a result of residual stress effects in the rock induced by the Timber Mountain caldera. Furthermore, the authors suggest that moderate earthquakes in this area could induce a sufficient change in geomechanical strain downstream of the current large hydraulic gradient to induce a similar gradient downstream of the repository. This would result in a large (150 m to 250 m) rise in the water table beneath the repository. However, the hypothesis regarding the residual stress effects of the 10 Ma Timber Mountain caldera contradicts extensive previous experience in the region of the Nevada Test Site (Stock et al. 1985 [DIRS 101027]). This composite experience is compiled from 14 sources reporting results from diverse methods, including hydraulic fracturing, overcoring stress measurements, earthquake focal mechanisms, borehole breakouts, orientations of explosion-produced fractures, and study of Quaternary faults and cinder-cone alignments. These studies show a reasonably uniform direction of extension between northwest and west, with a mixed potential-slip regime of normal faulting (mainly for shallow indicators) and strike-slip faulting (mainly for deep indicators). The Davies and Archambeau discussion is also inconsistent with stress measurements in borehole G-2 as reported by Stock and Healy (1988 [DIRS 101022]). Stock and Healy (1988 [DIRS 101022]) characterize G-2 as being within the same ("combined normal and strike-slip") faulting regime as that indicated by the results from the three holes that they tested south of the large gradient. Based on the stress measurements in the four holes, the tendency for strike-slip faulting is greatest in the southeastern hole, UE-25p#1, not in the northern Yucca Mountain area where G-2 is located, as Davies and Archambeau (1997 [DIRS 103180]) propose.

Stress measurements are also available from the ESF. Results from hydraulic fracturing experiments in two boreholes in the Thermal Test Facility alcove and one borehole in the Northern Ghost Dance Fault alcove indicate a west-northwest extensional stress regime. The relative magnitudes of the principal stresses are consistent with potential normal faulting (SNL 1996 [DIRS 163645]; DTNs: SN308F3710195.003 [DIRS 166458] and

SN37100195002.001 [DIRS 131356]). Principal stress orientations inferred from earthquake focal mechanism studies also indicate a west-northwesterly directed least principal stress. Observed focal mechanisms exhibit a mixture of normal and strike-slip faulting. The overall data suggest a uniform stress regime in the vicinity of Yucca Mountain (von Seggern et al. 2001 [DIRS 156297], Section 9).

Available data do not support a residual stress effect from the Timber Mountain caldera, do not support a modern stress field changing from strike-slip in northern Yucca Mountain to normal south of the large hydraulic gradient, and do not support a southward decrease of the least principal stress. Based on these findings, any changes in stress resulting from seismic activity would be expected to have a negligible effect on the location of the large hydraulic gradient. Therefore, migration of the large hydraulic gradient as a result of seismic activity is excluded from TSPA on the basis of low consequence.

Finally, the effect of a seismic-induced hydrologic response on saturated zone groundwater chemistry will be insignificant. Groundwater isotopic and geochemical signatures within the Yucca Mountain region are indicative of groundwater flow directions and flow paths that have existed over the past 10,000 years. Uncorrected groundwater ages determined from ^{14}C (percent modern carbon) data (SNL 2007 [DIRS 177391], Table A6-7 and Section B7) and an exponential decay relationship (SNL 2007 [DIRS 177391], Equation A6-3) range from about 12,000 to 18,000 years old in the vicinity of Yucca Mountain. The analysis of the geochemistry supports the conclusion that the bulk of the groundwater beneath Yucca Mountain is derived from local recharge (SNL 2007 [DIRS 177391], Sections A6.3.6.3 and A6.3.6.4). Therefore, the saturated zone groundwater under the repository and along the saturated zone transport path is primarily paleoclimate recharge water with a small component (2% to 15%) of young water less than 1,000 years old (SNL 2007 [DIRS 177391], Table A6-8). Given that the saturated zone groundwater below the repository comes from local recharge through the unsaturated zone, any saturated zone water that is temporarily forced less than 50 m into the unsaturated zone by seismic activity would be expected to have a negligible effect on chemical composition or temperature relative to natural variations.

For the unsaturated zone, the range of water compositions that is used to define radionuclide sorption coefficients is taken from the range of water compositions found in the unsaturated zone and saturated zone (SNL 2007 [DIRS 177396], Appendix A, Section A4). Therefore, any alteration of composition through mixing of unsaturated zone and saturated zone waters as a result of water table rise is expected to lie within the range of uncertainty for groundwater composition already included in the TSPA. For the unsaturated zone, any effects of water table rise are expected to have a negligible effect on temperature in comparison with the effects of repository heating, which is excluded in terms of unsaturated zone flow and transport in excluded FEPs 2.2.10.01.0A (Repository-Induced Thermal Effects on Flow in the UZ) and 2.2.10.06.0A (Thermo-Chemical Alteration in the UZ (Solubility, Speciation, Phase Changes, Precipitation_Dissolution)).

In summary, the direct effects of seismic activity on the water table are transient and are negligible considering the height of the repository above the water table (the maximum projected water table rise due to seismic activity is 50 m and the projected repository height is at least 300 m above the current water table over the majority of the repository area). Even taking into

account an increase in the water table elevation associated with wetter climates expected in the future (up to 120 m), seismic events are still unlikely to affect hydrologic conditions at the repository horizon. As a result, groundwater flow and radionuclide transport would not be significantly affected by the hydrologic effects of future seismic activity, and therefore the hydrologic response to seismic activity is excluded from the TSPA on the basis of low consequence. The effects of seismic activity on groundwater chemistry and temperature are also excluded from the TSPA on the basis of low consequence, because the changes in temperature caused by seismicity will be negligible compared to changes resulting from other natural variations in temperature or through repository heating. Changes in geochemical conditions will also be negligible in terms of the uncertainties in water chemsitry already included in the unsaturated zone and saturated zone models used in TSPA. Southward migration of the large hydraulic gradient, which currently lies to the north of the repository, is excluded from the TSPA on the basis of low consequence.

Based on the previous discussion, omission of FEP 1.2.10.01.0A (Hydrologic Response to Seismic Activity) will not result in a significant adverse change in the magnitude or timing of either radiological exposures to the RMEI or radionuclide releases to the accessible environment. Therefore, this FEP is excluded from the performance assessments conducted to demonstrate compliance with proposed 10 CFR 63.311 and 63.321 (70 FR 53313 [DIRS 178394]), and with 10 CFR 63.331 [DIRS 180319], on the basis of low consequence.

INPUTS:

Table 1.2.10.01.0A-1. Direct Inputs

Input	Source	Description
DTN: GS930108312312.003. Earthquake-Induced Water-Level Fluctuations at Yucca Mountain, Nevada, June, 1992. [DIRS 171974]	Files: S96143_001, S96143_002, and S96143_003	Data from groundwater monitoring wells describing earthquake-induced water-level fluctuations
DTN: SN0308F3710195.003. Hydraulic Fracturing Stress Measurements in Test Holes: ESF-GDJACK #1, and ESF-GDJACK #5, Exploratory Studies Facility at Yucca Mountain, Nevada. [DIRS 166458]	File: S03305_001	The relative magnitudes of the principal stresses are consistent with potential normal faulting
National Research Council 1992. *Ground Water at Yucca Mountain, How High Can It Rise? Final Report of the Panel on Coupled Hydrologic/Tectonic/Hydrothermal Systems at Yucca Mountain*. [DIRS 105162]	Chapter 5, p. 116	Results from the regional stress model approach indicated a maximum water table rise of 50 m
SNL 2007. Saturated Zone Site-Scale Flow Model. [DIRS 177391]	Table A6-7, Section B7	Uncorrected groundwater ages determined from ^{14}C
	Table A6-8	The SZ groundwater under the repository and along the SZ transport path is primarily paleoclimate recharge water with a small component (2% to 15%) of young water less than 1,000 years old
	Section 6.3.1.4	Hydraulic gradient of up to 0.13 just to the north of the repository

Table 1.2.10.01.0A-2. Indirect Inputs

Citation	Title	DIRS
10 CFR 63	Energy: Disposal of High-Level Radioactive Wastes in a Geologic Repository at Yucca Mountain, Nevada	180319
70 FR 53313	Implementation of a Dose Standard After 10,000 Years	178394
Carrigan et al. 1991	"Potential for Water-Table Excursions Induced by Seismic Events at Yucca Mountain, Nevada"	100967
Davies and Archambeau 1997	"Geohydrological Models and Earthquake Effects at Yucca Mountain, Nevada"	103180
DTN: SNF37100195002.001	Hydraulic Fracturing Stress Measurements in Test Hole: ESF-AOD-HDFR1, Thermal Test Facility, Exploratory Studies Facility at Yucca Mountain	131356
Gauthier et al. 1996	"Impacts of Seismic Activity on Long-Term Repository Performance at Yucca Mountain"	100447
National Research Council 1992	*Ground Water at Yucca Mountain, How High Can It Rise? Final Report of the Panel on Coupled Hydrologic/Tectonic/Hydrothermal Systems at Yucca Mountain*	105162
O'Brien 1993	*Earthquake-Induced Water-Level Fluctuations at Yucca Mountain, Nevada, June 1992*	101276
SNL 1996	*Hydraulic Fracturing Stress Measurements in Test Hole ESF-AOD-HDFR#1, Thermal Test Facility, Exploratory Studies Facility at Yucca Mountain*	163645
SNL 2007	*Saturated Zone Site-Scale Flow Model*	177391
SNL 2007	*Radionuclide Transport Models Under Ambient Conditions*	177396
Stock et al. 1985	"Hydraulic Fracturing Stress Measurements at Yucca Mountain, Nevada, and Relationship to the Regional Stress Field"	101027
Stock and Healy 1988	"Stress Field at Yucca Mountain, Nevada"	101022
Szymanski 1989	*Conceptual Considerations of the Yucca Mountain Groundwater System with Special Emphasis on the Adequacy of This System to Accommodate a High-Level Nuclear Waste Repository*	106963
von Seggern et al. 2001	*Seismicity in the Vicinity of Yucca Mountain, Nevada for the Period October 1, 1997, to September 30, 1999*	156297

FEP: 1.2.10.02.0A

FEP NAME:

Hydrologic Response to Igneous Activity

FEP DESCRIPTION:

Igneous activity includes magmatic intrusions, which may alter groundwater flow pathways, and thermal effects that may heat up groundwater and rock. Igneous activity may change the groundwater flow directions, water level, water chemistry, and temperature. Eruptive and extrusive phases may change the topography, surface drainage patterns, and surface soil conditions. This may affect infiltration rates and locations.

SCREENING DECISION:

Excluded – low consequence

SCREENING JUSTIFICATION:

Any future igneous activity in the Yucca Mountain region is expected to be basaltic (BSC 2004 [DIRS 169989], Section 6.2). The intrusion of a basalt dike at or near the repository block could locally alter the hydrological properties of the host rock and thereby affect flow-and-transport characteristics and radionuclide release to the accessible environment. The mean probability for the occurrence of a volcanic intrusion at Yucca Mountain is 1.7×10^{-8} per year (BSC 2004 [DIRS 169989], Table 7-1), which is not sufficiently low for exclusion from the TSPA on the basis of low probability (10 CFR 63.342 [DIRS 180319]). However, changes in hydrological properties caused by igneous activity are not expected to affect repository performance significantly, as discussed below.

The technical basis for exclusion from the TSPA of the hydrologic response to igneous activity relies on a variety of information including phenomena observed at analogue sites (such as thermal and geochemical effects on rock properties), analysis of effects of igneous activity on groundwater flow pathways, analysis of the potential for the development of a hydrothermal system, and analysis of the potential effects of eruptions on surface topography. These topics are discussed in the following paragraphs. Not all of the studies discussed here were performed for the purpose of assessing igneous impacts on hydrology, nevertheless, they still have considerable relevance to this subject and inferences from these studies may be drawn.

Observed Phenomena at Analogue Sites—Observations of mineral alterations around igneous intrusions at natural analogue sites show that alteration is limited to a zone that extends less than 10 m away from the intrusion/host rock contact (CRWMS M&O 1998 [DIRS 105347], pp. 5-41 to 5-71; Valentine et al. 1998 [DIRS 119132], p. 5-74). An appropriate analogue for understanding the characteristics of a volcanic event at Yucca Mountain is the Paiute Ridge intrusive/extrusive center (Byers and Barnes 1967 [DIRS 101859]) on the northeastern margin of the Nevada Test Site. The Paiute Ridge center is a small-volume Miocene volcanic center comparable in volume and composition to Quaternary volcanoes near Yucca Mountain (BSC 2004 [DIRS 169989], Section 6.3.2.1). Paleomagnetic, geochronologic, and geochemical

data indicate that the entire intrusive/extrusive complex formed during a brief magmatic pulse and thus represents a single volcanic event. The vents and associated dike system formed within a north-northwest-trending extensional graben, and there are excellent exposures of a variety of system depths. This includes remnants of surface lava flows, volcanic conduits, and dikes and sills intruded into tuff country rock at depths of up to 300 m. There is evidence of shallow structural control of dike emplacement at Paiute Ridge, including dike emplacement along fault planes (Byers and Barnes 1967 [DIRS 101859]). Dike lengths at Paiute Ridge range from less than 1 km to 5 km, comparable to the range estimated for post-Miocene volcanism near Yucca Mountain.

The margins of the Paiute Ridge dike complex are described in detail by Carter Krogh and Valentine (1996 [DIRS 160928], pp. 7 and 8) and are also discussed in the analysis of excluded FEP 1.2.04.02.0A (Igneous Activity Changes Rock Properties). In the region of an intrusion, zones of change in host-rock properties occur. Alterations include formation of vitrophyres and/or various degrees of contact welding of the host rock, vesicle formation, and formation of fiamme, which are flattened glassy inclusions. Carter Krogh and Valentine (1996 [DIRS 160928]) report that "Visible thermal effects on the wall rocks disappear within 1 m of the dike margin." The spatial extent of the alteration caused by dikes was also confirmed using x-ray diffraction, x-ray fluorescence, and ion chromatograph analytical methods to detect changes in mineralogical content and volatiles gained or lost during contact metamorphism (Valentine et al. 1998 [DIRS 119132], p. 5-44). Alteration effects were found to be limited to within 5 to 10 m of the dike margin (Valentine et al. 1998 [DIRS 119132], p. 5-41). Hydrologic changes are therefore also expected to be confined to within a few meters of the dike margin. As discussed in excluded FEP 1.2.04.02.0A (Igneous Activity Changes Rock Properties), dike orientations are expected to be subparallel to the major flow directions in the unsaturated zone and saturated zone, resulting in a negligible effect on unsaturated zone and saturated zone flow. A detailed discussion of the expected configuration of igneous intrusions and their effects on flow patterns and perched water is presented in excluded FEP 1.2.04.02.0A (Igneous Activity Changes Rock Properties).

There is no indication in the unsaturated zone of extensive hydrothermal circulation and alteration, brecciation, deformation related to magmatic intrusion, or vapor-phase recrystallization during the magmatic intrusions into the vitric and zeolitized tuffs (CRWMS M&O 1998 [DIRS 105347], p. 5-42). Further discussion concerning the effects of igneous intrusions on mineralogy is given in excluded FEP 1.2.04.02.0A (Igneous Activity Changes Rock Properties). Given the limited area of alteration around the intrusion, the impact of any geochemical changes are minimal in the unsaturated zone. Because saturated zone water chemistry is dominated by the chemical and atmospheric conditions and the large volume of paleoclimate recharge waters, the small volume of igneous-altered rock would have little impact on the characteristics of saturated zone water chemistry along groundwater flow paths as discussed in included FEP 2.2.08.01.0A (Chemical Characteristics of Groundwater in the Saturated Zone) and excluded FEP 2.2.08.03.0A (Geochemical Interactions and Evolution in the Saturated Zone). Thus, the regional saturated zone geochemistry in the Yucca Mountain vicinity will not be significantly affected by igneous activity.

Interaction with Repository Drifts—A dike intersecting a repository drift would result in magma entering the drift. A simple conduction-only cooling model indicates that if a drift is

instantaneously and entirely filled with basaltic magma at 1,150°C, it (and the surrounding rock) will cool to sub-boiling in less than three years, with boiling temperatures extending no more than 10 m from the drift (SNL 2007 [DIRS 177430], Figures 6-98 and 6-99; DTN: MO0408EG831811.008 [DIRS 173078]). Contact metamorphism caused by dikes appears to be confined to distances of less than 5 m from the dike (BSC 2004 [DIRS 169734], Section 4.2.3.5). With significant thermal perturbations limited to less than 100 years and alteration limited to zones of a few meters around the dike, the thermal and chemical effects of basaltic magmatism on unsaturatede zone processes in the vicinity of an intersected repository drift would be negligible.

Several configurations are possible as a result of post-intrusion in-drift conditions. One possible scenario is that the drift will be filled with cooled but fractured magma that will maintain the capillary barrier and flow diversion potential at the interface. A second scenario is that the magma may drain out of the interior, leaving an air space that would also maintain the capillary barrier. The third scenario is for the magma to encapsulate the waste, but with few cooling joints, thereby providing no capillary barrier. In the TSPA model, only the third scenario is invoked and is justified as an approximation that does not underestimate the impact of the event on system performance. After post-intrusive magma cooling, seepage water is expected to flow through the contact metamorphic aureole and react with the basalt in the intruded emplacement drifts. The geochemical interactions of the seepage water and rock and the resulting hydrochemistry are addressed in included FEP 1.2.04.04.0B (Chemical Effects of Magma and Magmatic Volatiles).

Potential for Development of a Hydrothermal System—Findings from the Paiute Ridge analogue site indicate that "the occurrence of low-temperature clinoptilolite and opal also suggests that thermal transfer into the adjacent country rock was minimal" (CRWMS M&O 1998 [DIRS 105347], p. 5-57). Findings from the Grants Ridge analogue site in New Mexico suggest the absence of a hydrothermal system at that location (CRWMS M&O 1998 [DIRS 105347], p. 5-74). Further, the study concluded that, "an intrusion at Yucca Mountain would not result in large amounts of hydrothermally driven mass transfer" (CRWMS M&O 1998 [DIRS 105347], p. 5-74). Consequently, the development of hydrothermal systems from igneous activity is excluded from the TSPA based on low consequence due to their limited size relative to the repository footprint. Hydrothermal activity is also discussed in excluded FEP 1.2.06.00.0A (Hydrothermal Activity).

Effects on the Water Table—Kuiper (1991 [DIRS 163417], p. 121) suggested that if a 10-km-long, 5-km-deep, and 100-m-wide disc-shaped dike initially intruded into the saturated zone, the maximum rise in the water table due to heat effects would be on the order of 25 m; not a sufficiently large increase to impact flow pathways or saturate the repository horizon (see included FEPs 1.3.07.02.0A (Water Table Rise Affects SZ) and 1.3.07.02.0B (Water Table Rise Affects UZ)). Furthermore, the dike analyzed by Kuiper (1991 [DIRS 163417]]) is much larger than the estimated size distributions for any potential future dikes at Yucca Mountain (SNL 2007 [DIRS 174260], Table 7-1).

Potential Topographic and Surface Effects Following an Eruption—There is a potential for igneous activity (primarily via eruption or effusive flow) to change surface topography, and subsequently affect drainage and infiltration. The effects could hypothetically result in

temporary obstruction of a drainage system by a lava flow at the surface or as a result of the sloughing of ash or soil materials from hill slopes into drainages. The steep topographic gradients at Yucca Mountain above the repository and the limited extent of effusive flow from small-scale volcanoes such as Lathrop Wells (SNL 2007 [DIRS 174260], Section C.9) would limit the consequences of any such topographic changes. Lava flows along the northern edge of the northeast lava field of the Lathrop Wells volcano did block a drainage channel resulting in a temporary, and possibly ephemeral, impoundment of water (SNL 2007 [DIRS 174260], Appendix C). Subsequent erosion produced new channels, allowing any drainage water to flow around the blockage. The formation of the impoundment was a result of the (1) relatively flat topography in the vicinity of the the Lathrop Wells volcano, (2) the geometry of the fault-block bounded valley where the volcano resides, and (3) the relatively large drainage area associated with the blocked channel. Even if a lava dam were to form in one of the washes that drain the repository block at Yucca Mountain, it would not produce a large surface-water impoundment relative to the repository emplacement area because of the steeper topography, narrower widths, and smaller drainage areas of these washes as compared with the Lathrop Wells case. Consequently, significant ponding and consequent increased infiltration are not anticipated. Included FEP 1.2.04.07.0C (Ash Redistribution via Soil and Sediment Transport) discusses assumptions regarding infiltration of radionuclides into underlying soil following ash flow and subsequent redistribution.

Another potential effect of igneous activity would be the deposition of an ash cover on the repository block. The range of mean particle size erupted during violent Strombolian eruptions is described by a log-triangular distribution with a minimum of 0.01 mm, a mode of 0.1 mm, and a maximum of 1.0 mm (SNL 2007 [DIRS 174260], Table 7-1). These values are typical of median grain sizes in silt, fine sand, and coarse sand, which typically have porosities of 40%, 35%, and 30%, respectively (Bear 1972 [DIRS 156269], pp. 40 and 46). Using these porosity and grain size ranges and the modified Kozeny-Carman equation for permeability (Bear 1972 [DIRS 156269], p. 166):

$$k = \frac{d_m^2}{180} \frac{n^3}{(1-n)^2}$$

where k is permeability, d_m is grain size, and n is porosity, the estimated permeability of the ash deposit ranges from 4×10^{-14} to 2×10^{-10} m^2. Mean bedrock saturated hydraulic conductivity in the infiltration model ranges from 6×10^{-7} to 3×10^{-5} m/s, corresponding to a permeability range of 7×10^{-14} to 3×10^{-12} m^2, and soil saturated hydraulic conductivity ranges from 7×10^{-7} to 11×10^{-7} m/s, corresponding to a permeability range of 7×10^{-14} to 1×10^{-13} m^2 (SNL 2008 [DIRS 182145], Tables 6.5.2.3-1 and 6.5.2.6-1). Therefore, an ash deposit is expected to have a permeability similar to or higher than that of the underlying bedrock and soil. Vertical flow will be limited by the lowest permeability units (the soil and bedrock in this case), and therefore the ash deposit would not cause a significant increase in infiltration rates. Based on the analyses in the net infiltration model report (SNL 2008 [DIRS 182145]), infiltration decreased as the soil thickness increased. The porous ash would behave hydraulically as an increase in soil thickness, and thus the deposited ash would be expected to decrease net infiltration, after vegetation is reestablished. The establishment of vegetation is important

because the increased soil thickness (or added ash) allows infiltrated water to be stored within the root zone of the plants, which then transpire the water back to the atmosphere.

Summary—Igneous intrusions that might occur in the time frame of 10,000 years after closure would affect a relatively small volume of the host rock and are expected to be oriented subparallel to existing flow directions. Consequently, future intrusions would not have a significant effect on groundwater flow patterns or water levels. Given the limited area of any thermal or geochemical alteration, and the consequent change of rock properties around an intrusion, any geochemical effects would be minimal. The potential development of a hydrothermal system from igneous activity is not expected based on analogue studies and would be of low consequence due to its limited size relative to the repository footprint. Any possible changes to topography and soils from extrusive activity are also of low consequence.

Based on the previous discussion, omission of FEP 1.2.10.02.0A (Hydrologic Response to Igneous Activity) will not result in a significant adverse change in the magnitude or timing of either radiological exposures to the RMEI or radionuclide releases to the accessible environment. Therefore, this FEP is excluded from the performance assessments conducted to demonstrate compliance with proposed 10 CFR 63.311 and 63.321 (70 FR 53313 [DIRS 178394]), and with 10 CFR 63.331 [DIRS 180319], on the basis of low consequence.

INPUTS:

Table 1.2.10.02.0A-1. Direct Inputs

Input	Source	Description
BSC 2004. *Characterize Framework for Igneous Activity at Yucca Mountain, Nevada*. [DIRS 169989]	Table 7-1	Probability of a volcanic event at Yucca Mountain
DTN: MO0408EG831811.008. Magma Cooling and Solidification. [DIRS 173078]	file: *MO0408EG831811.008. zip*	Simple conduction-only cooling model
SNL 2007. *Characterize Eruptive Processes at Yucca Mountain, Nevada*. [DIRS 174260]	Table 7-1	Describes the range of mean particle size erupted during violent Strombolian eruptions
SNL 2007. *Dike/Drift Interactions*. [DIRS 177430]	Figures 6-98, 6-99	Simple conduction-only cooling model
Valentine et al. 1998. "Physical Processes of Magmatism and Effects on the Potential Repository: Synthesis of Technical Work Through Fiscal Year 1995." [DIRS 119132]	p. 5-74	Mineral alterations around igneous intrusions at natural analogue sites show that alteration is limited to a zone that extends less than 10 m away from the intrusion/host rock contactaround igneous intrusions at natural analogue sites

Table 1.2.10.02.0A-2. Indirect Inputs

Citation	Title	DIRS
10 CFR 63	Energy: Disposal of High-Level Radioactive Wastes in a Geologic Repository at Yucca Mountain, Nevada	180319
70 FR 53313	Implementation of a Dose Standard After 10,000 Years	178394
Bear 1972	*Dynamics of Fluids in Porous Media. Environmental Science Series*	156269
BSC 2004	*Characterize Framework for Igneous Activity at Yucca Mountain, Nevada*	169989
BSC 2004	*Yucca Mountain Site Description*	169734
Byers and Barnes 1967	*Geologic Map of the Paiute Ridge Quadrangle, Nye and Lincoln Counties, Nevada*	101859
Carter Krogh and Valentine 1996	*Structural Control on Basaltic Dike and Sill Emplacement, Paiute Ridge Mafic Intrusion Complex, Southern Nevada*	160928
CRWMS M&O 1998	*Synthesis of Volcanism Studies for the Yucca Mountain Site Characterization Project*	105347
Kuiper 1991	"Water-Table Rise Due to Magma Intrusion Beneath Yucca Mountain"	163417
SNL 2007	*Characterize Eruptive Processes at Yucca Mountain, Nevada*	174260
SNL 2008	*Simulation of Net Infiltration for Present-Day and Potential Future Climates*	182145
Valentine et al. 1998	"Physical Processes of Magmatism and Effects on the Potential Repository: Synthesis of Technical Work Through Fiscal Year 1995"	119132

FEP: 1.3.01.00.0A

FEP NAME:

Climate Change

FEP DESCRIPTION:

Climate change may affect the long-term performance of the repository. This includes the effects of long-term change in global climate (e.g., glacial/interglacial cycles) and shorter-term change in regional and local climate. Climate is typically characterized by temporal variations in precipitation and temperature.

SCREENING DECISION:

Included

TSPA DISPOSITION:

Global climate change is addressed in TSPA, using a climate analysis based on paleoclimate information. That is, the record of climate changes in the past is used to predict the expected changes in climate for the future. Future climates are described in terms of discrete climate states that are used to approximate continuous variations in climate. The discussion in this FEP is limited to natural processes. The effects of human activity on climate change are addressed in excluded FEP 1.4.01.00.0A (Human Influences on Climate).

Future climate forecasts (BSC 2004 [DIRS 170002]) indicate that the climate at Yucca Mountain is predicted to evolve to the cooler, wetter conditions of a glacial-transition climate within the first 10,000 years after disposal. Within that period of time, the present-day climate is predicted to last for 400 to 600 years after present; a monsoon climate is predicted to last from the end of the present-day climate to between 900 and 1,400 years after present; and a glacial-transition (intermediate) climate state is predicted to last for the remainder of the 10,000-year period (BSC 2004 [DIRS 170002], Table 6-1). A fourth climate state is based on regulation (proposed 10 CFR 63.342(c)(2) (70 FR 53313 [DIRS 178394) and continues from 10,000 years to 1,000,000 years postclosure. To simplify how the climate change is implemented in the TSPA model for the first 10,000 years postclosure, only the maximum durations were used (i.e., 600 years for the present-day climate, 1,400 years for the monsoon climate, and 8,000 years for the glacial-transition climate) (SNL 2008 [DIRS 183478], Section 6.3.1.2). Proposed 10 CFR 63.305(c) (70 FR 53313 [DIRS 178394]) requires that the DOE vary factors related to climate based on cautious but reasonable assumptions. At the same time, changes in society, the biosphere (other than climate), human biology, or increases or decreases of human knowledge or technology should not be projected (10 CFR 63.305(b) [DIRS 180319]). The climate change FEP was evaluated and addressed from the perspective of natural processes and from the perspective of the factors that are related to human activity. In accordance with the proposed rule (70 FR 53313 [DIRS 178394], pp. 53315 and 53316), the effects of climate change after 10,000 years, but within the period of geologic stability, are assumed to be limited to the results of increased percolation of water through the repository, with percolation rates reflecting climate conditions that are wetter and cooler than present-day conditions.

Climate change is addressed in the unsaturated zone model and incorporated into TSPA through the use of unsaturated zone flow fields that have different surface water infiltration rates as a result of the four different climate states. For the pre-10,000-year climate states, climate conditions are addressed in the infiltration model (SNL 2008 [DIRS 182145], Section 6.5.1.1[a]) through the selection of analogues at other locations with present-day climates that are representative of the range of future climate conditions projected at Yucca Mountain (BSC 2004 [DIRS 170002], Section 6.6). The meteorological data from these analogues are then used for modeling infiltration under these future climate conditions at Yucca Mountain. A description of the modeling methods used for infiltration, and of how it is affected by climate, is given in *Simulation of Net Infiltration for Present-Day and Potential Future Climates* (SNL 2008 [DIRS 182145], Section 6.5).

For the post-10,000-year period, the climate change analysis is limited to the effects of increased water flow through the repository as a result of climate change, and the resulting transport and release of radionuclides to the accessible environment, in accordance with proposed 10 CFR 63.342(c)(2) (70 FR 53313 [DIRS 178394]), which defines the deep percolation rates for that period as based on a log-uniform probability distribution from 13 to 64 mm/yr. Unsaturated zone flow weighting factors were used to calibrate the unsaturated zone model using input from four infiltration maps representing the 10th, 30th, 50th, and 90th percentile infiltration scenarios for the present-day climate. The weighting factors were calculated to be 0.62, 0.16, 0.16, and 0.06 for the 10th, 30th, 50th, and 90th percentile infiltration scenarios. The midpoints of these probability ranges for a cumulative probability distribution are at 0.31, 0.70, 0.86, and 0.97, respectively. These midpoints were applied to the log-uniform proposed percolation flux range of 13 to 64 mm/yr resulting in targets of 21.29, 39.52, 51.05, and 61.03 mm/yr for the 10th, 30th, 50th, and 90th percentile infiltration scenarios, respectively. These midpoints were compared to the average infiltration calculated (over the repository footprint) for the 12 infiltration maps. Four maps were selected that most closely matched the midpoint values. The four infiltration maps that were selected and scaled are: the present-day 90th percentile, the glacial-transition 50th percentile, the glacial-transition 90th percentile, and the monsoon 90th percentile infiltration maps. These maps were scaled so that the average water flux rates through the repository footprint exactly matched the target values at the repository horizon. Once the infiltration boundary condition was determined, the methods used to generate the post-10,000-year flow fields were the same as used to generate the pre-10,000-year flow fields (SNL 2007 [DIRS 184614], Section 6.1.4).

The results of the infiltration model are then used for computing unsaturated zone flow throughout the UZ flow model domain, which includes the repository waste emplacement zone. The UZ flow model uses the infiltration results as top boundary conditions for unsaturated zone flow calculations (SNL 2007 [DIRS 184614], Section 6.1.4). The UZ flow fields are used directly in TSPA (SNL 2007 [DIRS 184614], Section 6.2.5). The output flow fields are in DTNs: LB0612PDFEHMFF.001 [DIRS 179296]; LB0701MOFEHMFF.001 [DIRS 179297]; LB0701GTFEHMFF.001 [DIRS 179160]; and LB0702PAFEM10K.002 [DIRS 179507], developed for use in performance assessment (SNL 2008 [DIRS 183478]).

Changes in net infiltration resulting from future climate change is also implicitly included in *Multiscale Thermohydrologic Model* (SNL 2008 [DIRS 184433], which predicts the expected range in the thermal-hydrologic parameters including: temperature and relative humidity. This

model uses the unsaturated zone flow fields as one of its inputs and therefore model results are affected by climate change.

Climate change is included in the treatment of radionuclide transport for the TSPA as discussed in *Particle Tracking Model and Abstraction of Transport Processes* (SNL 2008 [DIRS 184748], Section 6.4.8). The effect of climate change on repository performance was studied by using pre-generated flow fields under different climates (DTNs: LB0612PDFEHMFF.001 [DIRS 179296], LB0701MOFEHMFF.001 [DIRS 179297], LB0701GTFEHMFF.001 [DIRS 179160], and LB0702PAFEM10K.002 [DIRS 179507]). For the TSPA, the pregenerated flow fields are used by the finite element heat and mass (FEHM) model as described in *Particle Tracking Model and Abstraction of Transport Processes* (SNL 2008 [DIRS 184748], Section 6.4.9).

The effects of climate change are also included in the model for seepage water chemistry through changes in the percolation flux rates. The percolation flux values used in the model are based on fluxes at the PTn/TSw boundary predicted by the UZ flow model, given in the following four DTNs: LB0612PDPTNTSW.001 [DIRS 179150], LB0701MOPTNTSW.001 [DIRS 179156], LB0701GTPTNTSW.001 [DIRS 179153], and LB0702UZPTN10K.002 [DIRS 179332] representing each climate state. The approach used is a plug flow model that has a transport velocity equal to the percolation flux divided by the product of the average porosity and the average water saturation (SNL 2007 [DIRS 177412], Section 6.3.2.4.4). The effects of flow on the water chemistry are evaluated in terms of the amount of feldspar dissolution that occurs during flow through the TSw (SNL 2007 [DIRS 177412], Sections 6.3.2.4.5). This is a function of the ambient feldspar dissolution rate, the dissolution rate temperature dependence, the model for the thermal field, and the plug flow model for transport through the TSw (SNL 2007 [DIRS 177412], Section 6.3.2.4.5). The starting point for evaluating potential water compositions in the near field is the composition of ambient pore waters in the TSw. The available pore water data from the four repository host units (Tptpul, Tptpmn, Tptpll, Tptpln) were evaluated and grouped into four compositional groups (SNL 2007 [DIRS 177412], Section 6.3.2.3). The amount of feldspar dissolution is passed to TSPA in a lookup table, as the water–rock interaction parameter, or WRIP (SNL 2007 [DIRS 177412], Section 6.3.2.4.5; DTN: SN0703PAEBSPCE.006 [DIRS 181571]).

Potential effects of climate change on the amount of infiltration and percolation are similarly taken into account in *Abstraction of Drift Seepage* (SNL 2007 [DIRS 181244], Section 6.6.5). Seepage is calculated in the TSPA using percolation flux distributions based on results from the UZ flow and transport model (SNL 2007 [DIRS 184614], Section 6.4[a]) given in DTNs: LB0612PDPTNTSW.001 [DIRS 179150], LB0701MOPTNTSW.001 [DIRS 179156], LB0701GTPTNTSW.001 [DIRS 179153], and LB0702UZPTN10K.002 [DIRS 179332] representing each climate state. Condensation of water along the drift wall is affected by changes in climate and associated unsaturated zone flow as described in *In-Drift Natural Convection and Condensation* (SNL 2007 [DIRS 181648]), since percolation is used as an input to the drift wall condensation model.

The effects of climate change on radionuclide transport in the saturated zone are incorporated into the SZ flow and transport abstraction model and the SZ one-dimensional transport model as implemented in the TSPA by assuming instantaneous change from one steady-state flow

condition to another steady-state condition in the saturated zone. Changes in climate state are assumed to affect the magnitude of groundwater flux through the saturated zone system but have a negligible impact on flow paths. The effect of changes in groundwater flux is incorporated into the SZ flow and transport abstraction model by scaling the timing of radionuclide mass breakthrough curves proportionally to the change in SZ-specific discharge (SNL 2008 [DIRS 183750], Section 6.5).

In the biosphere model, the effect of climate change on the BDCFs for the groundwater exposure scenario must be weighed against two requirements. One requirement is not to project changes in society, the biosphere (other than climate), human biology, or increases or decreases of human knowledge or technology (10 CFR 63.305(b) [DIRS 180319]). The other requirement is to vary factors related to climate based on cautious but reasonable assumptions consistent with present knowledge (proposed 10 CFR 63.305(c) (70 FR 53313 [DIRS 178394])). Because BDCFs are a function of climate factors that depend on human activities and those that do not, the effect of climate change on BDCFs needed to be evaluated from the perspective of these two requirements. It was concluded that human activities, which should not be projected to change, have the largest effect on the BDCFs, and that the BDCFs are relatively insensitive to climate change effects on those parameters that are independent of human activities (SNL 2007 [DIRS 177399], Section 6.11.3). Therefore, consistent with the requirement not to project changes in human knowledge or technology, present-day climate BDCFs for the groundwater exposure scenario are used for both the pre-10,000-year and the post-10,000-year performance assessment calculations. This represents an appropriate balance between these two requirements, meets the requirements of 10 CFR 63.305(b) [DIRS 180319] and proposed 10 CFR 63.305(c) (70 FR 53313 [DIRS 178394]), and is appropriate for the assessment of doses to the RMEI for 10,000 years following disposal as well as after 10,000 years, but within the period of the geologic stability (SNL 2007 [DIRS 177399], Section 6.11.3).

BDCFs for the volcanic ash exposure scenario were relatively insensitive to the effects of the climate change on the model parameters. Therefore, the present-day climate BDCFs for the volcanic ash exposure scenario were used in the TSPA for the 10,000-year period following repository closure and beyond 10,000 years, within the period of geologic stability, as prescribed by proposed 10 CFR Part 63 (70 FR 53313 [DIRS 178394]) (SNL 2007 [DIRS 177399], Section 6.12.3).

The biosphere component of the climate change FEP is implemented in the TSPA through the groundwater and volcanic BDCFs. The BDCFs for all biosphere model realizations are provided as inputs to the TSPA model, which randomly samples the BDCFs to propagate uncertainty from the biosphere model into TSPA dose calculations.

In summary, climate change is included in the TSPA model of the geosphere and biosphere transport for the performance assessments that demonstrate compliance with the individual protection standards in proposed 10 CFR 63.311 and 10 CFR 63.321 (70 FR 53313 [DIRS 178394]). For the human intrusion event (proposed 10 CFR 63.321 (70 FR 53313 [DIRS 178394])), only the post-10,000-year climate is used, because the human intrusion event is not expected to occur before 10,000 years following disposal. For the performance assessment that demonstrates compliance with the groundwater protection standards (10 CFR 63.331

[DIRS 180319]), only those components of this FEP that address the geosphere transport are included.

INPUTS:

Table 1.3.01.00.0A-1. Indirect Inputs

Citation	Title	DIRS
10 CFR 63	Energy: Disposal of High-Level Radioactive Wastes in a Geologic Repository at Yucca Mountain, Nevada	180319
70 FR 53313	Implementation of a Dose Standard After 10,000 Years	178394
BSC 2004	*Future Climate Analysis*	170002
DTN: LB0612PDFEHMFF.001	Flow-Field Conversions from TOUGH2 to FEHM Format for Present Day 10-, 30-, 50-, and 90-Percentile Infiltration Maps	179296
DTN: LB0612PDPTNTSW.001	Vertical Flux at PTN/TSW Interface for Present-Day Climate of 10th, 30th, 50th, and 90-Percentile Infiltration Maps	179150
DTN: LB0701GTFEHMFF.001	Flow-Field Conversions from TOUGH2 to FEHM Format for Glacial Transition Climate 10th-, 30th-, 50th-, and 90th-Percentile Infiltration Maps	179160
DTN: LB0701GTPTNTSW.001	Vertical Flux at PTN/TSW Interface for Glacial Transition Climate of 10th, 30th, 50th, and 90th-Percentile Infiltration Maps	179153
DTN: LB0701MOFEHMFF.001	Flow-Field Conversions from TOUGH2 to FEHM Format for Monsoon Climate 10th-, 30th-, 50th-, and 90th-Percentile Infiltration Maps	179297
DTN: LB0701MOPTNTSW.001	Vertical Flux at PTN/TSW Interface for Monsoon Climate of 10th, 30th, 50th and 90th-Percentile Infiltration Maps	179156
DTN: LB0702PAFEM10K.002	Flow Field Conversions to FEHM Format for Post 10,000 Year Peak Dose Fluxes in the Unsaturated Zone for Four Selected Infiltration Rates	179507
DTN: LB0702UZPTN10K.002	Vertical Flux at PTN/TSW Interface for Post-10K-Year Climate Infiltration Maps	179332
DTN: SN0703PAEBSPCE.006	Physical and Chemical Environment (PCE) TDIP Water-Rock Interaction Parameter Table and Salt Separation Tables with Supporting Files	181571
SNL 2007	*Biosphere Model Report*	177399
SNL 2007	*Abstraction of Drift Seepage*	181244
SNL 2007	*Engineered Barrier System: Physical and Chemical Environment*	177412
SNL 2007	*In-Drift Natural Convection and Condensation*	181648
SNL 2007	*UZ Flow Models and Submodels*	184614
SNL 2008	*Multiscale Thermohydrologic Model*	184433
SNL 2008	*Particle Tracking Model and Abstraction of Transport Processes*	184748
SNL 2008	*Saturated Zone Flow and Transport Model Abstraction*	183750
SNL 2008	*Simulation of Net Infiltration for Present-Day and Potential Future Climates*	182145
SNL 2008	*Total System Performance Assessment Model/Analysis for the License Application*	183478

FEP: 1.3.04.00.0A

FEP NAME:

Periglacial Effects

FEP DESCRIPTION:

This FEP addresses the physical processes and associated landforms in cold but ice-sheet-free environments. Permafrost and seasonal freeze/thaw cycles are characteristic of periglacial environments. These effects could include erosion and deposition.

SCREENING DECISION:

Excluded – low consequence

SCREENING JUSTIFICATION:

This FEP refers to climate conditions that could produce a cold, but ice-sheet-free, environment at Yucca Mountain. The consequences of such a climate could include permafrost (permanently frozen ground), although paleoclimate records indicate that the climate conditions necessary to form permafrost are not expected at Yucca Mountain over the next 10,000 years (BSC 2004 [DIRS 170002], Section 6.6.2). This analysis forecasts that during the next 10,000 years the climate will evolve from the present interglacial climate through the monsoon to glacial-transition climate (BSC 2004 [DIRS 170002], Section 7.1). The glacial-transition climate (identified as "intermediate" in Sharpe 2003 [DIRS 161591], Table 6-6) has the lowest predicted mean annual temperatures for the 10,000-year period following repository closure (BSC 2004 [DIRS 170002], Section 6.6.2; Sharpe 2003 [DIRS 161591], Section 6.3.2). For the glacial-transition climate, analogue sites provide a basis for the conclusion that the estimated range of mean annual temperatures is 8.3°C to 10.1°C (DTN: UN0201SPA021SS.007 [DIRS 161588], file: *table 6-3.doc*; Sharpe 2003 [DIRS 161591], Table 6-3), which is too warm to sustain permafrost. Only the coldest scenario for the full glacial climate (Oxygen Isotope Stage 6/16) is expected to have a mean annual temperature of 0°C (Sharpe 2003 [DIRS 161591], Figure 6-4). The expected return to such a climate is 200,000 years after present (Sharpe 2003 [DIRS 161591], Table 6-5), although, even during the last glacial maximum, the mean annual temperature at Yucca Mountain exceeded 0°C (Thompson et al. 1999 [DIRS 109470], Figures 17 and 18).

The consequence of permafrost at Yucca Mountain can be evaluated using the risk-informed approach by considering the joint outcome of the probability of this process and its consequences. Considering the zero probability of the mean annual temperature in the Yucca Mountain region being 0°C or less during the 10,000-year period following repository closure (see excluded FEP 1.3.05.00.0A (Glacial and Ice Sheet Effects)), and the low consequence of permafrost (because the agriculture for the cooler and wetter conditions would rely less on irrigation than under the present-day climatic conditions), the impact of omitting this FEP from the TSPA would be insignificant.

Another process included in this FEP are the seasonal freeze/thaw cycles, which could influence soil erosion and deposition. Freeze/thaw mechanical erosion is expected to increase as the climate cools. However, the degree of erosion is expected to be insignificant even during the cooler climate condition. The time-averaged erosion at Yucca Mountain over a 10,000-year period is expected to be less than 10 cm (YMP 1993 [DIRS 100520], Section 3.4). This is based on estimates for erosion rates at Yucca Mountain over the last 12 million years (YMP 1993 [DIRS 100520], Section 3.4) and therefore includes the effects of cooler climates, including full glacial periods.

The erosion rate is an input parameter for the biosphere model. It is one of the parameters that influence the radionuclide concentration in surface soils (SNL 2007 [DIRS 177399], Sections 6.4.1.1 and 6.4.1.4). The value of this parameter, as used in the biosphere model, is characteristic of agricultural soils, unlike the erosion rate caused by natural processes discussed in the previous paragraph, including those in the Amargosa Valley area. The erosion rate is in the range from 0.2 to 1.1 $kg/m^2/yr$, which corresponds to 1.3×10^{-4} to 7.3×10^{-4} m/yr, when a soil bulk density of 1,500 kg/m^3 is used (DTN: MO0609SPASRPBM.004 [DIRS 179988], Sections 1 and 3). Over 10,000 years, this erosion rate would result in the removal/replacement of 1.3 to 7.3 m of cultivated soil. The erosion rate on noncultivated cropland and on pastureland is much lower than that for the cultivated cropland, even in the areas located farther north than southern Nevada that would experience freeze/thaw cycles (USDA 2000 [DIRS 160548], Tables 10 and 11). Therefore, the additional effect of the seasonal freeze/thaw cycles, if these occurred, would be insignificant on the erosion rate in comparison with the erosion caused by agricultural activities. Consequently, periglacial effects will not have a significant impact on the output of the biosphere model.

The effects of seasonal freeze/thaw cycles on deposition are expected to increase when the climate evolves from the present-day climate to a cooler and wetter climate. The compliance point is located within the depositional basin on the Fortymile Wash alluvial fan. The evolution of Fortymile Wash indicates that the overall process in this system during the Quaternary has been aggradation (i.e., the accumulation of deposits) (YMP 1993 [DIRS 100520], Section 3.4). The influx of uncontaminated material into the compliance location would lower the radionuclide concentration in the soil (and thus the dose to the RMEI) due to dilution.

Based on the preceding discussion, omission of FEP 1.3.04.00.0A (Periglacial Effects) will not result in a significant adverse change in the magnitude or time of radiological exposures to the RMEI or radionuclide releases to the accessible environment. Therefore, this FEP is excluded from the performance assessments conducted to demonstrate compliance with proposed 10 CFR 63.311 and 63.321 (70 FR 53313 [DIRS 178394]), and with 10 CFR 63.331 [DIRS 180319], on the basis of low consequence.

INPUTS:

Table 1.3.04.00.0A-1. Direct Inputs

Input	Source	Description
BSC 2004. *Future Climate Analysis*. [DIRS 170002]	Section 7.1	Analysis forecasts that during the next 10,000 years the climate will evolve from the present interglacial climate through the monsoon to glacial transition climate
DTN: MO0609SPASRPBM.004. Soil Related Parameters for the Biosphere Model. [DIRS 179988]	Sections 1 and 3	Range of erosion rates when soil density of 1,500 kg/m^3 is used
DTN: UN0201SPA021SS.007. Mean Annual Temperature and Precipitation for Select Western Regional Climate Locations. [DIRS 161588]	file: *table 6-3.doc*	Estimated range of mean annual temperatures for glacial-transition climate
Thompson et al. 1999. *Quantitative Paleoclimatic Reconstructions from Late Pleistocene Plant Macrofossils of the Yucca Mountain Region*. [DIRS 109470]	Figures 17, 18	During the last glacial maximum, the mean annual temperature at Yucca Mountain exceeded 0°C
USDA 2000. *Summary Report, 1997 National Resources Inventory (Revised December 2000)*. [DIRS 160548]	Tables 10, 11	Erosion rate on non-cultivated cropland and on pastureland is much lower than that for the cultivated cropland

Table 1.3.04.00.0A-2. Indirect Inputs

Citation	Title	DIRS
10 CFR 63	Energy: Disposal of High-Level Radioactive Wastes in a Geologic Repository at Yucca Mountain, Nevada	180319
70 FR 53313	Implementation of a Dose Standard After 10,000 Years	178394
BSC 2004	*Future Climate Analysis*	170002
Sharpe 2003	*Future Climate Analysis--10,000 Years to 1,000,000 Years After Present*	161591
SNL 2007	*Biosphere Model Report*	177399
YMP 1993	*Evaluation of the Potentially Adverse Condition "Evidence of Extreme Erosion During the Quaternary Period" at Yucca Mountain, Nevada*	100520

FEP: 1.3.05.00.0A

FEP NAME:

Glacial and Ice Sheet Effect

FEP DESCRIPTION:

This FEP addresses the effects of glaciers and ice sheets occurring within the region of the repository, including direct geomorphologic effects and hydrologic effects. These effects include changes in topography (due to glaciation and melt water), changes in flow fields, and isostatic depression and rebound. These effects could include erosion and deposition.

SCREENING DECISION:

Excluded – low probability

SCREENING JUSTIFICATION:

This FEP refers to the local effects of glaciers and ice sheets. Based on the paleoclimate records, the existence of glaciers or ice sheets at Yucca Mountain is not expected during the 10,000 years postclosure (BSC 2004 [DIRS 170002], Section 6.6). The analysis forecasts that during the next 10,000 years the climate will evolve from the present interglacial climate through the monsoon to glacial-transition climate (BSC 2004 [DIRS 170002], Section 7.1). The glacial-transition climate (identified as "intermediate" in Sharpe 2003 [DIRS 161591], Table 6-6) has the lowest predicted mean annual temperatures for the 10,000-year period following repository closure (BSC 2004 [DIRS 170002], Section 6.6.2; Sharpe 2003 [DIRS 161591], Section 6.3.2). For the glacial-transition climate, analogue sites provide a basis for the conclusion that the estimated range of mean annual temperatures is 8.3°C to 10.1°C (DTN: UN0201SPA021SS.007 [DIRS 161588], file: *table 6-3.doc*; Sharpe 2003 [DIRS 161591], Table 6-3), which is too warm to sustain glaciers or ice-sheets. Only the coldest scenario for the full glacial climate (Oxygen Isotope Stage 6/16) is expected to have a mean annual temperature of 0°C (Sharpe 2003 [DIRS 161591], Figure 6-4). The expected return for such a climate is 200,000 years-after-present (Sharpe 2003 [DIRS 161591], Table 6-5), although, even during the last glacial maximum, the mean annual temperature at Yucca Mountain exceeded 0°C (Thompson et al. 1999 [DIRS 109470], Figures 17 and 18).

The closest alpine glaciers to Yucca Mountain during the Pleistocene were in the White Mountains in California and possibly the Spring Range near Las Vegas (BSC 2004 [DIRS 169734], Section 6.4.1.4), both too far from Yucca Mountain to have any effect on site geomorphology or hydrology. Given the relatively low elevation of Yucca Mountain, there is no reasonable mechanism by which an alpine glacier could form at the site over the next 10,000 years. The geomorphologic and hydrological effects associated with glaciers, such as changes in topography resulting from erosion, deposition, and glacial transport, changes in flow fields, and isostatic depression and rebound, are therefore not expected to occur at Yucca Mountain.

An evaluation was made to demonstrate that this FEP is very unlikely to occur during the 10,000-year period following repository closure. As previously noted, the expected return of the maximum full glacial climate, when the mean annual temperature is at or below freezing, is approximately 200,000 years after present. This forecast is based on celestial mechanics involving earth-orbital cycles, which are corroborated by Devil's Hole and Owens Lake paleoclimatological records (BSC 2004 [DIRS 170002], Section 1; Sharpe 2003 [DIRS 161591], Section 1). The earth-orbital cycles result from the precession of the earth axis, variations in earth orbit eccentricity, and obliquity (i.e., changes in the Earth axis of rotation) (BSC 2004 [DIRS 170002], Section 6.4). The changes in these orbital parameters affect the total radiation received at the top of earth's atmosphere and thus the climate. Based on analysis of the timing of past climate changes associated with the Earth-orbital cycles it is very unlikely that an anomaly in the Earth's orbit would develop during the 10,000-year period following repository closure causing the full glacial climate. Because the climatic changes induced by changes in the Earth's orbit are not random, and the next maximum full glacial climate is not expected for approximately 200,000 years from present, the probability of glaciers and ice sheets forming at Yucca Mountain during the 10,000-year period following repository closure is considered to be zero.

Based on the preceding discussion, FEP 1.3.05.00.0A (Glacial and Ice Sheet Effects) is excluded from the performance assessments conducted to demonstrate compliance with proposed 10 CFR 63.311 and 63.321 (70 FR 53313 [DIRS 178394]), and with 10 CFR 63.331 [DIRS 180319], on the basis of low probability.

INPUTS:

Table 1.3.05.00.0A-1. Direct Inputs

Input	Source	Description
BSC 2004. *Future Climate Analysis*. [DIRS 170002]	Section 6.6	Description of future climate
	Section 7.1	Analysis forecasts that during the next 10,000 years the climate will evolve from the present interglacial climate through the monsoon to glacial transition climate
	Section 6.4	Description of earth orbital cycles and their causes
DTN: UN0201SPA021SS.007. Mean Annual Temperature and Precipitation for Select Western Regional Climate Locations. [DIRS 161588]	file: *table 6-3.doc*	Estimated range of mean annual temperatures for glacial-transition climate
Thompson et al. 1999. *Quantitative Paleoclimatic Reconstructions from Late Pleistocene Plant Macrofossils of the Yucca Mountain Region*. [DIRS 109470]	Figures 17, 18	During the last glacial maximum, the mean annual temperature at Yucca Mountain exceeded 0°C

Table 1.3.05.00.0A-2. Indirect Inputs

Citation	Title	DIRS
10 CFR 63	Energy: Disposal of High-Level Radioactive Wastes in a Geologic Repository at Yucca Mountain, Nevada	180319
70 FR 53313	Implementation of a Dose Standard After 10,000 Years	178394
BSC 2004	*Future Climate Analysis*	170002
BSC 2004	*Yucca Mountain Site Description*	169734
Sharpe 2003	*Future Climate Analysis—10,000 Years to 1,000,000 Years After Present*	161591

FEP: 1.3.07.01.0A

FEP NAME:

Water Table Decline

FEP DESCRIPTION:

Climate change could produce decreased infiltration (e.g., an extended drought), leading to a decline in the water table in the saturated zone, which would affect the release and exposure pathways from the repository.

SCREENING DECISION:

Excluded – low consequence

SCREENING JUSTIFICATION:

The Yucca Mountain region is a desert environment and future climate predictions indicate only increased precipitation (BSC 2004 [DIRS 170002], Sections 6.6 and 7.1; DTNs: GS000308315121.003 [DIRS 151139] and UN0201SPA021SS.007 [DIRS 161588]). Moreover, paleoclimate records indicate that arid conditions are short compared to wetter conditions while climatic conditions during the past two million years were wetter than current conditions 70% to 80% of the time (Forester et al. 1996 [DIRS 100148], p. 52). Analysis of Searles Lake deposits indicate that extremely dry conditions (resulting in lake desiccation) have occurred only twice within the past 600,000 years: once about 290,000 years ago and again in the past 10,000 years (Jannik et al. 1991 [DIRS 109434], p. 1,146 and Figure 10). This FEP examines the effects of a climate change over the next 10,000 years that lead to much drier conditions resulting in desertification of the surface environment, decreased infiltration, and declining water table elevation. It should be noted that the water table has been modeled to be higher for the post-10,000-year period because of the higher rate of deep infiltration required in 10 CFR 63.342(c) (70 FR 53313 [DIRS 178394]).

Present groundwater elevations in the Basin and Range province (which includes the Yucca Mountain region) reflect the current arid climatic conditions and the decrease in infiltration (i.e., decreased recharge) over the course of the present-day climate. The present-day climate extends for 600 years beyond the present in the TSPA. After the present-day climate, warmer and wetter monsoonal climatic conditions extend an additional 1,400 years. A cooler and wetter glacial-transition climatic condition will follow the brief monsoonal period and will persist for the remainder of the 10,000 years after repository closure (BSC 2004 [DIRS 170002], Section 7). *Future Climate Analysis* (BSC 2004 [DIRS 170002]) only predicts the average expected climate; however, this FEP addresses variability of future climates that could yield short-term, arid conditions that cause the current water table elevation to fall. However, these anomalously dry conditions are not expected to lower the water table elevation by more than a few meters (Luckey et al. 1996 [DIRS 100465], p. 29; Ervin et al. 1994 [DIRS 100633], pp. 11 to 13). Such small decreases to the water table elevation are well within the uncertainties included in both the unsaturated and saturated zone models and are therefore of low consequence.

Decreases in water table elevation would not degrade the performance of either the unsaturated or saturated zones. Specifically, a decreased water table elevation increases the unsaturated zone thickness. Decreases in the elevation of the water table result in a decrease in specific discharge because of the expected decrease in hydraulic gradient. Moreover, based on the saturated zone flow calculations, the transport pathways under current and expected wetter climatic conditions are confined to the following hydrostratigraphic units: the Crater Flat-Prow Pass, Crater Flat-Bullfrog, and Crater Flat-Tram, the Paintbrush Volcanic Aquifer, the Volcanic and Sedimentary Unit, and the Alluvium. Of these six units, most transport pathways pass through the Crater Flat-Bullfrog hydrostratigraphic unit (SNL 2007 [DIRS 177391], Figures 6-17 and 6-22). The Crater Flat-Prow Pass and -Bullfrog units are the most permeable volcanic units in the flowpath (SNL 2007 [DIRS 177391], Section 6.5.1.3 and Table 6-10; SNL 2007 [DIRS 177394], Section 6.2). Lowering the water table elevation in these volcanic units would result in a transport path increasingly in the Crater Flat-Tram unit and potentially in the Volcanic and Sedimentary unit. The permeabilities of these units are lower than the Crater Flat-Bullfrog. Therefore, if the water table elevation were lowered, transport times would increase because of the decreased permeabilities through which radionuclides would travel and the performance of the saturated zone would improve.

Based on the previous discussion, omission of FEP 1.3.07.01.0A (Water Table Decline) will not result in a significant adverse change in the magnitude or timing of either radiological exposure to the RMEI or radionuclide releases to the accessible environment. Therefore, this FEP is excluded from the performance assessments conducted to demonstrate compliance with proposed 10 CFR 63.311 and 63.321 (70 FR 53313 [DIRS 178394]), and with 10 CFR 63.331 [DIRS 180319], on the basis of low consequence.

INPUTS:

Table 1.3.07.01.0A-1. Direct Inputs

Input	Source	Description
BSC 2004. *Future Climate Analysis*. [DIRS 170002]	Section 7	Describes a glacial-transition climatic condition
SNL 2007. *Saturated Zone Site-Scale Flow Model*. [DIRS 177391]	Figures 6-17, 6-22	Transport pathways through the Crater Flat-Bullfrog hydrostratigraphic unit
	Section 6.5.1.3, Table 6-10	Prow Pass and Bullfrog units are the most permeable volcanic units in the flowpath
SNL 2007. *Saturated Zone In-Situ Testing*. [DIRS 177394]	Section 6.2	Prow Pass and Bullfrog units are the most permeable volcanic units in the flowpath

Table 1.3.07.01.0A-2. Indirect Inputs

Citation	Title	DIRS
10 CFR 63	Energy: Disposal of High-Level Radioactive Wastes in a Geologic Repository at Yucca Mountain, Nevada	180319
70 FR 53313	Implementation of a Dose Standard After 10,000 Years	178394
BSC 2004	*Future Climate Analysis*	170002
DTN: GS000308315121.003	Meteorological Stations Selected to Represent Future Climate States at Yucca Mountain, Nevada	151139
DTN: UN0201SPA021SS.007	Mean Annual Temperature and Precipitation for Select Western Regional Climate Locations	161588
Ervin et al. 1994	*Revised Potentiometric-Surface Map, Yucca Mountain and Vicinity, Nevada*	100633
Forester et al. 1996	*Synthesis of Quaternary Response of the Yucca Mountain Unsaturated and Saturated Zone Hydrology to Climate Change*	100148
Jannik et al. 1991	"A ^{36}Cl Chronology of Lacustrine Sedimentation in the Pleistocene Owens River System"	109434
Luckey et al. 1996	*Status of Understanding of the Saturated-Zone Ground-Water Flow System at Yucca Mountain, Nevada, as of 1995*	100465

FEP: 1.3.07.02.0A

FEP NAME:

Water Table Rise Affects SZ

FEP DESCRIPTION:

Climate change could produce increased infiltration, leading to a rise in the regional water table, possibly affecting radionuclide release from the repository by altering flow and transport pathways in the SZ. A regionally higher water table and change in SZ flow patterns might move discharge points closer to the repository.

SCREENING DECISION:

Included

TSPA DISPOSITION:

Water table rise is possible for the predicted future climates. The predicted future climates (monsoon and glacial transition) are wetter than present day and are expected to produce greater infiltration than the present day climate (SNL 2008 [DIRS 182145], Section 6.5.7[a]). Increased infiltration produces increased recharge to the groundwater system. The increased recharge will have two impacts on the groundwater system: (1) water levels will rise (D'Agnese et al. 1999 [DIRS 120425], p. 21), and (2) the amount of groundwater flowing past any location per unit time will increase (SNL 2008 [DIRS 183750], Section 6.5[a]). The groundwater flux, defined as the amount of groundwater flowing past any location per unit time per unit cross-sectional area, will also increase with the increase in recharge. As described later, the rise in water table leads to increases in radionuclide travel times in the saturated zone, while the increased groundwater fluxes lead to decreases in travel times.

The TSPA simulations of the saturated zone account for wetter climatic conditions with the use of a multiplicative factor that is the ratio of predicted groundwater flux under future climate conditions to the groundwater flux under present-day conditions while keeping the water table position at the present-day levels. An alternative conceptual model that included simulations with a higher water table elevation is described in later paragraphs. The multiplicative factor is called the saturated zone groundwater flux ratio (SNL 2008 [DIRS 183750], Section 6.5[a], Table 6-4[a]). The saturated zone groundwater multiplier scales the saturated zone radionuclide breakthrough curves, effectively modeling the impacts of increased groundwater flow that will exist for a higher water table condition (SNL 2008 [DIRS 183750], Section 5).

The TSPA simulations are performed for present-day, monsoon, and glacial-transition climates as well as the regulatory-based post-10,000-year case (proposed 10 CFR 63.342(c)(2) (70 FR 53313 [DIRS 178394])). For the early time when the present-day and monsoon climate dominate, the saturated zone groundwater multiplier will be used to scale the saturated zone radionuclide breakthrough curves from the glacial-transition results to the early climates. Three groundwater flux multipliers are used to characterize changes in the groundwater flow system reflective of future climatic conditions. For a monsoon climate, the groundwater flux is

1.9 times greater than that of the present-day climate. For a glacial-transition climate, the groundwater flux is 3.9 times greater than that of the present-day climate (SNL 2008 [DIRS 183750], Table 6-4[a]). For the post-10,000-year period, the saturated zone groundwater flux is maintained at 3.9 times greater than present day. This increased flux is a realistic representation of the assumed wetter and cooler climate conditions that are expected to exist during nearly two-thirds of the time after 10,000 years (Sharpe 2003 [DIRS 161591], Figure 6-8). The rationale for the use of the flux multiplier approach is provided in the following discussion.

Saturated zone transport times at the 18-km boundary using the flux multiplier method have been compared to transport times performed on an alternative model domain to corroborate the SZ flow model. The alternative model domain method allows the water table to be higher than present conditions (SNL 2007 [DIRS 177391], Section 6.6.4). The simulated water table rise varied from 20 m south of Highway 95 to 100 m north of the repository. The rise at the location of the Paleosprings at the southern end of Crater Flat was 30 m and beneath the repository was 50 m. Sorbing and nonsorbing radionuclide breakthrough curves show initial tracer breakthrough times (the leading edge of the radionuclide breakthrough curve) that are a factor of two to four times greater for the alternative model method compared with breakthrough times using the flux multiplier method. At the median (50%) breakthrough, the time is about a factor of 6 longer for the alternative model method. Additionally, radionuclide breakthrough curve trailing-edge times for the alternative model domain are well over an order of magnitude greater compared to those derived using a flux multiplier (SNL 2008 [DIRS 184806], Appendix E, Figures E-1 and E-2). Another simulation where the water table was assumed to rise 120 m beneath the repository produced similar results (BSC 2004 [DIRS 170036], Appendix E). The longer transport times using the alternative model are a function of several factors. The higher water table incorporated in the alternative model domain enables both sorbing and nonsorbing radionuclides to pass through less permeable upper volcanic confining units (that are above the water table in the present climate case), resulting in longer path lengths and transport times. Additionally, a higher water table promotes longer flow paths through the porous alluvium, equating to longer alluvium transport times.

Based on the comparison with results from the alternative model that simulates a higher water table, it is concluded that the simplified, flux multiplier method results in more rapid radionuclide transport to the 18-km boundary. That is, the flux multiplier method that accounts for the effect of climate change on water table elevations provides a conservative estimate of groundwater transport times in the saturated zone under wetter climate conditions compared to the case where the higher water table is simulated.

In summary, the saturated zone aspect of this FEP is included in TSPA by accounting for the effects of a higher water table on radionuclide transport in the saturated zone through the use of groundwater flux multipliers.

Water table rise associated with future climates is included in the radionuclide transport simulations for the unsaturated zone, and is discussed in included FEP 1.3.07.02.0B (Water Table Rise Affects UZ). To include this water table rise in TSPA calculations, the water table elevation is instantaneously increased by 120 m in the UZ model domain when the climate changes from present-day to monsoon climate. The same water table elevation is also used for

the glacial-transition climate. This approach uses the reasonable upper bound (120 m rise) from several estimates of the water table elevation under the repository in the past (SNL 2007 [DIRS 177391], Section 6.6.4). The water table rise of 120 m is maintained in the UZ model domain for the post-10,000-year period as a conservative representation of the effects of wetter and cooler climate conditions.

Water table rise could alter the location of groundwater discharge points, which could alter groundwater exposure pathways. Current natural groundwater discharge points along the saturated zone flow paths are several kilometers downstream from the 18-km accessible environment boundary. Also, modeling results indicate that, under the future climate states considered in the TSPA, the water table would not rise sufficiently to cause the formation of springs and the contamination of soils downgradient of the repository within the 18-km boundary (SNL 2007 [DIRS 177391], Section 6.6.4). The water table could rise to within 5 m of the ground surface at the location of paleospring deposits located southwest of the Yucca Mountain repository (SNL 2007 [DIRS 177391], Figure 6-21 as indicated by the blue shaded regions), but the Solitario Canyon and Windy Wash faults (SNL 2007 [DIRS 177391], Figure 6-12) serve as barriers between these paleosprings and potential flow paths from the repository (SNL 2007 [DIRS 177391], Figures 6-15 and 6-17). Therefore, even if springs were to develop in the shallow water table southwest of the repository, it is not expected that radionuclides released from the repository would be consituents of the spring water. Exposure via such pathways is insignificant compared to the exposure pathways considered in the biosphere model (see excluded FEP 2.2.08.11.0A (Groundwater Discharge to Surface Within the Reference Biosphere)).

However, given the depth to groundwater shown in *Information and Analyses to Support Selection of Critical Groups and Reference Biospheres for Yucca Mountain Exposure Scenarios* (LaPlante and Poor 1997 [DIRS 101079], Figure 2-2) and the possible paleodischarge locations identified in *Simulated Effects of Climate Change on the Death Valley Regional Ground-Water Flow System, Nevada and California* (D'Agnese et al. 1999 [DIRS 120425], p. 6), the possible effects of changes in groundwater level under future climate conditions are included in the biosphere model consistent with proposed 10 CFR 63.305(c) (70 FR 53313 [DIRS 178394]), which requires that the DOE vary factors related to hydrology and climate based on cautious but reasonable assumptions consistent with present knowledge. In addition, the use of such water needs to be included, consistent with 10 CFR 63.312(c) [DIRS 180319], which specifies the constraints for the radionuclide concentration in the groundwater used by the RMEI.

The biosphere model for the groundwater exposure scenario includes the effects of water table rise because the model calculates BDCFs for a unit activity concentration in the water, regardless of the origin of the water. If the groundwater entering the biosphere through a spring or other discharge point were an additional source of radionuclides in the biosphere, it would be treated in a manner similar to groundwater from a well. Therefore, water table rise is considered in the model, analogous to included FEP 1.4.07.02.0A (Wells), in the soil, air, plant, animal, fish, ^{14}C, and ingestion submodels (SNL 2007 [DIRS 177399], Sections 6.4.1 to 6.4.6 and 6.4.9).

The biosphere aspect of the water table rise is included in the biosphere component of the TSPA model through the use of groundwater exposure scenario BDCFs that are direct inputs to the TSPA for the scenario classes involving radionuclide release to the groundwater (SNL 2007

[DIRS 177399], Section 6.1.3). The annual doses are calculated as the product of radionuclide concentration in groundwater and the BDCFs.

The BDCFs for all biosphere model realizations are provided as inputs to the TSPA model, which randomly samples these inputs to propagate uncertainty from the biosphere model into TSPA dose calculations. The present-day climate BDCFs are used for the assessment of doses to the RMEI for 10,000 years following disposal as well as after 10,000 years, but within the period of geologic stability (SNL 2007 [DIRS 177399], Sections 6.11.3).

This FEP is included for the performance assessment to demonstrate compliance with the individual protection standard (proposed 10 CFR 63.311 (70 FR 53313 [DIRS 178394])) and the performance assessment to demonstrate compliance with the individual protection standard for human intrusion (proposed 10 CFR 63.321 (70 FR 53313 [DIRS 178394])). For the performance assessment that demonstrates compliance with the groundwater protection standards (10 CFR 63.331 [DIRS 180319]), only those components of this FEP that address the geosphere transport are included.

INPUTS:

Table 1.3.07.02.0A-1. Indirect Inputs

Citation	Title	DIRS
10 CFR 63	Energy: Disposal of High-Level Radioactive Wastes in a Geologic Repository at Yucca Mountain, Nevada	180319
70 FR 53313	Implementation of a Dose Standard After 10,000 Years	178394
BSC 2004	*Site-Scale Saturated Zone Transport*	170036
D'Agnese et al. 1999	*Simulated Effects of Climate Change on the Death Valley Regional Ground-Water Flow System, Nevada and California*	120425
LaPlante and Poor 1997	*Information and Analyses to Support Selection of Critical Groups and Reference Biospheres for Yucca Mountain Exposure Scenarios*	101079
Sharpe 2003	*Future Climate Analysis--10,000 Years to 1,000,000 Years After Present*	161591
SNL 2007	*Biosphere Model Report*	177399
SNL 2007	*Saturated Zone Site-Scale Flow Model*	177391
SNL 2008	*Saturated Zone Flow and Transport Model Abstraction*	183750
SNL 2008	*Simulation of Net Infiltration for Present-Day and Potential Future Climates*	182145
SNL 2008	*Site-Scale Saturated Zone Transport*	184806

FEP: 1.3.07.02.0B

FEP NAME:

Water Table Rise Affects UZ

FEP DESCRIPTION:

Climate change could produce increased infiltration, leading to a rise in the regional water table, possibly affecting radionuclide release from the repository by altering flow and transport pathways in the UZ. A regionally higher water table and change in UZ flow patterns might flood the repository.

SCREENING DECISION:

Included

TSPA DISPOSITION:

The water table will be higher in future climate states that have greater infiltration rates; these are discussed in included FEP 1.3.01.00.0A (Climate Change). To include this predicted water table rise in the TSPA calculations, the water table elevation is instantaneously increased by up to 120 m when the climate changes from present-day to monsoon climate. In the UZ flow model area, the present-day water table varies from less than 730 m to greater than 940 m above mean sea level (BSC 2004 [DIRS 169855], Figure 6.2). Within the repository footprint, the present-day water table varies from around 730 to 850 m above mean sea level (BSC 2004 [DIRS 169855], Figure 6.2). Note that the bottom boundary for the flow models of all climate states is the present-day water table. For use in conjunction with FEHM's multispecies particle tracking model the flow-field files for the monsoon, glacial-transition, and post-10,000-year climate flow fields from the UZ flow model abstraction are postprocessed to approximate the affects of a rising water table. The rising water table is approximated by constraining the water table to a minimum elevation of 850 m above mean sea level (SNL 2008 [DIRS 184748], Section 6.4.8). That is for future climates, any locations where the present-day water table is below 850 m it is set to 850 m and any locations where the present-day water table is above 850 m, the water table is not adjusted from the present-day level (BSC 2004 [DIRS 169855]). The same water table elevation is also used for the glacial-transition climate state.

Water table changes are implemented in the TSPA by allowing the water table to change elevation instantaneously upon change in climate, concurrent with changes in infiltration (implemented by the postprocessor software WTRISE (V2.0 2003 [DIRS 163453], STN: 105372.000) for radionuclide transport), thus affecting the unsaturated flow and pathways in the unsaturated zone. The original flow fields that are part of the UZ flow model abstraction are postprocessed with WTRISE, allowing the user to specify new water table locations in the flow field files. FEHM utilizes the updated flow fields and, as a result, particles will exit the unsaturated zone at the new water table (SNL 2008 [DIRS 184748], Section 6.4.8). At a time step where the water table rises, FEHM removes all the particles in the gridblocks between the old water table and the new water table (SNL 2007 [DIRS 184614], Section 6.6.2.2).

The particles removed from the volume between the old and new water tables immediately enter the saturated zone.

Paleoclimate data indicate that the historical water table has never risen to the level of the repository (Forester et al. 1999 [DIRS 109425], pp. 46 to 56). Based on analysis of mineralogic alteration (zeolitization and tridymite distribution) and strontium isotope ratios, and groundwater flow modeling, the water table for future climates (both monsoon and glacial transition) is specified in *Particle Tracking Model and Abstraction of Transport Processes* (SNL 2008 [DIRS 184748], Section 6.4.8). Future climate flow fields, implemented in the UZ flow model (SNL 2007 [DIRS 184614], Section 6.6.2.2), have been postprocessed using WTRISE.

In accordance with proposed 10 CFR 63.342(c) (70 FR 53313 [DIRS 178394]), the effects of climate change after 10,000 years, but within the period of geologic stability, are represented by the NRC-prescribed distribution of percolation rates at repository depth. The TSPA model simulations use four flow fields to represent this distribution (SNL 2007 [DIRS 184614], Section 6.6.2.2). The water table rise assumed in the TSPA for the post-10,000-year period is the same as that assumed for future climates in the pre-10,000-year period.

The effect of water table rise on the thermal regime is not included in the TSPA because the exact boundary condition values for temperature, gas pressure, and saturation are not important for thermal-hydrologic seepage model results. The temperature and gas pressure values that define the initial temperature and pressure fields, respectively, are significantly altered in the near-field rock early in the simulations once the drifts heat up.

INPUTS:

Table 1.3.07.02.0B-1. Indirect Inputs

Citation	Title	DIRS
70 FR 53313	Implementation of a Dose Standard After 10,000 Years	178394
BSC 2004	*Development of Numerical Grids for UZ Flow and Transport Modeling*	169855
Forester et al. 1999	*The Climatic and Hydrologic History of Southern Nevada During the Late Quaternary*	109425
WTRISE V. 2.0	PC/WINDOWS 2000/98; DEC ALPHA/OSF1 V5.1. 10537-2.0-00.	163453
SNL 2007	*UZ Flow Models and Submodels*	184614
SNL 2008	*Particle Tracking Model and Abstraction of Transport Processes*	184748

FEP: 1.4.01.00.0A

FEP NAME:

Human Influences on Climate

FEP DESCRIPTION:

Future human actions, either intentional or accidental, could influence global, regional, or local climate.

SCREENING DECISION:

Excluded – by regulation

SCREENING JUSTIFICATION:

The description of present-day climate, as discussed in included FEP 1.3.01.00.0A (Climate Change), is based on climate records that implicitly include effects of modern society over the duration of the historical record. Future changes in human influences on climate are excluded from postclosure assessment on the basis of requirements contained in 10 CFR 63.305(b) [DIRS 180319] and 10 CFR 63.305(c) [DIRS 178394], which provide as follows: "DOE should not project changes in society, the biosphere (other than climate), human biology, or increases or decreases of human knowledge or technology. In all analyses done to demonstrate compliance with this part, DOE must assume that all of those factors remain constant as they are at the time of submission of the license application" (10 CFR 63.305(b) [DIRS 180319]); and "DOE must vary factors related to the geology, hydrology, and climate based upon cautious, but reasonable assumptions consistent with present knowledge of factors that could affect the Yucca Mountain disposal system during the period of geologic stability and consistent with the requirements for performance assessment specified at § 63.342" (10 CFR 63.305(c) [DIRS 178394]).

The supplementary information portion of the preamble to 10 CFR Part 63 (66 FR 55732 [DIRS 156671]) provides rationale for the requirements in 10 CFR 63.305(b) and (c) and indicates that natural evolution of the geosphere and biosphere is to be included in the performance assessment but any impacts caused by future changes in human behaviors are not to be included. In response to comments made in the rulemaking proceeding associated with climate change (66 FR 55732 [DIRS 156671], p. 55757), the NRC emphasized the importance of including "climate change in both the geosphere and biosphere performance assessment calculations to ensure that the conceptual model of the environment is consistent with our scientific understanding of reasonably anticipated natural events." Similarly, in 67 FR 62628 [DIRS 162317], the NRC stated "DOE's performance assessments are required to consider the naturally occurring features, events and processes that could affect the performance of a geologic repository" (67 FR 62628 [DIRS 162317], p. 62629). In further response to comments, the NRC also stated that considering future economic growth trends and human behaviors would add inappropriate speculation into the requirements and would lead to problems deciding which alternative futures are credible and which are unrealistic (66 FR 55732 [DIRS 156671], p. 55757).

Prediction of human-induced climate changes would not only involve speculations about the local population, but also introduce inherently large uncertainties in prediction of the future global population behaviors and resulting consequences. In its discussion of the consideration of future economic growth trends, the NRC found that inclusion of such future predictions would not only add inappropriate speculation, but also "would not enhance public safety, and is likely inconsistent with the EPA standards" (66 FR 55732 [DIRS 156671], p. 55757).

Based on these requirements, the FEPs related to changes in or predictions of future human activities are excluded. Future climate analysis does not include potential changes that may occur as a result of future changes in human actions. Accordingly, this FEP is excluded from the TSPA by regulation.

INPUTS:

Table 1.4.01.00.0A-1. Direct Inputs

Input	Source	Description
10 CFR 63. 2007. Energy: Disposal of High-Level Radioactive Wastes in a Geologic Repository at Yucca Mountain, Nevada. [DIRS 180319]	10 CFR 63.331	Separate standards for protection of groundwater
	10 CFR 63.305(b)	DOE should not project changes in society, the biosphere (other than climate), human biology, or increases or decreases in human knowledge or technology
66 FR 55732. Disposal of High-Level Radioactive Wastes in a Proposed Geologic Repository at Yucca Mountain, NV, Final Rule. 10 CFR Parts 2, 19, 20, 21, 30, 40, 51, 60, 61, 63, 70, 72, 73, and 75. [DIRS 156671]	p. 55757	NRC discussion of future economic growth trends
	p. 55757	Rulemaking proceeding associated with climate change
67 FR 62628. Specification of a Probability for Unlikely Features, Events and Processes. [DIRS 162317]	p. 62,629	Specifies the requirement to consider naturally occurring FEPs
70 FR 53313. Implementation of a Dose Standard After 10,000 Years. [DIRS 178394]	10 CFR 63.305(c)	DOE must vary factors related to the geology, hydrology, and climate

Table 1.4.01.00.0A-2. Indirect Inputs

Citation	Title	DIRS
66 FR 55732	Disposal of High-Level Radioactive Wastes in a Proposed Geologic Repository at Yucca Mountain, NV, Final Rule. 10 CFR Parts 2, 19, 20, 21, 30, 40, 51, 60, 61, 63, 70, 72, 73, and 75.	156671

FEP: 1.4.01.01.0A

FEP NAME:

Climate Modification Increases Recharge

FEP DESCRIPTION:

Climate modification causes an increase in recharge in the Yucca Mountain region. Increased recharge might lead to increased flux through the repository, perched water, or water table rise.

SCREENING DECISION:

Included

TSPA DISPOSITION:

Future climate forecasts (BSC 2004 [DIRS 170002]) indicate that the climate at Yucca Mountain is predicted to evolve to the cooler, wetter conditions of a glacial-transition climate within the assessment timeframe. Monsoon and glacial-transition (intermediate) climate states are predicted to last about 38,000 years after waste emplacement (Sharpe 2003 [DIRS 161591]). Climate modification in the period up to 10,000 years is included in the TSPA through the use of three discrete climate states: present-day, monsoon, and glacial-transition. The effects of climate change after 10,000 years, but within the period of geologic stability, are assumed to be limited to the results of increased water flowing through the repository and the resulting transport and release of radionuclides to the accessible environment in accordance with proposed 10 CFR 63.342(c)(2) (70 FR 53313 [DIRS 178394], pp. 53315 to 53316). Increased deep percolation is reflective of wetter and cooler climate conditions than present-day conditions.

The effects of climate modification and increased recharge are considered by a number of processes represented by TSPA. The primary effect is to the calculation of net infiltration and associated percolation fluxes through the unsaturated zone. Percolation fluxes are used to calculate seepage fluxes into the repository and radionuclide transport from the repository to the saturated zone. Percolation fluxes also provide inputs to the calculation of drift-wall condensation and the evolution of thermal-hydrologic conditions in the unsaturated zone and repository, which affect chemical processes associated with radionuclide transport.

Spatially distributed net infiltration calculations provide inputs to the calculation of the spatial distribution of percolation fluxes in the unsaturated zone, otherwise know as UZ flow fields. A total of sixteen UZ flow fields are used in *Total System Performance Assessment Model/Analysis for the License Application* (SNL 2008 [DIRS 183478], Section 5.2). The flow conditions at the top boundary of the UZ flow model are provided from twelve net infiltration maps, four maps for the present-day, monsoon, and glacial-transition climate states that correspond to the 10th, 30th, 50th, and 90th infiltration percentiles for each of these climate states. For the post-10,000-year climate state, the development of the four utililized flow fields is described below. These infiltration maps are developed in *Simulation of Net Infiltration for Present-Day and Potential Future Climates* (SNL 2008 [DIRS 182145], Section 6.5.7[a]), and are used to propogate infiltration uncertainty through to the TSPA results. The probability weights for UZ flow fields

are calculated using the initial infiltration percentiles (monsoon and glacial transition climates) and UZ flow model calibration results (present-day climate) as described in *UZ Flow Models and Submodels* (SNL 2007 [DIRS 184614], Section 6.8). For the period from 10,000 years postclosure to the time of geologic stability, an additional four uncertainty cases are developed based on the prescribed percolation flux distribution through the repository footprint given in proposed 10 CFR 63.342(c) (70 FR 53313 [DIRS 178394]). The output flow fields are in DTNs: LB0612PDFEHMFF.001 [DIRS 179296], LB0701MOFEHMFF.001 [DIRS 179297], LB0701GTFEHMFF.001 [DIRS 179160], and LB0702PAFEM10K.002 [DIRS 179507], which were developed for use in performance assessment (SNL 2008 [DIRS 183478]).

For the post-10,000–year period, the climate change analysis is limited to the effects of increased water flow through the repository as a result of climate change, and the resulting transport and release of radionuclides to the accessible environment, in accordance with proposed 10 CFR 63.342(c)(2) (70 FR 53313 [DIRS 178394]). The proposed rule defines the deep percolation rates for that period as based on a log-uniform probability distribution from 13 to 64 mm/yr. This distribution was divided into four quantiles to develop four flow fields that most closely matched target rates based on proposed 10 CFR 63.342(c)(2) (70 FR 53313 [DIRS 178394]). The midpoint of each quantile was used to represent the average flux for the given flow field. The four midpoint values are 21.29, 39.52, 51.05, and 61.03 mm/yr (SNL 2007 [DIRS 184614], Section 6.1.4, Table 6.1-3). Four corresponding net infiltration maps representing present-day 90th percentile, glacial-transition 50th percentile, glacial-transition 90th percentile, and monsoon 90th percentile, respectively, are used to represent these quantiles. Net infiltration for these four cases was scaled so that the average water flux through the repository footprint matched the target values (quantile midpoints) at the repository horizon. Once the infiltration boundary condition was determined, the method used to generate the post-10,000-year flow fields was the same as that used to generate the pre-10,000-year flow fields (SNL 2007 [DIRS 184614], Section 6.1.4).

Calculations of seepage flux (flow into the repository drifts) are affected by increases in recharge caused by future climate changes because the drift seepage model uses unsaturated zone flow fields as input (SNL 2007 [DIRS 181244], Section 6.6.5). Seepage is calculated in the TSPA using percolation flux distributions based on results from the UZ flow model (SNL 2007 [DIRS 181244], Section 6.4[a]) given in DTNs: LB0612PDPTNTSW.001 [DIRS 179150], LB0701MOPTNTSW.001 [DIRS 179156], LB0701GTPTNTSW.001 [DIRS 179153], and LB0702UZPTN10K.002 [DIRS 179332] representing the three three climate states and the post-10,000-year fluxes, respectively.

The effect of future climate changes in the form of increased recharge is included in the UZ transport model for TSPA through the use of unsaturated zone flow fields as input to the model (SNL 2008 [DIRS 184748], Section 6.5.1; DTNs: LB0612PDFEHMFF.001 [DIRS 179296], LB0701MOFEHMFF.001 [DIRS 179297], LB0701GTFEHMFF.001 [DIRS 179160], and LB0702PAFEM10K.002 [DIRS 179507]).

Increased recharge from future climate change is included in *Multiscale Thermohydrologic Model* (SNL 2008 [DIRS 184433]), which predicts the expected range in the thermal-hydrologic parameters, including temperature and relative humidity (SNL 2008 [DIRS 184433]). This

model uses the unsaturated zone flow fields as one of its inputs, and therefore model results are affected by increases in recharge caused by future climate modifications.

In addition, condensation of water along the drift wall is affected by changes in recharge as described in *In-Drift Natural Convection and Condensation* (SNL 2007 [DIRS 181648]) as percolation is used as an input to the drift wall condensation model.

The effects of climate modification on the amount of percolation are also included in the model for seepage water chemistry through changes in the percolation flux (SNL 2007 [DIRS 177412]). The percolation flux values used in this model are based on fluxes at the PTn/TSw boundary predicted by the UZ flow model given in the following four DTNs: LB0612PDPTNTSW.001 [DIRS 179150], LB0701MOPTNTSW.001 [DIRS 179156], LB0701GTPTNTSW.001 [DIRS 179153], and LB0702UZPTN10K.002 [DIRS 179332], representing the three climate states and the post-10,000-year fluxes, respectively. The system is modeled assuming plug-flow with transport velocity equal to the percolation flux divided by the product of the average porosity and the average water saturation (SNL 2007 [DIRS 177412], Section 6.3.2.4.4). The effects of feldspar dissolution on the water chemistry are evaluated in terms of the amount of feldspar dissolution that occurs during flow through the TSw (SNL 2007 [DIRS 177412], Sections 6.3.2.4.4 and 6.3.2.4.5). The amount of feldspar dissolved is a primary parameter in determining the composition of potential seepage waters. This is a function of the ambient feldspar dissolution rate, the dissolution rate temperature dependence, the model for the thermal field, and the plug-flow model for transport through the TSw (SNL 2007 [DIRS 177412], Section 6.3.2.4.5). The starting point for evaluating potential water compositions in the near field is the composition of ambient pore waters in the TSw. The available pore-water data from the four repository host units (Tptpul, Tptpmn, Tptpll, Tptpln) were evaluated and grouped into four compositional groups (SNL 2007 [DIRS 177412], Section 6.3.2.3). The uncertainty in the amount of feldspar dissolution is propogated through to TSPA using a lookup table, as the water–rock interaction parameter, or WRIP (SNL 2007 [DIRS 177412], Section 6.3.2.4.5).

Perched water has not been observed in observation wells in the unsaturated zone above the repository horizon (BSC 2004 [DIRS 169734], Section 7.4.2). The potential effect of perched water above the repository is indirectly related to lateral diversion of percolation flux in the PTn unit above the repository. PTn effects on the flow fields are discussed in *UZ Flow Models and Submodels* (SNL 2007 [DIRS 184614], Section 6.2). The potential for water table rise caused by climate modification is included in TSPA calculations by adjusting the flow fields to the higher water tables, as implemented by the WTRISE software (LBNL 2003 [DIRS 163453]) and as modeled by *Saturated Zone Site-Scale Flow Model* (SNL 2007 [DIRS 177391], Section 6.6.4).

The effect of climate modification in the form of increased recharge is discussed in included FEPs 1.3.07.02.0A (Water Table Rise Affects SZ) and 1.3.07.02.0B (Water Table Rise Affects UZ).

INPUTS:

Table 1.4.01.01.0A-1. Indirect Inputs

Citation	Title	DIRS
70 FR 53313	Implementation of a Dose Standard After 10,000 Years	178394
BSC 2004	*Future Climate Analysis*	170002
BSC 2004	*Yucca Mountain Site Description*	169734
DTN: LB0612PDFEHMFF.001	Flow-Field Conversions from TOUGH2 to FEHM Format for Present Day 10-, 30-, 50-, and 90-Percentile Infiltration Maps	179296
DTN: LB0612PDPTNTSW.001	Vertical Flux at PTN/TSW Interface for Present-Day Climate of 10th, 30th, 50th, and 90-Percentile Infiltration Maps	179150
DTN: LB0701GTFEHMFF.001	Flow-Field Conversions from TOUGH2 to FEHM Format for Glacial Transition Climate 10th-, 30th-, 50th-, and 90th-Percentile Infiltration Maps	179160
DTN: LB0701GTPTNTSW.001	Vertical Flux at PTN/TSW Interface for Glacial Transition Climate of 10th, 30th, 50th, and 90th-Percentile Infiltration Maps	179153
DTN: LB0701MOFEHMFF.001	Flow-Field Conversions from TOUGH2 to FEHM Format for Monsoon Climate 10th-, 30th-, 50th-, and 90th-Percentile Infiltration Maps	179297
DTN: LB0701MOPTNTSW.001	Vertical Flux at PTN/TSW Interface for Monsoon Climate of 10th, 30th, 50th and 90th-Percentile Infiltration Maps	179156
DTN: LB0702PAFEM10K.002	Flow Field Conversions to FEHM Format for Post 10,000 Year Peak Dose Fluxes in the Unsaturated Zone for Four Selected Infiltration Rates	179507
DTN: LB0702UZPTN10K.002	Vertical Flux at PTN/TSW Interface for Post-10K-Year Climate Infiltration Maps	179332
WTRISE. V2.0.	PC/WINDOWS 2000/98; DEC ALPHA/OSF1 V5.1. STN: 10537-2.0-00.	163453
Sharpe 2003	*Future Climate Analysis—10,000 Years to 1,000,000 Years After Present*	161591
SNL 2007	*Saturated Zone Site-Scale Flow Model*	177391
SNL 2007	*Abstraction of Drift Seepage*	181244
SNL 2007	*Engineered Barrier System: Physical and Chemical Environment*	177412
SNL 2007	*In-Drift Natural Convection and Condensation*	181648
SNL 2007	*UZ Flow Models and Submodels*	184614
SNL 2008	*Multiscale Thermohydrologic Model*	184433
SNL 2008	*Particle Tracking Model and Abstraction of Transport Processes*	184748
SNL 2008	*Simulation of Net Infiltration for Present-Day and Potential Future Climates*	182145
SNL 2008	*Total System Performance Assessment Model/Analysis for the License Application*	183478

FEP: 1.4.01.02.0A

FEP NAME:

Greenhouse Gas Effects

FEP DESCRIPTION:

The Greenhouse Effect is the result of so-called 'greenhouse gases' allowing incoming solar radiation to pass through the Earth's atmosphere, but preventing much of the outgoing infrared radiation from the surface and lower atmosphere from escaping into outer space. Greenhouse gases include water vapor, carbon dioxide (CO_2), methane (CH_4), nitrous oxide (N_2O), halogenated fluorocarbons (HCFCs), ozone (O_3), perfluorinated carbons (PFCs), and hydrofluorocarbons (HFCs). Many of these gases are generated through various natural and physical processes, and have been responsible for maintaining habitable conditions on the planet. Human activities, such as burning fossil fuels, clearing forests (thereby increasing the oxidation of soil organic matter with the concurrent release of CO_2 as a decay product), most motorized transport and industrial processes have the potential to increase the levels of greenhouse gases, which could lead to changes in climate.

SCREENING DECISION:

Excluded – by regulation

SCREENING JUSTIFICATION:

The description of the present-day climate, as discussed in included FEP 1.3.01.00.0A (Climate Change), is based on climate records that implicitly include effects of modern society over the duration of the historical record as well as the greenhouse gas effects. Future changes in human influences on the concentrations of atmospheric gases are excluded from postclosure assessment on the basis of the requirements contained in 10 CFR 63.305(b) [DIRS 180319] and in proposed 10 CFR 63.305(c) (70 FR 53313 [DIRS 178394]), which provide as follows: "DOE should not project changes in society, the biosphere (other than climate), human biology, or increases or decreases of human knowledge or technology. In all analyses done to demonstrate compliance with this part, DOE must assume that all of those factors remain constant as they are at the time of submission of the license application" (10 CFR 63.305(b) [DIRS 180319]); and "DOE must vary factors related to the geology, hydrology, and climate based upon cautious, but reasonable assumptions consistent with present knowledge of factors that could affect the Yucca Mountain disposal system during the period of geologic stability and consistent with the requirements for performance assessment specified at § 63.342." (proposed 10 CFR 63.305(c) (70 FR 53313 [DIRS 178394])).

The supplementary information portion of the preamble to 10 CFR Part 63 (66 FR 55732 [DIRS 156671]) provides a rationale for the requirements in proposed 10 CFR 63.305(b) [DIRS 180319] and (c) (70 FR 53313 [DIRS 178394]) and indicates that natural evolution of the geosphere and biosphere is to be included in the performance assessment but any impactss caused by future changes in human behaviors are not to be included. In response to comments made in the rulemaking proceeding associated with climate change (66 FR 55732

[DIRS 156671], p. 55757), the NRC emphasized the importance of including "climate change in both the geosphere and the biosphere performance assessment calculations to ensure that the conceptual model of the environment is consistent with our scientific understanding of reasonably anticipated natural events." Similarly, in 67 FR 62628 ([DIRS 162317], p. 62629) the NRC states, "DOE's performance assessments are required to consider the naturally occurring features, events and processes that could affect the performance of a geologic repository." In further response to comments, the NRC stated that considering future economic growth trends and human behaviors would add inappropriate speculation into the requirements and would lead to problems deciding which alternative futures are credible and which are unrealistic (66 FR 55732 [DIRS 156671], p. 55757).

Prediction of the future human-induced emissions of greenhouse gases and their potential to effect climate change would not only involve speculation about the local population but also introduce inherently large uncertainties in prediction of the future global population behavior and resulting consequences. In their discussion of consideration of future economic growth trends, the NRC found that inclusion of such future predictions would not only add inappropriate speculation, but also "would not enhance public safety, and is likely inconsistent with the EPA standards" (66 FR 55732 [DIRS 156671], p. 55757).

Based on these requirements, the FEPs related to changes in or predictions of future human activities are excluded. Future climate analysis does not incorporate potential changes, including variations in greenhouse gas effects, that may occur as a result of changes in future human actions. Accordingly, this FEP is excluded from the TSPA by regulation.

INPUTS:

Table 1.4.01.02.0A-1. Direct Inputs

Input	Source	Description
10 CFR 63. 2007. Energy: Disposal of High-Level Radioactive Wastes in a Geologic Repository at Yucca Mountain, Nevada. [DIRS 180319]	10 CFR 63.305(b)	DOE should not project changes in society, the biosphere (other than climate), human biology, or increases or decreases in human knowledge or technology
66 FR 55732. Disposal of High-Level Radioactive Wastes in a Proposed Geologic Repository at Yucca Mountain, NV, Final Rule. 10 CFR Parts 2, 19, 20, 21, 30, 40, 51, 60, 61, 63, 70, 72, 73, and 75. [DIRS 156671]	p. 55757	NRC discussion of future economic growth trends
	p. 55757	Rulemaking proceeding associated with climate change
67 FR 62628. Specification of a Probability for Unlikely Features, Events and Processes. [DIRS 162317]	p. 62629	Specifies the requirement to consider naturally occurring FEPs
70 FR 53313. Implementation of a Dose Standard After 10,000 Years. [DIRS 178394]	10 CFR 63.305(c)	DOE must vary factors related to the geology, hydrology, and climate

Table 1.4.01.02.0A-2. Indirect Inputs

Citation	Title	DIRS
66 FR 55732	Disposal of High-Level Radioactive Wastes in a Proposed Geologic Repository at Yucca Mountain, NV, Final Rule. 10 CFR Parts 2, 19, 20, 21, 30, 40, 51, 60, 61, 63, 70, 72, 73, and 75.	156671

FEP: 1.4.01.03.0A

FEP NAME:

Acid Rain

FEP DESCRIPTION:

Acid rain refers to precipitation on a local to regional scale containing higher than normal amounts of nitric and sulfuric acids. This can result from man-made sources such as emissions produced from the burning of fossil fuels. Acid rain can detrimentally affect aquatic and terrestrial life by interfering with the growth, reproduction, and thus survival of affected organisms. It can influence the behavior and transport of contaminants in the biosphere, particularly by affecting surface water and soil chemistry and may also cause societal change due to contamination of water sources.

SCREENING DECISION:

Excluded – by regulation

SCREENING JUSTIFICATION:

The description of present-day climate, as discussed in included FEP 1.3.01.00.0A (Climate Change), includes the effects of acid rain and is based on climate records that implicitly include effects of modern society over the duration of the historical record. Future human influences on climate and other components of the reference biosphere are excluded on the basis of requirements contained in 10 CFR 63.305(b) [DIRS 180319] and proposed 10 CFR 63.305(c) (70 FR 53313 [DIRS 178394]), which provide as follows: "DOE should not project changes in society, the biosphere (other than climate), human biology, or increases or decreases of human knowledge or technology. In all analyses done to demonstrate compliance with this part, DOE must assume that all of those factors remain constant as they are at the time of submission of the license application" (10 CFR 63.305(b) [DIRS 180319]); and "DOE must vary factors related to the geology, hydrology, and climate based upon cautious, but reasonable assumptions consistent with present knowledge of factors that could affect the Yucca Mountain disposal system during the period of geologic stability and consistent with the requirements for performance assessments specified at § 63.342" (proposed 10 CFR 63.305(c) (70 FR 53313 [DIRS 178394])).

The supplementary information portion of the preamble to 10 CFR Part 63 (66 FR 55732 [DIRS 156671]) provides rationale for the requirements in 10 CFR 63.305(b) [DIRS 180319] and (c) (70 FR 53313 [DIRS 178394]) and indicates that only natural evolution of the geosphere and biosphere is to be included in the performance assessment but any impacts caused by the future changes in human behaviors are not to be included. In 67 FR 62628 [DIRS 162317], the NRC states, "DOE's performance assessments are required to consider the naturally occurring features, events and processes that could affect the performance of a geologic repository" (67 FR 62628 [DIRS 162317], p. 62629). In response to comments made in the rulemaking proceeding, the NRC stated that considering future economic growth trends and human behaviors would add inappropriate speculation into the requirements and would lead to problems

deciding which alternative futures are credible and which are unrealistic (66 FR 55732 [DIRS 156671], p. 55757).

The NRC stated further that the natural systems of the biosphere should be allowed to vary consistent with the geologic record, which provides the basis for predicting future biosphere changes (66 FR 55732 [DIRS 156671], p. 55757). The present knowledge of the factors related to climate does not allow prediction of the climate changes caused by future human behavior. The climate change predictions are based on the geologic record and concern the natural evolution of the reference biosphere.

Prediction of future human actions resulting in acid rain would not only involve speculations about the local population, but also introduce inherently large uncertainties in prediction of the future global population behaviors and resulting consequences. In the discussion of consideration of future economic growth trends, the NRC found that inclusion of such future predictions would not only add inappropriate speculation, but also "would not enhance public safety, and is likely inconsistent with the EPA standards" (66 FR 55732 [DIRS 156671], p. 55757).

Based on these requirements, the FEPs related to changes in the prediction of future human activities are excluded. Future climate analysis does not incorporate potential changes, including effects of acid rain, that may occur as a result of future changes in human actions. Therefore, acid rain as a consequence of future changes in human activities is excluded from consideration in the TSPA by regulation.

There also exists another potential source of acid rain. A volcanic eruption can, under certain conditions, lead to acid rain, although such conditions are not expected to occur at Yucca Mountain. When SO_2, initially dissolved in magma, escapes during a volcanic eruption, it interacts with moisture in air producing atmospheric aerosols in form of small sulfuric acid droplets (by atmospheric oxidation of sulfur dioxide in the presence of water). When atmospheric moisture is abundant, these fine sulfate aerosols combine and precipitate as acid rain. Other volcanic gases, such as hydrogen sulfide, hydrogen chloride, and hydrogen fluoride, can also contribute, although the most significant impact comes from SO_2.

The consequence of an acid rain event on radionuclide releases from the repository and radiological exposures to the RMEI can be evaluated by using a risk-informed approach. The risk-informed evaluation considers the joint outcome of the probability and the consequence of acid rain of volcanic origin. For the acid rain to influence the repository or the reference biosphere, the following conditions would have to occur: (1) an eruptive volcanic event would have to take place in the vicinity of Yucca Mountain, followed by (2) the atmospheric transport of aerosols containing sulfuric acid from the point of emission to Yucca Mountain or the reference biosphere, followed by (3) the wet deposition of these aerosols in form of acid rain at those locations. These events are independent, so the probability of the sequence of events is the product of their probabilities. Considering a low probability of a volcanic eruption in the Yucca Mountain region (BSC 2004 [DIRS 169989], Section 6.2), a relatively short eruption duration and small value (SNL 2007 [DIRS 174260], Table 7-1), a random location relative to Yucca Mountain and the reference biosphere, and a low humidity associated with arid and semi-arid climate, acid rain is not expected at Yucca Mountain or in the reference biosphere.

However, if acid rain occurred, any effects would be localized and of short duration. The effects of acid rain on the chemistry of precipitation that could reach the repository would be negligible considering the relative volumes of precipitation that would be affected by acid rain and that unaffected by acid rain over the period of repository performance. The effects of acid rain on the soil conditions and on subsequent radionuclide transport are implicitly included in the biosphere model through the distributions of soil-to-plant transfer factors. The uncertainty in these parameters accounts for the possible changes in soil conditions (e.g., due to addition of soil amendments), and is also appropriate for the volcanic conditions (BSC 2004 [DIRS 169672], Sections 6.2.1). An acid rain event would thus not significantly affect the radionuclide transport in the biosphere and the resulting exposures to the RMEI. Therefore, acid rain of volcanic origin would have a negligible effect on the results of performance assessment and, therefore, can be excluded.

Based on the regulatory requirements, the FEPs related to changes in, or the prediction of, future human activities are excluded. Future climate analysis does not incorproate potential changes including acid rain that may occur as a result of future changes in human actions. Accordingly, this FEP is excluded from the TSPA by regulation.

INPUTS:

Table 1.4.01.03.0A-1. Direct Inputs

Input	Source	Description
10 CFR 63. 2007. Energy: Disposal of High-Level Radioactive Wastes in a Geologic Repository at Yucca Mountain, Nevada. [DIRS 180319]	10 CFR 63.305(b)	DOE should not project changes in society, the biosphere (other than climate), human biology, or increases or decreases in human knowledge or technology
66 FR 55732. Disposal of High-Level Radioactive Wastes in a Proposed Geologic Repository at Yucca Mountain, NV, Final Rule. 10 CFR Parts 2, 19, 20, 21, 30, 40, 51, 60, 61, 63, 70, 72, 73, and 75. [DIRS 156671]	p. 55757	NRC discussion about natural systems of biosphere should be allowed to vary consistent with geologic record, which provide basis for predicting future biosphere changes
	p. 55757	NRC discussion of future economic growth trends
	p. 55757	NRC discussion of future economic growth trends
	p. 55757	Rulemaking proceeding associated with climate change
67 FR 62628. Specification of a Probability for Unlikely Features, Events and Processes. [DIRS 162317]	p. 62629	Specifies the requirement to consider naturally occurring FEPs
70 FR 53313. Implementation of a Dose Standard After 10,000 Years. [DIRS 178394]	10 CFR 63.305(c)	DOE must vary factors related to the geology, hydrology, and climate
BSC 2004. *Characterize Framework for Igneous Activity at Yucca Mountain, Nevada*. [DIRS 169989]	Section 6.2	Low probability of eruption at Yucca Mountain

Table 1.4.01.03.0A-1. Direct Inputs (Continued)

Input	Source	Description
BSC 2004. *Environmental Transport Input Parameters for the Biosphere Model*. [DIRS 169672]	Section 6.2.1	Uncertainty in distributions of transfer factors accounts for a wide range of soil conditions
SNL 2007. *Characterize Eruptive Processes at Yucca Mountain, Nevada*. [DIRS 174260]	Table 7-1	Short eruption duration and low volume

Table 1.4.01.03.0A-2. Indirect Inputs

Citation	Title	DIRS
66 FR 55732	Disposal of High-Level Radioactive Wastes in a Proposed Geologic Repository at Yucca Mountain, NV, Final Rule. 10 CFR Parts 2, 19, 20, 21, 30, 40, 51, 60, 61, 63, 70, 72, 73, and 75.	156671

FEP: 1.4.01.04.0A

FEP NAME:

Ozone Layer Failure

FEP DESCRIPTION:

Human actions (i.e., the use of certain industrial chemicals) may lead to destruction or damage to the earth's ozone layer. This may lead to significant changes to the climate locally and globally, affecting properties of the geosphere such as groundwater flow patterns.

SCREENING DECISION:

Excluded – by regulation

SCREENING JUSTIFICATION:

The description of present-day climate, as discussed in included FEP 1.3.01.00.0A (Climate Change), is based on climate records that implicitly include effects of modern society over the duration of the historical record. Future changes in human influences on climate are excluded from postclosure assessment on the basis of requirements contained in 10 CFR 63.305(b) [DIRS 180319] and proposed 10 CFR 63.305 (c) (70 FR 53313 [DIRS 178394]), which provide as follows: "DOE should not project changes in society, the biosphere (other than climate), human biology, or increases or decreases of human knowledge or technology. In all analyses done to demonstrate compliance with this part, DOE must assume that all of those factors remain constant as they are at the time of submission of the license application" (10 CFR 63.305(b) [DIRS 180319]); and "DOE must vary factors related to the geology, hydrology, and climate based upon cautious, but reasonable assumptions consistent with present knowledge of factors that could affect the Yucca Mountain disposal system during the period of geologic stability and consistent with the requirements for performance assessment specified at § 63.342" (proposed 10 CFR 63.305(c) (70 FR 53313 [DIRS 178394])).

The supplementary information portion of the preamble to 10 CFR Part 63 (66 FR 55732 [DIRS 156671]) provides rationale for the requirements in 10 CFR 63.305(b) [DIRS 180319] and (c) (70 FR 53313 [DIRS 178394])) and indicates that only natural evolution of the geosphere and biosphere is to be included in the performance assessment but any impacts caused by future changes in human behaviors are not to be included. In response to comments made in the rulemaking proceeding associated with climate change (66 FR 55732 [DIRS 156671], p. 55,757), the NRC emphasized the importance of including "climate change in both the geosphere and the biosphere performance assessment calculations to ensure that the conceptual model of the environment is consistent with our scientific understanding of reasonably anticipated natural events." Similarly, in 67 FR 62628 [DIRS 162317] the NRC states, "DOE's performance assessments are required to consider the naturally occurring features, events and processes that could affect the performance of a geologic repository…" (67 FR 62628 [DIRS 162317], p. 62629). In further response to comments, the NRC stated that considering future economic growth trends and human behaviors would add inappropriate speculation into

the requirements and would lead to problems deciding which alternative futures are credible and which are unrealistic (66 FR 55732 [DIRS 156671], p. 55757).

Prediction of ozone layer failure due to future human actions would not only involve speculation about the local population, but also introduce inherently large uncertainties in prediction of the future global population behavior and resulting consequences. In its discussion of consideration of future economic growth trends, the NRC found that inclusion of such future predictions would not only add inappropriate speculation, but also "would not enhance public safety, and is likely inconsistent with the EPA standards" (66 FR 55732 [DIRS 156671], p. 55757).

Based on these requirements, the FEPs related to changes in or predictions of future human activities are excluded. Future climate analysis does not incorporate potential changes, including ozone layer failure, that may occur as a result of future changes in human actions. Accordingly, this FEP is excluded from the TSPA by regulation.

INPUTS:

Table 1.4.01.04.0A-1. Direct Inputs

Input	Source	Description
10 CFR 63. 2007. Energy: Disposal of High-Level Radioactive Wastes in a Geologic Repository at Yucca Mountain, Nevada. [DIRS 180319]	10 CFR 63.305(b)	DOE should not project changes in society, the biosphere (other than climate), human biology, or increases or decreases in human knowledge or technology
66 FR 55732. Disposal of High-Level Radioactive Wastes in a Proposed Geologic Repository at Yucca Mountain, NV, Final Rule. 10 CFR Parts 2, 19, 20, 21, 30, 40, 51, 60, 61, 63, 70, 72, 73, and 75. [DIRS 156671]	p. 55757	NRC discussion of future economic growth trends
	p. 55757	Rulemaking proceeding associated with climate change
67 FR 62628. Specification of a Probability for Unlikely Features, Events and Processes. [DIRS 162317]	p. 62629	Specifies the requirement to consider naturally occurring FEPs
70 FR 53313. Implementation of a Dose Standard After 10,000 Years. [DIRS 178394]	10 CFR 63.305(c)	DOE must vary factors related to the geology, hydrology, and climate

Table 1.4.01.04.0A-2. Indirect Inputs

Citation	Title	DIRS
66 FR 55732	Disposal of High-Level Radioactive Wastes in a Proposed Geologic Repository at Yucca Mountain, NV, Final Rule. 10 CFR Parts 2, 19, 20, 21, 30, 40, 51, 60, 61, 63, 70, 72, 73, and 75.	156671

FEP: 1.4.02.01.0A

FEP NAME:

Deliberate Human Intrusion

FEP DESCRIPTION:

Humans could deliberately intrude into the repository, although without appropriate precautions, intruders could experience high radiation exposures. In addition, waste packages and other containment may be damaged during intrusion, thereby potentially increasing radionuclide release rates to the biosphere. Motivation for deliberate human intrusion includes mining for waste retrieval, site remediation/improvement activities, archaeological investigation, facility sabotage, and acts of war.

SCREENING DECISION:

Excluded – by regulation

SCREENING JUSTIFICATION:

Regulations indicate that deliberate human intrusion into the Yucca Mountain repository may be excluded from consideration in the TSPA. The approach to addressing potential future human intrusion into the repository is discussed in Subpart E of 10 CFR Part 63 ([DIRS 180319]). In particular, in discussing institutional controls, 10 CFR 63.102(k) [DIRS 180319] provides, in part, that:

> …because it is not possible to make scientifically sound forecasts of the long-term reliability of institutional controls, it is not appropriate to include consideration of human intrusion into a fully risk-based performance assessment for purposes of evaluating the ability of the geologic repository to achieve the performance objective at § 63.113(b). Hence, human intrusion is addressed in a stylized manner….

Further, in discussing the human intrusion analysis, 10 CFR 63.102(l) [DIRS 180319] provides, in part, that:

> Although the consequences of an assumed intrusion event would be a separate analysis, the analysis is similar to the performance assessment required by § 63.113(b) but subject to specific requirements for evaluation of human intrusion specified at §§ 63.321, 63.322 and 63.342.

Therefore, an assessment of human intrusion is required to demonstrate compliance with the individual protection standard for human intrusion (proposed 10 CFR 63.321 (70 FR 53313 [DIRS 178394])), but human intrusion does not require consideration within the demonstration of compliance with the individual protection standard after permanent closure (proposed 10 CFR 63.311 (70 FR 53313 [DIRS 178394])).

Future human intrusion may be intentional and deliberate or may be inadvertent and accidental. Supplementary discussion in the preamble to 40 CFR Part 197 [DIRS 155216] clarifies the point that consideration of deliberate human intrusion in the TSPA is not intended. In the supplementary information to 40 CFR Part 197 (66 FR 32074 [DIRS 155216], p. 32105, Item 3), the EPA, in response to comments regarding the human intrusion stylized analysis, states:

> Comments we received proposing alternative drilling frequencies and intentions, such as deliberately drilling into the repository, did not provide a sufficient rationale to abandon the NAS [National Academy of Science] recommendations and we therefore retained our original framing for the scenario.

The EPA amplifies on this point in 66 FR 32074 ([DIRS 155216], p. 32,127, Item 10). The EPA explicitly states that:

> Some comments suggested that there is a strong possibility for deliberate intrusion into the repository to access its content as possible resources. We believe that there is no useful purpose to assessing the consequences of deliberate intrusions because in that case the intruders would be aware of the risks and consequences and would have decided to assume the risks. This is consistent with NAS's [the National Academy of Science] conclusion regarding intentional intrusion (NAS Report, p. 14).

Further clarification that deliberate human intrusion may be excluded from the TSPA is provided in the requirements for the analysis of the human intrusion scenario (10 CFR 63.322 [DIRS 180319]). According to 10 CFR 63.322(a) [DIRS 180319], the DOE must assume that there is a single human intrusion as a result of exploratory drilling for groundwater. Therefore, deliberate human intrusion such as mining for waste retrieval, site remediation/improvement activities, archaeological investigation, facility sabotage, and acts of war may be may be excluded from the TSPA.

In summary, FEP 1.4.02.01.0A (Deliberate Human Intrusion) may be excluded from the TSPA based on regulation. Inadvertent human intrusion is discussed in included FEP 1.4.02.02.0A (Inadvertent Human Intrusion) and is included in the performance assessment to demonstrate compliance with the individual protection standard for human intrusion (proposed 10 CFR 63.321 (70 FR 53313 [DIRS 178394])).

INPUTS:

Table 1.4.02.01.0A-1. Direct Inputs

Input	Source	Description
10 CFR 63. 2007. Energy: Disposal of High-Level Radioactive Wastes in a Geologic Repository at Yucca Mountain, Nevada. [DIRS 180319]	10 CFR 63.322	Statement that excludes human intrusion
	10 CFR 63.102(k), 10 CFR 63.102(l)	Discusses the approach to addressing potential future human intrusion into the Yucca Mountain repository
66 FR 32074. 40 CFR Part 197, Public Health and Environmental Radiation Protection Standards for Yucca Mountain, NV; Final Rule. [DIRS 155216]	p. 32127, Item 10	Proposed change to 40 CFR Part 197 saying that there is no useful purpose in assessing the consequences of deliberate intrusions
	p. 32105, Item 3	Proposed change to 40 CFR Part 197 regarding deliberate human intrusion

Table 1.4.02.01.0A-2. Indirect Inputs

Citation	Title	DIRS
10 CFR 63	Energy: Disposal of High-Level Radioactive Wastes in a Geologic Repository at Yucca Mountain, Nevada	180319
66 FR 32074	40 CFR Part 197, Public Health and Environmental Radiation Protection Standards for Yucca Mountain, NV; Final Rule.	155216
70 FR 53313	Implementation of a Dose Standard After 10,000 Years	178394

FEP: 1.4.02.02.0A

FEP NAME:

Inadvertent Human Intrusion

FEP DESCRIPTION:

Humans could accidentally intrude into the repository. Without appropriate precautions, intruders could experience high radiation exposures. Moreover, containment may be left damaged, which could increase radionuclide release rates to the biosphere. Inadvertent human intrusion might occur during scientific, mineral or geothermal exploration.

SCREENING DECISION:

Included

TSPA DISPOSITION:

The approach to addressing potential future human intrusion into the Yucca Mountain repository is discussed in Subpart E of 10 CFR Part 63 [DIRS 180319]. In particular, in discussing institutional controls, 10 CFR 63.102(k) [DIRS 180319] provides, in part, that:

> …because it is not possible to make scientifically sound forecasts of the long-term reliability of institutional controls, it is not appropriate to include consideration of human intrusion into a fully risk-based performance assessment for purposes of evaluating the ability of the geologic repository to achieve the performance objective at § 63.113(b). Hence, human intrusion is addressed in a stylized manner….

Further, in discussing the human intrusion analysis, 10 CFR 63.102(l) [DIRS 180319] provides, in part, that:

> Although the consequences of an assumed intrusion event would be a separate analysis, the analysis is similar to the performance assessment required by § 63.113(b) but subject to specific requirements for evaluation of human intrusion specified at §§ 63.321, 63.322 and 63.342….

Therefore, an assessment of human intrusion is required to demonstrate compliance with the individual protection standard for human intrusion (proposed 10 CFR 63.321 (70 FR 53313 [DIRS 178394])), but human intrusion does not require consideration within the demonstration of compliance with the individual protection standard after permanent closure (proposed 10 CFR 63.311 (70 FR [DIRS 178394])) or within the demonstration of compliance with the groundwater protection standards (10 CFR 63.331 [DIRS 180319]).

The approach to assessing human intrusion is set out in Subpart L of 10 CFR Part 63 [DIRS 180319] and proposed 10 CFR Part 63 (70 FR 53313 [DIRS 178394]). A definition of human intrusion is provided in 10 CFR 63.302 [DIRS 180319], the individual protection

standard for human intrusion is provided in proposed 10 CFR 63.321 (70 FR 53313 [DIRS 178394]), and the approach to evaluating a human intrusion scenario is specified in 10 CFR 63.322 [DIRS 180319], as discussed below.

Human intrusion is defined as follows:

> Human intrusion means breaching of any portion of the Yucca Mountain disposal system, within the repository footprint, by any human activity.

Future human intrusion may be intentional and deliberate or may be inadvertent and accidental. The supplementary discussion in the preamble to 66 FR 32074 (40 CFR Part 197 [DIRS 155216]) clarifies the point that consideration of deliberate human intrusion in the TSPA is not intended, as discussed in detail in excluded FEP 1.4.02.01.0A (Deliberate Human Intrusion). Consideration of human intrusion into the repository is limited to inadvertent intrusion.

Inadvertent human intrusions are considered within the context of the regulatory requirements to demonstrate compliance with the human intrusion standard. Proposed 10 CFR 63.321 (70 FR 53313 [DIRS 178394]) states the following:

> (a) DOE must determine the earliest time after disposal that the waste package would degrade sufficiently that a human intrusion (see § 63.322) could occur without recognition by the drillers.
>
> (b) DOE must demonstrate that there is a reasonable expectation that the reasonably maximally exposed individual receives, as a result of human intrusion, no more than the following annual dose:
>
> (1) 0.15 mSv (15 mrem) for 10,000 years following disposal; and
>
> (2) 3.5 mSv (350 mrem) after 10,000 years, but within the period of geologic stability.
>
> (c) DOE's analysis must include all potential environmental pathways of radionuclide transport and exposure, subject to the requirements at § 63.322.

The assessment of inadvertent human intrusion is based on an evaluation of the dose resulting from a stylized human intrusion drilling scenario. This approach is documented in *Total System Performance Assessment Model/Analysis for the License Application* (SNL 2008 [DIRS 183478], Section 6.7) to demonstrate that the repository design will exhibit a measure of resilience against a typical human intrusion scenario. The scenario is not intended to represent all forms of human intrusion that could affect the repository. The stylized scenario for human intrusion makes use of the following assumptions (10 CFR 63.322 [DIRS 180319]):

> (a) There is a single human intrusion as a result of exploratory drilling for groundwater;

(b) The intruders drill a borehole directly through a degraded waste package into the uppermost aquifer underlying the Yucca Mountain repository;

(c) The drillers use the common techniques and practices that are currently employed in exploratory drilling for groundwater in the region surrounding Yucca Mountain;

(d) Careful sealing of the borehole does not occur, instead natural degradation processes gradually modify the borehole;

(e) No particulate waste material falls into the borehole;

(f) The exposure scenario includes only those radionuclides transported to the saturated zone by water (e.g., water enters the waste package, releases radionuclides, and transports radionuclides by way of the borehole to the saturated zone); and

(g) No releases are included which are caused by unlikely natural processes and events.

In particular, TSPA evaluation of the earliest time at which a waste package is expected to be breached is discussed in Section 6.7.2 of *Total System Performance Assessment Model/Analysis for the License Application* (SNL 2008 [DIRS 183478]); Section 6.7.2.1 of that report (SNL 2008 [DIRS 183478]) describes the analysis of drip shield and waste package degradation for this scenario; Section 6.7.2.2 describes unlikely events-related damage mechanisms; and Section 6.7.2.3 (describes the potential for waste package penetration by a drilling event. Implementation and the process for estimating the mean annual dose for the human intrusion scenario is discussed in Section 6.7.3 of *Total System Performance Assessment Model/Analysis for the License Application* (SNL 2008 [DIRS 183478]).

The requirement in 10 CFR 63.322(f) [DIRS 180319], that only radionuclides transported to the saturated zone need be considered, precludes consideration of exposure of the public, drillers, or other human intruders to radionuclides in cuttings, circulated materials, or tailings. The supplementary information in the preamble to 10 CFR Part 63 (66 FR 55732 [DIRS 156671], p. 55761, Supplementary Information, 3.10 Human Intrusion Standard) is clear regarding the intent of the NRC on this point:

> Human intrusion has the potential for releasing particulate HLW to the surface with drill cuttings or providing a fast pathway for radionuclides to be transported to the saturated zone by water (e.g., water enters the waste package, releases radionuclides, and transports radionuclides by way of the borehole to the saturated zone). NAS [The National Academy of Science] concluded, and the Commission agrees, that analysis of the risk to the public or the intruders (i.e., drilling crew) from radioactive drill cuttings left unattended at the surface for subsequent dispersal into the biosphere would not fulfill the purpose of the human intrusion calculation because it would not show how well a particular repository site and design would protect the public at large. Rather, an analysis of the hazard of particulate HLW left on the surface would be dominated by assumptions subject

> to significant speculation and uncertainty regardless of the particular site or design under evaluation. Additionally, the release to the surface represents a one-time release with no long-term effect on the repository barriers.

Therefore, consideration of the exposure of intruders to radioactive waste is specifically excluded. Exposure as a consequence of human intrusion is limited to the transport of radionuclides by water flowing through a borehole that intrudes through a waste package, which is sufficiently degraded that it goes undetected by the drill operators, directly into the saturated zone.

In summary, inadvertent human intrusion is included in the demonstration of compliance with the individual protection standard for human intrusion (proposed 10 CFR 63.321 (70 FR 53313 [DIRS 178394])), but does not require consideration within the demonstration of compliance with the individual protection standard after permanent closure (proposed 10 CFR 63.311 (70 FR 53313 [DIRS 178394])) or within the demonstration of compliance with the groundwater protection standards (10 CFR 63.331 [DIRS 180319]). The assessment of inadvertent human intrusion is based on an evaluation of the dose resulting from a stylized scenario, which is discussed in included FEPs 1.4.04.00.0A (Drilling Activities – Human Intrusion) and 1.4.04.01.0A (Effects of Drilling Intrusion).

INPUTS:

Table 1.4.02.02.0A-1. Direct Inputs

Input	Source	Description
10 CFR 63. 2007. Energy: Disposal of High-Level Radioactive Wastes in a Geologic Repository at Yucca Mountain, Nevada. [DIRS 180319]	10 CFR 63 Part 63.102(l)	Regulations indicate that analysis of deliberate human intrusion and exposure of the intruders is to be set aside as a separate analysis not included in the TSPA

Table 1.4.02.02.0A-2. Indirect Inputs

Citation	Title	DIRS
10 CFR 63	Energy: Disposal of High-Level Radioactive Wastes in a Geologic Repository at Yucca Mountain, Nevada	180319
66 FR 32074	40 CFR Part 197, Public Health and Environmental Radiation Protection Standards for Yucca Mountain, NV; Final Rule	155216
66 FR 55732	Disposal of High-Level Radioactive Wastes in a Proposed Geologic Repository at Yucca Mountain, NV, Final Rule. 10 CFR Parts 2, 19, 20, 21, 30, 40, 51, 60, 61, 63, 70, 72, 73, and 75	156671
70 FR 53313	Implementation of a Dose Standard After 10,000 Years	178394
SNL 2008	*Total System Performance Assessment Model/Analysis for the License Application*	183478

FEP: 1.4.02.03.0A

FEP NAME:

Igneous Event Precedes Human Intrusion

FEP DESCRIPTION:

An igneous event, such as a dike, could intersect the repository and significantly alter the material and structural properties of a drip shield and/or waste package. Because of the change in properties of these materials resulting from an igneous intrusion, an intruder, using groundwater exploration drilling techniques, may not be able to recognize that something other than naturally-occurring material has been encountered.

SCREENING DECISION:

Excluded – low probability

SCREENING JUSTIFICATION:

The probability of a dike intruding the repository has been determined to have a mean annualized probability of 1.7×10^{-8} (BSC 2004 [DIRS 169989], Table 7-1). An igneous event is therefore a "not expected event," as defined in proposed 10 CFR 63.342 (70 FR 53313 [DIRS 178394]). This FEP is applicable only to the performance assessment used to demonstrate compliance with the individual protection standard for human intrusion in proposed 10 CFR 63.321 (70 FR 53313 [DIRS 178394]). The human intrusion scenario is defined by 10 CFR 63.322 [DIRS 180319] as a single stylized scenario where a driller bores a single borehole into the repository. 10 CFR 63.322(g) [DIRS 180319] states, "no releases are included which are caused by unlikely natural processes and events." Proposed 10 CFR 63.342 (70 FR 53313 [DIRS 178394]) further states: "DOE's assessments for the human-intrusion and ground-water protection standards shall not include consideration of unlikely features, events, and processes, or sequences of events and processes, i.e., those that are estimated to have less than one chance in 10 and at least one chance in 10,000 of occurring within 10,000 years of disposal."

In conclusion, FEP 1.4.02.03.0A (Igneous Event Precedes Human Intrusion) is excluded from the performance assessments conducted to demonstrate compliance with proposed 10 CFR 63.311 and 63.321 (70 FR 53313 [DIRS 178394]), and with 10 CFR 63.331 [DIRS 180319], on the basis of low probability.

INPUTS:

Table 1.4.02.03.0A-1. Direct Inputs

Input	Source	Description
10 CFR 63. 2007. Energy: Disposal of High-Level Radioactive Wastes in a Geologic Repository at Yucca Mountain, Nevada. [DIRS 180319]	10 CFR 63.322	Human intrusion scenario is defined
BSC 2004. *Characterize Framework for Igneous Activity at Yucca Mountain, Nevada*. [DIRS 169989]	Table 7-1	Probability of a dike intruding the repository

Table 1.4.02.03.0A-2. Indirect Inputs

Citation	Title	DIRS
10 CFR 63	Energy: Disposal of High-Level Radioactive Wastes in a Geologic Repository at Yucca Mountain, Nevada	180319
70 FR 53313	Implementation of a Dose Standard After 10,000 Years	178394

FEP: 1.4.02.04.0A

FEP NAME:

Seismic Event Precedes Human Intrusion

FEP DESCRIPTION:

A seismic event of sufficient magnitude to significantly alter the material and structural properties of a drip shield and/or waste package could occur in the vicinity of the repository. Because of the change in properties, an intruder, using groundwater exploration drilling techniques, may not be able to recognize that something other than naturally-occurring material has been encountered.

SCREENING DECISION:

Excluded – low consequence

SCREENING JUSTIFICATION:

Human intrusion is not considered in the performance assessment used to demonstrate compliance with the individual protection standard of proposed 10 CFR 63.311 (70 FR 53313 [DIRS 178394]) or the groundwater protection standard of 10 CFR 63.331 [DIRS 180319], but is addressed separately in a stylized performance assessment used to demonstrate compliance with the human intrusion individual protection standard of proposed 10 CFR 63.321 (70 FR 53313 [DIRS 178394]). The stylized human intrusion performance assessment that is conducted to demonstrate compliance with proposed 10 CFR 63.321 (70 FR 53313 [DIRS 178394]) must include events with at least a 1 in 10 chance in 10,000 years of occurring (i.e., an approximate annual probability of 10^{-5} or greater) (proposed 10 CFR 63.342(b) (70 FR 53313 [DIRS 178394]), if these events are found to have a significant effect on the results of the performance assessment (proposed 10 CFR 63.342(a) and (c) (70 FR 53313 [DIRS 178394])). Lower probability events need not be considered (proposed 10 CFR 63.342 (70 FR 53313 [DIRS 178394])).

A seismic event may produce damage to drip shields or waste packages through effects from: (1) fault displacement along faults that intersect the repository, (2) damage induced by rockfall, and 3) mechanical damage induced by seismic ground motion.

The number of drip shields/waste packages estimated to lie on generic faults is 214 (SNL 2007 [DIRS 176828], Table 6-71) out of a total of 11,162 drip shields/waste packages (SNL 2007 [DIRS 176828], Table 6-62), to be stored in the repository. Waste package and drip shield failure due to fault displacement along faults intersecting the repository footprint has an annual probability of exceedance less than 2.2×10^{-7} [per year] for waste packages containing a TAD canister and less than 2.5×10^{-7} [per year] for codisposal waste packages (SNL 2007 [DIRS 176828], Table 6-67). Thus, failure of drip shields or waste packages from fault displacement is not relevant to the performance assessments conducted for proposed 10 CFR 63.321 (70 FR 53313 [DIRS 178394]), because the probability is lower than the regulatory threshold (see paragraph 1). For the same reason, waste package and drip shield

damage due to either rockfall or seismic ground motion associated with seismic events with probability less than 10^{-5} are not relevant.

Seismic events with an annual probability of 10^{-5} or above are associated with the potential for seismic-related damage to the drip shields and waste packages (SNL 2007 [DIRS 176828], Sections 5, 6.3, 6.4, and 6.5). For this magnitude of seismic event, corresponding to a response of 1.05 m/s PGV (SNL 2007 [DIRS 176828], Section 6.1.7), there is no possibility of rupture for 23-mm OCB TAD (SNL 2007 [DIRS 176828], Section 6.5.1.1) or codisposal (SNL 2007 [DIRS 176828], Section 6.6.1.1) waste packages with intact internals. The rupture probability for a 23-mm OCB TAD canister waste package with degraded internals is zero for single impacts (SNL 2007 [DIRS 176828], Section 6.5.1.1). Internals are degraded by multiple seismic events. The probability of failure for a drip shield depends on its plate thickness which slowly decreases with time because of general corrosion (modeled mean corrosion rate = 5 nm/yr ; SNL 2007 [DIRS 180778], Section 7.2.2) and on the rockfall loading factor for the 1.05 m/s PGV range. For a 15-mm plate thickness, which approximately corresponds to the plate thickness at 10,000 years, the probability of failure due to 100% rockfall loading (worst case) is zero (SNL 2007 [DIRS 176828], Table 6-36) and is only 0.001 when the drip shield thickness is reduced to 10 mm, which occurs on average at about 97,000 years. Thus, a seismic event only affects the timing or radiological exposure to the RMEI if a damaged drip shield or waste package is intersected by drilling.

For a 1.05 m/s PGV magnitude seismic event, the probability of damage to a 23 mm OCB TAD with intact internals is zero (SNL 2007 [DIRS 176828], Table 6-4) at a 90% residual stress threshold. The 90% residual stress threshold is the lower bound for the residual tensile stress threshold for potential crack initiation. The probability of damage to a codisposal waste package with a 23-mm OCB and intact internals is 0.559 (SNL 2007 [DIRS 176828], Tables 6-14 and 6-16). The mean and standard deviation of the damage at the 1.05 m/s PGV level is 0.120 and 0.144 m^2 (SNL 2007 [DIRS 176828], Section 6.5.4), which is a relatively small part of the total surface area of the TAD canister, 33.64 m^2 (SNL 2007 [DIRS 176828], Section 6.5.4), and as such the material properties (such as compressive strength), or the structural strength of the features will not have been significantly altered in terms of their ability to be recognized during drilling (SNL 2008 [DIRS 183478], Section 6.7.2.2). Figure 6-102 of *Total System Performance Assessment Model/Analysis for the License Application* (SNL 2008 [DIRS 183478] gives a nonconditional nonzero damaged area of approximately 0.15 m^2 for 15-mm drip shield plates, again corresponding to a small area compared to the total area of the drip shield.

Thus, the material properties (such as compressive strength), or the structural strength of the features will not have been significantly altered in terms of their ability to be recognized during drilling (SNL 2008 [DIRS 183478], Section 6.7.2.2). Since the materials retain their basic physical characteristics (compressive strength in particular), the drilling assembly will respond to material changes in a recognizable way. As the emplacement drift is penetrated, a loss of drilling fluid will alert the driller to a change of conditions (SNL 2008 [DIRS 183478], Section 6.7.2.3.2). Damage in the drift produced by seismic activity may produce rubble which would tend to cause uneven loading of the drill bit (SNL 2008 [DIRS 183478], Section 6.7.2.3.2). As an undamaged EBS component (drip shield or waste package) is encountered, the drill bit will tend to bounce or slide and would tend to slip off unless the drill bit were aligned on the apex of the drip shield, further signaling a response by the driller (SNL 2008

[DIRS 183478], Section 6.7.2.3.3). Encountering a damaged feature, the drill bit will catch on fractures or cracks in the surface of the material. In extreme cases, contact will prevent the drill bit from rotating as it becomes entangled with the metals and alloys of the various engineered features. Under these conditions, the significant differences in shear strength and modulus of elasticity between naturally occurring and engineered feature materials will be important factors in the recognition by the driller that metal has been contacted by the bit (SNL 2008 [DIRS 183478], Section 6.7.2.3.4). A more complete discussion on driller recognition of EBS components within the host rock is given in *Total System Performance Assessment Model/Analysis for the License Application* (SNL 2008 [DIRS 183478], Section 6.7.2.3.4).

DOE must determine the earliest time after disposal that a waste package would degrade sufficiently that a human intrusion could occur without recognition by the drillers (proposed 10 CFR 63.321 (70 FR 53313 [DIRS 178394])). The time until such degradation will depend most significantly on the rate of general corrosion of the drip shield and waste package materials. There is little expectation that a seismic event with an annual probability of 10^{-5} or more would affect this degradation time significantly. Based on the preceding discussion, seismic events with an annual probability of 10^{-5} or above would not induce significant changes in the material properties of the host rock or the engineered feature materials, or significantly affect the rate of degradation of engineered feature materials. These events are of low consequence because the magnitude and time of the resulting radiological exposures to the RMEI, or radionuclide releases to the accessible environment, would not be significantly adversely changed by their omission. Other seismic events of greater magnitude, which may occur with probability less than 10^{-5}, are not relevant as per proposed 10 CFR 63.342 (70 FR 53313 [DIRS 178394]).

Based on the previous discussion, omission of FEP 1.4.02.04.0A (Seismic Event Precedes Human Intrusion) will not result in a significant adverse change in the magnitude or timing of either radiological exposure to the RMEI or radionuclide releases to the accessible environment. Therefore, this FEP is excluded from the performance assessments conducted to demonstrate compliance with proposed 10 CFR 63.311 and 63.321 (70 FR 53313 [DIRS 178394]), and with 10 CFR 63.331 [DIRS 180319], on the basis of low consequence.

INPUTS:

Table 1.4.02.04.0A-1. Direct Inputs

Input	Source	Description
SNL 2007. *Seismic Consequence Abstraction*. [DIRS 176828]	Table 6-4	Probability of damage to a 23-mm OCB TAD with intact interna
	Table 6-36	Probability of failure due to 100% rockfall loading
	Sections 6.1.7, 6.5.1.1, 6.6.1.1	Magnitude of seismic event corresponding to a response of 1.05 m/s peak ground velocity
	Table 6-67	The number of drip shields/waste packages estimated to lie on generic displacement along faults intersecting the repository footprint
	Table 6-62	Number of drip shields/waste packages to be stored in the repository
	Table 6-71	Number of drip shields/waste packages estimated to lie on generic faults
	Sections 6.3, 6.4, 6.5	Seismic events with an annual probability of 10^{-5} or above are associated with the potential for seismic-related damage to the drip shields and waste packages
	Section 6.5.4	The mean and standard deviation of the damage of a seismic event
	Tables 6-14, 6-16	Probability of damage to a codisposal waste package with a 23-mm OCB and intact internals is 0.559

Table 1.4.02.04.0A-2. Indirect Inputs

Citation	Title	DIRS
10 CFR 63	Energy: Disposal of High-Level Radioactive Wastes in a Geologic Repository at Yucca Mountain, Nevada	180319
70 FR 53313	Implementation of a Dose Standard After 10,000 Years	178394
SNL 2007	*General Corrosion and Localized Corrosion of the Drip Shield*	180778
SNL 2008	*Total System Performance Assessment Model/Analysis for the License Application*	183478

FEP: 1.4.03.00.0A

FEP NAME:

Unintrusive Site Investigation

FEP DESCRIPTION:

This FEP concerns airborne, geophysical, or other surface-based investigations of a repository site area after its closure.

SCREENING DECISION:

Excluded – low consequence

SCREENING JUSTIFICATION:

Unintrusive activities have the potential to affect the repository. Activities that might produce deep excavation in the area of the repository are covered by excluded FEPs 1.4.05.00.0A (Mining and other Underground Activities) and 1.4.02.01.0A (Deliberate Human Intrusion), and in included FEPs 1.4.02.02.0A (Inadvertent Human Intrusion), 1.4.04.00.0A (Drilling activities), and 1.4.04.01.0A (Effects of Drilling Intrusion). Intrusive activities, whether deliberate or not, are considered human intrusion. Human intrusion is defined as (10 CFR 63.302 [DIRS 180319]):

> Human intrusion means breaching any portion of the Yucca Mountain disposal system, within the repository footprint, by any human activity.

This is an important concept in that any human activity that breaches the disposal system is included within the regulatory definition of human intrusion. Any human or human-induced activity (including surface-based site investigations, digs, grading, etc.) that breaches the natural barrier system is, by definition, a human intrusion. However, 10 CFR 63.113(d) [DIRS 180319] and 40 CFR 197.26 [DIRS 175755] stipulate that human intrusion shall be assessed only through the consideration of the human intrusion stylized analysis, which deals with the use of drilling techniques related to water well drilling.

There are a number of possible human activities with the potential to affect the repository that do not physically breach the Yucca Mountain disposal system. These might include surveys, mapping activities, and investigations using electromagnetic waves (sound, infrared, electromagnetic pulse events, lasers). Because the repository is located at least 200 m (656 ft) below the surface (SNL 2007 [DIRS 179466], Table 4-1, Parameter Number 01-06), these technologies in their present state do not produce sufficient energy to have a noticeable effect on the repository.

Based on the above discussion, omission of FEP 1.4.03.00.0A (Unintrusive Site Investigation) will not result in a significant adverse change in the magnitude or time of radiological exposures to the RMEI or radionuclide releases to the accessible environment. Therefore, this FEP is excluded from the performance assessments conducted to demonstrate compliance with the proposed 10 CFR 63.311 and

63.321 (70 FR 53313 [DIRS 178394]), and with 10 CFR 63.331 [DIRS 180319], on the basis of low consequence.

INPUTS:

Table 1.4.03.00.0A-1. Direct Inputs

Input	Source	Description
SNL 2007. *Total System Performance Assessment Data Input Package for Requirements Analysis for Subsurface Facilities*. [DIRS 179466]	Table 4-1, Parameter Number 01-06	Repository is located 200 m (656 ft) below the surface

Table 1.4.03.00.0A-2. Indirect Inputs

Citation	Title	DIRS
10 CFR 63	Energy: Disposal of High-Level Radioactive Wastes in a Geologic Repository at Yucca Mountain, Nevada	180319
40 CFR 197	Protection of Environment: Public Health and Environmental Radiation Protection Standards for Yucca Mountain, Nevada	175755
70 FR 53313	Implementation of a Dose Standard After 10,000 Years	178394

FEP: 1.4.04.00.0A

FEP NAME:

Drilling Activities (Human Intrusion)

FEP DESCRIPTION:

This FEP addresses any type of drilling activity in the repository environment. These activities may be taken with or without awareness of the presence of the repository and with or without consent of the repository licensee. Drilling activities may be associated with natural resource exploration (water, oil and gas, minerals, geothermal energy), waste disposal (liquid), fluid storage (hydrocarbon, gas), or reopening existing boreholes.

SCREENING DECISION:

Included

TSPA DISPOSITION:

An assessment of human intrusion is required as part of the Yucca Mountain repository license application to demonstrate compliance with the stylized human intrusion scenario based on exploratory drilling for groundwater in proposed 10 CFR 63.321 (70 FR 53313 [DIRS 178394]). The assessment of human intrusion is discussed in included FEP 1.4.02.02.0A (Inadvertent Human Intrusion). Compliance with the human intrusion standard involves evaluation of the dose resulting from a stylized inadvertent human intrusion analysis. Other drilling activities associated with natural resource exploration (oil and gas, minerals, geothermal energy), waste disposal (liquid), fluid storage (hydrocarbon, gas), or reopening existing boreholes are excluded by regulation.

The stylized human intrusion scenario is implemented to demonstrate that the repository design will exhibit a measure of resilience against a typical human intrusion scenario. The scenario is not intended to represent all forms of human intrusion that could affect the repository. The scope of the stylized scenario is set out in 10 CFR 63.322 [DIRS 180319], which requires that the analysis must assume the intrusion is the result of exploratory drilling for groundwater. Specifically, according to 10 CFR 63.322(a) [DIRS 180319], it should be assumed that:

> There is a single human intrusion as a result of exploratory drilling for ground water.

And according to 10 CFR 63.322(c) [DIRS 180319] it should be assumed that:

> The drillers use the common techniques and practices that are currently employed in exploratory drilling for ground water in the region surrounding Yucca Mountain.

In summary, FEP 1.4.04.00.0A (Drilling Activities (Human Intrusion)) is included in the demonstration of compliance with the individual protection standard for human intrusion

(proposed 10 CFR 63.321 (70 FR 53313 [DIRS 178394])), but does not require consideration within the demonstration of compliance with the individual protection standard after permanent closure (proposed 10 CFR 63.311 (70 FR 53313 [DIRS 178394])) or within the demonstration of compliance with the groundwater protection standards (10 CFR 63.331 [DIRS 180319]). The analysis conducted to demonstrate compliance with the individual protection standard for human intrusion is discussed in detail in included FEP 1.4.02.02.0A (Inadvertent Human Intrusion).

INPUTS:

Table 1.4.04.00.0A-1. Indirect Inputs

Citation	Title	DIRS
10 CFR 63	Energy: Disposal of High-Level Radioactive Wastes in a Geologic Repository at Yucca Mountain, Nevada	180319
70 FR 53313	Implementation of a Dose Standard After 10,000 Years	178394

FEP: 1.4.04.01.0A

FEP NAME:

Effects of Drilling Intrusion

FEP DESCRIPTION:

Drilling activities that intrude into the repository may create new release pathways to the biosphere and alter existing pathways. Possible effects of a drilling intrusion include interaction with waste packages, increased saturation in the repository leading to enhanced radionuclide transport to the SZ, changes to groundwater and EBS chemistry, and waste brought to the surface.

SCREENING DECISION:

Included

TSPA DISPOSITION:

An assessment of human intrusion is required as part of the Yucca Mountain repository license application. The effects of drilling intrusion are included in the demonstration of compliance with the individual protection standard for human intrusion (proposed 10 CFR 63.321 (70 FR 53313 [DIRS 178394])), but do not require consideration within the demonstration of compliance with the individual protection standard after permanent closure (proposed 10 CFR 63.311 (70 FR 53313 [DIRS 178394])) or within the demonstration of compliance with the groundwater protection standards (10 CFR 63.331 [DIRS 180319]). The analysis conducted to demonstrate compliance with the individual protection standard for human intrusion is discussed in detail in included FEP 1.4.02.02.0A (Inadvertent Human Intrusion). Compliance with the human intrusion standard involves evaluation of the dose resulting from a stylized inadvertent human intrusion scenario.

The stylized human intrusion scenario is implemented to demonstrate that the repository design will exhibit a measure of resilience against a typical human intrusion scenario. The scenario is not intended to represent all forms of human intrusion that could affect the repository. The scope of the stylized scenario is set out in 10 CFR 63.322 [DIRS 180319], which requires that the analysis must assume the intrusion is the result of exploratory drilling for groundwater, as discussed in included FEP 1.4.04.00.0A (Drilling Activities (Human Intrusion)). 10 CFR 63.322 [DIRS 180319] also specifies how the effects of drilling intrusion should be evaluated. In particular, according to 10 CFR 63.322 [DIRS 180319], it should be assumed that:

> (b) The intruders drill a borehole directly through a degraded waste package into the uppermost aquifer underlying the Yucca Mountain repository

and that:

> (d) Careful sealing of the borehole does not occur, instead natural degradation processes gradually modify the borehole;

> (e) No particulate waste material falls into the borehole;
>
> (f) The exposure scenario includes only those radionuclides transported to the saturated zone by water (e.g., water enters the waste package, releases radionuclides, and transports radionuclides by way of the borehole to the saturated zone); and
>
> (g) No releases are included which are caused by unlikely natural processes and events.

As part of the evaluation of the effects of drilling intrusion to demonstrate compliance with the human intrusion standard in proposed 10 CFR 63.321(a) (70 FR 53313 [DIRS 178394]) the NRC specifies that:

> DOE must determine the earliest time after disposal that the waste package would degrade sufficiently that a human intrusion could occur without recognition by the drillers.

As discussed in FEP 1.4.02.02.0A (Inadvertent Human Intrusion), inadvertent human intrusion is not considered to be possible while the drip shield and waste package remain intact. The rationale for this approach is given in *System Performance Assessment Model/Analysis for the License Application* (SNL 2008 [DIRS 183478], Section 6.7). Specifically, Section 6.7.2.3.4 of that report (SNL 2008 [DIRS 183478]) states:

> Selection of a bit for drilling involves knowledge of the characteristics of the rock. …there are significant differences between the tensile strengths and other material properties of the geologic units at Yucca Mountain and the materials for the drip shield and waste package. Because the materials used in the drip shield and waste packages have high tensile strengths, yield strengths and increased modulus of elasticity compared to the host rock properties, the tooth of a roller bit [typically used in drilling water wells due to their low cost and wide range of operational flexibility] cannot penetrate enough to cause sufficient strain for chipping to occur. Rather, if contact with the drip shield occurs, the rotation of the bit would result in a tearing or shearing action with associated and recognizable high torque values. Consequently, the ductility of the metals makes them nearly impenetrable by techniques used in drilling rock. Boring in metals typically utilizes a milling technique. The downhole milling tools needed to penetrate the drip shield and waste package are not typically used in groundwater exploration, and use of such tools would be a clear indicator of recognition of penetration of some type of metallic, anthropogenic structure.

Consequently, penetration of the drip shield or waste package without recognition by the driller prior to general corrosion failure of the engineered barriers is not feasible.

General corrosion failure of the drip shields is not expected to occur prior to 230,000 years (SNL 2008 [DIRS 183478], Section 6.7.2). Based on this analysis, unrecognized human intrusion is modeled conservatively to not occur prior to 200,000 years.

In conclusion, the effects of drilling intrusion are included in the TSPA for the stylized human intrusion scenario (proposed 10 CFR 63.321 (70 FR 53313 [DIRS 178394]); and 63.322 [DIRS 180319]). However, the assessment of human intrusion does not form part of the TSPA analyses for individual protection (proposed 10 CFR 63.311 (70 FR 53313 [DIRS 178394])) or groundwater protection (10 CFR 63.331 [DIRS 180319]). The human intrusion standard is discussed in detail in included FEP 1.4.02.02.0A (Inadvertent Human Intrusion).

INPUTS:

Table 1.4.04.01.0A-1. Direct Inputs

Input	Source	Description
10 CFR 63. 2007. Energy: Disposal of High-Level Radioactive Wastes in a Geologic Repository at Yucca Mountain, Nevada. [DIRS 180319]	10 CFR 63.322	Human intrusion scenario is defined

Table 1.4.04.01.0A-2. Indirect Inputs

Citation	Title	DIRS
10 CFR 63	Energy: Disposal of High-Level Radioactive Wastes in a Geologic Repository at Yucca Mountain, Nevada	180319
70 FR 53313	Implementation of a Dose Standard After 10,000 Years	178394
SNL 2008	*Total System Performance Assessment Model/Analysis for the License Application*	183478

FEP: 1.4.05.00.0A

FEP NAME:

Mining and Other Underground Activities (Human Intrusion)

FEP DESCRIPTION:

Mining and other underground human activities (e.g., tunneling, underground construction, quarrying) could disrupt the disposal system and affect predicted repository performance.

SCREENING DECISION:

Excluded – by regulation

SCREENING JUSTIFICATION:

Mining, tunneling, underground construction, and quarrying and any other human activity of this type intersecting the repository footprint is defined as a human intrusion as per 10 CFR 63.302 [DIRS 180319]:

> Human intrusion means breaching any portion of the Yucca Mountain disposal system, within the repository footprint, by any human activity.

This is an important concept in that any human activity that breaches the disposal system is included within the regulatory definition of human intrusion.

10 CFR 63.102(k) [DIRS 180319] states that "it is not appropriate to include consideration of human intrusion into a fully risk-based performance assessment for purposes of evaluating the ability of the geologic repository to achieve the performance objective at § 63.113(b). Hence, human intrusion is addressed in a stylized manner." The performance objectives for this stylized analysis are given in proposed 10 CFR 63.321 (70 FR 53313 [DIRS 178394]). In addition, the regulation specifies that the stylized analysis assume the intrusion is the result of exploration for groundwater. This is emphasized in 10 CFR 63.322 [DIRS 180319]. Therefore, all other types of intrusion of the repository footprint (including mining, tunneling, underground construction, and quarrying) are, by default, excluded due to the regulation.

Mining and other underground human activities outside the repository footprint are excluded on the grounds that they do not occur in the region today and 10 CFR 63.305(b) [DIRS 180319] specifies that "DOE should not project changes in society, the biosphere (other than climate), human biology, or increases or decreases in human knowledge or technology." Two related FEPs are included FEP 2.4.10.00.0A (Urban and Industrial Land and Water Use), which states that urban and industrial activities are included in the biosphere model to the extent that they occur today in the Amargosa Valley, and excluded FEP 1.4.08.00.0A (Social and Institutional Development), which excludes social and institutional development (activities, communities, and cities) in the vicinity of Yucca Mountain on the basis of regulation.

In summary FEP 1.4.05.00.0A (Mining and Other Underground Activities (Human Intrusion) is excluded from the performance assessments conducted to demonstrate compliance with the proposed 10 CFR 63.311 and 63.321 (70 FR 53313 [DIRS 178394]), and with 10 CFR 63.331 [DIRS 180319], on the basis of regulation.

INPUTS:

Table 1.4.05.00.0A-1. Direct Inputs

Input	Source	Description
10 CFR 63. 2007. Energy: Disposal of High-Level Radioactive Wastes in a Geologic Repository at Yucca Mountain, Nevada. [DIRS 180319]	10 CFR 63.302	Mining, tunneling, underground construction, and quarrying and any other human activity of this type intersecting the repository footprint is defined as a human intrusion
	10 CFR 63.305(b)	States DOE should not project changes in society, the biosphere (other than climate), human biology, or increases or decreases in human knowledge or technology
	10 CFR 63.322	Regulation specifies that the stylized analysis assume the intrusion is the result of exploration for groundwater
	10 CFR 63.102(k)	States it is not appropriate to include consideration of human intrusion into a fully risk-based performance assessment for purposes of evaluating the ability of the geologic repository to achieve the performance objective at 63.113(b)
66 FR 32074. 40 CFR Part 197, Public Health and Environmental Radiation Protection Standards for Yucca Mountain, NV; Final Rule. [DIRS 155216]	p. 32105, Item 3	Proposed change to 40 CFR Part 197 regarding deliberate human intrusion

Table 1.4.05.00.0A-2. Indirect Inputs

Citation	Title	DIRS
10 CFR 63	Energy: Disposal of High-Level Radioactive Wastes in a Geologic Repository at Yucca Mountain, Nevada	180319
70 FR 53313	Implementation of a Dose Standard After 10,000 Years	178394

FEP: 1.4.06.01.0A

FEP NAME:

Altered Soil or Surface Water Chemistry

FEP DESCRIPTION:

Human activities (e.g., those resulting in industrial pollution or those involving the use of agricultural chemicals) may produce local changes to the soil chemistry and, therefore, to the chemistry of water infiltrating Yucca Mountain. This could result in a contaminant plume of unspecified nature interacting with the repository and possibly with waste packages.

SCREENING DECISION:

Excluded – low consequence

SCREENING JUSTIFICATION:

Human activities may affect soil and surface water chemistry because of the use of chemicals in agricultural activities or the effects of pollution from industrial activities. Such effects on soil and surface water chemistry may impact the chemistry of infiltrating water. To the extent that agricultural and industrial activities currently practiced in the Yucca Mountain region (e.g., in Amargosa Valley) may affect repository performance, they are already included in the characterization of the natural barrier system and the biosphere. Future changes in these activities, including extensions of agricultural and industrial activities to Yucca Mountain itself, where they do not occur today, are excluded based on regulatory requirements. Specifically, 10 CFR 63.305(b) [DIRS 180319] states that "DOE should not project changes in society, the biosphere (other than climate), human biology, or increases or decreases in human knowledge or technology. In all analyses done to demonstrate compliance with this part, the DOE must assume that all of those factors remain constant as they are at the time of submission of the license application."

Industrial activities at the surface associated with the construction, operation, and closure of a repository at Yucca Mountain also have a potential to affect soil or water chemistry at the site. However, such activities will be designed and conducted in such a way to ensure that there are no significant adverse impacts on repository performance. As discussed in excluded FEPs 1.1.08.00.0A (Inadequate Quality Control and Deviations from Design) and 1.1.12.01.0A (Accidents and Unplanned Events during Construction and Operation), accidents and deviations from plans, designs, and accidents will be evaluated for potential impacts, and significant deviations will be corrected as needed. Impacts of industrial activities associated with the repository itself on soil and water chemistry will be minor and will have no significant adverse impacts on long-term repository performance. Potential effects of subsurface industrial activities associated with repository construction, operation, and closure are addressed separately (e.g., in excluded FEP 1.1.02.00.0A (Chemical Effects of Excavation and Construction in EBS)).

Consistent with the above discussion, omission of FEP 1.4.06.01.0A (Altered Soil or Surface Water Chemistry) will not result in a significant adverse change in the magnitude or time of

radiological exposures to the RMEI or radionuclide releases to the accessible environment. Therefore, this FEP is excluded from the performance assessments conducted to demonstrate compliance with proposed 10 CFR 63.311 and 63.321 (70 FR 53313 [DIRS 178394]), and with 10 CFR 63.331 [DIRS 180319], based on low consequence.

INPUTS:

Table 1.4.06.01.0A-1. Direct Inputs

Input	Source	Description
10 CFR 63. 2007. Energy: Disposal of High-Level Radioactive Wastes in a Geologic Repository at Yucca Mountain, Nevada. [DIRS 180319]	10 CFR 63.305(b)	Standards for FEP screening

Table 1.4.06.01.0A-2. Indirect Inputs

Citation	Title	DIRS
10 CFR 63	Energy: Disposal of High-Level Radioactive Wastes in a Geologic Repository at Yucca Mountain, Nevada	180319
70 FR 53313	Implementation of a Dose Standard After 10,000 Years	178394

FEP: 1.4.07.01.0A

FEP NAME:

Water Management Activities

FEP DESCRIPTION:

Water management is accomplished through a combination of dams, reservoirs, canals, pipelines, and collection and storage facilities. Water management activities could have a major influence on the behavior and transport of contaminants in the biosphere.

SCREENING DECISION:

Included

TSPA DISPOSITION:

The living style (called the lifestyle hereafter) and behaviors of the current residents of the Town of Amargosa Valley (called Amargosa Valley hereafter) explicitly include certain water management activities, such as irrigation and fish farming, and implicitly include the use of the associated infrastructure such as pipelines, storage and collection facilities, and ponds, as well as groundwater pumping wells.

10 CFR 63.305(a) [DIRS 180319] requires that the reference biosphere be consistent with present knowledge of the conditions in the region, and 10 CFR 63.305(b) [DIRS 180319] requires that the DOE "not project changes in society, the biosphere (other than climate), human biology, or increases or decreases in human knowledge or technology." Therefore, future water management activities in Amargosa Valley are assumed to be the same as the current activities.

The physical infrastructure for water management in Amargosa Valley, such as pipelines, storage and collection facilities, ponds and pumping wells, is considered under included FEP 1.4.07.02.0A (Wells). Climate change aspects are discussed in included FEP 1.3.01.00.0A (Climate Change). Fluctuations in the water table, which may affect water management, are discussed in excluded FEP 1.3.07.01.0A (Water Table Decline) and included FEPs 1.3.07.02.0B (Water Table Rise Affects UZ) and 1.3.07.02.0A (Water Table Rise Affects SZ). Water management activities related to irrigation are jointly addressed in this FEP and in included FEP 2.4.09.01.0B (Agricultural Land Use and Irrigation).

The effects of existing water management activities are implicitly included in the current potentiometric surface for Yucca Mountain and the surrounding vicinity. The potentiometric surface is based on the analysis of the current water-level data documented in *Water-Level Data Analysis for the Saturated Zone Site-Scale Flow and Transport Model* (BSC 2004 [DIRS 170009], Section 6.4). Future water management activities are presumed to be those currently in practice. Consequently, *Saturated Zone Flow and Transport Model Abstraction* (SNL 2008 [DIRS 183750]) assumes that the saturated zone flow domain is a steady-state system (SNL 2008 [DIRS 183750], Section 6.3.1[a]), thus implicitly accounting for the impact of future water management activities on the predicted flow and transport paths. This is consistent with

the statement above that future water management activities are assumed to be the same as the current activities. Water usage in Amargosa Valley varies seasonally, with the largest groundwater pumping occurring in the summer when the water needs of crops is largest. These seasonal fluctuations do not cause groundwater levels to fluctuate in the vicinity of the Yucca Mountain repository (BSC 2004 [DIRS 170009], Sections 6.2.1 and 6.3, Table 6-3). The future water use of the RMEI is assumed to be consistent with the current practices in Amargosa Valley. As the present groundwater levels account for the long term average impact of irrigation pumpage, and as seasonal irrigation pumpage does not impact water levels elsewhere in the groundwater model area, the impact of future water management activities is included in the simulation of the groundwater system.

Within the biosphere model, this FEP is included in the air, plant, and fish submodels of the groundwater exposure scenario through incorporation of parameters dealing with the fraction of overhead irrigation (BSC 2004 [DIRS 169673], Section 6.3) and the irrigation intensity (BSC 2004 [DIRS 169673], Section 6.6); of parameters related to the evaporative cooler use, such as the airflow rate, water use rate, and water transfer fraction (BSC 2004 [DIRS 169672], Section 6.5.2); and of the water concentration-modifying factor (BSC 2004 [DIRS 169672], Sections 6.4.3 and 6.4.5), which is used in the fish submodel. Parameter distributions were developed based in part on the types of water distribution and storage systems currently in use in Amargosa Valley for crop irrigation (BSC 2004 [DIRS 169673], Sections 6.3 and 6.6), evaporative cooler use, and fish farming (BSC 2004 [DIRS 169672], Section 6.4).

Groundwater exposure scenario BDCFs are direct inputs to the TSPA for the scenario classes involving radionuclide release to the groundwater (SNL 2007 [DIRS 177399], Section 6.1.3). The BDCFs for all biosphere model realizations are provided as inputs to the TSPA model, which randomly samples these inputs to propagate uncertainty from the biosphere model into TSPA dose calculations. The annual doses are calculated as the product of radionuclide concentration in groundwater and the BDCFs. The present-day climate BDCFs are used for the assessment of doses to the RMEI for 10,000 years following disposal as well as after 10,000 years, but within the period of geologic stability (SNL 2007 [DIRS 177399], Section 6.11.3).

All aspects of the water management activities FEP described above are included for the performance assessment to demonstrate compliance with the individual protection standard (proposed 10 CFR 63.311 (70 FR 53313 [DIRS 178394])) and the performance assessment to demonstrate compliance with the individual protection standard for human intrusion (proposed 10 CFR 63.321 (70 FR 53313 [DIRS 178394])). For the performance assessment that demonstrates compliance with the groundwater protection standards (10 CFR 63.331 [DIRS 180319]), only those components of this FEP that address the geosphere transport are included.

INPUTS:

Table 1.4.07.01.0A-1. Indirect Inputs

Citation	Title	DIRS
10 CFR 63	Energy: Disposal of High-Level Radioactive Wastes in a Geologic Repository at Yucca Mountain, Nevada	180319
70 FR 53313	Implementation of a Dose Standard After 10,000 Years	178394
BSC 2004	*Agricultural and Environmental Input Parameters for the Biosphere Model*	169673
BSC 2004	*Environmental Transport Input Parameters for the Biosphere Model*	169672
BSC 2004	*Water-Level Data Analysis for the Saturated Zone Site-Scale Flow and Transport Model*	170009
SNL 2007	*Biosphere Model Report*	177399
SNL 2008	*Saturated Zone Flow and Transport Model Abstraction*	183750

FEP: 1.4.07.02.0A

FEP NAME:

Wells

FEP DESCRIPTION:

One or more wells drilled for human use (e.g., drinking water, bathing) or agricultural use (e.g., irrigation, animal watering) may intersect the contaminant plume.

SCREENING DECISION:

Included

TSPA DISPOSITION:

Two postclosure quantitative requirements, the individual protection standard given in proposed 10 CFR 63.311 (70 FR 53313 [DIRS 178394]) and the individual protection standard for human intrusion given in proposed 10 CFR 63.321 (70 FR 53313 [DIRS 178394]), provide a limit the dose that may be received by the RMEI. Further guidance given in 10 CFR 63.312(c) [DIRS 180319] specifies that the RMEI uses well water with an average concentration of radionuclides based on an annual water demand of 3,000 acre-feet (3.7×10^6 m^3), which includes use of wells for both domestic and agricultural purposes. Therefore, the use of well water for domestic and agricultural purposes is included in the performance assessments for these two requirements. This FEP is also considered in the calculation of conversion factors for evaluating compliance with the dose portion of the groundwater protection standards of 10 CFR 63.331 [DIRS 180319] (SNL 2007 [DIRS 177399], Section 6.15.1).

Groundwater wells are the initial source of radionuclides entering the reference biosphere for the groundwater exposure scenario (SNL 2007 [DIRS 177399], Tables 6.2-1 and 6.7-1 and Section 6.3.1). Radionuclide concentration in groundwater is the corresponding parameter in the mathematical model used in the soil, air, plant, animal, fish, ^{14}C, and ingestion sub-models of the biosphere model (SNL 2007 [DIRS 177399], Sections 6.4.1 to 6.4.6, and 6.4.9).

The effects of wells on the dose to the RMEI are included by assuming that all of the radionuclide mass that reaches the accessible environment is contained in the annual water demand of 3,000 acre-feet, from which the RMEI obtains all required water (SNL 2008 [DIRS 183750], Section 6.3.3). As wells are the most common means of extracting groundwater, the approach used in *Saturated Zone Flow and Transport Abstraction Model* (SNL 2008 [DIRS 183750]) simulates the effect of one or more wells, located such that the wells completely intercept the radionuclide plume, but does not speculate about details of the wells such as discharge rates, diameter, screened intervals, etc. This approach accounts for wells used for domestic or agricultural purposes that may intersect the contaminant plume.

The effect of pumping wells on the groundwater flow system has been incorporated in *Saturated Zone Site-Scale Flow Model* (SNL 2007 [DIRS 177391]) via the configuration of the water table (BSC 2004 [DIRS 170009]) used as an upper boundary for the flow model and the amount of

flow crossing the model boundaries as provided by the *Death Valley Regional Groundwater Flow System Model* (Belcher 2005 [DIRS 173179]). The regional model specifically incorporated the irrigation wells located south of Yucca Mountain in the community of Amargosa Valley. The water table configuration used to define the top of the SZ flow model and the wells used to provide target water levels for calibration reflect average water levels near the community of Amargosa Valley, which includes the effect of pumping. Thus, *Saturated Zone Flow and Transport Abstraction Model* (SNL 2008 [DIRS 183750]) includes the effect of wells used to withdraw groundwater.

The assessment of annual doses is carried out in the TSPA model using the biosphere dose conversion factors (BDCFs) generated in the biosphere model as TSPA input parameters (SNL 2007 [DIRS 177399], Section 6.11 and 6.12). The BDCFs for all biosphere model realizations are provided as inputs to the TSPA model, which randomly samples these inputs to propagate uncertainty from the biosphere model into TSPA dose calculations. For the TSPA scenario classes involving groundwater withdrawn from a well as a source of radionuclides, the annual doses are calculated as the product of radionuclide concentration in groundwater and the BDCFs. Such an approach is possible because quantities calculated in the groundwater exposure scenario sub-models of the biosphere model, including radionuclide concentrations in the environmental media and the annual dose from various exposure pathways, are proportional to the radionuclide concentration in the groundwater (SNL 2007 [DIRS 177399], Section 6.4.10.2). Thus, for this exposure scenario, the biosphere model contribution to the dose assessment (i.e., BDCFs) can be separated from the source (i.e., radionuclide concentration in the groundwater). The BDCF for a radionuclide is numerically equal to the annual dose to the RMEI for a unit activity concentration of the radionuclide in the water (SNL 2007 [DIRS 177399], Section 6.4.10.2). To support the assessment of doses in TSPA for the scenario classes involving radionuclide release to the groundwater, the present-day climate BDCFs are used for the assessment of doses to the RMEI for 10,000 years following disposal as well as after 10,000 years, but within the period of geologic stability (SNL 2007 [DIRS 177399], Section 6.11.3).

Climate change, including treatment of long-term infiltration rates, is discussed in included FEP 1.3.01.00.0A (Climate Change). Fluctuations in the water table, which may affect well drilling, are discussed in excluded FEP 1.3.07.01.0A (Water Table Decline) and included FEPs 1.3.07.02.0B (Water Table Rise Affects UZ) and 1.3.07.02.0A (Water Table Rise Affects SZ).

All aspects of this FEP described above are included in the performance assessments that demonstrate compliance with the individual protection standards in proposed 10 CFR 63.311 and 63.321 (70 FR 53313 [DIRS 178394]) and with the groundwater protection standards in 10 CFR 63.331 [DIRS 180319].

INPUTS:

Table 1.4.07.02.0A-1. Indirect Inputs

Citation	Title	DIRS
10 CFR 63	Energy: Disposal of High-Level Radioactive Wastes in a Geologic Repository at Yucca Mountain, Nevada	180319
70 FR 53313	Implementation of a Dose Standard After 10,000 Years	178394
Belcher 2004	*Death Valley Regional Ground-Water Flow System, Nevada and California - Hydrogeologic Framework and Transient Ground-Water Flow Model*	173179
BSC 2004	*Water-Level Data Analysis for the Saturated Zone Site-Scale Flow and Transport Model*	170009
SNL 2007	*Biosphere Model Report*	177399
SNL 2007	*Saturated Zone Site-Scale Flow Model*	177391
SNL 2008	*Saturated Zone Flow and Transport Model Abstraction*	183750

FEP: 1.4.07.03.0A

FEP NAME:

Recycling of Accumulated Radionuclides from Soils to Groundwater

FEP DESCRIPTION:

Radionuclides that have accumulated in soils (e.g., from deposition of contaminated irrigation water) may leach out of the soil and be recycled back into the groundwater as a result of recharge (either from natural or agriculturally induced infiltration). The recycled radionuclides may lead to enhanced radionuclide exposure at the receptor.

SCREENING DECISION:

Excluded – low consequence

SCREENING JUSTIFICATION:

The estimated increase in the mean dose to the RMEI as a consequence of radionuclide recycling, averaged over the period of simulation, is calculated to be less than 11%, which is not significant compared with the range of uncertainty simulated by the TSPA model. Recycling of radionuclides accumulated in soils encompasses two pathways, irrigation recycling and capture of deep percolation from septic systems. The irrigation recycling pathway includes the leaching of radionuclides from agricultural soil irrigated with contaminated water, transport of the radionuclides by deep percolation to the water table, and recapture of the radionuclides by the water supply well. The potential recapture of deep percolation from septic systems is also included as a pathway to recycle radionuclides to the water where they are recaptured by the water supply well. The hypothetical community in which the RMEI resides is located in the accessible environment above the highest concentration of radionuclides in the plume of contamination, which is approximately 18 km from the repository. Such a community is assumed to practice irrigated agriculture, consistent with the regulatory construct that a rural community could be located at such a location; that the members of this community could grow some food using well water; and that other gardening, farming, and raising of domestic animals could occur (66 FR 32093 [DIRS 155216], p. 32093). Radionuclide recycling is a phenomenon that could reasonably result from irrigated farming, as inferred from observations of deep percolation beneath irrigated fields in Amargosa Valley (Stonestrom et al. 2003 [DIRS 165862]).

To consider the consequence of radionuclide recycling, an analysis was conducted based on a stylized agricultural and residential water use scenario for calculating the potential impact on dose to the RMEI as a result of radionuclide recycling at the location of the hypothetical community of which the RMEI is part. The analysis of the radionuclide recycling process consists of a quantitative process model that considers radionuclide recycling as a process that is coupled to the stylized biosphere model as applied in TSPA. The recycling model is developed in accordance with current and proposed regulatory requirements governing the RMEI (10 CFR 63.312 [DIRS 180319]) and the reference biosphere (10 CFR 63.305 [DIRS 180319] and 10 CFR 63.305c (70 FR 53313 [DIRS 178394])). The output of the recycling model, when coupled with the biosphere model in the TSPA, is the mean annual dose to the RMEI.

Recycling Process Model

The documentation of the recycling model, presented in *Irrigation Recycling Model* (SNL 2007 [DIRS 182130]), describes the conceptual model that was developed as its basis, model parameters (many of which are treated as probabilistic), the modeling assumptions that were made in the process of constructing the conceptual and mathematical models, and the numerical implementation with results.

The recycling model evaluates the potential impact of recycling of radionuclides contained within irrigation and residential water on the concentration of radionuclides in the groundwater at the location of the RMEI, based upon the current water use practices of individuals residing in the town of Amargosa Valley. The biosphere-based recycling process model was coupled with the biosphere model in the TSPA to conduct a sensitivity analysis of the impact of radionuclide recycling on the dose to the RMEI (SNL 2007 [DIRS 182130], Section 6.7).

Model Description—The conceptual recycling model assumes the existence of a single hypothetical water supply well located approximately 18 km from the repository at the location of the RMEI, which is at the point above of the highest concentration of radionuclides in the plume of contamination (10 CFR 63.312(a) [DIRS 180319]). The well is assumed to continuously withdraw groundwater at a constant rate equal to the annual rate of 3,000 acre-ft per year, consistent with the definition of the RMEI (10 CFR 63.312(c) [DIRS 180319]) and all of the radionuclide mass crossing the location of the RMEI is assumed to be captured in the 3,000 acre-ft per year of water withdrawn by the well. Of the water that is withdrawn by the well, at least 85% is used for irrigation and at least 4% is used for residential purposes (66 FR 32074 [DIRS 155216], p. 32112); the remaining 11% of withdrawn water is assumed to be distributed between irrigation and residential uses.

The portion of the well water that is applied to irrigated fields is simulated to move downward in the unsaturated zone using a piston-flow approach. This is a simplified representation that does not incorporate the relationships between the pressure, saturation, and hydraulic conductivity under unsaturated conditions. The piston flow rate is equal to the percolation rate in the unsaturated zone. These assumptions are reasonable because they lead to realistic transport velocities through the unsaturated zone (SNL 2007 [DIRS 182130], Section 7.2). The percolation rate in the unsaturated zone beneath the irrigated fields is estimated in the biosphere model (BSC 2004 [DIRS 169673], Table 6.9-1). This percolation rate is the result of all the processes occurring at the soil–atmosphere interface, such as crop evapo-transpiration, soil evaporation, irrigation, precipitation, and other processes. Because the percolation rate is available, the recycling model uses this rate directly and does not simulate the soil–atmosphere interface to estimate percolation rate. Advection, sorption, dispersion, and colloid transport processes are simulated in the unsaturated zone.

The residential portion of the withdrawn water is assumed to be recycled via septic leach fields. Transport from these leach fields to the water table is conservatively assumed to be instantaneous to simplify the analysis. This is reasonable because residential water volumes are much smaller than irrigation water volumes (as noted above, at least 85% of the withdrawn water is used for irrigated agriculture).

The residential and irrigation water use locations do not necessarily coincide with the location of the withdrawal well because residences and fields do not co-exist at the same location, and because the 3,000 acre-ft per year of groundwater withdrawn is sufficient to irrigate approximately four fields (SNL 2007 [DIRS 182130], Section 6.5.3.2.5), all of which occupy different locations within the farming community. The water that is withdrawn is assumed to be applied to irrigated fields and supplied to residences located at various distances from the pumping well. Probability distributions representing the distance from a pumping well to irrigated fields and to residences were developed from aerial photographs of the town of Amargosa Valley (SNL 2007 [DIRS 182130], Figures 6.5-3 and 6.5-5). The analysis implicitly assumes that contaminated well water is distributed to distant locations for use. The fields and residences are randomly located around the pumping well (i.e., no directional preference) and the distances are determined by sampling the distances from the probability distributions of distance.

Radionuclides in water that is applied to an irrigated field or used at a residence is recycled back to the pumping well if the field or residence lies above the capture zone of the well. The edges of the capture zone are defined by analytic solutions (SNL 2007 [DIRS 182130], Sections 6.5.3.3.1 and 6.5.3.3.2) based on the aquifer thickness, a uniform ambient specific discharge, and a parameter that represents the difference in the saturated thickness of the aquifer upgradient and downgradient of the well. These parameters are uncertain and are described by probability distributions. The simulations of the location of irrigated fields and the size of the capture zone are used to generate two parameters, the well recapture fraction cumulative distribution and the residential fraction cumulative distribution. These two parameters identify the fraction of irrigation or residential water that is recycled back to the pumping well (SNL 2007 [DIRS 182130], Sections 6.5.3.4.3 and 6.5.3.5.1).

To simplify the analyses, radionuclides that reach the water table and are within the well capture zone are returned to the well volume without accounting for transport within the saturated zone. This is a bounding assumption because the radionuclides from the distant irrigation locations will have to travel through the saturated zone to reach the pumping well.

To calculate the dose, the concentrations of radionuclides in the well water are supplied to the biosphere component (SNL 2007 [DIRS 177399]) in the TSPA model to determine the dose to the RMEI.

Three mechanisms of removing radionuclides from the recycling process were considered, leading to open-system behavior and placing limits on the long-term increase in concentrations within the aquifer. Some portion of the radionuclides will be permanently removed from the recycling process because:

(1) The fraction of the irrigation water that is used on fields located outside the capture zone of the water supply well will not be pumped back to the land surface. This will affect sorbing and nonsorbing radionuclides.

(2) The fraction of the residential water used outdoors and the fraction of residential water used indoors outside the well capture zone will not be pumped back to the land surface. This will affect sorbing and nonsorbing radionuclides.

(3) Erosion of soil from irrigated fields will transport the radionuclide mass sorbed to the soil out of the recycling system. This process will mostly affect sorbing radionuclides.

Parameters for the Recycling Model

The radionuclide recycling analysis utilizes parameters from a number of project sources. These include the alfalfa irrigation and overwatering rates (BSC 2004 [DIRS 169673], Tables 6.9-1 and 6.5-2), supporting parameters for the biosphere model analysis (SNL 2007 [DIRS 177399]), numerous flow and transport parameters related to transport in alluvium were obtained from the saturated zone flow and transport abstraction model (SNL 2008 [DIRS 183750]) and its output DTNs, and site specific parameters obtained from measurements in the vicinity of the RMEI location were used in the capture zone analysis (SNL 2007 [DIRS 182130], Section 6.5.3.3.3). For example, the specific discharge estimates were obtained from testing at wells NC-EWDP-19D and 22S. The aquifer thickness is based on observed stratigraphy at wells NC-EWDP-10SA, -23P, -2DB, -19D, and -22S (SNL 2007 [DIRS 182130], Section 6.5.3.3.3.1). The difference in saturated thickness (part of the capture zone analysis) comes from observed water levels and stratigraphy at wells NC-EWDP-19D and -22S.

The depth to the water table at the location of the RMEI, which also represents the length of the unsaturated zone flow path, was determined for the future glacial-transition climate state using predicted water table rise beneath the repository of 120 m and the simulated location and elevation of surface discharge downgradient of the RMEI (SNL 2007 [DIRS 182130], Section 6.5.3.7).

The parameters noted above, and others, are treated as uncertain and described by probability distributions (SNL 2007 [DIRS 182130], Section 6.5).

The radionuclides from the irrigation and residential pathways recaptured by the regulatory well are used in calculating groundwater concentrations at the RMEI location. These concentrations are passed to the biosphere component model in the TSPA sensitivity analysis using both the seismic ground motion and igneous intrusion scenarios to estimate the impacts of the increase in radionuclide concentrations in groundwater on mean annual doses (SNL 2007 [DIRS 182130], Sections 6.6 and 6.7). Transient effects in the calculations due to the radionuclide recycling process do not impact the results after a simulation time of about 5,000 years (SNL 2007 [DIRS 182130], Section 6.6). At early time, radionuclides recycled along the residential pathway arrive at the withdrawal well before radionuclides from the irrigation pathway. As the residential pathway accounts for less than 15% of the total water, the impact of radionuclide recycling at early time is very small. As time passes, radionuclides from the irrigation pathway arrive and the full effect of radionuclide recycling becomes apparent (SNL 2007 [DIRS 182130], Figures 6.6-4 to 6.6-6). The impact of radionuclide recycling is based on the later time results to incorporate both the residential and irrigation pathways.

The assumption of immediate transport to the well in the saturated zone is expected to have a similar impact. The transport processes in the saturated zone would be expected to delay the onset of recycling, but not significantly alter the long-term increase in concentrations.

Consequence—The simulations result in approximately an 11% average increase in mean dose for both the seismic ground motion and igneous intrusion scenarios over the 10,000-year period (SNL 2008 [DIRS 182130], Section 6.7, pp. 6-60 and 6-62).

Based on the previous discussion, omission of FEP 1.4.07.03.0A (Recycling of Accumulated Radionuclides from Soils to Groundwater) will not significantly change the magnitude or time of radiological exposures to the RMEI or radionuclide releases to the accessible environment when considered with respect to the uncertainty already incorporated in the TSPA model. Therefore, this FEP is excluded from the performance assessments conducted to demonstrate compliance with proposed 10 CFR 63.311 and 63.321 ([DIRS 178394]), and with 10 CFR 63.331 [DIRS 180319], on the basis of low consequence.

INPUTS:

Table 1.4.07.03.0A-1. Direct Inputs

Input	Source	Description
SNL 2007. *Irrigation Recycling Model*. [DIRS 182130]	Section 6.7, pp. 6-60 and 6-62	Model simulations showed that increases in the total mean annual dose due to irrigation recycling at the time of peak dose were about 11% for the seismic scenario and about 7% for the igneous scenario over a 1,000,000-year simulation period

Table 1.4.07.03.0A-2. Indirect Inputs

Citation	Title	DIRS
10 CFR 63	Energy: Disposal of High-Level Radioactive Wastes in a Geologic Repository at Yucca Mountain, Nevada	180319
66 FR 32074	40 CFR Part 197, Public Health and Environmental Radiation Protection Standards for Yucca Mountain, NV; Final Rule	155216
70 FR 53313	Implementation of a Dose Standard After 10,000 Years	178394
BSC 2004	*Agricultural and Environmental Input Parameters for the Biosphere Model*	169673
SNL 2007	*Biosphere Model Report*	177399
SNL 2007	*Irrigation Recycling Model*	182130
SNL 2008	*Saturated Zone Flow and Transport Model Abstraction*	183750
Stonestrom et al. 2003	*Estimates of Deep Percolation Beneath Native Vegetation, Irrigated Fields, and the Amargosa-River Channel, Amargosa Desert, Nye County, Nevada*	165862

FEP: 1.4.08.00.0A

FEP NAME:

Social and Institutional Developments

FEP DESCRIPTION:

Social and institutional developments could affect the long-term performance of the repository. The most likely is social and institutional development resulting in new activities, communities, or cities in the vicinity of Yucca Mountain.

SCREENING DECISION:

Excluded – by regulation

SCREENING JUSTIFICATION:

10 CFR 63.305(b) [DIRS 180319] states, "DOE should not project changes in society, the biosphere (other than climate), human biology, or increases or decreases in human knowledge or technology. In all analyses done to demonstrate compliance with this part, the DOE must assume that all of those factors remain constant as they are at the time of submission of the license application." Therefore, speculation concerning potential changes in society, including social and institutional development, are excluded on the basis of regulatory requirements in 10 CFR 63.305(b) [DIRS 180319].

INPUTS:

Table 1.4.08.00.0A-1. Direct Inputs

Input	Source	Description
10 CFR 63. 2007. Energy: Disposal of High-Level Radioactive Wastes in a Geologic Repository at Yucca Mountain, Nevada. [DIRS 180319]	10 CFR 63.305(b)	States DOE should not project changes in society, the biosphere (other than climate), human biology, or increases or decreases in human knowledge of technology

FEP: 1.4.09.00.0A

FEP NAME:

Technological Developments

FEP DESCRIPTION:

Technological developments may affect the long-term performance of the repository. These include changes in the ability of humans to intrude the site, and changes that might affect contaminant exposure and its health implications.

SCREENING DECISION:

Excluded – by regulation

SCREENING JUSTIFICATION:

10 CFR 63.305(b) [DIRS 180319] specifically states, "DOE should not project changes in society, the biosphere (other than climate), human biology, or increases or decreases in human knowledge or technology. In all analyses done to demonstrate compliance with this part, the DOE must assume that all of those factors remain constant as they are at the time of submission of the license application." Therefore, speculation concerning technological development is excluded on the basis of the regulatory requirements in 10 CFR 63.305(b) [DIRS 180319].

INPUTS:

Table 1.4.09.00.0A-1. Direct Inputs

Input	Source	Description
10 CFR 63. 2007. Energy: Disposal of High-Level Radioactive Wastes in a Geologic Repository at Yucca Mountain, Nevada. [DIRS 180319]	10 CFR 63.305(b)	States DOE should not project changes in society, the biosphere (other than cliamte), human biology, or increases or decreases in human knowledge of technology

FEP: 1.4.11.00.0A

FEP NAME:

Explosions and Crashes (Human Activities)

FEP DESCRIPTION:

Explosions or crashes resulting from future human activities may affect the long-term performance of the repository. Explosions may result from nuclear war, underground nuclear testing, or resource exploitation.

SCREENING DECISION:

Excluded – by regulation

SCREENING JUSTIFICATION:

Explosions or crashes that result from human activities are considered a form of human intrusion. Per 10 CFR 63.102(l) [DIRS 180319], human-intrusion related events are subject to specific requirements for evaluation of human intrusion, specified in proposed 10 CFR 63.321 (70 FR 53313 [DIRS 178394]) and in 10 CFR 63.322 [DIRS 180319]. These quantitative postclosure requirements specify that the consequences of human intrusion are to be evaluated via a stylized analysis. This stylized analysis includes the effect of a borehole that penetrates a single waste package, and does not include the effects of explosions and crashes. Nuclear or conventional wars and underground nuclear testing are excluded by 10 CFR 63.305(b) [DIRS 180319], which states, "DOE should not project changes in society, the biosphere (other than climate), human biology, or increases or decreases of human knowledge or technology. In all analyses done to demonstrate compliance with this part, DOE must assume that all of those factors remain constant as they are at the time of submission of the license application." For these reasons, this FEP is excluded on the basis of regulation.

INPUTS:

Table 1.4.11.00.0A-1. Direct Inputs

Input	Source	Description
10 CFR 63. 2007. Energy: Disposal of High-Level Radioactive Wastes in a Geologic Repository at Yucca Mountain, Nevada. [DIRS 180319]	10 CFR 63.102(1) and 10 CFR 63.305(b)	Definition of compliance regulation
70 FR 53313. Implementation of a Dose Standard After 10,000 Years. [DIRS 178394]	10 CFR 63.321	Individual protection standard for human intrusion

FEP: 1.5.01.01.0A

FEP NAME:

Meteorite Impact

FEP DESCRIPTION:

Meteorite impact close to the repository site might disturb or remove rock to such an extent that radionuclide transport to the surface is accelerated. Possible effects include alteration of flow patterns (by re-activation or formation of faults and fractures), changes in rock stress, cratering, and exhumation of waste.

SCREENING DECISION:

Excluded – low probability

SCREENING JUSTIFICATION:

Possible effects of a large meteorite impact near the repository include penetration of the repository and exhumation of waste. A meteorite associated with an impact crater not deep enough to exhume waste could reactivate or form faults and fractures, change the rock stress, and the associated shock wave could possibly cause damage to drifts and waste packages, or initiate an earthquake. Of particular interest for smaller meteorite impacts is the possibility of increased infiltration to the repository through damage to the geologic layers that limit infiltration. Analysis of a meteorite impact depends on the probability of occurrence of variously sized impact craters, the area and relative dimensions of the repository footprint, and the depth of the repository below the ground surface. The probability of an impact crater of a given size being formed directly above or adjacent to the repository depends on the total flux of meteors that penetrate the earth's atmosphere and impact the surface (hence becoming meteorites) and the area of the repository footprint (the target area). Two crater sizes of interest in the analysis are: (1) craters that are deep enough to exhume waste from the repository, and (2) craters that are deep enough to fracture or damage the Paintbrush nonwelded (PTn) tuff layer above the repository. Potential fracturing or damage to the overlying Tiva Canyon units is not of concern because of the damping effect of the PTn (SNL 2007 [DIRS 184614], Section 6.9[a]). The size of these craters is determined by the depth from ground surface to the top of the repository, as well as the depth to the Paintbrush nonwelded tuff. Detailed probability calculations and a discussion of meteorite impact probability and cratering information that provide the technical basis for exclusion are given in Appendix D.

The overburden thickness from the repository emplacement area to the topographic surface is specified to be a minimum of 200 m (SNL 2007 [DIRS 179466], Table 4-1, Parameter Number 01-06). Also of interest are the minimum depth to and thickness of the PTn. The PTn primarily consists of nonwelded to partially welded tuffs and extends from the base of the densely to moderately welded Tiva Canyon welded tuff (TCw) to the top of the TSw, which is densely welded (SNL 2007 [DIRS 184614], Section 6.2.2). With its high porosity and low fracture intensity, the PTn rock matrix has a large capacity for storing groundwater and effectively damps percolation transients at the base of the TCw unit. Water imbibing into the

PTn rock matrix, from rapid fracture flow in the TCw above, results in a more uniform distribution of groundwater flux at the base of the PTn such that unsaturated zone groundwater flow below the PTn is essentially steady (SNL 2007 [DIRS 184614], Section 6.9[a]). Geologic data indicate that the PTn ranges in thickness from greater than 125_m beneath northern Yucca Mountain to about 20 m in the south (Figure D-3), with breaks in area coverage along the Solitario Canyon, Iron Ridge, and Dune Wash fault systems. Within the repository area, the thickness of the PTn unit ranges from approximately 30 to 60 m (Appendix D). The depth to the PTn unit also varies from 0 where it outcrops in gullies in the northernmost portion of the repository to more than 120 m in the southern portion of the repository (Figure D-2).

Groundwater movement through specific rock units depends on the hydrogeologic properties of the rock units (SNL 2007 [DIRS 184614], Sections 6.1.2 and 6.2.2). Water that infiltrates into the Tiva Canyon welded unit can be transported rapidly through existing fractures as far as the underlying Paintbrush nonwelded unit, which limits flow transients, making flow through the unsaturated zone below this unit to the repository steady-state in character due to high porosity and low fracture density of this unit. The possibility of increased fracturing in the Paintbrush nonwelded unit due to a meteorite impact has the potential to increase transient flow through this unit and through the repository.

An evaluation (Appendix D) indicates that only small cratering effects needed to be considered, due to the low probability of large crater diameters being associated with complex cratering (Grieve et al. 1995 [DIRS 135260], p. 194; Wuschke et al. 1995 [DIRS 129326], p. 3). The information was translated from the the initial meteor radius to a resulting crater radius and other effects to produce a distribution of crater diameters based on meteorite flux to the earth. For impact probability calculation, a rectangular target area was designed that enclosed the repository footprint and was extended one-half crater diameter on each side to include near-miss impacts (Appendix D).

Appendix D provides cratering probability curves (based on two sources) in Figure D-5 and Figure D-6 for the frequency of cratering for the target area. The maximum crater diameter that corresponds to the 10^{-8} annualized exceedance probability over the target area is less than 60 m (Appendix D).

For a crater diameter of 60 m, the exhumation depth is 6 to 20 m, with a 0.1 to 0.33 ratio of exhumation depth to crater diameter (Appendix D). Because the overburden is at least 200 m, this crater size is insufficient to cause waste exhumation (Appendix D). The exhumation of waste from the repository can therefore be excluded based on low probability because the probability of a cratering event sufficiently large to cause waste exhumation is less than 10^{-8} per year.

In addition, given a fracturing depth to crater diameter ratio of 0.33 to 0.76, the maximum depth of induced fractures from a 60-m diameter cratering event (i.e., an estimate of the largest crater likely at the threshold probability of 10^{-8} events per year) would be no greater than 45 m based on a fracture depth to crater diameter ratio of 0.76 (Appendix D). Depths of less than 45 m would not affect infiltration into the repository because they are too shallow to reach the top of the PTn over most of the repository area. Figure D-1 shows that with the exception of the northwestern- and northern-most tip of the repository where the PTn outcrops, the distance to the

top of the PTn is at least 60 m. In these northern areas with a lesser distance between the ground surface and the PTn, the PTn itself is more than 90-m thick (Appendix D). Therefore, the PTn unit would maintain its original thickness even after the impact of a maximum-penetration cratering event that corresponds to the 10^{-8} annualized exceedance probability, and will continue to meet the 10-m thickness requirement set forth in the selection of the repository layout (BSC 2008 [DIRS 183627], Table 1, Parameter Number 01-21) that ensures that the unit will remain effective in damping the episodic infiltration transients (see excluded FEP 2.2.07.05.0A (Flow in the UZ from Episodic Infiltration)). The fracturing of the PTn can, therefore, be excluded based on low probability because the probability of a cratering event sufficiently large to cause fracturing the PTn to less than 10-m thick is less than 10^{-8} per year.

Smaller crater diameters occur more frequently, but these are of insufficient size to result in direct exhumation or fracturing to the depth of the repository and are excluded through *low consequence*. Larger crater diameters occur less frequently and are less probable than the exceedance probability, and are therefore excluded from the TSPA as low probability events (Appendix D). Effects on infiltration due to changes in ecological factors due to small meteor craters or the effects of a near-surface explosion associated with a meteorite are also excluded based on low consequence because such events are expected to have only transient effects or to have no means of affecting the subsurface postclosure repository (see also excluded FEPs 1.4.03.00.0A (Unintrusive Site Investigation) and 1.5.01.02.0A (Extraterrestrial Events)). A modern example of a site in which the ecology has recovered is the Tungunska site in Siberia.

Meteors that result in crater diameters of 60 m (corresponding to the threshold annual probability of 10^{-8}) could trigger earthquakes with Richter magnitudes ranging from magnitude 5 to slightly less than magnitude 7 (Hills and Goda 1993 [DIRS 135281], Figure 18). Existing seismic analyses cover this range of magnitude (CRWMS M&O 1998 [DIRS 103731], Figures 7-15 and 7-16). Therefore, an earthquake caused by meteorite impact is excluded based on low consequence because it would not provide a significant contribution to the overall earthquake hazard. Earthquake hazards are already included and probabilistically weighted in the TSPA. The effects of changes in rock stress, such as those caused by seismic activity, are addressed in multiple FEPs such as excluded FEPs 2.2.06.01.0A (Seismic Activity Changes Porosity and Permeability of Rock), 2.2.06.02.0A (Seismic Activity Changes Porosity and Permeability of Faults); and 2.2.06.02.0B (Seismic Activity Changes Porosity and Permeability of Fractures).

Because percolation is not significantly affected and no fracturing occurs down to the repository depth, with no associated waste exhumation, there is no mechanism for a meteorite impact at the threshold annual probability or greater to affect groundwater flux through the repository horizon. Therefore, the dose and release of radionuclides are not significantly changed.

Based on the preceding discussion, FEP 1.5.01.01.0A (Meteorite Impact) is excluded from the performance assessment conducted to demonstrate compliance with proposed 10 CFR 63.311 and 63.321 (70 FR 53313 [DIRS 178394]), and with 10 CFR 63.331 [DIRS 180319], on the basis of low probability for exhumation and fracturing to repository depth and to the PTn unit within the repository target area.

INPUTS:

Table 1.5.01.01.0A-1. Direct Inputs

Input	Source	Description
BSC 2008. *Postclosure Modeling and Analyses Design Parameters*. [DIRS 183627]	Table 1, Parameter Number 01-21	10-m thickness requirement set forth in the selection of the repository layout
Grieve et al. 1995. "The Record of Terrestrial Impact Cratering." [DIRS 135260]	pp. 194 to 196	Threshold for on-set of complex cratering
Hills and Goda 1993. "Fragmentation of Small Asteroids in the Atmosphere." [DIRS 135281]	Figure 18	Richter scale magnitude of the earthquake produced by impact or debris hitting the ground as a function of initial meteoroid radius
SNL 2007. *Total System Performance Assessment Data Input Package for Requirements Analysis for Subsurface Facilities*. [DIRS 179466]	Table 4-1, Parameter Number 01-06	200 m overburden thickness
SNL 2007. *UZ Flow Models and Submodels*. [DIRS 184614]	Section 6.2.2	Description of PTn
	Sections 6.1.2, 6.2.2	Groundwater movement through specific rock units depends on the hydrogeologic properties of the rock units
	Section 6.9[a]	Potential fracturing or damage to the overlying Tiva Canyon units is not of concern because of the damping effect of the PTn
	Section 6.9[a]	Discussion of groundwater flow below PTn
Wuschke et al. 1995. *Assessment of the Long-Term Risk of a Meteorite Impact on Hypothetical Canadian Nuclear Fuel Waste Disposal Vault Deep in Plutonic Rock*. [DIRS 129326]	p. 3	Low probability of large crater diameters being associated with complex cratering

Table 1.5.01.01.0A-2. Indirect Inputs

Citation	Title	DIRS
10 CFR 63	Energy: Disposal of High-Level Radioactive Wastes in a Geologic Repository at Yucca Mountain, Nevada	180319
70 FR 53313	Implementation of a Dose Standard After 10,000 Years	178394
CRWMS M&O 1998	*Probabilistic Seismic Hazard Analyses for Fault Displacement and Vibratory Ground Motion at Yucca Mountain, Nevada*	103731

FEP: 1.5.01.02.0A

FEP NAME:

Extraterrestrial Events

FEP DESCRIPTION:

Extraterrestrial events (e.g., supernova, solar flare, gamma-ray burster, and events associated with alien life forms) may affect long-term performance of the disposal system.

SCREENING DECISION:

Excluded – low consequence

SCREENING JUSTIFICATION:

Potential mechanisms linking extraterrestrial events to changes in the behavior of engineered and natural systems of an underground repository are not addressed in the scientific literature. Evaluating the effect of such events on the postclosure repository performance requires speculation and conceptualization of possible linkages between the event and repository performance.

High-energy radiation that enters the Earth's atmosphere from outer space is known as cosmic rays. Cosmic radiation of solar and galactic origin accounts for about 15% of the average natural background radiation dose (United Nations 1988 [DIRS 159566], p. 95) and is a part of the natural environment.

Proposed 10 CFR 63.311 and 63.321 (70 FR 53313 [DIRS 178394]) address the protection of individuals from future radionuclide releases from the repository by placing limits on the annual dose from radiation that may be received by the RMEI. Radiation doses that do not originate from repository releases are not included in these standards. Therefore, estimating the dose that the RMEI would receive directly from the radiations emitted by extraterrestrial events is not required. The following discussion concentrates on the potential effects of extraterrestrial events only to the extent that they may affect long-term performance of the disposal system.

The extraterrestrial events that are the subject of this FEP include the powerful but infrequent events, such as supernovae and gamma ray bursts that occur randomly in the Milky Way galaxy and beyond, and have a potential of producing high radiation levels on Earth. Supernovae and gamma ray bursts are the most energetic known events in the universe. Supernovae release between 10^{43} to 10^{45} J of energy (most of which occurs as neutrino energy and about 10^{42} J as gamma radiation), while gamma ray bursts release the isotropic equivalent of about 10^{45} to 10^{47} J of gamma energy (Karam 2002 [DIRS 167872], pp. 491 to 492). Solar flares, another category of events included in this FEP, are coronal mass ejections from the sun, with the average energy release of about 10^{23} to 10^{24} J (Karam 2003 [DIRS 184906], p. 323).

Gamma ray bursts appear to occur about once every 10^{6} to 10^{7} years in galaxies similar to the Milky Way with periods of maximum emission lasting on the order of minutes (Karam 2002

[DIRS 167872], p. 492). Therefore, all the gamma ray bursts that are routinely registered by orbiting spacecraft originate outside our galaxy. The overall rate of supernovae is much higher, with one to two events occurring per century in the Milky Way galaxy and the duration of these events is much longer than the gamma ray bursts (Karam 2002 [DIRS 167872], p. 492).

Because radiation emitted by any object in interstellar space must first travel a considerable distance to reach the Earth, the energy fluence received at Earth is substantially reduced, primarily because of its decrease with the inverse square of the distance (Karam 2002 [DIRS 167872], Table 1). The attenuation by the interstellar medium is insignificant (Karam 2002 [DIRS 167872], p. 492). The energy fluence from extraterrestrial events is further reduced by Earth's atmosphere. The energy deposited in rocks and other materials at the repository level from the extraterrestrial events would be negligible because of the additional attenuation (shielding) of the external radiation by the rocks above the repository. The overburden thickness from the emplacement area to the topographic surface at Yucca Mountain is at least 200 m (SNL 2007 [DIRS 179466], Table 4-1, Parameter Number 01-06), whereas 20 mm of rock thickness provides at least 7 orders of magnitude reduction in the photon energy absorbed by the rocks (i.e., the absorbed dose) (Karam 2002 [DIRS 167872], Table 2). The energy emitted in the form of neutrinos that is absorbed by Earth is insignificant.

In summary, extraterrestrial events would have a negligible effect on the performance of the repository from the direct energy deposition at the repository level. However, the energy released from nearby supernovae has a potential for causing climatic or other environmental changes that could indirectly affect the repository performance (Brakenridge 1981 [DIRS 167873], p. 81), as described below.

Studies of the potential effects of late Quaternary-Age supernovae on the terrestrial paleoenvironment have identified over 120 radio-emitting galactic supernovae remnants that occurred over the past 15,000 years, suggesting a rate of occurrence of approximately one such event per 100 years (Brakenridge 1981 [DIRS 167873], pp. 81 to 83). The largest inferred energy fluence received at Earth from these events was from the Vela supernova, which was calculated to have a peak energy fluence above Earth's atmosphere of about 40 J/m^2 (Brakenridge 1981 [DIRS 167873], Figure 1). It was postulated that the events of such magnitude have the potential to cause ozone depletion in the atmosphere for between two and six years, global cooling, and an increase in transfers of stratospheric nitrogen into tropospheric and fixed nitrogen on Earth's surface (Brakenridge 1981 [DIRS 167873], p. 85). Observable consequences of these effects include the existence of organic-rich zones in sediments (possibly caused by the influx of biologically available nitrogen), possible short-term global cooling caused by increased absorption of visible light in the stratosphere by NO_2 (Brakenridge 1981 [DIRS 167873], pp. 85 to 86), and possible increased ultraviolet-light penetration due to ozone layer depletion (Brakenridge 1981 [DIRS 167873], pp. 86 and 90 to 91). Others researchers observed nitrogen enrichment and ozone depletion (Ruderman 1974 [DIRS 167875], p. 1,079) as well as climate changes that occurred at the time of the Vela supernova (Arnold 2003 [DIRS 167638], p. 127; Novotna and Vitek 1991 [DIRS 167634], pp. 34 to 35). Alternative hypotheses exist that could explain the occurrence of the phenomena the Brackenridge attributes to that supernova (Brakenridge 1981 [DIRS 167873], p. 90); however, for the purposes of this evaluation it is conservative to assume that a supernova comparable to the Vela event could effect global climate.

The Vela supernova occurred 8,400 to 11,300 years ago (Brakenridge 1981 [DIRS 167873], p. 85), during a glacial transition (intermediate) climate (Sharpe 2003 [DIRS 161591], Table 6-5), and may have contributed to atmospheric cooling with an estimated range of 0.4 to 3 K (Brakenridge 1981 [DIRS 167873], p. 85). The postulated range of temperature decrease caused by the ionizing radiation from the supernova is comparable to the range of mean annual temperatures for the glacial transition climate, as represented by the future climate analogue locations (Sharpe 2003 [DIRS 161591], Table 6-3) and would not cause the climate transition to a different climate state. Other postulated changes such as ozone-layer depletion would be of lesser impact than small climate change itself. Therefore, the effect of such supernovae on the repository performance would not be significant.

Solar-related effects and their correlation with changes in natural systems on Earth are summarized in a conceptual statement by Lean (1997 [DIRS 167639], p. 61): "Numerous associations are evident between solar variability and terrestrial parameters that range from the Earth's surface to hundreds of kilometers above it, on the time scales from days to centuries." Lean (1997 [DIRS 167639], p. 61) points out that decadal cycles in sun activity are evident in temperatures at Earth surface and through the atmosphere, and also indicates that there is an apparent correlation between surface temperature and overall solar activity, but it is unclear whether variable solar radiation is responsible. Least certain is the extent to which changes in visible and infrared radiation, on the order of several orders of magnitude, modify global surface temperature and climate. Lean also suggests that there is a current inability to adequately quantify all climate and ozone controlling mechanisms, which adds ambiguities to assessments of global change (Lean 1997 [DIRS 167639], pp. 62 to 63).

Some of the examples of extraterrestrial events listed above (for example, supernovae, solar flares, gamma-ray bursts) are credible and could result in an influx of solar radiation, space radiation, or cosmic rays into the magnetosphere. Collectively, this can be referred to as "space weather." Maynard (1995 [DIRS 160888]), in discussing the uses of such "space weather" prediction, lists several types of operations that could be affected. They include spacecraft operations, satellite operations, GPS-locating operations (which are satellite based), space object tracking, over-the-horizon radar operations, high-frequency communications, telecommunications such as transatlantic fiber optic communications, geomagnetically induced currents in power transmission lines and transformers, applied direct currents for pipeline corrosion mitigation, and possible impacts on semiconductor manufacturing (likely related to power line fluctuations). This list of potentially affected systems is corroborated by Lean (1997 [DIRS 167639], pp. 57 to 61) and Cole (2003 [DIRS 167641], pp. 299 to 301). The potential effects of extraterrestrial events on these operations are not expected to affect postclosure performance.

This FEP definition also includes the potential effects of alien life forms. Aside from the hypothetical potential for microbial influx via meteorites, the presence of alien life forms has not been verified or documented in the scientific literature. The potential for effects from alien life forms (other than microbial activity) is, therefore, judged to be of low probability (not credible) based on the absence of verification of any such life forms in the scientific literature. The extraterrestrial transfer of microbes into the repository through a meteorite strike could be postulated. Meteorite strikes that are large enough to penetrate the repository are low-probability events based on excluded FEP 1.5.01.01.0A (Meteorite Impact). A few scientific papers have

postulated that microorganisms could have been transported to Earth within small meteorites (McKay 1996 [DIRS 184212]; Thomas-Keptra et al. 1998 [DIRS 184214]; Steele et al. 2000 [DIRS 184215]). These claims are, at present, controversial, but even if true, it is not credible that such microorganisms could escape their meteoric shell, be transported to the repository, and affect the repository performance in a significant manner. Based on this discussion, potential effects from alien life forms are of low probability to the long-term performance of the repository in the postclosure period.

In summary, omission of FEP 1.5.01.02.0A (Extraterrestrial Events) will have no significant adverse impact on long-term performance of the repository, and therefore, no significant impact to radiological exposure to the RMEI and radionuclide release to the accessible environment. Therefore, this FEP is excluded from the performance assessments conducted to demonstrate compliance with proposed 10 CFR 63.311 and 63.321 (70 FR 53313 [DIRS 178394]), and with 10 CFR 63.331 [DIRS 180319]), on the basis of low consequence.

INPUTS:

Table 1.5.01.02.0A-1. Direct Inputs

Input	Source	Description
Brakenridge 1981. "Terrestrial Paleoenvironmental Effects of a Late Quaternary-Age Supernova." [DIRS 167873]	p. 85	The postulated climatic and environmental effects of the supernovae, including the decrease in average temperature
Karam 2002. "Gamma and Neutrino Radiation Dose from Gamma Ray Bursts and Nearby Supernovae." [DIRS 167872]	Table 2	Dose reduction in top 20 mm of rock
SNL 2007. *Total System Performance Assessment Data Input Package for Requirements Analysis for Subsurface Facilities*. [DIRS 179466]	Table 4-1, Parameter Number 01-06	Overburden thickness

Table 1.5.01.02.0A-2. Indirect Inputs

Citation	Title	DIRS
10 CFR 63	Energy: Disposal of High-Level Radioactive Wastes in a Geologic Repository at Yucca Mountain, Nevada	180319
70 FR 53313	Implementation of a Dose Standard After 10,000 Years	178394
Arnold 2003	"Space Plasma Influences on the Earth's Atmosphere"	167638
Brakenridge 1981	"Terrestrial Paleoenvironmental Effects of a Late Quaternary-Age Supernova"	167873
Cole 2003	"Space Weather: Its Effects and Predictability"	167641
Karam 2002	"Gamma and Neutrino Radiation Dose from Gamma Ray Bursts and Nearby Supernovae"	167872
Karam 2003	"Inconstant Sun: How Solar Evolution Has Affected Cosmic and Ultraviolet Radiation Exposure over the History of Life on Earth"	184906
Lean 1997	"The Sun's Variable Radiation and its Relevance for Earth"	167639
Maynard 1995	"Space Weather Prediction"	160888

Table 1.5.01.02.0A-2. Indirect Inputs (Continued)

Citation	Title	DIRS
McKay et al. 1996	"Search for past life on Mars: Possible relic biogenic activity in martian meteorite ALH 84001"	184212
Novotna and Vitek 1991	"The Atmospheric Mean Energetic Level and External Forcing"	167634
Ruderman 1974	"Possible Consequences of Nearby Supernova Explosions for Atmospheric Ozone and Terrestrial Life"	167875
Sharpe 2003	*Future Climate Analysis—10,000 Years to 1,000,000 Years After Present*	161591
Steele et al. 2000	"Investigations into an Unknown Organism on the Martian Meteorite Allan Hills 84001"	184215
Thomas-Keprta et al. 1998	"Bacterial mineralization patterns in basaltic aquifers: Implications for possible life in martian meteorite ALH84001"	184214
United Nations 1988	*Sources, Effects and Risks of Ionizing Radiation, 1988 Report to the General Assembly, with Annexes*	159566

FEP: 1.5.02.00.0A

FEP NAME:

Species Evolution

FEP DESCRIPTION:

Humans and other species living at or near the repository site may evolve in the future and their new behavior patterns and physiological characteristics may affect their likelihood contaminant exposure and its consequent health implications.

SCREENING DECISION:

Excluded – by regulation

SCREENING JUSTIFICATION:

10 CFR 63.305(b) [DIRS 180319] states, "DOE should not project changes in society, the biosphere (other than climate), human biology, or increases or decreases in human knowledge or technology. In all analyses done to demonstrate compliance with this part, the DOE must assume that all of those factors remain constant as they are at the time of submission of the license application." Therefore, speculation concerning species evolution is excluded on the basis of regulatory requirements in 10 CFR 63.305(b) [DIRS 180319].

INPUTS:

Table 1.5.02.00.0A-1. Direct Inputs

Input	Source	Description
10 CFR 63. 2007. Energy: Disposal of High-Level Radioactive Wastes in a Geologic Repository at Yucca Mountain, Nevada. [DIRS 180319]	10 CFR 63.305(b)	States DOE should not project changes in society, the biosphere (other than climate), human biology, or increases or decreases in human knowledge or technology

FEP: 1.5.03.01.0A

FEP NAME:

Changes in the Earth's Magnetic Field

FEP DESCRIPTION:

Changes in the earth's magnetic field could affect the long-term performance of the repository.

SCREENING DECISION:

Excluded – low consequence

SCREENING JUSTIFICATION:

Changes and fluctuations in the earth's magnetic field are known to be relatively common in geologic history. Biggin and Thomas (2003 [DIRS 167876], pp. 409 to 412) suggest that changes in the earth's magnetic field result from global-scale tectonic processes such as slab subduction and from mantle processes. During the last 160 million years, the number of pole reversals varies from 0 to 50 (Biggin and Thomas 2003 [DIRS 167876], Figure 11). The frequency of pole reversals varies, but is thought to be on the order 2 to 3 per million years (Gubbins 1999 [DIRS 185112]). There has been a demonstrable decrease in the earth's magnetic field intensity over the last few thousand years, and there is some evidence to suggest that a pole reversal may occur sometime during the next several thousand years (Odenwald 2003 [DIRS 160892]). The frequency of magnetic pole reversals, and the variation in field intensity with time, are corroborated by Johnson et al. (1995 [DIRS 185111], Figure 3) and Odenwald (2003 [DIRS 160892]).

The potential mechanisms linking the effects of magnetic field changes to changes in the behavior of repository engineered and natural systems are not addressed in published scientific literature. The timeframe of any magnetic reversal event is expected to be in the thousands of years, and since flow and transport phenomena and repository barriers have no known dependence on the magnetic field, direct effects would be of low consequence (also see excluded FEP 1.4.02.01.0A (Unintrusive Site Investigation)). Odenwald (2003 [DIRS 160892]) indicates that there are no identifiable fossil mutations or extinction events associated with any previous reversals. Pechala (1985 [DIRS 167633], p. 406) discusses the linkage between the earth's magnetic field and tropospheric circulation, and indicates that some authors use this relationship as a basis for explaining past changes in climate.

Of the possible longer-term effects of changes in the earth's magnetic field, only climate change is expected to affect the repository. Linkage to the magnetic changes could hypothetically exist because of the complex coupling of the thermosphere, ionosphere, and magnetosphere (Pechala 1985 [DIRS 167633], p. 406). However, no clear evidence exists in the literature that long-term climate change is connected with magnetic reversals, and therefore no basis exists for evaluating the range of possible future effects. As noted, changes in the magnetic field are common in geologic history, and the effect of such past events is therefore reflected in the range of climatic properties determined from field studies and observations, which are included in the TSPA and

discussed in included FEP 1.3.01.00.0A (Climate Change). Because the existing climate data implicitly includes the effect of magnetic field fluctuations that have occurred in the past and because direct effects of the magnetic field on the repository are of low consequence to barriers, flow, and radionuclide transport, omission of FEP 1.5.03.01.0A (Changes in the Earth's Magnetic Field) will not result in a significant adverse change to the magnitude or time of radiological exposures to the RMEI or radionuclide releases to the accessible environment. Therefore, this FEP is excluded from the performance assessments conducted to demonstrate compliance with proposed 10 CFR 63.311 and 63.321 (70 FR 53313 [DIRS 178394]), and with 10 CFR 63.331 [DIRS 180319], on the basis of low consequence.

INPUTS:

Table 1.5.03.01.0A-1. Direct Inputs

Input	Source	Description
Biggin and Thomas 2003. "Analysis of Long-Term Variations in the Geomagnetic Polodial Field Intensity and Evaluation of Their Relationship with Global Geodynamics." [DIRS 167876]	Figure 11	Frequency of earth's magnetic pole reversals

Table 1.5.03.01.0A-2. Indirect Inputs

Citation	Title	DIRS
10 CFR 63	Energy: Disposal of High-Level Radioactive Wastes in a Geologic Repository at Yucca Mountain, Nevada	180319
70 FR 53313	Implementation of a Dose Standard After 10,000 Years	178394
Biggin and Thomas 2003	"Analysis of Long-Term Variations in the Geomagnetic Polodial Field Intensity and Evaluation of Their Relationship with Global Geodynamics"	167876
Johnson et al. 1995	"Geomagnetic Polarity Reversal Rate for the Phanerozoic"	185111
Odenwald 2003	"Earth – Magnetic Field"	160892
Pechala 1985	"The Effect of Extraterrestrial Interactions on Change of Tropospheric Circulation in the Polar Regions of the Earth"	167633

FEP: 1.5.03.02.0A

FEP NAME:

Earth Tides

FEP DESCRIPTION:

Small changes of the earth's gravitational field due to celestial movements (those of the sun and moon) cause earth tides and may, in turn, cause pressure variations in groundwater flow systems.

SCREENING DECISION:

Excluded – low consequence

SCREENING JUSTIFICATION:

Kies et al. (1999 [DIRS 160882]) describe earth tides as follows: "tidal forces deform the earth; effects induced on fluids near the surface of the earth are documented by the observations of water level changes in wells. These changes are driven by alterations of the pore pressure induced by tidal deformation of porous and fluid-saturated crustal material." The pressure changes can also result in related effects such as fluctuations in underground gas concentrations (Kies et al. 1999 [DIRS 160882]).

The fluctuations in groundwater pressure fields can be readily measured. At Yucca Mountain, the magnitude of the effect on water levels is on the order of centimeters. For example, earth tide effects in borehole UE-25 p#1 are cited by Bredehoeft (1997 [DIRS 100007], p. 2,460), with measured fluctuations in groundwater levels of 2.05 cm. Water levels in boreholes at Paiute Mesa (on the Nevada Test Site) exhibit similar if slightly smaller fluctuations (Fenelon 2000 [DIRS 160881], p. 14). Clearly, such fluctuations are of low magnitude when compared with the much larger fluctuations introduced by climate variations or groundwater extraction.

As noted by Kies et al. (1999 [DIRS 160882]), the strain variations induced by earth tides are small (less than on the order of 10^{-8}), but are periodic and generally of known magnitude. Therefore, any significant cumulative effects of earth tides will be reflected in the present existing data for the hydrogeological system (consistent with proposed 10 CFR 63.305(c) (70 FR 53313 [DIRS 178394], p. 53319)). Because the fluctuations associated with earth tides are of such a small magnitude, any effect on the flow system is accounted for in the water level data used in deriving the hydrologic flow fields for the TSPA (SNL 2007 [DIRS 177391]).

Based on the above discussion, omission of FEP 1.5.03.02.0A (Earth Tides) will not result in a significant adverse change in the magnitude or time of radiological exposures to the RMEI or radionuclide releases to the accessible environment. Therefore, this FEP is excluded from the performance assessments conducted to demonstrate compliance with proposed 10 CFR 63.311 and 63.321 (70 FR 53313 [DIRS 178394]), and with 10 CFR 63.331 [DIRS 180319], on the basis of low consequence.

INPUTS:

Table 1.5.03.02.0A-1. Direct Inputs

Input	Source	Description
Bredehoeft 1997. "Fault Permeability Near Yucca Mountain." [DIRS 100007]	p. 2,460	Earth tide water level fluctuations in borehole UE-25 p#1

Table 1.5.03.02.0A-2. Indirect Inputs

Citation	Title	DIRS
70 FR 53313	Implementation of a Dose Standard After 10,000 Years	178394
Fenelon 2000	*Quality Assurance and Analysis of Water Levels in Wells on Pahute Mesa and Vicinity, Nevada Test Site, Nye County, Nevada. Water-Resources Investigations Report 00-4014*	160881
Kies et al. 1999	"Underground Radon Gas Concentrations Related to Earth Tides"	160882
SNL 2007	*Saturated Zone Site-Scale Flow Model*	177391

FEP: 2.1.01.01.0A

FEP NAME:

Waste Inventory

FEP DESCRIPTION:

The waste inventory includes all potential sources of radio toxicity and chemical toxicity. It consists of the radionuclide inventory (typically in units of curies), by specific isotope, and the non-radionuclide inventory (typically in units of density or concentration), including chemical waste constituents. The radionuclide composition of the waste will vary due to initial enrichment, burn-up, the number of fuel assemblies per waste package, and the decay time subsequent to discharge of the fuel from the reactor.

SCREENING DECISION:

Included

TSPA DISPOSITION:

Modeling the waste inventory in the TSPA can be divided into two tasks. The first is to select those radionuclides important to dose calculations. The second is to determine which radionuclides are present in each type of waste and in what quantity.

The radionuclides of importance to dose calculations were assessed in *Radionuclide Screening* (SNL 2007 [DIRS 177424]). This information was incorporated in *Initial Radionuclide Inventories* (SNL 2007 [DIRS 180472]) and is reproduced in Table 6-1[a] of that report. Waste package quantities are also described in *Total System Performance Assessment Data Input Package for Requirements Analysis for DOE SNF/HLW and Navy SNF Waste Package Overpack Physical Attributes Basis for Performance Assessment* (SNL 2007 [DIRS 179567], Table 4-1, Parameter Number 03-02; SNL 2007 [DIRS 179394], Table 4-1, Parameter Number 03-02). Nonradioactive chemically toxic waste is not included in the repository disposal inventory; nonradiological toxicity is discussed further in excluded FEP 3.3.07.00.0A (Non-Radiological Toxicity and Effects).

Nominal average waste package inventories of the important radionuclides for each type of waste are documented in *Initial Radionuclide Inventories* (SNL 2007 [DIRS 180472]). Weighted average grams per package for the 32 important radionuclides and three waste types (commercial SNF, DOE SNF, and HLW) are listed in Table 7-1[a] of *Initial Radionuclide Inventories* (SNL 2007 [DIRS 180472]).

The weighted average waste inventory values (grams per package for each radionuclide for each waste type) (SNL 2007 [DIRS 180472], Table 7-1[a]), along with the uncertainty multipliers from Table 7-2 of *Initial Radionuclide Inventories* (SNL 2007 [DIRS 180472]), are input to GoldSim for use in the TSPA model. The uncertainty multipliers address uncertainties in the average waste package inventories due to factors such as uncertainties in the isotopic concentrations in spent fuel, uncertainties in the commercial SNF delivery forecasts,

uncertainties in the waste glass canister production estimates, and waste heterogeneity (SNL 2007 [DIRS 180472], Section 6.6).

INPUTS:

Table 2.1.01.01.0A-1. Indirect Inputs

Citation	Title	DIRS
SNL 2007	*Initial Radionuclides Inventory*	180472
SNL 2007	*Radionuclide Screening*	177424
SNL 2007	*Total System Performance Assessment Data Input Package for Requirements Analysis for DOE SNF/HLW and Navy SNF Waste Package Overpack Physical Attributes Basis for Performance Assessment*	179567
SNL 2007	*Total System Performance Assessment Data Input Package for Requirements Analysis for TAD Canister and Related Waste Package Overpack Physical Attributes Basis for Performance Assessment*	179394

FEP: 2.1.01.02.0A

FEP NAME:

Interactions Between Co-Located Waste

FEP DESCRIPTION:

Co-location refers to the disposal of CSNF, DSNF, HLW, and possibly other wastes in close proximity within the repository. Co-location might affect thermal outputs, chemical interactions, or radionuclide mobilization.

SCREENING DECISION:

Excluded – low consequence

SCREENING JUSTIFICATION:

The following types of waste form are represented in the TSPA:

- Commercial SNF from boiling-water and pressurized-water reactors
- DOE SNF (including naval SNF), approximately 85% by weight MTHM of which is the N Reactor SNF currently stored at Hanford (DOE 2002 [DIRS 158405])
- HLW in the form of glass logs in stainless steel canisters.

The HLW and the DOE SNF (with the exception of naval SNF) are combined in specially designed waste packages for emplacement (codisposal). Codisposal waste packages are designed to contain either two glass logs and two multicanister overpacks for N Reactor SNF or five glass logs and one DOE SNF canister for other DOE SNF (SNL 2007 [DIRS 179567], Section 4.1.1). A small fraction of the codisposal waste packages will be loaded with an empty center slot and with the five outer slots holding four 24-inch-diameter HLW canisters and one 24-inch-diameter DOE SNF canister. The codisposal waste packages will be colocated randomly within an array predominantly consisting of commercial SNF waste packages, and will contain a relatively small fraction of the total waste.

The codisposal waste packages (CRWMS M&O 2000 [DIRS 147650], Table 8-1; CRWMS M&O 2000 [DIRS 147651], Table 8-1) are expected to be generally cooler than commercial SNF waste packages (SNL 2007 [DIRS 179196], Sections 6.6 and 6.7). Condensation that could occur due to development of hotter and cooler zones in the EBS is addressed in included FEPs 2.1.08.04.0A (Condensation Forms on Roofs of Drifts (Drift-Scale Cold Traps)) and 2.1.08.04.0B (Condensation Forms at Repository Edges (Repository-Scale Cold Traps)). Considerations of the heat generated by radioactive decay of commercial SNF, DOE SNF, and HLW are addressed in included FEPs 2.1.11.01.0A (Heat Generated in EBS) and 2.1.11.02.0A (Non-Uniform Heat Distribution in EBS). Interactions among codisposed waste forms within a waste package are addressed in included FEP 2.1.01.02.0B (Interactions Between Co-disposed Waste).

The potential for chemical interactions between co-located waste packages will depend on the direction of groundwater flow in the vicinity of the waste packages. The waste packages will be distributed in horizontal tunnels in the repository and any water inflow into the EBS will move downward under the influence of gravity into the underlying invert and fractured rock (SNL 2007 [DIRS 177407], Section 6.3.1). Longitudinal dispersion of the radionuclide flux as it passes through the invert is expected to be negligible (SNL 2007 [DIRS 177407], Section 6.3.1.2). Therefore, any contaminants released from breached waste packages will migrate into the underlying rock and will not significantly interact with other waste packages along the tunnel. Hence, changes in the rates of waste package degradation and radionuclide mobilization due to chemical interactions between co-located waste packages is insignificant.

Based on the above discussion, omission of FEP 2.1.01.02.0A (Interactions Between Co-located Waste) will not result in a significant adverse change in the magnitude or timing of radiological exposure to the RMEI or radionuclide releases to the accessible environment. Therefore, this FEP is excluded from the performance assessments conducted to demonstrate compliance with proposed 10 CFR 63.311 and 63.321 (70 FR 53313 [DIRS 178394]), and with 10 CFR 63.331 [DIRS 180319], on the basis of low consequence.

INPUTS:

Table 2.1.01.02.0A-1. Direct Inputs

Input	Source	Description
SNL 2007. *EBS Radionuclide Transport Abstraction*. [DIRS 177407]	Sections 6.3.1 and 6.3.1.2	Direction of water flow in the EBS and longitudinal dispersion of radionuclide transport in the invert
SNL 2007. *Thermal Management Flexibility Analysis*. [DIRS 179196]	Sections 6.6, 6.7	Postclosure thermal analyses and results
SNL 2007. *Total System Performance Assessment Data Input Package for Requirements Analysis for DOE SNF/HLW and Navy SNF Waste Package Overpack Physical Attributes Basis for Performance Assessment*. [DIRS 179567]	Section 4.1.1	Waste canister loading of codisposal waste packages

Table 2.1.01.02.0A-2. Indirect Inputs

Citation	Title	DIRS
70 FR 53313	Implementation of a Dose Standard After 10,000 Years	178394
CRWMS M&O 2000	*Evaluation of Codisposal Viability for HEU Oxide (Shippingport PWR) DOE-Owned Fuel*	147651
CRWMS M&O 2000	*Evaluation of Codisposal Viability for UZrH (TRIGA) DOE-Owned Fuel*	147650
DOE 2002	*DOE Spent Nuclear Fuel Information in Support of TSPA-SR*	158405

FEP: 2.1.01.02.0B

FEP NAME:

Interactions Between Co-Disposed Waste

FEP DESCRIPTION:

Co-disposal refers to the disposal of different waste types within the same waste package. Co-disposal might affect chemical interactions or radionuclide mobilization. At Yucca Mountain, the DSNF will be combined with HLW canisters within a waste package. This co-disposal with HLW within a waste package is unique to the DSNF and does not apply to the CSNF or Naval SNF placement within waste packages.

The DSNF will be contained within canisters that will be placed within the waste packages. Some DSNF waste packages may contain only DSNF canisters, while others may contain both DSNF and HLW canisters.

SCREENING DECISION:

Included

TSPA DISPOSITION:

Codisposal waste packages are specially designed waste packages that will contain the HLW glass and DOE SNF waste forms. Current plans call for most codisposal waste packages to contain five HLW glass canisters and one DOE SNF canister, but some will contain two HLW glass canisters and two DSNF MCOs (SNL 2007 [DIRS 180472], Table 6-2[a]; SNL 2007 [DIRS 179567], Section 4.1.1 and Table 4-1, Parameter Number 04-07). The codisposal waste packages will not contain naval SNF as this will be emplaced separately. The codisposal packages will be emplaced randomly within an array comprised predominantly of commercial SNF waste packages.

Potential issues of concern regarding codisposal include chemical interactions between the two degrading waste forms and between the corroding HLW glass and DOE SNF disposal canisters that could occur within a breached waste package. The TSPA includes these interactions by accounting for the effects of waste form degradation and container corrosion on the in-package chemistry.

Interactions of vapor influx or liquid influx with DOE SNF and HLW glass in a breached codisposal waste package were simulated in *In-Package Chemistry Abstraction* (SNL 2007 [DIRS 180506], Section 6.3.1.3[a]), which used degradation models for DOE SNF (BSC 2004 [DIRS 172453], HLW glass (BSC 2004 [DIRS 169988], Section 8.1), and other waste package components. Condensed and seepage water compositions were used to calculate the range of potential water chemistries (e.g., pH) that could occur in a breached codisposal waste package. Calculations were performed for water interaction with HLW glass and for water interaction with HLW glass and DOE SNF. Degradation of HLW glass tends to generate high pH solutions, while DOE SNF degradation generates near-neutral pH solutions (SNL 2007 [DIRS 180506],

Sections 6.3.4[a] and 6.10.1[a]). These calculations indicate that the combined effects of degrading canisters, DOE SNF, and other waste package materials will moderate the pH values attained in condensed water and seepage water (SNL 2007 [DIRS 180506], Section 6.10.1[a]).

The resulting in-package water chemistry is made available to the TSPA as part of *In-Package Chemistry Abstraction* (SNL 2007 [DIRS 180506], Sections 8.2 and 8.2[a]). The DOE SNF release rate model has no explicit dependence on water chemistry effects and will not be affected by changes in the solution chemistry that occur due to chemical interactions between codisposal packages or between waste forms within a package (BSC 2004 [DIRS 172453]).

The HLW glass degradation rate model contains explicit pH dependence and will be affected by changes in the solution pH within a codisposal package (BSC 2004 [DIRS 169988], Section 8.1). The HLW glass model does not depend on other properties of the solution.

INPUTS:

Table 2.1.01.02.0B-1. Indirect Inputs

Citation	Title	DIRS
BSC 2004	*DSNF and Other Waste Form Degradation Abstraction*	172453
BSC 2004	*Defense HLW Glass Degradation Model*	169988
SNL 2007	*Initial Radionuclides Inventory*	180472
SNL 2007	*In-Package Chemistry Abstraction*	180506
SNL 2007	*Total System Performance Assessment Data Input Package for Requirements Analysis for DOE SNF/HLW and Navy SNF Waste Package Overpack Physical Attributes Basis for Performance Assessment*	179567

FEP: 2.1.01.03.0A

FEP NAME:

Heterogeneity of Waste Inventory

FEP DESCRIPTION:

CSNF, DSNF, and HLW shipped to the repository may contain quantities of radionuclides that vary from waste package to waste package, fuel assembly to fuel assembly, and canister to canister. The composition of each of these waste forms may vary due to initial uranium enrichment, possible plutonium enrichment, and fuel burn-up, among other factors. The physical state within the waste form may also vary. For example, damaged fuel pellets or extremely high-burn-up fuels may have greater surface area exposed to any water penetrating a waste package than undamaged, low burn-up spent fuel. Given these potential differences in isotopic composition and physical condition, the mass of radionuclides available for transport may vary significantly among waste packages.

The different physical (structure, geometry), chemical, and radiological properties of the many forms of CSNF, DSNF, and HLW could result in differences in the corrosion and alteration rates based on waste-package composition. This could affect repository chemistry, breach times, dissolution rates, and availability of radionuclides for transport.

SCREENING DECISION:

Included

TSPA DISPOSITION:

This FEP addresses how the heterogeneities in the radionuclide inventory and in physical and chemical properties of the waste types (commercial SNF, DOE SNF, and HLW) are addressed in the TSPA.

As discussed in *Initial Radionuclide Inventories* (SNL 2007 [DIRS 180472], Section 6.4) the repository waste forms are quite heterogeneous in radionuclide inventory (both isotopic content and radionuclide loading) per package, as a result of uranium enrichment, possible plutonium enrichment, and fuel burn-up among other factors. Heterogeneities in radionuclide inventory will occur at several scales (e.g., between individual fuel assemblies and waste form canisters) and will contribute to variability in radionuclide inventories in the waste packages (SNL 2007 [DIRS 179394], Table 4-1, Parameter Number 04-07; SNL 2007 [DIRS 179567], Table 4-1, Parameter Number 04-07). The package-to-package radionuclide inventory variability is not significant for the TSPA because it samples across many realizations. For this reason, the TSPA uses an average waste package inventory for each radionuclide; heterogeneities in the radionuclide inventory are included in the TSPA through the uncertainty distributions that are used for the average initial radionuclide inventories in the waste packages (SNL 2007 [DIRS 180472], Sections 6.4, 6.6, and 7.1).

The different physical, chemical, and radiological properties of the various commercial SNF, DOE SNF, and HLW glass waste forms could result in differences in their alteration or corrosion rates, which may subsequently affect the repository chemistry, waste form degradation rates and availability of radionuclides for transport. The TSPA uses separate models to describe the degradation rates of commercial SNF, DOE SNF, and HLW glass waste forms (BSC 2004 [DIRS 169987]; BSC 2004 [DIRS 172453]; BSC 2004 [DIRS 169988]). The effects of heterogeneities in the physical, chemical, and radiological properties of these waste form types on their degradation rates are included in uncertainty distributions for the parameters in the degradation rate models. Commercial SNF heterogeneities associated with burnup and linear power history influence the gap and grain boundary inventories. The effects of heterogeneities in commercial SNF burnup and linear power history are included in the uncertainty distributions for the instantaneous release fractions that are used to model release of the gap and grain boundary inventories (BSC 2004 [DIRS 169987], Section 6.3). Heterogeneity of the DOE SNF inventory is addressed in included FEP 2.1.02.28.0A (Grouping of DSNF Waste Types into Categories). As discussed in *Defense HLW Glass Degradation Model* (BSC 2004 [DIRS 169988]), one area where the heterogeneity of the waste form is particularly pronounced is in the variation in the composition of waste glasses made to immobilize specific wastes at different DOE sites. The effect of waste glass compositions on the calculated degradation rate is taken into account through the range of values of the model parameter k_E. Ranges for the values of k_E in acidic and alkaline solutions are selected based on the results of laboratory tests with glasses that provide a wide range of compositions that bounds the range of concentrations of key glass components in HLW glasses, such as aluminum (BSC 2004 [DIRS 169988], Section 6.5.2).

INPUTS:

Table 2.1.01.03.0A-1. Indirect Inputs

Citation	Title	DIRS
BSC 2004	*DSNF and Other Waste Form Degradation Abstraction*	172453
BSC 2004	*CSNF Waste Form Degradation: Summary Abstraction*	169987
BSC 2004	*Defense HLW Glass Degradation Model*	169988
SNL 2007	*Initial Radionuclides Inventory*	180472
SNL 2007	*Total System Performance Assessment Data Input Package for Requirements Analysis for DOE SNF/HLW and Navy SNF Waste Package Overpack Physical Attributes Basis for Performance Assessment*	179567
SNL 2007	*Total System Performance Assessment Data Input Package for Requirements Analysis for TAD Canister and Related Waste Package Overpack Physical Attributes Basis for Performance Assessment*	179394

FEP: 2.1.01.04.0A

FEP NAME:

Repository-Scale Spatial Heterogeneity of Emplaced Waste

FEP DESCRIPTION:

Waste placed in Yucca Mountain will have physical, chemical, and radiological properties that will vary spatially, resulting in variation in the mass of radionuclides available for transport from different parts of the repository.

SCREENING DECISION:

Included

TSPA DISPOSITION:

As discussed in *Initial Radionuclide Inventories* (SNL 2007 [DIRS 180472], Section 6.4.2) the repository waste forms are quite heterogeneous in radionuclide inventory (both isotopic content and radionuclide loading) per package, as a result of uranium enrichment, possible plutonium enrichment, and fuel burn-up among other factors. At the repository scale, waste form degradation and mobilization in the TSPA model is addressed using three representative waste forms: commercial SNF, which for modeling purposes also addresses naval SNF, DOE SNF, and defense HLW glass. These categories of waste will be placed in and disposed of in two types of waste packages: commercial SNF waste packages and codisposal waste packages, with the latter containing DOE SNF and defense HLW glass. Heterogeneity is greater for DOE SNF and defense HLW than it is for commercial SNF (SNL 2007 [DIRS 180472], Section 6.4.2).

For scenarios in which only a few packages breach, package-to-package heterogeneity could be important in quantifying exposure of the RMEI. This is discussed further in included FEP 2.1.01.03.0A (Heterogeneity of Waste Inventory). For the postclosure TSPA, however, these "few-package" scenarios are not significant to performance because only scenarios with many packages breached show calculated releases that approach the exposure limit. For multiple-package breach scenarios, package-to-package heterogeneity is directly addressed in the TSPA using uncertainty parameters for the average inventory within the commercial SNF and codisposal waste packages (SNL 2007 [DIRS 180472], Sections 6.4.2 and 6.6).

For the nominal scenario at the repository-scale, radionuclide dissolution and release depend more directly on groundwater infiltration than on the specific location of a waste package within the repository (since corrosion by groundwater is the primary mechanism for waste package degradation). Therefore, the resistance of the different waste forms to degradation is of key importance. The waste forms are treated as three representative categories: commercial SNF, DOE SNF and defense HLW (SNL 2008 [DIRS 183478], Section 6.3.7), since package-to-package heterogeneities are of less importance at the repository-scale (widespread degradation would average out any heterogeneities at the package-scale). Within the TSPA model, the generic waste types are coupled to spatial variations in percolation properties rather than to a specific location (SNL 2008 [DIRS 183478], Section 6.3.7.2.3). The process of waste form

degradation will be modeled by equations using empirical degradation rate formulae for the three representative waste form types: commercial SNF, DOE SNF, and defense HLW. Outputs from the waste form degradation and mobilization model component are provided for each representative waste package in seeping and nonseeping environments. For each percolation subregion, they provide the mass of radionuclides available for transport through the EBS; the concentration limits of radionuclides inside a failed waste package and in the invert; the concentrations of radionuclides, plutonium and americium, irreversibly attached (embedded in) waste form colloids; the concentrations of radionuclides, americium and plutonium, which are irreversibly attached to iron oxyhydroxide colloids; and the concentrations of radionuclides: americium, plutonium, protactinium, cesium, thorium, tin, radium, uranium, and neptunium, which are reversibly attached to colloids (SNL 2008 [DIRS 183478], Section 6.1.4.7). Various seepage and thermal-hydrologic environments are considered in the TSPA model.

INPUTS:

Table 2.1.01.04.0A-1. Indirect Inputs

Citation	Title	DIRS
SNL 2007	*Initial Radionuclides Inventory*	180472
SNL 2008	*Total System Performance Assessment Model/Analysis for the License Application*	183478

FEP: 2.1.02.01.0A

FEP NAME:

DSNF Degradation (Alteration, Dissolution, and Radionuclide Release)

FEP DESCRIPTION:

DSNF to be disposed in Yucca Mountain contains a variety of fuel types that include metallic uranium fuels; oxide and MOX fuels; Three Mile Island rubble; and heterogeneous fuels such as UAlx, U-ZrHx, and graphite fuels. In general, the composition and structure of these spent fuels are significantly different from CSNF, and the degradation, alteration, and dissolution may be different from the CSNF degradation.

Processes to be considered in this FEP include alteration and dissolution of the various DSNF waste forms, phase separation, oxidation of spent fuels, selective leaching, and the effects of the disposal canister on DSNF degradation.

SCREENING DECISION:

Included

TSPA DISPOSITION:

DOE SNF to be disposed of in Yucca Mountain is composed of a variety of fuel types including naval fuel (SNL 2007 [DIRS 179567], Table 4-1, Parameter Number 04-07, and Section 4.1). The various DOE SNF types are classified into eleven groups, which are outlined in *DOE Spent Nuclear Fuel Grouping in Support of Criticality, DBE, TSPA-LA* (DOE 2000 [DIRS 118968], Section 8.1). The largest single DOE SNF type is the N Reactor SNF, which comprises approximately 85% by weight expressed as MTHM of the total DOE SNF (DOE 2002 [DIRS 158405]). For the TSPA, the eleven groups of DOE SNF are being treated as two types: those waste packages containing naval fuel and all the rest (BSC 2004 [DIRS 172453], Section 8.1).

The degradation model for DOE SNF other than naval fuel is described in *DSNF and Other Waste Form Degradation Abstraction* (BSC 2004 [DIRS 172453], Section 6.1). Up to 50% of the cladding of non-naval DOE SNF may be perforated prior to repository emplacement (Rechard 1995 [DIRS 101084], Section 11.3.1, pp. 11 to 24). For the TSPA, it is conservatively assumed that all non-naval DOE SNF cladding is breached and neither protects the fuel from exposure to the repository environment after the waste package is breached nor inhibits radionuclide transport away from the fuel. The TSPA also takes no credit for the corrosion resistance of the disposal canister or the waste package inner vessel. Therefore, once the waste package outer shell has failed, it is conservatively assumed that the DOE SNF is directly exposed to the water or air of the repository environment. The model used in TSPA analyses for non-naval DOE SNF degradation is instantaneous degradation or dissolution of the waste form upon exposure of the waste form to groundwater, resulting in complete dissolution of the waste form during a single-code time step (BSC 2004 [DIRS 172453], Section 8.1).

Because of the robust design of naval SNF, it is assumed that commercial SNF can be used as a surrogate for naval SNF under the range of expected repository environmental conditions (BSC 2004 [DIRS 172453], Section 5.1). The classified *Naval Nuclear Propulsion Program Technical Support Document for the License Application* provides the technical basis for using this approach.

INPUTS:

Table 2.1.02.01.0A-1. Indirect Inputs

Citation	Title	DIRS
BSC 2004	*DSNF and Other Waste Form Degradation Abstraction*	172453
DOE 2000	*DOE Spent Nuclear Fuel Grouping in Support of Criticality, DBE, TSPA-LA*	118968
DOE 2002	*DOE Spent Nuclear Fuel Information in Support of TSPA-SR*	158405
Rechard 1995	*Methodology and Results*	101084
SNL 2007	*Total System Performance Assessment Data Input Package for Requirements Analysis for DOE SNF/HLW and Navy SNF Waste Package Overpack Physical Attributes Basis for Performance Assessment*	179567

FEP: 2.1.02.02.0A

FEP NAME:

CSNF Degradation (Alteration, Dissolution, and Radionuclide Release)

FEP DESCRIPTION:

Alteration of the original CSNF (under wet or dry conditions) and dissolution of the uranium-oxide matrix can influence the mobilization of radionuclides. The degradation of UO_2 could be affected by a number of variables, such as surface area, burn-up, temperature, overall solution electrochemical potential (Eh), pH, and especially solutions containing significant concentrations of calcium, sodium, carbonate, and silicate ions, as well as availability of organic complexing materials. In turn, these water properties are affected by the alteration of the cladding, fuel matrix and other waste package internals.

SCREENING DECISION:

Included

TSPA DISPOSITION:

For the TSPA, it is assumed that all commercial SNF cladding (stainless steel and Zircaloy) is breached upon emplacement in the repository as discussed in *Cladding Degradation Summary for LA* (SNL 2007 [DIRS 180616]). Furthermore, following waste package failure, cladding unzipping is assumed to result in immediate exposure of bare fuel to the waste package environment along the entire length of the fuel rod (included FEP 2.1.02.23.0A (Cladding Unzipping)). The TSPA also takes no credit for corrosion resistance of the TAD canister or the stainless steel inner vessel of the waste package. Therefore, once the waste package outer shell has failed, it is conservatively assumed that the commercial SNF is directly exposed to the water or air of the repository environment.

Commercial SNF degradation following waste package failure is addressed in *CSNF Waste Form Degradation: Summary Abstraction* (BSC 2004 [DIRS 169987]). The outputs from the report are the TSPA models for the instantaneous release fractions (f_i) and for the matrix fractional release rates (F_i) of radionuclides under acidic and basic conditions. The output also includes the parameter values used in the models and the associated distributions that capture the uncertainty in these parameters, notably, the uncertainties in the release of:

- Gap and grain-boundary inventory fractions of cesium, iodine, technetium, and strontium. These are modeled as an instantaneous release of the fraction (f_i) of the total inventory of each of these elements to be in the gap and grain-boundary regions.

- Fuel matrix inventory under basic and acidic conditions. An instantaneous radionuclide release rate model is to be used for any fuel that is exposed to humid air at temperatures greater than 100°C and is subsequently contacted by water.

As described in *CSNF Waste Form Degradation: Summary Abstraction* (BSC 2004 [DIRS 169987], Sections 6.1 and 6.2), the commercial SNF model is designed to provide the fractional release rate of radionuclides (F_i) when the commercial SNF matrix is dissolved or otherwise altered upon exposure to water or humid air. The mathematical form of the model has six model parameters (A, a_0, a_1, a_2, a_3, and a_4) and four independent variables (absolute temperature, pCO_3, pO_2, and pH) (BSC 2004 [DIRS 169987], Sections 1, 6.4.1). The effects of surface area are included through the effective specific surface area parameter (A) (BSC 2004 [DIRS 169987], Section 6.4.1.5). At temperatures greater than 100°C, potential fuel oxidation may increase the fuel surface area. This increase in surface area is accounted for by modeling an instantaneous release for any fuel in a waste package that is exposed to humid air at temperatures greater than 100°C and is subsequently contacted by water (BSC 2004 [DIRS 169987], Section 8.2).

Some factors are not accounted for in the commercial SNF degradation rate model because their effects have been found to have a negligible effect on the commercial SNF degradation rate. Potential oxidation of fuel during preclosure handling operations has been shown to have negligible consequences to the RMEI dose (DTN: MO0506MWDTLVAC.000 [DIRS 174811]) and is not modeled. Effects of other factors, including burnup, secondary phase formation, and selective or congruent release, are discussed in *CSNF Waste Form Degradation: Summary Abstraction* (BSC 2004 [DIRS 169987], Section 6.2.2.3). The burnup has a negligible effect on the commercial SNF degradation rate. Secondary phase formation and the resultant armoring of the waste form surface decrease the degradation rate and are not included in the conservative analysis.

In the TSPA, the commercial SNF degradation model parameters are used along with the in-package chemistry to calculate a commercial SNF degradation rate at each model time step. The degradation model parameters are determined by sampling from parameter distributions that incorporate uncertainty, while the in-package chemistry variables are calculated as part of the TSPA simulation.

INPUTS:

Table 2.1.02.02.0A-1. Indirect Inputs

Citation	Title	DIRS
BSC 2004	*CSNF Waste Form Degradation: Summary Abstraction*	169987
DTN: MO0506MWDTLVAC.000	TSPA-LA Validation and Analysis Cases	174811
SNL 2007	*Cladding Degradation Summary for LA*	180616

FEP: 2.1.02.03.0A

FEP NAME:

HLW Glass Degradation (Alteration, Dissolution, and Radionuclide Release)

FEP DESCRIPTION:

Glass waste forms are thermodynamically unstable over long time periods, and will alter on contact with water. Radionuclides can be mobilized from the glass waste by a variety of processes, including degradation and alteration of the glass, phase separation, congruent dissolution, precipitation of silicates, co-precipitation of other minerals (including iron corrosion products), and selective leaching.

SCREENING DECISION:

Included

TSPA DISPOSITION:

The expression for modeling the rate of glass degradation in the TSPA is provided in *Defense HLW Glass Degradation Model* (BSC 2004 [DIRS 169988], Section 8.1). The model addresses degradation of glass exposed to humid air or dripping water, and glass immersed in water. The glass degradation rate is calculated as a function of pH and temperature (BSC 2004 [DIRS 169988], Section 6.5.1 and Equation 13).

This rate accounts for the combined effects of water diffusion, ion exchange, and hydrolysis processes that lead to glass degradation when contacted by water. Explicit dependencies are given for variables tracked in TSPA calculations, including pH and temperature. A minimum relative humidity of 44% is required for glass degradation to occur (BSC 2004 [DIRS 169988], Section 6.5.5.3.2). The effects of environmental processes specific to the disposal conditions that affect glass degradation, such as water condensation and dripping, are captured in the model by the range of values of the k_E term. The results of tests in which those processes occur are used to determine bounding model parameter values. The range of the rate coefficient k_E also accounts for the range of glass durabilities (compositions) and the evolution of the solution chemistry contacting the glass. Although the rate equation is not explicitly time dependent, variables used in the model (pH, temperature, and relative humidity) depend on time so time dependence is implicitly addressed. The values for these parameters are obtained from other models. The release of radionuclides from HLW glass is modeled to be congruent with other glass matrix components. The release rates of boron measured in laboratory tests are used to determine the glass degradation rate. The radionuclide release rate is calculated as the product of the glass degradation rate, the exposed surface area, and the radionuclide inventory. *Defense HLW Glass Degradation Model* (BSC 2004 [DIRS 169988]) provides equations for calculating the glass degradation rate (described above) and the surface area; the radionuclide inventory is provided by another model report (SNL 2007 [DIRS 180472]).

Glasses having matrix compositions representative of HLW glasses were used in laboratory tests. These glasses provided levels of glass and glass phase separation and devitrification phases

representative of HLW glasses. The maximum rates calculated by the model were selected to bound the rates measured experimentally after the precipitation of silicate, iron silicate, and mineral phases. In this way, processes that affect the glass alteration rate, congruent dissolution, selective leaching, and precipitation of alteration phases, have been incorporated in the model through model parameters, even though only the temperature and pH dependencies are calculated. The range of values of the rate coefficient k_E provides rates consistent with those measured under various test conditions in which glasses were reacted in humid air, dripping water, and various immersion conditions. A triangular distribution of values for k_E is skewed to low values to reflect the greater likelihood that glass in the disposal system will be contacted by water vapor (which gives the lowest measured rates) rather than immersion (which gives the highest measured rates).

The range of k_E values also reflects the effects of glass composition and, to a large extent, the radionuclide inventory on glass degradation, since the waste glasses are formulated based on the waste compositions. Calculation of the radionuclide release rate accounts for the spatial heterogeneity of HLW glass (i.e., the distribution of various HLW glass) by using a representative glass log to represent all HLW glasses. The surface area of glass that is available for corrosion, and the average radionuclide inventory (BSC 2004 [DIRS 169988], Table 7.1), are calculated based on the characteristics and predicted numbers of glass logs to be received from different production facilities.

In the TSPA, the HLW glass degradation model is used along with the in-package chemistry to calculate a HLW glass degradation rate at each model time step. The degradation rate model parameters are determined by sampling from parameter distributions that incorporate uncertainty, while the in-package chemistry parameters are calculated as part of the TSPA simulation.

Because of the high temperatures that occur following an igneous intrusion, an instantaneous degradation rate is applied.

Glass cracking due to volume changes on cooling is another mechanism of degradation and is addressed in included FEP 2.1.02.05.0A (HLW Glass Cracking).

INPUTS:

Table 2.1.02.03.0A-1. Indirect Inputs

Citation	Title	DIRS
BSC 2004	*Defense HLW Glass Degradation Model*	169988
SNL 2007	*Initial Radionuclides Inventory*	180472

FEP: 2.1.02.04.0A

FEP NAME:

Alpha Recoil Enhances Dissolution

FEP DESCRIPTION:

During decay of certain radionuclides, alpha particles may be emitted with sufficiently high energies that the daughter nuclide recoils appreciably to conserve system momentum. A potential result of recoil is that certain radionuclides, such as ^{234}U, exhibit substantially greater dissolution rates (with the same solubility limits) and can be transported preferentially.

SCREENING DECISION:

Excluded – low consequence

SCREENING JUSTIFICATION:

Many of the heavy radionuclides decay by emitting alpha particles with energies greater than 4.0 MeV (Parrington et al. 1996 [DIRS 103896], p. 48). To conserve momentum, part of the decay energy is imparted to the daughter nuclide causing it to recoil from the position of the parent nuclide.

Alpha recoil may be analyzed according to the conservation of momentum in the center-of-mass frame of reference. Suppose a radionuclide X (e.g., ^{238}U), at rest in the lab-system frame of reference (Figure 2.1.02.04.0A-1a), decays to radionuclide Y (e.g., ^{234}Th) by emitting an alpha particle (see Figure 2.1.02.04.0A-1b for the center-of-mass frame).

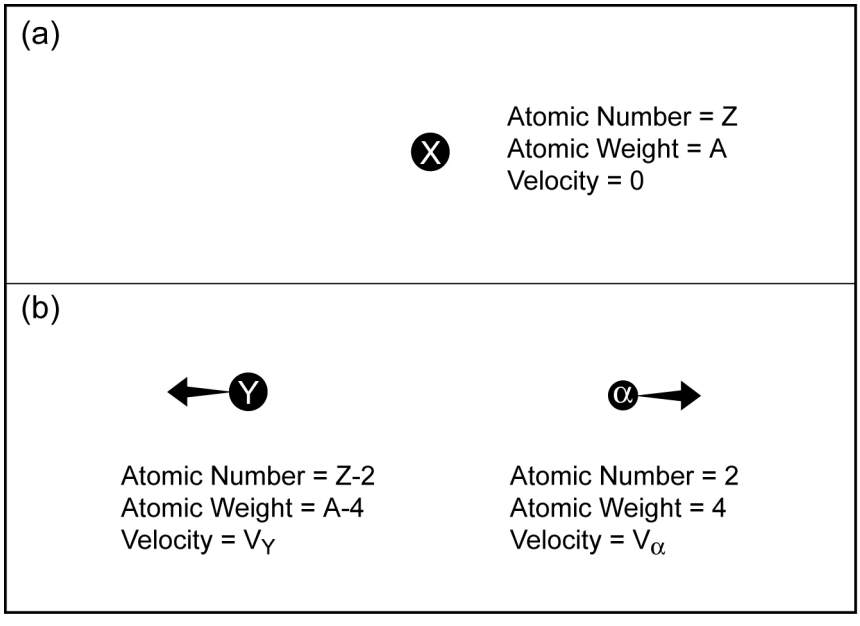

Figure 2.1.02.04.0A-1. Conceptual Illustration of Alpha Recoil Mechanics

Applying the conservation of momentum leads to Equations 2.1.02.04.0A-1 and 2.1.02.04.0A-2:

$$\text{Momentum Before} = \text{Momentum After} \qquad \text{(Eq. 2.1.02.04.0A-1)}$$

$$0 = M_Y V_Y + m_\alpha V_\alpha \qquad \text{(Eq. 2.1.02.04.0A-2)}$$

where

M_Y = Mass of the recoil nucleus

m_α = Mass of the alpha particle.

Therefore, the velocity of the recoil nucleus (in terms of the velocity of the alpha particle) is:

$$V_Y = -V_\alpha\left(\frac{m_\alpha}{M_Y}\right) \qquad \text{(Eq. 2.1.02.04.0A-3)}$$

The kinetic energy of the recoil nucleus can now be expressed in terms of the kinetic energy of the emitted alpha particle as:

$$KE(Y) = \frac{1}{2} M_Y V_Y^2 = \frac{m_\alpha}{M_Y}\left(\frac{1}{2} m_\alpha V_\alpha^2\right) = \frac{m_\alpha}{M_Y} KE(\alpha) \qquad \text{(Eq. 2.1.02.04.0A-4)}$$

Thus, the kinetic energy of the recoil nucleus is a small fraction of that given to the alpha particle. The energy of the alpha particle is dependent upon the proper mass defect value (the amount of mass converted into energy).

Both the emitted alpha particle and the recoiling daughter nucleus can displace other atoms. The number of atom displacements per alpha decay can be calculated by noting that when a recoil nucleus strikes an atom, it requires a minimum displacement energy, E_d, of approximately 25 eV to eject the struck atom from its lattice site (Foster and Wright 1973 [DIRS 144061], p. 296). The total number of displacements caused by a single alpha decay event is given by Equation 2.1.02.04.0A-5 (Foster and Wright 1973 [DIRS 144061], p. 296). Equation 2.1.02.04.0A-5 gives displacement units:

$$Disp(E) = \int_0^\infty P(T)K(E,T)\nu(T)dT = \int_{E_d}^{T_m} P(T)K(E,T)\nu(T)dT \qquad \text{(Eq. 2.1.02.04.0A-5)}$$

where

$P(T)$ = probability that an atom (primary knock-on), struck by either the emitted alpha or the alpha recoil atom, receiving energy T is displaced

$K(E,T)$ = probability for the transfer of kinetic energy T to the primary knock-on atom of energy E

$v(T)$ = total number of displacements in a cascade originating from a primary knock-on atom whose energy is T.

The expression is integrated over the energy range starting at the displacement threshold energy, E_d, and ending at the maximum energy that can be transferred to an atom, T_m. Because the displacement of atoms corresponds to a threshold event, $P(T)$ is modeled as a Heaviside step function (Foster and Wright 1973 [DIRS 144061], p. 297):

$$P(T) = \langle T - E_d \rangle^0 = \begin{cases} 0 & if \quad T < E_d \\ 1 & if \quad T \geq E_d \end{cases} \qquad \text{(Eq. 2.1.02.04.0A-6)}$$

To simplify the analysis, the probability for kinetic energy transfer is treated as being a uniform distribution over the applicable energy range:

$$K(E,T) = \frac{1}{T_m - E_d} \qquad \text{(Eq. 2.1.02.04.0A-7)}$$

The Kinchin-Pease model (Foster and Wright 1973 [DIRS 144061], p. 297) describes the total number of displacements that originate from a primary knock-on:

$$\nu(T) = \frac{T}{2E_d} + \frac{E_i - T}{2E_d}\langle T - E_i \rangle^0 = \begin{cases} T/2E_d & if \quad T \leq E_i \\ E_i/2E_d & if \quad T > E_i \end{cases} \qquad \text{(Eq. 2.1.02.04.0A-8)}$$

where

E_i = energy required for ionization.

The $2E_d$ in the denominator accounts for the displacement of the knock-on atom and the additional E_d for the striking atom to also leave the displacement site. The model also reasonably concludes there is an ionization threshold (E_i) below which displacements take place and above which only ionization takes place.

The total number of displacements is given by Equation 2.1.02.04.0A-9, which includes ionization interactions:

$$Disp(T_m) = \begin{cases} \int_{E_d}^{T_m} \frac{T}{2E_d T_m - 2E_d^2} dT & if \quad T_m \leq E_i \\ \int_{E_d}^{E_i} \frac{T}{2E_d T_m - 2E_d^2} dT + \int_{E_i}^{T_m} \frac{E_i}{2E_d T_m - 2E_d^2} dT & if \quad T_m > E_i \end{cases} \qquad \text{(Eq. 2.1.02.04.0A-9)}$$

$$= \begin{cases} \frac{T_m + E_d}{4E_d} & if\ T_m \leq E_i \\ \frac{E_i^2 - E_d^2}{4E_d(T_m - E_d)} + \frac{E_i T_m - E_i^2}{2E_d(T_m - E_d)} & if\ T_m > E_i \end{cases}$$

For the case of ^{238}U decaying to ^{234}Th, $KE(\alpha) = 4.196$ MeV (Lederer and Shirley 1978 [DIRS 142133]), $m_\alpha \cong 4.0$, and $M_{Th} \cong 234.0$, which results in a kinetic energy for the recoil nucleus of $KE(^{234}Th) = 0.072$ MeV. The kinetic energy of the recoil atom is much less than the ionization energy. Therefore, using the first version of Equation 2.1.02.04.0A-9 (with $E_d = 25$ eV), $Disp(^{234}Th)$ is equal to 720 displacements per alpha decay. This does not include replacement collisions along with focusing and channeling effects, which will significantly lower the estimate for displacements. If each of the secondary displacements follows a bifurcation process (i.e., 2^N equals 720), this would correspond to 9.49 bifurcation levels. This means that only those recoil nuclei originating within about 10 atom monolayers from the surface can escape directly into water. Given the isotropic nature of alpha recoil, only 50% of these recoil nuclei will initially be moving from the fuel towards the groundwater.

The emitted alpha particle can cause a much larger number of possible displacements owing to its larger kinetic energy. As noted above, the maximum energy for an alpha particle emitted from ^{238}U is 4.196 MeV. Since this energy is above the ionization value, the second version of Equation 2.1.02.04.0A-9 that contains two terms must be used to take into account the ionization by the alpha particles. Using the maximum alpha energy results in a value of 4,550 for $Disp(\alpha)$. When displacement from the emitted alpha particle is added to that of the recoil atom value, $Disp(^{234}Th)$, the net displacements are 5,270, which corresponds to approximately 12.4 bifurcation levels (i.e., the alpha recoils that can escape will occur in about the first 13 monolayers from the surface). Other estimates of the numbers of displacements per alpha decay in commercial SNF (Pelletier 2001 [DIRS 164034], Section 5.4.6.3.1) and defense HLW glasses (Wronkiewicz 1993 [DIRS 171709], Table 2) indicate that the number of displacements estimated above provides a conservative upper bound for the number of displacements that may be produced by alpha decay in commercial SNF and defense HLW glasses.

An upper bound to the enhancement of the dissolution rate due to direct escape of displaced atoms into groundwater contacting the waste forms may be determined based on the number of alpha decays per unit time within the first thirteen half-monolayers of the material surface that result in nuclei recoiling toward the groundwater. First, the mass of material in thirteen half-monolayers of SNF must be determined. The worst-case density for thorium (or even uranium) will be approximately that of pure plutonium metal, with a maximum density of 19.84 g/cm^3 (Wick 1980 [DIRS 143651], Table 7.1) and a monolayer thickness of approximately 3.0 Å (3.0×10^{-10} m). Therefore, over a surface area of 1.0 m^2, the first thirteen half-monolayers of SNF in the direction of the material surface have a mass of 0.0387 grams (19.84 g/cm^3 $\times$ 10^6 cm^3/m^3 $\times$ 13/2 monolayers $\times$ 3×10^{-10} m). The dissolution rate due to alpha decay is the product of the surface density (0.0387 g/m^2) and the fractional rate at which the SNF material experiences radioactive α-decay (the decay constant). Major constituents of final SNF and HLW on a mass basis have been determined to be ^{238}U, ^{235}U, ^{239}Pu, ^{236}U, and ^{240}Pu from inventory data in *Initial Radionuclide Inventories* (SNL 2007 [DIRS 180472], Table 7-1[a]), and the fractional rates of α-decay for these radionuclides have been determined from their radiological half-lives. These major radionuclides are analyzed in Table 2.1.02.04.0A-1. The maximum enhancement of the dissolution rate for each radionuclide due to alpha recoil (0.0387 g/m^2 $\times$ fractional decay rate) is shown in column 5. The fractional decay rate for each radionuclide is given by the decay constant ($\lambda = ln(2)/\tau_{½}$).

The dissolution rates shown in Table 2.1.02.04.0A-1 may be compared with the dissolution rates of different waste forms due to chemical (nonnuclear) processes. Commercial SNF flow-through test dissolution data show rates ranging from 0.15 to 109 mg/m^2 per day (DTNs: MO0304PNLLPHDD.000 [DIRS 163441]; file: *CSNF MR REV2.xls*, Sheet A3; and MO0302PNLDUFTD.000 [DIRS 162385], RUN # 66 Data). When converted to the same units as used in Table 2.1.02.04.0A-1 by assuming 365.25 days per year, the dissolution rates are 0.05 to 39.8 g/m^2 per year. For defense HLW glass the initial dissolution rates are approximately 1 to 5 g/m^2 per day (BSC 2004 [DIRS 169988], Table 7-2). The alpha recoil dissolution rates shown in column 5 of Table 2.1.02.04.0A-1 are, thus, much less than the values associated with chemical processes.

In the TSPA model, DOE SNF degradation (except naval SNF) is modeled as instantaneous degradation or dissolution of the waste form upon exposure of the waste form to groundwater. For all groups of DOE SNF (except naval SNF), the upper-limit model produces complete dissolution of the waste form during a single-code time step upon exposure of the waste form to groundwater (BSC 2004 [DIRS 172453], Section 8.1). Alpha recoil enhanced dissolution of DOE SNF is inconsequential for this bounding modeling approach.

Radiation damage effects that may accumulate in commercial SNF (Piron 2001 [DIRS 162396]) and defense HLW (Wronkiewicz 1993 [DIRS 171709], Section 5.0) due to alpha recoil are addressed in excluded FEP 2.1.13.02.0A (Radiation Damage in EBS).

In summary, even when it is assumed that all radioactive decays result in alpha recoil, calculated increases in the dissolution rates of the different waste forms are insignificant compared to the dissolution rates associated with chemical processes. Based on the above discussion, omission of FEP 2.1.02.04.0A (Alpha Recoil Enhances Dissolution) will not result in significant adverse changes in the magnitude or time of radiological exposures to the RMEI or radionuclide releases to the accessible environment. Therefore, this FEP is excluded from the performance assessments conducted to demonstrate compliance with proposed 10 CFR 63.311 and 63.321 (70 FR 53313 [DIRS 178394]), and with 10 CFR 63.331 [DIRS 180319], on the basis of low consequence.

Table 2.1.02.04.0A-1. Alpha Recoil Enhanced (from α and α-Recoil Atom) Dissolution Rates Due to the Major Mass-Based Constituents of SNF and HLW to be Disposed of in the Yucca Mountain Repository

Nuclide ID	Decay Mode	Half–Life [a] (years)	Fraction Decay Rate [b] (1/yr)	α–Decay Rate in 13 Half-Mono-Layers[c] ($g/m^2 \cdot yr$)
^{238}U	α, γ, SF	4.47×10^{9}	1.55×10^{-10}	6.00×10^{-12}
^{235}U	α, γ, SF	7.04×10^{8}	9.85×10^{-10}	3.81×10^{-11}
^{239}Pu	α, γ, SF	2.410×10^{4}	2.88×10^{-5}	1.11×10^{-6}
^{236}U	α, γ, SF	2.342×10^{7}	2.96×10^{-8}	1.15×10^{-9}
^{240}Pu	α, γ, SF	6.56×10^{3}	1.06×10^{-4}	4.09×10^{-6}

[a] Data obtained from Parrington et al. 1996 [DIRS 103896], p. 48.
[b] The fraction decay rate, also known as the decay constant, is given by $\lambda=\ln(2)/\iota½$, where $\iota½$ is the radionuclide half-life given by values in column 3.
[c] Each monolayer thickness is 3.0 Å (3.0×10^{-10} m), and the density has an upper bound of 19.84 g/cm^3 (theoretical density of pure plutonium metal (Wick 1980 [DIRS 143651])).

INPUTS:

Table 2.1.02.04.0A-2. Direct Inputs

Input	Source	Description
BSC 2004. *DSNF and Other Waste Form Degradation Abstraction*. [DIRS 172453]	Section 8.1	For all groups of DOE SNF (except naval DOE SNF), the upper-limit model produces complete dissolution of the waste form during a single-code time step upon exposure of the waste form to groundwater
BSC 2004. *Defense HLW Glass Degradation Model*. [DIRS 169988]	Table 7-2	Initial dissolution rates for defense HLW glass
DTN: MO0302PNLDUFTD.000. Flowthrough Dissolution Data. [DIRS 162385]	RUN # 66 data	Test dissolution data
DTN: MO0304PNLLPHDD.000. Low PH Dissolution Data. [DIRS 163441]	file: *CSNF MR REV2.xls*, Sheet A3	Test dissolution data
SNL 2007. *Initial Radionuclides Inventory*. [DIRS 180472]	Table 7-1[a]	Provides inventory data

Table 2.1.02.04.0A-3. Indirect Inputs

Citation	Title	DIRS
70 FR 53313	Implementation of a Dose Standard After 10,000 Years	178394
Foster and Wright 1973	*Basic Nuclear Engineering*	144061
Lederer and Shirley 1978	*Table of Isotopes*	142133
Parrington et al. 1996	*Nuclides and Isotopes, Chart of the Nuclides*	103896
Pelletier 2001	"State of the Art on the Potential Migration of Species"	164034
Piron 2001	"Presentation of the Key Scientific Issues for the Spent Nuclear Fuel Evolution in a Closed System"	162396
Wick 1980	*Plutonium Handbook: A Guide to the Technology.*	143651
Wronkiewicz 1993	*Effects of Radionuclide Decay on Waste Glass Behavior--A Critical Review*	171709

FEP: 2.1.02.05.0A

FEP NAME:

HLW Glass Cracking

FEP DESCRIPTION:

Cracking of the HLW glass on cooling and during handling means that the surface area of the glass is greater than the surface area of a monolithic block. The increase in the surface area could affect the rate of glass alteration and radionuclide dissolution.

SCREENING DECISION:

Included

TSPA DISPOSITION:

The expression for exposed glass surface area developed to address this FEP is provided in *Defense HLW Glass Degradation Model* (BSC 2004 [DIRS 169988]). The surface area used to calculate the radionuclide release rate accounts for the effects of thermal cracking during manufacture and impact cracking during subsequent handling. The exposure factor ($f_{exposure}$) is used to model the combined effects of the added surface area due to cracking, the fraction of the surface that is accessible to water, and the reactivity of glass in tight cracks relative to glass at a free surface. The value of $f_{exposure}$ is selected for each realization from a triangular distribution with a minimum and most probable value of 4 and a maximum value of 17. The initial exposed surface area is calculated by using the following equation (BSC 2004 [DIRS 169988], Section 6.5.4, Equation 44):

$$S_0 = f_{exposure} \times (2\pi r_o^2 + 2\pi r_o \times L_o) \qquad \text{(Eq. 2.1.02.05.0A-1)}$$

where r_o is the internal radius of the average glass canister, and L_o is the length of the average glass canister.

As the glass degrades, the surface area is calculated as the product of the specific surface area of an average glass log ($f_{exposure} \times 2.70 \times 10^{-3}$ m^2/kg) and the mass of glass available at the beginning of the time step using the following equation (BSC 2004 [DIRS 169988], Section 6.5.4, Equation 48):

$$S = f_{exposure} \times 2.70 \times 10^{-3} \text{ m}^2/\text{kg} \times (2{,}710 \text{ kg} - \Sigma M_t \text{ kg}) \qquad \text{(Eq. 2.1.02.05.0A-2)}$$

where ΣM_t gives the loss of mass of the average glass log during all previous time steps (which has an associated loss of surface area) and the initial mass of the average glass log is 2,710 kg.

The value of M at each time step is calculated as the product of the glass degradation rate used for that time step and duration of the time step. The mass loss is used to calculate the loss in surface area assuming the mass loss is uniform over all surfaces.

As discussed in included FEP 2.1.02.03.0A (HLW Glass Degradation), following an igneous intrusion event, an instantaneous degradation rate is applied. Therefore, the exposure factor ($f_{exposure}$) is not applied under those conditions.

INPUTS:

Table 2.1.02.05.0A-1. Indirect Inputs

Citation	Title	DIRS
BSC 2004	*Defense HLW Glass Degradation Model*	169988

FEP: 2.1.02.06.0A

FEP NAME:

HLW Glass Recrystallization

FEP DESCRIPTION:

HLW glass recrystallization could occur and would lead to a less corrosion-resistant waste form. Recrystallization is a slow process and typically occurs only if a high glass temperature is maintained over a prolonged period.

SCREENING DECISION:

Excluded – low consequence

SCREENING JUSTIFICATION:

The glass degradation model developed in *Defense HLW Glass Degradation Model* (BSC 2004 [DIRS 169988]) utilizes a range of model parameter values determined from experimentally measured dissolution rates of glasses having compositions similar to HLW glasses (BSC 2004 [DIRS 169988], Section 6.5.2.2). HLW glasses of various compositions will be disposed of in the repository and the value of the effective glass dissolution constant (k_E) takes into account uncertainty associated with glass composition, including the heterogeneity of the waste inventory, as well as the effect of the solution compositions (BSC 2004 [DIRS 169988], Section 6.5.1).

As part of the validation of the glass degradation model, the glass degradation rate has been shown to be insensitive to the presence of the crystalline phases formed by devitrification of the glass melt during manufacture. Published results show that the effects of devitrification on glass dissolution rates are included within the range of uncertainty in the rate measurements (BSC 2004 [DIRS 169988], Section 6.5.5).

In conclusion, glass recrystallization would have no effect on the overall HLW glass dissolution rate.

Based on the previous discussion, omission of FEP 2.1.02.06.0A (HLW Glass Recrystallization) will not result in a significant adverse change in the magnitude or timing of either radiological exposure to the RMEI or radionuclide releases to the accessible environment. Therefore, this FEP is excluded from the performance assessments conducted to demonstrate compliance with proposed 10 CFR 63.311 and 63.321 (70 FR 53313 [DIRS 178394]), and with 10 CFR 63.331 [DIRS 180319], on the basis of low consequence.

INPUTS:

Table 2.1.02.06.0A-1. Direct Inputs

Input	Source	Description
BSC 2004. *Defense HLW Glass Degradation Model*. [DIRS 169988]	Section 6.5.5	Published results show that the effects of devitrification on glass dissolution rates are within the range of uncertainty in the rate measurements

Table 2.1.02.06.0A-2. Indirect Inputs

Citation	Title	DIRS
10 CFR 63	Energy: Disposal of High-Level Radioactive Wastes in a Geologic Repository at Yucca Mountain, Nevada	180319
70 FR 53313	Implementation of a Dose Standard After 10,000 Years	178394
BSC 2004	*Defense HLW Glass Degradation Model*	169988

FEP: 2.1.02.07.0A

FEP NAME:

Radionuclide Release from Gap and Grain Boundaries

FEP DESCRIPTION:

While in the reactor at high temperatures, radionuclides such as I and Cs may migrate and preferentially accumulate in cracks in the fuel matrix, grain boundaries of the UO_2, and in the gap between the fuel and cladding. After the waste package fails and the cladding perforates, the release rate of this fraction of the radionuclides could be rapid.

SCREENING DECISION:

Included

TSPA DISPOSITION:

Radionuclide release from gap and grain boundaries applies mainly to commercial SNF and similar fuel designs (such as MOX), which are fabricated from UO_2-based fuel pellets. In such SNF, a portion of some of the volatile fission product radionuclides can migrate to the fuel pellet grain boundaries and open gap areas of the fuel rods under the influence of the high temperature gradients during reactor operation (BSC 2004 [DIRS 169987], Section 6.2.1.1). The gap and grain boundary inventory is assumed in the TSPA to be accessible for dissolution into any water that penetrates the fuel cladding.

For the TSPA, it is conservatively assumed that all commercial SNF fuel cladding (stainless steel and Zircaloy) is breached upon emplacement in the repository as discussed in *Cladding Degradation Summary for LA* (SNL 2007 [DIRS 180616], Section 6.2[a]). Furthermore, following waste package failure, cladding unzipping is assumed to result in immediate exposure of bare fuel to the waste package environment along the entire length of the fuel rod (SNL 2007 [DIRS 180616], Section 5.3; included FEP 2.1.02.23.0A (Cladding Unzipping)). Once the waste package outer shell has failed, it is conservatively assumed that the UO_2 fuel is directly exposed to the water or air of the repository environment and the gap and grain boundary inventories are immediately accessible for dissolution upon water contact.

As described in *CSNF Waste Form Degradation: Summary Abstraction* (BSC 2004 [DIRS 169987], Section 6.3), the release of the gap and grain boundary radionuclide inventory is modeled as an instantaneous release fraction (f_i) where the subscript i refers to ^{137}Cs, ^{129}I, ^{90}Sr, and ^{99}Tc. Available experimental data are used to estimate the mean values, the ranges, and the distribution functions for f_i (BSC 2004 [DIRS 169987], Section 6.3). The gap and grain boundary release is modeled as an instantaneous release in one time step. These distributions are sampled at the beginning of each TSPA realization to determine the values of f_i that are used for the instantaneous release fractions during the course of the realization. At the high temperatures fuel pellets experience during reactor operation, a significant migration of gaseous radionuclides to the gap and grain boundaries occurs. However, at the much lower temperatures expected after waste package emplacement, the thermally driven migration of radionuclides to the gap and

grain boundaries is expected to be low enough that it can be considered to be included in the uncertainties in the instantaneous release fraction of the commercial SNF (BSC 2004 [DIRS 169987], Section 6.2.1).

INPUTS:

Table 2.1.02.07.0A-1. Indirect Inputs

Citation	Title	DIRS
BSC 2004	*CSNF Waste Form Degradation: Summary Abstraction*	169987
SNL 2007	*Cladding Degradation Summary for LA*	180616

FEP: 2.1.02.08.0A

FEP NAME:

Pyrophoricity from DSNF

FEP DESCRIPTION:

DSNF can contain pyrophoric material. Pyrophoric material could ignite and produce an adverse effect on repository performance. Pyrophoric events could affect the thermal behavior of the system and could contribute to degradation of the waste package, waste form, and cladding.

SCREENING DECISION:

Excluded – low consequence

SCREENING JUSTIFICATION:

Uranium metal-based fuel, such as Hanford's N Reactor SNF, is a potentially pyrophoric material. For the purposes of this FEP, a pyrophoric material is understood to be capable of igniting spontaneously under temperature, chemical, or physical/mechanical conditions specific to the storage, handling, or transportation environments (ASTM C 1454-00 [DIRS 152779], Section 3.2.9). Occurrence of a pyrophoric event (i.e, an event that involves self-sustained rapid chemical oxidation or self-sustained burning) in the repository could produce an adverse effect on repository performance by producing heat and increasing waste form degradation and radionuclide release rates.

Uranium metal and uranium hydride are regarded as pyrophoric materials in the DOE handbook, *Primer on Spontaneous Heating and Pyrophoricity* (DOE-HDBK-1081-94 [DIRS 103327]), but uranium oxides and carbide are not. The DOE SNF inventory consists of SNF "groups" (DOE 2000 [DIRS 118968]) that include metal-, oxide-, and carbide-based fuels. The uranium metal-based N Reactor SNF group (which accounts for about 85% by weight MTHM of the total DOE SNF inventory (DOE 2002 [DIRS 158405], Appendix D)) is potentially pyrophoric. This fuel is expected to be loaded into about 219 waste packages (SNL 2007 [DIRS 180472], Table 7-3[a]). This represents less than 2% of the 11,629 (SNL 2007 [DIRS 180472], Table 7-3[a]) waste packages to be included in the TSPA analyses.

N Reactor SNF is composed primarily of Zircaloy-clad metallic uranium. A substantial amount of the cladding has been breached, thereby exposing the metallic uranium to the K-basin water (and any other subsequent canister or dry storage) environment. Metallic uranium-based SNF has shown pyrophoric behavior when exposed to air environments (Abrefah et al. 1999 [DIRS 151226], Appendix C). Such pyrophoric behavior has been observed when finely divided uranium metal or uranium hydride have been exposed to air; limiting the air supply has been used to limit the rate of reaction and achieve controlled oxidation and stabilization of the material involved (Abrefah et al. 1999 [DIRS 151226], Appendix C4). Pyrophoric behavior has been observed during past operations involving handling and processing of N Reactor SNF at West Valley (Schulz 1972 [DIRS 159406]). However, assessment of these events concluded that they were most likely initiated by rapid oxidation of a zirconium/beryllium alloy in the cladding

weld beads that had been sensitized by exposure to nitric acid in the fuel dissolution operations involved (Schulz 1972 [DIRS 159406]). This initiation source is not relevant to the repository because the cladding in the disposed fuel will not have been sensitized by exposure to nitric acid. Other factors that could cause the N Reactor fuel to ignite in the repository are discussed below.

When oxidized in an air or water environment, metallic uranium-based fuels will produce uranium hydride and oxide as corrosion products. The uranium hydride corrosion product can be pyrophoric, particularly when in a fine particulate form or when a substantial amount of hydride has formed in the uranium metal matrix. Examination and testing conducted at Pacific Northwest National Laboratory on damaged N Reactor zirconium-clad uranium metal fuel showed small but discernable amounts of uranium hydride formed as precipitates within the metal (Marschman et al. 1997 [DIRS 149429], Section 3.4.2). The presence of these hydrides is believed to be responsible for the decreased ignition temperature observed during ignition testing of damaged/corroded N Reactor SNF samples compared to unirradiated or undamaged samples (Abrefah et al. 1999 [DIRS 151226], Tables 4.2 and 4.3). While bulk uranium metal is not pyrophoric at temperatures below 600°C, ignition temperatures in the range 277°C to 500°C were observed for the fuel samples from damaged and corroded N Reactor fuel elements (Abrefah et al. 1999 [DIRS 151226], Summary). The possibility exists that additional uranium-hydride will form during interim storage (Reilly 1998 [DIRS 149433], p. 30). Uranium-hydride inclusions tend to be concentrated near the exposed uranium metal fuel surface of damaged SNF (Abrefah et al. 1999 [DIRS 151226]; Marschman et al. 1997 [DIRS 149429]). The fraction of N Reactor SNF with cladding that is damaged enough to expose the metallic uranium core was not well understood when the decision was made to remove the fuel from wet storage and package the fuel within the MCOs (Abrefah et al. 1995 [DIRS 151125]). A characterization program was conducted to assess the extent of fuel damage prior to fuel packaging and fuel inspection was conducted during the packaging operation to ensure that limits on exposed fuel surface area were not exceeded within individual MCOs. However, as discussed below, uranium hydride inclusions in the metallic uranium matrix of damaged N Reactor SNF (i.e., fuel elements with breached cladding) potentially provide an ignition mechanism.

Uranium hydride and uranium metal undergo exothermic reactions with oxygen and water. The reaction rates increase with temperature, and the presence of uranium hydride in uranium metal is known to greatly accelerate the oxidation rate even at low temperatures (Haschke 1998 [DIRS 174075]). As a result, oxidation initiated at a low temperature can generate sufficient heat locally near the hydride inclusions that the heat transfer rate is insufficient to remove the heat. This causes the temperature to increase locally at the reaction site, which then accelerates the reaction rate leading to a feedback situation that can initiate and sustain a pyrophoric event. At lower temperatures, humidity can increase the rate of uranium metal corrosion by a water-catalyzed cycle until a maximum is reached, and then the rate decreases at higher relative humidity. Humidity effects are absent in the autothermic regime above 500°C (Haschke 1998 [DIRS 174075]). For these reasons, and because the standard enthalpy of the reaction with water vapor is lower than that for the reaction with oxygen due to the enthalpy needed to split the water molecules (Grenthe et al. 1992 [DIRS 101671]), the reaction with oxygen is the focus of this analysis. Because the rate of oxidation increases with the specific surface area of the material and also because the rate of heat transfer away from the reaction site is slower for particulate material than for bulk uranium, the ignition temperatures are expected to be lower for fine

particulate material. Regardless of the ignition temperature, for a spontaneous ignition of metallic uranium or uranium-hydride inclusions, or both, to occur and become a sustained pyrophoric event, there must be sufficient oxygen to support the continuing oxidation reactions. In the repository, the sources of oxygen that are potentially available to initiate and sustain a pyrophoric event in the codisposal waste packages containing N Reactor fuel are:

- Oxygen that could be produced from residual and bound water left in the MCOs after they are dried and closed.
- Oxygen or air ingress into the waste package through waste package breaches.

These potential sources of oxygen and how they are expected to influence and limit the pyrophoric events that might occur in the repository are discussed in the following paragraphs.

Oxygen from Residual Water in the Codisposal Waste Packages: The codisposal DOE SNF waste packages will be dried and filled with helium prior to emplacement in the repository (SNL 2008 [DIRS 173869], Appendix I). The N Reactor SNF contained within MCOs emplaced inside the codisposal waste packages are also dried and filled with helium (Garvin 2002 [DIRS 169141], Section 4.1.3.2). The amount of free and bound water that may remain in the MCOs after they are dried and closed is uncertain. The dominant form of this water is bound water in uranium and aluminum oxide hydrates with the estimated acceptable amount per MCO ranging up to 4.64 kg (Garvin 2002 [DIRS 169141], Table 4-4). In the repository, this water could be released and converted to free hydrogen and oxygen due to thermal and radiolytic decomposition of the uranium and aluminum oxide hydrates involved. If free oxygen and hydrogen are produced inside the codisposal packages, the oxygen will probably be scavenged by reaction with exposed uranium metal in the breached fuel because of the rapid kinetics of the uranium-metal/oxygen reactions (Haschke 1998 [DIRS 174075], Table 1). The fate of the free hydrogen is less clear. In studies of uranium-metal corrosion in moist air, neither hydrides nor hydrogen gas formed (Haschke 1998 [DIRS 174075], p. 150) suggesting that any evolved hydrogen is rapidly transformed to water on the U-metal surface under the conditions of this study. The production and fate of hydrogen is discussed further in excluded FEPs 2.1.12.03.0A (Gas Generation (H_2) from Waste Package Corrosion) and 2.1.13.01.0A (Radiolysis). Even if both MCOs in a codisposal package are each assumed to contain 4.64 kg water and it is also assumed all of the oxygen in this water is available as free oxygen to convert uranium-metal to UO_2 in a rapid pyrophoric event, it would oxidize only a very small fraction (0.5%) of the fuel in the waste package (see excluded FEP 2.1.11.03.0A (Exothermic Reactions in the EBS)). The heat energy released would be about 2.8×10^5 kJ, which would cause a waste package temperature increase of only 21°C even under conservatively assumed adiabatic conditions and conservatively assumed zero heat capacities of the two MCO and two HLW glass steel canisters. This is calculated by dividing 4,640 g H_2O by the approximate molecular weight of water, 18 g/mol to obtain 258 moles per MCO and then multiplying by two to get 516 moles H_2O, which is equilivent to 258 moles O_2 per waste package. Assuming the end product of the oxidation reaction is UO_2 and ignoring O_2 consumption by the in-package steels, the total energy released is 258 moles × 1,085 kJ/mol (Grenthe et al. 1992 [DIRS 101671], Table III.1) = 2.8×10^5 kJ or 2.8×10^8 J. Assuming adiabatic conditions (all energy is available to increase the waste package temperature (i.e., no radiative heat losses)) a maximum temperature increase for the waste package can be calculated. There are 2.43×10^7 g steel per waste package, not

including the steel of the two MCO and two HLW glass canisters (SNL 2007 [DIRS 179567], Table 4-10) and 1.1×10^7 g uranium-metal per waste package assuming that the waste package contains two MCOs each containing Mark IV fuel and scrap baskets containing the maximum fuel (3,804 kg uranium) and scrap (1,832 kg uranium) loadings (Garvin 2002 [DIRS 169141], Table 4-4). The specific heat capacity for austenitic steels is 0.5 J/g·°C (ASM International 1990 [DIRS 106780], p. 871). This value is not considerably different from the Alloy 22 specific heat capacity used in the multiscale thermohydrologic model (0.423 J/g·°C) (SNL 2008 [DIRS 184433], Table 4.1-1). The specific heat capacity for uranium-metal is 27.66 J/mol K (Grenthe et al. 1992 [DIRS 101671], Section V.1.1), which is equivalent to 0.12 J/g·°C. An approximate weighted average of 0.38 J/g·°C is used here for the steel and uranium-metal combined. The maximum temperature increase for the waste package due to emplaced water is calculated as 2.8×10^8 J/ waste package ÷ (3.49×10^7 g metal/ waste package × 0.38 J/ g·°C) = 21°C, a negligible quantity. Including the masses of steel in the MCO and HLW glass canisters would have resulted in an even lower calculated maximum temperature increase.

The adverse consequences for such a pyrophoric event are expected to be small because the TSPA model uses a bounding instantaneous degradation rate for DOE SNF (BSC 2004 [DIRS 172453], Section 8.1), and because a very conservative bounding estimate of the overall temperature increase (i.e., the adiabatic estimate discussed above) is sufficiently small that it is not expected to melt or otherwise degrade the codisposed glass waste forms. Degradation of the uranium metal fuel as a result of its oxidation in a pyrophoric event may cause the radionuclides in the oxidized fuel to be available for dissolution and transport when that fuel is contacted by water. Even in the absence of oxidation in a pyrophoric event, the TSPA model uses a bounding instantaneous degradation rate for the uranium-metal DOE SNF (BSC 2004 [DIRS 172453], Section 8.1), which considers that the radionuclide inventory in this fuel is available for dissolution and transport when the fuel is contacted by water. Therefore, a pyrophoric event will not adversely affect radionuclide release because the pyrophoric event will not increase the rate of radionuclide release beyond that already included in the TSPA model. Also, because a bounding estimate of the overall temperature increase (i.e., the adiabatic estimate discussed above) is small, it is not expected to melt or otherwise significantly degrade the HLW glass that is codisposed with the uranium-metal fuel. The expected effects of small temperature increases on the rate of degradation of HLW glass are discussed in FEP 2.1.11.03.0A (Exothermic Reactions in EBS).

Oxygen Ingress after Waste Package Breaching: In the absence of disruptive events, the breaches in the waste package outer shell through which ingress of oxygen might occur are expected to be stress corrosion cracks. Following pressure equilibration between the waste package void space and the drift air, it is expected that the SCC may allow oxygen ingress by the following processes:

- Counter-diffusion process involving helium, nitrogen, oxygen, and water vapor
- Pumping due to barometric pressure fluctuations
- Advective flow driven by buoyancy differences between the gasses inside and outside the waste packages.

Each of these processes and their effects on potential pyrophoric events in the repository are discussed below.

Oxygen Ingress by Diffusion: Upper bound estimates for the diffusive mass transport rate of oxygen into the waste package through SCC can be calculated using the approach described in *EBS Radionuclide Transport Abstraction* (SNL 2008 [DIRS 177407], Section 6.6.2).

The oxygen diffusion rate is calculated by applying Fick's First Law and making a number of reasonably bounding assumptions. The first assumption is that the oxygen concentration in the waste package is zero (i.e., all oxygen in the package is consumed by oxidation reactions involving the in-package steels or by the uranium-metal). This assumption is conservative because it maximizes the oxygen diffusion rate and consequently the heat produced. The remaining assumptions are that oxygen behaves as an ideal gas in this system and that steady-state conditions apply. The oxygen flux is then given by:

$$J_{O_2} = -cD_{O_2}\frac{dX_{O_2}}{dz} \qquad \text{(Eq. 2.1.02.08.0A-1)}$$

Where J_{O2} is the oxygen flux, c is the molar density of an ideal gas at standard pressure and 50°C (37.712 mol/m^3) calculated from the ideal gas molar volume of 0.022414 m^3 mol^{-1} at standard temperature and pressure (Lide 2000 [DIRS 162229], P. 1-8), D_{O2} is the binary diffusion coefficient for O_2 in air (2.37×10^{-5} m^2 s^{-1}) (SNL 2008 [DIRS 177407], Section 6.6.2), X_{O2} is the mole fraction of O_2 in air (0.20946) (Weast 1984 [DIRS 106170], p. F-162), and z is the waste package wall thickness (0.0254 m) (SNL 2007 [DIRS 179394], Table 4-3). Assuming a steady state and integrating with respect to z yields:

$$J_{O_2} = -c\frac{D_{O_2}}{\Delta z}\ln\frac{1-X_{O_2 inside\ waste\ package}}{1-X_{O_2 in\ air}} \qquad \text{(Eq. 2.1.02.08.0A-2)}$$

The flux is then scaled to the total area of the SCCs in the waste package.

Disruptive seismic events may cause damage to the waste package outer shell that leads to stress corrosion cracking in the damaged areas. The total area of the stress corrosion cracking breaches in the outer shell following a bounding seismic event provides an upper bound estimate of the breach area that may be available for oxygen ingress. The damaged area on the OCB of the codisposal waste package is bounded by 0.792 m^2 for this screening analysis. The value of 0.792 m^2 corresponds to the mean damaged area on a codisposal waste package with a 23-mm-thick OCB and intact internals at the 4.07 m/s PGV level and the 90% RST (SNL 2007 [DIRS 176828], Table 6-18). The value of 0.792 m^2 (rounded up to 0.8 m^2 for the analyses in this FEP) is considered a reasonable upper bound because:

- The PGV level of 4.07 m/s corresponds to the lowest exceedance frequency, 10^{-8} per year that is considered in the seismic scenario class. Damaged areas are significantly smaller for the more frequent seismic events that are expected to occur during the 10,000-year period for FEP screening. For example, the mean damaged area is 0.120 m^2 for a seismic event at the 1.05 m/s PGV level (SNL 2007 [DIRS 176828], Table 6-18),

which corresponds to an exceedance frequency of about 10^{-5} per year on the bounded hazard curve (SNL 2007 [DIRS 176828], Table 6-3). This value, 0.120 m^2, is more than a factor of six below the bound of 0.8 m^2.

- The uncertainty in the RST for Alloy 22 is represented as a uniform distribution between 90% and 105% of the yield strength of Alloy 22. The 90% RST level is the lowest bound of the uniform distribution. Damaged areas are significantly smaller at the 100% and 105% RST levels. For example, the mean damaged areas are 0.006 m^2 and 0.0 m^2 at the 4.07 m/s PGV level for the 100% and 105% RST levels, respectively (SNL 2007 [DIRS 176828], Table 6-18). These values are more than two orders of magnitude less than the bound of 0.8 m^2.

- The 23-mm-thick OCB corresponds to a thickness reduction of 2.4 mm from the initial thickness of the OCB. The thickness reduction of 2.4 mm overestimates the general corrosion and hence the plastic deformation (i.e., the damaged area) of the OCB during the first 10,000 years after closure. For example, the median corrosion rate of Alloy 22 at 100°C is 30.8 nm per year, based on the median uncertainty level in the distributions for general corrosion rates of Alloy 22 (DTN: MO0612WPOUTERB.000 [DIRS 182035], file: *BaseCase GC CDFs2.xls*, worksheet: "Data," cell M71). The value of 100°C represents a reasonable average temperature for the first 10,000 years after repository closure. The median time for a thickness reduction of 2.4 mm is then estimated as $(2.4 \times 10^{-3}$ m)/$(30.8 \times 10^{-9}$ m/yr) = 77,000 years, which is well beyond the 10,000-year period for FEP screen analyses.

- Not all seismic events cause damage to the codisposal waste package with intact internals, as shown by the probabilities in *Seismic Consequence Abstraction* (SNL 2007 [DIRS 176828], Table 6-16). For example, the probability of damage is 0.559 for the 1.05 m/s PGV level at the 90% RST level. This probability goes to zero at the 100% and 105% RST levels.

Based on each of these factors, a damaged area of 0.8 m^2 for the codisposal waste package with intact internals provides a reasonable bound for the 10,000-year period for FEP screening. Assuming a bounding estimate of 1.31×10^{-2} for the SCC area density that could develop in the seismic damage region (SNL 2007 [DIRS 181953], Table 8-13), the breach surface area that would be available to admit oxygen into the waste package is about 1×10^{-2} m^2. Hence, a bounding estimate of the diffusive flux of oxygen is given by:

$$J_{O_2} = \frac{37.712 \frac{\text{mol}}{\text{m}^3} \cdot 2.37 \times 10^{-5} \frac{\text{m}^2}{\text{s}}}{0.0254\, m} \cdot \ln\left(\frac{1}{1 - 0.20946}\right) \cdot 1 \times 10^{-2} m^2 \cdot 3.156 \times 10^7 \frac{\text{s}}{\text{yr}} = 2610 \frac{\text{mol}}{\text{yr}}$$

(Eq. 2.1.02.08.0A-3)

If all of this oxygen is used to convert uranium metal to UO_2 for which the heat of formation is 1,085 kJ/mole uranium (Grenthe et al. 1992 [DIRS 101671], Table III.1), the corresponding heat generation rate is about 90 watts. This is calculated by converting the quantity of uranium-metal per MCO (3,804 kg uranium in the assembly baskets and 1,832 kg uranium in scrap baskets for

MCOs containing the maximum Mark IV fuel load with scrap basket, which was used because of initial exposed surfaces of uranium.) (Garvin 2002 [DIRS 169141], Table 4-4) to moles: (3,804 + 1,832) kg uranium × 1,000 g/kg ÷ 238 g uranium/mol = 23,689 moles uranium per MCO. Because there are two MCOs per waste package, there are 47,378 moles uranium metal per waste package. Therefore, the time required to complete the combustion of all the uranium metal in a waste package is approximately 18 years (47,378 moles uranium ÷ 2,610 moles O_2 per year) assuming the oxidation of one mole of uranium consumes one mole of O_2 to form UO_2. The corresponding heat generation is 2,610 moles/yr × 1,084.9 kJ/mol = 2.8×10^6 kJ/yr, which is equivalent to about 90 watts). This assumes that the pyrophoric reaction is self sustaining (i.e., that the heat energy is dissipated slowly enough from the reaction sites that the pyrophoric reaction continues and is limited only by the rate of oxygen supply). If it is assumed that U_3O_8 is the oxidation product (heat of formation on the basis of one uranium = 1,191.6 kJ/mol (Grenthe et al. 1992 [DIRS 101671], Section v.3.3.3.1)), then the oxidation of the fuel in the waste package occurs with a corresponding heat generation rate of approximately 74 watts.

As discussed above, the oxidation of the uranium metal fuel will not adversely affect radionuclide release because the TSPA model uses a bounding instantaneous degradation rate for DOE SNF other than naval SNF (BSC 2004 [DIRS 172453], Section 8.1). Because the heat output rate is small compared to the initial decay heat generation rates (SNL 2007 [DIRS 180472], Table 7-5[a]), the associated increase in the overall waste package temperature is expected to be small (see corroborating evidence below) and would therefore not lead to further degradation of the waste package outer shell that might increase the rate of oxygen ingress. Also, the small temperature increases involved are not expected to melt or otherwise degrade the codisposed glass waste.

Oxygen Ingress by Barometric Pumping: Barometric pressure fluctuations at the surface are transmitted to the repository horizon with some amplitude attenuation (BSC 2004 [DIRS 169734], Section 7.3.2). Pressure measurements made prior to excavation of the ESF indicated that the attenuated amplitude of the pressure fluctuations are less than 1% (BSC 2004 [DIRS 169734], Figure 7-27). For this analysis of oxygen ingress into a breached waste package due to barometric pressure fluctuations in the repository, it is conservatively assumed that the pressure fluctuations occur with a diurnal (twice daily) rhythm each involving a fluctuation of about 1%. Assuming that the pressures inside and outside the waste package are equilibrated in each of the twice-daily pressure fluctuations, the fractional rate at which the gasses in the void space of a breached waste are replaced by outside air is given by 1% × 2 per day = 2% per day. The void volume of the codisposal waste packages containing two MCOs packages is 7,400 liters (DTN: SN0702PAIPC1CA.001 [DIRS 180451], spreadsheet: *CDSP-2MCO Cell 1.xls*, sheet: "WP Cell 1 Moles & Surf Areas," cell: G11). Given that the mole fraction of oxygen in air is 0.20946 (Weast 1984 [DIRS 106170], p. F-162), the moles of oxygen ingress into a breached waste package as a result of barometric pumping can be calculated as: 7,400 liters × 0.02 × 365 days per year/22.4 liters per mole × 0.20946 (oxygen mole fraction in air) = 505 moles oxygen per year.

This is a relatively small rate of oxygen ingress compared to that calculated above for diffusion through SCCs. Hence, the effects of this source of oxygen ingress are small compared to those discussed above for oxygen ingress due to diffusion.

Oxygen Ingress by Flow Driven by Buoyancy Forces: The stress corrosion cracking that will lead to breaching of the waste package outer shell will develop over a period of time, which is expected to allow the initially slow rate of oxygen ingress to increase gradually as more through-wall SCCs develop. Hence, it is expected that any reactive uranium metal and uranium hydride will be stabilized as the SCCs are developing. However, it is instructive to examine the pyrophoric events that might ensue if all of the seismic-induced SCCs were to lead to through wall penetrations at one time.

An analysis of the quantitative response of the contents of a single MCO to hypothetical breaches and material/energy flow from the MCO (DOE 2004 [DIRS 173188]) provides corroborating evidence that pyrophoric events that are limited by the rate of oxygen ingress through large breaches (that may simulate buoyancy-driven flow through a large number of seismic-induced stress corrosion cracks) will not be highly energetic and will not lead to temperature increases in the waste package container that will cause the area of the container breaches to increase as the event unfolds. The analysis did not perform a mechanistic determination of the location, size, or quantity of hypothetical breaches in the MCO, but rather used a range of hole sizes arranged in a two-hole configuration to evaluate the response of the MCO. The two-hole configuration analyzed consisted of one lower and one upper hole in a vertically oriented MCO. This configuration maximizes the rate of air ingress by providing a chimney effect in which air flows in through the lower hole and out through the upper hole. Features of the MCO, basket internals, and the N Reactor SNF are modeled in the analysis. The Hanford interim storage safety basis data were used in the model, which represents the credible extremes of the characterization data. The reactive surface area (uranium metal and uranium hydride) was distributed to achieve the highest localized fuel temperatures. This configuration is similar to a match head, where the reactive surface area is concentrated at the tip of the fuel element. The objective was to determine if enough heat is generated by oxidation to heat the remaining bulk uranium (uranium unaffected by corrosion) in the fuel element to high enough temperatures that accelerated uranium oxidation would occur in the bulk uranium. More disperse distributions of the reactive surface area would lower peak temperatures, but increase the consumption of uranium metal over a greater period of event time. In the case of the two-hole breach, hole sizes of 0.75 inches and less show oxidation of only reactive material (uranium metal with reactive surface area and uranium hydride). Peak external MCO wall temperatures for the 0.75-inch two-hole breach are approximately 315°C (600°F), which is reached about 12 days after the event initiation and remains fairly constant until it drops rapidly with the extinction of the event after about 27 days (DOE 2004 [DIRS 173188], Figure A-20). The temperature of the bulk uranium in the fuel elements does not exceed the surface temperature where accelerated uranium oxidization would occur. Thus, if a more disperse distribution of the reactive surface area is present, the surface temperatures of the fuel elements would certainly not reach temperatures where accelerated oxidation would occur. There is no evidence of hydrogen accumulating in quantities permitting deflagration or detonation. These results demonstrate the event does not reach a highly energetic or an explosive state. Breaches with unequal sizes did not exacerbate the temperature response. The reaction is limited by flow through the smaller of the two holes regardless of whether the smaller hole was the lower or upper hole.

The results for two 0.75-inch holes are expected to overestimate the buoyancy-driven flow through SCCs because they allow more air inflow than the SCC breaches in the waste package even when the bounding estimates discussed above are used for SCC breaches following a

seismic event. The estimated brach area for a single SCC through the WPOB is 7.682 mm^2 (SNL 2008 [DIRS 177407], Section 6.6.2, Table 6.3-3). This corresponds to an equivalent radius of 0.156 cm or 0.061 inches. Because the gas inflow and outflow velocities are small (< 1 ft/s) the mass flow rates through the breach openings will scale approximately as the fourth power of the equivalent radius in accordance with Poiseuille's equation. Hence, an estimate of the number of SCCs needed to give the same mass flow rate as one 0.75-inch-diameter hole is:

$$((0.75/2)/0.061)^4 = 1{,}428$$

The SCC breach area of 1×10^{-2} m^2 discussed above for the waste package outer shell following a seismic event corresponds to about $1 \times 10^{-2} / 7.68 \times 10^{-6} = 1{,}302$ SCCs, which is less than the 1,428 number that would be equivalent to a 0.75-inch-diameter hole and much less than the 2,856 number that would be equivalent to two 0.75-inch holes.

Therefore, the uranium metal fuel meets the pyrophoricity acceptance requirements applicable to waste form postclosure performance (DOE 2007 [DIRS 169992], Section 4.2.5).

Based on the previous discussion, omission of FEP 2.1.02.08.0A (Pyrophoricity from DSNF) will not result in a significant adverse change in the magnitude or timing of either radiological exposures to the RMEI or radionuclide releases to the accessible environment. Therefore, this FEP is excluded from the performance assessments conducted to demonstrate compliance with proposed 10 CFR 63.311 and 63.321 (70 FR 53313 [DIRS 178394]), and with 10 CFR 63.331 [DIRS 180319], on the basis of low consequence.

INPUTS:

Table 2.1.02.08.0A-1. Direct Inputs

Input	Source	Description
ASM International 1990. *Properties and Selection: Irons, Steels, and High-Performance Alloys*. [DIRS 106780]	p. 871	The heat capacity of austenitic steel is 0.5 J/g C
BSC 2004. *DSNF and Other Waste Form Degradation Abstraction*. [DIRS 172453]	Sections 6.2, 8.1	Oxidation of the uranium metal fuel in the MCOs will not affect radionuclide release because a bounding instantaneous radionuclide release rate model is used for DSNF
DOE 2004. *GOTH_SNF MCO Chemical Reactivity Final Analysis*. [DIRS 173188]	Entire, Figure A-20	MCOs are dried and filled with helium. External MCO peak wall temperature and event duration for a two 0.75-inch hole configuration
DOE 2007. *Waste Acceptance System Requirements Document*. [DIRS 169992]	Section 4.2.5	Pyrophoricity acceptance requirements applicable to waste form postclosure performance
DTN: MO0612WPOUTERB.000. Output from General and Localized Corrosion of Waste Package Outer Barrier Report. [DIRS 182035]	file: *BaseCase GC CDFs2.xls*, worksheet: "Data," cell: M71	The median corrosion rate of Alloy 22 at 100°C is 30.8 nm/yr, based on the medium uncertainty level in the distributions for general corrosion rates of Alloy 22

Table 2.1.02.08.0A-1. Direct Inputs (Continued)

Input	Source	Description
DTN: SN0702PAIPC1CA.001. In-Package Chemistry Calculations and Abstractions. [DIRS 180451]	file: *CDSP-2MCO Cell 1.xls*, worksheet: "WP Cell 1 Moles & Surf Areas," cell: G11	The void volume of the co-disposal waste packages containing two MCOs packages is 7,400 liters
Garvin 2002. *Multi-Canister Overpack Topical Report*. [DIRS 169141]	Table 4-4	The estimated acceptable amount of water in a sealed MCO is 4.64 kg (bound in particulate), with less than 200 g being present as free water
	Section 4.1.3.2	MCOs will be dried and filled with helium
	Table 4-4	1.1×10^7 g uranium metal per waste package, assuming that the waste package contains two MCOs and each MCO contains Mark IV fuel (3,804 kg U) and scrap (1,832 kg U) for a total of 5,636 kg U
Grenthe et al. 1992. *Chemical Thermodynamics of Uranium*. [DIRS 101671]	Table III.1 and Sections v.3.3.3.1 and v.1.1	Heats of formation of UO_2 and U_3O_8. Specific heat capacity of uranium metal
Lide 2000. *CRC Handbook of Chemistry and Physics*. [DIRS 162229]	p. 1-8	Molar volume of an ideal gas at standard temperature and pressure
SNL 2007. *Seismic Consequence Abstraction*. [DIRS 176828]	Table 6-18	Estimates of the conditional damaged areas for the 23-mm-thick OCB with intact internals
	Table 6-3	1.05 m/s corresponds to an exceedance frequency of 10^{-5} per year on the bounded hazard curve
SNL 2008. *EBS Radionuclide Transport Abstraction*. [DIRS 177407]	Section 6.6.2	Approach for calculating diffusive mass transport rate of gasses through stress corrosion cracks in the waste package outer barrier. Number of stress corrosion cracks and the associated diffusion area. Including molar density of ideal gas (37.712 mol/m^3), and diffusion coefficient for O_2 in air (2.37×10^{-5} m^2/s)
SNL 2007. *Stress Corrosion Cracking of Waste Package Outer Barrier and Drip Shield Materials*. [DIRS 181953]	Table 8-13	Bounding estimate of the stress corrosion cracking area density following a seismic event
SNL 2007. *Total System Performance Assessment Data Input Package for Requirements Analysis for DOE SNF/HLW and Navy SNF Waste Package Overpack Physical Attributes Basis for Performance Assessment*. [DIRS 179567]	Table 4-10	Mass of steel per waste package (unloaded)
SNL 2007. *Total System Performance Assessment Data Input Package for Requirements Analysis for TAD Canister and Related Waste Package Overpack Physical Attributes Basis for Performance Assessment*. [DIRS 179394]	Table 4-3	Waste package outer barrier wall thickness
SNL 2008. *Screening Analysis of Criticality Features, Events, and Processes for License Application*. [DIRS 173869]	Appendix I	Waste package is dried and filled with helium
Weast 1984. *CRC Handbook of Chemistry and Physics*. [DIRS 106170]	p. F-162	Mole fraction of oxygen in air

Table 2.1.02.08.0A-2. Indirect Inputs

Citation	Title	DIRS
10 CFR 63	Energy: Disposal of High-Level Radioactive Wastes in a Geologic Repository at Yucca Mountain, Nevada	180319
70 FR 53313	Implementation of a Dose Standard After 10,000 Years	178394
Abrefah et al. 1995	*K-Basin Spent Nuclear Fuel Characterization Data Report*	151125
Abrefah et al. 1999	*Analysis of Ignition Testing on K-West Basin Fuel*	151226
ASTM C 1454-00	*Standard Guide for Pyrophoricity/Combustibility Testing in Support of Pyrophoricity Analyses of Metallic Uranium Spent Nuclear Fuel*	152779
BSC 2004	*Yucca Mountain Site Description*	169734
DOE 2000	*DOE Spent Nuclear Fuel Grouping in Support of Criticality, DBE, TSPA-LA*	118968
DOE 2002	*DOE Spent Nuclear Fuel Information in Support of TSPA-SR*	158405
DOE-HDBK-1081-94	*Primer on Spontaneous Heating and Pyrophoricity*	103327
Garvin 2002	*Multi-Canister Overpack Topical Report*	169141
Grenthe et al. 1992	*Chemical Thermodynamics of Uranium. Volume 1 of Chemical Thermodynamics*	101671
Haschke 1998	"Corrosion of Uranium in Air and Water Vapor: Consequences for Environmental Dispersal"	174075
Marschman et al. 1997	*Metallographic Examination of Damaged N Reactor Spent Nuclear Fuel Element SFEC5,4378*	149429
Reilly 1998	*Spent Nuclear Fuel Project Technical Databook*	149433
Schulz 1972	*Shear-Leach Processing of N-Reactor Fuel--Cladding Fires*	159406
SNL 2007	*Seismic Consequence Abstraction*	176828
SNL 2007	*Initial Radionuclides Inventory*	180472
SNL 2008	*Multiscale Thermohydrologic Model*	184433

FEP: 2.1.02.09.0A

FEP NAME:

Chemical Effects of Void Space in Waste Package

FEP DESCRIPTION:

If waste packages and/or DSNF canisters are not completely filled, then the unfilled inert gas or air-filled volume could influence water-chemistry calculations.

SCREENING DECISION:

Included

TSPA DISPOSITION:

This FEP evaluates the effects of the unfilled void space in the waste packages on in-package chemistry. Radionuclide accumulation in the gap between the waste form and cladding is addressed in included FEP 2.1.02.07.0A (Radionuclide Release from Gap and Grain Boundaries). The model for in-package chemistry is composed of two conceptual models, the vapor influx model and the liquid influx model (SNL 2007 [DIRS 180506], Section 6.3[a]). The vapor influx model addresses the situation in which water vapor enters the breached waste package and condenses. The liquid influx model addresses the situation in which liquid water seeps or drips into the breached waste package. These models differ from each other in the chemistry of the water to which the waste forms are exposed in a breached waste package. In evaluating the in-package water chemistry, the entire initial void volume in the waste package (derived from SNL 2007 [DIRS 179394], Table 4-1, Parameter Number 03-01; SNL 2007 [DIRS 179567], Table 4-1, Parameter Number 04-07), is taken to be filled with liquid and gas and includes any void volume in a canister and any void volume in the waste form. The in-package chemistry model, thus accounts for the unfilled void space in the waste package and its impact on the in-package chemistry. The inert gas (helium) is not expected to persist long after breach. Therefore, it is not expected to react materially with in-package fluids.

In the conceptual model, the void spaces within a waste package are filled by liquid water in equilibrium with atmospheric gases. This has the effect of putting the gas phase in close contact with the liquid and solid phase reactants in the system (SNL 2007 [DIRS 180506], Section 6.3.1[a]). Sensitivity studies were conducted that varied the ratio of water to reactants, which is equivalent to varying the ratio of water to air (SNL 2007 [DIRS 180506], Section 6.6.1[a]), and that varied the composition of the air in contact with the water (SNL 2007 [DIRS 180506], Section 6.6.4[a]). The effect of water–air ratio was not included in the abstraction because it is negligible compared to other uncertainties that were incorporated into the abstraction (SNL 2007 [DIRS 180506], Section 6.6.1[a]). The sensitivity of the composition of the air was included in the abstractions for pH and total carbonate by incorporating the functionality of CO_2 fugacity and relative humidity. Therefore, the chemical composition of the void space was investigated and incorporated into the model.

INPUTS:

Table 2.1.02.09.0A-1. Indirect Inputs

Citation	Title	DIRS
SNL 2007	*In-Package Chemistry Abstraction*	180506
SNL 2007	*Total System Performance Assessment Data Input Package for Requirements Analysis for DOE SNF/HLW and Naval SNF Waste Package Physical Attributes Basis for Performance Assessment*	179567
SNL 2007	*Total System Performance Assessment Data Input Package for Requirements Analysis for TAD Canister and Related Waste Package Overpack Physical Attributes Basis for Performance Assessment*	179394

FEP: 2.1.02.10.0A

FEP NAME:

Organic/Cellulosic Materials in Waste

FEP DESCRIPTION:

Degradation of cellulose in the waste could affect the long-term performance of the disposal system.

SCREENING DECISION:

Excluded – low consequence

SCREENING JUSTIFICATION:

The waste materials (i.e., commercial SNF, DOE SNF, and HLW glass) are not expected to contain organic/cellulosic materials other than trace amounts that might be included in the sealed canisters. Control and specification of technical information needs on the organic content of sealed waste form canisters (DOE 2007 [DIRS 169992], Sections 4.2.6, 5.4.1B(4), and 5.4.3.C) and waste form and TAD canister design parameters (SNL 2007 [DIRS 179394], Table 4-1) will be used to confirm consistency between the contents of the waste form canisters emplaced in the repository and the technical basis for the TSPA. The TSPA includes the expectation that organic materials, other than trace amounts, will not be included in the sealed waste form canisters.

The important factors that will influence the degradation of commercial SNF, DOE SNF, and HLW in the repository are addressed in Section 6 of the modeling reports for each of these waste forms (BSC 2004 [DIRS 169987]; BSC 2004 [DIRS 172453]; BSC 2004 [DIRS 169988]) and are included in the corresponding FEPs (2.1.02.02.0A (CSNF Degradation (Alteration, Dissolution, and Radionuclide Release)), 2.1.02.01.0A (DSNF Degradation (Alteration, Dissolution, and Radionuclide Release)), and 2.1.02.03.0A (HLW Glass Degradation (Alteration, Dissolution, and Radionuclide Release)). As documented in Section 6 of the reports cited above, the important waste form degradation processes are oxidation and dissolution of the commercial SNF and DOE SNF matrices and hydrolysis and dissolution of the HLW glass matrix. The effects of trace organic/cellulosic materials are relatively unimportant compared to these processes. The anticipated low activity of microbes (excluded FEP 2.1.10.01.0A (Microbial Activity in EBS)) indicates that significant conversion of organic/cellulosic materials to degradation-enhancing organic acids will not occur. Therefore, inclusion of trace amounts of organic/cellulosic materials in the waste is not expected to affect the waste form degradation.

The important factors that influence the dissolved concentrations of elements with radioactive isotopes and waste form and in-drift colloid concentrations are addressed in *Dissolved Concentration Limits of Elements with Radioactive Isotopes* (SNL 2007 [DIRS 177418], Section 6.4.1) and *Waste Form and In-Drift Colloids-Associated Radionuclide Concentrations: Abstraction and Summary* (SNL 2007 [DIRS 177423], Sections 6.3.1 and 6.3.13) and included FEPs 2.1.09.04.0A (Radionuclide Solubility, Solubility Limits, and Speciation in the Waste Form and EBS) and 2.1.09.16.0A (Formation of Pseudo-Colloids (Natural) in EBS). The effects

of trace amounts of organic/cellulosic materials on the dissolved and colloid concentrations are expected to be relatively unimportant compared to the effects of the factors that are included. Potential effects of organic materials on dissolved concentrations are also addressed in excluded FEP 2.1.09.13.0A (Complexation in EBS).

In summary, the emplaced waste is expected to contain only trace amounts of organic/cellulosic materials that will not affect the degradation of the waste forms or the dissolved and colloid concentrations of elements with radioactive isotopes.

Based on the previous discussion, omission of FEP 2.1.02.10.0A (Organic/Cellulosic Materials in Waste) will not result in a significant adverse change in the magnitude or timing of either radiological exposure to the RMEI or radionuclide releases to the accessible environment. Therefore, this FEP is excluded from the performance assessments conducted to demonstrate compliance with proposed 10 CFR 63.311 and 63.321 (70 FR 53313 [DIRS 178394]), and with 10 CFR 63.331 [DIRS 180319], on the basis of low consequence.

INPUTS:

Table 2.1.02.10.0A-1. Direct Inputs

Input	Source	Description
DOE 2007. *Waste Acceptance System Requirements Document*. [DIRS 169992]	Sections 4.2.6, 5.4.1B(4), 5.4.3.C	Provides specification of technical information needs on the organic content of sealed waste form canisters
SNL 2007. *Total System Performance Assessment Data Input Package for Requirements Analysis for TAD Canister and Related Waste Package Overpack Physical Attributes Basis for Performance Assessment*. [DIRS 179394]	Table 4-1	Waste form and TAD canister design parameters

Table 2.1.02.10.0A-2. Indirect Inputs

Citation	Title	DIRS
10 CFR 63	Energy: Disposal of High-Level Radioactive Wastes in a Geologic Repository at Yucca Mountain, Nevada	180319
70 FR 53313	Implementation of a Dose Standard After 10,000 Years	178394
BSC 2004	*DSNF and Other Waste Form Degradation Abstraction*	172453
BSC 2004	*CSNF Waste Form Degradation: Summary Abstraction*	169987
BSC 2004	*Defense HLW Glass Degradation Model*	169988
SNL 2007	*Dissolved Concentration Limits of Elements with Radioactive Isotopes*	177418
SNL 2007	*Waste Form and In-Drift Colloids-Associated Radionuclide Concentrations: Abstraction and Summary*	177423

FEP: 2.1.02.11.0A

FEP NAME:

Degradation of Cladding from Waterlogged Rods

FEP DESCRIPTION:

Failed fuel rods (attributed to breaches caused by manufacturing defects and reactor operations) comprise a small fraction of the fuel rods that are currently being stored in commercial reactor spent fuel pools. Failed fuel contains water in the fuel rod void space that may promote degradation of the spent fuel cladding. Such fuel is referred to as "waterlogged." The moisture remaining in a "dried" fuel rod is used to determine the extent of degradation of spent fuel cladding.

SCREENING DECISION:

Excluded – low consequence

SCREENING JUSTIFICATION:

For the performance assessments conducted to demonstrate compliance with proposed 10 CFR 63.311, 10 CFR 63.321 (70 FR 53313 [DIRS 178394]), and with 10 CFR 63.331 [DIRS 180319], it is considered that all commercial SNF cladding (stainless steel and Zircaloy) is breached on emplacement in the repository as discussed in included FEP 2.1.02.12.0A (Degradation of Cladding Prior to Disposal) and in *Cladding Degradation Summary for LA* (SNL 2007 [DIRS 180616], Section 6.2.1.2[a]). Furthermore, the zirconium-based (Zircaloy) and stainless steel SNF cladding is assumed to split instantly along the length of the fuel rods at the time of waste package failure. Cladding unzipping is assumed to result in immediate exposure of the commercial SNF fuel matrix to the failed waste package environment (included FEP 2.1.02.23.0A (Cladding Unzipping)). A waste package is considered to be failed at the time of the first penetration of the waste package by any process, including cracking, that allows ingress of oxygen and water vapour into the package.

Degradation of DOE SNF cladding (other than naval SNF cladding) is discussed in excluded FEP 2.1.02.25.0A (DSNF Cladding). As described in that FEP, DOE SNF cladding (with the exception of naval SNF cladding) is considered to be breached upon emplacement in the repository and will neither inhibit groundwater contacting the DOE SNF matrix nor the release of radionuclides from the DOE SNF after groundwater contact.

Using this approach, commercial SNF and DOE SNF (other than naval SNF) cladding does not prevent the release or substantially reduce the release rate of radionuclides from the waste. Based on the above discussion, even if further degradation of cladding in waterlogged rods were to occur, omission of FEP 2.1.02.11.0A (Degradation of Cladding from Waterlogged Rods) will not result in a significant adverse change in the magnitude or time of radiological exposure to the RMEI or radionuclide releases to the accessible environment. Therefore, this FEP is excluded from the performance assessments conducted to demonstrate compliance with proposed

10 CFR 63.311 and 63.321 (70 FR 53313 [DIRS 178394]), and with 10 CFR 63.331 [DIRS 180319], on the basis of low consequence.

Naval SNF cladding is discussed in included FEP 2.1.02.25.0B (Naval SNF Cladding).

INPUTS:

Table 2.1.02.11.0A-1. Direct Inputs

Input	Source	Description
SNL 2007. *Cladding Degradation Summary for LA*. [DIRS 180616]	Section 6.2.1.2[a]	Conservative assumption that all commercial SNF cladding (stainless steel and Zircaloy) is breached on receipt at the repository

Table 2.1.02.11.0A-2. Indirect Inputs

Citation	Title	DIRS
10 CFR 63	Energy: Disposal of High-Level Radioactive Wastes in a Geologic Repository at Yucca Mountain, Nevada	180319
70 FR 53313	Implementation of a Dose Standard After 10,000 Years	178394

FEP: 2.1.02.12.0A

FEP NAME:

Degradation of Cladding Prior to Disposal

FEP DESCRIPTION:

Certain aspects of cladding degradation may occur before the spent fuel arrives at Yucca Mountain. Possible mechanisms include rod cladding degradation during reactor operation, degradation during wet spent fuel pool storage, degradation during dry storage, and rod degradation during shipping (i.e., from creep and from vibration and impact) and fuel handling.

SCREENING DECISION:

Included

TSPA DISPOSITION:

Cladding degradation prior to receipt at the repository can occur during reactor operation, SNF pool storage, dry storage, transport, and handling. The condition of DOE SNF and commercial SNF cladding at the time of emplacement in the repository is discussed in the following paragraphs.

A significant but unquantified fraction of the N Reactor fuel, which constitutes about 85% of the MTHM of DOE SNF (BSC 2004 [DIRS 172453], Section 6.1.7), will have damaged cladding at the time of emplacement in disposal canisters (Abrefah et al. 1995 [DIRS 151125]). There has been insufficient characterization of the condition of the DSNF cladding to establish its initial condition and the effectiveness of the cladding as a barrier to radionuclide transport. For the purposes of TSPA it is considered that all DOE SNF cladding (with the exception of naval SNF cladding) is breached at the time of its arrival to the repository and will neither inhibit groundwater contacting the DOE SNF matrix nor the release of radionuclides from the DOE SNF after groundwater contact. DOE SNF cladding itself is further discussed in excluded FEP 2.1.02.25.0A (DSNF Cladding). Naval SNF cladding is discussed in included FEP 2.1.02.25.0B (Naval SNF Cladding).

The amount of initial "out of reactor" commercial SNF cladding damage is expected to be low, as documented in *Cladding Degradation Summary for LA* (SNL 2007 [DIRS 180616]), which is based on utility data collected from multiple sources. However, a decision has been made not to take cladding credit for the TSPA (SNL 2007 [DIRS 180616], Section 6.2.1.2[a]). For the purposes of TSPA it is considered that all commercial SNF cladding is breached at the time of its arrival at the repository and will neither inhibit groundwater contacting the commercial SNF fuel matrix nor the release of radionuclides from the commercial SNF after groundwater contact (SNL 2008 [DIRS 183478], Section 6.3.7.3).

INPUTS:

Table 2.1.02.12.0A-1. Direct Inputs

Input	Source	Description
SNL 2007. *Cladding Degradation Summary for LA*. [DIRS 180616]	Section 6.2.1.2[a]	Decision made not to take cladding credit for the compliance case

Table 2.1.02.12.0A-2. Indirect Inputs

Citation	Title	DIRS
Abrefah et al. 1995	*K-Basin Spent Nuclear Fuel Characterization Data Report*	151125
BSC 2004	*DSNF and Other Waste Form Degradation Abstraction*	172453
SNL 2007	*Cladding Degradation Summary for LA*	180616
SNL 2008	*Total System Performance Assessment Model/Analysis for the License Application*	183478

FEP: 2.1.02.13.0A

FEP NAME:

General Corrosion of Cladding

FEP DESCRIPTION:

General corrosion of cladding could expose large areas of fuel and produce hydrides.

SCREENING DECISION:

Excluded – low consequence

SCREENING JUSTIFICATION:

For the performance assessments conducted to demonstrate compliance with proposed 10 CFR 63.311, 10 CFR 63.321 (70 FR 53313 [DIRS 178394]), and with 10 CFR 63.331 [DIRS 180319], it is considered that all commercial SNF cladding (stainless steel and Zircaloy) is breached on emplacement in the repository as discussed in included FEP 2.1.02.12.0A (Degradation of Cladding Prior to Disposal) and in *Cladding Degradation Summary for LA* (SNL 2007 [DIRS 180616], Section 6.2.1.2[a]). Furthermore, the zirconium-based (Zircaloy) and stainless steel SNF cladding is assumed to split instantly along the length of the fuel rods at the time of waste package failure. Cladding unzipping is assumed to result in immediate exposure of the commercial SNF fuel matrix to the failed waste package environment (included FEP 2.1.02.23.0A (Cladding Unzipping)). A waste package is considered to be failed at the time of the first penetration of the waste package by any process, including cracking, that allows ingress of oxygen and water vapor into the package.

Degradation of DOE SNF cladding (other than naval SNF cladding) is discussed in excluded FEP 2.1.02.25.0A (DSNF Cladding). As described in that FEP, DOE SNF cladding (with the exception of naval SNF cladding) is considered to be breached upon emplacement in the repository and will neither inhibit groundwater contacting the DOE SNF matrix nor the release of radionuclides from the DOE SNF after groundwater contact.

Using this approach, commercial SNF and DOE SNF (other than naval SNF) cladding does not prevent the release or substantially reduce the release rate of radionuclides from the waste. Based on the above discussion, omission of FEP 2.1.02.13.0A (General Corrosion of Cladding) will not result in a significant adverse change in the magnitude or time of radiological exposureso to the RMEI or radionuclide releases to the accessible environment. Therefore, this FEP is excluded from the performance assessments conducted to demonstrate compliance with proposed 10 CFR 63.311 and 63.321 (70 FR 53313 [DIRS 178394]), and with 10 CFR 63.331 [DIRS 180319], on the basis of low consequence.

Naval SNF cladding is discussed in included FEP 2.1.02.25.0B (Naval SNF Cladding).

INPUTS:

Table 2.1.02.13.0A-1. Direct Inputs

Input	Source	Description
SNL 2007. *Cladding Degradation Summary for LA*. [DIRS 180616]	Section 6.2.1.2[a]	Conservative assumption that all commercial SNF cladding (stainless steel and Zircaloy) is breached on receipt at the repository

Table 2.1.02.13.0A-2. Indirect Inputs

Citation	Title	DIRS
10 CFR 63	Energy: Disposal of High-Level Radioactive Wastes in a Geologic Repository at Yucca Mountain, Nevada	180319
70 FR 53313	Implementation of a Dose Standard After 10,000 Years	178394

FEP: 2.1.02.14.0A

FEP NAME:

Microbially Influenced Corrosion (MIC) of Cladding

FEP DESCRIPTION:

Microbially influenced corrosion (MIC) of cladding is a potential localized corrosion mechanism where microbes produce a local acidic environment that could produce multiple penetrations through the fuel cladding.

SCREENING DECISION:

Excluded – low consequence

SCREENING JUSTIFICATION:

For the performance assessments conducted to demonstrate compliance with proposed 10 CFR 63.311, 10 CFR 63.321 (70 FR 53313 [DIRS 178394]), and with 10 CFR 63.331 [DIRS 180319], it is considered that all commercial SNF cladding (stainless steel and Zircaloy) is breached on emplacement in the repository as discussed in included FEP 2.1.02.12.0A (Degradation of Cladding Prior to Disposal) and in *Cladding Degradation Summary for LA* (SNL 2007 [DIRS 180616], Section 6.2.1.2[a]). Furthermore, the zirconium-based (Zircaloy) and stainless steel SNF cladding is assumed to split instantly along the length of the fuel rods at the time of waste package failure. Cladding unzipping is assumed to result in immediate exposure of the commercial SNF fuel matrix to the failed waste package environment (included FEP 2.1.02.23.0A (Cladding Unzipping)). A waste package is considered to be failed at the time of the first penetration of the waste package by any process, including cracking, that allows ingress of oxygen and water vapor into the package.

Degradation of DOE SNF cladding (other than naval SNF cladding) is discussed in excluded FEP 2.1.02.25.0A (DSNF Cladding). As described in that FEP, the TSPA model consideres that the DOE SNF cladding (with the exception of naval SNF cladding) will be breached upon emplacement in the repository and will neither inhibit groundwater contacting the DOE SNF matrix nor the release of radionuclides from the DOE SNF after groundwater contact.

Using this approach, commercial SNF and DOE SNF (other than naval SNF) cladding does not prevent the release or substantially reduce the release rate of radionuclides from the waste. Based on the above discussion, omission of FEP 2.1.02.14.0A (Microbially Influenced Corrosion (MIC) of Cladding) will not result in significant adverse change in the magnitude or time of radiological exposures to the RMEI or radionuclide releases to the accessible environment. Therefore, this FEP is excluded from the performance assessments conducted to demonstrate compliance with proposed 10 CFR 63.311 and 63.321 (70 FR 53313 [DIRS 178394]), and with 10 CFR 63.331 [DIRS 180319], on the basis of low consequence.

Naval SNF cladding is discussed in included FEP 2.1.02.25.0B (Naval SNF Cladding).

INPUTS:

Table 2.1.02.14.0A-1. Direct Inputs

Input	Source	Description
SNL 2007. *Cladding Degradation Summary for LA*. [DIRS 180616]	Section 6.2.1.2[a]	Conservative assumption that all commercial SNF cladding (stainless steel and Zircaloy) is breached on receipt at the repository

Table 2.1.02.14.0A-2. Indirect Inputs

Citation	Title	DIRS
10 CFR 63	Energy: Disposal of High-Level Radioactive Wastes in a Geologic Repository at Yucca Mountain, Nevada	180319
70 FR 53313	Implementation of a Dose Standard After 10,000 Years	178394

FEP: 2.1.02.15.0A

FEP NAME:

Localized (Radiolysis Enhanced) Corrosion of Cladding

FEP DESCRIPTION:

Radiolysis in a nitrogen/oxygen gas mixture with the presence of water film results in the formation of nitric acid (HNO_3). Hydrogen peroxide (H_2O_2) is formed in the water from radiolysis. These chemicals can enhance corrosion of the fuel cladding.

SCREENING DECISION:

Excluded – low consequence

SCREENING JUSTIFICATION:

For the performance assessments conducted to demonstrate compliance with proposed 10 CFR 63.311, 10 CFR 63.321(70 FR 53313 [DIRS 178394]), and with 10 CFR 63.331 [DIRS 180319], it is considered that all commercial SNF cladding (stainless steel and Zircaloy) is breached on emplacement in the repository as discussed in included FEP 2.1.02.12.0A (Degradation of Cladding Prior to Disposal) and in *Cladding Degradation Summary for LA* (SNL 2007 [DIRS 180616], Section 6.2.1.2[a]). Furthermore, the zirconium-based (Zircaloy) and stainless steel SNF cladding is assumed to split instantly along the length of the fuel rods at the time of waste package failure. Cladding unzipping is assumed to result in immediate exposure of the commercial SNF fuel matrix to the failed waste package environment (included FEP 2.1.02.23.0A (Cladding Unzipping)). A waste package is considered to be failed at the time of the first penetration of the waste package by any process, including cracking, that allows ingress of oxygen and water vapor into the package.

Degradation of DOE SNF cladding (other than naval SNF cladding) is discussed in excluded FEP 2.1.02.25.0A (DSNF Cladding). As described in that FEP, the TSPA model considers the DOE SNF cladding (with the exception of naval SNF cladding) will be breached upon emplacement in the repository and will neither inhibit groundwater contacting the DOE SNF matrix nor the release of radionuclides from the DOE SNF after groundwater contact.

Using this approach, commercial SNF and DOE SNF (other than naval SNF) cladding does not prevent the release or substantially reduce the release rate of radionuclides from the waste. Based on the above discussion, omission of FEP 2.1.02.15.0A (Localized (Radiolysis Enhanced) Corrosion of Cladding) will not result in a significant adverse change in the magnitude or time of radiological exposures to the RMEI or radionuclide releases to the accessible environment. Therefore, this FEP is excluded from the performance assessments conducted to demonstrate compliance with proposed 10 CFR 63.311 and 63.231 (70 FR 53313 [DIRS 178394]), and with 10 CFR 63.331 [DIRS 180319], on the basis of low consequence.

Naval SNF cladding is discussed in included FEP 2.1.02.25.0B (Naval SNF Cladding).

INPUTS:

Table 2.1.02.15.0A-1. Direct Inputs

Input	Source	Description
SNL 2007. *Cladding Degradation Summary for LA*. [DIRS 180616]	Section 6.2.1.2[a]	Assumption that all commercial SNF cladding (stainless steel and Zircaloy) is breached on emplacement in the repository

Table 2.1.02.15.0A-2. Indirect Inputs

Citation	Title	DIRS
10 CFR 63	Energy: Disposal of High-Level Radioactive Wastes in a Geologic Repository at Yucca Mountain, Nevada	180319
70 FR 53313	Implementation of a Dose Standard After 10,000 Years	178394

FEP: 2.1.02.16.0A

FEP NAME:

Localized (Pitting) Corrosion of Cladding

FEP DESCRIPTION:

Localized corrosion in pits could produce penetrations of cladding.

SCREENING DECISION:

Excluded – low consequence

SCREENING JUSTIFICATION:

For the performance assessments conducted to demonstrate compliance with proposed 10 CFR 63.311, 10 CFR 63.321 (70 FR 53313 [DIRS 178394]), and with 10 CFR 63.331 [DIRS 180319], it is considered that all commercial SNF cladding (stainless steel and Zircaloy) is breached on emplacement in the repository as discussed in included FEP 2.1.02.12.0A (Degradation of Cladding Prior to Disposal) and in *Cladding Degradation Summary for LA* (SNL 2007 [DIRS 180616], Section 6.2.1.2[a]). Furthermore, the zirconium-based (Zircaloy) and stainless steel SNF cladding is assumed to split instantly along the length of the fuel rods at the time of waste package failure. Cladding unzipping is assumed to result in immediate exposure of the commercial SNF fuel matrix to the failed waste package environment (included FEP 2.1.02.23.0A (Cladding Unzipping)). A waste package is considered to be failed at the time of the first penetration of the waste package by any process, including cracking, that allows ingress of oxygen and water vapor into the package.

Degradation of DOE SNF cladding (other than naval SNF cladding) is discussed in excluded FEP 2.1.02.25.0A (DSNF Cladding). As described in that FEP, the TSPA model considers that the DOE SNF cladding (with the exception of naval SNF cladding) will be breached upon emplacement in the repository and will neither inhibit groundwater contacting the DOE SNF matrix nor the release of radionuclides from the DOE SNF after groundwater contact.

Using this approach, commercial SNF and DOE SNF (other than naval SNF) cladding does not prevent the release or substantially reduce the release rate of radionuclides from the waste. Based on the above discussion, omission of FEP 2.1.02.16.0A (Localized (Pitting) Corrosion of Cladding) will not result in a significant adverse change in the magnitude or time of radiological exposures to the RMEI or radionuclide releases to the accessible environment. Therefore, this FEP is excluded from the performance assessments conducted to demonstrate compliance with proposed 10 CFR 63.311 and 63.321 (70 FR 53313 [DIRS 178394]), and with 10 CFR 63.331 [DIRS 180319], on the basis of low consequence.

Naval SNF cladding is discussed in included FEP 2.1.02.25.0B (Naval SNF Cladding).

INPUTS:

Table 2.1.02.16.0A-1. Direct Inputs

Input	Source	Description
SNL 2007. *Cladding Degradation Summary for LA*. [DIRS 180616]	Section 6.2.1.2[a]	Conservative assumption that all commercial SNF cladding (stainless steel and Zircaloy) is breached on receipt at the repository

Table 2.1.02.16.0A-2. Indirect Inputs

Citation	Title	DIRS
10 CFR 63	Energy: Disposal of High-Level Radioactive Wastes in a Geologic Repository at Yucca Mountain, Nevada	180319
70 FR 53313	Implementation of a Dose Standard After 10,000 Years	178394

FEP: 2.1.02.17.0A

FEP NAME:

Localized (Crevice) Corrosion of Cladding

FEP DESCRIPTION:

Localized corrosion in crevices could produce penetrations of cladding.

SCREENING DECISION:

Excluded – low consequence

SCREENING JUSTIFICATION:

For the performance assessments conducted to demonstrate compliance with proposed 10 CFR 63.311, 10 CFR 63.321 (70 FR 53313 [DIRS 178394]), and 10 CFR 63.331 [DIRS 180319], it is considered that all commercial SNF cladding (stainless steel and Zircaloy) is breached on emplacement in the repository as discussed in included FEP 2.1.02.12.0A (Degradation of Cladding Prior to Disposal) and in *Cladding Degradation Summary for LA* (SNL 2007 [DIRS 180616], Section 6.2.1.2[a]). Furthermore, the zirconium-based (Zircaloy) and stainless steel SNF cladding is assumed to split instantly along the length of the fuel rods at the time of waste package failure. Cladding unzipping is assumed to result in immediate exposure of the commercial SNF fuel matrix to the failed waste package environment (included FEP 2.1.02.23.0A (Cladding Unzipping)). A waste package is considered to be failed at the time of the first penetration of the waste package by any process, including cracking, that allows ingress of oxygen and water vapor into the package.

Degradation of DOE SNF cladding (other than naval SNF cladding) is discussed in excluded FEP 2.1.02.25.0A (DSNF Cladding). As described in that FEP, the TSPA model considers that the DOE SNF cladding (with the exception of naval SNF cladding) will be breached upon emplacement in the repository and will neither inhibit groundwater contacting the DOE SNF matrix nor the release of radionuclides from the DOE SNF after groundwater contact.

Using this approach, commercial SNF and DOE SNF (other than naval SNF) cladding does not prevent the release or substantially reduce the release rate of radionuclides from the waste. Therefore, even if localized (crevice) corrosion of cladding were to occur the additional impact of this FEP on cladding (other than naval SNF cladding) performance is of low consequence and will not affect the magnitude or timing of calculated radiological exposures to the RMEI or radionuclide releases to the accessible environment. Naval SNF cladding is discussed in included FEP 2.1.02.25.0B (Naval SNF Cladding).

Based on the previous discussion, omission of FEP 2.1.02.17.0A (Localized (Crevice) Corrosion of Cladding) will not result in a significant adverse change in the magnitude or timing of either radiological exposures to the RMEI or radionuclide releases to the accessible environment. Therefore, this FEP is excluded from the performance assessments conducted to demonstrate

compliance with proposed 10 CFR 63.311 and 63.321 (70 FR 53313 [DIRS 178394]), and with 10 CFR 63.331 [DIRS 180319], on the basis of low consequence.

INPUTS:

Table 2.1.02.17.0A-1. Direct Inputs

Input	Source	Description
SNL 2007. *Cladding Degradation Summary for LA*. [DIRS 180616]	Section 6.2.1.2[a]	Conservative assumption that all commercial SNF cladding (stainless steel and Zircaloy) is breached on receipt at the repository

Table 2.1.02.17.0A-2. Indirect Inputs

Citation	Title	DIRS
10 CFR 63	Energy: Disposal of High-Level Radioactive Wastes in a Geologic Repository at Yucca Mountain, Nevada	180319
70 FR 53313	Implementation of a Dose Standard After 10,000 Years	178394

FEP: 2.1.02.18.0A

FEP NAME:

Enhanced Corrosion of Cladding from Dissolved Silica

FEP DESCRIPTION:

High dissolved silica content of waters may enhance corrosion of cladding.

SCREENING DECISION:

Excluded – low consequence

SCREENING JUSTIFICATION:

For the performance assessments conducted to demonstrate compliance with proposed 10 CFR 63.311, 10 CFR 63.321 (70 FR 53313 [DIRS 178394]), and with 10 CFR 63.331 [DIRS 180319], it is considered that all commerical SNF cladding (stainless steel and Zircaloy) is breached on emplacement in the repository as discussed in included FEP 2.1.02.12.0A (Degradation of Cladding Prior to Disposal) and in *Cladding Degradation Summary for LA* (SNL 2007 [DIRS 180616], Section 6.2.1.2[a]). Furthermore, the zirconium-based (Zircaloy) and stainless steel SNF cladding is assumed to split instantly along the length of the fuel rods at the time of waste package failure. Cladding unzipping is assumed to result in immediate exposure of the commercial SNF fuel matrix to the failed waste package environment (included FEP 2.1.02.23.0A (Cladding Unzipping)). A waste package is considered to be failed at the time of the first penetration of the waste package by any process, including cracking, that allows ingress of oxygen and water vapor into the package.

Degradation of DOE SNF cladding (other than naval SNF cladding) is discussed in excluded FEP 2.1.02.25.0A (DSNF Cladding). As described in that FEP, the TSPA model considers that the DOE SNF cladding (with the exception of naval SNF cladding) will be breached upon emplacement in the repository and will neither inhibit groundwater contacting the DOE SNF matrix nor the release of radionuclides from the DOE SNF after groundwater contact.

Naval SNF cladding is discussed in included FEP 2.1.02.25.0B (Naval SNF Cladding).

Using this approach, commercial SNF and DOE SNF (other than naval SNF) cladding does not prevent the release or substantially reduce the release rate of radionuclides from the waste. Therefore, omission of FEP 2.1.02.18.0A (Enhanced Corrosion of Cladding from Dissolved Silica) will not result in a significant adverse change in the magnitude or timing of either radiological exposure to the RMEI or radionuclide releases to the accessible environment. Therefore, this FEP is excluded from the performance assessments conducted to demonstrate compliance with proposed 10 CFR 63.311 and 63.321 (70 FR 53313 [DIRS 178394]), and with 10 CFR 63.331 [DIRS 180319], on the basis of low consequence.

INPUTS:

Table 2.1.02.18.0A-1. Direct Inputs

Input	Source	Description
SNL 2007. *Cladding Degradation Summary for LA*. [DIRS 180616]	Section 6.1.1.2[a]	Conservative assumption that all commercial SNF cladding (stainless steel and Zircaloy) is breached on receipt at the repository

Table 2.1.02.18.0A-2. Indirect Inputs

Citation	Title	DIRS
10 CFR 63	Energy: Disposal of High-Level Radioactive Wastes in a Geologic Repository at Yucca Mountain, Nevada	180319
70 FR 53313	Implementation of a Dose Standard After 10,000 Years	178394

FEP: 2.1.02.19.0A

FEP NAME:

Creep Rupture of Cladding

FEP DESCRIPTION:

At high temperatures (>400°C) for sufficiently long time intervals, creep rupture of Zircaloy cladding on spent fuel can occur and produce small perforations in the cladding to relieve stress. After the waste package fails, the fuel can react with water and radionuclides can escape over time from the fuel rod.

SCREENING DECISION:

Excluded – low consequence

SCREENING JUSTIFICATION:

For the performance assessments conducted to demonstrate compliance with proposed 10 CFR 63.311, 10 CFR 63.321 (70 FR 53313 [DIRS 178394]), and with 10 CFR 63.331 [DIRS 180319], it is conservatively considered that all commercial SNF cladding (stainless steel and Zircaloy) is breached on emplacement in the repository as discussed in included FEP 2.1.02.12.0A (Degradation of Cladding Prior to Disposal) and in *Cladding Degradation Summary for LA* (SNL 2007 [DIRS 180616], Section 6.2.1.2[a]). Furthermore, the zirconium-based (Zircaloy) and stainless steel SNF cladding is assumed to split instantly along the length of the fuel rods at the time of waste package failure. Cladding unzipping is assumed to result in immediate exposure of the commercial SNF fuel matrix to the failed waste package environment (included FEP 2.1.02.23.0A (Cladding Unzipping)). A waste package is considered to be failed at the time of the first penetration of the waste package by any process, including cracking, that allows ingress of oxygen and water vapor into the package.

Degradation of DOE SNF cladding (other than naval SNF cladding) is discussed in excluded FEP 2.1.02.25.0A (DSNF Cladding). As described in that FEP, DOE SNF cladding (with the exception of naval SNF cladding) is considered to be breached upon emplacement in the repository and will neither inhibit groundwater contacting the DOE SNF matrix nor the release of radionuclides from the DOE SNF after groundwater contact.

Naval SNF cladding is discussed in included FEP 2.1.02.25.0B (Naval SNF Cladding).

Using this approach, commercial SNF and DOE SNF (other than naval SNF) cladding does not prevent the release or substantially reduce the release rate of radionuclides from the waste. Therefore, omission of FEP 2.1.02.19.0A (Creep Rupture of Cladding) will not result in a significant adverse change in the magnitude or timing of either radiological exposure to the RMEI or radionuclide releases to the accessible environment. Therefore, this FEP is excluded from the performance assessments conducted to demonstrate compliance with proposed 10 CFR 63.311 and 63.321 (70 FR 53313 [DIRS 178394]), and with 10 CFR 63.331 [DIRS 180319], on the basis of low consequence.

INPUTS:

Table 2.1.02.19.0A-1. Direct Inputs

Input	Source	Description
SNL 2007. *Cladding Degradation Summary for LA*. [DIRS 180616]	Section 6.2.1.2[a]	Conservative assumption that all commercial SNF cladding (stainless steel and Zircaloy) is breached on receipt at the repository

Table 2.1.02.19.0A-2. Indirect Inputs

Citation	Title	DIRS
10 CFR 63	Energy: Disposal of High-Level Radioactive Wastes in a Geologic Repository at Yucca Mountain, Nevada	180319
70 FR 53313	Implementation of a Dose Standard After 10,000 Years	178394

FEP: 2.1.02.20.0A

FEP NAME:

Internal Pressurization of Cladding

FEP DESCRIPTION:

Increased pressure within the fuel rod due to the production of helium gas could contribute to cladding failure.

SCREENING DECISION:

Excluded – low consequence

SCREENING JUSTIFICATION:

For the performance assessments conducted to demonstrate compliance with proposed 10 CFR 63.311, 10 CFR 63.321 (70 FR 53313 [DIRS 178394]), and with 10 CFR 63.331 [DIRS 180319], it is considered that all commercial SNF cladding (stainless steel and Zircaloy) is breached on emplacement in the repository as discussed included FEP 2.1.02.12.0A (Degradation of Cladding Prior to Disposal) and in *Cladding Degradation Summary for LA* (SNL 2007 [DIRS 180616], Section 6.2.1.2[a]). Furthermore, the zirconium-based (Zircaloy) and stainless steel SNF cladding is assumed to split instantly along the length of the fuel rods at the time of waste package failure. Cladding unzipping is assumed to result in immediate exposure of the commercial SNF fuel matrix to the failed waste package environment (included FEP 2.1.02.23.0A (Cladding Unzipping)). A waste package is considered to be failed at the time of the first penetration of the waste package by any process, including cracking, that allows ingress of oxygen and water vapor into the package.

Degradation of DOE SNF cladding (other than naval SNF cladding) is discussed in excluded FEP 2.1.02.25.0A (DSNF Cladding). As described in that FEP, the TSPA model considers that the DOE SNF cladding (with the exception of naval SNF cladding) will be breached upon emplacement in the repository and will neither inhibit groundwater contacting the DOE SNF matrix nor the release of radionuclides from the DOE SNF after groundwater contact.

Naval SNF cladding is discussed in included FEP 2.1.02.25.0B (Naval SNF Cladding).

Using this approach, commercial SNF and DOE SNF (other than naval SNF) cladding does not prevent the release or substantially reduce the release rate of radionuclides from the waste. Therefore, omission of FEP 2.1.02.20.0A (Internal Pressurization of Cladding) will not result in a significant adverse change in the magnitude or timing of either radiological exposure to the RMEI or radionuclide releases to the accessible environment. Therefore, this FEP is excluded from the performance assessments conducted to demonstrate compliance with proposed 10 CFR 63.311 and 63.321 (70 FR 53313 [DIRS 178394]), and with 10 CFR 63.331 [DIRS 180319], on the basis of low consequence.

INPUTS:

Table 2.1.02.20.0A-1. Direct Inputs

Input	Source	Description
SNL 2007. *Cladding Degradation Summary for LA*. [DIRS 180616]	Section 6.2.1.2[a]	Conservative assumption that all commercial SNF cladding (stainless steel and Zircaloy) is breached on receipt at the repository

Table 2.1.02.20.0A-2. Indirect Inputs

Citation	Title	DIRS
10 CFR 63	Energy: Disposal of High-Level Radioactive Wastes in a Geologic Repository at Yucca Mountain, Nevada	180319
70 FR 53313	Implementation of a Dose Standard After 10,000 Years	178394

FEP: 2.1.02.21.0A

FEP NAME:

Stress Corrosion Cracking (SCC) of Cladding

FEP DESCRIPTION:

Stress corrosion cracking (SCC) mechanisms can contribute to cladding failure. These mechanisms can operate both from the inside out from the action of fission products, or from the outside in from the actions of salts or other chemicals within the waste package.

SCREENING DECISION:

Excluded – low consequence

SCREENING JUSTIFICATION:

For the performance assessments conducted to demonstrate compliance with proposed 10 CFR 63.311, 10 CFR 63.321 (70 FR 53313 [DIRS 178394]), and with 10 CFR 63.331 [DIRS 180319], it is conservatively considered that all commercial SNF cladding (stainless steel and Zircaloy) is breached on emplacement in the repository as discussed in included FEP 2.1.02.12.0A (Degradation of Cladding Prior to Disposal) and in *Cladding Degradation Summary for LA* (SNL 2007 [DIRS 180616], Section 6.2.1.2[a]). Furthermore, the zirconium-based (Zircaloy) and stainless steel SNF cladding is assumed to split instantly along the length of the fuel rods at the time of waste package failure. Cladding unzipping is assumed to result in immediate exposure of the commercial SNF fuel matrix to the failed waste package environment (included FEP 2.1.02.23.0A (Cladding Unzipping)). A waste package is considered to be failed at the time of the first penetration of the waste package by any process, including cracking, that allows ingress of oxygen and water vapor into the package.

Degradation of DOE SNF cladding (other than naval SNF cladding) is discussed in excluded FEP 2.1.02.25.0A (DSNF Cladding). As described in that FEP, DOE SNF cladding (with the exception of naval SNF cladding) is considered to be breached upon emplacement in the repository and will neither inhibit groundwater contacting the DSNF fuel matrix nor the release of radionuclides from the DOE SNF after groundwater contact.

Naval SNF cladding is discussed in included FEP 2.1.02.25.0B (Naval SNF Cladding).

Using this approach, commercial SNF and DOE SNF (other than naval SNF) cladding does not prevent the release or substantially reduce the release rate of radionuclides from the waste. Therefore, omission of FEP 2.1.02.21.0A (Stress Corrosion Cracking (SCC) of Cladding) will not result in a significant adverse change in the magnitude or timing of either radiological exposure to the RMEI or radionuclide releases to the accessible environment. Therefore, this FEP is excluded from the performance assessments conducted to demonstrate compliance with proposed 10 CFR 63.311 and 63.321 (70 FR 53313 [DIRS 178394]), and with 10 CFR 63.331 [DIRS 180319], on the basis of low consequence.

INPUTS:

Table 2.1.02.21.0A-1. Direct Inputs

Input	Source	Description
SNL 2007. *Cladding Degradation Summary for LA*. [DIRS 180616]	Section 6.2.1.2[a]	Conservative assumption that all commercial SNF cladding (stainless steel and Zircaloy) is breached on receipt at the repository

Table 2.1.02.21.0A-2. Indirect Inputs

Citation	Title	DIRS
10 CFR 63	Energy: Disposal of High-Level Radioactive Wastes in a Geologic Repository at Yucca Mountain, Nevada	180319
70 FR 53313	Implementation of a Dose Standard After 10,000 Years	178394

FEP: 2.1.02.22.0A

FEP NAME:

Hydride Cracking of Cladding

FEP DESCRIPTION:

Cladding contains hydrogen after reactor operation. The cladding might pick up more hydrogen from cladding general corrosion (wet oxidation) after the waste package is breached. The hydrogen can exist both as zirconium hydride precipitates and as hydrogen in solid solution with zirconium. Hydrides might also form from UO_2 oxidation after waste package and cladding perforation. In addition, hydrides may dissolve in warmer areas of the cladding and migrate to cooler areas. Hydrogen can also move from places of low stress to places of high stress, causing hydride reorientation or delayed hydride cracking. The buildup of hydrides can cause existing cracks to propagate by delayed hydride cracking or hydride embrittlement.

SCREENING DECISION:

Excluded – low consequence

SCREENING JUSTIFICATION:

For the performance assessments conducted to demonstrate compliance with proposed 10 CFR 63.311 and 63.321 (70 FR 53313 [DIRS 178394]), and with 10 CFR 63.331 [DIRS 180319], it is considered that all commercial SNF cladding (stainless steel and Zircaloy) is breached on emplacement in the repository as discussed in included FEP 2.1.02.12.0A (Degradation of Cladding Prior to Disposal) and in *Cladding Degradation Summary for LA* (SNL 2007 [DIRS 180616], Section 6.2.1.2[a]). Furthermore, the zirconium-based (Zircaloy) and stainless steel SNF cladding is assumed to split instantly along the length of the fuel rods at the time of waste package failure. Cladding unzipping is assumed to result in immediate exposure of the commercial SNF fuel matrix to the failed waste package environment (included FEP 2.1.02.23.0A (Cladding Unzipping)). A waste package is considered to be failed at the time of the first penetration of the waste package by any process, including cracking, that allows ingress of oxygen and water vapor into the package.

Degradation of DOE SNF cladding (other than naval SNF cladding) is discussed in excluded FEP 2.1.02.25.0A (DSNF Cladding). As described in that FEP, DOE SNF cladding (with the exception of naval SNF cladding) is considered to be breached upon emplacement in the repository and will neither inhibit groundwater contacting the DOE SNF matrix nor the release of radionuclides from the DOE SNF after groundwater contact.

Naval SNF cladding is discussed in included FEP 2.1.02.25.0B (Naval SNF Cladding).

Using this approach, commercial SNF and DOE SNF (other than naval SNF) cladding does not prevent the release or substantially reduce the release rate of radionuclides from the waste. Therefore, omission of FEP 2.1.02.22.0A (Hydride Cracking of Cladding) will not result in a significant adverse change in the magnitude or timing of either radiological exposure to the

RMEI or radionuclide releases to the accessible environment. Therefore, this FEP is excluded from the performance assessments conducted to demonstrate compliance with proposed 10 CFR 63.311 and 63.321 (70 FR 53313 [DIRS 178394]), and with 10 CFR 63.331 [DIRS 180319], on the basis of low consequence.

INPUTS:

Table 2.1.02.22.0A-1. Direct Inputs

Input	Source	Description
SNL 2007. *Cladding Degradation Summary for LA*. [DIRS 180616]	Section 6.2.1.2[a]	Conservative assumption that all commercial SNF cladding (stainless steel and Zircaloy) is breached on receipt at the repository

Table 2.1.02.22.0A-2. Indirect Inputs

Citation	Title	DIRS
10 CFR 63	Energy: Disposal of High-Level Radioactive Wastes in a Geologic Repository at Yucca Mountain, Nevada	180319
70 FR 53313	Implementation of a Dose Standard After 10,000 Years	178394

FEP: 2.1.02.23.0A

FEP NAME:

Cladding Unzipping

FEP DESCRIPTION:

In either dry or wet oxidizing conditions and with perforated fuel cladding, the UO_2 fuel can oxidize. The volume increase of the fuel as it oxidizes can create stresses in the cladding that may cause gross rupture of the fuel cladding (unzipping).

SCREENING DECISION:

Included

TSPA DISPOSITION:

The axial splitting or "unzipping" of commercial SNF cladding is caused by the volume increase associated with the formation of fuel or cladding corrosion products (excluded FEP 2.1.09.03.0A (Volume Increase of Corrosion Products Impacts Cladding)). Unzipping of commercial SNF cladding is expected to occur after the fuel cladding is perforated, and it leaves fuel pellets exposed to the waste package internal environment.

For the TSPA, it is considered that all commercial SNF fuel cladding (stainless steel and Zircaloy) is breached on emplacement in the respository as discussed in included FEP 2.1.02.12.0A (Degradation of Cladding Prior to Disposal) and in *Cladding Degradation Summary for LA* (SNL 2007 [DIRS 180616], Section 6.1.2.2[a]).

Experiments carried out at Argonne National Laboratory involving two commercial SNF fuel rod segments with perforated cladding found that unzipping along the length of each fuel rod segment occurred in less than two years due to the fuel-side cladding corrosion (Cunnane et al. 2003 [DIRS 162406], Section 2a). Dry oxidation of the commercial SNF fuel (oxidation of UO_2 to U_3O_8) could also result in rapid cladding unzipping. Dry oxidation of the fuel in commercial SNF rods with breached cladding is expected to occur under the expected low humidity and high temperature conditions in the repository if the waste package fails soon after repository closure. Wet oxidation of the fuel in commercial SNF rods with breached cladding following waste package failure is also expected to result in rapid cladding unzipping.

Commercial SNF cladding unzipping is included in the TSPA model by assuming that the commercial SNF cladding is breached on emplacement in the repository and that cladding unzipping exposes bare fuel along the entire length of the fuel rod immediately following waste package failure. No credit is taken for the commercial SNF cladding playing any role in limiting exposure of the fuel to the repository environment or in limiting radionuclide release from the fuel.

DOE SNF and naval SNF cladding are discussed in excluded FEP 2.1.02.25.0A (DSNF Cladding) and in included FEP 2.1.02.25.0B (Naval SNF Cladding).

INPUTS:

Table 2.1.02.23.0A-1. Direct Inputs

Input	Source	Description
SNL 2007. *Cladding Degradation Summary for LA*. [DIRS 180616]	Section 6.2.2.2[a]	Conservative assumption that all commercial SNF cladding (stainless steel and Zircaloy) is breached on receipt at the repository

Table 2.1.02.23.0A-2. Indirect Inputs

Citation	Title	DIRS
Cunnane et al. 2003	*Yucca Mountain Project Report, Waste Form Testing Work*	162406

FEP: 2.1.02.24.0A

FEP NAME:

Mechanical Impact on Cladding

FEP DESCRIPTION:

Mechanical failure of cladding may result from external stresses, such as rockfall or impact from waste package internals. Seismic-induced impacts are addressed in several separate FEPs.

SCREENING DECISION:

Excluded – low consequence

SCREENING JUSTIFICATION:

For the performance assessments conducted to demonstrate compliance with proposed 10 CFR 63.311 and 63.321 (70 FR 53313 [DIRS 178394]), and with 10 CFR 63.331 [DIRS 180319], it is conservatively considered that all commercial SNF cladding (stainless steel and Zircaloy) is breached on emplacement in the repository as discussed in included FEP 2.1.02.12.0A (Degradation of Cladding Prior to Disposal) and in *Cladding Degradation Summary for LA* (SNL 2007 [DIRS 180616], Section 6.2.1.2[a]). Furthermore, the zirconium-based (Zircaloy) and stainless steel SNF cladding is assumed to split instantly along the length of the fuel rods at the time of waste package failure. Cladding unzipping is assumed to result in immediate exposure of the commercial SNF fuel matrix to the failed waste package environment (included FEP 2.1.02.23.0A (Cladding Unzipping)). A waste package is considered to be failed at the time of the first penetration of the waste package by any process, including cracking, that allows ingress of oxygen and water vapor into the package.

Degradation of DOE SNF cladding (other than naval SNF cladding) is discussed in excluded FEP 2.1.02.25.0A (DSNF Cladding). As described in that FEP, the TSPA model considers that the DOE SNF cladding (with the exception of naval SNF cladding) will be breached upon emplacement in the repository and will neither inhibit groundwater contacting the DOE SNF matrix nor the release of radionuclides from the DOE SNF after groundwater contact.

Naval SNF cladding is discussed in included FEP 2.1.02.25.0B (Naval SNF Cladding).

Using this approach, commercial SNF and DOE SNF (other than naval SNF) cladding does not prevent the release or substantially reduce the release rate of radionuclides from the waste. Therefore, omission of FEP 2.1.02.24.0A (Mechanical Impact on Cladding) will not result in a significant adverse change in the magnitude or timing of either radiological exposure to the RMEI or radionuclide releases to the accessible environment. Therefore, this FEP is excluded from the performance assessments conducted to demonstrate compliance with proposed 10 CFR 63.311 and 63.321 (70 FR 53313 [DIRS 178394]), and with 10 CFR 63.331 [DIRS 180319], on the basis of low consequence.

INPUTS:

Table 2.1.02.24.0A-1. Direct Inputs

Input	Source	Description
SNL 2007. *Cladding Degradation Summary for LA*. [DIRS 180616]	Section 6.2.1.2[a]	Conservative assumption that all commercial SNF cladding (stainless steel and Zircaloy) is breached on receipt at the repository

Table 2.1.02.24.0A-2. Indirect Inputs

Citation	Title	DIRS
10 CFR 63	Energy: D isposal of High-Level Radioactive Wastes in a Geologic Repository at Yucca Mountain, Nevada	180319
70 FR 53313	Implementation of a Dose Standard After 10,000 Years	178394

FEP: 2.1.02.25.0A

FEP NAME:

DSNF Cladding

FEP DESCRIPTION:

DSNF to be disposed in Yucca Mountain contains a variety of fuel types that may not be similar to CSNF. Some of the fuel types may have initial cladding-degradation characteristics that are different from those for CSNF. Therefore, the effectiveness of DSNF cladding as a barrier to radionuclide mobilization might be different from CSNF. This FEP addresses all types of DSNF cladding except Naval SNF cladding.

SCREENING DECISION:

Excluded – low consequence

SCREENING JUSTIFICATION:

About 85% by weight MTHM of the DOE SNF is from the N Reactor (DOE 2002 [DIRS 158405], Appendix D), a significant but unquantified fraction of which will have damaged cladding at the time of emplacement in their canisters (Abrefah et al. 1995 [DIRS 151125]). There has been insufficient characterization of the condition of the DOE SNF cladding (other than the observations of extensive damage to the N Reactor SNF cladding) to establish the effectiveness of the cladding. Because the cladding integrity of most DOE SNF will not be extensively characterized, the TSPA model uses an upper limit model for DOE SNF (with the exception of naval SNF) degradation that takes no credit for cladding in either protecting the fuel from exposure to the repository environment or in limiting radionuclide release as discussed in *DSNF and Other Waste Form Degradation* (BSC 2004 [DIRS 172453], Sections 6.2 and 8.1). Also, because the TSPA model takes no credit for DOE SNF canister integrity once the waste package has breached, it is modeled that the DOE SNF is directly exposed to repository water or air environment.

The TSPA model considers all DOE SNF (with the exception of naval fuel) cladding will be breached on emplacement in the repository and will neither inhibit groundwater contacting the DOE SNF matrix nor the release of radionuclides from the DOE SNF after groundwater contact as discussed in included FEP 2.1.02.12.0A (Degradation of Cladding Prior to Disposal). Naval SNF cladding is discussed in included FEP 2.1.02.25.0B (Naval SNF Cladding).

Based on the above discussion, omission of FEP 2.1.02.25.0A (DSNF Cladding) will not result in a significant adverse change in the magnitude or timing of either radiological exposure to the RMEI or radionuclide releases to the accessible environment. Therefore, this FEP is excluded from the performance assessments conducted to demonstrate compliance with proposed 10 CFR 63.311 and 63.321 (70 FR 53313 [DIRS 178394]), and with 10 CFR 63.331 [DIRS 180319], on the basis of low consequence.

INPUTS:

Table 2.1.02.25.0A-1. Direct Inputs

Input	Source	Description
BSC 2004. *DSNF and Other Waste Form Degradation Abstraction*. [DIRS 172453]	Sections 6.2, 8.1	TSPA uses an upper limit model for DOE SNF (with the exception of naval SNF) degradation that takes no credit for cladding in either protecting the fuel from exposure to the repository environment or in limiting radionuclide radionuclide release

Table 2.1.02.25.0A-2. Indirect Inputs

Citation	Title	DIRS
10 CFR 63	Energy: Disposal of High-Level Radioactive Wastes in a Geologic Repository at Yucca Mountain, Nevada	180319
70 FR 53313	Implementation of a Dose Standard After 10,000 Years	178394
Abrefah et al. 1995	*K-Basin Spent Nuclear Fuel Characterization Data Report*	151125
DOE 2002	*DOE Spent Nuclear Fuel Information in Support of TSPA-SR*	158405

FEP: 2.1.02.25.0B

FEP NAME:

Naval SNF Cladding

FEP DESCRIPTION:

DSNF to be disposed of in Yucca Mountain has a variety of fuel types that may not be similar to the CSNF to be disposed. Some of the fuel types may have initial cladding-degradation characteristics that are different from those for the CSNF. Therefore, the effectiveness of DSNF cladding as a barrier to radionuclide mobilization might be different from CSNF. This FEP addresses Naval SNF structure only.

SCREENING DECISION:

Included

TSPA DISPOSITION:

Naval Nuclear Propulsion Program cladding and SNF performance is discussed in *Naval Nuclear Propulsion Program Technical Support Document for the License Application*, Section 2.3.7, which is a classified document. Waste packages containing naval SNF are conservatively modeled in TSPA as commercial SNF waste packages.

FEP: 2.1.02.26.0A

FEP NAME:

Diffusion-Controlled Cavity Growth in Cladding

FEP DESCRIPTION:

Diffusion-controlled cavity growth is a possible creep rupture mechanism that could occur under the temperature and pressure conditions that prevail during dry storage of spent fuel. It might also occur during disposal.

SCREENING DECISION:

Excluded – low consequence

SCREENING JUSTIFICATION:

For the performance assessments conducted to demonstrate compliance with proposed 10 CFR 63.311 and 63.321 (70 FR 53313 [DIRS 178394]), and with with 10 CFR 63.331 [DIRS 180319], it is considered that all commercial SNF cladding (stainless steel and Zircaloy) is breached upon emplacement in the repository, as discussed in included FEP 2.1.02.12.0A (Degradation of Cladding Prior to Disposal) and in *Cladding Degradation Summary for LA* (SNL 2007 [DIRS 180616], Section 6.2.1.2[a]). Furthermore, the zirconium-based (Zircaloy) and stainless steel SNF cladding is assumed to split instantly along the length of the fuel rods at the time of waste package failure. Cladding unzipping is assumed to result in immediate exposure of the commercial SNF fuel matrix to the failed waste package environment (included FEP 2.1.02.23.0A (Cladding Unzipping)). A waste package is considered to be failed at the time of the first penetration of the waste package by any process, including cracking, that allows ingress of oxygen and water vapor into the package.

Degradation of DOE SNF cladding (other than naval SNF cladding) is discussed in excluded FEP 2.1.02.25.0A (DSNF Cladding). As described in that FEP, the TSPA model considers that the DOE SNF cladding (with the exception of naval SNF cladding) will be breached upon emplacement in the repository and will neither inhibit groundwater contacting the DOE SNF matrix nor the release of radionuclides from the DOE SNF after groundwater contact. Naval SNF cladding is discussed in included FEP 2.1.02.25.0B (Naval SNF Cladding).

Using this approach, commercial SNF and DOE SNF (other than naval SNF) cladding does not prevent the release or substantially reduce the release rate of radionuclides from the waste. Therefore, omission of FEP 2.1.02.26.0A (Diffusion-Controlled Cavity Growth in Cladding) will not result in a significant adverse change in the magnitude or timing of either radiological exposure to the RMEI or radionuclide releases to the accessible environment. Therefore, this FEP is excluded from the performance assessments conducted to demonstrate compliance with proposed 10 CFR 63.311 and 63.321 (70 FR 53313 [DIRS 178394]), and with 10 CFR 63.331 [DIRS 180319], on the basis of low consequence.

INPUTS:

Table 2.1.02.26.0A-1. Direct Inputs

Input	Source	Description
SNL 2007. *Cladding Degradation Summary for LA*. [DIRS 180616]	Section 6.2.1.2[a]	Conservative assumption that all commercial SNF cladding (stainless steel and Zircaloy) is breached on receipt at the repository

Table 2.1.02.26.0A-2. Indirect Inputs

Citation	Title	DIRS
10 CFR 63	Energy: Disposal of High-Level Radioactive Wastes in a Geologic Repository at Yucca Mountain, Nevada	180319
70 FR 53313	Implementation of a Dose Standard After 10,000 Years	178394

FEP: 2.1.02.27.0A

FEP NAME:

Localized (Fluoride Enhanced) Corrosion of Cladding

FEP DESCRIPTION:

Fluoride is present in Yucca Mountain groundwater, and zirconium has been observed to corrode in environments containing fluoride. Therefore, fluoride corrosion of cladding may occur in waste packages.

SCREENING DECISION:

Excluded – low consequence

SCREENING JUSTIFICATION:

For the performance assessments conducted to demonstrate compliance with proposed 10 CFR 63.311 and 63.321 (70 FR 53313 [DIRS 178394]), and with 10 CFR 63.331 [DIRS 180319], it is considered that all commercial SNF cladding (stainless steel and Zircaloy) is breached upon emplacement in at the repository, as discussed in included FEP 2.1.02.12.0A (Degradation of Cladding Prior to Disposal) and in *Cladding Degradation Summary for LA* (SNL 2007 [DIRS 180616], Section 6.2.1.2[a]). Furthermore, the zirconium-based (Zircaloy) and stainless steel SNF cladding is assumed to split instantly along the length of the fuel rods at the time of waste package failure. Cladding unzipping is assumed to result in immediate exposure of the commercial SNF fuel matrix to the failed waste package environment (included FEP 2.1.02.23.0A (Cladding Unzipping)). A waste package is considered to be failed at the time of the first penetration of the waste package by any process, including cracking, that allows ingress of oxygen and water vapor into the package.

Degradation of DOE SNF cladding (other than naval SNF cladding) is discussed in excluded FEP 2.1.02.25.0A (DSNF Cladding). As described in that FEP, the TSPA model considers that the DOE SNF cladding (with the exception of naval SNF cladding) will be breached upon emplacement in the repository and will neither inhibit groundwater contacting the DOE SNF matrix nor the release of radionuclides from the DOE SNF after groundwater contact. Naval SNF cladding is discussed in included FEP 2.1.02.25.0B (Naval SNF Cladding).

Using this approach, commercial SNF and DOE SNF (other than naval SNF) cladding does not prevent the release or substantially reduce the release rate of radionuclides from the waste. Therefore, omission of FEP 2.1.02.27.0A (Localized (Fluoride Enhanced) Corrosion of Cladding) will not result in a significant adverse change in the magnitude or timing of either radiological exposure to the RMEI or radionuclide releases to the accessible environment. Therefore, this FEP is excluded from the performance assessments conducted to demonstrate compliance with proposed 10 CFR 63.311 and 63.321 (70 FR 53313 [DIRS 178394]), and with 10 CFR 63.331 [DIRS 180319], on the basis of low consequence.

INPUTS:

Table 2.1.02.27.0A-1. Direct Inputs

Input	Source	Description
SNL 2007. *Cladding Degradation Summary for LA*. [DIRS 180616]	Section 6.2.1.2[a]	Conservative assumption that all commercial SNF cladding (stainless steel and Zircaloy) is breached on receipt at the repository

Table 2.1.02.27.0A-2. Indirect Inputs

Citation	Title	DIRS
10 CFR 63	Energy: Disposal of High-Level Radioactive Wastes in a Geologic Repository at Yucca Mountain, Nevada	180319
70 FR 53313	Implementation of a Dose Standard After 10,000 Years	178394

FEP: 2.1.02.28.0A

FEP NAME:

Grouping of DSNF Waste Types into Categories

FEP DESCRIPTION:

Several hundred distinct types of DSNF may potentially be stored in the repository. These represent many more types than can viably be examined for their individual effect on the repository. A limited number of representative or bounding degradation models must be selected and/or abstracted.

SCREENING DECISION:

Included

TSPA DISPOSITION:

DOE SNF to be disposed of in Yucca Mountain is composed of a variety of fuel types packaged in a number of configurations (BSC 2004 [DIRS 172453]; SNL 2007 [DIRS 179567], Table 4-1, Parameter Number 04-07). *Initial Radionuclide Inventories* (SNL 2007 [DIRS 180472]) considered all fuel types and the quantities of each fuel type when compiling the nominal radionuclide inventory in grams per package and uncertainty distributions for radionuclides important to dose calculations for the TSPA.

For degradation rate determination, the various DOE SNF types have been classified into eleven groups for the purpose of TSPA analyses (BSC 2004 [DIRS 172453]; DOE 2000 [DIRS 118968]). The largest single DOE SNF type is the N Reactor SNF uranium metal (Group 7), which comprises approximately 85% by weight expressed as MTHM of the total DOE SNF (DOE 2002 [DIRS 158405], Appendix D). N Reactor SNF degradation models are adopted as a surrogate for the entire DOE SNF inventory, except for the naval SNF (Group 1) (BSC 2004 [DIRS 172453]). Naval fuel is treated as commercial SNF in the TSPA. This grouping and implementation simplifies the TSPA model for computational efficiency while ensuring that the great majority of DOE SNF degradation is captured in a bounding fashion.

In addition to being the largest DOE SNF inventory type by weight, N Reactor SNF degradation can be used to represent degradation of the entire DOE SNF inventory because: (1) a significant fraction of the N Reactor SNF will be damaged at the time of emplacement in their canisters, and (2) the N Reactor SNF degradation rates are greater than those for most other groups (BSC 2004 [DIRS 172453], Section 6.2 and Table 6-9). The group that potentially has greater dissolution rates than N Reactor SNF is the mixed-carbide-fissile fuel waste particles in a nongraphite matrix (Group 3). Group 3 waste would not serve as an appropriate DOE SNF degradation surrogate because the total inventory of the Group 3 SNF is less than 0.001% of DOE SNF waste (DOE 2002 [DIRS 158405], Appendix D). The immobilized plutonium ceramic waste form is not included in this discussion because the DOE Office of Environmental Management has decided to use the majority of the excess defense plutonium as MOX fuel in commercial reactors

as the preferred disposition path rather than immobilization in a ceramic waste form (67 FR 19432 [DIRS 162618]).

As discussed in *DSNF and Other Waste Form Degradation Abstraction* (BSC 2004 [DIRS 172453], Section 6.3), a single conservative upper-bound model is used in TSPA to model degradation of the DOE SNF inventory other than naval SNF. This approach gives complete dissolution of the waste form during a single-code time step upon exposure of the waste form to groundwater.

INPUTS:

Table 2.1.02.28.0A-1. Indirect Inputs

Citation	Title	DIRS
67 FR 19432	Surplus Plutonium Disposition Program	162618
BSC 2004	*DSNF and Other Waste Form Degradation Abstraction*	172453
DOE 2000	*DOE Spent Nuclear Fuel Grouping in Support of Criticality, DBE, TSPA-LA*	118968
DOE 2002	*DOE Spent Nuclear Fuel Information in Support of TSPA-SR*	158405
SNL 2007	*Initial Radionuclides Inventory*	180472
SNL 2007	*Total System Performance Assessment Data Input Package for Requirements Analysis for DOE SNF/HLW and Navy SNF Waste Package Overpack Physical Attributes Basis for Performance Assessment*	179567

FEP: 2.1.02.29.0A

FEP NAME:

Flammable Gas Generation from DSNF

FEP DESCRIPTION:

DSNF to be disposed in Yucca Mountain will contain a small percentage of carbide fuel. When carbide is exposed to water, flammable gases such as methane and ethene, ethylene, and acetylene (the latter two are referred to as ethane and ethyne respectively by the International Union of Pure and Applied Chemistry) are generated. If these gases ignite, localized increases in temperature can occur, which might affect fuel degradation. The area around the ignition point may be mechanically and/or thermally perturbed, which could affect waste package or host-rock properties in the adjacent area of the EBS.

SCREENING DECISION:

Excluded – low consequence

SCREENING JUSTIFICATION:

The only fuel waste types capable of producing organic flammable gases, such as methane, and ethane, are the uranium-thorium carbide and the plutonium-uranium carbide DOE SNF because they are the only spent nuclear fuels containing more than trace quantities of carbon. These gases are formed by the reaction of the carbides with liquid water or water vapor. Only a small percentage (approximately 1% or 25 MTHM) of DOE SNF contains uranium/thorium carbide fuels. There is only about 100 kg of plutonium/uranium carbide DOE SNF (DOE 2002 [DIRS 158405], Table D-1). The carbide spent nuclear fuels will be present in about 5% of the waste packages (DOE 2004 [DIRS 169354], p. D-580). These carbide fuels will not be included in the 2-MCO/2-DHLW codisposal waste packages that will contain the potentially pyrophoric uranium metal fuel discussed in excluded FEP 2.1.02.08.0A (Pyrophoricity from DSNF) (SNL 2007 [DIRS 179567], Section 4.1). The effect of H_2 gas production is discussed in excluded FEPs 2.1.12.03.0A (Gas Generation (H_2) from Waste Package Corrosion) and 2.1.13.01.0A (Radiolysis).

Uranium/thorium carbide fuels were used in the Fort St. Vrain and Peach Bottom Unit 1, reactor Cores 1 and 2. The Peach Bottom Core-1 reactor pellets are relevant, since pellets from this reactor are not encased in the tough, corrosion-resistant, silicon-carbide shells used in the other reactor cores. As discussed in excluded FEP 2.1.02.25.0A (DSNF Cladding), it is considered in the TSPA that DOE SNF (with the exception of naval SNF) cladding is breached upon emplacement in at the repository and that the bare fuel is instantaneously exposed to the waste package environment when the waste package fails. The exposed fuel can possibly produce flammable hydrocarbons. Only 1.663 MTHM of Peach Bottom Core-1 pellets (DOE 1998 [DIRS 122980], Appendix B, p. 14) contained in 103 waste packages (DOE 1998 [DIRS 122980], Table 1-1, p.1-8) will be disposed in the repository. This is small compared to the 24.667 MTHM of high-integrity fuel (contained in 545 waste packages) from the Fort St.

Vrain and Peach Bottom cores (DOE 1998 [DIRS 122980], Appendix B, p. 14, and Table 1-1, p. 1-8). Thus, less than 7% {1.663/(1.663 + 24.667)} of the carbide fuel is low-integrity pellets.

An analysis of degradation and hydrocarbon production from graphite-matrix carbide fuels was conducted (Propp 1998 [DIRS 149395]). This study assessed the vulnerability of graphite-matrix SNF to oxidation by the ambient atmosphere in a geologic repository after fuel canister breach and examined the gases generated due to carbide combustion. Thermochemical and kinetic data were scrutinized for potential reactions between the graphite and the H_2O/O_2 system over the temperature range of 200°C to 400°C. This evaluation led to the following predictions and conclusions:

- Carbon dioxide is thermodynamically favored as the principal product of combustion of graphite in the presence of H_2O and/or O_2.
- Carbon monoxide may form; however, it will subsequently be consumed to form CO_2.
- The potential for direct reaction of water with graphite is small.
- Neglecting radiolysis, the decomposition of water into elemental hydrogen and oxygen is negligible and the reverse reaction (formation of water) is favored.
- Methane formation is not significant.

The kinetic analysis assumed an Arrhenius-type rate expression and concluded that the values of the reaction rate constant are very small but exhibit strong temperature dependence. The time required for a total carbon mass loss of 1 mg/cm^2 from a sample exposed under these conditions was calculated. Even at 400°C, the rate is "so small as to be of no practical consequence," it requires two years to produce this insignificant mass loss. This corresponds to a material thickness loss of 0.4 mm in 190 years. Therefore, oxidation of the carbide-bearing SNF upon waste package breach is not anticipated to be a concern (Propp 1998 [DIRS 149395], Summary).

Additionally, DOE SNF will be widely dispersed throughout the repository, as will any flammable gas produced. Like most of the DOE SNF waste packages, the carbide fuel will be placed in a DOE SNF canister and packaged with five HLW glass canisters in each waste package (SNL 2007 [DIRS 179567], Section 4.1.1). So the carbide fuel is inherently dispersed and any gas produced from carbide fuel would be dispersed as well. Since carbide can react to form flammable gases only in the presence of water, it is reasonable to assume that this process would be preceded by failure of the waste package and degradation of the fuel's graphite matrix. Therefore, pressure buildup following gas release in a waste package will be insignificant.

With the exception of intermittent perched zones, both the matrix and the fractures within the host rock above and below the repository horizon have a relatively high degree of gas-phase saturation and permeability (BSC 2004 [DIRS 170035], Section 6.1). Additionally, airflow through Yucca Mountain maintains repository pressures close to atmospheric pressure (SNL 2007 [DIRS 184614], Section 6.4). These conditions will promote a dispersive gas flow path between the repository and host rock, thus diluting any potential flammable-gas concentrations to levels below the ignition point. Given these conditions, any flammable gas

produced, once released, will quickly disperse and be diluted due to the presence of in situ non-flammable gases (nitrogen and argon in the air, and water vapor) in the repository (see excluded FEP 2.1.12.01.0A Gas Generation (Repository Pressurization)).

In summary, considering the small quantity of carbide fuel capable of generating flammable gas, the durability of the graphite fuel matrix used in these fuels, the dispersion of carbide waste among waste packages and across the repository and the low probability of ignition due to high rock permeability, and the fact that an upper bound instantaneous degradation rate model is used in TSPA for DOE SNF even in the absence of any hypothetical effects of flammable gas on radionuclide release, flammable gas generation from DOE SNF is insignificant.

Based on the previous discussion, omission of FEP 2.1.02.29.0A (Flammable Gas Generation from DSNF) will not result in a significant adverse change in the magnitude or timing of either radiological exposure to the RMEI or radionuclide releases to the accessible environment. Therefore, this FEP is excluded from the performance assessments conducted to demonstrate compliance with proposed 10 CFR 63.311 and 63.321 (70 FR 53313 [DIRS 178394]), and with 10 CFR 63.331 [DIRS 180319], on the basis of low consequence.

INPUTS:

Table 2.1.02.29.0A-1. Direct Inputs

Input	Source	Description
BSC 2004. *Conceptual Model and Numerical Approaches for Unsaturated Zone Flow and Transport*. [DIRS 170035]	Section 6.1	With the exception of intermittent perched zones, both the matrix and the fractures within the host rock above and below the repository horizon have a relatively high degree of gas-phase saturation and permeability

Table 2.1.02.29.0A-2. Indirect Inputs

Citation	Title	DIRS
10 CFR 63	Energy: Disposal of High-Level Radioactive Wastes in a Geologic Repository at Yucca Mountain, Nevada	180319
70 FR 53313	Implementation of a Dose Standard After 10,000 Years	178394
DOE 2002	*DOE Spent Nuclear Fuel Information in Support of TSPA-SR*	158405
DOE 1998	*Update to Assessment of Direct Disposal in Unsaturated Tuff of Spent Nuclear Fuel and High-Level Waste Owned by U.S. Department of Energy*	122980
DOE 2004	*Source Term Estimates for DOE Spent Nuclear Fuels*	169354
Propp 1998	*Graphite Oxidation Thermodynamics/Reactions*	149395
SNL 2007	*Total System Performance Assessment Data Input Package for Requirements Analysis for DOE SNF/HLW and Navy SNF Waste Package Overpack Physical Attributes Basis for Performance Assessment*	179567
SNL 2007	*UZ Flow Models and Submodels*	184614

FEP: 2.1.03.01.0A

FEP NAME:

General Corrosion of Waste Packages

FEP DESCRIPTION:

General corrosion may contribute to waste package failure.

SCREENING DECISION:

Included

TSPA DISPOSITION:

The outer corrosion barrier of the waste package, referred to here as the waste package outer barrier or WPOB, will be constructed of Alloy 22, a highly corrosion resistant Ni-Cr-Mo alloy. General corrosion of the WPOB is included in the TSPA. The effects of dry-air oxidation, humid-air and aqueous general corrosion, microbially influenced corrosion, and aging and phase instability on the WPOB are discussed in *General Corrosion and Localized Corrosion of Waste Package Outer Barrier* (SNL 2007 [DIRS 178519]). Initiation of aqueous corrosion processes requires the existence of a stable water film on the metal surface. The relative humidity at which this water layer forms is a strong function of the physical condition (e.g., cleanliness, surface roughness, etc.) of the metal surface (ASM International 1987 [DIRS 103753], pp. 80 to 82). As the surface condition of the waste package may vary in terms of the aforementioned characteristics, in the TSPA the onset of general corrosion of the WPOB is modeled as occurring independently of the in-drift temperature and relative humidity, and therefore is initiated at the time of repository closure (SNL 2007 [DIRS 178519], Section 8.2). Note that no barrier to flow performance credit is taken for the stainless steel liner or the TAD canister. Once the WPOB fails, it is assumed that these vessels fail in a manner that allows the in-drift environment to contact the waste form and allows water or water vapor to enter the failed waste package.

The WPOB general corrosion model was developed using data obtained from experiments conducted in mixed ionic environments as well as simple salt solutions including highly concentrated chloride brines and chloride brines containing nitrate ions. The general corrosion model has been validated against data obtained at temperatures as high as 180°C. For temperatures in excess of 180°C, the thin-film aqueous environment required to support general corrosion may not be sustainable under atmospheric pressures relevant to the repository. Therefore, application of any general corrosion rate at elevated temperature will consistently overestimate the rate of material degradation. The need to use this approach stems from the difficulty in defining a clear cut-off temperature where general corrosion would no longer be considered. Therefore, the general corrosion model should be applicable over all repository exposure environments (SNL 2007 [DIRS 178519], Sections 7.2.1 and 8.2). Because general corrosion is considered to be operative for the entire repository operation period, it could lead to degradation and breach of waste packages in the repository.

The effect of microbial activity on the general corrosion process of the WPOB is represented by a general corrosion rate-enhancement factor (SNL 2007 [DIRS 178519], Section 8.2). A more detailed discussion on the effect of microbial activity is provided in included FEP 2.1.03.05.0A (Microbially Influenced Corrosion (MIC) of Waste Packages) and in *General and Localized Corrosion of Waste Package Outer Barrier* (SNL 2007 [DIRS 178519], Sections 6.4.5 and 8.2).Thermal instability in metal alloys can result in the precipitation of secondary phases within the metal matrix; this process is sometimes referred to as phase instability. Phase instability was determined to have an insignificant effect (see excluded FEP 2.1.11.06.0A (Thermal Sensitization of Waste Packages)) on the general corrosion of the WPOB, and is therefore not included in the TSPA, as documented in *General and Localized Corrosion of Waste Package Outer Barrier* (SNL 2007 [DIRS 178519], Section 6.4.6.1).

Comparative analysis of the corrosion rates from the polarization resistance technique showed insignificant effects of welding and thermal aging of the waste WPOB on the general corrosion rates. It was determined that the aging of the base metal and welds of the WPOB under the thermal conditions expected in the repository would not affect the corrosion performance of the WPOB, and will not be specifically modeled in the TSPA (SNL 2007 [DIRS 178519], Section 6.4.6). Thermal aging (sensitization) of waste packages is discussed further in excluded FEP 2.1.11.06.0A (Thermal Sensitization of Waste Packages).

Penetration rates for general corrosion are provided in *General Corrosion and Localized Corrosion of Waste Package Outer Barrier* (SNL 2007 [DIRS 178519], Sections 6.4.3 and 8.2). General corrosion rates of the WPOB were estimated using the weight-loss of Alloy 22 crevice geometry specimens after a 5-year exposure in the LTCTF. The corrosion rate data were fit to a Weibull distribution and the uncertainty in the fitting process is represented as three distributions corresponding to low, medium and high levels of uncertainty in the fitting process. These distributions are randomly sampled such that the low and high general corrosion rate distributions are each used for 5% of realizations and the medium general corrosion rate distribution is used for 90% of realizations (DTN: MO0703PAGENCOR.001 [DIRS 182029], file: *BaseCase GC CDFs.xls*).

The temperature dependence of the general corrosion rate is represented by an apparent activation energy that was developed using data from polarization resistance tests (SNL 2007 [DIRS 178519], Sections 6.4.3.4 and 8.2). Data from several environments were used to calculate the temperature dependence using a linear mixed effects model with individual environments differentiated in the fitting procedure by use of a solution-dependent random effects vector. The temperature dependence is estimated by an apparent activation energy having a mean of 40.78 kJ/mol and a standard deviation of 11.75 kJ/mol with the range of sampled values restricted to −3 and +2 standard deviations (DTN: MO0703PAGENCOR.001 [DIRS 182029], file: *BaseCase GC CDFs.xls*). The entire variance in the values used to describe temperature dependence is attributed to uncertainty (SNL 2007 [DIRS 178519], Sections 6.4.3.3.2 and 8.2).

As discussed above, general corrosion of the WPOB is included in the TSPA. It is implemented for the groundwater protection standard (10 CFR 63.331 [DIRS 180319]), and the individual protection standard (proposed 10 CFR 63.311 (70 FR 53313 [DIRS 178394])). In the case of human intrusion (proposed 10 CFR 63.321 (70 FR 53313 [DIRS 178394])), general corrosion of

the WPOB is not implemented in the assessment of the earliest time at which intrusion would be recognized by the drillers because that is determined by drip shield corrosion rates (SNL 2008 [DIRS 183478], Section 6.7.2).

INPUTS:

Table 2.1.03.01.0A-1. Indirect Inputs

Citation	Title	DIRS
70 FR 53313	Implementation of a Dose Standard After 10,000 Years	178394
ASM International 1987	*Corrosion*	103753
DTN: MO0703PAGENCOR.001	Output from General Corrosion and Localized Corrosion of Waste Package Outer Barrier 2007 Second Version	182029
SNL 2007	*General Corrosion and Localized Corrosion of Waste Package Outer Barrier*	178519

FEP: 2.1.03.01.0B

FEP NAME:

General Corrosion of Drip Shields

FEP DESCRIPTION:

General corrosion may contribute to drip shield failure.

SCREENING DECISION:

Included

TSPA DISPOSITION:

The design requirements for drip shields include corrosion resistance as well as structural strength. Corrosion resistance is required so the drip shields can perform their seepage water diversion function with high reliability. Structural strength is required so the drip shield can protect the waste package against damage resulting from the impact and static load of rockfall and/or drift collapse weighing several tons, resulting from degradation of the drift walls and crown. Rockfall is discussed in excluded FEP 2.1.07.01.0A (Rockfall). The seepage water diversion function is performed by the Titanium Grade 7 drip shield plate material while the structural support function is performed by the Titanium Grade 29 support material (SNL 2007 [DIRS 179354], Table 4-2, Parameter Numbers 07-04).

General corrosion of the drip shield is included in the TSPA. The effects of dry-air oxidation, humid-air and aqueous general corrosion, microbially influenced corrosion, and aging and phase instability on the drip shield are discussed in *General Corrosion and Localized Corrosion of the Drip Shield* (SNL 2007 [DIRS 180778]). The corrosion resistance of titanium alloys is the result of a continuous, highly adherent, and protective oxide passive film on the metal surface. This passive film is stable over a wide range of potentials and pH values (SNL 2007 [DIRS 180778]). Initiation of aqueous corrosion processes requires the existence of a stable water film on the metal surface. The relative humidity at which this water layer forms is a strong function of the physical condition of the metal surface (ASM International 1987 [DIRS 103753], pp. 80 to 82), and thus it is assumed that a water layer will form at all relative humidities. As such, in the TSPA, general corrosion of the drip shield is modeled as being operative at the time of repository closure (SNL 2007 [DIRS 180778], Section 6.1.8[a]).

The penetration rates due to aqueous general corrosion for Titanium Grade 7 are estimated based on weight-loss measurements conducted at the LTCTF (DTN: LL030410012251.056 [DIRS 169583], file: *Ti-7 2 & one half Year Coupon Corrosion Rates Sup12 SN241.xls*). Testing was performed in a wide range of plausible generic test media including SDW, SCW and SAW. The compositions of these test media are summarized in DTN: LL040803112251.117 [DIRS 171362]. The general corrosion rates were higher for the samples exposed to aqueous SCW at 60°C and aqueous SCW at 90°C than for all other samples (SNL 2007 [DIRS 180778], Figures 6-2[a] and 6-3[a]). Based on these observations, the weight-loss data set was divided into three environmental groups with distinctively different rate distributions as follows:

aggressive condition (SCW aqueous at 90°C), intermediate condition (SCW aqueous at 60°C) and benign condition (all remaining included data) (SNL 2007 [DIRS 180778], Section 6.1.5[a]).

The higher corrosion rates calculated for samples exposed to the SCW environment may well be the result of the combined action of fluoride and chloride ions in solution. Fluoride additions to chloride-bearing solutions have been observed to cause an increase in the passive current density of Titanium Grade 7 measured under applied potential conditions (Brossia and Cragnolino 2001 [DIRS 162420], Figures 9 and 10; Brossia and Cragnolino 2004 [DIRS 180832], Figures 8 to 10). Thus, the weight-loss data collected in the fluoride-bearing SCW environment are the most appropriate data available for estimating the corrosion rate of titanium under aggressive repository conditions.

The concentration of fluoride within Yucca Mountain pore waters is anticipated to be very low (SNL 2007 [DIRS 177412], Table 4.1-3), but may be increased due to evaporative concentration (DTN: SN0701PAEBSPCE.001 [DIRS 180523]). Due to the low potential concentrations of fluoride in the environment on the drip shield surface both prior to and following evaporative concentration on the waste package surface, the impact of fluoride on the drip shield will be minimal (SNL 2007 [DIRS 180778], Section 6.5.7). The use of the aggressive condition data to represent general corrosion behavior under seepage conditions will therefore consistently overestimate the general corrosion rate of the outer surface of the drip shield on a time-averaged basis.

Because no long-term data from the LTCTF are available for general corrosion rate of Titanium Grade 29 in repository-relevant environments, the Titanium Grade 29 general corrosion rate is calculated from the long term Titanium Grade 7 data. Titanium Grades 7 and 29 were tested in four environments representing seepage and deliquescent brine environments expected in the repository (SNL 2007 [DIRS 180778], Table 6-7[a]), and from that data a CDF of conversion ratios was calculated (SNL 2007 [DIRS 180778], Table 6-8[a]). This CDF is sampled once per realization in TSPA and the value selected is used as a multiplier on the general corrosion rate determined for Titanium Grade 7 to calculate the general corrosion rate for Titanium Grade 29 (SNL 2007 [DIRS 180778], Section 6.2.2[a]).

While the outer surface of the drip shield may be exposed to seepage water and dust films, the inner surface will not (SNL 2007 [DIRS 180778], Sections 6.3, 6.5.2, and 6.5.3). Therefore, general corrosion of the inner and outer surfaces of the drip shield is modeled by using different sets of corrosion data: the outer surface corrosion rate is based on analysis of the aggressive condition data and the inner surface corrosion rate is based on analysis of the benign condition data as described in *General Corrosion and Localized Corrosion of the Drip Shield* (SNL 2007 [DIRS 180778], Section 6.1.2[a]). For each realization of TSPA (SNL 2008 [DIRS 183478], Section 6.3.5), a single general corrosion rate is sampled from each general corrosion rate distribution. The two sampled values are then applied once each to the outer and inner surfaces of each drip shield simulated during the given realization. Using this conceptual model for drip shield general corrosion, all drip shields in the repository fail by general corrosion at the same time.

General corrosion of the drip shield is included in the TSPA. It is implemented in TSPA for all three standards: the groundwater protection standard (10 CFR 63.331 [DIRS 180319]), the

individual protection standard (proposed 10 CFR 63.311 (70 FR 53313 [DIRS 178394])), and the human intrusion standard (proposed 10 CFR 63.321 (70 FR 53313 [DIRS 178394])). In the case of human intrusion (proposed 10 CFR 63.321 (70 FR 53313 [DIRS 178394])), the rate of general corrosion is used to determine the earliest time at which intrusion would be recognized by the drillers (SNL 2008 [DIRS 183478], Section 6.7.2).

INPUTS:

Table 2.1.03.01.0B-1. Indirect Inputs

Citation	Title	DIRS
70 FR 53313	Implementation of a Dose Standard After 10,000 Years	178394
ASM International 1987	*Corrosion*	103753
Brossia and Cragnolino 2001	"Effects of Environmental and Metallurgical Conditions on the Passive and Localized Dissolution of Ti-0.15%Pd"	162420
Brossia and Cragnolino 2004	"Effect of Palladium on the Corrosion Behavior of Titanium"	180832
DTN: LL030410012251.056	LTCTF Corrosion Rate Calculations for 2 1/2 - Year Exposed Titanium Alloy GR7 Specimens Cleaned Under TIP-CM-51	169583
DTN: LL040803112251.117	Target Compositions of Aqueous Solutions Used for Corrosion Testing	171362
DTN: SN0701PAEBSPCE.001	PCE TDIP Potential Seepage Water Chemistry Lookup Tables	180523
SNL 2007	*Total System Performance Assessment Data Input Package for Requirements Analysis for EBS In-Drift Configuration*	179354
SNL 2007	*Engineered Barrier System: Physical and Chemical Environment*	177412
SNL 2007	*General Corrosion and Localized Corrosion of the Drip Shield*	180778

FEP: 2.1.03.02.0A

FEP NAME:

Stress Corrosion Cracking (SCC) of Waste Packages

FEP DESCRIPTION:

Waste packages may become wet at specific locations that are stressed leading to stress corrosion cracking (SCC). The possibility of SCC under dry conditions or due to thermal stresses are also addressed as part of this FEP.

SCREENING DECISION:

Included

TSPA DISPOSITION:

Stress corrosion cracking of the waste package outer barrier is included in the TSPA. Stress corrosion cracking can occur via three possible mechanisms:

(1) Through propagation of fabrication flaws in the waste packages. This is included under nominal repository conditions and is discussed in included FEP 2.1.03.08.0A (Early Failure of Waste Packages).

(2) Through propagation of incipient cracks that can occur on the waste package outer barrier closure welds (since these cannot be annealed to relieve tensile stress). This is included under nominal repository conditions and is discussed in *Stress Corrosion Cracking of Waste Package and Drip Shield Materials* (SNL 2007 [DIRS 181953]).

(3) Through seismic events. This is discussed in *Seismic Consequence Abstraction* (SNL 2007 [DIRS 176828]). A network of through-wall cracks is assumed to form instantaneously following a seismic event of sufficient magnitude to induce residual stresses exceeding a threshold stress level. This network of cracks allows diffusive release of radionuclides through the waste package outer barrier. Seismic effects are discussed in included FEPs 1.2.03.02.0A (Seismic Ground Motion Damages EBS Components) and 1.2.03.02.0C (Seismic Induced Drift Collapse Damages EBS Components), as well as excluded FEP 1.2.03.02.0B (Seismic Induced Rockfall Damages EBS Components).

Stress corrosion cracking of the waste package outer barrier closure weld regions is included as part of the waste package degradation analyses. *Stress Corrosion Cracking of Waste Package Outer Barrier and Drip Shield Materials* (SNL 2007 [DIRS 181953], Section 8.4, Table 8-15) provides input for the treatment of waste package degradation by SCC of the waste package closure weld regions. Stress corrosion cracking of the TAD canister and stainless steel waste package inner vessel is not modeled because no flow performance credit is taken for these components after breach of the waste package outer barrier. Once the waste package outer

barrier fails, it is assumed that these vessels fail in a manner that allows the in-drift environment to contact the waste form and allows water or water vapor to enter the waste package.

As emplaced, stresses in the waste package Alloy 22 outer cylinder, including internal pressure stresses and contact stresses between waste package and pallet, are designed to be below the 0.9 to 1.05 times yield strength SCC-initiation criterion (SNL 2007 [DIRS 181953], Table 8-3; SNL 2007 [DIRS 179354], Table 4-3, Parameter Number 08-05). Therefore, in the absence of seismic activity, only the closure weld regions, where tensile residual stresses exist, are potentially susceptible to SCC initiation and propagation. The weld regions are susceptible to SCC because: (1) welding can produce high residual tensile stress in the weld area, (2) there is a much higher density of flaws due to fabrication and welding in the welds than in the base metal, and (3) welding could result in segregation and nonequilibrium brittle phases, the occurrence of which could enhance the susceptibility of materials to SCC. In the current design, all the welds, with the exception of the final closure welds, are subject to solution heat treatment to relieve the tensile residual stress when the entire Alloy 22 canister is heat-treated before the loading of the waste. Seismic events of a significant magnitude may lead to regions of plastic deformation that have the potential of leading to sustained residual tensile stresses. These resultant sustained residual tensile stresses may initiate cracks and drive them through the wall. The crack opening area for through-wall cracking initiated by seismic events has been developed for the waste package material and is described in *Stress Corrosion Cracking of Waste Package Outer Barrier and Drip Shield Materials* (SNL 2007 [DIRS 181953], Section 6.7). The breach criteria are based on a threshold stress, which is also discussed in *Stress Corrosion Cracking of Waste Package Outer Barrier and Drip Shield Materials* (SNL 2007 [DIRS 181953], Section 6.2). Seismic effects are discussed in included FEPs 1.2.03.02.0A (Seismic Ground Motion Damages EBS Components) and 1.2.03.02.0C (Seismic Induced Drift Collapse Damages EBS Components), as well as excluded FEP 1.2.03.02.0B (Seismic Induced Rockfall Damages EBS Components).

In the absence of seismic activity, weld residual stress is the only type of stress of concern for the waste package outer barrier. The stress mitigation of the outer lid closure weld will be by plasticity burnishing, which will impart a layer of compressive residual stress to a minimum depth of 3 mm (0.12 in.) (SNL 2007 [DIRS 179394], Table 4-1, Parameter Number 03-17; SNL 2007 [DIRS 179567], Table 4-1, Parameter Number 03-17). Based upon previous analyses using a compressive depth of 1.9 mm, a minimum mitigated depth of 4.6 mm (0.1811 in.) can be achieved for stress levels less than 90% of yield strength (BSC 2004 [DIRS 171499], Section 3.1.1.4.6). As described in *Waste Package Closure System Description Document* (BSC 2004 [DIRS 171499], Section 3.1.1.4.6), the performance acceptance criterion for stress mitigation is:

> Tensile stress from welding in the area near the intersection of the outer lid and outer barrier shall be mitigated by imparting a layer of compressive residual stress to a minimum depth of 1.9 mm (0.0748 in) and limiting tensile stress to 90 percent of yield stress to a minimum depth of 4.6 mm (0.1811 in).

According to the results of controlled plasticity burnishing in *Controlled Plasticity Burnishing (CPB) for Developing a Very Deep Layer of Compressive Residual Stresses in Rectangular Specimens of Alloy 22 for Yucca Mountain Nuclear Waste Package Closure Weld* (Woolf 2003

[DIRS 178059]), the desired through-wall stress profile at the closure weld can be produced by the plasticity burnishing process.

Stress Corrosion Cracking of Waste Package Outer Barrier and Drip Shield Materials (SNL 2007 [DIRS 181953]) provides stress and stress-intensity factor profiles; a threshold stress for crack initiation; a threshold stress-intensity factor for propagation; incipient crack size and density; and an estimate of crack-opening size. As discussed in the SCC report (SNL 2007 [DIRS 181953], Section 6.4), the slip dissolution–film rupture model is used to evaluate SCC crack propagation. *Analysis of Mechanisms for Early Waste Package/Drip Shield Failure* (SNL 2007 [DIRS 178765], Section 6.3) provides weld flaw size, density, and orientation distributions after non-destructive examination and repair.

Stress Corrosion Cracking of Waste Package Outer Barrier and Drip Shield Materials (SNL 2007 [DIRS 181953]) describes the results of SCC crack-initiation measurements under constant load conditions while immersed in a basic saturated water solution. Alloy 22 exhibits excellent SCC resistance, as cracking was not observed for any of the 120 Alloy 22 specimens covering a variety of metallurgical conditions (including the as-welded condition). The applied stress ratios used in the experiments were up to about 2.1 times the yield strength of the as-received material and up to 2.0 times the yield strength of the welded material. This stress ratio corresponds to an applied stress of about 89% to 95% of the ultimate tensile strength. The high degree of SCC-initiation resistance for Alloy 22 is corroborated by the results of high magnification visual examination of a number of Alloy 22 U-bend specimens exposed to a range of relevant environments at 60°C and 90°C in the LTCTF; no evidence of SCC initiation has been observed in these U-bend specimens after five years of exposure (SNL 2007 [DIRS 181953], Section 6.2.1.2.1).

Stress corrosion cracking can be initiated on a smooth weld surface (with incipient cracks) or at an existing weld flaw. Incipient cracks are considered to be 50-μm (0.05-mm) deep at the time of their nucleation and will be initiated on smooth surfaces when general corrosion has penetrated to the depth at which the tensile stress profile exceeds the threshold stress. Stress profiles reflect any stress mitigation performed, so stress mitigation is incorporated in the model. The threshold stress is taken to be 90% to 105% of the yield strength. Because weld flaws are already formed, they do not require a stress threshold to nucleate. However, most of the weld flaws are embedded within the material and are not exposed to the environment. As general corrosion proceeds, some initially embedded weld flaws may be exposed to the environment while others are corroded away. The evolution of the number of weld flaws is not considered in detail. Instead, only the fraction of weld flaws embedded within the outer one-fourth (0.25) of the weld thickness is considered capable of propagation.

The presence of stable “liquid” water is required to initiate corrosion processes (including SCC) that are supported by electrochemical corrosion reactions. Typically, a threshold relative humidity is used to simulate such a corrosion initiation condition (e.g., ASM International 1987 [DIRS 103753], pp. 80 to 82). In the waste package degradation analysis (SNL 2007 [DIRS 181953]), no threshold relative humidity is used (i.e., SCC occurs, if all stress and stress intensity factor criteria are satisfied, under any exposure conditions).

The discussion in excluded FEP 2.1.11.07.0A (Thermal Expansion/Stress of In-Drift EBS Components) indicates that thermal expansion is not a source of stress and, therefore, not a driving force for SCC in the repository.

In summary, SCC of the waste package outer barrier is included in performance assessments to demonstrate compliance with the individual protection standard after permanent closure at proposed 10 CFR 63.311 (70 FR 53313 [DIRS 178394]) and with the groundwater protection standard at 10 CFR 63.331 [DIRS 180319]. As opposed to general corrosion, waste package SCC is a localized effect and will not significantly affect overall waste package mechanical properties. Therefore, the earliest time after disposal that the waste package would degrade sufficiently that a human intrusion could occur without recognition by the drillers (SNL 2008 [DIRS 183478], Section 6.7.2) would not be affected, and SCC of the waste package is not included in the performance assessment to demonstrate compliance with the individual protection standard for human intrusion (proposed 10 CFR 63.321 (70 FR 53313 [DIRS 178394])) due to low consequence.

INPUTS:

Table 2.1.03.02.0A-1. Indirect Inputs

Citation	Title	DIRS
10 CFR 63	Energy: Disposal of High-Level Radioactive Wastes in a Geologic Repository at Yucca Mountain, Nevada	180319
70 FR 53313	Implementation of a Dose Standard After 10,000 Years	178394
ASM International 1987	*Corrosion*	103753
BSC 2004	*Waste Package Closure System Description Document*	171499
SNL 2007	*Seismic Consequence Abstraction*	176828
SNL 2007	*Analysis of Mechanisms for Early Waste Package/Drip Shield Failure*	178765
SNL 2007	*Stress Corrosion Cracking of Waste Package Outer Barrier and Drip Shield Materials*	181953
SNL 2007	*Total System Performance Assessment Data Input Package for Requirements Analysis for DOE SNF/HLW and Navy SNF Waste Package Overpack Physical Attributes Basis for Performance Assessment*	179567
SNL 2007	*Total System Performance Assessment Data Input Package for Requirements Analysis for TAD Canister and Related Waste Package Overpack Physical Attributes Basis for Performance Assessment*	179394
Woolf 2003	*Controlled Plasticity Burnishing (CPB) for Developing a Very Deep Layer of Compressive Residual Stresses in Rectangular Specimens of Alloy 22 for Yucca Mountain Nuclear Waste Package Closure Weld*	178059

FEP: 2.1.03.02.0B

FEP NAME:

Stress Corrosion Cracking (SCC) of Drip Shields

FEP DESCRIPTION:

Drip shields may become wet at specific locations that are stressed leading to stress corrosion cracking (SCC). The possibility of SCC under dry conditions or due to thermal stresses are also addressed as part of this FEP.

SCREENING DECISION:

Excluded – low consequence

SCREENING JUSTIFICATION:

The principal postclosure functions of the drip shield are to prevent: (1) rockfall from impacting and damaging the waste package, and (2) seepage waters from contacting the waste package. As explained below, if SCC were to occur in either the seepage diverting Titanium Grade 7 drip shield plate material or the Titanium Grade 29 structural support component material, it would not significantly subvert the drip shield functions. Stress corrosion cracking in the drip shield plate material is assumed to occur under repository conditions in regions where sustained tensile stresses exceed a threshold tensile stress value of 80% of the at-temperature yield strength, as discussed in *Stress Corrosion Cracking of Waste Package Outer Barrier and Drip Shield Materials* (SNL 2007 [DIRS 181953], Section 6.8.3.3, Table 6-32). If SCC is initiated, it is conservatively assumed that it will immediately propagate through-wall (SNL 2007 [DIRS 181953], Section 6.8.4.2.2). For the Titanium Grade 29 structural support component material, the threshold tensile stress value is 50% of the at-temperature yield strength (SNL 2007 [DIRS 181953], Table 6-32). The principal sources of stress that could result in SCC in the Titanium Grades 7 and 29 drip shield materials are: (1) weld-induced residual stress, (2) plasticity-induced residual stress caused by seismic events, and (3) stress produced by rockfalls and drift collapse (SNL 2007 [DIRS 181953], Section 6.8). In addition, thermal loading has the potential to induce stresses in the drip shield components.

Stress relief of tensile residual stresses in the welded regions of the drip shield will be accomplished by furnace heating at 1,100°F ± 50°F for a minimum of 2 hours (SNL 2007 [DIRS 179354], Table 4-2, Parameter Number 07-13). ASM Handbook data (Boyer et al. 2003 [DIRS 174636], pp. 608 to 609) indicates that this heat treatment will be sufficient to decrease stress levels below the threshold stresses for initiation of SCC in the drip shield materials. Therefore, properly annealed drip shields are not subject to SCC upon emplacement. The potential for early drip shield failure due to low probability manufacturing defects including improper drip shield heat treatment is considered in included FEP 2.1.03.08.0B (Early Failure of Drip Shields).

As summarized in excluded FEP 2.1.07.02.0A (Drift Collapse), non-seismic drift collapse will result in only minor degradation or collapse of the drift (including enlargement). This will result

in only minor and localized deviations from the currently predicted thermal and hydrologic conditions, and minimal consequences to the EBS components including the drip shield.

As discussed in excluded FEP 2.1.11.07.0A (Thermal Expansion/Stress of In-Drift EBS Components), the drip shield connectors are designed to allow for thermal expansion with no effect on drip shield performance up to at least 300°C. Since the drip shield is farther from the heat source (i.e., the decaying waste forms), its temperature will be lower than the waste package surface temperature. As discussed in excluded FEP 2.1.11.07.0A (Thermal Expansion/Stress of In-Drift EBS Components), the peak waste package surface temperature could exceed 300°C in the event of a low probability seismic-induced drift collapse with low thermal conductivity rubble occurring within the first 90 years following closure. However, the probability of generation of such conditions is less than one in 10,000 within the first 10,000 years of disposal. Within a few hundred years of closure, the waste package surface temperature drops below 200°C (SNL 2008 [DIRS 179962], Section 7.1). Therefore, no thermal expansion stresses high enough to initiate SCC will result from thermal loading in the repository. However, even if SCC were to initiate during this relatively short time period, as discussed later, the consequences relative to the seepage diversion function of the drip shield would be negligible.

Seismic effects on drip shield degradation are discussed in included FEP 1.2.03.02.0A (Seismic Ground Motion Damages EBS Components), included FEP 1.2.03.02.0C (Seismic Induced Drift Collapse Damages EBS Components), and excluded FEP 1.2.03.02.0B (Seismic Induced Rockfall Damage to EBS Components). Rockfall and early failure of the drip shield are discussed in more detail in excluded FEP 2.1.07.01.0A (Rockfall) and included FEP 2.1.03.08.0B (Early Failure of Drip Shields), respectively. More details on the treatment of SCC as a result of seismic effects on drip shield performance due to SCC are discussed in *Seismic Consequence Abstraction* (SNL 2007 [DIRS 176828], Sections 6.10, 6.12, and 7.1).

The tightness of stress corrosion cracks in passive alloys such as Titanium Grade 7 (i.e., small crack-opening displacement) as well as their tortuosity will preclude the advection of liquids and solids through these cracks as discussed in excluded FEP 2.1.03.10.0B (Advection of Liquids and Solids through Cracks in the Drip Shield). Therefore, since the primary role of the Titanium Grade 7 drip shield plates is to keep water from contacting the waste package, SCC of the Titanium Grade 7 drip shield plates does not compromise the design purpose of the drip shield.

Further, since propagation of SCC in Titanium Grade 7 is a result of repetitive passive film rupture, anodic dissolution, and repassivation events at the just-initiated or propagating crack tip (SNL 2007 [DIRS 181953], Section 6.8.4.1), there is no effect of SCC on the surrounding material that could lead to other corrosion degradation modes. However, since SCC does result in the formation of tight crevices, the potential effect of crevice corrosion in Titanium Grade 7 does need to be considered. Crevice corrosion of Titanium Grade 7 is evaluated in excluded FEP 2.1.03.03.0B (Localized Corrosion of Drip Shields) and excluded FEP 2.1.09.28.0B (Localized Corrosion on Drip Shield Surfaces Due to Deliquescence).

Under hot, dry conditions such as occur during about the first 100 years following repository closure, it may be possible for so-called hot salt cracking to occur on any tensile stressed regions of the drip shields in areas where salt deposits may be present. Unlike SCC, however, hot salt cracking is not observed below about 260°C (ASM International 1987 [DIRS 101992], p. 688),

which is above the maximum drift wall and drip shield temperatures under expected conditions (SNL 2008 [DIRS 179962], Section 6.4.3.3, Figure 6.4.3-3). If hot salt cracking occurs under unexpected conditions in which drip shield temperatures exceed 260°C, it will result in a crack morphology similar to SCC (ASM International 1987 [DIRS 101992], p. 688). Thus, if it were to occur, the expected impact on drip shield seepage diversion would be the same as for SCC (i.e., negligible).

Stress corrosion cracking, once initiated, is conservatively assumed to propagate immediately through-wall in the Titanium Grade 7 drip shield plate material. However, for the case of deformation-induced secondary type stresses that may result from rockfall or seismic impact, because of the high creep induced stress relaxation rate observed for Titanium Grade 7 (SNL 2007 [DIRS 181953], Section 6.8.5.1 and 6.8.3.1.2 and Figure 6-72) and the relatively low stress corrosion crack growth rates measured for Titanium Grade 7 (SNL 2007 [DIRS 181953], Section 6.8.4.2), it is expected that for regions with initiated SCC, the propagating crack tip stress intensity factor will decrease over time and drop below the threshold value, K_{ISCC}, needed to continue crack propagation. This is expected to lead to partial through-wall crack arrest (SNL 2007 [DIRS 181953], Section 6.8.5.1). In contrast to Titanium Grade 7, for the Titanium Grade 29 structural support material, the stress relaxation rate is lower because of its higher creep resistance (BSC 2005 [DIRS 174715], Attachment I, Figure I-13). However, the measured crack growth rate of annealed Titanium Grade 29 (approximately 5×10^{-9} to 6×10^{-9} mm/s at 25 ksi√in (27.5 MPa√m) at 150°C (SNL 2007 [DIRS 181953], Figure 6-78(a)) is much lower than that of annealed Titanium Grade 7 (approximately 1.3×10^{-8} mm/s at 110°C at 27.3 ksi√in (30 MPa√m)) (SNL 2007 [DIRS 181953], Figure 6-76(a)) even though the Titanium Grade 29 rate was measured at a higher temperature than that of Titanium Grade 7. Further, since it is observed that crack growth rates in Titanium Grade 7 drop by about two orders of magnitude as a result of 20% plastic deformation (SNL 2007 [DIRS 181953], Table 6-33), the growth rate for Titanium Grade 29 is also expected to drop significantly in regions of high residual stress levels (i.e., in regions deformed due to rockfall or seismic impacts). For a one order of magnitude drop in rate (i.e., to ~5×10^{-10} mm/s (~0.0158 mm/yr) at 25 ksi√in (27.5 MPa√m)), crack propagation through the 76-mm-thick Titanium Grade 29 structural supports (SNL 2007 [DIRS 179354], Table 4-2, Parameter Number 07-08) would take a significantly longer time, about 5,000 years, compensating for the lower stress relaxation rate. Further, at some stage of its propagation, when the crack becomes sufficiently large, it will affect the overall stiffness (compliance) of the drip shield resulting in crack blunting, or, in the case of a confined drip shield, in load and stress redistribution. This crack blunting or redistribution of stress will reduce stress concentrations and the resultant stress intensity factors and thus inhibit further crack propagation.

Thus, SCC does not affect the ability of the drip shield to maintain its seepage diversion function and it will continue to prevent rockfall from damaging the waste package. Therefore, omission of FEP 2.1.03.02.0B (Stress Corrosion Cracking (SCC) of Drip Shields) will not result in a significant adverse change in the magnitude or timing of either radiological exposure to the RMEI or radionuclide releases to the accessible environment. Therefore, this FEP is excluded from the performance assessments conducted to demonstrate compliance with proposed 10 CFR 63.311 and 63.321 (70 FR 53313 [DIRS 178394]), and with 10 CFR 63.331 [DIRS 180319], on the basis of low consequence.

INPUTS:

Table 2.1.03.02.0B-1. Direct Inputs

Input	Source	Description
ASM International 1987. *Corrosion*. [DIRS 101992]	p. 688	Hot salt cracking is not observed below about 260°C
Boyer et al. 2003. *Materials Properties Handbook: Titanium Alloys*. [DIRS 174636]	pp. 608 to 609	Stress relief heat treatment will be sufficient to decrease stress levels below the threshold stresses for initiation of SCC in the drip shield materials
SNL 2007. *Total System Performance Assessment Data Input Package for Requirements Analysis for EBS In-Drift Configuration*. [DIRS 179354]	Table 4-2, Parameter Number 07-13	Stress relieving heat treatment shall be by furnace heating at 1,100 F ± 50°F for a minimum of 2 hours
SNL 2007. *Stress Corrosion Cracking of Waste Package Outer Barrier and Drip Shield Materials*. [DIRS 181953]	Section 6.8.3.3, Table 6-32	SCC in the drip shield plate material is assumed to occur under repository conditions in regions where sustained tensile stresses exceed a threshold tensile stress value of 80% of the at-temperature yield strength
	Table 6-32	For the Titanium Grade 29 structural support material, the threshold tensile stress value is 50% of the at-temperature yield strength
	Section 6.8.4.2.2	If SCC is initiated, it is conservatively assumed that it will immediately propagate through-wall

Table 2.1.03.02.0B-2. Indirect Inputs

Citation	Title	DIRS
10 CFR 63	Energy: Disposal of High-Level Radioactive Wastes in a Geologic Repository at Yucca Mountain, Nevada	180319
70 FR 53313	Implementation of a Dose Standard After 10,000 Years	178394
ASM International 1987	*Corrosion*	101992
BSC 2005	*Creep Deformation of the Drip Shield*	174715
SNL 2007	*Seismic Consequence Abstraction*	176828
SNL 2007	*Total System Performance Assessment Data Input Package for Requirements Analysis for EBS In-Drift Configuration*	179354
SNL 2007	*Stress Corrosion Cracking of Waste Package Outer Barrier and Drip Shield Materials*	181953
SNL 2008	*Postclosure Analysis of the Range of Design Thermal Loadings*	179962

FEP: 2.1.03.03.0A

FEP NAME:

Localized Corrosion of Waste Packages

FEP DESCRIPTION:

Localized corrosion (pitting or crevice corrosion) could enhance degradation of the waste packages.

SCREENING DECISION:

Included

TSPA DISPOSITION:

Localized corrosion is corrosive attack at discrete sites or in a nonuniform manner. Based on a conservative linear growth model, the rate of localized corrosion penetration, if it occurs, is generally higher than the rate of general corrosion penetration and could lead to eventual breach of waste packages.

The two main routes through which an aqueous solution could come into contact with the waste package surface are dust deliquescence and seepage. The possibility of localized corrosion of the WPOB due to brines produced by dust deliquescence is discussed in excluded FEP 2.1.09.28.0A (Localized Corrosion on Waste Package Outer Surface due to Deliquescence). Localized corrosion initiation due to seepage water contact is discussed here. The potential impact of dripping condensate on waste package corrosion is discussed in excluded FEP 2.1.08.14.0A (Condensation on Underside of Drip Shield).

Localized corrosion of the WPOB is conservatively considered to be able to initiate regardless of relative humidity (SNL 2007 [DIRS 178519], Section 5.1), although in reality localized corrosion can only initiate under certain exposure conditions (SNL 2007 [DIRS 178519], Section 6.4.4). Localized corrosion requires the presence of at least a thin aqueous film in contact with the metal surface for a period of time. This is required to establish separate cathodic and anodic areas on the metal surface. The persistence of the thin aqueous film will depend on the temperature of the alloy surface. If the temperature of the alloy surface is significantly higher than the boiling point of pure water, then the water film–alloy interface may not exist because the aqueous film should evaporate upon contact with the alloy surface. However, seepage water can exist on the waste package surface at temperatures in excess of the normal boiling point of pure water due to elevation of boiling point by the presence of dissolved species. As mentioned in *General Corrosion and Localized Corrosion of Waste Package Outer Barrier* (SNL 2007 [DIRS 178519], Section 6.4.4.2), seepage water is not expected to contact the waste package surface if the waste package surface temperature exceeds 120°C. Even if the WPOB temperature is 120°C or lower, seepage water will not be able to contact the waste package surface if the drip shield is intact. Consequently, the localized corrosion model is evaluated only if the waste package temperature is below 120°C (SNL 2007 [DIRS 178519], Sections 8.3.1 and 6.4.4) and the overlying drip shield has failed. Drip shield degradation is discussed in included

FEPs 2.1.03.01.0B (General Corrosion of the Drip Shields) and 2.1.03.08.0B (Early Failure of Drip Shields), and excluded FEP 2.1.03.03.0B (Localized Corrosion of Drip Shields). Localized corrosion in the form of pitting generally occurs on boldly exposed surfaces whereas that in the form of crevice corrosion takes place in occluded regions as discussed in *General Corrosion and Localized Corrosion of the Waste Package Outer Barrier* (SNL 2007 [DIRS 178519], Section 6.4.4). Although both pitting and crevice corrosion can initiate on Alloy 22 surfaces, crevice corrosion is the only form of localized corrosion that is modeled. This is a conservative treatment because the initiation thresholds for crevice corrosion, in terms of exposure parameters such as chemistry and temperature, are lower than those required for pitting corrosion (SNL 2007 [DIRS 178519], Section 5.3). Crevices may be formed on the waste package surface at occluded regions such as in between the waste package and its supports and potentially beneath mineral scales, corrosion products, dust, rocks, etc. The chemical environment in a creviced region may be more severe than the near-field environment due to the buildup of metal cations in solution resulting from the corrosion process, as well as the migration of potentially aggressive anions from the near-field environment. Metal ion hydrolysis can lead to the accumulation of hydrogen ions and a corresponding decrease in pH. Electromigration of chloride ions (and other anions) into the crevice must occur to balance the charge within the creviced region. Chloride ions can cause initiation of crevice corrosion on the Alloy 22 WPOB and are, therefore, generally referred to as "aggressive" ions.

The WPOB localized corrosion model is used in the TSPA to evaluate the extent of WPOB degradation by localized corrosion under the expected repository environmental conditions over the regulatory performance period. The submodels included in the WPOB localized corrosion model are the crevice repassivation potential, long-term corrosion potential, and crevice corrosion propagation models (SNL 2007 [DIRS 178519], Section 6.4.4). If localized corrosion initiates, the fraction of the WPOB surface contacted by seepage water is considered to be affected by localized corrosion (SNL 2007 [DIRS 178519], Section 8.3.1).

According to *General Corrosion and Localized Corrosion of Waste Package Outer Barrier* (SNL 2007 [DIRS 178519], Section 8.3.1), localized corrosion of the WPOB may occur when the corrosion potential (E_{corr}) is equal to or greater than a threshold potential ($E_{critical}$), that is, $\Delta E = (E_{critical} - E_{corr}) \leq 0$. The magnitude of ΔE is an index of the localized corrosion resistance, i.e., the larger the positive difference, the greater the resistance to localized corrosion. The localized corrosion model uses the crevice repassivation potential (E_{rcrev}) as the critical potential for the crevice corrosion initiation analysis (i.e., $E_{critical} = E_{rcrev}$). The crevice corrosion initiation model components (i.e., E_{corr} and E_{rcrev}) are functions of the exposure conditions (temperature, pH (E_{corr} only), chloride ion concentration, and nitrate ion concentration, but not relative humidity as noted previously). The localized corrosion model assumes that, once initiated, localized corrosion of the waste package outer barrier propagates at a (time-independent) constant rate. This is a conservative assumption because it is known that the crevice corrosion propagation rate decreases with time (SNL 2007 [DIRS 178519], Section 6.4.4.8).

Anions containing nitrogen, carbon, and sulfur, which are present in the repository groundwater, exhibit varying degrees of inhibitive effects on localized corrosion (Thomas 1994 [DIRS 120498]; Dunn et al. 2004 [DIRS 173813]). Inhibitive anions counteract the effects of aggressive anions (e.g., chloride ions), which tend to accelerate dissolution and breakdown of the oxide passive films formed on Alloy 22. Nitrate ions have a strong inhibitive effect on localized

corrosion of Alloy 22 in chloride-containing solutions (SNL 2007 [DIRS 178519], Section 6.4.4.3). A study of welded Alloy 22 samples in 0.5 M NaCl solutions at 95°C demonstrated that the nitrate ion is an effective inhibitor of localized corrosion of Alloy 22, when the nitrate-to-chloride concentration ratio is greater than 0.2 (Dunn and Brossia 2002 [DIRS 162213]). Dunn et al. (2004 [DIRS 173813]) and Ilevbare (2005 [DIRS 173814]) have shown that sulfate ions decrease the localized corrosion susceptibility of Alloy 22 in chloride-containing solutions. Dunn et al. (2004 [DIRS 173813]) also concluded that carbonate anions were almost as effective as nitrate anions in inhibiting the initiation of localized corrosion on Alloy 22 and that bicarbonate anions inhibited localized corrosion to a lesser extent. The relationship between the inhibitive and aggressive anions corresponds to competitive adsorption or ion exchange at a fixed number of sites on the oxide surface (Thomas 1994 [DIRS 120498]). Inhibitive anions overcome the effects of aggressive anions through participation in competitive adsorption such that the adsorbed inhibitive anions reduce the surface concentration of aggressive anions below a critical value (Thomas 1994 [DIRS 120498]).

The WPOB crevice corrosion initiation model is used to evaluate the crevice corrosion initiation behavior of the Alloy 22 WPOB. The Alloy 22 WPOB contains solution-heat-treated welds and base metal that have had the solution-heat-treated film removed as well as low-plasticity-burnished closure weld regions (e.g., SNL 2007 [DIRS 179394], Section 4.1; Table 4-1, Parameter Number 03-17). Initiation of localized corrosion may be possible when seepage water contacts the waste package outer barrier surface. If the exposure temperature is greater than or equal to 20°C, and less than or equal to 120°C, then to implement the WPOB crevice corrosion initiation model, the empirical correlations for the long-term corrosion potential (E_{corr}) and crevice repassivation potential (E_{rcrev}) (SNL 2007 [DIRS 178519], Section 8.3.1) are evaluated in accordance with the following implementation rules.

(a) If the nitrate ion-to-chloride ion ratio in the environment exceeds 1, then evaluate E_{rcrev} and E_{corr} at a nitrate ion-to-chloride ion ratio of 1. If the molality of chloride ion is less than 0.0005 molal, the nitrate ion-to-chloride ion ratio should be evaluated with a chloride-ion concentration of 0.0005 molal.

(b) If the molality of chloride ion in the environment exceeds 20 molal, then evaluate E_{rcrev} and E_{corr} at a chloride-ion molality of 20 molal. If the molality of chloride ion is less than 0.0005 molal, then evaluate E_{rcrev} and E_{corr} at a chloride-ion molality of 0.0005 molal.

(c) If the pH in the environment exceeds 10, then evaluate E_{corr} at a pH of 10. If the pH in the environment is less than 1.9, then initiate localized corrosion.

If crevice corrosion initiates, then crevice corrosion propagates at a constant rate throughout the simulation period regardless of changes in the bulk chemical exposure environment. This is a conservative modeling assumption (SNL 2007 [DIRS 178519], Assumption 5.4) and is used because the localized corrosion model does not account for the possibility of crevice corrosion repassivation or stifling. Nitrate ions inhibit localized corrosion initiation (SNL 2007 [DIRS 178519], Section 6.4.4.3). In addition, carbonate and sulfate ions may have an inhibitive effect on localized corrosion. Therefore, because only nitrate ions are accounted for in the model, the results for solutions with significant amounts of other potentially inhibitive ions in addition to

nitrate are conservative (SNL 2007 [DIRS 178519], Section 8.3.1). The model results for the beneficial effects of the inhibitive ions combined with alkaline pH conditions of the typical carbonate-containing waters in the repository are consistent with the experimental observations on the immunity of Alloy 22 to localized corrosion in those waters (SNL 2007 [DIRS 178519], Section 7.2.3).

Before waste loading, the waste packages (base-metal and fabrication welds) will be solution-annealed for 20 minutes at about 1,120°C to 1,150°C and then quenched (SNL 2007 [DIRS 179394], Table 4-1, Parameter Number 03-16). This heat treatment results in the formation of a solution-annealed oxide film on the WPOB surface. Torres et al. (2006 [DIRS 182745], Figures 3.2.2.2(f) and 3.2.2.4(f)) observed that the crevice repassivation potentials of welded Alloy 22 specimens solution-annealed at about 1,120°C for 20 minutes with the solution-annealed oxide film removed were not significantly different from the crevice repassivation potentials of as-welded Alloy 22 specimens. The presence of the solution-annealed oxide films increases the Alloy 22 crevice repassivation potential in concentrated solutions, but decreases it in less concentrated solutions (Etien et al. 2005 [DIRS 182742]; Rebak et al. 2006 [DIRS 182744]). As the WPOB crevice repassivation potential model was developed using crevice repassivation potentials from Alloy 22 specimens without solution-annealed oxide films, and the solution-annealing oxide film could increase the uncertainty in predictions of localized corrosion initiation of the WPOB at lower chloride concentrations, the solution-annealing oxide film will be removed during waste package fabrication (SNL 2007 [DIRS 179394], Section 4.1).

The WPOB localized corrosion initiation model outputs consisting of mean values of model coefficients along with associated uncertainties are documented in Section 8 of *General Corrosion and Localized Corrosion of Waste Package Outer Barrier* (SNL 2007 [DIRS 178519], Table 8-2). The entire variance of the crevice corrosion initiation model (i.e., the crevice repassivation potential model and the long-term corrosion potential model) is attributed to uncertainty. Variability in the crevice repassivation potential and long-term corrosion potential is represented with the temporally and spatially varying waste package temperature and water chemistry contacting the waste packages. An appropriate distribution of the Alloy 22 crevice corrosion propagation rate is provided in Table 8-3 of *General Corrosion and Localized Corrosion of Waste Package Outer Barrier* (SNL 2007 [DIRS 178519]). The variation in crevice corrosion propagation rate is attributed to uncertainty.

Alloy 22 crevice samples were tested for over 5 years in three different solutions (simulated dilute water, simulated concentrated water , and simulated acidified water) at 60°C and 90°C in the LTCTF. The crevice corrosion data of the WPOB material (Alloy 22) that were generated in fully immersed conditions were assumed to be applicable to the crevice corrosion processes of the waste package in contact with thin water films (under porous layers of dust and mineral precipitates) having the same water chemistry as the fully immersed condition (SNL 2007 [DIRS 178519], Section 5.5). None of the crevice samples has shown any indication of localized corrosion attacks after being tested for over five years (SNL 2007 [DIRS 178519], Section 7.2.4). Stereomicroscope and scanning electron microscope examination of the crevice specimens tested in the LTCTF for five years clearly showed no preferential dissolution at any grain boundary, confirming the absence of intergranular attack (Wong et al. 2004 [DIRS 174800]).

In summary, localized corrosion of the WPOB is included in performance assessments to demonstrate compliance with the individual protection standard after permanent closure at proposed 10 CFR 63.311 (70 FR 53313 [DIRS 178394]) and with the groundwater protection standard at 10 CFR 63.331 [DIRS 180319]. Although pitting and crevice corrosion of Alloy 22 are possible, only crevice corrosion is represented in the WPOB degradation model. In the TSPA model, it is assumed that, once initiated, localized corrosion of the waste package outer barrier propagates at a constant rate. In the TSPA model, no credit is taken for the corrosion resistance of the disposal/TAD canister or the waste package inner vessel. Therefore, once the waste package outer barrier has failed, it is conservatively assumed that the waste form is directly exposed to the water or air of the repository environment. The crevice corrosion initiation model is intended exclusively for evaluating the long-term localized corrosion susceptibility of the WPOB and is not intended for short-term transient behavior.

As opposed to general corrosion, waste package localized corrosion is by definition a localized effect and will not significantly affect overall waste package mechanical properties. Therefore, the earliest time after disposal that the waste package would degrade sufficiently that a human intrusion could occur without recognition by the drillers (SNL 2008 [DIRS 183478], Section 6.7.2) would not be affected, and localized corrosion of the waste package is not included in the performance assessment to demonstrate compliance with the individual protection standard for human intrusion (proposed 10 CFR 63.321 (70 FR 53313 [DIRS 178394])) due to low consequence.

INPUTS:

Table 2.1.03.03.0A-1. Indirect Inputs

Citation	Title	DIRS
10 CFR 63	Energy: Disposal of High-Level Radioactive Wastes in a Geologic Repository at Yucca Mountain, Nevada	180319
70 FR 53313	Implementation of a Dose Standard After 10,000 Years	178394
Dunn and Brossia 2002	"Assessment of Passive and Localized Corrosion Processes for Alloy 22 as a High-Level Nuclear Waste Container Material"	162213
Dunn et al. 2004	"Effect of Inhibiting Oxyanions on the Localized Corrosion Susceptibility of Waste Package Container Materials"	173813
Etien et al. 2005	"Effect of Solution Annealing on Critical Potentials of Alloy 22"	182742
Ilevbare 2005	"The Effect of Sulfate Anions on the Crevice Breakdown and Repassivation Potentials of Alloy 22 in 4M NaCl"	173814
Rebak et al. 2006	"Influence of Black Annealing Oxide Scale on the Anodic Behavior of Alloy 22"	182744
SNL 2007	*General Corrosion and Localized Corrosion of Waste Package Outer Barrier*	178519
SNL 2007	*Total System Performance Assessment Data Input Package for Requirements Analysis for TAD Canister and Related Waste Package Overpack Physical Attributes Basis for Performance Assessment*	179394
Thomas 1994	"The Mechanism of Corrosion Prevention by Inhibitors"	120498
Torres et al. 2006	*Aging and Phase Stability of Alloy 22 Welds*	182745
Wong et al. 2004	"Surface Analysis of Alloy 22 Coupons Exposed for Five Years to Concentrated Ground Waters"	174800

FEP: 2.1.03.03.0B

FEP NAME:

Localized Corrosion of Drip Shields

FEP DESCRIPTION:

Localized corrosion (pitting or crevice corrosion) could enhance degradation of the drip shields.

SCREENING DECISION:

Excluded – low probability

SCREENING JUSTIFICATION:

Titanium and its alloys are resistant to general and localized corrosion due to the formation of a protective oxide layer on the metal surface in the presence of oxygen and moisture (Jones 1996 [DIRS 105076], p. 524). Both of these conditions are expected to be persistent within the repository. The drip shield plates are to be fabricated from Titanium Grade 7 (SNL 2007 [DIRS 179354], Table 4-2, Parameter Number 07-04), which is alloyed with 0.15% palladium for increased localized corrosion resistance. The drip shield structural support members are to be fabricated with Titanium Grade 29 (SNL 2007 [DIRS 179354], Table 4-2, Parameter Number 07-04), which is higher strength titanium containing approximately 6% aluminum, 4% vanadium, and 0.1% ruthenium, the latter of which is added to improve localized corrosion resistance, analogous to the impact that palladium has in Titanium Grade 7.

In *General Corrosion and Localized Corrosion of the Drip Shield* (SNL 2007 [DIRS 180778], Section 5.6), localized corrosion of the titanium drip shield is assumed to initiate when the corrosion potential (E_{corr}) equals or exceeds the threshold potential for breakdown of the passive film ($E_{critical}$). A correlation between exposure parameters (temperature, chloride ion concentration, and pH) and the difference between the critical potential ($E_{critical}$) and the corrosion potential (E_{corr}) (i.e., $\Delta E = E_{critical} - E_{corr}$) was developed to indicate when localized corrosion could be initiated. Localized corrosion initiates when ΔE is less than or equal to zero (i.e., when E_{corr} is greater than or equal to $E_{critical}$). The critical or threshold potential is defined as the potential where the current density in the forward portion of an anodic cyclic polarization scan rapidly increases, rather than the potential at which any specific value of the current density is achieved (SNL 2007 [DIRS 180778], Section 6.6.1). The results show, for Titanium Grade 7, that the mean ΔE is generally in excess of 1 V over all anticipated ranges of pH, chloride concentration, and temperature (SNL 2007 [DIRS 180778], Section 6.6.3) in the repository. Localized corrosion of Titanium Grade 7 is not expected to initiate in repository-relevant environments even at pH values as high as 14 (SNL 2007 [DIRS 180778], Section 8.4).

For the drip shield application in the repository, there is an early period of dry air exposure prior to aqueous exposure. During this time, the drip shield will be subjected to a long period of slow thermal oxidation resulting in the formation of a thick and relatively defect-free oxide coating on the Titanium Grades 7 and 29 components of the drip shield (SNL 2007 [DIRS 180778], Section 6.4.1). An increase in the oxide film thickness, coupled with a decrease in defect

concentration in the oxide film, will decrease the susceptibility of the passive film to fluoride-induced breakdown and, hence, fluoride-chloride-induced localized corrosion of the drip shield (SNL 2007 [DIRS 180778], Section 6.5.7). Handbooks (e.g., Revie 2000 [DIRS 159370], p. 865; ASM International 1987 [DIRS 103753], p. 669) indicate that damaged titanium oxide films can re-heal instantaneously if at least trace amounts of oxygen are present. Project analyses indicate that the repository will always support oxidizing exposure conditions (SNL 2007 [DIRS 177412], Section 8.1); therefore, such oxide films are expected to form, and be stable, in the period prior to the contact of the drip shield by any seepage water.

The presence of crevices and concentrated calcium and magnesium chloride solutions and their influences on corrosion were also evaluated in *General Corrosion and Localized Corrosion of the Drip Shield* (SNL 2007 [DIRS 180778], Sections 6.5.8, 6.6.4, and 6.6.5). The results in that report (SNL 2007 [DIRS 180778], Section 6.6.5) show that the passive film on Titanium Grade 7 is stable in concentrated calcium and magnesium chloride solutions and the passive current density is not increased under such conditions. The minimum ΔE observed in these studies (obtained in 9 *M* $CaCl_2$ at 150°C) is 1.4 V (SNL 2007 [DIRS 180778], Table 21), which supports the exclusion of localized corrosion in these environments.

As discussed in *General Corrosion and Localized Corrosion of the Drip Shield* (SNL 2007 [DIRS 180778], Section 6.5.7), the presence of dissolved fluoride ions can, under certain conditions, increase the general corrosion rate of titanium alloys, including Titanium Grades 7 and 29, and possibly destabilize the passive film. As discussed below, while certain fluoride-containing environments have been found to initiate localized corrosion, under repository-relevant exposure conditions the passive film on titanium is expected to remain stable.

Short-Term Tests and Fluoride Effects:

The literature results for fluoride effects on titanium corrosion include experiments conducted under a wide range of fluoride, chloride, nitrate, pH, and temperature conditions. In addition, the applied experimental approaches also vary, including both uninstrumented exposure testing as well as standard electrochemical techniques. It should be noted that the aforementioned combination of varying environmental and electrochemical conditions utilized throughout the literature hinder the establishment of general conclusions from any one result.

The scientific literature includes observations of both localized corrosion and enhanced general corrosion resulting from exposure of titanium alloys to certain fluoride bearing electrolytes (Pulvirenti et al. 2003 [DIRS 162574]; Pulvirenti et al. 2002 [DIRS 159841]; Lorenzo de Mele and Cortizo 2000 [DIRS 159833]; Brossia and Cragnolino 2001 [DIRS 162420]; Brossia and Cragnolino 2004 [DIRS 180832]; Lian et al. 2005 [DIRS 173979]; Lian et al. 2006 [DIRS 183947]).

Localized corrosion of Titanium Grade 7 in the form of pitting attack and, in one case, SCC has been reported by Pulvirenti et al. (2003 [DIRS 162574]; 2002 [DIRS 159841]) in a simulated groundwater environment augmented with both fluoride and chloride. In that study, samples were exposed under open circuit conditions to chloride-fluoride solutions at several temperatures and pH values. Pitting was observed in 1 *M* (35,500 ppm) chloride plus 0.1 *M* (1,900 ppm) fluoride at pH values from 6.5 to 7.2 at 105°C, but not in that same environment at 160°C

(Pulvirenti et al. 2002 [DIRS 159841], Tables 3 and 4). In cases where pitting was observed, initiation tended to be at mechanical defects on the metal surface, and Pulvirenti theorized that the initiation sites were probably contaminated with iron deposited during production of the sample based upon the experimental observation that pitting did not initiate at defects made with a diamond scribe. It should also be noted that pitting was not observed in an environment containing 48,000 ppm chloride and 14,400 ppm fluoride at 105°C, suggesting that the aggressiveness of such solutions is not a direct function of the fluoride content. Cyclic polarization testing revealed a decrease in repassivation potential with increasing chloride concentration for chloride-fluoride solutions, and suggested an inhibiting effect by nitrate but no inhibiting effect by sulfate (Pulvirenti et al. 2003 [DIRS 162574], Figure 1 and Table 2).

The behavior of Titanium Grade 7 in environments containing 1 *M* chloride with fluoride additions up to 0.1 *M* was evaluated using cyclic polarization and open circuit exposures of creviced samples by Lian et al. (2006 [DIRS 183947]). Results of this testing were consistent with that reported by Pulvirenti et al. (2003 [DIRS 162574]; 2002 [DIRS 159841]). Cyclic polarization in deaerated 1 *M* NaCl plus 0.1 *M* NaF at pH 8 and 95°C showed Titanium Grade 7 to be active during the reverse scan until E_{corr} was reached with localized attack reported following the polarization scan, indicating that Titanium Grade 7 will not remain passive in this environment under free-corrosion conditions (Lian et al. 2006 [DIRS 183947], Figure 7). This result was corroborated with open circuit testing in the same environment where localized attack was observed after two weeks of exposure (Lian et al. 2006 [DIRS 183947], Table 2).

Brossia and Cragnolino (2001 [DIRS 162420]; 2004 [DIRS 180832]) used short-term electrochemical testing in chloride-fluoride solutions to elucidate the effect of fluoride on the corrosion behavior of Titanium Grade 7. In contrast to the other studies cited above, Brossia and Cragnolino primarily observed an influence of fluoride on the passive current density. They found that increasing fluoride concentration in 1 *M* NaCl at 95°C resulted in increased passive current density up to values approaching 10^{-4} $A \cdot cm^{-2}$ (Brossia and Cragnolino 2004 [DIRS 180832], Figures 8 and 9). Addition of nitrate and sulfate to a chloride-fluoride solution did not appreciably alter the passive current density compared to the binary chloride-fluoride solution (Brossia and Cragnolino 2004 [DIRS 180832], Figure 10). In these experiments the samples were anodically polarized to 0 V versus saturated calomel electrode and the measured steady-state current reported as the passive corrosion rate. These results may not be directly applicable to the nominal conditions in the repository as the drip shield materials will be at open circuit rather than anodically polarized.

Localized corrosion of Titanium Grade 1 (unalloyed titanium containing neither platinum nor ruthenium) in the form of blisters was reported by de Mele and Cortizo following a 6-day exposure to synthetic saliva (pH equal to 6.5) with the addition of 0.2 *M* fluoride (Lorenzo de Mele and Cortizo (2000 [DIRS 159833]). They observed that if fluoride ions were added shortly after electrode immersion (while the oxide film was still growing and, hence, defective), the corrosion potential decreased rapidly (probably due to attack of the oxide). However, if the oxide film was allowed to grow for four days, then addition of the same amount of fluoride ions had no observable effect over the subsequent two days of exposure. These data suggest that growth or healing of the oxide prior to introduction of fluoride may decrease the initial susceptibility to oxide breakdown.

Corrosion of Titanium Grade 7 was measured by Lian et al. (2005 [DIRS 173979]) in 1 *M* NaCl + 0.1 *M* NaF at 95°C and pH values of 4, 8, and 11. Annealing samples for 3 hours at 593°C prior to exposure had the effect of decreasing the passive current density and increasing the open circuit potential. An annealed sample exposed under open circuit conditions in pH 8 solution had an initially low corrosion rate compared to a freshly polished sample; however, the corrosion rate of the annealed sample increased after 4 days of exposure to a value similar to that of the polished sample. Samples exposed to the pH 4 electrolyte underwent localized attack during a one-week open circuit exposure independent of the annealing treatment, although the annealed sample suffered less attack. It was concluded that the thick thermal oxide that forms during annealing can improve the corrosion resistance of Titanium Grade 7 but could not prevent the fluoride ion attack at low pH. It should be noted that the only samples reported to suffer localized corrosion in this study were those exposed to acidic conditions (pH 4). Extrapolation of this behavior to higher pH values representative of expected repository conditions is not appropriate, and localized corrosion is not expected at repository-relevant pH values.

Long-Term Tests and Fluoride Effects:

While the literature cited above suggests that under specific non-repository-relevant combinations of pH, temperature, [Cl^-] and [F^-], it is possible to initiate localized corrosion on Titanium Grade 7, as demonstrated below, localized corrosion will not initiate for repository-relevant environments. The influence of fluoride on titanium corrosion under repository-relevant conditions can be gained by examination of the localized corrosion results from multi-year tests conducted at the LTCTF, in which Titanium Grades 7 and 16 were evaluated.[1] Excellent corrosion behavior was observed on noncreviced and creviced Titanium Grade 7 and Grade 16 specimens during 2.5- and 5-year exposures, respectively; the general corrosion rates obtained were low, and no initiation of localized corrosion was observed (SNL 2007 [DIRS 180778], Section 6.5.1). Tests included exposure of samples to fluoride-bearing SCW (about 1,000× ionic concentration of J-13 well water with target composition of: 1,400 mg/L fluoride (0.07 *m*); 6,700 mg/L chloride (0.19 *m*); 6,400 mg/L nitrate (0.1 *m*); 16,700 mg/L sulfate (0.17 *m*); and 27 mg/L (0.001 *m*) to 49 mg/L (0.0017 *m*) silica at a pH value of ~9.8 to 10.2 (DTN: LL040803112251.117 [DIRS 171362], file: *LL040803112251.117 Table 1.pdf*)). The SCW environment contains nitrate and fluoride at a concentration ratio of 1.4:1 and contains other anions such as sulfate and bicarbonate; the resulting chemical composition is benign towards localized corrosion of titanium.

Repository Relevant Environments and Fluoride Effects:

Although the concentrations of fluoride and chloride that have been shown to cause initiation of localized corrosion on Titanium Grade 7 (e.g., 1 *M* chloride plus 0.1 *M* fluoride (Pulvirenti et al. 2003 [DIRS 162574]; Lian et al. 2006 [DIRS 183947])) are possible under normal repository conditions, the expected repository environments are more complex, containing additional cationic and anionic species, and are better represented by the SCW environment. A comparison of the SCW environment, the chloride-fluoride environment where localized corrosion has been

[1] It is important to emphasize that Titanium Grade 16 has less than half the level of palladium as Titanium Grade 7 and as such is considered to be less corrosion-resistant than Titanium Grade 7. This provides an additional level of confidence that Titanium Grade 7 will not be susceptible to localized corrosion over longer exposure times.

observed, and the Group 1 water predicted by the near-field chemistry model[2] is shown in Table 2.1.03.03.0B-1. While the chloride and fluoride concentrations of the evaporated in-drift waters are greater than the SCW, the presence of additional anions in the system inhibits localized corrosion from initiating. Therefore, the SCW environment is most appropriate in assessing the potential for initiation of localized corrosion under expected repository conditions.

Higher fluoride levels can result when potential seepage waters predicted by the near-field chemistry model are evaporatively concentrated on the drip shield surface (peak of 0.71 *m*, DTN: SN0701PAEBSPCE.001 [DIRS 180523], folder: Lookup Tables\ PCE Gp 1 LUT, files: *1jp2t30.xls* and *1lp2t30.xls*). However, a GoldSim analysis (DTN: MO0709TSPALOCO.000 [DIRS 182994], file: *LA_v5.000_LC_Initiation_Analysis_v2_ Conceptual_ Description.pdf*) demonstrates that the repository conditions required for highly elevated fluoride do not or only rarely occur. The simulation determines that an environmental boundary condition exists where water that has the highest WRIP, a parameter from the near-field chemistry model that typically lowers calcium and thereby increases fluoride, is unable to reach the repository horizon while the relative humidity is below 85%; these two conditions must occur simultaneously to begin to approach the 0.71 *m* fluoride levels cited previously, as seen by inspection of the evaporative seepage water lookup tables (DTN: SN0701PAEBSPCE.001 [DIRS 180523], folder: Lookup Tables).

Conceptually, this environmental boundary exists because to attain a high WRIP value, the water percolating through the mountain must see an extended thermal plume, which can only occur after peak in-drift temperatures have been reached and after which the relative humidity will be increasing. At both the expected and elevated WRIP levels, while temperatures are between 70°C and 100°C (no seepage is expected above 100°C), the concentrations of F^- are similar (compare the near-field chemistry water compositions in Table 2.1.03.03.0B-1). As the drip shield temperatures come down below 70°C, higher relative humidity prevails, such that while higher water–rock interaction may occur, resident seepage compositions are becoming more dilute. These environmental constraints, based on a GoldSim total system performance analysis in conjunction with inspection of the evaporative seepage water lookup tables (DTN: SN0701PAEBSPCE.001 [DIRS 180523]), constrain fluoride levels to below 0.2 *m*. For the expected repository conditions, the levels of fluoride achieved due to evaporative concentration appear constrained below 0.2 *m* for Group 1 seepage, and less than 0.01 *m* for seepage Groups 2 through 4.

[2] Extensive analysis of TSw porewater compositions from the four repository host units (Tptpul, Tptpmn, Tptpll, Tptpln) were evaluated and determined to fall into four compositional "groups" (SNL 2007 [DIRS 177412], Section 6.6). Group 1 water has distinctly lower calcium concentrations and higher pH (SNL 2007 [DIRS 177412], Figure 6.6 17); as such, it consistently has the highest potential fluoride concentrations of the four group waters when evaporated.

Table 2.1.03.03.0B-1. Comparison of Solutions from Corrosion Testing with the Expected Repository Compositions

Water Identity	a_w	T (°C)	pH	Cl	F	NO_3	SO_4	HCO_3	Na	K	Source
Lian et al. 2006	(0.964)	95	8	1.0	0.10	0	0	0	1.1	0	1
Pulvirenti et al. 2002	(0.964)	105	6.5	1.0	0.10	10^{-4}	2×10^{-4}	10^{-3}	1.1	2×10^{-4}	2
SCW	0.955	90	~10	0.2	0.06	0.1	0.3	0.6	2.0	0.1	3
NFC Group 1	0.960	100	9.2	0.3	0.06	0.1	0.1	0.7	1.5	0.3	4
NFC Group 1	0.960	70	9.3	0.2	0.04	0.1	0.06	0.8	1.3	0.4	4
NFC Group 1, evaporated	0.840	100	9.4	1.0	0.17	0.4	0.25	2.8	5.5	1.6	4
NFC Group 1, evaporated	0.840	70	9.4	0.9	0.16	0.4	0.2	2.7	5.1	1.5	4

Sources: 1. Lian et al. 2006 [DIRS 183947], Table 3.
2. Pulvirenti et. al. 2002 [DIRS 159841], Tables 1 and 4, source ppm converted to molal by simple division by species atomic or molecular weight.
3. DTN: LL031001023121.035 [DIRS 170502], file: *LLNL_molal_summary.xls,* sample ID: GH17; pH is the middle of the target value from DTN: LL040803112251.117 [DIRS 171362], file: *LL040803112251.117 Table 1.pdf*.
4. DTN: SN0701PAEBSPCE.001 [DIRS 180523], files: *1gp2t1.xls* and *1ip2t70.xls,* for the 100°C WRIP = "g", and the 70°C WRIP = "i" data, respectively.

NOTES: Activity of water (multiply by 100 to express as relative humidity) from DTN: LL060904312251.186 [DIRS 178283]. Lian et al. [DIRS 183947] and Pulvirenti et al. 2002 [DIRS 159841] activity is estimated as average of a similar monovalent mixture (1 *m* NaCl + 0.15/0.05 *m* KCl, files *19.3o* and *20.3o*). SCW from file: *2f.3o*. NFC results are directly from source 4.

Units of chemical species are in molar (*M*) for Lian et al. 2006 [DIRS 183947] and Pulvirenti et al. 2002 [DIRS 159841], and molal (*m,* mole solute per kg water) for all others. Values are rounded to simplify comparison.

This review of the experimentally observed influences of fluoride on titanium corrosion and comparison of the test environments to expected repository environments shows that while combinations of chloride and fluoride may cause localized corrosion initiation on titanium, no localized corrosion has been observed after up to 5 years of exposure to SCW, which is the most relevant fluoride-bearing test environment (SNL 2007 [DIRS 180778], Section 7.5). Additionally, similar long-term exposures were performed under two other aqueous conditions termed SAW and SDW, also with no observed initiation of localized corrosion (SNL 2007 [DIRS 180778], Section 6.6.4). In light of the above discussion, localized corrosion of Titanium Grade 7 is not expected to initiate under relevant repository exposure conditions. The passive film is expected to be stable even when crevices are present and the material is exposed to concentrated solution environments containing chloride (e.g., calcium or magnesium chloride) and fluoride ions alongside other species such as nitrate.

In addition to the Titanium Grade 7 plate material discussed previously, the drip shield will also have a series of Titanium Grade 29 structural members (SNL 2007 [DIRS 179354], Table 4-2, Parameter Numbers 07-01 and 07-04). Titanium Grade 29 differs compositionally from Titanium Grade 7 and, as such, can exhibit a different electrochemical response under certain environmental conditions. Cyclic polarization testing of noncreviced Titanium Grades 29 and 7 specimens at 120°C and 150°C in multi-ionic electrolytes containing various levels of $CaCl_2$, KCl, KNO_3, $NaNO_3$, NaCl, Na_2SO_4, NaF, and NaBr revealed similar behavior for the two alloys,

and specifically, that no localized attack was observed for either material following polarization (Andresen and Kim 2006 [DIRS 178239], Table 11 and Figures 46 to 53). Additionally, a limited set of cyclic polarization experiments were performed on creviced samples in concentrated NaCl plus KCl with and without KNO_3 and NaF at temperatures at or above 110°C (DTN: LL070800612251.197 [DIRS 183159], file: *Ti Gr 7 Gr 29 Electrochemical Developed Aug07*). In the case of Titanium Grade 7, the critical potentials were consistently high. In the case of the Titanium Grade 29, the passive current density was increased to greater than 20 mA/cm^2 in most cases (consistent with observations from the literature (Brossia and Cragnolino 2004 [DIRS 180832], Figures 8 and 9) discussed previously), hindering the use of critical potentials such as the E_{20} (i.e., the potential at which the measured current density exceeds 20 $\mu A/cm^2$). Furthermore, unlike Titanium Grade 7, crevice corrosion was initiated at large anodic polarizations ($E_{applied}$ > 1V versus SSC), and as a result, considerable hysteresis is present in the cyclic polarization scans, making the repassivation potential (i.e., E_{RCO} – the potential at which the return portion of the polarization scan crosses the upwards scan) the most appropriate critical potential to use in the case of Titanium Grade 29. If ΔE is calculated as $E_{RCO} - E_{corr}$, its magnitude is consistently large and greater than zero, with values ranging from 492 to 2,276 mV for the environments presented in DTN: LL070800612251.197 [DIRS 183159]. Given the large positive values observed for ΔE, initiation of localized corrosion for unpolarized samples under such conditions is not expected.

As discussed above, localized corrosion was observed on Titanium Grade 7 under certain specific combinations of pH, temperature, $[Cl^-]$, and $[F^-]$. As such, it follows that under similar conditions, localized corrosion could potentially initiate on Titanium Grade 29, given that it is less resistant to localized corrosion than Titanium Grade 7. Furthermore, there is no long-term data for Titanium Grade 29 as there is for Titanium Grade 7. Given this lack of data, it may be possible for localized corrosion to initiate on Titanium Grade 29 under some subset of repository environments, similar to those discussed above for Titanium Grade 7. This subset of environments is only considered possible when "aggressive" seepage water, as discussed in *General and Localized Corrosion of the Drip Shield* (SNL 2007 [DIRS 180778], Section 6.1.6[a]), is present on the drip shield surface. The only Titanium Grade 29 structure exposed to such conditions is the side support framework; the crown support framework of the drip shield is underneath the Titanium Grade 7 plates and therefore is in the benign environment, which is incapable of initiating localized corrosion.

The consequence of any localized corrosion of the Titanium Grade 29 side framework would be to make the drip shield more susceptible to failure under rock load and subsequent buckling of the sidewall, but there would not be any increase in the snap-through failure of the crown failure mode (SNL 2007 [DIRS 176828], Section 6.8.3.1). In the event of framework collapse where the Titanium Grade 7 plates are still intact, the drip shield continues to function as a barrier to seepage, as discussed in *Seismic Consequence Abstraction* (SNL 2007 [DIRS 176828], p. 6-232, item e). As this is the primary purpose of the drip shield in the performance assessment, an increase to the side framework failures under rock load due to possible localized corrosion of Titanium Grade 29 would not have a significant affect on dose calculations.

In conclusion, localized corrosion of the drip shield sufficient to affect the magnitude or timing of calculated radiological exposures to the RMEI or radionuclide releases to the accessible environment will not occur. Omission of FEP 2.1.03.03.0B (Localized Corrosion of Drip

Shields) will not result in a significant adverse change in the magnitude or timing of either radiological exposure to the RMEI or radionuclide releases to the accessible environment. Therefore, this FEP is excluded from the performance assessments conducted to demonstrate compliance with proposed 10 CFR 63.311 and 63.321 (70 FR 53313 [DIRS 178394]), and with 10 CFR 63.331 [DIRS 180319], on the basis of low consequence.

INPUTS:

Table 2.1.03.03.0B-2. Direct Inputs

Input	Source	Description
LL031001023121.035. Conversion of Corrosion Testing Solutions from Molar to Molal Concentration Units (II). [DIRS 170502]	file: *LLNL_molal_summary.xls*	Water chemistry for sample GH-17
LL060904312251.186. Modeling of Pitzer pH for Selected ECORR Test Solutions. [DIRS 178283]	files: *19.3o*, *20.3o*, *2f.3o*	Activity of water in corrosion test solutions
DTN: LL070800612251.197. Electrochemical Testing of Titanium Grade 7 and Titanium Grade 29 Alloys in Dust-Like Electrolytes - Developed. [DIRS 183159]	Ti Gr 7 Gr 29 Electrochemical Developed Aug07	Cyclic polarization testing of creviced samples in concentrated NaCl plus KCl with and without KNO_3 and NaF at temperatures at or above 110°C has shown high values for the critical potentials of both Titanium Grade 7 and Titanium Grade 29
DTN: MO0709TSPALOCO.000. TSPA Localized Corrosion Analysis. [DIRS 182994]	file: *LA_v5.000_LC_Initiation_Analysis_v2_Conceptual_Description.pdf*	Analysis demonstrates that the repository conditions required for highly elevated fluoride do not or only rarely occur
SNL 2007. *Total System Performance Assessment Data Input Package for Requirements Analysis for EBS In-Drift Configuration*. [DIRS 179354]	Table 4-2, Parameter Numbers 07-01, 07-04	Drip shield is designed with Titanium Grade 7 plates and Titanium Grade 29 support materials
SNL 2007. *Engineered Barrier System: Physical and Chemical Environment*. [DIRS 177412]	Section 8.1	Project analyses indicate that the repository will always support oxic exposure conditions
SNL 2007. *General Corrosion and Localized Corrosion of the Drip Shield*. [DIRS 180778]	Section 6.6.4	No localized corrosion observed in long-term exposures under aqueous conditions termed simulated acidified water and simulated dilute water
	Section 7.5	no localized corrosion has been observed after up to 5 years of exposure to SCW
	Table 21	The minimum delta E observed in 9 molar $CaCl_2$ at 150°C was 1.4 V
	Section 8.4	Localized corrosion of Titanium Grade 7 will not initiate at pH levels as high as 14

Table 2.1.03.03.0B-3. Indirect Inputs

Citation	Title	DIRS
10 CFR 63	Energy: Disposal of High-Level Radioactive Wastes in a Geologic Repository at Yucca Mountain, Nevada	180319
70 FR 53313	Implementation of a Dose Standard After 10,000 Years	178394
Andresen and Kim 2006	*Stress Corrosion Crack Initiation & Growth Measurements in Environments Relevant to High Level Nuclear Waste Packages*	178239
ASM International 1987	*Corrosion*	103753
Brossia and Cragnolino 2001	"Effects of Environmental and Metallurgical Conditions on the Passive and Localized Dissolution of Ti-0.15%Pd"	162420
Brossia and Cragnolino 2004	"Effect of Palladium on the Corrosion Behavior of Titanium"	180832
DTN: LL040803112251.117	Target Compositions of Aqueous Solutions Used for Corrosion Testing	171362
DTN: SN0701PAEBSPCE.001	PCE TDIP Potential Seepage Water Chemistry Lookup Tables	180523
Jones 1996	*Principles and Prevention of Corrosi*on. 2nd Edition.	105076
Lian et al. 2005	"Effects of Oxide Film on the Corrosion Resistance of Titanium Grade 7 in Fluoride-Containing NaCl Brines"	173979
Lian et al. 2006	"Comparative Corrosion Behavior of Two Palladium-Containing Titanium Alloys"	183947
Lorenzo de Mele and Cortizo 2000	"Electrochemical Behaviour of Titanium in Fluoride-Containing Saliva"	159833
Pulvirenti et al. 2002	"Corrosion of Titanium Grade 7 in Solutions Containing Fluoride and Chloride Salts"	159841
Pulvirenti et al. 2003	"Fluoride Corrosion of Ti-Grade 7: Effects of Other Ions"	162574
Revie 2000	*Uhlig's Corrosion Handbook*	159370
SNL 2007	*Seismic Consequence Abstraction*	176828
SNL 2007	*Engineered Barrier System: Physical and Chemical Environment*	177412
SNL 2007	*General Corrosion and Localized Corrosion of the Drip Shield*	180778

FEP: 2.1.03.04.0A

FEP NAME:

Hydride Cracking of Waste Packages

FEP DESCRIPTION:

The uptake of hydrogen and the formation of metal hydrides may mechanically weaken the waste packages and promote degradation.

SCREENING DECISION:

Excluded – low probability

SCREENING JUSTIFICATION:

Hydrogen generated at cathodic sites on a corroding metal may be absorbed into the metal and, if present at a sufficiently high concentration, could degrade the mechanical properties and potentially increase the metal's susceptibility to crack initiation and/or propagation. The hydrogen concentration achieved within a material is a direct function of the rate at which atomic hydrogen is generated at the metal surface (e.g., the rate of the water reduction reaction on a corroding metal), which in turn defines the surface coverage of adsorbed hydrogen. The subsurface absorbed hydrogen concentration (i.e., atomic hydrogen dissolved in the metal matrix at the metal surface) achieved is determined by this surface coverage combined with the efficiency through which it is absorbed into the metal. Once hydrogen has been absorbed into the metal, it will then migrate further into the material via diffusional processes. This migration will continue until there is no longer a chemical potential gradient to drive diffusion (i.e., the bulk hydrogen concentration is equivalent to the subsurface hydrogen concentration). The term hydrogen embrittlement is used to refer to the deleterious impact of hydrogen on the mechanical properties of a material. Hydrogen-induced cracking results from the combined action of absorbed hydrogen and residual or sustained applied tensile stresses, whereby crack initiation and/or propagation occurs at lower stress levels than in the absence of absorbed hydrogen. In the case of nickel-based alloys such as Alloy 22, hydrogen embrittlement typically manifests as a reduction in fracture toughness or an overall loss of ductility (ASM International 1987 [DIRS 103753], pp. 650 to 652). It should be noted that solid solution strengthened nickel-based alloys such as Alloy 22 do not form a hydride phase.

The Alloy 22 waste package, when emplaced, is protected by the drip shield. The drip shield will prevent any fallen ground support from contacting the waste package, thereby eliminating the chances of galvanic coupling. Likewise, the pallet will keep the waste package from contacting the invert (SNL 2007 [DIRS 179354], Table 4-3, Parameter Number 08-03), thereby precluding the galvanic coupling between the waste package and any material (such as carbon steel) in the invert. However, in the event that either the drip shield or the pallet fail to prevent electrical isolation of the waste package from the metals in the support structure or invert, hydrogen-induced cracking of Alloy 22 will still not take place due to the properties discussed in the following text. Hydrogen-induced cracking of the internal stainless steel components will not occur prior to waste package breach due to the insignificant degree of corrosion (excluded

FEP 2.1.03.06.0A (Internal Corrosion of Waste Packages Prior to Breach)), and thus, lack of sufficient hydrogen production (from the cathodic reactions supporting any metal oxidation).

Hydrogen-induced cracking of the waste package outer barrier (Alloy 22) will not occur under repository-relevant exposure conditions for the following reasons:

- The rate of general corrosion for Alloy 22 under repository-relevant conditions is extremely low (SNL 2007 [DIRS 178519], Sections 6.4.3 and 8.2). As such, the supporting cathodic reaction rate, even if assumed to be entirely due to the water reduction reaction, will not result in a sufficiently large absorbed hydrogen concentration to embrittle Alloy 22 (ASM International 1987 [DIRS 103753], p. 652).

- Fully annealed and uncoupled Ni-Cr-Mo alloys (such as Alloy 22) are effectively immune to hydrogen-induced cracking (ASM International 1987 [DIRS 103753], pp. 650 to 652; Gdowski 1991 [DIRS 100859], Section 5.12). Alloy 22 is a Ni-Cr-Mo alloy, and each waste package will be fully annealed (with the exception of the closure weld, which will be stress-mitigated).

- Although Ni-Cr-Mo alloys, such as Alloy 22, are susceptible to hydrogen-induced cracking when heavily cold-worked and cathodically charged with hydrogen (via an impressed current or galvanic couple to a more active material) in environments containing substantial concentrations of hydrogen recombination poisons such as hydrogen sulfide or arsenic trioxide, such conditions are not repository-relevant. These recombination poisons dramatically increase the surface coverage of the metal with adsorbed atomic hydrogen, thereby increasing the achievable subsurface hydrogen concentration (Asphahani 1978 [DIRS 160352], Section III.3 and Table 8; ASM International 1987 [DIRS 103753], p. 651). These environmental and electrochemical conditions are far outside the realm of what may take place on the waste package surface, including contact of the waste package with more active materials such as carbon steel from the invert or other features within the drift, which is not expected to occur. Even in cases where the microstructure could be rendered susceptible to hydrogen embrittlement, the cathodic reaction rate on the Alloy 22 surface is far too low to achieve an embrittling concentration (ASM International 1982 [DIRS 103753], p. 652).

- Aging of Ni-Cr-Mo alloys at temperatures around 500°C can lead to ordering, or grain-boundary segregation of deleterious elements such as phosphorus, which can increase susceptibility to hydrogen-induced cracking (ASM International 1987 [DIRS 103753], p. 169; Asphahani 1978 [DIRS 160352]). For the waste package surface to exceed 300°C, a seismic event of sufficient magnitude must occur within approximately 90 years after closure, resulting in drift collapse and subjecting a waste package to an unfavorable combination of a high thermal output surrounded by low-conductivity rubble (SNL 2008 [DIRS 179962], Section 6.5.1). Analyses have shown that the mean probability of these conditions occurring is about one in 10,000 within the first 10,000 years after closure (SNL 2008 [DIRS 179962], Table 6.5-5). Even if such ordering or grain-boundary segregation of deleterious elements were to occur, the hydrogen concentrations required to cause embrittlement of a Ni-Cr-Mo alloy that had

been thermally aged as described previously can not be achieved without a substantial externally applied cathodic current density in environments that promote hydrogen uptake.

- As discussed in excluded FEP 2.1.09.09.0A (Electrochemical Effects in EBS), contact between the Alloy 22 waste package outer barrier and Titanium Grade 7 drip shield is not expected. However, if it were to occur, galvanic corrosion would not be expected to take place. Both of these materials are electrochemically passive under repository-relevant conditions. As such, there will be little or no galvanic interactions between the two materials. (ASM International 1987 [DIRS 103753], p. 675), and thus there would be no significant increase in hydrogen uptake in either material due to metal-to-metal contact.

To summarize, (1) fully annealed Ni-Cr-Mo alloys (including Alloy 22) are highly resistant to hydrogen-induced cracking even when heavily cold-worked or thermally aged to induce ordering or grain boundary segregation of sulfur or phosphorus, requiring hydrogen concentrations far in excess of what might be achieved within Yucca Mountain to cause embrittlement; (2) the extremely low corrosion rates exhibited by Alloy 22 in repository environments will not generate sufficient hydrogen to cause hydrogen-induced cracking; and (3) if other materials from within the drift (e.g., drip shield, pallet, etc.) come into contact with the waste package, the resultant galvanic couples will not result in an increased rate of metal oxidation, and thus will not cause increased hydrogen production and uptake at the waste package surface. Therefore, hydrogen embrittlement will not occur, and hydrogen-induced cracking (e.g., hydride cracking) of the waste package is excluded from the performance assessments conducted to demonstrate compliance with proposed 10 CFR 63.311, 10 CFR 63.321 (70 FR 53313 [DIRS 178394]), and with 10 CFR 63.331 [DIRS 180319], on the basis of low probability.

INPUTS:

Table 2.1.03.04.0A-1. Direct Inputs

Input	Source	Description
ASM International 1987. *Corrosion*. [DIRS 103753]	pp. 169, 650 to 652	Fully annealed nickel-base alloys, such as Alloy 22, are essentially immune to hydrogen-induced cracking
SNL 2007. *General Corrosion and Localized Corrosion of Waste Package Outer Barrier*. [DIRS 178519]	Section 8.2	Alloy 22 waste package material exhibit extremely low corrosion rates under the repository environments
SNL 2008. *Postclosure Analysis of the Range of Design Thermal Loadings*. [DIRS 179962]	Table 6.5-5	Mean probability (TSPA base case) of key seismic event leading to waste package temp greater than 300°C is about 1 in 10,000 in 10,000 years

Table 2.1.03.04.0A-2. Indirect Inputs

Citation	Title	DIRS
10 CFR 63	Energy: Disposal of High-Level Radioactive Wastes in a Geologic Repository at Yucca Mountain, Nevada	180319
70 FR 53313	Implementation of a Dose Standard After 10,000 Years	178394
ASM International 1987	*Corrosion*	103753
Asphahani 1978	"Hydrogen Cracking of Nickel-Base Alloys"	160352
Gdowski 1991	*Survey of Degradation Modes of Four Nickel-Chromium-Molybdenum Alloys*	100859
SNL 2007	*Total System Performance Assessment Data Input Package for Requirements Analysis for EBS In-Drift Configuration*	179354
SNL 2007	*General Corrosion and Localized Corrosion of Waste Package Outer Barrier*	178519
SNL 2008	*Postclosure Analysis of the Range of Design Thermal Loadings*	179962

FEP: 2.1.03.04.0B

FEP NAME:

Hydride Cracking of Drip Shields

FEP DESCRIPTION:

The uptake of hydrogen and the formation of metal hydrides may mechanically weaken the drip shields and promote degradation.

SCREENING DECISION:

Excluded – low probability

SCREENING JUSTIFICATION:

The drip shield plates are to be fabricated from Titanium Grade 7, an α-titanium alloy, 15-mm thick (SNL 2007 [DIRS 179354], Table 4-2, Parameter Number 07-04). The drip shields are supported by Titanium Grade 29, an α+β titanium alloy, support beams (SNL 2007 [DIRS 179354], Table 4-2, Parameter Number 07-04). The Titanium Grade 29 drip shield support beams, which are external to the drip shield and exposed to seepage water and are more prone to hydrogen absorption than the crossmembers located on the underside of the drip shield (SNL 2007 [DIRS 179354], Table 4-2). Failure of the drip shields due to general corrosion is discussed in included FEP 2.1.03.01.0B (General Corrosion of Drip Shields).

Hydrogen absorption in both α-titanium and α-β titanium alloys can occur when three general conditions are simultaneously met (Covington 1979 [DIRS 151097], pp. 378 to 381; Schutz and Thomas 1987 [DIRS 144302], p. 673; SNL 2007 [DIRS 181339], Section 6.1.2):

(1) A mechanism exists for generating nascent (atomic) hydrogen on the surface (e.g., the water reduction reaction is a thermodynamically viable cathodic reaction).

(2) The temperature of the drip shield is above approximately 80°C (175°F) such that a surface film of hydride is not formed and the diffusion rate of hydrogen into α-titanium is significant.

(3) Either (a) the solution pH is less than 3 or greater than 12, or (b) impressed potentials are sufficiently cathodic to induce the redox transformation of Ti^{4+} to Ti^{3+} within the passive TiO_2 oxide (approximately −0.7 V versus the saturated calomel reference electrode under near neutral conditions).

By assuming that the only viable cathodic reaction on the titanium surface is the water reduction reaction, condition (1) is always met as long as aqueous corrosion occurs. At certain repository locations, where temperatures are greater than or equal to 80°C (175°F) and concentrated groundwater is present, conditions (2) and (3) may also be satisfied. However, it should be noted that while the aforementioned three conditions are necessary requirements for hydrogen absorption, they are not sufficient in determining if hydrogen embrittelment will take place. A

critical hydrogen concentration within the metal must be achieved in order to reduce the mechanical properties to the extent that hydrogen-induced cracking can occur (SNL 2007 [DIRS 181339], Section 8). It should also be noted that given the oxic conditions that will prevail within any given drift, the assumption that the cathodic current density is solely due to the water reduction reaction will consistently overestimate the hydrogen production rate as the oxygen reduction reaction, the expected cathodic reaction, is assumed not to occur.

The term hydrogen embrittlement is used to refer to the deleterious impact of hydrogen on the mechanical properties of a material. Hydrogen-induced cracking results from the combined action of hydrogen and residual or sustained applied tensile stresses, whereby crack initiation and/or propagation occur at lower stress levels than in the absence of absorbed hydrogen. The critical hydrogen concentration of Titanium Grade 7 is estimated as 1,000 ppm (μg/g) (SNL 2007 [DIRS 181339], Section 5.2). The critical hydrogen concentration of Titanium Grade 29 is estimated as between 400 and 600 ppm (μg/g) (SNL 2007 [DIRS 181339], Section 5.2[a]). The value of f_h, fractional hydrogen absorption efficiency, is conservatively selected as 0.015 (SNL 2007 [DIRS 181339], Sections 8.1 and 8.3.2). By using the 2.5-year general corrosion rates obtained for Titanium Grade 7 obtained at the LTCTF, the 0.999 probability value from the upper 97.5% uncertainty bound general corrosion rate of Titanium Grade 7 in the aggressive environment (90°C SCW) is about 58 nm/yr (SNL 2007 [DIRS 181339], Table 4-1[a]). At 10,000 years, the hydrogen content in the drip shield thus calculated is 105 μg/g (SNL 2007 [DIRS 181339], Section 8[a] and Table 8-1[a]), which is well below the critical hydrogen concentrations for Titanium Grade 7.

Because no long-term data from the LTCTF are available for general corrosion rate of Titanium Grade 29 in repository-relevant environments, the Titanium Grade 29 general corrosion rate is calculated from conversion factors based upon short-term experiments as discussed in *General and Localized Corrosion of the Drip Shield* (SNL 2007 [DIRS 180778], Section 6.2.2[a]). By using the Titanium Grade 29/Titanium Grade 7 corrosion rate ratio multiplier values, the absorbed hydrogen concentrations in Titanium Grade 29 drip shield support beam material are calculated in *Hydrogen-Induced Cracking of the Drip Shield* (SNL 2007 [DIRS 181339], Section 6.2[a]). Using the 75th percentile multiplier and the 0.999 probability value from the upper 97.5% uncertainty bound of the Titanium Grade 7 general corrosion rate in the specified aggressive environment, at 10,000 years, the hydrogen content in the drip shield structural support material (Titanium Grade 29) is 84 μg/g. Using the 95th percentile multiplier and the 0.999 probability value from the upper 97.5% uncertainty bound of the Titanium Grade 7 general corrosion rate in the specified aggressive environment, at 10,000 years, the hydrogen content in the drip shield structural support material (Titanium Grade 29) is 191 μg/g. These conservatively calculated hydrogen content values are well below the critical hydrogen concentrations for Titanium Grade 29 (400 to 600 ppm) (SNL 2007 [DIRS 181339], Section 8.1[a] and Table 8-2[a]).

The locally hydrided regions that may potentially result from galvanic effects (e.g., from failed rock bolts or ground supports contacting the drip shield surface) will not be sufficiently large in magnitude such that they result in hydrogen-induced cracking as illustrated in *Hydrogen-Induced Cracking of the Drip Shield* (SNL 2007 [DIRS 181339], Section 6.3.2). The rationale presented in the reference includes the following points: (1) the contact area is small and has a low anode-to-cathode area ratio, (2) the presence of seepage is anticipated to be intermittent at

temperatures greater than or equal to 80°C (175°F), (3) sustaining the water reduction reaction under the repository conditions is unexpected, and (4) the titanium drip shield and the steel component surfaces that may contact it will experience a long period of dry conditions where the temperature is greater than or equal to 85°C (185°F), resulting in the formation of a thermal oxide, in effect passivating both materials, thereby minimizing any potential galvanic interactions and preventing increased hydrogen absorption.

When a titanium alloy containing an appreciable concentration of aluminum (e.g., Titanium Grade 29) is welded with an aluminum-free alloy (e.g., Titanium Grade 7), an abrupt concentration gradient of aluminum is formed at the weld fusion line. This concentration gradient has been found to drive uphill diffusion of hydrogen from the aluminum-rich material to the aluminum-poor material, resulting in the formation of hydride bands along the weld fusion line, increasing the susceptibility of the weld region to hydrogen embrittlement (SNL 2007 [DIRS 181339], Section 6.3[a]). To eliminate the potential for hydride band formation due to hydrogen redistribution, the weld filler metal utilized will be Titanium Grade 28 (SNL 2007 [DIRS 179354], Table 4-2; SNL 2007 [DIRS 181339], Section 6.3[a]). That is, welds made between Titanium Grade 7 plates and Titanium Grade 29 support beams will be conducted utilizing Titanium Grade 28 filler material. Titanium Grade 28 has an aluminum content of 2.5% to 3.5 %, providing an intermediate level between the Titanium Grade 7 plates and Titanium Grade 29 support beams. As a result, the abrupt aluminum concentration gradient that has been found to result in hydrogen redistribution and the enhanced hydride formation can take place when high aluminum alloys are welded with a low aluminum filler metal is avoided (SNL 2007 [DIRS 181339], Section 6.3[a]; Kennedy 1993 [DIRS 177388]).

Based on the previous dicscussion, FEP 2.1.03.04.0B (Hydride Cracking of Drip Shields) is excluded from the performance assessments conducted to demonstrate compliance with proposed 10 CFR 63.311 and 63.321 (70 FR 53313 [DIRS 178394]), and with 10 CFR 63.331 [DIRS 180319], on the basis of low probability.

INPUTS:

Table 2.1.03.04.0B-1. Direct Inputs

Input	Source	Description
SNL 2007. *Hydrogen-Induced Cracking of the Drip Shield*. [DIRS 181339]	Section 8	A critical hydrogen concentration within the metal must be achieved in order to reduce the mechanical properties to the extent that hydrogen-induced cracking can occur
	Section 6.3.2	The locally hydrided regions which may potentially result from galvanic effects will not be sufficiently large in magnitude such that they result in hydrogen induced cracking
	Section 8.1[a] and Table 8-2[a]	Calculation of hydrogen content in Titanium Grade 29 support material is below critical concentration
	Section 8[a] and Table 8-1[a]	At 10,000 years, hydrogen content in the Titanium Grade 7 drip shield will be 105 micrograms/gram

Table 2.1.03.04.0B-2. Indirect Inputs

Citation	Title	DIRS
10 CFR 63	Energy: Disposal of High-Level Radioactive Wastes in a Geologic Repository at Yucca Mountain, Nevada	180319
Covington 1979	"The Influence of Surface Condition and Environment on the Hydriding of Titanium"	151097
Kennedy et al. 1993	"Effect of Activity Differences on Hydrogen Migration in Dissimilar Titanium Alloy Welds"	177388
Schutz and Thomas 1987	"Corrosion of Titanium and Titanium Alloys"	144302
SNL 2007	*Total System Performance Assessment Data Input Package for Requirements Analysis for EBS In-Drift Configuration*	179354
SNL 2007	*General Corrosion and Localized Corrosion of the Drip Shield*	180778
SNL 2007	*Hydrogen-Induced Cracking of the Drip Shield*	181339

FEP: 2.1.03.05.0A

FEP NAME:

Microbially Influenced Corrosion (MIC) of Waste Packages

FEP DESCRIPTION:

Microbial activity may either directly (e.g., direct enhancement of the dissolution rate) or indirectly (e.g., through the formation of chemical species, which in turn support increased metal oxidation) enhance the corrosion rate of the waste package, leading to an acceleration of the corrosion rate beyond the levels anticipated based upon the bulk environment to which it is exposed.

SCREENING DECISION:

Included

TSPA DISPOSITION:

Microbially influenced corrosion is the contribution to the corrosion rate of a metal or alloy due to the presence, activity, or both, of microorganisms. Limited microbial populations and effects are expected in the repository (SNL 2007 [DIRS 178519], Section 6.4.5), and microbial activity in the EBS is excluded on the basis of low consequence in FEP 2.1.10.01.0A (Microbial Activity in EBS).

Microbially influenced corrosion most often occurs due to the increase in anodic or cathodic reactions due to the direct impact of microorganisms on the alloy or by indirect chemical effects on the surrounding solution (SNL 2007 [DIRS 178519], Section 6.4.5). Microbially influenced corrosion of the waste package is discussed in *General Corrosion and Localized Corrosion of Waste Package Outer Barrier* (SNL 2007 [DIRS 178519], Section 6.4.5). The effect of MIC on waste package corrosion is incorporated via an MIC enhancement factor (i.e., MIC increases the general corrosion penetration rate). In this approach, the abiotic corrosion rate is multiplied by the MIC enhancement factor, f_{MIC}. The magnitude of the enhancement factor was determined by comparing the electrochemical behavior of Alloy 22 in a solution inoculated with bacteria cultured from the Yucca Mountain site, to its behavior in a sterile solution of the same chemical composition. The test solution was inoculated with microbes cultured from the Yucca Mountain site including sulfate-reducing, acid-producing, iron-oxidizing, and slime-producing bacteria. The range of the MIC enhancement factor is uniformly distributed between 1 and 2 and is attributed to variability (SNL 2007 [DIRS 178519], Sections 6.4.5 and 8.2). It is applied to the waste package outer barrier general corrosion rate when the relative humidity at the waste package outer barrier surface is greater than a threshold relative humidity value sampled from a uniform distribution between 75% and 90% (SNL 2007 [DIRS 178519], Sections 6.4.5 and 8.2), where the threshold relative humidity defines the minimum relative humidity required for bacterial colonization to take place and potentially impact the corrosion process. MIC has not been evaluated in detail for possible impacts on the stainless steel inner vessel because the TSPA model does not take credit for corrosion resistance of that material. This treatment of MIC is applied to all waste packages.

Despite the fact that microbial activity is expected to have little impact on the in-drift chemical environment, as discussed previously, MIC of waste packages is implemented for the groundwater protection standard (10 CFR 63.331 [DIRS 180319]), and the individual protection standard (proposed 10 CFR 63.311 (70 FR 53313 [DIRS 178394])). In the case of human intrusion (proposed 10 CFR 63.321 (70 FR 53313 [DIRS 178394])), MIC of waste packages is not implemented in the assessment of the earliest time at which intrusion would be recognized by the drillers because that is determined by drip shield corrosion rates (SNL 2008 [DIRS 183478], Section 6.7.2).

INPUTS:

Table 2.1.03.05.0A-1. Indirect Inputs

Citation	Title	DIRS
10 CFR 63	Energy: Disposal of High-Level Radioactive Wastes in a Geologic Repository at Yucca Mountain, Nevada	180319
70 FR 53313	Implementation of a Dose Standard After 10,000 Years	178394
SNL 2007	*General Corrosion and Localized Corrosion of Waste Package Outer Barrier*	178519

FEP: 2.1.03.05.0B

FEP NAME:

Microbially Influenced Corrosion (MIC) of Drip Shields

FEP DESCRIPTION:

Microbial activity may either directly (e.g., direct enhancement of the dissolution rate) or indirectly (e.g., through the formation of chemical species, which in turn support increased metal oxidation) enhance the dissolution rate of the drip shield, leading to an acceleration of the corrosion rate beyond the levels anticipated based upon the bulk environment to which it is exposed.

SCREENING DECISION:

Excluded – low consequence

SCREENING JUSTIFICATION:

Microbial activity in the EBS is discussed in detail in excluded FEP 2.1.10.01.0A (Microbial Activity in EBS). That evaluation concluded that the repository will impose severe environmental constraints upon the growth of any viable populations of microbes. FEP 2.1.10.01.0A (Microbial Activity in EBS) is excluded, therefore, on the basis of low consequence. However, even if microbial activity were to occur on the drip shield, MIC will not compromise the ability of the drip shields to perform in accordance with their design intent, and as such will not significantly change radionuclide releases to the accessible environment or radiological exposures to the RMEI.

The drip shield is to be composed of two titanium alloys: Titanium Grade 7 for the plate material, and Titanium Grade 29 for the structural support (SNL 2007 [DIRS 179354], Table 4-2). Microbially influenced corrosion of titanium is discussed in *General Corrosion and Localized Corrosion of the Drip Shield* (SNL 2007 [DIRS 180778], Section 6.7.2). Corrosion handbooks and literature reviews indicate that there have been no recorded case histories that document MIC of titanium and its alloys (Revie 2000 [DIRS 159370], Chapter 47; Little 1996 [DIRS 131533]; Brossia 2001 [DIRS 159836], Section 4.1.3). Titanium's immunity to microbially influenced corrosion stems from the stability of the TiO_2 passive film in environments containing the typical species present as the result of biogenic activity (Brossia 2001 [DIRS 159836], Section 4.1.3). Microbial activity can result in the formation of a wide variety of chemical species that have been associated with the enhanced corrosion of ferrous and other materials. As an example, sulfate-reducing bacteria biogenically reduce sulfate to sulfide (Borenstein 1994 [DIRS 118912], Section 2.3.1; Little 1997 [DIRS 100774], Figure 1). However, such bacterially generated species have not been demonstrated to induce enhanced corrosion of titanium. This includes the production of ammonia, sulfides, nitrites, ferrous ions, and organo-sulfur compounds that are often produced from anaerobic activity (Brossia 2001 [DIRS 159836], Section 4.1.3). Production of nitrates, polythionates, thiosulfates, and oxygen from biogenic activity associated with aerobic activity similarly does not significantly increase the corrosion rate of titanium alloys (Brossia 2001 [DIRS 159836], Section 4.1.3).

Typically, what has been observed in the case of titanium alloys exposed to biologically active environments during laboratory and in-service evaluations is the formation of a biofilm on the metal surface (Brossia 2001 [DIRS 159836], Section 4.1.3). While titanium may be susceptible to biofouling (i.e., accumulation of biologically produced material), the biofilm does not compromise the integrity of the passive film, and therefore biofouled titanium maintains its resistance to localized corrosion processes (Revie 2000 [DIRS 159370], Chapter 47).

Steep gradients in dissolved oxygen and pH can exist within biofilms, with aerobic and near-neutral pH in the outer layers becoming acidic and low in O_2 close to the metal surface (Shoesmith 1997 [DIRS 151179], Section 6). Biogenic production of hydrogen peroxide within biofilms has been observed experimentally at millimolar levels, the amount of which is thought to be controlled by bacterial enzymes generated during the aerobic respiration process (Shoesmith 1997 [DIRS 151179]). Hydrogen peroxide maintains a low pH (<3) near the metal by oxidizing metal cations that then undergo hydrolysis. These chemical changes have been demonstrated to ennoble (i.e., shift the corrosion potential to more positive values) high molybdenum stainless steels and superalloys by as much as 500 mV (Shoesmith 1997 [DIRS 151179], Section 6, Figure 16). It is reasonable to assume that a similar degree of ennoblement could take place for titanium, as it is also a highly polarizable material in the environments being considered here. As shown in Figures 19 and 20 of *General Corrosion and Localized Corrosion of the Drip Shield* (SNL 2007 [DIRS 180778], Section 6.6.3), the mean ΔE for Titanium Grade 7 in chloride solutions is at least 1,000 mV at acidic pH values (i.e., localized corrosion will not initiate even if the corrosion potential is increased by 1000 mV). Based upon this data, localized corrosion of Titanium Grade 7 will not be caused by bacterially induced ennoblement. Ennoblement can, however, lead to several beneficial effects, including thickening of the passive film and a decrease in the number and density of film defects (Shoesmith 1997 [DIRS 151179], Sections 3 and 6).

Based on the previous discussion, microbial activity will not significantly increase the kinetics of either anodic or cathodic reactions taking place on the drip shield surface. Consequently, there will be no significant impact of microbial activity on either the general or localized corrosion rates of titanium alloys (including Titanium Grades 7 and 29) under the exposure conditions anticipated within the repository. Omission of FEP 2.1.03.05.0B (Microbially Influenced Corrosion (MIC) of Drip Shields) will not result in a significant adverse change in the magnitude or timing of either radiological exposure to the RMEI or radionuclide releases to the accessible environment. Therefore, this FEP is excluded from the performance assessments conducted to demonstrate compliance with proposed 10 CFR 63.311 and 63.321 (70 FR 53313 [DIRS 178394]), and with 10 CFR 63.331 [DIRS 180319], on the basis of low consequence.

INPUTS:

Table 2.1.03.05.0B-1. Direct Inputs

Input	Source	Description
Revie 2000. *Uhlig's Corrosion Handbook*. [DIRS 159370]	Chapter 47	Biofouled titanium maintains its resistance to localized corrosion processes
	Chapter 47	Corrosion handbooks and literature reviews indicate that there have been no recorded case histories that document MIC of titanium and its alloys
SNL 2007. *General Corrosion and Localized Corrosion of the Drip Shield*. [DIRS 180778]	Section 6.7.2	Discussion of MIC of titanium
	Figures 19, 20	ΔE is at least 1,000 mV at low pH values

Table 2.1.03.05.0B-2. Indirect Inputs

Citation	Title	DIRS
10 CFR 63	Energy: Disposal of High-Level Radioactive Wastes in a Geologic Repository at Yucca Mountain, Nevada	180319
70 FR 53313	Implementation of a Dose Standard After 10,000 Years	178394
Borenstein 1994	*Microbiologically Influenced Corrosion Handbook*	118912
Brossia et al. 2001	*Effect of Environment on the Corrosion of Waste Package and Drip Shield Materials*	159836
Little and Wagner 1996	"An Overview of Microbiologically Influenced Corrosion of Metals and Alloys Used in the Storage of Nuclear Wastes"	131533
Little et al. 1997	"Spatial Relationships Between Bacteria and Mineral Surfaces"	100774
Shoesmith and Ikeda 1997	*The Resistance of Titanium to Pitting, Microbially Induced Corrosion and Corrosion in Unsaturated Conditions*	151179
SNL 2007	*Total System Performance Assessment Data Input Package for Requirements Analysis for EBS In-Drift Configuration*	179354

FEP: 2.1.03.06.0A

FEP NAME:

Internal Corrosion of Waste Packages Prior to Breach

FEP DESCRIPTION:

Aggressive chemical conditions within the waste package could contribute to corrosion from the inside out. Effects of different waste forms, including CSNF and DSNF, are considered in this FEP.

SCREENING DECISION:

Excluded – low consequence

SCREENING JUSTIFICATION:

The waste package design requirements preclude internal corrosion of the waste package and contained material prior to breach. As discussed below, the current waste package design requires all waste packages to be dried and inerted with helium gas (SNL 2007 [DIRS 179394], Table 4-1, Parameter Number 04-04). If a container is helium tight, no significant amount of oxidizing gases can enter it.

According to the current waste package design, all waste forms will be contained in waste form specific canisters. For example, the CSNF will be contained in TAD canisters made of 300 series stainless steel (e.g., Stainless Steel Type 316L) (SNL 2007 [DIRS 179394], Section 4.1.1.4). Individual TAD and naval canisters and combinations of DOE SNF and HLW canisters (referred to as codisposal) will be placed inside a waste package consisting of a Stainless Steel Type 316 inner vessel contained within an Alloy 22 waste package outer barrier (SNL 2007 [DIRS 179567], Section 4.1.1). All waste packages will be dried and backfilled with helium gas to achieve less than 0.43 mol (7.7 g) of H_2O in a 7 m^3 volume (e.g., a TAD canister volume) (SNL 2007 [DIRS 179394], Table 4-1, Parameter Number 04-04; SNL 2007 [DIRS 179567], Table 4-1, Parameter Number 04-04) in a manner similar to NUREG-1536 (NRC 1997 [DIRS 101903], Section 8.V.1). This amount of residual water can only cause a negligible amount of corrosion because 0.43 moles of water can produce 0.11 moles of Fe_3O_4 (per $3\ Fe + 4\ H_2O \rightarrow Fe_3O_4$) or about 4,800 mm^3 of Fe_3O_4 (given that the molar volume of Fe_3O_4 is 44.7 cm^3 (ASM International 1987 [DIRS 103753], p. 64, Table 2)). The inner vessel of the TAD canister waste package configuration has a nominal length, L, of 5,499.10 mm and a nominal diameter, d, of 1,821.2 mm (SNL 2007 [DIRS 179394], Table 4-3), so that the outer surface area of the inner vessel is about 3.7×10^7 mm^2 (calculating surface area as $2\pi(d/2)^2 + \pi dL$). Thus, 4,800 mm^3 of Fe_3O_4 corresponds to a layer of corrosion product about 0.13-µm thick ($4{,}800\ mm^3/3.7 \times 10^7\ mm^2$). This thickness is negligible compared to the thickness of the waste package outer barrier, inner vessel, or a TAD canister. Consideration of other corrosion products such as Fe_2O_3, Cr_2O_3, and NiO, or the surface areas of other waste package configurations or components would not alter this conclusion. Likewise, the potential presence of small quantities of residual boric acid (from the reactor SNF pools) cannot alter this conclusion, as the total corrosion of the waste package internals prior to breach is limited by the

water content alone. As discussed in excluded FEP 2.1.11.07.0A (Thermal Expansion/Stress of In-Drift EBS Components), the impact of this thin corrosion product layer is not expected to lead to significant thermal expansion stresses in the waste package. Therefore, the presence of an inert atmosphere inside the waste packages and TAD canisters will severely limit oxidation (by oxygen gas and water vapor) within waste packages, and thereby preserve the chemical and physical stability of the waste form. The presence of an inert gas atmosphere will also ensure negligible corrosion degradation prior to breach of the waste packages (i.e., breach of both the outer barrier and inner vessel).

Residual moisture contained in the waste packages at the time of emplacement could cause corrosion on the internal surface of the waste package inner vessel. Previously waterlogged SNF rods within the waste package may serve as the source of this residual moisture (Kohli and Pasupathi 1986 [DIRS 131519]). However, the amount of moisture available will cause a negligible amount of corrosion as shown above, and the potential for degradation of the waste form containers is expected to be very remote (Kohli and Pasupathi 1986 [DIRS 131519]). Consequently, significant corrosion damage to the internal surface of the Stainless Steel Type 316 inner vessel is not expected to occur and is even less probable for the inner surface of the waste package outer barrier.

The amount of residual water in the commercial SNF, DOE SNF, and HLW glass waste packages will be very small due to drying and inerting the waste packages (SNL 2007 [DIRS 179567], Table 4-1, Parameter Number 04-04). Consequently, due to scarcity of water, corrosion in the commercial SNF, DOE SNF, and HLW waste packages prior to breach will be insignificant. If any DOE SNF-containing waste packages, such as those containing N Reactor fuel (i.e., uranium metal-based fuel), have more water, this water would be scavenged by the waste form due to the rapid corrosion rate of the metallic uranium that is the matrix of N Reactor SNF compared with other SNF (BSC 2004 [DIRS 172453], Table 6-9; Gray and Einziger 1998 [DIRS 109691], Section 4). DSNF waste packages containing N Reactor SNF may have residual free and chemically bound water at the time of sealing prior to placement in storage. If the N Reactor SNF cladding is significantly damaged, it could expose chemically reactive uranium metal surfaces to residual water, producing uranium oxide and uranium hydride. This chemically scavenged water is not available for corrosion of the waste package inner vessel or the waste package outer barrier. Other forms of DOE SNF are less damaged, and will contain much lower quantities of residual water due to drying prior to sealing for storage.

No credit is taken in the TSPA for the ability of DOE SNF canisters (within the waste package) to delay fuel degradation and radionuclide mobilization because the canisters will be constructed of stainless steel, which will degrade relatively fast once the waste package fails. Therefore, mechanisms that might enhance canister degradation prior to breach do not impact the predicted radionuclide releases from waste packages containing DOE SNF. The effects of radiolytically produced gases and other impacts owing to waste package internal pressurizations are discussed in excluded FEPs 2.1.13.01.0A (Radiolysis) and 2.1.03.07.0A (Mechanical Impacts on Waste Package).

Based on above discussion, insignificant corrosion damage of DOE SNF waste packages, defense HLW waste packages, and commercial SNF waste packages will occur due to drying of the waste form before loading, and backfilling of the waste packages with an inert gas. Omission

of FEP 2.1.03.06.0A (Internal Corrosion of Waste Packages Prior to Breach) will not result in a significant adverse change in the magnitude or timing of either radiological exposure to the RMEI or radionuclide releases to the accessible environment. Therefore, this FEP is excluded from the performance assessments conducted to demonstrate compliance with proposed 10 CFR 63.311 and 63.321 (70 FR 53313 [DIRS 178394]), and with 10 CFR 63.331 [DIRS 180319], on the basis of low consequence.

INPUTS:

Table 2.1.03.06.0A-1. Direct Inputs

Input	Source	Description
ASM International 1987. *Corrosion*. [DIRS 103753]	p. 64, Table 2	Molar volume of Fe_3O_4
SNL 2007. *Total System Performance Assessment Data Input Package for Requirements Analysis for DOE SNF/HLW and Navy SNF Waste Package Overpack Physical Attributes Basis for Performance Assessment*. [DIRS 179567]	Table 4-1, Parameter Number 04-04	Waste package inner vessels will be backfilled with helium
SNL 2007. *Total System Performance Assessment Data Input Package for Requirements Analysis for TAD Canister and Related Waste Package Overpack Physical Attributes Basis for Performance Assessment*. [DIRS 179394]	Table 4-1, Parameter Number 04-04	Waste package inner vessels will be backfilled with helium
	Table 4-3	Dimensions of TAD waste package inner vessel

Table 2.1.03.06.0A-2. Indirect Inputs

Citation	Title	DIRS
10 CFR 63	Energy: Disposal of High-Level Radioactive Wastes in a Geologic Repository at Yucca Mountain, Nevada	180319
70 FR 53313	Implementation of a Dose Standard After 10,000 Years	178394
BSC 2004	*DSNF and Other Waste Form Degradation Abstraction*	172453
Gray and Einziger 1998	*Initial Results from Dissolution Rate Testing of N-Reactor Spent Fuel Over a Range of Potential Geologic Repository Aqueous Conditions*	109691
Kohli and Pasupathi 1986	*Investigation of Water-logged Spent Fuel Rods Under Dry Storage Conditions*	131519
NRC 1997	*Standard Review Plan for Dry Cask Storage Systems*	101903
SNL 2007	*Total System Performance Assessment Data Input Package for Requirements Analysis for DOE SNF/HLW and Navy SNF Waste Package Overpack Physical Attributes Basis for Performance Assessment*	179567
SNL 2007	*Total System Performance Assessment Data Input Package for Requirements Analysis for TAD Canister and Related Waste Package Overpack Physical Attributes Basis for Performance Assessment*	179394

FEP: 2.1.03.07.0A

FEP NAME:

Mechanical Impact on Waste Package

FEP DESCRIPTION:

Mechanical impact (dynamic loading) on the waste package may be caused by internal and external forces such as internal gas pressure, forces caused by swelling corrosion products, rockfall, and possible waste package or drip shield movement. Seismic-induced impacts are addressed in included FEP 1.2.03.02.0A, Seismic Ground Motion Damages EBS Components.

SCREENING DECISION:

Excluded – low consequence

SCREENING JUSTIFICATION:

Mechanical loads may be exerted on waste packages through a variety of external or internal phenomena, as listed in the FEP description. These phenomena are discussed below, beginning with the mechanisms that can lead to internal gas pressurization of a waste package.

Mechanisms leading to internal gas pressurization—A number of mechanisms may lead to internal pressurization of a waste package from gas generation and/or temperature increases. The relevant mechanisms potentially leading to gas generation include:

- Pyrophoricity. Pyrophoricity of DOE SNF could occur because of exothermic reactions of uranium hydride and uranium metal in the DOE SNF with any oxygen and water that is present inside the waste package. Pyrophoricity is analyzed in excluded FEP 2.1.02.08.0A (Pyrophoricity from DSNF).

- Production of organic flammable gases. The only fuel waste types capable of producing organic flammable gases, such as methane and ethane, are the uranium-thorium carbide and plutonium-uranium carbide in DOE SNF. The volume of combustible gases from DSNF is analyzed in excluded FEP 2.1.02.29.0A (Flammable Gas Generation from DSNF).

- Decay-derived helium gas. Alpha particles are generated by the decay of actinide isotopes within the fuel pellets, and a fraction of the resulting helium gas may be released into the gap between the pellets and cladding and ultimately into the waste package if the fuel rod cladding fails. The production of decay-derived helium gas is analyzed in excluded FEP 2.1.12.02.0A (Gas Generation (He) from Waste Form Decay).

- Prepressurization and gaseous fission products in fuel rods. The fission products krypton and xenon are generated during in-reactor operation and may be released from the spent-fuel matrix. Total internal pressures of fuel pins upon removal from reactor due to the combined effects of prepressurization (with helium) and in-reactor production

of these gaseous fission products is analyzed by Rothman (1984 [DIRS 100417], subsection: "Pressures and Stresses in Fuel Pins") and discussed in this FEP.

- Prepressurization of the waste packages. Waste packages will be cold vacuum dried and pre-pressurized with helium, as discussed below. The impact of temperature change on this initial pressurization is analyzed in this FEP.

- Residual moisture. Residual moisture contained on DOE SNF or on commercial SNF at the time of emplacement could generate or consume gases from corrosion on the internal surface of the waste package inner vessel. Gas generation from corrosion processes is analyzed in excluded FEP 2.1.03.06.0A (Internal Corrosion of Waste Packages Prior to Breach).

- Radiolysis. The potential pressurization caused by gases generated from radiolytic decomposition of free or chemically bound water inside a waste package is excluded on the basis of low consequence in excluded FEP 2.1.13.01.0A (Radiolysis). The potential for radiolysis to increase the pressure from water vapor in the waste package is also considered in this FEP.

- Microbial degradation. In-drift gas generation from microbial degradation is excluded on the basis of low consequence in excluded FEP 2.1.12.04.0A (Gas Generation (CO_2, CH_4, H_2S) from Microbial Degradation), and is not considered further. Gas generation within the waste packages will be insignificant because of the high radiation environment and the lack of nutrients within the waste packages.

Waste package temperature increases after ventilation ceases because the spent fuel continues to generate heat. Peak waste package temperature occurs within the first 100 years after ventilation ceases at repository closure (SNL 2008 [DIRS 184433], Figure 6.3-76[a]). The maximum value of the peak waste package temperature varies between 174.7°C and 211°C for the hottest waste package (SNL 2008 [DIRS 184433], Table 6.3-49[a]). At 10,000 years after repository closure waste package temperatures range from approximately 25°C to 60°C (SNL 2008 [DIRS 184433], Figures 6.3-76[a]). These temperatures are for an intact drift; the thermal effects from drift collapse are discussed later.

The combined impacts of gas generation and temperature increase on internal pressurization of a waste package with commercial SNF contained in a TAD canister are discussed next, followed by an analysis of internal pressurization for codisposal waste packages with DOE SNF and HLW glass canisters or with DOE SNF and MCOs.

Internal pressurization of waste packages with CSNF in TAD canisters—The individual sources of gas generation or gas pressure in the TAD canister-bearing waste packages are as follows:

- Pyrophoricity cannot occur in commercial SNF because this fuel type does not contain uranium hydride or uranium metal.

- Organic flammable gases are not produced by commercial SNF because this fuel type does not contain uranium-thorium carbide fuel or plutonium-uranium carbide fuel.

- Helium from prepressurization of the fuel rods, fission-derived gases, and decay-derived helium may be released from failed commercial SNF fuel rods within the TAD canister. The radionuclides that are the major sources of decay-derived helium in SNF are: ^{244}Cm, ^{238}Pu, ^{239}Pu, ^{240}Pu, and ^{241}Am (Piron 2001 [DIRS 162396], Section 5.1.2). The decay-derived helium will accumulate in the solid matrix of the fuel pellets because the radionuclides are embedded in the fuel matrix and because most of the alpha particles from their decay are stopped within the fuel matrix. The contribution to fuel rod pressure from decay-derived helium is small in the first 100 years (Rothman 1984 [DIRS 100417], subsection: "Pressures and Stresses in Fuel Pins"). Because of the long half lives of some of these radionuclides, the decay-derived helium will continue to accumulate in the fuel matrix for a long time after disposal. However, the potential pressure increase in the waste package is within the waste package design limit at all times after repository closure, as demonstrated here.

  Pressure in the fuel rods results from prepressurization of the rods with helium and from release of fission-derived gases and decay-derived helium from the fuel matrix. A pressure of 5.5 MPa is suggested as the 99th percentile end-of-reactor-life gas pressure for PWR SNF rods (Rothman 1984 [DIRS 100417], subsection: "Pressures and Stresses in Fuel Pins"). Similarly, a pressure of 2 MPa is recommended for the end-of-life gas pressure for the BWR SNF rods (Rothman 1984 [DIRS 100417], subsection: "Pressures and Stresses in Fuel Pins"). The following discussion focuses on the PWR fuel rods because they bound the response of the BWR fuel rods with respect to gas pressure.

  If the fuel rod cladding fails, helium and fission gases will be released into the void volume within the waste package. The resulting pressure is estimated from the ideal gas law, based on the gap volume per fuel rod, the void volume inside the waste package, and the gap pressure. These three parameters are defined as follows:

  - The gap volume or free volume per fuel rod is given as 13 cm^3 for a fuel rod with a burnup of 47.5 GWd/MTU (Piron and Pelletier 2001 [DIRS 165318], Section 5.3.2.4.1), 30 cm^3 for a fuel rod with a burnup of 36 MWd/kg-U (Rothman 1984 [DIRS 100417], subsection: "Pressures and Stresses in Fuel Pins"), and an average value of 35 cm^3 (BSC 2006 [DIRS 181534], Section 6). The value of 35 cm^3 is used in this analysis because it maximizes the internal pressure in the waste package. The total initial gap volume inside all of the fuel rods is calculated as 153 liters, based on 21-PWR fuel assemblies with 208 fuel rods per assembly and a 35 cm^3 gap volume per rod (i.e., $21 \times 208 \times 35 = 152{,}900$ $cm^3 \approx 153$ liters).

  - The free volume inside the waste package is 4,737 liters (SNL 2007 [DIRS 180506], Table 6-3[a]).

  - The gap pressure is 5.5 MPa at 25°C, the 99th percentile pressure from Rothman (1984 [DIRS 100417], subsection: "Pressures and Stresses in Fuel Pins"). This analysis is based on the 99th percentile gap pressure because each TAD canister will be loaded at a single reactor and the 4,368 SNF rods from a single reactor may not represent a statistical sampling of all SNF rods. Note that the gap

pressure of 8.3 MPa is not considered here because it is referred to as "rare" (Johnson 1977 [DIRS 101687]), corresponding to unique conditions in the fuel rods for the Maine Yankee reactor (Rothman 1984 [DIRS 100417], subsection: "Pressures and Stresses in Fuel Pins").

The resulting waste package pressure increase if the cladding on every fuel rod fails is estimated from a simplification of the ideal gas law, $P_2 = (P_1V_1)/V_2$, where the subscripts 1 and 2 denote conditions in the gap and in the waste package, respectively, and P and V denote pressure and volume, respectively. Numerically:

$$P_2 = (5.5 \text{ MPa})(153 \text{ liters})/(4{,}737 \text{ liters} + 153 \text{ liters}) = 0.172 \text{ MPa} \approx 25 \text{ psi}$$

at 25°C.

The maximum value of the peak waste package temperature for the hottest waste package with low percolation flux and low thermal conductivity of the host rock is 211.0°C (SNL 2008 [DIRS 184433], Table 6.3-49[a]). The resulting waste package pressure increase is estimated from a simplification of the ideal gas law, $P_3 = P_2(T_3/T_2)$, where the subscripts 2 and 3 denote conditions at 25°C and 211°C, respectively, and P and T denote pressure and temperature, respectively. Numerically, the waste package pressure increase is:

$$P_3 = (0.172 \text{ MPa})(211 + 273.15)(\text{K})/(25 + 273.15)(\text{K}) = 0.279 \text{ MPa} \approx 41 \text{ psi}$$

at the peak waste package temperature of 211°C. As a reminder, this peak temperature occurs within the first 100 years after repository closure, so the end-of-reactor-life gap pressure is an appropriate starting point for the analysis of waste package pressure at peak temperature. The pressure at 10,000 years is about 28 psi based on a similar calculation with a temperature of 65°C.

Decay-derived helium will continue to accumulate in the fuel matrix. Excluded FEP 2.1.12.02.0A (Gas Generation (He) from Waste Form Decay) provides a bounding estimate for the pressure resulting from the long-term buildup of helium in the gap. If the helium that accumulated for 10,000 years from alpha decay in a fuel rod with a burnup of 47.5 GWd/MTU is assumed to be completely released from the fuel matrix into the gap region between the fuel pellets and cladding, the pressure increase in the gap would be 90 bars at 20°C using a void volume of 13 cm^3/fuel rod (Piron and Pelletier 2001 [DIRS 165318], Section 5.3.2.4.1). This is an extreme upper bound because the release of fission gases from the fuel pellets into the gap is typically 3% or less for most fuel rods (Rothman 1984 [DIRS 100417], subsection: "Pressures and Stresses in Fuel Pins"). The total gap volume that would be estimated based on Piron and Pelletier (2001 [DIRS 165318], Section 5.3.2.4.1) is calculated as 57 liters (i.e., 21-PWR fuel assemblies with 208 fuel rods per assembly and a 13 cm^3 gap volume per rod ($21 \times 208 \times 13 = 56{,}784$ $cm^3 \approx 57$ liters)). The corresponding pressure inside the waste package for a temperature of 65°C at 10,000 years (with a total gap volume of 57 liters) is then given by a simplification of the ideal gas law, $P_5 = P_4(V_4T_5)/(V_5T_4)$, where the subscripts 4 and 5 denote conditions at 20°C for the gap volume and at 65°C for the void volume in the

waste package, respectively, and P, V, and T denote pressure, volume, and temperature, respectively. Numerically:

$$P_5 = (9\ \text{MPa})(57\ \text{liters})(65 + 273.15\ \text{K})/(4{,}737\ \text{liters} + 57\ \text{liters})/(20 + 273.15\ \text{K}) = 0.123\ \text{MPa} \approx 18\ \text{psi}.$$

Thus, at 65°C, the pressure inside a waste package from fission gases, helium from fuel rod prepressurization, and decay-derived helium is about 46 psi (28 psi + 18 psi). The total pressure from the fill gas, decay-derived helium, and the fission gas (mainly krypton and xenon) is analyzed by Rothman (1984 [DIRS 100417], Table 6), based on the assumption of a fill gas pressure of 500 psi at 20°C, 100% release of helium and 20% release of other gaseous fission products from the fuel pellets. The last three lines in the referenced table are relevant to the present analysis because the temperature at 100 years is 194°C, similar to the peak temperature of 211°C for this analysis, and because the temperature at 10,000 years is 30°C, similar to the temperature range used in TSPA for mean percolation flux and mean rock conductivity of 40°C to 55°C for this analysis. The total pressure increases by 2%, from 1,500 psi at 100 years to 1,530 psi at 10,000 years (Rothman 1984 [DIRS 100417], Table 6). The last line in the referenced table gives the total pressure inside a fuel rod at 10,000 years and 30°C as 1530 psi, assuming a gap volume of 30 cm^3 per fuel rod. Performing the same kind of calculation as done above (e.g., calculation of P_3) to calculate the pressure at 65°C yields a pressure inside a fuel rod of 1,707 psi. The total gap volume from all fuel rods inside a waste package (using the gap volume of 30 cm^3 given by Rothman (1984 [DIRS 100417, Table 6)) is about 131 liters ($21 \times 208 \times 30\ cm^3 = 131{,}040\ cm^3 \approx 131$ liters). Once again, performing the same kind of calculation as done above (e.g., calculation of P_2) to calculate the pressure at 65°C in a waste package that would result if every fuel rod failed yields a pressure of about 46 psi. This is the same as the pressure calculated above (46 psi) that used a measured gap pressure from fission gases and from helium from rod prepressurization of 5.5 MPa from Rothman (1984 [DIRS 100417], section: "Pressures and Stresses in Fuel Pins") and the calculated pressure from decay-derived helium of 90 bars (Piron and Pelletier 2001 [DIRS 165318], Section 5.3.2.4.1).

- The current waste package design requires the TAD canister-bearing waste packages to be dried and backfilled with helium gas (SNL 2007 [DIRS 179394], Table 4-1, Parameter Number 04-04): "All TAD canisters and waste packages shall be dried and backfilled with Helium to achieve less than 0.43 moles (7.7 g) of H_2O in a 7 m^3 TAD canister after drying in a manner similar to NUREG-1536, *Standard Review Plan for Dry Cask Storage Systems*" (NRC 1997 [DIRS 101903], Section 8.V.1). The procedure described in NUREG-1567, *Standard Review Plan for Spent Fuel Dry Storage Facilities* (NRC 2007 [DIRS 149756], Section 9.5.4.1) is equivalent to NUREG-1536, for moisture removal and is therefore acceptable. Some chemically bound and adsorbed water will also remain in the waste package, and may be converted to gases by radiolysis. The impact of radiolysis on emplaced water is discussed in excluded FEP 2.1.13.01.0A (Radiolysis).

  Based on the drying process, corrosion within a sealed TAD canister-bearing waste package is not expected to be significant for gas production, based on the analysis in excluded FEP 2.1.03.06.0A (Internal Corrosion of Waste Packages Prior to Breach). The

0.43 mol of residual water can only cause a negligible amount of corrosion, generating a uniform layer of corrosion product (Fe_3O_4) that is approximately 0.13-μm thick. The thickness of this corrosion layer is insignificant compared to the initial thicknesses of the waste package outer corrosion barrier and inner vessel. In addition, the presence of the inert helium atmosphere inside the waste packages and TAD canisters will severely limit oxidization by any oxygen gas and water vapor within waste packages, thereby preserving the chemical and physical stability of the waste form. The presence of an inert helium atmosphere will also ensure negligible corrosion degradation prior to breach of the waste packages (i.e., breach of both the outer barrier and inner vessel).

In the unexpected event that the free water remains unreacted by corrosion, it could generate gas pressure as water vapor. Assuming a maximum temperature of 211°C and an available void volume for gas in the waste package of 4,737 liters (SNL 2007 [DIRS 180506], Table 6-3[a]), the pressure of water vapor is estimated using the ideal gas law as 0.051 psi:

$$
\begin{aligned}
p &= \frac{n\mathrm{R}T}{V}, \\
&= \frac{(0.43\,\mathrm{mol})\left(8.3143\,\frac{\mathrm{N\cdot m}}{\mathrm{mol\cdot K}}\right)(273.15+211)(\mathrm{K})}{(4{,}737\,\mathrm{L})\left(\frac{1{,}000\,\mathrm{cc}}{\mathrm{L}}\right)\left(\frac{1\,\mathrm{m}^3}{10^6\,\mathrm{cc}}\right)}, \\
&= 365\,\mathrm{N/m^2}, \\
&= 365\,\mathrm{Pa}, \\
&= 0.051\,\mathrm{psi}.
\end{aligned}
$$

This pressure could increase by 50%, to 0.08 psi, if radiolysis splits each mole of water vapor into one mole of hydrogen gas and 0.5 mole of oxygen gas.

All waste packages will be cold vacuum dried and initially prepressurized with 1 to 2 atmospheres of helium, as noted earlier. Using the upper bound of 2 atmospheres, the resulting waste package prepressurization is defined by the Gay-Lussac's law, $P_7 = P_6(T_7/T_6)$, where the subscripts 6 and 7 denote conditions at 25°C and 211°C, respectively. Numerically, the waste package prepressurization is:

$$P_7 = 2(14.7\text{ psi})(211 + 273.15)(\mathrm{K})/(25 + 273.15)(\mathrm{K}) = 47.7\text{ psi} \approx 48\text{ psi}$$

at the peak waste package temperature of 211°C. The pressure at 10,000 years from prepressurization is 33 psi, based on a similar calculation for a maximum temperature of 65°C.

In summary, the time-dependent pressure increases within the TAD canister-bearing waste package with commercial SNF in an intact drift are bounded by the following sources:

- No contribution from pyrophoricity

- No contribution from organic flammable gases
- Within the first 100 years after closure, 41 psi from fuel rod prepressurization, fission product gases, and decay-derived helium plus 48 psi from waste package prepressurization for a total internal pressurization of 89 psi at a peak waste package temperature of 211°C
- At 10,000 years after closure, 28 psi from fuel rod prepressurization and fission product gases, 18 psi from 10,000 years of decay-derived helium plus 33 psi from waste package prepressurization for a total internal pressurization of 79 psi at a waste package temperature of 65°C
- The internal pressurization from residual moisture is 0.08 psi, including radiolysis. The pressure from residual moisture is very small in comparison to the pressurization from decay-derived helium, fission product gases, and prepressurization of the fuel rods and waste package.

These predictions are based on a number of bounding assumptions, including (1) failure of all cladding, (2) release of all decay-derived helium from the fuel matrix at 10,000 years, (3) an initial prepressurization pressure of 2 atm in the waste packages, and (4) maximum temperatures from the thermohydraulic analyses for waste package temperature.

The maximum value of the peak waste package temperature can be significantly greater than 211°C if a drift collapses from a high intensity seismic event during the first 100 years after repository closure. In a collapsed drift with rubble surrounding the drip shield, the peak waste package internal temperature may be conservatively bounded by adding 50°C to the maximum waste package surface temperature of 300°C (i.e., 350°C) (SNL 2008 [DIRS 179962], Sections 6.1.6 and 6.5.1). A maximum value of 350°C increases the pressure from prepressurization of the fuel rods, fission gases, and decay-derived helium from 41 psi at a temperature of 211°C to:

$$(41 \text{ psi})(350 + 273.15)(\text{K})/(211 + 273.15)(\text{K}) = 52.8 \approx 53 \text{ psi},$$

and increases the pressure from prepressurization of the waste package from 29.4 psi at 25°C to:

$$2(14.7 \text{ psi})(350 + 273.15)(\text{K})/(25 + 273.15)(\text{K}) = 61.4 \text{ psi} \approx 61 \text{ psi},$$

for a total pressurization of 114 psi within the first 100 years after closure. The pressure from fuel rod prepressurization, fission gases, decay-derived helium and waste package prepressurization at 10,000 years is unchanged from 79 psi because the waste package temperature for a collapsed drift at 10,000 years is essentially equal to the value for an intact drift (SNL 2008 [DIRS 184433], Figures 6.3-82[a]and 6.3-83[a]).

The waste package will be designed to meet applicable requirements in *2001 ASME Boiler and Pressure Vessel Code* (ASME 2001 [DIRS 158115]). The inner vessel of the waste package is designed to withstand internal pressures of up to 140 psia at 707°F (375°C) (BSC 2007

[DIRS 180190], Appendix B, B4.2.2). These same design requirements will be imposed on TAD canister-bearing waste packages.

The internal pressurization of the TAD canister-bearing waste package with commercial SNF is bounded by a pressure change of 114 psi for an intact or collapsed drift, as explained earlier. This pressure change is based on bounding assumptions and is less than the design pressure of 140 psia, so the processes that can result in internal pressurization of the TAD canister-bearing waste package are excluded based on low consequence.

CDSP Waste Packages with DSNF and high level glass waste canisters—The individual sources of gas generation or gas pressure in the codisposal waste packages with DOE SNF and HLW glass canisters are discussed here. The response for a codisposal waste package loaded with DOE SNF and two MCOs is discussed in the following section.

- A pyrophoric material is capable of igniting spontaneously under temperature, chemical, or physical/mechanical conditions specific to the storage, handling, or transportation environments (ASTM C 1454-00 [DIRS 152779], Section 3.2). Uranium metal-based fuel, such as Hanford's N Reactor SNF, is a pyrophoric material that accounts for about 85% by weight MTHM of the total DOE SNF inventory (DOE 2002 [DIRS 158405], Appendix D). The N Reactor SNF has been loaded into MCOs, so the effects of pyrophoricity are discussed in the next section. Pyrophoricity is not considered a significant source for gas generation or temperature increase that could lead to internal pressurization of the codisposal waste package with other DOE SNF and high level glass waste canisters.

- The only fuel waste types capable of producing organic flammable gases, such as methane and ethane, are the uranium-thorium carbide and the plutonium-uranium carbide DOE SNF because they are the only spent nuclear fuels containing more than trace quantities of carbon. These gases are formed by the reaction of the carbides with liquid water or water vapor.

  As documented in excluded FEP 2.1.02.29.0A (Flammable Gas Generation from DSNF), an analysis of degradation and hydrocarbon production from graphite-matrix carbide fuels was conducted (Propp 1998 [DIRS 149395]). This study assessed the vulnerability of graphite-matrix SNF to oxidation by the ambient atmosphere in a geologic repository after fuel canister breach and examined the gases generated due to carbide combustion. Thermochemical and kinetic data were scrutinized for potential reactions between the graphite and the H_2O/O_2 system over the temperature range of 200°C to 400°C. This evaluation led to the conclusion that, even at 400°C, the reaction rate is "so small as to be of no practical consequence." Therefore, oxidation of the carbide-bearing SNF upon waste package breach is not anticipated to be a concern (Propp 1998 [DIRS 149395], Summary), and should not be a significant source for gas generation within the waste package.

- Decay-derived helium may be released from the DOE SNF within codisposal waste packages. However, the codisposal waste packages containing HLW glass canisters and DOE SNF have a much smaller inventory of the radionuclides that can produce

decay-derived helium in comparison to the commercial SNF waste packages (SNL 2007 [DIRS 180472], Table 7-1[a]). It follows that the potential pressurization effects of decay-derived helium on the codisposal waste packages are bounded by the internal pressurization of the commercial SNF in a TAD canister-bearing waste package, and can therefore be excluded based on the low consequence justification given above.

- The current waste package design requires all waste packages to be dried and backfilled with helium gas (SNL 2007 [DIRS 179567], Table 4-1, Parameter Numbers 03-26 and 04-04): "All TAD canisters and waste packages shall be dried and backfilled with Helium to achieve less than 0.43 moles (7.7 g) of H_2O in a 7 m^3 TAD canister after drying in a manner similar to Standard Review Plan for Dry Cask Storage systems" (NRC 1997 [DIRS 101903], Section 8.V.1). The amount of residual water in the codisposal waste packages with DOE SNF and HLW glass canister waste will therefore be very small due to the process for drying and inerting the waste packages. Consequently, gas production from corrosion in the codisposal waste packages prior to breach will be insignificant because of the scarcity of water. If any DOE SNF-containing waste packages have excess water, this water would be at least partly scavenged by corrosion of the waste form. This chemically scavenged water is not available for corrosion of the waste package inner vessel or the waste package outer corrosion barrier.

  The cold vacuum drying process results in approximately 0.0004 to 0.0005 liters of free water in a 15-ft-long canister containing high level waste or DOE SNF (Wachs 2004 [DIRS 184624], Section 6). The free water in a codisposal waste package with six canisters is less than 6(0.0005 liters) = 0.003 liters = 3 grams = 0.17 moles of water. The void volume inside a long DOE SNF codisposal waste package (containing 5 DHLW canisters and 1 DOE SNF canister) is 6,430 liters (DTN: MO0705GEOMODEL.000 [DIRS 181798], folder: FFTF, file: *CDSP_Long WP_FFTF_REV02.xls*, tab: Void Volume). This does not include the void inside the six canisters. The maximum gas pressure from water vapor at the peak temperature of 211°C is given by:

$$
\begin{aligned}
p &= \frac{nRT}{V}, \\
&= \frac{(0.17\,\text{mol})\left(8.3143\,\frac{\text{N}\cdot\text{m}}{\text{mol}\cdot\text{K}}\right)(273.15+211)(\text{K})}{(6{,}430\,\text{L})\left(\frac{1{,}000\,\text{cc}}{\text{L}}\right)\left(\frac{1\,\text{m}^3}{10^6\,\text{cc}}\right)}, \\
&= 106\,\text{N/m}^2, \\
&= 106\,\text{Pa}, \\
&= 0.015\,\text{psi}.
\end{aligned}
$$

  This pressure increase is less than the corresponding value for the TAD canister-bearing waste package with codisposal, 0.051 psi.

  All waste packages will be cold vacuum dried and initially prepressurized with 1 to 2 atmospheres of helium, as noted above. Using the upper bound of 2 atmospheres for

prepressurization, the resulting waste package pressures within the first 100 years and at 10,000 years after closure are identical to those calculated for the TAD canister-bearing waste package.

In summary, the combined pressure increases within a codisposal waste package with DOE SNF and HLW glass should be no more than the pressure increase for a TAD canister-bearing waste package with commercial SNF. The total pressure increase for the commercial SNF waste package, 114 psi, is within the design pressure limit (140 psia) of the waste package inner vessel (BSC 2007 [DIRS 180190], Appendix B, B4.2.2), so the processes leading to internal pressurization of the codisposal waste package can also be excluded based on low consequence.

CDSP Waste Packages with DSNF and Multicanister Overpacks (MCOs)—The individual sources of gas generation or gas pressure in the codisposal waste packages with DOE SNF and MCOs are discussed here.

- A pyrophoric material is capable of igniting spontaneously under temperature, chemical, or physical/mechanical conditions specific to the storage, handling, or transportation environments (ASTM C 1454-00 [DIRS 152779], Section 3.2). Uranium metal-based fuel, such as Hanford's N Reactor SNF, is a pyrophoric material that accounts for about 85% by weight MTHM of the total DOE SNF inventory (DOE 2002 [DIRS 158405], Appendix D)). The incidence and consequences from a pyrophoric event are evaluated in excluded FEP 2.1.02.08.0A (Pyrophoricity from DSNF). Based on that FEP, the associated increase in the overall waste package temperature is expected to be small and would therefore not lead to further degradation of the waste package outer corrosion barrier that might increase the rate of oxygen ingress. These results are confirmed by a quantitative analysis for the response of the contents of a single MCO to hypothetical breaches and material/energy flow from the MCO (DOE 2004 [DIRS 173188]). The results of this analysis provide additional corroborating evidence that pyrophoric events that are limited by the rate of oxygen ingress will not be highly energetic and will not lead to temperature increases in the waste package container that will cause the area of the container breaches to increase as the event unfolds. Based on these results, pyrophoricity is not considered a significant source for gas generation or temperature increase that could lead to internal pressurization of the waste package.

- The only fuel waste types capable of producing organic flammable gases, such as methane, and ethane, are the uranium-thorium carbide and the plutonium-uranium carbide DOE SNF because they are the only spent nuclear fuels containing more than trace quantities of carbon. These gases are formed by the reaction of the carbides with liquid water or water vapor.

  As documented in excluded FEP 2.1.02.29.0A (Flammable Gas Generation from DSNF), an analysis of the degradation and hydrocarbon production from graphite-matrix carbide fuels was conducted (Propp 1998 [DIRS 149395]). This study assessed the vulnerability of graphite-matrix SNF to oxidation by the ambient atmosphere in a geologic repository after fuel canister breach and examined the gases generated due to carbide combustion. Thermochemical and kinetic data were scrutinized for potential reactions between the graphite and the H_2O/O_2 system over the temperature range of 200°C to 400°C. This

evaluation led to the conclusion that, even at 400°C, the reaction rate is "so small as to be of no practical consequence." Therefore, oxidation of the carbide-bearing SNF upon waste package breach is not anticipated to be a concern (Propp 1998 [DIRS 149395], Summary), and should not be a significant source for gas generation within the waste package.

- Decay-derived helium may be released from the DOE SNF within codisposal waste packages. However, the codisposal waste packages containing two MCOs and DOE SNF have a much smaller inventory of the radionuclides that can produce decay-derived helium in comparison to the commercial SNF waste packages (SNL 2007 [DIRS 180472], Table 7-1[a]). It follows that the potential pressurization effects of decay-derived helium on the codisposal waste packages are bounded by the internal pressurization of the commercial SNF in a TAD canister-bearing waste package, and can therefore be excluded based on the low consequence justification given above.

- The maximum pressure inside an MCO in the absence of a hydrogen deflagration has been estimated in excluded FEP 2.1.13.01.0A (Radiolysis). This analysis is based on the maximum amount of free and bound (hydrated) water that has been reported for all MCOs loaded to date. The pressure from release of all bound water and from prepressurization with 1.5 atm of helium gas is estimated to be 38 atmospheres (559 psia) at 211°C, the maximum value for the peak waste package temperature (SNL 2008 [DIRS 184433], Table 6.3-49[a]). This pressure is well beyond the design pressure for the MCO, 450 psig at 132°C (Garvin 2002 [DIRS 169141], Section 2.2.6.2). If an MCO fails from overpressurization, it will vent into the void volume inside the codisposal waste package. The resulting pressure is at most 104 psia at 211°C (see excluded FEP 2.1.13.01.0A (Radiolysis)), which is less than the design pressure of the waste package, 140 psia at 707°F (375°C) (BSC 2007 [DIRS 180190], Appendix B, B4.2.2).

  The maximum pressure in the event of a hydrogen deflagration is also analyzed in excluded FEP 2.1.13.01.0A (Radiolysis). The maximum pressure from a hydrogen deflagration is estimated to be about 16 atmospheres, or 235 psia, well below the MCO design pressure of 450 psig at 132°C (Garvin 2002 [DIRS 169141], Section 2.2.6.2). If the MCO canister fails from the hydrogen deflagration, the pressure is vented into the larger void volume inside the codisposal waste package, further reducing the pressure.

- The effects of radiolysis on the free water that remains inside an MCO and on the water that is bound in hydrides on the N reactor fuel in the MCO are analyzed in excluded FEP 2.1.13.01.0A (Radiolysis). The effects of radiolysis on the free and bound water are reflected in the predicted gas pressure inside an MCO in the absence of a hydrogen deflagration and in the event of a hydrogen deflagration, as discussed earlier.

In summary, the pressure increases within an MCO should be within the design pressure for the MCO or within the design pressure for the codisposal waste package containing the MCOs. The processes leading to internal pressurization of the codisposal waste package with two MCOs and DOE SNF can be excluded based on low consequence.

Swelling of corrosion products: As discussed in excluded FEP 2.1.09.03.0B (Volume Increase of Corrosion Products Impacts Waste Package), volume changes due to the corrosion of waste package internals from dry oxidation and from breaches in the waste package outer corrosion barrier caused by seismic events or the residual stresses in the waste package closure lid regions are excluded from the TSPA model based on low consequence under the exposure conditions in the repository.

Nominal Rockfall: The term "rockfall" as used in this discussion refers to the dislodging of relatively few, generally large blocks of rock from the sides or crown of an emplacement drift. Nominal rockfall may result from in situ conditions of gravitational stresses, excavation-induced stresses, and thermally induced stresses, as described in *Drift Degradation Analysis* (BSC 2004 [DIRS 166107], Section 6). Nominal rockfall does not include dynamic loading caused by seismic events.

Mechanical damage to the waste package by nominal rockfall that occurs as a result of gravitational-, excavation-, thermal- or corrosion-induced stresses, or weathering, is discussed in greater detail under excluded FEP 2.1.07.01.0A (Rockfall). Based on this discussion, the effects of nominal rockfall on the waste package are excluded from consideration on the basis of low consequence to the TSPA model for 10,000 years.

Seismic: Mechanical damage to the waste packages and drip shields by ground motion and rockfall during seismic events is discussed separately in included FEPs 1.2.03.02.0A (Seismic Ground Motion Damages EBS Components) and 1.2.03.02.0C (Seismic-Induced Drift Collapse Damages EBS Components), and in excluded FEP 1.2.03.02.0B (Seismic-Induced Rockfall Damages EBS Components).

The effects of mechanical impact on waste packages (except those resulting from seismic events) are therefore excluded from the TSPA based on the low consequence justifications given above.

Based on the previous discussion, omission of FEP 2.1.03.07.0A (Mechanical Impact on Waste Package) will not result in a significant adverse change in the magnitude or timing of either radiological exposure to the RMEI or radionuclide releases to the accessible environment. Therefore, this FEP is excluded from the performance assessments conducted to demonstrate compliance with proposed 10 CFR 63.311 and 63.321 (70 FR 53313 [DIRS 178394]), and with 10 CFR 63.331 [DIRS 180319], on the basis of low consequence.

INPUTS:

Table 2.1.03.07.0A-1. Direct Inputs

Input	Source	Description
BSC 2006. *21-PWR Waste Package Internal Pressure Estimate*. [DIRS 181534]	Section 6	The gap volume within a fuel rod is 35 cm^3
DTN: MO0705GEOMODEL.000. Input Files and Model Output Runs: Geochemistry Model Validation Report: Material Degradation and Release Model. [DIRS 181798]	folder: FFTF, file: *CDSP_Long WP_FFTF_REV02.xls*, tab: Void Volume	The void volume inside a long DOE SNF codisposal waste package (containing 5 defense HLW canisters and 1 DOE SNF canister) is 6,430 liters
Garvin 2002. *Multi-Canister Overpack Topical Report*. [DIRS 169141]	Section 2.2.6.2	The design pressure for the MCO is 450 psi at 132°C
Piron and Pelletier 2001. "State of the Art on the Helium Issues." [DIRS 165318]	Section 5.3.2.4.1	The decay helium gas pressure is 90 bars at 20°C in commercial spent nuclear fuel rods with a gap volume of 13 cm^3 and a burnup of 47.5 GWd/MTU after 10,000 years
SNL 2007. *Initial Radionuclides Inventory*. [DIRS 180472]	Table 7-1[a]	The codisposal waste packages containing HLW glass canisters and defense SNF have a much smaller inventory of the radionuclides that can produce decay-derived helium in comparison to the commercial SNF waste packages
SNL 2007. *In-Package Chemistry Abstraction*. [DIRS 180506]	Table 6-3[a]	The free volume inside a TAD-bearing waste package is 4,737 liters
SNL 2007. *Total System Performance Assessment Data Input Package for Requirements Analysis for TAD Canister and Related Waste Package Overpack Physical Attributes Basis for Performance Assessment*. [DIRS 179394]	Table 4-1, Parameter Number 04-04	Discussion of TAD canisters and waste packages drying specifications
SNL 2008. *Multiscale Thermohydrologic Model*. [DIRS 184433]	Figures 6.3-76[a]	The peak waste package temperature occurs within the first 100 years after closure and at 10,000 years after repository closure waste package temperatures range from approximately 25°C to 60°C
	Figures 6.3-82[a], and 6.3-83[a]	Waste package temperature for a collapsed drift at 10,000 years is essentially equal to the value for an intact drift
	Table 6.3-49[a]	Maximum value of the peak waste package temperature varies between 174.7°C and 211°C for the hottest waste package
SNL 2008. *Postclosure Analysis of the Range of Design Thermal Loadings*. [DIRS 179962]	Sections 6.1.6 and 6.5.1	Peak waste package temperature In a collapsed drift with rubble surrounding the drip shield
Wachs 2004. *Calculation of Amount of Free Water Required to Overpressurize DOE SNF Standardized Canister and RW Waste Package*. [DIRS 184624]	Section 6	The volume of free (unbound) water is approximately 0.0005 liters in a 15-ft-long DOE SNF Standardized Canister after cold vacuum drying

Table 2.1.03.07.0A-2. Indirect Inputs

Citation	Title	DIRS
10 CFR 63	Energy: Disposal of High-Level Radioactive Wastes in a Geologic Repository at Yucca Mountain, Nevada	180319
70 FR 53313	Implementation of a Dose Standard After 10,000 Years	178394
ASME 2001	*2001 ASME Boiler and Pressure Vessel Code (includes 2002 addenda)*	158115
ASTM C 1454-00 2000	*Standard Guide for Pyrophoricity/Combustibility Testing in Support of Pyrophoricity Analyses of Metallic Uranium Spent Nuclear Fuel*	152779
BSC 2004	*Drift Degradation Analysis*	166107
DOE 2002	*DOE Spent Nuclear Fuel Information in Support of TSPA-SR*	158405
DOE 2004	*GOTH_SNF MCO Chemical Reactivity Final Analysis*	173188
Johnson 1977	*Behavior of Spent Nuclear Fuel in Water Pool Storage*	101687
NRC 1997	*Standard Review Plan for Dry Cask Storage Systems*	101903
NRC 2000	*Standard Review Plan for Spent Fuel Dry Storage Facilities*	149756
Piron 2001	"Presentation of the Key Scientific Issues for the Spent Nuclear Fuel Evolution in a Closed System"	162396
Propp 1998	*Graphite Oxidation Thermodynamics/Reactions*	149395
Rothman 1984	*Potential Corrosion and Degradation Mechanisms of Zircaloy Cladding on Spent Nuclear Fuel in a Tuff Repository*	100417
SNL 2007	*Total System Performance Assessment Data Input Package for Requirements Analysis for DOE SNF/HLW and Navy SNF Waste Package Overpack Physical Attributes Basis for Performance Assessment*	179567

FEP: 2.1.03.07.0B

FEP NAME:

Mechanical Impact on Drip Shield

FEP DESCRIPTION:

Mechanical impact (dynamic loading) on the drip shield may be caused by forces such as rockfall and possible waste package or drip shield movement. Seismic-induced impacts are addressed in separate FEPs.

SCREENING DECISION:

Excluded – low consequence

SCREENING JUSTIFICATION:

The function of the drip shield is to prevent or reduce water flow that could contact the waste package (thus reducing waste package corrosion) and to prevent damage to the waste package from rockfall. The drip shield protects the waste package from rockfall during the first 10,000 years of the postclosure period (see excluded FEP 2.1.07.01.0A Rockfall). This FEP pertains specifically to the potential mechanical effects of non-seismic-induced rockfall (resulting from in situ conditions of gravitational stresses, excavation-induced stresses, thermally induced stresses, or time-dependent strength degradation of the rock mass) on the drip shield, and focuses on the potential for drip shield displacements that result in contact with the waste package, subsequently damaging the waste package (see also excluded FEP 2.1.03.07.0A (Mechanical Impact on Waste Package)). In the absence of seismic ground motion, mechanical impact on the drip shield from either waste package or drip shield movement is not expected. The effect of uneven invert settlement on drip shield stability as a result of seismic ground motion was analyzed in *Mechanical Assessment of Degraded Waste Packages and Drip Shields Subject to Vibratory Ground Motion* (SNL 2007 [DIRS 178851], Section 6.4.6). It was determined that the settlement of the invert is not expected to materially alter the drip shield function.

The effects of rockfall are discussed in more detail under excluded FEP 2.1.07.01.0A (Rockfall). The effects of seismic events on drip shield and waste package integrity are not considered here, but are discussed in included FEP 1.2.03.02.0A (Seismic Ground Motion Damages EBS Components), excluded FEP 1.2.03.02.0B (Seismic-Induced Rockfall Damages EBS Components), and included FEP 1.2.03.02.0C (Seismic-Induced Drift Collapse Damages EBS Components). Static loading to the drip shield resulting from either partial or complete collapse of the drifts is discussed in excluded FEP 2.1.07.02.0A (Drift Collapse).

Calculations of potential rockfall for the nonlithophysal and lithophysal layers of the repository for nominal and seismic loading conditions are described in detail in *Drift Degradation Analysis* (BSC 2004 [DIRS 166107], Sections 6.3 and 6.4). In the absence of seismic events, rockfall may result from in situ conditions of gravitational stresses, excavation-induced stresses, and thermally induced stresses. Varying degrees of drift collapse can be expected in the lithophysal rock resulting from in situ conditions of gravitational stresses, excavation-induced stresses,

thermally induced stresses, and time-dependent strength degradation of the rock mass. However, the rock block sizes are predicted to be small (i.e., only a few centimeters to decimeters on a side) due to the ubiquitous fracture fabric found in the Tptpll unit (BSC 2004 [DIRS 166107], Sections 6.1.4.1 and 8.1). Minor amounts of rockfall are expected in nonlithophysal rock units for the non-seismic case that considers thermally induced stresses and time-dependent strength degradation of the rock mass (BSC 2004 [DIRS 166107], Section 8.1). However, static fatigue failure of asperities along fracture surfaces is possible and would result in gravitationally induced failure of large blocks. Hence, potential rockfalls in nonlithophysal units will consist of much larger blocks than in the lithophysal units (SNL 2007 [DIRS 178851], Section 6.4.7.1), and are therefore more capable of causing significant damage to the drip shield.

The analysis of high-energy rock blocks due to seismic events is discussed in excluded FEP 1.2.03.02.0B (Seismic-Induced Rockfall Damages EBS Components). These results provide an upper bound to the expected mechanical effects of rockfall during the nominal scenario. Any SCC induced by non-seismic rockfall is of low consequence, as discussed in excluded FEP 2.1.03.02.0B (Stress Corrosion Cracking (SCC) of Drip Shields).

In conclusion, mechanical impacts on the drip shield have no effect on repository performance for 10,000 years after repository closure. Omission of FEP 2.1.03.07.0B (Mechanical Impact on Drip Shield) will not result in a significant adverse change in the magnitude or timing of either radiological exposure to the RMEI or radionuclide releases to the accessible environment. Therefore, this FEP is excluded from the performance assessments conducted to demonstrate compliance with proposed 10 CFR 63.311 and 63.321 (70 FR 53313 [DIRS 178394]), and with 10 CFR 63.331 [DIRS 180319], on the basis of low consequence.

INPUTS:

Table 2.1.03.07.0B-1. Direct Inputs

Input	Source	Description
BSC 2004. *Drift Degradation Analysis*. [DIRS 166107]	Section 8.1	Minor amounts of rockfall are expected in nonlithophysal rock units for the non-seismic case that considers thermally induced stresses and time-dependent strength degradation of the rock mass
	Sections 6.1.4.1, 8.1	Rock block sizes are predicted to be small (i.e., only a few centimeters to decimeters on a side) due to the ubiquitous fracture fabric found in the Tptpll unit
	Sections 6.3, 6.4	Calculations of potential rockfall for the nonlithophysal and lithophysal layers of the repository for nominal and seismic scenarios
SNL 2007. *Mechanical Assessment of Degraded Waste Packages and Drip Shields Subject to Vibratory Ground Motion*. [DIRS 178851]	Section 6.4.6	Discussion of the effect of uneven invert settlement on drip shield stability
	Section 6.4.7.1	Potential rockfalls in nonlithophysal units will consist of much larger blocks than in the lithophysal units

Table 2.1.03.07.0B-2. Indirect Inputs

Citation	Title	DIRS
10 CFR 63	Energy: Disposal of High-Level Radioactive Wastes in a Geologic Repository at Yucca Mountain, Nevada	180319
70 FR 53313	Implementation of a Dose Standard After 10,000 Years	178394

FEP: 2.1.03.08.0A

FEP NAME:

Early Failure of Waste Packages

FEP DESCRIPTION:

Waste packages may fail prematurely because of manufacturing defects, improper sealing, or other factors related to quality control during manufacture and emplacement.

SCREENING DECISION:

Included

TSPA DISPOSITION:

The type and rate of occurrence of potential manufacturing defects in waste packages and drip shields is based on information from analogous surrogate industrial operations. The various processes that could potentially lead to early failure of either a waste package or drip shield were reviewed, and eleven generic types of defects were identified from a literature search (SNL 2007 [DIRS 178765], Section 6.1.6). A complementary type of defect is added to the list of eleven, i.e., base metal flaw (improper material selection). This type of defect was not identified in the literature search; only instances of improper weld material were found. This particular defect mode is combined with those associated with base-metal flaws for the analysis report (SNL 2007 [DIRS 178765], Section 6.1.6). Planned repository design and operations (DOE 2006 [DIRS 176937]) indicated that the generic list should also include defects introduced by improper stress relief of the waste package outer corrosion barrier closure weld with a low-plasticity burnishing process and recognize that the drip shield or waste packages might be improperly emplaced. Thus, 13 processes or conditions were evaluated in the analysis of early waste package and drip shield failure. Note that early failure of drip shields is addressed in included FEP 2.1.03.08.0B. These processes are listed follows:

- Weld flaws
- Improper heat treatment
  - outer corrosion barrier shell
  - outer corrosion barrier closure lid
- Improper stress relief of outer corrosion barrier lid (low plasticity burnishing)
- Improper base metal selection
- Improper weld filler material
- Improper weld-flux material
- Poor weld-joint design
- Contaminants
- Improperly located welds
- Missing welds
- Waste package mishandling damage

- Emplacement errors
- Administrative or operational errors.

Of these 13 flaws or processes, six processes were screened from further analysis with respect to the waste package outer corrosion barrier on the basis of either very low likelihood of occurrence or low consequences. A seventh process, administrative or operational errors, was included within the analysis methodology. Six were identified as significant for the waste package outer corrosion barrier, requiring further analysis. The six processes retained for further analyses with respect to mechanisms for potential early failures of a waste package outer corrosion barrier are listed below. Heat treatment of the outer corrosion barrier involves two processes (SNL 2007 [DIRS 178765], Section 6.1.6).

- Weld flaws
- Improper heat treatment
  - outer corrosion barrier shell
  - outer corrosion barrier closure lid
- Improper stress relief of outer corrosion barrier lid (low plasticity burnishing)
- Waste package mishandling damage
- Improper base metal selection
- Improper weld filler material.

Information from the literature search cited in *Analysis of Mechanisms for Early Waste Package / Drip Shield Failure* (SNL 2007 [DIRS 178765], Section 6.1) on the rate and causes of manufacturing defects in welded metallic containers indicated that weld flaws (e.g., slag inclusions, porosity, lack of fusion, or hydrogen-induced cracking) have been a dominant contributor to early failure but usually required an external stimulus (e.g., cyclic fatigue) or environmental conditions to cause the flaw to propagate to failure. In many cases, components with unidentified defects entered service, not because the defect was missed by an inspection, but because no inspection for that type of defect was required at the time they were fabricated.

The weld flaw analysis applies only to the waste package outer corrosion barrier closure welds (SNL 2007 [DIRS 178765], Section 6.3). Other welds in the waste package outer corrosion barrier are heat treated for stress relief during the solution annealing of the outer corrosion barrier for phase control. In addition, these latter welds are examined with ultrasonic testing, radiographic testing, and visual penetrant testing methods that result in a lower (non-quantified) probability of non-detection.

Because the development of early failure modes from material defects is closely connected to the long-term environmental conditions, *Analysis of Mechanisms for Early Waste Package/Drip Shield Failure* (SNL 2007 [DIRS 178765]) addressed the probability that such defects exist, not the likelihood of failures due to defects. Accordingly, the information from the literature search on the fraction of components that experienced defect-related failure during their intended lifetime is not directly applicable to waste packages or drip shields. In addition, these population-based failure rates do not provide any insight into the time distribution of early failures. However, in some cases, information on the occurrence rate of particular types of defects was obtained from the literature search (SNL 2007 [DIRS 178765], Section 6.1).

Results from an uncertainty analysis of the six processes applicable to the waste package outer corrosion barrier evaluated by event tree/fault tree methods (SNL 2007 [DIRS 178765], Figure 6-9) were collected into individual and comprehensive entities. The comprehensive probability distribution for the presence of undetected defects per waste package was developed by running a large number of realizations for these various entities with Monte Carlo sampling of the individual distributions. A CDF from this information was developed for the waste package outer corrosion barrier (SNL 2007 [DIRS 178765], Figure 6-20).

A realistic estimate of when components with defects will fail would be difficult to develop and justify given the nature of the problem:

- Physical failure of highly corrosion resistant metallic structures with very small loads under nominal conditions
- The time frames involved—centuries to millennia or longer
- The lack of long-term experience with such engineered systems in standard industrial or engineering practice.

Because of such considerations, performance assessments to demonstrate compliance with the individual protection standard after permanent closure (proposed 10 CFR 63.311 (70 FR 53313 [DIRS 178394])) and the groundwater protection standards (10 CFR 63.331 [DIRS 180319]) assume a complete loss of function of the waste package barriers with respect to radionuclide containment at the time of repository closure for waste packages characterized as having defects.

However, an early failed waste package would only have an increased susceptibility to SCC (SNL 2007 [DIRS 178765], Section 6.5.2). Even with a network of stress corrosion cracks, the mechanical performance of the early failed waste package would be similar to an intact package and would not have degraded sufficiently that a human intrusion could occur without recognition by the drillers. Therefore, FEP 2.1.03.08.0A (Early Failure of Waste Packages) is not included in the performance assessment for the individual protection standard for human intrusion (proposed 10 CFR 63.321 (70 FR 53313 [DIRS 178394])) on the basis of low consequence.

INPUTS:

Table 2.1.03.08.0A-1. Indirect Inputs

Citation	Title	DIRS
10 CFR 63	Energy: Disposal of High-Level Radioactive Wastes in a Geologic Repository at Yucca Mountain, Nevada	180319
70 FR 53313	Implementation of a Dose Standard After 10,000 Years	178394
DOE 2006	*Yucca Mountain Project Conceptual Design Report*	176937
SNL 2007	*Analysis of Mechanisms for Early Waste Package/Drip Shield Failure*	178765

FEP: 2.1.03.08.0B

FEP NAME:

Early Failure of Drip Shields

FEP DESCRIPTION:

Drip shields may fail prematurely because of manufacturing defects, improper sealing, or other factors related to quality control during manufacture and emplacement.

SCREENING DECISION:

Included

TSPA DISPOSITION:

While intact, the titanium drip shields divert any moisture that might seep from the drift walls, including condensed water vapor, around the waste packages to the drift floor. Because of the low corrosion rates of titanium and the 15 mm thickness of the drip shields, breaches of the drip shields due to corrosion degradation processes are not expected to occur until at least 35,000 years after closure of the repository as discussed in *General and Localized Corrosion of the Drip Shield* (SNL 2007 [DIRS 180778], Section 1.3). Included FEP 2.1.03.01.0B (General Corrosion of Drip Shields) and excluded FEP 2.1.03.02.0B (Stress Corrosion Cracking (SCC) of Drip Shields) describe the potential causes of failure that are not related to flaws and errors in manufacturing and emplacement.

The various processes that could potentially lead to early failure of either a waste package or drip shield were reviewed, and eleven generic types of defects were identified from a literature search (SNL 2007 [DIRS 178765], Section 6.1.6). A complementary type of defect is added to the list of eleven, i.e., out-of-specification (improper) base metal. This type of defect was not identified in the literature search; only instances of improper weld material were found. This particular defect mode is combined with those associated with base-metal flaws for the analysis report (SNL 2007 [DIRS 178765]). Planned repository design and operations (DOE 2006 [DIRS 176937]) indicated that the generic list should also include defects introduced by stress annealing of the waste package outer corrosion barrier closure weld with a low-plasticity burnishing process and recognize that the drip shield or waste packages might be improperly installed. Thus, 13 processes or conditions were evaluated in the analysis of early waste package and drip shield failure. Early waste package failure is addressed in included FEP 2.1.03.08.0A (Early Failure of Waste Packages). The processes discussed are as follows:

- Weld flaws
- Base metal flaws
- Improper weld filler material
- Improper stress relief for lid (low plasticity burnishing)
- Improper heat treatment of outer corrosion barrier and closure lid
- Improper weld-flux material

- Poor weld-joint design
- Contaminants
- Improperly located welds
- Missing welds
- Handling-induced defects
- Emplacement errors
- Administrative or operational errors.

Of these 13 flaws or processes, four were identified as significant with respect to the drip shields, requiring further analysis. The remaining nine processes were screened from further analysis with respect to the drip shield on the basis of either being applicable only to the waste package outer corrosion barrier, or very low likelihood of occurrence, or low consequences, or for administrative or operational errors, because they are addressed within the analysis methodology. The four processes retained for further analyses with respect to mechanisms for potential early failures of a drip shield are as follows from *Analysis of Mechanisms for Early Waste Package/Drip Shield Failure* (SNL 2007 [DIRS 178765], Section 6.1.6):

- Improper heat treatment
- Base metal selection flaws
- Improper weld filler material
- Emplacement damage.

Because the development of early failure modes from material defects is closely connected to the long-term postclosure environmental conditions conducive to SCC, *Analysis of Mechanisms for Early Waste Package/Drip Shield Failure* (SNL 2007 [DIRS 178765]) addresses the probability that such defects exist, not the likelihood of failures due to defects. Failure is dependent on multiple factors and is anticipated to occur after degradation takes place, which may happen hundreds of years after emplacement.

Results from an uncertainty analysis of the four processes applicable to the drip shield evaluated by event tree/fault tree methods (SNL 2007 [DIRS 178765], Figure 6-15) were collected into a single uncertainty distribution. The comprehensive probability distribution for the presence of undetected defects per drip shield was developed by running a large number of realizations for these end states with Monte Carlo sampling of the distributions. A CDF from this information was developed for the drip shield (SNL 2007 [DIRS 178765], Figure 6-21).

A realistic estimate of when components with defects will fail would be difficult to develop and justify given the nature of the problem:

- Physical failure of highly corrosion resistant metallic structures with very small loads under nominal conditions

- The time frames involved—centuries to millennia or longer

- The lack of long-term experience with such engineered systems in standard industrial or engineering practice.

Because of such considerations, performance assessments to demonstrate compliance with the individual protection standard after permanent closure (proposed 10 CFR 63.311 (70 FR 53313 [DIRS 178394])) and the groundwater protection standards (10 CFR 63.331 [DIRS 180319]) assume complete loss of function of the drip shield with respect to seepage at the time of repository closure for drip shields characterized as having defects.

Because early failed drip shields will not result in changes in drip shield mechanical properties, the earliest time after disposal that the drip shield would degrade sufficiently that a human intrusion could occur without recognition by the drillers (SNL 2008 [DIRS 183478], Section 6.7.2) would not be affected. Therefore, FEP 2.1.03.08.0B (Early Failure of the Drip Shield) is not included in the performance assessment to demonstrate compliance with the individual protection standard for human intrusion (proposed 10 CFR 63.321 (70 FR 53313 [DIRS 178394])) on the basis of low consequence.

INPUTS:

Table 2.1.03.08.0B-1. Indirect Inputs

Citation	Title	DIRS
10 CFR 63	Energy: Disposal of High-Level Radioactive Wastes in a Geologic Repository at Yucca Mountain, Nevada	180319
70 FR 53313	Implementation of a Dose Standard After 10,000 Years	178394
DOE 2006	*Yucca Mountain Project Conceptual Design Report*	176937
SNL 2007	*Analysis of Mechanisms for Early Waste Package/Drip Shield Failure*	178765
SNL 2007	*General Corrosion and Localized Corrosion of the Drip Shield*	180778

FEP: 2.1.03.09.0A

FEP NAME:

Copper Corrosion in EBS

FEP DESCRIPTION:

Chemical reactions involving copper corrosion have been identified as being of potential interest for repository programs considering the use of copper containers.

SCREENING DECISION:

Excluded – low consequence

SCREENING JUSTIFICATION:

The repository does not use copper containers (SNL 2007 [DIRS 179567], Tables 4-6 through 4-10; SNL 2007 [DIRS 179394], Table 4-3); however, consideration of copper effects may be appropriate since a small amount of copper may be present in the emplacement drifts as part of the gantry rail system. The total mass of elemental copper per meter of emplacement drift is less than 5.0 kg/meter (SNL 2007 [DIRS 179354], Table 4-1, Parameter Number 02-06). Copper, when oxidized to copper oxide or copper sulfide, is a potentially significant sorbent for iodine and technetium. Copper in the invert could retard transport of iodine and technetium released from the waste packages (SNL 2008 [DIRS 177407], Sections 6.3.4.2.1 and 6.3.4.2.2), but the presence of copper is highly localized, so that the probability of iodine or technetium contacting the copper is low. Therefore, iodine and technetium are assumed not to sorb onto copper corrosion products in the invert.

Copper will have no adverse effects on the performance of the Alloy 22 waste package outer barrier or Titanium Grade 7 or Grade 29 drip shield material in the absence of seismic activity because the waste package or the drip shield will not come into contact with copper. The waste package is designed to rest on a pallet (SNL 2007 [DIRS 179354], Section 4.1.3) constructed of Alloy 22 bearing surfaces and stainless steel connector tubes. The pallet is designed to keep the waste package from contacting other dissimilar metals in the absence of seismic activity (SNL 2007 [DIRS 179354], Section 4.1.3 and Table 4-3). Similarly, the drip shields are designed to contact no other material except the Alloy 22 base (SNL 2007 [DIRS 179354], Table 4-2), which is attached to the bottom of the drip shields. Therefore, the effect of copper corrosion is of low consequence to the performance and integrity of the waste package and the drip shield.

If, however, the drip shield were to come into contact with copper due to the failure of the gantry system, there is a potential for galvanic interaction between the titanium and copper. If hydrogen generation were to result from galvanic coupling between copper and titanium, the potential for hydrogen absorption, or hydrogen-induced cracking, is considered low. This is because an oxide film forms on the surfaces of the Titanium Grade 7 drip shield plate material, which hinders hydrogen absorption (SNL 2007 [DIRS 181339], Section 6.1.5). When Titanium Grade 7 is cathodically polarized at −1.14 V (versus saturated calomel electrode), a more severe condition

than galvanically coupling to copper, the hydrogen absorption efficiency was found to be 0.015 and the resulting hydrogen absorption insignificant (SNL 2007 [DIRS 181339], Section 6.1.5). The Titanium Grade 29 drip shield support material is, for the same reasons as the Titanium Grade 7 drip shield plate material, also highly resistant to hydrogen embrittlement (SNL 2007 [DIRS 181339], Section 6.2[a]). Therefore, the potential for hydrogen-induced cracking of the Titanium Grade 29 drip shield support material, due to galvanic coupling with the limited amounts of copper in the emplacement drifts, is also considered to be low.

Based on the above discussion, omission of FEP 2.1.03.09.0A (Copper Corrosion in EBS) will not result in a significant adverse change in the magnitude or timing of either radiological exposure to the RMEI or radionuclide releases to the accessible environment. Therefore, this FEP is excluded from the performance assessments conducted to demonstrate compliance with proposed 10 CFR 63.311 and 63.321 (70 FR 53313 [DIRS 178394]), and with 10 CFR 63.331 [DIRS 180319], on the basis of low consequence.

INPUTS:

Table 2.1.03.09.0A-1. Direct Inputs

Input	Source	Description
SNL 2007. *Total System Performance Assessment Data Input Package for Requirements Analysis for EBS In-Drift Configuration*. [DIRS 179354]	Section 4.1.3, Table 4-3	Pallet is designed to keep the waste package from contacting other dissimilar metals in the absence of seismic activity
	Section 4.1.3	The waste package is designed to rest on a pallet which is constructed of Alloy 22 bearing surfaces and stainless steel connector tubes
	Table 4-1, Parameter Number 02-06	The total mass of elemental copper
	Table 4-2	Drip shields are designed to contact no other material except the Alloy 22 base
SNL 2007. Total System Performance Assessment Data Input Package for Requirements Analysis for TAD Canister and Related Waste Package Overpack Physical Attributes Basis for Performance Assessment. [DIRS 179394]	Table 4-3	Repository does not use copper containers

Table 2.1.03.09.0A-2. Indirect Inputs

Citation	Title	DIRS
10 CFR 63	Energy: Disposal of High-Level Radioactive Wastes in a Geologic Repository at Yucca Mountain, Nevada	180319
70 FR 53313	Implementation of a Dose Standard After 10,000 Years	178394
SNL 2007	*Total System Performance Assessment Data Input Package for Requirements Analysis for EBS In-Drift Configuration*	179354
SNL 2008	*EBS Radionuclide Transport Abstraction*	177407
SNL 2007	*Hydrogen-Induced Cracking of the Drip Shield*	181339
SNL 2007	*Total System Performance Assessment Data Input Package for Requirements Analysis for DOE SNF/HLW and Navy SNF Waste Package Overpack Physical Attributes Basis for Performance Assessment*	179567

FEP: 2.1.03.10.0A

FEP NAME:

Advection of Liquids and Solids Through Cracks in the Waste Package

FEP DESCRIPTION:

The presence of one or more cracks or other small openings of sufficient size in a waste package may provide a pathway for the advective flow of water (e.g., thin films or droplets) or solid material into the waste package. The resulting presence of sufficient water or solid material in the waste package may affect in-package chemistry and/or criticality. Partial or full plugging of the waste package cracks by chemical or physical reactions after their formation (i.e., healing) could also affect water flow and radionuclide transport through the waste package. Passivation by corrosion products is a potential mechanism for waste package healing.

SCREENING DECISION:

Excluded – low consequence

SCREENING JUSTIFICATION:

The waste packages may be subject to SCC under repository conditions. The potential sources of stress that could result in SCC in the Alloy 22 WPOB include: (1) weld-induced residual stress, and (2) plasticity-induced residual stress caused by small-probability severe seismic events, as discussed in *Stress Corrosion Cracking of Waste Package Outer Barrier and Drip Shield Materials* (SNL 2007 [DIRS 181953], Section 6.5.3.1).

Residual stresses in all regions of the waste package (including the fabrication welds), except the closure lid welds, are to be fully relieved by annealing before the waste packages are loaded with waste (SNL 2007 [DIRS 179567], Table 4-1, Parameter Number 03-16); therefore, the waste packages will not develop residual stress high enough for SCC to occur (SNL 2007 [DIRS 181953], Section 6.5.3). According to the current waste package design, the stress mitigation of the outer lid closure weld will be by low-plasticity burnishing (SNL 2007 [DIRS 179567], Table 4-1, Parameter Number 03-17; SNL 2007 [DIRS 181953], Section 6.5.5), which imparts a layer of compressive residual stress to a minimum depth of 3 mm (0.12 in.) (SNL 2007 [DIRS 181953], Section 6.5.3.3). Upon removal of the compressive stress layer by general corrosion, the closure-lid weld region may be subject to SCC (SNL 2007 [DIRS 181953], Sections 6.5.5 and 8.4.2.1). However, removal of the stress-mitigated layer by general corrosion is not expected in the first 10,000 years. Therefore, as discussed below, damage from seismic ground motion is the only significant potential cause for SCC breach in the WPOB within the first 10,000 years.

Waste packages could be subject to SCC under the action of seismic-induced loading and seismic-induced rockfall. Rockfall/seismic effects on waste package degradation are discussed in excluded FEPs 2.1.07.01.0A (Rockfall), and FEP 1.2.03.02.0B (Seismic-Induced Rockfall Damages EBS Components). Damage to the waste packages from seismic-induced ground motion could occur in response to the impact of waste packages on the emplacement pallets, and

from end-to-end impacts between adjacent waste packages. Seismic-induced damage could result in deformation and resultant sustained residual stresses that may initiate SCC cracks, depending on the corrosion environment. Through-wall cracks could develop if the residual tensile stress exceeds the residual threshold stress (i.e., 90% to 105% of the yield strength of Alloy 22), as discussed in *Seismic Consequence Abstraction* (SNL 2007 [DIRS 176828], Section 6.1.4). The potential for the seismic-induced damage is discussed in included FEP 1.2.03.02.0A (Seismic Ground Motion Damages EBS Components).

This FEP analyzes the potential for advective flow of liquid water into the waste package through SCC cracks; it does not address transport of water vapor through the cracks, which is included in the TSPA (SNL 2008 [DIRS 177407], Sections 1 and 6.4.2). The analysis considers SCC damage to the waste package subject to seismic-induced loading and rockfall impacts at the 1.05 m/s PGV level in the first 10,000 years of the repository. This PGV level corresponds to a mean annual exceedance frequency of approximately 10^{-5}/yr (DTN: MO0501BPVELEMP.001 [DIRS 172682], file: *Bounded Horizontal Peak Ground Velocity Hazard at the Repository Waste Emplacement Level.xls*, cells: A5 and B5), and was selected as representative.

This analysis provides quantitative estimates of the attenuation of seepage rates, when seepage contacts the surface of a waste package that has SCC damage. Seepage may contact the waste package surface as macroscopic "sheet" or rivulet flow, and as impinging drip ("falling drop") conditions. The analysis does not consider microscopic film flow along solid surfaces, under the impetus of gravity or in response to gradients of thermodynamic water potential, because such flows are considered to be much smaller than other modes of moisture movement such as gas-phase diffusion and condensation.

In addition, condensation on the underside of the drip shield, or directly on cooler waste packages, can provide a source of liquid water that could flow into SCC-damaged waste packages, but is excluded on low consequence as discussed in excluded FEP 2.1.08.14.0A (Condensation on Underside of Drip Shield).

This analysis shows that the potential for advective flow of liquids through waste package cracks caused by SCC damage is insignificant, following the logic below:

- As discussed in excluded FEP 2.1.03.10.0B (Advection of Liquids and Solids Through Cracks in the Drip Shield), SCC-damaged drip shields still divert seepage so that water flow through the drip shield, if any occurs, will be negligibly small. Using bounding values for the uncertain parameters of drip shield damage and flow, the analysis for that FEP shows that a damaged drip shield can still reduce the rate of seepage that contacts the underlying waste package by more than six orders of magnitude (output DTN: SN0705WFLOWSCC.001, file: *Bounding calc for water flow through SCC cracks.xls*, worksheet: "Impinging drip flow rate," cell B25).

- The size of the damaged area in the waste package from seismic-induced loading and ground motion is small relative to the surface area of the waste package (0.377 m^2, or 0.95% of the waste package surface; Section C.2.3.1).

- If through-wall SCC cracks were to develop in the WPOB, plugging of the tight, tortuous cracks by agglomerated mineral precipitates and corrosion products will limit the amount of water inside the cracks and the potential for advective water flow.

- If through-wall SCC cracks were to develop in the damaged waste package, only a small fraction of the through-wall cracks are expected to be spatially aligned with impinging seepage drips from the SCC-damaged drip shield.

Summary discussions for the factors listed above are presented below.

SCC Crack Morphology in Passive Alloys

As discussed in *Stress Corrosion Cracking of Waste Package Outer Barrier and Drip Shield Materials* (BSC 2007 [DIRS 181953], Section 6.7.1.1), SCC cracks in passive alloys such as Alloy 22 tend to be tight (i.e., small crack-opening displacement), and highly tortuous often with many branches. Figure 2.1.03.10.0A-1 shows typical examples of transgranular and intergranular SCC cracks in stainless steel. SCC crack morphology in Alloy 22 is expected to be similar to that in stainless steel because of the crystalline granular structure of these alloys (BSC 2007 [DIRS 181953], Section 6.7.1.1).

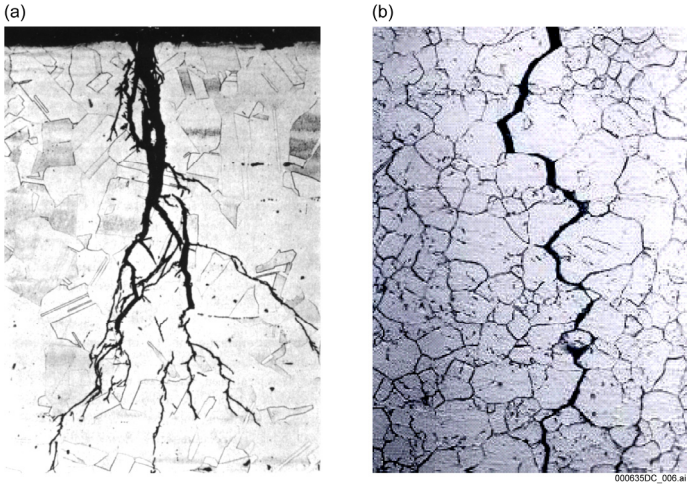

Sources: (a) Herrera 2004 [DIRS 168133], Figure 2-1.
(b) Herrera 2004 [DIRS 168133], Figure 2-2.

NOTE: This figure also appears in SNL 2007 [DIRS 181953], Figure 6-61.

Figure 2.1.03.10.0A-1. Typical Examples of (a) Transgranular SCC and (b) Intergranular SCC Cracks in Stainless Steel

Bounding Analysis for the Geometry and Number of Through-Wall SCC Cracks in Waste Package

As discussed in Section C.2.1, an SCC crack in the WPOB can be treated as a semi-elliptical crack. An initially semi-elliptical crack becomes a semi-circular crack as it grows to a through-wall crack (SNL 2007 [DIRS 181953], Section 6.6.2). See Figure C-1 for the simplified geometry of a through-wall crack in this analysis. The expected maximum length ($2c$) of the cracks is at least two times the wall thickness (SNL 2007 [DIRS 181953], Sections 6.6.2 and

6.8.5.2). The crack width and opening area are assumed to be the same through the wall thickness. Note that for an actual SCC crack propagating through the wall thickness, the crack width and opening area are expected to decrease with depth because of residual stress redistribution and relaxation near the crack tip as the crack grows. For waste packages that are damaged by seismic-induced events, the residual tensile stress in the WPOB tends to decrease from the outer surface (where the seismic impact occurs) to the inner surface of the WPOB (SNL 2007 [DIRS 181953], Sections 6.7.1.2 and 7.5.1.2). Therefore, the expected configuration of through-wall cracks that result from seismic damage is one with a larger opening at the outer surface and a much smaller opening at the penetration point on the inner surface. Those effects can be amplified when neighboring cracks propagate in parallel through the wall thickness (SNL 2007 [DIRS 181953], Section 6.7.1.3).

If SCC breach occurs during the first 10,000 years after repository closure when the WPOB maintains most of the design wall thickness of 25 mm (i.e., $2c$ = 50 mm), a reasonable upper-bound width for a through-wall crack in the WPOB is calculated to be approximately 195 μm, and the corresponding crack mouth area is approximately 7.68 mm^2 (Section C.2.1).

The seismic consequence abstraction analysis provides estimates of the damaged area on waste packages damaged by seismic ground motion (SNL 2007 [DIRS 176828]). The seismic-induced damaged area on a waste package is defined as the total area in which the residual tensile stress exceeds an uncertain threshold that varies from 90% to 105% of at-temperature yield strength of Alloy 22 (SNL 2007 [DIRS 181953], Section 8.1.1). This analysis assumes that seismic-induced damage to waste packages is distributed randomly over the package surface. As described in detail in Section C.2.3.1, the waste package with 23-mm thick WPOB was selected as appropriate for the first 10,000 years of the repository because degradation (or thinning) of the WPOB by general corrosion will be insignificant during this time period. A reasonably conservative estimate of the general corrosion penetration depth for the first 10,000 years is only 0.3 mm using the 50th percentile general corrosion rate (30.8 nm/yr) at 100°C for the expected case (the medium uncertainty level for R_o and the mean apparent activation energy of 40.78 kJ/mol) (DTN: MO0612WPOUTERB.000 [DIRS 182035], file: *BaseCase GC CDFs2.xls*, worksheet: "Data," cell: M71). An intact state of the waste package internals was selected as appropriate because earthquakes of sufficient magnitude to cause significant SCC damage to the WPOB occur relatively infrequently during this time period, and the internals will not undergo substantial degradation by corrosion until after the waste package experiences an extensive breach. The TAD canister-bearing waste package and 5-DHLW/DOE SNF codisposal waste package are the most abundant waste package types in the repository, and are considered in this analysis (Section C.2.3.1).

TAD canister-bearing waste packages with 23-mm-thick WPOB and intact internals are not subject to SCC damage from ground motion at the 1.05 m/s PGV level (DTN: MO0703PASDSTAT.001 [DIRS 183148], file: *Kinematic Damage Abstraction 23-mm Intact.xls*, worksheet: "WP Total"). Codisposal waste packages are subject to SCC damage from the same PGV level, and the 95th percentile of damaged area for this condition (0.377 m^2), conditioned on damage occurring, was selected as a reasonably conservative upper-bound value for the damage area of the waste package (DTN: MO0703PASDSTAT.001 [DIRS 183148], file: *CDSP Kinematic Damage Abstraction 23-mm Intact.xls*, worksheet: "Gamma for 90%_i23," cell I172). The probability of damage to the codisposal waste package occurring for the 1.05 m/s

PGV level is 0.559 at the RST of 90%, and significantly less at greater RST values (SNL 2007 [DIRS 176828], Section 6.6.1, Table 6-14). This codisposal waste package damaged area is used as a representative value for the waste package in the analysis (Section C.2.3.1). The damaged area is greater than the 50th percentile damaged area (0.253 m^2) at 2.44 m/s PGV (DTN: MO0703PASDSTAT.001 [DIRS 183148], file: *CDSP Kinematic Damage Abstraction 23-mm Intact.xls*, worksheet: "Gamma for 90%_i23," cell H178).

As discussed in Section C.2.3.1, the selected damage area corresponds to 0.95% of the total surface area of a codisposal waste package (output DTN: SN0705WFLOWSCC.001, file: *Bounding calc for water flow through SCC cracks.xls*, worksheet: "Sheet flow WP flow rate," cell B13). The upper-bound total number of through-wall SCC cracks per damaged waste package is then estimated to be 697 cracks, and the corresponding total crack-mouth opening area of through-wall SCC cracks per damaged waste package is approximately 5,351 mm^2 (output DTN: SN0705WFLOWSCC.001, file: *Bounding calc for water flow through SCC cracks.xls*, cells B17 and B16).

Laboratory Drip Tests

An analogue to the residual stress states and stress profiles from the stress calculation (BSC 2005 [DIRS 174052], Section 7) was created in stainless steel plates to evaluate the potential for such stresses to propagate through-wall cracks (Andresen et al. 2005 [DIRS 176653], Section 5). A series of stress corrosion crack tests was performed in which a simulated, rockfall-dented stainless steel plate was exposed to a boiling saturated aqueous solution of magnesium chloride. This is a highly corrosive environment that will initiate and propagate stress corrosion cracks in stainless steels even at low levels of residual tensile stress down to about 70 MPa (approximately 10 ksi) (ASM International 1987 [DIRS 101992], p. 272, Figure 54). The stress state in stainless steel was tested as an analogue to that of Alloy 22, which is extremely resistant to SCC and for which SCC is difficult to initiate under test conditions.

A series of tests was conducted to examine the potential for water flow through cracks (DTN: SN0506F4104405.003 [DIRS 174472]). These tests were designed to determine if water could penetrate real SCC cracks in the stainless steel plates described above, as well as simulated cracks formed between precision-ground blocks of Titanium Grade 7 and stainless steel. The simulated cracks had no tortuous pathways (i.e., machined internal surfaces), were empty, and free of any plugging matter. Flow testing was performed with the simulated, parallel-wall cracks, and with the real SCC cracks. Water was dripped onto both the simulated and real cracks from a height of 2.2 m (the maximum distance from the emplacement drift crown to the drip shield crown), and 0.4 m (the maximum distance between the drip shield crown and top of the waste package). The plates were held at different angles relative to the dripping water. A "sheet flow" test was also performed in which the water was dripped onto the plates a few inches above the cracks and allowed to flow over the cracks as a "sheet" flow.

For the real cracks in the stainless steel plate, the largest nominal aperture size (observed by inspection) in one location was approximately 381 μm, and that in the other location was approximately 127 μm; effective aperture sizes could be inferred from flow measurements, but were not characterized directly (Walton 2005 [DIRS 175407], pp. 110 and 145). The test results are summarized in DTN: SN0506F4104405.003 ([DIRS 174472], files: *Dynamic_Drop_Test_*

Summary_SCC_4-15-05.doc and *SCC_PhaseII_Test_Preliminary_Summary_9-21-05.doc*). The largest aperture used for simulated cracks with both the titanium and stainless steel blocks was 50.8 μm.

For the impinging drip ("falling drop") tests with real SCC cracks, two locations were identified as potential flow paths; one location did not yield any sign of water penetration, and the other yielded water flow through cracks in amounts ranging from 0.03% to 1.82% of the total amount of impinging water (with one exception, a test that yielded 4.02%) (DTN: SN0506F4104405.003 [DIRS 174472], file: *Dynamic_Drop_Test_Summary_SCC_4-15-05.doc*). Results from flow testing of the real SCC cracks are used to estimate potential leakage from the impinging-drip flow mode in Appendix C. Results from testing of the simulated cracks were used only to investigate behaviors such as the dependence on tilt angle and drop height and on material interactions. For the largest simulated crack aperture (50.8 μm) with the titanium blocks, less than 3% of the impinging drip water penetrated the crack when dripped from a height of 2.2 m (DTN: SN0506F4104405.003 [DIRS 174472], file: *SCC_PhaseII_Test_Preliminary_Summary_9-21-05.doc*).

A total of six test runs were conducted for the sheet flow condition, two runs for the titanium test blocks and four runs for the stainless steel test blocks. The titanium block test runs (both tilted at a 5° angle from horizontal) did not yield water penetration, and two (both tilted at a 5° angle) of the four stainless steel block test runs yielded water penetration (0.04% and 1.03%, respectively, of the total water dripped) (DTN: SN0506F4104405.003 [DIRS 174472], file: *SCC_PhaseII_Test_Preliminary_Summary_9-21-05.doc*).

The laboratory test results support the conclusion that only a small fraction of seepage flow is expected to penetrate cracks for both sheet flow and dripping conditions, even if dripping impinges directly on a crack. The results also demonstrate that the tilt angle of the block containing cracks strongly attenuates potential for water flow through the cracks under both sheet flow and impinging drip conditions.

Sustained dripping of seepage directly on the same cracks in the repository environment is not expected because the alignment of the drip impact location with the crack will vary. The tests also show that the tilt angle of the surface containing cracks strongly attenuates water flow through the cracks, for both sheet flow and impinging drip conditions. Furthermore, it is expected that these flow rates through actual SCC cracks will decrease significantly as a result of the plugging mechanisms discussed below and in Appendix C. Figure 2.1.03.10.0A-1 shows typical SCC cracks in stainless steel with highly branched (for transgranular crack) and tortuous crack morphology.

Crack Plugging with Mineral Precipitates and Corrosion Products

Stress corrosion cracking is a corrosion process that requires the presence of a corrosive environment (i.e., water with dissolved species such as chloride or fluoride) inside the crack and around the crack mouth for sustained operation. The SCC process will result in accumulation of corrosion products from associated corrosion reactions and mineral precipitates from evaporation (or evaporative equilibration) of water filling the crack. Detailed studies using high-resolution analytical electron microscopy have demonstrated the accumulation of corrosion products and

intrusion of the external environment water deep inside very fine SCC cracks of stainless steels and nickel-based alloys (Bruemmer and Thomas 2001 [DIRS 183685]).

As discussed in Section C.3, propagation of SCC cracks through the 25-mm thick WPOB could take a few hundreds years in the repository-relevant conditions. As SCC cracks grow through the WPOB wall, intermittent humidity cycles resulting from atmospheric fluctuations in the repository, or from variability in dripping rate and location (BSC 2004 [DIRS 169734], Sections 7.3.2 and 7.4.1), will promote mineral precipitation and accumulation of corrosion products inside the cracks.

Stress corrosion cracking cracks for corrosion-resistant materials like Alloy 22 are typically very tight and tortuous (BSC 2007 [DIRS 181953], Section 6.7.1.1; Bruemmer and Thomas 2001 [DIRS 183685]), and therefore require only small amounts of corrosion products and mineral precipitates to become filled. The corrosion product oxides tend to cement and agglomerate (Ishikawa et al. 2006 [DIRS 183682]; Ishikawa et al. 2007 [DIRS 181136]), especially in the presence of other minerals such as silica minerals (Milnes and Fitzpatrick 1995 [DIRS 105911], pp. 1,180 to 1,183). In addition, because of the larger molar volumes of the corrosion products than the base metal (e.g., nickel and chromium oxides from corrosion of Alloy 22), cracks will eventually be plugged by compacted corrosion products. The SCC cracks in the WPOB are expected to be continuously filled with compact cemented agglomerates of corrosion products and mineral precipitates as the cracks grow through the wall thickness.

A summary of the calculation of the expected rate of SCC plugging due to calcite precipitation from seepage is documented in *Plugging of Stress Corrosion Cracks by Precipitation* (BSC 2001 [DIRS 156807], Section 6.3). The calculation shows that water originating either as condensate or seepage, or water-dust mixtures that enter SCC cracks, will warm because of its closer proximity to the heat of the waste packages. This will cause enhanced precipitation of minerals such as calcite with retrograde solubility (depending on the availability of solutes). Over time, corrosion products, precipitated minerals, and particles of dust and rock in the environment will plug the cracks. The calculation employs a simplifying assumption that no corrosion products or mineral precipitates form inside a crack until the crack fully penetrates the wall thickness. Actually, as discussed earlier, SCC cracks will be continuously filled with corrosion products and mineral precipitates as they grow through the wall thickness. Dust on the waste package surface and CO_2 in the drift air will provide dissolved constituents for calcite and other minerals to form in water contacting the waste package surface. If there is fluctuation in humidity conditions on the waste package surface, more precipitation and faster plugging could occur (BSC 2001 [DIRS 156807], Section 6.3). Other assumptions of the calculation include: (1) that the corrosion products generated on the crack wall, as well as colloids, particulates, and any precipitated minerals, do not participate in resisting the water flow through the crack; and (2) that there is a uniform water seepage flow in space and time. It is concluded that, under these assumptions, the cracks will be sealed in a few hundred years at most when seepage water is allowed to flow at low sheet-flow rates. If the cracks are bridged by water, plugging may take thousands of years (limited by the delivery of solute), but no advective flow may occur if capillary forces hold the water.

Flow Rates in Through-Wall SCC Cracks Under Impinging Drips

For excluded FEP 2.1.03.10.0B (Advection of Liquids and Solids Through Cracks in the Drip Shield) estimated flow rates through a SCC-damaged drip shield in the sheet flow condition are found to be negligibly small (0.05 to 3.42 cm^3/yr; Section C.3.1). This range of flow rates is not sufficient to create sheet-flow conditions on the underlying waste package surface. Therefore, the potential for water flow through SCC cracks in the WPOB for sheet-flow conditions is not considered further in this FEP.

Analysis was conducted to evaluate the potential for the water flow in through-wall SCC cracks in the waste package, under impinging-drip conditions, below an SCC-damaged drip shield (Section C.5). The analysis assumes that waste packages are damaged from seismic-induced ground motion at the 1.05 m/s PGV level in the first 10,000 years of the repository, and that through-wall SCC cracks from the seismic damages are distributed randomly over the waste package surface. The analysis for the seismic-induced SCC damage to waste packages is detailed in Section C.2.3.1.

Using bounding values for the uncertain parameters, and the waste package damage from seismic-induced ground motion at the 1.05 m/s PGV level (Section C.2.3.1), analysis shows that the damaged waste package diverts the seepage from the SCC-damaged drip shield, reducing the seepage flux by more than five orders of magnitude (output DTN: SN0705WFLOWSCC.001, file: *Bounding calc for water flow through SCC cracks.xls*, worksheet: "Impinging drip flow rate," cell H25) (Section C.5). Combining diversion by the SCC-damaged drip shield and the SCC-damaged waste package, the drift seepage flux is reduced by at least ten orders of magnitude (output DTN: SN0705WFLOWSCC.001, file: *Bounding calc for water flow through SCC cracks.xls*, worksheet: "Impinging drip flow rate," cell H27). For comparison, the estimated upper-bound advective flow into a damaged waste package is negligible compared to the minimum advective liquid influx rate (100 mL/yr) into a breached waste package (SNL 2007 [DIRS 180506], Section 6.10.9.1[a]), or the threshold seepage rate per waste package (100 mL/yr; SNL 2007 [DIRS 181244], Section 6.4[a], p. 6-29[a]), that are defined for TSPA. Also, the TSPA model basis allows formation of corrosion products on the internal surfaces of the waste package to begin immediately after breach (SNL 2008 [DIRS 177407], Section 6.5.2.2.1), and the amount of water that is retained in those corrosion reactions greatly exceeds the potential advective leakage through a damaged waste package (e.g., SNL 2008 [DIRS 177407], Figure 6.5-8). Whereas gaseous diffusion of water vapor is the assumed mechanism that supplies this water, a small addition from advective flow would be inconsequential.

Screening Justification Summary

TAD canister-bearing waste packages are not subject to SCC damage in the first 10,000 years of the repository. Codisposal waste packages are subject to such damage, and the associated damaged area estimates are used in this analysis to represent potential waste package damage. Advective flow of water (and by inference, solids) in through-wall cracks in the SCC-damaged waste package is excluded on the basis of low consequence because the amount of advective water flow through the cracks will be severely limited by the combined effects of: (1) protection by drip shields (even damaged ones) against drift seepage; (2) limitations on the extent of waste

package damage from to seismic events; (3) tight and highly tortuous crack pathways for advective liquid flow; and (4) plugging of cracks by compact cemented agglomerates of corrosion products and mineral precipitates. The amount of liquid water that could flow advectively through cracks in the WPOB is small compared to the ingress of moisture by other modes such as diffusion, and the rates of moisture uptake by in-package degradation processes, as represented in TSPA.

Based on the above discussion, omission of FEP 2.1.03.10.0A (Advection of Liquids and Solids through Cracks in the Waste Package) will not result in a significant adverse change in the magnitude or timing of either radiological exposure to the RMEI or radionuclide releases to the accessible environment. Therefore, this FEP is excluded from the performance assessments conducted to demonstrate compliance with proposed 10 CFR 63.311 and 63.321 (70 FR 53313 [DIRS 178394]), and with 10 CFR 63.331 [DIRS 180319], on the basis of low consequence.

INPUTS:

Table 2.1.03.10.0A-1. Direct Inputs

Input	Source	Description
DTN: MO0703PASDSTAT.001. Statistical Analyses for Seismic Damage Abstractions. [DIRS 183148]	file: *CDSP Kinematic Damage Abstraction 23-mm Intact.xls*, worksheet: "Gamma for 90%_i23"	The CDSP waste packages can be subject to SCC-damage from the same PGV level ground motions, and selection of the 95th percentile value (0.377 m^2) as a reasonably conservative upper-bound value for the damage area of the waste package
	file: *Kinematic Damage Abstraction 23-mm Intact.xls*, worksheet: "WP Total"	The TAD-bearing waste packages of 23-mm-thick WPOB with intact internals are not subject to SCC damage from the 1.05 m/s PGV level ground motions
SNL 2007. *Abstraction of Drift Seepage*. [DIRS 181244]	Section 6.4[a]	Threshold seepage rate per waste package
SNL 2007. *In-Package Chemistry Abstraction*. [DIRS 180506]	Section 6.10.9.1[a]	Minimum advective liquid inflow rate into a breached waste package
SNL 2007. *Stress Corrosion Cracking of Waste Package Outer Barrier and Drip Shield Materials*. [DIRS 181953]	Sections 6.6.2 and 6.8.5.2	A reasonable upper-bound for maximum length of a through-wall cracks is two times the remaining wall thickness

Table 2.1.03.10.0A-2. Indirect Inputs

Citation	Title	DIRS
10 CFR 63	Energy: Disposal of High-Level Radioactive Wastes in a Geologic Repository at Yucca Mountain, Nevada	180319
70 FR 53313	Implementation of a Dose Standard After 10,000 Years	178394
Andresen et al. 2005	*Stress Corrosion Crack Initiation & Growth Measurements in Environments Relevant to High Level Nuclear Waste Packages*	176653
ASM International 1987	*Corrosion*	101992
Bruemmer and Thomas 2001	"High-Resolution Analytical Electron Microscopy Characterization of Corrosion and Cracking at Buried Interfaces"	183685
BSC 2001	*Plugging of Stress Corrosion Cracks by Precipitates*	156807
BSC 2004	*Yucca Mountain Site Description*	169734
BSC 2005	*Drip Shield Structural Response to Rock Fall Supplemental Calculation*	174052
DTN: MO0501BPVELEMP.001	Bounded Horizontal Peak Ground Velocity Hazard at the Repository Waste Emplacement Level	172682
DTN: MO0612WPOUTERB.000	Output from General and Localized Corrosion of Waste Package Outer Barrier Report	182035
DTN: SN0506F4104405.003	Analyses of Phase I and Phase II Data from the Stress Corrosion Crack Flow Tests (Data from 1/12/2005 to 5/13/2005)	174472
Herrera 2004	*Evaluation of the Potential Impact of Seismic Induced Deformation on the Stress Corrosion Cracking of the YMP Waste Packages*	168133
Ishikawa et al. 2006	"Characterization of Rust on Fe-Cr, Fe-Ni, and Fe-Cu Binary Alloys by Fourier Transform Infrared and N_2 Adsorption"	183682
Ishikawa et al. 2007	"Assessment of Protective Function of Steel Rust Layers by N_2 Adsorption"	181136
Milnes and Fitzpatrick 1995	"Titanium and Zirconium Minerals"	105911
SNL 2007	*Seismic Consequence Abstraction*	176828
SNL 2008	*EBS Radionuclide Transport Abstraction*	177407
SNL 2007	*Stress Corrosion Cracking of Waste Package Outer Barrier and Drip Shield Materials*	181953
SNL 2007	*Total System Performance Assessment Data Input Package for Requirements Analysis for DOE SNF/HLW and Navy SNF Waste Package Overpack Physical Attributes Basis for Performance Assessment*	179567
Walton 2005	Testing of Stress Crack Flow [final closure]. Scientific Notebook SN-SNL-SCI-032-V2	175407

FEP: 2.1.03.10.0B

FEP NAME:

Advection of Liquids and Solids Through Cracks in the Drip Shield

FEP DESCRIPTION:

The presence of one or more cracks or other small openings of sufficient size in a drip shield may provide a pathway for the advective flow of water (e.g., thin films or droplets) or solid material through the drip shield. The resulting flux may affect drip shield performance and/or subsequent dripping onto the waste packages. Partial or full plugging of the drip shield cracks by chemical or physical reactions after their formation (i.e., healing) could also affect water flow through the drip shield.

SCREENING DECISION:

Excluded – low consequence

SCREENING JUSTIFICATION:

Drip shields may be subject to SCC under repository conditions. The sources of stress that could result in SCC in the Titanium Grade 7 drip shields include: (1) welding-induced residual stress, (2) plasticity-induced residual stress from seismic-induced impacts, and (3) residual stress produced by rockfall impacts (SNL 2007 [DIRS 181953], Section 6.8, Introduction). Welding-induced residual stress in the drip shields will be relieved by heat treatment before placement in the drifts (SNL 2007 [DIRS 179354], Table 4-2, Parameter Number 07-13). Therefore, drip shields will not be subject to SCC on emplacement. However, the drip shields may be subject to SCC from damage induced by seismic and rockfall impacts. Rockfall/seismic effects on drip shield degradation are discussed in excluded FEPs 2.1.07.01.0A (Rockfall) and 1.2.03.02.0B (Seismic-Induced Rockfall Damages EBS Components). These FEPs are excluded from the TSPA on the basis of low-consequence for the first 10,000 years; exclusion of this FEP is used as one of the bases to support exclusion of the above two FEPs.

This FEP finds that residual stresses in the drip shield plates, made from Titanium Grade 7, will relax because of creep so that through-wall SCC cracks are not expected to result. For the unexpected situation in which through-wall cracks develop, this analysis also evaluates the potential for advective water flow through an SCC-damaged drip shield. The analysis considers SCC damage to drip shields subject to seismic-induced loading and reasonably bounding rock block size and energy at the 1.05 m/s PGV level in the first 10,000 years of the repository. This PGV level corresponds to a mean annual exceedance frequency of approximately 10^{-5}/yr (DTN: MO0501BPVELEMP.001 [DIRS 172682], file: *Bounded Horizontal Peak Ground Velocity Hazard at the Repository Waste Emplacement Level.xls*, cells: A5 and B5), and was selected as representative seismic ground motion in the first 10,000 years of the repository. The bounding block size used in this analysis (7.49 MT with an impact velocity of 4.81 m/s; SNL 2007 [DIRS 178851], Table 6-153) corresponds to greater than the 99th percentile of block size at PGV levels of 1.05 and 2.44 m/s (SNL 2007 [DIRS 178851], Table 6-154); these PGV levels correspond to mean annual exceedance frequencies of approximately 10^{-5} and

4.5×10^{-7} m/yr, respectively (DTN: MO0501BPVELEMP.001 [DIRS 172682]). The analysis of drip shield denting by rockfall (Appendix B) considers higher PGV levels.

This analysis provides quantitative estimates of the attenuation of seepage rates, when seepage contacts the surface of a drip shield that has SCC damage. Seepage may contact the drip shield surface as macroscopic "sheet" or rivulet flow, and impinging drip ("falling drop") conditions. The analysis does not consider microscopic film flow along solid surfaces, under the impetus of gravity or in response to gradients of thermodynamic water potential, because such flows are considered to be smaller than the minimum advective liquid inflow rate into a breached waste package (100 mL/yr; SNL 2007 [DIRS 180506], Section 6.10.9.1[a]), or the minimum seepage rate per waste package location (100 mL/yr; SNL 2007 [DIRS 181244], Section 6.4[a]), that are defined for TSPA. Below these low thresholds, the contribution to water availability at the waste package is not significant because other modes of moisture transport such as gaseous diffusion and condensation are more important.

This analysis shows that the potential for advective flow of liquids (and by analogy, solids) through drip shield cracks caused by SCC damage is insignificant, as follows:

- Much of the repository (80% to 85% of the repository emplacement area) will be in lithophysal rock zone (SNL 2007 [DIRS 179466], Table 4-1, Parameter Number 01-03) that does not produce rock blocks capable of causing sufficient SCC damage or denting of the drip shield (Section B.1), so the number of drip shields that could be affected by rockfall is small relative to the total number of drip shields in the repository. The impact of drift collapse (i.e., the en masse fall of rock fragments) on the drip shield is discussed in included FEP 1.2.03.02.0C (Seismic-Induced Drift Collapse Damages EBS Components).

- Relatively few rock blocks can fall in the nonlithophysal host rock that could damage drip shields or create dents that could act to funnel seepage. The probability for large rock blocks to fall in the nonlithophysal tuff is shown to be small due to the low probability of seismic events of sufficient magnitude (Section B.2.3). As discussed in detail in Appendix B, significant conservatisms were employed in the probability analysis.

- The size of the damaged area in the drip shield from seismic-induced rockfall is small relative to the surface area of the drip shield (0.064 m^2, or 0.48% of the drip shield topside surface; Section C.2.2.1).

- Residual stresses from seismic-induced rockfall are not expected to result in through-wall SCC cracks in the drip shield due to stress relaxation and low-temperature creep of Titanium Grade 7.

- If through-wall SCC cracks were to develop in the drip shield plate, only a small fraction of the through-wall cracks are expected to be spatially aligned with impinging seepage drips from the drift wall.

- If through-wall SCC cracks were to develop in the drip shield, plugging of the tight and highly tortuous cracks by mineral precipitates and corrosion products will limit the amount of water inside the cracks and the potential for advective water flow (a reasonable upper-bound volumetric flow rate of 4 mL/yr per damaged drip shield is estimated; Sections C.3.1 and C.4).

- The localized corrosion initiation uncertainty analysis for the WPOB shows that for the assumed condition that drip shields are completely removed and waste packages are exposed to the occurrence of drift seepage, only a fraction (approximately 10% or less at any point in time) of the waste packages are exposed to conditions that initiate localized corrosion (SNL 2008 [DIRS 183478], Appendix O).

- Even if leakage through a crack-damaged drip shield was to cause localized corrosion that penetrated the WPOB, and the 4 mL/yr leakage flowed directly into the waste package, the impact would be insignificant to repository performance.

In summary, the advection of liquids and solids through cracks in the drip shield is excluded on the basis of low consequence because: (1) SCC cracks resulting from damage by seismic-induced rockfall and/or ground motions at the 1.05 m/s PGV level are not expected to form or to fully penetrate the drip shield; and (2) if through-wall cracks develop, the additional factors described above and in Appendix C will limit the amount of advective water flow to amounts much less than the minimum liquid influx rate (100 mL/yr) into a breached waste package that is important in TSPA. A separate excluded FEP 2.1.03.02.0B (Stress Corrosion Cracking of Drip Shields) is also excluded on the basis of low consequence; exclusion of this FEP is used as one of the bases to support exclusion of that FEP. Summary discussions for each of those factors listed above are presented below.

Rockfall Damage Analysis

During a seismic event, large-block rockfall is predicted to occur in the nonlithophysal units only (BSC 2004 [DIRS 166107], Section 6.3). In the lithophysal units, large blocks are not expected to form due to the presence of lithophysal voids interconnected by densely spaced fractures (BSC 2004 [DIRS 166107], Sections 6.4.1.1 and 8.1). Approximately 80% to 85% of the repository emplacement area will be in lithophysal rock (SNL 2007 [DIRS 179466], Table 4-1, Parameter Number 01-03), so most drip shields will not be subject to large-block rockfall impacts that could lead to SCC. Some rock blocks released in the nonlithophysal tuff will have sufficient mass and energy to cause plastic deformation in the drip shield plates, and if the resulting residual tensile stress is sufficiently high and is not relaxed by creep, then the damaged area could be subject to SCC depending on the corrosion environment (SNL 2007 [DIRS 181953], Section 6.8).

Appendix B evaluates the potential for dents to occur to the drip shield that could impact its flow diversion function. The analysis in Appendix B evaluates the frequency of such rockfall events as a function of seismic event recurrence probability, and the consequences to the drip shields from rock block impacts. The results indicate that such damage will be rare, and additional confidence is assured because reasonable conservatisms are used in the consequence analysis, including:

- A large rock block is partly fractured and may break or crumble on impact with the drip shield, thus dispersing energy and attenuating the intensity of impact. However, the potential for block failure is not included in the structural response calculations.

- The orientation and shape of rock blocks are chosen to calculate an upper-bound damage to the drip shield by locating the center of mass directly above the impact point. Blocks have a cubic shape for the LS-DYNA calculations, with the center of mass directly above an edge that contacts the crown of the drip shield.

As shown in Appendix B, there are no blocks at the 1.05 and 2.44 m/s PGV levels that cause a significant dent (i.e., a dent that has a concave shape that can retain standing seepage liquid in the dent) to form on the drip shield crown (although residual stresses from these impacts may lead to SCC). The potential for SCC in the drip shield resulting from the damage areas associated with denting is addressed in subsequent sections within this FEP screening justification and in Appendix C. The tearing or rupture of drip shield plates from large block impacts is excluded from the TSPA model because of low consequence as discussed in excluded FEP 1.2.03.02.0B (Seismic-Induced Rockfall Damages EBS Components). For blocks simulated using seismic events with PGV levels greater than 2.44 m/s, the risk to performance is insignificant considering the low probability of occurrence, and the reasonable conservatisms in the consequence analysis (Section B.2.3). Based on the rockfall calculations, impacts by the highest energy blocks will be mitigated by the tendency toward shoulder impacts rather than crown impacts and by the irregular block shape, wherein the center of mass is not directly over the impact point.

The potential for SCC in the drip shield to result from the damage areas associated with denting is addressed in subsequent sections within this FEP screening justification and in Appendix C. Tearing or rupture of drip shield plates from large block impacts is excluded from the TSPA model because of low consequence as discussed in excluded FEP 1.2.03.02.0B (Seismic-Induced Rockfall Damages EBS Components).

Stress Mitigation by Low Temperature Creep of Titanium Alloy

In response to stresses induced by rockfall deformations, stress relief will occur via creep mechanisms or SCC of the drip shield. Unlike most metals and alloys, titanium and many of its alloys are susceptible to creep at lower temperatures, down to room temperature (ASM 1961 [DIRS 170284], pp. 537 to 539). Since stress relaxation is directly related to creep, relaxation of plasticity-induced residual stresses is expected and has been measured for titanium alloys. For example, titanium exhibits room temperature stress relaxation even after five minutes when held at a range of stresses from less than half of the yield strength to stresses in excess of the yield strength (Sargent and Conrad 1969 [DIRS 174054], Figure 3). Thus, even though residual stresses near the yield strength are calculated to be present following large-block rockfalls, these displacement-controlled stresses are expected to relax over time to stresses below the SCC initiation threshold of 80% of yield strength (SNL 2007 [DIRS 181953], Section 8.1.5) without initiation of cracking, or if cracks initiate, without propagation of cracks through the thickness.

This expectation is best corroborated by tests conducted on 182 U-bend test specimens of Titanium Grades 7 and 16, and welded Titanium Grade 12 (SNL 2007 [DIRS 181953],

Section 6.8.3.1.2). These U-bend specimens were bent approximately 180 degrees and then the legs were restrained to give an apex strain (cold-work level) of approximately 12%. Approximately half the specimens were exposed to liquid of representative composition, and half to vapor, for a range of relevant environments at 60°C and 90°C. These test conditions produced stress levels near or slightly above the yield strength. The exposure time was approximately 5 years for Titanium Grades 12 and 16 and approximately 2.5 years for Titanium Grade 7 (SNL 2007 [DIRS 181953], Section 6.8.3.1.2). Stress corrosion cracking initiation was not detected in any of the Titanium Grade 7 and 16 specimens. In all, only three of the welded Titanium Grade 12 specimens demonstrated cracking. These results show that the Titanium Grade 7 plates that serve as the flow diversion elements of the drip shield design are not expected to sustain any SCC damage at all, and that consideration of flow through such cracks is a conservative presumption.

The plastic deformation associated with the dented regions caused by rockfall will create residual stress gradients in the dented regions. An analysis of the resultant residual stress states is evaluated in *Drip Shield Structural Response to Rock Fall Supplemental Calculation* (BSC 2005 [DIRS 174052]). An evaluation of the time histories associated with these impacts shows that the stresses decrease as the material rebounds from the impact. The largest block of 28.29 MT, which is associated with unbounded ground motions with a PGV level of 5.35 m/s, leaves a residual first principal tensile stress of 140 MPa on the outer surface (also referred to as "top" surface) of the drip shield and a residual first principal tensile stress of 10 MPa on the inner surface (also referred to as "underside" surface) of the drip shield (BSC 2005 [DIRS 174052], Figure 7-60 and Table 7-9). The smaller block of 11.87 MT, which is associated with unbounded ground motions with a PGV level of 2.44 m/s, yields residual first principal tensile stresses of 125 MPa and 15 Mpa on the upper and lower surfaces of the drip, shield respectively (BSC 2005 [DIRS 174052], Figure 7-57 and Table 7-9).

These residual stress are well below the 209-MPa yield strength of Titanium Grade 7 at 150°C (the temperature for which the analysis was performed; BSC 2005 [DIRS 174052], Table 7-9). Because SCC also requires a corrosion environment (i.e., stable water to support corrosion reactions) in addition to sufficient tensile residual stress, the drip shield plate temperature has to decrease below approximately 100°C before SCC can initiate. Since the residual stress on the outer surface of the drip shield does not exceed the stress corrosion crack initiation threshold of 80% of yield strength (for example, 225 MPa at 90°C or 221 MPa at room temperature; SNL 2007 [DIRS 181953], Table 8-2), it is expected that cracks will not initiate in the dented regions. Because of the low temperature creep and resulting stress relief associated with Titanium Grade 7 discussed above, it is logical to expect gradual relief of these residual first principal stresses as the alloy undergoes creep.

Laboratory Tests

An analogue to the residual stress states and stress profiles from the stress calculation (BSC 2005 [DIRS 174052], Section 7) was created in stainless steel plates to evaluate the potential for such stresses to propagate through-wall cracks (Andresen et al. 2005 [DIRS 176653], Section 5). A series of stress corrosion crack tests was performed in which a simulated, rockfall-dented stainless steel plate was exposed to a boiling saturated aqueous solution of magnesium chloride. This is a highly corrosive environment that will initiate and propagate stress corrosion cracks in

stainless steels even at low levels of residual tensile stress down to about 70 MPa (approximately 10 ksi) (ASM International 1987 [DIRS 101992], p. 272, Figure 54). The stress state in stainless steel was tested as an analogue to that of Titanium Grade 7 because the titanium alloy is extremely resistant to SCC and it is difficult to initiate SCC under the test conditions.

A series of tests was conducted to examine the potential for water flow through cracks (DTN: SN0506F4104405.003 [DIRS 174472]). These tests were designed to determine if water could penetrate real SCC cracks formed in a stainless steel plate subject to point-loading and a boiling electrolyte, as well as simulated cracks formed between precision-ground blocks of Titanium Grade 7 and stainless steel. The simulated cracks had no tortuous pathways (i.e., machined internal surfaces), were empty, and free of any plugging matter. Flow testing was performed with the simulated, parallel-wall cracks, and with the real SCC cracks. Water was dripped onto both the simulated and real cracks from a height of 2.2 m (the maximum distance from the emplacement drift crown to the drip shield crown), and 0.4 m (the maximum distance between the drip shield crown and top of the waste package). The plates were held at different angles relative to the dripping water. A "sheet flow" test was also performed in which the water was dripped onto the plates a few inches above the cracks and allowed to flow over the cracks as a "sheet" flow.

The largest aperture used for the simulated cracks with both the titanium and stainless steel blocks was 50.8 μm. For the real cracks in the stainless steel plate, the largest nominal aperture size (observed by inspection) in one location was approximately 381 μm, and that in the other location was approximately 127 μm; effective aperture sizes could be inferred from flow measurements, but were not characterized directly (Walton 2005 [DIRS 175407], pp. 110 and 145). The test results are summarized in DTN: SN0506F4104405.003 ([DIRS 174472], files: *Dynamic_Drop_Test_Summary_SCC_4-15-05.doc* and *SCC_PhaseII_Test_Preliminary_Summary_9-21-05.doc*).

For the impinging drip ("falling drop") tests with real SCC cracks, two locations were identified as potential flow paths; one location did not yield any sign of water penetration, and the other yielded water flow through cracks in amounts ranging from 0.03% to 1.82% of the total amount of impinging water (with one exception, a test that yielded 4.02%) (DTN: SN0506F4104405.003 [DIRS 174472], file: *Dynamic_Drop_Test_Summary_SCC_4-15-05.doc*). Results from flow testing of the real SCC cracks are used to estimate potential leakage from the impinging-drip flow mode in Appendix C. Results from testing of the simulated cracks were used only to investigate behaviors such as the dependence on tilt angle and drop height and on material interactions. For the largest simulated crack aperture (50.8 μm) with the titanium blocks, less than 3% of the impinging drip water penetrated the crack when dripped from a height of 2.2 m (DTN: SN0506F4104405.003 [DIRS 174472], file: *SCC_PhaseII_Test_Preliminary_Summary_9-21-05.doc*).

A total of six test runs were conducted for the sheet flow condition, two runs for the titanium test blocks and four runs for the stainless steel test blocks. The titanium block test runs (both tilted at 5° angle from horizontal) did not yield water penetration, and two (both tilted at 5° angle) of the four stainless steel block test runs yielded water penetration (0.04% and 1.03%, respectively, of the total water dripped) (DTN: SN0506F4104405.003 [DIRS 174472], file: *SCC_PhaseII_Test_Preliminary_Summary_9-21-05.doc*).

The laboratory test results support the conclusion that only a small fraction of seepage flow is expected to penetrate cracks for sheet flow and dripping conditions, even if dripping impinges directly on a crack. Sustained dripping of seepage directly on the same cracks in the repository environment is not expected because the alignment of the drip impact location with the crack will vary. The tests also show that the tilt angle of the surface containing cracks strongly attenuates water flow through the cracks, for both sheet flow and impinging drip conditions. Furthermore, it is expected that these flow rates through actual SCC cracks will decrease significantly as a result of the plugging mechanisms discussed below and in Appendix C. Typical SCC cracks in stainless steel are highly branched (for transgranular cracks) and exhibit tortuous morphology (Figure 2.1.03.10.0B-1). It is expected that SCC morphology in Titanium Grade 7 is similar to that in stainless steel because of similarity in the crystalline granular structure of these alloys. Evidence of tight, highly branching intergranular and transgranular SCC cracks was observed from some Titanium Grade 7 U-bend samples tested in highly aggressive conditions with elevated dissolved fluoride and chloride concentrations (SNL 2007 [DIRS 181953], Section 6.8.2).

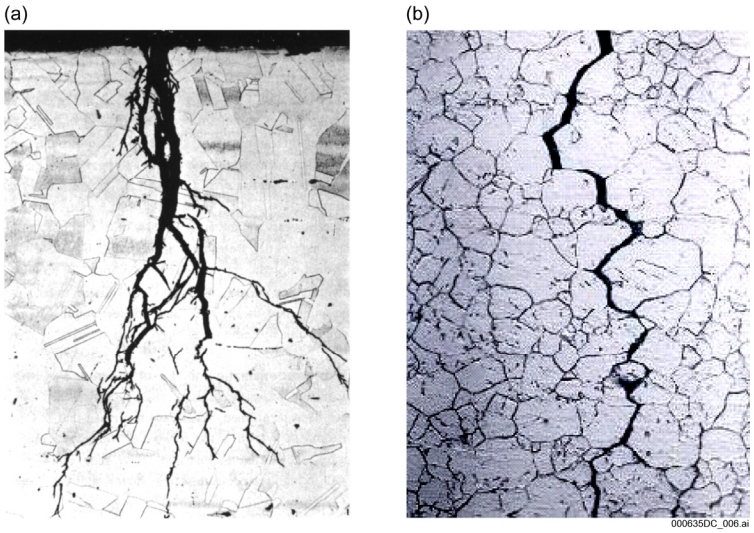

Sources: (a) Herrera 2004 [DIRS 168133], Figure 2-1.
(b) Herrera 2004 [DIRS 168133], Figure 2-2.

NOTE: This figure also appears in SNL 2007 [DIRS 181953], Figure 6-61.

Figure 2.1.03.10.0B-1. Typical Examples of (a) Transgranular SCC and (b) Intergranular SCC Cracks in Stainless Steel

Crack Plugging with Mineral Precipitates and Corrosion Products

SCC is a corrosion process that requires the presence of a corrosive environment (i.e., water with dissolved species such as chloride or fluoride) inside the crack and around the crack mouth for sustained operation. The SCC process will result in accumulation of corrosion products from associated corrosion reactions and mineral precipitates from evaporation (or evaporative equilibration) of water filling the crack. Detailed studies using high-resolution analytical electron microscopy have demonstrated the accumulation of corrosion products and intrusion of the external environment water deep inside very fine SCC cracks of stainless steels and nickel-based alloys (Bruemmer and Thomas 2001 [DIRS 183685]). Corrosion product particles are expected to be a few tens of nanometers in size as shown from electron microscope studies of

corrosion products formed on Titanium Grade 7 samples (He et al. 2007 [DIRS 183687], p. 789 and Figure 14-b).

As discussed in Section C.3, propagation of SCC cracks through the 15-mm-thick drip shield plates could take a few tens of years to thousands years in the repository environment. As SCC cracks grow through the drip shield plate thickness, intermittent humidity cycles resulting from atmospheric fluctuations in the repository, or from variability in dripping rate and location (BSC 2004 [DIRS 169734], Sections 7.3.2 and 7.4.1), will promote mineral precipitation and accumulation of corrosion products inside the cracks.

SCC cracks for corrosion resistant materials like Titanium Grade 7 are typically very tight and tortuous (SNL 2007 [DIRS 181953], Section 6.8.2), and therefore require only small amounts of corrosion products and/or mineral precipitates to become filled. The corrosion product oxides tend to cement and agglomerate (Ishikawa et al. 2006 [DIRS 183682]; Ishikawa et al. 2007 [DIRS 181136]), especially in the presence of other minerals such as silica minerals (Milnes and Fitzpatrick 1995 [DIRS 105911], pp. 1,180 to 1,183). In addition, because of greater molar volumes of corrosion product compounds compared to the base metal (e.g., titanium oxide from corrosion of Titanium Grade 7), cracks will eventually be plugged by compacted corrosion products in the presence of mineral precipitates. Any SCC cracks that form in the drip shield are expected to be filled with compact cemented agglomerates of corrosion products and mineral precipitates as the cracks grow through the plate wall thickness.

A summary of the calculation of the expected rate of SCC plugging due to calcite precipitation from seepage water is documented in *Plugging of Stress Corrosion Cracks by Precipitation* (BSC 2001 [DIRS 156807], Section 6.3). The calculation employs a simplifying assumption that no corrosion products or mineral precipitates form inside the crack until it fully penetrates the wall thickness. In reality, as discussed earlier, the SCC cracks will be continuously filled with corrosion products and mineral precipitates as they grow through the wall thickness. Other assumptions include: (1) that the corrosion products generated on the crack walls, as well as colloids, particulates, and any precipitated minerals, do not participate in resisting the water flow through the crack; and (2) that there is a uniform water seepage flow in space and time. It is concluded that, under these assumptions, the cracks will be sealed in a few hundred years at most when water is allowed to flow at low sheet-flow rates. If the cracks are bridged by water, plugging may take thousands of years (limited by the delivery of solute), but no flow will occur if capillary forces hold the water. In a more realistic case of nonuniform flow onto the drip shield, more precipitation and faster plugging could occur (BSC 2001 [DIRS 156807], Section 6.3).

Bounding Analysis for the Geometry and Number of Through-Wall SCC Cracks in Drip Shield

As discussed in Appendix C, an SCC crack in the drip shield can be treated as a semi-elliptical crack (SNL 2007 [DIRS 181953], Sections 6.6.2 and 6.8.5.2). An initially semi-elliptical crack becomes a semi-circular crack as it grows to a through-wall crack (SNL 2007 [DIRS 181953], Section 6.6.2). Figure C-1 presents the simplified geometry of a through-wall crack in this analysis. The expected maximum length ($2c$) of the cracks is at least two times the wall thickness (SNL 2007 [DIRS 181953], Sections 6.6.2 and 6.8.5.2). The crack width and opening

area are assumed to be the same through the wall thickness. Note that for an actual SCC crack propagating through the wall thickness, the crack width and opening area are expected to decrease with depth because of the residual stress redistribution and relaxation at the crack tip as the crack grows. For the drip shields that are damaged by seismic-induced events, the residual tensile stress tends to decrease from the outer surface (where the seismic impact occurs) to the inner surface of the drip shield (SNL 2007 [DIRS 181953], Sections 6.7.1.2 and 7.5.1.2). The expected configuration of through-wall cracks that result from seismic damage is one with a larger opening at the outer surface and a much smaller opening at the penetration point on the inner surface. Those effects can be amplified when neighboring cracks propagate in parallel through the wall thickness (SNL 2007 [DIRS 181953], Sections 6.7.1.2 and 6.7.1.3).

If SCC breach of the drip shield were to occur during the first 10,000 years after repository closure when the drip shields maintain most of the design wall thickness of 15 mm (i.e., $2c$ = 30 mm), a reasonable upper-bound width of a through-wall crack in the drip shield is calculated to be approximately 155 μm (Equation C-1), and the corresponding crack mouth area is approximately 3.65 mm^2 (Equation C-2), using the room temperature yield strength and modulus of elasticity of Titanium Grade 7 (Section C.2.1).

Seismic-induced SCC of the drip shield plates would require that the resultant residual tensile stress is greater than 80% of the yield strength of Titanium Grade 7 (SNL 2007 [DIRS 181953], Section 8.1.5). As described in detail in Section C.2.2.1, no damage to the drip shield with the 15-mm plate thickness is estimated in the lithophysal rock zone (also see DTN: MO0703PASDSTAT.001 [DIRS 183148], file: *DS Damaged Area with Rubble.xls*, worksheet: "1.05 ms PGV - Case 2 BCs," cells: M57 to M68, and worksheet: "1.05 ms PGV - Case 1 BCs," cells: M54 to M65). In the nonlithophysal zone, the upper-bound impact damage area in the drip shield with 15-mm thick plate by the largest rock block (the 99.9th percentile for all blocks ejected under the 1.05 m/s PGV) is estimated to be 0.064 m^2, which corresponds to 0.43% of the total upper surface area of the drip shield (output DTN: SN0705WFLOWSCC.001, file: *Bounding calc for water flow through SCC cracks.xls*, worksheet: "Sheet flow DS flow rate," cell: B12)) (see Section C.2.2.1 for details). The seismic damage areas are assumed to be distributed randomly over the drip shield surface. A reasonable upper-bound total number of through-wall SCC cracks per damaged drip shield is estimated to be 326 cracks, and the corresponding upper-bound total crack-mouth opening area of through-wall SCC cracks per damaged drip shield is approximately 1,190 mm^2 (output DTN: SN0705WFLOWSCC.001, file: *Bounding calc for water flow through SCC cracks.xls*, worksheet: "Sheet flow DS flow rate," cells: B16 and B17.

Water Flow Rates from Through-Wall SCC Cracks in Sheet Flow Condition

This analysis was conducted to bound the potential rate of gravity driven, liquid water flow through SCC cracks in a damaged drip shield in the sheet flow condition. The impinging drip ("falling drop") condition is discussed in the next section. The analysis assumes liquid-saturated conditions within a porous medium that fills the cracks in the path of sheet flow, bounding the potential flow rate. Note that 18 (about 6%) of 326 through-wall cracks (discussed earlier) are located on the top of the drip shield above the waste package, where leakage is potentially significant (Section C.3.1). The other through-wall cracks will not be fully saturated with water,

and thus will be more permeable to gases and water vapor (addressed in more detail for excluded FEP 2.1.03.10.0A (Advection of Liquids and Solids Through Cracks in the Waste Package)).

The Kozeny-Carman equation is a widely used derivation for permeability in granular media (Bear 1972 [DIRS 156269], pp. 165 to 167) and is used to estimate the saturated permeability of the porous filling for any SCC cracks that form in the drip shields (Section C.3). The Kozeny-Carman equation is based on a theory that treats a porous medium as a bundle of capillary tubes of equal length (Bear 1972 [DIRS 156269], p. 166) and this simplifying conceptual model gives rise to uncertainty in the estimation of permeability. An assumption is made that the porous medium inside a crack consists primarily of titanium oxide (TiO_2), a corrosion product of Titanium Grade 7. The corrosion product particles are expected to be a few tens of nanometers in size as shown from an electron microscopic study of corrosion products formed on Titanium Grade 7 samples (He et al. 2007 [DIRS 183687], p. 789 and Figure 14-b). Titanium oxide particles of the size have been estimated to have specific surface area on the order of 100 m^2/g (Yao and Zhang 1999 [DIRS 184766], Tables I and II (excluding those heat treated at 500°C and 600°C)). Compaction or cementation of the particles of corrosion products and mineral precipitates will further limit permeability. The density of natural rutile (4.26 g/cm^3; Lide 2000 [DIRS 131202], p. 4-108) and specific surface area of commercial-grade crystalline rutile and anatase (6 to 50 m^2/g; Siriwardane and Wightman 1983 [DIRS 183688], p. 504) are used in the analysis; the specific surface area used is conservative because, as discussed earlier, the surface area of titanium oxide corrosion product particles may be much higher.

The saturated hydraulic conductivity (calculated from permeability) of the titanium oxide particles filling cracks is estimated to be in a range of 7.44×10^{-4} m/yr (or 2.36×10^{-11} m/s for the lower bound of the specific surface area) to 5.17×10^{-2} m/yr (or 1.64×10^{-9} m/s for the upper bound of the specific surface area) (output DTN: SN0705WFLOWSCC.001, file: *Bounding calc for water flow through SCC cracks.xls*, worksheet: "Sheet flow DS flow rate," cells B29 and D29). The estimated hydraulic conductivity values fall in the range for clay, which range from 1.0×10^{-11} to 4.7×10^{-9} m/s (Domenico and Schwartz 1990 [DIRS 100569], Table 3-2, p. 65). Considering the high specific surface area of the corrosion products, the comparison with clays corroborates the estimated range for hydraulic conductivity. Clays typically have very fine particle sizes, rugged platy surface morphology, and high specific surface area. When settled or compacted, clays retain their high porosity but have very low permeability.

Applying a unit head gradient in the flowing cracks, the total volumetric flow rate through the SCC through-wall cracks in the drip shield is estimated to be in a range of 0.05 to 3.42 mL/yr (output DTN: SN0705WFLOWSCC.001, file: *Bounding calc for water flow through SCC cracks.xls*, worksheet: "Sheet flow DS flow rate," cells B31 and D31). The estimated flow rates through the damaged drip shield are negligibly small, so that no advective flow condition is expected on the waste package surface (Section C.3.1). These estimated flow rates are much smaller than the minimum advective liquid influx rate (100 mL/yr) into a breached waste package (SNL 2007 [DIRS 180506], Section 6.10.9.1[a]), or the threshold seepage rate per waste package (100 mL/yr; SNL 2007 [DIRS 181244], Section 6.4[a]), that are defined for TSPA.

Flow Rates in Through-Wall SCC Cracks Under Impinging Drips

This analysis was conducted to bound the potential rate of liquid flow through SCC cracks in a damaged drip shield, by impinging drips (Section C.4). As discussed earlier, the analysis considers that seismic damage area is distributed randomly over the drip shield surface. Twenty-five percent (82 cracks) of 326 through-wall cracks (reasonable upper-bound number of through-wall cracks per seismic-damaged drip shield) are estimated to potentially flow water under impinging drip conditions (Section C.3.1). The other through-wall cracks will not be fully saturated with water, and thus will be more permeable to gases and water vapor (addressed in more detail for excluded FEP 2.1.01.10.0A (Advection of Liquids and Solids Through Cracks in the Waste Package)).

Even for the bounding values for the uncertain parameters of the impinging drip condition analysis, the analysis shows that the SCC-damaged drip shield can still divert most of the drift seepage, reducing the seepage by more than six orders of magnitude (output DTN: SN0705WFLOWSCC.001, file: *Bounding calc for water flow through SCC cracks.xls*, worksheet: "Impinging drip flow rate," cell B25). For example, if the damaged drip shield were subject to a reasonable upper-bound drift seepage flux of 500 L/yr (DTN: MO0705TSPASEEP.000 [DIRS 183008], file: *v5.005_Seismic-FD_1Myr_CDSP_SeepRate_Bin5_stats.txt*; based on the mean drift seepage rate of approximately 460 L/yr from percolation subregion 5 (highest percolation rate subregion) at 10,000 years), a reasonable upper-bound volumetric flow rate through the damaged drip shield under impinging drip condition is estimated to be only 0.4 mL/yr, which is negligibly small (output DTN: SN0705WFLOWSCC.001, file: *Bounding calc for water flow through SCC cracks.xls*, worksheet: "Impinging drip flow rate," cell B24). Combining the sheet flow and impinging-drip modes for flow through cracks, the bounding estimate is approximately 4 mL/yr. As discussed above, this estimated upper-bound flow rate is much smaller than the minimum liquid influx rate (100 mL/yr) into a breached waste package, or the threshold seepage rate per waste package location (100 mL/yr) that are defined for TSPA (SNL 2007 [DIRS 181244], Section 6.4[a]).

Impact of Leakage through Crack-Damaged Drip Shield on the Waste Package

The effects from small rates of leakage through a crack-damaged drip shield on the potential for localized corrosion of the underlying WPOB are insignificant to repository performance because:

- Crack-damage is spatially distributed on the surface of the drip shield, so the leakage is also spatially distributed on the surface of the underlying waste package. In addition, much of the leakage would flow down the underside of the drip shield and not fall onto the waste package. These effects would combine to limit the salt load deposited on the waste package surface, so that the potential for localized corrosion initiation in the outer barrier is limited. This type of limitation is the same as that described for the effects of dust deliquescence (SNL 2007 [DIRS 181267], Section 6.5).

- Because only through-wall cracks in the upper surface of drip shield have the potential to flow seepage water, leakage, if any occurs, from an SCC-damaged drip shield is expected to fall onto the upper surface of the underlying waste package. Creviced conditions are not expected on the upper-surface area of the waste package, which will

be "boldly exposed" Alloy 22. Localized corrosion of boldly exposed Alloy 22 (i.e., pitting corrosion) requires much more aggressive corrosion conditions than the creviced conditions that are adopted in the localized corrosion initiation model for Alloy 22 for TSPA (SNL 2007 [DIRS 178519], Section 6.4.4.1). The small flow rates (4 mL/yr, reasonably conservative upper-bound) that are projected to result from leakage of a SCC-damaged drip shield are not expected to produce such aggressive corrosion environments on the upper surface of the waste package.

- The localized corrosion initiation uncertainty analysis for the WPOB shows that for the assumed condition that drip shields are completely removed and waste packages are exposed to the occurrence of drift seepage, only a fraction (approximately 10% or less at any point in time) of the waste packages are exposed to conditions that initiate localized corrosion (SNL 2008 [DIRS 183478], Appendix O).

Even if leakage through a crack-damaged drip shield were to cause localized corrosion that penetrated the WPOB, and the 4 mL/yr leakage flowed directly into the waste package, the impact would be insignificant to repository performance. The estimated upper-bound flow rate is much smaller than the minimum liquid influx rate (100 mL/yr) into a breached waste package that is important to the in-package chemistry for TSPA (SNL 2007 [DIRS 180506], Section 6.10.9.1[a]), or the threshold seepage rate per waste package location that is used to define the presence of seepage for TSPA (100 mL/yr; SNL 2007 [DIRS 181244], Section 6.4[a]). In addition, the TSPA model basis allows formation of corrosion products on the internal surfaces of the waste package to begin immediately after breach (SNL 2008 [DIRS 177407], Section 6.5.2.2.1), and the amount of water that is consumed by those corrosion reactions greatly exceeds 4 mL/yr (e.g., SNL 2008 [DIRS 177407], Figure 6.5-8). Whereas gaseous diffusion of water vapor is the assumed mechanism that supplies this water, a small addition from advective flow would be inconsequential. Thus even if localized corrosion under a crack-damaged drip shield were to penetrate the waste package, the amount of additional water that would be added to the in-package environment is negligible.

Screening Justification Summary

This FEP finds that residual stresses in the drip shield plates will relax because of creep so that through-wall SCC cracks are not expected to result. Stress relaxation is directly related to creep, so relaxation of rockfall-induced, displacement-controlled residual stresses will occur over time to stresses near or below the stress corrosion crack initiation threshold of 80% of the yield strength. For the unexpected situation in which through-wall cracks develop, this analysis shows that the impact to performance from SCC damage, leading to small amounts of seepage leaking through cracks, is insignificant.

A relatively small number of rock blocks are expected to fall in the repository in the first 10,000 years that could damage drip shields and create dents that could funnel seepage to through-wall cracks in the drip shield. The size of the SCC-damage area in the drip shield plate from seismic-induced rockfall will be small relative to the surface area of the drip shield. As shown in Appendix B, there are no blocks at the 1.05 and 2.44 m/s PGV levels that cause a significant dent to form on the drip shield. For blocks simulated using seismic events with PGV levels greater

than 2.44 m/s, the risk to performance is insignificant considering the low probability of occurrence, and the conservatisms in the consequence analysis (Section B.2.3).

Analysis detailed in Appendix C shows that, if through-wall SCC cracks were to develop in the drip shield, plugging of the tight and highly tortuous cracks by compact cemented agglomerates of mineral precipitates and corrosion products will limit the potential for advective water flow under sheet flow and impinging drip conditions to negligibly small levels. A reasonable upper-bound volumetric flow rate through a seismically damaged drip shield under these flow conditions combined is approximately 4 mL/yr. This rate is much smaller than the minimum liquid influx rate (100 mL/yr) into a breached waste package (SNL 2007 [DIRS 180506], Section 6.10.9.1[a]), or the threshold seepage rate per waste package (100 mL/yr; SNL 2007 [DIRS 181244], Section 6.4[a]) that are defined for TSPA.

The combined effects of: (1) few damaging rockfall events, (2) creep/stress relaxation in drip shield, (3) evaporation of seepage water contacting the drip shield, and (4) plugging of tight tortuous cracks will limit the amount of seepage water that can flow through cracks in the drip shields, to insignificant levels.

Based on this discussion, omission of FEP 2.1.03.10.0B (Advection of Liquids and Solids through Cracks in the Drip Shield) will not result in a significant adverse change in the magnitude or timing of either radiological exposure to the RMEI or radionuclide releases to the accessible environment. Therefore, this FEP is excluded from the performance assessments conducted to demonstrate compliance with proposed 10 CFR 63.311 and 63.321 (70 FR 53313 [DIRS 178394]), and with 10 CFR 63.331 [DIRS 180319], on the basis of low consequence.

INPUTS:

Table 2.1.03.10.0B-1. Direct Inputs

Input	Source	Description
DTN: MO0501BPVELEMP.001. Bounded Horizontal Peak Ground Velocity Hazard at the Repository Waste Emplacement Level. [DIRS 172682]	file: *Bounded Horizontal Peak Ground Velocity Hazard at the Repository Waste Emplacement Level.xls*, cells: A5 and B5	A PGV level selected as a representative seismic ground motion that corresponds to a mean annual exceedance frequency of approximately 10^{-5}
DTN: MO0705TSPASEEP.000. TSPA-LA Addendum, Seepage Results from the TSPA-LA Model. [DIRS 183008]	file: *v5.005_Seismic-FD_1Myr_CDSP_SeepRate_Bin5_stats.txt*	A reasonable upper-bound drift seepage flux
DTN: SN0506F4104405.003. Analyses of Phase I and Phase II Data from the Stress Corrosion Crack Flow Tests (Data from 1/12/2005 to 5/13/2005). [DIRS 174472]	file: *SCC_PhaseII_Test_Preliminary_Summary_9-21-05.doc*	Tilt angles of plate block containing a through-wall crack that is potentially subject to flow through cracks under impinging drips
	files: *Dynamic_Drop_Test_Summary_SCC_4-15-05.doc*, *Preliminary_Summary_9-21-05.doc*	Tilt angles of plate block containing a through-wall crack that can potentially flow water in sheet flow condition

Table 2.1.03.10.0B-1. Direct Inputs (Continued)

Input	Source	Description
Lide 1991. *CRC Handbook of Chemistry and Physics*. [DIRS 131202]	p. 4-108	Density of rutile (TiO_2)
Siriwardane and Wightman 1983. "Interaction of Hydrogen Chloride and Water with Oxide Surfaces. III. Titanium Dioxide." [DIRS 183688]	p. 504	Range of specific surface area of commercial grade crystalline rutile
SNL 2007. *Total System Performance Assessment Data Input Package for Requirements Analysis for EBS In-Drift Configuration*. [DIRS 179354]	Table 4-2, Parameter Number 07-13	Welding induced residual stress in the drip shields will be relieved by heat treatment before placement in the drifts
SNL 2007. *Abstraction of Drift Seepage*. [DIRS 181244]	Section 6.4[a]	Threshold seepage rate per waste package, 100 mL/yr
SNL 2007. *In-Package Chemistry Abstraction*. [DIRS 180506]	Section 6.10.9.1[a]	Minimum advective liquid inflow rate into a breached waste package (100 mL/yr) for liquid influx abstraction
SNL 2007. *Stress Corrosion Cracking of Waste Package Outer Barrier and Drip Shield Materials*. [DIRS 181953]	Sections 6.6.2, 6.8.5.2	A reasonable upper-bound maximum length of cracks is two times the wall thickness
	Section 8.1.5	Crack propagation rate in Titanium Grade 7 in repository condition
	Sections 6.6.2, 6.8.5.2	Treatment of SCC crack in the drip shield as a semi-elliptical crack, then as a semi-circular crack as it grows to a through-wall crack

Table 2.1.03.10.0B-2. Indirect Inputs

Citation	Title	DIRS
10 CFR 63	Energy: Disposal of High-Level Radioactive Wastes in a Geologic Repository at Yucca Mountain, Nevada	180319
70 FR 53313	Implementation of a Dose Standard After 10,000 Years	178394
Andresen et al. 2005	*Stress Corrosion Crack Initiation & Growth Measurements in Environments Relevant to High Level Nuclear Waste Packages*	176653
ASM 1961	"Properties and Selection of Metals"	170284
ASM International 1987	*Corrosion*	101992
Bear 1972	*Dynamics of Fluids in Porous Media. Environmental Science Series*	156269
Bruemmer and Thomas 2001	"High-Resolution Analytical Electron Microscopy Characterization of Corrosion and Cracking at Buried Interfaces"	183685
BSC 2001	*Plugging of Stress Corrosion Cracks by Precipitates*	156807
BSC 2004	*Drift Degradation Analysis*	166107
BSC 2004	*Yucca Mountain Site Description*	169734
BSC 2005	*Drip Shield Structural Response to Rock Fall Supplemental Calculation*	174052
Domenico and Schwartz 1990	*Physical and Chemical Hydrogeology*	100569
DTN: SN0506F4104405.003	Analyses of Phase I and Phase II Data from the Stress Corrosion Crack Flow Tests (Data from 1/12/2005 to 5/13/2005)	174472

Table 2.1.03.10.0B-2. Indirect Inputs (Continued)

Citation	Title	DIRS
He et al. 2007	"Temperature Effects on Oxide Film Properties of Grade-7 Titanium"	183687
Herrera 2004	*Evaluation of the Potential Impact of Seismic Induced Deformation on the Stress Corrosion Cracking of the YMP Waste Packages*	168133
Ishikawa et al. 2006	"Characterization of Rust on Fe-Cr, Fe-Ni, and Fe-Cu Binary Alloys by Fourier Transform Infrared and N_2 Adsorption"	183682
Ishikawa et al. 2007	"Assessment of Protective Function of Steel Rust Layers by N_2 Adsorption"	181136
Milnes and Fitzpatrick 1995	"Titanium and Zirconium Minerals"	105911
Sargent and Conrad 1969	"Stress Relaxation and Thermally Activated Deformation in Titanium"	174054
SNL 2007	*Analysis of Dust Deliquescence for FEP Screening*	181267
SNL 2008	*EBS Radionuclide Transport Abstraction*	177407
SNL 2007	*General Corrosion and Localized Corrosion of Waste Package Outer Barrier*	178519
SNL 2007	*Stress Corrosion Cracking of Waste Package Outer Barrier and Drip Shield Materials*	181953
SNL 2007	*Total System Performance Assessment Data Input Package for Requirements Analysis for Subsurface Facilities*	179466
Walton 2005	Testing of Stress Crack Flow [final closure]. Scientific Notebook SN-SNL-SCI-032-V2	175407
Yao and Zhang 1999	"Preparation and Characterization of Mesoporous Titania Gel-Monolith"	184766

FEP: 2.1.03.11.0A

FEP NAME:

Physical Form of Waste Package and Drip Shield

FEP DESCRIPTION:

The specific forms of the various drip shields, waste packages, and internal waste containers that are proposed for the Yucca Mountain repository can affect long-term performance. Waste package form may affect container strength through the shape and dimensions of the waste package and affect heat dissipation through waste package volume and surface area. Waste package and drip shield materials may affect physical and chemical behavior of the disposal area environment. Waste package and drip shield integrity will affect the releases of radionuclides from the disposal system. Waste packages may have both local effects and repository-scale effects. All types of waste packages and containers, including CSNF, DSNF, and DHLW, should be considered.

SCREENING DECISION:

Included

TSPA DISPOSITION:

The waste package, drip shield, and repository design configurations for the Yucca Mountain Project are shown in *Total System Performance Assessment Data Input Package for Requirements Analysis for Transportation Aging and Disposal Canister and Related Waste Package Physical Attributes Basis for Performance Assessment* (SNL 2007 [DIRS 179394]), *Total System Performance Assessment Data Input Package for Requirements Analysis for DOE SNF/HLW and Naval SNF Waste Package Physical Attributes Basis for Performance Assessment* (SNL 2007 [DIRS 179567]), and *Total System Performance Assessment Data Input Package for Requirements Analysis for Engineered Barrier System In-Drift Configuration* (SNL 2007 [DIRS 179354]). Only one drip shield configuration is used in the repository (SNL 2007 [DIRS 179354], Section 4.1.2), so the potential impacts from different drip shield configurations are not considered further. While different waste package configurations will be used in the repository, they are generally similar in their design and fabrication methodology. Dimensions and nominal quantities for the six major waste package configurations expected to be emplaced in the repository are shown in Table 2.1.03.11.0A-1.

Many analyses and models address the performance and characteristics of the waste package and drip shield as part of the performance assessment. For example, analyses that consider material properties, strength of the waste package, and shape and dimension of the waste package and drip shield are discussed in *Seismic Consequence Abstraction* (SNL 2007 [DIRS 176828]), *Stress Corrosion Cracking of Waste Package Outer Barrier and Drip Shield Materials* (SNL 2007 [DIRS 181953]), and *Analysis for Mechanisms of Early Waste Package/Drip Shield Failure* (SNL 2007 [DIRS 178765]). The effects of heat dissipation through the waste package are discussed in *In-Drift Natural Convection and Condensation* (SNL 2007 [DIRS 181648]) and *Multiscale Thermohydrologic Model* (SNL 2008 [DIRS 184433]). The effect of waste package

and drip shield materials on the physical and chemical behavior of the disposal area environment is discussed in *In-Package Chemistry Abstraction* (SNL 2007 [DIRS 180506]) and *EBS Radionuclide Transport Abstraction* (SNL 2008 [DIRS 177407]). The behavior of the waste package and drip shield materials is described in *General Corrosion and Localized Corrosion of the Waste Package Outer Barrier* (SNL 2007 [DIRS 178519]) and *General Corrosion and Localized Corrosion of the Drip Shield* (SNL 2007 [DIRS 180778]). For additional information, see included FEP 1.1.07.00.0A (Repository Design).

Table 2.1.03.11.0A-1. Waste Package Dimensions and Design Basis Inventory

Waste Package Configuration	Nominal Length (mm)	Outer Diameter of OCB (mm)	Nominal Quantity
TAD	5,850.1	1,881.6	7,483
Naval Fuel - Long	5,850.1	1,881.6	310
Naval Fuel - Short	5,215.1	1,881.6	90
5-DHLW/DOE SNF-Short	3,697.4	2,044.7	1,207
5-DHLW/DOE SNF-Long	5,303.9	2,044.7	1,862
2-MCO/2-DHLW	5,278.6	1,749.3	210

Sources: SNL 2007 [DIRS 179394], Table 4-3, for outside diameter of OCB and for nominal length of the TAD waste package; SNL 2007 [DIRS 179567], Tables 4-6 through 4-10, for outside diameter of OCB and nominal length of the other waste package types.

DTN: MO0702PASTREAM.001 [DIRS 179925], file: *DTN-Inventory-Rev00.xls*, worksheet: "UNIT CELL," cells B14:L15, for nominal quantity in design basis inventory.

NOTES: The nominal quantity of TAD waste packages includes all medium and small TAD waste packages in the design basis inventory.

The 5-DHLW/DOE SNF-Long waste package includes the 1S/5L and the 1D/4L codisposal waste packages in the design basis inventory.

TAD = transportation, aging, and disposal (canister); DHLW = defense HLW; DOE = U.S. Department of Energy; SNF = spent nuclear fuel; MCO = multicanister overpack; OCB = outer corrosion barrier.

INPUTS:

Table 2.1.03.11.0A-2. Indirect Inputs

Citation	Title	DIRS
DTN: MO0702PASTREAM.001	Waste Stream Composition and Thermal Decay Histories for LA	179925
SNL 2007	*Seismic Consequence Abstraction*	176828
SNL 2007	*Total System Performance Assessment Data Input Package for Requirements Analysis for EBS In-Drift Configuration*	179354
SNL 2007	*Analysis of Mechanisms for Early Waste Package/Drip Shield Failure*	178765
SNL 2008	*EBS Radionuclide Transport Abstraction*	177407
SNL 2007	*General Corrosion and Localized Corrosion of the Drip Shield*	180778
SNL 2007	*General Corrosion and Localized Corrosion of Waste Package Outer Barrier*	178519
SNL 2007	*In-Drift Natural Convection and Condensation*	181648
SNL 2007	*In-Package Chemistry Abstraction*	180506
SNL 2007	*Stress Corrosion Cracking of Waste Package Outer Barrier and Drip Shield Materials*	181953
SNL 2007	*Total System Performance Assessment Data Input Package for Requirements Analysis for DOE SNF/HLW and Navy SNF Waste Package Overpack Physical Attributes Basis for Performance Assessment*	179567
SNL 2007	*Total System Performance Assessment Data Input Package for Requirements Analysis for TAD Canister and Related Waste Package Overpack Physical Attributes Basis for Performance Assessment*	179394
SNL 2008	*Multiscale Thermohydrologic Model*	184433

FEP: 2.1.04.01.0A

FEP NAME:

Flow in the Backfill

FEP DESCRIPTION:

Preferential pathways for flow and diffusion may exist within the backfill and may affect long-term performance of the waste packages. Backfill may not preclude hydrological, chemical, and thermal interactions between waste packages within a drift.

SCREENING DECISION:

Excluded – low consequence

SCREENING JUSTIFICATION:

Backfill is not part of the design for the waste emplacement regions of the repository. Specifically, engineered backfill shall not be present in the space between the drip shield and the drift wall (SNL 2007 [DIRS 179354], Table 4-4, Parameter Number 05-04). Closure of shafts and ramps shall include backfill of the opening (SNL 2007 [DIRS 179466], Table 4-3, Parameter Number 09-01); however, because backfill in shafts and ramps will not be in close proximity to the waste emplacement region, flow and diffusion in the backfill will have a negligble impact on long-term performance. Based on the above discussion, omission of FEP 2.1.04.01.0A (Flow in the Backfill) will not result in significant adverse change in the magnitude of time or radiological exposures to the RMEI or radionuclide releases to the accessible environment. Therefore, this FEP is excluded from the performance assessments conducted to demonstrate compliance with proposed 10 CFR 63.311 and 63.321 (70 FR 53313 [DIRS 178394]), and with 10 CFR 63.331 [DIRS 180319], on the basis of low consequence.

INPUTS:

Table 2.1.04.01.0A-1. Direct Inputs

Input	Source	Description
SNL 2007. *Total System Performance Assessment Data Input Package for Requirements Analysis for EBS In-Drift Configuration*. [DIRS 179354]	Table 4-4, Parameter Number 05-04	There is no backfill in the space between the drip shield and the drift walls
SNL 2007. *Total System Performance Assessment Data Input Package for Requirements Analysis for Subsurface Facilities*. [DIRS 179466]	Table 4-3, Parameter Number 09-01	Closure shafts and ramps shall include backfill of the openings

Table 2.1.04.01.0A-2. Indirect Inputs

Citation	Title	DIRS
10 CFR 63	Energy: Disposal of High-Level Radioactive Wastes in a Geologic Repository at Yucca Mountain, Nevada	180319
70 FR 53313	Implementation of a Dose Standard After 10,000 Years	178394

FEP: 2.1.04.02.0A

FEP NAME:

Chemical Properties and Evolution of Backfill

FEP DESCRIPTION:

The chemical properties of the backfill may affect groundwater flow, waste package and drip shield durability, and radionuclide transport in the waste disposal region. Properties of the backfill may change through time, due to processes such as alteration of minerals.

SCREENING DECISION:

Excluded – low consequence

SCREENING JUSTIFICATION:

Backfill is not part of the design for the waste emplacement regions of the repository. Specifically, engineered backfill shall not be present in the space between the drip shield and the drift wall (SNL 2007 [DIRS 179354], Table 4-4, Parameter Number 05-04). Closure of shafts and ramps shall include backfill of the opening (SNL 2007]DIRS 179466], Table 4-3, Parameter Number 09-01); however, because backfill in shafts and ramps will not be in close proximity to the waste emplacement region, chemical properties of the backfill will have a negligible impact on long-term performance.

Backfill material is derived from the excavation and construction of the invert within the repository host horizon, and therefore would exhibit the same or similar chemical properties of the excavated invert material. Chemical degradation of the invert material (crushed tuff) has been excluded from the TSPA calculations (excluded FEP 2.1.06.05.0D (Chemical Degradation of Invert)), because it would not lead to significant changes in the hydrologic properties of the crushed tuff material. Thus the evolution of the backfill material is of little significance to the hydrologic properties in the access main and ventilation shaft openings.

Based on the this discussion, omission of FEP 2.1.04.02.0A (Chemical Properties and Evolution of Backfill) will not result in significant adverse change in the magnitude or time of radiological exposures to the RMEI or radionuclide releases to the accessible environment. Therefore, this FEP is excluded from the performance assessments conducted to demonstrate compliance with proposed 10 CFR 63.311 and 63.321 (70 FR 53313 [DIRS 178394]), and with 10 CFR 63.331 [DIRS 180319], on the basis of low consequence.

INPUTS:

Table 2.1.04.02.0A-1. Direct Inputs

Input	Source	Description
SNL 2007. *Total System Performance Assessment Data Input Package for Requirements Analysis for EBS In-Drift Configuration*. [DIRS 179354]	Table 4-4, Parameter Number 05-04	There is no backfill in the space between the drip shield and the drift walls
SNL 2007. *Total System Performance Assessment Data Input Package for Requirements Analysis for Subsurface Facilities*. [DIRS 179466]	Table 4-3, Parameter Number 09-01	Closure shafts and ramps shall include backfill of the openings

Table 2.1.04.02.0A-2. Indirect Inputs

Citation	Title	DIRS
10 CFR 63	Energy: Disposal of High-Level Radioactive Wastes in a Geologic Repository at Yucca Mountain, Nevada	180319
70 FR 53313	Implementation of a Dose Standard After 10,000 Years	178394

FEP: 2.1.04.03.0A

FEP NAME:

Erosion or Dissolution of Backfill

FEP DESCRIPTION:

Solid material in backfill may be carried away by flowing groundwater, either by erosion of particulate matter or by dissolution.

SCREENING DECISION:

Excluded – low consequence

SCREENING JUSTIFICATION:

Backfill is not part of the design for the waste emplacement regions of the repository. Specifically, engineered backfill shall not be present in the space between the drip shield and the drift wall (SNL 2007 [DIRS 179354], Table 4-4, Parameter Number 05-04). Closure of shafts and ramps shall include backfill of the opening (SNL 2007 [DIRS 179466], Table 4-3, Parameter Number 09-01); however, because backfill in shafts and ramps will not be in close proximity to the waste emplacement region, erosion or dissolution of backfill will have a negligible impact on long-term performance. In light of the above discussion, omission of FEP 2.1.04.03.0A (Erosion or Dissolution of the Backfill) will not result in a significant adverse change to the magnitude or time of radiological exposures to the RMEI or radionuclide release to the accessible environment. Therefore, this FEP is excluded from the performance assessments conducted to demonstrate compliance with proposed 10 CFR 63.311 and 63.321 (70 FR 53313 [DIRS 178394]), and with 10 CFR 63.331 [DIRS 180319], on the basis of low consequence.

INPUTS:

Table 2.1.04.03.0A-1. Direct Inputs

Input	Source	Description
SNL 2007. *Total System Performance Assessment Data Input Package for Requirements Analysis for EBS In-Drift Configuration*. [DIRS 179354]	Table 4-4, Parameter Number 05-04	There is no backfill in the space between the drip shield and the drift walls
SNL 2007. *Total System Performance Assessment Data Input Package for Requirements Analysis for Subsurface Facilities*. [DIRS 179466]	Table 4-3, Parameter Number 09-01	Closure shafts and ramps shall include backfill of the openings

Table 2.1.04.03.0A-2. Indirect Inputs

Citation	Title	DIRS
10 CFR 63	Energy: Disposal of High-Level Radioactive Wastes in a Geologic Repository at Yucca Mountain, Nevada	180319
70 FR 53313	Implementation of a Dose Standard After 10,000 Years	178394

FEP: 2.1.04.04.0A

FEP NAME:

Thermal-Mechanical Effects of Backfill

FEP DESCRIPTION:

Backfill may alter the mechanical evolution of the drift environment by providing resistance to rockfall and drift collapse, by changing the thermal properties of the drift, or by other means. Impacts of the evolution of the properties of the backfill itself should be considered.

SCREENING DECISION:

Excluded – low consequence

SCREENING JUSTIFICATION:

Backfill is not part of the design for the waste emplacement regions of the repository. Specifically, engineered backfill shall not be present in the space between the drip shield and the drift wall (SNL 2007 [DIRS 179354], Table 4-4, Parameter Number 05-04). Closure of shafts and ramps shall include backfill of the opening (SNL 2007 [DIRS 179466], Table 4-3, Parameter Number 09-01); however, because backfill in shafts and ramps will not be in close proximity to the waste emplacement region, thermal and mechanical effects of backfill will have a negligible impact on long-term performance. Based on this discussion, omission of FEP 2.1.04.04.0A (Thermal-Mechanical Effects of Backfill) will not result in a significant adverse change in the magnitude or time of radiological exposures to the RMEI or radionuclide releases to the accessible environment. Therefore, this FEP is excluded from the performance assessments conducted to demonstrate compliance with proposed 10 CFR 63.311 and 63.321 (70 FR 53313 [DIRS 178394]), and with 10 CFR 63.331 [DIRS 180319], on the basis of low consequence.

INPUTS:

Table 2.1.04.04.0A-1. Direct Inputs

Input	Source	Description
SNL 2007. *Total System Performance Assessment Data Input Package for Requirements Analysis for EBS In-Drift Configuration*. [DIRS 179354]	Table 4-4, Parameter Number 05-04	There is no backfill in the space between the drip shield and the drift walls
SNL 2007. *Total System Performance Assessment Data Input Package for Requirements Analysis for Subsurface Facilities*. [DIRS 179466]	Table 4-3, Parameter Number 09-01	Closure shafts and ramps shall include backfill of the openings

Table 2.1.04.04.0A-2. Indirect Inputs

Citation	Title	DIRS
10 CFR 63	Energy: Disposal of High-Level Radioactive Wastes in a Geologic Repository at Yucca Mountain, Nevada	180319
70 FR 53313	Implementation of a Dose Standard After 10,000 Years	178394

FEP: 2.1.04.05.0A

FEP NAME:

Thermal-Mechanical Properties and Evolution of Backfill

FEP DESCRIPTION:

The physical properties of the backfill may affect groundwater flow, waste package and drip shield durability, and radionuclide transport in the waste disposal region. Properties of the backfill may change through time, due to processes such as silica cementation, thermal effects, and physical compaction.

SCREENING DECISION:

Excluded – low consequence

SCREENING JUSTIFICATION:

Backfill is not part of the design for the waste emplacement regions of the repository. Specifically, engineered backfill shall not be present in the space between the drip shield and the drift wall (SNL 2007 [DIRS 179354], Table 4-4, Parameter Number 05-04). Closure of shafts and ramps shall include backfill of the opening (SNL 2007 [DIRS 179466], Table 4-3, Parameter Number 09-01); however, because backfill in shafts and ramps will not be in close proximity to the waste emplacement region, physical properties (thermal and mechanical) and evolution of the backfill will have a negligible impact on long-term performance. Based on the above discussion, omission of FEP 2.1.04.05.0A (Thermal-Mechanical Properties and Evolution of Backfill) will not result in a significant adverse change in the magnitude or time of radiological exposures to the RMEI or radionuclide releases to the accessible environment. Therefore, this FEP is excluded from the performance assessments conducted to demonstrate compliance with proposed 10 CFR 63.311 and 63.321 (70 FR 53313 [DIRS 178394]), and with 10 CFR 63.331 [DIRS 180319], on the basis of low consequence.

INPUTS:

Table 2.1.04.05.0A-1. Direct Inputs

Input	Source	Description
SNL 2007. *Total System Performance Assessment Data Input Package for Requirements Analysis for EBS In-Drift Configuration*. [DIRS 179354]	Table 4-4, Parameter Number 05-04	There is no backfill in the space between the drip shield and the drift walls
SNL 2007. *Total System Performance Assessment Data Input Package for Requirements Analysis for Subsurface Facilities*. [DIRS 179466]	Table 4-3, Parameter Number 09-01	Closure shafts and ramps shall include backfill of the openings

Table 2.1.04.05.0A-2. Indirect Inputs

Citation	Title	DIRS
10 CFR 63	Energy: Disposal of High-Level Radioactive Wastes in a Geologic Repository at Yucca Mountain, Nevada	180319
70 FR 53313	Implementation of a Dose Standard After 10,000 Years	178394

FEP: 2.1.04.09.0A

FEP NAME:

Radionuclide Transport in Backfill

FEP DESCRIPTION:

Radionuclide transport in the drift environment may be affected by the presence of backfill. Transport (i.e., advective and diffusive effects and sorption processes) of both dissolved and colloidal species should be considered.

SCREENING DECISION:

Excluded – low consequence

SCREENING JUSTIFICATION:

Backfill is not part of the design for the waste emplacement regions of the repository. Specifically, engineered backfill shall not be present in the space between the drip shield and the drift wall (SNL 2007 [DIRS 179354], Table 4-4, Parameter Number 05-04). Closure of shafts and ramps shall include backfill of the opening (SNL 2007 [DIRS 179466], Table 4-3, Parameter Number 09-01); however, because backfill in shafts and ramps will not be in close proximity to the waste emplacement region, radionuclide transport in the drift environment will have a negligible impact on long-term performance. Based on this discussion, omission of FEP 2.1.04.09.0A (Radionuclide Transport in Backfill) will not result in a significant adverse change to the magnitude or time of radiological exposure to the RMEI or radionuclide release to the accessible environment. Therefore, this FEP is excluded from the performance assessments conducted to demonstrate compliance with proposed 10 CFR 63.311 and 63.321 (70 FR 53313 [DIRS 178394]), and with 10 CFR 63.331 [DIRS 180319], on the basis of low consequence.

INPUTS:

Table 2.1.04.09.0A-1. Direct Inputs

Input	Source	Description
SNL 2007. *Total System Performance Assessment Data Input Package for Requirements Analysis for EBS In-Drift Configuration*. [DIRS 179354]	Table 4-4, Parameter Number 05-04	There is no backfill in the space between the drip shield and the drift walls
SNL 2007. *Total System Performance Assessment Data Input Package for Requirements Analysis for Subsurface Facilities*. [DIRS 179466]	Table 4-3, Parameter Number 09-01	Closure shafts and ramps shall include backfill of the openings

Table 2.1.04.09.0A-2. Indirect Inputs

Citation	Title	DIRS
10 CFR 63	Energy: Disposal of High-Level Radioactive Wastes in a Geologic Repository at Yucca Mountain, Nevada	180319
70 FR 53313	Implementation of a Dose Standard After 10,000 Years	178394

FEP: 2.1.05.01.0A

FEP NAME:

Flow Through Seals (Access Ramps and Ventilation Shafts)

FEP DESCRIPTION:

Long-term fluid flow through the shaft seal system, and uncertainty about long-term properties of the shaft seal system, may influence cumulative radionuclide releases from the disposal system.

SCREENING DECISION:

Excluded – low consequence

SCREENING JUSTIFICATION:

This FEP is very similar to FEP 2.1.05.02.0A (Radionuclide Transport through Seals), which is excluded on the basis of low consequence.

Closure of shafts and ramps shall include backfill of the opening (SNL 2007 [DIRS 179466], Table 4-3, Parameter Number 09-01). Deviations from backfill design are not relevant to the emplacement drift environment and would have no impact on repository performance as discussed in excluded FEP 1.1.03.01.0B (Error in Backfill Emplacement).

During construction of the emplacement drifts, and operation and closure of the repository, administrative controls will be imposed to prevent impact on waste isolation from materials used, lost, or left in the repository. These controls will be supported by technical evaluation. The entries for Parameter Number 02-03 (SNL 2007 [DIRS 179354], Table 4-1) point to the most recent documents that list committed materials (i.e., materials that are intended to be present in the repository at closure). The committed materials have been found to be acceptable by analysis.

Two justifications demonstrate that fluid flow through the seals, in the access ramps and ventilation shafts, will be of little consequence for the flow and transport of radionuclides. The first justification below shows that the flow through shafts and ramps is not expected to affect the flow and transport of water in the repository in any significant way. The second justification shows that long-term changes in the backfill material are not expected to impact repository performance.

First, the flow through the repository is expected to be predominantly vertical; water influx at the land surface percolates dominantly downward, with little lateral spread. *UZ Flow Models and Submodels* (SNL 2007 [DIRS 184614], p. 6-18) states, "Computations have shown that the average flux flowing to the repository is within three percent of the average flux specified at the ground surface over the projected repository area." Therefore, any flow down the ventilation shafts, which do not abut the emplacement drifts, should have little effect on flow into and through the emplacement drifts. Furthermore, the surface expressions of the ventilation shafts are such that the shafts should not be water-collection areas. The shafts will be positioned and

engineered to prevent flooding (SNL 2007 [DIRS 179466], Table 4-1, Parameter Number 01-19) (i.e., the shafts will not be in topographic lows expected to collect water).

Lateral drainage from perched-water zones is also not expected to impact flow through the repository via access ramps or the ventilation shafts (which only extend from the surface down to the repository). The North Construction Ramp is expected to intersect the Tptpv2, Tptpv1 and Tpbt1 (BSC 2003 [DIRS 165572], file: *subsurfaceladesign_i.dxf*; *Geologic Framework Model (GFM2000),* DTN: MO0012MWDGFM02.002 [DIRS 153777]). Two of these units have the potential for perched water, the Tptpv2 and the Tptpv1 (tsw38 = Tptpv3, tsw39 = Tptpv3, ch1z = Tptpv1 and Tpbt1, and ch2z is a component of Tac) (SNL 2007 [DIRS 184614], Sections 6.2.2, 6.2.3, 6.2.5). This study also indicates that there is evidence of perched water bodies along the base of the TSw in the northern region of the repository footprint (SNL 2007 [DIRS 184614], Sections 6.2.2.2 and 6.6.2.2). Perched waters that intersect a ramp could result in water being directed into the ramp and toward the emplacement drifts. However, drainage of perched water into the North Construction Ramp is not expected to significantly alter water flow to the emplacement drifts. The repository nonemplacement openings (such as access ramps) are designed to provide a repository grade so overall water drainage and accumulation travels away from waste package emplacement areas, as stated in *Total System Performance Assessment Data Input Package for Requirements Analysis for Subsurface Facilities* (SNL 2007 [DIRS 179466], Table 4-1, Parameter Number 01-02). Any water that enters the ramp and accumulates will eventually drain into the rock below before it can reach the emplacement drifts. A bounding analysis may be used to demonstrate this behavior.

First, consider the amount of lateral drainage that may occur into the North Construction Ramp in the perched water zone. The North Construction Ramp enters and exits the perched water zone near the curve where this ramp turns from a northerly heading to a southerly heading towards the repository. The portion of the turn within the potential perched-water zone is approximately 500 m (BSC 2003 [DIRS 165572], file: *subsurfaceladesign_i.dxf*; DTN: MO0012MWDGFM02.002 [DIRS 153777]). The maximum drainage may be estimated by the potential catchment area north of this segment of the ramp. The potential perched water zone is intercepted by other faults about 4,000 m north of the location of the North Construction Ramp (DTN: GS010908314221.001 [DIRS 162874]; BSC 2003 [DIRS 165572], file: *subsurfaceladesign_i.dxf*). Therefore, a maximum catchment area of about 500 m × 4,000 m = 2×10^6 m^2 is estimated for lateral flow into the 500-m segment of the North Construction Ramp. From infiltration maps for future climates (SNL 2008 [DIRS 182145], Figures 6.5.7.2-5[a] and 6.5.7.3-5[a]), a maximum infiltration rate of 100 mm/yr may be used. This infiltration rate is derived from the monsoon and glacial-transition climates using the 90th-percentile infiltration maps, which have about a 6% chance of occurrence in TSPA models (SNL 2007 [DIRS 184614], Table 6.8-1). Combining this rate with the catchment area gives a bounding value of 2×10^5 m^3/yr. This water will flow south from the North Construction Ramp to the Panel 3 Exhaust and Intake Mains (BSC 2003 [DIRS 165572], Section 8.4.3). From there, the water will move downward to Exhaust Shaft #2, the lowest point connecting these mains (BSC 2003 [DIRS 165572], Section 8.4.3). The Exhaust Shaft #2 East and West Access tunnels and a portion of the Panel 3 Exhaust Main are connected to Exhaust Shaft #2, and these three sections are at the lowest elevation in Panel 3 (BSC 2003 [DIRS 165572], file: *subsurfaceladesign_i.dxf*). The combined length of these tunnels is greater than 300 m, and the approximate width of each tunnel available for downward drainage is 8 m (BSC 2003

[DIRS 165572], Table 5 and Figure 8). Thus, the minimal area available for drainage of any accumulated water in these sections is 300 m × 8 m = 2,400 m^2.

Next, consider the area required to drain a continuous inflow of 2×10^5 m^3/yr (or 6.3×10^{-3} m^3/s) from the North Construction Ramp (calculated above). The fractured rock in these locations has a bulk permeability on the order of 10^{-12} m^2 (model units tsw35 through tsw38; SNL 2007 [DIRS 184614], Appendix B), which is equivalent to a hydraulic conductivity of about 9.8×10^{-6} m/s (bulk permeability is multiplied by the product of the liquid water density (1,000 kg/m^3) and the gravitational constant (9.81 m/s^2 and divided by the dynamic viscosity (10^{-3} kg/m-s). The required area to drain the inflow is therefore equal to 6.3×10^{-3} m^3/s ÷ 9.8×10^{-6} m/s = 640 m^2. Because the available area for downward drainage in the Exhaust Shaft #2 East and West Access tunnels and the lowest section of the Panel 3 Exhaust Main is significantly larger (2,400 m^2), any inflow from lateral drainage induced by perched water zones into the North Construction Ramp will eventually drain into the fractured rock near Exhaust Shaft #2 before entering the emplacement drifts.

Second, long-term changes in the backfill material are not expected to impact repository performance. There are no performance attributes assigned to backfill other than limiting ingress of animals (excluded FEP 2.3.09.01.0A (Animal Burrowing/Intrusion)). Therefore, any degradation of backfill material and subsequent change in hydraulic characteristics is not relevant to repository performance.

The conclusion of these two justifications is that the seals, and any long-term alteration of the seals, are not expected to have a significant effect on fluid flow through the repository.

Based on the previous discussion, omission of FEP 2.1.05.01.0A (Flow through Seals (Access Ramps and Ventilation Shafts)) from the performance assessment calculations will not result in a significant adverse change in the magnitude or timing of either radiological exposure to the RMEI or radionuclide releases to the accessible environment. Therefore, this FEP is excluded from the performance assessments conducted to demonstrate compliance with proposed 10 CFR 63.311 and 63.321 (70 FR 53313 [DIRS 178394]), and with 10 CFR 63.331 [DIRS 180319], on the basis of low consequence.

INPUTS:

Table 2.1.05.01.0A-1. Direct Inputs

Input	Source	Description
BSC 2003. *Underground Layout Configuration*. [DIRS 165572]	Table 5	The combined length of the Exhaust Shaft #2 East and West Access tunnels is greater than 300 m, and the approximate width of each tunnel available for downward drainage is 8 m
	file: *subsurfaceladesign_i_dxf.xls*	Location of the North Construction Ramp
	file: *subsurfaceladesign_i_dxf.xls*	The North Construction Ramp is expected to intersect the Tptpv2, Tptpv1, and Tpbt1
DTN: GS010908314221.001. Geologic Map of the Yucca Mountain Region, Nye County, Nevada. [DIRS 162874]	GIS Map I-2755	Fault locations in the Yucca Mountain area
SNL 2007. *Total System Performance Assessment Data Input Package for Requirements Analysis for Subsurface Facilities*. [DIRS 179466]	Table 4-1, Parameter Number 01-02	Repository non-emplacement openings are designed to provide a repository grade so overall water drainage and accumulation travels away from the waste package emplacement areas
	Table 4-1, Parameter Number 01-19	Shafts will be positioned and engineered to prevent flooding
	Table 4-3, Parameter Number 09-01	Requirement that closure of the shafts and ramps include backfilling of the opening
SNL 2007. *UZ Flow Models and Submodels*. [DIRS 184614]	Appendix B	The fractured rock in model units tsw35 through tsw38 has a bulk permeability on the order of at least 10^{-12} m^2, which is equivalent to a hydraulic conductivity of about 9.8×10^{-6} m/s
	Table 6.8-1	Maximum infiltration rate is derived from the monsoon and glacial-transition climates using the 90th-percentile infiltration maps, which have about a 6% chance of occurrence in TSPA models
	Sections 6.2.2.2 and 6.6.2.2	There is evidence of perched water bodies along the base of the TSw in the northern region of the repository footprint
	Sections 6.2.2, 6.2.3, and 6.2.5	The Tptpv2 and the Tptpv1 have the potential for perched water
	p. 6-18	Computations have shown that the average flux flowing to the repository is within three percent of the average flux specified at the ground surface over the projected repository area
SNL 2008. *Simulation of Net Infiltration for Present-Day and Potential Future Climates*. [DIRS 182145]	Figures 6.5.7.2-5[a] and 6.5.7.3-5[a]	Infiltration maps for future climates a maximum infiltration rate of 100 mm/yr may be used.

Table 2.1.05.01.0A-2. Indirect Inputs

Citation	Title	DIRS
10 CFR 63	Energy: Disposal of High-Level Radioactive Wastes in a Geologic Repository at Yucca Mountain, Nevada	180319
70 FR 53313	Implementation of a Dose Standard After 10,000 Years	178394
BSC 2003	*Underground Layout Configuration*	165572
DTN: MO0012MWDGFM02.002	Geologic Framework Model (GFM2000)	153777
SNL 2007	*Total System Performance Assessment Data Input Package for Requirements Analysis for EBS In-Drift Configuration*	179354

FEP: 2.1.05.02.0A

FEP NAME:

Radionuclide Transport Through Seals

FEP DESCRIPTION:

Groundwater flow through seals in the access ramps, ventilation shafts, and exploratory boreholes could affect long-term performance of the disposal system. Radionuclide transport through seals should be considered.

SCREENING DECISION:

Excluded – low consequence

SCREENING JUSTIFICATION:

This FEP is analogous in content to FEP 1.1.01.01.0A (Open Site Investigation Boreholes) and FEP 2.1.05.01.0A (Flow through Seals (Access Ramps and Ventilation Shafts)), both of which are excluded on the basis of low consequence and address the closure of shafts and ramps with backfill of the opening (SNL 2007 [DIRS 179466], Table 4-3, Parameter Number 09-01).

Therefore, omission of FEP 2.1.05.02.0A (Radionuclide Transport through Seals) will not result in a significant adverse change in the magnitude or timing of either radiological exposure to the RMEI or radionuclide releases to the accessible environment. Therefore, this FEP is excluded from the performance assessments conducted to demonstrate compliance with proposed 10 CFR 63.311 and 63.321 (70 FR 53313 [DIRS 178394]), and with 10 CFR 63.331 [DIRS 180319], on the basis of low consequence.

INPUTS:

Table 2.1.05.02.0A-1. Direct Inputs

Input	Source	Description
SNL 2007. *Total System Performance Assessment Data Input Package for Requirements Analysis for Subsurface Facilities*. [DIRS 179466]	Table 4-3, Parameter Number 09-01	Requirement that closure of the shafts and ramps include backfilling of the opening

Table 2.1.05.02.0A-2. Indirect Inputs

Citation	Title	DIRS
10 CFR 63	Energy: Disposal of High-Level Radioactive Wastes in a Geologic Repository at Yucca Mountain, Nevada	180319
70 FR 53313	Implementation of a Dose Standard After 10,000 Years	178394

FEP: 2.1.05.03.0A

FEP NAME:

Degradation of Seals

FEP DESCRIPTION:

Degradation of seals in the access ramps, ventilation shafts, and exploratory boreholes could modify flow and transport properties. Physical properties of the seals emplaced in the access ramps, ventilation shafts, and exploratory boreholes may affect the long-term performance of the disposal system. These properties include the location of the seals (and the openings they seal), and the physical and chemical characteristics of the sealing materials. Possible mechanisms for seal degradation include: chemical alteration from water interactions, wetting associated with condensation, and thermally-induced stress-strain changes.

SCREENING DECISION:

Excluded – low consequence

SCREENING JUSTIFICATION:

There are three other closely related excluded FEPs. The basis for excluding flow and radionuclide transport through seals is provided in FEP 2.1.05.01.0A (Flow through Seals (Access Ramps and Ventilation Shafts)) and FEP 2.1.05.02.0A (Radionuclide Transport through Seals). The degradation of seals in exploratory boreholes is discussed in FEP 1.1.01.01.0A (Open Site Investigation Boreholes), and is excluded on the basis of low consequence.

Closure of shafts and ramps shall include backfill of the opening (SNL 2007 [DIRS 179466], Table 4-3, Parameter Number 09-01). Deviations from backfill design are not relevant to the emplacement drift environment and would have no impact on repository performance as discussed in excluded FEP 1.1.03.01.0B (Error in Backfill Emplacement). Degradation of the seal material is not expected to increase permeability. Degradation of crushed tuff backfill will parallel that of the host rock and may lead to formation of clays and zeolites. These minerals have greater molar volumes than the initial, dominantly anhydrous minerals, and should be even less permeable than the initial material. In general, low-temperature alteration of primary phases in backfill results in higher volume hydrated alteration products. Condensation wetting would favor this. In the shorter term, the backfill may self-compact in the ventilation shafts under gravity; this physical degradation process should lower the permeability. If the backfill compacts to provide local, open pockets, such open spaces would act as capillary barriers to flow. Since the backfill is not brittle, it will respond to stress with granular flow or plastic deformation, and will not shatter or crack.

In conclusion, the effects of degradation of seals are considered to be negligible.

Based on the previous discussion, omission of FEP 2.1.05.03.0A (Degradation of Seals) will not result in a significant adverse change in the magnitude or timing of either radiological exposure to the RMEI or radionuclide releases to the accessible environment. Therefore, this FEP is

excluded from the performance assessments conducted to demonstrate compliance with proposed 10 CFR 63.311 and 63.321 (70 FR 53313 [DIRS 178394]), and with 10 CFR 63.331 [DIRS 180319], on the basis of low consequence.

INPUTS:

Table 2.1.05.03.0A-1. Direct Inputs

Input	Source	Description
SNL 2007. *Total System Performance Assessment Data Input Package for Requirements Analysis for Subsurface Facilities*. [DIRS 179466]	Table 4-3, Parameter Number 09-01	Closure of shafts and ramps shall include backfill of the opening

Table 2.1.05.03.0A-2. Indirect Inputs

Citation	Title	DIRS
10 CFR 63	Energy: Disposal of High-Level Radioactive Wastes in a Geologic Repository at Yucca Mountain, Nevada	180319
70 FR 53313	Implementation of a Dose Standard After 10,000 Years	178394

FEP: 2.1.06.01.0A

FEP NAME:

Chemical Effects of Rock Reinforcement and Cementitious Materials in EBS

FEP DESCRIPTION:

Degradation of ground support material (e.g., cement, rock bolts, wire mesh) used for any purpose in the disposal region may affect long-term performance through both chemical and physical processes. Degradation may occur by physical, chemical, and microbial processes.

SCREENING DECISION:

Excluded – low consequence

SCREENING JUSTIFICATION:

The discussion presented here focuses on potential impacts that ground support materials, left in the repository after closure, might have on the chemistry of seepage waters in the drifts, the transport of radionuclides, and the permeability of the surrounding rocks. The location and quantity of cemetitious materials and steels is obtainable from the design basis documents for TSPA (SNL 2007 [DIRS 179466]; SNL 2007 [DIRS 179354], Table 4-1, Parameter Numbers 01-15 and 02-03). These documents point to the most recent specifications, drawings and tables for the quantities of cementitious materials and steels used in the support materials. After closure of the repository, the vast majority of cementitious materials will be in the turnout intersections, exhaust air (ventilation) turnouts, and access ramps (SNL 2007 [DIRS 179354], Table 4-1, Parameter Number 01-15). Cementitious materials are specifically excluded from the emplacement drifts, but it is possible that cement leachates from other areas will disperse and interact with materials in the emplacement drifts. Excavation effects on chemistry of the near-field are addressed in excluded FEP 2.2.01.01.0B (Chemical Effects of Excavation and Construction in the Near-Field). The steel used in the emplacement drifts will be in the form of 3-mm-thick perforated sheets and friction-type rock bolts, both composed of Stainless Steel Type 316 or the equivalent; there will be no wire mesh in the emplacement drifts (SNL 2007 [DIRS 179466], Table 4-1, Parameter Number 01-15).

Corrosion of steel in the drift support materials could potentially affect performance in two ways: first, the degradation could alter the pH and general chemistry of the aqueous phase and second, the galvanic interaction of the perforated stainless steel plates, should they fall onto the drip shields, might cause galvanic corrosion. The first effect is evaluated in *Engineered Barrier System: Physical and Chemical Environment* (P&CE) (SNL 2007 [DIRS 177412], Section 6.8.4.1). The P&CE report (SNL 2007 [DIRS 177412]) demonstrates that wide variations in the available masses of Stainless Steel Type 316L merely result in the precipitation of more corrosion products and do not impact the aqueous phase chemistry significantly. These calculations were specifically designed to be corrosion-rate independent by adding masses of steels well beyond what would be expected for reasonable products of time, corrosion rate, and surface area. The second is discussed in excluded FEP 2.1.03.04.0B (Hydride Cracking of Drip Shields), and the potential galvanic action from contact with support materials is insufficient to

compromise the drip shields. Corrosion products from the ground support materials might also accumulate in the drift. Should radionuclides encounter these corrosion products, transport might be hindered.

Evaluation of Potential Impacts of Microbial Activity on Drift Chemistry (BSC 2004 [DIRS 169991], Section 7.1) discusses rock reinforcement materials and other introduced materials in the context of environmental constraints on in-drift microbial activity as sources of energy and nutrients. Microbial impacts on in-drift chemistry are expected to be minimal, as discussed in excluded FEP 2.1.10.01.0A (Microbial Activity in EBS). For this reason, microbes are not expected to accelerate degradation of ground support materials.

Two principal effects of cementitious materials on repository performance were identified by Ziegler (2004 [DIRS 171694], Section D.3). The first is an enhancement of transport that might result from an alkaline plume. This plume would result from leaching of the cementitious material and could enhance radionuclide transport to the accessible environment, either through the complexation of radionuclides or through the presence of pseudocolloids (i.e., radionuclides sorbed to preexisting solid phase colloids). Initially, any alkaline plume will be spatially separate from radionuclide-bearing plumes, because the principal locations of cementitious materials (the turnouts and ventilation shafts) are distant from the waste-bearing parts of the emplacement drifts. Standoff distances are established in *Total System Performance Assessment Data Input Package for Requirements Analysis for Subsurface Facilities* (SNL 2007 [DIRS 179466], Table 4-1, Parameter Number 01-18). Hence, the greatest possibility of radionuclide transport enhancement will come from potential overlapping of the plumes below the repository. For example, an increase in the pH of the radionuclide plume, from mixing with an alkaline plume, could conceivably lower sorption of radionuclides onto minerals in the saturated zone, simply because sorption coefficients are dependent on pH. The second effect is a potential porosity and permeability change in the surrounding rock due to calcite precipitation or caustic leaching of silicate phases in the tuff. Calcite precipitation is due to the addition of ambient CO_2 to the abundant CaO component of cements. Alkaline dissolution of silicates may occur if the pH stays high because most silicates are more soluble and dissolve faster at high pH. These changes would occur in the host rock near cementitious materials, particularly the shotcrete supporting the turnout intersections in the main access drifts and the intersections of the exhaust main drifts with the emplacement drifts. Such changes in hydrologic properties of the surrounding rock might alter the flow of water into and out of the drifts, and down to the saturated zone.

Before evaluating the two potential effects described above, it is necessary to establish the basic nature of the predicted flow near the repository. Water is expected to move in a generally vertical flow pattern through the waste emplacement horizon relative to the length scale of these drifts, with significant flow diversion around the drifts resulting from the capillary barrier effect. Water influx at the land surface percolates dominantly downward, with little lateral spread near the repository. *UZ Flow Models and Submodels* (SNL 2007 [DIRS 184614], p. 6-18) states, "Computations have shown that the average flux flowing to the repository is within three percent of the average flux specified at the ground surface over the projected repository area." Standoffs from the shotcrete portions of the turnouts and exhaust drift intersections are established (SNL 2007 [DIRS 179466], Table 4-1, Parameter Number 01-18) and will prevent contact between shotcrete or leachate, and waste packages in the emplacement drifts. As discussed

below, the rapid neutralization of the alkaline plumes combined with the calcium available in equilibrium with cement phases will result in rapid precipitation of calcite in close proximity to the location of the cement. Thus, there should be little chance for alkaline plumes to interact with the waste, at or below the repository horizon. However, flow below the repository horizon may be diverted laterally at the TSw–CHn contact or into a few fracture zones, with potential for mixing of the plumes.

The first effect, transport enhancement by alkaline plumes, will be negligible for long-term repository performance, for two reasons. First, as indicated above, there will be little opportunity for mixing of the alkaline plumes with the fluids in the EBS, hence, the plumes will have no effect on the generation of a mobile radionuclide source term. Second, any high-pH plumes in the unsaturated zone are expected to be short-lived and rapidly neutralized. The unsaturated zone is open to gas circulation; particularly, ambient CO_2 will dissolve into the plume and neutralize pH. The rapid neutralization of cement leachates by CO_2 gas is indicated by experiment (DTN: LL030211523125.006 [DIRS 172021], file: *LiquidCarbonationEQ36Modeling.doc*). These findings are consistent with the analysis reported by Ziegler (2004 [DIRS 171694], Table D-12). As discussed in Appendix J, the Ziegler data provide solubility values for portlandite. The solubility of portlandite is used in the assessment of the alkaline cement leachate stability. Exposure of the cement leachate to CO_2 leads to plume carbonation and thus its neutralization. It is assumed that the leachate is saturated with respect to portlandite and the total calcium concentration in solution is sufficient to allow for calcite precipitation as a result of the plume neutralization. The rapid rate of this reaction indicates that the generation of an alkaline plume which could effect radionuclide transport is not expected. Even in the northwestern end of the repository footprint, where the TSw–CHn contact is at its highest elevation, approximately 80 m below the repository horizon as read from a contour plot (source for the elevation of the top of the CHn: DTN: MO0610MWDHFM06.002 [DIRS 179352], file: *H06_18chvu_X.dat*; source for the repository outline and elevations: SNL 2007 [DIRS 179466], Table 4-1, Parameter Number 01-01) where lateral flow may occur, the flow path from the emplaced cement to that contact is more than sufficient to neutralize the potential plumes. Details regarding the impact of an alkaline plume in the unsaturated zone are considered as part of excluded FEP 2.2.08.03.0B (Geochemical Interactions and Evolution in the UZ).

For the reasons discussed above, calcite precipitation will not lead to changes in host-rock hydrologic properties that are sufficiently large or extensive enough to divert the dominantly vertical flow beneath the turnouts towards the emplacement drifts because it is expected to occur in close proximity to where the cement is located.

As stated earlier, cement will not be used in emplacement drifts, but will be used in turnout intersections, exhaust air (ventilation) turnouts, and access ramps. Resuspension of cement dust from these areas, prior to and during the ventilation period, could result in deposition of cement dust onto waste package surfaces. This could affect the dust composition, and in turn, the composition of brines that form by dust deliquescence on the waste package surface.

In general, dust deposited on the waste packages is anticipated to be similar to atmospheric dust collected at Yucca Mountain, or to dust collected from the Exploratory Studies Facility. Brines formed by deliquescence of these dusts is benign with respect to localized corrosion of Alloy 22 (excluded FEP 2.1.09.28.0A (Localized Corrosion on Waste Package Outer Surface due to

Deliquescence)). The effects of an added component of cement dust on deliquescent brine composition are uncertain. However, other aspects of the exclusion argument presented in excluded FEP 2.1.9.28.0A (Localized Corrosion on Waste Package Outer Surface due to Deliquescence) (e.g., capillary retention of brine in the dust inhibiting initiation of localized corrosion; limited extent of damage due to the limited mass of chloride) remain valid. Therefore, the cement dust is not expected to result in waste package failure due to localized corrosion. Also, the potential for deposition of cement dust on waste packages will be minimized by design requirements that limit the generation of concrete dust through the use of surface coatings and the use of dust suppression and ventilation control during concrete installation and removal (BSC 2008 [DIRS 183627], Parameter Number 02-03).

Based on this discussion, omission of FEP 2.1.06.01.0A (Chemical Effects of Rock Reinforcement and Cementitious Material in EBS) will not result in significant adverse change in the magnitude or time of radiological exposures to the RMEI or radionuclide releases to the accessible environment. Therefore, this FEP is excluded from the performance assessments conducted to demonstrate compliance with proposed 10 CFR 63.311 and 63.321 (70 FR 53313 [DIRS 178394]), and with 10 CFR 63.331 [DIRS 180319], on the basis of low consequence.

INPUTS:

Table 2.1.06.01.0A-1. Direct Inputs

Input	Source	Description
BSC 2004. *Evaluation of Potential Impacts of Microbial Activities on Drift Chemistry*. [DIRS 169991]	Section 7.1	Impacts of in-drift microbial activities
DTN: LL030211523125.006. EQ3/6 Modeling of Grout-Reacted Liquid Carbonation Experiments. [DIRS 172021]	file: *LiquidCarbonationEQ36 Modeling.doc*	High-pH plumes in the unsaturated zone are expected to be short-lived and rapidly neutralized
DTN: MO0610MWDHFM06.002. Hydrogeologic Framework Model (HFM2006) Stratigraphic Horizon Grids. [DIRS 179352]	file: *H06_18chvu_X.dat*	Elevation of the top of the CHn
SNL 2007. *Total System Performance Assessment Data Input Package for Requirements Analysis for EBS In-Drift Configuration*. [DIRS 179354]	Parameter Numbers 01-15 and 02-03	Commited materials description
SNL 2007. *Engineered Barrier System: Physical and Chemical Environment*. [DIRS 177412]	Section 6.8.4.1	The effect of stainless steel corrosion (including the degradation rate) on the chemistry of seepage entering the drift
SNL 2007. *Total System Performance Assessment Data Input Package for Requirements Analysis for Subsurface Facilities*. [DIRS 179466]	Table 4-1, Parameter Number 01-18	Standoffs from the shotcrete portions of the turnouts and exhaust drift intersections
	Table 4-1, Parameter Number 01-01	Repository outline and elevations
Ziegler 2004. " Transmittal of Appendix D of the Technical Basis Document No. 10: Unsaturated Zone Transport Addressing Key Technical Issue (KTI) Agreement Evolution of Near-Field Environment (ENFE) 1.04." [DIRS 171694]	Table D-12	Solubility values for portlandite

Table 2.1.06.01.0A-2. Indirect Inputs

Citation	Title	DIRS
10 CFR 63	Energy: Disposal of High-Level Radioactive Wastes in a Geologic Repository at Yucca Mountain, Nevada	180319
70 FR 53313	Implementation of a Dose Standard After 10,000 Years	178394
BSC 2008	*Postclosure Modeling and Analyses Design Parameters*	183627
SNL 2007	*Engineered Barrier System: Physical and Chemical Environment*	177412
SNL 2007	*Total System Performance Assessment Data Input Package for Requirements Analysis for Subsurface Facilities*	179466
SNL 2007	*UZ Flow Models and Submodels*	184614
Ziegler 2004	"Transmittal of Appendix D of the Technical Basis Document No. 10: Unsaturated Zone Transport Addressing Key Technical Issue (KTI) Agreement Evolution of Near-Field Environment (ENFE) 1.04."	171694

FEP: 2.1.06.02.0A

FEP NAME:

Mechanical Effects of Rock Reinforcement Materials in EBS

FEP DESCRIPTION:

Degradation of rock bolts, wire mesh, and other materials used in ground control may affect the long-term performance of the repository.

SCREENING DECISION:

Excluded – low consequence

SCREENING JUSTIFICATION:

Rock reinforcement, also called ground support, mitigates the potential for rockfall into repository emplacement drifts during construction and operations. After repository closure, ground support will continue to serve this function until it degrades and eventually fails (BSC 2004 [DIRS 166107], Section 1.1). Postclosure modeling of rock mechanical response to heating and ground motion, which estimates the amount of rockfall, takes no credit for the presence of functioning ground support (BSC 2004 [DIRS 166107], Section 6). This assumption is a bounding approach that simplifies the modeling and increases the extent of predicted drift degradation during preclosure and postclosure periods. The introduction of other materials will be governed by *Total System Performance Assessment Data Input Package for Requirements Analysis for Engineered Barrier System In-Drift Configuration* (SNL 2007 [DIRS 179354], Table 4-1, Parameter Numbers 01-15 and 02-03). Preclosure degradation that might affect postclosure conditions will also be addressed (SNL 2007 [DIRS 179354], Table 4-1, Parameter Numbers 01-17 and 02-03).

Analyses of multiple rockfall impacts (BSC 2004 [DIRS 171756]) suggest that the drip shield can withstand two 2-metric ton blocks hitting the same spot. The Bernold sheets will have a mass of approximately 40 kg (BSC 2007 [DIRS 181645]). Rock bolts will weigh roughly a third of that. Rock blocks falling onto the drip shield are calculated to acquire a kinetic energy approximately that gained by falling through a distance of 2.5 m (SNL 2007 [DIRS 176828], Section 6.10.2.2), reaching a maximum velocity of 7 m/s (SNL 2007 [DIRS 176828], Table 6-50). The energy imparted to the drip shield by rockfall, a Bernold sheet, or a rock bolt will be proportional to the mass of the falling object. Because the ground support material will possess less than one tenth the mass of a 2-metric ton rockfall it will impose less than a tenth the force of the non-damaging 2-ton rockfall onto the drip shield. The yield strength of the ground support material is expected to be marginally larger than that of the rock (roughly a factor of two greater), so falling ground support material will be expected to withstand an impact with the drip shield. Yet, the much larger difference between rock block mass and ground support mass outweighs this difference in material yield strength. It is therefore reasonable to expect falling ground support materials to not damage the drip shield.

Drift degradation (rockfall and ground support degradation) due to seismic, thermal, and time-dependent effects during the postclosure period is described in *Drift Degradation Analysis* (BSC 2004 [DIRS 166107], Sections 6.2 through 6.4). The impact of rockfall occurring during the postclosure period (when complete degradation of the ground support is assumed) is addressed in other FEPs: excluded FEP 1.2.03.02.0B (Seismic-induced Rockfall Damages EBS Components), included FEP 1.2.03.02.0C (Seismic-induced Drift Collapse Damages EBS Components), excluded FEP 2.1.07.01.0A (Rockfall), and excluded FEP 2.1.07.02.0A (Drift Collapse).

It should be noted that this FEP does not address the chemical effects that degradation of rock bolts or other ground support materials may have on repository performance. Those effects are addressed in excluded FEP 2.1.06.01.0A (Chemical Effects of Rock Reinforcement and Cementitious Materials in EBS). Also, as discussed in excluded FEP 2.1.06.04.0A (Flow through Rock Reinforcement Materials in EBS), the presence of rock bolts has minimal effect on seepage into the repository.

Based on the previous discussion, omission of FEP 2.1.06.02.0A (Mechanical Effects of Rock Reinforcement Materials in EBS) will not result in a significant adverse change in the magnitude or timing of either radiological exposure to the RMEI or radionuclide releases to the accessible environment. Therefore, this FEP is excluded from the performance assessments conducted to demonstrate compliance with proposed 10 CFR 63.311 and 63.321 (70 FR 53313 [DIRS 78394]), and with 10 CFR 63.331 [DIRS 180319], on the basis of low consequence.

INPUTS:

Table 2.1.06.02.0A-1. Direct Inputs

Input	Source	Description
BSC 2004. *Drift Degradation Analysis*. [DIRS 166107]	Section 1.1	Rock reinforcement materials will degrade and fail
	Sections 6.2 through 6.4	Degradation of rock-reinforcement material
SNL 2007. *Total System Performance Assessment Data Input Package for Requirements Analysis for EBS In-Drift Configuration*. [DIRS 179354]	Table 4-1, Parameter Numbers 01-17 and 02-03	Preclosure degradation that might affect postclosure will also be addressed
	Table 4-1, Parameter Numbers 01-15 and 02-03	Introduction of mechanical effects of rock reinforcement materials in the EBS

Table 2.1.06.02.0A-2. Indirect Inputs

Citation	Title	DIRS
10 CFR 63	Energy: Disposal of High-Level Radioactive Wastes in a Geologic Repository at Yucca Mountain, Nevada	180319
BSC 2004	*Drift Degradation Analysis*	166107
BSC 2004	*Multiple Rock Fall on Drip Shield*	171756
BSC 2007	*Ground Support Materials and Concrete Inverts - Committed and Non-Committed*	181645
SNL 2007	*Seismic Consequence Abstraction*	176828

FEP: 2.1.06.04.0A

FEP NAME:

Flow Through Rock Reinforcement Materials in EBS

FEP DESCRIPTION:

Groundwater flow may occur through the ground support materials (e.g., wire mesh, rock bolts, grout) and liner (if present).

SCREENING DECISION:

Excluded – low consequence

SCREENING JUSTIFICATION:

This FEP refers to the potential for ground support or its degradation products to enhance or decrease seepage (groundwater flow) into emplacement drifts, or to divert water flow within the drifts. Notice that cementitious materials will not be used for ground support in the emplacement areas (SNL 2007 [DIRS 179354], Table 4-1, Parameter Number 01-15). The Bernold-type sheets, which are bolted to the emplacement drift walls and roof (SNL 2007 [DIRS 179354], Table 4-1, Parameter Number 01-15), may be considered a liner. This FEP addresses groundwater flow and seepage; vapor transport and condensation are addressed by a separate included FEP 2.1.08.04.0A (Condensation Forms on Roofs of Drifts).

Groundwater flow into emplacement drifts (seepage) is modeled in the TSPA as being completely unhindered by any rock reinforcement materials. The impact of rock bolts on seepage was investigated using the predictive seepage model for performance assessment (BSC 2004 [DIRS 167652], Section 6.5). The results of these simulations are presented in Section 6.6.4 and Table 6-4 of that report (BSC 2004 [DIRS 167652]) and in *Abstraction of Drift Seepage* (SNL 2007 [DIRS 181244], Sections 6.4.2.5 and 6.5.1.6). These results indicate that the presence of rock bolts does not lead to significant seepage enhancement. This is understandable, considering that an open borehole without grout acts as a capillary barrier to unsaturated flow; that the cross-sectional area of the rock bolt borehole, onto which flow may be incident, is small; and that water that may have seeped into the borehole can imbibe back into the rock along its length (see excluded FEP 1.1.01.01.0B (Influx Through Holes Drilled in Drift Wall or Crown). Note that only ungrouted rock bolts will be used in emplacement drifts (SNL 2007 [DIRS 179354], Table 4-1, Parameter Number 01-15).

The Bernold-type sheets, which are bolted to the emplacement drift walls and roof (SNL 2007 [DIRS 179354], Table 4-1, Parameter Numbers 01-15 and 01-16), may act to divert some seepage away from waste packages either before or after the sheet installations fail due to corrosion or ground motion. However, these sheets are well perforated, so the potential diversion effect on seepage is limited and therefore not included in TSPA (consistent with SNL 2007 [DIRS 179354], Table 4-1, Parameter Number 01-16).

Friction-type carbon steel rock bolts with plates are planned for use as temporary ground support during construction of the emplacement drifts, and will be left in place between the rock and the permanent (Bernold-type) ground support (SNL 2007 [DIRS 179354], Table 4-1, Parameter Number 01-15). As discussed above, neither the rock bolts used as temporary ground support nor those holding the Berthold plates will have a significant effect on the seepage flow rate. Also, as discussed in *Drift Degradation Analysis* (BSC 2004 [DIRS 166107], Section 6) the ground support system is expected to degrade following repository closure. Therefore, not including the temporary ground support in the representation of seepage for TSPA is a realistic representation of the system with respect to groundwater flow into the drift.

In light of the above discussion, omission of FEP 2.1.06.04.0A (Flow Through Rock Reinforcement Materials in EBS) will not result in a significant adverse change in the magnitude or time of radiological exposures to the RMEI or radionuclide releases to the accessible environment. Therefore, this FEP is excluded from the performance assessments conducted to demonstrate compliance with proposed 10 CFR 63.311 and 63.321 (70 FR 53313 [DIRS 178394]), and with 10 CFR 63.331 [DIRS 180319], on the basis of low consequence.

INPUTS:

Table 2.1.06.04.0A-1. Direct Inputs

Input	Source	Description
BSC 2004. *Seepage Model for PA Including Drift Collapse*. [DIRS 167652]	Sections 6.5, 6.6.4, Table 6-4	Impact of rock bolts on seepage using the predictive seepage model for performance assessment
SNL 2007. *Total System Performance Assessment Data Input Package for Requirements Analysis for EBS In-Drift Configuration*. [DIRS 179354]	Table 4-1, Parameter Number 01-15	Friction-type carbon steel rock bolts with plates are planned for use as temporary ground support during construction of the emplacement drifts, and will be left in place between the rock and the permanent (Bernold-type) ground support
	Table 4 1, Parameter Numbers 01-15 and 01-16	Bernold-type sheets bolted to the emplacement drift walls and roof may divert some seepage away from waste packages before or after the plate installations fail due to corrosion or ground motion
	Table 4-1, Parameter Number 01-15	Bernold-type sheets which are bolted to the emplacement drift walls and roof may be considered a liner
	Table 4-1, Parameter Number 01-15	Cementitious materials will not be used for ground support in the emplacement areas
	Table 4 1, Parameter Number 01-15	Only ungrouted rock bolts will be used in emplacement drifts
SNL 2007. *Abstraction of Drift Seepage*. [DIRS 181244]	Sections 6.4.2.5, 6.5.1.6	Impact of rock bolts on seepage using the predictive seepage model for performance assessment

Table 2.1.06.04.0A-2. Indirect Inputs

Citation	Title	DIRS
10 CFR 63	Energy: Disposal of High-Level Radioactive Wastes in a Geologic Repository at Yucca Mountain, Nevada	180319
70 FR 53313	Implementation of a Dose Standard After 10,000 Years	178394
BSC 2004	*Drift Degradation Analysis*	166107

FEP: 2.1.06.05.0A

FEP NAME:

Mechanical Degradation of Emplacement Pallet

FEP DESCRIPTION:

Degradation of the materials used in the pallet supporting the waste package may occur by physical processes, and may affect the long-term performance of the repository. Degradation may be fast (e.g., from dynamic loading) or slow (e.g., from static loading).

SCREENING DECISION:

Excluded – low consequence

SCREENING JUSTIFICATION:

This FEP considers the potential for mechanical degradation of the emplacement pallets to affect long-term performance of the repository. Each emplacement pallet supports the static load of a waste package during handling and emplacement. The emplacement pallets raise the waste packages above the invert during the preclosure and postclosure time periods (SNL 2007 [DIRS 179354], Table 4-3, Parameter Number 08-02). If a seismic event occurs, the emplacement pallets are subjected to the static load of the waste packages plus the dynamic loads from waste package-to-pallet impacts. Both of these loading conditions are considered in this FEP.

Undisturbed Conditions—The emplacement pallet design consists of two cradles or pedestals, fabricated from Alloy 22, that are connected by tubing fabricated from Stainless Steel Type 316 (SNL 2007 [DIRS 179354], Table 4-3, Parameter Number 08-01). The tubing provides structural stability for the pallet as a lifting fixture for a waste package. The two pedestals are free-standing structures that can support a waste package without the tubing in the emplaced configuration. The dimensions and thicknesses of the key parts of the emplacement pallets are summarized in *Total System Performance Assessment Data Input Package for Requirements Analysis for Engineered Barrier System In-Drift Configuration* (SNL 2007 [DIRS 179354], Table 4-3, Parameter Number 08-01).

The load-bearing capacity of the pedestals will be virtually unaffected by general corrosion, and the pallets will continue to fulfill their function of supporting the waste packages during the 10,000-year period. General corrosion can reduce the thickness of the pedestals, but this is a very slow process. As an example, the median corrosion rate of Alloy 22 at 60°C is 6.35 nm/yr, based on a medium uncertainty level in the distributions for general corrosion rate (DTN: MO0612WPOUTERB.000 [DIRS 182035], file: *BaseCase GC CDFs2.xls*, worksheet: "Data," cell: L71). Over 10,000 years, the thickness reduction from double-sided corrosion on the pallets is estimated as (10,000 years)$(2 \times 7 \times 10^{-9}$ m/yr) = 1.4×10^{-4} m = 0.14 mm. This thickness reduction is not significant in comparison to the initial thicknesses of the sides, ends, or tops of the pallet, which are 17.5, 17.5, and 22.2 mm, respectively (SNL 2007 [DIRS 178851], Table 6-2). An average temperature of 100°C may be more appropriate for the first 10,000 years

after closure. The median corrosion rate increases by a factor of 4 to 5 between 60°C and 100°C (DTN: MO0612WPOUTERB.000 [DIRS 182035], file: *BaseCase GC CDFs2.xls*), equivalent to a thickness reduction of 0.56 mm to 0.70 mm after 10,000 years. In either case, the Alloy 22 pedestals remain structurally intact during the first 10,000 years after repository closure.

The pallet design requirements are also relevant to mechanical degradation of the pallets. The emplacement pallets provide structural support and isolation from the invert during the preclosure and postclosure repository periods (SNL 2007 [DIRS 179354], Table 4-3, Parameter Number 08-02). The pallet material thicknesses include allowance for specified corrosion rates for at least 10,000 years after repository closure (SNL 2007 [DIRS 179354], Table 4-3 Parameter Number 08-03). The fact that the pallet design provides a corrosion allowance for 10,000 years is confirmed by the median corrosion estimates calculated in a previous paragraph.

Possible impacts of thermal-mechanical stresses on in-drift EBS components are discussed under excluded FEP 2.1.11.07.0A (Thermal Expansion/Stress of In-drift EBS Components), which is excluded on the basis of low consequence.

Seismic-Induced Loads—Other FEPs evaluate the response of the engineered barrier system (EBS) components to seismic events. The EBS components are the waste package, drip shield, emplacement pallet, invert, waste form, cladding, and the emplacement drift. These FEPs generally focus on the response of the waste packages and drip shields because failure of these EBS components has the potential to form new transport pathways that release radionuclides and because TSPA does not take credit for the potential delay in radionuclide transport due to the presence of the emplacement pallets. However, two FEPs explicitly represent the chemical degradation of the pallets at the time of a seismic event. The effect of general corrosion of the Alloy 22 components of the emplacement pallet on the structural response to a seismic event is addressed in included FEP 2.1.06.05.0C (Chemical Degradation of Emplacement Pallet) and included FEP 1.2.03.02.0A (Seismic Induced Ground Motion Damages EBS Components). Included FEP 1.2.02.03.0A (Fault Displacement Damages EBS Components) discusses the potential for the emplacement pallets to change the clearance between the bottom of the drip shields and top of the waste packages in response to a fault displacement with an intact drip shield (SNL 2007 [DIRS 176828], Section 6.11.1.1).

A structural analysis of the pallets during seismic events is documented in *Structural Calculations of Waste Package Exposed to Vibratory Ground Motion* (BSC 2004 [DIRS 167083], Section 6.2.4). This analysis shows that the pallets will deform (bulge) but do not collapse under large dynamic loads imposed by waste package impacts during infrequent seismic events at the 5.35 m/s PGV level. This PGV level corresponds to less than the 10^{-8} annual exceedance frequency on the bounded hazard curve (SNL 2007 [DIRS 176828], Table 6-3). The dynamic deformation of the pallets reduces the damage to the waste packages from waste package-to-pallet/invert impacts (BSC 2004 [DIRS 167083], Section 6.2.4 and Figure 9). An additional assessment of the performance of the emplacement pallet connector tubes during seismic events with a PGV of 5.35 m/s, where the connector tube properties were those of 316 stainless steel instead of Alloy 22 as used in the original analysis, indicates that they will perform their function for at least 10,000 years (BSC 2005 [DIRS 173172], Attachment XI).

A complete suite of structural response calculations for waste package-to-pallet impacts during a seismic event has been performed with deformable pallets that are chemically degraded (SNL 2007 [DIRS 178851], Section 6.3.2.2). These calculations evaluate the damaged area on the waste packages' OCB for two OCB thicknesses, 23 and 17 mm, from the nominal 25.4-mm thickness (SNL 2007 [DIRS 179394], Table 4-1, Parameter Number 03-03), and for various impact velocities, impact locations, and impact angles between the pallet and the package. The corresponding thickness reduction for the Alloy 22 plates of the pallet is equal to the thickness reduction of the OCB for each analysis. The thickness reductions of 2.4 mm and 8.4 mm span the range of waste package structural response that is expected during the time frame for geologic stability (SNL 2007 [DIRS 176828], Sections 6.5.1.2 and 6.5.2.2). These calculations provide part of the basis for the seismic damage abstractions when the drip shields are intact and the waste packages and emplacement pallets can move kinematically beneath the drip shields (SNL 2007 [DIRS 176828], Sections 6.5 and 6.6).

Exclusion of the mechanical degradation of the pallets from the structural response calculations maximizes the plastic deformation of waste packages and maximizes the area with high residual stress that has the potential to form stress corrosion cracks in the OCB. For example, the presence of the stainless steel connector rods stiffens the pallets and maintains the pedestals in a vertical, as-emplaced configuration that maximizes plastic deformation from waste package-to-pallet impacts. As a second example, multiple waste package-to-pallet impacts will occur during many ground motions. However, the potential for damage to accumulate and reduce the mechanical stiffness of the pallets is excluded because an undamaged pallet maximizes the plastic deformation of a waste package. Finally, a severe ground motion could rupture the connector rods, allowing the individual pedestals to topple onto the invert. A toppled pedestal will lie flatter on the invert than a vertical pedestal, causing less plastic deformation of a waste package during waste package-to-pallet impacts than the pallets in their as-emplaced configuration. These examples show that screening out mechanical degradation of the pallets maximizes the damaged areas on the waste packages.

Based on the previous discussion, omission of FEP 2.1.06.05.0A (Mechanical Degradation of Emplacement Pallet) will not result in a significant adverse change in the magnitude or timing of either radiological exposure to the RMEI or radionuclide releases to the accessible environment. Therefore, this FEP is excluded from the performance assessments conducted to demonstrate compliance with proposed 10 CFR 63.311 and 63.321 (70 FR 53313 [DIRS 178394]), and with 10 CFR 63.331 [DIRS 180319], on the basis of low consequence.

INPUTS:

Table 2.1.06.05.0A-1. Direct Inputs

Input	Source	Description
BSC 2004. *Structural Calculations of Waste Package Exposed to Vibratory Ground Motion*. [DIRS 167083]	Section 6.2.4 and Figure 9	Structural response of the pallet during extreme seismic event; it will not collapse
DTN: MO0612WPOUTERB.000. Output from General and Localized Corrosion of Waste Package Outer Barrier Report. [DIRS 182035]	file: *BaseCase GC CDFs2.xls*	The median corrosion rate increases by a factor of 4 to 5 between 60°C and 100°C
	file: *BaseCase GC CDFs2.xls*, worksheet: "Data," cell: L71	The median corrosion rate of Alloy 22 at 60°C is 6.35 nm/yr
SNL 2007. *Total System Performance Assessment Data Input Package for Requirements Analysis for EBS In-Drift Configuration*. [DIRS 179354]	Table 4-3, Parameter Number 08-03	The material thicknesses of the pallet include allowance for specified corrosion rates for at least 10,000 years after disposal
	Table 4-3, Parameter Number 08-02	The emplacement pallet provides structural support and isolation from the invert during the preclosure and postclosure repository periods
	Table 4-3, Parameter Number 08-01	The dimensions and thicknesses of the key parts of the emplacement pallet and its total mass
	Table 4-3, Parameter Number 08-01	Emplacement pallet design
	Table 4-3, Parameter Number 08-02	Each emplacement pallet supports the static load of a waste package during handling and emplacement. The emplacement pallets raise the waste packages above the invert during the preclosure and postclosure time periods
SNL 2007. *Total System Performance Assessment Data Input Package for Requirements Analysis for TAD Canister and Related Waste Package Overpack Physical Attributes Basis for Performance Assessment*. [DIRS 179394]	Table 4-1, Parameter Number 03-03	Waste package nominal thickness of 25.4 mm

Table 2.1.06.05.0A-2. Indirect Inputs

Citation	Title	DIRS
10 CFR 63	Energy: Disposal of High-Level Radioactive Wastes in a Geologic Repository at Yucca Mountain, Nevada	180319
70 FR 53313	Implementation of a Dose Standard After 10,000 Years	178394
BSC 2005	*Mechanical Assessment of the Waste Package Subject to Vibratory Ground Motion*	173172
SNL 2007	*Seismic Consequence Abstraction*	176828
SNL 2007	*Mechanical Assessment of Degraded Waste Packages and Drip Shields Subject to Vibratory Ground Motion*	178851

FEP: 2.1.06.05.0B

FEP NAME:

Mechanical Degradation of Invert

FEP DESCRIPTION:

Degradation of the materials used in the invert may occur by physical processes, and may affect the long-term performance of the repository. Degradation may be fast (e.g., from dynamic loading) or slow (e.g., from static loading).

SCREENING DECISION:

Excluded – low consequence

SCREENING JUSTIFICATION:

The invert is composed of plain carbon steel components and crushed-tuff ballast (SNL 2007 [DIRS 179354], Table 4-1, Parameter Number 02-08). The invert provides structural support for other EBS components, namely the pallet, waste package, and drip shield (SNL 2007 [DIRS 179354], Table 4-1, Parameter Number 02-07). Degradation, bearing capacity, and long-term settlement properties are part of the design (SNL 2007 [DIRS 179354], Table 4-1, Parameter Number 02-08). Postclosure mechanical loads on the invert can result from thermal expansion of invert components (e.g., the steel structure), deformation of the host rock containing the invert, seismic loading, and loading from collapse-rubble. Postclosure thermal-mechanical effects on emplacement drift stability (i.e., rockfall) have been analyzed in *Drift Degradation Analysis* (BSC 2004 [DIRS 166107], Sections 6.3.1.3 and 6.4.2.3). EBS component responses to seismic events are discussed in included FEP 1.2.03.02.0A (Seismic Ground Motion Damages EBS Components), excluded FEP 1.2.03.02.0B (Seismic-Induced Rockfall Damages EBS Components), and in included FEP 1.2.03.02.0C (Seismic-Induced Drift Collapse Damages EBS Components). Invert damage due to drift collapse is also discussed in excluded FEP 2.1.07.02.0A (Drift Collapse).

Processes leading to postclosure mechanical loading, and the potential impacts of those processes on the EBS components, are summarized as follows:

- Thermal expansion of invert materials is accommodated in the invert design (SNL 2007 [DIRS 179354], Table 4-1, Parameter Number 02-04). Peak thermal deformation (e.g., of the invert steel) will occur when in-drift temperatures are at a maximum, within approximately 20 years after closure (SNL 2008 [DIRS 184433], Section 6.3.16[a]).

- The limited vertical displacement of the drift floor, as described in excluded FEP 2.1.07.06.0A (Floor Buckling), is not expected to result in invert degradation due to thermal-mechanical deformation of the host rock.

- Seismic ground motion could result in bulking and subsequent uneven settlement of the invert, potentially damaging the drip shield. This process is evaluated in *Mechanical*

Assessment of Degraded Waste Packages and Drip Shields Subject to Vibratory Ground Motion (SNL 2007 [DIRS 178851], Section 6.4.6). Stresses produced by uneven settlement of the invert do not exceed the drip shield tensile strength, and settlement of the invert is not expected to materially alter the drip shield function.

- In the absence of seismic ground motion, invert settlement is expected to be minor. The invert is graded and will be tightly compacted during placement, and most of the settlement will occur during construction. Further compaction is expected to be negligible (SNL 2007 [DIRS 179354], Table 4-1, Parameter Number 02-08), resulting in displacements that produce only minor shifting in the drip shields, which will not compromise their integrity because the overlap between adjacent drip shields is approximately 320 mm (SNL 2007 [DIRS 179354], Table 4-2, Parameter Number 07-01). The effect of settling on the position of the waste packages and pallet is also expected to be minor in the non-seismic case.

In addition to the effects listed above, the invert is part of the transport pathway for radionuclides as represented in TSPA (SNL 2008 [DIRS 177407], Section 6.5). Radionuclide transport through the invert is not significantly affected by mechanical degradation for the following reasons:

- Mechanical degradation or settling of the invert ballast could result in changes in the intergranular porosity and permeability. Uncertainty with respect to hydrologic properties of the invert could affect the predicted in-drift thermal-hydrologic environment (temperature, relative humidity, and invert liquid-phase saturation), which, in turn, controls the chemical environment in the drift (SNL 2007 [DIRS 177412], Section 6.9). This uncertainty was evaluated over a range of particle sizes (0.317 mm to 20 mm) in *Multiscale Thermohydrologic Model* (SNL 2008 [DIRS 184433], Section 6.3.11). The in-drift thermal-hydrologic environment is insensitive to the hydrologic properties of the intergranular porosity, indicating that mechanical degradation will have a negligible effect on predictions of in-drift chemistry.

- Consolidation of the invert ballast could change the hydrologic properties affecting advective radionuclide transport. Intragranular rewetting and degree of saturation are independent of grain size and intergranular hydrologic properties (SNL 2008 [DIRS 184433], Section 6.3.11); invert rewetting is largely a function of the capillary condensation in intragranular porosity as opposed to wicking, because the intergranular porosity has a negligible capillarity relative to that of fractures in the rock. Therefore, the invert provides little resistance to downward flow, regardless of grain size. The effects of hydrologic changes in the invert are discussed in excluded FEPs 2.1.08.09.0A (Saturated Flow in the EBS) and 2.1.08.12.0A (Induced Hydrologic Changes in Invert).

- Consolidation of the invert ballast could change the invert porosity and water content, affecting radionuclide diffusion rates. The uncertainty associated with the porosity of the invert is included in the uncertainty in the diffusion coefficient, which is based on measurements for a variety of geologic materials having a range of porosities. Thus, the porosity uncertainty can be considered to be accounted for in the effective diffusion coefficient. (SNL 2008 [DIRS 177407], Section 6.3.4.1.1). The anticipated porosity range of 0.27 to 0.39 (SNL 2008 [DIRS 177407], Equation 6.3.4.1.1-23) includes a

range of potential mechanical degradation effects. Therefore, small changes in invert porosity will not significantly affect calculation of the invert diffusion coefficient in TSPA.

Based on the previous discussion, omission of FEP 2.1.06.05.0B (Mechanical Degradation of Invert) will not result in a significant adverse change in the magnitude or time of radiological exposures to the RMEI or radionuclide releases to the accessible environment. Therefore, this FEP is excluded from the performance assessment conducted to demonstrate compliance with proposed 10 CFR 63.311 and 633.21 (70 FR 53313 [DIRS 178394]), and with 10 CFR 63.331 [DIRS 180319], on the basis of low consequence.

INPUTS:

Table 2.1.06.05.0B-1. Direct Inputs

Input	Source	Description
SNL 2008. *EBS Radionuclide Transport Abstraction*. [DIRS 177407]	Sections 6.3.4.1.1 and 6.5	The uncertainty associated with the porosity of the invert is included in the uncertainty in the diffusion coefficient, which is based on measurements for a variety of geologic materials having a range of porosities. Thus, the porosity uncertainty can be considered to be accounted for in the effective diffusion coefficient

Table 2.1.06.05.0B-2. Indirect Inputs

Citation	Title	DIRS
70 FR 53313	Implementation of a Dose Standard After 10,000 Years	178394
SNL 2007	*Engineered Barrier System: Physical and Chemical Environment*	177412
SNL 2008	*Implementation of a Dose Standard After 10,000 Years*	177407
SNL 2007	*Total System Performance Assessment Data Input Package for Requirements Analysis for EBS In-Drift Configuration*	179354
SNL 2008	*Multiscale Thermohydrologic Model*	184433

FEP: 2.1.06.05.0C

FEP NAME:

Chemical Degradation of Emplacement Pallet

FEP DESCRIPTION:

Degradation of the materials used in the pallet supporting the waste package may occur by chemical or microbial processes, and may affect the long-term performance of the repository.

SCREENING DECISION:

Included

TSPA DISPOSITION:

Mechanical degradation of the emplacement pallet is discussed in excluded FEP 2.1.06.05.0A (Mechanical Degradation of Emplacement Pallet). In addition, microbial activity in the EBS is of low consequence with respect to potential chemical degradation of EBS components, including emplacement pallets (see excluded FEP 2.1.10.01.0A (Microbial Activity in EBS)). Chemical degradation of the emplacement pallet is included by performing structural analyses with thinned emplacement pallet components.

The waste package emplacement pallet supports the waste package during handling, emplacement, preclosure, and postclosure periods. In the first 10,000 years after emplacement, in the absence of seismic or igneous activity, the emplacement pallet maintains a waste package in a nominally horizontal position (SNL 2007 [DIRS 179354], Table 4-3, Parameter Number 08-02). The emplacement pallet waste package supports are fabricated from Alloy 22 and the emplacement pallet connector tubes are fabricated from Stainless Steel Type 316 (SNL 2007 [DIRS 179354], Table 4-3, Parameter Number 08-01). The stainless steel tubes connect to the Alloy 22 waste package supports. Galvanic coupling between Alloy 22 and Stainless Steel Type 316 is discussed in excluded FEP 2.1.09.09.0A (Electrochemical Effects in EBS).

The Alloy 22 emplacement pallet supports are the main load-bearing members because the geometry of the emplacement pallet prevents direct contact between the waste package and non-Alloy 22 drift components (SNL 2007 [DIRS 179354], Table 4-3, Parameter Number 08-03). The emplacement pallet is designed with margins accounting for corrosion such that it meets the requirements to support the waste package (SNL 2007 [DIRS 179354], Table 4-3, Parameter Number 08-03) during the first 10,000 years after closure. The corrosion allowance for both the Alloy 22 and stainless steel components shall be at least 2 mm (SNL 2007 [DIRS 179354], Table 4-3, Parameter Number 08-03). As discussed below, the corrosion of the connector tubes over the first 10,000 years after closure is low enough that the connector tubes retain their structural integrity. The structural integrity of the connector tubes is only important in the case of a seismic event of sufficient acceleration to cause the waste package to separate from the emplacement pallet.

When the drip shield is intact, seepage water is prevented from contacting the emplacement pallet connector tubes. A bounding estimate of the drip shield failure time by general corrosion can be obtained by using the upper 97.5% uncertainty bound, 0.999 probability general corrosion rate for the outer surface of the Titanium Grade 7 drip shield plate material (DTN: SN0704PADSGCMT.001 [DIRS 182122], file: *DS GC Model Analysis_aggressive condition.xls*) and the upper 97.5% uncertainty bound, 0.999 probability general corrosion rate for the inner surface of the Titanium Grade 7 drip shield plate material (DTN: SN0704PADSGCMT.001 [DIRS 182122], file: *DS GC Model Analysis_benign condition.xls*). These general corrosion rates are about 58 nm/yr and 21 nm/yr, respectively. Using these general corrosion rates for the 15 mm drip shield plate material, the failure time by general corrosion is estimated to be about 190,000 years. Furthermore, drip shield localized corrosion is discussed in excluded FEP 2.1.03.03.0B (Localized Corrosion of Drip Shields). Thus, in the absence of seismic activity or igneous intrusion, the emplacement pallet will not experience seepage water contact during the first 10,000 years after closure. The potential for concentrated solutions formed as a result of dust deliquescence to materially influence localized corrosion is screened out for Alloy 22, as discussed in excluded FEP 2.1.09.28.0A (Localized Corrosion on Waste Package Outer Surface due to Deliquescence). Since similar justifications (small brine volume, sublimation of salts, acid degassing, capillary retention of deliquescent brine within the dust, retention of deliquescent brines by corrosion products) also apply to localized corrosion of the stainless steel connector tubes, these components of the emplacement pallet are not expected to experience significant amounts of localized corrosion while the drip shield is performing its water diversion function. The stresses imposed in the Alloy 22 components of both the waste package and the emplacement pallet, in the as-emplaced configuration, shall be lower than the stress level necessary to cause SCC of Alloy 22 (SNL 2007 [DIRS 179354], Table 4-3, Parameter Number 08-05). Therefore, in the absence of seismic activity of sufficient magnitude to disturb the as emplaced waste package/emplacement pallet geometry, the Alloy 22 components of the emplacement pallet are not expected to develop stresses large enough to cause SCC of these components.

A reasonable estimate for the aqueous phase general corrosion rate for the Stainless Steel Type 316 emplacement pallet supports is 0.2 μm/yr. This estimate is corroborated by the general corrosion rates of Stainless Steel Type 316L measured in J-13 water after over one year of exposure reported by McCright et al. (1984 [DIRS 159336], Table 6). These values are appropriate for corroboration of the aqueous phase general corrosion rates of the emplacement pallet supports because Stainless Steel Type 316L is a low carbon version of Stainless Steel Type 316, which is, therefore, a suitable analogue material for Stainless Steel Type 316. Furthermore, the bulk water that may contact the emplacement pallet supports under an intact drip shield will result from condensation and have a dilute chemistry, as does J-13 well water (McCright et al. 1984 [DIRS 159336], Table 5). Aqueous phase corrosion rates of Stainless Steel Type 316L at temperatures of 50°C, 80°C, and 100°C, for samples exposed for longer than one year, have been measured to be 0.154±0.008, 0.109±0.005 , and 0.037±0.011 μm/yr, respectively (McCright et al. 1984 [DIRS 159336], Table 6). The estimated aqueous phase general corrosion rate for the Stainless Steel Type 316 emplacement pallet supports of 0.2 μm/yr sufficiently bounds these reported general corrosion rate values. Furthermore, studies have shown that there is a continual decrease of the degradation rate of stainless steel over time (Gdowski and Bullen 1988 [DIRS 100860], Figure 19; Larrabee 1953 [DIRS 159337], pp. 259 to 271; Southwell et al. 1976 [DIRS 100927], Table 4), and therefore the values of corrosion rate

resulting from these shorter-term corrosion tests (1.2 to 1.3 years) are higher than the corrosion rates expected when averaged over the design life of the emplacement pallet. The highest Stainless Steel Type 316 corrosion rate used in *In-Package Chemistry Abstraction* (14.8 μm/yr) (SNL 2007 [DIRS 180506], Table 4-8) is higher than the rate used in the current analysis. However, this higher general corrosion rate, derived from salt-water conditions, is a bounding rate applicable only in a seepage scenario when the drip shield is no longer intact.

Marine atmosphere corrosion rates for Stainless Steel Type 316L have been compiled and found to have a mean of 0.113 μm/yr for atmospheric conditions (DTN: MO0705OXYBALAN.000 [DIRS 185041], file: *atmospheric May2007.xls*, worksheet: "316"). Using this vapor phase corrosion rate for the first 2,000 years during the hot, dry period, and using the aqueous phase corrosion rate of 0.2 μm/yr at 50°C for the remaining 8,000 years, the depth of corrosion is calculated to be approximately 1.8 mm (rounded to two significant figures), which is about 19% of the 9.5-mm connector tube wall thickness. Because this calculation is based on short-term corrosion measurements, and because general corrosion rates tend to decrease with time, this is an upper limit of corrosion penetration that would be expected.

Corrosion of the stainless steel ground support in the drifts does not significantly influence the in-drift chemistry (SNL 2007 [DIRS 177412], Section 6.8). Therefore, corrosion of the stainless steel pallet tubes can be excluded as a factor influencing in-drift chemistry on the basis of low consequence. Additionally, *EBS Radionuclide Transport Abstraction* (SNL 2008 [DIRS 177407], Section 8.1) uses the conceptual model that all of the flux from the waste package flows directly into the invert, independent of the breach location on the waste package. The emplacement pallet could interfere with flow into the invert; however, no performance credit is taken for this process. *EBS Radionuclide Transport Abstraction* (SNL 2008 [DIRS 177407], Section 5.6) also assumes that no corrosion products exist in the invert. This assumption maximizes the potential transport of radionuclides through the invert as metal oxide corrosion products are capable of sorbing large amounts of radionuclides (SNL 2008 [DIRS 177407], Section 5.6). Although the text of the assumption discusses the corrosion products of the carbon steel invert materials, similar processes involving corrosion products resulting from degradation of the emplacement pallet are not credited in TSPA either.

In summary, chemical degradation of the emplacement pallet during the first 10,000 years of closure is determined mostly by the expected corrosion behavior of the stainless steel connector tubes, which does not significantly influence structural integrity of the emplacement pallets or in-drift chemistry.

The following discussion summarizes the effect of the emplacement pallet on repository performance after the first 10,000 years of closure. Mechanical degradation of the emplacement pallet (including the effects of seismic loadings) is discussed in excluded FEP 2.1.06.05.0A (Mechanical Degradation of Emplacement Pallet). The seismic analyses documented in *Mechanical Assessment of Degraded TAD Canisters and Degraded Drip Shields Subject to Vibratory Ground Motion* (SNL 2007 [DIRS 178851], Section 6) are conducted on three degraded states: a 23-mm-thick WPOB with intact waste package internals; a 23-mm-thick WPOB with degraded waste package internals; and a 17-mm-thick WPOB with degraded waste package internals. The future states of the EBS components are represented by three conceptual configurations as discussed in *Seismic Consequence Abstraction* (SNL 2007 [DIRS 176828],

Section 6.1). These future configurations are defined largely by the physical condition of the drip shield and the presence of rubble in the drift. The first configuration represents the as-emplaced EBS configuration, with a substantially intact drip shield and minimal rockfall in the drifts. In this configuration, the waste packages can move freely beneath the drip shields. The second configuration represents an intermediate configuration of the system where the legs of the drip shield have buckled under combined rockfall/seismic load, but the drip shield plates remain intact. In this configuration, the drip shield may collapse onto the waste package, inhibiting free movement of the waste package and emplacement pallet during seismic events. When the waste package is free to move under the action of seismicity, analyses indicate that most of the damage to waste packages from vibratory ground motion is caused by waste package-to-pallet impacts as opposed to waste package-to-waste package impacts (SNL 2007 [DIRS 178851], Section 8). A thickness reduction equal to the WPOB thickness reduction is also applied to the Alloy 22 plates of the emplacement pallet for each analysis (SNL 2007 [DIRS 178851], Section 6.3.2.2.1). This approach is reasonable because there is no reason that the Alloy 22 components in the emplacement pallet should undergo corrosion rates that are significantly different from those of the WPOB. In this manner, chemical thinning of the emplacement pallet is included in these seismic analyses. In the third configuration of the system, rubble surrounds the waste package after failure of the drip shield plates. In the seismic analyses of this configuration, the emplacement pallet is as an elastic solid body with stiffness such that its deformability is negligible (SNL 2007 [DIRS 178851], Section 5.21). This treatment will result in overestimation of deformation and damage in the waste package (SNL 2007 [DIRS 178851], Section 5.21). The Alloy 22 waste packages and emplacement pallet supports are expected to last longer than the drip shields, which are fabricated from titanium, as explained in *Mechanical Assessment of Degraded TAD Canisters and Degraded Drip Shields Subject to Vibratory Ground Motion* (SNL 2007 [DIRS 178851], Section 1.2). Once the drip shield has degraded, mechanical system response is governed by the rubble surrounding the waste package and emplacement pallet (SNL 2007 [DIRS 178851], Section 6.5). In this final configuration, the interactions between the waste package and the surrounding rubble are not affected significantly by the emplacement pallet (SNL 2007 [DIRS 178851], Section 6.5.1.2.1). Thus, in the long-term, degradation of the emplacement pallet is a relatively small contributor to seismic performance of the waste package.

In an analysis representative of the drift configuration during the first 10,000 years of the postclosure period and for normal condition loads, the emplacement pallet design was evaluated using a reduction in plate thickness to represent the effects of corrosion. The emplacement pallet design was found to perform satisfactorily (i.e., the waste package remains on the emplacement pallet) under seismic events with an annual frequency of occurrence of 1×10^{-6} per year (SNL 2007 [DIRS 179354], Table 4-1, Parameter Number 03-08). As stated above, the function of the emplacement pallet becomes less important to mechanical performance at later times when the drip shield is collapsed and rubble accumulates adjacent to waste packages.

At some time beyond the first 10,000 years after waste package emplacement, the emplacement pallet will fail by corrosion of its components and/or mechanical damage. From the above discussion, degradation of the emplacement pallet is not considered from the standpoint of radionuclide release nor does it have a significant impact on long-term seismic performance. When the emplacement pallet does fail, the waste package may come to rest on the invert. The invert structure contains a carbon steel structure that provides a framework that supports the

emplacement pallets and is covered by a layer of crushed tuff (SNL 2007 [DIRS 179354], Table 4-1, Parameter Number 02-08). It is expected that the carbon steel invert structure will have degraded significantly by the time the emplacement pallet has failed (particularly its Alloy 22 components). Even if the waste package contacts the metallic components of the invert structure, as discussed in excluded FEP 2.1.09.09.0A (Electrochemical Effects in EBS), these contacts are not expected to result in enhanced degradation of the more corrosion-resistant Alloy 22 WPOB.

In conclusion, thinning of the waste package emplacement pallet due to chemical degradation is included in seismic analyses; however, the effect of the emplacement pallet on radionuclide release is not considered.

INPUTS:

Table 2.1.06.05.0C-1. Direct Inputs

Input	Source	Description
DTN: MO0705OXYBALAN.000. Oxygen Balance Analysis for Physical and Chemical Environment. [DIRS 185041]	file: *atmospheric May2007.xls*, worksheet: "316"	Marine condition used during hot mostly dry repository condition
SNL 2007. *Mechanical Assessment of Degraded Waste Packages and Drip Shields Subject to Vibratory Ground Motion*. [DIRS 178851]	Section 8	Analysis of damage to waste packages from vibratory ground motion

Table 2.1.06.05.0C-2. Indirect Inputs

Citation	Title	DIRS
DTN: SN0704PADSGCMT.001	Drip Shield General Corrosion Models Based on 2.5-Year Titanium Grade 7 Corrosion Rates	182122
Gdowski and Bullen 1988	*Oxidation and Corrosion*	100860
Larrabee 1953	"Corrosion Resistance of High-Strength Low-Alloy Steels as Influenced by Composition and Environment"	159337
McCright et al. 1987	*Progress Report on the Results of Testing Advanced Conceptual Design Metal Barrier Materials Under Relevant Environmental Conditions for a Tuff Repository*	159336
SNL 2007	*Seismic Consequence Abstraction*	176828
SNL 2007	*Mechanical Assessment of Degraded Waste Packages and Drip Shields Subject to Vibratory Ground Motion*	178851
SNL 2007	*Total System Performance Assessment Data Input Package for Requirements Analysis for EBS In-Drift Configuration*	179354
SNL 2008	*EBS Radionuclide Transport Abstraction*	177407
SNL 2007	*Engineered Barrier System: Physical and Chemical Environment*	177412
SNL 2007	*In-Package Chemistry Abstraction*	180506
Southwell et al. 1976	"Corrosion of Metals in Tropical Environments - Final Report of 16-Year Exposures"	100927

FEP: 2.1.06.05.0D

FEP NAME:

Chemical Degradation of Invert

FEP DESCRIPTION:

Degradation of the materials used in the invert may occur by chemical or microbial processes, and may affect the long-term performance of the repository.

SCREENING DECISION:

Excluded – low consequence

SCREENING JUSTIFICATION:

The invert is composed of plain carbon steel components and crushed-tuff ballast (SNL 2007 [DIRS 179354], Table 4-1, Parameter Number 02-08). The invert provides structural support for other EBS components, namely the pallet, waste package, and drip shield (SNL 2007 [DIRS 179354], Table 4-1, Parameter Number 02-07). Degradation, bearing capacity, and long-term settlement properties are part of the design (SNL 2007 [DIRS 179354], Table 4-1, Parameter Number 02-08).

One consequence of chemical degradation of the invert could be the loss of mechanical integrity. Mechanical degradation of the invert is discussed in excluded FEP 2.1.06.05.0B (Mechanical Degradation of Invert), floor buckling, or heave, is excluded in FEP 2.1.07.06.0A (Floor Buckling).

Potential chemical degradation products in the invert include metal oxides and oxyhydroxides from the corrosion of steels. Invert corrosion products are expected to be localized and widely spaced, with the possibility that seepage from the waste package could completely miss corrosion products in the invert (SNL 2008 [DIRS 177407], Section 6.3.4.2.2.2). In this case, even small sorption coefficient values could overestimate the amount of retardation of radionuclides in the invert. Therefore although steel corrosion products have the potential to retard both iodine and technetium, no credit is taken for radionuclide sorption onto these materials, which are expected to be present locally in the invert (SNL 2008 [DIRS 177407], Section 6.3.4.2.2.2), through which radionuclides must be transported to reach the accessible environment.

The impact of steel corrosion on seepage water chemistry is evaluated in *Engineered Barrier System: Physical and Chemical Environment* (SNL 2007 [DIRS 177412], Section 6.8.4.1). The P&CE report demonstrates that wide variations in the amount of low alloy steel that corrodes per liter of seepage (up to 0.1 mole per liter) merely result in differing amounts of corrosion products and do not impact the aqueous phase chemistry significantly. This conclusion is corrosion-rate independent, as the effect was evaluated for large masses of steel well beyond what would be expected for reasonable time scales, corrosion rates, and surface areas.

The lower part of the invert will be crushed tuff. Degradation of the crushed tuff can either result in increased porosity due to the dissolution of primary minerals or decrease in porosity through the precipitation secondary phases. Both scenarios would be limited by the availability of water. Increased porosity would increase repository performance by decreasing the likelihood of local ponding, and overall water availability. Reduced porosity might lead, at worst, to accumulation of water and an increase in the rate of radionuclide release by advection. However, as explained in excluded FEP 2.1.08.12.0A (Induced Hydrologic Changes in Invert), which is excluded on the basis of low consequence, the repository emplacement drift design will preclude wetting or ponding along the invert–rock interface. The effects of hydrologic changes in the invert are further discussed in excluded FEP 2.1.08.09.0A (Saturated Flow in the EBS).

In the absence of advective flow, radionuclide migration through the crushed tuff is evaluated as a diffusion-only process. The effects of variable porosity on radionuclide diffusion are captured in the range of values for the diffusion coefficient that are used in TSPA (SNL 2008 [DIRS 177407], Section 6.3.4.1.1). The anticipated porosity range of 0.27 to 0.39 (SNL 2008 [DIRS 177407], Equation 6.3.4.1.1-23) includes a range of potential invert degradation effects. Therefore, small changes in invert porosity will not significantly affect the magnitude of invert diffusion coefficients calculated by TSPA.

Chemical degradation of the crushed tuff ballast in the invert could lead to changes in the invert porewater chemistry. The thermally perturbed interactions between porewaters and tuff are evaluated by the near-field chemistry model as the water–rock interaction parameter (SNL 2007 [DIRS 177412], Section 6.3.2). The water–rock interaction parameter is utilized by the P&CE seepage dilution/evaporation abstraction model to provide a wide range of potential seepage water compositions to TSPA (SNL 2007 [DIRS 177412], Sections 6.3.3 and 6.9). Any additional chemical changes induced by pore water interactions with the invert are not expected to generate changes in chemistry that is outside the range of compositions already included in the TSPA. On this basis, the effects on invert water chemistry can be regarded as insignificant.

Carbon present as in-drift committed materials will be in a refractory, reduced state (e.g., graphite) as discussed in *Evaluation of Potential Impacts of Microbial Activity on Drift Chemistry* (BSC 2004 [DIRS 169991], Section 6.4.5). Therefore, introduced carbon will not be biodegradable and can not participate in microbial reactions. *Evaluation of Potential Impacts of Microbial Activity on Drift Chemistry* (BSC 2004 [DIRS 169991], Section 6.4.5) also evaluates the potential sources of carbon available as sources of energy and nutrients to bacteria and other microorganisms that might survive in the in-drift environment. Results of that analysis show that microbial activity is of low consequence with respect to the composition of the in-drift chemistry (BSC 2004 [DIRS 169991], Section 7.1; excluded FEP 2.1.12.04.0A (Gas Generation (CO_2, CH_4, H_2S) from Microbial Degradation) and excluded FEP 2.1.10.01.0A (Microbial Activity in EBS)).

In conclusion, degradation of the invert by chemical or microbial processes will not alter (a) the hydrologic properties of the invert sufficiently to affect the transport of radionuclides through the invert, and (b) the chemical environment of emplacement drifts sufficiently to affect predictions of repository chemistry.

Based on this discussion, omission of FEP 2.1.06.05.0D (Chemical Degradation of Invert) will not result in a significant adverse change in the magnitude or time of radiological exposures to the RMEI or radionuclide releases to the accessible environment. Therefore, this FEP is excluded from the performance assessments conducted to demonstrate compliance with proposed 10 CFR 63.311 and 63.321 (70 FR 53313 [DIRS 178394]), and with 10 CFR 63.331 [DIRS 180319], on the basis or low consequence.

INPUTS:

Table 2.1.06.05.0D-1. Direct Inputs

Input	Source	Description
BSC 2004. *Evaluation of Potential Impacts of Microbial Activities on Drift Chemistry*. [DIRS 169991]	Sections 6.4.5, 7.1	Impacts of in-drift microbial activities
SNL 2008. *EBS Radionuclide Transport Abstraction*. [DIRS 177407]	Equation 6.3.4.1.1-23	Diffusion coefficient is calculated to vary by a factor of approximately two over the anticipated porosity range of 0.27 to 0.39
	Section 6.3.4.1.1	Effects of variable porosity are included in calculating the invert diffusion coefficient

Table 2.1.06.05.0D-2. Indirect Inputs

Citation	Title	DIRS
10 CFR 63	Energy: Disposal of High-Level Radioactive Wastes in a Geologic Repository at Yucca Mountain, Nevada	180319
70 FR 53313	Implementation of a Dose Standard After 10,000 Years	178394
SNL 2007	*Total System Performance Assessment Data Input Package for Requirements Analysis for EBS In-Drift Configuration*	179354
SNL 2008	*EBS Radionuclide Transport Abstraction*	177407
SNL 2007	*Engineered Barrier System: Physical and Chemical Environment*	177412

FEP: 2.1.06.06.0A

FEP NAME:

Effects of Drip Shield on Flow

FEP DESCRIPTION:

The drip shield will affect the amount of water reaching the waste package. Effects of the drip shield on the disposal region environment (for example, changes in relative humidity and temperature below the shield) should be considered for both intact and degraded conditions.

SCREENING DECISION:

Included

TSPA DISPOSITION:

The EBS includes Titanium Grade 7 drip shield top and side plates supported by a Titanium Grade 29 framework, which is placed over the waste packages. The drip shield is a free-standing structure that sits on the invert transverse support beams and employs interlocking segments continually installed along the length of the drift. The drip shield design requirements and component details are summarized in *Total System Performance Assessment Data Input Package for Requirements Analysis for Engineered Barrier System In-Drift Configuration* (SNL 2007 [DIRS 179354], Section 4.1.2, Table 4-2). The effects of the drip shield on flow are included in TSPA models for in-drift natural convection and condensation as described in *In-Drift Natural Convection and Condensation* (SNL 2007 [DIRS 181648]) for in-drift thermal hydrology as described in *Multiscale Thermohydrologic Model* (SNL 2008 [DIRS 184433]), and for EBS radionuclide transport as described in *EBS Radionuclide Transport Abstraction* (SNL 2008 [DIRS 177407]).

The role of the drip shield on flow processes in the in-drift environment is addressed in *In-Drift Natural Convection and Condensation Model* (SNL 2007 [DIRS 181648]), which develops a computational fluid dynamics model of natural convection during the postclosure period (SNL 2007 [DIRS 181648], Sections 6.1.5 and 6.2.5). Axial dispersion coefficients of water vapor are derived from the natural convection model, and implemented in a simplified model of evaporation and condensation in the in-drift environment (SNL 2007 [DIRS 181648], Section 6.3.3). Condensation on the drift walls is discussed in more detail in included FEP 2.1.08.04.0A (Condensation Forms on Roofs of Drifts (Drift-Scale Cold Traps)). The results are included in the TSPA, as also described in included FEP 2.1.08.04.0A.

The drip shield limits the amount of water that contacts waste forms, and limit the rates of release of radionuclides from breached waste packages (as discussed for included FEP 2.1.08.07.0A (Unsaturated Flow in the EBS)).

Temperature and unsaturated relative humidity under intact drip shields are included in the multiscale model for TSPA (SNL 2008 [DIRS 184433], Sections 8.1 and 8.4). Diffusive vapor transport through gaps in the joints between drip shields, and through the invert ballast is

assumed to be rapid so that the partial pressure of water vapor is the same under and outside of the drip shield (SNL 2008 [DIRS 184433], Section 5.5). This is supported by results from scale-model testing to investigate condensation under the drip shield (as discussed for excluded FEP 2.1.08.14.0A (Condensation on Underside of Drip Shield)), in which water vapor readily migrated from inside to outside the drip shield, so that condensation was controlled by the cooler drift wall. In addition, the drip shield acts as a thermal radiation shield, causing the waste package to be warmer and thus drier than if no drip shield were present (SNL 2008 [DIRS 184433], Section 6.2.4). Similar behaviors are predicted in the event of seepage into collapsed drift openings, where coverage by collapse rubble increases the temperature of the drip shield and waste package, prolonging dryout. Seepage into collapse rubble will be diverted from contacting the drip shield until the waste package temperature cools to approximately 100°C or lower (SNL 2008 [DIRS 184433], Section 6.3.17[a]).

When seepage or drift wall condensation occurs, and the drip shield fails to perform its flow diversion function, liquid water may flow through breaches in the drip shield and contact the waste package (see included FEPs 2.2.07.20.0A (Flow Diversion Around Repository Drifts) and 2.1.08.04.0A (Condensation Forms on Roofs of Drifts (Drift-Scale Cold Traps)). Flow of water through breaches in the drip shield is described by the EBS flow component, of the EBS radionuclide transport abstraction model (SNL 2008 [DIRS 177407], Section 6.3.1.1), which quantifies the time-dependent radionuclide releases from a failed waste package and the subsequent transport through the EBS to the emplacement drift wall/unsaturated zone interface. Basic inputs to the EBS radionuclide transport abstraction model (SNL 2008 [DIRS 177407], Section 6.1) include the drift seepage and drift wall condensation rates, the environmental conditions in the drift (temperature, relative humidity, and water chemistry), and the degradation states of EBS components including the drip shield.

Water flow in the EBS comprises eight pathways (Figure 2.1.06.06.0A-1) and corresponding fluxes: total dripping flux, including any condensation on drift walls above the drip shield (F_1), flux through the failed drip shield (F_2), diversion around an intact drip shield (F_3), flux through the waste package (F_4), diversion around the waste package (F_5), flux from the waste package and drip shield into the invert (F_6), imbibition flux from the drift host-rock matrix to the invert (F_7), and flux from the invert to the unsaturated zone matrix and fractures (F_8). These pathways are time dependent, in that the total dripping flux and waste package penetrations will vary with time and local conditions in the repository. The primary source of inflow to the EBS is the dripping flux from the crown (roof) of the drift (F_1), and includes seepage flux and any condensation that may occur on the walls of the drift above the drip shield.

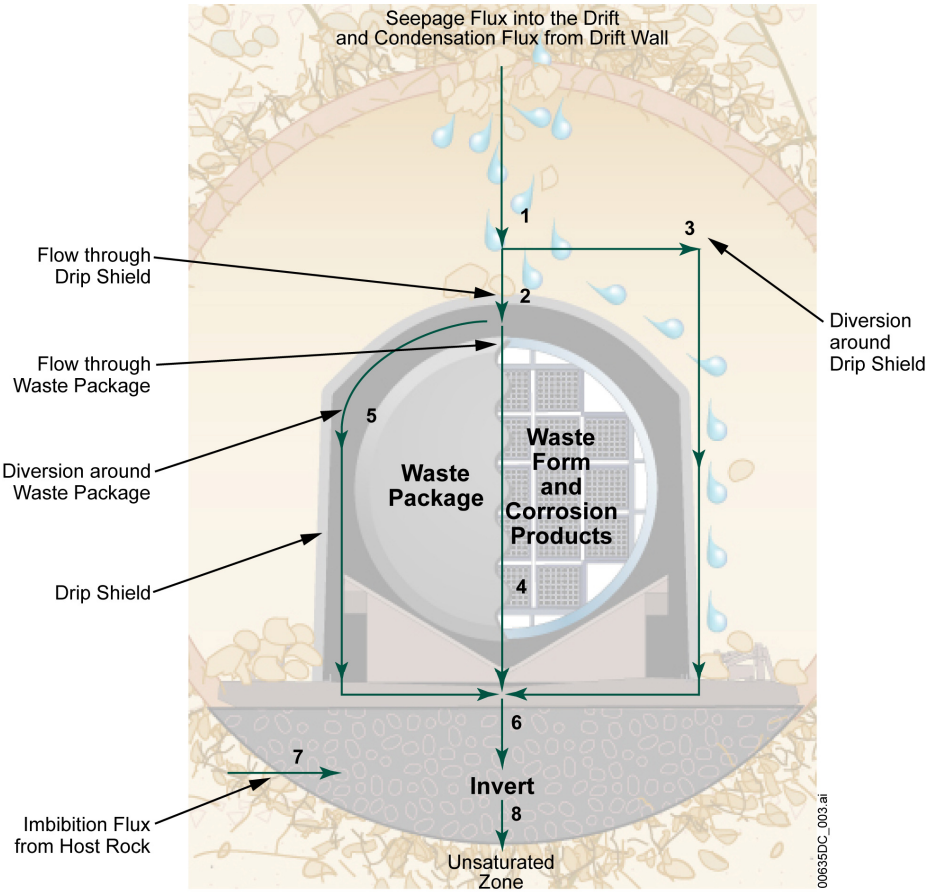

Source: SNL 2008 [DIRS 177407], Figure 6.3-1.

Figure 2.1.06.06.0A-1. Potential Flow Pathways in the EBS

Section 6.3.2 of *EBS Radionuclide Transport Abstraction* (SNL 2008 [DIRS 177407]) describes water flux through a failed drip shield (F_2) and around an intact drip shield (F_3). Once the drip shield has failed, all of the water flux ($F_2 = F_1$) will pass through the drip shield and have access to the waste package. Until the drip shield has failed, all of the flux is diverted around the drip shield ($F_3 = F_1$). Key assumptions include: (1) the dripping flux (seepage plus condensation) into the drift is assumed to fall as droplets from the top of the drift onto the crown of the drip shield; (2) droplets fall randomly along the length of the drip shield; (3) evaporation from the drip shield is assumed to be negligible; and (4) all water that flows through the failed drip shield flows onto or into the waste package.

This FEP is included in performance assessments to demonstrate compliance with the individual protection standard after permanent closure (proposed 10 CFR 63.311 (70 FR 53313 [DIRS 178394])) and the groundwater protection standards (10 CFR 63.331 [DIRS 180319]). It is not included in the human intrusion performance assessment (proposed 10 CFR 63.321 (70 FR 53313 [DIRS 178394])).

INPUTS:

Table 2.1.06.06.0A-1. Indirect Inputs

Citation	Title	DIRS
10 CFR 63	Energy: Disposal of High-Level Radioactive Wastes in a Geologic Repository at Yucca Mountain, Nevada	180319
70 FR 53313	Implementation of a Dose Standard After 10,000 Years	178394
SNL 2007	*Total System Performance Assessment Data Input Package for Requirements Analysis for EBS In-Drift Configuration*	179354
SNL 2008	*EBS Radionuclide Transport Abstraction*	177407
SNL 2007	*In-Drift Natural Convection and Condensation*	181648
SNL 2008	*Multiscale Thermohydrologic Model*	184433

FEP: 2.1.06.06.0B

FEP NAME:

Oxygen Embrittlement of Drip Shields

FEP DESCRIPTION:

A potential failure mechanism for drip shields is oxygen embrittlement, resulting from the diffusion of interstitial oxygen in the titanium at high temperatures.

SCREENING DECISION:

Excluded – low probability

SCREENING JUSTIFICATION:

Oxygen embrittlement of a titanium alloy results from the diffusion of oxygen into the titanium metal occurring at temperatures greater than 340°C to 370°C (i.e., 645°F to 700°F) (ASM International 1987 [DIRS 103753], p. 681). During diffusion through a titanium alloy, oxygen atoms insert themselves at interstitial positions in the crystal lattice and thereby increase the resistance to sliding of one part of the crystal past another. This effect, in turn, can impact mechanical properties of the titanium alloy (e.g., it can increase the hardness and strength but decrease the ductility) promoting embrittlement (Leyens and Peters 2004 [DIRS 181560], p. 187).

Without drift collapse, the waste package temperature will be below 300°C (SNL 2008 [DIRS 184433], Figure 6.3-76[a]) and decrease with time after achieving a peak value. Due to greater distance of the drip shield from the heat source (i.e., the waste form) than the waste package, surface temperatures of the drip shields will be lower than those for the waste packages. In order for the waste package surface to exceed 300°C, a seismic event must occur within approximately 90 years after closure, result in drift collapse, and affect a waste package with an unfavorable combination of a high thermal output surrounded by a low conductivity rubble (SNL 2008 [DIRS 179962], Section 6.5.1). Analyses have shown that the mean probability of these conditions occurring is about one in 10,000 within the first 10,000 years of disposal (SNL 2008 [DIRS 179962], Section 6.5.1). Therefore, a reasonably bounding drip shield exposure temperature in the repository is 300°C and is used in the analysis of oxygen embrittlement in this FEP.

To estimate the critical oxygen concentration below which oxygen embrittlement is not expected to occur, a reasonable approach is to use the maximum oxygen content specified for Titanium Grade 4, an oxygen-strengthened titanium metal, as the lower-bound value of this parameter for Titanium Grade 7 at 300°C. The specified maximum oxygen content in Titanium Grade 4 is 0.4 wt % (ASTM B265-02 [DIRS 162726], Table 2). Based on the above discussion, the lower-bound value of the critical oxygen concentration of Titanium Grade 7 could be considered as any value equal to or higher than the oxygen content of the oxygen-strengthened alloy Titanium Grade 4 (i.e., 0.4 wt %). Using this lower-bound value of the critical oxygen content, the amount of time required to increase the oxygen content of Titanium Grade 7 to 0.4 wt % at

300°C can be estimated if the oxygen diffusion coefficient at 300°C is known. The specified oxygen content in Titanium Grade 7 is 0.25 wt % (ASTM B265-02 [DIRS 162726], Table 2). The calculated time to reach the lower-bound oxygen content value of 0.4 wt % from 0.25 wt % represents the minimum period of time before oxygen embrittlement of titanium drip shield can occur.

The value of the oxygen diffusion coefficient in titanium at 300°C is 8.8×10^{-18} $cm^2 \cdot s^{-1}$ and has an uncertainty of 70% (Rogers et al. 1988 [DIRS 184108], Table 1 and p. 146). Using this value of the oxygen diffusion coefficient, the amount of time required to increase the oxygen content of Titanium Grade 7 to 0.4 wt % at 300°C at any depth, x, can be estimated from the following equation (Guy 1959 [DIRS 154917], p. 407):

$$\frac{C - C_0}{C_1 - C_0} = 1 - erf\left(\frac{x}{2\sqrt{Dt}}\right) \qquad \text{(Eq. 2.1.06.06.0B-1)}$$

Here, C is the oxygen concentration at a depth of x centimeters into the metal surface after diffusion has occurred for time t seconds, C_1 the surface oxygen concentration in wt %, C_0 the initial oxygen concentration in the metal plate in wt %, and D the diffusion coefficient of oxygen in the metal. A sensitivity analysis performed using various values of oxygen concentration on the drip shield surface (C_1 = 10 wt % to 40 wt %), the upper bound value of the diffusion coefficient of oxygen in titanium ($D = 1.7 \times 8.8 \times 10^{-18}$ $cm^2 \cdot s^{-1}$ at 300°C), a depth of 0.3 mm into the drip shield (x = 0.3 mm), the critical oxygen concentration beyond which oxygen embrittlement of drip shield could occur (C = 0.4 wt %), and the specified maximum oxygen concentration in Titanium Grade 7 (C_0 = 0.25 wt %), produced results as shown in Table 2.1.06.06.0B-1.

Table 2.1.06.06.0B-1. Results of Sensitivity Analysis for Oxygen Embrittlement of Drip Shield

C_1	Equation LHS Value	Required Time (Years)	Equation RHS Value
10%	1.54×10^{-2}	1.63×10^{5}	1.54×10^{-2}
20%	7.59×10^{-3}	1.34×10^{5}	7.59×10^{-3}
30%	5.04×10^{-3}	1.21×10^{5}	5.04×10^{-3}
40%	3.77×10^{-3}	1.14×10^{5}	3.77×10^{-3}

LHS = left-hand side; RHS = right-hand side.

As seen in Table 2.1.06.06.0B-1, a time on the order of 10^5 years would be required to increase the oxygen content of Titanium Grade 7 from 0.25 wt % to the critical oxygen content of 0.4 wt % at a depth of 0.3 mm into the drip shield. A thickness of 0.3 mm is very small compared to the intact drip shield total thickness of 15 mm. Thus, even if the mechanical properties of a 0.3 mm layer on each side of the drip shield were affected, there would be no significant impact on the mechanical properties of the drip shield. Therefore, the time needed to cause oxygen embrittlement of Titanium Grade 7 in the drip shield should be greater than 10^5 years even for a constant exposure temperature of 300°C. At temperatures below 300°C, the oxygen diffusivity in titanium would be lower so that the time needed to cause oxygen embrittlement of Titanium Grade 7 will be even longer. The value of the diffusion coefficient of

oxygen in titanium increases at higher temperatures (Rogers et al. 1988 [DIRS 184108], Table 1). As discussed earlier, the waste package temperature could possibly exceed 300°C due to a low probability drift collapse event. However, the waste package would be above 300°C only for a short time period and decrease at later times. Therefore, the drip shield temperature, which would be lower than the waste package temperature, could exceed 300°C for a short time period as well. Consequently, the use of a constant temperature of 300°C in this analysis is bounding.

Although a similar sensitivity analysis has not been performed for Titanium Grade 29, the drip shield structural support material, oxygen embrittlement of this material will not occur before 10^5 years for the following reasons:

- The drip shield surface temperature will be lower than 300°C except for the low-probability event of a drift collapse within the first approximately 90 years of emplacement (SNL 2008 [DIRS 184433], Figure 6.3-82[a]; SNL 2008 [DIRS 179962], Section 6.5.1).

- For drip shield surface temperatures below 300°C, the oxygen diffusivity in titanium, the base metal of Titanium Grade 29, is lower than that at 300°C. In light of the results of sensitivity analysis on Titanium Grade 7, the time required to cause oxygen embrittlement of Titanium Grade 29 at 300°C is expected to be approximately 1×10^5 years.

In conclusion, oxygen embrittlement of the titanium drip shields is not expected to occur under the relatively low temperature conditions of the drip shield in the repository.

According to 10 CFR 63.114(d) [DIRS 180319], only events that have at least one chance in 10,000 of occurring over 10,000 years need to be included in performance analysis.

Based on the previous discussion, FEP 2.1.06.06.0B (Oxygen Embrittlement of Drip Shields) will have less than one chance in 10,000 of occurring over 10,000 years based on the time required to achieve significant oxygen concentrations within the metal under repository thermal exposure conditions. Therefore, this FEP is excluded from the performance assessments conducted to demonstrate compliance with proposed 10 CFR 63.311 and 63.321 (70 FR 53313 [DIRS 178394]), and with 10 CFR 63.331 [DIRS 180319], on the basis of low probability.

Hydrogen embrittlement is discussed in excluded FEP 2.1.03.04.0B (Hydride Cracking of Drip Shields). The effects of potential acidification in creviced regions such as cracks are discussed in excluded FEP 2.1.03.03.0B (Localized Corrosion of Drip Shields).

INPUTS:

Table 2.1.06.06.0B-2. Direct Inputs

Input	Source	Description
ASM International 1987. *Corrosion*. [DIRS 103753]	p. 681	Temperature threshold for oxygen embrittlement of titanium
ASTM B 265-02. 2002. *Standard Specification for Titanium and Titanium Alloy Strip, Sheet, and Plate*. [DIRS 162726]	Table 2	Specified maximum oxygen content in various titanium grades
Rogers et al. 1988. "Low Temperature Diffusion of Oxygen in Titanium and Titanium Oxide Films." [DIRS 184108]	Table 1 and p. 146	The value of the oxygen diffusion coefficient in titanium at 300°C
SNL 2008. *Multiscale Thermohydrologic Model*. [DIRS 184433]	Figure 6.3-82[a]	The drip shield surface temperature will be lower than 300°C except for the low probability event of a drift collapse within the first approximately 90 years of emplacement
	Figure 6.3-76[a]	Waste package surface temperature profiles for nominal case
SNL 2008. *Postclosure Analysis of the Range of Design Thermal Loadings*. [DIRS 179962]	Section 6.5.1	Probability of seismically -induced drift collapse causing waste package (and drip shield) peak temperature to exceed 300°C is approximately one in 10,000 within the first 10,000 years of emplacement

Table 2.1.06.06.0B-3. Indirect Inputs

Citation	Title	DIRS
10 CFR 63	Energy: Disposal of High-Level Radioactive Wastes in a Geologic Repository at Yucca Mountain, Nevada	180319
70 FR 53313	Implementation of a Dose Standard After 10,000 Years	178394
Guy 1959	*Elements of Physical Metallurgy*. 2nd Edition.	154917
Leyens and Peters 2004	*Titanium and Titanium Alloys, Fundamentals and Applications*.	181560
SNL 2008	*Postclosure Analysis of the Range of Design Thermal Loadings*	179962

FEP: 2.1.06.07.0A

FEP NAME:

Chemical Effects at EBS Component Interfaces

FEP DESCRIPTION:

Chemical effects that occur at the interfaces between materials in the drift may affect the performance of the system.

SCREENING DECISION:

Excluded – low consequence

SCREENING JUSTIFICATION:

The EBS component interfaces addressed in this FEP are those that may involve solid-solid interactions. Solid–liquid interactions of EBS components are addressed in included FEPs 2.1.03.01.0A (General Corrosion of Waste Packages) and 2.1.03.03.0A (Localized Corrosion of Waste Package) for general and localized corrosion of the waste package, respectively. In addition, included FEP 2.1.03.01.0B (General Corrosion of Drip Shields) and excluded FEP 2.1.03.03.0B (Localized Corrosion of Drip Shields) address general and localized corrosion of the drip shield, respectively. As described in *Total System Performance Assessment Data Input Package for Requirements Analysis for Engineered Barrier System In-Drift Configuration* (SNL 2007 [DIRS 179354]), the base plates of the drip shield are fabricated from Alloy 22 (SNL 2007 [DIRS 181339], Section 6.3) to prevent direct contact between the titanium and steel members in the invert, thus minimizing electrochemical effects at this interface (SNL 2007 [DIRS 179354], Table 4-2, Parameter Number 07-07). This configuration prevents contact between the titanium and invert steel, to avoid hydrogen diffusion into the titanium (SNL 2007 [DIRS 181339], Section 6.3). The pallet pedestals are fabricated of Alloy 22, as is the waste package outer shell (SNL 2007 [DIRS 179354], Table 4-3, Parameter Numbers 08-01 and 08-03), thus precluding galvanic reactions at this interface. It should be noted that the pallet connector rods are made of stainless steel and will be in contact with the Alloy 22 pallet pedestals. If galvanic corrosion occurs, it will attack the invert steel rather than the Alloy 22 in the pallet pedestal because of the former's lower resistance to corrosion. Further discussions on the potential effects of galvanic interactions between EBS components are given in excluded FEP 2.1.09.09.0A (Electrochemical Effects in EBS). This FEP also concludes that enhanced degradation as a result of galvanic interactions would be negligible due to similarities in the corrosion potentials of the considered metals and alloys in the EBS that may come into contact with one another.

Interactions between various types of EBS components as a result of extensive degradation and subsequent consolidation of these assemblies is discussed in excluded FEP 2.1.08.15.0A (Consolidation of EBS Components). The only exception is the case of drift collapse as a result of seismically induced ground motion. In this case, rockfall could damage the drip shield and possibly the outer shells of the waste packages (assuming drip shield failure) as discussed in included FEP 1.2.03.02.0C (Seismic-induced Drift Collapse Damages EBS Components).

Included FEP 1.2.03.02.0A (Seismic Ground Motion Damages EBS Components) discusses the effects of ground motion damage on EBS components that mainly results in structural/mechanical interactions between adjacent waste packages. In-drift chemistry can be affected by modification of drift hydrological and thermal properties as a result of drift collapsed rock material and other related processes. These effects of rock collapsed on in-drift chemistry are discussed in excluded FEP 1.2.03.02.0E (Seismic-Induced Drift Collapse Alters In-Drift Chemistry). Mechanical effects at EBS component interfaces due to static loading are discussed in excluded FEP 2.1.06.07.0B (Mechanical Effects at EBS Component Interfaces). Interaction with magmatic fluids during an igneous intrusion is discussed in included FEPs 1.2.04.04.0A (Igneous Intrusion Interacts with EBS Components) and 1.2.04.04.0B (Chemical Effects of Magma and Magmatic Volatiles). According to that FEP, EBS components will be subjected to elevated temperatures diminishing the tensile strength of the metal components, making them susceptible to plastic deformation. Once the magma enters the drift, it will stagnate and magma flow would be insufficient to mobilize any of the waste packages. Excluded FEP 2.1.09.03.0B (Volume Increase of Corrosion Products Impacts Waste Packages) discusses the potential for mechanical damage as a result of volume change due to the formation of corrosion products relative to the metal. The lack of closely confined spaces in the EBS precludes any mechanical damage due to changes in corrosion product volume, and this process is therefore excluded on the basis of low consequence.

The effects of interactions of seepage waters with ground support materials (e.g., cement, rock bolts, wire mesh) remaining in the repository after closure were assessed by FEP 2.1.06.01.0A (Chemical Effects of Rock Reinforcement and Cementitious Materials in EBS); these effects were excluded on the basis of low consequence. Steel corrosion in the drift could potentially affect the pH and/or chemistry of aqueous solutions and the amount of precipitated steel corrosion products. The effect of steel corrosion on aqueous chemistry is examined in Section 6.8.4.1 of *Engineered Barrier System: Physical and Chemical Environment* (P&CE) (SNL 2007 [DIRS 177412]). This section of the P&CE model report indicates that significant changes in the masses of steel/alloy (Stainless Steel Type 316L and Carbon Steel Type A588) reacting with seepage essentially results in an increase of precipitated corrosion products and does not significantly affect aqueous solution chemistry. Therefore, the effect of these seepage-metal interactions on seepage chemistry in the drift is excluded on the basis of low consequence.

Telluric current flows induced by geomagnetic phenomena could result in the generation of significant electrical potentials and have been observed to cause corrosion of buried oil/gas pipelines. Enhancement of metal/alloy corrosion degradation in the EBS as a result of telluric currents is not expected. Both theoretical and measured pipe-to-soil potentials in buried pipelines indicate that the effects of telluric currents are expected to be more significant in long buried pipe-like structures having lengths in the order of tenths to hundreds of kilometers (Martin 1993 [DIRS 184437]; Boteler and Seager 1997 [DIRS 184439]). The combined length of EBS structures in a single drift does not add to a length of even one kilometer. A study of pipe-to-soil potentials in a segment of a ~450 km long gas pipeline in Canada (Ontario) shows that a peak value of about +200 mV only occurs within a pipeline segment of ~25 km; the rest of the pipeline experienced much smaller values. It is also expected that rocks in this locality will have larger degrees of saturation and, thus, larger conductivities than the tuffaceous rock in Yucca Mountain drifts. Based on EBS design configuration features (SNL 2007 [DIRS 179354],

Table 4-1, Parameter Number 02-05), it is expected that ground support assemblies including invert steel are sufficiently grounded to preclude any significant effect on potential build-up at the surface of EBS components. Also, the aforementioned metals/alloys used in the EBS components would remain passive under a wide range of applied potentials (SNL 2007 [DIRS 178519], Sections 8.2 and 8.3; SNL 2007 [DIRS 180778], Sections 6.6.1 and 6.6.2). Therefore, it is anticipated that any changes in surface potentials induced directly or indirectly by telluric currents would not significantly affect the corrosion rates of these materials. Moreover, the direct contact of EBS components with rock is to a large extent limited. This rock/metal interaction is mostly restricted to ground support and invert steel components, and the latter is more prone to corrosion degradation than the more noble metal components of the EBS. Any anticipated potentials between ground support and invert steel components, and a largely unsaturated rock in the invert domain, will not be significant enough as to affect corrosion rates on EBS components. Unsaturated tuffaceous gravel from Yucca Mountain, having a volumetric water content in the range 1% to 10%, has low electrical conductivities (Hu et al. 2004 [DIRS 184440]). It is expected that such low conductivity will influence the effective flow of telluric currents in this porous media and any potential interaction with EBS components. Even in the case where telluric currents can indeed affect rock-to-steel (e.g., invert steel) potentials as to enhance corrosion rates, this phenomenon will be largely limited to interface steel structures in contact with rock such as ground support and invert steel assemblies. The corrosion products produced from degradation of ground support and invert steel assemblies would provide a nonconductive interface, thus protecting EBS components from this effect.

In conclusion, chemical effects at EBS component interfaces will have little effect on repository performance.

Based on the previous discussion, omission of FEP 2.1.06.07.0A (Chemical Effects at EBS Component Interfaces) will not result in a significant adverse change in the magnitude or timing of either radiological exposure to the RMEI or radionuclide releases to the accessible environment. Therefore, this FEP is excluded from the performance assessments conducted to demonstrate compliance with proposed 10 CFR 63.311 and 63.321 (70 FR 53313 [DIRS 178394]), and with 10 CFR 63.331 [DIRS 180319], on the basis of low consequence.

INPUTS:

Table 2.1.06.07.0A-1. Direct Inputs

Input	Source	Description
SNL 2007. *Total System Performance Assessment Data Input Package for Requirements Analysis for EBS In-Drift Configuration*. [DIRS 179354]	Table 4-2, Parameter Number 07-07	Titanium drip shields will have Alloy 22 base plates
	Table 4-3, Parameter Numbers 08-01 and 08-03	Pallet pedestals and waste package outer barrier material

Table 2.1.06.07.0A-2. Indirect Inputs

Citation	Title	DIRS
10 CFR 63	Energy: Disposal of High-Level Radioactive Wastes in a Geologic Repository at Yucca Mountain, Nevada	180319
70 FR 53313	Implementation of a Dose Standard After 10,000 Years	178394
Boteler and Seager 1998	"Telluric Currents: A Meeting of Theory and Observation"	184439
Hu et al. 2004	"Characterizing Unsaturated Diffusion in Porous Tuff Gravel"	184440
Martin 1993	"Telluric Effects on a Buried Pipeline"	184437
SNL 2007	*Total System Performance Assessment Data Input Package for Requirements Analysis for EBS In-Drift Configuration*	179354
SNL 2007	*Engineered Barrier System: Physical and Chemical Environment*	177412
SNL 2007	*General Corrosion and Localized Corrosion of the Drip Shield*	180778
SNL 2007	*General Corrosion and Localized Corrosion of Waste Package Outer Barrier*	178519
SNL 2007	*Hydrogen-Induced Cracking of the Drip Shield*	181339

FEP: 2.1.06.07.0B

FEP NAME:

Mechanical Effects at EBS Component Interfaces

FEP DESCRIPTION:

Physical effects of steady-state contact (static loading) that occur at the interfaces between materials in the drift may affect the performance of the system.

SCREENING DECISION:

Excluded – low consequence

SCREENING JUSTIFICATION:

This FEP describes the physical (mechanical) effects of steady-state contact between EBS components (waste package, pallet, drip shield, and invert) and their respective contacting materials on projected long-term performance. Relevant design controls are described that minimize mechanical deformation and the potential for generating stresses sufficient to initiate stress corrosion cracking.

The effects of transient, non-steady-state loading have also been considered and evaluated in other FEPs. For example, the possibility of the drip shield contacting the waste package as a result of non-steady-state mechanical damage caused by rockfall is addressed in excluded FEP 2.1.03.07.0B (Mechanical Impact on Drip Shield). Other FEPs that discuss mechanical effects of non-steady-state seismic, rockfall, and igneous events are included FEP 1.2.03.02.0A (Seismic Ground Motion Damages EBS Components), excluded FEP 1.2.03.02.0B (Seismic Induced Rockfall Damages EBS Components), included FEP 1.2.03.02.0C (Seismic Induced Drift Collapse Damages EBS Components), and included FEP 1.2.04.04.0A (Igneous Intrusion Interacts with EBS Components).

The waste package and the drip shield, as designed and emplaced, contact other EBS components. Therefore, administrative, procedural, and design controls are required to maintain the analyzed configuration and basis. The need for such controls and the basis for the controls are identified in *Total System Performance Assessment Data Input Package for Requirements Analysis for Engineered Barrier System In-Drift Configuration* (SNL 2007 [DIRS 179354], Table 4-1, Parameter Number 02-03). The design basis for the configuration interface controls between the as-emplaced waste package and other EBS components is documented in *Total System Performance Assessment Data Input Package for Requirements Analysis for Engineered Barrier System In-Drift Configuration* (SNL 2007 [DIRS 179354], Table 4-1, Parameter Numbers 02-01 and 02-02).

For example, the waste package is designed to rest on an emplacement pallet (SNL 2007 [DIRS 179354], Table 4-3), which is constructed of Alloy 22 supports and designed to keep the waste package from contacting other dissimilar metals (SNL 2007 [DIRS 179354], Table 4-3, Parameter Number 08-03). The waste package outer corrosion barrier will only contact the

Alloy 22 emplacement pallet supports (SNL 2007 [DIRS 179354], Table 4-1, Parameter Number 02-05). In the case of the emplacement pallet, stainless steel tubes connect Alloy 22 waste package supports to form the structure (SNL 2007 [DIRS 179354], Table 4-3, Parameter Numbers 08-01 and 08-03). The function of the tubes is to facilitate handling of the emplacement pallet during the preclosure period. The emplacement pallet is also designed to keep the waste package supported in a horizontal position, and away from the invert and ground support under non-seismic scenarios (SNL 2007 [DIRS 179354], Table 4-3, Parameter Number 08-03). Structural failure or failure due to stress corrosion cracking of the connector tubes under non-seismic (static) conditions will not affect the emplacement pallet performance with respect to supporting the waste package. Thus, the emplacement pallet supports the waste package during handling, emplacement, preclosure, and postclosure periods (nominal position for 300 years, and nominally horizontal for 10,000 years) (SNL 2007 [DIRS 179354], Table 4-3, Parameter Number 08-02). After 300 years, stress due to temperature changes and settlement in the invert from mechanisms such as corrosion of carbon steel can result in changes from the original placement. Thus, the invert and other EBS components are designed to account for these potential in-situ stresses and thermal responses as discussed in excluded FEP 2,1.11.07.0A (Thermal Expansion/Stress of In-Drift EBS Components), excluded FEP 2.1.06.05.0B (Mechanical Degradation of Invert), excluded FEP 2.1.07.06.0A (Floor Buckling), and excluded FEP 2.1.09.03.0B (Volume Increase of Corrosion Products Impacts Other EBS Components). The effect of uneven invert settlement on drip shield stability as a result of seismic ground motion was analyzed in *Mechanical Assessment of Degraded Waste Packages and Drip Shields Subject to Vibratory Ground Motion* (SNL 2007 [DIRS 178851], Section 6.4.6). It was determined that the settlement of the invert is not expected to materially alter the drip shield function as discussed in excluded FEP 2.1.03.07.0B (Mechanical Impact on Drip Shield). Postclosure, the structural integrity of the stainless steel connector tubes is only important in the case of a seismic event of sufficient acceleration to cause the waste package to separate from the emplacement pallet as discussed in included FEP 2.1.06.05.0C (Chemical Degradation of Emplacement Pallet).

For the nominal scenario emplacement configuration, the design is constrained to ensure that the tensile stresses imposed on the Alloy 22 components of both the waste package and the emplacement pallet are less than 257 MPa, the approximate stress corrosion cracking threshold for Alloy 22 (SNL 2007 [DIRS 181953], Tables 8-2 and 8-3; SNL 2007 [DIRS 179354], Table 4-3, Parameter Numbers 08-03 and 08-05). This stress limit precludes deformation and stress corrosion cracking (SNL 2007 [DIRS 179354], Table 4-3, Parameter Numbers 08-03 and 08-05).

The drip shield is emplaced in a controlled manner and in the post-weld stress-relieved condition, which minimizes residual stresses generated from fabrication and welding as discussed in excluded FEP 2.1.03.02.0B (Stress Corrosion Cracking (SCC) of Drip Shields). The drip shield is designed for subsequent postclosure loadings that may occur due to thermal expansion, rockfall, drift collapse, and seismic effects (SNL 2007 [DIRS 179354], Table 4-2, Parameter Numbers 07-03, 07-04, 07-08, 07-14, and 07-15). The drip shield protects the waste package from rockfall as described in excluded FEP 2.1.07.01.0A (Rockfall). In the case of drift collapse, the quasi-static loading of rock rubble will occur as a result of slow, time-dependent strength reduction in the lithophysal rocks. Analyses summarized in excluded FEP 2.1.07.02.0A (Drift Collapse) conclude that drift collapse under nominal (static) loading conditions will not

have a significant effect on long-term performance of the repository. Stress corrosion cracking resulting from rockfall induced static residual stresses is discussed in excluded FEP 2.1.03.02.0B (Stress Corrosion Cracking (SCC) of Drip Shields).

Mechanical loading at the drip shield/invert interface occurs between the Alloy 22 drip shield base plates, which rest on the carbon steel components of the invert (SNL [DIRS 179354], Table 4-2, Parameter Number 07-07). The steel invert structure will provide a framework, consisting of a series of beams bolted to the invert rock mass, that supports the emplacement pallets, waste packages, and drip shields for static and dynamic loads, but excluding fault displacements (SNL 2007 [DIRS 179354], Table 4-1, Parameter Numbers 02-07 and 02-08). Loads can result from thermal expansion of the base plates, drip shield, or invert steel structure; rock movement due to in situ stress release from excavation; and rock deformation of the invert. The design of the carbon steel structure in the invert accounts for these loads as well as loads imposed by construction activities, the gantry crane, waste packages, waste package pallet, drip shield, and seismic and thermal loads, as discussed in *Total System Performance Assessment Data Input Package for Requirements Analysis for Engineered Barrier System In-Drift Configuration* (SNL 2007 [DIRS 179354], Table 4-1, Parameter Numbers 02-04, 02-07, and 02-08).

Similar to the waste package to pallet contact, the drip shields are designed to contact no other material except the Alloy 22 base (SNL 2007 [DIRS 179354], Table 4-2, Parameter Number 07-07), which is attached to the bottom of the drip shields. The Alloy 22 drip shield base is in resting contact with the invert, which is covered by crushed tuff as ballast. The mechanical loading at the interfaces between the waste package and degraded pallet (i.e., with removal of 2-mm/side corrosion allowance) has also been analyzed using 150°C mechanical properties (SNL 2007 [DIRS 179354], Table 4-3, Parameter Number 08-03). The maximum contact stresses (257 MPa) between the waste package and (degraded) emplacement pallet are less than 90% of the Alloy 22, 150°C yield strength, the minimum threshold stress for initiation of stress corrosion cracking (SNL 2007 [DIRS 179354], Table 4-3, Parameter Numbers 08-03 and 8-05; SNL 2007 [DIRS 181953], Section 6.2.2, Table 4-1, and Equation 42; FEP 2.1.03.02.0A (Stress Corrosion Cracking (SCC) of Waste Packages)). Further, since this stress is below 90% of the yield strength, plastic deformation is also very limited (SNL 2007 [DIRS 179354], Table 4-3, Parameter Number 08-03). On this basis, enhanced degradation due to mechanical loading at the waste package-emplacement pallet interfaces is not expected.

The analyses discussed here demonstrate that steady-state loading between EBS components has minimal impact on the long-term performance of these components. Therefore, FEP 2.1.06.07.0B (Mechanical Effects at EBS Component Interfaces) is excluded from the performance assessments conducted to demonstrate compliance with proposed 10 CFR 63.311 and 63.321 (70 FR 53313 [DIRS 178394]), and with 10 CFR 63.331 [DIRS 180319], on the basis of low consequence. This FEP will not adversely affect the magnitude or timing of calculated radiological exposures to the RMEI or radionuclide releases to the accessible environment.

INPUTS:

Table 2.1.06.07.0B-1. Direct Inputs

Input	Source	Description
SNL 2007. *Total System Performance Assessment Data Input Package for Requirements Analysis for EBS In-Drift Configuration*. [DIRS 179354]	Table 4-1, Parameter Numbers 02-07 and 02-08	The steel invert structure will provide a framework, consisting of a series of beams bolted to the invert rock mass, that supports the emplacement pallets, waste packages, and drip shields for static and dynamic loads, but excluding fault displacement
	Table 4-1, Parameter Numbers 02-01 and 02-02	Configuration between the as-emplaced Waste Package and other EBS components
	Table 4-2, Parameter Number 07-07	Design information on the base plates of the drip shield, fabricated from Alloy 22
	Table 4-1, Parameter Number 02-05	Waste package outer corrosion barrier will only contact the Alloy 22 emplacement pallet supports
	Table 4-3, Parameter Number 08-03	The waste package is designed to rest on a pallet which is constructed of Alloy 22 pedestals and is designed to keep the waste package from contacting other dissimilar metals
	Table 4-2, Parameter Numbers 07-03, 07-04, 07-08, 07-14, and 07-15	Drip shield is designed for subsequent postclosure loadings which may occur due to thermal expansion, rockfall, drift collapse, and seismic effects
	Table 4-2, Parameter Number 07-07	Mechanical loading at the drip shield/invert interface occurs between the Alloy 22 drip shield base plates and which rest upon the carbon steel components of the invert
	Table 4-3, Parameter Number 08-02	The emplacement pallet supports the waste package during handling, emplacement, preclosure, and postclosure periods (nominal position for 300 years, and nominally horizontal for 10,000 years)
	Table 4-1, Parameter Numbers 02-04, 02-07, and 02-08	The design of the carbon steel structure in the invert accounts for loads imposed by construction activities, the gantry crane, waste packages, waste package pallet, drip shield, and seismic and thermal loads
	Table 4-3, Parameter Number 08-03	Further, since this stress limit is less than 90% of the yield strength, plastic deformation is very limited
	Table 4-3, Parameter Numbers 08-03 and 08-05	Alloy 22 stress limit precludes deformation
	Table 4-3, Parameter Numbers 08-03 and 08-05	This stress limit precludes deformation and stress corrosion cracking

Table 2.1.06.07.0B-1. Direct Inputs (Continued)

Input	Source	Description
SNL 2007. *Total System Performance Assessment Data Input Package for Requirements Analysis for EBS In-Drift Configuration*. [DIRS 179354] (continued)	Table 4-3, Parameter Number 08-03	The pallet is designed to keep the waste package supported in a horizontal position, and away from the invert and ground support under non-seismic scenarios
	Table 4-3	Design information and functionality of the emplacement pallet
	Table 4-3, Parameter Numbers 08-01 and 08-03	In the case of the emplacement pallet, Stainless steel tubes connect Alloy 22 to waste package supports to form an emplacement pallet structure
SNL 2007. *Stress Corrosion Cracking of Waste Package Outer Barrier and Drip Shield Materials*. [DIRS 181953]	Section 6.2.2, Table 4-1, and Equation 42	The maximum contact stresses (257 MPa) between the waste package and (degraded) pallet are less than 90% of the Alloy 22, 150°C yield strength, the minimum threshold stress for initiation of stress corrosion cracking

Table 2.1.06.07.0B-2. Indirect Inputs

Citation	Title	DIRS
10 CFR 63	Energy: Disposal of High-Level Radioactive Wastes in a Geologic Repository at Yucca Mountain, Nevada	180319
70 FR 53313	Implementation of a Dose Standard After 10,000 Years	178394
SNL 2007	*Mechanical Assessment of Degraded Waste Packages and Drip Shields Subject to Vibratory Ground Motion*	178851
SNL 2007	*Total System Performance Assessment Data Input Package for Requirements Analysis for EBS In-Drift Configuration*	179354
SNL 2007	*Stress Corrosion Cracking of Waste Package Outer Barrier and Drip Shield Materials*	181953

FEP: 2.1.07.01.0A

FEP NAME:

Rockfall

FEP DESCRIPTION:

Rockfalls may occur with blocks that are large enough to mechanically tear or rupture drip shields and/or waste packages. Seismic-induced rockfall is addressed in separate FEPs.

SCREENING DECISION:

Excluded – low consequence

SCREENING JUSTIFICATION:

This FEP addresses the potential impact of rockfall on the EBS components, including waste packages and drip shields. The term "rockfall" as used in this discussion refers to the dislodging of relatively few, generally large blocks of rock from the sides or crown of an emplacement drift. "Drift collapse," in contrast, refers to the en masse fall of rock fragments into the emplacement drift. Nominal rockfall may result from in situ conditions of gravitational stresses, excavation-induced stresses, and thermally induced stresses, as described in *Drift Degradation Analysis* (BSC 2004 [DIRS 166107], Section 6). Nominal rockfall does not include dynamic loading caused by seismic events. Seismic induced rockfall and drift degradation and the impacts on the EBS are addressed in included FEP 1.2.03.02.0A (Seismic Ground Motion Damages EBS Components), excluded FEP 1.2.03.02.0B (Seismic-Induced Rockfall Damages EBS Components), and included FEP 1.2.03.02.0C (Seismic-Induced Drift Collapse Damages EBS Components). The impacts of rockfall on drift seepage are addressed in included FEP 1.2.03.02.0D (Seismic-Induced Drift Collapse Alters In-Drift Thermohydrology).

All emplacement drift areas will be circular in cross-section and excavated with a tunnel boring machine (SNL 2007 [DIRS 179466], Table 4-1, Parameter Numbers 01-09 and 01-10). This excavation method produces a nominally circular opening with a predominately smooth surface profile. This is the least destructive technique for excavation since excessive energy (as in blasting) is not used for breakage of the rock and therefore minimizes excavation-induced stresses. The impact of excavation and construction is discussed in more detail in excluded FEP 1.1.02.00.0B (Mechanical Effects of Excavation and Construction in EBS) and included FEP 2.2.01.01.0A (Mechanical Effects of Excavation and Construction in the Near-Field).

Calculations of potential rockfall for the nonlithophysal and lithophysal layers of the repository for nominal and seismic scenarios are described in detail in *Drift Degradation Analysis* (BSC 2004 [DIRS 166107], Sections 6.3 and 6.4). For both lithophysal and nonlithophysal zones, the potential consequences of rockfall are damage to the drip shields and waste packages. The rock mass surrounding the excavations may undergo over-stressing from thermal heating and/or time-dependent damage associated with static fatigue resulting from stress corrosion mechanisms (BSC 2004 [DIRS 166107], Section 6.3.1.5). Stress corrosion is a term used for time-dependent, sub-critical crack growth that occurs when existing material flaws in the rock

are subjected to stresses that are near the failure state of the material. This process may result in damage and yield of the rock mass at applied stresses that are less than the short-term rock strength (BSC 2004 [DIRS 166107], Section 1.1). Another possible long-term effect includes the increasing amounts of moisture/air induced weathering along the joints close to the tunnels. This damaged and/or weathered material may result in block fallout, particularly in the nonlithophysal units (BSC 2004 [DIRS 166107], Section 6.3.1.5).

Note that there is a 200°C drift wall temperature limit imposed during the repository postclosure period (SNL 2007 [DIRS 179466], Table 4-2, Parameter Number 06-02). The drift wall temperature limit will confine the extent of permanent changes in rock characteristics that could impact drift opening stability. It is noted that drift wall temperatures of 200°C and rock mass temperatures greater than 250°C were achieved in the Drift Scale Test with only minor effects observed (SNL 2008 [DIRS 179962], Section 6.1.1). Furthermore, analyses documented in *Postclosure Analysis of the Range of Design Thermal Loadings* (SNL 2008 [DIRS 179962], Section 7.1) indicate that the anticipated range of thermal loading will result in peak postclosure drift wall temperatures significantly less than 200°C.

The calculations that include the assessement of distinct fracture sets in the lithophysal rock mass (based on field mapping data) show that the formation of small blocks that fall under gravitational forces is expected to be the dominant potential failure mode of drifts in lithophysal rocks (BSC 2004 [DIRS 166107], Section 6.4.3). Small blocks do not have sufficient energy to cause damage, and thus the potential to tear or rupture drip shields or waste packages is precluded. The static load on the drip shield resulting from the en masse fall of small rock blocks is discussed in excluded FEP 2.1.07.02.0A (Drift Collapse) and included FEP 1.2.03.02.0C (Seismic-Induced Drift Collapse Damages EBS Components). Thermal effects on rockfall in the lithophysal units are discussed in excluded FEP 2.1.07.02.0A (Drift Collapse). Because rockfall in lithophysal units is predominated by small blocks, calculations regarding the effects of the impact of rockfall on drip shields and waste packages are performed in nonlithophysal rock, which has a greater potential for large block formation. Rockfall analyses in nonlithophysal rock that include thermal loading and exclude seismic loading result in a minor amount of rockfall. Static fatigue failure of asperities along fracture surfaces is possible and would result in gravitationally induced failure of large blocks. Hence, rockfall in nonlithophysal units has the *potential* to cause significant damage to the EBS.

In the calculations relating to rockfall in *Drift Degradation Analysis* (BSC 2004 [DIRS 166107], Section 6), the potential for drift stability afforded by ground control systems is conservatively not considered. As indicated in *Total System Performance Assessment Data Input Package for Requirements Analysis for Engineered Barrier System In-Drift Configuration* (SNL 2007 [DIRS 179354], Table 4-1, Parameter Numbers 01-15, 01-16, and 01-17), a substantial ground support system will be installed in the emplacement drifts to facilitate repository operations. The ground support structure will be fabricated of stainless steel for longevity (SNL 2007 [DIRS 179354], Table 4-1, Parameter Number 01-15). Rockfall results presented in *Drift Degradation Analysis* (BSC 2004 [DIRS 166107], Sections 6.3 and 6.4) provide input to analyses of possible damage to EBS components (SNL 2007 [DIRS 178851]) in the form of block size and impact energy.

The effects of high-energy blocks have been considered as part of the seismic rockfall analyses in excluded FEP 1.2.03.02.0B (Seismic-Induced Rockfall Damages EBS Components), and have been found to be insignificant. These results provide an upper bound to the expected mechanical effects of rockfall during the nominal scenario.

Analyses related to multiple rockfalls were conducted in *Multiple Rock Fall on Drip Shield* (BSC 2004 [DIRS 171756]). Bounding characteristics of the credible multiple rockfalls for postclosure were used in the calculation. The structural response of the drip shield to two identical 2-metric ton rock block impacts onto the same location was analyzed. Along the highly deformed area at the point of impact, the average stress intensity through the drip shield plate thickness (along a line perpendicular to the plate surface) was determined for several locations. It was concluded that at the location of highest average stress intensity, the wall-averaged total stress intensity through the drip shield top plate, and the maximum bending surface principal stress in the longitudinal stiffeners do not exceed the respective true tensile strengths of these titanium drip shield components, as discussed in *Multiple Rock Fall on Drip Shield* (BSC 2004 [DIRS 171756], Section 6.1).

The effects of rockfall on crack initiation in the drip shield are discussed in *Stress Corrosion Cracking of Waste Package Outer Barrier and Drip Shield Materials* (SNL 2007 [DIRS 181953], Section 8.1.6), excluded FEP 2.1.03.10.0B (Advection of Liquids and Solids Through Cracks in the Drip Shield), and excluded FEP 2.1.03.02.0B (Stress Corrosion Cracking (SCC) of Drip Shields). The tightness of stress corrosion cracks in passive alloys such as Titanium Grade 7 (i.e., small crack-opening displacement) and their tortuosity will lead to negligible water flow through these openings (SNL 2007 [DIRS 181953], Section 6.8.5.2). For the case of multiple rockfalls on the same drip shield location, the total damaged area from multiple block impacts during a ground motion is conservatively estimated as the sum of the damaged areas from the individual block impacts (SNL 2007 [DIRS 176828], Section 6.10.2.9). The consequence of stress corrosion cracking on drip shield water diversion performance is discussed in excluded FEP 2.1.03.10.0B (Advection of Liquids and Solids through Cracks in the Drip Shield).

Prior to closure (prior to the installation of the drip shield), waste packages that have come into contact with fallen rock will be inspected to ensure that any damage to the waste package outer corrosion barrier is within acceptable limits (SNL 2007 [DIRS 179354], Table 4-1, Parameter Number 03-24). Since the drip shield continues to function through rockfall events as described above, the waste package and cladding will be protected from rockfall during the postclosure period, for as long as the drip shield remains intact, and rockfall will therefore be of low consequence while this is the case.

TSPA considers all fuel cladding (with the exception of naval SNF cladding) to be breached at the time of its arrival at the repository, as discussed in included FEP 2.1.02.12.0A (Degradation of Cladding Prior to Disposal) and in *Cladding Degradation Summary for LA* (SNL 2007 [DIRS 180616], Table 7-2[a]). Furthermore, following waste package failure, clad unzipping is considered to result in the immediate exposure of bare fuel to the waste package environment along the entire length of the fuel rod (included FEP 2.1.02.23.0A (Cladding Unzipping)). Therefore, the impact of rockfall on cladding integrity is of low consequence.

In summary, rockfall, as a result of gravitational-, excavation-, thermal- or corrosion-induced stresses, or weathering, will not affect the dose to the RMEI or release of radionuclides to the environment for as long as the drip shield remains intact. As indicated above, rockfall generated from nominal processes is not sufficient to tear or rupture the drip shield plates. Therefore, the waste packages, cladding, and waste form are protected from rockfall damage. Rockfall can therefore be excluded from the TSPA on the basis of low consequence for 10,000 years.

Based on the previous discussion, omission of FEP 2.1.07.01.0A (Rockfall) will not result in a significant adverse change in the magnitude or timing of either radiological exposure to the RMEI or radionuclide releases to the accessible environment. Therefore, this FEP is excluded from the performance assessments conducted to demonstrate compliance with proposed 10 CFR 63.311 and 63.321 (70 FR 53313 [DIRS 178394]), and with 10 CFR 63.331 [DIRS 180319], on the basis of low consequence.

INPUTS:

Table 2.1.07.01.0A-1. Direct Inputs

Input	Source	Description
BSC 2004. *Drift Degradation Analysis*. [DIRS 166107]	Sections 6.3 and 6.4	Rockfall results provide input to analyses of possible damage to EBS components in form of block size and frequency of gravitationally induced failures
	Section 6.3.1.5	Rock mass surrounding excavations may undergo over-stressing from thermal heating and/or time-dependent damage associated with static fatigue resulting from stress corrosion mechanisms
	Section 6	Nominal rockfall may result from in situ conditions of gravitational stresses, excavation-induced stresses and thermally induced stresses
	Section 6.4.3	Formation of small blocks precludes potential to tear or rupture drip shields or waste packages
	Sections 6.3 and 6.4	Description of potential rockfall calculations for nonlithophysal and lithophysal layers of repository for nominal and seismic scenarios
	Section 6.3.1.5	Damaged and/or weathered material may result in block fallout particularly in nonlithophysal units
BSC 2004. *Multiple Rock Fall on Drip Shield*. [DIRS 171756]	Section 6.1	Wall-averaged total stress intensities through the drip shield top plate and the maximum bending surface principal stress in the longitudinal stiffeners do not exceed the respective true tensile strengths of these titanium drip shield components

Table 2.1.07.01.0A-1. Direct Inputs (Continued)

Input	Source	Description
SNL 2007. *Seismic Consequence Abstraction*. [DIRS 176828]	Section 6.10.2.9	For the case of multiple rockfalls on the same drip shield location, the total damaged area from multiple block impacts during a ground motion is conservatively estimated as the sum of the damaged areas from the individual block impacts
SNL 2007. *Cladding Degradation Summary for LA*. [DIRS 180616]	Table 7-2[a]	The TSPA assumes that all fuel cladding will be breached at the time of its emplacement in the repository
SNL 2007. *Total System Performance Assessment Data Input Package for Requirements Analysis for EBS In-Drift Configuration*. [DIRS 179354]	Table 4-1, Parameter Number 03-24	Prior to closure (prior to installation of drip shield), waste packages that have come into contact with fallen rock will be inspected to ensure that any damage to the waste package outer corrosion barrier is within acceptable limits
	Table 4-1, Parameter Numbers 01-15, 01-16, and 01-17	Ground support system will be installed in emplacement drifts to facilitate repository operations
	Table 4-1, Parameter Number 01-15	Ground support structure will be fabricated of stainless steel for longevity
SNL 2007. *Stress Corrosion Cracking of Waste Package Outer Barrier and Drip Shield Materials*. [DIRS 181953]	Section 6.8.5.2	Tightness of stress corrosion cracks in passive alloys such as Titanium Grade 7 and their tortuosity will limit the advection of liquids and solids through cracks
SNL 2007. *Total System Performance Assessment Data Input Package for Requirements Analysis for Subsurface Facilities*. [DIRS 179466]	Table 4-1, Parameter Numbers 01-09 and 01-10	All emplacement drift areas will be circular in cross-section and excavated with a tunnel boring machine

Table 2.1.07.01.0A-2. Indirect Inputs

Citation	Title	DIRS
10 CFR 63	Energy: Disposal of High-Level Radioactive Wastes in a Geologic Repository at Yucca Mountain, Nevada	180319
70 FR 53313	Implementation of a Dose Standard After 10,000 Years	178394
BSC 2004	*Drift Degradation Analysis*	166107
BSC 2004	*Multiple Rock Fall on Drip Shield*	171756
SNL 2007	*Mechanical Assessment of Degraded Waste Packages and Drip Shields Subject to Vibratory Ground Motion*	178851
SNL 2007	*Stress Corrosion Cracking of Waste Package Outer Barrier and Drip Shield Materials*	181953
SNL 2007	*Total System Performance Assessment Data Input Package for Requirements Analysis for Subsurface Facilities*	179466
SNL 2008	*Postclosure Analysis of the Range of Design Thermal Loadings*	179962

FEP: 2.1.07.02.0A

FEP NAME:

Drift Collapse

FEP DESCRIPTION:

Partial or complete collapse of the drifts, as opposed to discrete rockfall, could occur as a result of thermal effects, stresses related to excavation, or other mechanisms. Drift collapse could affect the stability of the engineered barriers and waste packages and/or result in static loading from rock overburden. Rockfalls of small blocks may produce rubble throughout part or all of the drifts. Seismic-induced drift collapse is addressed in a separate FEP.

SCREENING DECISION:

Excluded – low consequence

SCREENING JUSTIFICATION:

This FEP addresses nominal drift collapse effects. *Drift Degradation Analysis* (BSC 2004 [DIRS 166107]) provides analysis of drift degradation for both nonlithophysal and lithophysal rock. A summary of the analysis and results of the analysis are given in Section 8.1 of that report (BSC 2004 [DIRS 166107]). Section 6.3 of *Drift Degradation Analysis* (BSC 2004 [DIRS 166107]) provides a nonlithophysal rockfall model developed using the three-dimensional discontinuum code 3DEC, while Section 6.4 of that report (BSC 2004 [DIRS 166107]) provides a lithophysal rockfall model developed using the two-dimensional discontinuum code UDEC. The lithophysal rockfall model allows for the formation of stress-induced fractures between blocks (i.e., the formation of internal fracturing), and separation and instability (resulting from gravitational stresses, excavation-induced stresses, thermally induced stresses, and time-dependent strength degradation) of the rock mass around the drift (BSC 2004 [DIRS 166107], Section 6.4.2.1). In both models, appropriate thermal and mechanical properties of rock blocks and joints are used.

Seismic-induced drift collapse damage is addressed in included FEP 1.2.03.02.0C (Seismic Induced Drift Collapse Damages EBS Components), and seismic-induced drift collapse effects on thermal-hydrologic processes are addressed in included FEP 1.2.03.02.0D (Seismic-Induced Drift Collapse Alters In-Drift Thermohydrology). Seismic-induced drift collapse effects on seepage are discussed in excluded FEP 2.1.03.10.0B (Advection of Liquids and Solids through Cracks in the Drip Shield). Although seismic-induced drift collapse may alter in-drift chemistry as discussed in excluded FEP 1.2.03.02.0E (Seismic-Induced Drift Collapse Alters In-Drift Chemistry), this potential alteration is excluded on the basis of low consequence.

Thermally induced stresses at any location depend on the proximity and timing of waste emplacement, the amount of heat generated, the age of the waste, packaging and emplacement configuration, and the thermal-mechanical properties of the rock mass. Thermal stresses are time-dependent and are calculated over the first 10,000 years after repository closure (BSC 2004 [DIRS 166107], Section 6.2). Note that there is a 200°C drift wall temperature limit imposed

during the repository postclosure period (SNL 2007 [DIRS 179466], Table 4-2, Parameter Number 06-02). The drift wall temperature limit will confine the extent of permanent changes in rock characteristics that could impact drift opening stability. It is noted that drift wall temperatures of 200°C and rock mass temperatures greater than 250°C were achieved in the Drift Scale Test with only minor effects observed (SNL 2008 [DIRS 179962], Section 6.1.1). Furthermore, analyses documented in *Postclosure Analysis of the Range of Design Thermal Loadings* (SNL 2008 [DIRS 179962], Section 7.1) indicate that the anticipated range of thermal loading will result in peak postclosure drift wall temperatures significantly less than 200°C.

The rock mass surrounding the emplacement drifts may undergo over-stressing from thermal heating or time-dependent damage associated with static fatigue resulting from stress corrosion mechanisms. This damaged material may result in a slow unraveling (lithophysal rock) or block fallout (nonlithophysal rock). In the nonlithophysal rocks, static fatigue failure of asperities along fracture surfaces is possible and could result in gravitationally induced block failures. Fatigue failure would presumably initiate along asperities on fracture surfaces, reducing the effective friction angle along the fracture surfaces (BSC 2004 [DIRS 166107], Section 6.3.1.5). In the case of the lithophysal rocks, the uniaxial compressive elastic stressalong the immediate rib springline of the emplacement drifts is estimated to be 17.5 MPa (BSC 2004 [DIRS 166107], Section S2.2.5) and will be at or near the unconfined compressive strength of about 20 MPa (BSC 2004 [DIRS 166107], Table 6-41, Category 3), so static fatigue failure is possible. The analyses of the available static-fatigue test data indicate that an approximate 40% reduction in cohesive strength occurs over a 20,000-year period (BSC 2004 [DIRS 166107], Appendix S, Section S3.4.1). To model the lithophysal rock mass, a range of rock mass strength properties were considered, represented as rock mass strength categories 1 through 5 (BSC 2004 [DIRS 166107], Section 6.4.1.2). Depending on the rock mass strength category, varying degrees of drift collapse can be expected in the lithophysal rock resulting from in situ conditions of gravitational stresses, excavation-induced stresses, thermally induced stresses, and time-dependent strength degradation of the rock mass. However, the rock block sizes are predicted to be small (i.e., only a few centimeters to decimeters on a side) due to the ubiquitous fracture fabric found in the lithophysal rock (BSC 2004 [DIRS 166107], Sections 6.1.4.1 and 8.1).

In the calculations relating to rockfall in *Drift Degradation Analysis* (BSC 2004 [DIRS 166107], Section 6), the potential for drift stability afforded by ground control systems is conservatively not considered. This is a reasonably bounding approach that simplifies the modeling, while increasing the extent of predicted drift degradation. As indicated in *Total System Performance Assessment Data Input Package for Requirements Analysis for Engineered Barrier System In-Drift Configuration* (SNL 2007 [DIRS 179354], Table 4-1, Parameter Number 01-17), a ground support system will be installed in the emplacement drifts to facilitate repository operations. The ground support structure will be fabricated of stainless steel for longevity (SNL 2007 [DIRS 179354], Table 4-1, Parameter Number 01-15). The potential effects of ground support material on engineered barrier system components are addressed in excluded FEPs 2.1.06.01.0A (Chemical Effects of Rock Reinforcement and Cementitious Materials in EBS) and 2.1.06.02.0A (Mechanical Effects of Rock Reinforcement Materials in EBS).

Analyses presented in *Drift Degradation Analysis* (BSC 2004 [DIRS 166107], Sections 6.3 and 6.4) show that, for the base case thermal conditions, thermal stresses result in a thin yield zone

around the drifts for all cases of lithophysal and nonlithophysal rock strength, including accouting for time-dependent rock strength degradation. The nominal case for drift degradation (i.e., considering thermal and time-dependent effects, but excluding seismic effects) for both nonlithophysal and lithophysal rock results in only partial collapse of the drift (such that collapsed rock blocks do not cover the drip shield) for the first 10,000-year period of postclosure performance (BSC 2004 [DIRS 166107], Sections 6.3.1.3, 6.4.2.4.2.6, and 8.1).

Drift Degradation Analysis (BSC 2004 [DIRS 166107]) reports analyses of rockfall in the lithophysal and nonlithophysal units that provide time history of "expected" rockfall due to ongoing degradation of the drift. Furthermore, based on other analyses presented in that report (BSC 2004 [DIRS 166107], Sections 6.3 and 6.4), only minor degradation or partial collapse of the drift (including enlargement) will occur for the static (i.e., non-seismic) loading case, such that rubble settles around the sides of the drip shield and does not accumulate on the crown of the drip shield. The structural response calculations for an intact drip shield provide a reasonable representation of the potential for damage to the drip shield plates during the first 10,000 years after repository closure. The mean corrosion rate for Titanium Grade 7 under benign conditions, 5.15 nm/yr (SNL 2007 [DIRS 180778], Table 8-1[a]), is appropriate for the underside of the drip shield plates. The mean corrosion rate for Titanium Grade 7 under aggressive conditions, 46.1 nm/yr (SNL 2007 [DIRS 180778], Table 8-1[a]), is appropriate for the top side of the drip shield plates. The mean thickness reduction from double-sided corrosion during 10,000 years is given by (10,000 years) (5.15×10^{-9} m/yr + 46.1×10^{-9} m/yr) = 5.1×10^{-4} m = 0.51 mm, which is a small fraction of the initial plate thickness of 15 mm (SNL 2007 [DIRS 179354], Table 4-2, Parameter Number 07-04). It follows that the results in *Seismic Consequence Abstraction* (SNL 2007 [DIRS 176828], Sections 6.8.2 and 6.8.3) for the 15-mm-thick plate, with no thickness reduction, are applicable to the first 10,000 years after closure. The results from drip shield fragility analyses show that for seismic ground motion with a peak ground velocity of 1.05 m/s or less, and considering partial drift collapse with 50% rockfall load, the probability of drip shield failure is zero for the 15 mm thick plate and the intact framework (SNL 2007 [DIRS 176828], Tables 6-36 and 6-40). This seismic ground motion case, which considers nonuniform drip shield loads from a partially filled drift (SNL 2007 [DIRS 176828], Sections 6.8.2 and 6.8.3), provides an upper bound for the static load case. Therefore, it follows that the probability of drip shield failure is also zero for static loads.

Seepage analyses for degraded drifts that consider minor drift damage consistent with the static loading case show that there are no impacts to seepage, and therefore the magnitude of drift seepage for the nominal case (considering thermally induced stresses and time-dependent strength degradation of the rock mass) is determined using non-degraded drifts (SNL 2007 [DIRS 181244], Sections 6.4.2.4.2 and 8.1). To account for uncertainty in seepage simulation results and impacts of minor drift degredation, the intact drift seepage is increased by 20% (SNL 2007 [DIRS 181244], Section 6.2.4[a]). Minor drift damage associated with the static loading case will not significantly impact or alter the existing thermal conditions in the drift.

Thus, drift collapse under nominal (static) loading conditions will not have a significant effect on long-term performance of the repository.

Based on the previous discussion, omission of FEP 2.1.07.02.0A (Drift Collapse) will not result in a significant adverse change in the magnitude or timing of either radiological exposure to the

RMEI or radionuclide releases to the accessible environment. Therefore, this FEP is excluded from the performance assessments conducted to demonstrate compliance with proposed 10 CFR 63.311 and 63.321 (70 FR 53313 [DIRS 178394]), and with 10 CFR 63.331 [DIRS 180319], on the basis of low consequence.

INPUTS:

Table 2.1.07.02.0A-1. Direct Inputs

Input	Source	Description
BSC 2004. *Drift Degradation Analysis*. [DIRS 166107]	Sections 6.3 and 6.4	Analyses show that, for the base case thermal conditions, thermal stresses result in a thin yield zone around the drifts for all cases of lithophysal and nonlithophysal rock strength, including accounting for time-dependent rock strength degradation
	Section S2.2.5	Compressive stress concentrations along immediate rib springline of emplacement drifts are estimated in lithophysal rocks
	Section 6.3.1.5	Fatigue failure would presumably initiate along asperities on fracture surfaces, reducing the effective friction angle along the fracture surfaces
	Section 6.4.2.1	Lithophysal rockfall model allows formation of stress-induced fractures between blocks and separation and instability of rock mass around drift
	Sections 6.3 and 6.4	Minor degradation or collapse of drift will occur for the static loading case, such that rubble settles around the sides of the drip shield and does not accumulate on the crown of the drip shield
	Sections 6.3.1.3, 6.4.2.4.2.6, and 8.1	Nominal case for drift degradation results in partial collapse of drift for first 10,000-year period of postclosure performance
	Sections 6.1.4.1 and 8.1	The rock block sizes are predicted to be small (i.e., only a few centimeters to decimeters on a side) due to the ubiquitous fracture fabric found in the lithophysal rock
	Section 6.2	Thermal stresses are time-dependent and are calculated over the first 10,000 years after repository closure
	Appendix S, Section S3.4.1	Analyses of available static-fatigue test data
	Section 6.4.1.2	To model the lithophysal rock mass, a range of rock mass strength properties were considered, represented as rock mass strength categories 1 through 5
	Table 6-41, Category 3	Compressive stress will be at or near the uniaxial compressive strength

Table 2.1.07.02.0A-1. Direct Inputs (Continued)

Input	Source	Description
SNL 2007. *Seismic Consequence Abstraction*. [DIRS 176828]	Sections 6.8.2 and 6.8.3	Results of structural response calculations for an intact drip shield
	Tables 6-36 and 6-40	The results from drip shield fragility analyses show that for seismic ground motion with a peak ground velocity of 1.05 m/s or less, and considering partial drift collapse with 50% rockfall load, the probability of drip shield failure is zero for the 15-mm-thick plate and the intact framework
	Sections 6.8.2 and 6.8.3	The consideration of non-uniform drip shield loads from a partially filled drift
SNL 2007. *Total System Performance Assessment Data Input Package for Requirements Analysis for EBS In-Drift Configuration*. [DIRS 179354]	Table 4-2, Parameter Number 07-04	The drip shield initial plate thickness is 15 mm
	Table 4-1, Parameter Number 01-15	Ground support structure will be fabricated of stainless steel
	Table 4-1, Parameter Number 01-17	Ground support system will be installed in emplacement drifts to facilitate repository operations
SNL 2007. *Abstraction of Drift Seepage*. [DIRS 181244]	Sections 6.4.2.4.2 and 8.1	Seepage analyses for degraded drifts that consider minor drift damage consistent with the static loading case show that there are no impacts to seepage, and therefore the magnitude of drift seepage for the nominal case (considering thermally induced stresses and time-dependent strength degradation of the rock mass) is determined using non-degraded drifts
	Section 6.2.4[a]	To account for uncertainty in seepage simulation results and impacts of minor drift degredation, the intact drift seepage is increased by 20%
SNL 2007. *General Corrosion and Localized Corrosion of the Drip Shield*. [DIRS 180778]	Table 8-1[a]	The mean corrosion rate for Titanium Grade 7 under both benign and aggressive conditions

Table 2.1.07.02.0A-2. Indirect Inputs

Citation	Title	DIRS
10 CFR 63	Energy: Disposal of High-Level Radioactive Wastes in a Geologic Repository at Yucca Mountain, Nevada	180319
70 FR 53313	Implementation of a Dose Standard After 10,000 Years	178394
BSC 2004	*Drift Degradation Analysis*	166107
SNL 2007	*Total System Performance Assessment Data Input Package for Requirements Analysis for Subsurface Facilities*	179466
SNL 2008	*Postclosure Analysis of the Range of Design Thermal Loadings*	179962

FEP: 2.1.07.04.0A

FEP NAME:

Hydrostatic Pressure on Waste Package

FEP DESCRIPTION:

Waste packages emplaced in the saturated zone will be subjected to hydrostatic pressure in addition to stresses associated with the evolution of the waste and EBS.

SCREENING DECISION:

Excluded – low probability

SCREENING JUSTIFICATION:

Waste packages will be emplaced in the repository (located in the unsaturated zone), under atmospheric pressure, and will lie, on average, approximately 300 m above the present-day water table. The elevation of the repository will range from 1,039 to 1,107 m (SNL 2007 [DIRS 179466], Table 4-1, Parameter Number 01-01), while the measured water table elevation under the repository for present-day conditions varies from approximately 730 m to 850 m (BSC 2004 [DIRS 169855], Figure 6-2). Modeling (SNL 2007 [DIRS 177391], Figure 6-20) shows that water table elevation below the repository is expected to remain lower than 900 m. This is corroborated by Forester et al. (1999 [DIRS 109425], p. 57), who show that the historical water table (over a duration of approximately 500,000 years) has never risen to the level of the repository. Further corroboration is obtained by studies of mineralogic alteration (zeolitization and tridymite distribution) in the unsaturated zone at Yucca Mountain that place an upper limit of past water table rise below 60 m above its present position in the geologic past (Levy 1991 [DIRS 100053], p. 477); and by analysis of $^{87}Sr/^{86}Sr$ ratios in calcite veins of the unsaturated zone and saturated zone at Yucca Mountain indicating an upper limit of past water table rise below 85 m above the present level (Marshall et al. 1993 [DIRS 101142], p. 1,948). These studies, covering a historic time span of over 1 million years, include the effects of glacial climates, and future monsoon and glacial-transition climates are expected to be warmer and dryer than the glacial climate (Sharpe 2003 [DIRS 161591]). Hence, even under the extreme future climate conditions, the water table would not reach the repository horizon.

Water also occurs under fully saturated conditions as perched bodies in the unsaturated zone below the repository horizon. As shown in *UZ Flow Models and Submodels* (SNL 2007 [DIRS 184614], Section 6.2; DTNs: LB06123DPDUZFF.001 [DIRS 178587], GS031208312232.003 [DIRS 171287], GS031208312232.005 [DIRS 179284], and GS040108312312.001 [DIRS 181234]), even for high infiltration rates corresponding to future wetter climate scenarios of monsoon and glacial transition, the simulated extent and location of perched water is still consistent with observed moisture saturation and water potential. The elevation of the perched water is insensitive to the changes in infiltration rates corresponding to future wetter climates (SNL 2007 [DIRS 184614], Appendix D). Hence, even under the extreme wetter future climate conditions, the perched water bodies would not reach the repository horizon.

In conclusion, FEP 2.1.07.04.0A (Hydrostatic Pressure on Waste Package) can be excluded on the basis of low probability because the repository is designed such that waste will be emplaced within the unsaturated zone well above the water table, and it is very unlikely that the water table will rise to the level of the repository. Therefore, this FEP is excluded from the performance assessments conducted to demonstrate compliance with proposed 10 CFR 63.311 and 63.321 (70 FR 53313 [DIRS 178394]), and with 10 CFR 63.331 [DIRS 180319], on the basis of low probability.

INPUTS:

Table 2.1.07.04.0A-1. Direct Inputs

Input	Source	Description
BSC 2004. *Development of Numerical Grids for UZ Flow and Transport Modeling*. [DIRS 169855]	Figure 6-2	Water table elevation under the repository
DTN: GS040108312312.001. Water-Level, Discharge Rate and Related Data from the Pump Tests Conducted at Well USW UZ-14, August 12 through August 30, 1993. [DIRS 181234]	file: *Water level measurements.xls*	Water potential data from boreholes in the unsaturated zone
DTN: GS031208312232.003. Deep Unsaturated Zone Surface-Based Borehole Instrumentation Program Data from Boreholes USW NRG-7A, UE-25 UZ #4, USW NRG-6, UE-25 UZ #5, USW UZ-7A and USW SD-12 for the Time Period 10/01/97 - 03/31/98. [DIRS 171287]	file: *WATERPOT.txt*	Borehole testing data: water potentials
DTN: GS031208312232.005. Deep Unsaturated Zone Surface-Based Borehole Instrumentation Program Data from Boreholes USW NRG-7A, UE-25 UZ#4, UE-25 UZ#5, USW UZ-7A and USW SD-12 for the Time Period 1/1/97 - 6/30/97. [DIRS 179284]	file: *WATERPOT.txt*	Measured borehole data: water potentials
SNL 2007. *Saturated Zone Site-Scale Flow Model*. [DIRS 177391]	Figure 6-20	Water table elevation below the repository is expected to remain lower than 900 m
SNL 2007. *Total System Performance Assessment Data Input Package for Requirements Analysis for Subsurface Facilities*. [DIRS 179466]	Table 4-1, Parameter Number 01-01	Repository elevation
SNL 2007. *UZ Flow Models and Submodels*. [DIRS 184614]	Section 6.2	Water also occurs under fully saturated conditions as perched bodies

Table 2.1.07.04.0A-2. Indirect Inputs

Citation	Title	DIRS
70 FR 53313	Implementation of a Dose Standard After 10,000 Years	178394
Forester et al. 1999	*The Climatic and Hydrologic History of Southern Nevada During the Late Quaternary*	109425
Levy 1991	"Mineralogic Alteration History and Paleohydrology at Yucca Mountain, Nevada"	100053
Marshall et al. 1993	"Strontium Isotopic Evidence for a Higher Water Table at Yucca Mountain"	101142
Sharpe 2003	*Future Climate Analysis—10,000 Years to 1,000,000 Years After Present*	161591
SNL 2007	*UZ Flow Models and Submodels*	184614

FEP: 2.1.07.04.0B

FEP NAME:

Hydrostatic Pressure on Drip Shield

FEP DESCRIPTION:

Drip shields emplaced in the saturated zone will be subjected to hydrostatic pressure in addition to stresses associated with the evolution of the waste and EBS.

SCREENING DECISION:

Excluded – low probability

SCREENING JUSTIFICATION:

Drip shields will be emplaced in the repository (located in the unsaturated zone), under atmospheric pressure, and will lie, on average, approximately 300 m above the present-day water table. The elevation of the repository will range from 1,039 to 1,107 m (SNL 2007 [DIRS 179466], Table 4-1, Parameter Number 01-01), while the measured water table elevation under the repository for present-day conditions varies from approximately 730 m to 850 m (BSC 2004 [DIRS 169855], Figure 6-2). Modeling (SNL 2007 [DIRS 177391], Figure 6-20) shows that water table elevation below the repository is expected to remain lower than 900 m. This is corroborated by Forester et al. (1999 [DIRS 109425], p. 57), who show that the historical water table (over a duration of approximately 500,000 years) has never risen to the level of the repository. Further corroboration is obtained by studies of mineralogic alteration (zeolitization and tridymite distribution) in the unsaturated zone at Yucca Mountain that place an upper limit of past water table rise below 60 m above its present position in the geologic past (Levy 1991 [DIRS 100053], p. 477); and by analysis of $^{87}Sr/^{86}Sr$ ratios in calcite veins of the unsaturated zone and saturated zone at Yucca Mountain indicating an upper limit of past water table rise below 85 m above the present level (Marshall et al. 1993 [DIRS 101142], p. 1,948). These studies, covering a historic time span of over 1 million years, include the effects of glacial climates, and future monsoon and glacial-transition climates are expected to be warmer and dryer than the glacial climate (Sharpe 2003 [DIRS 161591]). Hence, even under the extreme future climate conditions, the water table would not reach the repository horizon.

Water also occurs under fully saturated conditions as perched bodies in the unsaturated zone below the repository horizon. As shown in *UZ Flow Models and Submodels* (SNL 2007 [DIRS 184614], Section 6.2), DTNs: LB06123DPDUZFF.001 [DIRS 178587], GS031208312232.003 [DIRS 171287], GS031208312232.005 [DIRS 179284], and GS040108312312.001 [DIRS 181234]), even for high infiltration rates corresponding to future wetter climate scenarios of monsoon and glacial transition, the simulated extent and location of perched water is still consistent with observed moisture saturation and water potential. The elevation of the perched water is insensitive to the changes in infiltration rates corresponding to future wetter climates (SNL 2007 [DIRS 184614], Appendix D). Hence, even under the extreme wetter future climate conditions, the perched water bodies would not reach the repository horizon.

In conclusion, FEP 2.1.07.04.0B (Hydrostatic Pressure on Drip Shield) can be excluded on the basis of low probability because the repository is designed such that drip shields will be emplaced within the unsaturated zone well above the water table, and it is very unlikely that the water table will rise to the level of the repository. Therefore, this FEP is excluded from the performance assessments conducted to demonstrate compliance with proposed 10 CFR 63.311 and 63.321 (70 FR 53313 [DIRS 178394]), and with 10 CFR 63.331 [DIRS 180319], on the basis of low probability.

INPUTS:

Table 2.1.07.04.0B-1. Direct Inputs

Input	Source	Description
BSC 2004. *Development of Numerical Grids for UZ Flow and Transport Modeling*. [DIRS 169855]	Figure 6-2	Water table elevation under the repository
DTN: GS040108312312.001. Water-Level, Discharge Rate and Related Data from the Pump Tests Conducted at Well USW UZ-14, August 12 through August 30, 1993. [DIRS 181234]	file: *Water level measurements.xls*	Water potential data from boreholes in the unsaturated zone
DTN: GS031208312232.003. Deep Unsaturated Zone Surface-Based Borehole Instrumentation Program Data from Boreholes USW NRG-7A, UE-25 UZ #4, USW NRG-6, UE-25 UZ #5, USW UZ-7A and USW SD-12 for the Time Period 10/01/97 - 03/31/98. [DIRS 171287]	file: *WATERPOT.txt*	Borehole testing data: water potentials
DTN: GS031208312232.005. Deep Unsaturated Zone Surface-Based Borehole Instrumentation Program Data from Boreholes USW NRG-7A, UE-25 UZ#4, UE-25 UZ#5, USW UZ-7A and USW SD-12 for the Time Period 1/1/97 - 6/30/97. [DIRS 179284]	file: *WATERPOT.txt*	Measured borehole data: water potentials
SNL 2007. *Saturated Zone Site-Scale Flow Model*. [DIRS 177391]	Figure 6-20	Water table elevation below the repository is expected to remain lower than 900 m
SNL 2007. *Total System Performance Assessment Data Input Package for Requirements Analysis for Subsurface Facilities*. [DIRS 179466]	Table 4-1, Parameter Number 01-01	Repository elevation
SNL 2007. *UZ Flow Models and Submodels*. [DIRS 184614]	Section 6.2	Water also occurs under fully saturated conditions as perched bodies

Table 2.1.07.04.0B-2. Indirect Inputs

Citation	Title	DIRS
70 FR 53313	Implementation of a Dose Standard After 10,000 Years	178394
Forester et al. 1999	*The Climatic and Hydrologic History of Southern Nevada During the Late Quaternary*	109425
Levy 1991	"Mineralogic Alteration History and Paleohydrology at Yucca Mountain, Nevada"	100053
Marshall et al. 1993	"Strontium Isotopic Evidence for a Higher Water Table at Yucca Mountain"	101142
Sharpe 2003	*Future Climate Analysis—10,000 Years to 1,000,000 Years After Present*	161591
SNL 2007	*UZ Flow Models and Submodels*	184614

FEP: 2.1.07.05.0A

FEP NAME:

Creep of Metallic Materials in the Waste Package

FEP DESCRIPTION:

Metals used in the waste package may deform by creep processes in response to deviatoric stress or internal void space.

SCREENING DECISION:

Excluded – low consequence

SCREENING JUSTIFICATION:

Creep of metallic materials in the waste package in response to deviatoric stress or internal void space is a function of temperature. A reasonable peak waste package surface temperature is 300°C. This peak temperature bounds all repository-relevant thermal exposure conditions (SNL 2008 [DIRS 184433], Figure 6.3-76[a]) except in the event of a drift collapse within approximately 90 years following closure (SNL 2008 [DIRS 184433], Figure 6.3-82[a]). For the waste package surface to exceed 300°C, a seismic event of sufficient magnitude must occur within approximately 90 years after closure, result in drift collapse and affect a waste package with an unfavorable combination of a high thermal output surrounded by a low conductivity rubble (SNL 2008 [DIRS 179962], Section 6.5.1). Analyses have shown that the mean probability of these conditions occurring is about one in 10,000 within the first 10,000 years after closure (SNL 2008 [DIRS 179962], Section 6.5.1). Adverse elevated-temperature responses of nickel-based alloys (i.e., creep deformation or creep fracture) are not expected for temperatures below 650°C (Boyer and Gall 1984 [DIRS 155318], Section 32). Although no directly relevant data exist for creep rupture (fracture) of Alloy 22 in this temperature regime, available Alloy 22 1,000-hour creep rupture data at 760°C and above indicate that the creep strength is high and would be expected to increase with decreasing temperature (BSC 2005 [DIRS 173802], Figure 2). Also, the melting point of Alloy 22 is approximately 1,370°C (1,643 K) (Haynes International 1997 [DIRS 100896], p. 13) and the maximum waste package surface temperature (less than 300°C or 573 K) represents a homologous temperature of approximately 0.35. Creep of metallic alloys is generally anticipated only for homologous temperatures of 0.5 or greater (Boyer and Gall 1984 [DIRS 155318]). Therefore, creep of WPOB at low temperatures (e.g., less than 300°C) is not expected, and this process will have no impact on the performance of the waste package. This treatment of creep of metallic materials in the waste package applies to all waste packages.

External stress, induced by rock displacements or ground motion, for example, may lead to plastic deformations and mechanical damage of the waste package. The drip shield is designed to protect the waste package during rockfall and ground motion events. Even if mechanical damage of the waste package were to occur, creep of metallic materials in the waste package will not occur unless an external factor raises the temperature of the waste package surface above 650°C (Boyer and Gall [DIRS 155318], Section 32) and will therefore have no impact on the

performance of the waste package. Based on the previous discussion, omission of, FEP 2.1.07.05.0A (Creep of Metallic Materials in the Waste Package) will not affect the magnitude or timing of calculated radiological exposures to the RMEI or radionuclide releases to the accessible environment. Therefore, this FEP is excluded from the performance assessments conducted to demonstrate compliance with proposed 10 CFR 63.311 and 63.321 (70 FR 53313 [DIRS 178394]), and with 10 CFR 63.331 [DIRS 180319], on the basis of low consequence.

INPUTS:

Table 2.1.07.05.0A-1. Direct Inputs

Input	Source	Description
Boyer and Gall 1984. *Metals Handbook*. [DIRS 155318]	Section 32	Temperature data expectations for creep of metallic alloys
SNL 2008. *Multiscale Thermohydrologic Model*. [DIRS 184433]	Figure 6.3-76[a]	A reasonable peak waste package surface temperature is 300°C. This peak temperature bounds all repository-relevant thermal exposure conditions
	Figure 6.3-82[a]	Maximum temperature that would be expected at the outer barrier surface of an emplaced waste package
SNL 2008. *Postclosure Analysis of the Range of Design Thermal Loadings*. [DIRS 179962]	Section 6.5.1	The mean probability of the waste package surface exceeding 300°C is about one in 10,000 within the first 10,000 years after closure

Table 2.1.07.05.0A-2. Indirect Inputs

Citation	Title	DIRS
10 CFR 63	Energy: Disposal of High-Level Radioactive Wastes in a Geologic Repository at Yucca Mountain, Nevada	180319
70 FR 53313	Implementation of a Dose Standard After 10,000 Years	178394
BSC 2005	*Waste Package Damage Due to Interaction with Magma*	173802
Haynes International 1997	*Hastelloy C-22 Alloy*	100896

FEP: 2.1.07.05.0B

FEP NAME:

Creep of Metallic Materials in the Drip Shield

FEP DESCRIPTION:

Metals used in the drip shield may deform by creep processes in response to deviatoric stress.

SCREENING DECISION:

Excluded – low consequence

SCREENING JUSTIFICATION:

The drip shield can be subjected to plastic deformation and mechanical damage due to stresses resulting from static and dynamic load resulting from rockfall or from vibratory ground motion. Mechanical damage of the drip shield by rockfall is discussed in excluded FEP 2.1.07.01.0A (Rockfall). Mechanical damage of the drip shield during seismic events is discussed in excluded FEP 1.2.03.02.0B (Seismic Induced Rockfall Damages EBS Components), and included FEPs 1.2.03.02.0A (Seismic Ground Motion Damages EBS Components) and 1.2.03.02.0C (Seismic-Induced Drift Collapse Damages EBS Components). Thus, this FEP only addresses creep of the metallic materials of the drip shield in response to static loads, which is temperature dependent. Due to the long duration of the regulatory period and the possibility of early drift collapse after the waste emplacement, it is important to analyze time-dependent deformation and the stability of the drip shield when non-uniformly loaded by the rock rubble mass.

Plastic deformation and mechanical damage of the drip shield are expected to be enhanced at elevated temperatures due to the combined effect of thermal and mechanical stresses. Without drift collapse, the waste package temperature will be below 300°C (SNL 2008 [DIRS 184433], Figure 6.3-76[a]). Due to greater distance of the drip shield from the heat source (i.e., the waste form) than the waste package, surface temperatures of the drip shields will be lower than those for the waste packages. For the waste package surface to exceed 300°C, a seismic event of sufficient magnitude must occur within approximately 90 years after closure, result in drift collapse, and affect a waste package with an unfavorable combination of a high thermal output surrounded by a low conductivity rubble (SNL 2008 [DIRS 179962], Section 6.5.1). Analyses have shown that the mean probability of these conditions occurring is about one in 10,000 within the first 10,000 years after closure (SNL 2008 [DIRS 179962], Section 6.5.1). Therefore, a reasonably bounding drip shield exposure temperature in the repository is 300°C and is used in the analysis of creep of metallic materials in the drip shield.

A review of scientific literature (Dutton 1995 [DIRS 173919], p. 8; Dutton 1996 [DIRS 174750], Section 2) reveals that Titanium Grades 7 and 29 can undergo creep deformation at temperatures as low as room temperature when subject to tensile stresses exceeding approximately 50% of the yield strength. Therefore, one of the important impediments to drip shield performance during the period of 10,000 years after closure is potential creep deformation under long-term applied loads. With the exception of the stresses imposed on the drip shield due to its own weight

(which represent a small fraction of the stress which the drip shield is designed to endure), the only long-term load on the drip shield could be due to pressure (weight) of the rock rubble mass that would cover the drip shield following collapse (degradation) of the emplacement drift. This can occur in cases of strong ground motions (e.g., ground motions with a peak ground velocity greater than about 2 m/s in lithophysal rock mass – an event with a mean annual exceedance frequency of ~8.8×10^{-7} per year (SNL 2007 [DIRS 176828], Table 6-3)) or as a result of time-dependent rock mass strength degradation (BSC 2004 [DIRS 166107], Section 6.4.2). Analyses presented in *Drift Degradation Analysis* (BSC 2004 [DIRS 166107], Attachment S, Section S3.4.2, Figures S-42 to S-44) suggest that total collapse of the emplacement drifts due to time-dependent strength degradation alone is not expected in the first 10,000 years. The load of the rock rubble resting on the drip shield structure is a consequence of the interaction between the structure and the surrounding rock rubble. The initial loads on the drip shield are calculated accounting for that interaction, and analysis of the drip shield stability for short-term loading conditions shows that the drip shield will be stable with a relatively large margin of safety (BSC 2004 [DIRS 169753], Section 5.4.3.2). Because of the long duration of the regulatory period and the possibility of early drift collapse after the waste emplacement, it is important to analyze time-dependent deformation and the stability of the drip shield non-uniformly loaded by the rock rubble mass. Such an analysis has been performed using creep equations that bound available literature and YMP-generated low-temperature creep results for both Titanium Grade 7 and the higher strength Titanium Grade 24 (or their analogues, Titanium Grades 2 and 5, respectively) over the range of temperatures and stresses of most interest (in BSC 2005 [DIRS 174715]). Titanium Grade 24 is similar to Titanium Grade 29 in that they are both platinum group metal-containing versions of Titanium Grade 5.

The initial loading of the rubble on the drip shield was derived from a series of realizations of discontinuum numerical analyses of complete drift collapse (BSC 2004 [DIRS 166107], Section 6.4). It should be noted that the rockfall estimates presented in the aforementioned document overestimate the actual extent of rockfall as the effect of ground support (which will serve to prevent rockfall), is not included in that analysis. These analyses showed the rubble loading to be highly non-uniform in nature. The non-uniform loads around the drip shield derived from these analyses were used as direct input to the creep analysis. Creep strain as a function of time in titanium and other metals follows three distinct stages—an initial, transient stage of primary creep; secondary or steady-state creep, which occurs at a relatively uniform rate; and tertiary creep, in which the creep strain rate rapidly accelerates until rupture occurs. In the creep analyses of the drip shield, the primary and secondary creep were simulated using a creep power law expression derived from a literature review of laboratory tensile creep tests on various grades of titanium (BSC 2005 [DIRS 174715], Section 5.6). Tertiary creep was not explicitly simulated because this is the point of rapid creep acceleration. When the magnitude of the creep strain at any point within the structure was equivalent to the onset of tertiary creep, it is assumed that the drip shield has failed. Based upon the literature, tertiary creep of Titanium Grades 7 and 24 (or analogous alloys such as Titanium Grade 29) could occur at creep strains of approximately 15% (Dutton 1996 [DIRS 174750], Section 5.1).

The drip shield creep analysis (BSC 2005 [DIRS 174715], Section 5.6) considered six rock rubble-loading scenarios derived from *Drift Degradation Analysis* (BSC 2004 [DIRS 166107], Section 6.4). These analyses applied the nonuniform rock rubble loading states, and assumed that the loads were constant with time (i.e., dead loads). Results of these analyses indicate that

the maximum resultant total creep strains remain below 5% during the 10,000-year period analyzed (BSC 2005 [DIRS 174715], Section 5.6). The maximum creep strains occur in the plates; the maximum creep strain in the support beams and the bulkheads are significantly less than that observed for the plate. These relatively low long-term strain levels, which are much less than the creep strains expected for the onset of tertiary creep, indicate that while some creep deformation may occur, it does not impact the drip shield seepage diversion function or the ability of the drip shield to protect the waste package from load (static or dynamic) by the rock overburden mass.

Based on the relatively low, structurally acceptable creep strains calculated for loading conditions more severe than those anticipated within Yucca Mountain both pre- and postclosure (BSC 2005 [DIRS 174715]), and the lack of potential resultant effects on dose, the effect of creep on the drip shield is negligible.

Based on the previous discussion, omission of FEP 2.1.07.05.0B (Creep of Metallic Materials in the Drip Shield) will not result in a significant adverse change in the magnitude or timing of either radiological exposure to the RMEI or radionuclide releases to the accessible environment. Therefore, this FEP is excluded from the performance assessments conducted to demonstrate compliance with proposed 10 CFR 63.311 and 63.321 (70 FR 53313 [DIRS 178394]), and with 10 CFR 63.331 [DIRS 180319], on the basis of low consequence.

INPUTS:

Table 2.1.07.05.0B-1. Direct Inputs

Input	Source	Description
BSC 2004. *Mechanical Assessment of the Drip Shield Subject to Vibratory Ground Motion and Dynamic and Static Rock Loading*. [DIRS 169753]	Section 5.4.3.2	Calculation of initial loads on drip shield
BSC 2005. *Creep Deformation of the Drip Shield*. [DIRS 174715]	Section 5.6	Anaysis of drip shield creep
SNL 2008. *Multiscale Thermohydrologic Model*. [DIRS 184433]	Figure 6.3-76[a]	Maximum waste package surface temperature will be less than 300°C

Table 2.1.07.05.0B-2. Indirect Inputs

Citation	Title	DIRS
10 CFR 63	Energy: Disposal of High-Level Radioactive Wastes in a Geologic Repository at Yucca Mountain, Nevada	180319
70 FR 53313	Implementation of a Dose Standard After 10,000 Years	178394
BSC 2004	*Drift Degradation Analysis*	166107
BSC 2005	*Creep Deformation of the Drip Shield*	174715
Dutton 1995	*A Methodology to Analyze the Creep Behaviour of Nuclear Fuel Waste Containers*	173919
Dutton 1996	*A Review of the Low-Temperature Creep Behaviour of Titanium*	174750
SNL 2007	*Seismic Consequence Abstraction*	176828
SNL 2008	*Postclosure Analysis of the Range of Design Thermal Loadings*	179962

FEP: 2.1.07.06.0A

FEP NAME:

Floor Buckling

FEP DESCRIPTION:

Buckling, or heave, of the drift floor may occur in response to changing stress. Floor buckling may affect the performance of EBS components such as the drip shield, the invert, and the pallet. Effects may include movement of EBS components and changes in the topography of the surface of the drift floor and invert that may affect water flow.

SCREENING DECISION:

Excluded – low consequence

SCREENING JUSTIFICATION:

Consideration of floor buckling (or heave) is centered on thermal stressing and excavation stress unloading. Ground motion associated with seismic activity and fault displacement and the impacts on EBS components are addressed in included FEPs 1.2.03.02.0A (Seismic Ground Motion Damages EBS Components) and 1.2.02.03.0A (Fault Displacement Damages EBS Components).

Drift response during the first 10,000 years after repository closure has been analyzed considering in situ stresses, excavation-induced stresses, thermally induced stresses, and time-dependent rock strength degradation (BSC 2004 [DIRS 166107], Sections 6.3 and 6.4). Stresses sufficient to cause floor buckling did not occur in the drift degradation models, which included appropriate stress changes and rock properties for the repository horizon. Calculations have demonstrated that prior to repository closure, the vertical displacement of the floor due to in situ stress and thermal response will be less than 1 mm per 6 m of drift (BSC 2004 [DIRS 168889], Table 6.4-3).

According to the U.S. Army Corps of Engineers manual for the planning, design, and construction of tunnels and shafts in rock for civil works, floor buckling is most common under the following conditions (Department of Army 1997 [DIRS 183771], pp. 6-18 to 6-19):

- Weak, laminated, clay-grade rock conducive to swelling
- Tunnels with a flat floor
- High in situ horizontal stresses.

In contrast to these conditions, the repository site at Yucca Mountain is located within a densely welded tuff unit with the following conditions:

- The rock is divided into two broad categories: nonlithophysal and lithophysal welded tuffs. The nonlithophysal rocks are hard, strong, fine-grained and fractured volcanic rocks. The lithophysal rocks are composed of the same strong, hard matrix material, but

have porosity in the form of lithophysal cavities (BSC 2004 [DIRS 166107], Section 1.1). Clay is not a common mineral in the crystallized rocks of the repository host horizon, nor are clay minerals a volumetrically significant fracture-coating material (BSC 2004 [DIRS 166107], Section 6.3.1.5).

- The excavated opening of all emplacement drifts will be circular in cross-section (SNL 2007 [DIRS 179466], Table 4-1, Parameter Number 01-10).

- While in situ horizontal stresses are initially approximately half of the vertical stresses at the repository site (BSC 2004 [DIRS 166107], Section 6.3.1.1), temperature increases anticipated in the repository result in thermally induced stresses such that horizontal stresses will exceed vertical stresses within the first 1,000 years after repository closure (BSC 2004 [DIRS 166107], Section 6.2). However, the stress states around the emplacement drift are generally well below the yield strength of the rock mass (BSC 2004 [DIRS 166107], Section 6.4.2.3).

Because of the limited vertical displacement of the floor expected as a result of in situ and thermal stresses, drip shield displacement, pallet displacement, and damage to invert will be minor. The limited vertical displacement of the floor will result in an insignificant impact to water flow. Seismic-induced impacts to water flow are addressed in excluded FEP 1.2.10.01.0A (Hydrologic Response to Seismic Activity) and included FEP 1.2.03.02.0D (Seismic-Induced Drift Collapse Alters In-Drift Thermohydrology).

Based on the previous discussion, omission of FEP 2.1.07.06.0A (Floor Buckling) will not result in a significant adverse change in the magnitude or time of radiological exposures to the RMEI or radionuclide releases to the accessible environment. Therefore, this FEP is excluded from the performance assessments conducted to demonstrate compliance with proposed 10 CFR 63.311 and 63.321 (10 FR 53313 [DIRS 178394]), and with 10 CFR 63.331 [DIRS 180319], on the basis of low consequence.

INPUTS:

Table 2.1.07.06.0A-1. Direct Inputs

Input	Source	Description
BSC 2004. *Drift Degradation Analysis*. [DIRS 166107]	Section 6.4.2.3	Stress states around the emplacement drift are generally well below the yield strength of the rock mass
	Sections 6.3 and 6.4	Drift response during the first 10,000 years after repository closure has been analyzed considering in situ stresses, excavation-induced stresses, thermally induced stresses, and time-dependent rock strength degradation
BSC 2004. *Evaluation of Emplacement Drift Stability for KTI Resolutions*. [DIRS 168889]	Table 6.4-3	Vertical displacement of drift floor

Table 2.1.07.06.0A-2. Indirect Inputs

Citation	Title	DIRS
10 CFR 63	Energy: Disposal of High-Level Radioactive Wastes in a Geologic Repository at Yucca Mountain, Nevada	180319
70 FR 53313	Implementation of a Dose Standard After 10,000 Years	178394
BSC 2004	*Drift Degradation Analysis*	166107
Department of Army 1997	*Engineering and Design Tunnels and Shafts in Rocks*	183771
SNL 2007	*Total System Performance Assessment Data Input Package for Requirements Analysis for Subsurface Facilities*	179466

FEP: 2.1.08.01.0A

FEP NAME:

Water Influx at the Repository

FEP DESCRIPTION:

An increase in the unsaturated water flux at the repository may affect thermal, hydrologic, chemical, and mechanical behavior of the system. Increases in flux could result from climate change, but the cause of the increase is not an essential part of the FEP.

SCREENING DECISION:

Included

TSPA DISPOSITION:

Long-term changes in ambient unsaturated zone flow in response to climate changes are incorporated in the infiltration maps developed in *Simulation of Net Infiltration for Present-Day and Potential Future Climates* (SNL 2008 [DIRS 182145], Section 6.5.7[a]), and in flow fields developed for use in the TSPA by *UZ Flow Models and Submodels* (SNL 2007 [DIRS 184614], Section 6.6.2). These flow fields incorporate different climate stages, and capture uncertainty in local percolation flux rates through use of infiltration maps representing the 10th, 30th, 50th, and 90th percentiles of infiltration. They are used in calculations of seepage flux into the drift in *Seepage Model for PA Including Drift Collapse* (BSC 2004 [DIRS 167652], Section 6.3.6) and *Abstraction of Drift Seepage* (SNL 2007 [DIRS 181244]), and in calculations that track radionuclide transport from the repository to the water table in *Particle Tracking Model and Abstraction of Transport Processes* (SNL 2008 [DIRS 184748]). Radionuclide transport in the unsaturated zone is strongly a function of the percolation flux at the repository level (SNL 2008 [DIRS 184748], Addendum Section 6.5.15).

Climate changes, and their impact on infiltration and percolation, are also considered in models simulating the thermal-hydrogical, chemical, and mechanical response of the repository rocks to the waste heat. This is done by setting infiltration or percolation rates at the top model boundaries that reflect the different climate stages and scenarios. Also, during the thermal period, waste heat causes water to boil and move as vapor to cooler regions, where it condenses and becomes available to locally increase the percolation flux. Flux increases related to climate change and/or thermal perturbation are directly accounted for in coupled process model simulations used for TSPA calculations or to evaluate FEPs for screening purposes, such as the multiscale thermohydrologic model (SNL 2008 [DIRS 184433]), the thermal-hydrological seepage model (BSC 2005 [DIRS 172232]), the thermal-hydrological-chemical seepage model (SNL 2007 [DIRS 177404]), the near-field chemistry model (SNL 2007 [DIRS 177412], Section 6.3.2), the in-drift condensation model (SNL 2007 [DIRS 181648]), and the drift-scale thermal-hydrological-mechanical model (BSC 2004 [DIRS 169864]). Most of these process models do not use the UZ flow fields directly, but parametrically evaluate the effects of changes in percolation flux in the abstractions provided to TSPA. The TSPA selects from the

abstractions using sampled infiltration conditions and the resulting percolation fluxes determined from the UZ flow fields.

INPUTS:

Table 2.1.08.01.0A-1. Indirect Inputs

Citation	Title	DIRS
BSC 2004	*Drift Scale THM Model*	169864
BSC 2004	*Seepage Model for PA Including Drift Collapse*	167652
BSC 2005	*Drift-Scale Coupled Process (DST and TH Seepage) Models*	172232
SNL 2007	*Abstraction of Drift Seepage*	181244
SNL 2007	*Drift-Scale THC Seepage Model*	177404
SNL 2007	*Engineered Barrier System: Physical and Chemical Environment*	177412
SNL 2007	*In-Drift Natural Convection and Condensation*	181648
SNL 2007	*UZ Flow Models and Submodels*	184614
SNL 2008	*Multiscale Thermohydrologic Model*	184433
SNL 2008	*Particle Tracking Model and Abstraction of Transport Processes*	184748
SNL 2008	*Simulation of Net Infiltration for Present-Day and Potential Future Climates*	182145

FEP: 2.1.08.01.0B

FEP NAME:

Effects of Rapid Influx into the Repository

FEP DESCRIPTION:

Extremely rapid influx could reduce temperatures below the boiling point during part or all of the thermal period. Increases in flux could result from climate change, but the cause of the increase is not an essential part of the FEP.

SCREENING DECISION:

Excluded – low consequence

SCREENING JUSTIFICATION:

This FEP evaluates the potential concern that influx of liquid water could cause rapid, localized temperature reduction during the thermal period, which could thermally perturb a waste package or drip shield leading to failure from the effects of thermal stresses. The thermal period is defined in this context as the time period during which the in-drift and near-field temperatures are elevated and thermally driven flow processes are induced in the host rock. The FEP allows that liquid water is the cause of the perturbation, and significant quantities of liquid water will be present in the repository only for temperatures up to approximately 100°C, thus limiting the temperature range for consideration.

A sudden or strong reduction of temperature can only result from very large influx of water to the repository. The percolation flux at the repository horizon is limited and transients are dampened by the overlying PTn unit (see excluded FEP 2.2.07.05.0A (Flow in the UZ from Episodic Infiltration)). Also, percolation flux has a limited effect on repository temperature, as shown by the multiscale model, for which variation of percolation between the 10th and 90th percentile conditions produced ranges of less than 10°C for peak temperature, among the coolest and hottest drip shields and waste packages (SNL 2008 [DIRS 184433], Table 6.3-49[a], uncertainty cases P10 and P90). Substantially higher flux rates than those considered in the multiscale model (which uses flux estimates from the unsaturated zone flow model) would be necessary to cause rapid, localized reduction in temperature. Such conditions could occur only for high magnitude, strongly episodic seepage flow, which is not expected for the reasons given below.

Episodic seepage requires episodic flow in the host rock. Episodic natural percolation is not significant and has been excluded from the performance assessment (see excluded FEP 2.2.07.05.0A (Flow in the UZ from Episodic Infiltration)). Simulations conducted in *UZ Flow Models and Submodels* (SNL 2007 [DIRS 184614], Sections 6.1.2 and 6.9[a]) show that the PTn unit dampens and homogenizes downward flowing transient pulses arising from episodic surface infiltration events.

Episodic flow in the host rock due to repository heating has also been evaluated, and was also found to be insignificant (BSC 2005 [DIRS 172232]). During the thermal period (while the drift wall temperature is above the boiling point of water) condensate in the host rock above the drift does not seep into the drift opening because of capillary diversion and vaporization effects. After the drift wall cools to below the boiling point, boiling no longer occurs anywhere in the host rock, and the amounts of evaporation and condensation are greatly decreased. These processes are addressed in *Drift-Scale Coupled Processes (DST and TH Seepage) Models* (BSC 2005 [DIRS 172232], Section 6.2) and in *Abstraction of Drift Seepage* (SNL 2007 [DIRS 181244], Section 6.4.3.2). These reports show that seepage during cooldown (after the drift wall has cooled below the boiling point) is bounded by the ambient seepage abstraction. The ambient seepage abstraction is then used for this condition (defined for this purpose as drift wall temperature less than 100°C) in TSPA. Factors potentially affecting flow and temperature conditions near drifts, such as climate change (included FEP 1.3.01.00.0A (Climate Change)) and flow focusing (included FEP 2.2.07.04.0A (Focusing of Unsaturated Flow (Fingers, Weeps))) are accounted for in the thermal seepage model (BSC 2005 [DIRS 172232]) and are included in TSPA drift seepage calculation (SNL 2007 [DIRS 181244]).

If seepage does enter the drift during cooldown (after the host rock cools below the boiling point of water), the drip shield will prevent direct contact with the waste package and pallet, thus protecting the waste package from transient thermal effects.

For the reasons discussed above, the potential for a large quantity of liquid water to contact a hot waste package during the thermal period is insignificant.

In the unexpected event that a significant quantity of liquid water would contact a waste package directly during cooldown, for example due to breach of the drip shield by seismically induced rockfall (included FEP 1.2.03.02.0C (Seismic Induced Drift Collapse Damages EBS Components)), the following two cases can be considered:

(1) Waste package surface temperature is slightly greater than the boiling point:

When seepage is possible (drift wall below 100°C), the waste package surface temperature is limited to only a few degrees above the boiling point of water. Water contacting the waste package for such conditions would initially boil, cooling the waste package surface to just below the boiling temperature. This would produce temperature variations of a only a few degrees Celsius on the waste package surface, because the water temperature would be close to that of the waste package. Temperature variations of similar magnitude are predicted for nominal performance of the waste package during the thermal period (for example, the thermal envelope calculated for naval SNF packages; BSC 2005 [DIRS 175761], Attachment I) and are inconsequential. Further discussion of thermal expansion effects is provided for excluded FEP 2.1.11.07.0A (Thermal Expansion/Stress of In-Drift EBS Components).

(2) Waste package temperature is below the boiling point:

Here, the same justification described in (1) is valid, with the exception that boiling will not occur on the WPOB surface.

These cases also apply to the drip shield, which is directly exposed to seepage but will not undergo significant degradation as a consequence.

In summary, rapid water influx into the repository with the possibility of contacting waste packages during the thermal period is not expected because of dampening of natural percolation in the unsaturated zone, capillary diversion and vaporization processes in the host rock, and the presence of the drip shield. Even if such contact occurred, its effects would be inconsequential.

Based on the above discussion, omission of FEP 2.1.08.01.0B (Effects of Rapid Influx into the Repository) will not result in a significant adverse change in the magnitude or time of radiological exposures to the RMEI or radionuclide releases to the accessible environment. Therefore, this FEP is excluded from the performance assessments conducted to demonstrate compliance with proposed 10 CFR 63.311 and 63.321 (70 FR 53313 [DIRS 178394]), and with 10 CFR 63.331 [DIRS 180319], on the basis of low consequence.

INPUTS:

Table 2.1.08.01.0B-1. Direct Inputs

Input	Source	Description
BSC 2005. *Drift-Scale Coupled Process (DST and TH Seepage) Models*. [DIRS 172232]	Section 6.2	Addresses episodic and preferential flow patterns
SNL 2007. *UZ Flow Models and Submodels*. [DIRS 184614]	Sections 6.1.2 and 6.9[a]	Dampening of episodic surface infiltration events
SNL 2008. *Multiscale Thermohydrologic Model*. [DIRS 184433]	Table 6.3-49[a]	The effect of infiltration flux on drift temperature variation

Table 2.1.08.01.0B-2. Indirect Inputs

Citation	Title	DIRS
10 CFR 63	Energy: Disposal of High-Level Radioactive Wastes in a Geologic Repository at Yucca Mountain, Nevada	180319
70 FR 53313	Implementation of a Dose Standard After 10,000 Years	178394
BSC 2005	*Calculation of the Naval Long Waste Package Two-Demensional Thermal Interface Temperatures*	175761
BSC 2005	*Drift-Scale Coupled Process (DST and TH Seepage) Models*	172232
SNL 2007	*Abstraction of Drift Seepage*	181244

FEP: 2.1.08.02.0A

FEP NAME:

Enhanced Influx at the Repository

FEP DESCRIPTION:

An opening in unsaturated rock may alter the hydraulic potential, affecting local saturation around the opening and redirecting flow. Some of the flow may be directed to the opening where it is available to seep into the opening.

SCREENING DECISION:

Included

TSPA DISPOSITION:

The impact of an underground opening on the unsaturated flow field (including a capillary barrier effect and flow diversion around the drifts) and its relevance for seepage is represented in the data acquired in *In Situ Field Testing of Processes* (BSC 2004 [DIRS 170004], Section 6.2). These data were used in *Seepage Calibration Model and Seepage Testing Data* (BSC 2004 [DIRS 171764], Sections 6.1.2, 6.3.3, and 6.6.3) for calibrating unsaturated flow parameters of the formation around the underground opening. The flow parameters derived in the seepage calibration model are used to evaluate the impact of an underground opening on the unsaturated flow field and seepage into the drift in *Seepage Model for PA Including Drift Collapse* (BSC 2004 [DIRS 167652], Section 6.3), and in *Drift-Scale Coupled Processes (DST and TH Seepage) Models* (BSC 2005 [DIRS 172232], Sections 6.1.1 and 6.2.1.4), for ambient and elevated temperatures, respectively. Results of these process models are abstracted for TSPA calculations in *Abstraction of Drift Seepage* (SNL 2007 [DIRS 181244], Sections 6.4.1, 6.4.2, and 6.4.3). Seepage model uncertainty is incorporated by sampling probability distributions for the rock hydrologic properties and using percolation fluxes based on multiple infiltration scenarios (SNL 2007 [DIRS 181244], Section 6.6).

This FEP is included in performance assessments to demonstrate compliance with the individual protection standard after permanent closure (proposed 10 CFR 63.311 (70 FR 53313 [DIRS 178394])) and the groundwater protection standards (10 CFR 63.331 [DIRS 180319]). It is not included in the human intrusion performance assessment (proposed 10 CFR 63.321 (70 FR 53313 [DIRS 178394])).

INPUTS:

Table 2.1.08.02.0A-1. Indirect Inputs

Citation	Title	DIRS
10 CFR 63	Energy: Disposal of High-Level Radioactive Wastes in a Geologic Repository at Yucca Mountain, Nevada	180319
70 FR 53313	Implementation of a Dose Standard After 10,000 Years	178394
BSC 2004	*In Situ Field Testing of Processes*	170004
BSC 2004	*Seepage Calibration Model and Seepage Testing Data*	171764
BSC 2004	*Seepage Model for PA Including Drift Collapse*	167652
BSC 2005	*Drift-Scale Coupled Process (DST and TH Seepage) Models*	172232
SNL 2007	*Abstraction of Drift Seepage*	181244

FEP: 2.1.08.03.0A

FEP NAME:

Repository Dry-Out Due to Waste Heat

FEP DESCRIPTION:

Repository heat evaporates water from the UZ rocks near the drifts, as the temperature exceeds the vaporization temperature. This zone of reduced water content (reduced saturation) could migrate outward during the heating phase and then migrate back to the waste package as heat diffuses throughout the mountain and the radioactive heat sources decay. This FEP addresses the effects of dry-out within the repository drifts.

SCREENING DECISION:

Included

TSPA DISPOSITION:

The postclosure in-drift thermal and hydrologic conditions are calculated in accordance with the methodology presented in *Multiscale Thermohydrologic Model* (SNL 2008 [DIRS 184433]). This includes a calculation of the postclosure thermohydrologic conditions including dryout during the heating phase and rewetting during the cooling phase. Using the modeling methodology described in *Multiscale Thermohydrologic Model* (SNL 2008 [DIRS 184433], Section 6.2[a]), the repository dryout is implemented in the TSPA by MSTHM output variables of temperature, relative humidity, and invert saturation at waste package locations throughout the repository. These output variables are used in the TSPA model.

Additional considerations of evaporation/condensation are discussed as part of included FEPs 2.1.08.04.0A (Condensation Forms on Roofs of Drifts (Drift-scale Cold Traps)) and 2.1.08.04.0B (Condensation Forms at Repository Edges (Repository-scale Cold Traps)).

Ventilation Model and Analysis Report (BSC 2004 [DIRS 169862], Section 8.1) calculates the preclosure thermal conditions in the host rock and characterizes the preclosure host rock response in terms of ventilation efficiency. The ventilation efficiency is the fraction of total decay heat removed from the repository by the vent air. The ventilation efficiency is determined through simulation of temporally and spatially dependent heat transfer processes (thermal radiation, convection, and conduction), which occur simultaneously in the drift and the surrounding rock mass during the ventilating or preclosure period. The ventilation efficiency is a direct input to *Multiscale Thermohydrologic Model* (SNL 2008 [DIRS 184433]), which in turn provides postclosure thermal, humidity, and saturation conditions to the TSPA.

Drift-Scale Coupled Processes (DST and TH Seepage) Models (BSC 2005 [DIRS 172232], Section 6.2) discusses the thermal-hydrologic seepage model and associated alternate conceptual models. The dual-permeability, integrated finite-difference code TOUGH2 V1.6 (Pruess 1991 [DIRS 100413]) specifically models thermal seepage including dryout and rewetting. Numerous saturation and temperature results are presented as functions of varied boundary and initial

conditions. Vertical liquid fluxes are presented along with various sensitivity analyses. The thermal-hydrologic seepage model results (DTN: LB0301DSCPTHSM.002 [DIRS 163689]) include these effects. *Abstraction of Drift Seepage* (SNL 2007 [DIRS 181244]) utilizes these modeling results to develop an appropriate seepage abstraction methodology for use in the TSPA.

INPUTS:

Table 2.1.08.03.0A-1. Indirect Inputs

Citation	Title	DIRS
BSC 2004	*Ventilation Model and Analysis Report*	169862
BSC 2005	*Drift-Scale Coupled Process (DST and TH Seepage) Models*	172232
DTN: LB0301DSCPTHSM.002	Drift-Scale Coupled Process Model for Thermohydrologic Seepage: Data Summary	163689
Pruess 1991	*TOUGH2—A General-Purpose Numerical Simulator for Multiphase Fluid and Heat Flow*	100413
SNL 2007	*Abstraction of Drift Seepage*	181244
SNL 2008	*Multiscale Thermohydrologic Model*	184433

FEP: 2.1.08.04.0A

FEP NAME:

Condensation Forms on Roofs of Drifts (Drift-Scale Cold Traps)

FEP DESCRIPTION:

Emplacement of waste in drifts creates thermal gradients within the repository. Such thermal gradients can lead to drift-scale cold traps characterized by latent heat transfer from warmer to cooler locations. This mechanism can result in condensation forming on the roof or other parts of the drifts, leading to enhanced dripping on the drip shields, waste packages, or exposed waste material.

SCREENING DECISION:

Included

TSPA DISPOSITION:

Cold-trap effects within the emplacement drift are represented in TSPA as documented in *In-Drift Natural Convection and Condensation* (SNL 2007 [DIRS 181648], Sections 6.3 and 6.1.2[a]). As discussed in that report (SNL 2007 [DIRS 181648], Section 6.3.3), three stages are identified during condensation within the emplacement drifts. Stage 1 designates the period when all locations are above the saturation temperature at the drift wall (and thus also all drip shields and waste packages) and condensation cannot occur. Stage 2 is a transitional stage where some locations are above the saturation temperature while others are below. Stage 3 condensation occurs when all waste packages and drip shields (and thus the drift wall) are below the saturation temperature. Abstractions are developed independently for stages 2 and 3 condensation for use in TSPA.

A bounding approach for predicting in-drift condensation rates during stage 2 has been developed in *In-Drift Natural Convection and Condensation* (SNL 2007 [DIRS 181648], Section 6.2[a]). The approach for stage 2 condensation requires that every waste package simulated in TSPA have two associated parameters: the onset time (in years) of stage 2, and the transition time from stages 2 to 3. For a given waste package location, the onset time of stage 2 is the time when the local drift wall temperature cools to 96°C (i.e., condensation is possible). The onset times for Stage 2 and for transition from Stages 2 to 3 are provided by *Multiscale Thermohydrologic Model* (SNL 2008 [DIRS 184433], Section 6.3.18[a]). These times are used in TSPA for each waste package to limit the period of time when stage 2 condensation can occur. Stage 2 condensation rates are developed for codisposal (codisposal, HLW-long, and HLW-short) packages and commercial SNF (commercial SNF, PWR, and BWR) packages in *In-Drift Natural Convection and Condensation* (SNL 2007 [DIRS 181648], Section 6.2.2[a]). Condensation rates represent a reasonable upper bound for drift wall condensation and are scaled to represent only condensation that forms over the drip shield (potential for enhanced dripping on the drip shields, waste packages, or exposed waste material).

The condensation model developed in *In-Drift Natural Convection and Condensation* (SNL 2007 [DIRS 181648], Section 6.3) applies to stage 3 condensation. This condensation model is a one-dimensional network model that produces estimates for the frequency and magnitude of condensation at waste package locations. Condensation on the drift walls is included in TSPA and is represented in the same manner as drift seepage, although with a different spatial distribution and flux rate. Drift wall seepage affects the transport of radionuclides through the drift invert and the partitioning of radionuclides onto the fractures and the matrix of the host rock.

Seven drifts in the repository are analyzed for condensation location and quantity as shown in *In-Drift Natural Convection and Condensation* (SNL 2007 [DIRS 181648], Figure 6-2 [a]). These drifts are chosen to reflect the range of conditions expected in the repository. Choices #1, #2, and #3 are collinear (having axes lying end to end in a straight line) and cut across the northern end of the repository. Choice #3 is shorter than most emplacement drifts and is at the edge of the repository. Choices #4, #5, and #6 are collinear and cut across the middle of the repository. Choice #7 is in the southern section of the repository. For each drift, the heated portion of the drift was identified using the nominal waste package end-point coordinates from *Total System Performance Assessment Data Input Package for Requirements Analysis for Subsurface Facilities* (SNL 2007 [DIRS 179466], Table 4-1, Parameter Number 01-02) and unheated drift length at each end of the emplacement drifts from *Total System Performance Assessment Data Input Package for Requirements Analysis for Subsurface Facilities* (SNL 2007 [DIRS 179466], Table 4-1, Parameter Number 01-18).

The stage 3 condensation model calculations consist of evaluating drift wall and drip shield condensation, for the seven drift choices, at six different times (1,000, 3,000, 10,000, 30,000, 100,000, and 300,000 years), and at three different percolation flux conditions (a range of average-flux values for each drift, representing uncertainty on percolation flux). The drift nearest the edge of the repository was also assessed at 300 years, as it reached stage 3 (all waste packages below 96°C) more rapidly that the other, hotter drifts. Additional parametric variations were used to quantify and bound model uncertainty, including:

- Two dispersion limits
- Two limits on the degree of mixing in the gas separated by the drip shield
- Two limits on invert transport.

The dispersion limits refer to the degree that water vapor is transported along the drift according to the one-dimensional axial dispersion coefficients calculated by the in-drift convection model (SNL 2007 [DIRS 181648], Section 6.3.5.1). Limits on the degree of mixing between gas volumes inside and outside the drip shield (i.e., perfect mixing and no-mixing) are used to capture the model uncertainty on the extent of such mixing. High and low invert transport cases use two different methods for determining the local vapor pressure at the invert surface. High-invert transport cases assume that the local vapor pressure is controlled by the temperature calculated at the top-center of the invert. Low-invert transport cases assume the local vapor pressure is controlled by the temperature of the drift wall. Calculations implemented in TSPA are for the "low invert transport" cases as discussed in the condensation analysis (SNL 2007 [DIRS 181648], Section 6.1.2[a]). Uncertainty in the occurrence and amount of condensation is

propagated to TSPA through the use of model outputs from all four "low invert transport" cases (low/high dispersion, ventilated/unventilated drip shield).

Condensate dripping from drift walls affects TSPA model calculations by adding additional water flow onto the drip shield. This flow is diverted to the invert, or it may flow through breaches in the drip shield where it interacts with the underyling waste package. The TSPA model calculates a probability of condensate on the drift walls at any location and, if condensation occurs, rate of condensation. The probability of condensation occurrence and condensation rate are abstracted as functions of the percolation flux, as described in *In-Drift Natural Convection and Condensation* (SNL 2007 [DIRS 181648], Section 8.3).

The model developed in *EBS Radionuclide Transport Abstraction* (SNL 2008 [DIRS 177407], Section 8.1) is used to quantify the release of radionuclides from the EBS to the unsaturated zone. Dripping flux comprises a major source of liquid flow into the EBS. Condensation represents one source of dripping flux into the radionuclide transport model (SNL 2008 [DIRS 177407], Section 8.1). The EBS flow model is implemented directly in TSPA (SNL 2008 [DIRS 177407], Section 8.1).

Related included FEP 2.1.08.04.0B (Condensation Forms at Repository Edges (Repository-scale Cold Traps)) considers larger-scale variability in condensation behavior.

This FEP is included in performance assessments to demonstrate compliance with the individual protection standard after permanent closure (proposed 10 CFR 63.311 (70 FR 53313 [DIRS 178394])) and the groundwater protection standards (10 CFR 63.331 [DIRS 180319]). It is not included in the human intrusion performance assessment (proposed 10 CFR 63.321 (70 FR 53313 [DIRS 178394])).

INPUTS:

Table 2.1.08.04.0A-1. Indirect Inputs

Citation	Title	DIRS
10 CFR 63	Energy: Disposal of High-Level Radioactive Wastes in a Geologic Repository at Yucca Mountain, Nevada	180319
70 FR 53313	Implementation of a Dose Standard After 10,000 Years	178394
SNL 2008	*EBS Radionuclide Transport Abstraction*	177407
SNL 2007	*In-Drift Natural Convection and Condensation*	181648
SNL 2007	*Total System Performance Assessment Data Input Package for Requirements Analysis for Subsurface Facilities*	179466
SNL 2008	*Multiscale Thermohydrologic Model*	184433

FEP: 2.1.08.04.0B

FEP NAME:

Condensation Forms at Repository Edges (Repository-Scale Cold Traps)

FEP DESCRIPTION:

Emplacement of waste in drifts creates thermal gradients within the repository. Such thermal gradients can lead to repository-scale cold traps characterized by latent heat transfer from warmer to cooler locations. This mechanism can result in condensation forming at repository edges or elsewhere in the EBS, leading to enhanced dripping on the drip shields, waste packages, or exposed waste material.

SCREENING DECISION:

Included

TSPA DISPOSITION:

Cold-trap effects within the repository are represented in TSPA as documented in *In-Drift Natural Convection and Condensation* (SNL 2007 [DIRS 181648]). As discussed in that report (SNL 2007 [DIRS 181648], Section 6.3.3), three stages are identified for the occurrence of condensation within the emplacement drifts. Stage 1 designates the period when all locations are above the saturation temperature at the drift wall (and thus, also all drip shields and waste packages) and condensation cannot occur. Stage 2 is a transitional stage in which some locations are above the saturation temperature while others are below the saturation temperature. Stage 3 condensation occurs when all waste packages and drip shields (and thus, the drift wall) are below the saturation temperature. Abstractions are developed independently for stages 2 and 3 condensation for use in TSPA.

A bounding approach for predicting in-drift condensation rates during the Stage 2 period has been developed in *In-Drift Natural Convection and Condensation* (SNL 2007 [DIRS 181648], Section 6.2[a]). The approach for stage 2 condensation requires that every waste package realized in TSPA have two parameters established, namely the time (in years) for onset of stage 2, and the time for transition from stage 2 to stage 3. For a given waste package location, the time for onset of stage 2 can be approximated by the time when the local drift wall temperature cools to 96°C and condensation becomes possible. The times for the onset of stage 2 and for transition from stage 2 to stage 3 are provided by *Multiscale Thermohydrologic Model* (SNL 2008 [DIRS 184433]). These times are used in TSPA as cutoffs for stage 2 condensation. Stage 2 condensation rates are developed for codisposal (codisposal, HLW-long, and HLW-short) packages and commercial SNF (commercial SNF, PWR, and BWR) packages in *In-Drift Natural Convection and Condensation* (SNL 2007 [DIRS 181648], Section 6.2.2[a]). Condensation rates represent a reasonable upper bound for drift wall condensation, and are scaled to represent only that condensation that forms over the drip shield, which may lead to enhanced dripping on the drip shields, waste packages, or exposed waste material.

The condensation model developed in *In-Drift Natural Convection and Condensation* (SNL 2007 [DIRS 181648], Section 6.3) applies to stage 3 condensation. This condensation model is a one-dimensional network model that produces estimates for the frequency and magnitude of condensation at waste package locations. Condensation on the drift walls is included in the TSPA and is represented in the same manner as drift seepage, although with a different spatial distribution and flux rate. As such, it affects the transport of radionuclides through the drift invert and the partitioning of that transport into the fractures and the matrix of the host rock.

Seven drifts in the repository are analyzed for condensation location and quantity as shown in *In-Drift Natural Convection and Condensation* (SNL 2007 [DIRS 181648], Figure 6-2 [a]). These drifts are chosen to reflect the range of conditions expected in the repository. Choices #1, #2, and #3 are collinear (having axes lying end to end in a straight line) and cut across the northern end of the repository. Choice #3 is shorter than most emplacement drifts and is at the edge of the repository. Choices #4, #5, and #6 are collinear and cut across the middle of the repository. Choice #7 is in the southern section of the repository. For each drift, the heated portion of the drift was identified using the nominal waste package end-point coordinates from *Total System Performance Assessment Data Input Package for Requirements Analysis for Subsurface Facilities* (SNL 2007 [DIRS 179466], Table 4-1, Parameter Number 01-02) and unheated drift length at each end of the emplacement drifts from *Total System Performance Assessment Data Input Package for Requirements Analysis for Subsurface Facilities* (SNL 2007 [DIRS 179466], Table 4-1, Parameter Number 01-18).

The stage 3 condensation model calculations consist of evaluating drift wall and drip shield condensation for the seven drift choices at six different times (1,000, 3,000, 10,000, 30,000, 100,000, and 300,000 yr) and at three different percolation flux conditions (a range of average-flux values for each drift, representing uncertainty in percolation flux). The drift nearest the edge of the repository was also assessed at 300 years, because it reached stage 3 (all waste packages below 96°C) more rapidly than the other, hotter drifts. Additional parametric variations were used to quantify and bound model uncertainty, including:

- Two dispersion limits
- Two limits on the degree of mixing in the gas separated by the drip shield
- Two limits on invert transport.

The dispersion limits refer to the degree that water vapor is transported along the drift by one-dimensional axial dispersion coefficients calculated by the in-drift convection model (SNL 2007 [DIRS 181648], Section 6.3.5.1). Limits on the degree of mixing in the gases separated by the drip shield are used to capture epistemic uncertainty associated with that aspect of the model. High- and low-invert transport cases use two different methods for determining the local vapor pressure at the invert surface. High-invert transport cases assume that the local vapor pressure is controlled by the temperature calculated at the top-center of the invert. Low-invert transport cases assume that the local vapor pressure is controlled by the temperature of the drift wall. Calculations implemented in TSPA are for the low-invert transport cases as discussed in the condensation analysis (SNL 2007 [DIRS 181648], Section 6.1.2[a]). Uncertainty in the occurrence and amount of condensation is propagated to TSPA through the

use of model outputs from all four "low-invert transport" cases (low/high dispersion, ventilated/unventilated drip shield).

The stage 3 condensation model described above is based on simulations of water vapor transport and condensation in single drifts, and is used to evaluate not only the location of condensation within the drift cross-section, but also the longitudinal location of condensation along a drift with an axial temperature gradient (see related included FEP 2.1.08.04.0A (Condensation Forms on Roofs of Drifts (Drift-Scale Cold Traps))). The effects of repository-scale cold traps are captured within the model, as the repository temperature field used in the simulations is calculated using the principle of superposition—the heat contribution from all 108 drifts, plus the natural geothermal gradient, is summed in calculating the thermal conditions along the drift of interest (SNL 2007 [DIRS 181648], Section 6.3.5.1.1). Thus, the temperature effects resulting from proximity to the repository edge are captured in the model, as described in the condensation model report (SNL 2007 [DIRS 181648], Section 6.3.5.1.1). Drifts at the north end of the repository reflect the cooler portion of the repository, and drifts in the middle reflect the hotter portions of the repository (SNL 2007 [DIRS 181648], Section 6.3.5.1.1 and Figure 6.3.5-2). The effects of moisture being driven from hot areas in the repository and becoming available for condensation in cooler regions are captured in the bounding percolation rates. The bounding percolation rates are incorporated for each of the times and each of the emplacement drifts. The percolation rates vary with both location and time (SNL 2007 [DIRS 181648], Section 6.1.1[a]). The stage 2 analysis does not model different locations within the repository because that analysis is based on a model of a single drift (SNL 2007 [DIRS 181648], Section 6.2.1[a]), but the edge effects within a single drift are modeled. Due to the bounding nature of the Stage 2 analysis, repository scale effects may be considered to be bounded within the results.

Condensate dripping from drift walls affects TSPA model calculations by adding additional water flow onto the drip shield. This flow is diverted to the invert, or it may flow through breaches in the drip shield where it interacts with the underlying waste package. The model implemented in the TSPA calculates a probability of condensate on the drift walls at any location and, if condensation occurs, rate of condensation. The probability of condensation occurrence and condensation rate are abstracted as functions of the percolation flux, as described in *In-Drift Natural Convection and Condensation* (SNL 2007 [DIRS 181648], Section 8.3).

The model developed in *EBS Radionuclide Transport Abstraction* (SNL 2008 [DIRS 177407], Section 8.1) is used to quantify the release of radionuclides from the EBS to the unsaturated zone. Dripping flux comprises a major source of liquid flow into the EBS. Condensation represents one source of dripping flux into the radionuclide transport model (SNL 2008 [DIRS 177407], Section 8.1). The EBS flow model is implemented directly in TSPA, as discussed in Section 8.1 of *EBS Radionuclide Transport Abstraction* (SNL 2008 [DIRS 177407]).

This FEP is included in performance assessments to demonstrate compliance with the individual protection standard after permanent closure (proposed 10 CFR 63.311 (70 FR 53313 [DIRS 178394])) and the groundwater protection standards (10 CFR 63.331 [DIRS 180319]). It is not included in the human intrusion performance assessment (proposed 10 CFR 63.321 (70 FR 53313 [DIRS 178394])).

INPUTS:

Table 2.1.08.04.0B-1. Indirect Inputs

Citation	Title	DIRS
10 CFR 63	Energy: Disposal of High-Level Radioactive Wastes in a Geologic Repository at Yucca Mountain, Nevada	180319
70 FR 53313	Implementation of a Dose Standard After 10,000 Years	178394
SNL 2008	*EBS Radionuclide Transport Abstraction*	177407
SNL 2007	*In-Drift Natural Convection and Condensation*	181648
SNL 2007	*Total System Performance Assessment Data Input Package for Requirements Analysis for Subsurface Facilities*	179466
SNL 2008	*Multiscale Thermohydrologic Model*	184433

FEP: 2.1.08.05.0A

FEP NAME:

Flow Through Invert

FEP DESCRIPTION:

The invert, a porous material consisting of crushed tuff, separates the waste package from the bottom of the drift. Flow and transport through and around the invert can influence radionuclide release to the UZ.

SCREENING DECISION:

Included

TSPA DISPOSITION:

Flow within the EBS is addressed within several included FEPs as follows: FEP 2.1.08.05.0A (Flow Through the Invert) (this FEP), FEP 2.1.08.06.0A (Capillary Effects (Wicking) in EBS), and FEP 2.1.08.07.0A (Unsaturated Flow in the EBS). FEP 2.1.08.09.0A (Saturated Flow in the EBS) is excluded.

Hydraulic properties of EBS components and flow pathways within the EBS are discussed in detail in *EBS Radionuclide Transport Abstraction* (SNL 2008 [DIRS 177407], Section 6.3). The EBS radionuclide transport abstraction model is used to quantify the time-dependent radionuclide releases from a failed waste package and their subsequent transport through the EBS to the emplacement drift wall/unsaturated zone interface. The basic inputs to the EBS radionuclide transport abstraction model consist of the drift seepage and drift wall condensation flux, the environmental conditions in the drift (temperature, relative humidity, and water chemistry), and the degradation state of the EBS components (SNL 2008 [DIRS 177407], Section 6.1). Outputs consist of the rates of radionuclide releases to the unsaturated zone as a result of advective and diffusive transport, accounting for the impact of colloids, radionuclide solubility and ingrowth/decay, retardation, and the degree of liquid saturation of the waste form and invert materials. The EBS radionuclide transport abstraction model is implemented directly into the TSPA GoldSim model to compute the radionuclide release rates from the EBS (SNL 2008 [DIRS 177407], Section 8).

The conceptual model for EBS flow used in the performance assessments to demonstrate compliance with the individual protection standard after permanent closure (proposed 10 CFR 63.311 (70 FR 53313 [DIRS 178394])) and the groundwater protection standard (10 CFR 63.331 [DIRS 180319]) is described in *EBS Radionuclide Transport Abstraction* (SNL 2008 [DIRS 177407], Section 6.3.1). The source of inflow to the EBS is the seepage flux that drips from the crown (roof) of the drift, drift wall condensation, and imbibition flux from the unsaturated zone into the invert. This inflow can flow through the EBS along eight pathways: (1) drift seepage and drift wall condensation flux, (2) flux through the drip shield, (3) diversion around the drip shield, (4) flux through the waste package, (5) diversion around the waste package, (6) flux from the waste package into the invert, (7) imbibition flux from the unsaturated

zone matrix to the invert, and (8) flux from the invert to the unsaturated zone (SNL 2008 [DIRS 177407], Section 6.3.1.1 and Figure 6.3-1). These pathways are time- and location-dependent, because drip shield penetrations and waste package penetrations will vary with time and local conditions in the repository.

The conceptual model for radionuclide transport through the EBS consists of transport through three separate domains: the waste form (e.g., fuel rods or defense high-level radioactive waste (defense HLW) glass), waste package corrosion products, and the invert (SNL 2008 [DIRS 177407], Section 6.3.4). Because the pallet is not considered to contribute to the EBS barrier capability in regards to the transport of radionuclides through the EBS, water and radionuclides pass directly from the waste package to the invert.

The EBS flow abstraction, which is a component of the EBS radionuclide transport abstraction model (SNL 2008 [DIRS 177407], Section 6.3.1), includes invert flows in the net flow of water from the EBS and the advective transport of radionuclides. Flow through the invert consists of the flux diverted by the drip shield and waste package and the flux through the waste package, and is reduced by any evaporation from the invert. Each of these terms is accounted for in the EBS flow abstraction, which is used directly in TSPA.

Advection and diffusion transport radionuclides into the invert from the corrosion products domain and from this domain to the unsaturated zone. Groundwater colloids are also available in this domain if there is any water flow. Reversible sorption of radionuclides is modeled on these colloids. Because the chemical environment of the invert may be different from the corrosion products domain, colloid stability may be affected and dissolution or precipitation of radionuclides may take place. The submodel for transport through the invert is summarized in transport pathway 3 of the transport abstraction summary in *EBS Radionuclide Transport Abstraction* (SNL 2008 [DIRS 177407], Table 8.1-2).

Water saturation in the invert is an input to the EBS radionuclide transport abstraction model and is provided by the MSTHM. The MSTHM determines the imbibition flux from the host rock matrix into the invert, as well as the water saturation in the invert (SNL 2008 [DIRS 177407], Section 6.3.3.4). Water saturation is used in calculating the diffusion coefficient both in the waste package and in the invert, and so it impacts radionuclide transport in the EBS. The amount of water that flows into the EBS by capillary effects and the resulting water saturation are documented in *Multiscale Thermohydrologic Model* (SNL 2008 [DIRS 184433], Section 6.3.3).

Multiscale Thermohydrologic Model (SNL 2008 [DIRS 184433], Appendix XV) also calculates the matrix saturation of the invert based on the inputs described in Table 4.1-1 of that report. These inputs include the hydrologic properties of the invert, which are consistent with *Total System Performance Assessment Data Input Package for Requirements Analysis for Engineered Barrier System In-Drift Configuration* (SNL 2007 [DIRS 179354], Table 4-1, Parameter Number 02-08). Unlike the EBS radionuclide transport abstraction model, the MSTHM simulates the invert as a dual-permeability medium consisting of “matrix” and “fracture” flow. This calculation develops the retention and unsaturated flow properties of the invert using a non-dimensionalized van Genuchten retention relation. The treatment of the invert as a single continuum for flow and transport is justified in *EBS Radionuclide Transport Abstraction*

(SNL 2008 [DIRS 177407], Section 6.5.2.3). Invert matrix saturations are then used in that report (SNL 2008 [DIRS 177407], Section 6.5.2.5) for the calculation of radionuclide transport.

This FEP is included in performance assessments to demonstrate compliance with the individual protection standard after permanent closure (proposed 10 CFR 63.311 (70 FR 53313 [DIRS 178394])) and the groundwater protection standards (10 CFR 63.331 [DIRS 180319]). For the performance assessment to demonstrate compliance with the individual protection standard for human intrusion (proposed 10 CFR 63.321 (70 FR 53313 [DIRS 178394])), an intrusion borehole is assumed to be drilled from the ground surface, through a drip shield and a single waste package to the water table. Radionuclide mass is released from the intruded waste package to the EBS Transport submodel (SNL 2008 [DIRS 183478], Section 6.3.8). Therefore, this FEP is not included in the human intrusion performance assessment (proposed 10 CFR 63.321 (70 FR 53313 [DIRS 178394])).

INPUTS:

Table 2.1.08.05.0A-1. Indirect Inputs

Citation	Title	DIRS
10 CFR 63	Energy: Disposal of High-Level Radioactive Wastes in a Geologic Repository at Yucca Mountain, Nevada	180319
70 FR 53313	Implementation of a Dose Standard After 10,000 Years	178394
SNL 2007	*Total System Performance Assessment Data Input Package for Requirements Analysis for EBS In-Drift Configuration*	179354
SNL 2008	*EBS Radionuclide Transport Abstraction*	177407
SNL 2008	*Multiscale Thermohydrologic Model*	184433

FEP: 2.1.08.06.0A

FEP NAME:

Capillary Effects (Wicking) in EBS

FEP DESCRIPTION:

Capillary rise, or wicking, is a potential mechanism for water to move through the waste and EBS.

SCREENING DECISION:

Included

TSPA DISPOSITION:

Flow within the EBS is addressed in several included FEPs as follows: Capillary Effects (Wicking) in EBS (this FEP), FEP 2.1.08.05.0A (Flow through Invert), and FEP 2.1.08.07.0A (Unsaturated Flow in the EBS). Related FEP 2.1.08.09.0A (Saturated Flow in the EBS) is excluded.

The effect of capillary flux of water from the host rock to the invert is captured by the analysis described in the MSTHM (SNL 2008 [DIRS 184433], Section 6.3.3). Chemistry of the water in the invert is represented by the P&CE model (SNL 2007 [DIRS 177412], Section 6.15.2). The invert matrix saturations calculated by the MSTHM and the invert water chemistry calculated by the P&CE model are used (along with other parameters such as the seepage flux rate) to calculate flow and transport in and around the invert (SNL 2008 [DIRS 177407], Section 6.5.2.3). Hydraulic properties of EBS components and flow pathways within the EBS are discussed in detail in that report.

Wicking is not modeled as a flow mechanism in *EBS Radionuclide Transport Abstraction* (SNL 2008 [DIRS 177407]). However, the abstraction does account for the mass of water brought into the invert because of wicking through the invert water saturation term (SNL 2008 [DIRS 177407], Section 6.5.2.3). The effects of water saturation on radionuclide transport are incorporated in the model in that water saturation is used to calculate the radionuclide diffusion coefficient both in the waste package and in the invert (SNL 2008 [DIRS 177407], Section 6.3.4).

This FEP is included in performance assessments to demonstrate compliance with the individual protection standard after permanent closure (proposed 10 CFR 63.311 (70 FR 53313 [DIRS 178394])) and the groundwater protection standards (10 CFR 63.331 [DIRS 180319]). It is not included in the human intrusion performance assessment (proposed 10 CFR 63.321 (70 FR 53313 [DIRS 178394])).

INPUTS:

Table 2.1.08.06.0A-1. Indirect Inputs

Citation	Title	DIRS
10 CFR 63	Energy: Disposal of High-Level Radioactive Wastes in a Geologic Repository at Yucca Mountain, Nevada	180319
70 FR 53313	Implementation of a Dose Standard After 10,000 Years	178394
SNL 2008	*EBS Radionuclide Transport Abstraction*	177407
SNL 2007	*Engineered Barrier System: Physical and Chemical Environment*	177412
SNL 2008	*Multiscale Thermohydrologic Model*	184433

FEP: 2.1.08.07.0A

FEP NAME:

Unsaturated Flow in the EBS

FEP DESCRIPTION:

Unsaturated flow may occur along preferential pathways in the waste and EBS. Physical and chemical properties of the EBS and waste form, in both intact and degraded states, should be considered in evaluating pathways.

SCREENING DECISION:

Included

TSPA DISPOSITION:

The emplacement drift will contain waste packages. A freestanding drip shield sits over the waste packages on the invert. The waste package sits on an emplacement pallet that raises the bottom of the waste package above the invert (SNL 2007 [DIRS 179354], Section 4.1). Flow within the EBS is addressed within several included FEPs as follows: FEP 2.1.08.06.0A (Capillary Effects (Wicking) in EBS), FEP 2.1.08.05.0A (Flow through Invert), FEP 2.1.06.06.0A (Effects of Drip Shield on Flow), and this FEP. Saturated flow is discussed in excluded FEP 2.1.08.09.0A (Saturated Flow in the EBS).

The conceptual model flow in the EBS is described in *EBS Radionuclide Transport Abstraction* (SNL 2008 [DIRS 177407], Sections 6.3 and 6.5). Hydraulic properties of EBS components and flow pathways within the EBS are discussed in detail in that report. The conceptual model for EBS flow is also described (SNL 2008 [DIRS 177407], Section 6.3). Sources of significant inflow of liquid water to the EBS are the seepage flux, plus any condensation that may occur on the walls of the drift and drip onto the drip shield, plus the small capillary imbibition flux that can flow from the host rock into the invert. This water can flow through the EBS along eight pathways: (1) seepage flux plus condensation, (2) flux through the drip shield, (3) diversion around the drip shield, (4) flux through the waste package, (5) diversion around the waste package, (6) flux from the waste package into the invert, (7) imbibition flux from the UZ matrix to the invert, and (8) flux from the invert to the unsaturated zone (SNL 2008 [DIRS 177407], Section 6.3.1.1 and Figure 6.3-1). These pathways are time- and location-dependent, in the sense that drip shield gaps, drip shield breaches, and waste package breaches will vary with time and local conditions in the repository.

The conceptual model for flow and transport of radionuclides through the EBS includes three domains: the waste form (e.g., fuel rods or defense HLW glass), waste package corrosion products, and the invert. The presence of the emplacement pallet is not considered; water and radionuclides pass directly from the waste package to the invert. Initially, water inside a breached waste package will encounter intact metallic supports and cladding, unoxidized fuel, and uncorroded defense HLW glass. Water is expected to move over these surfaces as a thin film. Ultimately the waste form will degrade to a high surface area, small particle size mixture

of iron oxides, clays (in defense HLW glass-containing packages), and oxidized fuel remnants. Water will move through this aggregate as it would a porous medium, such as a soil.

Because the repository is located above the water table, water movement in the EBS is conceptualized as flow under varying degrees of partial saturation. Pathways for liquid water inflow are modeled as described above (SNL 2008 [DIRS 177407], Section 6.3.1 and Table 6.3-1). When seepage occurs, advective transport pathways that include the waste package and drip shield are modeled as quasi-steady state (i.e., non-episodic) flow (SNL 2008 [DIRS 177407], Sections 6.3.3.2 and 6.3.2.4, respectively); within the waste package, the waste form and corrosion product domains are treated as being fully saturated (SNL 2008 [DIRS 177407], Section 6.3.3.2).

For conditions or locations for which seepage and drift wall condensation do not occur, unsaturated conditions control the mobility of radionuclides by diffusion (SNL 2008 [DIRS 177407], Section 6.3.3.2). For these no-seep conditions, the degree of water saturation in the waste package is calculated in *EBS Radionuclide Transport Abstraction* (SNL 2008 [DIRS 177407], Section 6.5.2.2) and used to modify the effective diffusion coefficient (SNL 2008 [DIRS 177407], Sections 6.3.4.1, 6.3.4.3, and 6.3.4.6). The effective diffusion coefficient is enhanced by greater liquid saturation, and is at maximum for fully saturated conditions.

For no-seep conditions, flow in the invert is described by *Multiscale Thermohydrologic Model* (SNL 2008 [DIRS 184433], Section 6.3.3), which represents the invert liquid saturation and the imbibition flux from the host rock, for use in *EBS Radionuclide Transport Abstraction* (SNL 2008 [DIRS 177407], Section 6.3.3.4). The in-drift temperature and humidity conditions provided by the multiscale model control the liquid saturation of degradation products within the waste package. Liquid saturation in the invert, and in the waste package, is used in calculating the effective diffusion coefficients for radionuclide transport. The multiscale model also provides the flux of water that wicks into the invert from the host rock (SNL 2008 [DIRS 184433], Section 6.3.3), and this small advective flux is incorporated in the EBS transport model (SNL 2008 [DIRS 177407], Section 6.5).

The composition of water in the EBS, whether present due to seepage, condensation, or capillary wicking, is represented in TSPA as discussed in *Engineered Barrier System: Physical and Chemical Environment* (SNL 2007 [DIRS 177412], Section 6.15). In-drift water composition is equilibrated to local conditions of temperature, relative humidity, and in-drift partial pressure of carbon dioxide. Seepage water and gas phase (carbon dioxide) compositions are abstracted from time-dependent outputs of the near-field chemistry model (SNL 2007 [DIRS 177412], Sections 6.7 and 6.9) corresponding to locations at or adjacent to the drift wall. In-drift evolution of seepage, condensation, and capillary waters is described by the seepage evaporation abstraction and the invert pore-water abstraction (SNL 2007 [DIRS 177412], Sections 6.9, 6.13, and 6.15).

Transport predictions are particularly sensitive to the porosity and pore volume, water saturation, interfacial diffusive areas, diffusive path lengths, and diffusion coefficients. Uncertainty in the output of the EBS flow and transport model is accounted for by using a range of these values as inputs (SNL 2008 [DIRS 177407], Sections 6.3.4 and 6.5.2.2).

For the performance assessment to demonstrate compliance with the individual protection standard for human intrusion (proposed 10 CFR 63.321 (70 FR 53313 [DIRS 178394])), an intrusion borehole is assumed to be drilled from the ground surface, through a drip shield and a single waste package to the water table. Radionuclide mass is released from the intruded waste package to the EBS Transport submodel (SNL 2008 [DIRS 183478], Section 6.3.8). The percolation flux is used to calculate a volumetric flux through the intrusion borehole. The volumetric flux is assumed to flow directly into the penetrated waste package; no diversion of the water by the drip shield or waste package is considered. Thus, the volumetric flux represents the flow through the waste package for the advective component of the EBS transport calculation. For the diffusive component of the EBS transport calculation, the diffusive area is set equal to the cross-sectional area of the borehole and, by giving the invert a very large water volume, the downstream concentration boundary condition is set to a zero concentration to maximize diffusion out of the waste package (SNL 2008 [DIRS 183478], Section 6.7.3.1). The radionuclide mass (dissolved and colloidal) released from the waste package is assumed to be transported down the intrusion borehole to the water table.

INPUTS:

Table 2.1.08.07.0A-1. Indirect Inputs

Citation	Title	DIRS
70 FR 53313	Implementation of a Dose Standard After 10,000 Years	178394
SNL 2007	*Total System Performance Assessment Data Input Package for Requirements Analysis for EBS In-Drift Configuration*	179354
SNL 2008	*EBS Radionuclide Transport Abstraction*	177407
SNL 2007	*Engineered Barrier System: Physical and Chemical Environment*	177412
SNL 2008	*Multiscale Thermohydrologic Model*	184433

FEP: 2.1.08.09.0A

FEP NAME:

Saturated Flow in the EBS

FEP DESCRIPTION:

Saturated flow and radionuclide transport may occur along preferential pathways in the waste and EBS. Physical and chemical properties of the EBS and waste form, in both intact and degraded states, should be considered in evaluating pathways.

SCREENING DECISION:

Excluded – low consequence

SCREENING JUSTIFICATION:

This FEP addresses the potential for localized conditions of full saturation and the significance for TSPA. Flow within the EBS is additionally addressed in part by included FEP 2.1.08.06.0A (Capillary Effects (Wicking) in EBS), included FEP 2.1.08.05.0A (Flow Through Invert), and included FEP 2.1.08.07.0A (Unsaturated Flow in the EBS). The potential for ponding in the invert is addressed by excluded FEP 2.1.08.12.0A (Induced Hydrologic Changes in Invert).

The model for flow in the EBS is described in *EBS Radionuclide Transport Abstraction* (SNL 2008 [DIRS 177407], Sections 6.3 and 6.5). Hydraulic properties of EBS components and flow pathways within the EBS are discussed in detail in that report. The source of groundwater inflow to the EBS is the seepage flux that drips from the crown (roof) of the drift and imbibition flux from the unsaturated zone into the invert. In addition, there is a condensation flux. The inflow can flow through the EBS along eight pathways: (1) seepage flux, plus any condensation that may occur on the walls of the drift above the drip shield, (2) flux through the drip shield, (3) diversion around the drip shield, (4) flux through the waste package, (5) diversion around the waste package, (6) flux from the waste package into the invert, (7) imbibition flux from the unsaturated zone matrix to the invert, and (8) flux from the invert to the unsaturated zone fractures (SNL 2008 [DIRS 177407], Section 6.3.1.1 and Figure 6.3-1).

The repository drifts will be located, on the average, approximately 300 m above the current water table. The elevation of the repository will range from 1,039 to 1107 m (SNL 2007 [DIRS 179466], Table 4-1, Parameter Number 01-01), while the measured water table elevation under the repository for present-day conditions varies from approximately 730 m to 850 m (BSC 2004 [DIRS 169855], Figure 6-2). *Particle Tracking Model and Abstraction of Transport Processes* (SNL 2008 [DIRS 184748], Section 6.4.8) estimates from evidence of past changes in the water table that the water table will rise no more than 120 m in response to climate change in the future. Because the repository is located above the water table, water movement in the EBS as described above is conceptualized as flow under varying degrees of partial saturation (see included FEP 2.1.08.07.0A (Unsaturated Flow in the EBS)). For the invert, which is the lowest point in the EBS and one of the first places where saturation buildup could occur, the EBS radionuclide transport abstraction model explicitly represents the effects from advective liquid

inflow on radionuclide transport (SNL 2008 [DIRS 177407], Section 6.5). Under seep conditions, the waste form is assumed to be fully saturated; under no-seep conditions, the saturation is calculated from the temperature, relative humidity, and material properties. The effects of ponding within waste packages (bathtub condition) are also addressed as an alternative conceptual model in *EBS Radionuclide Transport Abstraction* (SNL 2008 [DIRS 177407], Section 6.6.1). Specifically, calculated releases from a fully saturated "bathtub waste package" are found to be less than or equal to those predicted by the model. Hence, the latter bounds releases, and the bathtub model was not carried forward into TSPA calculations.

While transient liquid saturation may approach 100% locally, large persistent saturated flow pathways in the EBS are not expected to occur. As shown by results from *Multiscale Thermohydrologic Model* (SNL 2008 [DIRS 184433], Section 6.3.3), without seepage or drift wall condensation the liquid saturation in the invert is less than 100% at all times. With seepage or local drift wall condensation, more water is available to potentially saturate EBS materials. The repository emplacement drift is designed to promote drainage and preclude wetting or ponding along the invert–rock interface (SNL 2007 [DIRS 179466], Table 4-1, Parameter Number 01-02; also see excluded FEP 2.1.08.12.0A (Induced Hydrologic Changes in Invert)). It is conceivable that granular debris from tunnel boring machine cuttings created during excavation could accumulate in fractures in the floor and inhibit drainage locally. Similarly, crushed tuff in the invert might be ground finer by waste emplacement and find its way into fractures. Saturation buildup in the invert, if it occurs, will form at the bottom and spread up the curved surface, accessing additional fractures for drainage and unsaturated rock. Spreading of saturation axially down the drift will also access additional fractures and unsaturated rock. In this manner, localized seepage or condensation can readily drain downward into the host rock. Spreading of the flow will therefore ultimately decrease the maximum flux per unit area and thereby reduce the overall potential for local rock saturation, thus decreasing the potential for saturated transport of released radionuclides.

Based on the above discussion, omission of FEP 2.1.08.09.0A (Saturated Flow in the EBS) will not result in a significant adverse change to the magnitude or time of radiological exposures to the RMEI or radionuclide releases to the accessible environment. Therefore, this FEP is excluded from the performance assessments conducted to demonstrate compliance with proposed 10 CFR 63.311 and 63.321 (70 FR 53313 [DIRS 178394]), and with 10 CFR 63.331 [DIRS 180319], on the basis of low consequence.

INPUTS:

Table 2.1.08.09.0A-1. Direct Inputs

Input	Source	Description
BSC 2004. *Development of Numerical Grids for UZ Flow and Transport Modeling*. [DIRS 169855]	Figure 6-2	Measured water table elevation under the repository for present-day conditions varies from approximately 730 to 850 m
SNL 2008. *EBS Radionuclide Transport Abstraction*. [DIRS 177407]	Section 6.3.1.1 and Figure 6.3-1	Describes how inflow can flow through the EBS along eight pathways
	Sections 6.3 and 6.5	Describes hydraulic properties of EBS components and flow pathways within the EBS
SNL 2007. *Total System Performance Assessment Data Input Package for Requirements Analysis for Subsurface Facilities*. [DIRS 179466]	Table 4-1, Parameter Number 01-02	Repository emplacement drift design
	Table 4-1, Parameter Number 01-01	Repository location

Table 2.1.08.09.0A-2. Indirect Inputs

Citation	Title	DIRS
10 CFR 63	Energy: Disposal of High-Level Radioactive Wastes in a Geologic Repository at Yucca Mountain, Nevada	180319
70 FR 53313	Implementation of a Dose Standard After 10,000 Years	178394
SNL 2008	*EBS Radionuclide Transport Abstraction*	177407
SNL 2008	*Multiscale Thermohydrologic Model*	184433
SNL 2008	*Particle Tracking Model and Abstraction of Transport Processes*	184748

FEP: 2.1.08.11.0A

FEP NAME:

Repository Resaturation Due to Waste Cooling

FEP DESCRIPTION:

Following the peak thermal period, water in the condensation cap may flow downward, resaturating the geosphere dry-out zone and flowing into the drifts. This may lead to an increase in water content and/or resaturation in the repository.

SCREENING DECISION:

Included

TSPA DISPOSITION:

The thermal-hydrologic seepage model (BSC 2005 [DIRS 172232]) as abstracted for TSPA (SNL 2007 [DIRS 181244], Section 6.5.2) provides a detailed description of dryout, condensation, reflux, resaturation, and the potential impacts from these processes on seepage. This abstraction is incorporated into the TSPA along with thermal and hydrologic conditions provided by *Multiscale Thermohydrologic Model* (SNL 2008 [DIRS 184433]) to account for thermal effects on seepage (SNL 2007 [DIRS 181244], Section 6.5.2.1).

The MSTHM represents postclosure in-drift thermal-hydrologic conditions including the effects from host-rock dryout and resaturation, characterized by the output variables of temperature and liquid saturation at the drift wall (SNL 2008 [DIRS 184433], Section 6.2[a]). The effects of resaturation are represented at locations within the drift using MSTHM output, based on an assumption of uniform gas-phase composition at all points enclosed by the drift wall and above the invert (SNL 2008 [DIRS 184433], Section 5.5). Uncertainty in MSTHM results is propagated to TSPA calculations through the use of different rock thermal conductivities and a suite of percolation flux values (SNL 2008 [DIRS 184433], Section 6.3.16[a]). Other sources of uncertainty that could affect drift wall resaturation, and hence, in-drift thermal-hydrologic conditions, were evaluated using sensitivity analyses and found to be insignificant. These include uncertainties in rock hydrologic properties (SNL 2008 [DIRS 184433], Section 6.3.16[a]), in ventilation heat removal efficiency (SNL 2008 [DIRS 184433], Section 6.3.12), and in the effects of axial vapor transport (SNL 2008 [DIRS 184433], Section 6.3.18[a]).

Dryout conditions are explicitly represented by the maximum lateral extent of the boiling zone (dryout zone) in the pillars between drifts. The lateral extent of boiling is much smaller than the half-spacing between emplacement drifts (SNL 2008 [DIRS 184433], Figure 6.3-79[a]; SNL 2007 [DIRS 179466], Table 4-1, Parameter Number 01-13), enabling condensate and percolation flux to continuously drain between emplacement drifts. Storage of condensate in the rock will not be sufficient to augment seepage, nor will refluxing activity that converges on the drift opening as the dryout zone collapses (BSC 2005 [DIRS 172232], Section 6.2.4). These are significant factors in the thermal seepage model, in which seepage cannot occur until the drift

wall cools to below 100°C and resaturates. Uncertainty associated with the effect of the dryout zone on seepage was evaluated using sensitivity analyses varying the percolation flux, different fracture flow conceptual models, other thermal loads, and transient versus steady-state flow conditions (BSC 2005 [DIRS 172232], Section 6.2.4.2). The results of these calculations support the conclusion that seepage will not occur until the dryout zone resaturates to the drift wall.

The effect of resaturation on the composition of potential seepage is addressed in *Drift-Scale THC Seepage Model* (SNL 2007 [DIRS 177404], Section 6.5.5) and in the near-field chemistry model, described in *Engineered Barrier System: Physical and Chemical Environment* (SNL 2007 [DIRS 177412], Section 6.3.2). Sensitivity calculations have shown that seepage is dilute when it occurs after the drift wall cools to 100°C (SNL 2007 [DIRS 177413], Section 6.6.3). After cooldown, the composition of potential seepage waters converges to the composition of nearby pore waters in the host rock (SNL 2007 [DIRS 177413], Section 6.6.3). This behavior is represented in the near-field chemistry model (SNL 2007 [DIRS 177412], Section 6.3.2) by evaluating the evolution of in situ pore waters as they percolate downwards to the repository level, interacting with host-rock minerals. The predicted water compositions are used in performance assessment calculations to represent potential seepage after resaturation of the near field when seepage becomes possible.

INPUTS:

Table 2.1.08.11.0A-1. Indirect Inputs

Citation	Title	DIRS
BSC 2005	*Drift-Scale Coupled Process (DST and TH Seepage) Models*	172232
SNL 2007	*Abstraction of Drift Seepage*	181244
SNL 2007	*Drift-Scale THC Seepage Model*	177404
SNL 2007	*Engineered Barrier System: Physical and Chemical Environment*	177412
SNL 2007	*THC Sensitivity Study of Heterogeneous Permeability and Capillarity Effects*	177413
SNL 2007	*Total System Performance Assessment Data Input Package for Requirements Analysis for Subsurface Facilities*	179466
SNL 2008	*Multiscale Thermohydrologic Model*	184433

FEP: 2.1.08.12.0A

FEP NAME:

Induced Hydrologic Changes in Invert

FEP DESCRIPTION:

Drainage in the drifts may be altered by plugging of fractures or floor buckling. Possible effects include wetting or ponding in the invert until the water level reaches the fractures in the wall or until there is sufficient hydraulic head to clear the fractures. Wetting or ponding could provide a continuing source of water vapor for interaction with the drip shields, waste packages, and their supports.

SCREENING DECISION:

Excluded – low consequence

SCREENING JUSTIFICATION:

The repository horizon lies above the water table, as documented in *Total System Performance Assessment Data Input Package for Requirements Analysis for Subsurface Facilities* (SNL 2007 [DIRS 179466], Table 4-1, Parameter Number 01-04). The emplacement drifts will be configured as a series of tunnels in the mountain. As described in *Geologic Framework Model (GFM2000)* (BSC 2004 [DIRS 170029], Table 6-2), the repository lies within four host-rock units (Tptpul, Tptpmn, Tptpll, and Tptpln). For the range of hydrologic properties of the four host-rock units (see SNL 2007 [DIRS 179545], Table 6-6), fracture permeability is sufficiently large and fractures are sufficiently well-connected to allow gravity-driven drainage of percolation to occur in an unrestricted fashion, thus preventing wetting and ponding in the invert. Included FEP 2.1.08.05.0A (Flow Through the Invert) discusses flow through the invert and saturation properties. If water build-up in the invert occurs, the relatively large permeability in this region will cause the flow to spread along the curved surface towards adjacent fractures. Moreover, as described in *In-Drift Natural Convection and Condensation* (SNL 2007 [DIRS 181648], Section 6.3.3.2.9), condensate on the drift wall will tend to be imbibed into the host rock, away from the drift opening. Moreover, this report indicates that elevated saturation at the invert surface is not expected at representative in-drift conditions, and that axial transport will play an important role mobilizing water vapor into other regions of the drift (see excluded FEP 2.1.08.14.0A (Condensation on Underside of Drip Shield)).

It is conceivable that granular debris from tunnel-boring machine cuttings created during excavation could accumulate in fractures in the floor and inhibit drainage or affect infiltration in localized areas. However, the effect of dust filling fractures may be temporary since infiltration studies in Alcove 8 show stabilization of infiltration/seepage rates between 400 to 700 days as described in *Analysis of Alcove 8/Niche 3 Flow and Transport Tests* (BSC 2006 [DIRS 178275], Sections 6.2.1, 6.2.4, and 6.4.2). According to that report (BSC 2006 [DIRS 178275]), infiltrating water in these tests mobilized particles away from percolation paths leading to eventual stabilization of seepage rates. Excavation activities tend to increase fracture permeability by about an order of magnitude as described in *In Situ Field Testing of Processes*

(BSC 2004 [DIRS 170004], Section 6.1.2.2.1). This increase in fracture permeability upon excavation could counteract the effect of fracture plugging as a result of accumulating rock debris by excavation activities. Therefore, the effect of fracture plugging on fracture permeability should be considered transitory and minimal within the time scale of the repository performance.

To preclude "wetting or ponding" as described in this FEP, the repository is designed with horizontal emplacement drifts. *Total System Performance Assessment Data Input Package for Requirements Analysis for Subsurface Facilities* (SNL 2007 [DIRS 179466], Table 4-1, Parameter Numbers 01-11 and 01-12) specifies the emplacement drift design:

> The grade of the emplacement drift shall be nominally horizontal so that overall water drainage travels directly into the rock to prevent water accumulation…. The repository nonemplacement opening shall provide a repository grade so overall water drainage and accumulation travels away from emplacement areas.

Excluded FEP 2.1.07.06.0A (Floor Buckling) corroborates this justification as drift floor buckling is determined to be negligible with respect to creating conditions that would support ponding.

Thus, the repository emplacement drift is designed to preclude full wetting or ponding in the invert domain. Saturation buildup in the invert, if it occurs, will form at the bottom and spread up the curved surface, accessing additional fractures for drainage. Spreading of saturation axially down the drift will also access additional fractures. In this manner, localized seepage or condensation can readily drain downward into the host rock. Spreading of the flow and water vapor migration through axial transport in the drift will limit the maximum attainable flux and thereby reduce the potential for rapid transport of released radionuclides.

Consistent with the above discussion, omission of FEP 2.1.08.12.0A (Induced Hydrologic Changes in Invert) will not result in a significant adverse change to the magnitude or time of radiological exposures to the RMEI or radionuclide releases to the accessible environment. Therefore, this FEP is excluded from the performance assessments conducted to demonstrate compliance with proposed 10 CFR 63.311 and 63.321 (70 FR 53313 [DIRS 178394]), and with 10 CFR 63.331 [DIRS 180319], on the basis of low consequence.

INPUTS:

Table 2.1.08.12.0A-1. Direct Inputs

Input	Source	Description
BSC 2004. *Geologic Framework Model (GFM2000)*. [DIRS 170029]	Table 6-2	Describes the host-rock units where the repository lies (Tptpul, Tptpmn, Tptpll, and Tptpln)
SNL 2007. *Calibrated Unsaturated Zone Properties*. [DIRS 179545]	Table 6-6	Describes range of hydrologic properties of the four host-rock units
SNL 2007. *Total System Performance Assessment Data Input Package for Requirements Analysis for Subsurface Facilities*. [DIRS 179466]	Table 4-1, Parameter Numbers 01-11 and 01-12	Specifies the emplacement drifts design
	Table 4-1, Parameter Number 01-04	Repository location in relation to water table

Table 2.1.08.12.0A-2. Indirect Inputs

Citation	Title	DIRS
10 CFR 63	Energy: Disposal of High-Level Radioactive Wastes in a Geologic Repository at Yucca Mountain, Nevada	180319
70 FR 53313	Implementation of a Dose Standard After 10,000 Years	178394
BSC 2006	*Analysis of Alcove 8/Niche 3 Flow and Transport Tests*	178275
BSC 2004	*In Situ Field Testing of Processes*	170004
SNL 2007	*In-Drift Natural Convection and Condensation*	181648

FEP: 2.1.08.14.0A

FEP NAME:

Condensation on Underside of Drip Shield

FEP DESCRIPTION:

Condensation of water on the underside of the drip shield may affect the waste package hydrologic and chemical environment.

SCREENING DECISION:

Excluded – low consequence

SCREENING JUSTIFICATION:

In-Drift Natural Convection and Condensation (SNL 2007 [DIRS 181648], Section 8[a]) predicts condensation rates and probabilities within the EBS. Condensation rates and probabilities are predicted using bounding cases that address vapor transport, mixing of gas under the drip shield, and the availability of moisture to evaporate in the invert. These bounding analyses (SNL 2007 [DIRS 181648], Sections 6.3.7.2 and 6.1[a]) evaluate the occurrence of condensation under the drip shield for several different conditions, including "unventilated" cases in which the regions under the drip shield and outside the drip shield are isolated, and "ventilated" cases with a single well-mixed region. Simulations under both conditions provide inputs to TSPA, to ensure that the uncertainty in the efficiency of gas-phase mixing is fully captured (SNL 2007 [DIRS 181648], Section 6.1.2[a]). The location and amount of condensation was also evaluated using upper and lower bounding water vapor pressures, corresponding to the saturated vapor pressures for temperatures at the top and at the base of the invert—the "high-invert transport" and "low-invert transport" conditions, respectively. As discussed in the following sections, condensation under the drip shield occurs only in the "high-invert transport" case, which is not anticipated to occur (SNL 2007 [DIRS 181648], Section 6.1.2[a]).

Analysis of the potential for condensation on the underside of the drip shield and its possible effects leads to a conclusion that condensation under drip shields will not occur. Even if it does occur, the overall effect on dose will be insignificant. This screening justification addresses the following issues:

- Conditions needed for condensation to occur under drip shields
- Conditions that limit condensation under drip shields
- Effect of condensate on corrosion of the drip shield/waste package
- Effects from condensate dripping onto waste packages
- Effect of condensation on transport of radionuclides outside the waste package.

Conditions Needed for Condensation to Occur Under Drip Shields – Condensation under the drip shield (particularly where condensate could contact the waste package) requires the invert temperature where evaporation occurs to be greater than the temperature of the upper half of the drip shield. Other conditions also apply as discussed below. Using this invert temperature criterion actually overstates the likelihood of condensation because the partial pressure of water vapor in the invert is decreased, relative to the saturation vapor pressure at the invert temperature, due to capillary vapor pressure lowering—the vapor pressure is equal to the saturation vapor pressure at the invert temperature minus the capillary pressure exerted by the invert porosity. Temperatures of the drip shield crown and the top of the invert beneath the drip shield are always within a few degrees of each other (higher or lower) as calculated in *Multiscale Thermohydrologic Model* (SNL 2008 [DIRS 184433], Table 6.3-45). This result is corroborated by experimental data from a 44%-scale natural convection test of the in-drift configuration, reported in *In-Drift Natural Convection and Condensation* (SNL 2007 [DIRS 181648], Tables 7.4.1-23 and 7.4.1-24). Because the temperature difference is minor, the difference in relative humidity at the two locations is small, and condensation under the drip shield requires that the top of the invert be very moist. This condition is evident from the bounding cases in the condensation model (SNL 2007 [DIRS 181648], Table 6.2[a]), which predict drip shield condensation only for cases with "high-invert transport" and none for "low-invert transport." In the "low-invert transport" cases, the vapor pressure in the drift is controlled by the lower-temperature bottom of the invert, resulting in drier conditions (lower relative humidity) at the hotter top of the invert.

In the "high-invert transport" cases, the occurrence of condensation under drip shields in the first 10,000 years is restricted to conditions of limited gas-phase exchange with the air outside of the drip shield. The drift wall outside the drip shield is cooler than the invert, because the invert is closer to the waste package. If water vapor can readily migrate to the air space outside of the drip shield—either through the drip shield interfaces or through the invert—then condensation will occur at the drift wall rather than under the drip shield. This condition is evident from the condensation model, which predicts drip shield condensation within the first 10,000 years only for "high-invert transport" cases with an "unventilated" drip shield (SNL 2007 [DIRS 181648], Tables 6.2[a] and 6.3[a]).

Finally, condensation within the emplacement region is more likely under conditions of limited axial transport, as efficient axial transport results in water vapor migration to the unheated portions of the drift and condensation in that region (SNL 2007 [DIRS 181648], Section 6.1.2[a]).

In summary, condensation on the underside of the drip shields requires very moist conditions in the invert, restricted vapor movement from the volume enclosed by the drip shield to the gas phase within the drift, and limited axial transport of water vapor to the cool regions at the ends of the drifts. However, as detailed below, these conditions are not anticipated in the emplacement drifts, and the process has limited consequence to system performance.

Conditions that Limit Condensation Under Drip Shields – In analyses in *In-Drift Natural Convection and Condensation* (SNL 2007 [DIRS 181648], Sections 6.3.7.2 and 6.1[a]), condensation under the drip shield occurs only in the "high-invert transport" case, which is not considered representative of in-drift conditions. Thermal-hydrologic simulations (SNL 2007

[DIRS 181648], Sections 6.3.3.2.1, 6.1.2[a], and 8[a]) show that condensation under any drip shield does not occur when the local water vapor partial pressure is controlled by the temperature at the bottom of the invert (the "low-invert transport" case), which is always cooler than the top of the invert and than the crown of the drip shield (SNL 2008 [DIRS 184433], Section 6.3.11 and Table 6.3-45). This is the expected condition in the emplacement drifts. The dewpoint is controlled by the lower invert, unless vapor transport through the invert is limited or the invert is flooded. Both of these conditions are not anticipated, because the porous, coarse-grained invert is permeable to gases and has little capability for water retention. At even the highest seepage rates, water does not pool in the invert. Also, water shed from the drip shield travels downward through the invert instead of laterally underneath it. Thus, the top of the invert cannot be maintained in a moist state by lateral flow from edges of the drip shield. In addition, the "high invert transport" cases use predicted temperatures directly under the waste package, which are higher than the average value for the entire invert surface under the drip shield. For these reasons, the "high-invert transport" cases are not implemented by TSPA, and condensation on the underside of the drip shield is not anticipated to occur (SNL 2007 [DIRS 181648], Section 6.1.2[a]).

In the bounding "high-invert transport" cases, condensation on the underside of a drip shield may occur if water vapor evaporates from the invert at one waste package location, then migrates under the connected drip shield segments and condenses on the underside of a cooler drip shield at another location (SNL 2007 [DIRS 181648], Section 6.3.7.2). However, calculations in *Multiscale Thermohydrologic Model* (SNL 2008 [DIRS 184433], Section 6.3.11 and Table 6.3-45) show that for any given cross-section, the coolest and most humid location is always at the bottom of the invert. Thus, water vapor that is transported axially along the drift will have a greater tendency to condense near the bottom of the invert, where it is coolest, rather than at the top of the invert or the underside of the drip shield. Thus, condensation on the underside of the drip shield will be limited by the efficiency of axial water vapor migration as compared with radial mixing.

The radial thermal gradient is much greater than the axial thermal gradient (SNL 2007 [DIRS 181648], Figures 6.3.5-13 and J-1). Such thermal gradients drive mixing, promoting condensation on cooler surfaces such as the drift wall, the bottom of the invert, or possibly the sides of the drip shield. Experimental results reported in *In-Drift Natural Convection and Condensation* (SNL 2007 [DIRS 181648], Table 7.4.1-24) show that the drip shield sides are cooler than the top, because of proximity to the waste package surface and because of natural convection. Therefore, any condensation occurs preferentially on the sides, where it cannot contact the waste package. This effect is not represented in the condensation model, which represents the underside of each drip shield as a single node in a lumped-parameter network, and does not distinguish the top and sides (SNL 2007 [DIRS 181648], Section 6.3.5.1.3).

A test was conducted to corroborate predictions of condensation under the drip shield as discussed in *Engineered Barrier System – Pilot Scale Test #3, Heated Drip Shield Test Results* (Howard et al. 2001 [DIRS 153282], Section 4.3). The test was a 1/4-scale heated experiment intended to evaluate a seeping environment within a simulated emplacement drift that included a simulated waste package, drip shield, invert, and supporting components similar to the EBS design. Water was introduced through the top of the test cell and fell onto the drip shield, from which it drained to the invert. The test showed that the invert under the drip shield remained

consistently dryer than outside the drip shield. These observations support the assertion that boundary conditions for the condensation model are bounding with respect to the physical reality of the test. The coolest temperatures on the drip shield were hotter than the coolest temperatures of the invert, and no condensation was observed under the drip shield (Howard et al. 2001 [DIRS 153282], Section 5). The important findings of this test include: (1) the "high invert" condition evaluated in the condensation model is an extreme bound that is not anticipated to occur even with seepage; and (2) if water vapor can readily migrate from inside to outside the drip shield (i.e., the drift wall, which is cooler than the drip shield, controls the dewpoint), then condensation on the underside of the drip shield will not occur.

The thermal-hydrologic modeling in *In-Drift Natural Convection and Condensation* (SNL 2007 [DIRS 181648], Sections 6.3.7.2 and 6.1[a]) is not applicable under conditions of drift collapse. In this case, moisture transport is limited, and the processes of evaporation and condensation are localized, and tend to cancel each other out (SNL 2007 [DIRS 181648], Section 6.2.2[a]). Should the drip shield remain intact, effective radiative coupling between the waste package and drip shield will ensure that drip shield temperatures are elevated relative to the bottom of the invert. Hence, condensation on the underside of the drip shield is not expected to occur in the drift collapse case.

Effects of Condensate on Corrosion of the Drip Shield/Waste Package – Although condensation on the underside of the drip shield is not anticipated, should it occur, the impact with respect to drip shield or waste package corrosion is negligible. The potential existence of condensate on the underside of the drip shield is limited to drip shield temperatures below the boiling point of water at the repository level, 96°C. Condensate on the underside of the drip shield will have a composition similar to rain water (i.e., a very dilute solution of carbonic acid with a pH of approximately 5.6) (Stumm and Morgan 1996 [DIRS 125332], p. 161), varying somewhat with the temperature and the partial pressure of carbon dioxide in the drift. Such an environment is a significant deviation from the nominal environments expected to form on the WPOB by evaporative concentration of seepage, as the dissolved ionic content will be extremely low in the case of condensation, and the chloride load will be negligible.

Cyclic polarization testing of Titanium Grade 7 has been carried out over a range of pH, temperature, cation and anion types, and concentrations (SNL 2007 [DIRS 180778], Tables 19 to 21), representing much more potentially corrosive conditions than dilute condensation, and localized corrosion was not observed. By extension, no localized corrosion is expected in condensation. Localized corrosion of the drip shield is never anticipated to occur within the repository environment (excluded FEP 2.1.03.03.0B (Localized Corrosion of Drip Shields)).

The model used to predict the localized corrosion initiation on the Alloy 22 WPOB was developed using data primarily from mixed salt solutions with significant concentrations of chloride, nitrate, and other cations and anions (SNL 2007 [DIRS 178519], Section 6.4.4.6.6). The regression fit to the model is therefore weighted towards representing medium to high concentration brines rather than extremely dilute solutions. This modeling approach is appropriate because the model will best represent behavior in electrolytes that are more likely to support the electrochemical and chemical reactions associated with localized corrosion. Applying the model to extremely dilute solutions results in predicting high open circuit values and can lead to an overestimation of the probability of localized corrosion initiation.

However, experimental data do not support the occurrence of localized corrosion of either Titanium Grade 7 or Alloy 22 in dilute solutions representing condensation. Long-term exposure testing of creviced Titanium Grade 7 and Alloy 22 was performed in the LTCTF, with samples located both in the aqueous phase and suspended above the aqueous phase in the vapor-phase environment. The experimental configuration was such that the temperature of the lid of the chamber was less than that of the heated aqueous solution, and evaporated electrolyte continuously condensed and dripped back down into the test chamber. Samples hung in the vapor phase experienced this dripping condensate environment (SNL 2007 [DIRS 178519], Section 6.4.3) and, therefore, reasonably estimate the response of the materials to the condensing environments that could potentially develop under repository conditions. Optical examination of the creviced samples in the vapor phase revealed no indication of crevice initiation on either of the materials for exposure periods of up to five years (SNL 2007 [DIRS 178519], Section 6.4.3; SNL 2007 [DIRS 180778], Section 6.5.3). This result is confirmation that condensing environments, even those that form above concentrated, repository-relevant electrolytes, will not initiate crevice corrosion of either Alloy 22 or Titanium Grade 7.

Further support for the conclusion that Alloy 22 will not undergo crevice corrosion when exposed to the potential condensate environments is provided by the results of long-term exposure of Alloy C (UNS N06455), a less corrosion resistant material than Alloy 22, to a marine environment. Alloy C specimens exposed for 44 years to a marine environment at North Carolina's Kure Beach (i.e., with salt, air, and alternate wetting and drying, as well as the presence of surface deposits) (Baker 1988 [DIRS 154510], p. 134 and Table 6) indicated that passivity of this alloy was maintained over this long exposure period, as evidenced by the observation of a mirror-like surface finish after surface deposits were removed. Examination of specimens from this alloy after more than 50 years of exposure indicated that the samples continued to maintain a mirror-like finish indicative of passive behavior (McCright 1998 [DIRS 114637], Figure ES-1).

Brines formed by deliquescence of salts in dust on the waste package or drip shield may mix with condensate to yield somewhat more concentrated solutions than condensate alone. However, the resulting solutions are no more aggressive than the deliquescent brines without condensate. Brines formed by dust deliquescence are addressed by excluded FEPs 2.1.09.28.0A (Localized Corrosion on Waste Package Outer Surface Due to Deliquescence) and 2.1.09.28.0B (Localized Corrosion on Drip Shield Surfaces Due to Deliquescence).

Effects from Condensate Dripping Onto Waste Packages – Condensation on the underside of the drip shield could mobilize radionuclides out of the waste package if the water were to drip onto and penetrate the waste package wall, particularly the WPOB. Seismic ground motion and the resulting dynamic interaction of waste packages, pallets, and the drip shield can produce waste package damage from end-to-end impacts and package-pallet impacts (SNL 2007 [DIRS 176828], Section 6.5). Seismic damage occurs as stress corrosion cracks, and advective flow of liquid water through such cracks is addressed by excluded FEP 2.1.03.10.0A (Advection of Liquids and Solids Through Cracks in the Waste Package). General corrosion of the Alloy 22 WPOB will be very slow, and the lifetime will be well in excess of 10,000 years (SNL 2007 [DIRS 178519], Section 8.1); thus, the types of breaches that occur under intact drip shields (no seepage contact) are limited to stress corrosion cracks. In summary, condensate will not increase corrosion, and the gravity-influenced flow of any condensate under the drip shield will not

penetrate the waste package wall, thus limiting advective transport of radionuclides from the waste package. It is recognized that condensation can run down to the underside of the waste package, but this water would need to move against gravitational force, at that point, to enter the waste package. Consequently, condensation under the drip shield will not increase the net quantity of radionuclides exiting a waste package damaged by a seismic event, even were it to drip or condense on the WPOB.

Dripping of condensate is only possible if water droplets form near the top of the drip shield; otherwise they will flow down the underside of the drip shield. If drops contact the waste package, they will tend to evaporate because the waste package is warmer than the drip shield and the relative humidity at the waste package surface is lower, thus reducing the volume of condensate available for advective transport of radionuclides. As noted above, the most probable breaches are stress corrosion cracks. These cracks do not allow advective flow. By the time the waste package has degraded to allow general corrosion breaches, there are no drip shields present. In addition, in other cases (fault displacement and igneous intrusion) there is no drip shield that could be the location of condensation.

Effect of Condensation on Transport Outside the Waste Package – In *EBS Radionuclide Transport Abstraction* (SNL 2008 [DIRS 177407], Section 8.1), the gap between the waste package and the invert, which could inhibit diffusive transport of radionuclides, is ignored for transport purposes, and the waste package is assumed to contact the invert. Hence, the occurrence of condensate would have no effect on transport pathways from the waste package. Condensation under the drip shield could result in increased invert flux or saturation, potentially resulting in greater radionuclide transport through the invert. However, the effects of drift wall condensation on invert transport are accounted for in TSPA, and mass balance requirements ensure that any increased flux due to condensation under the drip shield is balanced by a corresponding decrease in drift wall condensation.

Based on the above discussion, omission of FEP 2.1.08.14.0A (Condensation on Underside of Drip Shield) will not result in a significant adverse change in the magnitude or time of radiological exposures to the RMEI or radionuclide releases to the accessible environment. Therefore, this FEP is excluded form the performance assessments conducted to demonstrate compliance with proposed 10 CFR 63.311 and 63.321 (70 FR 53313 [DIRS 178394]), and with 10 CFR 63.331 [DIRS 180319], on the basis of low consequence.

INPUTS:

Table 2.1.08.14.0A-1. Direct Inputs

Input	Source	Description
SNL 2007. *Seismic Consequence Abstraction*. [DIRS 176828]	Section 6.5	Description of waste package damage due to seismic ground motion
SNL 2007. *General Corrosion and Localized Corrosion of the Drip Shield*. [DIRS 180778]	Tables 19, 20, and 21	Range of testing conditions for cyclic polarization testing of Titanium Grade 7
	Section 6.5.3	Titanium samples from the vapor phase of localized corrosion experiments did not undergo localized corrosion
SNL 2007. *General Corrosion and Localized Corrosion of Waste Package Outer Barrier*. [DIRS 178519]	Section 6.4.4.6.6	General compositions of test solutions used to develop the localized corrosion model for Alloy 22
	Section 6.4.3	Alloy 22 samples in the vapor phase for localized corrosion experiments experienced condensation. Also, samples from the vapor phase did not undergo localized corrosion
	Section 8.1	General corrosion of the Alloy 22 outer barrier will not lead to failure within 10,000 years
SNL 2007. *In-Drift Natural Convection and Condensation*. [DIRS 181648]	Figures 6.3.5-13 and J-1	The radial thermal gradient is much greater than the axial thermal gradient
	Sections 6.3.7.2 and 6.1[a]	Bounding analysis showing conditions for condensation under the drip shield
	Table 6.2[a]	Condensation model predicts no drip shield condensation for the first 10,000 years, for all cases with a “ventilated” drip shield
	Section 6.3.7.2	Condensation under a drip shield may occur if water vapor evaporates from the invert at one waste package location, then migrates under the connected drip shield segments and condenses on the underside of a cooler drip shield at another location
	Table 7.4.1-24	Experimental results show that the drip shield sides are cooler than the top
	Section 6.1.2[a]	Both “ventilated” and “unventilated” condensation model results are used by TSPA, to ensure the efficiency in gas phase mixing is fully captured
	Section 6.1.2[a]	Condensation within the emplacement region is more likely under conditions of limited axial transport, as efficient axial transport results in water migration to the unheated portions of the drift and condensation in that region
	Section 6.1.2[a]	The “high-invert transport” cases are not used by TSPA, and condensation on the underside of the drip shield is not anticipated to occur

Table 2.1.08.14.0A-1. Direct Inputs (Continued)

Input	Source	Description
SNL 2007. *In-Drift Natural Convection and Condensation*. [DIRS 181648] (continued)	Section 6.2.2[a]	If moisture transport within the drift is limited (as in the drift collapse case), evaporation and condensation are localized and tend to cancel each other out
	Sections 6.3.3.2.1, 6.3.7.2, 6.1[a], 6.1.2[a], 8[a]; Tables 6.2[a], and 6.3[a]	Condensation under the drip shield only occurs in the "high invert transport" simulations, where the local water vapor partial pressure is controlled by the temperature at the top of the invert. It does not occur in the "low invert transport" simulations, where to vapor pressure is controlled by the temperature at the bottom of the invert
SNL 2008. *Multiscale Thermohydrologic Model*. [DIRS 184433]	Table 6.3-45	Calculated temperatures of the crown of the drip shield and the top of the invert beneath the drip shield are always within a few degrees of each other

Table 2.1.08.14.0A-2. Indirect Inputs

Citation	Title	DIRS
10 CFR 63	Energy: Disposal of High-Level Radioactive Wastes in a Geologic Repository at Yucca Mountain, Nevada	180319
70 FR 53313	Implementation of a Dose Standard After 10,000 Years	178394
Baker 1988	"Long-Term Corrosion Behavior of Materials in the Marine Atmosphere"	154510
Howard et al. 2001	*Engineered Barrier System–Pilot Scale Test #3, Heated Drip Shield Test Results*	153282
McCright 1998	*Corrosion Data and Modeling, Update for Viability Assessment*	114637
SNL 2008	*EBS Radionuclide Transport Abstraction*	177407
SNL 2007	*In-Drift Natural Convection and Condensation*	181648
SNL 2008	*Multiscale Thermohydrologic Model*	184433
Stumm and Morgan 1996	*Aquatic Chemistry, Chemical Equilibria and Rates in Natural Waters*	125332

FEP: 2.1.08.15.0A

FEP NAME:

Consolidation of EBS Components

FEP DESCRIPTION:

Physical and chemical degradation of the drip shield, invert, waste form, and waste package may cause collapse and settlement within the repository. This consolidation may affect the development of the chemical environment and, therefore, the radionuclide transport out of the EBS.

SCREENING DECISION:

Excluded – low consequence

SCREENING JUSTIFICATION:

This FEP addresses the nonseismic-induced consolidation of EBS components due to physical and chemical degradation processes. Seismic-induced collapse and subsequent settling are considered in included FEPs 1.2.03.02.0A (Seismic Ground Motion Damages EBS Components) and 1.2.03.02.0C (Seismic-induced Drift Collapse Damages EBS Components). Collapse and settlement of engineered barrier components as they weaken from continuous degradation processes such as corrosion have the potential to impact long-term repository performance. If the components are reduced to essentially granular form, the remnants of the engineered barrier could more readily interact with water in the drift and thereby alter the potential for chemical transport of radionuclides. Granular materials might better filter colloids and/or sorb dissolved radionuclides. Complete degradation of EBS components might also produce colloidal material. Chemical degradation of EBS components, however, tends to produce insoluble metal oxides and, other than to locally consume oxygen, to have minor impact on the chemistries of the fluids that contact them. The fact that degradation rates are low means that degradation impacts on fluid chemistry will be low as well. The net effect is that neglecting these secondary impacts of degradation of the EBS components (as opposed to degradation that opens up fluid pathways to and from the waste) will not affect dose.

Mechanical damage to the drip shield or waste package due to nonseismic rockfall or drift collapse has been excluded from the TSPA (see excluded FEPs 2.1.07.01.0A (Rockfall) and 2.1.07.02.0A (Drift Collapse)). Thus, EBS consolidation due to waste package or drip shield mechanical failure, or both, is excluded. The same conclusion holds for the invert. Degradation and consolidation of the invert are excluded from the TSPA, as documented in excluded FEPs 2.1.06.05.0B (Mechanical Degradation of Invert) and 2.1.06.05.0D (Chemical Degradation of Invert). Thus, EBS consolidation due to invert, waste package and/or drip shield failure is excluded from the TSPA.

The corrosion rates associated with the drip shield and waste package are very slow compared to the time-scale of interest, and these features will not collapse for at least 10,000 years. Analyses for the Alloy 22 WPOB demonstrate that general corrosion would lead to a loss of only

145 nm/yr of the wall thickness, or about 1.45 mm in 10,000 years (SNL 2007 [DIRS 178519], Section 8.1). Because the thickness of the WPOB is 25.4 mm (SNL 2007 [DIRS 179394], Table 4-1, Parameter Number 03-03), the corrosion lifetime of the WPOB will greatly exceed 10,000 years, and the corrosion impacts on ambient fluid chemistry will be minimal.

Analyses for the drip shield show that general corrosion would lead to loss of approximately 46 nm/yr of the wall thickness for the aggressive environment, or about 0.46 mm in 10,000 years (SNL 2007 [DIRS 180778], Table 6.5[a]). The nominal minimum thickness of the drip shield is 15 mm (SNL 2007 [DIRS 179354], Table 4-2, Parameter Number 07-04). Thus, the corrosion lifetime of the drip shield is expected to exceed 100,000 years and the corrosion impacts on ambient fluid chemistry will be minimal.

Localized corrosion of the drip shield is not expected to occur under repository conditions as discussed in excluded FEPs 2.1.03.03.0B (Localized Corrosion of Drip Shields) and 2.1.09.28.0B (Localized corrosion on Drip Shield Surfaces due to Deliquescence), both of which are excluded on the basis of low consequence. Localized corrosion of the waste package is discussed in included FEP 2.1.03.03.0A (Localized Corrosion of Waste Packages). As discussed in that analysis, localized corrosion of the waste package requires the presence of an aqueous phase on the waste package surface. Possible sources of such liquid are dust deliquescence and seepage. Localized corrosion from dust deliquescence on the waste package surface is excluded from TSPA as discussed in excluded FEP 2.1.09.28.0A (Localized Corrosion on Waste Package Outer Surface due to Deliquescence). Seepage water can contact the waste package only if the overlying drip shield has failed (included FEP 2.1.03.03.0A (Localized Corrosion of Waste Packages)). An analysis of the type of drip shield failure required to allow seepage to contact the waste package is presented in included FEP 1.2.02.03.0A (Fault Displacement Damages EBS Components), which addresses the effects of fault displacements on the EBS components.

Following waste package breach, in-package radionuclide transport is described in *EBS Radionuclide Transport Abstraction* (SNL 2008 [DIRS 177407], Section 6.3.4). Once the waste package is breached, the waste form inside will degrade, and consolidation of materials inside the waste package will eventually occur. This will ultimately result in some mixing of waste form and steel components and settling as the structural integrity of the package interior erodes. Consolidation of waste package internals is expected to lower net porosity and decrease the movement of water and radionuclides through the degraded waste form. Moreover, occlusion of reactive surface areas of the waste form by steel corrosion products would tend to lower releases of radionuclides by decreasing waste form degradation rates. For these reasons, excluding the consolidation of waste package internals will not overestimate predicted transport from the package.

Because collapse and extensive degradation of EBS components does not occur (except as seismically induced degradation processes described by other FEPs), any consolidation of these items will be minor.

Based on the previous discussion, omission of FEP 2.1.08.15.0A (Consolidation of EBS Components) will not result in a significant adverse change in the magnitude or time of radiological exposures to the RMEI or radionuclide releases to the accessible environment. Therefore, this FEP is excluded from the performance assessments conducted to demonstrate

compliance with proposed 10 CFR 63.311 and 63.321 (70 FR 53313 [DIRS 178394]), and with 10 CFR 63.331 [DIRS 180319], on the basis of low consequence.

INPUTS:

Table 2.1.08.15.0A-1. Direct Inputs

Input	Source	Description
SNL 2007. *Total System Performance Assessment Data Input Package for Requirements Analysis for EBS In-Drift Configuration*. [DIRS 179354]	Table 4-2, Parameter Number 07-04	Nominal thickness of the drip shield is 15 mm
SNL 2007. *General Corrosion and Localized Corrosion of the Drip Shield*. [DIRS 180778]	Table 6.5[a]	Drip shield corrosion rate
SNL 2007. *General Corrosion and Localized Corrosion of Waste Package Outer Barrier*. [DIRS 178519]	Section 8.1	Corrosion of the Alloy 22 waste package outer barrier
SNL 2007. *Total System Performance Assessment Data Input Package for Requirements Analysis for TAD Canister and Related Waste Package Overpack Physical Attributes Basis for Performance Assessment*. [DIRS 179394]	Table 4-1 Parameter Number 03-03	The thickness of the waste package outer barrier is 25.4 mm

Table 2.1.08.15.0A-2. Indirect Inputs

Citation	Title	DIRS
10 CFR 63	Energy: Disposal of High-Level Radioactive Wastes in a Geologic Repository at Yucca Mountain, Nevada	180319
70 FR 53313	Implementation of a Dose Standard After 10,000 Years	178394
SNL 2008	*EBS Radionuclide Transport Abstraction*	177407

FEP: 2.1.09.01.0A

FEP NAME:

Chemical Characteristics of Water in Drifts

FEP DESCRIPTION:

When flow in the drifts is re-established following the peak thermal period, water may have chemical characteristics influenced by the near-field host rock and EBS. Specifically, the water chemistry (pH and dissolved species in the groundwater) may be affected by interactions with cementitious materials or steel used in the disposal region. These point source contaminated waters may coalesce to form a larger volume of contaminated water. This altered groundwater is referred to as the carrier plume because dissolution and transport will occur in this altered chemical environment as contaminants move through the EBS, and down into the unsaturated zone. (Note: there is no defining limit as to what volume of contaminated water constitutes a plume.)

SCREENING DECISION:

Included

TSPA DISPOSITION:

The composition of seepage water entering the drift is used in the suite of models developed in *Engineered Barrier System: Physical and Chemical Environment* (SNL 2007 [DIRS 177412], Sections 6.3 and 6.9), referred to as the P&CE report hereafter. The potential seepage water composition inputs for in-drift chemistry modeling were selected from the available pore-water analyses for the TSw and utilized in the near-field chemistry (NFC) model. The NFC model is developed in and provides feeds to the P&CE report (SNL 2007 [DIRS 177412], Section 6.3.2). The pore-water selection process is also documented in the P&CE report, as is an analysis of the interaction between seepage waters and the steels of the ground support and the invert (SNL 2007 [DIRS 177412], Sections 6.6 and 6.8). This analysis concluded that there is no significant effect of corroding steel on incoming groundwater owing to the precipitation of various Fe-Ni-Cr-bearing solid phases. Ground support interactions with water chemistry are also discussed in FEP 2.1.06.01.0A (Chemical Effects of Rock Reinforcement and Cementitious Materials in EBS), which is excluded on the basis of low consequence. In the event that additional materials are introduced in the subsurface, their impact on water chemistry will be evaluated (SNL 2007 [DIRS 179466], Table 4-1, Parameter Number 02-03).

The starting point for evaluating potential water compositions in the near field is the composition of ambient pore waters in the TSw. The available pore-water data from the four repository host units (Tptpul, Tptpmn, Tptpll, Tptpln) were evaluated and grouped into four compositional groups. This analysis is documented in the P&CE report (SNL 2007 [DIRS 177412], Section 6.6). Representative waters for the four groups were selected statistically, by choosing the sample closest to the centroid of the group. The representative waters and their compositions are listed in the P&CE report (SNL 2007 [DIRS 177412], Tables 4.1-2 and 4.1-3) and discussed in included FEP 2.2.08.12.0A (Chemistry of Water Flowing Into the Drift). Once the potential

seepage waters were selected, the NFC model evaluated the ambient feldspar dissolution rate, the dissolution rate temperature dependence, the model for the thermal field, and the plug flow model for transport through the TSw, and combined these to evaluate the amount of feldspar that dissolves as the water percolates downward through the unit to the repository. The result is WRIP that is the quantity of alkali feldspar to be added to the starting waters (SNL 2007 [DIRS 177412], Table 6.3-5). The WRIP value was calculated by taking as inputs the location-specific thermal field, and the percolation flux values (SNL 2007 [DIRS 177412], Section 6.3.2.4.3 and Table 6.3-1). Because the TSw is represented as a single unit with averaged rock properties and the feldspar dissolution rate is calculated from average alteration mineral abundances, the results of the WRIP calculation represent water–rock interaction over an average flow path through the unit.

To determine the range of potential seepage water compositions, the calculated amount of feldspar (WRIP) was titrated into the starting waters and brought to the drift wall temperature (SNL 2007 [DIRS 177412], Sections 6.3.2.4.2 and 6.3.2.7). To model the evaporative evolution of these seepage waters, the IDPS process model was applied (SNL 2007 [DIRS 177411]). To cover the expected range of environmental conditions, each seepage water was equilibrated with three temperatures (30°C, 70°C, and 100°C) and three pCO_2 values (10^{-2}, 10^{-3}, and 10^{-4} bar) and then evaporated to the eutectic mineral assemblage (SNL 2007 [DIRS 177412], Section 6.9). In addition, each starting seepage composition was diluted by a factor of 100 in order to account for dilution by condensation. It was determined that 11 discrete WRIP values were required to adequately represent the expected range of water–rock interactions. This resulted in the generation of 396 lookup tables (4 starting waters × 11 WRIP × 3 T × 3 pCO_2) that present the water chemistry data from combined dilution and evaporation simulations as a function of relative humidity (SNL 2007 [DIRS 177412], Section 6.9).

These lookup tables are used to account for uncertainty in incoming water compositions for performance assessment by randomly choosing one of the four starting waters and implementing the P&CE dilution/evaporation abstraction model according to the instructions provided by the P&CE report (SNL 2007 [DIRS 177412], Section 6.15) The predicted temperature and partial pressure of CO_2 in the drift is then used to determine the appropriate lookup table for that starting water, and the water composition is determined as a function of predicted relative humidity in the drift (SNL 2007 [DIRS 177412], Section 6.15).

Parameters extracted from the water chemistries archived in the lookup tables and used by the TSPA are pH, ionic strength, and Cl^- and NO_3^- concentrations as a function of in-drift relative humidity. The Cl^- and NO_3^- concentrations are taken as total [Cl] and total [N].

The potential effects of cementitious materials on water chemistry and repository hydrology are described in excluded FEPs 2.1.06.01.0A (Chemical Effects of Rock Reinforcement and Cementitious Materials in EBS) and 2.2.01.01.0B (Chemical Effects of Excavation and Construction in the Near-Field). As discussed in these FEPs, leaching of cementitious materials used in the turnouts in the main access and exhaust drifts could modify the composition of seepage water from the surrounding rock immediately below the main turnoff intersection footprints. This will occur sufficiently far from emplacement drifts that repository performance will not be affected.

Chemical interactions with corrosion products in the drift are discussed in included FEP 2.1.09.02.0A (Chemical Interaction with Corrosion Products).

INPUTS:

Table 2.1.09.01.0A-1. Indirect Inputs

Citation	Title	DIRS
SNL 2007	*Engineered Barrier System: Physical and Chemical Environment*	177412
SNL 2007	*In-Drift Precipitates/Salts Model*	177411
SNL 2007	*Total System Performance Assessment Data Input Package for Requirements Analysis for Subsurface Facilities*	179466

FEP: 2.1.09.01.0B

FEP NAME:

Chemical Characteristics of Water in Waste Package

FEP DESCRIPTION:

Chemical characteristics of the water in the waste packages (pH and dissolved species) may be affected by interactions with steel and other materials used in the waste packages or waste forms, as well as by the inflowing water from the drifts and near-field host rock. The in-package chemistry, in turn may influence dissolution and transport as contaminants move through the waste, EBS, and down into the unsaturated zone.

SCREENING DECISION:

Included

TSPA DISPOSITION:

The chemical characteristics of water in the waste package are included in *In-Package Chemistry Abstraction* (IPC) (SNL 2007 [DIRS 180506]). *In-Package Chemistry Abstraction* (SNL 2007 [DIRS 180506]) develops a fully coupled reaction-path chemical model that includes the effects of waste form dissolution, metal alloy corrosion or dissolution, precipitation of metal oxide corrosion products, precipitation of complex mineral phases, reaction kinetics, interior waste package void space, oxidation–reduction reactions, heterogeneous chemical reactions, and seepage composition on the resulting fluid chemistry. The abstraction primarily provides the distributions of pH and ionic strength predicted to prevail in the inner portions (i.e., the waste form) of breached waste packages exposed to either incoming seepage or condensed fluids (SNL 2007 [DIRS 180506]). The chemistry of fluids outside of the waste form, in contact primarily with steel and corrosion products, is provided in *EBS Radionuclide Transport Abstraction* (SNL 2008 [DIRS 177407], Section 6.5.2.4.6).

The variability in the initial chemistry of incoming water is included by using five different types of groundwaters at Yucca Mountain and three different groundwaters from basalt aquifers in sensitivity analyses (SNL 2007 [DIRS 180506], Section 6.6.2[a]). Sensitivity studies considered include these compositions, variations in seepage flux, and the corrosion rates of the steels that make up the waste package internals (SNL 2007 [DIRS 179394], Table 4-1, Parameter Number 04-07; SNL 2007 [DIRS 179567], Table 4-1, Parameter Number 04-07). Uncertainty bands over pH and ionic strength were modified, as necessary, to incorporate results of sensitivity simulations that varied the incoming water composition and the degradation rates of the various materials in the waste form cells (SNL 2007 [DIRS 180506], Section 6.6[a]).

In-Package Chemistry Abstraction (SNL 2007 [DIRS 180506], Section 6.10[a]) produces abstractions (including uncertainty) of solution pH, ionic strength, fluoride ion concentration, and total carbonate concentration that set the ranges over which the dissolved concentrations model (SNL 2007 [DIRS 177418]) is used to evaluate radionuclide solubilities. Separate abstractions are developed for commercial SNF waste packages and codisposal waste packages.

EBS Radionuclide Transport Abstraction (SNL 2008 [DIRS 177407], Section 6.5.2.4.6) estimates pH in the outer portions of the waste form (the corrosion products domain). This calculation is done by numerically equilibrating a range of waste form effluents with corrosion products to parameterize pH as a function of ambient carbon dioxide levels and to estimate the distribution of radionuclides between colloids, stationary corrosion products, and the solution.

INPUTS:

Table 2.1.09.01.0B-1. Indirect Inputs

Citation	Title	DIRS
SNL 2007	*Dissolved Concentration Limits of Elements with Radioactive Isotopes*	177418
SNL 2008	*EBS Radionuclide Transport Abstraction*	177407
SNL 2007	*In-Package Chemistry Abstraction*	180506
SNL 2007	*Total System Performance Assessment Data Input Package for Requirements Analysis for DOE SNF/HLW and Navy SNF Waste Package Overpack Physical Attributes Basis for Performance Assessment*	179567
SNL 2007	*Total System Performance Assessment Data Input Package for Requirements Analysis for TAD Canister and Related Waste Package Overpack Physical Attributes Basis for Performance Assessment*	179394

FEP: 2.1.09.02.0A

FEP NAME:

Chemical Interaction with Corrosion Products

FEP DESCRIPTION:

Corrosion products produced during degradation of the waste form, metallic portions of the waste package, and metals in the drift (i.e., rock bolts, steel in the invert, gantry rails) may affect the mobilization and transport of radionuclides. Corrosion products may facilitate sorption/desorption and co-precipitation/dissolution processes. Corrosion products may form a "rind" around the fuel that could (1) restrict the availability of water for dissolution of radionuclides or (2) inhibit advective or diffusive transport of water and radionuclides from the waste form to the EBS. Corrosion products also have the potential to retard the transport of radionuclides to the EBS. Finally, corrosion products may alter the local chemistry, possibly enhancing dissolution rates for specific waste forms, or altering radionuclide solubility.

SCREENING DECISION:

Included

TSPA DISPOSITION:

Consideration is first given to chemical interaction with corrosion products in the waste form and waste package, followed by a discussion of the chemical interaction with corrosion products in the drift.

The in-package chemistry model developed in *In-Package Chemistry Abstraction* (SNL 2007 [DIRS 180506]) and the EBS radionuclide transport abstraction in *EBS Radionuclide Transport Abstraction* (SNL 2008 [DIRS 177407], Section 6.5.2.4.6) address in-package corrosion products (including gases) and their effect on in-package chemistry. The corrosion products of the steel and aluminum alloys in the waste package and their control on the concentration of aqueous species are of primary importance in determining the pH and ionic strength of the solution. In this way, the presence of steel corrosion products constitutes an indirect control over radionuclide solubilities.

As described in *Waste Form and In-Drift Colloids-Associated Radionuclide Concentrations: Abstraction and Summary* (SNL 2007 [DIRS 177423]), fixed and suspended colloidal corrosion products are modeled in the waste package. Suspended colloidal corrosion products are modeled in the drift. Corrosion colloids are assumed to form and are subject to concentration and stability constraints controlled by the aqueous chemistry. The potential development of rinds on fuel and glass waste surfaces has been included in the development of waste form degradation models by incorporating laboratory data derived from fuel and glass waste corrosion experiments. Clogging of stress corrosion cracks by corrosion products is considered in excluded FEP 2.1.03.10.0A (Advection of Liquids and Solids through Cracks in the Waste Package).

Model implementation of the following phenomena related to colloids and steel corrosion in the waste package is described in *Waste Form and In-Drift Colloids-Associated Radionuclide Concentrations: Abstraction and Summary* (SNL 2007 [DIRS 177423]):

- Formation of iron oxyhydroxide colloids and fixed corrosion products in the waste package (Section 6.3.1)
- Estimation of stability and mass concentration of iron oxyhydroxide colloids from experimental results and calculated ionic strength and pH of in-package and in-drift fluids (Section 6.3.2.1)
- Irreversible sorption of plutonium and americium onto iron oxyhydroxide colloids and fixed corrosion products (Section 6.3.12.2)
- Reversible sorption of dissolved plutonium, americium, protactinium, thorium, and cesium onto iron oxyhydroxide colloids using developed K_d values and the estimated colloid mass concentrations (Section 6.3.12.1).

The effects of dissolved iron on the glass dissolution rates are addressed by using the results of tests in which iron products were added to the test solution (BSC 2004 [DIRS 169988], Appendix A) when determining model parameter values for pH dependence in acidic and alkaline solutions (BSC 2004 [DIRS 169988], Sections 6.5.2.4 and 6.5.2.5). The effects of glass alteration phases on the glass dissolution rate (k_E) are addressed by including the results of tests in which alteration phases and/or alteration product rinds form when determining model parameter values for k_E (BSC 2004 [DIRS 169988], Section 6.5.3.3).

The effects of corrosion product formation on in-drift water chemistry and gas composition are evaluated in *Engineered Barrier System: Physical and Chemical Environment* (SNL 2007 [DIRS 177412], Sections 6.6 and 6.7, respectively). The report examines the effects of corrosion products and includes in-drift water chemistry and gas composition as part of the modeled chemical processes. In addition, the report accounts for corrosion in its oxygen mass balance analysis, where in-drift gas composition calculations are used to evaluate oxygen consumption due to corrosion of ground support materials and other committed materials (SNL 2007 [DIRS 177412], Section 6.7). In the physical and chemical environment model, water compositions abstracted from the thermal-hydrological-chemical seepage model are reacted with the Stainless Steel Type 316L ground support at the drift wall (SNL 2007 [DIRS 177412], Section 6.8). The general picture that emerges is that only under a limited range of early times can steel corrosion consume more oxygen than naturally advects into the drift. For this reason, it is reasonable to model the drift atmosphere as oxidizing.

The effect of corrosion products on the transport of radionuclides internal to the waste package is included in the TSPA model. However, no radionuclide sorption is modeled to occur on corrosion products in the invert. As discussed in *EBS Radionuclide Transport Abstraction* (SNL 2008 [DIRS 177407], Sections 6.3.4.2, 6.5.1.2, and 6.5.2), retardation of radionuclides in the waste package corrosion products is modeled by application of sorption coefficients on corrosion products. Sorption of dissolved radionuclides on corrosion products is discussed in included FEP 2.1.09.05.0A (Sorption of Dissolved Radionuclides in EBS), and

implementation in the TSPA is explained in *EBS Radionuclide Transport Abstraction* (SNL 2008 [DIRS 177407], Section 6.3.4.2).

Corrosion products can form pseudocolloids as discussed in included FEP 2.1.09.17.0A (Formation of Pseudo-colloids (Corrosion Product) in EBS).

The primary uncertainties associated with corrosion product behavior are the degradation rates of the absolute masses of the steels and the surface areas of the corrosion products (SNL 2007 [DIRS 179394], Table 4-1, Parameter Number 04-07; SNL 2007 [DIRS 179567], Table 4-1, Parameter Number 04-07; SNL 2007 [DIRS 179466], Section 4.1.1). Uncertainties are quantified by considering a broad range of laboratory-measured degradation rates and surface areas and are propagated in the model by sampling over this range. The effects of corrosion products and their uncertainties on EBS chemistry, glass dissolution, and the transport of radionuclides internal to the waste package are included in the TSPA model through the previously discussed processes.

INPUTS:

Table 2.1.09.02.0A-1. Indirect Inputs

Citation	Title	DIRS
BSC 2004	*Defense HLW Glass Degradation Model*	169988
SNL 2008	*EBS Radionuclide Transport Abstraction*	177407
SNL 2007	*Engineered Barrier System: Physical and Chemical Environment*	177412
SNL 2007	*In-Package Chemistry Abstraction*	180506
SNL 2007	*Total System Performance Assessment Data Input Package for Requirements Analysis for DOE SNF/HLW and Navy SNF Waste Package Overpack Physical Attributes Basis for Performance Assessment*	179567
SNL 2007	*Total System Performance Assessment Data Input Package for Requirements Analysis for Subsurface Facilities*	179466
SNL 2007	*Total System Performance Assessment Data Input Package for Requirements Analysis for TAD Canister and Related Waste Package Overpack Physical Attributes Basis for Performance Assessment*	179394
SNL 2007	*Waste Form and In-Drift Colloids-Associated Radionuclide Concentrations: Abstraction and Summary*	177423

FEP: 2.1.09.03.0A

FEP NAME:

Volume Increase of Corrosion Products Impacts Cladding

FEP DESCRIPTION:

Corrosion products have a higher molar volume than the intact, uncorroded material. Increases in volume during waste form and cladding corrosion could change the stress state in the material being corroded and lead to cladding unzipping.

SCREENING DECISION:

Excluded – low consequence

SCREENING JUSTIFICATION:

For the performance assessments conducted to demonstrate compliance with proposed 10 CFR 63.311 and 63.321 (70 FR 53313 [DIRS 178394]), and with 10 CFR 63.331 [DIRS 180319], it is considered that all commercial SNF cladding (stainless steel and Zircaloy) is breached on emplacement in the repository as discussed in included FEP 2.1.02.12.0A (Degradation of Cladding Prior to Disposal) and in *Cladding Degradation Summary for LA* (SNL 2007 [DIRS 180616], Sections 6.2.1.2[a] and 7.2[a]). Furthermore, the zirconium-based (Zircaloy) and stainless steel SNF cladding is assumed to split instantly along the length of the fuel rods at the time of waste package failure. Cladding unzipping is assumed to result in immediate exposure of the commercial SNF fuel matrix to the failed waste package environment (included FEP 2.1.02.23.0A (Cladding Unzipping)). A waste package is considered to be failed at the time of the first penetration of the waste package by any process, including cracking, that allows ingress of oxygen and water vapor into the package.

Degradation of DOE SNF cladding (other than naval SNF cladding) is discussed in excluded FEP 2.1.02.25.0A (DSNF Cladding). As described in that FEP, the TSPA model considers that the DOE SNF cladding (with the exception of naval SNF cladding) will be breached upon emplacement in the repository and will neither inhibit groundwater contacting the DOE SNF matrix nor the release of radionuclides from the DOE SNF after groundwater contact.

Using this approach, commercial SNF and DOE SNF (other than naval SNF) cladding does not prevent the release or substantially reduce the release rate of radionuclides from the waste. Therefore, even if the volume increase associated with formation of corrosion products were to degrade the cladding, the additional impact of this FEP on cladding performance is of low consequence and will not affect the magnitude or timing of calculated radiological exposures to the RMEI or radionuclide releases to the accessible environment. FEP 2.1.09.03.0A (Volume Increase of Corrosion Products Impacts Cladding) can be excluded from the performance assessments conducted to demonstrate compliance with proposed 10 CFR 63.311 and 63.321 (70 FR 53313 [DIRS 178394]), and with 10 CFR 63.331 [DIRS 180319].

Naval SNF cladding is discussed in included FEP 2.1.02.25.0B (Naval SNF Cladding).

INPUTS:

Table 2.1.09.03.0A-1. Direct Inputs

Input	Source	Description
SNL 2007. *Cladding Degradation Summary for LA*. [DIRS 180616]	Sections 6.2.1.2[a] and 7.2[a]	Conservative assumption that all commercial SNF cladding (stainless steel and Zircaloy) is breached on receipt at the repository

Table 2.1.09.03.0A-2. Indirect Inputs

Citation	Title	DIRS
10 CFR 63	Energy: Disposal of High-Level Radioactive Wastes in a Geologic Repository at Yucca Mountain, Nevada	180319
70 FR 53313	Implementation of a Dose Standard After 10,000 Years	178394

FEP: 2.1.09.03.0B

FEP NAME:

Volume Increase of Corrosion Products Impacts Waste Package

FEP DESCRIPTION:

Corrosion products have a higher molar volume than the intact, uncorroded material. Increases in volume during waste form, cladding, and waste package corrosion could change the stress state in the material being corroded and lead to waste package damage.

SCREENING DECISION:

Excluded – low consequence

SCREENING JUSTIFICATION:

In general, corrosion products have greater volume than the parent metal as they are (typically) oxides (i.e., oxygen atoms are present in the corrosion products as well as parent metal atoms). When the corrosion products form in a tightly confined space, their increase in volume may generate swelling pressures that could lead to mechanical damage of the surrounding material. This FEP discusses the potential impact of corrosion products formed prior to and after breach of the waste package outer corrosion barrier. The discussion evaluates the possible mechanisms by which the waste package outer corrosion barrier could be breached. Cracks formed in the waste package outer corrosion barrier closure weld region and those due to seismic events are considered. Crack propagation rates are used to estimate the time required for cracks to penetrate the waste package outer corrosion barrier and aspects of crack morphology are discussed. Estimates of the time required to form significant amounts of corrosion products are determined and the characteristics of these corrosion products are summarized. Finally, the insignificant consequences of stresses resulting from corrosion product volume increase are discussed.

The waste package outer corrosion barrier will be fabricated from Alloy 22 (UNS N06022) with additional elemental and chemical composition restrictions (SNL 2007 [DIRS 179394], Table 4-1, Parameter Number 03-19, and Table 4-3). The inner vessel of the waste package is fabricated from Stainless Steel Type 316 (UNS S31600) (SNL 2007 [DIRS 179394], Table 4-3). For commercial SNF waste package types, a TAD canister will be placed inside the double-walled waste package. The TAD canister shall be constructed of 300-series stainless steel (such as UNS S31603, which may also be designated as Stainless Steel Type 316L) (SNL 2007 [DIRS 179394], Section 4.1.1.4). The codisposal waste packages containing HLW and DOE SNF will consist of an internal structure that cannot act as a viable structural component exerting stresses on the inner vessel.

Volume changes due to corrosion of components internal to the inner vessel or TAD canister (e.g., the internal structures within the commercial SNF packages or the canisters within the codisposal packages that contain HLW and DOE SNF) are of little concern as there is ample void space within the waste package to accommodate the expected change in volume due to

corrosion of these materials. The impacts of volume changes due to corrosion on cladding are addressed in excluded FEP 2.1.09.03.0A (Volume Increase of Corrosion Products Impacts Cladding). This FEP, therefore, considers the possible impacts of corrosion of the stainless steel inner vessel and the TAD canister. The current waste package design precludes the use of shrink fitting for the outer and inner cylinder components of the waste packages and requires the radial gap between the inner vessel and the outer corrosion barrier for the as-fabricated waste packages to be at least 1 mm and could be a maximum of 5 mm (SNL 2007 [DIRS 179394], Table 4-1, Parameter Number 03-04). The minimum radial gap between the TAD canister and the waste package inner vessel is 0.60 in. (15 mm) (SNL 2007 [DIRS 179394], Section 4.1.2.5). The waste package barrier longitudinal gap will be at least 30 mm (between the stainless steel inner vessel lid and the Alloy 22 waste package outer corrosion barrier lid) (SNL 2007 [DIRS 179394], Table 4-1, Parameter Number 03-05; SNL 2007 [DIRS 179567], Table 4-1, Parameter Number 03-05). The inner vessel for the TAD waste package configuration has an exterior length of 5,499.10 mm and has 50.8-mm-thick top and bottom lids (SNL 2007 [DIRS 179394], Table 4-3). Therefore, the interior length of the inner vessel for the TAD canister waste package configuration is 5,397.5 mm (5,499.10 mm – 2 × 50.8 mm). The exterior length of the TAD canister is 5,385.00 mm (SNL 2007 [DIRS 179394], Table 4-3). Therefore, the longitudinal gap between the TAD canister and waste package inner vessel for the TAD canister waste package configuration is 6.25 mm. As the radial gap between the waste package outer corrosion barrier and the waste package inner vessel is smaller than the axial gaps and the radial gap between the waste package inner vessel and TAD canister, the analyses in this FEP focus on the radial gap between the waste package outer corrosion barrier and the waste package inner vessel.

Prior to breach of the waste package outer corrosion barrier, only dry oxidation is possible. As discussed in excluded FEP 2.1.03.06.0A (Internal Corrosion of Waste Packages Prior to Breach), residual moisture in the waste packages could result in formation of a thin (on the order of 0.13 μm) corrosion product layer prior to breach of the waste package outer corrosion barrier. The impact of this thin corrosion product layer is not expected to lead to significant thermal expansion stresses in the waste package, as discussed in excluded FEP 2.1.11.07.0A (Thermal Expansion/Stress of In-Drift EBS Components). Therefore, mechanical damage to the Alloy 22 waste package outer corrosion barrier or the waste package inner vessel (Stainless Steel Type 316) due to the pressure exerted by corrosion products (e.g., Cr_2O_3, NiO, and iron oxides) will not occur prior to breach of the waste package outer corrosion barrier.

In order for significant corrosion of the waste package outer corrosion barrier inner surface and the stainless steel inner vessel to occur, the waste package outer corrosion barrier must first be breached. In those cases where the breach is modeled as complete failure (e.g., by early failure processes, igneous intrusion, or localized corrosion), volume increase of corrosion products does not need to be accounted for. General corrosion, even under extreme exposure conditions (e.g., a constant exposure temperature of 150°C for 10,000 years), will not cause breach of the waste package outer corrosion barrier in the first 10,000 years after repository closure (SNL 2007 [DIRS 178519], Section 8.1). Consequently, stress generation from volume increase of corrosion products could only occur within the first 10,000 years after repository closure if the waste package outer corrosion barrier is penetrated by stress corrosion cracking resulting either from a seismic event or residual stresses in the waste package closure lid region as discussed in included FEP 2.1.03.02.0A (Stress Corrosion Cracking (SCC) of Waste Packages).

The waste package outer lid closure weld region will be stress mitigated by plasticity burnishing, which will limit residual tensile stresses to below 90% of yield stress (the lower bound of the threshold stress for initiation of SCC) for a minimum depth of about 5 mm (SNL 2007 [DIRS 181953], Section 8.1.3 and Figure 6-48). In the absence of weld flaws or seismic activity, this mitigated layer must be removed by general corrosion before SCC can initiate on the waste package outer corrosion barrier. Using the median Alloy 22 general corrosion rate value (determined using the median temperature dependence) at 150°C of about 145 nm/yr (DTN: MO0612WPOUTERB.000 [DIRS 182035], file: *BaseCase GC CDFs2.xls*, worksheet: "MedU_MedC_Chart"), 5 mm of Alloy 22 would be removed in about 34,000 years. Using the median Alloy 22 general corrosion rate value (determined using the median temperature dependence) at 100°C of about 31 nm/yr (DTN: MO0612WPOUTERB.000 [DIRS 182035], file: *BaseCase GC CDFs2.xls*, worksheet: "MedU_MedC_Chart"), 5 mm of Alloy 22 would be removed in about 160,000 years. However, Alloy 22 general corrosion and SCC crack growth rates are uncertain, and may be fast enough to cause crack penetration within 10,000 years. The minimum and maximum SCC crack growth rates for Alloy 22 measured in aggressive brines relevant to the repository are 4.94×10^{-12} and 4.23×10^{-9} mm/s, respectively (SNL 2007 [DIRS 181953], Table 7-4). At these crack growth rates, it takes between approximately 150 and 130,000 years to penetrate the remaining 20 mm of the 25-mm-thick WPOB, assuming a constant crack growth rate as the cracks propagate. For seismic-induced residual stresses, the crack growth rate slows down (and may arrest) as the tensile stress and the stress intensity factor at the crack tip redistributes (decreases) during the crack propagation (SNL 2007 [DIRS 181953], Sections 6.7.1.2 and 7.5.1.2). The model-predicted mean crack propagation rate at a stress intensity factor of 40 MPa$\sqrt{m}$ is 1.00×10^{-9} mm/s (DTN: MO0705CREEPSCC.000 [DIRS 183681], file: *SDFRvData.xls*, worksheet: "Graphs1", cell F32), requiring approximately 630 years to penetrate the remaining 20 mm of the 25 mm thick WPOB. The model-predicted mean crack propagation rate at a stress intensity factor of 20 MPa$\sqrt{m}$ is about 4×10^{-11} mm/s (DTN: MO0705CREEPSCC.000 [DIRS 183681], file: *SDFRvData.xls*, worksheet: "Graphs1", cell F12), requiring approximately 16,000 years to penetrate the remaining 20 mm of the 25-mm-thick WPOB. In summary, in the absence of weld flaws or seismic activity, cracks are not expected to penetrate the waste package outer corrosion barrier within 10,000 years of closure.

Cracks originating from weld flaws that extend beyond the stress mitigated layer can propagate without any general corrosion of the mitigated layer. However, analyses estimate that about 16% of waste packages may have one or more weld flaws after ultrasonic inspection and repair (SNL 2007 [DIRS 178765], Table 6-6). These remaining weld flaws will be generally small (SNL 2007 [DIRS 178765], p. A-11, Figure "Marginal Pre to Post Repair Flaw Size"), with less than a one percent being longer than 5 mm (SNL 2007 [DIRS 178765], top of p. A-12). Also, as discussed previously, in the absence of seismic activity, for cracks to penetrate the waste package outer corrosion barrier within 10,000 years of closure, the waste package must have an unfavorable combination of several parameters (e.g., a stress and stress intensity factor profile and crack growth rate).

Cracks due to seismic activity are considered in *Seismic Consequence Abstraction* (SNL 2007 [DIRS 176828], Section 6.5), which analyzes several degraded waste package states, the most intact of which has a waste package outer corrosion barrier thinned to 23 mm from its initial thickness of about 25 mm. A seismic event with a mean annual exceedance value of 4.3×10^{-4}/yr

or greater is needed to possibly cause damage to a waste package resulting in SCC. For earlier times, prior to the waste package thinning to 23 mm; therefore, a seismic event of greater magnitude would be required to cause damage to a waste package. Damage from a 4.3×10^{-4}/yr mean annual exceedance value seismic event has only a small probability of occurrence on a codisposal waste package (0.029 using the lower bound 90% of yield strength stress threshold) (SNL 2007 [DIRS 176828], Table 6-16) and zero probability for a TAD canister-containing waste package (SNL 2007 [DIRS 176828], Table 6-4). The probability of damage occurring on a codisposal waste package from a 4.3×10^{-4}/yr mean annual exceedance value seismic event using a stress threshold of 100% of the yield strength is zero (SNL 2007 [DIRS 176828], Table 6-16). Thus, for a codisposal waste package, a bounding overall probability of damage per year is about 1.2×10^{-5}/yr ($0.029 \times 4.3 \times 10^{-4}$/yr). In order for seismic activity to result in crack penetrations on the waste package outer corrosion barrier within 10,000 years of closure, a seismic event with a mean annual exceedance probability of 4.3×10^{-4}/yr or lower (particularly for a TAD canister-containing waste package) would have to occur.

The seismic damage model determines an area damaged by seismic activity and considers this damaged area to have a network of crack penetrations. In the seismic damage model: (1) cracks are considered to be arranged in a tight hexagonal array, (2) cracks instantly propagate through the waste package outer corrosion barrier, independent of local stress gradients, (3) the area of the crack opening is maximized, based on a stress difference given by the yield stress, (4) the crack opening is constant throughout the waste package outer corrosion barrier thickness, and (5) there is no stress relief when a crack forms, even though there is no internal pressure to drive the cracks through the waste package outer corrosion barrier (SNL 2007 [DIRS 176828], Section 6.1.4). These conservatisms are discussed further in *Stress Corrosion Cracking of Waste Package Outer Barrier and Drip Shield Materials* (SNL 2007 [DIRS 181953], Section 6.7). In regard to point (1), it has been determined that the minimum distance between through-wall cracks is the thickness of the component. This value is used in determining the density of the network of crack penetrations due to seismic activity. The same minimum crack distance is used to characterize the density of cracks resulting from residual stresses in the waste package outer corrosion barrier closure weld region (i.e., cracks not resulting from seismic activity). The crack density will be lower than is represented by the seismic damage model or the stress corrosion cracking models used to evaluate repository performance. In regard to point (2), as discussed above in relation to crack growth in the waste package outer corrosion barrier closure weld region, there may be a significant period of time before crack penetration occurs. In regard to points (3), (4), and (5), as discussed above, crack growth and penetration will decrease the residual stress state. Because the crack opening area is determined by the magnitude of the residual stress and the yield stress is conservatively used for this value, the crack opening area determined is conservative.

As discussed in excluded FEP 2.1.03.10.0A (Advection of Liquids and Solids Through Cracks in the Waste Package), stress corrosion cracks in passive alloys such as Alloy 22 tend to be tight (i.e., small crack-opening displacement) and tortuous, often with many branches. SCC is a corrosion process that requires the presence of water to support crack propagation. The SCC process will result in accumulation of corrosion products and mineral precipitates in the limited crack volume. The tight and tortuous SCC cracks in the WPOB are expected to be continuously filled with tightly compact cemented agglomerates of solid corrosion products and mineral

precipitates as the cracks grow through the wall thickness. These agglomerates will limit water transport through these cracks. However, analyses documented in *EBS Radionuclide Transport Abstraction* (SNL 2008 [DIRS 177407], Section 6.6.2) indicate that there is sufficient water vapor transport through stress corrosion cracks so as not to limit corrosion reactions on the stainless steel waste package inner vessel. For waste packages exposed to seepage, it was estimated that crack plugging could require anywhere from hundreds to thousands of years. In the absence of seepage, crack plugging could take longer times.

When SCC occurs, no corrosion performance credit is taken for the waste package inner vessel and TAD canisters. Once the waste package outer corrosion barrier is breached by SCC, these components are treated as degraded material with minimal strength and cohesion. This is a reasonable treatment because the waste package inner vessel and TAD canisters are not stress relief annealed rendering them susceptible to stress corrosion cracking, and the corrosion rates of these stainless steel components are expected to be greater than the Alloy 22 waste package outer corrosion barrier. Thus, it is expected that the stainless steel waste package inner vessel and TAD canister will not function as effective mechanical components after breach of the waste package outer corrosion barrier. This is consistent with the treatment in *Seismic Consequence Abstraction* (SNL 2007 [DIRS 176828], Section 6.1.3.2).

Once the waste package outer corrosion barrier is breached by SCC, a significant amount of time is required before the radial gap between the waste package outer corrosion barrier and inner vessel can become filled with corrosion products. As the Alloy 22 waste package outer corrosion barrier and Stainless Steel Type 316 inner vessel corrode, the radial gap between the remaining uncorroded metal, $gap(t)$, is increased by the removal of metal by the corrosion process. However, the overall radial gap is decreased by the formation of corrosion products. The radial gap between the remaining uncorroded metal as a function of time is:

$$gap(t) = igap + \left(CRA22 + CR316\right) t \qquad \text{(Eq. 2.1.09.03.0B-1)}$$

where t is exposure time in years, $igap$ is the initial radial gap (1 mm to 5 mm, as discussed above), $CRA22$ is the Alloy 22 corrosion rate and $CR316$ is the Stainless Steel Type 316 corrosion rate. The decrease in the radial gap from the formation of corrosion products is given by:

$$c(t) = \left(CRA22 + CR316\right) \sqrt[n]{PB}\, t \qquad \text{(Eq. 2.1.09.03.0B-2)}$$

where PB refers to the Pilling-Bedworth volume ratio (i.e., the volume ratio of the metal to its corrosion product) (ASM International 1987 [DIRS 133378], p. 65). The Pilling-Bedworth ratio for Cr_2O_3 is 2.02, that for NiO is 1.70, and that for Fe_3O_4 is 2.10 (ASM International 1987 [DIRS 133378], p. 64, Table 2). Thus, given that the aforementioned oxides are possible corrosion products of Alloy 22 and Stainless Steel Type 316, a reasonable choice for PB would be 2.10. The factor n is included in Equation 2.1.09.03.0B-2 to account for the degree of constraint on the corrosion products formed. If the corrosion product is constrained in all directions except for the radial direction, then all of the corrosion product volume expansion would result in a decrease in the radial gap and $n = 1$. If the corrosion product is unconstrained then $n = 3$. A realistic choice might be $n = 2$. Setting the right-hand sides of Equations 2.1.09.03.0B-1 and 2.1.09.03.0B-2 equal to each other and solving for time, yields the time

required to fill the radial gap between the Alloy 22 waste package outer corrosion barrier and Stainless Steel Type 316 inner vessel, t_{fill}.

$$t_{fill} = \frac{igap}{CRA22\left(\sqrt[n]{PB}-1\right)+CR316\left(\sqrt[n]{PB}-1\right)} \qquad \text{(Eq. 2.1.09.03.0B-3)}$$

The median Alloy 22 general corrosion rate value (determined using the median temperature dependence) at 150°C is about 145 nm/yr (DTN: MO0612WPOUTERB.000 [DIRS 182035], file: *BaseCase GC CDFs2.xls*) and decreases to 31 nm/yr at an exposure temperature of 100°C (DTN: MO0612WPOUTERB.000 [DIRS 182035], file: *BaseCase GC CDFs2.xls*). According to *EBS Radionuclide Transport Abstraction* (SNL 2008 [DIRS 177407], Section 6.3.4.3.4.3) the corrosion rate of Stainless Steel Type 316 is given by a truncated normal distribution (between 0.01 and 0.51 μm/yr) with a true mean of 0.267 μm/yr (DTN: SN0703PAEBSRTA.001 [DIRS 183217], file: *Bayesian Updating Short Term Fresh Water Corrosion Rate - 3-6-2007.xls*, worksheet: "A316 SS Short Term Fresh Water"). Using the parameter values discussed earlier, values of t_{fill} can be evaluated for various choices of input values as shown in Table 2.1.09.03.03.0B-1.

Table 2.1.09.03.0B-1. Parameter Values Used to Calculate t_{fill}

			igap = 1 mm	igap = 3 mm	igap = 5 mm
CRA22 nm/yr	CR316 nm/yr	n	t_{fill} yr	t_{fill} yr	t_{fill} yr
145	510	1	1,388	4,164	6,940
31	510	1	1,680	5,041	8,402
145	510	2	3,399	10,198	16,996
31	510	2	4,116	12,347	20,578
145	267	1	2,207	6,620	11,033
31	267	1	3,051	9,152	15,253
145	267	2	5,404	16,212	27,020
31	267	2	7,471	22,414	37,357

As can be seen from Table 2.1.09.03.03.0B-1, exposure times between about 1,400 and 37,000 years are required to fill the radial gap between the Alloy 22 waste package outer corrosion barrier and Stainless Steel Type 316 inner vessel with corrosion products depending on the values of *CRA22, CR316, n,* and *igap*. These fill times would be required in addition to the crack penetration times discussed previously before the volume increase of corrosion products could have any mechanical impact on the waste package outer corrosion barrier.

It would be expected that corrosion products under compressive stress would have a lower effective porosity than corrosion products that are not under compressive stress, and would be expected to limit water ingress and radionuclide egress from the waste package. The adherent stainless steel and Alloy 22 corrosion products are responsible for their passive behavior. Corrosion products of less corrosion resistant materials such as carbon steel have been found to be protective for periods of thousands of years. As discussed by Miller et al. (1994 [DIRS 126089], pp. 114 to 119), a hoard of over one million nails were buried in a five meter deep pit and then covered with compacted earth around 87 A.D. Nails in the outer regions of the

hoard, unearthed in the 1950s, were found to have undergone extensive corrosion presumably forming a low permeability solid crust of corrosion products resulting in minimal corrosion attack of nails in the hoard interior. Similar processes could significantly decrease the corrosion rates of the materials internal to the waste package outer corrosion barrier as well as decreasing the rate of diffusive radionuclide transport out of breached waste packages. Taking no credit for this process in performance assessment may be conservative.

Even if the gap between the waste package outer corrosion barrier and waste package inner vessel were to become filled with corrosion products, significant impacts to degradation of the waste package outer corrosion barrier and the rate of radionuclide release are not expected. As mentioned previously, once the waste package corrosion outer barrier is breached, the waste package inner vessel and TAD canisters are degraded materials with reduced strength. If the corrosion products formed could apply stress on the waste package outer corrosion barrier, stress would then also be applied to the degraded waste package inner vessel. It is expected that these stresses would result in enhanced degradation of the already degraded waste package inner vessel (e.g., more stress corrosion cracking than would occur in the absence of the corrosion products). This would lead to the already degraded waste package inner vessel failing to act as an effective mechanical substrate from which the corrosion products could exert stresses on the waste package outer corrosion barrier. Significant degradation of the waste package inner vessel would then allow the corrosion products to expand into the internal void volume of the waste package instead of exerting significant stress on the waste package outer corrosion barrier.

Even if the corrosion products exert pressure on the waste package outer corrosion barrier, the modeled releases from stress corrosion cracking would not be increased, because as mentioned previously, the stress corrosion crack opening area used to evaluate repository performance is maximized in that the highest crack density is used and the cracks are considered to be held open by a residual stress equal to the yield stress. Thus, if some amount of actual crack widening occurred on the Alloy 22 waste package outer corrosion barrier surface resulting from stresses induced by corrosion product formation, it has been sufficiently accounted for in performance evaluations through the use of a maximized stress corrosion crack opening area (SNL 2007 [DIRS 176828], Section 6.1.4; SNL 2007 [DIRS 181953], Section 6.7) and by taking no credit for the decreased rate of radionuclide transport through compressed corrosion products in the cracks.

Related excluded FEP 2.1.09.03.0A (Volume Increase of Corrosion Products Impacts Cladding) discusses volume increase of corrosion products that could impact cladding.

Based on the previous discussion, omission of FEP 2.1.09.03.0B (Volume Increase of Corrosion Products Impacts Waste Package) will not result in a significant adverse change in the magnitude or timing of either radiological exposure to the RMEI or radionuclide releases to the accessible environment. Therefore, this FEP is excluded from the performance assessments conducted to demonstrate compliance with proposed 10 CFR 63.311 and 63.321 (70 FR 53313 [DIRS 178394]), and with 10 CFR 63.331 [DIRS 180319], on the basis of low consequence.

INPUTS:

Table 2.1.09.03.0B-1. Direct Inputs

Input	Source	Description
ASM International 1987. *Corrosion*. [DIRS 133378]	p. 64, Table 2	Values of Pilling-Bedworth ratio
DTN: MO0612WPOUTERB.000. Output from General and Localized Corrosion of Waste Package Outer Barrier Report. [DIRS 182035]	file: *BaseCase GC CDFs2.xls*	Alloy 22 general corrosion rates
DTN: SN0703PAEBSRTA.001. Inputs Used in the Engineered Barrier System (EBS) Radionuclide Transport Abstraction. [DIRS 183217]	file: *Bayesian Updating Short Term Fresh Water Corrosion Rate - 3-6-2007.xls*, worksheet: "A316 SS Short Term Fresh Water"	Stainless steel general corrosion rates
SNL 2007. *Stress Corrosion Cracking of Waste Package Outer Barrier and Drip Shield Materials*. [DIRS 181953]	Table 7-4	Minimum and maximum measured crack growth rates
SNL 2007. *Total System Performance Assessment Data Input Package for Requirements Analysis for DOE SNF/HLW and Navy SNF Waste Package Overpack Physical Attributes Basis for Performance Assessment*. [DIRS 179567]	Table 4-1, Parameter Number 03-05	Current waste package design radial and longitudinal gaps
SNL 2007. *Total System Performance Assessment Data Input Package for Requirements Analysis for TAD Canister and Related Waste Package Overpack Physical Attributes Basis for Performance Assessment*. [DIRS 179394]	Tables 4-1 and 4-3; Parameter Number 03-19	The waste package outer barrier will be fabricated from Alloy 22 (UNS N06022) with additional elemental and chemical composition restrictions
	Section 4.1.2.5	Minimum radial gap of 0.60 in. between the stainless steel TAD canister and the inner vessel
	Table 4-3	Dimensions of Stainless Steel Type 316 waste package inner vessel and TAD canister
	Table 4-1, Parameter Number 03-04	Current waste package designs require the radial gap between the inner vessel and the outer barrier to be at least 1 mm and could be a maximum of 5 mm
	Table 4-1, Parameter Number 03-05	Current waste package design radial and longitudinal gaps

Table 2.1.09.03.0B-2. Indirect Inputs

Citation	Title	DIRS
10 CFR 63	Energy: Disposal of High-Level Radioactive Wastes in a Geologic Repository at Yucca Mountain, Nevada	180319
70 FR 53313	Implementation of a Dose Standard After 10,000 Years	178394
ASM International 1987	*Corrosion*	133378
DTN: MO0705CREEPSCC.000	Supplementary Output DTN from SCC AMR	183681
Miller et al. 1994	*Natural Analogue Studies in the Geological Disposal of Radioactive Wastes*	126089
SNL 2007	*Seismic Consequence Abstraction*	176828
SNL 2007	*Analysis of Mechanisms for Early Waste Package/Drip Shield Failure*	178765
SNL 2008	*EBS Radionuclide Transport Abstraction*	177407
SNL 2007	*General Corrosion and Localized Corrosion of Waste Package Outer Barrier*	178519
SNL 2007	*Stress Corrosion Cracking of Waste Package Outer Barrier and Drip Shield Materials*	181953
SNL 2007	*Total System Performance Assessment Data Input Package for Requirements Analysis for TAD Canister and Related Waste Package Overpack Physical Attributes Basis for Performance Assessment*	179394

FEP: 2.1.09.03.0C

FEP NAME:

Volume Increase of Corrosion Products Impacts other EBS Components

FEP DESCRIPTION:

Corrosion products have a higher molar volume than the intact, uncorroded material. This FEP addresses volume increase in all EBS components other than waste package, waste form, and cladding. Increases in volume during corrosion of steel in the invert may change the stress state or structural integrity of the invert.

SCREENING DECISION:

Excluded – low consequence

SCREENING JUSTIFICATION:

The effects of volume increase caused by corrosion of steel in the invert is excluded on the basis of low consequence, in accordance with proposed 10 CFR 63.342 (70 FR 53313 [DIRS 178394]). This FEP represents one mechanism by which corrosion might cause mechanical failure of the invert. Mechanical degradation of the invert is addressed under FEP 2.1.06.05.0B (Mechanical Degradation of Invert), which is excluded on the basis of low consequence. Corrosion product impacts on cladding, waste form, and waste packages are discussed in excluded FEPs 2.1.09.03.0A (Volume Increase of Corrosion Products Impacts Cladding) and 2.1.09.03.0B (Volume Increase of Corrosion Products Impacts Waste Package).

The bulk of EBS materials degrade slowly and with only minor volume changes. Carbon steel is the notable exception. As discussed in *Engineered Barrier System: Physical and Chemical Environment* (SNL 2007 [DIRS 177412], Section 6.5.2, Figure 6.5-3), the carbon steel components in the invert are predicted to corrode relatively rapidly (i.e., within a few hundred years) as compared to other in-drift committed materials. Moreover, it corrodes to iron oxide and hydroxides whose molar volume is larger than the original steel.

The ability of carbon steel mechanical supports, which comprise the invert substructure, to induce mechanical loads by volume expansion will not be large. As the steel invert structural components degrade, their total volume, including the corrosion products, will increase; however, as the volume of these materials increases, it can expand vertically without resistance into the drift, and thus, will create no increase in stresses in the support system. Any volume expansion in the invert of the drip shield due to corrosion will impose no added stress because the drip shield is not rigidly mounted to the invert and would move as a rigid body into the drift (SNL 2007 [DIRS 179354], Table 4-2, Parameter Number 07-01). Configuration of the invert steel structure is shown in *Total System Performance Assessment Data Input Package for Requirements Analysis for Engineered Barrier System In-Drift Configuration* (SNL 2007 [DIRS 179354], Table 4-1, Parameter Numbers 02-08 and 02-10).

Corrosion of steel rock bolts, plates, and Bernold sheets would result in the formation of corrosion products in the ground support system and possibly local buckling in the latter. This would not affect performance as no credit is taken for postclosure performance of the ground support system.

Based on the previous discussion, omission of FEP 2.1.09.03.0C (Volume Increase of Corrosion Products Impacts Other EBS Components) will not result in a significant adverse change in the magnitude or time of radiological exposures to the RMEI or radionuclide releases to the accessible environment. Therefore, this FEP is excluded from the performance assessments conducted to demonstrate compliance with proposed 10 CFR 63.311 and 63.321 (70 FR 53313 [DIRS 178394]), and with 10 CFR 63.331 [DIRS 180319], on the basis of low consequence.

INPUTS:

Table 2.1.09.03.0C-1. Direct Inputs

Input	Source	Description
SNL 2007. *Engineered Barrier System: Physical and Chemical Environment*. [DIRS 177412]	Section 6.5.2, Figure 6.5-3	Predicted corrosion of the carbon steel components in the invert

Table 2.1.09.03.0C-2. Indirect Inputs

Citation	Title	DIRS
10 CFR 63	Energy: Disposal of High-Level Radioactive Wastes in a Geologic Repository at Yucca Mountain, Nevada	180319
70 FR 53313	Implementation of a Dose Standard After 10,000 Years	178394
SNL 2007	*Total System Performance Assessment Data Input Package for Requirements Analysis for EBS In-Drift Configuration*	179354

FEP: 2.1.09.04.0A

FEP NAME:

Radionuclide Solubility, Solubility Limits, and Speciation in the Waste Form and EBS

FEP DESCRIPTION:

Degradation of the waste form will mobilize radionuclides in the aqueous phase. Factors to be considered in this FEP include the initial radionuclide inventory, justification of the limited inventory included in evaluations of aqueous concentrations, and the solubility limits for those radionuclides.

SCREENING DECISION:

Included

TSPA DISPOSITION:

Dissolved Concentration Limits of Elements with Radioactive Isotopes (SNL 2007 [DIRS 177418]) develops thermodynamic models for quantifying speciation, and estimating dissolved concentration limits of radionuclides, in the package and invert. TSPA uses these models to estimate maximal levels of sparingly soluble actinides over time. An initial assessment of radionuclide inventories is made to identify those radioelements that will be present in the repository and are expected to contribute to dose (SNL 2007 [DIRS 177424]). The speciation of, and solubility limits for, plutonium, neptunium, uranium, thorium, americium, protactinium, and tin are then calculated and tabulated as functions of pH and $\log f\mathrm{CO}_2$.

The primary uncertainties in calculated solubilities are temperature, fluoride levels, and the identity of the solubility-controlling phase(s). There are also uncertainties inherent in the thermodynamic functions describing the solubility of a given phase. Temperature and oxygen fugacity were conservatively bounded by using 25°C and 20% O_2 levels. Similarly, higher solubility phases were used to bound dissolved concentrations. A range of fluoride levels was used in the calculations. Lastly, uncertainties in thermodynamic data were accounted for by using a range of values.

For very soluble elements, solubility limits are not determined. Instead, their releases are considered to be controlled by the dissolution rate of waste forms and the waste inventory. Elements in this category are technetium, carbon, iodine, cesium, strontium, selenium, and chlorine. In part, because of the relatively short half-lives of ^{227}Ac and ^{210}Pb, solubility limits of actinium and lead were not investigated in the dissolved concentrations report. Instead their levels are conservatively set in TSPA to be in secular equilibrium with their parent isotopes.

INPUTS:

Table 2.1.09.04.0A-1. Indirect Inputs

Citation	Title	DIRS
SNL 2007	*Dissolved Concentration Limits of Elements with Radioactive Isotopes*	177418
SNL 2007	*Radionuclide Screening*	177424

FEP: 2.1.09.05.0A

FEP NAME:

Sorption of Dissolved Radionuclides in EBS

FEP DESCRIPTION:

Sorption of dissolved radionuclides within the waste package may affect the aqueous concentrations of radionuclides released to the EBS.

SCREENING DECISION:

Included

TSPA DISPOSITION:

Sorption of dissolved radionuclides in the EBS is an important component of the radionuclide transport abstraction model. Sorption parameters (sorption coefficients and distribution coefficients) appropriate for sorption onto corrosion products inside the waste package, onto colloids, and onto crushed tuff in the invert are developed or summarized in *EBS Radionuclide Transport Abstraction* (SNL 2008 [DIRS 177407], Sections 6.3.4.2 and 6.5.2.4). The sorption coefficients are uncertain parameters that are sampled in the TSPA. The radionuclide transport abstraction model, including sorption of dissolved radionuclides, is implemented directly in the TSPA, and thus has a direct impact on estimated releases of radionuclides from the EBS.

The radionuclide transport abstraction model is used to quantify the time-dependent radionuclide releases from a failed waste package and their subsequent transport through the EBS to the emplacement drift wall/unsaturated zone interface.

EBS Radionuclide Transport Abstraction (SNL 2008 [DIRS 177407], Sections 6.3.4.2 and 6.5.2.4) describes the model for sorption of radionuclides on the stationary corrosion products and iron oxyhydroxide colloids:

1. Both equilibrium and kinetic sorption-desorption processes are modeled.

2. Competition for a finite number of sorption sites among various species whose concentration varies as a function of pH and pCO_2 is considered. The elements considered for competitive sorption calculations are uranium, neptunium, plutonium, americium, thorium, and nickel. The competitive sorption calculations are done using single-site surface complexation reactions in PHREEQC V. 2.11 (STN: 10068-2.11-00 [DIRS 175698]).

3. Desorption reactions are implemented to account for desorption from stationary corrosion products.

4. For modeling radionuclide transport through the EBS, equilibrium sorption is modeled for uranium, neptunium, and thorium, while the kinetic sorption-desorption is applied to

plutonium and americium, because they also get transported while irreversibly sorbed onto iron oxyhydroxide colloids.

The conceptual model for flow through the EBS includes three domains: the waste form (e.g., fuel rods or defense HLW glass; this domain includes a small amount of corrosion products from steel components closely associated with the waste form, such as fuel basket tubes and glass pour canisters), waste package steel corrosion products, and the invert (SNL 2008 [DIRS 177407], Section 6.3.1.1). Because the presence of the emplacement pallet is not credited with any barrier capability, water and radionuclides pass directly from the waste package to the invert.

The sorption processes are implemented only in the corrosion products domain of the EBS transport model (SNL 2008 [DIRS 177407], Sections 6.3.4.2 and 6.5.2.4), where the majority of the corrosion products from degradation of steel components inside the waste package are expected to be present. The corrosion products from the degradation of steel are expected to be a mixture of goethite, ferrihydrite (referred to as hydrous ferric oxide), chromium oxide, and nickel oxide, among others. Radionuclide sorption is modeled only on the fraction of corrosion products that are represented by the goethite and ferrihydrite mineralogy. This approach is justified because the surface complexation constants on iron oxyhydroxide surfaces are known with a great degree of confidence and are bounding with respect to the other corrosion products.

The basic inputs to the radionuclide transport abstraction model consist of the drift seepage influx, the environmental conditions in the drift (temperature, relative humidity, and water chemistry) (SNL 2008 [DIRS 177407], Section 6.1), and the degradation state of the EBS components. Outputs consist of the rates of radionuclide releases to the unsaturated zone as a result of advective and diffusive transport, accounting for the impact of colloids, radionuclide solubility, retardation, and the degree of liquid saturation of the waste form and invert materials. The radionuclide transport abstraction model is implemented directly into the TSPA to compute the radionuclide release rates from the EBS.

INPUTS:

Table 2.1.09.05.0A-1. Indirect Inputs

Citation	Title	DIRS
PHREEQC V 2.11	WINDOWS 2000. STN: 10068-2.11-00.	175698
SNL 2008	*EBS Radionuclide Transport Abstraction*	177407

FEP: 2.1.09.06.0A

FEP NAME:

Reduction-Oxidation Potential in Waste Package

FEP DESCRIPTION:

The redox potential in the waste package influences the oxidation of waste-form materials and the in-package solubility of radionuclide species. Local variations in the in-package redox potential can occur.

SCREENING DECISION:

Included

TSPA DISPOSITION:

Oxidation of the metal waste package components is the primary process by which the waste packages corrode and the redox state of in-package water is potentially altered. The oxidation–reduction processes inside of the waste package are explicitly modeled in the in-package chemistry model and, thus, included in *In-Package Chemistry Abstraction* (SNL 2007 [DIRS 180506]). Waters entering the package and conditions inside the package are modeled to be uniformly oxidizing.

Also, the dissolved concentration model developed in *Dissolved Concentration Limits of Elements with Radioactive Isotopes* (SNL 2007 [DIRS 177418], Appendix V) examines redox potential as it pertains to repository conditions, and develops an adjusted-Eh model based on experimental data and natural analog information. This adjusted-Eh model is used only for the plutonium solubility calculation and accounts for the fact that solutions containing this actinide, in contact with air, are not expected to attain full equilibrium with atmospheric oxygen.

An oxidizing redox potential inside the waste package and its effect on in-package chemistry is included in the abstractions passed to the TSPA as part of *In-Package Chemistry Abstraction* (SNL 2007 [DIRS 180506]). Adjusted solubility lookup tables, which account for redox potential, are provided by *Dissolved Concentration Limits of Elements with Radioactive Isotopes* (SNL 2007 [DIRS 177418]) to the TSPA.

INPUTS:

Table 2.1.09.06.0A-1. Indirect Inputs

Citation	Title	DIRS
SNL 2007	*Dissolved Concentration Limits of Elements with Radioactive Isotopes*	177418
SNL 2007	*In-Package Chemistry Abstraction*	180506

FEP: 2.1.09.06.0B

FEP NAME:

Reduction-Oxidation Potential in Drifts

FEP DESCRIPTION:

The redox potential in the EBS influences the oxidation of the in-drift materials and the in-drift solubility of radionuclide species. Local variations in the in-drift redox potential can occur.

SCREENING DECISION:

Included

TSPA DISPOSITION:

Engineered Barrier System: Physical and Chemical Environment (SNL 2007 [DIRS 177412], Section 6.7) evaluates the reduction-oxidation (redox) potential in the EBS drifts as part of the modeled chemical processes. The report accounts for redox potential in its oxygen mass balance analysis (SNL 2007 [DIRS 177412], Section 6.7). Specifically, in-drift gas composition calculations evaluated oxygen composition due to corrosion of ground support materials and other committed materials. The estimate of oxygen flux begins with calculating the gas flux across the drift wall and into the drift (SNL 2007 [DIRS 177412], Section 6.7.1). Oxygen fugacities may drop to as low as 10^{-9} bar for a brief period of time, but they recover rapidly exceeding 10^{-2} bars after approximately 3,000 years and approach ambient values before 10,000 years (SNL 2007 [DIRS 177412], Figure 6.7-5). When the analysis considered the retardation of oxygen consumption by the formation of a corrosion layer, the fO_2 values do not fall below approximately 10^{-6} bar and return to ambient before 1,000 years (SNL 2007 [DIRS 177412], Figure 6.7-6 and Section 6.7.1.7). The analysis concludes that oxidizing conditions, relative to important redox couples such as goethite/magnetite and nitrate/nitrite (SNL 2007 [DIRS 177412], Section 6.7.1.6) will persist in the in-drift environment. Thus, the effects of redox reactions are included in the inputs provided to the TSPA.

The lower fO_2 conditions produced by the corrosion of materials in the EBS would be confined to a limited time during the thermal pulse (i.e., for a few thousand years) as shown in the P&CE report (SNL 2007 [DIRS 177412], Section 6.7.1.5 and Figures 6.7-5 and 6.7-6), which presents the fO_2 time histories. The potential for reducing conditions to occur in the drift is also examined and dismissed in *In-Drift Precipitates/Salts Model* (IDPS) (SNL 2007 [DIRS 177411], Section 4.1.2). The IDPS model is only validated for oxidizing conditions and all evaporation simulations are set for atmospheric conditions (SNL 2007 [DIRS 177411], Section 6.6.2). Oxidizing conditions prevail, with respect to the examined redox couples, for equilibrium fugacity of oxygen of 10^{-9} bars (SNL 2007 [DIRS 177411], Section 4.1.2). The IDPS model lookup table output includes boundary values, abstraction output, and supplemental calculations (SNL 2007 [DIRS 177411], Section 6.6.3.5). Boundary values include temperature, the fugacities of carbon dioxide and oxygen, and the reaction progress.

INPUTS:

Table 2.1.09.06.0B-1. Indirect Inputs

Citation	Title	DIRS
SNL 2007	*Engineered Barrier System: Physical and Chemical Environment*	177412
SNL 2007	*In-Drift Precipitates/Salts Model*	177411

FEP: 2.1.09.07.0A

FEP NAME:

Reaction Kinetics in Waste Package

FEP DESCRIPTION:

Chemical reactions, such as radionuclide dissolution/ precipitation reactions and reactions controlling the reduction-oxidation state, may not be at equilibrium within the waste package.

SCREENING DECISION:

Included

TSPA DISPOSITION:

Dissolution kinetics is included in the TSPA in-package chemistry model abstraction. The in-package chemistry model uses kinetic expressions—linear or transition state theory rate laws—to describe SNF degradation, defense HLW glass degradation, and steel degradation (SNL 2007 [DIRS 180506], Section 4.1.3[a]).

Kinetics are also taken into account in both the in-package chemistry model (SNL 2007 [DIRS 180506]) and the dissolved concentrations model (SNL 2007 [DIRS 177418]) when secondary phases that are kinetically inhibited from forming under repository conditions are suppressed in the calculations. The in-package chemistry model generally allows precipitation and/or corrosion reactions of non-kinetically inhibited reactions to reach thermodynamic equilibrium. The adjusted Eh model takes account of kinetic controls over plutonium speciation (SNL 2007 [DIRS 177418], Section 6.5.3). With these two exceptions, all other reactions are assumed to maintain equilibrium in an oxidized environment (SNL 2007 [DIRS 180506]).

INPUTS:

Table 2.1.09.07.0A-1. Indirect Inputs

Citation	Title	DIRS
SNL 2007	*Dissolved Concentration Limits of Elements with Radioactive Isotopes*	177418
SNL 2007	*In-Package Chemistry Abstraction*	180506

FEP: 2.1.09.07.0B

FEP NAME:

Reaction Kinetics in Drifts

FEP DESCRIPTION:

Chemical reactions, such as radionuclide dissolution/precipitation reactions and reactions controlling the reduction-oxidation state, may not be at equilibrium in the drifts.

SCREENING DECISION:

Included

TSPA DISPOSITION:

The effects of reaction kinetics are included in each geochemical submodel developed in *Engineered Barrier System: Physical and Chemical Environment* (SNL 2007 [DIRS 177412], Sections 6.2.3, 6.2.4, and 6.2.5), which takes its mineral suppressions from *In-Drift Precipitates/Salts Model* (IDPS) (SNL 2007 [DIRS 177411]). In particular, the IDPS model, which uses an EQ3/6 reaction path model to simulate evaporation of potential seepage waters, takes account of reaction kinetics when it suppresses individual mineral phases (SNL 2007 [DIRS 177412], Section 6.2.4.1 and Table 6.2-2).

Individual mineral phases were suppressed if those phases are kinetically inhibited from forming under repository conditions. A list of minerals inhibited during the modeling, including justification for the decision to suppress each mineral, is presented in Section 6.2.4.1 and Table 6.2-2 of the P&CE report (SNL 2007 [DIRS 177412]). The choice of mineral suppressions directly affects the modeled evolution of the in-drift waters, and hence the water compositions that are used by TSPA.

In addition, the kinetics of corrosion of steel in the drift was examined with respect to its effect on in-drift water and atmosphere compositions. Seepage water interactions with Stainless Steel Type 316L ground support components and low alloy invert steels were found to be of low consequence (SNL 2007 [DIRS 177412], Sections 6.7 and 6.8). A sensitivity analysis shows that increasing corrosion rates parametrically has no significant effect on in-drift water and atmospheric compositions (SNL 2007 [DIRS 177412], Sections 6.7 and 6.8). Oxygen consumption due to corrosion of ground support materials and other committed materials is evaluated using in-drift gas composition calculations that consider two different drift spacings (SNL 2007 [DIRS 177412], Section 6.7). A sensitivity study of in-drift oxygen fugacity showed that corrosion of invert steel will decrease oxygen fugacity, but as a transient phenomenon, and with insufficient magnitude to qualitatively change any important chemical reactions in the EBS (SNL 2007 [DIRS 177412], Section 6.7.1). Long-term conditions are expected to be oxidizing. Because of this, IDPS model calculations are done assuming atmospheric levels of oxygen and reduced phases (e.g., sulfides) are suppressed accordingly.

As stated above, the effects of reaction kinetics are implicitly included in the geochemical submodels developed in the P&CE report (SNL 2007 [DIRS 177412], Sections 6.2.3, 6.2.4, and 6.2.5) through the selection of mineral species allowed to form. Thus, the effects are propagated to the chemical composition data tables used by the TSPA. Reduction-oxidation potential in the drift is discussed in included FEP 2.1.09.06.0B (Reduction-oxidation Potential in the Drifts).

Radionuclide precipitation/dissolution kinetics are expected to happen rapidly and maintain equilibrium with in-drift fluids. The kinetics of sorption/desorption of americium and plutonium on colloids and corrosion products are included in the TSPA (SNL 2008 [DIRS 177407], Section 6.5.2.7). Uncertainty in sorption is considered by using a range of model input fluid chemistries and substrate abundance and area.

INPUTS:

Table 2.1.09.07.0B-1. Indirect Inputs

Citation	Title	DIRS
SNL 2008	*EBS Radionuclide Transport Abstraction*	177407
SNL 2007	*Engineered Barrier System: Physical and Chemical Environment*	177412
SNL 2007	*In-Drift Precipitates/Salts Model*	177411

FEP: 2.1.09.08.0A

FEP NAME:

Diffusion of Dissolved Radionuclides in EBS

FEP DESCRIPTION:

Radionuclide transport of dissolved radionuclides by diffusion, in response to chemical gradients, may occur within the EBS. Physical and chemical properties of the EBS and waste form, in both intact and degraded states, should be considered in evaluating diffusive transport.

SCREENING DECISION:

Included

TSPA DISPOSITION:

The model developed in *EBS Radionuclide Transport Abstraction* (RTA) (SNL 2007 [DIRS 177407], Section 6.3.4) is used to quantify the time-dependent radionuclide releases from a failed waste package and their subsequent transport through the EBS to the emplacement drift wall/unsaturated zone interface. The basic inputs to the RTA model consist of the drift seepage and drift wall condensation flux, the environmental conditions in the drift (temperature, relative humidity, and water chemistry), and the degradation state of the EBS components (SNL 2007 [DIRS 177407], Section 6.1). Outputs from the RTA model are used in the TSPA to calculate the rates of radionuclide releases to the unsaturated zone as a result of advective and diffusive transport, accounting for the impact of colloids, radionuclide solubility, retardation, and the degree of liquid saturation of the waste form and invert materials. The RTA model is implemented directly into the TSPA GoldSim model to compute the radionuclide release rates from the EBS. This FEP addresses diffusion of dissolved species in the EBS. Included FEP 2.1.09.24.0A (Diffusion of Colloids in EBS) addresses diffusion of colloids in the EBS. Advective transport of dissolved radionuclides is addressed in included FEP 2.1.09.08.0B (Advection of Dissolved Radionuclides in EBS).

The conceptual model for flow through the EBS includes three domains: the waste form (e.g., fuel rods or defense HLW glass; included in this domain is a small amount of corrosion products from steel components closely associated with the waste form, such as fuel basket tubes and glass pour canisters), waste package steel corrosion products, and the invert. The EBS domains are defined in *EBS Radionuclide Transport Abstraction* (SNL 2007 [DIRS 177407], Section 6.3.1.1). Because the presence of the emplacement pallet is not represented in TSPA for the purposes of estimating radionuclide transport path length, radionuclides pass directly from the waste package to the invert.

The source of inflow into the EBS is the seepage flux that drips from the crown (roof) of the drift, drift wall condensation, and imbibition flux from the unsaturated zone into the invert. This inflow can flow through the EBS along eight pathways: (1) seepage flux plus any drift wall condensation that may occur, (2) flux through the drip shield, (3) diversion around the drip shield, (4) flux through the waste package, (5) diversion around the waste package, (6) flux from

the waste package and drip shield into the invert, (7) imbibition flux from the drift host rock to the invert, and (8) flux from the invert to the unsaturated zone (SNL 2007 [DIRS 177407], Section 6.3.1.1 and Figure 6.3-1). These pathways are time dependent, because drip shield and waste package penetrations will vary with time and local conditions in the repository.

Diffusive transport of dissolved radionuclides in the EBS is a major component of the RTA model. The effects of saturation, temperature, porosity, and chemical potential gradient in the invert are discussed in *EBS Radionuclide Transport Abstraction* (SNL 2007 [DIRS 177407], Section 6.3.4.1). The effects of waste form properties and degradation state on diffusion in the waste package are modeled; diffusion from the waste form is dependent on the volume, effective surface area, and thickness of the "rind" of degraded waste form (SNL 2007 [DIRS 177407], Section 6.3.4.6), and the amount of corrosion products in the waste package determines both their saturation (and consequently, the diffusivity) (SNL 2007 [DIRS 177407], Section 6.3.4.3) and their sorptive capacity (SNL 2007 [DIRS 177407], Section 6.3.4.2.3). Note that the model of the commercial SNF waste form used in the abstraction model does not account for the cladding, consistent with the approach in the TSPA in which no credit is taken for the cladding.

The free water diffusion coefficient for each radionuclide species in water is used for all concentrations of radionuclides at a given temperature (DTN: LB0702PAUZMTDF.001 [DIRS 180776]). The diffusion coefficients for the corrosion products and waste form domains are modified for temperature, as is the invert diffusion coefficient (SNL 2007 [DIRS 177407], Section 6.3.4.1.2). Modification for the effect of concentrated aqueous solutions is not addressed in the TSPA (SNL 2007 [DIRS 177407], Section 6.3.4.1.3).

Uncertainty in diffusive transport is addressed by developing probability distribution functions that describe uncertainty, and then sampling from these probability distribution functions in implementing the RTA model in the performance assessment calculations. The following parameters are treated this way: invert diffusion coefficient uncertainty (SNL 2007 [DIRS 177407], Section 6.3.4.1.1), stainless steel and carbon steel corrosion rates (SNL 2007 [DIRS 177407], Section 6.3.4.3.4.3), water vapor adsorption isotherms for corrosion products (SNL 2007 [DIRS 177407], Sections 6.3.4.3.2), waste form rind (SNL 2007 [DIRS 177407], Section 6.3.4.6.1), density and porosity of commercial SNF rind materials (SNL 2007 [DIRS 177407], Section 6.3.4.6.1), and the specific surface area of corrosion products (SNL 2007 [DIRS 177407], Section 6.3.4.3.3).

INPUTS:

Table 2.1.09.08.0A-1. Indirect Inputs

Citation	Title	DIRS
DTN: LB0702PAUZMTDF.001	Unsaturated Zone Matrix Diffusion Coefficients	180776
SNL 2007	*EBS Radionuclide Transport Abstraction*	177407

FEP: 2.1.09.08.0B

FEP NAME:

Advection of Dissolved Radionuclides in EBS

FEP DESCRIPTION:

Radionuclide transport of dissolved radionuclides by advection with the flowing groundwater may occur within the EBS. Physical and chemical properties of the EBS and waste form, in both intact and degraded states, should be considered in evaluating advective transport.

SCREENING DECISION:

Included

TSPA DISPOSITION:

The model developed in *EBS Radionuclide Transport Abstraction* (SNL 2007 [DIRS 177407], Section 6.3.4) is used to quantify the time-dependent radionuclide releases from a failed waste package and their subsequent transport through the EBS to the emplacement drift wall/unsaturated zone interface. The basic inputs to the RTA model consist of the drift seepage and drift wall condensation flux, the environmental conditions in the drift (temperature, relative humidity, and water chemistry), and the degradation state of the EBS components (SNL 2007 [DIRS 177407], Section 6.1). Outputs from the RTA are used in the TSPA to calculate the rates of radionuclide releases to the unsaturated zone as a result of advective and diffusive transport, accounting for the impact of colloids, radionuclide solubility, retardation, and the degree of liquid saturation of the waste form and invert materials. The RTA model is implemented directly into the TSPA GoldSim model to compute the radionuclide release rates from the EBS. This FEP addresses advection of dissolved species in the EBS. Included FEP 2.1.09.19.0B (Advection of Colloids in EBS) addresses advection of colloids in the EBS.

The source of inflow to the EBS is the seepage flux that drips from the crown (roof) of the drift, drift wall condensation, and imbibition flux from the unsaturated zone into the invert. This inflow can flow through the EBS along eight pathways: (1) seepage flux plus any condensation that may occur on the walls of the drift above the drip shield, (2) flux through the drip shield, (3) diversion around the drip shield, (4) flux through the waste package, (5) diversion around the waste package, (6) flux from the waste package and drip shield into the invert, (7) imbibition flux from the drift host rock to the invert, and (8) flux from the invert to the unsaturated zone (SNL 2007 [DIRS 177407], Section 6.3.1.1 and Figure 6.3-1). These pathways are time dependent, in the sense that drip shield and waste package penetrations will vary with time and local conditions in the repository.

Radionuclide transport is modeled with three domains (SNL 2007 [DIRS 177407], Section 6.3.1.1). These are: (1) The waste form (e.g., fuel rods or defense HLW glass; included in this domain is a small amount of corrosion products from steel components closely associated with the waste form, such as fuel basket tubes and glass pour canisters); (2) waste package steel corrosion products; and (3) the invert. Radionuclides dissolved from the waste form are

transported from the waste form to the corrosion products and then to the invert via advection and diffusion; for simplicity, longitudinal and transverse dispersion are neglected in TSPA. Radionuclides interact with the crushed tuff in the invert by adsorption processes.

Radionuclide solubilities are specified in *Dissolved Concentration Limits of Radioactive Elements* (SNL 2007 [DIRS 177418], Sections 6.5 to 6.18) to provide radionuclide concentrations in each of the flow pathways in the RTA model, specifically in the waste form and waste package corrosion products. The seepage and drift wall condensation flux into a drift is also an input to the RTA model. The flux-splitting model determines the fraction of the seepage flux that flows through a failed drip shield and waste package. Fluxes that flow through a failed drip shield are split between those that flow around the waste package and those that flow into the waste package. Fluxes that are diverted around the waste package and the drip shield flow into the invert. These fluxes will not contain radionuclides. Water that flows into a waste package will contain radionuclides as it exits the waste package, as described in *EBS Radionuclide Transport Abstraction* (SNL 2007 [DIRS 177407], Section 6.3.4). The RTA model does not require or address details about the flow mechanisms or type of flow (such as film flow) that is occurring in the waste form. Uncertainty in advective transport through the waste form is addressed, in part, by sampling over a range of dissolved concentrations and sorption parameters (e.g., surface areas, corrosion product masses).

The invert cell is in intimate contact with the waste package and is 0.934 m in thickness (SNL 2007 [DIRS 177407], Section 6.5.2.3). This is the average thickness of the invert directly beneath the waste package. This value is appropriate because flow out of the waste package is primarily downward, centered over the thickest part of the invert. The presence of an emplacement pallet is not represented in TSPA for the purposes of estimating radionuclide transport path length. Consequently, radionuclides pass directly from the waste package to the invert.

The total mass flux of the radionuclides entering the unsaturated zone from the invert is the sum of radionuclides transported by advection and diffusion (SNL 2007 [DIRS 177407], Section 6.5.2). Flow through the invert is discussed in included FEP 2.1.08.05.0A (Flow through Invert).

INPUTS:

Table 2.1.09.08.0B-1. Indirect Inputs

Citation	Title	DIRS
SNL 2007	*Dissolved Concentration Limits of Elements with Radioactive Isotopes*	177418
SNL 2007	*EBS Radionuclide Transport Abstraction*	177407

FEP: 2.1.09.09.0A

FEP NAME:

Electrochemical Effects in EBS

FEP DESCRIPTION:

Electrochemical effects may establish an electric potential within the drift or between materials in the drift and more distant metallic materials. Migration of ions within such an electric field could affect corrosion of metals in the EBS and waste, and could also have a direct effect on the transport of radionuclides as charged ions.

SCREENING DECISION:

Excluded – low consequence

SCREENING JUSTIFICATION:

Electrochemical effects include electrophoresis and galvanic coupling. Electrophoresis is the movement of an electrically charged element or molecule (e.g., a radionuclide ion) under the influence of an electric field. Galvanic coupling refers to flow of electricity due to the potential differences that arise when two dissimilar metals or alloys are in electrical contact. In a galvanic couple consisting of two metals or alloys with significantly different corrosion potentials in the environment of concern, the metal or alloy that acts as the anode will corrode preferentially. The nobler of the two metals or alloys in the galvanic couple will act as the cathode.

A variety of materials are in the repository emplacement drifts. These materials are summarized in *Total System Performance Assessment Data Input Package for Requirements Analysis for EBS In-Drift Configuration* (SNL 2007 [DIRS 179354]).

The emplacement drifts include a ground support composed of Stainless Steel Type 316L (UNS S31603) drift liners and rock bolts (SNL 2007 [DIRS 179354], Table 4-1, Parameter Number 01-15). The waste package design is a double-walled waste package (inner vessel with outer corrosion barrier, SNL 2007 [DIRS 179394], Table 4-3) placed underneath a protective drip shield (SNL 2007 [DIRS 179354], Section 4.1.1). The WPOB will be constructed of Alloy 22 (UNS N06022) with additional elemental and chemical composition restrictions (SNL 2007 [DIRS 179567], Table 4-1, Parameter Number 03-19). The inner vessel of the waste package is constructed of Stainless Steel Type 316 (UNS S31600) (SNL 2007 [DIRS 179394], Table 4-3). The waste package rests on an emplacement pallet, which in turn rests on the invert structure, which is covered by crushed tuff as ballast. The waste package emplacement pallet is fabricated from Stainless Steel Type 316 and Alloy 22 (SNL 2007 [DIRS 179354], Table 4-3, Parameter Number 08-01). Stainless Steel Type 316 tubes connect to the Alloy 22 waste package supports to form the emplacement pallet (SNL 2007 [DIRS 179354], Table 4-3, Parameter Number 08-01). The drip shield plate material is Titanium Grade 7 (UNS R52400) and the drip shield structural support material is Titanium Grade 29 (UNS R56404) (SNL 2007 [DIRS 179354], Table 4-2, Parameter Number 07-04). The drip shields are designed to contact no other material except the Alloy 22 base (SNL 2007 [DIRS 179354], Table 4-2, Parameter

Number 07-07), which is attached to the bottom of the drip shields. The Alloy 22 drip shield base is in contact with the invert.

A commercial SNF TAD canister will be placed inside the double-walled waste package. The design characteristics used in modeling the TAD canister-bearing waste packages are documented in *Total System Performance Assessment (TSPA) Data Input Package for Requirements Analysis for TAD Canister and Related Waste Package Overpack Physical Attributes Basis for Performance Assessment* (SNL 2007 [DIRS 179394]). The TAD canister vessel and structural internals (i.e., basket) shall be constructed of 300-series stainless steel (such as UNS S31603, which may also be designated as Stainless Steel Type 316L).

The main codisposal waste package (N Reactor) components use the following materials: Alloy 22 for the outer corrosion barrier, Stainless Steel Type 316 for the inner vessel, Carbon Steel Type A516 for the divider plate fuel support plate assemblies, Stainless Steel Type 304L for the MCO and glass pour canisters , and Aluminum Alloy Type 1100 for the MCO spacer (SNL 2007 [DIRS 180506], Sections 4.1.4 and 4.1.4[a]).

In the 10,000 years following repository closure, the waste package emplacement pallet prevents direct contact of the waste package with the invert (SNL 2007 [DIRS 179354], Table 4-3, Parameter Number 08-02). The Alloy 22 waste package supports are the main load-bearing members because the geometry of the pallet and waste package supports prevents direct contact between the waste package and the emplacement pallet tubes (SNL 2007 [DIRS 179354], Table 4-3, Parameter Number 08-03). The emplacement pallet keeps the waste package from contacting other dissimilar metals in the absence of seismic activity (SNL 2007 [DIRS 179354], Table 4-3, Parameter Number 08-03). The affects of seismic activity on mechanical degradation of EBS components is addressed in included FEPs 1.2.03.02.0A (Seismic Ground Motion Damages EBS Components) and 1.2.03.02.0C (Seismic-induced Drift Collapse Damages EBS Components), and excluded FEP 1.2.03.02.0B (Seismic-induced Rockfall Damages EBS Components).

The carbon steel invert structure will provide a framework, consisting of a series of beams bolted to the invert rock mass, that supports the emplacement pallets, waste packages, and drip shields (SNL 2007 [DIRS 179354], Table 4-1, Parameter Number 02-08). The base plates of the drip shield are fabricated from Alloy 22 to prevent direct contact between the titanium and steel members in the invert, thus minimizing electrochemical effects at this interface (SNL 2007 [DIRS 179354], Table 4-2, Parameter Number 07-07). The corrosion resistance of the Alloy 22 WPOB, emplacement pallet components, and base plates of the drip shield, as well as the titanium drip shield components, is much greater than the carbon steel and, to a lesser extent, the stainless steel invert components. If any electrical contact were to be established between these Alloy 22 or titanium components and the invert materials, the invert materials would corrode preferentially. The potential for corrosion-generated hydrogen to embrittle the waste package or drip shield is discussed in excluded FEPs 2.1.03.04.0A (Hydride Cracking of Waste Packages) and 2.1.03.04.0B (Hydride Cracking of Drip Shields), respectively. If the invert components completely degrade before such electrical contacts were possible, no galvanic effects would occur.

Overall, the emplacement drift design is such that EBS materials shall be inert relative to each other so that physical contact between EBS materials minimizes dissimilar material interaction mechanisms (SNL 2007 [DIRS 179354], Table 4-2, Parameter Number 02-05). There are, however, a number of possible EBS component contacts between Alloy 22 and Stainless Steel Type 316 (e.g., between the Alloy 22 WPOB and the Stainless Steel Type 316 inner vessel or between the Alloy 22 emplacement pallet-bearing surfaces and the Stainless Steel Type 316 connector tubes). The corrosion potentials of Alloy 22 and Stainless Steel Type 316 are very close to each other under similar exposure conditions (e.g., Davison et al. 1987 [DIRS 162971], Figure 10; where Hastelloy C is comparable to Alloy 22), with Alloy 22 slightly more noble than Stainless Steel Type 316. After breach of the Alloy 22 WPOB, electrochemical coupling of the Alloy 22 WPOB with the Stainless Steel Type 316 waste package inner vessel could occur. Due to the similarity in corrosion potential of Alloy 22 and Stainless Steel Type 316 (e.g., Davison et al. 1987 [DIRS 162971], Figure 10), any enhanced degradation of either material due to galvanic interaction is expected to be negligible, although Alloy 22 would be expected to be the cathode relative to Stainless Steel Type 316 (SNL 2007 [DIRS 178519], Section 6.3.3).

A number of crevice corrosion studies of galvanically coupled specimens have been conducted in repository-relevant exposure conditions. Ikeda and Quinn (2003 [DIRS 162662]) studied the crevice corrosion of galvanically coupled Alloy 22 and Stainless Steel Type 316 in a simulated concentrated groundwater at about 90°C. The study found a limited amount of acidification in the creviced regions between Alloy 22 and Stainless Steel Type 316 and evidence of localized corrosion initiation on the Stainless Steel Type 316 surface. No enhanced degradation of the Alloy 22 was observed. This finding is consistent with the Alloy 22 functioning as the cathode and the Stainless Steel Type 316 as the anode in the galvanic couple. Stainless Steel Type 316 would also be expected to undergo localized corrosion even in the absence of electrical connection to Alloy 22 in the concentrated groundwater solution at 90°C. The results of Ikeda and Quinn (2003 [DIRS 162662]) are consistent with those of He et al. (2007 [DIRS 182722]), who also studied crevice corrosion of galvanically coupled Alloy 22 and Stainless Steel Type 316 and compared it to the behavior of uncoupled specimens. Their tests were conducted in 4 M NaCl solution at 95°C. They concluded that Stainless Steel Type 316 was susceptible to crevice corrosion in the test solution and did not significantly depend on the crevicing material (e.g., whether the crevicing material was Alloy 22 or a polytetrafluoroethylene washer). Given that no corrosion performance credit is taken for the Stainless Steel Type 316 inner vessel in evaluating waste package corrosion performance (SNL 2007 [DIRS 178519], Section 6.3.3), electrochemical coupling of the Alloy 22 WPOB and the Stainless Steel Type 316 waste package inner vessel is of low consequence with respect to potential degradation of the waste package. The same low consequence justification would apply to any galvanic coupling of Alloy 22 and any Stainless Steel Type 300 component within the waste package (e.g., the TAD and stainless steel pour canisters). Chemical degradation of the emplacement pallet connector tubes is discussed in included FEP 2.1.06.05.0C (Chemical Degradation of Emplacement Pallet), where it is concluded that the connector tubes retain their structural integrity during the first 10,000 years after closure. Also, as discussed in included FEP 2.1.06.05.0C (Chemical Degradation of Emplacement Pallet), the function of the emplacement pallet becomes less important to mechanical performance at later times when the drip shield is collapsed and rubble accumulates adjacent to waste packages.

The possibility of the drip shield contacting the waste package as a result of mechanical damage caused by rockfall was considered. This possibility is addressed in excluded FEP 2.1.03.07.0B (Mechanical Impact on Drip Shield). As emplaced, the only contact between Titanium Grade 7 and Alloy 22 occurs at the bottom of the drip shields where Alloy 22 feet are attached to prevent contact between titanium and the invert (SNL 2007 [DIRS 179354], Table 4-2, Parameter Number 07-07). The choice of Alloy 22 for the feet was based on similarity of the two materials in the electrochemical series (ASM International 1987 [DIRS 103753], p. 557, Figure 10), which indicates that any enhanced degradation of either material due to galvanic interaction would be negligible. After seismic drift collapse or mechanical failure of the drip shield, contact between the Alloy 22 WPOB and the Titanium Grade 7 drip shield plate material is possible. Ikeda and Quinn (2003 [DIRS 162662]) studied the crevice corrosion of galvanically coupled Alloy 22 and Titanium Grade 7 in a simulated concentrated groundwater at about 90°C. Although a limited amount of acidification was observed in the creviced region, no evidence of localized corrosion initiation was observed on either alloy. He et al. (2007 [DIRS 182722]) also studied crevice corrosion of galvanically coupled Alloy 22 and Titanium Grade 7 and compared it to the behavior of uncoupled specimens. Their tests were conducted primarily in 4 M NaCl solution at 95°C and a limited amount of testing was carried out in 0.5 M NaCl and 4 M $MgCl_2$ solutions. They concluded that metal-to-metal crevices were less susceptible to crevice corrosion than the corresponding metal-to-polytetrafluoroethylene crevices and that crevice repassivation models based on data from uncoupled specimens should bound crevice corrosion susceptibility determinations. Therefore, electrochemical coupling of the Alloy 22 WPOB and the Titanium Grade 7 drip shield is of low consequence with respect to potential degradation of the EBS and the waste package.

Another possible galvanic contact in the repository is between the Titanium Grade 7 drip shield plates and the Stainless Steel Type 316L (a low-carbon version of Stainless Steel Type 316) drift liners and rock bolts, which may fall on the drip shield surface after they degrade. Ikeda and Quinn (2003 [DIRS 162662]) studied the crevice corrosion of galvanically coupled Stainless Steel Type 316 and Titanium Grade 16 (an alloy similar to Titanium Grade 7 with a lower palladium content) in a simulated concentrated groundwater at about 90°C. Although a limited amount of acidification was observed in the creviced region, no evidence of localized corrosion initiation was observed on either alloy. Based on these results, deleterious effects of galvanic coupling between Titanium Grade 7 and Stainless Steel Type 316 are not expected under repository exposure conditions. Similar results would be expected for galvanic coupling between the Titanium Grade 29 drip shield supports and Stainless Steel Type 316, although galvanic contact between these materials in the repository will be limited due to the location of the drip shield supports in the drip shield configuration (SNL 2007 [DIRS 179354], Table 4-2, Parameter Number 07-01). The possibility of hydrogen-induced cracking of the drip shield due to galvanic contact with iron-based materials such as the Stainless Steel Type 316L drift liners and rock bolts is discussed in excluded FEP 2.1.03.04.0B (Hydride Cracking of Drip Shields).

Telluric currents (i.e., currents that move through the ground) can, under some conditions, affect corrosion rate in carbon steels, copper alloys, and other less corrosion-resistant alloy systems. This is especially true for cathodically protected buried carbon steel pipeline systems. In the case of the repository, the ground supports and invert are sufficiently grounded to prevent any significant build-up of telluric currents. The drip shields are grounded to the invert through the Alloy 22 feet. Also, in the case of the highly passive Alloy 22 WPOB material and the Titanium

Grade 7 drip shield material, telluric current effects would not be expected to affect corrosion response since these materials remain highly passive over a very broad range of applied potentials. Thus, small varying changes in local surface potentials that could potentially result from telluric currents or other stray current sources would not measurably affect the very low corrosion rates of these materials. The effect of telluric currents is also discussed in excluded FEP 2.1.06.07.0A (Chemical Effects at EBS Component Interfaces).

Commercial SNF and DOE SNF (other than naval SNF) cladding is considered to be breached upon emplacement in the repository and will neither inhibit groundwater contacting the fuel matrix nor the release of radionuclides from the fuel after groundwater contact (included FEPs 2.1.02.12.0A (Degradation of Cladding Prior to Disposal), 2.1.02.23.0A (Cladding Unzipping), and 2.1.02.25.0A (DSNF Cladding)).Zirconium is a highly corrosion-resistant material because it forms a protective and adherent oxide film when exposed to oxygen-containing environments (Yau and Webster 1987 [DIRS 165063], p. 707). This oxide film forms spontaneously in air or water at ambient temperatures, is self-healing, and protects the base metal from chemical and mechanical attack (Yau and Webster 1987 [DIRS 165063], p. 707). Zirconium-based cladding, with its thick oxide layer produced in reactor operation, is kinetically noble (Yau and Webster 1987 [DIRS 165063], Table 15, p. 717). Due to the self-healing properties of the oxide layer formed on zirconium-based cladding (Yau and Webster 1987 [DIRS 165063], pp. 707 and 718), any mechanical disruption of the oxide layer is not expected to have a significant impact on the corrosion behavior of this material. For instance, Hansson (1984 [DIRS 101676], p. 6) observed that zirconium-based cladding that had its oxide film scratched off reformed a passive oxide layer within seconds in a synthetic cement pore solution of pH values 12.0 to 13.8. Therefore, although the zirconium cladding is considered to be unzipped after a waste package breach, the cladding is still present in proximity to the waste forms and other waste package materials, which could influence radionuclide transport as discussed below.

Cragnolino (1999 [DIRS 152354], p. 4-13) surveyed various corrosion mechanisms for zirconium cladding under repository conditions and concluded:

> Zr is not susceptible to galvanic corrosion because the protective ZrO_2 passive film leads to E_{corr} values in the galvanic series in flowing seawater close to those of noble metals and graphite but slightly lower than that of Ag. However, local corrosion promoted by galvanic coupling to a more noble metal may occur if the film is mechanically disrupted. Nevertheless, the repassivation rate of Zr and its alloys is sufficiently fast in many aqueous solutions that unless fretting is continuously occurring no substantial corrosion can be expected.

If the oxidized zirconium cladding were to be electrically coupled to a less corrosion resistant material (e.g., the stainless steel fuel boxes), the corrosion rate of that material is expected to be accelerated (Yau and Webster 1987 [DIRS 165063], p. 717). Brossia et al. (2002 [DIRS 161988], Figure 4) showed that the resistance of the oxide film formed on zirconium increases by about three orders of magnitude (from 10^4 to 10^7 ohms) as the film thickness increases from about zero to 3.4 μm. Thus, it is reasonable to expect that the oxide film on zirconium cladding will serve to electrically isolate the cladding from other materials, limiting the possibility of galvanic coupling effects.

The lack of an observable galvanic effect is demonstrated within the radionuclide release rate model of *CSNF Waste Form Degradation: Summary Abstraction* (BSC 2004 [DIRS 169987], Section 8.1). A validation comparison of that model to cladded fuel rod segments (with potential for galvanic effect), and to fuel fragments (no possible galvanic effects) show radionuclide release rates do not indicate any obvious increase in these rates due to the presence of clad; in fact the fuel fragments are seen to have a greater release rate (BSC 2004 [DIRS 169987], Table 7-9). The effects of galvanic coupling on the corrosion and associated radionuclide release rate from DOE SNF are of no consequence to radionuclide release rates because the model for DOE SNF corrosion uses a bounding instantaneous radionuclide release rate (BSC 2004 [DIRS 172453], Section 8.1). As for electrochemical effects on defense HLW, these are negligible because the principal dissolution reactions involved are glass hydrolysis reactions that are not influenced by electrochemical effects.

Electrochemical effects on the waste form will also be minimal. The commercial SNF waste form is surrounded by the oxidized split zirconium cladding and would not be in direct contact with the waste package internals. If the UO_2 did contact the stainless steel fuel boxes and galvanic coupling were to occur, the steel boxes would see the accelerated reaction and not the fuel pellets. As the UO_2 corrodes, it coats itself with reaction products, which will minimize galvanic effects.

Electrophoresis is the movement of an electrically charged element or molecule (e.g., a radionuclide ion) under the influence of an electric field. The WPOB, inner vessel, TAD canister, and waste package internals are in electrical contact with each other and are in contact with the repository ground through the emplacement pallet. The drip shields are also in contact with the repository ground. The possibility of forming significant electric fields within the emplacement drifts owing to galvanic coupling is remote. As discussed earlier, the bulk of the materials in the emplacement drifts are titanium alloys, Alloy 22, and stainless steels that will all have similar corrosion potentials, and contact between these materials will not result in significant galvanic coupling effects. Thus, the movement of charged species such as radionuclides will be insignificant under these small electric fields. Therefore, omission of electrochemical effects (electrophoresis and galvanic coupling) would not have a significant effect on the resulting radionuclide exposures to the RMEI. The development of electric fields due to radiation effects (such as Compton scattering) is addressed in excluded FEP 2.1.09.27.0A (Coupled Effects on Radionuclide Transport in EBS).

Based on the previous discussion, omission of FEP 2.1.09.09.0A (Electrochemical Effects in EBS) will not result in a significant adverse change in the magnitude or timing of either radiological exposure to the RMEI or radionuclide releases to the accessible environment. Therefore, this FEP is excluded from the performance assessments conducted to demonstrate compliance with proposed 10 CFR 63.311 and 63.321 (70 FR 53313 [DIRS 178394]), and with 10 CFR 63.331 [DIRS 180319], on the basis of low consequence.

INPUTS:

Table 2.1.09.09.0A-1. Direct Inputs

Input	Source	Description
BSC 2004. *CSNF Waste Form Degradation: Summary Abstraction*. [DIRS 169987]	Section 8.1	Radionuclide release rate model and uncertainty
Davison et al. 1987. "Corrosion of Stainless Steels." [DIRS 162971]	Figure 10	The corrosion potentials of Alloy 22 and Stainless Steel Type 316 are very close to each other under similar exposure conditions
SNL 2007. *Total System Performance Assessment Data Input Package for Requirements Analysis for EBS In-Drift Configuration*. [DIRS 179354]	Table 4-3, Parameter Number 08-03	Emplacement pallet keeps the waste package from contacting other dissimilar metals in the absence of seismic activity
	Table 4-1, Parameter Number 02-08	Carbon steel invert structure framework
	Table 4-2, Parameter Number 07-07	Discussion of base plates of the drip shield, fabricated from Alloy 22
	Table 4-2, Parameter Number 07-04	Drip shield plate material is Titanium Grade 7 (UNS R52400) and the drip shield structural support material is Titanium Grade 29 (UNS R56404)
	Table 4-1, Parameter Number 01-15	Emplacement drifts include a ground support composed of Stainless Steel Type 316L drift liners and rock bolts
	Table 4-3, Parameter Number 08-02	In the 10,000 years following waste package emplacement, the pallet supports the waste package
	Table 4-3, Parameter Number 08-01	Stainless Steel Type 316 tubes connect to the Alloy 22 waste package supports to form the emplacement pallet
	Table 4-3, Parameter Number 08-01	Waste package emplacement pallet is fabricated from Stainless Steel Type 316 and Alloy 22
	Table 4-2, Parameter Number 02-05	Waste package outer corrosion barrier shall not contact EBS components other than the Alloy 22 support surfaces of the pallet
	Table 4-2, Parameter Number 07-01	Drip shield design configuration
	Section 4.1.1	Waste package is under a drip shield
	Table 4-2, Parameter Number 07-07	Drip shields are designed to contact no other material except the Alloy 22 base
SNL 2007. *General Corrosion and Localized Corrosion of Waste Package Outer Barrier*. [DIRS 178519]	Section 6.3.3	No corrosion credit is taken for inner vessel in evaluating waste package performance

Table 2.1.09.09.0A-1. Direct Inputs (Continued)

Input	Source	Description
SNL 2007. *Total System Performance Assessment Data Input Package for Requirements Analysis for DOE SNF/HLW and Navy SNF Waste Package Overpack Physical Attributes Basis for Performance Assessment*. [DIRS 179567]	Table 4-1, Parameter Number 03-19	WPOB will be constructed of Alloy 22 (UNS N06022) with additional elemental and chemical composition restrictions
SNL 2007. *Total System Performance Assessment Data Input Package for Requirements Analysis for TAD Canister and Related Waste Package Overpack Physical Attributes Basis for Performance Assessment*. [DIRS 179394]	Table 4-3	Construction of the inner vessel of the waste package with Stainless Steel Type 316
	Table 4-3	Waste package is double-walled (i.e., inner vessel and outer corrosion barrier)
Yau and Webster 1987. "Corrosion of Zirconium and Hafnium." [DIRS 165063]	p. 707	Oxide film forms spontaneously in air or water at ambient temperatures, is self-healing and protects the base metal from chemical and mechanical attack
	pp. 707, 718	Discussion of self-healing properties of oxide layer formed on zirconium-based cladding

Table 2.1.09.09.0A-2. Indirect Inputs

Citation	Title	DIRS
10 CFR 63	Energy: Disposal of High-Level Radioactive Wastes in a Geologic Repository at Yucca Mountain, Nevada	180319
70 FR 53313	Implementation of a Dose Standard After 10,000 Years	178394
ASM International 1987	*Corrosion*	103753
Brossia et al. 2002	"Effect of Oxide Thickness on the Localized Corrosion of Zircaloy"	161988
BSC 2004	*DSNF and Other Waste Form Degradation Abstraction*	172453
BSC 2004	*CSNF Waste Form Degradation: Summary Abstraction*	169987
Cragnolino et al. 1999	*Assessment of Performance Issues Related to Alternate Engineered Barrier System Materials and Design Options*	152354
Hansson 1984	*The Corrosion of Zircaloy 2 in Anaerobic Synthetic Cement Pore Solution*	101676
He et al. 2007	"Corrosion of Similar and Dissimilar Metal Crevices in the Engineered Barrier System of a Potential Nuclear Waste Repository"	182722
Ikeda and Quinn 2003	*Corrosion of Dissimilar Metal Crevices in Simulated Concentrated Ground Water Solutions at Elevated Temperature*	162662
SNL 2007	*In-Package Chemistry Abstraction*	180506
SNL 2007	*Total System Performance Assessment Data Input Package for Requirements Analysis for TAD Canister and Related Waste Package Overpack Physical Attributes Basis for Performance Assessment*	179394
SNL 2007	*General Corrosion and Localized Corrosion of Waste Package Outer Barrier*	178519
Yau and Webster 1987	"Corrosion of Zirconium and Hafnium"	165063

FEP: 2.1.09.10.0A

FEP NAME:

Secondary Phase Effects on Dissolved Radionuclide Concentrations

FEP DESCRIPTION:

Inclusion of radionuclides in secondary uranium mineral phases, such as neptunium in schoepite and uranium silicates, could affect radionuclide concentrations in water in contact with the waste form. During radionuclide alteration, the radionuclides could be chemically bound to immobile compounds and result in a reduction of available radionuclides for mobilization.

SCREENING DECISION:

Excluded – low consequence

SCREENING JUSTIFICATION:

Incorporation/sequestration of certain radionuclide(s) into corrosion products formed during the alteration of SNF may reduce concentrations of radionuclides in water that has contacted fuel and its corrosion products (SNL 2007 [DIRS 177418], Appendix IV). Simple mass-balance calculations (Werme and Spahiu 1998 [DIRS 113466]) on the results of spent fuel dissolution experiments as well as neptunium solubility experiments (Werme and Spahiu 1998 [DIRS 113466]; Quinones et al. 1996 [DIRS 161925]) revealed that the amount of neptunium in aqueous solution was a small portion of what should have been released from the dissolved nuclear fuel. One explanation for this observation is that released neptunium is included in uranyl solids that form during fuel degradation, as discussed in *Dissolved Concentration Limits of Elements with Radioactive Isotopes* (SNL 2007 [DIRS 177418], Appendix IV).

In conclusion, the inclusion of secondary uranyl mineral phases in the TSPA would reduce calculated doses because these solids would sequester actinides such as neptunium.

Based on the previous discussion, omission of FEP 2.1.09.10.0A (Secondary Phase Effects on Dissolved Radionuclide Concentrations) will not result in a significant adverse change in the magnitude or time of radiological exposures to the RMEI or radionuclide releases to the accessible environment. Therefore, this FEP is excluded from the performance assessments conducted to demonstrate compliance with proposed 10 CFR 63.311 and 63.321 (70 FR 53313 [DIRS 178394]), and with 10 CFR 63.331 [DIRS 180319], on the basis of low consequence.

INPUTS:

Table 2.1.09.10.0A-1. Direct Inputs

Input	Source	Description
SNL 2007. *Dissolved Concentration Limits of Elements with Radioactive Isotopes*. [DIRS 177418]	Appendix IV	Incorporation of certain radionuclide(s) into corrosion products formed during the alteration of spent nuclear fuel may reduce concentrations in water that has contacted fuel and its corrosion products

Table 2.1.09.10.0A-2. Indirect Inputs

Citation	Title	DIRS
10 CFR 63	Energy: Disposal of High-Level Radioactive Wastes in a Geologic Repository at Yucca Mountain, Nevada	180319
70 FR 53313	Implementation of a Dose Standard After 10,000 Years	178394
Quinones et al. 1996	"Coprecipitation Phenomena During Spent Fuel Dissolution. Part 1: Experimental Procedure and Initial Results on Trivalent Ion Behaviour"	161925
Werme and Spahiu 1998	"Direct Disposal of Spent Nuclear Fuel: Comparison Between Experimental and Modelled Actinide Solubiluties in Natural Waters"	113466

FEP: 2.1.09.11.0A

FEP NAME:

Chemical Effects of Waste–Rock Contact

FEP DESCRIPTION:

Waste (CSNF, DSNF, and HLW) and rock may be placed in direct contact by mechanical failure of the drip shields and/or waste packages. Chemical effects on the waste (e.g., dissolution) may be enhanced or altered in a system where waste, rock minerals, and water are all in physical contact with one another, relative to a system where only waste and water are in physical contact.

SCREENING DECISION:

Excluded – low consequence

SCREENING JUSTIFICATION:

The waste forms will have little chance of direct contact with the host rock because the canisters, the waste package stainless steel inner vessel, the Alloy 22 outer barrier, and the drip shield will prevent contact unless they are breached by early failure, or by igneous or seismic events.

For commercial SNF, even if contact of the UO_2 fuel with the rock were to occur, it would have little effect on the fuel corrosion. Uranium in the commercial SNF first oxidizes (U^{4+} to U^{6+}), dissolves, and then precipitates rapidly on the pellet surface as a U^{6+} mineral. Although proximity with the host rock might enhance availability of silicon to precipitate uranyl silicate minerals, this effect is not expected to influence the rate of the fuel's oxidative dissolution process (BSC 2004 [DIRS 169987], Section 6.2.2.3). DOE SNF and defense HLW are also not expected to come into contact with near-field rock. However, the possible direct effects of waste–rock contact, were it to occur, are also considered negligible. For defense HLW, indirect effects that could occur through the water chemistry (e.g., effects on dissolved silicon concentration), which would feed back into the rate of glass dissolution, are expected to be similar to those that will occur due to dissolution of the waste glass itself (BSC 2004 [DIRS 169988], Section 6.5.2.3) in the absence of waste glass and rock contact. The effects, if any, of rock contact would be to inhibit the initial dissolution rate of the glass (i.e., the dissolution rate during the period when the dissolved silicon concentration in the water contacting the glass is increasing due to dissolution of the glass itself). The choice of the k_E parameter value in the HLW glass dissolution model is designed to include the effect of the initial buildup of the dissolved silicon concentration (BSC 2004 [DIRS 169988], Section 6.5.2.6) regardless of whether the source of this silicon is the dissolution of the glass itself or the dissolution of rock with which the glass might come into contact. For DOE SNF (other than naval SNF), an upper-limit model that involves instantaneous degradation of the waste form is used in the TSPA model (see included FEP 2.1.02.01.0A (DSNF Degradation (Alteration, Dissolution, and Radionuclide Release)); direct contact of DOE SNF with the host rock would not affect this model.

Water that contacts SNF will have previously been in contact with the host rock, and therefore rock in physical contact with SNF will not affect the waste–rock–water system chemistry. Furthermore, *In-Package Chemistry Abstraction* (SNL 2007 [DIRS 180506], Sections 6.6.2[a], 6.10.1[a], and 6.10.5) demonstrated that variations in the chemistry of the water contacting the waste package internal components, including the SNF, had an insignificant effect on the pH and total carbonate content of the in-package fluids, the two key chemical parameters controlling the dissolution of commercial SNF and HLW.

Waste form and cladding interactions with igneous intrusions are addressed in included FEP 1.2.04.04.0A (Igneous Intrusion Interacts with EBS Components).

Based on the previous discussion, omission of FEP 2.1.09.11.0A (Chemical Effects of Waste–Rock Contact) will not result in a significant adverse change in the magnitude or timing of either radiological exposure to the RMEI or radionuclide releases to the accessible environment. Therefore, this FEP is excluded from the performance assessments conducted to demonstrate compliance with proposed 10 CFR 63.311 and 63.321 (70 FR 53313 [DIRS 178394]), and with 10 CFR 63.331 [DIRS 180319], on the basis of low consequence.

INPUTS:

Table 2.1.09.11.0A-1. Direct Inputs

Input	Source	Description
SNL 2007. *In-Package Chemistry Abstraction*. [DIRS 180506]	Sections 6.6.2[a], 6.10.1[a], and 6.10.5	Sensitivity of in-package chemistry (particularly pH and total carbonate) to composition of liquid influx

Table 2.1.09.11.0A-2. Indirect Inputs

Citation	Title	DIRS
10 CFR 63	Energy: Disposal of High-Level Radioactive Wastes in a Geologic Repository at Yucca Mountain, Nevada	180319
70 FR 53313	Implementation of a Dose Standard After 10,000 Years	178394
BSC 2004	*CSNF Waste Form Degradation: Summary Abstraction*	169987
BSC 2004	*Defense HLW Glass Degradation Model*	169988

FEP: 2.1.09.12.0A

FEP NAME:

Rind (Chemically Altered Zone) Forms in the Near-Field

FEP DESCRIPTION:

Thermal-chemical processes involving precipitation, condensation, and re-dissolution could alter the properties of the adjacent rock. These alterations may form a rind, or altered zone, in the rock, with hydrological, thermal, and mineralogical properties different from the initial conditions.

SCREENING DECISION:

Excluded – low consequence

SCREENING JUSTIFICATION:

The THC seepage model (SNL 2007 [DIRS 177404]) has been used to evaluate thermal-chemical interactions that will occur in the repository environment, and their impact on the composition of seepage entering the drift, and on the mineralogy and hydrologic properties of the host rock. This model captures the effects of changes in temperature, pH, Eh, ionic strength (and other compositional variables), time dependency, precipitation or dissolution effects, and effects of resaturation, and was used to examine near-field and drift seepage flow and chemistry (SNL 2007 [DIRS 177404], Section 6.2). Ion exchange reactions are not explicitly included in the THC seepage model but are represented by dissolution/precipitation of solid solutions for smectites and of pure end-member compositions for other clay minerals and zeolites (SNL 2007 [DIRS 177404], Section 6.2.1.2).

A wide range of fracture permeability data have been measured for the Topopah Spring units, from 10^{-10} to $10^{-13.2}$ m^2 (SNL 2007 [DIRS 181244], Table 7-2[a]). Changes in fracture permeabilities resulting from mineral precipitation or dissolution were found to be on the order of the natural variation in these permeabilities (SNL 2007 [DIRS 177404], Section 6.5.5.3; BSC 2004 [DIRS 170038], Table 6-5 and Section 6.1), with most of the substantial effects limited to regions above and to the side of the drift within about a drift diameter (SNL 2007 [DIRS 177404], Figures 6.5-8 to 6.5-9). The predicted mineral precipitation reduces permeability in the affected regions and leads to a reduction in flow around the drift and therefore less seepage. THC effects on fracture characteristics have been evaluated with the THC seepage model, which explicitly accounts for fracture flow affected by THC parameter alterations (SNL 2007 [DIRS 181244], Section 6.4.4.2). There is no indication that significant precipitation may occur immediately at the drift wall. This means that the local permeability and porosity in the boundary layer above the drift wall, important for the capillary barrier behavior, are not affected by THC processes.

It was demonstrated that the effects of these potential alterations on near-field and drift seepage flow can be excluded in the TSPA because the expected changes would lead to less seepage

(SNL 2007 [DIRS 181244], Section 6.5.1.4). Consequently, omission of this effect is expected to result in a slight increase in seepage and may enhance drift seepage and radionuclide transport.

Based on the previous discussion, omission of FEP 2.1.09.12.0A (Rind (Chemically Altered Zone) Forms in the Near Field) will not result in a significant adverse change in the magnitude or time of radiological exposures to the RMEI or radionuclide releases to the accessible environment. Therefore, this FEP is excluded from the performance assessments conducted to demonstrate compliance with proposed 10 CFR 63.311 and 63.321 (70 FR 53313 [DIRS 178394]), and with 10 CFR 63.331 [DIRS 180319], on the basis of low consequence.

INPUTS:

Table 2.1.09.12.0A-1. Direct Inputs

Input	Source	Description
SNL 2007. *Abstraction of Drift Seepage*. [DIRS 181244]	Section 6.5.1.4	The abstraction of THM and THC parameter alterations demonstrated that the effects of precipitation, condensation, and re-dissolution on near field and drift seepage flow can be excluded from the model because the expected changes would lead to less seepage
	Table 7-2[a]	Range of fracture permeability data measured for the Topopah Spring units

Table 2.1.09.12.0A-2. Indirect Inputs

Citation	Title	DIRS
10 CFR 63	Energy: Disposal of High-Level Radioactive Wastes in a Geologic Repository at Yucca Mountain, Nevada	180319
70 FR 53313	Implementation of a Dose Standard After 10,000 Years	178394
BSC 2004	*Analysis of Hydrologic Properties Data*	170038
SNL 2007	*Abstraction of Drift Seepage*	181244
SNL 2007	*Drift-Scale THC Seepage Model*	177404

FEP: 2.1.09.13.0A

FEP NAME:

Complexation in EBS

FEP DESCRIPTION:

The presence of organic complexants in water in the EBS could augment radionuclide transport by providing a transport mechanism in addition to simple diffusion and advection of dissolved material. Organic complexants may include materials found in natural groundwater such as humates and fulvates, or materials introduced with the waste or engineered materials.

SCREENING DECISION:

Excluded – low consequence

SCREENING JUSTIFICATION:

In the unexpected event of drip shield failure and waste package failure at the same location, seepage potentially containing organic complexants could enter the waste package. Organic compounds can form soluble complexes with radionuclides, complexes that are not expected to sorb, thereby enhancing their potential for transport. Humic acid and fulvic acid are of particular interest as they have been shown to complex strongly with actinides. Humic acid and fulvic acid are produced as a by-product of biologic activity and might accumulate in seepage. Because humic acid and fulvic acid production in the drift and waste package is expected to be minimal due to the early thermal pulse and long-term limits on nutrient availability (see excluded FEP 2.1.10.01.0A (Microbial Activity in EBS) and included FEP 2.1.11.08.0A (Thermal Effects on Chemistry and Microbial Activity in the EBS)) the analysis that follows focuses on humic acid and fulvic acid carried into the package by seepage. The bulk of the non-actinide radionuclides (e.g., ^{129}I, ^{99}Tc, $^{137,135}Cs$, ^{90}Sr) are predicted to be highly soluble (SNL 2007 [DIRS 177424], Table 6-4), in the absence of humic acid and fulvic acid. The presence of humic acid and fulvic acid that may potentially exist in seepage is, therefore, not expected to elevate their solubility any further (though it may inhibit sorption of cesium and strontium in the invert). The emphasis here is on the low solubility, highly sorbing actinides that might be mobilized by humic acid and fulvic acid.

A total organic carbon content of 0.58 mg/L is reported by Means et al. (1983 [DIRS 100797], Table 1) for well UE25b-1, 33% (0.19 mg/L) of which has a molecular weight greater than 1,000 (Means et al. (1983 [DIRS 100797], Table 3). Using as a maximum a ratio of one humic + fulvic carbon site per complexed actinide, 0.19 mg/L of carbon would correspond to 0.016 mM of complexed actinides.

Solubility limits of plutonium, neptunium, thorium, americium, uranium, and protactinium (SNL 2007 [DIRS 177418]) are much higher than 0.016 mM at high and low pH. Therefore the presence of humic and fulvic acids would have little effect on solubilities under these conditions. The addition of humic acid and/or fulvic acid might elevate actinide solubilities at near-neutral pH values. Humic acid and fulvic acid elevated actinide solubilities are unexpected, however,

because dissolved iron and uranium will compete with actinides for humic acid and fulvic acid complexation sites.

Many organic complexants coordinate with Fe(III), Cr(III), and Ni(II) produced by corrosion of steels (SNL 2007 [DIRS 180506], Table 4-7), and uranium that will leach from the fuels. Competition by Fe(III/II), Cr(III), and Ni(II) and dissolved uranium for binding sites on humic + fulvic acids introduced by seepage waters, or on organic residues in the waste package or EBS is therefore expected to inhibit coordination of actinides with organics, and thereby hinder organic-facilitated transport.In conclusion, because microbial activity in the repository is expected to be low (excluded FEP 2.1.10.01.0A (Microbial Activity in the EBS)), the formation of organic complexants in the EBS will also be low, and the impact of organic materials found in natural groundwater on radionuclide transport will be negligible.

Based on the previous discussion, omission of FEP 2.1.09.13.0A (Complexation in EBS) will not result in a significant adverse change in the magnitude or timing of either radiological exposure to the RMEI or radionuclide releases to the accessible environment. Therefore, this FEP is excluded from the performance assessments conducted to demonstrate compliance with proposed 10 CFR 63.311 and 63.321 (70 FR 53313 [DIRS 178394]), and with 10 CFR 63.331 [DIRS 180319], on the basis of low consequence.

INPUTS:

Table 2.1.09.13.0A-1. Direct Inputs

Input	Source	Description
Means et al. 1983. *The Organic Geochemistry of Deep Ground Waters and Radionuclide Partitioning Experiments under Hydrothermal Conditions*. [DIRS 100797]	Tables 1 and 3	Total organic carbon is 0.58 mg/L for well UE25b-1, 33% (0.19 mg/L) of which has a molecular weight greater than 1,000

Table 2.1.09.13.0A-2. Indirect Inputs

Citation	Title	DIRS
10 CFR 63	Energy: Disposal of High-Level Radioactive Wastes in a Geologic Repository at Yucca Mountain, Nevada	180319
70 FR 53313	Implementation of a Dose Standard After 10,000 Years	178394
SNL 2007	*Dissolved Concentration Limits of Elements with Radioactive Isotopes*	177418
SNL 2007	*In-Package Chemistry Abstraction*	180506
SNL 2007	*Radionuclide Screening*	177424

FEP: 2.1.09.15.0A

FEP NAME:

Formation of True (Intrinsic) Colloids in EBS

FEP DESCRIPTION:

True colloids are colloidal-sized assemblages (between approximately 1 nanometer and 1 micrometer in diameter) consisting of hydrolyzed and polymerized radionuclides. They may form in the waste package and EBS during waste form degradation and radionuclide transport. True colloids are also called primary colloids, real colloids, Type I colloids, Eigenkolloide, and intrinsic colloids (or actinide intrinsic colloids, for those including actinide elements).

SCREENING DECISION:

Excluded – low consequence

SCREENING JUSTIFICATION:

Of all the actinides, plutonium has the highest tendency to form stable intrinsic colloids, by virtue of polymerization (Choppin and Stout 1989 [DIRS 168379], p 209). If plutonium intrinsic colloids are shown to be of low importance for radionuclide transport relative to colloids included in system models, colloids of the other actinides of similar abundance should be of even lesser importance. Transport of radionuclides by groundwater colloids is more significant than transport by true colloids In fact, Rai and Swanson (1981 [DIRS 144599], p. 111) show that plutonium-colloidal suspensions (which may be polymers or very fine hydroxide solids) are generally unstable above pH = 5, whereas the pH of the natural system is expected to be higher, even for evolved fluid composition just around the drift (as discussed in excluded FEP 2.2.01.04.0A (Radionuclide Solubility in the Excavation Disturbed Zone)). As true colloids are thermodynamically unstable phases, they are expected to dissolve back into the aqueous phase; the radionuclides will subsequently be sorbed onto pseudocolloids and waste form colloids (or retarded via interaction with immobile substrates). For example, Kersting and Reimus (2003 [DIRS 162421], pp. 88 to 92) describe experiments in which plutonium polymer (an intrinsic colloid) was equilibrated with montmorillonite, silica, hematite, and goethite colloids (pseudocolloids). Sorption coefficients for plutonium onto these pseudocolloids were always at least 10^3 mL/g; and even after aggressive desorption, at least 50% of the plutonium remained bound to the pseudocolloids, demonstrating the dominance of these over the plutonium intrinsic colloids. Thus, plutonium intrinsic colloids, even if they existed after the sorption experiments, were relatively insignificant compared to the plutonium present as pseudocolloids (sorbed onto montmorillonite, silica, hematite and goethite). Near degrading fuel, plutonium may be associated with a zirconium-rich solid phase (conceptually identified as a mixed plutonium-zirconium-rare earth oxide and modeled as "ZrO_2" particles with irreversibly attached plutonium and americium with no additional sorption of other radionuclides), which is expected to transport as a waste form colloid, not as an intrinsic colloid (SNL 2007 [DIRS 177423], Section 6.3.1). Radionuclide transport by colloids formed through coprecipitation in the EBS is

discussed in included FEP 2.1.09.25.0A (Formation of Colloids (Waste-Form) by Co-precipitation in EBS).

Compared to plutonium, uranium shows a lower tendency to polymerize; yet, the much larger mass of uranium requires consideration of its intrinsic colloids. However, for uranium, unlike for plutonium where intrinsic colloids can dominate the mass of plutonium within the solution, the total colloid fraction represents only about 1% to 12% of the uranium dissolved in solution (Wronkiewicz et al. 1996 [DIRS 102047], p. 86). U(VI) hydroxides (polymerized intrinsic uranyl colloids) may initially form, but these will be unstable relative to U(VI) silicates in silica-containing groundwater (Finch and Ewing 1992 [DIRS 113030], Section 4.2.2), and even the U(VI) silicates are expected to be minor contributors to radionuclide transport even if they do not dissolve back into the groundwater over the duration of transport (SNL 2007 [DIRS 177423], Section 7.0).

Again, plutonium is the actinide that is most commonly observed to form true colloids. Because true plutonium colloids are not expected to affect dose, true colloids of the other actinides that are of similar abundance are not expected to affect dose either. For uranium, intrinsic colloids are expected to be neglible contributors to transport and are not expected to affect dose.

Consistent with the previous discussion, omission of FEP 2.1.09.15.0A (Formation of True (Intrinsic) Colloids in EBS) will not result in a significant adverse change in the magnitude or time of radiological exposures to the RMEI or radionuclide releases to the accessible environment. Therefore, this FEP is excluded from the performance assessments conducted to demonstrate compliance with proposed 10 CFR 63.311 and 63.321 (70 FR 53313 [DIRS 179394]), and with 10 CFR 63.331 [DIRS 180319], on the basis of low consequence.

INPUTS:

Table 2.1.09.15.0A-1. Direct Inputs

Input	Source	Description
Choppin and Stout 1989. "Actinide Behavior in Natural Waters." [DIRS 168379]	p. 209	For the higher charged actinides, hydrolysis can lead to formation of oligomers and polymers. At the low environmental concentrations of actinides, these are usually a problem only for Pu(IV) whose hydrolytic polymers are rather intractable
Finch and Ewing 1992. "The Corrosion of Uraninite Under Oxidizing Conditions." [DIRS 113030]	Section 4.2.2	The effect of dissolved silica on the alteration of the uranyl (VI) hydroxides is profound; the alteration of schoepite can result in the formation of uranyl silicates such as uranophane and sodyite
Rai and Swanson 1981. "Properties of Plutonium(IV) Polymer of Environmental Importance." [DIRS 144599]	p. 111	Pu(IV) polymer does not make stable suspensions at pH values above 5 and hence would not be expected to be mobile as polyer in the lithosphere
Wronkiewicz et al. 1996. "Ten-Year Results from Unsaturated Drip Tests with UO_2 at 90°C: Implications for the Corrosion of Spent Nuclear Fuel." [DIRS 102047]	p. 86	Between 1% and 12% of the total amount of uranium released was present as a >5 nm size-fraction

Table 2.1.09.15.0A-2. Indirect Inputs

Citation	Title	DIRS
10 CFR 63	Energy: Disposal of High-Level Radioactive Wastes in a Geologic Repository at Yucca Mountain, Nevada	180319
70 FR 53313	Implementation of a Dose Standard After 10,000 Years	178394
Kersting and Reimus 2003	*Colloid-Facilitated Transport of Low-Solubility Radionuclides: A Field, Experimental, and Modeling Investigation*	162421
SNL 2007	*Waste Form and In-Drift Colloids-Associated Radionuclide Concentrations: Abstraction and Summary*	177423

FEP: 2.1.09.16.0A

FEP NAME:

Formation of Pseudo-Colloids (Natural) in EBS

FEP DESCRIPTION:

Pseudo-colloids are colloidal-sized assemblages (between approximately 1 nanometer and 1 micrometer in diameter) of nonradioactive material that have radionuclides bound or sorbed to them. Natural pseudo-colloids include microbial colloids, mineral fragments (i.e., clay, silica, iron oxyhydroxides), and humic and fulvic acids. This FEP addresses radionuclide-bearing pseudo-colloids formed from host-rock materials and all interactions of the waste and EBS with the host rock environment except corrosion.

SCREENING DECISION:

Included

TSPA DISPOSITION:

Natural colloids are modeled as montmorillonite clay colloids as discussed in *Waste Form and In-Drift Colloids-Associated Radionuclide Concentrations: Abstraction and Summary* (SNL 2007 [DIRS 177423], Sections 6.3.1 and 6.3.11). Pseudocolloids generally form as a result of dissolved (aqueous) radionuclides sorbing to existing colloids (SNL 2007 [DIRS 177423], Section 6.3.1). K_d values are developed to model reversible sorption of plutonium, americium, thorium, neptunium, cesium, protactinium, uranium, radium, and tin onto natural groundwater colloids to form pseudocolloids (SNL 2007 [DIRS 177423], Section 6.3.12.1). Colloid stability (including pseudocolloids) is determined based on ionic strength and pH. Colloid concentration (including pseudocolloids) is modeled as an uncertain parameter based on field observations in the Yucca Mountain vicinity (SNL 2007 [DIRS 177423], Section 6.3.11).

In TSPA, seepage water colloids (including pseudocolloids) are modeled with reversible radionuclide attachment using linear sorption coefficients (K_ds) (SNL 2007 [DIRS 177423], Section 6.3.12.1). Model implementation and output parameters used by the TSPA are described in *Waste Form and In-Drift Colloids-Associated Radionuclide Concentrations: Abstraction and Summary* (SNL 2007 [DIRS 177423], Sections 6.5 and 8.1 and Table 8.1). Model parameter uncertainty associated with radionuclide adsorption onto colloids is discussed in *Waste Form and In-Drift Colloids-Associated Radionuclide Concentrations: Abstraction and Summary* (SNL 2007 [DIRS 177423], Section 6.6.8). The primary uncertainties in the colloid model are the abundances of this colloid type at a given solution composition and the sorption coefficients that are used to partition radionuclides onto this colloid type (SNL 2007 [DIRS 177423], Section 6.6). Laboratory measurement uncertainties are large contributors to both. Uncertainty is captured and propagated in the model by sampling over a range of colloid concentration and radionuclide uptake characteristics.

Natural colloids consisting of iron oxyhydroxides and silica may also be present (SNL 2007 [DIRS 177423], Section 6.3.1). However, these are not modeled. Silica colloids have such low sorptive properties that they can be ignored (SNL 2007 [DIRS 177423], Section 6.3.1), and waste package corrosion products will dwarf the quantity of natural groundwater iron oxyhydroxide colloids. Corrosion product colloids are the subject of included FEP 2.1.09.17.0A (Formation of Pseudo-colloids (Corrosion Product) in EBS) and are not discussed in this FEP.

INPUTS:

Table 2.1.09.16.0A-1. Indirect Inputs

Citation	Title	DIRS
SNL 2007	*Waste Form and In-Drift Colloids-Associated Radionuclide Concentrations: Abstraction and Summary*	177423

FEP: 2.1.09.17.0A

FEP NAME:

Formation of Pseudo-Colloids (Corrosion Product) in EBS

FEP DESCRIPTION:

Pseudo-colloids are colloidal-sized assemblages (between approximately 1 nanometer and 1 micrometer in diameter) of nonradioactive material that have radionuclides bound or sorbed to them. Corrosion product pseudo-colloids include iron oxyhydroxides from corrosion and degradation of the metals in the EBS and silica from degradation of cementitious materials.

SCREENING DECISION:

Included

TSPA DISPOSITION:

The model developed in *Waste Form and In-Drift Colloids-Associated Radionuclide Concentrations: Abstraction and Summary* (SNL 2007 [DIRS 177423], Sections 6.3.1 and 6.3.8) includes treatment of pseudocolloids associated with corrosion of steel components of the waste package. Silica colloids from the degradation of cementitious material is not treated in the colloids report (SNL 2007 [DIRS 177423], Section 6.3.1) because cementitious materials are not part of the EBS in-drift configuration (SNL 2007 [DIRS 179354], Table 4-1). Colloids formed from the corrosion of steel in the EBS are expected to be iron oxyhydroxides primarily consisting of three mineral species under the anticipated repository conditions: goethite, hematite, and ferrihydrite (also refered to as hydrous ferric oxide) (SNL 2007 [DIRS 177423], Section 6.3.8). Hematite is used in the model for constraining colloid stability, while the sorption properties of iron-oxide surfaces are modeled using hydrous ferric oxide and goethite. Estimated colloidal mass concentrations based on corrosion studies using miniature waste packages under repository-relevant conditions were used to constrain the model (SNL 2007 [DIRS 177423], Section 6.3.8). Iron oxyhydroxide corrosion colloids are subject to concentration and stability constraints controlled by the aqueous chemistry, chiefly determined from the ionic strength and pH of in-package and in-drift fluids (SNL 2007 [DIRS 177423], Section 6.5).

The sorption calculations for iron oxyhydroxide colloids are based on a mechanistic surface complexation-based competitive sorption model, where the sorption coefficients are calculated as a function of dissolved concentration of competing species, pCO_2, and sorption sites (SNL 2007 [DIRS 177407], Sections 6.3.4.2.3 and 6.5.2.4). The results of these calculations are implemented in TSPA by applying reversible sorption of thorium, uranium, and neptunium on iron oxyhydroxide colloids by computing an effective K_d at each timestep. The sorption of plutonium and americium on iron oxyhydroxide colloids is modeled as an irreversible sorption process by kinetic attachment (with no detachment) by applying a forward rate constant as decribed in *Waste Form and In-Drift Colloids-Associated Radionuclide Concentrations: Abstraction and Summary* (SNL 2007 [DIRS 177423], Section 6.3.12.2).

Model parameter uncertainty associated with colloid concentration is discussed in *Waste Form and In-Drift Colloids-Associated Radionuclide Concentrations: Abstraction and Summary* (SNL 2007 [DIRS 177423], Section 6.6.5). The primary uncertainties in the colloid model are the abundances of the colloid type for a given solution composition and the sorption coefficients that are used to partition radionuclides onto this colloid type. Uncertainty is captured and propagated in the model by sampling over a range of colloid concentrations and by computing the sorption coefficients from surface-complexation modeling performed over a range of dissolved concentrations, surface properties, and chemical conditions.

INPUTS:

Table 2.1.09.17.0A-1. Indirect Inputs

Citation	Title	DIRS
SNL 2007	*Total System Performance Assessment Data Input Package for Requirements Analysis for EBS In-Drift Configuration*	179354
SNL 2007	*EBS Radionuclide Transport Abstraction*	177407
SNL 2007	*Waste Form and In-Drift Colloids-Associated Radionuclide Concentrations: Abstraction and Summary*	177423

FEP: 2.1.09.18.0A

FEP NAME:

Formation of Microbial Colloids in EBS

FEP DESCRIPTION:

This FEP addresses the formation and transport of microbial colloids in the waste and EBS.

SCREENING DECISION:

Excluded – low consequence

SCREENING JUSTIFICATION:

For microbes to impact near-field performance, microbes must be present in significant quantities, which means that sufficient energy sources and nutrients must be available for microbial activity to be viable. However, due to severe environmental constraints, microbial activity in the EBS is expected to be low, and microbial activity impacts on drift chemistry will be insignificant (excluded FEP 2.1.10.01.0A (Microbial Activity in the EBS), which excludes microbial-activity impacts to the in-drift chemical environment in the TSPA on the basis of low consequence). By inference, the formation of microbial colloids in the EBS would be insignificant, and therefore of low consequence to the performance assessment.

To assess the potential effects on microbial populations within the EBS, *Evaluation of Potential Impacts of Microbial Activities on Drift Chemistry* (BSC 2004 [DIRS 169991]) considered the drift mineralogy; drift physical parameters; metals used in engineered barrier system components; waste dissolution rates and quantities; groundwater compositions and infiltration rates; and compositions and fluxes of gases (e.g., CO_2, water vapor). Environmental limits on microbial activity considered include redox conditions, temperature, radiation, hydrostatic pressure, water activity, pH, salinity, available nutrients, and others. The study evaluated the potential for radionuclide transport facilitated by suspended microbial cells, or biocolloids (BSC 2004 [DIRS 169991], Section 6.5.4). The study concluded that the potential effect of radionuclide-bearing colloids is negligible. The transport of those microbes that do exist will be limited by the scarcity of aqueous pathways. The transport and facilitated radionuclide migration are expected to be limited due to low liquid saturation, high ionic strength and low microbial activity in the EBS (SNL 2007 [DIRS 177423], Section 6.3.13.1). Microbes and organic compounds will not affect the generation of inorganic colloids. Any interactions will tend to destabilize inorganic colloids, possibly decreasing the mobility of associated radionuclides (SNL 2007 [DIRS 177423], Section 6.3.13).

Based on the previous discussion, omission of FEP 2.1.09.18.0A (Formation of Microbial Colloids in EBS) will not result in a significant adverse change in the magnitude or time of radiological exposures to the RMEI or radionuclide releases to the accessible environment. Therefore, this FEP is excluded from the performance assessments conducted to demonstrate compliance with proposed 10 CFR 63.311 and 63.321 (70 FR 53313 [DIRS 178394]), and with 10 CFR 63.331 [DIRS 180319], on the basis of low consequence.

INPUTS:

Table 2.1.09.18.0A-1. Direct Inputs

Input	Source	Description
BSC 2004. *Evaluation of Potential Impacts of Microbial Activities on Drift Chemistry*. [DIRS 169991]	Section 6.5.4	Microbial communities within the EBS
SNL 2007. *Waste Form and In-Drift Colloids-Associated Radionuclide Concentrations: Abstraction and Summary*. [DIRS 177423]	Section 6.3.13	Potential effects of microbes on inorganic colloids and microbial communities within the EBS

Table 2.1.09.18.0A-2. Indirect Inputs

Citation	Title	DIRS
10 CFR 63	Energy: Disposal of High-Level Radioactive Wastes in a Geologic Repository at Yucca Mountain, Nevada	180319
70 FR 53313	Implementation of a Dose Standard After 10,000 Years	178394
BSC 2004	*Evaluation of Potential Impacts of Microbial Activities on Drift Chemistry*	169991
SNL 2007	*Waste Form and In-Drift Colloids-Associated Radionuclide Concentrations: Abstraction and Summary*	177423

FEP: 2.1.09.19.0A

FEP NAME:

Sorption of Colloids in EBS

FEP DESCRIPTION:

Interactions between radionuclide-bearing colloids and the waste and EBS may result in retardation of the colloids during transport by sorption mechanisms.

SCREENING DECISION:

Excluded – low consequence

SCREENING JUSTIFICATION:

As discussed in *Waste Form and In-Drift Colloids-Associated Radionuclide Concentrations: Abstraction and Summary* (SNL 2007 [DIRS 177423], Section 6.5.2.1), the TSPA considers that colloids with embedded and sorbed radionuclides leave the failed waste package and enter the drift geochemical environment. The colloids exit the in-package chemical environment and enter the invert chemical environment. In the repository, interactions between radionuclide-bearing colloids and the waste and EBS may result in some retardation of the colloid transport by sorption mechanisms as discussed below.

Like physical filtration (see excluded FEP 2.1.09.20.0A (Filtration of Colloids in EBS) and gravitational settling of colloids (see excluded FEP 2.1.09.26.0A (Gravitational Settling of Colloids in EBS)), colloid sorption tends to retard colloid transport in the EBS. In *Waste Form and In-Drift Colloids-Associated Radionuclide Concentrations: Abstraction and Summary* (SNL 2007 [DIRS 177423], Sections 6.3.1 and 7.2), physical filtration of colloids is not explicitly included in the abstraction. Colloids that leave a failed waste package through the failure opening are not subsequently filtered out or settled out in the surrounding EBS material, including the invert. This assumption overestimates the potential consequences of colloid-facilitated transport of radionuclides and is, therefore, considered bounding. The effect of sorption is similar to filtration and settling, as all three processes result in immobilization of the colloids. Not crediting colloid sorption in the waste package and invert is therefore consistent with not crediting filtration and settling. This produces a bounding estimate of the consequences of colloid-facilitated transport of radionuclides in the EBS.

Based on the previous discussion, omission of FEP 2.1.09.19.0A (Sorption of Colloids in EBS) will not result in a significant adverse change in the magnitude or timing of either radiological exposure to the RMEI or radionuclide releases to the accessible environment. Therefore, this FEP is excluded from the performance assessments conducted to demonstrate compliance with proposed 10 CFR 63.311 and 63.321 (70 FR 53313 [DIRS 178394]), and with 10 CFR 63.331 [DIRS 180319], on the basis of low consequence.

INPUTS:

Table 2.1.09.19.0A-1. Direct Inputs

Input	Source	Description
SNL 2007. *Waste Form and In-Drift Colloids-Associated Radionuclide Concentrations: Abstraction and Summary*. [DIRS 177423]	Sections 6.3.1, 7.2	Physical filtration of colloids is not explicitly included in the abstraction
	Section 6.5.2.1	TSPA considers that colloids with embedded and sorbed radionuclides leave the failed waste package and enter the drift geochemical environment

Table 2.1.09.19.0A-2. Indirect Inputs

Citation	Title	DIRS
10 CFR 63	Energy: Disposal of High-Level Radioactive Wastes in a Geologic Repository at Yucca Mountain, Nevada	180319
70 FR 53313	Implementation of a Dose Standard After 10,000 Years	178394

FEP: 2.1.09.19.0B

FEP NAME:

Advection of Colloids in EBS

FEP DESCRIPTION:

Transport of radionuclide-bearing colloids in the waste and EBS may occur by advection.

SCREENING DECISION:

Included

TSPA DISPOSITION:

The formation, stability, and concentration of colloids are addressed in *Waste Form and In-Drift Colloids-Associated Radionuclide Concentrations: Abstraction and Summary* (SNL 2007 [DIRS 177423], Section 6.3.1). Three types of colloids are anticipated to exist in the EBS (SNL 2007 [DIRS 177423], Section 6.3.1): (1) waste form colloids from degradation of HLW glass and commercial SNF, (2) iron oxyhydroxide colloids due to products from the corrosion of steel waste packages, and (3) groundwater or seepage water colloids. On all three types of colloids, radionuclides may undergo reversible, or equilibrium, sorption. The waste form colloids may also contain embedded radionuclides that are not removable. Plutonium and americium can be strongly sorbed onto iron oxyhydroxide; for these radionuclides, sorption is modeled as a kinetic process.

The model developed in *EBS Radionuclide Transport Abstraction* (RTA) (SNL 2007 [DIRS 177407], Section 6.3.4) is used to quantify the time-dependent radionuclide releases from a failed waste package and their subsequent transport through the EBS to the emplacement drift wall/unsaturated zone interface. The basic inputs to the RTA model consist of the drift seepage and drift wall condensation flux, the environmental conditions in the drift (temperature, relative humidity, and water chemistry), and the degradation state of the EBS components (SNL 2007 [DIRS 177407], Section 6.1). Outputs consist of the rates of radionuclide releases to the unsaturated zone as a result of advective and diffusive transport, accounting for the impact of colloids, radionuclide solubility, retardation, and the degree of liquid saturation of the waste form and invert materials. The RTA model is implemented directly into the TSPA GoldSim model to compute the radionuclide release rates from the EBS (SNL 2007 [DIRS 177407], Section 6.5.2).

The source of inflow to the EBS is the seepage flux that drips from the crown (roof) of the drift, drift wall condensation, and imbibition flux from the unsaturated zone into the invert. This inflow can flow through the EBS along eight pathways: (1) seepage flux and drift wall condensation, (2) flux through the drip shield, (3) diversion around the drip shield, (4) flux through the waste package, (5) diversion around the waste package, (6) flux from the waste package into the invert, (7) imbibition flux from the unsaturated zone matrix to the invert, and (8) flux from the invert to the unsaturated zone (SNL 2007 [DIRS 177407], Section 6.3.1.1 and Figure 6.3-1). Pathways 4, 6, and 8 may cause advective flow of colloids bearing radionuclides.

These pathways are time dependent because drip shield penetrations and waste package penetrations will vary with time and local conditions in the repository.

The conceptual model for flow through the EBS also includes three domains: the waste form (e.g., fuel rods or defense HLW glass), waste package corrosion products, and the invert. The EBS domains are defined in *EBS Radionuclide Transport Abstraction* (SNL 2007 [DIRS 177407], Section 6.5.2). Because no barrier capability is credited to the emplacement pallet with respect to radionuclide transport, the water and radionuclides in this model pass directly from the waste package to the invert.

The total flux entering the invert is equal to: (1) the flux diverted around the drip shield, (2) the flux diverted around the waste package, and (3) the flux leaving the waste package. The concentration of radionuclide-bearing colloids in the invert is determined by the mass of colloids entering the invert and the total flux that leaves the invert (both described earlier). Except for the evaporative fluxes, all fluxes that enter the invert leave the invert to the unsaturated zone.

Radionuclide-bearing colloids are transported through the invert via advection and diffusion. Colloids are transported advectively at approximately the same velocity as the liquid flux leaving the waste package (SNL 2007 [DIRS 177407], Section 6.3.4.4). Longitudinal and transverse dispersion of colloids is ignored because of the short travel distance through the EBS (SNL 2007 [DIRS 177407], Section 6.3.4.4). A summary of the computational model provided to the TSPA, including model parameter uncertainty implementation, is described in *EBS Radionuclide Transport Abstraction* (SNL 2007 [DIRS 177407], Section 6.5.2 and Table 8.1-1).

The advective transport of dissolved radionuclides is addressed in included FEP 2.1.08.08.0B (Advection of Dissolved Radionuclides in EBS).

INPUTS:

Table 2.1.09.19.0B-1. Indirect Inputs

Citation	Title	DIRS
SNL 2007	*EBS Radionuclide Transport Abstraction*	177407
SNL 2007	*Waste Form and In-Drift Colloids-Associated Radionuclide Concentrations: Abstraction and Summary*	177423

FEP: 2.1.09.20.0A

FEP NAME:

Filtration of Colloids in EBS

FEP DESCRIPTION:

Filtration processes may affect transport of radionuclide-bearing colloids in the waste and EBS. Filtration includes physical and electrostatic processes in pores and fractures of natural and anthropogenic materials, such as concrete and the joints between invert segments.

SCREENING DECISION:

Excluded – low consequence

SCREENING JUSTIFICATION:

Colloid filtration, as discussed here, refers to the physical removal of colloids from a fluid flow system by physical and electrostatic processes. Filtration of colloids generally means the retention of suspended colloids moving with the groundwater in pores, channels, and fracture apertures that are too small or dry to allow passage of the colloids. Like sorption (see excluded FEP 2.1.09.19.0A (Sorption of Colloids in EBS)) and gravitational settling of colloids (see excluded FEP 2.1.09.26.0A (Gravitational Settling of Colloids in EBS)), colloid filtration tends to retard colloid transport in the EBS.

Within the waste package, colloids may form within the defense HLW glass at its outer surfaces (e.g., degraded defense HLW glass), from fuel, and from corroding steel. Colloids could be filtered within fractures in fuel pellets or trapped at the boundaries of disaggregating grains. Colloids forming within SNF rods whose cladding has been breached could be filtered at perforations in the cladding. Additionally, colloids could be filtered at perforations in the stainless steel containers. Colloids reaching the interior of the waste package could be filtered at perforations in the skin of the waste package. In the underlying invert material (crushed tuff), the colloids that do exit the waste package environment could be subjected to filtration in pores and channels that are too small or dry to allow further movement.

In the TSPA, the assumption is made that all stable colloids formed within the waste package (the calculated colloid source term) exit the package and enter the invert without filtration; these colloids will then move through the invert material without being subjected to filtration until they reach the underlying unsaturated zone (SNL 2007 [DIRS 177423], Section 6.3.1). Because filtration within the waste package and the invert will occur to some extent, excluding filtration overestimates the potential impact of colloid-facilitated transport of radionuclides in the TSPA dose calculations.

Based on the previous discussion, omission of FEP 2.1.09.20.0A (Filtration of Colloids in EBS) will not result in a significant adverse change in the magnitude or time of radiological exposures to the RMEI or radionuclide releases to the accessible environment. Therefore, this FEP is excluded from the performance assessments conducted to demonstrate compliance with proposed

10 CFR 63.311 and 63.321 (70 FR 53313 [DIRS 178394]), and with 10 CFR 63.331 [DIRS 180319], on the basis of low consequence.

INPUTS:

Table 2.1.09.20.0A-1. Direct Inputs

Input	Source	Description
SNL 2007. *Waste Form and In-Drift Colloids-Associated Radionuclide Concentrations: Abstraction and Summary*. [DIRS 177423]	Section 6.3.1	Filtration and sorption of colloids in EBS

Table 2.1.09.20.0A-2. Indirect Inputs

Citation	Title	DIRS
10 CFR 63	Energy: Disposal of High-Level Radioactive Wastes in a Geologic Repository at Yucca Mountain, Nevada	180319
70 FR 53313	Implementation of a Dose Standard After 10,000 Years	178394

FEP: 2.1.09.21.0A

FEP NAME:

Transport of Particles Larger than Colloids in EBS

FEP DESCRIPTION:

Groundwater flow through the waste could remove radionuclide-bearing particles by a rinse mechanism. Particles of radionuclide-bearing material larger than colloids could be entrained in suspension and then be transported in water flowing through the waste and EBS.

SCREENING DECISION:

Excluded – low consequence

SCREENING JUSTIFICATION:

Colloids by definition have at least one dimension between 1 nm and 1 μm. Particles larger than this inside a breached waste package might include metal and/or fuel fragments, and HLW glass shards. If these particles sorbed radionuclides and were transported from the waste package through the EBS, unsaturated zone, and saturated zone and into the biosphere, they might affect dose. However, transport of radionuclide-bearing particles larger than colloids in the EBS is not expected to have an adverse effect on performance because the size and density of these particles will favor settling from solution. In addition, particles with a relatively large radius are expected to become entrapped in pore throats and attach to immobile air-water interfaces in the EBS. Finally, inorganic particles larger than 1 μm will settle much more rapidly than they diffuse (Reimus 1995 [DIRS 144604], Section 3.2; see also excluded FEP 2.1.09.21.0B (Transport of Particles Larger than Colloids in the SZ)), so diffusion is not expected to contribute significantly to their transport through the EBS.

Although it cannot be ruled out that a small number of particles larger than colloids might transport through the EBS, for the reasons stated above, the number of such particles is expected to be very small compared to the number of colloids transported through the EBS. Colloid transport in the EBS is included in TSPA (FEPs 2.1.09.18.0B (Advection of Colloids in EBS) and 2.1.09.24.0A (Diffusion of Colloids in EBS)) because although colloids are subjected to the same transport processes as larger particles, they settle more slowly, diffuse more rapidly, fit through smaller pore throats, and advectively collide with air-water interfaces to a lesser extent than larger particles. .

Based on the previous discussion, omission of FEP 2.1.09.21.0A (Transport of Particles Larger than Colloids in EBS) will not result in a significant adverse change in the magnitude or time of radiological exposures to the RMEI or radionuclide releases to the accessible environment. Therefore, this FEP is excluded from the performance assessments conducted to demonstrate compliance with proposed 10 CFR 63.311 and 63.321 (70 FR 53313 [DIRS 178394]), and with 10 CFR 63.331 [DIRS 180319], on the basis of low consequence.

INPUTS:

Table 2.1.09.21.0A-1. Direct Inputs

Input	Source	Description
Reimus 1995. *Transport of Synthetic Colloids Through Single Saturated Fractures: A Literature Review*. [DIRS 144604]	Section 3.2	Equations and associated discussion describing normal and short-range forces and associated velocities affecting particles moving in a viscous fluid

Table 2.1.09.21.0A-2. Indirect Inputs

Citation	Title	DIRS
10 CFR 63	Energy: Disposal of High-Level Radioactive Wastes in a Geologic Repository at Yucca Mountain, Nevada	180319
70 FR 53313	Implementation of a Dose Standard After 10,000 Years	178394

FEP: 2.1.09.21.0B

FEP NAME:

Transport of Particles Larger than Colloids in the SZ

FEP DESCRIPTION:

Particles of radionuclide-bearing material larger than colloids could be entrained in suspension and then be transported in water flowing through the SZ.

SCREENING DECISION:

Excluded – low consequence

SCREENING JUSTIFICATION:

This FEP addresses particles larger than colloids (diameter > 1 μm) that could potentially transport radionuclides in the saturated zone. Particles larger than colloids that are generated in the waste package environment (SNL 2007 [DIRS 177423], Section 1.2) are not considered to move through the EBS (see excluded FEP 2.1.09.21.0A (Transport of Particles Larger than Colloids in the EBS)) or the unsaturated zone (see excluded FEP 2.1.09.21.0C (Transport of Particles Larger than Colloids in the UZ)), so particles larger than colloids with irreversibly sorbed radionuclides that originate in the waste package environment can be excluded from the saturated zone on these bases.

To assess the potential for radionuclide-bearing particles larger than colloids to transport over long distances in the saturated zone, it is convenient to compare the magnitudes of forces and velocities that dictate particle movement in a viscous fluid. Of particular interest are the competing forces that would tend to move particles toward or away from a rough surface upon which a particle is resting. The primary normal forces to be considered are listed below (Reimus 1995 [DIRS 144604], Sections 3.2 and 3.3). Particles will also experience a variety of short-range forces when they come in close proximity to fracture surfaces or collide with these surfaces (Reimus 1995 [DIRS 144604], Section 3.3). However, these short-range forces become less important as particle size increases (Reimus 1995 [DIRS 144604], Section 3.3), and they are expected to play a negligible role in the transport of particles larger than 1-μm diameter.

The primary forces acting on a spherical particle resting on a horizontal surface (these forces also apply to nonspherical particles and non-horizontal surfaces, but the force expressions are more complicated) are:

- Gravity Force (F_g) and Velocity (V_g)—acting toward surface (Reimus 1995 [DIRS 144604], Section 3.2.1):

$$F_g = \frac{4}{3}\pi R^3 \left(\rho_p - \rho_w\right) g \qquad \text{(Eq. 2.1.09.21.0B-1)}$$

$$V_g = \frac{2}{9} R^2 \left(\rho_p - \rho_w\right) \frac{g}{\mu} \qquad \text{(Eq. 2.1.09.21.0B-2)}$$

where, R = particle radius, cm

ρ_p = particle density, g/cm^3

ρ_w = water density, g/cm^3

g = gravitational constant = 980 cm/s^2

μ = water viscosity, g/cm-s (0.007 g/cm-s for water at 1 atm and 35°C (Fetter 2001 [DIRS 156668], Appendix 14)

- Hydrodynamic Drag Force (F_H) and Velocity (V_H)—acting away from surface (Reimus 1995 [DIRS 144604], Section 3.3.6 – Equation 51 of this reference defines the force, and the velocity is the force divided by the frictional drag force, 6πμR (per Equation 18 of this reference); note that the particle surface separation (h in Equation 51) is assumed here to be zero, and the asperity height is defined here as h instead of H):

$$F_H = 43.92 \sqrt{R^2 - (R-h)^2}\, \mu R \left(\frac{dV}{dz}\right)_{z=0} \qquad \text{(Eq. 2.1.09.21.0B-3)}$$

$$V_H = \frac{43.92}{6\pi} \sqrt{R^2 - (R-h)^2} \left(\frac{dV}{dz}\right)_{z=0} \qquad \text{(Eq. 2.1.09.21.0B-4)}$$

where

h = height of asperity on fracture surface, cm

$\left(\frac{dV}{dz}\right)_{z=0}$ = velocity shear at the fracture surface, s^{-1}

$\left(\frac{dV}{dz}\right) = 4V_{center}\left(\frac{1}{b} - \frac{2z}{b^2}\right) = \frac{4V_{center}}{b}$ when $z = 0$

z = distance from fracture surface, cm

V_{center} = water velocity at centerline of fracture (maximum velocity), cm/s

b = fracture aperture, cm.

Note that the expression for $\left(\frac{dV}{dz}\right)$ is calculated assuming a parabolic velocity profile for laminar flow in a parallel-plate channel (Reimus 1995 [DIRS 144604], Section 3.1.2): $V(z) = \frac{4V_{center}}{b^2}\left(bz - z^2\right)$

- Diffusion Force (F_d) and Characteristic Diffusion Velocity (V_d)—can act in both directions, but assumed to act away from the surface (Reimus 1995 [DIRS 144604], Section 3.2.1; note that the diffusion force is the thermal energy causing diffusion kT, divided by the distance over which diffusion acts, which in this case is h, the asperity height (the diffusion force is defined as **B**(t) on p. 28 of the reference); the diffusion velocity is the diffusion force divided by the frictional drag force, $6\pi\mu R$ (per Equations 18 and 26b of the reference)):

$$F_d = kT \qquad \text{(Eq. 2.1.09.21.0B-5)}$$

$$V_d = \frac{kT}{6\pi\mu Rh} \qquad \text{(Eq. 2.1.09.21.0B-6)}$$

where, k = Boltzmann's constant, 1.38×10^{-16} erg/K

T = absolute temperature, K.

Table 2.1.09.21.0B-1 lists the forces and velocities acting on 1-, 2- and 5-μm diameter spherical particles of density = 2.5 g/cm^3 (typical for a silicate) (SNL 2007 [DIRS 177423], Section I.1) at 35°C resting against an asperity with a height equal to half the particle diameter in an otherwise smooth horizontal parallel-plate fracture with an aperture of 1 mm and a flow velocity of 250 m/yr at the fracture centerline (considered to be at the high end of what would be experienced in a 1-mm fracture in the saturated zone). The physical situation is illustrated schematically in Figure 1.

Table 2.1.09.21.0B-1. Forces and Velocities Acting on a Spherical Particle Resting on a Horizontal Surface against an Asperity with Height Equal to Half the Particle Diameter (Figure 2.1.09.21.0B-1)

	Particle Diameter		
Force or Velocity	1 μm	2 μm	5 μm
F_g, dyne (g-cm/s^2)	7.7×10^{-10}	6.2×10^{-9}	9.6×10^{-8}
F_H, dyne	2.4×10^{-11}	9.7×10^{-11}	6.1×10^{-10}
F_d, dyne	8.5×10^{-10}	4.3×10^{-10}	1.7×10^{-10}
V_g, cm/s	1.2×10^{-4}	4.7×10^{-4}	2.9×10^{-3}
V_H, cm/s	3.7×10^{-6}	7.4×10^{-6}	1.8×10^{-6}
V_d, cm/s	1.3×10^{-4}	3.2×10^{-5}	5.2×10^{-6}

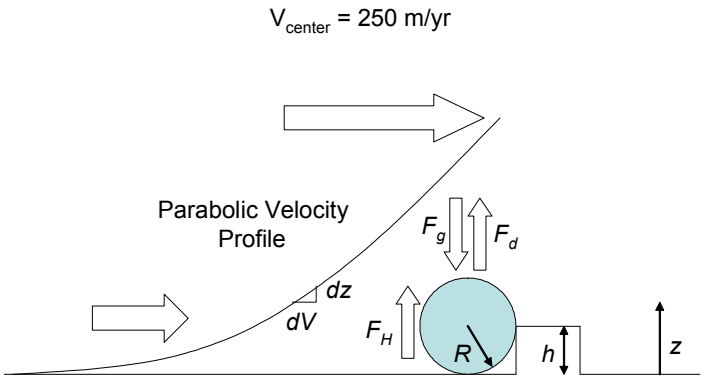

Figure 2.1.09.21.0B-1. Schematic Illustration of the Physical Situation Associated with the Forces and Velocities Calculated for Table 2.1.09.21.0B-1

Table 2.1.09.21.0B-1 shows that a 1-μm diameter particle can experience a diffusion velocity that is capable of freeing the particle from being pinned by gravity behind a 0.5-μm asperity. However, diffusion velocities *decrease* as R^l, while gravitational velocities *increase* as R^2. Thus, for a 2-μm-diameter particle, the gravitational velocity will be over an order of magnitude larger than the diffusion velocity, and for a 5-μm particle, the difference will be nearly 3 orders of magnitude. Therefore, gravity rapidly becomes the dominant force as particle sizes increase above 1-μm diameter. Also, as asperity height, l, increases, the diffusion velocity decreases, so the ability for diffusion to overcome gravity decreases.

It should be noted that the above analysis applies to inclined surfaces as well as horizontal surfaces. The only necessary correction for an inclined surface is that the gravity force vector must be separated into components parallel and perpendicular to the surface, and only the perpendicular component is considered (that is, $F_g(\cos\phi)$, where ϕ = angle between surface and horizontal). Although gravity becomes less important as fractures become more vertical, any particle larger than 1 μm in diameter will be incapable of transporting horizontally over long distances in rough-walled fractures that deviate even slightly from vertical, as expected over long distance scales. Furthermore, any particle that makes it through the volcanics will encounter saturated alluvium, which has numerous pores and asperities capable of trapping particles. Seismic events or flow transients could result in some particle remobilization, but the particle transport distances after remobilization would be limited by the processes described above.

Even if there were laterally extensive vertical fractures in the saturated zone, a sustained upward vertical component of groundwater velocity of ~25 m/yr would be required to keep a 1-μm-diameter particle of 2.5 g/cm^3 density translating horizontally through such a fracture. Upward vertical groundwater velocities this high are not expected in the saturated zone because there is no definitive geochemical signature from the carbonate aquifer in the volcanics or alluvium (SNL 2007 [DIRS 177391], Appendix A, Section A6.3.2) despite the significant upward vertical gradient from the carbonate aquifer to the overlying volcanics (SNL 2007 [DIRS 177391], Section 6.3.1.5). While upward groundwater velocities of ~25 m/yr cannot be completely discounted, they would have to be highly localized with low volumetric flow rates to preclude a geochemical signature.

The preceding paragraphs demonstrate that it is not expected that conditions will exist under which radionuclide-bearing particles larger than 1 μm might transport over long distances in the saturated zone. The number of radionuclide-bearing particles larger than colloids that could travel through the saturated zone to the compliance boundary is expected to be extremely small compared to the number of radionuclide-bearing colloids that travel through the saturated zone to the compliance boundary.

In conclusion, transport of particles larger than colloids is screened out on the basis of low consequence because: (1) the variable orientation and roughness of the fracture and alluvium surfaces along saturated zone transport pathways promote both settling and filtration of particles larger than colloids, and (2) vertical velocity components in the saturated zone are not expected to be large enough to keep particles larger than 1 μm in diameter suspended indefinitely.

Based on the previous discussion, omission of FEP 2.1.09.21.0B (Transport of Particles Larger Than Colloids in the SZ) will not result in a significant adverse change in the magnitude or time of radiological exposures to the RMEI or radionuclide releases to the accessible environment. Therefore, this FEP is excluded from the performance assessments conducted to demonstrate compliance with proposed 10 CFR 63.311 and 63.321 (70 FR 53313 [DIRS 178394]), and with 10 CFR 63.331 [DIRS 180319], on the basis of low consequence.

INPUTS:

Table 2.1.09.21.0B-2. Direct Inputs

Input	Source	Description
Fetter 2001. *Applied Hydrogeology*. [DIRS 156668]	Appendix 14	Water viscosity
Reimus 1995. *Transport of Synthetic Colloids Through Single Saturated Fractures: A Literature Review*. [DIRS 144604]	Sections 3.2 and 3.3, including subsections	Equations and associated discussion describing normal and short-range forces and associated velocities affecting particles moving in a viscous fluid
SNL 2007. *Saturated Zone Site-Scale Flow Model*. [DIRS 177391]	Section 6.3.1.5	There is a significant upward vertical gradient from the carbonate aquifer to the overlying volcanics near Yucca Mountain
	Section A6.3.2	No definitive geochemical signature from the carbonate aquifer in the volcanics or alluvium
SNL 2007. *Waste Form and In-Drift Colloids-Associated Radionuclide Concentrations: Abstraction and Summary*. [DIRS 177423]	Section I.1	Density (2,500 kg/m^3) for a typical silicate particle
	Section 1.2	Discussion of radionuclide-bearing particles larger than colloids generated in the waste package environment

Table 2.1.09.21.0B-3. Indirect Inputs

Citation	Title	DIRS
10 CFR 63	Energy: Disposal of High-Level Radioactive Wastes in a Geologic Repository at Yucca Mountain, Nevada	180319
70 FR 53313	Implementation of a Dose Standard After 10,000 Years	178394

FEP: 2.1.09.21.0C

FEP NAME:

Transport of Particles Larger than Colloids in the UZ

FEP DESCRIPTION:

Particles of radionuclide-bearing material larger than colloids could be entrained in suspension and then be transported in water flowing through the UZ.

SCREENING DECISION:

Excluded – low consequence

SCREENING JUSTIFICATION:

This FEP addresses particles larger than colloids (diameter > 1 μm) that could potentially facilitate the transport of radionuclides in the unsaturated zone. Particles larger than colloids that are generated in the waste package environment (SNL 2007 [DIRS 177423], Section 1.2) are not considered to move through the EBS (see excluded FEP 2.1.09.21.0A (Particles Larger than Colloids in Engineered Barrier System)), so particles with irreversibly sorbed radionuclides that originate in the waste package environment can be excluded from the unsaturated zone on this basis. Transport of other radionuclide-bearing particles larger than colloids in the unsaturated zone is not expected to have an adverse effect on performance because the size and density of these particles will favor settling from solution. In addition, particles with a relatively large radius are expected to become entrapped in pore throats and attach to immobile air-water interfaces in the unsaturated zone. Finally, inorganic particles larger than 1 μm will settle much more rapidly than they diffuse (Reimus 1995 [DIRS 144604], Section 3.2; see also excluded FEP 2.1.09.21.0B (Transport of Particles Larger than Colloids in the SZ)), so diffusion is not expected to contribute significantly to their transport in the unsaturated zone. Indeed, the small diffusivities and large settling velocities of particles will tend to cause particles that are advectively imbibed into the rock matrix from fractures during wetting/drying cycles to remain immobilized in the matrix instead of diffusing back into fractures.

Although it cannot be ruled out that a small number of particles larger than colloids might transport through the unsaturated zone, for the reasons stated above, the number of such particles is expected to be very small compared to the number of colloids transported through the unsaturated zone. Colloid transport in the unsaturated zone is included in TSPA (FEP 2.2.08.10.0B (Colloidal Transport in the UZ)) because although colloids are subjected to the same transport processes as larger particles, they settle more slowly, diffuse more rapidly, fit through smaller pore throats, and advectively collide with air-water interfaces to a lesser extent than larger particles.

Based on the previous discussion, omission of FEP 2.1.09.21.0C (Transport of Particles Larger Than Colloids in the UZ) will not result in a significant adverse change in the magnitude or time of radiological exposures to the RMEI or radionuclide releases to the accessible environment. Therefore, this FEP is excluded from the performance assessments conducted to demonstrate

compliance with proposed 10 CFR 63.311 and 63.321 (70 FR 53313 [DIRS 178394]), and with 10 CFR 63.331 [DIRS 180319], on the basis of low consequence.

INPUTS:

Table 2.1.09.21.0C-1. Direct Inputs

Input	Source	Description
Reimus 1995. *Transport of Synthetic Colloids Through Single Saturated Fractures: A Literature Review*. [DIRS 144604]	Section 3.2	Equations and associated discussion describing normal and short-range forces and associated velocities affecting particles moving in a viscous fluid
SNL 2007. *Waste Form and In-Drift Colloids-Associated Radionuclide Concentrations: Abstraction and Summary*. [DIRS 177423]	Section 1.2	Discussion of radionuclide-bearing particles larger than colloids generated in the waste package environment

Table 2.1.09.21.0C-2. Indirect Inputs

Citation	Title	DIRS
10 CFR 63	Energy: Disposal of High-Level Radioactive Wastes in a Geologic Repository at Yucca Mountain, Nevada	180319
70 FR 53313	Implementation of a Dose Standard After 10,000 Years	178394

FEP: 2.1.09.22.0A

FEP NAME:

Sorption of Colloids at Air-Water Interface

FEP DESCRIPTION:

Colloids may be sorbed irreversibly at the air-water interface under partially saturated conditions.

SCREENING DECISION:

Excluded – low consequence

SCREENING JUSTIFICATION:

Colloid sorption at the air-water interface may occur within the waste package and invert, as well as in the unsaturated zone and saturated zone. Both hydrophilic and hydrophobic colloids may be sorbed irreversibly at the air-water interface under partially saturated conditions. Colloid attachment to air-water interfaces commonly occurs in unsaturated environments and may limit mobile colloid generation and migration (SNL 2007 [DIRS 177423], Section 5.8). This phenomenon is dependent on the interface surface area, electrostatic charge on the particles, and the salinity of the aqueous phase (SNL 2007 [DIRS 177423], Section 5.8).

At low water saturations, air-water interfaces are extensive, and although colloid migration is retarded, colloids still diffuse through the adsorbed water films if these films are adequately thick. At intermediate water saturations, there is still an interconnected gas phase, but relative air-water interface areas are lower. The interface is expected to act as a static surface able to irreversibly sorb colloids, although this process is not credited in the model (SNL 2007 [DIRS 177423], Section 7.2). At high water saturations, the air is present as small bubbles, some of which are mobile in groundwater. Trapped bubbles will immobilize some colloids, potentially resulting in a net decrease in colloidal transport.

A number of features are expected to prevent transport of air interface-attached particles under fully saturated conditions. The interfacial area should be low. Increasing hydrostatic pressure with depth in the saturated zone should cause dissolution of small bubbles. Also, buoyant forces would hinder downward bubble movement in the saturated zone. Electrostatic interactions between the rock matrix and particles might likewise slow the transport of the latter.

In partially saturated media, liquid film straining would produce immobile air-water interfaces in confined domains (e.g., pendular rings in pores or fractures) as a result of capillary forces. Therefore, transport of colloid particles attached to these thin film interfaces are not expected to be mobile in unsaturated media (SNL 2007 ([DIRS 177407], Section 6.3.4.4, p. 6-101). Particles attached to air-water interfaces that are part of flowing films would tend to move rapidly through the unsaturated zone. However, flowing films are only expected if the matrix is nearly saturated and if water is tending to flow from the matrix into fractures (BSC 2004 [DIRS 170035], Section 6.1.3). These conditions may occur locally and for short periods of time, but it is not

considered plausible that they would persist over long distances or long times because fracture contact points will disrupt films. Also, continuous films would be difficult to maintain across lithological contacts that exist in the unsaturated zone because of the discontinuities in fractures that often occur at such contacts as well as the changes in matrix properties that give rise to differences in matrix potential and saturation across such contacts. Episodic flow events might cause short-term movement, but each flow event is expected to be followed by matrix imbibition of water and evaporation in the matrix, which will contribute to particle immobilization in pores. Furthermore, such episodic flow below the Paintbrush Tuff nonwelded hydrogeologic unit (PTn), which is above the repository horizon, is excluded in FEP 2.2.07.05.0A (Flow in the Unsaturated Zone from Episodic Infiltration).

Excluding consideration of retention at the air-water interface will overestimate the potential impact to radionuclide releases of colloid-facilitated transport of radionuclides.

Based on the previous discussion, omission of FEP 2.1.09.22.0A (Sorption of Colloids at Air–Water Interface) will not result in a significant adverse change in the magnitude or timing of either radiological exposure to the RMEI or radionuclide releases to the accessible environment. Therefore, this FEP is excluded from the performance assessments conducted to demonstrate compliance with proposed 10 CFR 63.311 and 63.321 (70 FR 53313 [DIRS 178394]), and with 10 CFR 63.331 [DIRS 180319], on the basis of low consequence.

INPUTS:

Table 2.1.09.22.0A-1. Direct Inputs

Input	Source	Description
SNL 2007. *EBS Radionuclide Transport Abstraction*. [DIRS 177407]	Section 6.3.4.4, p. 6-101	Colloid transport in partially saturated media is expected to be negligible as a result of liquid film straining and the effects of capillarity

Table 2.1.09.22.0A-2. Indirect Inputs

Citation	Title	DIRS
10 CFR 63	Energy: Disposal of High-Level Radioactive Wastes in a Geologic Repository at Yucca Mountain, Nevada	180319
70 FR 53313	Implementation of a Dose Standard After 10,000 Years	178394
BSC 2004	*Conceptual Model and Numerical Approaches for Unsaturated Zone Flow and Transport*	170035
SNL 2007	*Waste Form and In-Drift Colloids-Associated Radionuclide Concentrations: Abstraction and Summary*	177423

FEP: 2.1.09.23.0A

FEP NAME:

Stability of Colloids in EBS

FEP DESCRIPTION:

For radionuclide-bearing colloids to affect repository performance, they must remain suspended in the groundwater (i.e., be stable) for time scales that are long relative to the time required for groundwater travel. Further, they must carry significant concentrations of radionuclides. The stability of smectite colloids (applicable for natural groundwater colloids and waste form colloids) is determined primarily by ionic strength but also to an extent by pH. The stability of iron-(hydr)oxide colloids (applicable to corrosion-product colloids) is determined by both ionic strength and pH.

SCREENING DECISION:

Included

TSPA DISPOSITION:

Colloids in the model developed in *Waste Form and In-Drift Colloids-Associated Radionuclide Concentrations: Abstraction and Summary* (SNL 2007 [DIRS 177423], Section 6.3.1) are: waste form colloids (modeled as montmorillonite, "ZrO_2" and meta-autunite); corrosion product colloids (modeled as hematite, hydrous ferric oxide, and goethite); and in-drift/groundwater colloids (modeled as montmorillonite). Their stabilities are determined from ionic strength and pH of the in-package and in-drift fluids, as calculated in the TSPA model.

The colloid stabilities and mass concentrations are determined at each time step executed in the TSPA model calculations taking into account waste package and invert fluid properties (pH and ionic strength) to calculate the colloid mass concentrations entering the invert from the waste package (SNL 2007 [DIRS 177423], Section 6.5.2.1 and Figure 6-29). These determinations are then combined with the sorption analysis to calculate the colloid source term for radionuclides (SNL 2007 [DIRS 177423], Sections 6.5.2.2 to 6.5.2.3 and Figures 6-30 to 6-31). Colloid stability is governed by the Derjaguin-Landau-Verwey-Overbeek theory; which dictates that colloids become unstable at higher ionic strengths. The solution pH and the surface charge are utilized to determine the ionic strength threshold for colloid stability (SNL 2007 [DIRS 177423], Section 6.3.2). Uncertainty associated with colloid stability is discussed in *Waste Form and In-Drift Colloids-Associated Radionuclide Concentrations: Abstraction and Summary* (SNL 2007 [DIRS 177423], Section 6.6.7). The primary uncertainties in the colloid model are the abundances of the colloid type at a given solution composition and the sorption coefficients that are used to partition radionuclides onto the colloid type (SNL 2007 [DIRS 177423], Section 6.6). Laboratory measurement uncertainties are large contributors to both. Uncertainty is captured and propagated in the model by sampling over a range of colloid concentrations and radionuclide uptake characteristics.

INPUTS:

Table 2.1.09.23.0A-1. Indirect Inputs

Citation	Title	DIRS
SNL 2007	*Waste Form and In-Drift Colloids-Associated Radionuclide Concentrations: Abstraction and Summary*	177423

FEP: 2.1.09.24.0A

FEP NAME:

Diffusion of Colloids in EBS

FEP DESCRIPTION:

Colloidal particles, together with any associated actinides, that are sufficiently small may be transported through the EBS by diffusion.

SCREENING DECISION:

Included

TSPA DISPOSITION:

The formation, stability, and concentration of colloids are addressed in *Waste Form and In-Drift Colloids-Associated Radionuclide Concentrations: Abstraction and Summary* (SNL 2007 [DIRS 177423]). Three types of colloids are anticipated to exist in the EBS (SNL 2007 [DIRS 177423], Section 6.3.1): (1) waste form colloids from degradation of HLW glass and commercial SNF, (2) iron oxyhydroxide colloids due to products from the corrosion of steel waste packages, and (3) groundwater or seepage water colloids. On all three types of colloids, radionuclides may undergo reversible, or equilibrium, sorption. The waste form colloids may also contain embedded radionuclides that are not removable. Plutonium and americium can be strongly sorbed onto iron oxyhydroxide; for these radionuclides, sorption is modeled as a kinetic process.

The general colloid-facilitated diffusive transport model and implementation in the TSPA are described in *EBS Radionuclide Transport Abstraction* (SNL 2007 [DIRS 177407], Section 6.3.4.4). The concentration of colloids in each region of the EBS, specifically in the waste form domain, the waste package corrosion products domain, and the invert domain, is determined in part by the local chemical environment. The diffusion coefficient for colloidal particles (colloid diffusivity) is dependent on temperature and a sampled colloid particle size using the Stokes-Einstein equation (Bird et al. 1960 [DIRS 103524], Equation 16.5-4, p. 514). This is implemented accordingly in the TSPA. A discussion of colloid transport in the EBS is presented in Sections 6.3.4.4 and 6.5.1.2 of *EBS Radionuclide Transport Abstraction* (SNL 2007 [DIRS 177407]). Other factors involving diffusion areas and path lengths are also specified in the RTA model.

The RTA model developed in *EBS Radionuclide Transport Abstraction* (SNL 2007 [DIRS 177407]) is used to quantify the time-dependent radionuclide releases from a failed waste package and their subsequent transport through the EBS to the emplacement drift wall/unsaturated zone interface. The basic inputs to the RTA model consist of the drift seepage and drift wall condensation flux, the environmental conditions in the drift (temperature, relative humidity, water chemistry), and the degradation state of the EBS components (SNL 2007 [DIRS 177407], Section 6.1). Outputs consist of the rates of radionuclide releases to the unsaturated zone as a result of advective and diffusive transport, accounting for the impact of

colloids, radionuclide solubility, retardation, and the degree of liquid saturation of the waste form and invert materials (SNL 2007 [DIRS 177407], Section 8.2). The RTA model is implemented directly into the TSPA model to compute the radionuclide release rates from the EBS (SNL 2007 [DIRS 177407], Section 6.5.2). A summary of the computational model provided to the TSPA, including model parameter uncertainty implementation, is described in *EBS Radionuclide Transport Abstraction* (SNL 2007 [DIRS 177407], Section 6.5.2 and Table 8.1-1).

The source of inflow to the EBS is the seepage flux that drips from the crown (roof) of the drift, drift wall condensation, and imbibition flux from the unsaturated zone into the invert. This inflow can flow through the EBS along eight pathways: (1) seepage flux and drift wall condensation, (2) flux through the drip shield, (3) diversion around the drip shield, (4) flux through the waste package, (5) diversion around the waste package, (6) flux from the waste package into the invert, (7) imbibition flux from the unsaturated zone matrix to the invert, and (8) flux from the invert to the unsaturated zone (SNL 2007 [DIRS 177407], Section 6.3.1.1 and Figure 6.3-1). These pathways are time dependent, because drip shield penetrations and waste package penetrations will vary with time and local conditions in the repository. Diffusive transport may occur via flow pathways 4, 6, and 8 (SNL 2007 [DIRS 177407], Section 6.3.1.2).

The advective transport of colloids in the EBS is discussed in included FEP 2.1.09.19.0B (Advection of Colloids in EBS). The advective transport of dissolved radionuclides is addressed in included FEP 2.1.08.08.0B (Advection of Dissolved Radionuclides in EBS).

INPUTS:

Table 2.1.09.24.0A-1. Indirect Inputs

Citation	Title	DIRS
Bird et al. 1960	*Transport Phenomena*	103524
SNL 2007	*EBS Radionuclide Transport Abstraction*	177407
SNL 2007	*Waste Form and In-Drift Colloids-Associated Radionuclide Concentrations: Abstraction and Summary*	177423

FEP: 2.1.09.25.0A

FEP NAME:

Formation of Colloids (Waste-Form) by Co-Precipitation in EBS

FEP DESCRIPTION:

Dissolved radionuclides and other ions may coprecipitate to form colloids. Coprecipitates may consist of radionuclides bound in the crystal lattice of a dominating mineral phase or may consist of radionuclides engulfed by a dominating mineral phase.

SCREENING DECISION:

Included

TSPA DISPOSITION:

Colloids formed via coprecipitation during the degradation of defense HLW glass and SNF have been observed (SNL 2007 [DIRS 177423], Section 6.3.2.2 and Figure 6-2). Colloids produced from degradation of defense HLW glass are modeled as smectite colloids (SNL 2007 [DIRS 177423], Section 4.1) with "embedded" (assumed permanently attached) radionuclides, specifically those of plutonium and americium. These may, in a broad sense, be considered coprecipitates. SNF colloids are modeled as uranophane/meta-autunite and ZrO_2 (SNL 2007 [DIRS 177423], Section 6.3.2.5).

The concentrations of radionuclides associated with these colloids are based on empirical results from YMP-relevant defense HLW glass and SNF corrosion experiments (SNL 2007 [DIRS 177423], Sections 6.3.2.2). Mass concentrations of the particular colloids are based on those experiments with consideration of colloid mineralogy and the effects of ionic strength and pH on the stability of the colloids (SNL 2007 [DIRS 177423], Sections 6.3.2.3 and 6.3.2.4). Plutonium and americium associated with defense HLW colloids are modeled in the TSPA as "irreversibly attached" because they are embedded within the colloid matrix and can only be released upon the dissolution of the colloid. However, other radionuclides (thorium, protactinium, cesium, neptunium, radium, uranium, and tin) within the aqueous environment can reversibly attach to the surfaces of these colloids, and these colloid-radionuclide complexes can therefore be subject to transport in the TSPA model as pseudocolloids (i.e., when radionuclides attach to preexisting colloids) (SNL 2007 [DIRS 177423], Section 6.3.1). Radionuclide sorption onto these pseudocolloids is modeled by assigning K_d values (SNL 2007 [DIRS 177423], Section 6.3.2.5). Similar to natural groundwater smectite colloids, the pseudocolloid stability is controlled by ionic strength and pH.

The primary uncertainties in the colloid model are the abundances of this colloid type at a given solution composition and the sorption coefficients that are used to partition radionuclides onto this colloid type (SNL 2007 [DIRS 177423], Section 6.6). Laboratory measurement uncertainties are large contributors to both. Uncertainty is captured and propagated in the model by sampling over a range of colloid concentrations and radionuclide uptake characteristics.

INPUTS:

Table 2.1.09.25.0A-1. Indirect Inputs

Citation	Title	DIRS
SNL 2007	*Waste Form and In-Drift Colloids-Associated Radionuclide Concentrations: Abstraction and Summary*	177423

FEP: 2.1.09.26.0A

FEP NAME:

Gravitational Settling of Colloids in EBS

FEP DESCRIPTION:

Over the relatively short transport distances within the waste package, colloidal particles may experience gravitational settling, thereby inhibiting transport.

SCREENING DECISION:

Excluded – low consequence

SCREENING JUSTIFICATION:

The TSPA considers that all radionuclide-bearing colloids generated from waste form degradation within a failed waste package will leave the waste package and enter the drift and EBS minus any radionuclides that decay along the way. Settling of these radionuclide-bearing colloids could result in some retardation of colloid transport. Gravitational settling of colloids is assumed not to occur, resulting in all stable colloids formed within the waste package potentially being able to leave the breach to enter the invert (SNL 2007 [DIRS 177407], Section 5.7). Slow diffusion may limit this movement. Implementation of this assumption results in overestimates of the potential consequences of colloid-facilitated transport of radionuclides (SNL 2007 [DIRS 177407], Section 6.3.4.4, p. 6-101).

Based on the previous discussion, omission of FEP 2.1.09.26.0A (Gravitational Settling of Colloids in EBS) will not result in a significant adverse change in the magnitude or timing of either radiological exposure to the RMEI or radionuclide releases to the accessible environment. Therefore, this FEP is excluded from the performance assessments conducted to demonstrate compliance with proposed 10 CFR 63.311 and 63.321 (70 FR 53313 [DIRS 178394]), and with 10 CFR 63.331 [DIRS 180319], on the basis of low consequence.

INPUTS:

Table 2.1.09.26.0A-1. Direct Inputs

Input	Source	Description
SNL 2007. *EBS Radionuclide Transport Abstraction*. [DIRS 177407]	Section 6.3.4.4, p. 101	The exclusion of gravitational settling results in an over estimation of the potential consequences of colloid facilitated transport of radionuclides

Table 2.1.09.26.0A-2. Indirect Inputs

Citation	Title	DIRS
10 CFR 63	Energy: Disposal of High-Level Radioactive Wastes in a Geologic Repository at Yucca Mountain, Nevada	180319
70 FR 53313	Implementation of a Dose Standard After 10,000 Years	178394
SNL 2007	*EBS Radionuclide Transport Abstraction*	177407

FEP: 2.1.09.27.0A

FEP NAME:

Coupled Effects on Radionuclide Transport in EBS

FEP DESCRIPTION:

Repository induced changes to the physical and chemical properties of the EBS and waste form may be important for evaluating radionuclide transport in the EBS. The existence of chemical gradients within the disposal system, resulting from repository material, waste emplacement, and corrosion products, may influence the transport of dissolved and colloidal species. This could include: geochemical reactions that move (pump) radionuclides; effects on advection, diffusion, and sorption within and through failed waste packages; and microbial and electrochemical effects.

SCREENING DECISION:

Excluded – low consequence

SCREENING JUSTIFICATION:

Coupled processes refer to two or more physical and chemical processes interacting simultaneously to produce a physical or chemical effect, or to cases where a process is affected by chemical and physical processes at the same time. Onsager couplings refer specifically to chemical transport that is driven indirectly by gradients of thermodynamic state variables (e.g., temperature, pressure, chemical potential, and electrical potential). The coupled processes considered in the TSPA involve the transport of chemicals, including radionuclides, which can affect dose calculations. The bulk of the coupled processes are covered in other FEPs cited below. The present FEP covers the two coupled processes that are not covered elsewhere, specifically, thermal diffusion of water vapor and gas and the development of electric fields around waste packages.

Other FEPs listed here cover various combinations of coupling between thermal, hydrologic, mechanical, chemical, and microbial processes. Thermal-hydrologic processes are addressed in included FEPs 2.1.08.04.0A (Condensation Forms on Roofs of Drifts (Drift-Scale Cold Traps)) and 2.1.08.11.0A (Repository Resaturation due to Waste Cooling). Thermal-mechanical processes are addressed in excluded FEPs 2.2.01.02.0A (Thermally-Induced Stress Changes in the Near-Field), 2.2.10.04.0A (Thermo-Mechanical Stresses Alter Characteristics of Fractures Near Repository), 2.2.10.04.0B (Thermo-Mechanical Stresses Alter Characteristics of Faults Near Repository), and 2.2.10.05.0A (Thermo-Mechanical Stresses Alter Characteristics of Rocks Above and Below the Repository). Thermal effects on chemical equilibria are examined in *Engineered Barrier System: Physical and Chemical Environment* (SNL 2007 [DIRS 177412], Section 6.3), *Drift Scale THC Seepage Model* (SNL 2007 [DIRS 177404], Section 6.2.1) and *In-Drift Precipitates/Salts Model* (SNL 2007 [DIRS 177411], Section 6.3). Such effects are also discussed in included FEPs 2.1.09.01.0A (Chemical Characteristics of Water in Drifts) and 2.1.11.08.0A (Thermal Effects on Chemistry and Microbial Activity in the EBS). Thermal effects on chemical reaction rates are explicitly included in *Drift-Scale THC Seepage Model*

(SNL 2007 [DIRS 177404], Section 6.4), as well as in included FEP 2.1.09.07.0B (Reaction Kinetics in Drifts). Coupled effects concerning chemical reactions of the different waste forms are discussed in included FEPs 2.1.02.01.0A (DSNF Degradation (Alteration, Dissolution, and Radionuclide Release)), 2.1.02.02.0A (CSNF Degradation (Alteration, Dissolution, and Radionuclide Release)), and 2.1.02.03.0A (HLW Glass Degradation (Alteration, Dissolution, and Radionuclide Release)). The thermal diffusion effect (Soret effect) on radionuclide transport is discussed in excluded FEP 2.1.11.10.0A (Thermal Effects on Transport in EBS). Hydrologic-chemical processes are discussed in the following FEPs for the unsaturated zone, included FEPs 2.2.07.04.0A (Focusing of Unsaturated Flow (Fingers, Weeps)), 2.2.07.06.0B (Long-Term Release of Radionuclides from the Repository), 2.2.07.08.0A (Fracture Flow in the UZ), 2.2.10.10.0A (Two Phase Buoyant Flow/Heat Pipes), and 2.2.07.18.0A (Film Flow into the Repository); for the EBS, included FEPs 2.1.08.05.0A (Flow through Invert), 2.1.08.07.0A (Unsaturated Flow in the EBS), and excluded FEP 2.2.07.06.0A (Episodic or Pulse Release from Repository); and for the saturated zone, included FEP 2.2.08.08.0A (Matrix Diffusion in the SZ). Microbial effects on sorption in the EBS are considered to be of low consequence in excluded FEP 2.1.10.01.0A (Microbial Activity in EBS). Chemical-hydrologic processes are addressed in excluded FEP 2.2.08.03.0B (Geochemical Interactions and Evolution in the UZ) as part of the unsaturated zone and drift near-field analysis. Chemical effects on rock fracture permeability are considered in excluded FEP 2.2.10.06.0A (Thermo-Chemical Alteration in the UZ (Solubility, Speciation, Phase Changes, Precipitation/Dissolution)). Chemical-mechanical processes are addressed in included FEP 2.1.03.02.0A (Stress Corrosion Cracking (SCC) of Waste Packages).

Electrochemical processes of electrophoresis and galvanic coupling are considered in excluded FEP 2.1.09.09.0A (Electrochemical Effects in EBS). One additional Onsager coupled process that has not been addressed elsewhere is the development of electric fields around waste packages by Compton scattering and its exclusion is justified here. The generation of electric fields around waste packages is caused by Compton electron scattering was evaluated by Green et al. (1987 [DIRS 170174]). The authors (Green et al. 1987 [DIRS 170174]) calculated the field in direct contact with a wasteform representing a single PWR fuel assembly, assuming completely degraded canisters with no shielding effect by the cladding or the canister wall, and determined that a relatively strong electrical field could form in air, but only very weak fields in rock. Because radionuclide transport pathways from the waste package are through the invert, only weak electrical fields are anticipated. The geometry of the waste forms and waste packages at Yucca Mountain differs from that assumed by Green et al. (1987 [DIRS 170174]); however, their results are bounding for the external surface of a Yucca Mountain waste package. Yucca Mountain waste packages hold up to 21 PWR assemblies; however, the radiation flux at any given point within the package is much less than 21 times the flux on the surface of a single assembly because the flux decreases as a function of the square of the distance; more-distant assemblies contribute much less to the flux than those nearby. Although the net radiation flux within the package is greater than estimated by Green et al. (1987 [DIRS 170174]), the flux on the outside of the waste package, despite the presence of multiple assemblies, is less. In Yucca Mountain waste packages, dose rates will be severely limited by the steel and Alloy 22 waste package wall, which decreases the gamma dose by a factor of 30 to 50, based on a comparison of the gamma dose rate calculated for the inner radial waste package surface to that calculated for the same segment on the outer radial waste package surface (BSC 2004 [DIRS 172227] Tables 6.1-1 and 6.1-2). Furthermore, the Green et al. (1987 [DIRS 170174]) fluxes are overestimates because they assume a line source, resulting in extremely high gamma fluxes close

to the source and a steep radial gradient in flux with distance; this results in large electrical fields relative to those that would be expected around a waste package more than 1.5 m in diameter. Finally, the gamma dose rate decreases exponentially as a function of time making Compton scattering less significant over time. Because the electrical field generated by Compton scattering will be small in the invert, and the effect decreases rapidly with time, the effects of electrical fields generated by Compton scattering are expected to be insignificant and are excluded from the TSPA on the basis of low consequence.

The hydrologic-thermal coupled process that has not been screened above is thermal redistribution of water and gases, which might occur where steep thermal gradients exist. Its exclusion is justified here, and in excluded FEP 2.1.11.10.0A (Thermal Effects on Transport in EBS). In the EBS, areas with steep temperature gradients during the heating pulse will often have temperatures above the boiling point of water. Therefore, there will be little or no liquid available for thermal (Soret) diffusion. When temperatures are below the boiling point of water, the coupled effect of thermo-diffusion and thermo-gravitation (thermal convection of the gas phase) could affect relative humidity distributions. This coupling can cause the separation of water vapor and gas in empty spaces between hot and cold surfaces. This separation may induce the formation of spatially specific relative humidity environments with respect to the geometry of EBS components in the drift, and could therefore affect corrosion of EBS materials through the formation of water condensate. Vidal and Murphy (1999 [DIRS 171801]) conclude that gaps between the relatively hot and cold surfaces (i.e., waste package and drip shield or drip shield and drift wall) of less than 5 cm, coupled with thermal gradients greater than 1°C cm^{-1} can generate significant thermo-gravimetric and thermo-diffusive effects. However, the gaps between waste package and drip shield, and drip shield and drift wall, are very much larger than those considered in their study (SNL 2007 [DIRS 179354], Table 4-1, Parameter Numbers 02-01 and 02-02; Table 4-2, Parameter Number 07-01), and thermal gradients in the EBS are much smaller. Sensitivity analyses in *Multiscale Thermohydrologic Model* (SNL 2008 [DIRS 184433], Section 6.3.11), using different invert hydrologic parameters, indicate that a typical temperature difference just after the drift wall boiling period, from the top to the bottom of the invert (because of the insulating effect of the crushed tuff, thermal gradients in the invert are large relative to those in other parts of the EBS), a distance of approximately 1.3 m (SNL 2007 [DIRS 179354], Table 4-1, Parameter 01-10), is on the order of 5°C. The gradient decreases with time and after a few thousand years is less than a 1°C. Because the thermal gradients are so small within the EBS, this effect is excluded from TSPA on the basis of low consequence.

Based on the previous discussion, omission of FEP 2.1.09.27.0A (Coupled Effects on Radionuclide Transport in EBS) will not result in a significant adverse change in the magnitude or time of radiological exposures to the RMEI or radionuclide releases to the accessible environment. Therefore, this FEP is excluded from the performance assessments conducted to demonstrate compliance with proposed 10 CFR 63.311 and 6321 (70 FR 53313 [DIRS 178394]), and with 10 CFR 63.331 [DIRS 180319], on the basis of low consequence.

INPUTS:

Table 2.1.09.27.0A-1. Direct Inputs

Input	Source	Description
BSC 2004. *Dose Rate Calculation for 21-PWR Waste Package*. [DIRS 172227]	Tables 6.1-1 and 6.1-2	Dose fluxes to the inner and outer walls of the waste package
SNL 2007. *Total System Performance Assessment Data Input Package for Requirements Analysis for EBS In-Drift Configuration*. [DIRS 179354]	Table 4-1, Parameter Number 01-10	Thermal gradients in the invert are large relative to those in other parts of the EBS), a distance of approximately 1.3 m
SNL 2008. *Multiscale Thermohydrologic Model*. [DIRS 184433]	Section 6.3.11	Sensitivity analyses using different invert hydrologic parameters, indicate that a typical temperature difference just after the drift wall boiling period, from the top to the bottom of the invert (because of the insulating effect of the crushed tuff

Table 2.1.09.27.0A-2. Indirect Inputs

Citation	Title	DIRS
10 CFR 63	Energy: Disposal of High-Level Radioactive Wastes in a Geologic Repository at Yucca Mountain, Nevada	180319
70 FR 53313	Implementation of a Dose Standard After 10,000 Years	178394
Green et al. 1987	"Effect of Electric Fields on Vapor Transport Near a High-Level Waste Canister"	170174
SNL 2007	*Total System Performance Assessment Data Input Package for Requirements Analysis for EBS In-Drift Configuration*	179354
SNL 2007	*Drift-Scale THC Seepage Model*	177404
SNL 2007	*Engineered Barrier System: Physical and Chemical Environment*	177412
SNL 2007	*In-Drift Precipitates/Salts Model*	177411
Vidal and Murphy 1999	"Calculation of the Effect of Gaseous Thermodiffusion and Thermogravitation Processes on the Relative Humidity Surrounding a High Level Nuclear Waste Canister"	171801

FEP: 2.1.09.28.0A

FEP NAME:

Localized Corrosion on Waste Package Outer Surface Due to Deliquescence

FEP DESCRIPTION:

Salt-containing dust, which could accumulate on the waste package surface during the preclosure ventilation period, can absorb moisture from the drift atmosphere, even at low relative humidity, dissolving the salt and creating concentrated aqueous solutions. This deliquescence process may result in localized surface chemistry that could cause penetration of the waste package outer barrier by localized corrosion.

SCREENING DECISION:

Excluded – low consequence

SCREENING JUSTIFICATION:

The analysis for this FEP discusses the potential for dust deliquescence to influence the localized corrosion of the waste package. An analysis of the general corrosion of the waste package is presented in included FEP 2.1.03.01.0A (General Corrosion of Waste Packages), while an analysis of localized corrosion of the waste package due to other causes (such as seepage) is presented in included FEP 2.1.03.03.0A (Localized Corrosion of Waste Packages).

Dust will be deposited on the surfaces of waste packages in emplacement drifts primarily during the operational and the preclosure ventilation periods. After closure of the repository, there is a period of up to 1,000 years in which limited seepage is possible because much of the drift wall temperature is above the boiling point of water (SNL 2008 [DIRS 184433], Figure 6.3-78[a]). During this interval and for as long as the drip shields perform their function, the only aqueous phase that could potentially contact the waste package outer surface is brine that originates by deliquescence of soluble salts in dust residing on the waste package. The potential for brines formed by dust deliquescence to initiate and sustain localized corrosion that results in failure of the waste package outer corrosion barrier has been evaluated in *Analysis of Dust Deliquescence for FEP Screening* (SNL 2007 [DIRS 181267], Sections 7.1 and 7.1[a]). This evaluation shows that dust deliquescence-induced localized (primarily crevice) corrosion of the waste package outer corrosion barrier (Alloy 22) is of low consequence with respect to repository performance (SNL 2007 [DIRS 181267], Sections 7.1.5 and 7.1[a]).

Measured atmospheric and underground dust compositions are the basis of thermodynamic modeling and experimental studies used to evaluate the likelihood of brine formation (SNL 2007 [DIRS 181267], Sections 6.1 and 6.1[a]) and persistence (SNL 2007 [DIRS 181267], Sections 6.2 and 6.2[a]), the volume of brines that may form (SNL 2007 [DIRS 181267], Section 6.4), and the relative corrosivity of the initial deliquescent brines and of brines modified by processes on the waste package surface (SNL 2007 [DIRS 181267], Section 6.3). In addition, several mechanisms are evaluated that could inhibit or stifle localized corrosion should it initiate (SNL 2007 [DIRS 181267], Sections 6.5 and 6.5[a]).

The dust compositions considered include both tunnel and atmospheric dust samples from Yucca Mountain, as well as National Airfall Deposition Program precipitation data representing atmospheric dust compositions in southwestern Nevada. Also considered is the thermal decomposition of ammonium salts, a process that could affect soluble dust quantity and composition prior to deliquescence. Ammonium chlorides, nitrates, and, to some extent, sulfates thermally decompose into ammonia and acid gasses, and will be lost from the surface of the waste package prior to deliquescence (SNL 2007 [DIRS 181267], Section 6.1.2.3).

Justifications are developed using a logical framework approach, considering a wide range of dust and brine compositions, conditions on the waste package, and processes (SNL 2007 [DIRS 181267], Sections 1.1 and 7). Uncertainty or variation in the input parameter values, within a reasonable range, will not change the conclusions drawn in *Analysis of Dust Deliquescence for FEP Screening* (SNL 2007 [DIRS 181267], Section 7). In order for dust deliquescence-induced localized corrosion to significantly affect the performance of the waste package outer corrosion barrier, each of the following five propositions must be answered in the affirmative (SNL 2007 [DIRS 181267], Section 1.1). Analysis does not support an affirmative answer to all of these propositions, as shown below:

(1) *Can multiple-salt deliquescent brines form at elevated temperature?* Yes (see SNL 2007 [DIRS 181267], Table 7-2[a]). As discussed in *Analysis of Dust Deliquescence for FEP Screening* (SNL 2007 [DIRS 181267], Section 7.1.1), multiple-salt deliquescent brines can form at elevated temperatures (above 120°C). Ammonium salts can comprise a significant fraction of the salts in atmospheric dust, but most thermally decompose and will not persist long enough to contribute to deliquescent mineral assemblages, thus decreasing the salt load available for deliquescence. Boiling points of saturated salt solutions represent the maximum temperature of deliquescence at a given pressure. For most single-salt phases (nitrates, chlorides, and carbonates), boiling points at one atmosphere are limited to temperatures below 120°C. Saturated multiple-salt mixtures always boil at higher temperatures than the individual salt components. The boiling points for important salt assemblages predicted to occur on the waste package surface have been investigated experimentally. The two-salt mixture $NaCl + KNO_3$ boils at a maximum temperature of 134°C and both the three-salt mixture, $NaCl + KNO_3 + NaNO_3$, and four-salt mixture, $NaCl + KNO_3 + NaNO_3 + Ca(NO_3)_2$, with specific proportions can transition directly to anhydrous melts (i.e., they do not exhibit a maximum boiling temperature).

(2) *If deliquescent brines form at elevated temperature, will they persist?* Sometimes (see SNL 2007 [DIRS 181267], Table 7-2[a]). As discussed in *Analysis of Dust Deliquescence for FEP Screening* (SNL 2007 [DIRS 181267], Sections 7.1.2 and 7.1[a]), multiple-salt brines can persist on the waste package surface but are not stable. Acid degassing will occur rapidly at first, increasing the pH to near-neutral or alkaline conditions. Further acid degassing in conjunction with carbon dioxide uptake can result in decreasing brine volume, and will convert the four-salt calcium-containing mixture to the three-salt mixture (SNL 2007 [DIRS 181267], Section 6.2.2[a]). Degassing of HCl and HNO_3 from brines dominated by monovalent salts (e.g., NaCl, $NaNO_3$, KNO_3) also raises the pH, and the potential result is precipitation of less deliquescent salts (e.g., $NaHCO_3$). However, sufficient degassing

to result in complete dryout is not expected for monovalent brines. Should dryout occur, these salts may subsequently deliquesce at lower temperature and higher relative humidity, producing brines with higher pH than the original assemblage. Higher pH brines are generally more benign with respect to localized corrosion (SNL 2007 [DIRS 181267], Section 7.1.2) and the localized corrosion model for Alloy 22 reflects this in *General Corrosion and Localized Corrosion of Waste Package Outer Barrier* (SNL 2007 [DIRS 178519], Figures 6-49 and 6-50).

(3) *If deliquescent brines persist, will they be corrosive?* Not expected (see SNL 2007 [DIRS 181267], Table 7-2[a]). As discussed in *Analysis of Dust Deliquescence for FEP Screening* (SNL 2007 [DIRS 181267], Sections 7.1.3 and 7.1[a]), brines formed by deliquescence of tunnel dusts or atmospheric aerosols are generally benign, and will remain so as they are modified by processes that occur on the waste package surface. The effects of an added component of cement dust on deliquescent brine composition is discussed in excluded FEP 2.1.06.01.0A (Chemical Effects of Rock Reinforcement and Cementitious Material in EBS). Nitrate is a significant moderator of localized corrosion, as the YMP confirmed at 180°C (SNL 2007 [DIRS 181267], Section 6.4.2.2[a]). This conclusion is also supported by experimental observations by Dunn et al. (2004 [DIRS 173813]), which show that a nitrate-to-chloride ion concentration ratio greater than 0.1 can effectively inhibit localized corrosion of mill-annealed Alloy 22 in 4 M $MgCl_2$-based solutions at 110°C.

Nitrate is a major component of the soluble fraction of atmospheric air (as determined by samples from both cyclonic and rainout collectors). Initial brines formed by deliquescence of multiple-salt assemblages will have near-neutral pH, and they will be relatively nitrate-rich and chloride-poor. Experimental corrosion studies used to develop the localized corrosion model have verified that corrosion will not be initiated by nitrate-rich brines (nitrate-to-chloride ratio at 0.5 or greater) at temperatures below 120°C (SNL 2007 [DIRS 178519], Table 7-6). Higher-temperature data indicate that general corrosion mechanisms do not change up to temperatures of 220°C (SNL 2007 [DIRS 181267], Section 6.3.1.4). This suggests that the same chemical processes (thermodynamics and relative kinetics), which provide nitrate inhibition of localized corrosion, probably continue to be effective at similarly elevated temperatures. Processes occurring after deliquescence, including acid degassing and reactions with silicate minerals, do not result in corrosive brines (SNL 2007 [DIRS 181267], Section 6.3.4). Acid degassing has a beneficial effect, where even small degrees of degassing will result in increases in the brine pH, to values ranging from near-neutral to alkaline. Brine interactions with silicate minerals may also buffer the pH to near-neutral or slightly alkaline values, and may lead to dryout by precipitation of a less deliquescent salt or mineral assemblage.

In addition, as the pH rises due to acid degassing, carbonate and bicarbonate concentrations increase. According to Dunn et al. (2004 [DIRS 173813]) carbonate anions are almost as effective as nitrate anions at inhibiting the initiation of localized corrosion on Alloy 22, while bicarbonate anions inhibit localized corrosion of Alloy 22 to a lesser extent.

(4) *If deliquescent brines are potentially corrosive, will they initiate localized corrosion?* No (SNL 2007 [DIRS 181267], Table 7-2[a]). As stated above, the brines resulting from dust deliquescence are generally nitrate-rich, chloride-poor, with near-neutral pH and are, therefore, not considered to be corrosive. As discussed in *Analysis of Dust Deliquescence for FEP Screening* (SNL 2007 [DIRS 181267], Section 7.1.4), the volume of brines formed by deliquescence will be so limited that even if the brines were to be considered corrosive, they are not expected to initiate localized corrosion outside of tight crevices. Considering the effects of ammonium salt removal from dust, and assuming that the soluble component of repository dust derives from atmospheric aerosols, the maximum deliquescence brine volume is calculated to be 1.8 $\mu L/cm^2$ at 120°C or higher (SNL 2007 [DIRS 181267], Section 7.1.4). This value presumes that all salt components in the dust are in mutual contact so that eutectic salt mixtures occur. However, repository dust is heterogeneous and consists mostly of non-deliquescent minerals (e.g., rock-forming minerals) that can physically separate the salt components, so the brine volume estimate is potentially high.

Capillary and surface tension effects in the dust are expected to reduce brine contact with the waste package surface and inhibit brine flow into pores or crevices. Dust samples collected from the Exploratory Studies Facility have been characterized to evaluate the potential for capillary retention of the brine within the dust layer, decreasing the availability of brine for contact with the Alloy 22 surface. The results indicate that the capillary response of the dust is characterized by a typical dimension of about one micron (SNL 2007 [DIRS 181267], Section 7.1.4). This dimension suggests that brine mobility within the dust will be inhibited, and that roughness on the metal surface would need to have similar dimensions in order to compete successfully for the brine.

(5) *Once initiated, will localized corrosion penetrate the waste package outer barrier?* No (see SNL 2007 [DIRS 181267], Table 7-2[a]). Several processes will act to slow or stifle and often arrest localized corrosion before penetration of the waste package outer corrosion barrier can occur.

In order for a propagating crevice to remain active, the critical crevice solution contained within the crevice must be maintained such that the metal surface does not repassivate. As an active crevice propagates, material loss due to corrosion will lead to an increase in the crevice gap. If the resulting crevice gap becomes too large, the mass transport limitation required to maintain the critical crevice solution within the crevice will be lost and the localized corrosion will cease (SNL 2007 [DIRS 181267], Section 6.5.1[a]). Also, as corrosion products accumulate in the corrosion cell, cathodic limitation can result from secondary products that precipitate and coat the metal surface, causing the cessation of localized corrosion in that area.

A power-law description of localized crevice corrosion penetration, which is an alternative conceptual model in *General Corrosion and Localized Corrosion of Waste Package Outer Barrier* (SNL 2007 [DIRS 178519], Section 6.4.4.8), is applicable to Alloy 22, as well as many other materials. According to this power law, the corrosion rate slows with time. Laboratory data show that stifling of crevice corrosion in

Alloy 22 occurs (SNL 2007 [DIRS 181267], Section 7.1.5). Thus, the depth of localized corrosion penetration will be limited, with one extrapolation indicating that the localized-corrosion propagation rate would require approximately one-million years to penetrate 20 mm of Alloy 22 (SNL 2007 [DIRS 181267], Section 6.5.1[a]). All of the crevice corrosion stifling experiments to date have been performed under inundated conditions, the solutions representing a near-infinite source of reactive species (e.g., chloride). The brine quantity and the amount of reactive components are extremely limited in the environment produced by dust-deliquescence, and it is expected that stifling will be even more efficient under such conditions.

In summary, brines formed by deliquescence of tunnel and atmospheric dusts are not expected to be aggressive with respect to initiating localized corrosion. Processes that act to modify the brines on the waste package surface are beneficial with respect to corrosivity. Should corrosive brines form, scale factors related to brine volume will inhibit initiation of localized corrosion. Furthermore, should localized corrosion initiate, several processes will act to limit or stifle it, and would ensure that penetration of the waste package outer corrosion barrier will not occur (SNL 2007 [DIRS 181267], Sections 7 and 7.1[a]).

Based on the previous discussion, omission of FEP 2.1.09.28.0A (Localized Corrosion on Waste Package Outer Surface Due to Deliquescence) will not result in a significant adverse change in the magnitude or timing of either radiological exposure to the RMEI or radionuclide releases to the accessible environment. Therefore, this FEP is excluded from the performance assessments conducted to demonstrate compliance with proposed 10 CFR 63.311 and 63.321 (70 FR 53313 [DIRS 178394]), and with 10 CFR 63.331 [DIRS 180319], on the basis of low consequence.

INPUTS:

Table 2.1.09.28.0A-1. Direct Inputs

Input	Source	Description
SNL 2007. *Analysis of Dust Deliquescence for FEP Screening*. [DIRS 181267]	Section 7.1.4	Very low brine volumes and dimensional factors inhibit potential for localized corrosion initiation
	Section 6.4.2.2[a]	Nitrate demonstrated to inhibit localized corrosion initiation up to 180°C
	Section 7	Uncertainty or variation in the input parameter values will not affect the screening justification
	Sections 7.1.5 and 7.1[a]	Dust deliquecence analysis demonstrates low consequence of any potential localized corrosion from dust sources
	Sections 7.1 and 7.1[a]	Localized corrosion analysis conclusions here and will be of low consequence
	Table 7-2[a]	Logic tree responses to key process propositions for low-consequence

Table 2.1.09.28.0A-2. Indirect Inputs

Citation	Title	DIRS
10 CFR 63	Energy: Disposal of High-Level Radioactive Wastes in a Geologic Repository at Yucca Mountain, Nevada	180319
70 FR 53313	Implementation of a Dose Standard After 10,000 Years	178394
Dunn et al. 2004	"Effect of Inhibiting Oxyanions on the Localized Corrosion Susceptibility of Waste Package Container Materials"	173813
SNL 2007	*Analysis of Dust Deliquescence for FEP Screening*	181267
SNL 2007	*General Corrosion and Localized Corrosion of Waste Package Outer Barrier*	178519
SNL 2008	*Multiscale Thermohydrologic Model*	184433

FEP: 2.1.09.28.0B

FEP NAME:

Localized Corrosion on Drip Shield Surfaces Due to Deliquescence

FEP DESCRIPTION:

Salt-containing dust, which could accumulate on the drip shield surface during the preclosure ventilation period, can absorb moisture from the drift atmosphere, even at low relative humidity, dissolving the salt and creating concentrated aqueous solutions. This deliquescence process may result in localized surface chemistry that could cause penetration of the drip shield surface by localized corrosion.

SCREENING DECISION:

Excluded – low probability

SCREENING JUSTIFICATION:

The rationale for the exclusion of localized corrosion of the drip shields from the TSPA model under seepage conditions is presented under excluded FEP 2.1.03.03.0B (Localized Corrosion of Drip Shields). This FEP justifies exclusion from the TSPA model of localized corrosion of the drip shields in the absence of seepage, when the aqueous conditions upon the drip shield are due to deliquescence of material residing on the surfaces of the drip shield.

Dust will be deposited on the surfaces of drip shields primarily during their emplacement. Unlike the waste packages, which will see dust accumulation throughout the operational and preclosure ventilation periods, the drip shields will not be subject to such an extended accumulation period, as they are emplaced upon completion of the ventilation period. As such, the quantity of dust deposited on the surface of the drip shields will be lower than that on the waste package surface and be composed predominantly of tunnel dust, rather than atmospheric aerosols. Tunnel dust is composed primarily of powdered rock and contains a much lower soluble salt concentration (<<1%) than atmospheric aerosols (10% to 20%) (SNL 2007 [DIRS 181267], Section 6.1). As a result, the volume of brine produced by such dusts will be lower on a per mass basis than that present in the atmospheric aerosols that will reside on the surface of the waste packages following the ventilation period. Therefore, as the maximum brine quantity on the waste package surface has been calculated to be 1.8 $\mu l/cm^2$ at 120°C (SNL 2007 [DIRS 181267], Section 6.4.1.2), the quantity on the surface of the drip shields will be much lower due to the lower concentration of soluble salts in the dust on the surface of the drip shields combined with the much lower absolute quantity of dust present per unit area of drip shield surface.

Following closure of the repository, there is a period of up to 1,000 years in which limited seepage is possible because much of the drift wall temperature is above the boiling point of water (SNL 2008 [DIRS 184433], Figure 6.3-78[a]). During this interval, the only aqueous phase that could potentially contact the surface of any given drip shield is brine that originates by deliquescence of soluble salts in dust residing on the drip shields.

Justifications are developed using a logical framework approach, considering a wide range of dust and brine compositions, conditions on the waste package, and processes in the same manner in which this phenomenon was addressed in excluded FEP 2.1.09.28.0A (Localized Corrosion on Waste Package Outer Surface due to Deliquescence) for the waste package outer barrier. For dust deliquescence-induced localized corrosion to affect the performance of the drip shields, each of the following five propositions must be answered in the affirmative. Analysis does not support an affirmative answer to all of these propositions, as shown below:

(1) *Can multiple-salt deliquescent brines form at elevated temperature?* Yes (see SNL 2007 [DIRS 181267], Table 7-2[a]). As discussed in *Analysis of Dust Deliquescence for FEP Screening* (SNL 2007 [DIRS 181267], Section 7.1.1), multiple-salt deliquescent brines can form at elevated temperatures (above 120°C). Boiling points of saturated salt solutions represent the maximum temperature of deliquescence at a given pressure. For most single salt phases (nitrates, chlorides, and carbonates), boiling points at one atmosphere are limited to temperatures below 120°C. Saturated multi-salt mixtures always boil at higher temperatures than the individual salt components. The boiling points for important salt assemblages that are expected to occur on the drip shield surfaces have been investigated experimentally. The two-salt mixture $NaCl + KNO_3$ boils at a maximum temperature of 134°C and the three-salt mixture, $NaCl + KNO_3 + NaNO_3$, and four-salt mixture, $NaCl + KNO_3 + NaNO_3 + Ca(NO_3)_2$, with specific proportions can both transition directly to anhydrous melts (i.e., they do not exhibit a maximum boiling temperature).

(2) *If deliquescent brines form at elevated temperature, will they persist?* Sometimes (see SNL 2007 [DIRS 181267], Table 7-2[a]). As discussed in *Analysis of Dust Deliquescence for FEP Screening* (SNL 2007 [DIRS 181267], Sections 7.1.2 and 7.1[a]), multiple-salt brines can persist on the waste package surface but are not stable. Acid degassing will occur rapidly at first, increasing the pH to near-neutral or alkaline conditions. Further acid degassing in conjunction with carbon dioxide uptake can result in decreasing brine volume, and will convert the four-salt calcium-containing mixture to the three-salt mixture (SNL 2007 [DIRS 181267], Section 6.2.2[a]). Degassing of HCl and HNO_3 from brines dominated by monovalent salts (e.g., NaCl, $NaNO_3$, KNO_3), also raises the pH, and the potential result is precipitation of less deliquescent salts (e.g., $NaHCO_3$). However, sufficient degassing to result in complete dryout is not expected for monovalent brines. Should dryout occur, these salts may subsequently deliquesce at lower temperature and higher relative humidity, producing brines with higher pH than the original assemblage. Similar processes are expected to occur upon the surfaces of the drip shield. Higher pH brines are not of concern with respect to localized corrosion and the localized corrosion model for Titanium Grade 7 reflects this in *General Corrosion and Localized Corrosion of the Drip Shield* (SNL 2007 [DIRS 180778], Section 8.4, and Figures 19 and 20).

(3) *If deliquescent brines persist, will they be corrosive?* No. The environments that may form during the period where there is active deliquescence are predicted to be benign with respect to localized corrosion of the waste package outer barrier as discussed in *Analysis of Dust Deliquescence for FEP Screening* (SNL 2007 [DIRS 181267], Table 7-2[a]) and in excluded FEP 2.1.09.28.0A (Localized Corrosion on Waste Package Outer Surface due to Deliquescence). The postclosure brines initially formed on the drip shield surface are from tunnel (rock) dust and are expected to contain minimal fluoride (SNL 2007

[DIRS 181267], Table 6-3[a]). These brines will become increasingly benign with time due to processes that occur after deliquescence, such as acid degassing and carbonation (SNL 2007 [DIRS 181267], Sections 7.1.3 and 6.2[a]). The model for localized corrosion initiation on titanium was developed to predict the behavior of drip shield materials under seepage conditions. However, the model is based on experiments performed in electrolytes that also represent the dominant constituents of the predicted deliquescent brine chemistries. Tables 19 and 20 in *General Corrosion and Localized Corrosion of the Drip Shield* (SNL 2007 [DIRS 180778]) contain a catalogue of the test solutions used to develop the localized corrosion model for Titanium Grade 7, and Table 6.3-2 in *Analysis of Dust Deliquescence for FEP Screening* (SNL 2007 [DIRS 181267]) compares the predicted deliquescent brine chemistries to the corrosion test solutions that have been utilized. The corrosion performance of Titanium Grade 7 in $CaCl_2$-based brines is presented in *General Corrosion and Localized Corrosion of the Drip Shield* (SNL 2007 [DIRS 180778], Table 21), where the large positive values of ΔE preclude localized corrosion initiation. The localized corrosion model predicts a probability of much less than 1 in 10,000 in 10,000 years of localized corrosion initiation on Titanium Grade 7 across a wide range of chloride concentrations, temperatures, and pH levels, where initiation may occur if ΔE is less than zero (SNL 2007 [DIRS 180778], Figures 19 and 20). This is fully consistent with cyclic polarization tests performed on creviced Titanium Grade 7 specimens in 1 M NaCl over a range of temperatures from 90°C to 165°C by Brossia and Cragnolino (2000 [DIRS 162445]). The authors found that the measured repassivation potential exceeded the corrosion potential (measured at 95°C in aerated 1 M NaCl) by at least 1.2 volts. In another study, the same authors (Brossia and Cragnolino 2001 [DIRS 159840]) evaluated the effect of 0.1 to 10 M NaCl on the crevice repassivation potential of Titanium Grade 7 at 95°C. The potential dropped with increasing chloride content but was still over 4 V_{SCE} in 10 M NaCl, consistent with significant localized corrosion margin even in absence of nitrate. These results are also supported by YMP test results obtained in concentrated $CaCl_2$ and $CaCl_2 + Ca(NO_3)_2$ brines at temperatures up to 150°C, indicating that crevice corrosion is not expected to occur under these conditions (SNL 2007 [DIRS 180778], Table 21). These results demonstrate that localized corrosion of Titanium Grade 7 will not occur in environments representative of predicted deliquescent brine compositions.

According to the drip shield design (SNL 2007 [DIRS 179354], Table 4-2, Parameter Number 07-01), the drip shields will have Titanium Grade 29 structures mounted on the outer surface of the drip shield plates. While the exposed surface area is far less than for the plate material, dust may accumulate on the surface of the structural supports as well. Cyclic polarization testing of uncreviced samples at elevated temperature in multi-ionic electrolytes containing various levels of $CaCl_2$, KCl, KNO_3, $NaNO_3$, NaCl, Na_2SO_4, NaF, and NaBr has shown similar behavior for Titanium Grade 29 and Titanium Grade 7 with no localized attack reported for either grade of titanium following polarization (DTN: MO0705SCCIGM06.000 [DIRS 180869], Table 11 and Figures 46 to 53). Additionally, cyclic polarization testing of creviced samples in concentrated NaCl + KCl with and without KNO_3 and NaF at temperatures at or above 110°C has shown high values for the critical potentials of both Titanium Grade 7 and Titanium Grade 29 (DTN: LL070800612251.197 [DIRS 183159], file: *Ti Gr 7 Gr 29 Electrochemical Developed Aug07*). To evaluate the tabular data for the above tests, the critical potentials

were taken as the point in the polarization curve where the current density exceeds 200 $\mu A/cm^2$, designated as E_{200}. Although attack under the crevice former was noted for Titanium Grade 29 in some of the concentrated salt electrolytes, such attack only occurred after the samples had been polarized to high potentials (greater than 1 V versus SSC, a condition that cannot occur in the repository environment). Based on these experimental results, it is concluded that Titanium Grade 29 will not degrade due to localized corrosion processes when exposed to the anticipated deliquescent brines that may form on the surface of the drip shields.

(4) *If deliquescent brines are potentially corrosive, will they initiate localized corrosion?* No (SNL 2007 [DIRS 181267], Table 7-2[a]). As stated earlier, the brines resulting from dust deliquescence generally contain minimal fluoride with near-neutral pH, and are therefore not considered to be corrosive. As discussed in *Analysis of Dust Deliquescence for FEP Screening* (SNL 2007 [DIRS 181267], Section 7.1.4), the volume of brines formed by deliquescence will be so limited that even if the brines were to be considered corrosive, they are not expected to initiate localized corrosion outside of tight crevices. In the analysis of the dust on the waste package outer barrier, considering the effects of ammonium salt removal from dust, and assuming that the soluble component of repository dust derives from atmospheric aerosols, the maximum deliquescence brine volume is calculated to be 1.8 $\mu L/cm^2$ at 120°C or higher (SNL 2007 [DIRS 181267], Section 7.1.4). However, as discussed above, the dust on the surface of the drip shields will be predominantly tunnel dust. Tunnel dust is composed primarily of powdered rock and contains a much lower soluble salt concentration (<<1%) than atmospheric aerosols (10% to 20%) (SNL 2007 [DIRS 181267], Section 6.1). As a result, the volume of brine produced by such dusts will be lower on a per mass basis than that present in the atmospheric aerosols that will reside on the waste package surface following the ventilation period. Therefore, the quantity on the drip shield surfaces will be much lower than that on the waste package surface (i.e., <<1.8 $\mu l/cm^2$) due to the lower concentration of soluble salts in the dust on the surface of the drip shields combined with the much lower absolute quantity of dust present per unit area of drip shield surface. This value presumes that all salt components in the dust are in mutual contact so that eutectic salt mixtures occur. However, repository dust is heterogeneous and consists mostly of non-deliquescent minerals (e.g., rock-forming minerals) that can physically separate the salt components, so the brine volume estimate is potentially high.

Capillary and surface tension effects in the dust are expected to reduce contact with the drip shield surface and inhibit brine flow into pores or crevices. Dust samples collected from the Exploratory Studies Facility have been characterized to evaluate the potential for capillary retention of the brine within the dust layer, decreasing the availability of brine for contact with the surface of the drip shields. The results indicate that the capillary response of the dust is characterized by a typical dimension of about one micron (SNL 2007 [DIRS 181267], Section 7.1.4). This dimension suggests that brine mobility within the dust will be inhibited, and that roughness on the metal surface would need to have similar dimensions in order to compete successfully for the brine.

(5) *Once initiated, will localized corrosion penetrate the drip shield?* Not applicable. Localized corrosion will not initiate as discussed in proposition 4.

In summary, on the basis of the previous discussion, brines formed by deliquescence of the relevant tunnel dusts are not expected to be aggressive with respect to initiating localized corrosion. Processes that act to modify the brines on the waste package surface are beneficial with respect to corrosivity. Should corrosive brines form, scale factors related to brine volume will inhibit initiation of localized corrosion.

Therefore, significant localized corrosion of the drip shields due to dust deliquescence is not anticipated to occur, and FEP 2.1.09.28.0B (Localized Corrosion on Drip Shield Surfaces Due to Deliquescence**)** is excluded from the performance assessments conducted to demonstrate compliance with proposed 10 CFR 63.311 and 63.321 (70 FR 53313 [DIRS 178394]), and with 10 CFR 63.331 [DIRS 180319] on the basis of low probability.

INPUTS:

Table 2.1.09.28.0B-1. Direct Inputs

Input	Source	Description
DTN: MO0705SCCIGM06.000. Final Report for FY06: Stress Corrosion Crack Initiation & Growth Measurements in Environments Relevant to High Level Nuclear Waste Packages. [DIRS 180869]	Table 11 and Figures 46 to 53	Cyclic polarization testing of creviced samples at elevated temperature in multi-ionic electrolytes containing various levels of $CaCl_2$, KCl, KNO_3, $NaNO_3$, NaCl, Na_2SO_4, NaF, and NaBr has shown similar behavior for Titanium Grade 29 and Titanium Grade 7 with no localized attack reported for either grade of titanium following polarization
DTN: LL070800612251.197. Electrochemical Testing of Titanium Grade 7 and Titanium Grade 29 Alloys in Dust-Like Electrolytes – Developed. [DIRS 183159]	Ti Gr 7 Gr 29 Electrochemical Developed Aug07	Cyclic polarization testing of creviced samples in concentrated NaCl + KCl with and without KNO_3 and NaF at temperatures at or above 110°C has shown high values for the critical potentials of Titanium Grade 7 and Titanium Grade 29

Table 2.1.09.28.0B-2. Indirect Inputs

Citation	Title	DIRS
70 FR 53313	Implementation of a Dose Standard After 10,000 Years	178394
Brossia and Cragnolino 2000	"Effects of Environmental, Electrochemical, and Metallurgical Variables on the Passive and Localized Dissolution of Ti Grade 7"	162445
Brossia and Cragnolino 2001	"Effect of Palladium on the Localized and Passive Dissolution of Titanium"	159840
SNL 2007	*Total System Performance Assessment Data Input Package for Requirements Analysis for EBS In-Drift Configuration*	179354
SNL 2007	*Analysis of Dust Deliquescence for FEP Screening*	181267
SNL 2007	*General Corrosion and Localized Corrosion of the Drip Shield*	180778
SNL 2008	*Multiscale Thermohydrologic Model*	184433

FEP: 2.1.10.01.0A

FEP NAME:

Microbial Activity in EBS

FEP DESCRIPTION:

Biological activity is important to consider because of the potential impact on aqueous chemical conditions within the waste and EBS. In deep subsurface environments, biological activity is limited to microbiological activity and may include effects of natural and anthropogenic bacteria (e.g., anaerobic, methanogenic, sulfate reducers, etc.), protozoans, yeast, viruses, and algae. This FEP addresses a broad range of effects of biological impacts, including the effects of microbes on corrosion of waste packages, cladding, and waste form; bioreduction of multivalent contaminants, metals, and sulfate; generation of organic complexants and gases as metabolic by-products; and the formation of biofilms and their impact on transport.

SCREENING DECISION:

Excluded – low consequence

SCREENING JUSTIFICATION:

Early high temperatures and long-term nutrient scarcity will sharply limit microbial activity inside Yucca Mountain. Although microbial activity is expected to be insignificant and the effects of microbial activity are generally screened out, models of general waste package corrosion assign a rate-enhancement factor to bound any impact of microbes (BSC 2004 [DIRS 178519], Section 8.1). A more detailed discussion on the potential effect of microbes on corrosion of waste packages is provided separately in included FEP 2.1.03.05.0A (Microbially Influenced Corrosion (MIC) of Waste Packages). MIC of the drip shields is excluded (see excluded FEP 2.1.03.05.0B (Microbially Influenced Corrosion (MIC) of Drip Shields)). MIC of the cladding is addressed in excluded FEP 2.1.02.14.0A (Microbially Influenced Corrosion (MIC) of Cladding).

Evaluation of Potential Impacts of Microbial Activities on Drift Chemistry (BSC 2004 [DIRS 169991]) provides an analysis of in-drift biological activities and their potential impacts on EBS materials and processes. The discussion presented here is based on Sections 6.4, 6.5, and 7.1 of that report (BSC 2004 [DIRS 169991]). The following thermal and chemical factors will severely limit microbial activities in the repository:

Thermal

- The in-drift temperatures during the thermal pulse created by radioactive decay will exceed the temperature tolerance of many microbes in the repository environment for a period of time after repository closure, thus exerting an early sterilization effect on many, if not all, microorganisms.

- Microbial incubation experiments have demonstrated the importance of water availability for Yucca Mountain microbial growth. The relative humidity and the liquid-water saturation in the repository during the thermal period are predicted to be low, thus further limiting microbial activities during the thermal period.

- Evaporation of seepage waters in the low relative humidity environment of the thermal period will result in brine solutions in which only halophiles may be able to survive.

Chemical

- Although sub-oxic environments may persist locally while stainless steel in the waste package and in the ground support corrodes, an oxic environment will ultimately prevail in the repository over the growth-permissive period and prevent the generation and accumulation of reduced inorganic dissolved matter (in addition to nonreduced elements such as phosphate and nitrate) that are the prerequisite for autotrophic metabolism.

- Phosphate and organic carbon are important limiting factors for Yucca Mountain microbial growth. The extremely low organic carbon supply in the repository will limit heterotrophic microbial activities.

In short, thermal effects and water availability will limit microbial activity during, and for a period after, the thermal pulse; nutrient limitations will limit activity throughout. Because of the multiple and overlapping limitations on microbial growth, there will be no significant effects resulting from bio-reduction of multivalent contaminants, metals, or sulfate, nor will there be any significant potential to form organic complexants.

Evaluation of Potential Impacts of Microbial Activities on Drift Chemistry (BSC 2004 [DIRS 169991], Section 6.5) evaluates the potential impacts on repository chemistry, given the limitations of microbial activity. The report concludes that the effects on water chemistry are negligible (BSC 2004 [DIRS 169991], Section 6.5.1). Although microorganisms may release chemicals that complex with radionuclides, either the concentrations of complexing agents are small, or their binding sites will be dominated by iron (and other) ions, or both (BSC 2004 [DIRS 169991], Section 6.5.2). Section 6.5.3 of *Evaluation of Potential Impacts of Microbial Activities on Drift Chemistry* (BSC 2004 [DIRS 169991]) concludes that potential effects on radionuclide solubility are negligible, while Section 6.5.4 examines the potential for enhanced transport by radionuclides binding directly to the surface of unattached bacteria, concluding that long-distance biocolloid transport is not expected in the unsaturated zone. Gas generation from microbial degradation (FEP 2.1.12.04.0A (Gas Generation (CO_2, CH_4, H_2S) of Microbial Degradation)) is excluded as is radiological mutation of microbes (FEP 2.1.13.03.0A (Radiological Mutation of Microbes)).

In conclusion, due to severe environmental constraints, microbial activity in the repository is expected to be low, and its impacts on drift chemistry will be insignificant.

Based on the previous discussion, omission of FEP 2.1.10.01.0A (Microbial Activity in EBS) will not result in a significant adverse change in the magnitude or timing of either radiological exposure to the RMEI or radionuclide releases to the accessible environment. Therefore, this

FEP is excluded from the performance assessments conducted to demonstrate compliance with proposed 10 CFR 63.311 and 63.321 (70 FR 53313 [DIRS 178394]), and with 10 CFR 63.331 [DIRS 180319], on the basis of low consequence.

INPUTS:

Table 2.1.10.01.0A-1. Direct Inputs

Input	Source	Description
BSC 2004. *Evaluation of Potential Impacts of Microbial Activities on Drift Chemistry*. [DIRS 169991]	Section 7.1	Analysis of in-drift biological activities and their potential impacts on EBS materials and processes

Table 2.1.10.01.0A-2. Indirect Inputs

Citation	Title	DIRS
10 CFR 63	Energy: Disposal of High-Level Radioactive Wastes in a Geologic Repository at Yucca Mountain, Nevada	180319
70 FR 53313	Implementation of a Dose Standard After 10,000 Years	178394
BSC 2004	*Evaluation of Potential Impacts of Microbial Activities on Drift Chemistry*	169991
SNL 2007	*General Corrosion and Localized Corrosion of Waste Package Outer Barrier*	178519

FEP: 2.1.11.01.0A

FEP NAME:

Heat Generation in EBS

FEP DESCRIPTION:

Temperature in the waste and EBS will vary through time. Heat from radioactive decay will be the primary cause of temperature change, but other factors to be considered in determining the temperature history include the in-situ geothermal gradient, thermal properties of the rock, EBS, and waste materials, hydrological effects, and the possibility of exothermic reactions. Considerations of the heat generated by radioactive decay should take different properties of different waste types, including DSNF, into account.

SCREENING DECISION:

Included

TSPA DISPOSITION:

The temperature-time history of the waste and EBS is calculated as part of the model described in *Multiscale Thermohydrologic Model* (SNL 2008 [DIRS 184433]). The temperatures as predicted by the MSTHM are influenced by not only the heat of radionuclide decay, but also mountain-scale thermal-property stratigraphic variation, edge-cooling effects that result from lateral heat loss at the repository edges, the natural geothermal gradient from the water table to the ground surface, percolation flux, and rock hydrologic properties (SNL 2008 [DIRS 184433], Sections 6.1, 6.2.5, and 6.2.14[a]). Heat generated by exothermic reactions in the EBS is not considered in performance assessment, as discussed in excluded FEP 2.1.11.03.0A (Exothermic Reactions in the EBS).

The different waste packages considered in MSTHM calculations are summarized in Table 6.2-6[a] of the MSTHM report (SNL 2008 [DIRS 184433]). The thermal decay history of each of the waste package types is developed in *Initial Radionuclide Inventories* (SNL 2007 [DIRS 180472], Section 6.4.3[a]; SNL 2007 [DIRS 179567], Table 4-1, Parameter Number 03-11; SNL 2007 [DIRS 179394], Table 4-1, Parameter Number 03-11). The different waste packages fall in two major categories: commercial SNF waste packages, which include PWR and BWR waste packages, and codisposal waste packages, which contain both defense HLW and DOE SNF. Temperatures for different types of waste forms are captured in a submodel of the MSTHM. These waste forms include the 21-PWR, the 44-BWR, and long and short versions of the codisposal waste package, all of which produce heat at different rates. These effects are captured in the TSPA model by providing the temperatures as direct inputs. *Multiscale Thermohydrologic Model* (SNL 2008 [DIRS 184433], Section 6.2.17[a]) investigates the influence of waste package-to-waste package heat-generation variability on thermohydrologic conditions in the emplacement drifts.

In-Drift Natural Convection and Condensation (SNL 2007 [DIRS 181648]) deals with heat generation in the waste packages in several ways. The condensation analysis developed in that

report (SNL 2007 [DIRS 181648], Sections 6.3 and 6.1.1[a]) uses the thermal decay history of each of the waste package types developed in *Initial Radionuclide Inventories* (SNL 2007 [DIRS 180472], Section 6.4.3[a]) to establish temperatures and mass transfer rates (condensation and evaporation) within the drift. Drift wall and far-field temperatures are calculated by summing the heat contribution from all 108 drifts in the repository layout, each of which is simulated using a time-dependent thermal line load representing the heat of radionuclide decay. Correlations for condensation rates and condensation probabilities on the drift wall and other EBS components are developed for TSPA (SNL 2007 [DIRS 181648], Section 8.3). The convection and condensation model also calculates a dispersion coefficient that includes heat generation from individual waste packages for use in the condensation analysis. Dispersion coefficients are calculated for various cases using a computational fluid dynamics code that allows for mixing of the gasses in the drift to be enhanced by natural convection cells that form between hotter and cooler packages, and between waste packages and the cooler drift wall. An additional analysis presented in the convection and condensation report (SNL 2007 [DIRS 181648], Section 6.4) is used to generate an effective thermal conductivity within the drift for use by the MSTHM. The effective thermal conductivity is calculated using a two-dimensional computational fluid dynamics code that includes a steady-state heat source represented as a constant temperature boundary at the waste package. The feed to TSPA is indirect because it is through the average equivalent thermal conductivity correlation used by the MSTHM.

Heat generation in the EBS, as applied in the convection and condensation model and in the MSTHM, is closely coupled with heat transfer mechanisms. Conservation of energy dictates that all heat generated within the repository during postclosure must leave through the drift wall. Therefore, the temperature on the interior drift wall is dictated by the requirement to dissipate all the heat generated within the repository. The same energy balance applies to heat generated under the drip shield, which must be transferred from the drip shield to the drift wall. In fact, the temperatures on the surfaces of the waste packages, drip shields, and drift walls are all dependent on the heat transfer mechanisms available to satisfy conservation of energy. Heat transfer by conduction, turbulent natural convection, and thermal radiation are all included in the convection and condensation model such that each physical process occurring in the drift cavity during repository postclosure is simulated. The equivalent thermal conductivity, which is calculated in the convection and condensation model and fed to the MSTHM, does not include radiation because radiation is already included in the MSTHM. Heat transfer mechanisms are described in Sections 6.1.5.1 and 6.4.1.1 of *In-Drift Natural Convection and Condensation* (SNL 2007 [DIRS 181648]) and in Section 6.2.8.5 of *Multiscale Thermohydrologic Model* (SNL 2008 [DIRS 184433]).

The preclosure ventilation period is 50 years (SNL 2007 [DIRS 179466], Table 4-2, Parameter Number 06-01). As described in included FEP 1.1.02.02.0A (Preclosure Ventilation), during the ventilation period, a substantial amount of the decay heat generated by the waste packages is removed by the ventilation system. The balance of the heat is transferred into the rock. Ventilation efficiency is described in *Ventilation Model and Analysis Report* (BSC 2004 [DIRS 169862], Section 6.3.5). The waste package powers used by the MSTHM and the convection and condensation model are modified by multiplying them by the complement of the ventilation efficiency over the 50-year ventilation period.

Uncertainties associated with heat generation in the EBS are propagated to performance assessment calculations through the use of different waste package types, different rock thermal conductivities, and a suite of percolation flux values in the MSTHM (SNL 2008 [DIRS 184433], Sections 6.3.15[a] and 6.3.16[a]). In addition, uncertainties in rock hydrologic properties (SNL 2008 [DIRS 184433], Section 6.3.11[a]), ventilation heat removal efficiency (SNL 2008 [DIRS 184433], Section 6.3.12), and the effects of axial vapor transport (SNL 2008 [DIRS 184433], Section 6.3.18[a]) were evaluated using sensitivity analyses and found to be insignificant. Uncertainties in the in-drift natural convection and condensation model are propagated to TSPA through use of bounding values for the axial dispersion rate, for the degree of drip shield ventilation, and for the percolation rate at the repository horizon (SNL 2007 [DIRS 181648], Section 6.1.3[a]).

In performance assessment calculations, temperature and relative humidity conditions derived from the MSTHM (SNL 2008 [DIRS 184433]) are used to extract parameters of the in-drift chemical environment from the lookup tables generated by the in-drift seepage dilution/evaporation model developed in *Engineered Barrier System: Physical and Chemical Environment* (SNL 2007 [DIRS 177412], Section 6.3.3). In addition, drift wall temperatures predicted by the MSTHM are used to constrain the timing of potential seepage into the drift. As discussed in *Abstraction of Drift Seepage* (SNL 2007 [DIRS 181244], Section 6.5.2), seepage cannot occur until drift wall temperatures drop below 100°C.

INPUTS:

Table 2.1.11.01.0A-1. Indirect Inputs

Citation	Title	DIRS
BSC 2004	*Ventilation Model and Analysis Report*	169862
SNL 2007	*Abstraction of Drift Seepage*	181244
SNL 2007	*Engineered Barrier System: Physical and Chemical Environment*	177412
SNL 2007	*In-Drift Natural Convection and Condensation*	181648
SNL 2007	*Initial Radionuclides Inventory*	180472
SNL 2007	*Total System Performance Assessment Data Input Package for Requirements Analysis for DOE SNF/HLW and Navy SNF Waste Package Overpack Physical Attributes Basis for Performance Assessment*	179567
SNL 2007	*Total System Performance Assessment Data Input Package for Requirements Analysis for Subsurface Facilities*	179466
SNL 2007	*Total System Performance Assessment Data Input Package for Requirements Analysis for TAD Canister and Related Waste Package Overpack Physical Attributes Basis for Performance Assessment*	179394
SNL 2008	*Multiscale Thermohydrologic Model*	184433

FEP: 2.1.11.02.0A

FEP NAME:

Non-Uniform Heat Distribution in EBS

FEP DESCRIPTION:

Uneven heating and cooling at edges of the repository may lead to non-uniform thermal effects during both the thermal peak and the cool-down period.

SCREENING DECISION:

Included

TSPA DISPOSITION:

The calculation of the repository thermohydrologic environment, including thermal gradients from the repository center to the edges and corners of the repository, is described in *Multiscale Thermohydrologic Model* (SNL 2008 [DIRS 184433], Section 6.2.1). The increase in temperature from the ambient geothermal temperature as predicted by the MSTHM is influenced by: (1) the thermophysical properties of the rock and EBS components, and (2) the repository footprint shape, which influences the evolution of the edge-cooling effect (SNL 2008 [DIRS 184433], Section 1). *Multiscale Thermohydrologic Model* (SNL 2008 [DIRS 184433], Table 1-1) provides postclosure thermal-hydrologic parameters to the TSPA as functions of time and location in the drift or host rock. Uncertainty in MSTHM results is propagated to TSPA calculations through the use of simulation results using different rock thermal conductivities and a suite of percolation flux values (SNL 2008 [DIRS 184433], Sections 6.3.15[a] and 6.3-16[a]). Other sources of uncertainty, including rock hydrologic properties, ventilation heat removal efficiency, and the effects of axial vapor transport, were evaluated using sensitivity analyses and found to be insignificant (SNL 2008 [DIRS 184433], Sections 6.3.11[a], 6.3.12, and 6.3.18[a]).

In-Drift Natural Convection and Condensation (SNL 2007 [DIRS 181648], Section 6.3.5.1.1) includes the effects of heating and cooling at the repository edges. Seven drifts are chosen for the condensation/evaporation analysis. Two sets of three drifts span the width of the repository, capturing the temperature variations between the repository center and the repository edge. The three drifts at the north of the repository footprint reflect the cooler portion of the repository layout. The three drifts in the middle of the repository footprint capture the hotter portion of the layout. The seventh drift is in the narrowest portion of the repository. Condensation rates calculated in the model are influenced by the temperature profiles within each drift. The model implemented in the TSPA calculates a probability of condensate on the drift walls at any location and, if condensation occurs, rate of condensation. The probability of occurrence of condensation and the condensation rate are abstracted as functions of the percolation flux, as described in *In-Drift Natural Convection and Condensation* (SNL 2007 [DIRS 181648], Section 8.3). Uncertainties in the condensation model are propagated to TSPA through use of bounding values for the axial dispersion rate, the degree of drip shield ventilation, and the percolation rate at the repository horizon (SNL 2007 [DIRS 181648], Section 6.1.3[a]).

INPUTS:

Table 2.1.11.02.0A-1. Indirect Inputs

Citation	Title	DIRS
SNL 2007	*In-Drift Natural Convection and Condensation*	181648
SNL 2008	*Multiscale Thermohydrologic Model*	184433

FEP: 2.1.11.03.0A

FEP NAME:

Exothermic Reactions in the EBS

FEP DESCRIPTION:

Exothermic reactions liberate heat and will alter the temperature of the disposal system and affect the properties of the repository and surrounding materials. Examples of possible exothermic reactions include oxidation of uranium metal fuels such as represented by N Reactor fuels and hydration of concrete used in the underground environment.

SCREENING DECISION:

Excluded – low consequence

SCREENING JUSTIFICATION:

This FEP focuses on the effects of excess heat from exothermic reactions (other than pyrophoric reactions) on the properties of the repository and in the surrounding materials. The two exothermic reactions discussed in this FEP are the oxidation of uranium-metal fuel, which is significant because of the rapid O_2-scavenging ability of uranium-metal and the total quantity of specific heat generated is large; and the hydrolysis of cement, which is only significant if large quantities of cement are available to react. The oxidation of uranium-metal is considered to be bounding with respect to potential consequences as this reaction may occur extremely rapidly and thereby release significant heat essentially instantaneously. The N Reactor SNF, which is the uranium metal-based fuel, comprises the majority of DOE SNF by MTHM but only accounts for 6% of the codisposal waste packages and is expected to undergo oxidative degradation upon exposure to oxygen and/or water vapor. The oxidation of uranium-metal to form UO_2 is exothermic with a standard enthalpy of formation of −1,085 kJ/mol (Grenthe et al. 1992 [DIRS 101671], Table III.1). Uranium metal is also known to be pyrophoric under certain conditions. Pyrophoric materials are materials that can spontaneously ignite due to overheating as a result of oxidation, sparks, or mechanical trauma. A pyrophoric reaction is, thus, a rapid exothermic reaction resulting in fire. This FEP does not address pyrophoricity. The effects of pyrophoricity related to N Reactor fuel are addressed in excluded FEP 2.1.02.08.0A (Pyrophoricity from DSNF).

The reaction between uranium-metal and oxygen (as opposed to water vapor) is used in this analysis as it is the bounding case. In the repository, the sources of oxygen that are potentially available to react exothermically in the codisposal waste packages containing N Reactor fuel are:

- Oxygen or air ingress into the waste package through waste package breaches
- Oxygen that could be produced from radiolysis of residual and bound water left in the MCOs after they are dried and closed.

These potential sources of oxygen and how they are expected to influence and limit the exothermic reactions that might occur in the repository are discussed in the following paragraphs.

The breaches in the waste package outer shell through which ingress of oxygen might occur are expected to be SCCs (see included FEP 2.1.03.02.0A (Stress Corrosion Cracking (SCC) of Waste Packages)). A more rapid, advective flow of air into the MCOs could result in a pyrophoric event and that case is discussed in excluded FEP 2.1.02.08.0A (Pyrophoricity from DSNF). Following pressure equilibration between the waste package void space and the drift air, it is expected that the SCCs will allow oxygen ingress by a counter diffusion process involving helium, nitrogen, oxygen, and water vapor. Upper bound estimates for the diffusive mass transport rate of oxygen into the waste package through these SCCs can be calculated using the approach described in (SNL 2007 [DIRS 177407], Section 6.6.2). The analysis provided in the RTA report calculated water vapor diffusion through SCCs. Here that analysis is modified to maximize the amount of oxygen available for uranium oxidation by analyzing O_2 diffusion in air. This calculation shows that an upper bound estimate of the rate of diffusive ingress of oxygen into a waste package through SCCs is approximately 2,610 mol/yr. The details of this calculation are provided in excluded FEP 2.1.02.08.0A (Pyrophoricity from DSNF).

If all of this oxygen is used to covert uranium metal to UO_2, for which the heat of formation is 1,085 kJ/mole uranium (Grenthe et al. 1992 [DIRS 101671], Table III.1), the corresponding heat generation rate is about 90 watts with a reaction time of 18 years. In this analysis, every atom of uranium-metal in the waste packages is oxidized during the 18-year reaction time given the oxygen diffusion rate of 2,610 mol/yr (see details in excluded FEP 2.1.02.08.0A (Pyrophoricity from DSNF)).

Oxygen ingress by barometric pumping and by flow driven by buoyancy are both discussed in excluded FEP 2.1.02.08.0A (Pyrophoricity from DSNF).

At emplacement, a comparison of the calculated wattage increases due to uranium-metal oxidation to the average thermal power at emplacement for a 2-MCO/2-HLW-Long waste package, which is comprised of two MCOs and two HLW glass canisters, reveals that these values are insignificant to the total waste package heat generation due to radioactive decay (BSC 2004 [DIRS 166941], Table 2). At emplacement, the thermal output is 1,660 watts and the oxidation of uranium-metal contributes an additional 5.4% should a seismic event occur (90 watts ÷ 1,660 watts). Assuming that the MCO thermal output decays at a rate similar to the 5-HLW-Long waste package (Assumption 3.7 in BSC 2004 [DIRS 166941]), at 10,000 years the 2-MCO/2-HLW-Long waste package will have decayed to approximately 2 watts (0.001 × 1,660 watts; where 0.001 is estimated as the fraction of the heat remaining for a 5-HLW-Long waste package at 10,000 years (i.e., $1.42 \times 10^{-3} \div 9.9 \times 10^{-1}$ from SNL 2007 [DIRS 179466], Table 4-1, Parameter Number 01-02)) . At 10,000 years, the additional heat generated by the uranium-metal oxidation (approximately 90 watts) would result in an increase by a factor of 45 should a seismic event occur compared to the heat generated by an unbreached waste package. This increase over the nominal heat generation is considered inconsequential because it is so short lived (less than 20 years) and small relative to the initial heat at emplacement.

The impact of the increased heat generation on the repository performance and the surrounding materials is evaluated by examining the thermal output increase relative to an average thermal load. A comparison of these calculated values to the waste package decay heat generation along a 7-package segment (SNL 2007 [DIRS 179466], Table 4-1, Parameter Number 01-02) indicates that their relative contribution is small and their impact negligible. At emplacement, the average heat generation for the 7-packages segment is 51,200 W and the oxidation of uranium-metal should a seismic event occur contributes an additional 0.18% (90 watts ÷ 51,200 watts). At 10,000 years, the average heat generation for the 7-package segment is 603 W and the oxidation of uranium-metal should a seismic event occur contributes less than 15% (90 watts ÷ 603 watts).

The amount of free and bound water that may remain in the MCOs after they are dried and closed is uncertain. The dominant form of this water is bound water in uranium and aluminium oxide hydrates with the estimated amount per MCO ranging up to 4.64 kg or approximately 258 moles (Garvin 2002 [DIRS 169141], Table 4-4). In the repository, this water could be released and converted to free hydrogen and oxygen due to thermal and radiolytic decomposition of the uranium and aluminium oxide hydrates involved. If free oxygen and hydrogen are produced inside the codisposal packages, the oxygen will be scavenged by reaction with exposed uranium metal in the breached fuel because of the rapid kinetics of the uranium-metal/oxygen reactions at temperatures up to 1,440°C and at various O_2 and H_2O pressures (Haschke 1998 [DIRS 174075], Table 1). The fate of the free hydrogen is less clear. In studies of uranium-metal corrosion in moist air, neither hydrides nor hydrogen gas formed (Haschke 1998 [DIRS 174075], pp. 149 to 150), suggesting that any evolved hydrogen is rapidly transformed to water on the U-metal surface under the conditions of this study. The production and fate of hydrogen are discussed further in excluded FEPs 2.1.12.03.0A (Gas Generation (H_2) from Waste Package Corrosion) and 2.1.13.01.0A (Radiolysis). Even if both MCOs in a codisposal package are each assumed to contain 4.64 kg water, and it is also assumed all of the oxygen in this water is available as free oxygen to convert uranium-metal to UO_2 in a rapid exothermic reaction, it would oxidize only a very small fraction (0.5%) of the fuel in the waste package. This is calculated from 1.13×10^7 g uranium-metal per waste package assuming that the waste package contains two MCOs each containing Mark IV fuel and scrap baskets containing the maximum fuel (3,804 kg uranium) and scrap (1,832 kg uranium) loadings ($2 \times (3.804 \times 10^6 + 1.832 \times 10^6) = 1.13 \times 10^7$ g uranium-metal) (rounded)) (Garvin 2002 [DIRS 169141], Table 4-4), which is equivalent to 47,500 moles of uranium by conversion using the atomic weight of uranium = 238 (rounded) from DTN: SN0612T0502404.014 [DIRS 178850] (1.13×10^7 g ÷ 238 g/mol). The total O_2 available from the emplaced water is 258 moles per waste package (derived in excluded FEP 2.1.02.08.0A (Pyrophoricity from DSNF)). Thus, the fraction of uranium-metal that could be converted is approximately 0.5%. The heat energy released would be about 2.8×10^5 kJ, which would cause a waste package temperature increase of only 21°C even under assumed adiabatic conditions (see details of this calculation in excluded FEP 2.1.02.08.0A (Pyrophoricity from DSNF)).

Degradation of the uranium metal fuel as a result of its oxidation may cause the radionuclides in the oxidized fuel to be available for dissolution and transport when that fuel is contacted by water. Even in the absence of oxidation, the TSPA model uses a bounding instantaneous degradation rate for the uranium-metal DOE SNF (BSC 2004 [DIRS 172453]), which considers that the radionuclide inventory in this fuel is available for dissolution and transport when the fuel is contacted by water. Therefore, the heat generated during the oxidative alteration of the fuel

will not adversely affect radionuclide release because it will not increase the rate of radionuclide release beyond that already included in the TSPA model. Also, because a bounding estimate of the overall temperature increase (i.e., the adiabatic estimate discussed above) is small, it is not expected to melt or otherwise significantly degrade the HLW waste that is codisposed with the uranium-metal fuel.

An analysis of the impact of even a small temperature increase on the degradation rate of HLW glass is warranted because the rates are temperature dependant above a relative humidity of 44% (BSC 2004 [DIRS 169988], Section 8.1 and Equation 13). Note that this temperature-dependent increase in glass degradation rate affects only a small fraction of the codisposed waste packages. The temperature dependence follows an Arrhenius relationship:

$$\text{Rate} = K_E \text{B} \exp(-E_a/\text{RT})$$

where K_E is the ambient degradation rate, B contains a pH dependence, E_a is the activation energy for the degradation reaction, R is the molar gas constant (8.3145 J/K·mol) (rounded) (Grenthe et al. 1992 [DIRS 101671], Table II.7), and T is temperature in Kelvin. Thus, the increase in degradation rate as a function of temperature is calculated:

$$\text{Log K increase as } f(\text{T}) = \{\text{Log}[(K_E\text{B}) \times \text{EXP}(-E_a/\text{R} \times (1/\text{T}_2 - 1/\text{T}_1)]\}$$

$$- \text{Log}\,(K_E\text{B})$$

The E_a values used by the HLW degradation model are pH dependent with an "acidic" E_a equal to 31 kJ/mol and an "alkaline" E_a value of 69 kJ/mol (BSC 2004 [DIRS 169988], Table 8-1). Over the entire range of pH the faster of the two degradation rates is the rate implemented by the TSPA as described in *In-Package Chemistry Abstraction* (SNL 2007 [DIRS 180506], Section 6.3.1.3.4[a] and Figure 6-2[a]). Minimum (which is the most probable value) and maximum K_E values are provided for both the acidic and alkaline cases in Table 8-1 of the HLW glass degradation report (BSC 2004 [DIRS 169988]):

$$K_{E\_acidic} = 8.41 \times 10^3 \text{ g/m}^2\cdot\text{day to } 1.15 \times 10^7 \text{ g/m}^2\cdot\text{day}$$

$$K_{E\_alkaline} = 2.82 \times 10^1 \text{ g/m}^2\cdot\text{day to } 3.47 \times 10^4 \text{ g/m}^2\cdot\text{day}$$

Uncertainties are applied as a triangular distribution (BSC 2004 [DIRS 169988], Section 8.2.2). Using the most probable value for each set of rates the rate increase owing to a temperature rise of 21°C can be calculated (B cancels out):

$$0.80 = \{\text{Log}[(28.2) \times \text{EXP}(-69{,}000/8.3145 \times ((1/318.15) - (1/297.15))]\} - \text{Log}\,(28.2)$$

and

$$0.36 = \{\text{Log}[(8410) \times \text{EXP}(-31{,}000/8.3145 \times ((1/318.15) - (1/297.15))]\} - \text{Log}\,(8410)$$

Note that the activation energy alone accounts for the temperature-dependent rate increase; therefore, the increases in K_E calculated above are independent of the initial rate and the starting temperature.

For the alkaline case, the rate increase is 0.80 log units. For the acid case, the rate increase is 0.36 log units. The adverse consequences of the HLW glass degradation rate increase are expected to be small because both values are less than the range of uncertainty sampled by TSPA, which spans more than 3 log units for both the acidic and alkaline cases (BSC 2004 [DIRS 169988], Table 8-1).

As indicated in *Total System Performance Assessment Data Input Package for Requirements Analysis for Engineered Barrier System In-Drift Configuration* (SNL 2007 [DIRS 179354], Table 4-4, Parameter Number 05-04), cementitious and other backfill materials are not planned for use in the emplacement drifts, so exothermic reactions from hydration of concrete will not impact emplacement drift thermal conditions.

In conclusion, exothermic reactions in the EBS will not significantly increase heat generation beyond the expected thermal output from other sources.

Based on the previous discussion, omission of FEP 2.1.11.03.0A (Exothermic Reactions in the EBS) will not result in a significant adverse change in the magnitude or timing of either radiological exposure to the RMEI or radionuclide releases to the accessible environment. Therefore, this FEP is excluded from the performance assessments conducted to demonstrate compliance with proposed 10 CFR 63.311 and 63.321 (70 FR 53313 [DIRS 178394]), and with 10 CFR 63.331 [DIRS 180319], on the basis of low consequence.

INPUTS:

Table 2.1.11.03.0A-1. Direct Inputs

Input	Source	Description
BSC 2004. *Defense HLW Glass Degradation Model*. [DIRS 169988]	Table 8-1	The E_a values used by the HLW degradation model are pH dependent with an acidic E_a equal to 31 kJ/mol and an alkaline E_a value of 69 kJ/mol
	Table 8-1	Minimum (which is the most probable value) and maximum K_E values are provided for both the acidic and alkaline cases
	Table 8-1	The HLW glass degradation rate range of uncertainty sampled by TSPA spans more than 3 log units for both the acidic and alkaline cases
	Section 8.2.2	Uncertainties are applied as a triangular distribution
	Section 8.1; Equation 13	The degradation rate of HLW glass is temperature dependant above a RH of 44%
BSC 2004. *Waste Form, Heat Output, and Waste Package Spacing for an Idealized Drift Segment*. [DIRS 166941]	Table 2	At emplacemnt, output of a 2-MCO/2-HLW long waste package is 1,660 watts
Garvin 2002. *Multi-Canister Overpack Topical Report*. [DIRS 169141]	Table 4-4	The estimated acceptable amount of water in a sealed MCO is 4.64 kg (bound in particulate), with less than 200 g being present as free water

Table 2.1.11.03.0A-1. Direct Inputs (Continued)

Input	Source	Description
Garvin 2002. *Multi-Canister Overpack Topical Report*. [DIRS 169141] (continued)	Table 4-4	1.1 10^7 g uranium-metal per waste package, assuming that the waste package contains two MCOs and each MCO contains Mark IV fuel (3,804 kg uranium) and scrap (1,832 kg uranium) for a total of 5,636 kg uranium
Grenthe et al. 1992. *Chemical Thermodynamics of Uranium*. [DIRS 101671]	Table III.1	The oxidation of uranium-metal to form UO_2 is exothermic with a standard enthalpy of formation of –1,085 kJ/mol
	Table II.7	R is the molar gas constant (8.3145 J/K mol) (rounded)
SNL 2007. *Total System Performance Assessment Data Input Package for Requirements Analysis for EBS In-Drift Configuration*. [DIRS 179354]	Parameter Number 05-04	Cementitious and other backfill materials are not planned for use in the emplacement drifts, so exothermic reactions from hydration of concrete will not impact emplacement drift thermal conditions
SNL 2007. *EBS Radionuclide Transport Abstraction*. [DIRS 177407]	Section 6.6.2	Describes approach for calculating upper bound estimates for the diffusive mass transport rate of oxygen into the waste package through these stress corrosion cracks
SNL 2007. In-Package Chemistry Abstraction. [DIRS 180506]	Section 6.3.1.3.4[a] and Figure 6-2[a]	Over the entire range of pH the faster of the two degradation rates is the rate implemented by the TSPA
SNL 2007. *Total System Performance Assessment Data Input Package for Requirements Analysis for Subsurface Facilities*. [DIRS 179466]	Table 4-1, Parameter Number 01-02	At emplacement, the thermal output for the 7-package average is 51,200 watts and at 10,000 years it is 603 watts

Table 2.1.11.03.0A-2. Indirect Inputs

Citation	Title	DIRS
10 CFR 63	Energy: Disposal of High-Level Radioactive Wastes in a Geologic Repository at Yucca Mountain, Nevada	180319
70 FR 53313	Implementation of a Dose Standard After 10,000 Years	178394
BSC 2004	*DSNF and Other Waste Form Degradation Abstraction*	172453
BSC 2004	*Waste Form, Heat Output, and Waste Package Spacing for an Idealized Drift Segment*	166941
DTN: SN0612T0502404.014	Thermodynamic Database Input File for EQ3/6 - DATA0	178850
Haschke 1998	“Corrosion of Uranium in Air and Water Vapor: Consequences for Environmental Dispersal”	174075

FEP: 2.1.11.05.0A

FEP NAME:

Thermal Expansion/stress of In-Package EBS components

FEP DESCRIPTION:

Thermally induced stresses could alter the performance of the waste or EBS. For example, thermal stresses could cause the waste form to develop cracks and create pathways for preferential fluid flow and, thereby, accelerate degradation of the waste.

SCREENING DECISION:

Excluded – low consequence

SCREENING JUSTIFICATION:

Commercial SNF and defense SNF are designed for temperatures and the thermal cycles expected in reactors, which are more severe than the conditions that are anticipated to occur in the repository. As discussed in Section 6.2.1 of *CSNF Waste Form Degradation: Summary Abstraction* (BSC 2004 [DIRS 169987]), the in-reactor thermal cycles (principally that associated with the initial power escalation) cause stresses that result in extensive cracking of the fuel matrix. The effects of this cracking are included in the commercial SNF waste form degradation model through the specific surface area parameter (BSC 2004 [DIRS 169987], Section 6.4.1.5). Additional thermally induced cracking of the fuel pellets after they are emplaced in the repository is not expected because the temperatures and temperature gradients to which the fuel pellet fragments will be exposed are modest compared to those experienced during reactor operation. The HLW glass logs crack because of the stresses induced during cooldown following pouring into the glass canisters during manufacturing. The cracking that results from this cooldown is included in the defense HLW degradation model via a surface area parameter (see included FEP 2.1.02.05.0A (HLW Glass Cracking)). The cracking that results from this cooldown is included in the defense HLW model surface area parameter. This cooldown and the effects of the associated stresses on glass cracking is more severe than any cooldown anticipated under expected repository conditions; additional thermally induced cracking in the repository is not significant (BSC 2004 [DIRS 169988], Section 6.5.4). Waste form cracking prior to emplacement in the repository and the associated effects on the waste form surface areas available for alteration and dissolution are discussed in included FEPs 2.1.02.02.0A (CSNF Degradation) and 2.1.02.03.0A (HLW Glass Degradation). The effects of thermally induced cracking in the repository on the waste form surface area are not explicitly included in TSPA because these effects are small compared to the preemplacement waste form cracking effects that are included. In the TSPA, DOE SNF degradation (except naval SNF) is modeled as instantaneous degradation or dissolution of the waste form upon exposure of the waste form to groundwater. For all groups of DOE SNF (except naval SNF), the upper-limit model produces complete dissolution of the waste form during a single-code time step upon exposure of the waste form to groundwater (BSC 2004 [DIRS 172453], Section 8.1). Therefore, the impact of thermal expansion of the DOE SNF waste form on calculated dose will be insignificant.

The effects of thermal expansion on the waste of package outer barrier, the waste package inner vessel, the TAD canister, the emplacement pallet, drip shields, and invert are discussed in excluded FEP 2.1.11.07.0A (Thermal Expansion/Stress of In-Drift EBS Components).

Based on the previous discussion, omission of FEP 2.1.11.05.0A (Thermal Expansion and Stress of In-Package EBS Components) will not result in a significant adverse change in the magnitude or timing of either radiological exposure to the RMEI or radionuclide releases to the accessible environment. Therefore, this FEP is excluded from the performance assessments conducted to demonstrate compliance with proposed 10 CFR 63.311 and 63.321 (70 FR 53313 [DIRS 178394]), and with 10 CFR 63.331 [DIRS 180319], on the basis of low consequence.

INPUTS:

Table 2.1.11.05.0A-1. Direct Inputs

Input	Source	Description
BSC 2004. *DSNF and Other Waste Form Degradation Abstraction*. [DIRS 172453]	Section 8.1	For all groups of DOE SNF (except naval SNF), the upper-limit model produces complete dissolution of the waste form during a single-code time step upon exposure of the waste form to groundwater

Table 2.1.11.05.0A-2. Indirect Inputs

Citation	Title	DIRS
10 CFR 63	Energy: Disposal of High-Level Radioactive Wastes in a Geologic Repository at Yucca Mountain, Nevada	180319
70 FR 53313	Implementation of a Dose Standard After 10,000 Years	178394
BSC 2004	*CSNF Waste Form Degradation: Summary Abstraction*	169987
BSC 2004	*Defense HLW Glass Degradation Model*	169988

FEP: 2.1.11.06.0A

FEP NAME:

Thermal Sensitization of Waste Packages

FEP DESCRIPTION:

Phase changes in waste package materials can result from long-term storage at moderately hot temperatures in the repository. Stress corrosion cracking (SCC), intergranular corrosion, or mechanical degradation may ensue.

SCREENING DECISION:

Excluded – low consequence

SCREENING JUSTIFICATION:

Alloy 22 could be subject to aging and phase instability when exposed to elevated temperatures that are well above the anticipated maxima expected in the repository (BSC 2004 [DIRS 171924], Section 6.3). Aging and phase instability processes involve precipitation of different secondary phases and restructuring of the microstructure. The affected material may exhibit increased brittleness and decreased resistance to corrosion processes such as localized corrosion and stress corrosion cracking (BSC 2004 [DIRS 171924], Section 1.1).

Nominally, control of the heat treatment process and thermal loading of waste packages will avoid exposure to temperature ranges that can lead to degradation of the physical properties of the Alloy 22 WPOB through thermal sensitization (SNL 2007 [DIRS 179394], Table 4-1, Parameter Numbers 03-16 and 06-03; SNL 2007 [DIRS 179567], Table 4-1, Parameter Numbers 03-16 and 06-03). The effects of potential mechanisms leading to early failure of waste packages including improper heat treatment of waste packages are evaluated in *Analysis of Mechanisms for Early Waste Package/Drip Shield Failure* (SNL 2007 [DIRS 178765], Section 6.3) and discussed in included FEP 2.1.03.08.0A (Early Failure of Waste Packages). Before waste loading, the waste packages (base-metal and fabrication welds) are fully solution annealed (SNL 2007 [DIRS 179394], Table 4-1, Parameter Number 03-16; SNL 2007 [DIRS 179567], Table 4-1, Parameter Number 03-16). After waste loading, the closure lids are welded onto the waste package (SNL 2007 [DIRS 179394], Table 4-1, Parameter Number 03-17; SNL 2007 [DIRS 179567], Table 4-1, Parameter Number 03-17). Possible effects of aging and phase instability on the Alloy 22 WPOB closure lid weld regions are discussed later. *Aging and Phase Stability of Waste Package Outer Barrier* (BSC 2004 [DIRS 171924], Section 8) concluded that no effects of aging and phase instability on the Alloy 22 WPOB would be observed if the waste package were maintained at less than 300°C for a period of 500 years followed by temperatures less than 200°C for a period of 9,500 years. These thermal exposure conditions bound all repository-relevant thermal exposure conditions (SNL 2008 [DIRS 184433], Figure 6.3-76[a]) except in the event of a drift collapse within approximately 90 years after closure (SNL 2008 [DIRS 184433], Figure 6.3-82[a]). For the waste package surface to exceed 300°C, a seismic event of sufficient magnitude must occur within approximately 90 years after closure, result in drift collapse, and affect a waste package with an

unfavorable combination of a high thermal output surrounded by low conductivity rubble (SNL 2008 [DIRS 179962], Section 6.5.1). Analyses have shown that the mean probability of these conditions occurring is about one in 10,000 within the first 10,000 years after closure (SNL 2008 [DIRS 179962], Section 6.5.1). Therefore, with the exception of early failure-related processes, thermal sensitization of waste packages is not expected.

The ASTM specification for the composition of Alloy 22 is shown in Table 2.1.11.06.0A-1. *Aging and Phase Stability of Waste Package Outer Barrier* (BSC 2004 [DIRS 171924], Section 8.2) recommended the use of a more restricted compositional range based on the compositional range of Alloy 22 heats tested in that report. *Computational Modeling of Phase Stability in Alloy 22 Over a Range of Chemical Compositions for the Yucca Mountain Project* (Hu et al. 2005 [DIRS 181177], Figures 3a and 4a) shows that as the amount of alloying elements (in particular chromium and molybdenum) decrease, the phase stability of Alloy 22 is enhanced. Therefore, it is reasonable to extend the applicability of the conclusions of *Aging and Phase Stability of Waste Package Outer Barrier* (BSC 2004 [DIRS 171924], Section 8.2) to the ASTM specification minimums as shown in Table 2.1.11.06.0A-1. The compositional range of Alloy 22 used for waste package fabrication is constrained to these values (SNL 2007 [DIRS 179394], Table 4-1, Parameter Number 03-19; SNL 2007 [DIRS 179567], Table 4-1, Parameter Number 03-19).

Table 2.1.11.06.0A-1. Comparison of Alloy 22 ASTM Composition Specification to Range of Compositions Studied in Alloy 22 Aging and Phase Stability Model and Recommended Alloy 22 Composition Range of Applicability

Element	Alloy 22 ASTM Specification[a]		Alloy 22 Aging and Phase Stability Model Range[b]		Alloy 22 Composition Range of Applicability	
	Wt %		Wt %		Wt %	
	Low	High	Low	High	Low	High
Cr	20.0	22.5	21.2	21.4	20.0	21.4
Fe	2.0	6.0	3.6	4.5	2.0	4.5
Mo	12.5	14.5	13.3	13.5	12.5	13.5
W	2.5	3.5	2.8	3.0	2.5	3.0

Sources: [a] ASTM B 575-99a [DIRS 147465], Table 1, p. 2.
[b] BSC 2004 [DIRS 171924], Table 12.

The Alloy 22 WPOB closure lid welds cannot be solution annealed without risking damage to the waste form. Therefore, the closure welds of the WPOB could be more prone to thermal aging and phase instability than the base metal under long-term thermal exposure in the repository. Analyses conducted in *General Corrosion and Localized Corrosion of Waste Package Outer Barrier* (SNL 2007 [DIRS 178519], Section 6.4.6.1) studied the effect of thermal aging on corrosion of Alloy 22. Three metallurgical conditions of Alloy 22 were studied using creviced specimens: mill-annealed, as-welded, and as-welded plus thermally aged (at 700°C for 173 hours). The samples were tested in 5 M $CaCl_2$ solutions with and without 0.5 *M* $Ca(NO_3)_2$ at test temperatures varying from 30°C to 120°C (as-welded plus thermally aged specimens were tested at 120°C). Comparison of the calculated corrosion rates of the mill-annealed, as-welded, and as-welded plus thermally aged specimens showed no apparent enhancement of the general

corrosion rate (or any intergranular corrosion) due to the presence of welds or thermal aging of the welded specimens for the tested conditions. Also, the localized corrosion resistance of specimens taken from the longitudinal weld seam of a full-diameter, quarter-length mockup waste container that had undergone the fabrication process planned for the full-sized waste packages were evaluated (SNL 2007 [DIRS 178519], Section 6.4.6.2.2). It was concluded that the localized corrosion resistance (i.e., the crevice repassivation potential) of the specimens from the mock-up container was comparable to that of mill-annealed or as-welded specimens prepared from laboratory plates. Based on these results, it is expected that there will be insignificant impact of phase instability on general and localized corrosion of waste package closure lid welds under repository exposure conditions.

Stress corrosion cracking of the WPOB closure welds is discussed in *Stress Corrosion Cracking of Waste Package Outer Barrier and Drip Shield Materials* (SNL 2007 [DIRS 181953]) and included FEP 2.1.03.02.0A (Stress Corrosion Cracking (SCC) of Waste Packages). Data from thermally aged specimens (including welded and thermally aged specimens) were used to develop SCC initiation and crack growth models for the waste package outer barrier closure weld region (SNL 2007 [DIRS 181953], Sections 6.2.1 and 6.4.4). Therefore, although no significant amount of thermal aging is expected in the repository, the effects of potential thermal aging have been incorporated in the SCC models. In this respect, inclusion of an explicit dependence of SCC on thermal aging would not be expected to have a significant effect on predicted radiological exposure to the reasonably maximally exposed individual and radionuclide releases to the accessible environment.

Based on this analysis, insignificant aging and phase instability will occur under the thermal conditions expected in the repository, and the predicted corrosion performance of the waste package outer barrier material is not expected to be affected by aging and phase instability under the thermal conditions expected in the repository (SNL 2007 [DIRS 178519], Section 8).

Based on the previous discussion, omission of FEP 2.1.11.06.0A (Thermal Sensitization of Waste Packages) will not result in a significant adverse change in the magnitude or timing of either radiological exposure to the RMEI or radionuclide releases to the accessible environment. Therefore, this FEP is excluded from the performance assessments conducted to demonstrate compliance with proposed 10 CFR 63.311 and 63.321 (70 FR 53313 [DIRS 178394]), and with 10 CFR 63.331 [DIRS 180319], on the basis of low consequence.

INPUTS:

Table 2.1.11.06.0A-2. Direct Inputs

Input	Source	Description
ASTM B 575-99a. *Standard Specification for Low-Carbon Nickel-Molybdenum-Chromium, Low-Carbon Nickel-Chromium-Molybdenum, Low-Carbon Nickel-Chromium-Molybdenum-Copper, Low-Carbon Nickel-Chromium-Molybdenum-Tantalum, and Low-Carbon Nickel-Chromium-Molybdenum-Tungsten Alloy Plate, Sheet, and Strip* [DIRS 147465]	Table 1, p. 2	Alloy 22 ASTM specification
BSC 2004. *Aging and Phase Stability of Waste Package Outer Barrier*. [DIRS 171924]	Section 8	Discussion of aging and phase stability of waste package outer barrier
	Table 12	Alloy 22 aging and phase stability model range
	Section 8.2	Aging and phase stability of waste package outer barrier in regards to Alloy 22
SNL 2007. *General Corrosion and Localized Corrosion of Waste Package Outer Barrier*. [DIRS 178519]	Section 6.4.6.1	Effect of thermal aging on corrosion of Alloy 22 in welded region is no different than base material
	Section 8	Corrosion performance of the waste package outer barrier material is not expected to be affected by aging and phase stability under the thermal conditions expected in the repository
SNL 2007. *Total System Performance Assessment Data Input Package for Requirements Analysis for DOE SNF/HLW and Navy SNF Waste Package Overpack Physical Attributes Basis for Performance Assessment*. [DIRS 179567]	Table 4-1, Parameter Number 03-19	Alloy 22 waste package compositional range
	Table 4-1, Parameter Numbers 03-16 and 06-03	Discussion that before waste loading, waste packages (base-metal and fabrication welds) are fully solution annealed
	Table 4-1, Parameter Number 03-17	After waste loading, the closure lids are welded onto the waste package
SNL 2007. *Total System Performance Assessment Data Input Package for Requirements Analysis for TAD Canister and Related Waste Package Overpack Physical Attributes Basis for Performance Assessment*. [DIRS 179394]	Table 4-1, Parameter Number 03-19	Alloy 22 waste package compositional range
	Table 4-1, Parameter Number 03-16 and 06-03	Discussion that before waste loading, waste packages (base-metal and fabrication welds) are fully solution annealed
	Table 4-1, Parameter Number 03-17	After waste loading, the closure lids are welded onto the waste package
SNL 2008. *Multiscale Thermohydrologic Model*. [DIRS 184433]	Figures 6.3-76[a], 6.3-82[a]	Thermal exposure conditions bounding repository-relevant thermal exposure conditions
SNL 2008. *Postclosure Analysis of the Range of Design Thermal Loadings*. [DIRS 179962]	Section 6.5.1	Probability for waste package surface temperature to exceed 300°C

Table 2.1.11.06.0A-3. Indirect Inputs

Citation	Title	DIRS
10 CFR 63	Energy: Disposal of High-Level Radioactive Wastes in a Geologic Repository at Yucca Mountain, Nevada	180319
70 FR 53313	Implementation of a Dose Standard After 10,000 Years	178394
BSC 2004	*Aging and Phase Stability of Waste Package Outer Barrier*	171924
Hu et al. 2005	*Computational Modeling of Phase Stability in Alloy 22 Over a Range of Chemical Compositions for the Yucca Mountain Project*	181177
SNL 2007	*Analysis of Mechanisms for Early Waste Package/Drip Shield Failure*	178765
SNL 2007	*General Corrosion and Localized Corrosion of Waste Package Outer Barrier*	178519
SNL 2007	*Stress Corrosion Cracking of Waste Package Outer Barrier and Drip Shield Materials*	181953
SNL 2008	*Postclosure Analysis of the Range of Design Thermal Loadings*	179962

FEP: 2.1.11.06.0B

FEP NAME:

Thermal Sensitization of Drip Shields

FEP DESCRIPTION:

Phase changes in drip shield materials can result from long-term storage at moderately hot temperatures in the repository. Stress corrosion cracking (SCC), intergranular corrosion, or mechanical degradation may ensue.

SCREENING DECISION:

Excluded – low probability

SCREENING JUSTIFICATION:

Aging and phase stability of the Titanium Grade 7 drip shield plate material is discussed in *General Corrosion and Localized Corrosion of the Drip Shield* (SNL 2007 [DIRS 180778], Section 6.7.3), which concludes that aging and phase instability will not affect the corrosion performance of the Titanium Grade 7 drip shield material for properly fabricated drip shields. The effects of potential mechanisms leading to early failure of drip shields including improper heat treatment of drip shields are evaluated in *Analysis of Mechanisms for Early WastePackage/Drip Shield Failure* (SNL 2007 [DIRS 178765], Section 6.4) and discussed in included FEP 2.1.03.08.0B (Early Failure of Drip Shields).

Titanium Grade 7 is a stabilized alpha (α) phase alloy and possesses outstanding phase stability. Titanium Grade 7 contains small amounts of alloying elements (DTN: MO0003RIB00073.000 [DIRS 152926]), most notably palladium. The solubility of palladium in Titanium Grade 7 is about 1 wt % at 400°C. The nominal concentration of palladium in Titanium Grade 7 is well below the solubility limit at this temperature (Gdowski 1997 [DIRS 102789], pp. 1 to 8). Titanium –palladium intermetallic compounds capable of being formed in the titanium-palladium system have not been reported to occur in Titanium Grade 7 with normal heat treatments. Hua et al. (2002 [DIRS 160670]) tested the base and welded metals of Titanium Grade 7 in a highly concentrated basic environment at 60°C, 70°C, 80°C, 90°C, 100°C, and 105°C for up to eight weeks (Hua et al. 2002 [DIRS 160670]; Hua and Gordon 2003 [DIRS 163111]). No difference in weight loss and, therefore, in corrosion rate was observed between the base metal and welds. The boundaries between the welds and heat-affected zone, which experienced a range of temperatures during welding, as well as the boundaries between the heat-affected zone and base metal, were not visibly attacked.

Titanium Grade 29 (the drip shield support material) is a ruthenium-containing version of Titanium Grade 5 with extra-low interstitial elements (ASTM B 265-02 [DIRS 162726], Section 1.1.26 and Table 2). Titanium Grades 5 and 29 both contain about 6% aluminum and 4% vanadium, and are α-β alloys (Leyens and Peter 2003 [DIRS 181560], Chapter 1.5). The α-phase in the alloys is stablized by addition of 6% aluminum and β-phase is stablized by 4%

vanadium. The β-transus of Ti-6Al-4V alloys is about 980°C (Leyens and Peter 2003 [DIRS 181560], Chapter 1.5, Figure 1.12). In general, heating to a temperature higher than the β-transus will increase the initial β grain size, and slow cooling from this temperature will reduce the amount of fine acicular α that forms at high temperature. Below the β-transus, no significant β-phase grain growth is observed (Leyens and Peter 2003 [DIRS 181560], Chapter 1.5).

Stability of commercial α-β alloys, such as Titanium Grades 5 and 29, depends on composition and heat-treatment. In the mill-annealed condition, the α-β alloys can be considered thermally stable up to 315°C (600°F) to 370°C (700°F) (ASM 1990 [DIRS 141615], p. 628). Properly fabricated and heat treated, these α-β alloys are thermally stable up to 425°C (800°F) in the heat treated condition for periods of at least 1,000 hours (ASM 1990 [DIRS 141615], p. 628). These thermal exposure conditions bound all repository-relevant thermal exposure conditions (SNL 2008 [DIRS 184433], Figure 6.3-76[a]) except in the event of a drift collapse within approximately 90 years after closure (SNL 2008 [DIRS 184433], Figure 6.3-82[a]). For the waste package surface to exceed 300°C, a seismic event of sufficient magnitude must occur within approximately 90 years after closure, result in drift collapse and affect a waste package with an unfavorable combination of a high thermal output surrounded by a low conductivity rubble (SNL 2008 [DIRS 179962], Section 6.5.1). Analyses have shown that the mean probability of these conditions occurring is about 1 in 10,000 within the first 10,000 years after closure (SNL 2008 [DIRS 179962], Section 6.5.1). Therefore, given that the waste package exposure temperature will bound the drip shield exposure temperature (as the drip shield is further from the heat source (the decaying waste forms)), and that Titanium Grades 5 and 29 are expected to be thermally stable up to 315°C (600°F) to 370°C (700°F) (ASM 1990 [DIRS 141615], p. 628), thermal sensitization of these materials can be considered to be of low probability under repository exposure conditions.

Schutz et al. (2000 [DIRS 177257]) measured the mechanical properties of Titanium Grade 29 after 12 months of exposure at 210°C (410°F) and observed no changes in mechanical properties of Titanium Grade 29 after this long time exposure. Schutz et al. (2000 [DIRS 177257]) also concluded that the fully annealed, equilibrium, two-phase transformed β structure of Titanium Grade 29 exhibited no measurable changes in phases or phase composition after long-term exposure at 210°C. The low-ductility ordered phase α_2 (Ti_3Al) does not form below 400°C (750°F) (Jones 1992 [DIRS 178458], p. 269). No significant α_2 (Ti_3Al) precipitation was observed because of the low aluminum and interstitial content levels in Titanium Grade 29. Based on the previous discussion, it can be concluded that under the repository conditions, the precipitation of detrimental phases (e.g., α_2 (Ti_3Al) or coarsened β) is not expected to be a factor for the integrity of the material.

Therefore, based on the experimental evidence, FEP 2.1.11.06.0B (Thermal Sensitization of the Drip Shield) can be excluded from the performance assessments conducted to demonstrate compliance with proposed 10 CFR 63.311 and 63.321 (70 FR 53313 [DIRS 178394]), and with 10 CFR 63.331 [DIRS 180319], on the basis of low probability of occurrence under the exposure conditions in the repository.

INPUTS:

Table 2.1.11.06.0B-1. Direct Inputs

Input	Source	Description
ASM International 1990. *Properties and Selection: Nonferrous Alloys and Special-Purpose Materials*. [DIRS 141615]	p. 628	Thermal stability of alpha-beta alloys
ASTM B 265-02. 2002. *Standard Specification for Titanium and Titanium Alloy Strip, Sheet, and Plate*. [DIRS 162726]	Table 2, Section 1.1.26	Characteristics of Titanium Grades 5 and 29
DTN: MO0003RIB00073.000. Physical and Chemical Characteristics of Ti Grades 7 and 16. [DIRS 152926]	file: *s04197_001_001.pdf*	Titanium Grade 7 contains small amounts of alloying elements, most notably palladium
SNL 2008. *Multiscale Thermohydrologic Model*. [DIRS 184433]	Figures 6.3-76[a], 6.3-82[a]	Thermal exposure conditions bounding repository-relevant thermal exposure conditions
SNL 2008. *Postclosure Analysis of the Range of Design Thermal Loadings*. [DIRS 179962]	Section 6.5.1	Probability for waste package surface temperature to exceed 300°C

Table 2.1.11.06.0B-2. Indirect Inputs

Citation	Title	DIRS
70 FR 53313	Implementation of a Dose Standard After 10,000 Years	178394
Gdowski 1997	*Degradation Mode Survey Candidate Titanium - Base Alloys for Yucca Mountain Project Waste Package Materials*	102789
Hua and Gordon 2003	"On Apparent Bi-Linear Corrosion Rate Behavior of Ti Grade 7 in Basic Saturated Water (BSW-12) Below and Above 80°C"	163111
Hua et al. 2002	"General Corrosion Studies of Candidate Container Materials in Environments Relevant to Nuclear Waste Repository"	160670
Jones 1992	*Stress-Corrosion Cracking*	178458
Leyens and Peters 2004	*Titanium and Titanium Alloys, Fundamentals and Applications*	181560
Schutz et al. 2000	"Qualifications of Ti-6%Al-4%V-Ru Alloy Production Tubulars for Aggressive Fluoride-Containing Mobile Bay Well Service"	177257
SNL 2007	*Analysis of Mechanisms for Early Waste Package/Drip Shield Failure*	178765
SNL 2007	*General Corrosion and Localized Corrosion of the Drip Shield*	180778
SNL 2008	*Postclosure Analysis of the Range of Design Thermal Loadings*	179962

FEP: 2.1.11.07.0A

FEP NAME:

Thermal Expansion/Stress of In-Drift EBS Components

FEP DESCRIPTION:

Repository heat at Yucca Mountain could result in thermally induced stress changes that would affect the mechanical and chemical evolution of the repository. These stress changes could affect the EBS components, thus causing the formation of pathways for groundwater flow through the EBS or altering and/or enhancing existing pathways. Relevant processes include changes in physical properties of the drip shields, waste packages, pallet, and invert.

SCREENING DECISION:

Excluded – low consequence

SCREENING JUSTIFICATION:

Waste Package—According to the current waste package design, all waste forms except the codisposal canisters will be contained in TAD canisters made of 300-series stainless steel (e.g., Stainless Steel Type 316L (UNS S31603)) (SNL 2007 [DIRS 179394], Section 4.1.1.4). The TAD canisters will be placed inside the Stainless Steel Type 316 inner vessel contained inside the Alloy 22 waste package outer shell (SNL 2007 [DIRS 179394], Section 4.1). The codisposal canisters will be placed inside the Stainless Steel Type 316 inner vessel, which will be placed inside the Alloy 22 waste package outer shell (SNL 2007 [DIRS 179567], Sections 4.1.1). Since the thermal expansion coefficient of the TAD canister and the waste package inner vessel is expected to be the same, only stress induced from differing thermal expansion between the inner and the outer vessel is important for this FEP.

The coefficient of thermal expansion for Stainless Steel Type 316L (UNS S31603) (an analogue for the Stainless Steel Type 316 used for the waste package inner vessel) is larger than the coefficient of thermal expansion for Alloy 22 (e.g., Stainless Steel Type 316 NG [nuclear grade]: 17×10^{-6} m/m·K at 260°C, Alloy 22: 12.6×10^{-6} m/m·K from 24°C to 316°C, where K is temperature in Kelvin (BSC 2001 [DIRS 152655], Section 5.1)). Thus, changes in temperature could lead to contact stresses between the waste package inner vessel and outer shell. Consequently, a loose fit between the waste package outer shell and the inner vessel is required to accommodate the differing thermal expansion coefficients between Stainless Steel Type 316 and Alloy 22.

Under thermal expansion loading, tangential stresses are significantly higher than radial stresses (BSC 2001 [DIRS 152655], Section 1.0). The maximum tangential stress at the waste package outer shell inner and outer surfaces was evaluated for several waste package configurations (e.g., 5-DHLW/DOE SNF-Short, 2-MCO/2-DHLW, and naval SNF Long (which is similar to a TAD canister) and Short) as a function of temperature and shell gap size (i.e., difference in radius of the two shells evaluated at room temperature) and results documented in *Waste Package Outer Barrier Stresses Due to Thermal Expansion with Various Barrier Gap Sizes* (BSC 2001

[DIRS 152655], Section 6). These design calculations have shown that a shell gap size of about 1 mm (or greater) would result in no tangential stresses due to thermal expansion. Therefore, current waste package design requires the radial gap between the waste package inner vessel and the waste package outer shell to be a least 1 mm and could be increased to a maximum of 5 mm (SNL 2007 [DIRS 179394], Table 4-1, Parameter Number 03-04). Typical waste package design also requires a relatively large longitudinal shell gap of at least 30 mm (SNL 2007 [DIRS 179394], Table 4-1, Parameter Number 03-05). Therefore, no significant stress is expected to develop between the waste package inner and outer vessels due to differing thermal expansion of waste package components. Although, as discussed in excluded FEP 2.1.03.06.0A (Internal Corrosion of Waste Packages Prior to Breach), residual moisture in the waste packages could result in the formation of a thin (on the order of 0.13 μm) corrosion product layer prior to breach of the waste package outer shell, this small amount of corrosion product is not expected to generate significant stress between the waste package inner vessel and outer shell.

Pallet—The waste package pallet also contains components composed of stainless steel and Alloy 22 (SNL 2007 [DIRS 179354], Section 4.1.3). However, thermal expansion of the pallet would have negligible effect because it is not constrained laterally or longitudinally.

Drip Shields—The drip shield connectors are required to allow for thermal expansion with no impact on drip shield performance at temperatures up to 300°C (BSC 2007 [DIRS 179354], Table 4-2, Parameter Number 07-15). Since the drip shield is farther from the heat source (i.e., the decaying waste forms), its temperature will be lower than the waste package surface temperature. A temperature of 300°C on the waste package surface should bound all repository-relevant thermal exposure conditions (SNL 2008 [DIRS 184433], Figure 6.3-76[a]) except in the event of a drift collapse within approximately 90 years of closure (SNL 2008 [DIRS 184433], Figure 6.3-82[a]). For any waste package surface temperature to exceed 300°C, a seismic event causing drift collapse and subjecting that waste package to a high thermal output in a surrounding of a low thermal conductivity rubble is required to occur within approximately 90 years of closure (SNL 2008 [DIRS 179962], Section 6.5.1). However, analyses have shown that the mean probability of occurrence of such conditions is about one in 10,000 within the first 10,000 years of disposal (SNL 2008 [DIRS 179962], Section 6.5.1). Therefore, thermal expansion of the drip shield segments is expected to have no significant impact on drip shield performance in the repository. The space between the drip shield and waste package is large enough to accommodate deflection due to rockfall as discussed in excluded FEP 2.1.03.07.0B (Mechanical Impact on Drip Shield).

Invert—Any thermal expansion of the invert ballast material will not generate appreciable stress because the material is unconstrained vertically and will expand into the open spaces within the drift (see discussion in excluded FEP 2.1.06.05.0B (Mechanical Degradation of Invert)).

In conclusion, thermally induced stress changes as discussed above will not affect the aforementioned EBS in-drift components causing the formation of pathways for groundwater flow through the EBS or altering and/or enhancing existing pathways.

Based on the previous discussion, omission of FEP 2.1.11.07.0A (Thermal Expansion/Stress of In-Drift EBS Components) will not result in a significant adverse change in the magnitude or timing of either radiological exposure to the RMEI or radionuclide releases to the accessible

environment. Therefore, this FEP is excluded from the performance assessments conducted to demonstrate compliance with proposed 10 CFR 63.311 and 63.321 (70 FR 53313 [DIRS 178394]), and with 10 CFR 63.331 [DIRS 180319], on the basis of low consequence.

INPUTS:

Table 2.1.11.07.0A-1. Direct Inputs

Input	Source	Description
BSC 2001. *Waste Package Outer Barrier Stress Due to Thermal Expansion with Various Barrier Gap Sizes*. [DIRS 152655]	Section 6	The maximum tangential stress at the waste package outer barrier inner and outer surfaces evaluated for several waste package types
	Section 5.1	Thermal expansion coefficients of waste package materials
	Section 1.0	Thermal stresses in waste packages
SNL 2007. *Total System Performance Assessment Data Input Package for Requirements Analysis for EBS In-Drift Configuration*. [DIRS 179354]	Table 4-2, Parameter Number 07-15	Drip shield connector thermal expansion allowance
SNL 2007. *Total System Performance Assessment Data Input Package for Requirements Analysis for TAD Canister and Related Waste Package Overpack Physical Attributes Basis for Performance Assessment*. [DIRS 179394]	Table 4-1, Parameter Numbers 03-04 and 03-05	Typical waste package design: radial and longitudinal gaps
	Sections 4.1.1.4, 4.1	TAD waste package specifications and configurations
SNL 2008. *Multiscale Thermohydrologic Model*. [DIRS 184433]	Figures 6.3-76[a] and 6.3-82[a]	Predicted waste package surface temperatures under normal condition and after drift collapse
SNL 2008. *Postclosure Analysis of the Range of Design Thermal Loadings*. [DIRS 179962]	Section 6.5.1	Probability of waste package surface temperature reaching 300°C

Table 2.1.11.07.0A-2. Indirect Inputs

Citation	Title	DIRS
10 CFR 63	Energy: Disposal of High-Level Radioactive Wastes in a Geologic Repository at Yucca Mountain, Nevada	180319
70 FR 53313	Implementation of a Dose Standard After 10,000 Years	178394
SNL 2007	*Total System Performance Assessment Data Input Package for Requirements Analysis for EBS In-Drift Configuration*	179354
SNL 2007	*Total System Performance Assessment Data Input Package for Requirements Analysis for DOE SNF/HLW and Navy SNF Waste Package Overpack Physical Attributes Basis for Performance Assessment*	179567
SNL 2008	*Postclosure Analysis of the Range of Design Thermal Loadings*	179962

FEP: 2.1.11.08.0A

FEP NAME:

Thermal Effects on Chemistry and Microbial Activity in the EBS

FEP DESCRIPTION:

Temperature changes may affect chemical and microbial processes in the waste and EBS.

SCREENING DECISION:

Included

TSPA DISPOSITION:

Actinide solubilities in carbonate systems, such as those that will prevail in the EBS, decrease with increasing temperature (SNL 2007 [DIRS 177418], Section 6.3.3.3); the actinide solubilities used in TSPA are those calculated at 25°C. Conversely, the solubility of radium (using barium as an analog) increases with temperature (SNL 2007 [DIRS 177418], Section 6.3.3.3), and the radium solubilities used in TSPA are those calculated at 100°C. Tin solubilities are calculated at 25°C due to limited thermodynamic data; other radionuclides are not solubility-limited and their release rate is controlled by the dissolution rate of the waste form (SNL 2007 [DIRS 177418], Table 8-1). Sensitivity runs indicate that temperature influences in-package pH (SNL 2007 [DIRS 180506], Section 6.6.6), but has only a minor impact on ionic strength. To be consistent with the solubility model, and because of greater confidence in the 25°C thermo-kinetic inputs, all in-package pH and ionic strength abstractions are based on calculations performed at 25°C (SNL 2007 [DIRS 180506], Section 6.6[a]).

The effects of temperature on mineral stabilities and chemical reaction rates are included in each geochemical submodel of *Engineered Barrier System: Physical and Chemical Environment* (SNL 2007 [DIRS 177412], Section 6.2), which uses results from *In-Drift Precipitates/Salts Model* (SNL 2007 [DIRS 177411]); which is used to predict the temperature-dependent stabilities of precipitated phases in the drift.

Test data show that the reaction rates for commercial SNF and HLW glass degradation are temperature dependent. Temperature dependence was included in degradation abstraction models implemented in TSPA for both waste forms. Total carbonate concentration, which is an input for commercial SNF degradation, is also temperature dependent.

Evaluation of Potential Impacts of Microbial Activities on Drift Chemistry (BSC 2004 [DIRS 169991], Section 6.4) outlines several repository-specific environmental constraints on microbial activity. The conclusions from that analysis are summarized in excluded FEP 2.1.10.01.0A (Microbial Activity in EBS), which indicates that environmental factors will severely limit microbial activities in the repository. Microbial activity, therefore, need not be considered further.

INPUTS:

Table 2.1.11.08.0A-1. Indirect Inputs

Citation	Title	DIRS
BSC 2004	*Evaluation of Potential Impacts of Microbial Activities on Drift Chemistry*	169991
SNL 2007	*Dissolved Concentration Limits of Elements with Radioactive Isotopes*	177418
SNL 2007	*Engineered Barrier System: Physical and Chemical Environment*	177412
SNL 2007	*In-Drift Precipitates/Salts Model*	177411
SNL 2007	*In-Package Chemistry Abstraction*	180506

FEP: 2.1.11.09.0A

FEP NAME:

Thermal Effects on Flow in the EBS

FEP DESCRIPTION:

High temperatures in the EBS may influence seepage into, and flow within, the waste and EBS. Thermally-induced changes to fluid saturation and/or relative humidity could influence in-package chemistry. Thermal gradients in the repository could lead to localized accumulation of moisture. Wet zones could form below the areas of moisture accumulation.

SCREENING DECISION:

Included

TSPA DISPOSITION:

Multiscale Thermohydrologic Model (SNL 2008 [DIRS 184433]) calculates the thermohydrologic environment within and around the emplacement drifts. Based on the modeling methodology and inputs described in that report (SNL 2008 [DIRS 184433], Sections 6.2, 6.4, and 6.12[a], and Table 1-1), the MSTHM predicts the temperature, relative humidity, gas- and liquid-phase fluxes, and gas- and liquid-phase saturations in the near-field host rock, as well as within the emplacement drifts (SNL 2008 [DIRS 184433], Section 6.3[a]). The temperature and relative humidity directly affect the in-drift chemical environment calculated in the TSPA.

The thermal effects on flow within and around the drift are also simulated with the TH seepage model in *Drift-Scale Coupled Processes (DST and TH Seepage) Models* (BSC 2005 [DIRS 172232], Section 6.2). The TH seepage model evaluates seepage into the drift during the thermal pulse and concludes that (1) the volume of thermal seepage is always less than seepage under ambient conditions, and (2) seepage will not occur at drift wall temperatures over 100°C for the intact drifts. These conclusions are utilized to develop an appropriate seepage abstraction methodology in *Abstraction of Drift Seepage* (SNL 2007 [DIRS 181244], Section 6.5.2), which conservatively abstracts the larger ambient seepage rates determined by *Seepage Model for PA Including Drift Collapse* (BSC 2004 [DIRS 167652], Section 6.3.6) for use in TSPA. TSPA calculations incorporate seepage model uncertainty by sampling probability distributions for rock capillarity, permeability, and percolation flux (SNL 2007 [DIRS 181244], Section 6.6).

Thermal-hydrologic conditions calculated by the MSTHM (SNL 2008 [DIRS 184433], Section 6.3[a]), together with results described in *Abstraction of Drift Seepage* (SNL 2007 [DIRS 181244], Section 8[a]) and *In-Drift Natural Convection and Condensation* (SNL 2007 [DIRS 181648], Section 8[a]), are implemented in the TSPA and are also used as input by the EBS flow and transport model described in *EBS Radionuclide Transport Abstraction* (SNL 2007 [DIRS 177407], Section 6.3.1.1). Thus, thermal effects on flow into the EBS are accounted for in TSPA. However, with respect to advective fluxes of water through various EBS components, for the purpose of transporting radionuclides by advection, the potential effects of evaporation

within the drift are conservatively ignored. The total flux through the invert is set equal to the seepage flux into the drift, plus any contributions due to drift wall condensation and imbibition flux from the host rock.

Thermal gradients in the repository could lead to localized accumulation of moisture within the cooler regions of the emplacement drifts. Such effects are addressed in included FEPs 2.1.08.04.0A (Condensation Forms on Roofs of Drifts (Drift-scale Cold Traps)) and 2.1.08.04.0B (Condensation Forms at Repository Edges (Repository-scale Cold Traps)), and excluded FEP 2.1.08.14.0A (Condensation on Underside of Drip Shield). Locally saturated conditions are considered in the in-package chemistry abstraction provided to TSPA (SNL 2007 [DIRS 180506]).

The effects of evaporation and condensation are addressed in included FEP 2.1.08.04.0A (Condensation Forms on Roofs of Drifts (Drift-scale Cold Traps)), included FEP 2.1.08.04.0B (Condensation Forms at Repository Edges (Repository-scale Cold Traps)), and excluded FEP 2.1.08.14.0A (Condensation on Underside of Drip Shield).

INPUTS:

Table 2.1.11.09.0A-1. Indirect Inputs

Citation	Title	DIRS
BSC 2004	*Seepage Model for PA Including Drift Collapse*	167652
BSC 2005	*Drift-Scale Coupled Process (DST and TH Seepage) Models*	172232
SNL 2007	*Abstraction of Drift Seepage*	181244
SNL 2007	*EBS Radionuclide Transport Abstraction*	177407
SNL 2007	*In-Drift Natural Convection and Condensation*	181648
SNL 2007	*In-Package Chemistry Abstraction*	180506
SNL 2008	*Multiscale Thermohydrologic Model*	184433

FEP: 2.1.11.09.0B

FEP NAME:

Thermally-Driven Flow (Convection) in Waste Packages

FEP DESCRIPTION:

Temperature differentials may result in convective flow in the EBS. Convective flow within the waste packages could influence in-package chemistry.

SCREENING DECISION:

Excluded – low consequence

SCREENING JUSTIFICATION:

Convective flow in the gas phase or the aqueous phase within waste packages could occur as a result of local thermal gradients. Convective flow in the gas phase could affect the relative humidity or oxygen levels in waste packages. In the aqueous phase, such flow could serve to disperse corrosion by-products or dissolved radionuclides, potentially resulting in increased waste package releases. The effects of thermally driven convection in waste packages decrease with time, as the waste cools and temperature gradients within the packages decrease. There are few mechanisms for early waste package failure, limiting the potential occurrence of this process.

In TSPA, in-package chemistry is calculated using the in-drift gas phase composition, which is expected to be in equilibrium with the gas phase within the waste package; this equilibrium is maintained by diffusive and advective processes. The CO_2 partial pressure is set to the in-drift value; conditions are assumed to remain oxic; and the relative humidity at the waste package surface is taken to be representative of the interior relative humidity. Although not quantitatively evaluated, the effect of thermal convection in the gas phase within a waste package would be homogenization, reducing the possibility of compositional gradients. This is consistent with the existing TSPA implementation.

Convection in the aqueous phase is not anticipated to have a large effect on radionuclide releases from the waste package. Huge volumes of uranium secondary phases and steel corrosion products buffer the pH within the package (SNL 2007 [DIRS 180506], Section 6.3.4[a]), so little change in water chemistry can occur. Also, once packages have cooled sufficiently for water to exist in the package, thermal gradients and the resulting convective mixing will be minor. In addition, convection in the aqueous phase requires that water enters a waste package, and for convection to be important relative to advection, ponding must occur within the waste package. Water entry into a waste package requires both drip shield and waste package failure. The drip shield does not fail by localized corrosion (SNL 2007 [DIRS 180778], Section 8.4) or hydride cracking (excluded FEP 2.1.03.04.0B (Hydride Cracking of Drip Shields)), and will not breach by general corrosion within the first 10,000 years (SNL 2007 [DIRS 180778], Section 8.3). Waste packages do not fail by hydride cracking (excluded FEP 2.1.03.04.0A (Hydride Cracking of Waste Packages)), or by general corrosion within the first 10,000 years (SNL 2007

[DIRS 178519], Section 8.1). However, in the event of drip shield failure, waste packages may fail by localized corrosion if contacted by seepage. Seismic events may result in drip shield damage such as buckling, rupture, or displacement, allowing seepage to reach the waste package. Waste packages contacted by seepage may fail by localized corrosion, resulting in corrosion patches, which permit advective flow into the packages and ponding to occur.

If seepage is benign with respect to localized corrosion, ponding inside packages is not anticipated, because the types of waste package damage that occur due to seismic ground motion do not permit ponding of water in the waste package. Seismic ground motion and the resulting dynamic interaction of waste packages, pallets, and the drip shield, can produce waste package damage from end-to-end impacts and package-pallet impacts (SNL 2007 [DIRS 176828], Section 6.5). Breaches resulting from such damage are limited to stress corrosion cracks, and advective flow of liquid water through such cracks is excluded in FEP 2.1.03.10.0A (Advection of Liquids and Solids through Cracks in the Waste Package). Seismic fault displacement may result in shearing of waste packages, potentially allowing for flow into and radionuclide transport out of a damaged package (SNL 2007 [DIRS 176828], Section 6.1.4). However, fault displacement severely damages waste packages. In addition, seismic events sufficiently large to damage a waste package by fault displacement occur with a mean annual exceedance frequency of 2.5×10^{-7} or less (SNL 2007 [DIRS 176828], Section 6.11.4). Only 214 waste packages are intersected by faults in the consequence analyses reported in *Seismic Consequence Abstraction* (SNL 2007 [DIRS 176828], Section 6.11.2), and, generally, only a small fraction of that number are anticipated to be affected by any single faulting event. Because of the extensive damage to the waste package produced by fault displacement, ponding is not anticipated to occur.

An evaluation of the probability of ponding within waste packages, for several different combinations of drip shield and waste package failure mechanisms including early failures, failures due to seismic ground motion, rockfall and drift collapse, and waste package failure by localized corrosion, is presented in *Waste Package Flooding Probability Evaluation* (SNL 2008 [DIRS 184078], Table 7-4). The analysis concludes that, while ponding can occur if the drip shield fails and the waste package is subject to localized corrosion, the mean probability of ponding occurring in even a single waste package in 10,000 years is less than 10^{-4}.

Waste package failure will occur in the case of an igneous intrusion intersecting the respository. The effects of igneous intrusion are evaluated in *Dike/Drift Interactions* (SNL 2007 [DIRS 177430], Section 8.1.2). The damage to a waste package caused by magma intrusion is extensive, compromising the durability and even the shape of the entire waste package. High magma temperatures compromise the corrosion resistance of the waste package, and the cooling basaltic magma represents a corrosive environment, exsolving volatile gases such as H_2O, H_2, CO_2, CO, SO_2, S_2, HCl, HF, and H_2S, which has a large impact on waste package corrosion rates. Even if the waste package does not breach during the magma intrusion, subsequent rapid and ubiquitous failure will occur. Thus, ponding within the package is not plausible.

To summarize, convection in the gas phase will have little effect on gas-phase compositions, as diffusion and advective flow already provide driving forces for homogenization of the gas phase within a given waste package and with the in-drift gas phase. Convection in the aqueous phase is anticipated to occur only rarely because it requires ponding within a waste package. Should this

unlikely event occur, it will have little effect on water chemistry or radionuclide releases from a waste package.

Based on the previous discussion, omission of FEP 2.1.11.09.0B (Thermally Driven Flow (Convection) in Waste Packages) will not result in a significant adverse change in the magnitude or timing of either radiological exposure to the RMEI or radionuclide releases to the accessible environment. Therefore, this FEP is excluded from the performance assessments conducted to demonstrate compliance with proposed 10 CFR 63.311 and 63.321 (70 FR 53313 [DIRS 178394]), and with 10 CFR 63.331 [DIRS 180319], on the basis of low consequence.

INPUTS:

Table 2.1.11.09.0B-1. Direct Inputs

Input	Source	Description
SNL 2007. *Seismic Consequence Abstraction*. [DIRS 176828]	Section 6.11.2	The number of waste packages intersected by faults is 214, and only a small fraction of these are affected by any single event.
	Section 6.11.4	Mean annual exceedance frequency of a fault displacement large enough to damage a waste package by shearing is 2.5×10^{-7} or less
	Section 6.1.4	Seismic fault displacement can result in shearing of the waste package, potentially allowing for flow into and radionuclide transport out of the damaged package
	Section 6.5	Seismic ground motion and the resulting dynamic interaction of waste packages, pallets, and the drip shield, can produce waste package damage from end-to-end impacts and package-pallet impacts
SNL 2007. *Dike/Drift Interactions*. [DIRS 177430]	Section 8.1.2	Damage to a waste package caused by magma intrusion is extensive, compromising the durability and shape of the entire waste package. Magma intrusion also represents a corrosive environment, and rapid corrosion of the waste package occurs
SNL 2007. *General Corrosion and Localized Corrosion of the Drip Shield*. [DIRS 180778]	Section 8.3	The drip shield will not breach by general corrosion within the first 10,000 years
	Section 8.4	The drip shield does not fail by localized corrosion
SNL 2007. *General Corrosion and Localized Corrosion of Waste Package Outer Barrier*. [DIRS 178519]	Section 8.1	The waste package does not fail by general corrosion within the first 10,000 years
SNL 2007. *In-Package Chemistry Abstraction*. [DIRS 180506]	Section 6.3.4[a]	Uranium secondary minerals and steel corrosion products buffer the pH within the waste package
SNL 2008. *Waste Package Flooding Probability Due to Seismic Fault Displacement*. [DIRS 184078]	Table 7-4	The probability of ponding within a waste package in the repository is less than 10×10^{-4} in 10,000 years

Table 2.1.11.09.0B-2. Indirect Inputs

Citation	Title	DIRS
10 CFR 63	Energy: Disposal of High-Level Radioactive Wastes in a Geologic Repository at Yucca Mountain, Nevada	180319
70 FR 53313	Implementation of a Dose Standard After 10,000 Years	178394

FEP: 2.1.11.09.0C

FEP NAME:

Thermally Driven Flow (Convection) in Drifts

FEP DESCRIPTION:

Temperature differentials may result in convective flow in the EBS. Convective flow within the drifts could influence in-drift chemistry.

SCREENING DECISION:

Included

TSPA DISPOSITION:

Heat generated by decaying radioactive waste will produce temperature differences between the waste package, the drift wall, and other components of the engineered barrier system. Non-uniform heating will produce temperature differences between adjacent waste package locations. These temperature differences will cause natural convection within the open spaces in the drift. The effects of natural and forced convection during preclosure ventilation are addressed in *Ventilation Model and Analysis Report* (BSC 2004 [DIRS 169862], Sections 6.3.3 and 8.2). Natural convection in the drifts after closure is addressed by *In-Drift Natural Convection and Condensation* (SNL 2007 [DIRS 181648]).

The convection model presented in *In-Drift Natural Convection and Condensation* (SNL 2007 [DIRS 181648], Sections 6.1 and 6.2) includes explicit representation of two-dimensional and three-dimensional natural convection driven by temperature differences. Results from this model (SNL 2007 [DIRS 181648], Section 6.4) are used to develop an effective thermal conductivity for air that captures the heat transfer effects from natural convection, and is subsequently used in submodels of *Multiscale Thermohydrologic Model* (SNL 2008 [DIRS 184433], Appendix I[a]). Using this approach, the overall heat transfer rate from the waste package to the in-drift components and the drift wall is maintained. The three-dimensional convection model is also used to develop a dispersion coefficient (SNL 2007 [DIRS 181648], Section 6.2.7) that represents gas-phase mass transport by thermal convective mixing for use in simulating vapor transport in the emplacement drifts (SNL 2007 [DIRS 181648], Section 6.3.5; SNL 2008 [DIRS 184433], Sections 6.3.18[a] and 7.8[a]). Uncertainties in the in-drift natural convection and condensation model are propagated to TSPA through use of bounding values for the axial dispersion rate, for the degree of drip shield ventilation, and for the percolation rate at the repository horizon (SNL 2007 [DIRS 181648], Section 6.1.3[a]).

The output from the ventilation model (BSC 2004 [DIRS 169862], Section 8.2), modified and extended as described in *Thermal Management Flexibility Analysis* (SNL 2007 [DIRS 179196], Section 6.3), and output from the condensation model (SNL 2007 [DIRS 181648], Section 8.3.2) are used in the MSTHM (SNL 2008 [DIRS 184433]), which simulates thermal-hydrologic conditions in the drift. In TSPA calculations, temperature and relative humidity conditions derived from the MSTHM are used to extract parameters of the in-drift chemical environment

from the lookup-tables generated by the in-drift seepage dilution/evaporation model, developed in *Engineered Barrier System: Physical and Chemical Environment* (SNL 2007 [DIRS 177412], Section 6.3.3).

Condensation forming on the roof or other parts of the drift is input to the TSPA as described in included FEP 2.1.08.04.0A (Condensation Forms on Roofs of Drifts (Drift-Scale Cold Traps)). Condensation forming at the repository edges is discussed in included FEP 2.1.08.04.0B (Condensation Forms at Repository Edges (Repository-Scale Cold Traps)), and condensation forming on the underside of the drip shields is discussed in excluded FEP 2.1.08.14.0A (Condensation on Underside of Drip Shield). Preclosure ventilation is discussed in included FEP 1.1.02.02.0A (Preclosure Ventilation).

Finally, thermal convective mixing is also a factor in dispersion of acid-gas species that may evolve from liquid brines, such as those formed by salt deliquescence (SNL 2007 [DIRS 181267], Section 6.2). Dispersion from convective mixing is part of the justification for excluded FEP 2.1.09.28.0A (Localized Corrosion on Waste Package Outer Surface Due to Deliquescence).

INPUTS:

Table 2.1.11.09.0C-1. Indirect Inputs

Citation	Title	DIRS
BSC 2004	*Ventilation Model and Analysis Report*	169862
SNL 2007	*Analysis of Dust Deliquescence for FEP Screening*	181267
SNL 2007	*Engineered Barrier System: Physical and Chemical Environment*	177412
SNL 2007	*In-Drift Natural Convection and Condensation*	181648
SNL 2007	*Thermal Management Flexibility Analysis*	179196
SNL 2008	*Multiscale Thermohydrologic Model*	184433

FEP: 2.1.11.10.0A

FEP NAME:

Thermal Effects on Transport in EBS

FEP DESCRIPTION:

Temperature changes in the repository may influence advection, diffusion, and sorption in the EBS. The Soret effect is a diffusion process caused by a thermal gradient. In liquids having both light and heavy molecules (or ions) and a temperature or thermal gradient, the heavier solute molecules tend to concentrate in the colder region. Temperature differences in the waste and EBS may result in a component of diffusive solute flux that is proportional to the temperature gradient.

SCREENING DECISION:

Excluded – low consequence

SCREENING JUSTIFICATION:

This FEP addresses thermal effects on radionuclide transport by Soret diffusion and sorption. Other thermal effects are included in TSPA. In *EBS Radionuclide Transport Abstraction* (SNL 2007 [DIRS 177407], Section 6.3.4.1.2), the diffusion coefficient for the invert, corrosion products, and waste form domains is modified for temperature, but not for thermal gradient. The thermal effect on diffusion coefficients for species in an aqueous medium is based on hydrodynamic theory and is approximated by the Stokes-Einstein equation (Bird et al. 1960 [DIRS 103524], Section 16.5). The Stokes-Einstein equation shows that the diffusion coefficient in a liquid medium is directly proportional to the temperature divided by the viscosity of the medium. For aqueous media, the viscosity of water decreases with respect to increasing temperature so that the diffusion coefficient is seen to increase with increasing temperature (SNL 2007 [DIRS 177407], Section 6.3.4.1.2, Figure 6.3-5). The effect of temperature on diffusion rates is further discussed as part of included FEPs 2.1.09.08.0A (Diffusion of Dissolved Radionuclides in EBS) and 2.1.09.24.0A (Diffusion of Colloids in EBS). Diffusion rates in the invert are also indirectly coupled to thermal effects through the invert saturation (SNL 2007 [DIRS 177407], Sections 6.3.4.1, 6.3.4.3, and 6.3.4.6), which is determined by *Multiscale Thermohydrologic Model* (SNL 2008 [DIRS 184433], Section 6.2.12.1[a]). This effect is summarized in included FEPs 2.1.08.05.0A (Flow Through Invert) and 2.1.08.07.0A (Unsaturated Flow in the EBS).

In addition, thermal gradients and temperature effects relative to advection are addressed by evaluations of these transport-related processes, as summarized in included FEPs 2.1.11.09.0A (Thermal Effects of Flow in the EBS), 2.1.09.08.0B (Advection of Dissolved Radionuclides in EBS), and 2.1.09.19.0B (Advection of Colloids in EBS).

The Soret effect refers to the development of a concentration gradient in response to a temperature gradient. The magnitude of the effect is described by the Soret coefficient (S_T) (Duhr and Braun 2006 [DIRS 183865], p. 19,678):

$$S_T\,(\mathrm{K}^{-1}) = D_T/D \qquad \text{(Eq. 2.1.11.10.0A-1)}$$

where D_T is the thermodiffusion coefficient, and D is the diffusion coefficient. Because of thermodiffusion, a concentration gradient will develop in response to the temperature gradient, as described by Duhr and Braun (2006 [DIRS 183865], p. 19,678):

$$c / c_o = \exp\left[-S_T\left(T - T_o\right)\right] \qquad \text{(Eq. 2.1.11.10.0A-2)}$$

where the concentration c is normalized to the concentration c_o at temperature T_o. In general, ions diffuse from the hotter region to the cooler; therefore, in the EBS, the Soret effect could potentially result in more rapid diffusion of radionuclides out of the hot waste package or from the hotter top of the invert towards the cooler bottom. The magnitude of the effect is dependent upon, for any given species, the Soret coefficient and the magnitude of the thermal gradient ($T - To$). In general, this effect is small. According to Bird et al. (1960 [DIRS 103524], pp. 565 to 567), "The thermal diffusion term [Soret effect] describes the tendency for species to diffuse under the influence of a temperature gradient; this effect is quite small." This is corroborated by Hirschfelder et al. (1964 [DIRS 171800], p. 8), who state, "Diffusion may also result from a temperature gradient (thermal diffusion or the Soret effect), and the transfer of energy may also result from a concentration gradient (diffusion thermo or Dufour effect). These are small effects."

The small thermal conductivity of the invert results in large temperature gradients relative to other locations in the EBS (SNL 2008 [DIRS 184433], Section 6.3.11). Thermal gradients within the repository will be greatest soon after closure, when the maximum thermal response occurs in the repository. Later in time, as the repository cools, the thermal gradients within the EBS are reduced. Sensitivity analyses in *Multiscale Thermohydrologic Model* (SNL 2008 [DIRS 184433], Section 6.3.11), using different invert hydrologic parameters, indicate that a typical temperature difference just after the drift wall boiling period, from the top to the bottom of the invert, a distance of approximately 1.3 m (SNL 2007 [DIRS 179354], Table 4-1, Parameter Number 01-10), is on the order of 5°C. The gradient decreases with time and after a few thousand years is less than a 1°C.

Typical Soret coefficients for aqueous solutions are on the order of 0.001 to 0.01 K^{-1} (Platen 2006 [DIRS 183864], p. 5). These general values are corroborated by data from Snowden and Turner 1960 [DIRS 183867], Table 1), Thornton and Seyfried (1983 [DIRS 183866], Table 1), and Petit et al. (1986 [DIRS 183863], Table II). Using the maximum expected thermal gradient of 5°C, this corresponds to an increase in the diffusion rate through the invert of 0.5% to 5% (Equation 2.1.11.10.0A-1). This is negligible relative to the range of uncertainty in the invert diffusion coefficient that is implemented in *EBS Radionuclide Transport Abstraction* (SNL 2007 [DIRS 177407], Equation 6.3.4.1.1-22 and Figure 6.3-4), which spans a factor of 10. Hence, the Soret effect is considered to be insignificant and is not implemented by TSPA.

An evaluation to determine the potential for sorption coefficients to vary with temperature on substrates (tuff and hematite) relevant to the repository was done, as discussed in *Radionuclide Transport Models Under Ambient Conditions* (SNL 2007 [DIRS 177396], Appendix I). Measurements at various temperatures of K_d for sorption of barium (a proxy for radium), cesium, strontium, and neptunium on Yucca Mountain tuff are reported, respectively, in

DTNs: LA0010JC831341.001 [DIRS 162476], LA0010JC831341.002 [DIRS 153321], LA0010JC831341.003 [DIRS 153322], and LA0010JC831341.007 [DIRS 153319]. It was concluded that the effect of temperature on sorption coefficients is minor, and that sorption generally increases with increasing temperature. Hence, the use of sorption coefficients of the radioelements measured at ambient temperatures should be applicable and generally bounding, and the effect of temperature on sorption coefficients need not be considered in modeling radionuclide transport in the near-field of the repository.

Based on the previous discussion, omission of FEP 2.1.11.10.0A (Thermal Effects on Transport in EBS) will not result in a significant adverse change in the magnitude or timing of either radiological exposure to the RMEI or radionuclide releases to the accessible environment. Therefore, this FEP is excluded from the performance assessments conducted to demonstrate compliance with proposed 10 CFR 63.311 and 63.321 (70 FR 53313 [DIRS 178394]), and with 10 CFR 63.331 [DIRS 180319], on the basis of low consequence.

INPUTS:

Table 2.1.11.10.0A-1. Direct Inputs

Input	Source	Description
Bird et al. 1960. *Transport Phenomena*. [DIRS 103524]	pp. 565 to 567	The thermal diffusion term [Soret effect] describes the tendency for species to diffuse under the influence of a temperature gradient; this effect is quite small
DTN: LA0010JC831341.001. Radionuclide Retardation Measurements of Sorption Distribution Coefficients for Barium. [DIRS 162476]	file: *la0010jc831341_001_ S00420_001.zip*	Radionuclide retardation measurements of sorption distribution coefficients for barium
DTN: LA0010JC831341.002. Radionuclide Retardation Measurements of Sorption Distribution Coefficients for Cesium. [DIRS 153321]	Table S00421_001	Radionuclide retardation measurements of sorption distribution coefficients for cesium
DTN: LA0010JC831341.003. Radionuclide Retardation Measurements of Sorption Distribution Coefficients for Strontium. [DIRS 153322]	Table S00422_001	Radionuclide retardation measurements of sorption distribution coefficients for strontium
DTN: LA0010JC831341.007. Radionuclide Retardation Measurements of Sorption Distribution Coefficients for Neptunium. [DIRS 153319]	Table S00426_001	Radionuclide retardation measurements of sorption distribution coefficients for neptunium
Platten 2006. "The Soret Effect: A Review of Recent Experimental Results." [DIRS 183864]	p. 5	Typical range for Soret coefficients (0.01 to 0.001 K^{-1})
SNL 2007. *Total System Performance Assessment Data Input Package for Requirements Analysis for EBS In-Drift Configuration*. [DIRS 179354]	Table 4-1, Parameter Number 01-10	The top to the bottom of the invert is a distance of approximately 1.3 m

Table 2.1.11.10.0A-2. Indirect Inputs

Citation	Title	DIRS
70 FR 53313	Implementation of a Dose Standard After 10,000 Years	178394
Bird et al. 1960	*Transport Phenomena*	103524
Duhr and Braun 2006	"Why Molecules Move Along a Temperature Gradient."	183865
Hirschfelder et al. 1964	*Molecular Theory of Gases and Liquids*	171800
Petit et al. 1986	"The Soret Effect in Dilute Aqueous Alkaline Earth and Nickel Chloride Solutions at 25°C"	183863
SNL 2007	*EBS Radionuclide Transport Abstraction*	177407
SNL 2007	*Radionuclide Transport Models Under Ambient Conditions*	177396
SNL 2008	*Multiscale Thermohydrologic Model*	184433
Snowdon and Turner 1960	"The Soret Effect in Some 0·01 Normal Aqueous Electrolytes"	183867
Thornton and Seyfried 1983	"Thermodiffusional Transport in Pelagic Clay: Implications for Nuclear Waste Disposal in Geological Media"	183866

FEP: 2.1.12.01.0A

FEP NAME:

Gas Generation (Repository Pressurization)

FEP DESCRIPTION:

Gas generation in the repository might lead to pressurization of the repository, produce multiphase flow, and affect radionuclide transport. This FEP addresses repository pressurization.

SCREENING DECISION:

Excluded – low consequence

SCREENING JUSTIFICATION:

Gas may be generated in the repository by a variety of mechanisms. Waste form radioactive decay may result in helium gas production (excluded FEP 2.1.12.02.0A (Gas Generation (He) from Waste Form Decay)); waste package corrosion may generate hydrogen gas (excluded FEP 2.1.12.03.0A (Gas Generation (H_2) from Waste Package Corrosion)); microbial degradation of EBS materials may lead to the generation of gases (CO_2, CH_4, H_2S) (excluded FEP 2.1.12.04.0A (Gas Generation (CO_2, CH_4, H_2S) from Microbial Degradation)); and gas may be generated by radiolysis (excluded FEP 2.1.13.01.0A (Radiolysis)). After the waste packages are breached, gas release and continuing gas generation could conceivably lead to gas pressurization of the repository and affect radionuclide transport.

Gas is not expected to cause repository gas pressures to increase, given the repository's lithologic setting. As discussed in *Drift Degradation Analysis* (BSC 2004 [DIRS 166107], Section 6.1.4), the repository is situated in the Topopah Spring Welded Tuff, which is heavily fractured, allowing gases to escape the repository. Changes to the fluid-flow characteristics of the flow system in the mountain could be produced by thermally driven mechanical and chemical processes. This could produce a condensation cap in the drift (BSC 2005 [DIRS 172232], Section 6.1.1) that may result in gas accumulation under the cap. A condensation cap could form above the repository due to heat-driven reflux processes. With continuous heating, a hot dry zone may develop that is characterized by a continuous process of boiling, vapor transport, condensation, and migration of water back toward the heat source, either by capillary forces or gravity drainage. The dry out zone extends approximately 5 to 10 m from the drift wall. The drift spacing is large relative to the dry out zone, which allows the water above the repository to drain between drifts where the rock remains below boiling. The effects of condensation caps are confined to the thermal period, after which the maximum rock temperatures are always below boiling (BSC 2005 [DIRS 172232], Section 6.2.2.1.3). The relatively short-lived heat-driven reflux potentially resulting in the formation of a condensation cap is a dynamic process that does not preclude the diffusion of gasses through the drift wall, convection of gasses along thermal gradients within the drifts, and movement through fractures laterally and below the drifts. Thus, gases are not expected to accumulate under condensation caps.

Additional corroborative evidence for the relative permeability (with respect to gases) of the repository host unit and of the mountain as a whole is presented in *Hydrogeology of the Unsaturated Zone, North Ramp Area of the Exploratory Studies Facility, Yucca Mountain, Nevada* (Rousseau et al. 1999 [DIRS 102097], p. 55), which describes variations in the pressure of the gas phase in the unsaturated zone due to barometric pumping. Changes in gas and water vapor pressures at the repository level are driven by changes in the atmospheric barometric pressure, and are transmitted primarily through the connected fracture network (Rousseau et al. 1999 [DIRS 102097], p. 56). This shows that any gases generated in the repository horizon will migrate away from the emplacement drift into the unsaturated fractures of the host rock, thus preventing significant gas pressure buildup in the drift.

Based on the previous discussion, omission of FEP 2.1.12.01.0A (Gas Generation (Repository Pressurization)) will not result in a significant adverse change in the magnitude or timing of either radiological exposure to the RMEI or radionuclide releases to the accessible environment. Therefore, this FEP is excluded from the performance assessments conducted to demonstrate compliance with proposed 10 CFR 63.311 and 63.321 (70 FR 53313 [DIRS 178394]), and with 10 CFR 63.331 [DIRS 180319], on the basis of low consequence.

INPUTS:

Table 2.1.12.01.0A-1. Direct Inputs

Input	Source	Description
BSC 2004. *Drift Degradation Analysis*. [DIRS 166107]	Section 6.1.4	Pervasive fracture network in the rock mass
BSC 2005. *Drift-Scale Coupled Process (DST and TH Seepage) Models*. [DIRS 172232]	Section 6.2.2.1.3	The effects of condensation caps are confined to the thermal period, after which the maximum rock temperatures are always below boiling

Table 2.1.12.01.0A-2. Indirect Inputs

Citation	Title	DIRS
10 CFR 63	Energy: Disposal of High-Level Radioactive Wastes in a Geologic Repository at Yucca Mountain, Nevada	180319
70 FR 53313	Implementation of a Dose Standard After 10,000 Years	178394
BSC 2005	*Drift-Scale Coupled Process (DST and TH Seepage) Models*	172232
Rousseau et al. 1999	*Hydrogeology of the Unsaturated Zone, North Ramp Area of the Exploratory Studies Facility, Yucca Mountain, Nevada*	102097

FEP: 2.1.12.02.0A

FEP NAME:

Gas Generation (He) from Waste Form Decay

FEP DESCRIPTION:

Helium (He) gas production may occur by alpha decay in the waste. Helium production might cause local pressure buildup in cracks in the fuel and in the void between fuel and cladding, leading to cladding and waste package failure.

SCREENING DECISION:

Excluded – low consequence

SCREENING JUSTIFICATION:

Commercial SNF and DOE SNF (other than naval SNF) cladding is considered to be breached upon emplacement in the repository and will neither inhibit groundwater contacting the fuel matrix nor the release of radionuclides from the fuel after groundwater contact (included FEPs 2.1.02.12.0A (Degradation of Cladding Prior to Disposal); 2.1.02.23.0A (Cladding Unzipping), and 2.1.02.25.0A (DSNF Cladding)). Therefore, even if gas generation (helium) from waste form decay were to cause cladding degradation, the additional impact of this FEP on cladding (other than naval SNF cladding) performance is of low consequence and will not affect the magnitude or timing of calculated radiological exposures to the RMEI or radionuclide releases to the accessible environment. Naval SNF cladding is discussed in included FEP 2.1.02.25.0B (Naval SNF Cladding).

For failed rods, the helium would be released into the waste package, possibly increasing the pressure therein. However, as illustrated by the following discussion for a commercial SNF waste package, the potential addition of decay-derived helium gas to the waste package void volume would not have a significant effect on the internal waste package pressure.

The radionuclides that are the major sources of decay-derived helium in SNF are: ^{244}Cm, ^{238}Pu, ^{239}Pu, ^{240}Pu, and ^{241}Am (Piron 2001 [DIRS 162396], Section 5.1.2). The decay-derived helium will accumulate in the fuel pellet matrix because these radionuclides are embedded in the fuel matrix and the because most of the alpha particles from their decay are stopped within the fuel matrix. Because of the long half-lives of some of these radionuclides, the decay-derived helium will continue to accumulate in the fuel matrix for a long time after disposal. Even if the helium accumulated for 10,000 years from alpha decay in a fuel rod with a burnup of 47.5 GWd/MTU is assumed to be completely released from the fuel matrix into the gap region between the fuel pellets and the cladding, the pressure increase in the gap would be about 90 bars at 20°C (Piron and Pelletier 2001 [DIRS 165318], Section 5.3.2.4.1). If this helium were to be released from the fuel rods into the void volume of the waste package, the pressure increase in the waste package would be about one bar at 20°C, assuming that the gap volume is about 13 cm^3 (Piron and Pelletier 2001 [DIRS 165318], Section 5.3.2.4.1) and the available void volume for helium expansion in the waste package is about 4,737 liters (SNL 2007 [DIRS 180506], Table 6-3[a]).

This result is obtained when the ideal gas law is used to estimate the pressure in the waste package assuming release of the decay-derived helium that has accumulated for 10,000 years from the 4,368 fuel rods in a commercial SNF waste package containing 21 fuel assemblies each containing 208 fuel rods (i.e., 13 cm^3/rod × 4,368 rods = 56.8 liters). The pressure increase at 20°C is given by: 90 bar × 56.8 liters/waste package / (56.8 liters + 4,737 liters) = 1.1 bar. The corresponding pressure increase at a more relevant 10,000-year temperature of 50°C would be less than 1.2 bar or (1.2 bars × 14.504 psia per bar (Perry et al. 1984 [DIRS 125806], Table 1-6)) 17.4 psia. Such a pressure increase is small compared to the design pressure limit (140 psia at 707°F) (SNL 2007 [DIRS 179394], Table 4-1, Parameter Number 03-06) and would therefore have a negligible effect on the waste package. The combined effects of decay helium and other gasses on the internal waste package temperatures are addressed in included FEP 2.1.03.07.0A (Mechanical Impact on Waste Package). Because the codisposal waste packages containing HLW glass and DOE SNF (other than naval SNF) have a much smaller inventory of the radionuclides that can produce decay-derived helium compared to the commercial SNF waste packages (SNL 2008 [DIRS 180472], Table 7-1[a]), the potential pressurization effects of decay-derived helium on the codisposal waste packages is also expected to be negligible.

Helium is an inert gas and will not chemically react with in-package components (internals, cladding or UO_2 pellets). The effects of microcracking due to pressure buildup in gas bubbles within the fuel matrix on the rate of matrix corrosion are expected to be negligible. As described in Sections 6.2.1 and 6.2.2 of *CSNF Waste Form Degradation: Summary Abstraction* (BSC 2004 [DIRS 169987]), evidence from commercial SNF testing indicates that the corrosion process is a general corrosion process occurring predominantly at the periphery of the fuel fragments; the rate of the process is not significantly influenced by microcracks in the fuel matrix.

Based on the previous discussion, omission of FEP 2.1.12.02.0A (Gas Generation (He) from Waste Form Decay) will not result in a significant adverse change in the magnitude or timing of either radiological exposure to the RMEI or radionuclide releases to the accessible environment. Therefore, this FEP is excluded from the performance assessments conducted to demonstrate compliance with proposed 10 CFR 63.311 and 63.321 (70 FR 53313 [DIRS 178394]), and with 10 CFR 63.331 [DIRS 180319], on the basis of low consequence.

INPUTS:

Table 2.1.12.02.0A-1. Direct Inputs

Input	Source	Description
BSC 2004. *CSNF Waste Form Degradation: Summary Abstraction*. [DIRS 169987]	Sections 6.2.1, 6.2.2	Evidence from commercial SNF testing indicates corrosion process is a general corrosion process occurring predominantly at periphery of fuel fragments
Perry et al. 1984. *Perry's Chemical Engineers' Handbook*. [DIRS 125806]	Table 1-6	Conversion: 14.504 psia per bar
Piron and Pelletier 2001. "State of the Art on the Helium Issues." [DIRS 165318]	Section 5.3.2.4.1	The decay helium gas pressure is 90 bars at 20°C for a commercial spent nuclear fuel rod with a gap volume of 13 cm^3 and a burnup of 47.5 GWd/MTU after 10,000 years
SNL 2007. *In-Package Chemistry Abstraction*. [DIRS 180506]	Table 6-3[a]	Available void volume for helium expansion in the waste package is about 4,737 liters
SNL 2007. *Total System Performance Assessment Data Input Package for Requirements Analysis for TAD Canister and Related Waste Package Overpack Physical Attributes Basis for Performance Assessment*. [DIRS 179394]	Table 4-1, Parameter Number 03-06	Design pressure limit (140 psia at 707°F)

Table 2.1.12.02.0A-2. Indirect Inputs

Citation	Title	DIRS
10 CFR 63	Energy: Disposal of High-Level Radioactive Wastes in a Geologic Repository at Yucca Mountain, Nevada	180319
70 FR 53313	Implementation of a Dose Standard After 10,000 Years	178394
Piron 2001	"Presentation of the Key Scientific Issues for the Spent Nuclear Fuel Evolution in a Closed System"	162396
SNL 2007	*Initial Radionuclides Inventory*	180472

FEP: 2.1.12.03.0A

FEP NAME:

Gas Generation (H_2) from Waste Package Corrosion

FEP DESCRIPTION:

Gas generation can affect the mechanical behavior of the host rock and engineered barriers, chemical conditions, and fluid flow, and, as a result, the transport of radionuclides. Gas generation due to oxic corrosion of waste packages, cladding, and/or structural materials will occur at early times following closure of the repository. Anoxic corrosion may follow the oxic phase if all oxygen is depleted.

SCREENING DECISION:

Excluded – low consequence

SCREENING JUSTIFICATION:

This FEP discussion involves the potential impact of hydrogen gas generation on the waste package, cladding, and internal structure of the waste package through chemical processes. The screening justification is based on the kinetic aspect of hydrogen gas production due to metal corrosion, and the possible interaction of generated hydrogen with the waste package and cladding materials, and the surrounding atmosphere.

The waste package outer barrier material, Alloy 22 (UNS N06022) (SNL 2007 [DIRS 179567], Table 4-1, Parameter Number 03-03), is extremely corrosion resistant because it forms a highly protective oxide film that protects it from further corrosion, and the observed general corrosion rate of the waste package outer barrier under repository-relevant environments is very low, on the order of nanometers per year (SNL 2007 [DIRS 178519], Section 8.2, and Figures 6-26 to 6-27). The low general corrosion rate of Alloy 22 will lead to a very low rate of hydrogen gas generation in the oxic repository.

A fraction of the total amount of hydrogen produced will be adsorbed and then absorbed by the metals in the emplacement drift as atomic hydrogen (the extent of absorption will depend on the hydrogen absorption efficiency of the metal under the prevailing environmental conditions) potentially forming metal hydride phase(s), and the balance will evolve as hydrogen gas (i.e., as molecular hydrogen) into the surrounding environment. Almost all of the evolved hydrogen gas (i.e., undissolved molecular hydrogen) is expected to be diffused out (under a concentration gradient) and barometrically pumped out of the drift via fractures in the host rocks of the repository. Under this situation, hydrogen buildup leading to internal pressurization of the drift is not expected to occur (see also excluded FEP 2.1.12.01.0A (Gas Generation (Repository Pressurization)). Since the internal pressure of the repository remains unaltered, and there are no known chemical reactions between hydrogen and host rock materials, mechanical properties of the repository host rocks and hence fluid flow through these rocks will not be impacted. Further, due to lack of hydrogen pressure buildup in the repository, absorption of waste package general corrosion-produced hydrogen into the drip shield will be negligible. This is expected per

Sievert's law, which states that the concentration of absorbed hydrogen in a metal is directly proportional to the square root of hydrogen gas pressure outside the metal (ASM International 1987 [DIRS 103753], p. 329). Hydrogen incorporation into the waste package and drip shield materials is further evaluated in excluded FEPs 2.1.03.04.0A (Hydride Cracking of Waste Packages) and 2.1.03.04.0B (Hydride Cracking of Drip Shields).

In the event of waste package failure, water will gain access to the stainless steel inner vessel. If the inner vessel also breaches, then water will contact the waste package contents (e.g., TAD canister, structural components, and cladding). Corrosion of these materials will also produce hydrogen at a rate controlled by their corrosion rates and likely limited by the amount of water available, but with low consequence. Hydrogen production from aqueous corrosion of waste package materials (the TAD canister, waste package internals, and the cladding) will not have a significant impact on in-package chemistry, particularly in terms of radionuclide release from the waste form This is because the hydrogen gas is expected to quickly exit the through the openings of the failed waste package, also because a more-reducing environment (due to the presence of hydrogen gas) is expected to inhibit the dissolution of fuel (SNL 2007 [DIRS 177418]). In addition, corrosion-generated hydrogen will be consumed through the following physicochemical processes:

- A portion of the total hydrogen produced from aqueous corrosion of the waste package metal(s) will be first adsorbed onto the metal surface and then absorbed in the metal as atomic hydrogen, and the balance will be evolved as molecular hydrogen.

- A portion of molecular hydrogen evolved may exit the waste package without reacting with anything within the waste package and diffuse (under concentration gradient) out of the drift via fractures of the host rocks.

- As molecular hydrogen is slightly soluble (a few parts-per-million) in water (Lide 2006 [DIRS 178081], p. 8-81), a small portion of molecular hydrogen retained in the waste package will remain dissolved in water.

Commercial SNF and DOE SNF (other than naval SNF) cladding is considered to be breached upon emplacement in the repository and will neither inhibit groundwater contacting the fuel matrix nor the release of radionuclides from the fuel after groundwater contact (included FEPs 2.1.02.12.0A (Degradation of Cladding Prior to Disposal); 2.1.02.23.0A (Cladding Unzipping), and 2.1.02.25.0A (DSNF Cladding)). Furthermore, following waste package failure, immediate exposure of bare fuel to the waste package environment is assumed to take place (included FEP 2.1.02.23.0A (Cladding Unzipping)). Therefore, the incremental impact of corrosion-generated hydrogen gas on cladding will be insignificant.

The effect of hydrogen produced from radiolysis of water is discussed in excluded FEP 2.1.13.01.0A (Radiolysis).

In summary, hydrogen gas production due to oxic and anoxic corrosion of waste package materials is not expected to cause repository gas pressure to increase because the repository's fractured host rock is connected to the atmosphere. Pressurization of the repository due to gas pro duction is further discussed in excluded FEP 2.1.12.01.0A (Gas Generation (Repository

Pressurization)). Any credible potential for hydrogen gas leading to explosion is excluded by FEP 2.1.12.08.0A (Gas Explosions in EBS).

Based on the previous discussion, omission of FEP 2.1.12.03.0A (Gas Generation (H_2) From Waste Package Corrosion) will not result in a significant adverse change in the magnitude or timing of either radiological exposure to the RMEI or radionuclide releases to the accessible environment. Therefore, this FEP is excluded from the performance assessments conducted to demonstrate compliance with proposed 10 CFR 63.311 and 63.321 (70 FR 53313 [DIRS 178394]), and with 10 CFR 63.331 [DIRS 180319], on the basis of low consequence.

INPUTS:

Table 2.1.12.03.0A-1. Direct Inputs

Input	Source	Description
ASM International 1987. *Corrosion*. [DIRS 103753]	p. 329	Sievert's law, which states that the concentration of absorbed hydrogen in a metal is directly proportional to the square root of hydrogen gas pressure outside the metal
Lide 2006. *CRC Handbook of Chemistry and Physics*. [DIRS 178081]	p. 8-81	Molecular hydrogen is slightly soluble (a few parts-per-million) in water
SNL 2007. *General Corrosion and Localized Corrosion of Waste Package Outer Barrier*. [DIRS 178519]	Section 8.2	Discussion of general corrosion rate of waste package

Table 2.1.12.03.0A-2. Indirect Inputs

Citation	Title	DIRS
10 CFR 63	Energy: Disposal of High-Level Radioactive Wastes in a Geologic Repository at Yucca Mountain, Nevada	180319
70 FR 53313	Implementation of a Dose Standard After 10,000 Years	178394
SNL 2007	*Dissolved Concentration Limits of Elements with Radioactive Isotopes*	177418
SNL 2007	*Total System Performance Assessment Data Input Package for Requirements Analysis for DOE SNF/HLW and Navy SNF Waste Package Overpack Physical Attributes Basis for Performance Assessment*	179567

FEP: 2.1.12.04.0A

FEP NAME:

Gas Generation (CO_2, CH_4, H_2S) from Microbial Degradation

FEP DESCRIPTION:

Microbes are known to produce inorganic acids, methane, organic byproducts, carbon dioxide, and other chemical species that could change the longevity of materials in the repository and the transport of radionuclides from the near-field. The rate of microbial gas production will depend on the nature of the microbial populations established, the prevailing conditions (temperature, pressure, geochemical conditions), and the organic or inorganic substrates present. Initial analysis indicates the most important source of nutrient in the YMP repository will be metals. Other possible nutrients include cellulosic material, plastics, and synthetic materials. Minimal amounts of organics are mandated by regulation.

SCREENING DECISION:

Excluded – low consequence

SCREENING JUSTIFICATION:

The unsaturated zone communicates with the atmosphere, which will prevent any gas produced at the repository horizon from accumulating. This is discussed in more detail in excluded FEP 2.1.12.06.0A (Gas Transport in EBS). Microbiological activity inside the EBS, as discussed in excluded FEP 2.1.10.01.0A (Microbial Activity in EBS), is excluded from TSPA because early temperatures and long-term nutrient constraints will limit microbial activity. The presence of organic/cellulosic materials in the waste packages will be limited by design controls. Control and specification of technical information needs on the organic content of sealed waste form canisters (DOE 2007 [DIRS 169992], Sections 4.2.6, 5.4.1B(4), and 5.4.3.C) and waste form and TAD canister design parameters (SNL 2007 [DIRS 179394], Table 4-1) will be used to confirm consistency between the contents of the waste form canisters emplaced in the repository and the technical basis for the TSPA. Moreover, requirements have been established to prevent undesirable materials (e.g., organics/cellulosics) that could have an adverse impact on postclosure performance from being left in the drift. These requirements are discussed in *Total System Performance Assessment Data Input Package for Requirements Analysis for Subsurface Facilities* (SNL 2007 [DIRS 179466], Table 4-1, Parameter Number 02-03) and excluded FEP 1.1.02.03.0A (Undesirable Materials Left).

CO_2, CH_4, H_2S, and ammonia are gases that are produced by microbial activity. Under the oxidizing conditions of the repository, carbon dioxide would be most prevalent. Any generation of CO_2 by microorganisms present inside of breached waste packages would tend to be dissipated by diffusion and/or advection from waste packages. Moreover, calculations in *In-Package Chemistry Abstraction* (SNL 2007 [DIRS 180506], Section 6.6.3[a]) indicate that order of magnitude variations in carbon dioxide partial pressures have minor effects on in-package chemistry (i.e., pH and ionic strength). The CO_2 ranges over which TSPA calculates probability distributions for radionuclide solubilities (maximum values are 100 times

atmospheric levels) correspond to maximal levels seen in organic-rich soils. Therefore, any additional effects on radionuclide solubilities from high carbon dioxide levels from microbial degradation are expected to be minor.

Evaluation of Potential Impacts of Microbial Activity on Drift Chemistry (BSC 2004 [DIRS 169991], Section 6.5) suggests that the low levels of organic carbon in the system will limit any CO_2, CH_4, and H_2S elevation in the drift (BSC 2004 [DIRS 169991], Section 6.1.3 and Table 6.1-2). Furthermore, the oxidizing conditions in the repository will limit the formation of substantial quantities of H_2S (BSC 2004 [DIRS 169991], Section 6.4.2).

All waste packages will be dried and backfilled with helium, then sealed (SNL 2007 [DIRS 179394], Table 4-1, Parameter Number 04-04). This will result in low water availability, which will limit microbial activity inside the waste package prior to breach. Any postbreach microbial degradation of waste form and waste package materials will produce gases that will diffuse and disperse in the drift atmosphere.

Gas pressurization of the repository due to the production of gases such as CO_2, CH_4, and H_2S is discussed in excluded FEP 2.1.12.01.0A (Gas generation (Repository Pressurization)), which is excluded on the basis of low consequence. The possibility of chemical reaction between methane (and/or hydrogen sulfide) gas with atmospheric oxygen is discussed in excluded FEP 2.1.12.08.0A (Gas Explosions in EBS).

Based on the previous discussion, omission of FEP 2.1.12.04.0A (Gas Generation (CO_2, CH_4, H_2S) from Microbial Degradation) will not result in a significant adverse change in the magnitude or timing of either radiological exposure to the RMEI or radionuclide releases to the accessible environment. Therefore, this FEP is excluded from the performance assessments conducted to demonstrate compliance with proposed 10 CFR 63.311 and 63.321 (70 FR 53313 [DIRS 178394]), and with 10 CFR 63.331 [DIRS 180319], on the basis of low consequence.

INPUTS:

Table 2.1.12.04.0A-1. Direct Inputs

Input	Source	Description
BSC 2004. *Evaluation of Potential Impacts of Microbial Activities on Drift Chemistry*. [DIRS 169991]	Sections 6.1.3, 6.4.2, 6.5; Table 6.1-2	Environmental factors will limit microbial activity during/immediately after the thermal pulse; no significant impact on repositiry chemistry; oxidizing conditions preclude the formation of significant H_2S
DOE 2007. *Waste Acceptance System Requirements Document*. [DIRS 169992]	Sections 4.2.6, 5.4.1B(4), 5.4.3.C	Control and specification of technical information needs on the organic content of sealed waste form canisters
SNL 2007. *In-Package Chemistry Abstraction*. [DIRS 180506]	Section 6.6.3[a]	Calculations indicate that order of magnitude variations in carbon dioxide partial pressures have minor effects on in package chemistry
SNL 2007. *Total System Performance Assessment Data Input Package for Requirements Analysis for Subsurface Facilities*. [DIRS 179466]	Table 4-1, Parameter Number 02-03	All waste packages will be dried and backfilled with helium, then sealed
SNL 2007. *Total System Performance Assessment Data Input Package for Requirements Analysis for TAD Canister and Related Waste Package Overpack Physical Attributes Basis for Performance Assessment*. [DIRS 179394]	Table 4-1, Parameter Number 04-04	All waste packages will be dried and backfilled with helium, then sealed

Table 2.1.12.04.0A-2. Indirect Inputs

Citation	Title	DIRS
10 CFR 63	Energy: Disposal of High-Level Radioactive Wastes in a Geologic Repository at Yucca Mountain, Nevada	180319
70 FR 53313	Implementation of a Dose Standard After 10,000 Years	178394
SNL 2007	*Total System Performance Assessment Data Input Package for Requirements Analysis for TAD Canister and Related Waste Package Overpack Physical Attributes Basis for Performance Assessment*	179394

FEP: 2.1.12.06.0A

FEP NAME:

Gas Transport in EBS

FEP DESCRIPTION:

Gas in the waste and EBS could affect the long-term performance of the disposal system. Radionuclides may be transported as gases or in gases. Gas bubbles may affect flow paths, and two-phase flow conditions may be important.

SCREENING DECISION:

Excluded – low consequence

SCREENING JUSTIFICATION:

This FEP is focused on gas transport in the EBS. Related to this FEP is excluded FEP 2.2.11.03.0A (Gas Transport in Geosphere), which is concerned with the low consequence of gas transport in the geosphere. Gas pressurization of the repository is discussed under FEP 2.1.12.01.0A (Gas Generation (Repository Pressurization)), which is excluded on the basis of low consequence.

Several potential sources of gas in the waste package and EBS include: (1) air (O_2, N_2, Ar, CO_2, H_2, etc.), present at closure and circulated through convection and diffusion during the life of the repository; (2) gases produced from microbial processes (CO_2, CH_4, H_2S) (excluded FEP 2.1.12.04.0A (Gas Generation (CO_2, CH_4, H_2S) from Microbial Degradation)); (3) gases produced from waste form and EBS component degradation; (4) fission product gases (argon, xenon, krypton); (5) helium from initial fuel rod manufacture and waste form decay (excluded FEP 2.1.12.02.0A (Gas Generation (He) from Waste Form Decay)); (6) H_2 from waste package corrosion (excluded FEP 2.1.12.03.0A (Gas Generation (H_2) from Waste Package Corrosion)); and (7) gas generated by radiolysis – e.g., H_2 (excluded FEP 2.1.13.01.0A (Radiolysis)) – and radioactive decay ($^{14}CO_2$ and radon).

The following discussion is in two parts: (1) gas and performance; and (2) gas bubbles and two-phase flow.

Gas and performance—The results of THC seepage model simulations and the evidence for barometric pumping indicate that the minor gas generation that results from microbial respiration, corrosion, radiolysis, and other in-drift processes will not accumulate to the point of having any impact on long-term performance. Gases that may be present in the repository or formed from various processes are expected to convect and diffuse into the drift walls, become diluted, and disperse throughout the surrounding rock (gas transport in the geosphere is discussed under excluded FEP 2.2.11.03.0A (Gas Transport in Geosphere)). Despite the large volume change associated with the phase transition from liquid water to vapor (a factor of ~1,600 at 100°C and 1 atmosphere, as given by Keenan et al. (1969 [DIRS 134666]), THC seepage model simulations show that pressures in fractures adjacent to the drift (which are nearly identical to

pressures in the drift) do not significantly increase during the boiling period. This is documented in THC seepage model outputs (SNL 2007 [DIRS 177404], Table 6.5-5; spreadsheets "*fract_81_162_dr_wn.xls*" (n = 0, 8, 9, 10, for different starting waters), worksheets "data1" and "data2"), and points to the high permeability of the host rock to gases.

Additional corroborative evidence for the relative permeability with respect to gases of the repository host unit and of the mountain as a whole is presented in *Hydrogeology of the Unsaturated Zone, North Ramp Area of the Exploratory Studies Facility, Yucca Mountain, Nevada* (Rousseau et al. 1999 [DIRS 102097], p. 55), which describes variations in the pressure of the gas phase in the unsaturated zone due to barometric pumping. Changes in gas and water vapor pressures at the repository level are driven by changes in the atmospheric barometric pressure, and are transmitted primarily through the connected fracture network (Rousseau et al. 1999 [DIRS 102097], p. 56).

High early repository temperatures, the primarily oxic environment, and a relative scarcity of water and organic carbon will combine to limit microbial activity and biogenic gases in the emplacement drifts, as demonstrated in *Evaluation of Potential Impacts of Microbial Activity on Drift Chemistry* (BSC 2004 [DIRS 169991], Section 6.4).

Aqueous transport will fully encompass any dose effects of gas-phase transport in the geosphere. The only radionuclides that would have a potential for gas transport are $^{14}CO_2$ and ^{222}Rn as discussed in excluded FEP 2.2.11.03.0A (Gas Transport in Geosphere). An analysis of the potential dose from gas-phase geosphere transport of $^{14}CO_2$ has been done for the individual maximum radiological dose rate. It was found that the dose from aqueous geosphere transport of $^{14}CO_2$ bounds the dose from gas-phase geosphere transport pathways. Aqueous geosphere transport pathways will also bound the dose from ^{222}Rn, primarily through aqueous transport of uranium and generation of ^{222}Rn as a decay product at the accessible environment (excluded FEP 2.2.11.03.0A (Gas Transport in Geosphere)).

Gas bubbles and two-phase flow—If the waste package and invert were to become largely saturated, gas bubbles in advecting water in the waste package and invert could potentially affect advective and diffusive flow paths. The most plausible situation is one in which bubbles could lodge in pore spaces or fractures, forcing diversion of flow to neighboring flow paths. However, this would occur on a very localized scale, given the very small quantities of gas anticipated. Bubble effects in the unsaturated zone are described in excluded FEP 2.2.11.02.0A (Gas Effects in the UZ).

As discussed in part of included FEP 2.2.10.10.0A (Two-phase Buoyant Flow/heat Pipes), two-phase buoyant flow may occur as a result of waste-generated heat. Two-phase circulation continues until the heat source is too weak to provide the thermal gradients required to drive it. Therefore, this process would be temporary and would shut down at some point during cooldown.

Note that included FEP 2.1.11.09.0C (Thermally Driven Flow (Convection) in Drifts) describes thermally driven flow (convection) in drifts.

Based on the previous discussion, omission of FEP 2.1.12.06.0A (Gas Transport in EBS) will not result in a significant adverse change in the magnitude or timing of either radiological exposure to the RMEI or radionuclide releases to the accessible environment. Therefore, this FEP is excluded from the performance assessments conducted to demonstrate compliance with proposed 10 CFR 63.311 and 63.321 (70 FR 53313 [DIRS 178394]), and with 10 CFR 63.331 [DIRS 180319], on the basis of low consequence.

INPUTS:

Table 2.1.12.06.0A-1. Direct Inputs

Input	Source	Description
BSC 2004. *Evaluation of Potential Impacts of Microbial Activities on Drift Chemistry*. [DIRS 169991]	Section 6.4	Impacts of in-drift microbial activities
SNL 2007. *Drift-Scale THC Seepage Model*. [DIRS 177404]	Table 6.5-5; spreadsheets: *fract_81_162_dr_wn.xls* (n = 0, 8, 9, 10, for different starting waters), worksheets: "data1" and "data2"	Total gas pressure in fractures at the drift wall

Table 2.1.12.06.0A-2. Indirect Inputs

Citation	Title	DIRS
10 CFR 63	Energy: Disposal of High-Level Radioactive Wastes in a Geologic Repository at Yucca Mountain, Nevada	180319
70 FR 53313	Implementation of a Dose Standard After 10,000 Years	178394
Keenan et al. 1969	*Steam Tables, Thermodynamic Properties of Water Including Vapor, Liquid, and Solid Phases (English Units)*	134666
Rousseau et al. 1999	*Hydrogeology of the Unsaturated Zone, North Ramp Area of the Exploratory Studies Facility, Yucca Mountain, Nevada*	102097

FEP: 2.1.12.07.0A

FEP NAME:

Effects of Radioactive Gases in EBS

FEP DESCRIPTION:

Radioactive gases may exist or be produced in the repository. These gases may subsequently escape from the repository. Typical radioactive gases include ^{14}C (in $^{14}CO_2$ and $^{14}CH_4$ produced during microbial degradation), tritium, fission gases (Ar, Xe, Kr), and radon.

SCREENING DECISION:

Excluded – low consequence

SCREENING JUSTIFICATION:

Generation of radioactive gases due to activation of emplacement drift air and host rock is estimated to be low. By correcting the calculated activity in *Radiological Releases Due to Air and Silica Dust Activation in Emplacement Drifts* (BSC 2003 [DIRS 164562], Table 5-10) for an infinite irradiation time for stagnant air, activation of emplacement drift air generates approximately 9.0×10^{-11} μCi/mL of ^{16}N and 7.4×10^{-9} μCi/mL of ^{41}Ar. The ^{16}N activity is identical to the value in Table 5-10 of *Radiological Releases Due to Air and Silica Dust Activation in Emplacement Drifts* (BSC 2003 [DIRS 164562]) at the exhaust shaft inlet because it represents the saturation activity (the maximum activity produced by activation without radioactive decay). The ^{41}Ar activity includes a correction factor of $1/(1\text{-}e^{-0.3787*0.252}) = \sim 11.0$ (BSC 2003 [DIRS 164562], Section 5.7.1, example) for the saturated activity. The resulting ^{41}Ar activity is estimated as: 6.7×10^{-10} μCi/mL (BSC 2003 [DIRS 164562], Table 5-10, at the exhaust shaft inlet) $\times$ 11.0 = 7.4×10^{-9} μCi/ml. Activation of host rock produces a saturation activity of 2.1×10^{-7} μCi/mL of ^{16}N at the drift wall (BSC 2003 [DIRS 164562], Table 5-11).

In units of g/mL, this amounts to 9.0×10^{-28} g/mL of ^{16}N and 1.7×10^{-22} g/mL of ^{41}Ar from neutron activation of air, and 2.1×10^{-24} g/mL of ^{16}N from neutron activation of host rock. These concentration values are for onset of waste package emplacement and will be less at the time of closure and will decrease further with time. These estimated quantities are negligible (compare to the density of air - 1.204×10^{-3} g/mL; (Weast 1985 [DIRS 111561], p. F-10, for 20°C and 760 mm mercury) and are, therefore, considered to be non-contributors to in-drift conditions and to radionuclide releases to the accessible environment.

The major gas constituents trapped inside a waste package prior to disposal will be the result of fission and neutron-activation, predominantly radioactive isotopes of the noble gases argon, xenon, and krypton (Manaktala 1993 [DIRS 101719], Section 3.3.6). Gasses in the gap fraction will be available for release upon clad failure. There are several arguments that support the exclusion of radioactive gases from TSPA calculations, based on low consequence to waste package internal pressures (see excluded FEP 2.1.03.07.0A (Mechanical Impact on Waste Package)) and low consequence with respect to radionuclide releases from the EBS, discussed

further here. Radioactive gases residing in fuel rods and waste packages prior to postclosure or produced after postclosure times will either decay rapidly or quickly become negligible. Argon, krypton, and radon were screened out due to short half-lives or low activity (Baum et al. 2002 [DIRS 175238], pp. 53 and 54; see also SNL 2007 [DIRS 177424], Table 4-3). Likewise, xenon is also negligible, since the half-lives of the xenon isotopes are on the order of just a few days at most (Parrington et al. 1996 [DIRS 103896], p. 35). Specifically:

A. Xenon (^{135}Xe), a fission yield-product, is short-lived (with a half-life of 9.1 hours) and will not be produced during the regulatory time period. It will undergo decay to its long-lived daughter ^{135}Cs by the time of waste emplacement.

B. Argon (^{39}Ar) has a low activity and is screened out due to low consequence. It will not be produced during the regulatory time period.

C. Of the noble gases, ^{85}Kr has a significant initial inventory, but because of its short half-life (approximately 11 years), its concentration and radioactivity level would rapidly become insignificant.

D. Radon gas (^{222}Rn and ^{219}Rn) is short-lived (with half-lives of approximately 3.8 days and 4 seconds, respectively), as are its gaseous daughters (^{218}Po, half-life approximately 3.1 minutes and ^{215}Po, half-life of microseconds) and, thus, will be in secular equilibrium with, respectively, radium (^{226}Ra) and actinium (^{227}Ac). Geosphere transport of radon has been excluded as discussed in excluded FEP 2.2.11.03.0A (Gas Transport in Geosphere) because the radon will decay to insignificant levels before reaching the accessible environment.

E. Tritium may be present in SNF as a result of neutron activation of impurities present in the fuel assemblies. Tritium has a half-life of about 12 years (Dean 1992 [DIRS 100722], Table 4.16), and because of its short half-life, its concentration and radioactivity level would rapidly become insignificant.

F. ^{14}C is formed from nitrogen in reactors through neutron capture and proton decay. The generation of the radioactive gases $^{14}CH_4$ and $^{14}CO_2$ from microbial activity (BSC 2004 [DIRS 169991], Sections 6.4, 6.5, and 7.1) is not significant because organic levels in the waste are expected to be low, and microbial activity in the waste package and the EBS is expected to be negligible (see excluded FEP 2.1.10.01.0A (Microbial Activity in EBS)). Moreover, methane as $^{14}CH_4$ is not expected to be produced by microbes as sustained anaerobic conditions would be required (BSC 2004 [DIRS 169991], Section 6.1.3; and excluded FEP 2.1.12.04.0A (Gas generation (CO_2, CH_4, H_2S) from Microbial Degradation)) yet oxidizing conditions will prevail in the in-drift environment over the long-term (SNL 2007 [DIRS 177412], Section 6.7.1).

Once a waste package is breached, an oxidizing environment is created within the waste package enabling $^{14}CO_2$ to be formed via chemical oxidation of any ^{14}C species present in the waste form. The limited amount of ^{14}C remaining in the inventory limits the potential creation of $^{14}CO_2$ to small amounts. Furthermore, the dose from ^{14}C transported as a gas to the accessible

environment will be extremely small, so the risk consequence is negligible (see excluded FEP 2.2.11.03.0A (Gas Transport in the Geosphere)).

In summary, the effects of radioactive gases in the EBS are negligible compared to overall radionuclide releases to the accessible environment.

Based on the previous discussion, omission of FEP 2.1.12.07.0A (Effects of Radioactive Gases in EBS) will not result in a significant adverse change in the magnitude or timing of either radiological exposure to the RMEI or radionuclide releases to the accessible environment. Therefore, this FEP is excluded from the performance assessments conducted to demonstrate compliance with proposed 10 CFR 63.311 and 63.321 (70 FR 53313 [DIRS 178394]), and with 10 CFR 63.331 [DIRS 180319], on the basis of low consequence.

INPUTS:

Table 2.1.12.07.0A-1. Direct Inputs

Input	Source	Description
Baum et al. 2002 *Nuclides and Isotopes*. [DIRS 175238]	pp. 53 and 54	Established fact
BSC 2003. *Radiological Releases Due to Air and Silica Dust Activation in Emplacement Drifts*. [DIRS 164562]	Section 5.7.1; Tables 5-10, 5-11	Generation of radioactive gases due to activation of emplacement drift air and host rock is estimated to be low

Table 2.1.12.07.0A-2. Indirect Inputs

Citation	Title	DIRS
10 CFR 63	Energy: Disposal of High-Level Radioactive Wastes in a Geologic Repository at Yucca Mountain, Nevada	180319
70 FR 53313	Implementation of a Dose Standard After 10,000 Years	178394
BSC 2004	*Evaluation of Potential Impacts of Microbial Activities on Drift Chemistry*	169991
Dean 1992	*Lange's Handbook of Chemistry*	100722
Manaktala 1993	*Characteristics of Spent Nuclear Fuel and Cladding Relevant to High-Level Waste Source Term*	101719
Parrington et al. 1996	*Nuclides and Isotopes, Chart of the Nuclides*	103896
SNL 2007	*Engineered Barrier System: Physical and Chemical Environment*	177412
SNL 2007	*Radionuclide Screening*	177424
Weast 1985	*CRC Handbook of Chemistry and Physics*	111561

FEP: 2.1.12.08.0A

FEP NAME:

Gas Explosions in EBS

FEP DESCRIPTION:

Explosive gas mixtures could collect in the sealed repository. An explosion in the repository could have radiological consequences if the structure of the repository were damaged or near-field processes enhanced or inhibited.

SCREENING DECISION:

Excluded – low probability

SCREENING JUSTIFICATION:

This FEP focuses on potential flammable gas generation in the EBS external to the waste package. Potential flammable gas generation inside of waste packages is considered in excluded FEP 2.1.02.08.0A (Pyrophoricity from DSNF), excluded FEP 2.1.13.01.0A (Radiolysis), and excluded FEP 2.1.02.29.0A (Flammable Gas Generation from DSNF).

Flammable gases that may be produced in the EBS include hydrogen (H_2) and methane (CH_4). Hydrogen would be produced from the radiolysis of water (H_2O) (Glass et al. 1986 [DIRS 105021]) or oxidation of metals under anaerobic conditions. Methane could be produced from the microbial action on organics or the metal containers under anaerobic conditions.

However, negligible quantities of methane and hydrogen could be maintained in the EBS atmosphere because the necessary anaerobic conditions will only exist in the earliest stages of the repository (SNL 2007 [DIRS 177412], Section 6.7.1). Moreover, because the repository is located in unsaturated rock units that are connected by a pervasive fracture network to the ground surface (BSC 2004 [DIRS 166107], Section 6.1.4), flammable gases will be dispersed into the much larger gas volume residing in and above the rock mass surrounding the drift. The lower explosive limits are 4.1vol % and 5.3 vol % for hydrogen and methane, respectively, in air at 25°C and one atmosphere total pressure (Dean 1992 [DIRS 100722], Table 5.22). Because gas concentrations in the drift will largely reflect those in the atmosphere, the likelihood of exceeding the lower explosive limits (Dean 1992 [DIRS 100722], Table 5.22) is insignificant. Therefore, the probability of an explosion occurring is zero.

This FEP is therefore excluded from the performance assessments conducted to demonstrate compliance with proposed 10 CFR 63.311 and 63.321 (70 FR 53313 [DIRS 178394]), and with 10 CFR 63.331 [DIRS 180319] on the basis of low probability.

INPUTS:

Table 2.1.12.08.0A-1. Direct Inputs

Input	Source	Description
BSC 2004. *Drift Degradation Analysis*. [DIRS 166107]	Section 6.1.4	Pervasive fracture network in the rock mass
Dean 1992. *Lange's Handbook of Chemistry*. [DIRS 100722]	Table 5.22	Lower explosion limit of hydrogen and methane
SNL 2007. *Engineered Barrier System: Physical and Chemical Environment*. [DIRS 177412]	Section 6.7.1	Anaerobic conditions will only exist in the earliest stages of the repository

Table 2.1.12.08.0A-2. Indirect Inputs

Citation	Title	DIRS
70 FR 53313	Implementation of a Dose Standard After 10,000 Years	178394
Glass et al. 1986	"Gamma Radiation Effects on Corrosion-I. Electrochemical Mechanisms for the Aqueous Corrosion Processes of Austenitic Stainless Steels Relevant to Nuclear Waste Disposal in Tuff"	105021

FEP: 2.1.13.01.0A

FEP NAME:

Radiolysis

FEP DESCRIPTION:

Alpha, beta, gamma, and neutron irradiation of water can cause disassociation of molecules, leading to gas production and changes in chemical conditions (potential, pH, and concentration of reactive radicals).

SCREENING DECISION:

Excluded – low consequence

SCREENING JUSTIFICATION:

Potential pressurization and/or fire caused by gases generated from radiolytic decomposition of water inside a waste package is excluded on the basis of low consequence, because the small amount of water in a dried and inerted TAD canister-bearing waste package will not generate sufficient gas to cause a problem. Enhanced corrosion of waste packages and drip shields due to the effects of beta-gamma radiolysis is excluded because beta-gamma radiation is intense enough to cause a problem only while the repository temperature is above boiling when little or no liquid water will be present on waste package or drip shield surfaces. The effects of radiolysis on the corrosion of commercial SNF and other internal waste package components is excluded on the basis of low consequence, since neither nitric acid nor hydrogen peroxide (H_2O_2) are expected to have a significant impact on in-package chemistry. The potential influence on radionuclide concentrations and mobilities due to H_2O_2 accumulation caused by long-term alpha radiolysis is excluded on the basis of low consequence.

Background

Strong radiation fields (alpha, beta, gamma, and neutron) originating from HLW can cause radiolysis (molecular disintegration caused by radiation) of water and other molecules (e.g., molecular nitrogen in the air). These effects have the potential to adversely affect repository performance in several ways. Radiolysis of water leads to formation of ions, radicals, and other potentially reactive species that can alter water chemistry (e.g., pH), radionuclide speciation, and effective redox potential. Such changes can accelerate corrosion of metals (e.g., drip shields and waste packages) and waste forms (e.g., commercial SNF and HLW glass), as well as enhancing solubilities and/or mobilities of radionuclides (and other potentially toxic elements). This FEP addresses the aqueous-chemical effects of radiolysis (including gas generation). Direct radiation damage to solids is discussed in excluded FEP 2.1.13.02.0A (Radiation Damage in EBS).

Radiolysis of water leads to the production of charged and uncharged species, with proportions depending largely on radiation type (alpha, beta-gamma, or neutron). The number of radiolytic species produced is described by a radiation-specific "G-value," which expresses the number of

molecules produced as a function of energy deposited (in air or water). Note that beta and gamma radiations are not distinguished experimentally (because one can generate the other) and a single G-value applies to the beta-gamma field. Radiolysis of air can produce water-soluble nitrogen oxides that can form aqueous nitric acid. In the absence of a compensating acid-consuming reaction (e.g., dissolution of certain solids), nitric acid production can lower pH, potentially increasing corrosion rates (Reed and Bowers 1990 [DIRS 113577]) and enhancing solubilities of radionuclide-bearing solids. Hydrogen peroxide (H_2O_2) is a strong oxidant under most conditions and has the potential to accelerate corrosion of drip shields and waste packages, as well as enhancing the degradation rate of spent fuel. Under aqueous conditions (in bulk solutions), anodic shifts in the open-circuit potential of stainless steel in gamma-irradiated solutions have been observed experimentally, and these shifts in potential have been shown to be due to the formation of hydrogen peroxide (SNL 2007 [DIRS 180778], Section 6.7.1), which means that H_2O_2 might also enhance corrosion of stainless-steel TAD canisters.

Whereas beta-gamma radiation tends to produce large quantities of highly reactive free radicals and ionic species, alpha radiation tends to produce primarily molecular species, predominantly H_2 and H_2O_2. Thus, in addition to chemical changes, radiolytic production of hydrogen gas poses the risk of potentially flammable quantities of H_2 being generated.

Much of the discussion that follows focuses on the effects of radiolysis associated with commercial SNF because commercial SNF constitutes the vast majority of waste packages destined for disposal and contains most of the radionuclide inventory on a per-package basis (SNL 2007 [DIRS 180472], Table 7-1[a]). Furthermore, most commercial SNF waste packages are thermally hotter (SNL 2008 [DIRS 184433], Table 6.2-6[a] and Section 6.3.16[a]) and are more radioactive (BSC 2004 [DIRS 172227], Section 6.4.2) than most codisposal packages containing HLW glass and DOE SNF. Moreover, failure of an MCO-type codisposal package due to a pyrophoric event is addressed in excluded FEP 2.1.02.08.0A (Pyrophoricity from DSNF) and is shown to be of low consequence. The MCO canisters containing N Reactor fuel may contain considerably more water at emplacement than commercial SNF waste packages, and potential gas generation and pressurization of MCO-containing waste packages is addressed separately at the end of the following section.

Radiolytic Gas Production

Radiolysis of water has the potential to pressurize storage containers through the accumulation of radiolytically generated hydrogen and oxygen. The rate at which these gases are produced by radiolytic decomposition of water (and, potentially, of hydrous solids) will depend on a number of chemical and physical features and processes (e.g., exposed reactive metal surface area, radiation field, etc.). Perhaps most important is the availability of water, which limits the overall extent of H_2 and O_2 production. Even without an early breach, it is expected that TAD canister-bearing commercial SNF waste packages will contain some residual water upon emplacement (possibly including adsorbed, occluded, and chemically bound water, as well as water vapor). The potential consequences of hydrogen generation by radiolysis and a subsequent conflagration (either deflagration or detonation) in a waste package are discussed in more detail in Appendix I of *Screening Analysis of Criticality Features, Events, and Processes for License Application* (SNL 2008 [DIRS 173869]). From the standpoint of this FEP, the most serious effect due to

over-pressurization of the waste package is rupture and possible damage to one (or possibly two) neighboring waste packages.

Excluded FEPs that calculate pressure effects (e.g., FEPs 2.1.03.07.0A (Mechanical Impact on Waste Package) and 2.1.12.02.0A (Gas Generation (He) From Waste Form Decay)) use a TAD canister void volume of 4,737 L (from DTN: SN0702PAIPC1.001 [DIRS 180451], file: *CSNF WP Design Cell 1.xls*, worksheet: "TAD WP Total Moles and SA," cell: B48). This volume is based on a chemical "cell" inside a TAD canister-bearing waste package (c*ell 1* intended for in-package chemical calculations), and does not correspond to a physically defined volume that is potentially larger by as much as 70% (see SNL 2007 [DIRS 177407], Section 6.3.4.3.4.2, p. 6-90). There is uncertainty in estimating pressures inside a TAD canister-bearing waste package. Nevertheless, in order to help maintain consistency among FEPs, so that pressure calculations might be compared more directly, the in-package chemistry "cell 1" TAD canister void volume of 4,737 L (DTN: SN0702PAIPC1.001 [DIRS 180451]) is used in this FEP to estimate pressure inside a TAD canister-bearing waste package. All calculations of pressure performed in this document were conducted in units of atm and converted to psia according to 1 atm = 14.7 psia. No attempt was made to convert the resulting pressure in atm to psig (gauge pressure), although some specifications may be given in this unit (notably, the design pressure for an MCO canister from Garvin 2002 [DIRS 169141], Section 2.2.6.2). Because gauge pressure (psig) is less than or equal to absolute (psia), there is approximately a 1 atm (or less) margin of error in all calculated values when compared to psig (where applicable), such that the effect of this uncertainty on conclusions reached in this document is negligible.

The potential for over-pressurization and rupture of a TAD canister-bearing (commercial SNF) waste package due to waste package pressurization by several relevant processes (including gas generation by radiolysis) is addressed in excluded FEP 2.1.03.07.0A (Mechanical Impact on Waste Package). This FEP concludes that, even considering the upper limit of expected waste package temperatures (approximately 350°C for the drift-collapse case), rupture of a waste package due to over-pressurization is not expected to be a concern before 10,000 years after closure (pressure at 350°C is approximately 114 psia, from excluded FEP 2.1.03.07.0A (Mechanical Impact on Waste Package)). The safety margin is such that, in the absence of water or gases generated by radiolytic decomposition of water, the maximum expected pressure achievable inside a TAD canister-bearing (commercial SNF) waste package is on the order of 114 psia (0.8 MPa) at 350°C, whereas the design pressure for a commercial SNF waste package is 140 psia (0.97 MPa) at 375°C (SNL 2007 [DIRS 179394], Section 4.1.2.6; note that the temperature specified is 707°F rather than 375°C). In fact, a more reasonable maximum pressure – at 200°C – is not expected to exceed 70 psia (0.47 MPa), about one-half the design pressure.

According to *Total System Performance Assessment Data Input Package for Requirements Analysis for Transportation Aging and Disposal Canister and Related Waste Package Physical Attributes Basis for Performance Assessment* (SNL 2007 [DIRS 179394], Table 4-1, Parameter Number 04-04), "all TAD canisters and waste packages shall be dried and backfilled with Helium [sic] to achieve less than 0.43 mole (7.7 g) of H_2O in a 7 m^3 TAD canister after drying in a manner similar to *Standard Review Plan for Dry Cask Storage Systems* (NRC 1997 [DIRS 101903], Section 8.V.1)." The value of 0.43 mole in 7 m^3 is taken from Knoll and Gilbert (1987 [DIRS 123682] Table 3, p. 12), refers to the amount of H_2O in the gas phase only. The procedure described in NUREG-1567, *Standard Review Plan for Spent Fuel Dry Storage*

Facilities (NRC 2007 [DIRS 149756], Section 9.5.4.1) cites NUREG-1536 (NRC 1997 [DIRS 101903], Section 8.V.1) for moisture removal and is therefore acceptable. It is expected that compliance with this requirement will be accomplished according to specifications, and that there is no need to evaluate the potential for failing to meet that requirement, consistent with excluded FEP 1.1.08.00.0A (Inadequate Quality Control and Deviations from Design).

As discussed in excluded FEP 2.1.03.07.0A (Mechanical Impact on Waste Package), the complete conversion of 0.43 moles of water to 0.65 moles of H_2 and O_2 gas results in a pressure increase of only about 0.08 psia at 211°C (the temperature of the analysis). Water in the gas phase does not preclude (and in fact implies) some small quantity of adsorbed and potentially chemically bound water inside a properly dried and inerted TAD canister. To this vapor-phase water must be added any additional pressure that might be achieved if all adsorbed and chemically bound water (if present) were to also be converted to H_2 and O_2 gas. However, because the amount of water in the vapor phase is so small, only a few monolayers of water is expected to be adsorbed (e.g., less than about 10 to 15 nm). Spread over the approximately 1,200 m^2 surface area inside a 21-PWR waste package (SNL 2007 [DIRS 177407], Table 6.3-10) means that, at most, about one mole of additional water needs to be accounted for. Converting this to 1.5 moles of gas by radiolysis increases the pressure inside a TAD canister by only about 0.6% (0.2 psia). Thus, a reasonable assumption is that the potential pressure increase due to complete radiolytic conversion of water into gas might increase in-package pressure by less than one percent (at 211°C), so that the maximum expected pressure will still be approximately one-half the design pressure. The potential conservatism of this calculation should also be emphasized because, due to the high reactivity of radicals generated by radiolysis (many of which must recombine, rather than react with solids, in order to produce molecular O_2), it is highly doubtful that it will be possible to completely convert water into gas at a ratio of 1:1.5. Nevertheless, even if all water is converted into gas at a ratio of 1:1.5, the net effect on pressurizing a TAD canister-bearing waste package can be excluded on the basis of low consequence.

The maximum pressure that could be generated inside an MCO in the absence of a hydrogen fire can be estimated by assuming that one MCO in a codisposal waste package contains the maximum amount of free and bound water, as reported for all MCOs loaded to date: 4.3 kg or 239 moles H_2O (Sexton 2007 [DIRS 184742], Table 2-1). If pressurized at 25°C to 1.5 atm (0.15 MPa or 22 psia) with helium (24.5 mole helium in 400 L void volume; DTN: SN0702PAIPC1CA.001 [DIRS 180451], file: *CDSP – 2MCO Cell 1.xls*, worksheet: "Void Space," cell C51) and assuming all residual water is converted into H_2 and O_2 gas (358 mole gas = 1.5 × 239 mole H_2O) the design pressure of 450 psi (at 132°C; Garvin 2002 [DIRS 169141], Section 2.2.6.2) will be exceeded at about 117°C for a single MCO. The pressure inside the MCO at 211°C would reach 559 psia) (38 atm = 3.8 MPa), well beyond the design pressure. Therefore, it can be expected that an MCO containing the maximum amount of water will fail due to over-pressurization.

Failure of an over-pressurized MCO canister is not expected to damage the inner stainless-steel liner (two inches thick) and outer corrosion barrier (one inch thick) sufficiently to diminish the overall pressure rating of the codisposal waste package (140 psia; SNL 2007 [DIRS 179394], Section 4.1.2.6). Rather, a failed MCO is expected to vent into the surrounding codisposal waste package, which has a net void volume of 3,000 L (7,400 L minus the net volumes of two MCO

canisters at 1,000 L each and two HLW glass canisters at 1,200 L each; volumes from DTN: SN0702PAIPC1CA.001 [DIRS 180451], file: *CDSP – 2MCO Cell 1.xls*, worksheet: "Void Space"). It is assumed further here that the codisposal waste package will have also been pressurized to 1.5 atm with helium at 25°C (184 mole helium in 3,000 L of void volume). Combining the void volumes of the codisposal waste package and one MCO canister (3,000 + 400 = 3,400 L) indicates that the design pressure for the waste package will not be exceeded for temperatures below about 425°C, and that the pressure at 211°C would only be about 93 psia (6.3 atm = 0.64 MPa). Including the void volumes for both MCOs in the calculation increases the attainable pressure by only about 7% (e.g., 104 psia (7.1 atm = 0.71 MPa) at 211°C) if one MCO canister is assumed to contain the maximum amount of water (4.3 kg) and the second MCO canister is assumed to contain the average value of 1.03 kg (57 moles) total water (Sexton 2007 [DIRS 184742], Table 2-1). It should be noted that an MCO with only an average mass of water (1.03 kg; Sexton 2007 [DIRS 184742], Table 2-1) will not exceed its design pressure of 450 psig below about 1,000°C, so that the preceding calculation might tacitly assume damage to the second MCO canister caused by failure of the first.

The minimum hydrogen concentration that can support flammability varies, depending on the major constituents of the gaseous environment. A minimum hydrogen concentration of approximately 4 vol % in an air-hydrogen atmosphere at nominal (0.1 MPa) pressure is required to propagate a flame front (Coward and Jones 1952 [DIRS 182138], Figure 7). For a helium-hydrogen environment, the minimum hydrogen concentration that can support flammability is approximately 8 vol % (Coward and Jones 1952 [DIRS 182138], Table 3). A reasonably conservative estimate of the maximum concentration of hydrogen gas that could be generated inside a TAD canister due to radiolysis can be calculated by assuming that a TAD canister that has been dried according to procedure (no more than 0.43 moles H_2O in 7 m^3 volume of cover gas) has an estimated one mole of water that remains sorbed or chemically bound inside the TAD canister after backfilling with helium to 1.5 atm and sealing (moles of helium given by the ideal gas law: $n = PV/RT = \{1.5\ \text{atm} \times 4{,}737\ \text{L}\} \div \{0.082\ \text{L·atm·mol}^{-1}\ \text{K}^{-1} \times 298.15\ \text{K}\} = 291$ mole-helium). It is further assumed that all water inside the TAD canister (0.43 mole + 1 mole ≅ 1.5 moles H_2O = 27 grams H_2O) is converted to hydrogen and oxygen gas by radiolysis. Such a calculation demonstrates that, in the absence of any failure of the cladding, the maximum concentration of hydrogen is about one-half of one percent (0.005 ≅ 1.5 moles-H_2 ÷ [291 moles-He + 0.75 moles-O_2 + 1.5 moles-H_2]). Back-filling a TAD canister to 2 atm and potential rupture of cladding only reduces this concentration further, as does He generated due to alpha decay. Thus, as demonstrated by this bounding analysis, it is not possible to attain conditions capable of supporting a hydrogen fire inside a TAD canister-bearing waste package.

The average mass of residual water (free and bound) that has been determined to remain in an MCO after being dried and inerted is approximately 1.03 kg (57 moles H_2O) (Sexton 2007 [DIRS 184742], Table 2-1). Nearly all this water is present as chemically bound water in corrosion products (the most abundant corrosion product being aluminum hydroxide, $Al(OH)_3$, with lesser amounts of uranium oxy-hydroxides and aluminum and iron hydrates; Garvin 2002 [DIRS 169141], Table 4-4 and p. 4-30). This water could be released and converted to free hydrogen and oxygen due to thermal and/or radiolytic decomposition of these hydrated oxides. If free oxygen and hydrogen are produced inside an MCO, much of the oxygen may be scavenged by reaction with exposed uranium metal in the breached fuel because of the rapid kinetics of the uranium-metal/oxygen reactions (Haschke 1998 [DIRS 174075], Table 1), as well

as more moderate consumption by oxidation of iron in stainless steel and lower Fe alloys. The potential fate of free hydrogen is less clear. One experimental study of uranium-metal corrosion in moist air reported formation of neither hydrides nor hydrogen gas (Haschke 1998 [DIRS 174075], p. 150), suggesting that any hydrogen evolved was rapidly transformed to water on the uranium-metal surface under the experimental conditions. This study, however, was conducted using clean uranium-metal, and the reaction of hydrogen with partially oxidized uranium metal (as would be expected in an MCO with degraded fuel) is less certain (Plys and Duncan 1999 [DIRS 184687]).

A simplistic calculation, as outlined above for a TAD canister, demonstrates that, in the absence of mitigating reactions, ample gas could be generated in an MCO to support a hydrogen fire (400 L MCO void space, pressurized with 1.5 atm fill gas gives 24.5 moles helium at 25°C, from the ideal gas law), assuming the mean value of residual water (1.03 kg). That is, 48% ≅ 57 moles H_2 ÷ [24.5 moles-He + 29 moles O_2 + 57 moles H_2]. In fact, a hydrogen concentration in excess of 4% could be achieved inside an MCO canister if as little as 25 g residual water remains. Thus, a conflagration due to radiolytic generation of hydrogen and oxygen cannot be ruled out, and the potential consequences of such an event must be evaluated.

The consequence of a hydrogen fire inside an MCO would be to raise the temperature and pressure inside that MCO. The maximum achievable temperatures and pressures for such an event were calculated for a mixture of hydrogen in a mixture of oxygen (21%) and helium (79%) by Plys and Duncan (1999 [DIRS 184687], Figure 5-1), who assumed a conservative adiabatic, constant volume (isochoric) complete combustion ("AICC") model. Using the mean value for expected water content (1.03 kg = 57 moles) in an MCO canister inerted to 1.5 atm helium at 25°C (24.5 moles) and assuming complete conversion of all water to H_2 and O_2 gas (57 and 29 moles, respectively), gives a mixture of 48% H_2, 24% O_2, and 28% helium. This level of oxygen will be reduced due to reaction with uranium metal. To achieve a mixture comparable to that evaluated by Plys and Duncan (1999 [DIRS 184687], Figure 5-1) with 21% O_2 and 79% helium (ignoring H_2) requires that roughly 70% of this oxygen be consumed by oxidation reactions with, for example, uranium metal. In fact, highly reactive oxidizing radicals produced by radiolysis might be expected to reduce this oxygen content even further, suggesting this is a conservative estimate of O_2 concentration. Plys and Duncan (1999 [DIRS 184687], p. 6-7) also considered the fact that as H_2 pressures increased inside an MCO canister, this gas would be consumed by reaction with (primarily) uranium metal; however, due to insufficient data on the reactivity of partially corroded uranium metal to form hydrides, they ignored potential reduction in hydrogen concentration. They did note, however, that as H_2 pressure increases, the reaction of H_2 with even partially oxidized uranium metal should increase, becoming significant when the partial pressure of H_2 reaches between 10 and 20 atm, which is achievable for the mean residual mass of water in an MCO (1.03 kg) at temperatures near the upper limit of this analysis (i.e., greater than approximately 190°C).

Even if both MCOs in a codisposal waste package were assumed to contain the maximum 4.3 kg water each (Sexton 2007 [DIRS 184742], Table 2-1), and it is also assumed that all of the hydrogen in this water becomes available to burn, the heat energy released would be about 14×10^7 J, which would cause a waste package temperature increase of about 6°C, even under conservatively assumed adiabatic conditions. For the purposes of the following calculation, it is assumed that both MCOs in the waste package contain intact fuel elements, because these are

less susceptible to reacting with (and therefore consuming) radiolytically generated gases (as well as radicals and other reactive species) than are MCOs with scrap baskets (see excluded FEP 2.1.02.08.0A (Pyrophoricity from DSNF)).

The temperature increase is calculated by dividing 4,300 g H_2O by the approximate molecular weight of water, 18 g/mol to obtain 239 moles per MCO, and then multiplying by two to get 478 moles H_2O, which could produce 478 moles H_2 per codisposal waste package. Then, 478 moles × 285.83 kJ/mol (standard enthalpy of formation of water; Grenthe et al. 1992 [DIRS 101671], Table IV.1) equals 14×10^7 J. By assuming adiabatic conditions (all energy is available to increase the waste package temperature (i.e., no radiative heat losses)), a maximum temperature increase for the waste package can be calculated as follows. Each defense HLW glass canister will contain approximately 3×10^6 g HLW glass, which is calcuated by using the density (2.7 g/cm^3) and volume (1.1 m^3 = $\pi \times [0.3 \text{ m}]^2 \times [3.9 \text{ m}]$) from DTN: MO0502ANLGAMR1.016 [DIRS 172830], Table 8-1, making a total of 6×10^6 g defense HLW glass per waste package. Each MCO will contain approximately 6.34×10^6 g uranium-metal fuel and 4.43×10^5 g zirconium cladding (Garvin 2002 [DIRS 169141], Table 4-4, column 2), for a total of approximately 8.9×10^5 g zirconium cladding and 1.27×10^7 g uranium metal per waste package. Each waste package will also contain approximately 2.3×10^7 g steel. This includes 1.6×10^6 g steel in the (unloaded) waste package (SNL 2007 [DIRS 179567], Table 4-10), approximately 2.45×10^6 g steel in two HLW glass canisters (4.2×10^6 g per defense HLW glass canister, from SNL 2007 [DIRS 179567], Table 4-10, minus the mass of defense HLW glass noted above) plus approximately 4.8×10^6 g steel in the two MCOs (9.172×10^6 g per MCO, from SNL 2007 [DIRS 179567], Table 4-10, minus the mass of uranium fuel and zirconium cladding noted above). In addition, each waste package will contain approximately 1.6×10^7 g Alloy 22 (SNL 2007 [DIRS 179567], Table 4-10). A weighted average, or "net" heat capacity, is used here for calculating the temperature increase of a 2-MCO/2-DHLW codisposal waste package in the event of a hydrogen fire. The weighted-average heat capacity of 0.39 J/g·°C is calculated from the heat capacities of austenitic steels (0.5 J/g·°C; ASM International 1990 [DIRS 106780], p. 871), Alloy 22 (0.414 J/g·°C; DTN: MO0107TC239938.000 [DIRS 169995], p. 13), uranium metal (0.11 J/g·°C; Grenthe et al. 1992 [DIRS 101671], Section V.1.1), zirconium metal (0.278 J/g·°C; Lide 2006 [DIRS 178081] p. 4-127), and of sodium-aluminum silicate glass ($NaAlSi_3O_8$) as an analogue for borosilicate waste glass (0.78 J/g·°C; Robie et al. 1979 [DIRS 107109], p. 414). The maximum temperature increase for the waste package due to a hydrogen fire in two MCOs can now be calculated as follows: 14×10^7 J/waste package ÷ (5.8×10^7 g solids/waste package × 0.39 J/g·°C) equals 6°C, which is a negligible change.

In fact, any increase in temperature would only degrade the uranium-metal fuel, as discussed in excluded FEP 2.1.02.08.0A (Pyrophoricity from DSNF), which demonstrated that because this simply makes radionuclides from the DOE SNF available for immediate release (a consequence already assumed for DOE SNF inside a breached codisposal package because of the essentially instantaneous degradation rate already used for DOE SNF by TSPA), exclusion of such an event is of low consequence.

In the event of a hydrogen fire, the pressure increase in an MCO is expected to be considerably less than that calculated above, despite the heat of reaction (note that 1.5 moles of gas (H_2 plus O_2) are converted to one mole H_2O). For example, using their "AICC" model, Plys and Duncan

(1999 [DIRS 184687]) calculated pressures for the flammable gas mixtures noted above and found that the maximum pressure that can be achieved is approximately eleven times the initial pressure (i.e., ~16 atm or 235 psia) for a hydrogen concentration of about 30% (Plys and Duncan 1999 [DIRS 184687], Figure 5-1), also well below the design pressure for an MCO. Again, if this MCO canister were to fail, it would vent into the larger volume of the codisposal waste package, reducing the pressure substantially, as shown for the more conservative estimates calculated earlier.

Exclusion of Potentially Negative Effects on the EBS

As noted previously, radiolysis of air can produce water-soluble nitrogen oxides that can form aqueous nitric acid if sufficient water is present on the outer surfaces of waste packages and/or drip shields. However, a key limitation as to whether radiolysis might adversely affect waste package corrosion rates is the spatial extent (penetration) of radiation throughout the EBS. Radiolysis-enhanced corrosion can only occur if water is present and exposed to a radiation field. Therefore, the potential impact of beta-gamma radiolysis on the outer layers of waste packages will not be significant until relative humidity exceeds 95% (the threshold for forming a water film on surfaces) (SNL 2007 [DIRS 180506], Section 6.10.9.1[a]), or until after seepage water penetrates the drip shield. Maximum dose rates achievable within the drifts will be at the surfaces of a waste package that contain a bounding inventory of spent fuel (i.e., highest burnup). Because alpha and primary beta radiation cannot penetrate waste packages, gamma and secondary beta radiation will be the dominant contributor to dose rate at the waste package outer surface. Neutron-radiation levels are calculated to remain less than gamma levels by more than an order of magnitude for a 21-PWR commercial SNF waste package (BSC 2004 [DIRS 172227], Table 6.3-2).

For a waste package that contains 21 PWR high-burnup SNF assemblies (80 GWd/MTU burnup, and 5-year decay during storage), the maximum level of total radiation at the outer surface of the waste package has been estimated to be approximately 1,160 rad/hr (1,570 rad/hr at the outer surface of the waste package lid; BSC 2004 [DIRS 172227], Section 6.4.2 and Table 6.4-5). After 50 years (the anticipated ventilation period), this will have decreased by an order of magnitude to about 100 rad/hr at the outer surface of the waste package, and 100 years after emplacement the maximum calculated gamma dose will have dropped another third to less than 40 rad/hr at the outer surface of the waste package (BSC 2004 [DIRS 172227], Figure 6.4-1). The temperatures of even the coolest commercial SNF waste packages in the central region of the repository are currently estimated to remain above boiling, and the relative humidity to remain below about 95%, for approximately 1,000 years or more (SNL 2008 [DIRS 184433], Section 6.3.16[a]), so that, in the absence of deliquescent salts, no liquid water will be present on waste package or drip-shield surfaces exposed to high levels of gamma radiation (and secondary beta radiation).

Potential deliquescence of salts contained in dust that may settle on the waste package or drip-shield surfaces is discussed in excluded FEP 2.1.09.28.0A (Localized Corrosion on Waste Package Outer Surface Due to Deliquescence), although that FEP did not address potential radiation effects. Such effects were examined for Alloy C-4 and Titanium Grade 7 during long-term experiments (1 to 4 years) in especially corrosive Mg-Cl brines. These studies showed no observable influence on the corrosion behavior of Alloy C-4 (an analogue for Alloy 22) when

contacted by Mg-Cl brines exposed to gamma radiation doses of less than about 100 rad/hr (Shoesmith and King 1998 [DIRS 112178], p. 29); however, Alloy C-4 undergoes extensive pitting and crevice corrosion when contacted by brine exposed to a gamma dose above 100 rad/hr (Shoesmith and King 1998 [DIRS 112178], pp. 30 to 31). Titanium Grade 7 alloy showed exceptional corrosion resistance under these conditions, and even at dose rates above 1,000 rad/hr, only minor enhancement of film growth rates on Titanium Grade 7 was observed, and its passivity was not compromised (Shoesmith and King 1998 [DIRS 112178], p. 30). Based on these data and the discussion above, it is concluded that radiation levels in the repository after about 50 years will not be sufficiently high to significantly enhance corrosion of Alloy 22 or Titanium Grade 7, even in the presence of especially corrosive brines. (see excluded FEP 2.1.03.03.0B (Localized Corrosion of Drip Shield) for discussion of localized corrosion of Titanium Grade 29). Furthermore, most potentially corrosive deliquescent brine compositions are unstable in the drift environment, and those few that may be stable will degas acid phases in the presence of reactive products of radiolysis (SNL 2007 [DIRS 181267], Sections 7.2.1, 7.2.2, and 7.2.3, pp. 7-2 to 7-3).

Taken together, these conclusions suggest that radiation levels at the outer surface of a commercial SNF waste package, even for fuels with the highest potential burnups (considered here to be a bounding case for all waste packages), will be well below those for which radiolysis effects have been observed to negatively impact the corrosion of waste package or drip-shield metals. Furthermore, these maximum radiation levels are expected early, when most of the repository is anticipated to be dry. Later on, when liquid water is expected to be present (e.g., beyond several thousand years), beta-gamma radiation levels will have decreased enough that significant water radiolysis is not expected outside intact waste packages.

For those waste packages at the perimeter of the repository, exterior waste package and drip shield temperatures may never exceed boiling, so that liquid water (as condensate) may be present on those packages, and the potential that radiolytically generated nitric acid might accumulate in this condensate during the first few thousand years after closure cannot be excluded. However, as noted previously, even in relatively aggressive Mg-Cl brines, corrosion rates of Titanium Grade 7 are not substantially enhanced in a strong gamma field, and corrosion rates of Alloy 22 are negligible for dose rates below about 100 rad/hr in such brines (Shoesmith and King 1998 [DIRS 112178], pp. 29 and 30), which are not expected to exist, especially in lower-temperature regions of the repository. Furthermore, because beta-gamma dose decreases exponentially with time, even those few waste packages and drip shields that might not experience above-boiling temperatures are not expected to experience significant radiolytically enhanced corrosion during the period when beta-gamma dose rates are high. Thus, radiolytically enhanced corrosion of waste packages and drip shields is not expected to have a significant effect on repository performance.

The potential accumulation of radiolytically generated nitric acid inside a waste package is discussed separately in the following paragraphs.

Generation of Radiolytic Products within Waste Packages

Breaches to waste packages are the most common, but not the only way for water to exist within a waste package; because commercial SNF (and several types of DOE SNF) is cooled and stored

under water immediately after being removed from the reactor, water may be retained in fuel elements when loaded into TAD canisters and/or waste packages before being sealed for disposal. Radiolytically produced nitric acid can form only when both water and nitrogen are present, which would require failure to both dry (remove water) and inert (remove nitrogen) a TAD canister properly.

While most of the cladding is physically present (even if defective), alpha and beta radiation due to radioactive decay will be shielded and unable to affect internal steel corrosion of the TAD canister. Only after large-scale rod failure can substantial quantities of actinides and their decay products contact the interior of the steel TAD canister. If a waste package breaches while the temperature in the waste package is above boiling, any liquid water remaining in the TAD canister will evaporate and be unable to participate in further corrosion, and without liquid water, transport of dissolved radionuclides out of the waste package is impossible.

Under strongly oxidizing conditions, the effect of radiolysis on the degradation rate of spent fuel is most pronounced under the influence of beta-gamma radiation, since beta-gamma radiation produces the most reactive radiolytic products; however, as noted previously, the beta-gamma radiation field decreases exponentially to near-negligible levels (i.e., small fractions of a percent of initial levels) after a few thousand years (when waste package breaches are still unexpected and relative humidity is below 95%).

Nitric acid production is primarily a consequence of beta-gamma radiation, waste packages that breach later than about 1,000 years after closure will not be exposed to beta-gamma radiation fields strong enough to generate enough nitric acid to be of concern. According to *In-Package Chemistry Abstraction* (SNL 2007 [DIRS 180506], p. 6-53[a]), the acid-neutralizing capacity within a breached commercial SNF waste package can be described as the number of moles (of an acid-neutralizing component, specifically, the Ni-Fe spinel, trevorite, $NiFe_2O_4$) produced each year due to corrosion of waste-package internals (especially stainless steel). Because schoepite and iron corrosion products dominate the composition of the alteration products from about 500 years on (SNL 2007 [DIRS 180506], Section 6.7.2, p. 6-101) and the Stainless Steel Type 304L inside a 2-MCO/2-DHLW codisposal waste package is completely degraded after approximately 500 years (SNL 2007 [DIRS 180506], p. 6-46[a]), the following analysis considers the acid-neutralizing component inside a waste package at 500 years.

For example, the estimated production of acid-neutralizing capacity for a breached commercial SNF waste package at about 500 years after closure is 0.039 moles per kilogram of solution (molal) annually, and for a codisposal HLW glass-containing cell, it is about 0.0006 molal annually (SNL 2007 [DIRS 180506], p. 6-53[a]). This value can be converted to molecules·yr^{-1}·cm^{-3} of gas-filled porosity by using Equation 2.1.13.01.0A-1:

$$ANC\left(\frac{molecules}{yr \cdot cm^3(void)}\right) = ANC\left(\frac{molal}{yr}\right) \cdot \rho_w s_w A_v \qquad \text{(Eq. 2.1.13.01.0A-1)}$$

where A_v is Avogadro's constant (6.022×10^{23} molecules/mole), s_w is the base-case volumetric ratio of gas-filled porosity to total porosity (i.e., 50%; SNL 2007 [DIRS 180506], Table 6-1[a] and p. 6-4[a]), and ρ_w is the approximate density of the solution (for this calculation a density of 0.001 kg/cm^3 is used; however, a more concentrated aqueous solution will have a greater density,

so this may slightly underestimate acid-neutralizing capacity). This calculation gives an acid-neutralizing capacity production rate of 1.2×10^{19} molecules·yr^{-1}·cm^{-3} in a commercial SNF waste package and 1.8×10^{17} molecules·yr^{-1}·cm^{-3} in a codisposal waste package, for a 50% porous waste form. Therefore, the rates at which acid-neutralizing capacity is generated are several orders of magnitude higher than the annual rate of nitric acid production due to gamma radiolysis for the same time (BSC 2004 [DIRS 172017], Tables 19 and 22, and Figure 5). For comparison, the amount of nitric acid potentially generated by gamma radiolysis in a waste package breached 500 years after closure corresponds to about 3.6×10^{13} molecules·yr^{-1}·cm^{-3} of moist air. Furthermore, the rate of radiolytic nitric acid production decreases with decreasing beta-gamma field, which falls off exponentially over the first 500 years, after which the annual rate of nitric acid production (normalized fuel-rod surface area) remains fairly constant (BSC 2004 [DIRS 172017], Figure 5). Thus, the relatively small amount of nitric acid that will form due to radiolysis inside a waste package at early times will be neutralized by reaction with stainless steel and/or fuel, and the acid-neutralizing capacity of the waste-package corrosion products is expected to outpace the acid produced by radiolysis for all time.

As noted previously, hydrogen peroxide (H_2O_2) is a potentially strong oxidant that can enhance corrosion of many metals and spent fuel, and it is produced by both alpha and beta-gamma irradiation of water. However, the solubility in water of H_2O_2 decreases with increasing temperature. By using data from Stefanic and LaVerne (2002 [DIRS 166303]) the exponential decrease in H_2O_2 concentrations for temperatures between 25°C and 100°C was calculated (BSC 2004 [DIRS 170019], Section 6.2.5 and Table 6-3). At 25°C, the calculated "half-life" is 34 days; 3.79 days at 50°C, and 0.11 days at 100°C. Decomposition and/or degassing of dissolved H_2O_2 at elevated temperature is also implied by results of spent-fuel corrosion experiments, in which the uranyl peroxide solid, studtite, has been observed only in experiments conducted at near-room temperatures, but not in experiments conducted above about 60°C (McNamara et al. 2003 [DIRS 172673]). Because the temperature of waste packages is expected to remain above 100°C for several hundred years, and above 50°C for about 10,000 years or more (SNL 2008 [DIRS 184433], Figure 6.3-82[a]), a significant portion of H_2O_2 produced by radiolysis during the first 10,000 years is expected to decompose. Furthermore, and perhaps most important, elevated H_2O_2 concentrations have little influence on commercial SNF corrosion rates under the strongly oxidizing conditions expected in the repository (Shoesmith 2000 [DIRS 162405]). Finally, *In-Package Chemistry Abstraction* (SNL 2007 [DIRS 180506], Section 6.6.5[a], Figures 6-32[a] and 6-33[a]) reports on the influence to pH and ionic strength due to enhanced rates of steel and fuel oxidation. While the effect of higher degradation rates on predicted trajectories for pH and ionic strength can be discerned, higher degradation rates are not expected to significantly change the range of pH expected inside the waste package.

Based on the previous discussion, the effects of radiolysis on the corrosion of SNF and other internal waste package components are excluded from the TSPA on the basis of low consequence.

Potential Effects on Radionuclide Speciation and Transport

The potential that radiolysis may change in-package chemistry sufficiently to increase solubilities of radionuclide-bearing solids, alter the speciation of radionuclides, or otherwise enhance radionuclide concentrations and/or transport to the invert and unsaturated zone, must

also be considered. Generation of nitric acid during beta-gamma irradiation was shown above to have no significant effect on in-package pH, due to the buffering capacity (specifically acid-neutralizing capacity) of waste package corrosion products; besides, as noted previously, generation of nitric acid is most pronounced at early times when liquid water is not expected to be present. Although radiolytic decomposition of water produces an equal number of oxidizing and reducing species, H_2 gas (the most abundant reductant produced by alpha radiolysis) has a low solubility in water and is expected to diffuse rapidly out of a breached waste package to the drift environment, where it is expected to be diluted and to diffuse out through fractures in the surrounding rock. For this reason, once a waste package is breached, any change in the oxidation potential of water due to radiolysis is expected to be in a positive direction (i.e., more oxidizing), primarily due to radiolytic production of hydrogen peroxide. Hydrogen peroxide (H_2O_2) is considerably more soluble in water than H_2 gas; it is a potentially strong oxidant and is known to form stable solution species with certain actinides (notably plutonium; Katz et al. 1986 [DIRS 106312]).

It is first noted that concentrations of radiolytically produced H_2O_2 will be mitigated by at least four processes: (1) H_2O_2 will react with reduced iron in the stainless steel and in ferrous corrosion products, as well as with reduced uranium in the fuel (provided sufficient quantities of these reduced elements remain in waste packages); (2) even after complete oxidation of all waste package components, H_2O_2 will be catalytically decomposed by ferric iron in steel corrosion products such as goethite (Kremer 1985 [DIRS 184684]; Abbot and Brown 1990 [DIRS 184686]); (3) as noted, elevated temperatures promote decomposition of H_2O_2; and (4) the stability of H_2O_2 decreases with increasing pH. Such decomposition reactions will prevent H_2O_2 concentrations from increasing indefinitely. In fact, for a given alpha dose, the concentration of H_2O_2 generated by radiolysis is established within a few days and remains very nearly constant over time spans of hundreds to thousands of years, only gradually decreasing (on the order of thousands of years or more) as radiation levels decrease. Even during the first 10,000 years after closure, alpha-radiation levels change by little more than an order of magnitude between about 100 and 10,000 years, so that H_2O_2 concentrations will decrease by less than about 50% between 5,000 and 10,000 years (provided that decomposition reaction rates also remain approximately constant). It is this (poorly known) quasi-steady-state concentration of H_2O_2 that is of potential concern, and the reason it is expected to have little or no negative impact is addressed in the following paragraphs.

Once breached, a waste package is modeled as being fully exposed to the ambient drift atmosphere (i.e., partial pressure of oxygen equal to about 0.2 atmospheres, or $pO_2 = 0.2$ atm), and the dissolved concentrations of nearly all radionuclides are calculated by assuming equilibrium between the drift atmosphere, solubility-controlling solids, and water. The potential for increasing the oxidation potential (also known as the Eh) of water in equilibrium with 0.2 atm oxygen by increasing the dissolved concentration of radiolytic H_2O_2 will be negligible, because such a water is already close to the upper stability limit of water. Even so, most radionuclides are already assumed to be in their most oxidized valence states. However, two radionuclides are given somewhat special treatment: neptunium and plutonium (SNL 2007 [DIRS 177418], Appendix V). In the case of neptunium, the more reduced of two possible oxides, NpO_2, is used to calculate limits on dissolved neptunium concentrations inside a waste package until all waste-package internals are fully oxidized, at which time Np_2O_5, is assumed to limit dissolved neptunium concentrations. Therefore, as long as reductants (i.e., electron donors) exist in the

waste package, these can be assumed to be available to react with H_2O_2, and NpO_2 will remain the stable solubility-limiting solid for neptunium (although the rate at which radiolytic H_2O_2 might oxidize waste package internals is not considered, so that the time at which the TSPA model switches from the lower-solubility NpO_2 to higher-solubility Np_2O_5 may occur later than if radiolytic oxidation of waste package internals were accounted for; however, this delay is not expected to significantly impact calculated concentrations of dissolved neptunium downstream of the waste package because solubility limits on neptunium concentrations differ by just over an order of magnitude for either neptunium-bearing solid in equilibrium with the atmosphere in the pH range of concern).

Similar to the case for neptunium, radiolytic production of H_2O_2 is not expected to increase the dissolved concentration of plutonium releases under anticipated repository conditions. The treatment of plutonium differs from that of neptunium because limits on dissolved plutonium concentrations are calculated by using an "adjusted Eh" model, in which a lower-than-ambient oxidation potential is used to calculate dissolved concentrations of plutonium limited by PuO_2 solubility (SNL 2007 [DIRS 177418], Appendix V). This raises the question as to whether solubility is affected by radiolytically produced H_2O_2. The chemistry of H_2O_2 with plutonium means that H_2O_2 is not expected to adversely affect plutonium solubility, as discussed in the following paragraph.

Hydrogen peroxide (H_2O_2) is an oxidant; however, for certain elements H_2O_2 acts as a reducing agent (Stumm and Morgan 1996 [DIRS 125332], Chapter 11). This is the particular case for the reaction of H_2O_2 with plutonium, as demonstrated by well-documented studies using H_2O_2 to reduce Pu(V) and Pu(VI) to Pu(IV) (Katz et al. 1986 [DIRS 106312]). The vast majority of such work applies to highly acidic solutions containing high-levels of dissolved H_2O_2; that is, for solution chemistries not expected to exist within the repository under any scenario. One study, however, confirms the reduction at more representative conditions reporting reduction of Pu(V) to Pu(IV) in basic solutions with H_2O_2 concentrations closer to those that might be expected to occur due to alpha radiolysis ($7.9 \leq pH \leq 10.8$ and $0.00001 \leq [H_2O_2] \leq 0.04$ moles per liter (Morgenstern and Choppin 1999 [DIRS 184023], pp. 109 to 111). The authors found that not only was Pu(V) gradually reduced to Pu(IV), but the concentration of dissolved plutonium decreased as an unidentified plutonium solid was precipitated. The authors derived a redox half-life for Pu(V) as a function of pH and dissolved H_2O_2 that suggests 50% of Pu(V) would be reduced to Pu(IV) in about 55 years for $[H_2O_2]$ equals 10^{-7} moles per liter and a pH of 8 (and essentially 100% is reduced after 550 years). These experiments were conducted in high ionic-strength solutions (1.0 mole NaCl per kilogram of solution), and it is uncertain how quantitatively the results can be extrapolated to more dilute waters. Also, the pH range studied is on the high end and is above what is expected inside breached waste packages. The range of pH expected in a waste package should, in fact, stabilize H_2O_2 relative to the range reported by Morgenstern and Choppin (1999 [DIRS 184023]), potentially making plutonium reduction by radiolytic H_2O_2 somewhat more effective. Given that the qualitative chemistry demonstrates reduction of plutonium, it is not expected that radiolytic addition of H_2O_2 will increase the dissolved concentration of plutonium under the anticipated repository conditions.

Based on the previous discussion, the effects of radiolysis on the speciation and transport of radionuclides are not included in the TSPA on the basis of low consequence.

In summary, potential pressurization and/or fire caused by gases generated from radiolytic decomposition of water inside a waste package is excluded on the basis of low consequence: (1) the small amount of water in a dried and inerted TAD canister-bearing waste package will not generate sufficient gas to cause a problem; (2) although an MCO containing upwards of 4 kg residual water may fail, it would vent into the larger codisposal waste package, which would not fail; (3) a hydrogen fire in an MCO will not increase pressure sufficiently to fail the canister, and the maximum possible increase in temperature to the waste package would be negligible. Enhanced corrosion of waste packages and drip shields due to the effects of beta-gamma radiolysis is excluded because beta-gamma radiation is intense enough to cause a problem only while the repository temperature is above boiling when little or no liquid water will be present on waste package or drip-shield surfaces. The effects of nitric acid production by radiolysis on the corrosion of commercial SNF and other internal waste package components is excluded on the basis of low consequence because of the acid-neutralizing capacity of the waste package internal corrosion products. Similarly, potential generation of H_2O_2 by radiolysis and its potential enhancement of commercial SNF corrosion rates is excluded on the basis of low consequence, because increased H_2O_2 concentrations have little influence on commercial SNF corrosion rates under strongly oxidizing conditions. The potential influence on radionuclide concentrations and mobilities due to H_2O_2 accumulation caused by alpha radiolysis is excluded on the basis of low consequence.

Based on the previous discussion, omission of FEP 2.1.13.01.0A (Radiolysis) will not result in a significant adverse change in the magnitude or timing of either radiological exposure to the RMEI or radionuclide releases to the accessible environment. Therefore, this FEP is excluded from the performance assessments conducted to demonstrate compliance with proposed 10 CFR 63.311 and 63.321 (70 FR 53313 [DIRS 178394]), and with 10 CFR 63.331 [DIRS 180319], on the basis of low consequence.

INPUTS:

Table 2.1.13.01.0A-1. Direct Inputs

Input	Source	Description
ASM International 1990. *Properties and Selection: Irons, Steels, and High-Performance Alloys*. [DIRS 106780]	p. 871	The heat capacity of austenitic steel is 0.5 J/g • °C
BSC 2004. *Gamma and Neutron Radiolysis in the 21-PWR Waste Package from Ten to One Million Years*. [DIRS 172017]	Tables 19 and 22, and Figure 5	The annual rate of nitric acid production due to gamma radiolysis in a codisposal HLW glass-containing cell
Coward and Jones 1952. *Limits of Flammability of Gases and Vapors*. [DIRS 182138]	Figure 7	Minimal hydrogen concentration to propogate a flame front is 4 vol % in air at 0.1 Mpa
	Table 3	Minimal hydrogen concentration to propogate a flame front is 8 vol % in a helium-hydrogen atmosphere
DTN: MO0107TC239938.000. Hastelloy Alloy C-22, Nickel-Chromium-Molybdenum Alloy Available Today with Improved Resistance to Both Uniform and Localized Corrosion as Well as a Variety of Mixed Industrial Chemicals. [DIRS 169995]	p. 13	The heat capacity of Alloy 22 is 0.414 J/g • °C

Table 2.1.13.01.0A-1. Direct Inputs (Continued)

Input	Source	Description
DTN: MO0502ANLGAMR1.016. HLW Glass Degradation Model. [DIRS 172830]	Table 8-1	HLW glass density (2.7 g/cm^3) and volume (1.1 m^3 = π × [0.3 m]^2 × [3.9 m])
DTN: SN0702PAIPC1CA.001. In-Package Chemistry Calculations and Abstractions. [DIRS 180451]	file: *CDSP 2MCO Cell 1.xls*, worksheet: "Void Space"	The TAD canister void volume is 4,737 L
	file: *CDSP 2MCO Cell 1.xls*, worksheet: "Void Space," cell C51	The TAD canister void volume is 4,737 L
	file: *CSNF WP Design Cell 1.xls*, worksheet: "TAD WP Total Moles and SA," cell: B48	The TAD canister void volume is 4,737 L
Garvin 2002. *Multi-Canister Overpack Topical Report*. [DIRS 169141]	Table 4-4	443 kg zirconium cladding per MCO (Mark IV maximum fuel load without scrap basket)
	Table 4-4	6,340 kg uranium metal per MCO (Mark IV maximum fuel load without scrap basket)
	Table 4-4	443 kg zirconium cladding per MCO (Mark IV maximum fuel load without scrap basket)
	Table 4-4	6,340 kg uranium metal per MCO (Mark IV maximum fuel load without scrap basket)
Grenthe et al. 1992. *Chemical Thermodynamics of Uranium*. [DIRS 101671]	Table IV.1	285.83 kJ/mol is the standard enthalpy of formation of water
	Section V.1.1	The heat capacity of uranium metal is 0.11 J/g • °C
Lide 2006. *CRC Handbook of Chemistry and Physics*. [DIRS 178081]	p. 4-127	The heat capacity of zirconium metal is 0.278 J/g • °C
Morgenstern and Choppin 1999. "Kinetics of the Reduction of $Pu(V)O_2^+$ by Hydrogen Peroxide." [DIRS 184023]	pp. 109 to 111; Table 1	Reduction of Pu(V) to Pu(IV) in basic solutions having hydrogen peroxide (H_2O_2) concentrations on the order of 0.04 to 0.00001 moles per liter and pH 7.9 to 10.8.
NRC 1997. *Standard Review Plan for Dry Cask Storage Systems*. [DIRS 101903]	Section 8.V.1	Required procedures for vacuum drying of commercial spent fuel storage canisters
Plys and Duncan 1999. *FAI/99-14, Rev. 1, Hydrogen Combustion in an MCO During Interim Storage*. [DIRS 184687]	Figure 5-1, pp. 6 and 7	The maximum achievable temperatures and pressures (11 times the initial pressure) for a hydrogen fire in a mixture of oxygen (21%) and helium (79%) inside an MCO
Robie et al. 1979. *Thermodynamic Properties of Minerals and Related Substances at 298.15 K and 1 Bar (10^5 Pascals) Pressure and at Higher Temperatures*. [DIRS 107109]	p. 414	Analogue for borosilicate waste glass
Sexton 2007. *Particulate and Water in Multi-Canister Overpacks (OCRWM)*. [DIRS 184742]	Table 2-1	Maximum amount of free and bound water in an MCO is 4.3 kg
	Table 2-1	The average value of free and bound water in an MCO is 1.03 kg

Table 2.1.13.01.0A-1. Direct Inputs (Continued)

Input	Source	Description
Shoesmith and King 1998. *The Effects of Gamma Radiation on the Corrosion of Candidate Materials for the Fabrication of Nuclear Waste Packages*. [DIRS 112178]	pp. 29 to 31; Table 4	Effects of gamma radiolysis on waste package materials when in contact with Mg-Cl brines
SNL 2007. *Dissolved Concentration Limits of Elements with Radioactive Isotopes*. [DIRS 177418]	Appendix V	Limits on dissolved plutonium concentrations are calculated by using an Adjusted Eh model
SNL 2007. *EBS Radionuclide Transport Abstraction*. [DIRS 177407]	Table 6.3-10	A 21-PWR waste package has an inside surface area of 1,200 m^2
SNL 2007. *In-Package Chemistry Abstraction*. [DIRS 180506]	Section 6.6.5[a], Figures 6-32[a] and 6-33[a]	Reports on the influence to pH and ionic strength due to enhanced rates of steel and fuel oxidation
	p. 6-53[a]	Acid-neutralizing capacity within a breached commercial SNF waste package can be described as the number of moles (of an acid-neutralizing component, specifically, the Ni-Fe spinel, trevorite) produced each year due to corrosion of waste package internals (especially stainless steel)
SNL 2007. *Total System Performance Assessment Data Input Package for Requirements Analysis for DOE SNF/HLW and Navy SNF Waste Package Overpack Physical Attributes Basis for Performance Assessment*. [DIRS 179567]	Table 4-10	2-MCO/2-DHLW codisposal waste package dimensional envelope, weights and material masses
	Table 4-10	Description of steel and Alloy 22 in the unloaded waste package
SNL 2007. *Total System Performance Assessment Data Input Package for Requirements Analysis for TAD Canister and Related Waste Package Overpack Physical Attributes Basis for Performance Assessment*. [DIRS 179394]	Section 4.1.2.6	Design pressure rating for the as-manufactured waste package outer corrosion barrier, which is approximately 0.97 MPa (140 psia) at 375°C
	Table 4-1, Parameter Number 04-04	TAD canisters and waste packages shall be dried and backfilled with helium to achieve less than 0.43 mole (7.7 g) of H_2O in a 7 m^3 TAD canister
SNL 2008. *Multiscale Thermohydrologic Model*. [DIRS 184433]	Section 6.3.16[a]	The temperatures of even the coolest commercial SNF waste packages in the central region of the repository are currently estimated to remain above boiling, and the relative humidity to remain below about 95%, for approximately 1,000 years or more
	Figure 6.3-82[a]	The temperature of waste packages is expected to remain above 100°C for several hundred years and above 50°C for about 10,000 years or more

Table 2.1.13.01.0A-2. Indirect Inputs

Citation	Title	DIRS
10 CFR 63	Energy: Disposal of High-Level Radioactive Wastes in a Geologic Repository at Yucca Mountain, Nevada	180319
70 FR 53313	Implementation of a Dose Standard After 10,000 Years	178394
Abbot and Brown 1990	"Kinetics of Iron-Catalyzed Decomposition of Hydrogen Peroxide in Alkaline Solution"	184686
BSC 2004	*Dose Rate Calculation for 21-PWR Waste Package*	172227
BSC 2004	*Clad Degradation - FEPs Screening Arguments*	170019
Garvin 2002	*Multi-Canister Overpack Topical Report*	169141
Haschke 1998	"Corrosion of Uranium in Air and Water Vapor: Consequences for Environmental Dispersal"	174075
Katz et al. 1986	*The Chemistry of the Actinide Elements*	106312
Knoll et al. 1987	*Evaluation of Cover Gas Impurities and Their Effects on the Dry Storage of LWR Spent Fuel*	123682
Kremer 1985	"'Complex' versus 'Free Radical' Mechanism for the Catalytic Decomposition of H_2O_2 by Ferric Ions"	184684
McNamara et al. 2003	"Observation of Studtite and Metastudtite on Spent Fuel."	172673
NRC 2000	*Standard Review Plan for Spent Fuel Dry Storage Facilities*	149756
Plys and Duncan 1999	*FAI/99-14, Rev. 1, Hydrogen Combustion in an MCO During Interim Storage*	184687
Reed and Bowers 1990	"Alpha Particle-Induced Formation Of Nitrate in the Cm-Sulfate Aqueous System"	113577
Shoesmith 2000	"Fuel Corrosion Processes under Waste Disposal Conditions"	162405
SNL 2007	*Analysis of Dust Deliquescence for FEP Screening*	181267
SNL 2007	*EBS Radionuclide Transport Abstraction*	177407
SNL 2007	*General Corrosion and Localized Corrosion of the Drip Shield*	180778
SNL 2007	*Initial Radionuclides Inventory*	180472
SNL 2007	*In-Package Chemistry Abstraction*	180506
SNL 2008	*Screening Analysis of Criticality Features, Events, and Processes for License Application*	173869
SNL 2008	*Multiscale Thermohydrologic Model*	184433
Stefanic and LaVerne 2002	"Temperature Dependence of the Hydrogen Peroxide Production in the y-Radiolysis of Water"	166303
Stumm and Morgan 1996	*Aquatic Chemistry, Chemical Equilibria and Rates in Natural Waters*	125332

FEP: 2.1.13.02.0A

FEP NAME:

Radiation Damage in EBS

FEP DESCRIPTION:

Radiolysis due to the alpha, beta, gamma-ray, and neutron irradiation of water could result in enhancement of the radionuclide migration from the surface of a degraded waste form into groundwater. When radionuclides decay, the emitted high-energy particle could result in the production of radicals in the water or air surrounding the spent nuclear fuel. If these radicals migrate (diffuse) to the surface of the fuel, they may then enhance the degradation/corrosion rate of the fuel (UO_2). This effect would increase the dissolution rate for radionuclides from the fuel material (fuel matrix) into the groundwater. Strong radiation fields could lead to radiation damage to the waste forms (CSNF, DSNF, DHLW), waste packages, drip shield, seals, and surrounding rock.

SCREENING DECISION:

Excluded – low consequence

SCREENING JUSTIFICATION:

Radioactive decay can cause damage to the EBS directly and indirectly. Excluded FEP 2.1.02.04.0A (Alpha Recoil Enhances Dissolution) describes the enhancement of dissolution due to direct effects of alpha recoil. In addition, radiation can cause indirect damage to EBS components. For example, alpha-recoil nuclei can also cause damage (e.g., atom displacements, helium and oxygen bubble formation, and microcracking) particularly to the waste forms. Alpha, beta, and gamma radiation fields can also cause radiolysis of water and humid air, leading to the build-up of radicals, oxidizing species, and acids in the fluid surrounding the EBS, which may accelerate corrosion rates and may also lead to enhanced release rates (see excluded FEP 2.1.13.01.0A (Radiolysis)).

In general, the degree of irradiation in the EBS is highest in the waste form. Until the waste packages are breached, the waste forms degraded, and a major fraction of the radionuclide inventory is released, the radiation fields will decrease with distance from the waste form. In addition to the effects of distance from the source, each successive layer of the EBS (such as the waste package) will provide radiation shielding to EBS components that are further away from the waste. This screening justification addresses components of the EBS from the waste form outwards.

In the TSPA, DOE SNF degradation (except naval SNF) is modelled as instantaneous degradation or dissolution of the waste form upon exposure of the waste form to liquid water. For all groups of DOE SNF (except naval SNF), the upper-limit model produces complete dissolution of the waste form during a single-code time step upon exposure of the waste form to liquid water (BSC 2004 [DIRS 172453], Section 8.1). Radiation damage to the DOE SNF is inconsequential for this bounding modeling approach.

Effects of irradiation damage in commercial SNF freshly discharged from reactors are addressed within the scope of included FEP 2.1.02.02.0A (CSNF Degradation (Alteration, Dissolution, and Radionuclide Release)) and are included in the TSPA in so far as data used for the commercial SNF model development and validation were obtained from freshly discharged commercial SNF samples (BSC 2004 [DIRS 169987]). This FEP addresses the effects of radiation damage due to long-term self irradiation of commercial SNF in the repository. Review of the relative importance of the various types of self-irradiation (i.e., irradiation by α, β, γ, fast neutrons, and spontaneous fission) that can cause damage in CSNF indicates that most of the damage will be due to α-decay (Pelletier 2001 [DIRS 164034], Section 5.4.6.3). Unlike other ceramics, the UO_2 fuel matrix does not eventually become amorphous due to the atom displacements induced by radiation (Matzke 1992 [DIRS 113269]). However, accumulation of defect clusters, vacancies, and interstitials in the crystal lattice together with damage relaxation processes can lead to microstructural changes as exemplified in the fine-grained recrystallized structure seen in the peripheral region of high burnup commercial SNF (Dehaudt 2001 [DIRS 164019], Section 5.2.8.1.2.4). Potential effects of the commercial SNF recrystallized rim region on the effective specific surface area available for dissolution are within the scope of included FEP 2.1.02.02.0A (CSNF Degradation (Alteration, Dissolution, and Radionuclide Release)) and are included within the uncertainty range for this parameter in the commercial SNF model (BSC 2004 [DIRS 169987], Section 6.4.1.5). Self-irradiation damage in commercial SNF after it is emplaced in the repository will enhance the rate of diffusion of fission products in the fuel's matrix (Pelletier 2001 [DIRS 164034], Section 5.4). A recent assessment of the potential effect of radiation damage enhancement of fission product mobility in the commercial SNF matrix concluded that the effects on the commercial SNF gap and grain-boundary inventories are limited (Johnson 2005 [DIRS 178773]). This conclusion was based on calculations that showed that use of an upper estimate for the very uncertain radiation-enhanced diffusion coefficients indicates that self irradiation could cause about 5% of the inventory in the fuel matrix to migrate to the grain boundaries over 10,000 years (Johnson 2005 [DIRS 178773], Section 5). The theoretical approaches that have been used to estimate the alpha self-irradiation enhanced diffusion coefficients give estimates that range over three orders of magnitude (Johnson 2005 [DIRS 178773], Section 5); the effect of alpha self-irradiation on radionuclide migration in the fuel would be negligible if a value near the middle of the estimate range is used. Because the initial release fractions in the commercial SNF model (BSC 2004 [DIRS 169987], Section 6.3.2) are based on experimental data that are believed to already overestimate the gap and grain boundary inventory fractions (BSC 2004 [DIRS 169987], Sections 6.3.1 and 6.3.2), exclusion of explicit consideration of alpha irradiation damage effects is warranted. Other commercial SNF radiation damage effects (evolution of the fuel's chemical state, helium generation and accumulation, and evolution of the fuel's physical state including microcracking and grain decohesion) may accumulate in commercial SNF (Piron 2001 [DIRS 162396]). These effects are excluded from explicit inclusion in the TSPA because they are not expected to be significant given that the commercial SNF model considers that all of the gap and grain boundary inventories are part of the instantaneous release fraction (BSC 2004 [DIRS 169987], Section 6.4).

Radiation levels in the repository may damage defense HLW glass causing bond dissociation and atomic displacements, which may lead to devitrification, swelling and cracking, and consequently, enhanced degradation rates. Corrosion tests conducted on irradiated glasses have shown up to four-fold increases in the release rates of glass components (Wronkiewicz 1993

[DIRS 171709], Abstract). However, other authors have reported no significant change in the dissolution rate between actinide-doped and nonradioactive glasses (Advocat et al. 1998 [DIRS 160446]; Werme et al. 1990 [DIRS 163346]). While the experimental evidence indicates that there may be some effect, the effect appears to be small and the contribution to uncertainty in dissolution rate is small compared to the two orders of magnitude range of uncertainty in dissolution rates (BSC 2004 [DIRS 169988], Table 8-1). For these reasons, the effects of irradiation damage on defense HLW glass degradation are excluded from explicit inclusion in the TSPA.

For the TSPA, all commercial SNF and DOE SNF cladding (with the exception of naval SNF) is considered to be breached on emplacement in the repository, as discussed in included FEP 2.1.02.12.0A (Degradation of Cladding Prior to Disposal). Following waste package failure, commercial SNF cladding unzipping is assumed to result in immediate exposure of bare fuel to the waste package environment (included FEP 2.1.02.23.0A (Cladding Unzipping)). It is also considered that DOE SNF (with the exception of naval SNF) degrades instantaneously upon exposure to liquid water (included FEP 2.1.02.01.0A (DSNF Degradation (Alteration, Dissolution, and Radionuclide Release)). No credit is taken for retardation of radionuclide release by fuel cladding. Therefore, the impact of radiation damage to the cladding (with the exception of naval SNF cladding) is of low consequence and will not affect the magnitude or timing of calculated radiological exposures to the RMEI or radionuclide releases to the accessible environment.

The Waste Package Materials Performance Peer Review Panel addressed the possibility of radiation damage in the repository in its final report (Beavers et al. 2002 [DIRS 158781], Section 3.10). They stated that the waste package will be subjected to a flux of neutrons and gamma rays from the stored radioactive waste (Beavers et al. 2002 [DIRS 158781]). These fluxes could cause the following: (1) neutrons could produce atomic displacement damage in the metal, (2) neutrons could produce atomic displacement damage and gamma rays could cause electron-hole pairs in the protective oxide layer on the metal, and (3) gamma rays could cause radiolysis of the surrounding environment (Beavers et al. 2002 [DIRS 158781], Section 3.10). The report concluded that there is no evidence to suggest that radiation damage to the waste package will alter its mechanical properties or that radiation damage would alter the protective properties of the passive film on Alloy 22 (Beavers et al. 2002 [DIRS 158781], Section 3.10). The effects of radiolysis on waste package corrosion are addressed in excluded FEP 2.1.13.01.0A (Radiolysis).

The cumulative neutron fluence at the waste package emplacement pallet as a function of years after emplacement is determined in *Dose Rate Calculation for 21-PWR Waste Package* (BSC 2004 [DIRS 172227], Section 6.4.1). At 290 years and 340 years after emplacement (the two longest times reported), the cumulative neutron fluence at the emplacement pallet location was determined to be 3.83×10^{14} neutrons/cm^2 and 3.95×10^{14} neutrons/cm^2, respectively (BSC 2004 [DIRS 172227], Table 6.4-1). The cumulative neutron fluence at the emplacement pallet location can therefore be approximated to be increasing at a rate of 2.4×10^{11} neutrons/cm^2/yr. Using this approximation, the maximum cumulative neutron fluence at the emplacement pallet location after 10,000 years would be about 2.4×10^{15} neutrons/cm^2 (taking no account of the reduction in neutron irradiation due to radioactive decay). Due to the close proximity of the waste package and the waste package emplacement pallet, it is reasonable

to equate the cumulative neutron fluence at the emplacement pallet location to the cumulative neutron fluence at the waste package location. *Nuclear Engineering Handbook* (Etherington 1958 [DIRS 164789], p. 10-107) identifies neutron fluence levels below which there is no change in the mechanical properties of Stainless Steel Type 316, nickel, and molybdenum. These neutron fluence levels are 5×10^{19} neutrons/cm^2, 10^{20} neutrons/cm^2, and 10^{20} neutrons/cm^2, respectively. Because the estimated neutron fluence is many orders of magnitude below the neutron fluence thresholds for changes in the mechanical properties of stainless steel, nickel, and molybdenum, significant neutron-induced radiation damage is not expected for either the waste package or pallet. This conclusion is consistent with that presented for Alloy 22 in the preceding paragraph.

The drip shield is located farther away from the major source of radiation (the waste form) than the waste package. On this basis, the drip shield material will be subject to smaller neutron and gamma radiation fields than the waste package. Radiation damage is expected to be of even less consequence to drip shield performance than it is to waste package performance. The effects of radiolysis on corrosion of the drip shield are addressed in excluded FEP 2.1.13.01.0A (Radiolysis).

Gamma radiation will have a negligible effect on the host rock. This conclusion is based on data presented in *Effect of Radiation on the Mechanical Properties of Topopah Spring Tuff* (Blair et al. 1996 [DIRS 129637]), where tuff specimens were irradiated with large doses (9±1 MGy) of gamma radiation and uniaxially tested to measure maximum strength and Young's modulus. A cumulative dose of 9 MGy in 10,000 years corresponds to an average dose rate of 90,000 rad/yr. To put this dose rate in perspective, the calculated gamma dose rate at the outer surface of a waste package containing 21 high-burnup (80 GWd/MTU) assemblies at 100 years after emplacement in the repository is about 35 rad/hr or 306,600 rad/yr (BSC 2004 [DIRS 172227], Figure 6.4-1). The tuff irradiation results show that there is no dicernible difference in the peak strengths and Young's modulus between the irradiated and unirradiated samples (Blair et al. 1996 [DIRS 129637], Table 5).

Closure of the repository subsurface facilities requires closing and sealing all openings from the surface to the underground facilities. These openings consist of the north ramp, south ramp, north construction ramps and portals, ventilation shafts/raises, and exploratory boreholes within the repository footprint (the waste emplacement area projected vertically to the surface), and in a buffer zone around the footprint boundary. Radiation is not expected to damage seals within the repository because the seals are remote with respect to the radiation sources (SNL 2007 [DIRS 179466], Table 4-1, Parameter Number 01-02).

Based on the previous discussion, omission of FEP 2.1.13.02.0A (Radiation Damage in EBS) will not result in a significant adverse change in the magnitude or timing of either radiological exposure to the RMEI or radionuclide releases to the accessible environment. Therefore, this FEP is excluded from the performance assessments conducted to demonstrate compliance with proposed 10 CFR 63.311 and 63.321 (70 FR 53313 [DIRS 178394]), and with 10 CFR 63.331 [DIRS 180319], on the basis of low consequence.

INPUTS:

Table 2.1.13.02.0A-1. Direct Inputs

Input	Source	Description
BSC 2004. *Dose Rate Calculation for 21-PWR Waste Package*. [DIRS 172227]	Section 6.4.1; Table 6.4-1	Cumulative neutron fluence over time
BSC 2004. *DSNF and Other Waste Form Degradation Abstraction*. [DIRS 172453]	Section 8.1	It is conservatively assumed that DOE SNF degrades instantaneously upon exposure to liquid water
	Sections 6.4, 6.4.1.5, 6.3.1, 6.3.2	Effects of irradiation damage in commercial SNF including formation of a recrystallized rim region and effects on matrix degradation and on the initial release fractions
BSC 2004. *Defense HLW Glass Degradation Model*. [DIRS 169988]	Table 8-1	Range of uncertainty in waste glass dissolution rates
Etherington 1958. *Nuclear Engineering Handbook*. [DIRS 164789]	p. 10-107	Neutron fluence level thresholds for changes in mechanical properties

Table 2.1.13.02.0A-2. Indirect Inputs

Citation	Title	DIRS
10 CFR 63	Energy: Disposal of High-Level Radioactive Wastes in a Geologic Repository at Yucca Mountain, Nevada	180319
70 FR 53313	Implementation of a Dose Standard After 10,000 Years	178394
Advocat et al. 1998	"Borosilicate Nuclear Waste Glass Alteration Kinetics: Chemical Inhibition and Affinity Control"	160446
Beavers et al. 2002	*Final Report, Waste Package Materials Performance Peer Review Panel, February 28, 2002*	158781
Blair et al. 1996	*Effect of Radiation on the Mechanical Properties of Topopah Spring Tuff*	129637
BSC 2004	*Dose Rate Calculation for 21-PWR Waste Package*	172227
BSC 2004	*CSNF Waste Form Degradation: Summary Abstraction*	169987
Dehaudt 2001	"Physical and Chemical State of the Nuclear Spent Fuel After Irradiation"	164019
Johnson et al. 2005	"Spent Fuel Radionuclide Source-Term Model for Assessing Spent Fuel Performance in Geological Disposal. Part I: Assessment of the Instant Release Fraction"	178773
Matzke 1992	"Radiation Damage-Enhanced Dissolution of UO_2 in Water"	113269
Pelletier 2001	"State of the Art on the Potential Migration of Species"	164034
Piron 2001	"Presentation of the Key Scientific Issues for the Spent Nuclear Fuel Evolution in a Closed System"	162396
SNL 2007	*Total System Performance Assessment Data Input Package for Requirements Analysis for Subsurface Facilities*	179466
Werme et al. 1990	"Chemical Corrosion of Highly Radioactive Borosilicate Nuclear Waste Glass Under Simulated Repository Conditions"	163346
Wronkiewicz 1993	*Effects of Radionuclide Decay on Waste Glass Behavior—A Critical Review*	171709

FEP: 2.1.13.03.0A

FEP NAME:

Radiological Mutation of Microbes

FEP DESCRIPTION:

Radiation fields could cause mutation of microorganisms, leading to unexpected chemical reactions and impacts.

SCREENING DECISION:

Excluded – low consequence

SCREENING JUSTIFICATION:

Evaluation of Potential Impacts of Microbial Activity on Drift Chemistry (BSC 2004 [DIRS 169991], Section 6.4) considers the repository-specific environmental constraints of: temperature, pressure, oxic and anoxic conditions, relative humidity, water availability, pH, salinity, nutrient availability, and radiation on microbial activity. These are summarized in excluded FEP 2.1.10.01.0A (Microbial Activity in the EBS). High temperatures, low water availability, and high ionic strengths are predicted to limit microbial activity during the thermal pulse, while nutrient availability will limit microbial activity after the pulse has passed. These are fundamental controls over microbial growth that apply not only to those microbes found in the Yucca Mountain repository presently, but to any mutated forms that might potentially form in the future as well.

Based on the previous discussion, omission of FEP 2.1.13.03.0A (Radiological Mutation of Microbes) will not result in a significant adverse change in the magnitude or timing of either radiological exposure to the RMEI or radionuclide releases to the accessible environment. Therefore, this FEP is excluded from the performance assessments conducted to demonstrate compliance with proposed 10 CFR 63.311 and 63.321 (70 FR 53313 [DIRS 178394]), and with 10 CFR 63.331 [DIRS 180319], on the basis of low consequence.

INPUTS:

Table 2.1.13.03.0A-1. Direct Inputs

Input	Source	Description
BSC 2004. *Evaluation of Potential Impacts of Microbial Activities on Drift Chemistry*. [DIRS 169991]	Section 6.4	Impacts of in-drift microbial activities

Table 2.1.13.03.0A-2. Indirect Inputs

Citation	Title	DIRS
10 CFR 63	Energy: Disposal of High-Level Radioactive Wastes in a Geologic Repository at Yucca Mountain, Nevada	180319
70 FR 53313	Implementation of a Dose Standard After 10,000 Years	178394

FEP: 2.1.14.15.0A

FEP NAME:

In-Package Criticality (Intact Configuration)

FEP DESCRIPTION:

The waste package internal structures and the waste form remain intact. If there is a breach (or are breaches) in the waste package that allows water to either accumulate or flow-through the waste package, then criticality could occur in-situ.

SCREENING DECISION:

Excluded – low probability

SCREENING JUSTIFICATION:

A prerequisite for any of the SNF waste forms to have potential for criticality is the introduction of water in liquid or vapor form to the inside of the TAD or DOE SNF canister. Mechanisms considered that may lead to damage or failure of the waste package and allow water into the system have been idenitified in included FEPs 2.1.03.08.0A (Early Failure of Waste Packages) and 2.1.03.08.0B (Early Failure of Drip Shields). All postclosure criticality FEP scenarios, internal and external, require the presence of water in liquid or vapor form to degrade the waste package internals and/or the waste form as intact configurations are designed to remain subcritical if fabricated and loaded according to design specifications as demonstrated in *CSNF Loading Curve Sensitivity Analysis* (SNL 2008 [DIRS 182788], Section 6.2.2), *DOE SNF Phase I and II Summary Report* (Radulescu et al. 2004 [DIRS 165482], Sections 10 and 11.4), *Intact and Degraded Mode Criticality Calculations for the Codisposal of TMI-2 Spent Nuclear Fuel in a Waste Package* (BSC 2004 [DIRS 168935], Section 6), and *Intact and Degraded Mode Criticality Calculations for the Codisposal of ATR Spent Nuclear Fuel in a Waste Package* (BSC 2004 [DIRS 171926], Section 6).

For a criticality event to occur, the appropriate combination of materials (e.g., neutron moderators, neutron absorbers, or fissile materials) and geometric configurations favorable to criticality must exist. Therefore, for a configuration to have potential for criticality, all of the following conditions must occur: (1) sufficient mechanical or corrosive damage to the waste package OCB to cause a breach, (2) presence of a moderator (i.e., water), (3) separation of fissionable material from the neutron absorber material or an absorber material selection error during the canister fabrication process, and (4) the accumulation (external) or presence of a critical mass of fissionable material in a critical geometric configuration. The probability of developing a configuration with criticality potential is insignificant unless all four conditions are realized, and then is only representative of a conservative estimate since the probability values associated with the many other events required to generate a critical configuration that are less than one are not quantified, but rather are conservatively set to one.

As stated in Section 1 of *Screening Analysis of Criticality Features, Events, and Processes for License Application* (SNL 2008 [DIRS 173869]), an evaluation of the criticality FEP scenarios

from *Configuration Generator Model* (BSC 2004 [DIRS 172494], Section 7) for configurations with potential for criticality has identified two dominant sequences of events that must occur for a criticality event to be credible, and which are common to each of the in-package scenario classes. The two independent events are: (1) improper manufacturing, resulting in the absence and/or loss of efficacy of the neutron absorber material, and (2) improper loading of fuel assemblies. These independent events, coupled with the probability of an initiating event that could result in breaching the waste package are evaluated in *Screening Analysis of Criticality Features, Event, and Processes for License Application* (SNL 2008 [DIRS 173869]), and provide an upper-bound estimate for the probability of achieving a configuration with potential for criticality. An upper bound is provided because, for independent event (1), absorber material misload–the probability of criticality is conservatively set to the maximum value (i.e., 1.0) within the sequence of events that make up the scenario. For independent event (2), waste form misload–the calculated probability of a criticality from a waste form misload is based on a bounding design basis configuration that maximizes reactivity potential, whereas the actual scenario class limiting configuration would be a less reactive configuration than the design basis configuration, thus having a lower increase in reactivity from a waste form misload.

The processes that are relevant to this FEP that can breach a waste package during the first 10,000 years after repository closure are: (1) stress corrosion cracking initiated from manufacturing defects and (2) misplaced drip shields allowing advective seepage onto waste packages leading to breaching. Radiolytic gas generation is discussed in excluded FEP 2.1.13.01.0A (Radiolysis) and is not considered a potential mechanism for breach. The TAD canisters and DOE SNF MCO canisters are expected to be loaded in spent fuel pools. Intact TAD and DOE canisters and waste packages are expected to contain little moisture, per requirements for drying (SNL 2007 [DIRS 179394], Table 4-1, Parameter Number 04-04), but retention of water in a canister could possibly occur if the drying and inerting process is incomplete. The process controls for the drying and inerting process for commercial SNF and DOE SNF canisters are expected to be similar to NUREG-1536, *Standard Review Plan for Dry Cask Storage Systems* (NRC (1997 [DIRS 101903], Section 8.V.1) and, thus, sufficiently rigorous to reduce the likelihood of leaving residual water in the TADs to levels that, if quantified, would not significantly increase the overall probability of criticality in the repository.

Fabrication defects in the waste package OCB that can lead to stress corrosion cracking have been analyzed in *Analysis of Mechanisms for Early Waste Package/Drip Shield Failure* (SNL 2007 [DIRS 178765], Section 6). Such events include, for example, improper material selection, improper heat treatment, and waste package OCB lid closure weld flaws. The probabilities associated with the set of fabrication defects in the waste package OCB have been evaluated individually from the respective event tree/fault tree diagrams and collectively with the exception of the weld flaws in the latter case. Thus, probability values from the collective evaluation are used, for example, in the scenario where a waste package OCB breach could result from any one of several SCC initiators. Probability values from the individual evaluations are used where a waste package OCB breach could result from a specific SCC initiator such as failure of the low plasticity burnishing process for stress mitigation.

Certain DOE SNF waste forms have sufficient quantities of fissile material to support unmoderated (fast) criticality if the fissile material is concentrated beyond its design concentration in the waste form and the neutron absorber materials are removed. While

concentration of the fissile material beyond its nominal design concentration could result from degradation of the waste form by either water ingress or a disruptive event, removal of the neutron absorber materials from a DOE SNF waste package would require a breach of the waste package and a removal mechanism. Degradation in the presence of water would result in a moderated system. Likewise, there is no known mechanism that could reconfigure non-degraded fissile material into a compact configuration with unmoderated criticality potential. The most plausible neutron absorber material removal mechanism is through water ingress resulting in degradation of the waste package internal components, dissolving of the neutron absorber material in the water, and flushing of the material from the waste package. This mechanism is not expected to result in a critical configuration since the corrosion rate of the neutron absorber material is very low. In addition, the gadolinium absorber in the DOE SNF canisters forms phosphate or carbonate corrosion products (SNL 2007 [DIRS 181165], Section 6.3.16) that have very low solubility.

Sources of corrosion of the waste package OCB have been considered in the screening of processes affecting waste package degradation in included FEP 2.1.03.02.0A (Stress Corrosion Cracking of Waste Packages). This FEP identifies the propagation of incipient cracks that can occur on the waste package outer barrier closure welds (as these cannot be annealed to relieve tensile stress but stress mitigation processes will be employed (i.e., low plasticity burnishing)) and/or fabrication flaws in the waste packages as possible initiating mechanisms for the development of stress corrosion cracking of the waste package outer barrier. These mechanisms are discussed in *Stress Corrosion Cracking of Waste Package Outer Barrier and Drip Shield Materials* (SNL 2007 [DIRS 181953], Section 8.4.2.1) and *Analysis of Mechanisms for Early Waste Package/Drip Shield Failure* (SNL 2007 [DIRS 178765], Section 6.3). SCCs can be initiated on a smooth weld surface (with incipient cracks) or at existing weld flaws if the tensile stresses exceed the threshold stress for SCC nucleation that is taken to be 90% to 105% of the yield strength. Because weld flaws are already formed, they do not require a stress threshold to nucleate. However, most of the weld flaws are embedded within the material and not initially exposed to the environment. Thus, such flaws will not propagate until exposed to the environment. As general corrosion proceeds, some initially embedded weld flaws may be exposed to the environment while others are corroded away.

All regions of the Alloy 22 waste package outer barrier, except the outer-closure lid welds, are solution-annealed before the waste packages are loaded with SNF assemblies. Thus, the waste package OCB will not be expected to develop residual stresses or stress intensity factors sufficiently high for SCC to occur provided that fabrication defects in the waste package OCB are not present that can lead to stress corrosion cracking.

The criticality potential of the in-package intact configuration scenario is negligible since the EBS components and neutron absorber materials are designed to maintain their function in nominal repository environments over the first 10,000-year period after repository closure by specifying a corrosion allowance or minimum thickness (SNL 2007 [DIRS 179394], Table 4-1, Parameter Numbers 03-07 and 03-10). Although configurations not conforming to design specifications are applicable to both intact and degraded scenarios, configurations with potential for criticality require sufficient water for moderation.

Evaluation of the neutron absorber material misload failure mechanism is an important consideration for the determination of a configuration criticality potential. The probability that proper neutron absorber material is not used in the waste package (or waste form if integrally connected) or becomes separated from the fissile material must then be evaluated for configurations where absorber material is necessary for criticality control. Misloading of the waste forms is also an important consideration for the determination of a configuration criticality potential for commercial SNF that requires restricted loading configurations (i.e., specified loading curves). The probability that such waste forms are not loaded as required must then be evaluated.

The neutron absorber misload event represents the absence and/or loss of efficacy of the neutron absorber plates due to fabrication-related errors (e.g., incorrect material installed during fabrication, absorber content of plates outside specified range). These types of events can only occur during fabrication and/or loading of a canister due to process or procedural errors and are similar to waste package and drip shield early failure mechanisms (SNL 2007 [DIRS 178765], Section 6.2). Errors in fabrication and operational processes are primarily due to human factors that are common to the various processes. Surrogate fabrication and operational processes with associated human factor errors have been evaluated in *Analysis of Mechanisms for Early Waste Package/Drip Shield Failure* (SNL 2007 [DIRS 178765]) and results are used for such initiating events for the waste package and drip shield early failure mechanisms. The surrogate processes are:

1. Improper performance of the neutron absorber plates represented as a material selection error in the waste package component fabrication processes (SNL 2007 [DIRS 178765], Section 6.3.2)

2. Failure of the waste package and canister drying/inerting process represented as an operational process error (SNL 2007 [DIRS 178765], Section 6.3.5)

3. Drip shield misplacement allowing the possibility of advective seepage flow directly on a waste package OCB (SNL 2007 [DIRS 178765], Section 6.4.4)

4. Fabrication flaws allowing increased susceptibility to SCCs (SNL 2007 [DIRS 178765], Section 6.3).

Waste package fabrication and operational process error probabilities have been obtained from DTNs: MO0701PASHIELD.000 [DIRS 180508] and MO0705EARLYEND.000 [DIRS 180946]. The probability values assigned to absorber plate misloads due to material selection errors, waste package and canister operational process failures, waste package SCC mitigation process failures, and the occurrence of OCB closure lid weld flaws for this analysis are listed in Table 2.1.14.15.0A-1. The operational process failures include the drying and inerting process and OCB outer lid weld stress mitigation process. These processes are conceptually similar since each requires operator actions and the human error failure rate from the OCB outer lid weld stress mitigation process is assigned to each one in Table 2.1.14.15.0A-1.

Table 2.1.14.15.0A-1. Undetected Errors in Waste Package Fabrication and Operational Processes

Waste Package Operations	Probability per Canister
Absorber material selection error [a]	1.25×10^{-7} per canister
Outer closure lid weld stress mitigation process failure [a]	3.8×10^{-5} per canister
Emplacement error for drip shield [a]	4.36×10^{-9} per drip shield
Fraction of waste package OCB lid weld flaws oriented normally to surface [b]	0.008
Probability of undetected fabrication defects in a waste package OCB [b]	1.13×10^{-4} per waste package
Probability of at least one flaw in waste package OCB lid closure weld [c]	0.156

Sources: [a] DTN: MO0705EARLYEND.000 [DIRS 180946], file: *Table 1.doc*, Table 1.
[b] DTN: MO0701PASHIELD.000 [DIRS 180508], file: *Tables for DTN Readme.doc*, Table 1.
[c] DTN: MO0701PASHIELD.000 [DIRS 180508], file: *EarlyFail-WeldDefects.zip*, Section A.7.

The mean value for the probability that a waste package OCB has at least one such defect was estimated using a Monte Carlo sampling process on the collective set of waste package OCB fabrication flaws (excluding OCB closure lid weld flaws) resulting in a value of 1.13×10^{-4} per waste package (Table 2.1.14.15.0A-1).

The outer closure lid weld is plasticity burnished to produce a layer of compressive stress that prevents SCC initiation until general corrosion removes this layer. The probability of having at least one undetected flaw in the outer closure lid weld is 0.156 from Table 2.1.14.15.0A-1. However, such flaws are preferentially oriented in the circumferential direction along the weld, and as such they will not propagate when under residual hoop stress that would parallel most flaws. Only a small fraction (i.e., 0.008 from Table 2.1.14.15.0A-1) of these flaws would be oriented sufficiently normal to the residual hoop stress direction to permit propagation once the compressive stress layer is removed by corrosive action. Thus, the probability of a closure lid weld having a flaw that can propagate is given by $0.156 \times 0.008 = 1.25 \times 10^{-3}$. Specifications for controlled or low-plasticity burnishing of the waste package OCB closure lid call for the outer lid weld to be stress mitigated to a compressive depth of at least 3 mm (SNL 2007 [DIRS 179394], Table 4-1, Parameter Number 03-17). The upper values for the range of general corrosion rates for Alloy 22 from *General Corrosion and Localized Corrosion of Waste Package Outer Barrier* (SNL 2007 [DIRS 178519], Figure 6-10) is 15 nm/yr, which implies that the compressive layer will survive for $\geq 2 \times 10^5$ years in nominal repository conditions provided the low-plasticity burnishing process is properly performed.

The initiating events where the OCB is potentially breached include the failure of the low-plasticity burnishing process such that the compressive stress layer in the waste package OCB closure lid is not produced, failure of the waste package OCB stress mitigation processes to function properly, weld flaws in the waste package OCB lid, and failure to properly emplace drip shields. Weld flaws in the waste package OCB lid or a failure of the stress mitigation processes can lead to a waste package breach from either weld flaw propagation or SCCs initiated by the residual stresses. A drip shield emplacement error could result in an advective flow path to the waste package OCB, creating an environment for subsequent localized corrosion processes that

could breach the waste package OCB (included FEP 2.1.03.03.0A (Localized Corrosion of Waste Packages)).

Events requiring probability values for the screening calculation are listed as follows:

1. Probability of a failure for the low-plasticity burnishing process on the waste package OCB closure lid, or a failure of processes for stress mitigation for the waste package OCB, or a drip shield emplacement error

2. Probability of improper absorber material in a canister

3. Probability of a loading curve violation for a 21-PWR TAD canister.

The probabilities of events in this scenario are derived from preclosure activities, making those values independent of the postclosure period. The mean value of the probability distribution for failure of the low-plasticity burnishing process is given in Table 2.1.14.15.0A-1 as 3.8×10^{-5}. The probability that a waste package OCB closure weld has a flaw that can propagate through the OCB was estimated previously as 1.25×10^{-3} per waste package. The mean probability of waste package OCB fabrication defects as 1.13×10^{-4} per waste package and the mean probability value for improper emplacement of a drip shield is given in Table 2.1.14.15.0A-1 as 4.36×10^{-9} per drip shield. The probability of localized corrosion breaching the waste package OCB from advective seepage flow is conservatively set to 1.0. The probability of installing improper absorber plate material in a TAD or DOE canister is a fabrication related error. This type of error was evaluated in *Analysis of Mechanisms for Early Waste Package/Drip Shield Failure* (SNL 2007 [DIRS 178765], Section 6.3.2). The mean value of the probability distribution for a fabrication failure is given in Table 2.1.14.15.0A-1 as 1.25×10^{-7} per canister.

An analysis of commercial SNF misload probabilities was documented in *Commercial Spent Nuclear Fuels Waste Package Misload Analysis* (BSC 2003 [DIRS 166316]). Results from this analysis establish that the probability of a loading curve violation in a 21-PWR waste package is 1.18×10^{-5} (BSC 2003 [DIRS 166316], Table 41). The TAD canister specifications require the canisters for PWR SNF to contain 21 assemblies similar to the 21-PWR waste package (SNL 2007 [DIRS 179394], Section 4.1.1.2). The cited analysis is used as a surrogate for misloading waste forms in a TAD canister since the misloading of an assembly into a TAD canister requires the same improper selection of an assembly with characteristics (burnup and enrichment) in the unacceptable range of the loading curve. Thus, the probability of a loading curve violation for TAD canisters is expected to be similar in magnitude to the 21-PWR waste package value. However, neighboring assemblies that have low reactivity values may provide partial compensation for the excess reactivity from the incorrectly loaded assembly. Given that a misloading curve violation occurs, the likelihood of the misloaded configuration having potential for criticality has been shown to be 0.014 from results of a probabilistic calculation of that potential (SNL 2008 [DIRS 182788], Section 7). The probability of a potentially critical configuration resulting from an assembly misload of a 21-PWR TAD canister is $0.014 \times 1.18 \times 10^{-5} = 1.65 \times 10^{-7}$ per TAD canister.

The probability of misloading assemblies in the 44-BWR TAD canister is insignificant since the BWR waste stream inventory for the repository is in the acceptable region of the loading curve

map (SNL 2008 [DIRS 182788], Section 6.1.1.1.3). Misloading of waste forms in DOE SNF canisters is considered very improbable because the shape and size of the defense HLW glass canisters and the various DOE SNF canisters differ significantly and can be readily distinguished by visual inspection. Thus, the waste form misload probability for DOE SNF waste packages is considered to be sufficiently low such that, if quantified, would not significantly increase the overall probability of criticality in the repository.

The probability for the occurrence of configurations with potential for criticality is evaluated from a number of independent sets of sequences of events where all of the events in any specific sequence must happen for that configuration to occur. Since the events in any one sequence can also be considered as independent entities, the probability of the sequence is the product of the probability of each individual event. The expected probability of having a particular sequence occur in exactly *k* waste packages in the repository is a binomial process described by the binomial probability distribution, $P_B(k; p, N)$, with probability "p" for occurrence in a waste package and "q = 1 − p" for non-occurrence. The probability of having the sequence occur in at least "*k + 1*" waste packages is given by:

$$P(\text{at least } k+1 \text{ waste packages}) = 1 - \sum_{l=0 \text{ to } k} P_B(l; p, N) \quad \text{(Eq. 2.1.14.15.0A-1)}$$

where

k = number of items affected (e.g., waste packages, drip shields)

p = probability for occurrence of the event

N = number of possible items involved.

For large N and small "p" where N × p ≅ λ, the binomial distribution converges to the Poisson distribution (P_P) with a mean of λ = N × p. Then Equation 2.1.14.15.0A-1 can be rewritten as:

$$P(\text{at least } k+1 \text{ waste packages}) = 1 - \sum_{l=0,k} P_P(l; N \times p) = 1 - \sum_{l=0,k} \frac{\lambda^l \times \exp(-\lambda)}{l!}$$

(Eq. 2.1.14.15.0A-2)

The criterion for screening criticality scenarios from consideration in the repository as having a low probability for the occurrence of a criticality event sequence for any waste package in the repository (which can be stated as the probability of having at least one such sequence occur) is given by Equation 2.1.14.15.0A-2 with $k = 0$. For the case where $k = 0$ and λ is small, Equation 2.1.14.15.0A-2 can be approximated by λ. Then the probability of at least one waste package configuration with criticality potential occurring in the repository is given by λ ($= N \times p$).

Evaluating the event sequences for commercial SNF and DOE SNF with potential for criticality using the number of PWR TAD canisters as 4,568, the number of 44-BWR TAD canisters as 2,915, and DOE SNF canisters that require neutron absorber plates (DOE1, DOE2, and DOE7 groups) as 1,223 (SNL 2008 [DIRS 173869], Section 6.3.2), and setting the number of drip shields equal to the number of waste packages gives:

PWR TAD canister loading curve violation:

$$\{1 - P_B (0; ((3.8 \times 10^{-5} \times 1.25 \times 10^{-3} + 1.13 \times 10^{-4} + 4.36 \times 10^{-9} \times 1.0) \times 1.65 \times 10^{-7}), 4568)\} = 8.5 \times 10^{-8}$$

PWR TAD canister absorber misload:

$$\{1 - P_B (0; ((3.8 \times 10^{-5} \times 1.25 \times 10^{-3} + 1.13 \times 10^{-4} + 4.36 \times 10^{-9} \times 1.0) \times 1.25 \times 10^{-7}), 4568)\} = 6.5 \times 10^{-8}$$

44-BWR TAD canister absorber misload:

$$\{1 - P_B (0; ((3.8 \times 10^{-5} \times 1.25 \times 10^{-3} + 1.13 \times 10^{-4} + 4.36 \times 10^{-9} \times 1.0) \times 1.25 \times 10^{-7}), 2915)\} = 4.1 \times 10^{-8}$$

DOE SNF canister absorber misload (DOE1, DOE2, and DOE7):

$$\{1 - P_B (0; ((3.8 \times 10^{-5} \times 1.25 \times 10^{-3} + 1.13 \times 10^{-4} + 4.36 \times 10^{-9} \times 1.0) \times 1.25 \times 10^{-7}), 1223)\} = 1.7 \times 10^{-8}$$

Thus, a conservative estimate for the probability of achieving a configuration with criticality potential in the repository due to the presence of weld flaws in the OCB closure lid or other early failure mechanisms, based on summing this set of events, including the DOE1, DOE2, and DOE7 contributions is 2.1×10^{-7} for 10,000 years. Since the events in the above evaluation are all associated with operations during the preclosure period, the probabilities are constant over the postclosure time period. It should be noted that the other DOE criticality SNF groups do not pose a criticality concern because they do not need to rely on neutron absorber plates for criticality control. These evaluations are demonstrated in *DOE SNF Phase I and II Summary Report* (Radulescu et al. 2004 [DIRS 165482]), *Intact and Degraded Mode Criticality Calculations for the Codisposal of TMI-2 Spent Nuclear Fuel in a Waste Package* (BSC 2004 [DIRS 168935]), and *Intact and Degraded Mode Criticality Calculations for the Codisposal of ATR Spent Nuclear Fuel in a Waste Package* (BSC 2004 [DIRS 171926]).

Summary—As documented in *Screening Analysis of Criticality Features, Events, and Processes for License Application* (SNL 2008 [DIRS 173869]), the probability of criticality for the in-package location is much less than 1 chance in 10,000 of occurrence within 10,000 years after disposal. Accordingly, this FEP is excluded from the performance assessments conducted to demonstrate compliance with proposed 10 CFR 63.311 and 63.321 (70 FR 53313 [DIRS 178394]), and with 10 CFR 63.331 [DIRS 180319], on the basis of low probability.

In addition, as documented in *Screening Analysis of Criticality Features, Events, and Processes for License Application* (SNL 2008 [DIRS 173869]) the probability of criticality for all locations is less than 1 chance in 10,000 of occurrence within 10,000 years after disposal. The results documented in this analysis are applicable for all waste forms and waste package variants.

INPUTS:

Table 2.1.14.15.0A-2. Direct Inputs

Input	Source	Description
BSC 2003. *Commercial Spent Nuclear Fuel Waste Package Misload Analysis*. [DIRS 166316]	Table 41	Error probabilities for commercial SNF waste package loading violation
BSC 2004. *Intact and Degraded Mode Criticality Calculations for the Codisposal of ATR Spent Nuclear Fuel in a Waste Package*. [DIRS 171926]	Section 6	Criticality potential of DOE SNF waste forms
DTN: MO0701PASHIELD.000. Waste Package/Drip Shield Early Failure Probabilities. [DIRS 180508]	Tables for DTN *Readme.doc*, Table 1	Error probabilities for fabrication and operational processes representing waste package and drip shield early failure mechanisms
DTN: MO0705EARLYEND.000. Waste Package/Drip Shield Early Failure End State Probabilities. [DIRS 180946]	file: *Table 1.doc*, Table 1	Error probabilities for fabrication and operational processes representing waste package and drip shield early failure mechanisms
Radulescu et al. 2004. *DOE SNF Phase I and II Summary Report*. [DIRS 165482]	Sections 10 and 11.4	Criticality potential of DOE SNF waste forms
SNL 2007. *Stress Corrosion Cracking of Waste Package Outer Barrier and Drip Shield Materials*. [DIRS 181953]	Section 8.4.2.1	Initiating mechanisms for SCCs
SNL 2007. *Total System Performance Assessment Data Input Package for Requirements Analysis for TAD Canister and Related Waste Package Overpack Physical Attributes Basis for Performance Assessment*. [DIRS 179394]	Table 4-1, Parameter Numbers 03-07 and 03-10	Minimum thickness of materials to maintain material functionality after allowing for corrosion
SNL 2008. *CSNF Loading Curve Sensitivity Analysis*. [DIRS 182788]	Section 6.1.1.1.3	Probability of a critical configuration resulting from a BWR SNF waste package loading violation
	Section 7	Probability of a critical configuration resulting from a PWR SNF waste package loading violation
	Section 6.2.2	Criticality potential of commercial SNF waste forms
SNL 2008. *Screening Analysis of Criticality Features, Events, and Processes for License Application*. [DIRS 173869]	Section 6.3.2	Waste package inventory by type

Table 2.1.14.15.0A-3. Indirect Inputs

Citation	Title	DIRS
10 CFR 63	Energy: Disposal of High-Level Radioactive Wastes in a Geologic Repository at Yucca Mountain, Nevada	180319
70 FR 53313	Implementation of a Dose Standard After 10,000 Years	178394
BSC 2003	*Commercial Spent Nuclear Fuel Waste Package Misload Analysis*	166316
BSC 2004	*Configuration Generator Model*	172494
BSC 2004	*Intact and Degraded Mode Criticality Calculations for the Codisposal of TMI-2 Spent Nuclear Fuel in a Waste Package*	168935
NRC 1997	*Standard Review Plan for Dry Cask Storage Systems*	101903
SNL 2007	*Analysis of Mechanisms for Early Waste Package/Drip Shield Failure*	178765
SNL 2007	*General Corrosion and Localized Corrosion of Waste Package Outer Barrier*	178519
SNL 2007	*Geochemistry Model Validation Report: Material Degradation and Release Model*	181165
SNL 2007	*Total System Performance Assessment Data Input Package for Requirements Analysis for TAD Canister and Related Waste Package Overpack Physical Attributes Basis for Performance Assessment*	179394
SNL 2008	*Screening Analysis of Criticality Features, Events, and Processes for License Application*	173869

FEP: 2.1.14.16.0A

FEP NAME:

In-Package Criticality (Degraded Configurations)

FEP DESCRIPTION:

The waste package internal structures and the waste form may degrade. If a critical configuration (sufficient fissile material, and neutron moderator, lack of neutron absorbers) develops, a criticality event could occur in-situ. Potential in-situ critical configurations are defined in figures 3.2a and 3.2b of *Disposal Criticality Analysis Methodology Topical Report* (YMP 2003 [DIRS 165505]).

SCREENING DECISION:

Excluded – low probability

SCREENING JUSTIFICATION:

This FEP is analogous in content to excluded FEP 2.1.14.15.0A (In-Package Criticality (Intact Configuration)) with the exception of the configuration.

As noted in excluded FEP 2.1.14.15.0A (In-Package Criticality (Intact Configuration)), for a criticality event to occur, the appropriate combination of materials (e.g., neutron moderators, neutron absorbers, or fissile materials) and geometric configurations favorable to criticality must exist. Therefore, for a configuration to have potential for criticality, all of the following conditions must occur: (1) sufficient mechanical or corrosive damage to the waste package OCB to cause a breach, (2) presence of a moderator (i.e., water), (3) separation of fissionable material from the neutron absorber material or an absorber material selection error during the canister fabrication process, and (4) the accumulation (external) or presence of a critical mass of fissionable material in a critical geometric configuration.

Since this FEP considers degraded internal configurations, the cladding is considered breached within a damaged or failed waste package and the interior of the fuel rods are assumed to be exposed to the repository environment allowing the fissile material to convert to the mineral schoepite (UO_3:$2H_2O$) (SNL 2008 [DIRS 173869], Section 6.3.2). The criticality potential of the in-package degraded configuration scenario is negligible provided that waste packages are fabricated and loaded according to design specifications, as sensitivity studies have shown that the PWR SNF waste form in various degraded configurations, such as saturated porous schoepite, does not result in a more reactive configuration than the design basis configuration (SNL 2007 [DIRS 181373], Table A-12; SNL 2008 [DIRS 182788], Section 6.2.5). Although configurations not conforming to design specifications are applicable to intact and degraded scenarios, configurations with potential for criticality require sufficient water for moderation. These were considered in excluded FEP 2.1.14.15.0A (In-Package Criticality (Intact Configuration)) and show that the probability of criticality for the in-package location is much less than 1 chance in 10,000 of occurrence within 10,000 years after disposal. Accordingly, FEP 2.1.14.16.0A (In-Package Criticality (Degraded Configurations)) is excluded from the

performance assessments conducted to demonstrate compliance with proposed 10 CFR 63.311 and 63.321 (70 FR 53313 [DIRS 178394]), and with 10 CFR 63.331 [DIRS 180319], on the basis of low probability.

INPUTS:

Table 2.1.14.16.0A-1. Direct Inputs

Input	Source	Description
SNL 2007. *Commercial Spent Nuclear Fuel Igneous Scenario Criticality Evaluation*. [DIRS 181373]	Table A-12	Criticality potential of commercial SNF waste forms
SNL 2008. *CSNF Loading Curve Sensitivity Analysis*. [DIRS 182788]	Section 6.2.5	Criticality potential of commercial SNF waste forms

Table 2.1.14.16.0A-2. Indirect Inputs

Citation	Title	DIRS
10 CFR 63	Energy: Disposal of High-Level Radioactive Wastes in a Geologic Repository at Yucca Mountain, Nevada	180319
70 FR 53313	Implementation of a Dose Standard After 10,000 Years	178394
SNL 2008	*Screening Analysis of Criticality Features, Events, and Processes for License Application*	173869
YMP 2003	*Disposal Criticality Analysis Methodology Topical Report*	165505

FEP: 2.1.14.17.0A

FEP NAME:

Near-Field Criticality

FEP DESCRIPTION:

Near-field criticality could occur if fissile material-bearing solution from the waste package is transported into the drift and the fissile material is precipitated into a critical configuration. Potential near-field critical configurations are defined in *Disposal Criticality Analysis Methodology Topical Report* (YMP 2003 [DIRS 165505], Figure 3.3a).

SCREENING DECISION:

Excluded – low probability

SCREENING JUSTIFICATION:

This FEP justification accounts for external criticality for the near-field location for those conditions that may lead to damage or failure of the waste package and allow water into the system, as identified in included FEPs 2.1.03.08.0A (Early Failure of Waste Packages) and 2.1.03.08.0B (Early Failure of Drip Shields). A prerequisite for any of the spent fuel waste forms to have potential for criticality is the introduction of water in liquid or vapor form to the inside of the TAD or DOE SNF canister. All postclosure criticality FEP scenarios, internal and external, require the presence of water in liquid or vapor form to degrade the waste package internals and/or the waste form, as intact configurations are designed to remain subcritical if fabricated and loaded according to design specifications as demonstrated in *CSNF Loading Curve Sensitivity Analysis* (SNL 2008 [DIRS 182788], Section 6.2.2), *DOE SNF Phase I and II Summary Report* (Radulescu et al. 2004 [DIRS 165482], Sections 10 and 11.4), *Intact and Degraded Mode Criticality Calculations for the Codisposal of TMI-2 Spent Nuclear Fuel in a Waste Package* (BSC 2004 [DIRS 168935], Section 6), and *Intact and Degraded Mode Criticality Calculations for the Codisposal of ATR Spent Nuclear Fuel in a Waste Package* (BSC 2004 [DIRS 171926], Section 6).

For a criticality event to occur, the appropriate combination of materials (e.g., neutron moderators, neutron absorbers, or fissile materials) and geometric configurations favorable to criticality must exist. Therefore, for a configuration to have potential for criticality, all of the following conditions must occur: (1) sufficient mechanical or corrosive damage to the waste package OCB to cause a breach, (2) presence of a moderator (i.e., water), (3) separation of fissionable material from the neutron absorber material or an absorber material selection error during the canister fabrication process, and (4) the accumulation (external) or presence of a critical mass of fissionable material in a critical geometric configuration. The probability of developing a configuration with criticality potential is insignificant unless all four conditions are realized, and then is only representative of a conservative estimate since the probability values associated with the many other events required to generate a critical configuration that are less than one are not quantified, but rather are conservatively set to one.

Near-field criticality cannot occur unless the waste package and waste form are degraded. Water infiltration is required to degrade the waste package internals and waste form and transport them to the near-field location. Criticality cannot occur unless at least the minimum critical mass of a waste form can be accumulated in a favorable geometry. The probability of an external criticality event is expected to be lower than the probability of an in-package criticality event. This is because, in addition to the events evaluated to calculate the probability of water infiltrating a breached waste package, the probability of the following events or processes must also be considered for external criticality:

- Separation of the fissile materials from the degraded waste form
- Sufficient seepage water to transport fissile materials from the waste package
- Accumulating sufficient fissile material into a potentially critical configuration in the near-field environment.

Because the quantity of material released by diffusion would be small due to the tortuousity of the path, advective flow of water is necessary for transporting fissile materials from the waste package to the near-field in any appreciable quantities to be considered for criticality (SNL 2007 [DIRS 181165], Section 6.2). An advective seepage flow path to a waste package for nominal repository conditions would occur due to misplacement of a drip shield leading to breaching of the waste package from localized corrosion. However, the probability of this type of event is very low (4.36×10^{-9} per drip shield; DTN: MO0705EARLYEND.000 [DIRS 180946], file: *Table 1.doc*, Table 1). Since this type of event occurs during the preclosure time period, it is independent of the postclosure time period. Using the total number of waste packages (11,162; DTN: MO0702PASTREAM.001 [DIRS 179925], file: *DTN-Inventory-Rev00.xls*, worksheet "Unit Cell") as a conservative estimate for the number of drip shields (it is conservative because not all waste packages have sufficient quantities of fissile material to result in a criticality event) and multiplying by the probability of misplacing a drip shield results in an initiating event probability of 4.9×10^{-5}. This value is already below the regulatory screening criterion of 1 chance in 10,000 (10^{-4}) of occurrence within 10,000 years after disposal prior to consideration of probabilities (which would be less than 1.0) associated with the amount of degradation and accumulation into a favorable geometry for criticality that would only result in lowering the sequence probability.

As indicated in excluded FEP 2.1.14.26.0A (Near-Field Criticality Resulting from an Igneous Event) and excluded FEP 2.1.14.20.0A (Near-Field Criticality Resulting from a Seismic Event), the amount of fissile material accumulation in the near-field location is insufficient to pose a criticality concern. Note that the material degradation of the internals and subsequent accumulation in the near-field based on the seismic and igneous scenarios are bounding for nominal repository conditions because the seismic and igneous seepage fluxes are much higher. Therefore, under bounding seepage fluxes resulting from a seismic or igneous initiating event, an insufficient amount of fissile material could accumulate in the near-field to pose a criticality concern. It can be concluded that under nominal repository conditions, an insufficient amount of fissile material can accumulate in the near-field location to pose a criticality concern.

Accordingly, this FEP is excluded from the performance assessments conducted to demonstrate compliance with proposed 10 CFR 63.311 and 63.321 (70 FR 53313 [DIRS 178394]), and with 10 CFR 63.331 [DIRS 180319], on the basis of low probability.

In addition, as documented in *Screening Analysis of Criticality Features, Events, and Processes for License Application* (SNL 2008 [DIRS 173869], Section 7.1) the probability of criticality for all locations is less than 1 chance in 10,000 of occurrence within 10,000 years after disposal. The results documented in this analysis are applicable for all waste forms and waste package variants.

INPUTS:

Table 2.1.14.17.0A-1. Direct Inputs

Input	Source	Description
DTN: MO0702PASTREAM.001. Waste Stream Composition and Thermal Decay Histories for LA. [DIRS 179925]	file: *DTN-Inventory-Rev00.xls,* worksheet: "UNIT CELL"	Waste package inventory
DTN: MO0705EARLYEND.000. Waste Package/Drip Shield Early Failure End State Probabilities. [DIRS 180946]	file: *Table 1.doc*, Table 1	Probability of drip shield misplacement
SNL 2008. *Screening Analysis of Criticality Features, Events, and Processes for License Application*. [DIRS 173869]	Section 7.1	Probability of criticality for all locations below regulatory criterion

Table 2.1.14.17.0A-2. Indirect Inputs

Citation	Title	DIRS
10 CFR 63	Energy: Disposal of High-Level Radioactive Wastes in a Geologic Repository at Yucca Mountain, Nevada	180319
70 FR 53313	Implementation of a Dose Standard After 10,000 Years	178394
BSC 2004	*Intact and Degraded Mode Criticality Calculations for the Codisposal of ATR Spent Nuclear Fuel in a Waste Package*	171926
BSC 2004	*Intact and Degraded Mode Criticality Calculations for the Codisposal of TMI-2 Spent Nuclear Fuel in a Waste Package*	168935
Radulescu et al. 2004	*DOE SNF Phase I and II Summary Report*	165482
SNL 2007	*Geochemistry Model Validation Report: Material Degradation and Release Model*	181165
SNL 2008	*CSNF Loading Curve Sensitivity Analysis*	182788
YMP 2003	*Disposal Criticality Analysis Methodology Topical Report*	165505

FEP: 2.1.14.18.0A

FEP NAME:

In-Package Criticality Resulting from a Seismic Event (Intact Configuration)

FEP DESCRIPTION:

The waste package internal structures and the waste form remain intact either during or after a seismic disruptive event. If there is a breach (or are breaches) in the waste package that allow(s) water to either accumulate or flow through the waste package, then criticality could occur in-situ.

SCREENING DECISION:

Excluded – low probability

SCREENING JUSTIFICATION:

This FEP justification accounts for in-package criticality for the seismic scenario assuming an intact configuration. It is possible for in-package criticality to be analyzed as either an intact or degraded configuration. After a seismic event, the in-package, intact configuration is designed to remain subcritical, even under unanticipated fully flooded conditions; therefore, only degraded configurations are relevant for the assessment of criticality in the in-package location. Although configurations not conforming to design specifications are possible, these are evaluated in the degraded configuration class (SNL 2008 [DIRS 173869], Section 6.4). Accordingly, this FEP is excluded from the performance assessments conducted to demonstrate compliance with proposed 10 CFR 63.311 and 63.321 (70 FR 53313 [DIRS 178394]), and with 10 CFR 63.331 [DIRS 180319], on the basis of low probability. The in-package degraded configuration resulting from a seismic event is discussed in excluded FEP 2.1.14.19.0A (In-package Criticality Resulting from a Seismic Event (Degraded Configuration)).

In addition, as documented in *Screening Analysis of Criticality Features, Events, and Processes for License Application* (SNL 2008 [DIRS 173869], Section 7.1), the probability of criticality for all locations is less than 1 chance in 10,000 of occurrence within 10,000 years after disposal. The results documented in this analysis are applicable for all waste forms and waste package variants.

INPUTS:

Table 2.1.14.18.0A-1. Direct Inputs

Input	Source	Description
SNL 2008. *Screening Analysis of Criticality Features, Events, and Processes for License Application*. [DIRS 173869]	Section 6.4	Configurations not conforming to design specifications are evaluated in the degraded configuration class
	Section 7.1	Probability of criticality for allocations below the regulatory criterion

Table 2.1.14.18.0A-2. Indirect Inputs

Citation	Title	DIRS
10 CFR 63	Energy: Disposal of High-Level Radioactive Wastes in a Geologic Repository at Yucca Mountain, Nevada	180319
70 FR 53313	Implementation of a Dose Standard After 10,000 Years	178394

FEP: 2.1.14.19.0A

FEP NAME:

In-Package Criticality Resulting from a Seismic Event (Degraded Configurations)

FEP DESCRIPTION:

Either during or as a result of a seismic disruptive event, the waste package internal structures and the waste form may degrade. If a critical configuration develops, criticality could occur in-situ. Potential in-situ critical configurations are defined in *Disposal Criticality Analysis Methodology Topical Report* (YMP 2003 [DIRS 165505], Figures 3.2a and 3.2b).

SCREENING DECISION:

Excluded – low probability

SCREENING JUSTIFICATION:

This FEP justification accounts for in-package criticality for the seismic scenario. A prerequisite for any of the spent fuel waste forms to have potential for criticality is the introduction of water in liquid or vapor form to the inside of the TAD or DOE SNF canister. Vibratory ground motion (included FEP 1.2.03.02.0A (Seismic Ground Motion Damages EBS Components)), faulting (included FEP 1.2.02.03.0A (Fault Displacement Damages EBS Components)), seismic-induced drift collapse in the lithophysal units (included FEP 1.2.03.02.0C (Seismic-Induced Drift Collapse Damages EBS Components)), and seismic-induced rockfall (excluded FEP 1.2.03.02.0B (Seismic-Induced Rockfall Damages EBS Components)) are potential initiating events that could cause waste package or drip shield damage or drip shield failure leading to subsequent waste package failure from localized corrosion. Such failures may allow the influx of water (either advective or diffusive) into the waste package, which, in turn, has the potential to initiate processes leading to configurations with potential for criticality.

Note that excluded FEP 1.2.03.02.0B (Seismic-Induced Rockfall Damages EBS Components) has been screened from performance assessment on the basis of low consequence, which is not directly applicable to criticality potential evaluations. That FEP indicates that seismic-induced damage to the waste packages and its internals from rock block impacts in nonlithophysal units is screened out from the TSPA model on the basis of low probability. However, FEP 1.2.03.02.0B screens out tearing or rupture of the drip shield plates from large block impacts because of low consequence, which is not directly applicable to criticality potential evaluations. Drip shield failure could result in an advective flow path to the waste package OCB creating an environment for subsequent localized corrosion processes (included FEP 2.1.03.03.0A (Localized Corrosion of Waste Packages)) that could breach the waste package OCB. Therefore, this must be considered as an initiating event that can lead to a potentially critical configuration.

All postclosure criticality FEP scenarios, internal and external, require the presence of water in liquid or vapor form to degrade the waste package internals and/or the waste form as intact

configurations are designed to remain subcritical if fabricated and loaded according to design specifications as demonstrated in *CSNF Loading Curve Sensitivity Analysis* (SNL 2008 [DIRS 182788], Section 6.2.2), *DOE SNF Phase I and II Summary Report* (Radulescu et al. 2004 [DIRS 165482], Sections 10 and 11.4), *Intact and Degraded Mode Criticality Calculations for the Codisposal of TMI-2 Spent Nuclear Fuel in a Waste Package* (BSC 2004 [DIRS 168935], Section 6), and *Intact and Degraded Mode Criticality Calculations for the Codisposal of ATR Spent Nuclear Fuel in a Waste Package* (BSC 2004 [DIRS 171926], Section 6).

For a criticality event to occur, the appropriate combination of materials (e.g., neutron moderators, neutron absorbers, or fissile materials) and geometric configurations favorable to criticality must exist. Therefore, for a configuration to have potential for criticality, all of the following conditions must occur: (1) sufficient mechanical or corrosive damage to the waste package OCB to cause a breach, (2) presence of a moderator (i.e., water), (3) separation of fissionable material from the neutron absorber material or an absorber material selection error during the canister fabrication process, and (4) the accumulation (external) or presence of a critical mass of fissionable material in a critical geometric configuration. The probability of developing a configuration with criticality potential is insignificant unless all four conditions are realized, and then is only representative of a conservative estimate since the probability values associated with the many other events required to generate a critical configuration that are less than one are not quantified, but rather are conservatively set to one.

Seismic events that can cause significant displacement (> 0.1 cm) along fault lines that do intersect the drifts have a low probability of occurrence (i.e., mean annual exceedance frequencies of less than 10^{-6} per year) (SNL 2007 [DIRS 176828], Table 6-61). Damage to the drip shield causing loss of function is not expected to result from seismic faulting until sufficient displacement occurs to make contact between the drip shield and the drift. For seismic events with an annual exceedance frequency greater than 1.2×10^{-7} per year (i.e., less-severe earthquakes), no waste package damage is expected to occur due to faulting (DTN: MO0705FAULTABS.000 [DIRS 183150], file: *Fault Displacement Abstraction for Criticality.xls*, worksheet: "Tables by WP Type"). For seismic events with an annual exceedance frequency less than 1.2×10^{-7} per year (i.e., more severe earthquakes), waste package failure from seismically induced faulting is potentially initiated.

Under significant vibratory ground motions, impacts may occur between adjacent waste packages, between a waste package and its emplacement pallet, and between waste packages and the surrounding drip shield. Stress corrosion cracking from high residual stress is expected to be the cause of waste package damage from impact processes under vibratory ground motion (SNL 2007 [DIRS 178851], Section 8.2). Regions where the residual stress from mechanical damage exceeds the tensile failure criterion are expected to be severely cold-worked and, hence, potentially subject to enhanced SCC. However, if cracking were to occur as a result of specific environmental conditions coincident with the mechanical deformation, cracks would take time to develop after the shaking event.

The accumulation of rubble from multiple seismic events and the dynamic motion during a seismic event may generate damaged areas on the drip shield. The drip shields may accumulate damage from rockfall induced by vibratory ground motion from repository closure until the drip shield plates eventually rupture (SNL 2007 [DIRS 176828], Section 6.8). In the nonlithophysal

host rock, blocks released by seismic motion can impact the drip shield, and partial drift collapse may occur, but complete collapse is very unlikely. Rock block impacts may result in damaged areas on the drip shield plates and, in more extreme cases, may cause tearing or rupture of the plates (SNL 2007 [DIRS 176828], Section 6.10).

Waste packages may be contacted by limited amounts of water from condensation or slow leakage through damaged drip shields. However, flow of such condensation or leakage will be insignificant (excluded FEPs 2.1.08.14.0A (Condensation on the Underside of the Drip Shield) and 2.1.03.10.0B (Advection of Liquids and Solids through Cracks in the Drip Shield)). For failed drip shields, waste packages may be contacted directly by seepage from the host rock, which can induce localized corrosion (included FEP 2.1.03.03.0A (Localized Corrosion of Waste Packages)).

As stated in Section 1 of *Screening Analysis of Criticality Features, Events, and Processes for License Application* (SNL 2008 [DIRS 173869]), an evaluation of the criticality FEP scenarios from *Configuration Generator Model* (BSC 2004 [DIRS 172494], Section 7) for configurations with potential for criticality has identified two dominant sequences of events that must occur for a criticality event to be credible, and which are common to each of the in-package scenario classes. The two independent events are: (1) improper manufacturing, resulting in the absence and/or loss of efficacy of the neutron absorber material, and (2) for PWR SNF, improper loading of fuel assemblies. These independent events, coupled with the probability of an initiating event that could result in breaching the waste package are evaluated in *Screening Analysis of Criticality Features, Event, and Processes for License Application* (SNL 2008 [DIRS 173869]), and provide an upper bound estimate for the probability of achieving a configuration with potential for criticality. An upper bound is provided because, for independent event (1), absorber material misload–the probability of criticality is conservatively set to the maximum value (i.e., 1.0) within the sequence of events that make up the scenario. For independent event (2), waste form misload–the calculated probability of a criticality from a waste form misload is based on a bounding design basis configuration that maximizes reactivity potential, whereas the actual scenario class limiting configuration would be a less reactive configuration than the design basis configuration, thus having a lower increase in reactivity from a waste form misload.

Certain DOE SNF waste forms have sufficient quantities of fissile material to support unmoderated (fast) criticality if the fissile material is concentrated beyond its design concentration in the waste form and the neutron absorber materials are removed. While concentration of the fissile material beyond its nominal design concentration could result from degradation of the waste form by either water infiltration or a disruptive event, removal of the neutron absorber materials from a DOE SNF waste package would require a breach of the waste package and a removal mechanism. Degradation in the presence of water would result in a moderated system. Likewise, there is no known mechanism that could reconfigure non-degraded fissile material into a compact configuration with unmoderated criticality potential. The most plausible neutron absorber material removal mechanism is through water infiltration resulting in degradation of the waste package internal components, dissolving of the neutron absorber material in the water, and flushing of the material from the waste package. This mechanism is not expected to result in a critical configuration since the corrosion rate of the neutron absorber material is very low. In addition, the gadolinium absorber in the DOE SNF canisters forms

phosphate or carbonate corrosion products (SNL 2007 [DIRS 181165], Section 6.3.16), which have very low solubility.

Since this FEP considers degraded internal configurations, the cladding is considered breached within a damaged or failed waste package and the interior of the fuel rods are assumed to be exposed to the repository environment allowing the fissile material to convert to the mineral schoepite (UO_3:$2H_2O$) (SNL 2008 [DIRS 173869], Section 6.3.2). The criticality potential of the in-package degraded configuration scenario is negligible provided that waste packages are fabricated and loaded according to design specifications as sensitivity studies have shown that the PWR SNF waste form in various degraded configurations such as saturated porous schoepite does not result in a more reactive configuration than the design basis configuration (SNL 2007 [DIRS 181373], Table A-12; SNL 2008 [DIRS 182788], Section 6.2.5). Although configurations not conforming to design specifications are applicable to intact and degraded scenarios, configurations with potential for criticality require sufficient water for moderation.

The criticality potential of a seismic event that damages the waste package OCB and/or the drip shield is dependent upon the probability of a seismic event breaching a waste package in combination with other conditions, notably absorber misload and, for PWR SNF, loading curve violation probabilities. The probability for the occurrence of configurations with potential for criticality is evaluated from a number of independent sets of sequences of events where all of the events in any specific sequence must happen for that configuration to occur. Since the events in any one sequence can also be considered as independent entities, the probability of the sequence is the product of the probability of each individual event. The expected probability of having a particular sequence occur in exactly k waste packages in the repository is a binomial process described by the binomial probability distribution, $P_B(k; p, N)$, with probability "p" for occurrence in a waste package and "$q = 1 - p$" for non-occurrence. The probability of having the sequence occur in at least "$k + 1$" waste packages is given by:

$$P(\text{at least } k+1 \text{ waste packages}) = 1 - \sum_{l=0 \text{ to } k} P_B(l; p, N) \qquad \text{(Eq. 2.1.14.19.0A-1)}$$

where

k = number of items affected (e.g., waste packages, drip shields)

p = probability for occurrence of the event

N = number of possible items involved.

For large N and small "p" where $N \times p \cong \lambda$, the binomial distribution converges to the Poisson distribution (P_p) with a mean of $\lambda = N \times p$. Then, Equation 2.1.14.15.0A-1 can be rewritten as:

$$P(\textit{at least } 1 \textit{ waste packages}) = 1 - P_P(0; N \times p) = 1 - \frac{\lambda^k \times \exp(-\lambda)}{k!}$$

(Eq. 2.1.14.19.0A-2)

The criterion for screening criticality scenarios from consideration in the repository as having a low probability for the occurrence of a criticality event sequence for any waste package in the

repository (which can be stated as the probability of having at least one such sequence occur) and is given by Equation 2.1.14.19.0A-2 with $k = 0$. For the case where $k = 0$ and λ is small, Equation 2.1.14.19.0A-2 can be approximated by λ. Then, the probability of at least one waste package configuration with criticality potential occurring in the repository is given by λ $(= N \times p)$.

Events in the various seismic vibratory scenarios requiring probability values for the calculation are listed as follows:

1. Probability of a seismic vibratory ground motion event
2. Probability of waste package OCB damage from effects of the ground motion
3. Probability of improper absorber material in a commercial SNF or DOE SNF canister
4. Probability of a loading curve violation for a 21-PWR TAD canister
5. Probability of drip shield failure.

Probability of Seismic vibratory ground motion event—For seismic events causing waste package-pallet impacts that can damage a commercial SNF waste package at the 90% residual stress level, the probability of damage is zero at a PGV value of 2.44 m/s (exceedance frequency of 4.518×10^{-7} per year). At a PGV value of 4.07 (exceedance frequency of 1×10^{-8} per year), the probability of impact damage is 0.118 (DTN: MO0703PASDSTAT.001 [DIRS 183148], file: *Kinematic Damage Abstraction 23-mm Intact.xls*, sworksheet: "Probability of Damage"). Seismic events with the range of annual exceedance frequencies that can damage a TAD waste package are represented in the column labeled "PGV Value" in Table 2.1.14.19.0A-1. The probability of a seismic event is a random event in time following a Poisson distribution (SNL 2007 [DIRS 176828], Section 5.2), which increases linearly in log-time. Thus, the probabilities that one or more of these basic events occurs (i.e., one minus the probability that none occurs) is determined with Equation 2.1.14.19.0A-2 and the information provided in Table 2.1.14.19.0A-1.

Table 2.1.14.19.0A-1. Probability of Seismic Vibratory Ground Motion Events Causing Damage to TAD Canister-Bearing Waste Packages

PGV Value (m/s)	λ_1 (events/year)	λ_2 (events/year)	t_1 (years)	t_2 (years)	Probability
< 2.44	4.52×10^{-7}	NA	NA	NA	NA
2.44 - 4.07	1.0×10^{-8}	4.52×10^{-7}	10,000	0	4.41×10^{-3}

Source: DTN: MO0705CRITPROB.000 [DIRS 184958], file: *Fault Displacement Abstraction for Criticality Updated DTN 10-25-07.xls*, worksheet: "Tables by WP Type," rows 253 to 258.

Seismic events causing waste package-pallet impacts that can damage a codisposal waste package are shown in Table 2.1.14.19.0A-2. The range of the seismic events is shown in the column labeled "PGV Value" with the associated annual exceedance frequencies in columns 2 and 3.

Table 2.1.14.19.0A-2. Probability of Seismic Vibratory Ground Motion Events Causing Damage to Codisposal Waste Packages

PGV Value (m/s)	λ_1 (Events/year)	λ_2 (Events/year)	t_1 (years)	t_2 (years)	Probability
< 0.364	1.27×10^{-4}	NA	NA	NA	NA
0.364 to 0.4	9.30×10^{-5}	1.27×10^{-4}	10,000	0	2.87×10^{-1}
0.4 to 1.05	9.96×10^{-6}	9.30×10^{-5}	10,000	0	5.64×10^{-1}
1.05 to 2.44	4.52×10^{-7}	9.96×10^{-6}	10,000	0	9.07×10^{-2}
2.44 to 4.07	1.0×10^{-8}	4.52×10^{-7}	10,000	0	4.41×10^{-3}

Source: DTN: MO0705CRITPROB.000 [DIRS 184958], file: *Fault Displacement Abstraction for Criticality Updated DTN 10-25-07.xls*, worksheet: "Tables by WP Type," rows 250 to 256.

Probability of waste package OCB damage from effects of the ground motion—If a seismic vibratory ground motion event occurs, the estimated probability of damage to a TAD canister-bearing waste package from impacts is given as 0.118 (SNL 2007 [DIRS 176828], Section 6.5.1.2) at the 90% RST level at the 4.07 m/s PGV range, resulting in a probability of damage for a TAD canister-bearing waste package given by $4.41 \times 10^{-3} \times (0.0 + 0.118) \times 0.5 = 2.6 \times 10^{-4}$. The probability of damage at the 100% RST level is zero. Since the probability of damage (i.e., 0.118) is a point estimate evaluated at discrete PGV levels, the probability over the frequency range is assigned the average value. The 90% RST level data is used for conservatism for the initiating event probability values.

Similarly, the estimated probability of damage to a codisposal waste package from impacts is given in Table 2.1.14.19.0A-3 at the 90% RST level for PGV values between 0.4 and 4.07 m/s inclusively and at 100% RST level for PGV values between 2.44 and 4.07 m/s inclusively.

Table 2.1.14.19.0A-3. Probability of Damage for Intact Codisposal Waste Package

PGV Level (m/s)	Residual Stress Threshold as Percentage of Yield Strength		
	90%	100%	105%
0.364	0	0	0
0.4	0.029	0	0
1.05	0.559	0	0
2.44	0.941	0.147	0
4.07	1	0.412	0

Source: DTN: MO0703PASDSTST.001 [DIRS 183148], file: *CDSP Kinematic Damage Abstraction 23-mm Intact.xls*, worksheet: "Probability of Damage - New."

Combining the information from Tables 2.1.14.19.0A-2 and 2.1.14.19.0A-3 results in a probability of damage to a codisposal waste package at the 90% and 100% RST levels, respectively, of $(0.29 \times (0.0 + 0.03) + 0.56 \times (0.03 + 0.56) + 0.091 \times (0.56 + 0.94) + 0.0044 \times$

$(0.94 + 1.0)) \times 0.5 = 0.24$ and $(0.091 \times (0.0 + 0.147) + 0.0044 \times (0.147 + 0.412)) \times 0.5 = 7.9 \times 10^{-3}$. The estimated probability of damage from impacts for a codisposal waste package is zero for the 105% RST level. The 90% RST level data is used for conservatism for the initiating event probability values.

Probability of improper absorber material in a CSNF or DOE SNF canister—These types of events (e.g., incorrect material installed during fabrication, absorber content of plates outside specified range) can only occur during fabrication and/or loading of a canister due to process or procedural errors. Errors in fabrication and operational processes are primarily due to human factors that are common to the various processes. Surrogate fabrication and operational processes with associated human factor errors have been evaluated in *Analysis of Mechanisms for Early Waste Package/Drip Shield Failure* (SNL 2007 [DIRS 178765]), and results are used for such initiating events such as improper performance of the neutron absorber plates represented as a material selection error in the waste package component fabrication processes (SNL 2007 [DIRS 178765], Section 6.3.2). The mean value of the probability distribution for a fabrication failure is 1.25×10^{-7} per canister (DTN: MO0705EARLYEND.000 [DIRS 180946], file: *Table 1.doc*, Table 1).

Probability of Loading Curve Violation—An analysis of commercial SNF misload probabilities was documented in *Commercial Spent Nuclear Fuels Waste Package Misload Analysis* (BSC 2003 [DIRS 166316]). Results from this analysis establish that the probability of a loading curve violation in a 21-PWR waste package is 1.18×10^{-5} (BSC 2003 [DIRS 166316], Table 41). The TAD canister specifications require the canisters for PWR SNF to contain 21 assemblies similar to the 21-PWR waste package (SNL 2007 [DIRS 179394], Section 4.1.1.2). The cited analysis is used as a surrogate for misloading waste forms in a TAD canister since the misloading of an assembly into a TAD canister requires the same improper selection of an assembly with characteristics (burnup and enrichment) in the unacceptable range of the loading curve. Thus, the probability of a loading curve violation for TAD canisters is expected to be similar in magnitude to the 21-PWR waste package value. However, neighboring assemblies that have low reactivity values may provide partial compensation for the excess reactivity from the incorrectly loaded assembly. Given that a misloading curve violation occurs, the likelihood of the misloaded configuration having potential for criticality has been shown to be 0.014 from results of a probabilistic calculation of that potential (SNL 2008 [DIRS 182788], Section 7). The probability of a potentially critical configuration resulting from an assembly misload of a 21-PWR TAD canister is $0.014 \times 1.18 \times 10^{-5} = 1.65 \times 10^{-7}$ per TAD canister.

The probability of misloading assemblies in the 44-BWR TAD canister is insignificant since the entire expected BWR inventory for the repository is in the acceptable region of the loading curve map (SNL 2008 [DIRS 182788], Section 6.1.1.1.3). Misloading of waste forms in DOE SNF canisters is considered very improbable because the shape and size of the defense HLW glass canisters and the various DOE SNF canisters differ significantly and can be readily distinguished by visual inspection. Thus, the waste form misload probability for DOE SNF waste packages is considered to be sufficiently low such that, if quantified, would not significantly increase the overall probability of criticality in the repository.

Probability of drip shield failure—Significant rockfall onto and around the drip shields resulting in drip shield rupture is unlikely to occur (probability of 1.8×10^{-4} for PWR SNF repository

wide for 10,000 years in the lithophysal unit) (DTN: MO0712PBANLNWP.000 [DIRS 184664]). The likelihood of such damage in the lithophysal and nonlithophysal zones is discussed in *Seismic Consequence Abstraction* (SNL 2007 [DIRS 176828], Sections 6.8.2.2 and 6.10.2). The probability of the waste package OCB failing during the 10,000-year period following repository closure, given conditions for localized corrosion (included FEP 2.1.03.03.0A (Localized Corrosion of Waste Packages)), has been evaluated for both geologic units in DTNs: MO0712PANLNNWP.000 [DIRS 184480] and MO0712PBANLNWP.000 [DIRS 184664]. The combined probabilities associated with the events that would be necessary for criticality to be possible are presented in Table 2.1.14.19.0A-4. These probabilities are based on the TSPA localized corrosion model combined with seismic information for rockfall and drip shield fragility curves in conjunction with the probability of absorber misload and assembly misload for the 21-PWR TAD waste package.

Table 2.1.14.19.0A-4. Probability of Potential Criticality from Waste Package OCB Failure from Localized Corrosion due to Drip Shield Rupture from Rockfall Loading

Criticality Event Sequence	Probability
PWR TAD Canister Loading Curve Violation	5.9×10^{-10}
PWR TAD Canister Absorber Misload	4.4×10^{-10}
BWR TAD Canister Absorber Misload	2.8×10^{-10}
DOE SNF Canister Absorber Misload	2.8×10^{-10}

Source: SNL 2008 [DIRS 173869], Table 6.4-7.

Criticality following a seismic breach—Evaluating the event sequences resulting from breaches that are not fault induced or localized corrosion induced for commercial SNF and DOE SNF using the number of 21-PWR TAD canisters as 4,568, the number of 44-BWR TAD canisters as 2,915, and DOE SNF canisters that require neutron absorber plates (DOE1, DOE2, and DOE7 groups) as 1,223 (SNL 2008 [DIRS 173869], Section 6.4.2) and setting the number of drip shields equal to the number of waste packages gives:

21-PWR TAD canister loading curve violation:

$$2.6 \times 10^{-4} \times \{1-P_B\,(0;\,(1.65 \times 10^{-7}),\,4568)\} = 2.0 \times 10^{-7}$$

21-PWR TAD canister absorber misload:

$$2.6 \times 10^{-4} \times \{1-P_B\,(0;\,(1.25 \times 10^{-7}),\,4568)\} = 1.5 \times 10^{-7}$$

44-BWR TAD canister absorber misload:

$$2.6 \times 10^{-4} \times \{1-P_B\,(0;\,(1.25 \times 10^{-7}),\,2915)\} = 9.5 \times 10^{-8}$$

DOE SNF canister absorber misload (DOE1, DOE2, and DOE7):

$$0.24\,\{1-P_B\,(0;\,(1.25 \times 10^{-7}),\,1223)\} = 3.7 \times 10^{-5}$$

Thus, a conservative estimate for the probability of achieving a configuration with criticality potential in the repository resulting from seismic vibratory induced impact damage, assuming a damage threshold at the 90% RST level, with subsequent SCC breaching of the waste package

OCB for commercial SNF and DOE SNF, based on summing this set of events, including the DOE1, DOE2, and DOE7 contributions, is 3.7×10^{-5} for 10,000 years. In actuality, the number of DOE waste packages that have sufficient criticality potential to require absorber plate criticality control is much less than 1,223 packages. Therefore, an example estimate using only the DOE2 contribution (89 waste packages), is 3.1×10^{-6} for 10,000 years. These results have been developed on a very conservative basis (e.g., use of damage probabilities at the 90% RST level and a maximum of five intervals to represent the seismic hazard curve). The probabilities evaluated from complete event sequences are expected to be significantly lower than from using a truncated sequence of events to estimate the probability of achieving a configuration with potential for criticality. For example, using a maximum of 35 intervals in the hazard curve for estimating the probability of impact damage to codisposal waste packages reduced the estimated probability of vibratory impact damage to the codisposal waste packages by approximately 20% (DTN: MO0705CRITPROB.000 [DIRS 184958], file: *CSNF TAD & CDSP WP Impact damage.xls*).

Seismic Faulting

Results from analyses of waste package damage due to fault displacement during a seismic event are documented in *Seismic Consequence Abstraction* (SNL 2007 [DIRS 176828], Section 6.11.7) and FEP. The information for the criticality analysis is consistent with the methodology for the damage abstraction for fault displacement in the TSPA, but represents a finer level of detail. The finer level of detail is based on the damage abstraction for the TSPA being based on two waste package groups: the TAD canister group and the codisposal group. While this grouping is consistent with the representation of waste package groups in the TSPA, criticality studies require a more detailed analysis of waste package failures by individual waste package type. The calculations for the criticality analysis are given in *Fault Displacement Abstraction for Criticality.xls* derived from DTN: MO0705FAULTABS.000 [DIRS 183150]) updated to the waste package inventory from *Screening Analysis of Criticality Features, Events, and Processes for License Application* (SNL 2008 [DIRS 173869], Table 4.1-2).

Events considered in the seismic faulting scenario requiring probability values for the calculation are listed as follows:

1. Probability of a seismic faulting event over an exceedance range where sufficient displacement can shear waste packages

2. Number of failed waste packages for a seismic faulting event

3. Probability of improper absorber material in a TAD or DOE SNF canister

4. Probability of a loading curve violation for a 21-PWR TAD canister.

Fractional lengths of the various waste package types in the inventory, which are used to determine the expected number of waste package failures from faulting, are listed in Table 2.1.14.19.0A-5. Table 2.1.14.19.0A-6 provides the expected number of waste packages by type that are emplaced on each fault. Tables 2.1.14.19.0A-7 and 2.1.14.19.0A-8 show the result of combining the exceedance frequencies that cause failure and the number of packages

emplaced on faults in Table 2.1.14.19.0A-6 to determine the cumulative number of waste packages expected to fail by type as a function of annual exceedance frequency.

Table 2.1.14.19.0A-5. Fractional Length per Waste Package Variant

Waste Package Type	Nominal Quantity	Total Length of Waste Package Type (mm)	Fraction of Waste Packages (% of Total Length)
CSNF TAD Canister	7,483	4.378×10^7	74.7
CDSP Short	1,600	5.196×10^6	10.1
CDSP Long	1,474	7.818×10^6	13.3
CDSP MCO	210	1.109×10^6	1.9

Sources: DTN: MO0705CRITPROB.000 [DIRS 184958], file: *Fault Displacement Abstraction for Criticality Updated DTN 10-25-07.xls*, worksheet: "Tables by WP Type."

Table 2.1.14.19.0A-6. Expected Number of Waste Packages by Type Emplaced on Faults

Fault	Commercial SNF TAD Canister	Codisposal Short	Codisposal Long	Codisposal MCO
3 - Drill Hole Wash, Pagany Wash, & Sever Wash	19.4	2.6	3.5	1.5
4 – West Ghost Dance	8.2	1.1	1.5	0.2
5 – Sundance	4.5	0.6	0.8	0.1
Sites 7a/8a	127.7	17.3	22.8	3.2
Totals	159.8	21.6	28.5	4.0

Source: DTN: MO0705CRITPROB.000 [DIRS 184958], file: *Fault Displacement Abstraction for Criticality Updated DTN 10-25-07.xls*, worksheet: "Tables by WP Type", rows 177 to 187.

Table 2.1.14.19.0A-7. Cumulative Number of Failed Commercial SNF Waste Packages Expected versus Annual Exceedance Frequency

Exceedance Frequency Range (1/yr)	Commercial SNF TAD Canister
$> 8.2 \times 10^{-8}$	0
7.0×10^{-8} to 8.2×10^{-8}	19.4
2.7×10^{-8} to 7.0×10^{-8}	27.6
1.0×10^{-8} to 2.7×10^{-8}	32.1

Source: DTN: MO0705CRITPROB.000 [DIRS 184958], file: *Fault Displacement Abstraction for Criticality Updated DTN 10-25-07.xls*, worksheet: "Tables by WP Type," rows 189 to 197.

Table 2.1.14.19.0A-8. Cumulative Number of Failed Codisposal Waste Packages Expected versus Annual Exceedance Frequency

Exceedance Frequency Range (1/yr)	Expected Number of Failures Codisposal Short	Expected Number of Failures Codisposal Long	Exceedance Frequency Range (1/yr)	Expected Number of Failures Codisposal MCO
$> 1.2 \times 10^{-7}$	0	0	$> 6.3 \times 10^{-8}$	0
1.1×10^{-7} to 1.2×10^{-7}	2.6	3.5	5.4×10^{-8} to 6.3×10^{-8}	0.5
4.1×10^{-8} to 1.1×10^{-7}	3.7	4.9	2.1×10^{-8} to 5.4×10^{-8}	0.7
1.3×10^{-8} to 4.1×10^{-8}	4.3	5.7	1.0×10^{-8} to 2.1×10^{-8}	0.8
1.0×10^{-8} to 1.3×10^{-8}	21.6	28.5		

Source: DTN: MO0705CRITPROB.000 [DIRS 184958], file: *Fault Displacement Abstraction for Criticality Updated DTN 10-25-07.xls*, worksheet: "Tables by WP Type," rows 189 to 198.

For seismic events with an annual exceedance frequency greater than 1.2×10^{-7} per year (i.e., less severe earthquakes), no waste package damage is expected to occur due to faulting as shown in Tables 2.1.14.19.0A-7 and 2.1.14.19.0A-8. For seismic events with an annual exceedance frequency less than 1.2×10^{-7} per year (i.e., more severe earthquakes), waste package failure from seismically induced faulting is initiated. The number of failed waste packages increases with increasing seismic energy (decreasing annual exceedance frequency) to a maximum number that depends on waste package variant as shown in Tables 7 and 8. The annual exceedance frequency range for the commercial SNF TAD canister and codisposal waste packages is subdivided into three or four ranges for this analysis, depending on the waste package variant as shown in the column labeled "Exceedance Frequency Range" in Tables 2.1.14.19.0A-7 and 2.1.14.19.0A-8 for each waste package variant. The probabilities of these basic events are determined with Equation 2.1.14.19.0A-1 and the information provided in Table 2.1.14.19.0A-9.

Table 2.1.14.19.0A-9. Probabilities of Seismic Faulting Events with Waste Package Failure Capability

PGV Value (m/s)	λ_1 (events/year)	λ_2 (events/year)	t_1 (years)	t_2 (years)	Probability
Commercial SNF TAD Waste Package Variant					
4.07 to 3.77	1.0×10^{-8}	2.7×10^{-8}	10,000	0	1.7×10^{-4}
3.77 to 3.41	2.7×10^{-8}	7.0×10^{-8}	10,000	0	4.3×10^{-4}
3.41 to 3.34	7.0×10^{-8}	8.2×10^{-8}	10,000	0	1.2×10^{-4}
Codisposal Waste Package Variant					
4.07 to 4.00	1.0×10^{-8}	1.3×10^{-8}	10,000	0	3.0×10^{-5}
4.00 to 3.62	1.3×10^{-8}	4.1×10^{-8}	10,000	0	2.8×10^{-4}
3.62 to 3.21	4.1×10^{-8}	1.1×10^{-7}	10,000	0	6.9×10^{-4}
3.21 to 3.18	1.1×10^{-7}	1.2×10^{-7}	10,000	0	1.0×10^{-4}

Source: DTN: MO0705CRITPROB.000 [DIRS 184958], file: *Fault Displacement Abstraction for Criticality Updated DTN 10-25-07.xls*, worksheet: "Tables by WP Type," rows 203 to 209.

The mean probability of a seismic faulting event is a point value derived from the probability of a seismic event with faulting as given in Table 2.1.14.19.0A-9 multiplied by the incremental number of waste packages with criticality potential being impacted within each frequency range given in Tables 2.1.14.19.0A-7 and 2.1.14.19.0A-8.

The probabilities of the remaining events in this scenario were discussed above and resulted in the following: The probability of installing improper absorber plate material in a TAD canister is 1.25×10^{-7} per canister, and the probability of a potentially critical configuration resulting from an assembly misload of a 21-PWR TAD canister is 1.65×10^{-7} per TAD canister.

Evaluating the event sequences for commercial SNF and DOE SNF using the fractions of 21-PWR TAD canisters (4,568/7,483), 44-BWR TAD canisters (2,915/7,483), and DOE SNF canisters that require neutron absorber plates (DOE1, DOE2, and DOE7 groups) (1,223/3,074) (SNL 2008 [DIRS 173869], Section 6.4.3) gives:

PWR TAD canister loading curve violation:

$1.2 \times 10^{-4} \times (1-P_B (0; 1.65 \times 10^{-7}, (19.4 \times 4568/7483)) + 4.3 \times 10^{-4} \times (1-P_B (0; 1.65 \times 10^{-7}, (27.6 -19.4) \times 4568/7483)) +1.7 \times 10^{-4} \times (1-P_B (0; 1.65 \times 10^{-7}, (32.1 - 27.6) \times 4568/7483)) = 6.3 \times 10^{-10}$

PWR TAD canister absorber misload:

$1.2 \times 10^{-4} \times (1-P_B (0; 1.25 \times 10^{-7}, (19.4 \times 4568/7483)) + 4.3 \times 10^{-4} \times (1-P_B (0; 1.25 \times 10^{-7}, (27.6 -19.4) \times 4568/7483)) +1.7 \times 10^{-4} \times (1-P_B (0; 1.25 \times 10^{-7}, (32.1 - 27.6) \times 4568/7483)) = 4.8 \times 10^{-10}$

44-BWR TAD canister absorber misload:

$1.2 \times 10^{-4} \times (1\ P_B (0; 1.25 \times 10^{-7}, (19.4 \times 2915/7483)) + 4.3 \times 10^{-4} \times (1-P_B (0; 1.25 \times 10^{-7}, (27.6 - 19.4) \times 2915/7483)) +1.7 \times 10^{-4} \times (1-P_B (0; 1.25 \times 10^{-7}, (32.1 - 27.6) \times 2915/7483)) = 2.9 \times 10^{-10}$

DOE SNF canister absorber misload (DOE1, DOE2, and DOE7):

$1.0 \times 10^{-4} \times (1-P_B (0; 1.25 \times 10^{-7}, (2.6+3.5) \times 1223/3074)) + 6.9 \times 10^{-4} \times (1-P_B (0; 1.25 \times 10^{-7}, (3.7-2.6 + 4.9-3.5) \times 1223/3074)) + 2.8 \times 10^{-4} \times (1-P_B (0; 1.25 \times 10^{-7}, (4.3-3.7 + 5.7-4.9) \times 1223/3074)) + 3.0 \times 10^{-5} \times (1-P_B (0; 1.25 \times 10^{-7}, (21.6-4.3 + 28.5-5.7) \times 1223/3074)) = 8.1 \times 10^{-11}$

Thus, a conservative estimate for the probability of achieving a configuration with criticality potential in the repository resulting from a seismic faulting initiating event for commercial SNF and DOE SNF is 1.5×10^{-9} for 10,000 years.

Summary—The events in the short sequences are considered as the principal contributors to the probability of occurrence of configurations having criticality potential following a seismic initiating event. Extending the sequences to include additional events would further decrease the probability for the occurrence of configurations with potential for criticality. Summing the probabilities of potential criticality for the in-package location from the seismic vibratory, drip shield rupture inducing localized corrosion, and fault displacement initiating events results in a

probability of criticality of 3.7×10^{-5} over 10,000 years. This is less than 1 chance in 10,000 (1×10^{-4}) of occurrence within 10,000 years of disposal. Accordingly, FEP 2.1.14.19.0A (In-Package Criticality Resulting from a Seismic Event (Degraded Configurations) is excluded from the performance assessments conducted to demonstrate compliance with proposed 10 CFR 63.311 and 63.321 (70 FR 53313 [DIRS 178394]), and with 10 CFR 63.331 [DIRS 180319], on the basis of low probability.

In addition, as documented in *Screening Analysis of Criticality Features, Events, and Processes for License Application* (SNL 2008 [DIRS 173869], Section 7.1), the probability of criticality for all locations is less than 1 chance in 10,000 of occurrence within 10,000 years after disposal. The results documented in this analysis are applicable for all waste forms and waste package variants.

INPUTS:

Table 2.1.14.19.0A-10. Direct Inputs

Input	Source	Description
BSC 2003. *Commercial Spent Nuclear Fuel Waste Package Misload Analysis*. [DIRS 166316]	Table 41	Error probabilities for commercial SNF waste package loading violation
BSC 2004. *Intact and Degraded Mode Criticality Calculations for the Codisposal of ATR Spent Nuclear Fuel in a Waste Package*. [DIRS 171926]	Section 6	Criticality potential of DOE SNF waste forms
BSC 2004. *Intact and Degraded Mode Criticality Calculations for the Codisposal of TMI-2 Spent Nuclear Fuel in a Waste Package*. [DIRS 168935]	Section 6	Criticality potential of DOE SNF waste forms
DTN: MO0703PASDSTAT.001. Statistical Analyses for Seismic Damage Abstractions. [DIRS 183148]	file: *Kinematic Damage Abstraction 23-mm Intact.xls*, worksheet: "Probability of Damage"	For seismic events causing waste package-pallet impacts that can damage a commercial SNF waste package at the 90% residual stress level, at a PGV value of 4.07 (exceedance frequency of 1×10^{-8} per year), the probability of impact damage is 0.118
	file: *CDSP Kinematic Damage Abstraction 23-mm Intact.xls*, worksheet: "Probability of Damage – New"	Probability of seismic vibratory ground motion events causing damage to codisposal waste packages
DTN: MO0705CRITPROB.000. Probability of Criticality. [DIRS 184958]	file: *Fault Displacement Abstraction for Criticality Updated DTN 10-25-07.xls*, worksheet: "Tables by WP Type," rows: 250 to 256	Probability of seismic vibratory ground motion events causing damage to codisposal waste packages
	file: *Fault Displacement Abstraction for Criticality Updated DTN 10-25-07.xls*, worksheet: "Tables by WP Type," rows: 203 to 209	Commercial SNF TAD waste package variant

Table 2.1.14.19.0A-10. Direct Inputs (Continued)

Input	Source	Description
DTN: MO0705CRITPROB.000. Probability of Criticality. [DIRS 184958] (continued)	file: *Fault Displacement Abstraction for Criticality Updated DTN 10-25-07.xls*, worksheet: "Tables by WP Type," rows: 189 to 198	Cumulative number of failed codisposal waste packages expected versus annual exceedance frequency
	file: *Fault Displacement Abstraction for Criticality Updated DTN 10-25-07.xls*, worksheet: "Tables by WP Type," rows: 189 to 197	Cumulative number of failed CSNF waste packages expected versus anual exceedance frequency
	file: *CSNF TAD & CDSP WP Impact damage.xls*	Using a maximum of 35 intervals in the hazard curve for estimating the probability of impact damage to codisposal waste packages reduced the estimated probability of vibratory impact damage to the codisposal waste packages by approximately 20%
	file: *Fault Displacement Abstraction for Criticality Updated DTN 10-25-07.xls*, worksheet: "Tables by WP Type," rows: 253 to 258	TAD waste package variants
	file: *Fault Displacement Abstraction for Criticality Updated DTN 10-25-07.xls*, worksheet: "Tables by WP Type"	Fractional length per waste package variant
	file: *Fault Displacement Abstraction for Criticality Updated DTN 10-25-07.xls*, worksheet: "Tables by WP Type," rows: 177 to 187	Expected number of waste packages by type emplaced on faults
DTN: MO0705EARLYEND.000. Waste Package/Drip Shield Early Failure End State Probabilities. [DIRS 180946]	file: *Table 1.doc*, Table 1	Error probabilities for fabrication and operational processes representing waste package and drip shield early failure mechanisms
DTN: MO0705FAULTABS.000. Assessment of Waste Package Failure Due to Fault Displacement for Criticality. [DIRS 183150]	file: *Fault Displacement Abstraction for Criticality.xls*, worksheet: "Tables by WP Type"	Expected number of waste packages by type emplaced on faults
	file: *Fault Displacement Abstraction for Criticality.xls*, worksheet: "Tables by WP Type"	Cumulative number of failed commercial SNF waste packages expected versus annual exceedance frequency
	file: *Fault Displacement Abstraction for Criticality.xls*, worksheet: "Tables by WP Type"	For seismic events with an annual exceedance frequency greater than 1.2×10^{-7} per year (i.e., less-severe earthquakes), no waste package damage is expected to occur due to faulting

Table 2.1.14.19.0A-10. Direct Inputs (Continued)

Input	Source	Description
DTN: MO0705FAULTABS.000. Assessment of Waste Package Failure Due to Fault Displacement for Criticality. [DIRS 183150] (continued)	file: *Fault Displacement Abstraction for Criticality.xls*	Calculations for the criticality analysis
	file: *Fault Displacement Abstraction for Criticality.xls*, worksheet: "Tables by WP Type"	Cumulative number of failed codisposal waste packages expected versus annual exceedance frequency
	file: *Fault Displacement Abstraction for Criticality.xls*, worksheet: "Tables by WP Type"	Probabilities of seismic faulting events with waste package failure capability
	file: *Fault Displacement Abstraction for Criticality.xls*, worksheet: "Tables by WP Type"	Fractional length per waste package variant
Radulescu et al. 2004. *DOE SNF Phase I and II Summary Report*. [DIRS 165482]	Sections 10 and 11.4	Criticality potential of DOE SNF waste forms
SNL 2007. *Seismic Consequence Abstraction*. [DIRS 176828]	Section 6.10	Rock block impacts may result in damaged areas on the drip shield plates and, in more extreme cases, may cause tearing or rupture of the plates
	Section 6.5.1.2	If a seismic vibratory ground motion event occurs, the estimated probability of damage to a TAD waste package from impacts is given as 0.118
	Section 6.8	The drip shields may accumulate damage from rockfall induced by vibratory ground motion from repository closure until the drip shield plates eventually rupture
	Table 6-61	Seismic events that can cause significant displacement (>0.1 cm) along fault lines that do intersect the drifts have a low probability of occurrence (i.e., mean annual exceedance frequencies of less than 10^{-6} per year)
	Section 6.11.7	Results from analyses of waste package damage due to fault displacement during a seismic event
SNL 2007. *Mechanical Assessment of Degraded Waste Packages and Drip Shields Subject to Vibratory Ground Motion*. [DIRS 178851]	Section 8.2	Stress corrosion cracking from high residual stress is expected to be the cause of waste package damage from impact processes under vibratory ground motion
SNL 2007. *Commercial Spent Nuclear Fuel Igneous Scenario Criticality Evaluation*. [DIRS 181373]	Table A-12	The PWR SNF waste form in various degraded configurations such as saturated porous schoepite does not result in a more reactive configuration than the design basis configuration
SNL 2008. CSNF *Loading Curve Sensitivity Analysis*. [DIRS 182788]	Section 6.2.2	Criticality potential of commercial SNF waste forms
	Section 7	Probability of a critical configuration resulting from a PWR SNF waste package loading violation

Table 2.1.14.19.0A-10. Direct Inputs (Continued)

Input	Source	Description
SNL 2008. CSNF *Loading Curve Sensitivity Analysis*. [DIRS 182788] (continued)	Section 6.1.1.1.3	Probability of a critical configuration resulting from a BWR SNF waste package loading violation
	Section 6.2.5	The PWR SNF waste form in various degraded configurations such as saturated porous schoepite does not result in a more reactive configuration than the design basis configuration
SNL 2008. *Screening Analysis of Criticality Features, Events, and Processes for License Application*. [DIRS 173869]	Section 6.3.2	Cladding is considered breached within a damaged or failed waste package and the interior of the fuel rods are assumed to be exposed to the repository environment allowing the fissile material to convert to the mineral schoepite (UO_3:$2H_2O$)
	Section 6.3.2	Waste package inventory by type
	Section 7.1	Probability of criticality for all locations is less than 1 chance in 10,000 of occurrence within 10,000 years after disposal
	Table 6.4-7	Probability of potential criticality from waste package OCB failure from localized corrosion due to drip shield rupture from rockfall loading

Table 2.1.14.19.0A-11. Indirect Inputs

Citation	Title	DIRS
10 CFR 63	Energy: Disposal of High-Level Radioactive Wastes in a Geologic Repository at Yucca Mountain, Nevada	180319
70 FR 53313	Implementation of a Dose Standard After 10,000 Years	178394
BSC 2003	*Commercial Spent Nuclear Fuel Waste Package Misload Analysis*	166316
BSC 2004	*Configuration Generator Model*	172494
DTN: MO0712PANLNNWP.000	Probabilistic Analysis of Non-Navy Waste Packages	184480
DTN: MO0712PBANLNWP.000	Probabilistic Analysis of Navy Waste Packages	184664
SNL 2007	*Seismic Consequence Abstraction*	176828
SNL 2007	*Analysis of Mechanisms for Early Waste Package/Drip Shield Failure*	178765
SNL 2007	*Geochemistry Model Validation Report: Material Degradation and Release Model*	181165
SNL 2007	*Total System Performance Assessment Data Input Package for Requirements Analysis for TAD Canister and Related Waste Package Overpack Physical Attributes Basis for Performance Assessment*	179394
SNL 2008	*Screening Analysis of Criticality Features, Events, and Processes for License Application*	173869
YMP 2003	*Disposal Criticality Analysis Methodology Topical Report*	165505

FEP: 2.1.14.20.0A

FEP NAME:

Near-Field Criticality Resulting from a Seismic Event

FEP DESCRIPTION:

Either during or as a result of a seismic disruptive event, near-field criticality could occur if fissile material-bearing solution from the waste package is transported into the drift and the fissile material is precipitated into a critical configuration. Potential near-field critical configurations are defined in *Disposal Criticality Analysis Methodology Topical Report* (YMP 2003 [DIRS 165505], Figure 3.3a).

SCREENING DECISION:

Excluded – low probability

SCREENING JUSTIFICATION:

This FEP justification accounts for external criticality for the near-field location for the seismic scenario, where *near-field* is defined as the region inside the drift external to the waste package. A prerequisite for any of the spent fuel waste forms to have potential for criticality is the introduction of water in liquid or vapor form to the inside of the TAD or DOE SNF canister. All postclosure criticality FEP scenarios, internal and external, require the presence of water in liquid or vapor form to degrade the waste package internals and/or the waste form as intact configurations are designed to remain subcritical if fabricated and loaded according to design specifications as demonstrated in *CSNF Loading Curve Sensitivity Analysis* (SNL 2008 [DIRS 182788], Section 6.2.2), *DOE SNF Phase I and II Summary Report* (Radulescu et al. 2004 [DIRS 165482], Sections 10 and 11.4), *Intact and Degraded Mode Criticality Calculations for the Codisposal of TMI-2 Spent Nuclear Fuel in a Waste Package* (BSC 2004 [DIRS 168935], Section 6), and *Intact and Degraded Mode Criticality Calculations for the Codisposal of ATR Spent Nuclear Fuel in a Waste Package* (BSC 2004 [DIRS 171926], Section 6).

For a criticality event to occur, the appropriate combination of materials (e.g., neutron moderators, neutron absorbers, fissile materials, or isotopes) and geometric configurations favorable to criticality must exist. Therefore, for a configuration to have potential for criticality, all of the following conditions must occur: (1) sufficient mechanical or corrosive damage to the waste package OCB to cause a breach, (2) presence of a moderator (i.e., water), (3) separation of fissionable material from the neutron absorber material or an absorber material selection error during the canister fabrication process, and (4) the accumulation (external) or presence of a critical mass of fissionable material in a critical geometric configuration. The probability of developing a configuration with criticality potential is insignificant unless all four conditions are realized, and then is only representative of a conservative estimate since the probability values associated with the many other events required to generate a critical configuration that are less than one are not quantified, but rather are conservatively set to one.

Near-field criticality cannot occur unless the waste package and waste form are degraded. Water infiltration is required to degrade the waste package internals and waste form and transport them to the near-field location. Criticality cannot occur unless at least the minimum critical mass of a waste form can be accumulated. It then follows that the probability of near-field criticality must be less than the probability of water entering the waste package. This is because, in addition to the events evaluated to calculate the probability of water infiltrating a breached waste package, the probability of the following events or processes must also be considered for external criticality:

- Separation of the fissile materials from the degraded waste form
- Sufficient seepage water to transport fissile materials from the waste package
- Accumulating sufficient fissile material into a potentially critical configuration in the near-field environment.

If a waste package is breached, water and solutes might enter and leave the waste package by several mechanisms, including diffusion, condensation of vapor, and advection of liquid water. Leakage through a crack-damaged drip shield is an insignificant source for liquid water penetration through cracks in the underlying waste package especially when compared to the threshold flow rate (0.1 kg/yr) used in TSPA to define whether seepage occurs (excluded FEP 2.1.03.10.0 (Advection of Liquids and Solids through Cracks in the Waste Package)). Therefore, the predominant mechanism for water inflow and outflow through a breached waste package is through diffusive transport unless the drip shield has failed. *Geochemistry Model Validation Report: Material Degradation and Release Model* (SNL 2007 [DIRS 181165], Section 6.2) indicated that the quantity of material released by diffusion would be small due to the tortuosity of the path, and therefore the diffusion-only scenario is not considered a viable method for material transport. Thus, advective flow of water is necessary for transporting fissile materials from the waste package to the near-field in any appreciable quantities to be considered for criticality.

Vibratory ground motion (included FEP 1.2.03.02.0A (Seismic Ground Motion Damages EBS Components)), faulting (included FEP 1.2.02.03.0A (Fault Displacement Damages EBS Components)), seismic induced drift collapse in the lithophysal units (included FEP 1.2.03.02.0C (Seismic-Induced Drift Collapse Damages EBS Components)), and seismic induced rockfall (excluded FEP 1.2.03.02.0B (Seismic Induced Rockfall Damages EBS Components)) are potential initiating events that are capable of creating advective flow paths into the waste package. Such failures may allow the influx of water (either advective or diffusive) into the waste package, which, in turn, has the potential to initiate processes leading to degradation and transport of the fissile material to the near-field location.

Note that excluded FEP 1.2.03.02.0B (Seismic-Induced Rockfall Damages EBS Components) has been screened from performance assessment on the basis of low consequence, which is not directly applicable to criticality potential evaluations. FEP 1.2.03.02.0B indicates that seismic-induced damage to the waste packages and its internals from rock block impacts in nonlithophysal units is screened out from the TSPA model on the basis of low probability. However, FEP 1.2.03.02.0B screens out tearing or rupture of the drip shield plates from large

block impacts because of low consequence, which is not directly applicable to criticality potential evaluations. Drip shield failure could result in an advective flow path to the waste package OCB, creating an environment for subsequent localized corrosion processes (included FEP 2.1.03.03.0A (Localized Corrosion of Waste Packages)) that could breach the waste package OCB.

The probability of drip shield and waste package failure from a fault event varies with the magnitude of the earthquake but ranges from 1.2×10^{-4} to 4.3×10^{-4} for the commercial SNF waste packages and from 3.0×10^{-5} to 6.9×10^{-4} for the codisposal waste packages (SNL 2008 [DIRS 173869], Table 6.4-7).

There are several hundred distinct types of DOE SNF, and it is not practical to attempt to determine the impact of each individual type on repository performance. These fuels come from a wide range of reactor types, such as light- and heavy-water-moderated reactors, graphite-moderated reactors, and breeder reactors, with various cladding materials and enrichments, varying from depleted uranium to over 93% enriched ^{235}U. Many of these reactors, now decommissioned, had unique design features, such as core configuration, fuel element and assembly geometry, moderator and coolant materials, operational characteristics, and neutron spatial and spectral properties (DOE 2004 [DIRS 171271]).

Therefore, to facilitate DOE SNF waste form evaluations, the DOE SNF inventory was first reduced to 34 DOE SNF groups based on fuel matrix, cladding, cladding condition, and enrichment. These parameters are the fuel characteristics that were determined to have major impacts on the release of radionuclides from the DOE SNF and contributed to nuclear criticality scenarios (DOE 2000 [DIRS 118968], Section 5). Separate groups were further refined for the purposes of criticality, design basis events, and TSPA based on key parameters such as fuel matrix, cladding, and fuel condition, as well as fissile species and enrichment, and reactor and fuel design (DOE 2000 [DIRS 118968], Section 5.1). For criticality, nine DOE SNF criticality groups have been identified and are listed in *General Description of Database Information Version 5.0.1* (DOE 2007 [DIRS 182577], Table 6).

Within each of the nine DOE SNF criticality groups, a single fuel design was selected as being representative of the remaining fuel within each group. The term representative means that all fuels would perform similarly regarding chemical interactions within the waste package and basket, and that canister loading limits from the representative fuel (ranges of key parameters important to criticality such as linear fissile loading and total fissile mass) are established, which other fuels within the group can be shown to not exceed. Waste forms within a single criticality group that have configurations or key criticality parameters outside the range of applicability of the representative fuel will require supplemental analysis and/or additional reactivity control mechanisms.

Evaluations for naval fuel are conducted by the Naval Nuclear Propulsion Program. A miscellaneous waste form category, which has a variety of fuel matrix properties originating from various post-irradiation examinations and other testing are not included in the criticality evaluations for the fuel groups as they will need to be evaluated on a case-by-case basis. Thus, the disposal criticality analysis methodology (YMP 2003 [DIRS 165505]) can be applied to nine DOE SNF representative fuel groups for criticality evaluations.

The minimum fissile mass necessary for criticality external to the waste packages is discussed in *Geochemistry Model Validation Report: External Accumulation Model* (SNL 2007 [DIRS 181395], Section 8.1.4[a]), where it was concluded that insufficient fissile material can collect over 10,000 years to achieve a critical mass for the seismic scenario, where a critical mass is defined as one where k_{eff} (effective neutron multiplication factor) exceeds the critical limit for the material. Note that the material degradation of the internals and subsequent accumulation in the near-field based on the seismic scenario are bounding for localized corrosion because the seismic seepage flux is based on the entire waste package footprint area collecting seeps, whereas localized corrosion seeps would only be a fraction of the total area with a reduced seepage flux. In addition, these values are predicated on having an initiating event (i.e., seismic fault displacement rupturing the drip shield and waste package), which is an unlikely event (1.2×10^{-8} per year). The critical mass limits were evaluated for commercial SNF and DOE SNF waste forms using bounding parameters with regard to optimizing reactivity potential, so the actual masses that would be necessary to achieve criticality would most likely need to be far greater than what was identified (SNL 2007 [DIRS 181395], Section 8.1.4[a]).

Model abstractions were performed for commercial SNF and three DOE SNF waste forms in *Geochemistry Model Validation Report: External Accumulation Model* (SNL 2007 [DIRS 181395]) (i.e., N Reactor (DOE3), Three-Mile Island (DOE9), and FFTF (DOE1)) (SNL 2008 [DIRS 173869], Section 4.1.15), which make up approximately 90% of the metric tons of heavy metal in the DOE SNF inventory expected to be stored in the repository. In addition to these waste forms making up ~90% of the inventory by mass, they were selected because they provide degradation and accumulation characteristics of uranium-metal (N Reactor), mixed-oxide (FFTF), and damaged uranium dioxide (Three-Mile Island) waste forms that may be applicable to other representative DOE waste forms. Some of the other DOE SNF waste forms, such as Shippingport light-water breeder reactor (LWBR) (DOE5) and Ft. St. Vrain (DOE6), are not expected to be a concern for external criticality due to the corrosion resistance of the waste form (SNL 2007 [DIRS 181395], Section 6.9.3[a]).

Ft. St. Vrain fuels (DOE6) have an integral silicon carbide (SiC) protective layer that not only retains the fission products, but also protects the uranium and thorium dicarbide (ThC_2) from oxidation and hydrolysis (DOE 2003 [DIRS 166027], p. 48). Comparative analysis has indicated that the Ft. St. Vrain fuel has the lowest degradation rate of all DOE SNF and should behave significantly better in terms of fissile material dissolution, transport, and accumulation. In some residual quantities (< 250 grams per block), ^{233}U bred into the ThC_2 fertile particles. A canister loaded with five Ft. St. Vrain blocks contains sufficient quantities of ^{233}U to have criticality potential in solution; however, a mechanism to separate the uranium from within the SiC-coated fertile particles, and then a mechanism to accumulate in a concentrated fissile mass in a favorable geometry, is not credible.

For Shippingport LWBR fuel (DOE5), studies have indicated that both air and water oxidation of uranium and thorium oxide fuel pellets [$(Th, U)O_2$] proceed more slowly than in pure uranium oxide (UO_2), and decrease with decreasing UO_2 content in the $(Th, U)O_2$ (DOE 2003 [DIRS 166027], p. 33). Tests have shown that the thorium oxide pellets in the Shippingport LWBR fuel have excellent corrosion resistance with an estimated solubility of 10^{-14} mol/L at 25°C and pH > 5 (DOE 2003 [DIRS 166027], p. 32). With the less-reactive degradation rate, a

mechanism to separate the uranium, transporting, and accumulation into a favorable geometry is also not credible.

Table 2.1.14.20.0A-1 shows the ranges of minimum critical mass required to accumulate in the invert to achieve a critical limit of k_{eff} (effective neutron multiplication factor) equal to 0.96. Also shown is the calculated accumulation or mass released from the waste package for the waste forms evaluated for external criticality. For each of the waste forms evaluated, the results indicate that an insufficient amount of fissile material accumulates to pose a criticality concern.

Table 2.1.14.20.0A-1. Summary of Seismic Scenario External Criticality Results

Scenario	Waste Package Type	Calculated Accumulation or Mass Released from Waste Package (Uranium mass, unless otherwise noted (kg))	Mass of Uranium or Plutonium (for FFTF) Required to Achieve Critical Limit of k_{eff} = 0.96 in the Invert (kg)
Seismic	DOE3 (N Reactor)	Not calc[a]	266,000
	DOE9 (TMI II Fuel)	Not calc[a]	350
	Commercial SNF	90.3	126
	DOE1 (FFTF) (Plutonium mass)	0	1.66

[a] "Not calc" means that this scenario is bounded by another scenario. In most cases, this means that if commercial SNF waste is very subcritical, then Three-Mile Island and N Reactor had to be also.

Source: SNL 2007 [DIRS 181395], Table 6.9-1[a].

DOE fuel groups in DOE2, DOE4, DOE7, and DOE8 representing UZrHx (TRIGA), high enriched uranium oxide (Shippingport PWR), aluminum-based (ATR), and U-Zr/U-Mo alloy (Fermi), respectively (SNL 2008 [DIRS 173869], Table 4.1-2), have not been analyzed in detail for external fissile mass transport and accumulation as the other waste forms have. However, considering the processes that must occur to allow advective seepage into a DOE SNF canister without substantial drainage to allow degradation of the internal components and waste form, along with the other conservative modeling parameters that have been used to create a process to facilitate fissile material transport to the external environment, and the bounding modeling parameters respective to maximizing criticality potential, these waste forms are not expected to result in an increase in the total probability of criticality in the near-field location.

Some of the conservative modeling parameters are provided as follows:

- The material degradation and release model (SNL 2007 [DIRS 181165]) uses constant corrosion rates for the SNF; however, laboratory experiments on the surface structure of commercial SNF during dissolution have shown that UO_2 dissolution is accompanied by the formation of a protective layer of secondary phases that retards further corrosion (SNL 2007 [DIRS 181165], Section 6.6.2). Therefore, the release of uranium from the fuel would be slower and therefore less would be released.

- Experimental and field data indicate that actinides would be adsorbed on or incorporated into alteration products that form in the waste package (SNL 2007 [DIRS 181165], Section 6.6.3). This solid solution formation and adsorption would tend to lower

actinide concentrations below those predicted by EQ6 and would delay release from the waste package.

- The material degradation and release model (SNL 2007 [DIRS 181165]) considers the cladding and DOE SNF canister as breached upon emplacement in the repository, and unzipping immediately upon waste package breach, whereas a more likely scenario would be that the failure would take place over many years. This would also delay the release of actinides.

- Many conservative modeling approximations are used to simplify the critical mass calculations presented in Table 2.1.14.20.0A-1. For the commercial SNF and low-enriched DOE fuels analyzed in *Geochemistry Model Validation Report: External Accumulation Model* (SNL 2007 [DIRS 181395]), the conservatisms are appropriate, because the results show that a criticality is very unlikely. However, for the higher enriched DOE fuels, less conservative (increased detail) modeling parameters of the criticality potential are expected to generate similar conclusions.

Summary – The critical mass limits were evaluated for several waste forms using bounding parameters with regards to optimizing reactivity potential, so the actual masses that would be necessary to achieve criticality would most likely need to be far greater than what was identified (SNL 2007 [DIRS 181395], Section 8.1.4[a]). Model abstractions were performed for commercial SNF and three DOE SNF waste forms and resulted in insufficient fissile material accumulation in the near-field location to pose a criticality concern. Therefore, based on the analyzed waste forms representing the majority (>95% of the total metric tons) of the waste for disposal in the repository, and considering the conservative modeling parameters discussed above that would be further developed for other DOE representative fuel groups, in conjunction with the order of magnitude of the probability of a seismic faulting event causing waste package failure, the probability of near-field criticality is considered insignificant. Accordingly, this FEP is excluded from the performance assessments conducted to demonstrate compliance with proposed 10 CFR 63.311 and 63.321 (70 FR 53313 [DIRS 178394]), and with 10 CFR 63.331 [DIRS 180319], on the basis of low probability.

In addition, as documented in *Screening Analysis of Criticality Features, Events, and Processes for License Application* (SNL 2008 [DIRS 173869]), the probability of criticality for all locations is less than 1 chance in 10,000 of occurrence within 10,000 years after disposal. The results documented in this analysis are applicable for all waste forms and waste package variants.

INPUTS:

Table 2.1.14.20.0A-2. Direct Inputs

Input	Source	Description
DOE 2003. *Review of Oxidation Rates of DOE Spent Nuclear Fuel Part 2. Nonmetallic Fuel*. [DIRS 166027]	p. 32	Tests have shown that the thorium oxide pellets in the Shippingport LWBR fuel have excellent corrosion resistance with an estimated solubility of 10^{-14} mol/L at 25°C and pH > 5
	p. 33	For Shippingport LWBR fuel (DOE5), a number of studies has indicated both air and water oxidation of uranium and thorium oxide fuel pellets [(Th, U)O_2] proceed more slowly than in pure uranium oxide (UO_2), and decreases with decreasing UO_2 content in the (Th, U)O_2
	p. 48	Ft. St. Vrain fuels (DOE6) have an integral silicon carbide (SiC) protective layer that not only retains the fission products, but also protects the uranium and thorium dicarbide (ThC_2) from oxidation and hydrolysis
SNL 2007. *Geochemistry Model Validation Report: External Accumulation Model*. [DIRS 181395]	Section 8.1.4[a]	The critical mass limits were evaluated for several waste forms using bounding parameters with regards to optimizing reactivity potential, so the actual masses that would be necessary to achieve criticality would most likely need to be far greater than what was identified
	Table 6.9-1[a]	Summary of seismic scenario external criticality results
	Section 8.1.4[a]	Critical mass limits
SNL 2008. *CSNF Loading Curve Sensitivity Analysis*. [DIRS 182788]	Section 6.2.2	Design specifications
SNL 2008. *Screening Analysis of Criticality Features, Events, and Processes for License Application*. [DIRS 173869]	Table 6.4-7	The probability of drip shield and waste package failure from a fault event

Table 2.1.14.20.0A-3. Indirect Inputs

Citation	Title	DIRS
10 CFR 63	Energy: Disposal of High-Level Radioactive Wastes in a Geologic Repository at Yucca Mountain, Nevada	180319
70 FR 53313	Implementation of a Dose Standard After 10,000 Years	178394
BSC 2004	*Intact and Degraded Mode Criticality Calculations for the Codisposal of ATR Spent Nuclear Fuel in a Waste Package*	171926
BSC 2004	*Intact and Degraded Mode Criticality Calculations for the Codisposal of TMI-2 Spent Nuclear Fuel in a Waste Package*	168935
DOE 2000	*DOE Spent Nuclear Fuel Grouping in Support of Criticality, DBE, TSPA-LA*	118968
DOE 2004	*General Description of Database Information Version 5.0.1*	171271
DOE 2007	*General Description of Database Information Version 5.0.1*	182577
Radulescu et al. 2004	*DOE SNF Phase I and II Summary Report*	165482
SNL 2007	*Geochemistry Model Validation Report: External Accumulation Model*	181395
SNL 2007	*Geochemistry Model Validation Report: Material Degradation and Release Model*	181165
SNL 2008	*Screening Analysis of Criticality Features, Events, and Processes for License Application*	173869
YMP 2003	*Disposal Criticality Analysis Methodology Topical Report*	165505

FEP: 2.1.14.21.0A

FEP NAME:

In-Package Criticality Resulting from Rockfall (Intact Configuration)

FEP DESCRIPTION:

The waste package internal structures and the waste form remain intact either during or after a rockfall event. If there is a breach (or are breaches) in the waste package that allow(s) water to either accumulate or flow through the waste package, then criticality could occur in-situ.

SCREENING DECISION:

Excluded – low probability

SCREENING JUSTIFICATION:

This FEP justification accounts for in-package criticality resulting from a rockfall event. A prerequisite for any of the spent fuel waste forms to have potential for criticality is the introduction of water in liquid or vapor form to the inside of the waste package. Excluded FEP 2.1.07.01.0A (Rockfall) indicates that rockfall related to non-seismic processes such as drift degradation induced by in situ gravitational and excavation-induced stresses as well as thermally induced stresses do not generate rock block sizes sufficient to tear or rupture the drip shield plates. Drip shield damage from rockfall induced by thermal loading is found to be minor since the block sizes for such rockfall are small with a mean mass of less than 0.2 MT (BSC 2004 [DIRS 166107], p. 6-102). In addition, drift degradation (i.e., considering thermal and time-dependent effects on drift collapse, but excluding seismic effects) results in only partial collapse of the emplacement drifts at 20,000 years (see excluded FEP 2.1.07.02.0A (Drift Collapse)). The conclusion for the nominal scenario is that negligible drift degradation will occur over the initial 10,000-year postclosure period (BSC 2004 [DIRS 166107], Section 8.1 and Appendix S). Therefore, rockfall does not result in waste package outer barrier breaching. Without a waste package breach, there is no potential for in-package criticality.

Summary—Since the drip shield continues to function through rockfall events as described above, the waste package will be protected from advective water flow paths during the postclosure period, for as long as the drip shield remains intact. The probability of the occurrence of configurations with criticality potential for the in-package location resulting from rockfall is insignificant since no damage to the waste package OCBs is expected from the non-seismically initiated rockfall events. Accordingly, this FEP is excluded from the performance assessments conducted to demonstrate compliance with proposed 10 CFR 63.311 and 63.321 (70 FR 53313 [DIRS 178394]), and with 10 CFR 63.331 [DIRS 180319], on the basis of low probability. This result is applicable for all waste forms and waste package variants.

INPUTS:

Table 2.1.14.21.0A-1. Direct Inputs

Input	Source	Description
BSC 2004. *Drift Degradation Analysis*. [DIRS 166107]	Section 8.1, Appendix S	The conclusion for the nominal scenario is that negligible drift degradation will occur over the initial 10,000-year postclosure period
	p. 6-102	Drip shield damage from rockfall induced by thermal loading is found to be minor

Table 2.1.14.21.0A-2. Indirect Inputs

Citation	Title	DIRS
10 CFR 63	Energy: Disposal of High-Level Radioactive Wastes in a Geologic Repository at Yucca Mountain, Nevada	180319
70 FR 53313	Implementation of a Dose Standard After 10,000 Years	178394

FEP: 2.1.14.22.0A

FEP NAME:

In-Package Criticality Resulting from Rockfall (Degraded Configurations)

FEP DESCRIPTION:

Either during or as a result of a rockfall event, the waste package internal structures and the waste form may degrade. If a critical configuration develops, criticality could occur in situ. Potential in situ critical configurations are defined in *Disposal Criticality Analysis Methodology Topical Report* (YMP 2003 [DIRS 165505], Figures 3.2a and 3.2b).

SCREENING DECISION:

Excluded – low probability

SCREENING JUSTIFICATION:

This FEP justification accounts for in-package criticality resulting from a rockfall event. A prerequisite for any of the spent fuel waste forms to have potential for criticality is the introduction of water in liquid or vapor form to the inside of the waste package. Excluded FEP 2.1.07.01.0A (Rockfall) indicates that rockfall related to nonseismic processes such as drift degradation induced by in situ gravitational and excavation-induced stresses as well as thermally induced stresses do not generate rock block sizes sufficient to tear or rupture the drip shield plates. Drip shield damage from rockfall induced by thermal loading is found to be minor as the block sizes for such rockfall are small with a mean mass of less than 0.2 MT (BSC 2004 [DIRS 166107], p. 6-102). In addition, drift degradation (i.e., considering thermal and time-dependent effects on drift collapse, but excluding seismic effects) results in only partial collapse of the emplacement drifts at 20,000 years (see excluded FEP 2.1.07.02.0A (Drift Collapse)). The conclusion for the nominal scenario is that negligible drift degradation will occur over the initial 10,000-year postclosure period (BSC 2004 [DIRS 166107], Section 8.1 and Appendix S). Therefore, rockfall does not result in waste package outer barrier breaching. Without a waste package breach, there is no potential for in-package criticality.

Summary—Since the drip shield continues to function through rockfall events as described above, the waste package will be protected from advective water flow paths during the postclosure period, for as long as the drip shield remains intact. The probability of the occurrence of configurations with criticality potential for the in-package location resulting from rockfall is insignificant since no damage to the waste package OCBs is expected from the non-seismically initiated rockfall events. Accordingly, this FEP is excluded from the performance assessments conducted to demonstrate compliance with proposed 10 CFR 63.311 and 63.321 (70 FR 53313 [DIRS 178394]), and with 10 CFR 63.331 [DIRS 180319], on the basis of low probability. This result is applicable for all waste forms and waste package variants.

INPUTS:

Table 2.1.14.22.0A-1. Direct Inputs

Input	Source	Description
BSC 2004. *Drift Degradation Analysis*. [DIRS 166107]	Section 8.1, Appendix S	Negligible drift degradation will occur over the initial 10,000-year postclosure period
	p. 6-102	Drip shield damage from rockfall induced by thermal loading is found to be minor

Table 2.1.14.22.0A-2. Indirect Inputs

Citation	Title	DIRS
10 CFR 63	Energy: Disposal of High-Level Radioactive Wastes in a Geologic Repository at Yucca Mountain, Nevada	180319
70 FR 53313	Implementation of a Dose Standard After 10,000 Years	178394

FEP: 2.1.14.23.0A

FEP NAME:

Near-Field Criticality Resulting from Rockfall

FEP DESCRIPTION:

Either during or as a result of a rockfall event, near-field criticality could occur if fissile material-bearing solution from the waste package is transported into the drift and the fissile material is precipitated into a critical configuration. Potential near-field critical configurations are defined in *Disposal Criticality Analysis Methodology Topical Report* (YMP 2003 [DIRS 165505], Figure 3.3a).

SCREENING DECISION:

Excluded – low probability

SCREENING JUSTIFICATION:

This FEP justification accounts for external criticality for the near-field location resulting from rockfall, where *near-field* is defined as the region inside the drift external to the waste package. A prerequisite for any of the spent fuel waste forms to have potential for criticality is the introduction of water in liquid or vapor form to the inside of the TAD or DOE SNF canister. All postclosure criticality FEP scenarios, internal and external, require the presence of water in liquid or vapor form to degrade the waste package internals and/or the waste form as intact configurations are designed to remain subcritical if fabricated and loaded according to design specifications as demonstrated in *CSNF Loading Curve Sensitivity Analysis* (SNL 2008 [DIRS 182788], Section 6.2.2), *DOE SNF Phase I and II Summary Report* (Radulescu et al. 2004 [DIRS 165482], Sections 10 and 11.4), *Intact and Degraded Mode Criticality Calculations for the Codisposal of TMI-2 Spent Nuclear Fuel in a Waste Package* (BSC 2004 [DIRS 168935], Section 6), and *Intact and Degraded Mode Criticality Calculations for the Codisposal of ATR Spent Nuclear Fuel in a Waste Package* (BSC 2004 [DIRS 171926], Section 6).

For a criticality event to occur, the appropriate combination of materials (e.g., neutron moderators, neutron absorbers, fissile materials, or isotopes) and geometric configurations favorable to criticality must exist. Therefore, for a configuration to have potential for criticality, all of the following conditions must occur: (1) sufficient mechanical or corrosive damage to the waste package OCB to cause a breach, (2) presence of a moderator (i.e., water), (3) separation of fissionable material from the neutron absorber material or an absorber material selection error during the canister fabrication process, and (4) the accumulation (external) or presence of a critical mass of fissionable material in a critical geometric configuration. The probability of developing a configuration with criticality potential is insignificant unless all four conditions are realized, and then is only representative of a conservative estimate since the probability values associated with the many other events required to generate a critical configuration that are less than one are not quantified, but rather are conservatively set to one.

Near-field criticality cannot occur unless the waste package and waste form are degraded. Water infiltration is required to degrade the waste package internals and waste form and transport them to the near-field location. Criticality cannot occur unless at least the minimum critical mass of a waste form can be accumulated in a favorable geometry. It then follows that the probability of near-field criticality must be less than the probability of water entering the waste package. This is because, in addition to the events evaluated to calculate the probability of water infiltrating a breached waste package, the probability of the following events or processes must also be considered for external criticality:

- Separation of the fissile materials from the degraded waste form
- Sufficient seepage water to transport fissile materials from the waste package
- Accumulating sufficient fissile material into a potentially critical configuration in the near-field environment.

Excluded FEP 2.1.07.01.0A (Rockfall) indicates that rockfall related to nonseismic processes such as drift degradation induced by in situ gravitational and excavation-induced stresses as well as thermally induced stresses don't generate rock block sizes sufficient to tear or rupture the drip shield plates. Drip shield damage from rockfall induced by thermal loading is found to be minor since the block sizes for such rockfall are small with a mean mass of less than 0.2 metric tons (BSC 2004 [DIRS 166107], p. 6-102). In addition, drift degradation (i.e., considering thermal and time-dependent effects on drift collapse, but excluding seismic effects) results in only partial collapse of the emplacement drifts at 20,000 years (see excluded FEP 2.1.07.02.0A (Drift Collapse)). The conclusion for the nominal scenario is that negligible drift degradation will occur over the initial 10,000-year postclosure period (BSC 2004 [DIRS 166107], Section 8.1 and Appendix S).

A waste package must be breached in order to transport fissile material out. If a waste package is breached, water and solutes might enter and leave the waste package by several mechanisms, including diffusion, condensation of vapor, and advection of liquid water. Therefore, rockfall does not result in waste package outer barrier breaching. Without a waste package breach, there is no potential for external criticality.

Summary - Since the drip shield continues to function through rockfall events as described above, there is no advective flow of water to the waste package for as long as the drip shield remains intact. Therefore, there is no means to transport fissile material to the near field by precluding the introduction of water to the waste package, which is necessary to degrade the internals and transport material into the near-field location. The probability of the occurrence of configurations with criticality potential for the near-field location resulting from rockfall is insignificant since no damage to the waste package OCBs is expected from the non-seismically initiated rockfall events. Accordingly, this FEP is excluded from the performance assessments conducted to demonstrate compliance with proposed 10 CFR 63.311 and 63.321 (70 FR 53313 [DIRS 178394]), and with 10 CFR 63.331 [DIRS 180319], on the basis of low probability. This result is applicable for all waste forms and waste package variants.

INPUTS:

Table 2.1.14.23.0A-1. Direct Inputs

Input	Source	Description
BSC 2004. *Drift Degradation Analysis*. [DIRS 166107]	Section 8.1, Appendix S	Negligible drift degradation will occur over the initial 10,000-year postclosure period
	p. 6-102	Drip shield damage from rockfall induced by thermal loading is found to be minor
SNL 2008. *CSNF Loading Curve Sensitivity Analysis*. [DIRS 182788]	Section 6.2.2	All postclosure criticality FEP scenarios, internal and external, require the presence of water in liquid or vapor form to degrade the waste package internals and/or the waste form as intact configurations are designed to remain sub-critical if fabricated and loaded according to design specifications

Table 2.1.14.23.0A-2. Indirect Inputs

Citation	Title	DIRS
10 CFR 63	Energy: Disposal of High-Level Radioactive Wastes in a Geologic Repository at Yucca Mountain, Nevada	180319
70 FR 53313	Implementation of a Dose Standard After 10,000 Years	178394
BSC 2004	*Intact and Degraded Mode Criticality Calculations for the Codisposal of ATR Spent Nuclear Fuel in a Waste Package*	171926
BSC 2004	*Intact and Degraded Mode Criticality Calculations for the Codisposal of TMI-2 Spent Nuclear Fuel in a Waste Package*	168935
Radulescu et al. 2004	*DOE SNF Phase I and II Summary Report*	165482
YMP 2003	*Disposal Criticality Analysis Methodology Topical Report*	165505

FEP: 2.1.14.24.0A

FEP NAME:

In-Package Criticality Resulting from an Igneous Event (Intact Configuration)

FEP DESCRIPTION:

The waste package internal structures and the waste form remain intact either during or after an igneous disruptive event. If there is a breach (or are breaches) in the waste package that allow(s) water to either accumulate or flow through the waste package, then criticality could occur in situ.

SCREENING DECISION:

Excluded – low probability

SCREENING JUSTIFICATION:

This FEP justification accounts for in-package criticality for the igneous scenario. All postclosure criticality FEP scenarios, internal and external, require the presence of water in liquid or vapor form to degrade the waste package internals and/or the waste form as intact configurations are designed to remain subcritical if fabricated and loaded according to design specifications as demonstrated in *CSNF Loading Curve Sensitivity Analysis* (SNL 2008 [DIRS 182788], Section 6.2.2), *DOE SNF Phase I and II Summary Report* (Radulescu et al. 2004 [DIRS 165482], Sections 10 and 11.4), *Intact and Degraded Mode Criticality Calculations for the Codisposal of TMI-2 Spent Nuclear Fuel in a Waste Package* (BSC 2004 [DIRS 168935], Section 6), and *Intact and Degraded Mode Criticality Calculations for the Codisposal of ATR Spent Nuclear Fuel in a Waste Package* (BSC 2004 [DIRS 171926], Section 6).

For a criticality event to occur, the appropriate combination of materials (e.g., neutron moderators, neutron absorbers, fissile materials, or isotopes) and geometric configurations favorable to criticality must exist. Therefore, for a configuration to have potential for criticality, all of the following conditions must occur: (1) sufficient mechanical or corrosive damage to the waste package OCB to cause a breach, (2) presence of a moderator (i.e., water), (3) separation of fissionable material from the neutron absorber material or an absorber material selection error during the canister fabrication process, and (4) the accumulation (external) or presence of a critical mass of fissionable material in a critical geometric configuration. The probability of developing a configuration with criticality potential is insignificant unless all four conditions are realized, and then is only representative of a conservative estimate since the probability values associated with the many other events required to generate a critical configuration that are less than one are not quantified, but rather are conservatively set to one.

Included FEP 1.2.04.03.0A (Igneous Intrusion into Repository) describes an event where an igneous basaltic dike (magma-filled crack) intersects one or more repository drifts, followed by the intrusion of effusive (liquid) magma flow or pyroclastic flow (clots of melt in a stream of gas) into the drifts. The temperature of the waste package, the canister internals, and the SNF will heat up to near-magma temperatures in days to weeks (SNL 2007 [DIRS 177430], Figure 6-94) exceeding 700°C for one to nineteen months, depending on the temperature of the

magma and the decay heat generated by the waste (SNL 2007 [DIRS 177430], Section 6.4.6). At these high waste package temperatures, the fuel and the materials surrounding the fuel (i.e., cladding and structural materials) may be affected. Iron-zirconium and nickel-zirconium liquid eutectics are expected to form (starting at approximately 948°C (ASM International 1996 [DIRS 181641], iron-zirconium and nickel-zirconium phase diagrams)) but are not expected to provide any mechanisms causing appreciable removal of the neutron-absorber materials from their general locale in relation to the waste form since the eutectic is expected to contain both the absorber and waste form materials. In addition, thermal creep of the internal components resulting in internal slumping is also expected. In summary, it is expected that an igneous intrusion would sufficiently compromise the integrity of the waste packages, drip shields, and cladding in affected emplacement drifts to make them ineffective (i.e., a total loss of function in isolating waste packages and waste forms from seepage water when it returns after drifts have cooled), which is also indicated in *Dike/Drift Interactions* (SNL 2007 [DIRS 177430], Section 6.4.8.3). The damage is expected to be ubiquitous. Thus, it is improbable that a bathtub configuration (forming a closed-bottom container necessary for pooling) can be maintained or even created in a post-igneous intrusion environment.

During an igneous disruptive event, water, silica, and carbon are the only potential moderating materials for internal and external configurations. Carbon is not present within the magma composition, and the amount of silicon necessary to act as a moderator combined with its relatively low moderating effectiveness is insufficient to support criticality for low enriched systems. The physical and chemical environment around the waste package and waste form materials in contact with active magma will include abundant steam and other potentially corrosive or reactive volatiles (SNL 2007 [DIRS 177430], Section 6.4.8.3) where the estimated water content of potential magmas at Yucca Mountain ranges from 1.0 to 5.0 wt % with a uniform probability (DTN: LA0612DK831811.001 [DIRS 179987], file: *LA0612DK831811_001.xls*, worksheet: "EPAR_TPO-13Jan07"). As stated previously, temperatures could be in the range of $700 < T\ (°C) < 1{,}200$ for several months. The vapor pressures can be on the order of 7 MPa, giving a vapor density approximately double the density at atmospheric pressure. Thus, the water density during the igneous event will be too low to moderate the neutrons sufficiently to result in a criticality event for low enriched systems. In addition, the waste package internals are designed to preclude criticality when fully flooded with full density water. This fact, coupled with the fact that as fuel temperatures increase, the resonance absorption increases, which causes low enriched systems to decrease in reactivity, indicates that a criticality event during the igneous event is very improbable (i.e., physical conditions necessary are not present to support criticality). Therefore, the probability of sufficient moderating material to support criticality during an igneous event is considered to be sufficiently low such that, if quantified, would not significantly increase the overall probability of criticality in the repository.

The technical basis for inclusion of igneous intrusion into the repository in the TSPA is founded on the results of the probabilistic volcanic hazard analysis CRWMS M&O 1996 [DIRS 100116]) described in *Characterize Framework for Igneous Activity at Yucca Mountain, Nevada* (BSC 2004 [DIRS 169989], Table 7-1), which indicates that the computed mean annual frequency of intersection of the repository footprint by a dike is 1.7×10^{-8}. The computed 5th

and 95th percentiles of the uncertainty distribution for frequency of intersection are 7.4×10^{-10} and 5.5×10^{-8}, respectively.

This FEP is for the in-package location with intact configuration, which considers events such as canister and waste package OCB fabrication errors, neutron absorber misloads, and waste form misloads for configurations without degradation to evaluate those events for criticality potential. Each of these probabilities is less than 1 and some much less than 1 as identified in excluded FEP 2.1.14.15.0A (In-package Criticality (Intact Configuration)). Waste packages impacted by an igneous event are not expected to retain an intact internal configuration. In the unlikely event that it does, the intact configuration is designed to remain subcritical when fully flooded (SNL 2008 [DIRS 182788], Section 7; Radulescu et al. 2004 [DIRS 165482]; BSC 2004 [DIRS 168935], Section 6; BSC 2004 [DIRS 171926], Section 6). In addition, all packages shipped for disposal will have been required to meet the transportation requirements of 10 CFR 71.55 [DIRS 181967] in order to be shipped, which requires a demonstration that the fully flooded configuration remains subcritical. Although configurations not conforming to design specifications are applicable to both intact and degraded scenarios, these nonconformances would be based on probabilites associated with human reliability failures that occur during preclosure activities, making them independent of the postclosure period.

Considering that the igneous intrusive initiating event has a mean annual frequency of 1.7×10^{-8} (or a probability of 1.7×10^{-4} over 10,000 years), and the reasonable assurance implied by compliance with other NRC regulations and quality assurance programs (e.g., 10 CFR Parts 71 [DIRS 181967] and 72 [DIRS 181968], and 10 CFR Part 63 [DIRS 180319]), additional probability values associated with not meeting the design specifications because of human reliability failures would all be much less than 1 and result in a monotonically decreasing value of the overall probability for the igneous event sequence. Therefore, the resultant probability of criticality in the in-package location with intact configuration resulting from a disruptive igneous event is considered to be sufficiently low (below 1 chance in 10,000 (10^{-4}) of occurrence within 10,000 years of disposal) such that, if evaluated, would not change the conclusion, based on low probability, that a criticality event in the repository can be screened from further consideration in analyses for all waste forms. Accordingly, this FEP is excluded from the performance assessments conducted to demonstrate compliance with proposed 10 CFR 63.311 and 63.321 (70 FR 53313 [DIRS 178394]), and with 10 CFR 63.331 [DIRS 180319], on the basis of low probability.

INPUTS:

Table 2.1.14.24.0A-1. Direct Inputs

Input	Source	Description
ASM International 1996. *Binary Alloy Phase Diagrams*. [DIRS 181641]	Fe Zr and Ni Zr phase diagrams	Iron-zirconium and nickel-zirconium liquid eutectics are expected to form
BSC 2004. *Characterize Framework for Igneous Activity at Yucca Mountain, Nevada*. [DIRS 169989]	Table 7-1	The technical basis for inclusion of igneous intrusion into the repository in the TSPA is founded on the results of the Probabilistic Volcanic Hazard Analysis
DTN: LA0612DK831811.001. Magma and Eruption Properties for Potential Volcano at Yucca Mountain. [DIRS 179987]	file: *LA0612DK831811_001.xls*, worksheet: "EPAR_TPO-13Jan07"	The estimated water content of potential magmas at Yucca Mountain ranges from 1.0 to 5.0 wt %

Table 2.1.14.24.0A-1. Direct Inputs (Continued)

Input	Source	Description
SNL 2007. *Dike/Drift Interactions*. [DIRS 177430]	Section 6.4.8.3	The physical and chemical environment around the waste package and waste form materials in contact with active magma will include abundant steam and other potentially corrosive or reactive volatiles
	Section 6.4.8.3	It is expected that an igneous intrusion would sufficiently compromise the integrity of the waste packages, drip shields, and cladding in affected emplacement drifts to make them ineffective
	Section 6.4.6	The temperature of the magma and the decay heat generated by the waste
	Figure 6-94	The temperature of the waste package, the canister internals, and the SNF will heat up to near magma temperatures in days to weeks
SNL 2008. *CSNF Loading Curve Sensitivity Analysis*. [DIRS 182788]	Section 7	The intact configuration is designed to remain subcritical when fully flooded
	Section 6.2.2	All postclosure criticality FEP scenarios, internal and external, require the presence of water in liquid or vapor form to degrade the waste package internals and/or the waste form as intact configurations are designed to remain sub-critical if fabricated and loaded according to design specifications

Table 2.1.14.24.0A-2. Indirect Inputs

Citation	Title	DIRS
10 CFR 63	Energy: Disposal of High-Level Radioactive Wastes in a Geologic Repository at Yucca Mountain, Nevada	180319
10 CFR 71	Energy: Packaging and Transportation of Radioactive Material	181967
10 CFR 72	Energy: Licensing Requirements for the Independent Storage of Spent Nuclear Fuel, High-Level Radioactive Waste, and Reactor-Related Greater than Class C	181968
70 FR 53313	Implementation of a Dose Standard After 10,000 Years	178394
BSC 2004	*Intact and Degraded Mode Criticality Calculations for the Codisposal of ATR Spent Nuclear Fuel in a Waste Package*	171926
BSC 2004	*Intact and Degraded Mode Criticality Calculations for the Codisposal of TMI-2 Spent Nuclear Fuel in a Waste Package*	168935
CRWMS M&O 1996	*Probabilistic Volcanic Hazard Analysis for Yucca Mountain, Nevada*	100116
Radulescu et al. 2004	*DOE SNF Phase I and II Summary Report*	165482

FEP: 2.1.14.25.0A

FEP NAME:

In-Package Criticality Resulting from an Igneous Event (Degraded Configurations)

FEP DESCRIPTION:

Either during or as a result of an igneous disruptive event, the waste package internal structures and the waste form may degrade. If a critical configuration develops, criticality could occur in situ. Potential in situ critical configurations are defined in Disposal Criticality Analysis Methodology Topical Report (YMP 2003 [DIRS 165505], Figures 3.2a and 3.2b).

SCREENING DECISION:

Excluded – low probability

SCREENING JUSTIFICATION:

This FEP justification accounts for in-package criticality for the igneous scenario. All postclosure criticality FEP scenarios, internal and external, require the presence of water in liquid or vapor form to degrade the waste package internals and/or the waste form as intact configurations are designed to remain subcritical if fabricated and loaded according to design specifications as demonstrated in *CSNF Loading Curve Sensitivity Analysis* (SNL 2008 [DIRS 182788], Section 6.2.2), *DOE SNF Phase I and II Summary Report* (Radulescu et al. 2004 [DIRS 165482], Sections 10 and 11.4), *Intact and Degraded Mode Criticality Calculations for the Codisposal of TMI-2 Spent Nuclear Fuel in a Waste Package* (BSC 2004 [DIRS 168935], Section 6), and *Intact and Degraded Mode Criticality Calculations for the Codisposal of ATR Spent Nuclear Fuel in a Waste Package* (BSC 2004 [DIRS 171926], Section 6).

For a criticality event to occur, the appropriate combination of materials (e.g., neutron moderators, neutron absorbers, fissile materials, or isotopes) and geometric configurations favorable to criticality must exist. Therefore, for a configuration to have potential for criticality, all of the following conditions must occur: (1) sufficient mechanical or corrosive damage to the waste package OCB to cause a breach, (2) presence of a moderator (i.e., water), (3) separation of fissionable material from the neutron absorber material or an absorber material selection error during the canister fabrication process, and (4) the accumulation (external) or presence of a critical mass of fissionable material in a critical geometric configuration. The probability of developing a configuration with criticality potential is insignificant unless all four conditions are realized, and then is only representative of a conservative estimate since the probability values associated with the many other events required to generate a critical configuration that are less than one are not quantified, but rather are conservatively set to one.

Included FEP 1.2.04.03.0A (Igneous Intrusion into Repository) describes an event where an igneous basaltic dike (magma-filled crack) intersects one or more repository drifts, followed by the intrusion of effusive (liquid) magma flow or pyroclastic flow (clots of melt in a stream of gas) into the drifts. The temperature of the waste package, the canister internals, and the SNF will heat up to near-magma temperatures in days to weeks (SNL 2007 [DIRS 177430],

Figure 6-94), exceeding 700°C for one to nineteen months, depending on the temperature of the magma and the decay heat generated by the waste (SNL 2007 [DIRS 177430], Section 6.4.6). At these high waste package temperatures, the fuel and the materials surrounding the fuel (i.e., cladding and structural materials) may be affected. Iron-zirconium and nickel-zirconium liquid eutectics are expected to form (starting at approximately 948°C (ASM International 1996 [DIRS 181641], iron-zirconium and nickel-zirconium phase diagrams)) but are not expected to provide any mechanisms causing appreciable removal of the neutron-absorber materials from their general locale in relation to the waste form since the eutectic is expected to contain both the absorber and waste form materials. In addition, thermal creep of the internal components resulting in internal slumping is also expected. In summary, it is expected that an igneous intrusion would sufficiently compromise the integrity of the waste packages, drip shields, and cladding in affected emplacement drifts to make them ineffective (i.e., a total loss of function in isolating waste packages and waste forms from seepage water when it returns after drifts have cooled), which is also indicated in *Dike/Drift Interactions* (SNL 2007 [DIRS 177430], Section 6.4.8.3). The damage is expected to be ubiquitous. Thus, it is improbable that a bathtub configuration (forming a closed-bottom container necessary for pooling) can be maintained or even created in a post-igneous intrusion environment.

During an igneous disruptive event, water, silica, and carbon are the only potential moderating materials for internal and external configurations. Carbon is not present within the magma composition, and the amount of silicon necessary to act as a moderator combined with its relatively low moderating effectiveness is insufficient to support criticality for low enriched systems. The physical and chemical environment around the waste package and waste form materials in contact with active magma will include abundant steam and other potentially corrosive or reactive volatiles (SNL 2007 [DIRS 177430], Section 6.4.8.3) where the estimated water content of potential magmas at Yucca Mountain ranges from 1.0 wt % to 5.0 wt % with a uniform probability (DTN: LA0612DK831811.001 [DIRS 179987], file: *LA0612DK831811_001.xls*, worksheet: "EPAR_TPO-13Jan07"). As stated previously, temperatures could be in the range of $700 < T\ (°C) < 1{,}200$ for several months. The vapor pressures can be on the order of 7 MPa, giving a vapor density approximately double the density at atmospheric pressure. Thus, the water density during the igneous event will be too low to moderate the neutrons sufficiently to result in a criticality event for low enriched systems. In addition, the waste package internals are designed to preclude criticality when fully flooded with full density water. This fact, coupled with the fact that as fuel temperatures increase, the resonance absorption increases, which causes low enriched systems to decrease in reactivity, indicates that a criticality event during the igneous event is very improbable (i.e., physical conditions necessary are not present to support criticality). Therefore, the probability of sufficient moderating material to support criticality during an igneous event has been considered to be sufficiently low such that, if quantified, would not significantly increase the overall probability of criticality in the repository.

The technical basis for inclusion of igneous intrusion into the repository in the TSPA is founded on the results of the probabilistic volcanic hazard analysis (CRWMS M&O 1996 [DIRS 100116]) described in *Characterize Framework for Igneous Activity at Yucca Mountain, Nevada* (BSC 2004 [DIRS 169989], Table 7-1), which indicates that the computed mean annual frequency of intersection of the repository footprint by a dike is 1.7×10^{-8}. The computed 5th

and 95th percentiles of the uncertainty distribution for frequency of intersection are 7.4×10^{-10} and 5.5×10^{-8}, respectively.

In addition to the igneous disruptive event itself, additional events that must be considered, for which the probability is less than or equal to one but not necessarily quantifiable, that are necessary for a configuration to have criticality potential in the igneous disruptive scenario are as follows:

- Immediate or delayed waste package damage: The combined effects of plastic deformation, an enhanced corrosive environment, phase transformation, and ordering reactions (e.g., atomic dislocations or slippage), causing embrittlement and increased susceptibility to localized corrosion suggest that the waste packages will fail rather rapidly with respect to the time scale of interest (10,000 years).

- Separation of fissionable material from the neutron absorber material or lack of absorber material: During the igneous intrusive event and immediately following, temperatures will be elevated for a sufficiently long period to induce thermal creep and reconfiguration of the internal components. However, there is no expectation that most of the components or materials in CSNF waste packages will relocate from their locations relative to each other. This is reasonable given that intrusion temperatures do not exceed the melting temperatures of the majority of the waste package (SNL 2007 [DIRS 177430], Section 6.4.8.3) or waste form component materials (melting temperature of UO_2 is approximately 2,600°C (Todreas and Kazimi 1990 [DIRS 107735]), p. 306)), with the exception of the eutectics that are self limiting.

The specific geometry and composition of the numerous intermediate configurations are dependent on the environmental conditions and cannot all be defined individually for analysis. Considering the increased variability in the potential geometric reconfigurations, effects on material performance, and neutron spectrum changes resulting in varied neutron absorber effectiveness, the explicit detailed evaluations would be of limited value considering the high degree of uncertainty associated with any given scenario that may be evaluated. Therefore, the impact of an intrusive igneous event on waste packages and various SNF types has been evaluated for configurations with criticality potential (i.e., presence of fissile material, neutron moderator, lack of neutron absorbers) by considering a representative configuration in lieu of attempting to evaluate a range of specific environmental parameters and configurations, along with an estimate of their probability of occurrence, that could generate a large number of possible event sequences and outcomes. The single representative configuration is considered representative of ones having criticality potential following an initiating intrusive igneous event and provides a basis for demonstrating the additional events and processes that would be required to result in criticality following an intrusive igneous event. A detailed criticality assessment of configurations for the commercial SNF and various DOE SNF waste forms has been performed (SNL 2007 [DIRS 181373]; BSC 2006 [DIRS 181335]), with all configurations shown to be subcritical provided the SNF canisters were fabricated and loaded according to specifications. Although configurations not conforming to design specifications are applicable to both intact and degraded scenarios, these nonconformances would be based on probabilities associated with human reliability failures that occur during preclosure activities, making them independent of the postclosure period.

An evaluation documented in *DOE SNF Material Interaction Potentials during an Intrusive Igneous Event at Yucca Mountain* (Smith and Loo 2007 [DIRS 183392], Section 11) concluded that there was potential for some reconfigurations in most of the nine criticality fuel groups if immersed in magma. Results from the evaluation indicated that there is no obvious mechanism that can lead to liquefaction and reconfiguration of the mixed oxide waste form group. Other waste forms, particularly aluminum based SNF and uranium metal SNF, are expected to exhibit some geometry changes. However, results of criticality analyses for all of the representative DOE SNF waste forms in waste packages affected by an igneous intrusion showed that, for the range of reconfigurations considered, none exceeded the critical limit for the particular waste form (BSC 2006 [DIRS 181335], Section 7.10) provided the SNF canisters were fabricated and loaded according to specifications.

Several of the DOE SNF fuel types incorporate neutron poison that is necessary for criticality control for certain degraded scenarios. The poison is provided by basket material made of a nickel-gadolinium alloy and/or gadolinium-bearing shot composed of iron or aluminum. Temperatures during an igneous intrusive event scenario and immediately following will be sufficiently high such that the DOE aluminum fuels and gadolinium-containing aluminum shot used with certain DOE fuels for criticality control are expected to melt. Thus, these configurations are susceptible to fuel and absorber material reconfiguration by melting and collecting towards the bottom of the DOE SNF canister. Basket structure slumping due to the high temperature environment from the surrounding magma or from the formation of a mass either by melting or eutectic formation is not expected to lead to configurations where the fissile material is concentrated away from the bulk of the neutron absorber in the canisters. Melting or eutectic formation or slumping will always provide some mixing between the fissile materials and the neutron absorber.

Additionally, the commercial SNF fissionable material is not expected to separate significantly from the neutron absorber material in the commercial SNF waste packages. Sensitization of stainless steel and borated stainless steel can occur during heating and cooling, such as would occur from magmatic intrusion. In principle, heating of the stainless steel to magmatic temperatures might cause sensitization and a reduction in corrosion resistance. During sensitization, the chemical composition in the vicinity of the grain boundaries can be altered by the precipitation of chromium-containing carbides, which depletes chromium at the edges of the adjacent alloy grains (typically austenite) and increases potential for intergranular corrosion, since the chromium-depleted regions fail to produce a chromium-oxide passivating layer. Subsequent slow cooling at 500°C to 750°C may desensitize the steel, as chromium diffuses back into the depleted zones. However, the situation at lower temperatures is less clear, as the solubility of the carbide phase decreases. Fox and McCright (1983 [DIRS 159344]) argue that heating in the repository for years, at temperatures of 350°C and below, may cause desensitization, especially in Stainless Steel Type 304 alloys. Stainless Steel Type 304B does not suffer sensitization in the same way that Stainless Steel Type 304L is affected. The metal borides are actually boro-carbides of the form $(Cr,Fe)_2(B,C)$ or $(Cr,Fe)_{23}(B,C)_6$ and effectively soak up most excess carbon. The borides precipitate at rather high temperatures and are stable down to fairly low temperatures, so there is no formation of chromium carbide. For heat-treated Stainless Steel Type 304B, Moreno et al. (2004 [DIRS 179295]) conclude:

> …it is not possible to talk about a common sensitized state as no carbides are found at the grain boundaries.

Regardless of the sensitization effects on the corrosion resistance of the neutron absorber material, most of the boron is expected to remain between the assemblies.

Certain DOE SNF waste forms have sufficient quantities of fissile material to support unmoderated (fast) criticality if the fissile material is concentrated beyond its design concentration in the waste form and the neutron absorber materials are removed. While concentration of the fissile material beyond its nominal design concentration could result from degradation of the waste form by either water infiltration or a disruptive event, removal of the neutron absorber materials from a DOE SNF waste package would require a breach of the waste package and a removal mechanism. Degradation in the presence of water would result in a moderated system. Likewise, there is no known mechanism that could reconfigure nondegraded fissile material into a compact configuration with unmoderated criticality potential. The most likely neutron absorber material removal mechanism is through water infiltration resulting in degradation of the waste package internal components, dissolving of the neutron absorber material in the water, and flushing of the material from the waste package. This mechanism is not expected to result in a critical configuration since the corrosion rate of the neutron absorber material is very low. In addition, the gadolinium absorber in the DOE SNF canisters forms phosphate or carbonate corrosion products (SNL 2007 [DIRS 181165], Section 6.3.16), which have very low solubility.

Considering that the igneous intrusive initiating event has a mean annual frequency of 1.7×10^{-8} (or a probability of 1.7×10^{-4} over 10,000 years), and the reasonable assurance implied by compliance with other NRC regulations and quality assurance programs (e.g., 10 CFR Parts 71 [DIRS 181967] and 72 [DIRS 181968] and 10 CFR Part 63 [DIRS 180319]), additional probability values associated with not meeting the design specifications because of human reliability failures would all be much less than one and result in a monotonically decreasing value of the overall probability for the igneous event sequence (an example of these probabilities is identified in excluded FEP 2.1.14.15.0A (In-package Criticality (Intact Configuration)). Therefore, the resultant probability of criticality in the in-package location with degraded configurations resulting from a disruptive igneous event is considered to be sufficiently low (below 1 chance in 10,000 (10^{-4}) of occurrence within 10,000 years of disposal) such that, if evaluated, would not change the conclusion, based on low probability, that a criticality event in the repository can be screened from further consideration in analyses for all waste forms. Accordingly, this FEP is excluded from the performance assessments conducted to demonstrate compliance with proposed 10 CFR 63.311 and 63.321 (70 FR 53313 [DIRS 178394]), and with 10 CFR 63.331 [DIRS 180319], on the basis of low probability.

INPUTS:

Table 2.1.14.25.0A-1. Direct Inputs

Input	Source	Description
ASM International 1996. *Binary Alloy Phase Diagrams.* [DIRS 181641]	Fe Zr and Ni Zr phase diagrams	Formation of iron-zirconium and nickel-zirconium liquid eutectics (starting at approximately 948°C)
BSC 2004. *Characterize Framework for Igneous Activity at Yucca Mountain, Nevada*. [DIRS 169989]	Table 7-1	Description of probabilistic volcanic hazard analysis results
DTN: LA0612DK831811.001. Magma and Eruption Properties for Potential Volcano at Yucca Mountain. [DIRS 179987]	file: *LA0612DK831811_001.xls*, worksheet: "EPAR_TPO-13Jan07"	Estimated water content of potential magmas at Yucca Mountain ranges from 1.0 wt % to 5.0 wt % with a uniform probability
SNL 2007. *Dike/Drift Interactions*. [DIRS 177430]	Section 6.4.8.3	The physical and chemical environment around the waste package and waste form materials in contact with active magma will include abundant steam and other potentially corrosive or reactive volatiles
	Section 6.4.8.3	It is expected that an igneous intrusion would sufficiently compromise the integrity of the waste packages, drip shields, and cladding in affected emplacement drifts to make them ineffective (i.e., a total loss of function in isolating waste packages and waste forms from seepage water when it returns after drifts have cooled)
SNL 2007. *Geochemistry Model Validation Report: Material Degradation and Release Model*. [DIRS 181165]	Section 6.3.16	The gadolinium absorber in the DOE SNF canisters forms phosphate or carbonate corrosion products which have very low solubility
SNL 2008. *CSNF Loading Curve Sensitivity Analysis*. [DIRS 182788]	Section 6.2.2	All postclosure criticality FEP scenarios require the presence of water in liquid or vapor form to degrade the waste package internals and/or the waste form as intact configurations are designed to remain sub-critical if fabricated and loaded according to design specifications

Table 2.1.14.25.0A-2. Indirect Inputs

Citation	Title	DIRS
10 CFR 63	Energy: Disposal of High-Level Radioactive Wastes in a Geologic Repository at Yucca Mountain, Nevada	180319
10 CFR 72	Energy: Licensing Requirements for the Independent Storage of Spent Nuclear Fuel, High-Level Radioactive Waste, and Reactor-Related Greater than Class C	181968
70 FR 53313	Implementation of a Dose Standard After 10,000 Years	178394
BSC 2004	*Intact and Degraded Mode Criticality Calculations for the Codisposal of TMI-2 Spent Nuclear Fuel in a Waste Package*	168935
BSC 2006	*Criticality Potential of Waste Packages Affected by Igneous Intrusion*	181335
CRWMS M&O 1996	*Probabilistic Volcanic Hazard Analysis for Yucca Mountain, Nevada*	100116
Fox and McCright 1983	*An Overview of Low Temperature Sensitization*	159344
Moreno et al. 2004	"Microstructural Characterization and Pitting Corrosion Behavior of UNS S30466 Borated Stainless Steel"	179295
Radulescu et al. 2004	*DOE SNF Phase I and II Summary Report*	165482
Smith and Loo 2007	*DOE SNF Material Interaction Potentials during an Intrusive Igneous Event at Yucca Mountain*	183392
SNL 2007	*Commercial Spent Nuclear Fuel Igneous Scenario Criticality Evaluation*	181373
SNL 2007	*Dike/Drift Interactions*	177430
Todreas and Kazimi 1990	*Nuclear Systems I, Thermal Hydraulic Fundamentals*	107735
YMP 2003	*Disposal Criticality Analysis Methodology Topical Report*	165505

FEP: 2.1.14.26.0A

FEP NAME:

Near-Field Criticality Resulting from an Igneous Event

FEP DESCRIPTION:

Either during or as a result of an igneous disruptive event, near-field criticality could occur if fissile material-bearing solution from the waste package is transported into the drift and the fissile material is precipitated into a critical configuration. Potential near-field critical configurations are defined in *Disposal Criticality Analysis Methodology Topical Report* (YMP 2003 [DIRS 165505], Figure 3.3a).

SCREENING DECISION:

Excluded – low probability

SCREENING JUSTIFICATION:

This FEP justification accounts for external criticality for the near-field location for the igneous scenario, where *near-field* is defined as the region inside the drift external to the waste package. A prerequisite for any of the spent fuel waste forms to have potential for criticality is the introduction of water in liquid or vapor form to the inside of the TAD or DOE SNF canister. For a criticality event to occur, the appropriate combination of materials (e.g., neutron moderators, neutron absorbers, fissile materials, or isotopes) and geometric configurations favorable to criticality must exist. Therefore, for a configuration to have potential for criticality, all of the following conditions must occur: (1) sufficient mechanical or corrosive damage to the waste package OCB to cause a breach, (2) presence of a moderator (i.e., water), (3) separation of fissionable material from the neutron absorber material or an absorber material selection error during the canister fabrication process, and (4) the accumulation (external) or presence of a critical mass of fissionable material in a critical geometric configuration. The probability of developing a configuration with criticality potential is insignificant unless all four conditions are realized, and then is only representative of a conservative estimate since the probability values associated with the many other events required to generate a critical configuration that are less than one are not quantified, but rather are conservatively set to one.

Near-field criticality cannot occur unless the waste package and waste form are degraded. Water infiltration is required to degrade the waste package internals and waste form and transport them to the near-field location. Criticality cannot occur unless at least the minimum critical mass of a waste form can be accumulated in favorable geometry. It then follows that the probability of near-field criticality must be less than the probability of water entering the waste package. This is because, in addition to the events evaluated to calculate the probability of water infiltrating a breached waste package, the probability of the following events or processes must also be considered for external criticality:

- Separation of the fissile materials from the degraded waste form

- Sufficient seepage water to transport fissile materials from the waste package
- Accumulating sufficient fissile material into a potentially critical configuration in the near-field environment.

Included FEP 1.2.04.03.0A (Igneous Intrusion into Repository) is an event where an igneous basaltic dike (magma-filled crack) intersects one or more repository drifts, followed by the intrusion of effusive (liquid) magma flow or pyroclastic flow (clots of melt in a stream of gas) into the drifts. The temperature of the waste package, the canister internals, and the SNF will heat up to near-magma temperatures in days to weeks (SNL 2007 [DIRS 177430], Figure 6-94), exceeding 700°C for one to nineteen months, depending on the temperature of the magma and the radioactive decay heat generated by the waste (SNL 2007 [DIRS 177430], Section 6.4.6). At these high waste package temperatures, the fuel and the materials surrounding the fuel (i.e., cladding and structural materials) may be affected. Iron-zirconium and nickel-zirconium liquid eutectics will form (starting at approximately 948°C (ASM International 1996 [DIRS 181641], iron-zirconium and nickel-zirconium phase diagrams)), but are not expected to provide any mechanisms causing appreciable removal of the neutron-absorber materials from their general locale in relation to the waste form since the eutectic melt is expected to contain both the absorber and waste form materials. In addition, thermal creep of the internal components resulting in internal slumping is also expected. In summary, it is expected that an igneous intrusion would sufficiently compromise the integrity of the waste packages, drip shields, and cladding in affected emplacement drifts to make them ineffective (i.e., a total loss of function in isolating waste packages and waste forms from seepage water when it returns after drifts have cooled).

The technical basis for inclusion of igneous intrusion into the repository in the TSPA is founded on the results of the PVHA (CRWMS M&O 1996 [DIRS 100116]) described in *Characterize Framework for Igneous Activity at Yucca Mountain, Nevada* (BSC 2004 [DIRS 169989], Table 7-1), which indicates that the computed mean annual frequency of intersection of the repository footprint by a dike is 1.7×10^{-8}. The computed 5th and 95th percentiles of the uncertainty distribution for frequency of intersection are 7.4×10^{-10} and 5.5×10^{-8}, respectively.

An igneous intrusion is not expected to increase the criticality potential for the near-field scenario and is expected to reduce the near-field potential since the drift will be filled with magma. In addition, the temperatures in the invert fill supporting the pallets and waste packages will approach or exceed the glass transition temperature for the crushed tuff. This is expected to result in formation of tuff vitrophyre up to 3 m from the contact surface (SNL 2007 [DIRS 174260], Section F.2.2), which would have a significantly reduced void fraction within the invert for fissile material accumulation.

There are several hundred distinct types of DOE SNF. These fuels come from a wide range of reactor types, such as light- and heavy-water-moderated reactors, graphite-moderated reactors, and breeder reactors, with various cladding materials and enrichments, varying from depleted uranium to over 93% enriched ^{235}U. Many of these reactors, now decommissioned, had unique design features, such as core configuration, fuel element and assembly geometry, moderator and coolant materials, operational characteristics, and neutron spatial and spectral properties (DOE 2004 [DIRS 171271]).

Therefore, to facilitate DOE SNF waste form evaluations, the DOE SNF inventory was first reduced to 34 DOE SNF groups based on fuel matrix, cladding, cladding condition, and enrichment. These parameters are the fuel characteristics that were determined to have major impacts on the release of radionuclides from the DOE SNF and contributed to nuclear criticality scenarios (DOE 2000 [DIRS 118968], Section 5). Separate groups were further refined for the purposes of criticality, design basis events, and TSPA based on key parameters such as fuel matrix, cladding, and fuel condition, as well as fissile species and enrichment, and reactor and fuel design (DOE 2000 [DIRS 118968], Section 5.1). For criticality, nine DOE SNF criticality groups have been identified and are listed in *General Description of Database Information Version 5.0.1* (DOE 2007 [DIRS 182577], Table 6).

Within each of the nine DOE SNF criticality groups, a single fuel design was selected as being representative of the remaining fuel within each group. The term representative means that all fuels would perform similarly regarding chemical interactions within the waste package and basket, and that canister loading limits from the representative fuel (ranges of key parameters important to criticality such as linear fissile loading and total fissile mass) are established, which other fuels within the group can be shown to not exceed. Waste forms within a single criticality group that have configurations or key criticality parameters outside the range of applicability of the representative fuel will require supplemental analysis and/or additional reactivity control mechanisms.

Evaluations for naval fuel are conducted by the Naval Nuclear Propulsion Program. A miscellaneous waste form category that has a variety of fuel matrix properties originating from various post-irradiation examinations and other testing is not included in the criticality evaluations for the fuel groups as they will need to be evaluated on a case-by-case basis. Thus, the disposal criticality analysis methodology (YMP 2003 [DIRS 165505]) can be applied to nine DOE SNF representative fuel groups for criticality evaluations.

The minimum fissile mass necessary for criticality external to the waste packages is discussed in *Geochemistry Model Validation Report: External Accumulation Model* (SNL 2007 [DIRS 181395], Section 8.1.4[a]), where it was concluded that insufficient fissile material can collect over 10,000 years to achieve a critical mass for the igneous scenario, in which a critical mass is defined as one where k_{eff} (effective neutron multiplication factor) exceeds the critical limit for the material. The critical mass limits were evaluated for commercial SNF and DOE SNF waste forms using bounding parameters with regards to optimizing reactivity potential, so the actual masses that would be necessary to achieve criticality would need to be far greater than what was identified (SNL 2007 [DIRS 181395], Section 8.1.4[a]).

Model abstractions were performed for commercial SNF and three DOE SNF waste forms in *Geochemistry Model Validation Report: External Accumulation Model* (SNL 2007 [DIRS 181395]) (i.e., N Reactor (DOE3), TMI (DOE9), and FFTF (DOE1)) (SNL 2008 [DIRS 173869], Section 4.1.15), which make up a ~90% of the metric tons of heavy metal in the DOE SNF inventory expected to be stored in the repository. In addition to these waste forms making up ~90% of the inventory by mass, they were selected because they provide degradation and accumulation characteristics of uranium-metal (N Reactor), mixed-oxide (FFTF), and damaged uranium dioxide (TMI) waste forms which may be applicable to other representative DOE waste forms. Some of the other DOE SNF waste forms, such as Shippingport light-water

breeder reactor (LWBR) (DOE5) and Ft. St. Vrain (DOE6), are not expected to be a concern for external criticality due to the corrosion resistance of the waste form (SNL 2007 [DIRS 181395], Section 6.9.3[a]).

Ft. St. Vrain fuels (DOE6) have an integral silicon carbide (SiC) protective layer that not only retains the fission products but also protects the uranium and thorium dicarbide (ThC_2) from oxidation and hydrolysis (DOE 2003 [DIRS 166027], p. 48). Comparative analysis has indicated that the Ft. St. Vrain fuel has the lowest degradation rate of all DOE SNF and should behave significantly better in terms of fissile material dissolution, transport, and accumulation. In some residual quantities (<250 grams per block), ^{233}U bred into the ThC_2 fertile particles. A canister loaded with five Ft. St. Vrain blocks contains sufficient quantities of ^{233}U to have criticality potential in solution; however, a mechanism to separate the uranium from within the SiC-coated fertile particles, and then a mechanism to accumulate in a concentrated fissile mass in a favorable geometry, is not credible.

For Shippingport LWBR fuel (DOE5), a number of studies have indicated both air and water oxidation of uranium and thorium oxide fuel pellets [$(Th, U)O_2$] proceed more slowly than in pure uranium oxide (UO_2), and decrease with decreasing UO_2 content in the $(Th, U)O_2$ (DOE 2003 [DIRS 166027], p. 33). Tests have shown that the thorium oxide pellets in the Shippingport LWBR fuel have excellent corrosion resistance, with an estimated solubility of 10^{-14} mol/L at 25°C and pH > 5 (DOE 2003 [DIRS 166027], p. 32). With the less-reactive degradation rate, a mechanism to separate the uranium, transporting, and accumulation into a favorable geometry is also not credible.

Table 2.1.14.26.0A-1 shows the ranges of minimum critical mass required to accumulate in the invert to achieve a critical limit of k_{eff} (effective neutron multiplication factor) equal to 0.96. Also shown is the calculated accumulation or mass released from the waste package for the waste forms evaluated for external criticality. For each of the waste forms evaluated, the results indicate that an insufficient amount of fissile material accumulates to pose a criticality concern.

Table 2.1.14.26.0A-1. Summary of Igneous Scenario External Criticality Results

Scenario	Waste Package Type	Calculated Accumulation or Mass Released from Waste Package (uranium mass, unless otherwise noted (kg))	Mass of Uranium or Plutonium (for FFTF) Required to Achieve Critical Limit of k_{eff} = 0.96 in the Invert (kg)
Igneous	DOE3 (N Reactor)	0.109	Infinite[a]
	DOE9 (TMI II Fuel)	30.7	538
	Commercial SNF	74.8	159
	DOE1 (FFTF) (Plutonium mass)	6.34×10^{-3}	1.66

Source: SNL 2007 [DIRS 181395], Table 6.9-1[a].

[a] "Infinite" means that an infinite amount of fissile waste released in this model will not produce an arrangement that can reach the critical limit.

DOE fuel groups in DOE2, DOE4, DOE7, and DOE8 representing UZrHx (TRIGA), high enriched uranium oxide (Shippingport PWR), aluminum-based (ATR), and U-Zr/U-Mo alloy (Fermi), respectively (SNL 2008 [DIRS 173869], Table 4.1-2), have not been analyzed in detail

for external fissile mass transport and accumulation as the other waste forms have. However, considering the processes that must occur to allow advective seepage into a DOE SNF canister without substantial drainage to allow degradation of the internal components and waste form, along with the other conservative modeling parameters that have been used to create a process to facilitate fissile material transport to the external environment, and the bounding modeling parameters respective to maximizing criticality potential, these waste forms are not expected to result in an increase in the total probability of criticality in the near-field location.

Some of the conservative modeling parameters are provided as follows:

- The material degradation and release model (SNL 2007 [DIRS 181165]) uses constant corrosion rates for the SNF; however, laboratory experiments on the surface structure of commercial SNF during dissolution have shown that UO_2 dissolution is accompanied by the formation of a protective layer of secondary phases that retards further corrosion (SNL 2007 [DIRS 181165], Section 6.6.2). Therefore, the release of uranium from the fuel would be slower and therefore less would be released.

- Experimental and field data indicate that actinides would be adsorbed on or incorporated into alteration products that form in the waste package (SNL 2007 [DIRS 181165], Section 6.6.3). This solid solution formation and adsorption would tend to lower actinide concentrations below those predicted by EQ6 and would delay release from the waste package.

- The material degradation and release model (SNL 2007 [DIRS 181165]) considers that the cladding and DOE SNF canister as breached upon emplacement in the repository, and unzipping immediately upon waste package breach, whereas the expected scenario would be that the failure would take place over many years. This would also delay the release of actinides.

- Many conservative modeling approximations are used to simplify the critical mass calculations presented in Table 2.1.14.26.0A-1. For the commercial SNF and low-enriched DOE fuels analyzed in *Geochemistry Model Validation Report: External Accumulation Model* (SNL 2007 [DIRS 181395]), the conservatisms are appropriate, because the results show that a criticality is very unlikely. However, for the higher enriched DOE fuels, less conservative modeling parameters of the criticality potential are expected to generate similar conclusions.

Summary—The critical mass limits were evaluated for several waste forms using bounding parameters with regards to optimizing reactivity potential, so the actual masses that would be necessary to achieve criticality would need to be greater than what was identified in *Geochemistry Model Validation Report: External Accumulation Model* (SNL 2007 [DIRS 181395], Section 8.1.4[a]). Model abstractions were performed for commercial SNF and three DOE SNF waste forms and resulted in insufficient fissile material accumulation in the near-field location to pose a criticality concern. Therefore, based on the analyzed waste forms representing the majority (>95% of the total metric tons) of the waste for disposal in the repository, and considering the conservative modeling parameters discussed above that would be further developed for other DOE representative fuel groups, in conjunction with the probablity of

the igneous intrusive initiating event, the probability of near-field criticality is considered insignificant.

Accordingly, this FEP is excluded from the performance assessments conducted to demonstrate compliance with proposed 10 CFR 63.311 and CFR 63.321 (70 FR 53313 [DIRS 178394]), and with 10 CFR 63.331 [DIRS 180319], on the basis of low probability.

In addition, as documented in *Screening Analysis of Criticality Features, Events, and Processes for License Application* (SNL 2008 [DIRS 173869]), the probability of criticality for all locations is less than 1 chance in 10,000 of occurrence within 10,000 years after disposal. The results documented in this analysis are applicable for all waste forms and waste package variants.

INPUTS:

Table 2.1.14.26.0A-2. Direct Inputs

Input	Source	Description
ASM International 1996. *Binary Alloy Phase Diagrams*. [DIRS 181641]	Fe Zr and Ni Zr phase diagrams	Formation of iron-zirconium and nickel-zirconium liquid eutectics (starting at approximately 948°C)
DOE 2003. *Review of Oxidation Rates of DOE Spent Nuclear Fuel Part 2. Nonmetallic Fuel*. [DIRS 166027]	p. 33	For Shippingport LWBR fuel (DOE5), a number of studies have indicated both air and water oxidation of uranium and thorium oxide fuel pellets [(Th, U)O_2] proceed more slowly than in pure uranium oxide (UO_2), and decreases with decreasing UO_2 content in the (Th, U)O_2
	p. 48	Ft. St. Vrain fuels (DOE6) have an integral silicon carbide (SiC) protective layer that not only retains the fission products but also protects the uranium and thorium dicarbide (ThC_2) from oxidation and hydrolysis
	p. 32	Thorium oxide pellets in the Shippingport LWBR fuel have excellent corrosion resistance with an estimated solubility of 10^{-14} mol/L at 25°C and pH>5
SNL 2007. *Dike/Drift Interactions*. [DIRS 177430]	Section 6.4.6; Figure 6-94	The temperature of the waste package, the canister internals, and the SNF will heat up to near magma temperatures in days to weeks exceeding 700°C for one to nineteen months, depending on the temperature of the magma and the radioactive decay heat generated by the waste

Table 2.1.14.26.0A-2. Direct Inputs (Continued)

Input	Source	Description
SNL 2007. *Geochemistry Model Validation Report: External Accumulation Model*. [DIRS 181395]	Section 8.1.4[a]	Identifies masses that would be necessary to achieve criticality
	Table 6.9-1[a]	Summary of igneous scenario external criticality results
	Section 8.1.4[a]	The critical mass limits were evaluated for commercial SNF and DOE SNF waste forms using bounding parameters with regards to optimizing reactivity potential, so the actual masses that would be necessary to achieve criticality would most likely need to be far greater than what was identified
	Section 8.1.4[a]	The minimum fissile mass necessary for criticality external to the waste packages is discussed where it was concluded that insufficient fissile material can collect over 10,000 years to achieve a critical mass for the igneous scenario

Table 2.1.14.26.0A-3. Indirect Inputs

Citation	Title	DIRS
10 CFR 63	Energy: Disposal of High-Level Radioactive Wastes in a Geologic Repository at Yucca Mountain, Nevada	180319
70 FR 53313	Implementation of a Dose Standard After 10,000 Years	178394
BSC 2004	*Characterize Framework for Igneous Activity at Yucca Mountain, Nevada*	169989
CRWMS M&O 1996	*Probabilistic Volcanic Hazard Analysis for Yucca Mountain, Nevada*	100116
DOE 2000	*DOE Spent Nuclear Fuel Grouping in Support of Criticality, DBE, TSPA-LA*	118968
DOE 2004	*General Description of Database Information Version 5.0.1*	171271
DOE 2007	*General Description of Database Information Version 5.0.1*	182577
SNL 2007	*Characterize Eruptive Processes at Yucca Mountain, Nevada*	174260
SNL 2007	*Geochemistry Model Validation Report: External Accumulation Model*	181395
SNL 2007	*Geochemistry Model Validation Report: Material Degradation and Release Model*	181165
SNL 2008	*Screening Analysis of Criticality Features, Events, and Processes for License Application*	173869
YMP 2003	*Disposal Criticality Analysis Methodology Topical Report*	165505

FEP: 2.2.01.01.0A

FEP NAME:

Mechanical Effects of Excavation and Construction in the Near-Field

FEP DESCRIPTION:

Excavation will produce some disturbance of the rocks surrounding the drifts due to stress relief. Stresses associated directly with excavation (e.g., boring and blasting operations) may also cause some changes in rock properties. Properties that may be affected include rock strength, fracture spacing and block size, and hydrologic properties such as permeability.

SCREENING DECISION:

Included

TSPA DISPOSITION:

This disposition discusses two aspects of this FEP. The first aspect relates to changes in geomechanical properties caused by the mechanical effects of excavation and construction in the near-field rock. These have been shown to have a negligible effect on rock geomechanical properties. The second aspect relates to changes affecting hydrological properties, which have been included in the TSPA and are discussed in the following paragraphs.

The excavation-induced fracturing of the tunnel periphery is confined to a depth of influence of only a few centimeters. The depth of mechanically induced damage is therefore less than 1% of the tunnel diameter except where natural fractures are abundant and damage effects can penetrate up to 50 cm (Craig 2001 [DIRS 171411], p. 16). This is consistent with observations documented in *Drift Degradation Analysis* (BSC 2004 [DIRS 166107], Figure 7-25), which show that excavation-induced fracturing in the Exploratory Studies Facility (ESF) ranges from zero in good quality lithophysal rock to a maximum penetration of about 60 cm (2 ft) in poor quality lithophysal rock. In either case, no significant impacts on rock mass mechanical properties are expected to result from mechanical damage associated with excavation-related impacts (see excluded FEP 1.1.02.00.0B (Mechanical Effects of Excavation and Construction in EBS)). Likewise, no significant impacts on near-field rock mechanical properties are expected.

Fracture spacing data have been collected within the tunnel and analyzed in *Drift Degradation Analysis* (BSC 2004 [DIRS 166107], Section 6.1) to determine a range of block sizes. Excavation-induced changes associated with these block sizes have been accounted for in *Drift Degradation Analysis* (BSC 2004 [DIRS 166107], Sections 6.3 and 6.4), and are discussed in excluded FEP 1.2.03.02.0B (Seismic-Induced Rockfall Damages EBS Components) and included FEP 1.2.03.02.0C (Seismic-Induced Drift Collapse Damages EBS Components).

Mechanical effects of excavation on hydrologic properties and seepage are taken into account in the air injection tests and seepage tests conducted in the ESF (BSC 2004 [DIRS 170004]). Since the testing boreholes are located within the excavation-disturbed zone in the vicinity of ESF niches, the data derived from these tests implicitly reflect mechanical effects of excavation. The

measured post-excavation air permeability data are consistent with geomechanical model results (SNL 2007 [DIRS 181244], Section 6.3.3.1).

Based on the data from air injection and seepage tests, seepage-relevant parameters have been developed in *Seepage Calibration Model and Seepage Testing Data* (BSC 2004 [DIRS 171764], Sections 6.3, 6.5.2, and 6.6) and were then used for seepage predictions in *Seepage Model for PA Including Drift Collapse* (BSC 2004 [DIRS 167652], Sections 6.3.2 and 6.4). Results from these calibration and prediction efforts are included in the seepage abstraction through the use of the measured post-excavation air-permeability data (SNL 2007 [DIRS 181244], Section 6.6.3 and Table 6.6-3) and the calibrated capillary-strength data determined from seepage tests (SNL 2007 [DIRS 181244], Section 6.6.2 and Table 6.6-1). Statistics of these parameters, excavation-disturbed permeability and calibrated capillary strength, provide the basis for the probability distributions that are given in *Abstraction of Drift Seepage* (SNL 2007 [DIRS 181244], Sections 6.7.1). These probability distributions are used in the TSPA to calculate seepage from seepage lookup tables, using the methodology defined in *Abstraction of Drift Seepage* (SNL 2007 [DIRS 181244], Section 6.7.1). Simulations conducted with the thermal seepage model also incorporate the effects of excavation on seepage-relevant parameters (BSC 2005 [DIRS 172232], Section 6.2.2.1.4). Thus, the impact of excavation around a large opening (niche or drift) is included in the TSPA calculation of drift seepage. The impact of excavation on hydrologic properties near emplacement drifts is not considered in mountain-scale models, such as the UZ flow model or the UZ transport model, where these local changes are not relevant.

This FEP is included in performance assessments to demonstrate compliance with the individual protection standard after permanent closure (proposed 10 CFR 63.311 (70 FR 53313 [DIRS 178394])) and the groundwater protection standards (10 CFR 63.331 [DIRS 180319]). It is not included in the human intrusion performance assessment (proposed 10 CFR 63.321 (70 FR 53313 [DIRS 178394])).

INPUTS:

Table 2.2.01.01.0A-1. Indirect Inputs

Citation	Title	DIRS
10 CFR 63	Energy: Disposal of High-Level Radioactive Wastes in a Geologic Repository at Yucca Mountain, Nevada	180319
70 FR 53313	Implementation of a Dose Standard After 10,000 Years	178394
BSC 2004	*Drift Degradation Analysis*	166107
BSC 2004	*In Situ Field Testing of Processes*	170004
BSC 2004	*Seepage Calibration Model and Seepage Testing Data*	171764
BSC 2004	*Seepage Model for PA Including Drift Collapse*	167652
BSC 2005	*Drift-Scale Coupled Process (DST and TH Seepage) Models*	172232
Craig 2001	"Transmittal of Level 5 Deliverable SPW205M5, 'Excavation-Induced Fracture Study'"	171411
SNL 2007	*Abstraction of Drift Seepage*	181244

FEP: 2.2.01.01.0B

FEP NAME:

Chemical Effects of Excavation and Construction in the Near-Field

FEP DESCRIPTION:

Excavation may result in chemical changes to the incoming groundwater and to the rock in the excavation disturbed zone.

SCREENING DECISION:

Excluded – low consequence

SCREENING JUSTIFICATION:

FEP 2.2.01.01.0B concerns the chemical effects of excavation and construction in the host rock environment immediately surrounding the waste emplacement drifts. This FEP is focused on seepage water changes and near-field rock changes. Related excluded FEP 1.1.02.00.0A (Chemical Effects of Excavation and Construction in the EBS) is focused on the possible changes in the EBS. Excluded FEP 2.1.06.01.0A (Chemical Effects of Rock Reinforcement and Cementitious Materials in EBS) addresses the effect of cementitious material in the turnout intersections, exhaust air (ventilation) turnouts, and access ramps. Requirements have been established to identify, analyze, and control the use of any introduced or committed materials (including water) that could adversely impact postclosure performance, thus limiting undesired effects from excavation and construction. The application of these controls is described in *Total System Performance Assessment Data Input Package for Requirements Analysis for Engineered Barrier System In-Drift Configuration* (SNL 2007 [DIRS 179354], Table 4-1, Parameter Number 02-03). During construction of the emplacement drifts, and operation and closure of the repository, administrative controls will be imposed to prevent impact on waste isolation from materials used, lost, or left in the repository. These controls will be supported by technical evaluation. All tracers, fluids, and materials that may be used during construction, operation, and closure will be controlled. Various aspects of committed materials are discussed in excluded FEP 1.1.02.03.0A (Undesirable Materials Left).

The following constraints will be imposed on the administrative control of tracers, fluids, and materials; construction materials; and committed materials (SNL 2007 [DIRS 179354], Table 4-1, Parameter Number 02-03):

(A) All material not technically evaluated and determined acceptable prior to the permanent closure of the repository will be removed from subsurface facilities prior to permanent closure.

(B) Committed materials that are proposed to remain in the underground repository following the permanent closure period will be technically evaluated and determined acceptable prior to use.

(C) Administrative controls will include accounting and inspection, as appropriate, to confirm that controls on the approved TFM quantities and compositions are met.

Changes are expected in the rock fracture properties from excavation disturbance, stress relief around the opening, and ground support. However, these changes will not affect water chemistry; the effects of ground support on water chemistry are discussed later. Excavation will introduce water (for dust control), but it is not expected to have any significant effect on water chemistry. This is based on the controls on water use that limit the volumes of water that are lost during underground excavation as described in *Determination of Importance Evaluation for the Subsurface Exploratory Studies Facility* (BSC 2005 [DIRS 175089], Section 13.2.16). Furthermore, any water that remains local to the emplacement drifts and penetrates the unsaturated zone through fractures will have a dilute composition similar to that of nearby groundwater. Any salt solid forming as a result of evaporation would be present in relatively small quantities, even with additional dissolved solids from potential mixing of construction water with salt-bearing dust from the tunnel. *Drift-Scale THC Seepage Model* (SNL 2007 [DIRS 177404]) illustrates that upon rewetting, redissolution of salts has a minor effect on waters seeping into the drift. Therefore, even with the possible formation of salt solids as a result of evaporation, the effects on water chemistry are minimal upon rewetting. Salt-bearing dust could be generated by construction activities, and its potential effect on corrosion is discussed in excluded FEPs 2.1.09.28.0A (Geochemical Interactions and Evolution in the UZ), and 2.1.09.28.0B (Localized Corrosion on Drip Shield Surfaces due to Deliquescence). Included FEP 2.2.01.01.0A (Mechanical Effects of Excavation and Construction in the Near-field) describes the excavation-induced effects on rock properties and seepage in the near-field environment.

The principal ground supports in the emplacement drifts are expected to be Stainless Steel Type 316L rock bolts and steel sheets, while low-alloy Carbon Steel Type A588 comprises most of the invert structure (SNL 2007 [DIRS 179354], Table 4-1, Parameter Number 01-15). Sensitivity analyses of the effects of ground support and invert steels on aqueous chemistry are documented in *Engineered Barrier System: Physical and Chemical Environment* (SNL 2007 [DIRS 177412], Section 6.8). The P&CE report utilizes four initial water types that are provided by the NFC model to represent the range of water chemistries in the TSw (SNL 2007 [DIRS 177412], Sections 6.3.2 and 6.6). The steel sensitivity analyses considered the interaction of the two most chemically distinct of these starting waters ("Group 1" and "Group 3"), with and without alkali feldspar added (SNL 2007 [DIRS 177412], Section 6.8.2). Corrosion rates for Stainless Steel Type 316L and Carbon Steel Type A588 (approximated by Carbon Steel Type A516) were taken from *Aqueous Corrosion Rates for Waste Package Materials* (BSC 2004 [DIRS 169982]). Solubility limiting phases for Stainless Steel Type 316L corrosion products included goethite (FeOOH), Ni-ferrite ($NiFe_2O_4$), Ni-chromite ($NiCr_2O_4$), Ni-carbonate ($NiCO_3$), and nontronite clays. Solubility limiting phases for Carbon Steel Type A588 corrosion include goethite (FeOOH) and MnO_2. The effect of dissolving Stainless Steel Type 316L and Carbon Steel Type A588 into "Group 1" and "Group 3" waters was found to be negligible (SNL 2007 [DIRS 177412], Section 6.8.4.1 and Tables 6.8-3 to 6.8-6). Simulations aimed at characterizing the impact of invert steel corrosion on water chemistry were conducted using 100 g Carbon Steel Type A588 (1.77 moles per liter) and five times this amount for bounding calculations. Even with such large quantities of low-alloy steels, there were only negligible changes in water chemistries (SNL 2007 [DIRS 177412], Section 6.8.4.2, Tables 6.8-3 and 6.8-4). In general,

these conclusions indicate that if there is no limit to the oxygen supply, the result of adding more steel to the water is simply the formation of more corrosion product precipitates. The results of these simulations demonstrate that there is no impact on seepage water chemistry, as described in Section 6.8.3 of *Engineered Barrier System: Physical and Chemical Environment* (SNL 2007 [DIRS 177412]).

Chemical changes to the minerals in the EDZ rock as a result of excavation and construction are not expected to be significant given the little change expected in the aqueous water chemistry at the EDZ. Any construction water that penetrates the EDZ to flow through unsaturated zone fractures is not expected to cause any significant geochemical interactions involving mineral phase changes in the unsaturated zone host rock. See excluded FEP 2.2.08.03.0B (Geochemical Interactions and Evolution in the UZ) for additional discussion of this point.

Based on the previous discussion, omission of FEP 2.2.01.01.0B (Chemical Effects of Excavation and Construction in the Near-Field) will not result in a significant adverse change in the magnitude or timing of either radiological exposure to the RMEI or radionuclide releases to the accessible environment. Therefore, this FEP is excluded from the performance assessments conducted to demonstrate compliance with proposed 10 CFR 63.311 and 63.321 (70 FR 53313 [DIRS 178394]), and with 10 CFR 63.331 [DIRS 180319], on the basis of low consequence.

INPUTS:

Table 2.2.01.01.0B-1. Direct Inputs

Input	Source	Description
SNL 2007. *Total System Performance Assessment Data Input Package for Requirements Analysis for EBS In-Drift Configuration*. [DIRS 179354]	Table 4-1, Parameter Number 02-03	Constraints on the administrative control of tracers, fluids, and materials, construction materials, and committed materials
	Table 4-1, Parameter Number 02-03	Controls on the compositions and quantities for tracers, fluids, and materials used in the repository
SNL 2007. *Engineered Barrier System: Physical and Chemical Environment*. [DIRS 177412]	Section 6.8.3	Simulations demonstrate that there is no impact on seepage water chemistry
	Sections 6.8.4.1, 6.8.4.2; Tables 6.8-3 to 6.8-6	The effect of dissolving Stainless Steel Type 316L and A588 steel into Group 1 and Group 3 waters was found to be negligible
	Section 6.8	Sensitivity analyses of the effects of steel ground support and invert steels on aqueous chemistry

Table 2.2.01.01.0B-2. Indirect Inputs

Citation	Title	DIRS
10 CFR 63	Energy: Disposal of High-Level Radioactive Wastes in a Geologic Repository at Yucca Mountain, Nevada	180319
70 FR 53313	Implementation of a Dose Standard After 10,000 Years	178394
BSC 2004	*Aqueous Corrosion Rates for Waste Package Materials*	169982
BSC 2005	*Determination of Importance Evaluation for the Subsurface Exploratory Studies Facility*	175089
SNL 2007	*Total System Performance Assessment Data Input Package for Requirements Analysis for EBS In-Drift Configuration*	179354
SNL 2007	*Drift-Scale THC Seepage Model*	177404
SNL 2007	*Engineered Barrier System: Physical and Chemical Environment*	177412

FEP: 2.2.01.02.0A

FEP NAME:

Thermally-Induced Stress Changes in the Near-Field

FEP DESCRIPTION:

Changes in host rock properties may result from thermal effects or other factors related to emplacement of the waste. Properties that may be affected include rock strength, fracture spacing and block size, and hydrologic properties such as permeability and sorption.

SCREENING DECISION:

Excluded – low consequence

SCREENING JUSTIFICATION:

This FEP addresses the thermal-mechanical effects on drift seepage and thermal effects on rock strength, fracture spacing, and block size. The effects of thermal-mechanical stresses as a result of radioactive heating of the rock by the emplaced wastes may change the characteristics (e.g., permeability of the fractures) (see excluded FEP 2.2.10.04.0A (Thermo-Mechanical Stresses Alter Characteristics of Fractures Near Repository) for details) and the faults (see excluded FEP 2.2.10.04.0B (Thermo-mechanical Stresses Alter Characteristics of Faults Near Repository)). Furthermore, fracturing of the rocks above and below the repository might occur to affect vertical permeability and infiltration in the unsaturated zone (see excluded FEP 2.2.10.05.0A (Thermo-mechanical Stresses Alter Characteristics of Rocks Above and Below the Repository) for details). In addition, thermal effects on sorption, solubility, and precipitation/dissolution may be changed, and these are evaluated in excluded FEP 2.2.10.06.0A (Thermo-chemical Alteration in the UZ).

Thermal effects on rockfall in waste emplacement drifts are evaluated as part of *Drift Degradation Analysis* (BSC 2004 [DIRS 166107], Section 6.2). The analyses documented in that report (BSC 2004 [DIRS 166107]) use rockfall models that explicitly include rock strength, fracture spacing, and block size, as well as the potential impact of thermally induced stress changes in the rock mass. The effects of thermally induced stress changes are documented in *Drift Degradation Analysis* for nonlithophysal rock and for lithophysal rock (BSC 2004 [DIRS 166107], Sections 6.3.1.3 and 6.4.2.3, respectively). These effects are part of *Drift Degradation Analysis* (BSC 2004 [DIRS 166107], Section 8.1) and are incorporated into the rockfall calculations. Rockfall in the absence of seismic events (see excluded FEP 2.1.07.01.0A (Rockfall)) and seismic-induced rockfall (see excluded FEP 1.2.03.02.0B (Seismic-Induced Rockfall Damages EBS Components)) have been excluded with regard to effects on the EBS. However, the effects of seismic-induced drift collapse on the EBS are included in TSPA (see included FEP 1.2.03.02.0C (Seismic-Induced Drift Collapse Damages EBS Components)).

Thermal effects on rock strength are discussed in *Subsurface Geotechnical Parameters Report* (BSC 2007 [DIRS 178693], Figure 6-32), which shows that the temperature has little effect on rock strength. Variations in rock strength resulting from temperature are much smaller than the

natural variations found between samples at ambient conditions. Because of the high degree of fracturing in the lithophysal units, the rock mass will break into relatively small block sizes controlled by the spacing of natural fractures (BSC 2004 [DIRS 166107], Section 6.4.1.1). The character of fracturing in the nonlithophysal rock leads to discontinuous fractures. Although these discontinuities could lead to rock breakage under stress (BSC 2004 [DIRS 166107], Section 6.3.1), model results indicate that heating will not induce stress levels inside the blocks that are sufficient to cause damage (BSC 2004 [DIRS 166107], Section 6.3.1.3). Therefore, there are no thermal effects on fracture spacing or rock block size.

The Drift Scale Test is a large-scale, long-term thermal test designed to investigate coupled thermal-mechanical-hydrological-chemical behavior in a fractured, welded tuff rock mass (CRWMS M&O 1998 [DIRS 111115]). Simulations of the displacement response in the Drift Scale Test, based on elastic THM processes, were found to be in agreement with measurements. The dominant mode for stress-induced permeability change for THM processes was found to be elastic fracture opening or closing caused by changes in stress normal to the fractures (BSC 2004 [DIRS 169864], Section 8.2). The results of the drift-scale THM model show that thermal stress is not expected to induce failure at an emplacement drift located in the Tptpmn unit. For an emplacement drift located in the Tptpll unit, a limited yielding at the sidewalls of the drift is expected during excavation, but only for a drift located in low-quality lithophysal rock (BSC 2004 [DIRS 169864], Section 8.1). Low quality lithophysal rock is expected to be less than 10% of the waste emplacement areas (BSC 2004 [DIRS 166107], Figure S-50). Furthermore, the analysis indicates that the effects of stress-induced changes on hydrological properties and the flow field are small, particularly for the Tptpll, which occupies approximately 80% of repository emplacement area in the current design (BSC 2004 [DIRS 169864], Section 8.1; SNL 2007 [DIRS 179466], Table 4-1, Parameter Number 01-03). Furthermore, the changes in permeability around drifts from THM effects are either insignificant or result in decreases in the vertical permeability and increases in the horizontal permeability (BSC 2004 [DIRS 169864], Sections 6.5.5, 6.6.1, and 6.7.2)

The effects of thermally induced stress changes around the emplacement drifts on drift seepage were evaluated in *Abstraction of Drift Seepage* (SNL 2007 [DIRS 181244], Section 6.4.4). The drift-scale THM model was applied to assess the magnitude and distribution of stress-induced changes in hydrologic properties due to repository heating (SNL 2007 [DIRS 181244], Section 6.4.4). The report concludes that when comparing the fully coupled THM simulations with TH simulations, where the stress-induced property changes are neglected, the flow field differences are small to moderate. The changes in permeability resulting from THM effects appeared to give rise to less water reaching the drift crown (SNL 2007 [DIRS 181244], Figure 6.4-32). However, the identified impact on drift seepage was small and lies within the uncertainty of the seepage abstraction model (SNL 2007 [DIRS 181244], Figure 6.4-33 and Section 6.7.2). It was concluded in *Seepage Model for PA Including Drift Collapse* (BSC 2004 [DIRS 167652], Section 6.7) that these anisotropic THM property changes would increase the likelihood of flow being diverted around the drift, and thus would reduce the potential for seepage. Based upon these analyses, it is concluded that thermally induced stresses have a minimal impact on the hydrologic performance of the emplacement drift, and the impacts that it does have reduce the seepage of water into the drift.

Based on the previous discussion, omission of FEP 2.2.01.02.0A (Thermally-Induced Stress Changes in the Near Field) will not result in a significant adverse change in the magnitude or timing of either radiological exposure to the RMEI or radionuclide releases to the accessible environment. Therefore, this FEP is excluded from the performance assessments conducted to demonstrate compliance with proposed 10 CFR 63.311 and 63.321 (70 FR 53313 [DIRS 178394]), and with 10 CFR 63.331 [DIRS 180319], on the basis of low consequence.

INPUTS:

Table 2.2.01.02.0A-1. Direct Inputs

Input	Source	Description
BSC 2004. *Drift Degradation Analysis*. [DIRS 166107]	Figure S-50	Low quality lithophysal rock is expected to be less than 10% of the waste emplacement areas
	Sections 6.3.1, 6.3.1.3	Heating will not induce stress levels inside the blocks that are sufficient to cause damage in nonlithophysal rock; fractures are discontinuous in nonlithophysal rock
	Section 8.1	Rockfall calculations
BSC 2004. *Drift Scale THM Model*. [DIRS 169864]	Sections 6.5.5, 6.6.1, 6.7.2	Changes in permeability around drift from THM effects are either insignificant or result in decreases in the vertical permeability and increases in the horizontal permeability
	Section 8.1	Effects of stress-induced changes on hydrological properties and the flow field are small
	Section 8.1	For an emplacement drift located in the Tptpll unit, a limited yielding at the sidewalls of the drift is expected during excavation, but only for a drift located in low-quality lithophysal rock
	Section 8.2	Dominant mode for stress-induced permeability change for THM processes was found to be elastic fracture opening or closing caused by changes in stress normal to the fractures
BSC 2004. *Seepage Model for PA Including Drift Collapse*. [DIRS 167652]	Section 6.7	Impact of anisotropic THM property changes
BSC 2007. *Subsurface Geotechnical Parameters Report*. [DIRS 178693]	Figure 6-32	Temperature has little effect on rock strength
SNL 2007. *Abstraction of Drift Seepage*. [DIRS 181244]	Figure 6.4-32	Reduction in vertical permeability, combined with the essentially unchanged horizontal permeability, appeared to give rise to less water reaching the drift crown
	Section 6.4.4	Evaluated the effects of thermally induced stress changes around the emplacement drifts on drift seepage

Table 2.2.01.02.0A-1. Direct Inputs (Continued)

Input	Source	Description
SNL 2007. *Abstraction of Drift Seepage*. [DIRS 181244] (continued)	Figure 6.4-33 and Section 6.7.2	The identified impact of THM processes on drift seepage was small and lies within the uncertainty of the seepage abstraction model
SNL 2007. *Total System Performance Assessment Data Input Package for Requirements Analysis for Subsurface Facilities*. [DIRS 179466]	Table 4-1, Parameter Number 01-03	Tptpll occupies approximately 80% of repository emplacement area in the current design

Table 2.2.01.02.0A-2. Indirect Inputs

Citation	Title	DIRS
10 CFR 63	Energy: Disposal of High-Level Radioactive Wastes in a Geologic Repository at Yucca Mountain, Nevada	180319
70 FR 53313	Implementation of a Dose Standard After 10,000 Years	178394
BSC 2004	*Drift Degradation Analysis*	166107
CRWMS M&O 1998	*Drift Scale Test As-Built Report*	111115
SNL 2007	*Abstraction of Drift Seepage*	181244

FEP: 2.2.01.02.0B

FEP NAME:

Chemical Changes in the Near-Field from Backfill

FEP DESCRIPTION:

Changes in host rock properties may result from chemical effects of backfill. Properties that may be affected include permeability and sorption.

SCREENING DECISION:

Excluded – low consequence

SCREENING JUSTIFICATION:

Backfill is not part of the design for the waste emplacement regions of the repository. Specifically, engineered backfill shall not be present in the space between the drip shield and the drift wall (SNL 2007 [DIRS 179354], Table 4-4, Parameter Number 05-04). Closure of shafts and ramps shall include backfill of the opening (SNL 2007 [DIRS 179466], Table 4-3, Parameter Number 09-01); however, because backfill in shafts and ramps will not be in close proximity to the waste emplacement region, permeability and sorption and other host rock properties will have a negligible impact on long-term performance.

Based on the previous discussion, omission of FEP 2.2.01.02.0B (Chemical Changes in the Near-Field from Backfill) will not result in a significant adverse change in the magnitude or time of radiological exposures to the RMEI or radionuclide releases to the accessible environment. Therefore, this FEP is excluded from the performance assessments conducted to demonstrate compliance with proposed 10 CFR 63.311 and 63.321 (70 FR 53313 [DIRS 178394]), and with 10 CFR 63.3331 [DIRS 180319], on the basis of low consequence.

INPUTS:

Table 2.2.01.02.0B-1. Direct Inputs

Input	Source	Description
SNL 2007. *Total System Performance Assessment Data Input Package for Requirements Analysis for EBS In-Drift Configuration*. [DIRS 179354]	Table 4-4, Parameter Number 05-04	There is no backfill in the space between the drip shield and the drift walls
SNL 2007. *Total System Performance Assessment Data Input Package for Requirements Analysis for Subsurface Facilities*. [DIRS 179466]	Table 4-3, Parameter Number 09-01	Closure shafts and ramps shall include backfill of the openings

Table 2.2.01.02.0B-2. Indirect Inputs

Citation	Title	DIRS
10 CFR 63	Energy: Disposal of High-Level Radioactive Wastes in a Geologic Repository at Yucca Mountain, Nevada	180319
70 FR 53313	Implementation of a Dose Standard After 10,000 Years	178394

FEP: 2.2.01.03.0A

FEP NAME:

Changes in Fluid Saturations in the Excavation Disturbed Zone

FEP DESCRIPTION:

Fluid flow in the region near the repository may be affected by the presence of the excavation, waste, and EBS. Some dry-out will occur during excavation and operations.

SCREENING DECISION:

Excluded – low consequence

SCREENING JUSTIFICATION:

This FEP screening justification focuses on dryout caused by preclosure ventilation during excavation and operations. Other causes of changes in fluid saturations in the excavation disturbed zone are discussed elsewhere. The effects of the engineered barrier system (rock bolt holes) on fluid flow have been excluded in FEP 1.1.01.01.0B (Influx through Holes Drilled in Drift Wall or Crown). The mechanical effects of drift excavation on fluid flow are included as described in FEP 2.2.01.01.0A (Mechanical Effects of Excavation and Construction in the Near-Field). The effects of waste heat on fluid flow have been included in FEPs 2.2.10.10.0A (Two-Phase Buoyant Flow/Heat Pipes) and 2.2.10.12.0A (Geosphere Dry-Out due to Waste Heat).

Preclosure ventilation of the waste emplacement drifts will result in dryout of the surrounding rock. However, this dryout is not significant for the long-term evolution of flow and transport near emplacement drifts because thermal dryout and rewetting during and after the thermal period, respectively, will overlay nearly all the earlier effects of ventilation dryout. Dryout has been observed in the Exploratory Studies Facility (ESF) and Enhanced Characterization of the Repository Block (ECRB) tunnels during site characterization (BSC 2004 [DIRS 170004], Sections 6.10.1.2 and 6.10.2.1).

In general, the observed dryout region in the ESF and ECRB ranges from 1 to 3 m into the drift walls (BSC 2004 [DIRS 170004], Section 6.10.1.2.1). The zone of dryout is qualitatively identified as the zone where matrix saturation and/or water potential are noticeably reduced by dryout relative to natural fluctuations in these quantities. Observations of dryout in the ECRB at station 15+00 show an approximately 1.5 m zone of dryout (BSC 2004 [DIRS 170004], Figure 6-109(a)). These measurements were taken on July 29, 2000, approximately two years after completion of the ECRB tunnel excavation (BSC 2004 [DIRS 170004], Section 6.10.1.2.3). The preclosure subsurface ventilation period is planned to be a minimum of 50 years (SNL 2007 [DIRS 179466], Table 4-2). The rate of dryout is maximized in areas of low natural percolation flux. In the absence of natural percolation flux and negligible gas-phase advective transport, the rate of dryout is dependent on vapor diffusion and capillary imbibition to move water from regions of higher water saturation in the rock to the tunnel atmosphere. Capillary imbibition may be approximated as a diffusive process (Marshall and Holmes 1979 [DIRS 102532], Section 5.1).

A characteristic of diffusive mass transfer processes is that the cumulative mass transfer is proportional to the square root of time (Crank 1975 [DIRS 122990], Section 3.3; Marshall and Holmes 1979 [DIRS 102532], Section 5.1). Given the cylindrical geometry, this scaling is strictly correct only for a boundary condition at the drift center rather than the drift wall. In this case, the use of the square-root scaling may be considered a one-dimensional approximation to radial diffusion. Using the square-root scaling and the observation of a 1.5 m dryout zone after two years of ventilation, the estimated dryout zone after 50 years of preclosure ventilation is 7.5 m beyond the drift wall. Natural percolation flux will have a more pronounced effect slowing the expansion of the dryout zone as the size of the dryout zone increases. Therefore, natural percolation will cause the dryout zone to be smaller than 7.5 m as computed from the square-root scaling.

The majority of waste emplacement will be in the Tptpll geological unit, with a smaller amount in the Tptpmn and other units (SNL 2007 [DIRS 179466], Table 4-1, Parameter Number 01-03). A comparison of dryout in fractures around waste emplacement drifts in the Tptpmn and Tptpll geological units (BSC 2005 [DIRS 172232], Figures 6.2.2.1.7(a) and 6.2.3.1-3(a)) suggests that the dryout resulting from waste heat is similar in these two units. Furthermore, the size of the dryout in both units is expected to be greater than the size of the dryout zone resulting from the combined effects of ventilation and natural percolation. Therefore, thermal dryout effects will encompass a larger region than that affected by preclosure ventilation dryout. The small enhancement in dryout resulting from preclosure ventilation would lead to minor increases in the time to re-wet the rock around waste emplacement drifts and would not lead to an underestimate of seepage. Because the dryout zone and drift seepage in the postclosure period are not significantly affected by preclosure ventilation, the effects on radionuclide releases to the accessible environment or radiological exposures to the reasonably maximally exposed individual are also negligible.

Based on this analysis, preclosure ventilation dryout is not significant to the modeling studies investigating the potential for seepage during the thermal period (BSC 2005 [DIRS 172232], Section 6.2.1.3.3). Preclosure ventilation is even less important for ambient seepage at later stages when the near-field rock has cooled and resaturated. For the same reason, the effect of ventilation dryout on EBS radionuclide transport is insignificant.

Based on the previous discussion, omission of FEP 2.2.01.03.0A (Changes in Fluid Saturations in the Excavation Disturbed Zone) will not result in a significant adverse change in the magnitude or timing of either radiological exposure to the RMEI or radionuclide releases to the accessible environment. Therefore, this FEP is excluded from the performance assessments conducted to demonstrate compliance with proposed 10 CFR 63.311 and 63.321 (70 FR 53313 [DIRS 178394]), and with 10 CFR 63.331 [DIRS 180319], on the basis of low consequence.

INPUTS:

Table 2.2.01.03.0A-1. Direct Inputs

Input	Source	Description
BSC 2004. *In Situ Field Testing of Processes*. [DIRS 170004]	Sections 6.10.1.2, 6.10.1.2.1, 6.10.1.2.3, 6.10.2.1, Figure 6-109(a)	Observations of dryout during site characterization, approximately 1.5 m at station 15+00. Observations were 2 years after completion of ECRB tunnel
BSC 2005. *Drift-Scale Coupled Process (DST and TH Seepage) Models*. [DIRS 172232]	Figures 6.2.2.1.7(a) and 6.2.3.1-3(a)	Similar dryout from waste heat in Tptpln and Tptpmn
SNL 2007. *Total System Performance Assessment Data Input Package for Requirements Analysis for Subsurface Facilities*. [DIRS 179466]	Table 4-1, Parameter Number 01-03	The majority of waste emplacement will be in the Tptpll geological unit, with a smaller amount in the Tptpmn and other units
	Table 4-2	The preclosure subsurface ventilation period is planned to be a minimum of 50 years

Table 2.2.01.03.0A-2. Indirect Inputs

Citation	Title	DIRS
10 CFR 63	Energy: Disposal of High-Level Radioactive Wastes in a Geologic Repository at Yucca Mountain, Nevada	180319
70 FR 53313	Implementation of a Dose Standard After 10,000 Years	178394
BSC 2005	*Drift-Scale Coupled Process (DST and TH Seepage) Models*	172232
Crank 1975	*The Mathematics of Diffusion*	122990
Marshall and Holmes 1979	*Soil Physics*	102532

FEP: 2.2.01.04.0A

FEP NAME:

Radionuclide Solubility in the Excavation Disturbed Zone

FEP DESCRIPTION:

Radionuclide solubility limits in the excavation-disturbed zone may differ from those in the EBS.

SCREENING DECISION:

Excluded – low consequence

SCREENING JUSTIFICATION:

This FEP is excluded because the effects of potentially lower radionuclide solubility limits in the EDZ compared to those in the drifts will not have significant effect on radionuclide transport. If solubility limits are higher in the EDZ than in the emplacement drifts, then radionuclides entering the EDZ will remain in solution and there will be no retardation effect on radionuclide transport.

The EDZ is the zone around the drift where native materials have been disturbed from their natural conditions by excavation activities, resulting in chemical and/or hydrological alterations. The impact of this FEP may be qualitatively evaluated through a comparison of the different ranges of chemical environments estimated for the engineered barrier system, compared with the EDZ and unsaturated zone in general. The modeled pH of waters inside the drift ranges from approximately 5 to more than 11 (SNL 2007 [DIRS 177412], Figures 6.13-5 through 6.13-8). The evolution of water chemistry in the unsaturated zone, however, is not so broad because of the buffering effect of native rocks. For example, at the sides and crown of the drift, the pH ranges from roughly 7 to 10 (SNL 2007 [DIRS 177404], Figures 6.5-16, 6.6-1, 6.6-5, 6.6-7, 6.6-9, and 6.6-14). Given the much larger range of pH inside the drift, caused by the engineered materials, equilibrium solution concentrations for radionuclides inside the drift could be significantly larger than equilibrium solution concentrations in the unsaturated zone, including the EDZ. Excluded FEP 2.2.01.05.0A (Radionuclide Transport in the Excavation Disturbed Zone**)** provides additional information on this subject. If radionuclide solubility limits are lower in the EDZ than in the emplacement drifts, dissolved radionuclides could precipitate in the EDZ. This would occur only if the radionuclide concentrations entering the EDZ were higher than the solubility limits in the EDZ. However, contaminated water entering the EDZ is expected to be diluted by uncontaminated water and radionuclides will stay dissolved, even if the radionuclide concentration in the incoming water (before dilution) exceeds the solubility limit in the EDZ. Therefore, the effects of potentially lower radionuclide solubility limits in the EDZ compared to those in the drifts will not have a significant effect on radionuclide transport.

If solubility limits are higher in the EDZ than in the emplacement drifts, then radionuclides entering the EDZ will remain in solution and the difference in solubility limits between the EBS and the EDZ will not affect radionuclide transport.

Solubility limits, which depend on the solution chemistry, pH, and temperature, could also affect the formation of certain kinds of true colloids, such as polymeric forms of plutonium oxide (SNL 2007 [DIRS 177423], Section 6.3.1). However, only small quantities of true colloids have been observed to form in experiments on waste form degradation (SNL 2007 [DIRS 177423], Sections 6.3.1). Furthermore, these colloids are expected to dissolve into the aqueous phase with very little migration and provide radionuclides to be sorbed onto pseudocolloids (SNL 2007 [DIRS 177423], Section 6.3.1), the formation of which is not affected by solubility limits. Therefore, radionuclide solubility limits in the EDZ will not affect colloid-facilitated transport.

Based on the previous discussion, omission of FEP 2.2.01.04.0A (Radionuclide Solubility in the Excavation Disturbed Zone) will not result in a significant adverse change in the magnitude or timing of either radiological exposure to the RMEI or radionuclide releases to the accessible environment. Therefore, this FEP is excluded from the performance assessments conducted to demonstrate compliance with proposed 10 CFR 63.311 and 63.321 (70 FR 53313 [DIRS 178394]), and with 10 CFR 63.331 [DIRS 180319], on the basis of low consequence.

INPUTS:

Table 2.2.01.04.0A-1. Direct Inputs

Input	Source	Description
SNL 2007. *Drift-Scale THC Seepage Model*. [DIRS 177404]	Figures 6.5-16, 6.6-1, 6.6-5, 6.6-7, 6.6-9, and 6.6-14	pH ranges near the drift
SNL 2007. *Engineered Barrier System: Physical and Chemical Environment*. [DIRS 177412]	Figures 6.13-5 through 6.13-8	Modeled pH of waters inside the drift
SNL 2007. *Waste Form and In-Drift Colloids-Associated Radionuclide Concentrations: Abstraction and Summary*. [DIRS 177423]	Section 6.3.1	Observations of the formation of certain kinds of true colloids and their transformation

Table 2.2.01.04.0A-2. Indirect Inputs

Citation	Title	DIRS
10 CFR 63	Energy: Disposal of High-Level Radioactive Wastes in a Geologic Repository at Yucca Mountain, Nevada	180319
70 FR 53313	Implementation of a Dose Standard After 10,000 Years	178394

FEP: 2.2.01.05.0A

FEP NAME:

Radionuclide Transport in the Excavation Disturbed Zone

FEP DESCRIPTION:

Radionuclide transport through the excavation disturbed zone may differ from transport in the EBS and the undisturbed host rock. Transport processes such as dissolution and precipitation, sorption, and colloid filtration should be considered.

SCREENING DECISION:

Excluded – low consequence

SCREENING JUSTIFICATION:

The EDZ, which is the area immediately surrounding the waste emplacement drifts, may be characterized by larger apertures due to the mechanical effect of excavation and reduced apertures due to chemical alteration due to excavation. One aspect of this FEP refers to the effects of altered fracture properties in the EDZ immediately surrounding the waste emplacement drifts on radionuclide transport. The effects of changes in fracture aperture on radionuclide transport were investigated at the mountain scale (excluded FEP 2.2.06.02.0B (Seismic Activity Changes Porosity and Permeability of Fractures)). The results of this analysis indicate that radionuclide transport behavior is relatively insensitive to changes in fracture aperture by as much as a factor of ten. Investigations on the effects of stress relief on fracture permeability in the EDZ have found that the vertical permeability beneath the drift is affected over a very narrow zone, on the order of one to two meters for changes in permeability of more than a factor of two (BSC 2004 [DIRS 169864], Sections 6.5.1 and 6.6.1).

An important factor affecting radionuclide transport immediately below the waste emplacement drift is the partitioning of radionuclides exiting the drift between rock fractures and matrix. Aperture affects this partitioning through its influence on fracture water content, which affects diffusive mass flux at the interface (SNL 2007 [DIRS 177407], Equations 6.5.1.2-7 and 6.5.2.5-5). Large reductions in fracture aperture will lead to large reductions in fracture porosity and water content. However, reducing fracture water content increases the partitioning of radionuclides from the waste emplacement drift to the rock matrix, which can only result in reduced rates of radionuclide transport. Increases in fracture aperture are limited in terms of their effect on fracture water content because of limitations on the increase in fracture porosity and the trend for residual saturation to decrease with an increase in aperture or permeability (Dombrowski and Brownell 1954 [DIRS 163222], Figure 7). The potential increases and decreases in fracture aperture are within the range of uncertainty already considered within the current UZ transport model (SNL 2007 [DIRS 170806]). Due to limited information regarding functional dependencies between fracture aperture and residual saturation, residual saturation is not treated in the model as a function of fracture aperture. Given the limited potential range for increases in fracture aperture (i.e., porosity), the effects of the EDZ on fracture water content, and hence on fracture aperture, may be discounted.

The effects of precipitation of aqueous radionuclides on transport in the EDZ also are excluded based on low consequence (see excluded FEP 2.2.01.04.0A (Radionuclide Solubility in the Excavation Disturbed Zone)). The precipitation of radionuclides as a solid immobile phase slows the progress of radionuclide transport in the aqueous phase. Because of the relatively short transport distance in the EDZ and the slow release of radionuclide from the waste emplacement drifts, any remobilization of precipitated radionuclides in the EDZ will have negligible effects on the dose to the RMEI and the environment.

Thermal effects on sorption are evaluated in excluded FEP 2.2.10.06.0A (Thermo-Chemical Alteration in the unsaturated zone (Solubility, Speciation, Phase Changes, Precipitation/Dissolution)), where increased temperatures are found to slightly increase sorption, which means more retardation in the EDZ. Compositional variations found in *Drift-Scale THC* (SNL 2007 [DIRS 177404], Figures 6.5-13, 6.5-13, 6.5-16, 6.5-17, 6.5-18, 6.5-21, and 6.5-23) lie within the range of compositional variations expected in the unsaturated zone and are accounted for in terms of radionuclide sorption (SNL 2007 [DIRS 177396], Appendix A, Section A4).

The behavior of different colloids in the emplacement drifts and the near-field are discussed in *Waste Form and In-Drift Colloids-Associated Radionuclide Concentrations: Abstraction and Summary* (SNL 2007 [DIRS 177423], Section 6.3.1). Colloidal filtration in the EBS is excluded from the TSPA (excluded FEP 2.1.09.20.0A (Filtration of Colloids in EBS)). Once colloids have been transported into the EDZ from the EBS (included FEP 2.1.09.19.0B (Advection of Colloids in EBS) and included FEP 2.1.09.24.0A (Diffusion of colloids in EBS)), they become subject to advection and dispersion. See included FEP 2.2.08.10.0B (Colloidal Transport in the UZ), which treats radionuclide transport in the unsaturated zone via movement of colloids.

Therefore, the effects of altered fracture properties, precipitation, and other processes that might retard radionuclide transport in the EDZ are excluded from the TSPA.

Based on the previous discussion, omission of FEP 2.2.01.05.0A (Radionuclide Transport in the Excavation Disturbed Zone) will not result in a significant adverse change in the magnitude or timing of either radiological exposure to the RMEI or radionuclide releases to the accessible environment. Therefore, this FEP is excluded from the performance assessments conducted to demonstrate compliance with proposed 10 CFR 63.311 and 63.321 (70 FR 53313 [DIRS 178394]), and with 10 CFR 63.331 [DIRS 180319], on the basis of low consequence.

INPUTS:

Table 2.2.01.05.0A-1. Direct Inputs

Input	Source	Description
SNL 2007. *Drift-Scale THC Seepage Model*. [DIRS 177404]	Figures 6.5-13, 6.5-16, 6.5-17, 6.5-18, 6.5-21, and 6.5-23	Compositional variations found at the base of the drift lie within the range of compositional variations expected in the unsaturated zone and accounted for in terms of radionuclide sorption
SNL 2007. *EBS Radionuclide Transport Abstraction*. [DIRS 177407]	Equations 6.5.1.2-7, 6.5.2.5-5	Aperture affects partitioning on radionuclides through its influence on fracture water content, which affects diffusive mass flux at the interface
SNL 2007. *Radionuclide Transport Models Under Ambient Conditions*. [DIRS 177396]	Appendix A, Section A4	Compositional variations found at base of drift lie within range of compositional variations expected in unsaturated zone and accounted for in terms of radionuclide sorption
SNL 2007. *Waste Form and In-Drift Colloids-Associated Radionuclide Concentrations: Abstraction and Summary*. [DIRS 177423]	Section 6.3.1	Discusses behavior of different colloids in emplacement drifts and near-field

Table 2.2.01.05.0A-2. Indirect Inputs

Citation	Title	DIRS
10 CFR 63	Energy: Disposal of High-Level Radioactive Wastes in a Geologic Repository at Yucca Mountain, Nevada	180319
70 FR 53313	Implementation of a Dose Standard After 10,000 Years	178394
BSC 2004	*Drift Scale THM Model*	169864
Dombrowski and Brownell 1954	“Residual Equilibrium Saturation of Porous Media”	163222
DTN: LA0407BR831371.001	UZ Transport Abstraction Model, Transport Parameters and Base Case Simulation Results	170806

FEP: 2.2.03.01.0A

FEP NAME:

Stratigraphy

FEP DESCRIPTION:

Stratigraphic information is necessary information for the performance assessment. This information should include identification of the relevant rock units, soils and alluvium, and their thickness, lateral extents, and relationships to each other. Major discontinuities should be identified.

SCREENING DECISION:

Included

TSPA DISPOSITION:

This FEP is similar to included FEP 2.2.03.02.0A (Rock Properties of Host Rock and Other Units). For the sake of clarity, the unsaturated zone stratigraphy is discussed first and the saturated zone stratigraphy is discussed second.

The bases for the unsaturated zone and saturated zone stratigraphic models are different. The unsaturated zone uses the geologic framework model, GFM2000 (BSC 2004 [DIRS 170029]; DTN: MO0012MWDGFM02.002 [DIRS 153777]), and the saturated zone uses the hydrogeologic framework model, HFM, which has been documented in *Hydrogeologic Framework Model for the Saturated Zone Site-Scale Flow and Transport Model* (SNL 2007[DIRS 174109]). These different models for stratigraphy are used as a result of the different domains treated by the unsaturated zone and saturated zone models. The UZ model encompasses rock above the water table over a region around the repository that is roughly 5 km × 9 km (SNL 2007 [DIRS 184614], Figure 6.1-1). The unsaturated zone model depth is roughly 600 m (SNL 2007 [DIRS 184614], Figure 6.2-1). The saturated zone model encompasses rock below the water table over an area that is roughly 30 km × 45 km (SNL 2007 [DIRS 177391], Figure 6-1) and approximately 6 km deep (SNL 2007 [DIRS 177391], Table 6-4).

Unsaturated Zone Stratigraphy

Unsaturated zone stratigraphy is incorporated in the output from reports that develop different data sets for drifts in the Topopah Spring Tuff lower lithophysal zone (Tptpll) and Topopah Spring Tuff middle nonlithophysal zone (Tptpmn). This includes *Drift-Scale Coupled Processes (DST and TH Seepage) Models* (BSC 2005 [DIRS 172232]) and *Seepage Model for PA Including Drift Collapse* (BSC 2004 [DIRS 167652], Sections 6.3.2 through 6.3.4). Stratigraphy is also incorporated in *Analysis of Hydrologic Properties Data* (BSC 2004 [DIRS 170038]). Stratigraphy is incorporated in *Simulation of Net Infiltration for Present-Day and Future Climates* (SNL 2008 [DIRS 182145], Section 6.5.2.5[a]), because different strata are exposed at the soil-bedrock interface at different locations.

This FEP is included in the UZ flow model (SNL 2007 [DIRS 184614], Sections 6.1.1 and 6.1.2) by use of the grids developed with the information contained in *Geologic Framework Model (GFM2000)* (BSC 2004 [DIRS 170029]) and DTN: MO0012MWDGFM02.002 [DIRS 153777]. The stratigraphic unit and layers are developed into a model grid in *Development of Numerical Grids for UZ Flow and Transport Modeling* (BSC 2004 [DIRS 169855]). Because the assignment of hydrologic properties is associated with the grid used for the UZ flow model, the stratigraphy information is embedded in the TSPA through the flow fields. Aspects that affect hydrogeologic properties for flow are further discussed in *Development of Numerical Grids for UZ Flow and Transport Modeling* (BSC 2004 [DIRS 169855], Section 6). See also included FEP 2.2.03.02.0A (Rock Properties of Host Rock and Other Units).

The uncertainty in stratigraphic contact locations is not significant in comparisons with other uncertainties affecting unsaturated zone flow (SNL 2007 [DIRS 184614], Section 6.10), and its subsequent effects on radionuclide transport, drift seepage, and drift-scale coupled processes (see included FEP 2.2.07.02.0A (Unsaturated Groundwater Flow in the Geosphere)). Therefore, this uncertainty is not propagated into TSPA.

This FEP is also included for radionuclide transport in the unsaturated zone through the use of flow fields generated by the UZ flow model (DTNs: LB0612PDFEHMFF.001 [DIRS 179296], LB0701MOFEHMFF.001 [DIRS 179297], LB0701GTFEHMFF.001 [DIRS 179160], and LB0702PAFEM10K.002 [DIRS 179507]) and used by FEHM in TSPA multirealization runs (SNL 2008 [DIRS 184748], Section 6.5.1[b]).

Ambient seepage as a result of incomplete flow diversion around drifts is a local process simulated by the drift-scale seepage process model (SNL 2007 [DIRS 181244], Section 6.4). The stratigraphy of the repository host rock is included in the drift seepage models (SNL 2007 [DIRS 179466], Table 4-1, Parameter Number 01-03). The UZ flow model, which provides the percolation flux distributions used for seepage calculations, accounts for the effects of various geological units and major faults on the flow boundary condition for drift seepage (SNL 2007 [DIRS 184614], Sections 6.1.1 and 6.1.2). This is because the overall distribution of percolation flux at the repository horizon is influenced by stratigraphic layering and by major discontinuities. For example, the PTn unit overlying the Topopah Spring welded tuff units can divert a fraction of percolating water to intercepting faults and fault zones, thereby changing the spatial distribution of fluxes (SNL 2007 [DIRS 184614], Section 6.6.2.3), which could affect water–rock interaction and seepage water chemistry.

The drift-scale process models addressing thermal-hydrologic, THM, and THC processes (SNL 2007 [DIRS 181244], Sections 6.4.3.1, 6.4.4.1, and 6.4.4.2) also represent the stratigraphy in the unsaturated zone at Yucca Mountain in an explicit manner. This is needed because the thermal perturbation of the unsaturated rock extends far into the overlying and underlying geological units. Thus, the stratigraphy information is inherently embedded in the respective model results from the UZ flow and transport model and the thermal-hydrologic, THM, and THC drift-scale models. Finally, because the thermal perturbation affects the geologic units overlying and underlying the emplacement drifts, the THC seepage model includes the Yucca Mountain stratigraphy (SNL 2007 [DIRS 177404], Sections 4.1.2 and 6.5.1), using stratigraphic information from DTN: LB03023DKMGRID.001 [DIRS 162354] and mineralogical information from DTNs: LA9908JC831321.001 [DIRS 113495], LA9912SL831151.001

[DIRS 146447], LA9912SL831151.002 [DIRS 146449], and LA0009SL831151.001 [DIRS 153485].

The seepage water chemistry abstraction model includes the effects of stratigraphy within the TSw (SNL 2007 [DIRS 177412], Section 6.3.2.4.4), through the porosities and thicknesses of the stratigraphic units. The percolation flux values used in the model are based on fluxes at the PTn/TSw boundary predicted by the UZ flow model, given in DTNs: LB0612PDPTNTSW.001 [DIRS 179150], LB0701MOPTNTSW.001 [DIRS 179156], LB0701GTPTNTSW.001 [DIRS 179153], and LB0702UZPTN10K.002 [DIRS 179332], which represent each climate state. The approach used is a plug flow model that has a transport velocity equal to the percolation flux divided by the product of the average porosity and the average water saturation (SNL 2007 [DIRS 177412], Section 6.3.2.4.4).

Saturated Zone Stratigraphy

The stratigraphic (i.e., hydrologic) nature of the saturated zone rocks as it affects flow and transport is incorporated into the TSPA SZ site-scale flow and transport models (SNL 2007 [DIRS 177391]; SNL 2008 [DIRS 184806]). The primary hydrogeologic subdivisions are based on and coincide with (1) common permeability and porosity characteristics (on a regional scale) of the rock and (2) whether the rock's primary mode of origin is volcanic, clastic, sedimentary (carbonates), or alluvial in nature (SNL 2007 [DIRS 177391], Section 6.3.1.2). The hydrogeologic subdivisions employed for the TSPA are a synthesis of the hydrogeologic framework model, documented in *Hydrogeologic Framework Model for the Saturated Zone Site-Scale Flow and Transport Model* (SNL 2007 [DIRS 174109], Sections 4.1.1, 4.1.4, 6.1, and 6.3), and the calibrated SZ site-scale flow model as documented in *Saturated Zone Site-Scale Flow Model* (SNL 2007 [DIRS 177391], Sections 6.3.1.2, 6.4.3.1, 6.4.3.3, and 6.4.3.10).

Hydrogeologic Framework Model for the Saturated Zone Site-Scale Flow and Transport Model (SNL 2007 [DIRS 174109]]) documents HFM2006 (DTN: MO0610MWDHFM06.002 [DIRS 179352]). HFM2006 is used in *Saturated Zone Site-Scale Flow Model* (SNL 2007 [DIRS 177391]) to supply the spatial location of hydrogeologic units for the site-scale model. The 23 hydrogeologic units from HFM2006 (SNL 2007 [DIRS 174109]) are incorporated in the site-scale flow model (SNL 2007 [DIRS 177391], Section 6.5.1.3) via permeability zones. Additional permeability zones reflecting other features such as the altered permeability zone to the north, the regional horizontal anisotropy, and numerous faults are used to represent important structural or conceptual features. Ten additional zones representing faults and Lower Fortymile Wash alluvium were established to represent important structural or conceptual (large hydraulic gradient) features. The additional features reflect the degree of fracturing, faulting, fault orientation, and mineralogical alteration of glassy materials to zeolites and clay minerals. The site-scale saturated zone flow model is incorporated in the site-scale SZ transport model documented in *Site-Scale Saturated Zone Transport* (SNL 2008 [DIRS 184806]). The site-scale SZ transport model is used in SZ flow and transport model abstraction documented in *Saturated Zone Flow and Transport Model Abstraction* (SNL 2008 [DIRS 183750]). The SZ flow and transport model abstraction provides breakthrough curves and a one-dimensional transport model.

In all, there are 23 hydrogeologic units employed in the formulation of the SZ flow model (SNL 2007 [DIRS 177391], Section 6.4.3.1), and the SZ flow and transport abstraction (SNL 2008 [DIRS 183750], Section 6.5.2[b]). These same units are modeled in the SZ transport model (SNL 2008 [DIRS 184806]), as a result of the transport model being constructed from the SZ flow model. The uncertainty in transport parameters specific to stratigraphy, such as the effective diffusion coefficient, matrix porosity, and bulk density are described in *Saturated Zone Flow and Transport Model Abstraction* (SNL 2008 [DIRS 183750], Sections 6.5.2.6, 6.5.2.18, and 6.5.2.19).

In the hydrogeologic units where flow and transport are expected to take place, the alluvium units, Crater Flat Group, upper volcanic aquifer, and the upper volcanic confining units (SNL 2007 [DIRS 177391], Section 6.5.2.3), variability in transport properties between the major hydrogeologic units is implemented using a range of sampled parameters assigned to each unit for a particular realization (SNL 2008 [DIRS 183750], Section 6.5.2[b]). The primary stratigraphic uncertainty that has a significant effect on SZ flow and transport is the location of the contact between volcanic rocks and the alluvium (SNL 2008 [DIRS 183750], Section 6.5.2.2[a]). This is the only stratigraphic uncertainty propagated into TSPA for SZ flow and transport. Uncertainty in the contact between volcanic rocks and alluvium at the water table is addressed by a probability distribution function that represents the extent of the northwestern boundary of the alluvium uncertainty zone (SNL 2008 [DIRS 183750], Section 6.5.2.2[a]). For the fractured volcanic units, uncertainty in the spacing between intervals conducting significant quantities of groundwater flow is assessed in *Probability Distribution for Flowing Interval Spacing* (BSC 2004 [DIRS 170014]).

How the physical properties of stratigraphic units are modeled is discussed in included FEP 2.2.03.02.0A (Rock Properties of Host Rock and Other Units). Further discussions of the various aspects of stratigraphy affecting flow and transport in the saturated zone are found in *Saturated Zone Flow and Transport Model Abstraction* (SNL 2008 [DIRS 183750], Sections 6.5.2[b], 6.5.2.1[b], 6.5.2.2[a], 6.5.2.3[a], 6.5.2.6, 6.5.2.18, and 6.5.2.19), and *Site-Scale Saturated Zone Transport* (SNL 2008 [DIRS 184806], Section 6.3).

INPUTS:

Table 2.2.03.01.0A-1. Indirect Inputs

Citation	Title	DIRS
BSC 2004	*Probability Distribution for Flowing Interval Spacing*	170014
BSC 2004	*Analysis of Hydrologic Properties Data*	170038
BSC 2004	*Development of Numerical Grids for UZ Flow and Transport Modeling*	169855
BSC 2004	*Geologic Framework Model (GFM2000)*	170029
BSC 2004	*Seepage Model for PA Including Drift Collapse*	167652
BSC 2005	*Drift-Scale Coupled Process (DST and TH Seepage) Models*	172232
DTN: LA0009SL831151.001	Fracture Mineralogy of the ESF Single Heater Test Block, Alcove 5	153485
DTN: LA9908JC831321.001	Mineralogic Model “MM3”	113495
DTN: LA9912SL831151.001	Fracture Mineralogy of Drill Core ESF-HD-TEMP-2	146447

Table 2.2.03.01.0A-1. Indirect Inputs (Continued)

Citation	Title	DIRS
DTN: LA9912SL831151.002	Percent Coverage by Fracture-Coating Minerals in Core ESF-HD-TEMP-2	146449
DTN: LB03023DKMGRID.001	UZ 3-D Site Scale Model Grids	162354
DTN: LB0612PDFEHMFF.001	Flow-Field Conversions from TOUGH2 to FEHM Format for Present Day 10-, 30-, 50-, and 90-Percentile Infiltration Maps	179296
DTN: LB0612PDPTNTSW.001	Vertical Flux at PTN/TSW Interface for Present-Day Climate of 10th, 30th, 50th, and 90-Percentile Infiltration Maps	179150
DTN: LB0701GTFEHMFF.001	Flow-Field Conversions from TOUGH2 to FEHM Format for Glacial Transition Climate 10th-, 30th-, 50th-, and 90th-Percentile Infiltration Maps	179160
DTN: LB0701GTPTNTSW.001	Vertical Flux at PTN/TSW Interface for Glacial Transition Climate of 10th, 30th, 50th, and 90th-Percentile Infiltration Maps	179153
DTN: LB0701MOFEHMFF.001	Flow-Field Conversions from TOUGH2 to FEHM Format for Monsoon Climate 10th-, 30th-, 50th-, and 90th-Percentile Infiltration Maps	179297
DTN: LB0701MOPTNTSW.001	Vertical Flux at PTN/TSW Interface for Monsoon Climate of 10th, 30th, 50th and 90th-Percentile Infiltration Maps	179156
DTN: LB0702PAFEM10K.002	Flow Field Conversions to FEHM Format for Post 10,000 Year Peak Dose Fluxes in the Unsaturated Zone for Four Selected Infiltration Rates	179507
DTN: LB0702UZPTN10K.002	Vertical Flux at PTN/TSW Interface for Post-10K-Year Climate Infiltration Maps	179332
DTN: MO0012MWDGFM02.002	Geologic Framework Model (GFM2000)	153777
DTN: MO0610MWDHFM06.002	Hydrogeologic Framework Model (HFM2006) Stratigraphic Horizon Grids	179352
SNL 2007	*Saturated Zone Site-Scale Flow Model*	177391
SNL 2007	*Abstraction of Drift Seepage*	181244
SNL 2007	*Drift-Scale THC Seepage Model*	177404
SNL 2007	*Engineered Barrier System: Physical and Chemical Environment*	177412
SNL 2007	*Hydrogeologic Framework Model for the Saturated Zone Site Scale Flow and Transport Model*	174109
SNL 2007	*Total System Performance Assessment Data Input Package for Requirements Analysis for Subsurface Facilities*	179466
SNL 2007	*UZ Flow Models and Submodels*	184614
SNL 2008	*Particle Tracking Model and Abstraction of Transport Processes*	184748
SNL 2008	*Saturated Zone Flow and Transport Model Abstraction*	183750
SNL 2008	*Simulation of Net Infiltration for Present-Day and Potential Future Climates*	182145
SNL 2008	*Site-Scale Saturated Zone Transport*	184806

FEP: 2.2.03.02.0A

FEP NAME:

Rock Properties of Host Rock and Other Units

FEP DESCRIPTION:

Physical properties such as porosity and permeability of the relevant rock units, soils, and alluvium are necessary for the performance assessment. Possible heterogeneities in these properties should be considered. Questions concerning events and processes that may cause these physical properties to change over time are considered in other FEPs.

SCREENING DECISION:

Included

TSPA DISPOSITION:

This FEP is similar to included FEP 2.2.03.01.0A (Stratigraphy). For the sake of clarity, the unsaturated zone is discussed first and the saturated zone second. This FEP is implemented in TSPA by way of the infiltration model, the drift seepage abstraction, the EBS physical and chemical environment abstraction (via THM and THC seepage models), the unsaturated zone flow models and submodels, the unsaturated zone particle tracking transport abstraction, and the saturated zone flow and transport model abstraction.

Rock properties used are defined for each of the stratigraphic units/layers classified in *Geological Framework Model (GFM2000)* (BSC 2004 [DIRS 170029]; DTN: MO0012MWDGFM02.002 [DIRS 153777]), which are further developed into a model grid in *Development of Numerical Grids for Unsaturated Zone Flow and Transport Modeling* (BSC 2004 [DIRS 169855]). However, rock properties are not developed in the grid development report. For the unsaturated zone flow model, rock properties and their distributions are modeled in terms of the sequence of hydrogeologic units and discrete faults (SNL 2007 [DIRS 184614], Sections 6.1.1 and 6.1.5). Therefore, rock properties are embedded in the TSPA through the output flow fields, with site-scale layering and faults taken into account. Rock properties used as input for *Unsaturated Zone Flow Models and Submodels* (SNL 2007 [DIRS 184614]) are developed in *Analysis of Hydrologic Properties Data* (BSC 2004 [DIRS 170038], Section 6) and *Calibrated Unsaturated Zone Properties* (SNL 2007 [DIRS 179545], Section 6.3). Effects of rock property heterogeneity within a hydrogeologic unit on site-scale water flow processes are also evaluated and found to be insignificant (BSC 2004 [DIRS 170035], Section 6.3.4), which supports the use of the approach to represent subsurface heterogeneities (in the site-scale unsaturated zone model) by assigning uniform rock properties in a given unit.

Unsaturated Zone Rock Properties

The bedrock properties at the soil–rock interface, their spatial heterogeneities, and their uncertainties are employed in developing net-infiltration maps reported in *Simulation of Net*

Infiltration for Present-Day and Potential Future Climates (SNL 2008 [DIRS 182145], Section 6.5.2.6). For a given climate state, infiltration uncertainty is represented through four discrete infiltration scenarios, which are sampled in the TSPA model according to flow weighting factors (SNL 2007 [DIRS 184614], Section 6.8). These weighting factors are determined by the goodness of matches between simulated and observed chloride and temperature data in the unsaturated zone. The chloride and temperature data are used because they are relatively sensitive to the percolation flux in the unsaturated zone. The simulations used to determine these weighting factors are performed with the site-scale unsaturated zone flow model that, as previously discussed, includes rock properties and their heterogeneity.

The key rock-property data used in the three-dimensional unsaturated zone flow model and its submodel development include the following (SNL 2007 [DIRS 184614], Table 4.1-1):

- Fracture properties (frequency, permeability, van Genuchten α and *m* parameters, porosity, and interface area per unit volume rock) for each unsaturated zone model layer
- Matrix properties (porosity, permeability, and the van Genuchten α and *m* parameters) for each unsaturated zone model layer
- Thermal and transport properties (grain density, wet and dry thermal conductivity, grain specific heat, and tortuosity coefficients) for each unsaturated zone model layer
- Fault properties (fracture parameters) for each major hydrogeologic unit as defined by Table 6.1-1 of *Unsaturated Zone Flow Models and Submodels* (SNL 2007 [DIRS 184614]). Note that matrix properties in faults are the same as the adjacent matrix blocks of nonfault zones.

The calibrated parameter sets also include an estimate for each model layer of the active-fracture parameter, γ, that accounts for the reduction in interaction between matrix and fracture flow resulting from flow fingering and channelization (Liu et al. 1998 [DIRS 105729]). Uncertainty in the input data and parameters are addressed in Section 6.10 of *Unsaturated Zone Flow Models and Submodels* (SNL 2007 [DIRS 184614]). Specific input data sets and associated data tracking numbers (DTNs) are listed in Table 4.1-1 of *Unsaturated Zone Flow Models and Submodels* (SNL 2007 [DIRS 184614]).

Rock properties of host rock and other units are included and used in the simulations of radionuclide transport through the unsaturated zone. *Particle Tracking Model and Abstraction of Transport Processes* (SNL 2008 [DIRS 184748], Sections 6.5.3[b] and 6.5.7[b]; SNL 2008 [DIRS 184748], Addendum Section 4.1) documents the matrix porosity, rock density, fracture porosity, fracture spacing, and aperture data (DTNs: LB0205REVUZPRP.001 [DIRS 159525], LB0207REVUZPRP.001 [DIRS 159526], and LB0207REVUZPRP.002 [DIRS 159672]) and their uses in the particle tracking model. The generated distributions of fracture porosity and fracture frequency are given in DTN: LA0407BR831371.001 [DIRS 170806], and are used by the TSPA model in multirealization runs to determine aperature values as described in *Particle Tracking Model and Abstraction of Transport Processes* (SNL 2008 [DIRS 184748], Sections 6.5.3[b], 6.5.5[b], and 6.5.7[b]).

All the seepage process models that feed into seepage abstraction represent the physical properties of the unsaturated host rock and their heterogeneity (SNL 2007 [DIRS 181244], Section 6.4). Percolation flux distributions provided by *Unsaturated Zone Flow Models and Submodels* (SNL 2007 [DIRS 184614]) are used in *Abstraction of Drift Seepage* (SNL 2007 [DIRS 181244], Section 6.6.5.1; SNL 2007 [DIRS 181244], Section 6.4[a]), which accounts for rock properties and their variation on a larger scale (e.g., stemming from stratigraphy effects). Small-scale heterogeneity is accounted for by a stochastic continuum representation of fracture permeability. Thus, heterogeneity on this scale is embedded in the model output from the seepage calibration model (BSC 2004 [DIRS 171764], Section 6.5.2), the seepage model for performance assessment (BSC 2004 [DIRS 167652], Sections 6.3.2 through 6.3.4), and the thermal-hydrological seepage model (BSC 2005 [DIRS 172232]) provided respectively in DTNs: LB0407AMRU0120.001 [DIRS 173280], LB0706UZSEEP05.001 [DIRS 181445], and LB0301DSCPTHSM.002 [DIRS 163689]. The intermediate-scale spatial variability and uncertainty of seepage-relevant rock properties are accounted for by appropriate probability distributions that were developed in *Abstraction of Drift Seepage* (SNL 2007 [DIRS 181244], Sections 6.6.1 and 6.6.2; SNL 2007 [DIRS 181244], Section 6.3[a]).

Potential alterations of these properties, as a result of THM or THC processes, have been assessed using drift-scale process models (SNL 2007 [DIRS 181244], Sections 6.4.4.1 and 6.4.4.2). It was demonstrated that these potential alterations can be neglected in the TSPA model, because the expected changes would lead to less seepage (SNL 2007 [DIRS 181244], Section 6.5.1.4; see excluded FEP 2.1.09.12.0A (Rind (Chemically Altered Zone) Forms in the Near-Field) and excluded FEP 2.2.10.04.0A (Thermo-mechanical Stesses Alter Characteristics of Fractures Near Repository)). The THC seepage model represents the physical properties of the unsaturated rock (SNL 2007 [DIRS 177404], Section 6.4.7 and Table 6.4-2). Simulated chemical concentrations through time are presented in DTNs: LB0705DSTHC001.001 [DIRS 181217] and LB0705DSTHC001.002 [DIRS 180854]. These data are used to feed and/or provide the technical basis for *Engineered Barrier System: Physical and Chemical Environment* (SNL 2007 [DIRS 177412]), which generates lookup tables used in the TSPA model.

Small-scale fracture permeability heterogeneity was also investigated and determined not to significantly affect seepage water chemistry (SNL 2007 [DIRS 177404], Section 6.3). The THC seepage model includes rock properties from DTNs: LB0205REVUZPRP.001 [DIRS 159525] and LB0610UZDSCP30.002 [DIRS 179180]). Potential alterations of fracture permeability values as a result of THC processes are accounted for by the modeling of coupled THC processes, and result in reducing fracture permeability (SNL 2007 [DIRS 177404], Section 6.5.5.3).

Saturated Zone Rock Properties

Considering the saturated zone, geologic features and heterogeneous hydrostratigraphic units are included in *Saturated Zone Flow and Transport Abstraction Model* (SNL 2008 [DIRS 183750], Section 6.5[a]) as cells with specific hydrologic parameter values in a configuration based on the hydrogeologic framework used in *Saturated Zone Site-Scale Flow Model* (SNL 2007 [DIRS 177391], Section 6.4.3.1). Available geologic information on rock properties that affect saturated zone flow and transport in the Yucca Mountain region is used to determine the 23 hydrostratigraphic units modeled in the site-scale saturated zone flow domain (SNL 2007

[DIRS 177391], Table 6-5). The supporting geologic information is updated in *Hydrogeologic Framework Model for the Saturated Zone Site-Scale Flow and Transport Model* (SNL 2007 [DIRS 174109], Sections 6.2, 6.3, and 6.4).

Hydrogeologic Framework Model for the Saturated Zone Site-Scale Flow and Transport Model (SNL 2007 [DIRS 174109], Sections 6.2 to 6.4) documents HFM2006 (DTN: MO0610MWDHFM06.002 [DIRS 179352]). The TSPA disposition of this FEP is supported by *Hydrogeologic Framework Model for the Saturated Zone Site-Scale Flow and Transport Model* (SNL 2007 [DIRS 174109], Sections 6.2 to 6.4).

In *Saturated Zone Site-Scale Flow Model* (SNL 2007 [DIRS 177391], Section 6.6), base-case permeability and flow fields are generated. There are numerous broad and distinct zones in this model, categorized as "features," that affect or potentially affect flow. Many of these are directly or indirectly associated with faults, including zones of mineralogical alteration along faults and contact zones between offset units (SNL 2007 [DIRS 177391], Section 6.4.3.7, Table 6-7). The zones are categorized depending upon how their rock properties, most notably porosity and permeability, affect flow and transport. The rock properties in these zones can be specified to act as either barriers or conduits (or simultaneously as barriers in one direction and conduits in another direction (i.e., horizontal or vertical anisotropy)) to saturated zone flow (SNL 2007 [DIRS 177391], Section 6.4.3.7, Table 6-7). In all, 12 zones associated with 10 features plus a boundary separating a northern region of lower permeability from a southern region of higher permeability (attributed to geologic alteration associated with the Claim Canyon caldera north of Yucca Mountain and helping to account for the large hydraulic gradient north of Yucca Mountain) are built into the saturated zone site-scale flow model (SNL 2007 [DIRS 177391], Section 6.4.3.7). One feature, the Fortymile Wash fault, has two spatially separated zones in the model. The specified base-case flow properties and the effects of each feature/zone on flow are listed in Table 6-7 of *Saturated Zone Site-Scale Flow Model* (SNL 2007 [DIRS 177391], Section 6.4.3.7). Additional discussion of the features/zones is provided in included FEP 2.2.07.13.0A (Water-conducting Features in the Saturated Zone).

The saturated zone transport abstraction model and the saturated zone one-dimensional transport model (both described in SNL 2008 [DIRS 183750], Sections 6.3, 6.5[a], and 6.6) take the flow and transport model and indirectly account for additional uncertainty and heterogeneity in rock permeability through the stochastically sampled groundwater specific discharge multiplier parameter (SNL 2008 [DIRS 183750], Section 6.5.2.1[a]). Additional uncertainty and spatial variability in rock properties in the SZ transport abstraction model are accounted for in the flow and transport abstraction model by specifying uncertainty distributions for the following stochastically sampled parameters: (1) horizontal flow anisotropy in the volcanics; (2) effective porosity in the alluvium units 11 and 26; (3) flowing interval spacing in the volcanics; (4) flowing interval porosity; (5) sorption coefficients (K_d) for the sorbing radionuclides modeled in both the alluvium and volcanic units; and (6) longitudinal dispersivity. The above parameters are described in *Saturated Zone Flow and Transport Model Abstraction* (SNL 2008 [DIRS 183750], Section 6.5.2[b]). Uncertainty in the flowing interval spacing parameter is assessed in *Probability Distribution for Flowing Interval Spacing* (BSC 2004 [DIRS 170014], Sections 6.4 and 6.5). The basis for anisotropy in permeability in the volcanic units and assessment of groundwater specific discharge in the alluvium are discussed in *Saturated Zone In-Situ Testing* (SNL 2007 [DIRS 177394], Sections 6.2.6 and 6.5.5). Other parameters that are

stochastically varied to account for uncertainty in rock parameters include the location of the transition boundary from volcanic units to alluvium, and volcanic and alluvium porosities and bulk densities, which are discussed in *Saturated Zone Flow and Transport Model Abstraction* (SNL 2008 [DIRS 183750], Section 6.5.2[b]). The impacts of rock properties on the uncertainty of sorption coefficients are discussed in *Site-Scale Saturated Zone Transport* (SNL 2008 [DIRS 184806], Sections 6.3 and 6.4 and Appendix A). Impacts of rock properties on effective diffusion coefficients of radionuclides are discussed in *Saturated Zone Flow and Transport Model Abstraction* (SNL 2008 [DIRS 183750], Section 6.5.2.6).

The uncertainty in the location of the alluvium-volcanic contact boundary is accounted for through a probabilistically sampled parameter (SNL 2008 [DIRS 183750], Section 6.5.2.2[a]), which defines the northwestern boundary of the alluvial (valley-fill aquifer) uncertainty zone. This parameter determines whether nodes within the zone of uncertainty in the saturated zone flow and transport model(s) are assigned alluvium or volcanic rock properties.

INPUTS:

Table 2.2.03.02.0A-1. Indirect Inputs

Citation	Title	DIRS
BSC 2004	*Probability Distribution for Flowing Interval Spacing*	170014
BSC 2004	*Analysis of Hydrologic Properties Data*	170038
BSC 2004	*Conceptual Model and Numerical Approaches for Unsaturated Zone Flow and Transport*	170035
BSC 2004	*Development of Numerical Grids for UZ Flow and Transport Modeling*	169855
BSC 2004	*Geologic Framework Model (GFM2000)*	170029
BSC 2004	*Seepage Calibration Model and Seepage Testing Data*	171764
BSC 2004	*Seepage Model for PA Including Drift Collapse*	167652
BSC 2005	*Drift-Scale Coupled Process (DST and TH Seepage) Models*	172232
DTN: LA0407BR831371.001	UZ Transport Abstraction Model, Transport Parameters and Base Case Simulation Results	170806
DTN: LB0205REVUZPRP.001	Fracture Properties for UZ Model Layers Developed from Field Data	159525
DTN: LB0207REVUZPRP.001	Revised UZ Fault Zone Fracture Properties	159526
DTN: LB0207REVUZPRP.002	Matrix Properties for UZ Model Layers Developed from Field and Laboratory Data	159672
DTN: LB0301DSCPTHSM.002	Drift-Scale Coupled Process Model for Thermohydrologic Seepage: Data Summary	163689
DTN: LB0407AMRU0120.001	Supporting Calculations and Analysis for Seepage Abstraction and Summary of Abstraction Results.	173280
DTN: LB0610UZDSCP30.001	Drift-Scale Calibrated Property Set for the 30-Percentile Infiltration Map	179180
DTN: LB0705DSTHC001.001	Drift-Scale THC Simulation Results with Water HDPERM3 (W0)	181217
DTN: LB0705DSTHC001.002	Input and Output Files of Drift-Scale THC Simulations with Water HDPERM3 (W0)	180854
DTN: LB0706UZSEEP05.001	Mathcad 11 Spreadsheets for Probabilistic Seepage Evaluation	181445
DTN: MO0012MWDGFM02.002	Geologic Framework Model (GFM2000)	153777

Table 2.2.03.02.0A-1. Indirect Inputs (Continued)

Citation	Title	DIRS
DTN: MO0610MWDHFM06.002	Hydrogeologic Framework Model (HFM2006) Stratigraphic Horizon Grids	179352
Liu et al. 1998	"An Active Fracture Model for Unsaturated Flow and Transport in Fractured Rocks"	105729
SNL 2007	*Saturated Zone Site-Scale Flow Model*	177391
SNL 2007	*Abstraction of Drift Seepage*	181244
SNL 2007	*Calibrated Unsaturated Zone Properties*	179545
SNL 2007	*Drift-Scale THC Seepage Model*	177404
SNL 2007	*Engineered Barrier System: Physical and Chemical Environment*	177412
SNL 2007	*Hydrogeologic Framework Model for the Saturated Zone Site Scale Flow and Transport Model*	174109
SNL 2007	*Saturated Zone In-Situ Testing*	177394
SNL 2007	*UZ Flow Models and Submodels*	184614
SNL 2008	*Particle Tracking Model and Abstraction of Transport Processes*	184748
SNL 2008	*Saturated Zone Flow and Transport Model Abstraction*	183750
SNL 2008	*Simulation of Net Infiltration for Present-Day and Potential Future Climates*	182145
SNL 2008	*Site-Scale Saturated Zone Transport*	184806

FEP: 2.2.06.01.0A

FEP NAME:

Seismic Activity Changes Porosity and Permeability of Rock

FEP DESCRIPTION:

Seismic activity (fault displacement or vibratory ground motion) has a potential to change rock stresses and result in strains that affect flow properties in rock outside the excavation-disturbed zone. It could result in strains that alter the permeability in the rock matrix. These effects may decrease the transport times for potentially released radionuclides.

SCREENING DECISION:

Excluded – low consequence

SCREENING JUSTIFICATION:

Plate tectonic activity has imparted crustal extension stresses within the Basin and Range Province (which includes the Yucca Mountain region) during the past 12 million years. The height of this activity occurred between 10 and 12 million years ago, with estimated extension rates ranging between 10 and 30 mm per year (National Research Council 1992 [DIRS 105162], Chapter 2). During this period, major faults and fractures were created in the vicinity of Yucca Mountain. Approximately 5 million years ago, regional extension rates declined to 5 to 10 mm per year. At present, extension rates are still in a declining state (National Research Council 1992 [DIRS 105162], Chapter 2).

Regional extension imparts local extensional, compressional, and/or shear stresses on the crust, depending on location, depth, and the juxtaposition of parent rock units and existing faults and fractures. Release of stress results in seismic activity that creates faults (rupture), and causes fault displacement, vibratory motion, and/or spatial redistribution of stresses not associated with specific faults. Vibratory motion and spatial redistribution of stress in the rock matrix can alter the hydrologic properties of the parent rock by (1) causing a change in pore pressure, or (2) causing dilation, compression, or breakage of granular structures in the rock, leading to corresponding changes in permeability.

Pore pressure changes associated with seismic events are addressed in detail under excluded FEP 1.2.10.01.0A (Hydrologic Response to Seismic Activity) and are based on the results of an investigation conducted by the National Research Council (1992 [DIRS 105162], Chapter 5) that evaluated water table fluctuations for a predicted seismic event. It was concluded that a future seismic event would not alter the rock hydrologic properties on a regional scale.

Damage of the rock matrix material due to seismic loading would manifest itself in the form of inter-lithophysal tensile fractures that coalesce to form observable shear fractures with offset. The exposed lithophysal rocks in the ESF and the ECRB Cross-Drift show no fracturing of this type. Observed fracturing is consistent with typical cooling-fracture-related history (BSC 2005

[DIRS 170137], Sections 6 and 6.3). These findings indicate that the matrix material is largely unaffected by redistribution of strain introduced by seismic activity.

Given the relatively high strength of the matrix material and the extensive fracture network in the rock mass, the strain introduced by seismic activity would be expected to be accommodated by deformation of, and slip along, existing faults and fractures. The effects of seismic activity on the properties of faults and fractures are discussed under excluded FEP 2.2.06.02.0A (Seismic Activity Changes Porosity and Permeability of Faults) and excluded FEP 2.2.06.02.0B (Seismic Activity Changes Porosity and Permeability of Fractures). However, localized changes in hydrologic properties could occur adjacent to existing faults and fractures due to the creation of brecciation and gouge zones and possibly due to the creation of new fractures (outside of the brecciated zone). This disturbed rock zone, labeled herein as a "zone of alteration," is correlated with the amount of fault offset (Sweetkind et al. 1997 [DIRS 177047]). Faults with 1 to 5 m of cumulative offset have a zone of increased fracturing of only 1 to 2 m; faults with tens of meters of offset can have a zone of fracturing up to tens of meters wide (Sweetkind et al. 1997 [DIRS 177047], pp. 68 to 72). The hydrologic properties in the zone of alteration reflect the cumulative response of a dynamic seismic past, demonstrative of rapid extension rates in existence 10 to 12 million years ago and, to a lesser extent, the lower extension rates occurring today. In light of the cumulative nature of seismic stresses at Yucca Mountain over more than 10 million years, any changes in hydrologic properties resulting from seismic activity over the 10,000-year postclosure period are expected to be negligible.

The effects of a future seismic event on the hydrologic properties of the host rock are evaluated here based on the findings of the expert elicitation analysis documented in the PSHA report (CRWMS M&O 1998 [DIRS 103731], Sections 4 and 8). The PSHA group assessed the mean displacement for intact host rock in the vicinity of the repository to be less than 0.1 cm for a 10^{-8} annual-exceedance probability (DTN: MO0401MWDRPSHA.000 [DIRS 185014], file: *s7d.frac_mean*; CRWMS M&O 1998 [DIRS 103731], Section 8.2.1). Consequently, the rock matrix is largely unaffected by strain redistribution caused by seismic activity and no significant new faults or fractures are likely to form in the Yucca Mountain vicinity within the next 10,000 years. The small seismic displacement for intact rock, less than 0.1 cm, for an annual-exceedance probability of 10^{-8} corresponds to the level of displacement that occurred as a result of thermal stress in the Drift Scale Test, as measured in multiple-point borehole extensometers (BSC 2004 [DIRS 169864], Figure 7.4.2-2). The simulations of the displacement response in the Drift Scale Test, based on elastic thermal-hydrological-mechanical processes, were found to be in agreement with measurements. The dominant mode for stress-induced permeability change for THM processes was found to be elastic fracture opening or closing caused by changes in stress normal to the fractures, as opposed to changes in matrix permeability (BSC 2004 [DIRS 169864], Section 8.2). For similar displacements and stresses (as found in the Drift Scale Test) associated with seismic motion, the same conclusions apply to both the unsaturated zone and saturated zone. Therefore, the small seismic displacements in the intact rock matrix will have a negligible effect on rock-matrix hydrologic properties and may be excluded on the basis of low consequence.

In summary, any changes to hydrologic processes as a result of changes to rock matrix properties caused by seismic activity are expected to be negligible. Based on the previous discussion, omission of FEP 2.2.06.01.0A (Seismic Activity Changes Porosity and Permeability of Rock)

will not result in a significant adverse change in the magnitude or timing of either radiological exposures to the RMEI or radionuclide releases to the accessible environment. Therefore, this FEP is excluded from the performance assessments conducted to demonstrate compliance with proposed 10 CFR 63.311 and 63.321 (70 FR 53313 [DIRS 178394]), and with 10 CFR 63.331 [DIRS 180319], on the basis of low consequence.

INPUTS:

Table 2.2.06.01.0A-1. Direct Inputs

Input	Source	Description
BSC 2004. *Drift Scale THM Model*. [DIRS 169864]	Section 8.2	The dominant mode for stress-induced permeability change for THM processes was found to be elastic fracture opening or closing caused by changes in stress normal to the fractures
DTN: MO0401MWDRPSHA.000. Results of the Yucca Mountain Probabilistic Seismic Hazard Analysis (PSHA). [DIRS 185014]	file: *s7d.frac_mean*	Mean displacement for intact host rock in the vicinity of the repository to be less than 0.1 cm for a 10^{-8} annual-exceedance probability
National Research Council 1992. *Ground Water at Yucca Mountain, How High Can It Rise? Final Report of the Panel on Coupled Hydrologic/Tectonic/Hydrothermal Systems at Yucca Mountain*. [DIRS 105162]	Chapter 2	Plate tectonic activity imparted crustal extension stresses within the Yucca Mountain region during the past 12 million years. Extension rates between 10 and 12 million years ago ranged between 10 and 30 mm per year
	Chapter 5	Results of investigation of National Research Council of hydrologic responses to seismic events
	Chapter 2	Extension rates declined to 5 to 10 mm/yr at 5 Ma; extension rates are still in a declining state

Table 2.2.06.01.0A-2. Indirect Inputs

Citation	Title	DIRS
10 CFR 63	Energy: Disposal of High-Level Radioactive Wastes in a Geologic Repository at Yucca Mountain, Nevada	180319
70 FR 53313	Implementation of a Dose Standard After 10,000 Years	178394
BSC 2004	*Drift Scale THM Model*	169864
BSC 2004	*Peak Ground Velocities for Seismic Events at Yucca Mountain, Nevada*	170137
SNL 2007	*Saturated Zone Site-Scale Flow Model*	177391
Sweetkind et al. 1997	*Administrative Report: Integrated Fracture Data in Support of Process Models, Yucca Mountain, Nevada*	177047

FEP: 2.2.06.02.0A

FEP NAME:

Seismic Activity Changes Porosity and Permeability of Faults

FEP DESCRIPTION:

Seismic activity (fault displacement or vibratory ground motion) has a potential to produce jointed-rock motion and change stress and strains that alter the permeability along faults. This could result in reactivation of pre-existing faults or generation of significant new faults, which could significantly change the flow and transport paths, alter or short-circuit the flow paths and flow distributions close to the repository, and/or create new pathways through the repository. These effects may decrease the transport times for potentially released radionuclides.

SCREENING DECISION:

Excluded – low consequence

SCREENING JUSTIFICATION:

Fault displacements and concomitant formation or alteration of fractures can have a marked effect on hydrologic properties of the saturated and unsaturated zones. This FEP describes the processes by which seismic activity can alter the porosity and permeability of faults. The general topic of seismic hazard at Yucca Mountain has been investigated in detail in *Probabilistic Seismic Hazard Analyses for Fault Displacement and Vibratory Ground Motion at Yucca Mountain, Nevada* (CRWMS 1998 [DIRS 103731]), also known as the PSHA. Bates and Jackson (1987 [DIRS 164050], p. 257]) describe faults as a type of fracture, and as such, much of the discussion in excluded FEP 2.2.06.02.0B (Seismic Activity Changes Porosity and Permeability of Fractures) is also of considerable relevance here, as is the discussion contained in excluded FEP 2.2.06.01.0A (Seismic Activity Changes Porosity and Permeability of Rock). Direct hydrologic responses to seismic activity (such as transient changes in the water table) are discussed in excluded FEP 1.2.10.01.0A (Hydrologic Response to Seismic Activity). The seismic history of the Basin and Range Province is outlined in excluded FEP 1.2.01.01.0A (Tectonic Activity-Large Scale).

Movements produced by a fault displacement will result in changes in the rock stress in the vicinity of the fault (BSC 2004 [DIRS 169734], Section 4.3.4.1). The change in rock stress will decrease with distance from any given fault where movement occurs (BSC 2004 [DIRS 169734], Section 4.3.1). However, the magnitude of the changes in rock stress as a function of distance from the fault depends on the specific details of the fault displacement (e.g., magnitude of fault motion, direction of fault movement, extent of the fault that participates in the movement) and the mechanical properties of the surrounding rock (e.g., fracture spacing, fracture stiffness, geomechanical properties of the rock matrix). Given some change in rock stress, the fractured rock mass will respond to the change in stress through deformation, or strain, in the rock. This has the potential to alter hydrologic properties (BSC 2004 [DIRS 169864], Section 6.2.3).

Potential for the Development of New Faults—An aspect of faulting that could be important to repository performance is the formation of new faults. Expert elicitation, documented in the PSHA report (CRWMS M&O 1998 [DIRS 103731], Section 4), provides information that can be used to assess the effects of a seismic event on fault formation. As part of the PSHA, six teams of experts evaluated the available data to assess the fault displacement potential for nine sites that represent the range of fault conditions in the Yucca Mountain vicinity (CRWMS M&O 1998 [DIRS 103731], Figure 4-9). The teams also characterized the uncertainty in their assessment by defining alternative models and approaches and assigning weights. For each combination of alternatives, results for each site were provided as the annual frequency with which given levels of fault displacement would be exceeded. Uncertainty in the results was characterized by calculating the mean hazard and various percentile values. Results for each team were then combined using equal weights to determine the integrated fault displacement hazard (CRWMS M&O 1998 [DIRS 103731], Sections 4 and 8). The PSHA group assessed the mean displacement in the intact rock for the area between the Solitario Canyon and the Ghost Dance faults to be less than 0.1 cm for a 10^{-8} annual-exceedance probability. The development of new faults and fractures (which would have the potential to create new flow paths or significantly change the existing flow paths and flow directions) is inferred from the PSHA to be relatively inconsequential and is therefore of low consequence.

The major faults in the vicinity of the repository are the Solitario Canyon and Bow Ridge faults, which have been examined in terms of the probability distribution for fault displacement in the PSHA report (CRWMS M&O 1998 [DIRS 103731], Section 4). Extrapolating the PSHA results out to the annual exceedance probability of 10^{-8} results in a 13-m approximate mean displacement for the Solitario Canyon fault and a 6-m approximate mean displacement for the Bow Ridge fault (DTN: MO0401MWDRPSHA.000 [DIRS 185014], files: *s1.frac_mean* and *s2.frac_mean*; CRWMS M&O 1998 [DIRS 103731], Figures 8-2 and 8-3).

Current Solitario Canyon fault hydrologic properties reflect the cumulative effects of an active tectonic and seismic past that have resulted in a 260 m cumulative fault displacement where it intersects the ECRB Cross-Drift (Mongano et al. 1999 [DIRS 149850], pp. 48 to 65). An approximately 13-m displacement of the Solitario Canyon fault (and other faults) will release local stresses accumulated along the fault plane but will not alter the large and globally extensive stresses in effect over the past 10 to 12 million years incurred in the parent rock and embedded faults within the Yucca Mountain region (National Research Council 1992 [DIRS 105162], Chapter 5). The height of this activity occurred between 10 and 12 million years ago, with estimated extension rates ranging between 10 and 30 mm per year (National Research Council 1992 [DIRS 105162], Chapter 2). During this period, major faults and fractures were created in the vicinity of Yucca Mountain. Approximately 5 million years ago, regional extension rates declined to 5 to 10 mm per year. At present, extension rates are still in a declining state (National Research Council 1992 [DIRS 105162], Chapter 2) and are associated with a decline in seismic activity. It is these areally extensive stresses imposed on the fault that determine the hydrologic properties of the fault, such as permeability and porosity. The logical conclusion is that any changes in Solitario Canyon fault's hydrologic properties will be small, given an approximate 13-m displacement, as will any changes in hydrologic properties of other, smaller faults, which exhibit less extensive displacements. The Solitario Canyon fault will continue to serve as a groundwater divide between the Yucca Mountain and the Crater Flat regions (SNL 2007 [DIRS 177391], Section 6.3.2.3).

Changes in Fault Hydrologic Properties Due to Formation of Gouge/Brecciation Zones—Fault displacement can cause deformation and breakage of the parent rock, leading to the formation of gouge and brecciated zones in the vicinity of the fault. This is discussed in greater detail in excluded FEP 2.2.06.01.0A (Seismic Activity Changes Porosity and Permeability of Rock). The presence of gouge and brecciated zones only in close proximity to fault planes suggests that much of the strain introduced by seismic activity will be mechanically dissipated within or near the fault planes. The disturbed rock zone is correlated with the amount of fault offset. For instance, in the Solitario Canyon fault zone in the ECRB Cross-Drift, the total displacement is approximately 260 m, but the gouge and brecciated zones are limited to less than 20 m from the main fault trace (Mongano et al. 1999 [DIRS 149850], pp. 59 to 65). Other faults display less extensive fault offsets, so the corresponding gouge/brecciation zones are not expected to exceed that observed for the Solitario Canyon fault zone. Therefore, changes in hydrologic properties as a result of fault displacement are also expected to center within the fault zones.

Evaluation of Changes in Fault Zone Hydrologic Properties in the UZ—The effects of a given fault displacement on unsaturated zone hydrologic properties could be evaluated using process-level calculations for the effects of the induced stress and strain on fracture geometry. However, this direct approach was not used to specifically evaluate seismic effects because of the large uncertainty in the specification of the seismic event and complexity of translating seismic motion along faults into imposed stresses. An alternative bounding approach that employed two sensitivity studies was used to assess the potential effects of fault displacement on changes in fracture apertures and consequently on fracture hydrologic properties (Appendix I). Two bounding cases were considered. The first case considered changes in fracture aperture over the entire model domain (including faults). The second case, which considers change in fracture properties within the faults only, is directly applicable to this FEP. The results of the second sensitivity study have shown that fracture aperture changes confined to fault zones resulted in virtually no effect on transport behavior in the unsaturated zone (Appendix I, Section I3.3.1). Changes in fault properties would also have little effect on flow above the repository because faults carry about 1% of the flow in this region of the unsaturated zone (SNL 2007 [DIRS 184614], Tables 6.6-1 and 6.6-2). Fault permeabilities are high relative to the predicted flux. Changes in fault properties, other than a very substantial reduction in fault permeability, would not be expected to affect this flow percentage. This is because the percentage of flow in the faults above the repository is related to the fault area at the ground surface available for direct infiltration into faults and lateral flow processes in the unsaturated zone. A substantial reduction in fault permeability would result in flow redirection into more permeable zones near faults and would not have a signifcant effect on water arrival at the repository. A similar conclusion can be reached concerning transient flow between the ground surface and the repository. Any change in transient flow would be limited to the small fraction of flow that moves through faults.

This result is also supported by the parameter sensitivity study for unsaturated zone flow (BSC 2005 [DIRS 174116]) and corresponding effects on radionuclide transport (SNL 2008 [DIRS 184748], Section 6.6.3[b]). For this sensitivity, fracture permeability is varied by one standard deviation, which for the faults is a factor of 14. The sensitivity was conducted for both an increase and decrease in permeability by this factor, with changes to fracture permeability occurring globally over the entire model domain (BSC 2005 [DIRS 174116], Tables 6.2-1 and 6.2-4). The sensitivity calculation is not restricted to faults, but varies all fracture permeabilities

within the unsaturated zone model domain (note that the standard deviations for fracture permeability vary by hydrogeologic unit). The resulting flow fields were analyzed for effects on radionuclide transport. The transport results show that global variations in fracture permeability have only a small effect on transport relative to other uncertainties included in the TSPA (SNL 2008 [DIRS 184748], Section 6.6.3[b]). The effects of fracture permeability in these sensitivities are expected to be overestimated because the effects of changes in capillary strength, which are negatively correlated with permeability (SNL 2007 [DIRS 181244], Section 6.5.1.1), would tend to offset changes in permeability. This is because increased fracture permeability leads to greater flow in fractures, but the associated reduction in capillary strength (represented by an increase in the fracture α), leads to a reduction in fracture flow through enhanced matrix imbibition. This effect may be seen in the response to unsaturated zone flow distributions between fractures, matrix, and faults with changes in fracture α (BSC 2005 [DIRS 174116], Table 6.4-1(c)) and by the effects of changes in fracture α on radionuclide transport (SNL 2008 [DIRS 184748], Figures 6-25[b] and 6-26[b]).

The effects of changes in hydrologic properties of fractures on seepage into repository drifts are reported in *Abstraction of Drift Seepage* (SNL 2007 [DIRS 181244], Sections 6.5.1.1 and 6.8.2). Changes in fracture permeability and capillary strength above a drift as a result of seismic activity are expected to lead to either negligible changes in drift seepage or reduced seepage into drifts (BSC 2004 [DIRS 169864], Section 6.8.4; SNL 2007 [DIRS 181244], Section 6.4.4.1.2). This is a result of the fact that apertures above a drift tend to increase as a result of such a disturbance, and the resulting increase in permeability that permits greater drainage of water around the drift has more influence on seepage than the reduction in capillary strength. The effects of seismic activity on seepage into drifts is addressed in included FEP 1.2.03.02.0D (Seismic-Induced Drift Collapse Alters In-Drift Thermohydrology).

Evaluation of Changes in Fault Zone Hydrologic Properties in the Saturated Zone—As discussed in excluded FEP 1.2.10.01.0A (Hydrologic Response to Seismic Activity), the primary response of regional water levels to seismic events is a transient change (increase or decline) in the water table. The SZ flow and transport model abstraction (SNL 2008 [DIRS 183750], Section 6.5.2.3[a]) uses the flowing interval concept. The flowing interval concept, based on site data, indicates that only some of the fractures within the saturated zone contribute to the flow. Additionally, the saturated zone abstraction produces radionuclide breakthrough curves that implicitly include fracture zones (faults) by considering the horizontal anisotropy in permeability located in the fractured volcanic units downgradient of the repository (SNL 2008 [DIRS 183750], Section 6.5.2.10). The saturated zone abstraction does not explicitly address changes to fracture properties due to changes in stress (SNL 2008 [DIRS 183750], Section 6.5.2). However, the abstraction model includes a wide range of uncertatinty in the groundwater specific discharge multiplier (0.03 to 10), flowing interval spacing (1 m to 417 m), horizontal permeability anisotropy ratio (0.05 to 20), and fracture porosity of the volcanic units (10^{-5} to 0.1) (SNL 2008 [DIRS 183750], Table 6-8). These are factors that could potentially be affected by changes in fracture properties as a result of seismically-induced stress changes. The breadth of the uncertainty included in the model is expected to bound any changes that may result from seismic activity. A sensitivity study considers the effects of the addition of a high-permeability feature to the model (SNL 2008 [DIRS 183750], Section 6.9.3[a]). The feature added to the model is a 6-km long, 100-m wide, 30-m thick high-permeability zone oriented north-south along the transport pathway south of Yucca Mountain. The north-south

orientation is consistent with the approximate strike of major faults in this area (SNL 2008 [DIRS 183750], Section 6.9.3[a]). The permeability assigned to the feature is more than two orders of magnitude larger than the most permeable faults in the base model (SNL 2008 [DIRS 183750], Section 6.9.3[a]; SNL 2007 [DIRS 177391], Table 6-9). The resulting changes in SZ transport behavior was not significant in comparison to the range of transport results representing uncertainties included in the saturated zone abstraction model (SNL 2008 [DIRS 183750], Section 6.9.3[a] and Figure 6-18[a]). Therefore, changes in the hydrologic properties of faults in the saturated zone are of low consequence. Relevant aspects of modeling SZ flow and transport are discussed further in excluded FEP 2.2.06.02.0B (Seismic Activity Changes Porosity and Permeability of Fractures).

In summary, changes in the porosity and permeability of faults as a result of future seismic events will not significantly alter groundwater flow and radionuclide transport in the region of the Yucca Mountain Repository based on the following conclusions:

1. Current fault porosities and permeabilities reflect the effects of a seismically active past within the Yucca Mountain region. Past seismic activity is reflective of major plate extension and caldera formation phases in the Basin and Range Province, which includes the Yucca Mountain region. Seismic activity within the Yucca Mountain region is currently occurring at a reduced level relative to the period of most active extension 10 to 12 million years ago. Consequently, future seismic events are expected to have a relatively low impact on existing fault hydrologic properties.

2. Future seismic events are expected to rupture existing faults, rather than develop new faults.

3. Changes to fault properties (which implicitly affect the fault's hydrologic properties) will tend to occur in a relatively narrow zone, and be on the order of a few meters to, at most, tens of meters wide along the length of the fault. This is of low significance to the mountain-scale flow and transport properties.

4. Changes in fault permeability due to variation in the hydrologic properties of fractures contained within faults result in a negligible effect on radionuclide transport behavior in the unsaturated zone. In addition, the expected increase in fracture permeability and reduction in capillary strength associated with fracture dilation cause by seismic activity either leads to small or reduced seepage into drifts.

5. The uncertainty in the effective hydrologic properties incorporated in the SZ flow and transport model, coupled with uncertainty in specific discharge, overwhelms the changes that would be caused by small movements along existing faults.

Based on the previous discussion, omission of FEP 2.2.06.02.0A (Seismic Activity Changes Porosity and Permeability of Faults) will not result in a significant adverse change in the magnitude or timing of either radiological exposures to the RMEI or radionuclide releases to the accessible environment. Therefore, this FEP is excluded from the performance assessments conducted to demonstrate compliance with proposed 10 CFR 63.311 and 63.321 (70 FR 53313 [DIRS 178394]), and with 10 CFR 63.331 [DIRS 180319], on the basis of low consequence.

INPUTS:

Table 2.2.06.02.0A-1. Direct Inputs

Input	Source	Description
BSC 2004. *Drift Scale THM Model*. [DIRS 169864]	Section 6.8.4	Changes in fracture permeability and capillary strength above a drift as a result of seismic activity are expected to lead to either negligible changes in drift seepage or reduced seepage into drifts
BSC 2005. *Parameter Sensitivity Analysis for Unsaturated Zone Flow*. [DIRS 174116]	Tables 6.2-1, 6.2-4	Sensitivity was conducted for both an increase and decrease in permeability by this factor, with changes to fracture permeability occuring globally over the entire model domain
DTN: MO0401MWDRPSHA.000. Results of the Yucca Mountain Probabilistic Seismic Hazard Analysis (PSHA). [DIRS 185014]	files: *s1.frac_mean* and *s2.frac_mean*	Probability distribution for fault displacement
National Research Council 1992. *Ground Water at Yucca Mountain, How High Can It Rise? Final Report of the Panel on Coupled Hydrologic/Tectonic/Hydrothermal Systems at Yucca Mountain*. [DIRS 105162]	Chapter 2	Plate tectonic activity imparted crustal extension stresses within the Yucca Mountain region during the past 12 million years. Extension rates between 10 and 12 million years ago ranged between 10 and 30 mm/yr
	Chapter 2	Extension rates declined to 5 to 10 mm/yr at 5 Ma; extension rates are still in a declining state
	Chapter 5	Predicted seismic events within the Yucca Mountain region over the next 10,000 years will not alter the large and globally extensive stresses imposed in the rock and in effect over the past 10 to 12 million years
SNL 2007. *Abstraction of Drift Seepage*. [DIRS 181244]	Sections 6.5.1.1, 6.8.2	Studies on the effects of changes in hydrologic properties of fractures on seepage into repository drifts
	Section 6.4.4.1.2	Changes in fracture permeability and capillary strength above a drift as a result of seismic activity are expected to lead to either negligible changes in drift seepage or reduced seepage into drifts
SNL 2007. *UZ Flow Models and Submodels*. [DIRS 184614]	Tables 6.6-1, 6.6-2	Changes in fault properties would also have little effect on flow above the repository because faults carry about 1% of the flow in this region of the unsaturated zone
SNL 2008. *Particle Tracking Model and Abstraction of Transport Processes*. [DIRS 184748]	Figures 6-25[b], 6-26[b]	Effects of changes in fracture on radionuclide transport
	Section 6.6.3[b]	Effects on radionuclide transport
SNL 2008. *Saturated Zone Flow and Transport Model Abstraction*. [DIRS 183750]	Section 6.5.2.10	Radionuclide breakthrough curves
	Section 6.5.2.3[a]	The saturated zone model uses the flowing interval concept

Table 2.2.06.02.0A-2. Indirect Inputs

Citation	Title	DIRS
10 CFR 63	Energy: Disposal of High-Level Radioactive Wastes in a Geologic Repository at Yucca Mountain, Nevada	180319
70 FR 53313	Implementation of a Dose Standard After 10,000 Years	178394
Bates and Jackson 1987	*Glossary of Geology*	164050
BSC 2004	*Drift Scale THM Model*	169864
BSC 2004	*Yucca Mountain Site Description*	169734
CRWMS M&O 1998	*Probabilistic Seismic Hazard Analyses for Fault Displacement and Vibratory Ground Motion at Yucca Mountain, Nevada*	103731
Mongano et al. 1999	*Geology of the ECRB Cross Drift - Exploratory Studies Facility, Yucca Mountain Project, Yucca Mountain, Nevada*	149850
SNL 2007	*Saturated Zone Site-Scale Flow Model*	177391
SNL 2008	*Saturated Zone Flow and Transport Model Abstraction*	183750

FEP: 2.2.06.02.0B

FEP NAME:

Seismic Activity Changes Porosity and Permeability of Fractures

FEP DESCRIPTION:

Seismic activity (fault displacement or vibratory ground motion) has a potential to change stress and strains that alter the permeability along fractures. This could result in reactivation of pre-existing fractures or generation of new fractures, which could significantly change the flow and transport paths, alter or short-circuit the flow paths and flow distributions close to the repository, and/or create new pathways through the repository. These effects may decrease the transport times for potentially released radionuclides.

SCREENING DECISION:

Excluded – low consequence

SCREENING JUSTIFICATION:

Fractures involve a range from small cracks with no displacement, up to and including features with considerable displacement that are typically called faults. The potential for changes in the porosity and permeability of faults due to seismic activity is discussed more specifically in excluded FEP 2.2.06.02.0A (Seismic Activity Changes Porosity and Permeability of Faults). Features considered within this FEP are typically smaller, with little or no displacement, but may be strongly associated with regions of faulting. The spatial relationship between faults and other fracture features is discussed in excluded FEP 2.2.06.02.0A (Seismic Activity Changes Porosity and Permeability of Faults).

Future seismic activity could redistribute strain within the system. Movements produced by a fault displacement will result in changes in the rock stress in the vicinity of the fault. However, the magnitude of the changes in rock stress as a function of distance from the fault depends on the specific details of the fault displacement (e.g., magnitude of fault motion, direction of fault movement, extent of the fault that participates in the movement) and the mechanical properties of the surrounding rock (e.g., fracture spacing, fracture stiffness, geomechanical properties of the rock matrix). Given some change in rock stress, the fractured rock mass will respond to the change in stress through deformation, or strain, in the rock. This induced strain can affect the geometry of fractures in the rock.

This FEP describes the processes by which seismic activity can alter the porosity and permeability of fractures. The potential for formation of new fractures and reactivation of existing fractures is first considered, followed by a consideration of the effects of seismic activity on the hydrologic properties of existing fractures.

Potential for Fracture Reactivation or the Development of New Fractures—Redistribution of strain could open new fractures and close some existing fractures, as discussed by Gauthier et al. (1996 [DIRS 100447], p. 163). Much of this redistribution would be expected to occur within the

fault zones. Although an analysis of fractures was not the primary purpose of the study, the PSHA (CRWMS M&O 1998 [DIRS 103731], p. 8-7) examines the probability of movement along existing fractures and the development of new fractures. The results lead to the conclusion that the development of new fractures, given current geologic conditions and the existing stress field, is not expected and would be of low consequence.

The PSHA (CRWMS M&O 1998 [DIRS 103731], Section 8.2.1, Points 7 and 8 in Table 8-1) examined displacements at specific points along faults, including hypothetical points representing existing small faults, shears, and fractures. The PSHA indicates that for a 10^{-8} annual-exceedance probability, the mean displacement in the intact rock will be less than 0.1 cm (DTN: MO0401MWDRPSHA.000 [DIRS 185014], file: *s7d.frac_mean*; CRWMS M&O 1998 [DIRS 103731], p. 8-7, Point 7d in Table 8-1). Given the current network of small to large displacement fractures with varying apertures and other characteristics, the development of a few more very small displacement (less than 0.1 cm) fractures in presently intact rock will not noticeably affect groundwater flow or radionuclide transport. Therefore, based on the PSHA, the development of new fractures due to seismic activity (and associated fault displacement) is inconsequential, particularly given the existing extensive fracture network. The PSHA also indicates that fractures within the repository area having no measured displacements can be expected to experience on the order of 0.1 to 1 cm of displacement (reactivation) at the 10^{-8} annual-exceedance probability (DTN: MO0401MWDRPSHA.000 [DIRS 185014], files: *s7c.frac_mean* and *s8c.frac_mean*; CRWMS M&O 1998 [DIRS 103731], Figures 8-10 and 8-13 for points 7c and 8c). Thus, the results from the PSHA indicate that movement along existing fractures is expected to be the predominant effect of seismic activity on fractures rather than the development of new fractures.

The small seismic displacement for intact rock, less than 0.1 cm for an annual-exceedance probability of 10^{-8}, corresponds to the level of displacement that occurred as a result of thermal stress in the Drift Scale Test, as measured in multiple-point borehole extensometers (BSC 2004 [DIRS 169864], Figure 7.4.2-2). The simulations of the displacement response in the Drift Scale Test, based on elastic THM processes, were found to be in agreement with measurements. The dominant mode for stress-induced permeability change for THM processes was found to be elastic fracture opening or closing caused by changes in stress normal to the fractures, as opposed to changes in matrix permeability (BSC 2004 [DIRS 169864], Section 8.2). For similar displacements and stresses (as found in the DST) associated with seismic motion, the same conclusions apply to both the unsaturated zone and saturated zone. Therefore, the small seismic displacements in the intact rock matrix will have a negligible effect on rock-matrix hydrologic properties and may be excluded on the basis of low consequence.

Field observations indicate that the rock at Yucca Mountain is highly fractured and that existing fractures and joints have been subject to reactivation (BSC 2004 [DIRS 166107], Section 6.3). Evidence for reactivation of joints includes the presence of thin brecciated zones along cooling joints and observable slip lineations along joint surfaces (Sweetkind et al. 1996 [DIRS 106957]). Cooling joints, formed originally as tensional openings, have only normal displacement, not shear. However, thin selvages of tectonic breccia are locally present along the trace of cooling joints, indicating later slip. Formation of brecciated/gouge zones is discussed in excluded FEPs 2.2.06.01.0A (Seismic Activity Changes Porosity and Permeability of Rock) and 2.2.06.02.0A (Seismic Activity Changes Porosity and Permeability of Faults). Based on these

field observations, the fracture network appears to act as a significant preexisting weakness in the rock mass that can accommodate extensional strain through distributed slip along many reactivated joints. Coupled with the results of the PSHA for movement in the intact rock, it appears that changes in strain are expected to be accommodated through reactivation of existing fractures, rather than through the initiation of new fractures.

Evaluation of Changes in Fracture Hydrologic Properties for Infiltration as a Result of Reactivation—The reactivation of fractures can result in a change in fracture properties. The effects of changes in fracture system properties due to seismic activity on infiltration are negligible because of the high fracture bedrock permeabilities used in the infiltration model (SNL 2008 [DIRS 182145], Section 6.5.2.6). Sensitivity analyses indicate that futher increase in bedrock permeability would also have a negligible effect on infiltration (SNL 2008 [DIRS 182145], Section 7.1.4). Reduction in bedrock permeabilities could only result in decreased net infiltration, which would have no significant adverse effect on repository performance.

Evaluation of Changes in Fracture Hydrologic Properties in the Unsaturated Zone as a Result of Reactivation—The reactivation of fractures can result in a change in fracture properties. The effects of changes in fracture system properties due to seismic activity on mountain-scale flow and radionuclide transport in the unsaturated zone have been investigated using a sensitivity approach (Appendix I). Changes in fracture hydrologic properties were considered in terms of variation in fracture aperture induced by fault displacement. The effects of fracture aperture changes are examined because several fracture hydrologic properties (permeability, capillary pressure, and porosity) are functions of fracture aperture. The sensitivity study was performed (Appendix I) with the nominal UZ three-dimensional flow model using several approaches that together provided bounding cases for determining whether changes in fractures will significantly impact repository performance. The analysis was performed using a dual-permeability active-fracture flow model and was based on fracture aperture changes that could result from changes in strain conditions or other factors. Given a change in fracture aperture, other fracture hydrologic properties (permeability, capillary pressure, and porosity) were estimated using theoretical models (Appendix I). Calculations were then performed for unsaturated flow and transport using the modified fracture properties and the results were compared to the corresponding base case (Section I3.3). The sensitivity study (Appendix I) included two bounding cases: (1) uniform change in fracture properties throughout the UZ flow model domain and (2) change in fracture properties within the faults only. The first bounding case is particularly applicable to this FEP; the latter case is directly applicable to and is discussed in excluded FEP 2.2.06.02.0A (Seismic Activity Changes Porosity and Permeability of Faults). The two bounding cases were chosen to bound a range of fracture-aperture changes resulting from fault movement. No direct observations for Yucca Mountain relate stress caused by fault displacement to strain and the resultant changes in fracture aperture (Appendix I).

A potential upper bound for the sensitivity analysis lies in the estimated fracture aperture. A maximum ten-fold increase in fracture aperture was selected as the model's upper-bound value. The justification for this treatment (Appendix I) cites distance-strain relationships derived from models for a 1-m displacement along a strike-slip fault at Yucca Mountain, and for a 1-m displacement on a theoretical normal fault. The changes in fracture apertures for the sensitivity analysis were derived presuming a 10-m fault movement along the Solitario Canyon fault and

multiplying the strains cited in the justification for the 1-m faults. The potential upper bound is mentioned here, primarily because the presumed 10-m displacement, although a mean value, is greater than the probabilistically determined (median and 85th quantile) and observed fault displacements. The results of the PSHA (DTN: MO0401MWDRPSHA.000 [DIRS 185014], files: *s2.frac_mean*; CRWMS M&O 1998 [DIRS 103731], Figure 8-3) indicate that, for the Solitario Canyon fault, there is a large uncertainty range in the potential displacements from 3 m (the median value) to approximately 10 m (the 85th quantilevalue) at the 10^{-8} annual-exceedance probability. By contrast, the maximum measured single-event Quaternary displacement (i.e., during the past 1.6 million years) on the Solitario Canyon fault is only 1.3 m (Ramelli et al. 1996 [DIRS 101106], Table 4.7.3). Therefore, the sensitivity analysis parameterization bounds potential changes in fracture aperture that could result from any fault displacement at Yucca Mountain with an annual exceedance probability greater than 10^{-8}.

The results of geomechanical models used to investigate the amount of strain induced by fault movements in the rock at Yucca Mountain suggest that a factor of 10 change in facture aperture would bound the effects of tensile strain from such a fault movement (Appendix I, Section I3.2.4). Based on the cubic law for fracture permeability, a factor of 10 change in aperture leads to a factor of 1,000 change in permeability. Fracture permeabilities reduced by a factor of 1,000 were found to be inconsistent with the infiltration rates imposed on the model, because the bulk permeability was insufficient to accommodate the flow conditions. So, either reduced infiltration rates or a smaller reduction factor for the aperture would need to be used. Because the reduced apertures lead to reduced transport rates, this sensitivity does not show a potential adverse impact on performance. Therefore, a case with a reduction in aperture of a factor of 0.2 is considered sufficient.

The results of the sensitivity study have shown that fracture aperture changes confined to fault zones resulted in virtually no effect on transport behavior in the unsaturated zone (Appendix I, Section I3.3.1) and that increased fracture aperture applied over the entire unsaturated zone domain results in effects that are no more significant than other uncertainties related to infiltration that are included in the TSPA (Appendix I, Section I4).

This result is also supported by the parameter sensitivity study for unsaturated zone flow (BSC 2005 [DIRS 174116]) and corresponding effects on radionuclide transport (SNL 2008 [DIRS 184748], Section 6.6.3[b]). For this sensitivity, fracture permeability is varied by one standard deviation. The sensitivity was conducted for both an increase and decrease in permeability by this factor, with changes to fracture permeability occurring globally over the entire model domain (BSC 2005 [DIRS 174116], Tables 6.2-1 and 6.2-4). The resulting flow fields were analyzed for effects on radionuclide transport. The transport results show that global variations in fracture permeability have only a small effect on transport relative to other uncertainties (SNL 2008 [DIRS 184748], Section 6.6.3[b]). The effects of fracture permeability in these sensitivities are expected to be overestimated because the effects of changes in capillary strength, which are negatively correlated with permeability (SNL 2007 [DIRS 181244], Section 6.5.1.1), would tend to offset changes in permeability. This is because increased fracture permeability leads to greater flow in fractures, but the associated reduction in capillary strength (represented by an increase in the fracture α), leads to a reduction in fracture flow through enhanced matrix imbibition. This effect may be seen in the response to unsaturated zone flow distributions between fractures, matrix, and faults with changes in fracture α (BSC 2005

[DIRS 174116], Table 6.4-1 (c)) and by the effects of changes in fracture α on radionuclide transport (SNL 2008 [DIRS 184748], Figures 6-25[b] and 6-26[b]).

Evaluation of Changes in Fracture Hydrologic Properties in the Saturated Zone as a Result of Reactivation—The primary response of regional water levels to seismic events, as discussed in excluded FEP 1.2.10.01.0A (Hydrologic Response to Seismic Activity), is a transient change (increase or decline) in the water table. Flow and transport in the saturated zone is dominated by fault orientation and existing fractures, fracture clusters, and fracture spacing, collectively labeled as flowing intervals in the SZ flow and transport model (SNL 2008 [DIRS 183750], Section 6.5.2.4). This model (SNL 2008 [DIRS 183750], Section 6.5.2.4) uses the flowing intervals concept, which is based on site data and indicates that only some of the fractures within the saturated zone contribute to the flow. Additionally, the SZ flow and transport model abstraction produces radionuclide breakthrough curves that implicitly include fracture zones in the nominal case by considering the horizontal anisotropy in permeability located in the fractured volcanic units downgradient of the repository (SNL 2008 [DIRS 183750], Section 6.5.2.10).

The saturated zone model does not explicitly address changes to fracture or fault properties due to changes in stress. Rather, the model evaluates uncertainties assigned to flowing interval properties.

The uncertainty in the effective hydrologic properties incorporated in the SZ flow and transport model (SNL 2008 [DIRS 183750], Table 6-8), which reflects the cumulative changes in hydrologic properties since deposition, coupled with the scale of the model, overwhelms the changes in fracture properties, and their effects on flow paths and transport times, that would be caused by future seismic events. The SZ flow and transport model evaluates uncertainties, such as horizontal anisotropy in permeability, flowing interval spacing, flowing interval porosity in the volcanic units, and longitudinal dispersion (SNL 2008 [DIRS 183750], Table 6-8). Transport times through the saturated zone are sensitive to uncertainty in the specific discharge scaling parameter and flowing interval spacing. The uncertainty incorporated in the horizontal anisotropy (which accounts for the uncertainty in maximum and minimum in situ stresses imposed on fractures and faults) results in transport paths varying by several kilometers (SNL 2008 [DIRS 183750], Figure 6-6). Thus, the scale of the SZ flow and transport model, together with incorporated parameter uncertainties used for the analysis, overwhelms any potential changes in the hydrologic properties of fractures associated with future seismic activity. Therefore, the effects of changes in the hydrologic properties of fractures on groundwater flow and radionuclide transport in the saturated zone are excluded based on low consequence.

Furthermore, existing regional stresses imposed on fracture hydrologic properties reflect the crustal extension stresses in effect today. A fracture's physical properties (orientation, length, connectivity, and clustering) are reflective of a cumulative response to seismic events in existence in the last 10 to 12 million years. A change in regional fracture properties, given predicted seismic activity, will be minimal relative to the multiple seismic events imposed on the region over this period. Therefore, it is inferred that regional fracture hydrologic properties will not be significantly altered from current conditions by future seismic activity. As a result, effects of changes in fracture hydrologic properties, resulting from seismic activity, are excluded based on low consequence.

In summary, the effect of future seismic events on the porosity and permeability of fractures will not significantly alter flow and transport in the region of the Yucca Mountain repository. Reactivation of existing fractures is expected to be the main result of seismic activity rather than the opening of new fractures such that any new fractures formed would have a negligible effect on hydrologic or transport properties. The effects of changing the size of fracture apertures on the hydrologic properties of fractures and hence, on groundwater flow and radionuclide transport in the unsaturated zone, are small in comparison with the uncertainty in unsaturated zone flow and transport related to infiltration that is incorporated in the TSPA. Similarly, the uncertainty in hydrologic properties incorporated in the SZ flow and transport model are large in comparison with any changes in fracture hydrologic properties resulting from seismic activity.

Based on the previous discussion, omission of FEP 2.2.06.02.0B (Seismic Activity Changes Porosity and Permeability of Fractures) will not result in a significant adverse change in the magnitude or timing of either radiological exposure to the RMEI or radionuclide releases to the accessible environment. Therefore, this FEP is excluded from the performance assessments conducted to demonstrate compliance with proposed 10 CFR 63.311 and 63.321 (70 FR 53313 [DIRS 178394]), and with 10 CFR 63.331 [DIRS 180319], on the basis of low consequence.

INPUTS:

Table 2.2.06.02.0B-1. Direct Inputs

Input	Source	Description
BSC 2004. *Drift Scale THM Model*. [DIRS 169864]	Section 8.2	The dominant mode for stress-induced permeability change for THM processes was found to be elastic fracture opening or closing caused by changes in stress normal to the fractures, as opposed to changes in matrix permeability
BSC 2005. *Parameter Sensitivity Analysis for Unsaturated Zone Flow*. [DIRS 174116]	Table 6.4-1 (c)	Unsaturated zone flow distributions between fractures
DTN: MO0401MWDRPSHA.000. Results of the Yucca Mountain Probabilistic Seismic Hazard Analysis (PSHA). [DIRS 185014]	file: *s2.frac_mean*	for the Solitario Canyon fault, there is a large uncertainty range in the potential displacements from 3 m (the median value) to approximately 10 m (the 85th quantile value) at the 10^{-8} annual exceedance probability
	files: *s7c.frac_mean* and *s8c.frac_mean*	fractures within the repository area having no measured displacements can be expected to experience on the order of 0.1 to 1 cm of displacement (reactivation) at the 10^{-8} annual exceedance probability
	file: *s7d.frac_mean*	For a 10^{-8} annual-exceedance probability, the mean displacement in the intact rock will be less than 0.1 cm
SNL 2007. *Abstraction of Drift Seepage*. [DIRS 181244]	Section 6.5.1.1	Effect of changes in capillary strength

Table 2.2.06.02.0B-1. Direct Inputs (Continued)

Input	Source	Description
SNL 2008. *Particle Tracking Model and Abstraction of Transport Processes*. [DIRS 184748]	Section 6.6.3[b], Figures 6-25[b] and 6-26[b]	Radionuclide transport
SNL 2008. *Saturated Zone Flow and Transport Model Abstraction*. [DIRS 183750]	Section 6.5.2.10, Table 6-8, Figure 6-6	Flow and transport in the saturated zone
SNL 2008. *Simulation of Net Infiltration for Present-Day and Potential Future Climates*. [DIRS 182145]	Sections 6.5.2.6, 7.1.4	Sensitivity analyses indicate that futher increase in bedrock permeability would have a negligible effect on infiltration

Table 2.2.06.02.0B-2. Indirect Inputs

Citation	Title	DIRS
10 CFR 63	Energy: Disposal of High-Level Radioactive Wastes in a Geologic Repository at Yucca Mountain, Nevada	180319
70 FR 53313	Implementation of a Dose Standard After 10,000 Years	178394
BSC 2004	*Drift Degradation Analysis*	166107
BSC 2004	*Drift Scale THM Model*	169864
BSC 2005	*Parameter Sensitivity Analysis for Unsaturated Zone Flow*	174116
CRWMS M&O 1998	*Probabilistic Seismic Hazard Analyses for Fault Displacement and Vibratory Ground Motion at Yucca Mountain, Nevada*	103731
Gauthier et al. 1996	"Impacts of Seismic Activity on Long-Term Repository Performance at Yucca Mountain"	100447
Ramelli et al. 1996	"Quaternary Faulting on the Solitario Canyon Fault"	101106
Sweetkind et al. 1996	"Interaction Between Faults and the Fracture Network at Yucca Mountain, Nevada"	106957

FEP: 2.2.06.03.0A

FEP NAME:

Seismic Activity Alters Perched Water Zones

FEP DESCRIPTION:

Strain caused by stress changes from tectonic or seismic events could alter the rock permeabilities that allow formation and persistence of perched-water zones.

SCREENING DECISION:

Excluded – low consequence

SCREENING JUSTIFICATION:

A change in stress due to seismic activity has the potential to result in strains that affect groundwater flow and radionuclide transport properties, leading to increased or decreased dose. The question raised by this FEP is whether seismic activity and any associated changes in rock permeabilities could affect the formation and persistence of perched water. Perched water has only been found at Yucca Mountain near the TSw–CHn interface. In particular, the presence of perched water appears to be correlated with the presence of zeolitically altered minerals within the Calico Hills nonwelded unit (CHn) (SNL 2007 [DIRS 184614], Section 6.2.2.2). The presence of perched water appears to be a function of the lithology and local percolation flux. Seismic effects on permeability are discussed in excluded FEPs 2.2.06.01.0A (Seismic Activity Changes Porosity and Permeability of Rock), 2.2.06.02.0A (Seismic Activity Changes Porosity and Permeability of Faults), and 2.2.06.02.0B (Seismic Activity Changes Porosity and Permeability of Fractures). Zeolitic alteration is found primarily in the basal vitrophyre of the TSw, CHn, Prow Pass, and Bullfrog units (BSC 2004 [DIRS 170031], Section 6.2.2). The observed relationship of the vitric-zeolitic tuff contact and other stratigraphic contacts of vocanic units indicates that zeolitization occurred prior to uplift and rotation (Broxton et al. 1987 [DIRS 102004], p. 101). The timing of eruptions between 11.3 and 12.5 million years ago constrain the timing of uplift and rotation, leading to the conclusion that zeolitization occurred at least 11.3 million years ago (Broxton et al. 1987 [DIRS 102004], p. 101). This result is consistent with petrofabric constraints on the age of zeolitic alteration (Bish et al. 1984 [DIRS 106336], p. 72). Therefore, any effects of tectonic or seismic processes on the lithologic units associated with perched water should have already occurred. The process of zeolitic alteration occurs when the original volcanic glass dissolves and zeolites precipitate at ambient temperatures in a water-rich environment, and therefore is independent of seismic activity (BSC 2004 [DIRS 169734], Section 3.3.4.6). The fact that perched water occurrence is strongly correlated with zeolitic lithology indicates that the effects of seismic and tectonic processes do not play a significant role in the formation and persistence of perched water.

The concept that normal displacement along west-dipping faults on the east flank of Yucca Mountain could cause perching of water if fault displacement has created permeability contrasts on opposite sides of a fault was discussed by Montazer and Wilson (1984 [DIRS 100161], Figure 14, pp. 47 to 48). Given the declining extension rates and seismic activity described in

excluded FEP 2.2.06.02.0A (Seismic Activity Changes Porosity and Permeability of Faults), the existing contribution of permeability barriers at faults to perching of water should not be significantly changed by future fault displacement in response to tectonic or seismic events.

Based on the previous discussion, omission of FEP 2.2.06.03.0A (Seismic Activity Alters Perched Water Zones) will not result in a significant adverse change in the magnitude or timing of either radiological exposure to the RMEI or radionuclide releases to the accessible environment. Therefore, this FEP is excluded from the performance assessments conducted to demonstrate compliance with proposed 10 CFR 63.311 and 63.321 (70 FR 53313 [DIRS 178394]), and with 10 CFR 63.331 [DIRS 180319], on the basis of low consequence.

INPUTS:

Table 2.2.06.03.0A-1. Direct Inputs

Input	Source	Description
Broxton, et al. 1987. "Distribution and Chemistry of Diagenetic Minerals at Yucca Mountain, Nye County, Nevada." [DIRS 102004]	p. 101	Most of the zeolitic deposits at Yucca Mountain formed between 11.3 and 13.9 million years ago, and were largely contemporaneous with the most active period of silicic volcanism within the southwest Nevada volcanic field
SNL 2007. *UZ Flow Models and Submodels*. [DIRS 184614]	Section 6.6.2.2	The presence of perched water appears to be correlated with the presence of zeolitically altered minerals within the Calico Hills nonwelded

Table 2.2.06.03.0A-2. Indirect Inputs

Citation	Title	DIRS
10 CFR 63	Energy: Disposal of High-Level Radioactive Wastes in a Geologic Repository at Yucca Mountain, Nevada	180319
70 FR 53313	Implementation of a Dose Standard After 10,000 Years	178394
Bish et al. 1984	“Petrofabric Constraints of the Age of Zeolitization at Yucca Mountain"	106336
BSC 2004	*Mineralogic Model (MM3.0) Report*	170031
BSC 2004	*Yucca Mountain Site Description*	169734
Montazer and Wilson 1984	*Conceptual Hydrologic Model of Flow in the Unsaturated Zone, Yucca Mountain, Nevada*	100161

FEP: 2.2.06.04.0A

FEP NAME:

Effects of Subsidence

FEP DESCRIPTION:

Subsidence above the mined underground facility or other openings may affect the properties of the overlying rocks and surface topography. Changes in rock properties, such as enhanced permeability, may alter flow paths from the surface to the repository. Changes in surface topography may alter run-off and infiltration, and may perhaps create impoundments.

SCREENING DECISION:

Excluded – low consequence

SCREENING JUSTIFICATION:

Subsidence can occur as a result of underground excavations. Subsidence calculations for Yucca Mountain were done as the first step in the analysis of drift-scale thermal-hydrological-mechanical effects (BSC 2004 [DIRS 169864]). The model domain extends upward to the ground surface (BSC 2004 [DIRS 169864], Tables 4.1-3c and 4.1-3d). The simulation was conducted by first excavating the drift and then implementing a thermal line load into the drift opening (BSC 2004 [DIRS 169864], Sections 6.5.1 and 6.6). Subsidence data at the drift crown and at the ground surface directly above the drift were extracted from model results in DTNs: LB0306DRSCLTHM.001 [DIRS 169733] (files: *Fmn1_0.sav* and *Fll1_0.sav*) and LB0308DRSCLTHM.001 [DIRS 171567] (file: *Fll1c1_001y.sav*), and have been entered in a scientific notebook (Rutqvist 2006 [DIRS 183044], pp. 38 and 39). These results show that the simulated subsidence from excavation of a single drift, without input of heat, is greater at the drift crown than at the ground surface. The maximum subsidence in the absence of drift collapse predicted was 1.4 cm at the drift crown and 0.07 cm at the ground surface, for a drift in Tptpll low-quality rock. In the case of drift collapse, displacements of 8 to 12 cm were found about 12 m above the drift center, showing a trend of decreasing displacements with increasing distance from the drift (BSC 2004 [DIRS 166107], Figures V-1, V-5, and V-7). These calculated subsidence distances would be indistinguishable from natural variations in the ground surface, are far smaller than the absolute elevation uncertainty (7 m) in the model describing infiltration at Yucca Mountain (SNL 2008 [DIRS 182145], Section 6.5.2.1[a]), and are too small to affect run-off or infiltration, or to create impoundments. Based on these considerations, subsidence is expected to have a negligible impact on large-scale groundwater flow in the unsaturated zone, and on surface topography.

Brady and Brown (1985 [DIRS 126811], Figure 16.18) present an empirical correlation for the ratio of the maximum subsidence, S, to the extraction thickness, m (height of the opening), as a function of the width, w, of a rectangular opening and the depth of the opening below the ground surface, d. A circular drift, being smaller, will cause less subsidence than a rectangular opening; that is, the empirical correlation represents an upper bound. For repository drifts, $w = m = 5.5$ m and $d = 300$ m. For this combination of variables, the maximum subsidence is off the chart on

the low side; that is, *S/m* is substantially below the lowest curve presented at a value of 0.05, which corresponds to a value of *S* that is substantially below 27.5 cm.

Corroborative evidence comes from mining experience. In coal mining, subsidence has been found to occur when more than 50% of the coal bed was removed (Keller 1992 [DIRS 146831], p. 142). In the case of Yucca Mountain, the percentage of earth removal is very small. The emplacement drift diameter (5.5 m) is less than 10% of the drift spacing of 81 m between center lines (SNL 2007 [DIRS 179466], Table 4-1, Parameter Numbers 01-10 and 01-13). The effects of changes to fracture characteristics around emplacement drifts caused by stress relief have been found to be small to moderate and to have no adverse effects on seepage (BSC 2004 [DIRS 169864], Section 8.1; BSC 2004 [DIRS 167652], Section 6.6.3). Effects on permeability further from the drift have been shown to decrease (BSC 2004 [DIRS 169864], Figures 6.5.1-1 and 6.6.1-1).

Based on the previous discussion, omission of FEP 2.2.06.04.0A (Effects of Subsidence) will not result in a significant adverse change in the magnitude or timing of either radiological exposures to the RMEI or radionuclide releases to the accessible environment. Therefore, this FEP is excluded from the performance assessments conducted to demonstrate compliance with proposed 10 CFR 63.311 and 63.321 (70 FR 53313 [DIRS 178394]), and with 10 CFR 63.331 [DIRS 180319], on the basis of low consequence.

INPUTS:

Table 2.2.06.04.0A-1. Direct Inputs

Input	Source	Description
BSC 2004. *Drift Degradation Analysis*. [DIRS 166107]	Figures V-1, V-5, V-7	Displacements of 8 to 12 cm were found about 12 m above the drift center, showing a trend of decreasing displacements with increasing distance from the drift
BSC 2004. *Drift Scale THM Model*. [DIRS 169864]	Figures 6.5.1-1, 6.6.1-1	Effects of stress relief on permeability further from the drift have been shown to decrease
	Section 8.1	Effects of subsidence on fracture characterization and drift seepage
BSC 2004. *Seepage Model for PA Including Drift Collapse*. [DIRS 167652]	Section 6.6.3	The effects of changes to fracture characteristics around emplacement drifts caused by stress relief have been found to be small to moderate and to have no adverse effects on seepage
DTN: LB0306DRSCLTHM.001. Drift Scale THM Model Predictions: Simulations. [DIRS 169733]	files: *Fmn1_0.sav*, *Fll1_0.sav*	Subsidence calculations for drift in Tptpmn and Tptpll
DTN: LB0308DRSCLTHM.001. Drift Scale THM Model Predictions for Poor Quality Rock in Tptpll: Simulations. [DIRS 171567]	file: *Fll1c1_001y.sav*	Subsidence calculations for drift in Tptpll low-quality rock

Table 2.2.06.04.0A-1. Direct Inputs (Continued)

Input	Source	Description
SNL 2007. *Total System Performance Assessment Data Input Package for Requirements Analysis for Subsurface Facilities*. [DIRS 179466]	Table 4-1, Parameter Numbers 01-10 and 01-13	The emplacement drift diameter (5.5 m) is less than 10% of the drift spacing of 81 m between center lines
SNL 2008. *Simulation of Net Infiltration for Present-Day and Potential Future Climates*. [DIRS 182145]	Section 6.5.2.1[a]	Elevation uncertainty (7 m) in the model describing infiltration at Yucca Mountain

Table 2.2.06.04.0A-2. Indirect Inputs

Citation	Title	DIRS
10 CFR 63	Energy: Disposal of High-Level Radioactive Wastes in a Geologic Repository at Yucca Mountain, Nevada	180319
70 FR 53313	Implementation of a Dose Standard After 10,000 Years	178394
Brady and Brown 1985	*Rock Mechanics for Underground Mining*	126811
BSC 2004	*Drift Scale THM Model*	169864
Keller 1992	*Environmental Geology*	146831
Rutqvist 2006	MP-LBNL-JR-3, UZ AMRs for SR - Thermal-Hydrological-Mechanical Effects [final closure]. Scientific Notebook SN-LBNL-SCI-204-V3.	183044

FEP: 2.2.06.05.0A

FEP NAME:

Salt Creep

FEP DESCRIPTION:

Salt creep may lead to changes in the stress field, compaction of the waste packages, and consolidation of the long-term components of the sealing system.

SCREENING DECISION:

Excluded – low consequence

SCREENING JUSTIFICATION:

Salt creep is the continuous deformation of a salt formation as a response to an applied stress such as overburden pressure. Yucca Mountain is located in the southwestern Nevada volcanic field and consists of tilted fault blocks composed of layered sequences of ash flow, ash-fall, carbonates, and bedded tuffs of Miocene age (BSC 2004 [DIRS 170029], Sections 6 and 6.5, and Table 6-2; SNL 2007 [DIRS 174109], Sections 6.3 and 6.4, Table 6-2; BSC 2004 [DIRS 169734], Section 3.3.4; Day et al. 1998 [DIRS 100027]). Salt or evaporite deposits of sufficient volume to result in significant salt creep have not been reported to exist near Yucca Mountain. Any sizable deposit would be evident in well logs or high sodium or chloride measurements in groundwater. Measured sodium levels at the saturated zone site scale flow model range from 30 to 200 mg/L (SNL 2007 [DIRS 177391], Section A6.3.4.9) and measured chloride ranges from 3 to 125 mg/L (SNL 2007 [DIRS 177391], section A6.3.4.2). By comparison, at the Waste Isolation Pilot Plant site in Carlsbad, NM, sodium concentrations in the Rustler/Culebra dolomite (non-sodium) formation range from 54 mg/L to 63,000 mg/L with most wells containing more than 10,000 mg/L (Siegel et al. 1991 [DIRS 183944], Figure 1-8) reflecting dissolution of the underlying Salado (halite) formation and contamination of wells throughout the area. Thus, the presence of any sizable salt formation would be noticed in well logs or high sodium or chloride concentrations in wells.

The repository is not planned to be developed in a salt dome or cavern, and the related process of lithologic flow is therefore not relevant to the geologic setting for Yucca Mountain. Any salt formations in the area would necessarily be either too small or so far away as too not be of significance to flow and transport in the repository area, and there are no rocks in the repository that are sufficiently plastic to creep in a manner similar to salt.

Based on the previous discussion, omission of FEP 2.2.06.05.0A (Salt Creep) will not result in a significant adverse change in the magnitude or timing of either radiological exposure to the RMEI or radionuclide releases to the accessible environment. Therefore, this FEP is excluded from the performance assessments conducted to demonstrate compliance with proposed 10 CFR 63.311 and 63.321 (70 FR 53313 [DIRS 178394]), and with 10 CFR 63.331 [DIRS 180319], on the basis of low consequence.

INPUTS:

Table 2.2.06.05.0A-1. Direct Inputs

Input	Source	Description
SNL 2007. *Saturated Zone Site-Scale Flow Model*. [DIRS 177391]	Section A6.3.4.2	Measured chloride levels at the saturated zone site scale flow model ranges from 3 to 125 mg/L
	Section A6.3.4.9	Measured sodium levels at the saturated zone site scale flow model ranges from 30 to 200 mg/L

Table 2.2.06.05.0A-2. Indirect Inputs

Citation	Title	DIRS
10 CFR 63	Energy: Disposal of High-Level Radioactive Wastes in a Geologic Repository at Yucca Mountain, Nevada	180319
70 FR 53313	Implementation of a Dose Standard After 10,000 Years	178394
BSC 2004	*Geologic Framework Model (GFM2000)*	170029
BSC 2004	*Yucca Mountain Site Description*	169734
Day et al. 1998	*Bedrock Geologic Map of the Yucca Mountain Area, Nye County, Nevada*	100027
Siegel et al. 1991	*Hydrogeochemical Studies of the Rustler Formation and Related Rocks in the Waste Isolation Pilot Plant Area, Southeastern New Mexico*	183944
SNL 2007	*Hydrogeologic Framework Model for the Saturated Zone Site Scale Flow and Transport Model*	174109

FEP: 2.2.07.01.0A

FEP NAME:

Locally Saturated Flow at Bedrock/Alluvium Contact

FEP DESCRIPTION:

In arid areas and particularly in areas with shallow soils, infiltration can descend to the alluvium/bedrock interface and then proceed along that interface as a saturated flow system distinct from the surface water flow and distinct from the local water table. This phenomenon usually requires that the permeability of the bedrock be considerably less than that of the overlying soils.

SCREENING DECISION:

Excluded – Low consequence

SCREENING JUSTIFICATION:

The phenomenon of infiltration resulting in a saturated condition at the bedrock–alluvium contact, with water then either infiltrating into fractures or contributing to lateral drainage, is also referred to as interflow. This term refers to the lateral flow of liquid water in the unsaturated zone that can occur during and following precipitation events. This flow is driven by a lateral head gradient component, which is typically the result of a sloping bedrock surface (SNL 2008 [DIRS 182145], Section 5.1[a]).

Interflow is an excluded process on the basis of low consequence for the following reasons. First, most of the infiltration model domain is characterized by relatively low slopes. For example, the median slope for the infiltration model domain is approximately 10 degrees from horizontal and 90% of the domain has a slope less than 25 degrees. The lower the slope, the less the lateral head gradient (SNL 2008 [DIRS 182145], Section 5.1[a]). Second, bulk bedrock saturated hydraulic conductivity values are generally higher than the saturated hydraulic conductivity values in the overlying soil (SNL 2008 [DIRS 182145], Section 6.5.2.6), and therefore once water reaches the soil–bedrock interface, it would tend to enter bedrock instead of flowing laterally along the interface.

Observations also support this justification. For example, if significant interflow were occurring in the area of Yucca Mountain, one would expect that stream flows would continue for several days following large precipitation events, seeps would form at the toes of slopes, and mass wasting would occur when thin soils on steep slopes became saturated. None of these indicators of significant interflow characterize the site. Stream flows observed in the washes draining from Yucca Mountain tend to persist only as long as the significant precipitation events events that cause them (SNL 2008 [DIRS 182145], Section 7.1.3), seeps have only been described for areas tens of kilometers away from Yucca Mountain (BSC 2004 [DIRS 169734], Section 5.2.2.3), and recent mass wasting (debris flows) are rarely documented, such as that documented following a July 1984 storm (BSC 2004 [DIRS 169734], Section 3.4.6.4).

In areas that have low bedrock permeability, if the soil becomes completely saturated, then surface runoff will occur, which is described in included FEP 2.3.11.02.0A (Surface Runoff and Evapotranspiration). In areas that have low bedrock permeability, interflow can occur, but this flow is limited by the lateral permeability of the over-lying soil, and this layer of water is subject to depletion by evapotranspiration if the depth to bedrock is less than or equal to the rooting depth (SNL 2008 [DIRS 182145], Section 6.3.3). If interflow occurs in certain areas, as a result of low bedrock permeability, and subsequent increased net infiltration in down-gradient areas of the interflow with high bedrock permeability, this increased localized net infiltration will have an insignificant effect on seepage, as a result of the damping and homogenizing of downward-moving transient pulses by the Paintbrush nonwelded hydrogeologic unit (SNL 2007 [DIRS 184614], Section 6.1.2).

Based on the previous discussion, omission of FEP 2.2.07.01.0A (Locally Saturated Flow at Bedrock/Alluvium Contact) will not result in a significant adverse change in the magnitude or timing of either radiological exposure to the RMEI or radionuclide releases to the accessible environment. Therefore, this FEP is excluded from the performance assessments conducted to demonstrate compliance with proposed 10 CFR 63.311 and 63.321 (70 FR 53313 [DIRS 178394]), and with 10 CFR 63.331 [DIRS 180319], on the basis of low consequence.

INPUTS:

Table 2.2.07.01.0A-1. Direct Inputs

Input	Source	Description
SNL 2007. *UZ Flow Models and Submodels*. [DIRS 184614]	Section 6.1.2	Damping effect of Ptn layer in UZ model
SNL 2008. *Simulation of Net Infiltration for Present-Day and Potential Future Climates*. [DIRS 182145]	Section 6.5.2.6	Bulk bedrock conductivity values

Table 2.2.07.01.0A-2. Indirect Inputs

Citation	Title	DIRS
10 CFR 63	Energy: Disposal of High-Level Radioactive Wastes in a Geologic Repository at Yucca Mountain, Nevada	180319
70 FR 53313	Implementation of a Dose Standard After 10,000 Years	178394
BSC 2004	*Yucca Mountain Site Description*	169734
SNL 2008	*Simulation of Net Infiltration for Present-Day and Potential Future Climates*	182145

FEP: 2.2.07.02.0A

FEP NAME:

Unsaturated Groundwater Flow in the Geosphere

FEP DESCRIPTION:

Groundwater flow occurs in unsaturated rocks in most locations above the water table at Yucca Mountain, including at the location of the repository. See related FEPs for discussions of specific issues related to unsaturated flow.

SCREENING DECISION:

Included

TSPA DISPOSITION:

This FEP is included in the unsaturated zone process models for mountain-scale flow, radionuclide transport, drift seepage, and seepage chemistry. The mountain-scale flow model is for three-dimensional, steady flow in a heterogeneous dual-permeability system that includes discrete fault zones (SNL 2007 [DIRS 184614], Sections 6.1, 6.2, and 6.6). Flow fields generated by the UZ flow model are included in the TSPA via the abstractions for drift seepage (SNL 2007 [DIRS 181244], Section 6.6.5.1 and Table 4-1[a]) and radionuclide transport simulations (SNL 2008 [DIRS 184748], Addendum Section 6.5.1).

Parameter values needed to describe unsaturated flow are developed in several reports. Data input for model calibration is developed in *Analysis of Hydrologic Properties Data* (BSC 2004 [DIRS 170038], Section 6). The van Genuchten α and m parameter values, respectively for the saturation–capillary pressure and relative permeability functions, and the active-fracture parameter γ value for each model layer of the fracture and matrix continua are developed in *Calibrated Unsaturated Zone Properties* (SNL 2007 [DIRS 179545], Section 6.3). Further calibration of the parameters using the three-dimensional site-scale flow model is presented in *UZ Flow Models and Submodels* (SNL 2007 [DIRS 184614], Section 6.2). The active fracture model is described and validated in *Conceptual Model and Numerical Approaches for UZ Flow and Transport* (BSC 2004 [DIRS 170035], Sections 6.3.7 and 7). TSPA implementation for the UZ flow parameters is described in *UZ Flow Models and Submodels* (SNL 2007 [DIRS 184614], Sections 6.8, 8.6, and 8.8).

Unsaturated groundwater flow in the unsaturated zone is the driving force for radionuclide transport through the unsaturated zone. This FEP is addressed through the use of unsaturated zone flow fields (DTNs: LB0612PDFEHMFF.001 [DIRS 179296], LB0701MOFEHMFF.001 [DIRS 179297], LB0701GTFEHMFF.001 [DIRS 179160], and LB0702PAFEM10K.002 [DIRS 179507]) in TSPA multirealization simulations, as described in *Particle Tracking Model and Abstraction of Transport Processes* (SNL 2008 [DIRS 184748], Addendum Section 6.5.1). Local radionuclide transport velocities in the rock matrix and fractures are computed using the water flux and saturations provided by the UZ flow model (SNL 2008 [DIRS 184748], Addendum Section C1). This includes advective velocities within the fracture continuum and

matrix continuum, as well as advective velocities between the fracture and matrix continua (SNL 2008 [DIRS 184748], Addendum Section 6.4.3).

Seepage-relevant parameters for the drift-scale seepage model are based on measurements reported in *In Situ Field Testing of Processes* (BSC 2004 [DIRS 170004, Sections 6.1 and 6.2) and developed in *Seepage Calibration Model and Seepage Testing Data* (BSC 2004 [DIRS 171764], Sections 6.6.3.2 and 6.6.3.3). Unsaturated flow processes are accounted for in the seepage abstraction by using results from process models that account for various relevant aspects of unsaturated groundwater flow. All the seepage process models that feed into seepage abstraction simulate groundwater flow processes in unsaturated rock (SNL 2007 [DIRS 181244], Section 6.4). Percolation flux distributions are provided to the seepage abstraction model by the UZ flow model (SNL 2007 [DIRS 184614], Section 6.6.2.4), which accounts for groundwater flow on a larger scale than is treated by the drift-scale seepage model, influenced by climate changes, infiltration variability, and stratigraphy effects. For ambient seepage, the fracture flow processes in the drift vicinity and the resulting seepage rates are predicted by model simulations from the seepage model for performance assessment (BSC 2004 [DIRS 167652], Sections 6.2.1 and 6.6), and abstracted in *Abstraction of Drift Seepage* (SNL 2007 [DIRS 181244], Section 6.4.2). Results are available as lookup tables in DTNs: LB0702PASEEP01.001 [DIRS 179511] and LB0702PASEEP02.001 [DIRS 181635]. These are used in the TSPA model to calculate ambient seepage, by sampling parameter cases of seepage-relevant parameters from the probability distributions defined in *Abstraction of Drift Seepage* (SNL 2007 [DIRS 181244], Section 6.7.1).

During the thermal period, the ambient seepage rates will be adjusted based on the thermal-hydrologic-modeling results from *Drift-Scale Coupled Processes (DST and TH Seepage) Models* (BSC 2005 [DIRS 172232], Section 6.2), which simulates thermally perturbed groundwater flow processes. Results are given in DTN: LB0301DSCPTHSM.002 [DIRS 163689]. THM and THC effects on fracture flow processes are evaluated with process models that account for groundwater flow processes affected by THM and THC parameter alterations (SNL 2007 [DIRS 181244], Sections 6.4.4.1, 6.4.4.2, and 6.5[a]). It was demonstrated that these potential alterations can be neglected in the TSPA, as the expected changes would lead to less seepage (SNL 2007 [DIRS 181244], Sections 6.5.1.4 and 6.5[a]). See also excluded FEPs 2.1.09.12.0A (Rind (Chemically Altered Zone) Forms in the Near-Field) and 2.2.10.04.0A (Thermo-Mechanical Stresses Alter Characteristics of Fractures Near Repository).

The effects of unsaturated groundwater flow are also included in the model for seepage water chemistry. The approach used is a plug flow model that has a transport velocity equal to the percolation flux divided by the product of the average porosity and the average water saturation (SNL 2007 [DIRS 177412], Section 6.3.2.4.4). The effects of flow on the water chemistry are evaluated in terms of the amount of feldspar dissolution that occurs during flow through the TSw (SNL 2007 [DIRS 177412], Sections 6.3.2.4.4 and 6.3.2.4.5). This is a function of the ambient feldspar dissolution rate, the dissolution rate temperature dependence, the model for the thermal field, and the plug flow model for transport through the TSw (SNL 2007 [DIRS 177412], Section 6.3.2.4.5). The starting point for evaluating potential water compositions in the near field is the composition of ambient pore waters in the TSw. The available pore-water data from the four repository host units (Tptpul, Tptpmn, Tptpll, Tptpln) were evaluated and grouped into four compositional groups (SNL 2007 [DIRS 177412], Section 6.3.2.3). The amount of feldspar

dissolution is passed to TSPA in a lookup table, as the WRIP (SNL 2007 [DIRS 177412], Section 6.3.2.4.5; DTN: SN0703PAEBSPCE.006 [DIRS 181571]).

Uncertainty in unsaturated zone flow has been found to be primarily a result of the uncertainty in infiltration rates (SNL 2007 [DIRS 184614], Section 6.10). The uncertainty in infiltration is incorporated into unsaturated zone flow results through the use of a range of four infiltration boundary conditions (SNL 2007 [DIRS 184614], Section 6.1.4). Therefore, there are four unsaturated zone flow fields for each climate (present-day, monsoon, and glacial-transition) during the first 10,000 years (SNL 2007 [DIRS 184614], Section 6.1.4). The probabilities of each flow field are conditioned on results from the infiltration model, as well as temperature and chloride observations from the unsaturated zone (SNL 2007 [DIRS 184614], Section 6.8). For the post-10,000-year period, the infiltration is accounted for by prescribing the NRC-specified percolation rate at the repository horizon, using a range of four infiltration boundary conditions that approximate a log-uniform distribution of percolations rates from 13 to 64 mm/yr at the repository as specified by proposed 10 CFR 63.342(c) (70 FR 53313 [DIRS 178394]) (SNL 2007 [DIRS 184614], Section 6.1.4).

INPUTS:

Table 2.2.07.02.0A-1. Indirect Inputs

Citation	Title	DIRS
70 FR 53313	Implementation of a Dose Standard After 10,000 Years	178394
BSC 2004	*Analysis of Hydrologic Properties Data*	170038
BSC 2004	*Conceptual Model and Numerical Approaches for Unsaturated Zone Flow and Transport*	170035
BSC 2004	*In Situ Field Testing of Processes*	170004
BSC 2004	*Seepage Calibration Model and Seepage Testing Data*	171764
BSC 2004	*Seepage Model for PA Including Drift Collapse*	167652
BSC 2005	*Drift-Scale Coupled Process (DST and TH Seepage) Models*	172232
DTN: LB0301DSCPTHSM.002	Drift-Scale Coupled Process Model for Thermohydrologic Seepage: Data Summary	163689
DTN: LB0612PDFEHMFF.001	Flow-Field Conversions from TOUGH2 to FEHM Format for Present Day 10-, 30-, 50-, and 90-Percentile Infiltration Maps	179296
DTN: LB0701GTFEHMFF.001	Flow-Field Conversions from TOUGH2 to FEHM Format for Glacial Transition Climate 10th-, 30th-, 50th-, and 90th-Percentile Infiltration Maps	179160
DTN: LB0701MOFEHMFF.001	Flow-Field Conversions from TOUGH2 to FEHM Format for Monsoon Climate 10th-, 30th-, 50th-, and 90th-Percentile Infiltration Maps	179297
DTN: LB0702PAFEM10K.002	Flow Field Conversions to FEHM Format for Post 10,000 Year Peak Dose Fluxes in the Unsaturated Zone for Four Selected Infiltration Rates	179507
DTN: LB0702PASEEP01.001	New Extended-Range Seepage Look-Up Tables for Intact and Collapsed Drifts Plus Supporting Files	179511
DTN: LB0702PASEEP02.001	Seepage Abstraction for Degraded Drifts	181635
DTN: SN0703PAEBSPCE.006	Physical and Chemical Environment (PCE) TDIP Water-Rock Interaction Parameter Table and Salt Separation Tables with Supporting Files	181571

Table 2.2.07.02.0A-1. Indirect Inputs (Continued)

Citation	Title	DIRS
SNL 2007	*Abstraction of Drift Seepage*	181244
SNL 2007	*Calibrated Unsaturated Zone Properties*	179545
SNL 2007	*Engineered Barrier System: Physical and Chemical Environment*	177412
SNL 2007	*UZ Flow Models and Submodels*	184614
SNL 2008	*Particle Tracking Model and Abstraction of Transport Processes*	184748

FEP: 2.2.07.03.0A

FEP NAME:

Capillary Rise in the UZ

FEP DESCRIPTION:

Capillary rise involves the drawing up of water, above the water table or above locally saturated zones, in continuous pores of the unsaturated zone until the suction gradient is balanced by the gravitational pull downward.

SCREENING DECISION:

Included

TSPA DISPOSITION:

Capillary forces are included in the UZ flow model. These forces affect the distribution of water in the unsaturated zone through capillary effects on water flow, also known as capillary wicking (included FEP 2.2.07.02.0A, Unsaturated Groundwater Flow in the Geosphere). Parameters used for modeling capillarity are incorporated within the matrix properties (DTN: LB0207REVUZPRP.002 [DIRS 159672]) and fracture properties (DTN: LB0205REVUZPRP.001 [DIRS 159525]), as described in *UZ Flow Models and Submodels* (SNL 2007 [DIRS 184614], Section 6.1.5). These parameters are used as direct input to the UZ flow model and are incorporated into the output flow fields used in the TSPA model (flow fields are in DTNs: LB0612PDFEHMFF.001 [DIRS 179296], LB0701MOFEHMFF.001 [DIRS 179297], LB0701GTFEHMFF.001 [DIRS 179160], and LB0702PAFEM10K.002 [DIRS 179507]).

Capillary forces are also incorporated into the capillary-strength parameter ($1/\alpha$) that is implemented in *Seepage Model for PA Including Drift Collapse* (BSC 2004 [DIRS 167652]). All the seepage process models that feed into the seepage abstraction simulate groundwater flow processes in unsaturated rack (SNL 2007 [DIRS 181244], Section 6.4). Percolation flux distributions are provided to the seepage abstraction model by the UZ flow model (SNL 2007 [DIRS 184614], Section 6.6.2.4), which accounts for groundwater flow on a larger scale than is treated by the drift-scale seepage model, influenced by climate changes, infiltration variability, and stratigraphy effects. For ambient seepage, the fracture flow processes in the drift vicinity and the resulting seepage rates are predicted by model simulations from the seepage model for performance assessment (BSC 2004 [DIRS 167652], Sections 6.2.1 and 6.6), and abstracted in *Abstraction of Drift Seepage* (SNL 2007 [DIRS 181244], Section 6.4.2). Results are available as lookup tables in DTNs: LB0702PASEEP01.001 [DIRS 179511] and LB0702PASEEP02.001 [DIRS 181635], which are used in the TSPA model to calculate ambient seepage by sampling parameter cases of seepage-relevant parameters from the probability distributions defined in *Abstraction of Drift Seepage* (SNL 2007 [DIRS 181244], Section 6.7.1).

INPUTS:

Table 2.2.07.03.0A-1. Indirect Inputs

Citation	Title	DIRS
BSC 2004	*Seepage Model for PA Including Drift Collapse*	167652
DTN: LB0205REVUZPRP.001	Fracture Properties for UZ Model Layers Developed from Field Data	159525
DTN: LB0207REVUZPRP.002	Matrix Properties for UZ Model Layers Developed from Field and Laboratory Data	159672
DTN: LB0612PDFEHMFF.001	Flow-Field Conversions from TOUGH2 to FEHM Format for Present Day 10-, 30-, 50-, and 90-Percentile Infiltration Maps	179296
DTN: LB0701GTFEHMFF.001	Flow-Field Conversions from TOUGH2 to FEHM Format for Glacial Transition Climate 10th-, 30th-, 50th-, and 90th-Percentile Infiltration Maps	179160
DTN: LB0701MOFEHMFF.001	Flow-Field Conversions from TOUGH2 to FEHM Format for Monsoon Climate 10th-, 30th-, 50th-, and 90th-Percentile Infiltration Maps	179297
DTN: LB0702PAFEM10K.002	Flow Field Conversions to FEHM Format for Post 10,000 Year Peak Dose Fluxes in the Unsaturated Zone for Four Selected Infiltration Rates	179507
DTN: LB0702PASEEP01.001	New Extended-Range Seepage Look-Up Tables for Intact and Collapsed Drifts Plus Supporting Files	179511
DTN: LB0702PASEEP02.001	Seepage Abstraction for Degraded Drifts	181635
SNL 2007	*Abstraction of Drift Seepage*	181244
SNL 2007	*UZ Flow Models and Submodels*	184614

FEP: 2.2.07.04.0A

FEP NAME:

Focusing of Unsaturated Flow (Fingers, Weeps)

FEP DESCRIPTION:

Unsaturated flow can differentiate into zones of greater and lower saturation (fingers) that may persist as preferential flow paths. Heterogeneities in rock properties, including fractures and faults, may contribute to focusing. Focused flow may become locally saturated.

SCREENING DECISION:

Included

TSPA DISPOSITION:

Preferential flow paths, a possible result of heterogeneities in rock properties (including fractures and faults and their spatial variabilities), are accounted for in the predictive models that simulate flow and transport processes in the unsaturated zone. Mountain-scale models, such as the UZ flow model or the UZ transport model, address preferential flow in a different manner than near-field models (or drift-scale models), such as the seepage prediction models or the coupled-processes models for thermal-hydrological and THC processes. The respective ways of treating preferential flow processes for mountain-scale and drift-scale models are explained below.

The UZ flow model, a mountain-scale model comprising the entire unsaturated zone at Yucca Mountain, represents the redistribution of infiltrating water originated from the ground surface in the unsaturated zone, with the stratigraphic layers and their fracture characteristics as well as major faults explicitly taken into account (SNL 2007 [DIRS 184614], Sections 6.1.2, 6.6.2, and 6.7.3). The flux redistribution is based on tuff layer properties including the effects of fracture and matrix interaction. Faults are included in the UZ flow model as discrete features; therefore, flow in faults is also included in the UZ flow model (SNL 2007 [DIRS 184614]). Flow model results indicate that as flow moves downward through the unsaturated zone, the flow tends to focus into fault zones, with the fraction of flow in the faults increasing from about 30% to 40% at the repository horizon to about 60% at the water table (SNL 2007 [DIRS 184614], Section 6.6.2). Because of the resolution of the model, with grid block sizes on the order of tens of meters, small-scale preferential flow (such as the channelling of unsaturated flow into relatively few flowing fractures) is not explicitly simulated in the UZ flow model. Rather, the averaged effect of this small-scale preferential flow is captured in the active fracture model described and validated in *Conceptual Model and Numerical Approaches for UZ Flow and Transport* (BSC 2004 [DIRS 170035], Sections 6.1.7 and 6.3.7, description; Section 7, validation). The active-fracture parameter values for different model layers are calibrated in *Calibrated Unsaturated Zone Properties* (SNL 2007 [DIRS 179545], Tables 6-6 through 6-9 and 6-13 through 6-16).

For radionuclide transport in the unsaturated zone, the effect of preferential flow is implicitly included through the use of flow fields contained in DTNs: LB0612PDFEHMFF.001 [DIRS 179296], LB0701MOFEHMFF.001 [DIRS 179297], LB0701GTFEHMFF.001 [DIRS 179160], and LB0702PAFEM10K.002 [DIRS 179507] for simulations (SNL 2008 [DIRS 184748], Addendum Section 6.5.1 and Section 6.6.2[b]). In TSPA model runs, flow fields are used directly by the transport modeling code FEHM (FEHM V. 2.21 [DIRS 165741], STN: 10086-2.21-00). *Particle Tracking Model and Abstraction of Transport Processes* (SNL 2008 [DIRS 184748]) provides transport parameters in DTNs: LA0701PANS02BR.003 [DIRS 180497] and LB0702PAUZMTDF.001 [DIRS 180776] for use in the TSPA model, and provides transfer function data for the particle tracking algorithm for use in the TSPA model in DTN: MO0704PAPTTFBR.002 [DIRS 180442].

Drift-scale models focus on the vicinity of emplacement drifts. These models typically have a more refined grid resolution on the order of a few centimeters to decimeters that allows for explicit representation of preferential flows. Seepage models, for example, represent preferential flow of water into drifts (i.e., in "weeps") on two different scales. First, intermediate-scale focusing of flow from the site scale to the drift scale is accounted for in the seepage abstraction by using appropriate flow-focusing factors. These flow focusing factors increase the percolation fluxes predicted by the UZ flow model in some areas and reduce them in others, to generate appropriate flux boundary conditions for seepage models (SNL 2007 [DIRS 181244], Section 6.6.5.2). The distribution of flow-focusing factors used for seepage calculations is developed in *Seepage Model for PA Including Drift Collapse* (BSC 2004 [DIRS 167652], Sections 6.8), using property values calibrated in *Calibrated Unsaturated Zone Properties* (SNL 2007 [DIRS 179545], Section 6.3.2). Second, small-scale preferential flow is explicitly simulated in the seepage process model, developed in *Seepage Model for PA Including Drift Collapse* (BSC 2004 [DIRS 167652], Section 6.8), by use of heterogeneous fracture-permeability fields (SNL 2007 [DIRS 181244], Sections 6.4.1.1 and 6.4.2.1). Thus, preferential flow is inherently embedded in the seepage lookup tables for ambient seepage given in DTN: LB0702PASEEP01.001 [DIRS 179511]. Uncertainty in flow focusing is therefore propagated to TSPA models through the use of distributions of flow-focusing factors and lookup tables for seepage.

A similar methodology for representing preferential flows, using flow focusing factors and explicit representation of internal small-scale heterogeneity, is applied in the process model for thermal seepage, which evaluates seepage during thermally perturbed conditions, as described in *Drift-Scale Coupled Processes (DST and TH Seepage) Models* (BSC 2005 [DIRS 172232]). Thus, preferential flow is also inherently embedded in the thermal seepage results provided in DTN: LB0301DSCPTHSM.002 [DIRS 163689]. Furthermore, instead of using a continuum representation for fracture and matrix flow, an alternative conceptual model was developed that explicitly analyzed the episodic penetration of a single finger flow event in a heated fracture (BSC 2005 [DIRS 172232], Section 6.3). Results from this alternative conceptual model, which are not used in TSPA, are consistent with results from the thermal-hydrologic seepage model used for this abstraction (SNL 2007 [DIRS 181244], Section 6.4.3.2). The abstraction methodology for ambient and thermal seepage is described in *Abstraction of Drift Seepage* (SNL 2007 [DIRS 181244], Section 6.7.1).

Preferential-flow effects have also been evaluated in *THC Sensitivity Study of Heterogeneous Permeability and Capillarity Effects* (SNL 2007 [DIRS 177413]). The THC seepage model described in this report determines: (1) the effect of THC processes on water chemistry, and (2) the impact of mineral alteration on near-field hydrologic properties and seepage. Flow focusing and fracture permeability heterogeneity were determined to not significantly affect seepage water chemistry (SNL 2007 [DIRS 177413], Section 6.6.3). Also, mineral alteration was shown to have no significant effect on future seepage rates. Therefore, inclusion of these THC effects in the TSPA model was considered unnecessary.

FEP 2.2.07.4.0A (Focusing of Unsaturated Flow (Fingers, Weeps)) is included in the performance assessments conducted to demonstrate compliance with proposed 10 CFR 63.311 (70 FR 53313 [DIRS 178394]) and with 10 CFR 63.331 [DIRS 180319]. Flow focusing at the intermediate scale is not included in the performance assessment conducted to demonstrate compliance with proposed 10 CFR 63.321 (human intrusion) (70 FR 53313 [DIRS 178394]). Large scale focusing is included in human intrusion scenarios because percolation flux in the unsaturated zone above the repository at the base of the PTn is used to determine the flux downward through the borehole. Intermediate-scale focusing is not included in human intrusion because the seepage model is not implemented for that assessment.

INPUTS:

Table 2.2.07.04.0A-1. Indirect Inputs

Citation	Title	DIRS
10 CFR 63	Energy: Disposal of High-Level Radioactive Wastes in a Geologic Repository at Yucca Mountain, Nevada	180319
70 FR 53313	Implementation of a Dose Standard After 10,000 Years	178394
BSC 2004	*Conceptual Model and Numerical Approaches for Unsaturated Zone Flow and Transport*	170035
BSC 2004	*Seepage Model for PA Including Drift Collapse*	167652
BSC 2005	*Drift-Scale Coupled Process (DST and TH Seepage) Models*	172232
DTN: LA0701PANS02BR.003	UZ Transport Parameters	180497
DTN: LB0301DSCPTHSM.002	Drift-Scale Coupled Process Model for Thermohydrologic Seepage: Data Summary	163689
DTN: LB0612PDFEHMFF.001	Flow-Field Conversions from TOUGH2 to FEHM Format for Present Day 10-, 30-, 50-, and 90-Percentile Infiltration Maps	179296
DTN: LB0701GTFEHMFF.001	Flow-Field Conversions from TOUGH2 to FEHM Format for Glacial Transition Climate 10th-, 30th-, 50th-, and 90th-Percentile Infiltration Maps	179160
DTN: LB0701MOFEHMFF.001	Flow-Field Conversions from TOUGH2 to FEHM Format for Monsoon Climate 10th-, 30th-, 50th-, and 90th-Percentile Infiltration Maps	179297
DTN: LB0702PAFEM10K.002	Flow Field Conversions to FEHM Format for Post 10,000 Year Peak Dose Fluxes in the Unsaturated Zone for Four Selected Infiltration Rates	179507
DTN: LB0702PASEEP01.001	New Extended-Range Seepage Look-Up Tables for Intact and Collapsed Drifts Plus Supporting Files	179511
DTN: LB0702PAUZMTDF.001	Unsaturated Zone Matrix Diffusion Coefficients	180776

Table 2.2.07.04.0A-1. Indirect Inputs (Continued)

Citation	Title	DIRS
DTN: MO0704PAPTTFBR.002	Particle Tracking Transfer Functions	180442
FEHM V2.21	SUN, SunOS 5.8; PC, Windows 2000 and Linux 7.1. 10086-2.21-00.	165741
SNL 2007	*Abstraction of Drift Seepage*	181244
SNL 2007	*Calibrated Unsaturated Zone Properties*	179545
SNL 2007	*THC Sensitivity Study of Heterogeneous Permeability and Capillarity Effects*	177413
SNL 2007	*UZ Flow Models and Submodels*	184614
SNL 2008	*Particle Tracking Model and Abstraction of Transport Processes*	184748

FEP: 2.2.07.05.0A

FEP NAME:

Flow in the UZ from Episodic Infiltration

FEP DESCRIPTION:

Episodic flow could occur in the UZ as a result of episodic infiltration. Episodic flow may affect radionuclide transport.

SCREENING DECISION:

Excluded – low consequence

SCREENING JUSTIFICATION:

Although episodes of high precipitation and water percolation are expected to occur during future rain storms, modeling demonstrates that the porous rock matrix in the Paintbrush Tuff nonwelded hydrogeologic unit (PTn), which lies above the Topopah Spring welded hydrogeologic unit (TSw) containing the repository, would attenuate episodic percolation fluxes, smoothing out any near-surface transients (SNL 2007 [DIRS 184614], Section 6.9[a]). As a result, steady groundwater flow is predicted to occur below the PTn in the unsaturated zone. The influence of rapid flow through preferential pathways formed by fractures in the PTn is considered to be volumetrically insignificant compared to flow through the matrix (BSC 2004 [DIRS 169861], Appendix H). Episodic infiltration would therefore have no significant effect on radionuclide releases to the accessible environment (SNL 2007 [DIRS 184614], Section 6.9[a]). Climate change, which leads to transients with durations of hundreds to thousands of years, is addressed in included FEP 1.3.01.00.0A (Climate Change).

The process that drives infiltration is precipitation, which is episodic in nature. However, studies of episodic infiltration and percolation have found that groundwater flow in the PTn is dominated by porous flow (SNL 2007 [DIRS 184614], Section 6.9[a]). The PTn primarily consists of nonwelded to partially welded tuffs and extends from the base of the densely to moderately welded Tiva Canyon welded tuff (TCw) to the top of the TSw, which is densely welded (BSC 2004 [DIRS 169734], Section 3.3.6). Within the repository area, the thickness of the PTn unit ranges from approximately 21 m (70 ft) to over 120 m (400 ft) (Figure D-3). Water flow in the southern part of Solitario Canyon may be transient because the PTn unit is completely offset by the Solitario Canyon Fault in this area. Nevertheless, in these areas, episodic flow is not expected to be significant to performance assessment because the emplacement drifts are located away from Solitario Canyon (SNL 2007 [DIRS 179466], Table 4-1, Parameter 01-01). Furthermore, the southern part of Solitario Canyon Fault does not have a significant role in radionuclide transport (SNL 2007 [DIRS 177396], Figures 6-7 and 6-9 to 6-28). As a whole, the PTn unit exhibits different hydrogeologic properties than the TCw and TSw units that bound it respectively above and below. The TCw and the TSw units both display the low porosity and intense fracturing typical of the densely welded tuffs at Yucca Mountain (BSC 2004 [DIRS 170038], Tables 6-5 and 6-6). In contrast, with its high porosity and low fracture intensity, the PTn rock matrix has a large capacity for storing groundwater and

effectively damps percolation transients at the base of the TCw unit. Water imbibing into the PTn rock matrix, from rapid fracture flow in the TCw above, results in a more uniform distribution of groundwater flux at the base of the PTn after traveling through the entire PTn unit (SNL 2007 [DIRS 184614], Section 6.9[a]). Porous flow through the PTn rock matrix damps out the transient nature of the percolation such that unsaturated zone groundwater flow below the PTn is essentially steady (SNL 2007 [DIRS 184614], Section 6.9[a]).

The effects of transient infiltration events were investigated using a one-dimensional flow model (SNL 2007 [DIRS 184614], Section 6.9[a]). The episodic infiltration calculations used an average infiltration rate of 32 mm/yr, which is the mean percolation flux averaged over the repository for the post-10,000-year period (70 FR 53313 [DIRS 178394], p. 53316). Infiltration flux and percolation flux over the repository footprint have been shown to be quantitatively similar (SNL 2007 [DIRS 184614], Section 6.1.4). The calculations used episodic infiltration pulses of about 10,000 mm/yr over one week every 50 years in combination with a steady background infiltration flux of 28.1 mm/yr to give an average flux of 32 mm/yr (SNL 2007 [DIRS 184614], Section 6.9[a]). This boundary condition was used at two locations having different PTn thicknesses, 21 m and 81 m, representing the range in thickness for this unit over the model domain (SNL 2007 [DIRS 184614], Section 6.9[a]). The results of the episodic flow analyses show that episodic flow damping reduces the effects of episodic flow below the PTn to a maximum range of about 17 mm/yr, which is substantially less than the overall percolation flux uncertainty for the post-10,000-year period of 51 mm/yr (SNL 2007 [DIRS 184614], Figures 6.9-2 and 6.9-3[a] and Table 6.1-3). Lower average infiltration rates, which are representative of present-day, monsoon, and glacial-transition climates for the first 10,000 years, have also been investigated and show similar flow damping effects (BSC 2004 [DIRS 169861], Appendix G). The damping of episodic flow in the PTn is supported by additional calculations (Wu et al. 2000 [DIRS 154918], Section 4.1; Wu et al. 2002 [DIRS 161058]). Furthermore, the PTn overlies the entire repository block (Figure D-3). This damping of transient flow is due to capillary forces and high matrix permeability in the PTn that result in imbibition of water from fractures into the rock matrix. The concept of transient flow attenuation in the PTn is also supported by results of a water-release test at Alcove 4 and the results of line surveys of fracture minerals in the ESF and ECRB Cross-Drift (BSC 2004 [DIRS 170004], Sections 6.7 and 6.14.1).

A further systematic modeling study of damping effects in the unsaturated zone was conducted by Zhang et al. (2006 [DIRS 180273]), using both three-dimensional mountain-scale and one-dimensional vertical column models. The three-dimensional model incorporates a wide variety of field-specific data for the highly heterogeneous formation at the site and provides a more realistic representation, while the simplified one-dimensional flow and transport models are useful for examining the long-term response of the flow system to different infiltration pulses. In the three-dimensional model, the top pulse-infiltration boundary condition is set by concentrating a total amount of net infiltration that would occur in a 50-year period into a one-week infiltration pulse for an average infiltration rate of 4.43 mm/yr. The model's top boundary is subject to nonzero infiltration with a pulse of 2,609 times present-day mean infiltration (Zhang et al. 2006 [DIRS 180273], p. 238) for only one week every 50 years, while during the rest period of every 50 years, the surface boundary is subject to zero infiltration. The modeling results indicate that the PTn unit can attenuate the episodic infiltration flux significantly (Zhang et al. 2006 [DIRS 180273], Figures 5 and 6). Model results show that the total percolation fluxes at the PTn bottom gradually approach the average value of mean infiltration rate for the whole period, and

that eventually the system should reach a dynamic equilibrium condition under the uniform pulses of infiltration. In the areas without faults, vertical flux at the PTn bottom does not rapidly respond to top boundary infiltration pulses. The results indicate that the damping effect happens at the PTn1 through PTn4 subunits. Episodic infiltration pulses directly entering fault zones were found to penetrate to the base of the PTn with less attenuation than other locations, but reductions in peak flux rates were still on the order of 99% (Zhang et al. 2006 [DIRS 180273], Figure 6). Results from the one-dimensional model with higher-rate infiltration scenarios confirm that the damping effect will not be weakened by higher-rate infiltration pulses. The results also show that most percolating water is damped by the subunits at the top of PTn, and that a small percentage of percolation flux is diverted into faults. The highly porous PTn unit attenuates episodic infiltration flux by imbibing water into the rock matrix. Flux allocation analyses suggest that the damping effect at nonfault columns is mainly caused by matrix rock water storage, absorbing and releasing water at different periods. Along fault columns, both lateral flow and rock water storage play an integral role, with the relative importance of these two damping components being location-dependent.

Relatively small amounts of fracture flow may penetrate as fast pathways through fault zones between the ground surface and the repository elevation as evidenced by high ^{36}Cl concentrations in samples taken from the ESF (BSC 2006 [DIRS 179489]). Higher concentrations of this isotope found in the ESF are explained through surface deposition of ^{36}Cl from nuclear weapons testing and subsequent aqueous transport to certain ESF sampling locations in a period of approximately 50 years. Rapid transport could occur as a result of either steady or transient flow. In either case, the key to fast transport through the PTn is for solutes to move through fractures, thus bypassing transport through the rock matrix. However, the flow and transport models indicate that the quantity of water and dissolved constituents that penetrate the PTn as a result of fast pathways (approximately 1% of the total infiltration) is negligible with respect to repository performance (BSC 2004 [DIRS 169861], Appendix H).

Episodic flow resulting from episodic infiltration in the unsaturated zone at Yucca Mountain has also been investigated by Manepally et al. (2007 [DIRS 182155]), in which, longer-term transients that span up to thousands of years were investigated for a range of fluxes that roughly correspond with the 10,000-year percolation flux range required by the proposed regulations for time periods beyond 10,000 years after repository closure (Manepally et al. 2007 [DIRS 182155], Table 4-3; SNL 2007 [DIRS 184614], Section 6.1.4). As for the case with climate change, longer-term transients are expected to penetrate the PTn because of the finite storage capacity of the unit. The magnitude of the transients in the study by Manepally et al. (2007 [DIRS 182155], p. 5-2) were found to be characterized by a standard deviation of about 20% of the mean flux and a maximum range of 50%. By comparison, the standard deviation in the mean flux implemented for the post-10,000-year climate is about 60% and the range is 127% of the mean flux (SNL 2007 [DIRS 184614], Tables 6.1-3 and 6.8-1) over the repository footprint. Therefore, the transient fluctuations are small in comparison with the uncertainty in the mean already incorporated in the TSPA.

The analysis presented here indicates that episodic flow will be attenuated in the PTn, resulting in approximately steady-state flow in the repository host rock and below. Furthermore, the volume of flow through pathways that could lead to episodic flow in the repository host rock has been shown to be small.

Based on the previous discussion, omission of FEP 2.2.07.05.0A (Flow in the UZ from Episodic Infiltration) will not result in a significant adverse change in the magnitude or time of radiological exposures to the RMEI or radionuclide releases to the accessible environment. Therefore, this FEP is excluded from the performance assessments conducted to demonstrate compliance with proposed 10 CFR 63.311 and 63.321 (70 FR 53313 [DIRS 178394]), and with 10 CFR 63.331 [DIRS 180319], on the basis of low consequence.

INPUTS:

Table 2.2.07.05.0A-1. Direct Inputs

Input	Source	Description
SNL 2007. *Total System Performance Assessment Data Input Package for Requirements Analysis for Subsurface Facilities*. [DIRS 179466]	Table 4-1, Parameter Number 01-01	Emplacement drifts are located away from Solitario Canyon
SNL 2007. *UZ Flow Models and Submodels*. [DIRS 184614]	Section 6.9[a]; Figures 6.9-2, 6.9-3[a]; Table 6.1-3	Porous flow through the PTn rock matrix, damping of episodic infiltration
	Tables 6.1-3, 6.8-1	The standard deviation in the mean flux implemented for the post-10k climate is about 60% and the range is 127% of the mean flux over the repository footprint
	Section 6.1.4	Similarity of infiltration flux and percolation flux

Table 2.2.07.05.0A-2. Indirect Inputs

Citation	Title	DIRS
10 CFR 63	Energy: Disposal of High-Level Radioactive Wastes in a Geologic Repository at Yucca Mountain, Nevada	180319
70 FR 53313	Implementation of a Dose Standard After 10,000 Years	178394
BSC 2004	*Analysis of Hydrologic Properties Data*	170038
BSC 2004	*In Situ Field Testing of Processes*	170004
BSC 2004	*UZ Flow Models and Submodels*	169861
BSC 2004	*Yucca Mountain Site Description*	169734
BSC 2006	*Chlorine-36 Validation Study at Yucca Mountain, Nevada*	179489
Manepally et al. 2007	*The Nature of Flow in the Faulted and Fractured Paintbrush Nonwelded Hydrogeologic Unit*	182155
SNL 2007	*Radionuclide Transport Models Under Ambient Conditions*	177396
Wu et al. 2000	*Capillary Barriers in Unsaturated Fractured Rocks of Yucca Mountain, Nevada*	154918
Wu et al. 2002	"Modeling Capillary Barriers in Unsaturated Fractured Rock"	161058
Zhang et al. 2006	"Temporal Damping Effect of the Yucca Mountain Fractured Unsaturated Rock on Transient Infiltration Pulses"	180273

FEP: 2.2.07.06.0A

FEP NAME:

Episodic or Pulse Release from Repository

FEP DESCRIPTION:

Episodic or pulse release of radionuclides from the repository and radionuclide transport in the UZ may occur both because of episodic flow into the repository, and because of pulse releases from failed waste packages.

SCREENING DECISION:

Excluded – low consequence

SCREENING JUSTIFICATION:

Episodic or pulse release of radionuclides is of potential significance to the TSPA because this behavior could lead to the release of large quantities of radionuclides over relatively short time spans. Such behavior could occur as a result of fluctuations in the repository conditions and/or changes in the integrity of the EBS, which would affect flow and transport properties. If episodic or pulse release of radionuclides occurs, it could significantly impact the dose to the RMEI or the extent of release of radionuclides to the accessible environment.

Episodic and pulsed release of radionuclides is evaluated within the model developed in *EBS Radionuclide Transport Abstraction* (RTA) (SNL 2007 [DIRS 177407]). The abstraction outlines the principles and assumptions that guided the development of flow and transport models for the TSPA and is used to quantify the time-dependent radionuclide releases from a failed waste package and subsequent transport through the EBS to the emplacement drift wall/unsaturated zone interface. The basic inputs to the RTA model consist of the drift seepage influx, the environmental conditions in the drift (temperature, relative humidity, water chemistry), and the degradation state of the EBS components. Step changes in the seepage chemistry, such that the solubility of radionuclides might increase or decrease, are also considered. Outputs consist of the rates of radionuclide release to the unsaturated zone as a result of advective and diffusive transport, accounting for the impact of colloids, radionuclide solubility, retardation, and the degree of liquid saturation of the waste form and invert materials. The RTA model is implemented directly into the TSPA GoldSim model to compute radionuclide release rates from the EBS (SNL 2007 [DIRS 177407], Section 6.1).

The primary source of potential episodic or pulse inflow into the EBS is seepage and condensation flux that drips from the crown (roof) of the drift. Subsequent discussion in this FEP addresses specific sources of episodic or pulse release and their impact on the TSPA.

The RTA considered a “bathtub” model of flow as an alternative conceptual model to the continuous flow-through model that is implemented. The bathtub model simulates episodic releases of radionuclides (SNL 2007 [DIRS 177407], Sections 6.4.1 and 6.6.1) due to the uneven distribution of corroded patches and stress corrosion cracks on the surface of the waste package,

which may, in some cases, cause the accumulation of seepage water in the waste package after initial failure. However, if seepage water accumulates in a waste package prior to formation of a corroded patch below the water level, episodic release could occur, which would be well represented in the TSPA by the "bathtub" flow model. In this situation, matrix imbibition, sorption, and diffusion processes will damp out the effects of this episodic process, so it is of low consequence. The same processes are also expected to render variations in the time at which waste packages fail (due to variations in corrosion rates) to be inconsequential in terms of episodic or pulse releases. These processes are discussed in more detail in included FEP 2.2.07.09.0A (Matrix Imbibition in the UZ), excluded FEP 2.2.08.05.0A (Diffusion in the UZ), and included FEP 2.2.08.09.0B (Sorption in the UZ).

The effect of small-scale variation in permeability on flow channeling near the repository horizon is addressed by the UZ TH seepage model in *Abstraction of Drift Seepage* (SNL 2007 [DIRS 181244], Section 6.4.3.1; see also excluded FEP 2.2.07.05.0A (Flow in the UZ from Episodic Infiltration)). Although precipitation and infiltration are episodic, the percolation flux in the unsaturated zone is effectively steady at the repository horizon (below the PTn) and along radionuclide transport pathways (SNL 2007 [DIRS 181244], Section 6.6.5.1). This basis is developed in *UZ Flow Models and Submodels* (SNL 2007 [DIRS 184614], Section 6.1.2 and 6.9), which shows that the PTn unit is expected to dampen and homogenize downward-moving transient pulses arising from episodic surface infiltration events. This conclusion is based on a study by Wu et al. (2000 [DIRS 154918], Section 4.1 and Figure 4.1-11). Because the flow in the unsaturated zone at the repository horizon is steady, it follows that the seepage flux that enters the crown of the drift is relatively steady (SNL 2007 [DIRS 181244], Section 6.6.5.1).

In summary, episodic or pulse release of radionuclides from the repository and episodic or pulse transport in the unsaturated zone are excluded from the TSPA on the basis of low consequence. Any episodic/pulse release from the waste package, if it occurs, is expected to be damped out by imbibition, sorption, and diffusion processes in the EBS and unsaturated zone. Episodic precipitation and infiltration will have little effect on the seepage flux into the drift, so it can also be excluded on the basis of low consequence.

Based on the preceding discussion, omission of FEP 2.2.07.06.0A (Episodic or Pulse Release from Repository) will not result in a significant adverse change in the magnitude or timing of either radiological exposure to the RMEI or radionuclide releases to the accessible environment. Therefore, this FEP is excluded from the performance assessments conducted to demonstrate compliance with proposed 10 CFR 63.311 and 63.321 (70 FR 53313 [DIRS 178394]), and with 10 CFR 63.331 [DIRS 180319], on the basis of low consequence.

INPUTS:

Table 2.2.07.06.0A-1. Direct Inputs

Input	Source	Description
SNL 2007. *EBS Radionuclide Transport Abstraction*. [DIRS 177407]	Section 6.1	EBS RTA model is implemented directly into the TSPA GoldSim model to compute radionuclide release rates from the EBS
	Sections 6.4.1, 6.6.1	Bathtub model simulates episodic releases of radionuclides
SNL 2007. *UZ Flow Models and Submodels*. [DIRS 184614]	Sections 6.1.2 and 6.9	PTn unit is expected to dampen and homogenize downward-moving transient pulses arising from episodic surface infiltration events

Table 2.2.07.06.0A-2. Indirect Inputs

Citation	Title	DIRS
10 CFR 63	Energy: Disposal of High-Level Radioactive Wastes in a Geologic Repository at Yucca Mountain, Nevada	180319
70 FR 53313	Implementation of a Dose Standard After 10,000 Years	178394
SNL 2007	*Abstraction of Drift Seepage*	181244
SNL 2007	*EBS Radionuclide Transport Abstraction*	177407
Wu et al. 2000	*Capillary Barriers in Unsaturated Fractured Rocks of Yucca Mountain, Nevada*	154918

FEP: 2.2.07.06.0B

FEP NAME:

Long-Term Release of Radionuclides from the Repository

FEP DESCRIPTION:

The release of radionuclides from the repository may occur over a long period of time, as a result of the timing and magnitude of the waste packages and drip shield failures, waste form degradation, and radionuclide transport through the invert.

SCREENING DECISION:

Included

TSPA DISPOSITION:

The effects of waste package failures over a long period of time are included in the source term model for TSPA (SNL 2008 [DIRS 178871], Section 6.3.8). This is done by modeling the environmental conditions of the waste packages in different parts of the repository and by modeling corrosion processes under these environmental conditions that lead to waste package failure. The model developed in *EBS Radionuclide Transport Abstraction* (RTA) (SNL 2007 [DIRS 177407], Section 6.1) is used to quantify the time-dependent radionuclide releases from a failed waste package and subsequent transport through the EBS to the emplacement drift wall/unsaturated zone interface. The basic inputs to the RTA model consist of the drift seepage and drift wall condensation flux, the environmental conditions in the drift (temperature, relative humidity, water chemistry), and the degradation state of the EBS components. Outputs consist of the rates of radionuclide releases to the unsaturated zone as a result of advective and diffusive transport, accounting for the impact of colloids, radionuclide solubility, retardation, and the degree of liquid saturation of the waste form and invert materials. The RTA model, which is implemented directly into the TSPA GoldSim model, allows quantification of radionuclide releases from a failed waste package over the entire compliance period.

Releases from the waste package and engineered barrier system serve as a time-dependent boundary condition to the mountain-scale radionuclide transport model as discussed in *Particle Tracking Model and Abstraction of Transport Processes* (SNL 2008 [DIRS 184748], Section 6.4.7). This allows for a general time-dependent radionuclide source term that accounts for long-term releases. Releases from the waste package and engineered barrier system serve as a time-dependent boundary condition to the mountain-scale radionuclide transport model, regardless of when the release occurs, thus allowing for a general time-dependent radionuclide source term that accounts for long-term releases (SNL 2008 [DIRS 184748], Sections 6.4.6 and 6.4.7).

INPUTS:

Table 2.2.07.06.0B-1. Indirect Inputs

Citation	Title	DIRS
SNL 2007	*EBS Radionuclide Transport Abstraction*	177407
SNL 2008	*Particle Tracking Model and Abstraction of Transport Processes*	184748
SNL 2008	*Total System Performance Assessment Model/Analysis for the License Application*	178871

FEP: 2.2.07.07.0A

FEP NAME:

Perched Water Develops

FEP DESCRIPTION:

Zones of perched water may develop above the water table. If these zones occur above the repository, they may affect UZ flow between the surface and the waste packages. If they develop below the repository, e.g., at the base of the Topopah Spring welded unit, they may affect flow pathways and radionuclide transport between the waste packages and the saturated zone.

SCREENING DECISION:

Included

TSPA DISPOSITION:

The seepage abstraction model contains a wide range of seepage possibilities, including flow focusing and spatial variability (SNL 2007 [DIRS 181244], Section 6). Therefore, the potential for effects of perched water above the repository (diversion and subsequent drainage of flow) are indirectly captured in the seepage abstraction model through cases with high percolation flux, which can be as high as seven times the nominal flux (DTNs: LB06123DPDUZFF.001 [DIRS 178587], LB07013DMOUZFF.001 [DIRS 179064], LB07013DGTUZFF.001 [DIRS 179066], LB0702UZP10KFF.002 [DIRS 179324], LB0612PDFEHMFF.001 [DIRS 179296], LB0701MOFEHMFF.001 [DIRS 179297], LB0701GTFEHMFF.001 [DIRS 179160], and LB0702PAFEM10K.002 [DIRS 179507]) as described in *Abstraction of Drift Seepage* (SNL 2007 [DIRS 181244], Section 6). However, the flow fields predicted by the UZ flow model do not contain perched water bodies above the repository, and no perched water was observed in boreholes drilled through the unsaturated zone above the repository (BSC 2004 [DIRS 169734], Section 5.2.2.4.1).

The effects of existing perched water zones below the repository are also included, and potential changes in these perched-water zones caused by climate changes are also included in the mountain-scale UZ flow model (SNL 2007 [DIRS 184614], Sections 6.2.2, 6.2.5, and 6.6.2). The potential for this effect is captured in the output flow fields developed for use in the TSPA (output flow fields are in DTNs: LB06123DPDUZFF.001 [DIRS 178587], LB07013DMOUZFF.001 [DIRS 179064], LB07013DGTUZFF.001 [DIRS 179066], and LB0702UZP10KFF.002 [DIRS 179324]). UZ flow model results indicate that large-scale lateral diversion occurs in the vicinity of perched water zones because of the low fracture permeability associated with zeolitic alteration (SNL 2007 [DIRS 184614], Section 8.6). Lateral diversion can impact radionuclide transport to the water table, which is included in TSPA models.

This FEP is also included in the preliminary flow fields generated for radionuclide transport simulations in the unsaturated zone (DTNs: LB0612PDFEHMFF.001 [DIRS 179296], LB0701MOFEHMFF.001 [DIRS 179297], LB0701GTFEHMFF.001 [DIRS 179160], and

LB0702PAFEM10K.002 [DIRS 179507]). In TSPA model simulations, preliminary flow fields were used by FEHM and used in UZ transport simulations as described in *Particle Tracking Model and Abstraction of Transport Processes* (SNL 2008 [DIRS 184748], Addendum Section 6.5.1).

Uncertainty in the extent of perched water is captured through the use of a range of infiltration rates (SNL 2007 [DIRS 184614], Section 6.8.5). The resulting flow fields reflect the uncertainty in the infiltration rates, which subsequently impact the extent of perched water developoment in the flow fields used for TSPA.

This FEP is included in the performance assessments conducted to demonstrate compliance with the individual protection standard (proposed 10 CFR 63.311 (70 FR 53313 [DIRS 178394])) and the groundwater protection standard (10 CFR 63.331 [DIRS 180319]). However, the development of perched water is not included in the human-intrusion performance assessment (proposed 10 CFR 63.321 (70 FR 53313 [DIRS 178394])) because the flow and transport pathway considered in that assessment (through a borehole between the repository and saturated zone) is not impacted by the presence of perched water or low permeability layers in the unsaturated zone.

INPUTS:

Table 2.2.07.07.0A-1. Indirect Inputs

Citation	Title	DIRS
70 FR 53313	Implementation of a Dose Standard After 10,000 Years	178394
BSC 2004	*Yucca Mountain Site Description*	169734
DTN: LB06123DPDUZFF.001	3-D UZ Flow Fields for Present-Day Climate of 10th-, 30th-, 50th- and 90th -Percentile Infiltration Maps	178587
DTN: LB0612PDFEHMFF.001	Flow-Field Conversions from TOUGH2 to FEHM Format for Present Day 10-, 30-, 50-, and 90-Percentile Infiltration Maps	179296
DTN: LB07013DGTUZFF.001	3-D UZ Flow Fields for Glacial Transition Climate of 10th-, 30th-, 50th-, and 90th-Percentile Infiltration Maps	179066
DTN: LB07013DMOUZFF.001	3-D UZ Flow Fields for Monsoon Climate of 10th-, 30th-, 50th-, and 90th-Percentile Infiltration Maps	179064
DTN: LB0701GTFEHMFF.001	Flow-Field Conversions from TOUGH2 to FEHM Format for Glacial Transition Climate 10th-, 30th-, 50th-, and 90th-Percentile Infiltration Maps	179160
DTN: LB0701MOFEHMFF.001	Flow-Field Conversions from TOUGH2 to FEHM Format for Monsoon Climate 10th-, 30th-, 50th-, and 90th-Percentile Infiltration Maps	179297
DTN: LB0702PAFEM10K.002	Flow Field Conversions to FEHM Format for Post 10,000 Year Peak Dose Fluxes in the Unsaturated Zone for Four Selected Infiltration Rates	179507
DTN: LB0702UZP10KFF.002	3-D UZ Flow Fields for Post-10,000 Climate Infiltration Maps	179324
SNL 2007	*Abstraction of Drift Seepage*	181244
SNL 2007	*UZ Flow Models and Submodels*	184614
SNL 2008	*Particle Tracking Model and Abstraction of Transport Processes*	184748

FEP: 2.2.07.08.0A

FEP NAME:

Fracture Flow in the UZ

FEP DESCRIPTION:

Fractures or other analogous channels may act as conduits for fluids to move into the subsurface to interact with the repository and as conduits for fluids to leave the vicinity of the repository and be conducted to the saturated zone. Water may flow through only a portion of the fracture network, including flow through a restricted portion of a given fracture plane.

SCREENING DECISION:

Included

TSPA DISPOSITION:

The UZ flow model is based on the dual-permeability concept, with the fractures represented by a continuum (BSC 2004 [DIRS 170035], Section 6.3; SNL 2007 [DIRS 184614], Section 6.1.2). The fracture continuum represents the spatially averaged flow through discrete fractures. The fracture continuum interacts with the matrix continuum, which represents matrix blocks separated by fractures. Fracture continuum properties, including permeability, porosity, fracture-matrix interface area per unit rock volume, van Genuchten α and m parameters for the saturation–capillary pressure and relative permeability functions, and active fracture parameter γ, for each unsaturated zone model layer, are used as input to the UZ flow model (DTNs: LB0205REVUZPRP.001 [DIRS 159525], LB0611MTSCHP10.001 [DIRS 178586], LB0611MTSCHP30.001 [DIRS 180293], LB0612MTSCHP50.001 [DIRS 180294], and LB0612MTSCHP90.001 [DIRS 180295]) listed in *UZ Flow Models and Submodels* (SNL 2007 [DIRS 184614], Table 4.1-1). Permeabilities and values for van Genuchten α are calibrated as described in *Calibrated Unsaturated Zone Properties* (SNL 2007 [DIRS 179545], Section 6.3). The fracture-continuum properties are used as inputs to the UZ flow model, and their effects are incorporated into the output flow fields developed for use in the TSPA (output flow fields are in DTNs: LB06123DPDUZFF.001 [DIRS 178587], LB07013DMOUZFF.001 [DIRS 179064], LB07013DGTUZFF.001 [DIRS 179066], and LB0702UZP10KFF.002 [DIRS 179324]). Output flow fields for the fracture continuum are presented in *UZ Flow Models and Submodels* (SNL 2007 [DIRS 184614], Section 6.6.2).

The top boundary condition for the UZ flow model is set by the infiltration maps output by *Simulation of Net Infiltration for Present-Day and Potential Future Climates* (SNL 2008 [DIRS 182145], Section 6.5). When the water content at soil–bedrock contact reaches field capacity, fracture flow is initiated in the bedrock (SNL 2008 [DIRS 182145], Section 6.3.3). Channeling in the unsaturated zone fracture continuum is captured as discussed for included FEP 2.2.07.04.0A (Focusing of Unsaturated Flow (Fingers, Weeps)), including the use of the active fracture model in *Conceptual Model and Numerical Approaches for UZ Flow and Transport* (BSC 2004 [DIRS 170035], Section 6.3), and the development of the distribution of flow-focusing factors in *Abstraction of Drift Seepage* (SNL 2007 [DIRS 181244], Section 6.6.5).

In the unsaturated zone, fracture flow plays an important role in the transport of radionuclides. In TSPA model simulations, the effect of fracture flow on radionuclide transport (advection) is included through FEHM's use of pregenerated flow fields (DTNs: LB0612PDFEHMFF.001 [DIRS 179296]; LB0701MOFEHMFF.001 [DIRS 179297], LB0701GTFEHMFF.001 [DIRS 179160], and LB0702PAFEM10K.002 [DIRS 179507]) in unsaturated zone transport simulations as described in *Particle Tracking Model and Abstraction of Transport Processes* (SNL 2008 [DIRS 184748], Addendum Section 6.5.1). *Particle Tracking Model and Abstraction of Transport Processes* (SNL 2008 [DIRS 184748]) provides transport parameters in DTNs: LA0701PANS02BR.003 [DIRS 180497] and LB0702PAUZMTDF.001 [DIRS 180776] for use in the TSPA, and provides transfer function data for the particle tracking algorithm for use in the TSPA in DTN: MO0704PAPTTFBR.002 [DIRS 180442].

Percolation flux distributions are provided by the UZ flow model for use in the seepage abstraction model (SNL 2007 [DIRS 181244], Section 6.6.5.1). The UZ flow model accounts for fracture flow on a larger scale (influenced by climate changes), infiltration variability, and stratigraphy effects. Flow-focusing effects (channeling) are included, as discussed in *Abstraction of Drift Seepage* (SNL 2007 [DIRS 181244], Section 6.6.5.2). Flow processes in fractures or other channels are important for the seepage abstraction, because the amount of seepage is determined by the capacity of the fracture network to divert flow around the drifts as a result of capillary forces (SNL 2007 [DIRS 181244], Section 6.3.1). All the seepage process models that feed into seepage abstraction simulate flow processes in fractured rock (SNL 2007 [DIRS 181244], Section 6.4). Spatial variability in the fracture flow, potentially leading to water flow through only a portion of the fracture network, is accounted for by using a stochastic continuum representation. For ambient seepage, the fracture flow processes in the drift vicinity and the resulting seepage rates are predicted by model simulations from the seepage model for performance assessment (BSC 2004 [DIRS 167652], Sections 6.3.2 and 6.3.3) and abstracted in *Abstraction of Drift Seepage* (SNL 2007 [DIRS 181244], Sections 6.4.2 and 6[a]). Results are available as look-up tables in DTN: LB0702PASEEP01.001 [DIRS 179511]. These will be used in the TSPA to calculate ambient seepage; uncertainty in ambient seepage is accounted for by sampling parameter cases of seepage-relevant parameters from the probability distributions defined in *Abstraction of Drift Seepage* (SNL 2007 [DIRS 181244], Sections 6.7.1 and 6.3[a]).

During the thermal period, the ambient seepage rates will be adjusted based on the TH-modeling results from *Drift-Scale Coupled Processes (DST and TH Seepage) Models* (BSC 2005 [DIRS 172232]), which simulates thermally perturbed fracture flow conditions. In the TSPA model, thermal effects on seepage are represented in a simplified manner. When the temperature is under 100°C, ambient seepage is used. When the temperature is 100°C or above, seepage is not considered. Results are given in DTN: LB0301DSCPTHSM.002 [DIRS 163689]. The abstraction methodology for thermal seepage is developed in *Abstraction of Drift Seepage* (SNL 2007 [DIRS 181244], Section 6.5.2). THM and THC effects on fracture flow processes are evaluated with process models that account for fracture flow affected by THM and THC parameter alterations (SNL 2007 [DIRS 181244], Section 6.4.4). It was demonstrated that these potential alterations need not be addressed in the TSPA model (SNL 2007 [DIRS 181244], Section 6.5.1.4); see also excluded FEP 2.1.09.12.0A (Chemistry of Water Flowing into the Drift), excluded FEP 2.2.10.06.0A (Thermo-chemical Alteration in the UZ (Solubility, Speciation, Phase Changes, Precipitation/Dissolution)), and excluded FEP 2.2.10.04.0A (Thermo-mechanical Stresses Alter Characteristics of Faults near Repository).

Flow processes in fractures or other channels affect modeled THC coupled processes because of: (1) their strong effect on TH behavior (SNL 2007 [DIRS 181244], Section 6.4.4), and (2) their strong effect on water and gas chemistry (SNL 2007 [DIRS 177404], Section 6.2.1). The latter primarily involves volatilization of steam and CO_2 from the rock matrix-water and subsequent transport and condensation in fractures. The amount of mobilized CO_2 with steam directly affects the pH of the condensate, which in turn affects the degree of water–rock interaction and water chemistry. These THC processes are influenced by the fracture characteristics, such as orientation, aperture, asperity, length, connectivity, and fillings. The seepage chemistry abstraction uses a plug flow model that has a transport velocity equal to the percolation flux divided by the product of the average porosity and the average water saturation (SNL 2007 [DIRS 177412], Section 6.3.2.4.4). The effects of flow on the water chemistry are evaluated in terms of the amount of feldspar dissolution that occurs during flow through the TSw (SNL 2007 [DIRS 177412], Sections 6.3.2.4.4 and 6.3.2.4.5). This is a function of the ambient feldspar dissolution rate, the dissolution rate temperature dependence, the model for the thermal field, and the plug flow model for transport through the TSw (SNL 2007 [DIRS 177412], Section 6.3.2.4.5). The starting point for evaluating potential water compositions in the near field is the composition of ambient pore waters in the TSw. The available pore-water data from the four repository host units (Tptpul, Tptpmn, Tptpll, Tptpln) were evaluated and grouped into four compositional groups (SNL 2007 [DIRS 177412], Section 6.3.2.3). The amount of feldspar dissolution is passed to TSPA in a lookup table, as the WRIP (SNL 2007 [DIRS 177412], Section 6.3.2.4.5; DTN: SN0703PAEBSPCE.006 [DIRS 181571]). The effects of fracture flow are also included in the treatment of infiltration uncertainty for the TSPA (SNL 2007 [DIRS 184614], Section 6.8). Infiltration uncertainty is represented through four discrete infiltration scenarios (ranging from low to high infiltration), which are sampled in the TSPA model according to flow weighting factors (SNL 2007 [DIRS 184614], Section 6.8). This FEP is included in the determination of the flow weighting factors fed to the TSPA model (SNL 2007 [DIRS 184614], Section 6.8; DTN: LB0701PAWFINFM.001 [DIRS 179283]).

INPUTS:

Table 2.2.07.08.0A-1. Indirect Inputs

Citation	Title	DIRS
BSC 2004	*Conceptual Model and Numerical Approaches for Unsaturated Zone Flow and Transport*	170035
BSC 2004	*Seepage Model for PA Including Drift Collapse*	167652
BSC 2005	*Drift-Scale Coupled Process (DST and TH Seepage) Models*	172232
DTN: LA0701PANS02BR.003	UZ Transport Parameters	180497
DTN: LB0205REVUZPRP.001	Fracture Properties for UZ Model Layers Developed from Field Data	159525
DTN: LB0301DSCPTHSM.002	Drift-Scale Coupled Process Model for Thermohydrologic Seepage: Data Summary	163689
DTN: LB0611MTSCHP10.001	Mountain Scale Calibrated Property Set for the 10-Percentile Infiltration Map	178586
DTN: LB0611MTSCHP30.001	Mountain Scale Calibrated Property Set for the 30-Percentile Infiltration Map	180293

Table 2.2.07.08.0A-1. Indirect Inputs (Continued)

Citation	Title	DIRS
DTN: LB06123DPDUZFF.001	3-D UZ Flow Fields for Present-Day Climate of 10th-, 30th-, 50th- and 90th -Percentile Infiltration Maps	178587
DTN: LB0612MTSCHP50.001	Mountain Scale Calibrated Property Set for the 50-Percentile Infiltration Map	180294
DTN: LB0612MTSCHP90.001	Mountain Scale Calibrated Property Set for the 90-Percentile Infiltration Map	180295
DTN: LB0612PDFEHMFF.001	Flow-Field Conversions from TOUGH2 to FEHM Format for Present Day 10-, 30-, 50-, and 90-Percentile Infiltration Maps	179296
DTN: LB07013DGTUZFF.001	3-D UZ Flow Fields for Glacial Transition Climate of 10th-, 30th-, 50th-, and 90th-Percentile Infiltration Maps	179066
DTN: LB07013DMOUZFF.001	3-D UZ Flow Fields for Monsoon Climate of 10th-, 30th-, 50th-, and 90th-Percentile Infiltration Maps	179064
DTN: LB0701GTFEHMFF.001	Flow-Field Conversions from TOUGH2 to FEHM Format for Glacial Transition Climate 10th-, 30th-, 50th-, and 90th-Percentile Infiltration Maps	179160
DTN: LB0701MOFEHMFF.001	Flow-Field Conversions from TOUGH2 to FEHM Format for Monsoon Climate 10th-, 30th-, 50th-, and 90th-Percentile Infiltration Maps	179297
DTN: LB0701PAWFINFM.001	Weighting Factors for Infiltration Maps	179283
DTN: LB0702PAFEM10K.002	Flow Field Conversions to FEHM Format for Post 10,000 Year Peak Dose Fluxes in the Unsaturated Zone for Four Selected Infiltration Rates	179507
DTN: LB0702PASEEP01.001	New Extended-Range Seepage Look-Up Tables for Intact and Collapsed Drifts Plus Supporting Files	179511
DTN: LB0702PAUZMTDF.001	Unsaturated Zone Matrix Diffusion Coefficients	180776
DTN: LB0702UZP10KFF.002	3-D UZ Flow Fields for Post-10,000 Climate Infiltration Maps	179324
DTN: MO0704PAPTTFBR.002	Particle Tracking Transfer Functions	180442
SNL 2007	*Abstraction of Drift Seepage*	181244
SNL 2007	*Calibrated Unsaturated Zone Properties*	179545
SNL 2007	*Drift-Scale THC Seepage Model*	177404
SNL 2007	*Engineered Barrier System: Physical and Chemical Environment*	177412
SNL 2007	*UZ Flow Models and Submodels*	184614
SNL 2008	*Particle Tracking Model and Abstraction of Transport Processes*	184748
SNL 2008	*Simulation of Net Infiltration for Present-Day and Potential Future Climates*	182145

FEP: 2.2.07.09.0A

FEP NAME:

Matrix Imbibition in the UZ

FEP DESCRIPTION:

Water flowing in fractures or other channels in the unsaturated zone may be imbibed into the surrounding rock matrix. This may occur during steady flow, episodic flow, or into matrix pores that have been dried out during the thermal period.

SCREENING DECISION:

Included

TSPA DISPOSITION:

Matrix imbibition is included in the process model for unsaturated zone flow at the mountain scale (SNL 2007 [DIRS 184614], Section 6.1.2). Matrix imbibition refers to the movement of water into the matrix as a result of capillary forces. This process affects the distribution of flow between fractures and matrix in a dual-permeability flow model for fractured rock. The flow simulations in *UZ Flow Models and Submodels* (SNL 2007 [DIRS 184614], Section 6.6) are for steady-state flow. Imbibition is captured in the UZ flow model through capillarity modeling, which uses matrix and fracture properties as model input. Therefore, the effect of imbibition is incorporated in the output flow fields (DTNs: LB0612PDFEHMFF.001 [DIRS 179296], LB0701MOFEHMFF.001 [DIRS 179297], LB0701GTFEHMFF.001 [DIRS 179160], and LB0702PAFEM10K.002 [DIRS 179507]) used in the TSPA. Matrix imbibition is reflected in the increase in matrix saturation that is simulated when changing to a wetter climate state. Matrix imbibition is also important in damping the effect of episodic infiltration, as discussed in *UZ Flow Models and Submodels* (SNL 2007 [DIRS 184614], Section 6.9[a]). Also, see FEP 2.2.07.05.0A (Flow in the UZ from Episodic Infiltration), which is excluded from TSPA on the basis of low consequence. Matrix imbibition is also captured in the site-scale UZ flow model and the UZ flow fields that are used to prescribe the upper boundary condition water fluxes to the MSTHM process model simulations (SNL 2007 [DIRS 184614], Section 6.9[a]). The output flow fields DTNs given above are used by FEHM in unsaturated zone transport simulations as described in *Particle Tracking Model and Abstraction of Transport Processes* (SNL 2008 [DIRS 184748], Section 6.5.1 in AD01).

The effects of matrix imbibition are also included in the model for seepage water chemistry through changes in the percolation flux rates. The percolation flux values used in the model are based on fluxes at the PTn/TSw boundary predicted by the UZ flow model representing each climate state (SNL 2007 [DIRS 184614], Section 6.9[a]). The approach used is a plug flow model that has a transport velocity equal to the percolation flux divided by the product of the average porosity and the average water saturation (SNL 2007 [DIRS 177412], Section 6.3.2.4.4).

Ambient seepage into the repository drifts is mainly governed by flow in the fractures in the units of the repository horizon, as discussed in *Abstraction of Drift Seepage* (SNL 2007

[DIRS 181244], Section 6.4.1.1). Thus, in the predictive model for ambient seepage, that is, the seepage calibration model (BSC 2004 [DIRS 171764], Section 6.3.3.2) and the seepage model for performance assessment (BSC 2004 [DIRS 167652], Section 6.3), matrix imbibition is not modeled.

In contrast, *Drift-Scale Coupled Processes (DST and TH Seepage) Models* (BSC 2005 [DIRS 172232], Section 6.2.1.1.1) explicitly accounts for matrix imbibition using appropriate dual-permeability modeling concepts. This is needed because the thermal perturbation of the unsaturated rock results in significant transfer of liquid and gas from the matrix into the fractures and vice versa. The UZ flow model (which provides the percolation flux distributions used for seepage calculations; see SNL 2007 [DIRS 181244], Section 6.6.5.1) also accounts for the impact of matrix imbibition in an explicit manner. Thus, matrix imbibition effects are taken into account for seepage under thermal conditions as used in the seepage abstraction. Matrix imbibition tests are reported in *In-Situ Field Testing of Processes* (BSC 2004 [DIRS 170004], Section 6.4). The matrix properties used to simulate matrix imbibition are developed in *Calibrated Unsaturated Zone Properties* (SNL 2007 [DIRS 179545], Section 6.3).

INPUTS:

Table 2.2.07.09.0A-1. Indirect Inputs

Citation	Title	DIRS
BSC 2004	*In Situ Field Testing of Processes*	170004
BSC 2004	*Seepage Calibration Model and Seepage Testing Data*	171764
BSC 2004	*Seepage Model for PA Including Drift Collapse*	167652
BSC 2005	*Drift-Scale Coupled Process (DST and TH Seepage) Models*	172232
DTN: LB0302DSCPTHCS.002	Drift-Scale Coupled Processes (THC Seepage) Model: Data Summary	161976
DTN: LB0612PDFEHMFF.001	Flow-Field Conversions from TOUGH2 to FEHM Format for Present Day 10-, 30-, 50-, and 90-Percentile Infiltration Maps	179296
DTN: LB0701GTFEHMFF.001	Flow-Field Conversions from TOUGH2 to FEHM Format for Glacial Transition Climate 10th-, 30th-, 50th-, and 90th-Percentile Infiltration Maps	179160
DTN: LB0701MOFEHMFF.001	Flow-Field Conversions from TOUGH2 to FEHM Format for Monsoon Climate 10th-, 30th-, 50th-, and 90th-Percentile Infiltration Maps	179297
DTN: LB0702PAFEM10K.002	Flow Field Conversions to FEHM Format for Post 10,000 Year Peak Dose Fluxes in the Unsaturated Zone for Four Selected Infiltration Rates	179507
SNL 2007	*Abstraction of Drift Seepage*	181244
SNL 2007	*Calibrated Unsaturated Zone Properties*	179545
SNL 2007	*Engineered Barrier System: Physical and Chemical Environment*	177412
SNL 2007	*UZ Flow Models and Submodels*	184614
SNL 2008	*Particle Tracking Model and Abstraction of Transport Processes*	184748

FEP: 2.2.07.10.0A

FEP NAME:

Condensation Zone Forms Around Drifts

FEP DESCRIPTION:

Condensation of the two-phase flow generated by repository heat may form in the rock where the temperature drops below the local vaporization temperature. Waste package emplacement geometry and thermal loading may affect the scale at which condensation caps form (over waste packages, over panels, or over the entire repository), and the extent to which "shedding" will occur as water flows from the region above one drift to the region above another drift or into the rock between drifts.

SCREENING DECISION:

Included

TSPA DISPOSITION:

The coupled thermal-hydrologic processes resulting in water evaporation, vapor transport, and the formation of a condensation zone (or "condensation cap") in the fractured rock above the drifts are explicitly simulated, using an 81-m drift spacing (SNL 2007 [DIRS 179466], Parameter Number 01-13), with the TH seepage model as discussed in *Drift-Scale Coupled Processes (DST and TH Seepage) Models* (BSC 2005 [DIRS 172232], Section 6.2). As discussed in *Abstraction of Drift Seepage* (SNL 2007 [DIRS 181244], Section 6.5.2), the abstraction of thermal seepage (seepage at temperatures above ambient) uses the TH seepage modeling results to develop an appropriate thermal-seepage abstraction methodology. Thus, the TH modeling results include these effects. Using the TH seepage model, the impact of condensation and "shedding" between drifts (that is, diversion of vapor to cooler regions and drainage of condensation through the cooler region between drifts) on seepage is assessed for various simulation cases (SNL 2007 [DIRS 181244], Section 6.4.3.3) covering the expected range of values for rock capillarity, permeability, and percolation flux. These parameters control the development and magnitude of the condensation zone, and the relative importance of shedding. TSPA calculations incorporate thermal-hydrologic seepage model uncertainty through use of ambient seepage rates, which are shown to bound the seepage under thermal conditions (SNL 2007 [DIRS 181244], Section 6.4.3).

The coupled processes of vapor condensation forming a condensation cap above the drifts and occurrence of shedding between drifts are explicitly simulated with the THC seepage model (SNL 2007 [DIRS 177404], Sections 6.2.1 and 6.5.5.2). Using this model, the impact of condensation and drainage on seepage water chemistry is assessed for various simulation cases (SNL 2007 [DIRS 177404], Sections 6.2, 6.5, and 6.6). Condensation results in dilute pore waters in high saturation zones above the drift during the boiling period, but has negligible effect on water compositions once drift wall temperatures drop below 100°C. The effects of evaporation or condensation are negligible after the boiling period, and potential seepage waters rapidly return to ambient or near-ambient pore-water ionic strengths (SNL 2007 [DIRS 177404],

Section 6.5). These data provide the technical basis for the implementation of potential seepage chemistry in the near-field chemistry model in *Engineered Barrier System: Physical and Chemical Environment* (SNL 2007 [DIRS 177412], Section 6.3.2), which does not evaluate condensation. The near-field chemistry model provides potential seepage compositions to the seepage dilution/evaporation model, which generates lookup tables of in-drift water chemistry for use in the TSPA model (SNL 2007 [DIRS 177412], Sections 6.3.3 and 6.9).

Multiscale Thermohydrologic Model (SNL 2008 [DIRS 184433]) incorporates vapor condensation in the rock surrounding the drifts in calculating near field and in-drift thermal hydrology. This model provides in-drift temperature and relative humidity inputs used by TSPA to extract water composition data from the seepage/evaporation model lookup tables. Hence, the effects of vapor condensation in the rock surrounding the drift are implicitly incorporated in TSPA predictions of in-drift water chemistry through the multiscale model. The effect of uncertainties in the development and magnitude of a condensation zone are captured through the use of simulation results with different rock thermal conductivities and a suite of percolation flux values (SNL 2008 [DIRS 184433], Sections 6.3.15[a] and 6.3.16[a]). Uncertainties in rock hydrologic properties, ventilation heat removal efficiency, and the effects of axial vapor transport (SNL 2008 [DIRS 184433], Sections 6.3.11[a], 6.3.12, and 6.3.18[a]) were evaluated using sensitivity analyses and found to be insignificant with respect to predicted in-drift conditions.

INPUTS:

Table 2.2.07.10.0A-1. Indirect Inputs

Citation	Title	DIRS
BSC 2005	*Drift-Scale Coupled Process (DST and TH Seepage) Models*	172232
SNL 2007	*Abstraction of Drift Seepage*	181244
SNL 2007	*Drift-Scale THC Seepage Model*	177404
SNL 2007	*Engineered Barrier System: Physical and Chemical Environment*	177412
SNL 2007	*Total System Performance Assessment Data Input Package for Requirements Analysis for Subsurface Facilities*	179466
SNL 2008	*Multiscale Thermohydrologic Model*	184433

FEP: 2.2.07.11.0A

FEP NAME:

Resaturation of Geosphere Dry-Out Zone

FEP DESCRIPTION:

Following the peak thermal period, water in the condensation cap may flow downward into the drifts. Influx of cooler water from above, such as might occur from episodic flow, may accelerate return flow from the condensation cap by lowering temperatures below the condensation point. Percolating groundwater will also contribute to resaturation of the dry-out zone. Vapor flow, as distinct from liquid flow by capillary processes, may also contribute.

SCREENING DECISION:

Included

TSPA DISPOSITION:

Resaturation of the dryout zone around drifts, and the potential of return flow from the condensation zone back to the drifts, are explicitly simulated with the TH seepage model (BSC 2005 [DIRS 172232], Section 6.2). As discussed in *Abstraction of Drift Seepage* (SNL 2007 [DIRS 181244], Section 6.5.2), the abstraction of thermal seepage (seepage at temperatures above ambient) utilizes the TH seepage modeling results to develop an appropriate thermal-seepage abstraction methodology. Thus, the TH modeling results include these effects. Using this model, the impact of resaturation and reflux on seepage is assessed for various simulation cases (SNL 2007 [DIRS 181244], Section 6.4.3.3) covering the expected range of values for rock capillarity, permeability, and percolation flux. These parameters control resaturation of the dryout zone by both liquid flow and capillary condensation of water vapor. TSPA calculations incorporate seepage model uncertainty by sampling probability distributions for these parameters and interpolating between the results of the model simulations (SNL 2007 [DIRS 181244], Section 6.6). The impact of episodic flow, potentially resulting in finger flow penetrating the above-boiling dryout zone, was addressed with an alternative conceptual model for thermal seepage, as discussed in *Abstraction of Drift Seepage* (SNL 2007 [DIRS 181244], Section 6.4.3). It was shown that results from this alternative conceptual model are consistent with the process model results from the TH seepage model used for this abstraction.

During resaturation of the dryout zone, salts precipitated during dryout may redissolve and affect the chemistry of potential seepage waters. This transient process is screened from consideration in TSPA as discussed in excluded FEP 2.2.08.04.0A (Re-Dissolution of Precipitates Directs More Corrosive Fluids to Waste Packages).

Multiscale Thermohydrologic Model (SNL 2008 [DIRS 184433]) incorporates resaturation of the dryout zone around the drift, by both liquid flow and capillary condensation of water vapor, in calculating near-field and in-drift thermal hydrology. This model provides in-drift temperature and relative humidity inputs used by TSPA to extract water composition data from lookup tables generated by the seepage dilution/evaporation model (SNL 2007 [DIRS 177412], Sections 6.3.3

and 6.9), which evaluates in-drift processes and provides lookup tables for in-drift aqueous chemistry to TSPA. The effect of uncertainties in the development of the dryout zone and the timing of resaturation are captured through the use of multiscale model simulation results with different rock thermal conductivities and a suite of percolation flux values (SNL 2008 [DIRS 184433], Sections 6.3.15[a] and 6.3.16[a]). Uncertainties in rock hydrologic properties, ventilation heat removal efficiency, and the effects of axial vapor transport (SNL 2008 [DIRS 184433], Sections 6.3.11[a], 6.3.12, and 6.3.18[a]) were evaluated using sensitivity analyses and found to be insignificant with respect to predicted in-drift conditions. Hence, the effects of resaturation of the dryout zone are incorporated in TSPA predictions of in-drift chemistry through the multiscale model.

INPUTS:

Table 2.2.07.11.0A-1. Indirect Inputs

Citation	Title	DIRS
BSC 2005	*Drift-Scale Coupled Process (DST and TH Seepage) Models*	172232
SNL 2007	*Abstraction of Drift Seepage*	181244
SNL 2007	*Engineered Barrier System: Physical and Chemical Environment*	177412
SNL 2008	*Multiscale Thermohydrologic Model*	184433

FEP: 2.2.07.12.0A

FEP NAME:

Saturated Groundwater Flow in the Geosphere

FEP DESCRIPTION:

Groundwater flow in the saturated zone below the water table may affect long-term performance of the repository. The location, magnitude, and direction of flow under present and future conditions and the hydraulic properties of the rock are all relevant.

SCREENING DECISION:

Included

TSPA DISPOSITION:

Flows through geologic (rock) units below the water table (saturated) are the principal pathways for radionuclides released from the repository. Steady-state, saturated, three-dimensional, groundwater flow in the Yucca Mountain vicinity is modeled in *Saturated Zone Site-Scale Flow Model* (SNL 2007 [DIRS 177391]) with output data used by *Site-Scale Saturated Zone Transport* (SNL 2008 [DIRS 184806], Section 6.3) to estimate radionuclide transport. Both models are based on the numerical code FEHM (FEHM V. 2.24-02 [DIRS 179539], STN: 10086-2.24-02). Specified mass flow (kg/s) is assigned at the water table of the SZ site-scale flow model (SNL 2007 [DIRS 177391], Sections 6.3.1.7 and 6.4.3.9) using the technique outlined in *Recharge and Lateral Groundwater Flow Boundary Conditions for the Saturated Zone Site-Scale Flow and Transport Model* (BSC 2004 [DIRS 170015], Section 6). Specified mass flow data at the water table are derived from the 2004 Death Valley Regional Flow System model (Belcher 2004 [DIRS 173179]), the UZ flow model (SNL 2007 [DIRS 184614]), and data from Savard (1998 [DIRS 102213]). The hydrogeologic framework (SNL 2007 [DIRS 174109]) and additional faults and features (SNL 2007 [DIRS 177391], Section 6.4.3.7) are the strongest controlling factors on saturated zone flow (included FEPs 2.2.03.02.0A (Rock Properties of Host Rock and other Units) and 2.2.07.13.0A (Water-conducting Features in the SZ)). Saturated zone aquifers that are expected to transport radionuclides released from the repository include the volcanic Crater Flat Tuff hydrogeologic units and the shallow alluvial aquifer of Fortymile Wash. Targets for lateral flow at model boundaries are derived from the 2004 Death Valley Regional Flow System model (Belcher 2004 [DIRS 173179]).

As discussed in *Probability Distribution for Flowing Interval Spacing* (BSC 2004 [DIRS 170014]), only a subset of existing fractures is observed to transmit flow in the saturated zone. Flow through fractures is modeled as an effective continuum (SNL 2007 [DIRS 177391], Section 6.4.1). Uncertainty in the saturated flow through fractures is incorporated in the flow model abstraction with parameters of flowing interval spacing, specific discharge, and the horizontal anisotropy (SNL 2008 [DIRS 183750], Sections 6.5.2.3[a], 6.5.2.1[a], and 6.5.2.10). These parameters are described by probability distributions and sampled across multiple realizations to develop a range in radionuclide breakthroughs specified by a calculated

probability distribution function. For example, an uncertain parameter in saturated zone flow modeling is the groundwater specific discharge multiplier that ranges from 1/8.93 to 8.93 (SNL 2008 [DIRS 183750], Figure 6-2[a]).

Uncertainty in groundwater specific discharge in the alluvium is discussed in *Saturated Zone In-Situ Testing* (SNL 2007 [DIRS 177394], Section 6.5) and in *Saturated Zone Site-Scale Flow Model* (SNL 2007 [DIRS 177391], Section 6.7).

The impact of future climatic conditions on flow is modeled in *Saturated Zone Site-Scale Flow Model* (SNL 2007 [DIRS 177391], Section 6.6.4), *Site-Scale Saturated Zone Transport* (SNL 2008 [DIRS 184806], Section 6.6), and *Saturated Zone Flow and Transport Model Abstraction* (SNL 2008 [DIRS 183750], Section 6.5[a]). The radionuclide breakthrough curves are generated using glacial-transition climate flow rates and they are scaled back for present-day and monsoonal conditions using the convolution integral method. The simulated radionuclide mass breakthrough curves from the SZ flow and transport abstraction model are coupled to the TSPA analyses using the convolution integral method (SNL 2008 [DIRS 183750]). That is, plots of radionuclide normalized cumulative mass releases at the 18-km compliance boundary are developed from Latin-Hypercube-Sampled parameters with uncertainty distributions as specified in *Saturated Zone Flow and Transport Model Abstraction* (SNL 2008 [DIRS 183750], Section 6.5[a]) and are used by the convolution integral implementation in the TSPA analysis.

INPUTS:

Table 2.2.07.12.0A-1. Indirect Inputs

Citation	Title	DIRS
10 CFR 63	Energy: Disposal of High-Level Radioactive Wastes in a Geologic Repository at Yucca Mountain, Nevada	180319
Belcher 2004	*Death Valley Regional Ground-Water Flow System, Nevada and California – Hydrogeologic Framework and Transient Ground-Water Flow Model*	173179
BSC 2004	*Probability Distribution for Flowing Interval Spacing*	170014
BSC 2004	*Recharge and Lateral Groundwater Flow Boundary Conditions for the Saturated Zone Site-Scale Flow and Transport Model*	170015
FEHM V 2.24-02	WINDOWS XP. STN: 10086-2.24-02-00	179539
Savard 1998	*Estimated Ground-Water Recharge from Streamflow in Fortymile Wash Near Yucca Mountain, Nevada*	102213
SNL 2007	*Saturated Zone Site-Scale Flow Model*	177391
SNL 2007	*Hydrogeologic Framework Model for the Saturated Zone Site Scale Flow and Transport Model*	174109
SNL 2007	*Saturated Zone In-Situ Testing*	177394
SNL 2007	*UZ Flow Models and Submodels*	184614
SNL 2008	*Saturated Zone Flow and Transport Model Abstraction*	183750
SNL 2008	*Site-Scale Saturated Zone Transport*	184806

FEP: 2.2.07.13.0A

FEP NAME:

Water-Conducting Features in the SZ

FEP DESCRIPTION:

Geologic features in the saturated zone may affect groundwater flow by providing preferred pathways for flow.

SCREENING DECISION:

Included

TSPA DISPOSITION:

Geologic features in the saturated zone that may represent preferred pathways for flow are described in the *Hydrogeologic Framework Model for the Saturated Zone Site-Scale Flow and Transport Model* (SNL 2007 [DIRS 174109]), which updates the hydrogeologic framework model used in flow and transport modeling. These water-conducting features in the saturated zone are addressed in and incorporated into the *Saturated Zone Site-Scale Flow Model* (SNL 2007 [DIRS 177391]). Faults and features in the model domain are explicitly included through 10 discrete geologic features incorporated in the SZ site-scale flow model (SNL 2007 [DIRS 177391], Section 6.4.3.7 and Figure 6-12).

The impacts of these various features on saturated zone transport are evaluated in *Site-Scale Saturated Zone Transport* (SNL 2008 [DIRS 184806], Sections 6.2, 6.3, and 6.4). The variability and uncertainty due to the presence of fracture clusters, flowing intervals, and rubblized zones (all possible subsets of water-conducting features within the faulted and fractured system) are modeled in the SZ flow and transport abstraction model and the SZ one-dimensional transport model, both described in *Saturated Zone Flow and Transport Model Abstraction* (SNL 2008 [DIRS 183750]). The variability and uncertainty are quantified through the stochastically sampled probability distribution functions for values of several parameters in the performance assessment calculations. The parameters treated in such a manner include: groundwater specific discharge multiplier, flowing interval spacing in volcanic units, horizontal anisotropy in permeability, flowing interval porosity in volcanic units, and longitudinal dispersivity, as developed in *Saturated Zone Flow and Transport Model Abstraction* (SNL 2008 [DIRS 183750], Sections 6.5.2 and 6.5.2[a], and Tables 6-8 and 6-7[a]). The ranges of uncertainty in these parameters encompass the possibility of channelized flow along preferred pathways (SNL 2008 [DIRS 183750], Sections 6.5.2.1, 6.5.2.1[a], 6.5.2.4, 6.5.2.4[a], 6.5.2.5, 6.5.2.9, and 6.5.2.10).

Numerous broad and distinct zones in the SZ flow model are categorized as features and, depending upon their physical properties, these act as either barriers or conduits to saturated zone groundwater flow. These zones are directly or indirectly affected by faults, zones of mineralogical alteration along faults, or contact zones between units (SNL 2007 [DIRS 177391], Section 6.4.3.7). In total, there are 10 features defined in *Saturated Zone Site-Scale Flow Model*

for Yucca Mountain (SNL 2007 [DIRS 177391], Table 6-7) in addition to those geologic units specified in the hydrogeologic framework model (with 27 surfaces) employed as described in *Hydrogeologic Framework Model for the Saturated Zone Site-Scale Flow and Transport Model* (SNL 2007 [DIRS 174109], Section 6). Most of the 10 features are vertical, but some are areally extensive (SNL 2007 [DIRS 177391], Figure 6-12). Depending upon their hydrologic impact on groundwater flow patterns, these features fall under several distinct categories as follows: (1) zones of permeability enhancement parallel to faults, and zones of permeability reduction perpendicular to faults; (2) fault zones with generalized enhanced permeability; (3) juxtapositions of hydrogeologic units with different values of permeability; (4) the altered northern region and; (5) zones of enhanced or anisotropic permeability (SNL 2007 [DIRS 177391], Table 6-7). These features control the flow pattern in the saturated zone and also the specific discharge. Uncertainty in specific discharge is propagated through to TSPA in *Saturated Zone Flow and Transport Model Abstraction* (SNL 2008 [DIRS 183750], Table 6-8) through the uncertain parameter for groundwater specific discharge multiplier.

Smaller-scale water conducting features are assessed as flowing intervals in the fractured volcanic units, as described in *Probability Distribution for Flowing Interval Spacing* (BSC 2004 [DIRS 170014]). In-situ testing of smaller scale water conducting features was performed at the C-wells complex, as documented in *Saturated Zone In-Situ Testing* (SNL 2007 [DIRS 177394], Sections 6.2 and 6.3). These reports contain data used to formulate the flowing interval spacing parameter.

INPUTS:

Table 2.2.07.13.0A-1. Indirect Inputs

Citation	Title	DIRS
10 CFR 63	Energy: Disposal of High-Level Radioactive Wastes in a Geologic Repository at Yucca Mountain, Nevada	180319
70 FR 53313	Implementation of a Dose Standard After 10,000 Years	178394
BSC 2004	*Probability Distribution for Flowing Interval Spacing*	170014
SNL 2007	*Saturated Zone Site-Scale Flow Model*	177391
SNL 2007	*Hydrogeologic Framework Model for the Saturated Zone Site Scale Flow and Transport Model*	174109
SNL 2007	*Saturated Zone In-Situ Testing*	177394
SNL 2008	*Saturated Zone Flow and Transport Model Abstraction*	183750
SNL 2008	*Site-Scale Saturated Zone Transport*	184806

FEP: 2.2.07.14.0A

FEP NAME:

Chemically-Induced Density Effects on Groundwater Flow

FEP DESCRIPTION:

Chemically-induced spatial variation in groundwater density may affect groundwater flow.

SCREENING DECISION:

Excluded – low consequence

SCREENING JUSTIFICATION:

Large-scale, chemically induced variations in the density of groundwater, such as those related to the presence of natural brine, do not exist in the groundwater flow system at Yucca Mountain. Minor or transient variations in the chemical composition of groundwater related to unsaturated flow or repository thermal effects will occur in the flow system, but these will be of low consequence with regard to repository performance.

Water entering the saturated zone from the unsaturated zone under ambient conditions will tend to have a higher total dissolved solids concentration, and hence a higher density, than saturated zone groundwater because of evaporation in the unsaturated zone. However, the density differences are not expected to be large enough to result in density-driven flow of unsaturated zone water in the saturated zone. Indeed, unsaturated zone pore waters, though quite variable in composition, have total dissolved solids concentrations ranging from about 200 mg/L to as much as 1,300 to 1,400 mg/L, with an average of about 500 mg/L (derived from DTNs: GS020408312272.003 [DIRS 160899], GS020808312272.004 [DIRS 166569], GS030408312272.002 [DIRS 165226], GS031008312272.008 [DIRS 166570], GS041108312272.005 [DIRS 178057], and GS0703PA312272.001 [DIRS 182478]; the chemical constituent concentration data from analyses of unsaturated zone water samples in these data packages were summed to obtain total dissolved solids concentrations) whereas saturated zone samples from the volcanics near Yucca Mountain have an average total dissolved solids concentration of about 275 mg/L with a range from 246 to 288 mg/L (derived from DTNs: GS040108312322.001 [DIRS 179422] and GS980908312322.008 [DIRS 145412]; the chemical constituent concentration data from analyses of saturated zone water samples in these data packages were summed to obtain total dissolved solids concentrations.). Density contrasts of ~2,000 mg/L or greater are necessary for density-driven flow to occur (Zhang and Schwartz 1995 [DIRS 183479], pp. 837 to 847). Furthermore, perched waters in the unsaturated zone, which are considered to have water chemistries more representative of water that will flow through fractures in the unsaturated zone, tend to have total dissolved solids concentrations that are closer to that of saturated zone waters (derived from DTN: GS951208312272.004 [DIRS 165858]; the chemical constituent concentration data from analyses of perched water samples in this data package was summed to obtain total dissolved solids concentrations) than the more highly evaporated water from unsaturated zone rock matrices.

Once waste is emplaced in the repository, water seeping through the unsaturated zone and engineered barrier system will pick up additional dissolved solids as a result of evaporation (due to the radioactive decay heat in the near field) and interactions with host rock, waste package materials, invert materials, and dust introduced during mining and waste emplacement operations (SNL 2007 [DIRS 177412], Sections 6.3, 6.8, 6.9, 6.10 and 6.13). Depending on the extent of evaporation and the length of time the water remains in contact with these materials (a function of temperature and local water fluxes), dissolved solids concentrations could become high enough to result in brines in the near field (SNL 2007 [DIRS 177412], Section 6.3.3). However, the brines are predicted to persist for only a few thousand years or less after waste emplacement because of flushing by percolation flux that returns to the near field once temperatures drop below the water boiling point (SNL 2007 [DIRS 177412], Figure 7.1-11 (for predicted time periods of altered chemistry); and DTN: SN0701PAEBSPCE.001 [DIRS 180523], folder: "Lookup Tables" (for predicted temperature and concentration histories)). A short-duration pulse of brackish water (as much as 5,000 to 10,000 mg/L dissolved solids) may drain through the host rock when this flushing begins because of the dissolution of dry salts left behind by evaporation during the thermal pulse (SNL 2007 [DIRS 177404], Section 6.5.5.4. The dissolved solids concentrations were calculated from the peak molal concentrations plotted in Figures 6.5-13 to 6.5-23 of Section 6.5.5.4, with moles/kg converted to mg/L using appropriate values of elemental atomic weights and water density. The concentrations are presented here as a range because of the approximate nature of the values read from the plots and the uncertainties in the model predictions in Section 6.5.5.4.).

After the high temperature pulse has diminished and relatively steady-state flow is established through the repository, concentrated solutions may still develop in the immediate vicinity of waste packages due to water interactions with waste package materials and waste forms. The degree of dissolved solids buildup under these lower temperature conditions is predicted to be roughly inversely proportional to the water flux through the waste forms (SNL 2007 [DIRS 180506], Section 6.6.4[a]), and it has been shown that the water does not become highly concentrated at water fluxes greater than about 100 L/yr per waste package (SNL 2007 [DIRS 180506], Figures 6-27[a], 6-29[a], and 6-31[a]). Thus, only relatively low overall fluxes of high density solutions are possible out of the near-field environment.

The net result of all these processes is that radionuclide-bearing water leaving the unsaturated zone has the potential to be more dense than ambient saturated zone water and could thus tend to sink by density-driven flow when it enters the saturated zone. Such effects will be localized in the area beneath the repository and will be attenuated by dilution over the scale of transport from the repository to the accessible environment. The extent of this sinking will depend on a number of variables, including the density contrast between the waters, the downward water flow rate in the unsaturated zone relative to the horizontal flow rate at the top of the saturated zone, solute diffusivities and dispersivities, and the spatial heterogeneity in permeability at the top of the saturated zone (including fractures and horizontal layering).

The justification for excluding chemically induced density effects on groundwater flow relies on several consequence-based justifications:

1. The density contrast between unsaturated zone water entering the saturated zone and saturated zone water is not expected to be large enough to cause significant

density-driven flow except for possibly during the relatively short pulse associated with the repository thermal pulse. Zhang and Schwartz (1995 [DIRS 183479]) showed that for significant density-driven sinking of a plume entering a saturated zone to occur (their calculations were for a specific discharge of ~30 m/yr through a homogeneous isotropic porous medium with a flow porosity of 0.25, yielding a horizontal seepage velocity of ~120 m/yr), the concentration of the leachate (or contaminant plume) had to be at least 2,000 mg/L in a very dilute native groundwater at 20°C. Specifically, density-driven flow was evident only when they assumed a NaCl concentration greater than 2,000 mg/L, which corresponded to a solution density of 999.7 kg/m^3 at 20°C, in a native groundwater with a density of 998.2 kg/m^3 at 20°C (i.e., a density contrast of ~0.15%) (Zhang and Schwartz 1995 [DIRS 183479], pp. 839, 840, 843, and 844). For the temperatures and native dissolved solids concentrations in the upper part of the saturated zone at Yucca Mountain, a similar incremental dissolved solids concentration of 2,000 mg/L would be required for density-driven flow to occur. This incremental difference is greater than that expected and greater than what exists currently at Yucca Mountain under ambient conditions based on chemical analyses of unsaturated zone and saturated zone pore waters, which indicate, at most, a difference of about 1,000 mg/L (see above).

2. The higher density seepage water associated with the repository thermal pulse will move through the unsaturated zone soon after the repository near field becomes rewetted (between 1,000 and 10,000 years). However, this pulse is expected to be a one-time localized transient of relatively low volume (BSC 2007 [DIRS 177404], Section 6.5.5.2). In addition, the concentrated solutions that can potentially form in the vicinity of the drift after repository temperatures decrease below the boiling point of water will tend to become diluted by mixing with dilute unsaturated zone water. This mixing will occur over the several hundred meters that these waters must travel from the repository horizon to the water table or at the water table itself. The net result will be dilution of the concentrated solutions toward ambient pore-water concentrations before reaching the water table.

3. Even if relatively little mixing occurs in the unsaturated zone, the flux of the concentrated water reaching the saturated zone will be only a very small fraction of the horizontal flux in the saturated zone resulting from infiltration of dilute water and horizontal flux from through-flowing water. Indeed, percolation within the unsaturated zone flow model domain (which includes all of the repository horizon) amounts to only ~1% of the flow through the lateral boundaries of the site-scale saturated zone flow model domain, and it is only ~13% of the total recharge over the entire saturated zone flow model domain (SNL 2007 [DIRS 177391], Section 6.4.3.9). Under these conditions, a dense plume will not develop in the saturated zone because the solutes will be swept away faster than they arrive. Even in the unexpected event that the overall infiltration flux through the unsaturated zone *all* comes in contact with waste packages and is also low enough to result in elevated dissolved solids concentrations, this flux will be so low that dense plumes will not be able to develop except where the saturated zone water is nearly stagnant. In this case, the dense plume will move down through the stagnant zone until it reaches a horizontal flow zone, at which point sweeping/dilution will prevent further downward migration of the plume.

4. Although not expected for the reasons given in the three preceding paragraphs, if density-driven flow did occur, it would result in either an increase or a decrease in the rate of radionuclide migration through the fractured volcanics, depending on whether the increased downward flow causes radionuclides to move past a shallow high-flow layer/feature or to more quickly reach a deeper high-flow layer/feature. Thus, the consequences of density-driven flow in the saturated zone will ultimately be expressed as increased or decreased radionuclide travel times through the volcanics. The uncertainty in groundwater flow rates resulting from density-driven flow is small relative to the ranges of uncertainty in specific discharge and flowing interval porosity in the volcanic units of the saturated zone, as incorporated in the parameter uncertainty distributions for these parameters (SNL 2008 [DIRS 183750], Sections 6.5.2.1[a] and 6.5.2.5). Thus, while density-driven flow is not directly modeled or accounted for in TSPA, its consequences are expected to be minor relative to and, therefore, bounded by the modeled uncertainty in groundwater travel times through the volcanics that results from uncertainty in specific discharge and flowing interval porosity.

The TSPA model calculates the concentration of contaminants in groundwater by capturing all of the contaminants that annually cross the regulatory boundary (SNL 2008 [DIRS 183750], Section 6.3.3). This approach will tend to dampen any effects that density-driven flow may have on the contaminant plume (which would occur predominantly near the source because it is not considered plausible that density contrasts large enough to cause density-driven flow will persist in the saturated zone all the way to the compliance boundary). Although the timing of contaminant arrival at the compliance boundary could potentially be affected by density-driven flow near the source, the possible influence of density-driven flow on travel times is well bounded by the treatment of uncertainty in parameters that govern flow velocity in the saturated zone (see item 4).

In conclusion:

1 Density-driven flow will not occur under ambient unsaturated zone flow conditions because of insufficient density contrast between unsaturated zone and saturated zone pore waters.

2 The higher density seepage water associated with the repository thermal pulse will be a small flux, localized, and transient. These higher density seepage waters will mix with more dilute water in the unsaturated zone prior to reaching the water table such that the concentrated solutions will tend to shift toward ambient pore water concentrations before reaching the water table.

3. Even if relatively little mixing occurs in the unsaturated zone, the flux of the concentrated water reaching the saturated zone is expected to be only a small fraction of the horizontal flux in the saturated zone resulting from infiltration of dilute water and from through-flowing water.

4. While density-driven flow is not directly modeled or accounted for in TSPA, its consequences are expected to be minor relative to and, therefore, bounded by the

modeled uncertainty in groundwater travel times through the volcanics that results from uncertainty in specific discharge and flowing interval porosity.

Based on the previous discussion, omission of FEP 2.2.07.14.0A (Chemically-Induced Density Effects on Groundwater Flow) will not result in a significant adverse change in the magnitude or time of radiological exposures to the RMEI or radionuclide releases to the accessible environment. Therefore, this FEP is excluded from the performance assessments conducted to demonstrate compliance with proposed 10 CFR 63.311 and 63.321 (70 FR 53313 [DIRS 178394]), and with 10 CFR 63.331 [DIRS 180319], on the basis of low consequence.

INPUTS:

Table 2.2.07.14.0A-1. Direct Inputs

Input	Source	Description
DTN: GS020408312272.003. Collection and Analysis of Pore Water Samples for the Period from April 2001 to February 2002. [DIRS 160899]	Table S02133_001	Total dissolved solids concentrations in unsaturated zone waters
DTN: GS030408312272.002. Analysis of Water-Quality Samples for the Period from July 2002 to November 2002. [DIRS 165226]	Table S03203_001	Total dissolved solids concentrations in unsaturated zone waters
DTN: GS031008312272.008. Analysis of Pore Water and Miscellaneous Water Samples for the Period from December 2002 to July 2003. [DIRS 166570]	Tables S03370_001 and S03370_002	Total dissolved solids concentrations in unsaturated zone waters
DTN: GS040108312322.001. Field and Chemical Data Collected Between 10/4/01 and 10/3/02 and Isotopic Data Collected Between 5/19/00 and 5/22/03 from Wells in the Yucca Mountain Area, Nye County, Nevada. [DIRS 179422]	Table S04188_001	Total dissolved solids concentrations in saturated zone waters
DTN: GS041108312272.005. Analysis of Pore Water and Miscellaneous Water Samples for the Period from July 2003 to September 2004. [DIRS 178057]	Table S05038_001	Total dissolved solids concentrations in unsaturated zone waters
DTN: GS0703PA312272.001. Analysis of Pore Water Samples Collected from the ESF Cross Drift and Analyzed from November 1, 2005 through January 26, 2006. [DIRS 182478]	Table S07035_001	Total dissolved solids concentrations in unsaturated zone waters
SNL 2007. *Saturated Zone Site-Scale Flow Model*. [DIRS 177391]	Section 6.4.3.9	Percolation within the unsaturated zone flow model domain amounts to only ~1% of the flow through the lateral boundaries of the site-scale saturated zone flow model domain, and it is only ~13% of the total recharge over the entire saturated zone flow model domain
SNL 2007. D*rift-Scale THC Seepage Model*. [DIRS 177404]	Sections 6.5.5.2 and6.5.5.4	A short-duration pulse of concentrated solution is expected to move through the repository immediately after seepage is reestablished

Table 2.2.07.14.0A-1. Direct Inputs

Input	Source	Description
SNL 2007. *Engineered Barrier System: Physical and Chemical Environment*. [DIRS 177412]	Section 6.3.3	Brines could occur in the near field as a result of evaporation
	Sections 6.3, 6.8, 6.9, 6.10, 6.13	Seepage water will pick up total dissolved solids by a variety of processes
SNL 2007. *In-Package Chemistry Abstraction*. [DIRS 180506]	Section 6.6.4[a]	The degree of dissolved solids buildup under these lower temperature conditions is predicted to be roughly inversely proportional to the water flux through the waste forms
	Figures 6-27[a], 6-29[a], and 6-31[a]	Water does not become highly concentrated at water fluxes greater than about 100 L/yr per waste package (after the thermal pulse)
SNL 2008. *Saturated Zone Flow and Transport Model Abstraction*. [DIRS 183750]	Sections 6.5.2.1[a] and 6.5.2.5	Specific dischage and effective flow porosity in the volcanics have wide ranges of values in TSPA
	Section 6.3.3	At the downstream end of the SZ flow system, the TSPA model calculates the concentration of contaminants in groundwater by capturing all of the contaminants that cross the regulatory boundary in the representative groundwater volume at the compliance point
Zhang and Schwartz 1995. "Multispecies contaminant plumes in variable density flow systems." [DIRS 183479]	pp. 839, 840, 843, and 844	The chemical and physical properties of the leachate for a specified discharge and the medium

Table 2.2.07.14.0A-2. Indirect Inputs

Citation	Title	DIRS
10 CFR 63	Energy: Disposal of High-Level Radioactive Wastes in a Geologic Repository at Yucca Mountain, Nevada	180319
70 FR 53313	Implementation of a Dose Standard After 10,000 Years	178394
DTN: GS020808312272.004	Analysis of Water-Quality Samples for the Period from July 1999 to July 2002	166569
DTN: GS951208312272.004	Analysis for Chemical Composition of Perched-Water from Boreholes USW UZ-14, USW NRG-7A, USW SD-9, USW SD-7 and Groundwater from Boreholes UE-25 ONC#1 and USW G-2 from 8/18/89 to 3/21/95	165858
DTN: GS980908312322.008	Field, Chemical, and Isotopic Data from Precipitation Sample Collected Behind Service Station in Area 25 and Ground Water Samples Collected at Boreholes UE-25 C #2, UE-25 C #3, USW UZ-14, UE-25 WT #3, UE-25 WT #17, and USW WT-24	145412
DTN: SN0701PAEBSPCE.001	PCE TDIP Potential Seepage Water Chemistry Lookup Tables	180523
SNL 2007	*Engineered Barrier System: Physical and Chemical Environment*	177412
Zhang and Schwartz 1995	"Multispecies Contaminant Plumes in Variable Density Flow Systems"	183479

FEP: 2.2.07.15.0A

FEP NAME:

Advection and Dispersion in the SZ

FEP DESCRIPTION:

Advection and dispersion processes may affect radionuclide transport in the saturated zone.

SCREENING DECISION:

Included

TSPA DISPOSITION:

Advection and longitudinal dispersion of radionuclides in the saturated zone are explicitly included in the conceptual and mathematical models for radionuclide transport in the saturated zone (SNL 2008 [DIRS 184806], Sections 6.3 and 6.4). The numerical code FEHM is used to obtain a three-dimensional advective flow field that is calibrated to head observations and model boundary fluxes by adjusting permeabilities of geologic units within the model domain (SNL 2007 [DIRS 177391]). The estimated groundwater flow rates into the SZ site-scale flow model domain, both as recharge (infiltration) at the upper boundary (water table) and as underflow at the lateral boundaries, are determined from a larger scale regional model reported in *Recharge and Lateral Groundwater Flow Boundary Conditions for the Saturated Zone Site-Scale Flow and Transport Model* (BSC 2004 [DIRS 170015], Section 6). FEHM also implements, as part of the SZ site-scale transport model (SNL 2008 [DIRS 184806]), the dispersion tensor and random walk particle tracking method to simulate radionuclide dispersion in the saturated zone.

To address uncertainty in the flow field produced by the SZ site-scale flow model (SNL 2007 [DIRS 177391]), the HAVO (horizontal flow anisotropy in the volcanics) parameter is stochastically sampled to produce 200 unique three-dimensional permeability fields that result in 200 unique flow fields (SNL 2008 [DIRS 183750], Section 6.5.3.1), which are used in TSPA. This parameter determines the degree of anisotropy in permeability for the volcanic units, and its range of values is based on field-test analyses discussed in *Saturated Zone In-Situ Testing* (SNL 2007 [DIRS 177394], Section 6.2.6) as well as numerical analysis discussed in *Saturated Zone Site-Scale Flow Model* (SNL 2007 [DIRS 177391], Section 6.5.3). For each of the 200 flow field realizations, the recharge fluxes, boundary fluxes, and calibrated permeability field are scaled with the stochastically sampled parameter, GWSPD, to address uncertainty in advective transport velocities within the saturated zone model domain (SNL 2008 [DIRS 183750], Section 6.5.2.1[a]). The simultaneous scaling of the fluxes and permeabilities preserves the flow model calibration. GWSPD scales permeabilities in both the volcanic and alluvium units. The range for the GWSPD scaling parameter is based on field test analyses (SNL 2007 [DIRS 177394]), calibration of the "base-case" flow field to measured heads (SNL 2007 [DIRS 177391], Section 6.6.1.3), and expert elicitation (CRWMS M&O 1998 [DIRS 100353], Section 3.2). Detailed discussions of the GWSPD and HAVO parameter implementation are

provided in *Saturated Zone Flow and Transport Model Abstraction* (SNL 2008 [DIRS 183750], Sections 6.5.2.1[a] and 6.5.2.10).

Uncertainty in the dispersion tensor is modeled by stochastically varying the LDISP (SNL 2008 [DIRS 183750], Section 6.5.2.9[b]). The distribution of values for the LDISP is based on recommendations from the expert elicitation panel (CRWMS M&O 1998 [DIRS 100353], Section 3.2).

The transverse and vertical dispersivities are not varied independently but are scaled as a multiple (significantly less than 1) of the stochastically sampled LDISP. Further discussions on transverse and vertical dispersion are provided in *Saturated Zone Flow and Transport Model Abstraction* (SNL 2008 [DIRS 183750], Section 6.5.2.9).

INPUTS:

Table 2.2.07.15.0A-1. Indirect Inputs

Citation	Title	DIRS
BSC 2004	*Recharge and Lateral Groundwater Flow Boundary Conditions for the Saturated Zone Site-Scale Flow and Transport Model*	170015
CRWMS M&O 1998	*Saturated Zone Flow and Transport Expert Elicitation Project*	100353
SNL 2007	*Saturated Zone Site-Scale Flow Model*	177391
SNL 2007	*Saturated Zone In-Situ Testing*	177394
SNL 2008	*Saturated Zone Flow and Transport Model Abstraction*	183750
SNL 2008	*Site-Scale Saturated Zone Transport*	184806

FEP: 2.2.07.15.0B

FEP NAME:

Advection and Dispersion in the UZ

FEP DESCRIPTION:

Advection and dispersion processes may affect radionuclide transport in the UZ.

SCREENING DECISION:

Included

TSPA DISPOSITION:

Radionuclide transport through the unsaturated zone by advection is simulated using the RTTF method documented in *Particle Tracking Model and Abstraction of Transport Processes* (SNL 2008 [DIRS 184748], Section 6.4.1). Dispersion is incorporated into the RTTF algorithm through the use of a transfer function based on an analytical solution to the advection–dispersion equation (SNL 2008 [DIRS 184748], Section 6.4.2). In TSPA model runs, advection and dispersion are included through the use of FEHM (Finite Element Heat and Mass Transfer Code) RTTF model and the pregenerated flow fields as described in *Particle Tracking Model and Abstraction of Transport Processes* (SNL 2008 [DIRS 184748], Sections 6.4 and 6.5.1).

The fracture dispersivity is set at a fixed value of 10 m. This is discussed and justified in *Particle Tracking Model and Abstraction of Transport Processes* (SNL 2008 [DIRS 184748], Table 6-4).

Uncertainty in advection is handled by incorporating four infiltration scenarios for the first three climate states (present day, monsoon, and glacial-transition) into the UZ flow model (SNL 2008 [DIRS 184614], Section 6.1.4). For the post-10,000-year climate state, four corresponding net infiltration maps representing present-day 90th percentile, glacial-transition 50th percentile, glacial-transition 90th percentile, and monsoon 90th percentile, respectively, are used to develop the four flow fields for incorporation into the UZ abstraction model. Dispersion is represented by a single parameter value (SNL 2008 [DIRS 184748], Section 6.5.2).

INPUTS:

Table 2.2.07.15.0B-1. Indirect Inputs

Citation	Title	DIRS
SNL 2007	*UZ Flow Models and Submodels*	184614
SNL 2008	*Particle Tracking Model and Abstraction of Transport Processes*	184748

FEP: 2.2.07.16.0A

FEP NAME:

Dilution of Radionuclides in Groundwater

FEP DESCRIPTION:

Dilution due to mixing of contaminated and uncontaminated water may affect radionuclide concentrations in groundwater during transport in the saturated zone and during pumping at a withdrawal well.

SCREENING DECISION:

Included

TSPA DISPOSITION:

Dilution of radionuclides as a result of groundwater transport is included in the TSPA in two ways (SNL 2008 [DIRS 183750]): dispersion in flowing groundwater and dilution in the representative volume of groundwater. Dilution of simulated radionuclide concentrations within the contaminant plume is modeled through the longitudinal and transverse hydrodynamic dispersion parameters. Dispersion is caused, in part, by heterogeneities in permeability at all scales (SNL 2008 [DIRS 184806], Section 6.4.2.2). Longitudinal dispersivity will be important primarily at the leading edge of the advancing plume while transverse dispersion will occur along the entire length of the plume. Transverse dispersivity is a function of the stochastically sampled longitudinal dispersivity (SNL 2008 [DIRS 183750], Section 6.5.2.9).

Dilution in the volume of water used to calculate dose to the RMEI, which is defined as 3,000 acre-ft in accordance with 10 CFR 63.312(c) [DIRS 180319], or in the representative volume of groundwater used to demonstrate compliance with the groundwater protection standards, which is also 3,000 acre-ft in accordance with 10 CFR 63.332(a)(3) [DIRS 180319], is documented in *Saturated Zone Flow and Transport Model Abstraction* (SNL 2008 [DIRS 183750], Sections 5(3) and 6.3.3). It is assumed that all of the radionuclide mass crossing the accessible environment boundary in a year is dissolved in this volume of water.

INPUTS:

Table 2.2.07.16.0A-1. Indirect Inputs

Citation	Title	DIRS
10 CFR 63	Energy: Disposal of High-Level Radioactive Wastes in a Geologic Repository at Yucca Mountain, Nevada	180319
SNL 2008	*Saturated Zone Flow and Transport Model Abstraction*	183750
SNL 2008	*Site-Scale Saturated Zone Transport*	184806

FEP: 2.2.07.17.0A

FEP NAME:

Diffusion in the SZ

FEP DESCRIPTION:

Molecular diffusion processes may affect radionuclide transport in the SZ.

SCREENING DECISION:

Included

TSPA DISPOSITION:

This FEP addresses diffusive transport processes that are associated with hydrodynamic dispersion (part mechanical dispersion, part diffusion). The process of diffusion into the rock matrix of volcanic units is discussed in included FEP 2.2.08.08.0A (Matrix Diffusion in the SZ).

In the site-scale transport model diffusion is one of two components of a dispersion tensor. This tensor, denoted as D' (SNL 2008 [DIRS 184806], Section 6.4.2.1), is the sum of the mechanical dispersion tensor (D) for the flow system and the coefficient of molecular diffusion (D_0) in porous media. Uncertainty in the process of hydrodynamic dispersion is modeled using a stochastically sampled longitudinal dispersivity factor, LDISP (SNL 2008 [DIRS 183750], Sections 6.5.2.9 and 6.5.2[b]), and the transverse hydrodynamic dispersion parameters, which are a function of LDISP. The effects of molecular diffusion are explicitly included in the displacement matrix described in *Site-Scale Saturated Zone Transport* (SNL 2008 [DIRS 184806], Section 6.4.2.3 and Equation 20). The effects of molecular diffusion are, thus, explicitly included in the SZ site-scale transport model. The effects of matrix diffusion in the saturated zone are additionally considered in *Saturated Zone Flow and Transport Model Abstraction* (SNL 2008 [DIRS 183750], Figure 6-3). Moreover, the effective diffusion coefficient (tortuosity multiplied by free water diffusion coefficient) received detailed consideration in the one-dimensional abstraction to the three-dimensional flow model (SNL 2008 [DIRS 183750], Sections 6.5.2.6 and 6.5.2[b]) where radionuclide breakthrough curves are developed for use in TSPA. Molecular diffusion is not applied to colloids in the TSPA model.

INPUTS:

Table 2.2.07.17.0A-1. Indirect Inputs

Citation	Title	DIRS
10 CFR 63	Energy: Disposal of High-Level Radioactive Wastes in a Geologic Repository at Yucca Mountain, Nevada	180319
SNL 2008	*Saturated Zone Flow and Transport Model Abstraction*	183750
SNL 2008	*Site-Scale Saturated Zone Transport*	184806

FEP: 2.2.07.18.0A

FEP NAME:

Film Flow into the Repository

FEP DESCRIPTION:

Water may enter waste emplacement drifts by a film flow process. This differs from the traditional view of flow in a capillary network where the wetting phase exclusively occupies capillaries with apertures smaller than some level defined by the capillary pressure. A film flow process could allow water to enter a waste emplacement drift at non-zero capillary pressure. Dripping into the drifts could also occur through collection of the film flow on the local minima of surface roughness features along the crown of the drift.

SCREENING DECISION:

Included

TSPA DISPOSITION:

The potential effects of film flow are represented in the data acquired in *In Situ Field Testing of Processes* (BSC 2004 [DIRS 170004], Section 6.2), and developed by *Seepage Calibration Model and Seepage Testing Data* (BSC 2004 [DIRS 171764], Sections 6.1.2, 6.3.3, and 6.6.3). Water originating from film flow seeping into the opening during a liquid-release test is reflected in the corresponding seepage data point used for model calibration. Film flow is thus accounted for in the estimated seepage-related capillary-strength parameter from the seepage calibration model (BSC 2004 [DIRS 171764], Table 6-8). Therefore, the impact of film flow on seepage is included in the prediction of seepage into waste emplacement drifts performed in *Seepage Model for PA Including Drift Collapse* (BSC 2004 [DIRS 167652], Section 6.3) and developed for TSPA calculations by *Abstraction of Drift Seepage* (SNL 2007 [DIRS 181244], Section 6.4.1.1), because both of these models use capillary-strength parameter values developed by the seepage calibration model. Uncertainty due to the potential effects of film flow is incorporated into TSPA by sampling a probability distribution for the capillary-strength parameter (SNL 2007 [DIRS 181244], Section 6.6).

This FEP addresses film flow in fractures and pores in the rock around the drift, and does not apply to water films on the drift walls. Water traveling down the drift walls as a film cannot contact the drip shield or waste package, and is assumed to be resorbed by the sloping wall of the drift prior to reaching the invert, because drift wall saturations decrease progressing downwards along the wall (BSC 2005 [DIRS 172232], Section 6.2.2). Hence, water flowing as a film down the drift wall contributes neither to seepage nor to flux through the invert.

Transport of dissolved radionuclides through films in the EBS is discussed in included FEP 2.1.09.08.0B (Advection of Dissolved Radionuclides in EBS).

This FEP is included in performance assessments to demonstrate compliance with the individual protection standard after permanent closure (proposed 10 CFR 63.311 (70 FR 53313

[DIRS 178394])) and the groundwater protection standards (10 CFR 63.331 [DIRS 180319]). It is not included in the human intrusion performance assessment (proposed 10 CFR 63.321 (70 FR 53313 [DIRS 178394])).

INPUTS:

Table 2.2.07.18.0A-1. Indirect Inputs

Citation	Title	DIRS
10 CFR 63	Energy: Disposal of High-Level Radioactive Wastes in a Geologic Repository at Yucca Mountain, Nevada	180319
70 FR 53313	Implementation of a Dose Standard After 10,000 Years	178394
BSC 2004	*In Situ Field Testing of Processes*	170004
BSC 2004	*Seepage Calibration Model and Seepage Testing Data*	171764
BSC 2004	*Seepage Model for PA Including Drift Collapse*	167652
BSC 2005	*Drift-Scale Coupled Process (DST and TH Seepage) Models*	172232
SNL 2007	*Abstraction of Drift Seepage*	181244

FEP: 2.2.07.19.0A

FEP NAME:

Lateral Flow from Solitario Canyon Fault Enters Drifts

FEP DESCRIPTION:

Water movement down Solitario Canyon Fault could enter waste emplacement drifts through lateral flow mechanisms in the Topopah Spring welded hydrogeologic unit. This percolation pathway is more likely to transmit episodic transient flow to waste emplacement locations due to the major fault pathway through the overlying units.

SCREENING DECISION:

Included

TSPA DISPOSITION:

The UZ flow model contains hydrogeologic connections between the Solitario Canyon Fault and the waste emplacement horizon. Therefore, the UZ flow model is capable of computing lateral flow. The connection is captured using a property set of the Paintbrush nonwelded unit (PTn) with calibrated fracture-matrix properties that address expectations for lateral flow (SNL 2007 [DIRS 184614], Sections 6.2.2.1 and 6.2.2.2).

As for all percolation flux arriving at the repository, any water arriving at the repository through lateral flow in the PTn from Solitario Canyon Fault may seep into waste emplacement drifts if the flux is sufficient to overcome the capillary barrier calculated in the drift seepage | model (SNL 2007 [DIRS 181244]); however, this FEP is not explicitly called out in Table 6-1 of that report. Any associated lateral flow effect is implicitly incorporated in the output flow fields developed in *UZ Flow Models and Submodels* (SNL 2007 [DIRS 184614], Section 8.6). The effects of lateral flow from Solitario Canyon Fault on the percolation flux arriving at the waste emplacement drifts are included through the UZ flow model output of percolation flux at the PTn/TSw interface (DTNs: LB0612PDPTNTSW.001 [DIRS 179150], LB0701MOPTNTSW.001 [DIRS 179156], LB0701GTPTNTSW.001 [DIRS 179153], and LB0702UZPTN10K.002 [DIRS 179332]). This flux is the boundary condition used by the seepage abstraction in TSPA (SNL 2007 [DIRS 181244], Section 6.6.5.1). The effects of lateral flow from Solitario Canyon Fault on the percolation flux within the unsaturated zone model domain affect flow fields used by the radionuclide transport abstraction in TSPA (DTNs: LB0612PDFEHMFF.001 [DIRS 179296], LB0701MOFEHMFF.001 [DIRS 179297], LB0701GTFEHMFF.001 [DIRS 179160], and LB0702PAFEM10K.002 [DIRS 179507]).

Other aspects of flow focusing in faults (preferential flow in faults) are discussed in included FEP 2.2.07.04.0A (Focusing of Unsaturated Flow (Fingers, Weeps)). Perched water is discussed in included FEP 2.2.07.07.0A (Perched Water Develops). The potential effects of episodic flow through Solitario Canyon Fault are discussed in excluded FEP 2.2.07.05.0A (Flow in the UZ from Episodic Infiltration). FEP 2.2.07.19.0A (Lateral Flow from Solitario Canyon Fault Enters Drifts) is included in the performance assessments conducted to demonstrate compliance with

proposed 10 CFR 63.311 and 63.321 (70 FR 53313 [DIRS 178394]), and with 10 CFR 63.331 [DIRS 180319].

INPUTS:

Table 2.2.07.19.0A-1. Indirect Inputs

Citation	Title	DIRS
70 FR 53313	Implementation of a Dose Standard After 10,000 Years	178394
DTN: LB0612PDFEHMFF.001	Flow-Field Conversions from TOUGH2 to FEHM Format for Present Day 10-, 30-, 50-, and 90-Percentile Infiltration Maps	179296
DTN: LB0612PDPTNTSW.001	Vertical Flux at PTN/TSW Interface for Present-Day Climate of 10th, 30th, 50th, and 90-Percentile Infiltration Maps	179150
DTN: LB0701GTFEHMFF.001	Flow-Field Conversions from TOUGH2 to FEHM Format for Glacial Transition Climate 10th-, 30th-, 50th-, and 90th-Percentile Infiltration Maps	179160
DTN: LB0701GTPTNTSW.001	Vertical Flux at PTN/TSW Interface for Glacial Transition Climate of 10th, 30th, 50th, and 90th-Percentile Infiltration Maps	179153
DTN: LB0701MOFEHMFF.001	Flow-Field Conversions from TOUGH2 to FEHM Format for Monsoon Climate 10th-, 30th-, 50th-, and 90th-Percentile Infiltration Maps	179297
DTN: LB0701MOPTNTSW.001	Vertical Flux at PTN/TSW Interface for Monsoon Climate of 10th, 30th, 50th and 90th-Percentile Infiltration Maps	179156
DTN: LB0702PAFEM10K.002	Flow Field Conversions to FEHM Format for Post 10,000 Year Peak Dose Fluxes in the Unsaturated Zone for Four Selected Infiltration Rates	179507
SNL 2007	*Abstraction of Drift Seepage*	181244
SNL 2007	*UZ Flow Models and Submodels*	184614

FEP: 2.2.07.20.0A

FEP NAME:

Flow Diversion Around Repository Drifts

FEP DESCRIPTION:

Flow in unsaturated rock tends to be diverted by openings such as waste emplacement drifts due to the effects of capillary forces. The resulting diversion of flow could have an effect on seepage into the repository. Flow diversion around the drift openings could also lead to the development of a zone of lower flow rates and low saturation beneath the drift, known as the drift shadow.

SCREENING DECISION:

Included

TSPA DISPOSITION:

The drift diameter and the circular shape of the drift (SNL 2007 [DIRS 179354], Parameter Number 01-10) are used in the calculations of drift seepage and thermal-hydrologic conditions inside the drift. The drift spacing (SNL 2007 [DIRS 179354], Table 4-1, Parameter Number 01-13) is also considered for determining thermal-hydrologic conditions in the drift.

Liquid release tests performed at several locations at the Exploratory Studies Facility (ESF) were used to gain an understanding of the unsaturated zone flow process in the presence of openings, including flow diversion around drifts and seepage (BSC 2004 [DIRS 170004], Section 6.2; BSC 2004 [DIRS 171764], Section 6.5). These measured data sets were used in calibration and validation of seepage-relevant hydrologic parameters of the formation surrounding drifts. The calibrated seepage-relevant parameters were used in downstream seepage process models, which were designed to explicitly consider impact of underground openings (including flow diversion and seepage) (BSC 2004 [DIRS 171764], Sections 6.3, 6.6, and 6.8; BSC 2004 [DIRS 167652], Sections 6.2.1, 6.3.2, and 6.7; BSC 2005 [DIRS 172232]; SNL 2007 [DIRS 177404]). *Abstraction of Drift Seepage* (SNL 2007 [DIRS 181244]), which is based on the seepage procees models that capture the impact of underground openings, provides seepage predictions in the form of lookup tables and probability distributions of seepage-relevant parameters to be used in the TSPA. These lookup tables and probability distributions of seepage-relevant parameters also quantify the uncertainty in drift seepage propagated into the TSPA.

A drift shadow is a region of reduced flow velocity and water saturation that forms beneath the drift as a result of flow diversion around drifts. The formation of the drift shadow beneath drift openings is represented in the seepage simulations in *Seepage Calibration Model and Seepage Testing Data* (BSC 2004 [DIRS 171764], Sections 6.3, 6.6, and 6.8). The effect of a drift shadow on transport of radionuclides is not included in the TSPA (see excluded FEP 2.2.07.21.0A (Drift Shadow Forms Below Repository)).

The impact of flow diversion around the drifts due to capillary pressure differences and its relevance for thermal-hydrologic conditions in the EBS are captured in the MSTHM process

model simulations (SNL 2008 [DIRS 184433]). These simulations are used to develop the MSTHM abstraction implemented in TSPA.

INPUTS:

Table 2.2.07.20.0A-1. Indirect Inputs

Citation	Title	DIRS
BSC 2004	*In Situ Field Testing of Processes*	170004
BSC 2004	*Seepage Calibration Model and Seepage Testing Data*	171764
BSC 2004	*Seepage Model for PA Including Drift Collapse*	167652
BSC 2005	*Drift-Scale Coupled Process (DST and TH Seepage) Models*	172232
SNL 2007	*Total System Performance Assessment Data Input Package for Requirements Analysis for EBS In-Drift Configuration*	179354
SNL 2007	*Abstraction of Drift Seepage*	181244
SNL 2007	*Drift-Scale THC Seepage Model*	177404
SNL 2008	*Multiscale Thermohydrologic Model*	184433

FEP: 2.2.07.21.0A

FEP NAME:

Drift Shadow Forms Below Repository

FEP DESCRIPTION:

Flow in unsaturated rock tends to be diverted by openings such as waste emplacement drifts due to the effects of capillary forces. Flow diversion around the drift openings could lead to the development of a zone of lower flow rates and low saturation beneath the drift, known as the drift shadow. Radionuclide transport rates through the unsaturated rock may be dependent on whether or not radionuclide releases occur from drifts that are underlain by a drift shadow.

SCREENING DECISION:

Excluded – low consequence

SCREENING JUSTIFICATION:

As discussed in included FEP 2.2.07.20.0A (Flow Diversion Around Repository Drifts), flow diversion around drifts is explicitly captured in the data acquired for seepage process models, and is therefore implicitly included in the TSPA. In contrast, drift shadow formation is not incorporated in the TSPA and has been excluded on the basis of low consequence. In particular, the reduction in flow over a region beneath the waste emplacement drift of the approximate size of the drift is not further considered.

A repository drift shadow is a region of reduced flow velocity and water saturation beneath the drift (Philip et al. 1989 [DIRS 105743], pp. 21 to 22, Figure 1). The drift shadow effect is a result of flow diversion around drifts as discussed in included FEP 2.2.07.20.0A (Flow Diversion around Repository Drifts) and in *Abstraction of Drift Seepage* (SNL 2007 [DIRS 181244], Section 6). Drift shadow formation is considered within *Drift-Scale Radionuclide Transport* (BSC 2004 [DIRS 170040], Section 6.3). It documents drift-scale radionuclide transport, taking account of the effects of emplacement drifts on flow and transport in the vicinity of the drift, which are not accounted for elsewhere, for example in *UZ Flow Models and Submodels* (SNL 2007 [DIRS 184614), *Radionuclide Transport Models Under Ambient Conditions* (SNL 2007 [DIRS 177396]), and *Particle Tracking Model and Abstraction of Transport Process* (SNL 2008 [DIRS 184748]). Also, the models presented in *Drift-Scale Radionuclide Transport* (BSC 2004 [DIRS 170040]) are developed under ambient (unheated) conditions. Waste heat will also reduce water saturation in the vicinity of the drift, but the assessment of drift shadow only considers ambient conditions and flow fields. The impacts of waste heat on flow and repository dry-out are considered in included FEP 2.1.08.03.0A (Repository Dry-Out Due to Waste Heat).

The drift shadow model developed in *Drift-Scale Radionuclide Transport* (BSC 2004 [DIRS 170040], Sections 6.3) shows that a dryout zone forms primarily in the fracture continuum below the invert with two drip lobes (zones of increased magnitude of vertical water flux) that form within fractures on the sides of the emplacement drifts (BSC 2004 [DIRS 170040], Figure 6-2). The matrix continuum is less affected by the drift shadow than the

fracture continuum because the ratio of capillary forces to gravitational forces is much larger in the matrix, which reduces the extent of the drift shadow. Diversion of percolating water around a waste emplacement drift results in an environment of greatly diminished flow (seepage) inside the drift, and the primary transport mechanism for radionuclides to migrate from the drift to the surrounding rock is by diffusion in the drift shadow model. Because most of the fluid directly below the drift is within the matrix, radionuclides are released into the matrix. As a result, the transport behavior in the drift shadow model is very similar to transport in an unperturbed model with no drift shadow when radionuclides are released into the matrix (BSC 2004 [DIRS 170040], Figure 6-7). Therefore, the impact of the drift shadow is of low consequence when transport occurs via diffusion from the drift to the surrounding rock matrix. In addition, when advective transport occurs in the drift as a result of drift seepage, condensation, or wicking into the invert, the seepage that percolates to the bottom of the drift will mitigate the effects of a drift shadow, and the impact of the drift shadow during advective seepage is of low consequence as well. In all cases, the overall impact of the drift shadow, if present, will be to retard the transport of radionuclides as a result of the reduced saturation and water flux beneath the drift (BSC 2004 [DIRS 170040], Figure 6-2).

In summary, drift shadow formation below the repository is considered within *Drift-Scale Radionuclide Transport* (BSC 2004 [DIRS 170040]). Based on the previous discussion, omission of FEP 2.2.07.21.0A (Drift Shadow Forms below Repository) will not result in a significant adverse change in the magnitude or timing of either radiological exposure to the RMEI or radionuclide releases to the accessible environment. Therefore, this FEP is excluded from the performance assessments conducted to demonstrate compliance with proposed 10 CFR 63.311 and 63.321 (70 FR 53313 [DIRS 178394]), and with 10 CFR 63.331 [DIRS 180319], on the basis of low consequence.

INPUTS:

Table 2.2.07.21.0A-1. Direct Inputs

Input	Source	Description
BSC 2004. *Drift-Scale Radionuclide Transport*. [DIRS 170040]	Figure 6-7	Radionuclide transport in drift shadow model is similar to transport in unperturbed model when releases are from the matrix
	Section 6.3	Discusses drift shadow model and impacts on radionuclide transport
	Figure 6-2	Discussion of the drift shadow model's dryout zone

Table 2.2.07.21.0A-2. Indirect Inputs

Citation	Title	DIRS
10 CFR 63	Energy: Disposal of High-Level Radioactive Wastes in a Geologic Repository at Yucca Mountain, Nevada	180319
70 FR 53313	Implementation of a Dose Standard After 10,000 Years	178394
BSC 2004	*Drift-Scale Radionuclide Transport*	170040
Philip et al. 1989	"Unsaturated Seepage and Subterranean Holes: Conspectus, and Exclusion Problem for Circular Cylindrical Cavities"	105743
SNL 2007	*Abstraction of Drift Seepage*	181244
SNL 2007	*Radionuclide Transport Models Under Ambient Conditions*	177396
SNL 2007	*UZ Flow Models and Submodels*	184614
SNL 2008	*Particle Tracking Model and Abstraction of Transport Processes*	184748

FEP: 2.2.08.01.0A

FEP NAME:

Chemical Characteristics of Groundwater in the SZ

FEP DESCRIPTION:

Chemistry and other characteristics of groundwater in the saturated zone may affect groundwater flow and radionuclide transport of dissolved and colloidal species. Groundwater chemistry and other characteristics, including temperature, pH, Eh, ionic strength, and major ionic concentrations, may vary spatially throughout the system as a result of different rock mineralogy.

SCREENING DECISION:

Included

TSPA DISPOSITION:

Chemical characteristics of groundwater in the saturated zone are included in the TSPA model through variations in K_d values, and through variations of BDCF values used in the biosphere modeling.

Variations in temperature, pH, Eh, ionic strength, and major ion concentrations in the groundwater of the saturated zone affect the sorption of radionuclides onto the rock surface and onto colloids, which, in turn, affect the sorption coefficient, K_d, and thus, the retardation factor, R_f, for each radionuclide. Element-specific sorption coefficients and their associated retardation factors are used in the equations that describe radionuclide transport through fractured media (SNL 2008 [DIRS 184806], Section 6.4.2.4.1, Equations 21 (a, b) and 22) and through alluvium and other porous media (SNL 2008 [DIRS 184806], Section 6.4.2.5, Equations 42 and 43). Appropriate ranges and distributions of values for K_d (SNL 2008 [DIRS 184806], Appendices C and C[a]) are chosen based on laboratory measurements, thermodynamic modeling, and professional judgement (SNL 2008 [DIRS 184806], Appendix A). The translation of the laboratory measurements, thermodynamic modeling, and professional judgement into upscaled K_d distributions is described in *Site-Scale Saturated Zone Transport* (SNL 2008 [DIRS 184806], Appendices C and C[a]). Distributions are specified for radionuclides or radionuclide groups and for two rock types (volcanic tuff and alluvium). These distributions were developed taking into account both the range of groundwater chemistries and the range of tuff and alluvium mineralogies in the saturated zone (SNL 2008 [DIRS 184806], Appendix A), so they implicitly account for variations in the chemical characteristics of saturated zone waters. The only exception to this is that oxidizing conditions are conservatively assumed to exist everywhere in the saturated zone (SNL 2008 [DIRS 184806], Section 6.3, Items 4 and 7) despite the fact that reducing conditions (which result in larger K_d values for some radionuclides) have been observed in some wells near Yucca Mountain (BSC 2006 [DIRS 178672], Section 3 and Figure 2.1-2). The uncertainty in K_d values is propagated through to modeling results by sampling the K_d uncertainty distributions individually for each saturated zone transport realization so that a unique set of element-specific K_d values is used in each realization (SNL 2008 [DIRS 183750], Sections 6.5, 6.5.1.1[b], 6.5.1.2[b], 6.5.2[b], 6.5.2.1[b], and 6.5.3[b]).

The sorption coefficient parameter ranges are incorporated in the model abstraction through K_d distributions for uranium, neptunium, plutonium, cesium, americium, thorium, protactinium, strontium, radium, selenium, and tin (SNL 2008 [DIRS 183750], Section 6.5.2.8, Table 6-8). The equilibrium sorption partitioning of americium, cesium, plutonium, thorium, protactinium, and tin between the aqueous phase and stationary and colloidal solid phases is also accounted for through K_d distributions that describe sorption of these radionuclides onto colloids (SNL 2008 [DIRS 183750], Section 6.5.2.8 and Table 6-8). Distributions for colloid concentrations in the saturated zone and for colloid retardation factors in the saturated volcanics and alluvium, which inherently reflect the chemical characteristics of saturated zone groundwaters, are also used in the modeling of colloid-facilitated radionuclide transport (SNL 2008 [DIRS 183750], Section 6.5.2.11 and Table 6-8). Correlations in radionuclide K_d values for a given saturated zone transport simulation (realization) are implemented through a correlation matrix (DTN: LA0702AM150304.001 [DIRS 184763]), which is discussed in *Saturated Zone Flow and Transport Model Abstraction* (SNL 2008 [DIRS 183750], Section 6.5.2[a] and Table 6-7[a]) and *Site-Scale Saturated Zone Transport Model* (SNL 2008 [DIRS 184806], Section A9).

Regarding spatial variations of groundwater chemical characteristcs, geochemical analysis indicates that current saturated zone groundwater under the repository and along the saturated zone transport path is predominately oxidized paleoclimate recharge water with a swath of reducing conditions directly east of Yucca Mountain in wells H-3, H-4, WT-17, b#1, WT-10, WT-12, and WT-14 (BSC 2006 [DIRS 178672], Figure 2.1-2). This suggests the existence of a north−south zone of reducing groundwaters in the volcanic units (BSC 2006 [DIRS 178672], Section 3 and Figure 2.1-2). However, because of the uncertainty in the spatial extent of this zone and its temporal stability, oxidizing conditions are assumed in the development of radionuclide K_d distributions in the saturated zone. This assumption yields the lowest possible K_d values and hence the least potential retardation of redox-sensitive radioelements such as technetium, neptunium, and uranium in the saturated zone. Based on existing well water analyses, the variability in major ion water chemistry along saturated zone flowpaths (redox conditions notwithstanding) is bracketed reasonably well by the water chemistries of wells J-13 and UE-25p#1 (SNL 2008 [DIRS 184806], Section A3). These two water chemistries were used in batch laboratory sorption experiments to determine radionuclide K_d values, so variability in major ion groundwater chemistry in the saturated zone is implicitly accounted for when using the laboratory data in the development of radionuclide K_d distributions.

The potential effects of temporal variations of groundwater chemical characteristics on radionuclide transport in the saturated zone are considered to be bracketed by the K_d distributions used in TSPA. The possibility that temporal variations could cause radionuclide sorption parameters to go outside the limits of the K_d distributions is excluded, as discussed in FEP 2.2.08.03.0A (Geochemical Interactions and Evolution in the SZ).

The biosphere model for the groundwater exposure scenario implicitly includes this FEP because the model calculates BDCFs for a unit activity concentration in the water, in a manner that is inclusive of the chemical characteristics of groundwater. Several biosphere model input parameters are dependent on the chemical species present in groundwater and in other environmental media contaminated as a result of the groundwater use. These parameters include sorption coefficients (K_ds) (SNL 2007 [DIRS 179993], Section 6.3), soil-to-plant transfer factors (BSC 2004 [DIRS 169672], Section 6.2.1.2), transfer coefficients for animal products

(BSC 2004 [DIRS 169672], Section 6.3.3), bioaccumulation factors (BSC 2004 [DIRS 169672], Sections 6.4.3 and 6.4.4), irrigation interception fraction (SNL 2007 [DIRS 177399], Section 6.4.3.2), translocation factors (BSC 2004 [DIRS 169672], Section 6.2.2.2), and dose coefficients for radionuclide intakes by inhalation (SNL 2007 [DIRS 177399], Section 6.4.8.5).

The approach to developing values for these parameters is as follows. If a sufficient technical basis exists to develop a distribution of parameter values encompassing a range of values that would be expected in the environment for different chemical species, such an approach is preferred (BSC 2004 [DIRS 169672], Sections 6.2.1.1, 6.2.1.2, 6.3.3, and 6.4.3; SNL 2007 [DIRS 177399], Section 6.3). The advantage of this approach is that, where appropriate, such a distribution applies to multiple environmental media (not only for groundwater) and to all chemical species in these environmental media (e.g., transfer coefficients are used to model radionuclide transfer to animal products from water, animal feed, and soil). If a single value has to be assigned to a parameter that depends on chemical characteristics of a radionuclide, a value is selected for use in the biosphere model that is conservative with respect to the risk to the receptor. Such an approach ensures that if a parameter value is dependent on the chemical characteristics of a given environmental medium, including well water, by selecting the conservative value, the risk to the receptor is not underestimated. This approach is used to select the values of dose coefficients for inhalation of radionuclides (SNL 2007 [DIRS 177399], Section 6.4.8.5), and to select the values of empirical constants used in the equation for irrigation interception fraction for foliar uptake by crops (SNL 2007 [DIRS 177399], Section 6.4.3.2). For the parameters that are dependent on chemical properties of the environmental medium including the groundwater, and are fixed values, the model assumes parameter values such that the risk to the receptor is not underrepresented. This FEP is considered in the conceptual and mathematical models for the groundwater exposure scenario (SNL 2007 [DIRS 177399], Table 6.7-1) in the soil, plant, animal, fish, ^{14}C, and inhalation submodels (SNL 2007 [DIRS 177399], Sections 6.4.1 to 6.4.6, and 6.4.8).

The biosphere aspect of this FEP is included in the biosphere component of the TSPA model through the use of groundwater exposure scenario BDCFs that are direct inputs to the TSPA for the scenario classes involving radionuclide release to the groundwater (SNL 2007 [DIRS 177399], Section 6.1.3). The BDCFs for all biosphere model realizations are provided as inputs to the TSPA model, which randomly samples these inputs to propagate uncertainty from the biosphere model into TSPA dose calculations. Annual doses are calculated as the product of radionuclide concentration in groundwater and the BDCFs. The present-day climate BDCFs are used for the assessment of doses to the RMEI for 10,000 years following disposal as well as after 10,000 years, but within the period of geologic stability (SNL 2007 [DIRS 177399], Section 6.11.3).

All aspects of the chemical characteristics of groundwater in the saturated zone FEP described above are included in the performance assessments that demonstrate compliance with the individual protection standard (proposed 10 CFR 63.311 (70 FR 53313 [DIRS 178394])) and the performance assessment to demonstrate compliance with the individual protection standards for human intrusion (proposed 10 CFR 63.321 (70 FR 53313 [DIRS 178394])). For the performance assessment that demonstrates compliance with the groundwater protection standards (10 CFR 63.331 [DIRS 180319]), only those components of this FEP that address the geosphere transport are included.

INPUTS:

Table 2.2.08.01.0A-1. Indirect Inputs

Citation	Title	DIRS
10 CFR 63	Energy: Disposal of High-Level Radioactive Wastes in a Geologic Repository at Yucca Mountain, Nevada	180319
70 FR 53313	Implementation of a Dose Standard After 10,000 Years	178394
BSC 2004	*Environmental Transport Input Parameters for the Biosphere Model*	169672
BSC 2006	*Impacts of Solubility and Other Geochemical Processes on Radionuclide Retardation in the Natural System – Rev 01*	178672
DTN: LA0702AM150304.001	Probability Distribution Functions and Correlations for Sampling of Sorption Coefficient Probability Distributions of Radionuclides in the SZ at the YM	184763
SNL 2007	*Biosphere Model Report*	177399
SNL 2007	*Soil-Related Input Parameters for the Biosphere Model*	179993
SNL 2008	*Saturated Zone Flow and Transport Model Abstraction*	183750
SNL 2008	*Site-Scale Saturated Zone Transport*	184806

FEP: 2.2.08.01.0B

FEP NAME:

Chemical Characteristics of Groundwater in the UZ

FEP DESCRIPTION:

Chemistry and other characteristics of groundwater in the unsaturated zone may affect groundwater flow and radionuclide transport of dissolved and colloidal species. Groundwater chemistry and other characteristics, including temperature, pH, Eh, ionic strength, and major ionic concentrations, may vary spatially throughout the system as a result of different rock mineralogy. The chemistry of the groundwater in the UZ will affect the drift seepage composition and thereby the potential for localized corrosion on the waste package corrosion barrier.

SCREENING DECISION:

Included

TSPA DISPOSITION:

The groundwater chemical characteristics are important to determining potential in-drift seepage chemical compositions. The results of the near-field chemistry model are processed in TSPA along with the waste package localized corrosion model, where TSPA then calculates the potential for localized corrosion of the waste package corrosion barrier. The starting point for evaluating potential seepage water compositions in the near field was the chemical composition of ambient pore waters in the TSw. The available pore-water data from the four repository host units (Tptpul, Tptpmn, Tptpll, and Tptpln) were evaluated and statistically divided into four compositional groups. Each group is represented in the near-field chemistry model, which considers the water–rock interactions that will alter the composition of the waters percolating through the unsaturated zone. These waters represent potential drift seepage compositions that are the starting points for the in-drift seepage dilution/evaporation abstraction, which provides solution compositions inside the drift as a function of temperature, partial pressure of CO_2, and relative humidity, for use in the TSPA model. This is all done within *Engineered Barrier System: Physical and Chemical Environment* (SNL 2007 [DIRS 177412], Sections 6.3.2, 6.6, and 6.9). TSPA uses the predicted chemistry of evaporated seepage on the waste package surface to evaluate the potential for localized corrosion of the waste package outer barrier, using the localized corrosion model from *General and Localized Corrosion of the Waste Package Outer Barrier* (SNL 2007 [DIRS 178519], Section 8.3). If localized corrosion is initiated, the affected waste package will eventually be breached and open to advective flow and radionuclide transport.

The effects of groundwater chemical characteristics are included in the radionuclide sorption coefficients under ambient conditions. The sorption coefficient data on which the distributions are based are obtained in laboratory experiments in which crushed rock samples from the Yucca Mountain site are contacted with groundwaters (or simulated groundwaters) representative of the site, spiked with one or more of the radioelements (SNL 2007 [DIRS 177396], Sections A4 and

A5). The chemistry of pore waters and perched waters in the unsaturated zone along potential flowpaths to the accessible environment is discussed in *Yucca Mountain Site Description* (BSC 2004 [DIRS 169734]). In the insaturated zone, two distinct water types exist in the ambient system. One is perched water and the other is pore water. Perched water is generally more dilute than pore water. The J-13 and UE p#1 well waters were used in sorption experiments as end-member compositions intended to bracket the impact of water composition on sorption coefficients (SNL 2007 [DIRS 177396], Section A4). Some spatial trends in water composition through the TSw and CHn hydrogeologic units have been noted (BSC 2004 [DIRS 169734], Section 5.2.2.4.2). However, the uncertainty in these spatial variations (and the uncertainty with respect to the effects of the bounding water compositions on sorption (SNL 2007 [DIRS 177396], Sections A8.3, A8.4, and A8.9) have led to the treatment of natural variability in water composition as uncertainty. Sorption experiments have been carried out as a function of time, element concentration, atmospheric composition, particle size, and temperature. In some cases, the solids remaining from sorption experiments were contacted with unspiked groundwater in desorption experiments. The sorption and desorption experiments together provide information on the equilibration rates of the forward and backward sorption reactions. For elements that sorb primarily through surface complexation reactions, the experimental data are augmented with the results of modeling calculations using PHREEQC (PHREEQC V.2.3 [DIRS 155323], STN: 10068-2.3-00). The inputs for the modeling calculations include groundwater compositions, surface areas, binding constants for the elements of interest, and thermodynamic data for solution species. These modeling calculations provide a basis for interpolation and extrapolation of the experimentally derived sorption coefficient dataset. The effects of nonlinear sorption are approximated by capturing the effective K_d range (SNL 2007 [DIRS 177396], Section A8). In the case of a reactive or adsorbing radionuclide, several K_d values are used for different rock units in the unsaturated zone, as given in *Particle Tracking Model and Abstraction of Transport Processes* (SNL 2008 [DIRS 184748], Table 6-7). For a nonsorbing tracer, K_d is set to zero.

The effects of groundwater composition with respect to sorption coefficients are provided in terms of probability distributions for the sorption coefficient of each element of interest among the three major rock types (devitrified, zeolitic, and vitric) found in the unsaturated zone. The influence of expected variations in water chemistry, radionuclide concentrations, and variations in rock surface properties within one of the major rock types are incorporated into these probability distributions. These distributions are specified for each radionuclide–rock type combination (SNL 2007 [DIRS 177396], Section A8 and Appendix A[a]) and are sampled in the TSPA model to account for the effects of natural variations in pore-water chemistry and mineral surfaces on sorption. Correlations for sampling sorption coefficient probability distributions have been derived for the elements investigated (SNL 2007 [DIRS 177396], Appendix B[a]). To derive the correlations, a rating system was first developed to rate the impact of six different variables on the sorption coefficient for a given element in each of the three major rock types. The six variables are pH, Eh, water chemistry, rock composition, rock surface area, and radionuclide concentration. Water chemistry refers to the major ion concentrations and silica. Rock composition refers to both the mineralogical composition of the rocks and the chemical composition of the minerals (for example, zeolite compositions). The sorption coefficient uncertainty distributions, which include the effects of the chemical characteristics of groundwater, are used in the simulation of radionuclide transport in the TSPA model, as

described in *Particle Tracking Model and Abstraction of Transport Processes* (SNL 2008 [DIRS 184748], Section 6.5.4).

INPUTS:

Table 2.2.08.01.0B-1. Indirect Inputs

Citation	Title	DIRS
PHREEQC V. 2.3	WINDOWS 95/98/NT, Redhat 6.2. STN: 10068-2.3-00	155323
BSC 2004	*Yucca Mountain Site Description*	169734
SNL 2007	*Engineered Barrier System: Physical and Chemical Environment*	177412
SNL 2007	*General Corrosion and Localized Corrosion of Waste Package Outer Barrier*	178519
SNL 2007	*Radionuclide Transport Models Under Ambient Conditions*	177396
SNL 2008	*Particle Tracking Model and Abstraction of Transport Processes*	184748

FEP: 2.2.08.03.0A

FEP NAME:

Geochemical Interactions and Evolution in the SZ

FEP DESCRIPTION:

Groundwater chemistry and other characteristics, including temperature, pH, Eh, ionic strength, and major ionic concentrations, may change through time, as a result of the evolution of the disposal system or from mixing with other waters. Geochemical interactions may lead to dissolution and precipitation of minerals along the groundwater flow path, affecting groundwater flow, rock properties, and sorption of radionuclides. Effects on hydrologic flow properties of the rock, radionuclide solubilities, sorption processes, and colloidal transport are relevant. Kinetics of chemical reactions should be considered in the context of the time scale of concern.

SCREENING DECISION:

Excluded – low consequence

SCREENING JUSTIFICATION:

Geochemical analysis indicates that current saturated zone groundwater under the repository and along the saturated zone transport path is paleoclimate recharge water (SNL 2007 [DIRS 177391], Section A7.1.2). These waters represent a mixture of waters from past flow systems having different climatic signatures than those indicative of current dry climatic conditions. Corrected saturated zone groundwater ages based on ^{14}C data range from late Pleistocene to Holocene epochs (SNL 2007 [DIRS 177391], Section A6.3.6.6.2). Corrections to the groundwater ^{14}C ages to account for geochemical interactions are small (SNL 2007 [DIRS 177391], Section A6.3.6.6.2), and thus indicative of minor chemical reactions between carbonate minerals such as calcite and groundwaters. However, values for $\delta^{13}C$ and ^{14}C are negatively correlated (SNL 2007 [DIRS 177391], Section A6.3.6.6.2 and Figure A6-45) and could be interpreted as a result of various levels of calcite dissolution by infiltrating waters having different ages (SNL 2007 [DIRS 177391], Section A6.3.6.6.2). Bulk chemical and isotopic composition of perched and saturated zone groundwaters indicates that there are some geochemical variations associated with spatial variations that may be related to mixing. However, the overall aqueous species concentrations of perched waters and groundwaters are similar (SNL 2007 [DIRS 177391], Section A6.3.6.3). Therefore, it is expected that mixing of paleowaters and recharged waters under current climatic conditions, noting that the latter are a product of local recharge, would not result in major changes in the bulk water chemistry. Sufficiently large residence times of these waters in contact with silica-rich rock would produce near-neutral to mildly alkaline pH, inducing partitioning of $CO_2(g)$ into the aqueous phase.

The ranges in radionuclide sorption coefficients (K_d) and effective colloidal retardation factors were derived based on variations in water chemistry, radionuclide concentrations, and variations in rock surface properties (SNL 2008 [DIRS 184806], Section A3; BSC 2004 [DIRS 170006], Section 1). The groundwater ionic strength is expected to remain low, so it would not affect colloid stability over time. Moreover, temporal variations in water chemistry are expected to be

reasonably well bounded by current spatial variations in geochemical conditions. Hence, the effects of anticipated changes in K_d and retardation factors are effectively bounded by employing the ranges of transport parameter values used in the saturated zone transport model. Therefore, it is anticipated that temporal changes in water geochemistry exert little effects on geochemical interaction in the saturated zone. Specific details pertaining to variability in redox conditions are discussed below.

Hydrothermal activity is considered to be of low consequence to regional saturated zone flow and flow paths in the Yucca Mountain vicinity (see excluded FEP 1.2.06.00.0A (Hydrothermal Activity)). Also, temporal geochemical changes due to an increase in geothermal (hydrothermal) activity are not expected based on the characterization of mineral alteration in the rock and/or geochemical data (see excluded FEP 1.2.06.00.0A (Hydrothermal Activity)). The kinetics of heterogeneous chemical reaction, such as dissolution and precipitation, are also expected to be of low consequence. Results indicate that the temperature will peak at the present-day water table approximately 6,000 years after waste emplacement with the maximum temperature equal to 73°C and an average of the maximum at each of the 560 locations modeled of 63°C (as extracted from the 560 *.*wt* files in DTN: LL0702PA013MST.068 [DIRS 180553] in subfolder: /SDT/SDT-01/SDT55). Even subject to a wetter climate in the future, the estimated maximum temperature at the elevated water table is 80°C (see discussion in excluded FEP 2.2.10.02.0A (Thermal Convection Cell Develops in SZ)). The rates of water–rock reactions are still low at or below this temperature. As described in excluded FEP 2.2.10.08.0A (Thermo Chemical Alteration in the SZ (Solubility, Speciation, Phase Changes, Precipitation/Dissolution)), there is little volcanic glass remaining below the water table where the most common alteration products of this phase are sorptive zeolites. Therefore, any effect on the remaining volcanic glass with time would be towards zeolite formation and/or recrystallization of preexisting secondary mineral phases without the constraints of rate limiting processes. It is then concluded that these processes are insufficient as to cause any significant effect on the amount of sorptive minerals present below the water table and do not significantly affect the saturated zone. It should be noted that models describing radionuclide transport from the EBS to the unsaturated zone and then to the saturated zone do not account for radionuclide solubility (see excluded FEP 2.2.10.08.0A (Thermo Chemical Alteration in the SZ (Solubility, Speciation, Phase Changes, Precipitation/Dissolution)).

For the SZ site-scale transport model (SNL 2008 [DIRS 184806], Figures F-1 and F-2), it is assumed that the groundwaters along the transport path are oxidizing from the unsaturated zone–saturated zone water table interface to the boundary of the accessible environment. However, there is evidence of localized reducing zones along the saturated zone transport pathway east of Yucca Mountain, which may result in the reduction of redox-sensitive radionuclides such as technetium and neptunium (BSC 2006 [DIRS 178672], Section 2.1.3). These radionuclides are less soluble at lower oxidation states (i.e., reducing environments) and could precipitate out of solution and accumulate in localized reduction zones. Radionuclides such as technetium and neptunium also have significantly higher values of sorption coefficients under reducing conditions (BSC 2006 [DIRS 178672], Section 2.3). A subsequent return to oxidizing conditions within the localized reduction zones would favor dissolution of these precipitates back into solution or remobilization of sorbed species. If such a scenario occurs, this would cause radionuclide concentrations in the saturated zone groundwater to increase to levels above those that were present prior to the influx of more oxidized groundwater.

It is not expected that the local reduction zones will be oxidized during the 10,000 years after repository closure or that they will increase in size. A large-scale change in oxidation state from that measured currently at Yucca Mountain is excluded on the basis of low consequence. The rationale for this conclusion is as follows:

1. Reducing conditions found in Boreholes USW H-1, USW H-4, UE-25b#1 (Ogard and Kerrisk 1984 [DIRS 100783], Section IV), and USW WT-17 (SNL 2008 [DIRS 184806], Section F2.2) indicate that reducing conditions in this area extend from the shallow saturated zone to the lower Tram Tuff (BSC 2006 [DIRS 178672], Section 2.1.2.1). The reducing agents for groundwater in these wells could be located in the groundwater itself or in the rock matrix. Because the reducing zones are local in extent, the aquifer matrix most likely supplies most of the reduction capacity. Generally, in volcanic rocks the reduction capacity is associated with solid sulfides (e.g., pyrite), biotite, and other ferrous iron-bearing minerals. Pyrite has been identified as a mineral component of the lower Tram Tuff (Castor et al. 1994 [DIRS 102495]; SNL 2007 [DIRS 177394], Appendix O) and is believed to have been entrained in the ash-flow eruptions that produced the Tram Tuff (BSC 2006 [DIRS 178672], Section 2.1.2.1). Within the Yucca Mountain vicinity, the Tram Tuff spans west of Bare Mountain, eastward to Jackass Flats, and southward to within five miles of Highway 95 (Carr et al. 1984 [DIRS 101522], Figure 11). Given that pyrite is a mineral component of the Tram Tuff within the Yucca Mountain vicinity, it promotes reducing conditions in groundwater that comes into contact with that unit (BSC 2006 [DIRS 178672], Section 2.1.2.1). Given the age, areal extent, and mineral content of these volcanic hydrogeologic units, it is inferred that there is sufficient pyrite in these hydrogeologic units such that reducing conditions will be limited to their present-day location and persist for at least 10,000 years after repository closure.

2. Resident groundwaters along the projected groundwater flow path were exposed to relatively long residence times in contact with volcanic rock (SNL 2007 [DIRS 177391], Section A6.3.6.6.2). This would result in pH at near-neutral to mildly alkaline levels and an oxidation state to be largely determined by water–rock interactions. Consequently, it is not expected that future groundwaters will further oxidize localized reducing zones within the next 10,000 years after repository closure.

3. There is no current mechanism known to support the concept that reducing conditions will become more extensive along the saturated zone flow path. The total reduction capacities in the tuff are a function of the concentration of the rock's in situ reducing agents and the extent of these reducing zones. To date, only localized reducing zones have been produced over the past several million years (BSC 2006 [DIRS 178672], Section 2.1.2). It is reasonable to presume that this reduction capacity will remain localized over the relatively short 10,000 years after repository closure. Therefore, a significant increase in the size of these local reducing zones is not expected. Also, any effect on the redox state of the groundwaters on these reducing zones as a result of microbial activity is excluded on the basis of low consequence (see excluded FEP 2.2.09.01.0A (Microbial Activity in the SZ)). The reason for this is the small amount or absence of organic carbon in the groundwaters.

Detailed discussions pertaining to related FEPs in groundwater chemistry as they affect transport and sorption are addressed by included FEPs 2.2.08.01.0A (Chemical Characteristics of Groundwater in the SZ), 2.2.08.06.0A (Complexation in the SZ), 2.2.08.09.0A (Sorption in SZ), and 2.2.08.10.0A (Colloid Transport in the SZ), and by excluded FEP 2.2.08.07.0A (Radionuclide Solubility Limits in the SZ). They are also addressed in the following reports: *Saturated Zone In-Situ Testing* (SNL 2007 [DIRS 177394], Appendix O), *Saturated Zone Site-Scale Flow Model* (SNL 2007 [DIRS 177391], Appendix A), *Saturated Zone Colloid Transport* (BSC 2004 [DIRS 170006]), and *Site-Scale Saturated Zone Transport* (SNL 2008 [DIRS 184806], Appendices A, B, D and D[a], and F). The geochemical interactions in the saturated zone as a result of the thermal pulse from the repository are discussed in detail in excluded FEP 2.2.10.08.0A (Thermo-Chemical Alteration in the SZ (Solubility, Speciation, Phase Changes, Precipitation/Dissolution)). That FEP was excluded on the basis of low consequence.

Based on the previous discussion, omission of FEP 2.2.08.03.0A (Geochemical Interactions and Evolution in the SZ) will not result in a significant adverse change in the magnitude or timing of either radiological exposure to the RMEI or radionuclide releases to the accessible environment. Therefore, this FEP is excluded from the performance assessments conducted to demonstrate compliance with proposed 10 CFR 63.311 and 63.321 (70 FR 53313 [DIRS 178394]), and with 10 CFR 63.331 [DIRS 180319], on the basis of low consequence.

INPUTS:

Table 2.2.08.03.0A-1. Direct Inputs

Input	Source	Description
DTN: LL0702PA013MST.068. Input and Output Files for the SMT, SDT and DDT Submodels and MSTHAC Extract Output Files Used in ANL-EBS-MD-000049 Multiscale Thermohydrologic Model. [DIRS 180553]	560 *.wt files, subfolder /SDT/SDT-01/SDT55	Peak temperature at the water table during the thermal period
SNL 2008. *Site-Scale Saturated Zone Transport*. [DIRS 184806]	Appendix F, Figures F-1 and F-2.	Model assumes that the saturated zone groundwaters along the transport path are oxidizing from the unsaturated zone/saturated zone interface to the 18-km compliance boundary

Table 2.2.08.03.0A-2. Indirect Inputs

Citation	Title	DIRS
10 CFR 63	Energy: Disposal of High-Level Radioactive Wastes in a Geologic Repository at Yucca Mountain, Nevada	180319
70 FR 53313	Implementation of a Dose Standard After 10,000 Years	178394
BSC 2004	*Saturated Zone Colloid Transport*	170006
BSC 2006	*Impacts of Solubility and Other Geochemical Processes on Radionuclide Retardation in the Natural System – Rev 01*	178672
Carr et al. 1984	*Stratigraphic and Volcano-Tectonic Relations of Crater Flat Tuff and Some Older Volcanic Units, Nye County, Nevada*	101522
Castor et al. 1994	"Pyritic Ash-Flow Tuff, Yucca Mountain, Nevada"	102495
Ogard and Kerrisk 1984	*Groundwater Chemistry Along Flow Paths Between a Proposed Repository Site and the Accessible Environment*	100783
SNL 2007	*Saturated Zone Site-Scale Flow Model*	177391
SNL 2007	*Saturated Zone In-Situ Testing*	177394
SNL 2008	*Site-Scale Saturated Zone Transport*	184806

FEP: 2.2.08.03.0B

FEP NAME:

Geochemical Interactions and Evolution in the UZ

FEP DESCRIPTION:

Groundwater chemistry and other characteristics, including temperature, pH, Eh, ionic strength, and major ionic concentrations, may change through time, as a result of the evolution of the disposal system or from mixing with other waters. Geochemical interactions may lead to dissolution and precipitation of minerals along the groundwater flow path, affecting groundwater flow, rock properties, and sorption of radionuclides. Effects on hydrologic flow properties of the rock, radionuclide solubilities, sorption processes, and colloidal transport are relevant. Kinetics of chemical reactions should be considered in the context of the time scale of concern.

SCREENING DECISION:

Excluded – low consequence

SCREENING JUSTIFICATION:

This FEP is closely related to excluded FEP 2.2.10.06.0A (Thermo-Chemical Alteration in the UZ (Solubility, Speciation, Phase Changes, Precipitation/Dissolution)).

The thermo-chemical interactions that will occur in the repository environment have been studied with respect to effects on the seepage water entering the waste emplacement drifts using the THC seepage model (SNL 2007 [DIRS 177404]). This model, which explicitly captures the effects of changes in temperature, pH, Eh, ionic strength (and other compositional variables), time dependency, precipitation or dissolution effects, and effects of resaturation, was used to examine near-field and drift seepage flow and chemistry (SNL 2007 [DIRS 177404], Section 6.2). Changes in fracture permeabilities resulting from mineral precipitation or dissolution were found to be on the order of the natural variation in these properties (DTN: LB0302DSCPTHCS.001 [DIRS 164744]; SNL 2007 [DIRS 177404], Section 6.5.5.3; BSC 2004 [DIRS 170038], Table 6-5), with most of the substantial effects limited to regions above and to the side of the drift within about a drift diameter (SNL 2007 [DIRS 177404], Figures 6.5-8 to 6.5-9). The predicted mineral precipitation reduces the permeability in the affected regions, and leads to a reduction in flow into the drift. The effects of mineral precipitation on fracture permeability as it relates to near-field and drift seepage chemistry were also evaluated with the THC seepage model. A discussion of potential THC processes that could result in modification of fracture permeability is provided in included FEP 2.2.03.02.0A (Rock Properties of Host Rock and Other Units). The effects of mixing of waters are not explicitly accounted for by the THC seepage model or the near-field chemistry model in *Engineered Barrier System: Physical and Chemical Environment* (SNL 2007 [DIRS 177412], Section 6.3). However, *Engineered Barrier System: Physical and Chemical Environment* (SNL 2007 [DIRS 177412], Section 7.1.2.2) shows a near-field chemistry modeling validation case where the PTn pore waters percolate through the TSw hydrogeologic unit. The overall results of this modeling at various feldspar dissolution rates indicate that the evolutionary pathways of the PTn

pore-water chemistries closely progress towards those of the TSw hydrogeologic unit. Therefore, it is not expected that mixing of PTn and TSw pore waters would generate water chemistries that are different from those defined by the compositional range of the TSw pore waters.

Geochemical alteration of the PTn nonwelded unit above the repository host rock due to heat from the repository should not significantly change the PTn hydrologic properties. The reason for this is because the current alteration state of the unit represents the cumulative effects from similar heating of longer duration. Simulations show that the peak temperature at the bottom of the PTn unit from repository heating will be 43°C, or approximately 25°C hotter than the prerepository in situ temperature (SNL 2008 [DIRS 179962], Figure 6.4.2-30). The cited figure also shows that the duration of repository heating at the base of the PTn unit is on the order of 10,000 years. Significant mineralogical changes in the PTn unit are not expected since a combination of higher temperatures and high water saturation levels would be necessary for widespread rock alteration to zeolite and clay phases (see excluded FEP 2.2.10.07.0A (Thermochemical Alteration of the Calico Hills Unit)). The PTn strata (comprising several nonwelded lithostratigraphic units) are located between the underlying Topopah Spring Tuff and the overlying Tiva Canyon Tuff (BSC 2004 [DIRS 170029], Section 6.4, Table 6-2). In the geologic past, the pyroclastic section that includes both the host rock and the PTn has been subject to temperature excursions of greater magnitude and duration than those predicted as a result of repository heating (SNL 2007 [DIRS 177412], Section 6.12.2.2.1, p. 6-187). The effects from past heating events are represented in the current highly variable state of alteration in the PTn unit (BSC 2004 [170031], Figures 6-9, 6-17, and 6-18; Levy et al. 1996 [DIRS 104157], p. 788, Table 1, Figure 2). Because the past heating was greater than what is predicted from the repository, the repository-induced effects on PTn properties will be minor and within the range of variability of existing natural alteration. Thermal conditions associated with the eruption of the Timber Mountain Group heated the Topopah Spring Tuff, which directly underlies the PTn unit, to 50°C to 100°C for up to several millions of years (SNL 2007 [DIRS 177412], Section 6.12.2.2.1, p. 6-187). Similar temperatures may have existed in the PTn unit because of its close stratigraphic proximity.

The representation of geochemistry in the THC seepage model includes the major solid phases (minerals and glass) encountered in hydrogeologic units at Yucca Mountain with a range of possible reaction product minerals, CO_2 gas, and the aqueous species necessary to include these solid phases and pore-water compositions within the model (SNL 2007 [DIRS 177404], Table 6.2-2). Compositional changes of seepage are calculated by the drift-scale THC seepage model (SNL 2007 [DIRS 177404], Section 6.5.5.4) for matrix/fracture pore waters and gas at gridblocks near the drift wall boundary. Variations in pH (SNL 2007 [DIRS 177404], Figures 6.5-16, 6.6-1, 6.6-7, 6.6-9, and 6.6-14), a key compositional variable for sorption of some radionuclides (SNL 2007 [DIRS 177396], Appendix A), roughly lie within the range of variability investigated for radionuclide sorption (SNL 2007 [DIRS 177396], Appendix A).

Results were investigated for the THC seepage model applied to the Tptpll unit considering a range of initial pore-water compositions. In this model, four different initial pore-water compositions were investigated (SNL 2007 [DIRS 177404], Table 6.2-1). Peak concentrations usually found at the time of rewetting reflect mostly the small values of the first, nonzero, liquid-saturation output. In any case, elevated concentrations are predicted only for small liquid

saturations that are not subject to significant fluid movement. The model predicts, upon rewetting, more rapid return to near-ambient conditions for aqueous calcium, sodium, and chlorine. The findings indicate that most of the significant compositional variations are limited to the low saturation conditions near the drift wall. In areas with high saturation, compositional variations have little impact relative to the processes considered in this FEP. The effects of variations in potential seepage water composition on in-drift water chemistry are addressed in included FEP 2.2.08.12.0A (Chemistry of Water Flowing into the Drift).

The effects of colloid formation are accounted for in the colloid source term (SNL 2007 [DIRS 177423], Section 6.5.2.3). Colloids are formed from the degradation of the HLW and SNF waste forms, EBS materials, and rock (SNL 2007 [DIRS 177423], Section 6.3.1). Radionuclides associated with colloids are modeled as either irreversibly or reversibly attached to colloids to encompass the broadest range of potential radionuclide-colloid interactions (SNL 2008 [DIRS 184748], Section 6.4.5). Elevated temperatures are expected to result in fewer colloids due to the decrease in colloid stability. This is due to the greater energy of colloid motion at higher temperatures, which allows colloids to overcome the threshold associated with coagulation (SNL 2007 [DIRS 177423], Section 6.3.2). Modeling of colloid transport is discussed in *Particle Tracking Model and Abstraction of Transport Processes* (SNL 2008 ([DIRS 184748], Sections 6.4.5, 6.5.12, and 6.5.13). The cumulative probability distribution for colloid concentrations as a function of ionic strength, based on available data, spans five orders of magnitude for water with ionic strength less than 0.05 M (SNL 2008 [DIRS 184748], Section 6.5.12, Table 6-21), indicating that variability in ionic strength below this limit will not have a strong effect on colloid transport because colloid concentrations are so variable. Colloid concentration for water with ionic strength greater than 0.05 M is set to 10^{-6}, lower than the values for water with lower ionic strength (SNL 2008 [DIRS 184748], Section 6.5.12, Table 6-21). Therefore, higher ionic strength waters would inhibit colloid transport, but such waters are expected to be present in small amounts that don't last long, as described above.

In addition to natural materials, introduced materials may take part in geochemical interactions. Cementitious material (shotcrete) is planned for use as part of the ground support for the turnout intersections of the main access drifts and for the turnouts and intersections of the exhaust drifts with the emplacement drifts (BSC 2007 [DIRS 183406], Section 7.3). The incorporation of cementitious materials in the repository poses two potential effects. The first is that the leaching of cementitious materials, particularly the shotcrete supporting the turnout intersections in the main access drifts and the intersections of the exhaust main drifts with the emplacement drifts, will affect repository performance by modifying the hydrologic properties of the surrounding rock and diverting the flow of water entering the drifts. The second concern is that an alkaline plume resulting from leaching of the cementitious material could enhance radionuclide transport to the accessible environment, either through the complexation of radionuclides or through the presence of pseudocolloids.

No cementitious material will be used in the emplacement drifts (BSC 2007 [DIRS 183406], Section 7.3). In nonemplacement drifts, all cementitious material (concrete invert and shotcrete used in shafts) will be used only for ground support (BSC 2007 [DIRS 183406], Section 7.3). The only significant cementitious materials remaining in the repository after closure will be shotcrete in the emplacement drift turnouts, exhaust intersections, and other non-emplacement openings. Grout used for rock bolt placement will be present in non-emplacement drifts and

turnout intersections. Excluded FEP 2.1.06.01.0A (Chemical Effects of Rock Reinforcement and Cementitious Materials in EBS) addresses degradation of ground support material.

Transport enhancement by alkaline plumes will be negligible for long-term repository performance for two reasons. First, as discussed in excluded FEP 2.1.06.01.0A (Chemical Effects of Rock Reinforcement and Cementitious Materials in EBS), there will be little opportunity for mixing of the alkaline plumes with the fluids in the EBS; hence, the plumes will have no effect on the generation of a mobile radionuclide source term. Second, high-pH plumes in the unsaturated zone are expected to be short-lived and rapidly neutralized. The unsaturated zone is open to gas circulation; particularly, ambient CO_2 will dissolve into the plume and neutralize the high-pH fluids. The rapid neutralization of cement leachates by CO_2 gas is indicated by experiment (DTN: LL030211523125.006 [DIRS 172021], file: *LiquidCarbonationEQ3-6Modeling.doc*). These findings are consistent with the analysis reported by Ziegler (2004 [DIRS 171694], Section D.4). Even in the northwestern end of the repository footprint, where the TSw-CHn contact is approximately 80 m below the repository horizon (source for the elevation of the top of the CHn: DTN: MO0610MWDHFM06.002 [DIRS 179352], file: *H06_18chvu_X.dat*; source for the repository outline and elevations: SNL 2007 [DIRS 179466], Table 4-1, Parameter Number 01-01) where lateral flow may occur, the flow path from the emplaced cement to that contact is sufficient to neutralize the potential plumes. Additional details regarding the chemical effects of an alkaline plume are considered as part of excluded FEP 2.1.06.01.0A (Chemical Effects of Rock Reinforcement and Cementitious Materials in EBS).

The potential porosity and permeability changes in the surrounding rock are discussed in excluded FEP 2.1.06.01.0A (Chemical Effects of Rock Reinforcement and Cementitious Materials in EBS). Calcite precipitation will not lead to changes in host rock hydrologic properties that are sufficiently large or extensive enough to divert the dominantly vertical flow beneath the turnouts towards the emplacement drifts.

Based on the above discussion, omission of FEP 2.2.08.03.0B (Geochemical Interactions and Evolution in the UZ) will not result in a significant adverse change in the magnitude or timing of either radiological exposure to the RMEI or radionuclide releases to the accessible environment. Therefore, this FEP is excluded from the performance assessments conducted to demonstrate compliance with proposed 10 CFR 63.311 and 63.321 (70 FR 53313 [DIRS 178394]), and with 10 CFR 63.331 [DIRS 180319], on the basis of low consequence.

INPUTS:

Table 2.2.08.03.0B-1. Direct Inputs

Input	Source	Description
BSC 2004. *Mineralogic Model (MM3.0) Report*. [DIRS 170031]	Figures 6-9, 6-17, and 6-18	The effects from past heating events are represented in the current highly variable state of alteration in the PTn
BSC 2007. *Ground Control for Non-Emplacement Drifts for LA*. [DIRS 183406]	Section 7.3	Use of cementitious materials for ground support

Table 2.2.08.03.0B-1. Direct Inputs (Continued)

Input	Source	Description
DTN: LB0302DSCPTHCS.001. Drift-Scale Coupled Processes (THC Seepage) Model: Simulations. [DIRS 164744]	Files: *thc6_w0_rerun.tar.gz, thc6_w5_rerun.tar.gz*	Effects of mineral precipitation near waste emplacement drifts and changes in hydrologic properties due to THC processes
DTN: LB0302DSCPTHCS.002. Drift-Scale Coupled Processes (THC Seepage) Model: Data Summary. [DIRS 161976]	DTN: LB0302DSCPTHCS.002	Effects of THC processes on pH and water composition
DTN: LL030211523125.006. EQ3/6 Modeling of Grout-Reacted Liquid Carbonation Experiments. [DIRS 172021]	file: *LiquidCarbonationEQ36 Modeling.doc*	Rapid neutralization of cement leachates by CO_2 gas.
DTN: MO0610MWDHFM06.002. Hydrogeologic Framework Model (HFM2006) Stratigraphic Horizon Grids. [DIRS 179352]	file: *H06_18chvu_X.dat*	Location where the TSw-CHn contact is approximately 80 m below the repository horizon in the northwestern end of the repository footprint.
SNL 2007. *Drift-Scale THC Seepage Model*. [DIRS 177404]	Figures 6.5-16, 6.6-1, 6.6-7, 6.6-9, and 6.6-14	Variations in pH, a key compositional variable for sorption of some radionuclides roughly lie within the range of variability investigated for initial pore-water composition

Table 2.2.08.03.0B-2. Indirect Inputs

Citation	Title	DIRS
10 CFR 63	Energy: Disposal of High-Level Radioactive Wastes in a Geologic Repository at Yucca Mountain, Nevada	180319
70 FR 53313	Implementation of a Dose Standard After 10,000 Years	178394
BSC 2004	*Analysis of Hydrologic Properties Data*	170038
BSC 2004	*Seepage Model for PA Including Drift Collapse*	167652
Levy et al. 1996	"Alteration History Studies in the Exploratory Studies Facility, Yucca Mountain, Nevada, USA"	104157
SNL 2007	*Drift-Scale THC Seepage Model*	177404
SNL 2007	*Engineered Barrier System: Physical and Chemical Environment*	177412
SNL 2007	*Radionuclide Transport Models Under Ambient Conditions*	177396
SNL 2007	*Total System Performance Assessment Data Input Package for Requirements Analysis for Subsurface Facilities*	179466
SNL 2007	*Waste Form and In-Drift Colloids-Associated Radionuclide Concentrations: Abstraction and Summary*	177423
SNL 2008	*Particle Tracking Model and Abstraction of Transport Processes*	184748
SNL 2008	*Postclosure Analysis of the Range of Design Thermal Loadings*	179962
Ziegler 2004	"Transmittal of Appendix D of the Technical Basis Document No. 10: Unsaturated Zone Transport Addressing Key Technical Issue (KTI) Agreement Evolution of Near-Field Environment (ENFE) 1.04"	171694

FEP: 2.2.08.04.0A

FEP NAME:

Re-Dissolution of Precipitates Directs More Corrosive Fluids to Waste Packages

FEP DESCRIPTION:

Re-dissolution of precipitates that have plugged pores as a result of evaporation of groundwater in the dry-out zone, may produce a pulse of fluid reaching the waste packages when gravity-driven flow resumes, which is more corrosive than the original fluid in the rock.

SCREENING DECISION:

Excluded – low consequence

SCREENING JUSTIFICATION:

The process of redissolution of mineral precipitates is examined in the drift-scale thermal-hydrologic-chemical (THC) seepage model (SNL 2007 [DIRS 177404], Section 6.5.5.3). This model is used to evaluate the significance of coupled THC processes on the chemistry of seepage waters. In addition, a sensitivity study has been prepared (SNL 2007 [DIRS 177413]) that integrates features of the seepage model (SNL 2007 [DIRS 181244]; BSC 2005 [DIRS 172232]) with the drift-scale THC seepage model, to evaluate potential changes in seepage composition.

The results of these studies (primarily SNL 2007 [DIRS 177413], Section 6.6) show that:

- Precipitates form in the host rock during the thermal period, primarily consisting of silica and calcite, but also including halite, anhydrite, and minor amounts of sulfate, carbonate, and nitrate salts (SNL 2007 [DIRS 177404], Section 6.5.5.3).

- These precipitates redissolve when moisture returns to the dryout zone, with the most soluble species forming small amounts of concentrated brine when rewetting first occurs, at or before approximately 1,000 years after repository closure (SNL 2007 [DIRS 177404], Section 6.5.5.4).

- Seepage composition is dilute for conditions when seepage occurs, because relatively large local percolation flux is required to produce seepage, and the small amounts of brine that can be produced are insufficient to impact seepage chemistry (SNL 2007 [DIRS 177413], Section 6.1.2).

- After rewetting, seepage composition eventually returns to that of pore waters used for initial and boundary conditions (SNL 2007 [DIRS 177412], Section 6.3.2.4.5).

- THC processes affect seepage hydraulics, but the timing and magnitude of seepage are reasonably bounded by the abstraction used in TSPA (SNL 2007 [DIRS 181244]).

- The transient changes in the composition of seepage that occur immediately during or after rewetting of the dryout zone may involve re-dissolution of precipitated salts and temporary concentration of chloride and other soluble components relative to waters percolating through the rock around the dryout zone, but mostly involve dilution by condensation (SNL 2007 [DIRS 177413], Figure 6.6-7). For such transient changes to be significant, failure of the drip shield must occur during (or prior to) rewetting.

Drip Shield Performance during Rewetting – Seepage cannot contact the waste package if the drip shield performs its diversion function, so any transient flow of seepage that occurs during rewetting, and is concentrated in soluble salts, is not expected to contact the waste package. Drip shield corrosion will occur very slowly, and is not compositionally dependent (SNL 2007 [DIRS 180778], Section 8). The titanium alloy used in drip shield plates is not significantly affected by microbially influenced corrosion or localized corrosion (SNL 2007 [DIRS 180778], Section 8). Hence, the drip shield thickness will be substantially undegraded by corrosion during this early time period, and the drip shield will continue to perform its function.

Drip Shield Performance during Rewetting after an Early Failure Event – In the event of an early failure of a drip shield, the underlying waste package is assumed to fail by localized corrosion, so there is no additional dependence on seepage composition during rewetting (SNL 2008 [DIRS 183478], Section 6.4).

Drip Shield Performance during Rewetting after a Seismic Event – Vibratory ground motion effects are addressed in included FEP 1.2.03.02.0A (Seismic Ground Motion Damages EBS Components). Consequences of damage to the drip shield are generally insignificant because: (1) advective flow through stress corrosion cracks on the drip shield is excluded (see excluded FEP 2.1.03.10.0B (Advection of Liquids and Solids Through Cracks in the Drip Shield)), so the presence of stress corrosion cracks on the drip shield does not compromise its ability to divert seepage away from the waste package; (2) drip shield separation is not predicted to occur (SNL 2007 [DIRS 176828], Section 6.7.3); and (3) failure of the drip shield from waste package impacts is not predicted to occur (SNL 2007 [DIRS 176828], Section 6.8.5).

The direct effects of rockfall on drip shields are also excluded in FEP 1.2.03.02.0B (Seismic-Induced Rockfall Damages EBS Components). The screening justification (SNL 2007 [DIRS 176828], Section 6.10) focuses on the potential impacts on the drip shields and waste packages from rockfalls involving large rock blocks in the nonlithophysal zones, which bound the effects from small rock blocks in the lithophysal zones.

The direct effects of fault displacement on the EBS components are included, as discussed for FEP 1.2.02.03.0A (Fault Displacement Damages EBS Components). A conservative approximation is taken (neglecting the presence of the drip shield) to estimate damage to the waste package from fault displacement. Drip shield degradation from fault displacement occurs if the waste package is also damaged (SNL 2007 [DIRS 176828], Section 6.12.2, Item 27). This mitigates the effects from corrosion that might occur, for the unexpected circumstance of damage caused by fault displacement prior to rewetting of the near-field host rock (i.e., prior to approximately 1,000 to 3,000 years, depending on whether drift collapse has prolonged the boiling period in the EBS; SNL 2008 [DIRS 179962], Figure 6.4.2-28).

Drip Shield Performance during Rewetting after an Igneous Intrusion Event – An igneous intrusion in the form of a dike that may occur through the repository, as described in FEP 1.2.04.04.0A (Igneous Intrusion Interacts with EBS Components) is included in the TSPA and results in damage to the waste packages and mobilization of waste. This FEP leads to the assumption that drip shield and waste package are gone and therefore the impact of corrosive fluids on the waste package is irrelevant.

Summary – The above discussion shows that transient changes in seepage chemistry may occur during rewetting, although dilution is generally predicted by sensitivity analysis. These changes will have no significant effect on performance because the drip shields prevent seepage contact with waste packages, and performance of the drip shield does not depend on seepage composition.

Based on the preceding discussion, omission of FEP 2.2.08.04.0A (Re-Dissolution of Precipitates Directs More Corrosive Fluids to Waste Packages) will not result in a significant adverse change in the magnitude or timing of either radiological exposure to the RMEI or radionuclide releases to the accessible environment. Therefore, this FEP is excluded from the performance assessments conducted to demonstrate compliance with proposed 10 CFR 63.311 and 63.321 (70 FR 53313 [DIRS 178394]), and with 10 CFR 63.331 [DIRS 180319], on the basis of low consequence.

INPUTS:

Table 2.2.08.04.0A-1. Direct Inputs

Input	Source	Description
SNL 2007. *THC Sensitivity Study of Heterogeneous Permeability and Capillarity Effects*. [DIRS 177413]	Figure 6.6-7	The transient changes in composition of seepage that occur immediately during or after rewetting of the dryout zone, may involve temporary concentration of chloride and other soluble components but mostly involve dilution
	Section 6.6	Sensitivity study that integrates features of the seepage model with the drift-scale THC model, to evaluate potential changes in seepage composition
	Section 6.1.2	Seepage composition is dilute for conditions when seepage occurs, because relatively large local percolation flux is required to produce seepage, and the small amounts of brine that can be produced are insufficient

Table 2.2.08.04.0A-2. Indirect Inputs

Citation	Title	DIRS
10 CFR 63	Energy: Disposal of High-Level Radioactive Wastes in a Geologic Repository at Yucca Mountain, Nevada	180319
70 FR 53313	Implementation of a Dose Standard After 10,000 Years	178394
BSC 2005	*Drift-Scale Coupled Process (DST and TH Seepage) Models*	172232
SNL 2007	*Seismic Consequence Abstraction*	176828
SNL 2007	*Abstraction of Drift Seepage*	181244
SNL 2007	*Drift-Scale THC Seepage Model*	177404
SNL 2007	*Engineered Barrier System: Physical and Chemical Environment*	177412
SNL 2007	*General Corrosion and Localized Corrosion of the Drip Shield*	180778
SNL 2007	*THC Sensitivity Study of Heterogeneous Permeability and Capillarity Effects*	177413
SNL 2008	*Postclosure Analysis of the Range of Design Thermal Loadings*	179962
SNL 2008	*Total System Performance Assessment Model/Analysis for the License Application*	183478

FEP: 2.2.08.05.0A

FEP NAME:

Diffusion in the UZ

FEP DESCRIPTION:

Molecular diffusion processes may affect radionuclide transport in the UZ. This includes osmotic processes in response to chemical gradients.

SCREENING DECISION:

Excluded – low consequence

SCREENING JUSTIFICATION:

Although this FEP refers to diffusion in the unsaturated zone, it only addresses diffusion in faults and fractures in the unsaturated zone. Matrix diffusion in the unsaturated zone is described in included FEP 2.2.08.08.0B (Matrix Diffusion in the UZ).

The FEP description includes osmosis, which is a process that will not have a significant effect on radionuclide transport in the unsaturated zone compared to matrix diffusion. If groundwater present in a fault or fracture system in the unsaturated zone were to move across a mineral-based semi-permeable membrane into the rock matrix, the solutes present in the fracture or fault would be concentrated. Increased radionuclide concentrations could result in more matrix diffusion into the rock wall, a process that would tend to retard radionuclide transport in the unsaturated zone. Alternatively, if groundwater in the rock matrix were to move across a semi-permeable membrane into fractures or faults, the amount of water present in the fractures or faults would be increased, thus diluting the concentrations of radionuclides that are being transported to the water table, which may weaken matrix diffusion but not enough to impact transport times. In any case, a low volume of water may move across the boundary. Diffusion and osmosis into and from the fractures will eventually cancel each other. When radionuclides are present in fractures or faults, they can be transported by advection, dispersion, and diffusion. Transport by advection and dispersion are discussed in included FEP 2.2.07.15.0B (Advection and Dispersion in the UZ). Transport by diffusion, which is proportional to concentration gradient is not included in TSPA because under all scenarios, it is much less than transport by advection. The contribution of diffusion to total dispersion is negligible in comparison to that caused by advection related dispersion.

The free-water diffusion values for all radionuclides are defined in *Particle Tracking Model and Abstraction of Transport Processes* (SNL 2008 [DIRS 184748] Table 6.5.5-2). The largest value is for cesium and is 2.1×10^{-9} m^2/s. This can be compared with the corresponding value of the dispersion coefficient, which is the product of the flow velocity and the dispersivity. The fracture dispersivity has a fixed value of 10 m (SNL 2008 [DIRS 184748]). The flow velocity v depends upon the overall percolation flux q, the fraction of the flux which flows in fractures or faults (that is, not in the matrix) f, and the fracture porosity ϕ:

$$v = (q f)/\phi$$

Both q and f depend upon the flow field; that is, upon the climate (present-day, monsoon, or glacial-transition) and whatever percentile infiltration is imposed as a boundary condition. Porosity ϕ varies with the model layer, as shown in *Particle Tracking Model and Abstraction of Transport Processes* (SNL 2008 [DIRS 184748], Table 6-13). To minimize v, and therefore maximize the importance of diffusion relative to dispersion, q is taken from the slowest flow field, and f at the horizon where the greatest fraction of flow is through the matrix continuum. These are the lower bounds for present-day climate (probability distribution (pd10)), for which q = 3 mm/yr (SNL 2007 [DIRS 184614], Table 6.1-2) and f = 0.54 (SNL 2007 [DIRS 184614], Table 6.6-3), with f taken at the water table. For model layers below the repository, the greatest ϕ, giving the slowest v, is 0.025 (layer tswf; SNL 2008 [DIRS 184748], Table 6-13). Substituting these values, the minimum v = 65 mm/yr results in a minimum dispersion coefficient of 2.1×10^{-8} m^2/s. This minimum dispersion coefficient is still 10 times larger than the diffusion coefficient of 2.1×10^{-9} m^2/s for groundwater (Reimus et al. 2007 [DIRS 179246]). Because diffusion is at least one order of magnitude lower than the minimum dispersion, diffusion is excluded based on low consequence.

Free water diffusion represents an upper bound on radionuclide diffusion in faults and fractures (i.e., the transport of radionuclides by diffusion will be slower than the diffusional transport of water). Therefore, diffusional transport of radionuclides will be insignificant compared to transport by dispersion and advection.

Based on the previous discussion, omission of FEP 2.2.08.05.0A (Diffusion in the UZ) will not result in a significant adverse change in the magnitude or timing of either radiological exposure to the RMEI or radionuclide releases to the accessible environment. Therefore, this FEP is excluded from the performance assessments conducted to demonstrate compliance with proposed 10 CFR 63.311 and 63.321 (70 FR 53313 [DIRS 178394]), and with 10 CFR 63.331 [DIRS 180319], on the basis of low consequence.

INPUTS:

Table 2.2.08.05.0A-1. Direct Inputs

Input	Source	Description
SNL 2008. *Particle Tracking Model and Abstraction of Transport Processes*. [DIRS 184748]	Table 6-13	For model layers below the repository, the greatest porosity, giving the slowest v, is 0.025
	Table 6-13	Porosity varies with the model layer
	Table 6.5.5-2	Defined free water diffusion values for all radionuclides

Table 2.2.08.05.0A-2. Indirect Inputs

Citation	Title	DIRS
10 CFR 63	Energy: Disposal of High-Level Radioactive Wastes in a Geologic Repository at Yucca Mountain, Nevada	180319
70 FR 53313	Implementation of a Dose Standard After 10,000 Years	178394
Reimus et al. 2007	"Matrix Diffusion Coefficients in Volcanic Rocks at the Nevada Test Site: Influence of Matrix Porosity, Matrix Permeability, and Fracture Coating Minerals"	179246
SNL 2007	*UZ Flow Models and Submodels*	184614
SNL 2008	*Particle Tracking Model and Abstraction of Transport Processes*	184748

FEP: 2.2.08.06.0A

FEP NAME:

Complexation in the SZ

FEP DESCRIPTION:

Complexing agents such as carbonate, fluoride, and humic and fulvic acids present in natural groundwaters could affect radionuclide transport in the SZ.

SCREENING DECISION:

Included

TSPA DISPOSITION:

Inorganic complexing agents are included in the saturated zone transport model (SNL 2008 [DIRS 184806], Appendix A) in that the surface-complexation models used to develop radionuclide K_d distributions include the effects of these complexing agents as well as the effects of competing cations in solution, such as calcium, magnesium, sodium, potassium, and aluminum. In the saturated zone, inorganic complexing agents, such as carbonates, are dominant, whereas organic complexing agents are not found in significant amounts (see excluded FEP 2.2.09.01.0A (Microbial Activity in the SZ)).

Complexing agents can affect solubility and speciation of radionuclides in groundwater, and as a consequence, affect their sorption onto the rock surface and colloids. The effects of complexing agents on radionuclide sorption on rock surfaces, radionuclide sorption on inorganic colloids, and effective radionuclide sorption on rock surfaces in the presence of inorganic colloids are accounted for in TSPA through the use of sorption coefficients, K_ds, in the equations describing transport through fractures and porous media (SNL 2008 [DIRS 184806], Sections 6.4.2.4 to 6.4.2.6, Equations 21, 22, 42, 43, 45, and 46). Uncertainty in the values of these K_ds is accounted for by defining appropriate ranges of values for the sorption coefficients, as described in *Site-Scale Saturated Zone Transport* (SNL 2008 [DIRS 184806], Appendix A) and implemented in *Saturated Zone Flow and Transport Model Abstraction* (SNL 2008 [DIRS 183750], Sections 6.5.2.8, 6.5.2.11, 6.5.2.12, and Table 6-8). The sorption coefficient data on which these distributions are based were obtained in laboratory experiments in which crushed rock samples from the Yucca Mountain site were contacted with groundwaters (or simulated groundwaters) representative of the site (SNL 2008 [DIRS 184806], Appendix A), spiked with one or more of the elements of interest (SNL 2008 [DIRS 184806], Appendix A). The natural waters contained all the relevant inorganic complexants of interest in representative concentrations, and the synthetic groundwaters contained representative carbonate/bicarbonate concentrations. Carbonate ion is expected to be the dominant complexing agent in Yucca Mountain groundwaters.

Sorption experiments have been carried out as a function of time, element concentration, atmospheric composition, particle size, and temperature. In some cases, the solids remaining from sorption experiments were contacted with unspiked groundwater in desorption experiments.

The experimental data used to determine the sorption K_d distributions are discussed in Appendix A of *Site-Scale Saturated Zone Transport* (SNL 2008 [DIRS 184806]). The sorption and desorption experiments together provide information on the equilibration rates of the forward and backward sorption reactions. For elements that sorb primarily through surface complexation reactions, the experimental data are augmented with the results of modeling calculations using PHREEQC (PHREEQC V2.3 [DIRS 157837], STN: 10068-2.3-01) with the thermodynamic input data file *PHREEQCDATA025.dat* (DTN: MO0604SPAPHR25.001 [DIRS 176868]). The inputs for the modeling calculations include groundwater compositions, surface areas, binding constants for the elements of interest, and thermodynamic data for solution species. These modeling calculations provide a basis for interpolation and extrapolation of the experimentally derived sorption coefficient dataset.

Uncertainty in sorption coefficients is quantified in terms of probability distributions for the sorption coefficient of each element of interest among the three major rock types (devitrified, zeolitic, and vitric) found in the saturated zone. The influence of expected variations in water chemistry, radionuclide concentrations, and variations in rock surface properties within one of the major rock types are incorporated into these probability distributions (see included FEP 2.2.08.09.0A (Sorption in the SZ)). These distributions are specified for each radionuclide–rock type combination (SNL 2008 [DIRS 184806], Appendix A), and are sampled in the TSPA model to account for the effects of natural variations in pore-water chemistry and mineral surfaces on sorption. Correlations for sampling sorption coefficient probability distributions have been derived for the elements investigated (SNL 2008 [DIRS 184806], Section A9). To derive the correlations, a rating system was first developed to rate the impact of six different variables on the sorption coefficient for a given element in each of the three major rock types. The six variables are pH, Eh, water chemistry, rock composition, rock surface area, and radionuclide concentration. Water chemistry refers to the major ion concentrations and silica. Rock composition refers to both the mineralogic composition of the rocks and the chemical composition of the minerals (e.g., zeolite compositions). The DTNs for the sorption K_ds and correlations are LA0702AM150304.001 [DIRS 184763] and LA0311AM831341.001 [DIRS 167015].

Although naturally occurring organic complexing agents are not found in significant amounts in the saturated zone, they could still potentially affect radionuclide retardation if they form strong complexes with radionuclides, and these complexes sorb very weakly. The potential effects of organic complexing agents on sorption were investigated by Triay et al. (1997 [DIRS 100422], Section IV.B). Their experiments tested the effects of organic materials (dihydroxyphenylalanine and Nordic Aquatic Fulvic Acid) on the sorption of plutonium and neptunium on tuff materials. The results of these tests showed very little effect of the organic materials for sorption of these radionuclides in tuffs.

INPUTS:

Table 2.2.08.06.0A-1. Indirect Inputs

Citation	Title	DIRS
DTN: LA0311AM831341.001	Correlation Matrix for Sampling of Sorption Coefficient Probability Distributions	167015
DTN: LA0702AM150304.001	Probability Distribution Functions and Correlations for Sampling of Sorption Coefficient Probability Distributions of Radionuclides in the SZ at the YM	184763
DTN: MO0604SPAPHR25.001	PHREEQC Data 0 Thermodynamic Database for 25°C - File: PHREEQCDATA025	176868
SNL 2008	*Saturated Zone Flow and Transport Model Abstraction*	183750
SNL 2008	*Site-Scale Saturated Zone Transport*	184806
PHREEQC V 2.3.	PC. STN: 10068-2.3-01	157837
Triay et al. 1997	*Summary and Synthesis Report on Radionuclide Retardation for the Yucca Mountain Site Characterization Project*	100422

FEP: 2.2.08.06.0B

FEP NAME:

Complexation in the UZ

FEP DESCRIPTION:

Complexing agents such as humic and fulvic acids present in natural groundwaters could affect radionuclide transport in the UZ.

SCREENING DECISION:

Included

TSPA DISPOSITION:

Complexation of radionuclides by mobile complexing agents such as humic and fulvic acids is treated as part of colloid transport in *Radionuclide Transport Models Under Ambient Conditions* (SNL 2007 [DIRS 177396], Sections 6.1.3 and 6.18). Complexation on immobile mineral surfaces is treated as part of sorption of dissolved radionuclides in that same report (SNL 2007 [DIRS 177396], Section A7). Therefore, the effects of complexation are implicitly included in the radionuclide sorption coefficients under ambient conditions. For TSPA, radionuclide transport is simulated by a particle-tracking model that includes the effects of complexation, as described in *Particle Tracking Model and Abstraction of Transport Processes* (SNL 2008 [DIRS 184748], Section 6.5.4).

The sorption coefficient data on which the distributions are based are obtained in laboratory experiments in which crushed rock samples from the Yucca Mountain site are contacted with groundwaters (or simulated groundwaters) representative of the site (SNL 2007 [DIRS 177396], Section A4), spiked with one or more of the elements of interest (SNL 2007 [DIRS 177396], Section A5). As such, the sorption experiments contain representative ligands responsible for complex formation (Triay et al. 1997 [DIRS 100422], pp. 85 and 133). Sorption experiments have been carried out as a function of time, element concentration, atmospheric composition, particle size, and temperature. In some cases, the solids remaining from sorption experiments were contacted with unspiked groundwater in desorption experiments. The sorption and desorption experiments together provide information on the equilibration rates of the forward and backward sorption reactions. For elements that sorb primarily through surface complexation reactions, the experimental data are augmented with the results of modeling calculations using PHREEQC (PHREEQC V2.3 [DIRS 157837], STN: 10068-2.3-01). The inputs for the modeling calculations include groundwater compositions, surface areas, binding constants for the elements of interest, and thermodynamic data for solution species. These modeling calculations provide a basis for interpolation and extrapolation of the experimentally derived sorption coefficient dataset. The effects of nonlinear sorption are approximated by capturing the effective K_d range (SNL 2007 [DIRS 177396], Section A8 and Appendix A[a]).

The effects of complexation with respect to sorption coefficients are provided in terms of probability distributions for the sorption coefficient of each element of interest among the three

major rock types (devitrified, zeolitic, and vitric) found in the unsaturated zone. The influence of expected variations in water chemistry, radionuclide concentrations, and variations in rock surface properties within one of the major rock types are incorporated into these probability distributions. These distributions are specified for each radionuclide–rock type combination (SNL 2007 [DIRS 177396], Section A8 and Appendix A[a]), and are sampled in the TSPA model to account for the effects of natural variations in pore-water chemistry and mineral surfaces on sorption. Correlations for sampling sorption coefficient probability distributions have been derived for the elements investigated (SNL 2007 [DIRS 177396], Appendix B[a]). To derive the correlations, a rating system was first developed to rate the impact of six different variables on the sorption coefficient for a given element in each of the three major rock types. The six variables are pH, Eh, water chemistry, rock composition, rock surface area, and radionuclide concentration. Water chemistry refers to the major ion concentrations and silica. Rock composition refers to the mineralogic composition of the rocks and the chemical composition of the minerals (e.g., zeolite compositions).

The effects of organics on sorption were investigated by Triay et al. (1997 [DIRS 100422], Section IV.B). Their experiments tested the effects of organic materials (dihydroxyphenylalanine and Nordic Aquatic Fulvic Acid) on the sorption of plutonium and neptunium on tuff materials. The results of these tests showed very little effect of the organic materials for sorption of these radionuclides in tuffs.

INPUTS:

Table 2.2.08.06.0B-1. Indirect Inputs

Citation	Title	DIRS
PHREEQC V. 2.3	WINDOWS 95/98/NT, Redhat 6.2. STN: 10068-2.3-00	155323
SNL 2007	*Radionuclide Transport Models Under Ambient Conditions*	177396
SNL 2008	*Particle Tracking Model and Abstraction of Transport Processes*	184748
Triay et al. 1997	*Summary and Synthesis Report on Radionuclide Retardation for the Yucca Mountain Site Characterization Project*	100422

FEP: 2.2.08.07.0A

FEP NAME:

Radionuclide Solubility Limits in the SZ

FEP DESCRIPTION:

Solubility limits for radionuclides are different in saturated zone groundwater than in the water in the unsaturated zone or in the waste and EBS.

SCREENING DECISION:

Excluded – low consequence

SCREENING JUSTIFICATION:

Solubility determines the maximum concentration that a constituent can reach in the aqueous phase; therefore it is considered to be a bounding property. Once a particular radionuclide reaches its solubility limit, it will have the potential to precipitate or form a solid depending on kinetically related geochemical conditions in the local environment. The radionuclide constituent will then be at equilibrium between the solid and aqueous phase. The precipitate-forming solid phase will increase in mass until the concentration in the solution phase reaches the solubility limit. If the concentration in the aqueous phase decreases below the solubility limit, the solid phase will have the potential to dissolve into the aqueous phase depending on kinetically related geochemical conditions in the local environment.

Radionuclide solute concentrations entering the saturated zone from the unsaturated zone are not expected to exceed solubility limits because of the effects of dilution, dispersion, matrix diffusion, and sorption in the unsaturated zone (all of which will tend to decrease radionuclide concentrations below their concentrations at the source term, which are solubility-limited). Radionuclide concentrations will be further reduced in the saturated zone by the processes of dispersion, matrix diffusion, and sorption. Furthermore, throughout the saturated zone, the groundwater is primarily oxidizing, and is assumed to be such in the TSPA (SNL 2008 [DIRS 184806], Section 6.3). Redox-sensitive radionuclides introduced into the saturated zone from the unsaturated zone are more soluble in oxidizing waters than in reducing waters (SNL 2007 [DIRS 177418], Appendices V and VIII).

However, situated in the volcanic units (primarily the Tram Tuff), southeast of the repository footprint and within the first quarter of the predicted saturated zone flowpath length, there may exist a zone of reducing conditions (BSC 2006 [DIRS 178672], Figure 2.1-2). This zone cuts across the transport pathways from the repository that are predicted by the site-scale saturated zone flow model (SNL 2007 [DIRS 177391], Figure 6-17). If a solution containing a redox-sensitive constituent with lower solubility under reducing conditions passes through this reducing region, that constituent may precipitate out of solution, resulting in lower solution concentrations.

The effects of such a process are investigated in a sensitivity study reported in *Impacts of Solubility and Other Geochemical Processes on Radionuclide Retardation in the Natural System – Rev 01* (BSC 2006 [DIRS 178672]). In this study, the redox-sensitive radionuclide ^{99}Tc is introduced into oxidizing saturated zone groundwater and then transported through a thin reducing zone within the first quarter of the saturated zone flowpath length (BSC 2006 [DIRS 178672], Figure 2.6-1). When the technetium passes through the reducing zone, it is reduced from Tc(VII) to Tc(IV), and technetium precipitates may be formed if the solubility limit of one or more solid technetium phases is exceeded. This precipitation lowers the technetium concentrations in the groundwater. The aqueous technetium concentrations would be expected to remain at these lower levels downstream and well beyond the "exit point" of the reducing zone. Thus, the existence of the thin reducing zone would produce a significant delay in technetium peak concentrations at the compliance boundary (BSC 2006 [DIRS 178672], Section 3). The same result would be expected for other redox-sensitive radionuclides that have higher solubilities in oxidized groundwater than in reduced groundwater (e.g., nuclides of uranium, neptunium, plutonium), although the impact on dose is greatest for ^{99}Tc because of its high solubility and nonsorbing nature under oxidizing conditions. The study concludes that implementing solubility limits in the saturated zone, due to the presence of a zone of reducing conditions that may lie along the saturated zone transport path, could reduce concentrations of redox-sensitive constituents and significantly increase mean transport times to the accessible environment (BSC 2006 [DIRS 178672], Section 3).

The sensitivity study supports the supposition that if a solubility limit lower than that implemented in *Dissolved Concentration Limits of Radioactive Elements* (SNL 2007 [DIRS 177418], Section 6) were to be imposed in the saturated zone transport model, it could cause precipitates to form, dropping redox-sensitive radionuclide solutes out of the aqueous phase and reducing the maximum aqueous concentration capable of being transported to the accessible environment. No other changes in groundwater chemistry that may occur along flow paths in the saturated zone (e.g., pH, carbonate/bicarbonate concentration, ionic strength) are expected to be large enough (SNL 2007 [DIRS 177391], Sections A6.3.4.1, A6.3.5.1, and A6.3.4.4) to cause significant changes to radionuclide solubilities such that solubility limits would be exceeded in the saturated zone (SNL 2007 [DIRS 177418], Section 6). However, even if solubility limits were exceeded, this exceedance could only reduce radionuclide concentrations at the boundary of the accessible environment. The effect would be similar to, though presumably much lower in magnitude than, the effect of reducing conditions.

Potential precipitation of a radionuclide due to solubility limits in the saturated zone would increase the mean transport time and decrease the concentration of that radionuclide in the saturated zone relative to assuming no precipitation. Longer transport times in the saturated zone would allow radioactive decay to diminish the mass of radionuclides that are ultimately released to the accessible environment. Consequently, the process of precipitation due to solubility limits can only enhance the performance of the saturated zone with regard to its capability for retarding radionuclide migration. Thus, implementation of radionuclide solubility limits in the saturated zone can only be beneficial to repository performance. It follows that the exclusion of radionuclide solubility limits in the saturated zone is justified on the basis of low consequence because inclusion of these limits can only increase radionuclide travel times and decrease radionuclide releases to the accessible environment and radiation exposures to the RMEI.

Based on the previous discussion, omission of FEP 2.2.08.07.0A (Radionuclide Solubility Limits in the SZ) will not result in a significant adverse change to the magnitude or time of radiological exposures to the RMEI or radionuclide releases to the accessible environment. Therefore, this FEP is excluded from the performance assessments conducted to demonstrate compliance with proposed 10 CFR 63.311 and 63.321 (70 FR 53313 [DIRS 178394]), and with 10 CFR 63.331 [DIRS 180319], on the basis of low consequence.

INPUTS:

Table 2.2.08.07.0A-1. Direct Inputs

Input	Source	Description
SNL 2007. *Saturated Zone Site-Scale Flow Model*. [DIRS 177391]	Figure 6-17	Zone of reducing conditions cuts across the transport pathways from the repository that are predicted by the flow model
SNL 2007. *Dissolved Concentration Limits of Elements with Radioactive Isotopes*. [DIRS 177418]	Section 6	Radionuclide solubility limits

Table 2.2.08.07.0A-2. Indirect Inputs

Citation	Title	DIRS
10 CFR 63	Energy: Disposal of High-Level Radioactive Wastes in a Geologic Repository at Yucca Mountain, Nevada	180319
70 FR 53313	Implementation of a Dose Standard After 10,000 Years	178394
BSC 2006	*Impacts of Solubility and Other Geochemical Processes on Radionuclide Retardation in the Natural System – Rev 01*	178672
SNL 2007	*Saturated Zone Site-Scale Flow Model*	177391
SNL 2007	*Dissolved Concentration Limits of Elements with Radioactive Isotopes*	177418
SNL 2008	*Site-Scale Saturated Zone Transport*	184806

FEP: 2.2.08.07.0B

FEP NAME:

Radionuclide Solubility Limits in the UZ

FEP DESCRIPTION:

Solubility limits for radionuclides may be different in unsaturated zone groundwater than in the water in the waste and EBS.

SCREENING DECISION:

Excluded – low consequence

SCREENING JUSTIFICATION:

The conditions that control radionuclide solubility are identified in *Dissolved Concentration Limits of Radioactive Elements* (SNL 2007 [DIRS 177418]) and include pH, fugacity of CO_2, concentration of fluoride ion, redox conditions, and temperature. These variables are not all independent: at higher temperature, CO_2 gas is less soluble. This reduces the solubility of carbonate complexes, which at high pH are the species that contribute the most to actinide solubilities. The result is that actinides are less soluble at higher temperatures (SNL 2007 [DIRS 177418], Section 6.3.3.3; but note that only solubility limits at 25°C are used for TSPA). Non-actinide radionuclides that may be released include carbon, cesium, iodine, strontium, and technetium. For the most part, the unsaturated zone will be under oxidizing conditions, which are more favorable to solubility and therefore mobility of radionuclides. In general, the conditions that control the solubility of actinides in the invert of the EBS will be different than in the unsaturated zone. This is because the drift and the invert will be hotter than the surrounding rock. The justification for exclusion is presented here in two parts. First, actinides will be less soluble in the invert than in the unsaturated zone below the invert. Therefore, transport away from the drift will be limited by the relatively low actinide solubility in the invert, compared to the unsaturated zone. Despite the greater potential for actinide solubility away from the invert in the unsaturated zone, there will be no source of actinides in the unsaturated zone to increase the concentration to the greater solubility limit. Therefore, the expected difference in actinide solubility limits between the invert and the unsaturated zone will have no adverse effect on the release of actinides to the accessible environment. Second, if radionuclide solubility in the unsaturated zone groundwater were to be less than the solubility in the invert, the addition of uncontaminated water to the "plume" of radionuclides leaving the EBS will decrease concentrations in the unsaturated zone groundwater. The radionuclide mass flux will remain the same even if solubilities in the unsaturated zone are lower than solubilities in the waste form/EBS because of the addition. The lower solubilities in the unsaturated zone are compensated for by a higher water volume in the unsaturated zone such that precipitation does not occur and the mass flux does not decrease.

Solubility limits could also affect the formation of certain kinds of true colloids, such as polymeric forms of plutonium oxide (SNL 2007 [DIRS 177423], Section 6.3.1). However, only small quantities of true colloids have been observed to form in experiments on waste form

degradation (SNL 2007 [DIRS 177423], Section 6.3.1). Furthermore, these colloids are expected to undergo transformation to pseudocolloids in the near- or far-field aquifer system (SNL 2007 [DIRS 177423], Section 6.3.1).

Based on the above discussion, omission of FEP 2.2.08.07.0B (Radionuclide Solubility Limits in the UZ) will not result in a significant adverse change in the magnitude or timing of either radiological exposure to the RMEI or radionuclide releases to the accessible environment. Therefore, this FEP is excluded from the performance assessments conducted to demonstrate compliance with proposed 10 CFR 63.311 and 63.321 (70 FR 53313 [DIRS 178394]), and with 10 CFR 63.331 [DIRS 180319], on the basis of low consequence.

INPUTS:

Table 2.2.08.07.0B-1. Direct Inputs

Input	Source	Description
SNL 2007. *Dissolved Concentration Limits of Elements with Radioactive Isotopes*. [DIRS 177418]	Section 6.3.3.3	Actinides solubility at higher temperatures

Table 2.2.08.07.0B-2. Indirect Inputs

Citation	Title	DIRS
10 CFR 63	Energy: Disposal of High-Level Radioactive Wastes in a Geologic Repository at Yucca Mountain, Nevada	180319
70 FR 53313	Implementation of a Dose Standard After 10,000 Years	178394
SNL 2007	*Dissolved Concentration Limits of Elements with Radioactive Isotopes*	177418
SNL 2007	*Waste Form and In-Drift Colloids-Associated Radionuclide Concentrations: Abstraction and Summary*	177423

FEP: 2.2.08.07.0C

FEP NAME:

Radionuclide Solubility Limits in the Biosphere

FEP DESCRIPTION:

Solubility limits for radionuclides may be different in the biosphere pathways than in the water in the saturated zone.

SCREENING DECISION:

Excluded – low consequence

SCREENING JUSTIFICATION:

For the TSPA modeling cases involving radionuclide release to the groundwater, radionuclides are introduced into the biosphere with well water, either as dissolved species or in suspension attached to colloids. The conditions that dictate aqueous solubility levels in the saturated zone could be different from those prevailing in the surface soils of the biosphere. The degree of elemental solubility could potentially have an effect on the rate of removal of radionuclides from soils, thereby affecting the magnitude and duration of radionuclide accumulation in soil.

Radionuclide solute concentrations entering the saturated zone from the unsaturated zone are not expected to exceed solubility limits because of the effects of dilution, dispersion, matrix diffusion, and sorption in the unsaturated zone, all of which will tend to decrease radionuclide concentrations below their concentrations at the source, which are solubility-limited. Additional dilution is possible at the unsaturated zone–saturated zone interface, and radionuclide concentrations will be further reduced in the saturated zone by the processes of dispersion, matrix diffusion, and sorption. Furthermore, throughout the saturated zone, the groundwater is primarily oxidizing. Radionuclide constituents introduced into the saturated zone from the unsaturated zone are more soluble in oxidizing waters than in reducing waters (see excluded FEP 2.2.08.07.0A (Radionuclide Solubility Limits in the SZ)). The conditions in the biosphere are also expected to be predominantly oxidizing due to its proximity to the atmosphere. Therefore, it is not expected that the radionuclide concentrations in groundwater would exceed their solubility limits upon entering the biosphere. The concentration in the water may change when the water is used for irrigation, as discussed below. However, the conditions would still be oxidizing because the soils in the Yucca Mountain region have low organic matter content (SNL 2007 [DIRS 179993], Table 6.2-2), the agricultural soils are aerated by plowing, and the oxygen content of the irrigation water would be greater than that of the groundwater due to its contact with the atmosphere.

Precipitation of minerals is known to occur in the natural, not irrigated, soils in arid and semi-arid climates. This process results in a buildup of caliche layer, a hardened deposit of calcium carbonate and other minerals that forms when these minerals are leached from the upper soil layers and accumulate below as a result of water evaporation. If the volume of water in the soil significantly decreases due to evapotranspiration, the dissolved minerals will eventually

precipitate, regardless of their solubilities. This process will primarily occur in the natural systems in the arid and semi-arid climate when there is no excess water that would percolate below the region of soil where evaporation and plant uptake occur and prevent mineral buildup in the soil.

For the conditions where radionuclides are introduced into the biosphere from irrigation with contaminated groundwater, the solubility limits are not achieved (i.e., the rate of radionuclide removal from soil by leaching is proportional to the radionuclide concentration in the soil) (SNL 2007 [DIRS 177399], Sections 6.4.1.1 to 6.4.1.3). The biosphere model includes the overwatering parameter that represents the amount of irrigation water intentionally applied to soil to leach salts and the amount of precipitation that percolates below the root zone (BSC 2004 [DIRS 169673], Section 6.9). Because salts can impair root function and affect water uptake, salt buildup in soils in the plant root zone is undesirable. Overwatering is a common practice that prevents the soil buildup of salts from irrigation water, and there is evidence that it is practiced in Amargosa Valley (Stonestrom et al. 2003 [DIRS 165862]). In arid regions, the overwatering rate usually is determined by calculating the amount of water required to flush accumulated salts out of the surface soil to maintain long-term productivity (BSC 2004 [DIRS 169673], Section 6.9). The fraction of infiltrated water that must pass through the root zone to remove excess salts is a function of the salinity of the irrigation water and crop tolerance to salts. Soil salinity is measured by the electrical conductivity of the saturated soil solution. The crop salt tolerance is also expressed in terms of electrical conductivity.

Wells in the Amargosa and Yucca Mountain areas were drilled and monitored for salinity levels (among other variables) for the Nye County Early Warning Drilling Program (DTN: LA0206AM831234.001 [DIRS 160051]). Well number NC-EWDP-19D, located in the southwest corner of the Nevada Test Site, is the closest to the compliance location, as defined in 10 CFR 63.302 [DIRS 180319]. Average well water salinity, as reflected by the mean measurement of electrical conductivity, was 0.44 dS/m (BSC 2004 [DIRS 169673], Section 4.1.7). The electrical conductivity data from this source are corroborated by salinity measurements from 31 irrigation or domestic wells located in the town of Amargosa Valley or west of State Route 373 and south of Highway 95 in Amargosa Valley (BSC 2004 [DIRS 169673], Section 4.1.7). Average well water salinity for these 31 wells was 0.51 dS/m. Salinity tolerances for crops ranged from 1.0 to 2.8 dS/m for garden crops and alfalfa and from 6.0 to 8.0 dS/m for grains and grasses (Doorenbos and Pruit 1977 [DIRS 103062], Table 36, p. 78). Thus, to prevent garden crop and alfalfa yield reduction, the concentration of salts in the water can only increase by about a factor of 2 to 5. An average electrical conductivity for the water sampled from all the Nye County Early Warning Drilling Program wells that are included in DTN: LA0206AM831234.001 [DIRS 160051] is 0.76 dS/cm. If this value is used instead, the concentration in the soil water could increase only by a factor of 1 to 4. The tolerable concentration increase for alfalfa would be about 2 to 3 times. Alfalfa is the most common crop in Amargosa Valley and has the salt tolerance level of 2.0 dS/cm (Doorenbos and Pruitt 1977 [DIRS 103062], Table 36, p. 78).

Considering that the solubility limits in the groundwater would not be exceeded when the water enters the biosphere, it is also not expected that the limits would be exceeded in properly maintained agricultural soil. This is because agricultural practices in arid regions are specifically

designed to prevent precipitation of minerals in surface soil and, accordingly, the biosphere model excludes this process.

Those radionuclides that reach the biosphere irreversibly attached to colloidal particles will not take part in sorption exchange processes with soil and will, therefore, be transported through the soil system without any sorption buildup in soil. Because these radionuclides are not in solution, they are not available for plant uptake (via soil to plant transfer). However, in the biosphere model, radionuclide transfer from the soil to crops via root uptake is proportional to the radionuclide concentration in the surface soil (SNL 2007 [DIRS 177399], Section 6.4.3.1) (i.e., all radionuclides (solutes and colloids) in groundwater are assumed to be in solution and available for plant uptake). This is a conservative approach for cases where colloids are present because the activity associated with colloids is made available for plant uptake.

Based on the previous discussion, omission of FEP 2.2.08.07.0C (Radionuclide Solubility Limits in the Biosphere) will not result in a significant adverse change in the magnitude or timing of either radiological exposure to the RMEI or radionuclide releases to the accessible environment. Therefore, this FEP is excluded from the performance assessments conducted to demonstrate compliance with proposed 10 CFR 63.311 and 63.321 (70 FR 53313 [DIRS 178394]), and with 10 CFR 63.331 [DIRS 180319], on the basis of low consequence.

INPUTS:

Table 2.2.08.07.0C-1. Direct Inputs

Input	Source	Description
BSC 2004. *Agricultural and Environmental Input Parameters for the Biosphere Model*. [DIRS 169673]	Section 4.1.7	Average well water sallinity in well NC-EWDP-19D
Doorenbos and Pruitt 1977. *Crop Water Requirements*. [DIRS 103062]	Table 36, p. 78	Salinity tolerance for crops
DTN: LA0206AM831234.001. Eh-pH Field Measurements on Nye County EWDP Wells. [DIRS 160051]	Table of measured parameters	Electrical conductivity of well water
SNL 2007. *Soil-Related Input Parameters for the Biosphere Model*. [DIRS 179993]	Table 6.2-2	Low organic matter content of the soils in Yucca Mounain region

Table 2.2.08.07.0C-2. Indirect Inputs

Citation	Title	DIRS
10 CFR 63	Energy: Disposal of High-Level Radioactive Wastes in a Geologic Repository at Yucca Mountain, Nevada	180319
70 FR 53313	Implementation of a Dose Standard After 10,000 Years	178394
BSC 2004	*Agricultural and Environmental Input Parameters for the Biosphere Model*	169673
SNL 2007	*Biosphere Model Report*	177399
Stonestrom et al. 2003	*Estimates of Deep Percolation Beneath Native Vegetation, Irrigated Fields, and the Amargosa-River Channel, Amargosa Desert, Nye County, Nevada*	165862

FEP: 2.2.08.08.0A

FEP NAME:

Matrix Diffusion in the SZ

FEP DESCRIPTION:

Matrix diffusion is the process by which radionuclides and other species transported in the SZ by advective flow in fractures or other pathways move into the matrix of the porous rock by diffusion. Matrix diffusion can be a very efficient retarding mechanism, especially for strongly sorbed radionuclides, due to the increase in rock surface accessible to sorption.

SCREENING DECISION:

Included

TSPA DISPOSITION:

Matrix diffusion is the process by which radionuclides in fractures move into the matrix of the porous rock (SNL 2008 [DIRS 183750], Section 6.5.2.6). Diffusion into the rock matrix can occur from a subset of all fractures in the fractured volcanic units (i.e., flowing intervals), as described in *Probability Distribution for Flowing Interval Spacing* (BSC 2004 [DIRS 170014]). This process can be an effective retarding mechanism and is included in the conceptual model and equations describing radionuclide transport in volcanic rock in *Site-Scale Saturated Zone Transport* (SNL 2008 [DIRS 184806], Section 6.4.2.4.1, Equations (21a) and (21b)) and in the numerical implementation of the FEHM software code through the use of the diffusion coefficient and the random-walk particle-tracking method with a semi-analytical solution. The semi-analytical matrix diffusion equation obeys Fick's law and incorporates concentration gradients and the temporal and spatial changes in the gradient along the transport pathway.

Matrix diffusion is included in the SZ transport model abstraction (SNL 2008 [DIRS 183750], Section 6.3.1[a] and Table 6-8) through the parameter that represents the diffusion coefficient in volcanic units, which is sensitive to the volcanic matrix permeability and porosity (SNL 2008 [DIRS 183750], Section 6.5.2.6). This diffusion coefficient is specified with an uncertainty distribution so that uncertainty is captured in the characteristics of the breakthrough curves that are later propagated to TSPA. The uncertainty distribution for the diffusion coefficient in volcanic units is based on:

- Field and laboratory diffusion experiments performed in and on volcanic tuffs located within the Yucca Mountain vicinity (SNL 2008 [DIRS 183750], Section 6.5.2.6)
- A least-squares linear empirical equation fit to diffusion experiment results and measured values for matrix porosity and permeability (Reimus et al. 2002 [DIRS 163008], p. 2.25; 2007 [DIRS 179246], Figures 4 through 6).

The values of the effective matrix diffusion coefficient for diffusing radionuclides are stochastically sampled from this same cumulative distribution function. The process of matrix

diffusion is also a function of spacing between fractures with flowing groundwater, the fracture porosity, and matrix porosity (SNL 2008 [DIRS 184806], Section 6.4.2.4.1). The parameters for flowing interval spacing and flowing interval and average fracture porosity in volcanic units are represented by uncertainty distributions in the SZ flow and transport abstraction model (SNL 2008 [DIRS 183750], Sections 6.5.2.3[a] and 6.5.2.5).

Given the inhomogeneous nature of the alluvium, flow could preferentially occur through high permeability regions, and diffusion could potentially occur into the low permeability regions of the alluvium. Data are available from single-hole and cross-hole tracer tests conducted at the Alluvial Testing Complex and Site 22 (SNL 2007 [DIRS 177394], Sections 6.5.3 and 6.5.4). Based on these available data, the approach of not taking credit for matrix diffusion into low-permeability regions within the alluvium or for matrix diffusion of colloids in either the volcanic units or the alluvium does not underestimate dose to the RMEI because these effects would be small and would only retard transport.

INPUTS:

Table 2.2.08.08.0A-1. Indirect Inputs

Citation	Title	DIRS
10 CFR 63	Energy: Disposal of High-Level Radioactive Wastes in a Geologic Repository at Yucca Mountain, Nevada	180319
BSC 2004	*Probability Distribution for Flowing Interval Spacing*	170014
Reimus et al. 2002	*Diffusive and Advective Transport of ^{3}H, ^{14}C, and ^{99}Tc in Saturated, Fractured Volcanic Rocks from Pahute Mesa, Nevada*	163008
Reimus et al. 2007	"Matrix Diffusion Coefficients in Volcanic Rocks at the Nevada Test Site: Influence of Matrix Porosity, Matrix Permeability, and Fracture Coating Minerals"	179246
SNL 2008	*Saturated Zone Flow and Transport Model Abstraction*	183750
SNL 2007	*Saturated Zone In-Situ Testing*	177394
SNL 2008	*Site-Scale Saturated Zone Transport*	184806

FEP: 2.2.08.08.0B

FEP NAME:

Matrix Diffusion in the UZ

FEP DESCRIPTION:

Matrix diffusion is the process by which radionuclides and other species transported in the UZ by advective flow in fractures or other pathways move into the matrix of the porous rock by diffusion. This includes osmotic processes in response to chemical gradients. Matrix diffusion can be a very efficient retarding mechanism, especially for strongly sorbed radionuclides, due to the increase in rock surface accessible to sorption.

SCREENING DECISION:

Included

TSPA DISPOSITION:

Migration of radionuclides from water flowing in fractures into the surrounding rock matrix by diffusion could expose radionuclides to sorbing sites in the matrix. The diffusion into the matrix and its subsequent sorption into the matrix material will make these radionuclides unavailable for transport in the water flowing in the fracture for some times. Migration of radionuclides from fast flow fracture into surrounding slow flow matrix blocks by diffusion could play an important role in delaying the transport of radionuclides in fractures. Matrix diffusion is identified in *Conceptual Model and Numerical Approaches for UZ Flow and Transport* (BSC 2004 [DIRS 170035], Section 6.2.2) as a process to be included in transport modeling. The role of matrix diffusion is included through the development of the particle tracking approach as described in *Particle Tracking Model and Abstraction of Transport Processes* (SNL 2008 [DIRS 184748], Section 6.4.3). Transfer function curves (DTN: LA0311BR831229.001 [DIRS 166924]) that are generated are fed directly to the TSPA model. These curves are used by FEHM in simulating the effect of matrix diffusion on radionuclide transport in TSPA model simulations as described in *Particle Tracking Model and Abstraction of Transport Processes* (SNL 2008 [DIRS 184748], Section 6.4.3 and Appendix C). This particle tracking approach was used to simulate matrix diffusion of dissolved radionuclides. This treatment of matrix diffusion includes the effects of partial saturation of the matrix, radionuclide sorption in the matrix, and finite spacing of fractures. Diffusion in the unsaturated zone is treated separately in excluded FEP 2.2.08.05.0A (Diffusion in the UZ).

Osmosis would tend to cause water from fractures to flow into the matrix, if the matrix presents a suitable barrier to the migration of dissolved salts, but not a barrier to water migration. Osmosis is a process that is not expected to have a significant effect on radionuclide transport in the unsaturated zone compared to matrix diffusion (see excluded FEP 2.2.08.05.0A (Diffusion in the UZ)).

Matrix diffusion of colloids was assumed not to occur because its effects would be small because of the larger size of colloids compared to solutes and because diffusion coefficients of colloids

are significantly lower than values for solutes (SNL 2008 [DIRS 184748], Section 6.4.5). The potential for matrix diffusion of dissolved radionuclides is described by a matrix diffusion coefficient. The matrix diffusion coefficient can be presented as the product of the tortuosity and the free-water diffusion coefficient. The tortuosity is correlated to matrix water content, matrix effective permeability, and free-water diffusion coefficient through the relationship developed by Reimus et al. (2007 [DIRS 179246]). The free-water diffusion coefficients and the distribution of tortuosity are outputs from *Particle Tracking Model and Abstraction of Transport Processes* (SNL 2008 [DIRS 184748], Section 6.5.5 and Table 6-6; DTN: LA0407BR831371.001 [DIRS 170806]). The TSPA model uses these outputs in multiple realization simulations to randomly generate matrix diffusion coefficients (DTN: LA0407BR831371.001 [DIRS 170806]). Related to this FEP is included FEP 2.1.09.08.0A (Diffusion of Dissolved Radionuclides in EBS).

INPUTS:

Table 2.2.08.08.0B-1. Indirect Inputs

Citation	Title	DIRS
BSC 2004	*Conceptual Model and Numerical Approaches for Unsaturated Zone Flow and Transport*	170035
DTN: LA0311BR831229.001	UZ Transport Abstraction Model, Transfer Function Calculation Files	166924
DTN: LA0407BR831371.001	UZ Transport Abstraction Model, Transport Parameters and Base Case Simulation Results	170806
Reimus et al. 2002	*Diffusive and Advective Transport of ^{3}H, ^{14}C, and ^{99}Tc in Saturated, Fractured Volcanic Rocks from Pahute Mesa, Nevada*	163008
Reimus et al. 2007	"Matrix Diffusion Coefficients in Volcanic Rocks at the Nevada Test Site: Influence of Matrix Porosity, Matrix Permeability, and Fracture Coating Minerals"	179246
SNL 2008	*Particle Tracking Model and Abstraction of Transport Processes*	184748

FEP: 2.2.08.09.0A

FEP NAME:

Sorption in the SZ

FEP DESCRIPTION:

Sorption of dissolved and colloidal radionuclides in the SZ can occur on the surfaces of both fractures and matrix in rock or soil along the transport path. Sorption may be reversible or irreversible, and it may occur as a linear or nonlinear process. Sorption kinetics and the availability of sites for sorption should be considered. Sorption is a function of the radioelement type, mineral type, and groundwater composition.

SCREENING DECISION:

Included

TSPA DISPOSITION:

Sorption of dissolved radionuclides onto rock surfaces in the saturated zone can occur both in the volcanic rocks and the alluvium, as confirmed by field-scale tracer testing (SNL 2007 [DIRS 177394], Sections 6.3, 6.5.5, and G5.4.3). Radionuclides can be transported as a dissolved species, as well as a species attached to mobile colloids. Both of these mechanisms of transport are implemented in the TSPA model. Radionuclides can sorb onto the colloidal materials in two modes, either reversibly or irreversibly (SNL 2008 [DIRS 184806], Sections 6.4.2.6, 7.1.2.5, and 7.1.2.9). Uncertainties in radioelement sorption distributions are used in *Saturated Zone Flow and Transport Model Abstraction* (SNL 2008 [DIRS 183750], Table 6-8) and propagated to TSPA by way of their effects on the breakthrough curves.

Reversible Sorption of Dissolved Radioelements onto Rock Surfaces: The process of reversible sorption in the saturated zone is modeled using the sorption coefficient (K_d) approach in volcanic rocks (SNL 2008 [DIRS 184806], Section 6.4.2.4.1) and in alluvium (SNL 2008 [DIRS 184806], Section 6.4.2.5). In the volcanic rocks, sorption in the matrix is included in the model, but sorption onto fracture surfaces is not included in the model. Recognizing that sorption is a function of the radioelement type, mineral type, and groundwater composition, and that these vary over the transport domain of interest, probability distribution functions reflect uncertainty and variability in values of the sorption coefficients, and K_ds of various radioelements have been developed independently for volcanic formations and alluvium over the range of groundwater compositions expected to occur in the saturated zone (SNL 2008 [DIRS 184806], Sections A2, A3, A7, and Table C-14[a]). These probability distribution functions have been developed for use in stochastic simulations for the radioelements americium, cesium, neptunium, protactinium, plutonium, radium, selenium, strontium, thorium, tin, and uranium (SNL 2008 [DIRS 183750], Sections 6.5.2.8, 6.5.3.1, and Tables 6-8 and 6-7[a]).

Sorption coefficient distributions have been developed in the SZ transport report (SNL 2008 [DIRS 184806], Table 5-1 and Appendix A) assuming oxidizing conditions along the entire flowpaths to the accessible environment, not taking into account the reducing conditions that

potentially occur to the east of the Yucca Mountain (BSC 2005 [DIRS 174958], Figure 2.1-2). This introduces a bias towards lower values for the K_d distributions for neptunium and technetium used in the SZ transport model. Further, the SZ transport model treats the sorption as a reversible process. As discussed in *Site-Scale Saturated Zone Transport* (SNL 2008 [DIRS 184806], Table 6.6-1a, item 1), this introduces a bias towards lower values for the K_d distributions for uranium and neptunium used in the SZ transport model. The K_d approach used in the SZ transport model is based on treating the sorption as a linear, equilibrium process (SNL 2008 [DIRS 184806], Section 6.3). As discussed in *Site-Scale Saturated Zone Transport* (SNL 2008 [DIRS 184806], Table 6.6-1b, rows 1 and 2), the potential effects of nonlinear and nonequilibrium sorption are accounted for in the model by biasing the K_d distributions towards low values. This is because available data show that the rate of desorption of uranium and neptunium from the rock surfaces is slower than the rate of absorption. Sorption reactions that are not fully reversible result in rates of transport that are slower than would be the case for fully reversible reactions. Therefore, using unadjusted sorption coefficients would result in diminished total radionuclide mass breakthrough from the saturated zone, compared to the breakthrough based on the actual values used.

In the volcanic units, for radionuclides that are not transported by colloid-facilitated mechanisms (neptunium, radium, selenium, strontium, and uranium), sorption between the aqueous phase and the solid phase (parent rock) is modeled in the FEHM flow and transport code using sampled parameters (SNL 2008 [DIRS 183750], Section 6.5.2.8, Tables 6-8 and 6-7[a]); sorption for the same radionuclides in the alluvium is also modeled through sampled parameters (SNL 2008 [DIRS 183750], Section 6.5.2.8, Tables 6-8 and 6-7[a]).

Reversible Sorption of Radioelements onto Colloids: Equilibrium sorption between aqueous and solid phases and a colloidal phase is modeled (SNL 2008 [DIRS 184806], Section 6.4.2.6) for four radionuclide classes represented by partitioning of the radionuclides americium, thorium, protactinium, cesium, plutonium, and tin (SNL 2008 [DIRS 183750], Table 6-9[a]). Partitioning between the colloidal and aqueous phase is the same in both the volcanic units and the alluvium. Partitioning between the aqueous and solid phase (parent rock) for each species differs between the volcanic and alluvial units.

Irreversible Sorption of Radioelements onto Colloids: Only plutonium and americium are assumed to irreversibly sorb onto colloids. In the volcanic units, advectively transported colloids with irreversibly attached plutonium and americium (BSC 2004 [DIRS 170006], Section 6.4) undergo reversible filtration that results from a combination of physical processes and electrochemical interactions with media surfaces; this reversible filtration is modeled through the sampled colloid retardation factor (SNL 2008 [DIRS 183750], Section 6.5.2.11). These same colloids also undergo reversible filtration in the alluvium, which is modeled via a retardation factor sampled from a separate distribution (SNL 2008 [DIRS 183750], Section 6.5.2.11). The use of retardation factors to model filtration processes assumes that forward and reverse filtration rates are linear and fast relative to transport travel times and that there is no irreversible colloid filtration.

INPUTS:

Table 2.2.08.09.0A-1. Indirect Inputs

Citation	Title	DIRS
10 CFR 63	Energy: Disposal of High-Level Radioactive Wastes in a Geologic Repository at Yucca Mountain, Nevada	180319
BSC 2004	*Saturated Zone Colloid Transport*	170006
BSC 2005	*Impacts of Solubility and Other Geochemical Processes on Radionuclide Retardation in the Natural System*	174958
SNL 2007	*Saturated Zone In-Situ Testing*	177394
SNL 2008	*Saturated Zone Flow and Transport Model Abstraction*	183750
SNL 2008	*Site-Scale Saturated Zone Transport*	184806

FEP: 2.2.08.09.0B

FEP NAME:

Sorption in the UZ

FEP DESCRIPTION:

Sorption of dissolved and colloidal radionuclides in the UZ can occur on the surfaces of both fractures and matrix in rock or soil along the transport path. Sorption may be reversible or irreversible, and it may occur as a linear or nonlinear process. Sorption kinetics and the availability of sites for sorption should be considered. Sorption is a function of the radioelement type, mineral type, and groundwater composition.

SCREENING DECISION:

Included

TSPA DISPOSITION:

Sorption is identified in *Conceptual Model and Numerical Approaches for UZ Flow and Transport* (BSC 2004 [DIRS 170035], Section 6.2.3) as a process to be included in transport modeling. It is included in the TSPA model for mountain-scale UZ radionuclide transport as a linear equilibrium sorption (K_d) model in *Radionuclide Transport Models Under Ambient Conditions* (SNL 2007 [DIRS 177396], Section 6.1). K_d values and their basis in experimental data are presented in the same report (SNL 2007 [DIRS 177396], Appendix A[a]). In TSPA simulations, sorption coefficients are sampled and provided to FEHM.

The model implemented in FEHM can account for sorption in both the matrix continuum and the fracture continuum. While dissolved radionuclide sorption may occur in fractures, it is assumed that no sorption of dissolved radionuclides occurs on fracture surfaces (SNL 2008 [DIRS 184748], Section 6.5.8). This assumption will not result in underestimating radionuclide transport rates. Thus, a fracture surface retardation factor of one is set for use in TSPA model simulations (SNL 2008 [DIRS 184748], Section 6.5.8). A retardation factor of one assumes there is no radionuclide sorption onto fracture surfaces. Sorption characteristics of the rock minerals are assumed to be static in time. Sorption K_ds have been derived for the following eleven radioelements: americium, cesium, neptunium, protactinium, plutonium, radium, strontium, thorium, tin, selenium, and uranium as dissolved radionuclides; other dissolved radioelements treated by TSPA (for example, technetium) are modeled as nonsorbing.

The sorption coefficient data on which the distributions are based are obtained in laboratory experiments in which crushed rock samples from the Yucca Mountain site are contacted with groundwaters (or simulated groundwaters) representative of the site, spiked with one or more of the elements of interest (SNL 2007 [DIRS 177396], Sections A4 and A5). Sorption experiments have been carried out as a function of time, element concentration, atmospheric composition, particle size, and temperature. In some cases, the solids remaining from sorption experiments were contacted with unspiked groundwater in desorption experiments. The sorption and desorption experiments together provide information on the equilibration rates of the forward

and backward sorption reactions. For elements that sorb primarily through surface complexation reactions, the experimental data are augmented with the results of modeling calculations using PHREEQC (PHREEQC V2.3 [DIRS 157837], STN: 10068-2.3-01) with the thermodynamic input data file *PHREEQCDATA025.dat* (DTN: MO0604SPAPHR25.001 [DIRS 176868]). The inputs for the modeling calculations include groundwater compositions, surface areas, binding constants for the radioelements, and thermodynamic data for solution species. These modeling calculations provide a basis for interpolation and extrapolation of the experimentally derived sorption coefficient dataset. The effects of nonlinear sorption are approximated by the effective K_d range (SNL 2007 [DIRS 177396], Section A8, and Appendix A[a]).

Sorption coefficients are provided in terms of probability distributions for the sorption coefficient of each radioelement among the three major rock types (devitrified, zeolitic, and vitric) found in the unsaturated zone. The influence of expected variations in water chemistry, radionuclide concentrations, and variations in rock surface properties within one of the major rock types are incorporated into these probability distributions. These distributions are specified for each radionuclide–rock type combination (SNL 2007 [DIRS 177396], Section A8 and Appendix A[a]) and are sampled in the TSPA to account for the effects of natural variations in pore-water chemistry and mineral surfaces on sorption. Correlations for sampling sorption coefficient probability distributions have been derived for the elements investigated (SNL 2007 [DIRS 177396], Appendix B[a]). To derive the correlations, a rating system was first developed to rate the impact of six different variables on the sorption coefficient for a given element in each of the three major rock types. The six variables are pH, Eh, water chemistry, rock composition, rock surface area, and radionuclide concentration. Water chemistry refers to the major ion concentrations and silica. Rock composition refers to both the mineralogic composition of the rocks and the chemical composition of the minerals (for example, zeolite compositions).

Sorption in the unsaturated zone is treated as a linear reversible infinite capacity process in the radionuclide transport abstraction model (SNL 2008 [DIRS 184748], Section 6.5.4 in AD01). In the matrix, sorption is incorporated in the generation of transfer function curves and expressed as part of the defined dimensionless parameters (SNL 2008 [DIRS 184748], Section 6.4.3). For colloid facilitated radionuclide transport, radionuclide sorption onto colloids and its effect on transport are simulated through the colloid K_c factor (SNL 2008 [DIRS 184748], Section 6.4.5). The K_c factor is the product of the radionuclide sorption coefficient onto colloids and the colloid concentration (SNL 2008 [DIRS 184748], Section 6.5.12 in AD01). Radionuclide sorption coefficients that were used in the simulation of radionuclide transport in the unsaturated zone are documented in *Particle Tracking Model and Abstraction of Transport Processes* (SNL 2008 [DIRS 184748], Section 6.5.4 in AD01). Colloid concentration and radionuclide sorption coefficients onto colloids are documented in *Waste Form and In-Drift Colloids-Associated Radionuclide Concentrations: Abstraction and Summary* (SNL 2007 [DIRS 177423], Section 6.3) and used in *Particle Tracking Model and Abstraction of Transport Processes* (SNL 2008 [DIRS 184748], Section 6.5.12 in AD01). Sorption on colloids and the effects of colloid transport are addressed in *Radionuclide Transport Models under Ambient Conditions* (SNL 2007 [DIRS 177396], Sections 6.1.3 and 6.2.3), with simulation results presented in Section 6.18 of that report.

INPUTS:

Table 2.2.08.09.0B-1. Indirect Inputs

Citation	Title	DIRS
BSC 2004	*Conceptual Model and Numerical Approaches for Unsaturated Zone Flow and Transport*	170035
DTN: MO0604SPAPHR25.001	PHREEQC Data 0 Thermodynamic Database for 25°C - File: PHREEQCDATA025	176868
SNL 2007	*Radionuclide Transport Models Under Ambient Conditions*	177396
SNL 2007	*Waste Form and In-Drift Colloids-Associated Radionuclide Concentrations: Abstraction and Summary*	177423
SNL 2008	*Particle Tracking Model and Abstraction of Transport Processes*	184748
PHREEQC V2.3	PC. STN: 10068-2.3-01	157837

FEP: 2.2.08.10.0A

FEP NAME:

Colloidal Transport in the SZ

FEP DESCRIPTION:

Radionuclides may be transported in groundwater in the SZ as colloidal species. Types of colloids include true colloids, pseudo colloids, and microbial colloids.

SCREENING DECISION:

Included

TSPA DISPOSITION:

The colloid-facilitated transport of radionuclides is explicitly included in the SZ transport abstraction model and the SZ one-dimensional transport model (SNL 2008 [DIRS 183750], Sections 6.5.2.11 and 6.5.2.12). Colloids are subject to advection in the alluvium and fractures of tuff units and are assumed not to diffuse into the fractured rock matrix (SNL 2008 [DIRS 184806], Section 6.4.2.6 and Appendix B). Colloid transport in the saturated zone has been investigated at the field scale by tracer testing using carboxylate-modified latex microspheres in tracer tests in both the saturated volcanics and alluvium, as described in *Saturated Zone In-Situ Testing* (SNL 2007 [DIRS 177394], Sections 6.3 and 6.5).

Radionuclide transport in association with colloids is simulated in the TSPA to occur by two modes: (1) as solutes reversibly sorbed onto colloids, and (2) as solutes irreversibly attached to colloids or as true colloids (SNL 2008 [DIRS 183750], Sections 6.5.2.11 and 6.5.2.12). Natural or anthropogenic colloids with solutes reversibly sorbed or irreversibly attached onto them are called pseudocolloids. Reversible sorption of radionuclides may occur onto any colloidal material present in the groundwater. Measurements of natural colloid concentrations in groundwater of the saturated zone do not discriminate between mineral and microbial colloids, although available data on total organic carbon concentrations in saturated zone groundwaters (DTN: GS931100121347.007 [DIRS 149611], Table S96375_009); DTN: GS010308312322.003 [DIRS 154734], Table S01053_003) indicate that natural microbial colloid concentrations are insignificant in the saturated zone. The parameter distributions that are used to describe uncertainty related to reversible sorption onto colloids are based on field observations and laboratory experiments performed on colloids under geochemical conditions found in the vicinity of Yucca Mountain (BSC 2004 [DIRS 170006], Section 7). The key parameters for reversibly sorbed radionuclide transport in association with colloids are sorption coefficients onto colloids for americium, plutonium, cesium, and tin; colloid retardation factor in the volcanics; colloid retardation factor in the alluvium; and groundwater concentration of colloids as discussed in *Saturated Zone Flow and Transport Model Abstraction* (SNL 2008 [DIRS 183750], Tables 6-8 and 6-7[a]). These parameters are randomly sampled from probability distributions described in *Saturated Zone Flow and Transport Model Abstraction* (SNL 2008 [DIRS 183750], Tables 6-8 and 6-7[a]) to propagate uncertainties through to the results of the performance assessment.

Colloids with irreversibly attached radionuclides originate from the degradation of the glass waste form in the repository (SNL 2007 [DIRS 177423], Section 6.3.1), and are subject to retardation in the saturated zone both in the fractured tuff and the alluvium. However, a small fraction of colloids with irreversibly attached radionuclides are transported through the saturated zone with no retardation due to the kinetic nature of colloid attachment to the aquifer materials (BSC 2004 [DIRS 170006], Section 6.6). This small fraction is a result of inherent heterogeneity in natural colloid populations, which results in heterogeneous colloid transport properties, including a small fraction of colloids that transport unretarded over long time and distance scales because they have extremely low filtration rates. The parameters related to the retardation of colloids with irreversibly attached radionuclides are colloid retardation factors for fractured tuff and alluvium (SNL 2008 [DIRS 183750], Tables 6-8 and 6-7[a]). These parameters are randomly sampled from probability distributions described in *Saturated Zone Flow and Transport Model Abstraction* (SNL 2008 [DIRS 183750], Tables 6-8 and 6-7[a]) to propagate uncertainties associated with transport of radionuclides that are irreversibly sorbed to colloids through to the results of the performance assessment.

INPUTS:

Table 2.2.08.10.0A-1. Direct Inputs

Input	Source	Description
DTN: GS010308312322.003. Field, Chemical and Isotopic Data from Wells in Yucca Mountain Area, Nye County, Nevada, Collected Between 12/11/98 and 11/15/99. [DIRS 154734]	Table S01053_003	Geochemical analysis of groundwater samples taken from saturated zone wells within the Yucca Mountain vicinity

Table 2.2.08.10.0A-2. Indirect Inputs

Citation	Title	DIRS
BSC 2004	*Saturated Zone Colloid Transport*	170006
DTN: GS931100121347.007	Selected Ground-Water Data for Yucca Mountain Region, Southern Nevada and Eastern California, Through December 1992	149611
SNL 2007	*Saturated Zone In-Situ Testing*	177394
SNL 2007	*Waste Form and In-Drift Colloids-Associated Radionuclide Concentrations: Abstraction and Summary*	177423
SNL 2008	*Saturated Zone Flow and Transport Model Abstraction*	183750
SNL 2008	*Site-Scale Saturated Zone Transport*	184806

FEP: 2.2.08.10.0B

FEP NAME:

Colloidal Transport in the UZ

FEP DESCRIPTION:

Radionuclides may be transported in groundwater in the UZ as colloidal species. Types of colloids include true colloids, pseudo colloids, and microbial colloids.

SCREENING DECISION:

Included

TSPA DISPOSITION:

Colloidal transport of radionuclides is identified in *Conceptual Model and Numerical Approaches for UZ Flow and Transport* (BSC 2004 [DIRS 170035], Section 6.2.4) as a process to be included in transport modeling. The influence of colloid transport on radionuclide migration through the unsaturated zone is included and discussed in *Particle Tracking Model and Abstraction of Transport Processes* (SNL 2008 [DIRS 184748], Section 6.4.5). Parameters that can impact colloid transport in the unsaturated zone include colloid size (DTN: LL000122051021.116 [DIRS 142973]), colloid concentration (DTN: MO0701PAGROUND.000 [DIRS 179310]), radionuclide sorption coefficients onto colloid (DTN: MO0701PASORPTN.000 [DIRS 180391]) for plutonium, americium, thorium, protactium, and cesium; (DTN: MO0701PAKDSUNP.000 [DIRS 180392]) for tin; and colloid retardation factors (DTN: LA0303HV831352.002 [DIRS 163558]). The colloid concentration data and sorption-onto-colloid data are documented in *Waste Form and In-Drift Colloids-Associated Radionuclide Concentrations: Abstraction and Summary* (SNL 2007 [DIRS 177423], Sections 6.3.11 and 6.3.12). Colloid retardation factors are documented in *Saturated Zone Colloid Transport* (BSC 2004 [DIRS 170006], Section 6.4.3). These data are used in *Particle Tracking Model and Abstraction of Transport Processes* (SNL 2008 [DIRS 184748], Sections 6.5.9 to 6.5.13).

Colloid transport processes include advection and dispersion. In addition, colloids undergo a process by which certain size colloids are mechanically excluded from entering the matrix from the fractures (SNL 2008 [DIRS 184748], Section 6.5.9). Colloids can also be permanently removed from the system by a size-based filtration at matrix unit boundaries. The colloid retardation factor in the fracture continuum, R_{coll} (a function of physical and electrochemical processes collectively termed attachment), is evaluated on the basis of field experiments at the C-Well Complex using microspheres as analogues for natural colloids as well as laboratory experiments evaluating the transport of both microspheres and inorganic colloids (SNL 2008 [DIRS 184748], Section 6.5.13). Field experiments have also shown that a small percentage of colloidal particles are transported through the groundwater system essentially unretarded (BSC 2004 [DIRS 170006], Section 6.6). The fractions of unretarded colloids have been developed based on field data (BSC 2004 [DIRS 170006]). Included FEP 2.2.08.09.0B (Sorption in the UZ) addresses sorption of colloids in the unsaturated zone. Colloid matrix

diffusion is assumed not to occur because of the relatively larger size of colloids campared to solute, and therefore its effect would be small and would have little effect on dose. Included FEP 2.2.08.08.0B Matrix Diffusion in the UZ) discusses matrix diffusion in the unsaturated zone.

INPUTS:

Table 2.2.08.10.0B-1. Indirect Inputs

Citation	Title	DIRS
BSC 2004	*Conceptual Model and Numerical Approaches for Unsaturated Zone Flow and Transport*	170035
BSC 2004	*Saturated Zone Colloid Transport*	170006
DTN: LA0303HV831352.002	Colloid Retardation Factors for the Saturated Zone Fractured Volcanics	163558
DTN: LL000122051021.116	Summary of Analyses of Glass Dissolution Filtrates	142973
DTN: MO0701PAGROUND.000	Groundwater Colloid Concentration Parameters	179310
DTN: MO0701PAKDSUNP.000	Colloidal K_ds for U, Np, Ra and Sn	180392
DTN: MO0701PASORPTN.000	Colloidal Sorption Coefficients for Pu, Am, Th, Cs, and Pa	180391
SNL 2007	*Waste Form and In-Drift Colloids-Associated Radionuclide Concentrations: Abstraction and Summary*	177423
SNL 2008	*Particle Tracking Model and Abstraction of Transport Processes*	184748

FEP: 2.2.08.11.0A

FEP NAME:

Groundwater Discharge to Surface Within the Reference Biosphere

FEP DESCRIPTION:

Radionuclides transported in groundwater as solutes or solid materials (colloids) from the far-field may discharge at specific "entry" points that are within the reference biosphere. Natural surface discharge points, including those resulting from water table or capillary rise, may be surface water bodies (rivers, lakes), springs, wetlands, holding ponds, or unsaturated soils.

SCREENING DECISION:

Excluded – low consequence

SCREENING JUSTIFICATION:

Currently, groundwater discharge from the regional groundwater flow system in the area of Yucca Mountain occurs at Franklin Lake Playa (also known as Alkali Flat) and Ash Meadows (D'Agnese et al. 1997 [DIRS 100131], pp. 40 to 48); both are located over 10 km beyond the boundary of the accessible environment. There is evidence of paleospring discharge points within northern Amargosa Desert that could become reactivated during wetter climatic conditions. These are the paleospring deposits located in Crater Flat, Crater Flat Wash, Amargosa Valley Diatomite, Indian Pass, Scranton Well, Mesquite Wash, and the Amargosa River Snail Site (Paces et al. 1997 [DIRS 109148], Figure 18). The Stranton Wells, Mesquite Wash, and Amargosa River Snail Site paleospring deposits lie at the far terminus of Fortymile Wash and downstream from the projected flow path (from the repository to the 18-km boundary). The other paleospring deposits are separated from Fortymile Wash by faults and ridges and are not along the projected saturated zone transport path. Therefore, they would not contain contaminants originating from the repository if reactivated under wetter climatic conditions. 10 CFR 63.102(i) [DIRS 180319] defines the reference biosphere as "the environment inhabited by the [RMEI], along with associated human exposure pathways and parameters." Because these latter paleospring deposits do not contain repository contaminants and are not part of human exposure pathways, they would not be part of the reference biosphere.

Paleosprings along the far terminus of Fortymile Wash are not expected to be activated within 10,000 years after repository closure, based on geochemical evidence of previous groundwater discharge at these locations. With the exception of the Amargosa River Snail Site, geochemical dating indicates the last episode of paleospring activity for the majority of paleosprings occurred between 14,000 to 20,000 years ago (Paces et al. 1997 [DIRS 109148], Figure 18). Scranton Wells was active 40,000 to 60,000 years ago, Mesquite Wash active 30,000 years ago, and the Amargosa River Snail Site between 9,000 to 12,000 years ago (Paces et al. 1997 [DIRS 109148], Figure 18). There is some uncertainty regarding the activity that occurred 9,000 to 12,000 years ago at the Amargosa River Snail Site. Surface "lag" samples taken from this site and collected for dating indicate that plant petrifications may have tapped a subsided water source (a one-time discharge point that has been lowered below the ground surface). Thus, surface discharge may

have ceased much earlier than indicated from geochemical dating. Nevertheless, if the saturated zone plume potentially discharges at the historic discharge points located south of Fortymile Wash, it would contain lower radionuclide concentrations than at the 18-km boundary, because such discharge locations are over 10 km beyond the accessible environment boundary. Longer path lengths from the repository facilitate the processes of sorption and dispersion, which would lower the plume's radionuclide concentration levels as the path length increases. Additionally, a longer path length coupled with more sorption and dispersion equates to longer transport times, thus allowing more time for radioactive decay. More time for decay reduces the radionuclide activities in groundwater withdrawn from the community wells. Because of the distant location of these paleosprings relative to the accessible environment boundary (and thus the location of the hypothetical community that includes the RMEI), it is not expected that the exposures that could be potentially received from the discharges of groundwater to the surface at these distant locations would affect the average dose to the RMEI.

Flow and transport modeling was performed on the saturated zone site-scale model domain to assess water table elevations reflective of glacial-transition climatic conditions (SNL 2008 [DIRS 184806], Appendix E). For these simulations, the water table was allowed to rise under the repository by 50 m (SNL 2007 [DIRS 177391], Section 6.6.4.2). The higher water table estimated for use in these simulations does not indicate spring formation within the 18-km boundary, but does show a shallow water table within 5 m of the surface. The shallow water table corresponds to the three paleospring deposits located along Highway 95 and at the southern end of Crater Flat (SNL 2007 [DIRS 177391], Figure 6-21). Even if the water table were to rise to form springs, the Windy Wash fault and the Stagecoach fault (SNL 2007 [DIRS 177391], Figure 6-12) serve as barriers between Crater Flat and Fortymile Wash. It is in the Fortymile Wash where flow paths from the repository to the 18-km boundary converge. Consequently, if springs were to develop in the shallow water table area at the southern end of Crater Flat, radionuclides released from the repository are not expected to be constituents of the spring waters.

In summary, current natural groundwater discharge points along the saturated zone flow paths are greater than 10 km downstream from the 18-km boundary, and radionuclide concentrations at natural groundwater discharge locations would not be greater than concentrations at the 18-km boundary due to increased dispersion and sorption. Future discharge points, if they occur at all, would be located several kilometers downstream from the 18-km boundary, but would not contain contaminants originating from the repository because of the physical barriers, such as faults and ridges, which separate them from the projected path of radionuclide transport from the repository.

The biosphere model for the groundwater exposure scenario includes all exposure pathways expected to contribute to the annual dose to the RMEI (SNL 2007 [DIRS 177399], Section 6.3), as required by proposed 10 CFR 63.311 and 63.321 (70 FR 53313 [DIRS 178394]). Exposure is calculated for the radionuclide concentration in groundwater at the boundary of the accessible environment. Although not expected, if spring reactivation were to occur, the potential pathways from exposure to water flowing from such springs within the reference biosphere or other groundwater discharge points would be consumption of water, external exposure from contaminated soil around springs, and water immersion. These pathways are considered in the biosphere model because groundwater entering the biosphere from a spring or other discharge

point is assumed to be used in the same way as groundwater from a well. Because radionuclide concentrations at natural groundwater discharge locations would not be greater than concentrations at the 18-km boundary, radiological effects of exposure to groundwater discharged to surface are bounded by the radiological effects from exposure to groundwater withdrawn from wells at the compliance location. Therefore, the groundwater discharge to surface within the reference biosphere, if it occurred at all, would not need to be modeled separately. The groundwater release to the surface outside the reference biosphere (excluded FEP 2.3.11.04.0A (Groundwater Discharge to the Surface Outside the Reference Biosphere)) does not affect the dose to the RMEI and is, therefore, excluded.

Based on the previous discussion, omission of FEP 2.2.08.11.0A (Groundwater Discharge to Surface within the Reference Biosphere) will not result in a significant adverse change in the magnitude or timing of either radiological exposure to the RMEI or radionuclide releases to the accessible environment. Therefore, this FEP is excluded from the performance assessments conducted to demonstrate compliance with proposed 10 CFR 63.311 and 63.321 (70 FR 53313 [DIRS 178394]), and with 10 CFR 63.331 [DIRS 180319], on the basis of low consequence.

INPUTS:

Table 2.2.08.11.0A-1. Direct Inputs

Input	Source	Description
Paces et al. 1997. *Summary of Discharge Deposits in the Amargosa Valley*. [DIRS 109148]	Figure 18	Scranton Wells was active 40,000 to 60,000 years ago, Mesquite Wash active 30,000 years ago, and the Amargosa River Snail Site between 9,000 to 12,000 years ago
	Figure 18	With the exception of the Amargosa River Snail Site, geochemical dating indicates the last episode of paleospring activity for the majority of paleosprings occurred between 14 to 20 thousand years ago, or longer
SNL 2007. *Saturated Zone Site-Scale Flow Model*. [DIRS 177391]	Figure 6-12	Geologic features included in the SZ flow model and projected flow paths
	Figure 6-21	Projected locations of the surface discharges under the future climatic conditions

Table 2.2.08.11.0A-2. Indirect Inputs

Citation	Title	DIRS
10 CFR 63	Energy: Disposal of High-Level Radioactive Wastes in a Geologic Repository at Yucca Mountain, Nevada	180319
70 FR 53313	Implementation of a Dose Standard After 10,000 Years	178394
D'Agnese et al. 1997	*Hydrogeologic Evaluation and Numerical Simulation of the Death Valley Regional Ground-Water Flow System, Nevada and California*	100131
Paces et al. 1997	*Summary of Discharge Deposits in the Amargosa Valley*	109148
SNL 2007	*Biosphere Model Report*	177399
SNL 2007	*Saturated Zone Site-Scale Flow Model*	177391
SNL 2008	*Site-Scale Saturated Zone Transport*	184806

FEP: 2.2.08.12.0A

FEP NAME:

Chemistry of Water Flowing into the Drift

FEP DESCRIPTION:

Inflowing water chemistry may be used in analysis or modeling that requires initial water chemistry in the drift. Chemistry of water flowing into the drift is affected by initial water chemistry in the rock, mineral and gas composition in the rock, and thermal-hydrological-chemical processes in the rock.

SCREENING DECISION:

Included

TSPA DISPOSITION:

The near-field chemistry (NFC) process model in *Engineered Barrier System: Physical and Chemical Environment* (SNL 2007 [DIRS 177412], Section 6.3.2) predicts potential seepage water compositions at the drift wall, and was designed specifically to investigate the effects of thermal-hydrologic-chemical processes in the host rock, including the effects of initial water chemistry, and mineral and gas compositions in the rock (SNL 2007 [DIRS 177412], Sections 6.3.2 and 6.6). The near-field chemistry model evaluates water–rock interactions as the pore water percolates through the rock above the repository, using a repository depth and TSw unit thickness consistent with the repository geographic and geologic location within Yucca Mountain (SNL 2007 [DIRS 179466], Parameter Numbers 01-01 and 01-03). Therefore, these effects are accounted for in the potential seepage compositions predicted by the NFC model, which are in turn used as initial conditions for evaluating in-drift water chemistries in the seepage dilution/evaporation abstraction model (SNL 2007 [DIRS 177412], Sections 6.3.3 and 6.9). The seepage dilution/evaporation model provides lookup tables of in-drift water chemistry for TSPA calculations.

The NFC model does not simulate seepage into the drifts, but rather evaluates water compositions delivered to the evaporation front in the rock or at the drift wall. It is expected that these water compositions closely represent in-drift seepage chemistry. The evaluation of seepage flow rates into the drifts is discussed in included FEP 2.2.07.20.0A (Flow Diversion around Repository Drifts).

In the P&CE report (SNL 2007 [DIRS 177412], Section 6.6), available TSw pore-water analyses are screened for analysis quality (e.g., anion-cation charge balance) and for evidence of being affected by microbial processes during core storage. After eliminating those pore-water analyses with a poor charge balance or which showed evidence of having been modified by post-collection microbial activity, 34 TSw waters remained (SNL 2007 [DIRS 177412], Section 6.6.4). These were further evaluated to identify the number of waters required to adequately represent the observed compositional variability within the group. A statistical analysis of these water compositions and their evaporated equivalents, using the method of

principal components (SNL 2007 [DIRS 177412], Section 6.6.5), showed that they clustered into four compositional clusters or groups. After grouping the waters, a representative water composition was chosen for each group on the basis of statistical proximity to the cluster centroid. The NFC model outputs that are used by the seepage dilution/evaporation model are based on four initial pore-water compositions, corresponding to the four representative waters.

The statistical analysis and the observed similarities in evaporative evolution provide support that the four representative waters adequately cover the observed range in water compositions. While pore-water samples are not available from all possible locations in the repository, the available data are assumed to be representative of all water chemistries actually present in the repository units (SNL 2007 [DIRS 177412], Section 5.2.2). This assumption is supported by the chemical similarity of the four TSw lithostratigraphic units that host the repository (the Tptpll, Tptpul, Tptpmn, and Tptpln). The units are compositionally similar with respect to major oxides, trace elements, and normative mineral compositions (Peterman and Cloke 2002 [DIRS 162576], Erratum, Tables 4 and 5). The tight clustering also indicates that the effect of localized mineral heterogeneity on large-scale rock compositions, due to the presence of minerals which precipitated from the vapor phase during cooling of the tuff and low–temperature minerals, such as calcite and opal, is insignificant. Because the rocks are homogeneous, reaction with these rocks should result in similar pore-water evolution and large variations in the concentrations of nonconservative aqueous species in the TSw are not expected (SNL 2007 [DIRS 177412], Section 5.2.2).

The set of 34 pore waters represents samples from all four of the repository host units. They represent several different stratigraphic depths and degrees of water–rock interaction within the TSw, increasing the confidence that any new pore-water analysis would fall within that range. In addition, because the 34 TSw pore waters cluster into distinct groups, the potential that any new water will form a new, unrepresented group is reduced.

Uncertainty in the initial pore-water compositions is captured in the NFC and seepage dilution evaporation models and propagated to TSPA by use of the four water compositions, representing the four pore-water groups. Uncertainty in the nitrate-to-chloride ratio, an important parameter for evaluating localized corrosion of the waste package outer surface (SNL 2007 [DIRS 178519], Section 6.4.4), is treated specially. Following random selection of the starting water and determination of the in-drift water chemistry using the seepage dilution/evaporation model lookup tables and the nitrate-to-chloride ratio is sampled from a discrete distribution of all pore-water analyses that fall within that pore-water group. The resulting value is applied to predicted in-drift water chemistry (SNL 2007 [DIRS 177412], Section 6.12.3). Thus, the nitrate-to-chloride ratios for all 34 pore waters that passed the screening analysis, instead of just the four representative waters, are propagated to TSPA calculations.

To summarize, the near field chemistry model incorporates the effects of water–rock interactions and thermal-hydrologic-chemical processes. Uncertainty in the initial water chemistry is incorporated by using four starting waters in the P&CE models, representing the four chemically distinct groups of TSw pore-water compositions. Uncertainty in the nitrate-to-chloride ratio is propagated through use of the values for all 34 water analyses in the four groups. These pore waters are assumed to capture the range of actual pore-water compositions in the rock because they were collected throughout the entire stratigraphic interval of the TSw representing the

repository host horizon, and because of the compositional homogeneity of the TSw across that interval.

INPUTS:

Table 2.2.08.12.0A-1. Indirect Inputs

Citation	Title	DIRS
Peterman and Cloke 2002	"Geochemistry of Rock Units at the Potential Repository Level, Yucca Mountain, Nevada (includes Erratum)"	162576
SNL 2007	*Engineered Barrier System: Physical and Chemical Environment*	177412
SNL 2007	*General Corrosion and Localized Corrosion of Waste Package Outer Barrier*	178519
SNL 2007	*Total System Performance Assessment Data Input Package for Requirements Analysis for Subsurface Facilities*	179466

FEP: 2.2.08.12.0B

FEP NAME:

Chemistry of Water Flowing into the Waste Package

FEP DESCRIPTION:

Inflowing water chemistry may be used in analysis or modeling that requires initial water chemistry in the waste package.

SCREENING DECISION:

Included

TSPA DISPOSITION:

Eight different initial water compositions were used to represent the chemistry of the water flowing into the waste package in *In-Package Chemistry Abstraction* (SNL 2007 [DIRS 180506] Section 6.6.2[a]). The compositions included representative waters from four representative groundwater types from Yucca Mountain, mean J-13 well water, and three waters from basalt aquifers.

To account for igneous intrusion events, three groundwater samples from large fractured basalt reservoirs were selected for sensitivity analyses that examined pH and ionic strength of water that has reacted with cooled basalt (SNL 2007 [DIRS 180506], Section 4.1.2[a]). These sensitivity studies in *In-Package Chemistry Abstraction* (SNL 2007 [DIRS 180506], Section 6.6.2[a]) were used to estimate solution development during reactions between basalt-equilibrated water and the in-package materials and determined that in-package chemistry is insensitive to seepage water composition and subsequent reaction with basalt. Therefore, the in-package chemistry abstraction is used in TSPA to simulate the waste form chemical conditions following an igneous intrusion event.

The in-package chemistry model is used to predict pH, ionic strength, total carbonate, chloride, and fluoride in the waste form cells. Therefore, the variability of the incoming water composition is included in the in-package chemistry model and in the abstractions passed to the TSPA in *In-Package Chemistry Abstraction* (SNL 2007 [DIRS 180506]). The TSPA then feeds these results to the solubility, colloid, commercial SNF, and HLW glass submodels. The effects of the inflowing water chemistry are captured within the in-package chemistry model parameters: pH, ionic strength, total carbonate, chloride, and fluoride.

The TSPA parameters for pH and ionic strength have been described in *In-Package Chemistry Abstraction* (SNL 2007 [DIRS 180506], Section 8.2[a] and Table 6-21[a]), and the details for TSPA implementation of these abstractions are also provided (SNL 2007 [DIRS 180506], Section 6.10.9[a]). Uncertainties in the values of pH and ionic strength are quantified and propagated in TSPA, as described in *In-Package chemistry Abstraction* (SNL 2007 [DIRS 180506], Section 6.10.8[a]).

The dissolved concentration report considers the chemistry of the water potentially entering a waste package (SNL 2007 [DIRS 177418], Section 6.4). Examination of 25 pore-water compositions indicates that these pore waters are similar to the composition of the base-case water (J-13). The ratios of the average pore-water values to the base-case values of nine components (Na^+, K^+, Ca^{2+}, Mg^{2+}, SiO_2(aq), Cl^-, F^-, NO_3^-, and SO_4^{2-}) range from 0.83 (for SiO_2(aq)) to 8.51 (for Ca^{2+}), and the ratios of the maximum values of those nine components to the base-case values range from 1.07 to 18.46. Various sensitivities covering the range up to 1,000 times the base-case concentrations of Na^+, K^+, Ca^{2+}, Mg^{2+}, SiO_2(aq), Cl^-, F^-, NO_3^-, and SO_4^{2-} were performed to examine the effect that elevated concentrations of these components have on dissolved limits (SNL 2007 [DIRS 177418], Section 6.4.2.5). For the species that have an impact on solubility limits, an uncertainty term was developed (SNL 2007 [DIRS 177418], Sections 6.3.3.2 and 6.4.3.6) to account for the variation of the concentration of that species in the incoming water and its possible concentration within waste packages.

INPUTS:

Table 2.2.08.12.0B-1. Indirect Inputs

Citation	Title	DIRS
SNL 2007	*Dissolved Concentration Limits of Elements with Radioactive Isotopes*	177418
SNL 2007	*Engineered Barrier System: Physical and Chemical Environment*	177412
SNL 2007	*In-Package Chemistry Abstraction*	180506

FEP: 2.2.09.01.0A

FEP NAME:

Microbial Activity in the SZ

FEP DESCRIPTION:

Microbial activity in the SZ may affect radionuclide mobility in rock and soil through colloidal processes, by influencing the availability of complexing agents, or by influencing groundwater chemistry.

SCREENING DECISION:

Excluded – low consequence

SCREENING JUSTIFICATION:

Microbial activity can potentially change groundwater pH and Eh and introduce additional complexing agents, which could affect radionuclide K_d distributions in the saturated zone. Microbial activity can also potentially result in biotransformations and biocolloid-facilitated transport of radionuclides. Excluded FEP 2.1.10.01.0A (Microbial Activity in the EBS), and *Evaluation of Potential Impacts of Microbial Activity on Drift Chemistry* (BSC 2004 [DIRS 169991], Section 7) address these processes very thoroughly for the EBS, and it is concluded that microbial activity can be excluded in the EBS. The justifications for excluding the effects of microbial-produced complexing agents, biotransformation, and biocolloid transport in the EBS also apply in the saturated zone given that they are based on information obtained primarily from unsaturated zone and saturated zone rocks and saturated zone waters. These justifications are:

- Although microorganisms may release chemicals that complex with radionuclides, the concentrations of complexing agents are expected to be small, and their binding sites are expected to be dominated by iron ions, which these agents are designed to complex (BSC 2004 [DIRS 169991], Section 6.5.2).

- Reductive biotransformation reactions (the only kind that need be considered since redox-sensitive radionuclides are all assumed to be in oxidized states because of the oxidizing conditions at Yucca Mountain) will only decrease the solubility and increase the sorption of key redox-sensitive radionuclides, so their inclusion can only benefit performance (BSC 2004 [DIRS 169991], Section 6.5.3).

- Even if microbial cells can transport through rock fractures in the unsaturated and saturated zones, their impact on radionuclide transport is expected to be well bounded by the impact of inorganic groundwater colloids. Growing microbes have a propensity to attach to surfaces to remain in their favorable growth environment (BSC 2004 [DIRS 169991], Section 6.5.4), so they tend to be less mobile than inorganic colloids. Oligitrophic (i.e., starved) microbes can have dimensions as small as 0.2 to 0.3 μm (BSC 2004 [DIRS 169991], Section 6.5.4), which classifies them as biocolloids.

However, under oligitrophic conditions, cell concentrations will tend to be low; a concentration of ~7×10^6 cells/mL was observed in experiments conducted with Yucca Mountain tuff samples immersed in J-13 well water without the addition of a carbon source (DTN: LL040801512251.115 [DIRS 171476], Table S04340_001). This concentration translates to a mass concentration of ~0.1 mg/L if the cells have the dimensions stated above and are approximately the density of water. The range of saturated zone colloid mass concentrations used in TSPA is 0.001 to 200 mg/L (SNL 2008 [DIRS 183750], Figure 6-26), so the inclusion of cell mass concentrations would have an insignificant impact on these bounds, particularly on the upper end of the range where the effect on radionuclide transport and dose is greatest.

The remaining concern associated with microbial activity in the saturated zone is the effect on inorganic water chemistry, which can adversely affect radionuclide K_d values. The principal concerns are changes to pH and, more importantly, changes to bicarbonate/carbonate concentrations. The actinides (uranium, neptunium, plutonium, and americium) all have higher solubilities and lower K_d values as bicarbonate/carbonate concentrations increase.

In the saturated zone, heterotrophic microbial activity, which uses organic carbon as the sole energy source, is expected to be limited because geochemical analyses of groundwater samples taken from saturated zone wells within the Yucca Mountain vicinity indicate that there is little organic carbon in these waters (DTN: GS931100121347.007 [DIRS 149611], Table S96375_009; DTN: GS010308312322.003 [DIRS 154734], Table S01053_003; DTN: GS040108312322.001 [DIRS 179422], Table S04188_001; DTN: GS040808312322.006 [DIRS 179434], Table S04399_004). The maximum reported organic carbon concentration in pumped groundwater samples from the vicinity of Yucca Mountain (with the exception of samples from NC-EWDP-1DX, zone 2, which is located far to the west of any predicted groundwater flow pathways and was believed to be contaminanted by organic drilling fluids) is about 7.5 mg/L (DTN: GS040808312322.006 [DIRS 179434], Table S04399_004). Using the analysis approach in *Evaluation of Potential Impacts of Microbial Activity on Drift Chemistry* (BSC 2004 [DIRS 169991], Section 6.5.1), if 7.5 mg/L of organic carbon (assumed to be carbon, not CH_2O, as is often reported) were converted to HCO_3^- (bicarbonate), ~38 mg/L of HCO_3^- would be generated. Measured carbonate/bicarbonate concentrations in saturated zone groundwaters range from ~70 mg/L to several hundred mg/L (DTN: GS040808312322.006 [DIRS 179434], Table S04399_004), and the high-end concentration used to derive saturated zone radionuclide K_d distributions (UE-25p#1 water) is ~700 mg/L HCO_3^- (SNL 2008 [DIRS 184806], Table I-1). Thus, an increase of 38 mg/L of HCO_3^- is small compared to the range of uncertainty in carbonate/bicarbonate concentrations considered for radionuclide K_d values, and the impact of microbial activity on saturated zone water chemistry (pH and ΣCO_2) can be considered negligible. Furthermore, because the development of radionuclide K_d distributions was based on ranges of observed saturated zone pHs and bicarbonate/carbonate concentrations (SNL 2008 [DIRS 184806], Section A3), which reflect the influence of any naturally occurring processes on water chemistry, the K_d distributions used in TSPA should inherently reflect the influence of any naturally occurring microbial activity.

Based on the preceding discussion, omission of FEP 2.2.09.01.0A (Microbial Activity in the SZ) will not result in a significant adverse change in the magnitude or time of radiological exposures to the RMEI or radionuclide releases to the accessible environment. Therefore, this FEP is

excluded from the performance assessments conducted to demonstrate compliance with proposed 10 CFR 63.311 and 63.321 (70 FR 53313 [DIRS 178394]), and with 10 CFR 63.331 [DIRS 180319], on the basis of low consequence.

INPUTS:

Table 2.2.09.01.0A-1. Direct Inputs

Input	Source	Description
BSC 2004. *Evaluation of Potential Impacts of Microbial Activities on Drift Chemistry*. [DIRS 169991]	Section 6.5.4	Growing microbes have a propensity to attach to surfaces to remain in their favorable growth environment. Also, oligitrophic microbes can have dimensions as small as 0.2 to 0.3 microns
	Section 6.5.3	Reductive biotransformation reactions will only decrease the solubility and increase the sorption of key redox-sensitive radionuclides, so their inclusion can only benefit performance
	Section 6.5.2	The concentrations of complexing agents resulting from microbes are expected to be small, and their binding sites are expected to be dominated by iron ions, which these agents are designed to complex
	Section 7	Report addresses microbial processes in the EBS very throroughly, and concludes that microbial activity can be excluded from the EBS
	Section 6.5.1	Analysis converting organic carbon to carbonate or bicarbonate
DTN: GS010308312322.003. Field, Chemical and Isotopic Data from Wells in Yucca Mountain Area, Nye County, Nevada, Collected Between 12/11/98 and 11/15/99. [DIRS 154734]	Table S01053_003	Geochemical analysis of groundwater samples taken from saturated zone wells within the Yucca Mountain vicinity
DTN: GS040108312322.001. Field and Chemical Data Collected Between 10/4/01 and 10/3/02 and Isotopic Data Collected Between 5/19/00 and 5/22/03 from Wells in the Yucca Mountain Area, Nye County, Nevada. [DIRS 179422]	Table S04188_001	Geochemical analysis of groundwater samples taken from saturated zone wells within the Yucca Mountain vicinity
DTN: GS040808312322.006. Field, Chemical, and Isotope Data for Spring and Well Samples Collected Between 03/01/01 and 05/12/04 in the Yucca Mountain Area, Nye County, Nevada. [DIRS 179434]	Table S04399_004	Geochemical analysis of groundwater samples taken from saturated zone wells within the Yucca Mountain vicinity, including high organic carbon concentration in Well NC-EWDP-1DX
DTN: LL040801512251.115. Bacterial Growth Dynamics, Limiting Factors, and Community Diversity in a Proposed Geological Nuclear Waste Repository Environment. [DIRS 171476]	Table S04340_001	A concentration of ~7 × 10^6 cells/mL was observed in experiments conducted with Yucca Mountain tuff samples immersed in J-13 well water without the addition of a carbon source

Table 2.2.09.01.0A-1. Direct Inputs (Continued)

Input	Source	Description
SNL 2008. *Saturated Zone Flow and Transport Model Abstraction*. [DIRS 183750]	Figure 6-26	Range of colloid mass concentrations used in TSPA
SNL 2008. *Site-Scale Saturated Zone Transport*. [DIRS 184806]	Appendix I (Table I-1)	Bicarbonate concentration in UE-25p#1 water
	Appendix A, Section A3	Development of radionuclide K_d distributions was based on ranges of observed saturated zone pHs and bicarbonate/carbonate concentrations

Table 2.2.09.01.0A-2. Indirect Inputs

Citation	Title	DIRS
10 CFR 63	Energy: Disposal of High-Level Radioactive Wastes in a Geologic Repository at Yucca Mountain, Nevada	180319
70 FR 53313	Implementation of a Dose Standard After 10,000 Years	178394
DTN: GS931100121347.007	Selected Ground-Water Data for Yucca Mountain Region, Southern Nevada and Eastern California, Through December 1992	149611
SNL 2008	*Site-Scale Saturated Zone Transport*	184806

FEP: 2.2.09.01.0B

FEP NAME:

Microbial Activity in the UZ

FEP DESCRIPTION:

Microbial activity in the UZ may affect radionuclide mobility in rock and soil through colloidal processes, by influencing the availability of complexing agents, or by influencing groundwater chemistry. Changes in microbial activity could be caused by the response of the soil zone to changes in climate.

SCREENING DECISION:

Excluded – low consequence

SCREENING JUSTIFICATION:

Microbial activity can potentially change groundwater pH and Eh and introduce additional complexing agents, which could affect radionuclide K_d distributions in the unsaturated zone. Microbial activity can also potentially result in biotransformations and biocolloid-facilitated transport of radionuclides. Excluded FEP 2.1.10.01.0A (Microbial Activity in the EBS) and *Evaluation of Potential Impacts of Microbial Activity on Drift Chemistry* (BSC 2004 [DIRS 169991], Section 7) address these processes very thoroughly for the EBS, and it is concluded that microbial activity can be excluded in the EBS. The justifications for excluding the effects of microbial-produced complexing agents, biotransformation, and biocolloid transport in the EBS also apply in the unsaturated zone given that they are based on information obtained primarily from unsaturated zone and saturated zone rocks and saturated zone waters. These justifications are:

- Although microorganisms may release chemicals that complex with radionuclides, the concentrations of complexing agents are expected to be small, and their binding sites are expected to be dominated by iron ions, which these agents are designed to complex (BSC 2004 [DIRS 169991], Section 6.5.2).

- Reductive biotransformation reactions (the only kind that need be considered since redox-sensitive radionuclides are all assumed to be in oxidized states because of the oxidizing conditions at Yucca Mountain) will only decrease the solubility and increase the sorption of key redox-sensitive radionuclides, so their inclusion can only benefit performance (BSC 2004 [DIRS 169991], Section 6.5.3).

- Even if microbial cells can transport through rock fractures in the unsaturated and saturated zones, their impact on radionuclide transport is expected to be well bounded by the impact of inorganic groundwater colloids. Growing microbes have a propensity to attach to surfaces to remain in their favorable growth environment (BSC 2004 [DIRS 169991], Section 6.5.4), so they tend to be less mobile than inorganic colloids. Oligitrophic (i.e., starved) microbes can have dimensions as small as 0.2 to 0.3 μm

(BSC 2004 [DIRS 169991], Section 6.5.4), which classifies them as biocolloids. However, under oligitrophic conditions, cell concentrations will tend to be low; a concentration of ~7 × 10^6 cells/mL was observed in experiments conducted with Yucca Mountain tuff samples immersed in J-13 well water without the addition of a carbon source (DTN: LL040801512251.115 [DIRS 171476], Table S04340_001). This concentration translates to a mass concentration of ~0.1 mg/L if the cells have the dimensions stated above and are approximately the density of water. The range of unsaturated zone colloid mass concentrations used in TSPA is 0.001 to 200 mg/L (SNL 2008 [DIRS 184748], Table 6-21), so the inclusion of cell mass concentrations would have an insignificant effect on these bounds, particularly on the upper end of the range where the effect on radionuclide transport and dose is greatest.

The effects of changes in soil during future climates on microbial activity may be evaluated by considering the expected changes in soil depth and vegetation. Soil erosion and deposition are not expected to significantly affect soil depth over the next 10,000 years (see excluded FEPs 1.2.07.01.0A (Erosion/Denudation) and 1.2.07.02.0A (Deposition)). A significant change in microbial activity in the subsurface is not expected if the thin soils that exist over the repository footprint (SNL 2008 [DIRS 182145], Figure 6.5.2.4-1[a] and Tables 6.5.2.4-1[a] and 6.5.2.4-2[a]) do not develop into a thicker soil profile.

The remaining concern associated with microbial activity in the unsaturated zone is the effect on inorganic water chemistry, which can adversely affect radionuclide K_d values. The principal concerns are changes to pH and, more importantly, changes to bicarbonate/carbonate concentrations. The actinides (uranium, neptunium, plutonium, and americium) all have higher solubilities and lower K_d values as bicarbonate/carbonate concentrations increase.

In the saturated zone near Yucca Mountain, heterotrophic microbial activity, which uses organic carbon as the sole energy source, is expected to be limited because geochemical analyses of groundwater samples taken from saturated zone wells within the Yucca Mountain vicinity indicate that there is little organic carbon in these waters (DTNs: GS931100121347.007 [DIRS 149611], Table S96375_009; GS010308312322.003 [DIRS 154734], Table S01053_003; GS040108312322.001 [DIRS 179422], Table S04188_001; and GS040808312322.006 [DIRS 179434], Table S04399_004). Given that the source of saturated zone waters beneath the repository is primarily waters infiltrating from the unsaturated zone (SNL 2007 [DIRS 177391], Section A6.3.6.2), it is reasonable to expect that deeper unsaturated zone waters (at the repository level and below) will have similar organic carbon concentrations as saturated zone waters. The maximum reported organic carbon concentration in pumped groundwater samples from the vicinity of Yucca Mountain (with the exception of samples from NC-EWDP-1DX, zone 2, which is located far to the west of any predicted groundwater flow pathways and was believed to be contaminanted by organic drilling fluids) is about 7.5 mg/L (DTN: GS040808312322.006 [DIRS 179434], Table S04399_004). Using the analysis approach in *Evaluation of Potential Impacts of Microbial Activity on Drift Chemistry* (BSC 2004 [DIRS 169991], Section 6.5.1), if 7.5 mg/L of organic carbon (assumed to be carbon, not CH_2O, as is often reported) were converted to HCO_3^- (bicarbonate), ~38 mg/L of HCO_3^- would be generated. The lower and upper bound bicarbonate/carbonate concentrations used to derive unsaturated zone radionuclide K_d distributions are based on water chemistries from wells J-13 and UE-25p#1, with the latter well water providing an effective upper bound of ~700 mg/L HCO_3^- (SNL 2008 [DIRS 184806],

Table I-1). Thus, an increase of 38 mg/L of HCO_3^- is small compared to the range of uncertainty in carbonate/bicarbonate concentrations considered for radionuclide K_d values, and the impact of microbial activity on unsaturated zone water chemistry (pH and ΣCO_2) can be considered negligible. Furthermore, because the development of radionuclide K_d distributions was based on ranges of observed unsaturated zone pHs and bicarbonate/carbonate concentrations (SNL 2007 [DIRS 177396], Section A4), which reflect the influence of any naturally occurring processes on water chemistry, the K_d distributions used in TSPA should inherently reflect the influence of any naturally occurring microbial activity.

Based on the preceding discussion, omission of FEP 2.2.09.01.0B (Microbial Activity in the UZ) will not result in a significant adverse change in the magnitude or time of radiological exposures to the RMEI or radionuclide relases to the accessible environment. Therefore, this FEP is excluded from the performance assessments conducted to demonstrate compliance with proposed 10 CFR 63.311 and 63.321 (70 FR 53313 [DIRS 178394]), and with 10 CFR 63.331 [DIRS 180319], on the basis of low consequence.

INPUTS:

Table 2.2.09.01.0B-1. Direct Inputs

Input	Source	Description
BSC 2004. *Evaluation of Potential Impacts of Microbial Activities on Drift Chemistry*. [DIRS 169991]	Section 6.5.4	Growing microbes have a propensity to attach to surfaces to remain in their favorable growth environment. Also, oligitrophic microbes can have dimensions as small as 0.2 to 0.3 microns
	Section 6.5.3	Reductive biotransformation reactions will only decrease the solubility and increase the sorption of key redox-sensitive radionuclides, so their inclusion can only benefit performance
	Section 6.5.2	The concentrations of complexing agents resulting from microbes are expected to be small, and their binding sites will likely be dominated by iron ions, which these agents are designed to complex
	Section 7	Report addresses microbial processes in the EBS very throroughly, and concludes that microbial activity can be excluded from the EBS
	Section 6.5.1	Analysis converting organic carbon to carbonate or bicarbonate.
DTN: GS010308312322.003. Field, Chemical and Isotopic Data from Wells in Yucca Mountain Area, Nye County, Nevada, Collected Between 12/11/98 and 11/15/99. [DIRS 154734]	Table S01053_003	Geochemical analysis of groundwater samples taken from saturated zone wells within the Yucca Mountain vicinity
DTN: GS040108312322.001. Field and Chemical Data Collected Between 10/4/01 and 10/3/02 and Isotopic Data Collected Between 5/19/00 and 5/22/03 from Wells in the Yucca Mountain Area, Nye County, Nevada. [DIRS 179422]	Table S04188_001	Geochemical analysis of groundwater samples taken from saturated zone wells within the Yucca Mountain vicinity

Table 2.2.09.01.0B-1. Direct Inputs (Continued)

Input	Source	Description
DTN: GS040808312322.006. Field, Chemical, and Isotope Data for Spring and Well Samples Collected Between 03/01/01 and 05/12/04 in the Yucca Mountain Area, Nye County, Nevada. [DIRS 179434]	Table S04399_004	Geochemical analysis of groundwater samples taken from saturated zone wells within the Yucca Mountain vicinity, including high organic carbon concentration in Well NC-EWDP-1DX
DTN: LL040801512251.115. Bacterial Growth Dynamics, Limiting Factors, and Community Diversity in a Proposed Geological Nuclear Waste Repository Environment. [DIRS 171476]	Table S04340_001	A concentration of ~7 × 10^6 cells/mL was observed in experiments conducted with Yucca Mountain tuff samples immersed in J-13 well water without the addition of a carbon source
SNL 2007. *Saturated Zone Site-Scale Flow Model*. [DIRS 177391]	Section A6.3.6.2	Source of saturated zone waters beneath the repository is primarily waters infiltrating from the unsaturated zone
SNL 2007. *Radionuclide Transport Models Under Ambient Conditions*. [DIRS 177396]	Section A4	Development of radionuclide K_d distributions was based on ranges of observed unsaturated zone pHs and bicarbonate/carbonate concentrations
SNL 2008. *Particle Tracking Model and Abstraction of Transport Processes*. [DIRS 184748]	Table 6-21	Range of colloid mass concentrations used in TSPA
SNL 2008. *Site-Scale Saturated Zone Transport*. [DIRS 184806]	Appendix I (Table I-1)	Bicarbonate concentration in UE-25p#1 water

Table 2.2.09.01.0B-2. Indirect Inputs

Citation	Title	DIRS
70 FR 53313	Implementation of a Dose Standard After 10,000 Years	178394
DTN: GS931100121347.007	Selected Ground-Water Data for Yucca Mountain Region, Southern Nevada and Eastern California, Through December 1992	149611
SNL 2008	*Simulation of Net Infiltration for Present-Day and Potential Future Climates*	182145

FEP: 2.2.10.01.0A

FEP NAME:

Repository-Induced Thermal Effects on Flow in the UZ

FEP DESCRIPTION:

Thermal effects in the geosphere could affect the long-term performance of the disposal system, including effects on groundwater flow (e.g., density-driven flow), mechanical properties, and chemical effects in the UZ.

SCREENING DECISION:

Excluded – low consequence

SCREENING JUSTIFICATION:

This FEP addresses thermal effects on flow in the unsaturated zone with respect to water arrival at the repository and flow from the repository to the water table. Note that the effects of thermal-hydrologic processes on drift seepage and seepage water chemistry are addressed in included FEPs 2.2.07.10.0A (Condensation Zone Forms Around Drifts), 2.2.07.11.0A (Resaturation of Geosphere Dry-Out Zone), 2.2.08.12.0A (Chemistry of Water Flowing into the Drift), 2.2.10.10.0A (Two-Phase Buoyant Flow/Heat Pipes), and 2.2.10.12.0A (Geosphere Dry-Out Due to Waste Heat).

Heat from each emplacement drift dries out the rock surrounding the drift, and the resulting "vaporization barrier" diverts water around the drift. This thermal effect on flow is of limited temporal and spatial extent. Thermal-hydrologic modeling at the drift scale has been performed using a two-dimensional cross-sectional dual-permeability model in *Drift-Scale Coupled Processes (DST and TH Seepage) Models* (BSC 2005 [DIRS 172232]). Simulations by the TH seepage model (BSC 2005 [DIRS 172232], Figures 6.2.2.1-3 through 6.2.2.1-6) show that during the heating period vaporization of percolating water near hot emplacement drifts forms a dry-out zone around the drifts. A condensation cap forms above the dry-out zone where the rock is cooler. As a result of this vaporization and condensation, downward-percolating water above the drift is diverted laterally. A variety of simulations for base cases and sensitivity cases presented in *Drift-Scale Coupled Processes (DST and TH Seepage) Models* (BSC 2005 [DIRS 172232], Sections 6.2.2 and 6.2.3) show that the flow-field disturbance can extend to distances on the order of 10 m above the drift center. Above that elevation the vertical percolation flux is the same as imposed at the top boundary (e.g., BSC 2005 [DIRS 172232], Figure 6.2.2.1-7). Additional two-dimensional thermal-hydrologic simulation results in *Drift Scale THM Model* (BSC 2004 [DIRS 169864, Figures 6.5.5-3(b), 6.5.5-4(b), and 6.5.5-5(b); DTN: LB0306DRSCLTHM.002 [DIRS 174490]) also show redistribution of percolating water around heated drifts.

Numerical simulations of flow at 100 and 500 years after emplacement show reduced fracture saturation and diversion of percolating water inside the dryout zone (BSC 2005 [DIRS 172232], Section 6.2.2.1). Because of the flow diversion, the dryout is more extensive and longer lasting

beneath the drift; this is called the "drift shadow" effect. Note that there is no water flux through the fractures inside the dryout region, because fracture saturation is zero. After resaturation in 1,000 to 2,000 years, saturations below the drift remain smaller than above, because of the "shadow zone" created by the diversion of flow around the drift (BSC 2005 [DIRS 172232], Section 6.2.2.1; DTN: LB0306DRSCLTHM.002 [DIRS 174490]; BSC 2004 [DIRS 169864, Figures 6.5.5-3(b), 6.5.5-4(b), and 6.5.5-5(b)). The thermal-hydrologic dryout and associated coupled processes will lead to an environment where radionuclide transport in the vicinity of the drift is less likely (BSC 2005 [DIRS 172232], Section 6.2.2.1.1; DTN: LB0306DRSCLTHM.002 [DIRS 174490]; BSC 2004 [DIRS 169864], Figures 6.5.5-3(b), 6.5.5-4(b), and 6.5.5-5(b)).

Two-dimensional thermal-hydrologic simulations in *Mountain-Scale Coupled Processes (TH/THC/THM) Models* (BSC 2005 [DIRS 174101], Figures 6.5.13-1(a) to 6.5.13-6(a)) show the flow redistribution, with vertical percolation flux reduced beneath the drifts and increased around each drift. The limited extent of flow redistribution found in the mountain-scale modeling is consistent with drift-scale results discussed above (DTN: LB0306DRSCLTHM.002 [DIRS 174490]; BSC 2004 [DIRS 169864], Figures 6.5.5-3(b), 6.5.5-4(b), and 6.5.5-5(b)). Results from thermal-hydrologic modeling (BSC 2004 [DIRS 174101], Figures 6.2-10a and b, 6.3.1-18) show that the flow changes resulting from thermal-hydrologic processes are much smaller than those that result from climate change modeled to occur at 600 and 2,000 years after repository closure. The range of variation in flux resulting from climate change is similar in magnitude to the variation in flux resulting from infiltration and unsaturated zone flow uncertainty for the first 10,000 years (SNL 2007 [DIRS 184614], Tables 6.1-2 and 6.8-1). Therefore, the effects of thermal-hydrologic processes are much smaller than the range of variations resulting from existing uncertainties that are included in the flow and transport models (included FEP 1.3.01.00.0A (Climate Change)).

The effects of repository heat and the associated dryout on shallow infiltration at the surface of Yucca Mountain were investigated in *Final Report: Plant and Soil Related Processes Along a Natural Thermal Gradient at Yucca Mountain, Nevada* (CRWMS M&O 1999 [DIRS 105031]). The primary issue for thermal effects at the ground surface is the change in temperature and its associated effect on vegetation. Based on the detailed analysis of soil temperature changes documented in *Impact of Radioactive Waste Heat on Soil Temperatures* (CRWMS M&O 1999 [DIRS 103618], Figure 30), the temperature rise in the repository will have a negligible effect on vegetation, and hence on surface infiltration and groundwater flow in the unsaturated zone.

For thermal effects on chemical processes, see excluded FEPs 2.2.08.03.0B (Geochemical Interactions and Evolution in the UZ), 2.2.10.06.0A (Thermo-Chemical Alteration in the UZ (Solubility, Speciation, Phase Changes, Precipitation/Dissolution)), 2.2.10.07.0A (Thermo-Chemical Alteration of the Calico Hills Unit), and 2.2.10.09.0A (Thermo-Chemical Alteration of the Topopah Spring Basal Vitrophyre). For thermal effects on mechanical processes, see excluded FEPs 2.2.10.04.0A (Thermo-Mechanical Stresses Alter Characteristics of Fractures Near Repository), 2.2.10.04.0B (Thermo-Mechanical Stresses Alter Characteristics of Faults Near Repository), and 2.2.10.05.0A (Thermo-Mechanical Stresses Alter Characteristics of Rocks Above and Below the Repository).

Based on the preceding discussion, omission of FEP 2.2.10.01.0A (Repository-Induced Thermal Effects on Flow in the UZ) will not result in a significant adverse change in the magnitude or

time of radiological exposures to the RMEI or radionuclide releases to the accessible environment. Therefore, this FEP is excluded from the performance assessments conducted to demonstrate compliance with proposed 10 CFR 63.311 and 63.321 (70 FR 53313 [DIRS 178394]), and with 10 CFR 63.331 [DIRS 180319], on the basis of low consequence.

INPUTS:

Table 2.2.10.01.0A-1. Direct Inputs

Input	Source	Description
BSC 2005. *Drift-Scale Coupled Process (DST and TH Seepage) Models*. [DIRS 172232]	Section 6.2.2.1.1	Radionuclide transport in the vicinity of the drift
	Section 6.2.2.1	Numerical simulations of flow at 100 and 500 years after emplacement show reduced fracture saturation and diversion of percolating water inside the dryout zone. Discussion on the impact of the shadow zone
	Figure 6.2.2.1-7	Vertical percolation flux
	Figures 6.2.2.1-3 thru 6.2.2.1-6	Results from simulations by the TH seepage model
BSC 2005. *Mountain-Scale Coupled Processes (TH/THC/THM) Models*. [DIRS 174101]	Figures 6.2-10a and b, 6.3.1-18	Results from TH modeling show that the flow changes resulting from TH processes are much smaller than those that result from climate change modeled to occur at 600 and 2,000 years after repository closure
	Figures 6.5.13-1(a) thru 6.5.13-6(a)	Two-dimensional TH simulation results
DTN: LB0306DRSCLTHM.002. Drift Scale THM Model Predictions: Summary Plots. [DIRS 174490]	files: *Tmn1_10ky_th.tec*, *Tmn1_10ky_th_tm.tec*, *Tmn1_1ky.tec*, *Tmn1_1ky_m.tec*, *Tmn1_1ky_th.tec*, *Tmn1_1ky_th_tm.tec*	Two-dimensional TH simulation results
	files: *Tmn1_100t.tec*, *Tmn1_100y_m.tec*, *Tmn1_100y_th.tec*, *Tmn1_100y_th_m.tec*, *Tmn1_10y.tec*, *Tmn1_10ky_m.tec*	Two-dimensional TH simulation results
SNL 2007. *UZ Flow Models and Submodels*. [DIRS 184614]	Tables 6.1-2, 6.8-1	The range of variation in flux resulting from climate change is similar in magnitude to the variation in flux resulting from infiltration and UZ flow uncertainty for the first 10,000 years

Table 2.2.10.01.0A-2. Indirect Inputs

Citation	Title	DIRS
10 CFR 63	Energy: Disposal of High-Level Radioactive Wastes in a Geologic Repository at Yucca Mountain, Nevada	180319
70 FR 53313	Implementation of a Dose Standard After 10,000 Years	178394
BSC 2004	*Drift Scale THM Model*	169864
BSC 2005	*Drift-Scale Coupled Process (DST and TH Seepage) Models*	172232
CRWMS M&O 1999	*Final Report: Plant and Soil Related Processes Along a Natural Thermal Gradient at Yucca Mountain, Nevada*	105031
CRWMS M&O 1999	*Impact of Radioactive Waste Heat on Soil Temperatures*	103618

FEP: 2.2.10.02.0A

FEP NAME:

Thermal Convection Cell Develops in SZ

FEP DESCRIPTION:

Thermal effects due to waste emplacement result in convective flow in the saturated zone beneath the repository.

SCREENING DECISION:

Excluded – low consequence

SCREENING JUSTIFICATION:

To evaluate thermal effects in the saturated zone due to waste emplacement, two mechanisms that could potentially induce convective flow of groundwater are examined. The first mechanism evaluates the potential for convective flow cells to occur as a result of increasing temperatures from the repository. The second mechanism examines the potential for flow to occur due to mounding of the water table resulting from increased temperatures and decreased density of groundwater in the saturated zone below the repository. Either of these mechanisms could lead to greater migration rates of radionuclides in the saturated zone, and the convective outflow of groundwater would be additive to the ambient groundwater movement.

The three-dimensional multiscale thermohydrologic model (SNL 2008 [DIRS 184433]) estimates the temperature at the water table and within the saturated zone as a function of time following emplacement of the waste. Results indicate that temperature will peak at the present-day water table approximately 6,000 years after waste emplacement, with the maximum temperature equal to 73°C and an average of the maximum at each of the 560 locations modeled of 63°C (as extracted from the 560 **.wt* files in DTN: LL0702PA013MST.068 [DIRS 180553] in subfolder /SDT/SDT-01/SDT55). This represents an approximate, average 30°C increase in comparison with the ambient temperature of 30°C to 34°C observed at the water table in the general area of the repository (DTN: LB991201233129.001 [DIRS 146894], file: *INCON_thm_s32.dat*). *Multiscale Thermohydrologic Model* (SNL 2008 [DIRS 184433]) used an initial water-table temperature range of 26.7°C to 32.7°C with an average (and median) of 30°C (DTN: LL0702PA013MST.068 [DIRS 180553], file: *Twt.dat*). Although ambient groundwater flow will convect heat away from the area below the repository, it is assumed that the groundwater near the water table is stagnant and that none of the heat is swept downgradient by flow in the saturated zone. Consequently, this model overestimates the values of temperature at and below the water table.

Development of thermal convection cells in porous media is physically driven by an underlying heat source. In the case of the saturated zone at Yucca Mountain, the repository heat source is located above the saturated zone, in the unsaturated zone. Increased temperature in the saturated zone near the water table would decrease the potential for the development of classical thermally

driven convection cells by decreasing the magnitude of the ambient geothermal gradient in the upper part of the saturated zone.

The theoretical potential for the initiation of thermal convection currents in a horizontal porous medium heated from below is given by the modified Rayleigh number N_{RA} (e.g., Domenico and Schwartz 1990 [DIRS 100569], pp. 344 to 345):

$$N_{RA} = \frac{g\rho_o\left(c_w\rho_w\right)Hk\alpha_f\Delta T}{\mu\kappa_e}, \qquad \text{(Eq. 2.2.10.02.0A-1)}$$

where g is the acceleration of gravity, ρ_o is the reference density of water, c_w is the specific heat of water, ρ_w is the temperature-dependent density of water, H is the aquifer thickness, k is the intrinsic permeability, α_f is the coefficient of thermal expansion for water, ΔT is the difference in temperature between the bottom and top of the aquifer, μ is the viscosity of water, and κ_e is the effective thermal conductivity. The lower the Rayleigh number, the lower the likelihood of thermal convection. An increase in the temperature at the water table by repository-induced heating would decrease the value of ΔT in this expression, yielding decreased N_{RA} and a corresponding decrease in the potential for thermal convection compared to the potential for convection under ambient temperature conditions. Under ambient conditions, there is little or no evidence for vertical mixing in the saturated zone beneath Yucca Mountain due to any mechanism including heating from below (SNL 2007 [DIRS 177391], Appendices A and B); hence, it is reasonable to conclude that the Rayleigh number is below the critical value for the onset of convection and will remain below this critical value with additional repository-induced heating.

Mounding of the water table may occur due to the repository heating of the groundwater in the saturated zone. In addition to the ambient flow beneath the water table surface, a local rise in the water table would create a potential for lateral flow at or near the water table. The water-table gradient due to mounding will tend to increase the velocity of radionuclide transport in the saturated zone between the heated region beneath the repository and the downgradient edge of the heated region. The analysis presented below estimates an upper bound on the mound height by considering hydrostatic (no flow) conditions. Groundwater flow away from the water table mound would tend to dissipate the heat from the repository, and therefore lower the mound.

Consider a saturated column of permeable rock with the top at the water table (z = 0 m) and the bottom at a depth at which the temperature is relatively unchanged by the repository (z_d = 1,000 m, which is the maximum depth simulated in the MSTHM). The pressure at the bottom of the column is given by:

$$p_w = \int_0^{z_d} \rho(z) g dz, \qquad \text{(Eq. 2.2.10.02.0A-2)}$$

where $\rho(z)$ is the spatially dependent water density. Assuming a linear thermal gradient and linear relationship between the temperature and density, this equation becomes:

$$p_w = \frac{1}{2} z_d \left[\rho(0) + \rho(z_d) \right] g. \qquad \text{(Eq. 2.2.10.02.0A-3)}$$

Note that $\left[\rho(0)+\rho(z_d)\right]g/2$ represents an average water density within the column. The relationship between the water density and temperature is generally not linear; however, within the temperature range of interest (30°C to 74°C (Dean 1992 [DIRS 100722], Table 5.14)) it is nearly linear with best-fit equation:

$$\rho = 1010.5 - 0.46T. \qquad \text{(Eq. 2.2.10.02.0A-4)}$$

The temperature at the depth of 1,000 m (T_d) can be estimated as:

$$T_d = T_{wt}^0 + \frac{\mathrm{d}T}{\mathrm{d}z} \cdot 1000 \text{ m}, \qquad \text{(Eq. 2.2.10.02.0A-5)}$$

where T_{wt}^0 is the ambient temperature at the water table (30°C) and dT/dz = 25°C/km is the approximate ambient average thermal gradient (DTN: MO0102DQRBTEMP.001 [DIRS 154733], Figures 4, 5, 6, 7, 8, and 10). The resulting temperature at a depth of 1,000 m is 55°C. Consequently, the pressure at the bottom of the unheated vertical column can be written as:

$$p_w = \frac{1}{2} z_d \left[\rho\left(T = 30^\circ C\right) + \rho\left(T = 55^\circ C\right) \right] g. \qquad \text{(Eq. 2.2.10.02.0A-6)}$$

Based on MSTHM results, temperatures at the water table under the repository typically increase by 30°C at 6,000 years after repository closure. Assuming the temperature everywhere within the 1,000-m profile to be approximately 55°C is a reasonable and conservative approximation, given that the temperature at depth is 55°C and that the average temperature at the water table increases from 30°C to 60°C during the first 6,000 years of heating. This temperature is also maximized because the MSTHM does not take credit for any advective transport of heat away from the system due to flow in the saturated zone (in the MSTHM, the water table behaves only as a conducting medium).

The water pressure at the bottom of the 1,000-m vertical column under the repository is assumed constant, but the height of the column (z_{new}) will increase to reflect the increase in temperature and decrease in density. The increase can be found by equating the pressures under the repository with those of the ambient condition (the hydrostatic assumption):

$$p_w = \frac{1}{2} z_d \left[\rho\left(T = 30^\circ \mathrm{C}\right) + \rho\left(T = 55^\circ \mathrm{C}\right) \right] g = z_{new} \rho\left(T = 55^\circ \mathrm{C}\right) g. \qquad \text{(Eq. 2.2.10.02.0A-7)}$$

Rearranging the preceding equation, the following relationship is obtained:

$$z_{new} = \frac{z_d \left[\rho\left(T = 30^\circ \mathrm{C}\right) + \rho\left(T = 55^\circ \mathrm{C}\right) \right]}{2\rho\left(T = 55^\circ C\right)}. \qquad \text{(Eq. 2.2.10.02.0A-8)}$$

The following data from Dean (1992 [DIRS 100722], Table 5.14) were used as input in the formula for z_{new}:

$$\rho(T = 30°C) = 995.65 \text{ kg/m}^3,$$

$$\rho(T = 55°C) = 985.70 \text{ kg/m}^3 \text{ (linear interpolation).}$$

Using the equation for z_{new} results in a column height of 1,005 m. Consequently, the maximum water table mounding resulting from peak temperature at the water table surface is 5 m. To evaluate the effect of this potential increase in the water table above the heated repository, the associated change in the hydraulic gradient between the repository and the 18-km compliance boundary is estimated. The 18-km compliance boundary is at Nevada State Plane Northing 213,078 m (minimum Northing coordinate from DTN: MO0712DELNPCCA.001 ([DIRS 184172], file: *controlled.txt*). This Northing position is at approximately 4058250 m N in the UTM coordinate system. The potentiometric surface within the inferred flowpath, which is in the Lower Fortymile Wash Alluvium, is somewhere between UTM Easting 548017 and 551553 m. These easting coordinates were interpolated from the SZ site-scale flow model data set (DTN: SN0612T0510106.004 [DIRS 178956], file: *lower_fortymile_wash.zonn*). The average water table at Northing coordinate 4058250 between the Easting coordinate limits given above is about 711 m above mean sea level (DTN: SN0612T0510106.004 [DIRS 178956], file: *wt.dat*). The average water table over the repository, eighteen kilometers north of this location, and between UTM Easting 547800 and 548375 m, is about 732 m. Without heating, there is a change in potentiometric surface of 21 m yielding a hydraulic gradient of 1.2×10^{-3}. Adding the 5 m due to heating above the repository results in a hydraulic gradient of 1.5×10^{-3}, or an increase of approximately 24%. This additional increase in the hydraulic gradient resulting from the mounding of the water table is small relative to the uncertainty range for GWSPD multiplier, which goes as high as a factor of 8.93 (log-10-transformed value of 0.951) (SNL 2008 [DIRS 183750], Table 6.7[a]) and is linearly proportional to the hydraulic gradient times the hydraulic conductivity (permeability).

Subject to a wetter climate in the future, the water table below the repository is expected to rise by 120 m (SNL 2008 [DIRS 184748], Section 6.4.8) to an elevation of 850 m above sea level. Eighteen kilometers south and within the expected flowpaths, the water table is expected to be 739 m above sea level (DTN: SN0702T0510106.006 [DIRS 179575], file: *future_wt.dat*), which equates to a hydraulic gradient of 6.3×10^{-3}. The temperature in the nearby Calico Hills Formation reaches a maximum temperature of about 80°C, which is a reasonable approximation for the maximum temperature at the elevated water table (SNL 2008 [DIRS 179962], Figure 6.4.2-31; DTN: MO0707TH2D3DDC.000 [DIRS 182472], file: *p10-t_elws.dat*). Conservatively assuming a water-column mean temperature of 70°C (and corresponding density of 977.75 kg/m^3) yields Δz_{new} = 10 m and a new hydraulic gradient of 6.8×10^{-3}. This is a 9% relative increase still well within the maximum GWSPD multiplier of 8.93.

The potential for convective flow to occur in the saturated zone is decreased as a result of increasing temperatures from the repository heat source above. An increase in the temperature at the water table would decrease the value of the ΔT term in the Rayleigh expression, resulting in a smaller value for N_{RA} and a decrease in the potential for thermal convection. Mounding of the water table that may occur due to the repository serving as a heat source to the groundwater in

the saturated zone yields up to a 24% increase in the existing hydraulic gradient, which is small relative to the uncertainty range for GWSPD, as described above. Even subject to an elevated water table in a wetter climate, the increase is still much less than the maximum GWSPD multiplier.

Based on the previous discussion, omission of FEP 2.2.10.02.0A (Thermal Convection Cell Develops in SZ) will not result in a significant adverse change in the magnitude or timing of either radiological exposures to the RMEI or radionuclide releases to the accessible environment. Therefore, this FEP is excluded from the performance assessments conducted to demonstrate compliance with proposed 10 CFR 63.311 and 63.321 (70 FR 53313 [DIRS 178394]), and with 10 CFR 63.331 [DIRS 180319], on the basis of low consequence.

INPUTS:

Table 2.2.10.02.0A-1. Direct Inputs

Input	Source	Description
Dean 1992. *Lange's Handbook of Chemistry*. [DIRS 100722]	Table 5.14	Density as a function of temperature
Domenico and Schwartz 1990. *Physical and Chemical Hydrogeology*. [DIRS 100569]	pp. 344, 345	The theoretical potential for the initiation of thermal convection currents in a horizontal porous medium heated from below is given by the modified Rayleigh number N_{RA}
DTN: LL0702PA013MST.068. Input and Output Files for the SMT, SDT and DDT Submodels and MSTHAC Extract Output Files Used in ANL-EBS-MD-000049 Multiscale Thermohydrologic Model. [DIRS 180553]	*.wt files in subfolder /SDT/SDT-01/SDT55	Temperature at the water table and within the saturated zone as a function of time following emplacement of the waste
	file: *Twt.dat*	Initial water-table temperature range
DTN: MO0102DQRBTEMP.001. Temperature Data Collected from Boreholes Near Yucca Mountain in Early 1980s. [DIRS 154733]	Figures 4, 5, 6, 7, 8, and 10	Temperature at the depth of 1,000 m
DTN: MO0707TH2D3DDC.000. 2-D and 3-D Thermal-Hydrologic Analysis. [DIRS 182472]	file: *p10-t_elws.dat*	Calico Hills unit temperature
DTN: SN0612T0510106.004. Saturated Zone (SZ) Site-Scale Flow Model Pest and FEHM Files Using HFM2006. [DIRS 178956]	file: *wt.dat*	Potentiometric surface
	file: *lower_fortymile_ wash.zonn*	definition of the Lower Fortymile wash alluvial zone
DTN: SN0702T0510106.006. Saturated Zone (SZ) Site-Scale Flow Model with "Water Table Rise" Alternate Conceptual Model – FEHM Files Using HFM2006. [DIRS 179575]	file: *future_wt.dat*	Future potentiometric surface
SNL 2007. *Saturated Zone Site-Scale Flow Model*. [DIRS 177391]	Appendices A and B	No evidence of vertical mixing
SNL 2008. *Postclosure Analysis of the Range of Design Thermal Loadings*. [DIRS 179962]	Figure 6.4.2-31	Calico Hills unit temperature

Table 2.2.10.02.0A-1. Direct Inputs (Continued)

Input	Source	Description
SNL 2008. *Particle Tracking Model and Abstraction of Transport Processes*. [DIRS 184748]	Section 6.4.8	120-m water-table rise due to climate change
SNL 2008. *Saturated Zone Flow and Transport Model Abstraction*. [DIRS 183750]	Table 6.7[a]	Uncertainty range for groundwater specific discharge

Table 2.2.10.02.0A-2. Indirect Inputs

Citation	Title	DIRS
10 CFR 63	Energy: Disposal of High-Level Radioactive Wastes in a Geologic Repository at Yucca Mountain, Nevada	180319
70 FR 53313	Implementation of a Dose Standard After 10,000 Years	178394
DTN: LB991201233129.001	The Mountain-Scale Thermal-Hydrologic Model Simulations for AMR U0105, “Mountain-Scale Coupled Processes (TH) Models”	146894
DTN: MO0712DELNPCCA.001	Delineation of Postclosure Controlled Area	184172
SNL 2008	*Multiscale Thermohydrologic Model*	184433

FEP: 2.2.10.03.0A

FEP NAME:

Natural Geothermal Effects on Flow in the SZ

FEP DESCRIPTION:

The existing geothermal gradient, and spatial or temporal variability in that gradient, may affect groundwater flow in the saturated zones.

SCREENING DECISION:

Included

TSPA DISPOSITION:

Natural geothermal effects, as they influence fluid properties, are included in the SZ site-scale flow model. Groundwater flow is simulated in *Saturated Zone Site-Scale Flow Model* (SNL 2007 [DIRS 177391]) using conservation of mass and momentum equations in the numerical code FEHM. The fluid–rock momentum equation (simplified to Darcy's equation) is, in part, a function of permeability, density, viscosity, and temperature (SNL 2007 [DIRS 177391], Section 6.4.1). For temperatures that range between 20°C to 100°C, the density of water changes by only a few percent. In contrast, the variation in water viscosity changes by a factor of 3.3 over the same temperature range. Consequently, natural geothermal effects on groundwater flow are more effectively captured by spatially varying viscosity rather than density. *Saturated Zone Site-Scale Flow Model* (SNL 2007 [DIRS 177391], Section 6.4.3.10) assigns a specified temperature to each node, which varies with depth and is based on variable temperature measurements reported by Sass et al. (1988 [DIRS 100644]), using an average geothermal gradient. Temporal variations in the natural geothermal gradient are expected to be minor, as explained with regard to hydrothermal activity (see excluded FEP 1.2.06.00.0A (Hydrothermal Activity)). Specifically, studies of two-phase fluid inclusions in the unsaturated zone at Yucca Mountain using petrography, microthermometry, and uranium-lead dating indicate that temperatures have remained close to the current ambient values over the past 2 to 5 million years (Wilson et al. 2003 [DIRS 163589], Section 8). These findings show that significant or widespread alteration of the natural geothermal gradient has not occurred in the unsaturated zone in the recent geologic past, and imply that significant change to the geothermal gradient has likewise been absent from the saturated zone.

Permeability and viscosity are also assigned to each node. Temperatures are used to calculate nodal viscosities. Using both spatially varying viscosity and calibrated permeabilities, lumped fluid/rock property parameters can be calculated. Estimated hydraulic conductivity at each node is calibrated to hydraulic head measurements, while nodal viscosities and temperatures remain fixed (SNL 2007 [DIRS 177391], Section 6.4.3.10). Hydraulic heads are, in part, manifestations of multiple processes within the system, including geothermal effects. By calibrating permeabilities to hydraulic heads while maintaining temporally constant, spatially varying temperatures and viscosities, geothermal effects on flow are implicitly captured. The site-scale SZ transport model (SNL 2008 [DIRS 184806]) incorporates these effects by using the calibrated SZ site-scale flow

model as its basis. Furthermore, the uncertainty that temperature may have on matrix diffusion is implicitly captured in the range for effective diffusion coefficients adopted in the SZ flow and transport abstraction model (SNL 2008 [DIRS 183750], Section 6.5.2.6 and Table 7-1[b]). Because the natural geothermal gradient directly impacts the saturated zone flow field and groundwater specific discharge, its impact on TSPA is propagated through uncertainty in the groundwater specific discharge multiplier (SNL 2008 [DIRS 183750], Table 6-8).

INPUTS:

Table 2.2.10.03.0A-1. Indirect Inputs

Citation	Title	DIRS
10 CFR 63	Energy: Disposal of High-Level Radioactive Wastes in a Geologic Repository at Yucca Mountain, Nevada	180319
Sass et al. 1988	*Temperature, Thermal Conductivity, and Heat Flow Near Yucca Mountain, Nevada: Some Tectonic and Hydrologic Implications*	100644
SNL 2007	*Saturated Zone Site-Scale Flow Model*	177391
SNL 2008	*Saturated Zone Flow and Transport Model Abstraction*	183750
SNL 2008	*Site-Scale Saturated Zone Transport*	184806
Wilson et al. 2003	"Origin, Timing, and Temperature of Secondary Calcite--Silica Mineral Formation at Yucca Mountain, Nevada"	163589

FEP: 2.2.10.03.0B

FEP NAME:

Natural Geothermal Effects on Flow in the UZ

FEP DESCRIPTION:

The existing geothermal gradient, and spatial or temporal variability in that gradient, may affect groundwater flow in the UZ.

SCREENING DECISION:

Included

TSPA DISPOSITION:

Natural geothermal effects, observed as the natural temperature profile in the unsaturated zone, are included in the unsaturated zone model calibration. The temperature profile is primarily determined by the ground surface temperature, the water table temperature, water flux through the unsaturated zone, and the thermal conductivity from layer to layer (SNL 2007 [DIRS 184614], Section 6.3). The influence of water flux on temperature is utilized to calibrate the probabilities for different surface water flux boundary conditions for the unsaturated zone flow model. The calibration is based on the Generalized Likelihood Uncertainty Estimation methodology utilizing temperature observations and model predictions, as well as chloride observations and model predictions (SNL 2007 [DIRS 184614], Section 6.8). The probabilities for surface water flux are applied as flow weighting factors for unsaturated zone flow fields in TSPA, which are used for present-day, monsoon, glacial-transition, and post-10,000-year climates (SNL 2007 [DIRS 184614], Table 6.8-1).

The UZ flow fields, which are calibrated to the existing geothermal gradient, also provide percolation-flux boundary conditions in *Multiscale Thermohydrologic Model* (SNL 2008 [DIRS 184433], Section 5.1.2). Therefore, the effects of natural geothermal gradients are included in the multi-scale thermohydrologic model through the use of the calibrated flow fields. Subsequent effects caused by repository heating included in the TSPA model are discussed in that report (SNL 2008 [DIRS 184433], Sections 6.3 and 6.3[a]). The natural geothermal gradient in the unsaturated zone is explicitly included in boundary conditions for the thermal seepage model in *Drift-Scale Coupled Processes (DST and TH Seepage) Models* (BSC 2005 [DIRS 172232], Section 6.5.2).

INPUTS:

Table 2.2.10.03.0B-1. Indirect Inputs

Citation	Title	DIRS
10 CFR 63	Energy: Disposal of High-Level Radioactive Wastes in a Geologic Repository at Yucca Mountain, Nevada	180319
BSC 2005	*Drift-Scale Coupled Process (DST and TH Seepage) Models*	172232
SNL 2007	*UZ Flow Models and Submodels*	184614
SNL 2008	*Multiscale Thermohydrologic Model*	184433

FEP: 2.2.10.04.0A

FEP NAME:

Thermo-Mechanical Stresses Alter Characteristics of Fractures Near Repository

FEP DESCRIPTION:

Heat from the waste causes thermal expansion of the surrounding rock, generating changes in the stress field that may change the properties (both hydrologic and mechanical) of fractures in the rock. Cooling following the peak thermal period will also change the stress field, further affecting fracture properties near the repository.

SCREENING DECISION:

Excluded – low consequence

SCREENING JUSTIFICATION:

Changes to rock thermo-mechanical stresses due to heating by emplaced waste may alter rock hydro-mechanical characteristics (e.g., permeability, moisture retention) of the fractures near the repository. For this justification, the region near the repository is defined as the region below the Paintbrush non-welded unit (PTn) and above the water table. Changes to material properties at greater distances extending upward to the land surface and downward to the water table are presented in excluded FEP 2.2.10.05.0A (Thermo-mechanical Stresses Alter Characteristics of Rocks Above and Below the Repository). In addition, the thermal effects on sorption, solubility, and precipitation/dissolution are discussed in excluded FEP 2.2.10.06.0A (Thermal-chemical Alteration in the UZ (Solubility, Speciation, Phase Changes, Precipitation/Dissolution)). Thermally induced stress changes in the near-field are discussed in excluded FEP 2.2.01.02.0A (Thermally-Induced Stress Changes in the Near-Field), where they are determined to have a minimal impact on rockfall and the hydrologic performance of emplacement drifts.

The effects of thermo-mechanical loading on fractures within the vicinity of the repository drifts due to waste emplacement are evaluated in *Drift Scale THM Model* (BSC 2004 [DIRS 169864]). The results of the coupled drift-scale thermal-hydrological-mechanical (THM) model (BSC 2004 [DIRS 169864], Sections 6.5 and 6.6) indicate that time-dependent THM processes will last for more than 10,000 years. The thermo-mechanical processes have a small or moderate impact on the drift-scale behavior, including a negligible impact on the temperature evolution and small impact on the percolation flux as demonstrated by the comparison of thermal-hydrological (TH) and THM simulation results (BSC 2004 [DIRS 169864], Section 6.5.2, Figures 6.5.5-3, 6.5.5-4, 6.5.5-5, 6.6.2-1, 6.6.2-2, and 6.6.2-3). The THM simulation results were obtained by adopting parameters that emphasize the effect of THM coupling on hydrologic properties and the flow field. This included a bounding estimate of a thermal expansion coefficient (that emphasizes thermal stress) and a bounding estimate of a stress-versus-permeability function that emphasizes THM-induced permeability change. As fracture apertures are modified by the thermo-mechanical impact on the stress field, the permeability may be significantly altered because permeability varies as approximately the cube of the aperture (BSC 2004

[DIRS 169864], Equation 6.4-4). These parameter sets are sufficient for bounding the possible impact of the THM processes on permeability and percolation flux.

Overall, model results indicate that the impact of stress-induced changes in hydrological properties on the flow field is small as characterized by a slightly smaller extent of the dryout zone and a shorter time for resaturation of the rock to the drift wall for the THM case (BSC 2004 [DIRS 169864], Figure 6.5.5-4 and Section 8.1). In the long term, at around 10,000 years, vertical permeability is reduced just above the emplacement drift. The impact of this reduction in permeability is small, but tends to prevent vertical flux from reaching the drift wall at the drift crown (BSC 2004 [DIRS 169864], Figure 6.5.5-5). These changes in hydrological properties are not important because the impacts to the flow system are small. Impacts to the hydrologic property changes are not as important as impacts to the amount of seepage into the drifts. To assess the impact of hydrologic property changes, simulations were conducted to assess the impact to seepage at the repository horizon.

The THM simulations discussed in *Abstraction of Drift Seepage* (SNL 2007 [DIRS 181244], Section 6.4.4.1) indicate that temperature-induced stress changes give rise to changes in the vertical fracture permeability in the vicinity of waste emplacement drifts, particularly in the Tptpmn unit (Topopah Spring Tuff middle nonlithophysal zone) (SNL 2007 [DIRS 181244], Section 6.5.1.4). However, these permeability changes do not result in significant changes to the vertical percolation flux as noted in the paragraph above. In particular, the seepage rates calculated for a permeability field including THM permeability changes were similar to, but 10% less than, those calculated for a permeability field representative of the initial post-excavation conditions (SNL 2007 [DIRS 181244], Section 6.4.4.1.1). These simulations examine effects during the heating and cooling phases out to 10,000 years. It is concluded that an ambient seepage model with consideration of anisotropic THM property changes is only slightly different from the model with only TH considerations. Therefore, the thermo-mechanical impacts to fractures near the repository are insignificant.

Based on the previous discussion, omission of FEP 2.2.10.04.0A (Thermo-Mechanical Stresses Alter Characteristics of Fractures near Repository) will not result in a significant adverse change in the magnitude or timing of either radiological exposure to the RMEI or radionuclide releases to the accessible environment. Therefore, this FEP is excluded from the performance assessments conducted to demonstrate compliance with proposed 10 CFR 63.311 and 63.321 (70 FR 53313 [DIRS 178394]), and with 10 CFR 63.331 [DIRS 180319], on the basis of low consequence.

INPUTS:

Table 2.2.10.04.0A-1. Direct Inputs

Input	Source	Description
BSC 2004. *Drift Scale THM Model.* [DIRS 169864]	Section 6.5.2, Figures 6.5.5-3 to 6.5.5-5 and 6.6.2-2 to 6.6.2-3	Thermo-mechanical stresses caused by repository heat have an insignificant impact on percolation through the unsaturated zone
SNL 2007. *Abstraction of Drift Seepage*. [DIRS 181244]	Sections 6.4.4.1, 6.5.1.4	Effect of thermo-mechanical stresses on seepage

Table 2.2.10.04.0A-2. Indirect Inputs

Citation	Title	DIRS
10 CFR 63	Energy: Disposal of High-Level Radioactive Wastes in a Geologic Repository at Yucca Mountain, Nevada	180319
70 FR 53313	Implementation of a Dose Standard After 10,000 Years	178394
BSC 2004	*Drift Scale THM Model*	169864

FEP: 2.2.10.04.0B

FEP NAME:

Thermo-Mechanical Stresses Alter Characteristics of Faults Near Repository

FEP DESCRIPTION:

Heat from the waste causes thermal expansion of the surrounding rock, generating changes to the stress field that may change the properties (both hydrologic and mechanical) in and along faults. Cooling following the peak thermal period will also change the stress field, further affecting fault properties near the repository.

SCREENING DECISION:

Excluded – low consequence

SCREENING JUSTIFICATION:

Changes to rock thermo-mechanical stresses due to heating by emplaced waste may alter rock hydro-mechanical characteristics of faults (e.g., permeability) and may alter mechanical characteristics such as shear slip potential. Rock alteration above and below the repository from thermo-mechanical stresses caused by repository heat have been shown to have an insignificant impact on percolation through the unsaturated zone as demonstrated by the comparison of thermal-hydrological and THM simulation results (see excluded FEP 2.2.10.05.0A (Thermo-mechanical Stresses Alter Characteristics of Rocks Above and Below the Repository) and BSC 2004 [DIRS 169864], Section 6.5.2, Figures 6.5.5-3, 6.5.5-4, 6.5.5-5, 6.6.2-1, 6.6.2-2, and 6.6.2-3). As discussed in excluded FEP 2.2.01.02.0A (Thermally-Induced Stress Changes in the Near-field), thermally induced stress changes in the near-field have been shown to have a minimal effect on rockfall. Thermo-mechanical stress effects in the near-field are discussed in excluded FEP 2.2.10.04.0A (Thermo-Mechanical Stresses Alter Characteristics of Fractures Near Repository) and *Drift Scale THM Model* (BSC 2004 [DIRS 169864], Sections 6.5 and 6.6). These stress-related impacts are determined to have a minimal impact on the hydrologic performance of emplacement drifts. In addition, thermo-chemical effects on sorption, solubility, and precipitation/dissolution have been shown to be insignificant as discussed in excluded FEP 2.2.10.06.0A (Thermo-Chemical Alteration in the UZ (Solubility, Speciation, Phase Changes, Precipitation/Dissolution)). Stress changes in the cooling period are considered in excluded FEP 2.2.10.04.0A (Thermo-Mechanical Stresses Alter Characteristics of Fractures Near Repository) and are also shown to be insignificant.

Faults are treated as large fractures when assessing the impact of changes to thermo-mechanical stresses on faults. The primary differences between faults and fractures with respect to flow, transport, drift seepage, and coupled processes, are that faults may have greater permeability and continuity than fractures. Thermo-mechanical effects on fault-fractures are expected to be qualitatively similar to rock-mass fractures where thermal-hydrological-mechanical (THM) processes lead to reductions in vertical permeabilities (see excluded FEP 2.2.10.04.0A (Thermo-Mechanical Stresses Alter Characteristics of Fractures Near Repository) and SNL 2007 [DIRS 181244], Sections 6.4.4.1 and 6.5.1.4). As the faults are typically oriented vertical or near

vertical, the expected hydrologic impact of increased thermo-mechanical stresses due to heating on faults would be to decrease the vertical permeability of the faults as a result of rock expansion as a result of rock expansion.

The thermo-mechanical-induced stresses have no long-term effect on fracture properties that would affect long-term unsaturated zone flow and transport, as noted in excluded FEP 2.2.10.04.0A (Thermo-Mechanical Stresses Alter Characteristics of Fractures Near Repository) and SNL (2007 [DIRS 181244], Section 6.4.4.1.1). Thus, the thermo-mechanical stresses will have less of an impact on the block-bounding faults (Solitario Canyon Fault and Bow Ridge Fault), which will be further away from the heat source of the repository block. A block-bounding fault's response to the same thermo-mechanical-induced stresses imposed on fractures will be mitigated due to its size and distance from the heat source.

Based on the previous discussion, omission of FEP 2.2.10.04.0B (Thermo-Mechanical Stresses Alter Characteristics of Faults Near Repository) will not result in a significant adverse change in the magnitude or timing of either radiological exposures to the RMEI or radionuclide releases to the accessible environment. Therefore, this FEP is excluded from the performance assessments conducted to demonstrate compliance with proposed 10 CFR 63.311 and 63.321 (70 FR 53313 [DIRS 178394]), and with 10 CFR 63.331 [DIRS 180319], on the basis of low consequence.

INPUTS:

Table 2.2.10.04.0B-1. Direct Inputs

Input	Source	Description
BSC 2004. *Drift Scale THM Model*. [DIRS 169864]	Sections 6.5 and 6.6	Thermo-mechanical stress effects in the near field
	Section 6.5.2, Figures 6.5.5-3, 6.5.5-4, 6.5.5-5, 6.6.2-1, 6.6.2-2, and 6.6.2-3	Thermo-mechanical stresses caused by repository heat have an insignificant impact on percolation through the unsaturated zone
SNL 2007. *Abstraction of Drift Seepage*. [DIRS 181244]	Sections 6.4.4.1 and 6.5.1.4	Thermo mechanical effects on fault fractures are expected to be qualitatively similar to rock mass fractures where thermal

Table 2.2.10.04.0B-2. Indirect Inputs

Citation	Title	DIRS
10 CFR 63	Energy: Disposal of High-Level Radioactive Wastes in a Geologic Repository at Yucca Mountain, Nevada	180319
70 FR 53313	Implementation of a Dose Standard After 10,000 Years	178394

FEP: 2.2.10.05.0A

FEP NAME:

Thermo-Mechanical Stresses Alter Characteristics of Rocks Above and Below the Repository

FEP DESCRIPTION:

Thermal-mechanical compression at the repository may produce tension fracturing in the Paintbrush non-welded tuff and other units above the repository. These fractures may alter unsaturated zone flow between the surface and the repository. Extreme fracturing may propagate to the surface, affecting infiltration. Thermal fracturing in rocks below the repository may affect flow and radionuclide transport to the saturated zone.

SCREENING DECISION:

Excluded – low consequence

SCREENING JUSTIFICATION:

Changes to rock thermo-mechanical stresses due to heating by emplaced waste may alter rock hydro-mechanical characteristics (e.g., permeability). This FEP addresses rock fracturing above and below the repository as a result of thermo-mechanical stresses due to heating of the rock by emplaced wastes and examines the potential impacts on vertical permeability in the unsaturated zone. Other FEPs related to this one are excluded FEP 2.2.01.02.0A (Thermally-Induced Stress Changes in the Near-Field) and excluded FEP 2.2.10.04.0A (Thermo-Mechanical Stresses Alter Characteristics of Fractures Near Repository), which discuss thermo-mechanical stress effects in the near-field. These stress-related impacts are determined to have a minimal impact on rockfall and the hydrologic performance of emplacement drifts. Stress changes in the cooling period are considered in excluded FEP 2.2.10.04.0A (Thermo-Mechanical Stresses Alter Characteristics of Fractures Near Repository). Thermo-chemical alteration of the Calico Hills unit is addressed in excluded FEP 2.2.10.07.0A (Thermo-Chemical Alteration of the Calico Hills Unit).

The mountain-scale THM model (BSC 2005 [DIRS 174101], Section 6.5) assesses the magnitude and distribution of changes in hydrological properties and analyzes the potential impacts on the mountain-scale percolation flux through the repository horizon for a time period up to 10,000 years that includes both heating and cooling conditions. Calculations show that the vertical permeability changes much more than the horizontal permeability because the horizontal fractures remain open during the entire heating cycle and during cooling to 10,000 years. Thus, this discussion will focus on the changes to the vertical fractures. Results indicate that a maximum THM-induced change in hydrological properties occurs at about 1,000 years after emplacement of waste when the average temperature in the mountain is maximal. Near the ground surface, a zone of tensile stresses is caused by the redistribution of horizontal compressive stresses from the relatively cool regions near the ground surface towards hot regions near the repository horizon (BSC 2005 [DIRS 174101], Section 6.5.11). Compressive stresses transition to tensile stresses between about 260 and 330 m above the repository (BSC 2005 [DIRS 174101], Figure 6.5.11-1b).

At distances of about 190 to 230 m above the emplacement drifts, and again from 270 m above the emplacement drifts to the land surface, zones of tensile stresses with potential fracturing and shear slip were simulated in the THM model (BSC 2005 [DIRS 174101], Section 6.5.14). These zones may potentially represent strata where vertical permeability will be enhanced because fractures will tend to open under tension. The PTn unit, located between the land surface and the repository horizon, is expected to experience a smaller change in horizontal stress (BSC 2005 [DIRS 174101], Figures 6.1-2 and 6.5.11-1), but falls within a near-surface zone that may experience fracturing and shear slip that could result in permanent permeability changes (BSC 2005 [DIRS 174101], Section 6.5.14). Using estimates of input THM properties that would result in upper-bound changes in permeability and percolation rates, changes in permeability by elastic closure or opening of preexisting fractures are within a factor of 0.3 to 5, whereas calculated changes in capillary pressure range between a factor of 0.7 to 1.2 (BSC 2005 [DIRS 174101], Section 6.5.12). To assess the impact of the tensile zones, more extreme changes in vertical permeability and capillary pressure were assumed based on a wider range of observed values to assess the widest range of values possible. The vertical permeability of the tensile zones was increased by three orders of magnitude (representing an upper bound estimate of the increase in permeability expected during shear) and the capillary pressure was reduced by a factor of 10 to correct for the permeability change (BSC 2005 [DIRS 174101], Equation 6.5.5-6, Section 6.5.14). The simulated vertical percolation flux at 10,000 years across the repository horizon was no different, indicating that the potential increase in permeability above the repository horizon as a result of the thermo-mechanical-induced stresses does not impact the percolation flux at the repository level (BSC 2005 [DIRS 174101], Section 6.5.14, Figure 6.5.14-3).

The impact of thermo-mechanical stresses on units below the repository were also presented in *Mountain-Scale Coupled Processes (TH/THC/THM) Models* (BSC 2005 [DIRS 174101], Section 6.5). Beneath the repository horizon, thermo-mechanical impacts from repository heat will increase horizontal stresses (BSC 2005 [DIRS 174101], Figure 6.5.11-1), which lead to small decreases in vertical permeability relative to pre-emplacement values (0.7 to 0.9) (BSC 2005 [DIRS 174101], Figure 6.5.12-1). In the analysis of thermo-chemical alteration of the Calico Hills unit beneath the repository (excluded FEP 2.2.10.07.0A (Thermo-chemical Alteration of the Calico Hills Unit)), even larger increases or decreases in vertical fracture permeability, caused by chemical interactions, were shown to have an insignificant impact on the rate of radionuclide migration. Thus, the small changes in permeability of the Calico Hills unit due to thermo-mechanical stresses can also be excluded on the basis of low consequence.

The effects of seismic-induced mechanical disturbance of fractures along radionuclide transport pathways are discussed in excluded FEP 2.2.06.02.0B (Seismic Activity Changes Porosity and Permeability of Fractures). The conclusion reached in the screening justification of that FEP is that the effects of changes to fracture aperture or spacing on radionuclide transport are expected to be negligible over a wide range of permeability variation. The conclusions reached in that FEP are also applicable here because the analysis is based on a general sensitivity study of how fracture properties affect unsaturated zone flow and radionuclide transport.

Overall effects of thermal stresses on fluid flow due to repository heating above, around, and below the repository are evaluated in *Mountain-Scale Coupled Processes (TH/THC/THM) Models* (BSC 2005 [DIRS 174101], Section 6.5.13; DTN: LB0310MTSCLTHM.002

[DIRS 170718]). This analysis indicates that in the zones near and below the repository, the thermally induced stress changes do not impact the water flux at the repository level. Thus, it is appropriate to exclude thermal effects on mechanical coupling because fluid flow is unaffected by thermally induced stresses.

In the saturated zone, the impact of thermally induced stresses on the characteristics of fractures will also be small. Calculations (SNL 2008 [DIRS 184433], Figure 6.2-14[a]) were made assuming a fixed temperature boundary condition 1,000 m below the water table. The results of the calculation demonstrate that the average temperature change at the water table peaks at approximately 33°C above the initial temperature about 6,000 years after waste emplacement (as extracted from the 560 **.wt* files in DTN: LL0702PA013MST.068 [DIRS 180553], subfolder: /SDT.SDT-01/SDT55). This magnitude of temperature increase is not enough to produce thermo-mechanical stresses at the water table sufficient to produce compression stresses that would significantly affect fracture permeability in the saturated zone.

Based on the previous discussion, omission of FEP 2.2.10.05.0A (Thermo-Mechanical Stresses Alter Characteristics of Rocks Above and Below the Repository) will not result in a significant adverse change in the magnitude or timing of either radiological exposure to the RMEI or radionuclide releases to the accessible environment. Therefore, this FEP is excluded from the performance assessments conducted to demonstrate compliance with proposed 10 CFR 63.311 and 63.321 (70 FR 53313 [DIRS 178394]), and with 10 CFR 63.331 [DIRS 180319], on the basis of low consequence.

INPUTS:

Table 2.2.10.05.0A-1. Direct Inputs

Input	Source	Description
BSC 2005. *Mountain-Scale Coupled Processes (TH/THC/THM) Models*. [DIRS 174101]	Figure 6.5.12-1	The changes in permeability beneath the repository are approximately a factor of 0.7 to 0.9 due to heat induced increases in horizontal stresses
	Section 6.5.14	The change in permeability has little impact on the flux at the repository level
	Section 6.5.14, Figure 6.5.14-3	To investigate the impact of permeability changes
	Figure 6.5.11-1b	Compressive stresses transition to tensile stresses between 260 and 330 m above the repository
	Section 6.5.11	Near the ground surface, a zone of tensile stresses is caused by the redistribution of horizontal compressive stresses
	Figures 6.1-2, 6.5.11-1b	PTn unit, located between the land surface and the repository horizon, is expected to experience a smaller change in horizontal stress
	Section 6.5.14	PTn unit falls within a near-surface zone that may experience fracturing and shear slip that could result in permanent permeability

Table 2.2.10.05.0A-2. Indirect Inputs

Citation	Title	DIRS
10 CFR 63	Energy: Disposal of High-Level Radioactive Wastes in a Geologic Repository at Yucca Mountain, Nevada	180319
70 FR 53313	Implementation of a Dose Standard After 10,000 Years	178394
BSC 2005	*Mountain-Scale Coupled Processes (TH/THC/THM) Models*	174101
DTN: LB0310MTSCLTHM.002	Mountain Scale THM Predictions: Summary Plots	170718
DTN: LL0702PA013MST.068	Input and Output Files for the SMT, SDT and DDT Submodels and MSTHAC Extract Output Files Used in ANL-EBS-MD-000049 Multiscale Thermohydrologic Model	180553
SNL 2008	*Multiscale Thermohydrologic Model*	184433

FEP: 2.2.10.06.0A

FEP NAME:

Thermo-Chemical Alteration in the UZ (Solubility, Speciation, Phase Changes, Precipitation/Dissolution)

FEP DESCRIPTION:

Thermal effects may affect radionuclide transport directly, by causing changes in radionuclide speciation and solubility in the UZ, or indirectly, by causing changes in the host rock mineralogy that affect the flow path. Relevant processes include volume effects associated with silica phase changes, precipitation and dissolution of fracture-filling minerals (including silica and calcite), and alteration of zeolites and other minerals to clays.

SCREENING DECISION:

Excluded – low consequence

SCREENING JUSTIFICATION:

This FEP addresses thermal effects on water–rock interactions in the unsaturated zone. These effects could exert changes on heterogeneous chemical reactions such as mineral dissolution and precipitation. Such effects could also be manifested in changes on rock transport properties (e.g., fracture permeability) and modification of the chemistry of percolating waters. They could affect the sorption properties of radionuclides on tuff. The FEP description also raises some issues addressed in excluded FEPs 2.2.08.03.0B (Geochemical Interactions and Evolution in the UZ), 2.2.08.07.0B (Radionuclide Solubility Limits in the UZ), 2.2.10.07.0A (Thermo-Chemical Alteration of the Calico Hills Unit), 2.2.10.09.0A (Thermo-Chemical Alteration of the Topopah Spring Basal Vitrophyre), and 2.2.01.05.0A (Radionuclide Transport in the Excavation Disturbed Zone), and in included FEP 2.2.08.12.0A (Chemistry of Water Flowing into the Drift). The effects of colloid formation are accounted for in the colloid source term (SNL 2007 [DIRS 177423], Section 6.5.2.3), and are discussed in excluded FEP 2.2.08.03.0B (Geochemical Interactions and Evolution in the UZ).

Measurements at various temperatures of K_d for sorption of barium (a proxy for radium), cesium, strontium, and neptunium on Yucca Mountain tuff are reported, respectively, in DTNs: LA0010JC831341.001 [DIRS 162476], LA0010JC831341.002 [DIRS 153321], LA0010JC831341.003 [DIRS 153322], and LA0010JC831341.007 [DIRS 153319]. Plots of these data showing that K_d values for these elements are either unaffected by temperature or increase slightly with temperature are presented in *Radionuclide Transport Models Under Ambient Conditions* (SNL 2007 [DIRS 177396], Figure I-1). These data were combined with additional measurements of these elements, plus plutonium, americium, uranium, and europium and cerium (proxies for trivalent actinides), and analyzed in *Radionuclide Transport Models Under Ambient Conditions* (SNL 2007 [DIRS 177396], Appendix I) to estimate the enthalpy of sorption, ΔH_r (see also Equations I-6 to I-13b). ΔH_r greater than zero indicates that sorption increases with increasing temperature. The results of that analysis are shown in *Radionuclide Transport Models Under Ambient Conditions* (SNL 2007 [DIRS 177396], Figure I-5,

Table I-12). For cesium, barium, cerium, europium, plutonium, and americium, the values of ΔH_r were not statistically different from zero; that is, no dependence of K_d upon temperature could be inferred. For uranium, strontium, and neptunium, the ΔH_r values were somewhat greater than zero within their overall range. Given the overall weak dependency of sorption K_d values on temperature, the effect of temperature on radionuclide transport is, therefore, excluded on the basis of low consequence because it has no adverse effects on performance.

The thermal-chemical interactions that will occur in the repository environment have been studied with respect to effects on the seepage water entering the waste emplacement drifts in *Drift-Scale THC Seepage Model* (SNL 2007 [DIRS 177404]). This model captures the effects of changes in temperature, pH, ionic strength (and other compositional variables), time dependency, precipitation or dissolution effects, and effects of resaturation (SNL 2007 [DIRS 177404], Section 6.2). Changes in fracture permeabilities resulting from mineral precipitation or dissolution were found to be on the order of the natural variation in these properties (SNL 2007 [DIRS 177404], Section 6.5.5.3; BSC 2004 [DIRS 170038], Table 6-5), with most of the substantial effects spatially limited to localized regions above and to the side of the drift within about a drift diameter (SNL 2007 [DIRS 177404], Figure 6.5-8). The predicted mineral precipitation decreases permeability in the affected regions and leads to a diversion of flow into unaltered rocks further from the drift.

The geochemical model includes the major solid phases (minerals and glass) encountered in geologic units at Yucca Mountain, together with a range of possible reaction product minerals, CO_2 gas, and the aqueous species necessary to include these solid phases and the pore-water composition within the THC model (SNL 2007 [DIRS 177404], Table 6.2-2). Compositional changes of seepage are calculated by the drift-scale THC seepage model (SNL 2007 [DIRS 177404], Section 6.5.5.4) for matrix/fractures pore waters and gas at gridblocks nearby the drift wall boundary. Variations in pH (SNL 2007 [DIRS 177404], Figures 6.5-16, 6.6-1, 6.6-5, 6.6-7, 6.6-9, and 6.6-14), a key compositional variable for sorption of some radionuclides (SNL 2007 [DIRS 177396], Appendix A), roughly lie within the range of variability investigated for radionuclide sorption (SNL 2007 [DIRS 177396], Appendix A).

Results were also investigated for the Tptpll by considering a range of initial pore-water compositions. In this analysis, four different initial pore-water compositions were investigated (SNL 2007 [DIRS 177404], Table 6.2-1). Peak concentrations of aqueous species at the time of rewetting reflect mostly the small values of the first nonzero liquid-saturation output. Elevated concentrations are predicted only for small liquid saturations that are not subject to significant fluid movement. Overall, silica (and calcite) deposition at the boiling front is one of the main processes responsible for the long-term decrease in permeability (2007 [DIRS 177404], Section 6.5.5.3). Short-term effects on the decrease of fracture permeability are mainly restricted to the peak thermal period where salts precipitate as a result of dryout at the boiling front. As previously stated, fluid mobility during the thermal period is expected to be low since liquid saturations are also low.

The modeling results indicate that, at the drift wall, most of the significant compositional variations resulting from thermal-chemical processes are limited to low-saturation conditions over time periods that are short (approximately 1,400 years maximum) relative to a 10,000-year time period (SNL 2007 [DIRS 177404], Section 6.5.5.4). Included FEP 2.2.08.12.0A

(Chemistry of Water Flowing into the Drift) describes the chemistry of water percolating into the drift using the NFC model (SNL 2007 [DIRS 177412], Section 6.3.2). This model is used to predict the chemistry of potential seepage waters flowing into the repository drifts, and it is similar to the drift-scale THC model but differs conceptually in its implementation. The NFC model focuses more on the treatment of fluid–rock interactions as the water percolates through the TSw towards the evaporation front bounding the drift. Comparison of the two models in the validation presented in *Engineered Barrier System: Physical and Chemical Environment* (SNL 2007 [DIRS 177412], Section 7.1.3) shows that, overall, they provide similar results, capturing the major bounding mechanism responsible for changes in seepage chemistry. These analyses suggest that the effects of these changes upon water chemistry in the unsaturated zone are minimal in the long-term.

Based on the previous discussion, omission of FEP 2.2.10.06.0A (Thermo-Chemical Alteration in the UZ (Solubility, Speciation, Phase Changes, Precipitation/Dissolution)) will not result in a significant adverse change in the magnitude or timing of either radiological exposures to the RMEI or radionuclide releases to the accessible environment. Therefore, this FEP is excluded from the performance assessments conducted to demonstrate compliance with proposed 10 CFR 63.311 and 63.321 (70 FR 53313 [DIRS 178394]), and with 10 CFR 63.331 [DIRS 180319], on the basis of low consequence.

INPUTS:

Table 2.2.10.06.0A-1. Direct Inputs

Input	Source	Description
DTN: LA0010JC831341.001. Radionuclide Retardation Measurements of Sorption Distribution Coefficients for Barium. [DIRS 162476]	file: *la0010jc831341_001_S00420_001.zip*	Measurements at various temperatures of K_d for sorption of barium (a proxy for radium) on Yucca Mountain
DTN: LA0010JC831341.002. Radionuclide Retardation Measurements of Sorption Distribution Coefficients for Cesium. [DIRS 153321]	Table S00421_001	Effect of temperature on cesium sorption
DTN: LA0010JC831341.003. Radionuclide Retardation Measurements of Sorption Distribution Coefficients for Strontium. [DIRS 153322]	Table S00422_001	Measurements at various temperatures of K_d for sorption of strontium on Yucca Mountain
DTN: LA0010JC831341.007. Radionuclide Retardation Measurements of Sorption Distribution Coefficients for Neptunium. [DIRS 153319]	Table S00426_001	Effect of temperature on neptunium sorption
SNL 2007. *Drift-Scale THC Seepage Model*. [DIRS 177404]	Figure 6.5-8	Substantial effects spatially limited to regions above and to the side of the drift within about a drift diameter
	Figures 6.5-16, 6.6-1, 6.6-5, 6.6-7, 6.6-9, 6.6-14	Variations in pH lie within the range of variability investigated for radionuclide sorption

Table 2.2.10.06.0A-1. Direct Inputs (Continued)

Input	Source	Description
SNL 2007. *Drift-Scale THC Seepage Model*. [DIRS 177404]	Section 6.5.5.3	Changes in fracture permeabilities resulting from mineral precipitation or dissolution
	Section 6.2	Model captures the effects of changes in temperature, pH, Eh, ionic strength (and other compositional variables), time dependency, precipitation or dissolution effects, and effects of resaturation

Table 2.2.10.06.0A-2. Indirect Inputs

Citation	Title	DIRS
10 CFR 63	Energy: Disposal of High-Level Radioactive Wastes in a Geologic Repository at Yucca Mountain, Nevada	180319
70 FR 53313	Implementation of a Dose Standard After 10,000 Years	178394
BSC 2004	*Analysis of Hydrologic Properties Data*	170038
SNL 2007	*Drift-Scale THC Seepage Model*	177404
SNL 2007	*Engineered Barrier System: Physical and Chemical Environment*	177412
SNL 2007	*Radionuclide Transport Models Under Ambient Conditions*	177396
SNL 2007	*Waste Form and In-Drift Colloids-Associated Radionuclide Concentrations: Abstraction and Summary*	177423

FEP: 2.2.10.07.0A

FEP NAME:

Thermo-Chemical Alteration of the Calico Hills Unit

FEP DESCRIPTION:

Fracture pathways in the Calico Hills may be altered by the thermal and chemical properties of the water flowing out of the repository.

SCREENING DECISION:

Excluded – low consequence

SCREENING JUSTIFICATION:

The Calico Hills nonwelded unit (CHn) is composed of the Calico Hills vitric (CHv) and Calico Hills zeolitic (CHz) units. The CHn unit is situated below the repository horizon and is characterized by complex hydrologic properties for both fracture and matrix (SNL 2007 [DIRS 184614], Section 6.1.1; SNL 2007 [DIRS 177396], Section 6.1.1). Thermo-chemical alteration of fracture pathways in the Calico Hills unit might affect unsaturated zone flow and transport (1) by mineral dissolution and precipitation, which would change the fracture porosity and permeability of the fracture network (SNL 2007 [DIRS 177396], Section 6.1.1), (2) by changing the fraction of active fractures in the active fracture model (Liu et al. 1998 [DIRS 105729]), or (3) by changing the sorptive properties of minerals present on the fracture wall surfaces through mineral dissolution and precipitation, which would change the overall sorptive capacity, represented by K_d (SNL 2007 [DIRS 177396]). As discussed in the following paragraphs, sensitivity studies to examine these effects have shown that none of them significantly increases transport to the accessible environment or the dose to the RMEI.

Sensitivity of tracer transport to fracture porosity was studied by calculating breakthrough curves using (1) the base-case calibrated fracture porosity for each unit, and (2) fracture porosity reduced by a factor of ten everywhere (BSC 2004 [DIRS 169861], Section 6.8.2.2). *UZ Flow Models and Submodels* (BSC 2004 [DIRS 169861], Figure 6.8-4) shows that, with reduced fracture porosity, the fractional mass breakthrough of the tracer arriving at the water table is larger than the one obtained using the calibrated fracture porosity only during the first 50 years. However, in both cases, less than 15% of the released mass arrives during this period. After 100 years, both simulation cases give similar results: almost 50% of the tracer mass arrives at the groundwater table at about 3,400 years, and the two breakthrough curves are not distinguishable. Increasing the fracture porosity was not considered in that sensitivity study because it would retard tracer breakthrough and would, therefore, not be conservative. Comparison of the cases studied shows that transport is not sensitive to fracture porosity.

Sensitivity of tracer transport to the permeability of the fracture network in the Calico Hills unit was studied in *UZ Flow Models and Submodels* (BSC 2001 [DIRS 158726], Sections 6.2.2, 6.2.3, 6.2.5, and 6.7.3, Figures 6-54 to 6-56). Radionuclide breakthrough curves were evaluated for alternative perched water models presented in *UZ Flow Models and Submodels* (BSC 2001

[DIRS 158726], Section 6.7.3). Perched water conceptual models #1 and #2 are named the "flow-through" perched water model and "by-passing" perched water model, respectively (BSC 2001 [DIRS 158726], Section 6.2.2). For model #1, fracture permeability in some layers of the Calico Hills unit is set ten times as great as matrix permeability (BSC 2001 [DIRS 158726], Section 6.2.3, Table 6-6); this property set produces the known perched water. For model #2, fracture permeability is set equal to matrix permeability in all zeolitic units, effectively removing the fractures; this represents the case of fracture sealing. Comparisons for transport simulations between the repository and the water table for the two perched water models (and one other model not discussed here) were performed using sorbing and nonsorbing radionuclides (BSC 2001 [DIRS 158726], Section 6.7.2). The transport results for perched water models #1 and #2 have only minor differences (BSC 2001 [DIRS 158726], Figures 6-54 to 6-56). Transport is, therefore, not sensitive to fracture permeability in the zeolitic Calico Hills unit.

Based on evidence of past alteration, potential thermo-chemical alteration of the Calico Hills unit (CHn) falls into two categories: (1) zeolitization of vitric CHv tuff and (2) recrystallization of zeolitized CHz tuff. Vitric tuff exists mostly above the present water table and former high stands of the water table, suggesting that full saturation and slightly elevated temperatures are conducive to pervasive zeolitic alteration (Levy 1991 [DIRS 100053], Bish and Aronson 1993 [DIRS 100006]). Temperatures around 60°C to 65°C (Bish and Aronson, 1993 [DIRS 100006], Figure 6) and an elevated water table are the factors that would promote zeolitization of the vitric CHv unit. Recrystallization of clinoptilolite, the dominant zeolite in the CHz, to other zeolites may not occur at temperatures below about 100°C (Bish and Aronson, 1993 [DIRS 100006]. The top of the CHn unit will experience temperatures above ambient, exceeding ~60°C beginning at ~400 years and a peak of ~80°C at ~1,100 years during the thermal period (SNL 2008 [DIRS 179962], Figure 6.4.2-31). It is expected that, during the thermal pulse period, the hydraulic conductivity of the CHn will increase as a result of decreasing water viscosity thus promoting flow and drainage. This would lower the water content of the vitric CHv unit. For all these reasons, further alteration of this unit through fluid–rock interaction is not expected since the unit will not be fully saturated and average temperatures will not exceed 100°C. Therefore, significant changes in fracture and matrix permeability as a result of rock alteration during the thermal pulse period and beyond are not expected and are, thus, considered of low consequence in affecting radionuclide transport.

This conclusion differs from that of the mountain-scale thermal-hydrologic-chemical model presented in *Mountain-Scale Coupled Processes (TH/THC/THM) Models* (BSC 2005 [DIRS 174101], Section 6.4). The mountain-scale THC model concludes that significant mineralogic changes—glass alteration and changes in the abundance and mineralogy of the zeolite mineral assemblage—will occur in the Calico Hills unit during the thermal pulse. However, the mountain-scale model implements an older version of the THC seepage model, which differs from the current model. Specifically, dissolution/precipitation rates for several silicate minerals and for rhyolitic glass are 2 to 4 orders of magnitude lower in the current revision of the THC seepage model (SNL 2007 [DIRS 177404], Appendix H) than in the mountain-scale THC model (BSC 2005 [DIRS 174101], Section 4.1.12]). The slower rates implemented in the current THC seepage model are more consistent with field-based measurements of mineral dissolution (the older model used laboratory-derived rates) and with the site-specific observations of the degree of alteration at Yucca Mountain (SNL 2007

[DIRS 177404], Appendix H). If the mountain-scale model were implemented with the updated mineral dissolution/precipitation rates, considerably less alteration of the Calico Hills unit would be expected. Because a previous parameter set was used, and because the results with respect to alteration of the Calico Hills unit are inconsistent with the extended thermal history of that unit, the mountain-scale results do not represent the expected degree of alteration within that unit, and are not considered here.

Additional sensitivity studies concerning the effects of fracture permeability in the Calico Hills unit on radionuclide transport were discussed in *Particle Tracking Model and Abstraction of Transport Processes* (SNL 2008 [DIRS 184748], Figures 6-29 and 6-30). Two sensitivity cases were investigated for aqueous ^{99}Tc, ^{237}Np, and ^{242}Pu, and colloidal ^{242}Pu. In one case, the fracture permeabilities were increased throughout the model domain by one standard deviation and in the other case, the fracture permeabilities were decreased by one standard deviation. The results of these sensitivity analyses indicate that the effect of changing the permeability of the fracture continuum on the normalized cumulative breakthrough curves for the investigated actinides is small.

In the active fracture model conceptualization (Liu et al. 1998 [DIRS 105729], pp. 2,638 to 2,641), only a portion of fracture networks is active (hydraulically conductive) under unsaturated conditions. Numerically, this active portion is defined as a function of water saturation S and the active fracture parameter γ (Liu et al. 1998 [DIRS 105729], pp. 2,638 to 2,641). By definition, γ ranges between 0 and 1, with $\gamma = 0$ or $S = 1$ (corresponding to a saturated condition), signifying that all fractures are active, while $\gamma = 1$, signifying the smallest active fracture portion for a given saturation. Reducing γ increases the fraction of active fractures and allows more fracture–matrix interaction. Sensitivity of flow and transport to the active fracture parameter γ was studied by calculating flow fields and breakthrough curves for three cases: "base case" using the calibrated γ for each unit, "TSw" with γ reduced by half in the TSw units above and below the repository, including the repository layer, and "UnderRepo" with γ reduced by half in the TSw units below the repository, including the repository layer, and in all units below the TSw (DTN: LB0304RDTRNSNS.001 [DIRS 165992]; BSC 2004 [DIRS 169861], Table 6.8-1). The flow field was not sensitive to these changes in γ. Fracture fluxes at the repository layer and at the water table varied less than 2.5% from the base case (BSC 2004 [DIRS 169861], Table 6.8-2).

In the study of transport sensitivity to γ, the breakthrough curve for case "TSw" showed delayed tracer breakthrough at the water table compared to the base case. When a tracer is released as a pulse from the repository gridblocks, it travels faster in the fractures than in the matrix, causing a temporary concentration gradient between the fracture and matrix. Decreasing γ allows more tracer to diffuse into the matrix, where its transport is delayed (no sorption was modeled). In the base case, 20% of the total input mass arrives at the water table at (approximately) 150 years, and 50% of the total mass arrives at the water table at (approximately) 3,400 years. For case "TSw," there is 20% mass arrival at 1,900 years and 50% at (approximately) 7,100 years (BSC 2004 [DIRS 169861], Figure 6.8-3). The breakthrough curve for case "UnderRepo" was indistinguishable from that for case "TSw" (BSC 2004 [DIRS 169861], Figure 6.8-3). This indicates that increasing the fracture–matrix interaction in the Calico Hills unit does not further

delay tracer breakthrough; that is, fracture–matrix interaction in the TSw unit is more important in delaying transport than fracture-matrix interaction in the Calico Hills unit.

Additional sensitivity studies concerning the effects of the active-fracture parameter γ on radionuclide transport were conducted in *Particle Tracking Model and Abstraction of Transport Processes* (SNL 2008 [DIRS 184748], Figures 6-33 to 6-36). Five sensitivity cases were investigated for aqueous ^{99}Tc, ^{237}Np, and ^{242}Pu. The active fracture parameter γ in the TSw unit was set to values of 0.6, 0.5, 0.4, 0.3, and 0.2, with the base-case values for hydrogeologic units in and below the repository for the TSw unit (tsw33 through tsw38) ranging from 0.569 to 0.6 (SNL 2008 [DIRS 184748], Section 6.6.4 and Table 6-11). This uncertainty range for γ is discussed in *Conceptual Model and Numerical Approaches for Unsaturated Zone Flow and Transport* (BSC 2004 [DIRS 170035], Sections 7.4.1 and 7.4.2). The results show that transport is sensitive to γ only for the TSw unit; changes in γ for hydrogeologic units below the TSw unit had almost no effect on transport behavior (SNL 2008 [DIRS 184748], Figure 6-36).

Sensitivity of transport to K_d values was studied in *Radionuclide Transport Models Under Ambient Conditions* (SNL 2007 [DIRS 177396], Section 6.9.1.5; DTN: LB0310MR0060R1.010 [DIRS 174489]), which simulated transport of ^{237}Np for a base case and three alternative cases. For the base case, nonzero K_d values (SNL 2007 [DIRS 177396], Table 6-3) were used for TSw, CHv, and CHz units. In the alternative cases, K_d values for TSw, CHv, or CHz units were set to zero, leaving the others unchanged. Breakthrough curves for a mean present-day infiltration scenario (4.43 mm/yr; SNL 2007 [DIRS 177396], Table 6-5) are shown in *Radionuclide Transport Models Under Ambient Conditions* (SNL 2007 [DIRS 177396], Figure 6-37). Eliminating sorption in the TSw unit caused a portion of ^{237}Np to arrive at the water table significantly earlier, but eliminating sorption in the CHz or CHv units had little effect on the breakthrough curve.

These sensitivity studies show that alteration of fracture pathways in the Calico Hills unit would not significantly change the rate of radionuclide transport.

Based on the previous discussion, omission of FEP 2.2.10.07.0A (Thermo-Chemical Alteration of the Calico Hills Unit) will not result in a significant adverse change in the magnitude or timing of either radiological exposure to the RMEI or radionuclide releases to the accessible environment. Therefore, this FEP is excluded from the performance assessments conducted to demonstrate compliance with proposed 10 CFR 63.311 and 63.321 (70 FR 53313 [DIRS 178394]), and with 10 CFR 63.331 [DIRS 180319], on the basis of low consequence.

INPUTS:

Table 2.2.10.07.0A-1. Direct Inputs

Input	Source	Description
DTN: LB0304RDTRNSNS.001. Supporting Files of 3D Flow and Transport Sensitivity Analyses. [DIRS 165992]	files: *basecase_loporosity.tar.gz, reducedAFPforTSw.tar.gz, Underrep.tar.gz*, Entire	Sensitivity of transport to fracture porosity and active fracture parameters
DTN: LB0310MR0060R1.010. Supplemental Radionuclide Transport Simulations: Input/Output Files. [DIRS 174489]	File: *LB0310MR0060R1.010.zip*	Sensitivity of transport to sorption
SNL 2007. *Radionuclide Transport Models Under Ambient Conditions*. [DIRS 177396]	Figure 6-37	Breakthrough curves for a mean present-day infiltration scenario
	Table 6-3	Non-zero K_d values
	Section 6.9.1.5	Studied sensitivity of transport to K_d values
SNL 2008. *Particle Tracking Model and Abstraction of Transport Processes*. [DIRS 184748]	Figures 6-33 through 6-36	Conducted sensitivity studies concerning the effects of the active-fracture parameter on radionuclide transport
	Figures 6-29 and 6-30	Conducted sensitivity studies concerning the effects of fracture permeability on radionuclide transport
	Section 6.6.4 and Table 6-11	The active fracture parameter g in the TSw unit was set to values of 0.6, 0.5, 0.4, 0.3, and 0.2, with the base case values for hydrogeologic units in and below the repository for the TSw unit (tsw33 through tsw38) ranging from 0.569 to 0.6
SNL 2008. *Postclosure Analysis of the Range of Design Thermal Loadings*. [DIRS 179962]	Figure 6.4.2-31	Temperature profile of the top of the Calico Hills Unit

Table 2.2.10.07.0A-2. Indirect Inputs

Citation	Title	DIRS
10 CFR 63	Energy: Disposal of High-Level Radioactive Wastes in a Geologic Repository at Yucca Mountain, Nevada	180319
70 FR 53313	Implementation of a Dose Standard After 10,000 Years	178394
Bish and Aronson 1993	"Paleogeothermal and Paleohydrologic Conditions in Silicic Tuff from Yucca Mountain, Nevada"	100006
BSC 2001	*UZ Flow Models and Submodels*	158726
BSC 2004	*Conceptual Model and Numerical Approaches for Unsaturated Zone Flow and Transport*	170035
BSC 2004	*UZ Flow Models and Submodels*	169861
BSC 2005	*Mountain-Scale Coupled Processes (TH/THC/THM) Models*	174101
Levy 1991	"Mineralogic Alteration History and Paleohydrology at Yucca Mountain, Nevada"	100053
Liu et al. 1998	"An Active Fracture Model for Unsaturated Flow and Transport in Fractured Rocks"	105729
SNL 2007	*Drift-Scale THC Seepage Model*	177404
SNL 2007	*Radionuclide Transport Models Under Ambient Conditions*	177396
SNL 2007	*UZ Flow Models and Submodels*	184614

FEP: 2.2.10.08.0A

FEP NAME:

Thermo-Chemical Alteration in the SZ (Solubility, Speciation, Phase Changes, Precipitation/Dissolution)

FEP DESCRIPTION:

Thermal effects may affect radionuclide transport directly by causing changes in radionuclide speciation and solubility in the SZ, or, indirectly, by causing changes to host rock mineralogy that affect the flow path. Relevant processes include volume effects associated with silica phase changes, precipitation and dissolution of fracture filling minerals (including silica and calcite), and alteration of zeolites and other minerals to clays.

SCREENING DECISION:

Excluded – low consequence

SCREENING JUSTIFICATION:

Waste emplacement and subsequent heating of the rocks around the repository may increase the temperature of the groundwater at the water table and in the saturated zone below the repository footprint. An estimate of the potential temperature increase is predicted with the three-dimensional multiscale thermohydrologic model (SNL 2008 [DIRS 184433]). Average of the maximum water table temperatures at each of the 560 locations modeled is approximately 63°C at around 6,000 years after waste emplacement (as extracted from the 560 **.wt* files in DTN: LL0702PA013MST.068 [DIRS 180553], subfolder: /SDT/SDT-01/SDT55). This represents an approximate 33°C increase in comparison with the ambient temperature of 30°C to 34°C specified at the water table beneath the repository (Fridrich et al. 1994 [DIRS 100575], Figure 8). Available data show little statistical variation in the sorption coefficient values up to 80°C (DTN: LA0407AM831341.002 [DIRS 170621], file*: LA0407AM831341_002_S04296_001.TXT*, and DTN: LA0407AM831341.003 [DIRS 170626], file: *LA0407AM831341_003_S04297_001.TXT*). As long as temperatures at the water table do not consistently exceed the upper-bounding estimate of about 80°C, the thermal impact on host-rock mineralogy and water chemistry will not affect the saturated zone because these temperatures ranges were used when collecting sorption data.

Furthermore, CO_2 becomes less soluble at elevated temperatures. Small changes in CO_2 concentration may notably affect pH. These correlated constituents are the primary components that affect mineral/water interactions (SNL 2007 [DIRS 177404], Section 6.2.1.2). Therefore, as temperatures increase, CO_2 would exsolve from solution, and cause pH to rise with concomitant calcite precipitate in pores and fractures. Calcite precipitation in pores and along fractures would decrease permeability. Once temperatures start to drop, CO_2 dissolution will increase, and pH will decrease. This is because the temperature drop causes calcite that had precipitated in pores and fractures at elevated temperatures to dissolve. As a result, concomitant permeabilities would return to those in effect under ambient conditions. Thus, the net result of an increase in saturated

zone groundwater temperatures, induced by the expected heating from emplaced wastes, and a subsequent decrease in groundwater temperatures during repository cooling would be neutral with respect to saturated zone barrier capability. Regardless of the timing of the calcite precipitation, it serves to decrease permeability. This, in turn, decreases flux. As upstream gradients increase, flow will be forced through the units with decreased permeability or it will find alternate pathways. In any case, flow through the affected (heated) area is decreased, and with respect to precipitation/dissolution effects, thermo-chemical alteration in the saturated zone can beconsidered negligible.

At Yucca Mountain, the most sorptive zeolites (the mineral clinoptilolite) formed only from alteration of volcanic glass. However, there is almost no volcanic glass remaining below the water table that could alter to zeolites. If temperatures below the water table increase, the most likely mineralogic reaction would be recrystallization of clinoptilolite to the less sorptive zeolite analcime. Regardless, Bish and Aronson (1993 [DIRS 100006]) conclude that repository heating will be insufficient to cause clinoptilolite below the water table to recrystallize to less sorptive minerals.

Groundwater flow enters the saturated zone site-scale flow system primarily as underflow at the lateral boundaries of the model domain (lateral flows account for 90% of the flow through the system), with distributed recharge (infiltration or percolation) primarily in the northern part of the model domain and focused recharge along the Fortymile Wash channel (SNL 2007 [DIRS 177391], Section 6.4.3.9). Recharge through the footprint of the unsaturated zone model domain to the SZ flow model constitutes a small fraction of the entire groundwater budget of the site-scale flow system (10%); relative to the total water budget in the saturated zone flow domain, the distributed recharge from the UZ flow model to the saturated zone is only about 13% of total recharge (SNL 2007 [DIRS 177391], Section 6.4.3.9). Therefore, thermally induced changes in water chemistry would be diluted given the relatively small volume of unsaturated zone water that contributes to the total volume of water that passes through the saturated zone flow system (13% of 10%, which is about 1% of the total water budget flowing through the 30×45-km^2 saturated zone model domain).

In the case of no mixing, the analysis presented in excluded FEP 2.2.10.06.0A (Thermo-Chemical Alteration in the UZ (Solubility, Speciation, Phase Changes, Precipitation/Dissolution)) is relevant. This analysis considers the effects of THC processes on radionuclide transport in terms of radionuclide solubility, colloid stability, water composition, mineral precipitation and dissolution, and temperature. The results of this analysis indicate that the effects of THC processes on radionuclide transport between the repository and the water table are negligible. Therefore, the effects of THC processes on water composition entering the saturated zone from the unsaturated zone will also have a negligible effect on radionuclide transport in the saturated zone.

Radionuclides introduced in the unsaturated zone from the EBS are unconstrained; that is, the solubility is not reduced as radionuclides go from the higher temperature repository conditions to the unsaturated zone. Furthermore, neither does *Saturated Zone Flow and Transport Model Abstraction* (SNL 2008 [DIRS 183750]) implement a solubility limit for each transported radionuclide, so radionuclide concentration introduced into the saturated zone from the

unsaturated zone is also unconstrained. Therefore, saturated zone temperature variability will not alter the influx of radionuclides from the unsaturated zone to the saturated zone.

Excluded FEP 2.2.10.07.0A (Thermo-chemical Alteration of the Calico Hills Unit) evaluates the thermal-chemical effects on alteration in the Calico Hills unit (CHn) in the unsaturated zone below the repository. That analysis indicates that thermal-chemical effects are limited to the near-field environment and are of such short duration that they will not have a significant effect on unsaturated zone radionuclide transport or radionuclide release to the accessible environment. Because thermal-chemical effects can be excluded in the near-field, by deduction, thermal-chemical alteration will have less of an impact further away in the saturated zone. Therefore, thermal-chemical effects can also be excluded in the saturated zone.

Based on the previous discussion, omission of FEP 2.2.10.08.0A (Thermo-Chemical Alteration in the SZ (Solubility, Speciation, Phase Changes, Precipitation/Dissolution)) will not result in a significant adverse change in the magnitude or timing of either radiological exposure to the RMEI or radionuclide releases to the accessible environment. Therefore, this FEP is excluded from the performance assessments conducted to demonstrate compliance with proposed 10 CFR 63.311 and 63.321 (70 FR 53313 [DIRS 178394]), and with 10 CFR 63.331 [DIRS 180319], on the basis of low consequence.

INPUTS:

Table 2.2.10.08.0A-1. Direct Inputs

Input	Source	Description
DTN: LA0407AM831341.002. Batch Sorption Coefficient Data for Cesium on Yucca Mountain Tuffs in Representative Water Compositions. [DIRS 170621]	file: *LA0407AM831341_002_S04296_001.TXT*	Available data show little statistical variation in the sorption coefficient values up to 80°C
DTN: LA0407AM831341.003. Batch Sorption Coefficient Data for Strontium on Yucca Mountain Tuffs in Representative Water Compositions. [DIRS 170626]	file: *LA0407AM831341_003_S04297_001.TXT*	Available data show little statistical variation in the sorption coefficient values up to 80°C
DTN: LL0702PA013MST.068. Input and Output Files for the SMT, SDT and DDT Submodels and MSTHAC Extract Output Files Used in ANL-EBS-MD-000049 Multiscale Thermohydrologic Model. [DIRS 180553]	All *.wt files in subfolder /SDT/SDT-01/SDT55	Data for temperature at the water table
SNL 2007. *Saturated Zone Site-Scale Flow Model*. [DIRS 177391]	Section 6.4.3.9	Infiltration sources

Table 2.2.10.08.0A-2. Indirect Inputs

Citation	Title	DIRS
10 CFR 63	Energy: Disposal of High-Level Radioactive Wastes in a Geologic Repository at Yucca Mountain, Nevada	180319
70 FR 53313	Implementation of a Dose Standard After 10,000 Years	178394
Bish and Aronson 1993	"Paleogeothermal and Paleohydrologic Conditions in Silicic Tuff from Yucca Mountain, Nevada"	100006
Fridrich et al. 1994	"Hydrogeologic Analysis of the Saturated-Zone Ground-Water System, Under Yucca Mountain, Nevada"	100575
SNL 2007	*Drift-Scale THC Seepage Model*	177404
SNL 2008	*Multiscale Thermohydrologic Model*	184433

FEP: 2.2.10.09.0A

FEP NAME:

Thermo-Chemical Alteration of the Topopah Spring Basal Vitrophyre

FEP DESCRIPTION:

Heating the Topopah Spring basal vitrophyre with available water may cause alteration of the glasses to clays and zeolites. Possible effects include volume increases that plug fractures, changes in flow paths, creation of perched water zones, and an increase in the sorptive properties of the unit.

SCREENING DECISION:

Excluded – low consequence

SCREENING JUSTIFICATION:

The Topopah Spring Tuff basal vitrophyre is densely welded glassy tuff extending downward from the base of the lower nonlithophysal zone of the Topopah Spring Tuff into the crystal-poor vitric zone. The total thickness varies from about 3 to 30 m. Due to heat generated by radioactive decay, the rate of volcanic glass alteration to clays and zeolites will increase, potentially resulting in local changes to the hydrologic or sorptive properties of the unit. However, this effect is expected to be small, because the current degree of alteration represents exposure to elevated temperatures for extended periods of time—millions of years—since deposition. The thermal history of the Topopah Spring Tuff exposed in the Exploratory Studies Facility has been well characterized by fluid inclusion and isotopic (oxygen isotope and uranium-thorium series) studies of fracture minerals within the unit (BSC 2004 [DIRS 170004], Section 6.14.2.3.1). The highest temperatures (>80°C) occurred at times greater than or equal to 10 Ma, and temperatures cooled gradually to near-modern ambient temperatures over the next six or more million years where they have remained for the past 2 to 4 million years (BSC 2004 [DIRS 170004], Figure 6-199).

While no data are available prior to 10 Ma, Whelan et al. (2006 [DIRS 179305], Figure 8) present a thermal model that is consistent with the available data and suggest that the tuff cooled rapidly after eruption (12.8 Ma), but was reheated to temperatures of approximately 95°C by magmatic heat related to Timber Mountain group volcanism at 11.6 Ma. The thermal model predicts that temperatures above 80°C persisted until about 10 Ma, and then dropped gradually over the next several million years, consistent with the thermal history of the unit based on the measured data.

The overall thermal history of the tuff is corroborated by Evans et al. (2005 [DIRS 178836], p. 1,103), who performed (uranium-thorium)/helium dating of fluorite in the Topopah Spring Tuff. Two-phase fluid inclusions in fluorite were found to have trapping temperatures of 65°C to 80°C (Evans et al. 2005 [DIRS 178836], p. 1,100), which lies below the He closure temperature of 90°C. This implies that the fluorite was closed to He diffusion since deposition and that the average (uranium-thorium)/helium age of 9.7 Ma found for fluorite is the depositional age.

However, uncertainties regarding partial helium loss below the closure temperature suggest that the (uranium-thorium)/helium age may represent the time since the last period of heating, or the "cooling" age." Wilson et al. (2003 [DIRS 163589], p. 1,171) also provide corroborating information; they determined ages (uranium-lead dating) and temperatures (fluid inclusion homogenization temperatures) of calcite/silica mineral formation in the unsaturated zone at Yucca Mountain. They found that mineral deposition temperatures above 50°C persisted until about 6.3 Ma, and temperatures between 35°C to 45°C until about 5.3 Ma.

Thus, the Topopah Spring Tuff at the level of the Exploratory Studies Facility (where the fracture mineral samples were collected), and by implication, the underlying basal vitrophyre, was exposed to temperatures of approximately 80°C to 95°C for at least a million years, and temperatures above 50°C for several million years.

Much of the observed alteration in the basal vitrophyre occurred at 40°C to 100°C (Levy andO'Neil1989 [DIRS 133364], p. 322), apparently soon after eruption of the tuff (Levy and Valentine 1993 [DIRS 106681], p. 146). However, given the thermal history of the tuff, the relatively rapid rate of alteration associated with the initial cooling and devitrification of the tuff was not maintained in the long term; elevated temperatures later in the tuff history has lesser effect. The degree of alteration of the vitrophyre at the base of the unit reflects the total, extended thermal history of the tuff, with elevated temperatures lasting millions of years. During the period of repository thermal heating, the drift wall boiling duration will be at most 1,500 years (SNL 2008 [DIRS 184433], Figure 6.3-78[a], and drift wall temperatures drop below 50°C in less than 20,000 years (for most waste package locations, much less) (SNL 2008 [DIRS 184433], Figure 6.3-76[a]). These values offer bounds on conditions in the more distal Topopah Spring Tuff basal vitrophyre. Hence, the postclosure thermal pulse will be very brief relative to the extended thermal history of the tuff and will result in only minor changes in the abundance of secondary minerals in the vitrophyre. Therefore, thermally induced alteration of the basal vitrophyre will be limited and is not anticipated to significantly affect the sorptive or hydrologic properties of the unit.

This conclusion differs from that of the mountain-scale THC model presented in *Mountain-Scale Coupled Processes (TH/THC/THM) Models* (BSC 2005 [DIRS 174101], Section 6.4). The mountain-scale THC model concludes that significant glass alteration—up to nearly 20% in the first 7,000 years after closure—will occur in the basal vitrophyre of the Topopah Spring Tuff. However, the mountain-scale model implements an older version of the THC seepage model, which differs from the current model. Specifically, dissolution/precipitation rates for several silicate minerals and for rhyolitic glass are 2 to 4 orders of magnitude lower in the current revision of the THC seepage model (SNL 2007 [DIRS 177404], Appendix H) than in the mountain-scale THC model. The slower rates implemented in the current THC seepage model are more consistent with field-based measurements of mineral dissolution (the older model used laboratory-derived rates) and with the site-specific observations of the degree of alteration at Yucca Mountain (SNL 2007 [DIRS 177404], Appendix H). If the mountain-scale model were implemented with the updated mineral and glass dissolution/precipitation rates, considerably less alteration of the basal vitrophyre would be expected. Because a previous parameter set was used, and because the results with respect to alteration of the basal vitrophyre are inconsistent with the extended thermal history of that unit, the mountain-scale THC model results do not represent the expected degree of alteration within that unit, and are not considered here.

Based on the previous discussion, omission of FEP 2.2.10.09.0A (Thermo-Chemical Alteration of the Topopah Spring Basal Vitrophyre) will not result in a significant adverse change in the magnitude or timing of either radiological exposures to the RMEI or radionuclide releases to the accessible environment. Therefore, this FEP is excluded from the performance assessments conducted to demonstrate compliance with proposed 10 CFR 63.311 and 63.321 (70 FR 53313 [DIRS 178394]), and with 10 CFR 63.331 [DIRS 180319], on the basis of low consequence.

INPUTS:

Table 2.2.10.09.0A-1. Direct Inputs

Input	Source	Description
BSC 2004. *In Situ Field Testing of Processes*. [DIRS 170004]	Section 6.14.2.3.1, Figure 6-199	Thermal history of the TSw
SNL 2008. *Multiscale Thermohydrologic Model*. [DIRS 184433]	Figures 6.3-76[a] and 6.3-78[a]	Evolution of drift wall temperatures through time

Table 2.2.10.09.0A-2. Indirect Inputs

Citation	Title	DIRS
10 CFR 63	Energy: Disposal of High-Level Radioactive Wastes in a Geologic Repository at Yucca Mountain, Nevada	180319
70 FR 53313	Implementation of a Dose Standard After 10,000 Years	178394
BSC 2005	*Mountain-Scale Coupled Processes (TH/THC/THM) Models*	174101
Evans et al. 2005	"Fluorite (U-Th)/He Thermochronology: Constraints on the Low Temperature History of Yucca Mountain, Nevada"	178836
Levy and O'Neil 1986	"Moderate Temperature Zeolitic Alteration in a Cooling Pyroclastic Deposit"	133364
Levy and Valentine 1993	"Natural Alteration in the Cooling Topopah Spring Tuff, Yucca Mountain, Nevada, As an Analog to a Waste-Repository Hydrothermal Regime"	106681
SNL 2007	*Drift-Scale THC Seepage Model*	177404
Whelan et al. 2006	*Thermal History of the Unsaturated Zone at Yucca Mountain, Nevada, USA*	179305
Wilson et al. 2003	"Origin, Timing, and Temperature of Secondary Calcite—Silica Mineral Formation at Yucca Mountain, Nevada"	163589

FEP: 2.2.10.10.0A

FEP NAME:

Two-Phase Buoyant Flow/Heat Pipes

FEP DESCRIPTION:

Heat from waste can generate two phase buoyant flow. The vapor phase (water vapor) could escape from the mountain. A heat pipe consists of a system for transferring energy between a hot and a cold region (source and sink respectively) using the heat of vaporization and movement of the vapor as the transfer mechanism. Two phase circulation continues until the heat source is too weak to provide the thermal gradients required to drive it. Alteration of the rock adjacent to the drift may include dissolution that maintains the permeability necessary to support the circulation (as inferred for some geothermal systems).

SCREENING DECISION:

Included

TSPA DISPOSITION:

The coupled processes causing heat-pipe behavior are simulated with the TH seepage model described in *Drift-Scale Coupled Processes (DST and TH Seepage) Models* (BSC 2005 [DIRS 172232]) that provides input to *Abstraction of Drift Seepage* (SNL 2007 [DIRS 181244], Section 6.4.3). Using this model, the impact of heat-pipe behavior on seepage is assessed for several simulation cases in which percolation fluxes and rock properties are varied (BSC 2005 [DIRS 172232], Section 6.2.1.6). Thus, the TH seepage-modeling results include the effect of heat pipes and the resulting uncertainties in the conditions under which seepage occurs and in the volume of seepage. The TH seepage model results are used to develop an appropriate thermal-seepage methodology in the seepage abstraction (SNL 2007 [DIRS 181244], Section 6.5.2).

The effect of heat pipes on predicted in-drift thermal-hydrologic conditions is taken into account in the drift-scale submodels of *Multiscale Thermohydrologic Model* (SNL 2008 [DIRS 184433], Section 6.2.1). The MSTHM provides in-drift temperature and relative humidity values, which are used by the TSPA to extract in-drift water chemistry from lookup tables provided by the seepage dilution-evaporation abstraction, described in *Engineered Barrier System: Physical and Chemical Environment* (SNL 2007 [DIRS 177412], Sections 6.9 and 6.15.1).

Drift-Scale THC Seepage Model (SNL 2007 [DIRS 177404]) evaluates the effects of thermal-hydrologic-chemical coupled processes, including heat pipe behavior, on the composition of potential seepage waters. The development of a heat pipe results in evaporation and condensation above the drift, affecting potential seepage water compositions; however, these effects are largely confined to the boiling period, when seepage is not possible. After boiling ceases, heat pipe induced dilution-evaporation of potential seepage water compositions becomes negligible (SNL 2007 [DIRS 177404], Figure 6.5-13). The THC seepage model results provide the technical basis for the methodology used in the near-field chemistry model (SNL 2007

[DIRS 177412], Section 6.3.2) The near-field chemistry model provides initial seepage water compositions to the in-drift seepage dilution-evaporation model, and does not explicitly evaluate the effects of heat pipes.

INPUTS:

Table 2.2.10.10.0A-1. Indirect Inputs

Citation	Title	DIRS
BSC 2005	*Drift-Scale Coupled Process (DST and TH Seepage) Models*	172232
SNL 2007	*Abstraction of Drift Seepage*	181244
SNL 2007	*Drift-Scale THC Seepage Model*	177404
SNL 2007	*Engineered Barrier System: Physical and Chemical Environment*	177412
SNL 2008	*Multiscale Thermohydrologic Model*	184433

FEP: 2.2.10.11.0A

FEP NAME:

Natural Air Flow in the UZ

FEP DESCRIPTION:

Natural convective air circulation has been observed at a borehole at the top of the mountain. Repository heat may increase this flow.

SCREENING DECISION:

Excluded – low consequence

SCREENING JUSTIFICATION:

Natural air flow in the unsaturated zone may impact thermal hydrological processes in the host rock units and water vapor removal from the unsaturated zone during ambient conditions (not perturbed by repository heating). Gas flow in the host rock units may be radially directed toward or away from the emplacement drifts, or axially within emplacement drifts and connected openings. Radial gas flow in the host rock for thermally perturbed conditions is incorporated in models for thermal-hydrological response of the host rock (SNL 2008 [DIRS 184433], Section 6.1), thermal seepage (BSC 2005 [DIRS 172232], Section 6.2.2.1.1), and thermal-hydrological-chemical processes (SNL 2007 [DIRS 177404], Section 6.4.1). Potential effects from axial gas flow in the emplacement drifts on condensation (SNL 2007 [DIRS 181648], Section 6.3) and CO_2 fugacity (SNL 2007 [DIRS 177412], Section 6.15.1) are included in TSPA, while effects on the evolution of temperature and humidity in the emplacement areas are of limited magnitude and duration and are excluded (SNL 2008 [DIRS 184433], Section 7.8[a]).

Various aspects of gas-phase flow under thermally perturbed conditions are discussed in included FEPs 2.1.08.11.0A (Repository Resaturation due to Waste Cooling), 2.1.11.09.0A (Thermal Effects on Flow in the EBS), 2.2.07.10.0A (Condensation Zone Forms Around Drifts), 2.2.07.11.0A (Resaturation of Geosphere Dry-Out Zone), 2.2.10.10.0A (Two-Phase Buoyant Flow/Heat Pipes), and 2.2.10.12.0A (Geosphere Dry-Out Due to Waste Heat). The effects of natural air flow, or barometric pumping, on both thermal-hydrologic processes and water vapor removal are discussed below.

Barometric pumping is considered in the MSTHM (SNL 2008 [DIRS 184433]) and the in-drift convection and condensation model (SNL 2007 [DIRS 181648]). Although the effect is not explicitly included in either model as implemented in TSPA, both models have investigated ranges of three-dimensional axial transport behavior that cover the potential effects from barometric pumping. The following discusssion starts with the condensation model to develop the conceptual basis for describing the potential effects, followed by a discussion of three-dimensional validation test cases used in the multiscale thermohydrologic model which more clearly show the potential effects on the in-drift environment. The discussion then addresses the potential for moisture removal from the unsaturated zone by natural air flow.

Axial transport of water vapor in the emplacement drifts controls the potential for condensation. The in-drift convection and condensation model (SNL 2007 [DIRS 181648], Section 6.2) uses a three-dimensional thermal convection (dry air) simulation for a drift segment containing 14 waste packages to evaluate gas transport by convective mixing. Axial transport is represented using a one-dimensional dispersion approach, and the three-dimensional convection model produced a range of values for the effective dispersion coefficient for use in the one-dimensional model. The values can be conveniently expressed as multiples of the gaseous binary diffusion coefficient for water in air. A range of the diffusion coefficient multipliers from approximately 200 to 4,700 is developed, normalizing the values in Tables 6.2.7-2 and 6.2.7-3 by 2.13×10^{-5} m^2/s (SNL 2007 [DIRS 181648], Section 6.2.7), representing repository-center and -edge conditions, respectively. Barometric pumping could produce transport equivalent to extending the upper end of this range. However, the in-drift convection and condensation model shows that a value of 4,700 already causes condensation to occur predominantly in the unheated regions at the ends of the drifts, a result that would not change with greater dispersive transport.

A set of three-dimensional thermal-hydrological simulations was performed to further evaluate the effects from axial transport (SNL 2008 [DIRS 184433], Section 6.3.18[a]). This work was performed as a parametric sensitivity study, varying the axial dispersion factor well beyond the previous range (up to 10,000). The results are analyzed in *In-Drift Natural Convection and Condensation* (SNL 2007 ([DIRS 181648], Section 6.2) confirming that condensation within the emplacement area is not predicted for higher values of the dispersion factor. Using an intermediate value of 1,000, the validation test cases for the multiscale model demonstrate that axial transport lowers the relative humidity in the emplacement regions and delays the return of humidity by hundreds of years as the waste packages cool (SNL 2008 [DIRS 184433], Section 7.8[a]). These effects are not significant to the application of the multiscale model, which represents many thousands of years of repository thermal evolution.

Increased axial gas transport, as potentially induced by natural air flow, tends to dry out the near-field host rock in heated regions and deposit the resulting condensate at cooler or unheated regions of the drifts. Over the range of dispersion factor values investigated, the effect is limited in magnitude by other factors, such as the percolation flux (e.g., compare the gas-phase fluxes versus time for PWR waste packages in cases 1 and 4 of DTN: MO0703PAEVSIIC.000 [DIRS 181990], file: *Stage 2 Analysis.xls*). These results show that gas-phase transport of moisture from the rock is weakly related to the dispersion factor (and, therefore, natural air flow) because it is limited by availability of moisture as percolation and by the mass-transfer resistance within the host rock.

The effects of natural air flow due to barometric pumping and the associated removal of water through vapor transport under isothermal conditions have also been investigated. Estimates of the rate of water removal from Yucca Mountain through this mechanism range from 0.001 mm/yr to 0.3 mm/yr (Martinez and Nilson 1994 [DIRS 174095], p. 106; Tsang and Pruess 1990 [DIRS 172018], p. iii). These estimated rates are negligible in comparison with the estimates for average infiltration at Yucca Mountain, which range from 3 to 73 mm/yr (SNL 2007 [DIRS 184614], Table 6.1-2). During repository heating, enhanced flow of heated air will not increase the amount of water vapor removal from the mountain because water would condense upon reaching the cooler units above the repository.

In summary, barometric pumping may increase gas-phase axial transport of moisture in the emplacement drifts during the thermal period, with greater condensation occurring in cooler or unheated regions and lower relative humidity occurring in the heated regions. However, the potential effects are within the range of effects represented in the condensation model based on modeling of other processes, and are minor compared with the thermal-hydrological responses represented by the multiscale model. Also, the effects of natural air flow on moisture movement in the unsaturated zone are found to be small compared with the range of infiltration flux estimated for Yucca Mountain.

Based on the previous discussion, omission of FEP 2.2.10.11.0A (Natural Air Flow in the UZ) will not result in a significant adverse change in the magnitude or timing of either radiological exposure to the RMEI or radionuclide releases to the accessible environment. Therefore, this FEP is excluded from the performance assessments conducted to demonstrate compliance with proposed 10 CFR 63.311 and 63.321 (70 FR 53313 [DIRS 178394]), and with 10 CFR 63.331 [DIRS 180319], on the basis of low consequence.

INPUTS:

Table 2.2.10.11.0A-1. Direct Inputs

Input	Source	Description
BSC 2005. *Drift-Scale Coupled Process (DST and TH Seepage) Models*. [DIRS 172232]	Section 6.2.2.1.1	Base-case TH simulations that provide estimates of gas flux
DTN: MO0703PAEVSIIC.000. Evaluation of Stage II Condensation. [DIRS 181990]	Cases 1 and 4 in file *Stage 2 Analysis.xls*	These results show that gas-phase transport of moisture from the rock is weakly related to the dispersion factor (and, therefore, natural air flow) because it is limited by availability of moisture as percolation and by the mass-transfer resistance within the host rock
Martinez and Nilson 1999. "Estimates of Barometric Pumping of Moisture through Unsaturated Fractured Rock." [DIRS 174095]	p. 106	Estimated rate of water removal from Yucca Mountain through vapor transport
SNL 2007. *In-Drift Natural Convection and Condensation*. [DIRS 181648]	Sections 6.2.7, 6.2	Discussion of axial transport of water vapor in the emplacement drifts
	Section 6.2	Condensation report uses a three-dimensional thermal convection (dry air) simulation
SNL 2007. *UZ Flow Models and Submodels*. [DIRS 184614]	Table 6.1-2	Estimates for average infiltration at Yucca Mountain
SNL 2008. *Multiscale Thermohydrologic Model*. [DIRS 184433]	Section 7.8[a]	Using intermediate value of 1,000, multiscale validation test cases demonstrate axial transport lowers relative humidity in the emplacement regions, and delays return of humidity by hundreds of years as waste packages cool
	Section 6.3.18[a]	Three-dimensional thermal-hydrologic simulations was performed to evaluate the effects from axial transport

Table 2.2.10.11.0A-2. Indirect Inputs

Citation	Title	DIRS
10 CFR 63	Energy: Disposal of High-Level Radioactive Wastes in a Geologic Repository at Yucca Mountain, Nevada	180319
70 FR 53313	Implementation of a Dose Standard After 10,000 Years	178394
SNL 2007	*Drift-Scale THC Seepage Model*	177404
SNL 2007	*Engineered Barrier System: Physical and Chemical Environment*	177412
SNL 2007	*In-Drift Natural Convection and Condensation*	181648
SNL 2008	*Multiscale Thermohydrologic Model*	184433
Tsang and Pruess 1990	*Further Modeling Studies of Gas Movement and Moisture Migration at Yucca Mountain, Nevada*	172018

FEP: 2.2.10.12.0A

FEP NAME:

Geosphere Dry-Out Due to Waste Heat

FEP DESCRIPTION:

Repository heat evaporates water from the UZ rocks near the drifts as the temperature exceeds the vaporization temperature. This zone of reduced water content (reduced saturation) migrates outward during the heating phase (about the first 1000 years) and then migrates back to the waste packages as heat diffuses throughout the mountain and the radioactive sources decay. This FEP addresses the effects of dry-out within the rocks.

SCREENING DECISION:

Included

TSPA DISPOSITION:

Multiscale Thermohydrologic Model (SNL 2008 [DIRS 184433], Section 6.3[a]) provides histories for thermal-hydrologic conditions at key locations within the drifts. The multiscale model simulates dryout of the rock around the drift, and therefore includes its effect on in-drift thermal-hydrologic parameters used in performance assessment, such as temperature and relative humidity at the drift wall, drip shield, and waste package surface; the duration of drift wall boiling; and the temperature and liquid saturation in the invert. Following closure, dryout occurs in an expanding region in the rock around each drift where the rock temperatures exceed the boiling point of water; dryout is associated with higher temperatures and lower relative humidities within the emplacement drifts. Rewetting of the host rock occurs as the waste heat output decays and the rock temperature cools back toward the boiling point. The rate of rewetting at a particular location depends on the local temperature and percolation flux. Uncertainty associated with the timing and extent of dryout is propagated to TSPA calculations through the use of different rock thermal conductivities and a suite of percolation flux values (SNL 2008 [DIRS 184433], Sections 6.3.15[a] and 6.3.16[a]). Other sources of uncertainty that could affect the development and extent of the dryout zone, including rock hydrologic properties, ventilation heat removal efficiency, and the effects of axial vapor transport, were evaluated using sensitivity analyses and found to have an insignificant effect on multiscale model outputs (SNL 2008 [DIRS 184433], Sections 6.3.11[a], 6.3.12, and 6.3.18[a]).

The coupled processes of vaporization, dryout, and resaturation are simulated with the TH seepage model in *Drift-Scale Coupled Processes (DST and TH Seepage) Models* (BSC 2005 [DIRS 172232]). The TH seepage model assesses the impact of such coupled processes on seepage into the drift using several simulation cases (BSC 2005 [DIRS 172232], Section 6.2.4.2). Thus, the TH seepage model results (DTN: LB0301DSCPTHSM.002 [DIRS 163689]) include these effects. *Abstraction of Drift Seepage* (SNL 2007 [DIRS 181244]) utilizes these modeling results to develop an appropriate seepage abstraction methodology for use in the TSPA. An important feature of the seepage abstraction is that seepage does not occur when the drift wall

temperature exceeds 100°C, a bounding approximation that is consistent with the TH seepage conceptual model results (SNL 2007 [DIRS 181244], Section 6.5.2).

Uncertainty associated with the effect of the dryout zone on seepage was evaluated using sensitivity analyses varying the percolation flux, different fracture flow conceptual models, alternative thermal loads, and transient versus steady state flow conditions (BSC 2005 [DIRS 172232], Section 6.2.4.2). The results of these calculations support the conclusion that seepage will not occur until the drift wall cools below 100°C and the dryout zone no longer exists.

The coupled processes of vaporization, dryout, and resaturation are also simulated with the THC seepage model (SNL 2007 [DIRS 177404], Sections 6.2.1 and 6.5.5.1). These simulations are used to corroborate the near-field chemistry model (SNL 2007 [DIRS 177412], Section 7.1.3), which provides the composition of potential seepage waters. In the near-field chemistry model, the effect of dryout is implemented by adjusting the length of the flow pathway considered for water–rock interactions; however, the seepage compositions that are predicted during the boiling period are not used, because the abstraction of drift seepage does not predict seepage when the drift-wall temperature exceeds the boiling point.

Finally, the effects of dryout on larger-scale flow processes in the unsaturated zone are discussed in FEP 2.2.10.01.0A (Repository-Induced Thermal Effects on Flow in the UZ), which is excluded on the basis of low consequence.

INPUTS:

Table 2.2.10.12.0A-1. Indirect Inputs

Citation	Title	DIRS
BSC 2005	*Drift-Scale Coupled Process (DST and TH Seepage) Models*	172232
DTN: LB0301DSCPTHSM.002	Drift-Scale Coupled Process Model for Thermohydrologic Seepage: Data Summary	163689
SNL 2007	*Abstraction of Drift Seepage*	181244
SNL 2007	*Drift-Scale THC Seepage Model*	177404
SNL 2007	*Engineered Barrier System: Physical and Chemical Environment*	177412
SNL 2008	*Multiscale Thermohydrologic Model*	184433

FEP: 2.2.10.13.0A

FEP NAME:

Repository-Induced Thermal Effects on Flow in the SZ

FEP DESCRIPTION:

Thermal effects in the geosphere could affect the long-term performance of the disposal system, including effects on groundwater flow (e.g., density-driven flow), mechanical properties, and chemical effects in the SZ.

SCREENING DECISION:

Excluded – low consequence

SCREENING JUSTIFICATION:

Numerical modeling of the mountain-scale effects of thermal loading on the host rock due to waste emplacement is evaluated in *Mountain-Scale Coupled Processes (TH/THC/THM) Models* (BSC 2005 [DIRS 174101], Section 6.5), and results indicate that the host rock temperatures at the drift wall are about 100°C approximately 1,000 years after waste emplacement (BSC 2005 [DIRS 174101], Figure 6.5.10-2). These elevated temperatures produce a long-term heat pulse that originates at the repository and propagates outwards. A review of *Multiscale Thermohydrologic Model* (SNL 2008 [DIRS 184433]) indicates that temperature at the water table will peak at approximately 6,000 years after repository closure, with the maximum temperature equal to 73°C and an average of the maximum at each of the 560 locations modeled of 63°C (as extracted from the 560 *.*wt* files in DTN: LL0702PA013MST.068 [DIRS 180553], subfolder /SDT/SDT-01/SDT55). This represents an approximate 33°C increase in comparison with the ambient temperature of 30°C to 34°C specified at the water table beneath the repository (Fridrich et al. 1994 [DIRS 100575], Figure 8). Furthermore, saturated zone ambient temperatures increase with depth, with some temperatures as high as 45°C (depths of up to 1,000 m measured in well UE 25p#1; DTN: MO0102DQRBTEMP.001 [DIRS 154733]). Any changes in mechanical or chemical properties of the saturated zone due to repository heating are comparable to those due to ambient variability in temperature.

Heating of the water table from above will have the effect of decreasing fluid viscosity and density. For a given formation permeability, a decrease in kinematic viscosity (dynamic viscosity divided by density) will result in a corresponding increase in specific discharge. For example, if the specific discharge is 0.30 m/yr at 30°C, it will be 0.51 m/yr at 60°C due to the decrease in kinematic viscosity with temperature (Lide 2006 [DIRS 178081], p. 6-2). The peak temperature at the water table is uncertain and will depend, in part, on water-table elevation. However, even if the saturated zone temperature was to reach the theoretical upper bound of 96°C (vaporization point), the specific discharge would be 0.78 m/yr, a factor of 2.6 increase. This is still well within the factor of 8.93 (log-10-transformed value of 0.951) that is the upper limit of the uncertainty distribution for the specific discharge multiplier in the flow and transport model abstraction (SNL 2008 [DIRS 183750], Table 6-7[a]). Hence, repository-induced thermal effects on flow in the saturated zone are excluded due to low consequence because any such

effects are well within the uncertainty bounds provided by the flow and transport abstraction modeling.

Increased temperatures in the unsaturated zone can cause some changes in groundwater chemistry; however, recharge from the unsaturated zone to the SZ flow model domain constitutes a small fraction of the entire groundwater budget of the site-scale flow system (SNL 2007 [DIRS 177391], Section 6.4.3.9). Relative to the total water budget in the saturated zone flow domain, the distributed recharge (infiltration) to the saturated zone is approximately 10% of total flow through the model (SNL 2007 [DIRS 177391], Section 6.4.3.9), most of which is through the lateral boundaries. Therefore, thermally induced changes in saturated zone water chemistry would be diluted, given the relatively small volume of unsaturated zone water that is contributing to total volume of water that passes through the saturated zone flow system. Sorption is a temperature-dependent process, and an increase in groundwater temperatures could increase the sorption coefficient of cations and decrease the sorption of anions, but overall for temperatures below 80°C, corrections would be small (SNL 2007 [DIRS 177396], Appendix I). In the saturated zone models, radionuclide partitioning coefficients are based on ambient saturated zone temperatures and are not temperature dependent. Overall, including the effects of elevated saturated zone groundwater temperatures would introduce much less variability than is already included in the range of distribution coefficients used to model sorption.

This FEP is linked to excluded FEP 2.2.10.02.0A (Thermal Convection Cell Develops in SZ), which describes the low-consequence effects of temperature-induced density changes in the saturated zone groundwater and the resultant low-consequence effects of density-driven convection in the saturated zone.

The low-consequence effects of repository-induced thermal-mechanical stresses on the saturated zone rock characteristics are discussed in excluded FEPs 2.2.10.05.0A (Thermo-Mechanical Stresses Alter Characteristics of Rocks Above and Below the Repository), 2.2.10.04.0B (Thermo-Mechanical Stresses Alter Characteristics of Faults Near Repository), and 2.2.10.04.0A (Thermo-Mechanical Stresses Alter Characteristics of Fractures Near Repository).

Based on the previous discussion, omission of FEP 2.2.10.13.0A (Repository-Induced Thermal Effects on Flow in the SZ) will not result in a significant adverse change in the magnitude or timing of either radiological exposure to the RMEI or radionuclide releases to the accessible environment. Therefore, this FEP is excluded from the performance assessments conducted to demonstrate compliance with proposed 10 CFR 63.311 and 63.321 (70 FR 53313 [DIRS 178394]), and with 10 CFR 63.331 [DIRS 180319], on the basis of low consequence.

INPUTS:

Table 2.2.10.13.0A-1. Direct Inputs

Input	Source	Description
DTN: LL0702PA013MST.068. Input and Output Files for the SMT, SDT and DDT Submodels and MSTHAC Extract Output Files Used in ANL-EBS-MD-000049 Multiscale Thermohydrologic Model. [DIRS 180553]	560 *.wt files in subfolder /SDT/SDT-01/SDT5	Temperature will peak at approximately 6,000 years at the water table
DTN: MO0102DQRBTEMP.001. Temperature Data Collected from Boreholes Near Yucca Mountain in Early 1980's. [DIRS 154733]	S01035_001	Saturated zone vertical temperature gradient and temperature at the water table
DTN: LB991201233129.001. The Mountain-Scale Thermal-Hydrologic Model Simulations for AMR U0105, "Mountain-Scale Coupled Processes (TH) Models". [DIRS 146894]	file: *incon_thm_s32.dat*	Ambient water table temperature beneath the repository
Lide 2006. *CRC Handbook of Chemistry and Physics*. [DIRS 178081]	p. 6-2	Water tables (density and viscosity)
SNL 2007. *Saturated Zone Site-Scale Flow Model*. [DIRS 177391]	Section 6.4.3.9	The distributed recharge from the unsaturated zone to the saturated zone is approximately 10% of total

Table 2.2.10.13.0A-2. Indirect Inputs

Citation	Title	DIRS
10 CFR 63	Energy: Disposal of High-Level Radioactive Wastes in a Geologic Repository at Yucca Mountain, Nevada	180319
70 FR 53313	Implementation of a Dose Standard After 10,000 Years	178394
BSC 2005	*Mountain-Scale Coupled Processes (TH/THC/THM) Models*	174101
Fridrich et al. 1994	"Hydrogeologic Analysis of the Saturated-Zone Ground-Water System, Under Yucca Mountain, Nevada"	100575
SNL 2007	*Saturated Zone Site-Scale Flow Model*	177391
SNL 2007	*Radionuclide Transport Models Under Ambient Conditions*	177396
SNL 2008	*Multiscale Thermohydrologic Model*	184433

FEP: 2.2.10.14.0A

FEP NAME:

Mineralogic Dehydration Reactions

FEP DESCRIPTION:

Mineralogic dehydration reactions release water affecting hydrologic conditions. Dehydration of zeolites below the repository may lead to large-scale volume changes affecting flow and/or drift stability.

SCREENING DECISION:

Excluded – low consequence

SCREENING JUSTIFICATION:

The most common hydrous minerals and noncrystalline phases at Yucca Mountain are zeolites (predominantly clinoptilolite and mordenite), clays (predominantly smectite and illite), and volcanic glass (CRWMS M&O 2000 [DIRS 138960], Sections 1.4, 6.3.2, and 6.3.3). These phases are present both above and below the planned repository horizon (CRWMS M&O 2000 [DIRS 138960], Figures 12, 13, 20, 21, 22, and 23). The units of the repository horizon contain small quantities of zeolites (less than 0.10 wt %) and clay (less than 2.8 wt %) (DTN: LB0101DSTTHCR1.002 [DIRS 161277], file: *ecrb_cdtt_mindata.xls*, entries for Tsw 33 through Tsw 36). Dehydration of these small quantities is not expected to affect repository performance. Clays generally are of low abundance (CRWMS M&O 2000 [DIRS 138960], Section 6.3.3), and therefore are of little concern for dehydration reactions. Zeolites, principally clinoptilolite, are the minerals of greatest concern for dehydration reactions because they are widespread and abundant, especially below the planned repository. Volcanic glass is not a concern because it contains much less water compared to clinoptilolite and releases most of its water at much higher temperatures (Carey and Bish 1996 [DIRS 105200], p. 954; Vaniman et al. 1993 [DIRS 184332], p. 22,316, Table 3).

There is a prominent zone of zeolite-bearing tuffs in the lowermost Topopah Spring welded unit (tsw39) and in the underlying Calico Hills nonwelded unit (ch1, ch2, ch3, ch4, ch5, and ch6) (BSC 2004 [DIRS 169855], Section 5.2). The locations of these units below the planned repository are shown in Figure 6.1-2 of *Mountain-Scale Coupled Processes (TH/THC/THM) Models* (BSC 2005 [DIRS 174101]). Dehydration of zeolites below the repository would occur as zeolite water content decreases in response to any increase in temperature (Carey and Bish 1996 [DIRS 105200], p. 961). Such dehydration reactions could affect geohydrologic conditions in two ways: by release of water of hydration and by the resulting shrinkage of the zeolites. A mineralogic phase change from clinoptilolite, the most abundant zeolite, to analcime at temperatures above 85°C, could also occur, with greater shrinkage (Smyth and Caporuscio 1981 [DIRS 174060], pp. 11 and 12). Shrinkage could lead to formation of new rock fractures or expansion of existing fractures. Heating experiments (Bish 1984 [DIRS 104941], pp. 444, 449, and 451; 1990 [DIRS 183078], p. 773) suggest that long-term heating up to 100°C should not cause irreversible shrinkage of the clinoptilolite crystal lattice. However, the volumetric changes

in zeolitic rock due to dehydration and rehydration may not be fully reversible (Smyth and Caporuscio 1981 [DIRS 174060], pp. 25 and 26; Kranz et al. 1989 [DIRS 183167], p. 1,114).

Heating of the zeolitic tuffs below the repository could cause the zeolites to release water to the rock pores, especially if substantial rock dryout were to occur. Shrinkage of the zeolite crystal lattices due to heating and dehydration could change the rock porosity and permeability. Bulk shrinkage of the zeolitic tuff also could affect thermo-mechanical stresses in the zeolite-bearing tuffs and in the overlying repository host rock.

The amount of water held within zeolites in altered tuffs below the repository was estimated for a zeolitic tuff with bulk density of 1.57×10^3 kg/m^3 (DTN: GS960908312231.004 [DIRS 107065], Table S98219_002, Hydrologic Model Layer CHZ), mean porosity of 0.322, and 0.96 saturation (DTN: LB0207REVUZPRP.002 [DIRS 159672], file: *hydroprops_fin.xls*, worksheet: "summary," UZ model layer "ch[2-5]z"). One cubic meter of tuff contains 0.322 m^3 × 0.96 = 0.309 m^3 of pore water. If this tuff contains 60 wt % clinoptilolite with about 15 wt % intracrystalline water (Carey and Bish 1996 [DIRS 105200], p. 954), then the amount of water within the zeolite is about $1.57 \times 10^3 \times 0.60 \times 0.15 = 141$ kg or 0.141 m^3 of water per cubic meter of rock (assuming unit density of water). The water contained in zeolite is, thus, slightly less than one-half the amount of water in rock pores.

Dehydration of zeolitic tuff in response to predicted repository thermal-loading conditions has not been investigated, and the amount of zeolite dehydration as a function of temperature and pore-water saturation is not known. However, experimental data exist that allow bounds to be placed on the effects of dehydration. Experimental results suggest that loss of adsorbed zeolitic water increases in a linear manner with rising temperature up to the boiling point for clinoptilolite separates (Carey and Bish 1996 [DIRS 105200], Figure 10). Exploratory dehydration of saturated and unsaturated zeolitic tuffs with isothermal and step-wise heating was conducted without control or measurement of water-vapor pressure or initial water content (Smyth and Caporuscio 1981 [DIRS 174060], Appendices A and B). An approximate interpretation of the results is that rock weight loss upon heating reflects the progressive loss of a combination of rock-pore and zeolitic water. Pore water is more readily lost than zeolitic water. The composite rates of water loss from these two reservoirs show no large discontinuities with time for isothermal heating or with temperature for heating to 200°C (Smyth and Caporuscio [DIRS 174060], Figures A-1 and B-1). The zeolitic water behaves sufficiently like pore water that it would not need to be considered separately unless the rock were heated enough to cause a major decrease in pore-water saturation.

Results of the mountain-scale thermal-hydrologic model (BSC 2005 [DIRS 174101], Section 6.2.1.3, Figure 6.2-7c) indicate that matrix liquid saturation in zeolitic tuff at the base of the Topopah Spring welded unit (TSw) will remain between about 0.94 and 1.00 (full saturation) throughout the period of thermal perturbation. Peak temperatures at the base of TSw where the tuffs are zeolitized (northern part of Yucca Mountain) will remain below 75°C (BSC 2005 [DIRS 174101], Section 6.2.1.3, Figure 6.2-6c). The mountain-scale thermal-hydrologic model does not incorporate zeolite dehydration as a distinct process, but the potential effects are approximated by the incorporation of thermal and hydrologic property values (thermal conductivity, particle density, specific heat capacity, residual saturation) specific to zeolitic tuffs (BSC 2005 [DIRS 174101], Table 4.1-1; DTNs: LB0208UZDSCPMI.002 [DIRS 161243] and

LB0210THRMLPRP.001 [DIRS 160799]). Given that the matrix pores are near or at full saturation, and that pore water represents more than half the water in the tuff, the prediction of the mountain-scale thermal-hydrologic model still should be reasonably accurate. Zeolite dehydration is not expected to contribute significant additional water to the unsaturated-zone flow system.

Shrinkage of zeolitic tuffs from the combined effects of dehydration and heating has been investigated by laboratory experiments (Smyth and Caporuscio 1981 [DIRS 174060]; Kranz et al. 1989 [DIRS 183167]; and Bish et al. 2003 [DIRS 169638]). One study (Bish et al. 2003 [DIRS 169638]) provides shrinkage data for powdered clinoptilolite separates, and two studies (Smyth and Caporuscio 1981 [DIRS 174060], Appendices A and B; Kranz et al. 1989 [DIRS 183167]) provide data for intact zeolitic-tuff core. In all cases, the experimental conditions exceed the degree of dehydration or maximum temperatures predicted by the mountain-scale thermal-hydrologic model for zeolitic tuff below the repository. Therefore, tuff-shrinkage calculations based on the experimental results, presented below, place bounds on the effects of zeolite shrinkage if greater dehydration or higher temperatures than expected were to occur.

The powdered separate of a natural mixed-cation clinoptilolite from Yucca Mountain was equilibrated at 100% relative humidity and 23°C, then heated in the humid atmosphere (Bish et al. 2003 [DIRS 169638], p. 1,899). Volumetric shrinkage of the crystal lattice was measured in cubic angstroms ($Å^3$) at fifty-degree temperature increments, beginning at 50°C (Bish et al. 2003 [DIRS 169638], Figure 12, sample USW G-4 450.5). Approximate cumulative shrinkage values of $100(2{,}098Å^3 - 20{,}68Å^3)/2{,}098Å^3 = 1.43$ vol % at 50°C and $100(2{,}098Å^3 - 2{,}063Å^3)/2{,}098Å^3 = 1.67$ vol % at 100°C bound the zeolite crystal lattice shrinkage expected under conditions predicted by the mountain-scale thermal-hydrologic model.

The amount of rock shrinkage due to zeolite dehydration was estimated by considering the data from two experiments presented by Smyth and Caporuscio (1981 [DIRS 174060], Tables A-1 and B-1, sample YM-40), which record the volume and weight changes observed upon heating for two cylindrical rock samples from the zeolitized Calico Hills Formation. For the first experiment, the tuff was soaked in water at 91°C for 48 hours and then kept at approximately 95°C in a drying oven. The core was weighed and measured at the beginning of the experiment and periodically throughout the 32-hour dry-heating period. During the first hour of the heating period, the core expanded from its initial volume, possibly due to additional movement of water into the zeolite crystal lattice. Total volumetric shrinkage of the drying core, relative to the largest measured volume, amounted to $100(10.2814\ cm^3 - 10.1526\ cm^3)/10.2814\ cm^3 = 1.25$ vol %. However, the amount of water lost during the one-hour step between the highest measured volume (hour 1) and the next measurement (hour 2), relative to the total water lost during heating, was $100(19.7703\ g - 18.5134\ g)/(19.7703\ g - 17.9906\ g) = 70.6$ wt %. This step alone represents a greater drop in liquid saturation than that predicted by the mountain-scale thermal-hydrologic model (BSC 2005 [DIRS 174101], Section 6.2.1.3, Figure 6.2-7c). Therefore, the portion of core shrinkage associated with this step, $(10.2814\ cm^3 - 10.2028\ cm^3)/10.2814\ cm^3 = 0.76$ vol %, is a better bound on the amount of shrinkage that would occur under predicted repository conditions.

For the second experiment, air-dried zeolitic tuff was heated from 25°C to 500°C stepwise in increments of 75°C (first step) and 100°C (subsequent steps) (Smyth and Caporuscio 1981 [DIRS 174060], Table B-I, sample YM-40). The rock cylinder was initially equilibrated to room temperature and humidity, an indication that both the zeolites and the rock pores were under-saturated in water. This experiment thus under-represents the amount of water loss and shrinkage that could occur in nearly saturated zeolitic rocks below the repository. Therefore, the results of this experiment were not considered in evaluating the potential effects of zeolite dehydration.

In another experiment, a core of zeolitic tuff from the Calico Hills nonwelded unit was vacuum dehydrated and allowed to rehydrate at room temperature for 160 hours (Kranz et al. 1989 [DIRS 183167], p. 1,114). The cited reference does not provide data to calculate the volume change upon dehydration, but an approximate volume change during rehydration was estimated from the experimental procedure (Kranz et al. 1989 [DIRS 183167], p. 1,113) and Figure 2 of the cited paper (Kranz et al. 1989 [DIRS 183167]; note that Figures 1 and 2 are reversed with respect to their captions). Initial cylindrical core dimensions of 6.0 cm length and 2.54 cm diameter give a core volume of $\pi(2.54\ \text{cm}/2)^2 \times 6.0\ \text{cm} = 30.402\ \text{cm}^3$. From the final axial and radial expansive strains shown in Figure 2 of the cited paper, the calculated volume of the hydrated core would be $\pi[(2.54\ \text{cm}/2) + (2.54\ \text{cm}/2)(0.00196\ \text{cm})]^2 \times [6.0\ \text{cm} + (6.0\ \text{cm} \times 0.00226\ \text{cm})] = 30.591\ \text{cm}^3$. The volume increase upon hydration is $100(30.591\ \text{cm}^3 - 30.402\ \text{cm}^3)/(30.402\ \text{cm}^3) = 0.6$ vol %.

The 1.67 vol % shrinkage experienced by powdered clinoptilolite upon heating to 100°C under 100% relative humidity is a reasonable value for the maximum zeolite shrinkage that could occur under predicted repository heating conditions. However, the experimental data for cores of clinoptilolite-bearing tuff indicate that less shrinkage would occur in intact rock. The core shrinkage of 0.76 vol % upon heating is taken as a maximum value for rock shrinkage because it was observed under conditions of dehydration greater than predicted for the Calico Hills nonwelded unit. The core expansion of 0.6 vol % upon rehydration in another experiment is confirmatory and may be lower due to an irreversible component of shrinkage.

The potential effects of zeolite shrinkage on flow depend on how the shrinkage is accommodated by the zeolitic tuff. Physical changes in zeolitic tuff due to alternate wetting/drying cycles have been investigated for building stone (Colella et al. 2001 [DIRS 184454], p. 573, Figure 24). The weathering environment to which zeolitic building stone is subjected is much harsher than the expected conditions below the repository because the building blocks experience repeated wetting and drying that not only cause swelling and shrinkage but also result in salt deposition due to water evaporation. These processes lead to the possible formation of microcracks. A scanning-electron image of such a weathered zeolitic tuff shows microcracks with apertures of about one to two micrometers (Colella et al. 2001 [DIRS 184454], Figure 24). The microcracks formed largely along pre-existing intercrystalline pore spaces, without grain breakage.

Accommodation of zeolite shrinkage by aperture changes in scattered microcracks that largely correspond to preexisting porosity would be equivalent to a less than one percent change in matrix porosity. In the absence of strong preferred orientation of rock pores or microcracks, this process should not result in the formation of new throughgoing fractures. The apertures of preexisting fractures would be affected only by a subset of immediately adjacent microcracks. The overall effect of a less-than-one-percent change in matrix porosity is well within the range of

variability for matrix porosity in the affected units (DTN: LB0207REVUZPRP.002 [DIRS 159672], file: *hydroprops_fin.xls*, worksheet: "summary," UZ model layer "ch[2-5]z"). The permeability change associated with this small change in porosity also should be within the range of variability.

The potential effects of zeolite dehydration in rock below the repository on drift stability have not been explicitly investigated. However, this effect is implicitly addressed in excluded FEP 2.1.07.02.0A (Drift Collapse), which provides a summary of nonseismic processes affecting drift stability. *Drift Degradation Analysis* (BSC 2004 [DIRS 166107], Section 5.1.3) states an assumption that thermal expansion values used in the CHn1 and CHn2 (Calico Hills nonwelded unit) layers under the repository units (TSw2) are equal to those for the repository layers, which are densely welded and devitrified rather than nonwelded and zeolitic. The report states that temperature increase in the underlying layers is insignificant and thermally induced stresses are negligible. The cited discussion pertains to thermal expansion rather than contraction, but it verifies that other processes of volumetric change in the Calico Hills nonwelded unit are not part of the analysis.

As described above, the selected upper bounding value for volume reduction of initially saturated zeolitic tuff heated in air at 95°C was 0.76 vol % (Smyth and Caporuscio 1981 [DIRS 174060], Table A-1, sample YM-38). Actual rock shrinkage at Yucca Mountain should be less than that because predicted saturation will remain higher and temperatures will be lower than the experimental conditions. In addition, not all shrinkage will occur in a vertical direction, and this will reduce the potential effect on overlying rock. The combination of these factors should lead to insignificant or no subsidence of the rock containing the repository emplacement drifts.

Based on the previous discussion, omission of FEP 2.2.10.14.0A (Mineralogic Dehydration Reactions) will not result in a significant adverse change in the magnitude or timing of either radiological exposure to the RMEI or radionuclide releases to the accessible environment. Therefore, this FEP is excluded from the performance assessments conducted to demonstrate compliance with proposed 10 CFR 63.311 and 63.321 (70 FR 53313 [DIRS 178394]), and with 10 CFR 63.331 [DIRS 180319], on the basis of low consequence.

INPUTS:

Table 2.2.10.14.0A-1. Direct Inputs

Input	Source	Description
BSC 2005. *Mountain-Scale Coupled Processes (TH/THC/THM) Models*. [DIRS 174101]	Section 6.2.1.3, Figure 6.2-7c	Zeolitic tuff at the base of TSw will remain at close to full matrix liquid saturation (between 0.94 and 1.00) throughout the period of thermal perturbation
	Section 6.2.1.3, Figure 6.2-6c	Peak temperatures at the base of TSw where the tuffs are zeolitized (northern part of Yucca Mountain) will remain below 75°C
Colella et al. 2001. "Use of Zeolitic Tuff in the Building Industry." [DIRS 184454]	Figure 24	The SEM image of zeolitic tuff shows microcracks with apertures of about one to two micrometers

Table 2.2.10.14.0A-1. Direct Inputs (Continued)

Input	Source	Description
Smyth and Caporuscio 1981. *Review of the Thermal Stability and Cation Exchange Properties of the Zeolite Minerals Clinoptilolite, Mordenite, and Analcime: Applications to Radioactive Waste Isolation in Silicic Tuff*. [DIRS 174060]	Table A-1 (sample YM-38)	Upper bounding value for volume reduction of initially saturated zeolitic tuff under experimental heating conditions
	Tables A-1 and B-1 (sample YM-40)	Dehydration and shrinkage of zeolitic tuff under experimental heating conditions
	Table A-1 (sample YM-38)	Upper bounding value for volume reduction of initially saturated zeolitic tuff under experimental heating conditions
	Tables A-1 and B-1 (sample YM-40)	Dehydration and shrinkage of zeolitic tuff under experimental heating conditions

Table 2.2.10.14.0A-2. Indirect Inputs

Citation	Title	DIRS
10 CFR 63	Energy: Disposal of High-Level Radioactive Wastes in a Geologic Repository at Yucca Mountain, Nevada	180319
70 FR 53313	Implementation of a Dose Standard After 10,000 Years	178394
Bish 1984	"Effects of Exchangeable Cation Composition on the Thermal Expansion/Contraction of Clinoptilolite"	104941
Bish 1990	"Long-Term Thermal Stability of Clinoptilolite: The Development of a "B" Phase"	183078
Bish et al. 2003	"The Distribution of Zeolites and their Effects on the Performance of a Nuclear Waste Repository at Yucca Mountain, Nevada, U.S.A."	169638
BSC 2004	*Development of Numerical Grids for UZ Flow and Transport Modeling*	169855
BSC 2004	*Drift Degradation Analysis*	166107
BSC 2005	*Mountain-Scale Coupled Processes (TH/THC/THM) Models*	174101
Carey and Bish 1996	"Equilibrium in the Clinoptilolite-H_2O System"	105200
Colella et al. 2001	"Use of Zeolitic Tuff in the Building Industry"	184454
CRWMS M&O 2000	*Mineralogical Model (MM3.0)*	138960
DTN: GS960908312231.004	Characterization of Hydrogeologic Units Using Matrix Properties at Yucca Mountain, Nevada	107065
DTN: LB0101DSTTHCR1.002	Attachment II - Mineral Initial Volume Fractions for TPTPLL THC Model for AMR N0120/U0110 REV01, "Drift-Scale Coupled Processes (Drift-Scale Test and THC Seepage) Models"	161277
DTN: LB0207REVUZPRP.002	Matrix Properties for UZ Model Layers Developed from Field and Laboratory Data	159672
DTN: LB0208UZDSCPMI.002	Drift-Scale Calibrated Property Sets: Mean Infiltration Data Summary	161243
DTN: LB0210THRMLPRP.001	Thermal Properties of UZ Model Layers: Data Summary	160799
Kranz et al. 1989	"Hydration and Dehydration of Zeolitic Tuff from Yucca Mountain, Nevada"	183167
Smyth and Caporuscio 1981	*Review of the Thermal Stability and Cation Exchange Properties of the Zeolite Minerals Clinoptilolite, Mordenite, and Analcime: Applications to Radioactive Waste Isolation in Silicic Tuff*	174060
Vaniman et al. 1993	"Dehydration and Rehydration of a Tuff Vitrophyre"	184332

FEP: 2.2.11.01.0A

FEP NAME:

Gas Effects in the SZ

FEP DESCRIPTION:

Pressure variations due to gas generation may affect flow patterns and contaminant transport in the SZ. Degassing could affect flow and transport of gaseous contaminants. Potential gas sources include degradation of repository components and naturally occurring gases from clathrates, microbial degradation of organic material, or deep gases in general.

SCREENING DECISION:

Excluded – low consequence

SCREENING JUSTIFICATION:

The justification for exclusion is developed with respect to the low consequence effects of naturally occurring gases.

There is no evidence of large-scale gas build-up in or flow through the saturated zone. Additionally, no significant volumes of oil or gas have been found in the Yucca Mountain vicinity, and there are no proven source rocks in the region (French 2000 [DIRS 107425], p. 5). While the geologic elements required for a petroleum system are present in the Yucca Mountain region, stratigraphic seals (important in a viable hydrocarbon producing region) are not well developed in the Yucca Mountain area, causing the hydrocarbon potential to be classified as low (French 2000 [DIRS 107425], p. 39).

The presence of clathrates and microbial degradation of organic components are two potential sources of gas that could affect flow and transport in the saturated zone. Clathrates, methane gas molecules bound in a cage-like structure made up of water molecules, form under high pressures and low temperatures. Clathrates are found in polar and deep oceanic regions (Kvenvolden 1998 [DIRS 166162], pp. 9 to 11) and are, therefore, not a potential hydrocarbon source in the Yucca Mountain vicinity.

Microbial degradation of organic components is not considered a potential gas source in the saturated zone. Analysis of groundwater samples taken from saturated zone wells near Yucca Mountain have found little to no organic carbon (DTN: GS010308312322.003 [DIRS 154734], Table S01053_003; DTN: GS011108312322.006 [DIRS 162911]). Organic carbon is a byproduct of microbial activity. Because there is little organic carbon found in saturated zone waters, there is little microbial activity and, thus, it is not expected that sufficient CO_2 could be produced to affect saturated zone flow and transport.

In the unexpected event that natural gas-generating processes occur in the sedimentary rocks below the tuffs, the influence on the flow and transport pathways would tend to be highly localized. Moreover, such influences are too small to make a significant impact on flow fields

and such perturbations are accounted for in the heterogeneity and parameter uncertainties in *Saturated Zone Flow and Transport Model Abstraction* (SNL 2008 [DIRS 183750], Table 6-7[a]). Because gas-generating processes in the saturated zone do not have a significant effect on system parameters, there is negligible impact on radionuclide release to the accessible environment. In summary, the potential effects of naturally occurring gases in the geosphere can be excluded from the SZ flow and transport model on the basis of low consequence.

Degradation of repository components is a potential gas source for the saturated zone. Corrosion of EBS metal materials would mainly occur well beyond 10,000 years after repository closure and this would produce gas that might escape into the unsaturated zone. This process is considered by FEP 2.2.11.02.0A (Gas Effects in the UZ). However, gas pressurization in the unsaturated zone is not expected due to the presence of permeable fracture pathways that allow gas to flow away from its source and prevent formation of high-pressure gas pockets. Thus, if significant gas pressurization in the unsaturated zone due to the degradation of the waste is not expected, then it can be reasoned that such pressurization will also be unexpected in the saturated zone, where the water table is approximately 330 m below the repository sources of gas (DTN: SN0704T0510106.008 [DIRS 181283], file: *sz06_1302sur_10002.txt*; SNL 2007 [DIRS 179466]). In summary, degradation of repository components that would potentially produce gas will not affect flow and transport in the saturated zone.

Based on the previous discussion, omission of FEP 2.2.11.01.0A (Gas Effects in the SZ) will not result in a significant adverse change in the magnitude or timing of either radiological exposures to the RMEI or radionuclide releases to the accessible environment. Therefore, this FEP is excluded from the performance assessments conducted to demonstrate compliance with proposed 10 CFR 63.311 and 63.321 (70 FR 53313 [DIRS 178394]), and with 10 CFR 63.331 [DIRS 180319], on the basis of low consequence.

INPUTS:

Table 2.2.11.01.0A-1. Direct Inputs

Input	Source	Description
DTN: GS010308312322.003. Field, Chemical and Isotopic Data from Wells in Yucca Mountain Area, Nye County, Nevada, Collected Between 12/11/98 and 11/15/99. [DIRS 154734]	Table S01053_003	Analysis of groundwater samples taken from saturated zone wells near Yucca Mountain have found little to no organic carbon

Table 2.2.11.01.0A-2. Indirect Inputs

Citation	Title	DIRS
10 CFR 63	Energy: Disposal of High-Level Radioactive Wastes in a Geologic Repository at Yucca Mountain, Nevada	180319
70 FR 53313	Implementation of a Dose Standard After 10,000 Years	178394
DTN: GS011108312322.006	Field and Chemical Data Collected between 1/20/00 and 4/24/01 and Isotopic Data Collected between 12/11/98 and 11/6/00 from Wells in the Yucca Mountain Area, Nye County, Nevada	162911
DTN: SN0704T0510106.008	Flux, Head and Particle Track Output from the Qualified, Calibrated Saturated Zone (SZ) Site-Scale Flow Model	181283
French 2000	*Hydrocarbon Assessment of the Yucca Mountain Vicinity, Nye County, Nevada*	107425
Kvenvolden 1998	"A Primer on the Geological Occurrence of Gas Hydrate"	166162
SNL 2007	*Total System Performance Assessment Data Input Package for Requirements Analysis for Subsurface Facilities*	179466
SNL 2008	*Saturated Zone Flow and Transport Model Abstraction*	183750

FEP: 2.2.11.02.0A

FEP NAME:

Gas Effects in the UZ

FEP DESCRIPTION:

Pressure variations due to gas generation may affect flow patterns and contaminant transport in the UZ or may intrude into the repository. Degassing could affect flow and transport of gaseous contaminants. Gases could also affect other contaminants if water flow is driven by large gas bubbles forming in the repository. Potential gas sources include degradation of repository components and naturally occurring gases from clathrates, microbial degradation of organic material, or deep gases in general.

SCREENING DECISION:

Excluded – low consequence

SCREENING JUSTIFICATION:

In the Yucca Mountain unsaturated zone, the build-up of any significant gas pressure is expected to be of low consequence. Permeable fracture pathways would allow gas to flow away from its source, preventing the formation of high pressure gas pockets that might alter flow and transport patterns (SNL 2007 [DIRS 184614], Section 6.4). In addition, gas-phase radionuclide transport is excluded on the basis of low consequence (see excluded FEP 2.2.11.03.0A (Gas Transport in Geosphere)).

Studies have been performed to determine the potential impact of fracture sealing, caused by mineral precipitation during thermally induced processes, on pressure build-up and hydraulics. Thermal-hydrologic-chemical calculations that included gas transport and mineral precipitations during repository heating were performed, and results showed that potential sealing of fractures due to precipitation in the thermally perturbed repository environment would have a negligible effect on hydrogeologic response of the fractures (SNL 2007 [DIRS 177404], Section 8, Figure 8-1). The processes associated with this aspect of the FEP will not, therefore, significantly change radionuclide releases to the accessible environment and can be excluded on the basis of low consequence.

This FEP also addresses the possible effects of gas bubbles on the potential release of radionuclides from the repository to the accessible environment. Because the repository at Yucca Mountain is located within the unsaturated zone, gas bubbles would quickly be absorbed into the available gas phase surrounding the liquid. Therefore, bubbles could not drive substantial water flow. Thus, a bubble-release mechanism of radionuclides from the repository will be of low consequence relative to radionuclide transport to the accessible environment. This conclusion is valid regardless of the specific potential sources of gas generation (e.g., degradation of repository components over tens of thousands of years, or natural sources of gas). For more information on natural sources of gas, see excluded FEP 2.2.11.01.0A (Gas Effects in the SZ).

Based on the previous discussion, omission of FEP 2.2.11.02.0A (Gas Effects in the UZ) will not result in a significant adverse change in the magnitude or timing of either radiological exposure to the RMEI or radionuclide releases to the accessible environment. Therefore, this FEP is excluded from the performance assessments conducted to demonstrate compliance with proposed 10 CFR 63.311 and 63.321 (70 FR 53313 [DIRS 178394]), and with 10 CFR 63.331 [DIRS 180319], on the basis of low consequence.

INPUTS:

Table 2.2.11.02.0A-1. Direct Inputs

Input	Source	Description
SNL 2007. *UZ Flow Models and Submodels*. [DIRS 184614]	Section 6.4	Permeable fracture pathways would allow gas to flow away from its source, preventing the formation of high pressure gas pockets

Table 2.2.11.02.0A-2. Indirect Inputs

Citation	Title	DIRS
10 CFR 63	Energy: Disposal of High-Level Radioactive Wastes in a Geologic Repository at Yucca Mountain, Nevada	180319
70 FR 53313	Implementation of a Dose Standard After 10,000 Years	178394
SNL 2007	*Drift-Scale THC Seepage Model*	177404

FEP: 2.2.11.03.0A

FEP NAME:

Gas Transport in Geosphere

FEP DESCRIPTION:

Gas released from the drifts and gas generated in the near-field rock will flow through fracture systems in the near-field rock and in the geosphere. Certain gaseous or volatile radionuclides may be able to migrate through the far-field faster than the groundwater advection rate.

SCREENING DECISION:

Excluded – low consequence

SCREENING JUSTIFICATION:

Gas transport in the geosphere can occur either by gas-phase transport through unsaturated rock pores and fractures, or by aqueous-phase transport as dissolved gases in groundwater. Gases that are dissolved in groundwater would be transported by groundwater advection, with the rate of advection determining the rate of gas transport. Dissolved gas may exsolve from aqueous solution into the gaseous phase in unsaturated pores and fractures, and therefore become available for gas-phase migration to the accessible environment. This FEP is concerned with gas-phase transport through the geosphere, and its exclusion is based on the relatively low annual doses estimated for the gas-phase pathways compared to annual doses calculated for the aqueous-phase pathways.

The only radionuclides that would have a potential for gas transport are ^{14}C and ^{222}Rn. Although ^{129}I can exist in the gaseous phase, it is highly soluble, and therefore would be more likely to be dissolved in groundwater rather than exist as a gas. Other gas-phase isotopes have been eliminated in a screening analysis (DOE 2002 [DIRS 155970], Section I.3.3), primarily because they have short half-lives and are not decay products of long-lived isotopes. Note that for ^{14}C and ^{222}Rn, the process of inhalation is included in the biosphere model (SNL 2007 [DIRS 177399], Section 6.4.8).

Modeling of potential annual doses from gas-phase geosphere transport of ^{14}C shows that the individual maximum radiological dose is 1.8×10^{-10} mrem/yr, which corresponds to a maximum gas-phase release rate that occurs at 1,700 years following repository closure (DOE 2002 [DIRS 155970], Section I.7). This maximum annual dose from gas-phase ^{14}C releases may be compared with the maximum annual dose from aqueous releases of ^{14}C, which is calculated in TSPA to be approximately 10^{-3} mrem/yr for the early waste-package failure modeling case at 2,000 years following repository closure (SNL 2008 [DIRS 183478], Figure 8.2-6(a)). This comparison demonstrates that the predicted maximum annual dose of 1.8×10^{-10} mrem/yr for gas-phase geosphere transport of ^{14}C is insignificant relative to aqueous-phase transport.

In addition, about 2% of the ^{14}C in commercial SNF exists as a gas in the space between the fuel and the cladding (DOE 2002 [DIRS 155970], Section I.7). Even if the entire ^{14}C inventory were

released in the gas phase, the expected maximum annual dose from gas-phase geosphere transport of ^{14}C is only 9×10^{-9} mrem/yr ($50 \times 1.8 \times 10^{-10}$), which is still five orders of magnitude less than the peak annual dose from aqueous ^{14}C. Thus, the annual dose from the gas-phase release pathways is insignificant compared to the annual dose from the aqueous-phase pathways.

^{222}Rn is a decay product of the ^{238}U-decay series and would be generated for as long as any uranium remained in the repository. Based on gas flow studies, radon released from the repository in the gas phase is expected to radioactively decay before reaching the ground surface (DOE 2002 [DIRS 155970], Section I.7.3). Therefore, aqueous geosphere transport pathways will be the primary contributor to dose from ^{222}Rn, primarily through aqueous transport of uranium and generation of ^{222}Rn as a decay product in the accessible environment.

In summary, all radionuclides are transported in the aqueous phase between the repository and the accessible environment for all scenario classes except the eruptive modeling case of the igneous scenario class. The effects of gas-phase geosphere transport on radiological exposures and annual doses are insignificant relative to aqueous-phase geosphere transport.

Based on the previous discussion, omission of FEP 2.2.11.03.0A (Gas Transport in Geosphere) will not result in a significant adverse change in the magnitude or timing of either radiological exposure to the RMEI or radionuclide releases to the accessible environment. Therefore, this FEP is excluded from the performance assessments conducted to demonstrate compliance with proposed 10 CFR 63.311 and 63.321 (70 FR 53313 [DIRS 178394]), and with 10 CFR 63.331 [DIRS 180319], on the basis of low consequence.

INPUTS:

Table 2.2.11.03.0A-1. Direct Inputs

Input	Source	Description
DOE 2002. *Final Environmental Impact Statement for a Geologic Repository for the Disposal of Spent Nuclear Fuel and High-Level Radioactive Waste at Yucca Mountain, Nye County, Nevada*. [DIRS 155970]	Section I.7.3	Radon released from the repository in the gas phase is expected to radioactively decay before reaching the ground surface
	Section I.7	Modeling of potential annual doses from gas-phase geosphere transport of ^{14}C shows that the individual maximum radiological dose is 1.8×10^{-10}
SNL 2008. *Total System Performance Assessment Model /Analysis for the License Application*. [DIRS 183478]	Figure 8.2-6(a)[a]	^{14}C doses from aqueous release for early waste-package failure modeling case for 10,000 years

Table 2.2.11.03.0A-2. Indirect Inputs

Citation	Title	DIRS
10 CFR 63	Energy: Disposal of High-Level Radioactive Wastes in a Geologic Repository at Yucca Mountain, Nevada	180319
70 FR 53313	Implementation of a Dose Standard After 10,000 Years	178394
DOE 2002	*Final Environmental Impact Statement for a Geologic Repository for the Disposal of Spent Nuclear Fuel and High-Level Radioactive Waste at Yucca Mountain, Nye County, Nevada*	155970
SNL 2007	*Biosphere Model Report*	177399

FEP: 2.2.12.00.0A

FEP NAME:

Undetected Features in the UZ

FEP DESCRIPTION:

Undetected features in the UZ portion of the geosphere can affect long-term performance of the disposal system. Undetected but important features may be present, and may have significant impacts. These features include unknown active fracture zones, inhomogeneities, faults and features connecting different zones of rock, different geometries for fracture zones, and induced fractures due to the construction or presence of the repository.

SCREENING DECISION:

Excluded – low consequence

SCREENING JUSTIFICATION:

Two kinds of undetected features in the unsaturated zone are of concern: (1) features which, on the basis of previous investigations, could be potentially present, and (2) features that are totally unexpected. Features that could potentially be present on the basis of previous investigations include buried Plio-Pleistocene basaltic intrusions. As discussed in excluded FEP 1.2.04.02.0A (Igneous Activity Changes Rock Properties), the effects of small intrusions, or more generally, any heterogeneous features approximating meter scale intrusions (or smaller), are expected to have a negligible effect on flow and transport behavior in the unsaturated zone. Also, induced fractures may occur near waste emplacement drifts due to the disturbance of the rock stress field caused by the presence of the drift openings. Induced fractures are not unexpected features, and are evaluated in underground testing and included in drift seepage modeling, as discussed in included FEP 2.2.01.01.0A (Mechanical Effects of Excavation and Construction in the Near-Field).

The scenario that a major, critical feature in the vicinity of Yucca Mountain, such as a large seismogenic fault zone, has been overlooked is not expected given the extensive site characterization conducted at Yucca Mountain (BSC 2004 [DIRS 169734], p. 1-1), and falls into the second category of "totally unexpected" undetected features. Furthermore, subsequent repository development will involve the excavation of more than 170 km of waste emplacement drifts (BSC 2007 [DIRS 179640], Table 10), providing detailed geological information for the entire repository area. Actual subsurface conditions from site characterization excavations will be confirmed by mapping of these emplacement drifts and mains (BSC 2004 [DIRS 172452], p. 3-10). Any previously undetected features will be reported and evaluated with respect to performance assessment results (BSC 2004 [DIRS 172452], p. 2-16 and Section 4.3).

Small undetected features are always possible because a direct inspection of the entire UZ model domain is not possible. However, the results of an analysis of smaller-scale heterogeneity indicates that unsaturated zone flow and transport are governed primarily by large-scale stratigraphy, structure, and associated hydrological properties rather than by smaller-scale

heterogeneity (SNL 2007 [DIRS 184614], Section 7.8.3.1; Zhou et al. 2003 [DIRS 162133], Section 6). Therefore, smaller-scale undetected features are expected to have a negligible effect on unsaturated zone flow and transport processes.

Undetected features above the repository are also not expected to have significant effects on water arrival at the repository. This is supported by the UZ flow model results, which show that existing major fault features carry only a small fraction of the flow (about 1%) within the repository footprint above the repository (SNL 2007 [DIRS 184614], Tables 6.6-1 and 6.6-2). Undetected features would not be expected to significantly alter the fraction of flow through features (detected and undetected) within the repository footprint.

The corresponding FEP for the saturated zone, FEP 2.2.12.00.0B (Undetected Features in the SZ), is included. The reasons that undetected features in the unsaturated zone are excluded while undetected features in the saturated zone are included reflect the differences in the domains and degree of site characterization for these two zones, as well as differences in the types of measurements available. The unsaturated zone model domain consists of an area of less than 60 square kilometers (SNL 2007 [DIRS 184614], Figure 6.1-1) and a depth of less than 1 kilometer (BSC 2004 [DIRS 169855], Figure C3-2) for a volume of less than 60 cubic kilometers. By comparison, the SZ site-scale flow modeling domain consists of an area in excess of 1,300 square kilometers (SNL 2007 [DIRS 177391], Figure 6-5) and is approximately 6 kilometers in depth (SNL 2007 [DIRS 177391], Table 6-4) for a volume of more than 7,800 cubic kilometers. Therefore, the SZ site-scale flow model domain is more than two orders of magnitude larger than the unsaturated zone model domain. Furthermore, a greater intensity of site characterization has been performed for the unsaturated zone modeling domain as compared with the saturated zone modeling domain (BSC 2004 [DIRS 169734], Figures 7-2 and 8-10). Given these differences in the domains and site characterization, major undetected features in the unsaturated zone model domain are not expected, whereas major undetected features could be present in the saturated zone modeling domain. However, the ability to conduct pump tests in the saturated zone allows for the identification of the effects of major features on saturated zone flow processes, even if the features themselves have not been detected. In this way, the effects on groundwater flow of undetected features in the volcanic units in the saturated zone, such as fracture zones and smaller faults, have been incorporated into the distribution for horizontal anisotropy in permeability in the SZ flow and transport abstraction model (SNL 2008 [DIRS 183750], Section 6.5.2.10). These differences have led to the exclusion of undetected features in the unsaturated zone and inclusion of undetected features in the saturated zone.

Based on the previous discussion, omission of FEP 2.2.12.00.0A (Undetected Features in the UZ) will not result in a significant adverse change in the magnitude or timing of either radiological exposure to the RMEI or radionuclide releases to the accessible environment. Therefore, this FEP is excluded from the performance assessments conducted to demonstrate compliance with proposed 10 CFR 63.311 and 63.321 (70 FR 53313 [DIRS 178394]), and with 10 CFR 63.331 [DIRS 180319] on the basis of low consequence.

INPUTS:

Table 2.2.12.00.0A-1. Direct Inputs

Input	Source	Description
SNL 2007. *UZ Flow Models and Submodels*. [DIRS 184614]	Tables 6.6-1, 6.6-2	Existing major fault features carry only a small fraction of the flow (about 1%) within the repository footprint above the repository
Zhou et al. 2003. "Flow and Transport in Unsaturated Fractured Rock: Effects of Multiscale Heterogeneity of Hydrogeologic Properties." [DIRS 162133]	Section 6	An analysis of smaller-scale heterogeneity indicates that UZ flow and transport are governed primarily by large-scale stratigraphy, structure, and associated hydrological properties rather than by smaller-scale heterogeneity

Table 2.2.12.00.0A-2. Indirect Inputs

Citation	Title	DIRS
10 CFR 63	Energy: Disposal of High-Level Radioactive Wastes in a Geologic Repository at Yucca Mountain, Nevada	180319
70 FR 53313	Implementation of a Dose Standard After 10,000 Years	178394
BSC 2004	*Performance Confirmation Plan*	172452
BSC 2004	*Development of Numerical Grids for UZ Flow and Transport Modeling*	169855
BSC 2004	*Yucca Mountain Site Description*	169734
BSC 2007	*Underground Layout Configuration for LA*	179640
SNL 2007	*Saturated Zone Site-Scale Flow Model*	177391
SNL 2007	*UZ Flow Models and Submodels*	184614
SNL 2008	*Saturated Zone Flow and Transport Model Abstraction*	183750

FEP: 2.2.12.00.0B

FEP NAME:

Undetected Features in the SZ

FEP DESCRIPTION:

Undetected features in the SZ portion of the geosphere can affect long-term performance of the disposal system. Undetected but important features may be present, and may have significant impacts. These features include unknown active fracture zones, inhomogeneities, faults and features connecting different zones of rock, and different geometries for fracture zones.

SCREENING DECISION:

Included

TSPA DISPOSITION:

Potential impacts on groundwater flow from undetected features in the saturated zone, such as fracture zones, inhomogeneities, faults, gravel lenses, and channels in the alluvium, are incorporated in the SZ transport abstraction model and the SZ one-dimensional transport model through parameter distributions (SNL 2008 [DIRS 183750]), which ultimately propagate to TSPA through variation in radionuclide breakthrough curves. The generation of multiple flow and transport realizations, using stochastically sampled key parameters as input, significantly varies flow and transport pathways in the saturated zone (SNL 2008 [DIRS 183750]).

Modeling of natural processes is, in many instances, based on using scaled parameters. Scaled parameters are parameters that are based on empirical observations (i.e., not all processes or first order physics are explicitly understood or known). Hydraulic conductivity, permeability, and transmissivity are examples of scaled parameters. In matching hydraulic heads (a response to the system) with variable lumped parameters such as permeability, undetected features are implicitly incorporated into *Saturated Zone Site-Scale Flow Model* (SNL 2007 [DIRS 177391], Section 6.6.1). The site-scale SZ transport model (SNL 2008 [DIRS 184806]) incorporates these effects by using the calibrated SZ site-scale flow model as its basis.

Groundwater specific discharge in the saturated zone may be enhanced due to the presence of undetected features. In the alluvium, features could be undetected gravel lenses and channels, and in the volcanic units these could be undetected faults and fractures or fracture clusters. Uncertainty in parameters related to these features are applied to the hydrogeologic units defined in the hydrogeologic framework model documented in *Hydrogeologic Framework Model for the Saturated Zone Site Scale Flow and Transport Model* (BSC 2005 [DIRS 174109]). Uncertainty in groundwater specific discharge in the saturated zone is based on data gathered from single- and multiwell hydrologic testing in the volcanic units near Yucca Mountain and field testing in the alluvium at the alluvial tracer complex. In the TSPA, the groundwater specific discharge multiplier parameter is a multiplication factor applied to all saturated zone permeability values and specified boundary fluxes (SNL 2008 [DIRS 183750], Section 6.5.2.1[a]) to effectively scale the simulated specific discharge and model the effects that undetected features may have on

groundwater specific discharge. Uncertainty in the flowing interval spacing parameter (BSC 2004 [DIRS 170014]) accounts for smaller-scale undetected features that transmit significant quantities of groundwater in the saturated zone. The assessment of horizontal anisotropy in permeability, as documented in *Saturated Zone In-Situ Testing* (SNL 2007 [DIRS 177394]), potentially includes the effects of preferentially oriented undetected features on groundwater flow in the saturated zone.

Hydrogeologic Framework Model for the Saturated Zone Site-Scale Flow and Transport Model (SNL 2007 [DIRS 174109]) documents the development of the 2006 hydrogeologic framework model (DTN: MO0610MWDHFM06.002 [DIRS 179352]). The HFM output is used in the site-scale saturated zone flow model. The TSPA disposition of included FEP 2.2.12.00.0B (Undetected Features in the SZ), is supported by *Hydrogeologic Framework Model for the Saturated Zone Site-Scale Flow and Transport Model* (SNL 2007 [DIRS 174109], Sections 6.4.3 and 8).

Key parameters that model undetected features (SNL 2008 [DIRS 183750]) are: (1) groundwater specific discharge, (2) porosity, (3) flowing interval spacing in the volcanics, (4) longitudinal dispersion, (5) horizontal anisotropy of permeability, (6) alluvial bulk density, and (7) sorption coefficients (K_d) for the nine classes of radionuclides modeled in both the alluvium and volcanic units (parameters are described in SNL 2008 [DIRS 183750], Sections 6.5.2.1[a], 6.5.2.3[a], and Tables 6-7[a] and 7-1[b]).

Additionally, in the SZ transport abstraction model (SNL 2008 [DIRS 183750], Section 6.5.2.2[a]), undetected features are accounted for through the probabilistic boundaries of the alluvium uncertainty zone. The western and northern boundaries of the alluvium uncertainty zone are defined with the sampled parameters. The above parameters that model undetected features are described in *Saturated Zone Flow and Transport Model Abstraction* (SNL 2008 [DIRS 183750], Sections 6.5.2.1[a], 6.5.2.2[a], 6.5.2.3[a], 6.5.2.4[a], 6.5.2.5, 6.5.2.7, 6.5.2.8, 6.5.2.10, respectively; also see Table 6-7[a]).

INPUTS:

Table 2.2.12.00.0B-1. Indirect Inputs

Citation	Title	DIRS
BSC 2004	*Probability Distribution for Flowing Interval Spacing*	170014
DTN: MO0610MWDHFM06.002	Hydrogeologic Framework Model (HFM2006) Stratigraphic Horizon Grids	179352
SNL 2007	*Saturated Zone Site-Scale Flow Model*	177391
SNL 2007	*Hydrogeologic Framework Model for the Saturated Zone Site Scale Flow and Transport Model*	174109
SNL 2007	*Saturated Zone In-Situ Testing*	177394
SNL 2008	*Saturated Zone Flow and Transport Model Abstraction*	183750
SNL 2008	*Site-Scale Saturated Zone Transport*	184806

FEP: 2.2.14.09.0A

FEP NAME:

Far-Field Criticality

FEP DESCRIPTION:

Far-field criticality could occur if fissile material-bearing solution from the waste package is transported beyond the drift and the fissile material is precipitated into a critical configuration. Potential far-field critical configurations are defined in *Disposal Criticality Analysis Methodology Topical Report* (YMP 2003 [DIRS 165505], Figure 3.3.b).

SCREENING DECISION:

Excluded – low probability

SCREENING JUSTIFICATION:

This FEP justification accounts for external criticality for the far-field location for those conditions that may lead to damage or failure of the waste package and allow water into the system, as idenitified in included FEPs 2.1.03.08.0A (Early Failure of Waste Packages) and 2.1.03.08.0B (Early Failure of Drip Shields). A prerequisite for any of the spent fuel waste forms to have potential for criticality is the introduction of water in liquid or vapor form to the inside of the TAD or DOE SNF canister. All postclosure criticality FEP scenarios, internal and external, require the presence of water in liquid or vapor form to degrade the waste package internals and/or the waste form as intact configurations are designed to remain subcritical if fabricated and loaded according to design specifications as demonstrated in *CSNF Loading Curve Sensitivity Analysis* (SNL 2008 [DIRS 182788], Section 6.2.2), *DOE SNF Phase I and II Summary Report* (Radulescu et al. 2004 [DIRS 165482], Sections 10 and 11.4), *Intact and Degraded Mode Criticality Calculations for the Codisposal of TMI-2 Spent Nuclear Fuel in a Waste Package* (BSC 2004 [DIRS 168935]), and *Intact and Degraded Mode Criticality Calculations for the Codisposal of ATR Spent Nuclear Fuel in a Waste Package* (BSC 2004 [DIRS 171926]).

For a criticality event to occur, the appropriate combination of materials (e.g., neutron moderators, neutron absorbers, fissile materials, or isotopes) and geometric configurations favorable to criticality must exist. Therefore, for a configuration to have potential for criticality, all of the following conditions must occur: (1) sufficient mechanical or corrosive damage to the waste package OCB to cause a breach, (2) presence of a moderator (i.e., water), (3) separation of fissionable material from the neutron absorber material or an absorber material selection error during the canister fabrication process, and (4) the accumulation (external) or presence of a critical mass of fissionable material in a critical geometric configuration. The probability of developing a configuration with criticality potential is insignificant unless all four conditions are realized, and then is only representative of a conservative estimate since the probability values associated with the many other events required to generate a critical configuration that would be less than 1 are not evaluated, but are conservatively set to 1.

Far-field criticality cannot occur unless the waste package and waste form are degraded. Water infiltration is required to degrade the waste package internals and waste form and transport them to the far-field location. Criticality cannot occur unless at least the minimum critical mass of a waste form can be accumulated in a favorable geometry. It then follows that the probability of far-field criticality must be less than the probability of water entering the waste package. This is because, in addition to the events evaluated to calculate the probability of water infiltrating a breached waste package, the probability of the following events or processes must also be considered for external criticality:

- Separation of the fissile materials from the degraded waste form
- Sufficient seepage water to transport fissile materials from the waste package
- Accumulating sufficient fissile material into a potentially critical configuration in the far-field environment.

Because the quantity of material released by diffusion would be small due to the tortuousity of the path, advective flow of water is necessary for transporting fissile materials from the waste package to the near-field in any appreciable quantities to be considered for criticality (SNL 2007 [DIRS 181165], Section 6.2). An advective seepage flow path to a waste package for nominal repository conditions would occur due to misplacement of a drip shield leading to breaching of the waste package from localized corrosion. However, the probability of this type of event is very low (4.36×10^{-9} per drip shield; DTN: MO0705EARLYEND.000 [DIRS 180946], file: *Table 1.doc*, Table 1). Since this type of event occurs during the preclosure time period, it is independent of the postclosure time period. Using the total number of waste packages (11,162; MO0702PASTREAM.001 [DIRS 179925], file: *DTN-Inventory-Rev00.xls*, worksheet: "Unit Cell") as a conservative estimate for the number of drip shields (it is conservative because not all waste packages have sufficient quantities of fissile material to result in a criticality event) and multiplying by the probability of misplacing a drip shield results in an initiating event probability of 4.9×10^{-5}. This value is already below the regulatory screening criterion of 1 chance in 10,000 (10^{-4}) of occurrence within 10,000 years after disposal prior to consideration of probabilities (which would be less than 1.0) associated with the amount of degradation and accumulation into a favorable geometry for criticality that would only result in lowering the sequence probability.

As indicated in excluded FEP 2.1.14.12.0A (Far-Field Criticality Resulting from an Igneous Event) and excluded FEP 2.1.14.10.0A (Far-Field Criticality Resulting from a Seismic Event), the amount of fissile material accumulation in the far-field location is insufficient to pose a criticality concern. Note that the material degradation of the internals and subsequent accumulation in the far-field based on the seismic and igneous scenarios are bounding for nominal repository conditions because the seismic and igneous seepage fluxes are much higher. Therefore, under bounding seepage fluxes resulting from a sesimc or igneous initiating event, an insufficient amount of fissile material could accumulate in the far-field to pose a criticality concern, it can be concluded that under nominal reposity conditions, an insufficient amount of fissile material can accumulate in the far-field location to pose a criticality concern.

Accordingly, this FEP is excluded from the performance assessments conducted to demonstrate compliance with proposed 10 CFR 63.311 and 63.321 (70 FR 53313 [DIRS 178394]), and with 10 CFR 63.331 [DIRS 180319], on the basis of low probability.

In addition, as documented in *Screening Analysis of Criticality Features, Events, and Processes for License Application* (SNL 2008 [DIRS 173869]), the probability of criticality for all locations is less than 1 chance in 10,000 of occurrence within 10,000 years after disposal. The results documented in this analysis are applicable for all waste forms and waste package variants.

INPUTS:

Table 2.2.14.09.0A-1. Direct Inputs

Input	Source	Description
DTN: MO0702PASTREAM.001. Waste Stream Composition and Thermal Decay Histories for LA. [DIRS 179925]	Unit Cell in file *DTN_Inventory-Rev00.xls*	Total number of waste packages
DTN: MO0705EARLYEND.000. Waste Package/Drip Shield Early Failure End State Probabilities. [DIRS 180946]	file: *Table 1.doc*, Table 1	Probability of advective seepage flow path to a waste package for nominal repository conditions occuring due to misplacement of a drip shield leading to breaching of the waste package from localized corrosion
Radulescu et al. 2004. *DOE SNF Phase I and II Summary Report*. [DIRS 165482]	Sections 10 and 11.4	Reference to design specifications listed in DOE SNF Phase I and II Summary Report
SNL 2008. *CSNF Loading Curve Sensitivity Analysis*. [DIRS 182788]	Section 6.2.2	Reference to design specifications listed in CSNF Loading Curve Sensitivity Analysis

Table 2.2.14.09.0A-2. Indirect Inputs

Citation	Title	DIRS
10 CFR 63	Energy: Disposal of High-Level Radioactive Wastes in a Geologic Repository at Yucca Mountain, Nevada	180319
70 FR 53313	Implementation of a Dose Standard After 10,000 Years	178394
BSC 2004	*Intact and Degraded Mode Criticality Calculations for the Codisposal of ATR Spent Nuclear Fuel in a Waste Package*	171926
BSC 2004	*Intact and Degraded Mode Criticality Calculations for the Codisposal of TMI-2 Spent Nuclear Fuel in a Waste Package*	168935
SNL 2007	*Geochemistry Model Validation Report: Material Degradation and Release Model*	181165
SNL 2008	*Screening Analysis of Criticality Features, Events, and Processes for License Application*	173869
YMP 2003	*Disposal Criticality Analysis Methodology Topical Report*	165505

FEP: 2.2.14.10.0A

FEP NAME:

Far-Field Criticality Resulting from a Seismic Event

FEP DESCRIPTION:

Either during, or as a result of, a seismic disruptive event, far-field criticality could occur if fissile material-bearing solution from the waste package is transported beyond the drift and the fissile material is precipitated into a critical configuration. Potential far-field critical configurations are defined in *Disposal Criticality Analysis Methodology Topical Report* (YMP 2003 [DIRS 165505], Figure 3.3b).

SCREENING DECISION:

Excluded – low probability

SCREENING JUSTIFICATION:

This FEP justification accounts for external criticality for the far-field location for the seismic scenario, where far-field is defined as the region outside the drift. A prerequisite for any of the spent fuel waste forms to have potential for criticality is the introduction of water in liquid or vapor form to the inside of the TAD or DOE SNF canister. All postclosure criticality FEP scenarios, internal and external, require the presence of water in liquid or vapor form to degrade the waste package internals and/or the waste form as intact configurations are designed to remain subcritical if fabricated and loaded according to design specifications as demonstrated in *CSNF Loading Curve Sensitivity Analysis* (SNL 2008 [DIRS 182788], Section 6.2.2), *DOE SNF Phase I and II Summary Report* (Radulescu et al. 2004 [DIRS 165482], Sections 10 and 11.4), *Intact and Degraded Mode Criticality Calculations for the Codisposal of TMI-2 Spent Nuclear Fuel in a Waste Package* (BSC 2004 [DIRS 168935]), and *Intact and Degraded Mode Criticality Calculations for the Codisposal of ATR Spent Nuclear Fuel in a Waste Package* (BSC 2004 [DIRS 171926]).

For a criticality event to occur, the appropriate combination of materials (e.g., neutron moderators, neutron absorbers, fissile materials, or isotopes) and geometric configurations favorable to criticality must exist. Therefore, for a configuration to have potential for criticality, all of the following conditions must occur: (1) sufficient mechanical or corrosive damage to the waste package OCB to cause a breach, (2) presence of a moderator (i.e., water), (3) separation of fissionable material from the neutron absorber material or an absorber material selection error during the canister fabrication process, and (4) the accumulation (external) or presence of a critical mass of fissionable material. The probability of developing a configuration with criticality potential is insignificant unless all four conditions are realized, and then is only representative of a conservative estimate since the probability values associated with the many other events required to generate a critical configuration that would be less than 1 are not evaluated, but are conservatively set to 1.

Far-field criticality cannot occur unless the waste package and waste form are degraded. Water infiltration is required to degrade the waste package internals and waste form and transport them to the near-field location. Criticality cannot occur unless at least the minimum critical mass of a waste form can be accumulated in a favorable geometry. It then follows that the probability of near-field criticality must be less than the probability of water entering the waste package. This is because, in addition to the events evaluated to calculate the probability of water infiltrating a breached waste package, the probability of the following events or processes must also be considered for external criticality:

- Separation of the fissile materials from the degraded waste form
- Sufficient seepage water to transport fissile materials from the waste package
- Accumulating sufficient fissile material into a potentially critical configuration in the near-field environment.

If a waste package is breached, water and solutes might enter and leave the waste package by several mechanisms, including diffusion, condensation of vapor, and advection of liquid water. Leakage through a crack-damaged drip shield is an insignificant source for liquid water penetration through cracks in the underlying waste package especially when compared to the threshold flow rate (0.1 kg/yr) used in TSPA to define whether seepage occurs (excluded FEP 2.1.03.10.0 (Advection of Liquids and Solids through Cracks in the Waste Package)). Therefore, the predominant mechanism for water inflow and outflow through a breached waste package is through diffusive transport unless the drip shield has failed. *Geochemistry Model Validation Report: Material Degradation and Release Model* (SNL 2007 [DIRS 181165], Section 6.2) indicated that the quantity of material released by diffusion would be small due to the tortuosity of the path, and therefore the diffusion-only scenario is not considered a viable method for material transport. Thus, advective flow of water is necessary for transporting fissile materials from the waste package to the far-field in any appreciable quantities to be considered for criticality.

Vibratory ground motion (included FEP 1.2.03.02.0A (Seismic Ground Motion Damages EBS Components)), faulting (included FEP 1.2.02.03.0A (Fault Displacement Damages EBS Components)), seismic-induced drift collapse in the lithophysal units (included FEP 1.2.03.02.0C (Seismic-Induced Drift Collapse Damages EBS Components)), and seismic-induced rockfall (excluded FEP 1.2.03.02.0B (Seismic-Induced Rockfall Damages EBS Components)) are potential initiating events that are capable of creating advective flow paths into the waste package. Such failures may allow the influx of water (either advective or diffusive) into the waste package, which, in turn, has the potential to initiate processes leading to degradation and transport of the fissile material to the far-field location.

Note that excluded FEP 1.2.03.02.0B (Seismic-Induced Rockfall Damages EBS Components) has been screened from performance assessment on the basis of low consequence, which is not directly applicable to criticality potential evaluations. FEP 1.2.03.02.0B (Seismic-Induced Rockfall Damages EBS Components) indicates that seismic-induced damage to the waste package and its internals from rock block impacts in nonlithophysal units is screened out from the TSPA model on the basis of low probability. However, FEP 1.2.03.02.0B (Seismic-Induced

Rockfall Damages EBS Components) screens out tearing or rupture of the drip shield plates from large block impacts because of low consequence, which is not directly applicable to criticality potential evaluations. Drip shield failure could result in an advective flow path to the waste package OCB creating an environment for subsequent localized corrosion processes (FEP 2.1.03.03.0A (Localized Corrosion of Waste Packages)) that could breach the waste package OCB.

The probability of drip shield and waste package failure from a fault event varies with the magnitude of the earth quake but ranges from 1.2×10^{-4} to 4.3×10^{-4} for the TAD waste packages and from 3.0×10^{-5} to 6.9×10^{-4} for the codisposal waste packages (SNL 2008 [DIRS 173869], Table 6.4-7).

There are several hundred distinct types of DOE SNF and it is not practical to attempt to determine the impact of each individual type on repository performance. These fuels come from a wide range of reactor types, such as light- and heavy-water-moderated reactors, graphite-moderated reactors, and breeder reactors, with various cladding materials and enrichments, varying from depleted uranium to over 93% enriched ^{235}U. Many of these reactors, now decommissioned, had unique design features, such as core configuration, fuel element and assembly geometry, moderator and coolant materials, operational characteristics, and neutron spatial and spectral properties (DOE 2004 [DIRS 171271]).

Therefore, to facilitate DOE SNF waste form evaluations, the DOE SNF inventory was first reduced to 34 DOE SNF groups based on fuel matrix, cladding, cladding condition, and enrichment. These parameters are the fuel characteristics that were determined to have major impacts on the release of radionuclides from the DOE SNF and contributed to nuclear criticality scenarios (DOE 2000 [DIRS 118968], Section 5). Separate groups were further refined for the purposes of criticality, design basis events, and TSPA based on key parameters such as fuel matrix, cladding, and fuel condition, as well as fissile species and enrichment, and reactor and fuel design (DOE 2000 [DIRS 118968], Section 5.1). For criticality, nine DOE SNF criticality groups have been identified and are listed in *General Description of Database Information Version 5.0.1* (DOE 2007 [DIRS 182577], Table 6).

Within each of the nine DOE SNF criticality groups, a single fuel design was selected as being representative of the remaining fuel within each group. The term representative means that all fuels would perform similarly regarding chemical interactions within the waste package and basket, and that canister loading limits from the representative fuel (ranges of key parameters important to criticality such as linear fissile loading and total fissile mass) are established, which other fuels within the group can be shown to not exceed. Waste forms within a single criticality group that have configurations or key criticality parameters outside the range of applicability of the representative fuel will require supplemental analysis and/or additional reactivity control mechanisms.

Evaluations for naval fuel are conducted by the Naval Nuclear Propulsion Program. A miscellaneous waste form category which has a variety of fuel matrix properties originating from various postirradiation examinations and other testing are not included in the criticality evaluations for the fuel groups as they will need to be evaluated on a case-by-case basis. Thus,

the disposal criticality analysis methodology (YMP 2003 [DIRS 165505]) can be applied to nine DOE SNF representative fuel groups for criticality evaluations.

The minimum fissile mass necessary for criticality external to the waste packages is discussed in *Geochemistry Model Validation Report: External Accumulation Model* (SNL 2007 [DIRS 181395], Section 8.1.4[a]), where it was concluded that insufficient fissile material can collect over 10,000 years to achieve a critical mass for the seismic scenario. Note that the material degradation of the internals and subsequent accumulation in the near-field based on the seismic scenario are bounding for localized corrosion because the seismic seepage flux is based on the entire waste package footprint area collecting seeps whereas localized corrosion seeps would only be a fraction of the total area with a reduced seepage flux. In addition, these values are predicated on having an initiating event (i.e., seismic fault displacement rupturing the drip shield and waste package), which is an unlikely event (1.2×10^{-8} per year). The critical mass limits were evaluated for commercial SNF and DOE SNF waste forms using bounding parameters with regards to optimizing reactivity potential, so the actual masses that would be necessary to achieve criticality would need to be far greater than what was identified (SNL 2007 [DIRS 181395], Section 8.1.4[a]).

Model abstractions were performed for commercial SNF and three DOE SNF waste forms in *Geochemistry Model Validation Report: External Accumulation Model* (SNL 2007 [DIRS 181395]) (i.e., N Reactor (DOE3), TMI (DOE9), and FFTF (DOE1)) (SNL 2008 [DIRS 173869], Table 4.1-2), which make up approximately 90% of the metric tons of heavy metal in the DOE SNF inventory expected to be stored in the repository. In addition to these waste forms making up ~90% of the inventory by mass, they were selected because they provide degradation and accumulation characteristics of uranium-metal (N Reactor), mixed-oxide (FFTF), and damaged uranium dioxide (TMI) waste forms which may be applicable to other representative DOE waste forms. Some of the other DOE SNF waste forms, such as Shippingport light-water breeder reactor (LWBR) (DOE5) and Ft. St. Vrain (DOE6) are not expected to be a concern for external criticality due to the corrosion resistance of the waste form (SNL 2007 [DIRS 181395], Section 6.9.3[a]).

Ft. St. Vrain fuels (DOE6) have an integral silicon carbide (SiC) protective layer that not only retains the fission products but also protects the uranium and thorium dicarbide (ThC_2) from oxidation and hydrolysis (DOE 2003 [DIRS 166027], p. 48). Comparative analysis has indicated that the Ft. St. Vrain fuel has the lowest degradation rate of all DOE SNF and should behave significantly better in terms of fissile material dissolution, transport, and accumulation. In some residual quantities (< 250 grams per block), ^{233}U bred into the ThC_2 fertile particles. A canister loaded with five Ft. St. Vrain blocks contains sufficient quantities of ^{233}U to have criticality potential in solution; however, a mechanism to separate the uranium from within the SiC-coated fertile particles, and then a mechanism to accumulate in a concentrated fissile mass in a favorable geometry, is not credible.

For Shippingport LWBR fuel (DOE5), a number of studies has indicated both air and water oxidation of uranium and thorium oxide fuel pellets [(Th, U)O_2] proceed more slowly than in pure uranium oxide (UO_2), and decreases with decreasing UO_2 content in the (Th, U)O_2 (DOE 2003 [DIRS 166027], p. 33). Tests have shown that the thorium oxide pellets in the Shippingport LWBR fuel have excellent corrosion resistance with an estimated solubility of

10^{-14} mol/L at 25°C and pH > 5 (DOE 2003 [DIRS 166027], p. 32). With the less-reactive degradation rate, a mechanism to separate the uranium, transporting, and accumulation into a favorable geometry is also not credible.

Table 2.2.14.10.0A-1 shows the ranges of minimum critical mass required to accumulate in the invert as well as the calculated accumulation or mass released from the waste package for the waste forms evaluated for external criticality. For each of the waste forms evaluated, the results indicate that an insufficient amount of fissile material accumulates to pose a criticality concern.

Table 2.2.14.10.0A-1. Summary of Seismic Scenario External Criticality Results

Scenario	Waste Package Type	Calculated Accumulation or Mass Released from Waste Package	Mass of Uranium or Plutonium (for FFTF) required to achieve critical limit of k_{eff} = 0.96		
		Uranium Mass, Unless Otherwise Noted (kg)	Fractured Tuff	Lithophysae Array	Large Lithophysae
Seismic	DOE3 (N Reactor)	Not calculated[a]	Infinite[b]	Not calculated[a]	Not calculated[a]
	DOE9 (TMI II Fuel)	Not calculated[a]	Infinite[b]	Not calculated[a]	Not calculated[a]
	Commercial SNF	90.3	Infinite[b]	Not calculated[a]	Not calculated[a]
	DOE1 (FFTF) (Plutonium Mass)	0	4.3	Not calculated[a]	Not calculated[a]

[a] "Not calculated" means that this scenario is bounded by the igneous scenario (FEP 2.2.14.12.0A) . In most cases, this means that if commercial SNF waste is very subcritical, then TMI and N Reactor waste had to be also.
[b] "Infinite" means that an infinite amount of fissile waste released in this model will not produce an arrangement that can reach the critical limit.

Source: SNL 2007 [DIRS 181395], Table 6.9-1[a].

DOE fuel groups in DOE2, DOE4, DOE7, and DOE8 representing UZrHx (TRIGA), high enriched uranium oxide (Shippingport PWR), aluminum-based (ATR), and U-Zr/U-Mo alloy (Fermi), respectively (SNL 2008 [DIRS 173869], Table 4.1-2), have not been analyzed in detail for external fissile mass transport and accumulation as the other waste forms have. However, considering the processes that must occur to allow advective seepage into a DOE SNF canister without substantial drainage to allow degradation of the internal components and waste form, along with the other conservative modeling parameters that have been used to create a process to facilitate fissile material transport to the external environment, and the bounding modeling parameters respective to maximizing criticality potential, these waste forms are not expected to result in an increase in the total probability of criticality in the far-field location.

Some of the conservative modeling parameters are provided as follows:

- The material degradation and release model (SNL 2007 [DIRS 181165]) uses constant corrosion rates for the SNF; however, laboratory experiments on the surface structure of commercial SNF during dissolution have shown that UO_2 dissolution is accompanied by the formation of a protective layer of secondary phases that retards further corrosion

(SNL 2007 [DIRS 181165], Section 6.6.2). Therefore, the release of uranium from the fuel would be slower and therefore less would be released.

- Experimental and field data indicate that actinides would be adsorbed on or incorporated into alteration products that form in the waste package (SNL 2007 [DIRS 181165], Section 6.6.3). This solid solution formation and adsorption would tend to lower actinide concentrations below those predicted by EQ6 and would delay release from the waste package.

- The material degradation and release model (SNL 2007 [DIRS 181165]) assumes the cladding and DOE SNF canister fail immediately, whereas the expected scenario would be that the failure would take place over many years. This would also delay the release of actinides.

- Many conservative modeling approximations are used to simplify the critical mass calculations presented in Table 2.2.14.10.0A-1. For the commercial SNF and low-enriched DOE fuels analyzed in *Geochemistry Model Validation Report: External Accumulation Model* (SNL 2007 [DIRS 181395]), the conservatisms are appropriate, because the results show that a criticality event is very unlikely. However, for the higher enriched DOE fuels, less conservative (increased detail) modeling parameters of the criticality potential are expected to generate similar conclusions.

Summary—The critical mass limits were evaluated for several waste forms using bounding parameters with regards to optimizing reactivity potential, so the actual masses that would be necessary to achieve criticality would need to be far greater than what was identified (SNL 2007 [DIRS 181395], Section 8.1.4[a]). Model abstractions were performed for commercial SNF and three DOE SNF waste forms and resulted in insufficient fissile material accumulation in the near-field location to pose a criticality concern. Therefore, based on these waste forms representing the majority (>95% of the total metric tons) of the waste for disposal in the mountain, and considering the conservative modeling parameters discussed above that would be further developed for other DOE representative fuel groups, in conjunction with the order of magnitude of the probability of a seismic faulting event causing waste package failure, the probability of far-field criticality is considered insignificant. Accordingly, this FEP is excluded from the performance assessments conducted to demonstrate compliance with proposed 10 CFR 63.311 and 63.321 (70 FR 53313 [DIRS 178394]), and with 10 CFR 63.331 [DIRS 180319], on the basis of low probability.

In addition, as documented in *Screening Analysis of Criticality Features, Events, and Processes for License Application* (SNL 2008 [DIRS 173869]), the probability of criticality for all locations is less than 1 chance in 10,000 of occurrence within 10,000 years after disposal. The results documented in this analysis are applicable for all waste forms and waste package variants.

INPUTS:

Table 2.2.14.10.0A-2. Direct Inputs

Input	Source	Description
DOE 2003. *Review of Oxidation Rates of DOE Spent Nuclear Fuel Part 2. Nonmetallic Fuel*. [DIRS 166027]	p. 32	Thorium oxide pellets in the Shippingport LWBR fuel have excellent corrosion resistance with an estimated solubility of 10^{-14} mol/L at 25°C and pH > 5
Radulescu et al. 2004. *DOE SNF Phase I and II Summary Report*. [DIRS 165482]	Sections 10 and 11.4	Reference to design specifications listed in DOE SNF Phase I and II Summary Report
SNL 2007. *Geochemistry Model Validation Report: External Accumulation Model*. [DIRS 181395]	Section 8.1.4[a]	Critical mass limits were evaluated for several waste forms using bounding parameters with regards to optimizing reactivity potential
	Table 6.9-1[a]	Source for summary of seismic scenario external criticality results
	Section 8.1.4[a]	Critical mass limits were evaluated for commercial spent nuclear fuel and DOE SNF waste forms
	Section 8.1.4[a]	Minimum fissile mass necessary for criticality external to the waste packages is discussed
SNL 2008. *CSNF Loading Curve Sensitivity Analysis*. [DIRS 182788]	Section 6.2.2	Reference to design specifications listed in CSNF Loading Curve Sensitivity Analysis
SNL 2008. *Screening Analysis of Criticality Features, Events, and Processes for License Application*. [DIRS 173869]	Table 6.4-7	Gives probability of drip shield and waste package failure from a fault event varies with the magnitude of the earthquake

Table 2.2.14.10.0A-3. Indirect Inputs

Citation	Title	DIRS
10 CFR 63	Energy: Disposal of High-Level Radioactive Wastes in a Geologic Repository at Yucca Mountain, Nevada	180319
70 FR 53313	Implementation of a Dose Standard After 10,000 Years	178394
BSC 2004	*Intact and Degraded Mode Criticality Calculations for the Codisposal of ATR Spent Nuclear Fuel in a Waste Package*	171926
BSC 2004	*Intact and Degraded Mode Criticality Calculations for the Codisposal of TMI-2 Spent Nuclear Fuel in a Waste Package*	168935
DOE 2000	*DOE Spent Nuclear Fuel Grouping in Support of Criticality, DBE, TSPA-LA*	118968
DOE 2004	*General Description of Database Information Version 5.0.1*	171271
DOE 2003	*Review of Oxidation Rates of DOE Spent Nuclear Fuel Part 2. Nonmetallic Fuel*	166027
DOE 2007	*General Description of Database Information Version 5.0.1*	182577
SNL 2007	*Geochemistry Model Validation Report: External Accumulation Model*	181395
SNL 2007	*Geochemistry Model Validation Report: Material Degradation and Release Model*	181165
SNL 2008	*Screening Analysis of Criticality Features, Events, and Processes for License Application*	173869
YMP 2003	*Disposal Criticality Analysis Methodology Topical Report*	165505

FEP: 2.2.14.11.0A

FEP NAME:

Far-Field Criticality Resulting from Rockfall

FEP DESCRIPTION:

Either during or as a result of a rockfall event, far-field criticality could occur if fissile material-bearing solution from the waste package is transported beyond the drift and the fissile material is precipitated into a critical configuration. Potential far-field critical configurations are defined in *Disposal Criticality Analysis Methodology Topical Report* (YMP 2003 [DIRS 165505], Figure 3.3b).

SCREENING DECISION:

Excluded – low probability

SCREENING JUSTIFICATION:

This FEP justification accounts for external criticality for the far-field location resulting from rockfall, where *far-field* is defined as the region outside the drift. A prerequisite for any of the spent fuel waste forms to have potential for criticality is the introduction of water in liquid or vapor form to the inside of the TAD or DOE SNF canister. All postclosure criticality FEP scenarios, internal and external, require the presence of water in liquid or vapor form to degrade the waste package internals and/or the waste form as intact configurations are designed to remain subcritical if fabricated and loaded according to design specifications as demonstrated in *CSNF Loading Curve Sensitivity Analysis* (SNL 2008 [DIRS 182788], Section 6.2.2), *DOE SNF Phase I and II Summary Report* (Radulescu et al. 2004 [DIRS 165482], Sections 10 and 11.4), *Intact and Degraded Mode Criticality Calculations for the Codisposal of TMI-2 Spent Nuclear Fuel in a Waste Package* (BSC 2004 [DIRS 168935]), and *Intact and Degraded Mode Criticality Calculations for the Codisposal of ATR Spent Nuclear Fuel in a Waste Package* (BSC 2004 [DIRS 171926]).

For a criticality event to occur, the appropriate combination of materials (e.g., neutron moderators, neutron absorbers, fissile materials, or isotopes) and geometric configurations favorable to criticality must exist. Therefore, for a configuration to have potential for criticality, all of the following conditions must occur: (1) sufficient mechanical or corrosive damage to the waste package OCB to cause a breach, (2) presence of a moderator (i.e., water), (3) separation of fissionable material from the neutron absorber material or an absorber material selection error during the canister fabrication process, and (4) the accumulation (external) or presence of a critical mass of fissionable material in a critical geometric configuration. The probability of developing a configuration with criticality potential is insignificant unless all four conditions are realized, and then is only representative of a conservative estimate since the probability values associated with the many other events required to generate a critical configuration that are less than 1 are not quantified, but rather are conservatively set to 1.

Far-field criticality cannot occur unless the waste package and waste form are degraded. Water infiltration is required to degrade the waste package internals and waste form and transport them to the far-field location. Criticality cannot occur unless at least the minimum critical mass of a waste form can be accumulated. It then follows that the probability of far-field criticality must be less than the probability of water entering the waste package. This is because, in addition to the events evaluated to calculate the probability of water infiltrating a breached waste package, the probability of the following events or processes must also be considered for external criticality:

- Separation of the fissile materials from the degraded waste form
- Sufficient seepage water to transport fissile materials from the waste package
- Accumulating sufficient fissile material into a potentially critical configuration in the far-field environment.

Excluded FEP 2.1.07.01.0A (Rockfall) indicates that rockfall related to nonseismic processes such as drift degradation induced by in situ gravitational and excavation-induced stresses as well as thermally induced stresses do not generate rock block sizes sufficient to tear or rupture the drip shield plates. Drip shield damage from rockfall induced by thermal loading is found to be minor since the block sizes for such rockfall are small with a mean mass of less than 0.2 MT (BSC 2004 [DIRS 166107], p. 6-102). In addition, drift degradation (i.e., considering thermal and time-dependent effects on drift collapse, but excluding seismic effects) results in only partial collapse of the emplacement drifts at 20,000 years (see excluded FEP 2.1.07.02.0A (Drift Collapse)). The conclusion for the nominal scenario is that negligible drift degradation will occur over the initial 10,000-year postclosure period (BSC 2004 [DIRS 166107], p. x).

A waste package must be breached in order to transport fissile material out. If a waste package is breached, water and solutes might enter and leave the waste package by several mechanisms, including diffusion, condensation of vapor, and advection of liquid water. Therefore, rockfall does not result in waste package outer barrier breaching. Without a waste package breach, there is no potential for external criticality.

Summary—Since the drip shield continues to function through rockfall events as described previously, the waste package will be protected from rockfall during the postclosure period, for as long as the drip shield remains intact, thereby precluding the introduction of water to the waste package, which is necessary to degrade the internals and transport material into the far-field location. The probability of the occurrence of configurations with criticality potential for the far-field location resulting from rockfall is insignificant since no damage to the waste package OCBs is expected from the nonseismically initiated rockfall events. Accordingly, this FEP is excluded from the performance assessments conducted to demonstrate compliance with proposed 10 CFR 63.311 and 63.321 (70 FR 53313 [DIRS 178394]), and with 10 CFR 63.331 [DIRS 180319], on the basis of low probability. This result is applicable for all waste forms and waste package variants.

INPUTS:

Table 2.2.14.11.0A-1. Direct Inputs

Input	Source	Description
Radulescu et al. 2004. *DOE SNF Phase I and II Summary Report*. [DIRS 165482]	Sections 10 and 11.4	Waste package design specifications
SNL 2008. *CSNF Loading Curve Sensitivity Analysis*. [DIRS 182788]	Section 6.2.2	Waste package design specifications

Table 2.2.14.11.0A-2. Indirect Inputs

Citation	Title	DIRS
10 CFR 63	Energy: Disposal of High-Level Radioactive Wastes in a Geologic Repository at Yucca Mountain, Nevada	180319
70 FR 53313	Implementation of a Dose Standard After 10,000 Years	178394
BSC 2004	*Drift Degradation Analysis*	166107
BSC 2004	*Intact and Degraded Mode Criticality Calculations for the Codisposal of ATR Spent Nuclear Fuel in a Waste Package*	171926
BSC 2004	*Intact and Degraded Mode Criticality Calculations for the Codisposal of TMI-2 Spent Nuclear Fuel in a Waste Package*	168935
YMP 2003	*Disposal Criticality Analysis Methodology Topical Report*	165505

FEP: 2.2.14.12.0A

FEP NAME:

Far-Field Criticality Resulting from an Igneous Event

FEP DESCRIPTION:

Either during or as a result of an igneous disruptive event, far-field criticality could occur if fissile material-bearing solution from the waste package is transported beyond the drift and the fissile material is precipitated into a critical configuration. Potential far-field critical configurations are defined in *Disposal Criticality Analysis Methodology Topical Report* (YMP 2003 [DIRS 165505], Figure 3.3b).

SCREENING DECISION:

Excluded – low probability

SCREENING JUSTIFICATION:

This FEP justification accounts for external criticality for the far-field location for the igneous scenario, where *far-field* is defined as the region outside the drift. A prerequisite for any of the spent fuel waste forms to have potential for criticality is the introduction of water in liquid or vapor form to the inside of the TAD or DOE SNF canister. For a criticality event to occur, the appropriate combination of materials (e.g., neutron moderators, neutron absorbers, fissile materials, or isotopes) and geometric configurations favorable to criticality must exist. Therefore, for a configuration to have potential for criticality, all of the following conditions must occur: (1) sufficient mechanical or corrosive damage to the waste package OCB to cause a breach, (2) presence of a moderator (i.e., water), (3) separation of fissionable material from the neutron absorber material or an absorber material selection error during the canister fabrication process, and (4) the accumulation (external) or presence of a critical mass of fissionable material in a critical geometric configuration. The probability of developing a configuration with criticality potential is insignificant unless all four conditions are realized, and then is only representative of a conservative estimate since the probability values associated with the many other events required to generate a critical configuration that would be less than 1 are not evaluated, but are conservatively set to 1.

Far-field criticality cannot occur unless the waste package and waste form are degraded. Water infiltration is required to degrade the waste package internals and waste form and transport them to the far-field location. Criticality cannot occur unless at least the minimum critical mass of a waste form can be accumulated in a favorable geometry. It then follows that the probability of far-field criticality must be less than the probability of water entering the waste package. This is because, in addition to the events evaluated to calculate the probability of water infiltrating a breached waste package, the probability of the following events or processes must also be considered for external criticality:

- Separation of the fissile materials from the degraded waste form

- Sufficient seepage water to transport fissile materials from the waste package
- Accumulating sufficient fissile material into a potentially critical configuration in the far-field environment.

Included FEP 1.2.04.03.0A (Igneous Intrusion into Repository) is an event where an igneous basaltic dike (magma-filled crack) intersects one or more repository drifts, followed by the intrusion of effusive (liquid) magma flow or pyroclastic flow (clots of melt in a stream of gas) into the drifts. The temperature of the waste package, the canister internals, and the SNF will heat up to near-magma temperatures in days to weeks (SNL 2007 [DIRS 177430], Figure 6-94) exceeding 700°C for one to nineteen months, depending on the temperature of the magma and the radioactive decay heat generated by the waste (SNL 2007 [DIRS 177430], Section 6.4.6). At these high waste package temperatures, the fuel and the materials surrounding the fuel (i.e., cladding and structural materials) may be affected. Iron-zirconium and nickel-zirconium liquid eutectics will form (starting at approximately 948°C (ASM International 1996 [DIRS 181641], iron-zirconium and nickel-zirconium phase diagrams)) but are not expected to provide any mechanisms causing appreciable removal of the neutron-absorber materials from their general locale in relation to the waste form since the eutectic is expected to contain both the absorber and waste form materials. In addition, thermal creep of the internal components resulting in internal slumping is also expected. In summary, it is expected that an igneous intrusion would sufficiently compromise the integrity of the waste packages, drip shields, and cladding in affected emplacement drifts to make them ineffective (i.e., a total loss of function in isolating waste packages and waste forms from seepage water when it returns after drifts have cooled).

The technical basis for inclusion of igneous intrusion into the repository in the TSPA is founded on the results of the Probabilistic Volcanic Hazard Analysis (PVHA) (CRWMS M&O 1996 [DIRS 100116]) described in *Characterize Framework for Igneous Activity at Yucca Mountain, Nevada* (BSC 2004 [DIRS 169989], Table 7-1), which indicates that the computed mean annual frequency of intersection of the repository footprint by a dike is 1.7×10^{-8}. The computed 5th and 95th percentiles of the uncertainty distribution for frequency of intersection are 7.4×10^{-10} and 5.5×10^{-8}, respectively.

Potential accumulation sites for fissile material beneath a degrading waste package in the far-field are within fractures of the host rock and within lithophysae distributed throughout the host rock. Lithophysae are hollow, bubble-like structures in the rock composed of concentric shells of finely crystalline alkali feldspar, quartz, and other materials. The primary mechanisms for accumulation are: (1) adsorption and (2) mixing of the actinide-laden source term with resident water, thus changing the chemistry sufficiently for fissile minerals to become insoluble and precipitate (SNL 2007 [DIRS 181395], Section 1).

In order for fissile material to accumulate in the far-field, the waste package effluent containing dissolved uranium and plutonium must flow through the invert without interaction with invert materials, enter the fractured tuff, and mix with water that was diverted around the drift that is now in these same fractures or lithophysae. After the effluent and "new" water mixes, uranium and plutonium may precipitate within the fractures and lithophysae.

For lithophysae to be available for accumulation of fissile material, the lithophysae must be connected to fractures that could transport the waste package effluent. In the event effluent reaches the lithophysa, it must mix with uncontaminated seepage water that flows into the lithophysa via another fracture. The mixing of the two solutions can result in a chemistry change which allows the fissile minerals to precipitate. More realistically, the waste package effluent would be adsorbed or precipitated in the invert and fractures before it ever reached the lithophysa. Many of the fractures observed in the repository are deflected around lithohysae (SNL 2007 [DIRS 181395], Section 6.4.8.4), and therefore the chances are low of two fractures intersecting a large lithophysa, each carrying different water solutions. In addition, *UZ Flow Models and Submodels* (SNL 2007 [DIRS 184614], Section 6.1.5) states that little water is expected to flow through lithophysal cavities, owing to the strong capillary barrier effect on seepage into cavities. Therefore, the accumulation in a large lithophysa is not expected. However, in order to determine the criticality potential of accumulation in a large lithophysa, the scenario was evaluated in *Geochemistry Model Validation Report: External Accumulation Model* (SNL 2007 [DIRS 181395]).

There are several hundred distinct types of DOE SNF and it is not practical to attempt to determine the impact of each individual type on repository performance. These fuels come from a wide range of reactor types, such as light- and heavy-water-moderated reactors, graphite-moderated reactors, and breeder reactors, with various cladding materials and enrichments, varying from depleted uranium to over 93% enriched ^{235}U. Many of these reactors, now decommissioned, had unique design features, such as core configuration, fuel element and assembly geometry, moderator and coolant materials, operational characteristics, and neutron spatial and spectral properties (DOE 2004 [DIRS 171271]).

Therefore, to facilitate DOE SNF waste form evaluations, the DOE SNF inventory was first reduced to 34 DOE SNF groups based on fuel matrix, cladding, cladding condition, and enrichment. These parameters are the fuel characteristics that were determined to have major impacts on the release of radionuclides from the DOE SNF and contributed to nuclear criticality scenarios (DOE 2000 [DIRS 118968], Section 5). Separate groups were further refined for the purposes of criticality, design basis events, and TSPA based on key parameters such as fuel matrix, cladding, and fuel condition, as well as fissile species and enrichment, and reactor and fuel design. (DOE 2000 [DIRS 118968], Section 5.1). For criticality, nine DOE SNF criticality groups have been identified and are listed in *General Description of Database Information Version 5.0.1* (DOE 2007 [DIRS 182577], Table 6).

Within each of the nine DOE SNF criticality groups, a single fuel design was selected as being representative of the remaining fuel within each group. The term representative means that all fuels would perform similarly regarding chemical interactions within the waste package and basket, and that canister loading limits from the representative fuel (ranges of key parameters important to criticality such as linear fissile loading and total fissile mass) are established, which other fuels within the group can be shown to not exceed. Waste forms within a single criticality group that have configurations or key criticality parameters outside the range of applicability of the representative fuel will require supplemental analysis and/or additional reactivity control mechanisms.

Evaluations for naval fuel are conducted by the Naval Nuclear Propulsion Program. A miscellaneous waste form category which has a variety of fuel matrix properties originating from various postirradiation examinations and other testing is not included in the criticality evaluations for the fuel groups as they will need to be evaluated on a case-by-case basis. Thus, the disposal criticality analysis methodology (YMP 2003 [DIRS 165505]) can be applied to nine DOE SNF representative fuel groups for criticality evaluations.

The minimum fissile mass necessary for criticality external to the waste packages is discussed in *Geochemistry Model Validation Report: External Accumulation Model* (SNL 2007 [DIRS 181395], Section 8.1.4[a]), where it was concluded that insufficient fissile material can collect over 10,000 years to achieve a critical mass for the igneous scenario. In addition, these values are predicated on having an initiating event (i.e., igneous intrusive event causing drip shield and waste package failure), which is an unlikely event (1.7×10^{-8} per year). The critical mass limits were evaluated for commercial SNF and DOE SNF waste forms using bounding parameters with regards to optimizing reactivity potential, so the actual masses that would be necessary to achieve criticality would most likely need to be far greater than what was identified (SNL 2007 [DIRS 181395], Section 8.1.4[a]).

Model abstractions were performed for commercial SNF and three DOE SNF waste forms in *Geochemistry Model Validation Report: External Accumulation Model* (SNL 2007 [DIRS 181395]) (i.e., N Reactor (DOE3), TMI (DOE9), and FFTF (DOE1)) (SNL 2008 [DIRS 173869], Section 4.1.15), which make up approximately 90% of the metric tons of heavy metal in the DOE SNF inventory expected to be stored in the repository. In addition to these waste forms making up ~90% of the inventory by mass, they were selected because they provide degradation and accumulation characteristics of uranium-metal (N Reactor), mixed-oxide (FFTF), and damaged uranium dioxide (TMI) waste forms which may be applicable to other representative DOE waste forms. Some of the other DOE SNF waste forms, such as Shippingport light-water breeder reactor (LWBR) (DOE5) and Ft. St. Vrain (DOE6) are not expected to be a concern for external criticality due to the corrosion resistance of the waste form (SNL 2007 [DIRS 181395], Section 6.9.3[a]).

Ft. St. Vrain fuels (DOE6) have an integral silicon carbide (SiC) protective layer that not only retains the fission products but also protects the uranium and thorium dicarbide (ThC_2) from oxidation and hydrolysis (DOE 2003 [DIRS 166027], p. 48). Comparative analysis has indicated that the Ft. St. Vrain fuel has the lowest degradation rate of all DOE SNF and should behave significantly better in terms of fissile material dissolution, transport, and accumulation. In some residual quantities (< 250 grams per block), ^{233}U bred into the ThC_2 fertile particles. A canister loaded with five Ft. St. Vrain blocks contains sufficient quantities of ^{233}U to have criticality potential in solution; however, a mechanism to separate the uranium from within the SiC-coated fertile particles, and then a mechanism to accumulate in a concentrated fissile mass in a favorable geometry is not credible.

For Shippingport LWBR fuel (DOE5), a number of studies has indicated that air and water oxidation of uranium and thorium oxide fuel pellets [$(Th, U)O_2$] proceeds more slowly than in pure uranium oxide (UO_2), and decreases with decreasing UO_2 content in the $(Th, U)O_2$ (DOE 2003 [DIRS 166027], p. 33). Tests have shown that the thorium oxide pellets in the Shippingport LWBR fuel have excellent corrosion resistance with an estimated solubility of

10^{-14} mol/L at 25°C and pH > 5 (DOE 2003 [DIRS 166027], p. 32). With the less-reactive degradation rate, a mechanism to separate the uranium, transporting, and accumulation into a favorable geometry is also not credible.

Table 2.2.14.12.0A-1 shows the ranges of minimum critical mass required to accumulate as well as the calculated accumulation or mass released from the waste package for the waste forms evaluated for external criticality. For each of the waste forms evaluated, the results indicate that an insufficient amount of fissile material accumulates to pose a criticality concern.

Table 2.2.14.12.0A-1. Summary of Igneous Scenario External Criticality Results

Scenario	Waste Package Type	Calculated Accumulation or Mass Released from Waste Package	Mass of Uranium or Plutonium (for FFTF) Required to Achieve Critical Limit of k_{eff} = 0.96		
		Uranium Mass, Unless Otherwise Noted (kg)	Fractured Tuff	Lithophysae Array	Large Lithophysa
Igneous	DOE3 (N Reactor)	0.109	Infinite[a]	Infinite	Infinite
	DOE9 (TMI II Fuel)	30.7	Infinite	Infinite	Infinite
	CSNF	74.8	Infinite	1,390	Infinite
	DOE1 (FFTF) (Plutonium Mass)	6.34×10^{-3}	4.3	4.0	2.2

[a] "Infinite" means that an infinite amount of fissile waste released in this model will not produce an arrangement that can reach the critical limit.

Source: SNL 2007 [DIRS 181395], Table 6.9-1[a].

DOE fuel groups in DOE2, DOE4, DOE7, and DOE8 representing UZrHx (TRIGA), high enriched uranium oxide (Shippingport PWR), aluminum-based (ATR), and U-Zr/U-Mo alloy (Fermi), respectively (SNL 2008 [DIRS 173869], Table 4.1-2), have not been analyzed in detail for external fissile mass transport and accumulation as the other waste forms have. However, considering the processes that must occur to allow advective seepage into a DOE SNF canister without substantial drainage to allow degradation of the internal components and waste form, along with the other conservative modeling parameters that have been used to create a process to facilitate fissile material transport to the external environment, and the bounding modeling parameters respective to maximizing criticality potential, these waste forms are not expected to result in an increase in the total probability of criticality in the far-field location.

Some of the conservative modeling parameters are provided as follows:

- The material degradation and release model (SNL 2007 [DIRS 181165]) uses constant corrosion rates for the SNF; however, laboratory experiments on the surface structure of commercial SNF during dissolution have shown that UO_2 dissolution is accompanied by the formation of a protective layer of secondary phases that retards further corrosion (SNL 2007 [DIRS 181165], Section 6.6.2). Therefore, the release of uranium from the fuel would be slower and therefore less would be released.

- Experimental and field data indicate that actinides would be adsorbed on or incorporated into alteration products that form in the waste package (SNL 2007 [DIRS 181165], Section 6.6.3). This solid solution formation and adsorption would tend to lower actinide concentrations below those predicted by EQ6 and would delay release from the waste package.

- Many conservative modeling approximations are used to simplify the critical mass calculations presented in Table 2.2.14.12.0A-1. For the commercial SNF and low-enriched DOE fuels analyzed in *Geochemistry Model Validation Report: External Accumulation Model* (SNL 2007 [DIRS 181395], the conservatisms are appropriate, because the results show that a criticality event is very unlikely However, for the higher enriched DOE fuels, less conservative modeling parameters of the criticality potential are expected to generate similar conclusions.

Summary—The critical mass limits were evaluated for several waste forms using bounding parameters with regards to optimizing reactivity potential, so the actual masses that would be necessary to achieve criticality would most likely need to be far greater than what was identified (SNL 2007 [DIRS 181395], Section 8.1.4[a]). Model abstractions were performed for commercial SNF and three DOE SNF waste forms and resulted in insufficient fissile material accumulation in the far-field location to pose a criticality concern. Therefore, based on the analyzed waste forms representing the majority (>95% of the total metric tons) of the waste for disposal in the mountain, and considering the conservative modeling parameters discussed above that would be further developed for other DOE representative fuel groups, in conjunction with the probablity of the igneous intrusive initiating event, the probability of near-field criticality is considered insignificant.

Accordingly, this FEP is excluded from the performance assessments conducted to demonstrate compliance with proposed 10 CFR 63.311 and 63.321 (70 FR 53313 [DIRS 178394]), and with 10 CFR 63.331 [DIRS 180319], on the basis of low probability.

In addition, as documented in *Screening Analysis of Criticality Features, Events, and Processes for License Application* (SNL 2008 [DIRS 173869]), the probability of criticality for all locations is less than 1 chance in 10,000 of occurrence within 10,000 years after disposal. The results documented in this analysis are applicable for all waste forms and waste package variants.

INPUTS:

Table 2.2.14.12.0A-2. Direct Inputs

Input	Source	Description
ASM International 1996. *Binary Alloy Phase Diagrams.* [DIRS 181641]	Fe Zr and Ni Zr phase diagrams	Formation of iron-zirconium and nickel-zirconium liquid eutectics (starting at approximately 948°C)
DOE 2003. *Review of Oxidation Rates of DOE Spent Nuclear Fuel Part 2. Nonmetallic Fuel*. [DIRS 166027]	p. 33	For Shippingport LWBR fuel (DOE5), a number of studies have indicated both air and water oxidation of uranium and thorium oxide fuel pellets [(Th, U)O_2] proceed more slowly than in pure uranium oxide (UO_2), and decreases with decreasing UO_2 content in the (Th, U)O_2
	p. 48	Ft. St. Vrain fuels (DOE6) have an integral silicon carbide (SiC) protective layer that not only retains the fission products but also protects the uranium and thorium dicarbide (ThC_2) from oxidation and hydrolysis
SNL 2007. *Geochemistry Model Validation Report: External Accumulation Model*. [DIRS 181395]	Table 6.9-1[a]	Summary of igneous scenario external criticality results
	Section 8.1.4[a]	Discusses the minimum fissile mass necessary for criticality external to the waste packages

Table 2.2.14.12.0A-3. Indirect Inputs

Citation	Title	DIRS
10 CFR 63	Energy: Disposal of High-Level Radioactive Wastes in a Geologic Repository at Yucca Mountain, Nevada	180319
70 FR 53313	Implementation of a Dose Standard After 10,000 Years	178394
BSC 2004	*Characterize Framework for Igneous Activity at Yucca Mountain, Nevada*	169989
CRWMS M&O 1996	*Probabilistic Volcanic Hazard Analysis for Yucca Mountain, Nevada*	100116
DOE 2000	*DOE Spent Nuclear Fuel Grouping in Support of Criticality, DBE, TSPA-LA*	118968
DOE 2004	*General Description of Database Information Version 5.0.1*	171271
DOE 2003	*Review of Oxidation Rates of DOE Spent Nuclear Fuel Part 2. Nonmetallic Fuel*	166027
DOE 2007	*General Description of Database Information Version 5.0.1*	182577
SNL 2007	*Dike/Drift Interactions*	177430
SNL 2007	*Geochemistry Model Validation Report: External Accumulation Model*	181395
SNL 2007	*Geochemistry Model Validation Report: Material Degradation and Release Model*	181165
SNL 2007	*UZ Flow Models and Submodels*	184614
SNL 2008	*Screening Analysis of Criticality Features, Events, and Processes for License Application*	173869
YMP 2003	*Disposal Criticality Analysis Methodology Topical Report*	165505

FEP: 2.3.01.00.0A

FEP NAME:

Topography and Morphology

FEP DESCRIPTION:

This FEP is related to the topography and surface morphology of the disposal region. Topographical features include outcrops and hills, water-filled depressions, wetlands, recharge areas and discharge areas. Topography, precipitation, and surficial permeability distribution in the system will determine the flow boundary conditions (i.e., location and amount of recharge and discharge in the system).

SCREENING DECISION:

Included

TSPA DISPOSITION:

Topographical features (such as hillslopes, washes, and ridges), precipitation, and surficial permeability distribution are included in *Simulation of Net Infiltration for Present-Day and Potential Future Climates* (SNL 2008 [DIRS 182145], Section 6.5.2[a] and Appendix B[a]), and are incorporated into the MASSIF model (DTN: SN0701T0502206.037 [DIRS 184289]), which is used to model infiltration. Precipitation and surficial permeability distributions are incorporated into the infiltration uncertainty analysis. Ranges of uncertain precipitation, permeability and many other parameters are sampled for simulations that comprise the uncertainty analysis (SNL 2008 [DIRS 182145], Sections 6.5.5 and 6.6[a], and Appendix I). Topography is captured in the MASSIF model (DTN: SN0701T0502206.037 [DIRS 184289]) using data from the Shuttle Radar Topography Mission. The Shuttle Radar Topography Mission dataset of the Yucca Mountain area has absolute errors of 12.6 m in geolocation (which is less than the 30 × 30 m grid cell size) and 7.0 m in height. "Sinks" in topography are filled to enable flow to downslope grid cells (SNL 2008 [DIRS 182145], Section B2.1[a]). This uncertainty in topography is small and not propagated through the TSPA calculations. Any increased localized net infiltration caused by topographical features will have an insignificant effect on seepage as a result of the damping and homogenizing of downward-moving percolation fluxes by the Paintbrush nonwelded hydrogeologic unit (SNL 2007 [DIRS 184614], Section 6.1.2).

The effects of surface construction and characterization activities at the ground surface on topography will be negligible because of the planned reclamation of the site ground surface. As stated in *Reclamation Implementation Plan* (YMP 2001 [DIRS 154386], Section 5.2.2.1), "Recontouring and erosion control practices include backfilling spoil material and grading disturbed sites, so that a stable land form is created that blends with the surrounding topography. Following site decommissioning, disturbed areas will be graded such that the natural drainage pattern (predisturbance drainage) is restored. The sites will be stabilized and recontoured to blend into the natural topography of the area." In addition, reclamation of lands disturbed by the repository is a design constraint listed in *Total System Performance Assessment Data Input*

Package for Requirements Analysis for Subsurface Facilities (SNL 2007 [DIRS 179466], Table 4-1, Parameter Number 09-04).

The impacts of topography and morphology on preferential flow/percolation in the unsaturated zone are incorporated into the TSPA through the unsaturated zone flow fields, which use the infiltration model results (DTNs: SN0609T0502206.024 [DIRS 179063], SN0609T0502206.028 [DIRS 178753], and SN0609T0502206.029 [DIRS 178862]) as upper boundary conditions (SNL 2007 [DIRS 184614], Section 6.5.7 and Appendix I). Topographical features from GFM2000 (BSC 2004 [DIRS 170029]) are captured in the unsaturated zone model grid developed in *Development of Numerical Grids for UZ Flow and Transport Modeling* (BSC 2004 [DIRS 169855]) and used in *UZ Flow Models and Submodels* (SNL 2007 [DIRS 184614], Section 6.1.1). The incorporation of unsaturated zone flow fields into the TSPA is described in *UZ Flow Models and Submodels* (SNL 2007 [DIRS 184614], Section 6.6).

INPUTS:

Table 2.3.01.00.0A-1. Indirect Inputs

Citation	Title	DIRS
BSC 2004	*Development of Numerical Grids for UZ Flow and Transport Modeling*	169855
BSC 2004	*Geologic Framework Model (GFM2000)*	170029
DTN: SN0609T0502206.024	Monsoon Net Infiltration Results	179063
DTN: SN0609T0502206.028	Present-Day Net Infiltration Results	178753
DTN: SN0609T0502206.029	Glacial Transition Net Infiltration Results	178862
DTN: SN0701T0502206.037	Massif Calculation of Net Infiltration at Yucca Mountain, Rev 1	184289
SNL 2007	*Total System Performance Assessment Data Input Package for Requirements Analysis for Subsurface Facilities*	179466
SNL 2007	*UZ Flow Models and Submodels*	184614
SNL 2008	*Simulation of Net Infiltration for Present-Day and Potential Future Climates*	182145
YMP 2001	*Reclamation Implementation Plan*	154386

FEP: 2.3.02.01.0A

FEP NAME:

Soil Type

FEP DESCRIPTION:

Soil type is determined by many different factors (e.g., formative process, geology, climate, vegetation, land use). The physical and chemical attributes of the surficial soils (such as organic matter content and pH) may influence the mobility of radionuclides.

SCREENING DECISION:

Included

TSPA DISPOSITION:

Soil is a feature constituting part of the reference biosphere and is therefore included, consistent with the requirement that FEPs describing the reference biosphere be consistent with present knowledge of the conditions in the Yucca Mountain region (10 CFR 63.305(a) [DIRS 180319]). Soil is the biosphere medium containing the majority of the radionuclide inventory in the reference biosphere. Soil type is included in the biosphere model through the selection of the soil type-dependent values of model input parameters that may influence radionuclide transport to and from the surface soil. Specifically, the soil type is considered in the soil, plant, and ^{14}C submodels of the biosphere model. The characteristics of soils are based, in part, on the characteristics of soil types in northern Amargosa Valley (SNL 2007 [DIRS 179993]).

The biosphere model parameters relevant to soil type are surface soil (tillage) depth (BSC 2004 [DIRS 169673], Section 6.10), soil bulk density (SNL 2007 [DIRS 179993], Section 6.2), partition coefficients (SNL 2007 [DIRS 179993], Section 6.3), surface soil erosion rate (SNL 2007 [DIRS 179993], Section 6.4), enhancement factors for resuspension (SNL 2007 [DIRS 179993], Section 6.5), soil water content (SNL 2007 [DIRS 179993], Section 6.6), irrigation intensity (BSC 2004 [DIRS 169673], Section 6.6), and ^{14}C emission rate from soil (BSC 2004 [DIRS 169672], Section 6.7.1).

As described in included FEP 1.2.04.07.0C (Ash Redistribution via Soil and Sediment Transport), tephra redistribution may influence radionuclide transport to, and mobility in, soil at the RMEI location. Soil properties considered in the tephra redistribution model are ash density (SNL 2007 [DIRS 179347], Table 6.4-1) and effective diffusivity (SNL 2007 [DIRS 179347], Section 6.5.8).

This FEP is included in the biosphere component of the TSPA model through the use of groundwater exposure scenario biosphere dose conversion factors (BDCFs), which are direct inputs to the TSPA for the scenario classes involving radionuclide release to the groundwater (SNL 2007 [DIRS 177399], Section 6.11.3). The annual doses from the groundwater contamination are calculated as the product of radionuclide concentration in groundwater and the BDCFs. If a volcanic eruption occurs, this FEP is included through BDCFs for the volcanic ash

exposure scenario (SNL 2007 [DIRS 177399], Section 6.12.3). In the event of a volcanic eruption, the annual doses are calculated as the product of radionuclide concentration in the soil contaminated by radionuclides in volcanic tephra, the BDCF components, and the mass loading time decrease function. For the volcanic ash exposure scenario, three BDCF components are provided to the TSPA model that account for various RMEI exposure pathways (SNL 2007 [DIRS 177399], Section 6.12.3). See included FEP 3.3.04.02.0A (Inhalation) for a more detailed description of the volcanic BDCF components.

The BDCFs for all biosphere model realizations are provided as inputs to the TSPA model, which randomly samples these inputs to propagate uncertainty from the biosphere model into TSPA dose calculations. The present-day climate BDCFs are used for the assessment of doses to the RMEI for 10,000 years following disposal, as well as after 10,000 years, but within the period of geologic stability (SNL 2007 [DIRS 177399], Sections 6.11.3 and 6.12.3).

This FEP is included for the performance assessment to demonstrate compliance with the individual protection standards (proposed 10 CFR 63.311 (70 FR 53313 [DIRS 178394])) and the performance assessment to demonstrate compliance with the individual protection standards for human intrusion (proposed 10 CFR 63.321 (70 FR 53313 [DIRS 178394])) because both these standards implicitly require including the reference biosphere in the performance assessment calculations. This FEP is not included for the performance assessment to demonstrate compliance with the groundwater protection standards (10 CFR 63.331 [DIRS 180319]) because this standard does not require including the reference biosphere in the performance assessment calculations.

INPUTS:

Table 2.3.02.01.0A-1. Indirect Inputs

Citation	Title	DIRS
70 FR 53313	Implementation of a Dose Standard After 10,000 Years	178394
BSC 2004	*Agricultural and Environmental Input Parameters for the Biosphere Model*	169673
BSC 2004	*Environmental Transport Input Parameters for the Biosphere Model*	169672
SNL 2007	*Biosphere Model Report*	177399
SNL 2007	*Redistribution of Tephra and Waste by Geomorphic Processes Following a Potential Volcanic Eruption at Yucca Mountain, Nevada*	179347
SNL 2007	*Soil-Related Input Parameters for the Biosphere Model*	179993

FEP: 2.3.02.02.0A

FEP NAME:

Radionuclide Accumulation in Soils

FEP DESCRIPTION:

Radionuclide accumulation in soils may occur as a result of upwelling of contaminated groundwater (leaching, evaporation at discharge location), deposition of contaminated water or particulates (irrigation water, runoff), and/or atmospheric deposition.

SCREENING DECISION:

Included

TSPA DISPOSITION:

This FEP focuses on radionuclide accumulation in soils as a result of irrigation with the contaminated water. The potential for radionuclide accumulation in soils as a result of upwelling of contaminated groundwater is discussed in detail in excluded FEP 2.2.08.11.0A (Groundwater Discharge to Surface within the Reference Biosphere). The impacts of air deposition on the accumulation of radionuclides in soil are discussed in included FEP 3.2.10.00.0A (Atmospheric Transport of Contaminants). Radionuclide accumulation in soils resulting from atmospheric deposition is also addressed in included FEP 1.2.04.07.0C (Ashfall) and in included FEP 1.2.04.07.0C (Ash Redistribution via Soil and Sediment Transport).

Radionuclide accumulation in soil as a result of long-term irrigation is an integral process in the modeling of biosphere transport of radionuclides. Radionuclide accumulation in soil is accounted for in the soil submodel of the biosphere model for the groundwater exposure scenario by assuming that radionuclides build up in the soil as a result of long-term irrigation (SNL 2007 [DIRS 177399], Section 6.4.1). The concentrations of radionuclides in the soil are calculated as a function of groundwater concentrations; the annual irrigation duration and irrigation rate for crops; and loss by radionuclide decay, leaching, and soil erosion (SNL 2007 [DIRS 177399], Section 6.4.1). This calculation is based on the conservation of the mass of radionuclides in the surface soil. Leaching is included in the soil submodel to account for the residence time of radionuclides in the surface soil and their removal to deeper soil. The leaching rate is a function of the amount of water that percolates below the surface soil (i.e., the overwatering rate that depends on the overall water balance in the surface soil and considers storage capacity of the soil, precipitation, and evapotranspiration), element-specific solid-liquid partition coefficients, and other soil properties (e.g., bulk density, soil porosity, and soil moisture content). In the present-day arid conditions at Yucca Mountain, leaching occurs primarily when irrigation water is added to flush accumulated salts from the surface soil to maintain plant productivity. In wetter climates, such as those predicted to occur in the future at Yucca Mountain, leaching will also occur when excess precipitation flows through the surface soil, primarily during winter. Other mechanisms of radionuclide loss from surface soil, such as runoff, are not directly included in the biosphere model. Soil erosion accounts for the loss of deposited radionuclides from irrigated lands by wind and water erosion. The rate of soil loss from erosion is dependent on soil

characteristics, land use, and stewardship. To incorporate these influences, the minimum soil erosion rate used in the biosphere model was selected based on the soil loss by erosion on noncultivated cropland in Nevada (SNL 2007 179993], Section 6.4).

Radionuclide accumulation in soils is incorporated into the performance assessment calculations through the following parameters: the annual average irrigation rate (BSC 2004 [DIRS 169673], Section 6.5; SNL 2007 [DIRS 177399], Section 6.4.1.1), overwatering rate (BSC 2004 [DIRS 169673], Section 6.9), surface soil depth (tillage depth) (BSC 2004 [DIRS 169673], Section 6.10), soil solid-liquid partition coefficient (SNL 2007 [DIRS 179993], Section 6.3), soil bulk density (SNL 2007 [DIRS 179993], Section 6.2), soil water content (SNL 2007 [DIRS 179993], Section 6.6), surface soil erosion rate (SNL 2007 [DIRS 179993], Section 6.4), irrigation duration (SNL 2007 [DIRS 179993], Section 6.7), and the thickness of the soil layer that can become resuspended (BSC 2004 [DIRS 169672], Section 6.8).

The degree of elemental solubility may have an effect on the rate of removal of radionuclides from soils by leaching, thereby affecting the magnitude and duration of radionuclide accumulation in soil. For the groundwater exposure scenario, where radionuclides are introduced into the biosphere from groundwater use, the solubility limits are not achieved for radionuclides introduced as solutes (i.e., the rate of radionuclide removal from soil by leaching is proportional to the radionuclide concentration in the soil) (SNL 2007 [DIRS 177399], Sections 6.4.1.1 to 6.4.1.3).

Those radionuclides that reach the biosphere irreversibly attached to colloidal particles will not take part in sorption exchange processes with soil and will, therefore, be transported through the soil system without any sorption build-up in soil. Because these radionuclides are not dissolved, they are not available for plant uptake (via soil to plant transfer). However, in the biosphere model, radionuclide transfer from the soil to crops via root uptake is proportional to the radionuclide concentration in the surface soil (SNL 2007 [DIRS 177399], Section 6.4.3.1) (i.e., all radionuclides (solutes and colloids) in groundwater are assumed to be dissolved and available for plant uptake). This is a conservative approach for cases where colloids are present, because the activity associated with colloids is made available for plant uptake.

For the volcanic ash exposure scenario, the mode of radionuclide release into the biosphere is a volcanic eruption through the repository with the resulting entrainment of contaminated waste in the tephra, followed by the atmospheric transport, deposition, and redistribution of radioactive contaminants to the location of the RMEI (SNL 2007 [DIRS 177399], Section 6.12.3). These transport processes, leading to radionuclide accumulation on the soil, are addressed in the atmospheric tephra dispersion and deposition model (SNL 2007 [DIRS 177431]) and in the tephra redistribution model (SNL 2007 [DIRS 179347]). The contaminated tephra transported from the drainage basin, as well as the primary deposit of contaminated tephra at the RMEI location, provide the initial conditions for the redistribution of contaminants in the soil column at the RMEI location. The tephra redistribution model considers the migration of contaminants in the soil as a diffusion process that includes suspension and redeposition of fine particles by infiltration and physical mixing of soil particles by freeze-thaw cycles and bioturbation. The processes of radionuclide accumulation in soil as a result of a volcanic eruption through the repository are addressed in included FEP 1.2.04.07.0A (Ashfall) and in included FEP 1.2.04.07.0C (Ash Redistribution via Soil and Sediment Transport).

Radionuclide accumulation in soils is included in the biosphere component of the TSPA model through the use of groundwater exposure scenario biosphere dose conversion factors (BDCFs) that are direct inputs to the TSPA for the scenario classes involving radionuclide release to the groundwater (SNL 2007 [DIRS 177399], Section 6.11.3). The annual doses are calculated as the product of radionuclide concentration in groundwater and the BDCFs. In the event of a volcanic eruption, this FEP is included through BDCFs for the volcanic ash exposure scenario (SNL 2007 [DIRS 177399], Section 6.12.3). In the event of a volcanic eruption, the annual doses are calculated as the product of radionuclide concentration in the soil contaminated by radionuclides in volcanic tephra, the BDCF components, and the mass loading time decrease function. For the volcanic ash exposure scenario, three BDCF components are provided to the TSPA model that account for various RMEI exposure pathways (SNL 2007 [DIRS 177399], Section 6.12.3). See included FEP 3.3.04.02.0A (Inhalation) for a more detailed description of the volcanic BDCF components.

The BDCFs for all biosphere model realizations are provided as inputs to the TSPA model, which randomly samples these inputs to propagate uncertainty from the biosphere model into TSPA dose calculations. The present-day climate BDCFs are used for the assessment of doses to the RMEI for 10,000 years following disposal, as well as after 10,000 years, but within the period of the geologic stability (SNL 2007 [DIRS 177399], Sections 6.11.3 and 6.12.3).

This FEP is included for the performance assessment to demonstrate compliance with the individual protection standards (proposed 10 CFR 63.311 (70 FR 53313 [DIRS 178394])) and the performance assessment to demonstrate compliance with the individual protection standards for human intrusion (proposed 10 CFR 63.321 (70 FR 53313 [DIRS 178394])) because both these standards implicitly require including the reference biosphere in the performance assessment calculations. This FEP is not included for the performance assessment to demonstrate compliance with the groundwater protection standards (10 CFR 63.331 [DIRS 180319]) because this standard does not require including the reference biosphere in the performance assessment calculations.

INPUTS:

Table 2.3.02.02.0A-1. Indirect Inputs

Citation	Title	DIRS
10 CFR 63	Energy: Disposal of High-Level Radioactive Wastes in a Geologic Repository at Yucca Mountain, Nevada	180319
70 FR 53313	Implementation of a Dose Standard After 10,000 Years	178394
BSC 2004	*Agricultural and Environmental Input Parameters for the Biosphere Model*	169673
BSC 2004	*Environmental Transport Input Parameters for the Biosphere Model*	169672
SNL 2007	*Biosphere Model Report*	177399
SNL 2007	*Atmospheric Dispersal and Deposition of Tephra from a Potential Volcanic Eruption at Yucca Mountain, Nevada*	177431
SNL 2007	*Redistribution of Tephra and Waste by Geomorphic Processes Following a Potential Volcanic Eruption at Yucca Mountain, Nevada*	179347
SNL 2007	*Soil-Related Input Parameters for the Biosphere Model*	179993

FEP: 2.3.02.03.0A

FEP NAME:

Soil and Sediment Transport in the Biosphere

FEP DESCRIPTION:

Contaminated sediments can be transported to and through the biosphere by surface runoff and fluvial processes, and, to a lesser extent, by aeolian processes and bioturbation. Sediment transport and redistribution may cause concentration or dilution of radionuclides in the biosphere.

SCREENING DECISION:

Included

TSPA DISPOSITION:

Soil and sediment transport are processes currently occurring in the Yucca Mountain region, and are included in the TSPA. This is consistent with the requirement that FEPs describing the reference biosphere be consistent with present knowledge of the conditions in the region surrounding the Yucca Mountain site (10 CFR 63.305(a) [DIRS180319]). This FEP is addressed in the soil and air submodels of the biosphere model (SNL 2007 [DIRS 177399], Table 6.7-1). The soil and sediment transport processes are also included in the tephra redistribution model (SNL 2007 [DIRS 179347]) through included FEP 1.2.04.07.0C (Ash Redistribution via Soil and Sediment Transport).

Although the region around Yucca Mountain currently lacks permanent surface water bodies, sediment transport may occur by fluvial processes (e.g., during flash floods). The role of surface water in soil and sediment transport will increase if wetter climate conditions occur in the future. There are several environmental transport processes included in the biosphere model that result in soil and sediment transport. One of these processes is removal of radionuclides from the surface soil by erosion. Soil erosion in agricultural fields is incorporated into the soil submodel for the groundwater exposure scenario in calculation of the surface soil erosion removal rate constant (SNL 2007 [DIRS 177399], Section 6.4.1.4). Soil erosion includes soil loss and gain on farm fields (SNL 2007 [DIRS 179993], Section 6.4). The soil and sediment transport under the wetter climate would result in a greater rate of radionuclide removal from the surface soil than that for the present-day climate. This increased removal of contaminants from the reference biosphere was conservatively not accounted for in the biosphere model.

Bioturbation is the process of sediment or soil mixing by biological activity. However, in the case of a deep geologic repository, bioturbation cannot bring waste to the surface soil layer (see excluded FEP 2.3.09.01.0A (Animal Burrowing/Intrusion)). The process of bioturbation, although not explicitly included in the biosphere model, may contribute to radionuclide mixing in the soil, as modeled in the surface soil submodel of the biosphere model for the groundwater exposure scenario (SNL 2007 [DIRS 177399], Section 6.4.1.1). Bioturbation may also play a

role in radionuclide diffusion in the soil, as represented in the tephra redistribution model (SNL 2007 [DIRS 179347]).

For a volcanic radionuclide release, the soil and sediment transport occurs after contaminated volcanic ash settles to the ground. The tephra redistribution model (SNL 2007 [DIRS 179347]) uses a spatially distributed analysis of hillslopes and channels in the Fortymile Wash drainage basin (upstream of the alluvial fan apex) to estimate the mass of contaminated tephra that is transported from the drainage basin to the alluvial fan by hillslope and fluvial processes. Materials on slopes greater than a specified critical angle and in active channels are mobilized, mixed, and diluted as they are transported toward the RMEI location during flood events. Sediment mixing in channels is estimated with a scour-dilution-mixing model that explicitly includes the vertical mixing of contaminants with uncontaminated channel sediments within the scour zone, and the model is applicable for both tributary and distributary channels like the Fortymile Wash system. The mixing depths in channels are defined by the depths to the tops of the carbonate and clay-rich soil horizons of reduced permeability compared to the active zones (i.e., the depths to the petrocalcic horizon). The contaminated tephra transported from the drainage basin and the primary deposit of contaminated tephra at the RMEI location provide the initial conditions for the redistribution of contaminants in the soil at the RMEI location. The model considers the migration of contaminants in the soil as a diffusion process that includes suspension and redeposition of fine particles by infiltration and physical mixing of soil particles by freeze-thaw cycles and bioturbation. The processes of soil and sediment transport as a result of tephra redistribution are addressed in included FEP 1.2.04.07.0C (Ash Redistribution via Soil and Sediment Transport).

Soil and sediment transport is accounted for in the biosphere soil and air submodels as represented by the following parameters: surface soil erosion rate (SNL 2007 [DIRS 179993], Section 6.4), soil bulk density (SNL 2007 [DIRS 179993], Section 6.2), dry deposition velocity (BSC 2004 [DIRS 169672], Section 6.2.2.1), enhancement factor (SNL 2007 [DIRS 179993], Section 6.5), tillage depth (BSC 2004 [DIRS 169673], Section 6.10), and mass loading decrease constant (BSC 2006 [DIRS 177101], Section 6.4). Distributions of the mass loading decrease constants were developed based, in part, on the influence of ash redistribution on changes in mass loading through time (BSC 2006 [DIRS 177101], Section 6.4).

This FEP is included in the biosphere component of the TSPA model through the use of groundwater exposure scenario BDCFs that are direct inputs to TSPA for the scenario classes involving radionuclide release to the groundwater (SNL 2007 [DIRS 177399], Section 6.3.1). The annual doses are calculated as the product of radionuclide concentration in groundwater and the BDCFs. In the event of a volcanic eruption, this FEP is included through BDCFs for the volcanic ash exposure scenario (SNL 2007 [DIRS 177399], Section 6.12.3). The annual doses are calculated in TSPA as the product of radionuclide concentration in the soil contaminated by radionuclides in volcanic tephra, the BDCF components, and the mass loading time decrease function. For the volcanic ash exposure scenario, three BDCF components are provided to the TSPA model that account for various RMEI exposure pathways (SNL 2007 [DIRS 177399], Section 6.12.3). See included FEP 3.3.04.02.0A (Inhalation) for a more detailed description of the volcanic BDCF components.

The BDCFs for all biosphere model realizations are provided as inputs to the TSPA model, which randomly samples these inputs to propagate uncertainty from the biosphere model into TSPA dose calculations. The present-day climate BDCFs are used for the assessment of doses to the RMEI for 10,000 years following disposal, as well as after 10,000 years, but within the period of geologic stability (SNL 2007 [DIRS 177399], Sections 6.11.3 and 6.12.3).

This FEP is included for the performance assessment to demonstrate compliance with the individual protection standards (proposed 10 CFR 63.311 (70 FR 53313 [DIRS 178394])) and the performance assessment to demonstrate compliance with the individual protection standards for human intrusion (proposed 10 CFR 63.321 (70 FR 53313 [DIRS 178394])) because both these standards implicitly require including the reference biosphere in the performance assessment calculations. This FEP is not included for the performance assessment to demonstrate compliance with the groundwater protection standards (10 CFR 63.331 [DIRS 180319]) because this standard does not require including the reference biosphere in the performance assessment calculations.

INPUTS:

Table 2.3.02.03.0A-1. Indirect Inputs

Citation	Title	DIRS
10 CFR 63	Energy: Disposal of High-Level Radioactive Wastes in a Geologic Repository at Yucca Mountain, Nevada	180319
70 FR 53313	Implementation of a Dose Standard After 10,000 Years	178394
BSC 2004	*Agricultural and Environmental Input Parameters for the Biosphere Model*	169673
BSC 2004	*Environmental Transport Input Parameters for the Biosphere Model*	169672
BSC 2006	*Inhalation Exposure Input Parameters for the Biosphere Model*	177101
SNL 2007	*Biosphere Model Report*	177399
SNL 2007	*Redistribution of Tephra and Waste by Geomorphic Processes Following a Potential Volcanic Eruption at Yucca Mountain, Nevada*	179347
SNL 2007	*Soil-Related Input Parameters for the Biosphere Model*	179993

FEP: 2.3.04.01.0A

FEP NAME:

Surface Water Transport and Mixing

FEP DESCRIPTION:

Radionuclides released from an underground repository might enter the biosphere through discharge of deep groundwater into a lake or river. Transport and mixing within the surface water bodies affects the subsequent behavior and transport of radionuclides in the biosphere. Transport and mixing includes dilution, sedimentation, aeration, streamflow, and river meander.

SCREENING DECISION:

Included

TSPA DISPOSITION:

The region around Yucca Mountain currently lacks permanent surface water bodies. Future climate forecasts, based on the analysis of paleoclimatic conditions in the Yucca Mountain region (BSC 2004 [DIRS 170002], Section 7.1), indicate that the climate will evolve to a cooler, wetter state over the next 10,000 years, as discussed in included FEP 1.3.01.00.0A (Climate Change). The role of surface water in radionuclide transport will increase if wetter climate conditions occur in the future. However, any surface water that may discharge under future climate states would occur south of the accessible environment (D'Agnese et 1999 [DIRS 120425], Figure 11).

The biosphere model for the groundwater exposure scenario can accomodate surface water transport and mixing because the model applies to the use of any contaminated water, regardless of its origin (surface water body or well), as long as the reference biosphere, water use practices, and the characteristics of the RMEI remain essentially unchanged. The biosphere dose conversion factors (BDCFs) calculated by the biosphere model for the groundwater exposure scenario are developed for unit radionuclide concentration in the water, and therefore the results of biosphere modeling are independent of the actual radionuclide concentration in the water and its origin. Therefore, this FEP is included in the conceptual biosphere model and is considered in the model analogous to included FEP 1.4.07.02.0A (Wells), in the soil, air, plant, animal, fish, ^{14}C, and ingestion submodels (SNL 2007 [DIRS 177399], Table 6.7-1).

The biosphere model conservatively assumes that only contaminated water is used in agriculture, animal husbandry, and for human consumption. This assumption bounds the possible effects of surface water transport and mixing (e.g., as a result of flooding) because such processes would reasonably result in dilution of radionuclide concentrations in the soil.

This FEP is included in the biosphere component of the TSPA model through the use of groundwater exposure scenario BDCFs that are direct inputs to the TSPA for the scenario classes involving radionuclide release to the groundwater (SNL 2007 [DIRS 177399], Section 6.11.3). The BDCFs for all biosphere model realizations are provided as inputs to the TSPA model,

which randomly samples these inputs to propagate uncertainty from the biosphere model into TSPA dose calculations. The present-day climate BDCFs are used for the assessment of doses to the RMEI for 10,000 years following disposal, as well as after 10,000 years, but within the period of the geologic stability (SNL 2007 [DIRS 177399], Sections 6.11.3 and 6.12.3).

This FEP is included for the performance assessment to demonstrate compliance with the individual protection standards (proposed 10 CFR 63.311 (70 FR 53313 [DIRS 178394])) and the performance assessment to demonstrate compliance with the individual protection standards for human intrusion (proposed 10 CFR 63.321 (70 FR 53313 [DIRS 178394])) because both these standards implicitly require including the reference biosphere in the performance assessment calculations. This FEP is not included for the performance assessment to demonstrate compliance with the groundwater protection standards (10 CFR 63.331 [DIRS 180319]) because this standard does not require including the reference biosphere in the performance assessment calculations.

INPUTS:

Table 2.3.04.01.0A-1. Indirect Inputs

Citation	Title	DIRS
10 CFR 63	Energy: Disposal of High-Level Radioactive Wastes in a Geologic Repository at Yucca Mountain, Nevada	180319
70 FR 53313	Implementation of a Dose Standard After 10,000 Years	178394
BSC 2004	*Future Climate Analysis*	170002
D'Agnese et al. 1999	*Simulated Effects of Climate Change on the Death Valley Regional Ground-Water Flow System, Nevada and California*	120425
SNL 2007	*Biosphere Model Report*	177399

FEP: 2.3.06.00.0A

FEP NAME:

Marine Features

FEP DESCRIPTION:

This FEP addresses marine and coastal features and processes. Processes include erosion, sedimentation, deposition, sea-level change, and storms.

SCREENING DECISION:

Excluded – low consequence

SCREENING JUSTIFICATION:

Considering the location of Yucca Mountain relative to the continental boundaries of the United States (Stuckless and Levich 2007 [DIRS 181507], p. 10), the potential for impact of coastal or marine features and processes on the area around Yucca Mountain is considered to have negligible consequences.

Future climate forecasts based on the analysis of paleoclimatic conditions that have occurred in the Yucca Mountain region (BSC 2004 [DIRS 170002], Section 7.1) indicate that the climate will evolve to a cooler, wetter climate over the next 10,000 years. Monsoon and intermediate (glacial-transition) climate states are forecasted to last until 38,000 years after the present (Sharpe 2003 [DIRS 161591], Table 6-5). Although these climates are cooler and slightly wetter than the present-day interglacial climate, the changes are expected to have no effect on current coastlines relative to Yucca Mountain. Coastline evolution could also occur as a result of tectonic activity. However, the large scale tectonic events that would affect the physical properties of the Yucca Mountain region are not expected to occur, as discussed in exclude FEP 1.2.01.01.0A (Tectonic Activity – Large Scale).

Omission of FEP 2.3.06.00.0A (Marine Features) will not result in a significant adverse change in the magnitude or timing of either radiological exposure to the RMEI or radionuclide releases to the accessible environment. Therefore, this FEP is excluded from the performance assessments conducted to demonstrate compliance with proposed 10 CFR 63.311 and 10 CFR 63.321 (70 FR 53313 [DIRS 178394]), and with 10 CFR 63.331 [DIRS 180319], on the basis of low consequence.

INPUTS:

Table 2.3.06.00.0A-1. Direct Inputs

Input	Source	Description
Stuckless and Levich 2007. *The Geology and Climatology of Yucca Mountain and Vicinity, Southern Nevada and California*. [DIRS 181507]	p. 10	Map showing approximate location of Yucca Mountain relative to Pacific coast

Table 2.3.06.00.0A-2. Indirect Inputs

Citation	Title	DIRS
10 CFR 63	Energy: Disposal of High-Level Radioactive Wastes in a Geologic Repository at Yucca Mountain, Nevada	180319
70 FR 53313	Implementation of a Dose Standard After 10,000 Years	178394
BSC 2004	*Future Climate Analysis*	170002
Sharpe 2003	*Future Climate Analysis—10,000 Years to 1,000,000 Years After Present*	161591

FEP: 2.3.09.01.0A

FEP NAME:

Animal Burrowing/Intrusion

FEP DESCRIPTION:

Burrowing animals may intrude into the repository, promoting release and spread of contamination. Burrowing animals may also contact or ingest contaminated soil.

SCREENING DECISION:

Excluded – low consequence

SCREENING JUSTIFICATION:

The overburden thickness from the emplacement area to the topographic surface at Yucca Mountain is at least 200 m (SNL 2007 [DIRS 179466], Table 4-1, Parameter Number 01-06). The depth of soil above the bedrock in the immediate vicinity of Yucca Mountain is shallow, with most soils having a median depth of 0.25 m (SNL 2008 [DIRS 182145], Figure 6.5.2.4-1[a] and Table 6.5.2.4-2[a]). A small fraction of soils are categorized as moderately deep and intermediate with median depths of about 12 and 2 m, respectively (SNL 2008 [DIRS 182145], Figure 6.5.2.4-1[a] and Table 6.5.2.4-2[a]). Because the soil depth is a small fraction of the overburden thickness, it is reasonable to conclude that the animal burrows would not extend to the repository level. The observed maximum depth of animal burrows in the arid Yucca Mountain environment is about 3 m for vertebrates (e.g., gophers, moles, ground squirrels, and lizards) and about 10 m for invertebrates (e.g., ants and termites) (Cochran et al. 2001 [DIRS 163189], Section 5.8). Therefore, although burrowing species are known to occur at Yucca Mountain (Cochran et al. 2001 [DIRS 163189], Appendix H; DOE 2002 [DIRS 155970], Section 3.1.5.1.2), it is very unlikely that wildlife will burrow to 200 m or more, and move radioactive waste to the ground surface where it could be subjected to transport by surficial geomorphic processes to the accessible environment.

In the location of the reference biosphere, if burrowing animals come in contact with contaminated soil they can cause bioturbation and thus contribute to the mixing of the contaminants in the soil. Bioturbation is included in the soil submodel of the biosphere model for the groundwater release, where it is assumed that the radionuclide concentration in the surface soil cannot be less than that for the uniformly mixed surface soil (SNL 2007 [DIRS 177399], Section 6.4.1.1). The effect of bioturbation is also included in the tephra redistribution model for igneous eruptive events (SNL 2007 [DIRS 179347]), where this process is considered to contribute to the migration of contaminants in the soil. Bioturbation as a transport process is addressed in included FEP 2.3.02.02.0A (Soil and Sediment Transport in the Biosphere).

If burrowing animals ingest soil, they could potentially enter the food chain of some other species at a higher trophic level. As these animals are primarily rodents (Cochran et al. 2001 [DIRS 163189], Appendix H; DOE 2002 [DIRS 155970], Section 3.1.5.1.2), it is not expected

that this food chain would include humans directly. Therefore, ingestion of contaminated soil by burrowing animals would have a negligible effect on the dose to the RMEI.

Although not specifically discussed in the FEP description, intrusion by bats is potentially relevant to Yucca Mountain because of its location above the water table. Backfill in the shafts and ramps that connect the waste disposal regions with the land surface (SNL 2007 [DIRS 179466], Table 4-3, Parameter Number 09-01) will prevent bat intrusion. Even if such intrusion occurs and bats become contaminated, effects on the dose to the RMEI would be negligible because of the distance from Yucca Mountain to the compliance location and because bats are not expected to significantly contribute to human exposure pathways, including the human food chain.

In summary, animal intrusion directly into the repository is not expected, and even if should it occur, for example, by burrowing animals or bats, the effect on the dose to the RMEI would be negligible. The effects of animal burrowing in contaminated soil at the compliance location would likewise have negligible impact the dose to the RMEI, beyond the indirect effect of soil bioturbation that is included in the biosphere model.

Because omission of FEP 2.3.09.01.0A (Animal Burrowing/Intrusion) will not result in a significant adverse change in the magnitude or timing of either radiological exposure to the RMEI or radionuclide releases to the accessible environment, this FEP is excluded from the performance assessments conducted to demonstrate compliance with proposed 10 CFR 63.311 and 63.321 (70 FR 53313 [DIRS 178394]), and with 10 CFR 63.331 [DIRS 180319], on the basis of low consequence.

INPUTS:

Table 2.3.09.01.0A-1. Direct Inputs

Input	Source	Description
SNL 2007. *Total System Performance Assessment Data Input Package for Requirements Analysis for Subsurface Facilities*. [DIRS 179466]	Table 4-1, Parameter Number 01-06	The minimum overburden thickness at the repository is 200 m
SNL 2008. *Simulation of Net Infiltration for Present-Day and Potential Future Climates*. [DIRS 182145]	Figure 6.5.2.4-1[a] and Table 6.5.2.4-2[a]	Surface soil depth in the repository area

Table 2.3.09.01.0A-2. Indirect Inputs

Citation	Title	DIRS
10 CFR 63	Energy: Disposal of High-Level Radioactive Wastes in a Geologic Repository at Yucca Mountain, Nevada	180319
70 FR 53313	Implementation of a Dose Standard After 10,000 Years	178394
Cochran et al. 2001	*Compliance Assessment Document for the Transuranic Wastes in the Greater Confinement Disposal Boreholes at the Nevada Test Site, Volume 2: Performance Assessment, Version 2.0*	163189
DOE 2002	*Final Environmental Impact Statement for a Geologic Repository for the Disposal of Spent Nuclear Fuel and High-Level Radioactive Waste at Yucca Mountain, Nye County, Nevada*	155970
SNL 2007	*Biosphere Model Report*	177399
SNL 2007	*Redistribution of Tephra and Waste by Geomorphic Processes Following a Potential Volcanic Eruption at Yucca Mountain, Nevada*	179347
SNL 2007	*Total System Performance Assessment Data Input Package for Requirements Analysis for Subsurface Facilities*	179466

FEP: 2.3.11.01.0A

FEP NAME:

Precipitation

FEP DESCRIPTION:

Precipitation is an important control on the amount of infiltration, flow in the unsaturated zone, seepage into the repository, and groundwater recharge. It transports solutes with it as it flows downward through the subsurface or escapes as runoff. Precipitation influences agricultural practices of the receptor. The amount of precipitation depends on climate.

SCREENING DECISION:

Included

TSPA DISPOSITION:

Precipitation is included in the model of the unsaturated zone above the repository, consistent with the requirements of proposed 10 CFR 63.114(a)(5) (70 FR 53313 [DIRS 178394]), and in the reference biosphere model, consistent with the requirements of 10 CFR 63.305 [DIRS 180319 and DIRS 178394]. Precipitation levels are currently low, ranging from 100 to 250 mm/yr (DOE 2002 [DIRS 155970], Section 3.1.2.2). Future climate forecasts (BSC 2004 [DIRS 170002]) indicate that the climate at Yucca Mountain is predicted to evolve to the cooler, wetter conditions of a glacial transition climate within the first 10,000 years after disposal, as discussed in included FEP 1.3.01.00.0A (Climate Change).

Precipitation affects net infiltration into the unsaturated zone. Water balance, climate, and snowpack are included in *Simulation of Net Infiltration for Present-Day and Potential Future Climate* (SNL 2008 [DIRS 182145], Section 6.4), and precipitation under present-day and potential future climate states is represented in that same report (SNL 2008 [DIRS 182145], Section 6.5.1). Long-term (1,000-year) daily precipitation data are stochastically generated using local site-specific data to generate the precipitation records for the present-day climate and using analogue site data to generate records for the future climate states. A total of 120 realizations of 1,000-year daily precipitation records are generated for three climate states (40 for present-day, 40 for monsoon, and 40 for glacial-transition climate states) (SNL 2008 [DIRS 182145], Section 6.5 and Appendix F[a]). Ten representative years are selected from each of these realizations resulting in 40 10-year precipitation records for each of the three climate states predicted to occur in the first 10,000 years postclosure for use in simulating infiltration using the MASSIF model (SNL 2008 [DIRS 182145], Section 6.4). Long duration, low intensity precipitation events are expected to result in net infiltration while short duration, high intensity precipitation events are expected to result in runoff of surface water. The effect of rainfall intensity on surface water runoff is included in *Simulation of Net Infiltration for Present-Day and Potential Future Climate* (SNL 2008 [DIRS 182145], Section 7.1.3[a]).

The net infiltration map outputs (DTNs: SN0609T0502206.028 [DIRS 178753], SN0609T0502206.024 [DIRS 179063], and SN0609T0502206.029 [DIRS 178862] for

present-day, monsoon, and glacial-transition climates, respectively) are used as a boundary condition for the UZ flow model (SNL 2007 [DIRS 184614], Sections 6.1.3 and 6.1.4). Flow fields developed for use in the TSPA (DTNs: LB0612PDFEHMFF.001 [DIRS 179296], LB0701MOFEHMFF.001 [DIRS 179297], LB0701GTFEHMFF.001 [DIRS 179160], and LB0702PAFEM10K.002 [DIRS 179507]) using the UZ flow model, therefore, include the effects of precipitation and changes of precipitation under future climate conditions, including the 10th, 30th, 50th, and 90th percentile maps of infiltration rates for present-day, monsoon, and glacial-transition climate states.

For the period beyond 10,000 years, within the period of geologic stability, the effects of precipitation are accounted for in the distribution of deep percolation rates at the repository horizon for the post-10,000-year period, specified in proposed 10 CFR 63.342(c)(2) (70 FR 53313 [DIRS 178394]). The proposed rule defines the deep percolation rates for that period as represented by a log-uniform probability distribution from 13 to 64 mm/yr. Unsaturated zone flow weighting factors were used to calibrate the UZ model using input from 12 infiltration maps representing the 10th, 30th, 50th, and 90th percentile infiltration scenarios for each of the present-day, monsoon, and glacial-transition climates. The weighting factors were calculated to be 0.62, 0.16, 0.16, and 0.06 for the 10th, 30th, 50th, and 90th percentile infiltration scenarios. The midpoints of these probability ranges for a cumulative probability distribution are at 0.31, 0.70, 0.86, and 0.97, respectively. These midpoints were applied to the log-uniform proposed percolation flux range of 13 to 64 mm/yr, resulting in targets of 21.29, 39.52, 51.05, and 61.03 mm/yr for the 10th, 30th, 50th, and 90th percentile infiltration scenarios, respectively. These midpoints were compared to the average infiltration calculated (over the repository footprint) for the 12 infiltration maps. Four maps were selected that most closely matched the midpoint values. The four infiltration maps that were selected and scaled are: the present-day 90th percentile, the glacial-transition 50th percentile, the glacial-transition 90th percentile, and the monsoon 90th percentile infiltration maps. These maps were scaled so that the average water flux rates through the repository footprint exactly matched the target values at the repository horizon. Once the infiltration boundary condition was determined, the methods used to generate the post-10,000-year flow fields were the same as those used to generate the pre-10,000-year flow fields (SNL 2007 [DIRS 184614], Section 6.1.4).

Although precipitation is not directly used as input to the mathematical biosphere model, it is used to derive the values of parameters, such as leaching rate and irrigation rates, which depend on the overall water balance (SNL 2007 [DIRS 177399], Table 6.2-1). Specifically, precipitation rate, along with irrigation rate and evapotranspiration rate, are used to calculate the overwatering rate (BSC 2004 [DIRS 169673], Section 6.9), a parameter that controls infiltration of water, and thus radionuclide transport, below the root zone. Distributions of parameters were developed based in part on variation and uncertainty in precipitation for the present-day and predicted future climate states (BSC 2004 [DIRS 169673], Sections 6.5 and 6.7 to 6.9).

Within the biosphere model, precipitation is addressed in the soil, plant, and ^{14}C submodels. The relevant parameters are annual average irrigation rate (BSC 2004 [DIRS 169673], Section 6.5), overwatering rate (BSC 2004 [DIRS 169673], Section 6.9), irrigation amount per application (BSC 2004 [DIRS 169673], Section 6.7), and daily irrigation rate (BSC 2004 [DIRS 169673], Section 6.8).

Precipitation is assumed to cause the transport of radioactive waste-contaminated tephra following a potential volcanic eruption through the repository. Precipitation is inherently included in the tephra redistribution model (DOE 2007 [DIRS 179347]), which uses a spatially distributed analysis of hillslopes and channels in the Fortymile Wash drainage basin to provide an estimate of the mass of contaminated tephra that is transported from the drainage basin to the alluvial fan by hillslope and fluvial processes.

The effects of precipitation in the reference biosphere are included in the biosphere component of the TSPA model through the use of groundwater exposure scenario BDCFs that are direct inputs to the TSPA for the scenario classes involving radionuclide release to the groundwater (SNL 2007 [DIRS 177399]). The annual doses are calculated as the product of radionuclide concentration in groundwater and the BDCFs.

The effects of precipitation in the reference biosphere are also included in the event of a volcanic eruption through BDCFs for the volcanic ash exposure scenario (SNL 2007 [DIRS 177399], Section 6.1.3) (because the mass loading levels and some agricultural parameters may depend on precipitation) and the radioactive waste concentration in the soil calculated by the tephra redistribution model (SNL 2007 [DIRS 179347]). The annual doses are calculated in the TSPA as the product of radionuclide concentration in the soil contaminated by radionuclides in volcanic tephra, the BDCF components, and the mass loading time decrease function. For the volcanic ash exposure scenario, three BDCF components are provided to the TSPA model that account for various RMEI exposure pathways (SNL 2007 [DIRS 177399], Section 6.12.3). See included FEP 3.3.04.02.0A (Inhalation) for a more detailed description of the volcanic BDCF components.

The BDCFs for all biosphere model realizations are provided as inputs to the TSPA model, which randomly samples these inputs to propagate uncertainty from the biosphere model into TSPA dose calculations. The present-day climate BDCFs are used for the assessment of doses to the RMEI for 10,000 years following disposal, as well as after 10,000 years, but within the period of geologic stability (SNL 2007 [DIRS 177399], Sections 6.11.3 and 6.12.3).

In summary, precipitation is included in the TSPA model of the geosphere and biosphere transport for the performance assessments that demonstrate compliance with the individual protection standards in proposed 10 CFR 63.311 and 63.321 (70 FR 53313 [DIRS 178394]). For the human intrusion event (proposed 10 CFR 63.321 (70 FR 53313 [DIRS 178394])), only the post-10,000-year conditions are used, because the human intrusion event is not expected to occur before 10,000 years following disposal. For the performance assessment that demonstrates compliance with the groundwater protection standards (10 CFR 63.331 [DIRS 180319]), only those components of this FEP that address the geosphere transport are included.

INPUTS:

Table 2.3.11.01.0A-1. Indirect Inputs

Citation	Title	DIRS
10 CFR 63	Energy: Disposal of High-Level Radioactive Wastes in a Geologic Repository at Yucca Mountain, Nevada	180319
70 FR 53313	Implementation of a Dose Standard After 10,000 Years	178394
BSC 2004	*Agricultural and Environmental Input Parameters for the Biosphere Model*	169673
BSC 2004	*Future Climate Analysis*	170002
DOE 2002	*Final Environmental Impact Statement for a Geologic Repository for the Disposal of Spent Nuclear Fuel and High-Level Radioactive Waste at Yucca Mountain, Nye County, Nevada*	155970
DTN: LB0612PDFEHMFF.001	Flow-Field Conversions from TOUGH2 to FEHM Format for Present Day 10-, 30-, 50-, and 90-Percentile Infiltration Maps	179296
DTN: LB0701GTFEHMFF.001	Flow-Field Conversions from TOUGH2 to FEHM Format for Glacial Transition Climate 10th-, 30th-, 50th-, and 90th-Percentile Infiltration Maps	179160
DTN: LB0701MOFEHMFF.001	Flow-Field Conversions from TOUGH2 to FEHM Format for Monsoon Climate 10th-, 30th-, 50th-, and 90th-Percentile Infiltration Maps	179297
DTN: LB0702PAFEM10K.002	Flow Field Conversions to FEHM Format for Post 10,000 Year Peak Dose Fluxes in the Unsaturated Zone for Four Selected Infiltration Rates	179507
DTN: SN0609T0502206.024	Monsoon Net Infiltration Results	179063
DTN: SN0609T0502206.028	Present-Day Net Infiltration Results	178753
DTN: SN0609T0502206.029	Glacial Transition Net Infiltration Results	178862
SNL 2007	*Biosphere Model Report*	177399
SNL 2007	*Redistribution of Tephra and Waste by Geomorphic Processes Following a Potential Volcanic Eruption at Yucca Mountain, Nevada*	179347
SNL 2007	*UZ Flow Models and Submodels*	184614
SNL 2008	*Simulation of Net Infiltration for Present-Day and Potential Future Climates*	182145

FEP: 2.3.11.02.0A

FEP NAME:

Surface Runoff and Evapotranspiration

FEP DESCRIPTION:

Surface water runoff and evapotranspiration are components in the water balance, together with precipitation, infiltration, and change in soil water storage. Surface runoff produces erosion, and can feed washes, arroyos, and impoundments, where flooding may lead to increased recharge. Evapotranspiration removes water from soil and rock by evaporation and transpiration via plant root water uptake.

SCREENING DECISION:

Included

TSPA DISPOSITION:

Evapotranspiration and surface runoff affect net infiltration, as discussed in *Simulation of Net Infiltration for Present-Day and Potential Future Climates* (SNL 2008 [DIRS 182145], Section 6.4). The net infiltration map outputs (DTNs: SN0609T0502206.028 [DIRS 178753], SN0609T0502206.024 [DIRS 179063], and SN0609T0502206.029 [DIRS 178862]) are used as a boundary condition for the UZ flow model (SNL 2007 [DIRS 184614], Sections 6.1.3 and 6.1.4). Flow fields developed for use in the TSPA (DTNs: LB0612PDFEHMFF.001 [DIRS 179296], LB0701MOFEHMFF.001 [DIRS 179297], LB0701GTFEHMFF.001 [DIRS 179160], and LB0702PAFEM10K.002 [DIRS 179507]) using the UZ flow model, therefore, include the effects of runoff and evapotranspiration under present-day and future climate conditions. Four infiltration maps for each of the four climate states (present-day, monsoon, glacial transition, and post-10,000-year climate state) were used as boundary conditions for the calculation of the flow fields for TSPA. The four maps correspond to the 10th, 30th, 50th, and 90th percentiles of average annual net infiltration realizations for the present-day, monsoon, and glacial-transition climate states. For the post-10,000-year period, net infiltration maps representing present-day 90th percentile, glacial-transition 50th percentile, glacial-transition 90th percentile, and monsoon 90th percentile, respectively, are used to represent the four infiltration realizations.

INPUTS:

Table 2.3.11.02.0A-1. Indirect Inputs

Citation	Title	DIRS
DTN: LB0612PDFEHMFF.001	Flow-Field Conversions from TOUGH2 to FEHM Format for Present Day 10-, 30-, 50-, and 90-Percentile Infiltration Maps	179296
DTN: LB0701GTFEHMFF.001	Flow-Field Conversions from TOUGH2 to FEHM Format for Glacial Transition Climate 10th-, 30th-, 50th-, and 90th-Percentile Infiltration Maps	179160
DTN: LB0701MOFEHMFF.001	Flow-Field Conversions from TOUGH2 to FEHM Format for Monsoon Climate 10th-, 30th-, 50th-, and 90th-Percentile Infiltration Maps	179297
DTN: LB0702PAFEM10K.002	Flow Field Conversions to FEHM Format for Post 10,000 Year Peak Dose Fluxes in the Unsaturated Zone for Four Selected Infiltration Rates	179507
DTN: SN0609T0502206.024	Monsoon Net Infiltration Results	179063
DTN: SN0609T0502206.028	Present-Day Net Infiltration Results	178753
DTN: SN0609T0502206.029	Glacial Transition Net Infiltration Results	178862
SNL 2007	*UZ Flow Models and Submodels*	184614
SNL 2008	*Simulation of Net Infiltration for Present-Day and Potential Future Climates*	182145

FEP: 2.3.11.03.0A

FEP NAME:

Infiltration and Recharge

FEP DESCRIPTION:

Infiltration into the subsurface provides a boundary condition for groundwater flow in the unsaturated zone. The amount and location of the infiltration influences the amount of seepage entering the drifts; and the amount and location of recharge influences the height of the water table, the hydraulic gradient, and therefore specific discharge. Different sources of infiltration could change the composition of groundwater passing through the repository. Mixing of these waters with other groundwaters could result in mineral precipitation, dissolution, and altered chemical gradients in the subsurface.

SCREENING DECISION:

Included

TSPA DISPOSITION:

Infiltration—The infiltration process is simulated by the net infiltration model MASSIF, described in *Simulation of Net Infiltration for Present-Day and Potential Future Climates* (SNL 2008 [DIRS 182145]). This model includes the effects of seasonal and climate variations, climate change, evapotranspiration, surface-water runoff, and site topography such as hill slopes and washes to simulate the spatial distribution of infiltration. The time dependence of infiltration results is linked to the timing of climate change, as discussed in included FEP 1.3.01.00.0A (Climate Change). The infiltration model output is in the form of infiltration maps that are used to propogate infiltration uncertainty through to the TSPA results.

The results of the infiltration model (infiltration maps) provide input to the unsaturated zone flow model, which simulates the spatial distribution of percolation fluxes within the unsaturated zone. Specifically, the UZ flow model uses the infiltration results as the top boundary condition for unsaturated zone flow calculations (SNL 2007 [DIRS 184614], Section 6.1.4). A total of 16 unsaturated zone flow fields are used in *Total System Performance Assessment Model/Analysis for the License Application* (SNL 2008 [DIRS 183478], Section 6.3.1.3). The flow conditions at the top boundary of the UZ flow model are provided from twelve net infiltration maps (four maps for the present-day, monsoon, and glacial-transition climate states that correspond to the 10th, 30th, 50th, and 90th percentile infiltration scenarios for each of these climate states) and four maps for the period from 10,000 years postclosure to the time of geologic stability. Unsaturated zone flow weighting factors were used to calibrate the probabilities of the infiltration boundary conditions in the UZ model using input from the present-day infiltration maps. The weighting factors were calculated to be 0.62, 0.16, 0.16, and 0.06 for the 10th, 30th, 50th, and 90th percentile infiltration scenarios, respectively. The midpoints of these probability ranges for a cumulative probability distribution are at 0.31, 0.70, 0.86, and 0.97, respectively (SNL 2007 [DIRS 184614], Section 6.1.4).

For the post-10,000-year period, proposed rule 10 CFR 63.342(c) (70 CFR 53313 [DIRS 178394]) defines the deep percolation rates for that period as based on a log-uniform probability distribution from 13 to 64 mm/yr. This distribution was divided into four intervals to develop four flow fields that most closely matched target rates based on the proposed rule. The midpoint of each interval was used to represent the average flux for the given flow field. The four midpoint values are 21.29, 39.52, 51.05, and 61.03 mm/yr (SNL 2007 [DIRS 184614], Table 6.1-3). Four corresponding net infiltration maps representing present-day 90th percentile, glacial-transition 50th percentile, glacial-transition 90th percentile, and monsoon 90th percentile, respectively, are used to represent these intervals. Net infiltration for these four cases was scaled so that the average water flux through the repository footprint matched the target values (interval midpoints) at the repository horizon. Once the infiltration boundary condition was determined, the method used to generate the post-10,000-year flow fields was the same as that used to generate the pre-10,000-year flow fields (SNL 2007 [DIRS 184614], Section 6.1.4).

Percolation fluxes are used to calculate seepage fluxes into the repository, condensation onto the drift walls, evolution of thermal-hydrologic and chemical conditions in the unsaturated zone and repository, and radionuclide transport from the repository to the saturated zone. These processes are all affected by changes in infiltration and are discussed in more detail in other FEPs (e.g., included FEP 1.3.01.00.0A (Climate Change)).

The effects of present-day water composition infiltrating from the ground surface are accounted for in the analysis of seepage-water chemistry by using the measured pore-water chemistry in the unsaturated zone (SNL 2007 [DIRS 177404], Table 6.2-1). However, pore-water chemistry varies by hydrologic unit (SNL 2007 [DIRS 177404], Figure 6.2-4). Variation in the composition of infiltrating water is dominated by rock–water interaction.

Recharge—Recharge to the saturated zone is important because it impacts transport time of radionuclides that could potentially escape from the repository. The hydrological effects of recharge are included in *Saturated Zone Site-Scale Flow Model* (SNL 2007 [DIRS 177391]). The recharge to the flow model was derived from three sources: *Death Valley Regional Ground-Water Flow System, Nevada and California - Hydrogeologic Framework and Transient Ground-Water Flow Model* (Belcher 2004 [DIRS 173179]), *UZ Flow Models and Submodels* (SNL 2007 [DIRS 184614]), and Fortymile Wash data (Savard 1998 [DIRS 102213]). Recharge from the UZ site-scale model (percolation flux) was taken as the flow through the base of that model, the domain of which includes approximately 40 km^2 (19.3 mi^2) that encompasses only the footprint of Yucca Mountain, a very small fraction of the saturated zone model domain. The technique for estimated recharge from all three sources is summarized here:

- The distributed vertical recharge, limited to the northernmost portion of the SZ site-scale flow model domain for areas not covered by the unsaturated zone model domain and forty-mile wash, was extracted from the 2004 SZ regional-scale flow model (DTN: MO0602SPAMODAR.000 [DIRS 177371]).

- The recharge through each node of the UZ flow model is extracted and the corresponding recharge to the saturated zone site-scale flow model node was calculated. This is necessary because the UZ flow model grid is finer than the saturated zone site-scale grid.

- Estimates of recharge from the infiltration of surface flows in Fortymile Wash are given by linear reaches (discrete segments) along the wash. Recharge estimates were interpolated to at least a 500-m (1,640-ft) -wide recharge zone for most of the wash and a broader area of tributary channels in the Amargosa Desert (BSC 2004 [DIRS 170015], Table 6-3, Figure 6-6).

Details as to how recharge to the saturated zone site-scale flow model is calculated are described in *Recharge and Lateral Groundwater Flow Boundary Conditions for the Saturated Zone Site-Scale Flow and Transport Model* (BSC 2004 [DIRS 170015], Sections 6.5 and 6.7).

The effects of present-day water composition entering the saturated zone from recharge are accounted for in the analysis of water chemistry described in Appendices A and B of *Saturated Zone Site-Scale Flow Model* (SNL 2007 [DIRS 177391]) and the site-scale saturated zone transport model (SNL 2008 [DIRS 184806]).

This FEP is included in the performance assessments conducted to demonstrate compliance with proposed 10 CFR 63.311 and 10 CFR 63.321 (70 FR 53313 [DIRS 178394]), and with 10 CFR 63.331 [DIRS 180319]. Groundwater protection requirements specified in 10 CFR 63.331 [DIRS 180319] are only applicable to the 10,000-year period after disposal. Therefore, the post-10,000-year climate is not included in the performance assessment conducted to evaluate compliance with the groundwater protection requirements.

INPUTS:

Table 2.3.11.03.0A-1. Indirect Inputs

Citation	Title	DIRS
10 CFR 63	Energy: Disposal of High-Level Radioactive Wastes in a Geologic Repository at Yucca Mountain, Nevada	180319
70 FR 53313	Implementation of a Dose Standard After 10,000 Years	178394
Belcher 2004	*Death Valley Regional Ground-Water Flow System, Nevada and California - Hydrogeologic Framework and Transient Ground-Water Flow Model*	173179
BSC 2004	*Recharge and Lateral Groundwater Flow Boundary Conditions for the Saturated Zone Site-Scale Flow and Transport Model*	170015
DTN: MO0602SPAMODAR.000	Model Archives from USGS Special Investigations Report 2004-5205, Death Valley Regional Ground-Water Flow System, Nevada and California-Hydrogeologic Framework and Transient Ground-Water Flow Model	177371
Savard 1998	*Estimated Ground-Water Recharge from Streamflow in Fortymile Wash Near Yucca Mountain, Nevada*	102213
SNL 2007	*Saturated Zone Site-Scale Flow Model*	177391
SNL 2007	*Drift-Scale THC Seepage Model*	177404
SNL 2007	*UZ Flow Models and Submodels*	184614
SNL 2008	*Simulation of Net Infiltration for Present-Day and Potential Future Climates*	182145
SNL 2008	*Site-Scale Saturated Zone Transport*	184806
SNL 2008	*Total System Performance Assessment Model/Analysis for the License Application*	183478

FEP: 2.3.11.04.0A

FEP NAME:

Groundwater Discharge to Surface Outside the Reference Biosphere

FEP DESCRIPTION:

Radionuclides transported in groundwater as solutes or solid materials (colloids) from the far-field may discharge at specific "entry" points that are outside the reference biosphere. Natural surface discharge points, including those resulting from water table or capillary rise, may be surface water bodies (rivers, lakes), springs, wetlands, holding ponds, or unsaturated soils.

SCREENING DECISION:

Excluded – by regulation

SCREENING JUSTIFICATION:

The reference biosphere is defined as the description of the environment inhabited by the RMEI (10 CFR 63.2 [DIRS 180319]). The postclosure individual protection standard is formulated in terms of annual dose limits to the RMEI (proposed 10 CFR 63.311 and 10 CFR 63.321 (70 FR 53313 [DIRS 178394])). Only those FEPs that affect the reference biosphere can affect the RMEI and, thereby, be included in the performance assessment. Therefore, groundwater discharge to the surface outside the reference biosphere is excluded by regulation.

INPUTS:

Table 2.3.11.04.0A-1. Direct Inputs

Input	Source	Description
10 CFR 63. 2007. Energy: Disposal of High-Level Radioactive Wastes in a Geologic Repository at Yucca Mountain, Nevada. [DIRS 180319]	10 CFR 63.2	The reference biosphere is defined as the description of the environment inhabited by the RMEI

Table 2.3.11.04.0A-2. Indirect Inputs

Citation	Title	DIRS
70 FR 53313	Implementation of a Dose Standard After 10,000 Years	178394

FEP: 2.3.13.01.0A

FEP NAME:

Biosphere Characteristics

FEP DESCRIPTION:

The principal components, conditions, or characteristics of the biosphere system can influence radionuclide transport and affect the long-term performance of the disposal system. These include the characteristics of the reference biosphere such as climate, soils and microbes, flora and fauna, and their influences on human activities.

SCREENING DECISION:

Included

TSPA DISPOSITION:

Consideration of FEPs that describe the reference biosphere, and which are consistent with present knowledge of the conditions in the region surrounding Yucca Mountain, is required under 10 CFR 63.305(a) [DIRS 180319]. Biosphere characteristics based on cautious but reasonable assumptions consistent with present knowledge of potential changes in geology, hydrology, and climate are included in accordance with proposed 10 CFR 63.305(c) (70 FR 53313 [DIRS 178394]). Therefore, this FEP is included, consistent with the requirements of these regulatory sections.

Both the individual protection requirements (proposed 10 CFR 63.311 (70 FR 53313 [DIRS 178394])) and the individual protection requirements for human intrusion (proposed 10 CFR 63.321 (70 FR 53313 [DIRS 178394])) limit dose to the reasonably maximally exposed individual (RMEI). By definition, the RMEI lives in the reference biosphere (10 CFR 63.102(i) [DIRS 180319]). Therefore, biosphere characteristics are included in the performance assessments to demonstrate compliance with the individual protection and human intrusion requirements. In contrast, the groundwater protection standards do not limit the dose to the RMEI (10 CFR 63.331 [DIRS 180319]); therefore, this FEP is not included in the performance assessment to demonstrate compliance with the groundwater protection standard. The dose from drinking 2 liters of water per day from the representative volume is calculated by using a required daily consumption rate of water (10 CFR 63.331 [DIRS 180319]) without regard to the characteristics of the biosphere and the RMEI.

Biosphere characteristics encompass the principal components, conditions, and characteristics of the reference biosphere that influence contaminant transport from the point of release into the accessible environment to the receptor. This FEP includes the natural environment (e.g., climate, soils, flora, and fauna) and human activities, such as land and water use. The relationships among these components form the foundation of the biosphere model (SNL 2007 [DIRS 177399], Section 6.3.4). Some of these characteristics, particularly those relating to the soils, are also included in the tephra redistribution model (SNL 2007 [DIRS 179347]) (see included FEP 1.2.04.07.0C (Ash Redistribution via Soil and Sediment Transport)).

Distributions of parameter values were developed based in part on variation and uncertainty in site-specific characteristics of the reference biosphere, such as temperature, wind speed, and evaporation rate (BSC 2004 [DIRS 169673], Sections 6.4 to 6.9; BSC 2005 [DIRS 172827], Section 6.3.4.2; BSC 2004 [DIRS 169672], Sections 6.2.2.1, 6.4.3, 6.5.2, and 6.7.2). This FEP is addressed in the soil, air, plant, animal, fish, inhalation, and ^{14}C submodels (SNL 2007 [DIRS 177399], Table 6.7-1) through many parameters, such as the annual average irrigation rate (BSC 2004 [DIRS 169673], Section 6.5), overwatering rate (BSC 2004 [DIRS 169673], Section 6.9), water evaporation rate (use rate) for evaporative coolers (BSC 2004 [DIRS 169672], Section 6.5.2), dry deposition velocity (BSC 2004 [DIRS 169672], Section 6.2.2.1), daily irrigation rate (BSC 2004 [DIRS 169673], Section 6.8), irrigation application (BSC 2004 [DIRS 169673], Section 6.7), irrigation intensity (BSC 2004 [DIRS 169673], Section 6.6), growing time (BSC 2004 [DIRS 169673], Section 6.4), water concentration modifying factor (BSC 2004 [DIRS 169672], Sections 6.4.3 and 6.4.5), annual average wind speed (BSC 2004 [DIRS 169672], Section 6.7.2), and evaporative cooler use factor (BSC 2005 [DIRS 172827], Section 6.3.4.2). Additional biosphere characteristics are covered by other included FEPs, such as FEP 1.3.01.00.0A (Climate Change), FEP 2.3.02.01.0A (Soil Type), and FEP 2.3.11.01.0A (Precipitation).

This FEP is included in the biosphere component of the TSPA model through the use of groundwater exposure scenario BDCFs that are direct inputs to the TSPA for the scenario classes involving radionuclide release to the groundwater (SNL 2007 [DIRS 177399], Section 6.11.3). The annual doses are calculated as the product of radionuclide concentration in groundwater and the BDCFs. Such an approach is possible because quantities calculated in the groundwater exposure scenario submodels of the biosphere model, including radionuclide concentrations in the environmental media and the annual dose from various exposure pathways, are proportional to the radionuclide concentration in the groundwater (SNL 2007 [DIRS 177399], Section 6.4.10.2). Thus, for this exposure scenario, the biosphere model contribution to the dose assessment (i.e., BDCFs) can be separated from the source (i.e., radionuclide concentration in the groundwater). The BDCF for a radionuclide is numerically equal to the dose for a unit activity concentration of the radionuclide in the water (SNL 2007 [DIRS 177399], Section 6.4.10.2).

In the event of a volcanic eruption, this FEP is included in the TSPA through BDCFs for the volcanic ash exposure scenario (SNL 2007 [DIRS 177399], Section 6.12.3). The annual doses calculated in the event of a volcanic eruption depend primarily on radionuclide concentration in soil contaminated by radionuclides in volcanic tephra and the BDCFs. Because variation in radionuclide concentrations in the soil contaminated by deposited and redistributed volcanic tephra is not part of the biosphere model, BDCFs are calculated based on a unit radionuclide concentration in the soil (1 Bq/m^2 and 1 Bq/kg, depending on the exposure pathway) (SNL 2007 [DIRS 177399], Section 6.5). The TSPA model calculates radiation dose as a product of the time-dependent source terms, the source-independent BDCFs, and the mass loading time decay function. For the volcanic ash exposure scenario, three BDCF components are provided to the TSPA model that account for various RMEI exposure pathways (SNL 2007 [DIRS 177399], Section 6.12.3). See included FEP 3.3.04.02.0A (Inhalation) for a more detailed description of the volcanic BDCF components.

The BDCFs for all biosphere model realizations are provided as inputs to the TSPA model, which randomly samples these inputs to propagate uncertainty from the biosphere model into

TSPA dose calculations. The present-day climate BDCFs are used for the assessment of doses to the RMEI for 10,000 years following disposal, as well as after 10,000 years, but within the period of the geologic stability (SNL 2007 [DIRS 177399], Sections 6.11.3 and 6.12.3).

This FEP is included for the performance assessment to demonstrate compliance with the individual protection standard (proposed 10 CFR 63.311 (70 FR 53313 [DIRS 178394])) and the performance assessment to demonstrate compliance with the individual protection standard for human intrusion (proposed 10 CFR 63.321 (70 FR 53313 [DIRS 178394])) because both these standards require including the reference biosphere in the performance assessment calculations. This FEP is not included for the performance assessment to demonstrate compliance with the groundwater protection standards (10 CFR 63.331 [DIRS 180319]) because this standard does not require including the reference biosphere in the performance assessment calculations.

INPUTS:

Table 2.3.13.01.0A-1. Indirect Inputs

Citation	Title	DIRS
10 CFR 63	Energy: Disposal of High-Level Radioactive Wastes in a Geologic Repository at Yucca Mountain, Nevada	180319
70 FR 53313	Implementation of a Dose Standard After 10,000 Years	178394
BSC 2004	*Agricultural and Environmental Input Parameters for the Biosphere Model*	169673
BSC 2004	*Environmental Transport Input Parameters for the Biosphere Model*	169672
BSC 2005	*Characteristics of the Receptor for the Biosphere Model*	172827
SNL 2007	*Biosphere Model Report*	177399
SNL 2007	*Redistribution of Tephra and Waste by Geomorphic Processes Following a Potential Volcanic Eruption at Yucca Mountain, Nevada*	179347

FEP: 2.3.13.02.0A

FEP NAME:

Radionuclide Alteration During Biosphere Transport

FEP DESCRIPTION:

Once in the biosphere, radionuclides may be transported and transferred through and between different compartments of the biosphere. Temporally and spatially dependent physical and chemical environments in the biosphere may lead to alteration of both the physical and chemical properties of the radionuclides as they move through or between the different compartments of the biosphere. These alterations could consequently control exposure to the human population.

SCREENING DECISION:

Included

TSPA DISPOSITION:

The biosphere model is constructed around the radionuclide transfer interaction matrix (SNL 2007 [DIRS 177399], Sections 6.3.1.3 and 6.3.2.3, for the groundwater and volcanic ash exposure scenarios, respectively), which is constructed to identify the important processes leading to radionuclide transfer between biosphere components. Most of these transfer processes involve the change of physical and chemical forms of a radionuclide (alteration). Examples of processes involving the change of the physical form of radionuclides include the release of ^{14}C, initially present in groundwater, from the soil to the air as $^{14}CO_2$ (SNL 2007 [DIRS 177399], Section 6.4.6) and from the surface water (fish ponds) to the air (BSC 2004 [DIRS 169672], Section 6.4.4), the plant uptake of carbon dioxide from the air (SNL 2007 [DIRS 177399], Section 6.4.6.3), and release of gaseous species during operation of evaporative coolers (SNL 2007 [DIRS 177399], Section 6.4.2.2).

This FEP is also implicitly implemented through the use of element-specific partition coefficients (SNL 2007 [DIRS 179993], Section 6.3), radionuclide-specific and crop-type-specific soil-to-plant transfer factors (BSC 2004 [DIRS 169672], Section 6.2.1.2), correlation coefficients for the partition coefficients and transfer factors (BSC 2004 [DIRS 169672], Section 6.2.1.5), and radionuclide-specific and animal-product-specific transfer factors (BSC 2004 [DIRS 169672], Section 6.3.3) in the plant and animal submodels, respectively, as identified in *Biosphere Model Report* (SNL 2007 [DIRS 177399], Sections 6.4 and 6.5). In addition, this FEP is implemented in the following parameters: bioaccumulation factor for aquatic food (BSC 2004 [DIRS 169672], Sections 6.4.3 and 6.4.4), water concentration modification factor for fishpond water (BSC 2004 [DIRS 169672], Sections 6.4.3 and 6.4.5), fraction of radionuclides in evaporative cooler water transferred to air (BSC 2004 [DIRS 169672], Section 6.5.2), carbon emission rate constant for soil (BSC 2004 [DIRS 169672], Section 6.7.1), and fraction of air-derived and soil-derived carbon in plants (BSC 2004 [DIRS 169672], Section 6.7.3).

Radionuclide alteration during redistribution of volcanic tephra following a volcanic eruption (SNL 2007 [DIRS 179347]) is addressed in included FEP 1.2.04.07.0C (Ash Redistribution via Soil and Sediment Transport).

This FEP is included in the biosphere component of the TSPA model through the use of groundwater exposure scenario BDCFs that are direct inputs to the TSPA for the scenario classes involving radionuclide release to the groundwater (SNL 2007 [DIRS 177399], Section 6.11.3). The annual doses are calculated as the product of radionuclide concentration in groundwater and the BDCFs. This FEP is also included in the TSPA volcanic eruption modeling case through BDCFs for the volcanic ash exposure scenario (SNL 2007 [DIRS 177399], Section 6.12.3). The annual doses are calculated in this TSPA modeling case as the product of radionuclide concentration in soil contaminated by radionuclides in volcanic tephra, the BDCF components, and the mass loading time decrease function. For the volcanic ash exposure scenario, three BDCF components are provided to the TSPA model that account for various RMEI exposure pathways (SNL 2007 [DIRS 177399], Section 6.12.3). See included FEP 3.3.04.02.0A (Inhalation) for a more detailed description of the volcanic BDCF components.

The BDCFs for all biosphere model realizations are provided as inputs to the TSPA model, which randomly samples these inputs to propagate uncertainty from the biosphere model into TSPA dose calculations. The present-day climate BDCFs are used for the assessment of doses to the reasonably maximally exposed individual (RMEI) for 10,000 years following disposal, as well as after 10,000 years, but within the period of the geologic stability (SNL 2007 [DIRS 177399], Sections 6.11.3 and 6.12.3).

This FEP is included for the performance assessment to demonstrate compliance with the individual protection standards (proposed 10 CFR 63.311 (70 FR 53313 [DIRS 178394])) and the performance assessment to demonstrate compliance with the individual protection standards for human intrusion (proposed 10 CFR 63.321 (70 FR 53313 [DIRS 178394])) because both these standards implicitly require including the reference biosphere in the performance assessment calculations. This FEP is not included for the performance assessment to demonstrate compliance with the groundwater protection standards (10 CFR 63.331 [DIRS 180319]) because this standard does not require including the reference biosphere in the performance assessment calculations.

INPUTS:

Table 2.3.13.02.0A-1. Indirect Inputs

Citation	Title	DIRS
70 FR 53313	Implementation of a Dose Standard After 10,000 Years	178394
BSC 2004	*Environmental Transport Input Parameters for the Biosphere Model*	169672
SNL 2007	*Biosphere Model Report*	177399
SNL 2007	*Redistribution of Tephra and Waste by Geomorphic Processes Following a Potential Volcanic Eruption at Yucca Mountain, Nevada*	179347
SNL 2007	*Soil-Related Input Parameters for the Biosphere Model*	179993

FEP: 2.3.13.03.0A

FEP NAME:

Effects of Repository Heat on the Biosphere

FEP DESCRIPTION:

Heat released from radioactive decay of the waste may increase the temperatures at the surface above the repository. This could result in local or extensive changes in the ecological characteristics.

SCREENING DECISION:

Excluded – low consequence

SCREENING JUSTIFICATION:

The only effect on repository performance of an increase in surface heating due repository thermal loading is a possible change of net infiltration due to changes in vegetation at the surface above the repository footprint. The following paragraphs show that this FEP can be excluded based on low consequence because the change in future net infiltration rates due to ecological changes from repository heating will be much smaller than the range of infiltration rates already included in TSPA.

The approach to predicting temperature changes near the surface is to determine the flux of repository-generated heat, multiply by depth, and divide by the thermal conductivity (Carslaw and Jaegar 1959 [DIRS 100968], Equation 2):

$$\Delta T = \frac{Q \Delta z}{AK} \qquad \text{(Eq. 2.3.13.03.0A-1)}$$

where Q/A is the heat flux (W/m^2), Δz is depth (m), and K is thermal conductivity of the near-surface (W/m-K). The heat flux is determined from a one-dimensional "SDT" submodel of the multiscale model (SNL 2008 [DIRS 184433], Section 6.2.15[a]), by examining the temperature difference across the top (rock) model layer (the tcw12 hydrostratigraphic unit). The STD submodel used in this calculation applied the thermal loading equivalent to the postclosure thermal reference case (SNL 2008 [DIRS 184433], Section 6.2.4). A maximum heat flux of 0.4 W/m^2 through this layer is calculated using the layer thickness (10.122 m) and its thermal conductivity (1.81 W/m-K) (Figure 2.3.13.03.0A-1). The greatest change in surface temperature will occur when the flux of heat upward to the surface is greatest, which is predicted to occur approximately 1,700 years after closure (Figure 2.3.13.03.0A-1; based on calculations reported in DTN: LL0702PA013MST.068 [DIRS 180553], files: /SDT/SDT55/*P3W-13-g_SDT55-03.ext* and /include_overall/*SDT-1Dds-06*, SDT submodel, output for node g3) corresponding to the monsoonal climate state (SNL 2008 [DIRS 183478], Section 6.3.1.2). Equation 2.3.13.03.0A-1 computes only the temperature change at the surface when a repository is present. The air temperature at the ground surface does not change greatly from ambient conditions due to

repository heating because the heat flux from the repository (0.4 W/m^2) is small compared to the average solar insolation at Yucca Mountain. For instance, in 2006, an annual averge solar flux at the meteorological monitoring station at Site 9 was 255 W/m^2 (DTN: MO0706METMND06.000 [DIRS 181887], parameter SOLAR_M in table for Site 9). Because the heat equation, which determines heat flow through rock or soil at the repository, is linear, temperature changes due to sources may be superimposed (added). As the surface temperature does not change much in response to the repository heat, the temperature change computed from Equation 2.3.13.03.0A-1 may be used to compute the temperature change due to the repository heat source at points below the surface.

Infiltration values averaged over the infiltration model domain for the monsoonal climate state range from 5 to as much as 80 mm/yr, a factor of 16 (DTN: SN0609T0502206.024 [DIRS 179063], file: *Monsoon_R1-R2_Parameter_Inputs.xls*). In field observations at Yucca Mountain during active transpiration periods, shrubs removed about 31% of the total precipitation that fell during the period studied (with a range of 12% to 54% at the seven study locations exhibiting a full range of plant species common to the region) (CRWMS M&O 1999 [DIRS 105031], Executive Summary). Total shrub cover at the sites ranged from about 8% to 16% (CRWMS M&O 1999 [DIRS 105031], Figure 9). An analysis of the percentage of shrub cover and of soil temperature at a depth of 45 cm suggests that for each 1°C increase in temperature, the shrub cover decreases by 1.2% and that of annual grasses increases by 5.5% (CRWMS M&O 1999 [DIRS 105031], Section 3.3). The grass species currently found at each of the study sites (*Bromus rubens*) increased coverage by 2.3% for every 1°C increase. This focus only on the effects of shrub loss due to increasing temperature, neglecting the increase in grass species, as a conservative approach for bounding the effect of repository heating.

Applying Equation 2.3.13.03.0A-1 with a shrub root depth range of 0.5 to 2 m (CRWMS M&O 1999 [DIRS 105031], p. 5), with K = 1.81 W/m-K, gives a temperature change in the range 0.11°C to 0.44°C. For a near-surface soil with K = 0.18 W/m-K (typical of unsaturated sand; averaging the three recent values from Table 5.5 of Jury et al. 1991 [DIRS 102010] and converting units), the predicted temperature change is in the range 1.1°C to 4.4°C. This result is a slight overestimate because the heat flux is calculated by fixing the surface temperature, and because convective and evaporative mechanisms of heat exchange (which tend to attenuate temperature increases at the surface) are not considered.

Applying the maximum temperature change of 4.4°C (computed at a depth of 2 m) and using the 1.2% per °C scrub cover loss relationship of *Final Report: Plant and Soil Related Processes Along a Natural Thermal Gradient at Yucca Mountain, Nevada* (CRWMS M&O 1999 [DIRS 105031], Section 3.3), the resulting percent cover of shrubs could decrease by a maximum of about 5.3% (i.e., 1.2% change per °C, multiplied by 4.4°C). Noting that transpiration by shrubs is only part of the total evapotranspiration that determines net infiltration, the reported values for percentage of shrub cover are used to further constrain the thermally driven changes in net infiltration as shown in Table 2.3.13.03.0A-1. Multiplying the reduction in shrub coverage by the fraction of total evapotranspiration attributed to shrubs (CRWMS M&O 1999 [DIRS 105031], Executive Summary and Figure 9) yields the reduction in evapotranspiration due to repository heating for sites corresponding to the lower, mean, and upper bounds of scrub cover (CRWMS (1999 [DIRS 105031], Executive Summary). The

maximum in Table 2.3.13.03.0A-1, 2.9%, is insignificant compared to the factor of 16 difference between the low and high monsoon infiltration rates used in TSPA.

The results in Table 2.3.13.03.0A-1 are conservative in that they do not account for the offsetting contribution to evapotranspiration from the increase in coverage by annual grasses (i.e., 2.3% increase in annual grasses for each 1°C). Additionally, any shifts in plant species are expected to be transient, and would potentially reverse as the repository cooled with time. Also, studies indicate that the resulting temperature changes will be within the adaptive range of some plant species now at Yucca Mountain (CRWMS M&O 1999 [DIRS 105031], Figure 8 and p. 41). For example, *Final Report: Plant and Soil Related Processes Along a Natural Thermal Gradient at Yucca Mountain, Nevada* (CRWMS M&O 1999 [DIRS 105031], Figure 8 and p. 20) notes that big sagebrush presently grows most abundantly at mid-elevation sites with moderate soil temperatures (+0.5 – 2°C at 45-cm depth compared to Yucca Mountain) and white bursage grows at lower elevation sites with (+2 – 3.5°C at 45-cm depth compared to Yucca Mountain). These shrubs may replace shrubs that die out due to increased temperature above the repository. Ground surface temperature increases may cause snow to melt more readily than predicted by the infiltration model. However, since sublimation represents such a a small fraction of the water budget during the glacial transition climate, such an effect would not significantly increase net infiltration (SNL 2008 [DIRS 182145], Table 6.5.7.4-3). Thus, expected increases in infiltration would be significantly less than stated above and insignificant compared to the uncertainty and variability in infiltration that are included in the TSPA model.

Based on the above discussion, exclusion of FEP 2.3.13.03.0A (Effects of Repository Heat on the Biosphere) will not result in a significant adverse change in the magnitude or time of radiological exposures to the RMEI or radionuclide releases to the accessible environment. Therefore, this FEP is excluded from the performance assessments conducted to demonstrate compliance with proposed 10 CFR 63.311 and 63.321 (70 FR 53313 [DIRS 178394]), and with 10 CFR 63.331 [DIRS 180319], on the basis of low consequence.

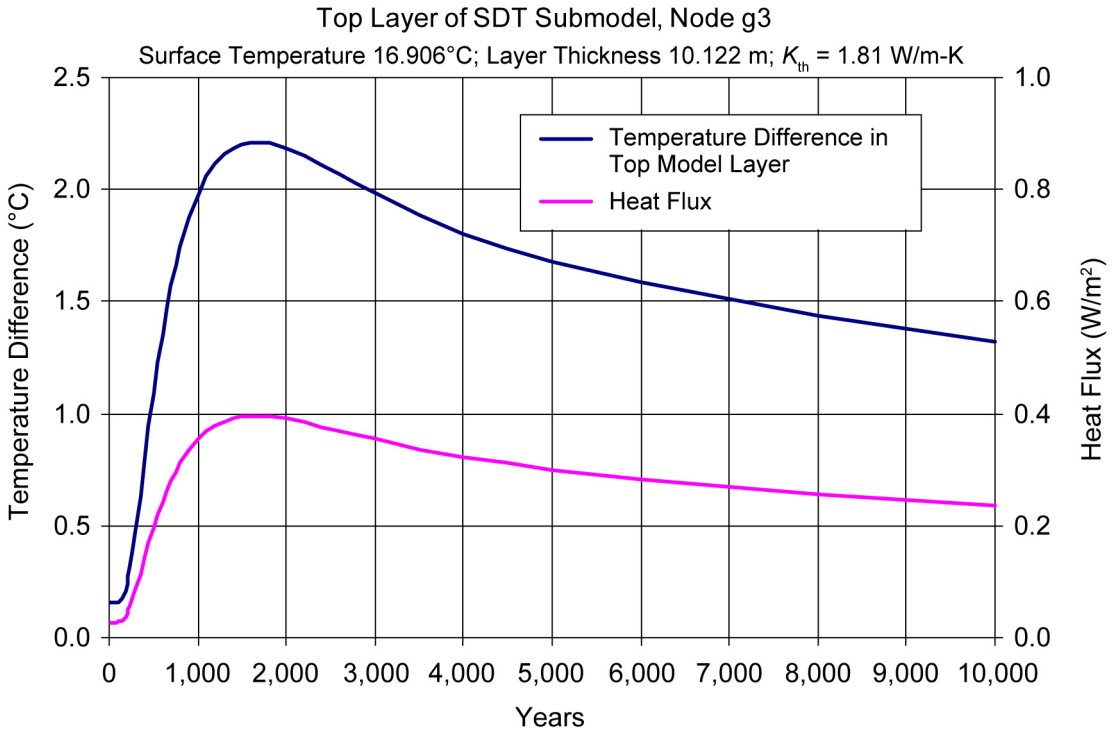

Source: The temperature difference history and thermal conductivity are obtained from DTN: LL0702PA013MST.068 [DIRS 180553], file: *P3W-13-g_9-SDT-03.ext* and file: *SDT-1Dds-06*, respectively.

NOTE: Temperature difference given for a 10.122-m layer, 2 m values given in the text.

Figure 2.3.13.03.0A-1. Time History of the Temperature Difference through the Top (surface) Layer (tcw12 hydrostratigraphic unit) in a Repository Thermal Model, and the Associated Heat Flux at the Repository Center (max heat flux point, node g3)

Table 2.3.13.03.0A-1. Fractional Change in Total Evapotranspiration Due to Thermally Induced Decrease in Shrub Coverage

Fraction of Precipitation Transpired by Shrubs [1] (Range for Existing Conditions)	**Change in Shrub Cover (see text)**	**Approximate Reduction in Total Evapotranspiration**
12% (low)	5.3%	0.64%
31% (mean)	5.3%	1.6%
54% (high)	5.3%	2.9%

[1]Data from CRWMS 1999 [DIRS 105031], Executive Summary, for the period from March to July 1998, corresponding to the time of the year in which the plants are actively transpiring.

INPUTS:

Table 2.3.13.03.0A-2. Direct Inputs

Input	Source	Description
CRWMS M&O 1999. *Final Report: Plant and Soil Related Processes Along a Natural Thermal Gradient at Yucca Mountain, Nevada*. [DIRS 105031]	Section 3.3	Relationshp between transpiration, percent shrub coverage, and temperature
	Executive Summary	Fractional change in total evapotranspiration due to thermally induced decrease in shrub coverage
DTN: LL0702PA013MST.068. Input and Output Files for the SMT, SDT and DDT Submodels and MSTHAC Extract Output Files Used in ANL-EBS-MD-000049 Multiscale Thermohydrologic Model. [DIRS 180553]	Entire	Time history of temperature difference through top (surface) layer in repository thermal model, and associated heat flux
	SDT submodel, node g3	Maximum heat flux to surface due to repository heating from SDT thermohydrologic model
DTN: MO0706METMND06.000. Meteorological Monitoring Data for 2006. [DIRS 181887]	Parameter Solar_M in table for site 9	Average solar flux at site 9 in 2006
DTN: SN0609T0502206.024. Monsoon Net Infiltration Results. [DIRS 179063]	file: *Monsoon_R1-R2_Parameter_ Inputs.xls*	Infiltration rate range for Monsoonal climate
Jury et al. 1991. *Soil Physics*. [DIRS 102010]	Table 5.5	Soil conductivity for unsaturated sand
SNL 2008. *Multiscale Thermohydrologic Model*. [DIRS 184433]	Section 6.2.4	Themal loading equivalent to postclosure thermal reference case
	Section 6.2.15[a]	Heat flux determination
SNL 2008. *Simulation of Net Infiltration for Present-Day and Potential Future Climates*. [DIRS 182145]	Table 6.5.7.4-3	Sublimation is small fraction of water budget of glacial transition climate
SNL 2008. *Total System Performance Assessment Model /Analysis for the License Application*. [DIRS 183478]	Section 6.3.1.2	1,700 years in Monsoonal climate state

Table 2.3.13.03.0A-3. Indirect Inputs

Citation	Title	DIRS
10 CFR 63	Energy: Disposal of High-Level Radioactive Wastes in a Geologic Repository at Yucca Mountain, Nevada	180319
70 FR 53313	Implementation of a Dose Standard After 10,000 Years	178394
Carslaw and Jaeger 1959	*Conduction of Heat in Solids*	100968
CRWMS M&O 1999	*Final Report: Plant and Soil Related Processes Along a Natural Thermal Gradient at Yucca Mountain, Nevada*	105031

FEP: 2.3.13.04.0A

FEP NAME:

Radionuclide Release Outside the Reference Biosphere

FEP DESCRIPTION:

Radionuclide releases outside the reference biosphere can occur. This could include areas surrounding distant springs and surface water bodies (such as at Ash Meadows), remote natural outfalls, discharge areas such as playas (e.g. Franklin Lake Playa), or forests, grasslands, or wetlands that occur in isolated areas in the region. This might also include withdrawal from wells in remote areas. Radionuclide accumulation could occur in these areas. Sediment transport and redistribution may cause concentration or dilution of radionuclides. Flora and fauna in these areas may be exposed and radionuclides be bioaccumulated and enter the food chain. Intermittent use of these areas by humans may also lead to exposure.

SCREENING DECISION:

Excluded – by regulation

SCREENING JUSTIFICATION:

The reference biosphere is defined as the description of the environment inhabited by the RMEI (10 CFR 63.2 [DIRS 180319]). FEPs that describe the reference biosphere are those that affect the dose to the RMEI. The postclosure individual protection standards are formulated in terms of annual dose limits to the RMEI (proposed 10 CFR 63.311 and 10 CFR 63.321 (70 FR 53313 [DIRS 178394])). Only those FEPs that affect the reference biosphere can affect the RMEI and, thereby, be included in the performance assessment. Therefore, radionuclide release outside the reference biosphere is excluded by regulation.

INPUTS:

Table 2.3.13.04.0A-1. Direct Inputs

Input	Source	Description
10 CFR 63. 2007. Energy: Disposal of High-Level Radioactive Wastes in a Geologic Repository at Yucca Mountain, Nevada. [DIRS 180319]	10 CFR 63.2	The reference biosphere is defined as the description of the environment inhabited by the RMEI
70 FR 53313. Implementation of a Dose Standard After 10,000 Years. [DIRS 178394]	10 CFR 63.311	Individual protection standard after permanent closure

FEP: 2.4.01.00.0A

FEP NAME:

Human Characteristics (Physiology, Metabolism)

FEP DESCRIPTION:

This FEP addresses human characteristics. These include physiology, metabolism, and variability among individual humans.

SCREENING DECISION:

Included

TSPA DISPOSITION:

A hypothetical human receptor, the RMEI, is used in the performance assessment calculations for both the individual protection standard (proposed 10 CFR 63.311 (70 FR 53313 [DIRS 178394])) and the individual protection standard for human intrusion (proposed 10 CFR 63.321 (70 FR 53313 [DIRS 178394])). Characteristics of the RMEI are representative of the physiology and metabolic characteristics of adults, consistent with 10 CFR 63.312(e) [DIRS 180319], which specifies that the RMEI is an adult. As a result, consideration is limited to the physiology and metabolic characteristics of adults. Elements of human physiology and metabolism are inherent in the dose coefficients for radionuclide intakes used in the biosphere model (SNL 2007 [DIRS 177399], Sections 6.4.7.2, 6.4.8.5, 6.4.9.6, and 6.5.5.2) and in the breathing rates (BSC 2005 [DIRS 172827], Section 6.3.3), which are based on adult human physiologic and metabolic characteristics. These parameters are used, and thus this FEP is addressed, in the external exposure, inhalation, and ingestion submodels (SNL 2007 [DIRS 177399], Table 6.7-1) to calculate the values of BDCFs. This FEP is also considered in the discussion of the dependence of inhalation dose coefficients on particle sizes (BSC 2005 [DIRS 172827], Section 6.5.5). Variability among individual humans adds to the uncertainty in the values of parameters that depend on human characteristics, such as dose coefficients. Uncertainty in these parameters is discussed in *Biosphere Model Report* (SNL 2007 [DIRS 177399], Section 6.6.3).

The groundwater protection standards (10 CFR 63.331 [DIRS 180319]) do not use the concept of the RMEI, but require an estimation of the dose from ingesting 2 liters per day of contaminated water. Physiology and metabolism of the human receptor are considered in the biokinetic models that are used to develop dose coefficients for ingestion. These dose coefficients are used as inputs in calculation of the conversion factors used in the performance assessment for demonstration of compliance with the groundwater protection standards (SNL 2007 [DIRS 177399], Section 6.15.1).

This FEP is included in the biosphere component of the TSPA model through the use of groundwater exposure scenario BDCFs that are direct inputs to the TSPA for the scenario classes involving radionuclide release to the groundwater (SNL 2007 [DIRS 177399], Section 6.1.3), and through the use of the conversion factors for demonstrating compliance with the

groundwater protection standards (SNL 2007 [DIRS 177399], Section 6.15.1). The annual doses are calculated as the product of radionuclide concentration in groundwater and the BDCFs or conversion factors. In the event of a volcanic eruption, this FEP is included in the TSPA through BDCFs for the volcanic ash exposure scenario (SNL 2007 [DIRS 177399], Section 6.1.3). The annual doses are calculated as the product of radionuclide concentration in the soil contaminated by radionuclides in volcanic tephra, the BDCF components, and the mass loading time decrease function. For the volcanic ash exposure scenario, three BDCF components are provided to the TSPA model that account for various RMEI exposure pathways (SNL 2007 [DIRS 177399], Section 6.12.3). See included FEP 3.3.04.02.0A (Inhalation) for a more detailed description of the volcanic BDCF components.

The BDCFs for all biosphere model realizations are provided as inputs to the TSPA model, which randomly samples these inputs to propagate uncertainty from the biosphere model into TSPA dose calculations. The present-day climate BDCFs are used for the assessment of doses to the RMEI for 10,000 years following disposal, as well as after 10,000 years, but within the period of the geologic stability (SNL 2007 [DIRS 177399], Sections 6.11.3 and 6.12.3).

This FEP is included for the performance assessments to demonstrate compliance with the individual protection standard (proposed 10 CFR 63.311 (70 FR 53313 [DIRS 178394])), the individual protection standards for human intrusion (proposed 10 CFR 63.321 (70 FR 53313 [DIRS 178394])), and with the groundwater protection standards (10 CFR 63.331 [DIRS 180319]).

INPUTS:

Table 2.4.01.00.0A-1. Indirect Inputs

Citation	Title	DIRS
70 FR 53313	Implementation of a Dose Standard After 10,000 Years	178394
BSC 2005	*Characteristics of the Receptor for the Biosphere Model*	172827
SNL 2007	*Biosphere Model Report*	177399

FEP: 2.4.04.01.0A

FEP NAME:

Human Lifestyle

FEP DESCRIPTION:

Human lifestyle, including everyday household activities and leisure activities, will influence the critical exposure pathways to humans.

SCREENING DECISION:

Included

TSPA DISPOSITION:

Work and leisure activities included in the TSPA are representative of the current residents of Amargosa Valley. This is consistent with 10 CFR 63.312(b) [DIRS 180319], which states that the lifestyle of the RMEI must be based on the people who reside in Amargosa Valley. Human lifestyle information is used to select values for exposure parameters, which, in addition to food and water consumption rates (included FEP 3.3.04.01.0A (Ingestion)), include the amount of time spent indoors and outdoors for work and recreation. The current lifestyle also includes certain uses of wild and natural resources (e.g., hunting and consumption of game products) (see included FEP 2.4.08.00.0A (Wild and Natural Land and Water Use)), but it is not intended to represent the hunter/gatherer lifestyle. This FEP is considered in the air, external exposure, inhalation, and ingestion submodels of the biosphere model (SNL 2007 [DIRS 177399], Table 6.7-1).

Distributions of the parameters related to human lifestyle are based, in part, on variation and uncertainty in the lifestyles and characteristics of people living in Amargosa Valley (BSC 2006 [DIRS 177101], Sections 6.2 and 6.3; BSC 2005 [DIRS 172827], Sections 6.3 and 6.4). Influence of human lifestyle on external exposure is considered in the biosphere models for the groundwater exposure scenario (SNL 2007 [DIRS 177399], Equation 6.4.7-1) and for the volcanic ash exposure scenario (SNL 2007 [DIRS 177399], Equation 6.5.5-1). Influence of human lifestyle on inhalation pathway is also considered in both models (SNL 2007 [DIRS 177399], Equations 6.4.8-2 to 6.4.8-7 for the groundwater exposure scenario; SNL 2007 [DIRS 177399], Equations 6.5.6-2 and 6.5.6-3 for the volcanic ash exposure scenario). Similarly, influences on the ingestion pathway are considered in both models (SNL 2007 [DIRS 177399], Equations 6.4.9-2 to 6.4.9-6 for the groundwater exposure scenario; SNL 2007 [DIRS 177399], Equations 6.5.7-2 to 6.5.7-4 for the volcanic ash exposure scenario). The following parameters address this FEP: mass loading for receptor environments (BSC 2006 [DIRS 177101], Sections 6.2 and 6.3), population proportion (BSC 2005 [DIRS 172827], Section 6.3.1), and exposure time (BSC 2005 [DIRS 172827], Section 6.3.2). The consumption rates of locally produced food are addressed in included FEP 3.3.04.01.0A (Ingestion).

This FEP is included in the biosphere component of the TSPA model through the use of groundwater exposure scenario BDCFs that are direct inputs to the TSPA for the scenario classes

involving radionuclide release to the groundwater (SNL 2007 [DIRS 177399], Section 6.1.3). The annual doses are calculated as the product of radionuclide concentration in groundwater and the BDCFs. In the event of a volcanic eruption, this FEP is included in the TSPA through BDCFs for the volcanic ash exposure scenario (SNL 2007 [DIRS 177399], Section 6.1.3). The annual doses are calculated as the product of radionuclide concentration in the soil contaminated by radionuclides in volcanic tephra and the BDCF components. For the volcanic ash exposure scenario, three BDCF components are provided to the TSPA model that account for various RMEI exposure pathways (SNL 2007 [DIRS 177399], Section 6.12.3). See included FEP 3.3.04.02.0A (Inhalation) for a more detailed description of the volcanic BDCF components.

The BDCFs for all biosphere model realizations are provided as inputs to the TSPA model, which randomly samples these inputs to propagate uncertainty from the biosphere model into TSPA dose calculations. The present-day climate BDCFs are used for the assessment of doses to the RMEI for 10,000 years following disposal, as well as after 10,000 years, but within the period of the geologic stability (SNL 2007 [DIRS 177399], Sections 6.11.3 and 6.12.3).

This FEP is included for the performance assessment to demonstrate compliance with the individual protection standard (proposed 10 CFR 63.311 (70 FR 53313 [DIRS 178394])) and the performance assessment to demonstrate compliance with the individual protection standard for human intrusion (proposed 10 CFR 63.321 (70 FR 53313 [DIRS 178394])) because both these standards require the use of the concept of the RMEI in the performance assessment calculations. This FEP is not included for the performance assessment to demonstrate compliance with the groundwater protection standards (10 CFR 63.331 [DIRS 180319]) because these standards do not require the use of the concept of the RMEI in the performance assessment calculations.

INPUTS:

Table 2.4.04.01.0A-1. Indirect Inputs

Citation	Title	DIRS
10 CFR 63	Energy: Disposal of High-Level Radioactive Wastes in a Geologic Repository at Yucca Mountain, Nevada	180319
70 FR 53313	Implementation of a Dose Standard After 10,000 Years	178394
BSC 2005	*Characteristics of the Receptor for the Biosphere Model*	172827
BSC 2006	*Inhalation Exposure Input Parameters for the Biosphere Model*	177101
SNL 2007	*Biosphere Model Report*	177399

FEP: 2.4.07.00.0A

FEP NAME:

Dwellings

FEP DESCRIPTION:

This FEP addresses human dwellings, and the ways in which dwellings might affect human exposures. Exposure pathways might be influenced by building materials and location.

SCREENING DECISION:

Included

TSPA DISPOSITION:

The choice of dwellings is one of the attributes of a lifestyle (see included FEP 2.4.04.01.0A (Human Lifestyle)). Characteristics of dwellings that are included in the TSPA are representative of the residences of Amargosa Valley, consistent with 10 CFR 63.312(b) [DIRS 180319], which states that the lifestyle of the RMEI must be based on the people who reside in the Town of Amargosa Valley. The location of dwellings that are included in the TSPA model is consistent with the location of the RMEI, above the highest concentration of radionuclides in the groundwater plume of contamination (10 CFR 63.312(a) [DIRS 180319]).

This FEP is incorporated into the biosphere model through consideration of the characteristics of the dwellings in Amargosa Valley and their effects on the inhalation and external exposure pathways. Data from *The 1997 "Biosphere" Food Consumption Survey Summary Findings and Technical Documentation* (DOE 1997 [DIRS 100332], Table 2.4.2) indicate that the predominant housing type is manufactured housing and that most residences have evaporative coolers. This information was used in selecting values for several pertinent parameters such as ventilation rate, evaporative cooler use factor, and evaporative cooler water evaporation rate. This FEP is addressed in the air, inhalation, and external exposure submodels by including characteristics of the dwellings in Amargosa Valley and their effects on the inhalation and external exposure pathways (SNL 2007 [DIRS 177399], Tables 6.2-1 and 6.7-1).

The parameter distributions used in the biosphere model are based, in part, on uncertainty and variation in the characteristics of types of dwellings in Amargosa Valley (BSC 2005 [DIRS 172827], Sections 6.3.4.1, 6.3.4.2, and 6.6; BSC 2004 [DIRS 169672], Sections 6.5.2 and 6.6.2). Specifically, this FEP is addressed through the following parameters: evaporative cooler water evaporation rate (BSC 2004 [DIRS 169672], Section 6.5.2), evaporative cooler air flow rate (BSC 2004 [DIRS 169672], Section 6.5.2), interior wall height (BSC 2004 [DIRS 169672], Sections 6.5.2 and 6.6.2), house ventilation rate (BSC 2004 [DIRS 169672], Section 6.6.2), correlation coefficient for airflow and water use in evaporative coolers (BSC 2004 [DIRS 169672], Section 6.5.2), building shielding factor (shielding provided by building materials) (BSC 2005 [DIRS 172827], Section 6.6), fraction of houses with evaporative coolers (BSC 2005 [DIRS 172827], Section 6.3.4.1), and evaporative cooler use factor (BSC 2005 [DIRS 172827], Section 6.3.4.2).

This FEP is included in the biosphere component of the TSPA model through the use of groundwater exposure scenario BDCFs that are direct inputs to the TSPA for the scenario classes involving radionuclide release to the groundwater (SNL 2007 [DIRS 177399], Section 6.1.3). The annual doses are calculated as the product of radionuclide concentration in groundwater and the BDCFs. In the event of a volcanic eruption, this FEP is included in the TSPA through BDCFs for the volcanic ash exposure scenarios (SNL 2007 [DIRS 177399], Section 6.1.3). The annual doses are calculated as the product of radionuclide concentration in soil contaminated by radionuclides, volcanic tephra, and the BDCF components. For the volcanic ash exposure scenario, three BDCF components are provided to the TSPA model that account for various RMEI exposure pathways (SNL 2007 [DIRS 177399], Section 6.12.3). See included FEP 3.3.04.02.0A (Inhalation) for a more detailed description of the volcanic BDCF components.

The BDCFs for all biosphere model realizations are provided as inputs to the TSPA model, which randomly samples these inputs to propagate uncertainty from the biosphere model into TSPA dose calculations. The present-day climate BDCFs are used for the assessment of doses to the RMEI for 10,000 years following disposal, as well as after 10,000 years, but within the period of the geologic stability (SNL 2007 [DIRS 177399], Sections 6.11.3 and 6.12.3).

This FEP is included for the performance assessment to demonstrate compliance with the individual protection standard (proposed 10 CFR 63.311 (70 FR 53313 [DIRS 178394])) and the performance assessment to demonstrate compliance with the individual protection standard for human intrusion (proposed 10 CFR 63.321 (70 FR 53313 [DIRS 178394])) because both these standards require the use of the concept of the RMEI in the performance assessment calculations. This FEP is not included for the performance assessment to demonstrate compliance with the groundwater protection standards (10 CFR 63.331 [DIRS 180319]) because these standards do not require the use of the concept of the RMEI in the performance assessment calculations.

INPUTS:

Table 2.4.07.00.0A-1. Indirect Inputs

Citation	Title	DIRS
10 CFR 63	Energy: Disposal of High-Level Radioactive Wastes in a Geologic Repository at Yucca Mountain, Nevada	180319
70 FR 53313	Implementation of a Dose Standard After 10,000 Years	178394
BSC 2004	*Environmental Transport Input Parameters for the Biosphere Model*	169672
BSC 2005	*Characteristics of the Receptor for the Biosphere Model*	172827
DOE 1997	*The 1997 "Biosphere" Food Consumption Survey Summary Findings and Technical Documentation*	100332
SNL 2007	*Biosphere Model Report*	177399

FEP: 2.4.08.00.0A

FEP NAME:

Wild and Natural Land and Water Use

FEP DESCRIPTION:

Human uses of wild and natural lands (forests, bush, coastlines) and water (lakes, rivers, oceans) may affect the long-term performance of the repository. Wild and natural land use will be primarily controlled by natural factors (topography, climate, etc.).

SCREENING DECISION:

Included

TSPA DISPOSITION:

The lifestyle and behavior of the current residents of Amargosa Valley implicitly include certain uses of wild and natural lands and water. Consistent with 10 CFR 63.312(b) [DIRS 180319], which states that the RMEI has a diet and lifestyle representative of the current residents of Amargosa Valley, and with 10 CFR 63.305(a) [DIRS 180319], which requires that the reference biosphere be consistent with present knowledge of the conditions in the region, future uses of wild and natural lands and water are assumed to be the same as the current uses.

This FEP is incorporated in the biosphere model by combining the consumption of game with the consumption rate for all meats, and by considering the time the RMEI spends in the outdoor environment (SNL 2007 [DIRS 177399], Sections 6.4.4 and 6.4.7). This FEP is addressed in the air, external exposure, inhalation, and ingestion submodels of the biosphere model. The parameters that address this FEP are mass loading for receptor environments (BSC 2006 [DIRS 177101], Sections 6.2 and 6.3), exposure time (BSC 2005 [DIRS 172827], Section 6.3.2), and annual consumption rate of locally produced animal products (BSC 2005 [DIRS 172827], Sections 6.4 and 6.4.2). Parameter distributions were developed and based in part on uncertainty and variation in the use of wild and natural lands, and the rate of consumption of wild game by the receptor (BSC 2006 [DIRS 177101], Sections 6.2 and 6.3; BSC 2005 [DIRS 172827], Sections 6.3.2 and 6.4.2).

This FEP is included in the biosphere component of the TSPA model through the use of groundwater exposure scenario BDCFs that are direct inputs to the TSPA for the scenario classes involving radionuclide release to the groundwater (SNL 2007 [DIRS 177399], Section 6.1.3). The annual doses are calculated as the product of radionuclide concentration in groundwater and the BDCFs. In the event of a volcanic eruption, this FEP is included in the TSPA through BDCFs for the volcanic ash exposure scenario (SNL 2007 [DIRS 177399], Section 6.1.3). The annual doses are calculated as the product of radionuclide concentration in soil contaminated by radionuclides in volcanic tephra, the BDCF components, and the mass loading time decrease function. For the volcanic ash exposure scenario, three BDCF components are provided to the TSPA model that account for various RMEI exposure pathways (SNL 2007 [DIRS 177399],

Section 6.12.3). See included FEP 3.3.04.02.0A (Inhalation) for a more detailed description of the volcanic BDCF components.

The BDCFs for all biosphere model realizations are provided as inputs to the TSPA model, which randomly samples these inputs to propagate uncertainty from the biosphere model into TSPA dose calculations. The present-day climate BDCFs are used for the assessment of doses to the RMEI for 10,000 years following disposal, as well as after 10,000 years, but within the period of the geologic stability (SNL 2007 [DIRS 177399], Sections 6.11.3 and 6.12.3).

This FEP is included for the performance assessment to demonstrate compliance with the individual protection standard (proposed 10 CFR 63.311 (70 FR 53313 [DIRS 178394])) and the performance assessment to demonstrate compliance with the individual protection standard for human intrusion (proposed 10 CFR 63.321 (70 FR 53313 [DIRS 178394])) because both these standards require the use of the concept of the RMEI in the performance assessment calculations. This FEP is not included for the performance assessment to demonstrate compliance with the groundwater protection standards (10 CFR 63.331 [DIRS 180319]) because these standards do not require the use of the concept of the RMEI in the performance assessment calculations.

INPUTS:

Table 2.4.08.00.0A-1. Indirect Inputs

Citation	Title	DIRS
10 CFR 63	Energy: Disposal of High-Level Radioactive Wastes in a Geologic Repository at Yucca Mountain, Nevada	180319
70 FR 53313	Implementation of a Dose Standard After 10,000 Years	178394
BSC 2005	*Characteristics of the Receptor for the Biosphere Model*	172827
BSC 2006	*Inhalation Exposure Input Parameters for the Biosphere Model*	177101
SNL 2007	*Biosphere Model Report*	177399

FEP: 2.4.09.01.0A

FEP NAME:

Implementation of New Agricultural Practices or Land Use

FEP DESCRIPTION:

Agricultural land use depends on many interrelated factors including climate, geology, topography, human lifestyle, and economics. Land use may include practices such as traditional crop farming, greenhouses, and hydroponics. Agricultural practices have the potential for radionuclide transfer through the food chain and may influence alternate pathways. Changes in current agricultural practices could change the significance of various exposure pathways.

SCREENING DECISION:

Excluded – by regulation

SCREENING JUSTIFICATION:

10 CFR 63.305(b) [DIRS 180319] specifically states, "DOE should not project changes in society, the biosphere (other than climate), human biology, or increases or decreases in human knowledge or technology. In all analyses done to demonstrate compliance with this part, the DOE must assume that all of those factors remain constant as they are at the time of submission of the license application." 10 CFR 63.312(b) [DIRS 180319] also states that the RMEI "has a diet and living style representative of the people who now reside in the Town of Amargosa Valley, Nevada." Therefore, speculation concerning changes in current agricultural practices or land use is excluded by regulation.

INPUTS:

Table 2.4.09.01.0A-1. Direct Inputs

Input	Source	Description
10 CFR 63. 2007. Energy: Disposal of High-Level Radioactive Wastes in a Geologic Repository at Yucca Mountain, Nevada. [DIRS 180319]	10 CFR 63.305(b)	DOE should not project changes in society, the biosphere (other than climate), human biology, or increases or decreases in human knowledge or technology

FEP: 2.4.09.01.0B

FEP NAME:

Agricultural Land Use and Irrigation

FEP DESCRIPTION:

Agricultural areas exist near Yucca Mountain, particularly in the direction of groundwater flow. Current practices include irrigation, plowing, fertilization, crop storage, and soil modification and amendment. Existing practices may play a significant role in determining exposure pathways and dose.

SCREENING DECISION:

Included

TSPA DISPOSITION:

Agricultural land use and irrigation form part of the lifestyle and behavior of the current residents of Amargosa Valley (BSC 2004 [DIRS 169673], Appendix A). In accordance with 10 CFR 63.312(b) [DIRS 180319], which states that the RMEI has a diet and lifestyle representative of the current residents of Amargosa Valley, and with 10 CFR 63.305(a) [DIRS 180319], which requires that the reference biosphere be consistent with present knowledge of the conditions in the region, future agricultural practices are assumed to be consistent with the current practices.

This FEP is considered in the soil, air, plant, animal, ^{14}C, fish, external exposure, and inhalation submodels of the biosphere model (SNL 2007 [DIRS 177399], Table 6.7-1). Agricultural land use and irrigation are represented in the model through the fraction of overhead irrigation (BSC 2004 [DIRS 169673], Section 6.3), exposure times for conducting outdoor and indoor activities (BSC 2005 [DIRS 172827], Section 6.3.2), annual average irrigation rate (BSC 2004 [DIRS 169673], Section 6.5; SNL 2007 [DIRS 177399], Section 6.4.1.1), overwatering rate (BSC 2004 [DIRS 169673], Section 6.9), mass loading for receptor environments (BSC 2006 [DIRS 177101], Sections 6.2 and 6.3), mass loading for crops (BSC 2006 [DIRS 177101], Sections 6.2.5 and 6.3.5), crop growing time (BSC 2004 [DIRS 169673], Section 6.4), tillage depth (BSC 2004 [DIRS 169673], Section 6.10), irrigation intensity (BSC 2004 [DIRS 169673], Section 6.6), irrigation amount per application (BSC 2004 [DIRS 169673], Section 6.7), daily irrigation rate (BSC 2004 [DIRS 169673], Section 6.8), animal consumption rate of water (BSC 2004 [DIRS 169672], Section 6.3.2), surface area of irrigated land (SNL 2007 [DIRS 177399], Section 6.4.6.2), water concentration modifying factor (BSC 2004 [DIRS 169672], Section 6.4.3), and duration of irrigation (SNL 2007 [DIRS 179993], Section 6.7).

Irrigation rates are developed based, in part, on variation and uncertainty in cultivated land and water use practices in Amargosa Valley (BSC 2004 [DIRS 169673], Sections 6.3 to 6.9; BSC 2004 [DIRS 169672], Section 6.7.2). Agricultural use of water, the rates and durations, is included in the soil (SNL 2007 [DIRS 177399], Section 6.4.1), plant (SNL 2007 [DIRS 177399],

Section 6.4.3), animal (SNL 2007 [DIRS 177399], Section 6.4.4), fish (SNL 2007 [DIRS 177399], Section 6.4.5), and ^{14}C (SNL 2007 [DIRS 177399], Section 6.4.7) submodels of the groundwater scenario. Irrigation of agricultural land with contaminated water may give rise to the leaching of radionuclides from the soil, the transport of radionuclides by deep percolation to the water table, and the recapture of the radionuclides by the water supply well. However, this process has been excluded, as discussed in FEP 1.4.07.03.0A (Recycling of Accumulated Radionuclides from Soil to Groundwater).

This FEP is included in the biosphere component of the TSPA model through the use of groundwater exposure scenario BDCFs that are direct inputs to the TSPA for the scenario classes involving radionuclide release to the groundwater (SNL 2007 [DIRS 177399], Section 6.1.3). The annual doses are calculated as the product of radionuclide concentration in groundwater and the BDCFs. In the event of a volcanic eruption, this FEP is included in the TSPA through BDCFs for the volcanic ash exposure scenario (SNL 2007 [DIRS 177399], Section 6.1.3). The annual doses are calculated as the product of radionuclide concentration in soil contaminated by radionuclides in volcanic tephra, the BDCF components, and the mass loading time decrease function. For the volcanic ash exposure scenario, three BDCF components are provided to the TSPA model that account for various RMEI exposure pathways (SNL 2007 [DIRS 177399], Section 6.12.3) (see included FEP 2.3.02.01.0A (Soil Type) for a more detailed description of the volcanic BDCF components).

The BDCFs for all biosphere model realizations are provided as inputs to the TSPA model, which randomly samples these inputs to propagate uncertainty from the biosphere model into TSPA dose calculations. The present-day climate BDCFs are used for the assessment of doses to the RMEI for 10,000 years following disposal, as well as after 10,000 years, but within the period of the geologic stability (SNL 2007 [DIRS 177399], Sections 6.11.3 and 6.12.3).

This FEP is included for the performance assessment to demonstrate compliance with the individual protection standard (proposed 10 CFR 63.311 (70 FR 53313 [DIRS 178394])) and the performance assessment to demonstrate compliance with the individual protection standard for human intrusion (proposed 10 CFR 63.321 (70 FR 53313 [DIRS 178394])) because both these standards require the use of the concept of the RMEI and the reference biosphere in the performance assessment calculations. This FEP is not included for the performance assessment to demonstrate compliance with the groundwater protection standards (10 CFR 63.331 [DIRS 180319]) because these standards do not require the use of the concept of the RMEI or the reference biosphere in the performance assessment calculations.

INPUTS:

Table 2.4.09.01.0B-1. Indirect Inputs

Citation	Title	DIRS
10 CFR 63	Energy: Disposal of High-Level Radioactive Wastes in a Geologic Repository at Yucca Mountain, Nevada	180319
70 FR 53313	Implementation of a Dose Standard After 10,000 Years	178394
BSC 2004	*Agricultural and Environmental Input Parameters for the Biosphere Model*	169673
BSC 2004	*Environmental Transport Input Parameters for the Biosphere Model*	169672
BSC 2005	*Characteristics of the Receptor for the Biosphere Model*	172827
BSC 2006	*Inhalation Exposure Input Parameters for the Biosphere Model*	177101
SNL 2007	*Biosphere Model Report*	177399
SNL 2007	*Soil-Related Input Parameters for the Biosphere Model*	179993

FEP: 2.4.09.02.0A

FEP NAME:

Animal Farms and Fisheries

FEP DESCRIPTION:

Domestic livestock or fish could become contaminated through the intake of contaminated feed, water, or soil. Such contamination could then enter the food chain.

SCREENING DECISION:

Included

TSPA DISPOSITION:

Animal farms and fisheries form part of the lifestyle and behavior of the current residents of Amargosa Valley. Socioeconomic and dietary survey data (DOE 1997 [DIRS 100332], Section 2.3) indicate that residents raise and consume locally produced domestic livestock and fish. Consistent with 10 CFR 63.312(b) [DIRS 180319], which states that the RMEI has a diet and lifestyle representative of the current residents of Amargosa Valley, and with 10 CFR 63.305(a) [DIRS 180319], which requires that the reference biosphere be consistent with present knowledge of the conditions in the region, future use of animal farms and fisheries is assumed to be the same as the current use.

This FEP is addressed in the animal and fish submodels of the biosphere model (SNL 2007 [DIRS 177399], Table 6.7-1) and is represented in the model by animal consumption rates of locally produced feed, contaminated water, and contaminated soil (BSC 2004 [DIRS 169672], Section 6.3.2), and water concentration modifying factor (BSC 2004 [DIRS 169672], Section 6.4.3). Relevant parameters are developed based in part on variation and uncertainty in animal and fish farming practices in Amargosa Valley (BSC 2004 [DIRS 169672], Sections 6.3.2, 6.4.3, and 6.4.5).

This FEP is included in the biosphere component of the TSPA model through the use of groundwater exposure scenario BDCFs that are direct inputs to the TSPA for the scenario classes involving radionuclide release to the groundwater (SNL 2007 [DIRS 177399], Section 6.1.3). The annual doses are calculated as the product of radionuclide concentration in groundwater and the BDCFs. In the event of a volcanic eruption, this FEP is included in the TSPA through BDCFs for the volcanic ash exposure scenario (SNL 2007 [DIRS 177399], Section 6.1.3). (For the volcanic ash scenario, a fish consumption pathway is not included because of its insignificant contribution to the BDCFs, and thus fisheries are not considered.) The annual doses are calculated as the product of radionuclide concentration in soil contaminated by radionuclides in volcanic tephra, the BDCF components, and the mass loading time decrease function. For the volcanic ash exposure scenario, three BDCF components are provided to the TSPA model that account for various RMEI exposure pathways (SNL 2007 [DIRS 177399], Section 6.12.3). See included FEP 3.3.04.02.0A (Inhalation) for a more detailed description of the volcanic BDCF components.

The BDCFs for all biosphere model realizations are provided as inputs to the TSPA model, which randomly samples these inputs to propagate uncertainty from the biosphere model into TSPA dose calculations. The present-day climate BDCFs are used for the assessment of doses to the RMEI for 10,000 years following disposal, as well as after 10,000 years, but within the period of the geologic stability (SNL 2007 [DIRS 177399], Sections 6.11.3 and 6.12.3).

This FEP is included for the performance assessment to demonstrate compliance with the individual protection standard (proposed 10 CFR 63.311 (70 FR 53313 [DIRS 178394])) and the performance assessment to demonstrate compliance with the individual protection standard for human intrusion (proposed 10 CFR 63.321 (70 FR 53313 [DIRS 178394])) because both these standards require the use of the concept of the RMEI and the reference biosphere in the performance assessment calculations. This FEP is not included for the performance assessment to demonstrate compliance with the groundwater protection standards (10 CFR 63.331 [DIRS 180319]) because these standards do not require the use of the concept of the RMEI or the reference biosphere in the performance assessment calculations.

INPUTS:

Table 2.4.09.02.0A-1. Indirect Inputs

Citation	Title	DIRS
10 CFR 63	Energy: Disposal of High-Level Radioactive Wastes in a Geologic Repository at Yucca Mountain, Nevada	180319
70 FR 53313	Implementation of a Dose Standard After 10,000 Years	178394
BSC 2004	*Environmental Transport Input Parameters for the Biosphere Model*	169672
DOE 1997	*The 1997 "Biosphere" Food Consumption Survey Summary Findings and Technical Documentation*	100332
SNL 2007	*Biosphere Model Report*	177399

FEP: 2.4.10.00.0A

FEP NAME:

Urban and Industrial Land and Water Use

FEP DESCRIPTION:

Urban and industrial uses of land and water (industry, urban development, earthworks, energy production, etc.) may affect the long-term performance of the repository. Urban and industrial land use will be controlled by both natural factors (topography, climate, etc.) and human factors (economics, population density, etc.).

SCREENING DECISION:

Included

TSPA DISPOSITION:

The lifestyle and behavior of the current residents of Amargosa Valley implicitly include certain uses of urban and industrial land and water. Consistent with 10 CFR 63.312(b) [DIRS 180319], which states that the RMEI has a diet and lifestyle representative of the current residents of Amargosa Valley, and with 10 CFR 63.305(a) [DIRS 180319], which requires that the reference biosphere be consistent with present knowledge of the conditions in the region, future uses of urban and industrial land and water are assumed to be the same as the current uses.

This FEP is addressed in the model by considering land and water use practices in residential and industrial settings in Amargosa Valley (BSC 2006 [DIRS 177101], Sections 6.2 and 6.3; BSC 2005 [DIRS 172827], Section 6.3.2; BSC 2004 [DIRS 169672], Section 6.5). The use of contaminated water in residential and urban environments is included in the soil submodel (SNL 2007 [DIRS 177399], Section 6.4.1) and air submodel (SNL 2007 [DIRS 177399], Section 6.4.2) of the groundwater exposure scenario. The biosphere model also implicitly includes urban industrial land and water use through the proportion of time that the RMEI spends away from the agricultural environment. Parameters that address urban and industrial land and water use are annual average irrigation rate (BSC 2004 [DIRS 169673], Section 6.5), mass loading for the receptor environments (BSC 2006 [DIRS 177101], Sections 6.2.1 to 6.2.4 and 6.3.1 to 6.3.4), evaporative cooler water evaporation rate (BSC 2004 [DIRS 169672], Section 6.5.2), and exposure time (BSC 2005 [DIRS 172827], Section 6.3.2).

This FEP is included in the biosphere component of the TSPA model through the use of groundwater exposure scenario BDCFs that are direct inputs to the TSPA for the scenario classes involving radionuclide release to the groundwater (SNL 2007 [DIRS 177399], Section 6.1.3). The annual doses are calculated as the product of radionuclide concentration in groundwater and the BDCFs. In the event of a volcanic eruption, this FEP is included in the TSPA through BDCFs for the volcanic ash exposure scenario (SNL 2007 [DIRS 177399], Section 6.1.3). The annual doses are calculated as the product of radionuclide concentration in soil contaminated by radionuclides in volcanic tephra, the BDCF components, and the mass loading time decrease function. For the volcanic ash exposure scenario, three BDCF components are provided to the

TSPA model that account for various RMEI exposure pathways (SNL 2007 [DIRS 177399], Section 6.12.3). See included FEP 3.3.04.02.0A (Inhalation) for a more detailed description of the volcanic BDCF components.

The BDCFs for all biosphere model realizations are provided as inputs to the TSPA model, which randomly samples these inputs to propagate uncertainty from the biosphere model into TSPA dose calculations. The present-day climate BDCFs are used for the assessment of doses to the RMEI for 10,000 years following disposal, as well as after 10,000 years, but within the period of the geologic stability (SNL 2007 [DIRS 177399], Sections 6.11.3 and 6.12.3).

This FEP is included for the performance assessment to demonstrate compliance with the individual protection standard (proposed 10 CFR 63.311 (70 FR 53313 [DIRS 178394])) and the performance assessment to demonstrate compliance with the individual protection standard for human intrusion (proposed 10 CFR 63.321 (70 FR 53313 [DIRS 178394])) because both these standards require the use of the concept of the RMEI and the reference biosphere in the performance assessment calculations. This FEP is not included for the performance assessment to demonstrate compliance with the groundwater protection standards (10 CFR 63.331 [DIRS 180319]) because these standards do not require the use of the concept of the RMEI or the reference biosphere in the performance assessment calculations.

INPUTS:

Table 2.4.10.00.0A-1. Indirect Inputs

Citation	Title	DIRS
70 FR 53313	Implementation of a Dose Standard After 10,000 Years	178394
BSC 2004	*Agricultural and Environmental Input Parameters for the Biosphere Model*	169673
BSC 2004	*Environmental Transport Input Parameters for the Biosphere Model*	169672
BSC 2005	*Characteristics of the Receptor for the Biosphere Model*	172827
BSC 2006	*Inhalation Exposure Input Parameters for the Biosphere Model*	177101
SNL 2007	*Biosphere Model Report*	177399

FEP: 3.1.01.01.0A

FEP NAME:

Radioactive Decay and Ingrowth

FEP DESCRIPTION:

Radioactivity is the spontaneous disintegration of an unstable atomic nucleus that results in the emission of subatomic particles. Radioactive species (isotopes) of a given element are known as radionuclides. Radioactive decay of the fuel in the repository changes the radionuclide content in the fuel with time and generates heat. Radionuclide quantities in the system at any time are the result of the radioactive decay and the ingrowth of decay products as a consequence of that decay. Over a 10,000-year performance period, these processes will produce decay products that need to be considered in order to adequately evaluate the release and transport of radionuclides to the accessible environment.

SCREENING DECISION:

Included

TSPA DISPOSITION:

Radionuclides originating in the waste form will decay at rates set by their half-lives. For TSPA, the subset of radionuclides that are potentially important dose contributors is identified (SNL 2007 [DIRS 177424], Table 7-1). Radioactive decay and ingrowth are modeled for these radionuclides in (1) the waste package and emplacement drift, (2) the unsaturated zone, (3) the saturated zone, and (4) the accessible environment or biosphere. The inclusion of radioactive decay and ingrowth in the TSPA is discussed as follows:

(1) *Waste Package and Emplacement Drift*: As discussed in included FEP 2.1.01.01.0A (Waste Inventory), initial average waste package inventories of each of the important radionuclides, together with the associated uncertainties in these inventories (SNL 2007 [DIRS 180472], Sections 6.4, 6.6, and 7.1[a]) are provided as input to the TSPA Model. The GoldSim contaminant transport module (GoldSim Technology Group 2007 [DIRS 183214]) in the TSPA model calculates and updates the radionuclide inventories in the waste packages and emplacement drift modeling cells at subsequent times to account for radioactive decay and ingrowth of decay products.

(2) *Unsaturated Zone*: In TSPA calculations, radioactive decay and ingrowth in the unsaturated zone are simulated through the use of the FEHM code (FEHM V. 2.24-01 [DIRS 179419], STN: 10086-2.24-01-00), which uses an effective integration algorithm described in *Particle Tracking Model and Abstraction of Transport Processes* (SNL 2008 [DIRS 184748], Section 6.4.4). This algorithm can handle multiple species decay and ingrowth processes. Radionuclide half-lives and decay products considered in the UZ transport abstraction model are documented in *Particle Tracking Model and Abstraction of Transport Processes* (SNL 2008 [DIRS 184748], Table 6-25 in AD01).

In the TSPA calculations for the human intrusion scenario, unsaturated zone transport, including radioactive decay and ingrowth, is modeled using the functions of the GoldSim radionuclide transport module. Specifically, radionuclide transport through the human intrusion borehole is modeled with a GoldSim pipe pathway (SNL 2008 [DIRS 183478], Section 6.7.3.2), which includes the decay and ingrowth calculations.

The output of the UZ radionuclide transport model is a boundary condition for the SZ radionuclide transport model, which accounts for decay and ingrowth during radionuclide transport as described in *Saturated Zone Flow and Transport Model Abstraction* (SNL 2008 [DIRS 183750], Section 6.3).

(3) *Saturated Zone*: Radionuclide transport in the saturated zone for the TSPA is simulated using two models, the SZ flow and transport abstraction model and the SZ one-dimensional transport model. The SZ flow and transport abstraction model is based on multiple realizations of radionuclide transport with the three-dimensional site-scale SZ transport model. The resulting radionuclide breakthrough curves are coupled to the TSPA model using the convolution integral method. The SZ one-dimensional transport model is implemented directly in the TSPA model and consists of streamtubes extracted from the three-dimensional site-scale SZ transport model. Both abstraction models are described in *Saturated Zone Flow and Transport Model Abstraction* (SNL 2008 [DIRS 183750], Section 6.3).

Radioactive decay during transport in the saturated zone is included in the TSPA. The convolution integral method, as implemented in the SZ flow and transport abstraction model, is not able to calculate radioactive ingrowth. Consequently, ingrowth is accounted for in two different ways in the TSPA saturated zone models. First, the radionuclide mass entering the saturated zone at the water table is adjusted to account for the potential ingrowth of some radioactive decay products, resulting in a "boosting" of the initial inventory of some radioactive decay products (SNL 2008 [DIRS 183750], Section 6.3.1[a]). This approach is a conservative simplification that overestimates the mass of these radioactive decay products being transported in the saturated zone. Second, a separate set of saturated zone transport calculations are performed to account for the decay and ingrowth for the four main radionuclide decay series chains. Within the TSPA, these calculations are performed using the SZ one-dimensional transport model (SNL 2008 [DIRS 183750], Sections 6.3.2 and 6.5.1.2[b]). The SZ one-dimensional transport model is used to calculate only the release of some decay products resulting from ingrowth in the saturated zone from the four decay series chains. These two ways of accounting for ingrowth in the saturated zone transport simulations differ from the approach used in the unsaturated zone transport simulations because of the differing numerical methods used.

(4) *Biosphere*: The biosphere model was constructed to estimate the dose from the primary long-lived radionuclides considered important for the TSPA (SNL 2007 [DIRS 177399], Section 6.1.3), and it includes consideration of the short-lived decay products of these radionuclides (SNL 2007 [DIRS 177399], Section 6.3.5). Radionuclide decay and ingrowth are included in the soil (SNL 2007 [DIRS 177399], Sections 6.4.1.1 and 6.4.1.2), external exposure (SNL 2007 [DIRS 177399],

Section 6.4.7), inhalation (SNL 2007 [DIRS 177399], Section 6.4.8), and ingestion (SNL 2007 [DIRS 177399], Section 6.4.9) submodels of the groundwater exposure scenario. They are also included in the external exposure (SNL 2007 [DIRS 177399], Section 6.5.5), inhalation (SNL 2007 [DIRS 177399], Section 6.5.6), and ingestion (SNL 2007 [DIRS 177399], Section 6.5.7) submodels of the volcanic ash exposure scenario for the biosphere model.

This FEP is included in the calculation of radionuclide buildup in the soil for the groundwater exposure scenario (SNL 2007 [DIRS 177399], Sections 6.4.1.1 and 6.4.1.2) and in the calculation of effective dose coefficients for external exposure, inhalation, and ingestion (SNL 2007 [DIRS 177399], Sections 6.4.7.2, 6.4.8.5, 6.4.9.6, and 6.5.5.2). These coefficients include dose contributions from short-lived decay products of the primary radionuclides. The contribution from long-lived and short-lived decay products of primary radionuclides is also considered in the calculations of the organ and the whole body conversion factors for evaluating compliance with the groundwater protection standards (SNL 2007 [DIRS 177399], Section 6.15.1). This is done through the use of effective dose coefficients for ingestion.

This FEP is dispositioned in the biosphere component of the TSPA model through the use of groundwater exposure scenario BDCFs that are direct inputs to the TSPA for the scenario classes involving radionuclide release to the groundwater (SNL 2007 [DIRS 177399], Section 6.1.3). Radioactive decay and ingrowth is also included in the TSPA through the use of the conversion factors for evaluating compliance with the groundwater protection standards (SNL 2007 [DIRS 177399], Section 6.15.1).

This FEP is also included in the TSPA volcanic eruption modeling case through BDCFs for the volcanic ash exposure scenario (SNL 2007 [DIRS 177399], Section 6.1.3), as described in included FEP 3.3.04.02.0A (Inhalation). Annual doses are calculated in the TSPA as the product of radionuclide concentrations in the soil contaminated by radionuclides in volcanic tephra, the BDCF components, and the mass loading time decrease function (SNL 2007 [DIRS 177399], Section 6.12.3). Radionuclide concentrations in the soil are adjusted for radionuclide decay and ingrowth using elements of the GoldSim radionuclide transport module. Decay and ingrowth factors for each radionuclide are calculated through time, and the radionuclide concentrations are adjusted by multiplying the calculated concentrations by the decay and ingrowth factors. These adjusted concentrations are used to determine dose.

INPUTS:

Table 3.1.01.01.0A-1. Indirect Inputs

Citation	Title	DIRS
GoldSim Technology Group 2007	*GoldSim Contaminant Transport Module*. Version 4.20.	183214
FEHM V. 2.24-01	WIN2003, 2000, & XP, Red Hat Linux 2.4.21, OS 5.9. STN: 10086-2.24-01-00	179419
SNL 2007	*Biosphere Model Report*	177399
SNL 2007	*Initial Radionuclides Inventory*	180472
SNL 2007	*Radionuclide Screening*	177424
SNL 2008	*Particle Tracking Model and Abstraction of Transport Processes*	184748
SNL 2008	*Saturated Zone Flow and Transport Model Abstraction*	183750
SNL 2008	*Total System Performance Assessment Model/Analysis for the License Application*	183478

FEP: 3.2.07.01.0A

FEP NAME:

Isotopic Dilution

FEP DESCRIPTION:

Mixing or dilution of the radioactive species from the waste with species of the same element from other sources (i.e., stable and/or naturally occurring isotopes of the same element) could lead to a reduction of the radiological consequences.

SCREENING DECISION:

Excluded – low consequence

SCREENING JUSTIFICATION:

Mixing of radionuclide isotopes from the repository waste with naturally occurring stable isotopes of the same element in groundwater would occur for some radionuclides (e.g., ^{129}I mixing with stable ^{127}I; ^{36}Cl mixing with stable ^{35}Cl and ^{37}Cl; and ^{90}Sr mixing with stable ^{84}Sr, ^{86}Sr, ^{87}Sr, and ^{88}Sr). Chemical and physical processes that result in competition among radioactive and stable isotopes may limit the uptake or retention of some radionuclides in the biosphere and the RMEI, leading to an isotopic dilution effect. The magnitude of the effect of isotopic dilution depends on the relative amounts of the radioactive and corresponding stable isotopes of the same element, as well as the competitive effects on uptake and retention for that element.

The effects of isotopic dilution from sources of stable isotopes specific to the natural system at Yucca Mountain are excluded from the TSPA model on the basis of low consequence. In general, for radionuclides that are rare in the natural environment, such as isotopes of technetium, plutonium, and americium, isotopic dilution of radionuclides of repository origin by natural sources would not occur, and, therefore it is appropriate to exclude possible effects of dilution for such radionuclides. Transport models used in the TSPA take into account the presence of multiple radioactive isotopes originating from the waste form (e.g., uranium, plutonium, americium, thorium, and other elements occur as multiple radionuclides) and account for possible competition affects by allocating individual isotopes of each element according to their relative abundance in the inventory (SNL 2008 [DIRS 183478], Section 6.3.7.5.3). Effects of mixing and competition among anthropogenic radionuclides, as opposed to dilution with naturally occurring isotopes, are therefore accounted for in the performance assessment.

For those radionuclides with common stable isotopes present in the environment, the potential effect of isotopic dilution was also not explicitly modeled, but has been taken into account through the regulatory specification of the stylized RMEI and the approach to calculating dose. Consistent with regulatory requirements (proposed 10 CFR 63.2 (70 FR 53313 [DIRS 178394])) and Federal Guidance Report 13 (EPA 2002 [DIRS 175544]), dose coefficients used in the biosphere model (SNL 2007 [DIRS 177399], Section 6.4.9.6) were developed using the International Commission on Radiological Protection metabolic and dosimetric models that

include, where appropriate, the stable element intake representative of a diet of a reference person (e.g., ICRP 1989 [DIRS 183654], Sections 2 and 7). The actual dietary intake of stable elements may be different than that for the reference diet, which could result in a different isotopic dilution, and thus, different metabolism of a radioactive isotope of an element. Because the locally produced food is a small fraction of the average diet for the Amargosa Valley population, site-specific conditions are not expected to strongly affect the intake of stable isotopes by an average person. Therefore, it is not appropriate to introduce a site-specific correction to the RMEI's dietary intake of stable isotopes.

Based on the previous discussion, omission of FEP 3.2.07.01.0A (Isotopic Dilution) will not result in a significant adverse change in the magnitude or timing of either radiological exposure to the RMEI or radionuclide releases to the accessible environment. Therefore, this FEP is excluded from the performance assessments conducted to demonstrate compliance with proposed 10 CFR 63.311 and 63.321 (70 FR 53313 [DIRS 178394]), and with 10 CFR 63.331 [DIRS 180319], on the basis of low consequence.

INPUTS:

Table 3.2.07.01.0A-1. Direct Inputs

Input	Source	Description
SNL 2007. *Biosphere Model Report.* [DIRS 177399]	Section 6.4.9.6	Dose coefficients used in the biosphere model were developed using the International Commission on Radiological Protection metabolic and dosimetric models that include, where appropriate, the stable element intake representative of a diet of a reference person

Table 3.2.07.01.0A-1. Indirect Inputs

Citation	Title	DIRS
10 CFR 63	Energy: Disposal of High-Level Radioactive Wastes in a Geologic Repository at Yucca Mountain, Nevada	180319
70 FR 53313	Implementation of a Dose Standard After 10,000 Years	178394
EPA 2002	*Federal Guidance Report 13, CD Supplement, Cancer Risk Coefficients for Environmental Exposure to Radionuclides, EPA*	175544
ICRP 1989	*"Age-Dependent Doses to Members of the Public from Intake of Radionuclides: Part 1"*	183654
SNL 2007	*Biosphere Model Report*	177399

FEP: 3.2.10.00.0A

FEP NAME:

Atmospheric Transport of Contaminants

FEP DESCRIPTION:

Atmospheric transport includes radiotoxic and chemotoxic species in the air as gas, vapor, particulates, or aerosol. Transport processes include wind, plowing and irrigation, degassing, saltation, and precipitation.

SCREENING DECISION:

Included

TSPA DISPOSITION:

Atmospheric transport of radionuclides is included in the biosphere model through the effects of resuspension of contaminated soil, gaseous emission of radionuclides from soil to air followed by atmospheric dispersion, deposition of airborne particulate matter, as well as generation of atmospheric aerosols (evaporative cooler), and gases (radon and $^{14}CO_2$). The biosphere model does not include processes related to long-range atmospheric transport and dispersion of airborne radionuclides because these have been excluded, as discussed in FEP 2.2.11.03.0A (Gas Transport in Geosphere). The biosphere model, however, does include the removal of radionuclides from the surface soil by erosion, which may involve atmospheric transport of contaminants. Soil erosion in agricultural fields is incorporated into the soil submodel for the groundwater exposure scenario (SNL 2007 [DIRS 177399], Section 6.4.1.4) in calculation of the surface soil removal constant (SNL 2007 [DIRS 177399], Section 6.4.1.4). Soil erosion includes soil loss and gain on farm fields (SNL 2007 [DIRS 179993], Section 6.4). For a volcanic eruption, the processes of long-range atmospheric transport are addressed in the atmospheric dispersion and tephra deposition model (SNL 2007 [DIRS 177431]) and in included FEP 1.2.04.07.0A (Ashfall). Aeolian transport following a volcanic eruption is addressed in the tephra redistribution model (SNL 2007 [DIRS 179347]) and in included FEP 1.2.04.07.0C (Ash Redistribution via Soil and Sediment Transport). These processes are not included in the biosphere model because they occur outside the reference biosphere.

Radiotoxic and chemotoxic species are outside the scope of performance assessment because the performance standards for the repository do not concern radiological or chemical toxicity (see excluded FEPs 3.3.06.00.0A (Radiological Toxicity and Effects) and 3.3.07.00.0A (Non-Radiological Toxicity and Effects)).

The process of atmospheric transport is included in the biosphere air submodel for the groundwater exposure scenario (SNL 2007 [DIRS 177399], Section 6.4.2), the air submodel for the volcanic ash exposure scenario (SNL 2007 [DIRS 177399], Section 6.5.2), and the ^{14}C special submodel for the groundwater exposure scenario (SNL 2007 [DIRS 177399], Section 6.4.6). The associated parameters include mass loading for crops (BSC 2006 [DIRS 177101], Sections 6.2.5 and 6.3.5), mass loading for the receptor environments

(BSC 2006 [DIRS 177101], Sections 6.2 and 6.3), soil bulk density (SNL 2007 [DIRS 179993], Section 6.2), tillage depth (BSC 2004 [DIRS 169673], Section 6.10), resuspension enhancement factor (SNL 2007 [DIRS 179993], Section 6.5), fraction of radionuclides in evaporative cooler water transferred to air (BSC 2004 [DIRS 169672], Section 6.5.2), water evaporation rate for evaporative coolers (BSC 2004 [DIRS 169672], Section 6.5.2), evaporative cooler air flow rate (BSC 2004 [DIRS 169672], Section 6.5.2), radon release factor (BSC 2004 [DIRS 169672], Section 6.6.1), interior wall height (BSC 2004 [DIRS 169672], Sections 6.5.2 and 6.6.2), house ventilation rate (BSC 2004 [DIRS 169672], Section 6.6.2), fraction of ^{222}Rn from soil entering the house (BSC 2004 [DIRS 169672], Section 6.6.2), ratio of ^{222}Rn concentration in air to flux density from soil (BSC 2004 [DIRS 169672], Section 6.6.1), ^{14}C emission rate for soil (BSC 2004 [DIRS 169672], Section 6.7.1), surface area of irrigated land (SNL 2007 [DIRS 177399], Section 6.4.6.2), annual average wind speed (BSC 2004 [DIRS 169672], Section 6.7.2), ^{14}C mixing height (BSC 2004 [DIRS 169672], Section 6.7.2), concentration of stable carbon in air (BSC 2004 [DIRS 169672], Section 6.7.3), and correlation coefficient for airflow and water use in evaporative coolers (BSC 2004 [DIRS 169672], Section 6.5.2).

This FEP is included in the biosphere component of the TSPA model through the use of groundwater exposure scenario BDCFs that are direct inputs to the TSPA for the scenario classes involving radionuclide release to the groundwater (SNL 2007 [DIRS 177399], Section 6.11.3). The annual doses are calculated as the product of radionuclide concentration in groundwater and the BDCFs. In the event of a volcanic eruption, this FEP is included in the TSPA through BDCFs for the volcanic ash exposure scenario (SNL 2007 [DIRS 177399], Section 6.12.3). The annual doses are calculated as the product of radionuclide concentration in soil contaminated by radionuclides in volcanic tephra, the BDCF components, and the mass loading time decrease function. For the volcanic ash exposure scenario, three BDCF components are provided to the TSPA model that account for various RMEI exposure pathways (SNL 2007 [DIRS 177399], Section 6.12.3). See included FEP 3.3.04.02.0A (Inhalation) for a more detailed description of the volcanic BDCF components.

The BDCFs for all biosphere model realizations are provided as inputs to the TSPA model, which randomly samples these inputs to propagate uncertainty from the biosphere model into TSPA dose calculations. The present-day climate BDCFs are used for the assessment of doses to the RMEI for 10,000 years following disposal, as well as after 10,000 years, but within the period of the geologic stability (SNL 2007 [DIRS 177399], Sections 6.11.3 and 6.12.3).

This FEP is included for the performance assessment to demonstrate compliance with the individual protection standard (proposed 10 CFR 63.311 (70 FR 53313 [DIRS 178394])) and the performance assessment to demonstrate compliance with the individual protection standard for human intrusion (proposed 10 CFR 63.321 (70 FR 53313 [DIRS 178394])) because both these standards require consideration of all potential pathways of radionuclide transport and exposure in the performance assessment calculations. This FEP is not included for the performance assessment to demonstrate compliance with the groundwater protection standards (10 CFR 63.331 [DIRS 180319]) because these standards do not require the consideration of all potential pathways of radionuclide transport and exposure in the performance assessment calculations; rather, only groundwater pathways must be included.

INPUTS:

Table 3.2.10.00.0A-1. Indirect Inputs

Citation	Title	DIRS
10 CFR 63	Energy: Disposal of High-Level Radioactive Wastes in a Geologic Repository at Yucca Mountain, Nevada	180319
70 FR 53313	Implementation of a Dose Standard After 10,000 Years	178394
BSC 2004	*Agricultural and Environmental Input Parameters for the Biosphere Model*	169673
BSC 2004	*Environmental Transport Input Parameters for the Biosphere Model*	169672
BSC 2006	*Inhalation Exposure Input Parameters for the Biosphere Model*	177101
SNL 2007	*Biosphere Model Report*	177399
SNL 2007	*Atmospheric Dispersal and Deposition of Tephra from a Potential Volcanic Eruption at Yucca Mountain, Nevada*	177431
SNL 2007	*Redistribution of Tephra and Waste by Geomorphic Processes Following a Potential Volcanic Eruption at Yucca Mountain, Nevada*	179347
SNL 2007	*Soil-Related Input Parameters for the Biosphere Model*	179993

FEP: 3.3.01.00.0A

FEP NAME:

Contaminated Drinking Water, Foodstuffs and Drugs

FEP DESCRIPTION:

This FEP addresses human diet and fluid intake. Consumption of food, water, soil, drugs, etc., will affect human exposure to radionuclides. Other influences include filtration of water, dilution of diet with uncontaminated food, and food preparation techniques.

SCREENING DECISION:

Included

TSPA DISPOSITION:

A hypothetical human receptor, the RMEI, is used in the performance assessment calculations for both the individual protection standard (proposed 10 CFR 63.311 (70 FR 53313 [DIRS 178394])) and the individual protection standard for human intrusion (proposed 10 CFR 63.321 321 (70 FR 53313 [DIRS 178394])). The diet and lifestyle of the RMEI are representative of the diet and lifestyle of the current residents of Amargosa Valley, consistent with 10 CFR 63.312(b) [DIRS 180319]. Dietary survey data (DOE 1997 [DIRS 100332], Section 2.3) indicate that residents consume locally grown foods and groundwater. The consumption of contaminated locally grown crops, animal products, fish, as well as water and soil, is addressed in the ingestion submodel of the biosphere model through the consumption rates of these media (BSC 2005 [DIRS 172827], Sections 6.4.2 and 6.4.3). Consumption rates used in the model only concern locally produced crops and animal products and are based on the survey of the Amargosa Valley population. Therefore, dilution of diet with uncontaminated food is not considered. The biosphere model conservatively also does not consider radioactivity loss due to filtration of water or food preparation. There is no evidence of the production of drugs in Amargosa Valley using local materials.

The ingestion submodel includes the intake of food, water, and soil for the groundwater scenario (SNL 2007 [DIRS 177399]), Section 6.4.9) and for the volcanic ash scenario (SNL 2007 [DIRS 177399]), Section 6.5.7). This FEP also considers the calculation of radionuclide concentrations in foodstuffs (SNL 2007 [DIRS 177399]), Sections 6.4.3 to 6.4.6, 6.5.3, and 6.5.4). The parameters related to consumption of contaminated drinking water and foodstuffs include consumption rates of well water and locally produced food (BSC 2005 [DIRS 172827], Section 6.4) and inadvertent soil ingestion rate (BSC 2005 [DIRS 172827], Section 6.4.3). Only the portion of this FEP that relates to ingestion in contaminated groundwater is considered in the calculations of conversion factors for demonstrating compliance with the groundwater protection standards (SNL 2007 [DIRS 177399], Section 6.15.1).

This FEP is included in the biosphere component of the TSPA model through the use of groundwater exposure scenario BDCFs that are direct inputs to the TSPA for the scenario classes involving radionuclide release to the groundwater (SNL 2007 [DIRS 177399], Section 6.11.3).

The annual doses are calculated as the product of radionuclide concentration in groundwater and the BDCFs. The contaminated water aspect of this FEP is also included in the TSPA through the use of the conversion factors for demonstrating compliance with the groundwater protection standards (SNL 2007 [DIRS 177399], Section 6.15.1). In the event of a volcanic eruption, this FEP is included in the TSPA through BDCFs for the volcanic ash exposure scenario (SNL 2007 [DIRS 177399], Section 6.12.3). The annual doses are calculated as the product of radionuclide concentration in soil contaminated by radionuclides in volcanic tephra, the BDCF components, and the mass loading time decrease function. For the volcanic ash exposure scenario, three BDCF components are provided to the TSPA model that account for various RMEI exposure pathways (SNL 2007 [DIRS 177399], Section 6.12.3). See included FEP 3.3.04.02.0A (Inhalation) for a more detailed description of the volcanic BDCF components.

The BDCFs for all biosphere model realizations are provided as inputs to the TSPA model, which randomly samples these inputs to propagate uncertainty from the biosphere model into TSPA dose calculations. The present-day climate BDCFs are used for the assessment of doses to the RMEI for 10,000 years following disposal, as well as after 10,000 years, but within the period of the geologic stability (SNL 2007 [DIRS 177399], Sections 6.11.3 and 6.12.3).

This FEP is included for the performance assessment to demonstrate compliance with the individual protection standard (proposed 10 CFR 63.311 (70 FR 53313 [DIRS 178394])) and the performance assessment to demonstrate compliance with the individual protection standard for human intrusion (proposed 10 CFR 63.321 (70 FR 53313 [DIRS 178394])) because both these standards require the use of the concept of the RMEI in the performance assessment calculations. Only the portion of this FEP that relates to ingestion in contaminated groundwater is included for the performance assessment to demonstrate compliance with the groundwater protection standards (10 CFR 63.331 [DIRS 180319]) because these standards do not require the use of the concept of the RMEI in the performance assessment calculations.

INPUTS:

Table 3.3.01.00.0A-1. Indirect Inputs

Citation	Title	DIRS
10 CFR 63	Energy: Disposal of High-Level Radioactive Wastes in a Geologic Repository at Yucca Mountain, Nevada	180319
70 FR 53313	Implementation of a Dose Standard After 10,000 Years	178394
BSC 2005	*Characteristics of the Receptor for the Biosphere Model*	172827
DOE 1997	*The 1997 "Biosphere" Food Consumption Survey Summary Findings and Technical Documentation*	100332
SNL 2007	*Biosphere Model Report*	177399

FEP: 3.3.02.01.0A

FEP NAME:

Plant Uptake

FEP DESCRIPTION:

Uptake and accumulation of contaminants by plants could affect potential exposure pathways. Plant uptake from contaminated soils and irrigation water is possible. Particulate deposition onto plant surfaces is also possible. These plants may be used as feed for livestock and/or consumed directly by humans.

SCREENING DECISION:

Included

TSPA DISPOSITION:

Consistent with 10 CFR 63.312(b) [DIRS 180319], which states that the RMEI has a diet and lifestyle representative of the current residents of Amargosa Valley, and with 10 CFR 63.305(a) [DIRS 180319], which requires that the reference biosphere be consistent with present knowledge of the conditions in the region, plant uptake is included in the TSPA model. A dietary survey (DOE 1997 [DIRS 100332], Section 2.3) indicates that Amargosa Valley residents consume locally grown crops from home gardens irrigated with water obtained from a local ground source. The human ingestion pathway represented by this consumption includes plant uptake of radionuclides, deposition of radionuclides on plant surfaces, and subsequent transfer to humans via ingestion. For all radionuclides, two plant uptake routes are included in the biosphere model: root uptake and direct deposition on crops due to the interception of irrigation water and resuspended soil particles. For ^{14}C, an additional uptake mechanism is considered because plants can acquire from the air gaseous $^{14}CO_2$, which is used in photosynthesis. Crops considered in the model include leafy vegetables, other vegetables, fruit, grain, and animal feed (SNL 2007 [DIRS 177399], Sections 6.3.1.6 and 6.3.2.6). The process of plant uptake of radionuclides (also referred to as radionuclide accumulation, bioconcentration, or biomagnification) is included in the plant submodel for the groundwater (SNL 2007 [DIRS 177399], Section 6.4.3) and volcanic ash exposure scenarios (SNL 2007 [DIRS 177399], Section 6.5.3), and in the ^{14}C special submodel for the groundwater exposure scenario (SNL 2007 [DIRS 177399], Section 6.4.6).

There are a number of model parameters related to plant uptake associated with these submodels, including soil-to-plant transfer factor (BSC 2004 [DIRS 169672], Sections 6.2.1.2 through 6.2.1.5), dry-to-wet ratio (BSC 2004 [DIRS 169673], Section 6.2), fraction of overhead irrigation (BSC 2004 [DIRS 169673], Section 6.3), translocation factor (BSC 2004 [DIRS 169672], Section 6.2.2.2), weathering rate constant (BSC 2004 [DIRS 169672], Section 6.2.2.3), crop growing time (BSC 2004 [DIRS 169673], Section 6.4), crop wet yield (BSC 2004 [DIRS 169673], Section 6.11), daily irrigation rate (BSC 2004 [DIRS 169673], Section 6.8), crop dry biomass (BSC 2004 [DIRS 169673], Section 6.1), irrigation amount per application (BSC 2004 [DIRS 169673], Section 6.7), irrigation intensity (BSC 2004 [DIRS 169673],

Section 6.6), dry deposition velocity (BSC 2004 [DIRS 169672], Section 6.2.2.1), soil bulk density (SNL 2007 [DIRS 179993], Section 6.2), tillage depth (BSC 2004 [DIRS 169673], Section 6.10), fraction of air-derived carbon in plants (BSC 2004 [DIRS 169672], Section 6.7.3), fraction of soil-derived carbon in plants (BSC 2004 [DIRS 169672], Section 6.7.3), fraction of stable carbon in crops (BSC 2004 [DIRS 169672], Section 6.7.3), fraction of stable carbon in soil (BSC 2004 [DIRS 169672], Section 6.7.3), concentration of stable carbon in air (BSC 2004 [DIRS 169672], Section 6.7.3), and correlation coefficient for transfer factors and partition coefficients (BSC 2004 [DIRS 169672], Section 6.2.1.5).

This FEP is included in the biosphere component of the TSPA model through the use of groundwater exposure scenario BDCFs that are direct inputs to the TSPA for the scenario classes involving radionuclide release to the groundwater (SNL 2007 [DIRS 177399], Section 6.11.3). The annual doses are calculated as the product of radionuclide concentration in groundwater and the BDCFs. In the event of a volcanic eruption, this FEP is included in the TSPA through BDCFs for the volcanic ash exposure scenario (SNL 2007 [DIRS 177399], Section 6.12.3). The annual doses are calculated as the product of radionuclide concentration in soil contaminated by radionuclides in volcanic tephra, the BDCF components, and the mass loading time decrease function. For the volcanic ash exposure scenario, three BDCF components are provided to the TSPA model that account for various RMEI exposure pathways (SNL 2007 [DIRS 177399], Section 6.12.3). See included FEP 3.3.04.02.0A (Inhalation) for a more detailed description of the volcanic BDCF components.

The BDCFs for all biosphere model realizations are provided as inputs to the TSPA model, which randomly samples these inputs to propagate uncertainty from the biosphere model into TSPA dose calculations. The present-day climate BDCFs are used for the assessment of doses to the RMEI for 10,000 years following disposal, as well as after 10,000 years, but within the period of the geologic stability (SNL 2007 [DIRS 177399], Sections 6.11.3 and 6.12.3).

This FEP is included for the performance assessment to demonstrate compliance with the individual protection standard (proposed 10 CFR 63.311 (70 FR 53313 [DIRS 178394])) and the performance assessment to demonstrate compliance with the individual protection standard for human intrusion (proposed 10 CFR 63.321 (70 FR 53313 [DIRS 178394])) because both these standards require consideration of all potential pathways of radionuclide transport and exposure in the performance assessment calculations. This FEP is not included for the performance assessment to demonstrate compliance with the groundwater protection standards (10 CFR 63.331 [DIRS 180319]) because these standards do not require the consideration of all potential pathways of radionuclide transport and exposure in the performance assessment calculations; rather, only the groundwater ingestion pathways must be included.

INPUTS:

Table 3.3.02.01.0A-1. Indirect Inputs

Citation	Title	DIRS
10 CFR 63	Energy: Disposal of High-Level Radioactive Wastes in a Geologic Repository at Yucca Mountain, Nevada	180319
70 FR 53313	Implementation of a Dose Standard After 10,000 Years	178394
BSC 2004	*Agricultural and Environmental Input Parameters for the Biosphere Model*	169673
BSC 2004	*Environmental Transport Input Parameters for the Biosphere Model*	169672
DOE 1997	*The 1997 "Biosphere" Food Consumption Survey Summary Findings and Technical Documentation*	100332
SNL 2007	*Biosphere Model Report*	177399
SNL 2007	*Soil-Related Input Parameters for the Biosphere Model*	179993

FEP: 3.3.02.02.0A

FEP NAME:

Animal Uptake

FEP DESCRIPTION:

Livestock may accumulate radionuclides as a result of ingestion (water, feed and soil/sediment) and inhalation (aerosols and particulates). Depending on the livestock, they may be used for human consumption directly, or their produce (milk, eggs, etc.) may be consumed.

SCREENING DECISION:

Included

TSPA DISPOSITION:

Consistent with 10 CFR 63.312(b) [DIRS 180319], which states that the RMEI has a diet and lifestyle representative of the current residents of Amargosa Valley, and with 10 CFR 63.305(a) [DIRS 180319], which requires that the reference biosphere be consistent with present knowledge of the conditions in the region, animal uptake is included in the TSPA model. A dietary survey (DOE 1997 [DIRS 100332], Section 2.3) indicates that Amargosa Valley residents consume locally produced animal products. The human ingestion pathway represented by this consumption includes radionuclide accumulation in animals and their products, and subsequent transfer to humans via ingestion. Three mechanisms of animal uptake are included in the model: consumption of contaminated water, feed, and soil. Radionuclide concentrations are calculated using equilibrium transfer factors, which relate daily animal intake of an element to the concentration of that element in animal tissue or product. Animal products include meat, milk, poultry, and eggs (SNL 2007 [DIRS 177399], Sections 6.3.1.6 and 6.3.2.6). This FEP is addressed in the animal and ^{14}C submodels of the biosphere model (SNL 2007 [DIRS 177399], Table 6.7-1).

For the groundwater exposure scenario, the animal uptake submodel includes ingestion of contaminated water, animal feed, and soil to assess the resulting radionuclide concentrations in animal products (SNL 2007 [DIRS 177399], Section 6.4.4). For the volcanic ash exposure scenario, the groundwater contains no radionuclides, so ingestion of contaminated water by animals is not included (SNL 2007 [DIRS 177399], Section 6.5.4). Animal uptake is also included in the ^{14}C special submodel for the groundwater exposure scenario (SNL 2007 [DIRS 177399], Section 6.4.6.4). The contribution of inhaled contaminated soil to the activity concentration in an animal product was evaluated and found to be small in comparison to the contributions from the ingestion pathways (SNL 2007 [DIRS 177399], Section 7.4.5). As a result, this subpathway was not further considered. Dermal exposure of animals to contaminated soil and dust with possible uptake of radionuclides through the skin is relatively insignificant and was not included because it would be small relative to the daily soil ingestion by animals, which for cows is, on average, 0.7 kg/day or more (SNL 2007 [DIRS 177399], Table 6.6-3).

The following input parameters support modeling of animal uptake: animal transfer coefficients (BSC 2004 [DIRS 169672], Section 6.3.3), animal consumption rate of feed, water, and soil (BSC 2004 [DIRS 169672], Section 6.3.2), fraction of stable carbon in animal products (BSC 2004 [DIRS 169672], Section 6.7.4), fraction of air-derived carbon in plants (BSC 2004 [DIRS 169672], Section 6.7.3), fraction of soil-derived carbon in plants (BSC 2004 [DIRS 169672], Section 6.7.3), and concentration of stable carbon in farm animal water (BSC 2004 [DIRS 169672], Section 6.7.4).

This FEP is included in the biosphere component of the TSPA model through the use of groundwater exposure scenario BDCFs that are direct inputs to the TSPA for the scenario classes involving radionuclide release to the groundwater (SNL 2007 [DIRS 177399], Section 6.11.3). The annual doses are calculated as the product of radionuclide concentration in groundwater and the BDCFs. In the event of a volcanic eruption, this FEP is included in the TSPA through BDCFs for the volcanic ash exposure scenario (SNL 2007 [DIRS 177399], Section 6.12.3). The annual doses are calculated as the product of radionuclide concentration in soil contaminated by radionuclides in volcanic tephra, the BDCF components, and the mass loading time decrease function. For the volcanic ash exposure scenario, three BDCF components are provided to the TSPA model that account for various RMEI exposure pathways (SNL 2007 [DIRS 177399], Section 6.12.3). See included FEP 3.3.04.02.0A (Inhalation) for a more detailed description of the volcanic BDCF components.

The BDCFs for all biosphere model realizations are provided as inputs to the TSPA model, which randomly samples these inputs to propagate uncertainty from the biosphere model into TSPA dose calculations. The present-day climate BDCFs are used for the assessment of doses to the RMEI for 10,000 years following disposal, as well as after 10,000 years, but within the period of the geologic stability (SNL 2007 [DIRS 177399], Sections 6.11.3 and 6.12.3).

This FEP is included for the performance assessment to demonstrate compliance with the individual protection standard (proposed 10 CFR 63.311 (70 FR 53313 [DIRS 178394])) and the performance assessment to demonstrate compliance with the individual protection standard for human intrusion (proposed 10 CFR 63.321 (70 FR 53313 [DIRS 178394])) because both these standards require consideration of all potential pathways of radionuclide transport and exposure in the performance assessment calculations. This FEP is not included for the performance assessment to demonstrate compliance with the groundwater protection standards (10 CFR 63.331 [DIRS 180319]) because these standards do not require the consideration of all potential pathways of radionuclide transport and exposure in the performance assessment calculations; rather, only the groundwater ingestion pathways must be included.

INPUTS:

Table 3.3.02.02.0A-1. Indirect Inputs

Citation	Title	DIRS
10 CFR 63	Energy: Disposal of High-Level Radioactive Wastes in a Geologic Repository at Yucca Mountain, Nevada	180319
70 FR 53313	Implementation of a Dose Standard After 10,000 Years	178394
BSC 2004	*Environmental Transport Input Parameters for the Biosphere Model*	169672
DOE 1997	*The 1997 "Biosphere" Food Consumption Survey Summary Findings and Technical Documentation*	100332
SNL 2007	*Biosphere Model Report*	177399

FEP: 3.3.02.03.0A

FEP NAME:

Fish Uptake

FEP DESCRIPTION:

Uptake and bioaccumulation of contaminants in aquatic organisms could affect potential exposure pathways.

SCREENING DECISION:

Included

TSPA DISPOSITION:

Consistent with 10 CFR 63.312(b) [DIRS 180319], which states that the RMEI has a diet and lifestyle representative of the current residents of Amargosa Valley, and with 10 CFR 63.305(a) [DIRS 180319], which requires that the reference biosphere be consistent with present knowledge of the conditions in the region, fish uptake is included in the TSPA model. Uptake of radionuclides by aquatic organisms is a process that is expected to occur during commercial fish farming. A dietary survey (DOE 1997 [DIRS 100332], Section 2.3) indicated that Amargosa Valley residents consumed locally grown fish; therefore, the accumulation of radionuclides in aquatic organisms is included.

This FEP applies to the uptake of radionuclides by fish due to the use of contaminated groundwater in fish farming. The fish uptake FEP is addressed in the fish submodel, which includes the bioaccumulation of radionuclides in fish (SNL 2007 [DIRS 177399], Section 6.4.5). The transfer process, as represented by the bioaccumulation factor, is based on equilibria between radionuclide concentrations in the water, the aquatic environment, and concentrations in the edible part of fish (BSC 2004 [DIRS 169672], Sections 6.4.3 and 6.4.4). Because the fish are fed uncontaminated, commercially produced feed (Roe 2002 [DIRS 160674], p. 2), bioaccumulation factors provide an upper bound of activity concentration in the fish. The parameters involved in modeling of this process include the bioaccumulation factor (BSC 2004 [DIRS 169672], Section 6.4.3) and fishpond water concentration-modifying factor (BSC 2004 [DIRS 169672], Sections 6.4.3 and 6.4.4).

This FEP is included in the biosphere component of the TSPA model through the use of groundwater exposure scenario BDCFs that are direct inputs to the TSPA for the scenario classes involving radionuclide release to the groundwater (SNL 2007 [DIRS 177399], Section 6.11.3). The annual doses are calculated as the product of radionuclide concentration in groundwater and the BDCFs. The ingestion of contaminated fish is not included in the volcanic ash exposure scenario because of its negligible dose contribution (SNL 2007 [DIRS 177399], Appendix E).

The BDCFs for all biosphere model realizations are provided as inputs to the TSPA model, which randomly samples these inputs to propagate uncertainty from the biosphere model into TSPA dose calculations. The present-day climate BDCFs are used for the assessment of doses to

the RMEI for 10,000 years following disposal, as well as after 10,000 years, but within the period of the geologic stability (SNL 2007 [DIRS 177399], Section 6.11.3).

This FEP is included for the performance assessment to demonstrate compliance with the individual protection standard (proposed 10 CFR 63.311 (70 FR 53313 [DIRS 178394])) and the performance assessment to demonstrate compliance with the individual protection standard for human intrusion (proposed 10 CFR 63.321 (70 FR 53313 [DIRS 178394])) because both these standards require consideration of all potential pathways of radionuclide transport and exposure in the performance assessment calculations. This FEP is not included for the performance assessment to demonstrate compliance with the groundwater protection standards (10 CFR 63.331 [DIRS 180319]) because these standards do not require the consideration of all potential pathways of radionuclide transport and exposure in the performance assessment calculations; rather, only the groundwater ingestion pathways must be included.

INPUTS:

Table 3.3.02.03.0A-1. Indirect Inputs

Citation	Title	DIRS
10 CFR 63	Energy: Disposal of High-Level Radioactive Wastes in a Geologic Repository at Yucca Mountain, Nevada	180319
70 FR 53313	Implementation of a Dose Standard After 10,000 Years	178394
BSC 2004	*Environmental Transport Input Parameters for the Biosphere Model*	169672
DOE 1997	*The 1997 "Biosphere" Food Consumption Survey Summary Findings and Technical Documentation*	100332
Roe 2002	"Summary of RDA Investigation ID: 4/10/02 Fish Farming in Amargosa Valley"	160674
SNL 2007	*Biosphere Model Report*	177399

FEP: 3.3.03.01.0A

FEP NAME:

Contaminated Non-Food Products and Exposure

FEP DESCRIPTION:

Contaminants may be concentrated in various products: clothing (e.g., hides, leather, linen, wool); furniture (e.g., wood, metal); building materials (e.g., stone, clay for bricks, wood, dung); fuel (e.g., peat), tobacco, pets.

SCREENING DECISION:

Included

TSPA DISPOSITION:

Various products, such as leather, wool, wood, or clay for bricks, could be produced locally using contaminated water and thus become contaminated. Contamination of non-food products could result in external exposure because such products are usually not ingested intentionally. Inadvertent soil ingestion is addressed in included FEP 3.3.04.01.0A (Ingestion).

Exposure to non-food products is not explicitly included in the biosphere model; rather, it is bounded by external exposure to contaminated soil. In general, exposure to contaminated non-food products would be lower than exposure to contaminated soil, which is the medium that contains the majority of the radionuclide inventory in the biosphere. Furthermore, exposure to contaminated soil occurrs at all times while the RMEI is indoors and outdoors in the contaminated area. Parameters that address this FEP are the same as those for included FEP 3.3.04.03.0A (External Exposure).

Other possible pathways resulting from exposure to contaminated non-food products include the use of locally grown tobacco products. However, the socioeconomic surveys conducted in Amargosa Valley (CRWMS M&O 1997 [DIRS 101090], Section 3.4; YMP 1999 [DIRS 158212], Section 3.4) and other biosphere studies (Horak and Carns 1997 [DIRS 124149]) did not provide evidence of this crop in Amargosa Valley. Therefore, inhalation exposure from smoking tobacco is not included in the model.

This FEP is included in the biosphere component of the TSPA model through the use of groundwater exposure scenario BDCFs that are direct inputs to the TSPA for the scenario classes involving radionuclide release to the groundwater (SNL 2007 [DIRS 177399], Section 6.11.3). The annual doses are calculated as the product of radionuclide concentration in groundwater and the BDCFs. In the event of a volcanic eruption, this FEP is included in the TSPA through BDCFs for the volcanic ash exposure scenario (SNL 2007 [DIRS 177399], Section 6.12.3). The annual doses are calculated as the product of radionuclide concentration in soil contaminated by radionuclides in volcanic tephra, the BDCF components, and the mass loading time decrease function. For the volcanic ash exposure scenario, three BDCF components are provided to the TSPA model that account for various RMEI exposure pathways (SNL 2007 [DIRS 177399],

Section 6.12.3). See included FEP 3.3.04.02.0A (Inhalation) for a more detailed description of the volcanic BDCF components.

The BDCFs for all biosphere model realizations are provided as inputs to the TSPA model, which randomly samples these inputs to propagate uncertainty from the biosphere model into TSPA dose calculations. The present-day climate BDCFs are used for the assessment of doses to the RMEI for 10,000 years following disposal, as well as after 10,000 years, but within the period of the geologic stability (SNL 2007 [DIRS 177399], Sections 6.11.3 and 6.12.3).

This FEP is included for the performance assessment to demonstrate compliance with the individual protection standard (proposed 10 CFR 63.311 (70 FR 53313 [DIRS 178394])) and the performance assessment to demonstrate compliance with the individual protection standard for human intrusion (proposed 10 CFR 63.321 (70 FR 53313 [DIRS 178394])) because both these standards require consideration of all potential pathways of radionuclide transport and exposure in the performance assessment calculations. This FEP is not included for the performance assessment to demonstrate compliance with the groundwater protection standards (10 CFR 63.331 [DIRS 180319]) because these standards do not require the consideration of all potential pathways of radionuclide transport and exposure in the performance assessment calculations; rather, only groundwater pathways must be included.

INPUTS:

Table 3.3.03.01.0A-1. Indirect Inputs

Citation	Title	DIRS
10 CFR 63	Energy: Disposal of High-Level Radioactive Wastes in a Geologic Repository at Yucca Mountain, Nevada	180319
70 FR 53313	Implementation of a Dose Standard After 10,000 Years	178394
CRWMS M&O 1997	*Yucca Mountain Site Characterization Project Summary of Socioeconomic Data Analyses Conducted in Support of the Radiological Monitoring Program First Quarter 1996 to First Quarter 1997*	101090
Horak and Carns 1997	*Amargosa Focus Group Report. Biosphere Study*	124149
SNL 2007	*Biosphere Model Report*	177399
YMP 1999	*Yucca Mountain Site Characterization Project: Summary of Socioeconomic Data Analyses Conducted in Support of the Radiological Monitoring Program, April 1998 to April 1999*	158212

FEP: 3.3.04.01.0A

FEP NAME:

Ingestion

FEP DESCRIPTION:

Ingestion is human exposure to repository-derived radionuclides through eating contaminated foodstuffs or drinking contaminated water.

SCREENING DECISION:

Included

TSPA DISPOSITION:

Consistent with 10 CFR 63.312(b) [DIRS 180319], which states that the RMEI has a diet and lifestyle representative of the current residents of Amargosa Valley, ingestion is included in the TSPA model. Dietary survey data collected in the Yucca Mountain area (DOE 1997 [DIRS 100332], Section 2.3) indicate that consumption of groundwater and locally grown produce, livestock, and fish does occur in Amargosa Valley. This FEP is addressed through the ingestion rates of locally produced food and groundwater in the ingestion submodel (SNL 2007 [DIRS 177399], Table 6.7-1). For the groundwater exposure scenario, the ingestion exposure pathways include consumption of water from a groundwater well; consumption of locally produced plant foodstuffs, animal products, and fish; as well as inadvertent soil ingestion (SNL 2007 [DIRS 177399], Section 6.3.1.6). For the volcanic ash scenario, only the ingestion of locally produced plant foodstuffs, animal products, and inadvertent soil ingestion are considered (SNL 2007 [DIRS 177399], Section 6.3.2.6).

Within the mathematical representation of the ingestion submodel for the groundwater exposure scenario (SNL 2007 [DIRS 177399], Section 6.4.9), the annual water consumption rate is defined at 2 liters per day, as specified in 10 CFR 63.312(d) [DIRS 180319]. Exposure to contaminated plant foodstuffs is addressed through annual consumption rates of each of four locally grown crop food types (leafy vegetables, other vegetables, fruits, and grains) (BSC 2005 [DIRS 172827], Section 6.4.2) and their associated radionuclide-specific activity concentration (SNL 2007 [DIRS 177399], Section 6.4.3). Selection of crop types used in the biosphere model is addressed by *Biosphere Model Report* (SNL 2007 [DIRS 177399], Section 6.4.3). Similarly, exposure to contaminated animal products is the product of the consumption rates of each of four types of locally produced animal products (meat, milk, poultry, and eggs) (BSC 2005 [DIRS 172827], Section 6.4.2) and their associated radionuclide-specific activity concentration (SNL 2007 [DIRS 177399], Section 6.4.4). Selection of animal product types used in the biosphere model is discussed in *Biosphere Model Report* (SNL 2007 [DIRS 177399], Section 6.4.4). Ingestion of fish is addressed within this submodel as the annual consumption rate of locally produced fish (BSC 2005 [DIRS 172827], Section 6.4.2) times the radionuclide-specific activity concentration in fish (SNL 2007 [DIRS 177399], Section 6.4.5). The inadvertent intake of soil, contaminated as a result of long-term irrigation of crops, is addressed in this submodel as the product of the mass activity concentration of each of the

primary radionuclides in soil (SNL 2007 [DIRS 177399], Section 6.4.1) times the annual consumption rate of soil (BSC 2005 [DIRS 172827], Section 6.4.3). Related parameters also include dose coefficients for ingestion of radionuclides (SNL 2007 [DIRS 177399], Section 6.4.9.6). Deliberate soil ingestion is not included (BSC 2005 [DIRS 172827], Section 6.4.3).

The mathematical representation of the ingestion submodel for the volcanic ash exposure scenario is similar to that for the groundwater exposure scenario (SNL 2007 [DIRS 177399], Section 6.5.7). The consumption of contaminated water, and crop and animal products, contaminated as a result of irrigation, are not considered because the groundwater is assumed to be uncontaminated for this exposure scenario.

Only the portion of this FEP that relates to ingestion of contaminated groundwater is considered in the calculations of conversion factors for calculating beta-photon dose from drinking 2 L per day of water taken from the representative volume, which are used for evaluating compliance with the groundwater protection standards (SNL 2007 [DIRS 177399], Section 6.15.1).

This FEP is included in the biosphere component of the TSPA model through the use of groundwater exposure scenario BDCFs that are direct inputs to the TSPA for the scenario classes involving radionuclide release to the groundwater (SNL 2007 [DIRS 177399], Section 6.1.3) and through the use of the conversion factors for evaluating compliance with the groundwater protection standards (SNL 2007 [DIRS 177399], Section 6.15.1). The annual doses are calculated as the product of radionuclide concentration in groundwater and the BDCFs. In the event of a volcanic eruption, this FEP is included in the TSPA through BDCFs for the volcanic ash exposure scenario (SNL 2007 [DIRS 177399], Section 6.12.3). The annual doses are calculated as the product of radionuclide concentration in soil contaminated by radionuclides in volcanic tephra, the BDCF components, and the mass loading time decrease function. For the volcanic ash exposure scenario, three BDCF components are provided to the TSPA model that account for various RMEI exposure pathways, including ingestion (SNL 2007 [DIRS 177399], Section 6.12.3). See included FEP 3.3.04.02.0A (Inhalation) for a more detailed description of the volcanic BDCF components.

The BDCFs for all biosphere model realizations are provided as inputs to the TSPA model, which randomly samples these inputs to propagate uncertainty from the biosphere model into TSPA dose calculations. The present-day climate BDCFs are used for the assessment of doses to the RMEI for 10,000 years following disposal, as well as after 10,000 years, but within the period of the geologic stability (SNL 2007 [DIRS 177399], Sections 6.11.3 and 6.12.3).

This FEP is included for the performance assessment to demonstrate compliance with the individual protection standard (proposed 10 CFR 63.311 (70 FR 53313 [DIRS 178394])) and the performance assessment to demonstrate compliance with the individual protection standard for human intrusion (proposed 10 CFR 63.321 (70 FR 53313 [DIRS 178394])) because both these standards require consideration of all potential pathways of radionuclide transport and exposure in the performance assessment calculations. This FEP is also included for the performance assessment to demonstrate compliance with the groundwater protection standards (10 CFR 63.331 [DIRS 180319]) because these standards require the consideration of the groundwater ingestion pathway.

INPUTS:

Table 3.3.04.01.0A-1. Indirect Inputs

Citation	Title	DIRS
10 CFR 63	Energy: Disposal of High-Level Radioactive Wastes in a Geologic Repository at Yucca Mountain, Nevada	180319
70 FR 53313	Implementation of a Dose Standard After 10,000 Years	178394
BSC 2005	*Characteristics of the Receptor for the Biosphere Model*	172827
DOE 1997	*The 1997 "Biosphere" Food Consumption Survey Summary Findings and Technical Documentation*	100332
SNL 2007	*Biosphere Model Report*	177399

FEP: 3.3.04.02.0A

FEP NAME:

Inhalation

FEP DESCRIPTION:

Inhalation pathways for repository-derived radionuclides should be considered. Two possible pathways are: inhalation of gases and vapors emanating directly from the ground after transport through the far-field; and inhalation of suspended, contaminated particulate matter (e.g., decay products of radon, dust, smoke, pollen, and soil particles).

SCREENING DECISION:

Included

TSPA DISPOSITION:

Inhalation of gases, vapors, and suspended particulate matter are processes by which the RMEI may be exposed to radionuclides in the reference biosphere. This FEP is addressed in the biosphere inhalation submodels for the groundwater (SNL 2007 [DIRS 177399], Section 6.4.8) and the volcanic ash (SNL 2007 [DIRS 177399], Section 6.5.6) exposure scenarios. The inhalation submodel for the groundwater exposure scenario includes inhalation of contaminated resuspended particles, aerosols from evaporative coolers, ^{14}C, and radon decay products (SNL 2007 [DIRS 177399], Section 6.4.8). For the volcanic ash exposure scenario (SNL 2007 [DIRS 177399], Section 6.5.6), inhalation of ^{14}C is not included because ^{14}C is not a primary radionuclide for this scenario. In addition, inhalation of atmospheric aerosols produced by evaporative coolers is not considered in the volcanic ash exposure scenario because the groundwater is assumed to be uncontaminated (SNL 2007 [DIRS 177399], Section 6.3.2). Transport of gases and vapors emanating directly from the ground after transport through the far-field and their radiological impact is evaluated in excluded FEP 2.2.11.03.0A (Gas Transport in Geosphere).

Within the mathematical representations of this FEP, human lifestyles, behavior, and physiology are accounted for through the use of the following parameters: environment-specific breathing rates (BSC 2005 [DIRS 172827], Section 6.3.3), fraction of houses with evaporative coolers (BSC 2005 [DIRS 172827], Section 6.3.4.1), evaporative cooler use factor (BSC 2005 [DIRS 172827], Section 6.3.4.2), population proportions (BSC 2005 [DIRS 172827], Section 6.3.1), and environment- and population group-specific exposure times (BSC 2005 [DIRS 172827], Section 6.3.2). The exposure source terms for the submodels are quantified, as applicable, by the following parameters: activity concentration in air for radionuclides attached to resuspended particles (SNL 2007 [DIRS 177399], Sections 6.4.2.1 and 6.5.2.1), activity concentration in air for radionuclides resulting from the use of an evaporative cooler (SNL 2007 [DIRS 177399], Section 6.4.2.2), activity concentration of ^{14}C in air (SNL 2007 [DIRS 177399], Section 6.4.6.2), and activity concentration of ^{222}Rn in air (SNL 2007 [DIRS 177399], Sections 6.4.2.3 and 6.5.2.2). The other parameters of the inhalation submodel include dose coefficient for inhalation of radon decay products (BSC 2005 [DIRS 172827], Section 6.5.4),

dose coefficients for inhalation of other radionuclides (SNL 2007 [DIRS 177399], Section 6.4.8.5), mass loading time function for the receptor environments (BSC 2006 [DIRS 177101], Section 6.4), equilibrium factor for ^{222}Rn decay products (BSC 2004 [DIRS 169672], Section 6.6.3), and critical thickness of soil for resuspension (BSC 2004 [DIRS 169672], Section 6.8).

This FEP is included in the biosphere component of the TSPA model through the use of groundwater exposure scenario BDCFs that are direct inputs to the TSPA for the scenario classes involving radionuclide release to the groundwater (SNL 2007 [DIRS 177399], Section 6.11.3). The annual doses are calculated as the product of radionuclide concentration in groundwater and the BDCFs. In the event of a volcanic eruption, this FEP is included in the TSPA through BDCFs for the volcanic ash exposure scenario (SNL 2007 [DIRS 177399], Section 6.12.3). The annual doses are calculated as the product of radionuclide concentration in soil contaminated by radionuclides in volcanic tephra, the BDCF components, and the mass loading time decrease function. For the volcanic ash exposure scenario, three BDCF components are provided to the TSPA model that account for various RMEI exposure pathways (SNL 2007 [DIRS 177399], Section 6.12.3). The first component accounts for exposure to sources external to the body, ingestion, and inhalation of radon decay products. The second and third BDCF components (the short-term and long-term inhalation components) account for inhaling airborne particulates. The short-term inhalation component is numerically equal to the incremental increase in inhalation exposure during the first year following a volcanic eruption. This term is used together with the time function to calculate short-term increase in inhalation exposure relative to the conditions existing before and long after an eruption. With time, particulate concentration in air returns to the preeruption level. These conditions are described by the long-term inhalation component, which represents inhalation of resuspended particulates under nominal conditions (i.e., when the mass loading is not elevated as the result of volcanic eruption) (SNL 2007 [DIRS 177399], Section 6.12.3).

The BDCFs for all biosphere model realizations are provided as inputs to the TSPA model, which randomly samples these inputs to propagate uncertainty from the biosphere model into TSPA dose calculations. The present-day climate BDCFs are used for the assessment of doses to the RMEI for 10,000 years following disposal, as well as after 10,000 years, but within the period of the geologic stability (SNL 2007 [DIRS 177399], Sections 6.11.3 and 6.12.3).

This FEP is included for the performance assessment to demonstrate compliance with the individual protection standard (proposed 10 CFR 63.311 (70 FR 53313 [DIRS 178394])) and the performance assessment to demonstrate compliance with the individual protection standard for human intrusion (proposed 10 CFR 63.321 (70 FR 53313 [DIRS 178394])) because both these standards require consideration of all potential pathways of radionuclide transport and exposure in the performance assessment calculations. This FEP is not included for the performance assessment to demonstrate compliance with the groundwater protection standards (10 CFR 63.331 [DIRS 180319]) because these standards do not require the consideration of all potential pathways of radionuclide transport and exposure in the performance assessment calculations; rather, only the groundwater ingestion pathways must be included.

INPUTS:

Table 3.3.04.02.0A-1. Indirect Inputs

Citation	Title	DIRS
10 CFR 63	Energy: Disposal of High-Level Radioactive Wastes in a Geologic Repository at Yucca Mountain, Nevada	180319
70 FR 53313	Implementation of a Dose Standard After 10,000 Years	178394
BSC 2004	*Environmental Transport Input Parameters for the Biosphere Model*	169672
BSC 2005	*Characteristics of the Receptor for the Biosphere Model*	172827
BSC 2006	*Inhalation Exposure Input Parameters for the Biosphere Model*	177101
SNL 2007	*Biosphere Model Report*	177399

FEP: 3.3.04.03.0A

FEP NAME:

External Exposure

FEP DESCRIPTION:

External exposure is human exposure to repository-derived radionuclides by contact, use, or exposure to contaminated materials.

SCREENING DECISION:

Included

TSPA DISPOSITION:

Amargosa Valley residents include people with lifestyles that bring them into contact with environmental media that may potentially become contaminated. Depending upon lifestyle, the RMEI may become externally exposed to radionuclides through the use of, contact with, or exposure to contaminated materials.

The biosphere model includes exposure to contaminated soil. Indoor exposures are mitigated by building materials providing shielding from contaminated soil. The model does not include other external exposure pathways (e.g., by air submersion, water immersion, and dermal absorption). Comparisons of the potential dose from air or water submersion pathways with that from exposure to contaminated soils indicate that the dose from air or water submersion is inconsequential (SNL 2007 [DIRS 177399], Section 7.4.8). Because the skin is generally an effective barrier against absorption of radionuclides, dermal absorption is also a very minor exposure pathway for the radionuclides included in the TSPA model (SNL 2007 177399], Section 7.3.7).

This FEP is addressed in the external exposure submodels for the groundwater (SNL 2007 [DIRS 177399], Section 6.4.7) and the volcanic ash (SNL 2007 [DIRS 177399], Section 6.5.5) exposure scenarios. For the groundwater exposure scenario, soil is considered contaminated to an infinite depth in order to account for the emissions from radionuclides that have been leached from the surface soil but still contribute to the external radiation field (SNL 2007 [DIRS 177399], Section 6.4.7.1). For the volcanic ash exposure scenario, it is assumed that all of the radioactivity deposited on the soil surface can be treated as the surface contamination regardless of the thickness of the contaminated layer (SNL 2007 [DIRS 177399], Section 6.5.5.1). Within the mathematical representation of this FEP (SNL 2007 [DIRS 177399], Sections 6.4.7 and 6.5.5), parameters such as building shielding factor (BSC 2005 [DIRS 172827], Section 6.6), exposure time (BSC 2005 [DIRS 172827], Section 6.3.2), and population proportion (BSC 2005 [DIRS 172827], Section 6.3.1) are used to account for receptor behavior and lifestyle. The exposure–dose relationship is represented through the dose coefficients for exposure to soil contaminated to an infinite depth and exposure to a contaminated ground surface (SNL 2007 [DIRS 177399], Sections 6.4.7.2 and 6.5.5.2).

Another parameter supporting this FEP is tillage depth (BSC 2004 [DIRS 169673], Section 6.10).

This FEP is included in the biosphere component of the TSPA model through the use of groundwater exposure scenario BDCFs that are direct inputs to the TSPA for the scenario classes involving radionuclide release to the groundwater (SNL 2007 [DIRS 177399], Section 6.1.3). The annual doses are calculated as the product of radionuclide concentration in groundwater and the BDCFs. The present-day climate BDCFs are used for the assessment of doses to the RMEI for the entire period of the geologic stability (SNL 2007 [DIRS 177399], Section 6.11.3). In the event of a volcanic eruption, this FEP is included in the TSPA through BDCFs for the volcanic ash exposure scenarios (SNL 2007 [DIRS 177399], Section 6.12.3). The annual doses are calculated as the product of radionuclide concentration in soil contaminated by radionuclides in volcanic tephra, the BDCF components, and the mass loading time decrease function. For the volcanic ash exposure scenario, three BDCF components are provided to the TSPA model that account for various RMEI exposure pathways, including external exposure (SNL 2007 [DIRS 177399], Section 6.12.3). See included FEP 3.3.04.02.0A (Inhalation) for a more detailed description of the volcanic BDCF components.

The BDCFs for all biosphere model realizations are provided as inputs to the TSPA model, which randomly samples these inputs to propagate uncertainty from the biosphere model into TSPA dose calculations. The present-day climate BDCFs are used for the assessment of doses to the RMEI for 10,000 years following disposal, as well as after 10,000 years, but within the period of the geologic stability (SNL 2007 [DIRS 177399], Sections 6.11.3 and 6.12.3).

This FEP is included for the performance assessment to demonstrate compliance with the individual protection standard (proposed 10 CFR 63.311 (70 FR 53313 [DIRS 178394])) and the performance assessment to demonstrate compliance with the individual protection standard for human intrusion (proposed 10 CFR 63.321 (70 FR 53313 [DIRS 178394])) because both these standards require consideration of all potential pathways of radionuclide transport and exposure in the performance assessment calculations. This FEP is not included for the performance assessment to demonstrate compliance with the groundwater protection standards (10 CFR 63.331 [DIRS 180319]) because these standards do not require the consideration of all potential pathways of radionuclide transport and exposure in the performance assessment calculations; rather, only the groundwater ingestion pathways must be included.

INPUTS:

Table 3.3.04.03.0A-1. Indirect Inputs

Citation	Title	DIRS
10 CFR 63	Energy: Disposal of High-Level Radioactive Wastes in a Geologic Repository at Yucca Mountain, Nevada	180319
70 FR 53313	Implementation of a Dose Standard After 10,000 Years	178394
BSC 2004	*Agricultural and Environmental Input Parameters for the Biosphere Model*	169673
BSC 2005	*Characteristics of the Receptor for the Biosphere Model*	172827
SNL 2007	*Biosphere Model Report*	177399

FEP: 3.3.05.01.0A

FEP NAME:

Radiation Doses

FEP DESCRIPTION:

The radiation dose is calculated from exposure rates (external, inhalation, and ingestion) and dose coefficients. The latter are based upon radiation type, human metabolism, metabolism of the element of concern in the human body, and duration of exposure.

SCREENING DECISION:

Included

TSPA DISPOSITION:

Regulations 10 CFR 63.113(b) and (d) [DIRS 180319] establish postclosure performance objectives for the repository in terms of limits on radiological exposure to the RMEI. The limits specified in proposed 10 CFR 63.311 and 10 CFR 63.321 (70 FR 53313 [DIRS 178394]) are expressed as an annual dose to the RMEI. In addition, 10 CFR 63.113(c) [DIRS 180319] establishes postclosure performance objectives for the repository in terms of limits on radionuclides in the representative volume of groundwater. The limits are specified in 10 CFR 63.331 [DIRS 180319] and include a limit on dose from ingesting 2 L/day of water from the representative volume. The dietary and lifestyle characteristics of the RMEI are representative of the current residents of Amargosa Valley, consistent with 10 CFR 63.312(b) [DIRS 180319]; the metabolic and physiological characteristics of the RMEI are those of an adult, consistent with 10 CFR 63.312(e) [DIRS 180319].

Within the biosphere model, the external exposure, ingestion, and inhalation submodels address this FEP (SNL 2007 [DIRS 177399], Table 6.7-1). The exposure rates depend on radionuclide concentrations in environmental media and on the dietary and lifestyle characteristics of the receptor. The doses arising from these exposures depend on radiation type, physiology, metabolism, and the biometrics of the receptor. In the model, the annual radiation dose from each of the primary radionuclides is the sum of the annual effective dose from the external exposure to each radionuclide and the annual committed effective dose from the ingestion and inhalation of each radionuclide (SNL 2007 [DIRS 177399], Section 6.4.10 for the groundwater exposure scenario, and Section 6.5.8 for the volcanic ash exposure scenario). For the annual dose from the ingestion or inhalation of each of the radionuclides of interest, the dose is the product of the individual radionuclide annual activity intakes into the body times the appropriate radionuclide-specific effective dose coefficient (SNL 2007 [DIRS 177399], Sections 6.4.8, 6.4.9, 6.5.6, and 6.5.7; BSC 2005 [DIRS 172827], Section 6.5.4). Effective dose coefficients for inhalation and ingestion are calculated using the appropriate dose coefficients and radionuclide branching fractions to account for the contribution from the short-lived decay products (SNL 2007 [DIRS 177399], Sections 6.4.8.5 and 6.4.9.6). External exposure is calculated using the radionuclide concentration in contaminated soil, various times of exposure to the contaminated soil, and radionuclide-specific effective dose coefficients (SNL 2007

[DIRS 177399], Sections 6.4.7 and 6.5.5). Effective dose coefficients for external exposure are also calculated using the appropriate dose coefficients and radionuclide branching fractions to account for the contribution from the short-lived decay products (SNL 2007 [DIRS 177399], Sections 6.4.7.2 and 6.5.5.2). This FEP is also considered in the calculations of conversion factors for evaluating compliance with the groundwater protection standards (SNL 2007 [DIRS 177399], Section 6.15.1).

This FEP is included in the biosphere component of the TSPA model through the use of groundwater exposure scenario BDCFs and through the use of the conversion factors for groundwater protection standards (SNL 2007 [DIRS 177399], Sections 6.1.3 and 6.15.1). For the TSPA scenario classes involving groundwater as a source of radionuclides, annual doses are calculated as the product of radionuclide concentration in groundwater and BDCFs generated in the biosphere model (or conversion factors for the groundwater protection requirements calculation). Such an approach is possible because quantities calculated in the submodels of the biosphere model for the groundwater exposure scenario, including radionuclide concentrations in the environmental media and the annual dose from various exposure pathways, are proportional to the radionuclide concentration in the groundwater (SNL 2007 [DIRS 177399], Section 6.4.10.2). Thus, for this exposure scenario, the biosphere model contribution to the dose assessment (i.e., BDCFs) can be separated from the source (i.e., radionuclide concentration in the groundwater). The BDCF for a radionuclide is numerically equal to the dose for a unit activity concentration of the radionuclide in the water (SNL 2007 [DIRS 177399], Section 6.4.10.2).

In the event of a volcanic eruption, this FEP is included in the TSPA through BDCFs for the volcanic ash exposure scenario (SNL 2007 [DIRS 177399], Section 6.12.3). Because variation in radionuclide concentrations in deposited and redistributed volcanic tephra is not part of the biosphere model, BDCFs are calculated based on a unit radionuclide concentration in the soil (1 Bq/m^2 and 1 Bq/kg, depending on the exposure pathway) (SNL 2007 [DIRS 177399], Section 6.5). The TSPA model calculates annual radiation dose as a product of the time-dependent source terms, the source-independent BDCFs, and the mass loading time decay function. For the volcanic ash exposure scenario, three BDCF components are provided to the TSPA model. The first component accounts for exposure to sources external to the body, ingestion, and inhalation of radon decay products. The second and third BDCF components (the short-term and long-term inhalation components) account for inhaling airborne particulates. The short-term inhalation component is numerically equal to the incremental increase in inhalation exposure during the first year following a volcanic eruption. This term is used together with the time function to calculate short-term increase in inhalation exposure relative to the conditions existing before and long after an eruption. With time, particulate concentration in air returns to the preeruption level. These conditions are described by the long-term inhalation component, which represents inhalation of resuspended particulates under nominal conditions (i.e., when the mass loading is not elevated as the result of volcanic eruption) (SNL 2007 [DIRS 177399], Section 6.12.3).

The BDCFs for all biosphere model realizations are provided as inputs to the TSPA model, which randomly samples these inputs to propagate uncertainty from the biosphere model into TSPA dose calculations. The present-day climate BDCFs are used for the assessment of doses to the RMEI for 10,000 years following disposal, as well as after 10,000 years, but within the period of the geologic stability (SNL 2007 [DIRS 177399], Sections 6.11.3 and 6.12.3).

INPUTS:

Table 3.3.05.01.0A-1. Indirect Inputs

Citation	Title	DIRS
10 CFR 63	Energy: Disposal of High-Level Radioactive Wastes in a Geologic Repository at Yucca Mountain, Nevada	180319
70 FR 53313	Implementation of a Dose Standard After 10,000 Years	178394
BSC 2005	*Characteristics of the Receptor for the Biosphere Model*	172827
SNL 2007	*Biosphere Model Report*	177399

FEP: 3.3.06.00.0A

FEP NAME:

Radiological Toxicity and Effects

FEP DESCRIPTION:

This FEP addresses the estimation of human health effects resulting from radiation doses.

SCREENING DECISION:

Excluded – by regulation

SCREENING JUSTIFICATION:

Proposed 10 CFR 63.311 and 10 CFR 63.321 (70 FR 53313 [DIRS 178394]) address the protection of individuals from future radionuclide releases by placing limits on the annual dose from radiation that may be received by the RMEI. The RMEI, per 10 CFR 63.312(e) [DIRS 180319], is an adult with metabolic and physiological characteristics consistent with present knowledge of adults. The dose limits reflect the risk to the health and safety of the public, using the RMEI as a conservative surrogate for the public. The groundwater protection standards in 10 CFR 63.331 [DIRS 180319] are based on radionuclide concentrations in groundwater and on a radiation dose from drinking water.

No performance standards for possible radiological toxicity effects of radiation on human health have been imposed by the NRC. The regulations require calculation of radiation doses and radionuclide concentrations in the groundwater. They do not require estimating radiological health effects resulting from exposure to radiation. Therefore, this FEP is excluded on the basis of inconsistency with the regulations in proposed 10 CFR 63.311 and 10 CFR 63.321 (70 FR 53313 [DIRS 178394]), and 10 CFR 63.331 [DIRS 180319].

INPUTS:

Table 3.3.06.00.0A-1. Direct Inputs

Input	Source	Description
10 CFR 63. 2007. Energy: Disposal of High-Level Radioactive Wastes in a Geologic Repository at Yucca Mountain, Nevada. [DIRS 180319]	10 CFR 63.331	Separate standards for protection of groundwater
	10 CFR 63.312(e)	Definition of the RMEI as an adult with metabolic and physiological considerations consistent with present knowledge of adults
70 FR 53313. Implementation of a Dose Standard After 10,000 Years. [DIRS 178394]	10 CFR 63.321	Individual protection standard for human intrusion
	10 CFR 63.311	Individual protection standard after permanent closure

FEP: 3.3.06.01.0A

FEP NAME:

Repository Excavation

FEP DESCRIPTION:

Excavation of the repository and/or its contents may result in the production of tailings, which may subsequently release toxic contaminants.

SCREENING DECISION:

Excluded – by regulation

SCREENING JUSTIFICATION:

The handling of excavation spoils during construction of the repository is a preclosure operational concern, whereas the TSPA focus for FEP inclusion and exclusion is on postclosure assessment. Therefore, the effects of excavation spoils associated with the construction of the repository are excluded from the TSPA based on regulation. Future mining of the repository for its waste content constitutes human intrusion, and postclosure excavation of repository contents would constitute deliberate human intrusion. These activities are discussed in excluded FEPs 1.4.02.01.0A (Deliberate Human Intrusion) and 1.4.05.00.0A (Mining and Other Underground Activities (Human Intrusion)), both of which are excluded by regulation.

The NRC states that a performance assessment is to demonstrate compliance with postclosure performance objectives (10 CFR 63.102(j) [DIRS 180319]). The creation and handling of excavation spoils is part of preclosure operations; the surface facilities will be removed and the surface restored prior to repository closure (SNL 2007 [DIRS 179466], Table 4-3, Parameter Number 09-04). Also, the NRC indicates that the postclosure performance objectives are to be based on protecting the RMEI against radiation exposures and releases of radioactive material to the accessible environment (proposed 10 CFR 63.311 and 63.321 (70 FR 53313 [DIRS 178394]), and with 10 CFR 63.331 [DIRS 180319]). The regulation does not specify chemical toxicity as a postclosure performance criterion, nor does it require the estimation of health effects resulting from non-radiological toxicity. This is consistent with exclusion of FEP 3.3.07.00.0A (Non-Radiological Toxicity and Effects). In conclusion, the effects of repository excavation are excluded from the TSPA based on regulation.

INPUTS:

Table 3.3.06.01.0A-1. Direct Inputs

Input	Source	Description
SNL 2007. *Total System Performance Assessment Data Input Package for Requirements Analysis for Subsurface Facilities*. [DIRS 179466]	Table 4-3, Parameter Number 09-04)	The creation and handling of excavation spoils is part of preclosure operations; the surface facilities will be removed and the surface restored prior to repository closure

Table 3.3.06.01.0A-2. Indirect Inputs

Citation	Title	DIRS
70 FR 53313	Implementation of a Dose Standard After 10,000 Years	178394

FEP: 3.3.06.02.0A

FEP NAME:

Sensitization to Radiation

FEP DESCRIPTION:

Human and other organisms may become sensitized to radiation exposure so that its effects are more severe.

SCREENING DECISION:

Excluded – by regulation

SCREENING JUSTIFICATION:

Proposed 10 CFR 63.311 and 10 CFR 63.321 (70 FR 53313 [DIRS 178394]) address protection of individuals from future radionuclide releases by placing limits on the annual dose from radiation that may be received by the RMEI. The RMEI, per 10 CFR 63.312(e) [DIRS 180319], is an adult with metabolic and physiological characteristics consistent with present knowledge of adults. The dose limits reflect the risk to the health and safety of the public, using the RMEI as a conservative surrogate for the public. The groundwater protection standards in 10 CFR 63.331 [DIRS 180319] are based on radionuclide concentrations in groundwater and on a radiation dose from drinking water.

No performance standards for possible effects of sensitization to radiation on human health and on other organisms have been imposed by the NRC. The regulations require calculation of radiation doses and radionuclide concentrations in the groundwater. They do not require estimating radiological health or other effects, such as the sensitization to radiation, resulting from radiation exposure. Therefore this FEP is excluded on the basis of inconsistency with the regulations in proposed 10 CFR 63.311 and 10 CFR 63.321 (70 FR 53313 [DIRS 178394]), and 10 CFR 63.331 [DIRS 180319].

INPUTS:

Table 3.3.06.02.0A-1. Direct Inputs

Input	Source	Description
10 CFR 63. 2007. Energy: Disposal of High-Level Radioactive Wastes in a Geologic Repository at Yucca Mountain, Nevada. [DIRS 180319]	10 CFR 63.331	The regulation that defines the groundwater protection standards
	10 CFR 63.331	Separate standards for protection of groundwater
	10 CFR 63.312(e)	Definition of the RMEI as an adult with metabolic and physiological considerations consistent with present knowledge of adults
70 FR 53313. Implementation of a Dose Standard After 10,000 Years. [DIRS 178394]	10 CFR 63.321	Individual protection standard for human intrusion
	10 CFR 63.311	Individual protection standard after permanent closure

FEP: 3.3.07.00.0A

FEP NAME:

Non-Radiological Toxicity and Effects

FEP DESCRIPTION:

This FEP addresses the estimation of human health effects resulting from the non-radiological toxicity of the waste.

SCREENING DECISION:

Excluded – by regulation

SCREENING JUSTIFICATION:

Proposed 10 CFR 63.311 and 10 CFR 63.321 (70 FR 53313 [DIRS 178394]) address the protection of individuals from future radionuclide releases by placing limits on the annual dose from radiation that may be received by the RMEI. The RMEI, per 10 CFR 63.312(e) [DIRS 180319], is an adult with metabolic and physiological characteristics consistent with present knowledge of adults. The dose limits reflect the risk to the health and safety of the public, using the RMEI as a conservative surrogate for the public. The groundwater protection standards in 10 CFR 63.331 [DIRS 180319] are based on radionuclide concentrations in groundwater and on a radiation dose from drinking water.

No performance standards for possible non-radiological toxicity and effects on human health have been imposed by the NRC. The regulations require calculation of radiation doses and radionuclide concentrations in the groundwater. They do not require estimating non-radiological health effects resulting from exposure to the waste. Therefore, this FEP is excluded on the basis of inconsistency with the regulations in proposed 10 CFR 63.311 and 10 CFR 63.321 (70 FR 53313 [DIRS 178394]), and 10 CFR 63.331 [DIRS 180319].

INPUTS:

Table 3.3.07.00.0A-1. Direct Inputs

Input	Source	Description
10 CFR 63. 2007. Energy: Disposal of High-Level Radioactive Wastes in a Geologic Repository at Yucca Mountain, Nevada. [DIRS 180319]	10 CFR 63.331	Separate standards for protection of groundwater
	10 CFR 63.312(e)	Definition of the RMEI as an adult with metabolic and physiological considerations consistent with present knowledge of adults
70 FR 53313. Implementation of a Dose Standard After 10,000 Years. [DIRS 178394]	10 CFR 63.321	Individual protection standard for human intrusion
	10 CFR 63.311	Individual protection standard after permanent closure

FEP: 3.3.08.00.0A

FEP NAME:

Radon and Radon Decay Product Exposure

FEP DESCRIPTION:

This FEP addresses human exposure to radon and radon decay products. ^{226}Ra occurs in nuclear fuel waste and it gives rise to ^{222}Rn gas, the radioactive decay products of which can result in radiation doses to humans upon inhalation.

SCREENING DECISION:

Included

TSPA DISPOSITION:

Radon (^{222}Rn) is a decay product of one of the primary radionuclides considered in the TSPA (SNL 2007 [DIRS 177399], Table 6.3-7). Human exposure to radon and radon decay products occurs through inhalation.

Exposure to radon (^{222}Rn) and radon decay products is included in the air and inhalation submodels of the groundwater (SNL 2007 [DIRS 177399], Sections 6.4.2.3 and 6.4.8.4) and volcanic ash (SNL 2007 [DIRS 177399], Sections 6.5.2.2 and 6.5.6.2) exposure scenarios. Concentrations of radon and radon decay products are calculated in the air submodels for the groundwater exposure scenario (SNL 2007 [DIRS 177399], Section 6.4.2.3) and volcanic ash exposure scenario (SNL 2007 [DIRS 177399], Section 6.5.2.2). The consequences of inhalation of radon and the decay products are included in the inhalation submodels for the groundwater exposure scenario (SNL 2007 [DIRS 177399], Section 6.4.8.4) and the volcanic ash exposure scenario (SNL 2007 [DIRS 177399], Section 6.5.6.2). The parameters supporting this FEP include radon release factor (BSC 2004 [DIRS 169672], Section 6.6.1), interior wall height (BSC 2004 [DIRS 169672], Sections 6.5.2 and 6.6.2), house ventilation rate (BSC 2004 [DIRS 169672], Section 6.6.2), fraction of ^{222}Rn from soil entering the house (BSC 2004 [DIRS 169672], Section 6.6.2), ratio of ^{222}Rn concentration in air to flux density from soil (BSC 2004 [DIRS 169672], Section 6.6.1), equilibrium factor for ^{222}Rn decay products (BSC 2004 [DIRS 169672], Section 6.6.3), fraction of radionuclide transfer from water to air for evaporative coolers (BSC 2004 [DIRS 169672], Section 6.5.2), and dose coefficient for inhalation of radon decay products (BSC 2005 [DIRS 172827], Section 6.5.4). As discussed in excluded FEP 2.2.11.03.0A (Gas Transport in Geosphere), exposure to ^{222}Rn that migrates directly from the repository to the land surface in the gas phase is negligible and is not included in the pathways evaluated in the biosphere model.

This FEP is included in the biosphere component of the TSPA model through the use of groundwater exposure scenario BDCFs that are direct inputs to the TSPA for the scenario classes involving radionuclide release to the groundwater (SNL 2007 [DIRS 177399], Section 6.11.3). The annual doses are calculated as the product of radionuclide concentration in groundwater and the BDCFs. In the event of a volcanic eruption, this FEP is included in the TSPA through

BDCFs for the volcanic ash exposure scenarios (SNL 2007 [DIRS 177399], Section 6.12.3). The annual doses are calculated as the product of radionuclide concentration in soil contaminated by radionuclides in volcanic tephra, the BDCF components, and the mass loading time decay function. For the volcanic ash exposure scenario, three BDCF components are provided to the TSPA model that account for various RMEI exposure pathways, including inhalation of radon and its decay products (SNL 2007 [DIRS 177399], Section 6.12.3). See included FEP 3.3.04.02.0A (Inhalation) for a more detailed description of the volcanic BDCF components.

The BDCFs for all biosphere model realizations are provided as inputs to the TSPA model, which randomly samples these inputs to propagate uncertainty from the biosphere model into TSPA dose calculations. The present-day climate BDCFs are used for the assessment of doses to the RMEI for 10,000 years following disposal, as well as after 10,000 years, but within the period of the geologic stability (SNL 2007 [DIRS 177399], Sections 6.11.3 and 6.12.3).

This FEP is included for the performance assessment to demonstrate compliance with the individual protection standard (proposed 10 CFR 63.311 (70 FR 53313 [DIRS 178394])) and the performance assessment to demonstrate compliance with the individual protection standard for human intrusion (proposed 10 CFR 63.321 (70 FR 53313 [DIRS 178394])) because these standards require consideration of all potential pathways of radionuclide transport and exposure in the performance assessment calculations. This FEP is also included for the performance assessment to demonstrate compliance with the groundwater protection standards (10 CFR 63.331 [DIRS 180319]). These standards do not require the consideration of all potential pathways of radionuclide transport and exposure in the performance assessment calculations; rather, only the groundwater ingestion pathway must be included. Radon decay products contribute to the beta-photon dose for that pathway.

INPUTS:

Table 3.3.08.00.0A-1. Indirect Inputs

Citation	Title	DIRS
10 CFR 63	Energy: Disposal of High-Level Radioactive Wastes in a Geologic Repository at Yucca Mountain, Nevada	180319
70 FR 53313	Implementation of a Dose Standard After 10,000 Years	178394
BSC 2004	*Environmental Transport Input Parameters for the Biosphere Model*	169672
BSC 2005	*Characteristics of the Receptor for the Biosphere Model*	172827
SNL 2007	*Biosphere Model Report*	177399

7. CONCLUSIONS

This analysis report documents the screening decisions for the current Yucca Mountain disposal system FEPs, along with their technical bases. The results of these FEP screening analyses, documented in Section 6.2, are summarized in Table 7-1. The included FEPs become part of the total system performance assessment described in *Total System Performance Assessment Model/Analysis for the License Application* (SNL 2008 [DIRS 183478]).

The technical product output from these screening analyses is contained in the electronic database *FY 2007 LA FEP List and Screening* (DTN: MO0706SPAFEPLA.001). This database is useful to catalog and display the screening decisions and detailed FEP information. It is acknowledged that the FEP justification and implementation text provided in Section 6.2 may differ from that contained within the output DTN, but only at an editorial level.

Other technical product output from this report includes:

- DTN: SN0705WFLOWSCC.001—Output from Appendix C containing seepage flux analyses for flow through cracks (support exclusion justification for FEPs 2.1.03.10.0A (Advection of Liquids and Solids Through Cracks in the Waste Package) and 2.1.03.10.0B (Advection of Liquids and Solids Through Cracks in the Drip Shield)).

- DTN: MO0707NONLITHO.000—Output from Appendix E calculations demonstrating low consequence from seismic-induced rock block impacts in the nonlithophysal units (support exclusion justification for FEP 1.2.03.02.0B (Seismic-Induced Rockfall Damages EBS Components)).

- DTN: SN0712CEMENTEQ.001—Output from Appendix J used to corroborate and thereby qualify a direct input source of data.

Section 7.1 presents a discussion of the applicable NUREG-1804 (NRC 2003 [DIRS 163274]) acceptance criteria, which were identified in Section 4.2, and how these criteria are met.

Table 7-1. Yucca Mountain Project FEP List and Screening Decisions Listed by FEP Number

FEP Number	FEP Name	Screening Decision
0.1.02.00.0A	Timescales of Concern	Included
0.1.03.00.0A	Spatial Domain of Concern	Included
0.1.09.00.0A	Regulatory Requirements and Exclusions	Included
0.1.10.00.0A	Model and Data Issues	Included
1.1.01.01.0A	Open Site Investigation Boreholes	Excluded
1.1.01.01.0B	Influx Through Holes Drilled in Drift Wall or Crown	Excluded
1.1.02.00.0A	Chemical Effects of Excavation and Construction in EBS	Excluded
1.1.02.00.0B	Mechanical Effects of Excavation and Construction in EBS	Excluded
1.1.02.01.0A	Site Flooding (During Construction and Operation)	Excluded
1.1.02.02.0A	Preclosure Ventilation	Included
1.1.02.03.0A	Undesirable Materials Left	Excluded

Table 7-1. Yucca Mountain Project Features, Events, and Processes List and Screening Decisions Listed by FEP Number (Continued)

FEP Number	FEP Name	Screening Decision
1.1.03.01.0A	Error in Waste Emplacement	Excluded
1.1.03.01.0B	Error in Backfill Emplacement	Excluded
1.1.04.01.0A	Incomplete Closure	Excluded
1.1.05.00.0A	Records and Markers for the Repository	Excluded
1.1.07.00.0A	Repository Design	Included
1.1.08.00.0A	Inadequate Quality Control and Deviations from Design	Excluded
1.1.09.00.0A	Schedule and Planning	Included
1.1.10.00.0A	Administrative Control of the Repository Site	Excluded
1.1.11.00.0A	Monitoring of the Repository	Excluded
1.1.12.01.0A	Accidents and Unplanned Events During Construction and Operation	Excluded
1.1.13.00.0A	Retrievability	Included
1.2.01.01.0A	Tectonic Activity - Large Scale	Excluded
1.2.02.01.0A	Fractures	Included
1.2.02.02.0A	Faults	Included
1.2.02.03.0A	Fault Displacement Damages EBS Components	Included
1.2.03.02.0A	Seismic Ground Motion Damages EBS Components	Included
1.2.03.02.0B	Seismic-Induced Rockfall Damages EBS Components	Excluded
1.2.03.02.0C	Seismic-Induced Drift Collapse Damages EBS Components	Included
1.2.03.02.0D	Seismic-Induced Drift Collapse Alters In-Drift Thermohydrology	Included
1.2.03.02.0E	Seismic-Induced Drift Collapse Alters In-Drift Chemistry	Excluded
1.2.03.03.0A	Seismicity Associated With Igneous Activity	Included
1.2.04.02.0A	Igneous Activity Changes Rock Properties	Excluded
1.2.04.03.0A	Igneous Intrusion Into Repository	Included
1.2.04.04.0A	Igneous Intrusion Interacts With EBS Components	Included
1.2.04.04.0B	Chemical Effects of Magma and Magmatic Volatiles	Included
1.2.04.05.0A	Magma Or Pyroclastic Base Surge Transports Waste	Excluded
1.2.04.06.0A	Eruptive Conduit to Surface Intersects Repository	Included
1.2.04.07.0A	Ashfall	Included
1.2.04.07.0B	Ash Redistribution in Groundwater	Excluded
1.2.04.07.0C	Ash Redistribution Via Soil and Sediment Transport	Included
1.2.05.00.0A	Metamorphism	Excluded
1.2.06.00.0A	Hydrothermal Activity	Excluded
1.2.07.01.0A	Erosion/Denudation	Excluded
1.2.07.02.0A	Deposition	Excluded
1.2.08.00.0A	Diagenesis	Excluded
1.2.09.00.0A	Salt Diapirism and Dissolution	Excluded
1.2.09.01.0A	Diapirism	Excluded
1.2.09.02.0A	Large-Scale Dissolution	Excluded
1.2.10.01.0A	Hydrologic Response to Seismic Activity	Excluded
1.2.10.02.0A	Hydrologic Response to Igneous Activity	Excluded
1.3.01.00.0A	Climate Change	Included
1.3.04.00.0A	Periglacial Effects	Excluded
1.3.05.00.0A	Glacial and Ice Sheet Effect	Excluded

Table 7-1. Yucca Mountain Project Features, Events, and Processes List and Screening Decisions Listed by FEP Number (Continued)

FEP Number	FEP Name	Screening Decision
1.3.07.01.0A	Water Table Decline	Excluded
1.3.07.02.0A	Water Table Rise Affects SZ	Included
1.3.07.02.0B	Water Table Rise Affects UZ	Included
1.4.01.00.0A	Human Influences on Climate	Excluded
1.4.01.01.0A	Climate Modification Increases Recharge	Included
1.4.01.02.0A	Greenhouse Gas Effects	Excluded
1.4.01.03.0A	Acid Rain	Excluded
1.4.01.04.0A	Ozone Layer Failure	Excluded
1.4.02.01.0A	Deliberate Human Intrusion	Excluded
1.4.02.02.0A	Inadvertent Human Intrusion	Included
1.4.02.03.0A	Igneous Event Precedes Human Intrusion	Excluded
1.4.02.04.0A	Seismic Event Precedes Human Intrusion	Excluded
1.4.03.00.0A	Unintrusive Site Investigation	Excluded
1.4.04.00.0A	Drilling Activities (Human Intrusion)	Included
1.4.04.01.0A	Effects of Drilling Intrusion	Included
1.4.05.00.0A	Mining and Other Underground Activities (Human Intrusion)	Excluded
1.4.06.01.0A	Altered Soil Or Surface Water Chemistry	Excluded
1.4.07.01.0A	Water Management Activities	Included
1.4.07.02.0A	Wells	Included
1.4.07.03.0A	Recycling of Accumulated Radionuclides from Soils to Groundwater	Excluded
1.4.08.00.0A	Social and Institutional Developments	Excluded
1.4.09.00.0A	Technological Developments	Excluded
1.4.11.00.0A	Explosions and Crashes (Human Activities)	Excluded
1.5.01.01.0A	Meteorite Impact	Excluded
1.5.01.02.0A	Extraterrestrial Events	Excluded
1.5.02.00.0A	Species Evolution	Excluded
1.5.03.01.0A	Changes in the Earth's Magnetic Field	Excluded
1.5.03.02.0A	Earth Tides	Excluded
2.1.01.01.0A	Waste Inventory	Included
2.1.01.02.0A	Interactions Between Co-Located Waste	Excluded
2.1.01.02.0B	Interactions Between Co-Disposed Waste	Included
2.1.01.03.0A	Heterogeneity of Waste Inventory	Included
2.1.01.04.0A	Repository-Scale Spatial Heterogeneity of Emplaced Waste	Included
2.1.02.01.0A	DSNF Degradation (Alteration, Dissolution, and Radionuclide Release)	Included
2.1.02.02.0A	CSNF Degradation (Alteration, Dissolution, and Radionuclide Release)	Included
2.1.02.03.0A	HLW Glass Degradation (Alteration, Dissolution, and Radionuclide Release)	Included
2.1.02.04.0A	Alpha Recoil Enhances Dissolution	Excluded
2.1.02.05.0A	HLW Glass Cracking	Included
2.1.02.06.0A	HLW Glass Recrystallization	Excluded
2.1.02.07.0A	Radionuclide Release from Gap and Grain Boundaries	Included
2.1.02.08.0A	Pyrophoricity from DSNF	Excluded
2.1.02.09.0A	Chemical Effects of Void Space in Waste Package	Included

Table 7-1. Yucca Mountain Project Features, Events, and Processes List and Screening Decisions Listed by FEP Number (Continued)

FEP Number	FEP Name	Screening Decision
2.1.02.10.0A	Organic/Cellulosic Materials in Waste	Excluded
2.1.02.11.0A	Degradation of Cladding from Waterlogged Rods	Excluded
2.1.02.12.0A	Degradation of Cladding Prior to Disposal	Included
2.1.02.13.0A	General Corrosion of Cladding	Excluded
2.1.02.14.0A	Microbially Influenced Corrosion (MIC) of Cladding	Excluded
2.1.02.15.0A	Localized (Radiolysis Enhanced) Corrosion of Cladding	Excluded
2.1.02.16.0A	Localized (Pitting) Corrosion of Cladding	Excluded
2.1.02.17.0A	Localized (Crevice) Corrosion of Cladding	Excluded
2.1.02.18.0A	Enhanced Corrosion of Cladding from Dissolved Silica	Excluded
2.1.02.19.0A	Creep Rupture of Cladding	Excluded
2.1.02.20.0A	Internal Pressurization of Cladding	Excluded
2.1.02.21.0A	Stress Corrosion Cracking (SCC) of Cladding	Excluded
2.1.02.22.0A	Hydride Cracking of Cladding	Excluded
2.1.02.23.0A	Cladding Unzipping	Included
2.1.02.24.0A	Mechanical Impact on Cladding	Excluded
2.1.02.25.0A	DSNF Cladding	Excluded
2.1.02.25.0B	Naval SNF Cladding	Included
2.1.02.26.0A	Diffusion-Controlled Cavity Growth in Cladding	Excluded
2.1.02.27.0A	Localized (Fluoride Enhanced) Corrosion of Cladding	Excluded
2.1.02.28.0A	Grouping of DSNF Waste Types Into Categories	Included
2.1.02.29.0A	Flammable Gas Generation from DSNF	Excluded
2.1.03.01.0A	General Corrosion of Waste Packages	Included
2.1.03.01.0B	General Corrosion of Drip Shields	Included
2.1.03.02.0A	Stress Corrosion Cracking (SCC) of Waste Packages	Included
2.1.03.02.0B	Stress Corrosion Cracking (SCC) of Drip Shields	Excluded
2.1.03.03.0A	Localized Corrosion of Waste Packages	Included
2.1.03.03.0B	Localized Corrosion of Drip Shields	Excluded
2.1.03.04.0A	Hydride Cracking of Waste Packages	Excluded
2.1.03.04.0B	Hydride Cracking of Drip Shields	Excluded
2.1.03.05.0A	Microbially Influenced Corrosion (MIC) of Waste Packages	Included
2.1.03.05.0B	Microbially Influenced Corrosion (MIC) of Drip Shields	Excluded
2.1.03.06.0A	Internal Corrosion of Waste Packages Prior to Breach	Excluded
2.1.03.07.0A	Mechanical Impact on Waste Package	Excluded
2.1.03.07.0B	Mechanical Impact on Drip Shield	Excluded
2.1.03.08.0A	Early Failure of Waste Packages	Included
2.1.03.08.0B	Early Failure of Drip Shields	Included
2.1.03.09.0A	Copper Corrosion in EBS	Excluded
2.1.03.10.0A	Advection of Liquids and Solids Through Cracks in the Waste Package	Excluded
2.1.03.10.0B	Advection of Liquids and Solids Through Cracks in the Drip Shield	Excluded
2.1.03.11.0A	Physical Form of Waste Package and Drip Shield	Included
2.1.04.01.0A	Flow in the Backfill	Excluded
2.1.04.02.0A	Chemical Properties and Evolution of Backfill	Excluded
2.1.04.03.0A	Erosion or Dissolution of Backfill	Excluded

Table 7-1. Yucca Mountain Project Features, Events, and Processes List and Screening Decisions Listed by FEP Number (Continued)

FEP Number	FEP Name	Screening Decision
2.1.04.04.0A	Thermal-Mechanical Effects of Backfill	Excluded
2.1.04.05.0A	Thermal-Mechanical Properties and Evolution of Backfill	Excluded
2.1.04.09.0A	Radionuclide Transport in Backfill	Excluded
2.1.05.01.0A	Flow Through Seals (Access Ramps and Ventilation Shafts)	Excluded
2.1.05.02.0A	Radionuclide Transport Through Seals	Excluded
2.1.05.03.0A	Degradation of Seals	Excluded
2.1.06.01.0A	Chemical Effects of Rock Reinforcement and Cementitious Materials in EBS	Excluded
2.1.06.02.0A	Mechanical Effects of Rock Reinforcement Materials in EBS	Excluded
2.1.06.04.0A	Flow Through Rock Reinforcement Materials in EBS	Excluded
2.1.06.05.0A	Mechanical Degradation of Emplacement Pallet	Excluded
2.1.06.05.0B	Mechanical Degradation of Invert	Excluded
2.1.06.05.0C	Chemical Degradation of Emplacement Pallet	Included
2.1.06.05.0D	Chemical Degradation of Invert	Excluded
2.1.06.06.0A	Effects of Drip Shield on Flow	Included
2.1.06.06.0B	Oxygen Embrittlement of Drip Shields	Excluded
2.1.06.07.0A	Chemical Effects at EBS Component Interfaces	Excluded
2.1.06.07.0B	Mechanical Effects at EBS Component Interfaces	Excluded
2.1.07.01.0A	Rockfall	Excluded
2.1.07.02.0A	Drift Collapse	Excluded
2.1.07.04.0A	Hydrostatic Pressure on Waste Package	Excluded
2.1.07.04.0B	Hydrostatic Pressure on Drip Shield	Excluded
2.1.07.05.0A	Creep of Metallic Materials in the Waste Package	Excluded
2.1.07.05.0B	Creep of Metallic Materials in the Drip Shield	Excluded
2.1.07.06.0A	Floor Buckling	Excluded
2.1.08.01.0A	Water Influx at the Repository	Included
2.1.08.01.0B	Effects of Rapid Influx into the Repository	Excluded
2.1.08.02.0A	Enhanced Influx at the Repository	Included
2.1.08.03.0A	Repository Dry-Out Due to Waste Heat	Included
2.1.08.04.0A	Condensation Forms on Roofs of Drifts (Drift-Scale Cold Traps)	Included
2.1.08.04.0B	Condensation Forms at Repository Edges (Repository-Scale Cold Traps)	Included
2.1.08.05.0A	Flow Through Invert	Included
2.1.08.06.0A	Capillary Effects (Wicking) in EBS	Included
2.1.08.07.0A	Unsaturated Flow in the EBS	Included
2.1.08.09.0A	Saturated Flow in the EBS	Excluded
2.1.08.11.0A	Repository Resaturation Due to Waste Cooling	Included
2.1.08.12.0A	Induced Hydrologic Changes in Invert	Excluded
2.1.08.14.0A	Condensation on Underside of Drip Shield	Excluded
2.1.08.15.0A	Consolidation of EBS Components	Excluded
2.1.09.01.0A	Chemical Characteristics of Water in Drifts	Included
2.1.09.01.0B	Chemical Characteristics of Water in Waste Package	Included
2.1.09.02.0A	Chemical Interaction With Corrosion Products	Included

Table 7-1. Yucca Mountain Project Features, Events, and Processes List and Screening Decisions Listed by FEP Number (Continued)

FEP Number	FEP Name	Screening Decision
2.1.09.03.0A	Volume Increase of Corrosion Products Impacts Cladding	Excluded
2.1.09.03.0B	Volume Increase of Corrosion Products Impacts Waste Package	Excluded
2.1.09.03.0C	Volume Increase of Corrosion Products Impacts Other EBS Components	Excluded
2.1.09.04.0A	Radionuclide Solubility, Solubility Limits, and Speciation in the Waste Form and EBS	Included
2.1.09.05.0A	Sorption of Dissolved Radionuclides in EBS	Included
2.1.09.06.0A	Reduction-Oxidation Potential in Waste Package	Included
2.1.09.06.0B	Reduction-Oxidation Potential in Drifts	Included
2.1.09.07.0A	Reaction Kinetics in Waste Package	Included
2.1.09.07.0B	Reaction Kinetics in Drifts	Included
2.1.09.08.0A	Diffusion of Dissolved Radionuclides in EBS	Included
2.1.09.08.0B	Advection of Dissolved Radionuclides in EBS	Included
2.1.09.09.0A	Electrochemical Effects in EBS	Excluded
2.1.09.10.0A	Secondary Phase Effects on Dissolved Radionuclide Concentrations	Excluded
2.1.09.11.0A	Chemical Effects of Waste-Rock Contact	Excluded
2.1.09.12.0A	Rind (Chemically Altered Zone) Forms in the Near-Field	Excluded
2.1.09.13.0A	Complexation in EBS	Excluded
2.1.09.15.0A	Formation of True (Intrinsic) Colloids in EBS	Excluded
2.1.09.16.0A	Formation of Pseudo-Colloids (Natural) in EBS	Included
2.1.09.17.0A	Formation of Pseudo-Colloids (Corrosion Product) in EBS	Included
2.1.09.18.0A	Formation of Microbial Colloids in EBS	Excluded
2.1.09.19.0A	Sorption of Colloids in EBS	Excluded
2.1.09.19.0B	Advection of Colloids in EBS	Included
2.1.09.20.0A	Filtration of Colloids in EBS	Excluded
2.1.09.21.0A	Transport of Particles Larger Than Colloids in EBS	Excluded
2.1.09.21.0B	Transport of Particles Larger Than Colloids in the SZ	Excluded
2.1.09.21.0C	Transport of Particles Larger Than Colloids in the UZ	Excluded
2.1.09.22.0A	Sorption of Colloids at Air-Water Interface	Excluded
2.1.09.23.0A	Stability of Colloids in EBS	Included
2.1.09.24.0A	Diffusion of Colloids in EBS	Included
2.1.09.25.0A	Formation of Colloids (Waste-Form) By Co-Precipitation in EBS	Included
2.1.09.26.0A	Gravitational Settling of Colloids in EBS	Excluded
2.1.09.27.0A	Coupled Effects on Radionuclide Transport in EBS	Excluded
2.1.09.28.0A	Localized Corrosion on Waste Package Outer Surface Due to Deliquescence	Excluded
2.1.09.28.0B	Localized Corrosion on Drip Shield Surfaces Due to Deliquescence	Excluded
2.1.10.01.0A	Microbial Activity in EBS	Excluded
2.1.11.01.0A	Heat Generation in EBS	Included
2.1.11.02.0A	Non-Uniform Heat Distribution in EBS	Included
2.1.11.03.0A	Exothermic Reactions in the EBS	Excluded
2.1.11.05.0A	Thermal Expansion/Stress of in-Package EBS Components	Excluded
2.1.11.06.0A	Thermal Sensitization of Waste Packages	Excluded

Table 7-1. Yucca Mountain Project Features, Events, and Processes List and Screening Decisions Listed by FEP Number (Continued)

FEP Number	FEP Name	Screening Decision
2.1.11.06.0B	Thermal Sensitization of Drip Shields	Excluded
2.1.11.07.0A	Thermal Expansion/Stress of in-Drift EBS Components	Excluded
2.1.11.08.0A	Thermal Effects on Chemistry and Microbial Activity in the EBS	Included
2.1.11.09.0A	Thermal Effects on Flow in the EBS	Included
2.1.11.09.0B	Thermally-Driven Flow (Convection) in Waste Packages	Excluded
2.1.11.09.0C	Thermally Driven Flow (Convection) in Drifts	Included
2.1.11.10.0A	Thermal Effects on Transport in EBS	Excluded
2.1.12.01.0A	Gas Generation (Repository Pressurization)	Excluded
2.1.12.02.0A	Gas Generation (He) from Waste Form Decay	Excluded
2.1.12.03.0A	Gas Generation (H_2) from Waste Package Corrosion	Excluded
2.1.12.04.0A	Gas Generation (CO_2, CH_4, H_2S) from Microbial Degradation	Excluded
2.1.12.06.0A	Gas Transport in EBS	Excluded
2.1.12.07.0A	Effects of Radioactive Gases in EBS	Excluded
2.1.12.08.0A	Gas Explosions in EBS	Excluded
2.1.13.01.0A	Radiolysis	Excluded
2.1.13.02.0A	Radiation Damage in EBS	Excluded
2.1.13.03.0A	Radiological Mutation of Microbes	Excluded
2.1.14.15.0A	In-Package Criticality (Intact Configuration)	Excluded
2.1.14.16.0A	In-Package Criticality (Degraded Configurations)	Excluded
2.1.14.17.0A	Near-Field Criticality	Excluded
2.1.14.18.0A	In-Package Criticality Resulting from a Seismic Event (Intact Configuration)	Excluded
2.1.14.19.0A	In-Package Criticality Resulting from a Seismic Event (Degraded Configurations)	Excluded
2.1.14.20.0A	Near-Field Criticality Resulting from a Seismic Event	Excluded
2.1.14.21.0A	In-Package Criticality Resulting from Rockfall (Intact Configuration)	Excluded
2.1.14.22.0A	In-Package Criticality Resulting from Rockfall (Degraded Configurations)	Excluded
2.1.14.23.0A	Near-Field Criticality Resulting from Rockfall	Excluded
2.1.14.24.0A	In-Package Criticality Resulting from an Igneous Event (Intact Configuration)	Excluded
2.1.14.25.0A	In-Package Criticality Resulting from an Igneous Event (Degraded Configurations)	Excluded
2.1.14.26.0A	Near-Field Criticality Resulting from an Igneous Event	Excluded
2.2.01.01.0A	Mechanical Effects of Excavation and Construction in the Near-Field	Included
2.2.01.01.0B	Chemical Effects of Excavation and Construction in the Near-Field	Excluded
2.2.01.02.0A	Thermally-Induced Stress Changes in the Near-Field	Excluded
2.2.01.02.0B	Chemical Changes in the Near-Field from Backfill	Excluded
2.2.01.03.0A	Changes In Fluid Saturations in the Excavation Disturbed Zone	Excluded
2.2.01.04.0A	Radionuclide Solubility in the Excavation Disturbed Zone	Excluded
2.2.01.05.0A	Radionuclide Transport in the Excavation Disturbed Zone	Excluded
2.2.03.01.0A	Stratigraphy	Included
2.2.03.02.0A	Rock Properties of Host Rock and Other Units	Included
2.2.06.01.0A	Seismic Activity Changes Porosity and Permeability of Rock	Excluded

Table 7-1. Yucca Mountain Project Features, Events, and Processes List and Screening Decisions Listed by FEP Number (Continued)

FEP Number	FEP Name	Screening Decision
2.2.06.02.0A	Seismic Activity Changes Porosity and Permeability of Faults	Excluded
2.2.06.02.0B	Seismic Activity Changes Porosity and Permeability of Fractures	Excluded
2.2.06.03.0A	Seismic Activity Alters Perched Water Zones	Excluded
2.2.06.04.0A	Effects of Subsidence	Excluded
2.2.06.05.0A	Salt Creep	Excluded
2.2.07.01.0A	Locally Saturated Flow at Bedrock/Alluvium Contact	Excluded
2.2.07.02.0A	Unsaturated Groundwater Flow in the Geosphere	Included
2.2.07.03.0A	Capillary Rise in the UZ	Included
2.2.07.04.0A	Focusing of Unsaturated Flow (Fingers, Weeps)	Included
2.2.07.05.0A	Flow in the UZ from Episodic Infiltration	Excluded
2.2.07.06.0A	Episodic Or Pulse Release from Repository	Excluded
2.2.07.06.0B	Long-Term Release of Radionuclides from The Repository	Included
2.2.07.07.0A	Perched Water Develops	Included
2.2.07.08.0A	Fracture Flow in the UZ	Included
2.2.07.09.0A	Matrix Imbibition in the UZ	Included
2.2.07.10.0A	Condensation Zone Forms Around Drifts	Included
2.2.07.11.0A	Resaturation of Geosphere Dry-Out Zone	Included
2.2.07.12.0A	Saturated Groundwater Flow in the Geosphere	Included
2.2.07.13.0A	Water-Conducting Features in the SZ	Included
2.2.07.14.0A	Chemically-Induced Density Effects on Groundwater Flow	Excluded
2.2.07.15.0A	Advection and Dispersion in the SZ	Included
2.2.07.15.0B	Advection and Dispersion in the UZ	Included
2.2.07.16.0A	Dilution of Radionuclides in Groundwater	Included
2.2.07.17.0A	Diffusion in the SZ	Included
2.2.07.18.0A	Film Flow into the Repository	Included
2.2.07.19.0A	Lateral Flow from Solitario Canyon Fault Enters Drifts	Included
2.2.07.20.0A	Flow Diversion Around Repository Drifts	Included
2.2.07.21.0A	Drift Shadow Forms Below Repository	Excluded
2.2.08.01.0A	Chemical Characteristics of Groundwater in the SZ	Included
2.2.08.01.0B	Chemical Characteristics of Groundwater in the UZ	Included
2.2.08.03.0A	Geochemical Interactions and Evolution in the SZ	Excluded
2.2.08.03.0B	Geochemical Interactions and Evolution in the UZ	Excluded
2.2.08.04.0A	Re-Dissolution of Precipitates Directs More Corrosive Fluids to Waste Packages	Excluded
2.2.08.05.0A	Diffusion in the UZ	Excluded
2.2.08.06.0A	Complexation in the SZ	Included
2.2.08.06.0B	Complexation in the UZ	Included
2.2.08.07.0A	Radionuclide Solubility Limits in the SZ	Excluded
2.2.08.07.0B	Radionuclide Solubility Limits in the UZ	Excluded
2.2.08.07.0C	Radionuclide Solubility Limits in the Biosphere	Excluded
2.2.08.08.0A	Matrix Diffusion in the SZ	Included
2.2.08.08.0B	Matrix Diffusion in the UZ	Included
2.2.08.09.0A	Sorption in the SZ	Included

Table 7-1. Yucca Mountain Project Features, Events, and Processes List and Screening Decisions Listed by FEP Number (Continued)

FEP Number	FEP Name	Screening Decision
2.2.08.09.0B	Sorption in the UZ	Included
2.2.08.10.0A	Colloidal Transport in the SZ	Included
2.2.08.10.0B	Colloidal Transport in the UZ	Included
2.2.08.11.0A	Groundwater Discharge to Surface Within The Reference Biosphere	Excluded
2.2.08.12.0A	Chemistry of Water Flowing into the Drift	Included
2.2.08.12.0B	Chemistry of Water Flowing into the Waste Package	Included
2.2.09.01.0A	Microbial Activity in the SZ	Excluded
2.2.09.01.0B	Microbial Activity in the UZ	Excluded
2.2.10.01.0A	Repository-Induced Thermal Effects on Flow in the UZ	Excluded
2.2.10.02.0A	Thermal Convection Cell Develops in SZ	Excluded
2.2.10.03.0A	Natural Geothermal Effects on Flow in the SZ	Included
2.2.10.03.0B	Natural Geothermal Effects on Flow in the UZ	Included
2.2.10.04.0A	Thermo-Mechanical Stresses Alter Characteristics of Fractures Near Repository	Excluded
2.2.10.04.0B	Thermo-Mechanical Stresses Alter Characteristics of Faults Near Repository	Excluded
2.2.10.05.0A	Thermo-Mechanical Stresses Alter Characteristics of Rocks Above and Below The Repository	Excluded
2.2.10.06.0A	Thermo-Chemical Alteration in the UZ (Solubility, Speciation, Phase Changes, Precipitation/Dissolution)	Excluded
2.2.10.07.0A	Thermo-Chemical Alteration of the Calico Hills Unit	Excluded
2.2.10.08.0A	Thermo-Chemical Alteration in the SZ (Solubility, Speciation, Phase Changes, Precipitation/Dissolution)	Excluded
2.2.10.09.0A	Thermo-Chemical Alteration of the Topopah Spring Basal Vitrophyre	Excluded
2.2.10.10.0A	Two-Phase Buoyant Flow/Heat Pipes	Included
2.2.10.11.0A	Natural Air Flow in the UZ	Excluded
2.2.10.12.0A	Geosphere Dry-Out Due to Waste Heat	Included
2.2.10.13.0A	Repository-Induced Thermal Effects on Flow in the SZ	Excluded
2.2.10.14.0A	Mineralogic Dehydration Reactions	Excluded
2.2.11.01.0A	Gas Effects in the SZ	Excluded
2.2.11.02.0A	Gas Effects in the UZ	Excluded
2.2.11.03.0A	Gas Transport in Geosphere	Excluded
2.2.12.00.0A	Undetected Features in the UZ	Excluded
2.2.12.00.0B	Undetected Features in the SZ	Included
2.2.14.09.0A	Far-Field Criticality	Excluded
2.2.14.10.0A	Far-Field Criticality Resulting from a Seismic Event	Excluded
2.2.14.11.0A	Far-Field Criticality Resulting from Rockfall	Excluded
2.2.14.12.0A	Far-Field Criticality Resulting from an Igneous Event	Excluded
2.3.01.00.0A	Topography and Morphology	Included
2.3.02.01.0A	Soil Type	Included
2.3.02.02.0A	Radionuclide Accumulation in Soils	Included
2.3.02.03.0A	Soil and Sediment Transport in the Biosphere	Included
2.3.04.01.0A	Surface Water Transport and Mixing	Included
2.3.06.00.0A	Marine Features	Excluded

Table 7-1. Yucca Mountain Project Features, Events, and Processes List and Screening Decisions Listed by FEP Number (Continued)

FEP Number	FEP Name	Screening Decision
2.3.09.01.0A	Animal Burrowing/Intrusion	Excluded
2.3.11.01.0A	Precipitation	Included
2.3.11.02.0A	Surface Runoff and Evapotranspiration	Included
2.3.11.03.0A	Infiltration and Recharge	Included
2.3.11.04.0A	Groundwater Discharge to Surface Outside The Reference Biosphere	Excluded
2.3.13.01.0A	Biosphere Characteristics	Included
2.3.13.02.0A	Radionuclide Alteration During Biosphere Transport	Included
2.3.13.03.0A	Effects of Repository Heat on The Biosphere	Excluded
2.3.13.04.0A	Radionuclide Release Outside The Reference Biosphere	Excluded
2.4.01.00.0A	Human Characteristics (Physiology, Metabolism)	Included
2.4.04.01.0A	Human Lifestyle	Included
2.4.07.00.0A	Dwellings	Included
2.4.08.00.0A	Wild and Natural Land and Water Use	Included
2.4.09.01.0A	Implementation of New Agricultural Practices Or Land Use	Excluded
2.4.09.01.0B	Agricultural Land Use and Irrigation	Included
2.4.09.02.0A	Animal Farms and Fisheries	Included
2.4.10.00.0A	Urban and Industrial Land and Water Use	Included
3.1.01.01.0A	Radioactive Decay and Ingrowth	Included
3.2.07.01.0A	Isotopic Dilution	Excluded
3.2.10.00.0A	Atmospheric Transport of Contaminants	Included
3.3.01.00.0A	Contaminated Drinking Water, Foodstuffs and Drugs	Included
3.3.02.01.0A	Plant Uptake	Included
3.3.02.02.0A	Animal Uptake	Included
3.3.02.03.0A	Fish Uptake	Included
3.3.03.01.0A	Contaminated Non-Food Products and Exposure	Included
3.3.04.01.0A	Ingestion	Included
3.3.04.02.0A	Inhalation	Included
3.3.04.03.0A	External Exposure	Included
3.3.05.01.0A	Radiation Doses	Included
3.3.06.00.0A	Radiological Toxicity and Effects	Excluded
3.3.06.01.0A	Repository Excavation	Excluded
3.3.06.02.0A	Sensitization to Radiation	Excluded
3.3.07.00.0A	Non-Radiological Toxicity and Effects	Excluded
3.3.08.00.0A	Radon and Radon Decay Product Exposure	Included

Output DTN: MO0706SPAFEPLA.001.

7.1 RELEVANT ACCEPTANCE CRITERIA

The following acceptance criterion from NUREG-1804 (NRC 2003 [DIRS 163274], Section 2.2.1.2.1.3), identified previously in Section 4.2, is addressed in this report:

NUREG-1804 Section 2.2.1.2.1.3, Acceptance Criterion 2: Screening of the List of Features, Events, and Processes Is Appropriate.

1. The U.S. Department of Energy has identified all features, events, and processes related to either the geologic setting or to the degradation, deterioration, or alteration of engineered barriers (including those processes that would affect the performance of natural barriers) that have been excluded;

2. The U.S. Department of Energy has provided justification for those features, events, and processes that have been excluded. An acceptable justification for excluding features, events, and processes is that either the feature, event, and process is specifically excluded by regulation; probability of the feature, event, and process (generally an event) falls below the regulatory criterion; or omission of the feature, event, and process does not significantly change the magnitude and time of the resulting radiological exposures to the reasonably maximally exposed individual, or radionuclide releases to the accessible environment; and

3. The U.S. Department of Energy has provided an adequate technical basis for each feature, event, and process, excluded from the performance assessment, to support the conclusion that either the feature, event, or process is specifically excluded by regulation; the probability of the feature, event, and process falls below the regulatory criterion; or omission of the feature, event, and process does not significantly change the magnitude and time of the resulting radiological exposures to the reasonably maximally exposed individual, or radionuclide releases to the accessible environment.

How Addressed

1. Complete identification of the excluded FEPs.

2. As described in Section 6.1, each FEP was evaluated against regulatory-based screening criteria and documented in Section 6.2 with a screening decision, screening justification (for excluded FEPs), or TSPA disposition (for included FEPs). A FEP that satisfied any one of the exclusion screening criteria (low probability, low consequence, or by regulation) was excluded from the TSPA model. A FEP that did not satisfy any of the exclusion screening criteria was included in the TSPA model. These screening decisions are summarized in Table 7-1.

3. The documentation in Section 6.2 provides the appropriate justification and technical basis of exclusion, or a TSPA model implementation description of inclusion, for each FEP. The screening decisions and technical bases consider site-specific information, design, and regulations.

INTENTIONALLY LEFT BLANK

8. INPUTS AND REFERENCES

8.1 DOCUMENTS CITED

184686 Abbot, J. and Brown, D.G. 1990. "Kinetics of Iron-Catalyzed Decomposition of Hydrogen Peroxide in Alkaline Solution." *International Journal of Chemical Kinetics, 22,* 963-974. New York, New York: John Wiley & Sons. TIC: 260000.

151125 Abrefah, J.; Gray, W.J.; Ketner, G.L.; Marschman, S.C.; Pyecha, T.D.; and Thornton, T.A. 1995. *K-Basin Spent Nuclear Fuel Characterization Data Report.* PNL-10778. Richland, Washington: Pacific Northwest National Laboratory. TIC: 243197.

151226 Abrefah, J.; Huang, F.H.; Gerry, W.M.; Gray, W.J.; Marschman, S.C.; and Thornton, T.A. 1999. *Analysis of Ignition Testing on K-West Basin Fuel.* PNNL-11816. Richland, Washington: Pacific Northwest National Laboratory. TIC: 248558.

160446 Advocat, T.; Chouchan, J.L.; Crovisier, J.L.; Guy, C.; Daux, V.; Jegou, C.; Gin, S.; and Vernaz, E. 1998. "Borosilicate Nuclear Waste Glass Alteration Kinetics: Chemical Inhibition and Affinity Control." *Scientific Basis for Nuclear Waste Management XXI, Symposium held September 28-October 3, 1997, Davos, Switzerland.* McKinley, I.G. and McCombie, C., eds. *506,* 63-70. Warrendale, Pennsylvania: Materials Research Society. TIC: 240702.

101367 Albin, A.L.; Singleton, W.L.; Moyer, T.C.; Lee, A.C.; Lung, R.C.; Eatman, G.L.W.; and Barr, D.L. 1997. *Geology of the Main Drift - Station 28+00 to 55+00, Exploratory Studies Facility, Yucca Mountain Project, Yucca Mountain, Nevada.* Milestone SPG42AM3. Denver, Colorado: Bureau of Reclamation and U.S. Geological Survey. ACC: MOL.19970625.0096.

103597 Altman, W.D.; Donnelly, J.P.; and Kennedy, J.E. 1988. *Peer Review for High-Level Nuclear Waste Repositories: Generic Technical Position.* NUREG-1297. Washington, D.C.: U.S. Nuclear Regulatory Commission. TIC: 200651.

103750 Altman, W.D.; Donnelly, J.P.; and Kennedy, J.E. 1988. *Qualification of Existing Data for High-Level Nuclear Waste Repositories: Generic Technical Position.* NUREG-1298. Washington, D.C.: U.S. Nuclear Regulatory Commission. TIC: 200652.

183684 Amer, F.; Mahmoud, A.A.; and Sabet, V. 1985. "Zeta Potential and Surface Area of Calcium Carbonate as Related to Phosphate Sorption." *Soil Science Society of America Journal, 49,* 1137-1142. Madison, Wisconsin: Soil Science Society of America. TIC: 259832.

178239 Andresen, P.L. and Kim, Y.J. 2006. *Stress Corrosion Crack Initiation & Growth Measurements in Environments Relevant to High Level Nuclear Waste Packages.* Report Number: GE-GRC-Bechtel-2006-2. Niskayuna, New York: General Electric Global Research Center. ACC: MOL.20061109.0070; MOL.20061108.0004.

176653 Andresen, P.L.; Kim, Y.J.; Emigh, P.W.; Catlin, G.M.; and Martiniano, P.J. 2005. *Stress Corrosion Crack Initiation & Growth Measurements in Environments Relevant to High Level Nuclear Waste Packages.* Report Number: GE-GRC-Bechtel-2005-1. Niskayuna, New York: General Electric Global Research Center. ACC: MOL.20060112.0042.

167623 Arakel, A.V. 1996. "Quaternary Vadose Calcretes Revisited." *AGSO Journal of Australian Geology & Geophysics, 16,* (3), 223-229. Canberra, Australia: Australian Government Public Service. TIC: 255481.

167638 Arnold, N.F. 2003. "Space Plasma Influences on the Earth's Atmosphere." *Philosophical Transactions of the Royal Society of London. Series A, Mathematical and Physical Sciences, 361,* 127-132. London, England: Royal Society of London. TIC: 255613.

170284 ASM (American Society for Metals) 1961. "Properties and Selection of Metals." Volume 1 of *Metals Handbook.* 8th Edition. Lyman, T.; ed. Metals Park, Ohio: American Society for Metals. TIC: 257281.

141615 ASM International 1990. *Properties and Selection: Nonferrous Alloys and Special-Purpose Materials.* Volume 2 of *ASM Handbook.* Formerly Tenth Edition, Metals Handbook. 5th Printing 1998. Materials Park, Ohio: ASM International. TIC: 241059.

101992 ASM International 1987. *Corrosion.* Volume 13 of *ASM Handbook.* 9th Edition. Materials Park, Ohio: ASM International. TIC: 240704.

133378 ASM International 1987. *Corrosion.* Volume 13 of *ASM Handbook.* Formerly 9th Edition, Metals Handbook. Materials Park, Ohio: ASM International. TIC: 240704.

103753 ASM International 1987. *Corrosion.* Volume 13 of *Metals Handbook.* 9th Edition. Metals Park, Ohio: ASM International. TIC: 209807.

106780 ASM International 1990. *Properties and Selection: Irons, Steels, and High-Performance Alloys.* Volume 1 of *Metals Handbook.* 10th Edition. Materials Park, Ohio: ASM International. TIC: 245666.

181641 ASM International 1996. *Binary Alloy Phase Diagrams.* 2nd Edition. Plus Updates. Version 1.0. Materials Park, Ohio: ASM International. TIC: 259552.

155708 ASME (American Society of Mechanical Engineers) 1998. "Rules for Construction of Nuclear Power Plant Components, Division 1, Subsection NB." Section III of *1995 ASME Boiler and Pressure Vessel Code.* New York, New York: American Society of Mechanical Engineers. TIC: 247429.

158115 ASME 2001. *2001 ASME Boiler and Pressure Vessel Code (includes 2002 addenda).* New York, New York: American Society of Mechanical Engineers. TIC: 251425.

160352 Asphahani, A.I. 1978. "Hydrogen Cracking of Nickel-Base Alloys." *Hydrogen in Metals, Proceedings of the 2nd International Congress, Paris, France, 6-10 June, 1977. 1,* Paper 3C2. New York, New York: Pergamon. ACC: NNA.19910419.0006.

154510 Baker, E.A. 1988. "Long-Term Corrosion Behavior of Materials in the Marine Atmosphere." *Degradation of Metals in the Atmosphere, Proceedings of the Symposium on Corrosion of Metals, Philadelphia, Pennsylvania, 12-13 May 1986.* Dean, S.W. and Lee, T.S., eds. ASTM STP 965. Pages 125-144. Philadelphia, Pennsylvania: American Society for Testing and Materials. TIC: 224019.

167871 Baldwin, B. and Butler, C.O. 1985. "Compaction Curve." *American Association of Petroleum Geologists Bulletin, 69,* (4), 622-626. Tulsa, Oklahoma: American Association of Petroleum Geologists. TIC: 255917.

128109 Bates, R.L. and Jackson, J.A., eds. 1984. *Dictionary of Geological Terms.* 3rd Edition. Garden City, New York: Anchor Books/Doubleday. TIC: 206591.

164050 Bates, R.L. and Jackson, J.A., eds. 1987. *Glossary of Geology.* 3rd Edition. Alexandria, Virginia: American Geological Institute. TIC: 8832.

175238 Baum, E.M.; Knox, H.D.; and Miller, T.R. 2002. *Nuclides and Isotopes.* 16th edition. Schenectady, New York: Knolls Atomic Power Laboratory. TIC: 255130.

156269 Bear, J. 1972. *Dynamics of Fluids in Porous Media.* Environmental Science Series. Biswas, A.K., ed. New York, New York: Elsevier. TIC: 217356.

171953 Beason, S. 2003. Collection of Underground Site Characterization Data [final submittal]. Scientific Notebook SN-USGS-SCI-084-V1. Pages 1-155. ACC: MOL.20040112.0121.

158781 Beavers, J.A.; Devine, T.M., Jr.; Frankel, G.S.; Jones, R.H.; Kelly, R.G.; Latanision, R.M.; and Payer, J.H. 2002. *Final Report, Waste Package Materials Performance Peer Review Panel, February 28, 2002.* Las Vegas, Nevada: Waste Package Materials Performance Peer Review Panel. ACC: MOL.20020614.0035.

173179 Belcher, W.R. 2004. *Death Valley Regional Ground-Water Flow System, Nevada and California - Hydrogeologic Framework and Transient Ground-Water Flow Model.* Scientific Investigations Report 2004-5205. Reston, Virginia: U.S. Geological Survey. ACC: MOL.20050323.0070.

135236 Berry, L.G. and Mason, B. 1959. *Mineralogy: Concepts, Descriptions, Determinations.* San Francisco, California: W.H. Freeman and Company. TIC: 238767.

167876 Biggin, A.J. and Thomas, D.N. 2003. "Analysis of Long-Term Variations in the Geomagnetic Polodial Field Intensity and Evaluation of Their Relationship with Global Geodynamics." *Geophysical Journal International, 152,* (2), 392-415. Oxford, England: Blackwell Publishing. TIC: 255680.

103524 Bird, R.B.; Stewart, W.E.; and Lightfoot, E.N. 1960. *Transport Phenomena.* New York, New York: John Wiley & Sons. TIC: 208957.

104941 Bish, D.L. 1984. "Effects of Exchangeable Cation Composition on the Thermal Expansion/Contraction of Clinoptilolite." *Clays and Clay Minerals, 32,* (6), 444-452. Long Island City, New York: Pergamon Press. TIC: 212510.

183078 Bish, D.L. 1990. "Long-Term Thermal Stability of Clinoptilolite: The Development of a "B" Phase." *European Journal of Mineralogy, 2,* 771-777. Stuttgart, Germany: E. Schweizerbart'sche Verlagsbuchhandlung. TIC: 225940.

100006 Bish, D.L. and Aronson, J.L. 1993. "Paleogeothermal and Paleohydrologic Conditions in Silicic Tuff from Yucca Mountain, Nevada." *Clays and Clay Minerals, 41,* (2), 148-161. Long Island City, New York: Pergamon Press. TIC: 224613.

106336 Bish, D.L.; Broxton, D.E.; Byers, F.M., Jr.; Caporuscio, F.A.; Carlos, B.A.; Levy, S.S.; and Vaniman, D.T. 1984. "Petrofabric Constraints of the Age of Zeolitization at Yucca Mountain." Chapter VIII, Section C of *Research and Development Related to the Nevada Nuclear Waste Storage Investigations, July 1—September 30, 1983.* Bryant, E.A. and Vaniman, D.T., eds. LA-10006-PR. Los Alamos, New Mexico: Los Alamos National Laboratory. ACC: HQS.19880517.1962.

169638 Bish, D.L.; Vaniman, D.T.; Chipera, S.J.; and Carey, J.W. 2003. "The Distribution of Zeolites and their Effects on the Performance of a Nuclear Waste Repository at Yucca Mountain, Nevada, U.S.A." *American Mineralogist, 88,* (11-12, Part 2), 1889–1902. Washington, D.C.: Mineralogical Society of America. TIC: 255986.

183582 Blackwell, D.D.; Wisian, K.W.; Richards, M.C.; and Steele, J.L. 2000. *Geothermal Resource/Reservoir Investigations Based on Heat Flow and Thermal Gradient Data for the United States.* DOE/ID/13504. Washington, D.C.: U.S. Department of Energy. ACC: LLR.20070919.0006.

129637 Blair, S.C.; Kelly, J.M.; Pine, O.; Pletcher, R.; and Berge, P.A. 1996. *Effect of Radiation on the Mechanical Properties of Topopah Spring Tuff.* UCRL-ID-122899. Livermore, California: Lawrence Livermore National Laboratory. ACC: MOL.19961021.0132.

118912 Borenstein, S.W. 1994. *Microbiologically Influenced Corrosion Handbook.* New York, New York: Industrial Press. TIC: 241092.

184439 Boteler, D.H. and Seager, W.H. 1998. "Telluric Currents: A Meeting of Theory and Observation." *Corrosion, 54,* (9), 751-755. Houston, Texas: NACE International. TIC: 259884.

155318 Boyer, H.E. and Gall, T.L., eds. 1984. *Metals Handbook.* Desk Edition. 10th Printing 1997. Metals Park, Ohio: American Society for Metals. TIC: 250192.

174636 Boyer, R.; Welsch, G.; and Collings, E.W. 2003. *Materials Properties Handbook: Titanium Alloys.* Materials Park, Ohio: ASM International. TIC: 257276.

126811 Brady, B.H.G. and Brown, E.T. 1985. *Rock Mechanics for Underground Mining.* London, United Kingdom: George Allen and Unwin. TIC: 226226.

167873 Brakenridge, G.R. 1981. "Terrestrial Paleoenvironmental Effects of a Late Quaternary-Age Supernova." *Icarus, 46,* (1), 81-93. New York, New York: Academic Press. TIC: 255707.

100007 Bredehoeft, J.D. 1997. "Fault Permeability Near Yucca Mountain." *Water Resources Research, 33,* (11), 2459-2463. Washington, D.C.: American Geophysical Union. TIC: 236570.

162445 Brossia, C.S. and Cragnolino, G.A. 2000. "Effects of Environmental, Electrochemical, and Metallurgical Variables on the Passive and Localized Dissolution of Ti Grade 7." *Corrosion/2000, 55th Annual Conference & Exposition, March 26-31, 2000, Orlando, Florida.* Paper No. 00211. Houston, Texas: NACE International. TIC: 254067.

159840 Brossia, C.S. and Cragnolino, G.A. 2001. "Effect of Palladium on the Localized and Passive Dissolution of Titanium." *Corrosion/2001 56th Annual Conference & Exposition, March 11-16, 2001, Houston, Texas, USA.* Paper No. 01127. Houston, Texas: NACE International. TIC: 253171.

162420 Brossia, C.S. and Cragnolino, G.A. 2001. "Effects of Environmental and Metallurgical Conditions on the Passive and Localized Dissolution of Ti-0.15%Pd." *Corrosion, 57,* (9), 768-776. Houston, Texas: National Association of Corrosion Engineers. TIC: 254028.

180832 Brossia, C.S. and Cragnolino, G.A. 2004. "Effect of Palladium on the Corrosion Behavior of Titanium." *Corrosion Science, 46,* 1693-1711. New York, New York: Elsevier. TIC: 259423.

159836 Brossia, C.S.; Browning, L.; Dunn, D.S.; Moghissi, O.C.; Pensado, O.; and Yang, L. 2001. *Effect of Environment on the Corrosion of Waste Package and Drip Shield Materials.* CNWRA 2001-003. San Antonio, Texas: Center for Nuclear Waste Regulatory Analyses. TIC: 252324.

161988 Brossia, C.S.; Cragnolino, G.A.; and Dunn, D.S. 2002. "Effect of Oxide Thickness on the Localized Corrosion of Zircaloy." *Corrosion/2002, 57th Annual Conference & Exposition, April 7-11, 2002, Denver, Colorado.* Paper No. 02549. Houston, Texas: NACE International. TIC: 253839.

162569 Brown, P.; Spalding, R.E.; ReVelle, D.O.; Tagliaferri, E.; and Worden, S.P. 2002. "The Flux of Small Near-Earth Objects Colliding with the Earth." *Nature, 420,* (6913), 294-296. London, England: Macmillan Journals. TIC: 254145.

102004 Broxton, D.E.; Bish, D.L.; and Warren, R.G. 1987. "Distribution and Chemistry of Diagenetic Minerals at Yucca Mountain, Nye County, Nevada." *Clays and Clay Minerals, 35,* (2), 89-110. Long Island City, New York: Pergamon Press. TIC: 203900.

183685 Bruemmer, S.M. and Thomas, L.E. 2001. "High-Resolution Analytical Electron Microscopy Characterization of Corrosion and Cracking at Buried Interfaces." *Surface and Interface Analysis, 31,* 571-581. New York, New York: John Wiley & Sons. TIC: 259834.

156807 BSC (Bechtel SAIC Company) 2001. *Plugging of Stress Corrosion Cracks by Precipitates.* CAL-EBS-MD-000017 REV 00. Las Vegas, Nevada: Bechtel SAIC Company. ACC: MOL.20011010.0168.

158726 BSC 2001. *UZ Flow Models and Submodels.* MDL-NBS-HS-000006 REV 00 ICN 01. Las Vegas, Nevada: Bechtel SAIC Company. ACC: MOL.20020417.0382.

152655 BSC 2001. *Waste Package Outer Barrier Stress Due to Thermal Expansion with Various Barrier Gap Sizes.* CAL-EBS-ME-000011 REV 00. Las Vegas, Nevada: Bechtel SAIC Company. ACC: MOL.20011212.0222.

157928 BSC 2002. *Preliminary Hydrologic Engineering Studies for the North Portal Pad and Vicinity.* ANL-EBS-MD-000060 REV 00. Las Vegas, Nevada: Bechtel SAIC Company. ACC: MOL.20021028.0123.

165991 BSC 2003. *Analysis of Infiltration Uncertainty.* ANL-NBS-HS-000027 REV 01. Las Vegas, Nevada: Bechtel SAIC Company. ACC: DOC.20031030.0003.

166316 BSC 2003. *Commercial Spent Nuclear Fuel Waste Package Misload Analysis.* CAL-WHS-MD-000003 REV 00A. Las Vegas, Nevada: Bechtel SAIC Company. ACC: DOC.20031002.0005; DOC.20050728.0004.

164562 BSC 2003. *Radiological Releases Due to Air and Silica Dust Activation in Emplacement Drifts.* 800-00C-EBS0-00100-000-00A. Las Vegas, Nevada: Bechtel SAIC Company. ACC: ENG.20030509.0001; ENG.20050816.0006; ENG.20080131.0004.

165572 BSC 2003. *Underground Layout Configuration.* 800-P0C-MGR0-00100-000-00E. Las Vegas, Nevada: Bechtel SAIC Company. ACC: ENG.20031002.0007; ENG.20050817.0005.

171924 BSC 2004. *Aging and Phase Stability of Waste Package Outer Barrier.* ANL-EBS-MD-000002 REV 02. Las Vegas, Nevada: Bechtel SAIC Company. ACC: DOC.20041005.0003.

169673 BSC 2004. *Agricultural and Environmental Input Parameters for the Biosphere Model.* ANL-MGR-MD-000006 REV 02. Las Vegas, Nevada: Bechtel SAIC Company. ACC: DOC.20040915.0007.

170038 BSC 2004. *Analysis of Hydrologic Properties Data.* ANL-NBS-HS-000042 REV 00. Las Vegas, Nevada: Bechtel SAIC Company. ACC: DOC.20041005.0004; DOC.20050815.0003.

169982 BSC 2004. *Aqueous Corrosion Rates for Waste Package Materials.* ANL-DSD-MD-000001 REV 01. Las Vegas, Nevada: Bechtel SAIC Company. ACC: DOC.20041012.0003; DOC.20060403.0001.

169989 BSC 2004. *Characterize Framework for Igneous Activity at Yucca Mountain, Nevada.* ANL-MGR-GS-000001 REV 02. Las Vegas, Nevada: Bechtel SAIC Company. ACC: DOC.20041015.0002; DOC.20050718.0007.

168030 BSC 2004. *Characterize Framework for Seismicity and Structural Deformation at Yucca Mountain, Nevada.* ANL-CRW-GS-000003 REV 00 [Errata 001]. Las Vegas, Nevada: Bechtel SAIC Company. ACC: MOL.20000510.0175; DOC.20040223.0007.

170019 BSC 2004. *Clad Degradation – FEPs Screening Arguments.* ANL-WIS-MD-000008 REV 02. Las Vegas, Nevada: Bechtel SAIC Company. ACC: DOC.20041020.0014; DOC.20060213.0007.

169766 BSC 2004. *Commercial SNF Waste Package Design Report.* 000-00C-DSU0-02800-000-00B. Las Vegas, Nevada: Bechtel SAIC Company. ACC: ENG.20040709.0001; ENG.20050817.0021.

170035 BSC 2004. *Conceptual Model and Numerical Approaches for Unsaturated Zone Flow and Transport.* MDL-NBS-HS-000005 REV 01. Las Vegas, Nevada: Bechtel SAIC Company. ACC: DOC.20040922.0006; DOC.20050307.0009.

172494 BSC 2004. *Configuration Generator Model.* CAL-DS0-NU-000002 REV 00B. Las Vegas, Nevada: Bechtel SAIC Company. ACC: DOC.20041122.0004; DOC.20050801.0004.

169987 BSC 2004. *CSNF Waste Form Degradation: Summary Abstraction.* ANL-EBS-MD-000015 REV 02. Las Vegas, Nevada: Bechtel SAIC Company. ACC: DOC.20040908.0001; DOC.20050620.0004.

169988 BSC 2004. *Defense HLW Glass Degradation Model.* ANL-EBS-MD-000016 REV 02. Las Vegas, Nevada: Bechtel SAIC Company. ACC: DOC.20041020.0015; DOC.20050922.0002.

170027 BSC 2004. *Development of Earthquake Ground Motion Input for Preclosure Seismic Design and Postclosure Performance Assessment of a Geologic Repository at Yucca Mountain, NV.* MDL-MGR-GS-000003 REV 01. Las Vegas, Nevada: Bechtel SAIC Company. ACC: DOC.20041111.0006; DOC.20051130.0003.

169855 BSC 2004. *Development of Numerical Grids for UZ Flow and Transport Modeling.* ANL-NBS-HS-000015 REV 02. Las Vegas, Nevada: Bechtel SAIC Company. ACC: DOC.20040901.0001.

172227 BSC 2004. *Dose Rate Calculation for 21-PWR Waste Package.* 000-00C-DSU0-01800-000-00C. Las Vegas, Nevada: Bechtel SAIC Company. ACC: ENG.20041102.0003; ENG.20050815.0017.

166107 BSC 2004. *Drift Degradation Analysis.* ANL-EBS-MD-000027 REV 03. Las Vegas, Nevada: Bechtel SAIC Company. ACC: DOC.20040915.0010; DOC.20050419.0001; DOC.20051130.0002; DOC.20060731.0005.

169864 BSC 2004. *Drift Scale THM Model.* MDL-NBS-HS-000017 REV 01. Las Vegas, Nevada: Bechtel SAIC Company. ACC: DOC.20041012.0001; DOC.20060103.0002.

170040 BSC 2004. *Drift-Scale Radionuclide Transport.* MDL-NBS-HS-000016 REV 01. Las Vegas, Nevada: Bechtel SAIC Company. ACC: DOC.20040927.0031; DOC.20050927.0003.

172453 BSC 2004. *DSNF and Other Waste Form Degradation Abstraction.* ANL-WIS-MD-000004 REV 04. Las Vegas, Nevada: Bechtel SAIC Company. ACC: DOC.20041201.0007.

169672 BSC 2004. *Environmental Transport Input Parameters for the Biosphere Model.* ANL-MGR-MD-000007 REV 02. Las Vegas, Nevada: Bechtel SAIC Company. ACC: DOC.20040913.0003.

168889 BSC 2004. *Evaluation of Emplacement Drift Stability for KTI Resolutions.* 800-KMC-SSE0-00200-000-00A. Las Vegas, Nevada: Bechtel SAIC Company. ACC: ENG.20040520.0001; ENG.20050816.0023.

169991 BSC 2004. *Evaluation of Potential Impacts of Microbial Activity on Drift Chemistry.* ANL-EBS-MD-000038 REV 01. Las Vegas, Nevada: Bechtel SAIC Company. ACC: DOC.20041118.0005; DOC.20050505.0001; DOC.20050609.0001.

170013 BSC 2004. *Features, Events, and Processes in SZ Flow and Transport.* ANL-NBS-MD-000002 REV 03. Las Vegas, Nevada: Bechtel SAIC Company. ACC: DOC.20041116.0007.

170012 BSC 2004. *Features, Events, and Processes in UZ Flow and Transport.* ANL-NBS-MD-000001 REV 03. Las Vegas, Nevada: Bechtel SAIC Company. ACC: DOC.20041108.0004; DOC.20050525.0007.

170021 BSC 2004. *Features, Events, and Processes: System Level.* ANL-WIS-MD-000019 REV 02. Las Vegas, Nevada: Bechtel SAIC Company. ACC: DOC.20041020.0009; DOC.20051206.0019.

170002 BSC 2004. *Future Climate Analysis.* ANL-NBS-GS-000008 REV 01. Las Vegas, Nevada: Bechtel SAIC Company. ACC: DOC.20040908.0005.

172017 BSC 2004. *Gamma and Neutron Radiolysis in the 21-PWR Waste Package from Ten to One Million Years.* 000-00C-DSU0-00700-000-00A. Las Vegas, Nevada: Bechtel SAIC Company. ACC: ENG.20041013.0008; ENG.20070924.0024.

170029 BSC 2004. *Geologic Framework Model (GFM2000).* MDL-NBS-GS-000002 REV 02. Las Vegas, Nevada: Bechtel SAIC Company. ACC: DOC.20040827.0008.

170003 BSC 2004. *Heat Capacity Analysis Report.* ANL-NBS-GS-000013 REV 01. Las Vegas, Nevada: Bechtel SAIC Company. ACC: DOC.20041101.0003.

170004 BSC 2004. *In Situ Field Testing of Processes.* ANL-NBS-HS-000005 REV 03. Las Vegas, Nevada: Bechtel SAIC Company. ACC: DOC.20041109.0001; DOC.20051010.0001.

171926 BSC 2004. *Intact and Degraded Mode Criticality Calculations for the Codisposal of ATR Spent Nuclear Fuel in a Waste Package.* CAL-DSD-NU-000007 REV 00A. Las Vegas, Nevada: Bechtel SAIC Company. ACC: DOC.20041018.0001; DOC.20050728.0002.

168935 BSC 2004. *Intact and Degraded Mode Criticality Calculations for the Codisposal of TMI-2 Spent Nuclear Fuel in a Waste Package.* CAL-DSD-NU-000004 REV 00A. Las Vegas, Nevada: Bechtel SAIC Company. ACC: DOC.20040329.0002; DOC.20050601.0003; DOC.20050801.0001.

169753 BSC 2004. *Mechanical Assessment of the Drip Shield Subject to Vibratory Motion and Dynamic and Static Rock Loading.* CAL-WIS-AC-000002 REV 00A. Las Vegas, Nevada: Bechtel SAIC Company. ACC: DOC.20041028.0004; DOC.20050830.0003; DOC.20051121.0010.

170031 BSC 2004. *Mineralogic Model (MM3.0) Report.* MDL-NBS-GS-000003 REV 01. Las Vegas, Nevada: Bechtel SAIC Company. ACC: DOC.20040908.0006; DOC.20050914.0001.

171756 BSC 2004. *Multiple Rock Fall on Drip Shield.* 000-00C-SSE0-00200-000-00A. Las Vegas, Nevada: Bechtel SAIC Company. ACC: ENG.20040407.0009; ENG.20050817.0025.

172452 BSC 2004. *Performance Confirmation Plan.* TDR-PCS-SE-000001 REV 05. Las Vegas, Nevada: Bechtel SAIC Company. ACC: DOC.20041122.0002.

170014 BSC 2004. *Probability Distribution for Flowing Interval Spacing.* ANL-NBS-MD-000003 REV 01. Las Vegas, Nevada: Bechtel SAIC Company. ACC: DOC.20040923.0003.

170015 BSC 2004. *Recharge and Lateral Groundwater Flow Boundary Conditions for the Saturated Zone Site-Scale Flow and Transport Model.* ANL-NBS-MD-000010 REV 01. Las Vegas, Nevada: Bechtel SAIC Company. ACC: DOC.20041008.0004.

170006 BSC 2004. *Saturated Zone Colloid Transport.* ANL-NBS-HS-000031 REV 02. Las Vegas, Nevada: Bechtel SAIC Company. ACC: DOC.20041008.0007; DOC.20051215.0005.

171764 BSC 2004. *Seepage Calibration Model and Seepage Testing Data.* MDL-NBS-HS-000004 REV 03. Las Vegas, Nevada: Bechtel SAIC Company. ACC: DOC.20040922.0003; DOC.20051121.0012.

167652 BSC 2004. *Seepage Model for PA Including Drift Collapse.* MDL-NBS-HS-000002 REV 03. Las Vegas, Nevada: Bechtel SAIC Company. ACC: DOC.20040922.0008; DOC.20051205.0001.

170036 BSC 2004. *Site-Scale Saturated Zone Transport.* MDL-NBS-HS-000010 REV 02. Las Vegas, Nevada: Bechtel SAIC Company. ACC: DOC.20041103.0004; DOC.20050405.0008.

167083 BSC 2004. *Structural Calculations of Waste Package Exposed to Vibratory Ground Motion.* 000-00C-WIS0-01400-000-00A. Las Vegas, Nevada: Bechtel SAIC Company. ACC: ENG.20040217.0008; ENG.20050817.0038; ENG.20050823.0023.

169861 BSC 2004. *UZ Flow Models and Submodels.* MDL-NBS-HS-000006 REV 02. Las Vegas, Nevada: Bechtel SAIC Company. ACC: DOC.20041101.0004; DOC.20050629.0003.

169862 BSC 2004. *Ventilation Model and Analysis Report.* ANL-EBS-MD-000030 REV 04. Las Vegas, Nevada: Bechtel SAIC Company. ACC: DOC.20041025.0002.

170020 BSC 2004. *Waste Form Features, Events, and Processes.* ANL-WIS-MD-000009 REV 02. Las Vegas, Nevada: Bechtel SAIC Company. ACC: DOC.20041028.0006; DOC.20050214.0004.

166941 BSC 2004. *Waste Form, Heat Output, and Waste Package Spacing for an Idealized Drift Segment.* 000-00C-WIS0-00500-000-00A. Las Vegas, Nevada: Bechtel SAIC Company. ACC: ENG.20040121.0007; ENG.20050817.0031; ENG.20051019.0002.

171499 BSC 2004. *Waste Package Closure System Description Document.* 100-3YD-HW00-00100-000-003. Las Vegas, Nevada: Bechtel SAIC Company. ACC: ENG.20040927.0003.

170009 BSC 2004. *Water-Level Data Analysis for the Saturated Zone Site-Scale Flow and Transport Model.* ANL-NBS-HS-000034 REV 02. Las Vegas, Nevada: Bechtel SAIC Company. ACC: DOC.20041012.0002; DOC.20050214.0002.

169734 BSC 2004. *Yucca Mountain Site Description.* TDR-CRW-GS-000001 REV 02 ICN 01. Two volumes. Las Vegas, Nevada: Bechtel SAIC Company. ACC: DOC.20040504.0008.

175761 BSC 2005. *Calculation of the Naval Long Waste Package Two-Demensional Thermal Interface Temperatures.* 000-00C-WIS0-02600-000-00A. Las Vegas, Nevada: Bechtel SAIC Company. ACC: ENG.20050721.0006.

172827 BSC 2005. *Characteristics of the Receptor for the Biosphere Model.* ANL-MGR-MD-000005 REV 04. Las Vegas, Nevada: Bechtel SAIC Company. ACC: DOC.20050405.0005.

174715 BSC 2005. *Creep Deformation of the Drip Shield.* CAL-WIS-AC-000004 REV 0A. Las Vegas, Nevada: Bechtel SAIC Company. ACC: DOC.20050830.0007.

175089 BSC 2005. *Determination of Importance Evaluation for the Subsurface Exploratory Studies Facility.* BAB000000-01717-2200-00005 REV 07 ICN 05. Las Vegas, Nevada: Bechtel SAIC Company. ACC: DOC.20050822.0011.

173800 BSC 2005. *Development of the Total System Performance Assessment-License Application Features, Events, and Processes.* TDR-WIS-MD-000003 REV 02. Las Vegas, Nevada: Bechtel SAIC Company. ACC: DOC.20050829.0004.

172232 BSC 2005. *Drift-Scale Coupled Processes (DST and TH Seepage) Models.* MDL-NBS-HS-000015 REV 02. Las Vegas, Nevada: Bechtel SAIC Company. ACC: DOC.20050114.0004; DOC.20051115.0002.

174052 BSC 2005. *Drip Shield Structural Response to Rock Fall Supplemental Calculation.* 000-00C-SSE0-00700-000-00A. Las Vegas, Nevada: Bechtel SAIC Company. ACC: ENG.20050707.0002.

175014 BSC 2005. *Engineered Barrier System Features, Events, and Processes.* ANL-WIS-PA-000002 REV 05. Las Vegas, Nevada: Bechtel SAIC Company. ACC: DOC.20050829.0003; DOC.20050830.0006.

174107 BSC 2005. *Evaluation of Features, Events, and Processes (FEP) for the Biosphere Model.* ANL-MGR-MD-000011 REV 05. Las Vegas, Nevada: Bechtel SAIC Company. ACC: DOC.20050718.0006.

174190 BSC 2005. *Features, Events, and Processes in SZ Flow and Transport.* ANL-NBS-MD-000002 REV 04. Las Vegas, Nevada: Bechtel SAIC Company. ACC: DOC.20050822.0012.

174191 BSC 2005. *Features, Events, and Processes in UZ Flow and Transport.* ANL-NBS-MD-000001 REV 04. Las Vegas, Nevada: Bechtel SAIC Company. ACC: DOC.20050809.0002.

173981 BSC 2005. *Features, Events, and Processes: Disruptive Events.* ANL-WIS-MD-000005 REV 03. Las Vegas, Nevada: Bechtel SAIC Company. ACC: DOC.20050830.0008.

174958 BSC 2005. *Impacts of Solubility and Other Geochemical Processes on Radionuclide Retardation in the Natural System.* Las Vegas, Nevada: Bechtel SAIC Company. ACC: MOL.20050804.0120.

174070 BSC 2005. *Magma Dynamics at Yucca Mountain, Nevada.* ANL-MGR-GS-000005 REV 00. Las Vegas, Nevada: Bechtel SAIC Company. ACC: DOC.20050829.0006.

173172 BSC 2005. *Mechanical Assessment of the Waste Package Subject to Vibratory Ground Motion.* CAL-WIS-AC-000001 REV 0B. Las Vegas, Nevada: Bechtel SAIC Company. ACC: DOC.20050823.0001; DOC.20050830.0005.

174101 BSC 2005. *Mountain-Scale Coupled Processes (TH/THC/THM) Models.* MDL-NBS-HS-000007 REV 03. Las Vegas, Nevada: Bechtel SAIC Company. ACC: DOC.20050825.0007.

174116 BSC 2005. *Parameter Sensitivity Analysis for Unsaturated Zone Flow.* ANL-NBS-HS-000049 REV 00. Las Vegas, Nevada: Bechtel SAIC Company. ACC: DOC.20050808.0005; DOC.20060329.0020.

170137 BSC 2005. *Peak Ground Velocities for Seismic Events at Yucca Mountain, Nevada.* ANL-MGR-GS-000004 REV 00. Las Vegas, Nevada: Bechtel SAIC Company. ACC: DOC.20050223.0002; DOC.20050725.0002.

174995 BSC 2005. *Screening of Features, Events, and Processes in Drip Shield and Waste Package Degradation.* ANL-EBS-PA-000002 REV 05. Las Vegas, Nevada: Bechtel SAIC Company. ACC: DOC.20050817.0003; DOC.20050826.0002; DOC.20050929.0007.

173802 BSC 2005. *Waste Package Damage Due to Interaction with Magma.* CAL-WIS-MD-000013 REV 00A. Las Vegas, Nevada: Bechtel SAIC Company. ACC: DOC.20050706.0006.

181534 BSC 2006. *21-PWR Waste Package Internal Pressure Estimate.* 000-00C-DSU0-03500-000-00B. Las Vegas, Nevada: Bechtel SAIC Company. ACC: ENG.20061108.0004; ENG.20070402.0003.

178275 BSC 2006. *Analysis of Alcove 8/Niche 3 Flow and Transport Tests.* ANL-NBS-HS-000056 REV 00. Las Vegas, Nevada: Bechtel SAIC Company. ACC: DOC.20060901.0003.

179489 BSC 2006. *Chlorine-36 Validation Study at Yucca Mountain, Nevada.* TDR-NBS-HS-000017 REV 00. Las Vegas, Nevada: Bechtel SAIC Company. ACC: DOC.20060829.0002.

181335 BSC 2006. *Criticality Potential of Waste Packages Affected by Igneous Intrusion.* CAL-DS0-NU-000005 REV 00B. Las Vegas, Nevada: Bechtel SAIC Company. ACC: DOC.20061201.0001.

178672 BSC 2006. *Impacts of Solubility and Other Geochemical Processes on Radionuclide Retardation in the Natural System – Rev 01.* Las Vegas, Nevada: Bechtel SAIC Company. ACC: MOL.20060105.0022.

177101 BSC 2006. *Inhalation Exposure Input Parameters for the Biosphere Model.* ANL-MGR-MD-000001 REV 04. Las Vegas, Nevada: Bechtel SAIC Company. ACC: DOC.20060605.0011.

183416 BSC 2007. *Concepts for Waste Retrieval and Alternate Storage of Radioactive Waste.* 800-30R-HER0-00100-000 REV 006. Las Vegas, Nevada: Bechtel SAIC Company. ACC: ENG.20071024.0003.

183406 BSC 2007. *Ground Control for Non-Emplacement Drifts for LA.* 800-K0C-SSD0-00400-000-00A. Las Vegas, Nevada: Bechtel SAIC Company. ACC: ENG.20071001.0042; ENG.20071218.0001.

181645 BSC 2007. *Ground Support Materials and Concrete Inverts - Committed and Non-Committed.* 800-K0C-SSD0-00300-000-00A. Las Vegas, Nevada: Bechtel SAIC Company. ACC: ENG.20070627.0001.

182746 BSC 2007. *IED Emplacement Drift Invert.* 800-IED-MGR0-00601-000 REV 00B. Las Vegas, Nevada: Bechtel SAIC Company. ACC: ENG.20071120.0004.

182926 BSC 2007. *IED Subsurface Facilities Geological Data.* 800-IED-WIS0-01801-000-00C. Las Vegas, Nevada: Bechtel SAIC Company. ACC: ENG.20070913.0012.

183743 BSC 2007. *IED Subsurface Facilities Layout Geographical Data.* 800-IED-WIS0-01701-000 REV 00C. Las Vegas, Nevada: Bechtel SAIC Company. ACC: ENG.20071211.0007.

184446 BSC 2007. *Regulatory Guidance Agreement, Agreement for NUREG-1297, February 1988, Peer Review for High Level Nuclear Waste Repositories - Generic Technical Position.* REG-CRW-RG-000387 REV 00. Las Vegas, Nevada: Bechtel SAIC Company. ACC: DOC.20070618.0013.

184422 BSC 2007. *Regulatory Guidance Agreement, Agreement for NUREG/CR 5485, November, 1998, Guidelines on Modeling Common-Cause Failures in Probabilistic Risk Assessment.* REG-CRW-RG-000437 REV 01. Las Vegas, Nevada: Bechtel SAIC Company. ACC: DOC.20071010.0011.

178693 BSC 2007. *Subsurface Geotechnical Parameters Report.* ANL-SSD-GE-000001 REV 00. Las Vegas, Nevada: Bechtel SAIC Company. ACC: ENG.20070115.0006.

179640 BSC 2007. *Underground Layout Configuration for LA.* 800-KMC-SS00-00200-000-00B. Las Vegas, Nevada: Bechtel SAIC Company. ACC: ENG.20070727.0004; ENG.20071214.0002.

180190 BSC 2007. *Waste Package Fabrication.* 000-3SS-DSC0-00100-000-001. Las Vegas, Nevada: Bechtel SAIC Company. ACC: ENG.20070315.0001.

185102 BSC 2008. *HLW/DOE SNF Co-Disposal Waste Package Design Report.* 000-00C-DS00-00600-000-00F. Las Vegas, Nevada: Bechtel SAIC Company. ACC: ENG.20080222.0016.

183627 BSC 2008. *Postclosure Modeling and Analyses Design Parameters.* TDR-MGR-MD-000037 REV 02. Las Vegas, Nevada: Bechtel SAIC Company. ACC: ENG.20080108.0002.

101859 Byers, F.M., Jr. and Barnes, H. 1967. *Geologic Map of the Paiute Ridge Quadrangle, Nye and Lincoln Counties, Nevada.* Map GQ-577. Washington, D.C.: U.S. Geological Survey. ACC: HQS.19880517.1104.

105200 Carey, J.W. and Bish, D.L. 1996. "Equilibrium in the Clinoptilolite-H2O System." *American Mineralogist, 81,* 952-962. Washington, D.C.: Mineralogical Society of America. TIC: 233145.

101522 Carr, W.J.; Byers, F.M., Jr.; and Orkild, P.P. 1984. *Stratigraphic and Volcano-Tectonic Relations of Crater Flat Tuff and Some Older Volcanic Units, Nye County, Nevada.* Open-File Report 84-114. Denver, Colorado: U.S. Geological Survey. ACC: NNA.19870518.0075.

100967 Carrigan, C.R.; King, G.C.P.; Barr, G.E.; and Bixler, N.E. 1991. "Potential for Water-Table Excursions Induced by Seismic Events at Yucca Mountain, Nevada." *Geology, 19,* (12), 1157-1160. Boulder, Colorado: Geological Society of America. TIC: 242407.

100968 Carslaw, H.S. and Jaeger, J.C. 1959. *Conduction of Heat in Solids.* 2nd Edition. Oxford, Great Britain: Oxford University Press. TIC: 206085.

160928 Carter Krogh, K.E. and Valentine, G.A. 1996. *Structural Control on Basaltic Dike and Sill Emplacement, Paiute Ridge Mafic Intrusion Complex, Southern Nevada.* LA-13157-MS. Los Alamos, New Mexico: Los Alamos National Laboratories. ACC: MOL.20030828.0138.

102495 Castor, S.B.; Tingley, J.V.; and Bonham, H.F., Jr. 1994. "Pyritic Ash-Flow Tuff, Yucca Mountain, Nevada." *Economic Geology, 89,* 401-407. El Paso, Texas: Economic Geology Publishing. TIC: 234278.

135243 Ceplecha, Z. 1994. "Impacts of Meteoroids Larger than 1m into the Earth's Atmosphere." *Astronomy and Astrophysics, 286,* (3), 967-970. New York, New York: Springer-Verlag. TIC: 246761.

167626 Chadwick, O.A.; Nettleton, W.D.; and Staidl, G.J. 1995. "Soil Polygenesis as a Function of Quaternary Climate Change, Northern Great Basin, USA." *Geoderma, 68,* (1-2), 1-26. New York, New York: Elsevier. TIC: 255603.

135245 Chapman, C.R. and Morrison, D. 1994. "Impacts on the Earth by Asteroids and Comets: Assessing the Hazard." *Nature, 367,* (6458), 33-40. New York, New York: Nature America. TIC: 246781.

160802 Cho, Y.I.; Ganic, E.N.; Hartnett, J.P.; and Rohsenow, W.M. 1998. "Basic Concepts of Heat Transfer." Chapter 1 of *Handbook of Heat Transfer.* 3rd Edition. Rohsenow, W.M.; Hartnett, J.P.; and Cho, Y.I., eds. New York, New York: McGraw-Hill. TIC: 253612.

168395 Choppin, G.R. 1983. "Aspects of Plutonium Solution Chemistry." Chapter 14 of *Plutonium Chemistry.* Carnall, W.T. and Choppin, G.R., eds. ACS Symposium Series 216. Washington, D.C.: American Chemical Society. TIC: 219103.

100717 Choppin, G.R. 1992. "The Role of Natural Organics in Radionuclide Migration in Natural Aquifer Systems." *Radiochimica Acta, 58/59,* 113-120. New York, New York: Academic Press. TIC: 222387.

168308 Choppin, G.R. 2003. "Actinide Speciation in the Environment." *Radiochimica Acta, 91,* (11), 645-649. München, Germany: Oldenbourg Wissenschaftsverlag. TIC: 255776.

168379 Choppin, G.R. and Stout, B.E. 1989. "Actinide Behavior in Natural Waters." *Science of the Total Environment, 83,* (3), 203-216. Amsterdam, The Netherlands: Elsevier. TIC: 255706.

168377 Choppin, G.R.; Roberts, R.A.; and Morse, J.W. 1986. "Effects of Humic Substances on Plutonium Speciation in Marine Systems." *Organic Marine Geochemistry.* Sohn, M.L., ed. ACS Symposium Series 305. Pages 382-388. Washington, D.C.: American Chemical Society. TIC: 255705.

135248 Chyba, C.F. 1993. "Explosions of Small Spacewatch Objects in Earth's Atmosphere." *Nature, 363,* (6431), 701-703. London, United Kingdom: Macmillan Journals. TIC: 246762.

163189 Cochran, J.R.; Beyeler, W.E.; Brosseau, D.A.; Brush, L.H.; Brown, T.J.; Crowe, B.M.; Conrad, S.H.; Davis, P.A.; Ehrhorn, T.; Feeney, T.; Fogleman, B.; Gallegos, D.P.; Haaker, R.; Kalinina, E.; Price, L.L.; Thomas, D.P.; and Wirth, S. 2001. *Compliance Assessment Document for the Transuranic Wastes in the Greater Confinement Disposal Boreholes at the Nevada Test Site, Volume 2: Performance Assessment, Version 2.0.* SAND2001-2977. Albuquerque, New Mexico: Sandia National Laboratories. TIC: 254267.

167641 Cole, D.G. 2003. "Space Weather: Its Effects and Predictability." *Space Science Reviews, 107,* (1-2), 295-302. Dordrecht, The Netherlands: Kluwer Academic. TIC: 255616.

184454 Colella, C.; de' Gennaro, M.; and Aiello, R. 2001. "Use of Zeolitic Tuff in the Building Industry." *Reviews in Mineralogy and Geochemistry, 45,* 551-587. Washington, D.C.: Mineralogical Society of America. TIC: 259937.

135969 Connor, C.B.; Stamatakos, J.; Ferrill, D.; Hill, B.E.; Magsino, S.B.L.; La Femina, P.; and Martin, R.H. 1996. "Integrating Structural Models into Probabilistic Volcanic Hazard Analyses: An Example from Yucca Mountain, NV." *Abstracts with Programs - Geological Society of America, 28,* (7), A-192. Boulder, Colorado: Geological Society of America. TIC: 247409.

151097 Covington, L.C. 1979. "The Influence of Surface Condition and Environment on the Hydriding of Titanium." *Corrosion, 35,* (8), 378-382. Houston, Texas: National Association of Corrosion Engineers. TIC: 226671.

182138 Coward, H.F. and Jones, G.W. 1952. *Limits of Flammability of Gases and Vapors.* Bulletin 503. Washington, D.C.: U.S. Government Printing Office. TIC: 241049.

152354 Cragnolino, G.A.; Dunn, D.S.; Brossia, C.S.; Jain, V.; and Chan, K.S. 1999. *Assessment of Performance Issues Related to Alternate Engineered Barrier System Materials and Design Options.* CNWRA 99-003. San Antonio, Texas: Center for Nuclear Waste Regulatory Analyses. TIC: 248875.

171411 Craig, R.W. 2001. "Transmittal of Level 5 Deliverable SPW205M5, 'Excavation-Induced Fracture Study'." Letter from R.W. Craig (USGS) to T.C. Gunter (DOE/YMSCO), September 26, 2001, with enclosure. ACC: MOL.20011114.0003.

122990 Crank, J. 1975. *The Mathematics of Diffusion.* 2nd Edition. 1983 Reprint. Oxford, England: Clarendon Press. TIC: 9662.

101234 Cranwell, R.M.; Guzowski, R.V.; Campbell, J.E.; and Ortiz, N.R. 1990. *Risk Methodology for Geologic Disposal of Radioactive Waste, Scenario Selection Procedure.* NUREG/CR-1667. Washington, D.C.: U.S. Nuclear Regulatory Commission. ACC: NNA.19900611.0073.

101532 Crowe, B.M.; Owlets, K.H.; Vaniman, D.T.; Gladney, E.; and Bower, N. 1986. *Status of Volcanic Hazard Studies for the Nevada Nuclear Waste Storage Investigations.* LA-9325-MS. Volume II. Los Alamos, New Mexico: Los Alamos National Laboratory. ACC: NNA.19890501.0157.

129957 CRWMS (Civilian Radioactive Waste Management System) M&O (Management and Operating Contractor) 1996. *Forensic Evaluation of Geophysical Log Data for Borehole USW SD-7 in Support of the Yucca Mountain Site Characterization Project.* BAAA00000-01717-0200-00007 REV 00. Las Vegas, Nevada: CRWMS M&O. ACC: MOL.19971023.0133.

114799 CRWMS M&O 1996. *Forensic Evaluation of Geophysical Log Data for Borehole USW SD-9 in Support of the Yucca Mountain Site Characterization Project.* BAAA00000-01717-0200-00005 REV 00. Las Vegas, Nevada: CRWMS M&O. ACC: MOL.19970606.0345.

130425 CRWMS M&O 1996. *Forensic Evaluation of Geophysical Log Data for Borehole USW SZ-7a in Support of the Yucca Mountain Site Characterization Project.* BAAA00000-01717-0200-00004 REV 00. Las Vegas, Nevada: CRWMS M&O. ACC: MOL.19960517.0080.

130429 CRWMS M&O 1996. *Forensic Evaluation of Geophysical Log Data for Borehole USW UZ-14 in Support of the Yucca Mountain Site Characterization Project.* BAAA00000-01717-0200-00012 REV 00. Las Vegas, Nevada: CRWMS M&O. ACC: MOL.19960522.0169.

100116 CRWMS M&O 1996. *Probabilistic Volcanic Hazard Analysis for Yucca Mountain, Nevada.* BA0000000-01717-2200-00082 REV 0. Las Vegas, Nevada: CRWMS M&O. ACC: MOL.19971201.0221.

101090 CRWMS M&O 1997. *Yucca Mountain Site Characterization Project Summary of Socioeconomic Data Analyses Conducted in Support of the Radiological Monitoring Program First Quarter 1996 to First Quarter 1997.* Las Vegas, Nevada: CRWMS M&O. ACC: MOL.19971117.0460.

111115 CRWMS M&O 1998. *Drift Scale Test As-Built Report.* BAB000000-01717-5700-00003 REV 01. Las Vegas, Nevada: CRWMS M&O. ACC: MOL.19990107.0223.

123201 CRWMS M&O 1998. "Physical Processes of Magmatism and Effects on the Potential Repository: Synthesis of Technical Work through Fiscal Year 1995." Chapter 5 of *Synthesis of Volcanism Studies for the Yucca Mountain Site Characterization Project.* Deliverable 3781MR1. Las Vegas, Nevada: CRWMS M&O. ACC: MOL.19990511.0400.

103731 CRWMS M&O 1998. *Probabilistic Seismic Hazard Analyses for Fault Displacement and Vibratory Ground Motion at Yucca Mountain, Nevada.* Milestone SP32IM3, September 23, 1998. Three volumes. Las Vegas, Nevada: CRWMS M&O. ACC: MOL.19981207.0393.

100353 CRWMS M&O 1998. *Saturated Zone Flow and Transport Expert Elicitation Project.* Deliverable SL5X4AM3. Las Vegas, Nevada: CRWMS M&O. ACC: MOL.19980825.0008.

105347 CRWMS M&O 1998. *Synthesis of Volcanism Studies for the Yucca Mountain Site Characterization Project.* Deliverable 3781MR1. Las Vegas, Nevada: CRWMS M&O. ACC: MOL.19990511.0400.

105031 CRWMS M&O 1999. *Final Report: Plant and Soil Related Processes Along a Natural Thermal Gradient at Yucca Mountain, Nevada.* B00000000-01717-5705-00109 REV 00. Las Vegas, Nevada: CRWMS M&O. ACC: MOL.19990513.0037.

103618 CRWMS M&O 1999. *Impact of Radioactive Waste Heat on Soil Temperatures.* BA0000000-01717-5700-00030 REV 0. Las Vegas, Nevada: CRWMS M&O. ACC: MOL.19990309.0403.

144426 CRWMS M&O 2000. *Calibrated Properties Model.* MDL-NBS-HS-000003 REV 00. Las Vegas, Nevada: CRWMS M&O. ACC: MOL.19990721.0520.

147651 CRWMS M&O 2000. *Evaluation of Codisposal Viability for HEU Oxide (Shippingport PWR) DOE-Owned Fuel.* TDR-EDC-NU-000003 REV 00. Las Vegas, Nevada: CRWMS M&O. ACC: MOL.20000227.0240.

147650 CRWMS M&O 2000. *Evaluation of Codisposal Viability for UZrH (TRIGA) DOE-Owned Fuel.* TDR-EDC-NU-000001 REV 00. Las Vegas, Nevada: CRWMS M&O. ACC: MOL.20000207.0689.

138960 CRWMS M&O 2000. *Mineralogical Model (MM3.0).* MDL-NBS-GS-000003 REV 00 ICN 01. Las Vegas, Nevada: CRWMS M&O. ACC: MOL.20000120.0477.

162406 Cunnane, J.; Ebert, W.; Goldberg, M.; Finch, R.; and Mertz, C. 2003. *Yucca Mountain Project Report, Waste Form Testing Work.* Argonne, Illinois: Argonne National Laboratory, Chemical Technology Division. ACC: MOL.20030630.0418.

100131 D'Agnese, F.A.; Faunt, C.C.; Turner, A.K.; and Hill, M.C. 1997. *Hydrogeologic Evaluation and Numerical Simulation of the Death Valley Regional Ground-Water Flow System, Nevada and California.* Water-Resources Investigations Report 96-4300. Denver, Colorado: U.S. Geological Survey. ACC: MOL.19980306.0253.

120425 D'Agnese, F.A.; O'Brien, G.M.; Faunt, C.C.; and San Juan, C.A. 1999. *Simulated Effects of Climate Change on the Death Valley Regional Ground-Water Flow System, Nevada and California.* Water-Resources Investigations Report 98-4041. Denver, Colorado: U.S. Geological Survey. TIC: 243555.

182090 Dartevelle, S. and Valentine, G. A. 2007. *Interaction of Multiphase Magmatic Flows with Underground Openings at the Proposed Yucca Mountain Radioactive Waste Repository (Southern Nevada, USA).* LA-UR-07-3579. Los Alamos, New Mexico: Los Alamos National Laboratory. ACC: LLR.20070807.0153.

103180 Davies, J.B. and Archambeau, C.B. 1997. "Geohydrological Models and Earthquake Effects at Yucca Mountain, Nevada." *Environmental Geology, 32,* (1), 23-35. New York, New York: Springer-Verlag. TIC: 237118.

162971 Davison, R.M.; DeBold, T.; and Johnson, M.J. 1987. "Corrosion of Stainless Steels." In *Corrosion,* Volume 13, Pages 547-565 of *ASM Handbook.* Formerly 9th Edition, Metals Handbook. Materials Park, Ohio: ASM International. TIC: 240704.

100027 Day, W.C.; Dickerson, R.P.; Potter, C.J.; Sweetkind, D.S.; San Juan, C.A.; Drake, R.M., II; and Fridrich, C.J. 1998. *Bedrock Geologic Map of the Yucca Mountain Area, Nye County, Nevada.* Geologic Investigations Series I-2627. Denver, Colorado: U.S. Geological Survey. ACC: MOL.19981014.0301.

101557 Day, W.C.; Potter, C.J.; Sweetkind, D.S.; Dickerson, R.P.; and San Juan, C.A. 1998. *Bedrock Geologic Map of the Central Block Area, Yucca Mountain, Nye County, Nevada.* Miscellaneous Investigations Series Map I-2601. Washington, D.C.: U.S. Geological Survey. ACC: MOL.19980611.0339.

118615 de Groot, S.R. and Mazur, P. 1962. *Non-Equilibrium Thermodynamics.* Amsterdam, The Netherlands: North-Holland Publishing Company. TIC: 234710.

100722 Dean, J.A. 1992. *Lange's Handbook of Chemistry.* 14th Edition. New York, New York: McGraw-Hill. TIC: 240690.

164019 Dehaudt, P. 2001. "Physical and Chemical State of the Nuclear Spent Fuel After Irradiation." Section 5.2 of *Synthesis on the Long Term Behavior of the Spent Nuclear Fuel.* Poinssot, C., ed. CEA-R-5958(E). Volume I. Paris, France: Commissariat à l'Énergie Atomique. TIC: 253976.

183771 Department of Army 1997. *Engineering and Design Tunnels and Shafts in Rocks.* CECW-EG Engineer Manual 1110-2-2901. Washington, D.C.: Department of Army, U. S. Army Corps of Engineers. ACC: LLR.20071102.0100.

104855 dePolo, C.M. 1994. "Estimating Fault Slip Rates in the Great Basin, USA." *Proceedings of the Workshop on Paleoseismology, 18-22 September, 1994, Marshall, California.* Prentice, C.S.; Schwartz, D.P.; and Yeats, R.S., eds. Open-File Report 94-568. Pages 48-49. Menlo Park, California: U.S. Geological Survey. TIC: 234812.

102793 Dixon, T.H.; Robaudo, S.; Lee, J.; and Reheis, M.C. 1995. "Constraints on Present-Day Basin and Range Deformation from Space Geodesy." *Tectonics, 14,* (4), 755-772. Washington, D.C.: American Geophysical Union. TIC: 234271.

100282 DOE (U.S. Department of Energy) 1988. *Site Characterization Plan Yucca Mountain Site, Nevada Research and Development Area, Nevada.* DOE/RW-0199. Nine volumes. Washington, D.C.: U.S. Department of Energy, Office of Civilian Radioactive Waste Management. ACC: HQO.19881201.0002.

171970 DOE 1997. *Quality Assurance Surveillance Record, Verify Compliance with USGS Procedures in the Preparation of "Memorandum Report" Milestone SPC333M4 "Evaluation of Paleo Groundwater Discharge."* Surveillance No. USGS-SR-97-061. Las Vegas, Nevada: U.S. Department of Energy, Office of Civilian Radioactive Waste Management. ACC: MOL.19980204.0201.

100332 DOE 1997. *The 1997 "Biosphere" Food Consumption Survey Summary Findings and Technical Documentation.* Las Vegas, Nevada: U.S. Department of Energy, Office of Civilian Radioactive Waste Management. ACC: MOL.19981021.0301.

122980 DOE 1998. *Update to Assessment of Direct Disposal in Unsaturated Tuff of Spent Nuclear Fuel and High-Level Waste Owned by U.S. Department of Energy.* DOE/SNF/REP-015. Washington, D.C.: U.S. Department of Energy. TIC: 243859.

118968 DOE 2000. *DOE Spent Nuclear Fuel Grouping in Support of Criticality, DBE, TSPA-LA.* DOE/SNF/REP-046, Rev. 0. Idaho Falls, Idaho: U.S. Department of Energy, Idaho Operations Office. ACC: DOC.20030905.0021.

158405 DOE 2002. *DOE Spent Nuclear Fuel Information in Support of TSPA-SR.* DOE/SNF/REP-047, Rev. 2. Idaho Falls, Idaho: U.S. Department of Energy, Idaho Operations Office. TIC: 252089.

155970 DOE 2002. *Final Environmental Impact Statement for a Geologic Repository for the Disposal of Spent Nuclear Fuel and High-Level Radioactive Waste at Yucca Mountain, Nye County, Nevada.* DOE/EIS-0250. Washington, D.C.: U.S. Department of Energy, Office of Civilian Radioactive Waste Management. ACC: MOL.20020524.0314; MOL.20020524.0315; MOL.20020524.0316; MOL.20020524.0317; MOL.20020524.0318; MOL.20020524.0319; MOL.20020524.0320.

155943 DOE 2002. *Yucca Mountain Science and Engineering Report.* DOE/RW-0539, Rev. 1. Washington, D.C.: U.S. Department of Energy, Office of Civilian Radioactive Waste Management. ACC: MOL.20020404.0042.

166027 DOE 2003. *Review of Oxidation Rates of DOE Spent Nuclear Fuel Part 2. Nonmetallic Fuel.* DOE/SNF/REP-068, Rev. 0. Idaho Falls, Idaho: U.S. Department of Energy, Idaho Operations Office. ACC: DOC.20030905.0009.

171271 DOE 2004. *General Description of Database Information Version 5.0.1.* DOE/SNF/REP-094, Rev. 0. Idaho Falls, Idaho: U.S. Department of Energy, Idaho Operations Office. ACC: MOL.20040812.0117.

173188 DOE 2004. *GOTH_SNF MCO Chemical Reactivity Final Analysis.* DOE/SNF/REP-77, Rev. 1. Idaho Falls, Idaho: U.S. Department of Energy, Idaho Operations Office. ACC: DOC.20040503.0003.

171539 DOE 2004. *Quality Assurance Requirements and Description.* DOE/RW-0333P, Rev. 16. Washington, D.C.: U.S. Department of Energy, Office of Civilian Radioactive Waste Management. ACC: DOC.20040907.0002.

169354 DOE 2004. *Source Term Estimates for DOE Spent Nuclear Fuels.* DOE/SNF/REP-078, Rev. 1. Three volumes. Idaho Falls, Idaho: U.S. Department of Energy, Idaho Operations Office. ACC: MOL.20040524.0451.

177173 DOE 2006. *Augmented Quality Assurance Program (AQAP).* DOE/RW-0565, Rev. 1. Washington, D.C.: U.S. Department of Energy, Office of Civilian Radioactive Waste Management. ACC: DOC.20060713.0007.

176937 DOE 2006. *Yucca Mountain Project Conceptual Design Report.* TDR-MGR-MD-000014, Rev. 05. Las Vegas, Nevada: U.S. Department of Energy, Office of Repository Development. ACC: ENG.20060505.0003.

182577 DOE 2007. *General Description of Database Information Version 5.0.1.* DOE/SNF/REP-094, Rev. 1. Idaho Falls, Idaho: U.S. Department of Energy, National Spent Nuclear Fuel Program. ACC: MOL.20070823.0010.

182051 DOE 2007. *Quality Assurance Requirements and Description.* DOE/RW-0333P, Rev. 19. Washington, D. C.: U.S. Department of Energy, Office of Civilian Radioactive Waste Management. ACC: DOC.20070717.0006.

169992 DOE 2007. *Waste Acceptance System Requirements Document.* DOE/RW-0351, Rev. 5. Washington, D.C.: U.S. Department of Energy, Office of Civilian Radioactive Waste Management. ACC: DOC.20070522.0007.

163222 Dombrowski, H.S. and Brownell, L.E. 1954. "Residual Equilibrium Saturation of Porous Media." *Industrial & Engineering Chemistry, 46,* (6), 1207-1219. Easton, Pennsylvania: American Chemical Society. TIC: 254309.

100569 Domenico, P.A. and Schwartz, F.W. 1990. *Physical and Chemical Hydrogeology.* New York, New York: John Wiley & Sons. TIC: 234782.

103062 Doorenbos, J. and Pruitt, W.O. 1977. *Crop Water Requirements.* FAO Irrigation and Drainage Paper 24. Rome, Italy: Food and Agriculture Organization of the United Nations. TIC: 245199.

185029 Dublyansky, Y. 2007. "Analysis of the Treatment, by the U.S. Department of Energy, of the FEP Hydrothermal Activity in the Yucca Mountain Performance Assessment." *Risk Analysis, 27,* (6), 1455-1468. McLean, Virginia: Society for Risk Analysis. TIC: 260048.

183865 Duhr, S. and Braun, D. 2006. "Why Molecules Move Along a Temperature Gradient." *Proceedings of the National Academy of Sciences of the United States of America, 103,* (52), 19678-19682. Washington, D.C.: National Academy of Sciences. TIC: 259839.

162213 Dunn, D.S. and Brossia, C.S. 2002. "Assessment of Passive and Localized Corrosion Processes for Alloy 22 as a High-Level Nuclear Waste Container Material." *Corrosion/2002, 57th Annual Conference & Exposition, April 7-11, 2002, Denver, Colorado.* Paper No. 02548. Houston, Texas: NACE International. TIC: 254579.

173813 Dunn, D.S.; Yang, L.; Wu, C.; and Cragnolino, G.A. 2004. "Effect of Inhibiting Oxyanions on the Localized Corrosion Susceptibility of Waste Package Container Materials." *Scientific Basis for Nuclear Waste Management XXVIII, Symposium held April 13-16, 2004, San Francisco, California, U.S.A.* Hanchar, J.M.; Stroes-Gascoyne, S.; and Browning, L., eds. *824,* 33-38. Warrendale, Pennsylvania: Materials Research Society. TIC: 256855.

173919 Dutton, R. 1995. *A Methodology to Analyze the Creep Behaviour of Nuclear Fuel Waste Containers.* AECL-11249. Pinawa, Manitoba, Canada: Whiteshell Laboratories, Atomic Energy of Canada Limited. TIC: 226154.

174750 Dutton, R. 1996. *A Review of the Low-Temperature Creep Behaviour of Titanium.* AECL-11544. Pinawa, Manitoba, Canada: Whiteshell Laboratories, Atomic Energy of Canada Limited. TIC: 231204.

105655 Dyer, J.R. 1999. "Revised Interim Guidance Pending Issuance of New U.S. Nuclear Regulatory Commission (NRC) Regulations (Revision 01, July 22, 1999), for Yucca Mountain, Nevada." Letter from J.R. Dyer (DOE/YMSCO) to D.R. Wilkins (CRWMS M&O), September 3, 1999, OL&RC:SB-1714, with enclosure, "Interim Guidance Pending Issuance of New NRC Regulations for Yucca Mountain (Revision 01)." ACC: MOL.19990910.0079.

157677 Eatman, G.L.W.; Singleton, W.L.; Moyer, T.C.; Barr, D.L.; Albin, A.L.; Lung, R.C.; and Beason, S.C. 1997. *Geology of the South Ramp - Station 55+00 to 78+77, Exploratory Studies Facility, Yucca Mountain Project, Yucca Mountain, Nevada.* Denver, Colorado: U.S. Department of Energy. ACC: MOL.19980127.0396.

167625 Eghbal, M.K. and Southard, R.J. 1993. "Micromorphological Evidence of Polygenesis of Three Aridisols, Western Mohave Desert, California." *Soil Science Society of America Journal, 57,* (4), 1041-1050. Madison, Wisconsin: Soil Science Society of America. TIC: 255602.

167624 Eghbal, M.K. and Southard, R.J. 1993. "Stratigraphy and Genesis of Durorthids and Haplargids on Dissected Alluvial Fans, Western Mojave Desert, California." *Geoderma, 59,* (1-4), 151-174. Amsterdam, The Netherlands: Elsevier. TIC: 255601.

167802 Ehlers, E.G. and Blatt, H. 1982. *Petrology, Igneous, Sedimentary, and Metamorphic.* New York, New York: W.H. Freeman and Company. TIC: 255657.

175544 EPA (U.S. Environmental Protection Agency) 2002. *Federal Guidance Report 13, CD Supplement, Cancer Risk Coefficients for Environmental Exposure to Radionuclides, EPA.* EPA-402-C-99-001, Rev. 1. Washington, D.C.: U.S. Environmental Protection Agency. ACC: MOL.20051013.0016.

100633 Ervin, E.M.; Luckey, R.R.; and Burkhardt, D.J. 1994. *Revised Potentiometric-Surface Map, Yucca Mountain and Vicinity, Nevada.* Water-Resources Investigations Report 93-4000. Denver, Colorado: U.S. Geological Survey. ACC: NNA.19930212.0018.

164789 Etherington, H., ed. 1958. *Nuclear Engineering Handbook.* 1st Edition. New York, New York: McGraw-Hill. TIC: 231758.

182742 Etien, R.A.; Gordon, S.R.; and Ilevbare, G.O. 2005. "Effect of Solution Annealing on Critical Potentials of Alloy 22." *2005 ASME Pressure Vessels and Piping Conference (PVP2005), Technologies for Safe and Efficient Energy Conversion, July 17-21, 2005, Denver, Colorado, USA.* PVP2005-71652. New York, New York: American Society of Mechanical Engineers. TIC: 257583.

178836 Evans, N.J.; Wilson, N.S.F.; Cline, J.S.; McInnes, B.I.A.; and Byrne, J. 2005. "Fluorite (U-Th)/He Thermochronology: Constraints on the Low Temperature History of Yucca Mountain, Nevada." *Applied Geochemistry, 20,* 1099-1105. New York, New York: Elsevier. TIC: 259246.

153024 Farmer, G.L.; Broxton, D.E.; Warren, R.G.; and Pickthorn, W. 1991. "Nd, Sr, and O Isotopic Variations in Metaluminius Ash-Flow Tuffs and Related Volcanic Rocks at the Timber Mountain/Oasis Valley Caldera, Complex, SW Nevada: Implications for the Origin and Evolution of Large-Volume Silicic Magma Bodies." *Contributions to Mineralogy and Petrology, 109,* 53-68. New York, New York: Springer-Verlag. TIC: 249053.

105126 Faulds, J.E.; Bell, J.W.; Feuerbach, D.L.; and Ramelli, A.R. 1994. *Geologic Map of the Crater Flat Area, Nevada.* Geophysical Investigations Map 101. Reno, Nevada: University of Nevada, Reno. TIC: 211484.

160881 Fenelon, J.M. 2000. *Quality Assurance and Analysis of Water Levels in Wells on Pahute Mesa and Vicinity, Nevada Test Site, Nye County, Nevada.* Water-Resources Investigations Report 00-4014. Carson City, Nevada: U.S. Geological Survey. ACC: MOL.20030904.0304.

101238 Fenix & Scisson 1986. *NNWSI Hole Histories, UE-25 WT #3, UE-25 WT #4, UE-25 WT #5, UE-25 WT #6, UE-25 WT #12, UE-25 WT #13, UE-25 WT #14, UE-25 WT #15, UE-25 WT #16, UE-25 WT #17, UE-25 WT #18, USW WT-1, USW WT-2, USW WT-7, USW WT-10, USW WT-11.* DOE/NV/10322-10. Mercury, Nevada: Fenix & Scisson. ACC: NNA.19870317.0155.

103102 Fenix & Scisson 1987. *NNWSI Hole Histories, USW G-1, USW G-2, USW G-3, USW G-4, USW GA-1, USW GU-3.* DOE/NV/10322-19. Mercury, Nevada: Fenix & Scisson. ACC: HQS.19880517.1194.

126415 Fenix & Scisson 1987. *NNWSI Hole Histories, USW H-1, USW H-3, USW H-4, USW H-5, USW H-6.* DOE/NV/10322-18. Washington, D.C.: U.S. Department of Energy, Office of Civilian Radioactive Waste Management. ACC: NNA.19871006.0069.

165939 Fenix & Scisson 1987. *NNWSI Hole Histories, USW UZ-1, UE-25 UZ #4, UE-25 UZ #5, USW UZ-6, USW UZ-6s, USW UZ-7, USW UZ-8, USW UZ-13.* DOE/NV/10322-20. Washington, D.C.: U.S. Department of Energy, Office of Civilian Radioactive Waste Management. ACC: HQS.19880517.1193.

171196 Ferrill, D.A.; Morris, A.P.; Evans, M.A.; Burkhard, M.; Groshong,R.H.,Jr.; and Onasch, C.M. 2004. "Calcite Twin Morphology: A Low-Temperature Deformation Geothermometer." *Journal of Structural Geology, 26,* (8), 1521-1529. New York, New York: Elsevier. TIC: 256408.

156668 Fetter, C.W. 2001. *Applied Hydrogeology.* 4th Edition. Upper Saddle River, New Jersey: Prentice Hall. TIC: 251142.

113030 Finch, R.J. and Ewing, R.C. 1992. "The Corrosion of Uraninite Under Oxidizing Conditions." *Journal of Nuclear Materials, 190,* 133-156. Amsterdam, The Netherlands: Elsevier. TIC: 246369.

151875 Finsterle, S. 2000. "Using the Continuum Approach to Model Unsaturated Flow in Fractured Rock." *Water Resources Research, 36,* (8), 2055-2066. Washington, D.C.: American Geophysical Union. TIC: 248769.

162806 Fisher, R.V. and Schmincke, H.-U. 1984. *Pyroclastic Rocks.* New York, New York: Springer-Verlag. TIC: 223562.

100033 Flint, L.E. 1998. *Characterization of Hydrogeologic Units Using Matrix Properties, Yucca Mountain, Nevada.* Water-Resources Investigations Report 97-4243. Denver, Colorado: U.S. Geological Survey. ACC: MOL.19980429.0512.

112530 Flynn, T.; Buchanan, P.; Trexler, D.; Shevenell, L.; and Garside, L. 1996. *Geothermal Resource Assessment of the Yucca Mountain Area, Nye County, Nevada.* BA0000000-03255-5705-00002. Las Vegas, Nevada: University and Community College System of Nevada. ACC: MOL.19960903.0027.

100148 Forester, R.M.; Bradbury, J.P.; Carter, C.; Elvidge, A.B.; Hemphill, M.L.; Lundstrom, S.C.; Mahan, S.A.; Marshall, B.D.; Neymark, L.A.; Paces, J.B.; Sharpe, S.E.; Whelan, J.F.; and Wigand, P.E. 1996. *Synthesis of Quaternary Response of the Yucca Mountain Unsaturated and Saturated Zone Hydrology to Climate Change.* Milestone 3GCA102M. Las Vegas, Nevada: U.S. Geological Survey. ACC: MOL.19970211.0026.

109425 Forester, R.M.; Bradbury, J.P.; Carter, C.; Elvidge-Tuma, A.B.; Hemphill, M.L.; Lundstrom, S.C.; Mahan, S.A.; Marshall, B.D.; Neymark, L.A.; Paces, J.B.; Sharpe, S.E.; Whelan, J.F.; and Wigand, P.E. 1999. *The Climatic and Hydrologic History of Southern Nevada During the Late Quaternary.* Open-File Report 98-635. Denver, Colorado: U.S. Geological Survey. TIC: 245717.

144061 Foster, A.R. and Wright, R.L., Jr. 1973. *Basic Nuclear Engineering.* 2nd Edition. Boston, Massachusetts: Allyn and Bacon. TIC: 247586.

159344 Fox, M.J. and McCright, R.D. 1983. *An Overview of Low Temperature Sensitization.* UCRL-15619. Livermore, California: Lawrence Livermore National Laboratory. ACC: HQS.19880517.2438.

154365 Freeze, G.A.; Brodsky, N.S.; and Swift, P.N. 2001. *The Development of Information Catalogued in REV00 of the YMP FEP Database.* TDR-WIS-MD-000003 REV 00 ICN 01. Las Vegas, Nevada: Bechtel SAIC Company. ACC: MOL.20010301.0237.

101173 Freeze, R.A. and Cherry, J.A. 1979. *Groundwater.* Englewood Cliffs, New Jersey: Prentice-Hall. TIC: 217571.

107425 French, D.E. 2000. *Hydrocarbon Assessment of the Yucca Mountain Vicinity, Nye County, Nevada.* Open-File Report 2000-2. Reno, Nevada: Nevada Bureau of Mines and Geology. ACC: MOL.20000609.0298.

118942 Fridrich, C.J. 1999. "Tectonic Evolution of the Crater Flat Basin, Yucca Mountain Region, Nevada." Chapter 7 of *Cenozoic Basins of the Death Valley Region.* Wright, L.A. and Troxel, B.W., eds. Special Paper 333. Boulder, Colorado: Geological Society of America. TIC: 248054.

100575 Fridrich, C.J.; Dudley, W.W., Jr.; and Stuckless, J.S. 1994. "Hydrogeologic Analysis of the Saturated-Zone Ground-Water System, Under Yucca Mountain, Nevada." *Journal of Hydrology, 154,* 133-168. Amsterdam, The Netherlands: Elsevier. TIC: 224606.

164051 Fridrich, C.J.; Whitney, J.W.; Hudson, M.R.; and Crowe, B.M. 1998. *Space-Time Patterns of Late Cenozoic Extension, Vertical-Axis Rotation, and Volcanism in the Crater Flat Basin, Southwest Nevada.* Open-File Report 98-461. Denver, Colorado: U.S. Geological Survey. ACC: MOL.19981014.0299.

184915 Fridrich, C.J.; Whitney, J.W.; Hudson, M.R.; and Crowe, B.M. 2003. *Documentation for USGS Review of Chapter 2, Section 2 of the Seismotectonic Framework Report Entitled "Space-Time Patterns of Extension, Vertical-Axis Rotation, and Volcanism in the Crater Flat Basin, Southern Nevada."* Las Vegas, Nevada: U.S. Geological Survey. ACC: MOL.20030627.0043.

105086 Fridrich, C.J.; Whitney, J.W.; Hudson, M.R.; Keefer, W.R.; and Crowe, B.M. 1996. "Space-Time Patterns of Extension, Vertical-Axis Rotation, and Volcanism in the Crater Flat Basin." Chapter 2.II of *Seismotectonic Framework and Characterization of Faulting at Yucca Mountain, Nevada.* Whitney, J.W., ed. Milestone 3GSH100M. Denver, Colorado: U.S. Geological Survey. TIC: 237980. ACC: MOL.19970129.0041.

113267 Frondel, C. 1958. *Systematic Mineralogy of Uranium and Thorium.* Bulletin 1064. Washington, D.C.: U.S. Geological Survey. TIC: 246837.

156826 Galloway, D. and Rojstaczer, S. 1988. "Analysis of the Frequency Response of Water Levels in Wells to Earth Tides and Atmospheric Loading." *Proceedings, Fourth Canadian/American Conference on Hydrogeology, Fluid Flow, Heat Transfer, and Mass Transport in Fractured Rocks, Banff, Alberta, Canada, June 21-24, 1988.* Hitchon, B. and Bachu, S., eds. Pages 100-113. Dublin, Ohio: National Water Well Association. TIC: 222289.

169141 Garvin, L.J. 2002. *Multi-Canister Overpack Topical Report.* HNF-SD-SNF-SARR-005, Rev. 3. Richland, Washington: Fluor Hanford. ACC: MOL.20040510.0106.

103258 Gauthier, J.H.; Wilson, M.L.; Borns, D.J.; and Arnold, B.W. 1995. *Impacts of Seismic Activity on Long-Term Repository Performance at Yucca Mountain.* SAND95-1917C. Albuquerque, New Mexico: Sandia National Laboratories. ACC: MOL.19960327.0356.

100447 Gauthier, J.H.; Wilson, M.L.; Borns, D.J.; and Arnold, B.W. 1996. "Impacts of Seismic Activity on Long-Term Repository Performance at Yucca Mountain." *Proceedings of the Topical Meeting on Methods of Seismic Hazards Evaluation, Focus '95, September 18-20, 1995, Las Vegas, Nevada.* Pages 159-168. La Grange Park, Illinois: American Nuclear Society. TIC: 232628.

100859 Gdowski, G.E. 1991. *Survey of Degradation Modes of Four Nickel-Chromium-Molybdenum Alloys.* UCRL-ID-108330. Livermore, California: Lawrence Livermore National Laboratory. ACC: NNA.19910521.0010.

102789 Gdowski, G.E. 1997. *Degradation Mode Survey Candidate Titanium - Base Alloys for Yucca Mountain Project Waste Package Materials.* UCRL-ID-121191, Rev. 1. Livermore, California: Lawrence Livermore National Laboratory. ACC: MOL.19980120.0053.

100860 Gdowski, G.E. and Bullen, D.B. 1988. *Oxidation and Corrosion.* Volume 2 of *Survey of Degradation Modes of Candidate Materials for High-Level Radioactive-Waste Disposal Containers.* UCID-21362. Livermore, California: Lawrence Livermore National Laboratory. ACC: MOL.19980715.0384.

129721 Geldon, A.L.; Umari, A.M.A.; Earle, J.D.; Fahy, M.F.; Gemmell, J.M.; and Darnell, J. 1998. *Analysis of a Multiple-Well Interference Test in Miocene Tuffaceous Rocks at the C-Hole Complex, May-June 1995, Yucca Mountain, Nye County, Nevada.* Water-Resources Investigations Report 97-4166. Denver, Colorado: U.S. Geological Survey. TIC: 236724.

100397 Geldon, A.L.; Umari, A.M.A.; Fahy, M.F.; Earle, J.D.; Gemmell, J.M.; and Darnell, J. 1997. *Results of Hydraulic and Conservative Tracer Tests in Miocene Tuffaceous Rocks at the C-Hole Complex, 1995 to 1997, Yucca Mountain, Nye County, Nevada.* Milestone SP23PM3. Las Vegas, Nevada: U.S. Geological Survey. ACC: MOL.19980122.0412.

105021 Glass, R.S.; Overturf, G.E.; Van Konynenburg, R.A.; and McCright, R.D. 1986. "Gamma Radiation Effects on Corrosion-I. Electrochemical Mechanisms for the Aqueous Corrosion Processes of Austenitic Stainless Steels Relevant to Nuclear Waste Disposal in Tuff." *Corrosion Science, 26,* (8), 577-590. Oxford, Great Britain: Pergamon. TIC: 226179.

183214 GoldSim Technology Group 2007. *GoldSim Contaminant Transport Module.* Version 4.20. Issaquah, Washington: GoldSim Technology Group. TIC: 259223.

170725 Gosse, J.C.; Harrington, C.D.; and Whitney, J.W. 1996. "Applications of In Situ Cosmogenic Nuclides in the Geologic Site Characterization of Yucca Mountain, Nevada." *Scientific Basis for Nuclear Waste Management XIX, Symposium held November 27-December 1, 1995, Boston, Massachusetts.* Murphy, W.M. and Knecht, D.A., eds. *412,* 799-806. Pittsburgh, Pennsylvania: Materials Research Society. TIC: 233877.

171202 Gray, M.B.; Stamatakos, J.A.; and Ferrill, D.A. 2000. "Polygenetic Secondary Calcite Mineralization in Yucca Mountain, NV." *Abstracts with Programs - Geological Society of America, 32,* (7), A-260. Boulder, Colorado: Geological Society of America. TIC: 249113.

109691 Gray, W.J. and Einziger, R.E. 1998. *Initial Results from Dissolution Rate Testing of N-Reactor Spent Fuel Over a Range of Potential Geologic Repository Aqueous Conditions.* DOE/SNF/REP-022, Rev. 0. Washington, D.C.: U.S. Department of Energy. TIC: 245380.

170174 Green, R.T.; Evans, D.D.; and Filippone, W.L. 1987. "Effect of Electric Fields on Vapor Transport Near a High-Level Waste Canister." Chapter 32 of *Coupled Processes Associated with Nuclear Waste Repositories.* Tsang, C-F., ed. Orlando, Florida: Academic Press. TIC: 200325.

101671 Grenthe, I.; Fuger, J.; Konings, R.J.M.; Lemire, R.J.; Muller, A.B.; Nguyen-Trung, C.; and Wanner, H. 1992. *Chemical Thermodynamics of Uranium.* Volume 1 of *Chemical Thermodynamics.* Wanner, H. and Forest, I., eds. Amsterdam, The Netherlands: North-Holland Publishing Company. TIC: 224074.

135260 Grieve, R.; Rupert, J.; and Therriault, A. 1995. "The Record of Terrestrial Impact Cratering." *GSA Today, 5,* (10), 194-196. Boulder, Colorado: Geological Society of America. TIC: 246688.

163385 Grieve, R.A.F. 1998. "Extraterrestrial Impacts on Earth: The Evidence and the Consequences." *Meteorites: Flux with Time and Impact Effects.* Grady, M.M.; Hutchinson, R.; McCall, G.J.H.; and Rothery, D.A., eds. Geological Society Special Publication No. 140. Pages 105-131. London, England: Geological Society. TIC: 254143.

185030 Grieve, R.A.F. and Robertson, P.B. 1984. "The Potential for the Disturbance of a Buried Nuclear Waste Vault by a Large-Scale Meteorite Impact." *Workshop on Transitional Processes Proceedings, held in Ottawa, 1982 November 4 and 5.* AECL-7822. Pages 231-269. Pinawa, Manitoba, Canada: Whiteshell Nuclear Research Establishment. TIC: 227319.

135254 Grieve, R.F. 1987. "Terrestrial Impact Structures." *Annual Review of Earth and Planetary Sciences, 15,* 245-269. Palo Alto, California: Annual Reviews. TIC: 246788.

185112 Gubbins, D. 1999. "The Distinction between Geomagnetic Excursions and Reversals." *Geophysical Journal International, 137,* F1-F3. Oxford, England: Blackwell Publishing. TIC: 260079.

109207 Guenther, R.J.; Blahnik, D.E.; Jenquin, U.P.; Mendel, J.E.; Thomas, L.E.; and Thornhill, C.K. 1991. *Characterization of Spent Fuel Approved Testing Material--ATM-104.* PNL-5109-104. Richland, Washington: Pacific Northwest Laboratory. TIC: 203846.

154917 Guy, A.G. 1959. *Elements of Physical Metallurgy.* 2nd Edition. Reading, Massachusetts: Addison-Wesley Publishing. TIC: 231760.

185095 Hala, J. and Miyamoto, H. 2007. "IUPAC-NIST Solubility Data Series. 84. Solubility of Inorganic Actinide Compounds." *Journal of Physical and Chemical Reference Data, 36,* (4), 1417-1736. College Park, Maryland: American Institute of Physics. TIC: 260073.

145228 Haldeman, D.L. and Amy, P.S. 1993. "Bacterial Heterogeneity in Deep Subsurface Tunnels at Rainier Mesa, Nevada Test Site." *Microbial Ecology, 25,* (2), 185-194. New York, New York: Springer-Verlag. TIC: 238373.

101676 Hansson, C.M. 1984. *The Corrosion of Zircaloy 2 in Anaerobic Synthetic Cement Pore Solution.* SKB TR-84-13. Stockholm, Sweden: Svensk Kärnbränsleförsörjning A.B. TIC: 206293.

100534 Hardin, E.L. and Chesnut, D.A. 1997. *Synthesis Report on Thermally Driven Coupled Processes.* Milestone SPL8BM4. Livermore, California: Lawrence Livermore National Laboratory. ACC: MOL.19980113.0395.

106095 Harrington, C.D. and Whitney, J.W. 1987. "Scanning Electron Microscope Method for Rock-Varnish Dating." *Geology, 15,* 967-970. Boulder, Colorado: Geological Society of America. TIC: 203298.

174075 Haschke, J.M. 1998. "Corrosion of Uranium in Air and Water Vapor: Consequences for Environmental Dispersal." *Journal of Alloys and Compounds, 278,* 149-160. New York, New York: Elsevier. TIC: 257449.

100896 Haynes International 1997. Hastelloy C-22 Alloy. Kokomo, Indiana: Haynes International. TIC: 238121.

182722 He, X.; Dunn, D.S.; and Csontos, A.A. 2007. "Corrosion of Similar and Dissimilar Metal Crevices in the Engineered Barrier System of a Potential Nuclear Waste Repository." *Electrochimica Acta, 52,* 7556-7569. New York, New York: Elsevier. TIC: 259704.

183687 He, X.; Noël, J.J.; and Shoesmith, D.W. 2007. "Temperature Effects on Oxide Film Properties of Grade-7 Titanium." *Corrosion, 63,* (8), 781-792. Houston, Texas: NACE International. TIC: 259836.

107255 Heizler, M.T.; Perry, F.V.; Crowe, B.M.; Peters, L.; and Appelt, R. 1999. "The Age of Lathrop Wells Volcanic Center: An $^{40}Ar/^{39}Ar$ Dating Investigation." *Journal of Geophysical Research, 104,* (B1), 767-804. Washington, D.C.: American Geophysical Union. TIC: 243399.

168133 Herrera, M.L. 2004. *Evaluation of the Potential Impact of Seismic Induced Deformation on the Stress Corrosion Cracking of the YMP Waste Packages.* SIR-04-015, Rev. 1. San Jose, California: Structural Integrity Associates. ACC: MOL.20040311.0149.

135281 Hills, J.G. and Goda, P.M. 1993. "Fragmentation of Small Asteroids in the Atmosphere." *The Astronomical Journal, 105,* (3), 1114-1144. Woodbury, New York: American Institute of Physics. TIC: 246798.

171800 Hirschfelder, J.O.; Curtiss, C.F.; and Bird, R.B 1964. *Molecular Theory of Gases and Liquids.* New York, New York: John Wiley & Sons. TIC: 103052.

183686 Holford, I.C.R. and Mattingly, G.E.G. 1975. "Surface Areas of Calcium Carbonate in Soils." *Geoderma, 13,* 247-255. Amsterdam, The Netherlands: Elsevier. TIC: 259835.

162326 Holt, E.W. 2002. "$^{18}0/^{16}0$ Evidence for an Early, Short-Lived (~10 yr), Fumarolic Event in the Topopah Spring Tuff Near the Proposed High-Level Nuclear Waste Repository Within Yucca Mountain, Nevada, USA." *Earth and Planetary Science Letters, 201,* (3-4), 559-573. New York, New York: Elsevier. TIC: 255127.

124149 Horak, C. and Carns, D. 1997. *Amargosa Focus Group Report.* Biosphere Study. Las Vegas, Nevada: University of Nevada, Las Vegas. TIC: 241712.

171058 Horn, J.M.; Masterson, B.A.; Rivera, A.; Miranda, A.; Davis, M.A.; and Martin, S. 2004. "Bacterial Growth Dynamics, Limiting Factors, and Community Diversity in a Proposed Geological Nuclear Waste Repository Environment." *Geomicrobiology Journal, 21,* 273-286. London, England: Taylor & Francis Group. TIC: 256356.

153282 Howard, C.L.; Finley, R.L.; Johnston, R.L.; Taylor, R.S.; George, J.T.; Lowry, W.E.; and Mason, N.G. 2001. *Engineered Barrier System—Pilot Scale Test #3, Heated Drip Shield Test Results.* TDR-EBS-SE-000001 REV 00. Las Vegas, Nevada: Bechtel SAIC Company. ACC: MOL.20010529.0330.

181177 Hu, H.; Turchi, P.E.A.; and Wong, F. 2005. *Computational Modeling of Phase Stability in Alloy 22 Over a Range of Chemical Compositions for the Yucca Mountain Project.* UCRL-MI-212471. Livermore, California: Lawrence Livermore National Laboratory. ACC: LLR.20070627.0002.

161623 Hu, Q.; Kneafsey, T.; Wang, J.S.Y.; Roberts, J.; and Carlson, S. 2001. *Summary Report on Phase I Feasibility Study of In-Drift Diffusion.* LBNL-49063. Berkeley, California: Lawrence Berkeley National Laboratory. ACC: MOL.20030225.0125.

184440 Hu, Q.; Kneafsey, T.J.; Roberts, J.J.; Tomutsa, L.; and Wang, J.S.Y. 2004. "Characterizing Unsaturated Diffusion in Porous Tuff Gravel." *Vadose Zone Journal, 3,* 1425-1438. Madison, Wisconsin: Soil Science Society of America. TIC: 259886.

163111 Hua, F. and Gordon, G. 2003. "On Apparent Bi-Linear Corrosion Rate Behavior of Ti Grade 7 in Basic Saturated Water (BSW-12) Below and Above 80°C." *Corrosion/2003, 58th Annual Conference & Exposition, March 16-20, 2003, San Diego, California.* Paper No. 03687. Houston, Texas: NACE International. TIC: 254248.

160670 Hua, F.; Sarver, J.; Jevec, J.; and Gordon, G. 2002. "General Corrosion Studies of Candidate Container Materials in Environments Relevant to Nuclear Waste Repository." *Corrosion/2002, 57th Annual Conference & Exposition, April 7-11, 2002, Denver, Colorado.* Paper No. 02530. Houston, Texas: NACE International. TIC: 252067.

162562 Hughes, D.W. 1998. "The Mass Distribution of Crater-Producing Bodies." *Meteorites: Flux with Time and Impact Effects.* Geological Society Special Publication No. 140. Grady, M.M.; Hutchison, R.; McCall, G.J.H.; and Rothery, D.A., eds. Pages 31-42. Bath, England: Geological Society of London. TIC: 254143.

150295 Hyndman, D.W. 1972. *Petrology of Igneous and Metamorphic Rocks.* International Series in the Earth and Planetary Sciences. New York, New York: McGraw-Hill. TIC: 248141.

183654 ICRP (International Commission on Radiological Protection) 1989. "Age-Dependent Doses to Members of the Public from Intake of Radionuclides: Part 1." Volume 20, No. 2 of *Annals of the ICRP.* New York, New York: Pergamon Press. TIC: 234780.

162662 Ikeda, B.M. and Quinn, M.J. 2003. *Corrosion of Dissimilar Metal Crevices in Simulated Concentrated Ground Water Solutions at Elevated Temperature.* AECL-12167, Rev. 00. Pinawa, Manitoba, Canada: Atomic Energy of Canada Limited, Whiteshell Laboratories. ACC: MOL.20051017.0161.

173814 Ilevbare, G.O. 2005. "The Effect of Sulfate Anions on the Crevice Breakdown and Repassivation Potentials of Alloy 22 in 4M NaCl." *Corrosion/2005, 60th Annual Conference & Exposition, 1945-2005, April 3-7, 2005, George R. Brown Convention Center, Houston, Texas.* Paper No. 05611. Houston, Texas: NACE International. TIC: 257165.

183682 Ishikawa, T.; Maeda, A.; Kandori, K.; and Tahara, A. 2006. "Characterization of Rust on Fe-Cr, Fe-Ni, and Fe-Cu Binary Alloys by Fourier Transform Infrared and N_2 Adsorption." *Corrosion, 62,* (7), 559-567. Houston, Texas: NACE International. TIC: 259833.

181136 Ishikawa, T.; Yoshida, T.; Kandori, K.; Nakayma, T.; and Hara, S. 2007. "Assessment of Protective Function of Steel Rust Layers by N_2 Adsorption." *Corrosion Science, 49,* 1468-1477. New York, New York: Elsevier. TIC: 259431.

109434 Jannik, N.O.; Phillips, F.M.; Smith, G.I.; and Elmore, D. 1991. "A 36Cl Chronology of Lacustrine Sedimentation in the Pleistocene Owens River System." *Geological Society of America Bulletin, 103,* 1146-1159. Boulder, Colorado: Geological Society of America. TIC: 245705.

100987 Jarzemba, M.S.; LaPlante, P.A.; and Poor, K.J. 1997. *ASHPLUME Version 1.0—A Code for Contaminated Ash Dispersal and Deposition, Technical Description and User's Guide.* CNWRA 97-004, Rev. 1. San Antonio, Texas: Center for Nuclear Waste Regulatory Analyses. ACC: MOL.20010727.0162.

101687 Johnson, A.B., Jr. 1977. *Behavior of Spent Nuclear Fuel in Water Pool Storage.* BNWL-2256. Richland, Washington: Pacific Northwest Laboratory. TIC: 234703.

185111 Johnson, H.P.; Van Patten, D.; Tivey, M.; and Sager, W.W. 1995. "Geomagnetic Polarity Reversal Rate for the Phanerozoic." *Geophysical Research Letters, 22,* (3), 231-234. Washington, D.C.: American Geophysical Union. TIC: 260076.

178773 Johnson, L.; Ferry, C.; Poinssot, C.; and Lovera, P. 2005. "Spent Fuel Radionuclide Source-Term Model for Assessing Spent Fuel Performance in Geological Disposal. Part I: Assessment of the Instant Release Fraction." *Journal of Nuclear Materials, 346,* 56-65. New York, New York: Elsevier. TIC: 259052.

105076 Jones, D.A. 1996. *Principles and Prevention of Corrosion.* 2nd Edition. Upper Saddle River, New Jersey: Prentice Hall. TIC: 241233.

178458 Jones, R.H., ed. 1992. *Stress-Corrosion Cracking.* Materials Park, Ohio: ASM International. TIC: 9221.

102010 Jury, W.A.; Gardner, W.R.; and Gardner, W.H. 1991. *Soil Physics.* 5th Edition. New York, New York: John Wiley & Sons. TIC: 241000.

167872 Karam, P.A. 2002. "Gamma and Neutrino Radiation Dose from Gamma Ray Bursts and Nearby Supernovae." *Health Physics, 82,* (4), 491-499. Philadelphia, Pennsylvania: Lippincott Williams & Wilkins. TIC: 255918.

184906 Karam, P.A. 2003. "Inconstant Sun: How Solar Evolution Has Affected Cosmic and Ultraviolet Radiation Exposure over the History of Life on Earth." *Health Physics, 84,* (3), 322-333. Philadelphia, Pennsylvania: Lippincott Williams & Wilkins. TIC: 260031.

106312 Katz, J.J.; Seaborg, G.T.; and Morss, L.R., eds. 1986. *The Chemistry of the Actinide Elements.* 2nd Edition. Two volumes. New York, New York: Chapman and Hall. TIC: 243942.

134666 Keenan, J.H.; Keyes, F.G.; Hill, P.G.; and Moore, J.G. 1969. *Steam Tables, Thermodynamic Properties of Water Including Vapor, Liquid, and Solid Phases (English Units).* New York, New York: John Wiley & Sons. TIC: 246766.

146831 Keller, E.A. 1992. *Environmental Geology.* Sixth Edition. New York, New York: Macmillan Publishing. TIC: 247330.

177388 Kennedy, J.R.; Adler, P.N.; and Margolin, H. 1993. "Effect of Activity Differences on Hydrogen Migration in Dissimilar Titanium Alloy Welds." *Metallurgical Transactions A, 24A,* (12), 2763-2771. New York, New York: Metallurgical Society of AIME. TIC: 258524.

162421 Kersting, A.P. and Reimus, P.W., eds. 2003. *Colloid-Facilitated Transport of Low-Solubility Radionuclides: A Field, Experimental, and Modeling Investigation.* UCRL-ID-149688. Livermore, California: Lawrence Livermore National Laboratory. TIC: 254176.

100767 Kieft, T.L.; Kovacik, W.P., Jr.; Ringelberg, D.B.; White, D.C.; Haldeman, D.L.; Amy, P.S.; and Hersman, L.E. 1997. "Factors Limiting Microbial Growth and Activity at a Proposed High-Level Nuclear Repository, Yucca Mountain, Nevada." *Applied and Environmental Microbiology, 63,* (8), 3128-3133. Washington, D.C.: American Society for Microbiology. TIC: 236444.

160882 Kies, A.; Majerus, J.; and de Lantremange, N.D. 1999. "Underground Radon Gas Concentrations Related to Earth Tides." *Il Nuovo Cimento della Società Italiana di Fisica, 22C,* (3-4), 287-293. Bologna, Italy: Editrice Compositori. TIC: 253721.

133347 Kistler, R.W. 1968. "Potassium-Argon Ages of Volcanic Rocks in Nye and Esmeralda Counties, Nevada." *Nevada Test Site.* Memoir 110. Eckel, E.B., ed. Boulder, Colorado: Geological Society of America. TIC: 221562.

123682 Knoll, R.W. and Gilbert, E.R. 1987. *Evaluation of Cover Gas Impurities and Their Effects on the Dry Storage of LWR Spent Fuel.* PNL-6365. Richland, Washington: Pacific Northwest Laboratory. TIC: 213789.

131519 Kohli, R. and Pasupathi, V. 1986. *Investigation of Water-logged Spent Fuel Rods Under Dry Storage Conditions.* PNL-5987. Richland, Washington: Pacific Northwest Laboratory. TIC: 246472.

100909 Kotra, J.P.; Lee, M.P.; Eisenberg, N.A.; and DeWispelare, A.R. 1996. *Branch Technical Position on the Use of Expert Elicitation in the High-Level Radioactive Waste Program.* NUREG-1563. Washington, D.C.: U.S. Nuclear Regulatory Commission. TIC: 226832.

183167 Kranz, R.L.; Bish, D.L.; and Blacic, J.D. 1989. "Hydration and Dehydration of Zeolitic Tuff from Yucca Mountain, Nevada." *Geophysical Research Letters, 16,* (10), 1113-1116. Washington, D.C.: American Geophysical Union. TIC: 221910.

184684 Kremer, M.L. 1985. "'Complex' versus 'Free Radical' Mechanism for the Catalytic Decomposition of H_2O_2 by Ferric Ions." *International Journal of Chemical Kinetics, 17,* 1299-1314. New York, New York: John Wiley & Sons. TIC: 260001.

135295 Krystinik, L.F. 1990. "Early Diagenesis in Continental Eolian Deposits." Chapter 8 of *Modern and Ancient Eolian Deposits: Petroleum Exploration and Production.* Fryberger, S.G.; Krystinik, L.F.; and Schenk, C.J., eds. Denver, Colorado: Society of Economic Paleontologists and Mineralogists, Rocky Mountain Section. TIC: 247781.

163417 Kuiper, L.K. 1991. "Water-Table Rise Due to Magma Intrusion Beneath Yucca Mountain." *EOS, Transactions, 72,* (1-26), 121. Washington, D.C.: American Geophysical Union. TIC: 255727.

166162 Kvenvolden, K.A. 1998. "A Primer on the Geological Occurrence of Gas Hydrate." *Gas Hydrates, Relevance to World Margin Stability and Climate Change.* Henriet, J.-P. and Mienert, J., eds. Geological Society Special Publication No. 137. Pages 9-30. London, England: Geological Society of London. TIC: 255726.

142990 Lachenbruch, A.H. and Sass, J.H. 1978. "Models of an Extending Lithosphere and Heat Flow in the Basin and Range Province." Chapter 9 of *Cenozoic Tectonics and Regional Geophysics of the Western Cordillera.* Smith, R.B. and Eaton, G.P., eds. Memoir 152. Pages 209-250. Boulder, Colorado: Geological Society of America. TIC: 225059.

185002 LANL (Los Alamos National Laboratory) 1993. *Review Sheets, Transport of Synthetic Colloids through Single Saturated Fractures: A Literature Review.* Las Vegas, Nevada: Los Alamos, Yucca Mountain Site Characterization Project. ACC: MOL.19951027.0219.

185000 LANL 1994. *Publication Traveler, Transport of Synthetic Colloids through Single Saturated Fractures: A Literature Review.* Las Vegas, Nevada: Los Alamos, Yucca Mountain Site Characterization Project. ACC: MOL.19951027.0218.

101079 LaPlante, P.A. and Poor, K. 1997. *Information and Analyses to Support Selection of Critical Groups and Reference Biospheres for Yucca Mountain Exposure Scenarios.* CNWRA 97-009. San Antonio, Texas: Center for Nuclear Waste Regulatory Analyses. ACC: MOL.20010721.0035.

159337 Larrabee, C.P. 1953. "Corrosion Resistance of High-Strength Low-Alloy Steels as Influenced by Composition and Environment." *Corrosion, 9,* 259-271. Houston, Texas: National Association of Corrosion Engineers. TIC: 223386.

167815 Lattman, L.H. 1983. "Effect of Caliche on Desert Processes." Chapter 4 of *Origin and Evolution of Deserts.* Wells, S.G. and Haragan, D.R., eds. 1st Edition. Albuequerque, New Mexico: University of New Mexico Press. TIC: 255700.

167813 Lattman, L.H. 1972. "Relation of Caliche (Calcrete) Horizons to Alluvial Fan Processes in Southern Nevada." *Abstracts with Programs - Geological Society of America, 4,* (7), 574. Boulder, Colorado: Geological Society of America. TIC: 255828.

129305 Lattman, L.H. 1973. "Calcium Carbonate Cementation of Alluvial Fans in Southern Nevada." *Geological Society of America Bulletin, 84,* (9), 3013-3028. Boulder, Colorado: Geological Society of America. TIC: 235904.

129306 Lattman, L.H. and Simonberg, E.M. 1971. "Case-Hardening of Carbonate Alluvium and Colluvium, Spring Mountains, Nevada." *Journal of Sedimentary Petrology, 41,* (1), 274-281. Tulsa, Oklahoma: Society of Economic Paleontologists and Mineralogists. TIC: 223189.

167639 Lean, J. 1997. "The Sun's Variable Radiation and its Relevance for Earth." *Annual Review of Astronomy and Astrophysics, 35,* 33-67. Palo Alto, California: Annual Reviews. TIC: 255614.

142133 Lederer, C.M. and Shirley, V.S., eds. 1978. *Table of Isotopes.* 7th Edition. New York, New York: John Wiley & Sons. TIC: 243883.

133364 Levy, S. and O'Neil, J. 1986. "Moderate Temperature Zeolitic Alteration in a Cooling Pyroclastic Deposit." *Fifth International Symposium on Water-Rock Interaction, Reykjavik, 8-17 August 1986, Extended Abstracts.* LA-UR-86-1248. Pages 361-364. Los Alamos, New Mexico: Los Alamos National Laboratory. TIC: 223793.

106681 Levy, S. and Valentine, G. 1993. "Natural Alteration in the Cooling Topopah Spring Tuff, Yucca Mountain, Nevada, As an Analog to a Waste-Repository Hydrothermal Regime." *Proceedings of the Topical Meeting on Site Characterization and Model Validation, FOCUS '93, September 26-29, 1993, Las Vegas, Nevada.* Pages 145-149. La Grange Park, Illinois: American Nuclear Society. TIC: 102245.

100053 Levy, S.S. 1991. "Mineralogic Alteration History and Paleohydrology at Yucca Mountain, Nevada." *High Level Radioactive Waste Management, Proceedings of the Second Annual International Conference, Las Vegas, Nevada, April 28-May 3, 1991. 1,* 477-485. La Grange Park, Illinois: American Nuclear Society. TIC: 204272.

104157 Levy, S.S.; Norman, D.I.; and Chipera, S.J. 1996. "Alteration History Studies in the Exploratory Studies Facility, Yucca Mountain, Nevada, USA." *Scientific Basis for Nuclear Waste Management XIX, Symposium held November 27-December 1, 1995, Boston, Massachusetts.* Murphy, W.M. and Knecht, D.A., eds. *412,* 783-790. Pittsburgh, Pennsylvania: Materials Research Society. TIC: 233877.

181560 Leyens, C. and Peters, M., eds. 2004. *Titanium and Titanium Alloys, Fundamentals and Applications.* 1st Edition. 1st Reprint. Weinhein, Germany: Wiley-VCH Verlag GmbH & Co. KGaA. TIC: 257010.

173979 Lian, T.; Whalen, M.T.; and Wong, L.L 2005. "Effects of Oxide Film on the Corrosion Resistance of Titanium Grade 7 in Fluoride-Containing NaCl Brines." *Corrosion/2005, 60th Annual Conference & Exposition, 1945-2005, April 3-7, 2005, George R. Brown Convention Center, Houston, Texas.* Paper No. 05609. Houston, Texas: NACE International. TIC: 257165.

183947 Lian, T.; Yashiki, T.; Nakayama, T.; Nakanishi, T.; and Rebak, R.B. 2006. "Comparative Corrosion Behavior of Two Palladium-Containing Titanium Alloys." *Proceeding of ASME PVP 2006 and ICPVT-11 Conference, July 23-27, 2006, Vancouver, British Columbia, Canada.* PVP2006-ICPVT-11-93418. Pages 1-9. New York, New York: American Society of Mechanical Engineers. TIC: 258646.

131202 Lide, D.R., ed. 1991. *CRC Handbook of Chemistry and Physics.* 72nd Edition. Boca Raton, Florida: CRC Press. TIC: 3595.

162229 Lide, D.R., ed. 2000. *CRC Handbook of Chemistry and Physics.* 81st Edition. Boca Raton, Florida: CRC Press. TIC: 253056.

178081 Lide, D.R., ed. 2006. *CRC Handbook of Chemistry and Physics.* 87th Edition. Boca Raton, Florida: CRC Press. TIC: 258634.

131533 Little B. and Wagner P. 1996. "An Overview of Microbiologically Influenced Corrosion of Metals and Alloys Used in the Storage of Nuclear Wastes." *Canadian Journal of Microbiology, 42,* (4), 367-374. Ottawa, Canada: National Research Council of Canada. TIC: 246614.

100774 Little, B.J.; Wagner, P.A.; and Lewandowski, Z. 1997. "Spatial Relationships Between Bacteria and Mineral Surfaces." Chapter 4 of *Geomicrobiology: Interactions Between Microbes and Minerals.* Banfield, J.F. and Nealson, K.H., eds. Reviews in Mineralogy Volume 35. Washington, D.C.: Mineralogical Society of America. TIC: 236757.

105729 Liu, H.H.; Doughty, C.; and Bodvarsson, G.S. 1998. "An Active Fracture Model for Unsaturated Flow and Transport in Fractured Rocks." *Water Resources Research, 34,* (10), 2633-2646. Washington, D.C.: American Geophysical Union. TIC: 243012.

159833 Lorenzo de Mele, M.F. and Cortizo, M.C. 2000. "Electrochemical Behaviour of Titanium in Fluoride-Containing Saliva." *Journal of Applied Electrochemistry, 30,* (1), 95-100. Dordrecht, The Netherlands: Kluwer Academic Publishers. TIC: 253126.

100465 Luckey, R.R.; Tucci, P.; Faunt, C.C.; Ervin, E.M.; Steinkampf, W.C.; D'Agnese, F.A.; and Patterson, G.L. 1996. *Status of Understanding of the Saturated-Zone Ground-Water Flow System at Yucca Mountain, Nevada, as of 1995.* Water-Resources Investigations Report 96-4077. Denver, Colorado: U.S. Geological Survey. ACC: MOL.19970513.0209.

167814 Machette, M.N. 1982. "Morphology, Age, and Rate of Accumulation of Pedogenic $CaCO_3$ in Some Calcareous Soils and Pedogenic Calcretes of Southwestern United States." *Abstracts with Programs - Geological Society of America, 14,* (4), 182-183. Boulder, Colorado: Geological Society of America. TIC: 209942.

101719 Manaktala, H.K. 1993. *Characteristics of Spent Nuclear Fuel and Cladding Relevant to High-Level Waste Source Term.* CNWRA 93-006. San Antonio, Texas: Center for Nuclear Waste Regulatory Analyses. TIC: 208034.

182155 Manepally, C.; Bradbury, K.; Colton, S.; Dinwiddle, C.; Green, R.; McGinnis, R.; Sims, D.; Smart, K.; and Walter, G. 2007. *The Nature of Flow in the Faulted and Fractured Paintbrush Nonwelded Hydrogeologic Unit.* San Antonio, Texas: Center for Nuclear Waste Regulatory Analyses. ACC: LLR.20070725.0014.

149429 Marschman, S.C.; Pyecha, T.D.; and Abrefah, J. 1997. *Metallographic Examination of Damaged N Reactor Spent Nuclear Fuel Element SFEC5,4378.* PNNL-11438. Richland, Washington: Pacific Northwest National Laboratory. TIC: 248059.

129308 Marsden, B.G. and Steel, D.I. 1994. "Warning Times and Impact Probabilities for Long-Period Comets." *Hazards Due to Comets and Asteroids.* Gehrels, T., ed. Pages 221-237. Tucson, Arizona: University of Arizona Press. TIC: 246879.

154415 Marshall, B.D. and Whelan, J.F. 2000. "Isotope Geochemistry of Calcite Coatings and the Thermal History of the Unsaturated Zone at Yucca Mountain, Nevada." *Abstracts with Programs - Geological Society of America, 32,* (7), A-259. Boulder, Colorado: Geological Society of America. TIC: 249113.

171061 Marshall, B.D. and Whelan, J.F. 2001. *Simulating the Thermal History of the Unsaturated Zone at Yucca Mountain, Nevada.* Denver, Colorado: U.S. Geological Survey. ACC: MOL.20040505.0491.

101142 Marshall, B.D.; Peterman, Z.E.; and Stuckless, J.S. 1993. "Strontium Isotopic Evidence for a Higher Water Table at Yucca Mountain." *High Level Radioactive Waste Management, Proceedings of the Fourth Annual International Conference, Las Vegas, Nevada, April 26-30, 1993. 2,* 1948-1952. La Grange Park, Illinois: American Nuclear Society. TIC: 208542.

102532 Marshall, T.J. and Holmes, J.W. 1979. *Soil Physics.* Melbourne, Australia: Cambridge University Press. TIC: 240992.

184437 Martin, B.A. 1993. "Telluric Effects on a Buried Pipeline." *Corrosion, 49,* (4), 343-350. Houston, Texas: National Association of Corrosion Engineers. TIC: 259885.

174095 Martinez M.J. and Nilson, R.H. 1999. "Estimates of Barometric Pumping of Moisture through Unsaturated Fractured Rock." *Transport in Porous Media, 36,* (1), 85-119. Dordrecht, The Netherlands: Kluwer Academic Publishers. TIC: 257394.

113269 Matzke, Hj. 1992. "Radiation Damage-Enhanced Dissolution of UO2 in Water." *Journal of Nuclear Materials, 190,* 101-106. Amsterdam, The Netherlands: Elsevier. TIC: 246435.

160888 Maynard, N.C. 1995. "Space Weather Prediction." *Reviews of Geophysics (Supplement), 33,* (Part 1), 547-557. Washington, D.C.: American Geophysical Union. TIC: 253729.

104770 McCalpin, J.P. 1995. "Short Notes Frequency Distribution of Geologically Determined Slip Rates for Normal Faults in the Western United States." *Bulletin of the Seismological Society of America, 85,* (6), 1867-1872. El Cerrito, California: Seismological Society of America. TIC: 236669.

114637 McCright, R.D. 1998. *Corrosion Data and Modeling, Update for Viability Assessment.* Volume 3 of *Engineered Materials Characterization Report.* UCRL-ID-119564, Rev. 1.1. Livermore, California: Lawrence Livermore National Laboratory. ACC: MOL.19980806.0177.

159336 McCright, R.D.; Halsey, W.G.; and Van Konynenburg, R.A. 1987. *Progress Report on the Results of Testing Advanced Conceptual Design Metal Barrier Materials Under Relevant Environmental Conditions for a Tuff Repository.* UCID-21044. Livermore, California: Lawrence Livermore National Laboratory. ACC: HQX.19880201.0016.

184212 McKay, D.S.; Gibson, E.K., Jr.; Thomas-Keprta, K.L.; Vali, H.; Romanek, C.S.; Clemett, S.J.; Chillier, X.D.F; Maechling, C.R.; and Zare, R.N. 1996. "Search for Past Life on Mars: Possible Relic Biogenic Activity in Martian Meteorite ALH84001." *Science,* (273), 924-930. Washington, D.C.: American Association for the Advancement of Science. TIC: 259921.

106339 McKee, E.H. and Bergquist, J.R. 1993. *New Radiometric Ages Related to Alteration and Mineralization in the Vicinity of Yucca Mountain, Nye County, Nevada.* Open-File Report 93-538. Menlo Park, California: U.S. Geological Survey. TIC: 211265.

185042 McKenna, J.R. and Blackwell, D.D. 2004. "Numerical Modeling of Transient Basin and Range Extensional Geothermal Systems." *Geothermics, 33,* 457-476. New York, New York: Pergamon. TIC: 260054.

172673 McNamara, B.; Buck, E.; and Hanson, B. 2003. "Observation of Studtite and Metastudtite on Spent Fuel." *Scientific Basis for Nuclear Waste Management XXVI, Symposium held December 2-5, 2002, Boston, Massachusetts.* Finch, R.J. and Bullen, D.B., eds. *757,* 401-406. Warrendale, Pennsylvania: Materials Research Society. TIC: 254940.

100797 Means, J.L.; Maest, A.S.; and Crerar, D.A. 1983. *The Organic Geochemistry of Deep Ground Waters and Radionuclide Partitioning Experiments under Hydrothermal Conditions.* ONWI-448. Columbus, Ohio: Battelle Memorial Institute, Office of Nuclear Waste Isolation. TIC: 209098.

126089 Miller, W.; Alexander, R.; Chapman, N.; McKinley, I.; and Smellie, J. 1994. *Natural Analogue Studies in the Geological Disposal of Radioactive Wastes.* Studies in Environmental Science 57. New York, New York: Elsevier. TIC: 101822.

105911 Milnes, A.R. and Fitzpatrick, R.W. 1995. "Titanium and Zirconium Minerals." Chapter 23 of *Minerals in Soil Environments.* 2nd Edition. Dixon, J.B. and Weed, S.B., eds. SSSA Book Series, No. 1. Madison, Wisconsin: Soil Science Society of America. TIC: 237222.

100801 Minai, Y.; Choppin, G.R.; and Sisson, D.H. 1992. "Humic Material in Well Water from the Nevada Test Site." *Radiochimica Acta, 56,* 195-199. München, Germany: R. Oldenbourg Verlag. TIC: 238763.

149850 Mongano, G.S.; Singleton, W.L.; Moyer, T.C.; Beason, S.C.; Eatman, G.L.W.; Albin, A.L.; and Lung, R.C. 1999. *Geology of the ECRB Cross Drift - Exploratory Studies Facility, Yucca Mountain Project, Yucca Mountain, Nevada.* Deliverable SPG42GM3. Denver, Colorado: U.S. Geological Survey. ACC: MOL.20000324.0614.

100161 Montazer, P. and Wilson, W.E. 1984. *Conceptual Hydrologic Model of Flow in the Unsaturated Zone, Yucca Mountain, Nevada.* Water-Resources Investigations Report 84-4345. Lakewood, Colorado: U.S. Geological Survey. ACC: NNA.19890327.0051.

179295 Moreno, D.A.; Molina, B.; Ranninger, C.; Montero, F.; and Izquierdo, J. 2004. "Microstructural Characterization and Pitting Corrosion Behavior of UNS S30466 Borated Stainless Steel." *Corrosion, 60,* (6), 573-583. Houston, Texas: NACE International. TIC: 258529.

184023 Morgenstern, A. and Choppin, G.R. 1999. "Kinetics of the Reduction of $Pu(V)O_2^+$ by Hydrogen Peroxide." *Radiochim Acta, 36,* 109-113. München, Germany: Oldenbourg Wissenschaftsverlag. TIC: 259871.

184817 Nag, M.; Basak, P.; and Manorama, S.V. 2007. "Low-Temperature Hydrothermal Synthesis of Phase-Pure Rutile Titania Nanocrystals: Time Temperature Tuning of Morphology and Photocatalytic Activity." *Materials Research Bulletin, 42,* 1691-1704. New York, New York: Elsevier. TIC: 260014.

105162 National Research Council. 1992. *Ground Water at Yucca Mountain, How High Can It Rise? Final Report of the Panel on Coupled Hydrologic/Tectonic/Hydrothermal Systems at Yucca Mountain.* Washington, D.C.: National Academy Press. TIC: 204931.

100018 National Research Council. 1995. *Technical Bases for Yucca Mountain Standards.* Washington, D.C.: National Academy Press. TIC: 217588.

185174 NEA (Nuclear Energy Agency) 2006. *The NEA International FEP Database: Version 2.1.* Paris, France: Nuclear Energy Agency.

121510 Neukum, G. and Ivanov, B.A. 1994. "Crater Size Distributions and Impact Probabilities on Earth from Lunar, Terrestrial-Planet, and Asteroid Cratering Data." *Hazards Due to Comets and Asteroids.* Gehrels, T., ed. Pages 359-416. Tucson, Arizona: The University of Arizona Press. TIC: 246879.

163681 Neymark, L.A.; Paces, J.B.; and Amelin, Y.V. 2003. "Reliability of U-Th-Pb Dating of Secondary Silica at Yucca Mountain, Nevada." *Proceedings of the 10th International High-Level Radioactive Waste Management Conference (IHLRWM), March 30-April 2, 2003, Las Vegas, Nevada.* Pages 1-12. La Grange Park, Illinois: American Nuclear Society. TIC: 254559.

167634 Novotna, D. and Vitek, V. 1991. "The Atmospheric Mean Energetic Level and External Forcing." *Studia Geophysica et Geodaetica, 35,* (1), 33-38. Prague, Czechoslovakia: Geophysical Institute of the Czechoslovak Academy of Sciences. TIC: 255610.

101903 NRC (U.S. Nuclear Regulatory Commission) 1997. *Standard Review Plan for Dry Cask Storage Systems.* NUREG-1536. Washington, D.C.: U.S. Nuclear Regulatory Commission. ACC: MOL.20010724.0307.

149756 NRC 2000. *Standard Review Plan for Spent Fuel Dry Storage Facilities.* NUREG-1567. Washington, D.C.: U.S. Nuclear Regulatory Commission. TIC: 247929.

163274 NRC 2003. *Yucca Mountain Review Plan, Final Report.* NUREG-1804, Rev. 2. Washington, D.C.: U.S. Nuclear Regulatory Commission, Office of Nuclear Material Safety and Safeguards. TIC: 254568.

101276 O'Brien, G.M. 1993. *Earthquake-Induced Water-Level Fluctuations at Yucca Mountain, Nevada, June 1992.* Open-File Report 93-73. Denver, Colorado: U.S. Geological Survey. ACC: NNA.19930326.0022.

160892 Odenwald, S. 2003. "Earth - Magnetic Field." *Poetry Space Science Education: Ask the Space Scientist.* Washington, D.C.: National Aeronautics and Space Administration. Accessed February 25, 2003. TIC: 253712. URL: http://image.gsfc.nasa.gov/poetry/ask/askmag.html

152952 OECD (Organisation for Economic Co-Operation and Development) 2000. *Features, Events and Processes (FEPs) for Geologic Disposal of Radioactive Waste: An International Database.* Paris, France: Organisation for Economic Co-Operation and Development. TIC: 249037.

100783 Ogard, A.E. and Kerrisk, J.F. 1984. *Groundwater Chemistry Along Flow Paths Between a Proposed Repository Site and the Accessible Environment.* LA-10188-MS. Los Alamos, New Mexico: Los Alamos National Laboratory. ACC: HQS.19880517.2031.

184800 ORD (Office of Repository Development) 2007. *Management Plan for Development of the Yucca Mountain License Application.* YMP/04-01, Rev. 05. Las Vegas, Nevada: U.S. Department of Energy, Office of Repository Development. ACC: DOC.20070731.0006.

103446 Oversby, V.M. 1987. "Spent Fuel as a Waste Form – Data Needs to Allow Long Term Performance Assessment under Repository Disposal Conditions." *Scientific Basis for Nuclear Waste Management X, Symposium held December 1-4, 1986, Boston, Massachusetts.* Bates, J.K. and Seefeldt, W.B., eds. *84,* 87-101. Pittsburgh, Pennsylvania: Materials Research Society. TIC: 203663.

156507 Paces, J.B.; Neymark, L.A.; Marshall, B.D.; Whelan, J.F.; and Peterman, Z.E. 2001. *Ages and Origins of Calcite and Opal in the Exploratory Studies Facility Tunnel, Yucca Mountain, Nevada.* Water-Resources Investigations Report 01-4049. Denver, Colorado: U.S. Geological Survey. TIC: 251284.

109148 Paces, J.B.; Whelan, J.F.; Forester, R.M.; Bradbury, J.P.; Marshall, B.D.; and Mahan, S.A. 1997. *Summary of Discharge Deposits in the Amargosa Valley.* Milestone SPC333M4. Denver, Colorado: U.S. Geological Survey. ACC: MOL.19981104.0151.

118483 Palmer, S.N. and Barton, M.E. 1987. "Porosity Reduction, Microfabric and Resultant Lithification in UK Uncemented Sands." *Geological Society Special Publication, 36,* 29-40. Oxford, United Kingdom: Blackwell Scientific Publications. TIC: 246095.

103896 Parrington, J.R.; Knox, H.D.; Breneman, S.L.; Baum, E.M.; and Feiner, F. 1996. *Nuclides and Isotopes, Chart of the Nuclides.* 15th Edition. San Jose, California: General Electric Company and KAPL, Inc. TIC: 233705.

167633 Pechala, F. 1985. "The Effect of Extraterrestrial Interactions on Change of Tropospheric Circulation in the Polar Regions of the Earth." *Studia Geophysica et Geodaetica, 29,* (4), 405-412. Prague, Czechoslovakia: Geophycial Institute of the Czechoslovak Academy of Sciences. TIC: 255609.

164034 Pelletier, M. 2001. "State of the Art on the Potential Migration of Species." Section 5.4 of *Synthesis on the Long Term Behavior of the Spent Nuclear Fuel.* Poinssot, C., ed. CEA-R-5958(E). Volume I. Paris, France: Commissariat à l'Énergie Atomique. TIC: 253976.

106488 Perry, F.V. and Crowe, B.M. 1992. "Geochemical Evidence for Waning Magmatism and Polycyclic Volcanism at Crater Flat, Nevada." *High Level Radioactive Waste Management, Proceedings of the Third International Conference, Las Vegas, Nevada, April 12-16, 1992. 2,* 2356-2365. La Grange Park, Illinois: American Nuclear Society. TIC: 204231.

144335 Perry, F.V.; Crowe, B.M.; Valentine, G.A.; and Bowker, L.M., eds. 1998. *Volcanism Studies: Final Report for the Yucca Mountain Project.* LA-13478. Los Alamos, New Mexico: Los Alamos National Laboratory. TIC: 247225.

125806 Perry, R.H.; Green, D.W.; and Maloney, J.O., eds. 1984. *Perry's Chemical Engineers' Handbook.* 6th Edition. New York, New York: McGraw-Hill. TIC: 246473.

162576 Peterman, Z.E. and Cloke, P.L. 2002. "Geochemistry of Rock Units at the Potential Repository Level, Yucca Mountain, Nevada (includes Erratum)." *Applied Geochemistry, 17,* (6, 7), 683-698, 955-958. New York, New York: Pergamon. TIC: 252516; 252517; 254046.

183863 Petit, C. J.; Hwang, M.-H.; and Lin, J.-L. 1986. "The Soret Effect in Dilute Aqueous Alkaline Earth and Nickel Chloride Solutions at 25°C." *International Journal of Thermophysics, 7,* (3), 687-697. New York, New York: Plenum Publishing. TIC: 259842.

105743 Philip, J.R.; Knight, J.H.; and Waechter, R.T. 1989. "Unsaturated Seepage and Subterranean Holes: Conspectus, and Exclusion Problem for Circular Cylindrical Cavities." *Water Resources Research, 25,* (1), 16-28. Washington, D.C.: American Geophysical Union. TIC: 239117.

162396 Piron, J.P. 2001. "Presentation of the Key Scientific Issues for the Spent Nuclear Fuel Evolution in a Closed System." Section 5.1 of *Synthesis on the Long Term Behavior of the Spent Nuclear Fuel.* Poinssot, C., ed. CEA-R-5958(E). Volume I. Paris, France: Commissariat à l'Énergie Atomique. TIC: 253976.

165318 Piron, J.P. and Pelletier, M. 2001. "State of the Art on the Helium Issues." Section 5.3 of *Synthesis on the Long Term Behavior of the Spent Nuclear Fuel.* Poinssot, C., ed. CEA-R-5958(E). Volume 1. Paris, France: Commissariat à l'Énergie Atomique. TIC: 253976.

183864 Platten, J.K. 2006. "The Soret Effect: A Review of Recent Experimental Results." *Journal of Applied Mechanics, 73,* 5-15. New York, New York: American Society of Mechanical Engineers. TIC: 259838.

184687 Plys, M.G. and Duncan, D.R. 1999. *FAI/99-14, Rev. 1, Hydrogen Combustion in an MCO During Interim Storage.* SNF-3951, Rev. 0. Richland, Washington: Duke Engineering & Services Hanford. ACC: LLR.20080115.0173.

106582 Potter, C.J.; Day, W.C.; and Sweetkind, D.S. 1996. "Structural Evolution of the Potential High-Level Nuclear Waste Repository Site at Yucca Mountain, Nevada." *Abstracts with Programs - Geological Society of America, 28,* (7), A-191. Boulder, Colorado: Geological Society of America. TIC: 233271.

106583 Potter, C.J.; Day, W.C.; Sweetkind, D.S.; and Dickerson, R.P. 1996. "Fault Styles and Strain Accommodation in the Tiva Canyon Tuff, Yucca Mountain, Nevada." *Eos, Transactions (Supplement), 77,* (17), S265. Washington, D.C.: American Geophysical Union. TIC: 234819.

167965 Press, F. and Siever, R. 1978. *Earth.* 2nd Edition. San Francisco, California: W.H. Freeman and Company. TIC: 255856.

149395 Propp, W.A. 1998. *Graphite Oxidation Thermodynamics/Reactions.* DOE/SNF/REP-018, Rev. 0. Idaho Falls, Idaho: U.S. Department of Energy. TIC: 247663.

100413 Pruess, K. 1991. *TOUGH2—A General-Purpose Numerical Simulator for Multiphase Fluid and Heat Flow.* LBL-29400. Berkeley, California: Lawrence Berkeley Laboratory. ACC: NNA.19940202.0088.

160778 Pruess, K.; Oldenburg, C.; and Moridis, G. 1999. *TOUGH2 User's Guide, Version 2.0.* LBNL-43134. Berkeley, California: Lawrence Berkeley National Laboratory. TIC: 253038.

159841 Pulvirenti, A.L.; Needham, K.M.; Adel-Hadadi, M.A.; Barkatt, A.; Marks, C.R.; and Gorman, J.A. 2002. "Corrosion of Titanium Grade 7 in Solutions Containing Fluoride and Chloride Salts." *Corrosion/2002, 57th Annual Conference & Exposition, April 7-11, 2002, Denver, Colorado.* Paper No. 02552. Houston, Texas: NACE International. TIC: 253169.

162574 Pulvirenti, A.L.; Needham, K.M.; Wong, D.S.; Adel-Hadadi, M.A.; Barkatt, A.; Marks, C.R.; and Gorman, J.A. 2003. "Fluoride Corrosion of Ti-Grade 7: Effects of Other Ions." *Corrosion/2003, 58th Annual Conference & Exposition, March 16-20, 2003, San Diego, California.* Paper No. 03686. Houston, Texas: NACE International. TIC: 254029.

161925 Quinones, J.; Grambow, B.; Loida, A.; and Geckeis, H. 1996. "Coprecipitation Phenomena During Spent Fuel Dissolution. Part 1: Experimental Procedure and Initial Results on Trivalent Ion Behaviour." *Journal of Nuclear Materials, 238,* (1), 38-43. Amsterdam, The Netherlands: Elsevier. TIC: 252663.

165482 Radulescu, H.; Moscalu, D.; and Saglam, M. 2004. *DOE SNF Phase I and II Summary Report.* TDR-DSD-MD-000001 REV 00. Las Vegas, Nevada: Bechtel SAIC Company. ACC: DOC.20040303.0005.

144599 Rai, D. and Swanson, J.L. 1981. "Properties of Plutonium(IV) Polymer of Environmental Importance." *Nuclear Technology, 54,* (1), 107-112. La Grange Park, Illinois: American Nuclear Society. TIC: 221390.

101106 Ramelli, A.R.; Oswald, J.A.; Vadurro, G.; Menges, C.M.; and Paces, J.B. 1996. "Quaternary Faulting on the Solitario Canyon Fault." Chapter 4.7 of *Seismotectonic Framework and Characterization of Faulting at Yucca Mountain, Nevada.* Whitney, J.W., ed. Milestone 3GSH100M. Denver, Colorado: U.S. Geological Survey. TIC: 237980. ACC: MOL.19970129.0041.

119693 Reamer, C.W. 1999. "Issue Resolution Status Report (Key Technical Issue: Igneous Activity, Revision 2)." Letter from C.W. Reamer (NRC) to Dr. S. Brocoum (DOE/YMSCO), July 16, 1999, with enclosure. ACC: MOL.19990810.0639.

182744 Rebak, R.B.; Etien, R.A.; Gordon, S.R.; and Ilevbare, G.O. 2006. "Influence of Black Annealing Oxide Scale on the Anodic Behavior of Alloy 22." *Corrosion 2006, 61st Annual Conference & Exposition, San Diego Convention Center, March 12-16, 2006.* Paper No. 06624. Houston, Texas: NACE International. TIC: 258178.

101084 Rechard, R.P., ed. 1995. *Methodology and Results.* Volume 2 of *Performance Assessment of the Direct Disposal in Unsaturated Tuff of Spent Nuclear Fuel and High-Level Waste Owned by U.S. Department of Energy.* SAND94-2563/2. Albuquerque, New Mexico: Sandia National Laboratories. TIC: 237102.

113577 Reed, D.T. and Bowers, D.L. 1990. "Alpha Particle-Induced Formation Of Nitrate in the Cm-Sulfate Aqueous System." *Radiochimica Acta, 51,* 119-125. München, Germany: R. Oldenbourg Verlag. TIC: 245894.

104303 Reeves, C.C. 1976. *Caliche: Origin, Classification, Morphology and Uses.* Lubbock, Texas: Estacado Books. TIC: 245928.

149433 Reilly, M.A. 1998. *Spent Nuclear Fuel Project Technical Databook.* HNF-SD-SNF-TI-015, Rev. 5. Richland, Washington: Fluor Daniel Hanford. TIC: 247814.

144604 Reimus, P.W. 1995. *Transport of Synthetic Colloids Through Single Saturated Fractures: A Literature Review.* LA-12707-MS. Los Alamos, New Mexico: Los Alamos National Laboratory. ACC: MOL.19950302.0063.

179246 Reimus, P.W.; Callahan, T.J.; Ware, S.D.; Haga, M.J.; and Counce, D.A. 2007. "Matrix Diffusion Coefficients in Volcanic Rocks at the Nevada Test Site: Influence of Matrix Porosity, Matrix Permeability, and Fracture Coating Minerals." *Journal of Contaminant Hydrology, 93,* 85-95. New York, New York: Elsevier. TIC: 259673.

163008 Reimus, P.W.; Ware, S.D.; Benedict, F.C.; Warren, R.G.; Humphrey, A.; Adams, A.; Wilson, B.; and Gonzales, D. 2002. *Diffusive and Advective Transport of ^{3}H, ^{14}C, and ^{99}Tc in Saturated, Fractured Volcanic Rocks from Pahute Mesa, Nevada.* LA-13891-MS. Los Alamos, New Mexico: Los Alamos National Laboratory. TIC: 253905.

167870 Retallack, G.J. 1991. "Untangling the Effects of Burial Alteration and Ancient Soil Formation." *Annual Review of Earth and Planetary Sciences, 19*, 183-206. Palo Alto, California: Annual Reviews. TIC: 255912.

159370 Revie, R.W., ed. 2000. *Uhlig's Corrosion Handbook.* 2nd Edition. New York, New York: John Wiley & Sons. TIC: 248360.

107109 Robie, R.A.; Hemingway, B.S.; and Fisher, J.R. 1979. *Thermodynamic Properties of Minerals and Related Substances at 298.15 K and 1 Bar (10^5 Pascals) Pressure and at Higher Temperatures.* U.S. Geological Survey Bulletin 1452. Washington, D.C.: U.S. Government Printing Office. ACC: NNA.19900702.0002.

160674 Roe, L.K. 2002. "Summary of RDA Investigation ID: 4/10/02 Fish Farming in Amargosa Valley." Interoffice memorandum from L.K. Roe (BSC) to File, November 5, 2002, 1105024986, with an attachment. ACC: MOL.20021107.0091; MOL.20020821.0002.

184108 Rogers, J.W., Jr.; Erickson, K.L.; Belton, D.N.; Springer, R.W.; Taylor, T.N.; and Beery, J.G. 1988. "Low Temperature Diffusion of Oxygen in Titanium and Titanium Oxide Films." *Applied Surface Science, 35,* 137-152. Amsterdam, The Netherlands: North-Holland. TIC: 259889.

100417 Rothman, A.J. 1984. *Potential Corrosion and Degradation Mechanisms of Zircaloy Cladding on Spent Nuclear Fuel in a Tuff Repository.* UCID-20172. Livermore, California: Lawrence Livermore National Laboratory. ACC: NNA.19870903.0039.

102097 Rousseau, J.P.; Kwicklis, E.M.; and Gillies, D.C., eds. 1999. *Hydrogeology of the Unsaturated Zone, North Ramp Area of the Exploratory Studies Facility, Yucca Mountain, Nevada.* Water-Resources Investigations Report 98-4050. Denver, Colorado: U.S. Geological Survey. ACC: MOL.19990419.0335.

100178 Rousseau, J.P.; Loskot, C.L.; Thamir, F.; and Lu, N. 1997. *Results of Borehole Monitoring in the Unsaturated Zone Within the Main Drift Area of the Exploratory Studies Facility, Yucca Mountain, Nevada.* Milestone SPH22M3. Denver, Colorado: U.S. Geological Survey. ACC: MOL.19970626.0351.

167875 Ruderman, M.A. 1974. "Possible Consequences of Nearby Supernova Explosions for Atmospheric Ozone and Terrestrial Life." *Science, 184,* 1079-1081. Washington, D.C.: American Association for the Advancement of Science. TIC: 255914.

183044 Rutqvist, J. 2006. YMP-LBNL-JR-3, UZ AMRs for SR - Thermal-Hydrological-Mechanical Effects [final closure]. Scientific Notebook SN-LBNL-SCI-204-V3. TOC, Pages 1-53. ACC: MOL.20060621.0162.

167869 Salem, A.M.K.; Abdel-Wahab, A.; and McBride, E.F. 1998. "Diagenesis of Shallowly Buried Cratonic Sandstones, Southwest Sinai, Egypt." *Sedimentary Geology, 119,* (3-4), 311-335. New York, New York: Elsevier. TIC: 255708.

139333 SAM (Safety Assessment Management) 1997. Safety Assessment of Radioactive Waste Repositories, An International Database of Features, Events and Processes. Unpublished Draft, June 24, 1997. ACC: MOL.19991214.0522.

174054 Sargent G. and Conrad H. 1969. "Stress Relaxation and Thermally Activated Deformation in Titanium." *Scripta Metallurgica, 3,* (1), 43-50. New York, New York: Pergamon Press. TIC: 257403.

109161 Sarna-Wojcicki, A.M.; Meyer, C.M.; and Wan, E. 1997. "Age and Correlation of Tephra Layers, Position of the Matuyama-Brunhes Chron Boundary, and Effects of Bishop Ash Eruption on Owens Lake, as Determined from Drill Hole OL-92, Southeast California." Chapter 7 of *An 800,000-Year Paleoclimatic Record from Core OL-92, Owens Lake, Southeast California.* Smith, G.I. and Bischoff, J.L., eds. Special Paper 317. Boulder, Colorado: Geological Society of America. TIC: 236857.

100644 Sass, J.H.; Lachenbruch, A.H.; Dudley, W.W., Jr.; Priest, S.S.; and Munroe, R.J. 1988. *Temperature, Thermal Conductivity, and Heat Flow Near Yucca Mountain, Nevada: Some Tectonic and Hydrologic Implications.* Open-File Report 87-649. Denver, Colorado: U.S. Geological Survey. TIC: 203195.

118952 Savage, J.C.; Svarc, J.L.; and Prescott, W.H. 1999. "Strain Accumulation at Yucca Mountain, Nevada, 1983-1998." *Journal of Geophysical Research, 104,* (B8), 17627-17631. Washington, D.C.: American Geophysical Union. TIC: 245645.

183366 Savage, J.C.; Svarc, J.L.; and Prescott, W.H. 2001. "Strain Accumulation Near Yucca Mountain, Nevada, 1993-1998." *Journal of Geophysical Research, 106,* (B8), 16483-16488. Washington, D.C.: American Geophysical Union. TIC: 256881.

102213 Savard, C.S. 1998. *Estimated Ground-Water Recharge from Streamflow in Fortymile Wash Near Yucca Mountain, Nevada.* Water-Resources Investigations Report 97-4273. Denver, Colorado: U.S. Geological Survey. TIC: 236848.

100075 Sawyer, D.A.; Fleck, R.J.; Lanphere, M.A.; Warren, R.G.; Broxton, D.E.; and Hudson, M.R. 1994. "Episodic Caldera Volcanism in the Miocene Southwestern Nevada Volcanic Field: Revised Stratigraphic Framework, $^{40}Ar/^{39}Ar$ Geochronology, and Implications for Magmatism and Extension." *Geological Society of America Bulletin, 106,* (10), 1304-1318. Boulder, Colorado: Geological Society of America. TIC: 222523.

159406 Schulz, W.W. 1972. *Shear-Leach Processing of N-Reactor Fuel--Cladding Fires.* ARH-2351. Richland, Washington: Atlantic Richfield Hanford. TIC: 243079.

144302 Schutz, R.W. and Thomas, D.E. 1987. "Corrosion of Titanium and Titanium Alloys." In *Corrosion,* Volume 13, Pages 669-706 of *Metals Handbook.* 9th Edition. Metals Park, Ohio: ASM International. TIC: 209807.

177257 Schutz, R.W.; Porter, R.L.; and Horrigan, J.M. 2000. "Qualifications of Ti-6%Al-4%V-Ru Alloy Production Tubulars for Aggressive Fluoride-Containing Mobile Bay Well Service." *Corrosion, 56,* (11), 1170-1179. Houston, Texas: NACE International. TIC: 258489.

106751 Scott, R.B. 1990. "Tectonic Setting of Yucca Mountain, Southwest Nevada." Chapter 12 of *Basin and Range Extensional Tectonics Near the Latitude of Las Vegas, Nevada.* Wernicke, B.P., ed. Memoir 176. Boulder, Colorado: Geological Society of America. TIC: 222540.

104181 Scott, R.B. and Bonk, J. 1984. *Preliminary Geologic Map of Yucca Mountain, Nye County, Nevada, with Geologic Sections.* Open-File Report 84-494. Denver, Colorado: U.S. Geological Survey. ACC: HQS.19880517.1443.

184742 Sexton, R.A. 2007. *Particulate and Water in Multi-Canister Overpacks (OCRWM).* KBC-33403, Rev. 0. Richland, Washington: Fluor Hanford. ACC: LLR.20080116.0003.

161591 Sharpe, S. 2003. *Future Climate Analysis—10,000 Years to 1,000,000 Years After Present.* MOD-01-001 REV 01. Reno, Nevada: Desert Research Institute. ACC: MOL.20030407.0055.

127299 Shleien, B., ed. 1992. *The Health Physics and Radiological Health Handbook.* Revised Edition. Silver Spring, Maryland: Scinta. TIC: 9360.

135308 Shoemaker, E.M. 1983. "Asteroid and Comet Bombardment of the Earth." *Annual Review of Earth and Planetary Sciences, 11,* 461-494. Palo Alto, California: Annual Reviews. TIC: 246922.

162405 Shoesmith, D.W. 2000. "Fuel Corrosion Processes under Waste Disposal Conditions." *Journal of Nuclear Materials, 282,* (1), 1-31. Amsterdam, The Netherlands: North-Holland. TIC: 254043.

151179 Shoesmith, D.W. and Ikeda, B.M. 1997. *The Resistance of Titanium to Pitting, Microbially Induced Corrosion and Corrosion in Unsaturated Conditions.* AECL-11709. Pinawa, Manitoba, Canada: Whiteshell Laboratories. TIC: 236226.

112178 Shoesmith, D.W. and King, F. 1998. *The Effects of Gamma Radiation on the Corrosion of Candidate Materials for the Fabrication of Nuclear Waste Packages.* AECL-11999. Pinawa, Manitoba, Canada: Atomic Energy of Canada Limited. ACC: MOL.19990311.0212.

183944 Siegel, M.D.; Lambert, S.J.; and Robinson, K.L., eds. 1991. *Hydrogeochemical Studies of the Rustler Formation and Related Rocks in the Waste Isolation Pilot Plant Area, Southeastern New Mexico.* SAND88-0196. Albuquerque, New Mexico: Sandia National Laboratories. ACC: LLR.20080215.0248.

183688 Siriwardane, R.V. and Wightman, J.P. 1983. "Interaction of Hydrogen Chloride and Water with Oxide Surfaces. III. Titanium Dioxide." *Journal of Colloid and Interface Science, 94,* (2), 502-513. New York, New York: Academic Press. TIC: 259837.

106815 Slemmons, D.B. and dePolo, C.M. 1986. "Evaluation of Active Faulting and Associated Hazards." Chapter 3 of *Active Tectonics.* Studies in Geophysics. Washington, D.C.: National Academy Press. TIC: 209251.

159774 Smailos, E. and Köster, R. 1987. "Corrosion Studies on Selected Packaging Materials for Disposal of High Level Wastes." *Materials Reliability in the Back End of the Nuclear Fuel Cycle, Proceedings of a Technical Committee Meeting, Vienna, 2-5 September 1986. IAEA TECHDOC-421,* 7-24. Vienna, Austria: International Atomic Energy Agency. TIC: 252877.

154820 Smailos, E.; Schwarzkopf, W.; Köster, R.; Fiehn, B.; and Halm, G. 1990. *Corrosion Testing of Selected Packaging Materials for Disposal of High-Level Waste Glass in Rock Salt Formations.* KfK 4723. Karlsruhe, Germany: Kernforschungszentrum Karlsruhe GmbH. TIC: 215124.

183392 Smith, R.E. and Loo, H.H. 2007. *DOE SNF Material Interaction Potentials during an Intrusive Igneous Event at Yucca Mountain.* DOE/SNF/REP-108, Rev. 0. Idaho Falls, Idaho: U.S. Department of Energy, Idaho Operations Office. ACC: CCU.20070906.0009.

118967 Smith, R.P.; Jackson, S.M.; and Hackett, W.R. 1998. "Magma Intrusion and Seismic-Hazards Assessment in the Basin and Range Province." *Proceedings Volume, Basin and Range Province (BRP) Seismic-Hazards Summit, Reno, Nevada, May 13-15, 1997.* Miscellaneous Publication 98-2. Pages 155-166. Salt Lake City, Utah: Utah Geological Survey. TIC: 246749.

174060 Smyth, J.R. and Caporuscio, F.A. 1981. *Review of the Thermal Stability and Cation Exchange Properties of the Zeolite Minerals Clinoptilolite, Mordenite, and Analcime: Applications to Radioactive Waste Isolation in Silicic Tuff.* LA-8841-MS. Los Alamos, New Mexico: Los Alamos Scientific Laboratory. ACC: HQS.19880517.2065.

163645 SNL (Sandia National Laboratories) 1996. *Hydraulic Fracturing Stress Measurements in Test Hole ESF-AOD-HDFR#1, Thermal Test Facility, Exploratory Studies Facility at Yucca Mountain.* WA-0065. Albuquerque, New Mexico: Sandia National Laboratories. ACC: MOL.19970717.0008.

181244 SNL 2007. *Abstraction of Drift Seepage.* MDL-NBS-HS-000019 REV 01 ADD 01. Las Vegas, Nevada: Sandia National Laboratories. ACC: DOC.20070807.0001.

181267 SNL 2007. *Analysis of Dust Deliquescence for FEP Screening.* ANL-EBS-MD-000074 REV 01 AD 01. Las Vegas, Nevada: Sandia National Laboratories. ACC: DOC.20070911.0004; DOC.20070824.0001; DOC.20080109.0005.

178765 SNL 2007. *Analysis of Mechanisms for Early Waste Package/Drip Shield Failure.* ANL-EBS-MD-000076 REV 00. Las Vegas, Nevada: Sandia National Laboratories. ACC: DOC.20070629.0002; DOC.20071003.0015.

177431 SNL 2007. *Atmospheric Dispersal and Deposition of Tephra from a Potential Volcanic Eruption at Yucca Mountain, Nevada.* MDL-MGR-GS-000002 REV 03. Las Vegas, Nevada: Sandia National Laboratories. ACC: DOC.20071010.0003.

177399 SNL 2007. *Biosphere Model Report.* MDL-MGR-MD-000001 REV 02. Las Vegas, Nevada: Sandia National Laboratories. ACC: DOC.20070830.0007.

179545 SNL 2007. *Calibrated Unsaturated Zone Properties.* ANL-NBS-HS-000058 REV 00. Las Vegas, Nevada: Sandia National Laboratories. ACC: DOC.20070530.0013.

174260 SNL 2007. *Characterize Eruptive Processes at Yucca Mountain, Nevada.* ANL-MGR-GS-000002 REV 03. Las Vegas, Nevada: Sandia National Laboratories. ACC: DOC.20070301.0001.

180616 SNL 2007. *Cladding Degradation Summary for LA.* ANL-WIS-MD-000021 REV 03 ADD 01. Las Vegas, Nevada: Sandia National Laboratories. ACC: DOC.20050815.0002; DOC.20070614.0002.

181373 SNL 2007. *Commercial Spent Nuclear Fuel Igneous Scenario Criticality Evaluation.* ANL-EBS-NU-000009 REV 00. Las Vegas, Nevada: Sandia National Laboratories. ACC: DOC.20070711.0003.

177430 SNL 2007. *Dike/Drift Interactions.* MDL-MGR-GS-000005 REV 02. Las Vegas, Nevada: Sandia National Laboratories. ACC: DOC.20071009.0015.

177418 SNL 2007. *Dissolved Concentration Limits of Elements with Radioactive Isotopes.* ANL-WIS-MD-000010 REV 06. Las Vegas, Nevada: Sandia National Laboratory. ACC: DOC.20070918.0010.

177404 SNL 2007. *Drift-Scale THC Seepage Model.* MDL-NBS-HS-000001 REV 05. Las Vegas, Nevada: Sandia National Laboratories. ACC: DOC.20071010.0004.

177407 SNL 2007. *EBS Radionuclide Transport Abstraction.* ANL-WIS-PA-000001 REV 03. Las Vegas, Nevada: Sandia National Laboratories. ACC: DOC.20071004.0001.

177412 SNL 2007. *Engineered Barrier System: Physical and Chemical Environment.* ANL-EBS-MD-000033 REV 06. Las Vegas, Nevada: Sandia National Laboratories. ACC: DOC.20070907.0003.

180778 SNL 2007. *General Corrosion and Localized Corrosion of the Drip Shield.* ANL-EBS-MD-000004 REV 02 ADD 01. Las Vegas, Nevada: Sandia National Laboratories. ACC: DOC.20060427.0002; DOC.20070807.0004; DOC.20071003.0019.

178519 SNL 2007. *General Corrosion and Localized Corrosion of Waste Package Outer Barrier.* ANL-EBS-MD-000003 REV 03. Las Vegas, Nevada: Sandia National Laboratories. ACC: DOC.20070730.0003; DOC.20070807.0007.

181395 SNL 2007. *Geochemistry Model Validation Report: External Accumulation Model.* ANL-EBS-GS-000002 REV 01 AD 01. Las Vegas, Nevada: Sandia National Laboratories. ACC: DOC.20071106.0015.

181165 SNL 2007. *Geochemistry Model Validation Report: Material Degradation and Release Model.* ANL-EBS-GS-000001 REV 02. Las Vegas, Nevada: Sandia National Laboratories. ACC: DOC.20070928.0010.

181339 SNL 2007. *Hydrogen-Induced Cracking of the Drip Shield.* ANL-EBS-MD-000006 REV 02 ADD 01. Las Vegas, Nevada: Sandia National Laboratories. ACC: DOC.20060306.0007; DOC.20070807.0005.

174109 SNL 2007. *Hydrogeologic Framework Model for the Saturated Zone Site-Scale Flow and Transport Model.* MDL-NBS-HS-000024 REV 01. Las Vegas, Nevada: Sandia National Laboratories. ACC: DOC.20070411.0003.

181648 SNL 2007. *In-Drift Natural Convection and Condensation.* MDL-EBS-MD-000001 REV 00 AD 01. Las Vegas, Nevada: Sandia National Laboratories. ACC: DOC.20050330.0001; DOC.20051122.0005; DOC.20070907.0004.

177411 SNL 2007. *In-Drift Precipitates/Salts Model.* ANL-EBS-MD-000045 REV 03. Las Vegas, Nevada: Sandia National Laboratories. ACC: DOC.20070306.0037.

180506 SNL 2007. *In-Package Chemistry Abstraction.* ANL-EBS-MD-000037 REV 04 ADD 01. Las Vegas, Nevada: Sandia National Laboratories. ACC: DOC.20070816.0004.

180472 SNL 2007. *Initial Radionuclide Inventories.* ANL-WIS-MD-000020 REV 01 ADD 01. Las Vegas, Nevada: Sandia National Laboratories. ACC: DOC.20050927.0005; DOC.20070801.0001.

182130 SNL 2007. *Irrigation Recycling Model.* MDL-MGR-HS-000001 REV 00. Las Vegas, Nevada: Sandia National Laboratories. ACC: DOC.20071105.0005; DOC.20080117.0001.

178851 SNL 2007. *Mechanical Assessment of Degraded Waste Packages and Drip Shields Subject to Vibratory Ground Motion.* MDL-WIS-AC-000001 REV 00. Las Vegas, Nevada: Sandia National Laboratories. ACC: DOC.20070917.0006.

177432 SNL 2007. *Number of Waste Packages Hit by Igneous Events.* ANL-MGR-GS-000003 REV 03. Las Vegas, Nevada: Sandia National Laboratories. ACC: DOC.20071002.0001.

177424 SNL 2007. *Radionuclide Screening.* ANL-WIS-MD-000006 REV 02. Las Vegas, Nevada: Sandia National Laboratories. ACC: DOC.20070326.0003.

177396 SNL 2007. *Radionuclide Transport Models Under Ambient Conditions.* MDL-NBS-HS-000008 REV 02 ADD 01. Las Vegas, Nevada: Sandia National Laboratories. ACC: DOC.20050823.0003; DOC.20070718.0003.

179347 SNL 2007. *Redistribution of Tephra and Waste by Geomorphic Processes Following a Potential Volcanic Eruption at Yucca Mountain, Nevada.* MDL-MGR-GS-000006 REV 00. Las Vegas, Nevada: Sandia National Laboratories. ACC: DOC.20071220.0004.

177394 SNL 2007. *Saturated Zone In-Situ Testing.* ANL-NBS-HS-000039 REV 02. Las Vegas, Nevada: Sandia National Laboratories. ACC: DOC.20070608.0004.

177391 SNL 2007. *Saturated Zone Site-Scale Flow Model.* MDL-NBS-HS-000011 REV 03. Las Vegas, Nevada: Sandia National Laboratories. ACC: DOC.20070626.0004; DOC.20071001.0013.

176828 SNL 2007. *Seismic Consequence Abstraction.* MDL-WIS-PA-000003 REV 03. Las Vegas, Nevada: Sandia National Laboratories. ACC: DOC.20070928.0011.

179993 SNL 2007. *Soil-Related Input Parameters for the Biosphere Model.* ANL-NBS-MD-000009 REV 03 AD 01. Las Vegas, Nevada: Sandia National Laboratories. ACC: DOC.20070927.0004.

181953 SNL 2007. *Stress Corrosion Cracking of Waste Package Outer Barrier and Drip Shield Materials.* ANL-EBS-MD-000005 REV 04. Las Vegas, Nevada: Sandia National Laboratories. ACC: DOC.20070913.0001.

184327 SNL 2007. *Technical Work Plan for the Performance Assessment Features, Events, and Processes.* TWP-MGR-MD-000036 REV 03. Las Vegas, Nevada: Sandia National Laboratories. ACC: DOC.20071207.0001.

177413 SNL 2007. *THC Sensitivity Study of Heterogeneous Permeability and Capillarity Effects.* ANL-NBS-HS-000047 REV 01. Las Vegas, Nevada: Sandia National Laboratories. ACC: DOC.20070807.0006; DOC.20080129.0001.

179196 SNL 2007. *Thermal Management Flexibility Analysis.* ANL-EBS-MD-000075 REV 01. Las Vegas, Nevada: Sandia National Laboratories. ACC: DOC.20070207.0001.

179567 SNL 2007. *Total System Performance Assessment Data Input Package for Requirements Analysis for DOE SNF/HLW and Naval SNF Waste Package Physical Attributes Basis for Performance Assessment.* TDR-TDIP-ES-000009 REV 00. Las Vegas, Nevada: Sandia National Laboratories. ACC: DOC.20070921.0009.

179354 SNL 2007. *Total System Performance Assessment Data Input Package for Requirements Analysis for Engineered Barrier System In-Drift Configuration.* TDR-TDIP-ES-000010 REV 00. Las Vegas, Nevada: Sandia National Laboratories. ACC: DOC.20070921.0008.

179466 SNL 2007. *Total System Performance Assessment Data Input Package for Requirements Analysis for Subsurface Facilities.* TDR-TDIP-PA-000001 REV 00. Las Vegas, Nevada: Sandia National Laboratories. ACC: DOC.20070921.0007.

179394 SNL 2007. *Total System Performance Assessment Data Input Package for Requirements Analysis for Transportation Aging and Disposal Canister and Related Waste Package Physical Attributes Basis for Performance Assessment.* TDR-TDIP-ES-000006 REV 00. Las Vegas, Nevada: Sandia National Laboratories. ACC: DOC.20070918.0005.

182846 SNL 2007. *TSPA Information Package for the Draft Supplemental Environmental Impact Statement.* TDR-WIS-PA-000014 REV 00. Las Vegas, Nevada: Sandia National Laboratories. ACC: LLR.20071004.0002.

184614 SNL 2007. *UZ Flow Models and Submodels.* MDL-NBS-HS-000006 REV 03 AD 01. Las Vegas, Nevada: Sandia National Laboratories. ACC: DOC.20080108.0003; DOC.20080114.0001.

177423 SNL 2007. *Waste Form and In-Drift Colloids-Associated Radionuclide Concentrations: Abstraction and Summary.* MDL-EBS-PA-000004 REV 03. Las Vegas, Nevada: Sandia National Laboratories. ACC: DOC.20071018.0019.

182788 SNL 2008. *CSNF Loading Curve Sensitivity Analysis.* ANL-EBS-NU-000010 REV 00. Las Vegas, Nevada: Sandia National Laboratories. ACC: DOC.20080211.0001.

179476 SNL 2008. *Features, Events, and Processes for the Total System Performance Assessment: Methods.* ANL-WIS-MD-000026 REV 00. Las Vegas, Nevada: Sandia National Laboratories. ACC: DOC.20080211.0010.

184433 SNL 2008. *Multiscale Thermohydrologic Model.* ANL-EBS-MD-000049 REV 03 AD 02. Las Vegas, Nevada: Sandia National Laboratories. ACC: DOC.20080201.0003.

184748 SNL 2008. *Particle Tracking Model and Abstraction of Transport Processes.* MDL-NBS-HS-000020 REV 02 AD 02. Las Vegas, Nevada: Sandia National Laboratories. ACC: DOC.20080129.0008.

179962 SNL 2008. *Postclosure Analysis of the Range of Design Thermal Loadings.* ANL-NBS-HS-000057 REV 00. Las Vegas, Nevada: Sandia National Laboratories. ACC: DOC.20080121.0002.

183750 SNL 2008. *Saturated Zone Flow and Transport Model Abstraction.* MDL-NBS-HS-000021 REV 03 AD 02. Las Vegas, Nevada: Sandia National Laboratories. ACC: DOC.20080107.0006.

173869 SNL 2008. *Screening Analysis of Criticality Features, Events, and Processes for License Application.* ANL-DS0-NU-000001 REV 00. Las Vegas, Nevada: Sandia National Laboratories. ACC: DOC.20080208.0001.

182145 SNL 2008. *Simulation of Net Infiltration for Present-Day and Potential Future Climates.* MDL-NBS-HS-000023 REV 01 AD 01. Las Vegas, Nevada: Sandia National Laboratories. ACC: DOC.20080201.0002.

184806 SNL 2008. *Site-Scale Saturated Zone Transport.* MDL-NBS-HS-000010 REV 03 AD 01. Las Vegas, Nevada: Sandia National Laboratories. ACC: DOC.20080121.0003.

178871 SNL 2008. *Total System Performance Assessment Model/Analysis for the License Application.* MDL-WIS-PA-000005 REV 00. Las Vegas, Nevada: Sandia National Laboratories. ACC: DOC.20080204.0003.

183478 SNL 2008. *Total System Performance Assessment Model/Analysis for the License Application.* MDL-WIS-PA-000005 REV 00 AD 01. Las Vegas, Nevada: Sandia National Laboratories.

184078 SNL 2008. *Waste Package Flooding Probability Evaluation.* CAL-DN0-NU-000002 REV 00C. Las Vegas, Nevada: Sandia National Laboratories. ACC: DOC.20080222.0002.

183867 Snowdon, P.N. and Turner, J.C.R. 1960. "The Soret Effect in Some 0·01 Normal Aqueous Electrolytes." *Transactions of the Faraday Society, 56,* 1409-1418. Aberdeen, England: Aberdeen University Press, Faraday Society. TIC: 259841.

101296 Sonnenthal, E.L.; DePaolo, D.J.; and Bodvarsson, G.S. 1997. "Modeling the Strontium Geochemistry and Isotopic Ratio in the Unsaturated Zone." Chapter 17 of *The Site-Scale Unsaturated Zone Model of Yucca Mountain, Nevada, for the Viability Assessment.* Bodvarsson, G.S.; Bandurraga, T.M.; and Wu, Y.S., eds. LBNL-40376. Berkeley, California: Lawrence Berkeley National Laboratory. ACC: MOL.19971014.0232.

100927 Southwell, C.R.; Bultman, J.D.; and Alexander, A.L. 1976. "Corrosion of Metals in Tropical Environments - Final Report of 16-Year Exposures." *Materials Performance, 15,* (7), 9-25. Houston, Texas: National Association of Corrosion Engineers. TIC: 224022.

101623 Spaulding, W.G. 1983. *Vegetation and Climates of the Last 45,000 Years in the Vicinity of the Nevada Test Site, South-Central Nevada.* Open-File Report 83-535. Denver, Colorado: U.S. Geological Survey. ACC: NNA.19890523.0110.

184215 Steele, A.; Goddard, D.T.; Stapleton, D.; Toporski, J.K.W.; Peters, V.; Bassinger, V.; Sharples, G.; Wynn-Williams, D.D.; and McKay, D.S. 2000. "Investigations into an Unknown Organism on the Martian Meteorite Allan Hills 84001." *Meteoritics & Planetary Science,* (35), 237-241. Tucson, Arizona: Meteoritical Society. TIC: 259920.

166303 Štefanic I. and LaVerne, J.A. 2002. "Temperature Dependence of the Hydrogen Peroxide Production in the y-Radiolysis of Water." *Journal of Physical Chemistry, 106,* (2), 447-452. Washington, D.C.: American Chemical Society. TIC: 255323.

101022 Stock, J.M. and Healy, J.H. 1988. "Stress Field at Yucca Mountain, Nevada." Chapter 6 of *Geologic and Hydrologic Investigations of a Potential Nuclear Waste Disposal Site at Yucca Mountain, Southern Nevada.* Carr, M.D. and Yount, J.C., eds. Bulletin 1790. Denver, Colorado: U.S. Geological Survey. TIC: 203085.

101027 Stock, J.M.; Healy, J.H.; Hickman, S.H.; and Zoback, M.D. 1985. "Hydraulic Fracturing Stress Measurements at Yucca Mountain, Nevada, and Relationship to the Regional Stress Field." *Journal of Geophysical Research, 90,* (B10), 8691-8706. Washington, D.C.: American Geophysical Union. TIC: 219009.

165862 Stonestrom, D.A.; Prudic, D.E.; Laczniak, R.J.; Akstin, K.C.; Boyd, R.A.; and Henkelman, K.K. 2003. *Estimates of Deep Percolation Beneath Native Vegetation, Irrigated Fields, and the Amargosa-River Channel, Amargosa Desert, Nye County, Nevada.* Open-File Report 03-104. Denver, Colorado: U.S. Geological Survey. TIC: 255088.

119051 Stuckless, J.S. 1996. "Current Status of Paleohydrologic Studies at Yucca Mountain and Vicinity, Nevada." *High Level Radioactive Waste Management, Proceedings of the Seventh Annual International Conference, Las Vegas, Nevada, April 29-May 3, 1996.* Pages 98-101. La Grange Park, Illinois: American Nuclear Society. TIC: 226494.

181507 Stuckless, J.S. and Levich, R.A., eds. 2007. *The Geology and Climatology of Yucca Mountain and Vicinity, Southern Nevada and California.* Memoir 199. Boulder, Colorado: Geological Society of America. TIC: 259378.

125332 Stumm, W. and Morgan, J.J. 1996. *Aquatic Chemistry, Chemical Equilibria and Rates in Natural Waters.* 3rd Edition. New York, New York: John Wiley & Sons. TIC: 246296.

100489 Suzuki, T. 1983. "A Theoretical Model for Dispersion of Tephra." *Arc Volcanism: Physics and Tectonics, Proceedings of a 1981 IAVCEI Symposium, August-September, 1981, Tokyo and Hakone.* Shimozuru, D. and Yokoyama, I., eds. Pages 95-113. Tokyo, Japan: Terra Scientific Publishing Company. TIC: 238307.

177047 Sweetkind, D.S.; Barr, D.L.; Polacsek, D.K.; and Anna, L.O. 1997. *Administrative Report: Integrated Fracture Data in Support of Process Models, Yucca Mountain, Nevada.* Milestone SPG32M3. Denver, Colorado: U.S. Geological Survey. ACC: MOL.19990825.0109.

106957 Sweetkind, D.S.; Potter, C.J.; and Verbeek, E.R. 1996. "Interaction Between Faults and the Fracture Network at Yucca Mountain, Nevada." *Eos Transactions,* S266. Washington, D.C.: American Geophysical Union. TIC: 236789.

106963 Szymanski, J.S. 1989. *Conceptual Considerations of the Yucca Mountain Groundwater System with Special Emphasis on the Adequacy of This System to Accommodate a High-Level Nuclear Waste Repository.* Three volumes. Las Vegas, Nevada: U.S. Department of Energy, Nevada Operations Office. ACC: NNA.19890831.0152.

167756 Tada, H.; Paris, P.C.; and Irwin, G.R. 2000. *The Stress Analysis of Cracks Handbook.* 3rd Edition. New York, New York: American Society of Mechanical Engineers. TIC: 255547.

102864 Taylor, E.M. 1986. *Impact of Time and Climate on Quaternary Soils in the Yucca Mountain Area of the Nevada Test Site.* Master's thesis. Boulder, Colorado: University of Colorado. TIC: 218287.

120498 Thomas, J.G.N. 1994. "The Mechanism of Corrosion Prevention by Inhibitors." In *Corrosion Control,* 3rd Edition. Volume 2, Chapter 17.3 of *Corrosion.* Reprinted 1998. Sheir, L.L.; Jarman, R.A.; and Burstein, G.T., eds. Woburn, Massachusetts: Butterworth-Heinemann. TIC: 244694.

184214 Thomas-Keprta, K.L.; McKay, D.S.; Wentworth, S.J.; Stevens, T.O.; Taunton, A.E.; Allen, C.C.; Coleman, A.; Gibson, E.K., Jr.; and Romanek, C.S. 1998. "Bacterial Mineralization Patterns in Basaltic Aquifers: Implications for Possible Life in Martian Meteorite ALH84001." *Geology, 26,* (11), 1031-1034. Boulder, Colorado: Geological Society of America. TIC: 259919.

109470 Thompson, R.S.; Anderson, K.H.; and Bartlein, P.J. 1999. *Quantitative Paleoclimatic Reconstructions from Late Pleistocene Plant Macrofossils of the Yucca Mountain Region.* Open-File Report 99-338. Denver, Colorado: U.S. Geological Survey. ACC: MOL.19991015.0296.

183866 Thornton, E.C. and Seyfried, W.E., Jr. 1983. "Thermodiffusional Transport in Pelagic Clay: Implications for Nuclear Waste Disposal in Geological Media." *Science, 220,* (4602), 1156-1158. Washington, D.C.: American Association for the Advancement of Science. TIC: 259840.

107735 Todreas, N.E. and Kazimi, M.S. 1990. *Nuclear Systems I, Thermal Hydraulic Fundamentals.* New York, New York: Hemisphere Publishing. TIC: 226511.

182745 Torres, S.G.; El-Dasher, B.; McGregor, M.; Etien, R.; Edgecumbe, T.S.; Gdowski, G.; Yang, N.; Headley, T.; Chames, J.; Yio, J.L.; and Gardea, A. 2006. *Aging and Phase Stability of Alloy 22 Welds.* UCRL-TR-217339. Livermore, California: Lawrence Livermore National Laboratory. ACC: LLR.20070829.0001.

168394 Toth, L.M.; Friedman, H.A.; and Osborne, M.M. 1983. "Aspects of Plutonium(IV) Hydrous Polymer Chemistry." Chapter 15 of *Plutonium Chemistry.* Carnall, W.T. and Choppin, G.R., eds. ACS Symposium Series 216. Washington, D.C.: American Chemical Society. TIC: 219103.

100422 Triay, I.R.; Meijer, A.; Conca, J.L.; Kung, K.S.; Rundberg, R.S.; Strietelmeier, B.A.; and Tait, C.D. 1997. *Summary and Synthesis Report on Radionuclide Retardation for the Yucca Mountain Site Characterization Project.* Eckhardt, R.C., ed. LA-13262-MS. Los Alamos, New Mexico: Los Alamos National Laboratory. ACC: MOL.19971210.0177.

172018 Tsang, Y.W. and Pruess, K. 1990. *Further Modeling Studies of Gas Movement and Moisture Migration at Yucca Mountain, Nevada.* LBL-29127. Berkeley, California: Lawrence Berkeley Laboratory. ACC: NNA.19910405.0037.

184794 Tsang, Y.W. and Pruess, K. [n.d.]. *Preliminary Studies of Gas Phase Flow Effects and Moisture Migration at Yucca Mountain, Nevada.* Berkeley, California: Lawrence Berkeley Laboratory. ACC: MOL.20060814.0385.

159566 United Nations 1988. *Sources, Effects and Risks of Ionizing Radiation, 1988 Report to the General Assembly, with Annexes.* New York, New York: United Nations. TIC: 209701.

160548 USDA (U.S. Department of Agriculture) 2000. *Summary Report, 1997 National Resources Inventory (Revised December 2000).* Washington, D.C.: U.S. Department of Agriculture. TIC: 253006.

183277 USGS (U.S.Geological Survey) 2000. *Ground Water in Hawaii.* FS 126-00. Honolulu, Hawaii: U.S.Geological Survey. ACC: LLR.20071004.0011.

177282 Valentine, G.A. and Krogh, K.E.C. 2006. "Emplacement of Shallow Dikes and Sills Beneath a Small Basaltic Volcanic Center - The Role of Pre-Existing Structure (Paiute Ridge, Southern Nevada, USA)." *Earth and Planetary Science Letters, 246,* 217-230. New York, New York: Elsevier. TIC: 258400.

177495 Valentine, G.A. and Perry, F.V. 2006. "Decreasing Magmatic Footprints on Individual Volcanoes in a Waning Basaltic Field." *Geophysical Research Letters, 33,* 1-5. Washington, D.C.: American Geophysical Union. TIC: 258439.

119132 Valentine, G.A.; WoldeGabriel, G.; Rosenberg, N.D.; Carter Krogh, K.E.; Crowe, B.M.; Stauffer, P.; Auer, L.H.; Gable, C.W.; Goff, F.; Warren, R.; and Perry, F.V. 1998. "Physical Processes of Magmatism and Effects on the Potential Repository: Synthesis of Technical Work Through Fiscal Year 1995." Chapter 5 of *Volcanism Studies: Final Report for the Yucca Mountain Project.* Perry, F.V.; Crowe, B.M.; Valentine, G.A.; and Bowker, L.M., eds. LA-13478. Los Alamos, New Mexico: Los Alamos National Laboratory. TIC: 247225.

100610 van Genuchten, M.T. 1980. "A Closed-Form Equation for Predicting the Hydraulic Conductivity of Unsaturated Soils." *Soil Science Society of America Journal, 44,* (5), 892-898. Madison, Wisconsin: Soil Science Society of America. TIC: 217327.

184332 Vaniman, D.; Bish, D.; and Chipera, S. 1993. "Dehydration and Rehydration of a Tuff Vitrophyre." *Journal of Geophysical Research, 98,* (B12), 22,309 - 22,320. Washington, D.C.: American Geophysical Union. TIC: 224612.

171801 Vidal, O. and Murphy, W.M. 1999. "Calculation of the Effect of Gaseous Thermodiffusion and Thermogravitation Processes on the Relative Humidity Surrounding a High Level Nuclear Waste Canister." *Waste Management, 19,* 189-198. New York, New York: Pergamon. TIC: 256580.

156297 von Seggern, D.H.; Smith, K.D.; and Biasi, G.P. 2001. *Seismicity in the Vicinity of Yucca Mountain, Nevada for the Period October 1, 1997, to September 30, 1999.* Reno, Nevada: University of Nevada, Reno, Nevada Seismological Laboratory. ACC: MOL.20010731.0293.

184624 Wachs, G. 2004. *Calculation of Amount of Free Water Required to Overpressurize DOE SNF Standardized Canister and RW Waste Package.* EDF-NSNF-017, Rev. 1. Washington, D.C.: U.S. Department of Energy, National Spent Nuclear Fuel Program. ACC: LLR.20080109.0001.

175407 Walton, Z.P. 2005. Testing of Stress Crack Flow [final closure]. Scientific Notebook SN-SNL-SCI-032-V2. Cover-150. ACC: MOL.20060724.0109.

106170 Weast, R.C., ed. 1984. *CRC Handbook of Chemistry and Physics.* 65th Edition. Boca Raton, Florida: CRC Press. TIC: 206666.

111561 Weast, R.C., ed. 1985. *CRC Handbook of Chemistry and Physics.* 66th Edition. Boca Raton, Florida: CRC Press. TIC: 216054.

163346 Werme, L.; Björner, I.K.; Bart, G.; Zwicky, H.U.; Grambow, B.; Lutze, W.; Ewing, R.C.; and Magrabi, C. 1990. "Chemical Corrosion of Highly Radioactive Borosilicate Nuclear Waste Glass Under Simulated Repository Conditions." *Journal of Material Research, 5,* (5), 1130-1146. Warrendale, Pennsylvania: Materials Research Society. TIC: 254313.

113466 Werme, L.O. and Spahiu, K. 1998. "Direct Disposal of Spent Nuclear Fuel: Comparison Between Experimental and Modelled Actinide Solubiluties in Natural Waters." *Journal of Alloys and Compounds, 271-273,* 194-200. Lausanne, Switzerland: Elsevier. TIC: 243085.

103485 Wernicke, B.; Davis, J.L.; Bennett, R.A.; Elosegui, P.; Abolins, M.J.; Brady, R.J.; House, M.A.; Niemi, N.A.; and Snow, J.K. 1998. "Anomalous Strain Accumulation in the Yucca Mountain Area, Nevada." *Science, 279,* 2096-2100. New York, New York: American Association for the Advancement of Science. TIC: 235956.

175199 Wernicke, B.; Davis, J.L.; Bennett, R.A.; Normandeau, J.E.; Friedrich, A.M.; and Niemi, N.A. 2004. "Tectonic Implications of a Dense Continuous GPS Velocity Field at Yucca Mountain, Nevada." *Journal of Geophysical Research, 109,* (B12404), 1-13. Washington, D.C.: American Geophysical Union. TIC: 257651.

170697 Whelan, J.F. 2004. *Secondary Mineral Deposits and Evidence of Past Seismicity and Heating of the Proposed Repository Horizon at Yucca Mountain, Nevada.* Water-Resources Investigations Report 03-4321. Reston, Virginia: U.S. Geological Survey. ACC: MOL.20040902.0236.

109179 Whelan, J.F. and Moscati, R.J. 1998. "9 M.Y. Record of Southern Nevada Climate from Yucca Mountain Secondary Minerals." *High-Level Radioactive Waste Management, Proceedings of the Eighth International Conference, Las Vegas, Nevada, May 11-14, 1998.* Pages 12-15. La Grange Park, Illinois: American Nuclear Society. TIC: 237082.

179305 Whelan, J.F.; Neymark, L.A.; Moscati, R.J.; Marshall, B.D.; and Roedder, E. 2006. *Thermal History of the Unsaturated Zone at Yucca Mountain, Nevada, USA.* Denver, Colorado: U.S. Geological Survey. ACC: MOL.20070508.0200.

163590 Whelan, J.F.; Neymark, L.A.; Roedder, E.; and Moscati, R.J. 2003. "Thermochronology of Secondary Minerals from the Yucca Mountain Unsaturated Zone." *Proceedings of the 10th International High-Level Radioactive Waste Management Conference (IHLRWM), March 30-April 2, 2003, Las Vegas, Nevada.* Pages 357-366. La Grange Park, Illinois: American Nuclear Society. TIC: 254368.

160442 Whelan, J.F.; Paces, J.B.; and Peterman, Z.E. 2002. "Physical and Stable-Isotope Evidence for Formation of Secondary Calcite and Silica in the Unsaturated Zone, Yucca Mountain, Nevada." *Applied Geochemistry, 17,* (6), 735-750. New York, New York: Elsevier. TIC: 253462.

100091 Whelan, J.F.; Vaniman, D.T.; Stuckless, J.S.; and Moscati, R.J. 1994. "Paleoclimatic and Paleohydrologic Records from Secondary Calcite: Yucca Mountain, Nevada." *High Level Radioactive Waste Management, Proceedings of the Fifth Annual International Conference, Las Vegas, Nevada, May 22-26, 1994. 4,* 2738-2745. La Grange Park, Illinois: American Nuclear Society. TIC: 210984.

143651 Wick, O.J., ed. 1980. *Plutonium Handbook: A Guide to the Technology.* Volumes I & II. La Grange Park, Illinois: American Nuclear Society. TIC: 248002.

163589 Wilson, N.S.F.; Cline, J.S.; and Amelin, Y.V. 2003. "Origin, Timing, and Temperature of Secondary Calcite–Silica Mineral Formation at Yucca Mountain, Nevada." *Geochimica et Cosmochimica Acta, 67,* (6), 1145-1176. New York, New York: Pergamon. TIC: 254369.

105544 Wohletz, K. and Heiken, G. 1992. *Volcanology and Geothermal Energy.* Berkeley, California: University of California Press. TIC: 241603.

110071 WoldeGabriel, G.; Keating, G.N.; and Valentine, G.A. 1999. "Effects of Shallow Basaltic Intrusion into Pyroclastic Deposits, Grants Ridge, New Mexico, USA." *Journal of Volcanology and Geothermal Research, 92,* (3), 389-411. New York, New York: Elsevier. TIC: 246037.

107327 Wollenberg, H.A.; Asaro, F.; Bowman, H.; McEvilly, T.; Morrison, F.; and Witherspoon, P. 1975. *Geothermal Energy Resource Assessment.* UCID-3762. Berkeley, California: Lawrence Berkeley Laboratory. TIC: 237549.

174800 Wong, L.L.; Lian, T.; Fix, D.V.; Sutton, M.; and Rebak, R.B. 2004. "Surface Analysis of Alloy 22 Coupons Exposed for Five Years to Concentrated Ground Waters." *Corrosion/2004, 59th Annual Conference & Exposition, March 28 - April 1, 2004, New Orleans.* Paper No. 04701. Houston, Texas: NACE International. TIC: 255943.

178059 Woolf, R. 2003. *Controlled Plasticity Burnishing (CPB) for Developing a Very Deep Layer of Compressive Residual Stresses in Rectangular Specimens of Alloy 22 for Yucca Mountain Nuclear Waste Package Closure Weld.* SET Job No.: 37. Cincinnati, Ohio: Surface Enhancement Technologies. ACC: ENG.20030729.0002.

171709 Wronkiewicz, D.J. 1993. *Effects of Radionuclide Decay on Waste Glass Behavior--A Critical Review.* ANL-93/45. Argonne, Illinois: Argonne National Laboratory. TIC: 210799.

176891 Wronkiewicz, D.J.; Bates, J.K.; Gerding, T.J.; Veleckis, E.; and Tani, B.S. 1991. *Leaching Action of EJ-13 Water on Unirradiated UO_2 Surfaces Under Unsaturated Conditions at 90°C: Interim Report.* ANL-91/11. Argonne, Illinois: Argonne National Laboratory. ACC: NNA.19910314.0091.

100493 Wronkiewicz, D.J.; Bates, J.K.; Gerding, T.J.; Veleckis, E.; and Tani, B.S. 1992. "Uranium Release and Secondary Phase Formation During Unsaturated Testing of UO2 at 90°C." *Journal of Nuclear Materials, 190,* 107-127. Amsterdam, The Netherlands: North-Holland Publishing Company. TIC: 236558.

102047 Wronkiewicz, D.J.; Bates, J.K.; Wolf, S.F.; and Buck, E.C. 1996. "Ten-Year Results from Unsaturated Drip Tests with UO_2 at 90°C: Implications for the Corrosion of Spent Nuclear Fuel." *Journal of Nuclear Materials, 238,* (1), 78-95. Amsterdam, The Netherlands: North-Holland. TIC: 243361.

153972 Wu, Y-S. and Pruess, K. 2000. "Numerical Simulation of Non-Isothermal Multiphase Tracer Transport in Heterogeneous Fractured Porous Media." *Advances in Water Resources, 23,* (7), 699-723. New York, New York: Elsevier. TIC: 249626.

154918 Wu, Y-S.; Zhang, W.; Pan, L.; Hinds, J.; and Bodvarsson, G.S. 2000. *Capillary Barriers in Unsaturated Fractured Rocks of Yucca Mountain, Nevada.* LBNL-46876. Berkeley, California: Lawrence Berkeley National Laboratory. TIC: 249912.

161058 Wu, Y-S.; Zhang, W.; Pan, L.; Hinds, J.; and Bodvarsson, G.S. 2002. "Modeling Capillary Barriers in Unsaturated Fractured Rock." *Water Resources Research, 38,* (11), 35-1 through 35-12. Washington, D.C.: American Geophysical Union. TIC: 253854.

103690 Wu, Y.S.; Chen, G.; and Bodvarsson, G. 1995. *Preliminary Analysis of Effects of Thermal Loading on Gas and Heat Flow Within the Framework of the LBNL/USGS Site-Scale Model.* LBL-37729. Berkeley, California: Lawrence Berkeley National Laboratory. TIC: 222270.

129326 Wuschke, D.M.; Whitaker, S.H.; Goodwin, B.W.; and Rasmussen, L.R. 1995. *Assessment of the Long-Term Risk of a Meteorite Impact on a Hypothetical Canadian Nuclear Fuel Waste Disposal Vault Deep in Plutonic Rock.* AECL-11014. Pinawa, Manitoba, Canada: Atomic Energy of Canada Limited, Whiteshell Laboratories. TIC: 221413.

167622 Yaalon, D.H. 1967. "Factors Affecting the Lithification of Eolianite and Interpretation of Its Environmental Significance in the Coastal Plain of Israel." *Journal of Sedimentary Petrology, 37,* (4), 1189-1199. Tulsa, Oklahoma: Society of Economic Paleontologists and Mineralogists. TIC: 255600.

184766 Yao, B. and Zhang, L. 1999. "Preparation and Characterization of Mesoporous Titania Gel-Monolith." *Journal of Materials Science, 34,* 5983-5987. Boston, Massachusetts: Kluwer Academic Publishers. TIC: 260011.

165063 Yau, T.L. and Webster, R.T. 1987. "Corrosion of Zirconium and Hafnium." In *Corrosion,* Volume 13, Pages 707-721 of *Metals Handbook.* 9th Edition. Metals Park, Ohio: ASM International. TIC: 209807.

100520 YMP (Yucca Mountain Site Characterization Project) 1993. *Evaluation of the Potentially Adverse Condition "Evidence of Extreme Erosion During the Quaternary Period" at Yucca Mountain, Nevada.* Topical Report YMP/92-41-TPR. Las Vegas, Nevada: Yucca Mountain Site Characterization Office. ACC: NNA.19930316.0208.

102215 YMP 1995. *Technical Basis Report for Surface Characteristics, Preclosure Hydrology, and Erosion.* YMP/TBR-001, Rev. 0. Las Vegas, Nevada: Yucca Mountain Site Characterization Office. ACC: MOL.19951201.0049.

166080 YMP 1999. *Borehole USW SD-6.* Field Work Package FWP-SB-97-002, Rev. 2. Las Vegas, Nevada: Yucca Mountain Site Characterization Office. ACC: MOL.19990414.0267.

158212 YMP 1999. *Yucca Mountain Site Characterization Project: Summary of Socioeconomic Data Analyses Conducted in Support of the Radiological Monitoring Program, April 1998 to April 1999.* North Las Vegas, Nevada: Yucca Mountain Site Characterization Office. ACC: MOL.19991021.0188.

154386 YMP 2001. *Reclamation Implementation Plan.* YMP/91-14, Rev. 2. Las Vegas, Nevada: Yucca Mountain Site Characterization Office. ACC: MOL.20010301.0238.

165505 YMP 2003. *Disposal Criticality Analysis Methodology Topical Report.* YMP/TR-004Q, Rev. 02. Las Vegas, Nevada: Yucca Mountain Site Characterization Office. ACC: DOC.20031110.0005.

183479 Zhang, H. and Schwartz, F.W. 1995. "Multispecies Contaminant Plumes in Variable Density Flow Systems." *Water Resources Research, 31,* (4), 837-847. Washington, D.C.: American Geophysical Union. TIC: 252318.

180273 Zhang, K.; Wu, Y-S.; and Pan, L. 2006. "Temporal Damping Effect of the Yucca Mountain Fractured Unsaturated Rock on Transient Infiltration Pulses." *Journal of Hydrology, 327,* 235-248. New York, New York: Elsevier. TIC: 259283.

162133 Zhou, Q.; Liu, H-H.; Bodvarsson, G.S.; and Oldenburg, C.M. 2003. "Flow and Transport in Unsaturated Fractured Rock: Effects of Multiscale Heterogeneity of Hydrogeologic Properties." *Journal of Contaminant Hydrology, 60,* (1-2), 1-30. New York, New York: Elsevier. TIC: 253978.

171694 Ziegler, J.D. 2004. "Transmittal of Appendix D of the Technical Basis Document No. 10: Unsaturated Zone Transport Addressing Key Technical Issue (KTI) Agreement Evolution of Near-Field Environment (ENFE) 1.04." Letter from J.D. Ziegler (DOE/ORD) to the NRC, August 31, 2004, 0902043035, OLA&S:JCP-1434 with enclosure. ACC: MOL.20041027.0242.

8.2 CODES, STANDARDS, REGULATIONS, AND PROCEDURES

181964 10 CFR 50. 2007. Energy: Domestic Licensing of Production and Utilization Facilities. Internet Accessible.

100015 10 CFR 60 Subpart G. 1998. Energy: Quality Assurance. TIC: 238475.

180319 10 CFR 63. 2007. Energy: Disposal of High-Level Radioactive Wastes in a Geologic Repository at Yucca Mountain, Nevada. Internet Accessible.

181967 10 CFR 71. 2007. Energy: Packaging and Transportation of Radioactive Material. ACC: MOL.20070829.0114. Internet Accessible.

181968 10 CFR 72. 2007. Energy: Licensing Requirements for the Independent Storage of Spent Nuclear Fuel, High-Level Radioactive Waste, and Reactor-Related Greater than Class C Waste. Internet Accessible.

175755 40 CFR 197. 2005. Protection of Environment: Public Health and Environmental Radiation Protection Standards for Yucca Mountain, Nevada. ACC: MOL.20051121.0084.

105065 64 FR 46976. Environmental Radiation Protection Standards for Yucca Mountain, Nevada. Proposed rule 40 CFR Part 197. ACC: MOL.20050420.0206.

155216 66 FR 32074. 40 CFR Part 197, Public Health and Environmental Radiation Protection Standards for Yucca Mountain, NV; Final Rule. ACC: MOL.20050418.0113.

156671 66 FR 55732. Disposal of High-Level Radioactive Wastes in a Proposed Geologic Repository at Yucca Mountain, NV, Final Rule. 10 CFR Parts 2, 19, 20, 21, 30, 40, 51, 60, 61, 63, 70, 72, 73, and 75. ACC: MOL.20050324.0102; MOL.20050418.0124.

162618 67 FR 19432. Surplus Plutonium Disposition Program. ACC: MOL.20050418.0137.

162317 67 FR 62628. Specification of a Probability for Unlikely Features, Events and Processes. ACC: MOL.20050418.0143.

178394 70 FR 53313. Implementation of a Dose Standard After 10,000 Years. Internet Accessible.

AP-SIII.1Q, Rev. 2, ICN 0. *Scientific Notebooks*. Washington, D.C.: U.S. Department of Energy, Office of Civilian Radioactive Waste Management. ACC: MOL.20021202.0026.

162726 ASTM B 265-02. 2002. *Standard Specification for Titanium and Titanium Alloy Strip, Sheet, and Plate.* West Conshohocken, Pennsylvania: American Society for Testing and Materials. TIC: 254000.

147465 ASTM B 575-99a. 1999. *Standard Specification for Low-Carbon Nickel-Molybdenum-Chromium, Low-Carbon Nickel-Chromium-Molybdenum, Low-Carbon Nickel-Chromium-Molybdenum-Copper, Low-Carbon Nickel-Chromium-Molybdenum-Tantalum, and Low-Carbon Nickel-Chromium-Molybdenum-Tungsten Alloy Plate, Sheet, and Strip.* West Conshohocken, Pennsylvania: American Society for Testing and Materials. TIC: 247534.

152779 ASTM C 1454-00. 2000. *Standard Guide for Pyrophoricity/Combustibility Testing in Support of Pyrophoricity Analyses of Metallic Uranium Spent Nuclear Fuel.* West Conshohocken, Pennsylvania: American Society for Testing and Materials. TIC: 248977.

103327 DOE-HDBK-1081-94. 1994. *Primer on Spontaneous Heating and Pyrophoricity.* Washington, D.C.: U.S. Department of Energy. TIC: 213578.

IM-PRO-002, Rev. 1, ICN 0. *Control of the Electronic Management of Information*. Las Vegas, NV: Sandia National Laboratories. ACC: DOC.20070912.0012.

IM-PRO-003, Rev. 5, ICN 0. *Software Management*. Las Vegas, NV: Sandia National Laboratories. ACC: DOC.20080227.0005.

151873 NAC (Nevada Administrative Code) 534. 2006. Underground Water and Wells. 258960.

100016 Nuclear Waste Policy Amendments Act of 1987. Public Law No. 100-203, 101 Stat. 1330. TIC: 223717.

PI-PRO-005, Rev. 1, ICN 0. *Requirements Management*. Las Vegas, NV: Sandia National Laboratories. ACC: DOC.20080131.0050.

QAP-SIII-2, Rev. 1. *Review of Scientific Documents and Data*. Las Vegas, Nevada: CRWMS M&O. ACC: MOL.19980219.0733.

SCI-PRO-001, Rev. 5, ICN 0. *Qualification of Unqualified Data*. Las Vegas, NV: Sandia National Laboratories. ACC: DOC.20071106.0020.

SCI-PRO-002, Rev. 4, ICN 0. *Planning for Science Activities*. Las Vegas, NV: Sandia National Laboratories. ACC: DOC.20071213.0005.

SCI-PRO-003, Rev. 2, ICN 0. *Document Review*. Las Vegas, NV: Sandia National Laboratories. ACC: DOC.20070418.0002.

SCI-PRO-004, Rev. 6, ICN 0. *Managing Technical Product Inputs*. Las Vegas, NV: Sandia National Laboratories. ACC: DOC.20071018.0015.

SCI-PRO-005, Rev. 9, ICN 0. *Scientific Analyses and Calculations*. Las Vegas, NV: Sandia National Laboratories. ACC: DOC.20080221.0004.

SCI-PRO-006, Rev. 9, ICN 0. *Models*. Las Vegas, NV: Sandia National Laboratories. ACC: DOC.20080221.0005.

SCI-PRO-007, Rev. 2, ICN 0. *Determination of Importance and Site Performance Protection Evaluations*. Las Vegas, NV: Sandia National Laboratories. ACC: DOC.20071009.0010.

YMP-USGS-GP-32, R2. Underground Geologic Mapping. Denver, Colorado: U.S. Geological Survey. ACC: MOL.19980930.0086.

8.3 SOURCE DATA, LISTED BY DATA TRACKING NUMBER

151139 GS000308315121.003. Meteorological Stations Selected to Represent Future Climate States at Yucca Mountain, Nevada. Submittal date: 03/14/2000.

154734 GS010308312322.003. Field, Chemical and Isotopic Data from Wells in Yucca Mountain Area, Nye County, Nevada, Collected Between 12/11/98 and 11/15/99. Submittal date: 03/29/2001.

155307 GS010608312332.001. Potentiometric-Surface Map, Assuming Perched Conditions North of Yucca Mountain, in the Saturated Site-Scale Model. Submittal date: 06/19/2001.

162874 GS010908314221.001. Geologic Map of the Yucca Mountain Region, Nye County, Nevada. Submittal date: 01/23/2002.

162911 GS011108312322.006. Field and Chemical Data Collected between 1/20/00 and 4/24/01 and Isotopic Data Collected between 12/11/98 and 11/6/00 from Wells in the Yucca Mountain Area, Nye County, Nevada. Submittal date: 11/20/2001.

160899 GS020408312272.003. Collection and Analysis of Pore Water Samples for the Period from April 2001 to February 2002. Submittal date: 04/24/2002.

166569 GS020808312272.004. Analysis of Water-Quality Samples for the Period from July 1999 to July 2002. Submittal date: 09/18/2002.

164846 GS020908315215.003. Fluid Inclusion Homogenization Temperatures from the ESF and ECRB, 10/01 to 5/02. Submittal date: 09/26/2001.

164847 GS020908315215.004. Stable Carbon and Oxygen Isotope Analyses of ESF/ECRB Calcite and USW SD-6 and USW WT-24 Whole Rock; 1/1999-6/2002. Submittal date: 10/16/2002.

164750 GS021208315215.009. U Abundances, 238U-234U-230TH-232TH Activity Ratios, and Calculated 230TH/U Ages, and Initial 234U/238U Activity Ratios Determined for Sequential In-Situ Microdigestions of Opal Hemispheres from the ESF by Thermal Ionization Mass Spectrometry. Submittal date: 12/19/2002.

165226 GS030408312272.002. Analysis of Water-Quality Samples for the Period from July 2002 to November 2002. Submittal date: 05/07/2003.

163745 GS030608312272.005. Anion Data from Leach Samples Collected for the Chlorine-36 Validation Study. Submittal date: 06/17/2003.

166570 GS031008312272.008. Analysis of Pore Water and Miscellaneous Water Samples for the Period from December 2002 to July 2003. Submittal date: 11/13/2003.

171287 GS031208312232.003. Deep Unsaturated Zone Surface-Based Borehole Instrumentation Program Data from Boreholes USW NRG-7A, UE-25 UZ #4, USW NRG-6, UE-25 UZ #5, USW UZ-7A and USW SD-12 for the Time Period 10/01/97 - 03/31/98. Submittal date: 07/29/2004.

179284 GS031208312232.005. Deep Unsaturated Zone Surface-Based Borehole Instrumentation Program Data from Boreholes USW NRG-7A, UE-25 UZ#4, UE-25 UZ#5, USW UZ-7A and USW SD-12 for the Time Period 1/1/97 - 6/30/97. Submittal date: 05/24/2004.

181234 GS040108312312.001. Water-Level, Discharge Rate and Related Data from the Pump Tests Conducted at Well USW UZ-14, August 12 through August 30, 1993. Submittal date: 02/12/2004.

179422 GS040108312322.001. Field and Chemical Data Collected Between 10/4/01 and 10/3/02 and Isotopic Data Collected Between 5/19/00 and 5/22/03 from Wells in the Yucca Mountain Area, Nye County, Nevada. Submittal date: 06/07/2004.

179434 GS040808312322.006. Field, Chemical, and Isotope Data for Spring and Well Samples Collected Between 03/01/01 and 05/12/04 in the Yucca Mountain Area, Nye County, Nevada. Submittal date: 11/15/2004.

178057 GS041108312272.005. Analysis of Pore Water and Miscellaneous Water Samples for the Period from July 2003 to September 2004. Submittal date: 02/25/2005.

182478 GS0703PA312272.001. Analysis of Pore Water Samples Collected from the ESF Cross Drift and Analyzed from November 1, 2005 through January 26, 2006. Submittal date: 03/23/2007.

171974 GS930108312312.003. Earthquake-Induced Water-Level Fluctuations at Yucca Mountain, Nevada, June, 1992. Submittal date: 01/21/1993.

149611 GS931100121347.007. Selected Ground-Water Data for Yucca Mountain Region, Southern Nevada and Eastern California, Through December 1992. Submittal date: 11/30/1993.

165858 GS951208312272.004. Analysis for Chemical Composition of Perched-Water from Boreholes USW UZ-14, USW NRG-7A, USW SD-9, USW SD-7 and Groundwater from Boreholes UE-25 ONC#1 and USW G-2 from 8/18/89 to 3/21/95. Submittal date: 09/12/2001.

107065 GS960908312231.004. Characterization of Hydrogeologic Units Using Matrix Properties at Yucca Mountain, Nevada. Submittal date: 09/12/1996.

145412 GS980908312322.008. Field, Chemical, and Isotopic Data from Precipitation Sample Collected Behind Service Station in Area 25 and Ground Water Samples Collected at Boreholes UE-25 C #2, UE-25 C #3, USW UZ-14, UE-25 WT #3, UE-25 WT #17, and USW WT-24, 10/06/97 to 07/01/98. Submittal date: 09/15/1998.

149593 LA0004FP831811.002. Volume of Volcanic Centers in the Yucca Mountain Region. Submittal date: 04/14/2000.

153485 LA0009SL831151.001. Fracture Mineralogy of the ESF Single Heater Test Block, Alcove 5. Submittal date: 09/28/2000.

162476 LA0010JC831341.001. Radionuclide Retardation Measurements of Sorption Distribution Coefficients for Barium. Submittal date: 10/19/2000.

153321 LA0010JC831341.002. Radionuclide Retardation Measurements of Sorption Distribution Coefficients for Cesium. Submittal date: 10/19/2000.

153322 LA0010JC831341.003. Radionuclide Retardation Measurements of Sorption Distribution Coefficients for Strontium. Submittal date: 10/19/2000.

153319 LA0010JC831341.007. Radionuclide Retardation Measurements of Sorption Distribution Coefficients for Neptunium. Submittal date: 10/19/2000.

160051 LA0206AM831234.001. Eh-pH Field Measurements on Nye County EWDP Wells. Submittal date: 06/21/2002.

163558 LA0303HV831352.002. Colloid Retardation Factors for the Saturated Zone Fractured Volcanics. Submittal date: 03/31/2003.

163422 LA0305RR831222.001. Chlorine-36 and Cl in Salts Leached from Rock Samples for the Chlorine-36 Validation Study. Submittal date: 05/22/2003.

164090 LA0307RR831222.002. Chloride, Bromide, Sulfate, and Chlorine-36 Analyses of Salts Leached from ESF 36Cl Validation Drillcore Samples in FY99. Submittal date: 07/09/2003.

167015 LA0311AM831341.001. Correlation Matrix for Sampling of Sorption Coefficient Probability Distributions. Submittal date: 11/06/2003.

166924 LA0311BR831229.001. UZ Transport Abstraction Model, Transfer Function Calculation Files. Submittal date: 11/17/2003.

170621 LA0407AM831341.002. Batch Sorption Coefficient Data for Cesium on Yucca Mountain Tuffs in Representative Water Compositions. Submittal date: 07/12/2004.

170626 LA0407AM831341.003. Batch Sorption Coefficient Data for Strontium on Yucca Mountain Tuffs in Representative Water Compositions. Submittal date: 07/12/2004.

170806 LA0407BR831371.001. UZ Transport Abstraction Model, Transport Parameters and Base Case Simulation Results. Submittal date: 07/13/2004.

179987 LA0612DK831811.001. Magma and Eruption Properties for Potential Volcano at Yucca Mountain. Submittal date: 03/23/2007.

180497 LA0701PANS02BR.003. UZ Transport Parameters. Submittal date: 04/23/2007.

184763 LA0702AM150304.001. Probability Distribution Functions and Correlations for Sampling of Sorption Coefficient Probability Distributions of Radionuclides in the SZ at the YM. Submittal date: 01/17/2008.

180322 LA0702PANS02BR.001. Repository and Water Table Bins. Submittal date: 04/16/2007.

113495 LA9908JC831321.001. Mineralogic Model "MM3.0" Version 3.0. Submittal date: 08/16/1999.

146447 LA9912SL831151.001. Fracture Mineralogy of Drill Core ESF-HD-TEMP-2. Submittal date: 01/04/2000.

146449 LA9912SL831151.002. Percent Coverage by Fracture-Coating Minerals in Core ESF-HD-TEMP-2. Submittal date: 01/05/2000.

161277 LB0101DSTTHCR1.002. Attachment II - Mineral Initial Volume Fractions for TPTPLL THC Model for AMR N0120/U0110 REV01, "Drift-Scale Coupled Processes (Drift-Scale Test and THC Seepage) Models." Submittal date: 01/26/2001.

159525 LB0205REVUZPRP.001. Fracture Properties for UZ Model Layers Developed from Field Data. Submittal date: 05/14/2002.

159526 LB0207REVUZPRP.001. Revised UZ Fault Zone Fracture Properties. Submittal date: 07/03/2002.

159672 LB0207REVUZPRP.002. Matrix Properties for UZ Model Layers Developed from Field and Laboratory Data. Submittal date: 07/15/2002.

161243 LB0208UZDSCPMI.002. Drift-Scale Calibrated Property Sets: Mean Infiltration Data Summary. Submittal date: 08/26/2002.

160799 LB0210THRMLPRP.001. Thermal Properties of UZ Model Layers: Data Summary. Submittal date: 10/25/2002.

163689 LB0301DSCPTHSM.002. Drift-Scale Coupled Process Model for Thermohydrologic Seepage: Data Summary. Submittal date: 01/29/2003.

162354 LB03023DKMGRID.001. UZ 3-D Site Scale Model Grids. Submittal date: 02/26/2003.

164744 LB0302DSCPTHCS.001. Drift-Scale Coupled Processes (THC Seepage) Model: Simulations. Submittal date: 02/11/2003.

161976 LB0302DSCPTHCS.002. Drift-Scale Coupled Processes (THC Seepage) Model: Data Summary. Submittal date: 02/11/2003.

165992 LB0304RDTRNSNS.001. Supporting Files of 3D Flow and Transport Sensitivity Analyses. Submittal date: 04/29/2003.

173235 LB0304SMDCREV2.001. Seepage Modeling for Performance Assessment, Including Drift Collapse: Input/Output Files. Submittal date: 04/11/2003.

169733 LB0306DRSCLTHM.001. Drift Scale THM Model Predictions: Simulations. Submittal date: 06/26/2003.

174490 LB0306DRSCLTHM.002. Drift Scale THM Model Predictions: Summary Plots. Submittal date: 06/26/2003.

165541 LB0307DSTTHCR2.002. Drift-Scale Coupled Processes (DST Seepage) Model: Data Summary. Submittal date: 07/24/2003.

171567 LB0308DRSCLTHM.001. Drift Scale THM Model Predictions for Poor Quality Rock in Tptpll: Simulations. Submittal date: 08/29/2003.

174489 LB0310MR0060R1.010. Supplemental Radionuclide Transport Simulations: Input/Output Files. Submittal date: 10/23/2003.

170718 LB0310MTSCLTHM.002. Mountain Scale THM Predictions: Summary Plots. Submittal date: 10/21/2003.

166714 LB0311ABSTHCR2.001. Drift Scale Coupled Process Abstraction Model (for Intact-Drift Case). Submittal date: 11/07/2003.

173280 LB0407AMRU0120.001. Supporting Calculations and Analysis for Seepage Abstraction and Summary of Abstraction Results. Submittal date: 07/29/2004.

171706 LB0408CMATUZFT.004. Leaching of Altered Cementitious Materials - EQ3/6 Simulations for Cementitious Material Transport. Submittal date: 08/31/2004.

171595 LB0408U0170FEP.001. Sensitivity Study of Fracture Width Influence on UZ Flow and Transport: Simulations. Submittal date: 09/01/2004.

171596 LB0408U0170FEP.002. Sensitivity Study of Fracture Width Influence on UZ Flow and Transport: Summaries. Submittal date: 09/01/2004.

179180 LB0610UZDSCP30.001. Drift-Scale Calibrated Property Set for the 30-Percentile Infiltration Map. Submittal date: 11/02/2006.

178586 LB0611MTSCHP10.001. Mountain Scale Calibrated Property Set for the 10-Percentile Infiltration Map. Submittal date: 11/28/2006.

180293 LB0611MTSCHP30.001. Mountain Scale Calibrated Property Set for the 30-Percentile Infiltration Map. Submittal date: 11/28/2006.

178587 LB06123DPDUZFF.001. 3-D UZ Flow Fields for Present-Day Climate of 10th-, 30th-, 50th- and 90th -Percentile Infiltration Maps. Submittal date: 12/19/2006.

180294 LB0612MTSCHP50.001. Mountain Scale Calibrated Property Set for the 50-Percentile Infiltration Map. Submittal date: 12/19/2006.

180295 LB0612MTSCHP90.001. Mountain Scale Calibrated Property Set for the 90-Percentile Infiltration Map. Submittal date: 12/20/2006.

180296 LB0612MTSCHPFT.001. Calibrated UZ Fault Property Sets. Submittal date: 12/07/2006.

179296 LB0612PDFEHMFF.001. Flow-Field Conversions from TOUGH2 to FEHM Format for Present Day 10-, 30-, 50-, and 90-Percentile Infiltration Maps. Submittal date: 12/19/2006.

179150 LB0612PDPTNTSW.001. Vertical Flux at PTN/TSW Interface for Present-Day Climate of 10th, 30th, 50th, and 90-Percentile Infiltration Maps. Submittal date: 12/19/2006.

179066 LB07013DGTUZFF.001. 3-D UZ Flow Fields for Glacial Transition Climate of 10th-, 30th-, 50th-, and 90th-Percentile Infiltration Maps. Submittal date: 01/03/2007.

179064 LB07013DMOUZFF.001. 3-D UZ Flow Fields for Monsoon Climate of 10th-, 30th-, 50th-, and 90th-Percentile Infiltration Maps. Submittal date: 01/03/2007.

179160 LB0701GTFEHMFF.001. Flow-Field Conversions from TOUGH2 to FEHM Format for Glacial Transition Climate 10th-, 30th-, 50th-, and 90th-Percentile Infiltration Maps. Submittal date: 01/05/2007.

179153 LB0701GTPTNTSW.001. Vertical Flux at PTN/TSW Interface for Glacial Transition Climate of 10th, 30th, 50th, and 90th-Percentile Infiltration Maps. Submittal date: 01/03/2007.

179297 LB0701MOFEHMFF.001. Flow-Field Conversions from TOUGH2 to FEHM Format for Monsoon Climate 10th-, 30th-, 50th-, and 90th-Percentile Infiltration Maps. Submittal date: 01/05/2007.

179156 LB0701MOPTNTSW.001. Vertical Flux at PTN/TSW Interface for Monsoon Climate of 10th, 30th, 50th and 90th-Percentile Infiltration Maps. Submittal date: 01/03/2007.

179283 LB0701PAWFINFM.001. Weighting Factors for Infiltration Maps. Submittal date: 01/25/2007.

179507 LB0702PAFEM10K.002. Flow Field Conversions to FEHM Format for Post 10,000 Year Peak Dose Fluxes in the Unsaturated Zone for Four Selected Infiltration Rates. Submittal date: 02/15/2007.

179511 LB0702PASEEP01.001. New Extended-Range Seepage Look-Up Tables for Intact and Collapsed Drifts Plus Supporting Files. Submittal date: 02/20/2007.

181635 LB0702PASEEP02.001. Seepage Abstraction for Degraded Drifts. Submittal date: 06/29/2007.

180776 LB0702PAUZMTDF.001. Unsaturated Zone Matrix Diffusion Coefficients. Submittal date: 05/10/2007.

179324 LB0702UZP10KFF.002. 3-D UZ Flow Fields for Post-10,000 Climate Infiltration Maps. Submittal date: 02/15/2007.

179332 LB0702UZPTN10K.002. Vertical Flux at PTN/TSW Interface for Post-10K-Year Climate Infiltration Maps. Submittal date: 02/15/2007.

181217 LB0705DSTHC001.001. Drift-Scale THC Simulation Results with Water HDPERM3 (W0). Submittal date: 05/02/2007.

180854 LB0705DSTHC001.002. Input and Output Files of Drift-Scale THC Simulations with Water HDPERM3 (W0). Submittal date: 05/02/2007.

181300 LB0705TRAVTIME.001. Simulated Breakthrough Curves and Travel Times. Submittal date: 05/18/2007.

181445 LB0706UZSEEP05.001. Mathcad 11 Spreadsheets for Probabilistic Seepage Evaluation. Submittal date: 06/05/2007.

106785 LB990701233129.001. 3-D UZ Model Grids for Calculation of Flow Fields for PA for AMR U0000, "Development of Numerical Grids for UZ Flow and Transport Modeling". Submittal date: 09/24/1999.

122757 LB990801233129.003. TSPA Grid Flow Simulations for AMR U0050, "UZ Flow Models and Submodels" (Flow Field #3). Submittal date: 11/29/1999.

118717 LB990801233129.009. TSPA Grid Flow Simulations for AMR U0050, "UZ Flow Models and Submodels" (Flow Field #9). Submittal date: 11/29/1999.

147115 LB9908T1233129.001. Transport Simulations for the Low, Mean, and Upper Infiltration Scenarios of the Present-Day, Monsoon, and Glacial Transition Climates for AMR U0050, "UZ Flow Models and Submodels." Submittal date: 03/11/2000.

146894 LB991201233129.001. The Mountain-Scale Thermal-Hydrologic Model Simulations for AMR U0105, "Mountain-Scale Coupled Processes (TH) Models". Submittal date: 12/03/1999.

142973 LL000122051021.116. Summary of Analyses of Glass Dissolution Filtrates. Submittal date: 01/27/2000.

172021 LL030211523125.006. EQ3/6 Modeling of Grout-Reacted Liquid Carbonation Experiments. Submittal date: 07/01/2003.

162949 LL030408023121.027. Cl Abundance and Cl Ratios of Leachates from ESF Core Samples. Submittal date: 04/17/2003.

169583 LL030410012251.056. LTCTF Corrosion Rate Calculations for 2 1/2 - Year Exposed Titanium Alloy GR7 Specimens Cleaned Under TIP-CM-51. Submittal date: 07/16/2003.

170502 LL031001023121.035. Conversion of Corrosion Testing Solutions from Molar to Molal Concentration Units (II). Submittal date: 04/23/2004.

171476 LL040801512251.115. Bacterial Growth Dynamics, Limiting Factors, and Community Diversity in a Proposed Geological Nuclear Waste Repository Environment. Submittal date: 08/18/2004.

171362 LL040803112251.117. Target Compositions of Aqueous Solutions Used for Corrosion Testing. Submittal date: 08/14/2004.

178283 LL060904312251.186. Modeling of Pitzer pH for Selected ECORR Test Solutions. Submittal date: 11/02/2006.

180553 LL0702PA013MST.068. Input and Output Files for the SMT, SDT and DDT Submodels and MSTHAC Extract Output Files Used in ANL-EBS-MD-000049 Multiscale Thermohydrologic Model. Submittal date: 04/27/2007.

183159 LL070800612251.197. Electrochemical Testing of Titanium Grade 7 and Titanium Grade 29 Alloys in Dust-Like Electrolytes - Developed. Submittal date: 08/28/2007.

185101 LL960905751021.019. Ten Year Results from Unsaturated Drip Tests with UO2 at 90C: Implications for the Geologic Disposal of Spent Nuclear Fuel. Submittal date: 09/25/1996.

152926 MO0003RIB00073.000. Physical and Chemical Characteristics of Ti Grades 7 and 16. Submittal date: 03/13/2000.

152554 MO0004QGFMPICK.000. Lithostratigraphic Contacts from MO9811MWDGFM03.000 to be Qualified Under the Data Qualification Plan, TDP-NBS-GS-000001. Submittal date: 04/04/2000.

149806 MO0004YMP98132.004. Flood Inundation Areas in the Vicinity of Yucca Mountain. Submittal date: 03/31/2000.

155959 MO0010CPORGLOG.003. Calculated Porosity Values at Depth Derived from Qualified Geophysical Log Data from Modern Boreholes. Submittal date: 10/16/2000.

171565 MO0011YMP00114.000. Potential Repository Site. Submittal date: 11/21/2000.

153777 MO0012MWDGFM02.002. Geologic Framework Model (GFM2000). Submittal date: 12/18/2000.

154733 MO0102DQRBTEMP.001. Temperature Data Collected from Boreholes Near Yucca Mountain in Early 1980's. Submittal date: 02/21/2001.

169995 MO0107TC239938.000. Hastelloy Alloy C-22, the Most Versatile Nickel-Chromium-Molybdenum Alloy Available Today with Improved Resistance to Both Uniform and Localized Corrosion as Well as a Variety of Mixed Industrial Chemicals. Submittal date: 07/23/2001.

161845 MO0209EBSPMFSD.029. Probable Maximum Flood Study Data. Submittal date: 09/18/2002.

161496 MO0301SEPFEPS1.000. LA FEP List. Submittal date: 01/21/2003.

162385 MO0302PNLDUFTD.000. Flowthrough Dissolution Data. Submittal date: 02/28/2003.

163441 MO0304PNLLPHDD.000. Low PH Dissolution Data. Submittal date: 04/09/2003.

185014 MO0401MWDRPSHA.000. Results of the Yucca Mountain Probabilistic Seismic Hazard Analysis (PSHA). Submittal date: 02/20/2008.

173078 MO0408EG831811.008. Magma Cooling and Solidification. Submittal date: 09/13/2004.

171483 MO0408MWDDDMIO.002. Drift Degradation Model Inputs and Outputs. Submittal date: 08/31/2004.

172682 MO0501BPVELEMP.001. Bounded Horizontal Peak Ground Velocity Hazard at the Repository Waste Emplacement Level. Submittal date: 01/11/2005.

172601 MO0501SEPFEPLA.001. LA FEP List and Screening. Submittal date: 01/17/2005.

172830 MO0502ANLGAMR1.016. HLW Glass Degradation Model. Submittal date: 02/08/2005.

174811 MO0506MWDTLVAC.000. TSPA-LA Validation and Analysis Cases. Submittal date: 06/30/2005.

175064 MO0508SEPFEPLA.002. LA FEP List and Screening. Submittal date: 08/22/2005.

177371 MO0602SPAMODAR.000. Model Archives from USGS Special Investigations Report 2004-5205, Death Valley Regional Ground-Water Flow System, Nevada and California-Hydrogeologic Framework and Transient Ground-Water Flow Model. Submittal date: 02/10/2006.

176868 MO0604SPAPHR25.001. PHREEQC Data 0 Thermodynamic Database for 25 Degrees C - File: PHREEQCDATA025.DAT. Submittal date: 04/10/2006.

179988 MO0609SPASRPBM.004. Soil Related Parameters for the Biosphere Model. Submittal date: 03/28/2007.

179352 MO0610MWDHFM06.002. Hydrogeologic Framework Model (HFM2006) Stratigraphic Horizon Grids. Submittal date: 11/01/2006.

182035 MO0612WPOUTERB.000. Output from General and Localized Corrosion of Waste Package Outer Barrier Report. Submittal date: 07/18/2007.

179310 MO0701PAGROUND.000. Groundwater Colloid Concentration Parameters. Submittal date: 01/18/2007.

180392 MO0701PAKDSUNP.000. Colloidal KDS for U, NP, RA and SN. Submittal date: 04/17/2007.

180508 MO0701PASHIELD.000. Waste Package/Drip Shield Early Failure Probabilities. Submittal date: 04/24/2007.

180391 MO0701PASORPTN.000. Colloidal Sorption Coefficients for PU, AM, TH, CS, and PA. Submittal date: 04/17/2007.

179925 MO0702PASTREAM.001. Waste Stream Composition and Thermal Decay Histories for LA. Submittal date: 02/15/2007.

180514 MO0702PASTRESS.002. Output DTN of Model Report, "Stress Corrosion Cracking of Waste Package Outer Barrier and Drip Shield Materials," ANL-EBS-MD-000005. Submittal date: 04/24/2007.

181990 MO0703PAEVSIIC.000. Evaluation of Stage II Condensation. Submittal date: 07/16/2007.

182029 MO0703PAGENCOR.001. Output from General Corrosion and Localized Corrosion of Waste Package Outer Barrier 2007 Second Version. Submittal date: 07/18/2007.

183148 MO0703PASDSTAT.001. Statistical Analyses for Seismic Damage Abstractions. Submittal date: 09/21/2007.

183156 MO0703PASEISDA.002. Seismic Damage Abstractions for TSPA Compliance Case. Submittal date: 09/21/2007.

180442 MO0704PAPTTFBR.002. Particle Tracking Transfer Functions. Submittal date: 04/12/2007.

183681 MO0705CREEPSCC.000. Supplementary Output DTN from SCC AMR. Submittal date: 05/14/2007.

184958 MO0705CRITPROB.000. Probability of Criticality. Submittal date: 02/05/2008.

180946 MO0705EARLYEND.000. Waste Package/Drip Shield Early Failure End State Probabilities. Submittal date: 05/16/2007.

183150 MO0705FAULTABS.000. Assessment of Waste Package Failure Due to Fault Displacement for Criticality. Submittal date: 09/21/2007.

181798 MO0705GEOMODEL.000. Input Files and Model Output Runs: Geochemistry Model Validation Report: Material Degradation and Release Model. Submittal date: 05/23/2007.

185041 MO0705OXYBALAN.000. Oxygen Balance Analysis for Physical and Chemical Environment. Submittal date: 05/23/2007.

180869 MO0705SCCIGM06.000. Final Report for FY06: Stress Corrosion Crack Initiation & Growth Measurements in Environments Relevant to High Level Nuclear Waste Packages. Submittal date: 05/14/2007.

183008 MO0705TSPASEEP.000. TSPA-LA Addendum, Seepage Results from the TSPA-LA Model. Submittal date: 01/15/2008.

181887 MO0706METMND06.000. Meteorological Monitoring Data for 2006. Submittal date: 06/19/2007.

182472 MO0707TH2D3DDC.000. 2-D and 3-D Thermal-Hydrologic Analysis. Submittal date: 08/15/2007.

182994 MO0709TSPALOCO.000. TSPA Localized Corrosion Analysis. Submittal date: 09/13/2007.

182976 MO0709TSPAREGS.000. TSPA-LA Model (GW & E) Used for Regulatory Compliance. Submittal date: 09/04/2007.

184172 MO0712DELNPCCA.001. Delineation of Postclosure Controlled Area. Submittal date: 12/03/2007.

184480 MO0712PANLNNWP.000. Probabilistic Analysis of Drip Shield Failure and CSNF and CDSP Package OCB Localized Corrosion. Submittal date: 12/17/2007.

184664 MO0712PBANLNWP.000. Probabilistic Analysis of Navy Waste Packages. Submittal date: 12/13/2007.

109059 MO9906GPS98410.000. Yucca Mountain Project (YMP) Borehole Locations. Submittal date: 06/23/1999.

165922 MO9912GSC99492.000. Surveyed USW SD-6 As-Built Location. Submittal date: 12/21/1999.

166458 SN0308F3710195.003. Hydraulic Fracturing Stress Measurements in Test Holes: ESF-GDJACK #1, and ESF-GDJACK #5, Exploratory Studies Facility at Yucca Mountain, Nevada. Submittal date: 08/29/2003.

168761 SN0310T0505503.004. Initial Radionuclide Inventories for TSPA-LA. Submittal date: 10/27/2003.

174472 SN0506F4104405.003. Analyses of Phase I and Phase II Data from the Stress Corrosion Crack Flow Tests (Data from 1/12/2005 to 5/13/2005). Submittal date: 06/20/2005.

179063 SN0609T0502206.024. Monsoon Net Infiltration Results. Submittal date: 09/18/2006.

178753 SN0609T0502206.028. Present-Day Net Infiltration Results. Submittal date: 09/22/2006.

178862 SN0609T0502206.029. Glacial Transition Net Infiltration Results. Submittal date: 09/28/2006.

178850 SN0612T0502404.014. Thermodynamic Database Input File for EQ3/6 - DATA0.YMP.R5. Submittal date: 12/15/2006.

178956 SN0612T0510106.004. Saturated Zone (SZ) Site-Scale Flow Model Pest and FEHM Files Using HFM2006. Submittal date: 01/17/2007.

180523 SN0701PAEBSPCE.001. PCE TDIP Potential Seepage Water Chemistry Lookup Tables. Submittal date: 04/25/2007.

184289 SN0701T0502206.037. Massif Calculation of Net Infiltration at Yucca Mountain, Rev 1. Submittal date: 12/10/2007.

180451 SN0702PAIPC1CA.001. In-Package Chemistry Calculations and Abstractions. Submittal date: 04/19/2007.

179575 SN0702T0510106.006. Saturated Zone (SZ) Site-Scale Flow Model with "Water Table Rise" Alternate Conceptual Model - FEHM Files Using HFM2006. Submittal date: 02/19/2007.

181571 SN0703PAEBSPCE.006. Physical and Chemical Environment (PCE) TDIP Water-Rock Interaction Parameter Table and Salt Separation Tables with Supporting Files. Submittal date: 06/27/2007.

183217 SN0703PAEBSRTA.001. Inputs Used in the Engineered Barrier System (EBS) Radionuclide Transport Abstraction. Submittal date: 09/28/2007.

182122 SN0704PADSGCMT.001. Drip Shield General Corrosion Models Based on 2.5-Year Titanium Grade 7 Corrosion Rates. Submittal date: 07/24/2007.

181283 SN0704T0510106.008. Flux, Head and Particle Track Output from the Qualified, Calibrated Saturated Zone (SZ) Site-Scale Flow Model. Submittal date: 05/01/2007.

131356 SNF37100195002.001. Hydraulic Fracturing Stress Measurements in Test Hole: ESF-AOD-HDFR1, Thermal Test Facility, Exploratory Studies Facility at Yucca Mountain. Submittal date: 12/18/1996.

107372 SNF40060298001.001. Unsaturated Zone Lithostratigraphic Contacts in Borehole USW SD-6. Submittal date: 10/15/1998.

105627 TM000000SD12RS.012. USW SD-12 Composite Borehole Log (0.0'-1435.3') and Weight Logs (1,438.8-2,151.7'). Submittal date: 09/08/1995.

166424 TMUSWNRG7A0096.002. Geophysical Logs for Borehole USW NRG-7/7A. Submittal date: 11/27/1996.

161588 UN0201SPA021SS.007. Mean Annual Temperature and Precipitation for Select Western Regional Climate Locations. Submittal date: 01/11/2002.

8.4 OUTPUT DATA, LISTED BY DATA TRACKING NUMBER

MO0706SPAFEPLA.001. FY 2007 LA FEP List and Screening. Submittal date: 03/05/2008.

MO0707NONLITHO.000. Estimated Expected Seismic Dose from Nonlithophysal Units, Twenty Thousand Year Duration. Submittal date: 07/24/2007.

SN0705WFLOWSCC.001. Analysis for Water Flow through Stress Corrosion Cracking (SCC) Cracks in Waste Package and Drip Shield. Submittal date: 05/16/2007.

SN0712CEMENTEQ.001. EQ3/6 Code Run to Evaluate Portlandite-Hillebrandite Equilibria. Submittal date: 12/10/2007.

8.5 SOFTWARE CODES

178870 ASHPLUME_DLL_LA. V. 2.1. 2006. WinDOWS 2000/XP. STN: 11117-2.1-00.

184835 EarthVision V. 7.5.2. 2007. Windows 2000. STN: 607871-7.5.2-00.

176889 EQ3/6 V. 8.1. 2005. WINDOWS 2000. STN: 10813-8.1-00.

182225 FAR V. 1.2. 2007. WINDOWS 2000 & WINDOWS 2003. STN: 11190-1.2-00.

165741 FEHM V. 2.21. 2003. SUN OS 5.8, Windows 2000 and Linux 7.1. STN: 10086-2.21-00.

179419 FEHM V. 2.24-01. 2007. WIN2003, 2000, & XP, Red Hat Linux 2.4.21, OS 5.9. STN: 10086-2.24-01-00.

179539 FEHM V. 2.24-02. 2006. WINDOWS XP. STN: 10086-2.24-02-00.

159684 FEPS Database Software Program V. . 2. 2002. WINDOWS 2000. STN: 10418-.2-00.

181089 FEPS Viewer V. 1.0. 2007. Windows 2000/XP. STN: 611664-1.0-00.

175698 PHREEQC V. 2.11. 2006. WINDOWS 2000. STN: 10068-2.11-00.

155323 PHREEQC V. 2.3. 2001. WINDOWS 95/98/NT, Redhat 6.2. STN: 10068-2.3-00.

157837 PHREEQC V. 2.3. 2002. PC. STN: 10068-2.3-01.

163453 WTRISE V. 2.0. 2003. PC/WINDOWS 2000/98; DEC ALPHA/OSF1 V5.1. STN: 10537-2.0-00.

APPENDIX A

REPOSITORY DESIGN USE IN PERFORMANCE ASSESSMENT

The use of the repository design in performance assessment can be demonstrated by identification of representative FEPs that have been either excluded or included based on that design. The design elements are represented as parameters that define the physical dimensions, characteristics, and long-term behavior of the waste form, waste packages, emplacement drift, drip shields, and other components of the repository system. A mapping of these parameters to representative FEPs relying on those parameters is contained in Table A-1.

These control parameters, as well as the resulting design based on these control parameters, have been used as the basis to exclude or include repository design-related FEPs. Table A-1 depicts how the repository design has been included in the performance assessment. It is relevant to note that in some cases the repository design supports the basis to exclude FEPs while in other cases the repository design has been used to support the spatial domain of concern, boundary conditions, or initial conditions used in models and analyses that are abstracted in the TSPA model. Representative FEPs are selected based on either the control parameter being explicitly identified in the FEP Screening Justification or TSPA Disposition in Section 6, or by inference when a FEP Screening Justification or TSPA Disposition is based on additional detailed modeling and analysis. Representative FEPs selected based on inference are noted with an asterisk (*) in the table. Note that Table A-1 is not intended to be all inclusive.

Table A-1. Repository Design Use in Performance Assessment

Control Parameter	Representative FEPs Relying on Design/Control Parameter	Control Parameter Use in Performance Assessment
01-01 Repository Geographic and Geologic Location	• FEP 0.1.03.00.0A – Spatial Domain of Concern* • FEP 1.1.01.01.0A – Open Site Investigation Boreholes (Excluded) • FEP 1.1.07.00.0A – Repository Design • FEP 2.1.06.01.0A – Chemical Effects of Rock Reinforcement and Cementitious Materials in EBS (Excluded) • FEP 2.1.07.04.0A – Hydrostatic Pressure on Waste Package (Excluded) • FEP 2.1.07.04.0B – Hydrostatic Pressure on Drip Shield (Excluded) • FEP 2.1.08.09.0A – Saturated Flow in the EBS (Excluded) • FEP 2.2.08.03.0B – Geochemical Interactions and Evolution in the UZ (Excluded) • FEP 2.2.08.12.0A – Chemistry of Water Flowing into the Drift	Supports spatial domain of concern and boundary conditions for various mountain-scale, repository-scale, and drift-scale models Supports basis for FEP exclusion
01-02 Repository Layout	• FEP 1.1.07.00.0A – Repository Design • FEP 1.2.04.03.0A – Igneous Intrusion into Repository* • FEP 2.1.05.01.0A – Flow Through Seals (Access Ramps and Ventilation Shafts) (Excluded) • FEP 2.1.08.04.0A – Condensation Forms on Roofs of Drifts (Drift-Scale Cold Traps) • FEP 2.1.08.04.0B – Condensation Forms at Repository Edges (Repository-Scale Cold Traps) • FEP 2.1.08.09.0A – Saturated Flow in the EBS (Excluded) • FEP 2.1.11.03.0A – Exothermic Reactions in the EBS (Excluded) • FEP 2.1.13.02.0A – Radiation Damage in EBS (Excluded)	Supports spatial domain of concern and boundary conditions for various mountain-scale, repository-scale, and drift-scale models Supports basis for FEPs exclusion
01-03 Repository Geologic Location	• FEP 1.1.01.01.0A – Open Site Investigation Boreholes • FEP 1.2.03.02.0B – Seismic Induced Rockfall Damages EBS Components (Excluded) • FEP 1.2.03.02.0C – Seismic-Induced Drift Collapse Damages EBS Components • FEP 2.2.01.02.0A – Thermally-Induced Stress Changes in the Near-Field (Excluded) • FEP 2.2.01.03.0A – Changes in Fluid Saturations in the Excavation Disturbed Zone (Excluded) • FEP 2.2.03.01.0A – Stratigraphy • FEP 2.2.08.12.0A – Chemistry of Water Flowing into the Drift • FEP 2.1.03.10.0B – Advection of Liquids and Solids Through Cracks in the Drip Shield (Excluded)	Supports spatial domain of concern and boundary conditions for various mountain-scale, repository-scale, and drift-scale models Supports basis for FEPs exclusion
01-04 Repository Elevation – Standoff from Water Table	• FEP 2.1.08.12.0A – Induced Hydrologic Changes in Invert (Excluded) • FEP 2.2.10.04.0A – Thermal-Mechanical Stresses Alter Characteristics of Fractures Near Repository (Excluded)* • FEP 2.2.11.01.0A – Gas Effects in the SZ (Excluded)*	Supports basis for FEPs exclusion

Table A-1. Repository Design Use in Performance Assessment (Continued)

Control Parameter	Representative FEPs Relying on Design/Control Parameter	Control Parameter Use in Performance Assessment
01-05 Repository Standoff from Quaternary Fault	• FEP 1.2.02.03.0A – Fault Displacement Damages EBS Components • FEP 2.2.07.05.0A – Flow in the UZ from Episodic Infiltration (Excluded)*	Supports spatial domain of concern and boundary conditions for various mountain-scale, repository-scale, and drift-scale models Supports basis for FEP exclusion
01-06 Repository Elevation – Overburden Thickness	• FEP 1.2.02.03.0A – Fault Displacement Damages EBS Components • FEP 1.2.07.01.0A – Erosion/Denudation (Excluded) • FEP 1.4.03.00.0A – Unintrusive Site Investigation (Excluded) • FEP 1.4.11.00.0A – Explosions and Crashes (Human Activities) (Excluded) • FEP 1.5.01.01.0A – Meteorite Impact (Excluded) • FEP 1.5.01.02.0A – Extraterrestrial Events (Excluded) • FEP 2.3.09.01.0A – Animal Burrowing/Intrusion (Excluded)	Supports spatial domain of concern and boundary conditions for various mountain-scale, repository-scale, and drift-scale models Supports basis for FEP exclusion
01-07 Repository Standoff from Perched Water	• FEP 2.2.06.03.0A – Seismic Activity Alters Perched Water Zones (Excluded)*	Supports basis for FEP exclusion
01-08 Orientation of Emplacement Drifts	• FEP 2.1.07.01.0A – Rockfall (Excluded)* • FEP 2.1.07.02.0A – Drift Collapse (Excluded)*	Supports basis for FEP exclusion
01-09 Excavation Methods	• FEP 1.1.02.00.0A – Chemical Effects of Excavation and Construction in EBS (Excluded) • FEP 1.1.02.00.0B – Mechanical Effects of Excavation and Construction in EBS (Excluded) • FEP 2.1.07.01.0A – Rockfall (Excluded) • FEP 2.2.01.01.0A – Mechanical Effects of Excavation and Construction in the Near Field*	Supports the basis for performance assessment initial conditions Supports basis for FEP exclusion
01-10 Emplacement Drift Configuration	• FEP 1.1.02.00.0B – Mechanical Effects of Excavation and Construction in EBS (Excluded) • FEP 1.1.07.00.0A – Repository Design • FEP 2.1.07.01.0A – Rockfall (Excluded) • FEP 2.1.07.06.0A – Floor Buckling (Excluded) • FEP 2.1.11.10.0A – Thermal Effects on Transport in EBS (Excluded) • FEP 2.2.06.04.0A – Effects of Subsidence (Excluded) • FEP 2.2.07.20.0A – Flow Diversion Around Repository Drifts	Supports spatial domain of concern and boundary conditions for various repository-scale and drift-scale models Supports basis for FEP exclusion

Table A-1. Repository Design Use in Performance Assessment (Continued)

Control Parameter	Representative FEPs Relying on Design/Control Parameter	Control Parameter Use in Performance Assessment
01-11 Emplacement Drift Gradient	• FEP 2.1.08.12.0A – Induced Hydrologic Changes in Invert (Excluded)	Supports basis for FEP exclusion
01-12 Non-Emplacement Opening Gradient	• FEP 2.1.08.12.0A – Induced Hydrologic Changes in Invert (Excluded)*	Supports basis for FEP exclusion
01-13 Emplacement Drift Spacing	• FEP 2.1.08.11.0A – Repository Resaturation Due to Waste Cooling • FEP 2.2.06.04.0A – Effects of Subsidence (Excluded) • FEP 2.2.07.10.0A – Condensation Zone Forms Around Drifts • FEP 2.2.07.20.0A – Flow Diversion Around Repository Drifts • FEP 2.2.10.01.0A – Repository-Induced Thermal Effects on Flow in the UZ (Excluded)*	Supports spatial domain of concern and boundary conditions for various repository-scale and drift-scale models Supports basis for FEP exclusion
01-14 Verification of Design Rock Properties	• FEP 2.1.07.01.0A – Rockfall (Excluded)* • FEP 2.1.07.02.0A – Drift Collapse (Excluded)*	Supports basis for FEP exclusion
01-15 Design of Ground Support System	• FEP 1.1.01.01.0B – Influx Through Holes Drilled in Drift Wall or Crown (Excluded) • FEP 2.1.06.01.0A – Chemical Effects of Rock Reinforcement and Cementitious Materials in EBS (Excluded) • FEP 2.1.06.02.0A – Mechanical Effects of Rock Reinforcement Materials in EBS (Excluded) • FEP 2.1.06.04.0A – Flow Through Rock Reinforcement Materials in EBS (Excluded) • FEP 2.1.07.01.0A – Rockfall (Excluded) • FEP 2.1.07.02.0A – Drift Collapse (Excluded) • FEP 2.1.09.09.0A – Electrochemical Effects in EBS (Excluded) • FEP 2.1.09.17.0A – Formation of Pseudo-Colloids (Corrosion Product) in EBS* • FEP 2.2.01.01.0B – Chemical Effects of Excavation and Construction in the Near-Field (Excluded) • FEP 2.2.08.03.0B – Geotechnical Interactions and Evolution in the UZ (Excluded)	Supports the basis for performance assessment initial conditions Supports basis for FEP exclusion
01-16 Air Circulation through Ground Support	• FEP 1.1.01.01.0B – Influx Through Holes Drilled in Drift Wall or Crown (Excluded) • FEP 2.1.06.04.0A – Flow Through Rock Reinforcement Materials in EBS (Excluded) • FEP 2.1.07.01.0A – Rockfall (Excluded)	Supports basis for FEP exclusion
01-17 Emplacement Drift Ground Support	• FEP 2.1.06.02.0A – Mechanical Effects of Rock Reinforcement Materials in EBS (Excluded) • FEP 2.1.07.01.0A – Rockfall (Excluded) • FEP 2.1.07.02.0A – Drift Collapse (Excluded)	Supports basis for FEP exclusion

Table A-1. Repository Design Use in Performance Assessment (Continued)

Control Parameter	Representative FEPs Relying on Design/Control Parameter	Control Parameter Use in Performance Assessment
01-18 Unheated Drift Length	• FEP 2.1.06.01.0A – Chemical Effects of Rock Reinforcement and Cementitious Materials in EBS (Excluded) • FEP 2.1.08.04.0A – Condensation Forms on Roofs of Drifts (Drift-Scale Cold Traps) • FEP 2.1.08.04.0B – Condensation Forms at Repository Edges (Repository-Scale Cold Traps)	Supports the basis for performance assessment initial and boundary conditions Supports basis for FEP exclusion
01-19 Flood Protection	• FEP 1.1.02.01.0A – Site Flooding (During Construction and Operation) (Excluded) • FEP 2.1.05.01.0A – Flow Through Seals (Access Ramps and Ventilation Shafts) (Excluded)	Supports basis for FEP exclusion
01-20 Repository Standoff from Paintbrush Nonwelded Hydrogeologic Unit	• FEP 2.2.10.05.0A – Thermo-Mechanical Stresses Alter Characteristics of Rocks above and below the Repository (Excluded)* • FEP 2.2.10.06.0A – Thermo-Chemical Alteration in the UZ (Solubility, Speciation, Phase Changes, Precipitation/Dissolution) (Excluded)*	Supports basis for FEP exclusion
01-21 Minimum Thickness of the Paintbrush Nonwelded Hydrogeologic Unit above the Repository	• FEP 2.2.07.05.0A – Flow in the UZ from Episodic Infiltration (Excluded)*	Supports basis for FEP exclusion
01-22 Repository Standoff from Calico Hills Nonwelded Hydrogeologic Unit	• FEP 2.2.10.07.0A – Thermo-Chemical Alteration of the Calico Hills Unit (Excluded)* • FEP 2.2.10.14.0A – Mineralogic Dehydration Reactions (Excluded)*	Supports basis for FEP exclusion
02-01 As-Emplaced Waste Configuration	• FEP 1.1.09.00.0A – Schedule and Planning* • FEP 1.2.03.02.0A – Seismic-Induced Rockfall Damages EBS Components* • FEP 2.1.06.05.0B – Mechanical Degradation of Emplacement Pallet (Excluded)* • FEP 2.1.06.07.0B – Mechanical Effects at EBS Component Interfaces (Excluded) • FEP 2.1.09.09.0A – Electrochemical Effects in EBS (Excluded)*	Supports the basis for performance assessment initial conditions Supports basis for FEP exclusion

Table A-1. Repository Design Use in Performance Assessment (Continued)

Control Parameter	Representative FEPs Relying on Design/Control Parameter	Control Parameter Use in Performance Assessment
02-02 As-Emplaced Waste Package-Drip Shield Configuration	• FEP 1.2.03.02.0A – Seismic Ground Motion Damages EBS Components* • FEP 1.2.03.02.0B – Seismic-Induced Rockfall Damages EBS Components (Excluded)* • FEP 2.1.03.07.0B – Mechanical Impact on Drip Shield (Excluded)* • FEP 2.1.06.07.0B – Mechanical Effects at EBS Component Interfaces (Excluded) • FEP 2.1.07.01.0A – Rockfall (Excluded)* • FEP 2.1.09.09.0A – Electrochemical Effects in EBS (Excluded)*	Supports the basis for performance assessment initial and boundary conditions Supports basis for FEP exclusion
02-03 Committed Materials	• FEP 1.1.02.00.0A – Chemical Effects of Excavation and Construction in EBS (Excluded) • FEP 1.1.02.03.0A – Undesirable Materials Left (Excluded) • FEP 1.1.08.00.0A – Inadequate Quality Control and Deviations from Design (Excluded) • FEP 2.1.05.01.0A – Flow Through Seals (Access Ramps and Ventilation Shafts) (Excluded) • FEP 2.1.06.01.0A – Chemical Effects of Rock Reinforcement and Cementitious Materials in EBS (Excluded) • FEP 2.1.06.02.0A – Mechanical Effects of Rock Reinforcement Materials in EBS (Excluded) • FEP 2.1.06.07.0B – Mechanical Effects at EBS Component Interfaces (Excluded) • FEP 2.1.09.01.0A – Chemical Characteristics of Water in Drifts • FEP 2.1.09.02.0A – Chemical Interaction with Corrosion Products • FEP 2.1.09.17.0A – Formation of Pseudo-Colloids (Corrosion Product) in EBS • FEP 2.1.09.28.0A – Localized Corrosion on Waste Package Outer Surface Due to Deliquescence (Excluded)* • FEP 2.1.12.04.0A – Gas Generation (CO_2, CH_4, H_2S) from Microbial Degradation (Excluded) • FEP 2.2.01.01.0B – Chemical Effects of Excavation and Construction in the Near-Field (Excluded)	Supports the basis for performance assessment initial and boundary conditions Supports basis for FEP exclusion
02-04 Invert and EBS Components in Situ Stress and Thermal Response	• FEP 2.1.06.05.0B – Mechanical Degradation of Invert (Excluded) • FEP 2.1.06.07.0B – Mechanical Effects at EBS Component Interfaces (Excluded) • FEP 2.1.11.07.0A – Thermal Expansion/Stress of In-Drift EBS Components (Excluded)*	Supports basis for FEP exclusion
02-05 EBS In-Drift Materials Interactions	• FEP 2.1.03.04.0A – Hydride Cracking of Waste Packages (Excluded)* • FEP 2.1.03.04.0B – Hydride Cracking of Drip Shields (Excluded)* • FEP 2.1.06.07.0A – Chemical Effects at EBS Component Interfaces (Excluded) • FEP 2.1.06.07.0B – Mechanical Effects at EBS Component Interfaces (Excluded) • FEP 2.1.09.02.0A – Chemical Interaction with Corrosion Products • FEP 2.1.09.09.0A – Electrochemical Effects in EBS (Excluded)	Supports the basis for performance assessment initial conditions Supports basis for FEP exclusion

Table A-1. Repository Design Use in Performance Assessment (Continued)

Control Parameter	Representative FEPs Relying on Design/Control Parameter	Control Parameter Use in Performance Assessment
02-06 EBS Material Interactions – Copper	• FEP 2.1.03.09.0A – Copper Corrosion in EBS (Excluded) • FEP 2.1.09.02.0A – Chemical Interaction with Corrosion Products	Supports the basis for performance assessment initial conditions Supports basis for FEP exclusion
02-07 Emplacement Drift Invert Function	• FEP 2.1.06.05.0B – Mechanical Degradation of Invert (Excluded) • FEP 2.1.06.07.0B – Mechanical Effects at EBS Component Interfaces (Excluded)	Supports basis for FEP exclusion
02-08 Invert Materials	• FEP 1.1.02.00.0A – Chemical Effects of Excavation and Construction in EBS (Excluded) • FEP 1.1.07.00.0A – Repository Design • FEP 2.1.06.05.0B – Mechanical Degradation of Invert (Excluded) • FEP 2.1.06.05.0C – Chemical Degradation of Emplacement Pallet • FEP 2.1.06.05.0D – Chemical Degradation of Invert (Excluded) • FEP 2.1.06.07.0B – Mechanical Effects at EBS Component Interfaces (Excluded) • FEP 2.1.08.05.0A – Flow Through Invert • FEP 2.1.09.02.0A – Chemical Interaction with Corrosion Products • FEP 2.1.09.03.0C – Volume Increase of Corrosion Products Impacts Other EBS Components (Excluded) • FEP 2.1.09.09.0A – Electrochemical Effects in EBS (Excluded)	Supports the basis for performance assessment initial conditions Supports basis for FEP exclusion
02-09		Not used
02-10 Emplacement Drift Invert Configuration	• FEP 2.1.06.05.0B – Mechanical Degradation of Invert (Excluded)* • FEP 2.1.09.03.0C – Volume Increase of Corrosion Products Impacts Other EBS Components (Excluded)	Supports the basis for performance assessment initial and boundary conditions Supports basis for FEP exclusion

Table A-1. Repository Design Use in Performance Assessment (Continued)

Control Parameter	Representative FEPs Relying on Design/Control Parameter	Control Parameter Use in Performance Assessment
03-01 Waste Package Dimensions and Component Masses	• FEP 1.1.07.00.0A – Repository Design • FEP 1.1.08.00.0A – Inadequate Quality Control and Deviations from Design (Excluded) • FEP 2.1.02.08.0A – Pyrophoricity from DSNF (Excluded) • FEP 2.1.03.06.0A – Internal Corrosion of Waste Packages Prior To Breach (Excluded) • FEP 2.1.03.11.0A – Physical Form of Waste Package and Drip Shield • FEP 2.1.09.03.0B – Volume Increase of Corrosion Products Impacts Waste Package (Excluded) • FEP 2.1.09.09.0A – Electrochemical Effects in EBS (Excluded) • FEP 2.1.11.07.0A – Thermal Expansion/Stress of In-Drift EBS Components (Excluded) • FEP 2.1.12.03.0A – Gas Generation (H_2) from Waste Package Corrosion (Excluded) • FEP 2.1.13.01.0A – Radiolysis (Excluded)	Supports the basis for performance assessment initial and boundary conditions Supports basis for FEP exclusion
03-02 Waste Package Quantities	• FEP 2.1.01.01.0A – Waste Inventory	Supports the basis for performance assessment initial conditions
03-03 Waste Package Outer Barrier Material and Thickness	• FEP 1.1.08.00.0A – Inadequate Quality Control and Deviations from Design (Excluded) • FEP 1.2.03.02.0A – Seismic Ground Motion Damages EBS Components • FEP 2.1.03.01.0A – General Corrosion of Waste Packages* • FEP 2.1.03.03.0A – Localized Corrosion of Waste Packages* • FEP 2.1.12.03.0A – Gas Generation (H_2) from Waste Package Corrosion (Excluded)	Supports the basis for performance assessment initial conditions Supports basis for FEP exclusion
03-04 Waste Package Radial Gap	• FEP 2.1.11.05.0A – Thermal Expansion/Stress of In-Package EBS Components (Excluded)* • FEP 2.1.11.07.0A – Thermal Expansion/Stress of In-Drift EBS Components (Excluded) • FEP 2.1.03.07.0A – Mechanical Impact on Waste Package (Excluded)* • FEP 2.1.09.03.0B – Volume Increase of Corrosion Products Impacts Waste Package (Excluded)*	Supports basis for FEP exclusion
03-05 Waste Package Longitudinal Gap	• FEP 2.1.09.03.0B – Volume Increase of Corrosion Products Impacts Waste Package (Excluded) • FEP 2.1.11.05.0A – Thermal Expansion/Stress of In-Package EBS Components (Excluded)* • FEP 2.1.11.07.0A – Thermal Expansion/Stress of In-Drift EBS Components (Excluded)	Supports basis for FEP exclusion
03-06 Waste Package Internal Pressurization	• FEP 2.1.03.07.0A – Mechanical Impact on Waste Package (Excluded) • FEP 2.1.12.02.0A – Gas Generation (He) from Waste Form Decay (Excluded) • FEP 2.1.13.01.0A – Radiolysis (Excluded)	Supports basis for FEP exclusion

Table A-1. Repository Design Use in Performance Assessment (Continued)

Control Parameter	Representative FEPs Relying on Design/Control Parameter	Control Parameter Use in Performance Assessment
03-07 Waste Package Corrosion Allowance	• FEP 1.2.03.02.0A – Seismic Ground Motion Damages EBS Components* • FEP 2.1.03.01.0A – General Corrosion of Waste Packages* • FEP 2.1.14.15.0A – In-Package Criticality (Intact Configuration) (Excluded)	Supports the basis for performance assessment initial conditions Supports basis for FEP exclusion
03-08 Seismic Design of Waste Package	• FEP 1.2.03.02.0A – Seismic Ground Motion Damages EBS Components* • FEP 2.1.06.05.0C – Chemical Degradation of Emplacement Pallet	Supports the basis for performance assessment initial conditions
03-09 Waste Package Worst-Case Dose Rate	• FEP 1.1.07.00.0A – Repository Design • FEP 2.1.13.01.0A – Radiolysis (Excluded)* • FEP 2.1.13.02.0A – Radiation Damage in EBS (Excluded)*	Supports the basis for performance assessment initial conditions Supports basis for FEP exclusion
03-10 Waste Package Design Basis Bounding Dose Rate	• FEP 1.1.07.00.0A – Repository Design • FEP 2.1.13.01.0A – Radiolysis (Excluded) • FEP 2.1.13.02.0A – Radiation Damage in EBS (Excluded)* • FEP 2.1.14.15.0A – In-Package Criticality (Intact Configuration) (Excluded)	Supports the basis for performance assessment initial and boundary conditions Supports basis for FEP exclusion
03-11 Waste Package Decay Heat	• FEP 2.1.11.01.0A – Heat Generation in EBS	Supports the basis for performance assessment initial conditions
03-12 Waste Package Fabrication	• FEP 2.1.03.08.0A – Early Failure of Waste Packages*	Supports bases for early failure event probability
03-13 Waste Package Fabrication Weld Inspections	• FEP 2.1.03.08.0A – Early Failure of Waste Packages*	Supports bases for early failure event probability
03-14 Waste Package Welding Materials	• FEP 2.1.03.02.0A – Stress Corrosion Cracking (SCC) of Waste Packages* • FEP 2.1.03.08.0A – Early Failure of Waste Packages*	Supports bases for early failure event probability
03-15 Waste Package Fabrication Welding Flaws	• FEP 2.1.03.02.0A – Stress Corrosion Cracking (SCC) of Waste Packages* • FEP 2.1.03.08.0A – Early Failure of Waste Packages*	Supports bases for early failure event probability

Table A-1. Repository Design Use in Performance Assessment (Continued)

Control Parameter	Representative FEPs Relying on Design/Control Parameter	Control Parameter Use in Performance Assessment
03-16 Waste Package Annealing	• FEP 2.1.03.02.0A – Stress Corrosion Cracking (SCC) of Waste Packages* • FEP 2.1.03.03.0A – Localized Corrosion of Waste Packages • FEP 2.1.03.08.0A – Early Failure of Waste Packages* • FEP 2.1.03.10.0A – Advection of Liquids and Solids Through Cracks in the Waste Package (Excluded) • FEP 2.1.11.06.0A – Thermal Sensitization of Waste Packages (Excluded)	Supports bases for early failure event probability Supports the basis for performance assessment initial conditions Supports basis for FEP exclusion
03-17 Waste Package Closure	• FEP 2.1.03.02.0A – Stress Corrosion Cracking (SCC) of Waste Packages • FEP 2.1.03.03.0A – Localized Corrosion of Waste Packages • FEP 2.1.03.10.0A – Advection of Liquids and Solids Through Cracks in the Waste Package (Excluded) • FEP 2.1.11.06.0A – Thermal Sensitization of Waste Packages (Excluded) • FEP 2.1.14.15.0A – In-Package Criticality (Intact Configuration) (Excluded)	Supports the basis for performance assessment initial conditions Supports basis for FEP exclusion
03-18 Waste Package Surface Marring Prior to Emplacement	• FEP 2.1.03.02.0A – Stress Corrosion Cracking (SCC) of Waste Packages • FEP 2.1.03.08.0A – Early Failure of Waste Packages*	Supports the basis for performance assessment initial conditions
03-19 Waste Package Outer Corrosion Barrier Material Specifications	• FEP 2.1.03.01.0A – General Corrosion of Waste Packages* • FEP 2.1.03.03.0A – Localized Corrosion of Waste Packages* • FEP 2.1.09.03.0B – Volume Increase of Corrosion Products Impacts Waste Package (Excluded) • FEP 2.1.09.09.0A – Electrochemical Effects in EBS (Excluded) • FEP 2.1.11.06.0A – Thermal Sensitization of Waste Packages (Excluded)	Supports the basis for performance assessment initial conditions Supports basis for FEP exclusion
03-20 Materials Contacting the Waste Package	• FEP 2.1.09.09.0A – Electrochemical Effects in EBS (Excluded)	Supports basis for FEP exclusion
03-21 Waste Package Handling	• FEP 2.1.03.08.0A – Early Failure of Waste Packages*	Supports bases for early failure event probability
03-22 Waste Package Handling and Emplacement	• FEP 1.1.03.01.0A – Error in Waste Emplacement (Excluded)* • FEP 2.1.03.08.0A – Early Failure of Waste Packages*	Supports bases for early failure event probability Supports thermal analyses
03-23 Waste Package Surface Finish	• FEP 2.1.03.08.0A – Early Failure of Waste Packages*	Supports bases for early failure event probability

Table A-1. Repository Design Use in Performance Assessment (Continued)

Control Parameter	Representative FEPs Relying on Design/Control Parameter	Control Parameter Use in Performance Assessment
03-24 Waste Package Surface Damage Prior to Closure	• FEP 2.1.03.08.0A – Early Failure of Waste Packages* • FEP 2.1.03.07.0A – Mechanical Impact on Waste Package (Excluded)* • FEP 2.1.07.01.0A – Rockfall (Excluded)	Supports the basis for performance assessment initial conditions
03-25 Waste Package Early Failure		Not used
03-26 Waste Form Moisture Removal and Inerting	• FEP 2.1.02.09.0A – Chemical Effects of Void Space in Waste Package • FEP 2.1.03.06.0A – Internal Corrosion of Waste Packages Prior to Breach (Excluded) • FEP 2.1.03.07.0A – Mechanical Impact on Waste Package (Excluded) • FEP 2.1.13.01.0A – Radiolysis (Excluded) • FEP 2.1.14.15.0A – In-Package Criticality (Intact Configuration) • FEP 2.2.12.04.0A – Gas Generation (CO_2, CH_4, H_2S) from Microbial Degradation (Excluded)	Supports the basis for performance assessment initial conditions Supports basis for FEP exclusion
04-01 Loading of Waste Forms	• FEP 2.1.03.06.0A – Internal Corrosion of Waste Packages Prior To Breach (Excluded) • FEP 2.1.11.07.0A – Thermal Expansion/Stress of In-Drift EBS Components (Excluded)	Supports basis for FEP exclusion
04-02 Handling of Uncanistered Spent Nuclear Fuel	• FEP 2.1.02.02.0A – CSNF Degradation (Alteration, Dissolution, and Radionuclide Release)*	Supports the basis for performance assessment initial conditions
04-03 Waste Form CSNF Fuel Rod Maximum Burnup Limit	• FEP 2.1.01.01.0A – Waste Inventory* • FEP 2.1.14.15.0A – In-Package Criticality (Intact Configuration) (Excluded)*	Supports the basis for performance assessment initial conditions Supports basis for FEP exclusion
04-04 Waste Form Moisture Removal and Inerting	• FEP 2.1.02.09.0A – Chemical Effects of Void Space in Waste Package • FEP 2.1.03.06.0A – Internal Corrosion of Waste Packages Prior to Breach (Excluded) • FEP 2.1.03.07.0A – Mechanical Impact on Waste Package (Excluded) • FEP 2.1.13.01.0A – Radiolysis (Excluded) • FEP 2.1.14.15.0A – In-Package Criticality (Intact Configuration) • FEP 2.2.12.04.0A – Gas Generation (CO_2, CH_4, H_2S) from Microbial Degradation (Excluded)	Supports the basis for performance assessment initial conditions Supports basis for FEP exclusion
04-05 Cladding Temperature Limit – Waste Form		Not relevant because the performance assessment does not take credit for cladding performance

Table A-1. Repository Design Use in Performance Assessment (Continued)

Control Parameter	Representative FEPs Relying on Design/Control Parameter	Control Parameter Use in Performance Assessment
04-06 Maximum Temperature of HLW Glass Canisters – Waste Form	• FEP 2.1.02.03.0A – HLW Glass Degradation (Alteration, Dissolution, and Radionuclide Release)* • FEP 2.1.02.06.0A – HLW Glass Recrystallization (Excluded)*	Supports basis for HLW degradation rate in performance assessment Supports basis for FEP exclusion
04-07 Waste Package Capacities	• FEP 2.1.01.01.0A – Waste Inventory • FEP 2.1.01.02.0A – Interactions Between Co-Located Waste (Excluded) • FEP 2.1.01.03.0A – Heterogeneity of Waste Inventory • FEP 2.1.01.02.0B – Interactions Between Co-Disposed Waste • FEP 2.1.02.01.0A – DSNF Degradation (Alteration, Dissolution, and Radionuclide Release) • FEP 2.1.02.09.0A – Chemical Effects of Void Space in Waste Package • FEP 2.1.02.28.0A – Grouping of DSNF Waste Types into Categories • FEP 2.1.02.29.0A – Flammable Gas Generation from DSNF (Excluded) • FEP 2.1.03.06.0A – Internal Corrosion of Waste Packages Prior To Breach (Excluded) • FEP 2.1.09.01.0B – Chemical Characteristics of Water in Waste Package • FEP 2.1.09.02.0A – Chemical Interaction with Corrosion Products • FEP 2.1.11.07.0A – Thermal Expansion/Stress of In-Drift EBS Components (Excluded) • FEP 2.1.14.15.0A – In-Package Criticality (Intact Configuration) (Excluded)	Supports the basis for performance assessment initial conditions Supports basis for FEP exclusion
04-08 Handling of Waste Forms	• FEP 2.1.02.01.0A – DSNF Degradation (Alteration, Dissolution, and Radionuclide Release)* • FEP 2.1.02.02.0A – CSNF Degradation (Alteration, Dissolution, and Radionuclide Release)* • FEP 2.1.02.03.0A – HLW Glass Degradation (Alteration, Dissolution, and Radionuclide Release)*	Supports the basis for performance assessment initial conditions
04-09 Waste Package & TAD Canister Excluded Materials	• FEP 2.1.02.10.0A – Organic/Cellulosic Materials in Waste (Excluded) • FEP 2.1.09.03.0B – Volume Increase of Corrosion Products Impacts Waste Package (Excluded) • FEP 2.1.12.04.0A – Gas Generation (CO_2, CH_4, H_2S) from Microbial Degradation (Excluded)	Supports basis for FEP exclusion
05-01 Waste Package Handling and Emplacement	• FEP 1.1.03.01.0A – Error in Waste Emplacement (Excluded)* • FEP 2.1.03.08.0A – Early Failure of Waste Packages*	Supports bases for early failure event probability Supports basis for FEP exclusion analyses
05-02 Waste Package Spacing	• FEP 1.1.07.00.0A – Repository Design • FEP 1.2.03.02.0A – Seismic Ground Motion Damages EBS Components*	Supports the basis for performance assessment initial conditions

Table A-1. Repository Design Use in Performance Assessment (Continued)

Control Parameter	Representative FEPs Relying on Design/Control Parameter	Control Parameter Use in Performance Assessment
05-03 Waste Package Thermal Limits	• FEP 1.1.07.00.0A – Repository Design • FEP 2.1.01.04.0A – Repository-Scale Spatial Heterogeneity of Emplaced Waste* • FEP 2.1.08.03.0A – Repository Dry-Out Due to Waste Heat* • FEP 2.1.11.06.0A – Thermal Sensitization of Waste Packages (Excluded)* • FEP 2.1.11.06.0B – Thermal Sensitization of Drip Shields (Excluded)*	Supports the basis for performance assessment initial conditions Supports basis for FEP exclusion
05-04 No Backfill in Emplacement Drifts	• FEP 1.1.03.01.0B – Error in Backfill Emplacement (Excluded) • FEP 2.1.04.01.0A – Flow in the Backfill (Excluded) • FEP 2.1.04.02.0A – Chemical Properties and Evolution of Backfill (Excluded) • FEP 2.1.04.03.0A – Erosion or Dissolution of Backfill (Excluded) • FEP 2.1.04.04.0A – Thermal-Mechanical Effects of Backfill (Excluded) • FEP 2.1.04.05.0A – Thermal-Mechanical Properties and Evolution of Backfill (Excluded) • FEP 2.1.04.09.0A – Radionuclide Transport in Backfill (Excluded) • FEP 2.1.11.03.0A – Exothermic Reactions in the EBS (Excluded) • FEP 2.2.01.02.0B – Chemical Changes in the Near-Field from Backfill (Excluded)	Supports basis for FEP exclusion
06-01 Duration of Ventilation Period	• FEP 1.1.02.00.0A – Chemical Effects of Excavation and Construction in EBS (Excluded) • FEP 1.1.02.02.0A – Preclosure Ventilation • FEP 1.1.07.00.0A – Repository Design • FEP 1.1.09.00.0A – Schedule and Planning • FEP 2.1.11.01.0A – Heat Generation in EBS • FEP 2.2.01.03.0A – Changes in Fluid Saturations in the Excavation Disturbed Zone (Excluded)	Supports the basis for performance assessment initial conditions Supports basis for FEP exclusion
06-02 Drift Wall Temperature	• FEP 1.1.02.02.0A – Preclosure Ventilation* • FEP 2.1.07.01.0A – Rockfall (Excluded) • FEP 2.1.07.02.0A – Drift Collapse (Excluded) • FEP 2.1.11.01.0A – Heat Generation in EBS*	Supports the basis for performance assessment initial conditions Supports basis for FEP exclusion
06-03 Waste Package Temperature Limit	• FEP 2.1.11.06.0A – Thermal Sensitization of Waste Packages (Excluded)	Supports basis for FEP exclusion
06-04 Cladding Temperature Limit – Ventilation		Not relevant because the performance assessment does not take credit for cladding performance

Table A-1. Repository Design Use in Performance Assessment (Continued)

Control Parameter	Representative FEPs Relying on Design/Control Parameter	Control Parameter Use in Performance Assessment
06-05 Maximum Temperature of HLW Glass Canisters – Ventilation	• FEP 2.1.02.03.0A – HLW Glass Degradation (Alteration, Dissolution, and Radionuclide Release)* • FEP 2.1.02.06.0A – HLW Glass Recrystallization (Excluded)*	Supports basis for HLW degradation rate in performance assessment Supports basis for FEP exclusion
06-06 Average Airflow Rate for Preclosure Ventilation Period	• FEP 1.1.02.00.0A – Chemical Effects of Excavation and Construction in EBS (Excluded) • FEP 1.1.02.02.0A – Preclosure Ventilation* • FEP 2.1.11.01.0A – Heat Generation in EBS* • FEP 2.2.10.13.0A – Repository-Induced Thermal Effects on Flow in the SZ (Excluded)*	Supports the basis for performance assessment initial conditions
07-01 Drip Shield Design	• FEP 1.2.03.02.0B – Seismic-Induced Rockfall Damages EBS Components (Excluded) • FEP 2.1.03.03.0B – Localized Corrosion of Drip Shields (Excluded) • FEP 2.1.03.04.0B – Hydride Cracking of Drip Shields (Excluded) • FEP 2.1.06.05.0B – Mechanical Degradation of Invert (Excluded) • FEP 2.1.06.06.0A – Effects of Drip Shield on Flow • FEP 2.1.09.03.0C – Volume Increase of Corrosion Products Impacts Other EBS Components (Excluded) • FEP 2.1.09.09.0A – Electrochemical Effects in EBS (Excluded) • FEP 2.1.03.10.0B – Advection of Liquids and Solids Through Cracks in the Drip Shield (Excluded)* • FEP 2.1.03.11.0A – Physical Form of Waste Package and Drip Shield	Supports the basis for performance assessment initial conditions Supports basis for FEP exclusion
07-02 Drip Shield Design and Installation	• FEP 1.1.07.00.0A – Repository Design • FEP 2.1.06.06.0A – Effects of Drip Shield on Flow	Supports the basis for performance assessment initial conditions
07-03 Drip Shield Corrosion Allowance	• FEP 1.2.03.02.0A – Seismic Ground Motion Damages EBS Components* • FEP 2.1.03.01.0B – General Corrosion of Drip Shields* • FEP 2.1.06.07.0B – Mechanical Effects at EBS Component Interfaces (Excluded)	Supports the basis for performance assessment initial conditions Supports basis for FEP exclusion

Table A-1. Repository Design Use in Performance Assessment (Continued)

Control Parameter	Representative FEPs Relying on Design/Control Parameter	Control Parameter Use in Performance Assessment
07-04 Drip Shield Materials and Thicknesses	• FEP 1.1.07.00.0A – Repository Design • FEP 1.2.03.02.0A – Seismic Ground Motion Damages EBS Components* • FEP 1.2.03.02.0B – Seismic-Induced Rockfall Damages EBS Components (Excluded)* • FEP 2.1.03.01.0B – General Corrosion of Drip Shields • FEP 2.1.03.03.0B – Localized Corrosion of Drip Shields (Excluded) • FEP 2.1.03.04.0B – Hydride Cracking of Drip Shields (Excluded) • FEP 2.1.03.05.0B – Microbially Influenced Corrosion (MIC) of Drip Shields (Excluded) • FEP 2.1.06.07.0B – Mechanical Effects at EBS Component Interfaces (Excluded) • FEP 2.1.07.02.0A – Drift Collapse (Excluded) • FEP 2.1.08.15.0A – Consolidation of EBS Components (Excluded) • FEP 2.1.09.09.0A – Electrochemical Effects in EBS (Excluded) • FEP 2.1.09.28.0B – Localized Corrosion on Drip Shield Surfaces Due to Deliquescence (Excluded)	Supports the basis for performance assessment initial conditions Supports basis for FEP exclusion
07-05		Not used
07-06		Not used
07-07 EBS Drip Shield/Emplacement Drift Invert Materials Interactions	• FEP 1.1.07.00.0A – Repository Design • FEP 2.1.03.04.0B – Hydride Cracking of Drip Shields (Excluded) • FEP 2.1.03.09.0A – Copper Corrosion in EBS (Excluded) • FEP 2.1.06.07.0A – Chemical Effects at EBS Component Interfaces (Excluded) • FEP 2.1.06.07.0B – Mechanical Effects at EBS Component Interfaces (Excluded) • FEP 2.1.09.09.0A – Electrochemical Effects in EBS (Excluded)	Supports the basis for performance assessment initial conditions Supports basis for FEP exclusion
07-08 Drip Shield Seismic Performance	• FEP 1.2.03.02.0A – Seismic Ground Motion Damages EBS Components* • FEP 2.1.03.02.0B – Stress Corrosion Cracking (SCC) of Drip Shields (Excluded) • FEP 2.1.06.07.0B – Mechanical Effects at EBS Component Interfaces (Excluded)	Supports the basis for performance assessment initial conditions Supports basis for FEP exclusion
07-09 Drip Shield Fabrication	• FEP 2.1.03.08.0B – Early Failure of Drip Shields*	Supports bases for early failure event probability
07-10 Drip Shield Fabrication Weld Inspections	• FEP 2.1.03.08.0B – Early Failure of Drip Shields*	Supports bases for early failure event probability

Table A-1. Repository Design Use in Performance Assessment (Continued)

Control Parameter	Representative FEPs Relying on Design/Control Parameter	Control Parameter Use in Performance Assessment
07-11 Drip Shield Fabrication Welding Flaws	• FEP 2.1.03.08.0B – Early Failure of Drip Shields*	Supports bases for early failure event probability
07-12 Drip Shield Fabrication Weld Materials	• FEP 2.1.03.04.0B – Hydride Cracking of Drip Shields (Excluded) • FEP 2.1.03.08.0B – Early Failure of Drip Shields*	Supports bases for early failure event probability Supports basis for FEP exclusion
07-13 Drip Shield Heat Treatment	• FEP 2.1.03.02.0B – Stress Corrosion Cracking (SCC) of Drip Shields (Excluded) • FEP 2.1.03.10.0B – Advection of Liquids and Solids Through Cracks in the Drip Shield (Excluded)	Supports basis for FEP exclusion
07-14 Drip Shield Handling	• FEP 2.1.06.07.0B – Mechanical Effects at EBS Component Interfaces (Excluded) • FEP 2.1.03.07.0A – Mechanical Impact on Waste Package (Excluded)* • FEP 2.1.03.08.0B – Early Failure of Drip Shields*	Supports bases for early failure event probability Supports basis for FEP exclusion
07-15 Drip Shield Thermal Expansion Constraint	• FEP 2.1.06.07.0B – Mechanical Effects at EBS Component Interfaces (Excluded) • FEP 2.1.11.07.0A – Thermal Expansion/Stress of In-Drift EBS Components (Excluded)	Supports basis for FEP exclusion
07-16 As-emplaced Waste Configuration – Waste Package/Drip Shield Clearance	• FEP 1.2.03.02.0A – Seismic Ground Motion Damages EBS Components* • FEP 1.2.03.02.0B – Seismic-Induced Rockfall Damages EBS Components (Excluded)	Supports the basis for performance assessment initial conditions Supports basis for FEP exclusion
07-17 Drip Shield Early Failure		Not used
08-01 Emplacement Pallet Design	• FEP 1.2.03.02.0B – Seismic-Induced Rockfall Damages EBS Components (Excluded) • FEP 2.1.03.09.0A – Copper Corrosion in EBS (Excluded) • FEP 2.1.06.05.0A – Mechanical Degradation of Emplacement Pallet (Excluded) • FEP 2.1.06.05.0C – Chemical Degradation of Emplacement Pallet • FEP 2.1.06.07.0A – Chemical Effects at EBS Component Interfaces (Excluded) • FEP 2.1.06.07.0B – Mechanical Effects at EBS Component Interfaces (Excluded) • FEP 2.1.08.07.0A – Unsaturated Flow in the EBS • FEP 2.1.09.09.0A – Electrochemical Effects in EBS (Excluded) • FEP 2.1.11.07.0A – Thermal Expansion/Stress of In-Drift EBS Components (Excluded)	Supports the basis for performance assessment initial conditions Supports basis for FEP exclusion

Table A-1. Repository Design Use in Performance Assessment (Continued)

Control Parameter	Representative FEPs Relying on Design/Control Parameter	Control Parameter Use in Performance Assessment
08-02 Emplacement Pallet Function	• FEP 2.1.03.09.0A – Copper Corrosion in EBS (Excluded) • FEP 2.1.06.05.0A – Mechanical Degradation of Emplacement Pallet (Excluded) • FEP 2.1.06.05.0C – Chemical Degradation of Emplacement Pallet • FEP 2.1.06.07.0B – Mechanical Effects at EBS Component Interfaces (Excluded) • FEP 2.1.08.07.0A – Unsaturated Flow in the EBS • FEP 2.1.09.09.0A – Electrochemical Effects in EBS (Excluded)	Supports the basis for performance assessment initial conditions Supports basis for FEP exclusion
08-03 Emplacement Pallet Fabrication and Corrosion Allowance	• FEP 1.2.03.02.0A – Seismic Ground Motion Damages EBS Components* • FEP 2.1.03.04.0A – Hydride Cracking of Waste Packages (Excluded) • FEP 2.1.03.09.0A – Copper Corrosion in EBS (Excluded) • FEP 2.1.06.05.0A – Mechanical Degradation of Emplacement Pallet (Excluded) • FEP 2.1.06.05.0C – Chemical Degradation of Emplacement Pallet • FEP 2.1.06.07.0A – Chemical Effects at EBS Component Interfaces (Excluded) • FEP 2.1.06.07.0B – Mechanical Effects at EBS Component Interfaces (Excluded) • FEP 2.1.09.09.0A – Electrochemical Effects in EBS (Excluded)	Supports the basis for performance assessment initial conditions Supports basis for FEP exclusion
08-04 EBS Materials Interactions – Emplacement Pallet Function	• FEP 2.1.06.05.0C – Chemical Degradation of Emplacement Pallet* • FEP 2.1.06.07.0A – Chemical Effects at EBS Component Interfaces (Excluded)* • FEP 2.1.09.09.0A – Electrochemical Effects in EBS (Excluded)*	Supports the basis for performance assessment initial conditions Supports basis for FEP exclusion
08-05 Waste Package and Emplacement Pallet Static Stresses	• FEP 2.1.03.02.0A – Stress Corrosion Cracking (SCC) of Waste Packages • FEP 2.1.06.05.0C – Chemical Degradation of Emplacement Pallet • FEP 2.1.06.07.0B – Mechanical Effects at EBS Component Interfaces (Excluded)	Supports the basis for performance assessment initial conditions Supports basis for FEP exclusion

Table A-1. Repository Design Use in Performance Assessment (Continued)

Control Parameter	Representative FEPs Relying on Design/Control Parameter	Control Parameter Use in Performance Assessment
09-01 Closure of Shafts and Ramps	• FEP 1.1.03.01.0B – Error in Backfill Emplacement (Excluded) • FEP 1.1.09.00.0A – Schedule and Planning • FEP 2.1.04.01.0A – Flow in the Backfill (Excluded) • FEP 2.1.04.02.0A – Chemical Properties and Evolution of Backfill (Excluded) • FEP 2.1.04.03.0A – Erosion or Dissolution of Backfill (Excluded) • FEP 2.1.04.04.0A – Thermal-Mechanical Effects of Backfill (Excluded) • FEP 2.1.04.05.0A – Thermal-Mechanical Properties and Evolution of Backfill (Excluded) • FEP 2.1.04.09.0A – Radionuclide Transport in Backfill (Excluded) • FEP 2.1.05.01.0A – Flow Through Seals (Access Ramps and Ventilation Shafts) (Excluded) • FEP 2.1.05.02.0A – Radionuclide Transport Through Seals (Excluded) • FEP 2.1.05.03.0A – Degradation of Seals (Excluded) • FEP 2.2.01.02.0B – Chemical Changes in the Near-Field from Backfill (Excluded) • FEP 2.3.09.01.0A – Animal Burrowing/Intrusion (Excluded)	Supports the basis for performance assessment initial conditions Supports basis for FEP exclusion
09-02		Not used
09-03 Sealing of Boreholes	• FEP 1.1.01.01.0A – Open Site Investigation Boreholes (Excluded) • FEP 1.1.11.00.0A – Monitoring of the Repository (Excluded)	Supports basis for FEP exclusion
09-04 Reclamation of Lands Disturbed by Repository	• FEP 1.2.07.01.0A – Erosion/Denudation (Excluded) • FEP 2.3.01.00.0A – Topography and Morphology • FEP 2.3.11.02.0A – Surface Runoff and Flooding* • FEP 2.3.11.03.0A – Infiltration and Recharge* • FEP 3.3.06.01.0A – Repository Excavation (Excluded)	Supports the basis for performance assessment initial and boundary conditions Supports basis for FEP exclusion

Sources: BSC 2008 [DIRS 183627]; SNL 2007 [DIRS 179354]; SNL 2007 [DIRS 179466]; SNL 2007 [DIRS 179567]; SNL [DIRS 179394].

Table A-2. Indirect Inputs for Appendix A

Citation	Title	DIRS
SNL 2007	*Total System Performance Assessment Data Input Package for Requirements Analysis for EBS In-Drift Configuration*	179354
SNL 2007	*Total System Performance Assessment Data Input Package for Requirements Analysis for DOE SNF/HLW and Navy SNF Waste Package Overpack Physical Attributes Basis for Performance Assessment*	179567
SNL 2007	*Total System Performance Assessment Data Input Package for Requirements Analysis for Subsurface Facilities*	179466
SNL 2007	*Total System Performance Assessment Data Input Package for Requirements Analysis for TAD Canister and Related Waste Package Overpack Physical Attributes Basis for Performance Assessment*	179394
BSC 2008	*Postclosure Modeling and Analyses Design Parameters*	183627

INTENTIONALLY LEFT BLANK

APPENDIX B

ANALYSIS OF ROCKFALL AND ITS IMPACT TO DRIP SHIELD DENTING

B.1 INTRODUCTION

This appendix provides an analysis of data on rockfalls capable of denting a drip shield. The results from this analysis support the screening justification for excluded FEP 2.1.03.10.0B (Advection of Liquids and Solids Through Cracks in the Drip Shield). The potential for SCC in the drip shield resulting from the damage areas associated with denting is addressed in the FEP screening justification and in Appendix C. The tearing or rupture of drip shield plates from large block impacts is excluded from the TSPA model because of low consequence as discussed in excluded FEP 1.2.03.02.0B (Seismic-Induced Rockfall Damages EBS Components).

The response of the rock mass surrounding a repository emplacement drift to a seismic event is a function of the structural characteristics of the rock. In the repository, lithophysal units (including the upper lithophysal zone (Tptpul) and lower lithophysal zone (Tptpll)) are characterized by lithophysal voids interconnected by intense fracturing (BSC 2004 [DIRS 166107], Section 6.4.1.1). The strength of the lithophysal rock ranges from approximately 10 to 40 MPa (BSC 2004 [DIRS 166107], Table E-9). Postclosure ground motion in lithophysal rock results in rock failure, with fragmented rock particle sizes on the order of centimeters to decimeters (BSC 2004 [DIRS 166107], Section 8.1). The individual fragments are too small to damage the drip shield; the drip shields in the lithophysal rock zone are damaged from the static loading due to rubble accumulation and seismic-induced dynamic loading (SNL 2007 [DIRS 176828], Section 6.10.1). Approximately 85% of the repository emplacement area will be in lithophysal rock (SNL 2007 [DIRS 179466], Table 4-1, Parameter Number 01-03). Therefore, approximately 85% of the drip shields will not be subject to denting from rockfall.

The nonlithophysal units (including the middle nonlithophysal zone (Tptpmn) and the lower nonlithophysal zone (Tptpln)) are composed of strong, intact blocks of welded tuff that are separated by fracture planes (BSC 2004 [DIRS 166107], Section 6.4.1.1). The strength of the nonlithophysal rock ranges from approximately 40 to 360 MPa (BSC 2004 [DIRS 166107], Table E-8). Postclosure ground motion in nonlithophysal rock results in a varying extent of drift damage due to rockfall (BSC 2004 [DIRS 166107], Section 8.1), with the rockfall results described in *Drift Degradation Analysis* (BSC 2004 [DIRS 166107], Section 6.3.1.2). Some of the rock blocks ejected from the walls or back of the emplacement drifts will impact the drip shield and could result in mechanically stressed areas. If the stress is sufficiently high, the damaged area may be susceptible to stress corrosion cracking (SNL 2007 [DIRS 181953], Section 6.2.2). This appendix provides a reasonable estimate of the potential for damage (i.e., denting and cracking) to occur to the drip shield relative to its performance as a barrier to seepage contacting the waste packages. This analysis is designed to estimate the rockfall events that could result in such dents or cracking as a function of seismic event probabilities.

B.2 PROBABILITY ANALYSIS FOR EBS FEP JUSTIFICATION RELATED TO DRIP SHIELD DENTING

The probability that seismic-induced rockfall causes a significant dent on the drip shield can be evaluated from structural response calculations for large rock blocks impacting the drip shield and from the bounded hazard curve for horizontal peak ground velocity (PGV) at the

emplacement drifts. A dent is considered significant if it has a concave shape that can retain a significant amount of standing liquid (seepage) in the dent.

The rockfall and denting probability analysis is based on three types of information:

- Analysis of rockfall induced by vibratory ground motions in the nonlithophysal zones
- Structural response of the drip shield to individual rock block impacts
- The bounded hazard curve for PGV.

The occurrence of multiple rockfalls impacting the drip shield at the same location is addressed in excluded FEP 2.1.07.01.0A (Rockfall). The probability analysis is reasonable and conservative because of the issues discussed in Section B.2.4.

B.2.1 Analysis of Rockfall Data in Nonlithophysal Zones

Rockfall calculations for the nonlithophysal zones have been performed (BSC 2004 [DIRS 166107], Section 6.3) using vibratory ground motions at the 1.05, 2.44, and 5.35 m/s PGV levels (BSC 2004 [DIRS 170027], Tables 6.3-14, 6.3-16, and 6.3-18). A total of 50 realizations were performed at the 1.05 and 2.44 m/s PGV levels and 44 realizations were performed at the 5.35 m/s PGV level. Each realization analyzes the response of a 21.74-m-long section of drift (Figure B-1) with a randomly sampled fracture pattern. The output from each realization includes the impact parameters (location, relative velocity, block kinetic energy, block momentum, etc.) of the individual rock blocks on the top and sides of the drip shield. The shape of the drip shield, depicted in Figure B-2, in the rockfall calculations has been simplified to a rectangular cross-section as depicted in Figure B-3, ignoring the curvature of the top of the drip shield. This geometric simplification is not significant for the probability analysis that follows, since the simplified drip shield is only used as a marker for collecting rockfall data (i.e., locations and relative velocities of the rockfall impacts) (BSC 2004 [DIRS 166107], Section 6.3.1.1).

The impact data for the rock blocks at the 1.05, 2.44, and 5.35 m/s PGV levels have been filtered to retain only the blocks that contact the top of the drip shield, including the top corners of the rectangular cross-section (Table B-1). Table B-1 contains a truncated list of blocks (sorted by impact energy) beginning with the rock block with the highest impact energy. A review of these data indicates that the blocks with the greatest impact energies impact the shoulders (i.e., the top corners of the rectangular cross-section) of the drip shield. The list of blocks in Table B-1 has been truncated at a point coincident to the block with the highest impact energy that impacts the center third of the drip shield. For example:

- At the 1.05 m/s PGV level, the two blocks with the greatest impact energies of 87 and 84 kJ are shoulder impacts; the block with the third highest impact energy, 32 kJ, contacts the top of the drip shield, toward the center.

- At the 2.44 m/s PGV level, the blocks with the seven greatest impact energies, ranging from 153 to 45 kJ, are shoulder impacts. The block with the eighth greatest impact energy, 44 kJ, contacts the top of the drip shield, toward the center.

- At the 5.35 m/s PGV level, the blocks with the twenty-four greatest impact energies, ranging from 707 to 48 kJ, are shoulder impacts. The block with the twenty-fifth greatest impact energy, 48 kJ, contacts the top of the drip shield, toward the center.

Blocks that impact the shoulders of the drip shield are likely to form a crease where the slope of the drip shield is large. The creases are expected to allow seepage to run down the side of the drip shield, rather than retaining a "pool" of liquid in the dent. The blocks impacting the center third of the drip shield (Figure B-2) could form dents that can pool water (since the slope of the drip shield increases away from the crown).

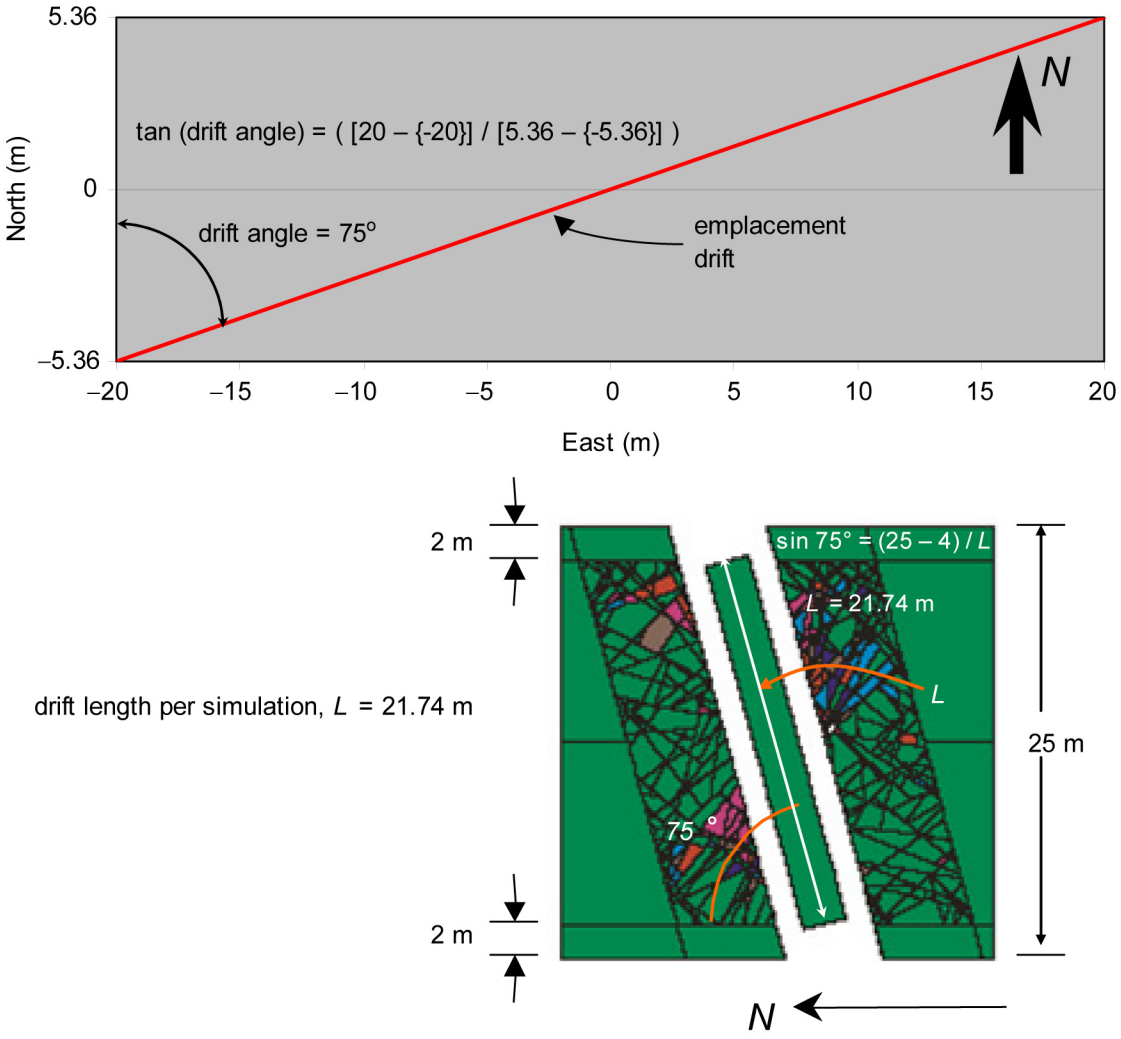

Sources: DTN: MO0408MWDDDMIO.002 [DIRS 171483], folder: 3DEC Inputs and Outputs\Nonlithophysal\Base Case\3DEC 1e-5\Case14, file: *driver.dat*, coordinates of the emplacement drift (*north1 = −5.36 m*; *east1 = −0 m*; *north2 = 5.36 m*; *east2 = 20 m*), model size (*modelSize = 25 m*), and boundary edge (*edge = 2 m*); BSC 2004 [DIRS 166107], Figure 6-34, plan view drift sketch.

Figure B-1. Drift Length per Simulation

Table B-1. Selection of Blocks with Highest Impact Energy That Could Dent Drip Shield Crown Area

Case	Volume (m^3)	Impact Velocity, x-component (longitudinal) (m/s)	Impact Velocity, y-component (vertical) (m/s)	Impact Velocity, z-component (lateral) (m/s)	Impact Location, x-coordinate (m)	Impact Location, y-coordinate (m)	Impact Location, z-coordinate (m)	Mass (metric ton)	Velocity (m/s)	Impact Angle (degree)	Impact Momentum (kg*m/s)	Impact Energy (kJ)	Drip Shield Crown Area Impact Location
Impact information:	*Unbounded ground motion with 10^{-4} annual exceedance frequency; – No blocks of sufficient energy (i.e., greater than approximately 20 kJ) were simulated.*												
Impact information:	*Unbounded ground motion with 10^{-5} Annual Exceedance Frequency. PGV = 1.05 m/s (BSC 2004 [DIRS 170027], Table 6.3-14). Total simulated drift length = 1,087 m.*												
40	3.11	4×10^{-2}	−4.77	5.74×10^{-1}	−6.63	1.44	−1.27	7.49	4.81	131	36,017	87	shoulder
53	3.03	4.20×10^{-1}	−4.74	-5.22×10^{-1}	3.52	1.44	−1.27	7.31	4.78	131	34,967	84	shoulder
40	5.57×10^{-1}	3.83×10^{-1}	−6.86	2.51×10^{-1}	−6.52	1.44	3.17×10^{-1}	1.34	6.87	78	9,224	32	center 1/3
Impact information:	*Unbounded ground motion with 10^{-6} annual exceedance frequency; PGV = 2.44 m/s (BSC 2004 [DIRS 170027], Table 6.3-16). Total simulated drift length = 1,087 m.*												
61	4.92	−1.34	−3.98	2.85	4.64	1.44	−1.27	11.87	5.07	131	60,231	153	shoulder
40	5.50	5.13×10^{-1}	−4.17	6.21×10^{-1}	−7.26	1.44	−1.26	13.28	4.24	131	56,344	120	shoulder
67	4.45×10^{-1}	−5.54	−6.01	8.83	3.28	1.44	−1.27	1.07	12.03	131	12,909	78	shoulder
40	2.85	−1.17	−3.80	4.32×10^{-1}	−5.60	1.44	1.27	6.86	4.00	49	27,469	55	shoulder
33	4.77	4.30×10^{-1}	−2.89	-5.72×10^{-1}	−3.98	1.44	1.27	11.50	2.98	49	34,257	51	shoulder
64	1.40	1.41	−5.05	1.25	5.45	1.44	−1.25	3.36	5.39	131	18,147	49	shoulder
32	1.67	−2.68	−3.85	7.72×10^{-1}	8.62	1.44	−1.27	4.02	4.76	131	19,125	45	shoulder
39	1.34	−1.70	−4.94	3.77×10^{-1}	−8.55	1.44	2.82×10^{-1}	3.23	5.23	79	16,882	44	center 1/3
Impact information:	*Unbounded ground motion with 10^{-7} annual exceedance frequency; PGV = 5.35 m/s (BSC 2004 [DIRS 170027], Table 6.3-18). Total simulated drift length = 957 m.*												
42	1.17×10^{1}	-5.68×10^{-1}	−6.76	1.98	2.75	1.44	−1.27	28.29	7.07	131	199,979	707	shoulder
42	6.15	−3.58	−5.76	1.25	−2.28	1.44	−1.27	14.82	6.90	131	102,216	353	shoulder
60	4.55	−1.42	−3.23	4.91	−3.22	1.44	−1.27	10.98	6.04	131	66,346	200	shoulder
67	1.71	−1.00	−7.39	3.95×10^{-1}	4.58	1.44	1.27	4.12	7.47	49	30,789	115	shoulder
44	3.99×10^{-1}	−6.46	−6.78	1.23×10^{2}	−1.96	1.44	6.58×10^{-1}	0.96	15.46	66	14,874	115	shoulder
53	2.48	-3.43×10^{-2}	−5.94	1.60	3.36	1.44	-9.06×10^{-1}	5.98	6.15	122	36,791	113	shoulder
61	4.92	−1.88	−3.59	8.99×10^{-1}	2.96	1.44	−1.27	11.86	4.16	131	49,300	102	shoulder
53	7.10	-7.50×10^{-1}	−2.95	−1.46	3.42	1.44	−1.08	17.11	3.37	127	57,713	97	shoulder
15	1.81	−3.46	−3.52	3.54	−7.87	1.44	−1.23	4.35	6.07	131	26,432	80	shoulder
53	9.81×10^{-1}	4.45	−5.63	−3.59	8.30	1.44	8.57×10^{-1}	2.36	8.02	59	18,970	76	shoulder
33	4.77	−1.02	−2.98	−1.76	−5.60	1.44	1.27	11.49	3.61	49	41,434	75	shoulder

Table B-1. Selection of Blocks with Highest Impact Energy that Could Dent Drip Shield Crown Area (Continued)

Case	Volume (m^3)	Impact Velocity, x-component (longitudinal) (m/s)	Impact Velocity, y-component (vertical) (m/s)	Impact Velocity, z-component (lateral) (m/s)	Impact Location, x-coordinate (m)	Impact Location, y-coordinate (m)	Impact Location, z-coordinate (m)	Mass (metric ton)	Velocity (m/s)	Impact Angle (degree)	Impact Momentum (kg*m/s)	Impact Energy (kJ)	Drip Shield Crown Area Impact Location
64	8.67×10^{-1}	3.55	−7.28	1.98	−4.79	1.44	−1.26	2.09	8.34	131	17,427	73	shoulder
59	2.82	-2.94×10^{-2}	−4.32	-7.30×10^{-1}	−3.43	1.44	1.27	6.79	4.38	49	29,725	65	shoulder
15	4.40	1.53	−1.85	−2.44	−3.49	1.44	1.26	10.60	3.43	49	36,318	62	shoulder
17	1.23	1.36	−5.99	2.12×10^{-1}	1.04×10^{1}	1.44	−1.27	2.98	6.15	131	18,291	56	shoulder
49	1.28	3.10	−1.92	4.53	3.02	1.44	−1.24	3.08	5.82	131	17,955	52	shoulder
48	1.38	−1.17	−5.24	−1.54	6.90	1.44	1.17	3.31	5.58	51	18,504	52	shoulder
67	8.68×10^{-1}	7.28×10^{-1}	−6.90	-9.69×10^{-1}	1.59	1.44	-7.50×10^{-1}	2.09	7.00	118	14,653	51	shoulder
27	8.09×10^{-1}	−3.96	−5.96	6.60×10^{-1}	−5.01	1.44	1.27	1.95	7.19	49	14,010	50	shoulder
64	1.53	7.61×10^{-1}	−5.01	−1.04	5.68	1.44	1.16	3.68	5.18	51	19,037	49	shoulder
29	2.26×10^{-1}	−8.87	−6.95	7.06	−8.89	1.44	-4.59×10^{-1}	0.54	13.30	108	7243	48	shoulder
27	7.69×10^{-1}	−3.96	−5.98	5.30×10^{-1}	−5.00	1.44	1.23	1.85	7.19	50	13,327	48	shoulder
58	2.09	2.59	−2.59	−2.36	−4.52	1.44	1.27	5.04	4.35	49	21,930	48	shoulder
55	3.99×10^{-1}	−5.66	−4.02	7.13	6.17	1.44	−1.27	0.96	9.96	131	9,581	48	shoulder
66	4.19×10^{-1}	4.02	−7.31	4.94	−1.16	1.44	-6.29×10^{-2}	1.01	9.70	93	9,796	48	center 1/3

Source: DTN: MO0408MWDDDMIO.002 [DIRS 171483].

NOTES: To download data from the source DTN: (1) Select "Download files." (2) Copy the segmented zip file (10 files total) into a folder with approximately 140 GB of available space (the download requires 45 GB on one drive and the extraction requires 95 GB on that drive or another drive. If sufficient disk space is not available, contact the Model Warehouse Data Administrator using the link provided within the DTN). (3) Select file: *MO0408MWDDDMIO_002RPC1.zip*, to extract the data from the DTN (note that WinZip version 9.0 or higher must be used to extract the compressed files; select "Use folder names" from the WinZip "Extract" dialog box). Source data are provided by the following Excel spreadsheets within the extracted data from the source DTN (the files are located in folder: Calculation Files\3DEC rockfall results):

- *nonlith rockfall characteristics in emplacement drifts with 1e-4 gm.xls*
- *nonlith rockfall characteristics in emplacement drifts with 1e-5 gm.xls*
- *nonlith rockfall characteristics in emplacement drifts with 1e-6 gm.xls*
- *nonlith rockfall characteristics in emplacement drifts with 1e-7 gm.xls.*

The data in this table are provided in the worksheet "Impact Information," located within each of the Excel spreadsheets listed above. This table contains a truncated list of blocks (sorted by impact energy) beginning with the rock block with the highest impact energy. The list of blocks has been truncated to show the block with the highest impact energy that impacts center 1/3 of the drip shield. Note that the drip shield has been represented by a simplified, rectangular geometry. Only those rockfalls impacting the top of the simplified rectangular drip shield have been included. The coordinate system and impact angle are illustrated in Figure B-3. Based on the local coordinate system used (see Figure B-3), the rock blocks impacting the crown of the drip shield will have a y-coordinate (column "y-imp" in the Excel file) of 1.44 m. The center one-third of the crown is in the range of z-coordinate (column "z-imp" in the Excel file) of −0.426 to 0.426. Note that the total simulated drift length is calculated knowing the number of simulations as provided by the source DTN (i.e., either 50 or 44 simulations) and the length of drift per simulation (i.e., 21.74 m, Figure B-1).

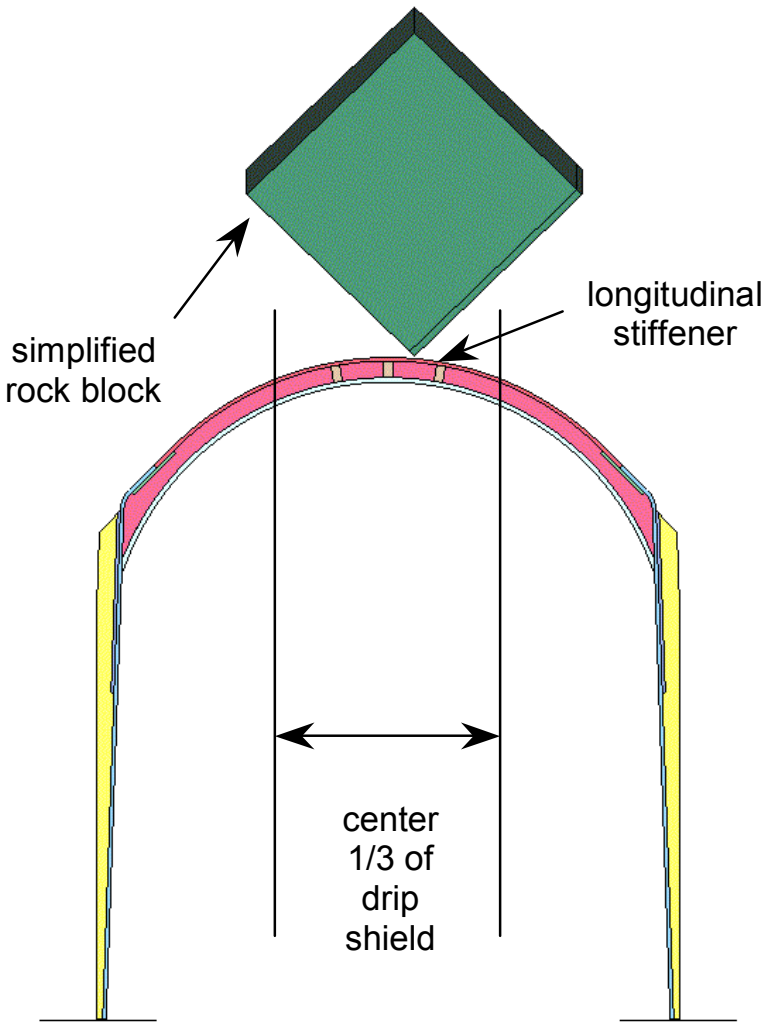

Source: BSC 2005 [DIRS 174052], Figure 6-3.

Figure B-2. Section View of Drip Shield

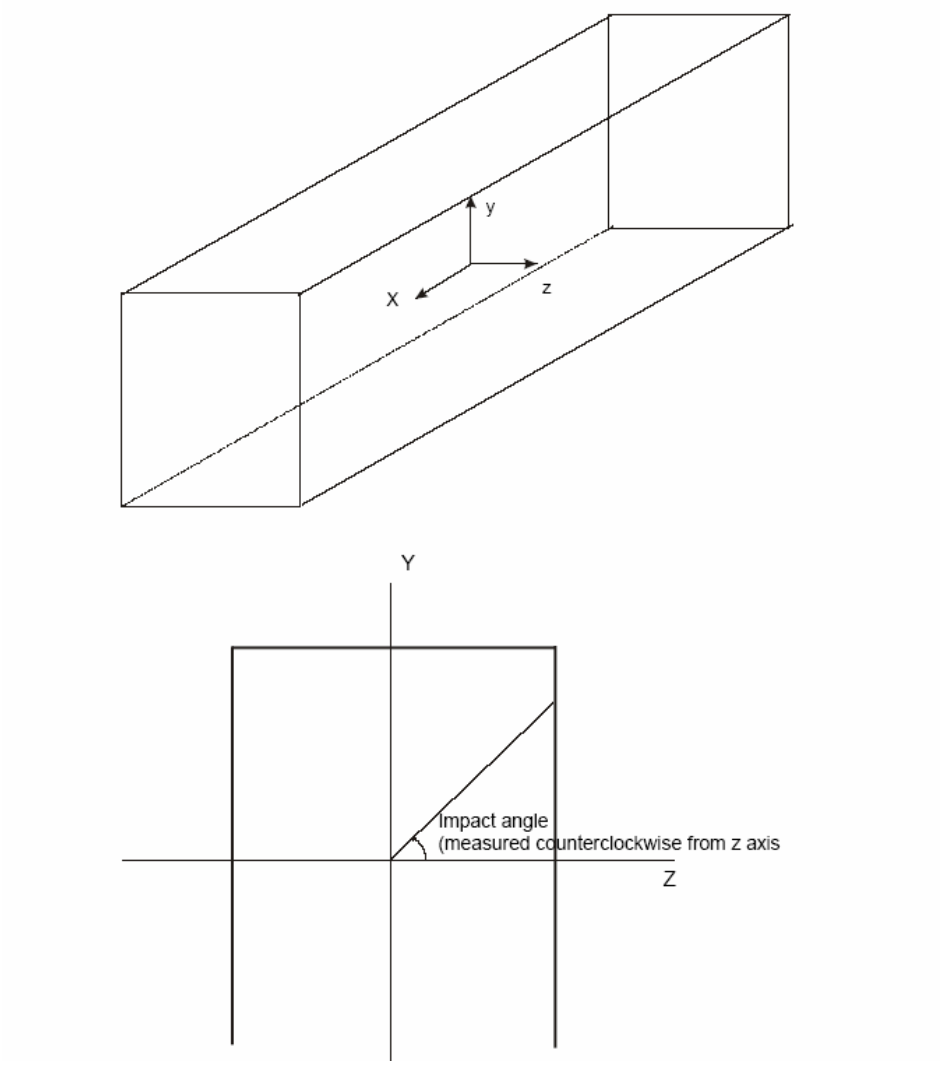

Source: BSC 2004 [DIRS 166107], Figure 6-42.

Figure B-3. Definition of Impact Angle and Drip Shield Block Local Coordinate System

B.2.2 Structural Response of the Drip Shield to Individual Rock Blocks

The structural response of the drip shield to impacts by individual rock blocks has already been calculated using a three-dimensional representation of the drip shield as discussed in *Drip Shield Structural Response to Rock Fall Supplemental Calculation* (BSC 2005 [DIRS 174052]). The individual rock blocks are idealized as cubic in shape with two possible orientations: an edge-on impact to the crown of the drip shield and a corner-on impact to the crown of the drip shield. The edge-on impact has the edge perpendicular to the longitudinal axis of the drip shield. The corner-on impact has the corner impacting between the longitudinal stiffeners that support the crown of the drip shield. In either case, the center of mass is located directly over the impact point.

The impact energy of the individual rock blocks has been selected to span the range of impact energies that are expected to result in a significant dent on the crown of the drip shield. The six individual cases are described as follows (BSC 2005 [DIRS 174052], Section 3.2.2):

- 880 Joule/0.28 metric ton block that corresponds to the 50th percentile of impact energy for the 2.44 m/s PGV level (unbounded ground motion with 10^{-6} annual exceedance frequency)
- 2,569 Joule/0.69 metric ton block that corresponds to the 75th percentile of impact energy for the 2.44 m/s PGV level (unbounded ground motion with 10^{-6} annual exceedance frequency)
- 12,894 Joule/0.96 metric ton block that corresponds to the 95th percentile of impact energy for the 2.44 m/s PGV level (unbounded ground motion with 10^{-6} annual exceedance frequency)
- 86,559 Joule/7.49 metric ton block that corresponds to the maximum impact energy for the 1.05 m/s PGV level (unbounded ground motion with 10^{-5} annual exceedance frequency)
- 152,775 Joule/11.87 metric ton block that corresponds to the maximum impact energy for the 2.44 m/s PGV level (unbounded ground motion with 10^{-6} annual exceedance frequency)
- 706,914 Joule/28.29 metric ton block that corresponds to the maximum impact energy for the 5.35 m/s PGV level (unbounded ground motion with 10^{-7} annual exceedance frequency).

The computational results for the edge-on impacts are summarized in Table B-2. Based on the results in Table B-2, the 152,775-Joule impact corresponds to the maximum rock block impact energy at the 2.44 m/s PGV level. This did not result in a dent that would retain water. It follows then that only edge-on impacts with energies greater than 152,775 Joules could result in a dent that could catch or retain seepage. The computational results for the corner-on impacts are presented in *Drip Shield Structural Response to Rock Fall Supplemental Calculation* (BSC 2005 [DIRS 174052], Figures 7-21 to 7-25).

A corner-on impact, between the longitudinal stiffeners, results in significant denting to the drip shield plates at lower impact energies than for the edge-on impacts in Table B-2. However, this corner-on geometry is considered unlikely, particularly for blocks that are 1 metric ton or larger. As represented in the drip shield structural response calculation (BSC 2005 [DIRS 174052], Section 6.3), those blocks with corner impacts are assumed to have a resultant centroid velocity vector that is directly in line with the impacting block corner (Figure B-2). In other words, all of the force of the accelerated block is assumed to be concentrated directly through the block corner. This assumption is highly improbable as the model predictions of rockfall (BSC 2004 [DIRS 166107], Section 6.3) show that blocks have complex, irregular geometries (BSC 2004 [DIRS 166107], Appendix I), and that the applied complex earthquake vibratory motion results in blocks that rotate as they fall (BSC 2004 [DIRS 166107], Figure 6-38). The blocks then

impact the curving drip shield crown with glancing impacts that have not only normal, but also tangential force components. Thus, the assumed corner impacts are considered to be an extreme case. Additionally, contacts of a rock block corner to the stiff drip shield structure will result in shearing or fragmentation and disintegration of the contact point, which will consume some of the block kinetic energy. This fragmentation potential was not accounted for in the analysis of denting (BSC 2005 [DIRS 174052], Section 6.5). The result of fragmentation is that, in reality, contact forces and energies would be far smaller than represented in the corner impact analyses. The results for the corner-on impacts are excluded from further consideration.

Table B-2. Results for Edge-On Impacts

Impact Energy (Block Mass)	Location in Source	Structural Response
880 Joule (0.28 MT)	Figure 7-14	No measurable dent—seepage will run off.
2,569 Joule (0.69 MT)	Figure 7-15	No significant deformation—seepage will run off.
12,894 Joule (0.96 MT)	Figure 7-16	Small deformation, but the slope within the dent allows seepage to run off.
86,559 Joule (7.49 MT)	Figure 7-17	Significant dent, but the remaining slope within the dent allows seepage to run off.
152,775 Joule (11.87 MT)	Figure 7-18	Significant dent, with a small flat at the top of the crown but no depression. Droplets of seepage may remain on the flat, but should runoff before forming a "pool" with significant depth.
706,914 Joule (28.29 MT)	Figure 7-19	Significant denting, with a small depression between the longitudinal stiffeners. Seepage can pool in this dent. The dent is 63.5 mm long in the axial direction. The volume of the small depression is about 5.35×10^{-5} m^3 or 1.8 ounces.

Source: BSC 2005 [DIRS 174052], Section 7.

B.2.3 Bounded Hazard Curve for Peak Ground Velocity

There are no blocks from the simulations at the 1.05 m/s and 2.44 m/s PGV levels that cause a significant dent to form on the drip shield. The probability that seismic events with PGV levels greater than 2.44 m/s will occur can be calculated from the hazard curve for PGV. A hazard curve defines the annual frequency of seismic events that exceed a given intensity level. Intensity is often measured in peak ground acceleration or peak ground velocity. Intensity is measured by horizontal PGV. The bounded hazard curve for PGV indicates that the annual exceedance frequency for all seismic events with PGV greater than 2.44 m/s is 4.52×10^{-7} per year (DTN: MO0501BPVELEMP.001 [DIRS 172682]).

This exceedance frequency includes very unlikely seismic events, including those with exceedance frequencies less than 10^{-8} per year, and this corresponds to the 5.35 PGV level with the 706,914-Joule impact energy by a 28.29 metric ton block. However, the performance assessment for the repository must consider only those events with probabilities greater than 1 in 10,000 over a 10,000-year period (10 CFR 63.114 [DIRS 180319]), corresponding to events with an annual probability[1] greater than 10^{-8}. It follows that the very unlikely seismic events can be

[1] The exceedance frequency from the hazard curve and the exceedance probability are essentially equal for very low frequency events. The probability of one or more events for a random (Poisson) process with annual rate λ over duration T is given by $(1 - e^{-\lambda T})$. When λ is small enough, the probability that one or more events occur in an interval T becomes $(1 - e^{-\lambda T}) = 1 - (1 - \lambda T + (\lambda T)^2 - \ldots) \approx \lambda T$ (Taylor series expansion for an exponential, Bolz and Tuve 1973 [DIRS 148520], Table 9-47, exponential series, p. 892). The annual probability for one or more events is then given by $(\lambda T)/T = \lambda$, the annual frequency of events.

excluded from this probability analysis. These very unlikely events can be eliminated from consideration by subtracting the exceedance frequency for the very unlikely events from that for all the events with PGV greater than 2.44 m/s:

$$\textit{Final Frequency} = 4.52 \times 10^{-7}\ \textit{per year} - 10^{-8}\ \textit{per year} = 4.42 \times 10^{-7}\ \textit{per year} \qquad \text{(Eq. B-1)}$$

The annual probability of seismic events that can cause a significant dent to form in the drip shield is then 4.42×10^{-7} per year, and the corresponding probability over 10,000 years[2] is given by:

$$\textit{Probability Over 10,000 Years} = (4.42 \times 10^{-7}\ \textit{per year})(10{,}000\ \textit{years}) = 4.42 \times 10^{-3} \sim 0.004 \qquad \text{(Eq. B-2)}$$

This probability (alone) cannot be used to screen denting of the drip shield out of TSPA because it exceeds 1 chance in 10,000. However, the reasonable conservatisms in the probability calculation are considered next.

B.2.4 Conservatisms in Probability Analysis

The probability analysis for denting from rockfall induced by seismic events has the following reasonable conservative assumptions:

- A large rock block is a partly fractured structure that is likely to crumble or partly shatter on impact with the drip shield. However, the potential for block failure is not included in the structural response calculations.

- The orientation and shape of rock blocks are chosen to increase damage by locating the center of mass directly above the impact point. Blocks have a cubic shape for the calculations, with the center of mass directly above an edge that contacts the crown of the drip shield. Based on the rockfall calculations, impacts by the highest energy blocks are likely to be mitigated by the tendency toward shoulder impacts rather than crown impacts and by the irregular block shape, wherein the center of mass is not directly over the impact point.

It should be noted that the ratio of the damaged area on the drip shield to the total drip shield area within the repository is very small. The largest dent capable of pooling water is 63.5 mm long (Table B-2) in the axial direction. Given the 21.74-m rockfall model domain (Section B.2.1), there is 0.0635-m dent length per 21.74 m of drip shield. Furthermore, 85% of the drip shields in the repository will not be subject to denting from rockfall since they will be located in lithophysal rocks (Section B.1).

A typical criterion for the accuracy of this expansion is that $\lambda T \leq 0.1$. This criterion is satisfied for this analysis because $\lambda = 4.4 \times 10^{-7}$ per year and $T = 10{,}000$ years, so that $\lambda T = 4.4 \times 10^{-3}$.

[2] FEP screening justifications are based on the initial 10,000 years after closure.

Table B-3. Direct Inputs for Appendix B

Input	Source	Description
BSC 2004. *Development of Earthquake Ground Motion Input for Preclosure Seismic Design and Postclosure Performance Assessment of a Geologic Repository at Yucca Mountain, NV*. [DIRS 170027]	Table 6.3-18	Unbounded ground motion with 1×10^{-7} annual exceedance frequency; PGV = 5.35 m/s
	Table 6.3-16	Unbounded ground motion with 1×10^{-6} annual exceedance frequency; PGV = 2.44 m/s
	Table 6.3-14	Unbounded ground motion with 1×10^{-5} annual exceedance frequency; PGV = 1.05 m/s
	Tables 6.3-14, 6.3-16, 6.3-18	Rockfall calculations for the nonlithophysal zones using vibratory ground motions at the 1.05 m/s, 2.44 m/s, and 5.35 m/s PGV levels
BSC 2004. *Drift Degradation Analysis*. [DIRS 166107]	Section 6.3, Appendix I, Figure 6-38	Model predictions of rockfall show that blocks have complex, irregular geometries and that the applied complex earthquake vibratory motion results in blocks that rotate as they fall
	Section 6.3	Rockfall calculations for the nonlithophysal zones
BSC 2005. *Drip Shield Structural Response to Rock Fall Supplemental Calculation*. [DIRS 174052]	Section 7, Figures 7-14 through 7-19	Results for edge-on impacts
	Section 6.3	Drip shield structural response calculation
	Figures 7-21 to 7-25	Computational results for the corner-on impacts
	Section 3.2.2	Six cases for the impact energy of the individual rock blocks
DTN: MO0408MWDDDMIO.002. Drift Degradation Model Inputs and Outputs. [DIRS 171483]	*MO0408MWDDDMIO_002RPC1.zip*, file: Calculation Files\3DEC rockfall results	Degradation of rock mass surrounding the emplacement drifts

Table B-4. Indirect Inputs for Appendix B

Citation	Title	DIRS
10 CFR 63	Energy: Disposal of High-Level Radioactive Wastes in a Geologic Repository at Yucca Mountain, Nevada	180319
BSC 2004	*Drift Degradation Analysis*	166107
BSC 2005	*Drip Shield Structural Response to Rock Fall Supplemental Calculation*	174052
DTN: MO0408MWDDDMIO.002	Drift Degradation Model Inputs and Outputs	171483
DTN: MO0501BPVELEMP.001	Bounded Horizontal Peak Ground Velocity Hazard at the Repository Waste Emplacement Level	172682
SNL 2007	*Seismic Consequence Abstraction*	176828
SNL 2007	*Stress Corrosion Cracking of Waste Package Outer Barrier and Drip Shield Materials*	181953
SNL 2007	*Total System Performance Assessment Data Input Package for Requirements Analysis for Subsurface Facilities*	179466

APPENDIX C

BOUNDING ANALYSIS OF WATER FLOW THROUGH SCC CRACKS IN DRIP SHIELD AND WASTE PACKAGE UNDER SHEET FLOW AND IMPINGING SEEPAGE CONDITIONS

C.1 INTRODUCTION

This appendix provides bounding analysis to evaluate the potential for water flow through seismically induced SCC-damaged drip shields and waste packages, for sheet flow (static) and impinging drip (dynamic) conditions. The analysis is conducted for the following two cases:

- Effect of sheet flow (static) water over through-wall cracks in SCC-damaged drip shields and waste packages. This condition represents the flow of water in sheets, or equivalently, rivulets, and also from "pooling" of seepage in the vicinity of the cracks.

- Effect of impinging drips (falling drops) directly on through-wall cracks in SCC-damaged drip shields and waste packages.

The analysis does not consider microscopic "film flow" along solid surfaces (as investigated by Hu et al. 2001 [DIRS 161623]) because it involves small liquid flow rates and is considered to have negligible effect on drip shield performance, by comparison to the advective water flow rate thresholds that are important to the repository performance:

- TSPA considers "no seepage" for the locations with less than a threshold seepage rate of 0.1 kg/yr per waste package location (SNL 2007 [DIRS 181244], Section 6.4[a]). Such small seepage rates are rare in the seepage abstraction and mainly a result of the interpolation procedure.

- A liquid influx rate into a breached waste package less than 100 mL/yr is negligible, compared to vapor influx, for ionic strength and pH changes of the in-package water (SNL 2007 [DIRS 180506], Section 6.10.9.1[a]).

These flow rate thresholds are also used to evaluate the significance of estimated water flow rates through cracks in the drip shield. The results from this analysis support the screening justification for excluded FEP 2.1.03.10.0A (Advection of Liquids and Solids Through Cracks in the Waste Package) and excluded FEP 2.1.03.10.0B (Advection of Liquids and Solids Through Cracks in the Drip Shield).

C.2 BOUNDING ANALYSIS FOR THROUGH-WALL SCC CRACKS IN DRIP SHIELD AND WASTE PACKAGE OUTERBARRIER

This section provides bounding analysis for: (1) the geometry of a through-wall SCC cracks in drip shield and WPOB, and (2) reasonable upper-bound numbers of through-wall SCC cracks in the drip shield and WPOB damaged by seismic-induced events (e.g., ground motion, rockfall, and rock rubble loading).

C.2.1 Width and Opening Area of a Through-Wall SCC Crack

Stress corrosion cracks in the drip shield and WPOB can be treated as semi-elliptical (SNL 2007 [DIRS 181953], Sections 6.6.2 and 6.8.5.2). Figure C-1 presents the simplified geometry of through-wall cracks. The opening displacement of a crack in an infinite sheet for a plane stress condition can be calculated using the equation given by Tada et al. (2000 [DIRS 167756], p. 125):

$$b = \frac{2(2c)\sigma}{E} \quad \text{(Eq. C-1)}$$

where b = crack width (mm), $2c$ = crack length (mm), σ = residual tensile stress (Pa), and E = the modulus of elasticity (Pa). The opening area, A_{SCC}, for an elliptical crack can be estimated by:

$$A_{SCC} = \pi\left(\frac{b}{2}\right)\left(\frac{2c}{2}\right) = \frac{(2\pi c^2)\sigma}{E} \quad \text{(Eq. C-2)}$$

When Equations C-1 and C-2 are used to estimate the width and opening area of a through-wall crack, σ is the maximum tensile stress across the wall thickness of the dominant stress plane (SNL 2007 [DIRS 181953], Section 6.6.2).

An initially semi-elliptical crack becomes a semi-circular crack as it grows to a through-wall crack (Figure C-1) (SNL 2007 [DIRS 181953], Section 6.6.2). Therefore, the expected maximum length ($2c$) of the cracks is at least two times the wall thickness (SNL 2007 [DIRS 181953], Sections 6.6.2 and 6.8.5.2). The crack width and opening area are assumed to be the same through the wall thickness. For an actual SCC crack propagating through the wall thickness, the crack width and opening area are likely to decrease along the wall thickness because of the residual stress redistribution and relaxation at the crack tip as the crack grows through the wall thickness. For the drip shield and waste package that are damaged by seismic-induced events, the residual tensile stress tends to decrease from the outer surface (where the seismic impact occurs) to the inner surface of the drip shield or WPOB. The likely shape of the through-wall cracks that result from seismic damage would be one with a larger opening in the outer surface side and a much smaller opening size at the penetration point in the inner wall surface. Those effects can be amplified when neighboring cracks propagate in parallel through the wall thickness (SNL 2007 [DIRS 181953], Sections 6.7.1.2 and 6.7.1.3).

For this analysis, the room-temperature yield strength (σ_{YS}) of Titanium Grade 7 or Alloy 22 is used for the residual stress, σ, in Equations C-1 and C-2. Values for σ_{YS} and E for the titanium alloy and Alloy 22 at room temperature are found in DTN: MO0702PASTRESS.002 [DIRS 180514] (file: *Model Output DTN.doc*) and listed in Table C-1. The use of room-temperature values is justified because SCC is a corrosion process that requires the presence of water inside and around the crack mouth to support associated corrosion reactions and is therefore operative below the water boiling temperature at the repository. In addition, using the property values from DTN: MO0702PASTRESS.002 [DIRS 180514] (file: *Model Output DTN.doc*, Table 8-1), the σ_{YS}/E ratios in Equations C-1 and C-2 for Alloy 22 and Titanium Grade 7 are larger for the room temperature values than the values at 93°C for Alloy 22 and those at 149°C for Titanium Grade 7; the use of the room temperature values results in a larger crack opening size and therefore is reasonable and conservative.

If SCC breach of the drip shield occurs during the first 10,000 years after repository closure when the drip shields maintain most of the design wall thickness of 15 mm (i.e., $2c$ = 30 mm), the maximum width of a through-wall crack in the drip shield is calculated to be approximately

155 μm (Equation C-1), and the maximum crack mouth area is approximately 3.65 mm^2 (Equation C-2).

For the waste packages, if SCC breach occurs during the first 10,000 years after repository closure when the WPOB maintains most of the design wall thickness of 25 mm (i.e., $2c = 50$ mm), the maximum width of a through-wall crack in the WPOB is calculated to be approximately 195 μm (Equation C-1), and the maximum crack mouth area is approximately 7.68 mm^2 (Equation C-2).

Table C-1. Yield Strength and Modulus of Elasticity of Titanium Grade 7 and Alloy 22 Used in This Analysis

Materials	Yield Strength (MPa) at Room Temperature	Modulus of Elasticity (GPa) at Room Temperature
Titanium Grade 7	276	107
Alloy 22	403	206

Source: DTN: MO0702PASTRESS.002 [DIRS 180514], file: *Model Output DTN.doc,* Table 8-1.

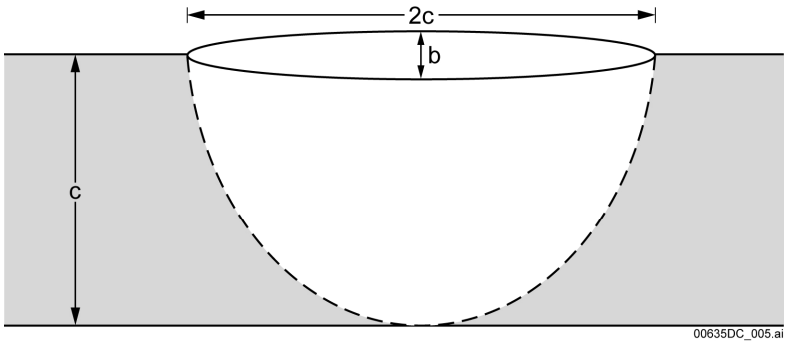

2c = maximum length of through-wall crack
c = thickness of wall
b = maximum crack width

NOTE: Illustration purpose only.

Figure C-1. A Schematic Showing Simplified Geometry of a Through-wall Crack

C.2.2 Drip Shield SCC Damage Induced by Seismic Events

Seismic-induced SCC of the drip shield plate can occur when the resultant residual tensile stress is greater than 80% of the yield strength of Titanium Grade 7 (SNL 2007 [DIRS 181953], Section 8.1.5). The seismic consequence abstraction analysis provides the areas on the drip shields damaged by seismic loading and rockfall (DTN: MO0703PASDSTAT.001 [DIRS 183148], files: *DS Damaged Areas with Rubble.xls* and *Nonlith Damage Abstraction for DS.xls*), and the summary of the analysis results is found in DTN: MO0703PASEISDA.002 [DIRS 183156]. The seismic-induced damaged area on the drip shield is defined as the residual tensile stress exceeding 80% of the at-temperature yield strength of Titanium Grade 7 (SNL 2007 [DIRS 181953], Section 8.1.5). This analysis assumes that the damage to drip shields due to seismic ground motion is distributed randomly over the surface of the drip shield.

Considering two bounding arrangements for the through-wall cracks in the drip shields (SNL 2007 [DIRS 181953], Section 6.8.5.2), the crack opening area density (crack opening area per unit seismically damaged area) (ρ_{SCCA}) is calculated as follows:

$$\rho_{SCCA} = C \times \frac{\pi \sigma_{YS}}{\sqrt{3}\, E} \qquad \text{(Eq. C-3)}$$

$$C = uniform(1, 4) \qquad \text{(Eq. C-4)}$$

where C is an epistemic uncertainty factor given by a uniform distribution between 1 and 4. Details of this bounding crack arrangement and geometry are given in *Stress Corrosion Cracking of Waste Package Outer Barrier and Drip Shield Materials* (SNL 2007 [DIRS 181953], Section 6.8.5.2). The total through-wall SCC crack opening area per drip shield (A_{DS_SCC}) that results from the seismic damage is calculated as:

$$A_{DS\_SCC} = C \frac{\pi \sigma_{YS\_DS}}{\sqrt{3}\, E_{DS}} \cdot A_{SD\_DS} \qquad \text{(Eq. C-5)}$$

where A_{SD_DS} is the seismically damaged area on the drip shield (similar to SNL 2007 [DIRS 181953], Equation 32 in Section 6.7.2), and is provided by the seismic consequence abstraction analysis (DTN: MO0703PASDSTAT.001 [DIRS 183148], files: *DS Damaged Areas with Rubble.xls* and *Nonlith Damage Abstraction for DS.xls*; DTN: MO0703PASEISDA.002 [DIRS 183156]). Regions of seismic damage are assumed to be distributed randomly over the drip shield surface.

C.2.2.1 Seismic-induced damage area of drip shield

Damage to a drip shield could occur in either the lithophysal or nonlithophysal host rock. The nonlithophysal zone comprises approximately 15% of the repository area (SNL 2007 [DIRS 179466], Table 4-1, Parameter Number 01-03). To evaluate drift degradation and rockfall impact damage on drip shields, from seismic ground motion in the first 10,000 years, a peak ground velocity (PGV) of 1.05 m/s was selected as a representative seismic ground motion. This corresponds to a mean annual exceedance frequency of approximately 10^{-5}/yr (DTN: MO0501BPVELEMP.001 [DIRS 172682]), which roughly equates to 1 chance in 10 of occurring in the first 10,000 years. The full plate thickness for drip shields was selected as appropriate for the first 10,000 years because the extent of general corrosion of Titanium Grade 7 during this time will be very small, and will not markedly alter structural performance.

For drift degradation in the lithophysal zone at the 1.05 m/s PGV level, the resulting degraded drift volume, on a per meter basis (also the volume of rock needed to fill the drift) is quantified as a uniform distribution between 30 and 120 m^3 (DTN: MO0703PASEISDA.002 [DIRS 183156], Section 1.1, step 5.e.). For this evaluation, the median value (75 m^3 per meter of drift length) was selected for a nominal collapsed drift volume. An estimate of how much rock volume is produced during such an event is quantified in *Seismic Consequence Abstraction* (SNL 2007 [DIRS 176828], Figure 6-57) and, at the 1.05 m/s PGV, has a mean value of 7.47 m^3

and a standard deviation of 8.37 m^3, which are both per meter of drift length (SNL 2007 [DIRS 176828], Table 6-30).

The total rubble accumulation on the drip shield for the time up to the point of the evaluation was estimated by selecting the 99th percentile value of the analysis for the selected PGV level. This is calculated to be 38.7 m^3 per meter of drift length (DTN: MO0703PASDSTAT.001 [DIRS 183148], file: *Lith Rubble Abstraction.xls*, worksheet: "Gamma Abstraction," cell: AE11), and is also shown in Figure 6-57 of *Seismic Consequence Abstraction* (SNL 2007 [DIRS 176828]).

Combining the estimate of rock rubble volume accumulation with the volume needed to fill a degraded drift, an estimate of the percentage fill of the drift is found by dividing 38.7 m^3 by 75 m^3, or approximately 52%. At this drift fill volume, no damage to the drip shield with the 15-mm plate thickness is estimated, as shown in DTN: MO0703PASDSTAT.001 [DIRS 183148] (file: *DS Damaged Area with Rubble.xls*, worksheet: "1.05 ms PGV - Case 2 BCs," cells: M57 to M68, and worksheet: "1.05 ms PGV - Case 1 BCs," cells: M54 to M65).

In the nonlithophysal zone, the impact damage to a drip shield due to the six largest rock blocks ejected during a 1.05 m/s PGV event was evaluated as indicated in *Mechanical Assessment of Degraded Waste Packages and Drip Shields Subject to Vibratory Ground Motion* (SNL 2007 [DIRS 178851], Table 6-153). The largest rock block considered for this analysis was at the 99.9th percentile for all blocks ejected for the 1.05 m/s PGV event (SNL 2007 [DIRS 178851], Table 6-154), and the impact by the block was estimated to result in a damage area of 0.0159 m^2 for the 15-mm drip shield plate thickness (SNL 2007 [DIRS 178851], Table 6-157). Because the estimated damage area is for one-quarter of the drip shield, the damage area for the entire drip shield is obtained by multiplying the estimate by 4, for a total damage area of 0.064 m^2.

The upper-bound damage area in the drip shield with 15-mm plate thickness that could result from seismic ground motion at the 1.05 m/s PGV level in the first 10,000 years in the repository is estimated to be 0.064 m^2, which corresponds to 0.48% of the total topside surface area of the drip shield (output DTN: SN0705WFLOWSCC.001, file: *Bounding calc for water flow through SCC cracks.xls*). A reasonable upper-bound total number of through-wall SCC cracks per damaged drip shield is estimated to be 326 cracks, and the corresponding upper-bound total crack-mouth opening area of through-wall SCC cracks per damaged drip shield is approximately 1,190 mm^2 (output DTN: SN0705WFLOWSCC.001, file: *Bounding calc for water flow through SCC cracks.xls*).

C.2.3 Waste Package SCC Damage Induced by Seismic Events

The seismic consequence abstraction analysis provides the areas on the waste packages damaged by the seismic ground motion (DTN: MO0703PASEISDA.002 [DIRS 183156]). The seismic-induced damaged area on the waste package is defined as the residual tensile stress exceeding 90% to 105% of at-temperature yield strength of Alloy 22 (SNL 2007 [DIRS 181953], Section 8.1.1).

Considering two bounding arrangements for the through-wall cracks in the waste packages (SNL 2007 [DIRS 181953], Section 6.7.3), the crack opening area density (crack opening area

per unit seismically damaged area) (ρ_{SCCA}) is calculated using Equations C-3 and C-4 and using the yield strength and elastic modulus of Alloy 22. As for the drip shield, C in Equation C-6 is an epistemic uncertainty factor given by a uniform distribution between 1 and 4 (as defined in Equation C-4). The total through-wall SCC crack opening area per waste package (A_{WP_SCC}) that results from the seismic damage is calculated as follows:

$$A_{WP\_SCC} = C \frac{\pi \sigma_{YS\_WP}}{\sqrt{3}\, E_{WP}} \times A_{SD\_WP} \qquad \text{(Eq. C-6)}$$

Where, A_{SD_WP} is the seismically damaged area on the waste package, and is provided by the seismic consequence abstraction analysis (DTN: MO0703PASEISDA.002 [DIRS 183156]). This analysis assumes that regions of damage to the WPOB due to seismic ground motion are distributed randomly over the surface of the waste package.

C.2.3.1 Seismic-Induced Damage Area of Waste Package

As for the drip shield, seismic ground motion at a PGV of 1.05 m/s was selected as a representative condition for evaluating seismic-induced damage to waste packages in the first 10,000 years in the repository. This PGV level corresponds to a mean annual exceedance frequency of approximately 10^{-5} (DTN: MO0501BPVELEMP.001 [DIRS 172682]), which roughly equates to 1 chance in 10 of occurring in the first 10,000 years.

As recommended by *Seismic Consequence Abstraction* (SNL 2007 [DIRS 176828], Section 6.5.1.2) the WPOB thickness of 23-mm, with intact internals, was selected as appropriate for the first 10,000 years of the repository. Degradation or thinning of the WPOB by general corrosion will be insignificant during this time period, and will not markedly alter structural performance. A reasonably conservative estimate of the general corrosion penetration depth for the first 10,000 years is only 0.3 mm using the 50th percentile general corrosion rate (30.8 nm/yr) at 100°C for the expected case (the medium uncertainty level for R_o and the mean apparent activation energy of 40.78 kJ/mol) (DTN: MO0612WPOUTERB.000 [DIRS 182035], file: *BaseCase GC CDFs2.xls*).

Seismic Consequence Abstraction (SNL 2007 [DIRS 176828], example in Section 6.8.3.1) provides the seismic damage analysis for two states of the waste package internals: intact and degraded state. The degraded state requires breach of the waste package and subsequent corrosion of the internals. An intact state of the internals was selected as appropriate for the first 10,000 years of the repository because earthquakes of sufficient magnitude to cause significant damage to the WPOB occur relatively infrequently during this time period, and the internals will not undergo substantial degradation by corrosion until a package experiences an extensive breach. Because they are the most abundant waste package types in the repository, the TAD-bearing waste package and the 5-DHLW/DOE SNF codisposal waste package are considered in this analysis.

Analyses have shown that the TAD-bearing waste packages of 23-mm-thick WPOB with intact internals are not subject to SCC damage from the 1.05 m/s PGV level ground motions (DTN: MO0703PASDSTAT.001 [DIRS 183148], file: *Kinematic Damage Abstraction 23-mm*

Intact.xls, worksheet: "WP Total"), and the results are also discussed in *Seismic Consequence Abstraction* (SNL 2007 [DIRS 176828], Section 6.5.1.2, Table 6-4). Therefore, no TAD-bearing waste packages are considered for this analysis.

The codisposal waste packages can be subject to SCC-damage from the same PGV level ground motions, and the 95th percentile value (0.377 m^2) was selected as a reasonably conservative upper-bound value for the damage area of the waste package (DTN: MO0703PASDSTAT.001 [DIRS 183148], file: *CDSP Kinematic Damage Abstraction 23-mm Intact.xls*, worksheet: "Gamma for 90%_i23"), and the analysis results are also shown in Figure 6-33 of *Seismic Consequence Abstraction* (SNL 2007 [DIRS 176828]). This codisposal waste package damage area is used as a representative value for the waste package in the analysis.

The selected damage area corresponds to 0.95% of the total surface area of the codisposal waste package (output DTN: SN0705WFLOWSCC.001, file: *Bounding calc for water flow through SCC cracks.xls*). A reasonably conservative upper-bound total number of through-wall SCC cracks per damaged waste package is estimated to be 697 cracks, and the corresponding upper-bound total crack-mouth opening area of through-wall SCC cracks per damaged waste package is approximately 5,351 mm^2 (output DTN: SN0705WFLOWSCC.001, file: *Bounding calc for water flow through SCC cracks.xls*).

C.3 BOUNDING ANALYSIS FOR WATER FLOW RATE IN SCC THROUGH-WALL CRACKS IN SHEET FLOW

This analysis evaluates the water flow rate in through-wall SCC cracks in the drip shield and waste package for sheet flow. This condition represents those such as a slowly moving water layer, or equivalently, rivulet flow, or limited "pooling" of seepage drips in the vicinity of a crack, but not impinging drips directly onto the cracks. The analysis assumes full liquid saturation for the tight, compact porous medium filling the cracks that are in the path of sheet flow. The initial transient unsaturated condition for the porous medium filling cracks is not included. The SCC cracks that are not affected by sheet flow are expected not to be fully saturated with water, and are permeable to gases and water vapor in the drift.

The SCC process will result in accumulation of corrosion products from associated corrosion reactions and mineral precipitates from evaporation of the water filling the crack. As discussed later, propagation of SCC cracks through the thickness of drip shield plates or the WPOB could take hundreds to thousands of years to occur for repository-relevant conditions. As SCC cracks grow through the wall, intermittent wetting and drying cycles (e.g., from episodic drips) will promote precipitation, and accumulation of corrosion products and mineral particles inside the crack. In particular, episodic drips on the drip shield surface are enhanced by spatial and temporal movements of seeps in the drift. It is further enhanced by gas pressure fluctuations and moisture redistribution in the host rock in response to barometric changes (BSC 2004 [DIRS 169734], Sections 7.3.2 and 7.4.1).

The expected SCC crack propagation rate for Titanium Grade 7 under repository conditions is approximately 10^{-10} mm/s (SNL 2007 [DIRS 181953], Section 8.1.5), and at this rate, it will take approximately 4,700 years to penetrate the 15-mm thick drip shield, assuming conservatively a constant crack growth rate as it propagates through the wall thickness. The upper-bound crack

propagation rate is approximately 10^{-8} mm/s (SNL 2007 [DIRS 181953], Section 8.1.5), and it still takes approximately 50 years for through-wall penetration. For Alloy 22 the maximum measured SCC crack growth rate in an aggressive corrosion condition relevant to the repository environments is 4.23×10^{-9} mm/s (DTN: MO0705CREEPSCC.000 [DIRS 183681], file: *SDFRvData.xls*, worksheet: "Graphs1;" SNL 2007 [DIRS 181953], Table 7-4), and at this rate, it will take approximately 190 years to penetrate the 25-mm-thick WPOB, assuming conservatively a constant crack growth rate as it propagates through the wall thickness. The model-predicted mean crack propagation rate at a reasonably bounding stress intensity factor of 40 MPa√m is 1.00×10^{-9} mm/s (DTN: MO0705CREEPSCC.000 [DIRS 183681], file: *SDFRvData.xls*, worksheet: "Graphs1"), and it will take approximately 800 years for through-wall penetration at this rate, assuming a constant crack growth rate through the wall thickness.

A detailed study using high-resolution analytical electron microscopy showed accumulation of corrosion products and presence of water from the external environment deep inside very fine SCC cracks in stainless steels and nickel-based alloys (Bruemmer and Thomas 2001 [DIRS 183685]). The corrosion product oxides tend to cement and agglomerate, especially in the presence of other minerals such as silica (Milnes and Fitzpatrick 1995 [DIRS 105911], pp. 1,180 to 1,183). SCC cracks for corrosion resistant materials like Alloy 22 and Titanium Grade 7 are typically tight and tortuous, and require only small amounts of corrosion products or mineral precipitates to become filled. In addition, because of the larger molar volumes for corrosion products compared with the base metal (e.g., titanium oxide from corrosion of Titanium Grade 7, and nickel and chromium oxides from Alloy 22), the corrosion products and mineral precipitates will be compacted inside the crack as more corrosion products form from general corrosion of the crack walls. This analysis considers that the SCC cracks in the drip shield and waste package are continuously filled with compact cemented corrosion products and mineral precipitates as the cracks grow through the wall thickness.

The saturated hydraulic conductivity of the compact, cemented porous material filling the cracks is estimated using the Kozeny-Carman equation (Bear 1972 [DIRS 156269], pp. 165 to 167) for the permeability, and using the relationship between the permeability and hydraulic conductivity (Domenico and Schwartz 1990 [DIRS 100569], pp. 61 to 63):

$$K = \left(\frac{\rho_w g}{\mu_w} \right) k = \frac{1}{5M^2} \left(\frac{\rho_w g}{\mu_w} \right) \frac{\phi^3}{(1-\phi)^2} \qquad \text{(Eq. C-7)}$$

where

K = Saturated hydraulic conductivity (cm/s)

k = permeability (cm^2)

M = Specific surface area of porous medium (surface area of solid per unit volume of solid, cm^2/cm^3)

ϕ = Porosity of medium

ρ_w = Density of water (g/cm^3)

μ_w = Absolute viscosity of water (Poise, g/cm-s)

g = Gravitational constant (981 cm/s^2).

The Kozeny-Carman equation is a widely used predictive equation for permeability, and its dependence on particle size (Bear 1972 [DIRS 156269], p. 165). The equation is based on a theory that treats a porous medium as a bundle of capillary tubes of equal length (Bear 1972 [DIRS 156269], p. 166), and this simplifying assumption gives rise to uncertainty in the estimation of permeability for real porous media. The specific surface area (M) for the porous medium filling the cracks is estimated by multiplying the density of the medium (g solid porous medium/cm^3 solid porous medium) by another type of specific surface area (cm^2 solid porous medium/g solid porous medium). The latter is measured typically by the gas absorption method. The porosity (0.4) of unconsolidated corrosion products (DTN: SN0703PAEBSRTA.001 [DIRS 183217], file: *SN0703PAEBSRTA.001 - RTA Input Tables.doc*, Table 8.2-6) is used as a reasonable conservative upper-bound in the analysis. Porosity of consolidated, compact corrosion products (and mineral precipitates) inside cracks would likely be less, and result in a lower saturated hydraulic conductivity value in Equation C-7. The density of pure water (0.965 g/cm^3) and the viscosity of pure water (0.00315 g/(cm s)) at 90°C (Lide 2000 [DIRS 131202], p. 6-9) are used in the analysis, and the effect of dissolved solutes on these properties is not considered.

Assuming unit static head gradient in the crack, the volumetric water flow rate (Q, cm^3/s) through the through-wall cracks is calculated as follows:

$$Q = K\, n_{SCC}\, A_{SCC} \qquad \text{(Eq. C-8)}$$

where

n_{SCC} = Number of through-wall cracks in the path of sheet flow that potentially flow water

A_{SCC} = Crack mouth opening area of a single through-wall crack from Equation C-2.

Parameter n_{SCC} is estimated using laboratory drip test results, which indicate that only through-wall cracks in the top part of the drip shield or waste package, where the surface is within 10 to 20 degrees of horizontal, can potentially flow in response to sheet flow conditions (DTN: SN0506F4104405.003 [DIRS 174472], file: *SCC_PhaseII_Test_Preliminary_Summary_9-21-05.doc*, table: "Sheet Flow Block Tests"). This corresponds to 2.8% to 5.6% of the total number of through-wall cracks in the drip shield and WPOB, approximating their surface area to an equivalent circular geometry and assuming the seismic-damage areas are randomly distributed over the drip shield and waste package surface.

C.3.1 Water Flow Rate in SCC Through-Wall Cracks in Sheet Flow Condition in Drip Shield

For estimating the saturated hydraulic conductivity of the porous medium inside cracks in the drip shield using the Kozeny-Carman equation (Equation C-7), a simplifying assumption is made that the porous medium consists primarily of titanium oxide (TiO_2), a corrosion product of Titanium Grade 7. The titanium oxide particles are expected to be a few tens of nanometers in size as shown from electron microscopy studies of corrosion products formed on Titanium Grade 7 samples (He et al. 2007 [DIRS 183687], p. 789 and Figure 14-b). As described previously, the titanium corrosion products inside the cracks are expected to form cemented agglomerates of poorly crystalline or polycrystalline precipitated particles. Specific surface area of 6 to 50 m^2/g for commercial grade crystalline rutile and anatase (Siriwardane and Wightman 1983 [DIRS 183688]) are used for the titanium oxide corrosion products. The specific surface area used is conservative because, as discussed previously, the surface areas of titanium oxide corrosion product particles are expected to be much higher. The density of natural rutile (4.26 g/cm^3; Lide 2000 [DIRS 131202], p. 4-108) is used for titanium oxide.

A previous study considered calcite as the crack filling material (BSC 2001 [DIRS 156807]). The specific surface area of calcium carbonate precipitates or weathered calcium carbonates in soil environments is equivalent to, or greater than, the values used for titanium corrosion products in this analysis. The specific surface area for calcium carbonate in soil environments was reported to range from a few tens to a few hundreds of m^2/g (Holford and Mattingly 1975 [DIRS 183686]). Typical commercial reagent-grade crystalline calcium carbonate powders have a specific surface area that ranges from 0.4 to 13 m^2/g (Amer et al. 1985 [DIRS 183684], Table 1). The density (2.71 g/cm^3) of natural calcite (Lide 2000 [DIRS 131202], p. 4-47) is a factor of two less than that of rutile used for the titanium corrosion products, but this makes only a minor difference in the saturated hydraulic conductivity estimates using Equation C-7. Therefore, use of calcium carbonate precipitates or weathered calcium carbonate as the crack filling materials will not make much difference in the hydraulic conductivity estimates.

With the values for the parameters of the Kozeny-Carman equation described previously, the saturated hydraulic conductivity of the titanium oxide filling inside cracks is estimated to range from 7.44×10^{-4} m/yr (or 2.36×10^{-11} m/s for the lower bound of the specific surface area) to 5.17×10^{-2} m/yr (or 1.64×10^{-9} m/s for the upper bound of the specific surface area) (output DTN: SN0705WFLOWSCC.001, file: *Bounding calc for water flow through SCC cracks.xls*, worksheet: "Sheet flow DS flow rate," cells: B29 and D29). The estimated hydraulic conductivity values fall in the range for clay, from 1.0×10^{-11} to 4.7×10^{-9} m/s (Domenico and Schwartz 1990 [DIRS 100569], Table 3-2). Considering the high specific surface area of the corrosion products, the good match with the values for clays shows that the estimated range for the hydraulic conductivity is reasonable. Clays are characterized as having very fine particle sizes, rugged platy surface morphology, and high specific surface area. Clay-rich media have very low permeability when wet, even when settled or compacted.

Using the upper-bound value of 18 for n_{SCC} in Equation C-8, the volumetric flow rate of water through the SCC through-wall cracks in the drip shield is estimated to be in the range 0.05 to 3.42 cm^3/yr (output DTN: SN0705WFLOWSCC.001, file: *Bounding calc for water flow through SCC cracks.xls*, worksheet: "Sheet flow DS flow rate," cells: B31 and D31). The

estimated flow rates through damaged drip shields for sheet flow conditions are small enough that this flow need not be considered as a potential source of flow through SCC cracks in the underlying waste package outer barrier. These estimated flow rates are much less than the threshold seepage rate of 100 mL/yr per waste package that is important to the repository performance as determined by TSPA (SNL 2007 [DIRS 181244], Section 6.4[a]; SNL 2007 [DIRS 180506], Section 6.10.9.1[a]).

C.3.2 Water Flow Rate in SCC Through-Wall Cracks in the WPOB for Sheet Flow Conditions, under Completely Failed Drip Shields

A similar bounding analysis is conducted for a SCC-damaged waste package with completely failed drip shield that does not perform the seepage diversion function. The affected waste package is assumed to be exposed directly to the drift seepage. This is not an expected condition for the drip shield in the first 10,000 years of the repository because it requires a mechanism such as drip shield early failure (SNL 2007 [DIRS 178765], Section 7).

As detailed in Section C.2.3.1, the upper-bound total number of through-wall SCC cracks per damaged waste package from the seismic ground motions at the 1.05 m/s PGV level is estimated to be 697 cracks, and the upper-bound total crack-mouth opening area of through-wall SCC cracks per damaged waste package is approximately 5,351 mm^2 (output DTN: SN0705WFLOWSCC.001, file: *Bounding calc for water flow through SCC cracks.xls*). Approximating the waste package surface to a circular geometry and assuming the seismic-damage areas are randomly distributed over the waste package surface, the upper-bound number of through-wall cracks that potentially flow water in sheet flow condition is 39 cracks (output DTN: SN0705WFLOWSCC.001, file: *Bounding calc for water flow through SCC cracks.xls*, worksheet: "Sheet flow WP flow rate," cell: B19).

For estimation of the permeability (and hydraulic conductivity) of the crack filling medium using the Kozeny-Carman equation (Equation C-7), a simplifying assumption is made that nickel oxide (NiO) is the representative corrosion product of Alloy 22 that fills the cracks. Calcium carbonate precipitates or weathered calcium carbonate in soil environment can also be considered as an alternative crack filling material, but this does not make much difference in the hydraulic conductivity estimate for the reasons discussed previously. The parameter values that are specific to this analysis are:

- Density of nickel oxide, 6.72 g/cm^3 (DTN: SN0703PAEBSRTA.001 [DIRS 183217], file: *SN0703PAEBSRTA.001 - RTA Input Tables.doc*, Table 8.2-6).

- Specific surface area of nickel oxide, 1 to 30 m^2/g (DTN: SN0703PAEBSRTA.001 [DIRS 183217], file: *SN0703PAEBSRTA.001 - RTA Input Tables.doc*, Table 8.2-4).

- Porosity of crack filling medium, 0.4 (DTN: SN0703PAEBSRTA.001 [DIRS 183217], file: *SN0703PAEBSRTA.001 - RTA Input Tables.doc*, Table 8.2-6). The porosity value used in the analysis is for unconsolidated corrosion products and considered as a reasonably conservative upper bound in the analysis. Porosity of consolidated, compact corrosion products (and mineral precipitates) inside crack would be lower and result in a lower saturated hydraulic conductivity estimate.

Using the density and viscosity of pure water at 90°C, the saturated hydraulic conductivity of the nickel oxide filling inside cracks is estimated to range from 8.30×10^{-4} m/yr (or 2.63×10^{-11} m/s for the upper bound of the specific surface area) to 7.47×10^{-1} m/yr (or 2.37×10^{-8} m/s for the lower bound of the specific surface area) (output DTN: SN0705WFLOWSCC.001, file: *Bounding calc for water flow through SCC cracks.xls*, worksheet: "Sheet flow WP flow rate," cells: D29 and B29, respectively).

Using the upper-bound value of 39 for n_{SCC} in Equation C-8, the volumetric flow rate for liquid water in SCC through-wall cracks in the WPOB for sheet flow conditions, exposed directly to drift seepage (i.e., no seepage protection by the drip shield) is estimated to be in a range of 0.25 to 222.18 cm^3/yr (output DTN: SN0705WFLOWSCC.001, file: *Bounding calc for water flow through SCC cracks.xls*, worksheet: "Sheet flow WP flow rate," cells: B31 and D31). As discussed earlier, these estimated flow rates are for conditions that are unexpected for the first 10,000 years of the repository. Much of the estimated flow rate range is less than the threshold seepage rate of 100 mL/yr per waste package location as determined for TSPA (SNL 2007 [DIRS 181244], Section 6.4[a]; SNL 2007 [DIRS 180506], Section 6.10.9.1[a]). Note also that advection of water into the inner canister of the waste package will be further hindered by the presence of the 50-mm Stainless Steel Type 316 inner vessel, and the 25-mm TAD canister.

C.4 WATER FLOW RATES THROUGH SCC CRACKS IN DRIP SHIELD BY IMPINGING DRIPS

The laboratory drip tests (DTN: SN0506F4104405.003 [DIRS 174472], files: *Dynamic_Drop_Test_Summary_SCC_4-15-05.doc*, and *SCC_PhaseII_Test_Preliminary_Summary_9-21-05.doc*, table: "Dynamic Drop Block Tests") showed that dripping onto a through-wall crack can cause water to flow through the crack. This analysis evaluates the water flow rate through a drip shield damaged by through-wall cracks, with seepage drips impinging onto the cracks. The analysis considers that drip shields are damaged from seismic-induced rockfall and ground motion at the 1.05 m/s PGV level for the first 10,000 years of the repository, and that regions of SCC crack damage are distributed uniformly over the drip shield surface. This analysis uses the same characterization of seismic-induced SCC damage as detailed in Section C.2.2.1. The SCC cracks that are not affected by drips and resulting sheet flow are expected not to be fully saturated with water, and will be permeable to gases and water vapor in the drift.

The amount of the drift seepage that potentially impinges on the through-wall cracks in a drip shield is estimated as follows:

$$F_{DS\_impinging\_drips} = F_{drift\_seepage} \times f_{DS\_drip\_angle} \times f_{DS\_crack\_area} \quad \text{(Eq. C-9)}$$

where

$F_{DS\_impinging\_drips}$ = Amount of the drift seepage flux that impinges on to through-wall cracks in drip shield

$F_{drift\_seepage}$ = Drift seepage flux

$f_{DS\_drip\_angle}$ = Fraction of the drip shield area that is potentially subject to flow through cracks under impinging drips

$f_{DS\_crack\_area}$ = Fraction of the drip shield area that corresponds to the total opening area of through-wall cracks from seismic damage, calculated by dividing the total crack opening areas in the drip shield (Equation C-5) by the total drip shield surface area.

Parameter $f_{DS\_drip\_angle}$ corresponds to the top 40- to 90-degree angle of the drip shield (DTN: SN0506F4104405 [DIRS 174472], file: *Dynamic_Drop_Test_ Summary_SCC_4-15-05.doc*, tables: "Summary of Dynamic Sample Block Test Results" and "Summary of SCC Dynamic Drop Test Results;" file: *SCC_PhaseII_Test_ Preliminary_Summary_9-21-05.doc*, table: "Dynamic Drop Block Tests"). Approximating the drip shield surface area to an equivalent circular geometry, the area associated with the top 40- to 90-degree angle corresponds to 0.11 to 0.25 of the total drip shield outer surface area. The range is characterized as an epistemic uncertainty with a uniform distribution between the bounds (0.11 and 0.25).

The flow rate through the cracks in the drip shield ($F_{DS\_seepage}$) is estimated by multiplying the impinging drift seepage flux ($F_{impinging\_drips}$) with a crack seepage scaling factor (f_{crack_seeps}), which is the fraction of the total amount of drips that flows through the cracks. The factor is based on the data from the dynamic drip tests on Stainless Steel Type 316 and Titanium Grade 7 test samples with varying shapes and aperture sizes of cracks, including actual SCC cracks in a large stainless steel plate (DTN: SN0506F4104405.003 [DIRS 174472], files: *Dynamic_Drop_Test_Summary_SCC_4-15-05.doc* and *SCC_PhaseII_Test_Preliminary_ Summary_9-21-05.doc*).

$$F_{DS\_seepage} = f_{crack\_seeps} \times F_{DS\_impinging\_drips} \quad \text{(Eq. C-10)}$$

The largest aperture size of the cracks in one location of the stainless steel plate is approximately 381 µm, and the largest aperture size in other location is approximately 127 µm (Walton 2005 [DIRS 175407], pp. 110 and 145). The crack seepage scaling factor ranges from 0.0 to 0.04, and is characterized as an epistemic uncertainty with a uniform distribution between the bounds (0.0 and 0.04).

Using the bounding values for the parameters of this analysis, and for the drip shield SCC-damage from seismic-induced rockfall and ground motion at the 1.05 m/s PGV level (Section C.2.2.1), the damaged drip shield can still reduce the drift seepage flux by more than six orders of magnitude (output DTN: SN0705WFLOWSCC.001, file: *Bounding calc for water flow through SCC cracks.xls*, worksheet: "Impinging drip flow rate," cell: B25). For example, if the damaged drip shield were subject to a reasonable-bound drift seepage flux of 500 L/yr (DTN: MO0705TSPASEEP.000 [DIRS 183008], file: *v5.005_Seismic-FD_1Myr_CDSP_ SeepRate_Bin5_stats.txt*; based on the mean drift seepage rate of approximately 460 L/yr from percolation subregion 5 (highest percolation rate subregion) at 10,000 years) the maximum volumetric flow rate through the damaged drip shield is estimated to be only 0.4 mL/yr, which is negligibly small (output DTN: SN0705WFLOWSCC.001, file: *Bounding calc for water flow*

through SCC cracks.xls, worksheet: "Impinging drip flow rate," cell: B24). The estimated upper-bound flow rate is much less than the threshold seepage rate of 100 mL/yr per waste package that is important to repository performance as determined by TSPA (SNL 2007 [DIRS 181244], Section 6.4[a]; SNL 2007 [DIRS 180506], Section 6.10.9.1[a]).

C.5 WATER FLOW RATES THROUGH SCC CRACKS IN WASTE PACKAGE BY IMPINGING DRIPS

This analysis evaluates the water flow rate in through-wall SCC cracks in the WPOB, for impinging-drip conditions, underneath SCC-damaged drip shields. The analysis assumes that waste packages are damaged from seismic-induced ground motion at the 1.05 m/s PGV level in the first 10,000 years of the repository, and that the resulting through-wall SCC cracks are distributed uniformly over the waste package surface. This analysis uses the same characterization of seismic-induced SCC damage as detailed in Section C.2.3.1. The SCC cracks that are not affected by drips or resulting sheet flow are expected not to be fully saturated with water, and will remain permeable to gases and water vapor in the drift.

The amount of the seepage from an SCC-damaged drip shield that potentially impinges on through-wall cracks in the underlying waste package is estimated as follows:

$$F_{WP\_impinging\_drips} = F_{DS\_seepage} \times f_{WP\_drip\_angle} \times f_{WP\_crack\_area} \quad \text{(Eq. C-11)}$$

where

$F_{WP\_impinging\_drips}$ = Amount of the seepage flux from an SCC-damaged drip shield that impinges on through-wall cracks in the underlying waste package

$F_{DS\_seepage}$ = Seepage flux from SCC-damaged drip shield (see analysis in Sections C.4 and C.3.1)

$f_{WP\_drip\_angle}$ = Fraction of the waste package area that is potentially subject to flow through cracks under impinging drips

$f_{WP\_crack\_area}$ = Fraction of the waste package area that corresponds to the total opening area of through-wall cracks from seismic damage, calculated by dividing the total crack opening areas in the waste package (Equation C-6) by the total waste package surface area.

As in the analysis for the drip shield (Section C-4), $f_{WP\_drip\_angle}$ corresponds to the top 40- to 90-degree angle of the waste package (DTN: SN0506F4104405.003 [DIRS 174472], file: *Dynamic_Drop_Test_Summary_SCC_4-15-05.doc*, tables: "Summary of Dynamic Sample Block Test Results and Summary of SCC Dynamic Drop Test Results;" file: *SCC_PhaseII_Test_Preliminary_Summary_9-21-05.doc*, table: "Dynamic Drop Block Tests"). The area associated with the top 40- to 90-degree angle corresponds to 0.11 to 0.25 of the total waste package surface area. The range is characterized as an epistemic uncertainty with a uniform distribution between the bounds (0.11 and 0.25).

The flow rate through the cracks ($F_{WP\_seepage}$) is estimated by multiplying the impinging drift seepage flux ($F_{WP\_impinging\_drips}$) with a crack seepage scaling factor (f_{crack_seeps}) that is based on the data from the dynamic drip tests on Stainless Steel Type 316 and Titanium Grade 7 test blocks with varying shapes and aperture sizes of cracks, including actual SCC cracks in a large stainless steel plate (DTN: SN0506F4104405.003 [DIRS 174472], files: *Dynamic_Drop_Test_Summary_SCC_4-15-05.doc* and *SCC_PhaseII_Test_Preliminary_Summary_9-21-05.doc*).

$$F_{WP\_seepage} = f_{crack\_seeps} \times F_{WP\_impinging\_drips} \quad \text{(Eq. C-12)}$$

The crack seepage factor ranges from 0.0 to 0.04, and is characterized as epistemic uncertainty with a uniform distribution between the bounds (0.0 and 0.04).

Using the bounding values for the parameters of this analysis, and the waste package damage from ground motion at the 1.05 m/s PGV level (Section C.2.3.1), the damaged waste package reduces the seepage flux from the SCC-damaged drip shield by more than five orders of magnitude (output DTN: SN0705WFLOWSCC.001, file: *Bounding calc for water flow through SCC cracks.xls*, worksheet: "Impinging drip flow rate," cell: H25). Combined, the SCC-damaged drip shield and waste package can reduce the drift seepage flux on to the drip shield by at least ten orders of magnitude (output DTN: SN0705WFLOWSCC.001, file: *Bounding calc for water flow through SCC cracks.xls*, worksheet: "Impinging drip flow rate," cell: H27). This means that advective flow of seepage through seismic-induced SCC damage in the drip shield and the underlying waste package, is much less than the amount of water that is retained in the corrosion reactions in a breached waste package (SNL 2007 [DIRS 177404], Figure 6.5-8), and is therefore negligible.

Table C-2. Direct Inputs for Appendix C

Input	Source	Description
DTN: MO0702PASTRESS.002. Output DTN of Model Report, "Stress Corrosion Cracking of Waste Package Outer Barrier and Drip Shield Materials," ANL-EBS-MD-000005. [DIRS 180514]	File: *Model Output DTN.doc*, Table 8-1	Values for yield strength and modulus of elasticity for Titanium Grade 7 and Alloy 22 at room temperature
DTN: MO0703PASDSTAT.001. Statistical Analyses for Seismic Damage Abstractions. [DIRS 183148]	File: *DS Damaged Area with Rubble.xls*, worksheet: "1.05 ms PGV - Case 2 BCs," cells: M57 to M68; worksheet: "1.05 ms PGV - Case 1 BCs," cells: M54 to M65	No damage to the drip shield with the 15-mm plate thickness by rock rubble accumulation and seismic loading in the lithophysal rock zone
	File: *Kinematic Damage Abstraction 23-mm Intact.xls*, worksheet: "WP Total"	No seismic-induced SCC damage to the TAD-bearing waste packages of 23-mm-thick WPOB with intact internals from the 1.05 m/s PGV level ground motions

Table C-2. Direct Inputs (Continued)

Input	Source	Description
DTN: MO0703PASDSTAT.001. Statistical Analyses for Seismic Damage Abstractions. [DIRS 183148]	File: *CDSP Kinematic Damage Abstraction 23-mm Intact.xls*, worksheet: "Gamma for 90%_i23"	The 95th percentile value (0.377 m^2) selected as a reasonably conservative upper-bound value for the seismic-induced SCC damage area of the codisposal waste package from the selected PGV level ground motions
DTN: MO0703PASEISDA.002. Seismic Damage Abstractions for TSPA Compliance Case. [DIRS 183156]	Section 1.1, Step 5.e	Uniform distribution between 30 and 120 m^3 for the degraded drift volume, on a per meter basis (also the volume of rock needed to fill the drift) in the lithophysal zone at the 1.05 m/s PGV level
DTN: MO0705TSPASEEP.000. TSPA-LA Addendum, Seepage Results from the TSPA-LA Model. Submittal date: 01/15/2008. [DIRS 183008]	File: *v5.005_Seismic-FD_1Myr_CDSP_SeepRate_Bin 5_stats.txt*	A reasonable upper-bound drift seepage flux
DTN: SN0506F4104405.003. Analyses of Phase I and Phase II Data from the Stress Corrosion Crack Flow Tests (Data from 1/12/2005 to 5/13/2005). [DIRS 174472]	File: *SCC_PhaseII_Test_ Preliminary_ Summary_9-21-05.doc*, table: Sheet Flow Block Tests	Through-wall SCC cracks in the top part of the drip shield or waste package, where the surface is within 10 to 20 degrees of horizontal, can potentially flow in response to sheet flow conditions
	File: *Dynamic_Drop_Test_ Summary_SCC_4-15-05.doc*, tables: "Summary of Dynamic Sample Block Test Results" and "Summary of SCC Dynamic Drop Test Results"; file: *SCC_PhaseII_Test_ Preliminary_Summary_9-21*	Fraction of the drip shield area that is potentially subject to flow through cracks under impinging drips, which corresponds to the top 40 to 90 degrees angle of the drip shield
	File: *Dynamic_Drop_Test_ Summary_SCC_4-15-05.doc*, tables: "Summary of Dynamic Sample Block Test Results" and "Summary of SCC Dynamic Drop Test Results"; file: *SCC_PhaseII_Test_Preliminary_ Summary_9-21*	The fraction of the waste package area that is potentially subject to flow through cracks under impinging drips, which corresponds to the top 40 to 90 degrees angle of the waste package
DTN: SN0703PAEBSRTA.001. Inputs Used in the Engineered Barrier System (EBS) Radionuclide Transport Abstraction. [DIRS 183217]	File: *SN0703PAEBSRTA.001 - RTA Input Tables.doc*, Table 8.2-6	Porosity of crack filling medium, 0.4
	File: *SN0703PAEBSRTA.001 - RTA Input Tables.doc*, Table 8.2-6	The porosity (0.4) of unconsolidated corrosion products used as a reasonable conservative upper-bound in the analysis
	File: *SN0703PAEBSRTA.001 - RTA Input Tables.doc*, Table 8.2-4	Specific surface area of nickel oxide, 1 to 30 m^2/g
	File: *SN0703PAEBSRTA.001 - RTA Input Tables.doc*, Table 8.2-6	Density of nickel oxide, 6.72 g/cm^3

Table C-2. Direct Inputs (Continued)

Input	Source	Description
Lide 1991. *CRC Handbook of Chemistry and Physics*. 72nd Edition. [DIRS 131202]	p. 4-108	The density of natural rutile (4.26 g/cm^3) is used for titanium oxide
	p. 6-9	The density of pure water (0.965 g/cm3) and the viscosity of pure water (0.00315 g/(cm sec)) at 90°C
SNL 2007. *In-Package Chemistry Abstraction.* [DIRS 180506]	Section 6.10.9.1[a]	A threshold water flow rate of 100 mL/yr into a breached waste package that is important to the repository performance as determined by TSPA
SNL 2007. *Seismic Consequence Abstraction*. [DIRS 176828]	Section 6.5.1.2, Table 6-4	Analysis results showing that the TAD canister-bearing waste packages of 23-mm-thick WPOB with intact internals are not subject to SCC damage from the 1.05 m/s PGV level ground motions
	Figure 6-33	The 95th percentile value (0.377 m^2) selected as a reasonably conservative upper-bound value for the damage area of the codisposal waste package subject to SCC-damage from the 1.05 m/s PGV level ground motions
	Figure 6-57	An estimate of how much rock volume is produced from drift degradation in the lithophysal zone during the 1.05 m/s PGV-level seismic event
	Table 6-30	Drift degradation in the lithophysal zone at the 1.05 m/s PGV has a mean value of 7.47 m^3 and a standard deviation of 8.37 m^3, both per meter of drift length
	Figure 6-57	The total rubble accumulation on the drip shield for the time up to the point of the evaluation (the 99th percentile value of the analysis for the 1.05 m/s PGV level). This is calculated to be 38.7 m^3 per meter of drift length
SNL 2007. *Mechanical Assessment of Degraded Waste Packages and Drip Shields Subject to Vibratory Ground Motion*. [DIRS 178851]	Table 6-153	Evaluation of the impact damage to a drip shield due to the six largest rock blocks ejected during a 1.05 m/s PGV event in the non-lithophysal rock zone
	Table 6-157	A damage area of 0.0159 m^2 for one-quarter size drip shield with the 15-mm plate thickness, impacted by the largest rock block (the 99.9th percentile for all blocks ejected for the 1.05 m/s PGV event)

Table C-2. Direct Inputs (Continued)

Input	Source	Description
SNL 2007. *Mechanical Assessment of Degraded Waste Packages and Drip Shields Subject to Vibratory Ground Motion*. [DIRS 178851]	Table 6-154	The largest rock block (the 99.9th percentile for all blocks ejected for the 1.05 m/s PGV event) considered for this analysis
SNL 2007. *Drift-Scale THC Seepage Model*. [DIRS 177404]	Figure 6.5-8	Amount of water that is retained in the corrosion reactions inside a breached waste package
SNL 2007. *Stress Corrosion Cracking of Waste Package Outer Barrier and Drip Shield Materials*. [DIRS 181953]	Sections 6.6.2, 6.8.5.2	SCC cracks in the drip shield and WPOB can be treated as semi-elliptical. The expected maximum length (2c in Equations C-1 and C-2) of a semi-circular crack as it grows to a through-wall crack is at least two times the wall thickness
	Section 6.6.2	Maximum tensile stress across the wall thickness of the dominant stress plane for the yield strength term in Equation C-2

Table C-3. Indirect Inputs for Appendix C

Citation	Title	DIRS
Amer et al. 1985	"Zeta Potential and Surface Area of Calcium Carbonate as Related to Phosphate Sorption"	183684
Bear 1972	*Dynamics of Fluids in Porous Media*	156269
Bruemmer and Thomas 2001	"High-Resolution Analytical Electron Microscopy Characterization of Corrosion and Cracking at Buried Interfaces"	183685
BSC 2001	*Plugging of Stress Corrosion Cracks by Precipitates*	156807
BSC 2004	*Yucca Mountain Site Description*	169734
Domenico and Schwartz 1990	*Physical and Chemical Hydrogeology*	100569
DTN: MO0612WPOUTERB.000	Output from General and Localized Corrosion of Waste Package Outer Barrier Report	182035
DTN: MO0703PASEISDA.002	Seismic Damage Abstractions for TSPA Compliance Case	183156
DTN: MO0705CREEPSCC.000	Supplementary Output DTN from SCC AMR	183681
DTN: SN0506F4104405.003	Analyses of Phase I and Phase II Data from the Stress Corrosion Crack Flow Tests (Data from 1/12/2005 to 5/13/2005)	174472
He et al. 2007	"Temperature Effects on Oxide Film Properties of Grade-7 Titanium"	183687
Holford and Mattingly 1975	"Surface Areas of Calcium Carbonate in Soils"	183686
Hu et al. 2001	*Summary Report on Phase I Feasibility Study of In-Drift Diffusion*	161623
Lide 1991	*CRC Handbook of Chemistry and Physics*	131202
Milnes and Fitzpatrick 1995	"Titanium and Zirconium Minerals"	105911
Siriwardane and Wightman 1983	"Interaction of Hydrogen Chloride and Water with Oxide Surfaces. III. Titanium Dioxide"	183688
SNL 2007	*Seismic Consequence Abstraction*	176828

Table C-3. Indirect Inputs for Appendix C (Continued)

Citation	Title	DIRS
SNL 2007	*Analysis of Mechanisms for Early Waste Package/Drip Shield Failure*	178765
SNL 2007	*Stress Corrosion Cracking of Waste Package Outer Barrier and Drip Shield Materials*	181953
SNL 2007	*Total System Performance Assessment Data Input Package for Requirements Analysis for Subsurface Facilities*	179466
Tada et al. 2000	*The Stress Analysis of Cracks Handbook*	167756
Walton 2005	*Testing of Stress Crack Flow [final closure]. Scientific Notebook SN-SNL-SCI-032-V2.*	175407

INTENTIONALLY LEFT BLANK

APPENDIX D

SCIENTIFIC ANALYSES DISCUSSION AND SUPPORTING DOCUMENTATION FOR METEORITE IMPACT AND CRATERING PROBABILITY AND CONSEQUENCES

This appendix is referenced in FEP 1.5.01.01.0A (Meteorite Impact). It provides a detailed calculation and discussion regarding meteorite impact and provides the technical basis for exclusion based on probability for meteorite crater diameters larger than the threshold diameter associated with a frequency of one per 10,000 per 10,000 years.

Possible effects of a large meteorite impact near the repository include penetration of the repository and exhumation of waste. A meteorite associated with an impact crater not deep enough to exhume waste could reactivate or form faults and fractures, change the rock stress, and the associated shock wave could possibly cause damage to drifts and waste packages, or initiate an earthquake. Of particular interest for smaller meteorite impacts is the possibility of increased water percolation in the unsaturated zone to the repository through damage to the geologic layers that limit percolation.

Analysis of a meteorite impact depends on the probability of occurrence of variously sized impact craters, the area and relative dimensions of the repository footprint, and the depth of the repository below the ground surface. The probability of an impact crater of a given size occurring directly over or adjacent to the repository is dependent on the total flux of meteorites to the earth surface and on the repository footprint area. The size of the craters of interest is determined by the depth from ground surface to the top of the repository and/or any intervening geologic layers of particular interest due to their physical or hydrologic properties, and the spatial relationship of crater diameter to exhumation depth and fracturing depth. Accordingly, this appendix specifically examines the waste emplacement drifts and the probability of crater diameters sufficient to exhume waste, to fracture overlying rock units down to the repository depth, and to fracture to a depth less than the repository depth but sufficient to impair performance. Two crater sizes of interest in the analysis are: (1) craters that are deep enough to exhume waste from the repository, and (2) craters that are deep enough to fracture or damage the Paintbrush non-welded tuff (PTn) layer above the repository. Potential fracturing or damage to the overlying Tiva Canyon units is not of concern because of the damping effect of the PTn (SNL 2007 [DIRS 184614], Section 6.9[a]).

Section D1 lists the assumptions used in the analysis. Sections D2 and D3 describe the repository target area and the depth to and thickness of the PTn unit, respectively, which are the key site characteristics that are of interest to this analysis. Section D4 presents the development of the probability of meteorite impact. The probability of meteorite impact is based on cratering frequency distributions (annualized number of events per km^2) from observed earth and lunar cratering data (Sections D4.2.1 through D4.2.3). These distributions are then adjusted based on meteoroid influx after considering atmospheric shielding effects (Section D4.2.4). The slope and power constant of the modified distributions are obtained after regression analyses for the upper and lower portions of the distribution and for two air entry velocities of 15 and 20 km/s, which bound the range of cratering rate distributions for the FEP screening analysis (Section D4). Using the slope and power constant obtained, the probability of meteorite impact is calculated by integrating the frequency distribution over the target area. The maximum-impact crater diameter is then identified from the probability curve for the threshold of occurrence of 1×10^{-8} per year over the target area. Using correlation relationships identified in Section D4.3.5 between the crater diameter and the exhumation depth or the fracturing depth, the threshold exhumation and fracturing depths are then estimated from the maximum-impact crater diameter. Finally, the threshold exhumation depth is compared to the overburden thickness above the repository, and

the threshold fracturing depth is compared to the depth to and thickness of the PTn unit within the repository area. Results of these comparisons provide the technical basis to screen out the FEP based on low probability (Section D5). Section D5 also presents consideration of other additional impacts before reaching the final screening decision. Direct inputs are listed in Table D-5 and indirect inputs in Table D-6. The qualification of previously unqualified data for its intended use in this appendix is documented in Section D6.

For clarity, the following terms are used in the discussions: *Meteoroid* refers generically to a non-anthropogenic space object prior to entry to earth's atmosphere, *meteor* refers to the object once it enters earth's atmosphere and prior to impact, and *meteorite* refers to the object (or fragments of the object) impacting on (or in the case of aerial explosion, occurring near) the earth's surface. The terms *bolide* and *fireball* are also used. A *bolide* is defined as a meteor that shows signs of explosion or fragmentation, and a *fireball* is defined as a bright meteor with luminosity that equals or exceeds that of the brightest planets (generally magnitude of −3 or brighter).

A summary of velocity information from the reviewed literature is provided in Table D-1, which lists point values or average values where distributions were given. Calculated impact velocities of known meteoroids and comets range from 12.9 km/sec for small Earth-crossing objects with diameters less than 50 m (Chyba 1993 [DIRS 135248], Table 1a) to over 70 km/sec for long-period comets (Marsden and Steel 1994 [DIRS 129308], Table VI). The entry velocity of meteoroids is typically about 20 km/s (Hills and Goda 1993 [DIRS 135281], Section 2.1). Note that the extremes given above are values from an ensemble. However, a velocity of 15 km/s, in addition to being conservative with respect to crater formation, is consistent with the average impact velocities (Table D-1, Column 4) of observed meteors with diameters of particular interest (i.e., producing craters with frequencies at or greater than the screening criterion) (Chyba 1993 [DIRS 135248], Table 1a; Ceplecha 1994 [DIRS 135243], Table 2). Table D-1 is provided for informational purposes as the crater impact analysis is based on crater diameter distributions.

Table D-1. Summary of Velocity Data from Reviewed Literature

Velocity (km/s)				Source
Asteroids	Long-Period Comets	Short-Period Comets	Not Specified	
—	—	—	20.3	Brown et al. 2002 [DIRS 162569], p. 294.
20	60	40	—	Chapman and Morrison 1994 [DIRS 135245], p. 34 and Figure 1.
—	—	—	14.3	Chyba 1993 [DIRS 135248], p. 701. Average value (excluding object 1991-VG as human artifact).
20.8	45	38.5	—	Hughes 1998 [DIRS 162562], pp. 35 and 37.
—	—	—	20.7	Ceplecha 1994 [DIRS 135243], Table 2; Chyba 1993 [DIRS 135248], Table 1a. Derived average for 1 to 10 m.
—	—	—	15.8	Ceplecha 1994 [DIRS 135243], Table 2; Chyba 1993 [DIRS 135248], Table 1a. Derived average for 11 to 60 m.
—	58.2	—	—	Marsden and Steel 1994 [DIRS 129308], Table V.
—	—	—	25	Grieve 1987 [DIRS 135254], p. 250.
20.1	—	—	—	Shoemaker 1983 [DIRS 135308], p. 468. Weighted by probability.
20.3	54.4	39.3	19.2	Average.
30.7				Average of all values regardless of type.

D1 ASSUMPTIONS

The following assumption is used in the analysis. For the meteorite analysis (provided in this appendix), assumptions are made to ensure that the analysis is conservative in nature and that the range of uncertainty in values is covered. The justification for the assumption are explained in later sections.

D1.1 ZONE OF FRACTURING IS CYLINDRICAL WITH DEPTH, RATHER THAN PARABOLIC

For analysis purposes, the vertical extent of effects (e.g., exhumation or fracturing) is represented as a cylinder.

The diameter of the cylinder is assumed to correspond to the crater diameter, and the depth corresponds to the depth of interest derived from the crater diameter. In reality, the effects are more likely parabolic in nature (inferred from Wuschke et al. 1995 [DIRS 129326], Figure 1). By assuming a cylindrical zone, the maximum depth of the effect (exhumation or fracturing) is applied throughout the area below the crater diameter and, thereby, conservatively considers a larger volume of the material overlying the repository.

D2 REPOSITORY FOOTPRINT AND TARGET AREA

The repository emplacement area is of primary interest to the analysis of meteorite impact. The target area to be used for this FEP screening includes the TSPA-LA emplacement drifts and surrounding areas. Figure D-1 shows the emplacement drifts and nearby boring locations.

Information of the repository layout for the TSPA-LA, including endpoint coordinates of emplacement drifts, can be found in subsurface facilities drawings (BSC 2007 [DIRS 183743], Tables 2 to 5). The maximum extent of the emplacement drifts is shown in Table D-2.

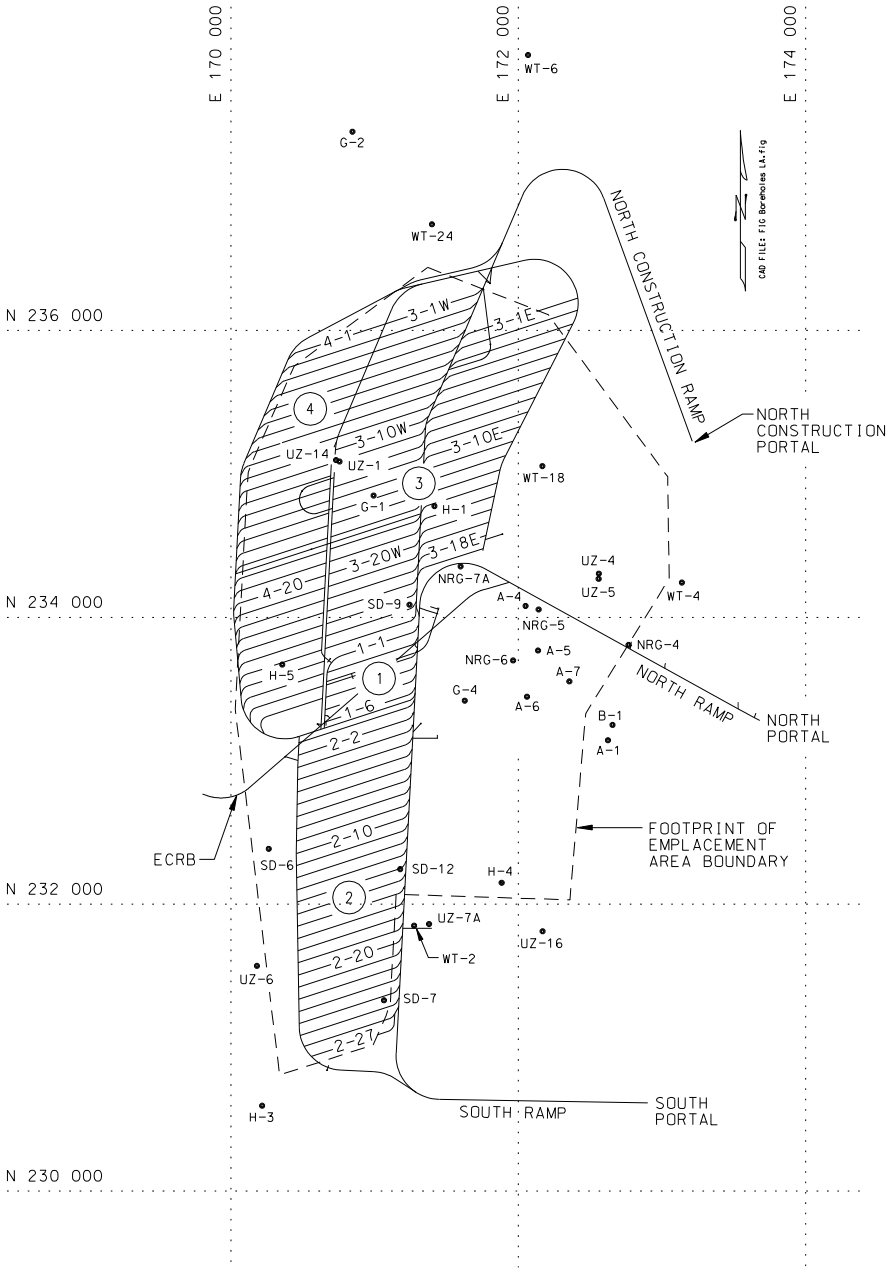

Sources: SNL 2007 [DIRS 179466], Table 4-1, Parameter 01-03; BSC 2007 [DIRS 182926], Figure 2.

Figure D-1. Waste Emplacement and Repository Target Area and Surrounding Boreholes

Table D-2. Emplacement Drift Endpoint Coordinates

Drift Number and Basis	Drift End Coordinate (m)
(3-1W) northernmost drift end	N236237
(2-27) southernmost drift end	N230944
(3-4E) easternmost drift end	E172309
(4-20) westernmost drift end	E170085

Source: BSC 2007 [DIRS 183743], Tables 2 to 5.

The total emplacement area is 6,004,074 m^2 (BSC 2003 [DIRS 165572], Table II-1) or ~6.0 km^2. For this analysis, a larger rectangular area containing the emplacement drifts is considered using original dimensions as follows.

North/South Length (L) (236237 m to 230944 m) = 5.3 km
East/West Width (W) (172309 m to 170085m) = 2.2 km
Approximate Area (A) 5.3 km × 2.2 km = 11.7 km^2

The measured distances are rounded upward to the nearest tenth of a kilometer, and the rounding is inconsequential because a rectangular repository area is used as a calculational simplification. Also, the repository length was extended by 0.1 km to account for the construction ramp location. Using the adjusted value of 5.4 km, the rectangular area is approximately 11.9 km^2. This is defined as the target area that represents the repository emplacement drifts and surrounding areas that could potentially be impacted by meteorites. Use of this rectangular target area with adjustments of lengths as simplifications to the repository footprint will result in a conservative overestimation of the repository emplacement area by a factor of about 2, which in turn will lead to a conservative overestimation of the meteorite impact probability.

D3 DEPTH AND THICKNESS OF THE PAINTBRUSH NONWELDED TUFF UNIT

The Paintbrush non-welded tuff (PTn) primarily consists of nonwelded to partially welded tuffs and extends from the base of the densely to moderately welded Tiva Canyon welded tuff (TCw) to the top of the Topopah Spring welded unit (TSw), which is densely welded (BSC 2004 [DIRS 170029], Table 6-2). It is stated in *UZ Flow Models and Submodels* (SNL 2007 [DIRS 184614], Section 6.2.2[a]) about the paintbrush (PTn) unit that:

> The PTn unit, as described by the current geological model, consists primarily of non- to partially welded tuffs. The dip of these layers is generally less than 10° to the east or southeast. The combined thickness of the PTn layers ranges from 150 m in the north of the model area to 30 m or less, even completely disappearing in several areas of the south. However, the PTn unit is present over the entire repository area, where the thickness of the PTn unit ranges from approximately 30 to 60 m, and it is even thicker to the north of the repository. The PTn unit as a whole exhibits very different hydrogeologic properties from the TCw and TSw units that bound it above and below. The TCw and TSw units have low porosity and intense fracturing typical of the densely welded tuffs at Yucca Mountain. In contrast, the PTn has high porosity and low fracture intensity, and its matrix

system has a large capacity for storing groundwater. It has been shown to effectively damp spatial and temporal variations in percolation flux.

The large storage capacity and low fracture frequency of the highly porous PTn unit may effectively dampen transient pulses of infiltration and more evenly distribute the downward flow of water. Geologic data indicate that the PTn ranges in thickness from greater than 125 m beneath northern Yucca Mountain to about 20 m in the south, with breaks in area coverage along the Solitario Canyon, Iron Ridge, and Dune Wash fault systems. The depth to the top of the PTn unit is shown in Figure D-2, the thickness of the PTn unit in Figure D-3, and the depth to the base of the PTn in Figure D-4. The repository underground layout incorporates a minimum PTn thickness of 10 m (BSC 2008 [DIRS 183627], Table 1, Parameter 01-21). Therefore, the meteorite impact on the PTn unit and thereby UZ flow and transport can be considered insignificant if one of the following conditions is met within the repository target area defined in Section D2:

(a) The overburden thickness above the PTn exceeds the exhumation or fracturing depth of the crater.

(b) The combined thickness of the PTn unit and the overburden above it exceeds the sum of the crater exhumation or fracturing depth plus 10 m that is required to maintain the effectiveness of the PTn unit in damping episodic infiltration pulses.

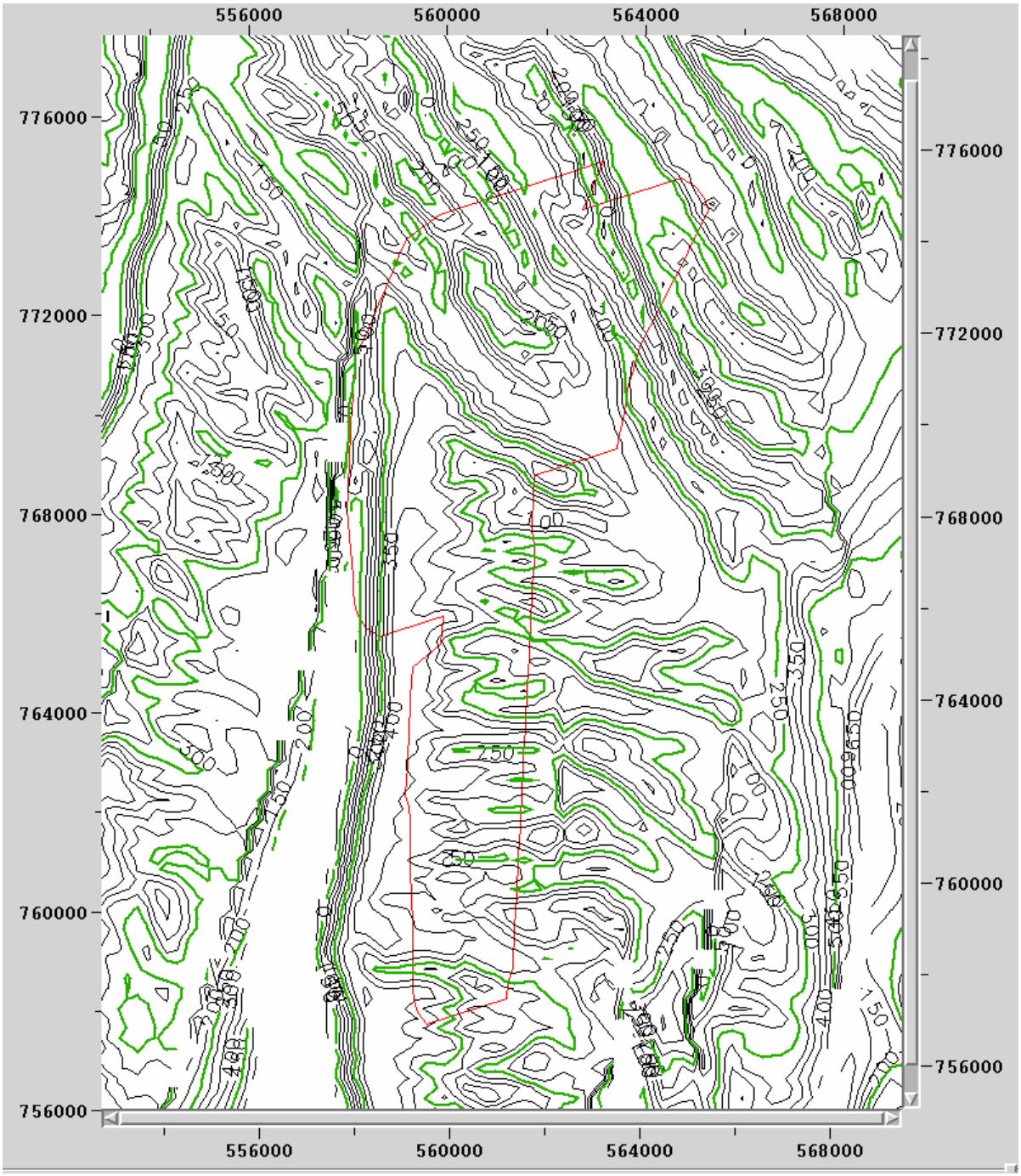

Sources: Geologic information from DTN: MO0012MWDGFM02.002 [DIRS 153777]. Repository footprint converted from m to ft from SNL 2007 [DIRS 179466], Table 4-1, Parameters 01-01 and 01-03.

NOTE: All dimensions in units of feet. Plot generated using EarthVision (7.5.2) on the Windows 2000 platform, in accordance with Section 2.0 of IM-PRO-003, *Software Management*.

Figure D-2. Contours of Depth to the Top of the PTn Unit

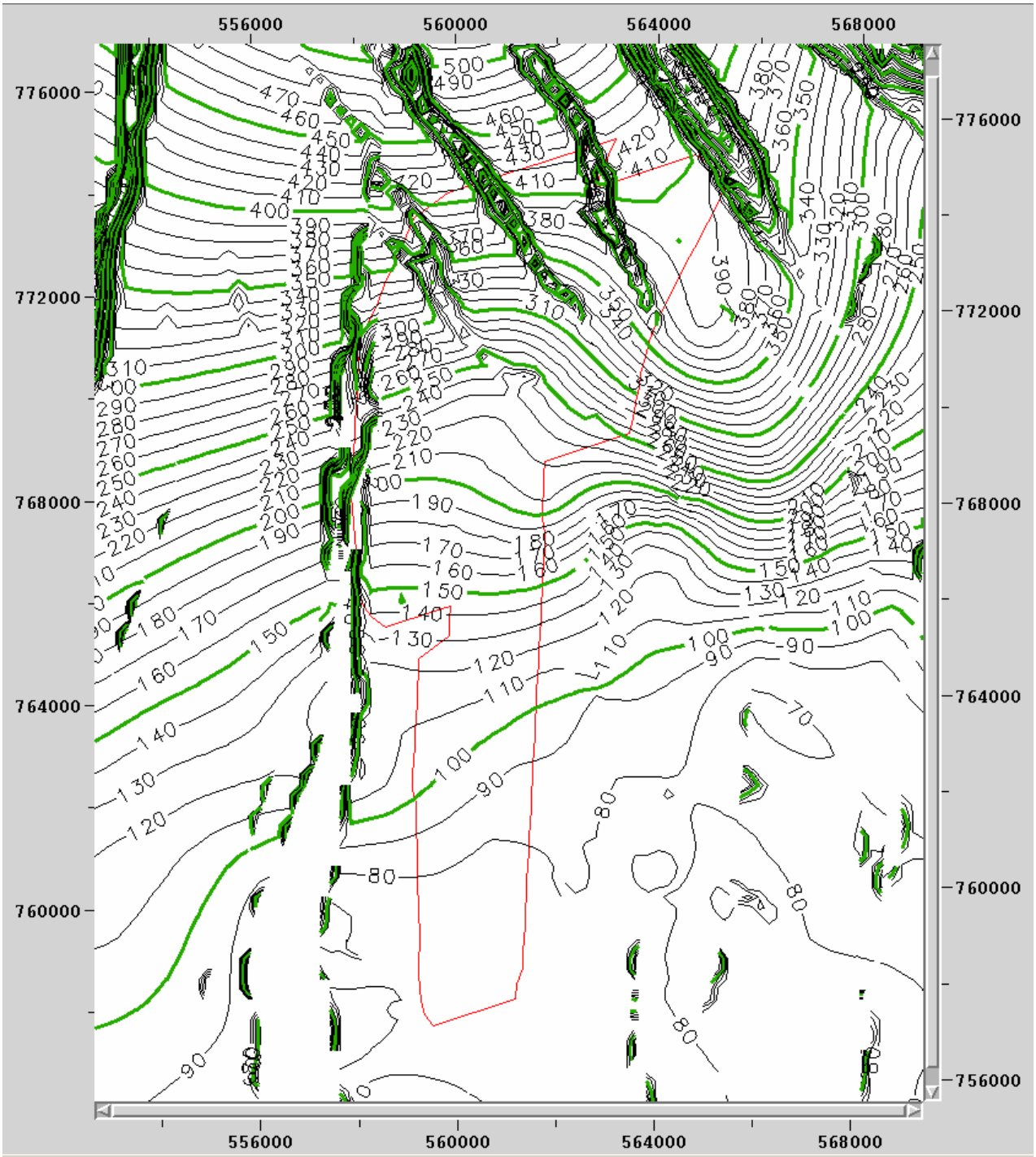

Sources: Geologic information from DTN: MO0012MWDGFM02.002 [DIRS 153777]. Repository footprint converted from m to ft from SNL 2007 [DIRS 179466], Table 4-1, Parameters 01-01 and 01-03.

NOTE: All dimensions in units of feet. Plot generated using EarthVision (7.5.2) on the Windows 2000 platform, in accordance with Section 2.0 of IM-PRO-003, *Software Management*.

Figure D-3. Contours of Thickness of the PTn Unit

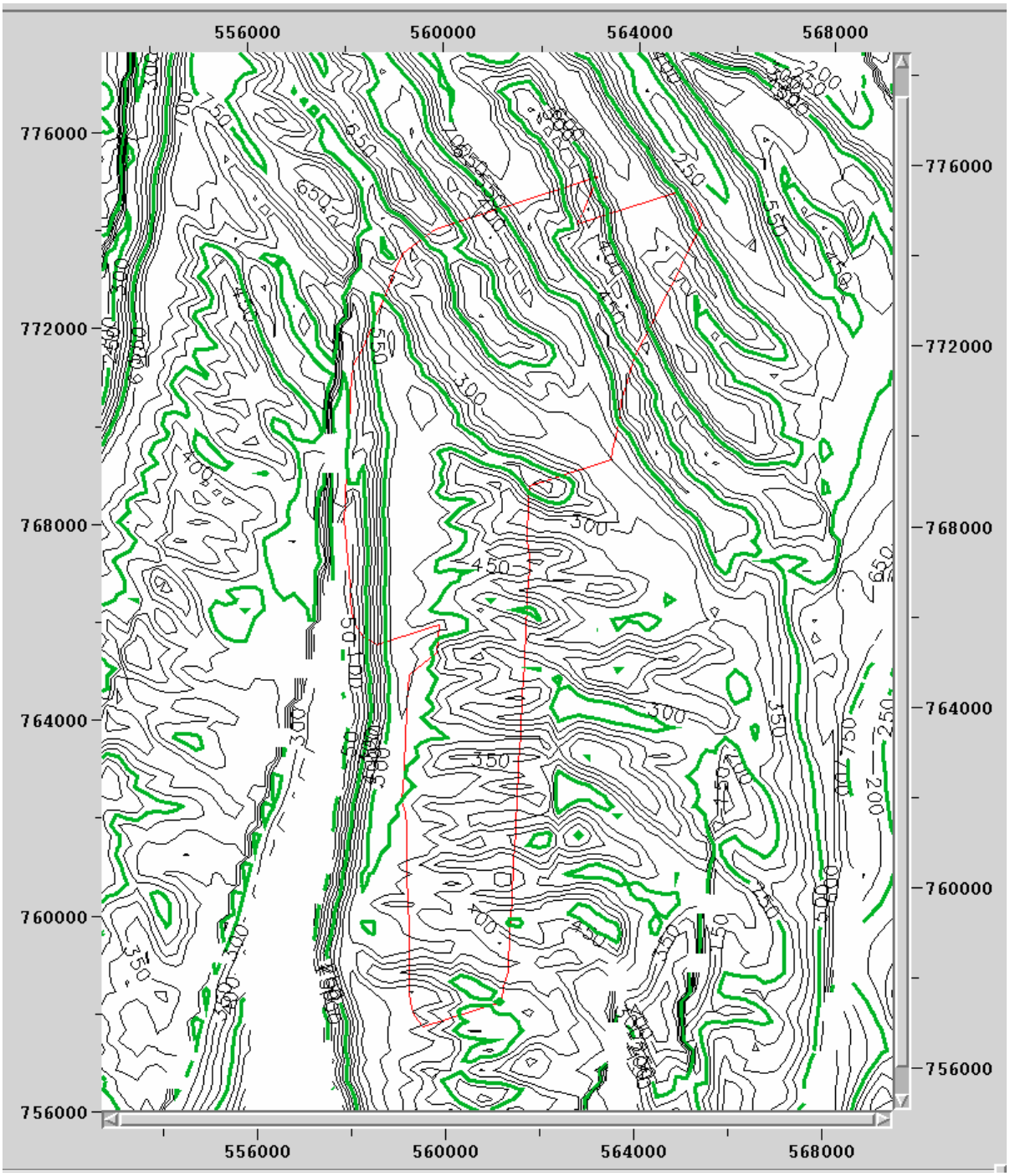

Source: Geologic information from DTN: MO0012MWDGFM02.002 [DIRS 153777]. Repository footprint converted from m to ft from SNL 2007 [DIRS 179466], Table 4-1, Parameters 01-01 and 01-03.

NOTE: All dimensions in units of feet. Plot generated using EarthVision (7.5.2) on the Windows 2000 platform, in accordance with Section 2.0 of IM-PRO-003, *Software Management*.

Figure D-4. Contours of Depth to the Base of the PTn Unit

D4 CRATERING RATE DISTRIBUTIONS

D4.1 PROBABILITY OF IMPACT BASED ON INDIVIDUAL OBJECTS

Various authors have calculated the probability of entry of known individual interplanetary bodies into the earth's atmosphere. These probabilities are for any entry into the earth's atmosphere. However, the interest here concerns the cumulative probability of impact of all objects, not just for individual objects, so the following information is considered as corroborative-use only.

Chyba (1993 [DIRS 135248], Table 1a) addresses 12 objects with diameters of less than 55 m that have been observed to date. Excluding object 1991-VG (a suspected possible human artifact), the mean calculated probability of impact on the earth's atmosphere for the known bodies is 29 per gigayear, suggesting rates on the order of 3×10^{-8} per year, or on the order of 3×10^{-4} in 10,000 years (Chyba 1993 [DIRS 135248], p. 701) for the whole earth surface, and it is stated to be a factor of approximately seven greater than for other earth-crossing asteroids. Since impact is a spatially random process (Grieve 1987 [DIRS 135254], p. 257), dividing this value by the surface area of the earth (5.1×10^{8} km^2), and multiplying by the maximum area of the repository footprint (approximated by a 12 km^2 rectangular area; see Section D2), yields a probability of impact above the repository on the order of 10^{-15} per year, or approximately 10^{-11} in 10,000 years.

Marsden and Steel (1994 [DIRS 129308], p. 235, Figure 4) provide the calculated atmospheric entry probabilities, defined as crossing within 0.1 to 1 astronomical unit (AU) (1 AU = 149,598,000 km) of earth's orbit, for all observed long-period comets (i.e., orbit duration of greater than 200 years). The greatest calculated probability is 2.6×10^{-7} per orbit (Marsden and Steel 1994 [DIRS 129308], Figure 4) and the estimated mean impact probability is 2×10^{-9} to 3×10^{-9} per orbit (Marsden and Steel 1994 [DIRS 129308], Table V). Dividing by the minimum orbital period of 200 years (by definition of a long-period comet) yields a maximum probability of approximately 1.3×10^{-11} per year, or on the order of 10^{-7} in 10,000 years for the whole earth. If one neglects atmospheric shielding effects, the probability of impact above the repository can be estimated by dividing the probability by 5.1×10^{8} km^2, the approximate surface area of the earth, and multiplying by the maximum repository area (12 km^2). This yields a maximum probability of approximately 3.1×10^{-19} per year or about 3.1×10^{-15} in 10,000 years.

The probability of the impact of any individual known object is, therefore, at least ten or eleven orders of magnitude less than the regulatory threshold of an annualized event frequency of about 10^{-8} or, more specifically, a probability of 10^{-4} in 10,000 years. Thus, cratering from these objects is not considered in the crater impact analysis.

D4.2 CRATERING RATE DISTRIBUTIONS FROM EARTH AND LUNAR OBSERVATIONS

The FEP screening considers the cratering rate distributions derived from Grieve et al. (1995 [DIRS 135260]), which are based on world-wide cratering information (Section D4.2.1). It also considers the distribution from Wuschke et al. (1995 [DIRS 129326]), which is based on

cratering of the Canadian shield, and serves as a "realistic case" (Section D4.2.2). In addition, the analysis examines the distribution proposed by Neukum and Ivanov (1994 [DIRS 121510]), which is based on lunar cratering data (Section D4.2.3). Because the Neukum and Ivanov distribution was developed assuming an "atmosphereless earth," it serves as an upper bound for earth cratering. However, this distribution is only used for corroboration purposes, as it is unrealistic to expect that the atmosphere has no effect on the cratering distribution.

D4.2.1 Crater Diameter Frequency Distributions

Existing distributions in the literature are stated, generally, to apply to crater diameters on the scale of kilometers, rather than within the primary range of interest for this analysis (79 to 625 m as discussed in Section D4.3.2). Accordingly, this analysis develops a cratering distribution applicable to the smaller diameter range. This flux-derived distribution is developed based on meteoroid flux, meteoroid properties, and on meteoroid radius to crater diameter relationships (Section D4.2.4).

An applicable cumulative cratering rate (and one commonly used for these types of analyses) can be derived from a power law derived by Grieve and Robertson (1984 [DIRS 185030], Abstract), and Grieve (1987 [DIRS 135254], p. 257 and Figure 8). The cumulative number of impact craters, $F(D)$, larger than a crater of diameter D, (in units of km), produced per year per square km, can be represented by a power law proportional to the apparent crater diameter to the k power (Grieve 1987 [DIRS 135254], p. 257 and Figure 8):

$$F(D) = K \times D^k \qquad \text{(Eq. D-1)}$$

The value for K can be derived by fixing $F(D)$ at 5.5×10^{-15} per km^2 per year for D = 20 km (Grieve et al. 1995 [DIRS 135260], p. 196). Thus:

$$F(20) = K(20)^{-1.8} = 5.5 \times 10^{-15}\ (1/\text{km}^2\text{-yr}) \qquad \text{(Eq. D-2)}$$

which gives a value of 1.2×10^{-12} for K, and giving the equation for the cumulative number of craters per year per km^2 with diameters larger than D as

$$F(D) = 1.2 \times 10^{-12} \times D^{-1.8} \qquad \text{(Eq. D-3)}$$

The given proportionality ($D^{-1.8}$) applies for earth crater diameters greater than 10 km, per analysis by Neukum and Ivanov (1994 [DIRS 121510], p. 404). The departure of the cumulative size-frequency distribution from the proportionality below diameters of 10 km is shown in Figure 8 of Grieve (1987 [DIRS 135254], p. 257). The slope change represents a decreased number of small crater observations, which indicates a shortage of known craters (Grieve 1987 [DIRS 135254], Figure 8) due to recognition and crater retention problems.

Using a repository emplacement area of no greater than 11.9 km^2, the cratering diameter of interest is that associated with a probability of $1 \times 10^{-8}/11.9 = 8.4 \times 10^{-10}$/km^2/yr (i.e., the regulatory threshold for consideration). From Equation D-3, this gives a crater diameter of no more than 30 m.

The respective distributions based on observed earth and lunar cratering are shown in Figure D-5 where Equation D-3 is extrapolated back to a crater diameter of 0.01 km. Given the distribution of crater diameters by Grieve (1998 [DIRS 163385], Figure 8), it is conservative (in relation to observed craters) to extend the distribution to smaller diameters, which overstates the number of craters used in this analysis compared to the actual number observed to date.

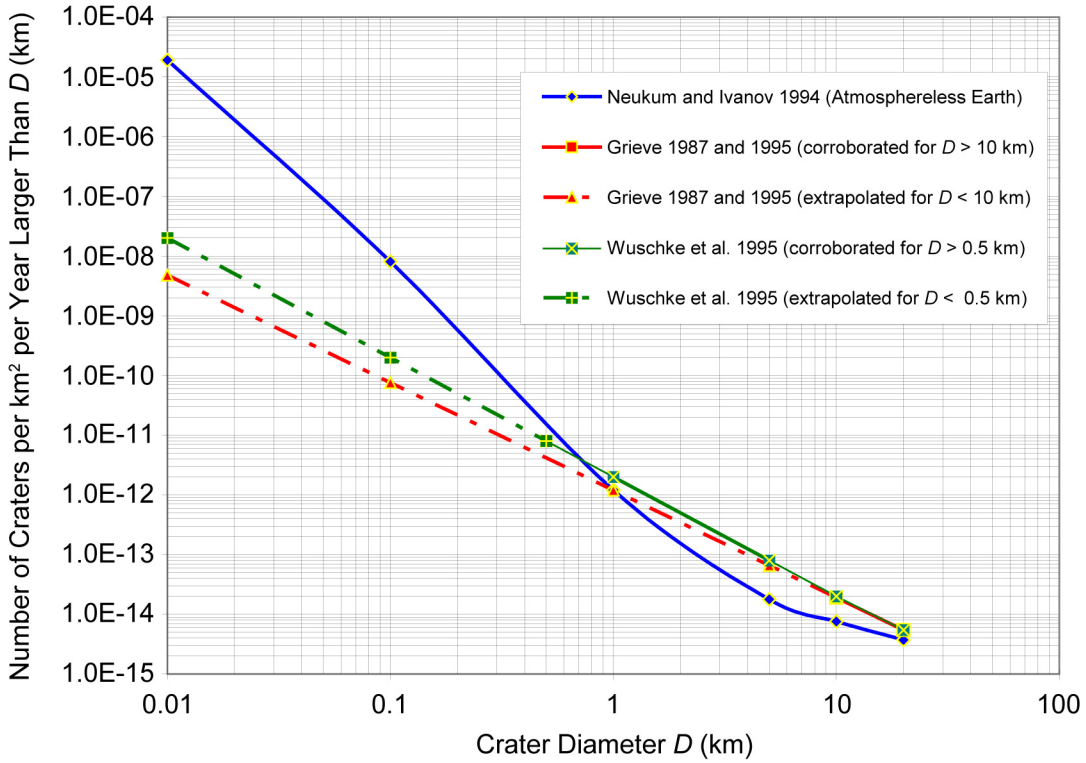

Source: Neukum and Ivanov 1994 [DIRS 121510]; Grieve 1987 [DIRS 135254]; Grieve et al. 1995 [DIRS 135260]; and Wuschke et al. 1995 [DIRS 129326].

Figure D-5. Cratering Rate Distribution from Four Sources

D4.2.2 Wuschke et al. (1995)

A particular example of the use of Grieve's distribution and the consideration of exhumation and fracturing depths is presented by Wuschke et al. (1995 [DIRS 129326]). The analyses presented in this study was for a hypothetical depository deep in plutonic rock of the Canadian shield, located at least 500 m below ground surface with a total area of 4 km^2. The curve from Wuschke et al. (1995 [DIRS 129326]), if comparable to the information used by Hughes (1998 [DIRS 162562], p. 34), may only be valid down to diameters of 1 km. For Wuschke et al. (1995 [DIRS 129326], p. 4), the distribution is derived from subsets of the observed earth cratering distribution used by Grieve (1987 [DIRS 135254]), and is given as:

$$F(D) = 2.0 \times 10^{-12} D^{-2} \quad \text{(Eq. D-4)}$$

where D is km, and $F(D)$ in $1/km^2/yr$. This denotes a slightly steeper slope compared to Grieve (2.0×10^{-12} compared to 1.2×10^{-12}). Wuschke's approach results in a slightly decreased annual frequency for a 20-km diameter crater (5.0×10^{-15} per km^2 compared to the values from Grieve of 5.5×10^{-15} km^2). This difference is reflected in the plot in Figure D-5.

The findings of this study are presented in Table 1 of Wuschke et al. (1995 [DIRS 129326], p. 26) and provide the annual probability and cumulative probability for 10,000 years for meteorite impact events. The results indicate that the annualized probability of impact for the Canadian repository design sufficient to cause damage by exhumation and fracturing is approximately 7.6×10^{-12} to 6.5×10^{-11} per year, respectively. This is associated with crater diameters of 7.6 to 0.66 km for exhumation and fracturing, respectively. Given the parameters used for the hypothetical Canadian repository (area of 4 km^2 and depth of 500 m), the reported probabilities should be less than the probability of impact for the Yucca Mountain repository (depths greater than 200 m below the surface and total area not to exceed 11.9 km^2 (SNL 2007 [DIRS 179466], Table 4-1, Parameters 01-02 and 01-06)) for the same effects of exhumation and fracturing. For exhumation of the Yucca Mountain repository, the least frequent and maximum crater diameter that could cause such an event is a crater diameter of 2 km (i.e., 200 m/0.10), and the most frequent would be a crater diameter of 625 m (200 m/0.32). Based on Figure D-6, and using a siting area of 11.9 km^2, such events occur with annual frequencies on the order of 10^{-10}, or about an order of magnitude more frequently than for the hypothetical Canadian design. For fracturing to repository depth, the crater diameter of interest is 263 m (i.e., 200 m/0.76). This occurs, based on Figure D-6, with an annual frequency of on the order of 10^{-9}, and again this is more frequent than predicted for the Canadian repository as expected.

D4.2.3 Neukum and Ivanov (1994)

The plot of the Neukum and Ivanov (1994 [DIRS 121510]) information represents a true upper bound (i.e., an "atmosphereless" earth which neglects effects of ablation and fragmentation). Because it is unrealistic due to an "atmosphereless" earth, it is discussed for corroborative purposes only, but it also provides a true upper bound.

Neukum and Ivanov (1994 [DIRS 121510], Table IV) provide a tabulation of impact accumulation rates and mean time intervals between impacts for earth, based on lunar craters and adjusted for gravity differences. This table includes the mean interval between events with energies equal to or greater than that required to form a crater of a given diameter. The cumulative cratering rate (or frequency) of such events can be derived from the calculated mean intervals by using the inverse of the mean interval. The frequency per square kilometer of the earth's surface can be derived by dividing the frequency by the area of earth's surface. This curve represents an extreme upper bound for the cratering rate on earth in the range of crater diameters of interest as it accounts for gravity differences between the lunar and earth surfaces and includes data for small-diameter craters. It does not take into account atmospheric shielding effects, which are known to exist and are significant in reducing crater frequency and size. The data used in plotting Figure D-5 is given in Table D-3.

Given that the footprint area is no greater than 11.9 km^2 as previously mentioned, the cratering diameter of interest is that associated with an annualized probability of $8.4 \times 10^{-10}/km^2$ (i.e., $8.4 \times 10^{-10}/km^2$ multiplied by an area of 11.9 km^2 equates to an annualized probability of 1×10^{-8}).

Based on Figure D-5, this equates to a crater diameter of less than 200 m. Using the exhumation depth relationship mentioned above, such a crater diameter could result in exhumation depths greater than 20 m and less than 64 m, which are insufficient to exhume waste at the depth of the proposed repository (i.e., greater than 200 m below ground surface (SNL 2006 [DIRS 179466], Table 4-1, Parameter 01-06)) or to exhume significant portions of the Paintbrush hydrogeologic unit. With regard to fracturing, the depth could be as little as 70 m to as great as 150 m. These depths are insufficient to reach to the proposed repository depth, although the values may represent depths that are sufficient to fracture the Paintbrush nonwelded unit in certain portions of the repository area, depending on the choice of factors (0.3 or 0.76). However, it must be kept in mind that the stated values represent the "worst-case" model proposed in the literature for exhumation and fracturing, coupled with the "upper bound" for crater diameter distribution. They are not realistic in that they are based on an "atmosphereless" earth.

D4.3 PROBABILITY OF A CRATER DIAMETER OF INTEREST OCCURRING WITHIN THE REPOSITORY TARGET AREA

Figure D-5 represents the range of possible frequencies of impacts resulting in a given or larger crater diameter per km^2. All frequency curves fall below the Neukum and Ivanov curve. This is to be expected since the curve derived from Neukum and Ivanov (1994 [DIRS 121510], Table IV) is based on the lunar cratering rate and neglects any atmospheric shielding effects. The relationship of the Neukum and Ivanov curve to the other curves shows that the Neukum and Ivanov curve is an upper bound within the range of interest. As discussed below, the bounding nature is used to divide the mass flux curves and to define the related coefficients and integration limits for those curves. The Neukum and Ivanov curve is not further used in the probability calculations, since it would unrealistically overestimate the frequency of occurrence.

D4.3.1 Simple and Complex Cratering

The amount of meteor kinetic energy acting in combination with the impacted rock properties determines the features, shape, size, and depth of any crater and any related cratering effects such as fracturing. The potential consequences are divided at the first level based on two types of observed cratering. Simple craters consist of an elevated rim and central depression. Complex cratering involves the uplift and significant vertical displacement of the central portion of the crater. Complex cratering can be initiated with crater diameters of 2 km in sedimentary rocks; however, terrestrial simple craters may also exhibit crater diameters up to 4 km, which is the threshold for simple-to-complex cratering in crystalline rocks based on the direct inputs justified for use in Section D6 (Grieve 1987 [DIRS 135254], p. 249; Grieve et al. 1995 [DIRS 135260], p. 194; Wuschke et al. 1995 [DIRS 129326], p. 3). The threshold for FEP screening based on probability is stated as an annualized equivalence of 10^{-8} events per year for the repository area (Section D1). Based on the cratering rate distributions given in Figure D-6, a 2-km crater diameter occurs at a frequency of approximately 10^{-10} or less per year, which is two orders of magnitude less frequent than the threshold for consideration. Consequently, complex cratering features, which can onset at a crater diameter of 2 km, do not occur with sufficient frequency to be of concern for FEP screening. Because such large diameter craters are very unlikely events, complex cratering is not further considered in the FEP analysis.

D4.3.2 Derivation of Cratering Distributions Adjusted for Target Area

The target area is initially assumed rectangular in shape, with the dimensions described in Section D2. However, if a meteorite were to impact exterior to the repository boundary, but within one-half of the crater diameter from the boundary, the repository could still potentially be affected. This affects the boundaries on each side of the repository. Assuming fracturing and exhumation effects are cylindrical below the entire crater, the target area can be expressed as:

$$\text{Area (A)} = (L + (2 \times D/2))(W + (2 \times D/2)) = (L+D)(W+D) \qquad \text{(Eq. D-5)}$$

Equation D-5 further simplifies to:

$$\text{Area (A)} = LW + (L+W)D + D^2 \qquad \text{(Eq. D-5a)}$$

where:

L	=	length of target area (km)
W	=	width of target area (km)
D	=	diameter of crater (km)

Starting with Equation D-1, the overall annual probability of meteorite impacts that could disrupt or fracture the repository is given by the product of the frequency of impact and the target area integrated over the range of possible crater diameters:

$$P(D) = \int F(D)\, A\, dD \qquad \text{(Eq. D-6)}$$

From Equations D-2 and D-5a and with k equaling the power of the distribution for a given meteorite crater distribution:

$$P(D) = \int (-k\, K\, D^{k-1})\, (LW + (L+W)\, D + D^2)\, dD \qquad \text{(Eq. D-7)}$$

By removing the constants k and K and using the additive properties of integrals and exponents, the resulting integral is in the form of $\int u^n\, du$

$$P(D) = -k\, K \int (LWD^{k-1} + (L+W)D^k + D^{k+1})\, dD \qquad \text{(Eq. D-7a)}$$

Equation D-7a simplifies to:

$$Pf(D) = -kK\left(\frac{LWD^k}{k} + \frac{(L+W)D^{k+1}}{k+1} + \frac{D^{k+2}}{k+2}\right)\Bigg|_{D\,\min}^{D\,\max} \qquad \text{(Eq. D-7b)}$$

where:

P(D)	=	frequency of meteorite impacts per year capable of creating crater of diameter D
K	=	the proportionality constant
k	=	power of the distribution
L	=	length of the repository (km)
W	=	width of the repository (km)
D	=	diameter of the crater (km).

The lower limit (D_{min}) to the integral is assumed to be 0.001 km (1 m), based on the need to capture very small crater diameters. The choice is arbitrary based on the possible scale of interest, and larger or smaller values could have been chosen. The upper limit (D_{max}) was set at 100 km, which is on the order of the largest recognized crater diameter on the earth's surface. The choice for an upper limit value only affects the shape and magnitude of frequency curves for the largest values of the crater diameters.

D4.3.3 Calculation of Cratering Distribution for the Repository Target Area

Equation D-7b is applied below to calculate the cratering probability distribution for the target area for the Grieve (1987 [DIRS 135254]) distribution (Section D4.2.1) and the Wuschke et al. (1995 [DIRS 129326]) distribution (Section D4.2.2). For the Grieve (1987 [DIRS 135254]) distribution, the value for *k* is –1.8 and the value for K is 1.2×10^{-12}, as shown in Equation D-2. Table D-3 provides the annual probability calculations for cratering above the repository for the repository target area. The results are shown in Figure D-6, which indicates that for a threshold probability of 10^{-8} events per year, the diameter of the largest crater is estimated to be conservatively less than 60 m.

D4.3.4 Exhumation Depth within the Target Area

D4.3.4.1 Relationship Exhumation Depth and Crater Diameter

A range of exhumation depth-to-crater diameter ratios of 0.10 to 0.33 is assumed in this appendix, and a value of 0.32 based on Wuschke et al. (1995 [DIRS 129326], Figure 1) and 0.28 from Grieve (1998 [DIRS 163385], p. 113).

D4.3.4.2 Estimation of Exhumation Depth within the Target Area

For a maximum crater diameter of 60 m that corresponds to a cratering probability of 10^{-8} within the target area (Section D4.3.3), the exhumation depth ranges from 6 to 20 m, given an exhumation depth-to-crater diameter ratio of 0.10 to 0.33 as described above. Because the overburden thickness above the repository within the target area is at least 200 m as discussed in Section D2 (see also SNL 2007 [DIRS 179466], Table 4-1, Parameter 01-06), the probability of waste exhumation from cratering is less than 10^{-8} within the target area.

D4.3.5 Estimation of Fracturing Depth within the Target Area

D4.3.5.1 Relationship Fracturing Depth and Crater Diameter

The fracturing depth-to-crater diameter ratios assumed in this appendix ranges from 0.33 to 0.76 based on values of 0.75-0.76 (Wuschke et al. 1995 [DIRS 129326], Section 2.2 and Figure 1). Because the intended use is for the FEP screening, the conservative value of increased fracturing depth to 0.76 of the crater diameter, as indicated by Wuschke et al. (1995 [DIRS 129326]), is used to ensure that the range of uncertainty in this relationship is covered.

The use of this value based on effects in plutonic rock is somewhat contrary to the observation made by Grieve (1998 [DIRS 163385], p. 113) that depths in sedimentary rocks tend to be shallower than in plutonic rock. However, the use of these values is consistent with use of cratering rate and crater diameter distributions from these same sources.

D4.3.5.2 Estimation of Fracturing Depth within the Target Area

For a maximum crater diameter of 60 m that corresponds to a cratering probability of 10^{-8} per year within the target area (Section D4.3.3), the fracturing depth ranges from about 20 to 45 m, given a fracturing depth–to–crater diameter ratio of 0.33 to 0.76 as described in Section D4.3.5.1. Because the distance overburden thickness above the repository within the target area is at least 200 m as given in *Total System Performance Assessment Data Input Package for Requirements Analysis for Subsurface Facilities* (SNL 2007 [DIRS 179466], Table 4-1, Parameter 01-06), the probability of waste exhumation from cratering is less than 10^{-8} within the target area. Fracturing depths of less than 45 m would not affect infiltration into the repository because they are too shallow to reach the top of the PTn over most of the repository area. Figure D-2 shows that with the exception of the northwestern- and northern-most tip of the repository where the PTn outcrops, the distance to the top of the PTn is at least 60 m. In these northern areas with a lesser distance between the ground surface and the PTn, the PTn itself is more than 90 m thick (Figure D-3). Therefore, the PTn unit would maintain its original thickness (Figure D-4) even after the impact of a maximum-penetration cratering event that corresponds to the 10^{-8} annualized exceedance probability, and will continue to meet the 10-m thickness requirement set forth in the selection of the repository layout (BSC 2008 [DIRS 183627], Table 1, Parameter 01-21) that ensures that the unit will remain effective in damping the episodic infiltration transients (see excluded FEP 2.2.07.05.0A (Flow in the UZ from Episodic Infiltration)). The fracturing of the PTn can, therefore, be excluded based on low probability because the probability of fracturing the PTn to less than 10 m thick is less than 10^{-8} per year.

Table D-3. Annual Frequency of Cratering above Repository for TSPA-LA Emplacement Area

Power Law from Grieve (1987 [DIRS 135254])		L = 5.4	W = 2.2	k = −1.8	K = 1.2E−12
Crater Diameter (km)	$\frac{LWD^{k}}{(k)}$	$\frac{(L+W) \times D^{k+1}}{(k+1)}$	$\frac{D^{k+2}}{(k+2)}$	G(D)	$k \times K \times [G(D) - G(D_{max})]$
1.00E−03	-1.66E+06	-2.39E+03	1.26E+00	-1.66E+06	3.59E-06
.000E−03	-4.76E+05	-1.37E+03	1.44E+00	-4.77E+05	1.03E-06
.000E−03	-9.15E+04	-6.58E+02	1.73E+00	-9.22E+04	1.99E-07
.000E−03	-4.99E+04	-5.03E+02	1.85E+00	-5.04E+04	1.09E-07
9.00E−03	-3.18E+04	-4.11E+02	1.95E+00	-3.22E+04	6.95E-08
1.00E−02	-2.63E+04	-3.78E+02	1.99E+00	-2.67E+04	5.76E-08
2.00E−02	-7.55E+03	-2.17E+02	2.29E+00	-7.76E+03	1.68E-08
3.00E−02	-3.64E+03	-1.57E+02	2.48E+00	-3.79E+03	8.22E-09
4.00E−02	-2.17E+03	-1.25E+02	2.63E+00	-2.29E+03	4.97E-09
5.00E−02	-1.45E+03	-1.04E+02	2.75E+00	-1.55E+03	3.38E-09
6.00E−02	-1.04E+03	-9.02E+01	2.85E+00	-1.13E+03	2.47E-09
7.00E−02	-7.91E+02	-7.97E+01	2.94E+00	-8.68E+02	1.90E-09
8.00E−02	-6.22E+02	-7.17E+01	3.02E+00	-6.91E+02	1.52E-09
1.00E−01	-4.16E+02	-5.99E+01	3.15E+00	-4.73E+02	1.05E-09
2.00E−01	-1.20E+02	-3.44E+01	3.62E+00	-1.50E+02	3.51E-10
5.00E−01	-2.30E+01	-1.65E+01	4.35E+00	-3.52E+01	1.03E-10
7.50E−01	-1.11E+01	-1.20E+01	4.72E+00	-1.83E+01	6.62E-11
1.00E+00	-6.60E+00	-9.50E+00	5.00E+00	-1.11E+01	5.06E-11
2.00E+00	-1.90E+00	-5.46E+00	5.74E+00	-1.61E+00	3.01E-11
5.00E+00	-3.64E-01	-2.62E+00	6.90E+00	3.91E+00	1.82E-11
7.50E+00	-1.76E-01	-1.90E+00	7.48E+00	5.41E+00	1.49E-11
1.00E+01	-1.05E-01	-1.51E+00	7.92E+00	6.31E+00	1.30E-11

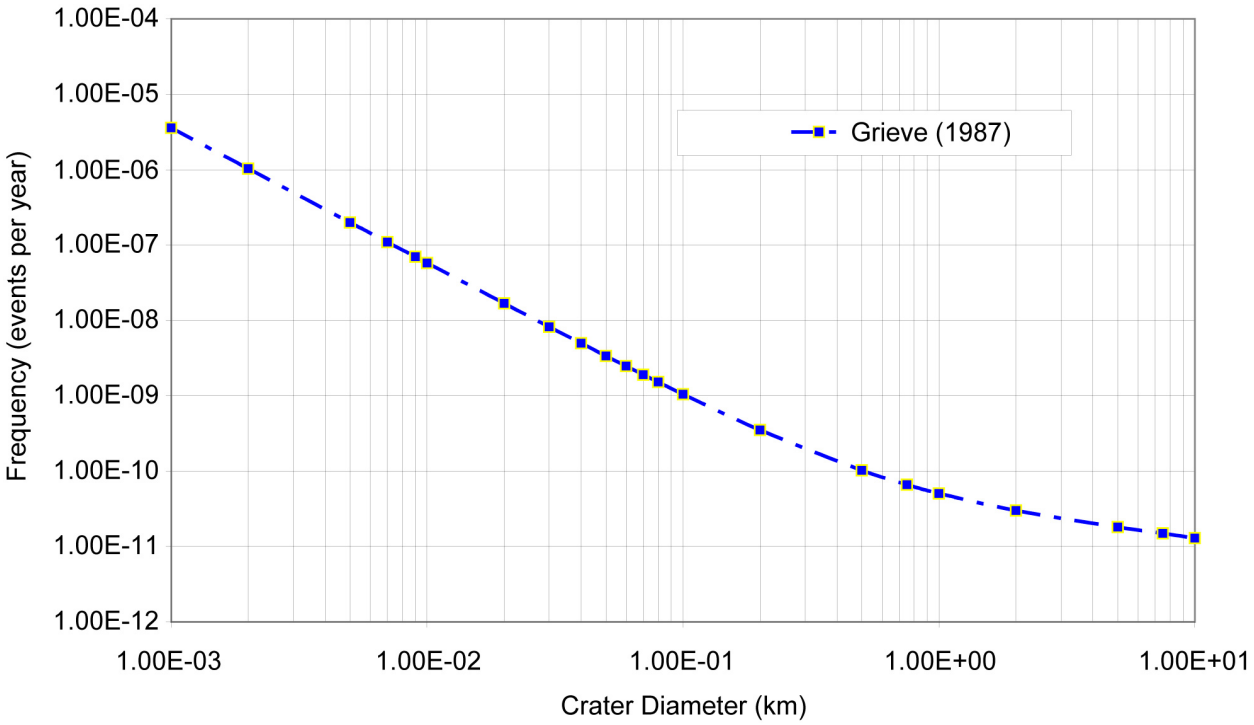

Source: Grieve 1987 [DIRS 135254]

Figure D-6. Annualized Frequency of Cratering above the Repository for the Target Area

D5. CONCLUSIONS

The probability of the occurrence of crater diameters of interest (i.e., the diameters that define whether the repository is affected by direct exhumation, fracturing to repository depth, or fracturing of other overlying units of interest) is compared to the FEP screening threshold diameter of one chance in 10,000 of occurring in 10,000 years (or an annualized occurrence of 10^{-8}). If the probability of occurrence is less than this threshold, the effect can be excluded from further consideration in TSPA.

The above analysis shows that at an annualized probability of 10^{-8} (the FEP screening probability threshold), the corresponding crater diameter resulting from impact of the largest meteor fragment is less than 60 m (Figure D-6).

As discussed in Section D4.3, the probability of the formation of such craters within the repository target area sufficient to result in exhumation to the depth of the repository falls below the regulatory criterion of 10^{-8} per year. Likewise, maximum fracturing induced by a threshold cratering event will not be sufficient to reduce the thickness of the PTn unit to less than 10 m, which is the requirement set forth in the selection of the repository layout (BSC 2008 [DIRS 183627], Table 1, Parameter 01-21) to ensure that the unit is effective in damping the episodic infiltration transients (see excluded FEP 2.2.07.05.0A (Flow in the UZ from Episodic Infiltration)). Significant fracturing of the PTn can, therefore, be excluded based on low probability because the probability of reducing the PTn to a thickness of less than 10 m is less than 10^{-8} per year.

Smaller crater diameters occur more frequently, but these are of insufficient size to result in direct exhumation or fracturing to the depth of the repository and are excluded based on low consequence. Larger crater diameters occur less frequently and are less probable than the exceedance probability, and are therefore excluded from the TSPA as low probability events. Effects on infiltration due to changes in ecological factors due to small meteor craters or the effects of a near-surface explosion associated with a meteorite are also excluded based on low consequence because such events would likely have only transient effects or have no means of affecting the subsurface postclosure repository (see also excluded FEPs 1.4.03.00.0A (Unintrusive Site Investigation) and 1.5.01.02.0A (Extraterrestrial Events)). A modern example of a site in which the ecology has recovered is the Tunguska site in Siberia.

Meteors that result in crater diameters of 60 m (corresponding to the threshold annual probability of 10^{-8}) could trigger earthquakes with Richter magnitudes ranging from Magnitude 5 to slightly less than Magnitude 7 (Hills and Goda 1993 [DIRS 135281], Figure 18). Existing seismic analyses cover this range of magnitude (CRWMS M&O 1998 [DIRS 103731], Section 4). Therefore, an earthquake caused by meteorite impact is excluded based on low consequence because it would not provide a significant contribution to the overall earthquake hazard. Earthquake hazards are already included and probabilistically weighted in the TSPA. The effects of changes in rock stress, such as those caused by seismic activity, are addressed in multiple FEPs such as excluded FEPs 2.2.06.01.0A (Seismic Activity Changes Porosity and Permeability of Rock), 2.2.06.02.0A (Seismic Activity Changes Porosity and Permeability of Faults), and 2.2.06.02.0B (Seismic Activity Changes Porosity and Permeability of Fractures).

Because percolation is not significantly affected and no fracturing occurs down to the repository depth, with no associated waste exhumation, there is no mechanism for a meteorite impact at the threshold annual probability or greater to affect groundwater flux through the repository horizon. Therefore, the dose and release of radionuclides are not significantly changed.

Based on the preceding discussion, meteorite impact is excluded from the performance assessment conducted to demonstrate compliance with proposed 10 CFR 63.311 and 10 CFR 63.321 (70 FR 53313 [DIRS 178394]), and with 10 CFR 63.331 [DIRS 180319], on the basis of low probability for exhumation and fracturing to repository depth and to the PTn unit within the repository target area.

D6 DATA QUALIFICATION

This section provides the data qualification for unqualified external sources used as direct input only for the screening analysis of FEP 1.5.01.01.0A (Meteorite Impact) in this appendix. Data qualifications are performed in accordance with SCI-PRO-005, *Scientific Analyses and Calculations*.

D6.1 DATA FOR QUALIFICATION

There are six external sources of data used as direct input for this screening analysis listed in Table D-4.

D6.1.1 Qualification Method

The data to be evaluated have been extracted from non-YMP-specific sources and will be qualified for intended use. The method for qualification of the six external sources of data is the technical assessment method (SCI-PRO-001, Attachment 3, Method 5. The rationale for using this method is that it is the most suitable considering the methodology, data acquisition or development results, and use in similar applications are applicable. Qualification process attributes used in the technical assessment of each external source are selected from the list provided in Attachment 4 of SCI-PRO-001. Attributes specifically applicable as data qualification attributes in this appendix are:

1. Qualifications of personnel or organizations generating the data are comparable to qualification requirements of personnel generating similar data under an approved program that supports the YMP license application process or postclosure science.

2. The extent to which the data demonstrate the properties of interest (e.g., physical, chemical, geologic, mechanical)

Table D-4. Data Sets for Use within this Technical Product

Item	Source	Description of Direct Input	Summary of Source
1	Grieve and Robertson 1984 [DIRS 185030]	Power law for distribution for terrestrial craters Abstract, p. 231	Introduction of a size-frequency power law relationship for analyzing terrestrial and lunar crater diameters. This power law was further improved and used in later publications concerning crater impacts.
2	Grieve 1987 [DIRS 135254]	Use of a power law for cratering rate distribution based on observed earth cratering and threshold size for onset of complex cratering. pp. 248 and 257, Figure 8	This is a seminal work in the area of impact cratering and lists observed craters, crater characteristics, and cratering rates. The paper provides relationships of crater diameter to crater depth and provides a cratering rate estimate for large-diameter craters that are generally used in hazard estimates. This paper was taken from a peer-reviewed journal. The documentation is somewhat limited, but is generally accepted as reliable.
3	Grieve et al. 1995 [DIRS 135260]	Crater rate distribution based on observed earth cratering. pp. 194 to 196	This is an update to the 1987 paper by the primary author. It provides updated cratering information, defines the constants, and addresses the limits for simple and complex cratering. This paper was taken from a technical journal. Acknowledgments are given to peer-reviewers on an earlier version of the document. This paper provides a listing of observed cratering impact structures and their diameters and ages, allowing independent confirmation of the developed distribution. A thorough reference list is also provided.
4	Grieve 1998 [DIRS 163385]	Crater diameter to depth of effect relationships. Depth of exhumation is approximately 0.28 times the crater diameter. p. 113, Figure 8	This is an update and summary of previous papers and summarizes the results of studies to date, and provides a distinction of the cratering effect data based on craters in sedimentary and crystalline materials. This paper is focused on updating the “state of knowledge” regarding the number of craters, cratering mechanics, shock metamorphism, and effect of impacts on biological evolution. This paper was taken from a compendium addressing flux with time and impact effects. An extensive reference list is provided.
5	Hills and Goda 1993 [DIRS 135281]	Earthquake magnitudes due to a meteoroid impact range from magnitude 5 to slightly less than magnitude 7 on the Richter scale. Figure 18	This paper focuses on evaluating effects of small asteroids impacting the Earth. The paper provides a relationship between crater diameters and earthquake energy. This paper was taken from a peer-reviewed journal. Los Alamos National Laboratory prepared the work, and the development of the models is well documented and supporting equations are provided. No information is provided on quality control or development procedures
6	Wuschke et al. 1995 [DIRS 129326]	Spatial relationships of crater diameter to extents and depth of fracturing and exhumation. p. 3 Spatial extent of fracturing is assumed to be spherical. Figure 1 Cratering rate data for the Canadian shield and application to a hypothetical Canadian repository. pp. 4 and 26	This paper is directly applicable as it presents a well-documented evaluation equivalent to the evaluation needed for the YMP. The paper provides a detailed analysis of the hazard and risk associated with meteorite impact above an underground repository. Assumptions, spatial relationships, mathematical formulations, and uncertainty analysis are all documented within the report. This paper was prepared by AECL Research to evaluate risk from meteorite impact on a hypothetical underground repository. The paper reports results of a specific technical analysis. Citations are provided for all sources and uncertainty analyses are provided.

D6.1.2 Technical Assessment of External Data from Grieve 1987

The action taken to qualify the meteoroid impact data from "Terrestrial Impact Structures" (Grieve 1987 [DIRS 135254]) is from SCI-PRO-001, Attachment 3, Method 5(b) as follows:

> Determination that confidence in the data acquisition or developmental results is warranted. A discussion and justification that the data acquisition and/or subsequent data development (e.g., reduction or extrapolation) discussed in source documentation was appropriate for the type of data under consideration. This could include assurances that processes were conducted by qualified professionals; data were collected under proper environmental conditions; collected results and/or data development are appropriate, reasonable, and suitable for their intended use; etc.

The following criteria were used to assess the external data from "Terrestrial Impact Structures" (Grieve 1987 [DIRS 135254]):

1. Qualifications of personnel or organizations generating the data are comparable to qualification requirements of personnel generating similar data under an approved program that supports the YMP license application process or postclosure science.

2. The extent to which the data demonstrate the properties of interest (e.g., physical, chemical, geologic, mechanical).

Justification for the appropriate use of data from "Terrestrial Impact Structures" (Grieve 1987 [DIRS 135254]):

> R.A.F. Grieve has been on the faculty for the Department of Geological Sciences at Brown University and a member of the Geophysics Division for the Geological Survey of Canada. These associations demonstrate an appropriate technical level of competence for qualification of publications authored by Grieve for their intended use in this appendix.
>
> The report is a seminal work in the area of impact cratering and lists observed craters, crater characteristics, and cratering rates. The paper builds on earlier relationships of crater diameter to crater depth and provides a cratering rate estimate for large-diameter craters that are generally used in hazard estimates. This paper was taken from a peer-reviewed journal. The documentation is somewhat limited, but is generally accepted as reliable and has been updated on a periodic basis.

Based on the assessment made above, data from "Terrestrial Impact Structures" (Grieve 1987 [DIRS 135254]) are qualified for use as direct input for this appendix.

D6.1.3 Technical Assessment of External Data from Grieve and Robertson 1984

The action taken to qualify the meteoroid impact data from "The Potential for the Disturbance of a Buried Nuclear Waste Vault by a Large-Scale Meteorite Impact" (Grieve and Robertson 1984 [DIRS 185030]) is from SCI-PRO-001, Attachment 3, Method 5(b) as follows:

Determination that confidence in the data acquisition or developmental results is warranted. A discussion and justification that the data acquisition and/or subsequent data development (e.g., reduction or extrapolation) discussed in source documentation was appropriate for the type of data under consideration. This could include assurances that processes were conducted by qualified professionals; data were collected under proper environmental conditions; collected results and/or data development are appropriate, reasonable, and suitable for their intended use; etc.

The following criteria were used to assess the external data from "The Potential for the Disturbance of a Buried Nuclear Waste Vault by a Large-Scale Meteorite Impact" (Grieve and Robertson 1984 [DIRS 185030]):

1. Qualifications of personnel or organizations generating the data are comparable to qualification requirements of personnel generating similar data under an approved program that supports the YMP license application process or postclosure science.

2. The extent to which the data demonstrate the properties of interest (e.g., physical, chemical, geologic, mechanical).

Justification for the appropriate use of data from "The Potential for the Disturbance of a Buried Nuclear Waste Vault by a Large-Scale Meteorite Impact" (Grieve and Robertson 1984 [DIRS 185030]):

R.A.F. Grieve has been on the faculty for the Department of Geological Sciences at Brown University and a member of the Geophysics Division for the Geological Survey of Canada. P. B. Robertson has been a member of the Earth Sciences Branch of The Department of Energy, Mines and Resources for Ontario Canada. These associations demonstrate an appropriate technical level of competence for qualification of publications authored by Grieve and Robertson for their intended use in this appendix.

The report introduces the size-frequency power law relationship for analyzing terrestrial and lunar crater diameters used in this appendix. This power law was further improved and used in later publications concerning crater impacts.

Based on the assessment made above, data from "The Potential for the Disturbance of a Buried Nuclear Waste Vault by a Large-Scale Meteorite Impact" (Grieve and Robertson 1984 [DIRS 185030]) are qualified for use as direct input for this appendix.

D6.1.4 Technical Assessment of External Data from Grieve 1998

The action taken to qualify the meteoroid impact data from "Extraterrestrial Impacts on Earth: The Evidence and the Consequences" (Grieve 1998 [DIRS 163385]) is from SCI-PRO-001, Attachment 3, Method 5(b) as follows:

Determination that confidence in the data acquisition or developmental results is warranted. A discussion and justification that the data acquisition and/or subsequent data development (e.g., reduction or extrapolation) discussed in source documentation was appropriate for the type of data under consideration. This could include assurances that processes were

conducted by qualified professionals; data were collected under proper environmental conditions; collected results and/or data development are appropriate, reasonable, and suitable for their intended use; etc.

The following criteria were used to assess the external data from "Extraterrestrial Impacts on Earth: The Evidence and the Consequences" (Grieve 1998 [DIRS 163385]):

1. Qualifications of personnel or organizations generating the data are comparable to qualification requirements of personnel generating similar data under an approved program that supports the YMP license application process or postclosure science.

2. The extent to which the data demonstrate the properties of interest (e.g., physical, chemical, geologic, mechanical).

Justification for the appropriate use of data from "Extraterrestrial Impacts on Earth: The Evidence and the Consequences" (Grieve 1998 [DIRS 163385]):

R.A.F. Grieve has been on the faculty for the Department of Geological Sciences at Brown University and a member of the Geophysics Division for the Geological Survey of Canada. These associations demonstrate an appropriate technical level of competence for qualification of publications authored by Grieve for their intended use in this appendix.

This report is an update and summary of previous papers and summarizes the results of studies to date, and provides a distinction of the cratering effect data based on craters in sedimentary and crystalline materials. This paper is focused on updating the "state of knowledge" regarding the number of craters, cratering mechanics, shock metamorphism, and effect of impacts on biological evolution.

Based on the assessment made above, data from "Extraterrestrial Impacts on Earth: The Evidence and the Consequences" (Grieve 1998 [DIRS 163385]) are qualified for use as direct input for this appendix.

D6.1.5 Technical Assessment of External Data from Hills and Goda 1993

The action taken to qualify the meteoroid impact data from "Fragmentation of Small Asteroids in the Atmosphere" (Hills and Goda 1993 [DIRS 135281]) is from SCI-PRO-001, Attachment 3, Method 5(b) as follows:

Determination that confidence in the data acquisition or developmental results is warranted. A discussion and justification that the data acquisition and/or subsequent data development (e.g., reduction or extrapolation) discussed in source documentation was appropriate for the type of data under consideration. This could include assurances that processes were conducted by qualified professionals; data were collected under proper environmental conditions; collected results and/or data development are appropriate, reasonable, and suitable for their intended use; etc.

The following criteria were used to assess the external data from "Fragmentation of Small Asteroids in the Atmosphere" (Hills and Goda 1993 [DIRS 135281]):

1. Qualifications of personnel or organizations generating the data are comparable to qualification requirements of personnel generating similar data under an approved program that supports the YMP license application process or postclosure science.

2. The extent to which the data demonstrate the properties of interest (e.g., physical, chemical, geologic, mechanical).

Justification for the appropriate use of data from "Fragmentation of Small Asteroids in the Atmosphere" (Hills and Goda 1993 [DIRS 135281]):

> J. G. Hills and M.P. Goda have been members of the Theoretical Astrophysics Group at Los Alamos National Laboratory. These associations demonstrate an appropriate technical level of competence for qualification of publications authored by Hills and Gods for their intended use in this appendix.
>
> The report relates the earthquake energy level from a meteoroid impact as determined from the Richter scale to the impact crater diameter, thus providing a link to the repository seismic analyses.

Based on the assessment made above, data from "Fragmentation of Small Asteroids in the Atmosphere" (Hills and Goda 1993 [DIRS 135281]) are qualified for use as direct input for this appendix and FEP 1.5.01.01.0A (Meteorite Impact).

D6.1.6 Technical Assessment of External Data from Grieve et al. 1995

The action taken to qualify the meteoroid impact data from "The Record of Terrestrial Impact Cratering" (Grieve et al. 1995 [DIRS 135260]) is from SCI-PRO-001, Attachment 3, Method 5(b) as follows:

> Determination that confidence in the data acquisition or developmental results is warranted. A discussion and justification that the data acquisition and/or subsequent data development (e.g., reduction or extrapolation) discussed in source documentation was appropriate for the type of data under consideration. This could include assurances that processes were conducted by qualified professionals; data were collected under proper environmental conditions; collected results and/or data development are appropriate, reasonable, and suitable for their intended use; etc.

The following criteria were used to assess the external data from "The Record of Terrestrial Impact Cratering" (Grieve et al.1995 [DIRS 135260]):

1. Qualifications of personnel or organizations generating the data are comparable to qualification requirements of personnel generating similar data under an approved program that supports the YMP license application process or postclosure science.

2. The extent to which the data demonstrate the properties of interest (e.g., physical, chemical, geologic, mechanical).

Justification for the appropriate use of data from "The Record of Terrestrial Impact Cratering" (Grieve et al.1995 [DIRS 135260]):

> R.A.F. Grieve has been on the faculty for the Department of Geological Sciences at Brown University and a member of the Geophysics Division for the Geological Survey of Canada. These associations demonstrate an appropriate technical level of competence for qualification of publications authored by Grieve for their intended use in this appendix.
>
> This report is an update and summary of previous papers and summarizes the results of studies to date, and provides a distinction of the cratering effect data based on craters in sedimentary and crystalline materials. This paper is focused on updating the "state of knowledge" regarding the number of craters, cratering mechanics, shock metamorphism, and effect of impacts on biological evolution.

Based on the assessment made above, data from "The Record of Terrestrial Impact Cratering" (Grieve et al. 1995 [DIRS 135260]) are qualified for use as direct input for this appendix and FEP 1.5.01.01.0A (Meteorite Impact).

D6.1.7 Technical Assessment of External Data from Wuschke et al. 1995

The action taken to qualify the meteoroid impact data from *Assessment of the Long-Term Risk of a Meteorite Impact on a Hypothetical Canadian Nuclear Fuel Waste Disposal Vault Deep in Plutonic Rock* (Wuschke et al. 1995 [DIRS 129326]) is from SCI-PRO-001, Attachment 3, Method 5(b) as follows:

> Determination that confidence in the data acquisition or developmental results is warranted. A discussion and justification that the data acquisition and/or subsequent data development (e.g., reduction or extrapolation) discussed in source documentation was appropriate for the type of data under consideration. This could include assurances that processes were conducted by qualified professionals; data were collected under proper environmental conditions; collected results and/or data development are appropriate, reasonable, and suitable for their intended use; etc.

The following criteria were used to assess the external data from *Assessment of the Long-Term Risk of a Meteorite Impact on a Hypothetical Canadian Nuclear Fuel Waste Disposal Vault Deep in Plutonic Rock* (Wuschke et al. 1995 [DIRS 129326]):

1. Qualifications of personnel or organizations generating the data are comparable to qualification requirements of personnel generating similar data under an approved program that supports the YMP license application process or postclosure science.

2. The extent to which the data demonstrate the properties of interest (e.g., physical, chemical, geologic, mechanical).

Justification for the appropriate use of data from *Assessment of the Long-Term Risk of a Meteorite Impact on a Hypothetical Canadian Nuclear Fuel Waste Disposal Vault Deep in Plutonic Rock* (Wuschke et al. 1995 [DIRS 129326]):

D.M. Wuschke, S.H. Whitaker, B.W. Goodwin, and L.R. Rasmussen have been staff members of Atomic Energy of Canada, Limited (AECL). These associations demonstrate an appropriate technical level of competence for qualification of publications authored by Hills and Gods for their intended use in this appendix.

This paper is directly applicable as it presents a well-documented evaluation equivalent to the evaluation needed for YMP. The paper provides a detailed analysis of the hazard and risk associated with meteorite impact above an underground repository. Assumptions, spatial relationships, mathematical formulations, and uncertainty analysis are all documented within the report.

Based on the assessment made above, data from *Assessment of the Long-Term Risk of a Meteorite Impact on a Hypothetical Canadian Nuclear Fuel Waste Disposal Vault Deep in Plutonic Rock* (Wuschke et al. 1995 [DIRS 129326]) are qualified for use as direct input for this appendix and FEP 1.5.01.01.0A (Meteorite Impact).

Table D-5. Direct Inputs for Appendix D

Input	Source	Description
Grieve 1987. "Terrestrial Impact Structures." [DIRS 135254]	pp. 248 and 257, Figure 8	Cratering rate distribution based on observed earth cratering (i.e., proportional to $D_{crater}^{-1.8}$) and threshold size for onset of complex cratering (4 km)
Grieve 1998. "Extraterrestrial Impacts on Earth: The Evidence and the Consequences." [DIRS 163385]	p. 113, Figure 8	Range of exhumation depth to crater diameter ratios justified for use as direct input
Grieve et al. 1995. "The Record of Terrestrial Impact Cratering." [DIRS 135260]	pp. 194 to 196	Crater rate distribution based on observed earth cratering
Hills and Goda 1993. "Fragmentation of Small Asteroids in the Atmosphere." [DIRS 135281]	Figure 18	Richter scale magnitude of the earthquake produced by impact or debris hitting the ground as a function of initial meteoroid radius
Wuschke et al. 1995. "Assessment of the Long-Term Risk of a Meteorite Impact on a Hypothetical Canadian Nuclear Fuel Waste Disposal Vault Deep in Plutonic Rock." [DIRS 129326]	p. 3 and Figure 1 pp. 4 and 26	Crater diameter to depth of effect relationships and ratio of crater diameter-to-fracture depth and the ratio are used as direct input Cratering rate data for the Canadian shield and application to a hypothetical Canadian repository
Grieve and Robertson 1984. "*The Potential for the Disturbance of a Buried Nuclear Waste Vault by a Large-Scale Meteorite Impact*. *Proceedings of a Workshop on Transitional Processes*." [DIRS 185030]	Abstract, p. 231	Power law for distribution for terrestrial craters

Table D-6. Indirect Inputs for Appendix D

Citation	Title	DIRS
10 CFR 63	Energy: Disposal of High-Level Radioactive Wastes in a Geologic Repository at Yucca Mountain, Nevada	180319
70 FR 53313	Implementation of a Dose Standard After 10,000 Years	178394
Brown et al. 2002	"The Flux of Small Near-Earth Objects Colliding with the Earth"	162569
BSC 2003	*Underground Layout Configuration*	165572
BSC 2004	*Geologic Framework Model (GFM2000)*	170029
BSC 2007	*IED Subsurface Facilities Geological Data*	182926
BSC 2007	*IED Subsurface Facilities Layout Geographical Data*	183743
BSC 2008	*Postclosure Modeling and Analyses Design Parameters*	183627
Ceplecha 1994	"Impacts of Meteoroids Larger than 1m into the Earth's Atmosphere"	135243
Chapman and Morrison 1994	"Impacts on the Earth by Asteroids and Comets: Assessing the Hazard"	135245
Chyba 1993	"Explosions of Small Spacewatch Objects in Earth's Atmosphere"	135248
CRWMS M&O 1998	*Probabilistic Seismic Hazard Analyses for Fault Displacement and Vibratory Ground Motion at Yucca Mountain, Nevada*	103731
Grieve 1987	"Terrestrial Impact Structures"	135254
Grieve 1998	"Extraterrestrial Impacts on Earth: The Evidence and the Consequences"	163385
Grieve et al. 1995	"The Record of Terrestrial Impact Cratering"	135260
Hughes 1998	"The Mass Distribution of Crater-Producing Bodies"	162562
Marsden and Steel 1994	"Warning Times and Impact Probabilities for Long-Period Comets"	129308
Neukum and Ivanov 1994	"Crater Size Distributions and Impact Probabilities on Earth from Lunar, Terrestrial-Planet, and Asteroid Cratering Data"	121510
Shoemaker 1983	"Asteroid and Comet Bombardment of the Earth"	135308
SNL 2007	*Total System Performance Assessment Data Input Package for Requirements Analysis for Subsurface Facilities*	179466
SNL 2007	*UZ Flow Models and Submodels*	184614
Wuschke et al. 1995	*Assessment of the Long-Term Risk of a Meteorite Impact on Hypothetical Canadian Nuclear Fuel Waste Disposal Vault Deep in Plutonic Rock*	129326

INTENTIONALLY LEFT BLANK

APPENDIX E

LOW CONSEQUENCE CALCULATION FOR RUPTURE OF DRIP SHIELD PLATES FROM SEISMIC-INDUCED ROCK BLOCK IMPACTS

E.1 PURPOSE

This calculation demonstrates that drip shield plate failures due to seismic-induced rock block impacts in the nonlithophysal units of the repository have low consequence for repository performance. This calculation supports the screening justification for excluded FEP 1.2.03.02.0B (Seismic-Induced Rockfall Damages EBS Components).

E.1.1 Scope

The scope of this calculation is limited to estimating the dose to the reasonably maximally exposed individual within the first 10,000 years after repository closure due to drip shield plate failures caused by seismic-induced rock block impacts in nonlithophysal units of the repository. This calculation does not address the performance of naval spent nuclear fuel during seismic events. This calculation also does not address the preclosure response of the drip shield to seismic-induced rockfall.

E.1.2 Limitation

The maximum dose from drip shield plate failures is estimated using the results from the drip shield early failure modeling case (SNL 2008 [DIRS 183478], Sections 6.4 and 6.4.1). The drip shield early failure modeling case assumes that a single drip shield and its associated waste package fail simultaneously. This approach overestimates the dose from drip shield plate failures from seismic-induced rock block impacts because it ignores the potential for a delay between the time that localized corrosion could occur and the time that the drip shield fails due to rock block impacts. As shown by the last term in Equation E-2, the dose estimate begins from t_{LC}, the earliest time that localized corrosion could occur. In actuality, no dose would be possible until after a seismic event occurs, which could be later than t_{LC} because both localized corrosion and a seismic event that causes the drip shield plates to fail are required for a release, as explained in Section E.6.1. The potential delay in releases for a seismic event that occurs after t_{LC} is not included in the dose estimate in Equation E-2.

E.2 QUALITY ASSURANCE

Calculations performed under the technical work plan (SNL 2007 [DIRS 184327], Section 4) are subject to the requirements of SCI-PRO-005, *Scientific Analyses and Calculations*.

E.3 USE OF SOFTWARE

No qualified software is used to perform this calculation.

As already indicated in Section 3, MathCad Version 13.1 (STN: 611161-13.1-00), running under the Microsoft Windows 2000 Professional operating system, has been used to perform the calculation documented in this appendix. The standard features of MathCad are sufficient for these calculations. No macros, codes, or software routines are required for or developed during this work. As used here, MathCad Version 13.1 is not required to be qualified or documented in accordance with IM-PRO-003, *Software Management*. The formulas, inputs to the formulas, and outputs from the formulas in the MathCad calculation are identified in this appendix and in the MathCad file.

All MathCad files that are relevant for the calculation are included in output DTN: MO0707NONLITHO.000.

E.4 INPUTS

E.4.1 Direct Input

Table E-1 presents the direct input information for this calculation. The numerical values in Table E-1 are presented with the same number of significant figures and in the same units as the data in the source, unless otherwise noted. The technical product inputs identified in Table E-1 are appropriate for the development of a scientific analysis for the dose related to failures of drip shield plates in the nonlithophysal units of the repository.

E.4.2 Criteria

No criteria are specific to the calculation in this appendix.

E.4.3 Codes, Standards, and Regulations

No additional codes, standards, or regulations apply to the calculation in this appendix.

Table E-1. Direct Inputs for Appendix E

Input Data or Information	Value	Source
Bounded hazard curve at the emplacement drifts	See Table 1-1 or parameter PGV in Table 1-15 in the DTN	DTN: MO0703PASEISDA.002 [DIRS 183156], file: *Seismic Damage Abstractions for TSPA Compliance Case.doc*
Maximum annual exceedance frequency on the bounded hazard curve	4.287×10^{-4} per year	DTN: MO0703PASEISDA.002 [DIRS 183156], Step 2 or parameter LAMBDA_MAX in Table 1-15 in file: *Seismic Damage Abstractions for TSPA Compliance Case.doc*
Minimum annual exceedance frequency on the bounded hazard curve	10^{-8} per year	DTN: MO0703PASEISDA.002 [DIRS 183156], Step 2 or parameter LAMBDA_MIN in Table 1-15 in file: *Seismic Damage Abstractions for TSPA Compliance Case.doc*
Probability of damage to the drip shield or failure of the drip shield plates from seismic-induced rock block impacts in the nonlithophysal units	Values are tabulated in the DTN	DTN: MO0703PASEISDA.002 [DIRS 183156], Table 1-10 or parameter PD_DSNL in Table 1-18 in file: *Seismic Damage Abstractions for TSPA Compliance Case.doc*
Probability of the number of drip shields with failed plates from seismic-induced rock block impacts in the nonlithophysal units. This probability is conditional on the occurrence of drip shield damage or drip shield plate failures.	Values are tabulated in the DTN	DTN: MO0703PASEISDA.002 [DIRS 183156], Table 1-11 or parameters: PD_DSNL-STATE1, PD_DSNL_STATE2, PD_DSNL_STATE3, PD_DSNL_STATE4, and PD_DSNL-STATE5 in Table 1-18 in file: *Seismic Damage Abstractions for TSPA Compliance Case.doc*
Mean corrosion rate for Titanium Grade 7 under aggressive conditions, which applies to the top side of the drip shield plates	46.1 nm/yr	DTN: SN0704PADSGCMT.001 [DIRS 182122], Section 2 in file: *TSPA Implementation_DS GC Model.pdf*

Table E-1. Direct Inputs for Appendix E (Continued)

Input Data or Information	Value	Source
Mean corrosion rate for Titanium Grade 7 under benign conditions, which applies to the bottom side of the drip shield plates	5.15 nm/yr	DTN: SN0704PADSGCMT.001 [DIRS 182122], Section 3 in file: *TSPA Implementation_DS GC Model.pdf*
Initial thickness of drip shield plates	0.59 in (15 mm)	SNL 2007 [DIRS 179354], Section 4.1.2, Table 4-2, Parameter 07-04A
Number of repository percolation subregions (seepage bins)	5	DTN: LA0702PANS02BR.001 [DIRS 180322], file: *README*, second bullet under the heading Repository Node Lists
Fraction of waste packages in repository percolation subregions 1 through 5	**Bin # Fraction of Waste Package** 1 0.05 2 0.25 3 0.40 4 0.25 5 0.05	SNL 2008 [DIRS 183478], Section 6.3.2.2.1, bottom of first paragraph
Fraction of each repository percolation subregion in the nonlithophysal units	**Bin # Fraction in Nonlithophysal Units** 1 0.319018 2 0.237454 3 0.173077 4 0.0414634 5 0.109756	DTN: MO0709TSPALOCO.000 [DIRS 182994], TSPA parameter: NonLith_Frac_CSNF_out
Number of epistemic vectors for the drip shield early failure modeling case	300	SNL 2008 [DIRS 183478], Section 7.3.1.2
Number of waste package types for each epistemic vector in the drip shield early failure modeling case	2 (commercial SNF or codisposal)	SNL 2008 [DIRS 183478], Section 6.3.7
Number of commercial spent nuclear fuel waste packages in the inventory for the TSPA model	8,213	DTN: MO0702PASTREAM.001 [DIRS 179925] file: *DTN-Inventory-Rev00.xlsl*, worksheet: "UNIT CELL," cell: G49
Number of codisposal waste packages in the inventory for the TSPA model	3,416	DTN: MO0702PASTREAM.001 [DIRS 179925] file: *DTN-Inventory-Rev00.xlsl*, worksheet: "UNIT CELL," cell: K49
Timing of localized corrosion by waste package type and by seepage bin	See files in DTN for data	DTN: MO0709TSPALOCO.000 [DIRS 182994], files: *LC_Initiation_Analysis_v2_CSNF_Bin1.TXT* *LC_Initiation_Analysis_v2_CSNF_Bin2.TXT* *LC_Initiation_Analysis_v2_CSNF_Bin3.TXT* *LC_Initiation_Analysis_v2_CSNF_Bin4.TXT* *LC_Initiation_Analysis_v2_CSNF_Bin5.TXT* *LC_Initiation_Analysis_v2_CDSP_Bin1.TXT* *LC_Initiation_Analysis_v2_CDSP_Bin2.TXT* *LC_Initiation_Analysis_v2_CDSP_Bin3.TXT* *LC_Initiation_Analysis_v2_CDSP_Bin4.TXT* *LC_Initiation_Analysis_v2_CDSP_Bin5.TXT*
Dose time histories for the drip shield early failure modeling case	See file in DTN for data	DTN: MO0709TSPAREGS [DIRS 182976], file: *LA_v5.000_ED_003000_007_Dose_Total.txt*

Table E-1. Direct Inputs for Appendix E (Continued)

Input Data or Information	Value	Source
Expected annual dose for the drip shield early failure modeling case for 1,000,000 years after repository closure	Dose gradually decreases during the 1,000,000-year period	SNL 2008 [DIRS 183478], Figure 8.2-3(b)[a]
Expected annual dose for the seismic ground motion modeling case for 10,000 years after repository closure	See Table E-3 for numerical values from Figure 8.2-11(a)[a]	SNL 2008 [DIRS 183478], Figure 8.2-11(a)[a]
Expected annual dose for the seismic ground motion modeling case for 1,000,000 years after repository closure	0.1 to 1 mrem	SNL 2008 [DIRS 183478], Figure 8.2-11(b)[a]
Maximum duration of localized corrosion	12,000 years	SNL 2008 [DIRS 183478], Section 6.3.5.2.3

E.5 ASSUMPTIONS

Several supporting documents identify assumptions that are relevant to this calculation:

- Assumption 5.2, Randomness of Seismic Events, from *Seismic Consequence Abstraction* (SNL 2007 [DIRS 176828], Section 5.2) is relevant to this calculation.

- Assumptions 5.1, 5.3, 5.4, and 5.5 from *General Corrosion and Localized Corrosion of Waste Package Outer Barrier* (SNL 2007 [DIRS 180778], Sections 5.1, 5.3, 5.4, and 5.5) are relevant to the initiation, duration, and rate of localized corrosion on the outer corrosion barrier of the waste package.

- Sections 6.4.1.2 and 6.4.1.3 of *Total System Performance Assessment Model/Analysis for the License Application* (SNL 2008 [DIRS 183478]) describe the assumptions that are relevant to the drip shield early failure modeling case, which forms the basis for this low consequence analysis.

There are no additional assumptions for this calculation.

E.6 DISCUSSION

The following discussions address the technical approach, mathematical formulation, and the computational results of this analysis. A list of references used as indirect inputs is provided in Table E-2.

Table E-2. Indirect Inputs for Appendix E

Citation	Title	DIRS
70 FR 53313	Implementation of a Dose Standard After 10,000 Years	178394
SNL 2007	*Seismic Consequence Abstraction*	176828
SNL 2007	*General Corrosion and Localized Corrosion of the Drip Shield*	180778
SNL 2007	*Technical Work Plan for the Performance Assessment Features, Events, and Processes*	184327

E.6.1 Technical Approach

The dose from drip shield plate failures is estimated using the results of the drip shield early failure modeling case (SNL 2008 [DIRS 183478], Section 6.4). The drip shield early failure modeling case computes the dose that results from manufacturing defects or emplacement damage to drip shields. This modeling case simulates the effects of an early failure by removing a single drip shield as an impediment to seepage. If seepage occurs in a location with an early failed drip shield, the associated waste package is conservatively assumed to also be failed. Hence, the drip shield early failure modeling case describes the dose that may result if a drip shield and its associated waste package fail simultaneously.

The estimate of dose from drip shield plate failure accounts for the frequency of occurrence of rock block impacts in the nonlithophysal units, and the extent of ruptured drip shields caused by these impacts. Although the impacts may rupture the drip shield, the associated waste package is not expected to be breached from rock block impacts (SNL 2008 [DIRS 183478], Section 6.4.7.3). However, failure of the drip shield plates allows seepage to contact the waste package, potentially failing the waste package if localized corrosion initiates on the waste package outer corrosion barrier. This estimate considers localized corrosion as the process that may compromise the waste package subsequent to rupture of the drip shield plates. Other processes that affect the waste package outer corrosion barrier, such as damage from seismic ground motion, are not relevant because they are not altered by the rupture of the drip shield plates by rock block impacts.

The dose histories from the drip shield early failure modeling case (DTN: MO0709TSPAREGS.000 [DIRS 182976], file: *LA_v5.000_ED_003000_007_Dose_Total.txt*) are a function of the epistemic uncertainty in the TSPA model, the type of waste package that fails, and the seepage bin with the failed waste package. Each realization of the TSPA model has a unique "vector" of sampled values for random variables with epistemic uncertainty. There are a total of 300 epistemic vectors, denoted as $\mathbf{e}_i$ for i = 1, 2, 3, ..., 300, in the drip shield early failure modeling case (SNL 2008 [DIRS 183478], Section 7.3.1.2). The total number of epistemic vectors was selected to produce a stable mean dose, based on computational testing with the drip shield early failure modeling case. Each epistemic vector generates a total of 10 dose histories because the TSPA model has five repository percolation subregions (i.e., seepage bins) (DTN: LA0702PANS02BR.001 [DIRS 180322], file: README, second bullet under the heading: Repository Node Lists) with two different waste package types (SNL 2008 [DIRS 183478], Section 6.3.7) in each bin, for a total of 10 combinations.

These dose histories provide a basis for estimating the dose from tearing of drip shield plates due to large rock block impacts. Since the drip shield early failure modeling case computes the dose resulting from a single simultaneous failure of drip shield and waste package, the estimated dose must account for: (1) the number of drip shields damaged by the rock block impacts during a seismic event, (2) the timing of the seismic event relative to the occurrence of localized corrosion, (3) the two waste package types, and (4) the five repository percolation subregions (i.e., seepage bins). The first two factors are important because releases can only occur if the drip shield plates fail and if the associated waste package fails from localized corrosion. Stated differently, a seismic event that fails the drip shield plates must occur before or simultaneously with localized corrosion in order to have a radionuclide release. The type of waste package is important because it determines the radionuclide source term and the waste package temperature, which influences the timing of localized corrosion. The seepage bin is important because it determines, in part, the flow rates for radionuclide transport as well as influencing the chemistry of the seepage water and the waste package temperature.

E.6.2 Mathematical Formulation

Let $\overline{\overline{D}}_{NL}(\tau)$ denote the mean dose at time τ resulting from radionuclides released due to nonlithophysal rockfall induced by a seismic event. The quantity $\overline{\overline{D}}_{NL}(\tau)$ is estimated by:

$$\overline{\overline{D}}_{NL}(\tau) = \frac{1}{N}\sum_{i=1}^{N} \overline{D}_{NL}(\tau \mid \mathbf{e}_i) \qquad \text{(Eq. E-1)}$$

where $\overline{D}_{NL}(\tau|\mathbf{e}_i)$ is the expected dose at time τ due to nonlithophysal rockfall, conditional on a vector of samples values, $\mathbf{e}_i$, for epistemic uncertain parameters. The quantity $\overline{D}_{NL}(\tau|\mathbf{e}_i)$ is termed an expected dose because it is averaged over the aleatory uncertainty in the seismic events as well as the spatial variability between waste packages. The vectors $\mathbf{e}_i$ are determined by a Latin hypercube sample of size *N*. The value of *N* is 300 for this analysis.

The quantity $\overline{D}_{NL}(\tau|\mathbf{e}_i)$ is defined, in turn, as:

$$\overline{D}_{NL}(\tau|\mathbf{e}_i) = \sum_{p=1}^{2}\sum_{b=1}^{5} E\left(n_{LC}(p,b,\mathbf{e}_i)\right) \times D_{ED}(\tau - t_{LC}|1,p,b,\mathbf{e}_i) \qquad \text{(Eq. E-2)}$$

where:

$E\left(n_{LC}(p,b,\mathbf{e}_i)\right)$ is the expected number of waste packages of type p in bin b that fail due to drip shield plate failure and localized corrosion for the epistemic vector $\mathbf{e}_i$. The drip shield plate failures are the result of seismic-induced rock block impacts in the nonlithophysal units. These failures are a function of the intensity of the seismic event, measured as a function of horizontal peak ground velocity. The occurrence and timing of

localized corrosion is a function of the seepage bin. There are two waste package types, and five seepage bins in the TSPA model, which define the limits of the summations in Equation E-2.

$D_{ED}\left(\tau \middle| 1, p, b, \mathbf{e}_i\right)$ is the dose at time τ conditional on a single failed drip shield colocated with a failed waste package of type p in seepage bin b for the epistemic vector $\mathbf{e}_i$. This dose history is based on the results for the epistemic vector, $\mathbf{e}_i$, from the drip shield early failure modeling case (DTN: MO0709TSPAREGS.000 [DIRS 182976], file: *LA_v5.000_ED_003000_007_Dose_Total.txt*).

$t_{LC} = t_{LC}\left(p, b, \mathbf{e}_i\right)$ is the earliest time that localized corrosion is possible on a waste package of type p in bin b for the epistemic vector $\mathbf{e}_i$, based on DTN: MO0709TSPALOCO.000 [DIRS 182994], files:
LC_Initiation_Analysis_v2_CSNF_Bin1.TXT
LC_Initiation_Analysis_v2_CSNF_Bin2.TXT
LC_Initiation_Analysis_v2_CSNF_Bin3.TXT
LC_Initiation_Analysis_v2_CSNF_Bin4.TXT
LC_Initiation_Analysis_v2_CDSP_Bin1.TXT
LC_Initiation_Analysis_v2_CDSP_Bin2.TXT
LC_Initiation_Analysis_v2_CDSP_Bin3.TXT
LC_Initiation_Analysis_v2_CDSP_Bin4.TXT.

The term t_{LC} is necessary because localized corrosion requires seepage to be present, which may not occur until some time after repository closure. The inclusion of t_{LC} in $D_{ED}\left(\tau - t_{LC} \middle| 1, p, b, \mathbf{e}_i\right)$ shifts the beginning of radionuclide transport to the earliest time that localized corrosion could result in waste package failure. The use of the earliest time that localized corrosion is possible provides a conservative bias to the estimated dose because the seismic event that causes drip shield plate failure may occur after t_{LC}.

The term $E\left(n_{LC}\left(p, b, \mathbf{e}_i\right)\right)$ is estimated by:

$$E(n_{LC}(p,b,\mathbf{e}_i)) = \lambda_F \times T_{LC}(p,b,\mathbf{e}_i) \times (f_p \times f_b \times N_{WP} \times f_{NL}(b)) \times f_{LC}(p,b,\mathbf{e}_i) \quad \text{(Eq. E-3)}$$

where

λ_F is the frequency of drip shield failure due to rock block impacts caused by seismic events. This frequency is a calculated parameter in the MathCad file, based on 100,000 realizations

$T_{LC}(p,b,\mathbf{e}_i)$ is the latest time that localized corrosion could occur on a waste package of type p in bin b for epistemic vector $\mathbf{e}_i$, based on data in DTN: MO0709TSPALOCO.000 [DIRS 182994], files:
LC_Initiation_Analysis_v2_CSNF_Bin1.TXT
LC_Initiation_Analysis_v2_CSNF_Bin2.TXT
LC_Initiation_Analysis_v2_CSNF_Bin3.TXT
LC_Initiation_Analysis_v2_CSNF_Bin4.TXT
LC_Initiation_Analysis_v2_CDSP_Bin1.TXT
LC_Initiation_Analysis_v2_CDSP_Bin2.TXT
LC_Initiation_Analysis_v2_CDSP_Bin3.TXT
LC_Initiation_Analysis_v2_CDSP_Bin4.TXT.

$(f_p \times f_b \times N_{WP})$ is the total number of waste packages of type p in seepage bin b

f_p is the fraction of waste packages of type p in the inventory for the TSPA model, based on DTN: MO0702PASTREAM.001 [DIRS 179925], file: *DTN-Inventory-Rev00.xlsI*, worksheet: "UNIT CELL," cells: "G49 and K49"

f_b is the fraction of waste packages in seepage bin b

$f_{NL}(b)$ is the fraction of seepage bin b that is in the nonlithophysal units (DTN: MO0709TSPALOCO.000 [DIRS 182994], TSPA parameter: NonLith_Frac_CSNF_out)

$\boldsymbol{N_{WP}}$ is the total number of waste packages in the repository, based on DTN: MO0702PASTREAM.001 [DIRS 179925], file: *DTN-Inventory-Rev00.xlsI*, worksheet: "UNIT CELL," cells: G49 and K49

$f_{LC}(p,b,\mathbf{e}_i)$ is the maximum fraction of waste packages of type p in bin b on which localized corrosion may occur for epistemic vector $\mathbf{e}_i$.

Equation E-3 assumes that $\lambda_F \times T_{LC}$ represents the expected number of seismic events that cause drip shield failure and that can occur during the time when localized corrosion can occur. This is a conservative formulation because it assumes that localized corrosion can begin at time zero, rather than after rewetting occurs in percolation subregion *b*.

The MathCad calculation for λ_F, the frequency of drip shield failure due to rock block impacts, is a function of the following parameters: (1) the bounded hazard curve at the emplacement drifts, (2) the maximum and minimum annual exceedance frequencies on the bounded hazard curve, (3) the probability of damage/failure of the drip shield plates from seismic-induced rock block impacts in the nonlithophysal units, and (4) the conditional probability for the number of drip shields with failed plates from seismic-induced rock block impacts in the nonlithophysal units. These quantities are defined by Table 1-1, Step 2, Table 1-10, and Table 1-11, respectively, in DTN: MO0703PASEISDA.002 [DIRS 183156]. λ_F is also a function of the thickness of the drip shield plates as a function of time, based on mean corrosion rates for Titanium Grade 7 under aggressive and benign conditions (DTN: SN0704PADSGCMT.001 [DIRS 182122], Sections 2 and 3 in file: *TSPA Implementation_DS GC Model.pdf*) and the initial thickness of the plates (SNL 2007 [DIRS 179354], Section 4.1.2, Table 4-2, Parameter 07-04A).

E.6.3 Computational Results

Table E-3 presents the mean annual dose due to nonlithophysal rockfall, $\bar{\bar{D}}_{NL}(\tau)$, at 1,000, 2,000, 5,000, and 10,000 years. Table E-3 also presents the corresponding values for the seismic ground motion modeling case. The seismic ground motion modeling case represents the dose from damage to EBS components caused by vibratory ground motion and caused by rockfall induced in the lithophysal zones by vibratory ground motion. The mean annual dose due to nonlithophysal rockfall would be included as a component of the seismic ground motion modeling case if it is included in TSPA. A comparison of the mean annual doses from nonlithophysal rockfall and from the seismic ground motion modeling case is therefore appropriate for demonstrating low consequence.

Table E-3. Comparison of Mean Annual Dose Due to Nonlithophysal Rockfall with the Dose from the Seismic Ground Motion Modeling Case

Time after Repository Closure (years)	Mean Annual Dose – Nonlithophysal Rockfall (mrem)	Mean Annual Dose – Seismic Ground Motion Modeling Case (mrem)	Ratio of Nonlithophysal Rockfall Dose to Seismic Ground Motion Modeling Case Dose (%)
1,000	0.00098	0.002	49
2,000	0.00096	0.03	3.2
5,000	0.00037	0.1	0.37
10,000	0.00031	0.2	0.16

Sources: Output DTN: MO0707NONLITHO.000, file: *LA_v5_ED_003000_007_NL_LC_Dose.txt* for the nonlithophysal rock. Numerical values estimated from Figure 8.2-11(a)[a] in SNL 2008 [DIRS 183478] for the seismic ground motion modeling case.

A comparison of the ratios in Table E-3 demonstrates that: (1) the mean annual dose from the seismic ground motion modeling case is always greater than the estimated dose due to nonlithophysal rockfall; (2) at 1,000 years, the mean annual dose due to nonlithophysal rockfall is about 50% of the dose from the seismic ground motion modeling case, although the magnitude of the nonlithophysal-related dose is very small compared to the individual protection standard of 15 mrem during the first 10,000 years after closure (proposed 10 CFR 63.311(a)(1) [DIRS 178394]); and (3) after 2,000 years, the mean annual dose due to nonlithophysal rockfall is about 3% or less of the dose from the seismic ground motion modeling case. These results

indicate that the effects of nonlithophysal rockfall can be screened out of the performance assessment on the basis of low consequence to the seismic ground motion modeling case and to TSPA for the first 10,000 years after repository closure.

This same conclusion is valid for the period of geologic stability after repository closure because of the timing of localized corrosion and because the long-term dose from early dip shield failures is approximately constant. The timing of localized corrosion is important because a pathway for advective release through the EBS is only formed when the drip shield plates fail from seismic-induced nonlithophysal rockfall before or during a period when localized corrosion is active. In other words, a seismic event that causes plate failures after the period when localized corrosion is active will have no impact on dose because the waste package's outer corrosion barrier remains intact and can deflect seepage away from the waste form. As localized corrosion only occurs within the first 12,000 years after repository closure (SNL 2008 [DIRS 183478], Section 6.3.5.2.3), seismic events after this time will not affect the dose due to nonlithophysal rockfall. In addition, the expected dose for the drip shield early failure modeling case decreases gradually during the first 1,000,000 years after repository closure (SNL 2008 [DIRS 183478], Figure 8.2-3(b)[a]). The lack of new advective pathways after 12,000 years, and the gradual decrease in the expected annual dose for the drip shield early failure modeling case, means that the mean annual dose throughout the period of geologic stability that results from nonlithophysal rockfall within the first 12,000 years will remain less than or equal to its early-time maximum value of 0.001466 mrem at 1,240 years (output DTN: MO0707NONLITHO.000, file: *LA_v5_ED_003000_007_NL_LC_Dose.txt*) throughout the period of geologic stability.

The mean annual dose from the seismic ground motion modeling case varies between 0.1 and 1 mrem between 10,000 years and 1,000,000 years after repository closure (SNL 2008 [DIRS 183478], Figure 8.2-11(b)[a]). It follows that the mean annual dose from nonlithophysal rockfall is about 1% of the seismic ground motion modeling case (0.001466 mrem/0.1 mrem = 0.015) for the period from 10,000 years to 1,000,000 years after repository closure. This result indicates that the effects of nonlithophysal rockfall can be excluded from performance assessment on the basis of low consequence to the seismic ground motion modeling case during the period of geologic stability.

E.7 CONCLUSION

The effects of nonlithophysal rockfall on the drip shield can be excluded from the performance assessment on the basis of low consequence because the maximum mean dose from drip shield plate failures and seismic-induced nonlithophysal rockfall is a small fraction of the mean annual dose from seismic ground motion during the period of geologic stability.

The computational files and output from this calculation are documented in output DTN: MO0707NONLITHO.000.

APPENDIX F

CROSS-REFERENCE OF YMP LA FEPS TO INTERNATIONAL AND OTHER FEP DATABASES

F1. INTRODUCTION

As described in *Development of the Total System Performance Assessment-License Application Features, Events, and Processes* (BSC 2005 [DIRS 173800]), one of the major sources of FEP information was the list of FEPs in the Organisation for Economic Co-operation and Development database (OECD 2000 [DIRS 152952], Appendix D). During the process of analyzing FEPs for the TSPA-LA, each FEP contained in the OECD database (OECD 2000 [DIRS 152952], Appendix D) or identified from other sources (Freeze et al. 2001 [DIRS 154365], Tables 3 through 6) collectively referred to as "Source FEPs" was reviewed to determine if it had any possible relevance to the Yucca Mountain disposal system and, if it did, to ensure that it was addressed by one or more FEPs in the TSPA-LA FEP list. Version 2.1 of the OECD database (NEA 2006 [DIRS 185174]) was reviewed. It was determined that the FEPs introduced by the two new projects noted in Version 2.1 presented no additional scope beyond FEPs already addressed in the TSPA-LA FEP list. Details of this evaluation can be found in the Potential FEP Log in output DTN: MO0706SPAFEPLA.001.

Those FEPs in the OECD database (OECD 2000 [DIRS 152952], Appendix D) that addressed specific geographic features not located in the Yucca Mountain region (for example, specific geographic features of the Rhine river), were not included. However, those FEPs that addressed properties of specific features that could be applicable to similar features in the Yucca Mountain region were retained for consideration. The cross-referencing of FEPs between the OECD database (OECD 2000 [DIRS 152952], Appendix D) and the FEPs presented in this analysis report does not imply that there is an exact one-to-one or one-to-many correspondence among those FEPs.

The cross-referencing from TSPA-LA FEPs to Source FEPs (Table F-2) indicates that the TSPA-LA FEP addresses issues contained within the Source FEP(s). The cross-referencing from Source FEPs to TSPA-LA FEPs (Table F-3) indicates that the aggregate of all TSPA-LA FEPs tied to that specific Source FEP addresses all the major issues raised by the Source FEP.

These tables are provided to assist in demonstrating that the TSPA-LA FEP list is, in fact, both complete and comprehensive with respect to the source FEPs.

F1.1 DATA SOURCE

The information presented in Tables F-2 and F-3 is taken from the FEP Database output DTN: MO0706SPAFEPLA.001, tables: "FEPS," "SourceFEPs," and "FEPMapping NEAtoLA." The table "SourceFEPs" was imported directly from *Features, Events, and Processes (FEPs) for Geologic Disposal of Radioactive Waste: An International Database* (OECD 2000 [DIRS 152952], Appendix D) and then updated with FEPs from various other sources such as the 1999 system workshops. These tables were imported directly without editing and, therefore, reproduce typographical errors that were in the source. The source of each FEP in the "Source FEPs" table can be determined from the FEP identifier and format. The explanation is presented in Table F-1.

Table F-1. Source FEP Information

Source FEP Category	Number of Source FEPs	Source Identifier and Format
From OECD 2000 [DIRS 152952] , Appendix D, The NEA FEP Database: Included Projects		
Sweden - Joint SKI/SKB Scenario Development Project, 1989	158*	Jx.x.xx
International - NEA Systematic Approaches to Scenario Development, 1992	146*	Nx.x.xx
Canada - AECL Scenario Analysis for Canadian Disposal Concept, 1994	281	Ax.xxx
U.K. - HMIP Assessment of Nirex Proposals–System Concept Group, 1993	79	Hx.x.x
Sweden - SKI SITE-94 Deep Repository Performance Assessment Project, 1995	106*	Sxxx
Switzerland - NAGRA Scenario Development for Kristallin-I, 1994	258*	Kx.xx
USA - DOE Waste Isolation Pilot Plant, CCA, 1996	246*	Wx.xxx
Canada - AECL Intrusion Resistant Underground Structure (IRUS) Study, 1997	144	Ixxx
From Freeze et al. (2001 [DIRS 154365], Tables 3 through 6)		
YMP Site Characterization Plan	91	YSCPxx
Other YMP Documents	201	YMxx
DSNF Workshop, 1999	40	CA-x, MLD-x
WF Workshop, 1999	12	WF/xxxx
DE Workshop, 1999	24	DE/xxxx, ISC-x, NFC-x, FFC-x
SZ Workshop, 1999	1	SZ/xxxx
TH Workshop, 1999	1	TH/xxxx
IDGE Workshop, 1999	2	ID/xxxx
WP Workshop, 1999	2	WP/xxxx
WF Cladding AMR for TSPA-SR	2	WFClad AMR-x
WF Colloid AMR for TSPA-SR	4	WFCol AMR-x
WF Miscellaneous FEP AMR for TSPA-SR	4	WFMisc AMR-x
EBS FEP AMR for TSPA-SR	3	EBS-x
Igneous Activity (NRC) Meeting, 2000	3	NRC IA-x
NRC NFE Audit, 1999	2	NRC NFE-x
NRC Structural Deformation and Seismicity IRSR, 1999	1	NRC SDS-x
Unsaturated and Saturated Flow under Isothermal Conditions KTI Meeting, 2000	2	NRC USFIC-x
Total	**1813**	

Source: Adapted from BSC 2005 [DIRS 173800], Table G-1.

* Slight differences between number of source FEPs from the OECD (OECD 2000 [DIRS 152952] , Appendix D, The NEA FEP Database: Included Projects) and number of FEPs indicated in Tables 2-2 and 2-4 of BSC 2005 [DIRS 173800] are due to alternate interpretations of the same information (e.g., classification headings may or may not be counted as FEPs).

Table F-2. Cross Reference of TSPA-LA FEPs to Source FEPs

TSPA-LA FEP Number	TSPA-LA FEP Name	Source FEP No.	Source FEP Name
0.1.02.00.0A	Timescales of concern	K S1.4	Local and Regional Surface Environment
0.1.03.00.0A	Spatial domain of concern	I 320	Vault orientation (with respect to groundwater flow)
		K S1.4	Local and Regional Surface Environment
		K S1.5	Geographical Location
0.1.09.00.0A	Regulatory requirements and exclusions	I 271	Regulatory does limit lowered
		K 10.01	Present-day climatic conditions
		K S2.4	No Consideration of Deliberate Human Intrusion
		K S2.5	No Consideration of Future Human Society and Technology
		K S2.6.1	Consideration of radiological impacts to man (only)
		K S2.6.2	Basis for consideration of radiological impacts to man
		K S2.7	No Consideration of Future Evolution of Man and Other Species
		W 4.001	Assessment basis FEPs
		W 4.002	Assessment basis FEPs
0.1.10.00.0A	Model and data issues	A 1.04	Boundary conditions
		A 1.23	Correlation
		A 1.85	Uncertainties
		A 1.87	Unmodelled design features
		A 2.10	Conceptual model - hydrology
		A 2.12	Correlation
		A 2.68	Uncertainties
		A 3.028	Correlation
		A 3.111	Uncertainties
		H 2.2.3	Groundwater flow
		I 042	Chemical speciation (wrong assumption for model)
		I 062c	Concrete performance (incorrect modelling)
		I 070	Correlation of model parameters
		I 072	Modelling (SYVAC/NSURE adequacy)
		I 094	Modelling (diffusion)
		I 153	Groundwater flow model (geosphere model validity)
		I 161	Incomplete filling of containers
		I 177	Kd values (wrong value for model)
		I 180	Surface waster bodies (non-uniform mixing of)
		I 202	Modelling (evaluation of construction changes)
		I 273	Container performance(incorrect modelling)
		I 278	Soil characteristics (wrong value for model)

Table F-2. Cross Reference of TSPA-LA FEPs to Source FEPs (Continued)

TSPA-LA FEP Number	TSPA-LA FEP Name	Source FEP No.	Source FEP Name
0.1.10.00.0A	Model and data issues (continued)	I 286	Source term model (vault model validity)
		I 314	Uncertainties (in values of model parameters)
		I 323	Waste form performance (incorrect modelling)
		I 349	Wrong input data
		I 351	Biosphere model (biosphere model validity)
		K S1.4	Local and Regional Surface Environment
		K S2.2	No Consideration of Global and Regional Disasters
		K S2.6.1	Consideration of radiological impacts to man (only)
		W 2.001	Disposal Geometry
		W 4.008	Model and data issues
1.1.01.01.0A	Open site investigation boreholes	A 2.47	Open boreholes
		H 5.1.1	Loss of integrity of borehole seals
		J 5.21	Future boreholes and undetected past boreholes
		K 4.17	Shaft and tunnel seals
		K 5.25	Exploratory boreholes (sealing)
		N 2.1.2	Investigation borehole seal failure and degradation
		W 2.038	Investigation boreholes
		W 2.039	Underground boreholes
		W 3.031	Natural borehole fluid flow
		W 3.032	Waste-induced borehole flow
		W 3.033	Flow through undetected boreholes
		W 3.035	Borehole-induced mineralization
		W 3.036	Borehole-induced geochemical changes
		YSCP38	Container lies in the trace of an old borehole
		YSCP42	Exploratory borehole creates flow pathway
1.1.01.01.0B	Influx through holes drilled in drift wall or crown	A 2.47	Open boreholes
		I 203	Monitoring shaft (failure to close)
1.1.02.00.0A	Chemical effects of excavation and construction in EBS	I 071	Corrosive chemicals (in vault)
		J 4.1.08	Change of groundwater chemistry in nearby rock
		K 4.05	Geochemical alteration
		K 4.06	Groundwater chemistry
		K 5.19	Influx of oxidising water
		K 6.19	Influx of oxidising water
		N 2.1	DESIGN AND CONSTRUCTION
		N 3.1.4	Induced hydrological changes (fluid pressure, density convection, viscosity)

Table F-2. Cross Reference of TSPA-LA FEPs to Source FEPs (Continued)

TSPA-LA FEP Number	TSPA-LA FEP Name	Source FEP No.	Source FEP Name
1.1.02.00.0B	Mechanical effects of excavation and construction in EBS	A 1.52	Long-term transients
		A 2.01	Blasting and vibration
		H 2.2.2	Rock property changes
		I 022	Explosions/bombs/blasting/collision/impacts/vibration
		I 143	Groundwater (redirection of)
		N 2.1	DESIGN AND CONSTRUCTION
		N 3.1.4	Induced hydrological changes (fluid pressure, density convection, viscosity)
		S 015	Creeping of rock mass, near-field
		W 2.019	Excavation-induced changes in stress
1.1.02.01.0A	Site flooding (during construction and operation)	A 3.052	Flooding
		I 115	Flooding (localized, short-term, surface flooding)
		I 178	Surface water bodies (flooding of Lake 233)
		I 337	Water contacting waste in vault
		N 1.5.2	Site flooding
		N 2.1	DESIGN AND CONSTRUCTION
		N 2.2.8	Repository flooding during operation
1.1.02.02.0A	Preclosure ventilation	ID/Hydro-1	Effects of pre-closure ventilation
		N 2.1	DESIGN AND CONSTRUCTION
		S 046	Gas generation, near-field rock
		S 092	Temperature, near-field rock
1.1.02.03.0A	Undesirable materials left	J 5.03	Stray materials left
		J 5.04	Decontamination materials left
		K 3.24	Organics/contamination of bentonite
		K 4.18	Oil or organic fluid spill
		N 2.1	DESIGN AND CONSTRUCTION
		N 2.2.4	Inadvertant inclusion of undesirable materials
1.1.03.01.0A	Error in waste emplacement	I 173	Inventory (inadequate control)
		K 1.26	Handling accidents
		K 2.12b	Canister failure (reference)
		K S1.2	Waste Emplacement and Repository
		N 2.1	DESIGN AND CONSTRUCTION
		N 2.2.1	Radioactive waste disposal error
		YSCP25	Emplacement error - containers placed in wet zone
		YSCP27	Containers are improperly placed - on drift floor
		YSCP28	Containers are placed too close together
		YSCP39	Undiscovered mine shaft (an old prospect hole) in a wash acts as a source for increased local infiltration
1.1.03.01.0B	Error in backfill emplacement	A 1.33	Faulty buffer emplacement
		I 011a	Backfill (properties)
		I 029	Buffer (faulty emplacement)
		J 3.2.11	Backfill material deficiencies

Table F-2. Cross Reference of TSPA-LA FEPs to Source FEPs (Continued)

TSPA-LA FEP Number	TSPA-LA FEP Name	Source FEP No.	Source FEP Name
1.1.03.01.0B	Error in backfill emplacement (continued)	K 3.01	Bentonite emplacement and composition
		K 3.21	Inhomogeneities (properties and evolution)
		K 3.22	Quality Control
		K 3.23	Poor emplacement of buffer
		K 3.24	Organics/contamination of bentonite
		K S1.2	Waste Emplacement and Repository
		N 2.1	DESIGN AND CONSTRUCTION
		N 2.2.2	Inadequate backfill or compaction, voidage
1.1.04.01.0A	Incomplete closure	A 1.45	Incomplete closure
		A 2.70	Vault closure (incomplete)
		I 352	IRUS closure system
		J 5.02	Non-sealed repository
		J 5.09	Unsealed boreholes and/or shafts
		J 5.21	Future boreholes and undetected past boreholes
		K 4.17	Shaft and tunnel seals
		K S2.1	Appropriate Repository Design and Closure
		N 2.1.2	Investigation borehole seal failure and degradation
		N 2.2	OPERATION AND CLOSURE
		N 2.2.10	Poor closure
		N 2.2.9	Abandonment of unsealed repository
		W 2.006	Seal geometry
		W 3.031	Natural borehole fluid flow
		W 3.032	Waste-induced borehole flow
		W 3.033	Flow through undetected boreholes
		W 3.036	Borehole-induced geochemical changes
1.1.05.00.0A	Records and markers for the repository	I 189	Loss of markers (misinterpretation)
		I 190	Loss of records
		I 223	Political (loss of institutional control)
		J 5.28	Underground dwellings
		J 7.09	Loss of records
		K 11.10	Repository records, markers
		N 2.4.1	Loss of records
		W 3.057	Loss of records
1.1.07.00.0A	Repository design	I 062a1	Concrete (incorrect structural design)
		I 320	Vault orientation (with respect to groundwater flow)
		I 352	IRUS closure system
		J 5.07	Poorly designed repository
		K 4.14	HLW panels (siting)
		K 4.15	TRU silos (siting)
		K 4.16	Access tunnels and shafts
		K S1.4	Local and Regional Surface Environment

Table F-2. Cross Reference of TSPA-LA FEPs to Source FEPs (Continued)

TSPA-LA FEP Number	TSPA-LA FEP Name	Source FEP No.	Source FEP Name
1.1.07.00.0A	Repository design (continued)	K S1.5	Geographical Location
		K S2.1	Appropriate Repository Design and Closure
		N 2.1	DESIGN AND CONSTRUCTION
		N 2.1.9	Design modification
		W 4.003	Design and construction FEPs
		W 4.004	Design and construction FEPs
1.1.08.00.0A	Inadequate quality control and deviations from design	I 062a1	Concrete (incorrect structural design)
		I 062a2	Concrete (incorrect mix design)
		I 062b	Concrete (incorrect preparation/emplacement)
		I 062c	Concrete performance (incorrect modelling)
		I 062f	Concrete (poor quality - procurement)
		I 173	Inventory (inadequate control)
		I 202	Modelling (evaluation of construction changes)
		I 320	Vault orientation (with respect to groundwater flow)
		I 323	Waste form performance (incorrect modelling)
		I 351	Biosphere model (biosphere model validity)
		J 3.2.02	Movement of canister in buffer/backfill
		J 5.08	Poorly constructed repository
		K 1.25	Quality control
		K 2.12b	Canister failure (reference)
		K 2.21	Quality control
		K 3.22	Quality Control
		K 3.24	Organics/contamination of bentonite
		K 4.18	Oil or organic fluid spill
		K S2.1	Appropriate Repository Design and Closure
		K S2.2	No Consideration of Global and Regional Disasters
		N 2.1	DESIGN AND CONSTRUCTION
		N 2.1.6	Material defects
		N 2.1.7	Common cause failures
		N 2.1.8	Poor quality construction
		YSCP26	Drains, installed to divert water around containers, are improperly placed
1.1.09.00.0A	Schedule and planning	N 2.2.12	Effects of phased operation
1.1.10.00.0A	Administrative control of the repository site	I 223	Political (loss of institutional control)
		K 11.11	Planning restrictions
1.1.11.00.0A	Monitoring of the repository	A 1.56	Monitoring and remedial activities
		I 195	Monitoring program - criteria and response
		J 5.21	Future boreholes and undetected past boreholes

Table F-2. Cross Reference of TSPA-LA FEPs to Source FEPs (Continued)

TSPA-LA FEP Number	TSPA-LA FEP Name	Source FEP No.	Source FEP Name
1.1.11.00.0A	Monitoring of the repository (continued)	J 5.39	Postclosure monitoring
		K S2.1	Appropriate Repository Design and Closure
		N 2.1.2	Investigation borehole seal failure and degradation
		N 2.2.11	Post-closure monitoring
		W 2.011	Postclosure monitoring
1.1.12.01.0A	Accidents and unplanned events during construction and operation	A 1.44	Improper operation
		A 1.61	Preclosure events
		A 1.70	Sabotage and improper operation
		I 057	Weather (hurricanes and tornadoes)
		J 5.10	Accidents during operation
		K 1.26	Handling accidents
		K 4.18	Oil or organic fluid spill
		K S2.1	Appropriate Repository Design and Closure
		K S2.2	No Consideration of Global and Regional Disasters
		K S2.3	No Consideration of Malicious Acts and Acts of War
		N 2.1	DESIGN AND CONSTRUCTION
		N 2.2.6	Accidents during operation
1.1.13.00.0A	Retrievability	A 1.69	Retrievability
		I 253	Retrievability
		K S2.1	Appropriate Repository Design and Closure
1.2.01.01.0A	Tectonic activity - large scale	H 2.1.1	Regional tectonic activity
		J 5.16	Uplift and subsidence
		J 5.19	Effect of plate movements
		J 6.14	Tectonic activity - large scale
		K 9.01	Regional horizontal movements
		K 9.02	Regional vertical movements
		N 1.2	GEOLOGICAL
		N 1.2.1	Plate movement/tectonic change
		N 1.2.6	Uplift and subsidence
		N 3.1.4	Induced hydrological changes (fluid pressure, density convection, viscosity)
		W 1.004	Regional tectonics
		W 1.005	Regional uplift and subsidence
		YM200	Aseismic alteration of permeability along and across faults
		YSCP95	Tectonic changes to local geothermal flux causes convective flow in SZ and elevates water table
		YSCP96	Tectonic folding alters dip of tuff beds, changing percolation flux
		YSCP97	Uplift or subsidence changes drainage at the site, increasing infiltration
		YSCP98	Folding, uplift or subsidence lowers facility w/r/t current water table

Table F-2. Cross Reference of TSPA-LA FEPs to Source FEPs (Continued)

TSPA-LA FEP Number	TSPA-LA FEP Name	Source FEP No.	Source FEP Name
1.2.02.01.0A	Fractures	A 3.045	Earthquakes
		H 2.1.7	Faulting/fracturing
		H 2.2.3	Groundwater flow
		I 317	Unsaturated transport
		N 3.3.5	Fracturing
		S 049	Groundwater flow
		S 064	Properties of far-field rock
		S 065	Properties of near-field rock
		W 1.008	Formation of fractures
		W 1.009	Changes in fracture properties
		W 1.025	Fracture flow
1.2.02.02.0A	Faults	A 2.24	Faulting
		A 2.72	Volcanism
		H 2.1.7	Faulting/fracturing
		I 317	Unsaturated transport
		J 4.2.06	Faulting
		K 7.05	Boundary conditions for flow
		K 9.03	Movements along major faults
		K 9.04	Movements along small-scale faults
		N 1.2.10	Fault generation
		N 1.2.9	Fault activation
		NRC SDS-1	Faulting exhumes waste container
		S 036	Faulting
		S 064	Properties of far-field rock
		W 1.010	Formation of new faults
		W 1.011	Fault movement
		YM162b	Degradation of the liner
		YM163	Strike/slip faulting occurs or exists at Yucca Mountain.
		YM164	Detachment faulting occurs or exists at Yucca Mountain
		YM165	Dip/slip faulting occurs at Yucca Mountain
		YM166	New fault occurs at Yucca Mountain
		YM167	Old fault strand is reactivated at Yucca Mountain
		YM168	New fault strand is activated at Yucca Mountain
1.2.02.03.0A	Fault displacement damages EBS components	H 2.1.6	Seismicity
		H 2.1.7	Faulting/fracturing
		I 066	Waste container (corrosion/collapse)
		K 2.12b	Canister failure (reference)
		S 058	Movement of canister in buffer/backfill
		YSCP12	Fault movement shears waste container

Table F-2. Cross Reference of TSPA-LA FEPs to Source FEPs (Continued)

TSPA-LA FEP Number	TSPA-LA FEP Name	Source FEP No.	Source FEP Name
1.2.03.02.0A	Seismic ground motion damages EBS components	A 1.29	Earthquakes
		A 2.21	Earthquakes
		A 3.045	Earthquakes
		H 2.1.6	Seismicity
		I 022	Explosions/bombs/blasting/collision/impacts/vibration
		I 066	Waste container (corrosion/collapse)
		I 100	Seismic events
		J 5.15	Earthquakes
		K 9.05	Seismic activity
		N 1.2.8	Seismicity
		W 1.012	Seismic activity
		YM1	Seismic vibration causes container failure
		YM35	Container failure induced by microseisms associated with dike emplacement
1.2.03.02.0B	Seismic-induced rockfall damages EBS components	A 1.29	Earthquakes
		A 2.21	Earthquakes
		A 3.045	Earthquakes
		H 2.1.6	Seismicity
		I 022	Explosions/bombs/blasting/collision/impacts/vibration
		I 066	Waste container (corrosion/collapse)
		I 100	Seismic events
		J 5.15	Earthquakes
		K 2.12b	Canister failure (reference)
		K 9.05	Seismic activity
		N 1.2.8	Seismicity
		W 1.012	Seismic activity
		YM1	Seismic vibration causes container failure
		YM3	Rockfall (large block) WFClad--Rockfall
1.2.03.02.0C	Seismic-induced drift collapse damages EBS components	A 2.21	Earthquakes
		I 022	Explosions/bombs/blasting/collision/impacts/vibration
		K 2.12b	Canister failure (reference)
		N 3.3	MECHANICAL
		W 2.022	Roof falls
		YM13	Rockfall (rubble) (in waste and EBS)
		YM169	Mechanical degradation or collapse of drift
1.2.03.02.0D	Seismic-induced drift collapse alters in-drift thermohydrology	I 022	Explosions/bombs/blasting/collision/impacts/vibration
		I 100	Seismic events
		N 3.3	MECHANICAL
		W 2.022	Roof falls

Table F-2. Cross Reference of TSPA-LA FEPs to Source FEPs (Continued)

TSPA-LA FEP Number	TSPA-LA FEP Name	Source FEP No.	Source FEP Name
1.2.03.02.0D	Seismic-induced drift collapse alters in-drift thermohydrology (continued)	YM13	Rockfall (rubble) (in waste and EBS)
		YM169	Mechanical degradation or collapse of drift
1.2.03.02.0E	Seismic-induced drift collapse alters in-drift chemistry	N 3.3	MECHANICAL
		YM13	Rockfall (rubble) (in waste and EBS)
		YM169	Mechanical degradation or collapse of drift
1.2.03.03.0A	Seismicity associated with igneous activity	A 2.72	Volcanism
		A 3.045	Earthquakes
		DE/Seismic-1	Seismicity associated with igneous activity
		H 2.1.6	Seismicity
		K 9.05	Seismic activity
		K 9.09	Magmatic activity (volcanism and plutonism)
		N 1.2.3	Magmatic activity
		N 1.2.8	Seismicity
		W 1.012	Seismic activity
		W 1.013	Volcanic activity
		YM35	Container failure induced by microseisms associated with dike emplacement
1.2.04.02.0A	Igneous activity changes rock properties	A 2.36	Intrusion (magmatic)
		A 2.39	Magmatic activity
		A 2.72	Volcanism
		H 2.1.2	Magmatic activity
		H 2.1.7	Faulting/fracturing
		H 2.2.2	Rock property changes
		I 013	Bedrock fracture
		K 9.09	Magmatic activity (volcanism and plutonism)
		N 1.2.3	Magmatic activity
		N 3.1.4	Induced hydrological changes (fluid pressure, density convection, viscosity)
		S 064	Properties of far-field rock
		S 065	Properties of near-field rock
		W 1.013	Volcanic activity
		W 2.030	Thermally-induced stress changes
		YM190	Dike related fractures alter flow
		YM195	Dike provides a permeable flow path
		YM196	Dike provides a barrier to flow
		YSCP91	Igneous activity causes changes to rock properties
		YSCP92	Igneous activity causes extreme changes to rock geochemical properties
1.2.04.03.0A	Igneous intrusion into repository	A 2.72	Volcanism
		H 2.1.2	Magmatic activity
		I 066	Waste container (corrosion/collapse)
		I 143	Groundwater (redirection of)

Table F-2. Cross Reference of TSPA-LA FEPs to Source FEPs (Continued)

TSPA-LA FEP Number	TSPA-LA FEP Name	Source FEP No.	Source FEP Name
1.2.04.03.0A	Igneous intrusion into repository (continued)	I 322	Volcanic activity
		J 5.13	Volcanism
		J 6.11	Intruding dykes
		K 2.12b	Canister failure (reference)
		K 9.09	Magmatic activity (volcanism and plutonism)
		N 1.2.3	Magmatic activity
		W 1.013	Volcanic activity
		W 1.014	Magmatic activity
		YM197	Sill provides a permeable flow path
		YM198	Sill provides a flow barrier
		YM30	Magma interacts with waste
		YM34	Magmatic volatiles attack waste
		YSCP90	Igneous intrusion into repository
		YSCP90a	Sill intrudes repository openings
1.2.04.04.0A	Igneous intrusion interacts with EBS components	A 1.82	Temperature rises (unexpected effects)
		A 2.72	Volcanism
		DE/Igneous-3	Fragmentation
		H 2.1.2	Magmatic activity
		I 322	Volcanic activity
		K 2.12b	Canister failure (reference)
		K 9.09	Magmatic activity (volcanism and plutonism)
		N 1.2.3	Magmatic activity
		W 1.013	Volcanic activity
		W 1.014	Magmatic activity
		YM191	Heating of waste container by magma (without contact)
		YM192	Failure of waste container by direct contact w/magma
		YM30	Magma interacts with waste
1.2.04.04.0B	Chemical effects of magma and magmatic volatiles	YM30	Magma interacts with waste
		YM34	Magmatic volatiles attack waste
1.2.04.05.0A	Magma or pyroclastic base surge transports waste	A 2.72	Volcanism
		H 2.1.2	Magmatic activity
		I 322	Volcanic activity
		W 1.014	Magmatic activity
		YM187	Dissolution of spent fuel in magma
		YM188	Volatile radionuclides plate out in the surrounding rock
		YM189	Entrainment of SNF in a flowing dike
		YM199	Dissolution of other waste in magma
		YM30	Magma interacts with waste
		YM31	Magmatic transport of waste
		YM33	Direct exposure of waste in dike apron

Table F-2. Cross Reference of TSPA-LA FEPs to Source FEPs (Continued)

TSPA-LA FEP Number	TSPA-LA FEP Name	Source FEP No.	Source FEP Name
1.2.04.06.0A	Eruptive conduit to surface intersects repository	A 2.72	Volcanism
		H 2.1.2	Magmatic activity
		H 2.1.8	Major incision
		I 322	Volcanic activity
		YM193	Vent erosion
		YM194	Vent jump
		YSCP24	Basaltic cinder cone erupts through the repository
1.2.04.07.0A	Ashfall	A 3.039	Deposition (wet and dry)
		YM32	Ashfall
1.2.04.07.0B	Ash redistribution in groundwater	A 3.027	Convection, turbulence and diffusion (atmospheric)
		A 3.039	Deposition (wet and dry)
		NRC IA-1	Soil leaching following ashfall
1.2.04.07.0C	Ash redistribution via soil and sediment transport	A 3.027	Convection, turbulence and diffusion (atmospheric)
		A 3.039	Deposition (wet and dry)
		A 3.047	Erosion (wind)
		A 3.091	Sediment resuspension in water bodies
		NRC IA-1	Soil leaching following ashfall
1.2.05.00.0A	Metamorphism	A 2.42	Metamorphic activity
		H 2.1.3	Regional metamorphism
		H 2.2.2	Rock property changes
		N 1.2.4	Metamorphic activity
		S 064	Properties of far-field rock
		S 065	Properties of near-field rock
		W 1.015	Metamorphic activity
1.2.06.00.0A	Hydrothermal activity	H 2.2.3	Groundwater flow
		K 9.10	Hydrothermal activity
		S 049	Groundwater flow
		S 064	Properties of far-field rock
		S 065	Properties of near-field rock
		W 2.030	Thermally-induced stress changes
1.2.07.01.0A	Erosion/denudation	A 2.22	Erosion
		A 3.027	Convection, turbulence and diffusion (atmospheric)
		A 3.042	Dispersion
		A 3.046	Erosion - lateral transport
		A 3.047	Erosion (wind)
		H 2.1.8	Major incision
		H 2.2.1	Changes in geometry and driving forces of the flow system
		H 2.4.1	Generalised denudation
		H 2.4.2	Localised denudation
		H 4.1.2	Solid discharge via erosional processes
		I 057	Weather (hurricanes and tornadoes)
		I 105	Erosion (of sand ridge by wind)

Table F-2. Cross Reference of TSPA-LA FEPs to Source FEPs (Continued)

TSPA-LA FEP Number	TSPA-LA FEP Name	Source FEP No.	Source FEP Name
1.2.07.01.0A	Erosion/denudation (continued)	I 112b	Denuding of the site
		I 280	Soil slumping
		I 305	Topography (changes)
		J 5.26	Erosion on surface/sediments
		K 10.11	Fluvial erosion/sedimentation
		K 10.12	Surface denudation
		K 5.18	Hydraulic gradient changes (magnitude, direction)
		K 6.18	Hydraulic gradient changes (magnitude, direction)
		K 7.11	Erosion
		K 8.22	Erosion/deposition
		K 9.07	Erosion/denudation
		K 9.08	Basement alteration
		N 1.4.1	Land slide
		N 1.4.2	Denudation
		N 1.4.3	River, stream, channel erosion
		N 1.4.9	Chemical denudation and weathering
		W 1.041	Mechanical weathering
		W 1.042	Chemical weathering
		W 1.043	Aeolian erosion
		W 1.044	Fluvial erosion
		W 1.045	Mass wasting
		W 1.049	Mass wasting
		YSCP7	Stream erosion of Amargosa River lowers base levels and increases gradient in SZ
		YSCP8	Ephemeral stream erosion cuts Tiva Canyon units to underlying nonwelded units
1.2.07.02.0A	Deposition	A 3.027	Convection, turbulence and diffusion (atmospheric)
		A 3.039	Deposition (wet and dry)
		I 305	Topography (changes)
		N 1.4.5	Freshwater sediment transport and deposition
		W 1.046	Aeolian deposition
		W 1.047	Fluvial deposition
		W 1.048	Lacustrine deposition
1.2.08.00.0A	Diagenesis	H 2.1.4	Diagenesis
		I 012	Biological activity (bacteria & microbes)
		J 7.10	Diagenesis
		N 1.2.5	Diagenesis
		S 064	Properties of far-field rock
		S 065	Properties of near-field rock
		W 1.022	Fracture infills
1.2.09.00.0A	Salt diapirism and dissolution	S 064	Properties of far-field rock
		S 065	Properties of near-field rock

Table F-2. Cross Reference of TSPA-LA FEPs to Source FEPs (Continued)

TSPA-LA FEP Number	TSPA-LA FEP Name	Source FEP No.	Source FEP Name
1.2.09.01.0A	Diapirism	H 2.1.5	Diapirism
		H 2.2.3	Groundwater flow
		I 143	Groundwater (redirection of)
		J 4.2.05	Changes in Groundwater Flow
		N 1.2.7	Diapirism
		S 049	Groundwater flow
		S 064	Properties of far-field rock
		S 065	Properties of near-field rock
		W 1.006	Salt deformation
		W 1.007	Diapirism
1.2.09.02.0A	Large-scale dissolution	S 064	Properties of far-field rock
		S 065	Properties of near-field rock
		W 1.016	Shallow dissolution
		W 1.017	Lateral dissolution
		W 1.018	Deep dissolution
		W 1.019	Solution chimneys
		W 1.020	Breccia pipes
		W 1.021	Collapse breccias
1.2.10.01.0A	Hydrologic response to seismic activity	A 2.21	Earthquakes
		A 3.045	Earthquakes
		H 2.1.6	Seismicity
		I 091	Watertable changes
		I 100	Seismic events
		I 143	Groundwater (redirection of)
		J 5.15	Earthquakes
		K 9.05	Seismic activity
		N 1.2.8	Seismicity
		N 3.1.4	Induced hydrological changes (fluid pressure, density convection, viscosity)
		W 1.012	Seismic activity
		W 1.031	Hydrological response to earthquakes
		YM173	Seismically-induced water table changes
		YM174	Fault movement connects tuff and carbonate aquifers
		YM175	Fault pathway through the altered Topopah Spring basal vitrophyre
		YM180	Fault establishes pathway through the UZ
		YM181	Fault establishes pathway through the SZ
		YM182	Fluid supplied by a fault migrates down the drift
		YM183	Fault intersects and drains condensate zone
		YM186	Head-driven flow up from Carbonates

Table F-2. Cross Reference of TSPA-LA FEPs to Source FEPs (Continued)

TSPA-LA FEP Number	TSPA-LA FEP Name	Source FEP No.	Source FEP Name
1.2.10.01.0A	Hydrologic response to seismic activity (continued)	YSCP14	Normal faulting produces a trap for laterally moving moisture in the Tiva Canyon unit
		YSCP15	New faulting breaches flow barrier controlling large hydraulic gradient to the north
		YSCP16	Flow barrier south of site blocks flow, causing water table to rise
		YSCP3	Short circuit of a flow barrier in the saturated zone because of a water table rise
		YSCP51	Climate modification raises water table to short circuit flow barrier in SZ
		YSCP89	Fault creep causes short term fluctuations of the water table
		YSCP94	Fault movement pumps fluid from SZ to UZ (seismic pumping)
1.2.10.02.0A	Hydrologic response to igneous activity	A 2.72	Volcanism
		DE/Igneous-1	Interaction of WT with Magma
		DE/Igneous-2	Interaction of UZ Pore Water with Magma
		H 2.2.3	Groundwater flow
		I 091	Watertable changes
		I 098	Drain gutters plug
		I 143	Groundwater (redirection of)
		I 305	Topography (changes)
		J 4.2.05	Changes in Groundwater Flow
		K 9.09	Magmatic activity (volcanism and plutonism)
		N 1.2.3	Magmatic activity
		N 3.1.4	Induced hydrological changes (fluid pressure, density convection, viscosity)
		S 049	Groundwater flow
		W 1.013	Volcanic activity
		W 1.014	Magmatic activity
		YSCP3	Short circuit of a flow barrier in the saturated zone because of a water table rise
		YSCP51	Climate modification raises water table to short circuit flow barrier in SZ
		YSCP87	Volcanic activity in the vicinity produces an impoundment
		YSCP93	Hydrologic response to igneous activity
1.3.01.00.0A	Climate change	A 1.12	Climate change
		A 1.39	Global effects
		A 2.07	Climate change
		A 2.25	Flood
		A 3.023	Climate
		A 3.024	Climate change

Table F-2. Cross Reference of TSPA-LA FEPs to Source FEPs (Continued)

TSPA-LA FEP Number	TSPA-LA FEP Name	Source FEP No.	Source FEP Name
1.3.01.00.0A	Climate change (continued)	A 3.043	Dust storms and desertification
		A 3.090	Seasons
		H 2.3.13	Far-field transport: Biogeochemical changes
		H 3.1.2	Climate change: Natural
		H 3.1.3	Exit from glacial/interglacial cycling
		H 3.1.4	Intensification of natural climate change
		I 292	Surface water bodies (physical/chemical changes)
		J 5.32	Desert and unsaturation
		J 6.10	No ice age
		K 10.01	Present-day climatic conditions
		K 10.02	Effective moisture (recharge)
		K 10.03	Seasonality of climate
		K 10.04	Future climatic conditions
		K 10.07	Warmer climate - arid
		K 10.08	Warmer climate - seasonal humid
		K 10.09	Warmer climate - equable humid
		K 8.26	Surface water bodies
		N 1.1.2	Solar insolation
		N 1.3	CLIMATOLOGICAL
		N 1.3.7	No ice age
		W 1.060	Temperature
		W 1.061	Climate change
1.3.04.00.0A	Periglacial effects	A 3.023	Climate
		A 3.024	Climate change
		H 2.2.1	Changes in geometry and driving forces of the flow system
		H 3.1.2	Climate change: Natural
		H 3.1.3	Exit from glacial/interglacial cycling
		H 3.1.4	Intensification of natural climate change
		I 049	Climate change
		I 268	Freeze/thaw cycles
		J 5.17	Permafrost
		J 5.22	Accumulation of gases under permafrost
		K 10.01	Present-day climatic conditions
		K 10.05	Tundra climate
		K 10.13	Permafrost
		K 8.26	Surface water bodies
		N 1.3.5	Periglacial effects
		N 1.4.10	Frost weathering
		N 1.4.8	Solifluction
		S 059	Permafrost
		W 1.060	Temperature
		W 1.063	Permafrost

Table F-2. Cross Reference of TSPA-LA FEPs to Source FEPs (Continued)

TSPA-LA FEP Number	TSPA-LA FEP Name	Source FEP No.	Source FEP Name
1.3.05.00.0A	Glacial and ice sheet effect	A 1.38	Glaciation
		A 2.30	Glaciation
		A 2.38	Isostatic rebound
		A 3.023	Climate
		A 3.024	Climate change
		A 3.057	Glaciation
		H 2.1.8	Major incision
		H 2.2.1	Changes in geometry and driving forces of the flow system
		H 3.1.2	Climate change: Natural
		H 3.1.3	Exit from glacial/interglacial cycling
		H 3.1.4	Intensification of natural climate change
		I 049	Climate change
		I 268	Freeze/thaw cycles
		I 305	Topography (changes)
		J 5.42	Glaciation
		K 10.01	Present-day climatic conditions
		K 10.06	Glacial climate
		K 10.07	Warmer climate - arid
		K 10.14	Glacial erosion/sedimentation
		K 10.15	Glacial-fluvial erosion/sedimentation
		K 10.16	Ice sheet effects (loading, melt water recharge)
		K 8.26	Surface water bodies
		N 1.3.6	Glaciation
		N 3.1.4	Induced hydrological changes (fluid pressure, density convection, viscosity)
		S 047	Glaciation
		W 1.060	Temperature
		W 1.062	Glaciation
1.3.07.01.0A	Water table decline	A 2.19	Drought
		A 3.023	Climate
		A 3.024	Climate change
		A 3.043	Dust storms and desertification
		A 3.097	Soil depth
		I 049	Climate change
		I 091	Watertable changes
		J 5.32	Desert and unsaturation
		K 10.01	Present-day climatic conditions
1.3.07.02.0A	Water table rise affects SZ	A 3.023	Climate
		A 3.024	Climate change
		H 2.2.1	Changes in geometry and driving forces of the flow system
		I 049	Climate change
		I 091	Watertable changes
		I 143	Groundwater (redirection of)
		K 10.01	Present-day climatic conditions

Table F-2. Cross Reference of TSPA-LA FEPs to Source FEPs (Continued)

TSPA-LA FEP Number	TSPA-LA FEP Name	Source FEP No.	Source FEP Name
1.3.07.02.0A	Water table rise affects SZ (continued)	W 1.030	Freshwater intrusion
		YSCP3	Short circuit of a flow barrier in the saturated zone because of a water table rise
		YSCP4	Water table rise
		YSCP49	Climate modification raises water table
		YSCP50	Climate modification raises water table to flood repository
		YSCP51	Climate modification raises water table to short circuit flow barrier in SZ
1.3.07.02.0B	Water table rise affects UZ	A 3.017	Capillary rise in soil
		A 3.023	Climate
		A 3.024	Climate change
		A 3.052	Flooding
		A 3.097	Soil depth
		H 2.2.1	Changes in geometry and driving forces of the flow system
		I 049	Climate change
		I 091	Watertable changes
		I 115	Flooding (localized, short-term, surface flooding)
		I 143	Groundwater (redirection of)
		I 178	Surface water bodies (flooding of Lake 233)
		I 292	Surface water bodies (physical/chemical changes)
		I 317	Unsaturated transport
		I 337	Water contacting waste in vault
		K 10.01	Present-day climatic conditions
		K 8.26	Surface water bodies
		N 1.5.2	Site flooding
		YSCP4	Water table rise
		YSCP51	Climate modification raises water table to short circuit flow barrier in SZ
1.4.01.00.0A	Human influences on climate	A 3.023	Climate
		H 3.1.1	Climate change: Human induced
		I 049	Climate change
		J 6.08	Human induced climate change
		K 10.01	Present-day climatic conditions
		K 11.09	Human-induced climate change
		N 2.4.9	Anthropogenic climate change
		W 1.060	Temperature
1.4.01.01.0A	Climate modification increases recharge	A 3.023	Climate
		A 3.024	Climate change
		I 049	Climate change
		I 091	Watertable changes
		K 10.01	Present-day climatic conditions
		W 1.060	Temperature
		YSCP48	Climate modification increases recharge

Table F-2. Cross Reference of TSPA-LA FEPs to Source FEPs (Continued)

TSPA-LA FEP Number	TSPA-LA FEP Name	Source FEP No.	Source FEP Name
1.4.01.01.0A	Climate modification increases recharge	YSCP49	Climate modification raises water table
		YSCP50	Climate modification raises water table to flood repository
		YSCP51	Climate modification raises water table to short circuit flow barrier in SZ
		YSCP52	Climate modification causes perched water to develop above repository
		YSCP53	Climate modification causes perched water to develop at base of Topopah Spring unit
1.4.01.02.0A	Greenhouse gas effects	A 2.31	Greenhouse effect
		A 3.023	Climate
		A 3.059	Greenhouse effect
		H 3.1.1	Climate change: Human induced
		I 049	Climate change
		K 10.01	Present-day climatic conditions
		K 10.07	Warmer climate - arid
		K 10.10	Greenhouse effect
		W 3.047	Greenhouse gas effects
1.4.01.03.0A	Acid rain	A 3.001	Acid rain
		A 3.023	Climate
		A 3.103	Surface water bodies
		A 3.104	Surface water pH
		I 001	Acid rain
		I 049	Climate change
		I 292	Surface water bodies (physical/chemical changes)
		K 10.01	Present-day climatic conditions
		W 3.048	Acid rain
1.4.01.04.0A	Ozone layer failure	A 2.48	Ozone layer
		A 3.023	Climate
		A 3.078	Ozone layer failure
		H 2.2.3	Groundwater flow
		I 049	Climate change
		I 143	Groundwater (redirection of)
		J 4.2.05	Changes in Groundwater Flow
		K 10.01	Present-day climatic conditions
		S 049	Groundwater flow
		W 3.049	Damage to the ozone layer
1.4.02.01.0A	Deliberate human intrusion	A 1.49	Intrusion (human)
		A 1.70	Sabotage and improper operation
		A 2.56	Sabotage
		A 3.070	Intrusion (deliberate)
		A 3.109	Toxicity of mined rock
		H 5.2.2	Deliberate intrusion
		H 5.2.3	Malicious intrusion

Table F-2. Cross Reference of TSPA-LA FEPs to Source FEPs (Continued)

TSPA-LA FEP Number	TSPA-LA FEP Name	Source FEP No.	Source FEP Name
1.4.02.01.0A	Deliberate human intrusion (continued)	I 008a	Archaeology (a find during construction)
		I 008b	Archaeology (a find during post-closure period)
		I 074d	Combination exposure scenario
		I 167	Intrusion (human/deliberate)
		I 200	Minerals (exploration, exploitation)
		I 252	Remediation of other sites
		J 1.4	Sudden energy release
		J 5.05	Chemical sabotage
		J 5.33	Waste retrieval, mining
		J 5.35	Other future uses of crystalline rock
		J 5.37	Archeological intrusion
		J 5.40	Unsuccessful attempt of site improvement
		J 7.03	Intrusion into accumulation zone in the biosphere
		K S2.3	No Consideration of Malicious Acts and Acts of War
		K S2.4	No Consideration of Deliberate Human Intrusion
		N 2.2.7	Sabotage
		N 2.3	POST-CLOSURE SUB-SURFACE ACTIVITIES (INTRUSION)
		N 2.3.1	Recovery of repository materials
		N 2.3.2	Malicious intrusion
		N 2.3.9	Archaeological investigation
		W 3.006	Archeological investigations
		W 3.012	Deliberate drilling intrusion
1.4.02.02.0A	Inadvertent human intrusion	A 3.071	Intrusion (inadvertent)
		A 3.109	Toxicity of mined rock
		H 5.2.4	Accidental intrusion
		I 074d	Combination exposure scenario
		I 169	Intrusion (human/inadvertent)
		I 200	Minerals (exploration, exploitation)
		I 252	Remediation of other sites
		W 3.031	Natural borehole fluid flow
1.4.02.03.0A	Igneous event precedes human intrusion	H 2.1.2	Magmatic activity
		W 1.013	Volcanic activity
		W 1.014	Magmatic activity
1.4.02.04.0A	Seismic event precedes human intrusion	A 1.29	Earthquakes
		A 2.21	Earthquakes
		A 3.045	Earthquakes
		I 100	Seismic events
		J 5.15	Earthquakes
		K 9.05	Seismic activity
		W 1.012	Seismic activity

Table F-2. Cross Reference of TSPA-LA FEPs to Source FEPs (Continued)

TSPA-LA FEP Number	TSPA-LA FEP Name	Source FEP No.	Source FEP Name
1.4.03.00.0A	Unintrusive site investigation	I 008b	Archaeology (a find during post-closure period)
		W 3.017	Archeological excavations
1.4.04.00.0A	Drilling activities (human intrusion)	A 2.03	Borehole - well
		A 2.05	Boreholes - exploration
		A 3.109	Toxicity of mined rock
		I 167	Intrusion (human/deliberate)
		I 169	Intrusion (human/inadvertent)
		I 200	Minerals (exploration, exploitation)
		J 5.21	Future boreholes and undetected past boreholes
		J 5.34	Geothermal energy production
		J 5.36	Reuse of boreholes
		K 11.01	Exploratory drilling
		K 11.03	Geothermal exploitation
		K 11.04	Liquid waste injection
		N 2.3.10	Injection of liquid wastes
		N 2.3.3	Exploratory drilling
		N 2.3.4	Exploitation drilling
		N 2.3.5	Geothermal energy production
		W 3.001	Oil and gas exploration
		W 3.002	Potash exploration
		W 3.003	Water resources exploration
		W 3.004	Oil and gas exploitation
		W 3.005	Groundwater exploitation
		W 3.007	Geothermal
		W 3.008	Other resources
		W 3.009	Enhanced oil and gas recovery
		W 3.010	Liquid waste disposal
		W 3.011	Hydrocarbon storage
		W 3.025	Oil and gas extraction
		W 3.027	Liquid waste disposal
		W 3.028	Enhanced oil and gas production
		W 3.029	Hydrocarbon storage
		W 3.031	Natural borehole fluid flow
		W 3.032	Waste-induced borehole flow
		W 3.036	Borehole-induced geochemical changes
		YM36	Exploratory drilling for hydrocarbons
		YM38	Exploratory drilling for metals
1.4.04.01.0A	Effects of drilling intrusion	A 3.109	Toxicity of mined rock
		I 143	Groundwater (redirection of)
		W 2.084	Cuttings
		W 2.085	Cavings
		W 2.086	Spallings
		W 3.021	Drilling fluid flow
		W 3.022	Drilling fluid loss
		W 3.023	Blowouts

Table F-2. Cross Reference of TSPA-LA FEPs to Source FEPs (Continued)

TSPA-LA FEP Number	TSPA-LA FEP Name	Source FEP No.	Source FEP Name
1.4.04.01.0A	Effects of drilling intrusion (continued)	W 3.024	Drilling-induced geochemical changes
		W 3.030	Fluid injection-induced geochemical changes
		YM37	Direct exposure to waste in mud pit
		YM39	Flooding of drifts with drilling fluids
		YSCP40	Effects of drilling intrusion
		YSCP41	Drilling fluid interacts with waste
		YSCP43	Drilling introduces surfactants
1.4.05.00.0A	Mining and other underground activities (human intrusion)	A 2.37	Intrusion (mines)
		A 2.46	Mines
		A 2.61	Solution mining
		A 3.061	Heat storage in lakes or underground
		A 3.109	Toxicity of mined rock
		I 167	Intrusion (human/deliberate)
		I 169	Intrusion (human/inadvertent)
		I 200	Minerals (exploration, exploitation)
		I 252	Remediation of other sites
		J 5.28	Underground dwellings
		K 11.02	Mining activities
		N 2.3.6	Resource mining
		N 2.3.7	Tunnelling
		N 2.3.8	Underground construction
		N 2.4.10	Quarrying, near surface extraction
		W 3.013	Potash mining
		W 3.014	Other resources
		W 3.015	Tunneling
		W 3.016	Construction of underground facilities (for example storage, disposal, accommodation)
		W 3.017	Archeological excavations
		W 3.018	Deliberate mining intrusion
		W 3.037	Changes in groundwater flow due to mining
		W 3.038	Changes in geochemistry due to mining
		YSCP44	Mine shaft intersects waste container
		YSCP45	Water from mining above the repository drains through repository.
		YSCP46	A mine shaft creates a preferential path thru the upper nonwelded unit and a wetter zone develops
1.4.06.01.0A	Altered soil or surface water chemistry	A 3.103	Surface water bodies
		H 4.2.2	Surface water mixing
		I 002	Alkali Flats
		I 046a	Waste management sites adjacent (additive effects of contaminants)
		I 046b	Waste management sites adjacent (effects on vault)

Table F-2. Cross Reference of TSPA-LA FEPs to Source FEPs (Continued)

TSPA-LA FEP Number	TSPA-LA FEP Name	Source FEP No.	Source FEP Name
1.4.06.01.0A	Altered soil or surface water chemistry (continued)	I 292	Surface water bodies (physical/chemical changes)
		J 6.03	Far field hydrochemistry – acids, oxides, nitrate
		J 7.08	Altered surface water chemistry by humans
		K 11.07	Groundwater pollution
		K 11.08	Surface pollution (soils, rivers)
		K 8.26	Surface water bodies
		N 2.4.5	Altered soil or surface water chemistry
		S 087	Surface water chemistry
		W 3.046	Altered soil or water surface chemistry by human activities
		W 3.053	Arable farming
1.4.07.01.0A	Water management activities	A 2.14	Dams
		A 2.15	Dewatering
		A 3.073	Irrigation
		A 3.115	Water management projects
		H 4.3.1	Land and surface water use: Terrestrial
		H 4.3.2	Land and surface water use: Estuarine
		H 4.3.3	Land and surface water use: Coastal waters
		H 4.3.4	Land and surface water use: Seas
		I 085a	Dams (filling, draining)
		I 175	Irrigation (dose pathway)
		J 5.27	Human induced actions on groundwater recharge
		J 7.07	Human induced changes in surface hydrology
		K 11.06	Water management schemes
		K 8.26	Surface water bodies
		K 8.33	Irrigation
		N 2.4.2	Dams and reservoirs, built/drained
		N 2.4.3	River rechannelled
		W 3.042	Damming of streams or rivers
		W 3.043	Reservoirs
		W 3.045	Lake usage
		YSCP32	Water collection in cisterns over repository
		YSCP35	Water table drawdown by down gradient pumping increases hydraulic gradient
		YSCP37	Water management of nearby ground water basins
		YSCP88	Surface water impoundment is constructed near the site, increasing percolation

Table F-2. Cross Reference of TSPA-LA FEPs to Source FEPs (Continued)

TSPA-LA FEP Number	TSPA-LA FEP Name	Source FEP No.	Source FEP Name
1.4.07.02.0A	Wells	A 2.73	Wells
		A 2.74	Wells (high-demand)
		A 3.003	Animal diets
		A 3.004	Animal grooming and fighting
		A 3.005	Animal soil ingestion
		A 3.073	Irrigation
		A 3.115	Water management projects
		H 4.3.1	Land and surface water use: Terrestrial
		H 4.3.2	Land and surface water use: Estuarine
		I 007	Animals (external contamination)
		I 074b	Well exposure scenario
		I 175	Irrigation (dose pathway)
		J 5.41	Water producing well
		K 11.05	Deep groundwater abstraction
		K 8.07	Water resource exploitation
		K 8.33	Irrigation
		N 2.3.11	Groundwater abstraction
		W 3.026	Groundwater extraction
		YSCP31	Irrigation wells in Midway Valley increase moisture flux through repository
		YSCP33	Irrigation wells in Midway Valley reduce distance to accessible environment
		YSCP34	Irrigation wells in Crater Flats or Jackass Flats increase hydraulic gradient under repository
1.4.07.03.0A	Recycling of accumulated radionuclides from soils to groundwater	A 3.039	Deposition (wet and dry)
		A 3.085	Recycling
		H 4.1.2	Solid discharge via erosional processes
		H 4.2.1	Soil moisture and evaporation.
		I 010	Recycling process (biomass)
		I 175	Irrigation (dose pathway)
		J 4.1.06	Reconcentration
		S 073	Reconcentration
1.4.08.00.0A	Social and institutional developments	A 3.112	Urbanization on the discharge site
		H 4.3.1	Land and surface water use: Terrestrial
		H 4.3.2	Land and surface water use: Estuarine
		H 4.3.3	Land and surface water use: Coastal waters
		H 4.3.4	Land and surface water use: Seas
		I 099	Earth moving projects (civil)
		I 227	Urbanization (demographics)
		J 7.11	City on the site
		N 2.4.8	Demographic change, urban development
		W 3.056	Demographic change and urban development

Table F-2. Cross Reference of TSPA-LA FEPs to Source FEPs (Continued)

TSPA-LA FEP Number	TSPA-LA FEP Name	Source FEP No.	Source FEP Name
1.4.09.00.0A	Technological developments	A 3.038	Cure for cancer
		A 3.106	Technological advances in food production
		I 084	Cure for cancer
		I 299	Technological advances in food production
		K S2.5	No Consideration of Future Human Society and Technology
		K S2.7	No Consideration of Future Evolution of Man and Other Species
1.4.11.00.0A	Explosions and crashes (human activities)	A 2.02	Bomb blast
		A 3.025	Collisions, explosions and impacts
		H 2.1.8	Major incision
		I 022	Explosions/bombs/blasting/collision/impacts/vibration
		I 167	Intrusion (human/deliberate)
		I 169	Intrusion (human/inadvertent)
		I 200	Minerals (exploration, exploitation)
		J 5.30	Underground test of nuclear devices
		J 5.38	Explosions
		J 6.07	Nuclear war
		N 2.3.12	Underground nuclear testing
		W 3.019	Explosions for resource recovery
		W 3.020	Underground nuclear device testing
		W 3.039	Changes in groundwater flow due to explosions
1.5.01.01.0A	Meteorite impact	A 2.43	Meteorite impact
		A 3.025	Collisions, explosions and impacts
		H 2.1.7	Faulting/fracturing
		H 2.1.8	Major incision
		H 5.2.1	Meteorite impact
		I 013	Bedrock fracture
		I 022	Explosions/bombs/blasting/collision/impacts/vibration
		I 143	Groundwater (redirection of)
		I 197	Meteorite impact
		J 5.29	Meteorite
		N 1.1.1	Meteorite Impact
		W 1.040	Impact of a large meteorite
1.5.01.02.0A	Extraterrestrial events	A 3.023	Climate
		I 049	Climate change
		I 143	Groundwater (redirection of)
		K 10.01	Present-day climatic conditions
		K 9.11	Extraterrestrial events
		N 1.1	EXTRA-TERRESTRIAL
1.5.02.00.0A	Species evolution	A 3.011	Biological evolution
		A 3.031	Critical group - evolution
		I 017	Biological evolution

Table F-2. Cross Reference of TSPA-LA FEPs to Source FEPs (Continued)

TSPA-LA FEP Number	TSPA-LA FEP Name	Source FEP No.	Source FEP Name
1.5.02.00.0A	Species evolution (continued)	K S2.5	No Consideration of Future Human Society and Technology
		K S2.7	No Consideration of Future Evolution of Man and Other Species
		N 1.7.10	Plant and animal evolution
		W 1.072	Natural ecological development
1.5.03.01.0A	Changes in the earth's magnetic field	A 2.40	Magnetic poles (reversal)
		A 3.023	Climate
		A 3.051	Flipping of earth's magnetic poles
		I 049	Climate change
		J 5.20	Changes of the magnetic field
		K 10.01	Present-day climatic conditions
		N 1.2.2	Changes in the Earth's magnetic field
1.5.03.02.0A	Earth tides	H 2.2.3	Groundwater flow
		I 143	Groundwater (redirection of)
		J 4.2.05	Changes in Groundwater Flow
		S 028	Earth tides
		S 049	Groundwater flow
2.1.01.01.0A	Waste inventory	A 1.50	Inventory
		CA-11	DOE SNF gap radionuclide inventory
		CA-12	DOE SNF initial radionuclide inventory
		CA-13	DOE SNF structure
		I 173	Inventory (inadequate control)
		I 347	Inventory database (WIP III)
		K 1.01	Waste product (glass)
		K 1.02	Radionuclide inventory
		MLD-1	DOE SNF initial radionuclide inventory
		MLD-5	DOE SNF hazardous chemical inventory
		S 005	Changes in radionuclide inventory
		W 2.002	Waste inventory
		WF//Inv-1	Exotic Fuels
2.1.01.02.0A	Interactions between co-located waste	A 1.58	Other waste (other than used fuel)
		CA-1	DOE SNF waste package placement
		CA-4	DOE SNF canister arrangement within waste package
		I 039	Vault chemical interactions
		J 5.06	Co-storage of other waste
		J 5.12	Near storage of other waste
		K 3.20	Interaction and diffusion between canisters
		MLD-7	DOE SNF waste package placement
		N 2.2.3	Co-disposal of reactive wastes
2.1.01.02.0B	Interactions between co-disposed waste	CA-5	DOE SNF colocation with HLW
		CA-8	DOE SNF geometry
		I 039	Vault chemical interactions
		J 5.06	Co-storage of other waste
		K 1.03	Stainless steel fabrication flask

Table F-2. Cross Reference of TSPA-LA FEPs to Source FEPs (Continued)

TSPA-LA FEP Number	TSPA-LA FEP Name	Source FEP No.	Source FEP Name
2.1.01.02.0B	Interactions between co-disposed waste (continued)	K 1.04	Void space
		K 3.20	Interaction and diffusion between canisters
		MLD-16	DOE SNF colocation with HLW (waste form degradation impact)
		MLD-20	DOE SNF colocation with HLW (radionuclide mobilization impact)
		MLD-23	DOE SNF colocation with HLW (cladding degradation impact)
		WF//DSNF-2	DOE SNF/HLW Glass Interactions
		WF//DSNF-6	High Integrity Canisters for DOE SNF
2.1.01.03.0A	Heterogeneity of waste inventory	CA-7	DOE SNF canister atmosphere
		I 347	Inventory database (WIP III)
		J 1.3	Damaged or deviating fuel
		K 1.02	Radionuclide inventory
		K 1.27	Deviant inventory flask
		N 2.2.5	Heterogeneity of waste forms
		W 2.003	Heterogeneity of wasteforms
2.1.01.04.0A	Repository-scale spatial heterogeneity of emplaced waste	WFMisc AMR-2	Spatial Heterogeneity of Emplaced Waste
2.1.02.01.0A	DSNF degradation (alteration, dissolution, and radionuclide release)	J 1.5	Release of radionuclides from the failed canister
		MLD-15	DSNF degradation, alteration, and dissolution
		MLD-21	DOE SNF dissolution
		S 019	Degradation of fuel elements
		S 060	Precipitation/dissolution
		WF/DSNF-3	Alteration/Dissolution of DOE SNF
		WF/DSNF-4	Oxidation of DOE SNF
		WF/DSNF-5	Alteration/Dissolution of Pu Ceramic Waste
		WF/DSNF-6	High-Integrity Canisters for DOE SNF
2.1.02.02.0A	CSNF degradation (alteration, dissolution, and radionuclide release)	A 1.75	Source terms (expected)
		A 1.76	Source terms (other)
		A 1.79	Stability of UO2
		J 1.2.09	Dissolution chemistry
		J 1.5	Release of radionuclides from the failed canister
		S 012	Corrosion of metal parts
		S 014	Corrosion prior to wetting
		S 019	Degradation of fuel elements
		S 038	Fuel dissolution and conversion
		S 060	Precipitation/dissolution
		S 076	Release from fuel matrix
		S 077	Release from metal parts
		S 095	Total release from fuel elements

Table F-2. Cross Reference of TSPA-LA FEPs to Source FEPs (Continued)

TSPA-LA FEP Number	TSPA-LA FEP Name	Source FEP No.	Source FEP Name
2.1.02.02.0A	CSNF degradation (alteration, dissolution, and radionuclide release) (continued)	S 106	Water turnover, steel vessel
		W 2.058	Dissolution of waste
		YSCP70	Selective dissolution of contaminants contained in SNF
2.1.02.03.0A	HLW glass degradation (alteration, dissolution, and radionuclide release)	J 1.5	Release of radionuclides from the failured canister
		K 1.03	Stainless steel fabrication flask
		K 1.04	Void space
		K 1.07	Phase separation
		K 1.11a	Glass alteration/dissolution
		K 1.11b	Congruent dissolution
		K 1.12	Rate of glass dissolution
		K 1.13	Selective leaching
		K 1.14	Coprecipitates/solid solutions
		K 1.17	Iron corrosion products
		K 1.18	Precipitation of silicates/silica gel
		K 1.19	Radionuclide release from glass
		S 019	Degradation of fuel elements
		S 060	Precipitation/dissolution
		WF/HLW-1	Composition of DHLW Glass
		YM102	Degradation and alteration of glass waste form
2.1.02.04.0A	Alpha recoil enhances dissolution	J 1.1.03	Recoil of alpha-decay
		W 2.099	Alpha recoil
2.1.02.05.0A	HLW glass cracking	K 1.05	Glass cracking and surface area
		K 1.16	Solute transport resistance
		K 1.26	Handling accidents
2.1.02.06.0A	HLW glass recrystallization	K 1.06	Glass recrystallisation
2.1.02.07.0A	Radionuclide release from gap and grain boundaries	A 1.75	Source terms (expected)
		J 1.2.03	Pb-I reactions
		J 1.2.05	I, Cs-migration to fuel surface
		S 039	Gap and grain boundary release
		S 050	I, Cs-migration to fuel surface
		S 095	Total release from fuel elements
2.1.02.08.0A	Pyrophoricity from DSNF	CA-14	DOE SNF pyrophoricity
		I 146	Heat generation in IRUS vault(B)
		K 2.12b	Canister failure (reference)
		MLD-13	DOE SNF pyrophoric event (waste package degradation impact)
		MLD-18	DOE SNF pyrophoric event (waste form degradation impact)
		MLD-24	DOE SNF pyrophoric event (cladding degradation impact)
		MLD-8	DOE SNF pyrophoric event (waste heat impact)
		W 2.030	Thermally-induced stress changes
		WF//DSNF-1	Pyrophoricity

Table F-2. Cross Reference of TSPA-LA FEPs to Source FEPs (Continued)

TSPA-LA FEP Number	TSPA-LA FEP Name	Source FEP No.	Source FEP Name
2.1.02.09.0A	Chemical effects of void space in waste package	J 2.1.04	Role of the eventual channeling within the canister
		K 1.04	Void space
2.1.02.10.0A	Organic/cellulosic materials in waste	N 3.2.5	Cellulosic degradation
		W 2.053	Radiolysis of cellulose
2.1.02.11.0A	Degradation of cladding from waterlogged rods	S 019	Degradation of fuel elements
		WF//Cladd-1	Waterlogged Rods
2.1.02.12.0A	Degradation of cladding prior to disposal	K 1.26	Handling accidents
		YM130	Cladding degradation before YMP receives it
		YM131	Pin Degradation During Reactor Operation
		YM132	Pin Degradation During Spent Fuel Pool Storage
		YM133	Pin Degradation During Dry Storage
		YM134	Pin Degradation During Fuel Shipment and Handling
		YM135	Cladding Degradation Mechanisms at YMP, Pre-Pin Failure
2.1.02.13.0A	General corrosion of cladding	I 300	Termperature effects (on transport)
		S 012	Corrosion of metal parts
		S 013	Corrosion of steel vessel
		S 014	Corrosion prior to wetting
		S 019	Degradation of fuel elements
		YM136	Corrosion (of cladding)
		YM137	General corrosion of cladding
2.1.02.14.0A	Microbially influenced corrosion (MIC) of cladding	A 1.54	Microbes
		A 2.45	Microbes
		I 012	Biological activity (bacteria & microbes)
		J 2.1.10	Microbes
		J 4.1.02	pH-deviations
		S 013	Corrosion of steel vessel
		S 019	Degradation of fuel elements
		YM138	Microbial corrosion (MIC) of cladding WFClad--Microbiologically
2.1.02.15.0A	Localized (radiolysis enhanced) corrosion of cladding	I 071	Corrosive chemicals (in vault)
		I 238	Radiation effects
		J 4.1.02	pH-deviations
		S 013	Corrosion of steel vessel
		S 019	Degradation of fuel elements
		YM139	Acid corrosion of cladding from radiolysis
2.1.02.16.0A	Localized (pitting) corrosion of cladding	S 012	Corrosion of metal parts
		S 013	Corrosion of steel vessel
		S 014	Corrosion prior to wetting
		S 019	Degradation of fuel elements
		YM140	Localized corrosion (pitting) of cladding

Table F-2. Cross Reference of TSPA-LA FEPs to Source FEPs (Continued)

TSPA-LA FEP Number	TSPA-LA FEP Name	Source FEP No.	Source FEP Name
2.1.02.17.0A	Localized (crevice) corrosion of cladding	S 013	Corrosion of steel vessel
		S 014	Corrosion prior to wetting
		S 019	Degradation of fuel elements
		YM141	Localized corrosion (crevice corrosion) of cladding
2.1.02.18.0A	Enhanced corrosion of cladding from dissolved silica	S 013	Corrosion of steel vessel
		S 019	Degradation of fuel elements
		YSCP72	High dissolved silica content of waters enhances corrosion of cladding
2.1.02.19.0A	Creep rupture of cladding	J 2.3.01	Thermal cracking
		S 019	Degradation of fuel elements
		YM142	Creep rupture of cladding
2.1.02.20.0A	Internal pressurization of cladding	S 019	Degradation of fuel elements
		YM143	Pressurization from He production causes cladding failure
2.1.02.21.0A	Stress corrosion cracking (SCC) of cladding	S 013	Corrosion of steel vessel
		S 014	Corrosion prior to wetting
		S 019	Degradation of fuel elements
		YM145	Stress corrosion cracking (SCC) of cladding
		YM146	Inside Out from fission products (iodine) (failure of cladding)
		YM147	Outside In from Salts or WP Chemicals (failure of cladding)
		YSCP68	Stress-corrosion cracking of Zircaloy cladding
2.1.02.22.0A	Hydride cracking of cladding	I 126	Corrosion (galvanic coupling)
		S 013	Corrosion of steel vessel
		S 019	Degradation of fuel elements
		YM148	Hydride Embrittlement of Cladding
		YM149	Hydride Embrittlement From Zirconium Corrosion (of cladding)
		YM150	Hydride Embrittlement From WP Corrosion & H2 Absorption (of cladding)
		YM151	Hydride Embrittlement From Galvanic Corrosion of WP contacting Cladding
		YM152	Delayed Hydride Cracking (of cladding) WFClad—Delayed Hydride
		YM153	Hydride Reorientation (of cladding)
		YM154	Hydrogen Axial Migration (of cladding)
		YM159	Hydride Embrittlement from Fuel Reaction (causes failure of cladding)
2.1.02.23.0A	Cladding unzipping	S 013	Corrosion of steel vessel
		S 019	Degradation of fuel elements
		YM155	Cladding Degradation after Initial Cladding Perforation
		YM156	Cladding unzipping

Table F-2. Cross Reference of TSPA-LA FEPs to Source FEPs (Continued)

TSPA-LA FEP Number	TSPA-LA FEP Name	Source FEP No.	Source FEP Name
2.1.02.23.0A	Cladding unzipping (continued)	YM157	Dry Oxidation of Fuel (causes failure of cladding) WFClad—Dry Oxidation of Fuel
		YM158	Wet Oxidation of Fuel (causes failure of cladding) WFClad—Wet Oxidation of Fuel
2.1.02.24.0A	Mechanical impact on cladding	A 3.045	Earthquakes
		H 2.1.6	Seismicity
		K 9.05	Seismic activity
		N 1.2.8	Seismicity
		S 019	Degradation of fuel elements
		W 1.012	Seismic activity
		YM144	Mechanical failure of cladding
2.1.02.25.0A	DSNF cladding	CA-10	DOE SNF cladding condition
		CA-9	DOE SNF cladding material
		MLD-22	DSNF cladding degradation
		S 019	Degradation of fuel elements
		WF//DSNF-7	Internal Canister/Cladding Corrosion due to DOE SNF
2.1.02.25.0B	Naval SNF Cladding	MLD-22	DSNF cladding degradation
		S 019	Degradation of fuel elements
2.1.02.26.0A	Diffusion-controlled cavity growth in cladding	S 019	Degradation of fuel elements
		WFClad AMR-2	Diffusion-controlled cavity growth WFClad—Diffusion Controlled Cavity Growth (DCCG)
2.1.02.27.0A	Localized (fluoride enhanced) corrosion of cladding	S 013	Corrosion of steel vessel
		S 019	Degradation of fuel elements
		WFClad AMR-1	Localized corrosion perforation from fluoride
2.1.02.28.0A	Grouping of DSNF waste types into categories	CA-8	DOE SNF geometry
		WFMisc AMR-3	Various Features of the Approximately 250 DSNF Types and Grouping into Waste Categories
2.1.02.29.0A	Flammable gas generation from DSNF	I 039	Vault chemical interactions
		I 130	Gas (from waste containing a gas cylinder)
		K 0.3	Gaseous and volatile isotopes
		MLD-17	Acetylene generation from DSNF WFMisc—Flammable Gases Generation from DSNF - YMP
		S 046	Gas generation, near-field rock
		WFMisc AMR-4	Flammable Gas Generation from DSNF
2.1.03.01.0A	General corrosion of waste packages	A 1.18	Container failure (long-term)
		A 1.24	Corrosion
		A 1.51	Long-term physical stability
		A 1.86	Uniform corrosion
		H 1.1.1	Container metal corrosion
		I 066	Waste container (corrosion/collapse)

Table F-2. Cross Reference of TSPA-LA FEPs to Source FEPs (Continued)

TSPA-LA FEP Number	TSPA-LA FEP Name	Source FEP No.	Source FEP Name
2.1.03.01.0A	General corrosion of waste packages (continued)	J 2.1.08	Corrosive agents, Sulphides, oxygen, etc.
		K 2.03	Corrosion on wetting
		K 2.04	Oxic corrosion
		K 2.06	Anoxic corrosion
		K 2.08	Total corrosion rate
		K 2.12b	Canister failure (reference)
		N 3.2.1	Metallic corrosion
		S 013	Corrosion of steel vessel
		S 014	Corrosion prior to wetting
		S 105	Water turnover, copper canister
		YSCP64	Corrosion of waste containers
2.1.03.01.0B	General corrosion of drip shields	A 1.86	Uniform corrosion
		WP/Chem-1	Effects and degradation of drip shield
		YSCP64	Corrosion of waste containers
2.1.03.02.0A	Stress corrosion cracking (SCC) of waste packages	A 1.18	Container failure (long-term)
		I 066	Waste container (corrosion/collapse)
		J 2.3.03	Stress corrosion cracking
		K 2.09	Stress corrosion cracking
		K 2.12b	Canister failure (reference)
		S 013	Corrosion of steel vessel
		S 014	Corrosion prior to wetting
		W 2.030	Thermally-induced stress changes
		YSCP55	Stress corrosion cracking induced by secondary stress (container failure)
		YSCP65	Stress corrosion cracking of waste containers and drip shields
		YSCP66	Stress corrosion cracking - dry waste container
2.1.03.02.0B	Stress corrosion cracking (SCC) of drip shields	K 2.09	Stress corrosion cracking
		S 014	Corrosion prior to wetting
		W 2.030	Thermally-induced stress changes
		YSCP65	Stress corrosion cracking of waste containers and drip shields
2.1.03.03.0A	Localized corrosion of waste packages	A 1.18	Container failure (long-term)
		A 1.60	Pitting
		I 066	Waste container (corrosion/collapse)
		J 2.1.07	Pitting
		K 2.07	Localised corrosion
		K 2.12b	Canister failure (reference)
		S 013	Corrosion of steel vessel
		S 014	Corrosion prior to wetting
		YM46	Pitting corrosion develops on containers
		YSCP64	Corrosion of waste containers
2.1.03.03.0B	Localized corrosion of drip shields	A 1.60	Pitting
		J 2.1.07	Pitting
		K 2.07	Localised corrosion
		S 014	Corrosion prior to wetting
		WP/Crack-1	Oxygen embrittlement of Ti drip shield

Table F-2. Cross Reference of TSPA-LA FEPs to Source FEPs (Continued)

TSPA-LA FEP Number	TSPA-LA FEP Name	Source FEP No.	Source FEP Name
2.1.03.04.0A	Hydride cracking of waste packages	A 1.18	Container failure (long-term)
		A 1.42	Hydride cracking
		I 066	Waste container (corrosion/collapse)
		I 126	Corrosion (galvanic coupling)
		K 2.10	Other canister degradation processes
		K 2.12b	Canister failure (reference)
		N 3.3.3	Embrittlement and cracking
		S 013	Corrosion of steel vessel
		S 014	Corrosion prior to wetting
2.1.03.04.0B	Hydride cracking of drip shields	A 1.42	Hydride cracking
		I 126	Corrosion (galvanic coupling)
		S 014	Corrosion prior to wetting
		WP/Crack-1	Oxygen embrittlement of Ti drip shield
2.1.03.05.0A	Microbially influenced corrosion (MIC) of waste packages	A 1.18	Container failure (long-term)
		A 1.54	Microbes
		A 2.45	Microbes
		I 066	Waste container (corrosion/collapse)
		J 2.1.10	Microbes
		K 2.05	Microbially-mediated corrosion
		K 2.12b	Canister failure (reference)
		S 013	Corrosion of steel vessel
2.1.03.05.0B	Microbially influenced corrosion (MIC) of drip shields	A 1.54	Microbes
		A 2.45	Microbes
		J 2.1.10	Microbes
		K 2.05	Microbially-mediated corrosion
2.1.03.06.0A	Internal corrosion of waste packages prior to breach	I 066	Waste container (corrosion/collapse)
		I 071	Corrosive chemicals (in vault)
		I 238	Radiation effects
		J 2.1.03	Internal corrosion due to waste
		K 2.12b	Canister failure (reference)
		MLD-12	DOE SNF waste package internal corrosion
		S 013	Corrosion of steel vessel
		S 014	Corrosion prior to wetting
		S 072	Radiolysis prior to wetting
		S 105	Water turnover, copper canister
		WF//DSNF-7	Internal Canister/Cladding Corrosion due to DOE SNF
2.1.03.07.0A	Mechanical impact on waste package	A 1.19	Container failure (mechanical processes)
		A 3.045	Earthquakes
		DE/Seismic-2	Falling rock hits container, increased seepage occurs, speeds corrosion of container
		H 2.1.6	Seismicity
		I 066	Waste container (corrosion/collapse)
		J 3.2.02	Movement of canister in buffer/backfill
		K 2.12b	Canister failure (reference)

Table F-2. Cross Reference of TSPA-LA FEPs to Source FEPs (Continued)

TSPA-LA FEP Number	TSPA-LA FEP Name	Source FEP No.	Source FEP Name
2.1.03.07.0A	Mechanical impact on waste package (continued)	K 9.05	Seismic activity
		N 1.2.8	Seismicity
		S 035	Failure of steel vessel
		S 055	Mechanical impact on canister
		S 058	Movement of canister in buffer/backfill
		S 075	Reduced mechanical strength
		W 1.012	Seismic activity
		W 2.033	Movement of containers
2.1.03.07.0B	Mechanical impact on drip shield	A 1.19	Container failure (mechanical processes)
		A 3.045	Earthquakes
		DE/Seismic-2	Falling rock hits container, increased seepage occurs, speeds corrosion of container
		H 2.1.6	Seismicity
		K 9.05	Seismic activity
		N 1.2.8	Seismicity
		S 055	Mechanical impact on canister
		S 058	Movement of canister in buffer/backfill
		W 1.012	Seismic activity
		W 2.033	Movement of containers
		WP/Chem-1	Effects and degradation of drip shield
2.1.03.08.0A	Early failure of waste packages	A 1.17	Container failure (early)
		I 066	Waste container (corrosion/collapse)
		J 2.3.06	Cracking along welds
		J 2.5.01	Random canister defects - quality control
		J 2.5.02	Common cause canister defects - quality control
		K 2.12a	Canister failure (alternative modes)
		K 2.12b	Canister failure (reference)
		K 2.22	Mis-sealed canister
		S 013	Corrosion of steel vessel
		YSCP29	Juvenile and Early Failure of Waste Containers and Drip Shields
2.1.03.08.0B	Early failure of drip shields	YSCP29	Juvenile and Early Failure of Waste Containers and Drip Shields
2.1.03.09.0A	Copper corrosion in EBS	J 2.1.01	Chemical reactions (copper corrosion)
		J 2.1.05	Role of chlorides in copper corrosion
		J 2.2	Creeping of copper
		S 011	Corrosion of copper canister
		S 034	Failure of copper canister
2.1.03.10.0A	Advection of liquids and solids through cracks in the waste package	A 1.20	Container healing
		K 2.18	Corrosion products (physical effects)
2.1.03.10.0B	Advection of liquids and solids through cracks in the drip shield	A 1.20	Container healing

Table F-2. Cross Reference of TSPA-LA FEPs to Source FEPs (Continued)

TSPA-LA FEP Number	TSPA-LA FEP Name	Source FEP No.	Source FEP Name
2.1.03.11.0A	Physical form of waste package and drip shield	A 1.18	Container failure (long-term)
		A 1.51	Long-term physical stability
		CA-3	DOE SNF waste package design
		CA-6	DOE SNF canister design
		I 066	Waste container (corrosion/collapse)
		K 1.03	Stainless steel fabrication flask
		K 2.01	Cast steel canister
		K 2.02	Canister thickness
		K 2.12b	Canister failure (reference)
		K S1.1	Waste Form and Packaging
		MLD-11	DOE SNF waste package design
		W 2.004	Container form
		W 2.034	Container integrity
2.1.04.01.0A	Flow in the backfill	A 3.017	Capillary rise in soil
		I 011a	Backfill (properties)
		I 011b	Backfill (faulty emplacement)
		I 025	Buffer (plugging by bitumen, slime molds, waste degradation products, etc.
		I 027	Buffer (channelling)
		I 030	Buffer (washout of clay)
		J 3.1.02	Saturation of sorption sites
		J 3.1.05	Coagulation of bentonite
		J 3.2.08	Preferential pathways in the buffer/backfill
		J 3.2.09	Flow through buffer/backfill
		J 3.2.11	Backfill material deficiencies
		K 3.03	Bentonite saturation
		K 3.05	Bentonite plasticity
		K 3.08	Buffer impermeability
		S 007	Coagulation of bentonite
		S 025	Dilution of buffer/backfill
		S 037	Flow through buffer/backfill
		S 062	Properties of bentonite buffer
		S 079	Resaturation of bentonite buffer
		S 080	Resaturation of tunnel backfill
2.1.04.02.0A	Chemical properties and evolution of backfill	A 1.02	Backfill evolution
		A 1.05	Buffer additives
		A 1.06	Buffer characteristics
		A 1.07	Buffer evolution
		A 1.43	Hydrothermal alteration
		H 2.2.3	Groundwater flow
		I 011a	Backfill (properties)
		I 011b	Backfill (faulty emplacement)
		I 028b	Buffer (quality)
		I 030	Buffer (washout of clay)
		I 048	Buffer (degradation by concrete)
		I 182	Buffer (chemical saturation)

Table F-2. Cross Reference of TSPA-LA FEPs to Source FEPs (Continued)

TSPA-LA FEP Number	TSPA-LA FEP Name	Source FEP No.	Source FEP Name
2.1.04.02.0A	Chemical properties and evolution of backfill (continued)	J 2.1.09	Backfill effects on Cu corrosion
		J 3.1.01	Degradation of the bentonite by chemical reactions
		J 3.1.02	Saturation of sorption sites
		J 3.1.03	Effects of bentonite on groundwater chemistry
		J 3.1.05	Coagulation of bentonite
		J 3.1.08	Near field buffer chemistry
		J 3.1.12	Perturbed buffer material chemistry
		J 3.2.11	Backfill material deficiencies
		J 4.2.05	Changes in Groundwater Flow
		K 2.12b	Canister failure (reference)
		K 3.01	Bentonite emplacement and composition
		K 3.05	Bentonite plasticity
		K 3.09	Bentonite porewater chemistry
		K 3.12a	Mineralogical alteration - short term
		K 3.12b	Mineralogical alteration - long term
		K 3.14	Canister/bentonite interaction
		K 3.21	Inhomogeneities (properties and evolution)
		K 3.25	Interaction with cement components
		S 006	Chemical alteration of buffer/backfill
		S 025	Dilution of buffer/backfill
		S 049	Groundwater flow
		S 062	Properties of bentonite buffer
		S 066	Properties of tunnel backfill
		S 094	Thermal degradation of buffer/backfill
		S 101	Water chemistry, bentonite buffer
		S 104	Water chemistry, tunnel backfill
		W 2.010	Backfill chemical composition
		W 2.075	Chemical degradation of backfill
2.1.04.03.0A	Erosion or dissolution of backfill	I 011a	Backfill (properties)
		I 011b	Backfill (faulty emplacement)
		I 028a	Buffer(degradation)
		I 030	Buffer (washout of clay)
		J 3.1.01	Degradation of the bentonite by chemical reactions
		J 3.1.06	Sedimentation of bentonite
		J 3.2.04	Erosion of buffer/backfill
		K 3.06	Bentonite erosion
		S 025	Dilution of buffer/backfill
		S 031	Erosion of buffer/backfill
		S 062	Properties of bentonite buffer
2.1.04.04.0A	Thermal-mechanical effects of backfill	A 1.80	Swelling pressure
		I 011a	Backfill (properties)
		I 011b	Backfill (faulty emplacement)
		J 3.2.01.1	Swelling of bentonite into tunnels and cracks

Table F-2. Cross Reference of TSPA-LA FEPs to Source FEPs (Continued)

TSPA-LA FEP Number	TSPA-LA FEP Name	Source FEP No.	Source FEP Name
2.1.04.04.0A	Thermal-mechanical effects of backfill (continued)	J 3.2.01.2	Uneven swelling of bentonite
		J 3.2.03	Mechanical failure of buffer/backfill
		J 3.2.05	Thermal effects on the buffer material
		K 2.16	Hydrogen production
		K 3.04	Bentonite swelling pressure
		K 3.07	Canister sinking
		K 4.04	Effect of bentonite swelling on EDZ
		S 003	Bentonite swelling, buffer
		S 056	Mechanical impact/failure, buffer/backfill
		S 062	Properties of bentonite buffer
		S 066	Properties of tunnel backfill
		S 088	Swelling of tunnel backfill
		W 2.035	Mechanical effects of backfill
2.1.04.05.0A	Thermal-mechanical properties and evolution of backfill	A 1.01	Backfill characteristics
		A 1.02	Backfill evolution
		A 1.07	Buffer evolution
		A 1.33	Faulty buffer emplacement
		A 1.80	Swelling pressure
		H 2.2.3	Groundwater flow
		I 011b	Backfill (faulty emplacement)
		J 3.1.01	Degradation of the bentonite by chemical reactions
		J 3.1.05	Coagulation of bentonite
		J 3.1.06	Sedimentation of bentonite
		J 3.2.01.1	Swelling of bentonite into tunnels and cracks
		J 3.2.01.2	Uneven swelling of bentonite
		J 3.2.05	Thermal effects on the buffer material
		J 4.2.05	Changes in Groundwater Flow
		K 2.12b	Canister failure (reference)
		K 3.01	Bentonite emplacement and composition
		K 3.02	Thermal evolution
		K 3.03	Bentonite saturation
		K 3.04	Bentonite swelling pressure
		K 3.05	Bentonite plasticity
		K 3.07	Canister sinking
		K 3.08	Buffer impermeability
		K 3.12a	Mineralogical alteration - short term
		K 3.12b	Mineralogical alteration - long term
		K 3.13	Bentonite cementation
		K 3.20	Interaction and diffusion between canisters
		S 003	Bentonite swelling, buffer
		S 007	Coagulation of bentonite
		S 049	Groundwater flow
		S 062	Properties of bentonite buffer
		S 066	Properties of tunnel backfill

Table F-2. Cross Reference of TSPA-LA FEPs to Source FEPs (Continued)

TSPA-LA FEP Number	TSPA-LA FEP Name	Source FEP No.	Source FEP Name
2.1.04.05.0A	Thermal-mechanical properties and evolution of backfill (continued)	S 079	Resaturation of bentonite buffer
		S 080	Resaturation of tunnel backfill
		S 082	Sedimentation of bentonite
		S 088	Swelling of tunnel backfill
		W 2.009	Backfill physical composition
		YM48	Small pieces of backfill under go phase changes when heated and weld together
2.1.04.09.0A	Radionuclide transport in backfill	A 1.06	Buffer characteristics
		A 1.22	Convection
		A 3.026	Colloids
		I 011a	Backfill (properties)
		I 011b	Backfill (faulty emplacement)
		J 2.3.06	Cracking along welds
		J 3.1.04	Colloid generation - source
		J 3.2.06	Diffusion - surface diffusion
		J 3.2.12	Gas transport in bentonite
		J 4.1.04	Sorption
		K 3.16	Radionuclide transport through buffer
		K 3.20	Interaction and diffusion between canisters
		S 042	Gas flow and transport, near-field rock/far-field
		S 062	Properties of bentonite buffer
		S 085	Sorption on filling material
		S 096	Transport and release of nuclides, bentonite buffer
		S 099	Transport and release of nuclides, tunnel backfill
2.1.05.01.0A	Flow through seals (access ramps and ventilation shafts)	A 1.59	Percolation in shafts
		A 2.04	Borehole seal failure
		H 5.1.1	Loss of integrity of borehole seals
		H 5.1.2	Loss of integrity of shaft or access tunnel seals
		I 203	Monitoring shaft (failure to close)
		K 4.17	Shaft and tunnel seals
		N 2.1.2	Investigation borehole seal failure and degradation
		W 2.006	Seal geometry
		W 2.007	Seal physical properties
2.1.05.02.0A	Radionuclide transport through seals	A 1.59	Percolation in shafts
		A 2.04	Borehole seal failure
		H 2.2.3	Groundwater flow
		H 5.1.1	Loss of integrity of borehole seals
		H 5.1.2	Loss of integrity of shaft or access tunnel seals
		I 203	Monitoring shaft (failure to close)
		I 317	Unsaturated transport
		S 049	Groundwater flow

Table F-2. Cross Reference of TSPA-LA FEPs to Source FEPs (Continued)

TSPA-LA FEP Number	TSPA-LA FEP Name	Source FEP No.	Source FEP Name
2.1.05.02.0A	Radionuclide transport through seals (continued)	W 2.006	Seal geometry
		W 3.031	Natural borehole fluid flow
		W 3.032	Waste-induced borehole flow
		W 3.036	Borehole-induced geochemical changes
2.1.05.03.0A	Degradation of seals	A 1.59	Percolation in shafts
		A 1.71	Seal evolution
		A 1.72	Seal failure
		A 2.04	Borehole seal failure
		A 2.60	Shaft seal failure
		H 5.1.1	Loss of integrity of borehole seals
		H 5.1.2	Loss of integrity of shaft or access tunnel seals
		I 203	Monitoring shaft (failure to close)
		J 5.11	Degradation of hole- and shaft seals
		K 4.17	Shaft and tunnel seals
		N 2.1.2	Investigation borehole seal failure and degradation
		N 2.1.3	Shaft or access tunnel seal failure and degradation
		S 020	Degradation of hole and shaft seals
		W 2.008	Seal chemical composition
		W 2.030	Thermally-induced stress changes
		W 2.036	Consolidation of seals
		W 2.037	Mechanical degradation of seals
		W 2.074	Chemical degradation of seals
		W 3.031	Natural borehole fluid flow
		W 3.032	Waste-induced borehole flow
		W 3.036	Borehole-induced geochemical changes
2.1.06.01.0A	Chemical effects of rock reinforcement and cementitious materials in EBS	A 1.15	Concrete
		A 1.54	Microbes
		A 2.45	Microbes
		H 1.1.2	Physico-chemical degradation of concrete
		I 062d	Concrete (degradation–natural, artificial)
		I 062e	Concrete (rebar corrosion)
		I 071	Corrosive chemicals (in vault)
		I 127	Gas absorption (14C in CO2) into concrete walls
		J 2.1.10	Microbes
		J 4.2.10	Chemical effects of rock reinforcement
		S 021	Degradation of rock reinforcement and grout
		W 2.008	Seal chemical composition
		W 2.076	Microbial growth on concrete
		YM72	Hyperalkaline carrier plume forms

Table F-2. Cross Reference of TSPA-LA FEPs to Source FEPs (Continued)

TSPA-LA FEP Number	TSPA-LA FEP Name	Source FEP No.	Source FEP Name
2.1.06.02.0A	Mechanical effects of rock reinforcement materials in EBS	H 1.1.2	Physico-chemical degradation of concrete
		I 062e	Concrete (rebar corrosion)
		J 4.2.10	Chemical effects of rock reinforcement
		S 021	Degradation of rock reinforcement and grout
2.1.06.04.0A	Flow through rock reinforcement materials in EBS	H 2.2.3	Groundwater flow
		S 049	Groundwater flow
		YM162b	Degradation of the liner
		YM71	Fracture flow through the liner
		YM99	Flow through the liner
2.1.06.05.0A	Mechanical degradation of emplacement pallet	J 3.2.02	Movement of canister in buffer/backfill
		K 3.07	Canister sinking
		N 3.3.1	Canister or container movement
		S 058	Movement of canister in buffer/backfill
		W 2.033	Movement of containers
		YM17	Degradation of invert and pedestal
2.1.06.05.0B	Mechanical degradation of invert	W 2.033	Movement of containers
		YM162a	Normal faulting occurs or exists at Yucca Mountain
		YM17	Degradation of invert and pedestal
2.1.06.05.0C	Chemical degradation of emplacement pallet	A 1.54	Microbes
		A 2.45	Microbes
		I 071	Corrosive chemicals (in vault)
		J 2.1.10	Microbes
		YM17	Degradation of invert and pedestal
2.1.06.05.0D	Chemical degradation of invert	A 1.54	Microbes
		A 2.45	Microbes
		I 071	Corrosive chemicals (in vault)
		J 2.1.10	Microbes
		YM161	Cementitious invert
		YM162a	Normal faulting occurs or exists at Yucca Mountain
		YM17	Degradation of invert and pedestal
2.1.06.06.0A	Effects of drip shield on flow	WP/Chem-1	Effects and degradation of drip shield
2.1.06.06.0B	Oxygen embrittlement of drip shields	WP/Chem-1	Effects and degradation of drip shield
		WP/Crack-1	Oxygen embrittlement of Ti drip shield
2.1.06.07.0A	Chemical effects at EBS component interfaces	A 1.47	Interfaces (boundary conditions)
		I 071	Corrosive chemicals (in vault)
		I 126	Corrosion (galvanic coupling)
		I 165	Interfaces (boundary conditions)
2.1.06.07.0B	Mechanical effects at EBS component interfaces	A 1.47	Interfaces (boundary conditions)
		I 165	Interfaces (boundary conditions)
2.1.07.01.0A	Rockfall	A 1.08	Cave ins
		I 066	Waste container (corrosion/collapse)
		K 2.12b	Canister failure (reference)
		N 3.3	MECHANICAL

Table F-2. Cross Reference of TSPA-LA FEPs to Source FEPs (Continued)

TSPA-LA FEP Number	TSPA-LA FEP Name	Source FEP No.	Source FEP Name
2.1.07.01.0A	Rockfall (continued)	S 004	Cave in
		S 058	Movement of canister in buffer/backfill
		W 2.022	Roof falls
		YM3	Rockfall (large block) WFClad--Rockfall
		YSCP63	Rockbursts in container holes
2.1.07.02.0A	Drift collapse	A 1.08	Cave ins
		A 1.78	Stability
		A 3.045	Earthquakes
		H 1.4.2	Vault collapse
		H 2.1.6	Seismicity
		I 066	Waste container (corrosion/collapse)
		I 093	Differential settling (inside IRUS)
		J 4.2.01	Mechanical failure of repository
		J 4.2.09	Creeping of rock mass
		K 9.05	Seismic activity
		N 1.2.8	Seismicity
		N 2.1.4	Stress field changes, settling, subsidence or caving
		N 3.3	MECHANICAL
		N 3.3.4	Subsidence/collapse
		S 004	Cave in
		S 058	Movement of canister in buffer/backfill
		W 1.012	Seismic activity
		W 2.022	Roof falls
		YM13	Rockfall (rubble) (in waste and EBS)
		YM169	Mechanical degradation or collapse of drift
		YM185	Rockfall stopes up fault
2.1.07.04.0A	Hydrostatic pressure on waste package	A 1.19	Container failure (mechanical processes)
		A 1.31	Excessive hydrostatic pressures
		I 298	Swelling pressure (clay)
		J 2.3.07.2	Hydrostatic pressure on canister
		J 5.23	Changed hydrostatic pressure on canister
		K 2.12a	Canister failure (alternative modes)
2.1.07.04.0B	Hydrostatic pressure on drip shield	I 298	Swelling pressure (clay)
		J 2.3.07.2	Hydrostatic pressure on canister
		J 5.23	Changed hydrostatic pressure on canister
2.1.07.05.0A	Creep of metallic materials in the waste package	A 1.46	Incomplete filling of containers
		I 066	Waste container (corrosion/collapse)
		I 161	Incomplete filling of containers
		J 2.2	Creeping of copper
		J 2.3.01	Thermal cracking

Table F-2. Cross Reference of TSPA-LA FEPs to Source FEPs (Continued)

TSPA-LA FEP Number	TSPA-LA FEP Name	Source FEP No.	Source FEP Name
2.1.07.05.0A	Creep of metallic materials in the waste package (continued)	J 2.3.04	Loss of ductility
		J 2.4	Voids in the lead filling
		K 2.10	Other canister degradation processes
		S 016	Creeping of steel/copper
2.1.07.05.0B	Creep of metallic materials in the drip shield	J 2.3.01	Thermal cracking
		J 2.3.07.1	External stress
		S 016	Creeping of steel/copper
2.1.07.06.0A	Floor buckling	N 2.1.4	Stress field changes, settling, subsidence or caving
		N 3.3.1	Canister or container movement
		S 058	Movement of canister in buffer/backfill
		YM103	Accumulation of clays and sediments in basin (in EBS)
		YM107	Pu accumulates in basin pool (in waste and EBS)
		YM83	Floor buckling
		YM86	Basin formation (in waste and EBS)
2.1.08.01.0A	Water influx at the repository	I 071	Corrosive chemicals (in vault)
		K 10.01	Present-day climatic conditions
		N 3.1.4	Induced hydrological changes (fluid pressure, density convection, viscosity)
		YSCP1	Increased unsaturated water flux at the repository
2.1.08.01.0B	Effects of rapid influx into the repository	A 2.06	Cavitation
		S 078	Resaturation, near-field rock
		YM184	Waste container is thermally quenched by rapid influx of water
		YSCP1	Increased unsaturated water flux at the repository
2.1.08.02.0A	Enhanced influx at the repository	YM96	Enhanced influx (Philip's drip)
2.1.08.03.0A	Repository dry-out due to waste heat	A 2.15	Dewatering
		H 1.5.1	Desaturation (pumping) effects
		I 300	Termperature effects (on transport)
		N 2.1.5	Dewatering of host rock
		YM43	Repository dry-out due to waste heat
2.1.08.04.0A	Condensation forms on roofs of drifts (drift-scale cold traps)	A 1.89	Vault geometry
		EBS AMR-3	Cold traps
		YSCP60	Condensation forms on backs of drifts
2.1.08.04.0B	Condensation forms at repository edges (repository-scale cold traps)	A 1.89	Vault geometry
		EBS AMR-3	Cold traps
		YM52	Condensation zone forms around drifts
		YM57	Shedding of condensation cap over one drift to another drift
		YM59	Return flow from condensation cap / resaturation of dry-out zone
		YM67	Unsaturated flow plume returns flow from the condensation cap
		YSCP59	Condensation cap forms above repository
		YSCP60	Condensation forms on backs of drifts

Table F-2. Cross Reference of TSPA-LA FEPs to Source FEPs (Continued)

TSPA-LA FEP Number	TSPA-LA FEP Name	Source FEP No.	Source FEP Name
2.1.08.05.0A	Flow through invert	I 317	Unsaturated transport
		YM70	Fracture flow through the invert
		YM97	Flow through invert
		YM98	UZ flow through/around the collapsed invert
2.1.08.06.0A	Capillary effects (wicking) in EBS	A 3.017	Capillary rise in soil
		I 032	Capillary rise in soil
		W 2.041	Wicking
2.1.08.07.0A	Unsaturated flow in the EBS	A 1.21	Containers - partial corrosion
		A 1.40	Hydraulic conductivity
		A 1.88	Unsaturated transport
		H 1.5.3	Unsaturated flow due to gas production
		H 2.2.3	Groundwater flow
		I 317	Unsaturated transport
		J 2.1.04	Role of the eventual channeling within the canister
		K 2.13	Residual canister (crack/hole effects)
		K 8.20	Groundwater flow (alluvium of Rhine valley)
		S 061	Preferential pathways in canister
		S 106	Water turnover, steel vessel
2.1.08.09.0A	Saturated flow in the EBS	A 1.41	Hydraulic head
		A 2.06	Cavitation
		H 1.5.4	Saturated groundwater flow
		H 2.2.3	Groundwater flow
		K 8.20	Groundwater flow (alluvium of Rhine valley)
		S 049	Groundwater flow
		S 106	Water turnover, steel vessel
2.1.08.11.0A	Repository resaturation due to waste cooling	A 1.68	Reflooding
		J 5.14	Resaturation
		W 2.040	Brine inflow
2.1.08.12.0A	Induced hydrologic changes in invert	EBS AMR-1	Drainage with Transport - Sealing and Plugging
		EBS AMR-2	Drains
		I 098	Drain gutters plug
		N 3.1.4	Induced hydrological changes (fluid pressure, density convection, viscosity)
		W 2.040	Brine inflow
		YM103	Accumulation of clays and sediments in basin (in EBS)
2.1.08.14.0A	Condensation on underside of drip shield	N 3.1.4	Induced hydrological changes (fluid pressure, density convection, viscosity)
		NRC NFE-2	Condensation on underside of drip shield

Table F-2. Cross Reference of TSPA-LA FEPs to Source FEPs (Continued)

TSPA-LA FEP Number	TSPA-LA FEP Name	Source FEP No.	Source FEP Name
2.1.08.15.0A	Consolidation of EBS components	H 1.4.1	Waste-form and backfill consolidation
		I 066	Waste container (corrosion/collapse)
		I 093	Differential settling (inside IRUS)
		K 3.07	Canister sinking
		N 2.1.4	Stress field changes, settling, subsidence or caving
		S 058	Movement of canister in buffer/backfill
		W 2.032	Consolidation of waste
		W 2.033	Movement of containers
2.1.09.01.0A	Chemical characteristics of water in drifts	H 1.5.5	Transport of chemically-active substances into the near-field
		H 5.1.3	Incomplete near-field chemical conditioning
		I 071	Corrosive chemicals (in vault)
		I 317	Unsaturated transport
		J 3.1.07	Reactions with cement pore water
		J 4.1.02	pH-deviations
		J 4.1.04	Sorption
		J 5.01	Saline (or fresh) groundwater intrusion
		K 4.19	TRU silos cementitious plume
		K 5.11	Intrusion of saline groundwater
		K 5.20	TRU alkaline or organic plume
		K 6.11	Intrusion of saline groundwater
		K 6.20	TRU alkaline or organics plume
		N 1.5.7	Saline or freshwater intrusion
		N 1.5.8	Effects at saline-freshwater interface
		N 3.1.5	Induced chemical changes
		N 3.2	CHEMICAL
		N 3.2.2	Interactions of host materials and groundwater with repository material
		N 3.2.3	Interactions of waste and repository materials with host materials
		S 018	Deep saline water intrusion
		W 1.029	Saline intrusion
		W 1.034	Saline intrusion
		YM15	Rind (altered zone) formation in waste, EBS, and adjacent rock
		YM4	Properties of the potential carrier plume in the waste and EBS
		YM72	Hyperalkaline carrier plume forms
2.1.09.01.0B	Chemical characteristics of water in waste package	A 1.10	Chemical interactions
		H 1.5.5	Transport of chemically-active substances into the near-field
		H 5.1.3	Incomplete near-field chemical conditioning
		I 071	Corrosive chemicals (in vault)
		I 337	Water contacting waste in vault
		J 4.1.02	pH-deviations

Table F-2. Cross Reference of TSPA-LA FEPs to Source FEPs (Continued)

TSPA-LA FEP Number	TSPA-LA FEP Name	Source FEP No.	Source FEP Name
2.1.09.01.0B	Chemical characteristics of water in waste package (continued)	N 3.2.2	Interactions of host materials and groundwater with repository material
		N 3.2.3	Interactions of waste and repository materials with host materials
		S 102	Water chemistry, canister
		YM15	Rind (altered zone) formation in waste, EBS, and adjacent rock
2.1.09.02.0A	Chemical interaction with corrosion products	A 1.16	Container corrosion products
		I 039	Vault chemical interactions
		I 058	Colloid formation (natural and vault generated)
		I 065	Waste container (metal corrosion products)
		J 1.5	Release of radionuclides from the failured canister
		J 3.1.02	Saturation of sorption sites
		J 3.1.10	Interactions with corrosion products and waste
		J 4.1.04	Sorption
		K 1.21	Colloid formation
		K 2.14	Chemical buffering (canister corrosion products)
		S 051	Interaction with corrosion products
		W 2.064	Effect of metal corrosion
		YM49	Fe control of oxidation state of contaminants
2.1.09.03.0A	Volume increase of corrosion products impacts cladding	J 3.2.07	Swelling of corrosion products
		S 055	Mechanical impact on canister
		S 100	Volume increase of corrosion products
2.1.09.03.0B	Volume increase of corrosion products impacts waste package	J 3.2.07	Swelling of corrosion products
		S 055	Mechanical impact on canister
		S 100	Volume increase of corrosion products
		K 2.18	Corrosion products (physical effects)
2.1.09.03.0C	Volume increase of corrosion products impacts other EBS components	J 3.2.07	Swelling of corrosion products
		S 100	Volume increase of corrosion products
2.1.09.04.0A	Radionuclide solubility, solubility limits, and speciation in the waste form and EBS	A 1.37	Geochemical pump
		A 1.62	Precipitation and dissolution
		A 2.64	Speciation
		H 1.1.3	Waste corrosion and solubility and speciation of radionuclides
		I 042	Chemical speciation (wrong assumption for model)
		I 233	Source term & solubility limits
		J 1.2.06	Solubility within fuel matrix
		J 5.44	Solubility and precipitation
		K 0.2	Speciation
		K 1.15	Elemental solubility limits

Table F-2. Cross Reference of TSPA-LA FEPs to Source FEPs (Continued)

TSPA-LA FEP Number	TSPA-LA FEP Name	Source FEP No.	Source FEP Name
2.1.09.04.0A	Radionuclide solubility, solubility limits, and speciation in the waste form and EBS (continued)	K 1.20	Radionuclide source term
		K 3.18	Elemental solubility/precipitation
		N 1.6.6	Solubility limit
		W 2.056	Speciation
		W 2.059	Precipitation
		YM104	Differential solubility or neutron poisons
		YM105	Differential solubility of fissile isotopes
		YM11	Speciation (in waste and EBS)
		YM7	Speciation control of contaminants by hyperalkaline plume formed in the EBS
		YSCP70	Selective dissolution of contaminants contained in SNF
2.1.09.05.0A	Sorption of dissolved radionuclides in EBS	A 1.73	Sorption
		A 3.021	Chemical precipitation
		J 4.1.04	Sorption
		K 2.20	Radionuclide transport
		K 3.10	Radionuclide retardation
		S 063	Properties of failed canister
		S 085	Sorption on filling material
		YM117	Selective sorption of Pu from solution
		YM87	In-drift sorption WFMisc—In-Package Sorption
2.1.09.06.0A	Reduction-oxidation potential in waste package	I 233	Source term & solubility limits
		J 1.2.08	Redox potential
		J 3.1.11	Redox front
		J 4.1.02	pH-deviations
		K 2.14	Chemical buffering (canister corrosion products)
		S 074	Redox front
		W 2.065	Reduction-oxidation fronts
		W 2.067	Localized reducing zones
		YM49	Fe control of oxidation state of contaminants
2.1.09.06.0B	Reduction-oxidation potential in drifts	I 233	Source term & solubility limits
		J 1.2.08	Redox potential
		J 3.1.11	Redox front
		J 4.1.02	pH-deviations
2.1.09.07.0A	Reaction kinetics in waste package	A 1.11	Chemical kinetics
		W 2.066	Reduction-oxidation kinetics
2.1.09.07.0B	Reaction kinetics in drifts	A 1.11	Chemical kinetics
		W 2.066	Reduction-oxidation kinetics
2.1.09.08.0A	Diffusion of dissolved radionuclides in EBS	A 1.21	Containers - partial corrosion
		A 1.88	Unsaturated transport
		A 3.021	Chemical precipitation
		H 1.5.5	Transport of chemically-active substances into the near-field
		I 317	Unsaturated transport
		K 1.16	Solute transport resistance

Table F-2. Cross Reference of TSPA-LA FEPs to Source FEPs (Continued)

TSPA-LA FEP Number	TSPA-LA FEP Name	Source FEP No.	Source FEP Name
2.1.09.08.0A	Diffusion of dissolved radionuclides in EBS (continued)	K 2.13	Residual canister (crack/hole effects)
		K 2.20	Radionuclide transport
		S 024	Diffusion in and through failed canister
		S 063	Properties of failed canister
		S 097	Transport and release of nuclides, failed canister
		W 2.097	Chemical gradients
		YM160	Radionuclide Release (Diffusion) Through Failed Cladding
2.1.09.08.0B	Advection of dissolved radionuclides in EBS	A 1.21	Containers - partial corrosion
		A 1.88	Unsaturated transport
		A 3.021	Chemical precipitation
		I 317	Unsaturated transport
		K 2.13	Residual canister (crack/hole effects)
		K 2.20	Radionuclide transport
		S 063	Properties of failed canister
		S 097	Transport and release of nuclides, failed canister
		W 2.097	Chemical gradients
2.1.09.09.0A	Electrochemical effects in EBS	A 1.30	Electrochemical gradients
		A 1.36	Galvanic coupling
		A 1.47	Interfaces (boundary conditions)
		H 1.1.4	Electrochemical effects of metal corrosion
		I 126	Corrosion (galvanic coupling)
		J 2.1.02	Coupled effects (electrophoresis)
		J 2.1.06.1	Repository induced Pb/Cu electrochemical reactions
		J 2.1.06.2	Natural telluric electrochemical reactions
		J 2.3.02	Electro-chemical cracking
		S 029	Electrochemical effects/gradients
		W 2.050	Galvanic coupling
		W 2.094	Electrochemical effects
		W 2.095	Galvanic coupling
		W 2.096	Electrophoresis
2.1.09.10.0A	Secondary phase effects on dissolved radionuclide concentrations	K 1.15	Elemental solubility limits
		W 2.059	Precipitation
		WF//Solub-1	Secondary phase effects on dissolved radionuclide concentrations at the waste form
2.1.09.11.0A	Chemical effects of waste-rock contact	H 2.3.4	Far-field transport: Solubility constraints
		I 071	Corrosive chemicals (in vault)
		YSCP71	Waste-rock contact
2.1.09.12.0A	Rind (chemically altered zone) forms in the near-field	J 4.1.04	Sorption
		N 3.1.4	Induced hydrological changes (fluid pressure, density convection, viscosity)
		YM128	Deep alteration of the porosity of drift walls

Table F-2. Cross Reference of TSPA-LA FEPs to Source FEPs (Continued)

TSPA-LA FEP Number	TSPA-LA FEP Name	Source FEP No.	Source FEP Name
2.1.09.12.0A	Rind (chemically altered zone) forms in the near-field (continued)	YM15	Rind (altered zone) formation in waste, EBS, and adjacent rock
		YM94	Locally-saturated carrier plume forms (in geosphere)
		YM95	Unsaturated carrier plume forms (in geosphere)
2.1.09.13.0A	Complexation in EBS	A 1.14	Complexation by organics
		A 1.53	Methylation
		A 2.09	Complexation by organics
		A 2.26	Fulvic acid
		A 2.34	Humic acid
		H 1.5.5	Transport of chemically-active substances into the near-field
		I 317	Unsaturated transport
		J 4.1.03	Colloids, complexing agents
		K 3.17	Microbial activity
		K 4.12	Colloids
		K 5.21	Organics
		K 6.21	Organics
		N 1.6.10	Complexing agents
		N 1.6.9	Colloid formation, dissolution and transport
		N 3.2.6	Introduced complexing agents and cellulosics
		S 008	Colloid generation and transport
		W 2.068	Organic complexation
		W 2.069	Organic ligands
		W 2.070	Humic and fulvic acids
		W 2.071	Kinetics of organic complexation
2.1.09.15.0A	Formation of true (intrinsic) colloids in EBS	A 3.026	Colloids
		I 058	Colloid formation (natural and vault generated)
		J 4.1.03	Colloids, complexing agents
		J 5.45	Colloid generation and transport
		K 1.21	Colloid formation
		K 4.12	Colloids
		N 1.6.9	Colloid formation, dissolution and transport
		S 008	Colloid generation and transport
		S 009	Colloid generation-source
		W 2.079	Colloid formation and stability
		YM118	Agglomeration of Pu colloids
		YM45	Formation of true colloids in waste and EBS
2.1.09.16.0A	Formation of pseudo-colloids (natural) in EBS	A 1.13	Colloids
		A 1.63	Psuedo-colloids
		A 2.08	Colloid formation
		A 2.50	Pseudo-colloids

Table F-2. Cross Reference of TSPA-LA FEPs to Source FEPs (Continued)

TSPA-LA FEP Number	TSPA-LA FEP Name	Source FEP No.	Source FEP Name
2.1.09.16.0A	Formation of pseudo-colloids (natural) in EBS (continued)	A 3.026	Colloids
		I 058	Colloid formation (natural and vault generated)
		J 4.1.03	Colloids, complexing agents
		J 5.45	Colloid generation and transport
		K 1.21	Colloid formation
		K 4.12	Colloids
		K 5.15	Natural colloids
		K 6.15	Natural colloids
		N 1.6.9	Colloid formation, dissolution and transport
		S 008	Colloid generation and transport
		S 009	Colloid generation-source
		W 2.079	Colloid formation and stability
		YM118	Agglomeration of Pu colloids
		YSCP73	Formation of pseudo-colloids (natural) in waste and EBS
2.1.09.17.0A	Formation of pseudo-colloids (corrosion product) in EBS	A 1.13	Colloids
		A 2.08	Colloid formation
		A 3.026	Colloids
		I 058	Colloid formation (natural and vault generated)
		J 4.1.03	Colloids, complexing agents
		J 5.45	Colloid generation and transport
		K 1.21	Colloid formation
		K 4.12	Colloids
		N 1.6.9	Colloid formation, dissolution and transport
		S 008	Colloid generation and transport
		S 009	Colloid generation-source
		S 010	Colloids/particles in canister
		W 2.079	Colloid formation and stability
		YM118	Agglomeration of Pu colloids
		YM44	Colloid formation is associated with container hydrolysis products
		YSCP69	Formation of pseudo-colloids (corrosion products) in waste and EBS
2.1.09.18.0A	Formation of microbial colloids in EBS	A 1.13	Colloids
		A 3.026	Colloids
		I 058	Colloid formation (natural and vault generated)
		I 317	Unsaturated transport
		J 4.1.03	Colloids, complexing agents
		J 5.45	Colloid generation and transport
		K 1.21	Colloid formation
		K 4.12	Colloids
		N 1.6.9	Colloid formation, dissolution and transport

Table F-2. Cross Reference of TSPA-LA FEPs to Source FEPs (Continued)

TSPA-LA FEP Number	TSPA-LA FEP Name	Source FEP No.	Source FEP Name
2.1.09.18.0A	Formation of microbial colloids in EBS (continued)	S 008	Colloid generation and transport
		S 009	Colloid generation-source
		S 010	Colloids/particles in canister
		W 2.087	Microbial transport
2.1.09.19.0A	Sorption of colloids in EBS	A 3.026	Colloids
		I 317	Unsaturated transport
		J 4.1.03	Colloids, complexing agents
		J 4.1.04	Sorption
		J 5.45	Colloid generation and transport
		K 4.12	Colloids
		N 1.6.9	Colloid formation, dissolution and transport
		S 008	Colloid generation and transport
		S 009	Colloid generation-source
		W 2.078	Colloid transport
		W 2.081	Colloid sorption
2.1.09.19.0B	Advection of colloids in EBS	A 3.026	Colloids
		I 317	Unsaturated transport
		J 4.1.03	Colloids, complexing agents
		J 5.45	Colloid generation and transport
		K 4.12	Colloids
		N 1.6.9	Colloid formation, dissolution and transport
		S 008	Colloid generation and transport
		S 097	Transport and release of nuclides, failed canister
		W 2.078	Colloid transport
2.1.09.20.0A	Filtration of colloids in EBS	A 3.026	Colloids
		J 4.1.03	Colloids, complexing agents
		J 5.45	Colloid generation and transport
		K 3.11	Colloid filtration
		K 4.12	Colloids
		N 1.6.9	Colloid formation, dissolution and transport
		S 008	Colloid generation and transport
		W 2.080	Colloid filtration
		YM119	Colloid filtration by the invert
		YM9	Colloid filtration (in pores and fractures)
2.1.09.21.0A	Transport of particles larger than colloids in EBS	A 3.026	Colloids
		H 2.2.3	Groundwater flow
		I 317	Unsaturated transport
		K 8.36	Suspended sediment transport
		S 049	Groundwater flow
		W 2.082	Suspensions of particles
		W 2.083	Rinse
2.1.09.21.0B	Transport of particles larger than colloids in the SZ	A 3.026	Colloids
		K 8.36	Suspended sediment transport
		W 2.082	Suspensions of particles
		W 2.083	Rinse

Table F-2. Cross Reference of TSPA-LA FEPs to Source FEPs (Continued)

TSPA-LA FEP Number	TSPA-LA FEP Name	Source FEP No.	Source FEP Name
2.1.09.21.0C	Transport of particles larger than colloids in the UZ	A 3.026	Colloids
		K 8.36	Suspended sediment transport
		W 2.082	Suspensions of particles
2.1.09.22.0A	Sorption of colloids at air-water interface	A 3.026	Colloids
		J 4.1.03	Colloids, complexing agents
		J 4.1.04	Sorption
		J 5.45	Colloid generation and transport
		K 4.12	Colloids
		N 1.6.9	Colloid formation, dissolution and transport
		S 008	Colloid generation and transport
		WFCol AMR-1	Colloid Sorption at the Air-Water Interface
2.1.09.23.0A	Stability of colloids in EBS	A 3.026	Colloids
		J 4.1.03	Colloids, complexing agents
		J 5.45	Colloid generation and transport
		K 4.12	Colloids
		N 1.6.9	Colloid formation, dissolution and transport
		S 008	Colloid generation and transport
		W 2.079	Colloid formation and stability
		WFCol AMR-2	Colloidal stability and concentration dependence on aqueous chemistry
2.1.09.24.0A	Diffusion of colloids in EBS	A 3.026	Colloids
		I 317	Unsaturated transport
		J 4.1.03	Colloids, complexing agents
		J 5.45	Colloid generation and transport
		K 1.16	Solute transport resistance
		K 4.12	Colloids
		N 1.6.9	Colloid formation, dissolution and transport
		S 008	Colloid generation and transport
		S 097	Transport and release of nuclides, failed canister
		WFCol AMR-3	Colloidal diffusion
		YM160	Radionuclide Release (Diffusion) Through Failed Cladding
2.1.09.25.0A	Formation of colloids (waste-form) by co-precipitation in EBS	A 3.026	Colloids
		I 058	Colloid formation (natural and vault generated)
		J 4.1.03	Colloids, complexing agents
		J 5.45	Colloid generation and transport
		K 1.14	Coprecipitates/solid solutions
		K 1.21	Colloid formation
		K 4.12	Colloids
		N 1.6.9	Colloid formation, dissolution and transport

Table F-2. Cross Reference of TSPA-LA FEPs to Source FEPs (Continued)

TSPA-LA FEP Number	TSPA-LA FEP Name	Source FEP No.	Source FEP Name
2.1.09.25.0A	Formation of colloids (waste-form) by co-precipitation in EBS (continued)	S 008	Colloid generation and transport
		S 009	Colloid generation-source
		S 010	Colloids/particles in canister
		YSCP74	Colloidal phases are produced by coprecipitation (in waste and EBS)
2.1.09.26.0A	Gravitational settling of colloids in EBS	A 3.026	Colloids
		I 317	Unsaturated transport
		J 4.1.03	Colloids, complexing agents
		J 5.45	Colloid generation and transport
		K 4.12	Colloids
		N 1.6.9	Colloid formation, dissolution and transport
		S 008	Colloid generation and transport
		WFCol AMR-4	Colloid gravitational settling
2.1.09.27.0A	Coupled effects on radionuclide transport in EBS	A 1.09	Chemical gradients
		A 1.16	Container corrosion products
		A 1.25	Coupled processes
		A 1.37	Geochemical pump
		H 1.5.5	Transport of chemically-active substances into the near-field
		I 065	Waste container (metal corrosion products)
		I 317	Unsaturated transport
		J 2.1.02	Coupled effects (electrophoresis)
		J 4.1.04	Sorption
		K 2.15	Radionuclide sorption and co-precipitation
		W 2.097	Chemical gradients
		W 2.100	Enhanced diffusion
		YM49	Fe control of oxidation state of contaminants
2.1.09.28.0A	Localized corrosion on waste package outer surface due to deliquescence	A 1.60	Pitting
		I 261	Salt (road salt, CaCl2, etc.)
		K 2.12b	Canister failure (reference)
		YSCP64	Corrosion of waste containers
		YSCP65	Stress corrosion cracking of waste containers and drip shields
2.1.09.28.0B	Localized corrosion on drip shield surfaces due to deliquescence	A 1.60	Pitting
		I 261	Salt (road salt, CaCl2, etc.)
		YSCP64	Corrosion of waste containers
		YSCP65	Stress corrosion cracking of waste containers and drip shields
2.1.10.01.0A	Microbial activity in EBS	A 1.03	Biological activity
		A 1.54	Microbes
		A 1.55	Microorganisms
		A 2.45	Microbes
		A 3.026	Colloids
		I 015	Gas generation (CH4, CO2, H2)

Table F-2. Cross Reference of TSPA-LA FEPs to Source FEPs (Continued)

TSPA-LA FEP Number	TSPA-LA FEP Name	Source FEP No.	Source FEP Name
2.1.10.01.0A	Microbial activity in EBS (continued)	I 270	Seeds in vault/water
		J 2.1.10	Microbes
		J 4.1.04	Sorption
		K 1.22	Microbial activity
		K 3.17	Microbial activity
		N 1.7.7	Microbial interactions
		N 3.2.7	Microbiological effects
		S 057	Microbial activity
		W 2.045	Effect of temperature on microbial gas generation
		W 2.076	Microbial growth on concrete
		W 2.088	Biofilms
		YSCP82	Microbial activity accelerates corrosion of containers
		YSCP83	Microbial activity accelerates corrosion of cladding
		YSCP84	Microbial activity accelerates corrosion of contaminants
2.1.11.01.0A	Heat generation in EBS	A 1.52	Long-term transients
		A 1.81	Temperature effects
		A 1.83	Time dependence
		A 2.71	Vault heating effects
		CA-2	DOE SNF expected waste heat generation
		I 146	Heat generation in IRUS vault(B)
		J 1.1.02	Radioactive decay; heat
		J 4.1.07	Thermochemical change
		K 1.08	Heat output (RN decay heat)
		K 1.09	Glass temperature
		K 2.19	Canister temperature
		MLD-6	DOE SNF expected waste heat generation
		N 3.1	THERMAL
		N 3.1.4	Induced hydrological changes (fluid pressure, density convection, viscosity)
		S 089	Temperature, bentonite buffer
		S 090	Temperature, canister
		S 093	Temperature, tunnel backfill
		W 2.013	Heat from radioactive decay
		W 2.030	Thermally-induced stress changes
		YM63a	Heat generation from waste containers
2.1.11.02.0A	Non-uniform heat distribution in EBS	A 2.71	Vault heating effects
		N 3.1	THERMAL
		YM89	Panel/repository edge effects - thermal
		YM90	Panel/repository edge effects - post-thermal
		YSCP61	Nonuniform heat distribution / edge effects in repository

Table F-2. Cross Reference of TSPA-LA FEPs to Source FEPs (Continued)

TSPA-LA FEP Number	TSPA-LA FEP Name	Source FEP No.	Source FEP Name
2.1.11.03.0A	Exothermic reactions in the EBS	I 061	Concrete (influence on vault chemistry)
		I 146	Heat generation in IRUS vault(B)
		N 3.1	THERMAL
		W 2.030	Thermally-induced stress changes
		W 2.072	Exothermic reactions
		W 2.073	Concrete hydration
2.1.11.05.0A	Thermal expansion/stress of in-package EBS components	I 143	Groundwater (redirection of)
		I 146	Heat generation in IRUS vault(B)
		N 3.1	THERMAL
		W 2.030	Thermally-induced stress changes
		W 2.031	Differing thermal expansion of repository components
		YSCP55	Stress corrosion cracking induced by secondary stress (container failure)
2.1.11.06.0A	Thermal sensitization of waste packages	I 146	Heat generation in IRUS vault(B)
		K 2.12b	Canister failure (reference)
		N 3.1	THERMAL
		YSCP67	Thermal sensitization of waste containers and drip shields increases their fragility
2.1.11.06.0B	Thermal sensitization of drip shields	N 3.1	THERMAL
		YSCP67	Thermal sensitization of waste containers and drip shields increases their fragility
2.1.11.07.0A	Thermal expansion/stress of in-drift EBS components	A 2.71	Vault heating effects
		H 2.2.3	Groundwater flow
		I 143	Groundwater (redirection of)
		K 2.12b	Canister failure (reference)
		N 3.1.1	Differential elastic response
		N 3.1.2	Non-elastic response
		N 3.3.2	Changes in in-situ stress field
		S 022	Differential thermal expansion of near-field barriers
		S 049	Groundwater flow
		W 2.030	Thermally-induced stress changes
		W 2.031	Differing thermal expansion of repository components
		YM89	Panel/repository edge effects - thermal
		YM90	Panel/repository edge effects - post-thermal
		YSCP55	Stress corrosion cracking induced by secondary stress (container failure)
		YSCP56	Shearing of waste containers by secondary stresses from thermal expansion of the rock
2.1.11.08.0A	Thermal effects on chemistry and microbial activity in the EBS	H 1.6.3	Thermal effects: Chemical and microbiological changes
		J 4.1.07	Thermochemical change
		N 3.1	THERMAL

Table F-2. Cross Reference of TSPA-LA FEPs to Source FEPs (Continued)

TSPA-LA FEP Number	TSPA-LA FEP Name	Source FEP No.	Source FEP Name
2.1.11.09.0A	Thermal effects on flow in the EBS	A 1.25	Coupled processes
		A 2.71	Vault heating effects
		K 5.13	Geothermal regime
		N 1.6.5	Multiphase flow and gas driven flow
		N 3.1	THERMAL
		N 3.1.4	Induced hydrological changes (fluid pressure, density convection, viscosity)
		TH/Flow-1	Convection effects on transport (Enhanced vapor diffusion)
		W 1.028	Thermal effects on groundwater flow
		W 2.043	Convection
		YSCP61	Nonuniform heat distribution / edge effects in repository
		YSCP62	Thermal convection cell develops in SZ
2.1.11.09.0B	Thermally-driven flow (convection) in waste packages	A 2.71	Vault heating effects
		N 1.6.5	Multiphase flow and gas driven flow
		N 3.1	THERMAL
		TH/Flow-1	Convection effects on transport (Enhanced vapor diffusion)
		W 2.043	Convection
2.1.11.09.0C	Thermally driven flow (convection) in drifts	A 2.71	Vault heating effects
		K 5.13	Geothermal regime
		N 1.6.5	Multiphase flow and gas driven flow
		N 3.1	THERMAL
		TH/Flow-1	Convection effects on transport (Enhanced vapor diffusion)
		W 2.043	Convection
2.1.11.10.0A	Thermal effects on transport in EBS	A 1.25	Coupled processes
		H 1.6.4	Thermal effects: Transport (diffusion) effects
		I 300	Termperature effects (on transport)
		I 317	Unsaturated transport
		J 3.2.10	Soret effect
		J 4.1.04	Sorption
		J 4.1.07	Thermochemical change
		N 3.1	THERMAL
		S 083	Soret effect
		TH/Flow-1	Convection effects on transport (Enhanced vapor diffusion)
		W 2.093	Soret effect
2.1.12.01.0A	Gas generation (repository pressurization)	A 1.35	Formation of gases
		H 1.2.6	Gas transport
		H 1.2.8	Thermo-chemical effects
		H 1.5.3	Unsaturated flow due to gas production
		I 130	Gas (from waste containing a gas cylinder)
		I 317	Unsaturated transport
		I 328	Swelling pressure(bales)

Table F-2. Cross Reference of TSPA-LA FEPs to Source FEPs (Continued)

TSPA-LA FEP Number	TSPA-LA FEP Name	Source FEP No.	Source FEP Name
2.1.12.01.0A	Gas generation (repository pressurization) (continued)	K 0.3	Gaseous and volatile isotopes
		N 3.3.6	Gas effects
		S 046	Gas generation, near-field rock
		W 2.026	Pressurization
		YM12	Gas generation
2.1.12.02.0A	Gas generation (He) from waste form decay	H 1.2.5	Chemotoxic gases
		H 1.5.3	Unsaturated flow due to gas production
		I 015	Gas generation (CH4, CO2, H2)
		I 039	Vault chemical interactions
		I 130	Gas (from waste containing a gas cylinder)
		J 1.1.04	Gas generation: He production
		J 1.2.04	Gas generation
		J 2.3.08	Internal pressure
		K 1.24	He gas production
		S 045	Gas generation, canister
		S 046	Gas generation, near-field rock
		S 053	Internal pressure
		W 2.054	Helium gas production
		YM12	Gas generation
2.1.12.03.0A	Gas generation (H2) from waste package corrosion	A 1.35	Formation of gases
		H 1.2.1	Hydrogen by metal corrosion
		H 1.2.5	Chemotoxic gases
		H 1.2.8	Thermo-chemical effects
		H 1.5.3	Unsaturated flow due to gas production
		I 015	Gas generation (CH4, CO2, H2)
		I 039	Vault chemical interactions
		I 130	Gas (from waste containing a gas cylinder)
		I 317	Unsaturated transport
		J 1.2.04	Gas generation
		K 2.16	Hydrogen production
		K 2.17	Effect of hydrogen on corrosion
		S 046	Gas generation, near-field rock
		W 2.005	Container material inventory
		W 2.049	Gases from metal corrosion
		W 2.051	Chemical effects of corrosion
		YM12	Gas generation
2.1.12.04.0A	Gas generation (CO2, CH4, H2S) from microbial degradation	A 1.54	Microbes
		A 2.45	Microbes
		H 1.2.1	Hydrogen by metal corrosion
		H 1.2.2	Methane and carbon dioxide by microbial degradation
		H 1.2.3	Gas generation from concrete
		H 1.2.5	Chemotoxic gases
		H 1.5.3	Unsaturated flow due to gas production
		I 012	Biological activity (bacteria & microbes)

Table F-2. Cross Reference of TSPA-LA FEPs to Source FEPs (Continued)

TSPA-LA FEP Number	TSPA-LA FEP Name	Source FEP No.	Source FEP Name
2.1.12.04.0A	Gas generation (CO_2, CH_4, H_2S) from microbial degradation (continued)	I 015	Gas generation (CH_4, CO_2, H_2)
		I 061	Concrete (influence on vault chemistry)
		I 130	Gas (from waste containing a gas cylinder)
		I 317	Unsaturated transport
		J 1.2.04	Gas generation
		J 2.1.10	Microbes
		N 3.2.5	Cellulosic degradation
		S 043	Gas generation and gas sources, far-field
		S 044	Gas generation, buffer/backfill
		S 046	Gas generation, near-field rock
		W 2.044	Degradation of organic material
		W 2.045	Effect of temperature on microbial gas generation
		W 2.046	Effect of pressure on microbial gas generation
		W 2.047	Effect of radiation on microbial gas generation
		W 2.048	Effect of biofilms on microbial gas generation
		W 2.053	Radiolysis of cellulose
		W 2.076	Microbial growth on concrete
		YM12	Gas generation
2.1.12.06.0A	Gas transport in EBS	A 1.84	Transport in gases or of gases
		H 1.2.6	Gas transport
		H 1.2.8	Thermo-chemical effects
		H 1.5.3	Unsaturated flow due to gas production
		I 130	Gas (from waste containing a gas cylinder)
		I 317	Unsaturated transport
		J 3.2.12	Gas transport in bentonite
		J 6.02	Gas transport
		K 3.15	Gas permeability
		K 4.11	Gas transport/dissolution
		N 3.3.6	Gas effects
		S 040	Gas escape from canister
		S 041	Gas flow and transport, buffer/backfill
		S 042	Gas flow and transport, near-field rock/far-field
2.1.12.07.0A	Effects of radioactive gases in EBS	H 1.2.4	Radioactive gases
		H 1.2.5	Chemotoxic gases
		H 1.2.6	Gas transport
		H 1.2.8	Thermo-chemical effects
		H 1.5.3	Unsaturated flow due to gas production
		I 130	Gas (from waste containing a gas cylinder)
		J 6.02	Gas transport

Table F-2. Cross Reference of TSPA-LA FEPs to Source FEPs (Continued)

TSPA-LA FEP Number	TSPA-LA FEP Name	Source FEP No.	Source FEP Name
2.1.12.07.0A	Effects of radioactive gases in EBS (continued)	K 0.3	Gaseous and volatile isotopes
		K 2.12b	Canister failure (reference)
		N 3.3.6	Gas effects
		S 042	Gas flow and transport, near-field rock/far-field
		S 046	Gas generation, near-field rock
		W 2.055	Radioactive gases
2.1.12.08.0A	Gas explosions in EBS	A 1.32	Explosions
		A 1.82	Temperature rises (unexpected effects)
		A 2.23	Explosion
		A 3.025	Collisions, collisions and impacts
		H 1.2.7	Flammability
		I 022	Explosions/bombs/blasting/collision/impacts/vibration
		J 1.2.02	Hydrogen/oxygen explosions
		K 0.3	Gaseous and volatile isotopes
		MLD-17	Acetylene generation from DSNF WFMisc—Flammable Gases Generation from DSNF - YMP
		W 1.032	Natural gas intrusion
		W 2.027	Gas explosions
2.1.13.01.0A	Radiolysis	A 1.35	Formation of gases
		A 1.66	Radiolysis
		A 2.52	Radiation effects
		H 1.2.3	Gas generation from concrete
		H 1.2.5	Chemotoxic gases
		I 130	Gas (from waste containing a gas cylinder)
		I 238	Radiation effects
		J 1.2.01	Radiolysis
		J 1.2.04	Gas generation
		J 1.2.08	Redox potential
		J 3.1.09	Radiolysis
		J 3.1.11	Redox front
		J 4.1.02	pH-deviations
		J 4.1.08	Change of groundwater chemistry in nearby rock
		K 0.3	Gaseous and volatile isotopes
		K 1.23	Radiolysis
		K 2.10	Other canister degradation processes
		K 2.11	Radiation shielding
		K 3.19	Radiolysis
		N 3.4	RADIOLOGICAL
		N 3.4.1	Radiolysis
		S 044	Gas generation, buffer/backfill
		S 046	Gas generation, near-field rock
		S 069	Radioactive Decay, fuel

Table F-2. Cross Reference of TSPA-LA FEPs to Source FEPs (Continued)

TSPA-LA FEP Number	TSPA-LA FEP Name	Source FEP No.	Source FEP Name
2.1.13.01.0A	Radiolysis (continued)	S 071	Radiolysis
		S 072	Radiolysis prior to wetting
		S 074	Redox front
		W 2.052	Radiolysis of brine
		W 2.053	Radiolysis of cellulose
		YM12	Gas generation
		YM146	Inside Out from fission products (iodine) (failure of cladding)
2.1.13.02.0A	Radiation damage in EBS	A 1.64	Radiation damage
		A 2.52	Radiation effects
		H 2.2.3	Groundwater flow
		I 238	Radiation effects
		J 1.1.03	Recoil of alpha-decay
		J 2.3.05	Radiation effects on canister
		J 3.1.13	Radiation effects on bentonite
		K 1.10	Radiation damage
		K 2.10	Other canister degradation processes
		K 2.11	Radiation shielding
		N 3.4	RADIOLOGICAL
		N 3.4.2	Material property changes
		S 049	Groundwater flow
		S 067	Radiation effects on buffer/backfill
		S 068	Radiation effects on canister
		S 069	Radioactive Decay, fuel
		W 2.015	Radiological effects on waste
		W 2.016	Radiological effects on containers
		W 2.017	Radiological effects on seals
2.1.13.03.0A	Radiological mutation of microbes	A 1.57	Mutation
		A 3.011	Biological evolution
		A 3.022	Chemical toxicity
		I 012	Biological activity (bacteria & microbes)
		I 130	Gas (from waste containing a gas cylinder)
		W 2.047	Effect of radiation on microbial gas generation
2.1.14.15.0A	In-package criticality (intact configuration)	A 1.26	Criticality
		CA-15	DOE SNF criticality in-situ
		H 1.3.2	Nuclear criticality
		I 081	Criticality event
		J 1.1.01	Criticality
		K 0.4	Nuclear criticality
		MLD-14	DOE SNF criticality in-situ (waste package degradation impact)
		MLD-19	DOE SNF criticality in-situ (waste form degradation impact)
		MLD-2	DOE SNF criticality in-situ (radionuclide inventory impact)

Table F-2. Cross Reference of TSPA-LA FEPs to Source FEPs (Continued)

TSPA-LA FEP Number	TSPA-LA FEP Name	Source FEP No.	Source FEP Name
2.1.14.15.0A	In-package criticality (intact configuration) (continued)	MLD-25	DOE SNF criticality in-situ (cladding degradation impact)
		MLD-9	DOE SNF criticality in-situ (waste heat impact)
		N 3.4.3	Nuclear criticality
		S 017	Criticality
		W 2.014	Nuclear criticality: heat
		W 2.028	Nuclear explosions
		YM18	Criticality - MPC flooded
		YM25	Criticality in-situ, nominal configuration, top breach
		YM26	Criticality - nominal configuration, partially flooded, otherwise intact
		YM27	Criticality - clad and disintegrated pellets, optimally mixed, flooded
2.1.14.16.0A	In-package criticality (degraded configurations)	A 1.26	Criticality
		CA-15	DOE SNF criticality in-situ
		H 1.3.2	Nuclear criticality
		I 081	Criticality event
		ISC-1	Criticality in-situ, WP internal structures degrade faster than waste form, top breach
		ISC-2	Criticality in-situ, WP internal structures degrade at same rate as waste form, top breach
		ISC-3	Criticality in-situ, WP internal structures degrade slower than waste form, top breach
		ISC-4	Criticality in-situ, bottom breach allows flow through WP, fissile material collects at bottom of WP
		ISC-5	Criticality in-situ, bottom breach allows flow through WP, waste form degrades in place
		ISC-6	Criticality in-situ, waste form degrades in place and swells, top breach
		J 1.1.01	Criticality
		K 0.4	Nuclear criticality
		MLD-14	DOE SNF criticality in-situ (waste package degradation impact)
		MLD-19	DOE SNF criticality in-situ (waste form degradation impact)
		MLD-25	DOE SNF criticality in-situ (cladding degradation impact)
		MLD-3	DOE SNF criticality near-field (radionuclide inventory impact)
		MLD-9	DOE SNF criticality in-situ (waste heat impact)
		N 3.4.3	Nuclear criticality
		S 017	Criticality

Table F-2. Cross Reference of TSPA-LA FEPs to Source FEPs (Continued)

TSPA-LA FEP Number	TSPA-LA FEP Name	Source FEP No.	Source FEP Name
2.1.14.16.0A	In-package criticality (degraded configurations) (continued)	W 2.014	Nuclear criticality: heat
		W 2.028	Nuclear explosions
		YM104	Differential solubility of neutron poisons
		YM105	Differential solubility of fissile isotopes
		YM115	Selective leaching of neutron sorbers
		YM116	Selective leaching of fissile materials
		YM120	Waste package internal structures degrade slower than waste form
		YM121	Waste package internal structures degrade faster than waste form
		YM122	Waste package internal structures and the waste form degrade at the same rate
		YM123	Neutron absorber system selectively degrades
		YM124	Neutron sorbers selectively flushed from containers
		YM125	Waste package internal structures collapse
		YM24	Criticality - container partially gone, optimal rod configuration, flooded
		YM27	Criticality - clad and disintegrated pellets, optimally mixed, flooded
2.1.14.17.0A	Near-field criticality	H 1.3.2	Nuclear criticality
		J 1.1.01	Criticality
		K 0.4	Nuclear criticality
		MLD-2	DOE SNF criticality in-situ (radionuclide inventory impact)
		MLD-3	DOE SNF criticality near-field (radionuclide inventory impact)
		N 3.4.3	Nuclear criticality
		NFC-1	Near-field criticality, fissile solution is adsorbed or reduced in invert
		NFC-2	Near-field criticality, fissile material deposited in near-field pond
		NFC-3a	Near-field criticality associated with colloidal deposits
		NFC-4	Near-field criticality, fissile solution flows into drift lowpoint
		NFC-5	Near-field criticality, filtered slurry or colloidal stream collects on invert surface
		S 017	Criticality
		W 2.014	Nuclear criticality: heat
		YM103	Accumulation of clays and sediments in basin (in EBS)
		YM106	Formation of a critical assembly in a pool (in waste and EBS)
		YM107	Pu accumulates in basin pool (in waste and EBS)

Table F-2. Cross Reference of TSPA-LA FEPs to Source FEPs (Continued)

TSPA-LA FEP Number	TSPA-LA FEP Name	Source FEP No.	Source FEP Name
2.1.14.17.0A	Near-field criticality (continued)	YM108	Accumulated 239Pu decays to 235U in basin pool (in waste and EBS)
		YM19	Criticality - container gone, intact rods, flooded
		YM20	Criticality - container and cladding gone, fuel powder, dry
		YM21	Criticality - container gone, intact rods, dry
		YM22	Criticality - container gone, pile of fuel pellets, dry
		YM23	Criticality - container gone, pile of fuel pellets, flooded
		YM28	Criticality - container and cladding gone, fuel powder, flooded
2.1.14.18.0A	In-package criticality resulting from a seismic event (intact configuration)	DE/Crit-1	Out-of-package criticality, fuel/magma mixture
		H 1.3.2	Nuclear criticality
		I 081	Criticality event
		I 100	Seismic events
		J 1.1.01	Criticality
		K 0.4	Nuclear criticality
		N 3.4.3	Nuclear criticality
		S 017	Criticality
		W 2.014	Nuclear criticality: heat
2.1.14.19.0A	In-package criticality resulting from a seismic event (degraded configurations)	DE/Crit-1	Out-of-package criticality, fuel/magma mixture
		H 1.3.2	Nuclear criticality
		I 081	Criticality event
		I 100	Seismic events
		J 1.1.01	Criticality
		K 0.4	Nuclear criticality
		N 3.4.3	Nuclear criticality
		S 017	Criticality
		W 2.014	Nuclear criticality: heat
2.1.14.20.0A	Near-field criticality resulting from a seismic event	DE/Crit-1	Out-of-package criticality, fuel/magma mixture
		H 1.3.2	Nuclear criticality
		J 1.1.01	Criticality
		K 0.4	Nuclear criticality
		N 3.4.3	Nuclear criticality
		S 017	Criticality
		W 2.014	Nuclear criticality: heat
2.1.14.21.0A	In-package criticality resulting from rockfall (intact configuration)	DE/Crit-1	Out-of-package criticality, fuel/magma mixture
		H 1.3.2	Nuclear criticality
		I 081	Criticality event
		J 1.1.01	Criticality

Table F-2. Cross Reference of TSPA-LA FEPs to Source FEPs (Continued)

TSPA-LA FEP Number	TSPA-LA FEP Name	Source FEP No.	Source FEP Name
2.1.14.21.0A	In-package criticality resulting from rockfall (intact configuration) (continued)	K 0.4	Nuclear criticality
		N 3.4.3	Nuclear criticality
		S 017	Criticality
		W 2.014	Nuclear criticality: heat
2.1.14.22.0A	In-package criticality resulting from rockfall (degraded configurations)	DE/Crit-1	Out-of-package criticality, fuel/magma mixture
		H 1.3.2	Nuclear criticality
		I 081	Criticality event
		J 1.1.01	Criticality
		K 0.4	Nuclear criticality
		N 3.4.3	Nuclear criticality
		S 017	Criticality
		W 2.014	Nuclear criticality: heat
2.1.14.23.0A	Near-field criticality resulting from rockfall	DE/Crit-1	Out-of-package criticality, fuel/magma mixture
		H 1.3.2	Nuclear criticality
		J 1.1.01	Criticality
		K 0.4	Nuclear criticality
		N 3.4.3	Nuclear criticality
		S 017	Criticality
		W 2.014	Nuclear criticality: heat
2.1.14.24.0A	In-package criticality resulting from an igneous event (intact configuration)	DE/Crit-1	Out-of-package criticality, fuel/magma mixture
		H 1.3.2	Nuclear criticality
		I 081	Criticality event
		J 1.1.01	Criticality
		K 0.4	Nuclear criticality
		N 3.4.3	Nuclear criticality
		S 017	Criticality
		W 2.014	Nuclear criticality: heat
2.1.14.25.0A	In-package criticality resulting from an igneous event (degraded configurations)	DE/Crit-1	Out-of-package criticality, fuel/magma mixture
		H 1.3.2	Nuclear criticality
		I 081	Criticality event
		J 1.1.01	Criticality
		K 0.4	Nuclear criticality
		N 3.4.3	Nuclear criticality
		S 017	Criticality
		W 2.014	Nuclear criticality: heat
2.1.14.26.0A	Near-field criticality resulting from an igneous event	DE/Crit-1	Out-of-package criticality, fuel/magma mixture
		H 1.3.2	Nuclear criticality
		J 1.1.01	Criticality
		K 0.4	Nuclear criticality
		N 3.4.3	Nuclear criticality
		S 017	Criticality
		W 2.014	Nuclear criticality: heat

Table F-2. Cross Reference of TSPA-LA FEPs to Source FEPs (Continued)

TSPA-LA FEP Number	TSPA-LA FEP Name	Source FEP No.	Source FEP Name
2.2.01.01.0A	Mechanical effects of excavation and construction in the near-field	A 1.34	Formation of cracks
		A 2.01	Blasting and vibration
		A 2.13	Damaged zone
		H 1.5.2	Disturbed zone (hydromechanical) effects
		I 013	Bedrock fracture
		I 022	Explosions/bombs/blasting/collision/impacts/vibration
		J 4.2.02.1	Excavation/backfilling effects on nearby rock
		J 4.2.02.2	Hydraulic conductivity change - Excavation/backfilling effect
		J 4.2.02.3	Mechanical effects - Excavation/backfilling effects
		J 4.2.08	Enhanced rock fracturing
		K 4.01	Excavation-disturbed zone (EDZ)
		N 2.1	DESIGN AND CONSTRUCTION
		N 3.1.4	Induced hydrological changes (fluid pressure, density convection, viscosity)
		S 032	Excavation effects on nearby rock
		W 2.018	Disturbed rock zone
		W 2.019	Excavation-induced changes in stress
2.2.01.01.0B	Chemical effects of excavation and construction in the near-field	A 1.34	Formation of cracks
		K 4.01	Excavation-disturbed zone (EDZ)
		N 2.1	DESIGN AND CONSTRUCTION
		N 3.1.4	Induced hydrological changes (fluid pressure, density convection, viscosity)
2.2.01.02.0A	Thermally-induced stress changes in the near-field	I 013	Bedrock fracture
		J 4.1.04	Sorption
		J 4.2.02.2	Hydraulic conductivity change - Excavation/backfilling effect
		J 5.24	Stress changes of conductivity
		N 3.1.4	Induced hydrological changes (fluid pressure, density convection, viscosity)
		S 030	Enhanced rock fracturing
		S 065	Properties of near-field rock
		W 2.030	Thermally-induced stress changes
2.2.01.02.0B	Chemical changes in the near-field from backfill	H 2.2.2	Rock property changes
		I 011a	Backfill (properties)
		I 011b	Backfill (faulty emplacement)
		J 4.1.04	Sorption
		K 4.07	Water flow at the bentonite-host rock interface
		S 062	Properties of bentonite buffer
2.2.01.03.0A	Changes in fluid saturations in the excavation disturbed zone	A 2.13	Damaged zone
		A 2.15	Dewatering
		H 1.5.1	Desaturation (pumping) effects
		K 4.03	Desaturation/resaturation of EDZ
		K 4.07	Water flow at the bentonite-host rock interface

Table F-2. Cross Reference of TSPA-LA FEPs to Source FEPs (Continued)

TSPA-LA FEP Number	TSPA-LA FEP Name	Source FEP No.	Source FEP Name
2.2.01.04.0A	Radionuclide solubility in the excavation disturbed zone	H 2.3.4	Far-field transport: Solubility constraints
		I 233	Source term & solubility limits
		K 4.10	Elemental solubility
2.2.01.05.0A	Radionuclide transport in the excavation disturbed zone	A 2.13	Damaged zone
		J 4.1.04	Sorption
		K 4.08	Radionuclide migration
		K 4.09	Radionuclide retardation
		K 4.11	Gas transport/dissolution
		K 4.13	Radionuclide release from EDZ
2.2.03.01.0A	Stratigraphy	A 3.097	Soil depth
		H 2.2.2	Rock property changes
		K 7.02	Mesozoic sedimentary cover
		K 7.03	Permo-Carbonferous Trough
		K S1.3	Host Geology
		S 064	Properties of far-field rock
		S 065	Properties of near-field rock
		W 1.001	Stratigraphy
		W 1.002	Brine reservoirs
2.2.03.02.0A	Rock properties of host rock and other units	A 2.54	Rock properties
		H 2.2.2	Rock property changes
		K 5.01	LPD effective hydraulic properties
		K 6.01	MWCF effective hydraulic properties
		K 7.01	HPD effective hydraulic properties
		N 1.2.11	Rock heterogeneity
		S 064	Properties of far-field rock
		S 065	Properties of near-field rock
2.2.06.01.0A	Seismic activity changes porosity and permeability of rock	A 3.045	Earthquakes
		H 2.1.6	Seismicity
		H 2.2.2	Rock property changes
		I 100	Seismic events
		I 277	Soil liquefaction (seismic)
		J 4.2.07	Thermo-hydro-mechanical effects
		J 5.15	Earthquakes
		K 5.14	Regional stress regime
		K 6.14	Regional stress regime
		K 7.10	Stress regime
		K 9.05	Seismic activity
		K 9.06	Stress changes - hydrogeological effects
		N 1.2.8	Seismicity
		S 064	Properties of far-field rock
		S 065	Properties of near-field rock
		S 086	Stress field
		W 1.003	Changes in regional stress
		W 1.012	Seismic activity
		W 2.021	Changes in the stress field
		YM171	Stress-produced porosity changes
		YM172	Stress-produced permeability changes
		YM179	Stress-produced permeability changes

Table F-2. Cross Reference of TSPA-LA FEPs to Source FEPs (Continued)

TSPA-LA FEP Number	TSPA-LA FEP Name	Source FEP No.	Source FEP Name
2.2.06.02.0A	Seismic activity changes porosity and permeability of faults	A 3.045	Earthquakes
		H 2.1.6	Seismicity
		H 2.1.7	Faulting/fracturing
		H 2.2.2	Rock property changes
		I 100	Seismic events
		I 143	Groundwater (redirection of)
		J 5.15	Earthquakes
		K 9.05	Seismic activity
		N 1.2.8	Seismicity
		S 036	Faulting
		S 064	Properties of far-field rock
		S 065	Properties of near-field rock
		W 1.010	Formation of new faults
		W 1.011	Fault movement
		W 1.012	Seismic activity
		YM127a	Relaxation of thermal stresses by fault movement
		YM127b	Relaxation of thermal stresses by fault movement
		YM166	New fault occurs at Yucca Mountain
		YM167	Old fault strand is reactivated at Yucca Mountain
		YM168	New fault strand is activated at Yucca Mountain
		YM170	Seismically-stimulated release of thermo-mechanical stress on bounding faults
		YM171	Stress-produced porosity changes
		YM172	Stress-produced permeability changes
		YM176	Changes in stress (due to thermal, seismic, or tectonic effects) produce change in
		YM179	Stress-produced permeability changes
		YM200	Aseismic alteration of permeability along and across faults
		YSCP13	Fracture dilation along faults creates zones of enhanced permeability
2.2.06.02.0B	Seismic activity changes porosity and permeability of fractures	A 3.045	Earthquakes
		H 2.1.6	Seismicity
		H 2.1.7	Faulting/fracturing
		H 2.2.2	Rock property changes
		I 013	Bedrock fracture
		I 143	Groundwater (redirection of)
		J 5.15	Earthquakes
		K 9.05	Seismic activity
		N 1.2.8	Seismicity
		W 1.008	Formation of fractures
		W 1.009	Changes in fracture properties

Table F-2. Cross Reference of TSPA-LA FEPs to Source FEPs (Continued)

TSPA-LA FEP Number	TSPA-LA FEP Name	Source FEP No.	Source FEP Name
2.2.06.02.0B	Seismic activity changes porosity and permeability of fractures (continued)	W 1.012	Seismic activity
		YM171	Stress-produced porosity changes
		YM172	Stress-produced permeability changes
		YM176	Changes in stress (due to thermal, seismic, or tectonic effects) produce change in
		YM179	Stress-produced permeability changes
		YSCP13	Fracture dilation along faults creates zones of enhanced permeability
2.2.06.03.0A	Seismic activity alters perched water zones	A 3.045	Earthquakes
		H 2.1.6	Seismicity
		I 100	Seismic events
		J 5.15	Earthquakes
		K 9.05	Seismic activity
		N 1.2.8	Seismicity
		W 1.012	Seismic activity
		YM177	Changes in stress (due to seismic or tectonic effects) alter perched water zones
		YM178	Perched zones develop as a result of stress changes
2.2.06.04.0A	Effects of subsidence	H 2.2.2	Rock property changes
		I 013	Bedrock fracture
		I 034	Void formation (cave-ins, cavitation-outside the vault)
		I 143	Groundwater (redirection of)
		I 280	Soil slumping
		I 305	Topography (changes)
		N 2.1.4	Stress field changes, settling, subsidence, or caving
		S 064	Properties of far-field rock
		S 065	Properties of near-field rock
		W 2.023	Subsidence
		W 2.024	Large-scale rock fracturing
		W 3.034	Borehole-induced solution and subsidence
		YSCP99	Effects of subsidence
2.2.06.05.0A	Salt creep	I 261	Salt (road salt, CaCl2, etc.)
		W 2.020	Salt creep
		W 2.022	Roof falls
		W 2.032	Consolidation of waste
2.2.07.01.0A	Locally saturated flow at bedrock/alluvium contact	K 8.20	Groundwater flow (alluvium of Rhine valley)
		W 1.027	Effects of preferential pathways
		YM54	Locally saturated flow at bedrock/alluvium contact

Table F-2. Cross Reference of TSPA-LA FEPs to Source FEPs (Continued)

TSPA-LA FEP Number	TSPA-LA FEP Name	Source FEP No.	Source FEP Name
2.2.07.02.0A	Unsaturated groundwater flow in the geosphere	A 2.69	Unsaturated rock
		A 3.097	Soil depth
		H 2.2.3	Groundwater flow
		H 2.2.3	Groundwater flow
		K 8.20	Groundwater flow (alluvium of Rhine valley)
		S 049	Groundwater flow
		W 1.024	Unsaturated groundwater flow
2.2.07.03.0A	Capillary rise in the UZ	A 3.017	Capillary rise in soil
		A 3.097	Soil depth
		I 032	Capillary rise in soil
		I 317	Unsaturated transport
		K 8.31	Capillary rise
		YM61	Resaturation of dry-out zone is effected by liquid under capillary forces
2.2.07.04.0A	Focusing of unsaturated flow (fingers, weeps)	H 2.1.7	Faulting/fracturing
		W 1.025	Fracture flow
		W 1.027	Effects of preferential pathways
		YM29	Fault control of fluid entrance to and movement away from the repository
		YM53	Focusing of unsaturated flow (fingers, weeps)
		YM56	Seeps and weeps form as a locally saturated flow system
		YM63b	Fingering – contaminant transport in fingers in UZ
2.2.07.05.0A	Flow in the UZ from episodic infiltration	I 317	Unsaturated transport
		YM58	Flow and transport in the UZ from episodic infiltration
2.2.07.06.0A	Episodic or pulse release from repository	I 317	Unsaturated transport
		ID/EBS-1	Episodic / pulse release from repository
		J 1.5	Release of radionuclides from the failured canister
		WF//Coll	Episodic infiltration enhances colloid transport
2.2.07.06.0B	Long-term release of radionuclides from the repository	I 317	Unsaturated transport
		ID/EBS-1	Episodic / pulse release from repository
		J 1.5	Release of radionuclides from the failured canister
2.2.07.07.0A	Perched water develops	I 143	Groundwater (redirection of)
		YM110	Accumulation of solute in topographic lows of the altered TSbv
		YM53	Focusing of unsaturated flow (fingers, weeps)
		YM74	Formation of perched water on the altered Topopah Spring basal vitrophyre
		YSCP5	Perched water develops

Table F-2. Cross Reference of TSPA-LA FEPs to Source FEPs (Continued)

TSPA-LA FEP Number	TSPA-LA FEP Name	Source FEP No.	Source FEP Name
2.2.07.07.0A	Perched water develops (continued)	YSCP52	Climate modification causes perched water to develop above repository
		YSCP53	Climate modification causes perched water to develop at base of Topopah Spring unit
		YSCP6	Perched water develops at base of Topopah Spring welded unit
2.2.07.08.0A	Fracture flow in the UZ	H 2.1.7	Faulting/fracturing
		J 4.2.03	Extreme channel flow of oxidants and nuclides
		W 1.025	Fracture flow
		YM50	Fracture flow in the unsaturated zone
2.2.07.09.0A	Matrix imbibition in the UZ	YM55	Matrix imbibition in the unsaturated zone
		YM68	Resaturation due to matrix imbibition of episodic fracture flow
2.2.07.10.0A	Condensation zone forms around drifts	A 1.89	Vault geometry
		YM52	Condensation zone forms around drifts
		YM57	Shedding of condensation cap over one drift to another drift
		YM69	Return of condensate to same panel
		YM78	Formation of condensate over individual containers
		YM79	Formation of condensate over individual panels
		YM80	Formation of condensate over the entire repository
		YSCP59	Condensation cap forms above repository
2.2.07.11.0A	Resaturation of geosphere dry-out zone	S 078	Resaturation, mear-field rock
		YM42	Auto-catalytic drainage of locally saturated flow thru condensation cap
		YM59	Return flow from condensation cap / resaturation of dry-out zone
		YM60	Resaturation of dry-out zone is affected by vapor flow
		YM61	Resaturation of dry-out zone is effected by liquid under capillary forces
		YM67	Unsaturated flow plume returns flow from the condensation cap
		YM69	Return of condensate to same panel
		YM94	Locally-saturated carrier plume forms (in geosphere)
		YM95	Unsaturated carrier plume forms (in geosphere)
2.2.07.12.0A	Saturated groundwater flow in the geosphere	A 2.67	Turbulence
		H 2.2.3	Groundwater flow
		I 313	Turbulence (groundwater flow)
		J 4.2.05	Changes in Groundwater Flow
		J 5.18	Enhanced groundwater flow

Table F-2. Cross Reference of TSPA-LA FEPs to Source FEPs (Continued)

TSPA-LA FEP Number	TSPA-LA FEP Name	Source FEP No.	Source FEP Name
2.2.07.12.0A	Saturated groundwater flow in the geosphere (continued)	K 5.03	Groundwater flow in LPD
		K 5.04	Groundwater flow path
		K 6.03	Groundwater flow in MWCF
		K 6.04	Groundwater flow path
		K 7.04	Groundwater flow
		K 7.05	Boundary conditions for flow
		K 7.06	Groundwater flow path
		K 7.12	Hydraulic gradient (magnitude, regional direction)
		N 1.5	HYDROLOGICAL
		N 1.5.5	Groundwater flow
		S 049	Groundwater flow
		W 1.023	Saturated groundwater flow
		YSCP51	Climate modification raises water table to short circuit flow barrier in SZ
2.2.07.13.0A	Water-conducting features in the SZ	H 2.1.7	Faulting/fracturing
		H 2.2.3	Groundwater flow
		I 143	Groundwater (redirection of)
		K 5.02	Water-conducting features (types)
		K 6.02	Water-conducting features (types)
		S 049	Groundwater flow
		W 1.025	Fracture flow
2.2.07.14.0A	Chemically-induced density effects on groundwater flow	A 2.57	Salinity effects on flow
		H 2.2.3	Groundwater flow
		I 143	Groundwater (redirection of)
		J 4.2.05	Changes in Groundwater Flow
		K 6.11	Intrusion of saline groundwater
		S 049	Groundwater flow
		W 1.026	Density effects on groundwater flow
		W 1.029	Saline intrusion
2.2.07.15.0A	Advection and dispersion in the SZ	A 1.28	Dispersion
		A 2.11	Convection
		A 2.18	Dispersion
		A 3.042	Dispersion
		H 2.3.1	Far-field transport: Advection
		H 2.3.3	Far-field transport: Hydrodynamic dispersion
		J 6.04	Dispersion
		K 8.20	Groundwater flow (alluvium of Rhine valley)
		N 1.6.1	Advection and dispersion
		S 026	Dispersion
		S 098	Transport and release of nuclides, near-field rock
		W 2.077	Solute transport
		W 2.090	Advection

Table F-2. Cross Reference of TSPA-LA FEPs to Source FEPs (Continued)

TSPA-LA FEP Number	TSPA-LA FEP Name	Source FEP No.	Source FEP Name
2.2.07.15.0B	Advection and dispersion in the UZ	A 2.11	Convection
		A 2.18	Dispersion
		A 2.69	Unsaturated rock
		A 3.042	Dispersion
		H 2.3.1	Far-field transport: Advection
		H 2.3.3	Far-field transport: Hydrodynamic dispersion
		J 4.2.03	Extreme channel flow of oxidants and nuclides
		N 1.6.1	Advection and dispersion
		W 1.054	Groundwater recharge
		YM63b	Fingering - contaminant transport in fingers in UZ
2.2.07.16.0A	Dilution of radionuclides in groundwater	H 2.3.3	Far-field transport: Hydrodynamic dispersion
		I 180	Surface waster bodies (non-uniform mixing of)
		J 6.05	Dilution
		K 5.23	Dilution of radionuclides in groundwater (LPD to HPD or MWCF)
		K 6.23	Dilution of radionuclides in groundwater (MWCF to HPD & Biosph.)
		K 7.07	Dilution of radionuclides in HPD
		K 8.03	Exfiltration to a local aquifer
		K 8.20	Groundwater flow (alluvium of Rhine valley)
		K 8.21	Dilution of radionuclides in surface water (aquifer, river, lake, etc.)
2.2.07.17.0A	Diffusion in the SZ	A 1.27	Diffusion
		A 2.16	Diffusion
		H 2.3.2	Far-field transport: Diffusion
		N 1.6.2	Diffusion
		S 023	Diffusion
		S 098	Transport and release of nuclides, near-field rock
		W 2.077	Solute transport
		W 2.091	Diffusion
2.2.07.18.0A	Film flow into the repository	NRC USFIC-1	Film flow into drifts
2.2.07.19.0A	Lateral flow from Solitario Canyon Fault enters drifts	NRC USFIC-2	Lateral Flow from Solitario Canyon Fault Enters Potential Waste Emplacement Drifts
		W 1.027	Effects of preferential pathways
		YM29	Fault control of fluid entrance to and movement away from the repository
2.2.07.20.0A	Flow diversion around repository drifts	A 1.34	Formation of cracks
		A 1.40	Hydraulic conductivity
		YM98	UZ flow through/around the collapsed invert

Table F-2. Cross Reference of TSPA-LA FEPs to Source FEPs (Continued)

TSPA-LA FEP Number	TSPA-LA FEP Name	Source FEP No.	Source FEP Name
2.2.07.21.0A	Drift shadow forms below repository	H 1.5.1	Desaturation (pumping) effects
		YM43	Repository dry-out due to waste heat
2.2.08.01.0A	Chemical characteristics of groundwater in the SZ	A 2.32	Groundwater composition
		A 2.33	Groundwater - evolution
		A 3.021	Chemical precipitation
		H 2.2.3	Groundwater flow
		H 2.3.6	Far-field transport: Changes in sorptive surfaces
		I 143	Groundwater (redirection of)
		J 4.1.02	pH-deviations
		J 4.1.04	Sorption
		J 4.2.05	Changes in Groundwater Flow
		K 5.07	Mineralogy
		K 5.08	Groundwater chemistry
		K 6.07	Mineralogy
		K 7.08	Groundwater chemistry
		N 1.5.6	Groundwater conditions
		N 1.6.14	Chemical gradients
		N 3.2.4	Non-radioactive solute plume in geosphere
		S 018	Deep saline water intrusion
		S 048	Groundwater chemistry
		S 049	Groundwater flow
		S 052	Interface different waters
		W 1.033	Groundwater geochemistry
		YM81	Radionuclide transport occurs in a carrier plume in geosphere SZ—Radioactive Transport in a Carrier Plume
		YM82	Colloid transport occurs in a carrier plume (in geosphere)
2.2.08.01.0B	Chemical characteristics of groundwater in the UZ	A 1.67	Recharge groundwater
		A 2.29	Geochemical interactions
		A 2.32	Groundwater composition
		A 2.33	Groundwater - evolution
		A 2.53	Recharge groundwater
		A 3.021	Chemical precipitation
		H 1.5.5	Transport of chemically-active substances into the near-field
		H 2.2.3	Groundwater flow
		H 2.3.6	Far-field transport: Changes in sorptive surfaces
		I 143	Groundwater (redirection of)
		I 317	Unsaturated transport
		J 4.1.02	pH-deviations
		J 4.1.04	Sorption
		J 4.2.05	Changes in Groundwater Flow
		K 5.07	Mineralogy

Table F-2. Cross Reference of TSPA-LA FEPs to Source FEPs (Continued)

TSPA-LA FEP Number	TSPA-LA FEP Name	Source FEP No.	Source FEP Name
2.2.08.01.0B	Chemical characteristics of groundwater in the UZ (continued)	K 5.08	Groundwater chemistry
		K 6.07	Mineralogy
		K 7.08	Groundwater chemistry
		N 1.5.6	Groundwater conditions
		N 1.6.14	Chemical gradients
		N 3.2.4	Non-radioactive solute plume in geosphere
		S 049	Groundwater flow
		S 052	Interface different waters
		S 087	Surface water chemistry
		S 103	Water chemistry in near-field rock
		W 1.033	Groundwater geochemistry
		YM81	Radionuclide transport occurs in a carrier plume in geosphere SZ—Radionuclide Transport in a Carrier Plume
2.2.08.03.0A	Geochemical interactions and evolution in the SZ	A 1.77	Speciation
		A 2.29	Geochemical interactions
		A 2.32	Groundwater composition
		A 2.35	Hydraulic properties - evolution
		A 2.49	Precipitation and dissolution
		A 2.64	Speciation
		A 3.021	Chemical precipitation
		H 2.2.2	Rock property changes
		H 2.2.3	Groundwater flow
		H 2.3.6	Far-field transport: Changes in sorptive surfaces
		H 2.3.7	Far-field transport: Changes in groundwater chemistry and flow direction
		I 040	Farfield chemical interactions
		I 042	Chemical speciation (wrong assumption for model)
		I 143	Groundwater (redirection of)
		J 1.2.07	Recrystallization
		J 4.1.01	Oxidizing conditions
		J 4.1.02	pH-deviations
		J 4.1.04	Sorption
		J 4.2.05	Changes in Groundwater Flow
		J 5.01	Saline (or fresh) groundwater intrusion
		J 5.25	Dissolution of fracture fillings/precipitations
		J 6.06	Weathering of flow paths
		K 0.2	Speciation
		K 5.08	Groundwater chemistry
		K 5.11	Intrusion of saline groundwater
		K 6.08	Groundwater chemistry
		K 6.11	Intrusion of saline groundwater

Table F-2. Cross Reference of TSPA-LA FEPs to Source FEPs (Continued)

TSPA-LA FEP Number	TSPA-LA FEP Name	Source FEP No.	Source FEP Name
2.2.08.03.0A	Geochemical interactions and evolution in the SZ (continued)	K 7.08	Groundwater chemistry
		N 1.5.7	Saline or freshwater intrusion
		N 1.5.8	Effects at saline-freshwater interface
		N 1.6.11	Fracture mineralisation and weathering
		N 1.6.8	Dissolution, precipitation and crystallisation
		N 3.1.4	Induced hydrological changes (fluid pressure, density convection, viscosity)
		N 3.2.4	Non-radioactive solute plume in geosphere
		S 001	Alteration/weathering of flow paths
		S 018	Deep saline water intrusion
		S 048	Groundwater chemistry
		S 049	Groundwater flow
		S 060	Precipitation/dissolution
		W 1.029	Saline intrusion
		W 1.033	Groundwater geochemistry
		W 1.034	Saline intrusion
		W 1.035	Freshwater intrusion
		W 1.036	Changes in groundwater Eh
		W 1.037	Changes in groundwater pH
		W 1.038	Effects of dissolution
		W 2.057	Kinetics of speciation
		W 2.060	Kinetics of precipitation and dissolution
		YM81	Radionuclide transport occurs in a carrier plume in geosphere SZ—Radionuclide Transport in a Carrier Plume
		YM82	Colloid transport occurs in a carrier plume (in geosphere)
		YSCP78	Redissolution of precipitates directs more corrosive fluids to containers
2.2.08.03.0B	Geochemical interactions and evolution in the UZ	A 1.77	Speciation
		A 2.29	Geochemical interactions
		A 2.32	Groundwater composition
		A 2.35	Hydraulic properties - evolution
		A 2.49	Precipitation and dissolution
		A 2.64	Speciation
		A 3.021	Chemical precipitation
		H 2.2.2	Rock property changes
		H 2.2.3	Groundwater flow
		H 2.3.6	Far-field transport: Changes in sorptive surfaces
		H 2.3.7	Far-field transport: Changes in groundwater chemistry and flow direction
		I 040	Farfield chemical interactions
		I 042	Chemical speciation (wrong assumption for model)

Table F-2. Cross Reference of TSPA-LA FEPs to Source FEPs (Continued)

TSPA-LA FEP Number	TSPA-LA FEP Name	Source FEP No.	Source FEP Name
2.2.08.03.0B	Geochemical interactions and evolution in the UZ (continued)	I 143	Groundwater (redirection of)
		I 317	Unsaturated transport
		J 1.2.07	Recrystallization
		J 4.1.01	Oxidizing conditions
		J 4.1.02	pH-deviations
		J 4.1.04	Sorption
		J 4.1.08	Change of groundwater chemistry in nearby rock
		J 4.2.05	Changes in Groundwater Flow
		J 5.25	Dissolution of fracture fillings/precipitations
		J 6.06	Weathering of flow paths
		K 0.2	Speciation
		K 5.08	Groundwater chemistry
		K 6.08	Groundwater chemistry
		K 7.08	Groundwater chemistry
		N 1.6.11	Fracture mineralisation and weathering
		N 1.6.8	Dissolution, precipitation and crystallisation
		N 3.2.4	Non-radioactive solute plume in geosphere
		S 001	Alteration/weathering of flow paths
		S 049	Groundwater flow
		S 060	Precipitation/dissolution
		S 103	Water chemistry in near-field rock
		W 1.033	Groundwater geochemistry
		W 1.035	Freshwater intrusion
		W 2.057	Kinetics of speciation
		W 2.060	Kinetics of precipitation and dissolution
		YM81	Radionuclide transport occurs in a carrier plume in geosphere SZ—Radionuclide Transport in a
		YM94	Locally-saturated carrier plume forms (in geosphere)
		YM95	Unsaturated carrier plume forms (in geosphere)
2.2.08.04.0A	Re-dissolution of precipitates directs more corrosive fluids to waste packages	I 071	Corrosive chemicals (in vault)
		S 060	Precipitation/dissolution
		YSCP78	Redissolution of precipitates directs more corrosive fluids to containers
2.2.08.05.0A	Diffusion in the UZ	A 3.021	Chemical precipitation
		H 2.3.2	Far-field transport: Diffusion
		I 317	Unsaturated transport
		J 3.2.06	Diffusion - surface diffusion
		W 1.054	Groundwater recharge
		W 2.098	Osmotic processes
2.2.08.06.0A	Complexation in the SZ	A 2.32	Groundwater composition
		I 044	Chealting agents
		J 2.1.10	Microbes
		J 4.1.09	Complexing agents

Table F-2. Cross Reference of TSPA-LA FEPs to Source FEPs (Continued)

TSPA-LA FEP Number	TSPA-LA FEP Name	Source FEP No.	Source FEP Name
2.2.08.06.0B	Complexation in the UZ	A 2.32	Groundwater composition
		I 044	Chealting agents
		I 317	Unsaturated transport
		J 2.1.10	Microbes
		J 4.1.09	Complexing agents
2.2.08.07.0A	Radionuclide solubility limits in the SZ	A 1.77	Speciation
		A 2.64	Speciation
		H 2.3.4	Far-field transport: Solubility constraints
		I 042	Chemical speciation (wrong assumption for model)
		I 143	Groundwater (redirection of)
		I 233	Source term & solubility limits
		J 1.2.07	Recrystallization
		K 0.2	Speciation
		K 5.05	Radionuclide transport through LPD
		K 5.16	Solubility limits/colloid formation
		K 6.05	Radionuclide transport through MWCF
		K 6.16	Solubility limits/colloid formation
		S 060	Precipitation/dissolution
		W 2.057	Kinetics of speciation
2.2.08.07.0B	Radionuclide solubility limits in the UZ	A 1.77	Speciation
		A 2.64	Speciation
		H 2.3.4	Far-field transport: Solubility constraints
		I 042	Chemical speciation (wrong assumption for model)
		I 143	Groundwater (redirection of)
		I 233	Source term & solubility limits
		I 317	Unsaturated transport
		J 1.2.07	Recrystallization
		K 0.2	Speciation
		K 5.05	Radionuclide transport through LPD
		K 6.05	Radionuclide transport through MWCF
		S 060	Precipitation/dissolution
		W 2.057	Kinetics of speciation
2.2.08.07.0C	Radionuclide solubility limits in the biosphere	H 2.3.4	Far-field transport: Solubility constraints
2.2.08.08.0A	Matrix diffusion in the SZ	A 2.41	Matrix diffusion
		A 3.021	Chemical precipitation
		H 2.3.2	Far-field transport: Diffusion
		J 4.1.04	Sorption
		J 4.1.05	Matrix diffusion
		K 5.06	Matrix diffusion
		K 5.09	Sorption
		K 6.06	Matrix diffusion
		N 1.6.3	Matrix diffusion
		S 054	Matrix diffusion

Table F-2. Cross Reference of TSPA-LA FEPs to Source FEPs (Continued)

TSPA-LA FEP Number	TSPA-LA FEP Name	Source FEP No.	Source FEP Name
2.2.08.08.0A	Matrix diffusion in the SZ (continued)	W 1.025	Fracture flow
		W 2.092	Matrix diffusion
		YM100	Matrix diffusion in geosphere SZ—Matrix Diffusion
		YM101	Matrix diffusion (water transport)
2.2.08.08.0B	Matrix diffusion in the UZ	A 3.021	Chemical precipitation
		H 2.3.2	Far-field transport: Diffusion
		I 317	Unsaturated transport
		J 4.1.04	Sorption
		J 4.1.05	Matrix diffusion
		W 1.025	Fracture flow
		YM100	Matrix diffusion in geosphere SZ—Matrix Diffusion
		YM101	Matrix diffusion (water transport)
2.2.08.09.0A	Sorption in the SZ	A 1.74	Sorption - nonlinear
		A 2.58	Saturation
		A 2.62	Sorption
		A 2.63	Sorption - nonlinear
		A 3.021	Chemical precipitation
		A 3.026	Colloids
		A 3.072	Ion exchange in soil
		A 3.099	Soil porewater pH
		A 3.100	Soil sorption
		H 2.3.5	Far-field transport: Sorption including ion-exchange
		H 2.3.6	Far-field transport: Changes in sorptive surfaces
		H 2.3.7	Far-field transport: Changes in groundwater chemistry and flow direction
		I 174	Ion exchanges in soil
		J 4.1.04	Sorption
		K 5.09	Sorption
		K 5.10	Non-linear sorption
		K 6.09	Sorption
		K 6.10	Non-linear sorption
		K 7.09	Radionuclide sorption
		K 8.17	Radionuclide sorption
		N 1.6.7	Sorption
		S 002	Anion-exclusion
		S 084	Sorption
		W 1.036	Changes in groundwater Eh
		W 1.037	Changes in groundwater pH
		W 1.054	Groundwater recharge
		W 2.061	Actinide sorption
		W 2.062	Kinetics of sorption
		W 2.063	Changes in sorptive surfaces
		YM8	Sorption (reversible and irreversible)
		YM88	Sorption in UZ and SZ

Table F-2. Cross Reference of TSPA-LA FEPs to Source FEPs (Continued)

TSPA-LA FEP Number	TSPA-LA FEP Name	Source FEP No.	Source FEP Name
2.2.08.09.0B	Sorption in the UZ	A 1.74	Sorption - nonlinear
		A 2.62	Sorption
		A 2.63	Sorption - nonlinear
		A 3.021	Chemical precipitation
		A 3.026	Colloids
		H 2.3.5	Far-field transport: Sorption including ion-exchange
		H 2.3.6	Far-field transport: Changes in sorptive surfaces
		I 174	Ion exchanges in soil
		I 317	Unsaturated transport
		J 4.1.04	Sorption
		K 5.10	Non-linear sorption
		K 6.09	Sorption
		K 6.10	Non-linear sorption
		N 1.6.7	Sorption
		S 084	Sorption
		W 2.061	Actinide sorption
		W 2.062	Kinetics of sorption
		W 2.063	Changes in sorptive surfaces
		YM8	Sorption (reversible and irreversible)
		YM88	Sorption in UZ and SZ
2.2.08.10.0A	Colloidal transport in the SZ	A 3.026	Colloids
		H 2.3.8	Far-field transport: Colloid transport
		H 2.3.9	Far-field transport: Transport of radionuclides bound to microbes
		J 4.1.03	Colloids, complexing agents
		J 4.1.04	Sorption
		K 4.12	Colloids
		K 5.16	Solubility limits/colloid formation
		K 6.16	Solubility limits/colloid formation
		N 1.6.9	Colloid formation, dissolution and transport
		S 008	Colloid generation and transport
		S 098	Transport and release of nuclides, near-field rock
		W 1.036	Changes in groundwater Eh
		W 1.037	Changes in groundwater pH
		W 1.038	Effects of dissolution
		W 1.054	Groundwater recharge
2.2.08.10.0B	Colloidal transport in the UZ	A 3.026	Colloids
		H 1.5.5	Transport of chemically-active substances into the near-field
		H 2.3.8	Far-field transport: Colloid transport
		J 4.1.03	Colloids, complexing agents
		J 4.1.04	Sorption
		K 4.12	Colloids

Table F-2. Cross Reference of TSPA-LA FEPs to Source FEPs (Continued)

TSPA-LA FEP Number	TSPA-LA FEP Name	Source FEP No.	Source FEP Name
2.2.08.10.0B	Colloidal transport in the UZ (continued)	N 1.6.9	Colloid formation, dissolution and transport
		S 008	Colloid generation and transport
		WF//Coll	Episodic infiltration enhances colloid transport
		YM82	Colloid transport occurs in a carrier plume (in geosphere)
2.2.08.11.0A	Groundwater discharge to surface within the reference biosphere	A 2.17	Discharge zones
		A 3.017	Capillary rise in soil
		A 3.021	Chemical precipitation
		A 3.026	Colloids
		A 3.103	Surface water bodies
		H 4.2.2	Surface water mixing
		I 074a	Lake exposure scenario
		I 180	Surface waster bodies (non-uniform mixing of)
		I 292	Surface water bodies (physical/chemical changes)
		K 8.03	Exfiltration to a local aquifer
		K 8.04	Exfiltration to surface waters
		K 8.21	Dilution of radionuclides in surface water (aquifer, river, lake, etc.)
		N 1.5.1	River flow and lake level changes
		N 1.6	TRANSPORT AND GEOCHEMICAL
		S 027	Distribution and release of nuclides from the geosphere
2.2.08.12.0A	Chemistry of water flowing into the drift	A 1.67	Recharge groundwater
		I 071	Corrosive chemicals (in vault)
		J 5.01	Saline (or fresh) groundwater intrusion
		K 5.11	Intrusion of saline groundwater
		K 6.11	Intrusion of saline groundwater
		NRC USFIC-1	Film flow into drifts
		S 018	Deep saline water intrusion
		WFMisc AMR-1	Use of J-13 well water as a surrogate for water flowing into the EBS and waste
2.2.08.12.0B	Chemistry of water flowing into the waste package	A 1.67	Recharge groundwater
		I 071	Corrosive chemicals (in vault)
		NRC USFIC-1	Film flow into drifts
		WFMisc AMR-1	Use of J-13 well water as a surrogate for water flowing into the EBS and waste
2.2.09.01.0A	Microbial activity in the SZ	A 1.54	Microbes
		A 2.45	Microbes
		A 2.49	Precipitation and dissolution
		A 3.007	Bacteria and microbes in soil
		A 3.021	Chemical precipitation

Table F-2. Cross Reference of TSPA-LA FEPs to Source FEPs (Continued)

TSPA-LA FEP Number	TSPA-LA FEP Name	Source FEP No.	Source FEP Name
2.2.09.01.0A	Microbial activity in the SZ (continued)	H 2.3.13	Far-field transport: Biogeochemical changes
		H 2.3.9	Far-field transport: Transport of radionuclides bound to microbes
		J 2.1.10	Microbes
		J 4.1.04	Sorption
		K 5.22	Microbial activity
		K 6.22	Microbial activity
		N 1.7.6	Chemical transformations
2.2.09.01.0B	Microbial activity in the UZ	A 1.54	Microbes
		A 2.45	Microbes
		A 2.49	Precipitation and dissolution
		A 3.007	Bacteria and microbes in soil
		A 3.021	Chemical precipitation
		H 2.3.13	Far-field transport: Biogeochemical changes
		H 2.3.9	Far-field transport: Transport of radionuclides bound to microbes
		J 2.1.10	Microbes
		J 4.1.04	Sorption
		K 5.22	Microbial activity
		K 6.22	Microbial activity
		N 1.7.6	Chemical transformations
2.2.10.01.0A	Repository-induced thermal effects on flow in the UZ	A 2.33	Groundwater - evolution
		A 3.021	Chemical precipitation
		H 1.6.1	Thermal effects: Rock-mass changes
		H 1.6.2	Thermal effects: Hydrogeological changes
		H 2.2.3	Groundwater flow
		I 143	Groundwater (redirection of)
		I 300	Termperature effects (on transport)
		J 4.2.05	Changes in Groundwater Flow
		N 2.1.10	Thermal effects
		S 049	Groundwater flow
		S 092	Temperature, near-field rock
		W 2.029	Thermal effects on material properties
		YSCP61	Nonuniform heat distribution / edge effects in repository
2.2.10.02.0A	Thermal convection cell develops in SZ	A 2.28	Geothermal gradient effects
		S 092	Temperature, near-field rock
		YSCP62	Thermal convection cell develops in SZ
2.2.10.03.0A	Natural geothermal effects on flow in the SZ	A 2.28	Geothermal gradient effects
		H 2.2.3	Groundwater flow
		I 143	Groundwater (redirection of)
		J 4.2.04	Thermal buoyancy
		J 4.2.05	Changes in Groundwater Flow
		J 6.13	Geothermally induced flow .

Table F-2. Cross Reference of TSPA-LA FEPs to Source FEPs (Continued)

TSPA-LA FEP Number	TSPA-LA FEP Name	Source FEP No.	Source FEP Name
2.2.10.03.0A	Natural geothermal effects on flow in the SZ (continued)	K 5.12	Density-driven groundwater flow (thermal)
		K 5.13	Geothermal regime
		K 6.12	Density-driven groundwater flows (thermal)
		K 6.13	Geothermal regime
		K 7.13	Density-driven groundwater flows (temperature/salinity differences)
		N 1.5.9	Natural thermal effects
		S 049	Groundwater flow
		S 091	Temperature, far-field
		S 092	Temperature, near-field rock
		W 1.028	Thermal effects on groundwater flow
2.2.10.03.0B	Natural geothermal effects on flow in the UZ	A 2.28	Geothermal gradient effects
		H 2.2.3	Groundwater flow
		I 143	Groundwater (redirection of)
		J 4.2.05	Changes in Groundwater Flow
		J 6.13	Geothermally induced flow .
		N 1.5.9	Natural thermal effects
		S 049	Groundwater flow
		S 092	Temperature, neaer-field rock
2.2.10.04.0A	Thermo-mechanical stresses alter characteristics of fractures near repository	I 013	Bedrock fracture
		N 2.1.4	Stress field changes, settling, subsidence or caving
		N 3.1.3	Host rock fracture aperture changes
		N 3.1.4	Induced hydrological changes (fluid pressure, density convection, viscosity)
		S 064	Properties of far-field rock
		S 065	Properties of near-field rock
		S 092	Temperature, near-field rock
		W 1.008	Formation of fractures
		W 1.009	Changes in fracture properties
		W 2.030	Thermally-induced stress changes
		YM10	Thermo-mechanical alteration of fractures near repository
		YM176	Changes in stress (due to thermal, seismic, or tectonic effects) produce change in permeability of faults
		YSCP54	Thermal expansion closes most fractures close to repository
		YSCP57	Thermal expansion of rocks below repository opens fractures in Paint Brush unwelded
		YSCP58	Thermally-induced fracturing around containers creates a capillary barrier

Table F-2. Cross Reference of TSPA-LA FEPs to Source FEPs (Continued)

TSPA-LA FEP Number	TSPA-LA FEP Name	Source FEP No.	Source FEP Name
2.2.10.04.0B	Thermo-mechanical stresses alter characteristics of faults near repository	I 013	Bedrock fracture
		N 2.1.4	Stress field changes, settling, subsidence or caving
		N 3.1.4	Induced hydrological changes (fluid pressure, density convection, viscosity)
		S 036	Faulting
		S 064	Properties of far-field rock
		S 065	Properties of near-field rock
		S 092	Temperature, near-field rock
		W 2.030	Thermally-induced stress changes
		YM176	Changes in stress (due to thermal, seismic, or tectonic effects) produce changes in permeability of faults
2.2.10.05.0A	Thermo-mechanical stresses alter characteristics of rocks above and below the repository	A 3.021	Chemical precipitation
		H 2.2.2	Rock property changes
		I 013	Bedrock fracture
		J 4.2.07	Thermo-hydro-mechanical effects
		S 064	Properties of far-field rock
		S 065	Properties of near-field rock
		S 092	Temperature, near-field rock
		W 2.030	Thermally-induced stress changes
		YM126	Thermo-mechanical alteration of rocks above and below the repository
		YM129	Thermo-mechanical alteration of surface infiltration
		YSCP57	Thermal expansion of rocks below repository opens fractures in Paint Brush unwelded
2.2.10.06.0A	Thermo-chemical alteration in the UZ (solubility, speciation, phase changes, precipitation/dissolution)	A 3.021	Chemical precipitation
		H 2.3.12	Far-field transport: Thermal effects on hydrochemistry
		H 2.3.4	Far-field transport: Solubility constraints
		I 143	Groundwater (redirection of)
		I 233	Source term & solubility limits
		I 317	Unsaturated transport
		J 4.1.07	Thermochemical change
		N 3.1.3	Host rock fracture aperture changes
		S 001	Alteration/weathering of flow paths
		S 060	Precipitation/dissolution
		S 092	Temperature, near-field rock
		YM62	Alteration of rock properties because of 2-phase flow
		YM66	Silica phase changes (accompanied by volume change) occur due to elevated temperature
		YSCP75	Alteration of minerals to clays (in geosphere)

Table F-2. Cross Reference of TSPA-LA FEPs to Source FEPs (Continued)

TSPA-LA FEP Number	TSPA-LA FEP Name	Source FEP No.	Source FEP Name
2.2.10.06.0A	Thermo-chemical alteration in the UZ (solubility, speciation, phase changes, precipitation/dissolution) (continued)	YSCP77	Precipitates from dissolved constituents of tuff and repository materials form by evaporation
		YSCP80	Heat-induced chemical reactions plug small fractures; flow is preferentially redirect to large fractures
		YSCP81	Calcite precipitation in hot region produces fluids depleted in calcite which dissolve calcite below the repository
2.2.10.07.0A	Thermo-chemical alteration of the Calico Hills unit	A 3.021	Chemical precipitation
		YM77	Thermo-chemical alteration of the Calico Hills unit SZ—Repository Induced Thermal Effects
2.2.10.08.0A	Thermo-chemical alteration in the SZ (solubility, speciation, phase changes, precipitation/dissolution)	A 3.021	Chemical precipitation
		H 2.3.12	Far-field transport: Thermal effects on hydrochemistry
		H 2.3.4	Far-field transport: Solubility constraints
		I 143	Groundwater (redirection of)
		I 233	Source term & solubility limits
		S 001	Alteration/weathering of flow paths
		S 060	Precipitation/dissolution
		S 092	Temperature, near-field rock
		YM51	Thermo chemical alteration of the saturated zone SZ—Repository Induced Thermal Effects
		YSCP17	Precipitation of zeolites in the saturated zone plug pores
2.2.10.09.0A	Thermo-chemical alteration of the Topopah Spring basal vitrophyre	A 3.021	Chemical precipitation
		I 143	Groundwater (redirection of)
		S 001	Alteration/weathering of flow paths
		YM109	Sorption of actinides on altered Topopah Spring basal vitrophyre
		YM203	Alteration of the Topopah Spring basal vitrophyre
		YM73	Thermo-chemical alteration of the Topopah Spring basal vitrophyre
		YM74	Formation of perched water on the altered Topopah Spring basal vitrophyre
		YM75	Sorption of contaminants by the altered Topopah Spring basal vitrophyre
		YM76	Redirection of transport paths by the altered Topopah Spring basal vitrophyre
2.2.10.10.0A	Two-phase buoyant flow/heat pipes	H 1.6.2	Thermal effects: Hydrogeological changes
		H 2.3.11	Far-field transport: Gas induced groundwater transport
		YM40	Two-phase buoyant flow / heat pipes

Table F-2. Cross Reference of TSPA-LA FEPs to Source FEPs (Continued)

TSPA-LA FEP Number	TSPA-LA FEP Name	Source FEP No.	Source FEP Name
2.2.10.10.0A	Two-phase buoyant flow/heat pipes (continued)	YM60	Resaturation of dry-out zone is affected by vapor flow
		YM62	Alteration of rock properties because of 2-phase flow
		YM64a	Heat pipe formation, 2-phase system
		YM91	Heat pipe -evolving
		YM92	Heat pipe -continuing
2.2.10.11.0A	Natural air flow in the UZ	YM41	Natural air flow in unsaturated zone
2.2.10.12.0A	Geosphere dry-out due to waste heat	I 300	Termperature effects (on transport)
		YM93	Geosphere dry-out due to waste heat
2.2.10.13.0A	Repository-induced thermal effects on flow in the SZ	H 1.6.2	Thermal effects: Hydrogeological changes
		I 143	Groundwater (redirection of)
		I 300	Termperature effects (on transport)
		J 4.2.04	Thermal buoyancy
		J 4.2.05	Changes in Groundwater Flow
		J 6.13	Geothermally induced flow .
		K 5.12	Density-driven groundwater flow (thermal)
		S 091	Temperature, far-field
		W 2.029	Thermal effects on material properties
2.2.10.14.0A	Mineralogic dehydration reactions	N 3.1.4	Induced hydrological changes (fluid pressure, density convection, viscosity)
		NRC NFE-1	Mineralogic dehydration reactions
2.2.11.01.0A	Gas effects in the SZ	A 2.44	Methane
		A 3.007	Bacteria and microbes in soil
		H 2.1.9	Effects of natural gases.
		H 2.3.11	Far-field transport: Gas induced groundwater transport
		I 015	Gas generation (CH4, CO2, H2)
		J 5.43	Methane intrusion
		K 5.24	Geogas
		K 6.24	Geogas
		N 1.2.13	Natural gas intrusion
		S 042	Gas flow and transport, near-field rock/far-field
		S 043	Gas generation and gas sources, far-field
		W 1.032	Natural gas intrusion
		W 2.025	Disruption due to gas effects
2.2.11.02.0A	Gas effects in the UZ	A 2.27	Gases and gas transport
		A 3.007	Bacteria and microbes in soil
		H 2.1.9	Effects of natural gases.
		I 015	Gas generation (CH4, CO2, H2)
		I 317	Unsaturated transport
		K 5.17	Gas pressure effects
		K 6.17	Gas pressure effects
		N 1.2.13	Natural gas intrusion

Table F-2. Cross Reference of TSPA-LA FEPs to Source FEPs (Continued)

TSPA-LA FEP Number	TSPA-LA FEP Name	Source FEP No.	Source FEP Name
2.2.11.02.0A	Gas effects in the UZ (continued)	N 1.6.4	Gas mediated transport
		N 1.6.5	Multiphase flow and gas driven flow
		S 042	Gas flow and transport, near-field rock/far-field
		S 043	Gas generation and gas sources, far-field
		S 046	Gas generation, near-field rock
		W 1.032	Natural gas intrusion
		W 2.025	Disruption due to gas effects
		W 2.042	Fluid flow due to gas production
2.2.11.03.0A	Gas transport in geosphere	A 2.27	Gases and gas transport
		H 2.3.10	Far-field transport: Transport of radioactive gases
		H 2.3.11	Far-field transport: Gas induced groundwater transport
		H 4.1.3	Gas discharge
		K 4.11	Gas transport/dissolution
		N 1.6.4	Gas mediated transport
		S 042	Gas flow and transport, near-field rock/far-field
		S 098	Transport and release of nuclides, near-field rock
		W 2.089	Transport of radioactive gases
2.2.12.00.0A	Undetected features in the UZ	A 2.55	Rock properties - undetected features
		H 2.1.7	Faulting/fracturing
		J 6.01	Undetected fracture zones
		J 6.12	Undetected discontinuities
		N 1.2.12	Undetected features
		N 2.1.1	Undetected past intrusions
		S 064	Properties of far-field rock
		S 065	Properties of near-field rock
		YSCP19	Perched water escapes detection and waste is put in it
		YSCP20	Undetected fault dips below the repository providing a highly permeable flow path
		YSCP21	Undetected fault beneath the repository acts as a flow barrier altering the flow system
		YSCP22	Undetected fault connects tuff aquifers to carbonate aquifers; providing a fast path
		YSCP23	Undetected dike beneath the repository passing thru the Calico Hills provides a highly permeable flow path
		YSCP39	Undiscovered mine shaft (an old prospect hole) in a wash acts as a source for increased local infiltration

Table F-2. Cross Reference of TSPA-LA FEPs to Source FEPs (Continued)

TSPA-LA FEP Number	TSPA-LA FEP Name	Source FEP No.	Source FEP Name
2.2.12.00.0B	Undetected features in the SZ	H 2.1.7	Faulting/fracturing
		S 064	Properties of far-field rock
		S 065	Properties of near-field rock
		YSCP19	Perched water escapes detection and waste is put in it
		YSCP20	Undetected fault dips below the repository providing a highly permeable flow path
		YSCP21	Undetected fault beneath the repository acts as a flow barrier altering the flow system
		YSCP22	Undetected fault connects tuff aquifers to carbonate aquifers; providing a fast path
		YSCP23	Undetected dike beneath the repository passing thru the Calico Hills provides a highly permeable flow path
		YSCP39	Undiscovered mine shaft (an old prospect hole) in a wash acts as a source for increased local infiltration
2.2.14.09.0A	Far-field criticality	FFC-1	Far-field criticality, precipitation in organic reducing zone in or near water table
		FFC-2	Far-field criticality, sorption on clay/zeolite in TSbv
		FFC-3	Far-field criticality, precipitation caused by hydrothermal upwell or redox front in the SZ
		FFC-4	Far-field criticality, precipitation in perched water above TSbv
		FFC-5	Far-field criticality, precipitation in fractures of TSw rock
		FFC-6	Far-field criticality, dryout produces fissile salt in a perched water basin
		H 1.3.2	Nuclear criticality
		J 1.1.01	Criticality
		J 4.1.06	Reconcentration
		K 0.4	Nuclear criticality
		MLD-10	DOE SNF criticality far-field (waste heat impact)
		MLD-4	DOE SNF criticality far-field (radionuclide inventory impact)
		N 3.4.3	Nuclear criticality
		NFC-3b	Far-field criticality associated with colloidal deposits
		S 017	Criticality
		S 073	Reconcentration
		W 2.014	Nuclear criticality: heat
		YM110	Accumulation of solute in topographic lows of the altered TSbv

Table F-2. Cross Reference of TSPA-LA FEPs to Source FEPs (Continued)

TSPA-LA FEP Number	TSPA-LA FEP Name	Source FEP No.	Source FEP Name
2.2.14.09.0A	Far-field criticality (continued)	YM111	Precipitation of U in the upwelling zone along some faults
		YM112	Precipitation of U below the redox front in the SZ
		YM113	Precipitation of U at reducing zone associated w/organics in alluvial aquifer
		YM114	Precipitation of U at reducing zone associated w/organics in Franklin Lake playa
		YM14	Critical assembly forms away from repository
2.2.14.10.0A	Far-field criticality resulting from a seismic event	DE/Crit-1	Out-of-package criticality, fuel/magma mixture
		H 1.3.2	Nuclear criticality
		J 1.1.01	Criticality
		K 0.4	Nuclear criticality
		N 3.4.3	Nuclear criticality
		S 017	Criticality
		W 2.014	Nuclear criticality: heat
2.2.14.11.0A	Far-field criticality resulting from rockfall	DE/Crit-1	Out-of-package criticality, fuel/magma mixture
		H 1.3.2	Nuclear criticality
		J 1.1.01	Criticality
		K 0.4	Nuclear criticality
		N 3.4.3	Nuclear criticality
		S 017	Criticality
		W 2.014	Nuclear criticality: heat
2.2.14.12.0A	Far-field criticality resulting from an igneous event	DE/Crit-1	Out-of-package criticality, fuel/magma mixture
		H 1.3.2	Nuclear criticality
		J 1.1.01	Criticality
		K 0.4	Nuclear criticality
		N 3.4.3	Nuclear criticality
		S 017	Criticality
		W 2.014	Nuclear criticality: heat
2.3.01.00.0A	Topography and morphology	A 2.65	Topography (current)
		A 2.66	Topography (future)
		A 2.72	Volcanism
		A 3.108	Terrestrial surface
		H 2.2.1	Changes in geometry and driving forces of the flow system
		I 102	Ecological successions
		I 143	Groundwater (redirection of)
		I 280	Soil slumping
		I 305	Topography (changes)
		K S1.3	Host Geology
		K S1.4	Local and Regional Surface Environment

Table F-2. Cross Reference of TSPA-LA FEPs to Source FEPs (Continued)

TSPA-LA FEP Number	TSPA-LA FEP Name	Source FEP No.	Source FEP Name
2.3.01.00.0A	Topography and morphology (continued)	N 1.4	GEOMORPHOLOGICAL
		S 033	External flow boundary conditions
		W 1.039	Physiography
2.3.02.01.0A	Soil type	A 3.002	Alkali flats
		A 3.007	Bacteria and microbes in soil
		A 3.021	Chemical precipitation
		A 3.101	Soil type
		I 280	Soil slumping
		K 8.24	Soil formation
		K 8.25	Soil
		K S1.3	Host Geology
		K S1.4	Local and Regional Surface Environment
		N 1.7.5	Pedogenesis
		W 1.050	Soil development
2.3.02.02.0A	Radionuclide accumulation in soils	A 3.002	Alkali flats
		A 3.018	Carcasses
		A 3.039	Deposition (wet and dry)
		A 3.073	Irrigation
		A 3.096	Soil
		A 3.097	Soil depth
		A 3.098	Soil leaching
		H 4.1.1	Groundwater discharge to soils and surface waters
		H 4.1.2	Solid discharge via erosional processes
		H 4.2.1	Soil moisture and evaporation.
		I 002	Alkali Flats
		I 175	Irrigation (dose pathway)
		J 7.01	Accumulation in sediments
		J 7.02	Accumulation in peat
		K 8.05	Radionuclide accumulation in sediments
		K 8.06	Radionuclide accumulation in soils
		K 8.33	Irrigation
		N 1.6.12	Accumulation in soils and organic debris
		NRC IA-2	Soil leaching to groundwater
		W 2.103	Accumulation in soil
		YM16	Radionuclide accumulation in sediments at Franklin Lake Playa (water transport)
2.3.02.03.0A	Soil and sediment transport in the biosphere	A 3.014	Bioturbation of soil and sediment
		A 3.016	Burrowing animals
		A 3.021	Chemical precipitation
		A 3.027	Convection, turbulence, and diffusion (atmospheric)
		A 3.039	Deposition (wet and dry)
		A 3.046	Erosion - lateral transport
		A 3.047	Erosion (wind)
		A 3.052	Flooding

Table F-2. Cross Reference of TSPA-LA FEPs to Source FEPs (Continued)

TSPA-LA FEP Number	TSPA-LA FEP Name	Source FEP No.	Source FEP Name
2.3.02.03.0A	Soil and sediment transport in the biosphere (continued)	A 3.086	Rivercourse meander
		A 3.087	Runoff
		A 3.091	Sediment resuspension in water bodies
		H 4.2.3	Sediment transport including bioturbation
		H 4.2.4	Sediment/water/gas interaction with the atmosphere.
		I 021	Bioturbation (soil & sediment)
		I 069	Atmospheric pathways (dispersion)
		K 8.05	Radionuclide accumulation in sediments
		K 8.26	Surface water bodies
		K 8.28	Interface effects
		K 8.34	Surface run-off
		K 8.35	Bioturbation
		N 1.4.5	Freshwater sediment transport and deposition
		N 1.7.4	Soil and sediment bioturbation
		W 1.046	Aeolian deposition
2.3.04.01.0A	Surface water transport and mixing	A 3.053	Flushing of water bodies
		A 3.075	Lake mixing (artificial)
		A 3.086	Rivercourse meander
		A 3.091	Sediment resuspension in water bodies
		A 3.092	Sedimentation in water bodies
		A 3.103	Surface water bodies
		H 4.2.2	Surface water mixing
		H 4.2.4	Sediment/water/gas interaction with the atmosphere.
		I 009	Sediments (in water bodies)
		I 116	Flushing of water bodies
		I 180	Surface waster bodies (non-uniform mixing of)
		I 235	Precipitation (wet deposition)
		I 258	Surface runoff
		I 292	Surface water bodies (physical/chemical changes)
		J 6.09	River meandering
		K 8.04	Exfiltration to surface waters
		K 8.05	Radionuclide accumulation in sediments
		K 8.19	Surface water flow (river Rhine)
		K 8.21	Dilution of radionuclides in surface water (aquifer, river, lake, etc.)
		K 8.23	Sedimentation
		K 8.26	Surface water bodies
		K 8.28	Interface effects
		N 1.4.4	River meander
		N 1.4.5	Freshwater sediment transport and deposition

Table F-2. Cross Reference of TSPA-LA FEPs to Source FEPs (Continued)

TSPA-LA FEP Number	TSPA-LA FEP Name	Source FEP No.	Source FEP Name
2.3.04.01.0A	Surface water transport and mixing (continued)	N 1.5.1	River flow and lake level changes
		W 1.051	Stream and river flow
		W 1.052	Surface water bodies
		W 1.057	Lake formation
2.3.06.00.0A	Marine features	A 2.59	Sea level change
		A 3.039	Deposition (wet and dry)
		A 3.091	Sediment resuspension in water bodies
		A 3.092	Sedimentation in water bodies
		H 4.3.3	Land and surface water use: Coastal waters
		H 4.3.4	Land and surface water use: Seas
		I 009	Sediments (in water bodies)
		I 178	Surface water bodies (flooding of Lake 233)
		I 266	Sea level (rising)
		I 292	Surface water bodies (physical/chemical changes)
		J 5.31	Change in sealevel
		K 8.23	Sedimentation
		N 1.3.3	Coastal surge, storms and hurricanes
		N 1.3.4	Sea-level rise/fall
		N 1.4.6	Coastal erosion and estuarine development
		N 1.4.7	Marine sediment transport and deposition
		S 081	Sea level changes
		W 1.064	Seas and oceans
		W 1.065	Estuaries
		W 1.066	Coastal erosion
		W 1.067	Marine sediment transport and deposition
		W 1.068	Sea level changes
2.3.09.01.0A	Animal burrowing/intrusion	A 1.48	Intrusion (animal)
		A 3.003	Animal diets
		A 3.004	Animal grooming and fighting
		A 3.005	Animal soil ingestion
		A 3.016	Burrowing animals
		H 4.2.4	Sediment/water/gas interaction with the atmosphere.
		I 021	Bioturbation (soil & sediment)
		K 8.28	Interface effects
2.3.11.01.0A	Precipitation	A 2.25	Flood
		A 3.023	Climate
		A 3.024	Climate change
		A 3.087	Runoff
		I 057	Weather (hurricanes and tornadoes)
		I 235	Precipitation (wet deposition)

Table F-2. Cross Reference of TSPA-LA FEPs to Source FEPs (Continued)

TSPA-LA FEP Number	TSPA-LA FEP Name	Source FEP No.	Source FEP Name
2.3.11.01.0A	Precipitation (continued)	I 258	Surface runoff
		K 10.01	Present-day climatic conditions
		K 8.29	Precipitation
		N 1.3.1	Precipitation, temperature and soil water balance
		N 1.3.2	Extremes of precipitation, snow melt and associated flooding
		W 1.059	Precipitation (for example, rainfall)
2.3.11.02.0A	Surface runoff and evapotranspiration	A 3.046	Erosion - lateral transport
		A 3.052	Flooding
		A 3.087	Runoff
		I 115	Flooding (localized, short-term surface flooding)
		I 258	Surface runoff
		K 8.19	Surface water flow (river Rhine)
		K 8.26	Surface water bodies
		K 8.30	Evapotranspiration
		K 8.34	Surface run-off
		N 1.5.2	Site flooding
		W 1.052	Surface water bodies
		W 1.057	Lake formation
		W 1.058	River flooding
		YM201	Equilibrated flow system
		YM64b	Flow in ephemeral streams tends to be in channels and is a source of recharge
		YM65	Runoff is intercepted by wash terraces
		YSCP85	Flooding occurs in Drill Hole Wash and increases percolation below the wash
		YSCP86	Faulting at the surface produces a scarp causing an impoundment
		YSCP9	Runoff to washes infiltrates and maintains a zone of higher flux to the UZ
2.3.11.03.0A	Infiltration and recharge	A 1.67	Recharge groundwater
		A 2.53	Recharge groundwater
		A 3.023	Climate
		A 3.024	Climate change
		H 2.2.3	Groundwater flow
		H 4.2.2	Surface water mixing
		I 235	Precipitation (wet deposition)
		I 258	Surface runoff
		I 261	Salt (road salt, CaCl2, etc.)
		I 337	Water contacting waste in vault
		J 5.46	Groundwater recharge/discharge
		K 10.02	Effective moisture (recharge)
		K 8.20	Groundwater flow (alluvium of Rhine valley)
		K 8.26	Surface water bodies
		K 8.32	Percolation

Table F-2. Cross Reference of TSPA-LA FEPs to Source FEPs (Continued)

TSPA-LA FEP Number	TSPA-LA FEP Name	Source FEP No.	Source FEP Name
2.3.11.03.0A	Infiltration and recharge (continued)	N 1.5.3	Recharge to groundwater
		S 049	Groundwater flow
		S 087	Surface water chemistry
		SZ/Coupl-1	Coupling of surface water flow to climate/hydrologic modeling system
		W 1.030	Freshwater intrusion
		W 1.054	Groundwater recharge
		W 1.055	Infiltration
		W 1.056	Changes in groundwater recharge and discharge
		YM201	Equilibrated flow system
		YM202	Draining flow system
		YM64b	Flow in ephemeral streams tends to be in channels and is a source of recharge
		YM65	Runoff is intercepted by wash terraces
		YSCP9	Runoff to washes infiltrates and maintains a zone of higher flux to the UZ
2.3.11.04.0A	Groundwater discharge to surface outside the reference biosphere	A 2.17	Discharge zones
		A 3.017	Capillary rise in soil
		A 3.021	Chemical precipitation
		A 3.026	Colloids
		A 3.103	Surface water bodies
		H 4.1.1	Groundwater discharge to soils and surface waters
		H 4.2.2	Surface water mixing
		I 180	Surface waster bodies (non-uniform mixing of)
		I 235	Precipitation (wet deposition)
		I 292	Surface water bodies (physical/chemical changes)
		I 317	Unsaturated transport
		K 8.03	Exfiltration to a local aquifer
		K 8.04	Exfiltration to surface waters
		N 1.5.1	River flow and lake level changes
		N 1.5.4	Groundwater discharge
		W 1.053	Groundwater discharge
		YSCP4	Water table rise
2.3.13.01.0A	Biosphere characteristics	A 3.007	Bacteria and microbes in soil
		A 3.023	Climate
		A 3.049	Fires (forest and grass)
		A 3.074	Lake infilling
		A 3.117	Wetlands
		H 4.3.1	Land and surface water use: Terrestrial
		H 4.3.2	Land and surface water use: Estuarine
		H 4.3.3	Land and surface water use: Coastal waters
		H 4.3.4	Land and surface water use: Seas
		I 049	Climate change

Table F-2. Cross Reference of TSPA-LA FEPs to Source FEPs (Continued)

TSPA-LA FEP Number	TSPA-LA FEP Name	Source FEP No.	Source FEP Name
2.3.13.01.0A	Biosphere characteristics (continued)	I 351	Biosphere model (biosphere model validity)
		K 8.01	Present-day biosphere
		K 8.02	Future biosphere conditions
		K S2.5	No Consideration of Future Human Society and Technology
		N 1.7	ECOLOGICAL
		N 1.7.8	Ecological change
		N 1.7.9	Ecological response to climate (e.g. desert formation)
		W 1.060	Temperature
		W 1.069	Plants
		W 1.070	Animals
		W 1.071	Microbes
		W 1.072	Natural ecological development
2.3.13.02.0A	Radionuclide alteration during biosphere transport	A 3.042	Dispersion
		H 4.2.4	Sediment/water/gas interaction with the atmosphere.
		H 4.2.6	Biogeochemical processes
		I 317	Unsaturated transport
		K 8.28	Interface effects
2.3.13.03.0A	Effects of repository heat on the biosphere	A 3.113	Vault heating effects
		K S2.6.1	Consideration of radiological impacts to man (only)
		W 2.030	Thermally-induced stress changes
2.3.13.04.0A	Radionuclide release outside the reference biosphere	A 2.73	Wells
		A 2.74	Wells (high-demand)
		A 3.021	Chemical precipitation
		A 3.049	Fires (forest and grass)
		A 3.103	Surface water bodies
		A 3.117	Wetlands
		H 4.3.1	Land and surface water use: Terrestrial
		H 4.3.2	Land and surface water use: Estuarine
		H 4.3.3	Land and surface water use: Coastal waters
		I 235	Precipitation (wet deposition)
		I 292	Surface water bodies (physical/chemical changes)
		I 317	Unsaturated transport
		YM16	Radionuclide accumulation in sediments at Franklin Lake Playa (water transport)
2.4.01.00.0A	Human characteristics (physiology, metabolism)	A 3.011	Biological evolution
		A 3.033	Critical group – individuality
		K S2.5	No Consideration of Future Human Society and Technology
2.4.04.01.0A	Human lifestyle	A 3.034	Critical group - leisure pursuits
		A 3.063	Household dust and fumes
		A 3.077	Outdoor spraying of water

Table F-2. Cross Reference of TSPA-LA FEPs to Source FEPs (Continued)

TSPA-LA FEP Number	TSPA-LA FEP Name	Source FEP No.	Source FEP Name
2.4.04.01.0A	Human lifestyle	I 074c	Swamp exposure scenario
		I 074e	Artificial lake exposure scenario
		I 113	Food chain (dose pathway)
		I 272	Showers and humidifiers (atmospheric dose pathway)
		K 8.14	Human lifestyle
		K 8.41	Hunter/gathering lifestyle
		K S2.5	No Consideration of Future Human Society and Technology
2.4.07.00.0A	Dwellings	A 3.015	Building materials
		A 3.032	Critical group - house location
		A 3.056	Gas leakage into basements
		A 3.063	Household dust and fumes
		A 3.064	Houseplants
		A 3.077	Outdoor spraying of water
		A 3.094	Showers and humidifiers
		A 3.102	Space heating
		A 3.114	Water leaking into basements
		I 128	Gas leakage into basements
		I 150	Household plants (dose pathway)
		I 272	Showers and humidifiers (atmospheric dose pathway)
		J 5.28	Underground dwellings
		NRC IA-3	Evaporative coolers
2.4.08.00.0A	Wild and natural land and water use	A 3.023	Climate
		H 4.3.1	Land and surface water use: Terrestrial
		H 4.3.2	Land and surface water use: Estuarine
		H 4.3.3	Land and surface water use: Coastal waters
		H 4.3.4	Land and surface water use: Seas
		I 074a	Lake exposure scenario
		I 113	Food chain (dose pathway)
		K 8.40	Natural and semi-natural environments
		N 1.5.1	River flow and lake level changes
		W 3.050	Coastal water use
		W 3.051	Sea water use
		W 3.052	Estuarine water use
2.4.09.01.0A	Implementation of new agricultural practices or land use	A 3.006	Ashes and sewage sludge fertilizers
		A 3.023	Climate
		A 3.029	Critical group - agricultural labour
		A 3.036	Crop fertilizers and soil conditioners
		A 3.037	Crop storage
		A 3.048	Fires (agricultural)
		A 3.058	Greenhouse food production
		A 3.062	Herbicides, pesticides, and fungicides
		A 3.067	Hydroponics
		A 3.073	Irrigation

Table F-2. Cross Reference of TSPA-LA FEPs to Source FEPs (Continued)

TSPA-LA FEP Number	TSPA-LA FEP Name	Source FEP No.	Source FEP Name
2.4.09.01.0A	Implementation of new agricultural practices or land use (continued)	A 3.079	Peat and leaf litter harvesting
		H 4.3.1	Land and surface water use: Terrestrial
		H 4.3.2	Land and surface water use: Estuarine
		I 112a	Fire (atmospheric dose pathway)
		I 113	Food chain (dose pathway)
		I 148	Herbicides, pesticides, and fungicides (dose pathway)
		I 157	Hydroponics (dose pathway)
		I 299	Technological advances in food production
		K 8.33	Irrigation
		K 8.38	Ploughing
		K 8.39	Agricultural practices
		K S2.5	No Consideration of Future Human Society and Technology
		N 2.4.4	Irrigation
		N 2.4.7	Agricultural and fisheries practice changes
		W 3.044	Irrigation
2.4.09.01.0B	Agricultural land use and irrigation	A 3.006	Ashes and sewage sludge fertilizers
		A 3.036	Crop fertilizers and soil conditioners
		A 3.037	Crop storage
		A 3.048	Fires (agricultural)
		A 3.058	Greenhouse food production
		A 3.062	Herbicides, pesticides, and fungicides
		A 3.073	Irrigation
		A 3.079	Peat and leaf litter harvesting
		H 4.3.1	Land and surface water use: Terrestrial
		H 4.3.2	Land and surface water use: Estuarine
		I 010	Recycling process (biomass)
		I 021	Bioturbation (soil & sediment)
		I 082	Crop storage
		I 113	Food chain (dose pathway)
		I 148	Herbicides, pesticides, and fungicides (dose pathway)
		I 175	Irrigation (dose pathway)
		I 211	Ooutdoor spraying of water (atmospheric dose pathway)
		K 8.28	Interface effects
		K 8.33	Irrigation
		K 8.38	Ploughing
		K 8.39	Agricultural practices
2.4.09.02.0A	Animal farms and fisheries	A 3.003	Animal diets
		A 3.004	Animal grooming and fighting
		A 3.005	Animal soil ingestion
		A 3.050	Fish farming
		A 3.055	Game ranching

Table F-2. Cross Reference of TSPA-LA FEPs to Source FEPs (Continued)

TSPA-LA FEP Number	TSPA-LA FEP Name	Source FEP No.	Source FEP Name
2.4.09.02.0A	Animal farms and fisheries (continued)	H 4.3.1	Land and surface water use: Terrestrial
		H 4.3.2	Land and surface water use: Estuarine
		H 4.3.3	Land and surface water use: Coastal waters
		H 4.3.4	Land and surface water use: Seas
		I 004	Animals (intrusion)/ plants (root uptake)
		I 007	Animals (external contamination)
		I 009	Sediments (in water bodies)
		I 113	Food chain (dose pathway)
		W 3.054	Ranching
		W 3.055	Fish farming
2.4.10.00.0A	Urban and industrial land and water use	A 2.20	Earthmoving
		A 3.010	Biogas production
		A 3.023	Climate
		A 3.044	Earthmoving projects
		A 3.068	Industrial water use
		H 4.3.1	Land and surface water use: Terrestrial
		H 4.3.2	Land and surface water use: Estuarine
		H 4.3.3	Land and surface water use: Coastal waters
		H 4.3.4	Land and surface water use: Seas
		I 099	Earth moving projects (civil)
		K 8.37	Earthworks (human actions, dredging, etc.)
		N 2.4	POST-CLOSURE SURFACE ACTIVITIES
		N 2.4.6	Land use changes
		W 3.040	Land use changes
		W 3.041	Surface disruptions
3.1.01.01.0A	Radioactive decay and ingrowth	A 1.65	Radioactive decay
		A 2.51	Radioactive decay
		A 3.082	Radioactive decay
		H 1.3.1	Radioactive decay and ingrowth
		I 045	Progency nuclides (critical radionuclides)
		K 0.1	Radioactive decay
		K 0.3	Gaseous and volatile isotopes
		N 3.4	RADIOLOGICAL
		N 3.4.4	Radioactive decay and ingrowth
		S 069	Radioactive Decay, fuel
		S 070	Radioactive decay of mobile nuclides
		W 2.012	Radionuclide decay and ingrowth
		YM108	Accumulated 239Pu decays to 235U in basin pool (in waste and EBS)
3.2.07.01.0A	Isotopic dilution	A 3.046	Erosion - lateral transport
		H 4.2.2	Surface water mixing
		I 180	Surface waster bodies (non-uniform mixing of)

Table F-2. Cross Reference of TSPA-LA FEPs to Source FEPs (Continued)

TSPA-LA FEP Number	TSPA-LA FEP Name	Source FEP No.	Source FEP Name
3.2.07.01.0A	Isotopic dilution (continued)	J 7.05	Isotopic dilution
		K 4.02	Natural radionuclides/elements
		K 5.16	Solubility limits/colloid formation
		K 6.16	Solubility limits/colloid formation
		N 1.6.13	Mass, isotopic and species dilution
3.2.10.00.0A	Atmospheric transport of contaminants	A 3.027	Convection, turbulence, and diffusion (atmospheric)
		A 3.039	Deposition (wet and dry)
		A 3.042	Dispersion
		A 3.049	Fires (forest and grass)
		A 3.073	Irrigation
		A 3.077	Outdoor spraying of water
		A 3.081	Precipitation (meteoric)
		A 3.088	Saltation
		A 3.103	Surface water bodies
		A 3.105	Suspension in air
		A 3.118	Wind
		I 021	Bioturbation (soil & sediment)
		I 211	Outdoor spraying of water (atmospheric dose pathway)
		I 235	Precipitation (wet deposition)
		K 8.12	Radionuclide volatilisation/aerosol/dust production
		K 8.27	Atmosphere
		K 8.28	Interface effects
		K 8.33	Irrigation
3.3.01.00.0A	Contaminated drinking water, foodstuffs and drugs	A 3.054	Food preparation
		A 3.065	Human diet
		A 3.066	Human soil ingestion
		A 3.069	Intake of drugs
		A 3.116	Water source
		I 113	Food chain (dose pathway)
		K 8.08	Filtration
		K 8.44	Consumption of uncontaminated products
		W 2.108	Injection
3.3.02.01.0A	Plant uptake	A 3.006	Ashes and sewage sludge fertilizers
		A 3.008	Bioaccumulation
		A 3.009	Bioconcentration
		A 3.012	Biomagnification
		A 3.021	Chemical precipitation
		A 3.039	Deposition (wet and dry)
		A 3.062	Herbicides, pesticides, and fungicides
		A 3.073	Irrigation
		A 3.080	Plant roots
		A 3.085	Recycling
		A 3.110	Tree sap

Table F-2. Cross Reference of TSPA-LA FEPs to Source FEPs (Continued)

TSPA-LA FEP Number	TSPA-LA FEP Name	Source FEP No.	Source FEP Name
3.3.02.01.0A	Plant uptake (continued)	H 4.2.5	Bioaccumulation and translocation
		I 004	Animals (intrusion)/ plants (root uptake)
		I 014	Bioaccumulation/bioconcentration/biomagnification
		I 069	Atmospheric pathways (dispersion)
		I 113	Food chain (dose pathway)
		I 175	Irrigation (dose pathway)
		K 8.09	Uptake by crops
		K 8.16	Foodchain equilibrium
		K 8.43	Removal mechanisms
		N 1.7.1	Plant uptake
		N 1.7.3	Uptake by deep rooting species
		W 2.101	Plant uptake
3.3.02.02.0A	Animal uptake	A 3.003	Animal diets
		A 3.004	Animal grooming and fighting
		A 3.005	Animal soil ingestion
		A 3.006	Ashes and sewage sludge fertilizers
		A 3.008	Bioaccumulation
		A 3.009	Bioconcentration
		A 3.012	Biomagnification
		A 3.018	Carcasses
		A 3.062	Herbicides, pesticides, and fungicides
		A 3.069	Intake of drugs
		A 3.089	Scavengers and predators
		H 4.2.5	Bioaccumulation and translocation
		I 003	Animal diets (domestic and wild)
		I 004	Animals (intrusion)/ plants (root uptake)
		I 007	Animals (external contamination)
		I 009	Sediments (in water bodies)
		I 014	Bioaccumulation/bioconcentration/biomagnification
		I 113	Food chain (dose pathway)
		I 163	Insect pathways
		K 8.10	Uptake by livestock
		K 8.11	Uptake in fish
		K 8.16	Foodchain equilibrium
		K 8.43	Removal mechanisms
		N 1.7.2	Animal uptake
		W 1.070	Animals
		W 2.102	Animal uptake
3.3.02.03.0A	Fish uptake	A 3.003	Animal diets
		A 3.008	Bioaccumulation
		A 3.009	Bioconcentration
		A 3.012	Biomagnification
		A 3.018	Carcasses
		A 3.085	Recycling
		A 3.089	Scavengers and predators

Table F-2. Cross Reference of TSPA-LA FEPs to Source FEPs (Continued)

TSPA-LA FEP Number	TSPA-LA FEP Name	Source FEP No.	Source FEP Name
3.3.02.03.0A	Fish uptake (continued)	H 4.2.5	Bioaccumulation and translocation
		I 004	Animals (intrusion)/ plants (root uptake)
		I 009	Sediments (in water bodies)
		I 014	Bioaccumulation/bioconcentration/biomagnification
		I 113	Food chain (dose pathway)
		I 163	Insect pathways
		K 8.11	Uptake in fish
		K 8.43	Removal mechanisms
3.3.03.01.0A	Contaminated non-food products and exposure	A 3.004	Animal grooming and fighting
		A 3.015	Building materials
		A 3.018	Carcasses
		A 3.020	Charcoal production
		A 3.030	Critical group - clothing and home furnishings
		A 3.035	Critical group - pets
		A 3.036	Crop fertilizers and soil conditioners
		A 3.062	Herbicides, pesticides, and fungicides
		A 3.066	Human soil ingestion
		A 3.085	Recycling
		A 3.095	Smoking
		A 3.102	Space heating
		A 3.110	Tree sap
		I 010	Recycling process (biomass)
		I 090	Dermal sorption (tritium and others)
		I 113	Food chain (dose pathway)
		I 276	Smoking (dose pathway)
		J 7.02	Accumulation in peat
		K 8.42	Contaminated products (non-food)
3.3.04.01.0A	Ingestion	A 3.006	Ashes and sewage sludge fertilizers
		A 3.008	Bioaccumulation
		A 3.009	Bioconcentration
		A 3.012	Biomagnification
		A 3.065	Human diet
		A 3.066	Human soil ingestion
		A 3.089	Scavengers and predators
		A 3.110	Tree sap
		H 4.2.5	Bioaccumulation and translocation
		H 4.4.2	Human exposure: Ingestion
		I 074c	Swamp exposure scenario
		I 074d	Combination exposure scenario
		I 074e	Artificial lake exposure scenario
		I 113	Food chain (dose pathway)
		I 163	Insect pathways
		K 8.11	Uptake in fish
		K 8.13	Exposure pathways
		W 2.104	Ingestion

Table F-2. Cross Reference of TSPA-LA FEPs to Source FEPs (Continued)

TSPA-LA FEP Number	TSPA-LA FEP Name	Source FEP No.	Source FEP Name
3.3.04.02.0A	Inhalation	A 3.063	Household dust and fumes
		H 4.4.3	Human exposure: Inhalation
		I 074d	Combination exposure scenario
		I 112a	Fire (atmospheric dose pathway)
		I 211	Ooutdoor spraying of water (atmospheric dose pathway)
		I 272	Showers and humidifiers (atmospheric dose pathway)
		K 8.13	Exposure pathways
		W 2.105	Inhalation
3.3.04.03.0A	External exposure	A 3.004	Animal grooming and fighting
		A 3.040	Dermal sorption (except tritium)
		A 3.041	Dermal sorption (tritium)
		A 3.060	Groundshine
		A 3.094	Showers and humidifiers
		H 4.4.1	Human exposure: External
		I 007	Animals (external contamination)
		I 074c	Swamp exposure scenario
		I 074d	Combination exposure scenario
		I 074e	Artificial lake exposure scenario
		I 090	Dermal sorption (tritium and others)
		I 139	Groundshine
		I 211	Ooutdoor spraying of water (atmospheric dose pathway)
		I 272	Showers and humidifiers (atmospheric dose pathway)
		K 8.13	Exposure pathways
		W 2.106	Irradiation
		W 2.107	Dermal sorption
		W 2.108	Injection
3.3.05.01.0A	Radiation doses	A 3.008	Bioaccumulation
		A 3.082	Radioactive decay
		I 045	Progency nuclides (critical radionuclides)
		I 074d	Combination exposure scenario
		K 8.15	Radiation doses
		K 8.18	Secular equilibrium of radionuclide chains
		K S2.6.1	Consideration of radiological impacts to man (only)
		K S2.6.2	Basis for consideration of radiological impacts to man
		W 4.005	Radionuclide uptake and dosimetry FEPs
		W 4.006	Radionuclide uptake and dosimetry FEPs
		W 4.007	Radionuclide uptake and dosimetry FEPs

Table F-2. Cross Reference of TSPA-LA FEPs to Source FEPs (Continued)

TSPA-LA FEP Number	TSPA-LA FEP Name	Source FEP No.	Source FEP Name
3.3.06.00.0A	Radiological toxicity and effects	A 3.013	Biotoxicity
		A 3.019	Carcinogenic contaminants
		A 3.022	Chemical toxicity
		A 3.076	Mutagenic contaminants
		A 3.083	Radiotoxic contaminants
		A 3.107	Teratogenic contaminants
		K S2.6.1	Consideration of radiological impacts to man (only)
3.3.06.01.0A	Repository excavation	A 3.109	Toxicity of mined rock
		I 167	Intrusion (human/deliberate)
3.3.06.02.0A	Sensitization to radiation	A 3.022	Chemical toxicity
		A 3.093	Sensitization to radiation
		I 020	Non radiological toxicity
		I 350	Non-human biota effects
		K S2.6.1	Consideration of radiological impacts to man (only)
3.3.07.00.0A	Non-radiological toxicity and effects	A 3.013	Biotoxicity
		A 3.022	Chemical toxicity
		A 3.076	Mutagenic contaminants
		J 7.04	Chemical toxicity of wastes
		K S2.6.1	Consideration of radiological impacts to man (only)
		W 4.009	Non-radiological toxicity FEPs
3.3.08.00.0A	Radon and radon decay product exposure	A 3.003	Animal diets
		A 3.056	Gas leakage into basements
		A 3.084	Radon emission
		K 0.3	Gaseous and volatile isotopes
		K 8.13	Exposure pathways
		K 8.45	Radon pathways and doses

Source: Output DTN: MO0706SPAFEPLA.001.

Table F-3. Cross Reference of Source FEPs to TSPA-LA FEPs

Source FEP No.	Source FEP Name	TSPA-LA FEP Number	TSPA-LA FEP Name
A 1.01	Backfill characteristics	2.1.04.05.0A	Thermal-mechanical properties and evolution of backfill
A 1.02	Backfill evolution	2.1.04.02.0A	Chemical properties and evolution of backfill
		2.1.04.05.0A	Thermal-mechanical properties and evolution of backfill
A 1.03	Biological activity	2.1.10.01.0A	Microbial activity in EBS
A 1.04	Boundary conditions	0.1.10.00.0A	Model and data issues
A 1.05	Buffer additives	2.1.04.02.0A	Chemical properties and evolution of backfill
A 1.06	Buffer characteristics	2.1.04.02.0A	Chemical properties and evolution of backfill
		2.1.04.09.0A	Radionuclide transport in backfill
A 1.07	Buffer evolution	2.1.04.05.0A	Thermal-mechanical properties and evolution of backfill
		2.1.04.02.0A	Chemical properties and evolution of backfill
A 1.08	Cave ins	2.1.07.02.0A	Drift collapse
		2.1.07.01.0A	Rockfall
A 1.09	Chemical gradients	2.1.09.27.0A	Coupled effects on radionuclide transport in EBS
A 1.10	Chemical interactions	2.1.09.01.0B	Chemical characteristics of water in waste package
A 1.11	Chemical kinetics	2.1.09.07.0A	Reaction kinetics in waste package
		2.1.09.07.0B	Reaction kinetics in drifts
A 1.12	Climate change	1.3.01.00.0A	Climate change
A 1.13	Colloids	2.1.09.18.0A	Formation of microbial colloids in EBS
		2.1.09.16.0A	Formation of pseudo-colloids (natural) in EBS
		2.1.09.17.0A	Formation of pseudo-colloids (corrosion product) in EBS
A 1.14	Complexation by organics	2.1.09.13.0A	Complexation in EBS
A 1.15	Concrete	2.1.06.01.0A	Chemical effects of rock reinforcement and cementitious materials in EBS
A 1.16	Container corrosion products	2.1.09.02.0A	Chemical interaction with corrosion products
		2.1.09.27.0A	Coupled effects on radionuclide transport in EBS
A 1.17	Container failure (early)	2.1.03.08.0A	Early failure of waste packages
A 1.18	Container failure (long-term)	2.1.03.02.0A	Stress corrosion cracking (SCC) of waste packages
		2.1.03.03.0A	Localized corrosion of waste packages
		2.1.03.01.0A	General corrosion of waste packages
		2.1.03.04.0A	Hydride cracking of waste packages
		2.1.03.11.0A	Physical form of waste package and drip shield
		2.1.03.05.0A	Microbially influenced corrosion (MIC) of waste packages
A 1.19	Container failure (mechanical processes)	2.1.03.07.0B	Mechanical impact on drip shield
		2.1.07.04.0A	Hydrostatic pressure on waste package
		2.1.03.07.0A	Mechanical impact on waste package
A 1.20	Container healing	2.1.03.10.0A	Advection of liquids and solids through cracks in the waste package
		2.1.03.10.0B	Advection of liquids and solids through cracks in the drip shield

Table F-3. Cross Reference of Source FEPs to TSPA-LA FEPs (Continued)

Source FEP No.	Source FEP Name	TSPA-LA FEP Number	TSPA-LA FEP Name
A 1.21	Containers - partial corrosion	2.1.09.08.0B	Advection of dissolved radionuclides in EBS
		2.1.08.07.0A	Unsaturated flow in the EBS
		2.1.09.08.0A	Diffusion of dissolved radionuclides in EBS
A 1.22	Convection	2.1.04.09.0A	Radionuclide transport in backfill
A 1.23	Correlation	0.1.10.00.0A	Model and data issues
A 1.24	Corrosion	2.1.03.01.0A	General corrosion of waste packages
A 1.25	Coupled processes	2.1.09.27.0A	Coupled effects on radionuclide transport in EBS
		2.1.11.10.0A	Thermal effects on transport in EBS
		2.1.11.09.0A	Thermal effects on flow in the EBS
A 1.26	Criticality	2.1.14.15.0A	In-package criticality (intact configuration)
		2.1.14.16.0A	In-package criticality (degraded configurations)
A 1.27	Diffusion	2.2.07.17.0A	Diffusion in the SZ
A 1.28	Dispersion	2.2.07.15.0A	Advection and dispersion in the SZ
A 1.29	Earthquakes	1.4.02.04.0A	Seismic event precedes human intrusion
		1.2.03.02.0B	Seismic-induced rockfall damages EBS components
		1.2.03.02.0A	Seismic ground motion damages EBS components
A 1.30	Electrochemical gradients	2.1.09.09.0A	Electrochemical effects in EBS
A 1.31	Excessive hydrostatic pressures	2.1.07.04.0A	Hydrostatic pressure on waste package
A 1.32	Explosions	2.1.12.08.0A	Gas explosions in EBS
A 1.33	Faulty buffer emplacement	2.1.04.05.0A	Thermal-mechanical properties and evolution of backfill
		1.1.03.01.0B	Error in backfill emplacement
A 1.34	Formation of cracks	2.2.01.01.0B	Chemical effects of excavation and construction in the near-field
		2.2.01.01.0A	Mechanical effects of excavation and construction in the near-field
		2.2.07.20.0A	Flow diversion around repository drifts
A 1.35	Formation of gases	2.1.13.01.0A	Radiolysis
		2.1.12.03.0A	Gas generation (H2) from waste package corrosion
		2.1.12.01.0A	Gas generation (repository pressurization)
A 1.36	Galvanic coupling	2.1.09.09.0A	Electrochemical effects in EBS
A 1.37	Geochemical pump	2.1.09.04.0A	Radionuclide solubility, solubility limits, and speciation in the waste form and EBS
		2.1.09.27.0A	Coupled effects on radionuclide transport in EBS
A 1.38	Glaciation	1.3.05.00.0A	Glacial and ice sheet effect
A 1.39	Global effects	1.3.01.00.0A	Climate change
A 1.40	Hydraulic conductivity	2.2.07.20.0A	Flow diversion around repository drifts
		2.1.08.07.0A	Unsaturated flow in the EBS
A 1.41	Hydraulic head	2.1.08.09.0A	Saturated flow in the EBS
A 1.42	Hydride cracking	2.1.03.04.0A	Hydride cracking of waste packages
		2.1.03.04.0B	Hydride cracking of drip shields
A 1.43	Hydrothermal alteration	2.1.04.02.0A	Chemical properties and evolution of backfill
A 1.44	Improper operation	1.1.12.01.0A	Accidents and unplanned events during construction and operation
A 1.45	Incomplete closure	1.1.04.01.0A	Incomplete closure

Table F-3. Cross Reference of Source FEPs to TSPA-LA FEPs (Continued)

Source FEP No.	Source FEP Name	TSPA-LA FEP Number	TSPA-LA FEP Name
A 1.46	Incomplete filling of containers	2.1.07.05.0A	Creep of metallic materials in the waste package
A 1.47	Interfaces (boundary conditions)	2.1.06.07.0A	Chemical effects at EBS component interfaces
		2.1.06.07.0B	Mechanical effects at EBS component interfaces
		2.1.09.09.0A	Electrochemical effects in EBS
A 1.48	Intrusion (animal)	2.3.09.01.0A	Animal burrowing/intrusion
A 1.49	Intrusion (human)	1.4.02.01.0A	Deliberate human intrusion
A 1.50	Inventory	2.1.01.01.0A	Waste inventory
A 1.51	Long-term physical stability	2.1.03.01.0A	General corrosion of waste packages
		2.1.03.11.0A	Physical form of waste package and drip shield
A 1.52	Long-term transients	2.1.11.01.0A	Heat generation in EBS
		1.1.02.00.0B	Mechanical effects of excavation and construction in EBS
A 1.53	Methylation	2.1.09.13.0A	Complexation in EBS
A 1.54	Microbes	2.1.03.05.0B	Microbially influenced corrosion (MIC) of drip shields
		2.2.09.01.0A	Microbial activity in the SZ
		2.2.09.01.0B	Microbial activity in the UZ
		2.1.03.05.0A	Microbially influenced corrosion (MIC) of waste packages
		2.1.10.01.0A	Microbial activity in EBS
		2.1.12.04.0A	Gas generation (CO_2, CH_4, H_2S) from microbial degradation
		2.1.02.14.0A	Microbially influenced corrosion (MIC) of cladding
		2.1.06.01.0A	Chemical effects of rock reinforcement and cementitious materials in EBS
		2.1.06.05.0D	Chemical degradation of invert
		2.1.06.05.0C	Chemical degradation of emplacement pallet
A 1.55	Microorganisms	2.1.10.01.0A	Microbial activity in EBS
A 1.56	Monitoring and remedial activities	1.1.11.00.0A	Monitoring of the repository
A 1.57	Mutation	2.1.13.03.0A	Radiological mutation of microbes
A 1.58	Other waste (other than used fuel)	2.1.01.02.0A	Interactions between co-located waste
A 1.59	Percolation in shafts	2.1.05.03.0A	Degradation of seals
		2.1.05.02.0A	Radionuclide transport through seals
		2.1.05.01.0A	Flow through seals (access ramps and ventilation shafts)
A 1.60	Pitting	2.1.09.28.0A	Localized corrosion on waste package outer surface due to deliquescence
		2.1.03.03.0A	Localized corrosion of waste packages
		2.1.03.03.0B	Localized corrosion of drip shields
		2.1.09.28.0B	Localized corrosion on drip shield surfaces due to deliquescence
A 1.61	Preclosure events	1.1.12.01.0A	Accidents and unplanned events during construction and operation
A 1.62	Precipitation and dissolution	2.1.09.04.0A	Radionuclide solubility, solubility limits, and speciation in the waste form and EBS
A 1.63	Psuedo-colloids	2.1.09.16.0A	Formation of pseudo-colloids (natural) in EBS
A 1.64	Radiation damage	2.1.13.02.0A	Radiation damage in EBS

Table F-3. Cross Reference of Source FEPs to TSPA-LA FEPs (Continued)

Source FEP No.	Source FEP Name	TSPA-LA FEP Number	TSPA-LA FEP Name
A 1.65	Radioactive decay	3.1.01.01.0A	Radioactive decay and ingrowth
A 1.66	Radiolysis	2.1.13.01.0A	Radiolysis
A 1.67	Recharge groundwater	2.3.11.03.0A	Infiltration and recharge
		2.2.08.12.0B	Chemistry of water flowing into the waste package
		2.2.08.01.0B	Chemical characteristics of groundwater in the UZ
		2.2.08.12.0A	Chemistry of water flowing into the drift
A 1.68	Reflooding	2.1.08.11.0A	Repository resaturation due to waste cooling
A 1.69	Retrievability	1.1.13.00.0A	Retrievability
A 1.70	Sabotage and improper operation	1.4.02.01.0A	Deliberate human intrusion
		1.1.12.01.0A	Accidents and unplanned events during construction and operation
A 1.71	Seal evolution	2.1.05.03.0A	Degradation of seals
A 1.72	Seal failure	2.1.05.03.0A	Degradation of seals
A 1.73	Sorption	2.1.09.05.0A	Sorption of dissolved radionuclides in EBS
A 1.74	Sorption - nonlinear	2.2.08.09.0A	Sorption in the SZ
		2.2.08.09.0B	Sorption in the UZ
A 1.75	Source terms (expected)	2.1.02.02.0A	CSNF degradation (alteration, dissolution, and radionuclide release)
		2.1.02.07.0A	Radionuclide release from gap and grain boundaries
A 1.76	Source terms (other)	2.1.02.02.0A	CSNF degradation (alteration, dissolution, and radionuclide release)
A 1.77	Speciation	2.2.08.07.0B	Radionuclide solubility limits in the UZ
		2.2.08.07.0A	Radionuclide solubility limits in the SZ
		2.2.08.03.0A	Geochemical interactions and evolution in the SZ
		2.2.08.03.0B	Geochemical interactions and evolution in the UZ
A 1.78	Stability	2.1.07.02.0A	Drift collapse
A 1.79	Stability of UO2	2.1.02.02.0A	CSNF degradation (alteration, dissolution, and radionuclide release)
A 1.80	Swelling pressure	2.1.04.04.0A	Thermal-mechanical effects of backfill
		2.1.04.05.0A	Thermal-mechanical properties and evolution of backfill
A 1.81	Temperature effects	2.1.11.01.0A	Heat generation in EBS
A 1.82	Temperature rises (unexpected effects)	2.1.12.08.0A	Gas explosions in EBS
		1.2.04.04.0A	Igneous intrusion interacts with EBS components
A 1.83	Time dependence	2.1.11.01.0A	Heat generation in EBS
A 1.84	Transport in gases or of gases	2.1.12.06.0A	Gas transport in EBS
A 1.85	Uncertainties	0.1.10.00.0A	Model and data issues
A 1.86	Uniform corrosion	2.1.03.01.0A	General corrosion of waste packages
		2.1.03.01.0B	General corrosion of drip shields
A 1.87	Unmodelled design features	0.1.10.00.0A	Model and data issues

Table F-3. Cross Reference of Source FEPs to TSPA-LA FEPs (Continued)

Source FEP No.	Source FEP Name	TSPA-LA FEP Number	TSPA-LA FEP Name
A 1.88	Unsaturated transport	2.1.08.07.0A	Unsaturated flow in the EBS
		2.1.09.08.0B	Advection of dissolved radionuclides in EBS
		2.1.09.08.0A	Diffusion of dissolved radionuclides in EBS
A 1.89	Vault geometry	2.2.07.10.0A	Condensation zone forms around drifts
		2.1.08.04.0A	Condensation forms on roofs of drifts (drift-scale cold traps)
		2.1.08.04.0B	Condensation forms at repository edges (repository-scale cold traps)
A 2.01	Blasting and vibration	2.2.01.01.0A	Mechanical effects of excavation and construction in the near-field
		1.1.02.00.0B	Mechanical effects of excavation and construction in EBS
A 2.02	Bomb blast	1.4.11.00.0A	Explosions and crashes (human activities)
A 2.03	Borehole - well	1.4.04.00.0A	Drilling activities (human intrusion)
A 2.04	Borehole seal failure	2.1.05.01.0A	Flow through seals (access ramps and ventilation shafts)
		2.1.05.02.0A	Radionuclide transport through seals
		2.1.05.03.0A	Degradation of seals
A 2.05	Boreholes - exploration	1.4.04.00.0A	Drilling activities (human intrusion)
A 2.06	Cavitation	2.1.08.01.0B	Effects of rapid influx into the repository
		2.1.08.09.0A	Saturated flow in the EBS
A 2.07	Climate change	1.3.01.00.0A	Climate change
A 2.08	Colloid formation	2.1.09.16.0A	Formation of pseudo-colloids (natural) in EBS
		2.1.09.17.0A	Formation of pseudo-colloids (corrosion product) in EBS
A 2.09	Complexation by organics	2.1.09.13.0A	Complexation in EBS
A 2.10	Conceptual model - hydrology	0.1.10.00.0A	Model and data issues
A 2.11	Convection	2.2.07.15.0A	Advection and dispersion in the SZ
		2.2.07.15.0B	Advection and dispersion in the UZ
A 2.12	Correlation	0.1.10.00.0A	Model and data issues
A 2.13	Damaged zone	2.2.01.05.0A	Radionuclide transport in the excavation disturbed zone
		2.2.01.03.0A	Changes in fluid saturations in the excavation disturbed zone
		2.2.01.01.0A	Mechanical effects of excavation and construction in the near-field
A 2.14	Dams	1.4.07.01.0A	Water management activities
A 2.15	Dewatering	2.1.08.03.0A	Repository dry-out due to waste heat
		2.2.01.03.0A	Changes in fluid saturations in the excavation disturbed zone
		1.4.07.01.0A	Water management activities
A 2.16	Diffusion	2.2.07.17.0A	Diffusion in the SZ
A 2.17	Discharge zones	2.2.08.11.0A	Groundwater discharge to surface within the reference biosphere
		2.3.11.04.0A	Groundwater discharge to surface outside the reference biosphere
A 2.18	Dispersion	2.2.07.15.0A	Advection and dispersion in the SZ
		2.2.07.15.0B	Advection and dispersion in the UZ

Table F-3. Cross Reference of Source FEPs to TSPA-LA FEPs (Continued)

Source FEP No.	Source FEP Name	TSPA-LA FEP Number	TSPA-LA FEP Name
A 2.19	Drought	1.3.07.01.0A	Water table decline
A 2.20	Earthmoving	2.4.10.00.0A	Urban and industrial land and water use
A 2.21	Earthquakes	1.2.03.02.0C	Seismic-induced drift collapse damages EBS components
		1.4.02.04.0A	Seismic event precedes human intrusion
		1.2.03.02.0B	Seismic-induced rockfall damages EBS components
		1.2.10.01.0A	Hydrologic response to seismic activity
		1.2.03.02.0A	Seismic ground motion damages EBS components
A 2.22	Erosion	1.2.07.01.0A	Erosion/denudation
A 2.23	Explosion	2.1.12.08.0A	Gas explosions in EBS
A 2.24	Faulting	1.2.02.02.0A	Faults
A 2.25	Flood	2.3.11.01.0A	Precipitation
		1.3.01.00.0A	Climate change
A 2.26	Fulvic acid	2.1.09.13.0A	Complexation in EBS
A 2.27	Gases and gas transport	2.2.11.02.0A	Gas effects in the UZ
		2.2.11.03.0A	Gas transport in geosphere
A 2.28	Geothermal gradient effects	2.2.10.02.0A	Thermal convection cell develops in SZ
		2.2.10.03.0A	Natural geothermal effects on flow in the SZ
		2.2.10.03.0B	Natural geothermal effects on flow in the UZ
A 2.29	Geochemical interactions	2.2.08.03.0B	Geochemical interactions and evolution in the UZ
		2.2.08.01.0B	Chemical characteristics of groundwater in the UZ
		2.2.08.03.0A	Geochemical interactions and evolution in the SZ
A 2.30	Glaciation	1.3.05.00.0A	Glacial and ice sheet effect
A 2.31	Greenhouse effect	1.4.01.02.0A	Greenhouse gas effects
A 2.32	Groundwater composition	2.2.08.01.0A	Chemical characteristics of groundwater in the SZ
		2.2.08.01.0B	Chemical characteristics of groundwater in the UZ
		2.2.08.03.0A	Geochemical interactions and evolution in the SZ
		2.2.08.03.0B	Geochemical interactions and evolution in the UZ
		2.2.08.06.0A	Complexation in the SZ
		2.2.08.06.0B	Complexation in the UZ
A 2.33	Groundwater – evolution	2.2.10.01.0A	Repository-induced thermal effects on flow in the UZ
		2.2.08.01.0B	Chemical characteristics of groundwater in the UZ
		2.2.08.01.0A	Chemical characteristics of groundwater in the SZ
A 2.34	Humic acid	2.1.09.13.0A	Complexation in EBS

Table F-3. Cross Reference of Source FEPs to TSPA-LA FEPs (Continued)

Source FEP No.	Source FEP Name	TSPA-LA FEP Number	TSPA-LA FEP Name
A 2.35	Hydraulic properties – evolution	2.2.08.03.0B	Geochemical interactions and evolution in the UZ
		2.2.08.03.0A	Geochemical interactions and evolution in the SZ
A 2.36	Intrusion (magmatic)	1.2.04.02.0A	Igneous activity changes rock properties
A 2.37	Intrusion (mines)	1.4.05.00.0A	Mining and other underground activities (human intrusion)
A 2.38	Isostatic rebound	1.3.05.00.0A	Glacial and ice sheet effect
A 2.39	Magmatic activity	1.2.04.02.0A	Igneous activity changes rock properties
A 2.40	Magnetic poles (reversal)	1.5.03.01.0A	Changes in the earth's magnetic field
A 2.41	Matrix diffusion	2.2.08.08.0A	Matrix diffusion in the SZ
A 2.42	Metamorphic activity	1.2.05.00.0A	Metamorphism
A 2.43	Meteorite impact	1.5.01.01.0A	Meteorite impact
A 2.44	Methane	2.2.11.01.0A	Gas effects in the SZ
A 2.45	Microbes	2.1.06.05.0C	Chemical degradation of emplacement pallet
		2.1.03.05.0B	Microbially influenced corrosion (MIC) of drip shields
		2.1.06.01.0A	Chemical effects of rock reinforcement and cementitious materials in EBS
		2.1.06.05.0D	Chemical degradation of invert
		2.1.10.01.0A	Microbial activity in EBS
		2.1.12.04.0A	Gas generation (CO2, CH4, H2S) from microbial degradation
		2.2.09.01.0A	Microbial activity in the SZ
		2.2.09.01.0B	Microbial activity in the UZ
		2.1.03.05.0A	Microbially influenced corrosion (MIC) of waste packages
		2.1.02.14.0A	Microbially influenced corrosion (MIC) of cladding
A 2.46	Mines	1.4.05.00.0A	Mining and other underground activities (human intrusion)
A 2.47	Open boreholes	1.1.01.01.0A	Open site investigation boreholes
		1.1.01.01.0B	Influx through holes drilled in drift wall or crown
A 2.48	Ozone layer	1.4.01.04.0A	Ozone layer failure
A 2.49	Precipitation and dissolution	2.2.09.01.0A	Microbial activity in the SZ
		2.2.09.01.0B	Microbial activity in the UZ
		2.2.08.03.0A	Geochemical interactions and evolution in the SZ
		2.2.08.03.0B	Geochemical interactions and evolution in the UZ
A 2.50	Pseudo-colloids	2.1.09.16.0A	Formation of pseudo-colloids (natural) in EBS
A 2.51	Radioactive decay	3.1.01.01.0A	Radioactive decay and ingrowth
A 2.52	Radiation effects	2.1.13.02.0A	Radiation damage in EBS
		2.1.13.01.0A	Radiolysis
A 2.53	Recharge groundwater	2.2.08.01.0B	Chemical characteristics of groundwater in the UZ
		2.3.11.03.0A	Infiltration and recharge
A 2.54	Rock properties	2.2.03.02.0A	Rock properties of host rock and other units

Table F-3. Cross Reference of Source FEPs to TSPA-LA FEPs (Continued)

Source FEP No.	Source FEP Name	TSPA-LA FEP Number	TSPA-LA FEP Name
A 2.55	Rock properties - undetected features	2.2.12.00.0A	Undetected features in the UZ
A 2.56	Sabotage	1.4.02.01.0A	Deliberate human intrusion
A 2.57	Salinity effects on flow	2.2.07.14.0A	Chemically-induced density effects on groundwater flow
A 2.58	Saturation	2.2.08.09.0A	Sorption in the SZ
A 2.59	Sea level change	2.3.06.00.0A	Marine features
A 2.60	Shaft seal failure	2.1.05.03.0A	Degradation of seals
A 2.61	Solution mining	1.4.05.00.0A	Mining and other underground activities (human intrusion)
A 2.62	Sorption	2.2.08.09.0B	Sorption in the UZ
		2.2.08.09.0A	Sorption in the SZ
A 2.63	Sorption – nonlinear	2.2.08.09.0A	Sorption in the SZ
		2.2.08.09.0B	Sorption in the UZ
A 2.64	Speciation	2.2.08.07.0B	Radionuclide solubility limits in the UZ
		2.2.08.07.0A	Radionuclide solubility limits in the SZ
		2.1.09.04.0A	Radionuclide solubility, solubility limits, and speciation in the waste form and EBS
		2.2.08.03.0B	Geochemical interactions and evolution in the UZ
		2.2.08.03.0A	Geochemical interactions and evolution in the SZ
A 2.65	Topography (current)	2.3.01.00.0A	Topography and morphology
A 2.66	Topography (future)	2.3.01.00.0A	Topography and morphology
A 2.67	Turbulence	2.2.07.12.0A	Saturated groundwater flow in the geosphere
A 2.68	Uncertainties	0.1.10.00.0A	Model and data issues
A 2.69	Unsaturated rock	2.2.07.02.0A	Unsaturated groundwater flow in the geosphere
		2.2.07.15.0B	Advection and dispersion in the UZ
A 2.70	Vault closure (incomplete)	1.1.04.01.0A	Incomplete closure
A 2.71	Vault heating effects	2.1.11.07.0A	Thermal expansion/stress of in-drift EBS components
		2.1.11.09.0C	Thermally driven flow (convection) in drifts
		2.1.11.09.0B	Thermally-driven flow (convection) in waste packages
		2.1.11.02.0A	Non-uniform heat distribution in EBS
		2.1.11.09.0A	Thermal effects on flow in the EBS
		2.1.11.01.0A	Heat generation in EBS
A 2.72	Volcanism	1.2.04.02.0A	Igneous activity changes rock properties
		1.2.02.02.0A	Faults
		1.2.03.03.0A	Seismicity associated with igneous activity
		1.2.04.03.0A	Igneous intrusion into repository
		1.2.04.05.0A	Magma or pyroclastic base surge transports waste
		1.2.04.06.0A	Eruptive conduit to surface intersects repository
		2.3.01.00.0A	Topography and morphology
		1.2.10.02.0A	Hydrologic response to igneous activity
		1.2.04.04.0A	Igneous intrusion interacts with EBS components

Table F-3. Cross Reference of Source FEPs to TSPA-LA FEPs (Continued)

Source FEP No.	Source FEP Name	TSPA-LA FEP Number	TSPA-LA FEP Name
A 2.73	Wells	2.3.13.04.0A	Radionuclide release outside the reference biosphere
		1.4.07.02.0A	Wells
A 2.74	Wells (high-demand)	2.3.13.04.0A	Radionuclide release outside the reference biosphere
		1.4.07.02.0A	Wells
A 3.001	Acid rain	1.4.01.03.0A	Acid rain
A 3.002	Alkali flats	2.3.02.01.0A	Soil type
		2.3.02.02.0A	Radionuclide accumulation in soils
A 3.003	Animal diets	3.3.08.00.0A	Radon and radon decay product exposure
		2.4.09.02.0A	Animal farms and fisheries
		3.3.02.03.0A	Fish uptake
		3.3.02.02.0A	Animal uptake
		1.4.07.02.0A	Wells
		2.3.09.01.0A	Animal burrowing/intrusion
A 3.004	Animal grooming and fighting	2.3.09.01.0A	Animal burrowing/intrusion
		3.3.04.03.0A	External exposure
		3.3.03.01.0A	Contaminated non-food products and exposure
		2.4.09.02.0A	Animal farms and fisheries
		1.4.07.02.0A	Wells
		3.3.02.02.0A	Animal uptake
A 3.005	Animal soil ingestion	2.3.09.01.0A	Animal burrowing/intrusion
		3.3.02.02.0A	Animal uptake
		1.4.07.02.0A	Wells
		2.4.09.02.0A	Animal farms and fisheries
A 3.006	Ashes and sewage sludge fertilizers	3.3.04.01.0A	Ingestion
		2.4.09.01.0A	Implementation of new agricultural practices or land use
		3.3.02.02.0A	Animal uptake
		2.4.09.01.0B	Agricultural land use and irrigation
		3.3.02.01.0A	Plant uptake
A 3.007	Bacteria and microbes in soil	2.2.09.01.0A	Microbial activity in the SZ
		2.3.13.01.0A	Biosphere characteristics
		2.3.02.01.0A	Soil type
		2.2.11.02.0A	Gas effects in the UZ
		2.2.11.01.0A	Gas effects in the SZ
		2.2.09.01.0B	Microbial activity in the UZ
A 3.008	Bioaccumulation	3.3.02.01.0A	Plant uptake
		3.3.04.01.0A	Ingestion
		3.3.02.02.0A	Animal uptake
		3.3.05.01.0A	Radiation doses
		3.3.02.03.0A	Fish uptake
A 3.009	Bioconcentration	3.3.04.01.0A	Ingestion
		3.3.02.03.0A	Fish uptake
		3.3.02.02.0A	Animal uptake
		3.3.02.01.0A	Plant uptake

Table F-3. Cross Reference of Source FEPs to TSPA-LA FEPs (Continued)

Source FEP No.	Source FEP Name	TSPA-LA FEP Number	TSPA-LA FEP Name
A 3.010	Biogas production	2.4.10.00.0A	Urban and industrial land and water use
A 3.011	Biological evolution	1.5.02.00.0A	Species evolution
		2.4.01.00.0A	Human characteristics (physiology, metabolism)
		2.1.13.03.0A	Radiological mutation of microbes
A 3.012	Biomagnification	3.3.02.03.0A	Fish uptake
		3.3.04.01.0A	Ingestion
		3.3.02.01.0A	Plant uptake
		3.3.02.02.0A	Animal uptake
A 3.013	Biotoxicity	3.3.07.00.0A	Non-radiological toxicity and effects
		3.3.06.00.0A	Radiological toxicity and effects
A 3.014	Bioturbation of soil and sediment	2.3.02.03.0A	Soil and sediment transport in the biosphere
A 3.015	Building materials	3.3.03.01.0A	Contaminated non-food products and exposure
		2.4.07.00.0A	Dwellings
A 3.016	Burrowing animals	2.3.02.03.0A	Soil and sediment transport in the biosphere
		2.3.09.01.0A	Animal burrowing/intrusion
A 3.017	Capillary rise in soil	2.2.08.11.0A	Groundwater discharge to surface within the reference biosphere
		2.1.04.01.0A	Flow in the backfill
		2.1.08.06.0A	Capillary effects (wicking) in EBS
		1.3.07.02.0B	Water table rise affects UZ
		2.2.07.03.0A	Capillary rise in the UZ
		2.3.11.04.0A	Groundwater discharge to surface outside the reference biosphere
A 3.018	Carcasses	2.3.02.02.0A	Radionuclide accumulation in soils
		3.3.02.02.0A	Animal uptake
		3.3.03.01.0A	Contaminated non-food products and exposure
		3.3.02.03.0A	Fish uptake
A 3.019	Carcinogenic contaminants	3.3.06.00.0A	Radiological toxicity and effects
A 3.020	Charcoal production	3.3.03.01.0A	Contaminated non-food products and exposure
A 3.021	Chemical precipitation	2.2.08.09.0B	Sorption in the UZ
		2.2.08.08.0A	Matrix diffusion in the SZ
		2.2.08.05.0A	Diffusion in the UZ
		2.2.08.03.0B	Geochemical interactions and evolution in the UZ
		2.3.02.01.0A	Soil type
		2.2.10.01.0A	Repository-induced thermal effects on flow in the UZ
		2.1.09.08.0A	Diffusion of dissolved radionuclides in EBS
		2.2.08.08.0B	Matrix diffusion in the UZ
		3.3.02.01.0A	Plant uptake
		2.3.13.04.0A	Radionuclide release outside the reference biosphere
		2.3.11.04.0A	Groundwater discharge to surface outside the reference biosphere
		2.3.02.03.0A	Soil and sediment transport in the biosphere
		2.2.10.09.0A	Thermo-chemical alteration of the Topopah Spring basal vitrophyre

Table F-3. Cross Reference of Source FEPs to TSPA-LA FEPs (Continued)

Source FEP No.	Source FEP Name	TSPA-LA FEP Number	TSPA-LA FEP Name
A 3.021	Chemical precipitation (continued)	2.2.10.07.0A	Thermo-chemical alteration of the Calico Hills unit
		2.2.08.01.0B	Chemical characteristics of groundwater in the UZ
		2.2.10.05.0A	Thermo-mechanical stresses alter characteristics of rocks above and below the repository
		2.2.08.03.0A	Geochemical interactions and evolution in the SZ
		2.2.09.01.0B	Microbial activity in the UZ
		2.2.09.01.0A	Microbial activity in the SZ
		2.2.08.11.0A	Groundwater discharge to surface within the reference biosphere
		2.2.10.08.0A	Thermo-chemical alteration in the SZ (solubility, speciation, phase changes)
		2.2.08.09.0A	Sorption in the SZ
		2.2.08.01.0A	Chemical characteristics of groundwater in the SZ
		2.1.09.05.0A	Sorption of dissolved radionuclides in EBS
		2.1.09.08.0B	Advection of dissolved radionuclides in EBS
		2.2.10.06.0A	Thermo-chemical alteration in the UZ (solubility, speciation, phase changes)
A 3.022	Chemical toxicity	3.3.06.00.0A	Radiological toxicity and effects
		3.3.06.02.0A	Sensitization to radiation
		3.3.07.00.0A	Non-radiological toxicity and effects
		2.1.13.03.0A	Radiological mutation of microbes
A 3.023	Climate	1.5.01.02.0A	Extraterrestrial events
		1.3.01.00.0A	Climate change
		1.3.05.00.0A	Glacial and ice sheet effect
		1.3.07.02.0A	Water table rise affects SZ
		1.4.01.00.0A	Human influences on climate
		1.4.01.03.0A	Acid rain
		2.4.08.00.0A	Wild and natural land and water use
		1.4.01.04.0A	Ozone layer failure
		1.3.04.00.0A	Periglacial effects
		1.5.03.01.0A	Changes in the earth's magnetic field
		2.3.11.01.0A	Precipitation
		2.3.11.03.0A	Infiltration and recharge
		2.3.13.01.0A	Biosphere characteristics
		1.4.01.02.0A	Greenhouse gas effects
		2.4.09.01.0A	Implementation of new agricultural practices or land use
		2.4.10.00.0A	Urban and industrial land and water use
		1.3.07.02.0B	Water table rise affects UZ
		1.4.01.01.0A	Climate modification increases recharge
		1.3.07.01.0A	Water table decline

Table F-3. Cross Reference of Source FEPs to TSPA-LA FEPs (Continued)

Source FEP No.	Source FEP Name	TSPA-LA FEP Number	TSPA-LA FEP Name
A 3.024	Climate change	1.3.07.01.0A	Water table decline
		2.3.11.03.0A	Infiltration and recharge
		1.3.01.00.0A	Climate change
		1.3.04.00.0A	Periglacial effects
		1.3.05.00.0A	Glacial and ice sheet effect
		1.3.07.02.0A	Water table rise affects SZ
		1.3.07.02.0B	Water table rise affects UZ
		1.4.01.01.0A	Climate modification increases recharge
		2.3.11.01.0A	Precipitation
A 3.025	Collisions, explosions, and impacts	1.5.01.01.0A	Meteorite impact
		2.1.12.08.0A	Gas explosions in EBS
		1.4.11.00.0A	Explosions and crashes (human activities)
A 3.026	Colloids	2.1.09.24.0A	Diffusion of colloids in EBS
		2.1.09.19.0A	Sorption of colloids in EBS
		2.2.08.09.0B	Sorption in the UZ
		2.2.08.09.0A	Sorption in the SZ
		2.1.09.23.0A	Stability of colloids in EBS
		2.2.08.10.0B	Colloidal transport in the UZ
		2.1.09.18.0A	Formation of microbial colloids in EBS
		2.1.09.21.0A	Transport of particles larger than colloids in EBS
		2.3.11.04.0A	Groundwater discharge to surface outside the reference biosphere
		2.1.09.21.0B	Transport of particles larger than colloids in the SZ
		2.1.09.20.0A	Filtration of colloids in EBS
		2.1.09.19.0B	Advection of colloids in EBS
		2.2.08.10.0A	Colloidal transport in the SZ
		2.1.09.26.0A	Gravitational settling of colloids in EBS
		2.1.09.25.0A	Formation of colloids (waste-form) by co-precipitation in EBS
		2.1.09.22.0A	Sorption of colloids at air-water interface
		2.1.09.17.0A	Formation of pseudo-colloids (corrosion product) in EBS
		2.1.09.21.0C	Transport of particles larger than colloids in the UZ
		2.1.04.09.0A	Radionuclide transport in backfill
		2.1.09.15.0A	Formation of true (intrinsic) colloids in EBS
		2.1.09.16.0A	Formation of pseudo-colloids (natural) in EBS
		2.2.08.11.0A	Groundwater discharge to surface within the reference biosphere
		2.1.10.01.0A	Microbial activity in EBS
A 3.027	Convection, turbulence and diffusion (atmospheric)	3.2.10.00.0A	Atmospheric transport of contaminants
		2.3.02.03.0A	Soil and sediment transport in the biosphere
		1.2.07.01.0A	Erosion/denudation
		1.2.04.07.0C	Ash redistribution via soil and sediment transport
		1.2.04.07.0B	Ash redistribution in groundwater
		1.2.07.02.0A	Deposition

Table F-3. Cross Reference of Source FEPs to TSPA-LA FEPs (Continued)

Source FEP No.	Source FEP Name	TSPA-LA FEP Number	TSPA-LA FEP Name
A 3.028	Correlation	0.1.10.00.0A	Model and data issues
A 3.029	Critical group - agricultural labour	2.4.09.01.0A	Implementation of new agricultural practices or land use
A 3.030	Critical group - clothing and home furnishings	3.3.03.01.0A	Contaminated non-food products and exposure
A 3.031	Critical group - evolution	1.5.02.00.0A	Species evolution
A 3.032	Critical group - house location	2.4.07.00.0A	Dwellings
A 3.033	Critical group - individuality	2.4.01.00.0A	Human characteristics (physiology, metabolism)
A 3.034	Critical group - leisure pursuits	2.4.04.01.0A	Human lifestyle
A 3.035	Critical group - pets	3.3.03.01.0A	Contaminated non-food products and exposure
A 3.036	Crop fertilizers and soil conditioners	2.4.09.01.0B	Agricultural land use and irrigation
		3.3.03.01.0A	Contaminated non-food products and exposure
		2.4.09.01.0A	Implementation of new agricultural practices or land use
A 3.037	Crop storage	2.4.09.01.0A	Implementation of new agricultural practices or land use
		2.4.09.01.0B	Agricultural land use and irrigation
A 3.038	Cure for cancer	1.4.09.00.0A	Technological developments
A 3.039	Deposition (wet and dry)	1.2.04.07.0B	Ash redistribution in groundwater
		1.2.07.02.0A	Deposition
		3.2.10.00.0A	Atmospheric transport of contaminants
		2.3.02.03.0A	Soil and sediment transport in the biosphere
		2.3.02.02.0A	Radionuclide accumulation in soils
		1.2.04.07.0A	Ashfall
		1.4.07.03.0A	Recycling of accumulated radionuclides from soils to groundwater
		1.2.04.07.0C	Ash redistribution via soil and sediment transport
		3.3.02.01.0A	Plant uptake
		2.3.06.00.0A	Marine features
A 3.040	Dermal sorption (except tritium)	3.3.04.03.0A	External exposure
A 3.041	Dermal sorption (tritium)	3.3.04.03.0A	External exposure
A 3.042	Dispersion	3.2.10.00.0A	Atmospheric transport of contaminants
		2.3.13.02.0A	Radionuclide alteration during biosphere transport
		2.2.07.15.0B	Advection and dispersion in the UZ
		1.2.07.01.0A	Erosion/denudation
		2.2.07.15.0A	Advection and dispersion in the SZ
A 3.043	Dust storms and desertification	1.3.07.01.0A	Water table decline
		1.3.01.00.0A	Climate change
A 3.044	Earthmoving projects	2.4.10.00.0A	Urban and industrial land and water use
A 3.045	Earthquakes	1.2.03.02.0A	Seismic ground motion damages EBS components
		2.2.06.02.0A	Seismic activity changes porosity and permeability of faults
		1.2.02.01.0A	Fractures
		2.1.03.07.0A	Mechanical impact on waste package
		2.2.06.01.0A	Seismic activity changes porosity and permeability of rock

Table F-3. Cross Reference of Source FEPs to TSPA-LA FEPs (Continued)

Source FEP No.	Source FEP Name	TSPA-LA FEP Number	TSPA-LA FEP Name
A 3.045	Earthquakes (continued)	1.4.02.04.0A	Seismic event precedes human intrusion
		1.2.03.03.0A	Seismicity associated with igneous activity
		1.2.03.02.0B	Seismic-induced rockfall damages EBS components
		2.1.03.07.0B	Mechanical impact on drip shield
		2.2.06.02.0B	Seismic activity changes porosity and permeability of fractures
		2.1.02.24.0A	Mechanical impact on cladding
		2.2.06.03.0A	Seismic activity alters perched water zones
		2.1.07.02.0A	Drift collapse
		1.2.10.01.0A	Hydrologic response to seismic activity
A 3.046	Erosion - lateral transport	3.2.07.01.0A	Isotopic dilution
		2.3.11.02.0A	Surface runoff and evapotranspiration
		2.3.02.03.0A	Soil and sediment transport in the biosphere
		1.2.07.01.0A	Erosion/denudation
A 3.047	Erosion (wind)	1.2.07.01.0A	Erosion/denudation
		1.2.04.07.0C	Ash redistribution via soil and sediment transport
		2.3.02.03.0A	Soil and sediment transport in the biosphere
A 3.048	Fires (agricultural)	2.4.09.01.0B	Agricultural land use and irrigation
		2.4.09.01.0A	Implementation of new agricultural practices or land use
A 3.049	Fires (forest and grass)	2.3.13.04.0A	Radionuclide release outside the reference biosphere
		2.3.13.01.0A	Biosphere characteristics
		3.2.10.00.0A	Atmospheric transport of contaminants
A 3.050	Fish farming	2.4.09.02.0A	Animal farms and fisheries
A 3.051	Flipping of earth's magnetic poles	1.5.03.01.0A	Changes in the earth's magnetic field
A 3.052	Flooding	2.3.02.03.0A	Soil and sediment transport in the biosphere
		2.3.11.02.0A	Surface runoff and evapotranspiration
		1.1.02.01.0A	Site flooding (during construction and operation)
		1.3.07.02.0B	Water table rise affects UZ
A 3.053	Flushing of water bodies	2.3.04.01.0A	Surface water transport and mixing
A 3.054	Food preparation	3.3.01.00.0A	Contaminated drinking water, foodstuffs and drugs)
A 3.055	Game ranching	2.4.09.02.0A	Animal farms and fisheries
A 3.056	Gas leakage into basements	2.4.07.00.0A	Dwellings
		3.3.08.00.0A	Radon and radon decay product exposure
A 3.057	Glaciation	1.3.05.00.0A	Glacial and ice sheet effect
A 3.058	Greenhouse food production	2.4.09.01.0A	Implementation of new agricultural practices or land use
		2.4.09.01.0B	Agricultural land use and irrigation
A 3.059	Greenhouse effect	1.4.01.02.0A	Greenhouse gas effects
A 3.060	Groundshine	3.3.04.03.0A	External exposure
A 3.061	Heat storage in lakes or underground	1.4.05.00.0A	Mining and other underground activities (human intrusion)

Table F-3. Cross Reference of Source FEPs to TSPA-LA FEPs (Continued)

Source FEP No.	Source FEP Name	TSPA-LA FEP Number	TSPA-LA FEP Name
A 3.062	Herbicides, pesticides and fungicides	3.3.02.01.0A	Plant uptake
		2.4.09.01.0B	Agricultural land use and irrigation
		2.4.09.01.0A	Implementation of new agricultural practices or land use
		3.3.03.01.0A	Contaminated non-food products and exposure
		3.3.02.02.0A	Animal uptake
A 3.063	Household dust and fumes	2.4.04.01.0A	Human lifestyle
		3.3.04.02.0A	Inhalation
		2.4.07.00.0A	Dwellings
A 3.064	Houseplants	2.4.07.00.0A	Dwellings
A 3.065	Human diet	3.3.04.01.0A	Ingestion
		3.3.01.00.0A	Contaminated drinking water, foodstuffs and drugs
A 3.066	Human soil ingestion	3.3.03.01.0A	Contaminated non-food products and exposure
		3.3.04.01.0A	Ingestion
		3.3.01.00.0A	Contaminated drinking water, foodstuffs and drugs
A 3.067	Hydroponics	2.4.09.01.0A	Implementation of new agricultural practices or land use
A 3.068	Industrial water use	2.4.10.00.0A	Urban and industrial land and water use
A 3.069	Intake of drugs	3.3.02.02.0A	Animal uptake
		3.3.01.00.0A	Contaminated drinking water, foodstuffs and drugs
A 3.070	Intrusion (deliberate)	1.4.02.01.0A	Deliberate human intrusion
A 3.071	Intrusion (inadvertent)	1.4.02.02.0A	Inadvertent human intrusion
A 3.072	Ion exchange in soil	2.2.08.09.0A	Sorption in the SZ
A 3.073	Irrigation	1.4.07.02.0A	Wells
		1.4.07.01.0A	Water management activities
		2.3.02.02.0A	Radionuclide accumulation in soils
		2.4.09.01.0A	Implementation of new agricultural practices or land use
		2.4.09.01.0B	Agricultural land use and irrigation
		3.3.02.01.0A	Plant uptake
		3.2.10.00.0A	Atmospheric transport of contaminants
A 3.074	Lake infilling	2.3.13.01.0A	Biosphere characteristics
A 3.075	Lake mixing (artificial)	2.3.04.01.0A	Surface water transport and mixing
A 3.076	Mutagenic contaminants	3.3.07.00.0A	Non-radiological toxicity and effects
		3.3.06.00.0A	Radiological toxicity and effects
A 3.077	Outdoor spraying of water	2.4.04.01.0A	Human lifestyle
		2.4.07.00.0A	Dwellings
		3.2.10.00.0A	Atmospheric transport of contaminants
A 3.078	Ozone layer failure	1.4.01.04.0A	Ozone layer failure
A 3.079	Peat and leaf litter harvesting	2.4.09.01.0B	Agricultural land use and irrigation
		2.4.09.01.0A	Implementation of new agricultural practices or land use
A 3.080	Plant roots	3.3.02.01.0A	Plant uptake
A 3.081	Precipitation (meteoric)	3.2.10.00.0A	Atmospheric transport of contaminants

Table F-3. Cross Reference of Source FEPs to TSPA-LA FEPs (Continued)

Source FEP No.	Source FEP Name	TSPA-LA FEP Number	TSPA-LA FEP Name
A 3.082	Radioactive decay	3.1.01.01.0A	Radioactive decay and ingrowth
		3.3.05.01.0A	Radiation doses
A 3.083	Radiotoxic contaminants	3.3.06.00.0A	Radiological toxicity and effects
A 3.084	Radon emission	3.3.08.00.0A	Radon and radon decay product exposure
A 3.085	Recycling	3.3.02.01.0A	Plant uptake
		3.3.02.03.0A	Fish uptake
		1.4.07.03.0A	Recycling of accumulated radionuclides from soils to groundwater
		3.3.03.01.0A	Contaminated non-food products and exposure
A 3.086	Rivercourse meander	2.3.04.01.0A	Surface water transport and mixing
		2.3.02.03.0A	Soil and sediment transport in the biosphere
A 3.087	Runoff	2.3.02.03.0A	Soil and sediment transport in the biosphere
		2.3.11.02.0A	Surface runoff and evapotranspiration
		2.3.11.01.0A	Precipitation
A 3.088	Saltation	3.2.10.00.0A	Atmospheric transport of contaminants
A 3.089	Scavengers and predators	3.3.02.02.0A	Animal uptake
		3.3.02.03.0A	Fish uptake
		3.3.04.01.0A	Ingestion
A 3.090	Seasons	1.3.01.00.0A	Climate change
A 3.091	Sediment resuspension in water bodies	1.2.04.07.0C	Ash redistribution via soil and sediment transport
		2.3.02.03.0A	Soil and sediment transport in the biosphere
		2.3.04.01.0A	Surface water transport and mixing
		2.3.06.00.0A	Marine features
A 3.092	Sedimentation in water bodies	2.3.06.00.0A	Marine features
		2.3.04.01.0A	Surface water transport and mixing
A 3.093	Sensitization to radiation	3.3.06.02.0A	Sensitization to radiation
A 3.094	Showers and humidifiers	2.4.07.00.0A	Dwellings
		3.3.04.03.0A	External exposure
A 3.095	Smoking	3.3.03.01.0A	Contaminated non-food products and exposure
A 3.096	Soil	2.3.02.02.0A	Radionuclide accumulation in soils
A 3.097	Soil depth	2.3.02.02.0A	Radionuclide accumulation in soils
		2.2.03.01.0A	Stratigraphy
		2.2.07.02.0A	Unsaturated groundwater flow in the geosphere
		1.3.07.01.0A	Water table decline
		2.2.07.03.0A	Capillary rise in the UZ
		1.3.07.02.0B	Water table rise affects UZ
A 3.098	Soil leaching	2.3.02.02.0A	Radionuclide accumulation in soils
A 3.099	Soil porewater pH	2.2.08.09.0A	Sorption in the SZ
A 3.100	Soil sorption	2.2.08.09.0A	Sorption in the SZ
A 3.101	Soil type	2.3.02.01.0A	Soil type
A 3.102	Space heating	3.3.03.01.0A	Contaminated non-food products and exposure
		2.4.07.00.0A	Dwellings
A 3.103	Surface water bodies	2.3.11.04.0A	Groundwater discharge to surface outside the reference biosphere
		2.3.04.01.0A	Surface water transport and mixing
		1.4.01.03.0A	Acid rain

Table F-3. Cross Reference of Source FEPs to TSPA-LA FEPs (Continued)

Source FEP No.	Source FEP Name	TSPA-LA FEP Number	TSPA-LA FEP Name
A 3.103	Surface water bodies (continued)	1.4.06.01.0A	Altered soil or surface water chemistry
		2.3.13.04.0A	Radionuclide release outside the reference biosphere
		2.2.08.11.0A	Groundwater discharge to surface within the reference biosphere
		3.2.10.00.0A	Atmospheric transport of contaminants
A 3.104	Surface water pH	1.4.01.03.0A	Acid rain
A 3.105	Suspension in air	3.2.10.00.0A	Atmospheric transport of contaminants
A 3.106	Technological advances in food production	1.4.09.00.0A	Technological developments
A 3.107	Teratogenic contaminants	3.3.06.00.0A	Radiological toxicity and effects
A 3.108	Terrestrial surface	2.3.01.00.0A	Topography and morphology
A 3.109	Toxicity of mined rock	1.4.02.02.0A	Inadvertent human intrusion
		1.4.04.00.0A	Drilling activities (human intrusion)
		1.4.05.00.0A	Mining and other underground activities (human intrusion)
		3.3.06.01.0A	Repository excavation
		1.4.02.01.0A	Deliberate human intrusion
		1.4.04.01.0A	Effects of drilling intrusion
A 3.110	Tree sap	3.3.04.01.0A	Ingestion
		3.3.02.01.0A	Plant uptake
		3.3.03.01.0A	Contaminated non-food products and exposure
A 3.111	Uncertainties	0.1.10.00.0A	Model and data issues
A 3.112	Urbanization on the discharge site	1.4.08.00.0A	Social and institutional developments
A 3.113	Vault heating effects	2.3.13.03.0A	Effects of repository heat on the biosphere
A 3.114	Water leaking into basements	2.4.07.00.0A	Dwellings
A 3.115	Water management projects	1.4.07.01.0A	Water management activities
		1.4.07.02.0A	Wells
A 3.116	Water source	3.3.01.00.0A	Contaminated drinking water, foodstuffs and drugs
A 3.117	Wetlands	2.3.13.04.0A	Radionuclide release outside the reference biosphere
		2.3.13.01.0A	Biosphere characteristics
A 3.118	Wind	3.2.10.00.0A	Atmospheric transport of contaminants
CA-1	DOE SNF waste package placement	2.1.01.02.0A	Interactions between co-located waste
CA-10	DOE SNF cladding condition	2.1.02.25.0A	DSNF cladding
CA-11	DOE SNF gap radionuclide inventory	2.1.01.01.0A	Waste inventory
CA-12	DOE SNF initial radionuclide inventory	2.1.01.01.0A	Waste inventory
CA-13	DOE SNF structure	2.1.01.01.0A	Waste inventory
CA-14	DOE SNF pyrophoricity	2.1.02.08.0A	Pyrophoricity from DSNF
CA-15	DOE SNF criticality in-situ	2.1.14.15.0A	In-package criticality (intact configuration)
		2.1.14.16.0A	In-package criticality (degraded configurations)

Table F-3. Cross Reference of Source FEPs to TSPA-LA FEPs (Continued)

Source FEP No.	Source FEP Name	TSPA-LA FEP Number	TSPA-LA FEP Name
CA-2	DOE SNF expected waste heat generation	2.1.11.01.0A	Heat generation in EBS
CA-3	DOE SNF waste package design	2.1.03.11.0A	Physical form of waste package and drip shield
CA-4	DOE SNF canister arrangement within waste package	2.1.01.02.0A	Interactions between co-located waste
CA-5	DOE SNF colocation with HLW	2.1.01.02.0B	Interactions between co-disposed waste
CA-6	DOE SNF canister design	2.1.03.11.0A	Physical form of waste package and drip shield
CA-7	DOE SNF canister atmosphere	2.1.01.03.0A	Heterogeneity of waste inventory
CA-8	DOE SNF geometry	2.1.01.02.0B	Interactions between co-disposed waste
		2.1.02.28.0A	Grouping of DSNF waste types into categories
CA-9	DOE SNF cladding material	2.1.02.25.0A	DSNF cladding
DE/Crit-1	Out-of-package criticality, fuel/magma mixture	2.2.14.10.0A	Far-field criticality resulting from a seismic event
		2.1.14.18.0A	In-package criticality resulting from a seismic event (intact configuration)
		2.2.14.12.0A	Far-field criticality resulting from an igneous event
		2.1.14.22.0A	In-package criticality resulting from rockfall (degraded configurations)
		2.2.14.11.0A	Far-field criticality resulting from rockfall
		2.1.14.19.0A	In-package criticality resulting from a seismic event (degraded configurations)
		2.1.14.25.0A	In-package criticality resulting from an igneous event (degraded configurations)
		2.1.14.23.0A	Near-field criticality resulting from rockfall
		2.1.14.21.0A	In-package criticality resulting from rockfall (intact configuration)
		2.1.14.20.0A	Near-field criticality resulting from a seismic event
		2.1.14.24.0A	In-package criticality resulting from an igneous event (intact configuration)
		2.1.14.26.0A	Near-field criticality resulting from an igneous event
DE/Igneous-1	Interaction of WT with Magma	1.2.10.02.0A	Hydrologic response to igneous activity
DE/Igneous-2	Interaction of UZ Pore Water with Magma	1.2.10.02.0A	Hydrologic response to igneous activity
DE/Igneous-3	Fragmentation	1.2.04.04.0A	Igneous intrusion interacts with EBS components
DE/Seismic-1	Seismicity associated with igneous activity	1.2.03.03.0A	Seismicity associated with igneous activity
DE/Seismic-2	Falling rock hits container, increased seepage occurs, speeds corrosion of container	2.1.03.07.0A	Mechanical impact on waste package
		2.1.03.07.0B	Mechanical impact on drip shield
EBS AMR-1	Drainage with Transport - Sealing and Plugging	2.1.08.12.0A	Induced hydrologic changes in invert
EBS AMR-2	Drains	2.1.08.12.0A	Induced hydrologic changes in invert
EBS AMR-3	Cold traps	2.1.08.04.0A	Condensation forms on roofs of drifts (drift-scale cold traps)
		2.1.08.04.0B	Condensation forms at repository edges (repository-scale cold traps)

Table F-3. Cross Reference of Source FEPs to TSPA-LA FEPs (Continued)

Source FEP No.	Source FEP Name	TSPA-LA FEP Number	TSPA-LA FEP Name
FFC-1	Far-field criticality, precipitation in organic reducing zone in or near water table	2.2.14.09.0A	Far-field criticality
FFC-2	Far-field criticality, sorption on clay/zeolite in TSbv	2.2.14.09.0A	Far-field criticality
FFC-3	Far-field criticality, precipitation caused by hydrothermal upwell or redox front in the SZ	2.2.14.09.0A	Far-field criticality
FFC-4	Far-field criticality, precipitation in perched water above TSbv	2.2.14.09.0A	Far-field criticality
FFC-5	Far-field criticality, precipitation in fractures of TSw rock	2.2.14.09.0A	Far-field criticality
FFC-6	Far-field criticality, dryout produces fissile salt in a perched water basin	2.2.14.09.0A	Far-field criticality
H 1.1.1	Container metal corrosion	2.1.03.01.0A	General corrosion of waste packages
H 1.1.2	Physico-chemical degradation of concrete	2.1.06.01.0A	Chemical effects of rock reinforcement and cementitious materials in EBS
		2.1.06.02.0A	Mechanical effects of rock reinforcement materials in EBS
H 1.1.3	Waste corrosion and solubility and speciation of radionuclides	2.1.09.04.0A	Radionuclide solubility, solubility limits, and speciation in the waste form and EBS
H 1.1.4	Electrochemical effects of metal corrosion	2.1.09.09.0A	Electrochemical effects in EBS
H 1.2.1	Hydrogen by metal corrosion	2.1.12.04.0A	Gas generation (CO2, CH4, H2S) from microbial degradation
		2.1.12.03.0A	Gas generation (H2) from waste package corrosion
H 1.2.2	Methane and carbon dioxide by microbial degradation	2.1.12.04.0A	Gas generation (CO2, CH4, H2S) from microbial degradation
H 1.2.3	Gas generation from concrete	2.1.12.04.0A	Gas generation (CO2, CH4, H2S) from microbial degradation
		2.1.13.01.0A	Radiolysis
H 1.2.4	Radioactive gases	2.1.12.07.0A	Effects of radioactive gases in EBS
H 1.2.5	Chemotoxic gases	2.1.12.03.0A	Gas generation (H2) from waste package corrosion
		2.1.12.04.0A	Gas generation (CO2, CH4, H2S) from microbial degradation
		2.1.12.02.0A	Gas generation (He) from waste form decay
		2.1.13.01.0A	Radiolysis
		2.1.12.07.0A	Effects of radioactive gases in EBS
H 1.2.6	Gas transport	2.1.12.01.0A	Gas generation (repository pressurization)
		2.1.12.06.0A	Gas transport in EBS
		2.1.12.07.0A	Effects of radioactive gases in EBS
H 1.2.7	Flammability	2.1.12.08.0A	Gas explosions in EBS
H 1.2.8	Thermo-chemical effects	2.1.12.03.0A	Gas generation (H2) from waste package corrosion
		2.1.12.06.0A	Gas transport in EBS
		2.1.12.01.0A	Gas generation (repository pressurization)
		2.1.12.07.0A	Effects of radioactive gases in EBS

Table F-3. Cross Reference of Source FEPs to TSPA-LA FEPs (Continued)

Source FEP No.	Source FEP Name	TSPA-LA FEP Number	TSPA-LA FEP Name
H 1.3.1	Radioactive decay and ingrowth	3.1.01.01.0A	Radioactive decay and ingrowth
H 1.3.2	Nuclear criticality	2.1.14.26.0A	Near-field criticality resulting from an igneous event
		2.1.14.21.0A	In-package criticality resulting from rockfall (intact configuration)
		2.1.14.22.0A	In-package criticality resulting from rockfall (degraded configurations)
		2.2.14.12.0A	Far-field criticality resulting from an igneous event
		2.2.14.11.0A	Far-field criticality resulting from rockfall
		2.1.14.16.0A	In-package criticality (degraded configurations)
		2.2.14.10.0A	Far-field criticality resulting from a seismic event
		2.2.14.09.0A	Far-field criticality
		2.1.14.19.0A	In-package criticality resulting from a seismic event (degraded configurations)
		2.1.14.23.0A	Near-field criticality resulting from rockfall
		2.1.14.20.0A	Near-field criticality resulting from a seismic event
		2.1.14.17.0A	Near-field criticality
		2.1.14.18.0A	In-package criticality resulting from a seismic event (intact configuration)
		2.1.14.15.0A	In-package criticality (intact configuration)
		2.1.14.24.0A	In-package criticality resulting from an igneous event (intact configuration)
		2.1.14.25.0A	In-package criticality resulting from an igneous event (degraded configurations)
H 1.4.1	Waste-form and backfill consolidation	2.1.08.15.0A	Consolidation of EBS components
H 1.4.2	Vault collapse	2.1.07.02.0A	Drift collapse
H 1.5.1	Desaturation (pumping) effects	2.2.01.03.0A	Changes in fluid saturations in the excavation disturbed zone
		2.1.08.03.0A	Repository dry-out due to waste heat
		2.2.07.21.0A	Drift shadow forms below repository
H 1.5.2	Disturbed zone (hydromechanical) effects	2.2.01.01.0A	Mechanical effects of excavation and construction in the near-field
H 1.5.3	Unsaturated flow due to gas production	2.1.12.03.0A	Gas generation (H2) from waste package corrosion
		2.1.12.02.0A	Gas generation (He) from waste form decay
		2.1.12.01.0A	Gas generation (repository pressurization)
		2.1.08.07.0A	Unsaturated flow in the EBS
		2.1.12.07.0A	Effects of radioactive gases in EBS
		2.1.12.06.0A	Gas transport in EBS
		2.1.12.04.0A	Gas generation (CO2, CH4, HS2) from microbial degradation
H 1.5.4	Saturated groundwater flow	2.1.08.09.0A	Saturated flow in the EBS

Table F-3. Cross Reference of Source FEPs to TSPA-LA FEPs (Continued)

Source FEP No.	Source FEP Name	TSPA-LA FEP Number	TSPA-LA FEP Name
H 1.5.5	Transport of chemically-active substances into the near-field	2.1.09.01.0B	Chemical characteristics of water in waste package
		2.1.09.27.0A	Coupled effects on radionuclide transport in EBS
		2.1.09.13.0A	Complexation in EBS
		2.2.08.01.0B	Chemical characteristics of groundwater in the UZ
		2.1.09.08.0A	Diffusion of dissolved radionuclides in EBS
		2.1.09.01.0A	Chemical characteristics of water in drifts
		2.2.08.10.0B	Colloidal transport in the UZ
H 1.6.1	Thermal effects: Rock-mass changes	2.2.10.01.0A	Repository-induced thermal effects on flow in the UZ
H 1.6.2	Thermal effects: Hydrogeological changes	2.2.10.13.0A	Repository-induced thermal effects on flow in the SZ
		2.2.10.10.0A	Two-phase buoyant flow/heat pipes
		2.2.10.01.0A	Repository-induced thermal effects on flow in the UZ
H 1.6.3	Thermal effects: Chemical and microbiological changes	2.1.11.08.0A	Thermal effects on chemistry and microbial activity in the EBS
H 1.6.4	Thermal effects: Transport (diffusion) effects	2.1.11.10.0A	Thermal effects on transport in EBS
H 2.1.1	Regional tectonic activity	1.2.01.01.0A	Tectonic activity - large scale
H 2.1.2	Magmatic activity	1.2.04.06.0A	Eruptive conduit to surface intersects repository
		1.2.04.05.0A	Magma or pyroclastic base surge transports waste
		1.4.02.03.0A	Igneous event precedes human intrusion
		1.2.04.02.0A	Igneous activity changes rock properties
		1.2.04.04.0A	Igneous intrusion interacts with EBS components
		1.2.04.03.0A	Igneous intrusion into repository
H 2.1.3	Regional metamorphism	1.2.05.00.0A	Metamorphism
H 2.1.4	Diagenesis	1.2.08.00.0A	Diagenesis
H 2.1.5	Diapirism	1.2.09.01.0A	Diapirism
H 2.1.6	Seismicity	1.2.03.02.0B	Seismic-induced rockfall damages EBS components
		2.2.06.01.0A	Seismic activity changes porosity and permeability of rock
		1.2.02.03.0A	Fault displacement damages EBS components
		2.1.07.02.0A	Drift collapse
		2.2.06.02.0A	Seismic activity changes porosity and permeability of faults
		1.2.03.02.0A	Seismic ground motion damages EBS components
		1.2.10.01.0A	Hydrologic response to seismic activity
		2.1.02.24.0A	Mechanical impact on cladding
		2.1.03.07.0A	Mechanical impact on waste package
		2.1.03.07.0B	Mechanical impact on drip shield
		2.2.06.03.0A	Seismic activity alters perched water zones
		2.2.06.02.0B	Seismic activity changes porosity and permeability of fractures
		1.2.03.03.0A	Seismicity associated with igneous activity

Table F-3. Cross Reference of Source FEPs to TSPA-LA FEPs (Continued)

Source FEP No.	Source FEP Name	TSPA-LA FEP Number	TSPA-LA FEP Name
H 2.1.7	Faulting/fracturing	2.2.07.13.0A	Water-conducting features in the SZ
		2.2.07.04.0A	Focusing of unsaturated flow (fingers, weeps)
		2.2.12.00.0A	Undetected features in the UZ
		2.2.07.08.0A	Fracture flow in the UZ
		2.2.06.02.0B	Seismic activity changes porosity and permeability of fractures
		1.2.04.02.0A	Igneous activity changes rock properties
		1.2.02.03.0A	Fault displacement damages EBS components
		1.2.02.02.0A	Faults
		1.2.02.01.0A	Fractures
		2.2.06.02.0A	Seismic activity changes porosity and permeability of faults
		2.2.12.00.0B	Undetected features in the SZ
		1.5.01.01.0A	Meteorite impact
H 2.1.8	Major incision	1.3.05.00.0A	Glacial and ice sheet effect
		1.2.07.01.0A	Erosion/denudation
		1.4.11.00.0A	Explosions and crashes (human activities)
		1.5.01.01.0A	Meteorite impact
		1.2.04.06.0A	Eruptive conduit to surface intersects repository
H 2.1.9	Effects of natural gases.	2.2.11.02.0A	Gas effects in the UZ
		2.2.11.01.0A	Gas effects in the SZ
H 2.2.1	Changes in geometry and driving forces of the flow system	1.3.04.00.0A	Periglacial effects
		2.3.01.00.0A	Topography and morphology
		1.3.07.02.0B	Water table rise affects UZ
		1.3.07.02.0A	Water table rise affects SZ
		1.3.05.00.0A	Glacial and ice sheet effect
		1.2.07.01.0A	Erosion/denudation
H 2.2.2	Rock property changes	2.2.03.02.0A	Rock properties of host rock and other units
		2.2.01.02.0B	Chemical changes in the near-field from backfill
		1.2.04.02.0A	Igneous activity changes rock properties
		1.2.05.00.0A	Metamorphism
		2.2.06.01.0A	Seismic activity changes porosity and permeability of rock
		2.2.08.03.0B	Geochemical interactions and evolution in the UZ
		2.2.03.01.0A	Stratigraphy
		2.2.06.02.0B	Seismic activity changes porosity and permeability of fractures
		2.2.08.03.0A	Geochemical interactions and evolution in the SZ
		2.2.06.02.0A	Seismic activity changes porosity and permeability of faults
		2.2.10.05.0A	Thermo-mechanical stresses alter characteristics of rocks above and below the repository
		1.1.02.00.0B	Mechanical effects of excavation and construction in EBS
		2.2.06.04.0A	Effects of subsidence

Table F-3. Cross Reference of Source FEPs to TSPA-LA FEPs (Continued)

Source FEP No.	Source FEP Name	TSPA-LA FEP Number	TSPA-LA FEP Name
H 2.2.3	Groundwater flow	0.1.10.00.0A	Model and data issues
		2.2.07.12.0A	Saturated groundwater flow in the geosphere
		2.1.09.21.0A	Transport of particles larger than colloids in EBS
		2.2.10.03.0B	Natural geothermal effects on flow in the UZ
		2.2.08.01.0A	Chemical characteristics of groundwater in the SZ
		1.4.01.04.0A	Ozone layer failure
		1.2.10.02.0A	Hydrologic response to igneous activity
		1.2.09.01.0A	Diapirism
		2.1.11.07.0A	Thermal expansion/stress of in-drift EBS components
		1.2.02.01.0A	Fractures
		2.2.08.03.0B	Geochemical interactions and evolution in the UZ
		1.5.03.02.0A	Earth tides
		1.2.06.00.0A	Hydrothermal activity
		2.2.07.02.0A	Unsaturated groundwater flow in the geosphere
		2.2.08.01.0B	Chemical characteristics of groundwater in the UZ
		2.1.04.02.0A	Chemical properties and evolution of backfill
		2.1.04.05.0A	Thermal-mechanical properties and evolution of backfill
		2.1.05.02.0A	Radionuclide transport through seals
		2.2.10.01.0A	Repository-induced thermal effects on flow in the UZ
		2.1.08.07.0A	Unsaturated flow in the EBS
		2.1.13.02.0A	Radiation damage in EBS
		2.2.07.13.0A	Water-conducting features in the SZ
		2.2.07.14.0A	Chemically-induced density effects on groundwater flow
		2.1.08.09.0A	Saturated flow in the EBS
		2.2.10.03.0A	Natural geothermal effects on flow in the SZ
		2.2.08.03.0A	Geochemical interactions and evolution in the SZ
		2.3.11.03.0A	Infiltration and recharge
		2.1.06.04.0A	Flow through rock reinforcement materials in EBS
H 2.3.1	Far-field transport: Advection	2.2.07.15.0B	Advection and dispersion in the UZ
		2.2.07.15.0A	Advection and dispersion in the SZ
H 2.3.10	Far-field transport: Transport of radioactive gases	2.2.11.03.0A	Gas transport in geosphere
H 2.3.11	Far-field transport: Gas induced groundwater transport	2.2.10.10.0A	Two-phase buoyant flow/heat pipes
		2.2.11.01.0A	Gas effects in the SZ
		2.2.11.03.0A	Gas transport in geosphere
H 2.3.12	Far-field transport: Thermal effects on hydrochemistry	2.2.10.08.0A	Thermo-chemical alteration in the SZ (solubility, speciation and phase change)
		2.2.10.06.0A	Thermo-chemical alteration in the UZ (solubility, speciation and phase change)

Table F-3. Cross Reference of Source FEPs to TSPA-LA FEPs (Continued)

Source FEP No.	Source FEP Name	TSPA-LA FEP Number	TSPA-LA FEP Name
H 2.3.13	Far-field transport: Biogeochemical changes	2.2.09.01.0B	Microbial activity in the UZ
		2.2.09.01.0A	Microbial activity in the SZ
		1.3.01.00.0A	Climate change
H 2.3.2	Far-field transport: Diffusion	2.2.07.17.0A	Diffusion in the SZ
		2.2.08.08.0A	Matrix diffusion in the SZ
		2.2.08.08.0B	Matrix diffusion in the UZ
		2.2.08.05.0A	Diffusion in the UZ
H 2.3.3	Far-field transport: Hydrodynamic dispersion	2.2.07.15.0B	Advection and dispersion in the UZ
		2.2.07.16.0A	Dilution of radionuclides in groundwater
		2.2.07.15.0A	Advection and dispersion in the SZ
H 2.3.4	Far-field transport: Solubility constraints	2.2.08.07.0C	Radionuclide solubility limits in the biosphere
		2.2.10.08.0A	Thermo-chemical alteration in the SZ (solubility, speciation, phase changes)
		2.2.10.06.0A	Thermo-chemical alteration in the UZ (solubility, speciation, phase changes)
		2.2.08.07.0B	Radionuclide solubility limits in the UZ
		2.2.08.07.0A	Radionuclide solubility limits in the SZ
		2.1.09.11.0A	Chemical effects of waste-rock contact
		2.2.01.04.0A	Radionuclide solubility in the excavation disturbed zone
H 2.3.5	Far-field transport: Sorption including ion-exchange	2.2.08.09.0A	Sorption in the SZ
		2.2.08.09.0B	Sorption in the UZ
H 2.3.6	Far-field transport: Changes in sorptive surfaces	2.2.08.09.0A	Sorption in the SZ
		2.2.08.03.0B	Geochemical interactions and evolution in the UZ
		2.2.08.03.0A	Geochemical interactions and evolution in the SZ
		2.2.08.01.0B	Chemical characteristics of groundwater in the UZ
		2.2.08.01.0A	Chemical characteristics of groundwater in the SZ
		2.2.08.09.0B	Sorption in the UZ
H 2.3.7	Far-field transport: Changes in groundwater chemistry and flow direction	2.2.08.03.0A	Geochemical interactions and evolution in the SZ
		2.2.08.03.0B	Geochemical interactions and evolution in the UZ
		2.2.08.09.0A	Sorption in the SZ
H 2.3.8	Far-field transport: Colloid transport	2.2.08.10.0A	Colloidal transport in the SZ
		2.2.08.10.0B	Colloidal transport in the UZ
H 2.3.9	Far-field transport: Transport of radionuclides bound to microbes	2.2.08.10.0A	Colloidal transport in the SZ
		2.2.09.01.0B	Microbial activity in the UZ
		2.2.09.01.0A	Microbial activity in the SZ
H 2.4.1	Generalised denudation	1.2.07.01.0A	Erosion/denudation
H 2.4.2	Localised denudation	1.2.07.01.0A	Erosion/denudation
H 3.1.1	Climate change: Human induced	1.4.01.00.0A	Human influences on climate
		1.4.01.02.0A	Greenhouse gas effects
H 3.1.2	Climate change: Natural	1.3.04.00.0A	Periglacial effects
		1.3.01.00.0A	Climate change
		1.3.05.00.0A	Glacial and ice sheet effect

Table F-3. Cross Reference of Source FEPs to TSPA-LA FEPs (Continued)

Source FEP No.	Source FEP Name	TSPA-LA FEP Number	TSPA-LA FEP Name
H 3.1.3	Exit from glacial/interglacial cycling	1.3.04.00.0A	Periglacial effects
		1.3.05.00.0A	Glacial and ice sheet effect
		1.3.01.00.0A	Climate change
H 3.1.4	Intensification of natural climate change	1.3.01.00.0A	Climate change
		1.3.05.00.0A	Glacial and ice sheet effect
		1.3.04.00.0A	Periglacial effects
H 4.1.1	Groundwater discharge to soils and surface waters	2.3.11.04.0A	Groundwater discharge to surface outside the reference biosphere
		2.3.02.02.0A	Radionuclide accumulation in soils
H 4.1.2	Solid discharge via erosional processes	2.3.02.02.0A	Radionuclide accumulation in soils
		1.2.07.01.0A	Erosion/denudation
		1.4.07.03.0A	Recycling of accumulated radionuclides from soils to groundwater
H 4.1.3	Gas discharge	2.2.11.03.0A	Gas transport in geosphere
H 4.2.1	Soil moisture and evaporation.	1.4.07.03.0A	Recycling of accumulated radionuclides from soils to groundwater
		2.3.02.02.0A	Radionuclide accumulation in soils
H 4.2.2	Surface water mixing	2.2.08.11.0A	Groundwater discharge to surface within the reference biosphere
		2.3.11.04.0A	Groundwater discharge to surface outside the reference biosphere
		1.4.06.01.0A	Altered soil or surface water chemistry
		2.3.11.03.0A	Infiltration and recharge
		3.2.07.01.0A	Isotopic dilution
		2.3.04.01.0A	Surface water transport and mixing
H 4.2.3	Sediment transport including bioturbation	2.3.02.03.0A	Soil and sediment transport in the biosphere
H 4.2.4	Sediment/water/gas interaction with the atmosphere.	2.3.13.02.0A	Radionuclide alteration during biosphere transport
		2.3.04.01.0A	Surface water transport and mixing
		2.3.02.03.0A	Soil and sediment transport in the biosphere
		2.3.09.01.0A	Animal burrowing/intrusion
H 4.2.5	Bioaccumulation and translocation	3.3.02.03.0A	Fish uptake
		3.3.02.02.0A	Animal uptake
		3.3.04.01.0A	Ingestion
		3.3.02.01.0A	Plant uptake
H 4.2.6	Biogeochemical processes	2.3.13.02.0A	Radionuclide alteration during biosphere transport
H 4.3.1	Land and surface water use: Terrestrial	2.4.09.02.0A	Animal farms and fisheries
		1.4.07.01.0A	Water management activities
		2.4.09.01.0A	Implementation of new agricultural practices or land use
		2.4.08.00.0A	Wild and natural land and water use
		1.4.07.02.0A	Wells
		2.4.10.00.0A	Urban and industrial land and water use
		2.4.09.01.0B	Agricultural land use and irrigation

Table F-3. Cross Reference of Source FEPs to TSPA-LA FEPs (Continued)

Source FEP No.	Source FEP Name	TSPA-LA FEP Number	TSPA-LA FEP Name
H 4.3.1	Land and surface water use: Terrestrial (continued)	1.4.08.00.0A	Social and institutional developments
		2.3.13.04.0A	Radionuclide release outside the reference biosphere
		2.3.13.01.0A	Biosphere characteristics
H 4.3.2	Land and surface water use: Estuarine	1.4.08.00.0A	Social and institutional developments
		2.4.10.00.0A	Urban and industrial land and water use
		2.4.09.01.0B	Agricultural land use and irrigation
		1.4.07.02.0A	Wells
		2.4.09.01.0A	Implementation of new agricultural practices or land use
		2.4.08.00.0A	Wild and natural land and water use
		2.3.13.01.0A	Biosphere characteristics
		1.4.07.01.0A	Water management activities
		2.4.09.02.0A	Animal farms and fisheries
		2.3.13.04.0A	Radionuclide release outside the reference biosphere
H 4.3.3	Land and surface water use: Coastal waters	2.4.09.02.0A	Animal farms and fisheries
		2.4.10.00.0A	Urban and industrial land and water use
		1.4.07.01.0A	Water management activities
		2.3.13.04.0A	Radionuclide release outside the reference biosphere
		2.3.13.01.0A	Biosphere characteristics
		2.3.06.00.0A	Marine features
		1.4.08.00.0A	Social and institutional developments
		2.4.08.00.0A	Wild and natural land and water use
H 4.3.4	Land and surface water use: Seas	2.3.06.00.0A	Marine features
		1.4.07.01.0A	Water management activities
		2.4.10.00.0A	Urban and industrial land and water use
		2.4.09.02.0A	Animal farms and fisheries
		2.4.08.00.0A	Wild and natural land and water use
		2.3.13.01.0A	Biosphere characteristics
		1.4.08.00.0A	Social and institutional developments
H 4.4.1	Human exposure: External	3.3.04.03.0A	External exposure
H 4.4.2	Human exposure: Ingestion	3.3.04.01.0A	Ingestion
H 4.4.3	Human exposure: Inhalation	3.3.04.02.0A	Inhalation
H 5.1.1	Loss of integrity of borehole seals	2.1.05.01.0A	Flow through seals (access ramps and ventilation shafts)
		1.1.01.01.0A	Open site investigation boreholes
		2.1.05.03.0A	Degradation of seals
		2.1.05.02.0A	Radionuclide transport through seals
H 5.1.2	Loss of integrity of shaft or access tunnel seals	2.1.05.02.0A	Radionuclide transport through seals
		2.1.05.01.0A	Flow through seals (access ramps and ventilation shafts)
		2.1.05.03.0A	Degradation of seals
H 5.1.3	Incomplete near-field chemical conditioning	2.1.09.01.0B	Chemical characteristics of water in waste package
		2.1.09.01.0A	Chemical characteristics of water in drifts

Table F-3. Cross Reference of Source FEPs to TSPA-LA FEPs (Continued)

Source FEP No.	Source FEP Name	TSPA-LA FEP Number	TSPA-LA FEP Name
H 5.2.1	Meteorite impact	1.5.01.01.0A	Meteorite impact
H 5.2.2	Deliberate intrusion	1.4.02.01.0A	Deliberate human intrusion
H 5.2.3	Malicious intrusion	1.4.02.01.0A	Deliberate human intrusion
H 5.2.4	Accidental intrusion	1.4.02.02.0A	Inadvertent human intrusion
I 001	Acid rain	1.4.01.03.0A	Acid rain
I 002	Alkali Flats	1.4.06.01.0A	Altered soil or surface water chemistry
		2.3.02.02.0A	Radionuclide accumulation in soils
I 003	Animal diets (domestic and wild)	3.3.02.02.0A	Animal uptake
I 004	Animals (intrusion)/ plants (root uptake)	3.3.02.02.0A	Animal uptake
		3.3.02.03.0A	Fish uptake
		3.3.02.01.0A	Plant uptake
		2.4.09.02.0A	Animal farms and fisheries
I 007	Animals (external contamination)	2.4.09.02.0A	Animal farms and fisheries
		3.3.02.02.0A	Animal uptake
		3.3.04.03.0A	External exposure
		1.4.07.02.0A	Wells
I 008a	Archaeology (a find during construction)	1.4.02.01.0A	Deliberate human intrusion
I 008b	Archaeology (a find during post-closure period)	1.4.03.00.0A	Unintrusive site investigation
		1.4.02.01.0A	Deliberate human intrusion
I 009	Sediments (in water bodies)	2.4.09.02.0A	Animal farms and fisheries
		2.3.04.01.0A	Surface water transport and mixing
		3.3.02.02.0A	Animal uptake
		3.3.02.03.0A	Fish uptake
		2.3.06.00.0A	Marine features
I 010	Recycling process (biomass)	3.3.03.01.0A	Contaminated non-food products and exposure
		2.4.09.01.0B	Agricultural land use and irrigation
		1.4.07.03.0A	Recycling of accumulated radionuclides from soils to groundwater
I 011a	Backfill (properties)	1.1.03.01.0B	Error in backfill emplacement
		2.1.04.09.0A	Radionuclide transport in backfill
		2.1.04.02.0A	Chemical properties and evolution of backfill
		2.2.01.02.0B	Chemical changes in the near-field from backfill
		2.1.04.04.0A	Thermal-mechanical effects of backfill
		2.1.04.01.0A	Flow in the backfill
		2.1.04.03.0A	Erosion or dissolution of backfill
I 011b	Backfill (faulty emplacement)	2.2.01.02.0B	Chemical changes in the near-field from backfill
		2.1.04.04.0A	Thermal-mechanical effects of backfill
		2.1.04.09.0A	Radionuclide transport in backfill
		2.1.04.03.0A	Erosion or dissolution of backfill
		2.1.04.02.0A	Chemical properties and evolution of backfill
		2.1.04.01.0A	Flow in the backfill
		2.1.04.05.0A	Thermal-mechanical properties and evolution of backfill

Table F-3. Cross Reference of Source FEPs to TSPA-LA FEPs (Continued)

Source FEP No.	Source FEP Name	TSPA-LA FEP Number	TSPA-LA FEP Name
I 012	Biological activity (bacteria & microbes)	2.1.13.03.0A	Radiological mutation of microbes
		1.2.08.00.0A	Diagenesis
		2.1.02.14.0A	Microbially influenced corrosion (MIC) of cladding
		2.1.12.04.0A	Gas generation (CO2, CH4, H2S) from microbial degradation
I 013	Bedrock fracture	2.2.01.02.0A	Thermally-induced stress changes in the near-field
		1.2.04.02.0A	Igneous activity changes rock properties
		2.2.10.05.0A	Thermo-mechanical stresses alter characteristics of rocks above and below the repository
		2.2.01.01.0A	Mechanical effects of excavation and construction in the near-field
		2.2.10.04.0B	Thermo-mechanical stresses alter characteristics of faults near repository
		2.2.06.02.0B	Seismic activity changes porosity and permeability of fractures
		2.2.06.04.0A	Effects of subsidence
		2.2.10.04.0A	Thermo-mechanical stresses alter characteristics of fractures near repository
		1.5.01.01.0A	Meteorite impact
I 014	Bioaccumulation/ bioconcentration/ biomagnification	3.3.02.01.0A	Plant uptake
		3.3.02.03.0A	Fish uptake
		3.3.02.02.0A	Animal uptake
I 015	Gas generation (CH4, CO2, H2)	2.1.10.01.0A	Microbial activity in EBS
		2.1.12.02.0A	Gas generation (He) from waste form decay
		2.1.12.03.0A	Gas generation (H2) from waste package corrosion
		2.1.12.04.0A	Gas generation (CO2, CH4, H2S) from microbial degradation
		2.2.11.01.0A	Gas effects in the SZ
		2.2.11.02.0A	Gas effects in the UZ
I 017	Biological evolution	1.5.02.00.0A	Species evolution
I 020	Non radiological toxicity	3.3.06.02.0A	Sensitization to radiation
I 021	Bioturbation (soil & sediment)	2.4.09.01.0B	Agricultural land use and irrigation
		2.3.09.01.0A	Animal burrowing/intrusion
		3.2.10.00.0A	Atmospheric transport of contaminants
		2.3.02.03.0A	Soil and sediment transport in the biosphere
I 022	Explosions/bombs/blasting/ collision/impacts/vibration	1.2.03.02.0D	Seismic-induced drift collapse alters in-drift thermohydrology
		1.4.11.00.0A	Explosions and crashes (human activities)
		2.2.01.01.0A	Mechanical effects of excavation and construction in the near-field
		1.5.01.01.0A	Meteorite impact
		1.2.03.02.0B	Seismic-induced rockfall damages EBS components

Table F-3. Cross Reference of Source FEPs to TSPA-LA FEPs (Continued)

Source FEP No.	Source FEP Name	TSPA-LA FEP Number	TSPA-LA FEP Name
I 022	Explosions/bombs/blasting/ collision/impacts/vibration (continued)	1.2.03.02.0A	Seismic ground motion damages EBS components
		1.1.02.00.0B	Mechanical effects of excavation and construction in EBS
		1.2.03.02.0C	Seismic-induced drift collapse damages EBS components
		2.1.12.08.0A	Gas explosions in EBS
I 025	Buffer (plugging by bitumen, slime molds, waste degradation products, etc.)	2.1.04.01.0A	Flow in the backfill
I 027	Buffer (channelling)	2.1.04.01.0A	Flow in the backfill
I 028a	Buffer(degradation)	2.1.04.03.0A	Erosion or dissolution of backfill
I 028b	Buffer (quality)	2.1.04.02.0A	Chemical properties and evolution of backfill
I 029	Buffer (faulty emplacement)	1.1.03.01.0B	Error in backfill emplacement
I 030	Buffer (washout of clay)	2.1.04.01.0A	Flow in the backfill
		2.1.04.02.0A	Chemical properties and evolution of backfill
		2.1.04.03.0A	Erosion or dissolution of backfill
I 032	Capillary rise in soil	2.1.08.06.0A	Capillary effects (wicking) in EBS
		2.2.07.03.0A	Capillary rise in the UZ
I 034	Void formation (cave-ins, cavitation-outside the vault)	2.2.06.04.0A	Effects of subsidence
I 039	Vault chemical interactions	2.1.01.02.0B	Interactions between co-disposed waste
		2.1.12.03.0A	Gas generation (H2) from waste package corrosion
		2.1.12.02.0A	Gas generation (He) from waste form decay
		2.1.09.02.0A	Chemical interaction with corrosion products
		2.1.01.02.0A	Interactions between co-located waste
		2.1.02.29.0A	Flammable gas generation from DSNF
I 040	Farfield chemical interactions	2.2.08.03.0B	Geochemical interactions and evolution in the UZ
		2.2.08.03.0A	Geochemical interactions and evolution in the SZ
I 042	Chemical speciation (wrong assumption for model)	2.1.09.04.0A	Radionuclide solubility, solubility limits, and speciation in the waste form and EBS
		0.1.10.00.0A	Model and data issues
		2.2.08.03.0A	Geochemical interactions and evolution in the SZ
		2.2.08.07.0A	Radionuclide solubility limits in the SZ
		2.2.08.07.0B	Radionuclide solubility limits in the UZ
		2.2.08.03.0B	Geochemical interactions and evolution in the UZ
I 044	Chealting agents	2.2.08.06.0B	Complexation in the UZ
		2.2.08.06.0A	Complexation in the SZ
I 045	Progency nuclides (critical radionuclides)	3.1.01.01.0A	Radioactive decay and ingrowth
		3.3.05.01.0A	Radiation doses
I 046a	Waste management sites adjacent (additive effects of contaminants)	1.4.06.01.0A	Altered soil or surface water chemistry

Table F-3. Cross Reference of Source FEPs to TSPA-LA FEPs (Continued)

Source FEP No.	Source FEP Name	TSPA-LA FEP Number	TSPA-LA FEP Name
I 046b	Waste management sites adjacent (effects on vault)	1.4.06.01.0A	Altered soil or surface water chemistry
I 048	Buffer (degradation by concrete)	2.1.04.02.0A	Chemical properties and evolution of backfill
I 049	Climate change	2.3.13.01.0A	Biosphere characteristics
		1.3.04.00.0A	Periglacial effects
		1.4.01.02.0A	Greenhouse gas effects
		1.5.01.02.0A	Extraterrestrial events
		1.5.03.01.0A	Changes in the earth's magnetic field
		1.4.01.00.0A	Human influences on climate
		1.3.07.02.0B	Water table rise affects UZ
		1.3.05.00.0A	Glacial and ice sheet effect
		1.4.01.03.0A	Acid rain
		1.4.01.01.0A	Climate modification increases recharge
		1.3.07.02.0A	Water table rise affects SZ
		1.4.01.04.0A	Ozone layer failure
		1.3.07.01.0A	Water table decline
I 057	Weather (hurricanes and tornadoes)	2.3.11.01.0A	Precipitation
		1.2.07.01.0A	Erosion/denudation
		1.1.12.01.0A	Accidents and unplanned events during construction and operation
I 058	Colloid formation (natural and vault generated)	2.1.09.16.0A	Formation of pseudo-colloids (natural) in EBS
		2.1.09.15.0A	Formation of true (intrinsic) colloids in EBS
		2.1.09.02.0A	Chemical interaction with corrosion products
		2.1.09.18.0A	Formation of microbial colloids in EBS
		2.1.09.25.0A	Formation of colloids (waste-form) by co-precipitation in EBS
		2.1.09.17.0A	Formation of pseudo-colloids (corrosion product) in EBS
I 061	Concrete (influence on vault chemistry)	2.1.12.04.0A	Gas generation (CO_2, CH_4, H_2S) from microbial degradation
		2.1.11.03.0A	Exothermic reactions in the EBS
I 062a1	Concrete (incorrect structural design)	1.1.08.00.0A	Inadequate quality control and deviations from design
		1.1.07.00.0A	Repository design
I 062a2	Concrete (incorrect mix design)	1.1.08.00.0A	Inadequate quality control and deviations from design
I 062b	Concrete (incorrect preparation/emplacement)	1.1.08.00.0A	Inadequate quality control and deviations from design
I 062c	Concrete performance (incorrect modelling)	1.1.08.00.0A	Inadequate quality control and deviations from design
		0.1.10.00.0A	Model and data issues
I 062d	Concrete (degradation–natural, artificial	2.1.06.01.0A	Chemical effects of rock reinforcement and cementitious materials in EBS
I 062e	Concrete (rebar corrosion)	2.1.06.01.0A	Chemical effects of rock reinforcement and cementitious materials in EBS
		2.1.06.02.0A	Mechanical effects of rock reinforcement materials in EBS
I 062f	Concrete (poor quality - procurement)	1.1.08.00.0A	Inadequate quality control and deviations from design

Table F-3. Cross Reference of Source FEPs to TSPA-LA FEPs (Continued)

Source FEP No.	Source FEP Name	TSPA-LA FEP Number	TSPA-LA FEP Name
I 065	Waste container (metal corrosion products)	2.1.09.27.0A	Coupled effects on radionuclide transport in EBS
		2.1.09.02.0A	Chemical interaction with corrosion products
I 066	Waste container (corrosion/collapse)	2.1.07.02.0A	Drift collapse
		1.2.03.02.0A	Seismic ground motion damages EBS components
		1.2.02.03.0A	Fault displacement damages EBS components
		2.1.03.04.0A	Hydride cracking of waste packages
		2.1.07.05.0A	Creep of metallic materials in the waste package
		2.1.07.01.0A	Rockfall
		2.1.03.11.0A	Physical form of waste package and drip shield
		2.1.03.08.0A	Early failure of waste packages
		2.1.03.05.0A	Microbially influenced corrosion (MIC) of waste packages
		2.1.03.03.0A	Localized corrosion of waste packages
		2.1.03.02.0A	Stress corrosion cracking (SCC) of waste packages
		2.1.03.01.0A	General corrosion of waste packages
		1.2.04.03.0A	Igneous intrusion into repository
		1.2.03.02.0B	Seismic-induced rockfall damages EBS components
		2.1.03.06.0A	Internal corrosion of waste packages prior to breach
		2.1.03.07.0A	Mechanical impact on waste package
		2.1.08.15.0A	Consolidation of EBS components
I 069	Atmospheric pathways (dispersion)	2.3.02.03.0A	Soil and sediment transport in the biosphere
		3.3.02.01.0A	Plant uptake
I 070	Correlation of model parameters	0.1.10.00.0A	Model and data issues
I 071	Corrosive chemicals (in vault)	2.1.06.05.0D	Chemical degradation of invert
		2.2.08.12.0B	Chemistry of water flowing into the waste package
		2.1.08.01.0A	Water influx at the repository
		1.1.02.00.0A	Chemical effects of excavation and construction in EBS
		2.1.02.15.0A	Localized (radiolysis enhanced) corrosion of cladding
		2.1.03.06.0A	Internal corrosion of waste packages prior to breach
		2.1.06.05.0C	Chemical degradation of emplacement pallet
		2.1.06.01.0A	Chemical effects of rock reinforcement and cementitious materials in EBS
		2.2.08.12.0A	Chemistry of water flowing into the drift
		2.2.08.04.0A	Re-dissolution of precipitates directs more corrosive fluids to waste packages
		2.1.09.11.0A	Chemical effects of waste-rock contact
		2.1.09.01.0B	Chemical characteristics of water in waste package
		2.1.09.01.0A	Chemical characteristics of water in drifts
		2.1.06.07.0A	Chemical effects at EBS component interfaces

Table F-3. Cross Reference of Source FEPs to TSPA-LA FEPs (Continued)

Source FEP No.	Source FEP Name	TSPA-LA FEP Number	TSPA-LA FEP Name
I 072	Modelling (SYVAC/NSURE adequacy)	0.1.10.00.0A	Model and data issues
I 074a	Lake exposure scenario	2.4.08.00.0A	Wild and natural land and water use
		2.2.08.11.0A	Groundwater discharge to surface within the reference biosphere
I 074b	Well exposure scenario	1.4.07.02.0A	Wells
I 074c	Swamp exposure scenario	3.3.04.03.0A	External exposure
		3.3.04.01.0A	Ingestion
		2.4.04.01.0A	Human lifestyle
I 074d	Combination exposure scenario	1.4.02.01.0A	Deliberate human intrusion
		3.3.04.02.0A	Inhalation
		3.3.04.01.0A	Ingestion
		1.4.02.02.0A	Inadvertent human intrusion
		3.3.05.01.0A	Radiation doses
		3.3.04.03.0A	External exposure
I 074e	Artificial lake exposure scenario	2.4.04.01.0A	Human lifestyle
		3.3.04.01.0A	Ingestion
		3.3.04.03.0A	External exposure
I 081	Criticality event	2.1.14.18.0A	In-package criticality resulting from a seismic event (intact configuration)
		2.1.14.19.0A	In-package criticality resulting from a seismic event (degraded configurations)
		2.1.14.25.0A	In-package criticality resulting from an igneous event (degraded configurations)
		2.1.14.24.0A	In-package criticality resulting from an igneous event (intact configuration)
		2.1.14.21.0A	In-package criticality resulting from rockfall (intact configuration)
		2.1.14.15.0A	In-package criticality (intact configuration)
		2.1.14.16.0A	In-package criticality (degraded configurations)
		2.1.14.22.0A	In-package criticality resulting from rockfall (degraded configurations)
I 082	Crop storage	2.4.09.01.0B	Agricultural land use and irrigation
I 084	Cure for cancer	1.4.09.00.0A	Technological developments
I 085a	Dams (filling, draining)	1.4.07.01.0A	Water management activities
I 090	Dermal sorption (tritium and others)	3.3.04.03.0A	External exposure
		3.3.03.01.0A	Contaminated non-food products and exposure
I 091	Watertable changes	1.2.10.01.0A	Hydrologic response to seismic activity
		1.4.01.01.0A	Climate modification increases recharge
		1.3.07.02.0B	Water table rise affects UZ
		1.3.07.02.0A	Water table rise affects SZ
		1.2.10.02.0A	Hydrologic response to igneous activity
		1.3.07.01.0A	Water table decline
I 093	Differential settling (inside IRUS)	2.1.07.02.0A	Drift collapse
		2.1.08.15.0A	Consolidation of EBS components
I 094	Modelling (diffusion)	0.1.10.00.0A	Model and data issues
I 098	Drain gutters plug	1.2.10.02.0A	Hydrologic response to igneous activity
		2.1.08.12.0A	Induced hydrologic changes in invert

Table F-3. Cross Reference of Source FEPs to TSPA-LA FEPs (Continued)

Source FEP No.	Source FEP Name	TSPA-LA FEP Number	TSPA-LA FEP Name
I 099	Earth moving projects (civil)	1.4.08.00.0A	Social and institutional developments
		2.4.10.00.0A	Urban and industrial land and water use
I 100	Seismic events	2.2.06.03.0A	Seismic activity alters perched water zones
		2.2.06.02.0A	Seismic activity changes porosity and permeability of faults
		1.2.03.02.0B	Seismic-induced rockfall damages EBS components
		1.2.10.01.0A	Hydrologic response to seismic activity
		1.2.03.02.0D	Seismic-induced drift collapse alters in-drift thermohydrology
		1.4.02.04.0A	Seismic event precedes human intrusion
		1.2.03.02.0A	Seismic ground motion damages EBS components
		2.2.06.01.0A	Seismic activity changes porosity and permeability of rock
		2.1.14.18.0A	In-package criticality resulting from a seismic event (intact configuration)
		2.1.14.19.0A	In-package criticality resulting from a seismic event (degraded configurations)
I 102	Ecological successions	2.3.01.00.0A	Topography and morphology
I 105	Erosion (of sand ridge by wind)	1.2.07.01.0A	Erosion/denudation
I 112a	Fire (atmospheric dose pathway)	2.4.09.01.0A	Implementation of new agricultural practices or land use
		3.3.04.02.0A	Inhalation
I 112b	Denuding of the site	1.2.07.01.0A	Erosion/denudation
I 113	Food chain (dose pathway)	2.4.09.01.0B	Agricultural land use and irrigation
		3.3.03.01.0A	Contaminated non-food products and exposure
		2.4.09.02.0A	Animal farms and fisheries
		3.3.02.03.0A	Fish uptake
		3.3.02.02.0A	Animal uptake
		2.4.09.01.0A	Implementation of new agricultural practices or land use
		2.4.08.00.0A	Wild and natural land and water use
		2.4.04.01.0A	Human lifestyle
		3.3.02.01.0A	Plant uptake
		3.3.01.00.0A	Contaminated drinking water, foodstuffs and drugs
		3.3.04.01.0A	Ingestion
I 115	Flooding (localized, short-term surface flooding)	2.3.11.02.0A	Surface runoff and evapotranspiration
		1.3.07.02.0B	Water table rise affects UZ
		1.1.02.01.0A	Site flooding (during construction and operation)
I 116	Flushing of water bodies	2.3.04.01.0A	Surface water transport and mixing
I 126	Corrosion (galvanic coupling)	2.1.09.09.0A	Electrochemical effects in EBS
		2.1.02.22.0A	Hydride cracking of cladding
		2.1.03.04.0A	Hydride cracking of waste packages
		2.1.03.04.0B	Hydride cracking of drip shields
		2.1.06.07.0A	Chemical effects at EBS component interfaces

Table F-3. Cross Reference of Source FEPs to TSPA-LA FEPs (Continued)

Source FEP No.	Source FEP Name	TSPA-LA FEP Number	TSPA-LA FEP Name
I 127	Gas absorption (14C in CO2) into concrete walls	2.1.06.01.0A	Chemical effects of rock reinforcement and cementitious materials in EBS
I 128	Gas leakage into basements	2.4.07.00.0A	Dwellings
I 130	Gas (from waste containing a gas cylinder)	2.1.12.03.0A	Gas generation (H2) from waste package corrosion
		2.1.12.04.0A	Gas generation (CO2, CH4, H2S) from microbial degradation
		2.1.12.01.0A	Gas generation (repository pressurization)
		2.1.02.29.0A	Flammable gas generation from DSNF
		2.1.12.06.0A	Gas transport in EBS
		2.1.12.07.0A	Effects of radioactive gases in EBS
		2.1.13.01.0A	Radiolysis
		2.1.13.03.0A	Radiological mutation of microbes
		2.1.12.02.0A	Gas generation (He) from waste form decay
I 139	Groundshine	3.3.04.03.0A	External exposure
I 143	Groundwater (redirection of)	1.2.10.01.0A	Hydrologic response to seismic activity
		2.2.10.08.0A	Thermo-chemical alteration in the SZ (solubility, speciation, phase changes)
		1.5.01.01.0A	Meteorite impact
		2.3.01.00.0A	Topography and morphology
		2.2.07.14.0A	Chemically-induced density effects on groundwater flow
		2.2.10.13.0A	Repository-induced thermal effects on flow in the SZ
		2.2.08.07.0A	Radionuclide solubility limits in the SZ
		2.2.08.01.0B	Chemical characteristics of groundwater in the UZ
		1.4.04.01.0A	Effects of drilling intrusion
		1.1.02.00.0B	Mechanical effects of excavation and construction in EBS
		1.2.09.01.0A	Diapirism
		2.1.11.05.0A	Thermal expansion/stress of in-package EBS components
		1.2.10.02.0A	Hydrologic response to igneous activity
		1.3.07.02.0A	Water table rise affects SZ
		1.3.07.02.0B	Water table rise affects UZ
		2.2.10.01.0A	Repository-induced thermal effects on flow in the UZ
		1.2.04.03.0A	Igneous intrusion into repository
		2.2.07.07.0A	Perched water develops
		2.2.08.03.0A	Geochemical interactions and evolution in the SZ
		1.5.01.02.0A	Extraterrestrial events
		1.5.03.02.0A	Earth tides
		1.4.01.04.0A	Ozone layer failure
		2.1.11.07.0A	Thermal expansion/stress of in-drift EBS components

Table F-3. Cross Reference of Source FEPs to TSPA-LA FEPs (Continued)

Source FEP No.	Source FEP Name	TSPA-LA FEP Number	TSPA-LA FEP Name
I 143	Groundwater (redirection of) (continued)	2.2.06.02.0A	Seismic activity changes porosity and permeability of faults
		2.2.06.04.0A	Effects of subsidence
		2.2.10.06.0A	Thermo-chemical alteration in the UZ (solubility, speciation, phase changes)
		2.2.08.07.0B	Radionuclide solubility limits in the UZ
		2.2.08.03.0B	Geochemical interactions and evolution in the UZ
		2.2.10.09.0A	Thermo-chemical alteration of the Topopah Spring basal vitrophyre
		2.2.08.01.0A	Chemical characteristics of groundwater in the SZ
		2.2.07.13.0A	Water-conducting features in the SZ
		2.2.10.03.0A	Natural geothermal effects on flow in the SZ
		2.2.10.03.0B	Natural geothermal effects on flow in the UZ
		2.2.06.02.0B	Seismic activity changes porosity and permeability of fractures
I 146	Heat generation in IRUS vault(B)	2.1.11.03.0A	Exothermic reactions in the EBS
		2.1.11.01.0A	Heat generation in EBS
		2.1.11.06.0A	Thermal sensitization of waste packages
		2.1.02.08.0A	Pyrophoricity from DSNF
		2.1.11.05.0A	Thermal expansion/stress of in-package EBS components
I 148	Herbicides, pesticides & fungicides (dose pathway)	2.4.09.01.0B	Agricultural land use and irrigation
		2.4.09.01.0A	Implementation of new agricultural practices or land use
I 150	Household plants (dose pathway)	2.4.07.00.0A	Dwellings
I 153	Groundwater flow model (geosphere model validity)	0.1.10.00.0A	Model and data issues
I 157	Hydroponics (dose pathway)	2.4.09.01.0A	Implementation of new agricultural practices or land use
I 161	Incomplete filling of containers	0.1.10.00.0A	Model and data issues
		2.1.07.05.0A	Creep of metallic materials in the waste package
I 163	Insect pathways	3.3.02.03.0A	Fish uptake
		3.3.02.02.0A	Animal uptake
		3.3.04.01.0A	Ingestion
I 165	Interfaces (boundary conditions)	2.1.06.07.0B	Mechanical effects at EBS component interfaces
		2.1.06.07.0A	Chemical effects at EBS component interfaces
I 167	Intrusion (human/deliberate)	1.4.02.01.0A	Deliberate human intrusion
		1.4.04.00.0A	Drilling activities (human intrusion)
		1.4.11.00.0A	Explosions and crashes (human activities)
		3.3.06.01.0A	Repository excavation
		1.4.05.00.0A	Mining and other underground activities (human intrusion)
I 169	Intrusion (human/inadvertent)	1.4.05.00.0A	Mining and other underground activities (human intrusion)
		1.4.11.00.0A	Explosions and crashes (human activities)
		1.4.04.00.0A	Drilling activities (human intrusion)
		1.4.02.02.0A	Inadvertent human intrusion

Table F-3. Cross Reference of Source FEPs to TSPA-LA FEPs (Continued)

Source FEP No.	Source FEP Name	TSPA-LA FEP Number	TSPA-LA FEP Name
I 173	Inventory (inadequate control)	1.1.08.00.0A	Inadequate quality control and deviations from design
		1.1.03.01.0A	Error in waste emplacement
		2.1.01.01.0A	Waste inventory
I 174	Ion exchanges in soil	2.2.08.09.0A	Sorption in the SZ
		2.2.08.09.0B	Sorption in the UZ
I 175	Irrigation (dose pathway)	2.3.02.02.0A	Radionuclide accumulation in soils
		1.4.07.03.0A	Recycling of accumulated radionuclides from soils to groundwater
		1.4.07.02.0A	Wells
		1.4.07.01.0A	Water management activities
		3.3.02.01.0A	Plant uptake
		2.4.09.01.0B	Agricultural land use and irrigation
I 177	Kd values (wrong value for model)	0.1.10.00.0A	Model and data issues
I 178	Surface water bodies (flooding of Lake 233)	2.3.06.00.0A	Marine features
		1.3.07.02.0B	Water table rise affects UZ
		1.1.02.01.0A	Site flooding (during construction and operation)
I 180	Surface waster bodies (non-uniform mixing of)	2.3.04.01.0A	Surface water transport and mixing
		2.2.07.16.0A	Dilution of radionuclides in groundwater
		0.1.10.00.0A	Model and data issues
		2.2.08.11.0A	Groundwater discharge to surface within the reference biosphere
		2.3.11.04.0A	Groundwater discharge to surface outside the reference biosphere
		3.2.07.01.0A	Isotopic dilution
I 182	Buffer (chemical saturation)	2.1.04.02.0A	Chemical properties and evolution of backfill
I 189	Loss of markers (misinterpretation)	1.1.05.00.0A	Records and markers for the repository
I 190	Loss of records	1.1.05.00.0A	Records and markers for the repository
I 195	Monitoring program - criteria and response	1.1.11.00.0A	Monitoring of the repository
I 197	Meteorite impact	1.5.01.01.0A	Meteorite impact
I 200	Minerals (exploration, exploitation)	1.4.02.01.0A	Deliberate human intrusion
		1.4.04.00.0A	Drilling activities (human intrusion)
		1.4.05.00.0A	Mining and other underground activities (human intrusion)
		1.4.11.00.0A	Explosions and crashes (human activities)
		1.4.02.02.0A	Inadvertent human intrusion
I 202	Modelling (evaluation of construction changes)	0.1.10.00.0A	Model and data issues
		1.1.08.00.0A	Inadequate quality control and deviations from design
I 203	Monitoring shaft (failure to close)	2.1.05.03.0A	Degradation of seals
		2.1.05.01.0A	Flow through seals (access ramps and ventilation shafts)
		1.1.01.01.0B	Influx through holes drilled in drift wall or crown
		2.1.05.02.0A	Radionuclide transport through seals

Table F-3. Cross Reference of Source FEPs to TSPA-LA FEPs (Continued)

Source FEP No.	Source FEP Name	TSPA-LA FEP Number	TSPA-LA FEP Name
I 211	Outdoor spraying of water (atmospheric dose pathway)	2.4.09.01.0B	Agricultural land use and irrigation
		3.2.10.00.0A	Atmospheric transport of contaminants
		3.3.04.02.0A	Inhalation
		3.3.04.03.0A	External exposure
I 223	Political (loss of institutional control)	1.1.10.00.0A	Administrative control of the repository site
		1.1.05.00.0A	Records and markers for the repository
I 227	Urbanization (demographics)	1.4.08.00.0A	Social and institutional developments
I 233	Source term & solubility limits	2.2.10.06.0A	Thermo-chemical alteration in the UZ (solubility, speciation, phase changes)
		2.2.10.08.0A	Thermo-chemical alteration in the SZ (solubility, speciation, phase changes)
		2.2.08.07.0B	Radionuclide solubility limits in the UZ
		2.1.09.06.0A	Reduction-oxidation potential in waste package
		2.2.08.07.0A	Radionuclide solubility limits in the SZ
		2.1.09.04.0A	Radionuclide solubility, solubility limits, and speciation in the waste form and EBS
		2.1.09.06.0B	Reduction-oxidation potential in drifts
		2.2.01.04.0A	Radionuclide solubility in the excavation disturbed zone
I 235	Precipitation (wet deposition)	2.3.11.01.0A	Precipitation
		2.3.04.01.0A	Surface water transport and mixing
		2.3.11.03.0A	Infiltration and recharge
		2.3.13.04.0A	Radionuclide release outside the reference biosphere
		2.3.11.04.0A	Groundwater discharge to surface outside the reference biosphere
		3.2.10.00.0A	Atmospheric transport of contaminants
I 238	Radiation effects	2.1.02.15.0A	Localized (radiolysis enhanced) corrosion of cladding
		2.1.13.02.0A	Radiation damage in EBS
		2.1.03.06.0A	Internal corrosion of waste packages prior to breach
		2.1.13.01.0A	Radiolysis
I 252	Remediation of other sites	1.4.02.01.0A	Deliberate human intrusion
		1.4.05.00.0A	Mining and other underground activities (human intrusion)
		1.4.02.02.0A	Inadvertent human intrusion
I 253	Retrievability	1.1.13.00.0A	Retrievability
I 258	Surface runoff	2.3.11.01.0A	Precipitation
		2.3.11.03.0A	Infiltration and recharge
		2.3.11.02.0A	Surface runoff and evapotranspiration
		2.3.04.01.0A	Surface water transport and mixing
I 261	Salt (road salt, CaCl2, etc.)	2.1.09.28.0A	Localized corrosion on waste package outer surface due to deliquescence
		2.1.09.28.0B	Localized corrosion on drip shield surfaces due to deliquescence
		2.2.06.05.0A	Salt creep
		2.3.11.03.0A	Infiltration and recharge

Table F-3. Cross Reference of Source FEPs to TSPA-LA FEPs (Continued)

Source FEP No.	Source FEP Name	TSPA-LA FEP Number	TSPA-LA FEP Name
I 266	Sea level (rising)	2.3.06.00.0A	Marine features
I 268	Freeze/thaw cycles	1.3.04.00.0A	Periglacial effects
		1.3.05.00.0A	Glacial and ice sheet effect
I 270	Seeds in vault/wate	2.1.10.01.0A	Microbial activity in EBS
I 271	Regulatory does limit lowered	0.1.09.00.0A	Regulatory requirements and exclusions
I 272	Showers and humidifiers (atmospheric dose pathway)	2.4.04.01.0A	Human lifestyle
		3.3.04.03.0A	External exposure
		2.4.07.00.0A	Dwellings
		3.3.04.02.0A	Inhalation
I 273	Container performance(incorrect modelling)	0.1.10.00.0A	Model and data issues
I 276	Smoking (dose pathway)	3.3.03.01.0A	Contaminated non-food products and exposure
I 277	Soil liquefaction (seismic)	2.2.06.01.0A	Seismic activity changes porosity and permeability of rock
I 278	Soil characteristics (wrong value for model)	0.1.10.00.0A	Model and data issues
I 280	Soil slumping	2.3.01.00.0A	Topography and morphology
		2.3.02.01.0A	Soil type
		2.2.06.04.0A	Effects of subsidence
		1.2.07.01.0A	Erosion/denudation
I 286	Source term model (vault model validity)	0.1.10.00.0A	Model and data issues
I 292	Surface water bodies (physical/chemical changes)	2.3.04.01.0A	Surface water transport and mixing
		1.3.01.00.0A	Climate change
		1.3.07.02.0B	Water table rise affects UZ
		1.4.01.03.0A	Acid rain
		1.4.06.01.0A	Altered soil or surface water chemistry
		2.3.06.00.0A	Marine features
		2.3.11.04.0A	Groundwater discharge to surface outside the reference biosphere
		2.3.13.04.0A	Radionuclide release outside the reference biosphere
		2.2.08.11.0A	Groundwater discharge to surface within the reference biosphere
I 298	Swelling pressure (clay)	2.1.07.04.0B	Hydrostatic pressure on drip shield
		2.1.07.04.0A	Hydrostatic pressure on waste package
I 299	Technological advances in food production	1.4.09.00.0A	Technological developments
		2.4.09.01.0A	Implementation of new agricultural practices or land use
I 300	Temperature effects (on transport)	2.2.10.01.0A	Repository-induced thermal effects on flow in the UZ
		2.2.10.13.0A	Repository-induced thermal effects on flow in the SZ
		2.1.02.13.0A	General corrosion of cladding
		2.1.08.03.0A	Repository dry-out due to waste heat
		2.2.10.12.0A	Geosphere dry-out due to waste heat
		2.1.11.10.0A	Thermal effects on transport in EBS

Table F-3. Cross Reference of Source FEPs to TSPA-LA FEPs (Continued)

Source FEP No.	Source FEP Name	TSPA-LA FEP Number	TSPA-LA FEP Name
I 305	Topography (changes)	1.2.10.02.0A	Hydrologic response to igneous activity
		1.2.07.01.0A	Erosion/denudation
		2.3.01.00.0A	Topography and morphology
		2.2.06.04.0A	Effects of subsidence
		1.3.05.00.0A	Glacial and ice sheet effect
		1.2.07.02.0A	Deposition
I 313	Turbulence (groundwater flow)	2.2.07.12.0A	Saturated groundwater flow in the geosphere
I 314	Uncertainties (in values of model parameters)	0.1.10.00.0A	Model and data issues
I 317	Unsaturated transport	2.1.12.03.0A	Gas generation (H2) from waste package corrosion
		2.2.08.01.0B	Chemical characteristics of groundwater in the UZ
		2.2.08.03.0B	Geochemical interactions and evolution in the UZ
		2.2.08.05.0A	Diffusion in the UZ
		2.1.09.19.0B	Advection of colloids in EBS
		2.3.13.02.0A	Radionuclide alteration during biosphere transport
		2.2.08.07.0B	Radionuclide solubility limits in the UZ
		2.1.09.19.0A	Sorption of colloids in EBS
		2.1.09.18.0A	Formation of microbial colloids in EBS
		2.1.09.13.0A	Complexation in EBS
		2.1.09.08.0B	Advection of dissolved radionuclides in EBS
		2.1.09.08.0A	Diffusion of dissolved radionuclides in EBS
		2.1.09.01.0A	Chemical characteristics of water in drifts
		2.1.08.07.0A	Unsaturated flow in the EBS
		2.1.08.05.0A	Flow through invert
		2.1.05.02.0A	Radionuclide transport through seals
		1.3.07.02.0B	Water table rise affects UZ
		2.2.07.06.0B	Long-term release of radionuclides from the repository
		1.2.02.01.0A	Fractures
		2.1.12.04.0A	Gas generation (CO2, CH4, H2S) from microbial degradation
		1.2.02.02.0A	Faults
		2.2.08.09.0B	Sorption in the UZ
		2.1.09.21.0A	Transport of particles larger than colloids in EBS
		2.1.09.24.0A	Diffusion of colloids in EBS
		2.1.09.26.0A	Gravitational settling of colloids in EBS
		2.1.09.27.0A	Coupled effects on radionuclide transport in EBS
		2.3.13.04.0A	Radionuclide release outside the reference biosphere
		2.1.12.01.0A	Gas generation (repository pressurization)
		2.2.07.05.0A	Flow in the UZ from episodic infiltration
		2.1.12.06.0A	Gas transport in EBS

Table F-3. Cross Reference of Source FEPs to TSPA-LA FEPs (Continued)

Source FEP No.	Source FEP Name	TSPA-LA FEP Number	TSPA-LA FEP Name
I 317	Unsaturated transport (continued)	2.2.07.03.0A	Capillary rise in the UZ
		2.2.08.08.0B	Matrix diffusion in the UZ
		2.3.11.04.0A	Groundwater discharge to surface outside the reference biosphere
		2.2.10.06.0A	Thermo-chemical alteration in the UZ (solubility, speciation, phase changes)
		2.2.11.02.0A	Gas effects in the UZ
		2.2.08.06.0B	Complexation in the UZ
		2.2.07.06.0A	Episodic or pulse release from repository
		2.1.11.10.0A	Thermal effects on transport in EBS
I 320	Vault orientation (with respect to groundwater flow)	1.1.08.00.0A	Inadequate quality control and deviations from design
		0.1.03.00.0A	Spatial domain of concern
		1.1.07.00.0A	Repository design
I 322	Volcanic activity	1.2.04.04.0A	Igneous intrusion interacts with EBS components
		1.2.04.06.0A	Eruptive conduit to surface intersects repository
		1.2.04.05.0A	Magma or pyroclastic base surge transports waste
		1.2.04.03.0A	Igneous intrusion into repository
I 323	Waste form performance (incorrect modelling)	1.1.08.00.0A	Inadequate quality control and deviations from design
		0.1.10.00.0A	Model and data issues
I 328	Swelling pressure(bales)	2.1.12.01.0A	Gas generation (repository pressurization)
I 337	Water contacting waste in vault	1.1.02.01.0A	Site flooding (during construction and operation)
		1.3.07.02.0B	Water table rise affects UZ
		2.3.11.03.0A	Infiltration and recharge
		2.1.09.01.0B	Chemical characteristics of water in waste package
I 347	Inventory database (WIP III)	2.1.01.03.0A	Heterogeneity of waste inventory
		2.1.01.01.0A	Waste inventory
I 349	Wrong input data	0.1.10.00.0A	Model and data issues
I 350	Non-human biota effects	3.3.06.02.0A	Sensitization to radiation
I 351	Biosphere model (biosphere model validity)	2.3.13.01.0A	Biosphere characteristics
		0.1.10.00.0A	Model and data issues
		1.1.08.00.0A	Inadequate quality control and deviations from design
I 352	IRUS closure system	1.1.07.00.0A	Repository design
		1.1.04.01.0A	Incomplete closure
ID/EBS-1	Episodic / pulse release from repository	2.2.07.06.0A	Episodic or pulse release from repository
		2.2.07.06.0B	Long-term release of radionuclides from the repository
ID/Hydro-1	Effects of pre-closure ventilation	1.1.02.02.0A	Preclosure ventilation
ISC-1	Criticality in-situ, WP internal structures degrade faster than waste form, top breach	2.1.14.16.0A	In-package criticality (degraded configurations)
ISC-2	Criticality in-situ, WP internal structures degrade at same rate as waste form, top breach	2.1.14.16.0A	In-package criticality (degraded configurations)

Table F-3. Cross Reference of Source FEPs to TSPA-LA FEPs (Continued)

Source FEP No.	Source FEP Name	TSPA-LA FEP Number	TSPA-LA FEP Name
ISC-3	Criticality in-situ, WP internal structures degrade slower than waste form, top breach	2.1.14.16.0A	In-package criticality (degraded configurations)
ISC-4	Criticality in-situ, bottom breach allows flow through WP, fissile material collects at bottom of WP	2.1.14.16.0A	In-package criticality (degraded configurations)
ISC-5	Criticality in-situ, bottom breach allows flow through WP, waste form degrades in place	2.1.14.16.0A	In-package criticality (degraded configurations)
ISC-6	Criticality in-situ, waste form degrades in place and wells, top breach	2.1.14.16.0A	In-package criticality (degraded configurations)
J 1.1.01	Criticality	2.1.14.26.0A	Near-field criticality resulting from an igneous event
		2.1.14.18.0A	In-package criticality resulting from a seismic event (intact configuration)
		2.1.14.15.0A	In-package criticality (intact configuration)
		2.1.14.22.0A	In-package criticality resulting from rockfall (degraded configurations)
		2.2.14.12.0A	Far-field criticality resulting from an igneous event
		2.2.14.11.0A	Far-field criticality resulting from rockfall
		2.2.14.10.0A	Far-field criticality resulting from a seismic event
		2.2.14.09.0A	Far-field criticality
		2.1.14.16.0A	In-package criticality (degraded configurations)
		2.1.14.23.0A	Near-field criticality resulting from rockfall
		2.1.14.21.0A	In-package criticality resulting from rockfall (intact configuration)
		2.1.14.20.0A	Near-field criticality resulting from a seismic event
		2.1.14.19.0A	In-package criticality resulting from a seismic event (degraded configurations)
		2.1.14.17.0A	Near-field criticality
		2.1.14.24.0A	In-package criticality resulting from an igneous event (intact configuration)
		2.1.14.25.0A	In-package criticality resulting from an igneous event (degraded configurations)
J 1.1.02	Radioactive decay; heat	2.1.11.01.0A	Heat generation in EBS
J 1.1.03	Recoil of alpha-decay	2.1.02.04.0A	Alpha recoil enhances dissolution
		2.1.13.02.0A	Radiation damage in EBS
J 1.1.04	Gas generation: He production	2.1.12.02.0A	Gas generation (He) from waste form decay
J 1.2.01	Radiolysis	2.1.13.01.0A	Radiolysis
J 1.2.02	Hydrogen/oxygen explosions	2.1.12.08.0A	Gas explosions in EBS
J 1.2.03	Pb-I reactions	2.1.02.07.0A	Radionuclide release from gap and grain boundaries
J 1.2.04	Gas generation	2.1.12.04.0A	Gas generation (CO2, CH4, H2S) from microbial degradation
		2.1.12.03.0A	Gas generation (H2) from waste package corrosion
		2.1.12.02.0A	Gas generation (He) from waste form decay
		2.1.13.01.0A	Radiolysis

Table F-3. Cross Reference of Source FEPs to TSPA-LA FEPs (Continued)

Source FEP No.	Source FEP Name	TSPA-LA FEP Number	TSPA-LA FEP Name
J 1.2.05	I, Cs-migration to fuel surface	2.1.02.07.0A	Radionuclide release from gap and grain boundaries
J 1.2.06	Solubility within fuel matrix	2.1.09.04.0A	Radionuclide solubility, solubility limits, and speciation in the waste form and EBS
J 1.2.07	Recrystallization	2.2.08.07.0A	Radionuclide solubility limits in the SZ
		2.2.08.03.0B	Geochemical interactions and evolution in the UZ
		2.2.08.03.0A	Geochemical interactions and evolution in the SZ
		2.2.08.07.0B	Radionuclide solubility limits in the UZ
J 1.2.08	Redox potential	2.1.09.06.0A	Reduction-oxidation potential in waste package
		2.1.13.01.0A	Radiolysis
		2.1.09.06.0B	Reduction-oxidation potential in drifts
J 1.2.09	Dissolution chemistry	2.1.02.02.0A	CSNF degradation (alteration, dissolution, and radionuclide release)
J 1.3	Damaged or deviating fuel	2.1.01.03.0A	Heterogeneity of waste inventory
J 1.4	Sudden energy release	1.4.02.01.0A	Deliberate human intrusion
J 1.5	Release of radionuclides from the failured canister	2.1.02.03.0A	HLW glass degradation (alteration, dissolution, and radionuclide release)
		2.1.02.01.0A	DSNF degradation (alteration, dissolution, and radionuclide release)
		2.1.09.02.0A	Chemical interaction with corrosion products
		2.2.07.06.0A	Episodic or pulse release from repository
		2.1.02.02.0A	CSNF degradation (alteration, dissolution, and radionuclide release)
		2.2.07.06.0B	Long-term release of radionuclides from the repository
J 2.1.01	Chemical reactions (copper corrosion)	2.1.03.09.0A	Copper corrosion in EBS
J 2.1.02	Coupled effects (electrophoresis)	2.1.09.27.0A	Coupled effects on radionuclide transport in EBS
		2.1.09.09.0A	Electrochemical effects in EBS
J 2.1.03	Internal corrosion due to waste	2.1.03.06.0A	Internal corrosion of waste packages prior to breach
J 2.1.04	Role of the eventual channeling within the canister	2.1.08.07.0A	Unsaturated flow in the EBS
		2.1.02.09.0A	Chemical effects of void space in waste package
J 2.1.05	Role of chlorides in copper corrosion	2.1.03.09.0A	Copper corrosion in EBS
J 2.1.06.1	Repository induced Pb/Cu electrochemical reactions	2.1.09.09.0A	Electrochemical effects in EBS
J 2.1.06.2	Natural telluric electrochemical reactions	2.1.09.09.0A	Electrochemical effects in EBS
J 2.1.07	Pitting	2.1.03.03.0A	Localized corrosion of waste packages
		2.1.03.03.0B	Localized corrosion of drip shields
J 2.1.08	Corrosive agents, Sulphides, oxygen, etc.	2.1.03.01.0A	General corrosion of waste packages
J 2.1.09	Backfill effects on Cu corrosion	2.1.04.02.0A	Chemical properties and evolution of backfill

Table F-3. Cross Reference of Source FEPs to TSPA-LA FEPs (Continued)

Source FEP No.	Source FEP Name	TSPA-LA FEP Number	TSPA-LA FEP Name
J 2.1.10	Microbes	2.2.09.01.0A	Microbial activity in the SZ
		2.2.08.06.0B	Complexation in the UZ
		2.2.08.06.0A	Complexation in the SZ
		2.1.06.01.0A	Chemical effects of rock reinforcement and cementitious materials in EBS
		2.1.10.01.0A	Microbial activity in EBS
		2.1.02.14.0A	Microbially influenced corrosion (MIC) of cladding
		2.1.03.05.0B	Microbially influenced corrosion (MIC) of drip shields
		2.1.12.04.0A	Gas generation (CO2, CH4, H2S) from microbial degradation
		2.2.09.01.0B	Microbial activity in the UZ
		2.1.06.05.0D	Chemical degradation of invert
		2.1.06.05.0C	Chemical degradation of emplacement pallet
		2.1.03.05.0A	Microbially influenced corrosion (MIC) of waste packages
J 2.2	Creeping of copper	2.1.07.05.0A	Creep of metallic materials in the waste package
		2.1.03.09.0A	Copper corrosion in EBS
J 2.3.01	Thermal cracking	2.1.07.05.0B	Creep of metallic materials in the drip shield
		2.1.07.05.0A	Creep of metallic materials in the waste package
		2.1.02.19.0A	Creep rupture of cladding
J 2.3.02	Electro-chemical cracking	2.1.09.09.0A	Electrochemical effects in EBS
J 2.3.03	Stress corrosion cracking	2.1.03.02.0A	Stress corrosion cracking (SCC) of waste packages
J 2.3.04	Loss of ductility	2.1.07.05.0A	Creep of metallic materials in the waste package
J 2.3.05	Radiation effects on canister	2.1.13.02.0A	Radiation damage in EBS
J 2.3.06	Cracking along welds	2.1.03.08.0A	Early failure of waste packages
		2.1.04.09.0A	Radionuclide transport in backfill
J 2.3.07.1	External stress	2.1.07.05.0B	Creep of metallic materials in the drip shield
J 2.3.07.2	Hydrostatic pressure on canister	2.1.07.04.0A	Hydrostatic pressure on waste package
		2.1.07.04.0B	Hydrostatic pressure on drip shield
J 2.3.08	Internal pressure	2.1.12.02.0A	Gas generation (He) from waste form decay
J 2.4	Voids in the lead filling	2.1.07.05.0A	Creep of metallic materials in the waste package
J 2.5.01	Random canister defects - quality control	2.1.03.08.0A	Early failure of waste packages
J 2.5.02	Common cause canister defects - quality control	2.1.03.08.0A	Early failure of waste packages
J 3.1.01	Degradation of the bentonite by chemical reactions	2.1.04.05.0A	Thermal-mechanical properties and evolution of backfill
		2.1.04.03.0A	Erosion or dissolution of backfill
		2.1.04.02.0A	Chemical properties and evolution of backfill
J 3.1.02	Saturation of sorption sites	2.1.04.01.0A	Flow in the backfill
		2.1.04.02.0A	Chemical properties and evolution of backfill
		2.1.09.02.0A	Chemical interaction with corrosion products
J 3.1.03	Effects of bentonite on groundwater chemistry	2.1.04.02.0A	Chemical properties and evolution of backfill
J 3.1.04	Colloid generation - source	2.1.04.09.0A	Radionuclide transport in backfill

Table F-3. Cross Reference of Source FEPs to TSPA-LA FEPs (Continued)

Source FEP No.	Source FEP Name	TSPA-LA FEP Number	TSPA-LA FEP Name
J 3.1.05	Coagulation of bentonite	2.1.04.05.0A	Thermal-mechanical properties and evolution of backfill
		2.1.04.02.0A	Chemical properties and evolution of backfill
		2.1.04.01.0A	Flow in the backfill
J 3.1.06	Sedimentation of bentonite	2.1.04.05.0A	Thermal-mechanical properties and evolution of backfill
		2.1.04.03.0A	Erosion or dissolution of backfill
J 3.1.07	Reactions with cement pore water	2.1.09.01.0A	Chemical characteristics of water in drifts
J 3.1.08	Near field buffer chemistry	2.1.04.02.0A	Chemical properties and evolution of backfill
J 3.1.09	Radiolysis	2.1.13.01.0A	Radiolysis
J 3.1.10	Interactions with corrosion products and waste	2.1.09.02.0A	Chemical interaction with corrosion products
J 3.1.11	Redox front	2.1.13.01.0A	Radiolysis
		2.1.09.06.0A	Reduction-oxidation potential in waste package
		2.1.09.06.0B	Reduction-oxidation potential in drifts
J 3.1.12	Perturbed buffer material chemistry	2.1.04.02.0A	Chemical properties and evolution of backfill
J 3.1.13	Radiation effects on bentonite	2.1.13.02.0A	Radiation damage in EBS
J 3.2.01.1	Swelling of bentonite into tunnels and cracks	2.1.04.04.0A	Thermal-mechanical effects of backfill
		2.1.04.05.0A	Thermal-mechanical properties and evolution of backfill
J 3.2.01.2	Uneven swelling of bentonite	2.1.04.04.0A	Thermal-mechanical effects of backfill
		2.1.04.05.0A	Thermal-mechanical properties and evolution of backfill
J 3.2.02	Movement of canister in buffer/backfill	2.1.03.07.0A	Mechanical impact on waste package
		1.1.08.00.0A	Inadequate quality control and deviations from design
		2.1.06.05.0A	Mechanical degradation of emplacement pallet
J 3.2.03	Mechanical failure of buffer/backfill	2.1.04.04.0A	Thermal-mechanical effects of backfill
J 3.2.04	Erosion of buffer/backfill	2.1.04.03.0A	Erosion or dissolution of backfill
J 3.2.05	Thermal effects on the buffer material	2.1.04.04.0A	Thermal-mechanical effects of backfill
		2.1.04.05.0A	Thermal-mechanical properties and evolution of backfill
J 3.2.06	Diffusion - surface diffusion	2.2.08.05.0A	Diffusion in the UZ
		2.1.04.09.0A	Radionuclide transport in backfill
J 3.2.07	Swelling of corrosion products	2.1.09.03.0A	Volume increase of corrosion products impacts cladding
		2.1.09.03.0C	Volume increase of corrosion products impacts other EBS components
		2.1.09.03.0B	Volume increase of corrosion products impacts waste package
J 3.2.08	Preferential pathways in the buffer/backfill	2.1.04.01.0A	Flow in the backfill
J 3.2.09	Flow through buffer/backfill	2.1.04.01.0A	Flow in the backfill
J 3.2.10	Soret effect	2.1.11.10.0A	Thermal effects on transport in EBS
J 3.2.11	Backfill material deficiencies	2.1.04.01.0A	Flow in the backfill
		2.1.04.02.0A	Chemical properties and evolution of backfill
		1.1.03.01.0B	Error in backfill emplacement

Table F-3. Cross Reference of Source FEPs to TSPA-LA FEPs (Continued)

Source FEP No.	Source FEP Name	TSPA-LA FEP Number	TSPA-LA FEP Name
J 3.2.12	Gas transport in bentonite	2.1.12.06.0A	Gas transport in EBS
		2.1.04.09.0A	Radionuclide transport in backfill
J 4.1.01	Oxidizing conditions	2.2.08.03.0B	Geochemical interactions and evolution in the UZ
		2.2.08.03.0A	Geochemical interactions and evolution in the SZ
J 4.1.02	pH-deviations	2.1.09.06.0B	Reduction-oxidation potential in drifts
		2.1.09.01.0A	Chemical characteristics of water in drifts
		2.1.09.01.0B	Chemical characteristics of water in waste package
		2.1.02.14.0A	Microbially influenced corrosion (MIC) of cladding
		2.1.09.06.0A	Reduction-oxidation potential in waste package
		2.1.13.01.0A	Radiolysis
		2.1.02.15.0A	Localized (radiolysis enhanced) corrosion of cladding
		2.2.08.03.0B	Geochemical interactions and evolution in the UZ
		2.2.08.01.0A	Chemical characteristics of groundwater in the SZ
		2.2.08.01.0B	Chemical characteristics of groundwater in the UZ
		2.2.08.03.0A	Geochemical interactions and evolution in the SZ
J 4.1.03	Colloids, complexing agents	2.1.09.19.0A	Sorption of colloids in EBS
		2.1.09.23.0A	Stability of colloids in EBS
		2.1.09.18.0A	Formation of microbial colloids in EBS
		2.1.09.13.0A	Complexation in EBS
		2.1.09.15.0A	Formation of true (intrinsic) colloids in EBS
		2.1.09.16.0A	Formation of pseudo-colloids (natural) in EBS
		2.1.09.19.0B	Advection of colloids in EBS
		2.1.09.22.0A	Sorption of colloids at air-water interface
		2.1.09.24.0A	Diffusion of colloids in EBS
		2.1.09.25.0A	Formation of colloids (waste-form) by co-precipitation in EBS
		2.1.09.26.0A	Gravitational settling of colloids in EBS
		2.2.08.10.0A	Colloidal transport in the SZ
		2.2.08.10.0B	Colloidal transport in the UZ
		2.1.09.20.0A	Filtration of colloids in EBS
		2.1.09.17.0A	Formation of pseudo-colloids (corrosion product) in EBS
J 4.1.04	Sorption	2.2.01.02.0B	Chemical changes in the near-field from backfill
		2.2.09.01.0A	Microbial activity in the SZ
		2.2.08.08.0B	Matrix diffusion in the UZ
		2.1.09.27.0A	Coupled effects on radionuclide transport in EBS

Table F-3. Cross Reference of Source FEPs to TSPA-LA FEPs (Continued)

Source FEP No.	Source FEP Name	TSPA-LA FEP Number	TSPA-LA FEP Name
J 4.1.04	Sorption (continued)	2.1.09.22.0A	Sorption of colloids at air-water interface
		2.1.09.19.0A	Sorption of colloids in EBS
		2.1.09.12.0A	Rind (chemically altered zone) forms in the near-field
		2.1.09.05.0A	Sorption of dissolved radionuclides in EBS
		2.2.08.10.0B	Colloidal transport in the UZ
		2.1.09.01.0A	Chemical characteristics of water in drifts
		2.1.04.09.0A	Radionuclide transport in backfill
		2.1.09.02.0A	Chemical interaction with corrosion products
		2.2.01.02.0A	Thermally-induced stress changes in the near-field
		2.2.08.10.0A	Colloidal transport in the SZ
		2.1.10.01.0A	Microbial activity in EBS
		2.2.08.09.0A	Sorption in the SZ
		2.2.09.01.0B	Microbial activity in the UZ
		2.2.01.05.0A	Radionuclide transport in the excavation disturbed zone
		2.2.08.01.0A	Chemical characteristics of groundwater in the SZ
		2.2.08.01.0B	Chemical characteristics of groundwater in the UZ
		2.2.08.03.0A	Geochemical interactions and evolution in the SZ
		2.2.08.03.0B	Geochemical interactions and evolution in the UZ
		2.2.08.08.0A	Matrix diffusion in the SZ
		2.1.11.10.0A	Thermal effects on transport in EBS
		2.2.08.09.0B	Sorption in the UZ
J 4.1.05	Matrix diffusion	2.2.08.08.0A	Matrix diffusion in the SZ
		2.2.08.08.0B	Matrix diffusion in the UZ
J 4.1.06	Reconcentration	2.2.14.09.0A	Far-field criticality
		1.4.07.03.0A	Recycling of accumulated radionuclides from soils to groundwater
J 4.1.07	Thermochemical change	2.1.11.01.0A	Heat generation in EBS
		2.1.11.10.0A	Thermal effects on transport in EBS
		2.2.10.06.0A	Thermo-chemical alteration in the UZ (solubility, speciation, phase changes)
		2.1.11.08.0A	Thermal effects on chemistry and microbial activity in the EBS
J 4.1.08	Change of groundwater chemistry in nearby rock	1.1.02.00.0A	Chemical effects of excavation and construction in EBS
		2.2.08.03.0B	Geochemical interactions and evolution in the UZ
		2.1.13.01.0A	Radiolysis
J 4.1.09	Complexing agents	2.2.08.06.0A	Complexation in the SZ
		2.2.08.06.0B	Complexation in the UZ
J 4.2.01	Mechanical failure of repository	2.1.07.02.0A	Drift collapse
J 4.2.02.1	Excavation/backfilling effects on nearby rock	2.2.01.01.0A	Mechanical effects of excavation and construction in the near-field

Table F-3. Cross Reference of Source FEPs to TSPA-LA FEPs (Continued)

Source FEP No.	Source FEP Name	TSPA-LA FEP Number	TSPA-LA FEP Name
J 4.2.02.2	Hydraulic conductivity change - Excavation/backfilling effect	2.2.01.01.0A	Mechanical effects of excavation and construction in the near-field
		2.2.01.02.0A	Thermally-induced stress changes in the near-field
J 4.2.02.3	Mechanical effects - Excavation/backfilling effects	2.2.01.01.0A	Mechanical effects of excavation and construction in the near-field
J 4.2.03	Extreme channel flow of oxidants and nuclides	2.2.07.15.0B	Advection and dispersion in the UZ
		2.2.07.08.0A	Fracture flow in the UZ
J 4.2.04	Thermal buoyancy	2.2.10.13.0A	Repository-induced thermal effects on flow in the SZ
		2.2.10.03.0A	Natural geothermal effects on flow in the SZ
J 4.2.05	Changes in Groundwater Flow	2.2.10.13.0A	Repository-induced thermal effects on flow in the SZ
		2.2.10.03.0A	Natural geothermal effects on flow in the SZ
		2.1.04.05.0A	Thermal-mechanical properties and evolution of backfill
		1.2.09.01.0A	Diapirism
		2.1.04.02.0A	Chemical properties and evolution of backfill
		1.2.10.02.0A	Hydrologic response to igneous activity
		1.4.01.04.0A	Ozone layer failure
		1.5.03.02.0A	Earth tides
		2.2.07.14.0A	Chemically-induced density effects on groundwater flow
		2.2.08.01.0A	Chemical characteristics of groundwater in the SZ
		2.2.08.01.0B	Chemical characteristics of groundwater in the UZ
		2.2.08.03.0A	Geochemical interactions and evolution in the SZ
		2.2.10.03.0B	Natural geothermal effects on flow in the UZ
		2.2.08.03.0B	Geochemical interactions and evolution in the UZ
		2.2.10.01.0A	Repository-induced thermal effects on flow in the UZ
		2.2.07.12.0A	Saturated groundwater flow in the geosphere
J 4.2.06	Faulting	1.2.02.02.0A	Faults
J 4.2.07	Thermo-hydro-mechanical effects	2.2.06.01.0A	Seismic activity changes porosity and permeability of rock
		2.2.10.05.0A	Thermo-mechanical stresses alter characteristics of rocks above and below the repository
J 4.2.08	Enhanced rock fracturing	2.2.01.01.0A	Mechanical effects of excavation and construction in the near-field
J 4.2.09	Creeping of rock mass	2.1.07.02.0A	Drift collapse
J 4.2.10	Chemical effects of rock reinforcement	2.1.06.02.0A	Mechanical effects of rock reinforcement materials in EBS
		2.1.06.01.0A	Chemical effects of rock reinforcement and cementitious materials in EBS

Table F-3. Cross Reference of Source FEPs to TSPA-LA FEPs (Continued)

Source FEP No.	Source FEP Name	TSPA-LA FEP Number	TSPA-LA FEP Name
J 5.01	Saline (or fresh) groundwater intrusion	2.2.08.12.0A	Chemistry of water flowing into the drift
		2.2.08.03.0A	Geochemical interactions and evolution in the SZ
		2.1.09.01.0A	Chemical characteristics of water in drifts
J 5.02	Non-sealed repository	1.1.04.01.0A	Incomplete closure
J 5.03	Stray materials left	1.1.02.03.0A	Undesirable materials left
J 5.04	Decontamination materials left	1.1.02.03.0A	Undesirable materials left
J 5.05	Chemical sabotage	1.4.02.01.0A	Deliberate human intrusion
J 5.06	Co-storage of other waste	2.1.01.02.0A	Interactions between co-located waste
		2.1.01.02.0B	Interactions between co-disposed waste
J 5.07	Poorly designed repository	1.1.07.00.0A	Repository design
J 5.08	Poorly constructed repository	1.1.08.00.0A	Inadequate quality control and deviations from design
J 5.09	Unsealed boreholes and/or shafts	1.1.04.01.0A	Incomplete closure
J 5.10	Accidents during operation	1.1.12.01.0A	Accidents and unplanned events during construction and operation
J 5.11	Degradation of hole- and shaft seals	2.1.05.03.0A	Degradation of seals
J 5.12	Near storage of other waste	2.1.01.02.0A	Interactions between co-located waste
J 5.13	Volcanism	1.2.04.03.0A	Igneous intrusion into repository
J 5.14	Resaturation	2.1.08.11.0A	Repository resaturation due to waste cooling
J 5.15	Earthquakes	2.2.06.02.0A	Seismic activity changes porosity and permeability of faults
		2.2.06.02.0B	Seismic activity changes porosity and permeability of fractures
		2.2.06.01.0A	Seismic activity changes porosity and permeability of rock
		1.4.02.04.0A	Seismic event precedes human intrusion
		1.2.10.01.0A	Hydrologic response to seismic activity
		1.2.03.02.0A	Seismic ground motion damages EBS components
		2.2.06.03.0A	Seismic activity alters perched water zones
		1.2.03.02.0B	Seismic-induced rockfall damages EBS components
J 5.16	Uplift and subsidence	1.2.01.01.0A	Tectonic activity - large scale
J 5.17	Permafrost	1.3.04.00.0A	Periglacial effects
J 5.18	Enhanced groundwater flow	2.2.07.12.0A	Saturated groundwater flow in the geosphere
J 5.19	Effect of plate movements	1.2.01.01.0A	Tectonic activity - large scale
J 5.20	Changes of the magnetic field	1.5.03.01.0A	Changes in the earth's magnetic field
J 5.21	Future boreholes and undetected past boreholes	1.1.04.01.0A	Incomplete closure
		1.1.11.00.0A	Monitoring of the repository
		1.4.04.00.0A	Drilling activities (human intrusion)
		1.1.01.01.0A	Open site investigation boreholes
J 5.22	Accumulation of gases under permafrost	1.3.04.00.0A	Periglacial effects
J 5.23	Changed hydrostatic pressure on canister	2.1.07.04.0B	Hydrostatic pressure on drip shield
		2.1.07.04.0A	Hydrostatic pressure on waste package
J 5.24	Stress changes of conductivity	2.2.01.02.0A	Thermally-induced stress changes in the near-field

Table F-3. Cross Reference of Source FEPs to TSPA-LA FEPs (Continued)

Source FEP No.	Source FEP Name	TSPA-LA FEP Number	TSPA-LA FEP Name
J 5.25	Dissolution of fracture fillings/precipitations	2.2.08.03.0B	Geochemical interactions and evolution in the UZ
		2.2.08.03.0A	Geochemical interactions and evolution in the SZ
J 5.26	Erosion on surface/sediments	1.2.07.01.0A	Erosion/denudation
J 5.27	Human induced actions on groundwater recharge	1.4.07.01.0A	Water management activities
J 5.28	Underground dwellings	2.4.07.00.0A	Dwellings
		1.4.05.00.0A	Mining and other underground activities (human intrusion)
		1.1.05.00.0A	Records and markers for the repository
J 5.29	Meteorite	1.5.01.01.0A	Meteorite impact
J 5.30	Underground test of nuclear devices	1.4.11.00.0A	Explosions and crashes (human activities)
J 5.31	Change in sealevel	2.3.06.00.0A	Marine features
J 5.32	Desert and unsaturation	1.3.01.00.0A	Climate change
		1.3.07.01.0A	Water table decline
J 5.33	Waste retrieval, mining	1.4.02.01.0A	Deliberate human intrusion
J 5.34	Geothermal energy production	1.4.04.00.0A	Drilling activities (human intrusion)
J 5.35	Other future uses of crystalline rock	1.4.02.01.0A	Deliberate human intrusion
J 5.36	Reuse of boreholes	1.4.04.00.0A	Drilling activities (human intrusion)
J 5.37	Archeological intrusion	1.4.02.01.0A	Deliberate human intrusion
J 5.38	Explosions	1.4.11.00.0A	Explosions and crashes (human activities)
J 5.39	Postclosure monitoring	1.1.11.00.0A	Monitoring of the repository
J 5.40	Unsuccessful attempt of site improvement	1.4.02.01.0A	Deliberate human intrusion
J 5.41	Water producing well	1.4.07.02.0A	Wells
J 5.42	Glaciation	1.3.05.00.0A	Glacial and ice sheet effect
J 5.43	Methane intrusion	2.2.11.01.0A	Gas effects in the SZ
J 5.44	Solubility and precipitation	2.1.09.04.0A	Radionuclide solubility, solubility limits, and speciation in the waste form and EBS
J 5.45	Colloid generation and transport	2.1.09.19.0A	Sorption of colloids in EBS
		2.1.09.23.0A	Stability of colloids in EBS
		2.1.09.15.0A	Formation of true (intrinsic) colloids in EBS
		2.1.09.22.0A	Sorption of colloids at air-water interface
		2.1.09.20.0A	Filtration of colloids in EBS
		2.1.09.19.0B	Advection of colloids in EBS
		2.1.09.17.0A	Formation of pseudo-colloids (corrosion product) in EBS
		2.1.09.16.0A	Formation of pseudo-colloids (natural) in EBS
		2.1.09.25.0A	Formation of colloids (waste-form) by co-precipitation in EBS
		2.1.09.24.0A	Diffusion of colloids in EBS
		2.1.09.26.0A	Gravitational settling of colloids in EBS
		2.1.09.18.0A	Formation of microbial colloids in EBS
J 5.46	Groundwater recharge/discharge	2.3.11.03.0A	Infiltration and recharge
J 6.01	Undetected fracture zones	2.2.12.00.0A	Undetected features in the UZ

Table F-3. Cross Reference of Source FEPs to TSPA-LA FEPs (Continued)

Source FEP No.	Source FEP Name	TSPA-LA FEP Number	TSPA-LA FEP Name
J 6.02	Gas transport	2.1.12.06.0A	Gas transport in EBS
		2.1.12.07.0A	Effects of radioactive gases in EBS
J 6.03	Far field hydrochemistry – acids, oxidants, nitrate	1.4.06.01.0A	Altered soil or surface water chemistry
J 6.04	Dispersion	2.2.07.15.0A	Advection and dispersion in the SZ
J 6.05	Dilution	2.2.07.16.0A	Dilution of radionuclides in groundwater
J 6.06	Weathering of flow paths	2.2.08.03.0A	Geochemical interactions and evolution in the SZ
		2.2.08.03.0B	Geochemical interactions and evolution in the UZ
J 6.07	Nuclear war	1.4.11.00.0A	Explosions and crashes (human activities)
J 6.08	Human induced climate change	1.4.01.00.0A	Human influences on climate
J 6.09	River meandering	2.3.04.01.0A	Surface water transport and mixing
J 6.10	No ice age	1.3.01.00.0A	Climate change
J 6.11	Intruding dykes	1.2.04.03.0A	Igneous intrusion into repository
J 6.12	Undetected discontinuities	2.2.12.00.0A	Undetected features in the UZ
J 6.13	Geothermally induced flow .	2.2.10.03.0A	Natural geothermal effects on flow in the SZ
		2.2.10.03.0B	Natural geothermal effects on flow in the UZ
		2.2.10.13.0A	Repository-induced thermal effects on flow in the SZ
J 6.14	Tectonic activity - large scale	1.2.01.01.0A	Tectonic activity - large scale
J 7.01	Accumulation in sediments	2.3.02.02.0A	Radionuclide accumulation in soils
J 7.02	Accumulation in peat	2.3.02.02.0A	Radionuclide accumulation in soils
		3.3.03.01.0A	Contaminated non-food products and exposure
J 7.03	Intrusion into accumulation zone in the biosphere	1.4.02.01.0A	Deliberate human intrusion
J 7.04	Chemical toxicity of wastes	3.3.07.00.0A	Non-radiological toxicity and effects
J 7.05	Isotopic dilution	3.2.07.01.0A	Isotopic dilution
J 7.07	Human induced changes in surface hydrology	1.4.07.01.0A	Water management activities
J 7.08	Altered surface water chemistry by humans	1.4.06.01.0A	Altered soil or surface water chemistry
J 7.09	Loss of records	1.1.05.00.0A	Records and markers for the repository
J 7.10	Diagenesis	1.2.08.00.0A	Diagenesis
J 7.11	City on the site	1.4.08.00.0A	Social and institutional developments
K 0.1	Radioactive decay	3.1.01.01.0A	Radioactive decay and ingrowth
K 0.2	Speciation	2.2.08.07.0B	Radionuclide solubility limits in the UZ
		2.2.08.03.0B	Geochemical interactions and evolution in the UZ
		2.1.09.04.0A	Radionuclide solubility, solubility limits, and speciation in the waste form and EBS
		2.2.08.07.0A	Radionuclide solubility limits in the SZ
		2.2.08.03.0A	Geochemical interactions and evolution in the SZ
K 0.3	Gaseous and volatile isotopes	2.1.12.07.0A	Effects of radioactive gases in EBS
		3.3.08.00.0A	Radon and radon decay product exposure
		2.1.12.01.0A	Gas generation (repository pressurization)

Table F-3. Cross Reference of Source FEPs to TSPA-LA FEPs (Continued)

Source FEP No.	Source FEP Name	TSPA-LA FEP Number	TSPA-LA FEP Name
K 0.3	Gaseous and volatile isotopes (continued)	2.1.12.08.0A	Gas explosions in EBS
		3.1.01.01.0A	Radioactive decay and ingrowth
		2.1.13.01.0A	Radiolysis
		2.1.02.29.0A	Flammable gas generation from DSNF
K 0.4	Nuclear criticality	2.1.14.23.0A	Near-field criticality resulting from rockfall
		2.1.14.22.0A	In-package criticality resulting from rockfall (degraded configurations)
		2.1.14.20.0A	Near-field criticality resulting from a seismic event
		2.1.14.15.0A	In-package criticality (intact configuration)
		2.1.14.16.0A	In-package criticality (degraded configurations)
		2.1.14.17.0A	Near-field criticality
		2.1.14.18.0A	In-package criticality resulting from a seismic event (intact configuration)
		2.1.14.19.0A	In-package criticality resulting from a seismic event (degraded configurations)
		2.1.14.21.0A	In-package criticality resulting from rockfall (intact configuration)
		2.1.14.24.0A	In-package criticality resulting from an igneous event (intact configuration)
		2.1.14.25.0A	In-package criticality resulting from an igneous event (degraded configurations)
		2.1.14.26.0A	Near-field criticality resulting from an igneous event
		2.2.14.09.0A	Far-field criticality
		2.2.14.11.0A	Far-field criticality resulting from rockfall
		2.2.14.10.0A	Far-field criticality resulting from a seismic event
		2.2.14.12.0A	Far-field criticality resulting from an igneous event
K 1.01	Waste product (glass)	2.1.01.01.0A	Waste inventory
K 1.02	Radionuclide inventory	2.1.01.03.0A	Heterogeneity of waste inventory
		2.1.01.01.0A	Waste inventory
K 1.03	Stainless steel fabrication flask	2.1.01.02.0B	Interactions between co-disposed waste
		2.1.02.03.0A	HLW glass degradation (alteration, dissolution, and radionuclide release)
		2.1.03.11.0A	Physical form of waste package and drip shield
K 1.04	Void space	2.1.01.02.0B	Interactions between co-disposed waste
		2.1.02.09.0A	Chemical effects of void space in waste package
		2.1.02.03.0A	HLW glass degradation (alteration, dissolution, and radionuclide release)
K 1.05	Glass cracking and surface area	2.1.02.05.0A	HLW glass cracking
K 1.06	Glass recrystallisation	2.1.02.06.0A	HLW glass recrystallization
K 1.07	Phase separation	2.1.02.03.0A	HLW glass degradation (alteration, dissolution, and radionuclide release)
K 1.08	Heat output (RN decay heat)	2.1.11.01.0A	Heat generation in EBS
K 1.09	Glass temperature	2.1.11.01.0A	Heat generation in EBS
K 1.10	Radiation damage	2.1.13.02.0A	Radiation damage in EBS
K 1.11a	Glass alteration/dissolution	2.1.02.03.0A	HLW glass degradation (alteration, dissolution, and radionuclide release)

Table F-3. Cross Reference of Source FEPs to TSPA-LA FEPs (Continued)

Source FEP No.	Source FEP Name	TSPA-LA FEP Number	TSPA-LA FEP Name
K 1.11b	Congruent dissolution	2.1.02.03.0A	HLW glass degradation (alteration, dissolution, and radionuclide release)
K 1.12	Rate of glass dissolution	2.1.02.03.0A	HLW glass degradation (alteration, dissolution, and radionuclide release)
K 1.13	Selective leaching	2.1.02.03.0A	HLW glass degradation (alteration, dissolution, and radionuclide release)
K 1.14	Coprecipitates/solid solutions	2.1.02.03.0A	HLW glass degradation (alteration, dissolution, and radionuclide release)
		2.1.09.25.0A	Formation of colloids (waste-form) by co-precipitation in EBS
K 1.15	Elemental solubility limits	2.1.09.04.0A	Radionuclide solubility, solubility limits, and speciation in the waste form and EBS
		2.1.09.10.0A	Secondary phase effects on dissolved radionuclide concentrations
K 1.16	Solute transport resistance	2.1.02.05.0A	HLW glass cracking
		2.1.09.08.0A	Diffusion of dissolved radionuclides in EBS
		2.1.09.24.0A	Diffusion of colloids in EBS
K 1.17	Iron corrosion products	2.1.02.03.0A	HLW glass degradation (alteration, dissolution, and radionuclide release)
K 1.18	Precipitation of silicates/silica gel	2.1.02.03.0A	HLW glass degradation (alteration, dissolution, and radionuclide release)
K 1.19	Radionuclide release from glass	2.1.02.03.0A	HLW glass degradation (alteration, dissolution, and radionuclide release)
K 1.20	Radionuclide source term	2.1.09.04.0A	Radionuclide solubility, solubility limits, and speciation in the waste form and EBS
K 1.21	Colloid formation	2.1.09.18.0A	Formation of microbial colloids in EBS
		2.1.09.25.0A	Formation of colloids (waste-form) by co-precipitation in EBS
		2.1.09.17.0A	Formation of pseudo-colloids (corrosion product) in EBS
		2.1.09.16.0A	Formation of pseudo-colloids (natural) in EBS
		2.1.09.15.0A	Formation of true (intrinsic) colloids in EBS
		2.1.09.02.0A	Chemical interaction with corrosion products
K 1.22	Microbial activity	2.1.10.01.0A	Microbial activity in EBS
K 1.23	Radiolysis	2.1.13.01.0A	Radiolysis
K 1.24	He gas production	2.1.12.02.0A	Gas generation (He) from waste form decay
K 1.25	Quality control	1.1.08.00.0A	Inadequate quality control and deviations from design
K 1.26	Handling accidents	2.1.02.05.0A	HLW glass cracking
		1.1.12.01.0A	Accidents and unplanned events during construction and operation
		2.1.02.12.0A	Degradation of cladding prior to disposal
		1.1.03.01.0A	Error in waste emplacement
K 1.27	Deviant inventory flask	2.1.01.03.0A	Heterogeneity of waste inventory
K 10.01	Present-day climatic conditions	1.4.01.00.0A	Human influences on climate
		1.3.01.00.0A	Climate change
		1.3.04.00.0A	Periglacial effects
		1.3.05.00.0A	Glacial and ice sheet effect

Table F-3. Cross Reference of Source FEPs to TSPA-LA FEPs (Continued)

Source FEP No.	Source FEP Name	TSPA-LA FEP Number	TSPA-LA FEP Name
K 10.01	Present-day climatic conditions (continued)	1.3.07.01.0A	Water table decline
		1.3.07.02.0A	Water table rise affects SZ
		1.3.07.02.0B	Water table rise affects UZ
		1.4.01.01.0A	Climate modification increases recharge
		1.4.01.03.0A	Acid rain
		1.4.01.04.0A	Ozone layer failure
		1.5.01.02.0A	Extraterrestrial events
		1.5.03.01.0A	Changes in the earth's magnetic field
		2.3.11.01.0A	Precipitation
		0.1.09.00.0A	Regulatory requirements and exclusions
		2.1.08.01.0A	Water influx at the repository
		1.4.01.02.0A	Greenhouse gas effects
K 10.02	Effective moisture (recharge)	1.3.01.00.0A	Climate change
		2.3.11.03.0A	Infiltration and recharge
K 10.03	Seasonality of climate	1.3.01.00.0A	Climate change
K 10.04	Future climatic conditions	1.3.01.00.0A	Climate change
K 10.05	Tundra climate	1.3.04.00.0A	Periglacial effects
K 10.06	Glacial climate	1.3.05.00.0A	Glacial and ice sheet effect
K 10.07	Warmer climate - arid	1.4.01.02.0A	Greenhouse gas effects
		1.3.01.00.0A	Climate change
		1.3.05.00.0A	Glacial and ice sheet effect
K 10.08	Warmer climate - seasonal humid	1.3.01.00.0A	Climate change
K 10.09	Warmer climate - equable humid	1.3.01.00.0A	Climate change
K 10.10	Greenhouse effect	1.4.01.02.0A	Greenhouse gas effects
K 10.11	Fluvial erosion/sedimentation	1.2.07.01.0A	Erosion/denudation
K 10.12	Surface denudation	1.2.07.01.0A	Erosion/denudation
K 10.13	Permafrost	1.3.04.00.0A	Periglacial effects
K 10.14	Glacial erosion/sedimentation	1.3.05.00.0A	Glacial and ice sheet effect
K 10.15	Glacial-fluvial erosion/sedimentation	1.3.05.00.0A	Glacial and ice sheet effect
K 10.16	Ice sheet effects (loading, melt water recharge)	1.3.05.00.0A	Glacial and ice sheet effect
K 11.01	Exploratory drilling	1.4.04.00.0A	Drilling activities (human intrusion)
K 11.02	Mining activities	1.4.05.00.0A	Mining and other underground activities (human intrusion)
K 11.03	Geothermal exploitation	1.4.04.00.0A	Drilling activities (human intrusion)
K 11.04	Liquid waste injection	1.4.04.00.0A	Drilling activities (human intrusion)
K 11.05	Deep groundwater abstraction	1.4.07.02.0A	Wells
K 11.06	Water management schemes	1.4.07.01.0A	Water management activities
K 11.07	Groundwater pollution	1.4.06.01.0A	Altered soil or surface water chemistry
K 11.08	Surface pollution (soils, rivers)	1.4.06.01.0A	Altered soil or surface water chemistry
K 11.09	Human-induced climate change	1.4.01.00.0A	Human influences on climate
K 11.10	Repository records, markers	1.1.05.00.0A	Records and markers for the repository
K 11.11	Planning restrictions	1.1.10.00.0A	Administrative control of the repository site
K 2.01	Cast steel canister	2.1.03.11.0A	Physical form of waste package and drip shield
K 2.02	Canister thickness	2.1.03.11.0A	Physical form of waste package and drip shield
K 2.03	Corrosion on wetting	2.1.03.01.0A	General corrosion of waste packages

Table F-3. Cross Reference of Source FEPs to TSPA-LA FEPs (Continued)

Source FEP No.	Source FEP Name	TSPA-LA FEP Number	TSPA-LA FEP Name
K 2.04	Oxic corrosion	2.1.03.01.0A	General corrosion of waste packages
K 2.05	Microbially-mediated corrosion	2.1.03.05.0A	Microbially influenced corrosion (MIC) of waste packages
		2.1.03.05.0B	Microbially influenced corrosion (MIC) of drip shields
K 2.06	Anoxic corrosion	2.1.03.01.0A	General corrosion of waste packages
K 2.07	Localised corrosion	2.1.03.03.0A	Localized corrosion of waste packages
		2.1.03.03.0B	Localized corrosion of drip shields
K 2.08	Total corrosion rate	2.1.03.01.0A	General corrosion of waste packages
K 2.09	Stress corrosion cracking	2.1.03.02.0A	Stress corrosion cracking (SCC) of waste packages
		2.1.03.02.0B	Stress corrosion cracking (SCC) of drip shields
K 2.10	Other canister degradation processes	2.1.13.01.0A	Radiolysis
		2.1.13.02.0A	Radiation damage in EBS
		2.1.07.05.0A	Creep of metallic materials in the waste package
		2.1.03.04.0A	Hydride cracking of waste packages
K 2.11	Radiation shielding	2.1.13.01.0A	Radiolysis
		2.1.13.02.0A	Radiation damage in EBS
K 2.12a	Canister failure (alternative modes)	2.1.03.08.0A	Early failure of waste packages
		2.1.07.04.0A	Hydrostatic pressure on waste package
K 2.12b	Canister failure (reference)	2.1.02.08.0A	Pyrophoricity from DSNF
		2.1.04.02.0A	Chemical properties and evolution of backfill
		2.1.03.08.0A	Early failure of waste packages
		2.1.03.07.0A	Mechanical impact on waste package
		2.1.03.05.0A	Microbially influenced corrosion (MIC) of waste packages
		2.1.03.03.0A	Localized corrosion of waste packages
		2.1.03.01.0A	General corrosion of waste packages
		2.1.12.07.0A	Effects of radioactive gases in EBS
		2.1.03.11.0A	Physical form of waste package and drip shield
		2.1.11.07.0A	Thermal expansion/stress of in-drift EBS components
		2.1.04.05.0A	Thermal-mechanical properties and evolution of backfill
		2.1.03.02.0A	Stress corrosion cracking (SCC) of waste packages
		1.2.04.04.0A	Igneous intrusion interacts with EBS components
		2.1.03.04.0A	Hydride cracking of waste packages
		2.1.11.06.0A	Thermal sensitization of waste packages
		2.1.09.28.0A	Localized corrosion on waste package outer surface due to deliquescence
		1.2.03.02.0C	Seismic-induced drift collapse damages EBS components
		1.2.03.02.0B	Seismic-induced rockfall damages EBS components
		1.2.02.03.0A	Fault displacement damages EBS components

Table F-3. Cross Reference of Source FEPs to TSPA-LA FEPs (Continued)

Source FEP No.	Source FEP Name	TSPA-LA FEP Number	TSPA-LA FEP Name
K 2.12b	Canister failure (reference) (continued)	1.1.08.00.0A	Inadequate quality control and deviations from design
		2.1.03.06.0A	Internal corrosion of waste packages prior to breach
		1.1.03.01.0A	Error in waste emplacement
		1.2.04.03.0A	Igneous intrusion into repository
		2.1.07.01.0A	Rockfall
K 2.13	Residual canister (crack/hole effects)	2.1.09.08.0A	Diffusion of dissolved radionuclides in EBS
		2.1.09.08.0B	Advection of dissolved radionuclides in EBS
		2.1.08.07.0A	Unsaturated flow in the EBS
K 2.14	Chemical buffering (canister corrosion products)	2.1.09.06.0A	Reduction-oxidation potential in waste package
		2.1.09.02.0A	Chemical interaction with corrosion products
K 2.15	Radionuclide sorption and co-precipitation	2.1.09.27.0A	Coupled effects on radionuclide transport in EBS
K 2.16	Hydrogen production	2.1.04.04.0A	Thermal-mechanical effects of backfill
		2.1.12.03.0A	Gas generation (H2) from waste package corrosion
K 2.17	Effect of hydrogen on corrosion	2.1.12.03.0A	Gas generation (H2) from waste package corrosion
K 2.18	Corrosion products (physical effects)	2.1.09.03.0B	Volume increase of corrosion products impacts waste package
		2.1.03.10.0A	Advection of liquids and solids through cracks in the waste package
K 2.19	Canister temperature	2.1.11.01.0A	Heat generation in EBS
K 2.20	Radionuclide transport	2.1.09.05.0A	Sorption of dissolved radionuclides in EBS
		2.1.09.08.0A	Diffusion of dissolved radionuclides in EBS
		2.1.09.08.0B	Advection of dissolved radionuclides in EBS
K 2.21	Quality control	1.1.08.00.0A	Inadequate quality control and deviations from design
K 2.22	Mis-sealed canister	2.1.03.08.0A	Early failure of waste packages
K 3.01	Bentonite emplacement and composition	1.1.03.01.0B	Error in backfill emplacement
		2.1.04.02.0A	Chemical properties and evolution of backfill
		2.1.04.05.0A	Thermal-mechanical properties and evolution of backfill
K 3.02	Thermal evolution	2.1.04.05.0A	Thermal-mechanical properties and evolution of backfill
K 3.03	Bentonite saturation	2.1.04.01.0A	Flow in the backfill
		2.1.04.05.0A	Thermal-mechanical properties and evolution of backfill
K 3.04	Bentonite swelling pressure	2.1.04.05.0A	Thermal-mechanical properties and evolution of backfill
		2.1.04.04.0A	Thermal-mechanical effects of backfill
K 3.05	Bentonite plasticity	2.1.04.02.0A	Chemical properties and evolution of backfill
		2.1.04.05.0A	Thermal-mechanical properties and evolution of backfill
		2.1.04.01.0A	Flow in the backfill
K 3.06	Bentonite erosion	2.1.04.03.0A	Erosion or dissolution of backfill

Table F-3. Cross Reference of Source FEPs to TSPA-LA FEPs (Continued)

Source FEP No.	Source FEP Name	TSPA-LA FEP Number	TSPA-LA FEP Name
K 3.07	Canister sinking	2.1.04.05.0A	Thermal-mechanical properties and evolution of backfill
		2.1.08.15.0A	Consolidation of EBS components
		2.1.04.04.0A	Thermal-mechanical effects of backfill
		2.1.06.05.0A	Mechanical degradation of emplacement pallet
K 3.08	Buffer impermeability	2.1.04.05.0A	Thermal-mechanical properties and evolution of backfill
		2.1.04.01.0A	Flow in the backfill
K 3.09	Bentonite porewater chemistry	2.1.04.02.0A	Chemical properties and evolution of backfill
K 3.10	Radionuclide retardation	2.1.09.05.0A	Sorption of dissolved radionuclides in EBS
K 3.11	Colloid filtration	2.1.09.20.0A	Filtration of colloids in EBS
K 3.12a	Mineralogical alteration - short term	2.1.04.05.0A	Thermal-mechanical properties and evolution of backfill
		2.1.04.02.0A	Chemical properties and evolution of backfill
K 3.12b	Mineralogical alteration - long term	2.1.04.05.0A	Thermal-mechanical properties and evolution of backfill
		2.1.04.02.0A	Chemical properties and evolution of backfill
K 3.13	Bentonite cementation	2.1.04.05.0A	Thermal-mechanical properties and evolution of backfill
K 3.14	Canister/bentonite interaction	2.1.04.02.0A	Chemical properties and evolution of backfill
K 3.15	Gas permeability	2.1.12.06.0A	Gas transport in EBS
K 3.16	Radionuclide transport through buffer	2.1.04.09.0A	Radionuclide transport in backfill
K 3.17	Microbial activity	2.1.09.13.0A	Complexation in EBS
		2.1.10.01.0A	Microbial activity in EBS
K 3.18	Elemental solubility/precipitation	2.1.09.04.0A	Radionuclide solubility, solubility limits, and speciation in the waste form and EBS
K 3.19	Radiolysis	2.1.13.01.0A	Radiolysis
K 3.20	Interaction and diffusion between canisters	2.1.04.05.0A	Thermal-mechanical properties and evolution of backfill
		2.1.04.09.0A	Radionuclide transport in backfill
		2.1.01.02.0B	Interactions between co-disposed waste
		2.1.01.02.0A	Interactions between co-located waste
K 3.21	Inhomogeneities (properties and evolution)	1.1.03.01.0B	Error in backfill emplacement
		2.1.04.02.0A	Chemical properties and evolution of backfill
K 3.22	Quality Control	1.1.08.00.0A	Inadequate quality control and deviations from design
		1.1.03.01.0B	Error in backfill emplacement
K 3.23	Poor emplacement of buffer	1.1.03.01.0B	Error in backfill emplacement
K 3.24	Organics/contamination of bentonite	1.1.08.00.0A	Inadequate quality control and deviations from design
		1.1.02.03.0A	Undesirable materials left
		1.1.03.01.0B	Error in backfill emplacement
K 3.25	Interaction with cement components	2.1.04.02.0A	Chemical properties and evolution of backfill
K 4.01	Excavation-disturbed zone (EDZ)	2.2.01.01.0A	Mechanical effects of excavation and construction in the near-field
		2.2.01.01.0B	Chemical effects of excavation and construction in the near-field

Table F-3. Cross Reference of Source FEPs to TSPA-LA FEPs (Continued)

Source FEP No.	Source FEP Name	TSPA-LA FEP Number	TSPA-LA FEP Name
K 4.02	Natural radionuclides/elements	3.2.07.01.0A	Isotopic dilution
K 4.03	Desaturation/resaturation of EDZ	2.2.01.03.0A	Changes in fluid saturations in the excavation disturbed zone
K 4.04	Effect of bentonite swelling on EDZ	2.1.04.04.0A	Thermal-mechanical effects of backfill
K 4.05	Geochemical alteration	1.1.02.00.0A	Chemical effects of excavation and construction in EBS
K 4.06	Groundwater chemistry	1.1.02.00.0A	Chemical effects of excavation and construction in EBS
K 4.07	Water flow at the bentonite-host rock interface	2.2.01.03.0A	Changes in fluid saturations in the excavation disturbed zone
		2.2.01.02.0B	Chemical changes in the near-field from backfill
K 4.08	Radionuclide migration	2.2.01.05.0A	Radionuclide transport in the excavation disturbed zone
K 4.09	Radionuclide retardation	2.2.01.05.0A	Radionuclide transport in the excavation disturbed zone
K 4.10	Elemental solubility	2.2.01.04.0A	Radionuclide solubility in the excavation disturbed zone
K 4.11	Gas transport/dissolution	2.1.12.06.0A	Gas transport in EBS
		2.2.11.03.0A	Gas transport in geosphere
		2.2.01.05.0A	Radionuclide transport in the excavation disturbed zone
K 4.12	Colloids	2.1.09.13.0A	Complexation in EBS
		2.1.09.26.0A	Gravitational settling of colloids in EBS
		2.1.09.25.0A	Formation of colloids (waste-form) by co-precipitation in EBS
		2.1.09.24.0A	Diffusion of colloids in EBS
		2.1.09.23.0A	Stability of colloids in EBS
		2.1.09.19.0B	Advection of colloids in EBS
		2.1.09.16.0A	Formation of pseudo-colloids (natural) in EBS
		2.1.09.15.0A	Formation of true (intrinsic) colloids in EBS
		2.1.09.20.0A	Filtration of colloids in EBS
		2.1.09.22.0A	Sorption of colloids at air-water interface
		2.1.09.19.0A	Sorption of colloids in EBS
		2.1.09.17.0A	Formation of pseudo-colloids (corrosion product) in EBS
		2.2.08.10.0B	Colloidal transport in the UZ
		2.2.08.10.0A	Colloidal transport in the SZ
		2.1.09.18.0A	Formation of microbial colloids in EBS
K 4.13	Radionuclide release from EDZ	2.2.01.05.0A	Radionuclide transport in the excavation disturbed zone
K 4.14	HLW panels (siting)	1.1.07.00.0A	Repository design
K 4.15	TRU silos (siting)	1.1.07.00.0A	Repository design
K 4.16	Access tunnels and shafts	1.1.07.00.0A	Repository design
K 4.17	Shaft and tunnel seals	1.1.04.01.0A	Incomplete closure
		1.1.01.01.0A	Open site investigation boreholes
		2.1.05.03.0A	Degradation of seals
		2.1.05.01.0A	Flow through seals (access ramps and ventilation shafts)

Table F-3. Cross Reference of Source FEPs to TSPA-LA FEPs (Continued)

Source FEP No.	Source FEP Name	TSPA-LA FEP Number	TSPA-LA FEP Name
K 4.18	Oil or organic fluid spill	1.1.02.03.0A	Undesirable materials left
		1.1.08.00.0A	Inadequate quality control and deviations from design
		1.1.12.01.0A	Accidents and unplanned events during construction and operation
K 4.19	TRU silos cementitious plume	2.1.09.01.0A	Chemical characteristics of water in drifts
K 5.01	LPD effective hydraulic properties	2.2.03.02.0A	Rock properties of host rock and other units
K 5.02	Water-conducting features (types)	2.2.07.13.0A	Water-conducting features in the SZ
K 5.03	Groundwater flow in LPD	2.2.07.12.0A	Saturated groundwater flow in the geosphere
K 5.04	Groundwater flow path	2.2.07.12.0A	Saturated groundwater flow in the geosphere
K 5.05	Radionuclide transport through LPD	2.2.08.07.0B	Radionuclide solubility limits in the UZ
		2.2.08.07.0A	Radionuclide solubility limits in the SZ
K 5.06	Matrix diffusion	2.2.08.08.0A	Matrix diffusion in the SZ
K 5.07	Mineralogy	2.2.08.01.0A	Chemical characteristics of groundwater in the SZ
		2.2.08.01.0B	Chemical characteristics of groundwater in the UZ
K 5.08	Groundwater chemistry	2.2.08.03.0B	Geochemical interactions and evolution in the UZ
		2.2.08.01.0A	Chemical characteristics of groundwater in the SZ
		2.2.08.03.0A	Geochemical interactions and evolution in the SZ
		2.2.08.01.0B	Chemical characteristics of groundwater in the UZ
K 5.09	Sorption	2.2.08.09.0A	Sorption in the SZ
		2.2.08.08.0A	Matrix diffusion in the SZ
K 5.10	Non-linear sorption	2.2.08.09.0A	Sorption in the SZ
		2.2.08.09.0B	Sorption in the UZ
K 5.11	Intrusion of saline groundwater	2.2.08.03.0A	Geochemical interactions and evolution in the SZ
		2.1.09.01.0A	Chemical characteristics of water in drifts
		2.2.08.12.0A	Chemistry of water flowing into the drift
K 5.12	Density-driven groundwater flow (thermal)	2.2.10.03.0A	Natural geothermal effects on flow in the SZ
		2.2.10.13.0A	Repository-induced thermal effects on flow in the SZ
K 5.13	Geothermal regime	2.1.11.09.0A	Thermal effects on flow in the EBS
		2.2.10.03.0A	Natural geothermal effects on flow in the SZ
		2.1.11.09.0C	Thermally driven flow (convection) in drifts
K 5.14	Regional stress regime	2.2.06.01.0A	Seismic activity changes porosity and permeability of rock
K 5.15	Natural colloids	2.1.09.16.0A	Formation of pseudo-colloids (natural) in EBS
K 5.16	Solubility limits/colloid formation	2.2.08.10.0A	Colloidal transport in the SZ
		2.2.08.07.0A	Radionuclide solubility limits in the SZ
		3.2.07.01.0A	Isotopic dilution
K 5.17	Gas pressure effects	2.2.11.02.0A	Gas effects in the UZ
K 5.18	Hydraulic gradient changes (magnitude, direction)	1.2.07.01.0A	Erosion/denudation

Table F-3. Cross Reference of Source FEPs to TSPA-LA FEPs (Continued)

Source FEP No.	Source FEP Name	TSPA-LA FEP Number	TSPA-LA FEP Name
K 5.19	Influx of oxidising water	1.1.02.00.0A	Chemical effects of excavation and construction in EBS
K 5.20	TRU alkaline or organic plume	2.1.09.01.0A	Chemical characteristics of water in drifts
K 5.21	Organics	2.1.09.13.0A	Complexation in EBS
K 5.22	Microbial activity	2.2.09.01.0B	Microbial activity in the UZ
		2.2.09.01.0A	Microbial activity in the SZ
K 5.23	Dilution of radionuclides in groundwater (LPD to HPD or MWCF)	2.2.07.16.0A	Dilution of radionuclides in groundwater
K 5.24	Geogas	2.2.11.01.0A	Gas effects in the SZ
K 5.25	Exploratory boreholes (sealing)	1.1.01.01.0A	Open site investigation boreholes
K 6.01	MWCF effective hydraulic properties	2.2.03.02.0A	Rock properties of host rock and other units
K 6.02	Water-conducting features (types)	2.2.07.13.0A	Water-conducting features in the SZ
K 6.03	Groundwater flow in MWCF	2.2.07.12.0A	Saturated groundwater flow in the geosphere
K 6.04	Groundwater flow path	2.2.07.12.0A	Saturated groundwater flow in the geosphere
K 6.05	Radionuclide transport through MWCF	2.2.08.07.0A	Radionuclide solubility limits in the SZ
		2.2.08.07.0B	Radionuclide solubility limits in the UZ
K 6.06	Matrix diffusion	2.2.08.08.0A	Matrix diffusion in the SZ
K 6.07	Mineralogy	2.2.08.01.0A	Chemical characteristics of groundwater in the SZ
		2.2.08.01.0B	Chemical characteristics of groundwater in the UZ
K 6.08	Groundwater chemistry	2.2.08.03.0A	Geochemical interactions and evolution in the SZ
		2.2.08.03.0B	Geochemical interactions and evolution in the UZ
K 6.09	Sorption	2.2.08.09.0A	Sorption in the SZ
		2.2.08.09.0B	Sorption in the UZ
K 6.10	Non-linear sorption	2.2.08.09.0A	Sorption in the SZ
		2.2.08.09.0B	Sorption in the UZ
K 6.11	Intrusion of saline groundwater	2.2.08.03.0A	Geochemical interactions and evolution in the SZ
		2.2.08.12.0A	Chemistry of water flowing into the drift
		2.2.07.14.0A	Chemically-induced density effects on groundwater flow
		2.1.09.01.0A	Chemical characteristics of water in drifts
K 6.12	Density-driven groundwater flows (thermal)	2.2.10.03.0A	Natural geothermal effects on flow in the SZ
K 6.13	Geothermal regime	2.2.10.03.0A	Natural geothermal effects on flow in the SZ
K 6.14	Regional stress regime	2.2.06.01.0A	Seismic activity changes porosity and permeability of rock
K 6.15	Natural colloids	2.1.09.16.0A	Formation of pseudo-colloids (natural) in EBS
K 6.16	Solubility limits/colloid formation	2.2.08.07.0A	Radionuclide solubility limits in the SZ
		2.2.08.10.0A	Colloidal transport in the SZ
		3.2.07.01.0A	Isotopic dilution
K 6.17	Gas pressure effects	2.2.11.02.0A	Gas effects in the UZ
K 6.18	Hydraulic gradient changes (magnitude, direction)	1.2.07.01.0A	Erosion/denudation

Table F-3. Cross Reference of Source FEPs to TSPA-LA FEPs (Continued)

Source FEP No.	Source FEP Name	TSPA-LA FEP Number	TSPA-LA FEP Name
K 6.19	Influx of oxidising water	1.1.02.00.0A	Chemical effects of excavation and construction in EBS
K 6.20	TRU alkaline or organics plume	2.1.09.01.0A	Chemical characteristics of water in drifts
K 6.21	Organics	2.1.09.13.0A	Complexation in EBS
K 6.22	Microbial activity	2.2.09.01.0A	Microbial activity in the SZ
		2.2.09.01.0B	Microbial activity in the UZ
K 6.23	Dilution of radionuclides in groundwater (MWCF to HPD & Biosph.)	2.2.07.16.0A	Dilution of radionuclides in groundwater
K 6.24	Geogas	2.2.11.01.0A	Gas effects in the SZ
K 7.01	HPD effective hydraulic properties	2.2.03.02.0A	Rock properties of host rock and other units
K 7.02	Mesozoic sedimentary cover	2.2.03.01.0A	Stratigraphy
K 7.03	Permo-Carboniferous Trough	2.2.03.01.0A	Stratigraphy
K 7.04	Groundwater flow	2.2.07.12.0A	Saturated groundwater flow in the geosphere
K 7.05	Boundary conditions for flow	2.2.07.12.0A	Saturated groundwater flow in the geosphere
		1.2.02.02.0A	Faults
K 7.06	Groundwater flow path	2.2.07.12.0A	Saturated groundwater flow in the geosphere
K 7.07	Dilution of radionuclides in HPD	2.2.07.16.0A	Dilution of radionuclides in groundwater
K 7.08	Groundwater chemistry	2.2.08.01.0A	Chemical characteristics of groundwater in the SZ
		2.2.08.03.0B	Geochemical interactions and evolution in the UZ
		2.2.08.03.0A	Geochemical interactions and evolution in the SZ
		2.2.08.01.0B	Chemical characteristics of groundwater in the UZ
K 7.09	Radionuclide sorption	2.2.08.09.0A	Sorption in the SZ
K 7.10	Stress regime	2.2.06.01.0A	Seismic activity changes porosity and permeability of rock
K 7.11	Erosion	1.2.07.01.0A	Erosion/denudation
K 7.12	Hydraulic gradient (magnitude, regional direction)	2.2.07.12.0A	Saturated groundwater flow in the geosphere
K 7.13	Density-driven groundwater flows (temperature/salinity differences)	2.2.10.03.0A	Natural geothermal effects on flow in the SZ
K 8.01	Present-day biosphere	2.3.13.01.0A	Biosphere characteristics
K 8.02	Future biosphere conditions	2.3.13.01.0A	Biosphere characteristics
K 8.03	Exfiltration to a local aquifer	2.2.07.16.0A	Dilution of radionuclides in groundwater
		2.2.08.11.0A	Groundwater discharge to surface within the reference biosphere
		2.3.11.04.0A	Groundwater discharge to surface outside the reference biosphere
K 8.04	Exfiltration to surface waters	2.3.11.04.0A	Groundwater discharge to surface outside the reference biosphere
		2.3.04.01.0A	Surface water transport and mixing
		2.2.08.11.0A	Groundwater discharge to surface within the reference biosphere
K 8.05	Radionuclide accumulation in sediments	2.3.04.01.0A	Surface water transport and mixing
		2.3.02.02.0A	Radionuclide accumulation in soils
		2.3.02.03.0A	Soil and sediment transport in the biosphere

Table F-3. Cross Reference of Source FEPs to TSPA-LA FEPs (Continued)

Source FEP No.	Source FEP Name	TSPA-LA FEP Number	TSPA-LA FEP Name
K 8.06	Radionuclide accumulation in soils	2.3.02.02.0A	Radionuclide accumulation in soils
K 8.07	Water resource exploitation	1.4.07.02.0A	Wells
K 8.08	Filtration	3.3.01.00.0A	Contaminated drinking water, foodstuffs and drugs
K 8.09	Uptake by crops	3.3.02.01.0A	Plant uptake
K 8.10	Uptake by livestock	3.3.02.02.0A	Animal uptake
K 8.11	Uptake in fish	3.3.04.01.0A	Ingestion
		3.3.02.02.0A	Animal uptake
		3.3.02.03.0A	Fish uptake
K 8.12	Radionuclide volatilisation/aerosol/dust production	3.2.10.00.0A	Atmospheric transport of contaminants
K 8.13	Exposure pathways	3.3.04.03.0A	External exposure
		3.3.04.01.0A	Ingestion
		3.3.04.02.0A	Inhalation
		3.3.08.00.0A	Radon and radon decay product exposure
K 8.14	Human lifestyle	2.4.04.01.0A	Human lifestyle
K 8.15	Radiation doses	3.3.05.01.0A	Radiation doses
K 8.16	Foodchain equilibrium	3.3.02.02.0A	Animal uptake
		3.3.02.01.0A	Plant uptake
K 8.17	Radionuclide sorption	2.2.08.09.0A	Sorption in the SZ
K 8.18	Secular equilibrium of radionuclide chains	3.3.05.01.0A	Radiation doses
K 8.19	Surface water flow (river Rhine)	2.3.11.02.0A	Surface runoff and evapotranspiration
		2.3.04.01.0A	Surface water transport and mixing
K 8.20	Groundwater flow (alluvium of Rhine valley)	2.2.07.15.0A	Advection and dispersion in the SZ
		2.2.07.16.0A	Dilution of radionuclides in groundwater
		2.3.11.03.0A	Infiltration and recharge
		2.2.07.02.0A	Unsaturated groundwater flow in the geosphere
		2.2.07.01.0A	Locally saturated flow at bedrock/alluvium contact
		2.1.08.07.0A	Unsaturated flow in the EBS
		2.1.08.09.0A	Saturated flow in the EBS
K 8.21	Dilution of radionuclides in surface water (aquifer, river, lake etc.)	2.2.07.16.0A	Dilution of radionuclides in groundwater
		2.2.08.11.0A	Groundwater discharge to surface within the reference biosphere
		2.3.04.01.0A	Surface water transport and mixing
K 8.22	Erosion/deposition	1.2.07.01.0A	Erosion/denudation
K 8.23	Sedimentation	2.3.06.00.0A	Marine features
		2.3.04.01.0A	Surface water transport and mixing
K 8.24	Soil formation	2.3.02.01.0A	Soil type
K 8.25	Soil	2.3.02.01.0A	Soil type
K 8.26	Surface water bodies	1.3.04.00.0A	Periglacial effects
		1.3.05.00.0A	Glacial and ice sheet effect
		1.4.07.01.0A	Water management activities
		1.3.01.00.0A	Climate change

Table F-3. Cross Reference of Source FEPs to TSPA-LA FEPs (Continued)

Source FEP No.	Source FEP Name	TSPA-LA FEP Number	TSPA-LA FEP Name
K 8.26	Surface water bodies (continued)	2.3.02.03.0A	Soil and sediment transport in the biosphere
		2.3.04.01.0A	Surface water transport and mixing
		2.3.11.03.0A	Infiltration and recharge
		1.4.06.01.0A	Altered soil or surface water chemistry
		1.3.07.02.0B	Water table rise affects UZ
		2.3.11.02.0A	Surface runoff and evapotranspiration
K 8.27	Atmosphere	3.2.10.00.0A	Atmospheric transport of contaminants
K 8.28	Interface effects	2.3.02.03.0A	Soil and sediment transport in the biosphere
		3.2.10.00.0A	Atmospheric transport of contaminants
		2.3.04.01.0A	Surface water transport and mixing
		2.4.09.01.0B	Agricultural land use and irrigation
		2.3.09.01.0A	Animal burrowing/intrusion
		2.3.13.02.0A	Radionuclide alteration during biosphere transport
K 8.29	Precipitation	2.3.11.01.0A	Precipitation
K 8.30	Evapotranspiration	2.3.11.02.0A	Surface runoff and evapotranspiration
K 8.31	Capillary rise	2.2.07.03.0A	Capillary rise in the UZ
K 8.32	Percolation	2.3.11.03.0A	Infiltration and recharge
K 8.33	Irrigation	2.3.02.02.0A	Radionuclide accumulation in soils
		1.4.07.02.0A	Wells
		2.4.09.01.0A	Implementation of new agricultural practices or land use
		2.4.09.01.0B	Agricultural land use and irrigation
		3.2.10.00.0A	Atmospheric transport of contaminants
		1.4.07.01.0A	Water management activities
K 8.34	Surface run-off	2.3.02.03.0A	Soil and sediment transport in the biosphere
		2.3.11.02.0A	Surface runoff and evapotranspiration
K 8.35	Bioturbation	2.3.02.03.0A	Soil and sediment transport in the biosphere
K 8.36	Suspended sediment transport	2.1.09.21.0C	Transport of particles larger than colloids in the UZ
		2.1.09.21.0B	Transport of particles larger than colloids in the SZ
		2.1.09.21.0A	Transport of particles larger than colloids in EBS
K 8.37	Earthworks (human actions, dredging, etc.)	2.4.10.00.0A	Urban and industrial land and water use
K 8.38	Ploughing	2.4.09.01.0B	Agricultural land use and irrigation
		2.4.09.01.0A	Implementation of new agricultural practices or land use
K 8.39	Agricultural practices	2.4.09.01.0A	Implementation of new agricultural practices or land use
		2.4.09.01.0B	Agricultural land use and irrigation
K 8.40	Natural and semi-natural environments	2.4.08.00.0A	Wild and natural land and water use
K 8.41	Hunter/gathering lifestyle	2.4.04.01.0A	Human lifestyle
K 8.42	Contaminated products (non-food)	3.3.03.01.0A	Contaminated non-food products and exposure
K 8.43	Removal mechanisms	3.3.02.02.0A	Animal uptake
		3.3.02.03.0A	Fish uptake
		3.3.02.01.0A	Plant uptake

Table F-3. Cross Reference of Source FEPs to TSPA-LA FEPs (Continued)

Source FEP No.	Source FEP Name	TSPA-LA FEP Number	TSPA-LA FEP Name
K 8.44	Consumption of uncontaminated products	3.3.01.00.0A	Contaminated drinking water, foodstuffs and drugs
K 8.45	Radon pathways and doses	3.3.08.00.0A	Radon and radon decay product exposure
K 9.01	Regional horizontal movements	1.2.01.01.0A	Tectonic activity - large scale
K 9.02	Regional vertical movements	1.2.01.01.0A	Tectonic activity - large scale
K 9.03	Movements along major faults	1.2.02.02.0A	Faults
K 9.04	Movements along small-scale faults	1.2.02.02.0A	Faults
K 9.05	Seismic activity	1.4.02.04.0A	Seismic event precedes human intrusion
		2.2.06.02.0B	Seismic activity changes porosity and permeability of fractures
		2.1.02.24.0A	Mechanical impact on cladding
		2.1.03.07.0A	Mechanical impact on waste package
		2.1.03.07.0B	Mechanical impact on drip shield
		2.1.07.02.0A	Drift collapse
		2.2.06.03.0A	Seismic activity alters perched water zones
		1.2.03.02.0B	Seismic-induced rockfall damages EBS components
		2.2.06.02.0A	Seismic activity changes porosity and permeability of faults
		1.2.03.03.0A	Seismicity associated with igneous activity
		1.2.03.02.0A	Seismic ground motion damages EBS components
		1.2.10.01.0A	Hydrologic response to seismic activity
		2.2.06.01.0A	Seismic activity changes porosity and permeability of rock
K 9.06	Stress changes - hydrogeological effects	2.2.06.01.0A	Seismic activity changes porosity and permeability of rock
K 9.07	Erosion/denudation	1.2.07.01.0A	Erosion/denudation
K 9.08	Basement alteration	1.2.07.01.0A	Erosion/denudation
K 9.09	Magmatic activity (volcanism and plutonism)	1.2.03.03.0A	Seismicity associated with igneous activity
		1.2.10.02.0A	Hydrologic response to igneous activity
		1.2.04.04.0A	Igneous intrusion interacts with EBS components
		1.2.04.02.0A	Igneous activity changes rock properties
		1.2.04.03.0A	Igneous intrusion into repository
K 9.10	Hydrothermal activity	1.2.06.00.0A	Hydrothermal activity
K 9.11	Extraterrestrial events	1.5.01.02.0A	Extraterrestrial events
K S1.1	Waste Form and Packaging	2.1.03.11.0A	Physical form of waste package and drip shield
K S1.2	Waste Emplacement and Repository	1.1.03.01.0B	Error in backfill emplacement
		1.1.03.01.0A	Error in waste emplacement
K S1.3	Host Geology	2.3.01.00.0A	Topography and morphology
		2.3.02.01.0A	Soil type
		2.2.03.01.0A	Stratigraphy
K S1.4	Local and Regional Surface Environment	1.1.07.00.0A	Repository design
		2.3.01.00.0A	Topography and morphology
		0.1.02.00.0A	Timescales of concern

Table F-3. Cross Reference of Source FEPs to TSPA-LA FEPs (Continued)

Source FEP No.	Source FEP Name	TSPA-LA FEP Number	TSPA-LA FEP Name
K S1.4	Local and Regional Surface Environment (continued)	0.1.03.00.0A	Spatial domain of concern
		0.1.10.00.0A	Model and data issues
		2.3.02.01.0A	Soil type
K S1.5	Geographical Location	0.1.03.00.0A	Spatial domain of concern
		1.1.07.00.0A	Repository design
K S2.1	Appropriate Repository Design and Closure	1.1.13.00.0A	Retrievability
		1.1.12.01.0A	Accidents and unplanned events during construction and operation
		1.1.11.00.0A	Monitoring of the repository
		1.1.07.00.0A	Repository design
		1.1.08.00.0A	Inadequate quality control and deviations from design
		1.1.04.01.0A	Incomplete closure
K S2.2	No Consideration of Global and Regional Disasters	1.1.08.00.0A	Inadequate quality control and deviations from design
		1.1.12.01.0A	Accidents and unplanned events during construction and operation
		0.1.10.00.0A	Model and data issues
K S2.3	No Consideration of Malicious Acts and Acts of War	1.4.02.01.0A	Deliberate human intrusion
		1.1.12.01.0A	Accidents and unplanned events during construction and operation
K S2.4	No Consideration of Deliberate Human Intrusion	1.4.02.01.0A	Deliberate human intrusion
		0.1.09.00.0A	Regulatory requirements and exclusions
K S2.5	No Consideration of Future Human Society and Technology	2.4.04.01.0A	Human lifestyle
		0.1.09.00.0A	Regulatory requirements and exclusions
		1.4.09.00.0A	Technological developments
		1.5.02.00.0A	Species evolution
		2.4.01.00.0A	Human characteristics (physiology, metabolism)
		2.4.09.01.0A	Implementation of new agricultural practices or land use
		2.3.13.01.0A	Biosphere characteristics
K S2.6.1	Consideration of radiological impacts to man (only)	3.3.05.01.0A	Radiation doses
		3.3.07.00.0A	Non-radiological toxicity and effects
		3.3.06.02.0A	Sensitization to radiation
		3.3.06.00.0A	Radiological toxicity and effects
		0.1.09.00.0A	Regulatory requirements and exclusions
		0.1.10.00.0A	Model and data issues
		2.3.13.03.0A	Effects of repository heat on the biosphere
K S2.6.2	Basis for consideration of radiological impacts to man	0.1.09.00.0A	Regulatory requirements and exclusions
		3.3.05.01.0A	Radiation doses
K S2.7	No Consideration of Future Evolution of Man and Other Species	1.5.02.00.0A	Species evolution
		0.1.09.00.0A	Regulatory requirements and exclusions
		1.4.09.00.0A	Technological developments
MLD-1	DOE SNF initial radionuclide inventory	2.1.01.01.0A	Waste inventory
MLD-10	DOE SNF criticality far-field (waste heat impact)	2.2.14.09.0A	Far-field criticality

Table F-3. Cross Reference of Source FEPs to TSPA-LA FEPs (Continued)

Source FEP No.	Source FEP Name	TSPA-LA FEP Number	TSPA-LA FEP Name
MLD-11	DOE SNF waste package design	2.1.03.11.0A	Physical form of waste package and drip shield
MLD-12	DOE SNF waste package internal corrosion	2.1.03.06.0A	Internal corrosion of waste packages prior to breach
MLD-13	DOE SNF pyrophoric event (waste package degradation impact)	2.1.02.08.0A	Pyrophoricity from DSNF
MLD-14	DOE SNF criticality in-situ (waste package degradation impact)	2.1.14.15.0A	In-package criticality (intact configuration)
		2.1.14.16.0A	In-package criticality (degraded configurations)
MLD-15	DSNF degradation, alteration, and dissolution	2.1.02.01.0A	DSNF degradation (alteration, dissolution, and radionuclide release)
MLD-16	DOE SNF colocation with HLW (waste form degradation impact)	2.1.01.02.0B	Interactions between co-disposed waste
MLD-17	Acetylene generation from DSNF, WFMisc – Flammable Gasses Generation from DSNF – YMP	2.1.02.29.0A	Flammable gas generation from DSNF
		2.1.12.08.0A	Gas explosions in EBS
MLD-18	DOE SNF pyrophoric event (waste form degradation impact)	2.1.02.08.0A	Pyrophoricity from DSNF
MLD-19	DOE SNF criticality in-situ (waste form degradation impact)	2.1.14.16.0A	In-package criticality (degraded configurations)
		2.1.14.15.0A	In-package criticality (intact configuration)
MLD-2	DOE SNF criticality in-situ (radionuclide inventory impact)	2.1.14.15.0A	In-package criticality (intact configuration)
		2.1.14.17.0A	Near-field criticality
MLD-20	DOE SNF colocation with HLW (radionuclide mobilization impact)	2.1.01.02.0B	Interactions between co-disposed waste
MLD-21	DOE SNF dissolution	2.1.02.01.0A	DSNF degradation (alteration, dissolution, and radionuclide release)
MLD-22	DSNF cladding degradation	2.1.02.25.0B	Naval SNF Cladding
		2.1.02.25.0A	DSNF cladding
MLD-23	DOE SNF colocation with HLW (cladding degradation impact)	2.1.01.02.0B	Interactions between co-disposed waste
MLD-24	DOE SNF pyrophoric event (cladding degradation impact)	2.1.02.08.0A	Pyrophoricity from DSNF
MLD-25	DOE SNF criticality in-situ (cladding degradation impact)	2.1.14.16.0A	In-package criticality (degraded configurations)
		2.1.14.15.0A	In-package criticality (intact configuration)
MLD-3	DOE SNF criticality near-field (radionuclide inventory impact)	2.1.14.16.0A	In-package criticality (degraded configurations)
		2.1.14.17.0A	Near-field criticality
MLD-4	DOE SNF criticality far-field (radionuclide inventory impact)	2.2.14.09.0A	Far-field criticality
MLD-5	DOE SNF hazardous chemical inventory	2.1.01.01.0A	Waste inventory
MLD-6	DOE SNF expected waste heat generation	2.1.11.01.0A	Heat generation in EBS
MLD-7	DOE SNF waste package placement	2.1.01.02.0A	Interactions between co-located waste
MLD-8	DOE SNF pyrophoric event (waste heat impact)	2.1.02.08.0A	Pyrophoricity from DSNF
MLD-9	DOE SNF criticality in-situ (waste heat impact)	2.1.14.15.0A	In-package criticality (intact configuration)
		2.1.14.16.0A	In-package criticality (degraded configurations)
N 1.1	EXTRA-TERRESTRIAL	1.5.01.02.0A	Extraterrestrial events
N 1.1.1	Meteorite Impact	1.5.01.01.0A	Meteorite impact
N 1.1.2	Solar insolation	1.3.01.00.0A	Climate change

Table F-3. Cross Reference of Source FEPs to TSPA-LA FEPs (Continued)

Source FEP No.	Source FEP Name	TSPA-LA FEP Number	TSPA-LA FEP Name
N 1.2	GEOLOGICAL	1.2.01.01.0A	Tectonic activity - large scale
N 1.2.1	Plate movement/tectonic change	1.2.01.01.0A	Tectonic activity - large scale
N 1.2.10	Fault generation	1.2.02.02.0A	Faults
N 1.2.11	Rock heterogeneity	2.2.03.02.0A	Rock properties of host rock and other units
N 1.2.12	Undetected features	2.2.12.00.0A	Undetected features in the UZ
N 1.2.13	Natural gas intrusion	2.2.11.01.0A	Gas effects in the SZ
		2.2.11.02.0A	Gas effects in the UZ
N 1.2.2	Changes in the Earth's magnetic field	1.5.03.01.0A	Changes in the earth's magnetic field
N 1.2.3	Magmatic activity	1.2.10.02.0A	Hydrologic response to igneous activity
		1.2.03.03.0A	Seismicity associated with igneous activity
		1.2.04.03.0A	Igneous intrusion into repository
		1.2.04.02.0A	Igneous activity changes rock properties
		1.2.04.04.0A	Igneous intrusion interacts with EBS components
N 1.2.4	Metamorphic activity	1.2.05.00.0A	Metamorphism
N 1.2.5	Diagenesis	1.2.08.00.0A	Diagenesis
N 1.2.6	Uplift and subsidence	1.2.01.01.0A	Tectonic activity - large scale
N 1.2.7	Diapirism	1.2.09.01.0A	Diapirism
N 1.2.8	Seismicity	2.1.03.07.0B	Mechanical impact on drip shield
		2.2.06.03.0A	Seismic activity alters perched water zones
		2.1.02.24.0A	Mechanical impact on cladding
		1.2.10.01.0A	Hydrologic response to seismic activity
		1.2.03.02.0A	Seismic ground motion damages EBS components
		1.2.03.02.0B	Seismic-induced rockfall damages EBS components
		1.2.03.03.0A	Seismicity associated with igneous activity
		2.1.03.07.0A	Mechanical impact on waste package
		2.2.06.02.0B	Seismic activity changes porosity and permeability of fractures
		2.2.06.02.0A	Seismic activity changes porosity and permeability of faults
		2.2.06.01.0A	Seismic activity changes porosity and permeability of rock
		2.1.07.02.0A	Drift collapse
N 1.2.9	Fault activation	1.2.02.02.0A	Faults
N 1.3	CLIMATOLOGICAL	1.3.01.00.0A	Climate change
N 1.3.1	Precipitation, temperature and soil water balance	2.3.11.01.0A	Precipitation
N 1.3.2	Extremes of precipitation, snow melt and associated flooding	2.3.11.01.0A	Precipitation
N 1.3.3	Coastal surge, storms and hurricanes	2.3.06.00.0A	Marine features
N 1.3.4	Sea-level rise/fall	2.3.06.00.0A	Marine features
N 1.3.5	Periglacial effects	1.3.04.00.0A	Periglacial effects
N 1.3.6	Glaciation	1.3.05.00.0A	Glacial and ice sheet effect
N 1.3.7	No ice age	1.3.01.00.0A	Climate change
N 1.4	GEOMORPHOLOGICAL	2.3.01.00.0A	Topography and morphology

Table F-3. Cross Reference of Source FEPs to TSPA-LA FEPs (Continued)

Source FEP No.	Source FEP Name	TSPA-LA FEP Number	TSPA-LA FEP Name
N 1.4.1	Land slide	1.2.07.01.0A	Erosion/denudation
N 1.4.10	Frost weathering	1.3.04.00.0A	Periglacial effects
N 1.4.2	Denudation	1.2.07.01.0A	Erosion/denudation
N 1.4.3	River, stream, channel erosion	1.2.07.01.0A	Erosion/denudation
N 1.4.4	River meander	2.3.04.01.0A	Surface water transport and mixing
N 1.4.5	Freshwater sediment transport and deposition	1.2.07.02.0A	Deposition
		2.3.04.01.0A	Surface water transport and mixing
		2.3.02.03.0A	Soil and sediment transport in the biosphere
N 1.4.6	Coastal erosion and estuarine development	2.3.06.00.0A	Marine features
N 1.4.7	Marine sediment transport and deposition	2.3.06.00.0A	Marine features
N 1.4.8	Solifluction	1.3.04.00.0A	Periglacial effects
N 1.4.9	Chemical denudation and weathering	1.2.07.01.0A	Erosion/denudation
N 1.5	HYDROLOGICAL	2.2.07.12.0A	Saturated groundwater flow in the geosphere
N 1.5.1	River flow and lake level changes	2.3.04.01.0A	Surface water transport and mixing
		2.3.11.04.0A	Groundwater discharge to surface outside the reference biosphere
		2.2.08.11.0A	Groundwater discharge to surface within the reference biosphere
		2.4.08.00.0A	Wild and natural land and water use
N 1.5.2	Site flooding	1.3.07.02.0B	Water table rise affects UZ
		1.1.02.01.0A	Site flooding (during construction and operation)
		2.3.11.02.0A	Surface runoff and evapotranspiration
N 1.5.3	Recharge to groundwater	2.3.11.03.0A	Infiltration and recharge
N 1.5.4	Groundwater discharge	2.3.11.04.0A	Groundwater discharge to surface outside the reference biosphere
N 1.5.5	Groundwater flow	2.2.07.12.0A	Saturated groundwater flow in the geosphere
N 1.5.6	Groundwater conditions	2.2.08.01.0B	Chemical characteristics of groundwater in the UZ
		2.2.08.01.0A	Chemical characteristics of groundwater in the SZ
N 1.5.7	Saline or freshwater intrusion	2.1.09.01.0A	Chemical characteristics of water in drifts
		2.2.08.03.0A	Geochemical interactions and evolution in the SZ
N 1.5.8	Effects at saline-freshwater interface	2.1.09.01.0A	Chemical characteristics of water in drifts
		2.2.08.03.0A	Geochemical interactions and evolution in the SZ
N 1.5.9	Natural thermal effects	2.2.10.03.0A	Natural geothermal effects on flow in the SZ
		2.2.10.03.0B	Natural geothermal effects on flow in the UZ
N 1.6	TRANSPORT AND GEOCHEMICAL	2.2.08.11.0A	Groundwater discharge to surface within the reference biosphere
N 1.6.1	Advection and dispersion	2.2.07.15.0A	Advection and dispersion in the SZ
		2.2.07.15.0B	Advection and dispersion in the UZ
N 1.6.10	Complexing agents	2.1.09.13.0A	Complexation in EBS
N 1.6.11	Fracture mineralisation and weathering	2.2.08.03.0A	Geochemical interactions and evolution in the SZ
		2.2.08.03.0B	Geochemical interactions and evolution in the UZ

Table F-3. Cross Reference of Source FEPs to TSPA-LA FEPs (Continued)

Source FEP No.	Source FEP Name	TSPA-LA FEP Number	TSPA-LA FEP Name
N 1.6.12	Accumulation in soils and organic debris	2.3.02.02.0A	Radionuclide accumulation in soils
N 1.6.13	Mass, isotopic and species dilution	3.2.07.01.0A	Isotopic dilution
N 1.6.14	Chemical gradients	2.2.08.01.0B	Chemical characteristics of groundwater in the UZ
		2.2.08.01.0A	Chemical characteristics of groundwater in the SZ
N 1.6.2	Diffusion	2.2.07.17.0A	Diffusion in the SZ
N 1.6.3	Matrix diffusion	2.2.08.08.0A	Matrix diffusion in the SZ
N 1.6.4	Gas mediated transport	2.2.11.02.0A	Gas effects in the UZ
		2.2.11.03.0A	Gas transport in geosphere
N 1.6.5	Multiphase flow and gas driven flow	2.2.11.02.0A	Gas effects in the UZ
		2.1.11.09.0C	Thermally driven flow (convection) in drifts
		2.1.11.09.0A	Thermal effects on flow in the EBS
		2.1.11.09.0B	Thermally-driven flow (convection) in waste packages
N 1.6.6	Solubility limit	2.1.09.04.0A	Radionuclide solubility, solubility limits, and speciation in the waste form and EBS
N 1.6.7	Sorption	2.2.08.09.0B	Sorption in the UZ
		2.2.08.09.0A	Sorption in the SZ
N 1.6.8	Dissolution, precipitation and crystallisation	2.2.08.03.0B	Geochemical interactions and evolution in the UZ
		2.2.08.03.0A	Geochemical interactions and evolution in the SZ
N 1.6.9	Colloid formation, dissolution and transport	2.1.09.19.0B	Advection of colloids in EBS
		2.2.08.10.0B	Colloidal transport in the UZ
		2.1.09.20.0A	Filtration of colloids in EBS
		2.2.08.10.0A	Colloidal transport in the SZ
		2.1.09.25.0A	Formation of colloids (waste-form) by co-precipitation in EBS
		2.1.09.22.0A	Sorption of colloids at air-water interface
		2.1.09.26.0A	Gravitational settling of colloids in EBS
		2.1.09.24.0A	Diffusion of colloids in EBS
		2.1.09.18.0A	Formation of microbial colloids in EBS
		2.1.09.17.0A	Formation of pseudo-colloids (corrosion product) in EBS
		2.1.09.16.0A	Formation of pseudo-colloids (natural) in EBS
		2.1.09.15.0A	Formation of true (intrinsic) colloids in EBS
		2.1.09.13.0A	Complexation in EBS
		2.1.09.19.0A	Sorption of colloids in EBS
		2.1.09.23.0A	Stability of colloids in EBS
N 1.7	ECOLOGICAL	2.3.13.01.0A	Biosphere characteristics
N 1.7.1	Plant uptake	3.3.02.01.0A	Plant uptake
N 1.7.10	Plant and animal evolution	1.5.02.00.0A	Species evolution
N 1.7.2	Animal uptake	3.3.02.02.0A	Animal uptake
N 1.7.3	Uptake by deep rooting species	3.3.02.01.0A	Plant uptake
N 1.7.4	Soil and sediment bioturbation	2.3.02.03.0A	Soil and sediment transport in the biosphere
N 1.7.5	Pedogenesis	2.3.02.01.0A	Soil type

Table F-3. Cross Reference of Source FEPs to TSPA-LA FEPs (Continued)

Source FEP No.	Source FEP Name	TSPA-LA FEP Number	TSPA-LA FEP Name
N 1.7.6	Chemical transformations	2.2.09.01.0A	Microbial activity in the SZ
		2.2.09.01.0B	Microbial activity in the UZ
N 1.7.7	Microbial interactions	2.1.10.01.0A	Microbial activity in EBS
N 1.7.8	Ecological change	2.3.13.01.0A	Biosphere characteristics
N 1.7.9	Ecological response to climate (e.g. desert formation)	2.3.13.01.0A	Biosphere characteristics
N 2.1	DESIGN AND CONSTRUCTION	1.1.03.01.0A	Error in waste emplacement
		1.1.02.00.0A	Chemical effects of excavation and construction in EBS
		1.1.12.01.0A	Accidents and unplanned events during construction and operation
		1.1.08.00.0A	Inadequate quality control and deviations from design
		1.1.03.01.0B	Error in backfill emplacement
		1.1.02.03.0A	Undesirable materials left
		1.1.02.02.0A	Preclosure ventilation
		2.2.01.01.0A	Mechanical effects of excavation and construction in the near-field
		1.1.02.00.0B	Mechanical effects of excavation and construction in EBS
		2.2.01.01.0B	Chemical effects of excavation and construction in the near-field
		1.1.02.01.0A	Site flooding (during construction and operation)
		1.1.07.00.0A	Repository design
N 2.1.1	Undetected past intrusions	2.2.12.00.0A	Undetected features in the UZ
N 2.1.10	Thermal effects	2.2.10.01.0A	Repository-induced thermal effects on flow in the UZ
N 2.1.2	Investigation borehole seal failure and degradation	2.1.05.03.0A	Degradation of seals
		2.1.05.01.0A	Flow through seals (access ramps and ventilation shafts)
		1.1.01.01.0A	Open site investigation boreholes
		1.1.04.01.0A	Incomplete closure
		1.1.11.00.0A	Monitoring of the repository
N 2.1.3	Shaft or access tunnel seal failure and degradation	2.1.05.03.0A	Degradation of seals
N 2.1.4	Stress field changes, settling, subsidence or caving	2.1.07.02.0A	Drift collapse
		2.1.07.06.0A	Floor buckling
		2.1.08.15.0A	Consolidation of EBS components
		2.2.06.04.0A	Effects of subsidence
		2.2.10.04.0A	Thermo-mechanical stresses alter characteristics of fractures near repository
		2.2.10.04.0B	Thermo-mechanical stresses alter characteristics of faults near repository
N 2.1.5	Dewatering of host rock	2.1.08.03.0A	Repository dry-out due to waste heat
N 2.1.6	Material defects	1.1.08.00.0A	Inadequate quality control and deviations from design
N 2.1.7	Common cause failures	1.1.08.00.0A	Inadequate quality control and deviations from design
N 2.1.8	Poor quality construction	1.1.08.00.0A	Inadequate quality control and deviations from design

Table F-3. Cross Reference of Source FEPs to TSPA-LA FEPs (Continued)

Source FEP No.	Source FEP Name	TSPA-LA FEP Number	TSPA-LA FEP Name
N 2.1.9	Design modification	1.1.07.00.0A	Repository design
N 2.2	OPERATION AND CLOSURE	1.1.04.01.0A	Incomplete closure
N 2.2.1	Radioactive waste disposal error	1.1.03.01.0A	Error in waste emplacement
N 2.2.10	Poor closure	1.1.04.01.0A	Incomplete closure
N 2.2.11	Post-closure monitoring	1.1.11.00.0A	Monitoring of the repository
N 2.2.12	Effects of phased operation	1.1.09.00.0A	Schedule and planning
N 2.2.2	Inadequate backfill or compaction, voidage	1.1.03.01.0B	Error in backfill emplacement
N 2.2.3	Co-disposal of reactive wastes	2.1.01.02.0A	Interactions between co-located waste
N 2.2.4	Inadvertant inclusion of undesirable materials	1.1.02.03.0A	Undesirable materials left
N 2.2.5	Heterogeneity of waste forms	2.1.01.03.0A	Heterogeneity of waste inventory
N 2.2.6	Accidents during operation	1.1.12.01.0A	Accidents and unplanned events during construction and operation
N 2.2.7	Sabotage	1.4.02.01.0A	Deliberate human intrusion
N 2.2.8	Repository flooding during operation	1.1.02.01.0A	Site flooding (during construction and operation)
N 2.2.9	Abandonment of unsealed repository	1.1.04.01.0A	Incomplete closure
N 2.3	POST-CLOSURE SUB-SURFACE ACTIVITIES (INTRUSION)	1.4.02.01.0A	Deliberate human intrusion
N 2.3.1	Recovery of repository materials	1.4.02.01.0A	Deliberate human intrusion
N 2.3.10	Injection of liquid wastes	1.4.04.00.0A	Drilling activities (human intrusion)
N 2.3.11	Groundwater abstraction	1.4.07.02.0A	Wells
N 2.3.12	Underground nuclear testing	1.4.11.00.0A	Explosions and crashes (human activities)
N 2.3.2	Malicious intrusion	1.4.02.01.0A	Deliberate human intrusion
N 2.3.3	Exploratory drilling	1.4.04.00.0A	Drilling activities (human intrusion)
N 2.3.4	Exploitation drilling	1.4.04.00.0A	Drilling activities (human intrusion)
N 2.3.5	Geothermal energy production	1.4.04.00.0A	Drilling activities (human intrusion)
N 2.3.6	Resource mining	1.4.05.00.0A	Mining and other underground activities (human intrusion)
N 2.3.7	Tunnelling	1.4.05.00.0A	Mining and other underground activities (human intrusion)
N 2.3.8	Underground construction	1.4.05.00.0A	Mining and other underground activities (human intrusion)
N 2.3.9	Archaeological investigation	1.4.02.01.0A	Deliberate human intrusion
N 2.4	POST-CLOSURE SURFACE ACTIVITIES	2.4.10.00.0A	Urban and industrial land and water use
N 2.4.1	Loss of records	1.1.05.00.0A	Records and markers for the repository
N 2.4.10	Quarrying, near surface extraction	1.4.05.00.0A	Mining and other underground activities (human intrusion)
N 2.4.2	Dams and reservoirs, built/drained	1.4.07.01.0A	Water management activities
N 2.4.3	River rechannelled	1.4.07.01.0A	Water management activities
N 2.4.4	Irrigation	2.4.09.01.0A	Implementation of new agricultural practices or land use
N 2.4.5	Altered soil or surface water chemistry	1.4.06.01.0A	Altered soil or surface water chemistry
N 2.4.6	Land use changes	2.4.10.00.0A	Urban and industrial land and water use

Table F-3. Cross Reference of Source FEPs to TSPA-LA FEPs (Continued)

Source FEP No.	Source FEP Name	TSPA-LA FEP Number	TSPA-LA FEP Name
N 2.4.7	Agricultural and fisheries practice changes	2.4.09.01.0A	Implementation of new agricultural practices or land use
N 2.4.8	Demographic change, urban development	1.4.08.00.0A	Social and institutional developments
N 2.4.9	Anthropogenic climate change	1.4.01.00.0A	Human influences on climate
N 3.1	THERMAL	2.1.11.08.0A	Thermal effects on chemistry and microbial activity in the EBS
		2.1.11.09.0C	Thermally driven flow (convection) in drifts
		2.1.11.01.0A	Heat generation in EBS
		2.1.11.02.0A	Non-uniform heat distribution in EBS
		2.1.11.03.0A	Exothermic reactions in the EBS
		2.1.11.05.0A	Thermal expansion/stress of in-package EBS components
		2.1.11.06.0B	Thermal sensitization of drip shields
		2.1.11.10.0A	Thermal effects on transport in EBS
		2.1.11.09.0B	Thermally-driven flow (convection) in waste packages
		2.1.11.09.0A	Thermal effects on flow in the EBS
		2.1.11.06.0A	Thermal sensitization of waste packages
N 3.1.1	Differential elastic response	2.1.11.07.0A	Thermal expansion/stress of in-drift EBS components
N 3.1.2	Non-elastic response	2.1.11.07.0A	Thermal expansion/stress of in-drift EBS components
N 3.1.3	Host rock fracture aperture changes	2.2.10.04.0A	Thermo-mechanical stresses alter characteristics of fractures near repository
		2.2.10.06.0A	Thermo-chemical alteration in the UZ (solubility, speciation, phase changes)
N 3.1.4	Induced hydrological changes (fluid pressure, density convection, viscosity)	1.1.02.00.0A	Chemical effects of excavation and construction in EBS
		1.1.02.00.0B	Mechanical effects of excavation and construction in EBS
		1.2.01.01.0A	Tectonic activity – large scale
		1.2.04.02.0A	Igneous activity changes rock properties
		1.2.10.01.0A	Hydrologic response to seismic activity
		1.2.10.02.0A	Hydrologic response to igneous activity
		1.3.05.00.0A	Glacial and ice sheet effect
		2.1.08.01.0A	Water influx at the repository
		2.1.08.12.0A	Induced hydrologic changes in invert
		2.1.08.14.0A	Condensation on underside of drip shield
		2.1.09.12.0A	Rind (chemically altered zone) forms in the near field
		2.1.11.01.0A	Heat generation in EBS
		2.1.11.09.0A	Thermal effects on flow in the EBS
		2.2.01.01.0A	Mechanical effects of excavation and construction in the near-field
		2.2.01.01.0B	Chemical effects of excavation and construction in the near-field

Table F-3. Cross Reference of Source FEPs to TSPA-LA FEPs (Continued)

Source FEP No.	Source FEP Name	TSPA-LA FEP Number	TSPA-LA FEP Name
N 3.1.4	Induced hydrological changes (fluid pressure, density convection, viscosity) (continued)	2.2.01.02.0A	Thermally-induced stress changes in the near-field
		2.2.08.03.0A	Geochemical interactions and evolution in the SZ
		2.2.10.04.0A	Thermo-mechanical stresses alter characteristics of fractures near repository
		2.2.10.04.0B	Thermo-mechanical stresses alter characteristics of faults near repository
		2.2.10.14.0A	Mineralogic dehydration reactions
N 3.1.5	Induced chemical changes	2.1.09.01.0A	Chemical characteristics of water in drifts
N 3.2	CHEMICAL	2.1.09.01.0A	Chemical characteristics of water in drifts
N 3.2.1	Metallic corrosion	2.1.03.01.0A	General corrosion of waste packages
N 3.2.2	Interactions of host materials and groundwater with repository material	2.1.09.01.0A	Chemical characteristics of water in drifts
		2.1.09.01.0B	Chemical characteristics of water in waste package
N 3.2.3	Interactions of waste and repository materials with host materials	2.1.09.01.0B	Chemical characteristics of water in waste package
		2.1.09.01.0A	Chemical characteristics of water in drifts
N 3.2.4	Non-radioactive solute plume in geosphere	2.2.08.03.0B	Geochemical interactions and evolution in the UZ
		2.2.08.01.0A	Chemical characteristics of groundwater in the SZ
		2.2.08.03.0A	Geochemical interactions and evolution in the SZ
		2.2.08.01.0B	Chemical characteristics of groundwater in the UZ
N 3.2.5	Cellulosic degradation	2.1.12.04.0A	Gas generation (CO2, CH$, H2S) from microbial degradation
		2.1.02.10.0A	Organic/cellulosic materials in waste
N 3.2.6	Introduced complexing agents and cellulosics	2.1.09.13.0A	Complexation in EBS
N 3.2.7	Microbiological effects	2.1.10.01.0A	Microbial activity in EBS
N 3.3	MECHANICAL	1.2.03.02.0E	Seismic-induced drift collapse alters in-drift chemistry
		1.2.03.02.0C	Seismic-induced drift collapse damages EBS components
		2.1.07.02.0A	Drift collapse
		2.1.07.01.0A	Rockfall
		1.2.03.02.0D	Seismic-induced drift collapse alters in-drift thermohydrology
N 3.3.1	Canister or container movement	2.1.06.05.0A	Mechanical degradation of emplacement pallet
		2.1.07.06.0A	Floor buckling
N 3.3.2	Changes in in-situ stress field	2.1.11.07.0A	Thermal expansion/stress of in-drift EBS components
N 3.3.3	Embrittlement and cracking	2.1.03.04.0A	Hydride cracking of waste packages
N 3.3.4	Subsidence/collapse	2.1.07.02.0A	Drift collapse
N 3.3.5	Fracturing	1.2.02.01.0A	Fractures
N 3.3.6	Gas effects	2.1.12.06.0A	Gas transport in EBS
		2.1.12.01.0A	Gas generation (repository pressurization)
		2.1.12.07.0A	Effects of radioactive gases in EBS

Table F-3. Cross Reference of Source FEPs to TSPA-LA FEPs (Continued)

Source FEP No.	Source FEP Name	TSPA-LA FEP Number	TSPA-LA FEP Name
N 3.4	RADIOLOGICAL	2.1.13.02.0A	Radiation damage in EBS
		2.1.13.01.0A	Radiolysis
		3.1.01.01.0A	Radioactive decay and ingrowth
N 3.4.1	Radiolysis	2.1.13.01.0A	Radiolysis
N 3.4.2	Material property changes	2.1.13.02.0A	Radiation damage in EBS
N 3.4.3	Nuclear criticality	2.1.14.20.0A	Near-field criticality resulting from a seismic event
		2.1.14.16.0A	In-package criticality (degraded configurations)
		2.1.14.17.0A	Near-field criticality
		2.1.14.18.0A	In-package criticality resulting from a seismic event (intact configuration)
		2.2.14.09.0A	Far-field criticality
		2.1.14.19.0A	In-package criticality resulting from a seismic event (degraded configurations)
		2.1.14.23.0A	Near-field criticality resulting from rockfall
		2.1.14.15.0A	In-package criticality (intact configuration)
		2.1.14.24.0A	In-package criticality resulting from an igneous event (intact configuration)
		2.1.14.26.0A	Near-field criticality resulting from an igneous event
		2.2.14.10.0A	Far-field criticality resulting from a seismic event
		2.2.14.11.0A	Far-field criticality resulting from rockfall
		2.2.14.12.0A	Far-field criticality resulting from an igneous event
		2.1.14.21.0A	In-package criticality resulting from rockfall (intact configuration)
		2.1.14.25.0A	In-package criticality resulting from an igneous event (degraded configurations)
		2.1.14.22.0A	In-package criticality resulting from rockfall (degraded configurations)
N 3.4.4	Radioactive decay and ingrowth	3.1.01.01.0A	Radioactive decay and ingrowth
NFC-1	Near-field criticality, fissile solution is adsorbed or reduced in invert	2.1.14.17.0A	Near-field criticality
NFC-2	Near-field criticality, fissile material deposited in near-field pond	2.1.14.17.0A	Near-field criticality
NFC-3a	Near-field criticality associated with colloidal deposits	2.1.14.17.0A	Near-field criticality
NFC-3b	Far-field criticality associated with colloidal deposits	2.2.14.09.0A	Far-field criticality
NFC-4	Near-field criticality, fissile solution flows into drift lowpoint	2.1.14.17.0A	Near-field criticality
NFC-5	Near-field criticality, filtered slurry or colloidal stream collects on invert surface	2.1.14.17.0A	Near-field criticality
NRC IA-1	Soil leaching following ashfall	1.2.04.07.0C	Ash redistribution via soil and sediment transport
		1.2.04.07.0B	Ash redistribution in groundwater
NRC IA-2	Soil leaching to groundwater	2.3.02.02.0A	Radionuclide accumulation in soils
NRC IA-3	Evaporative coolers	2.4.07.00.0A	Dwellings

Table F-3. Cross Reference of Source FEPs to TSPA-LA FEPs (Continued)

Source FEP No.	Source FEP Name	TSPA-LA FEP Number	TSPA-LA FEP Name
NRC NFE-1	Mineralogic dehydration reactions	2.2.10.14.0A	Mineralogic dehydration reactions
NRC NFE-2	Condensation on underside of drip shield	2.1.08.14.0A	Condensation on underside of drip shield
NRC SDS-1	Faulting exhumes waste container	1.2.02.02.0A	Faults
NRC USFIC-1	Film flow into drifts	2.2.07.18.0A	Film flow into the repository
		2.2.08.12.0A	Chemistry of water flowing into the drift
		2.2.08.12.0B	Chemistry of water flowing into the waste package
NRC USFIC-2	Lateral Flow from Solitario Canyon Fault Enters Potential Waste Emplacement Drifts	2.2.07.19.0A	Lateral flow from Solitario Canyon Fault enters drifts
S 001	Alteration/weathering of flow paths	2.2.10.06.0A	Thermo-chemical alteration in the UZ (solubility, speciation, phase changes)
		2.2.10.08.0A	Thermo-chemical alteration in the SZ (solubility, speciation, phase changes)
		2.2.08.03.0B	Geochemical interactions and evolution in the UZ
		2.2.08.03.0A	Geochemical interactions and evolution in the SZ
		2.2.10.09.0A	Thermo-chemical alteration of the Topopah Spring basal vitrophyre
S 002	Anion-exclusion	2.2.08.09.0A	Sorption in the SZ
S 003	Bentonite swelling, buffer	2.1.04.05.0A	Thermal-mechanical properties and evolution of backfill
		2.1.04.04.0A	Thermal-mechanical effects of backfill
S 004	Cave in	2.1.07.01.0A	Rockfall
		2.1.07.02.0A	Drift collapse
S 005	Changes in radionuclide inventory	2.1.01.01.0A	Waste inventory
S 006	Chemical alteration of buffer/backfill	2.1.04.02.0A	Chemical properties and evolution of backfill
S 007	Coagulation of bentonite	2.1.04.05.0A	Thermal-mechanical properties and evolution of backfill
		2.1.04.01.0A	Flow in the backfill
S 008	Colloid generation and transport	2.1.09.25.0A	Formation of colloids (waste-form) by co-precipitation in EBS
		2.1.09.17.0A	Formation of pseudo-colloids (corrosion product) in EBS
		2.1.09.23.0A	Stability of colloids in EBS
		2.1.09.24.0A	Diffusion of colloids in EBS
		2.1.09.13.0A	Complexation in EBS
		2.2.08.10.0B	Colloidal transport in the UZ
		2.2.08.10.0A	Colloidal transport in the SZ
		2.1.09.20.0A	Filtration of colloids in EBS
		2.1.09.15.0A	Formation of true (intrinsic) colloids in EBS
		2.1.09.22.0A	Sorption of colloids at air-water interface

Table F-3. Cross Reference of Source FEPs to TSPA-LA FEPs (Continued)

Source FEP No.	Source FEP Name	TSPA-LA FEP Number	TSPA-LA FEP Name
S 008	Colloid generation and transport (continued)	2.1.09.19.0B	Advection of colloids in EBS
		2.1.09.18.0A	Formation of microbial colloids in EBS
		2.1.09.16.0A	Formation of pseudo-colloids (natural) in EBS
		2.1.09.26.0A	Gravitational settling of colloids in EBS
		2.1.09.19.0A	Sorption of colloids in EBS
S 009	Colloid generation-source	2.1.09.25.0A	Formation of colloids (waste-form) by co-precipitation in EBS
		2.1.09.16.0A	Formation of pseudo-colloids (natural) in EBS
		2.1.09.15.0A	Formation of true (intrinsic) colloids in EBS
		2.1.09.17.0A	Formation of pseudo-colloids (corrosion product) in EBS
		2.1.09.18.0A	Formation of microbial colloids in EBS
		2.1.09.19.0A	Sorption of colloids in EBS
S 010	Colloids/particles in canister	2.1.09.18.0A	Formation of microbial colloids in EBS
		2.1.09.25.0A	Formation of colloids (waste-form) by co-precipitation in EBS
		2.1.09.17.0A	Formation of pseudo-colloids (corrosion product) in EBS
S 011	Corrosion of copper canister	2.1.03.09.0A	Copper corrosion in EBS
S 012	Corrosion of metal parts	2.1.02.13.0A	General corrosion of cladding
		2.1.02.16.0A	Localized (pitting) corrosion of cladding
		2.1.02.02.0A	CSNF degradation (alteration, dissolution, and radionuclide release)
S 013	Corrosion of steel vessel	2.1.02.15.0A	Localized (radiolysis enhanced) corrosion of cladding
		2.1.03.08.0A	Early failure of waste packages
		2.1.03.06.0A	Internal corrosion of waste packages prior to breach
		2.1.03.05.0A	Microbially influenced corrosion (MIC) of waste packages
		2.1.02.22.0A	Hydride cracking of cladding
		2.1.02.14.0A	Microbially influenced corrosion (MIC) of cladding
		2.1.03.03.0A	Localized corrosion of waste packages
		2.1.02.27.0A	Localized (fluoride enhanced) corrosion of cladding
		2.1.02.23.0A	Cladding unzipping
		2.1.02.13.0A	General corrosion of cladding
		2.1.02.16.0A	Localized (pitting) corrosion of cladding
		2.1.02.17.0A	Localized (crevice) corrosion of cladding
		2.1.03.02.0A	Stress corrosion cracking (SCC) of waste packages
		2.1.02.21.0A	Stress corrosion cracking (SCC) of cladding
		2.1.02.18.0A	Enhanced corrosion of cladding from dissolved silica
		2.1.03.01.0A	General corrosion of waste packages
		2.1.03.04.0A	Hydride cracking of waste packages

Table F-3. Cross Reference of Source FEPs to TSPA-LA FEPs (Continued)

Source FEP No.	Source FEP Name	TSPA-LA FEP Number	TSPA-LA FEP Name
S 014	Corrosion prior to wetting	2.1.02.17.0A	Localized (crevice) corrosion of cladding
		2.1.03.02.0A	Stress corrosion cracking (SCC) of waste packages
		2.1.02.02.0A	CSNF degradation (alteration, dissolution and radionuclide release)
		2.1.02.13.0A	General corrosion of cladding
		2.1.02.16.0A	Localized (pitting) corrosion of cladding
		2.1.03.06.0A	Internal corrosion of waste packages prior to breach
		2.1.03.02.0B	Stress corrosion cracking (SCC) of drip shields
		2.1.03.03.0B	Localized corrosion of drip shields
		2.1.03.03.0A	Localized corrosion of waste packages
		2.1.03.04.0B	Hydride cracking of drip shields
		2.1.03.04.0A	Hydride cracking of waste packages
		2.1.02.21.0A	Stress corrosion cracking (SCC) of cladding
		2.1.03.01.0A	General corrosion of waste packages
S 015	Creeping of rock mass, near-field	1.1.02.00.0B	Mechanical effects of excavation and construction in EBS
S 016	Creeping of steel/copper	2.1.07.05.0B	Creep of metallic materials in the drip shield
		2.1.07.05.0A	Creep of metallic materials in the waste package
S 017	Criticality	2.1.14.23.0A	Near-field criticality resulting from rockfall
		2.2.14.10.0A	Far-field criticality resulting from a seismic event
		2.2.14.09.0A	Far-field criticality
		2.1.14.26.0A	Near-field criticality resulting from an igneous event
		2.1.14.25.0A	In-package criticality resulting from an igneous event (degraded configurations)
		2.1.14.17.0A	Near-field criticality
		2.1.14.24.0A	In-package criticality resulting from an igneous event (intact configuration)
		2.1.14.20.0A	Near-field criticality resulting from a seismic event
		2.2.14.11.0A	Far-field criticality resulting from rockfall
		2.1.14.21.0A	In-package criticality resulting from rockfall (intact configuration)
		2.2.14.12.0A	Far-field criticality resulting from an igneous event
		2.1.14.18.0A	In-package criticality resulting from a seismic event (intact configuration)
		2.1.14.16.0A	In-package criticality (degraded configurations)
		2.1.14.15.0A	In-package criticality (intact configuration)
		2.1.14.22.0A	In-package criticality resulting from rockfall (degraded configurations)
		2.1.14.19.0A	In-package criticality resulting from a seismic event (degraded configurations)

Table F-3. Cross Reference of Source FEPs to TSPA-LA FEPs (Continued)

Source FEP No.	Source FEP Name	TSPA-LA FEP Number	TSPA-LA FEP Name
S 018	Deep saline water intrusion	2.1.09.01.0A	Chemical characteristics of water in drifts
		2.2.08.03.0A	Geochemical interactions and evolution in the SZ
		2.2.08.12.0A	Chemistry of water flowing into the drift
		2.2.08.01.0A	Chemical characteristics of groundwater in the SZ
S 019	Degradation of fuel elements	2.1.02.21.0A	Stress corrosion cracking (SCC) of cladding
		2.1.02.18.0A	Enhanced corrosion of cladding from dissolved silica
		2.1.02.15.0A	Localized (radiolysis enhanced) corrosion of cladding
		2.1.02.27.0A	Localized (fluoride enhanced) corrosion of cladding
		2.1.02.26.0A	Diffusion-controlled cavity growth in cladding
		2.1.02.25.0A	DSNF cladding
		2.1.02.24.0A	Mechanical impact on cladding
		2.1.02.22.0A	Hydride cracking of cladding
		2.1.02.11.0A	Degradation of cladding from waterlogged rods
		2.1.02.19.0A	Creep rupture of cladding
		2.1.02.20.0A	Internal pressurization of cladding
		2.1.02.17.0A	Localized (crevice) corrosion of cladding
		2.1.02.16.0A	Localized (pitting) corrosion of cladding
		2.1.02.01.0A	DSNF degradation (alteration, dissolution, and radionuclide release)
		2.1.02.02.0A	CSNF degradation (alteration, dissolution, and radionuclide release)
		2.1.02.03.0A	HLW glass degradation (alteration, dissolution, and radionuclide release)
		2.1.02.25.0B	Naval SNF Cladding
		2.1.02.13.0A	General corrosion of cladding
		2.1.02.14.0A	Microbially influenced corrosion (MIC) of cladding
		2.1.02.23.0A	Cladding unzipping
S 020	Degradation of hole and shaft seals	2.1.05.03.0A	Degradation of seals
S 021	Degradation of rock reinforcement and grout	2.1.06.01.0A	Chemical effects of rock reinforcement and cementitious materials in EBS
		2.1.06.02.0A	Mechanical effects of rock reinforcement materials in EBS
S 022	Differential thermal expansion of near-field barriers	2.1.11.07.0A	Thermal expansion/stress of in-drift EBS components
S 023	Diffusion	2.2.07.17.0A	Diffusion in the SZ
S 024	Diffusion in and through failed canister	2.1.09.08.0A	Diffusion of dissolved radionuclides in EBS
S 025	Dilution of buffer/backfill	2.1.04.02.0A	Chemical properties and evolution of backfill
		2.1.04.01.0A	Flow in the backfill
		2.1.04.03.0A	Erosion or dissolution of backfill
S 026	Dispersion	2.2.07.15.0A	Advection and dispersion in the SZ
S 027	Distribution and release of nuclides from the geosphere	2.2.08.11.0A	Groundwater discharge to surface within the reference biosphere

Table F-3. Cross Reference of Source FEPs to TSPA-LA FEPs (Continued)

Source FEP No.	Source FEP Name	TSPA-LA FEP Number	TSPA-LA FEP Name
S 028	Earth tides	1.5.03.02.0A	Earth tides
S 029	Electrochemical effects/gradients	2.1.09.09.0A	Electrochemical effects in EBS
S 030	Enhanced rock fracturing	2.2.01.02.0A	Thermally-induced stress changes in the near-field
S 031	Erosion of buffer/backfill	2.1.04.03.0A	Erosion or dissolution of backfill
S 032	Excavation effects on nearby rock	2.2.01.01.0A	Mechanical effects of excavation and construction in the near-field
S 033	External flow boundary conditions	2.3.01.00.0A	Topography and morphology
S 034	Failure of copper canister	2.1.03.09.0A	Copper corrosion in EBS
S 035	Failure of steel vessel	2.1.03.07.0A	Mechanical impact on waste package
S 036	Faulting	2.2.10.04.0B	Thermo-mechanical stresses alter characteristics of faults near repository
		2.2.06.02.0A	Seismic activity changes porosity and permeability of faults
		1.2.02.02.0A	Faults
S 037	Flow through buffer/backfill	2.1.04.01.0A	Flow in the backfill
S 038	Fuel dissolution and conversion	2.1.02.02.0A	CSNF degradation (alteration, dissolution, and radionuclide release)
S 039	Gap and grain boundary release	2.1.02.07.0A	Radionuclide release from gap and grain boundaries
S 040	Gas escape from canister	2.1.12.06.0A	Gas transport in EBS
S 041	Gas flow and transport, buffer/backfill	2.1.12.06.0A	Gas transport in EBS
S 042	Gas flow and transport, near-field rock/far-field	2.1.04.09.0A	Radionuclide transport in backfill
		2.1.12.06.0A	Gas transport in EBS
		2.1.12.07.0A	Effects of radioactive gases in EBS
		2.2.11.01.0A	Gas effects in the SZ
		2.2.11.02.0A	Gas effects in the UZ
		2.2.11.03.0A	Gas transport in the geosphere
S 043	Gas generation and gas sources, far-field	2.2.11.02.0A	Gas effects in the UZ
		2.1.12.04.0A	Gas generation (CO2, CH4, H2S) from microbial degradation
		2.2.11.01.0A	Gas effects in the SZ
S 044	Gas generation, buffer/backfill	2.1.12.04.0A	Gas generation (CO2, CH4, H2S) from microbial degradation
		2.1.13.01.0A	Radiolysis
S 045	Gas generation, canister	2.1.12.02.0A	Gas generation (He) from waste form decay
S 046	Gas generation, near-field rock	1.1.02.02.0A	Preclosure ventilation
		2.2.11.02.0A	Gas effects in the UZ
		2.1.13.01.0A	Radiolysis
		2.1.12.07.0A	Effects of radioactive gases in EBS
		2.1.12.04.0A	Gas generation (CO2, CH4, H2S) from microbial degradation
		2.1.12.03.0A	Gas generation (H2) from waste package corrosion
		2.1.12.02.0A	Gas generation (He) from waste form decay
		2.1.12.01.0A	Gas generation (repository pressurization)
		2.1.02.29.0A	Flammable gas generation from DSNF

Table F-3. Cross Reference of Source FEPs to TSPA-LA FEPs (Continued)

Source FEP No.	Source FEP Name	TSPA-LA FEP Number	TSPA-LA FEP Name
S 047	Glaciation	1.3.05.00.0A	Glacial and ice sheet effect
S 048	Groundwater chemistry	2.2.08.01.0A	Chemical characteristics of groundwater in the SZ
		2.2.08.03.0A	Geochemical interactions and evolution in the SZ
S 049	Groundwater flow	1.5.03.02.0A	Earth tides
		2.2.10.01.0A	Repository-induced thermal effects on flow in the UZ
		2.2.07.12.0A	Saturated groundwater flow in the geosphere
		2.2.08.03.0A	Geochemical interactions and evolution in the SZ
		2.2.08.01.0B	Chemical characteristics of groundwater in the UZ
		2.2.08.01.0A	Chemical characteristics of groundwater in the SZ
		1.2.06.00.0A	Hydrothermal activity
		1.2.02.01.0A	Fractures
		2.3.11.03.0A	Infiltration and recharge
		1.2.09.01.0A	Diapirism
		1.2.10.02.0A	Hydrologic response to igneous activity
		1.4.01.04.0A	Ozone layer failure
		2.2.10.03.0B	Natural geothermal effects on flow in the UZ
		2.2.07.14.0A	Chemically-induced density effects on groundwater flow
		2.1.04.05.0A	Thermal-mechanical properties and evolution of backfill
		2.2.07.13.0A	Water-conducting features in the SZ
		2.1.06.04.0A	Flow through rock reinforcement materials in EBS
		2.1.08.09.0A	Saturated flow in the EBS
		2.1.09.21.0A	Transport of particles larger than colloids in EBS
		2.1.11.07.0A	Thermal expansion/stress of in-drift EBS components
		2.1.13.02.0A	Radiation damage in EBS
		2.2.07.02.0A	Unsaturated groundwater flow in the geosphere
		2.2.10.03.0A	Natural geothermal effects on flow in the SZ
		2.2.08.03.0B	Geochemical interactions and evolution in the UZ
		2.1.05.02.0A	Radionuclide transport through seals
		2.1.04.02.0A	Chemical properties and evolution of backfill
S 050	I, Cs-migration to fuel surface	2.1.02.07.0A	Radionuclide release from gap and grain boundaries
S 051	Interaction with corrosion products	2.1.09.02.0A	Chemical interaction with corrosion products
S 052	Interface different waters	2.2.08.01.0A	Chemical characteristics of groundwater in the SZ
		2.2.08.01.0B	Chemical characteristics of groundwater in the UZ
S 053	Internal pressure	2.1.12.02.0A	Gas generation (He) from waste form decay
S 054	Matrix diffusion	2.2.08.08.0A	Matrix diffusion in the SZ

Table F-3. Cross Reference of Source FEPs to TSPA-LA FEPs (Continued)

Source FEP No.	Source FEP Name	TSPA-LA FEP Number	TSPA-LA FEP Name
S 055	Mechanical impact on canister	2.1.03.07.0A	Mechanical impact on waste package
		2.1.03.07.0B	Mechanical impact on drip shield
		2.1.09.03.0A	Volume increase of corrosion products impacts cladding
		2.1.09.03.0B	Volume increase of corrosion products impacts waste package
S 056	Mechanical impact/failure, buffer/backfill	2.1.04.04.0A	Thermal-mechanical effects of backfill
S 057	Microbial activity	2.1.10.01.0A	Microbial activity in EBS
S 058	Movement of canister in buffer/backfill	2.1.07.02.0A	Drift collapse
		2.1.03.07.0A	Mechanical impact on waste package
		2.1.08.15.0A	Consolidation of EBS components
		2.1.07.06.0A	Floor buckling
		2.1.06.05.0A	Mechanical degradation of emplacement pallet
		2.1.03.07.0B	Mechanical impact on drip shield
		1.2.02.03.0A	Fault displacement damages EBS components
		2.1.07.01.0A	Rockfall
S 059	Permafrost	1.3.04.00.0A	Periglacial effects
S 060	Precipitation/dissolution	2.2.08.03.0A	Geochemical interactions and evolution in the SZ
		2.2.08.03.0B	Geochemical interactions and evolution in the UZ
		2.2.10.08.0A	Thermo-chemical alteration in the SZ (solubility, speciation, phase changes)
		2.2.10.06.0A	Thermo-chemical alteration in the UZ (solubility, speciation, phase changes)
		2.2.08.04.0A	Re-dissolution of precipitates directs more corrosive fluids to waste packages
		2.1.02.03.0A	HLW glass degradation (alteration, dissolution, and radionuclide release)
		2.1.02.02.0A	CSNF degradation (alteration, dissolution, and radionuclide release)
		2.1.02.01.0A	DSNF degradation (alteration, dissolution, and radionuclide release)
		2.2.08.07.0A	Radionuclide solubility limits in the SZ
		2.2.08.07.0B	Radionuclide solubility limits in the UZ
S 061	Preferential pathways in canister	2.1.08.07.0A	Unsaturated flow in the EBS
S 062	Properties of bentonite buffer	2.2.01.02.0B	Chemical changes in the near-field from backfill
		2.1.04.01.0A	Flow in the backfill
		2.1.04.05.0A	Thermal-mechanical properties and evolution of backfill
		2.1.04.02.0A	Chemical properties and evolution of backfill
		2.1.04.03.0A	Erosion or dissolution of backfill
		2.1.04.09.0A	Radionuclide transport in backfill
		2.1.04.04.0A	Thermal-mechanical effects of backfill
S 063	Properties of failed canister	2.1.09.08.0B	Advection of dissolved radionuclides in EBS
		2.1.09.05.0A	Sorption of dissolved radionuclides in EBS
		2.1.09.08.0A	Diffusion of dissolved radionuclides in EBS

Table F-3. Cross Reference of Source FEPs to TSPA-LA FEPs (Continued)

Source FEP No.	Source FEP Name	TSPA-LA FEP Number	TSPA-LA FEP Name
S 064	Properties of far-field rock	2.2.12.00.0B	Undetected features in the SZ
		1.2.09.02.0A	Large-scale dissolution
		1.2.09.01.0A	Diapirism
		1.2.09.00.0A	Salt diapirism and dissolution
		1.2.06.00.0A	Hydrothermal activity
		1.2.04.02.0A	Igneous activity changes rock properties
		2.2.03.01.0A	Stratigraphy
		1.2.02.02.0A	Faults
		1.2.05.00.0A	Metamorphism
		1.2.02.01.0A	Fractures
		1.2.08.00.0A	Diagenesis
		2.2.03.02.0A	Rock properties of host rock and other units
		2.2.10.05.0A	Thermo-mechanical stresses alter characteristics of rocks above and below the repository
		2.2.12.00.0A	Undetected features in the UZ
		2.2.10.04.0B	Thermo-mechanical stresses alter characteristics of faults near repository
		2.2.10.04.0A	Thermo-mechanical stresses alter characteristics of fractures near repository
		2.2.06.04.0A	Effects of subsidence
		2.2.06.02.0A	Seismic activity changes porosity and permeability of faults
		2.2.06.01.0A	Seismic activity changes porosity and permeability of rock
S 065	Properties of near-field rock	1.2.05.00.0A	Metamorphism
		1.2.04.02.0A	Igneous activity changes rock properties
		2.2.12.00.0B	Undetected features in the SZ
		2.2.12.00.0A	Undetected features in the UZ
		2.2.10.05.0A	Thermo-mechanical stresses alter characteristics of rocks above and below the repository
		1.2.08.00.0A	Diagenesis
		2.2.10.04.0B	Thermo-mechanical stresses alter characteristics of faults near repository
		2.2.10.04.0A	Thermo-mechanical stresses alter characteristics of fractures near repository
		1.2.02.01.0A	Fractures
		2.2.06.04.0A	Effects of subsidence
		1.2.06.00.0A	Hydrothermal activity
		1.2.09.00.0A	Salt diapirism and dissolution
		2.2.06.01.0A	Seismic activity changes porosity and permeability of rock
		2.2.06.02.0A	Seismic activity changes porosity and permeability of faults
		1.2.09.02.0A	Large-scale dissolution
		2.2.03.02.0A	Rock properties of host rock and other units

Table F-3. Cross Reference of Source FEPs to TSPA-LA FEPs (Continued)

Source FEP No.	Source FEP Name	TSPA-LA FEP Number	TSPA-LA FEP Name
S 065	Properties of near-field rock (continued)	2.2.03.01.0A	Stratigraphy
		2.2.01.02.0A	Thermally-induced stress changes in the near-field
		1.2.09.01.0A	Diapirism
S 066	Properties of tunnel backfill	2.1.04.05.0A	Thermal-mechanical properties and evolution of backfill
		2.1.04.04.0A	Thermal-mechanical effects of backfill
		2.1.04.02.0A	Chemical properties and evolution of backfill
S 067	Radiation effects on buffer/backfill	2.1.13.02.0A	Radiation damage in EBS
S 068	Radiation effects on canister	2.1.13.02.0A	Radiation damage in EBS
S 069	Radioactive Decay, fuel	2.1.13.02.0A	Radiation damage in EBS
		3.1.01.01.0A	Radioactive decay and ingrowth
		2.1.13.01.0A	Radiolysis
S 070	Radioactive decay of mobile nuclides	3.1.01.01.0A	Radioactive decay and ingrowth
S 071	Radiolysis	2.1.13.01.0A	Radiolysis
S 072	Radiolysis prior to wetting	2.1.03.06.0A	Internal corrosion of waste packages prior to breach
		2.1.13.01.0A	Radiolysis
S 073	Reconcentration	1.4.07.03.0A	Recycling of accumulated radionuclides from soils to groundwater
		2.2.14.09.0A	Far-field criticality
S 074	Redox front	2.1.13.01.0A	Radiolysis
		2.1.09.06.0A	Reduction-oxidation potential in waste package
S 075	Reduced mechanical strength	2.1.03.07.0A	Mechanical impact on waste package
S 076	Release from fuel matrix	2.1.02.02.0A	CSNF degradation (alteration, dissolution, and radionuclide release)
S 077	Release from metal parts	2.1.02.02.0A	CSNF degradation (alteration, dissolution, and radionuclide release)
S 078	Resaturation, near-field rock	2.2.07.11.0A	Resaturation of geosphere dry-out zine
		2.1.08.01.0B	Effects of rapid influx into the repository
S 079	Resaturation of bentonite buffer	2.1.04.05.0A	Thermal-mechanical properties and evolution of backfill
		2.1.04.01.0A	Flow in the backfill
S 080	Resaturation of tunnel backfill	2.1.04.05.0A	Thermal-mechanical properties and evolution of backfill
		2.1.04.01.0A	Flow in the backfill
S 081	Sea level changes	2.3.06.00.0A	Marine features
S 082	Sedimentation of bentonite	2.1.04.05.0A	Thermal-mechanical properties and evolution of backfill
S 083	Soret effect	2.1.11.10.0A	Thermal effects on transport in EBS
S 084	Sorption	2.2.08.09.0A	Sorption in the SZ
		2.2.08.09.0B	Sorption in the UZ
S 085	Sorption on filling material	2.1.09.05.0A	Sorption of dissolved radionuclides in EBS
		2.1.04.09.0A	Radionuclide transport in backfill
S 086	Stress field	2.2.06.01.0A	Seismic activity changes porosity and permeability of rock

Table F-3. Cross Reference of Source FEPs to TSPA-LA FEPs (Continued)

Source FEP No.	Source FEP Name	TSPA-LA FEP Number	TSPA-LA FEP Name
S 087	Surface water chemistry	2.2.08.01.0B	Chemical characteristics of groundwater in the UZ
		2.3.11.03.0A	Infiltration and recharge
		1.4.06.01.0A	Altered soil or surface water chemistry
S 088	Swelling of tunnel backfill	2.1.04.05.0A	Thermal-mechanical properties and evolution of backfill
		2.1.04.04.0A	Thermal-mechanical effects of backfill
S 089	Temperature, bentonite buffer	2.1.11.01.0A	Heat generation in EBS
S 090	Temperature, canister	2.1.11.01.0A	Heat generation in EBS
S 091	Temperature, far-field	2.2.10.13.0A	Repository-induced thermal effects on flow in the SZ
		2.2.10.03.0A	Natural geothermal effects on flow in the SZ
S 092	Temperature, near-field rock	2.2.10.02.0A	Thermal convection cell develops in SZ
		2.2.10.04.0B	Thermo-mechanical stresses alter characteristics of faults near repository
		2.2.10.08.0A	Thermo-chemical alteration in the SZ (solubility, speciation, phase changes)
		2.2.10.04.0A	Thermo-mechanical stresses alter characteristics of fractures near repository
		2.2.10.03.0A	Natural geothermal effects on flow in the SZ
		2.2.10.01.0A	Repository-induced thermal effects on flow in the UZ
		2.2.10.05.0A	Thermo-mechanical stresses alter characteristics of rocks above and below the repository
		1.1.02.02.0A	Preclosure ventilation
		2.2.10.06.0A	Thermo-chemical alteration in the UZ (solubility, speciation, phase changes)
		2.2.10.03.0B	Natural geothermal effects on flow in the UZ
S 093	Temperature, tunnel backfill	2.1.11.01.0A	Heat generation in EBS
S 094	Thermal degradation of buffer/backfill	2.1.04.02.0A	Chemical properties and evolution of backfill
S 095	Total release from fuel elements	2.1.02.07.0A	Radionuclide release from gap and grain boundaries
		2.1.02.02.0A	CSNF degradation (alteration, dissolution, and radionuclide release)
S 096	Transport and release of nuclides, bentonite buffer	2.1.04.09.0A	Radionuclide transport in backfill
S 097	Transport and release of nuclides, failed canister	2.1.09.08.0A	Diffusion of dissolved radionuclides in EBS
		2.1.09.24.0A	Diffusion of colloids in EBS
		2.1.09.19.0B	Advection of colloids in EBS
		2.1.09.08.0B	Advection of dissolved radionuclides in EBS
S 098	Transport and release of nuclides, near-field rock	2.2.07.17.0A	Diffusion in the SZ
		2.2.11.03.0A	Gas transport in geosphere
		2.2.07.15.0A	Advection and dispersion in the SZ
		2.2.08.10.0A	Colloidal transport in the SZ
S 099	Transport and release of nuclides, tunnel backfill	2.1.04.09.0A	Radionuclide transport in backfill

Table F-3. Cross Reference of Source FEPs to TSPA-LA FEPs (Continued)

Source FEP No.	Source FEP Name	TSPA-LA FEP Number	TSPA-LA FEP Name
S 100	Volume increase of corrosion products	2.1.09.03.0B	Volume increase of corrosion products impacts waste package
		2.1.09.03.0C	Volume increase of corrosion products impacts other EBS components
		2.1.09.03.0A	Volume increase of corrosion products impacts cladding
S 101	Water chemistry, bentonite buffer	2.1.04.02.0A	Chemical properties and evolution of backfill
S 102	Water chemistry, canister	2.1.09.01.0B	Chemical characteristics of water in waste package
S 103	Water chemistry in near-field rock	2.2.08.03.0B	Geochemical interactions and evolution in the UZ
		2.2.08.01.0B	Chemical characteristics of groundwater in the UZ
S 104	Water chemistry, tunnel backfill	2.1.04.02.0A	Chemical properties and evolution of backfill
S 105	Water turnover, copper canister	2.1.03.01.0A	General corrosion of waste packages
		2.1.03.06.0A	Internal corrosion of waste packages prior to breach
S 106	Water turnover, steel vessel	2.1.08.09.0A	Saturated flow in the EBS
		2.1.08.07.0A	Unsaturated flow in the EBS
		2.1.02.02.0A	CSNF degradation (alteration, dissolution, and radionuclide release)
SZ/Coupl-1	Coupling of surface water flow to climate/hydrologic modeling system	2.3.11.03.0A	Infiltration and recharge
TH/Flow-1	Convection effects on transport (Enhanced vapor diffusion)	2.1.11.09.0C	Thermally driven flow (convection) in drifts
		2.1.11.09.0A	Thermal effects on flow in the EBS
		2.1.11.10.0A	Thermal effects on transport in EBS
		2.1.11.09.0B	Thermally-driven flow (convection) in waste packages
W 1.001	Stratigraphy	2.2.03.01.0A	Stratigraphy
W 1.002	Brine reservoirs	2.2.03.01.0A	Stratigraphy
W 1.003	Changes in regional stress	2.2.06.01.0A	Seismic activity changes porosity and permeability of rock
W 1.004	Regional tectonics	1.2.01.01.0A	Tectonic activity - large scale
W 1.005	Regional uplift and subsidence	1.2.01.01.0A	Tectonic activity - large scale
W 1.006	Salt deformation	1.2.09.01.0A	Diapirism
W 1.007	Diapirism	1.2.09.01.0A	Diapirism
W 1.008	Formation of fractures	2.2.06.02.0B	Seismic activity changes porosity and permeability of fractures
		2.2.10.04.0A	Thermo-mechanical stresses alter characteristics of fractures near repository
		1.2.02.01.0A	Fractures
W 1.009	Changes in fracture properties	2.2.06.02.0B	Seismic activity changes porosity and permeability of fractures
		1.2.02.01.0A	Fractures
		2.2.10.04.0A	Thermo-mechanical stresses alter characteristics of fractures near repository
W 1.010	Formation of new faults	2.2.06.02.0A	Seismic activity changes porosity and permeability of faults
		1.2.02.02.0A	Faults

Table F-3. Cross Reference of Source FEPs to TSPA-LA FEPs (Continued)

Source FEP No.	Source FEP Name	TSPA-LA FEP Number	TSPA-LA FEP Name
W 1.011	Fault movement	2.2.06.02.0A	Seismic activity changes porosity and permeability of faults
		1.2.02.02.0A	Faults
W 1.012	Seismic activity	1.2.03.03.0A	Seismicity associated with igneous activity
		2.2.06.02.0B	Seismic activity changes porosity and permeability of fractures
		2.1.07.02.0A	Drift collapse
		2.1.03.07.0B	Mechanical impact on drip shield
		2.1.03.07.0A	Mechanical impact on waste package
		1.2.10.01.0A	Hydrologic response to seismic activity
		1.2.03.02.0B	Seismic-induced rockfall damages EBS components
		2.2.06.02.0A	Seismic activity changes porosity and permeability of faults
		1.4.02.04.0A	Seismic event precedes human intrusion
		2.2.06.03.0A	Seismic activity alters perched water zones
		2.1.02.24.0A	Mechanical impact on cladding
		2.2.06.01.0A	Seismic activity changes porosity and permeability of rock
		1.2.03.02.0A	Seismic ground motion damages EBS components
W 1.013	Volcanic activity	1.2.04.02.0A	Igneous activity changes rock properties
		1.2.03.03.0A	Seismicity associated with igneous activity
		1.4.02.03.0A	Igneous event precedes human intrusion
		1.2.10.02.0A	Hydrologic response to igneous activity
		1.2.04.04.0A	Igneous intrusion interacts with EBS components
		1.2.04.03.0A	Igneous intrusion into repository
W 1.014	Magmatic activity	1.2.04.03.0A	Igneous intrusion into repository
		1.2.04.04.0A	Igneous intrusion interacts with EBS components
		1.2.04.05.0A	Magma or pyroclastic base surge transports waste
		1.2.10.02.0A	Hydrologic response to igneous activity
		1.4.02.03.0A	Igneous event precedes human intrusion
W 1.015	Metamorphic activity	1.2.05.00.0A	Metamorphism
W 1.016	Shallow dissolution	1.2.09.02.0A	Large-scale dissolution
W 1.017	Lateral dissolution	1.2.09.02.0A	Large-scale dissolution
W 1.018	Deep dissolution	1.2.09.02.0A	Large-scale dissolution
W 1.019	Solution chimneys	1.2.09.02.0A	Large-scale dissolution
W 1.020	Breccia pipes	1.2.09.02.0A	Large-scale dissolution
W 1.021	Collapse breccias	1.2.09.02.0A	Large-scale dissolution
W 1.022	Fracture infills	1.2.08.00.0A	Diagenesis
W 1.023	Saturated groundwater flow	2.2.07.12.0A	Saturated groundwater flow in the geosphere
W 1.024	Unsaturated groundwater flow	2.2.07.02.0A	Unsaturated groundwater flow in the geosphere

Table F-3. Cross Reference of Source FEPs to TSPA-LA FEPs (Continued)

Source FEP No.	Source FEP Name	TSPA-LA FEP Number	TSPA-LA FEP Name
W 1.025	Fracture flow	1.2.02.01.0A	Fractures
		2.2.08.08.0A	Matrix diffusion in the SZ
		2.2.08.08.0B	Matrix diffusion in the UZ
		2.2.07.04.0A	Focusing of unsaturated flow (fingers, weeps)
		2.2.07.13.0A	Water-conducting features in the SZ
		2.2.07.08.0A	Fracture flow in the UZ
W 1.026	Density effects on groundwater flow	2.2.07.14.0A	Chemically-induced density effects on groundwater flow
W 1.027	Effects of preferential pathways	2.2.07.19.0A	Lateral flow from Solitario Canyon Fault enters drifts
		2.2.07.04.0A	Focusing of unsaturated flow (fingers, weeps)
		2.2.07.01.0A	Locally saturated flow at bedrock/alluvium contact
W 1.028	Thermal effects on groundwater flow	2.1.11.09.0A	Thermal effects on flow in the EBS
		2.2.10.03.0A	Natural geothermal effects on flow in the SZ
W 1.029	Saline intrusion	2.2.07.14.0A	Chemically-induced density effects on groundwater flow
		2.1.09.01.0A	Chemical characteristics of water in drifts
		2.2.08.03.0A	Geochemical interactions and evolution in the SZ
W 1.030	Freshwater intrusion	2.3.11.03.0A	Infiltration and recharge
		1.3.07.02.0A	Water table rise affects SZ
W 1.031	Hydrological response to earthquakes	1.2.10.01.0A	Hydrologic response to seismic activity
W 1.032	Natural gas intrusion	2.2.11.01.0A	Gas effects in the SZ
		2.1.12.08.0A	Gas explosions in EBS
		2.2.11.02.0A	Gas effects in the UZ
W 1.033	Groundwater geochemistry	2.2.08.01.0A	Chemical characteristics of groundwater in the SZ
		2.2.08.01.0B	Chemical characteristics of groundwater in the UZ
		2.2.08.03.0A	Geochemical interactions and evolution in the SZ
		2.2.08.03.0B	Geochemical interactions and evolution in the UZ
W 1.034	Saline intrusion	2.2.08.03.0A	Geochemical interactions and evolution in the SZ
		2.1.09.01.0A	Chemical characteristics of water in drifts
W 1.035	Freshwater intrusion	2.2.08.03.0A	Geochemical interactions and evolution in the SZ
		2.2.08.03.0B	Geochemical interactions and evolution in the UZ
W 1.036	Changes in groundwater Eh	2.2.08.09.0A	Sorption in the SZ
		2.2.08.10.0A	Colloidal transport in the SZ
		2.2.08.03.0A	Geochemical interactions and evolution in the SZ
W 1.037	Changes in groundwater pH	2.2.08.03.0A	Geochemical interactions and evolution in the SZ
		2.2.08.09.0A	Sorption in the SZ
		2.2.08.10.0A	Colloidal transport in the SZ

Table F-3. Cross Reference of Source FEPs to TSPA-LA FEPs (Continued)

Source FEP No.	Source FEP Name	TSPA-LA FEP Number	TSPA-LA FEP Name
W 1.038	Effects of dissolution	2.2.08.03.0A	Geochemical interactions and evolution in the SZ
		2.2.08.10.0A	Colloidal transport in the SZ
W 1.039	Physiography	2.3.01.00.0A	Topography and morphology
W 1.040	Impact of a large meteorite	1.5.01.01.0A	Meteorite impact
W 1.041	Mechanical weathering	1.2.07.01.0A	Erosion/denudation
W 1.042	Chemical weathering	1.2.07.01.0A	Erosion/denudation
W 1.043	Aeolian erosion	1.2.07.01.0A	Erosion/denudation
W 1.044	Fluvial erosion	1.2.07.01.0A	Erosion/denudation
W 1.045	Mass wasting	1.2.07.01.0A	Erosion/denudation
W 1.046	Aeolian deposition	2.3.02.03.0A	Soil and sediment transport in the biosphere
		1.2.07.02.0A	Deposition
W 1.047	Fluvial deposition	1.2.07.02.0A	Deposition
W 1.048	Lacustrine deposition	1.2.07.02.0A	Deposition
W 1.049	Mass wasting	1.2.07.01.0A	Erosion/denudation
W 1.050	Soil development	2.3.02.01.0A	Soil type
W 1.051	Stream and river flow	2.3.04.01.0A	Surface water transport and mixing
W 1.052	Surface water bodies	2.3.04.01.0A	Surface water transport and mixing
		2.3.11.02.0A	Surface runoff and evapotranspiration
W 1.053	Groundwater discharge	2.3.11.04.0A	Groundwater discharge to surface outside the reference biosphere
W 1.054	Groundwater recharge	2.2.08.10.0A	Colloidal transport in the SZ
		2.2.08.09.0A	Sorption in the SZ
		2.2.08.05.0A	Diffusion in the UZ
		2.2.07.15.0B	Advection and dispersion in the UZ
		2.3.11.03.0A	Infiltration and recharge
W 1.055	Infiltration	2.3.11.03.0A	Infiltration and recharge
W 1.056	Changes in groundwater recharge and discharge	2.3.11.03.0A	Infiltration and recharge
W 1.057	Lake formation	2.3.11.02.0A	Surface runoff and evapotranspiration
		2.3.04.01.0A	Surface water transport and mixing
W 1.058	River flooding	2.3.11.02.0A	Surface runoff and evapotranspiration
W 1.059	Precipitation (for example, rainfall)	2.3.11.01.0A	Precipitation
W 1.060	Temperature	1.4.01.01.0A	Climate modification increases recharge
		2.3.13.01.0A	Biosphere characteristics
		1.4.01.00.0A	Human influences on climate
		1.3.05.00.0A	Glacial and ice sheet effect
		1.3.04.00.0A	Periglacial effects
		1.3.01.00.0A	Climate change
W 1.061	Climate change	1.3.01.00.0A	Climate change
W 1.062	Glaciation	1.3.05.00.0A	Glacial and ice sheet effect
W 1.063	Permafrost	1.3.04.00.0A	Periglacial effects
W 1.064	Seas and oceans	2.3.06.00.0A	Marine features
W 1.065	Estuaries	2.3.06.00.0A	Marine features
W 1.066	Coastal erosion	2.3.06.00.0A	Marine features

Table F-3. Cross Reference of Source FEPs to TSPA-LA FEPs (Continued)

Source FEP No.	Source FEP Name	TSPA-LA FEP Number	TSPA-LA FEP Name
W 1.067	Marine sediment transport and deposition	2.3.06.00.0A	Marine features
W 1.068	Sea level changes	2.3.06.00.0A	Marine features
W 1.069	Plants	2.3.13.01.0A	Biosphere characteristics
W 1.070	Animals	2.3.13.01.0A	Biosphere characteristics
		3.3.02.02.0A	Animal uptake
W 1.071	Microbes	2.3.13.01.0A	Biosphere characteristics
W 1.072	Natural ecological development	1.5.02.00.0A	Species evolution
		2.3.13.01.0A	Biosphere characteristics
W 2.001	Disposal Geometry	0.1.10.00.0A	Model and data issues
W 2.002	Waste inventory	2.1.01.01.0A	Waste inventory
W 2.003	Heterogeneity of wasteforms	2.1.01.03.0A	Heterogeneity of waste inventory
W 2.004	Container form	2.1.03.11.0A	Physical form of waste package and drip shield
W 2.005	Container material inventory	2.1.12.03.0A	Gas generation (H2) from waste package corrosion
W 2.006	Seal geometry	2.1.05.02.0A	Radionuclide transport through seals
		1.1.04.01.0A	Incomplete closure
		2.1.05.01.0A	Flow through seals (access ramps and ventilation shafts)
W 2.007	Seal physical properties	2.1.05.01.0A	Flow through seals (access ramps and ventilation shafts)
W 2.008	Seal chemical composition	2.1.06.01.0A	Chemical effects of rock reinforcement and cementitious materials in EBS
		2.1.05.03.0A	Degradation of seals
W 2.009	Backfill physical composition	2.1.04.05.0A	Thermal-mechanical properties and evolution of backfill
W 2.010	Backfill chemical composition	2.1.04.02.0A	Chemical properties and evolution of backfill
W 2.011	Postclosure monitoring	1.1.11.00.0A	Monitoring of the repository
W 2.012	Radionuclide decay and ingrowth	3.1.01.01.0A	Radioactive decay and ingrowth
W 2.013	Heat from radioactive decay	2.1.11.01.0A	Heat generation in EBS
W 2.014	Nuclear criticality: heat	2.1.14.15.0A	In-package criticality (intact configuration)
		2.1.14.22.0A	In-package criticality resulting from rockfall (degraded configurations)
		2.1.14.17.0A	Near-field criticality
		2.1.14.18.0A	In-package criticality resulting from a seismic event (intact configuration)
		2.1.14.19.0A	In-package criticality resulting from a seismic event (degraded configurations)
		2.1.14.21.0A	In-package criticality resulting from rockfall (intact configuration)
		2.1.14.23.0A	Near-field criticality resulting from rockfall
		2.1.14.20.0A	Near-field criticality resulting from a seismic event
		2.1.14.26.0A	Near-field criticality resulting from an igneous event
		2.1.14.25.0A	In-package criticality resulting from an igneous event (degraded configurations)
		2.2.14.09.0A	Far-field criticality

Table F-3. Cross Reference of Source FEPs to TSPA-LA FEPs (Continued)

Source FEP No.	Source FEP Name	TSPA-LA FEP Number	TSPA-LA FEP Name
W 2.014	Nuclear criticality: heat (continued)	2.2.14.10.0A	Far-field criticality resulting from a seismic event
		2.2.14.11.0A	Far-field criticality resulting from rockfall
		2.2.14.12.0A	Far-field criticality resulting from an igneous event
		2.1.14.24.0A	In-package criticality resulting from an igneous event (intact configuration)
		2.1.14.16.0A	In-package criticality (degraded configurations)
W 2.015	Radiological effects on waste	2.1.13.02.0A	Radiation damage in EBS
W 2.016	Radiological effects on containers	2.1.13.02.0A	Radiation damage in EBS
W 2.017	Radiological effects on seals	2.1.13.02.0A	Radiation damage in EBS
W 2.018	Disturbed rock zone	2.2.01.01.0A	Mechanical effects of excavation and construction in the near-field
W 2.019	Excavation-induced changes in stress	2.2.01.01.0A	Mechanical effects of excavation and construction in the near-field
		1.1.02.00.0B	Mechanical effects of excavation and construction in EBS
W 2.020	Salt creep	2.2.06.05.0A	Salt creep
W 2.021	Changes in the stress field	2.2.06.01.0A	Seismic activity changes porosity and permeability of rock
W 2.022	Roof falls	1.2.03.02.0D	Seismic-induced drift collapse alters in-drift thermohydrology
		2.1.07.01.0A	Rockfall
		2.1.07.02.0A	Drift collapse
		2.2.06.05.0A	Salt creep
		1.2.03.02.0C	Seismic-induced drift collapse damages EBS components
W 2.023	Subsidence	2.2.06.04.0A	Effects of subsidence
W 2.024	Large-scale rock fracturing	2.2.06.04.0A	Effects of subsidence
W 2.025	Disruption due to gas effects	2.2.11.01.0A	Gas effects in the SZ
		2.2.11.02.0A	Gas effects in the UZ
W 2.026	Pressurization	2.1.12.01.0A	Gas generation (repository pressurization)
W 2.027	Gas explosions	2.1.12.08.0A	Gas explosions in EBS
W 2.028	Nuclear explosions	2.1.14.15.0A	In-package criticality (intact configuration)
		2.1.14.16.0A	In-package criticality (degraded configurations)
W 2.029	Thermal effects on material properties	2.2.10.01.0A	Repository-induced thermal effects on flow in the UZ
		2.2.10.13.0A	Repository-induced thermal effects on flow in the SZ
W 2.030	Thermally-induced stress changes	2.2.10.05.0A	Thermo-mechanical stresses alter characteristics of rocks above and below the repository
		2.3.13.03.0A	Effects of repository heat on the biosphere
		2.2.10.04.0B	Thermo-mechanical stresses alter characteristics of faults near repository
		2.2.10.04.0A	Thermo-mechanical stresses alter characteristics of fractures near repository

Table F-3. Cross Reference of Source FEPs to TSPA-LA FEPs (Continued)

Source FEP No.	Source FEP Name	TSPA-LA FEP Number	TSPA-LA FEP Name
W 2.030	Thermally-induced stress changes (continued)	2.2.01.02.0A	Thermally-induced stress changes in the near-field
		2.1.11.07.0A	Thermal expansion/stress of in-drift EBS components
		2.1.11.03.0A	Exothermic reactions in the EBS
		2.1.05.03.0A	Degradation of seals
		2.1.03.02.0B	Stress corrosion cracking (SCC) of drip shields
		2.1.03.02.0A	Stress corrosion cracking (SCC) of waste packages
		2.1.02.08.0A	Pyrophoricity from DSNF
		2.1.11.05.0A	Thermal expansion/stress of in-package EBS components
		1.2.06.00.0A	Hydrothermal activity
		1.2.04.02.0A	Igneous activity changes rock properties
		2.1.11.01.0A	Heat generation in EBS
W 2.031	Differing thermal expansion of repository components	2.1.11.07.0A	Thermal expansion/stress of in-drift EBS components
		2.1.11.05.0A	Thermal expansion/stress of in-package EBS components
W 2.032	Consolidation of waste	2.1.08.15.0A	Consolidation of EBS components
		2.2.06.05.0A	Salt creep
W 2.033	Movement of containers	2.1.03.07.0B	Mechanical impact on drip shield
		2.1.08.15.0A	Consolidation of EBS components
		2.1.06.05.0A	Mechanical degradation of emplacement pallet
		2.1.03.07.0A	Mechanical impact on waste package
		2.1.06.05.0B	Mechanical degradation of invert
W 2.034	Container integrity	2.1.03.11.0A	Physical form of waste package and drip shield
W 2.035	Mechanical effects of backfill	2.1.04.04.0A	Thermal-mechanical effects of backfill
W 2.036	Consolidation of seals	2.1.05.03.0A	Degradation of seals
W 2.037	Mechanical degradation of seals	2.1.05.03.0A	Degradation of seals
W 2.038	Investigation boreholes	1.1.01.01.0A	Open site investigation boreholes
W 2.039	Underground boreholes	1.1.01.01.0A	Open site investigation boreholes
W 2.040	Brine inflow	2.1.08.11.0A	Repository resaturation due to waste cooling
		2.1.08.12.0A	Induced hydrologic changes in invert
W 2.041	Wicking	2.1.08.06.0A	Capillary effects (wicking) in EBS
W 2.042	Fluid flow due to gas production	2.2.11.02.0A	Gas effects in the UZ
W 2.043	Convection	2.1.11.09.0C	Thermally driven flow (convection) in drifts
		2.1.11.09.0B	Thermally-driven flow (convection) in waste packages
		2.1.11.09.0A	Thermal effects on flow in the EBS
W 2.044	Degradation of organic material	2.1.12.04.0A	Gas generation (CO2, CH4, H2S) from microbial degradation
W 2.045	Effect of temperature on microbial gas generation	2.1.10.01.0A	Microbial activity in EBS
		2.1.12.04.0A	Gas generation (CO2, CH4, H2S) from microbial degradation
W 2.046	Effect of pressure on microbial gas generation	2.1.12.04.0A	Gas generation (CO2, CH4, H2S) from microbial degradation
W 2.047	Effect of radiation on microbial gas generation	2.1.13.03.0A	Radiological mutation of microbes
		2.1.12.04.0A	Gas generation (CO2, CH4, H2S) from microbial degradation

Table F-3. Cross Reference of Source FEPs to TSPA-LA FEPs (Continued)

Source FEP No.	Source FEP Name	TSPA-LA FEP Number	TSPA-LA FEP Name
W 2.048	Effect of biofilms on microbial gas generation	2.1.12.04.0A	Gas generation (CO2, CH4, H2S) from microbial degradation
W 2.049	Gases from metal corrosion	2.1.12.03.0A	Gas generation (H2) from waste package corrosion
W 2.050	Galvanic coupling	2.1.09.09.0A	Electrochemical effects in EBS
W 2.051	Chemical effects of corrosion	2.1.12.03.0A	Gas generation (H2) from waste package corrosion
W 2.052	Radiolysis of brine	2.1.13.01.0A	Radiolysis
W 2.053	Radiolysis of cellulose	2.1.13.01.0A	Radiolysis
		2.1.02.10.0A	Organic/cellulosic materials in waste
		2.1.12.04.0A	Gas generation (CO2, CH4, H2S) from microbial degradation
W 2.054	Helium gas production	2.1.12.02.0A	Gas generation (He) from waste form decay
W 2.055	Radioactive gases	2.1.12.07.0A	Effects of radioactive gases in EBS
W 2.056	Speciation	2.1.09.04.0A	Radionuclide solubility, solubility limits, and speciation in the waste form and EBS
W 2.057	Kinetics of speciation	2.2.08.07.0B	Radionuclide solubility limits in the UZ
		2.2.08.03.0A	Geochemical interactions and evolution in the SZ
		2.2.08.03.0B	Geochemical interactions and evolution in the UZ
		2.2.08.07.0A	Radionuclide solubility limits in the SZ
W 2.058	Dissolution of waste	2.1.02.02.0A	CSNF degradation (alteration, dissolution, and radionuclide release)
W 2.059	Precipitation	2.1.09.10.0A	Secondary phase effects on dissolved radionuclide concentrations
		2.1.09.04.0A	Radionuclide solubility, solubility limits, and speciation in the waste form and EBS
W 2.060	Kinetics of precipitation and dissolution	2.2.08.03.0A	Geochemical interactions and evolution in the SZ
		2.2.08.03.0B	Geochemical interactions and evolution in the UZ
W 2.061	Actinide sorption	2.2.08.09.0A	Sorption in the SZ
		2.2.08.09.0B	Sorption in the UZ
W 2.062	Kinetics of sorption	2.2.08.09.0B	Sorption in the UZ
		2.2.08.09.0A	Sorption in the SZ
W 2.063	Changes in sorptive surfaces	2.2.08.09.0A	Sorption in the SZ
		2.2.08.09.0B	Sorption in the UZ
W 2.064	Effect of metal corrosion	2.1.09.02.0A	Chemical interaction with corrosion products
W 2.065	Reduction-oxidation fronts	2.1.09.06.0A	Reduction-oxidation potential in waste package
W 2.066	Reduction-oxidation kinetics	2.1.09.07.0B	Reaction kinetics in drifts
		2.1.09.07.0A	Reaction kinetics in waste package
W 2.067	Localized reducing zones	2.1.09.06.0A	Reduction-oxidation potential in waste package
W 2.068	Organic complexation	2.1.09.13.0A	Complexation in EBS
W 2.069	Organic ligands	2.1.09.13.0A	Complexation in EBS
W 2.070	Humic and fulvic acids	2.1.09.13.0A	Complexation in EBS
W 2.071	Kinetics of organic complexation	2.1.09.13.0A	Complexation in EBS
W 2.072	Exothermic reactions	2.1.11.03.0A	Exothermic reactions in the EBS

Table F-3. Cross Reference of Source FEPs to TSPA-LA FEPs (Continued)

Source FEP No.	Source FEP Name	TSPA-LA FEP Number	TSPA-LA FEP Name
W 2.073	Concrete hydration	2.1.11.03.0A	Exothermic reactions in the EBS
W 2.074	Chemical degradation of seals	2.1.05.03.0A	Degradation of seals
W 2.075	Chemical degradation of backfill	2.1.04.02.0A	Chemical properties and evolution of backfill
W 2.076	Microbial growth on concrete	2.1.12.04.0A	Gas generation (CO2, CH4, H2S) from microbial degradation
		2.1.06.01.0A	Chemical effects of rock reinforcement and cementitious materials in EBS
		2.1.10.01.0A	Microbial activity in EBS
W 2.077	Solute transport	2.2.07.17.0A	Diffusion in the SZ
		2.2.07.15.0A	Advection and dispersion in the SZ
W 2.078	Colloid transport	2.1.09.19.0A	Sorption of colloids in EBS
		2.1.09.19.0B	Advection of colloids in EBS
W 2.079	Colloid formation and stability	2.1.09.16.0A	Formation of pseudo-colloids (natural) in EBS
		2.1.09.15.0A	Formation of true (intrinsic) colloids in EBS
		2.1.09.23.0A	Stability of colloids in EBS
		2.1.09.17.0A	Formation of pseudo-colloids (corrosion product) in EBS
W 2.080	Colloid filtration	2.1.09.20.0A	Filtration of colloids in EBS
W 2.081	Colloid sorption	2.1.09.19.0A	Sorption of colloids in EBS
W 2.082	Suspensions of particles	2.1.09.21.0A	Transport of particles larger than colloids in EBS
		2.1.09.21.0B	Transport of particles larger than colloids in the SZ
		2.1.09.21.0C	Transport of particles larger than colloids in the UZ
W 2.083	Rinse	2.1.09.21.0B	Transport of particles larger than colloids in the SZ
		2.1.09.21.0A	Transport of particles larger than colloids in EBS
W 2.084	Cuttings	1.4.04.01.0A	Effects of drilling intrusion
W 2.085	Cavings	1.4.04.01.0A	Effects of drilling intrusion
W 2.086	Spallings	1.4.04.01.0A	Effects of drilling intrusion
W 2.087	Microbial transport	2.1.09.18.0A	Formation of microbial colloids in EBS
W 2.088	Biofilms	2.1.10.01.0A	Microbial activity in EBS
W 2.089	Transport of radioactive gases	2.2.11.03.0A	Gas transport in geosphere
W 2.090	Advection	2.2.07.15.0A	Advection and dispersion in the SZ
W 2.091	Diffusion	2.2.07.17.0A	Diffusion in the SZ
W 2.092	Matrix diffusion	2.2.08.08.0A	Matrix diffusion in the SZ
W 2.093	Soret effect	2.1.11.10.0A	Thermal effects on transport in EBS
W 2.094	Electrochemical effects	2.1.09.09.0A	Electrochemical effects in EBS
W 2.095	Galvanic coupling	2.1.09.09.0A	Electrochemical effects in EBS
W 2.096	Electrophoresis	2.1.09.09.0A	Electrochemical effects in EBS
W 2.097	Chemical gradients	2.1.09.27.0A	Coupled effects on radionuclide transport in EBS
		2.1.09.08.0A	Diffusion of dissolved radionuclides in EBS
		2.1.09.08.0B	Advection of dissolved radionuclides in EBS
W 2.098	Osmotic processes	2.2.08.05.0A	Diffusion in the UZ
W 2.099	Alpha recoil	2.1.02.04.0A	Alpha recoil enhances dissolution
W 2.100	Enhanced diffusion	2.1.09.27.0A	Coupled effects on radionuclide transport in EBS
W 2.101	Plant uptake	3.3.02.01.0A	Plant uptake
W 2.102	Animal uptake	3.3.02.02.0A	Animal uptake
W 2.103	Accumulation in soil	2.3.02.02.0A	Radionuclide accumulation in soils

Table F-3. Cross Reference of Source FEPs to TSPA-LA FEPs (Continued)

Source FEP No.	Source FEP Name	TSPA-LA FEP Number	TSPA-LA FEP Name
W 2.104	Ingestion	3.3.04.01.0A	Ingestion
W 2.105	Inhalation	3.3.04.02.0A	Inhalation
W 2.106	Irradiation	3.3.04.03.0A	External exposure
W 2.107	Dermal sorption	3.3.04.03.0A	External exposure
W 2.108	Injection	3.3.01.00.0A	Contaminated drinking water, foodstuffs, and drugs
		3.3.04.03.0A	External exposure
W 3.001	Oil and gas exploration	1.4.04.00.0A	Drilling activities (human intrusion)
W 3.002	Potash exploration	1.4.04.00.0A	Drilling activities (human intrusion)
W 3.003	Water resources exploration	1.4.04.00.0A	Drilling activities (human intrusion)
W 3.004	Oil and gas exploitation	1.4.04.00.0A	Drilling activities (human intrusion)
W 3.005	Groundwater exploitation	1.4.04.00.0A	Drilling activities (human intrusion)
W 3.006	Archeological investigations	1.4.02.01.0A	Deliberate human intrusion
W 3.007	Geothermal	1.4.04.00.0A	Drilling activities (human intrusion)
W 3.008	Other resources	1.4.04.00.0A	Drilling activities (human intrusion)
W 3.009	Enhanced oil and gas recovery	1.4.04.00.0A	Drilling activities (human intrusion)
W 3.010	Liquid waste disposal	1.4.04.00.0A	Drilling activities (human intrusion)
W 3.011	Hydrocarbon storage	1.4.04.00.0A	Drilling activities (human intrusion)
W 3.012	Deliberate drilling intrusion	1.4.02.01.0A	Deliberate human intrusion
W 3.013	Potash mining	1.4.05.00.0A	Mining and other underground activities (human intrusion)
W 3.014	Other resources	1.4.05.00.0A	Mining and other underground activities (human intrusion)
W 3.015	Tunneling	1.4.05.00.0A	Mining and other underground activities (human intrusion)
W 3.016	Construction of underground facilities (for example storage, disposal, accommodation)	1.4.05.00.0A	Mining and other underground activities (human intrusion)
W 3.017	Archeological excavations	1.4.03.00.0A	Unintrusive site investigation
		1.4.05.00.0A	Mining and other underground activities (human intrusion)
W 3.018	Deliberate mining intrusion	1.4.05.00.0A	Mining and other underground activities (human intrusion)
W 3.019	Explosions for resource recovery	1.4.11.00.0A	Explosions and crashes (human activities)
W 3.020	Underground nuclear device testing	1.4.11.00.0A	Explosions and crashes (human activities)
W 3.021	Drilling fluid flow	1.4.04.01.0A	Effects of drilling intrusion
W 3.022	Drilling fluid loss	1.4.04.01.0A	Effects of drilling intrusion
W 3.023	Blowouts	1.4.04.01.0A	Effects of drilling intrusion
W 3.024	Drilling-induced geochemical changes	1.4.04.01.0A	Effects of drilling intrusion
W 3.025	Oil and gas extraction	1.4.04.00.0A	Drilling activities (human intrusion)
W 3.026	Groundwater extraction	1.4.07.02.0A	Wells
W 3.027	Liquid waste disposal	1.4.04.00.0A	Drilling activities (human intrusion)
W 3.028	Enhanced oil and gas production	1.4.04.00.0A	Drilling activities (human intrusion)
W 3.029	Hydrocarbon storage	1.4.04.00.0A	Drilling activities (human intrusion)
W 3.030	Fluid injection-induced geochemical changes	1.4.04.01.0A	Effects of drilling intrusion

Table F-3. Cross Reference of Source FEPs to TSPA-LA FEPs (Continued)

Source FEP No.	Source FEP Name	TSPA-LA FEP Number	TSPA-LA FEP Name
W 3.031	Natural borehole fluid flow	1.4.04.00.0A	Drilling activities (human intrusion)
		2.1.05.02.0A	Radionuclide transport through seals
		1.1.04.01.0A	Incomplete closure
		1.1.01.01.0A	Open site investigation boreholes
		2.1.05.03.0A	Degradation of seals
		1.4.02.02.0A	Inadvertent human intrusion
W 3.032	Waste-induced borehole flow	2.1.05.02.0A	Radionuclide transport through seals
		1.4.04.00.0A	Drilling activities (human intrusion)
		2.1.05.03.0A	Degradation of seals
		1.1.04.01.0A	Incomplete closure
		1.1.01.01.0A	Open site investigation boreholes
W 3.033	Flow through undetected boreholes	1.1.04.01.0A	Incomplete closure
		1.1.01.01.0A	Open site investigation boreholes
W 3.034	Borehole-induced solution and subsidence	2.2.06.04.0A	Effects of subsidence
W 3.035	Borehole-induced mineralization	1.1.01.01.0A	Open site investigation boreholes
W 3.036	Borehole-induced geochemical changes	1.1.04.01.0A	Incomplete closure
		2.1.05.03.0A	Degradation of seals
		2.1.05.02.0A	Radionuclide transport through seals
		1.4.04.00.0A	Drilling activities (human intrusion)
		1.1.01.01.0A	Open site investigation boreholes
W 3.037	Changes in groundwater flow due to mining	1.4.05.00.0A	Mining and other underground activities (human intrusion)
W 3.038	Changes in geochemistry due to mining	1.4.05.00.0A	Mining and other underground activities (human intrusion)
W 3.039	Changes in groundwater flow due to explosions	1.4.11.00.0A	Explosions and crashes (human activities)
W 3.040	Land use changes	2.4.10.00.0A	Urban and industrial land and water use
W 3.041	Surface disruptions	2.4.10.00.0A	Urban and industrial land and water use
W 3.042	Damming of streams or rivers	1.4.07.01.0A	Water management activities
W 3.043	Reservoirs	1.4.07.01.0A	Water management activities
W 3.044	Irrigation	2.4.09.01.0A	Implementation of new agricultural practices or land use
W 3.045	Lake usage	1.4.07.01.0A	Water management activities
W 3.046	Altered soil or water surface chemistry by human activities	1.4.06.01.0A	Altered soil or surface water chemistry
W 3.047	Greenhouse gas effects	1.4.01.02.0A	Greenhouse gas effects
W 3.048	Acid rain	1.4.01.03.0A	Acid rain
W 3.049	Damage to the ozone layer	1.4.01.04.0A	Ozone layer failure
W 3.050	Coastal water use	2.4.08.00.0A	Wild and natural land and water use
W 3.051	Sea water use	2.4.08.00.0A	Wild and natural land and water use
W 3.052	Estuarine water use	2.4.08.00.0A	Wild and natural land and water use
W 3.053	Arable farming	1.4.06.01.0A	Altered soil or surface water chemistry
W 3.054	Ranching	2.4.09.02.0A	Animal farms and fisheries
W 3.055	Fish farming	2.4.09.02.0A	Animal farms and fisheries
W 3.056	Demographic change and urban development	1.4.08.00.0A	Social and institutional developments
W 3.057	Loss of records	1.1.05.00.0A	Records and markers for the repository
W 4.001	Assessment basis FEPs	0.1.09.00.0A	Regulatory requirements and exclusions

Table F-3. Cross Reference of Source FEPs to TSPA-LA FEPs (Continued)

Source FEP No.	Source FEP Name	TSPA-LA FEP Number	TSPA-LA FEP Name
W 4.002	Assessment basis FEPs	0.1.09.00.0A	Regulatory requirements and exclusions
W 4.003	Design and construction FEPs	1.1.07.00.0A	Repository design
W 4.004	Design and construction FEPs	1.1.07.00.0A	Repository design
W 4.005	Radionuclide uptake and dosimetry FEPs	3.3.05.01.0A	Radiation doses
W 4.006	Radionuclide uptake and dosimetry FEPs	3.3.05.01.0A	Radiation doses
W 4.007	Radionuclide uptake and dosimetry FEPs	3.3.05.01.0A	Radiation doses
W 4.008	Model and data issues	0.1.10.00.0A	Model and data issues
W 4.009	Non-radiological toxicity FEPs	3.3.07.00.0A	Non-radiological toxicity and effects
WF//Cladd-1	Waterlogged Rods	2.1.02.11.0A	Degradation of cladding from waterlogged rods
WF//Coll	Episodic infiltration enhances colloid transport	2.2.07.06.0A	Episodic or pulse release from repository
		2.2.08.10.0B	Colloidal transport in the UZ
WF//DSNF-1	Pyrophoricity	2.1.02.08.0A	Pyrophoricity from DSNF
WF//DSNF-2	DOE SNF/HLW Glass Interactions	2.1.01.02.0B	Interactions between co-disposed waste
WF//DSNF-3	Alteration/Dissolution of DOE SNF	2.1.02.01.0A	DSNF degradation (alteration, dissolution, and radionuclide release)
WF//DSNF-4	Oxidation of DOE SNF	2.1.02.01.0A	DSNF degradation (alteration, dissolution, and radionuclide release)
WF//DSNF-5	Alteration/Dissolution of Pu Ceramic Waste	2.1.02.01.0A	DSNF degradation (alteration, dissolution, and radionuclide release)
WF//DSNF-6	High Integrity Canisters for DOE SNF	2.1.01.02.0B	Interactions between co-disposed waste
		2.1.02.01.0A	DSNF degradation (alteration, dissolution, and radionuclide release)
WF//DSNF-7	Internal Canister/Cladding Corrosion due to DOE SNF	2.1.03.06.0A	Internal corrosion of waste packages prior to breach
		2.1.02.25.0A	DSNF cladding
WF//HLW-1	Composition of DHLW Glass	2.1.02.03.0A	HLW glass degradation (alteration, dissolution, and radionuclide release)
WF//Inv-1	Exotic Fuels	2.1.01.01.0A	Waste inventory
WF//Solub-1	Secondary phase effects on dissolved radionuclide concentrations at the waste form	2.1.09.10.0A	Secondary phase effects on dissolved radionuclide concentrations
WFClad AMR-1	Localized corrosion perforation from fluoride	2.1.02.27.0A	Localized (fluoride enhanced) corrosion of cladding
WFClad AMR-2	Diffusion-controlled cavity growth WFClad—Diffusion-Controlled Cavity Growth (DCCG)	2.1.02.26.0A	Diffusion-controlled cavity growth in cladding
WFCol AMR-1	Colloid Sorption at the Air-Water Interface	2.1.09.22.0A	Sorption of colloids at air-water interface
WFCol AMR-2	Colloidal stability and concentration dependence on aqueous chemistry	2.1.09.23.0A	Stability of colloids in EBS
WFCol AMR-3	Colloidal diffusion	2.1.09.24.0A	Diffusion of colloids in EBS
WFCol AMR-4	Colloid gravitational settling	2.1.09.26.0A	Gravitational settling of colloids in EBS

Table F-3. Cross Reference of Source FEPs to TSPA-LA FEPs (Continued)

Source FEP No.	Source FEP Name	TSPA-LA FEP Number	TSPA-LA FEP Name
WFMisc AMR-1	Use of J-13 well water as a surrogate for water flowing into the EBS and waste	2.2.08.12.0B	Chemistry of water flowing into the waste package
		2.2.08.12.0A	Chemistry of water flowing into the drift
WFMisc AMR-2	Spatial Heterogeneity of Emplaced Waste	2.1.01.04.0A	Repository-scale spatial heterogeneity of emplaced waste
WFMisc AMR-3	Various Features of the Approximately 250 DSNF Types and Grouping into Waste Categories	2.1.02.28.0A	Grouping of DSNF waste types into categories
WFMisc AMR-4	Flammable Gas Generation from DSNF	2.1.02.29.0A	Flammable gas generation from DSNF
WP/Chem -1	Effects and degradation of drip shield	2.1.06.06.0B	Oxygen embrittlement of drip shields
		2.1.03.07.0B	Mechanical impact on drip shield
		2.1.03.01.0B	General corrosion of drip shields
		2.1.06.06.0A	Effects of drip shield on flow
WP/Crack -1	Oxygen embrittlement of Ti drip shield	2.1.06.06.0B	Oxygen embrittlement of drip shields
		2.1.03.04.0B	Hydride cracking of drip shields
		2.1.03.03.0B	Localized corrosion of drip shields
YM1	Seismic vibration causes container failure	1.2.03.02.0B	Seismic-induced rockfall damages EBS components
		1.2.03.02.0A	Seismic ground motion damages EBS components
YM10	Thermo-mechanical alteration of fractures near repository	2.2.10.04.0A	Thermo-mechanical stresses alter characteristics of fractures near repository
YM100	Matrix diffusion in geosphere SZ—Matrix Diffusion	2.2.08.08.0A	Matrix diffusion in the SZ
		2.2.08.08.0B	Matrix diffusion in the UZ
YM101	Matrix diffusion (water transport)	2.2.08.08.0A	Matrix diffusion in the SZ
		2.2.08.08.0B	Matrix diffusion in the UZ
YM102	Degradation and alteration of glass waste form	2.1.02.03.0A	HLW glass degradation (alteration, dissolution, and radionuclide release)
YM103	Accumulation of clays and sediments in basin (in EBS)	2.1.07.06.0A	Floor buckling
		2.1.08.12.0A	Induced hydrologic changes in invert
		2.1.14.17.0A	Near-field criticality
YM104	Differential solubility of neutron poisons	2.1.14.16.0A	In-package criticality (degraded configurations)
		2.1.09.04.0A	Radionuclide solubility, solubility limits, and speciation in the waste form and EBS
YM105	Differential solubility of fissile isotopes	2.1.09.04.0A	Radionuclide solubility, solubility limits, and speciation in the waste form and EBS
		2.1.14.16.0A	In-package criticality (degraded configurations)
YM106	Formation of a critical assembly in a pool (in waste and EBS)	2.1.14.17.0A	Near-field criticality
YM107	Pu accumulates in basin pool (in waste and EBS)	2.1.14.17.0A	Near-field criticality
		2.1.07.06.0A	Floor buckling
YM108	Accumulated 239Pu decays to 235U in basin pool (in waste and EBS)	2.1.14.17.0A	Near-field criticality
		3.1.01.01.0A	Radioactive decay and ingrowth
YM109	Sorption of actinides on altered Topopah Spring basal vitrophyre	2.2.10.09.0A	Thermo-chemical alteration of the Topopah Spring basal vitrophyre
YM11	Speciation (in waste and EBS)	2.1.09.04.0A	Radionuclide solubility, solubility limits, and speciation in the waste form and EBS

Table F-3. Cross Reference of Source FEPs to TSPA-LA FEPs (Continued)

Source FEP No.	Source FEP Name	TSPA-LA FEP Number	TSPA-LA FEP Name
YM110	Accumulation of solute in topographic lows of the altered TSbv	2.2.14.09.0A	Far-field criticality
		2.2.07.07.0A	Perched water develops
YM111	Precipitation of U in the upwelling zone along some faults	2.2.14.09.0A	Far-field criticality
YM112	Precipitation of U below the redox front in the SZ	2.2.14.09.0A	Far-field criticality
YM113	Precipitation of U at reducing zone associated w/organics in alluvial aquifer	2.2.14.09.0A	Far-field criticality
YM114	Precipitation of U at reducing zone associated w/organics in Franklin Lake playa	2.2.14.09.0A	Far-field criticality
YM115	Selective leaching of neutron sorbers	2.1.14.16.0A	In-package criticality (degraded configurations)
YM116	Selective leaching of fissile materials	2.1.14.16.0A	In-package criticality (degraded configurations)
YM117	Selective sorption of Pu from solution	2.1.09.05.0A	Sorption of dissolved radionuclides in EBS
YM118	Agglomeration of Pu colloids	2.1.09.17.0A	Formation of pseudo-colloids (corrosion product) in EBS
		2.1.09.16.0A	Formation of pseudo-colloids (natural) in EBS
		2.1.09.15.0A	Formation of true (intrinsic) colloids in EBS
YM119	Colloid filtration by the invert	2.1.09.20.0A	Filtration of colloids in EBS
YM12	Gas generation	2.1.12.03.0A	Gas generation (H2) from waste package corrosion
		2.1.12.04.0A	Gas generation (CO2, CH4, H2S) from microbial degradation
		2.1.13.01.0A	Radiolysis
		2.1.12.02.0A	Gas generation (He) from waste form decay
		2.1.12.01.0A	Gas generation (repository pressurization)
YM120	Waste package internal structures degrade slower than waste form	2.1.14.16.0A	In-package criticality (degraded configurations)
YM121	Waste package internal structures degrade faster than waste form	2.1.14.16.0A	In-package criticality (degraded configurations)
YM122	Waste package internal structures and the waste form degrade at the same rate	2.1.14.16.0A	In-package criticality (degraded configurations)
YM123	Neutron absorber system selectively degrades	2.1.14.16.0A	In-package criticality (degraded configurations)
YM124	Neutron sorbers selectively flushed from containers	2.1.14.16.0A	In-package criticality (degraded configurations)
YM125	Waste package internal structures collapse	2.1.14.16.0A	In-package criticality (degraded configurations)
YM126	Thermo-mechanical alteration of rocks above and below the repository	2.2.10.05.0A	Thermo-mechanical stresses alter characteristics of rocks above and below the repository
YM127a	Relaxation of thermal stresses by fault movement	2.2.06.02.0A	Seismic activity changes porosity and permeability of faults

Table F-3. Cross Reference of Source FEPs to TSPA-LA FEPs (Continued)

Source FEP No.	Source FEP Name	TSPA-LA FEP Number	TSPA-LA FEP Name
YM127b	Relaxation of thermal stresses by fault movement	2.2.06.02.0A	Seismic activity changes porosity and permeability of faults
YM128	Deep alteration of the porosity of drift walls	2.1.09.12.0A	Rind (chemically altered zone) forms in the near-field
YM129	Thermo-mechanical alteration of surface infiltration	2.2.10.05.0A	Thermo-mechanical stresses alter characteristics of rocks above and below the repository
YM13	Rockfall (rubble) (in waste and EBS)	1.2.03.02.0E	Seismic-induced drift collapse alters in-drift chemistry
		2.1.07.02.0A	Drift collapse
		1.2.03.02.0C	Seismic-induced drift collapse damages EBS components
		1.2.03.02.0D	Seismic-induced drift collapse alters in-drift thermohydrology
YM130	Cladding degradation before YMP receives it	2.1.02.12.0A	Degradation of cladding prior to disposal
YM131	Pin Degradation During Reactor Operation	2.1.02.12.0A	Degradation of cladding prior to disposal
YM132	Pin Degradation During Spent Fuel Pool Storage	2.1.02.12.0A	Degradation of cladding prior to disposal
YM133	Pin Degradation During Dry Storage	2.1.02.12.0A	Degradation of cladding prior to disposal
YM134	Pin Degradation During Fuel Shipment and Handling	2.1.02.12.0A	Degradation of cladding prior to disposal
YM135	Cladding Degradation Mechanisms at YMP, Pre-Pin Failure	2.1.02.12.0A	Degradation of cladding prior to disposal
YM136	Corrosion (of cladding)	2.1.02.13.0A	General corrosion of cladding
YM137	General corrosion of cladding	2.1.02.13.0A	General corrosion of cladding
YM138	Microbial corrosion (MIC) of cladding WFClad—Microbiologically	2.1.02.14.0A	Microbially influenced corrosion (MIC) of cladding
YM139	Acid corrosion of cladding from radiolysis	2.1.02.15.0A	Localized (radiolysis enhanced) corrosion of cladding
YM14	Critical assembly forms away from repository	2.2.14.09.0A	Far-field criticality
YM140	Localized corrosion (pitting) of cladding	2.1.02.16.0A	Localized (pitting) corrosion of cladding
YM141	Localized corrosion (crevice corrosion) of cladding	2.1.02.17.0A	Localized (crevice) corrosion of cladding
YM142	Creep rupture of cladding	2.1.02.19.0A	Creep rupture of cladding
YM143	Pressurization from He production causes cladding failure	2.1.02.20.0A	Internal pressurization of cladding
YM144	Mechanical failure of cladding	2.1.02.24.0A	Mechanical impact on cladding
YM145	Stress corrosion cracking (SCC) of cladding	2.1.02.21.0A	Stress corrosion cracking (SCC) of cladding
YM146	Inside Out from fission products (iodine) (failure of cladding)	2.1.02.21.0A	Stress corrosion cracking (SCC) of cladding
		2.1.13.01.0A	Radiolysis
YM147	Outside In from Salts or WP Chemicals (failure of cladding)	2.1.02.21.0A	Stress corrosion cracking (SCC) of cladding

Table F-3. Cross Reference of Source FEPs to TSPA-LA FEPs (Continued)

Source FEP No.	Source FEP Name	TSPA-LA FEP Number	TSPA-LA FEP Name
YM148	Hydride Embrittlement of Cladding	2.1.02.22.0A	Hydride cracking of cladding
YM149	Hydride Embrittlement From Zirconium Corrosion (of cladding)	2.1.02.22.0A	Hydride cracking of cladding
YM15	Rind (altered zone) formation in waste, EBS, and adjacent rock	2.1.09.01.0A	Chemical characteristics of water in drifts
		2.1.09.01.0B	Chemical characteristics of water in waste packages
		2.1.09.12.0A	Rind (chemically altered zone) forms in the near-field
YM150	Hydride Embrittlement From WP Corrosion & H2 Absorption (of cladding)	2.1.02.22.0A	Hydride cracking of cladding
YM151	Hydride Embrittlement From Galvanic Corrosion of WP contacting Cladding	2.1.02.22.0A	Hydride cracking of cladding
YM152	Delayed Hydride Cracking (of cladding) WFClad—Delayed Hydride	2.1.02.22.0A	Hydride cracking of cladding
YM153	Hydride Reorientation (of cladding)	2.1.02.22.0A	Hydride cracking of cladding
YM154	Hydrogen Axial Migration (of cladding)	2.1.02.22.0A	Hydride cracking of cladding
YM155	Cladding Degradation after Initial Cladding Perforation	2.1.02.23.0A	Cladding unzipping
YM156	Cladding unzipping	2.1.02.23.0A	Cladding unzipping
YM157	Dry Oxidation of Fuel (causes failure of cladding) WFClad—Dry Oxidation of Fuel	2.1.02.23.0A	Cladding unzipping
YM158	Wet Oxidation of Fuel (causes failure of cladding) WFClad—Wet Oxidation of Fuel	2.1.02.23.0A	Cladding unzipping
YM159	Hydride Embrittlement from Fuel Reaction (causes failure of cladding)	2.1.02.22.0A	Hydride cracking of cladding
YM16	Radionuclide accumulation in sediments at Franklin Lake Playa (water transport)	2.3.13.04.0A	Radionuclide release outside the reference biosphere
		2.3.02.02.0A	Radionuclide accumulation in soils
YM160	Radionuclide Release (Diffusion) Through Failed Cladding	2.1.09.24.0A	Diffusion of colloids in EBS
		2.1.09.08.0A	Diffusion of dissolved radionuclides in EBS
YM161	Cementitious invert	2.1.06.05.0D	Chemical degradation of invert
YM162a	Normal faulting occurs or exists at Yucca Mountain	2.1.06.05.0B	Mechanical degradation of invert
		2.1.06.05.0D	Chemical degradation of invert
YM162b	Degradation of the liner	1.2.02.02.0A	Faults
		2.1.06.04.0A	Flow through rock reinforcement materials in EBS
YM163	Strike/slip faulting occurs or exists at Yucca Mountain.	1.2.02.02.0A	Faults
YM164	Detachment faulting occurs or exists at Yucca Mountain	1.2.02.02.0A	Faults

Table F-3. Cross Reference of Source FEPs to TSPA-LA FEPs (Continued)

Source FEP No.	Source FEP Name	TSPA-LA FEP Number	TSPA-LA FEP Name
YM165	Dip/slip faulting occurs at Yucca Mountain	1.2.02.02.0A	Faults
YM166	New fault occurs at Yucca Mountain	1.2.02.02.0A	Faults
		2.2.06.02.0A	Seismic activity changes porosity and permeability of faults
YM167	Old fault strand is reactivated at Yucca Mountain	2.2.06.02.0A	Seismic activity changes porosity and permeability of faults
		1.2.02.02.0A	Faults
YM168	New fault strand is activated at Yucca Mountain	1.2.02.02.0A	Faults
		2.2.06.02.0A	Seismic activity changes porosity and permeability of faults
YM169	Mechanical degradation or collapse of drift	2.1.07.02.0A	Drift collapse
		1.2.03.02.0E	Seismic-induced drift collapse alters in-drift chemistry
		1.2.03.02.0D	Seismic-induced drift collapse alters in-drift thermohydrology
		1.2.03.02.0C	Seismic-induced drift collapse damages EBS components
YM17	Degradation of invert and pedestal	2.1.06.05.0D	Chemical degradation of invert
		2.1.06.05.0C	Chemical degradation of emplacement pallet
		2.1.06.05.0B	Mechanical degradation of invert
		2.1.06.05.0A	Mechanical degradation of emplacement pallet
YM170	Seismically-stimulated release of thermo-mechanical stress on bounding faults	2.2.06.02.0A	Seismic activity changes porosity and permeability of faults
YM171	Stress-produced porosity changes	2.2.06.01.0A	Seismic activity changes porosity and permeability of rock
		2.2.06.02.0B	Seismic activity changes porosity and permeability of fractures
		2.2.06.02.0A	Seismic activity changes porosity and permeability of faults
YM172	Stress-produced permeability changes	2.2.06.02.0A	Seismic activity changes porosity and permeability of faults
		2.2.06.02.0B	Seismic activity changes porosity and permeability of fractures
		2.2.06.01.0A	Seismic activity changes porosity and permeability of rock
YM173	Seismically-induced water table changes	1.2.10.01.0A	Hydrologic response to seismic activity
YM174	Fault movement connects tuff and carbonate aquifers	1.2.10.01.0A	Hydrologic response to seismic activity
YM175	Fault pathway through the altered Topopah Spring basal vitrophyre	1.2.10.01.0A	Hydrologic response to seismic activity

Table F-3. Cross Reference of Source FEPs to TSPA-LA FEPs (Continued)

Source FEP No.	Source FEP Name	TSPA-LA FEP Number	TSPA-LA FEP Name
YM176	Changes in stress (due to thermal, seismic, or tectonic effects) produce change in permeability of faults	2.2.06.02.0A	Seismic activity changes porosity and permeability of faults
		2.2.06.02.0B	Seismic activity changes porosity and permeability of fractures
		2.2.10.04.0A	Thermo-mechanical stresses alter characteristics of fractures near repository
		2.2.10.04.0B	Thermo-mechanical stresses alter characteristics of faults near repository
YM177	Changes in stress (due to seismic or tectonic effects) alter perched water zones	2.2.06.03.0A	Seismic activity alters perched water zones
YM178	Perched zones develop as a result of stress changes	2.2.06.03.0A	Seismic activity alters perched water zones
YM179	Stress-produced permeability changes	2.2.06.02.0A	Seismic activity changes porosity and permeability of faults
		2.2.06.02.0B	Seismic activity changes porosity and permeability of fractures
		2.2.06.01.0A	Seismic activity changes porosity and permeability of rock
YM18	Criticality - MPC flooded	2.1.14.15.0A	In-package criticality (intact configuration)
YM180	Fault establishes pathway through the UZ	1.2.10.01.0A	Hydrologic response to seismic activity
YM181	Fault establishes pathway through the SZ	1.2.10.01.0A	Hydrologic response to seismic activity
YM182	Fluid supplied by a fault migrates down the drift	1.2.10.01.0A	Hydrologic response to seismic activity
YM183	Fault intersects and drains condensate zone	1.2.10.01.0A	Hydrologic response to seismic activity
YM184	Waste container is thermally quenched by rapid influx of water	2.1.08.01.0B	Effects of rapid influx into the repository
YM185	Rockfall stopes up fault	2.1.07.02.0A	Drift collapse
YM186	Head-driven flow up from Carbonates	1.2.10.01.0A	Hydrologic response to seismic activity
YM187	Dissolution of spent fuel in magma	1.2.04.05.0A	Magma or pyroclastic base surge transports waste
YM188	Volatile radionuclides plate out in the surrounding rock	1.2.04.05.0A	Magma or pyroclastic base surge transports waste
YM189	Entrainment of SNF in a flowing dike	1.2.04.05.0A	Magma or pyroclastic base surge transports waste
YM19	Criticality - container gone, intact rods, flooded	2.1.14.17.0A	Near-field criticality
YM190	Dike related fractures alter flow	1.2.04.02.0A	Igneous activity changes rock properties
YM191	Heating of waste container by magma (without contact)	1.2.04.04.0A	Igneous intrusion interacts with EBS components
YM192	Failure of waste container by direct contact w/magma	1.2.04.04.0A	Igneous intrusion interacts with EBS components
YM193	Vent erosion	1.2.04.06.0A	Eruptive conduit to surface intersects repository
YM194	Vent jump	1.2.04.06.0A	Eruptive conduit to surface intersects repository
YM195	Dike provides a permeable flow path	1.2.04.02.0A	Igneous activity changes rock properties
YM196	Dike provides a barrier to flow	1.2.04.02.0A	Igneous activity changes rock properties

Table F-3. Cross Reference of Source FEPs to TSPA-LA FEPs (Continued)

Source FEP No.	Source FEP Name	TSPA-LA FEP Number	TSPA-LA FEP Name
YM197	Sill provides a permeable flow path	1.2.04.03.0A	Igneous intrusion into repository
YM198	Sill provides a flow barrier	1.2.04.03.0A	Igneous intrusion into repository
YM199	Dissolution of other waste in magma	1.2.04.05.0A	Magma or pyroclastic base surge transports waste
YM20	Criticality - container and cladding gone, fuel powder, dry	2.1.14.17.0A	Near-field criticaltiy
YM200	Aseismic alteration of permeability along and across faults	1.2.01.01.0A	Tectonic activity - large scale
		2.2.06.02.0A	Seismic activity changes porosity and permeability of faults
YM201	Equilibrated flow system	2.3.11.02.0A	Surface runoff and evapotranspiration
		2.3.11.03.0A	Infiltration and recharge
YM202	Draining flow system	2.3.11.03.0A	Infiltration and recharge
YM203	Alteration of the Topopah Spring basal vitrophyre	2.2.10.09.0A	Thermo-chemical alteration of the Topopah Spring basal vitrophyre
YM21	Criticality - container gone, intact rods, dry	2.1.14.17.0A	Near-field criticality
YM22	Criticality - container gone, pile of fuel pellets, dry	2.1.14.17.0A	Near-field criticality
YM23	Criticality - container gone, pile of fuel pellets, flooded	2.1.14.17.0A	Near-field criticality
YM24	Criticality - container partially gone, optimal rod configuration, flooded	2.1.14.16.0A	In-package criticality (degraded configurations)
YM25	Criticality in-situ, nominal configuration, top breach	2.1.14.15.0A	In-package criticality (intact configuration)
YM26	Criticality - nominal configuration, partially flooded, otherwise intact	2.1.14.15.0A	In-package criticality (intact configuration)
YM27	Criticality - clad and disintegrated pellets, optimally mixed, flooded	2.1.14.15.0A	In-package criticality (intact configuration)
		2.1.14.16.0A	In-package criticality (degraded configurations)
YM28	Criticality - container and cladding gone, fuel powder, flooded	2.1.14.17.0A	Near-field criticaltiy
YM29	Fault control of fluid entrance to and movement away from the repository	2.2.07.04.0A	Focusing of unsaturated flow (fingers, weeps)
		2.2.07.19.0A	Lateral flow from Solitario Canyon Fault enters drifts
YM3	Rockfall (large block) WFClad--Rockfall	1.2.03.02.0B	Seismic-induced rockfall damages EBS components
		2.1.07.01.0A	Rockfall
YM30	Magma interacts with waste	1.2.04.03.0A	Igneous intrusion into repository
		1.2.04.04.0B	Chemical effects of magma and magmatic volatiles
		1.2.04.05.0A	Magma or pyroclastic base surge transports waste
		1.2.04.04.0A	Igneous intrusion interacts with EBS components
YM31	Magmatic transport of waste	1.2.04.05.0A	Magma or pyroclastic base surge transports waste
YM32	Ashfall	1.2.04.07.0A	Ashfall
YM33	Direct exposure of waste in dike apron	1.2.04.05.0A	Magma or pyroclastic base surge transports waste

Table F-3. Cross Reference of Source FEPs to TSPA-LA FEPs (Continued)

Source FEP No.	Source FEP Name	TSPA-LA FEP Number	TSPA-LA FEP Name
YM34	Magmatic volatiles attack waste	1.2.04.04.0B	Chemical effects of magma and magmatic volatiles
		1.2.04.03.0A	Igneous intrusion into repository
YM35	Container failure induced by microseisms associated with dike emplacement	1.2.03.02.0A	Seismic ground motion damages EBS components
		1.2.03.03.0A	Seismicity associated with igneous activity
YM36	Exploratory drilling for hydrocarbons	1.4.04.00.0A	Drilling activities (human intrusion)
YM37	Direct exposure to waste in mud pit	1.4.04.01.0A	Effects of drilling intrusion
YM38	Exploratory drilling for metals	1.4.04.00.0A	Drilling activities (human intrusion)
YM39	Flooding of drifts with drilling fluids	1.4.04.01.0A	Effects of drilling intrusion
YM4	Properties of the potential carrier plume in the waste and EBS	2.1.09.01.0A	Chemical characteristics of water in drifts
YM40	Two-phase buoyant flow / heat pipes	2.2.10.10.0A	Two-phase buoyant flow/heat pipes
YM41	Natural air flow in unsaturated zone	2.2.10.11.0A	Natural air flow in the UZ
YM42	Auto-catalytic drainage of locally saturated flow thru condensation cap	2.2.07.11.0A	Resaturation of geosphere dry-out zone
YM43	Repository dry-out due to waste heat	2.2.07.21.0A	Drift shadow forms below repository
		2.1.08.03.0A	Repository dry-out due to waste heat
YM44	Colloid formation is associated with container hydrolysis products	2.1.09.17.0A	Formation of pseudo-colloids (corrosion product) in EBS
YM45	Formation of true colloids in waste and EBS	2.1.09.15.0A	Formation of true (intrinsic) colloids in EBS
YM46	Pitting corrosion develops on containers	2.1.03.03.0A	Localized corrosion of waste packages
YM48	Small pieces of backfill under go phase changes when heated and weld together	2.1.04.05.0A	Thermal-mechanical properties and evolution of backfill
YM49	Fe control of oxidation state of contaminants	2.1.09.27.0A	Coupled effects on radionuclide transport in EBS
		2.1.09.02.0A	Chemical interaction with corrosion products
		2.1.09.06.0A	Reduction-oxidation potential in waste package
YM50	Fracture flow in the unsaturated zone	2.2.07.08.0A	Fracture flow in the UZ
YM51	Thermo-chemical alteration of the saturated zone SZ—Repository Induced Thermal Effects	2.2.10.08.0A	Thermo-chemical alteration in the SZ (solubility, speciation, phase changes)
YM52	Condensation zone forms around drifts	2.2.07.10.0A	Condensation zone forms around drifts
		2.1.08.04.0B	Condensation forms at repository edges (repository-scale cold traps)
YM53	Focusing of unsaturated flow (fingers, weeps)	2.2.07.04.0A	Focusing of unsaturated flow (fingers, weeps)
		2.2.07.07.0A	Perched water develops
YM54	Locally saturated flow at bedrock/alluvium contact	2.2.07.01.0A	Locally saturated flow at bedrock/alluvium contact

Table F-3. Cross Reference of Source FEPs to TSPA-LA FEPs (Continued)

Source FEP No.	Source FEP Name	TSPA-LA FEP Number	TSPA-LA FEP Name
YM55	Matrix imbibition in the unsaturated zone	2.2.07.09.0A	Matrix imbibition in the UZ
YM56	Seeps and weeps form as a locally saturated flow system	2.2.07.04.0A	Focusing of unsaturated flow (fingers, weeps)
YM57	Shedding of condensation cap over one drift to another drift	2.1.08.04.0B	Condensation forms at repository edges (repository-scale cold traps)
		2.2.07.10.0A	Condensation zone forms around drifts
YM58	Flow and transport in the UZ from episodic infiltration	2.2.07.05.0A	Flow in the UZ from episodic infiltration
YM59	Return flow from condensation cap / resaturation of dry-out zone	2.1.08.04.0B	Condensation forms at repository edges (repository-scale cold traps)
		2.2.07.11.0A	Resaturation of geosphere dry-out zone
YM60	Resaturation of dry-out zone is affected by vapor flow	2.2.07.11.0A	Resaturation of geosphere dry-out zone
		2.2.10.10.0A	Two-phase buoyant flow/heat pipes
YM61	Resaturation of dry-out zone is effected by liquid under capillary forces	2.2.07.11.0A	Resaturation of geosphere dry-out zone
		2.2.07.03.0A	Capillary rise in the UZ
YM62	Alteration of rock properties because of 2-phase flow	2.2.10.06.0A	Thermo-chemical alteration in the UZ (solubility, speciation, phases changes)
		2.2.10.10.0A	Two-phase buoyant flow/heat pipes
YM63a	Heat generation from waste containers	2.1.11.01.0A	Heat generation in EBS
YM63b	Fingering - contaminant transport in fingers in UZ	2.2.07.15.0B	Advection and dispersion in the UZ
		2.2.07.04.0A	Focusing of unsaturated flow (fingers, weeps)
YM64a	Heat pipe formation, 2-phase system	2.2.10.10.0A	Two-phase buoyant flow/heat pipes
YM64b	Flow in ephemeral streams tends to be in channels and is a source of recharge	2.3.11.03.0A	Infiltration and recharge
		2.3.11.02.0A	Surface runoff and evapotranspiration
YM65	Runoff is intercepted by wash terraces	2.3.11.02.0A	Surface runoff and evapotranspiration
		2.3.11.03.0A	Infiltration and recharge
YM66	Silica phase changes (accompanied by volume change) occur due to elevated temperature	2.2.10.06.0A	Thermo-chemical alteration in the UZ (solubility, speciation, phase changes)
YM67	Unsaturated flow plume returns flow from the condensation cap	2.1.08.04.0B	Condensation forms at repository edges (repository-scale cold traps)
		2.2.07.11.0A	Resaturation of geosphere dry-out zone
YM68	Resaturation due to matrix imbibition of episodic fracture flow	2.2.07.09.0A	Matrix imbibition in the UZ
YM69	Return of condensate to same panel	2.2.07.11.0A	Resaturation of geosphere dry-out zone
		2.2.07.10.0A	Condensation zone forms around drifts
YM7	Speciation control of contaminants by hyperalkaline plume formed in the EBS	2.1.09.04.0A	Radionuclide solubility, solubility limits, and speciation in the waste form and EBS
YM70	Fracture flow through the invert	2.1.08.05.0A	Flow through invert
YM71	Fracture flow through the liner	2.1.06.04.0A	Flow through rock reinforcement materials in EBS

Table F-3. Cross Reference of Source FEPs to TSPA-LA FEPs (Continued)

Source FEP No.	Source FEP Name	TSPA-LA FEP Number	TSPA-LA FEP Name
YM72	Hyperalkaline carrier plume forms	2.1.06.01.0A	Chemical effects of rock reinforcement and cementitious materials in EBS
		2.1.09.01.0A	Chemical characteristics of water in drifts
YM73	Thermo-chemical alteration of the Topopah Spring basal vitrophyre	2.2.10.09.0A	Thermo-chemical alteration of the Topopah Spring basal vitrophyre
YM74	Formation of perched water on the altered Topopah Spring basal vitrophyre	2.2.10.09.0A	Thermo-chemical alteration of the Topopah Spring basal vitrophyre
		2.2.07.07.0A	Perched water develops
YM75	Sorption of contaminants by the altered Topopah Spring basal vitrophyre	2.2.10.09.0A	Thermo-chemical alteration of the Topopah Spring basal vitrophyre
YM76	Redirection of transport paths by the altered Topopah Spring basal vitrophyre	2.2.10.09.0A	Thermo-chemical alteration of the Topopah Spring basal vitrophyre
YM77	Thermo-chemical alteration of the Calico Hills unit SZ—Repository Induced Thermal Effects	2.2.10.07.0A	Thermo-chemical alteration of the Calico Hills unit
YM78	Formation of condensate over individual containers	2.2.07.10.0A	Condensation zone forms around drifts
YM79	Formation of condensate over individual panels	2.2.07.10.0A	Condensation zone forms around drifts
YM8	Sorption (reversible and irreversible)	2.2.08.09.0B	Sorption in the UZ
		2.2.08.09.0A	Sorption in the SZ
YM80	Formation of condensate over the entire repository	2.2.07.10.0A	Condensation zone forms around drifts
YM81	Radionuclide transport occurs in a carrier plume in geosphere SZ—Radionuclide Transport in a Carrier Plume	2.2.08.01.0A	Chemical characteristics of groundwater in the SZ
		2.2.08.01.0B	Chemical characteristics of groundwater in the UZ
		2.2.08.03.0A	Geochemical interactions and evolution in the SZ
		2.2.08.03.0B	Geochemical interactions and evolution in the UZ
YM82	Colloid transport occurs in a carrier plume (in geosphere)	2.2.08.10.0B	Colloidal transport in the UZ
		2.2.08.01.0A	Chemical characteristics of groundwater in the SZ
		2.2.08.03.0A	Geochemical interactions and evolution in the SZ
YM83	Floor buckling	2.1.07.06.0A	Floor buckling
YM86	Basin formation (in waste and EBS)	2.1.07.06.0A	Floor buckling
YM87	In-drift sorption WFMisc—In-Package Sorption	2.1.09.05.0A	Sorption of dissolved radionuclides in EBS
YM88	Sorption in UZ and SZ	2.2.08.09.0A	Sorption in the SZ
		2.2.08.09.0B	Sorption in the UZ
YM89	Panel/repository edge effects - thermal	2.1.11.07.0A	Thermal expansion/stress of in-drift EBS components
		2.1.11.02.0A	Non-uniform heat distribution in EBS
YM9	Colloid filtration (in pores and fractures)	2.1.09.20.0A	Filtration of colloids in EBS

Table F-3. Cross Reference of Source FEPs to TSPA-LA FEPs (Continued)

Source FEP No.	Source FEP Name	TSPA-LA FEP Number	TSPA-LA FEP Name
YM90	Panel/repository edge effects - post-thermal	2.1.11.02.0A	Non-uniform heat distribution in EBS
		2.1.11.07.0A	Thermal expansion/stress of in-drift EBS components
YM91	Heat pipe -evolving	2.2.10.10.0A	Two-phase buoyant flow/heat pipes
YM92	Heat pipe -continuing	2.2.10.10.0A	Two-phase buoyant flow/heat pipes
YM93	Geosphere dry-out due to waste heat	2.2.10.12.0A	Geosphere dry-out due to waste heat
YM94	Locally-saturated carrier plume forms (in geosphere)	2.2.07.11.0A	Resaturation of geosphere dry-out zone
		2.2.08.03.0B	Geochemical interactions and evolution in the UZ
		2.1.09.12.0A	Rind (chemically altered zone) forms in the near-field
YM95	Unsaturated carrier plume forms (in geosphere)	2.2.08.03.0B	Geochemical interactions and evolution in the UZ
		2.2.07.11.0A	Resaturation of geosphere dry-out zone
		2.1.09.12.0A	Rind (chemically altered zone) forms in the near-field
YM96	Enhanced influx (Philip's drip)	2.1.08.02.0A	Enhanced influx at the repository
YM97	Flow through invert	2.1.08.05.0A	Flow through invert
YM98	UZ flow through/around the collapsed invert	2.1.08.05.0A	Flow through invert
		2.2.07.20.0A	Flow diversion around repository drifts
YM99	Flow through the liner	2.1.06.04.0A	Flow through rock reinforcement materials in EBS
YSCP1	Increased unsaturated water flux at the repository	2.1.08.01.0A	Water influx at the repository
		2.1.08.01.0B	Effects of rapid influx into the repository
YSCP12	Fault movement shears waste container	1.2.02.03.0A	Fault displacement damages EBS components
YSCP13	Fracture dilation along faults creates zones of enhanced permeability	2.2.06.02.0B	Seismic activity changes porosity and permeability of fractures
		2.2.06.02.0A	Seismic activity changes porosity and permeability of faults
YSCP14	Normal faulting produces a trap for laterally moving moisture in the Tiva Canyon unit	1.2.10.01.0A	Hydrologic response to seismic activity
YSCP15	New faulting breaches flow barrier controlling large hydraulic gradient to the north	1.2.10.01.0A	Hydrologic response to seismic activity
YSCP16	Flow barrier south of site blocks flow, causing water table to rise	1.2.10.01.0A	Hydrologic response to seismic activity
YSCP17	Precipitation of zeolites in the saturated zone plugs pores	2.2.10.08.0A	Thermo-chemical alteration in the SZ (solubility, speciation, phase changes)
YSCP19	Perched water escapes detection and waste is put in it	2.2.12.00.0A	Undetected features in the UZ
		2.2.12.00.0B	Undetected features in the SZ
YSCP20	Undetected fault dips below the repository providing a highly permeable flow path	2.2.12.00.0A	Undetected features in the UZ
		2.2.12.00.0B	Undetected features in the SZ
YSCP21	Undetected fault beneath the repository acts as a flow barrier altering the flow system	2.2.12.00.0A	Undetected features in the UZ
		2.2.12.00.0B	Undetected features in the SZ

Table F-3. Cross Reference of Source FEPs to TSPA-LA FEPs (Continued)

Source FEP No.	Source FEP Name	TSPA-LA FEP Number	TSPA-LA FEP Name
YSCP22	Undetected fault connects tuff aquifers to carbonate aquifers; providing a fast path	2.2.12.00.0A	Undetected features in the UZ
		2.2.12.00.0B	Undetected features in the SZ
YSCP23	Undetected dike beneath the repository passing thru the Calico Hills provides a highly permeable flow path	2.2.12.00.0A	Undetected features in the UZ
		2.2.12.00.0B	Undetected features in the SZ
YSCP24	Basaltic cinder cone erupts through the repository	1.2.04.06.0A	Eruptive conduit to surface intersects repository
YSCP25	Emplacement error - containers placed in wet zone	1.1.03.01.0A	Error in waste emplacement
YSCP26	Drains, installed to divert water around containers, are improperly placed	1.1.08.00.0A	Inadequate quality control and deviations from design
YSCP27	Containers are improperly placed - on drift floor	1.1.03.01.0A	Error in waste emplacement
YSCP28	Containers are placed too close together	1.1.03.01.0A	Error in waste emplacement
YSCP29	Juvenile and Early Failure of Waste Containers and Drip Shields	2.1.03.08.0A	Early failure of waste packages
		2.1.03.08.0B	Early failure of drip shields
YSCP3	Short circuit of a flow barrier in the saturated zone because of a water table rise	1.2.10.02.0A	Hydrologic response to igneous activity
		1.2.10.01.0A	Hydrologic response to seismic activity
		1.3.07.02.0A	Water table rise affects SZ
YSCP31	Irrigation wells in Midway Valley increase moisture flux through repository	1.4.07.02.0A	Wells
YSCP32	Water collection in cisterns over repository	1.4.07.01.0A	Water management activities
YSCP33	Irrigation wells in Midway Valley reduce distance to accessible environment	1.4.07.02.0A	Wells
YSCP34	Irrigation wells in Crater Flats or Jackass Flats increase hydraulic gradient under repository	1.4.07.02.0A	Wells
YSCP35	Water table drawdown by down gradient pumping increases hydraulic gradient	1.4.07.01.0A	Water management activities
YSCP37	Water management of nearby ground water basins	1.4.07.01.0A	Water management activities
YSCP38	Container lies in the trace of an old borehole	1.1.01.01.0A	Open site investigation boreholes
YSCP39	Undiscovered mine shaft (an old prospect hole) in a wash acts as a source for increased local infiltration	1.1.03.01.0A	Error in waste emplacement
		2.2.12.00.0A	Undetected features in the UZ
		2.2.12.00.0B	Undetected features in the SZ
YSCP4	Water table rise	2.3.11.04.0A	Groundwater discharge to surface outside the reference biosphere
		1.3.07.02.0B	Water table rise affects UZ
		1.3.07.02.0A	Water table rise affects SZ
YSCP40	Effects of drilling intrusion	1.4.04.01.0A	Effects of drilling intrusion
YSCP41	Drilling fluid interacts with waste	1.4.04.01.0A	Effects of drilling intrusion

Table F-3. Cross Reference of Source FEPs to TSPA-LA FEPs (Continued)

Source FEP No.	Source FEP Name	TSPA-LA FEP Number	TSPA-LA FEP Name
YSCP42	Exploratory borehole creates flow pathway	1.1.01.01.0A	Open site investigation boreholes
YSCP43	Drilling introduces surfactants	1.4.04.01.0A	Effects of drilling intrusion
YSCP44	Mine shaft intersects waste container	1.4.05.00.0A	Mining and other underground activities (human intrusion)
YSCP45	Water from mining above the repository drains through repository.	1.4.05.00.0A	Mining and other underground activities (human intrusion)
YSCP46	A mine shaft creates a preferential path thru the upper nonwelded unit and a wetter zone develops	1.4.05.00.0A	Mining and other underground activities (human intrusion)
YSCP48	Climate modification increases recharge	1.4.01.01.0A	Climate modification increases recharge
YSCP49	Climate modification raises water table	1.3.07.02.0A	Water table rise affects SZ
		1.4.01.01.0A	Climate modification increases recharge
YSCP5	Perched water develops	2.2.07.07.0A	Perched water develops
YSCP50	Climate modification raises water table to flood repository	1.3.07.02.0A	Water table rise affects SZ
		1.4.01.01.0A	Climate modification increases recharge
YSCP51	Climate modification raises water table to short circuit flow barrier in SZ	1.3.07.02.0B	Water table rise affects UZ
		1.4.01.01.0A	Climate modification increases recharge
		1.2.10.01.0A	Hydrologic response to seismic activity
		2.2.07.12.0A	Saturated groundwater flow in the geosphere
		1.3.07.02.0A	Water table rise affects SZ
		1.2.10.02.0A	Hydrologic response to igneous activity
YSCP52	Climate modification causes perched water to develop above repository	1.4.01.01.0A	Climate modification increases recharge
		2.2.07.07.0A	Perched water develops
YSCP53	Climate modification causes perched water to develop at base of Topopah Spring unit	1.4.01.01.0A	Climate modification increases recharge
		2.2.07.07.0A	Perched water develops
YSCP54	Thermal expansion closes most fractures close to repository	2.2.10.04.0A	Thermo-mechanical stresses alter characteristics of fractures near repository
YSCP55	Stress corrosion cracking induced by secondary stress (container failure)	2.1.03.02.0A	Stress corrosion cracking (SCC) of waste packages
		2.1.11.05.0A	Thermal expansion/stress of in-package EBS components
		2.1.11.07.0A	Thermal expansion/stress of in-drift EBS components
YSCP56	Shearing of waste containers by secondary stresses from thermal expansion of the rock	2.1.11.07.0A	Thermal expansion/stress of in-drift EBS components
YSCP57	Thermal expansion of rocks below repository opens fractures in Paint Brush unwelded	2.2.10.04.0A	Thermo-mechanical stresses alter characteristics of fractures near repository
		2.2.10.05.0A	Thermo-mechanical stresses alter characteristics of rocks above and below the repository
YSCP58	Thermally-induced fracturing around containers creates a capillary barrier	2.2.10.04.0A	Thermo-mechanical stresses alter characteristics of fractures near repository

Table F-3. Cross Reference of Source FEPs to TSPA-LA FEPs (Continued)

Source FEP No.	Source FEP Name	TSPA-LA FEP Number	TSPA-LA FEP Name
YSCP59	Condensation cap forms above repository	2.1.08.04.0B	Condensation forms at repository edges (repository-scale cold traps)
		2.2.07.10.0A	Condensation zone forms around drifts
YSCP6	Perched water develops at base of Topopah Spring welded unit	2.2.07.07.0A	Perched water develops
YSCP60	Condensation forms on backs of drifts	2.1.08.04.0B	Condensation forms at repository edges (repository-scale cold traps)
		2.1.08.04.0A	Condensation forms on roofs of drifts (drift-scale cold traps)
YSCP61	Nonuniform heat distribution / edge effects in repository	2.2.10.01.0A	Repository-induced thermal effects on flow in the UZ
		2.1.11.02.0A	Non-uniform heat distribution in EBS
		2.1.11.09.0A	Thermal effects on flow in the EBS
YSCP62	Thermal convection cell develops in SZ	2.2.10.02.0A	Thermal convection cell develops in SZ
		2.1.11.09.0A	Thermal effects on flow in the EBS
YSCP63	Rockbursts in container holes	2.1.07.01.0A	Rockfall
YSCP64	Corrosion of waste containers	2.1.03.03.0A	Localized corrosion of waste packages
		2.1.09.28.0B	Localized corrosion on drip shield surfaces due to deliquescence
		2.1.03.01.0A	General corrosion of waste packages
		2.1.09.28.0A	Localized corrosion on waste package outer surface due to deliquescence
		2.1.03.01.0B	General corrosion of drip shields
YSCP65	Stress corrosion cracking of waste containers and drip shields	2.1.03.02.0A	Stress corrosion cracking (SCC) of waste packages
		2.1.03.02.0B	Stress corrosion cracking (SCC) of drip shields
		2.1.09.28.0B	Localized corrosion on drip shield surfaces due to deliquescence
		2.1.09.28.0A	Localized corrosion on waste package outer surface due to deliquescence
YSCP66	Stress corrosion cracking - dry waste container	2.1.03.02.0A	Stress corrosion cracking (SCC) of waste packages
YSCP67	Thermal sensitization of waste containers and drip shields increases their fragility	2.1.11.06.0A	Thermal sensitization of waste packages
		2.1.11.06.0B	Thermal sensitization of drip shields
YSCP68	Stress-corrosion cracking of Zircaloy cladding	2.1.02.21.0A	Stress corrosion cracking (SCC) of cladding
YSCP69	Formation of pseudo-colloids (corrosion products) in waste and EBS	2.1.09.17.0A	Formation of pseudo-colloids (corrosion product) in EBS
YSCP7	Stream erosion of Amargosa River lowers base levels and increases gradient in SZ	1.2.07.01.0A	Erosion/denudation
YSCP70	Selective dissolution of contaminants contained in SNF	2.1.09.04.0A	Radionuclide solubility, speciation, and phase changes in the waste form and EBS
		2.1.02.02.0A	CSNF degradation (alteration, dissolution, and radionuclide release)
YSCP71	Waste-rock contact	2.1.09.11.0A	Chemical effects of waste-rock contact
YSCP72	High dissolved silica content of waters enhances corrosion of cladding	2.1.02.18.0A	Enhanced corrosion of cladding from dissolved silica

Table F-3. Cross Reference of Source FEPs to TSPA-LA FEPs (Continued)

Source FEP No.	Source FEP Name	TSPA-LA FEP Number	TSPA-LA FEP Name
YSCP73	Formation of pseudo-colloids (natural) in waste and EBS	2.1.09.16.0A	Formation of pseudo-colloids (natural) in EBS
YSCP74	Colloidal phases are produced by coprecipitation (in waste and EBS)	2.1.09.25.0A	Formation of colloids (waste-form) by co-precipitation in EBS
YSCP75	Alteration of minerals to clays (in geosphere)	2.2.10.06.0A	Thermo-chemical alteration in the UZ (solubility, speciation, phase changes)
YSCP77	Precipitates from dissolved constituents of tuff and repository materials form by evaporation during thermal period	2.2.10.06.0A	Thermo-chemical alteration in the UZ (solubility, speciation, phase changes)
YSCP78	Redissolution of precipitates directs more corrosive fluids to containers	2.2.08.04.0A	Re-dissolution of precipitates directs more corrosive fluids to waste packages
		2.2.08.03.0A	Geochemical interactions and evolution in the SZ
YSCP8	Ephemeral stream erosion cuts Tiva Canyon units to underlying nonwelded units	1.2.07.01.0A	Erosion/denudation
YSCP80	Heat-induced chemical reactions plug small fractures; flow is preferentially redirected to large fractures	2.2.10.06.0A	Thermo-chemical alteration in the UZ (solubility, speciation, phase changes)
YSCP81	Calcite precipitation in hot region produces fluids depleted in calcite which dissolve calcite below the repository	2.2.10.06.0A	Thermo-chemical alteration in the UZ (solubility, speciation, phase changes)
YSCP82	Microbial activity accelerates corrosion of containers	2.1.10.01.0A	Microbial activity in EBS
YSCP83	Microbial activity accelerates corrosion of cladding	2.1.10.01.0A	Microbial activity in EBS
YSCP84	Microbial activity accelerates corrosion of contaminants	2.1.10.01.0A	Microbial activity in EBS
YSCP85	Flooding occurs in Drill Hole Wash and increases percolation below the wash	2.3.11.02.0A	Surface runoff and evapotranspiration
YSCP86	Faulting at the surface produces a scarp causing an impoundment	2.3.11.02.0A	Surface runoff and evapotranspiration
YSCP87	Volcanic activity in the vicinity produces an impoundment	1.2.10.02.0A	Hydrologic response to igneous activity
YSCP88	Surface water impoundment is constructed near the site, increasing percolation	1.4.07.01.0A	Water management activities
YSCP89	Fault creep causes short term fluctuations of the water table	1.2.10.01.0A	Hydrologic response to seismic activity
YSCP9	Runoff to washes infiltrates and maintains a zone of higher flux to the UZ	2.3.11.02.0A	Surface runoff and evapotranspiration
		2.3.11.03.0A	Infiltration and recharge
YSCP90	Igneous intrusion into repository	1.2.04.03.0A	Igneous intrusion into repository
YSCP90a	Sill intrudes repository openings	1.2.04.03.0A	Igneous intrusion into repository
YSCP91	Igneous activity causes changes to rock properties	1.2.04.02.0A	Igneous activity changes rock properties

Table F-3. Cross Reference of Source FEPs to TSPA-LA FEPs (Continued)

Source FEP No.	Source FEP Name	TSPA-LA FEP Number	TSPA-LA FEP Name
YSCP92	Igneous activity causes extreme changes to rock geochemical properties	1.2.04.02.0A	Igneous activity changes rock properties
YSCP93	Hydrologic response to igneous activity	1.2.10.02.0A	Hydrologic response to igneous activity
YSCP94	Fault movement pumps fluid from SZ to UZ (seismic pumping)	1.2.10.01.0A	Hydrologic response to seismic activity
YSCP95	Tectonic changes to local geothermal flux causes convective flow in SZ and elevates water table	1.2.01.01.0A	Tectonic activity - large scale
YSCP96	Tectonic folding alters dip of tuff beds, changing percolation flux	1.2.01.01.0A	Tectonic activity – large scale
YSCP97	Uplift or subsidence changes drainage at the site, increasing infiltration	1.2.01.01.0A	Tectonic activity – large scale
YSCP98	Folding, uplift or subsidence lowers facility w/r/t current water table	1.2.01.01.0A	Tectonic activity – large scale
YSCP99	Effects of subsidence	2.2.06.04.0A	Effects of subsidence

Source: Technical Product Output DTN: MO0706SPAFEPLA.001.

Table F-4. Direct Inputs for Appendix F

Input	Source	Description
OECD 2000. *Features, Events, and Processes (FEPs) for Geologic Disposal of Radioactive Waste: An International Database*. [DIRS 152952]	Appendix D	Source of FEPs to be considered for Yucca Mountain

Table F-5. Indirect Inputs for Appendix F

Citation	Title	DIRS
BSC 2005	*Development of the Total System Performance Assessment-License Application Features, Events, and Processes*	173800
Freeze et al. 2001	*The Development of Information Catalogued in REV00 of the YMP FEP Database*	154365

INTENTIONALLY LEFT BLANK

APPENDIX G

CROSS-REFERENCE BETWEEN YMP LICENSE APPLICATION FEPS AND SITE RECOMMENDATION FEPS

G1. INTRODUCTION

The iterative process for FEP analysis was initiated to support TSPA-SR and continued through the TSPA-LA. For TSPA-SR, an initial list of FEPs relevant to Yucca Mountain was developed from a comprehensive list of FEPs from radioactive waste disposal programs in other countries (Freeze et al. 2001 [DIRS 154365], Section 2.1) and was supplemented with additional YMP-specific FEPs from YMP literature, technical workshops, and reviews (Freeze et al. 2001 [DIRS 154365], Sections 2.2 to 2.4).

The all-inclusive TSPA-SR FEP identification approach produced 1,656 specific FEPs and 152 associated classifications (derived from Version 1.0 of the NEA International FEP Database (SAM 1997 [DIRS 139333]) and from YMP-specific information), and resulted in considerable redundancy in the FEPs list because the same FEPs were frequently identified by multiple sources. To eliminate the redundancy and to create a more efficient aggregation of FEPs to carry forward into the TSPA-SR screening process, each of the 1,808 FEP entries was subjected to a classification process (Freeze et al. 2001 [DIRS 154365], Section 3.2). After further refinement, this classification process produced a list of 328 primary FEPs. Each of these primary FEPs encompassed a single process or event or a few closely related or coupled processes or events that could be addressed by a specific screening decision (BSC 2005 [DIRS 173800], Section 3).

The NRC and other agencies reviewed the list of FEPs and presented a number of recommendations for improvement. One specific recommendation was to eliminate all FEPs with multiple (that is, included and excluded) screening decisions. Another enhancement was to eliminate the secondary FEPs after ensuring that the concepts represented by them were included in FEPs on the TSPA-LA FEP list.

The cross-reference tables (Tables G-1 and G-2) present the relationship between the TSPA-LA FEPs and the TSPA-SR FEPs (primary and secondary). The cross-referencing from TSPA-LA FEPs to TSPA-SR FEPs (Table G-1) shows that the TSPA-LA FEP addressed issues contained within the TSPA-SR FEP(s). The cross-referencing from TSPA-SR FEPs to TSPA-LA FEPs (Table G-2) indicates that the aggregate of all TSPA-LA FEPs tied to that specific TSPA-SR FEP addresses all the major issues raised by the TSPA-SR FEP.

These tables are provided to assist in demonstrating that the TSPA-LA FEP list is complete and comprehensive.

Table G-1. Cross-Reference of TSPA-LA FEPs to TSPA-SR FEPs

LA FEP Number	LA FEP Name	SR FEP Number	SR FEP Name
0.1.02.00.0A	Timescales of Concern	0.1.02.00.00	Timescales of Concern
0.1.03.00.0A	Spatial Domain of Concern	0.1.03.00.00	Spatial Domain of Concern
0.1.09.00.0A	Regulatory Requirements and Exclusions	0.1.09.00.00	Regulatory Requirements and Exclusions
		0.1.09.00.01	Assessment Basis FEP
		0.1.09.00.02	Assessment Basis FEP (Atmospheric Processes)
0.1.10.00.0A	Model and Data Issues	0.1.10.00.00	Model and Data Issues
		0.1.10.00.01	Boundary Conditions
		0.1.10.00.02	Uncertainties (Repository)
		0.1.10.00.03	Correlation
		0.1.10.00.04	Uncertainties (Geosphere)
		0.1.10.00.05	Correlation
		0.1.10.00.06	Uncertainties (Biosphere)
		0.1.10.00.07	Model and Data Issues
		0.1.10.00.08	Unmodeled Design Features
		0.1.10.00.09	Disposal Geometry
		0.1.10.00.10	Conceptual Model - Hydrology
		0.1.10.00.11	Correlation (Contaminant Speciation and Solubility)
1.1.01.01.0A	Open Site Investigation Boreholes	1.1.01.01.00	Open Site Investigation Boreholes
		1.1.01.01.01	Exploratory Boreholes (Sealing)
		1.1.01.01.02	Investigation Boreholes
		1.1.01.01.03	Underground Boreholes
		1.1.01.02.00	Loss of Integrity of Borehole Seals
		1.1.01.02.01	Investigation Borehole Seal Failure and Degradation
		1.1.04.01.00	Incomplete Closure
		1.4.04.02.00	Abandoned and Undetected Boreholes
		1.4.04.02.01	Exploratory Borehole Creates Flow Pathway
		1.4.04.02.02	Container Lies in the Trace of an Old Borehole
		1.4.04.02.03	Waste-Induced Borehole Flow (In Waste and EBS)
		1.4.04.02.04	Flow Through Undetected Boreholes
		1.4.04.02.05	Natural Borehole Fluid Flow
		1.4.04.02.06	Borehole-Induced Mineralization
		1.4.04.02.07	Borehole-Induced Geochemical Changes
1.1.01.01.0B	Influx Through Holes Drilled in Drift Wall or Crown	1.1.01.01.00	Open Site Investigation Boreholes

Table G-1. Cross-Reference of TSPA-LA FEPs to TSPA-SR FEPs (Continued)

LA FEP Number	LA FEP Name	SR FEP Number	SR FEP Name
1.1.02.00.0A	Chemical Effects of Excavation and Construction in EBS	1.1.02.00.00	Excavation/Construction
		1.1.02.00.02	Geochemical Alteration (Excavation)
		1.1.02.00.03	Groundwater Chemistry (Excavation)
		1.1.02.00.04	Influx of Oxidizing Water
		1.1.02.00.05	Influx of Oxidizing Water
		2.1.08.08.00	Induced Hydrological Changes in the Waste and EBS
		2.2.08.01.13	Change of Groundwater Chemistry in Nearby Rock
1.1.02.00.0B	Mechanical Effects of Excavation and Construction in EBS	1.1.02.00.00	Excavation/Construction
		1.1.02.00.01	Blasting and Vibration
		2.1.08.08.00	Induced Hydrological Changes in the Waste and EBS
		2.2.01.01.08	Creeping of Rock Mass, Near-Field
		2.2.01.01.11	Excavation-Induced Changes in Stress
1.1.02.01.0A	Site Flooding (During Construction and Operation)	1.1.02.01.00	Site Flooding (During Construction and Operation)
		1.1.02.01.01	Repository Flooding During Operation
1.1.02.02.0A	Preclosure Ventilation	1.1.02.02.00	Effects of Pre-Closure Ventilation
		2.2.10.01.02	Temperature, Near-Field Rock
1.1.02.03.0A	Undesirable Materials Left	1.1.02.03.00	Undesirable Materials Left
		1.1.02.03.01	Decontamination Materials Left
		1.1.02.03.02	Inadvertent Inclusion of Undesirable Materials
		1.1.12.01.06	Oil or Organic Fluid Spill
		2.1.04.06.10	Organics/Contamination of Bentonite
1.1.03.01.0A	Error in Waste Emplacement	1.1.03.01.00	Error in Waste or Backfill Emplacement
		1.1.03.01.02	Containers Are Improperly Placed - on Drift Floor
		1.1.03.01.03	Containers Are Placed Too Close Together
		1.1.03.01.04	Emplacement Error - Containers Placed in Wet Zone
1.1.03.01.0B	Error in Backfill Emplacement	1.1.03.01.01	Inadequate Backfill or Compaction, Voidage
		2.1.04.02.02	Inhomogeneities (Properties and Evolution) (In Buffer/Backfill)
		2.1.04.02.07	Backfill Materials Deficiencies
		2.1.04.06.08	Quality Control (In Buffer/Backfill)
		2.1.04.06.09	Poor Emplacement of Buffer

Table G-1. Cross-Reference of TSPA-LA FEPs to TSPA-SR FEPs (Continued)

LA FEP Number	LA FEP Name	SR FEP Number	SR FEP Name
1.1.03.01.0B	Error in Backfill Emplacement (continued)	2.1.04.06.10	Organics/Contamination of Bentonite
		2.1.04.06.23	Bentonite Emplacement and Composition
		2.1.04.07.03	Faulty Buffer Emplacement
1.1.04.01.0A	Incomplete Closure	1.1.04.01.00	Incomplete Closure
		1.1.04.01.01	Vault Closure (Geosphere)
		1.1.04.01.02	Non-Sealed Repository
		1.1.04.01.03	Poor Closure
		1.1.04.01.04	Abandonment of Unsealed Repository
		1.1.04.01.05	Unsealed Boreholes And/Or Shafts
		1.1.04.01.06	Operation and Closure
		1.4.04.02.00	Abandoned and Undetected Boreholes
		1.4.04.02.04	Flow Through Undetected Boreholes
1.1.05.00.0A	Records and Markers For the Repository	1.1.05.00.00	Records and Markers, Repository
		1.1.05.00.01	Loss of Records
		1.1.05.00.02	Repository Records, Markers
		1.1.05.00.03	Loss of Records
		1.1.05.00.04	Loss of Records
1.1.07.00.0A	Repository Design	1.1.07.00.00	Repository Design
		1.1.07.00.01	Poorly Designed Repository
		1.1.07.00.02	Design Modification
		1.1.07.00.03	HLW Panels (Siting)
		1.1.07.00.04	TRU Silos (Siting)
		1.1.07.00.05	Access Tunnels and Shafts
		1.1.07.00.06	Design and Construction FEPs
		1.1.07.00.07	Design and Construction
		1.1.07.00.08	Design and Construction FEPs
1.1.08.00.0A	Inadequate Quality Control and Deviations from Design	1.1.08.00.00	Quality Control
		1.1.08.00.01	Poorly Constructed Repository
		1.1.08.00.02	Material Defects
		1.1.08.00.03	Common Cause Failures
		1.1.08.00.04	Poor Quality Construction
		1.1.08.00.05	Quality Control
		1.1.08.00.06	Quality Control
		1.1.08.00.07	Drains, Installed to Divert Water Around Containers, Are Improperly Placed

Table G-1. Cross-Reference of TSPA-LA FEPs to TSPA-SR FEPs (Continued)

LA FEP Number	LA FEP Name	SR FEP Number	SR FEP Name
1.1.09.00.0A	Schedule and Planning	1.1.09.00.00	Schedule and Planning
		1.1.09.00.01	Effects of Phased Operation
1.1.10.00.0A	Administrative Control of the Repository Site	1.1.10.00.00	Administrative Control, Repository Site
		1.1.10.00.01	Planning Restrictions
1.1.11.00.0A	Monitoring of the Repository	1.1.11.00.00	Monitoring of Repository
		1.1.11.00.01	Monitoring and Remedial Activities
		1.1.11.00.02	Postclosure Monitoring
		1.1.11.00.03	Post-Closure Monitoring
		1.1.11.00.04	Postclosure Monitoring
		1.4.04.02.00	Abandoned and Undetected Boreholes
1.1.12.01.0A	Accidents and Unplanned Events During Construction and Operation	1.1.12.01.00	Accidents and Unplanned Events During Operation
		1.1.12.01.01	Preclosure Events
		1.1.12.01.02	Sabotage and Improper Operation
		1.1.12.01.03	Accidents During Operation
		1.1.12.01.04	Accidents During Operation
		1.1.12.01.05	Handling Accidents
		1.1.12.01.06	Oil or Organic Fluid Spill
1.1.13.00.0A	Retrievability	1.1.13.00.00	Retrievability
		1.1.13.00.01	Retrievability
1.2.01.01.0A	Tectonic Activity - Large Scale	1.2.01.01.00	Tectonic Activity - Large Scale
		1.2.01.01.01	Folding, Uplift or Subsidence Lowers Facility W/R/T Current Water Table
		1.2.01.01.02	Tectonic Changes to Local Geothermal Flux Causes Convective Flow in SZ and Elevates Water Table
		1.2.01.01.03	Tectonic Folding Alters Dip of Tuff Beds, Changing Percolation Flux
		1.2.01.01.04	Uplift or Subsidence Changes Drainage At the Site, Increasing Infiltration
		1.2.01.01.05	Uplift and Subsidence
		1.2.01.01.06	Effect of Plate Movements
		1.2.01.01.07	Plate Movement/Tectonic Change
		1.2.01.01.08	Uplift and Subsidence
		1.2.01.01.09	Regional Vertical Movements
		1.2.01.01.10	Regional Tectonic Activity

Table G-1. Cross-Reference of TSPA-LA FEPs to TSPA-SR FEPs (Continued)

LA FEP Number	LA FEP Name	SR FEP Number	SR FEP Name
1.2.01.01.0A	Tectonic Activity - Large Scale (continued)	1.2.01.01.11	Regional Tectonics
		1.2.01.01.12	Regional Horizontal Movements
		1.2.01.01.13	Regional Uplift and Subsidence
		1.2.01.01.14	Geological (Events)
1.2.02.01.0A	Fractures	1.2.02.01.00	Fractures
		1.2.02.01.01	Changes in Fracture Properties
		1.2.02.01.02	Fracturing
		1.2.03.01.02	Earthquakes
1.2.02.02.0A	Faults	1.2.02.02.00	Faulting
		1.2.02.02.01	Faulting
		1.2.02.02.02	Fault Generation
		1.2.02.02.03	Fault Activation
		1.2.02.02.04	Movements Along Small-Scale Faults
		1.2.02.02.05	Faulting/Fracturing
		1.2.02.02.06	Formation of New Faults
		1.2.02.02.07	Fault Movement
		1.2.02.02.08	Normal Faulting Occurs or Exists at Yucca Mountain
		1.2.02.02.09	Strike/Slip Faulting Occurs or Exists at Yucca Mountain.
		1.2.02.02.10	Detachment Faulting Occurs or Exists at Yucca Mountain
		1.2.02.02.11	Dip/Slip Faulting Occurs at Yucca Mountain
		1.2.02.02.12	New Fault Occurs at Yucca Mountain
		1.2.02.02.13	Old Fault Strand Is Reactivated at Yucca Mountain
		1.2.02.02.14	New Fault Strand Is Activated at Yucca Mountain
		1.2.02.02.15	Movements Along Major Faults
		1.2.02.02.16	Faulting (Large Scale, in Geosphere)
		1.2.02.02.17	Faulting Exhumes Waste Container
		1.2.04.01.01	Volcanism
1.2.02.03.0A	Fault Displacement Damages EBS Components	1.2.02.03.00	Fault Movement Shears Waste Container
		1.2.03.01.06	Seismicity
1.2.03.02.0A	Seismic Ground Motion Damages EBS Components	1.2.03.01.00	Seismic Activity
		1.2.03.01.01	Earthquakes
		1.2.03.01.03	Earthquakes
		1.2.03.01.04	Seismicity

Table G-1. Cross-Reference of TSPA-LA FEPs to TSPA-SR FEPs (Continued)

LA FEP Number	LA FEP Name	SR FEP Number	SR FEP Name
1.2.03.02.0A	Seismic Ground Motion Damages EBS Components (continued)	1.2.03.01.05	Seismicity
		1.2.03.01.07	Seismic Activity
		1.2.03.02.00	Seismic Vibration Causes Container Failure
		1.2.03.02.01	Container Failure Induced by Microseisms Associated With Dike Emplacement
1.2.03.02.0B	Seismic-Induced Rockfall Damages EBS Components	1.2.03.01.00	Seismic Activity
		1.2.03.01.01	Earthquakes
		1.2.03.01.03	Earthquakes
		1.2.03.01.04	Seismicity
		1.2.03.01.05	Seismicity
		1.2.03.01.07	Seismic Activity
		1.2.03.02.00	Seismic Vibration Causes Container Failure
		2.1.07.01.00	Rockfall (Large Block) Wfclad--Rockfall
1.2.03.02.0C	Seismic-Induced Drift Collapse Damages EBS Components	1.2.03.01.00	Seismic Activity
		2.1.07.02.00	Mechanical Degradation or Collapse of Drift
		2.1.07.02.02	Mechanical (Events and Processes in the Waste and EBS)
		2.1.07.02.04	Rockfall (Rubble) (In Waste and EBS)
1.2.03.02.0D	Seismic-Induced Drift Collapse Alters In-Drift Thermohydrology	2.1.07.02.00	Mechanical Degradation or Collapse of Drift
		2.1.07.02.02	Mechanical (Events and Processes in the Waste and EBS)
		2.1.07.02.04	Rockfall (Rubble) (In Waste and EBS)
1.2.03.02.0E	Seismic-Induced Drift Collapse Alters In-Drift Chemistry	2.1.07.02.00	Mechanical Degradation or Collapse of Drift
		2.1.07.02.02	Mechanical (Events and Processes in the Waste and EBS)
		2.1.07.02.04	Rockfall (Rubble) (In Waste and EBS)
1.2.03.03.0A	Seismicity Associated With Igneous Activity	1.2.03.02.01	Container Failure Induced by Microseisms Associated With Dike Emplacement
		1.2.03.03.00	Seismicity Associated With Igneous Activity

Table G-1. Cross-Reference of TSPA-LA FEPs to TSPA-SR FEPs (Continued)

LA FEP Number	LA FEP Name	SR FEP Number	SR FEP Name
1.2.04.02.0A	Igneous Activity Changes Rock Properties	1.2.04.01.01	Volcanism
		1.2.04.01.02	Magmatic Activity
		1.2.04.01.03	Magmatic Activity
		1.2.04.01.05	Volcanic Activity
		1.2.04.02.00	Igneous Activity Causes Changes to Rock Properties
		1.2.04.02.01	Dike Provides a Permeable Flow Path
		1.2.04.02.02	Dike Provides a Barrier to Flow
		1.2.04.02.04	Igneous Activity Causes Extreme Changes to Rock Geochemical Properties
		1.2.04.02.05	Intrusion (Magmatic)
		1.2.04.02.06	Dike Related Fractures Alter Flow
		1.2.04.02.07	Magmatic Activity
		2.1.11.07.00	Thermally-Induced Stress Changes in Waste and EBS
1.2.04.03.0A	Igneous Intrusion Into Repository	1.2.04.01.00	Igneous Activity
		1.2.04.01.02	Magmatic Activity
		1.2.04.01.03	Magmatic Activity
		1.2.04.03.00	Igneous Intrusion Into Repository
		1.2.04.03.01	Sill Provides a Permeable Flow Path
		1.2.04.03.02	Sill Provides a Flow Barrier
		1.2.04.03.03	Sill Intrudes Repository Openings
		1.2.04.03.04	Volcanism
		1.2.04.03.05	Intruding Dikes
		1.2.04.04.00	Magma Interacts With Waste
		1.2.04.04.01	Magmatic Volatiles Attack Waste
1.2.04.04.0A	Igneous Intrusion Interacts With EBS Components	1.2.04.01.00	Igneous Activity
		1.2.04.01.01	Volcanism
		1.2.04.04.00	Magma Interacts With Waste
		1.2.04.04.04	Heating of Waste Container by Magma (Without Contact)
		1.2.04.04.05	Failure of Waste Container by Direct Contact W/Magma
		1.2.04.04.06	Fragmentation
		2.1.11.04.02	Temperature Effects (Unexpected Effects) (In Waste and EBS)
1.2.04.04.0B	Chemical Effects of Magma and Magmatic Volatiles	1.2.04.04.00	Magma Interacts With Waste
		1.2.04.04.01	Magmatic Volatiles Attack Waste

Table G-1. Cross-Reference of TSPA-LA FEPs to TSPA-SR FEPs (Continued)

LA FEP Number	LA FEP Name	SR FEP Number	SR FEP Name
1.2.04.05.0A	Magma or Pyroclastic Base Surge Transports Waste	1.2.04.01.00	Igneous Activity
		1.2.04.04.00	Magma Interacts With Waste
		1.2.04.04.02	Dissolution of Spent Fuel in Magma
		1.2.04.04.03	Dissolution of Other Waste in Magma
		1.2.04.05.00	Magmatic Transport of Waste
		1.2.04.05.01	Direct Exposure of Waste in Dike Apron
		1.2.04.05.02	Volatile Radionuclides Plate Out in the Surrounding Rock
		1.2.04.05.03	Entrainment of SNF in a Flowing Dike
1.2.04.06.0A	Eruptive Conduit to Surface Intersects Repository	1.2.04.01.04	Magmatic Activity
		1.2.04.06.00	Basaltic Cinder Cone Erupts Through the Repository
		1.2.04.06.01	Vent Jump
		1.2.04.06.02	Vent Erosion
1.2.04.07.0A	Ashfall	1.2.04.07.00	Ashfall
		3.2.10.00.00	Atmospheric Transport of Contaminants
1.2.04.07.0B	Ash Redistribution in Groundwater	1.2.04.07.01	Soil Leaching Following Ashfall
		3.2.10.00.00	Atmospheric Transport of Contaminants
1.2.04.07.0C	Ash Redistribution via Soil and Sediment Transport	1.2.04.07.01	Soil Leaching Following Ashfall
		3.2.10.00.00	Atmospheric Transport of Contaminants
1.2.05.00.0A	Metamorphism	1.2.05.00.00	Metamorphism
		1.2.05.00.01	Metamorphic Activity
		1.2.05.00.02	Regional Metamorphism
		1.2.05.00.03	Metamorphic Activity
		1.2.05.00.04	Metamorphic Activity
1.2.06.00.0A	Hydrothermal Activity	1.2.06.00.00	Hydrothermal Activity
		1.2.06.00.01	Hydrothermal Activity
		2.1.11.07.00	Thermally-Induced Stress Changes in Waste and EBS
1.2.07.01.0A	Erosion/Denudation	1.2.07.01.00	Erosion/Denudation
		1.2.07.01.01	Major Incision
		1.2.07.01.02	Generalized Denudation
		1.2.07.01.03	Localized Denudation
		1.2.07.01.04	Solid Discharge via Erosional Processes
		1.2.07.01.05	Basement Alteration

Table G-1. Cross-Reference of TSPA-LA FEPs to TSPA-SR FEPs (Continued)

LA FEP Number	LA FEP Name	SR FEP Number	SR FEP Name
1.2.07.01.0A	Erosion/Denudation (continued)	1.2.07.01.06	Hydraulic Gradient Changes (Magnitude, Direction) (In Geosphere)
		1.2.07.01.07	Hydraulic Gradient Changes (Magnitude, Direction)
		1.2.07.01.08	Ephemeral Stream Erosion Cuts Tiva Canyon Units to Underlying Nonwelded Units
		1.2.07.01.09	Land Slide
		1.2.07.01.10	Stream Erosion of Amargosa River Lowers Base Levels and Increases Gradient in SZ
		1.2.07.01.11	Erosion
		1.2.07.01.12	Erosion - Lateral Transport
		1.2.07.01.13	Erosion (Wind)
		1.2.07.01.14	Erosion on Surface/Sediments
		1.2.07.01.15	Denudation
		1.2.07.01.16	River, Stream Channel Erosion
		1.2.07.01.17	Chemical Denudation and Weathering
		1.2.07.01.18	Erosion
		1.2.07.01.19	Erosion/Deposition
		1.2.07.01.20	Fluvial Erosion/Sedimentation
		1.2.07.01.21	Surface Denudation
		1.2.07.01.22	Chemical Weathering
		1.2.07.01.23	Aeolian Erosion
		1.2.07.01.24	Fluvial Erosion
		1.2.07.01.25	Mass Wasting
		1.2.07.01.26	Mass Wasting
		1.2.07.01.27	Mechanical Weathering
1.2.07.02.0A	Deposition	1.2.07.02.00	Deposition
		1.2.07.02.01	Aeolian Deposition
		1.2.07.02.02	Lacustrine Deposition
1.2.08.00.0A	Diagenesis	1.2.08.00.00	Diagenesis
		1.2.08.00.01	Diagenesis
		1.2.08.00.02	Diagenesis
		1.2.08.00.03	Fracture Infills
		1.2.08.00.04	Diagenesis
1.2.09.00.0A	Salt Diapirism and Dissolution	1.2.09.00.00	Salt Diapirism and Dissolution
1.2.09.01.0A	Diapirism	1.2.09.01.00	Diapirism
		1.2.09.01.01	Diapirism
		1.2.09.01.02	Salt Deformation
		1.2.09.01.03	Diapirism

Table G-1. Cross-Reference of TSPA-LA FEPs to TSPA-SR FEPs (Continued)

LA FEP Number	LA FEP Name	SR FEP Number	SR FEP Name
1.2.09.02.0A	Large-Scale Dissolution	1.2.09.02.00	Large-Scale Dissolution
		1.2.09.02.01	Shallow Dissolution
		1.2.09.02.02	Lateral Dissolution
		1.2.09.02.03	Solution Chimneys
		1.2.09.02.04	Breccia Pipes
		1.2.09.02.05	Collapse Breccias
1.2.10.01.0A	Hydrologic Response to Seismic Activity	1.2.03.01.00	Seismic Activity
		1.2.10.01.00	Hydrological Response to Seismic Activity
		1.2.10.01.01	Fault Movement Pumps Fluid from SZ to UZ (Seismic Pumping)
		1.2.10.01.02	Fault Creep Causes Short Term Fluctuations of the Water Table
		1.2.10.01.03	New Faulting Breaches Flow Barrier Controlling Large Hydraulic Gradient to the North
		1.2.10.01.04	Normal Faulting Produces a Trap For Laterally Moving Moisture in the Tiva Canyon Unit
		1.2.10.01.05	Head-Driven Flow Up from Carbonates
		1.2.10.01.06	Seismically-Induced Water Table Changes
		1.2.10.01.07	Fault Pathway Through the Altered Topopah Spring Basal Vitrophyre
		1.2.10.01.08	Fault Movement Connects Tuff and Carbonate Aquifers
		1.2.10.01.09	Fault Establishes Pathway Through the UZ
		1.2.10.01.10	Fault Establishes Pathway Through the SZ
		1.2.10.01.11	Fluid Supplied by a Fault Migrates Down the Drift
		1.2.10.01.12	Fault Intersects and Drains Condensate Zone
		1.2.10.01.13	Flow Barrier South of Site Blocks Flow, Causing Water Table to Rise
		1.3.07.02.01	Short Circuit of a Flow Barrier in the Saturated Zone Because of a Water Table Rise
		1.4.01.01.05	Climate Modification Raises Water Table to Short Circuit Flow Barrier in SZ
		2.1.08.08.00	Induced Hydrological Changes in the Waste and EBS

Table G-1. Cross-Reference of TSPA-LA FEPs to TSPA-SR FEPs (Continued)

LA FEP Number	LA FEP Name	SR FEP Number	SR FEP Name
1.2.10.02.0A	Hydrologic Response to Igneous Activity	1.2.04.01.00	Igneous Activity
		1.2.04.01.01	Volcanism
		1.2.04.01.02	Magmatic Activity
		1.2.04.02.03	Volcanic Activity in the Vicinity Produces an Impoundment
		1.2.10.02.00	Hydrologic Response to Igneous Activity
		1.2.10.02.01	Interaction of WT With Magma
		1.2.10.02.02	Interaction of UZ Pore Water With Magma
		1.3.07.02.01	Short Circuit of a Flow Barrier in the Saturated Zone Because of a Water Table Rise
		1.4.01.01.05	Climate Modification Raises Water Table to Short Circuit Flow Barrier in SZ
		2.1.08.08.00	Induced Hydrological Changes in the Waste and EBS
1.3.01.00.0A	Climate Change	1.3.01.00.00	Climate Change, Global
		1.3.01.00.01	Climate Change
		1.3.01.00.02	No Ice Age
		1.3.01.00.03	Solar Insolation
		1.3.01.00.04	No Ice Age
		1.3.01.00.05	Climate Change: Natural
		1.3.01.00.06	Exit from Glacial/Interglacial Cycling
		1.3.01.00.07	Intensification of Natural Climate Change
		1.3.01.00.08	Climatological (Effects)
		1.3.01.00.09	Climate Change
		1.3.01.00.10	Present-Day Climatic Conditions
		1.3.01.00.11	Seasonality of Climate
		1.3.01.00.12	Future Climatic Conditions
		1.3.01.00.13	Warmer Climate - Arid
		1.3.01.00.14	Warmer Climate - Seasonal Humid
		1.3.01.00.15	Warmer Climate - Equable Humid
		1.3.01.00.16	Climate Change (Effects on Repository)
		1.3.01.00.17	Global Effects
		1.3.01.00.18	Climate (Meteorology)
		1.3.01.00.19	Seasons (Meteorology)
		1.3.01.00.20	Temperature (Meteorology)
		1.3.01.00.21	Climate Change (Meteorology)

Table G-1. Cross-Reference of TSPA-LA FEPs to TSPA-SR FEPs (Continued)

LA FEP Number	LA FEP Name	SR FEP Number	SR FEP Name
1.3.01.00.0A	Climate Change (continued)	1.3.07.01.01	Desert and Unsaturation
		1.3.07.01.02	Dust Storms and Desertification
		2.3.11.03.14	Effective Moisture (Recharge)
1.3.04.00.0A	Periglacial Effects	1.3.04.00.00	Periglacial Effects
		1.3.04.00.01	Permafrost
		1.3.04.00.02	Accumulation of Gases Under Permafrost
		1.3.04.00.03	Periglacial Effects
		1.3.04.00.04	Frost Weathering
		1.3.04.00.05	Solifluction
		1.3.04.00.06	Tundra Climate
		1.3.04.00.07	Permafrost
		1.3.04.00.08	Permafrost
		1.3.04.00.09	Permafrost
1.3.05.00.0A	Glacial and Ice Sheet Effect	1.2.07.01.01	Major Incision
		1.3.05.00.00	Glacial and Ice Sheet Effects, Local
		1.3.05.00.01	Glaciation
		1.3.05.00.02	Glaciation
		1.3.05.00.03	Glaciation
		1.3.05.00.04	Glaciation
		1.3.05.00.05	Glacial Climate
		1.3.05.00.06	Glacial Erosion/Sedimentation
		1.3.05.00.07	Glacial-Fluvial Erosion/Sedimentation
		1.3.05.00.08	Ice Sheet Effects (Loading, Melt Water Recharge)
		1.3.05.00.09	Glaciation
		1.3.05.00.10	Glaciation
		1.3.05.00.11	Glaciation
		1.3.05.00.12	Isostatic Rebound
1.3.07.01.0A	Water Table Decline	1.3.07.01.00	Drought / Water Table Decline
		1.3.07.01.01	Desert and Unsaturation
		1.3.07.01.02	Dust Storms and Desertification
1.3.07.02.0A	Water Table Rise Affects SZ	1.3.07.02.00	Water Table Rise
		1.3.07.02.01	Short Circuit of a Flow Barrier in the Saturated Zone Because of a Water Table Rise
		1.4.01.01.03	Climate Modification Raises Water Table
		1.4.01.01.04	Climate Modification Raises Water Table to Flood Repository

Table G-1. Cross-Reference of TSPA-LA FEPs to TSPA-SR FEPs (Continued)

LA FEP Number	LA FEP Name	SR FEP Number	SR FEP Name
1.3.07.02.0A	Water Table Rise Affects SZ (continued)	1.4.01.01.05	Climate Modification Raises Water Table to Short Circuit Flow Barrier in SZ
		2.3.11.03.01	Freshwater Intrusion (In Geosphere)
1.3.07.02.0B	Water Table Rise Affects UZ	1.1.02.01.00	Site Flooding (During Construction and Operation)
		1.3.07.02.00	Water Table Rise
		2.2.07.03.00	Capillary Rise
1.4.01.00.0A	Human Influences on Climate	1.4.01.00.00	Human Influences on Climate
		1.4.01.00.01	Human-Induced Climate Change
		1.4.01.00.02	Anthropogenic Climate Change
		1.4.01.00.03	Human-Induced Climate Change
		1.4.01.00.04	Climate Change: Human Induced
1.4.01.01.0A	Climate Modification Increases Recharge	1.4.01.01.00	Climate Modification Increases Recharge
		1.4.01.01.01	Climate Modification Causes Perched Water to Develop at Base of Topopah Spring Unit
		1.4.01.01.02	Climate Modification Causes Perched Water to Develop Above Repository
		1.4.01.01.03	Climate Modification Raises Water Table
		1.4.01.01.04	Climate Modification Raises Water Table to Flood Repository
		1.4.01.01.05	Climate Modification Raises Water Table to Short Circuit Flow Barrier in SZ
1.4.01.02.0A	Greenhouse Gas Effects	1.4.01.02.00	Greenhouse Gas Effects
		1.4.01.02.01	Greenhouse Effect
		1.4.01.02.02	Greenhouse Gas Effects
		1.4.01.02.03	Greenhouse Effect
1.4.01.03.0A	Acid Rain	1.4.01.03.00	Acid Rain
		1.4.01.03.01	Acid Rain
		1.4.01.03.02	Surface Water Ph
		2.3.04.01.00	Surface Water Transport and Mixing
1.4.01.04.0A	Ozone Layer Failure	1.4.01.04.00	Ozone Layer Failure
		1.4.01.04.01	Damage to the Ozone Layer
		1.4.01.04.02	Ozone Layer
1.4.02.01.0A	Deliberate Human Intrusion	1.4.02.01.00	Deliberate Human Intrusion
		1.4.02.01.01	Chemical Sabotage
		1.4.02.01.02	Waste Retrieval, Mining
		1.4.02.01.03	Archeological Intrusion

Table G-1. Cross-Reference of TSPA-LA FEPs to TSPA-SR FEPs (Continued)

LA FEP Number	LA FEP Name	SR FEP Number	SR FEP Name
1.4.02.01.0A	Deliberate Human Intrusion (continued)	1.4.02.01.04	Recovery of Repository Materials
		1.4.02.01.05	Malicious Intrusion
		1.4.02.01.06	Archaeological Investigation
		1.4.02.01.07	Deliberate Intrusion
		1.4.02.01.08	Malicious Intrusion
		1.4.02.01.09	Deliberate Drilling Intrusion
		1.4.02.01.10	Archeological Investigations
		1.4.02.01.11	Post-Closure Subsurface Activities (Intrusion)
		1.4.02.01.12	Intrusion Into Accumulation Zone in the Biosphere
		1.4.02.01.13	Unsuccessful Attempt of Site Improvement
		1.4.02.01.14	Sabotage
		1.4.02.01.15	Sabotage
		1.4.02.01.16	Sudden Energy Release (In Waste and EBS)
		1.4.02.01.17	Other Future Uses of Crystalline Rock
		1.4.02.01.18	Intrusion (Human)
		3.3.06.01.00	Toxicity of Mined Rock
1.4.02.02.0A	Inadvertent Human Intrusion	1.4.02.02.00	Inadvertent Human Intrusion
		1.4.02.02.01	Accidental Intrusion
		3.3.06.01.00	Toxicity of Mined Rock
1.4.02.03.0A	Igneous Event Precedes Human Intrusion	1.2.04.01.00	Igneous Activity
1.4.02.04.0A	Seismic Event Precedes Human Intrusion	1.2.03.01.00	Seismic Activity
1.4.03.00.0A	Unintrusive Site Investigation	1.4.03.00.00	Un-Intrusive Site Investigation
1.4.04.00.0A	Drilling Activities (Human Intrusion)	1.4.04.00.00	Drilling Activities (Human Intrusion)
		1.4.04.00.01	Geothermal
		1.4.04.00.02	Other Resources
		1.4.04.00.03	Enhanced Oil and Gas Recovery
		1.4.04.00.04	Liquid Waste Disposal
		1.4.04.00.05	Hydrocarbon Storage
		1.4.04.00.06	Exploratory Drilling For Hydrocarbons
		1.4.04.00.07	Exploratory Drilling For Metals
		1.4.04.00.08	Boreholes - Exploration
		1.4.04.00.09	Injection of Liquid Wastes
		1.4.04.00.10	Exploratory Drilling
		1.4.04.00.11	Exploitation Drilling
		1.4.04.00.12	Exploratory Drilling

Table G-1. Cross-Reference of TSPA-LA FEPs to TSPA-SR FEPs (Continued)

LA FEP Number	LA FEP Name	SR FEP Number	SR FEP Name
1.4.04.00.0A	Drilling Activities (Human Intrusion) (continued)	1.4.04.00.13	Geothermal Exploitation
		1.4.04.00.14	Liquid Waste Injection
		1.4.04.00.15	Oil and Gas Exploration
		1.4.04.00.16	Potash Exploration
		1.4.04.00.17	Water Resource Exploration
		1.4.04.00.18	Oil and Gas Exploitation
		1.4.04.00.19	Groundwater Exploitation
		1.4.04.00.20	Geothermal Energy Production
		1.4.04.00.21	Geothermal Energy Production
		1.4.04.00.22	Borehole-Well
		1.4.04.00.23	Reuse of Boreholes
		1.4.04.00.24	Oil and Gas Extraction
		1.4.04.00.25	Liquid Waste Disposal
		1.4.04.00.26	Enhanced Oil and Gas Production
		1.4.04.00.27	Hydrocarbon Storage
		1.4.04.02.00	Abandoned and Undetected Boreholes
		3.3.06.01.00	Toxicity of Mined Rock
1.4.04.01.0A	Effects of Drilling Intrusion	1.4.04.01.00	Effects of Drilling Intrusion
		1.4.04.01.01	Drilling Fluid Interacts With Waste
		1.4.04.01.02	Drilling Introduces Surfactants
		1.4.04.01.03	Direct Exposure to Waste in Mud Pit
		1.4.04.01.04	Flooding of Drifts With Drilling Fluids
		1.4.04.01.05	Drilling Fluid Flow
		1.4.04.01.06	Drilling Fluid Loss
		1.4.04.01.07	Blowouts
		1.4.04.01.08	Drilling-Induced Geochemical Changes
		1.4.04.01.09	Fluid Injection-Induced Geochemical Changes
		1.4.04.01.10	Cuttings
		1.4.04.01.11	Cavings
		1.4.04.01.12	Spallings
		3.3.06.01.00	Toxicity of Mined Rock
1.4.05.00.0A	Mining and Other Underground Activities (Human Intrusion)	1.4.05.00.00	Mining and Other Underground Activities (Human Intrusion)
		1.4.05.00.01	Mine Shaft Intersects Waste Container
		1.4.05.00.02	A Mine Shaft Creates a Preferential Path Thru the Upper Nonwelded Unit and a Wetter Zone Develops

Table G-1. Cross-Reference of TSPA-LA FEPs to TSPA-SR FEPs (Continued)

LA FEP Number	LA FEP Name	SR FEP Number	SR FEP Name
1.4.05.00.0A	Mining and Other Underground Activities (Human Intrusion) (continued)	1.4.05.00.03	Intrusion (Mining)
		1.4.05.00.04	Mines
		1.4.05.00.05	Solution Mining
		1.4.05.00.06	Water from Mining Above the Repository Drains Through Repository.
		1.4.05.00.07	Underground Dwellings
		1.4.05.00.08	Resource Mining
		1.4.05.00.09	Tunneling
		1.4.05.00.10	Underground Construction
		1.4.05.00.11	Quarrying, Near Surface Extraction
		1.4.05.00.12	Mining Activities
		1.4.05.00.13	Potash Mining
		1.4.05.00.14	Other Resources
		1.4.05.00.15	Tunneling
		1.4.05.00.16	Construction of Underground Facilities
		1.4.05.00.17	Archaeological Excavations
		1.4.05.00.18	Deliberate Mining Intrusion
		1.4.05.00.19	Heat Storage in Lakes or Underground
		1.4.05.00.20	Changes in Groundwater Flow Due to Mining
		1.4.05.00.21	Changes in Geochemistry Due to Mining
		3.3.06.01.00	Toxicity of Mined Rock
1.4.06.01.0A	Altered Soil or Surface Water Chemistry	1.4.06.01.00	Altered Soil or Surface Water Chemistry
		1.4.06.01.01	Altered Soil or Surface Water Chemistry
		1.4.06.01.02	Groundwater Pollution
		1.4.06.01.03	Surface Pollution (Soils, Rivers)
		1.4.06.01.04	Altered Soil or Surface Water Chemistry by Human Activities
		1.4.06.01.05	Far Field Hydrochemistry – Acids, Oxidants, Nitrate
		1.4.06.01.06	Arable Farming
		2.3.04.01.00	Surface Water Transport and Mixing
1.4.07.01.0A	Water Management Activities	1.4.07.01.00	Water Management Activities
		1.4.07.01.01	Water Collection in Cisterns Over Repository
		1.4.07.01.02	Water Management of Nearby Ground Water Basins

Table G-1. Cross-Reference of TSPA-LA FEPs to TSPA-SR FEPs (Continued)

LA FEP Number	LA FEP Name	SR FEP Number	SR FEP Name
1.4.07.01.0A	Water Management Activities (continued)	1.4.07.01.03	Water Table Drawdown by Down Gradient Pumping Increases Hydraulic Gradient
		1.4.07.01.04	Surface Water Impoundment Is Constructed Near the Site, Increasing Percolation
		1.4.07.01.05	Dams
		1.4.07.01.06	Human Induced Actions on Groundwater Recharge
		1.4.07.01.07	Human-Induced Changes in Surface Hydrology
		1.4.07.01.08	Dams and Reservoirs, Built and Drained
		1.4.07.01.09	River Rechannelled
		1.4.07.01.10	Damming of Streams or Rivers
		1.4.07.01.11	Reservoirs
		1.4.07.01.12	Lake Usage
		1.4.07.01.13	Water Management Schemes
1.4.07.02.0A	Wells	1.4.07.01.00	Water Management Activities
		1.4.07.02.00	Wells
		1.4.07.02.01	Irrigation Wells in Midway Valley Increase Moisture Flux Through Repository
		1.4.07.02.02	Irrigation Wells in Midway Valley Reduce Distance to Accessible Environment
		1.4.07.02.03	Irrigation Wells in Crater Flats or Jackass Flats Increase Hydraulic Gradient Under Repository
		1.4.07.02.04	Wells (High Demand)
		1.4.07.02.05	Groundwater Abstraction
		1.4.07.02.06	Water Resource Exploitation
		1.4.07.02.07	Deep Groundwater Abstraction
		1.4.07.02.08	Water Producing Well
		1.4.07.02.09	Groundwater Extraction
1.4.07.03.0A	Recycling of Accumulated Radionuclides from Soils to Groundwater	3.3.02.03.04	Recycling (Exposure Factors)
1.4.08.00.0A	Social and Institutional Developments	1.4.08.00.00	Social and Institutional Developments
		1.4.08.00.01	Demographic Change and Urban Development
		1.4.08.00.02	City On the Site
		1.4.08.00.03	Urbanization On the Discharge Site
		1.4.08.00.04	Demographic Change, Urban Development

Table G-1. Cross-Reference of TSPA-LA FEPs to TSPA-SR FEPs (Continued)

LA FEP Number	LA FEP Name	SR FEP Number	SR FEP Name
1.4.09.00.0A	Technological Developments	1.4.09.00.00	Technological Developments
		1.4.09.00.01	Cure For Cancer
		1.4.09.00.02	Technological Advances in Food Production
1.4.11.00.0A	Explosions and Crashes (Human Activities)	1.4.11.00.00	Explosions and Crashes (Human Activities)
		1.4.11.00.01	Bomb Blast
		1.4.11.00.02	Collisions, Explosions and Impacts
		1.4.11.00.03	Underground Test of Nuclear Devices
		1.4.11.00.04	Explosions
		1.4.11.00.05	Nuclear War
		1.4.11.00.06	Underground Nuclear Testing
		1.4.11.00.07	Explosions For Resource Recovery
		1.4.11.00.08	Underground Nuclear Device Testing
		1.4.11.00.09	Changes in Groundwater Flow Due to Explosions
1.5.01.01.0A	Meteorite Impact	1.5.01.01.00	Meteorite Impact
		1.5.01.01.01	Meteorite Impact
		1.5.01.01.02	Meteorite
		1.5.01.01.03	Meteorite Impact
		1.5.01.01.04	Impact of a Large Meteorite
1.5.01.02.0A	Extraterrestrial Events	1.5.01.02.00	Extraterrestrial Events
		1.5.01.02.01	Extraterrestrial (Events)
1.5.02.00.0A	Species Evolution	1.5.02.00.00	Species Evolution
		1.5.02.00.01	Biological Evolution
		1.5.02.00.02	Critical Group - Evolution
		1.5.02.00.03	Plant and Animal Evolution
1.5.03.01.0A	Changes in the Earth's Magnetic Field	1.5.03.01.00	Changes in the Earth's Magnetic Field
		1.5.03.01.01	Flipping of the Earth's Magnetic Poles
		1.5.03.01.02	Changes of the Magnetic Field
		1.5.03.01.03	Magnetic Pole Reversal
1.5.03.02.0A	Earth Tides	1.5.03.02.00	Earth Tides
2.1.01.01.0A	Waste Inventory	2.1.01.01.00	Waste Inventory
		2.1.01.01.01	Inventory
		2.1.01.01.02	Inventory
		2.1.01.01.03	Changes in Radionuclide Inventory (In Waste Form)

Table G-1. Cross-Reference of TSPA-LA FEPs to TSPA-SR FEPs (Continued)

LA FEP Number	LA FEP Name	SR FEP Number	SR FEP Name
2.1.01.01.0A	Waste Inventory (continued)	2.1.01.01.04	Waste Product (Glass)
		2.1.01.01.05	Exotic Fuels
		2.1.01.01.06	DOE SNF Gap Radionuclide Inventory
		2.1.01.01.07	DOE SNF Initial Radionuclide Inventory
		2.1.01.01.08	DOE SNF Structure
		2.1.01.01.09	DOE SNF Initial Radionuclide Inventory
		2.1.01.01.10	DOE SNF Hazardous Chemical Inventory
2.1.01.02.0A	Interactions Between Co-Located Waste	2.1.01.02.00	Co-Disposal/Co-Location of Waste
		2.1.01.02.01	Other Waste
		2.1.01.02.02	Co-Disposal of Reactive Wastes
		2.1.01.02.03	Near Storage of Other Waste
		2.1.01.02.05	DOE SNF Waste Package Placement
		2.1.01.02.06	DOE SNF Canister Arrangement Within Waste Package
		2.1.01.02.09	DOE SNF Waste Package Placement
2.1.01.02.0B	Interactions Between Co-Disposed Waste	2.1.01.02.00	Co-Disposal/Co-Location of Waste
		2.1.01.02.04	DOE SNF/HLW Glass Interactions
		2.1.01.02.07	DOE SNF Colocation With HLW
		2.1.01.02.08	DOE SNF Geometry
		2.1.01.02.10	DOE SNF Colocation With HLW (Waste Form Degradation Impact)
		2.1.01.02.11	DOE SNF Colocation With HLW (Radionuclide Mobilization Impact)
		2.1.01.02.12	DOE SNF Colocation With HLW (Cladding Degradation Impact)
		2.1.02.01.05	High Integrity Canisters For DOE SNF
		2.1.02.09.00	Void Space (In Glass Container)
		2.1.03.11.01	Stainless Steel Fabrication Flask
2.1.01.03.0A	Heterogeneity of Waste Inventory	2.1.01.03.00	Heterogeneity of Waste Forms
		2.1.01.03.01	Damaged or Deviating Fuel
		2.1.01.03.02	Heterogeneity of Waste Form
		2.1.01.03.03	Deviant Inventory Flask
		2.1.01.03.04	DOE SNF Canister Atmosphere

Table G-1. Cross-Reference of TSPA-LA FEPs to TSPA-SR FEPs (Continued)

LA FEP Number	LA FEP Name	SR FEP Number	SR FEP Name
2.1.01.04.0A	Repository-Scale Spatial Heterogeneity of Emplaced Waste	2.1.01.04.00	Spatial Heterogeneity of Emplaced Waste
2.1.02.01.0A	DSNF Degradation (Alteration, Dissolution, and Radionuclide Release)	2.1.02.01.00	DSNF Degradation, Alteration, and Dissolution
		2.1.02.01.01	DOE SNF Dissolution
		2.1.02.01.02	Alteration/Dissolution of DOE SNF
		2.1.02.01.03	Oxidation of DOE SNF
		2.1.02.01.04	Alteration/Dissolution of Pu Ceramic Waste
		2.1.02.01.05	High-Integrity Canisters For DOE SNF
2.1.02.02.0A	CSNF Degradation (Alteration, Dissolution, and Radionuclide Release)	2.1.02.02.00	CSNF Alteration, Dissolution, and Radionuclide Release
		2.1.02.02.01	Source Terms (Expected)
		2.1.02.02.02	Source Terms (Other) (In Waste Form)
		2.1.02.02.03	Stability of UO2 (In Waste Form)
		2.1.02.02.04	Degradation of Fuel Elements
		2.1.02.02.05	Corrosion of Metal Parts (In Waste Form)
		2.1.02.02.06	Corrosion Prior to Wetting
		2.1.02.02.08	Water Turnover, Steel Vessel
		2.1.02.02.09	Dissolution Chemistry (In Waste and EBS)
		2.1.02.02.10	Release from Fuel Matrix (Release/Migration Factors)
		2.1.02.02.11	Release from Metal Parts
		2.1.02.02.12	Total Release from Fuel Elements
		2.1.02.02.13	Dissolution of Waste (Release/Migration Factors)
		2.1.02.02.14	Release of Radionuclides from the Failed Canister
		2.1.09.04.05	Selective Dissolution of Contaminants Contained in SNF
2.1.02.03.0A	HLW Glass Degradation (Alteration, Dissolution and Radionuclide Release)	2.1.02.03.00	Glass Degradation, Alteration, and Dissolution
		2.1.02.03.01	Degradation and Alteration of Glass Waste Form
		2.1.02.03.02	Phase Separation (In Waste Form)
		2.1.02.03.03	Congruent Dissolution (In Waste Form)
		2.1.02.03.04	Rate of Glass Dissolution
		2.1.02.03.05	Selective Leaching (In Waste Form)

Table G-1. Cross-Reference of TSPA-LA FEPs to TSPA-SR FEPs (Continued)

LA FEP Number	LA FEP Name	SR FEP Number	SR FEP Name
2.1.02.03.0A	HLW Glass Degradation (Alteration, Dissolution and Radionuclide Release) (continued)	2.1.02.03.06	Coprecipitates/Solid Solutions (In Waste Form)
		2.1.02.03.07	Precipitation of Silicates/Silica Gel (In Waste Form)
		2.1.02.03.08	Iron Corrosion Products
		2.1.02.03.09	Radionuclide Release from Glass
		2.1.02.03.10	Composition of DHLW Glass
		2.1.02.09.00	Void Space (In Glass Container)
		2.1.03.11.01	Stainless Steel Fabrication Flask
2.1.02.04.0A	Alpha Recoil Enhances Dissolution	2.1.02.04.00	Alpha Recoil Enhances Dissolution
		2.1.02.04.01	Recoil of Alpha-Decay
2.1.02.05.0A	HLW Glass Cracking	2.1.02.05.00	Glass Cracking and Surface Area
		2.1.02.05.01	Solute Transport Resistance (In Waste Form)
2.1.02.06.0A	HLW Glass Recrystallization	2.1.02.06.00	Glass Recrystallization
2.1.02.07.0A	Radionuclide Release from Gap and Grain Boundaries	2.1.02.02.01	Source Terms (Expected)
		2.1.02.02.12	Total Release from Fuel Elements
		2.1.02.07.00	Gap and Grain Release of Cs, I
		2.1.02.07.01	Gap and Grain Release
		2.1.02.07.02	Pb-I Reactions (In Waste Form)
		2.1.02.07.03	I, Cs-Migration to Fuel Surface
2.1.02.08.0A	Pyrophoricity from DSNF	2.1.02.08.00	Pyrophoricity
		2.1.02.08.01	DOE SNF Pyrophoricity
		2.1.02.08.02	DOE SNF Pyrophoric Event (Waste Heat Impact)
		2.1.02.08.03	DOE SNF Pyrophoric Event (Waste Package Degradation Impact)
		2.1.02.08.05	DOE SNF Pyrophoric Event (Waste Form Degradation Impact)
		2.1.02.08.06	DOE SNF Pyrophoric Event (Cladding Degradation Impact)
		2.1.11.07.00	Thermally-Induced Stress Changes in Waste and EBS
2.1.02.09.0A	Chemical Effects of Void Space in Waste Package	2.1.02.09.00	Void Space (In Glass Container)
2.1.02.10.0A	Organic/Cellulosic Materials in Waste	2.1.02.10.00	Cellulosic Degradation
		2.1.13.01.07	Radiolysis of Cellulose (In Waste and EBS)
2.1.02.11.0A	Degradation of Cladding from Waterlogged Rods	2.1.02.11.00	Waterlogged Rods

Table G-1. Cross-Reference of TSPA-LA FEPs to TSPA-SR FEPs (Continued)

LA FEP Number	LA FEP Name	SR FEP Number	SR FEP Name
2.1.02.12.0A	Degradation of Cladding Prior to Disposal	2.1.02.12.00	Cladding Degradation Before YMP Receives It
		2.1.02.12.01	Pin Degradation During Reactor Operation
		2.1.02.12.02	Pin Degradation During Spent Fuel Pool Storage
		2.1.02.12.03	Pin Degradation During Dry Storage
		2.1.02.12.04	Pin Degradation During Fuel Shipment and Handling
		2.1.02.13.01	Cladding Degradation Mechanisms at YMP, Pre-Pin Failure
2.1.02.13.0A	General Corrosion of Cladding	2.1.02.13.00	General Corrosion of Cladding
		2.1.02.13.02	Corrosion (Of Cladding)
2.1.02.14.0A	Microbially Influenced Corrosion (MIC) of Cladding	2.1.02.14.00	Microbial Corrosion (MIC) of Cladding Wfclad—Microbiologically Influenced Corrosion (MIC) of Cladding
2.1.02.15.0A	Localized (Radiolysis Enhanced) Corrosion of Cladding	2.1.02.15.00	Acid Corrosion of Cladding from Radiolysis
2.1.02.16.0A	Localized (Pitting) Corrosion of Cladding	2.1.02.02.05	Corrosion of Metal Parts (In Waste Form)
		2.1.02.16.00	Localized Corrosion (Pitting) of Cladding
2.1.02.17.0A	Localized (Crevice) Corrosion of Cladding	2.1.02.17.00	Localized Corrosion (Crevice Corrosion) of Cladding
2.1.02.18.0A	Enhanced Corrosion of Cladding from Dissolved Silica	2.1.02.18.00	High Dissolved Silica Content of Waters Enhances Corrosion of Cladding
2.1.02.19.0A	Creep Rupture of Cladding	2.1.02.19.00	Creep Rupture of Cladding
		2.1.02.19.01	Thermal Cracking (In Waste and EBS)
2.1.02.20.0A	Internal Pressurization of Cladding	2.1.02.20.00	Pressurization from He Production Causes Cladding Failure
2.1.02.21.0A	Stress Corrosion Cracking (SCC) of Cladding	2.1.02.21.00	Stress Corrosion Cracking (SCC) of Cladding
		2.1.02.21.01	Inside Out from Fission Products (Iodine) (Failure of Cladding)
		2.1.02.21.02	Outside in from Salts or WP Chemicals (Failure of Cladding)
		2.1.02.21.03	Stress-Corrosion Cracking of Zircaloy Cladding

Table G-1. Cross-Reference of TSPA-LA FEPs to TSPA-SR FEPs (Continued)

LA FEP Number	LA FEP Name	SR FEP Number	SR FEP Name
2.1.02.22.0A	Hydride Cracking of Cladding	2.1.02.22.00	Hydride Embrittlement of Cladding
		2.1.02.22.01	Hydride Embrittlement from Zirconium Corrosion (Of Cladding)
		2.1.02.22.02	Hydride Embrittlement from WP Corrosion & H2 Absorption (Of Cladding)
		2.1.02.22.03	Hydride Embrittlement from Galvanic Corrosion of WP Contacting Cladding
		2.1.02.22.04	Delayed Hydride Cracking (Of Cladding) Wfclad—Delayed Hydride Cracking (DHC) of Cladding
		2.1.02.22.05	Hydride Reorientation (Of Cladding)
		2.1.02.22.06	Hydrogen Axial Migration (Of Cladding)
		2.1.02.22.07	Hydride Embrittlement from Fuel Reaction (Causes Failure of Cladding) Wfclad—Hydride Embrittlement from Fuel Reaction
2.1.02.23.0A	Cladding Unzipping	2.1.02.23.00	Cladding Unzipping
		2.1.02.23.01	Cladding Degradation After Initial Cladding Perforation
		2.1.02.23.02	Dry Oxidation of Fuel (Causes Failure of Cladding) Wfclad—Dry Oxidation of Fuel
		2.1.02.23.03	Wet Oxidation of Fuel (Causes Failure of Cladding) Wfclad—Wet Oxidation of Fuel
2.1.02.24.0A	Mechanical Impact on Cladding	2.1.02.24.00	Mechanical Failure of Cladding
2.1.02.25.0A	DSNF Cladding	2.1.02.25.00	DSNF Cladding Degradation
		2.1.02.25.01	DOE SNF Cladding Material
		2.1.02.25.02	DOE SNF Cladding Condition
		2.1.02.25.03	Internal Canister/Cladding Corrosion Due to DOE SNF
2.1.02.25.0B	Naval SNF Cladding	2.1.02.25.00	DSNF Cladding Degradation
2.1.02.26.0A	Diffusion-Controlled Cavity Growth in Cladding	2.1.02.26.00	Diffusion-Controlled Cavity Growth Wfclad—Diffusion-Controlled Cavity Growth (DCCG)
2.1.02.27.0A	Localized (Fluoride Enhanced) Corrosion of Cladding	2.1.02.27.00	Localized Corrosion Perforation from Fluoride

Table G-1. Cross-Reference of TSPA-LA FEPs to TSPA-SR FEPs (Continued)

LA FEP Number	LA FEP Name	SR FEP Number	SR FEP Name
2.1.02.28.0A	Grouping of DSNF Waste Types Into Categories	2.1.01.02.08	DOE SNF Geometry
		2.1.02.28.00	Various Features of the Approximately 250 DSNF Types and Grouping Into Waste Categories
2.1.02.29.0A	Flammable Gas Generation from DSNF	2.1.02.08.04	Acetylene Generation from DSNF Wfmisc—Flammable Gasses Generation from DSNF - YMP
		2.1.02.29.00	Flammable Gas Generation from DSNF
2.1.03.01.0A	General Corrosion of Waste Packages	2.1.03.01.00	Corrosion of Waste Containers
		2.1.03.01.01	Metallic Corrosion
		2.1.03.01.02	Corrosion on Wetting (Of Waste Container)
		2.1.03.01.03	Oxic Corrosion (Of Waste Container)
		2.1.03.01.04	Anoxic Corrosion (Of Waste Container)
		2.1.03.01.05	Total Corrosion Rate (Of Waste Container)
		2.1.03.01.07	Corrosion of Steel Vessel
		2.1.03.01.08	Container Metal Corrosion
		2.1.03.01.09	Corrosion (Of Waste Container)
		2.1.03.01.10	Uniform Corrosion (Of Waste Container)
		2.1.03.01.11	Corrosive Agents, Sulfides, Oxygen, Etc.
		2.1.03.01.12	Water Turnover, Copper Canister
		2.1.03.12.00	Container Failure (Long-Term)
		2.1.03.12.01	Canister Failure (Reference)
		2.1.03.12.02	Long-Term Physical Stability (In Waste and EBS)
2.1.03.01.0B	General Corrosion of Drip Shields	2.1.03.01.00	Corrosion of Waste Containers
		2.1.06.06.00	Effects and Degradation of Drip Shield
2.1.03.02.0A	Stress Corrosion Cracking (SCC) of Waste Packages	2.1.03.02.00	Stress Corrosion Cracking of Waste Containers and Drip Shields
		2.1.03.02.01	Stress Corrosion Cracking (Of Waste Container)
		2.1.03.02.02	Stress Corrosion Cracking - Dry Waste Container
		2.1.03.02.03	Stress Corrosion Cracking Induced by Secondary Stress (Container Failure)

Table G-1. Cross-Reference of TSPA-LA FEPs to TSPA-SR FEPs (Continued)

LA FEP Number	LA FEP Name	SR FEP Number	SR FEP Name
2.1.03.02.0A	Stress Corrosion Cracking (SCC) of Waste Packages (continued)	2.1.03.02.04	Stress Corrosion Cracking (In Waste and EBS)
		2.1.03.12.00	Container Failure (Long-Term)
		2.1.11.07.00	Thermally-Induced Stress Changes in Waste and EBS
2.1.03.02.0B	Stress Corrosion Cracking (SCC) of Drip Shields	2.1.03.02.00	Stress Corrosion Cracking of Waste Containers and Drip Shields
		2.1.03.02.01	Stress Corrosion Cracking (Of Waste Container)
		2.1.11.07.00	Thermally-Induced Stress Changes in Waste and EBS
2.1.03.03.0A	Localized Corrosion of Waste Packages	2.1.03.01.00	Corrosion of Waste Containers
		2.1.03.03.00	Pitting of Waste Containers and Drip Shields
		2.1.03.03.01	Localized Corrosion (Of Waste Container)
		2.1.03.03.02	Pitting (Of Waste Container)
		2.1.03.03.03	Pitting Corrosion Develops on Containers
		2.1.03.12.00	Container Failure (Long-Term)
2.1.03.03.0B	Localized Corrosion of Drip Shields	2.1.03.03.00	Pitting of Waste Containers and Drip Shields
		2.1.03.03.01	Localized Corrosion (Of Waste Container)
		2.1.06.06.01	Oxygen Embrittlement of Ti Drip Shield
2.1.03.04.0A	Hydride Cracking of Waste Packages	2.1.03.04.00	Hydride Cracking of Waste Containers and Drip Shields
		2.1.03.04.01	Embrittlement and Cracking
		2.1.03.07.01	Other Canister Degradation Processes
		2.1.03.12.00	Container Failure (Long-Term)
2.1.03.04.0B	Hydride Cracking of Drip Shields	2.1.03.04.00	Hydride Cracking of Waste Containers and Drip Shields
		2.1.06.06.01	Oxygen Embrittlement of Ti Drip Shield
2.1.03.05.0A	Microbially Influenced Corrosion (MIC) of Waste Packages	2.1.03.05.00	Microbially-Mediated Corrosion of Waste Container and Drip Shield
		2.1.03.12.00	Container Failure (Long-Term)
2.1.03.05.0B	Microbially Influenced Corrosion (MIC) of Drip Shields	2.1.03.05.00	Microbially-Mediated Corrosion of Waste Container and Drip Shield

Table G-1. Cross-Reference of TSPA-LA FEPs to TSPA-SR FEPs (Continued)

LA FEP Number	LA FEP Name	SR FEP Number	SR FEP Name
2.1.03.06.0A	Internal Corrosion of Waste Packages Prior to Breach	2.1.02.25.03	Internal Canister/Cladding Corrosion Due to DOE SNF
		2.1.03.01.12	Water Turnover, Copper Canister
		2.1.03.06.00	Internal Corrosion of Waste Container
		2.1.03.06.01	DOE SNF Waste Package Internal Corrosion
2.1.03.07.0A	Mechanical Impact on Waste Package	2.1.03.07.00	Mechanical Impact on Waste Container and Drip Shield
		2.1.03.07.03	Failure of Steel Canister
		2.1.03.07.04	Reduced Mechanical Strength
		2.1.03.07.05	Container Failure (Mechanical)
		2.1.03.07.06	Falling Rock Hits Container, Increased Seepage Occurs, Speeds Corrosion of Container
		2.1.07.03.00	Movement of Containers
2.1.03.07.0B	Mechanical Impact on Drip Shield	2.1.03.07.00	Mechanical Impact on Waste Container and Drip Shield
		2.1.03.07.05	Container Failure (Mechanical)
		2.1.03.07.06	Falling Rock Hits Container, Increased Seepage Occurs, Speeds Corrosion of Container
		2.1.06.06.00	Effects and Degradation of Drip Shield
		2.1.07.03.00	Movement of Containers
2.1.03.08.0A	Early Failure of Waste Packages	2.1.03.08.00	Juvenile and Early Failure of Waste Containers and Drip Shields
		2.1.03.08.01	Canister Failure (Alternative Modes)
		2.1.03.08.02	Mis-Sealed Canister
		2.1.03.08.03	Container Failure (Early)
		2.1.03.08.04	Cracking Along Welds (Of Waste Container)
		2.1.03.08.05	Random Canister Defects - Quality Control
		2.1.03.08.06	Common Cause Canister Defects - Quality Control
2.1.03.08.0B	Early Failure of Drip Shields	2.1.03.08.00	Juvenile and Early Failure of Waste Containers and Drip Shields
2.1.03.09.0A	Copper Corrosion in EBS	2.1.03.01.06	Corrosion of Copper Canister
		2.1.03.07.02	Failure of Copper Canister
		2.1.03.09.00	Copper Corrosion
		2.1.03.09.01	Role of Chlorides in Copper Corrosion
		2.1.07.05.01	Creeping of Copper

Table G-1. Cross-Reference of TSPA-LA FEPs to TSPA-SR FEPs (Continued)

LA FEP Number	LA FEP Name	SR FEP Number	SR FEP Name
2.1.03.10.0A	Advection of Liquids and Solids Through Cracks in the Waste Package	2.1.03.10.00	Container Healing
		2.1.03.10.01	Corrosion Products (Physical Effects)
2.1.03.10.0B	Advection of Liquids and Solids Through Cracks in the Drip Shield	2.1.03.10.00	Container Healing
2.1.03.11.0A	Physical Form of Waste Package and Drip Shield	2.1.03.11.00	Container Form
		2.1.03.11.01	Stainless Steel Fabrication Flask
		2.1.03.11.02	Cast Steel Canister
		2.1.03.11.03	Canister Thickness
		2.1.03.11.04	Container Integrity
		2.1.03.11.05	DOE SNF Waste Package Design
		2.1.03.11.06	DOE SNF Canister Design
		2.1.03.11.07	DOE SNF Waste Package Design
		2.1.03.12.00	Container Failure (Long-Term)
		2.1.03.12.01	Canister Failure (Reference)
		2.1.03.12.02	Long-Term Physical Stability (In Waste and EBS)
2.1.04.01.0A	Flow in the Backfill	2.1.04.01.00	Preferential Pathways in the Backfill
		2.1.04.01.02	Flow Through Buffer/Backfill
		2.1.04.01.03	Flow Through Buffer/Backfill
		2.1.04.02.07	Backfill Materials Deficiencies
		2.1.04.06.00	Properties of Bentonite
		2.1.04.06.28	Resaturation of Bentonite Buffer
		2.1.04.06.29	Resaturation of Tunnel Backfill
		2.2.07.03.00	Capillary Rise
2.1.04.02.0A	Chemical Properties and Evolution of Backfill	2.1.04.02.00	Physical and Chemical Properties of Backfill
		2.1.04.02.02	Inhomogeneities (Properties and Evolution) (In Buffer/Backfill)
		2.1.04.02.03	Chemical Alteration of Buffer/Backfill
		2.1.04.02.05	Backfill Chemical Composition
		2.1.04.02.06	Chemical Degradation of Backfill
		2.1.04.02.07	Backfill Materials Deficiencies
		2.1.04.02.08	Near-Field Buffer Chemistry
		2.1.04.02.09	Water Chemistry, Tunnel Backfill
		2.1.04.02.10	Backfill Effects on Cu Corrosion
		2.1.04.05.00	Backfill Evolution
		2.1.04.05.01	Hydrothermal Alteration (In Buffer/Backfill)
		2.1.04.05.03	Thermal Degradation of Buffer/Backfill

Table G-1. Cross-Reference of TSPA-LA FEPs to TSPA-SR FEPs (Continued)

LA FEP Number	LA FEP Name	SR FEP Number	SR FEP Name
2.1.04.02.0A	Chemical Properties and Evolution of Backfill (continued)	2.1.04.06.00	Properties of Bentonite
		2.1.04.06.04	Bentonite Porewater Chemistry
		2.1.04.06.05	Mineralogical Alteration - Short Term (In Buffer/Backfill)
		2.1.04.06.06	Mineralogical Alteration - Long Term (In Buffer/Backfill)
		2.1.04.06.12	Dilution of Buffer/Backfill
		2.1.04.06.16	Degradation of Bentonite by Chemical Reactions
		2.1.04.06.30	Effects of Bentonite on Groundwater Chemistry
		2.1.04.06.31	Canister/Bentonite Interaction
		2.1.04.06.32	Interaction With Cement Components
		2.1.04.06.33	Water Chemistry, Bentonite Buffer
		2.1.04.07.00	Buffer Characteristics
		2.1.04.07.01	Buffer Additives
		2.1.04.07.04	Saturation of Sorption Sites
		2.1.04.07.05	Perturbed Buffer Material Chemistry
2.1.04.03.0A	Erosion or Dissolution of Backfill	2.1.04.03.00	Erosion or Dissolution of Backfill
		2.1.04.03.01	Erosion of Buffer/Backfill
		2.1.04.06.00	Properties of Bentonite
		2.1.04.06.02	Bentonite Erosion
2.1.04.04.0A	Thermal-Mechanical Effects of Backfill	2.1.04.02.00	Physical and Chemical Properties of Backfill
		2.1.04.04.00	Mechanical Effects of Backfill
		2.1.04.04.01	Mechanical Failure of Buffer/Backfill
		2.1.04.04.02	Mechanical Impact/Failure, Buffer/Backfill
		2.1.04.06.00	Properties of Bentonite
		2.1.04.06.01	Bentonite Swelling Pressure
		2.1.04.06.14	Swelling of Tunnel Backfill
		2.1.04.06.15	Swelling Pressure (In Buffer/Backfill)
		2.1.04.06.20	Swelling of Bentonite Into Tunnels and Cracks
		2.1.04.06.21	Uneven Swelling of Bentonite
		2.1.04.06.27	Bentonite Swelling
		2.1.04.06.35	Effect of Bentonite Swelling on EDZ

Table G-1. Cross-Reference of TSPA-LA FEPs to TSPA-SR FEPs (Continued)

LA FEP Number	LA FEP Name	SR FEP Number	SR FEP Name
2.1.04.05.0A	Thermal-Mechanical Properties and Evolution of Backfill	2.1.04.01.01	Interaction and Diffusion Between Canisters (And Buffer/Backfill)
		2.1.04.02.00	Physical and Chemical Properties of Backfill
		2.1.04.02.01	Backfill Characteristics
		2.1.04.02.04	Backfill Physical Composition
		2.1.04.05.00	Backfill Evolution
		2.1.04.05.02	Small Pieces of Backfill Under Go Phase Changes When Heated and Weld Together
		2.1.04.06.00	Properties of Bentonite
		2.1.04.06.03	Bentonite Plasticity
		2.1.04.06.07	Bentonite Cementation
		2.1.04.06.11	Coagulation of Bentonite
		2.1.04.06.13	Sedimentation of Bentonite
		2.1.04.06.18	Coagulation of Bentonite
		2.1.04.06.19	Sedimentation of Bentonite
		2.1.04.06.22	Thermal Effects On the Buffer Material
		2.1.04.06.24	Thermal Evolution (In Buffer/Backfill)
		2.1.04.06.25	Bentonite Saturation
		2.1.04.06.26	Buffer Impermeability
		2.1.04.07.02	Buffer Evolution
2.1.04.09.0A	Radionuclide Transport in Backfill	2.1.04.01.01	Interaction and Diffusion Between Canisters (And Buffer/Backfill)
		2.1.04.06.00	Properties of Bentonite
		2.1.04.06.17	Colloid Generation (In Buffer/Backfill)
		2.1.04.06.34	Gas Transport in Bentonite
		2.1.04.07.00	Buffer Characteristics
		2.1.04.08.00	Diffusion in Backfill
		2.1.04.09.00	Radionuclide Transport Through Backfill
		2.1.04.09.01	Transport and Release of Nuclides, Bentonite Buffer
		2.1.04.09.02	Transport and Release of Nuclides, Tunnel Backfill
		2.2.07.15.06	Convection (Water Transport)
		2.2.11.03.00	Gas Transport in Geosphere
2.1.05.01.0A	Flow Through Seals (Access Ramps and Ventilation Shafts)	2.1.05.01.00	Seal Physical Properties
		2.1.05.01.01	Seal Geometry
		2.1.05.01.03	Shaft and Tunnel Seals
		2.1.05.02.00	Groundwater Flow and Radionuclide Transport in Seals

Table G-1. Cross-Reference of TSPA-LA FEPs to TSPA-SR FEPs (Continued)

LA FEP Number	LA FEP Name	SR FEP Number	SR FEP Name
2.1.05.02.0A	Radionuclide Transport Through Seals	2.1.05.02.00	Groundwater Flow and Radionuclide Transport in Seals
2.1.05.03.0A	Degradation of Seals	1.1.01.02.00	Loss of Integrity of Borehole Seals
		1.1.01.02.02	Borehole Seal Failure
		2.1.05.01.02	Consolidation of Seals
		2.1.05.02.00	Groundwater Flow and Radionuclide Transport in Seals
		2.1.05.03.00	Seal Degradation
		2.1.05.03.01	Seal Evolution
		2.1.05.03.02	Seal Failure
		2.1.05.03.03	Degradation of Hole and Shaft Seals
		2.1.05.03.04	Shaft or Access Tunnel Seal Failure and Degradation
		2.1.05.03.05	Degradation of Hole and Shaft Seals
		2.1.05.03.06	Loss of Integrity of Shaft or Access Tunnel Seals
		2.1.05.03.07	Mechanical Degradation of Seals
		2.1.05.03.08	Chemical Degradation of Seals
		2.1.06.01.02	Seal Chemical Composition
		2.1.11.07.00	Thermally-Induced Stress Changes in Waste and EBS
2.1.06.01.0A	Chemical Effects of Rock Reinforcement and Cementitious Materials in EBS	2.1.06.01.00	Degradation of Cementitious Materials in Drift
		2.1.06.01.01	Physio-Chemical Degradation of Concrete
		2.1.06.01.02	Seal Chemical Composition
		2.1.06.01.03	Microbial Growth on Concrete
		2.1.06.02.00	Effects of Rock Reinforcement Materials
		2.1.06.02.01	Degradation of Rock Reinforcement and Grout
		2.1.09.01.10	Hyperalkaline Carrier Plume Forms
2.1.06.02.0A	Mechanical Effects of Rock Reinforcement Materials in EBS	2.1.06.01.01	Physio-Chemical Degradation of Concrete
		2.1.06.02.00	Effects of Rock Reinforcement Materials
		2.1.06.02.01	Degradation of Rock Reinforcement and Grout
2.1.06.04.0A	Flow Through Rock Reinforcement Materials in EBS	2.1.06.03.00	Degradation of the Liner
		2.1.06.04.00	Flow Through the Liner
		2.1.06.04.01	Fracture Flow Through the Liner

Table G-1. Cross-Reference of TSPA-LA FEPs to TSPA-SR FEPs (Continued)

LA FEP Number	LA FEP Name	SR FEP Number	SR FEP Name
2.1.06.05.0A	Mechanical Degradation of Emplacement Pallet	2.1.06.05.00	Degradation of Invert and Pedestal
		2.1.07.03.00	Movement of Containers
		2.1.07.03.01	Movement of Canister in Buffer/Backfill
		2.1.07.03.02	Canister or Container Movement
		2.1.07.03.03	Movement of Canister in Buffer/Backfill
		2.1.07.03.04	Canister Sinking
2.1.06.05.0B	Mechanical Degradation of Invert	2.1.06.03.00	Degradation of the Liner
		2.1.06.05.00	Degradation of Invert and Pedestal
		2.1.07.03.00	Movement of Containers
2.1.06.05.0C	Chemical Degradation of Emplacement Pallet	2.1.06.05.00	Degradation of Invert and Pedestal
2.1.06.05.0D	Chemical Degradation of Invert	2.1.06.03.00	Degradation of the Liner
		2.1.06.05.00	Degradation of Invert and Pedestal
		2.1.06.05.01	Cementitious Invert
2.1.06.06.0A	Effects of Drip Shield on Flow	2.1.06.06.00	Effects and Degradation of Drip Shield
2.1.06.06.0B	Oxygen Embrittlement of Drip Shields	2.1.06.06.00	Effects and Degradation of Drip Shield
2.1.06.07.0A	Chemical Effects at EBS Component Interfaces	2.1.06.07.00	Effects at Material Interfaces
2.1.06.07.0B	Mechanical Effects at EBS Component Interfaces	2.1.06.07.00	Effects at Material Interfaces
2.1.07.01.0A	Rockfall	2.1.07.01.00	Rockfall (Large Block) Wfclad--Rockfall
		2.1.07.01.01	Rockbursts in Container Holes
		2.1.07.01.02	Cave Ins
		2.1.07.01.03	Cave in (In Waste and EBS)
		2.1.07.01.04	Roof Falls
		2.1.07.02.02	Mechanical (Events and Processes in the Waste and EBS)
2.1.07.02.0A	Drift Collapse	2.1.07.01.03	Cave in (In Waste and EBS)
		2.1.07.02.00	Mechanical Degradation or Collapse of Drift
		2.1.07.02.01	Stability (In Waste and EBS)
		2.1.07.02.02	Mechanical (Events and Processes in the Waste and EBS)
		2.1.07.02.03	Rockfall Slopes Up Fault
		2.1.07.02.04	Rockfall (Rubble) (In Waste and EBS)
		2.1.07.02.05	Mechanical Failure of Repository

Table G-1. Cross-Reference of TSPA-LA FEPs to TSPA-SR FEPs (Continued)

LA FEP Number	LA FEP Name	SR FEP Number	SR FEP Name
2.1.07.02.0A	Drift Collapse (continued)	2.1.07.02.06	Subsidence/Collapse
		2.1.07.02.07	Vault Collapse
		2.1.07.02.08	Creeping of Rock Mass
2.1.07.04.0A	Hydrostatic Pressure on Waste Package	2.1.03.07.05	Container Failure (Mechanical)
		2.1.03.08.01	Canister Failure (Alternative Modes)
		2.1.07.04.00	Hydrostatic Pressure on Container
		2.1.07.04.01	Excessive Hydrostatic Pressures (In Waste and EBS)
		2.1.07.04.02	Changed Hydrostatic Pressure on Canister
2.1.07.04.0B	Hydrostatic Pressure on Drip Shield	2.1.07.04.00	Hydrostatic Pressure on Container
2.1.07.05.0A	Creep of Metallic Materials in the Waste Package	2.1.02.19.01	Thermal Cracking (In Waste and EBS)
		2.1.03.07.01	Other Canister Degradation Processes
		2.1.07.05.00	Creeping of Metallic Materials in the EBS
		2.1.07.05.01	Creeping of Copper
		2.1.07.05.03	Voids in the Lead Filling
		2.1.07.05.04	Loss of Ductility (Of Waste Container)
		2.1.07.05.05	Incomplete Filling of Containers
2.1.07.05.0B	Creep of Metallic Materials in the Drip Shield	2.1.02.19.01	Thermal Cracking (In Waste and EBS)
		2.1.07.05.00	Creeping of Metallic Materials in the EBS
		2.1.07.05.02	External Stress (In Waste and EBS)
2.1.07.06.0A	Floor Buckling	2.1.07.06.00	Floor Buckling
		2.1.07.06.01	Basin Formation (In Waste and EBS)
2.1.08.01.0A	Water Influx At the Repository	2.1.08.01.00	Increased Unsaturated Water Flux At the Repository
		2.1.08.08.00	Induced Hydrological Changes in the Waste and EBS
2.1.08.01.0B	Effects of Rapid Influx Into the Repository	2.1.08.01.00	Increased Unsaturated Water Flux At the Repository
		2.1.08.01.01	Waste Container Is Thermally Quenched by Rapid Influx of Water
		2.1.08.09.02	Cavitation
		2.2.07.11.02	Resaturation, Near-Field Rock
2.1.08.02.0A	Enhanced Influx At the Repository	2.1.08.02.00	Enhanced Influx (Philip's Drip)

Table G-1. Cross-Reference of TSPA-LA FEPs to TSPA-SR FEPs (Continued)

LA FEP Number	LA FEP Name	SR FEP Number	SR FEP Name
2.1.08.03.0A	Repository Dry-Out Due to Waste Heat	2.1.08.03.00	Repository Dry-Out Due to Waste Heat
		2.1.08.10.00	Desaturation/Dewatering of the Repository
		2.1.08.10.01	Dewatering of Host Rock (In Waste and EBS)
		2.1.08.10.02	Dewatering
2.1.08.04.0A	Condensation Forms on Roofs of Drifts (Drift-Scale Cold Traps)	2.1.08.04.00	Cold Traps
		2.1.08.04.01	Condensation Forms on Backs of Drifts
		2.2.07.10.06	Vault Geometry
2.1.08.04.0B	Condensation Forms at Repository Edges (Repository-Scale Cold Traps)	2.1.08.04.00	Cold Traps
		2.2.07.10.00	Condensation Zone Forms Around Drifts
		2.2.07.10.06	Vault Geometry
		2.2.07.11.00	Return Flow from Condensation Cap / Resaturation of Dry-Out Zone
2.1.08.05.0A	Flow Through Invert	2.1.08.05.00	Flow Through Invert
		2.1.08.05.01	Fracture Flow Through the Invert
		2.1.08.05.02	UZ Flow Through/Around the Collapsed Invert
2.1.08.06.0A	Capillary Effects (Wicking) in EBS	2.1.08.06.00	Wicking in Waste and EBS
		2.2.07.03.00	Capillary Rise
2.1.08.07.0A	Unsaturated Flow in the EBS	2.1.02.02.08	Water Turnover, Steel Vessel
		2.1.08.07.00	Pathways For Unsaturated Flow and Transport in the Waste and EBS
		2.1.08.07.01	Residual Canister (Crack/Holes Effects)
		2.1.08.07.03	Container-Partial Corrosion
		2.1.08.07.04	Hydraulic Conductivity (In Waste and EBS)
		2.1.08.07.06	Channeling Within the Waste
		2.1.12.06.07	Unsaturated Flow Due to Gas Production (In Waste and EBS)
2.1.08.09.0A	Saturated Flow in the EBS	2.1.02.02.08	Water Turnover, Steel Vessel
		2.1.08.09.00	Saturated Groundwater Flow in Waste and EBS
		2.1.08.09.01	Hydraulic Head (In Waste and EBS)
		2.1.08.09.02	Cavitation
2.1.08.11.0A	Repository Resaturation Due to Waste Cooling	2.1.08.11.00	Resaturation of Repository
		2.1.08.11.01	Reflooding (In Waste and EBS)
		2.1.08.11.02	Brine Inflow (In Waste and EBS)

Table G-1. Cross-Reference of TSPA-LA FEPs to TSPA-SR FEPs (Continued)

LA FEP Number	LA FEP Name	SR FEP Number	SR FEP Name
2.1.08.12.0A	Induced Hydrologic Changes in Invert	2.1.08.08.00	Induced Hydrological Changes in the Waste and EBS
		2.1.08.12.00	Drainage With Transport - Sealing and Plugging
		2.1.08.13.00	Drains
2.1.08.14.0A	Condensation on Underside of Drip Shield	2.1.08.08.00	Induced Hydrological Changes in the Waste and EBS
		2.1.08.14.00	Condensation on Underside of Drip Shield
2.1.08.15.0A	Consolidation of EBS Components	2.1.07.03.00	Movement of Containers
		2.1.08.07.05	Consolidation of Waste
		2.1.08.15.00	Waste-Form and Backfill Consolidation
2.1.09.01.0A	Chemical Characteristics of Water in Drifts	2.1.09.01.00	Properties of the Potential Carrier Plume in the Waste and EBS
		2.1.09.01.01	Reactions With Cement Pore Water
		2.1.09.01.02	Reactions With Cement Pore Water
		2.1.09.01.03	Induced Chemical Changes (In Waste and EBS)
		2.1.09.01.04	Interactions of Host Materials and Ground Water With Repository Material
		2.1.09.01.05	TRU Silos Cementitious Plume
		2.1.09.01.07	Transport of Chemically-Active Substances Into the Near-Field
		2.1.09.01.08	Incomplete Near-Field Chemical Conditioning
		2.1.09.01.09	Chemical Processes (In Waste and EBS)
		2.1.09.01.10	Hyperalkaline Carrier Plume Forms
		2.1.09.01.12	TRU Alkaline or Organic Plume
		2.1.09.01.13	Interactions of Waste and Repository Materials With Host Materials
		2.1.09.01.14	TRU Alkaline or Organic Plume
		2.1.09.12.00	Rind (Altered Zone) Formation in Waste, EBS, and Adjacent Rock
2.1.09.01.0B	Chemical Characteristics of Water in Waste Package	2.1.09.01.04	Interactions of Host Materials and Ground Water With Repository Material
		2.1.09.01.06	Water Chemistry, Canister
		2.1.09.01.07	Transport of Chemically-Active Substances Into the Near-Field

Table G-1. Cross-Reference of TSPA-LA FEPs to TSPA-SR FEPs (Continued)

LA FEP Number	LA FEP Name	SR FEP Number	SR FEP Name
2.1.09.01.0B	Chemical Characteristics of Water in Waste Package (continued)	2.1.09.01.11	Chemical Interactions (In Waste and EBS)
		2.1.09.01.13	Interactions of Waste and Repository Materials With Host Materials
		2.1.09.12.00	Rind (Altered Zone) Formation in Waste, EBS, and Adjacent Rock
2.1.09.02.0A	Chemical Interaction With Corrosion Products	2.1.04.07.04	Saturation of Sorption Sites
		2.1.09.02.00	Interaction With Corrosion Products
		2.1.09.02.01	Interactions With Corrosion Products and Waste
		2.1.09.02.02	Effects of Metal Corrosion (In Waste and EBS)
		2.1.09.02.03	Container Corrosion Products
		2.1.09.02.04	Chemical Buffering (Canister Corrosion Products)
		2.1.09.06.05	Fe Control of Oxidation State of Contaminants
		2.1.09.14.00	Colloid Formation in Waste and EBS
2.1.09.03.0A	Volume Increase of Corrosion Products Impacts Cladding	2.1.03.07.00	Mechanical Impact on Waste Container and Drip Shield
		2.1.09.03.00	Volume Increase of Corrosion Products
		2.1.09.03.01	Swelling of Corrosion Products (In Waste and EBS)
2.1.09.03.0B	Volume Increase of Corrosion Products Impacts Waste Package	2.1.03.07.00	Mechanical Impact on Waste Container and Drip Shield
		2.1.09.03.00	Volume Increase of Corrosion Products
2.1.09.03.0C	Volume Increase of Corrosion Products Impacts Other EBS Components	2.1.09.03.00	Volume Increase of Corrosion Products
2.1.09.04.0A	Radionuclide Solubility, Solubility Limits, and Speciation in the Waste Form and EBS	2.1.09.04.00	Radionuclide Solubility, Solubility Limits, and Speciation in the Waste Form and EBS
		2.1.09.04.01	Elemental Solubility (In Waste and EBS)
		2.1.09.04.02	Speciation (In Waste and EBS)
		2.1.09.04.03	Geochemical Pump (In Waste and EBS)
		2.1.09.04.04	Precipitation and Dissolution (In Waste and EBS)
		2.1.09.04.05	Selective Dissolution of Contaminants Contained in SNF

Table G-1. Cross-Reference of TSPA-LA FEPs to TSPA-SR FEPs (Continued)

LA FEP Number	LA FEP Name	SR FEP Number	SR FEP Name
2.1.09.04.0A	Radionuclide Solubility, Solubility Limits, and Speciation in the Waste Form and EBS (continued)	2.1.09.04.06	Precipitation (Release/Migration Factors)
		2.1.09.04.07	Speciation Control of Contaminants by Hyperalkaline Plume Formed in the EBS
		2.1.09.04.08	Solubility Within Fuel Matrix
		2.1.09.04.09	Solubility and Precipitation (Contaminant Speciation and Solubility)
		2.1.09.04.10	Solubility Limit (Contaminant Speciation and Solubility)
		2.1.09.04.11	Radionuclide Source Term (Contaminant Speciation and Solubility)
		2.1.09.04.12	Elemental Solubility/Precipitation (Contaminant Speciation and Solubility)
		2.1.09.04.13	Speciation (Contaminant Speciation and Solubility)
2.1.09.05.0A	Sorption of Dissolved Radionuclides in EBS	2.1.08.07.02	Properties of Failed Canister
		2.1.08.07.08	Radionuclide Transport (Water Transport)
		2.1.09.05.00	In-Drift Sorption Wfmisc—In Package Sorption
		2.1.09.05.01	Selective Sorption of Pu from Solution
		2.1.09.05.02	Sorption
		2.1.09.05.03	Radionuclide Retardation
		2.1.09.05.04	Sorption on Filling Material
2.1.09.06.0A	Reduction-Oxidation Potential in Waste Package	2.1.09.02.04	Chemical Buffering (Canister Corrosion Products)
		2.1.09.06.00	Reduction-Oxidation Potential in Waste and EBS
		2.1.09.06.01	Redox Front (In Waste and EBS)
		2.1.09.06.02	Reduction-Oxidation Fronts (In Waste and EBS)
		2.1.09.06.03	Localized Reducing Zones (In Waste and EBS)
		2.1.09.06.04	Redox Front (In Buffer/Backfill)
		2.1.09.06.05	Fe Control of Oxidation State of Contaminants
2.1.09.06.0B	Reduction-Oxidation Potential in Drifts	2.1.09.06.00	Reduction-Oxidation Potential in Waste and EBS
		2.1.09.06.04	Redox Front (In Buffer/Backfill)

Table G-1. Cross-Reference of TSPA-LA FEPs to TSPA-SR FEPs (Continued)

LA FEP Number	LA FEP Name	SR FEP Number	SR FEP Name
2.1.09.07.0A	Reaction Kinetics in Waste Package	2.1.09.07.00	Reaction Kinetics in Waste and EBS
		2.1.09.07.01	Chemical Kinetics (In Waste and EBS)
2.1.09.07.0B	Reaction Kinetics in Drifts	2.1.09.07.00	Reaction Kinetics in Waste and EBS
2.1.09.08.0A	Diffusion of Dissolved Radionuclides in EBS	2.1.02.02.07	Radionuclide Release (Diffusion) Through Failed Cladding
		2.1.02.02.15	Transport and Release of Nuclides, Failed Canister
		2.1.02.05.01	Solute Transport Resistance (In Waste Form)
		2.1.08.07.01	Residual Canister (Crack/Holes Effects)
		2.1.08.07.02	Properties of Failed Canister
		2.1.08.07.03	Container-Partial Corrosion
		2.1.08.07.07	Unsaturated Transport (Water Transport)
		2.1.08.07.08	Radionuclide Transport (Water Transport)
		2.1.09.01.07	Transport of Chemically-Active Substances Into the Near-Field
		2.1.09.08.00	Chemical Gradients/Enhanced Diffusion in Waste and EBS
		2.1.09.08.03	Diffusion in and Through Failed Canister
2.1.09.08.0B	Advection of Dissolved Radionuclides in EBS	2.1.02.02.15	Transport and Release of Nuclides, Failed Canister
		2.1.08.07.01	Residual Canister (Crack/Holes Effects)
		2.1.08.07.02	Properties of Failed Canister
		2.1.08.07.03	Container-Partial Corrosion
		2.1.08.07.07	Unsaturated Transport (Water Transport)
		2.1.08.07.08	Radionuclide Transport (Water Transport)
		2.1.09.08.00	Chemical Gradients/Enhanced Diffusion in Waste and EBS
2.1.09.09.0A	Electrochemical Effects in EBS	2.1.06.07.00	Effects at Material Interfaces
		2.1.09.09.00	Electrochemical Effects (Electrophoresis, Galvanic Coupling) in Waste and EBS WP—Electrochemical Effects in Waste Package
		2.1.09.09.01	Repository Induced Pb/Cu Electrochemical Reactions

Table G-1. Cross-Reference of TSPA-LA FEPs to TSPA-SR FEPs (Continued)

LA FEP Number	LA FEP Name	SR FEP Number	SR FEP Name
2.1.09.09.0A	Electrochemical Effects in EBS (continued)	2.1.09.09.02	Natural Telluric Electrochemical Reactions (In Waste and EBS)
		2.1.09.09.03	Electro-Chemical Cracking (In Waste and EBS)
		2.1.09.09.04	Electrochemical Effects/Gradients (In Waste and EBS)
		2.1.09.09.05	Electrochemical Effects of Metal Corrosion
		2.1.09.09.06	Electrochemical Effects (In Waste and EBS)
		2.1.09.09.07	Galvanic Coupling (In Waste and EBS)
		2.1.09.09.08	Electrophoresis (In Waste and EBS)
		2.1.09.09.09	Electrochemical Gradients (In Waste and EBS)
		2.1.09.09.10	Galvanic Coupling (In Waste and EBS)
		2.1.09.09.11	Galvanic Coupling (In Waste and EBS)
2.1.09.10.0A	Secondary Phase Effects on Dissolved Radionuclide Concentrations	2.1.09.04.01	Elemental Solubility (In Waste and EBS)
		2.1.09.04.06	Precipitation (Release/Migration Factors)
		2.1.09.10.00	Secondary Phase Effects on Dissolved Radionuclide Concentrations At the Waste Form
2.1.09.11.0A	Chemical Effects of Waste-Rock Contact	2.1.09.11.00	Waste-Rock Contact
2.1.09.12.0A	Rind (Chemically Altered Zone) Forms in the Near-Field	2.1.08.08.00	Induced Hydrological Changes in the Waste and EBS
		2.1.09.12.00	Rind (Altered Zone) Formation in Waste, EBS, and Adjacent Rock
		2.1.09.12.01	Deep Alteration of the Porosity of Drift Walls
		2.2.08.02.01	Locally-Saturated Carrier Plume Forms (In Geosphere)
		2.2.08.02.02	Unsaturated Carrier Plume Forms (In Geosphere)
2.1.09.13.0A	Complexation in EBS	2.1.09.13.00	Complexation by Organics in Waste and EBS
		2.1.09.13.01	Methylation (In Waste and EBS)
		2.1.09.13.02	Humic and Fulvic Acids
		2.1.09.13.03	Complexation by Organics
		2.1.09.13.04	Fulvic Acid

Table G-1. Cross-Reference of TSPA-LA FEPs to TSPA-SR FEPs (Continued)

LA FEP Number	LA FEP Name	SR FEP Number	SR FEP Name
2.1.09.13.0A	Complexation in EBS (continued)	2.1.09.13.05	Humic Acid
		2.1.09.13.06	Complexing Agents
		2.1.09.13.07	Organics (Complexing Agents)
		2.1.09.13.08	Organics (Complexing Agents)
		2.1.09.13.09	Organic Complexation
		2.1.09.13.10	Organic Ligands
		2.1.09.13.11	Kinetics of Organic Complexation
		2.1.09.13.12	Introduced Complexing Agents
		2.1.09.14.07	Colloids, Complexing Agents
		2.1.10.01.08	Microbial Activity (In Waste and EBS)
2.1.09.15.0A	Formation of True (Intrinsic) Colloids in EBS	2.1.09.14.00	Colloid Formation in Waste and EBS
		2.1.09.14.02	Agglomeration of Pu Colloids
		2.1.09.14.06	Colloids
		2.1.09.14.07	Colloids, Complexing Agents
		2.1.09.14.08	Colloid Generation and Transport
		2.1.09.14.09	Colloid Formation, Dissolution and Transport
		2.1.09.14.10	Colloid Generation and Transport
		2.1.09.14.11	Colloid Formation and Stability
		2.1.09.15.00	Formation of True Colloids in Waste and EBS
2.1.09.16.0A	Formation of Pseudo-Colloids (Natural) in EBS	2.1.09.14.00	Colloid Formation in Waste and EBS
		2.1.09.14.01	Colloid Generation-Source (In Waste and EBS)
		2.1.09.14.02	Agglomeration of Pu Colloids
		2.1.09.14.03	Colloids (In Waste and EBS)
		2.1.09.14.05	Colloid Formation
		2.1.09.14.06	Colloids
		2.1.09.14.07	Colloids, Complexing Agents
		2.1.09.14.08	Colloid Generation and Transport
		2.1.09.14.09	Colloid Formation, Dissolution and Transport
		2.1.09.14.10	Colloid Generation and Transport
		2.1.09.14.11	Colloid Formation and Stability
		2.1.09.16.00	Formation of Pseudo-Colloids (Natural) in Waste and EBS
		2.1.09.16.01	Pseudo-Colloids
		2.1.09.16.02	Pseudo-Colloids
		2.1.09.16.03	Natural Colloids
		2.1.09.16.04	Natural Colloids
		2.2.08.10.03	Colloids (In Geosphere)

Table G-1. Cross-Reference of TSPA-LA FEPs to TSPA-SR FEPs (Continued)

LA FEP Number	LA FEP Name	SR FEP Number	SR FEP Name
2.1.09.17.0A	Formation of Pseudo-Colloids (Corrosion Product) in EBS	2.1.09.14.00	Colloid Formation in Waste and EBS
		2.1.09.14.02	Agglomeration of Pu Colloids
		2.1.09.14.03	Colloids (In Waste and EBS)
		2.1.09.14.04	Colloids/Particles in Canister
		2.1.09.14.05	Colloid Formation
		2.1.09.14.06	Colloids
		2.1.09.14.07	Colloids, Complexing Agents
		2.1.09.14.08	Colloid Generation and Transport
		2.1.09.14.09	Colloid Formation, Dissolution and Transport
		2.1.09.14.10	Colloid Generation and Transport
		2.1.09.14.11	Colloid Formation and Stability
		2.1.09.17.00	Formation of Pseudo-Colloids (Corrosion Products) in Waste and EBS
		2.1.09.17.01	Colloid Formation Is Associated With Container Hydrolysis Products
2.1.09.18.0A	Formation of Microbial Colloids in EBS	2.1.09.14.00	Colloid Formation in Waste and EBS
		2.1.09.14.03	Colloids (In Waste and EBS)
		2.1.09.14.04	Colloids/Particles in Canister
		2.1.09.18.00	Microbial Colloid Transport in the Waste and EBS.
2.1.09.19.0A	Sorption of Colloids in EBS	2.1.09.19.00	Colloid Transport and Sorption in the Waste and EBS.
		2.1.09.19.01	Colloid Transport
2.1.09.19.0B	Advection of Colloids in EBS	2.1.02.02.15	Transport and Release of Nuclides, Failed Canister
		2.1.09.14.08	Colloid Generation and Transport
		2.1.09.14.09	Colloid Formation, Dissolution and Transport
		2.1.09.14.10	Colloid Generation and Transport
		2.1.09.19.01	Colloid Transport
2.1.09.20.0A	Filtration of Colloids in EBS	2.1.09.20.00	Colloid Filtration in the Waste and EBS Wfcol—Colloid Filtration
		2.1.09.20.01	Colloid Filtration By the Invert
		2.1.09.20.02	Colloid Filtration (In Pores and Fractures)
		2.1.09.20.03	Colloid Filtration
2.1.09.21.0A	Transport of Particles Larger Than Colloids in EBS	2.1.09.21.00	Suspensions of Particles Larger Than Colloids
		2.1.09.21.01	Suspended Sediment Transport
		2.1.09.21.02	Rinse

Table G-1. Cross-Reference of TSPA-LA FEPs to TSPA-SR FEPs (Continued)

LA FEP Number	LA FEP Name	SR FEP Number	SR FEP Name
2.1.09.21.0B	Transport of Particles Larger Than Colloids in the SZ	2.1.09.21.00	Suspensions of Particles Larger Than Colloids
		2.1.09.21.01	Suspended Sediment Transport
		2.1.09.21.02	Rinse
2.1.09.21.0C	Transport of Particles Larger Than Colloids in the UZ	2.1.09.21.00	Suspensions of Particles Larger Than Colloids
		2.1.09.21.01	Suspended Sediment Transport
2.1.09.22.0A	Sorption of Colloids at Air-Water Interface	2.1.09.22.00	Colloid Sorption At the Air-Water Interface
2.1.09.23.0A	Stability of Colloids in EBS	2.1.09.14.11	Colloid Formation and Stability
		2.1.09.23.00	Colloidal Stability and Concentration Dependence on Aqueous Chemistry
2.1.09.24.0A	Diffusion of Colloids in EBS	2.1.02.02.07	Radionuclide Release (Diffusion) Through Failed Cladding
		2.1.02.02.15	Transport and Release of Nuclides, Failed Canister
		2.1.02.05.01	Solute Transport Resistance (In Waste Form)
		2.1.09.24.00	Colloidal Diffusion
2.1.09.25.0A	Formation of Colloids (Waste-Form) by Co-Precipitation in EBS	2.1.02.03.06	Coprecipitates/Solid Solutions (In Waste Form)
		2.1.09.14.00	Colloid Formation in Waste and EBS
		2.1.09.14.04	Colloids/Particles in Canister
		2.1.09.25.00	Colloidal Phases Are Produced by Coprecipitation (In Waste and EBS)
2.1.09.26.0A	Gravitational Settling of Colloids in EBS	2.1.09.26.00	Colloid Gravitational Settling
2.1.09.27.0A	Coupled Effects on Radionuclide Transport in EBS	2.1.09.01.07	Transport of Chemically-Active Substances Into the Near-Field
		2.1.09.02.03	Container Corrosion Products
		2.1.09.02.05	Radionuclide Sorption and Co-Precipitation (In EBS)
		2.1.09.04.03	Geochemical Pump (In Waste and EBS)
		2.1.09.06.05	Fe Control of Oxidation State of Contaminants
		2.1.09.08.00	Chemical Gradients/Enhanced Diffusion in Waste and EBS
		2.1.09.08.01	Enhanced Diffusion (In Waste and EBS)
		2.1.09.08.02	Chemical Gradients (In Waste and EBS)

Table G-1. Cross-Reference of TSPA-LA FEPs to TSPA-SR FEPs (Continued)

LA FEP Number	LA FEP Name	SR FEP Number	SR FEP Name
2.1.09.27.0A	Coupled Effects on Radionuclide Transport in EBS (continued)	2.1.09.09.00	Electrochemical Effects (Electrophoresis, Galvanic Coupling) in Waste and EBS WP—Electrochemical Effects in Waste Package
		2.1.11.04.06	Coupled Processes (In Waste and EBS)
2.1.09.28.0A	Localized Corrosion on Waste Package Outer Surface Due to Deliquescence	2.1.03.01.00	Corrosion of Waste Containers
		2.1.03.02.00	Stress Corrosion Cracking of Waste Containers and Drip Shields
		2.1.03.03.00	Pitting of Waste Containers and Drip Shields
2.1.09.28.0B	Localized Corrosion on Drip Shield Surfaces Due to Deliquescence	2.1.03.01.00	Corrosion of Waste Containers
		2.1.03.02.00	Stress Corrosion Cracking of Waste Containers and Drip Shields
		2.1.03.03.00	Pitting of Waste Containers and Drip Shields
2.1.10.01.0A	Microbial Activity in EBS	2.1.06.01.03	Microbial Growth on Concrete
		2.1.10.01.00	Biological Activity in Waste and EBS
		2.1.10.01.01	Microbial Activity Accelerates Corrosion of Containers
		2.1.10.01.02	Microbial Activity Accelerates Corrosion of Cladding
		2.1.10.01.03	Microbial Activity Accelerates Corrosion of Contaminants
		2.1.10.01.04	Microbes (In Waste and EBS)
		2.1.10.01.05	Microorganisms (In Waste and EBS)
		2.1.10.01.06	Microbiological Effects (In Waste and EBS)
		2.1.10.01.07	Microbial Activity (In Waste and EBS)
		2.1.10.01.08	Microbial Activity (In Waste and EBS)
		2.1.10.01.09	Microbial Activity (In Waste and EBS)
		2.1.10.01.10	Microbial Interactions
		2.1.10.01.11	Biofilms
		2.1.12.04.01	Effect of Temperature on Microbial Gas Generation
2.1.11.01.0A	Heat Generation in EBS	2.1.08.08.00	Induced Hydrological Changes in the Waste and EBS
		2.1.11.01.00	Heat Output / Temperature in Waste and EBS

Table G-1. Cross-Reference of TSPA-LA FEPs to TSPA-SR FEPs (Continued)

LA FEP Number	LA FEP Name	SR FEP Number	SR FEP Name
2.1.11.01.0A	Heat Generation in EBS (continued)	2.1.11.01.01	Glass Temperature (In Waste and EBS)
		2.1.11.01.02	Canister Temperature
		2.1.11.01.03	Temperature, Bentonite Buffer
		2.1.11.01.04	Temperature, Canister
		2.1.11.01.05	Temperature, Tunnel Backfill
		2.1.11.01.06	Heat Generation from Waste Containers
		2.1.11.01.07	Radioactive Decay Heat
		2.1.11.01.08	DOE SNF Expected Waste Heat Generation
		2.1.11.01.09	DOE SNF Expected Waste Heat Generation
		2.1.11.02.03	Vault Heating Effects
		2.1.11.04.00	Temperature Effects / Coupled Processes in Waste and EBS
		2.1.11.04.01	Thermal (Processes)
		2.1.11.04.03	Heat from Radioactive Decay (In Waste and EBS)
		2.1.11.04.04	Long-Term Transients (In Waste and EBS)
		2.1.11.04.05	Time Dependence (In Waste and EBS)
		2.1.11.07.00	Thermally-Induced Stress Changes in Waste and EBS
2.1.11.02.0A	Non-Uniform Heat Distribution in EBS	2.1.11.02.00	Nonuniform Heat Distribution / Edge Effects in Repository
		2.1.11.02.01	Panel/Repository Edge Effects - Thermal
		2.1.11.02.02	Panel/Repository Edge Effects - Post-Thermal
2.1.11.03.0A	Exothermic Reactions in the EBS	2.1.11.03.00	Exothermic Reactions in Waste and EBS Wfmisc—Exothermic Reactions and Other Thermal Effects in Waste and EBS
		2.1.11.03.01	Concrete Hydration
		2.1.11.07.00	Thermally-Induced Stress Changes in Waste and EBS
2.1.11.05.0A	Thermal Expansion/Stress of In-Package EBS Components	2.1.03.02.03	Stress Corrosion Cracking Induced by Secondary Stress (Container Failure)
		2.1.11.05.00	Differing Thermal Expansion of Repository Components
		2.1.11.07.00	Thermally-Induced Stress Changes in Waste and EBS

Table G-1. Cross-Reference of TSPA-LA FEPs to TSPA-SR FEPs (Continued)

LA FEP Number	LA FEP Name	SR FEP Number	SR FEP Name
2.1.11.06.0A	Thermal Sensitization of Waste Packages	2.1.11.06.00	Thermal Sensitization of Waste Containers and Drip Shields Increases Their Fragility
2.1.11.06.0B	Thermal Sensitization of Drip Shields	2.1.11.06.00	Thermal Sensitization of Waste Containers and Drip Shields Increases Their Fragility
2.1.11.07.0A	Thermal Expansion/Stress of In-Drift EBS Components	2.1.03.02.03	Stress Corrosion Cracking Induced by Secondary Stress (Container Failure)
		2.1.11.02.01	Panel/Repository Edge Effects - Thermal
		2.1.11.02.02	Panel/Repository Edge Effects - Post-Thermal
		2.1.11.02.03	Vault Heating Effects
		2.1.11.05.00	Differing Thermal Expansion of Repository Components
		2.1.11.05.01	Differential Thermal Expansion of Near-Field Barriers
		2.1.11.05.02	Shearing of Waste Containers by Secondary Stresses from Thermal Expansion of the Rock
		2.1.11.05.03	Differential Elastic Response (In Waste and EBS)
		2.1.11.05.04	Non-Elastic Response (In Waste and EBS)
		2.1.11.07.00	Thermally-Induced Stress Changes in Waste and EBS
		2.1.11.07.01	Changes in In-Situ Stress Field (In Waste and EBS)
2.1.11.08.0A	Thermal Effects on Chemistry and Microbial Activity in the EBS	2.1.11.08.00	Thermal Effects: Chemical and Microbiological Changes in the Waste and EBS
2.1.11.09.0A	Thermal Effects on Flow in the EBS	2.1.11.02.00	Nonuniform Heat Distribution / Edge Effects in Repository
		2.1.11.04.06	Coupled Processes (In Waste and EBS)
		2.1.11.09.00	Thermal Effects on Liquid or Two-Phase Fluid Flow in the Waste and EBS
		2.1.11.09.02	Multiphase Flow and Gas-Driven Transport (Water Transport)
		2.2.10.02.00	Thermal Convection Cell Develops in SZ
2.1.11.09.0B	Thermally-Driven Flow (Convection) in Waste Packages	2.1.11.02.03	Vault Heating Effects
		2.1.11.09.00	Thermal Effects on Liquid or Two-Phase Fluid Flow in the Waste and EBS
		2.1.11.09.01	Convection Effects on Transport (Enhanced Vapor Diffusion)

Table G-1. Cross-Reference of TSPA-LA FEPs to TSPA-SR FEPs (Continued)

LA FEP Number	LA FEP Name	SR FEP Number	SR FEP Name
2.1.11.09.0C	Thermally Driven Flow (Convection) in Drifts	2.1.11.02.03	Vault Heating Effects
		2.1.11.09.00	Thermal Effects on Liquid or Two-Phase Fluid Flow in the Waste and EBS
		2.1.11.09.01	Convection Effects on Transport (Enhanced Vapor Diffusion)
2.1.11.10.0A	Thermal Effects on Transport in EBS	2.1.11.09.01	Convection Effects on Transport (Enhanced Vapor Diffusion)
		2.1.11.10.00	Thermal Effects on Diffusion (Soret Effect) in Waste and EBS
		2.1.11.10.01	Soret Effect (In Waste and EBS)
		2.1.11.10.02	Thermal Effects: Transport(Diffusion) Effects (In Waste and EBS)
		2.1.11.10.03	Soret Effect (Water Transport)
2.1.12.01.0A	Gas Generation (Repository Pressurization)	2.1.12.01.00	Gas Generation
		2.1.12.01.01	Formation of Gases (In Wastes and EBS)
		2.1.12.01.05	Pressurization (In Waste and EBS)
		2.1.12.06.01	Thermo-Chemical Effects (Related to Gas in Waste and EBS)
		2.1.12.06.03	Gas Effects (In Waste and EBS)
		2.1.12.06.06	Gas Transport
		2.1.12.06.07	Unsaturated Flow Due to Gas Production (In Waste and EBS)
2.1.12.02.0A	Gas Generation (He) from Waste Form Decay	2.1.12.01.00	Gas Generation
		2.1.12.01.02	Gas Generation
		2.1.12.01.04	Chemotoxic Gases (In Waste and EBS)
		2.1.12.02.00	Gas Generation (He) from Fuel Decay
		2.1.12.02.01	Helium Gas Production
		2.1.12.02.02	Internal Pressure (In Waste and EBS)
		2.1.12.02.03	Gas Generation, Canister
		2.1.12.02.04	Internal Pressure (In Waste and EBS)
		2.1.12.02.05	He Gas Production (In Waste and EBS)
2.1.12.03.0A	Gas Generation (H2) from Waste Package Corrosion	2.1.12.01.00	Gas Generation
		2.1.12.01.01	Formation of Gases (In Wastes and EBS)
		2.1.12.01.02	Gas Generation
		2.1.12.01.04	Chemotoxic Gases (In Waste and EBS)

Table G-1. Cross-Reference of TSPA-LA FEPs to TSPA-SR FEPs (Continued)

LA FEP Number	LA FEP Name	SR FEP Number	SR FEP Name
2.1.12.03.0A	Gas Generation (H2) from Waste Package Corrosion (continued)	2.1.12.03.00	Gas Generation (H2) from Metal Corrosion
		2.1.12.03.01	Chemical Effects of Corrosion
		2.1.12.03.02	Effect of Hydrogen on Corrosion
		2.1.12.03.03	Hydrogen Production (In Waste and EBS)
		2.1.12.03.04	Hydrogen Production by Metal Corrosion
		2.1.12.03.05	Container Material Inventory
		2.1.12.06.01	Thermo-Chemical Effects (Related to Gas in Waste and EBS)
2.1.12.04.0A	Gas Generation (CO2, CH4, H2S) from Microbial Degradation	2.1.02.10.00	Cellulosic Degradation
		2.1.06.01.03	Microbial Growth on Concrete
		2.1.12.01.00	Gas Generation
		2.1.12.01.02	Gas Generation
		2.1.12.01.03	Gas Generation, Buffer/Backfill
		2.1.12.01.04	Chemotoxic Gases (In Waste and EBS)
		2.1.12.03.04	Hydrogen Production by Metal Corrosion
		2.1.12.04.00	Gas Generation (CO2, CH4, H2S) from Microbial Degradation
		2.1.12.04.01	Effect of Temperature on Microbial Gas Generation
		2.1.12.04.02	Effect of Pressure on Microbial Gas Generation
		2.1.12.04.03	Effect of Radiation on Microbial Gas Generation
		2.1.12.04.04	Effect of Biofilms on Microbial Gas Generation
		2.1.12.04.05	Methane and Carbon Dioxide by Microbial Degradation
		2.1.12.05.00	Gas Generation from Concrete
		2.1.13.01.07	Radiolysis of Cellulose (In Waste and EBS)
2.1.12.06.0A	Gas Transport in EBS	2.1.12.06.00	Gas Transport in Waste and EBS
		2.1.12.06.01	Thermo-Chemical Effects (Related to Gas in Waste and EBS)
		2.1.12.06.02	Gas Transport
		2.1.12.06.03	Gas Effects (In Waste and EBS)
		2.1.12.06.04	Gas Escape from Canister
		2.1.12.06.05	Gas Flow and Transport, Buffer/Backfill
		2.1.12.06.06	Gas Transport

Table G-1. Cross-Reference of TSPA-LA FEPs to TSPA-SR FEPs (Continued)

LA FEP Number	LA FEP Name	SR FEP Number	SR FEP Name
2.1.12.06.0A	Gas Transport in EBS (continued)	2.1.12.06.07	Unsaturated Flow Due to Gas Production (In Waste and EBS)
		2.1.12.06.08	Gas Permeability (In Buffer/Backfill)
		2.2.01.03.01	Gas Transport/Dissolution (In the EDZ)
		2.2.11.03.00	Gas Transport in Geosphere
2.1.12.07.0A	Effects of Radioactive Gases in EBS	2.1.12.06.01	Thermo-Chemical Effects (Related to Gas in Waste and EBS)
		2.1.12.06.02	Gas Transport
		2.1.12.06.03	Gas Effects (In Waste and EBS)
		2.1.12.06.06	Gas Transport
		2.1.12.06.07	Unsaturated Flow Due to Gas Production (In Waste and EBS)
		2.1.12.07.00	Radioactive Gases in Waste and EBS
		2.1.12.07.01	Radioactive Gas (In Waste and EBS)
		2.1.12.07.02	Gaseous and Volatile Isotopes
		2.2.11.03.00	Gas Transport in Geosphere
2.1.12.08.0A	Gas Explosions in EBS	2.1.02.08.04	Acetylene Generation from DSNF Wfmisc—Flammable Gases Generation from DSNF - YMP
		2.1.11.04.02	Temperature Effects (Unexpected Effects) (In Waste and EBS)
		2.1.12.07.02	Gaseous and Volatile Isotopes
		2.1.12.08.00	Gas Explosions
		2.1.12.08.01	H2/O2 Explosions (In Waste and EBS)
		2.1.12.08.02	Flammability (In Waste and EBS)
		2.1.12.08.03	Explosions
		2.1.12.08.04	Explosion
2.1.13.01.0A	Radiolysis	2.1.02.21.01	Inside Out from Fission Products (Iodine) (Failure of Cladding)
		2.1.03.07.01	Other Canister Degradation Processes
		2.1.09.06.00	Reduction-Oxidation Potential in Waste and EBS
		2.1.09.06.01	Redox Front (In Waste and EBS)
		2.1.09.06.04	Redox Front (In Buffer/Backfill)
		2.1.12.01.00	Gas Generation
		2.1.12.01.01	Formation of Gases (In Wastes and EBS)

Table G-1. Cross-Reference of TSPA-LA FEPs to TSPA-SR FEPs (Continued)

LA FEP Number	LA FEP Name	SR FEP Number	SR FEP Name
2.1.13.01.0A	Radiolysis (continued)	2.1.12.01.02	Gas Generation
		2.1.12.01.03	Gas Generation, Buffer/Backfill
		2.1.12.01.04	Chemotoxic Gases (In Waste and EBS)
		2.1.12.05.00	Gas Generation from Concrete
		2.1.13.01.00	Radiolysis
		2.1.13.01.01	Radiolysis (In Waste and EBS)
		2.1.13.01.02	Radiolysis
		2.1.13.01.03	Radiolysis (In Waste and EBS)
		2.1.13.01.04	Radiolysis (In Waste and EBS)
		2.1.13.01.05	Radiolysis Prior to Wetting (In Waste and EBS)
		2.1.13.01.06	Radiolysis of Brine
		2.1.13.01.07	Radiolysis of Cellulose (In Waste and EBS)
		2.1.13.01.08	Radiolysis
		2.1.13.01.09	Radiolysis
		2.1.13.02.01	Radiation Effects (In Waste and EBS)
		2.1.13.02.05	Radiation Shielding (In Waste and EBS)
		2.2.08.01.13	Change of Groundwater Chemistry in Nearby Rock
		3.1.01.01.06	Radioactive Decay
		3.1.01.01.09	Radiological Events and Processes
2.1.13.02.0A	Radiation Damage in EBS	2.1.02.04.01	Recoil of Alpha-Decay
		2.1.03.07.01	Other Canister Degradation Processes
		2.1.13.02.00	Radiation Damage in Waste and EBS
		2.1.13.02.01	Radiation Effects (In Waste and EBS)
		2.1.13.02.02	Radiation Effects on Bentonite
		2.1.13.02.03	Material Property Changes (Due to Radiation in Waste and EBS)
		2.1.13.02.04	Radiation Damage (In Waste and EBS)
		2.1.13.02.05	Radiation Shielding (In Waste and EBS)
		2.1.13.02.06	Radiation Effects on Buffer/Backfill
		2.1.13.02.07	Radiation Effects on Canister
		2.1.13.02.08	Radiological Effects on Waste
		2.1.13.02.09	Radiological Effects on Containers

Table G-1. Cross-Reference of TSPA-LA FEPs to TSPA-SR FEPs (Continued)

LA FEP Number	LA FEP Name	SR FEP Number	SR FEP Name
2.1.13.02.0A	Radiation Damage in EBS (continued)	2.1.13.02.10	Radiological Effects on Seals
		2.1.13.02.11	Radiation Effects on Canister
		3.1.01.01.06	Radioactive Decay
		3.1.01.01.09	Radiological Events and Processes
2.1.13.03.0A	Radiological Mutation of Microbes	2.1.12.04.03	Effect of Radiation on Microbial Gas Generation
		2.1.13.03.00	Mutation
2.1.14.15.0A	In-Package Criticality (Intact Configuration)	2.1.14.01.00	Criticality in Waste and EBS
		2.1.14.02.00	Criticality In-Situ, Nominal Configuration, Top Breach
		2.1.14.02.01	Criticality - MPC Flooded
		2.1.14.02.02	Criticality - Nominal Configuration, Partially Flooded, Otherwise Intact
2.1.14.16.0A	In-Package Criticality (Degraded Configurations)	2.1.14.01.00	Criticality in Waste and EBS
		2.1.14.01.01	Criticality (In Waste and EBS)
		2.1.14.01.02	Criticality (In Waste and EBS)
		2.1.14.01.03	Nuclear Criticality (In Waste and EBS)
		2.1.14.01.04	Nuclear Criticality (In Waste and EBS)
		2.1.14.01.05	Nuclear Criticality (In Waste and EBS)
		2.1.14.01.06	Nuclear Criticality: Heat (In Waste and EBS)
		2.1.14.01.07	Nuclear Explosions (In Waste and EBS)
		2.1.14.01.08	DOE SNF Criticality In-Situ
		2.1.14.01.10	DOE SNF Criticality Near-Field (Radionuclide Inventory Impact)
		2.1.14.01.11	DOE SNF Criticality In-Situ (Waste Heat Impact)
		2.1.14.01.12	DOE SNF Criticality In-Situ (Waste Package Degradation Impact)
		2.1.14.01.13	DOE SNF Criticality In-Situ (Waste Form Degradation Impact)
		2.1.14.01.14	DOE SNF Criticality In-Situ (Cladding Degradation Impact)
		2.1.14.01.15	Differential Solubility of Neutron Poisons
		2.1.14.01.16	Selective Leaching of Fissile Materials

Table G-1. Cross-Reference of TSPA-LA FEPs to TSPA-SR FEPs (Continued)

LA FEP Number	LA FEP Name	SR FEP Number	SR FEP Name
2.1.14.16.0A	In-Package Criticality (Degraded Configurations) (continued)	2.1.14.01.17	Differential Solubility of Fissile Isotopes
		2.1.14.03.00	Criticality In-Situ, WP Internal Structures Degrade Faster Than Waste Form, Top Breach
		2.1.14.03.01	Waste Package Internal Structures Degrade Faster Than Waste Form
		2.1.14.03.02	Waste Package Internal Structures Collapse
		2.1.14.03.03	Criticality - Container Partially Gone, Optimal Rod Configuration, Flooded
		2.1.14.04.00	Criticality In-Situ, WP Internal Structures Degrade at Same Rate As Waste Form, Top Breach
		2.1.14.04.01	Waste Package Internal Structures and the Waste Form Degrade At the Same Rate
		2.1.14.04.02	Criticality - Clad and Disintegrated Pellets, Optimally Mixed, Flooded
		2.1.14.05.00	Criticality In-Situ, WP Internal Structures Degrade Slower Than Waste Form, Top Breach
		2.1.14.05.01	Waste Package Internal Structures Degrade Slower Than Waste Form
		2.1.14.06.00	Criticality In-Situ, Waste Form Degrades in Place and Swells, Top Breach
		2.1.14.07.00	Criticality In-Situ, Bottom Breach Allows Flow Through WP, Fissile Material Collects at Bottom of WP
		2.1.14.08.00	Criticality In-Situ, Bottom Breach Allows Flow Through WP, Waste Form Degrades in Place
		2.1.14.08.01	Neutron Absorber System Selectively Degrades
		2.1.14.08.02	Neutron Sorbers Selectively Flushed from Containers
		2.1.14.08.03	Selective Leaching of Neutron Sorbers

Table G-1. Cross-Reference of TSPA-LA FEPs to TSPA-SR FEPs (Continued)

LA FEP Number	LA FEP Name	SR FEP Number	SR FEP Name
2.1.14.17.0A	Near-Field Criticality	2.1.14.01.00	Criticality in Waste and EBS
		2.1.14.01.09	DOE SNF Criticality In-Situ (Radionuclide Inventory Impact)
		2.1.14.09.00	Near-Field Criticality, Fissile Material Deposited in Near-Field Pond
		2.1.14.09.01	Criticality - Container Gone, Intact Rods, Flooded
		2.1.14.09.02	Criticality - Container Gone, Intact Rods, Dry
		2.1.14.09.03	Criticality - Container Gone, Pile of Fuel Pellets, Dry
		2.1.14.09.04	Criticality - Container Gone, Pile of Fuel Pellets, Flooded
		2.1.14.09.05	Criticality - Container and Cladding Gone, Fuel Powder, Flooded
		2.1.14.09.06	Criticality - Container and Cladding Gone, Fuel Powder, Dry
		2.1.14.09.07	Formation of a Critical Assembly in a Pool (In Waste and EBS)
		2.1.14.09.08	Pu Accumulates in Basin Pool (In Waste and EBS)
		2.1.14.09.09	Accumulated 239Pu Decays to 235U in Basin Pool (In Waste and EBS)
		2.1.14.10.00	Near-Field Criticality, Fissile Solution Flows Into Drift Lowpoint
		2.1.14.10.01	Accumulation of Clays and Sediments in Basin (In EBS)
		2.1.14.11.00	Near-Field Criticality, Fissile Solution Is Adsorbed or Reduced in Invert
		2.1.14.12.00	Near-Field Criticality, Filtered Slurry or Colloidal Stream Collects on Invert Surface
		2.1.14.13.00	Near-Field Criticality Associated With Colloidal Deposits
2.1.14.18.0A	In-Package Criticality Resulting from a Seismic Event (Intact Configuration)	2.1.14.01.00	Criticality in Waste and EBS
		2.1.14.14.00	Out-of-Package Criticality, Fuel/Magma Mixture
2.1.14.19.0A	In-Package Criticality Resulting from a Seismic Event (Degraded Configurations)	2.1.14.01.00	Criticality in Waste and EBS
		2.1.14.14.00	Out-of-Package Criticality, Fuel/Magma Mixture
2.1.14.20.0A	Near-Field Criticality Resulting from a Seismic Event	2.1.14.01.00	Criticality in Waste and EBS
		2.1.14.14.00	Out-of-Package Criticality, Fuel/Magma Mixture

Table G-1. Cross-Reference of TSPA-LA FEPs to TSPA-SR FEPs (Continued)

LA FEP Number	LA FEP Name	SR FEP Number	SR FEP Name
2.1.14.21.0A	In-Package Criticality Resulting from Rockfall (Intact Configuration)	2.1.14.01.00	Criticality in Waste and EBS
		2.1.14.14.00	Out-of-Package Criticality, Fuel/Magma Mixture
2.1.14.22.0A	In-Package Criticality Resulting from Rockfall (Degraded Configurations)	2.1.14.01.00	Criticality in Waste and EBS
		2.1.14.14.00	Out-of-Package Criticality, Fuel/Magma Mixture
2.1.14.23.0A	Near-Field Criticality Resulting from Rockfall	2.1.14.01.00	Criticality in Waste and EBS
		2.1.14.14.00	Out-of-Package Criticality, Fuel/Magma Mixture
2.1.14.24.0A	In-Package Criticality Resulting from an Igneous Event (Intact Configuration)	2.1.14.01.00	Criticality in Waste and EBS
		2.1.14.14.00	Out-of-Package Criticality, Fuel/Magma Mixture
2.1.14.25.0A	In-Package Criticality Resulting from an Igneous Event (Degraded Configurations)	2.1.14.01.00	Criticality in Waste and EBS
		2.1.14.14.00	Out-of-Package Criticality, Fuel/Magma Mixture
2.1.14.26.0A	Near-Field Criticality Resulting from an Igneous Event	2.1.14.01.00	Criticality in Waste and EBS
		2.1.14.14.00	Out-of-Package Criticality, Fuel/Magma Mixture
2.2.01.01.0A	Mechanical Effects of Excavation and Construction in the Near-Field	1.1.02.00.01	Blasting and Vibration
		1.1.02.00.03	Groundwater Chemistry (Excavation)
		2.1.08.08.00	Induced Hydrological Changes in the Waste and EBS
		2.2.01.01.00	Excavation and Construction-Related Changes in the Adjacent Host Rock
		2.2.01.01.01	Disturbed Rock Zone
		2.2.01.01.02	Mechanical Effects - Excavation/Backfilling Effects
		2.2.01.01.03	Formation of Cracks (Host Rock Disturbed Zone)
		2.2.01.01.04	Damaged Zone (Host Rock Disturbed Zone)
		2.2.01.01.05	Excavation/Backfilling Effects on Nearby Rock
		2.2.01.01.06	Mechanical Effects - Excavation/Backfilling Effects
		2.2.01.01.07	Enhanced Rock Fracturing
		2.2.01.01.09	Excavation Effects on Nearby Rock
		2.2.01.01.10	Disturbed Zone (Hydromechanical) Effects
		2.2.01.01.11	Excavation-Induced Changes in Stress
		2.2.01.02.01	Hydraulic Conductivity Change (Host Rock Disturbed Zone)

Table G-1. Cross-Reference of TSPA-LA FEPs to TSPA-SR FEPs (Continued)

LA FEP Number	LA FEP Name	SR FEP Number	SR FEP Name
2.2.01.01.0B	Chemical Effects of Excavation and Construction in the Near-Field	2.1.08.08.00	Induced Hydrological Changes in the Waste and EBS
		2.2.01.01.00	Excavation and Construction-Related Changes in the Adjacent Host Rock
		2.2.01.01.03	Formation of Cracks (Host Rock Disturbed Zone)
2.2.01.02.0A	Thermally-Induced Stress Changes in the Near-Field	2.1.11.07.00	Thermally-Induced Stress Changes in Waste and EBS
		2.2.01.02.00	Thermal and Other Waste and EBS-Related Changes in the Adjacent Host Rock
		2.2.01.02.01	Hydraulic Conductivity Change (Host Rock Disturbed Zone)
		2.2.01.02.03	Properties of Near-Field Rock (Host Rock Disturbed Zone)
		2.2.01.02.04	Stress Changes of Conductivity
2.2.01.02.0B	Chemical Changes in the Near-Field from Backfill	2.1.04.06.00	Properties of Bentonite
		2.2.01.02.02	Water Flow At the Bentonite-Host Rock Interface
2.2.01.03.0A	Changes in Fluid Saturations in the Excavation Disturbed Zone	2.2.01.01.04	Damaged Zone (Host Rock Disturbed Zone)
		2.2.01.02.02	Water Flow At the Bentonite-Host Rock Interface
		2.2.01.03.00	Changes in Fluid Saturations in the Excavation Disturbed Zone
2.2.01.04.0A	Radionuclide Solubility in the Excavation Disturbed Zone	2.2.01.04.00	Elemental Solubility in Excavation Disturbed Zone
2.2.01.05.0A	Radionuclide Transport in the Excavation Disturbed Zone	2.2.01.01.04	Damaged Zone (Host Rock Disturbed Zone)
		2.2.01.03.01	Gas Transport/Dissolution (In the EDZ)
		2.2.01.05.00	Radionuclide Transport in Excavation Disturbed Zone
		2.2.01.05.01	Radionuclide Retardation (Excavation-Disturbed Zone)
		2.2.01.05.02	Radionuclide Release from EDZ
2.2.03.01.0A	Stratigraphy	2.2.03.01.00	Stratigraphy
		2.2.03.01.01	Mesozoic Sedimentary Cover
		2.2.03.01.02	Permo-Carboniferous Trough
		2.2.03.01.03	Brine Reservoirs
2.2.03.02.0A	Rock Properties of Host Rock and Other Units	2.2.03.02.00	Rock Properties of Host Rock and Other Units
		2.2.03.02.01	Rock Heterogeneity (Host Rock)
		2.2.03.02.02	LPD Effective Hydraulic Properties
		2.2.03.02.03	MWCF Effective Hydraulic Properties

Table G-1. Cross-Reference of TSPA-LA FEPs to TSPA-SR FEPs (Continued)

LA FEP Number	LA FEP Name	SR FEP Number	SR FEP Name
2.2.03.02.0A	Rock Properties of Host Rock and Other Units (continued)	2.2.03.02.04	HPD Effective Hydraulic Properties
		2.2.03.02.05	Properties of Far-Field Rock
2.2.06.01.0A	Seismic Activity Changes Porosity and Permeability of Rock	2.2.06.01.00	Changes in Stress (Due to Thermal, Seismic, or Tectonic Effects) Change Porosity and Permeability of Rock
		2.2.06.01.01	Stress-Produced Porosity Changes
		2.2.06.01.02	Stress-Produced Permeability Changes
		2.2.06.01.03	Stress-Produced Permeability Changes
		2.2.06.01.04	Regional Stress Regime
		2.2.06.01.05	Regional Stress Regime
		2.2.06.01.06	Regional Stress Regime
		2.2.06.01.07	Stress Field (In Geosphere)
		2.2.06.01.08	Changes in the Stress Field
		2.2.06.01.09	Changes in Regional Stress
		2.2.06.01.10	Stress Changes - Hydrogeological Effects
2.2.06.02.0A	Seismic Activity Changes Porosity and Permeability of Faults	1.2.02.02.00	Faulting
		2.2.06.02.00	Changes in Stress (Due to Thermal, Seismic, or Tectonic Effects) Produce Changes in Permeability of Faults
		2.2.06.02.01	Aseismic Alteration of Permeability Along and Across Faults
		2.2.06.02.02	Fracture Dilation Along Faults Creates Zones of Enhanced Permeability
		2.2.06.02.03	Relaxation of Thermal Stresses by Fault Movement
		2.2.06.02.04	Seismically-Stimulated Release of Thermo-Mechanical Stress on Bounding Faults
		2.2.06.02.05	Relaxation of Thermal Stresses by Fault Movement
2.2.06.02.0B	Seismic Activity Changes Porosity and Permeability of Fractures	1.2.02.01.00	Fractures
		2.2.06.02.00	Changes in Stress (Due to Thermal, Seismic, or Tectonic Effects) Produce Changes in Permeability of Faults
		2.2.06.02.02	Fracture Dilation Along Faults Creates Zones of Enhanced Permeability

Table G-1. Cross-Reference of TSPA-LA FEPs to TSPA-SR FEPs (Continued)

LA FEP Number	LA FEP Name	SR FEP Number	SR FEP Name
2.2.06.03.0A	Seismic Activity Alters Perched Water Zones	2.2.06.03.00	Changes in Stress (Due to Seismic or Tectonic Effects) Alter Perched Water Zones
		2.2.06.03.01	Perched Zones Develop As a Result of Stress Changes
2.2.06.04.0A	Effects of Subsidence	2.1.11.07.02	Stress Field Changes, Settling, Subsidence, or Caving
		2.2.06.04.00	Effects of Subsidence
		2.2.06.04.01	Subsidence
		2.2.06.04.02	Large-Scale Rock Fracturing
		2.2.06.04.03	Borehole-Induced Solution and Subsidence
2.2.06.05.0A	Salt Creep	2.2.06.05.00	Salt Creep
2.2.07.01.0A	Locally Saturated Flow at Bedrock/Alluvium Contact	2.2.07.01.00	Locally Saturated Flow at Bedrock/Alluvium Contact
		2.2.07.04.01	Effects of Preferential Flow Paths
2.2.07.02.0A	Unsaturated Groundwater Flow in the Geosphere	2.2.07.02.00	Unsaturated Groundwater Flow in Geosphere
		2.2.07.02.01	Unsaturated Rock
2.2.07.03.0A	Capillary Rise in the UZ	2.2.07.02.02	Soil Depth
		2.2.07.03.00	Capillary Rise
		2.2.07.03.01	Capillary Rise (Near Surface Hydrology)
		2.2.07.11.05	Resaturation of Dry-Out Zone Is Effected by Liquid Under Capillary Forces
2.2.07.04.0A	Focusing of Unsaturated Flow (Fingers, Weeps)	2.2.07.04.00	Focusing of Unsaturated Flow (Fingers, Weeps)
		2.2.07.04.01	Effects of Preferential Flow Paths
		2.2.07.04.02	Seeps and Weeps Form As a Locally Saturated Flow System
		2.2.07.04.03	Fault Control of Fluid Entrance To and Movement Away from the Repository
		2.2.07.04.04	Fingering – Contaminant Transport in Fingers in UZ
2.2.07.05.0A	Flow in the UZ from Episodic Infiltration	2.2.07.05.00	Flow and Transport in the UZ from Episodic Infiltration
2.2.07.06.0A	Episodic or Pulse Release from Repository	2.2.07.05.01	Episodic Infiltration Enhances Colloid Transport
		2.2.07.06.00	Episodic / Pulse Release from Repository
2.2.07.06.0B	Long-Term Release of Radionuclides from the Repository	2.2.07.06.00	Episodic / Pulse Release from Repository

Table G-1. Cross-Reference of TSPA-LA FEPs to TSPA-SR FEPs (Continued)

LA FEP Number	LA FEP Name	SR FEP Number	SR FEP Name
2.2.07.07.0A	Perched Water Develops	1.4.01.01.01	Climate Modification Causes Perched Water to Develop at Base of Topopah Spring Unit
		1.4.01.01.02	Climate Modification Causes Perched Water to Develop Above Repository
		2.2.07.04.00	Focusing of Unsaturated Flow (Fingers, Weeps)
		2.2.07.07.00	Perched Water Develops
		2.2.07.07.01	Perched Water Develops at Base of Topopah Spring Welded Unit
2.2.07.08.0A	Fracture Flow in the UZ	2.2.07.08.00	Fracture Flow in the Unsaturated Zone
		2.2.07.08.01	Fracture Flow (In Geosphere)
		2.2.07.08.02	Extreme Channel Flow of Oxidants and Nuclides (In Geosphere)
2.2.07.09.0A	Matrix Imbibition in the UZ	2.2.07.09.00	Matrix Imbibition in the Unsaturated Zone
		2.2.07.09.01	Resaturation Due to Matrix Imbibition of Episodic Fracture Flow
2.2.07.10.0A	Condensation Zone Forms Around Drifts	2.2.07.10.00	Condensation Zone Forms Around Drifts
		2.2.07.10.01	Condensation Cap Forms Above Repository
		2.2.07.10.02	Formation of Condensate Over Individual Containers
		2.2.07.10.03	Formation of Condensate Over Individual Panels
		2.2.07.10.04	Formation of Condensate Over the Entire Repository
		2.2.07.10.05	Shedding of Condensation Cap Over One Drift to Another Drift
		2.2.07.10.06	Vault Geometry
2.2.07.11.0A	Resaturation of Geosphere Dry-Out Zone	2.2.07.11.00	Return Flow from Condensation Cap / Resaturation of Dry-Out Zone
		2.2.07.11.01	Auto-Catalytic Drainage of Locally Saturated Flow Thru Condensation Cap
		2.2.07.11.02	Resaturation, Near-Field Rock
		2.2.07.11.03	Return of Condensate to Same Panel
		2.2.07.11.04	Resaturation of Dry-Out Zone Is Affected by Vapor Flow

Table G-1. Cross-Reference of TSPA-LA FEPs to TSPA-SR FEPs (Continued)

LA FEP Number	LA FEP Name	SR FEP Number	SR FEP Name
2.2.07.11.0A	Resaturation of Geosphere Dry-Out Zone (continued)	2.2.07.11.05	Resaturation of Dry-Out Zone Is Effected by Liquid Under Capillary Forces
		2.2.07.11.06	Unsaturated Flow Plume Returns Flow from the Condensation Cap
		2.2.08.02.01	Locally-Saturated Carrier Plume Forms (In Geosphere)
		2.2.08.02.02	Unsaturated Carrier Plume Forms (In Geosphere)
2.2.07.12.0A	Saturated Groundwater Flow in the Geosphere	1.4.01.01.05	Climate Modification Raises Water Table to Short Circuit Flow Barrier in SZ
		2.2.07.12.00	Saturated Groundwater Flow
		2.2.07.12.01	Groundwater Flow (In Geosphere)
		2.2.07.12.02	Groundwater Flow in LPD
		2.2.07.12.03	Groundwater Flow Path
		2.2.07.12.04	Groundwater Flow in MWCF
		2.2.07.12.05	Groundwater Flow Path (In Geosphere)
		2.2.07.12.06	Groundwater Flow (In Geosphere)
		2.2.07.12.07	Boundary Conditions For Flow
		2.2.07.12.08	Groundwater Flow Path (In Geosphere)
		2.2.07.12.09	Hydraulic Gradient Changes (Magnitude, Regional Direction)
		2.2.07.12.10	Groundwater Flow (In Geosphere)
		2.2.07.12.11	Groundwater Flow (In Geosphere)
		2.2.07.12.12	Hydrological (Processes)
		2.2.07.12.13	Turbulence (In Groundwater)
		2.2.07.12.14	Changes in Groundwater Flow
		2.2.07.12.15	Enhanced Groundwater Flow
2.2.07.13.0A	Water-Conducting Features in the SZ	2.2.07.13.00	Water-Conducting Features in the Saturated Zone SZ—Water-Conducting Features
		2.2.07.13.01	Water-Conducting Features (Types) (In Geosphere)
2.2.07.14.0A	Chemically-Induced Density Effects on Groundwater Flow	2.2.07.14.00	Density Effects on Groundwater Flow
		2.2.07.14.01	Saline Intrusion (In Geosphere)
		2.2.07.14.02	Salinity Effects on Flow
		2.2.07.14.03	Intrusion of Saline Groundwater

Table G-1. Cross-Reference of TSPA-LA FEPs to TSPA-SR FEPs (Continued)

LA FEP Number	LA FEP Name	SR FEP Number	SR FEP Name
2.2.07.15.0A	Advection and Dispersion in the SZ	2.2.07.15.00	Advection and Dispersion
		2.2.07.15.01	Far-Field Transport: Advection
		2.2.07.15.02	Far-Field Transport: Hydrodynamic Dispersion
		2.2.07.15.03	Dispersion (Water Transport)
		2.2.07.15.04	Solute Transport (Water Transport)
		2.2.07.15.05	Advection (Water Transport)
		2.2.07.15.07	Dispersion (Water Transport)
		2.2.07.15.08	Convection (Water Transport)
		2.2.07.15.09	Dispersion (Water Transport)
		2.2.07.15.10	Dispersion (Water Transport)
		2.2.07.15.11	Dispersion (Water Transport)
		2.2.07.15.12	Transport and Release of Nuclides, Near-Field Rock
		2.2.07.15.13	Groundwater Flow (Alluvium of Rhine Valley)
2.2.07.15.0B	Advection and Dispersion in the UZ	2.2.07.02.01	Unsaturated Rock
		2.2.07.04.04	Fingering - Contaminant Transport in Fingers in UZ
		2.2.07.08.02	Extreme Channel Flow of Oxidants and Nuclides (In Geosphere)
		2.2.07.15.00	Advection and Dispersion
		2.3.11.03.11	Groundwater Recharge
2.2.07.16.0A	Dilution of Radionuclides in Groundwater	2.2.07.15.14	Exfiltration to a Local Aquifer
		2.2.07.16.00	Dilution of Radionuclides in Groundwater
		2.2.07.16.01	Dilution (Water Transport)
		2.2.07.16.02	Dilution of Radionuclides in Groundwater (Water Transport)
		2.2.07.16.03	Dilution of Radionuclides in HPD
2.2.07.17.0A	Diffusion in the SZ	2.2.07.15.04	Solute Transport (Water Transport)
		2.2.07.15.12	Transport and Release of Nuclides, Near-Field Rock
		2.2.07.17.00	Diffusion in the Saturated Zone
		2.2.07.17.01	Far-Field Transport: Diffusion
		2.2.07.17.02	Diffusion (Water Transport)
		2.2.07.17.03	Diffusion (Water Transport)
		2.2.07.17.04	Diffusion (Water Transport)
		2.2.07.17.05	Diffusion (Water Transport)
2.2.07.18.0A	Film Flow Into the Repository	2.2.07.18.00	Film Flow Into Drifts

Table G-1. Cross-Reference of TSPA-LA FEPs to TSPA-SR FEPs (Continued)

LA FEP Number	LA FEP Name	SR FEP Number	SR FEP Name
2.2.07.19.0A	Lateral Flow from Solitario Canyon Fault Enters Drifts	2.2.07.04.01	Effects of Preferential Flow Paths
		2.2.07.04.03	Fault Control of Fluid Entrance To and Movement Away from the Repository
		2.2.07.19.00	Lateral Flow from Solitario Canyon Fault Enters Potential Waste Emplacement Drifts
2.2.07.20.0A	Flow Diversion Around Repository Drifts	2.1.08.05.02	UZ Flow Through/Around the Collapsed Invert
2.2.07.21.0A	Drift Shadow Forms Below Repository	2.1.08.03.00	Repository Dry-Out Due to Waste Heat
2.2.08.01.0A	Chemical Characteristics of Groundwater in the SZ	2.2.08.01.00	Groundwater Chemistry / Composition in UZ and SZ SZ—Groundwater Chemistry FEPs
		2.2.08.01.01	Groundwater Chemistry (In Geosphere)
		2.2.08.01.03	Interface Different Waters (In Geosphere)
		2.2.08.01.05	Groundwater Geochemistry (In Geosphere)
		2.2.08.01.17	Chemical Gradients
		2.2.08.01.19	Groundwater Chemistry (In Geosphere)
		2.2.08.01.21	Groundwater Conditions
		2.2.08.01.22	Mineralogy (Host Rock)
		2.2.08.01.23	Mineralogy (Host Rock)
		2.2.08.02.00	Radionuclide Transport Occurs in a Carrier Plume in Geosphere SZ—Radionuclide Transport in a Carrier Plume
		2.2.08.10.02	Colloid Transport Occurs in a Carrier Plume (In Geosphere)
2.2.08.01.0B	Chemical Characteristics of Groundwater in the UZ	2.2.08.01.01	Groundwater Chemistry (In Geosphere)
		2.2.08.01.03	Interface Different Waters (In Geosphere)
		2.2.08.01.04	Water Chemistry in Near-Field Rock
		2.2.08.01.17	Chemical Gradients
		2.2.08.01.19	Groundwater Chemistry (In Geosphere)
		2.2.08.01.21	Groundwater Conditions
		2.2.08.01.22	Mineralogy (Host Rock)
		2.2.08.01.23	Mineralogy (Host Rock)

Table G-1. Cross-Reference of TSPA-LA FEPs to TSPA-SR FEPs (Continued)

LA FEP Number	LA FEP Name	SR FEP Number	SR FEP Name
2.2.08.01.0B	Chemical Characteristics of Groundwater in the UZ (continued)	2.2.08.02.00	Radionuclide Transport Occurs in a Carrier Plume in Geosphere SZ—Radionuclide Transport in a Carrier Plume
		2.2.08.03.00	Geochemical Interactions in Geosphere (Dissolution, Precipitation, Weathering) and Effects on Radionuclide Transport SZ—Groundwater Chemistry FEPs
		2.3.11.03.05	Recharge Groundwater
		2.3.11.03.06	Surface Water Chemistry
		2.3.11.03.13	Recharge Groundwater (Affects Waste and EBS)
2.2.08.03.0A	Geochemical Interactions and Evolution in the SZ	2.2.08.01.00	Groundwater Chemistry / Composition in UZ and SZ SZ—Groundwater Chemistry FEPs
		2.2.08.01.01	Groundwater Chemistry (In Geosphere)
		2.2.08.01.02	Deep Saline Water Intrusion
		2.2.08.01.06	Saline Intrusion (In Geosphere)
		2.2.08.01.07	Freshwater Intrusion (In Geosphere)
		2.2.08.01.08	Changes in Groundwater Eh
		2.2.08.01.09	Changes in Groundwater Ph
		2.2.08.01.10	Oxidizing Conditions
		2.2.08.01.11	Groundwater Composition
		2.2.08.01.12	Ph-Deviations
		2.2.08.01.14	Saline (Or Fresh) Groundwater Intrusion
		2.2.08.01.15	Saline or Freshwater Intrusion
		2.2.08.01.16	Effects at Saline-Freshwater Interface
		2.2.08.01.18	Non-Radioactive Solute Plume in Geosphere
		2.2.08.01.19	Groundwater Chemistry (In Geosphere)
		2.2.08.01.20	Intrusion of Saline Groundwater
		2.2.08.02.00	Radionuclide Transport Occurs in a Carrier Plume in Geosphere SZ—Radionuclide Transport in a Carrier Plume
		2.2.08.02.03	Precipitation/Dissolution (Release/Migration Factors)

Table G-1. Cross-Reference of TSPA-LA FEPs to TSPA-SR FEPs (Continued)

LA FEP Number	LA FEP Name	SR FEP Number	SR FEP Name
2.2.08.03.0A	Geochemical Interactions and Evolution in the SZ (continued)	2.2.08.03.00	Geochemical Interactions in Geosphere (Dissolution, Precipitation, Weathering) and Effects on Radionuclide Transport SZ—Groundwater Chemistry FEPs
		2.2.08.03.01	Far-Field Transport: Changes in Groundwater Chemistry and Flow Direction
		2.2.08.03.02	Effects of Dissolution (In Geosphere)
		2.2.08.03.03	Rock Property Changes (In Geosphere)
		2.2.08.03.04	Hydraulic Properties-Evolution
		2.2.08.03.05	Dissolution of Fracture Fillings/Precipitations (In Geosphere)
		2.2.08.03.06	Weathering of Flow Paths (In Geosphere)
		2.2.08.03.07	Fracture Mineralization and Weathering (In Geosphere)
		2.2.08.03.08	Alteration/Weathering of Flow Paths
		2.2.08.03.09	Precipitation and Dissolution (Release/Migration Factors)
		2.2.08.03.10	Chemical Precipitation (Release/Migration Factors)
		2.2.08.03.11	Dissolution, Precipitation, and Crystallization (Release/Migration Factors)
		2.2.08.03.12	Kinetics of Precipitation and Dissolution (Release/Migration Factors)
		2.2.08.03.13	Speciation (Contaminant Speciation and Solubility)
		2.2.08.03.14	Speciation (Geosphere) (Contaminant Speciation and Solubility)
		2.2.08.03.15	Recrystallization (Contaminant Speciation and Solubility)
		2.2.08.03.16	Speciation (Contaminant Speciation and Solubility)
		2.2.08.03.17	Kinetics of Speciation (Contaminant Speciation and Solubility)
		2.2.08.03.18	Groundwater Chemistry (Sorption/Desorption Processes)
		2.2.08.10.02	Colloid Transport Occurs in a Carrier Plume (In Geosphere)

Table G-1. Cross-Reference of TSPA-LA FEPs to TSPA-SR FEPs (Continued)

LA FEP Number	LA FEP Name	SR FEP Number	SR FEP Name
2.2.08.03.0B	Geochemical Interactions and Evolution in the UZ	2.2.08.01.01	Groundwater Chemistry (In Geosphere)
		2.2.08.01.04	Water Chemistry in Near-Field Rock
		2.2.08.01.10	Oxidizing Conditions
		2.2.08.01.11	Groundwater Composition
		2.2.08.01.13	Change of Groundwater Chemistry in Nearby Rock
		2.2.08.01.18	Non-Radioactive Solute Plume in Geosphere
		2.2.08.01.19	Groundwater Chemistry (In Geosphere)
		2.2.08.02.00	Radionuclide Transport Occurs in a Carrier Plume in Geosphere SZ—Radionuclide Transport in a Carrier Plume
		2.2.08.02.01	Locally-Saturated Carrier Plume Forms (In Geosphere)
		2.2.08.02.02	Unsaturated Carrier Plume Forms (In Geosphere)
		2.2.08.02.03	Precipitation/Dissolution (Release/Migration Factors)
		2.2.08.03.00	Geochemical Interactions in Geosphere (Dissolution, Precipitation, Weathering) and Effects on Radionuclide Transport SZ—Groundwater Chemistry FEPs
		2.2.08.03.03	Rock Property Changes (In Geosphere)
		2.2.08.03.04	Hydraulic Properties-Evolution
		2.2.08.03.05	Dissolution of Fracture Fillings/Precipitations (In Geosphere)
		2.2.08.03.06	Weathering of Flow Paths (In Geosphere)
		2.2.08.03.07	Fracture Mineralization and Weathering (In Geosphere)
		2.2.08.03.08	Alteration/Weathering of Flow Paths
		2.2.08.03.09	Precipitation and Dissolution (Release/Migration Factors)
		2.2.08.03.10	Chemical Precipitation (Release/Migration Factors)
		2.2.08.03.11	Dissolution, Precipitation, and Crystallization (Release/Migration Factors)

Table G-1. Cross-Reference of TSPA-LA FEPs to TSPA-SR FEPs (Continued)

LA FEP Number	LA FEP Name	SR FEP Number	SR FEP Name
2.2.08.03.0B	Geochemical Interactions and Evolution in the UZ (continued)	2.2.08.03.12	Kinetics of Precipitation and Dissolution (Release/Migration Factors)
		2.2.08.03.13	Speciation (Contaminant Speciation and Solubility)
		2.2.08.03.14	Speciation (Geosphere) (Contaminant Speciation and Solubility)
		2.2.08.03.15	Recrystallization (Contaminant Speciation and Solubility)
		2.2.08.03.16	Speciation (Contaminant Speciation and Solubility)
		2.2.08.03.17	Kinetics of Speciation (Contaminant Speciation and Solubility)
		2.2.08.03.18	Groundwater Chemistry (Sorption/Desorption Processes)
2.2.08.04.0A	Re-Dissolution of Precipitates Directs More Corrosive Fluids to Waste Packages	2.2.08.04.00	Redissolution of Precipitates Directs More Corrosive Fluids to Containers
2.2.08.05.0A	Diffusion in the UZ	2.2.08.05.00	Osmotic Processes
		2.3.11.03.11	Groundwater Recharge
2.2.08.06.0A	Complexation in the SZ	2.2.08.01.11	Groundwater Composition
		2.2.08.06.00	Complexation in Geosphere
		2.2.09.01.02	Microbes (In Geosphere)
2.2.08.06.0B	Complexation in the UZ	2.2.08.01.11	Groundwater Composition
		2.2.08.06.00	Complexation in Geosphere
2.2.08.07.0A	Radionuclide Solubility Limits in the SZ	2.2.08.03.13	Speciation (Contaminant Speciation and Solubility)
		2.2.08.03.14	Speciation (Geosphere) (Contaminant Speciation and Solubility)
		2.2.08.03.15	Recrystallization (Contaminant Speciation and Solubility)
		2.2.08.03.16	Speciation (Contaminant Speciation and Solubility)
		2.2.08.03.17	Kinetics of Speciation (Contaminant Speciation and Solubility)
		2.2.08.07.00	Radionuclide Solubility Limits in the Geosphere
		2.2.08.07.01	Radionuclide Transport Through LPD (Water Transport)
		2.2.08.07.02	Radionuclide Transport Through MWCF (Water Transport)
		2.2.08.07.03	Solubility Limits/Colloid Formation
		2.2.08.07.04	Solubility Limits/Colloid Formation

Table G-1. Cross-Reference of TSPA-LA FEPs to TSPA-SR FEPs (Continued)

LA FEP Number	LA FEP Name	SR FEP Number	SR FEP Name
2.2.08.07.0B	Radionuclide Solubility Limits in the UZ	2.2.08.03.13	Speciation (Contaminant Speciation and Solubility)
		2.2.08.03.14	Speciation (Geosphere) (Contaminant Speciation and Solubility)
		2.2.08.03.15	Recrystallization (Contaminant Speciation and Solubility)
		2.2.08.03.16	Speciation (Contaminant Speciation and Solubility)
		2.2.08.03.17	Kinetics of Speciation (Contaminant Speciation and Solubility)
		2.2.08.07.00	Radionuclide Solubility Limits in the Geosphere
		2.2.08.07.01	Radionuclide Transport Through LPD (Water Transport)
		2.2.08.07.02	Radionuclide Transport Through MWCF (Water Transport)
2.2.08.07.0C	Radionuclide Solubility Limits in the Biosphere	2.2.08.07.00	Radionuclide Solubility Limits in the Geosphere
2.2.08.08.0A	Matrix Diffusion in the SZ	2.2.07.17.01	Far-Field Transport: Diffusion
		2.2.08.08.00	Matrix Diffusion in Geosphere SZ—Matrix Diffusion
		2.2.08.08.01	Matrix Diffusion (Water Transport)
		2.2.08.08.02	Matrix Diffusion (Water Transport)
		2.2.08.08.03	Matrix Diffusion (Water Transport)
		2.2.08.08.04	Matrix Diffusion (Water Transport)
		2.2.08.08.05	Matrix Diffusion (Water Transport)
		2.2.08.08.06	Matrix Diffusion (Water Transport)
		2.2.08.08.07	Matrix Diffusion (Water Transport)
		2.2.08.08.08	Matrix Diffusion
		2.2.08.09.12	Sorption
2.2.08.08.0B	Matrix Diffusion in the UZ	2.2.08.08.00	Matrix Diffusion in Geosphere SZ—Matrix Diffusion
		2.2.08.08.03	Matrix Diffusion (Water Transport)
2.2.08.09.0A	Sorption in the SZ	2.2.08.01.08	Changes in Groundwater Eh
		2.2.08.01.09	Changes in Groundwater Ph
		2.2.08.03.01	Far-Field Transport: Changes in Groundwater Chemistry and Flow Direction

Table G-1. Cross-Reference of TSPA-LA FEPs to TSPA-SR FEPs (Continued)

LA FEP Number	LA FEP Name	SR FEP Number	SR FEP Name
2.2.08.09.0A	Sorption in the SZ (continued)	2.2.08.09.00	Sorption in UZ and SZ
		2.2.08.09.01	Far-Field Transport: Sorption Including Ion-Exchange
		2.2.08.09.02	Far-Field Transport: Changes in Sorptive Surfaces
		2.2.08.09.03	Anion-Exclusion General: (In Geosphere)
		2.2.08.09.04	Soil Pore Water Ph
		2.2.08.09.05	Soil Sorption
		2.2.08.09.06	Ion Exchange in Soil
		2.2.08.09.07	Sorption (Reversible and Irreversible)
		2.2.08.09.08	Sorption - Nonlinear
		2.2.08.09.09	Saturation (Of Sorption Sites)
		2.2.08.09.10	Sorption (Geosphere)
		2.2.08.09.11	Sorption
		2.2.08.09.12	Sorption
		2.2.08.09.13	Nonlinear Sorption
		2.2.08.09.14	Sorption
		2.2.08.09.15	Nonlinear Sorption
		2.2.08.09.16	Sorption
		2.2.08.09.17	Radionuclide Sorption
		2.2.08.09.18	Sorption
		2.2.08.09.19	Actinide Sorption
		2.2.08.09.20	Kinetics of Sorption
		2.2.08.09.21	Changes in Sorptive Surfaces
		2.2.08.09.22	Sorption - Nonlinear (Geosphere)
		2.3.11.03.11	Groundwater Recharge
2.2.08.09.0B	Sorption in the UZ	2.2.08.09.00	Sorption in UZ and SZ
		2.2.08.09.07	Sorption (Reversible and Irreversible)
		2.2.08.09.14	Sorption
2.2.08.10.0A	Colloidal Transport in the SZ	2.2.07.15.12	Transport and Release of Nuclides, Near-Field Rock
		2.2.08.01.08	Changes in Groundwater Eh
		2.2.08.01.09	Changes in Groundwater Ph
		2.2.08.03.02	Effects of Dissolution (In Geosphere)
		2.2.08.07.03	Solubility Limits/Colloid Formation
		2.2.08.07.04	Solubility Limits/Colloid Formation
		2.2.08.10.00	Colloidal Transport in Geosphere

Table G-1. Cross-Reference of TSPA-LA FEPs to TSPA-SR FEPs (Continued)

LA FEP Number	LA FEP Name	SR FEP Number	SR FEP Name
2.2.08.10.0A	Colloidal Transport in the SZ (continued)	2.2.08.10.01	Far-Field Transport: Transport of Radionuclides Bound to Microbes
		2.3.11.03.11	Groundwater Recharge
2.2.08.10.0B	Colloidal Transport in the UZ	2.2.07.05.01	Episodic Infiltration Enhances Colloid Transport
		2.2.08.10.00	Colloidal Transport in Geosphere
		2.2.08.10.02	Colloid Transport Occurs in a Carrier Plume (In Geosphere)
		2.2.08.10.03	Colloids (In Geosphere)
2.2.08.11.0A	Groundwater Discharge to Surface Within the Reference Biosphere	2.2.07.03.00	Capillary Rise
		2.2.08.11.00	Distribution and Release of Nuclides from the Geosphere SZ—Distribution and Release of Nuclides
		2.2.08.11.01	Transport and Geochemical (Processes)
		2.3.04.01.00	Surface Water Transport and Mixing
2.2.08.12.0A	Chemistry of Water Flowing Into the Drift	2.2.07.18.00	Film Flow Into Drifts
		2.2.08.12.00	Use of J-13 Well Water As a Surrogate For Water Flowing Into the EBS and Waste
2.2.08.12.0B	Chemistry of Water Flowing Into the Waste Package	2.2.08.12.00	Use of J-13 Well Water As a Surrogate For Water Flowing Into the EBS and Waste
2.2.09.01.0A	Microbial Activity in the SZ	2.2.08.03.09	Precipitation and Dissolution (Release/Migration Factors)
		2.2.08.10.01	Far-Field Transport: Transport of Radionuclides Bound to Microbes
		2.2.09.01.00	Microbial Activity in Geosphere SZ—Groundwater Chemistry FEPs
		2.2.09.01.01	Microbes (In Geosphere)
		2.2.09.01.02	Microbes (In Geosphere)
		2.2.09.01.03	Microbial Activity (In Geosphere)
		2.2.09.01.04	Far-Field Transport: Biogeochemical Changes
		2.2.09.01.05	Bacteria and Microbes in Soil
		2.2.09.01.06	Chemical Transformations (Biological Processes)
2.2.09.01.0B	Microbial Activity in the UZ	2.2.08.03.09	Precipitation and Dissolution (Release/Migration Factors)
		2.2.09.01.00	Microbial Activity in Geosphere SZ—Groundwater Chemistry FEPs
		2.2.09.01.01	Microbes (In Geosphere)

Table G-1. Cross-Reference of TSPA-LA FEPs to TSPA-SR FEPs (Continued)

LA FEP Number	LA FEP Name	SR FEP Number	SR FEP Name
2.2.09.01.0B	Microbial Activity in the UZ (continued)	2.2.09.01.02	Microbes (In Geosphere)
		2.2.09.01.03	Microbial Activity (In Geosphere)
		2.2.09.01.04	Far-Field Transport: Biogeochemical Changes
		2.2.09.01.05	Bacteria and Microbes in Soil
		2.2.09.01.06	Chemical Transformations (Biological Processes)
2.2.10.01.0A	Repository-Induced Thermal Effects on Flow in the UZ	2.1.11.02.00	Nonuniform Heat Distribution / Edge Effects in Repository
		2.2.10.01.00	Repository-Induced Thermal Effects in Geosphere
		2.2.10.01.02	Temperature, Near-Field Rock
		2.2.10.01.04	Groundwater - Evolution
		2.2.10.01.05	Thermal Effects on Material Properties (In Waste and EBS)
		2.2.10.01.06	Thermal Effects: Rock-Mass Changes
		2.2.10.01.07	Thermal Effects: Hydrogeological Changes
2.2.10.02.0A	Thermal Convection Cell Develops in SZ	2.2.10.02.00	Thermal Convection Cell Develops in SZ
		2.2.10.03.04	Geothermal Gradient Effects
2.2.10.03.0A	Natural Geothermal Effects on Flow in the SZ	2.2.10.01.01	Temperature, Far-Field
		2.2.10.01.03	Thermal Effects on Groundwater Flow
		2.2.10.03.00	Natural Geothermal Effects SZ—Geothermal Effects
		2.2.10.03.01	Natural Thermal Effects (In Geosphere)
		2.2.10.03.02	Geothermal Regime
		2.2.10.03.03	Geothermal Regime
		2.2.10.03.04	Geothermal Gradient Effects
		2.2.10.13.00	Density-Driven Groundwater Flow (Thermal)
		2.2.10.13.01	Density-Driven Groundwater Flow (Thermal) SZ—Repository Induced Thermal Effects
		2.2.10.13.02	Density-Driven Groundwater Flows (Temperature/Salinity Differences)
		2.2.10.13.03	Thermal Buoyancy
2.2.10.03.0B	Natural Geothermal Effects on Flow in the UZ	2.2.10.03.00	Natural Geothermal Effects SZ—Geothermal Effects
		2.2.10.03.01	Natural Thermal Effects (In Geosphere)

Table G-1. Cross-Reference of TSPA-LA FEPs to TSPA-SR FEPs (Continued)

LA FEP Number	LA FEP Name	SR FEP Number	SR FEP Name
2.2.10.04.0A	Thermo-Mechanical Stresses Alter Characteristics of Fractures Near Repository	1.2.02.01.00	Fractures
		2.1.11.07.00	Thermally-Induced Stress Changes in Waste and EBS
		2.1.11.07.02	Stress Field Changes, Settling, Subsidence, or Caving
		2.2.06.02.00	Changes in Stress (Due to Thermal, Seismic, or Tectonic Effects) Produce Change in Permeability of Faults
		2.2.10.04.00	Thermo-Mechanical Alteration of Fractures Near Repository
		2.2.10.04.01	Thermal Expansion Closes Most Fractures Close to Repository
		2.2.10.04.02	Thermally-Induced Fracturing Around Containers Creates a Capillary Barrier
2.2.10.04.0B	Thermo-Mechanical Stresses Alter Characteristics of Faults Near Repository	1.2.02.02.00	Faulting
		2.1.11.07.00	Thermally-Induced Stress Changes in Waste and EBS
		2.1.11.07.02	Stress Field Changes, Settling, Subsidence, or Caving
		2.2.06.02.00	Changes in Stress (Due to Thermal, Seismic, or Tectonic Effects) Produce Change in Permeability of Faults
2.2.10.05.0A	Thermo-Mechanical Stresses Alter Characteristics of Rocks Above and Below the Repository	2.1.11.07.00	Thermally-Induced Stress Changes in Waste and EBS
		2.2.06.01.00	Changes in Stress (Due to Thermal, Seismic, or Tectonic Effects) Change Porosity and Permeability of Rock
		2.2.10.05.00	Thermo-Mechanical Alteration of Rocks Above and Below the Repository
		2.2.10.05.01	Thermal Expansion of Rocks Below Repository Opens Fractures in Paint Brush Unwelded
		2.2.10.05.02	Thermo-Mechanical Alteration of Surface Infiltration
2.2.10.06.0A	Thermo-Chemical Alteration in the UZ (Solubility, Speciation, Phase Changes, Precipitation/Dissolution)	2.2.10.04.03	Host Rock Fracture Aperture Changes
		2.2.10.06.00	Thermo-Chemical Alteration (Solubility Speciation, Phase Changes, Precipitation/Dissolution)
		2.2.10.06.01	Silica Phase Changes (Accompanied by Volume Change) Occur Due to Elevated Temperature

Table G-1. Cross-Reference of TSPA-LA FEPs to TSPA-SR FEPs (Continued)

LA FEP Number	LA FEP Name	SR FEP Number	SR FEP Name
2.2.10.06.0A	Thermo-Chemical Alteration in the UZ (Solubility, Speciation, Phase Changes, Precipitation/Dissolution) (continued)	2.2.10.06.02	Thermochemical Change
		2.2.10.06.03	Alteration of Rock Properties Because of 2-Phase Flow
		2.2.10.06.04	Heat-Induced Chemical Reactions Plug Small Fractures; Flow Is Preferentially Redirected to Large Fractures
		2.2.10.06.05	Alteration of Minerals to Clays (In Geosphere)
		2.2.10.06.06	Calcite Precipitation in Hot Region Produces Fluids Depleted in Calcite Which Dissolve Calcite Below the Repository
		2.2.10.06.07	Precipitates from Dissolved Constituents of Tuff and Repository Materials Form by Evaporation During Thermal Period
2.2.10.07.0A	Thermo-Chemical Alteration of the Calico Hills Unit	2.2.10.07.00	Thermo-Chemical Alteration of the Calico Hills Unit SZ—Repository Induced Thermal Effects
2.2.10.08.0A	Thermo-Chemical Alteration in the SZ (Solubility, Speciation, Phase Changes, Precipitation/Dissolution)	2.2.10.06.00	Thermo-Chemical Alteration (Solubility Speciation, Phase Changes, Precipitation/Dissolution)
		2.2.10.08.00	Thermo-Chemical Alteration of the Saturated Zone SZ—Repository Induced Thermal Effects
		2.2.10.08.01	Precipitation of Zeolites in the Saturated Zone Plugs Pores
2.2.10.09.0A	Thermo-Chemical Alteration of the Topopah Spring Basal Vitrophyre	2.2.10.09.00	Thermo-Chemical Alteration of the Topopah Spring Basal Vitrophyre
		2.2.10.09.01	Formation of Perched Water On the Altered Topopah Spring Basal Vitrophyre
		2.2.10.09.02	Sorption of Contaminants By the Altered Topopah Spring Basal Vitrophyre
		2.2.10.09.03	Redirection of Transport Paths By the Altered Topopah Spring Basal Vitrophyre
		2.2.10.09.04	Sorption of Actinides on Altered Topopah Spring Basal Vitrophyre
		2.2.10.09.05	Alteration of the Topopah Spring Basal Vitrophyre

Table G-1. Cross-Reference of TSPA-LA FEPs to TSPA-SR FEPs (Continued)

LA FEP Number	LA FEP Name	SR FEP Number	SR FEP Name
2.2.10.10.0A	Two-Phase Buoyant Flow/Heat Pipes	2.2.07.11.04	Resaturation of Dry-Out Zone Is Affected by Vapor Flow
		2.2.10.01.07	Thermal Effects: Hydrogeological Changes
		2.2.10.10.00	Two-Phase Buoyant Flow / Heat Pipes
		2.2.10.10.01	Heat Pipe -Evolving
		2.2.10.10.02	Heat Pipe -Continuing
		2.2.10.10.03	Heat Pipe Formation, 2-Phase System
		2.2.11.03.02	Far-Field Transport: Gas Induced Groundwater Transport
2.2.10.11.0A	Natural Air Flow in the UZ	2.2.10.11.00	Natural Air Flow in Unsaturated Zone
2.2.10.12.0A	Geosphere Dry-Out Due to Waste Heat	2.2.10.12.00	Geosphere Dry-Out Due to Waste Heat
2.2.10.13.0A	Repository-Induced Thermal Effects on Flow in the SZ	2.2.10.01.01	Temperature, Far-Field
		2.2.10.01.05	Thermal Effects on Material Properties (In Waste and EBS)
		2.2.10.01.07	Thermal Effects: Hydrogeological Changes
		2.2.10.03.00	Natural Geothermal Effects SZ—Geothermal Effects
		2.2.10.13.00	Density-Driven Groundwater Flow (Thermal) SZ—Repository Induced Thermal Effects
		2.2.10.13.03	Thermal Buoyancy
2.2.10.14.0A	Mineralogic Dehydration Reactions	2.2.10.14.00	Mineralogic Dehydration Reactions
2.2.11.01.0A	Gas Effects in the SZ	1.1.02.02.01	Gas Generation, Near-Field Rock
		2.2.11.01.00	Naturally-Occurring Gases in Geosphere
		2.2.11.01.01	Methane Intrusion (In Geosphere)
		2.2.11.01.02	Natural Gas Intrusion
		2.2.11.01.03	Geogas
		2.2.11.01.04	Geogas
		2.2.11.01.05	Gas Generation and Gas Sources, Far-Field
		2.2.11.01.06	Natural Gas Intrusion
		2.2.11.01.07	Methane
		2.2.11.03.00	Gas Transport in Geosphere
		2.2.11.03.02	Far-Field Transport: Gas Induced Groundwater Transport

Table G-1. Cross-Reference of TSPA-LA FEPs to TSPA-SR FEPs (Continued)

LA FEP Number	LA FEP Name	SR FEP Number	SR FEP Name
2.2.11.02.0A	Gas Effects in the UZ	2.2.11.01.00	Naturally-Occurring Gases in Geosphere
		2.2.11.01.05	Gas Generation and Gas Sources, Far-Field
		2.2.11.02.00	Gas Pressure Effects
		2.2.11.02.01	Gas Pressure Effects
		2.2.11.02.02	Fluid Flow Due to Gas Pressurization (In Waste and EBS)
		2.2.11.02.03	Disruption Due to Gas Effects
		2.2.11.03.00	Gas Transport in Geosphere
		2.2.11.03.01	Gases and Gas Transport (In Geosphere)
		2.2.11.03.03	Gas Mediated Transport
2.2.11.03.0A	Gas Transport in Geosphere	2.2.07.15.12	Transport and Release of Nuclides, Near-Field Rock
		2.2.11.03.00	Gas Transport in Geosphere
		2.2.11.03.01	Gases and Gas Transport (In Geosphere)
		2.2.11.03.02	Far-Field Transport: Gas Induced Groundwater Transport
		2.2.11.03.03	Gas Mediated Transport
		2.2.11.03.04	Far-Field Transport: Transport of Radioactive Gases
		2.2.11.03.05	Gas Discharge
		2.2.11.03.06	Transport of Radioactive Gases
2.2.12.00.0A	Undetected Features in the UZ	2.2.12.00.00	Undetected Features (In Geosphere) SZ—Undetected Features
		2.2.12.00.01	Undetected Dike Beneath the Repository Passing Thru the Calico Hills Provides a Highly Permeable Flow Path
		2.2.12.00.02	Undetected Fault Dips Below the Repository Providing a Highly Permeable Flow Path
		2.2.12.00.03	Undetected Fault Beneath the Repository Acts As a Flow Barrier Altering the Flow System
		2.2.12.00.04	Undetected Fault Connects Tuff Aquifers to Carbonate Aquifers; Providing a Fast Path
		2.2.12.00.05	Perched Water Escapes Detection and Waste Is Put in It
		2.2.12.00.06	Undiscovered Mine Shaft (An Old Prospect Hole) in a Wash Acts As a Source For Increased Local Infiltration

Table G-1. Cross-Reference of TSPA-LA FEPs to TSPA-SR FEPs (Continued)

LA FEP Number	LA FEP Name	SR FEP Number	SR FEP Name
2.2.12.00.0A	Undetected Features in the UZ (continued)	2.2.12.00.07	Rock Properties-Undetected Features
		2.2.12.00.08	Undetected Fracture Zone
		2.2.12.00.09	Undetected Features
		2.2.12.00.10	Undetected Past Intrusions
		2.2.12.00.11	Undetected Discontinuities (In Geosphere)
2.2.12.00.0B	Undetected Features in the SZ	2.2.12.00.00	Undetected Features (In Geosphere) SZ—Undetected Features
2.2.14.09.0A	Far-Field Criticality	2.2.14.01.00	Critical Assembly Forms Away from Repository
		2.2.14.01.01	Reconcentration (Release/Migration Factors)
		2.2.14.01.02	Reconcentration (Release/Migration Factors)
		2.2.14.01.03	DOE SNF Criticality Far-Field (Radionuclide Inventory Impact)
		2.2.14.01.04	DOE SNF Criticality Far-Field (Waste Heat Impact)
		2.2.14.02.00	Far-Field Criticality, Precipitation in Organic Reducing Zone in or Near Water Table
		2.2.14.02.01	Precipitation of U at Reducing Zone Associated W/Organics in Alluvial Aquifer
		2.2.14.02.02	Precipitation of U at Reducing Zone Associated W/Organics in Franklin Lake Playa
		2.2.14.03.00	Far-Field Criticality, Sorption on Clay/Zeolite in Tsbv
		2.2.14.04.00	Far-Field Criticality, Precipitation Caused by Hydrothermal Upwell or Redox Front in the SZ
		2.2.14.04.01	Precipitation of U in the Upwelling Zone Along Some Faults
		2.2.14.04.02	Precipitation of U Below the Redox Front in the SZ
		2.2.14.05.00	Far-Field Criticality, Precipitation in Perched Water Above Tsbv
		2.2.14.05.01	Accumulation of Solute in Topographic Lows of the Altered Tsbv
		2.2.14.06.00	Far-Field Criticality, Precipitation in Fractures of Tsw Rock
		2.2.14.07.00	Far-Field Criticality, Dryout Produces Fissile Salt in a Perched Water Basin

Table G-1. Cross-Reference of TSPA-LA FEPs to TSPA-SR FEPs (Continued)

LA FEP Number	LA FEP Name	SR FEP Number	SR FEP Name
2.2.14.09.0A	Far-Field Criticality (continued)	2.2.14.08.00	Far-Field Criticality Associated With Colloidal Deposits
2.2.14.10.0A	Far-Field Criticality Resulting from a Seismic Event	2.1.14.14.00	Out-of-Package Criticality, Fuel/Magma Mixture
2.2.14.11.0A	Far-Field Criticality Resulting from Rockfall	2.1.14.14.00	Out-of-Package Criticality, Fuel/Magma Mixture
2.2.14.12.0A	Far-Field Criticality Resulting from an Igneous Event	2.1.14.14.00	Out-of-Package Criticality, Fuel/Magma Mixture
2.3.01.00.0A	Topography and Morphology	1.2.04.01.01	Volcanism
		2.3.01.00.00	Topography and Morphology
		2.3.01.00.01	Topography (Current)
		2.3.01.00.02	Topography (Future)
		2.3.01.00.03	Terrestrial Surface
		2.3.01.00.04	Physiography
		2.3.01.00.05	Geomorphological (Processes)
		2.3.01.00.06	External Flow Boundaries (Surface Environment)
		2.3.01.00.07	Changes in Geometry and Driving Forces of the Flow System
2.3.02.01.0A	Soil Type	2.3.02.01.00	Soil Type
		2.3.02.01.01	Pedogenesis
		2.3.02.01.02	Soil Formation
		2.3.02.01.03	Soil Development
		2.3.02.01.04	Soil
2.3.02.02.0A	Radionuclide Accumulation in Soils	2.2.07.02.02	Soil Depth
		2.3.02.02.00	Radionuclide Accumulation in Soils
		2.3.02.02.01	Soil Moisture and Evaporation (Water Transport)
		2.3.02.02.02	Radionuclide Accumulation in Sediments at Franklin Lake Playa (Water Transport)
		2.3.02.02.03	Accumulation in Sediments (Sorption/Desorption Processes)
		2.3.02.02.04	Accumulation in Soils and Organic Debris (Sorption/Desorption Processes)
		2.3.02.02.05	Soil
		2.3.02.02.06	Soil Leaching
		2.3.02.02.07	Accumulation in Peat
		2.3.02.02.08	Alkali Flats (And Other Playa Deposits)
		2.3.02.02.09	Accumulation in Soil (Exposure Factors)
		2.3.02.02.10	Soil Leaching to Groundwater

Table G-1. Cross-Reference of TSPA-LA FEPs to TSPA-SR FEPs (Continued)

LA FEP Number	LA FEP Name	SR FEP Number	SR FEP Name
2.3.02.02.0A	Radionuclide Accumulation in Soils (continued)	2.3.11.04.00	Groundwater Discharge to Surface
2.3.02.03.0A	Soil and Sediment Transport in the Biosphere	1.2.07.01.12	Erosion - Lateral Transport
		1.2.07.01.13	Erosion (Wind)
		1.2.07.02.01	Aeolian Deposition
		2.3.02.03.00	Soil and Sediment Transport
		2.3.02.03.01	Soil and Sediment Bioturbation
		2.3.02.03.02	Bioturbation
		2.3.02.03.03	Sediment Transport Including Bioturbation
		2.3.09.01.00	Animal Burrowing/Intrusion
		2.3.11.02.00	Surface Runoff and Flooding
		2.3.11.02.01	Runoff (Near Surface Hydrology)
		2.3.11.02.02	Flooding (Near Surface Hydrology)
		2.3.13.02.00	Biosphere Transport
2.3.04.01.0A	Surface Water Transport and Mixing	2.3.04.01.00	Surface Water Transport and Mixing
		2.3.04.01.01	Flushing of Water Bodies
		2.3.04.01.02	Lake Mixing (Artificial)
		2.3.04.01.03	Sediment Resuspension in Water Bodies
		2.3.04.01.04	Sedimentation in Water Bodies
		2.3.04.01.05	River Meandering
		2.3.04.01.06	River Meander
		2.3.04.01.07	Freshwater Sediment Transport and Deposition
		2.3.04.01.08	River Flow and Lake Level Changes
		2.3.04.01.09	Surface Water Flow (River Rhine)
		2.3.04.01.10	Sedimentation
		2.3.04.01.11	River Course Meander
		2.3.04.01.12	Surface Water Bodies
		2.3.04.01.13	Surface Water Mixing
		2.3.04.01.14	Stream and River Flow
		2.3.04.01.15	Surface Water Bodies
		2.3.04.01.16	Exfiltration to Surface Waters
		2.3.04.01.17	Lake Formation
		2.3.04.01.18	Dilution of Radionuclides in Surface Water (Aquifer, River, Lake, Etc.)
		2.3.04.01.19	Radionuclide Accumulation in Sediments (Water Transport)
		2.3.13.02.00	Biosphere Transport

Table G-1. Cross-Reference of TSPA-LA FEPs to TSPA-SR FEPs (Continued)

LA FEP Number	LA FEP Name	SR FEP Number	SR FEP Name
2.3.06.00.0A	Marine Features	2.3.06.00.00	Marine Features
		2.3.06.00.01	Marine Sediment Transport and Deposition
		2.3.06.00.02	Seas and Oceans
		2.3.06.00.03	Marine Sediment Transport and Deposition
		2.3.06.00.04	Coastal Surge, Storms and Hurricanes
		2.3.06.00.05	Coastal Erosion and Estuarine Development
		2.3.06.00.06	Estuaries
		2.3.06.00.07	Coastal Erosion
		2.3.06.00.08	Sea Level Change
		2.3.06.00.09	Change in Sea Level
		2.3.06.00.10	Sea-Level Rise/Fall
		2.3.06.00.11	Sea Level Changes
		2.3.06.00.12	Sea Level Changes
2.3.09.01.0A	Animal Burrowing/Intrusion	2.3.09.01.00	Animal Burrowing/Intrusion
		2.3.09.01.01	Intrusion (Animal)
		2.3.13.02.00	Biosphere Transport
2.3.11.01.0A	Precipitation	2.3.11.01.00	Precipitation
		2.3.11.01.01	Precipitation, Temperature and Soil Water Balance
		2.3.11.01.02	Flood (Meteorology)
		2.3.11.01.03	Extremes of Precipitation, Snow Melt and Associated Flooding (Meteorology)
		2.3.11.01.04	Precipitation (Meteorology)
2.3.11.02.0A	Surface Runoff and Evapotranspiration	1.1.02.01.00	Site Flooding (During Construction and Operation)
		2.3.11.02.00	Surface Runoff and Flooding
		2.3.11.02.01	Runoff (Near Surface Hydrology)
		2.3.11.02.02	Flooding (Near Surface Hydrology)
		2.3.11.02.03	Evapotranspiration (Near Surface Hydrology)
		2.3.11.02.04	Flooding Occurs in Drill Hole Wash and Increases Percolation Below the Wash
		2.3.11.02.05	Faulting At the Surface Produces a Scarp Causing an Impoundment
		2.3.11.02.06	River Flooding
		2.3.11.03.03	Equilibrated Flow System

Table G-1. Cross-Reference of TSPA-LA FEPs to TSPA-SR FEPs (Continued)

LA FEP Number	LA FEP Name	SR FEP Number	SR FEP Name
2.3.11.02.0A	Surface Runoff and Evapotranspiration (continued)	2.3.11.03.07	Runoff Is Intercepted by Wash Terraces
		2.3.11.03.08	Runoff to Washes Infiltrates and Maintains a Zone of Higher Flux to the UZ
		2.3.11.03.09	Flow in Ephemeral Streams Tends to Be in Channels and Is a Source of Recharge
2.3.11.03.0A	Infiltration and Recharge	2.3.11.03.00	Infiltration and Recharge (Hydrologic and Chemical Effects)
		2.3.11.03.01	Freshwater Intrusion (In Geosphere)
		2.3.11.03.02	Groundwater Recharge/Discharge
		2.3.11.03.03	Equilibrated Flow System
		2.3.11.03.04	Draining Flow System
		2.3.11.03.05	Recharge Groundwater
		2.3.11.03.06	Surface Water Chemistry
		2.3.11.03.07	Runoff Is Intercepted by Wash Terraces
		2.3.11.03.08	Runoff to Washes Infiltrates and Maintains a Zone of Higher Flux to the UZ
		2.3.11.03.09	Flow in Ephemeral Streams Tends to Be in Channels and Is a Source of Recharge
		2.3.11.03.10	Percolation (Near Surface Hydrology)
		2.3.11.03.11	Groundwater Recharge
		2.3.11.03.12	Infiltration (Near Surface Hydrology)
		2.3.11.03.13	Recharge Groundwater (Affects Waste and EBS)
		2.3.11.03.14	Effective Moisture (Recharge)
		2.3.11.03.15	Changes in Groundwater Recharge and Discharge
		2.3.11.03.16	Coupling of Surface Water Flow to Climate/Hydrologic Modeling System
2.3.11.04.0A	Groundwater Discharge to Surface Outside the Reference Biosphere	1.3.07.02.00	Water Table Rise
		2.2.07.03.00	Capillary Rise
		2.3.04.01.00	Surface Water Transport and Mixing
		2.3.11.04.00	Groundwater Discharge to Surface
		2.3.11.04.01	Discharge Zones

Table G-1. Cross-Reference of TSPA-LA FEPs to TSPA-SR FEPs (Continued)

LA FEP Number	LA FEP Name	SR FEP Number	SR FEP Name
2.3.11.04.0A	Groundwater Discharge to Surface Outside the Reference Biosphere (continued)	2.3.11.04.02	Groundwater Discharge
		2.3.11.04.03	Groundwater Discharge
2.3.13.01.0A	Biosphere Characteristics	2.3.13.01.00	Biosphere Characteristics
		2.3.13.01.01	Fires (Forest and Grass)
		2.3.13.01.02	Wetlands
		2.3.13.01.03	Ecological Change
		2.3.13.01.04	Microbes (Ecological Systems)
		2.3.13.01.05	Ecological (Processes)
		2.3.13.01.06	Lake Infilling
		2.3.13.01.07	Plants
		2.3.13.01.08	Future Biosphere Conditions
		2.3.13.01.09	Ecological Response to Climate (E.G. Desert Formation)
		2.3.13.01.10	Natural Ecological Development
2.3.13.02.0A	Radionuclide Alteration During Biosphere Transport	2.3.13.02.00	Biosphere Transport
		2.3.13.02.01	Sediment/Water/Gas Interaction With the Atmosphere
		2.3.13.02.02	Biogeochemical Processes
2.3.13.03.0A	Effects of Repository Heat On the Biosphere	2.3.13.03.00	Effects of Repository Heat on Biosphere
2.3.13.04.0A	Radionuclide Release Outside the Reference Biosphere	1.4.07.02.00	Wells
		2.3.02.02.02	Radionuclide Accumulation in Sediments at Franklin Lake Playa (Water Transport)
		2.3.04.01.00	Surface Water Transport and Mixing
		2.3.13.01.01	Fires (Forest and Grass)
		2.3.13.01.02	Wetlands
2.4.01.00.0A	Human Characteristics (Physiology, Metabolism)	2.4.01.00.00	Human Characteristics (Physiology, Metabolism)
		2.4.01.00.01	Critical Group - Individuality
2.4.04.01.0A	Human Lifestyle	2.4.04.01.00	Human Lifestyle
		2.4.04.01.01	Hunter/Gathering Lifestyle
		2.4.04.01.02	Critical Group - Leisure Pursuits
		2.4.07.00.00	Dwellings
2.4.07.00.0A	Dwellings	2.4.07.00.00	Dwellings
		2.4.07.00.01	Building Materials
		2.4.07.00.02	Critical Group - House Location
		2.4.07.00.03	Gas Leakage Into Basements
		2.4.07.00.04	Household Dust and Fumes
		2.4.07.00.05	Houseplants
		2.4.07.00.06	Showers and Humidifiers

Table G-1. Cross-Reference of TSPA-LA FEPs to TSPA-SR FEPs (Continued)

LA FEP Number	LA FEP Name	SR FEP Number	SR FEP Name
2.4.07.00.0A	Dwellings (continued)	2.4.07.00.07	Space Heating
		2.4.07.00.08	Water Leaking Into Basements
		2.4.07.00.09	Outdoor Spraying of Water
		2.4.07.00.10	Evaporative Coolers
2.4.08.00.0A	Wild and Natural Land and Water Use	2.4.08.00.00	Wild and Natural Land and Water Use
		2.4.08.00.01	Natural and Semi-Natural Environments
		2.4.08.00.02	Land and Surface Water Use: Terrestrial
		2.4.08.00.03	Coastal Water Use
		2.4.08.00.04	Sea Water Use
		2.4.08.00.05	Estuarine Water Use
		2.4.08.00.06	Land and Surface Water Use: Estuarine
		2.4.08.00.07	Land and Surface Water Use: Coastal Waters
		2.4.08.00.08	Land and Surface Water Use: Seas
2.4.09.01.0A	Implementation of New Agricultural Practices or Land Use	2.4.09.01.00	Agricultural Land Use and Irrigation
		2.4.09.01.01	Crop Fertilizers and Soil Conditioners
		2.4.09.01.02	Crop Storage
		2.4.09.01.03	Fires (Agricultural)
		2.4.09.01.04	Greenhouse Food Production
		2.4.09.01.05	Hydroponics
		2.4.09.01.06	Peat and Leaf Harvesting
		2.4.09.01.07	Irrigation
		2.4.09.01.08	Agricultural and Fisheries Practice Changes
		2.4.09.01.09	Irrigation
		2.4.09.01.10	Ploughing
		2.4.09.01.11	Irrigation
		2.4.09.01.12	Critical Group - Agricultural Labor
		2.4.09.01.13	Ashes and Sewage Sludge Fertilizer
		2.4.09.01.14	Irrigation
		2.4.09.01.15	Herbicides, Pesticides, and Fungicides
2.4.09.01.0B	Agricultural Land Use and Irrigation	2.3.13.02.00	Biosphere Transport
		2.4.09.01.00	Agricultural Land Use and Irrigation

Table G-1. Cross-Reference of TSPA-LA FEPs to TSPA-SR FEPs (Continued)

LA FEP Number	LA FEP Name	SR FEP Number	SR FEP Name
2.4.09.02.0A	Animal Farms and Fisheries	2.4.09.02.00	Animal Farms and Fisheries
		2.4.09.02.01	Fish Farming
		2.4.09.02.02	Ranching
		2.4.09.02.03	Fish Farming
2.4.10.00.0A	Urban and Industrial Land and Water Use	2.4.10.00.00	Urban and Industrial Land and Water Use
		2.4.10.00.01	Industrial Water Use
		2.4.10.00.02	Earthmoving
		2.4.10.00.03	Earthmoving Projects
		2.4.10.00.04	Earthworks
		2.4.10.00.05	Land Use Changes
		2.4.10.00.06	Land Use Changes
		2.4.10.00.07	Post-Closure Surface Activities
		2.4.10.00.08	Surface Disruptions
		2.4.10.00.09	Biogas Production
3.1.01.01.0A	Radioactive Decay and Ingrowth	3.1.01.01.00	Radioactive Decay and Ingrowth
		3.1.01.01.01	Radioactive Decay
		3.1.01.01.02	Radioactive Decay
		3.1.01.01.03	Radioactive Decay
		3.1.01.01.04	Radioactive Decay and Ingrowth
		3.1.01.01.05	Radioactive Decay
		3.1.01.01.06	Radioactive Decay
		3.1.01.01.07	Radioactive Decay of Mobile Nuclides
		3.1.01.01.08	Radionuclide Decay and Ingrowth
		3.1.01.01.09	Radiological Events and Processes
3.2.07.01.0A	Isotopic Dilution	2.2.08.07.03	Solubility Limits/Colloid Formation
		2.2.08.07.04	Solubility Limits/Colloid Formation
		3.2.07.01.00	Isotopic Dilution
		3.2.07.01.01	Mass, Isotopic and Species Dilution
		3.2.07.01.02	Natural Radionuclides/Elements (In Host Rock Disturbed Zone)
3.2.10.00.0A	Atmospheric Transport of Contaminants	2.3.04.01.00	Surface Water Transport and Mixing
		2.3.13.02.00	Biosphere Transport
		3.2.10.00.01	Suspension in Air
		3.2.10.00.02	Wind
		3.2.10.00.03	Radionuclide Volatilization/Aerosol/Dust Production

Table G-1. Cross-Reference of TSPA-LA FEPs to TSPA-SR FEPs (Continued)

LA FEP Number	LA FEP Name	SR FEP Number	SR FEP Name
3.2.10.00.0A	Atmospheric Transport of Contaminants (continued)	3.2.10.00.04	Convection, Turbulence and Diffusion (Atmospheric)
		3.2.10.00.05	Deposition (Atmospheric)
		3.2.10.00.06	Saltation
		3.2.10.00.07	Atmosphere
		3.2.10.00.08	Precipitation (Meteoric)
3.3.01.00.0A	Contaminated Drinking Water, Foodstuffs and Drugs	2.4.03.00.00	Diet and Fluid Intake
		2.4.03.00.01	Intake of Drugs
		2.4.03.00.02	Human Diet
		2.4.03.00.03	Human Soil Ingestion
		2.4.03.00.04	Consumption of Uncontaminated Products
		2.4.03.00.05	Filtration (Water Processing)
		2.4.03.00.06	Food Preparation
		3.3.01.00.00	Drinking Water, Foodstuffs and Drugs, Contaminant Concentrations In
		3.3.01.00.01	Water Source (Exposure Factors)
3.3.02.01.0A	Plant Uptake	3.3.02.01.00	Plant Uptake
		3.3.02.01.01	Plant Roots (Foodchains)
		3.3.02.01.02	Uptake by Crops (Foodchains)
		3.3.02.01.03	Plant Uptake
		3.3.02.01.04	Uptake by Deep Rooting Species
		3.3.02.03.01	Bioconcentration (Foodchains)
		3.3.02.03.02	Foodchain Equilibrium
		3.3.02.03.04	Recycling (Exposure Factors)
		3.3.02.03.05	Removal Mechanisms (Exposure Factors)
		3.3.02.03.06	Bioaccumulation and Translocation
3.3.02.02.0A	Animal Uptake	3.3.02.02.00	Animal Uptake
		3.3.02.02.01	Carcasses
		3.3.02.02.02	Uptake by Livestock (Foodchains)
		3.3.02.02.04	Animal Diets
		3.3.02.02.05	Animal Grooming and Fighting
		3.3.02.02.06	Scavengers and Predators
		3.3.02.02.07	Animal Uptake
		3.3.02.02.08	Animals
		3.3.02.02.09	Animal Soil Ingestion
		3.3.02.03.01	Bioconcentration (Foodchains)
		3.3.02.03.02	Foodchain Equilibrium

Table G-1. Cross-Reference of TSPA-LA FEPs to TSPA-SR FEPs (Continued)

LA FEP Number	LA FEP Name	SR FEP Number	SR FEP Name
3.3.02.02.0A	Animal Uptake (continued)	3.3.02.03.03	Biomagnification (Foodchains)
		3.3.02.03.05	Removal Mechanisms (Exposure Factors)
		3.3.02.03.06	Bioaccumulation and Translocation
3.3.02.03.0A	Fish Uptake	3.3.02.02.03	Uptake in Fish (Foodchains)
3.3.03.01.0A	Contaminated Non-Food Products and Exposure	3.3.03.01.00	Contaminated Non-Food Products and Exposure
		3.3.03.01.01	Charcoal Production (Exposure Factors)
		3.3.03.01.02	Critical Group - Clothing and Home Furnishings (Exposure Factors)
		3.3.03.01.03	Tree Sap (Exposure Factors)
		3.3.03.01.04	Critical Group - Pets
		3.3.03.01.05	Smoking
3.3.04.01.0A	Ingestion	3.3.02.03.00	Bioaccumulation
		3.3.02.03.01	Bioconcentration (Foodchains)
		3.3.02.03.06	Bioaccumulation and Translocation
		3.3.04.01.00	Ingestion
		3.3.04.01.01	Ingestion
3.3.04.02.0A	Inhalation	3.3.04.02.00	Inhalation
		3.3.04.02.01	Inhalation
3.3.04.03.0A	External Exposure	3.3.04.03.00	External Exposure
		3.3.04.03.01	Dermal Sorption (Except Tritium)
		3.3.04.03.02	Dermal Sorption (Tritium)
		3.3.04.03.03	Groundshine
		3.3.04.03.04	Exposure Pathways
		3.3.04.03.05	Irradiation
		3.3.04.03.06	Dermal Sorption
		3.3.04.03.07	Injection
3.3.05.01.0A	Radiation Doses	3.1.01.01.03	Radioactive Decay
		3.3.02.03.00	Bioaccumulation
		3.3.05.01.00	Radiation Doses
		3.3.05.01.01	Secular Equilibrium of Radionuclide Chains
		3.3.05.01.02	Radionuclide Uptake and Dosimetry FEPs
		3.3.05.01.03	Radionuclide Uptake and Dosimetry FEPs
		3.3.05.01.04	Radionuclide Uptake and Dosimetry FEPs (Exposure Factors)

Table G-1. Cross-Reference of TSPA-LA FEPs to TSPA-SR FEPs (Continued)

LA FEP Number	LA FEP Name	SR FEP Number	SR FEP Name
3.3.06.00.0A	Radiological Toxicity and Effects	3.3.06.00.00	Radiological Toxicity /Effects
		3.3.06.00.01	Mutagenic Contaminants
		3.3.06.00.02	Biotoxicity
		3.3.06.00.03	Carcinogenic Contaminants
		3.3.06.00.04	Radiotoxic Contaminants
		3.3.06.00.05	Teratogenic Contaminants
3.3.06.01.0A	Repository Excavation	3.3.06.01.00	Toxicity of Mined Rock
3.3.06.02.0A	Sensitization to Radiation	3.3.06.02.00	Sensitization to Radiation
3.3.07.00.0A	Non-Radiological Toxicity and Effects	3.3.07.00.00	Non-Radiological Toxicity/Effects
		3.3.07.00.01	Chemical Toxicity of Wastes
		3.3.07.00.02	Chemical Toxicity
		3.3.07.00.03	Non-Radiological Toxicity FEPs
3.3.08.00.0A	Radon and Radon Decay Product Exposure	3.3.08.00.00	Radon and Radon Daughter Exposure
		3.3.08.00.01	Radon Emission
		3.3.08.00.02	Radon Pathways and Doses

Source: Technical Product Output DTN: MO0706SPAFEPLA.001, Tables: FEPS, FEPS_REV00_ICN02, FEPMappingSRtoLA.

Table G-2. Cross Reference of TSPA-SR FEPs to TSPA-LA FEPs

SR FEP Number	SR FEP Name	LA FEP Number	LA FEP Name
0.1.02.00.00	Timescales of Concern	0.1.02.00.0A	Timescales of Concern
0.1.03.00.00	Spatial Domain of Concern	0.1.03.00.0A	Spatial Domain of Concern
0.1.09.00.00	Regulatory Requirements and Exclusions	0.1.09.00.0A	Regulatory Requirements and Exclusions
0.1.09.00.01	Assessment Basis FEP	0.1.09.00.0A	Regulatory Requirements and Exclusions
0.1.09.00.02	Assessment Basis FEP (Atmospheric Processes)	0.1.09.00.0A	Regulatory Requirements and Exclusions
0.1.10.00.00	Model and Data Issues	0.1.10.00.0A	Model and Data Issues
0.1.10.00.01	Boundary Conditions	0.1.10.00.0A	Model and Data Issues
0.1.10.00.02	Uncertainties (Repository)	0.1.10.00.0A	Model and Data Issues
0.1.10.00.03	Correlation	0.1.10.00.0A	Model and Data Issues
0.1.10.00.04	Uncertainties (Geosphere)	0.1.10.00.0A	Model and Data Issues
0.1.10.00.05	Correlation	0.1.10.00.0A	Model and Data Issues
0.1.10.00.06	Uncertainties (Biosphere)	0.1.10.00.0A	Model and Data Issues
0.1.10.00.07	Model and Data Issues	0.1.10.00.0A	Model and Data Issues
0.1.10.00.08	Unmodeled Design Features	0.1.10.00.0A	Model and Data Issues
0.1.10.00.09	Disposal Geometry	0.1.10.00.0A	Model and Data Issues
0.1.10.00.10	Conceptual Model - Hydrology	0.1.10.00.0A	Model and Data Issues
0.1.10.00.11	Correlation (Contaminant Speciation and Solubility)	0.1.10.00.0A	Model and Data Issues
1.1.01.01.00	Open Site Investigation Boreholes	1.1.01.01.0A	Open Site Investigation Boreholes
		1.1.01.01.0B	Influx Through Holes Drilled in Drift Wall or Crown
1.1.01.01.01	Exploratory Boreholes (Sealing)	1.1.01.01.0A	Open Site Investigation Boreholes
1.1.01.01.02	Investigation Boreholes	1.1.01.01.0A	Open Site Investigation Boreholes
1.1.01.01.03	Underground Boreholes	1.1.01.01.0A	Open Site Investigation Boreholes
1.1.01.02.00	Loss of Integrity of Borehole Seals	1.1.01.01.0A	Open Site Investigation Boreholes
		2.1.05.03.0A	Degradation of Seals
1.1.01.02.01	Investigation Borehole Seal Failure and Degradation	1.1.01.01.0A	Open Site Investigation Boreholes
1.1.01.02.02	Borehole Seal Failure	2.1.05.03.0A	Degradation of Seals
1.1.02.00.00	Excavation/Construction	1.1.02.00.0A	Chemical Effects of Excavation and Construction in EBS
		1.1.02.00.0B	Mechanical Effects of Excavation and Construction in EBS
1.1.02.00.01	Blasting and Vibration	1.1.02.00.0B	Mechanical Effects of Excavation and Construction in EBS
		2.2.01.01.0A	Mechanical Effects of Excavation and Construction in the Near-Field
1.1.02.00.02	Geochemical Alteration (Excavation)	1.1.02.00.0A	Chemical Effects of Excavation and Construction in EBS
1.1.02.00.03	Groundwater Chemistry (Excavation)	1.1.02.00.0A	Chemical Effects of Excavation and Construction in EBS
		2.2.01.01.0A	Mechanical Effects of Excavation and Construction in the Near-Field

Table G-2. Cross Reference of TSPA-SR FEPs to TSPA-LA FEPs (Continued)

SR FEP Number	SR FEP Name	LA FEP Number	LA FEP Name
1.1.02.00.04	Influx of Oxidizing Water	1.1.02.00.0A	Chemical Effects of Excavation and Construction in EBS
1.1.02.00.05	Influx of Oxidizing Water	1.1.02.00.0A	Chemical Effects of Excavation and Construction in EBS
1.1.02.01.00	Site Flooding (During Construction and Operation)	1.1.02.01.0A	Site Flooding (During Construction and Operation)
		1.3.07.02.0B	Water Table Rise Affects UZ
		2.3.11.02.0A	Surface Runoff and Evapotranspiration
1.1.02.01.01	Repository Flooding During Operation	1.1.02.01.0A	Site Flooding (During Construction and Operation)
1.1.02.02.00	Effects of Pre-Closure Ventilation	1.1.02.02.0A	Preclosure Ventilation
1.1.02.02.01	Gas Generation, Near-Field Rock	2.2.11.01.0A	Gas Effects in the SZ
1.1.02.03.00	Undesirable Materials Left	1.1.02.03.0A	Undesirable Materials Left
1.1.02.03.01	Decontamination Materials Left	1.1.02.03.0A	Undesirable Materials Left
1.1.02.03.02	Inadvertent Inclusion of Undesirable Materials	1.1.02.03.0A	Undesirable Materials Left
1.1.03.01.00	Error in Waste or Backfill Emplacement	1.1.03.01.0A	Error in Waste Emplacement
1.1.03.01.01	Inadequate Backfill or Compaction, Voidage	1.1.03.01.0B	Error in Backfill Emplacement
1.1.03.01.02	Containers Are Improperly Placed - on Drift Floor	1.1.03.01.0A	Error in Waste Emplacement
1.1.03.01.03	Containers Are Placed Too Close Together	1.1.03.01.0A	Error in Waste Emplacement
1.1.03.01.04	Emplacement Error - Containers Placed in Wet Zone	1.1.03.01.0A	Error in Waste Emplacement
1.1.04.01.00	Incomplete Closure	1.1.01.01.0A	Open Site Investigation Boreholes
		1.1.04.01.0A	Incomplete Closure
1.1.04.01.01	Vault Closure (Geosphere)	1.1.04.01.0A	Incomplete Closure
1.1.04.01.02	Non-Sealed Repository	1.1.04.01.0A	Incomplete Closure
1.1.04.01.03	Poor Closure	1.1.04.01.0A	Incomplete Closure
1.1.04.01.04	Abandonment of Unsealed Repository	1.1.04.01.0A	Incomplete Closure
1.1.04.01.05	Unsealed Boreholes And/Or Shafts	1.1.04.01.0A	Incomplete Closure
1.1.04.01.06	Operation and Closure	1.1.04.01.0A	Incomplete Closure
1.1.05.00.00	Records and Markers, Repository	1.1.05.00.0A	Records and Markers For the Repository
1.1.05.00.01	Loss of Records	1.1.05.00.0A	Records and Markers For the Repository
1.1.05.00.02	Repository Records, Markers	1.1.05.00.0A	Records and Markers For the Repository
1.1.05.00.03	Loss of Records	1.1.05.00.0A	Records and Markers For the Repository
1.1.05.00.04	Loss of Records	1.1.05.00.0A	Records and Markers For the Repository
1.1.07.00.00	Repository Design	1.1.07.00.0A	Repository Design
1.1.07.00.01	Poorly Designed Repository	1.1.07.00.0A	Repository Design
1.1.07.00.02	Design Modification	1.1.07.00.0A	Repository Design

Table G-2. Cross Reference of TSPA-SR FEPs to TSPA-LA FEPs (Continued)

SR FEP Number	SR FEP Name	LA FEP Number	LA FEP Name
1.1.07.00.03	HLW Panels (Siting)	1.1.07.00.0A	Repository Design
1.1.07.00.04	TRU Silos (Siting)	1.1.07.00.0A	Repository Design
1.1.07.00.05	Access Tunnels and Shafts	1.1.07.00.0A	Repository Design
1.1.07.00.06	Design and Construction FEPs	1.1.07.00.0A	Repository Design
1.1.07.00.07	Design and Construction	1.1.07.00.0A	Repository Design
1.1.07.00.08	Design and Construction FEPs	1.1.07.00.0A	Repository Design
1.1.08.00.00	Quality Control	1.1.08.00.0A	Inadequate Quality Control and Deviations from Design
1.1.08.00.01	Poorly Constructed Repository	1.1.08.00.0A	Inadequate Quality Control and Deviations from Design
1.1.08.00.02	Material Defects	1.1.08.00.0A	Inadequate Quality Control and Deviations from Design
1.1.08.00.03	Common Cause Failures	1.1.08.00.0A	Inadequate Quality Control and Deviations from Design
1.1.08.00.04	Poor Quality Construction	1.1.08.00.0A	Inadequate Quality Control and Deviations from Design
1.1.08.00.05	Quality Control	1.1.08.00.0A	Inadequate Quality Control and Deviations from Design
1.1.08.00.06	Quality Control	1.1.08.00.0A	Inadequate Quality Control and Deviations from Design
1.1.08.00.07	Drains, Installed to Divert Water Around Containers, Are Improperly Placed	1.1.08.00.0A	Inadequate Quality Control and Deviations from Design
1.1.09.00.00	Schedule and Planning	1.1.09.00.0A	Schedule and Planning
1.1.09.00.01	Effects of Phased Operation	1.1.09.00.0A	Schedule and Planning
1.1.10.00.00	Administrative Control, Repository Site	1.1.10.00.0A	Administrative Control of the Repository Site
1.1.10.00.01	Planning Restrictions	1.1.10.00.0A	Administrative Control of the Repository Site
1.1.11.00.00	Monitoring of Repository	1.1.11.00.0A	Monitoring of the Repository
1.1.11.00.01	Monitoring and Remedial Activities	1.1.11.00.0A	Monitoring of the Repository
1.1.11.00.02	Postclosure Monitoring	1.1.11.00.0A	Monitoring of the Repository
1.1.11.00.03	Post-Closure Monitoring	1.1.11.00.0A	Monitoring of the Repository
1.1.11.00.04	Postclosure Monitoring	1.1.11.00.0A	Monitoring of the Repository
1.1.12.01.00	Accidents and Unplanned Events During Operation	1.1.12.01.0A	Accidents and Unplanned Events During Construction and Operation
1.1.12.01.01	Preclosure Events	1.1.12.01.0A	Accidents and Unplanned Events During Construction and Operation
1.1.12.01.02	Sabotage and Improper Operation	1.1.12.01.0A	Accidents and Unplanned Events During Construction and Operation
1.1.12.01.03	Accidents During Operation	1.1.12.01.0A	Accidents and Unplanned Events During Construction and Operation
1.1.12.01.04	Accidents During Operation	1.1.12.01.0A	Accidents and Unplanned Events During Construction and Operation
1.1.12.01.05	Handling Accidents	1.1.12.01.0A	Accidents and Unplanned Events During Construction and Operation

Table G-2. Cross Reference of TSPA-SR FEPs to TSPA-LA FEPs (Continued)

SR FEP Number	SR FEP Name	LA FEP Number	LA FEP Name
1.1.12.01.06	Oil or Organic Fluid Spill	1.1.02.03.0A	Undesirable Materials Left
		1.1.12.01.0A	Accidents and Unplanned Events During Construction and Operation
1.1.13.00.00	Retrievability	1.1.13.00.0A	Retrievability
1.1.13.00.01	Retrievability	1.1.13.00.0A	Retrievability
1.2.01.01.00	Tectonic Activity - Large Scale	1.2.01.01.0A	Tectonic Activity - Large Scale
1.2.01.01.01	Folding, Uplift or Subsidence Lowers Facility W/R/T Current Water Table	1.2.01.01.0A	Tectonic Activity – Large Scale
1.2.01.01.02	Tectonic Changes to Local Geothermal Flux Causes Convective Flow in SZ and Elevates Water Table	1.2.01.01.0A	Tectonic Activity - Large Scale
1.2.01.01.03	Tectonic Folding Alters Dip of Tuff Beds, Changing Percolation Flux	1.2.01.01.0A	Tectonic Activity – Large Scale
1.2.01.01.04	Uplift or Subsidence Changes Drainage At the Site, Increasing Infiltration	1.2.01.01.0A	Tectonic Activity – Large Scale
1.2.01.01.05	Uplift and Subsidence	1.2.01.01.0A	Tectonic Activity - Large Scale
1.2.01.01.06	Effect of Plate Movements	1.2.01.01.0A	Tectonic Activity - Large Scale
1.2.01.01.07	Plate Movement/Tectonic Change	1.2.01.01.0A	Tectonic Activity - Large Scale
1.2.01.01.08	Uplift and Subsidence	1.2.01.01.0A	Tectonic Activity - Large Scale
1.2.01.01.09	Regional Vertical Movements	1.2.01.01.0A	Tectonic Activity - Large Scale
1.2.01.01.10	Regional Tectonic Activity	1.2.01.01.0A	Tectonic Activity - Large Scale
1.2.01.01.11	Regional Tectonics	1.2.01.01.0A	Tectonic Activity - Large Scale
1.2.01.01.12	Regional Horizontal Movements	1.2.01.01.0A	Tectonic Activity - Large Scale
1.2.01.01.13	Regional Uplift and Subsidence	1.2.01.01.0A	Tectonic Activity - Large Scale
1.2.01.01.14	Geological (Events)	1.2.01.01.0A	Tectonic Activity - Large Scale
1.2.02.01.00	Fractures	1.2.02.01.0A	Fractures
		2.2.06.02.0B	Seismic Activity Changes Porosity and Permeability of Fractures
		2.2.10.04.0A	Thermo-Mechanical Stresses Alter Characteristics of Fractures Near Repository
1.2.02.01.01	Changes in Fracture Properties	1.2.02.01.0A	Fractures
1.2.02.01.02	Fracturing	1.2.02.01.0A	Fractures
1.2.02.02.00	Faulting	1.2.02.02.0A	Faults
		2.2.06.02.0A	Seismic Activity Changes Porosity and Permeability of Faults
		2.2.10.04.0B	Thermo-Mechanical Stresses Alter Characteristics of Faults Near Repository
1.2.02.02.01	Faulting	1.2.02.02.0A	Faults
1.2.02.02.02	Fault Generation	1.2.02.02.0A	Faults

Table G-2. Cross Reference of TSPA-SR FEPs to TSPA-LA FEPs (Continued)

SR FEP Number	SR FEP Name	LA FEP Number	LA FEP Name
1.2.02.02.03	Fault Activation	1.2.02.02.0A	Faults
1.2.02.02.04	Movements Along Small-Scale Faults	1.2.02.02.0A	Faults
1.2.02.02.05	Faulting/Fracturing	1.2.02.02.0A	Faults
1.2.02.02.06	Formation of New Faults	1.2.02.02.0A	Faults
1.2.02.02.07	Fault Movement	1.2.02.02.0A	Faults
1.2.02.02.08	Normal Faulting Occurs or Exists at Yucca Mountain	1.2.02.02.0A	Faults
1.2.02.02.09	Strike/Slip Faulting Occurs or Exists at Yucca Mountain.	1.2.02.02.0A	Faults
1.2.02.02.10	Detachment Faulting Occurs or Exists at Yucca Mountain	1.2.02.02.0A	Faults
1.2.02.02.11	Dip/Slip Faulting Occurs at Yucca Mountain	1.2.02.02.0A	Faults
1.2.02.02.12	New Fault Occurs at Yucca Mountain	1.2.02.02.0A	Faults
1.2.02.02.13	Old Fault Strand Is Reactivated at Yucca Mountain	1.2.02.02.0A	Faults
1.2.02.02.14	New Fault Strand Is Activated at Yucca Mountain	1.2.02.02.0A	Faults
1.2.02.02.15	Movements Along Major Faults	1.2.02.02.0A	Faults
1.2.02.02.16	Faulting (Large Scale, in Geosphere)	1.2.02.02.0A	Faults
1.2.02.02.17	Faulting Exhumes Waste Container	1.2.02.02.0A	Faults
1.2.02.03.00	Fault Movement Shears Waste Container	1.2.02.03.0A	Fault Displacement Damages EBS Components
1.2.03.01.00	Seismic Activity	1.2.03.02.0A	Seismic Ground Motion Damages EBS Components
		1.2.03.02.0B	Seismic-Induced Rockfall Damages EBS Components
		1.2.03.02.0C	Seismic-Induced Drift Collapse Damages EBS Components
		1.2.10.01.0A	Hydrologic Response to Seismic Activity
		1.4.02.04.0A	Seismic Event Precedes Human Intrusion
1.2.03.01.01	Earthquakes	1.2.03.02.0A	Seismic Ground Motion Damages EBS Components
		1.2.03.02.0B	Seismic-Induced Rockfall Damages EBS Components
1.2.03.01.02	Earthquakes	1.2.02.01.0A	Fractures
1.2.03.01.03	Earthquakes	1.2.03.02.0A	Seismic Ground Motion Damages EBS Components
		1.2.03.02.0B	Seismic-Induced Rockfall Damages EBS Components
1.2.03.01.04	Seismicity	1.2.03.02.0A	Seismic Ground Motion Damages EBS Components
		1.2.03.02.0B	Seismic-Induced Rockfall Damages EBS Components

Table G-2. Cross Reference of TSPA-SR FEPs to TSPA-LA FEPs (Continued)

SR FEP Number	SR FEP Name	LA FEP Number	LA FEP Name
1.2.03.01.05	Seismicity	1.2.03.02.0A	Seismic Ground Motion Damages EBS Components
		1.2.03.02.0B	Seismic-Induced Rockfall Damages EBS Components
1.2.03.01.06	Seismicity	1.2.02.03.0A	Fault Displacement Damages EBS Components
1.2.03.01.07	Seismic Activity	1.2.03.02.0A	Seismic Ground Motion Damages EBS Components
		1.2.03.02.0B	Seismic-Induced Rockfall Damages EBS Components
1.2.03.02.00	Seismic Vibration Causes Container Failure	1.2.03.02.0A	Seismic Ground Motion Damages EBS Components
		1.2.03.02.0B	Seismic-Induced Rockfall Damages EBS Components
1.2.03.02.01	Container Failure Induced by Microseisms Associated With Dike Emplacement	1.2.03.02.0A	Seismic Ground Motion Damages EBS Components
		1.2.03.03.0A	Seismicity Associated With Igneous Activity
1.2.03.03.00	Seismicity Associated With Igneous Activity	1.2.03.03.0A	Seismicity Associated With Igneous Activity
1.2.04.01.00	Igneous Activity	1.2.04.03.0A	Igneous Intrusion Into Repository
		1.2.04.04.0A	Igneous Intrusion Interacts With EBS Components
		1.2.04.05.0A	Magma or Pyroclastic Base Surge Transports Waste
		1.2.10.02.0A	Hydrologic Response to Igneous Activity
		1.4.02.03.0A	Igneous Event Precedes Human Intrusion
1.2.04.01.01	Volcanism	1.2.02.02.0A	Faults
		1.2.04.02.0A	Igneous Activity Changes Rock Properties
		1.2.04.04.0A	Igneous Intrusion Interacts With EBS Components
		1.2.10.02.0A	Hydrologic Response to Igneous Activity
		2.3.01.00.0A	Topography and Morphology
1.2.04.01.02	Magmatic Activity	1.2.04.02.0A	Igneous Activity Changes Rock Properties
		1.2.04.03.0A	Igneous Intrusion Into Repository
		1.2.10.02.0A	Hydrologic Response to Igneous Activity
1.2.04.01.03	Magmatic Activity	1.2.04.02.0A	Igneous Activity Changes Rock Properties
		1.2.04.03.0A	Igneous Intrusion Into Repository
1.2.04.01.04	Magmatic Activity	1.2.04.06.0A	Eruptive Conduit to Surface Intersects Repository
1.2.04.01.05	Volcanic Activity	1.2.04.02.0A	Igneous Activity Changes Rock Properties
1.2.04.02.00	Igneous Activity Causes Changes to Rock Properties	1.2.04.02.0A	Igneous Activity Changes Rock Properties
1.2.04.02.01	Dike Provides a Permeable Flow Path	1.2.04.02.0A	Igneous Activity Changes Rock Properties
1.2.04.02.02	Dike Provides a Barrier to Flow	1.2.04.02.0A	Igneous Activity Changes Rock Properties
1.2.04.02.03	Volcanic Activity in the Vicinity Produces an Impoundment	1.2.10.02.0A	Hydrologic Response to Igneous Activity

Table G-2. Cross Reference of TSPA-SR FEPs to TSPA-LA FEPs (Continued)

SR FEP Number	SR FEP Name	LA FEP Number	LA FEP Name
1.2.04.02.04	Igneous Activity Causes Extreme Changes to Rock Geochemical Properties	1.2.04.02.0A	Igneous Activity Changes Rock Properties
1.2.04.02.05	Intrusion (Magmatic)	1.2.04.02.0A	Igneous Activity Changes Rock Properties
1.2.04.02.06	Dike Related Fractures Alter Flow	1.2.04.02.0A	Igneous Activity Changes Rock Properties
1.2.04.02.07	Magmatic Activity	1.2.04.02.0A	Igneous Activity Changes Rock Properties
1.2.04.03.00	Igneous Intrusion Into Repository	1.2.04.03.0A	Igneous Intrusion Into Repository
1.2.04.03.01	Sill Provides a Permeable Flow Path	1.2.04.03.0A	Igneous Intrusion Into Repository
1.2.04.03.02	Sill Provides a Flow Barrier	1.2.04.03.0A	Igneous Intrusion Into Repository
1.2.04.03.03	Sill Intrudes Repository Openings	1.2.04.03.0A	Igneous Intrusion Into Repository
1.2.04.03.04	Volcanism	1.2.04.03.0A	Igneous Intrusion Into Repository
1.2.04.03.05	Intruding Dikes	1.2.04.03.0A	Igneous Intrusion Into Repository
1.2.04.04.00	Magma Interacts With Waste	1.2.04.03.0A	Igneous Intrusion Into Repository
		1.2.04.04.0A	Igneous Intrusion Interacts With EBS Components
		1.2.04.04.0B	Chemical Effects of Magma and Magmatic Volatiles
		1.2.04.05.0A	Magma or Pyroclastic Base Surge Transports Waste
1.2.04.04.01	Magmatic Volatiles Attack Waste	1.2.04.03.0A	Igneous Intrusion Into Repository
		1.2.04.04.0B	Chemical Effects of Magma and Magmatic Volatiles
1.2.04.04.02	Dissolution of Spent Fuel in Magma	1.2.04.05.0A	Magma or Pyroclastic Base Surge Transports Waste
1.2.04.04.03	Dissolution of Other Waste in Magma	1.2.04.05.0A	Magma or Pyroclastic Base Surge Transports Waste
1.2.04.04.04	Heating of Waste Container by Magma (Without Contact)	1.2.04.04.0A	Igneous Intrusion Interacts With EBS Components
1.2.04.04.05	Failure of Waste Container by Direct Contact W/Magma	1.2.04.04.0A	Igneous Intrusion Interacts With EBS Components
1.2.04.04.06	Fragmentation	1.2.04.04.0A	Igneous Intrusion Interacts With EBS Components
1.2.04.05.00	Magmatic Transport of Waste	1.2.04.05.0A	Magma or Pyroclastic Base Surge Transports Waste
1.2.04.05.01	Direct Exposure of Waste in Dike Apron	1.2.04.05.0A	Magma or Pyroclastic Base Surge Transports Waste
1.2.04.05.02	Volatile Radionuclides Plate Out in the Surrounding Rock	1.2.04.05.0A	Magma or Pyroclastic Base Surge Transports Waste
1.2.04.05.03	Entrainment of SNF in a Flowing Dike	1.2.04.05.0A	Magma or Pyroclastic Base Surge Transports Waste
1.2.04.06.00	Basaltic Cinder Cone Erupts Through the Repository	1.2.04.06.0A	Eruptive Conduit to Surface Intersects Repository
1.2.04.06.01	Vent Jump	1.2.04.06.0A	Eruptive Conduit to Surface Intersects Repository

Table G-2. Cross Reference of TSPA-SR FEPs to TSPA-LA FEPs (Continued)

SR FEP Number	SR FEP Name	LA FEP Number	LA FEP Name
1.2.04.06.02	Vent Erosion	1.2.04.06.0A	Eruptive Conduit to Surface Intersects Repository
1.2.04.07.00	Ashfall	1.2.04.07.0A	Ashfall
1.2.04.07.01	Soil Leaching Following Ashfall	1.2.04.07.0B	Ash Redistribution in Groundwater
		1.2.04.07.0C	Ash Redistribution via Soil and Sediment Transport
1.2.05.00.00	Metamorphism	1.2.05.00.0A	Metamorphism
1.2.05.00.01	Metamorphic Activity	1.2.05.00.0A	Metamorphism
1.2.05.00.02	Regional Metamorphism	1.2.05.00.0A	Metamorphism
1.2.05.00.03	Metamorphic Activity	1.2.05.00.0A	Metamorphism
1.2.05.00.04	Metamorphic Activity	1.2.05.00.0A	Metamorphism
1.2.06.00.00	Hydrothermal Activity	1.2.06.00.0A	Hydrothermal Activity
1.2.06.00.01	Hydrothermal Activity	1.2.06.00.0A	Hydrothermal Activity
1.2.07.01.00	Erosion/Denudation	1.2.07.01.0A	Erosion/Denudation
1.2.07.01.01	Major Incision	1.2.07.01.0A	Erosion/Denudation
		1.3.05.00.0A	Glacial and Ice Sheet Effect
1.2.07.01.02	Generalized Denudation	1.2.07.01.0A	Erosion/Denudation
1.2.07.01.03	Localized Denudation	1.2.07.01.0A	Erosion/Denudation
1.2.07.01.04	Solid Discharge via Erosional Processes	1.2.07.01.0A	Erosion/Denudation
1.2.07.01.05	Basement Alteration	1.2.07.01.0A	Erosion/Denudation
1.2.07.01.06	Hydraulic Gradient Changes (Magnitude, Direction) (In Geosphere)	1.2.07.01.0A	Erosion/Denudation
1.2.07.01.07	Hydraulic Gradient Changes (Magnitude, Direction)	1.2.07.01.0A	Erosion/Denudation
1.2.07.01.08	Ephemeral Stream Erosion Cuts Tiva Canyon Units to Underlying Nonwelded Units	1.2.07.01.0A	Erosion/Denudation
1.2.07.01.09	Land Slide	1.2.07.01.0A	Erosion/Denudation
1.2.07.01.10	Stream Erosion of Amargosa River Lowers Base Levels and Increases Gradient in SZ	1.2.07.01.0A	Erosion/Denudation
1.2.07.01.11	Erosion	1.2.07.01.0A	Erosion/Denudation
1.2.07.01.12	Erosion - Lateral Transport	1.2.07.01.0A	Erosion/Denudation
		2.3.02.03.0A	Soil and Sediment Transport in the Biosphere
1.2.07.01.13	Erosion (Wind)	1.2.07.01.0A	Erosion/Denudation
		2.3.02.03.0A	Soil and Sediment Transport in the Biosphere
1.2.07.01.14	Erosion on Surface/Sediments	1.2.07.01.0A	Erosion/Denudation
1.2.07.01.15	Denudation	1.2.07.01.0A	Erosion/Denudation
1.2.07.01.16	River, Stream Channel Erosion	1.2.07.01.0A	Erosion/Denudation
1.2.07.01.17	Chemical Denudation and Weathering	1.2.07.01.0A	Erosion/Denudation
1.2.07.01.18	Erosion	1.2.07.01.0A	Erosion/Denudation
1.2.07.01.19	Erosion/Deposition	1.2.07.01.0A	Erosion/Denudation

Table G-2. Cross Reference of TSPA-SR FEPs to TSPA-LA FEPs (Continued)

SR FEP Number	SR FEP Name	LA FEP Number	LA FEP Name
1.2.07.01.20	Fluvial Erosion/Sedimentation	1.2.07.01.0A	Erosion/Denudation
1.2.07.01.21	Surface Denudation	1.2.07.01.0A	Erosion/Denudation
1.2.07.01.22	Chemical Weathering	1.2.07.01.0A	Erosion/Denudation
1.2.07.01.23	Aeolian Erosion	1.2.07.01.0A	Erosion/Denudation
1.2.07.01.24	Fluvial Erosion	1.2.07.01.0A	Erosion/Denudation
1.2.07.01.25	Mass Wasting	1.2.07.01.0A	Erosion/Denudation
1.2.07.01.26	Mass Wasting	1.2.07.01.0A	Erosion/Denudation
1.2.07.01.27	Mechanical Weathering	1.2.07.01.0A	Erosion/Denudation
1.2.07.02.00	Deposition	1.2.07.02.0A	Deposition
1.2.07.02.01	Aeolian Deposition	1.2.07.02.0A	Deposition
		2.3.02.03.0A	Soil and Sediment Transport in the Biosphere
1.2.07.02.02	Lacustrine Deposition	1.2.07.02.0A	Deposition
1.2.08.00.00	Diagenesis	1.2.08.00.0A	Diagenesis
1.2.08.00.01	Diagenesis	1.2.08.00.0A	Diagenesis
1.2.08.00.02	Diagenesis	1.2.08.00.0A	Diagenesis
1.2.08.00.03	Fracture Infills	1.2.08.00.0A	Diagenesis
1.2.08.00.04	Diagenesis	1.2.08.00.0A	Diagenesis
1.2.09.00.00	Salt Diapirism and Dissolution	1.2.09.00.0A	Salt Diapirism and Dissolution
1.2.09.01.00	Diapirism	1.2.09.01.0A	Diapirism
1.2.09.01.01	Diapirism	1.2.09.01.0A	Diapirism
1.2.09.01.02	Salt Deformation	1.2.09.01.0A	Diapirism
1.2.09.01.03	Diapirism	1.2.09.01.0A	Diapirism
1.2.09.02.00	Large-Scale Dissolution	1.2.09.02.0A	Large-Scale Dissolution
1.2.09.02.01	Shallow Dissolution	1.2.09.02.0A	Large-Scale Dissolution
1.2.09.02.02	Lateral Dissolution	1.2.09.02.0A	Large-Scale Dissolution
1.2.09.02.03	Solution Chimneys	1.2.09.02.0A	Large-Scale Dissolution
1.2.09.02.04	Breccia Pipes	1.2.09.02.0A	Large-Scale Dissolution
1.2.09.02.05	Collapse Breccias	1.2.09.02.0A	Large-Scale Dissolution
1.2.10.01.00	Hydrological Response to Seismic Activity	1.2.10.01.0A	Hydrologic Response to Seismic Activity
1.2.10.01.01	Fault Movement Pumps Fluid from SZ to UZ (Seismic Pumping)	1.2.10.01.0A	Hydrologic Response to Seismic Activity
1.2.10.01.02	Fault Creep Causes Short Term Fluctuations of the Water Table	1.2.10.01.0A	Hydrologic Response to Seismic Activity
1.2.10.01.03	New Faulting Breaches Flow Barrier Controlling Large Hydraulic Gradient to the North	1.2.10.01.0A	Hydrologic Response to Seismic Activity
1.2.10.01.04	Normal Faulting Produces a Trap For Laterally Moving Moisture in the Tiva Canyon Unit	1.2.10.01.0A	Hydrologic Response to Seismic Activity
1.2.10.01.05	Head-Driven Flow Up from Carbonates	1.2.10.01.0A	Hydrologic Response to Seismic Activity

Table G-2. Cross Reference of TSPA-SR FEPs to TSPA-LA FEPs (Continued)

SR FEP Number	SR FEP Name	LA FEP Number	LA FEP Name
1.2.10.01.06	Seismically-Induced Water Table Changes	1.2.10.01.0A	Hydrologic Response to Seismic Activity
1.2.10.01.07	Fault Pathway Through the Altered Topopah Spring Basal Vitrophyre	1.2.10.01.0A	Hydrologic Response to Seismic Activity
1.2.10.01.08	Fault Movement Connects Tuff and Carbonate Aquifers	1.2.10.01.0A	Hydrologic Response to Seismic Activity
1.2.10.01.09	Fault Establishes Pathway Through the UZ	1.2.10.01.0A	Hydrologic Response to Seismic Activity
1.2.10.01.10	Fault Establishes Pathway Through the SZ	1.2.10.01.0A	Hydrologic Response to Seismic Activity
1.2.10.01.11	Fluid Supplied by a Fault Migrates Down the Drift	1.2.10.01.0A	Hydrologic Response to Seismic Activity
1.2.10.01.12	Fault Intersects and Drains Condensate Zone	1.2.10.01.0A	Hydrologic Response to Seismic Activity
1.2.10.01.13	Flow Barrier South of Site Blocks Flow, Causing Water Table to Rise	1.2.10.01.0A	Hydrologic Response to Seismic Activity
1.2.10.02.00	Hydrologic Response to Igneous Activity	1.2.10.02.0A	Hydrologic Response to Igneous Activity
1.2.10.02.01	Interaction of WT With Magma	1.2.10.02.0A	Hydrologic Response to Igneous Activity
1.2.10.02.02	Interaction of UZ Pore Water With Magma	1.2.10.02.0A	Hydrologic Response to Igneous Activity
1.3.01.00.00	Climate Change, Global	1.3.01.00.0A	Climate Change
1.3.01.00.01	Climate Change	1.3.01.00.0A	Climate Change
1.3.01.00.02	No Ice Age	1.3.01.00.0A	Climate Change
1.3.01.00.03	Solar Insolation	1.3.01.00.0A	Climate Change
1.3.01.00.04	No Ice Age	1.3.01.00.0A	Climate Change
1.3.01.00.05	Climate Change: Natural	1.3.01.00.0A	Climate Change
1.3.01.00.06	Exit from Glacial/Interglacial Cycling	1.3.01.00.0A	Climate Change
1.3.01.00.07	Intensification of Natural Climate Change	1.3.01.00.0A	Climate Change
1.3.01.00.08	Climatological (Effects)	1.3.01.00.0A	Climate Change
1.3.01.00.09	Climate Change	1.3.01.00.0A	Climate Change
1.3.01.00.10	Present-Day Climatic Conditions	1.3.01.00.0A	Climate Change
1.3.01.00.11	Seasonality of Climate	1.3.01.00.0A	Climate Change
1.3.01.00.12	Future Climatic Conditions	1.3.01.00.0A	Climate Change
1.3.01.00.13	Warmer Climate - Arid	1.3.01.00.0A	Climate Change
1.3.01.00.14	Warmer Climate - Seasonal Humid	1.3.01.00.0A	Climate Change
1.3.01.00.15	Warmer Climate - Equable Humid	1.3.01.00.0A	Climate Change
1.3.01.00.16	Climate Change (Effects on Repository)	1.3.01.00.0A	Climate Change
1.3.01.00.17	Global Effects	1.3.01.00.0A	Climate Change
1.3.01.00.18	Climate (Meteorology)	1.3.01.00.0A	Climate Change

Table G-2. Cross Reference of TSPA-SR FEPs to TSPA-LA FEPs (Continued)

SR FEP Number	SR FEP Name	LA FEP Number	LA FEP Name
1.3.01.00.19	Seasons (Meteorology)	1.3.01.00.0A	Climate Change
1.3.01.00.20	Temperature (Meteorology)	1.3.01.00.0A	Climate Change
1.3.01.00.21	Climate Change (Meteorology)	1.3.01.00.0A	Climate Change
1.3.04.00.00	Periglacial Effects	1.3.04.00.0A	Periglacial Effects
1.3.04.00.01	Permafrost	1.3.04.00.0A	Periglacial Effects
1.3.04.00.02	Accumulation of Gases Under Permafrost	1.3.04.00.0A	Periglacial Effects
1.3.04.00.03	Periglacial Effects	1.3.04.00.0A	Periglacial Effects
1.3.04.00.04	Frost Weathering	1.3.04.00.0A	Periglacial Effects
1.3.04.00.05	Solifluction	1.3.04.00.0A	Periglacial Effects
1.3.04.00.06	Tundra Climate	1.3.04.00.0A	Periglacial Effects
1.3.04.00.07	Permafrost	1.3.04.00.0A	Periglacial Effects
1.3.04.00.08	Permafrost	1.3.04.00.0A	Periglacial Effects
1.3.04.00.09	Permafrost	1.3.04.00.0A	Periglacial Effects
1.3.05.00.00	Glacial and Ice Sheet Effects, Local	1.3.05.00.0A	Glacial and Ice Sheet Effect
1.3.05.00.01	Glaciation	1.3.05.00.0A	Glacial and Ice Sheet Effect
1.3.05.00.02	Glaciation	1.3.05.00.0A	Glacial and Ice Sheet Effect
1.3.05.00.03	Glaciation	1.3.05.00.0A	Glacial and Ice Sheet Effect
1.3.05.00.04	Glaciation	1.3.05.00.0A	Glacial and Ice Sheet Effect
1.3.05.00.05	Glacial Climate	1.3.05.00.0A	Glacial and Ice Sheet Effect
1.3.05.00.06	Glacial Erosion/Sedimentation	1.3.05.00.0A	Glacial and Ice Sheet Effect
1.3.05.00.07	Glacial-Fluvial Erosion/Sedimentation	1.3.05.00.0A	Glacial and Ice Sheet Effect
1.3.05.00.08	Ice Sheet Effects (Loading, Melt Water Recharge)	1.3.05.00.0A	Glacial and Ice Sheet Effect
1.3.05.00.09	Glaciation	1.3.05.00.0A	Glacial and Ice Sheet Effect
1.3.05.00.10	Glaciation	1.3.05.00.0A	Glacial and Ice Sheet Effect
1.3.05.00.11	Glaciation	1.3.05.00.0A	Glacial and Ice Sheet Effect
1.3.05.00.12	Isostatic Rebound	1.3.05.00.0A	Glacial and Ice Sheet Effect
1.3.07.01.00	Drought / Water Table Decline	1.3.07.01.0A	Water Table Decline
1.3.07.01.01	Desert and Unsaturation	1.3.01.00.0A	Climate Change
		1.3.07.01.0A	Water Table Decline
1.3.07.01.02	Dust Storms and Desertification	1.3.01.00.0A	Climate Change
		1.3.07.01.0A	Water Table Decline
1.3.07.02.00	Water Table Rise	1.3.07.02.0A	Water Table Rise Affects SZ
		1.3.07.02.0B	Water Table Rise Affects UZ
		2.3.11.04.0A	Groundwater Discharge to Surface Outside the Reference Biosphere
1.3.07.02.01	Short Circuit of a Flow Barrier in the Saturated Zone Because of a Water Table Rise	1.2.10.01.0A	Hydrologic Response to Seismic Activity
		1.2.10.02.0A	Hydrologic Response to Igneous Activity
		1.3.07.02.0A	Water Table Rise Affects SZ
1.4.01.00.00	Human Influences on Climate	1.4.01.00.0A	Human Influences on Climate
1.4.01.00.01	Human-Induced Climate Change	1.4.01.00.0A	Human Influences on Climate

Table G-2. Cross Reference of TSPA-SR FEPs to TSPA-LA FEPs (Continued)

SR FEP Number	SR FEP Name	LA FEP Number	LA FEP Name
1.4.01.00.02	Anthropogenic Climate Change	1.4.01.00.0A	Human Influences on Climate
1.4.01.00.03	Human-Induced Climate Change	1.4.01.00.0A	Human Influences on Climate
1.4.01.00.04	Climate Change: Human Induced	1.4.01.00.0A	Human Influences on Climate
1.4.01.01.00	Climate Modification Increases Recharge	1.4.01.01.0A	Climate Modification Increases Recharge
1.4.01.01.01	Climate Modification Causes Perched Water to Develop at Base of Topopah Spring Unit	1.4.01.01.0A	Climate Modification Increases Recharge
		2.2.07.07.0A	Perched Water Develops
1.4.01.01.02	Climate Modification Causes Perched Water to Develop Above Repository	1.4.01.01.0A	Climate Modification Increases Recharge
		2.2.07.07.0A	Perched Water Develops
1.4.01.01.03	Climate Modification Raises Water Table	1.3.07.02.0A	Water Table Rise Affects SZ
		1.4.01.01.0A	Climate Modification Increases Recharge
1.4.01.01.04	Climate Modification Raises Water Table to Flood Repository	1.3.07.02.0A	Water Table Rise Affects SZ
		1.4.01.01.0A	Climate Modification Increases Recharge
1.4.01.01.05	Climate Modification Raises Water Table to Short Circuit Flow Barrier in SZ	1.2.10.01.0A	Hydrologic Response to Seismic Activity
		1.2.10.02.0A	Hydrologic Response to Igneous Activity
		1.3.07.02.0A	Water Table Rise Affects SZ
		1.4.01.01.0A	Climate Modification Increases Recharge
		2.2.07.12.0A	Saturated Groundwater Flow in the Geosphere
1.4.01.02.00	Greenhouse Gas Effects	1.4.01.02.0A	Greenhouse Gas Effects
1.4.01.02.01	Greenhouse Effect	1.4.01.02.0A	Greenhouse Gas Effects
1.4.01.02.02	Greenhouse Gas Effects	1.4.01.02.0A	Greenhouse Gas Effects
1.4.01.02.03	Greenhouse Effect	1.4.01.02.0A	Greenhouse Gas Effects
1.4.01.03.00	Acid Rain	1.4.01.03.0A	Acid Rain
1.4.01.03.01	Acid Rain	1.4.01.03.0A	Acid Rain
1.4.01.03.02	Surface Water Ph	1.4.01.03.0A	Acid Rain
1.4.01.04.00	Ozone Layer Failure	1.4.01.04.0A	Ozone Layer Failure
1.4.01.04.01	Damage to the Ozone Layer	1.4.01.04.0A	Ozone Layer Failure
1.4.01.04.02	Ozone Layer	1.4.01.04.0A	Ozone Layer Failure
1.4.02.01.00	Deliberate Human Intrusion	1.4.02.01.0A	Deliberate Human Intrusion
1.4.02.01.01	Chemical Sabotage	1.4.02.01.0A	Deliberate Human Intrusion
1.4.02.01.02	Waste Retrieval, Mining	1.4.02.01.0A	Deliberate Human Intrusion
1.4.02.01.03	Archeological Intrusion	1.4.02.01.0A	Deliberate Human Intrusion
1.4.02.01.04	Recovery of Repository Materials	1.4.02.01.0A	Deliberate Human Intrusion
1.4.02.01.05	Malicious Intrusion	1.4.02.01.0A	Deliberate Human Intrusion
1.4.02.01.06	Archaeological Investigation	1.4.02.01.0A	Deliberate Human Intrusion
1.4.02.01.07	Deliberate Intrusion	1.4.02.01.0A	Deliberate Human Intrusion
1.4.02.01.08	Malicious Intrusion	1.4.02.01.0A	Deliberate Human Intrusion
1.4.02.01.09	Deliberate Drilling Intrusion	1.4.02.01.0A	Deliberate Human Intrusion
1.4.02.01.10	Archeological Investigations	1.4.02.01.0A	Deliberate Human Intrusion

Table G-2. Cross Reference of TSPA-SR FEPs to TSPA-LA FEPs (Continued)

SR FEP Number	SR FEP Name	LA FEP Number	LA FEP Name
1.4.02.01.11	Post-Closure Subsurface Activities (Intrusion)	1.4.02.01.0A	Deliberate Human Intrusion
1.4.02.01.12	Intrusion Into Accumulation Zone in the Biosphere	1.4.02.01.0A	Deliberate Human Intrusion
1.4.02.01.13	Unsuccessful Attempt of Site Improvement	1.4.02.01.0A	Deliberate Human Intrusion
1.4.02.01.14	Sabotage	1.4.02.01.0A	Deliberate Human Intrusion
1.4.02.01.15	Sabotage	1.4.02.01.0A	Deliberate Human Intrusion
1.4.02.01.16	Sudden Energy Release (In Waste and EBS)	1.4.02.01.0A	Deliberate Human Intrusion
1.4.02.01.17	Other Future Uses of Crystalline Rock	1.4.02.01.0A	Deliberate Human Intrusion
1.4.02.01.18	Intrusion (Human)	1.4.02.01.0A	Deliberate Human Intrusion
1.4.02.02.00	Inadvertent Human Intrusion	1.4.02.02.0A	Inadvertent Human Intrusion
1.4.02.02.01	Accidental Intrusion	1.4.02.02.0A	Inadvertent Human Intrusion
1.4.03.00.00	Un-Intrusive Site Investigation	1.4.03.00.0A	Unintrusive Site Investigation
1.4.04.00.00	Drilling Activities (Human Intrusion)	1.4.04.00.0A	Drilling Activities (Human Intrusion)
1.4.04.00.01	Geothermal	1.4.04.00.0A	Drilling Activities (Human Intrusion)
1.4.04.00.02	Other Resources	1.4.04.00.0A	Drilling Activities (Human Intrusion)
1.4.04.00.03	Enhanced Oil and Gas Recovery	1.4.04.00.0A	Drilling Activities (Human Intrusion)
1.4.04.00.04	Liquid Waste Disposal	1.4.04.00.0A	Drilling Activities (Human Intrusion)
1.4.04.00.05	Hydrocarbon Storage	1.4.04.00.0A	Drilling Activities (Human Intrusion)
1.4.04.00.06	Exploratory Drilling For Hydrocarbons	1.4.04.00.0A	Drilling Activities (Human Intrusion)
1.4.04.00.07	Exploratory Drilling For Metals	1.4.04.00.0A	Drilling Activities (Human Intrusion)
1.4.04.00.08	Boreholes - Exploration	1.4.04.00.0A	Drilling Activities (Human Intrusion)
1.4.04.00.09	Injection of Liquid Wastes	1.4.04.00.0A	Drilling Activities (Human Intrusion)
1.4.04.00.10	Exploratory Drilling	1.4.04.00.0A	Drilling Activities (Human Intrusion)
1.4.04.00.11	Exploitation Drilling	1.4.04.00.0A	Drilling Activities (Human Intrusion)
1.4.04.00.12	Exploratory Drilling	1.4.04.00.0A	Drilling Activities (Human Intrusion)
1.4.04.00.13	Geothermal Exploitation	1.4.04.00.0A	Drilling Activities (Human Intrusion)
1.4.04.00.14	Liquid Waste Injection	1.4.04.00.0A	Drilling Activities (Human Intrusion)
1.4.04.00.15	Oil and Gas Exploration	1.4.04.00.0A	Drilling Activities (Human Intrusion)
1.4.04.00.16	Potash Exploration	1.4.04.00.0A	Drilling Activities (Human Intrusion)
1.4.04.00.17	Water Resource Exploration	1.4.04.00.0A	Drilling Activities (Human Intrusion)
1.4.04.00.18	Oil and Gas Exploitation	1.4.04.00.0A	Drilling Activities (Human Intrusion)
1.4.04.00.19	Groundwater Exploitation	1.4.04.00.0A	Drilling Activities (Human Intrusion)
1.4.04.00.20	Geothermal Energy Production	1.4.04.00.0A	Drilling Activities (Human Intrusion)
1.4.04.00.21	Geothermal Energy Production	1.4.04.00.0A	Drilling Activities (Human Intrusion)
1.4.04.00.22	Borehole-Well	1.4.04.00.0A	Drilling Activities (Human Intrusion)
1.4.04.00.23	Reuse of Boreholes	1.4.04.00.0A	Drilling Activities (Human Intrusion)
1.4.04.00.24	Oil and Gas Extraction	1.4.04.00.0A	Drilling Activities (Human Intrusion)
1.4.04.00.25	Liquid Waste Disposal	1.4.04.00.0A	Drilling Activities (Human Intrusion)

Table G-2. Cross Reference of TSPA-SR FEPs to TSPA-LA FEPs (Continued)

SR FEP Number	SR FEP Name	LA FEP Number	LA FEP Name
1.4.04.00.26	Enhanced Oil and Gas Production	1.4.04.00.0A	Drilling Activities (Human Intrusion)
1.4.04.00.27	Hydrocarbon Storage	1.4.04.00.0A	Drilling Activities (Human Intrusion)
1.4.04.01.00	Effects of Drilling Intrusion	1.4.04.01.0A	Effects of Drilling Intrusion
1.4.04.01.01	Drilling Fluid Interacts With Waste	1.4.04.01.0A	Effects of Drilling Intrusion
1.4.04.01.02	Drilling Introduces Surfactants	1.4.04.01.0A	Effects of Drilling Intrusion
1.4.04.01.03	Direct Exposure to Waste in Mud Pit	1.4.04.01.0A	Effects of Drilling Intrusion
1.4.04.01.04	Flooding of Drifts With Drilling Fluids	1.4.04.01.0A	Effects of Drilling Intrusion
1.4.04.01.05	Drilling Fluid Flow	1.4.04.01.0A	Effects of Drilling Intrusion
1.4.04.01.06	Drilling Fluid Loss	1.4.04.01.0A	Effects of Drilling Intrusion
1.4.04.01.07	Blowouts	1.4.04.01.0A	Effects of Drilling Intrusion
1.4.04.01.08	Drilling-Induced Geochemical Changes	1.4.04.01.0A	Effects of Drilling Intrusion
1.4.04.01.09	Fluid Injection-Induced Geochemical Changes	1.4.04.01.0A	Effects of Drilling Intrusion
1.4.04.01.10	Cuttings	1.4.04.01.0A	Effects of Drilling Intrusion
1.4.04.01.11	Cavings	1.4.04.01.0A	Effects of Drilling Intrusion
1.4.04.01.12	Spallings	1.4.04.01.0A	Effects of Drilling Intrusion
1.4.04.02.00	Abandoned and Undetected Boreholes	1.1.01.01.0A	Open Site Investigation Boreholes
		1.1.04.01.0A	Incomplete Closure
		1.1.11.00.0A	Monitoring of the Repository
		1.4.04.00.0A	Drilling Activities (Human Intrusion)
1.4.04.02.01	Exploratory Borehole Creates Flow Pathway	1.1.01.01.0A	Open Site Investigation Boreholes
1.4.04.02.02	Container Lies in the Trace of an Old Borehole	1.1.01.01.0A	Open Site Investigation Boreholes
1.4.04.02.03	Waste-Induced Borehole Flow (In Waste and EBS)	1.1.01.01.0A	Open Site Investigation Boreholes
1.4.04.02.04	Flow Through Undetected Boreholes	1.1.01.01.0A	Open Site Investigation Boreholes
		1.1.04.01.0A	Incomplete Closure
1.4.04.02.05	Natural Borehole Fluid Flow	1.1.01.01.0A	Open Site Investigation Boreholes
1.4.04.02.06	Borehole-Induced Mineralization	1.1.01.01.0A	Open Site Investigation Boreholes
1.4.04.02.07	Borehole-Induced Geochemical Changes	1.1.01.01.0A	Open Site Investigation Boreholes
1.4.05.00.00	Mining and Other Underground Activities (Human Intrusion)	1.4.05.00.0A	Mining and Other Underground Activities (Human Intrusion)
1.4.05.00.01	Mine Shaft Intersects Waste Container	1.4.05.00.0A	Mining and Other Underground Activities (Human Intrusion)
1.4.05.00.02	A Mine Shaft Creates a Preferential Path Thru the Upper Nonwelded Unit and a Wetter Zone Develops	1.4.05.00.0A	Mining and Other Underground Activities (Human Intrusion)
1.4.05.00.03	Intrusion (Mining)	1.4.05.00.0A	Mining and Other Underground Activities (Human Intrusion)

Table G-2. Cross Reference of TSPA-SR FEPs to TSPA-LA FEPs (Continued)

SR FEP Number	SR FEP Name	LA FEP Number	LA FEP Name
1.4.05.00.04	Mines	1.4.05.00.0A	Mining and Other Underground Activities (Human Intrusion)
1.4.05.00.05	Solution Mining	1.4.05.00.0A	Mining and Other Underground Activities (Human Intrusion)
1.4.05.00.06	Water from Mining Above the Repository Drains Through Repository.	1.4.05.00.0A	Mining and Other Underground Activities (Human Intrusion)
1.4.05.00.07	Underground Dwellings	1.4.05.00.0A	Mining and Other Underground Activities (Human Intrusion)
1.4.05.00.08	Resource Mining	1.4.05.00.0A	Mining and Other Underground Activities (Human Intrusion)
1.4.05.00.09	Tunneling	1.4.05.00.0A	Mining and Other Underground Activities (Human Intrusion)
1.4.05.00.10	Underground Construction	1.4.05.00.0A	Mining and Other Underground Activities (Human Intrusion)
1.4.05.00.11	Quarrying, Near Surface Extraction	1.4.05.00.0A	Mining and Other Underground Activities (Human Intrusion)
1.4.05.00.12	Mining Activities	1.4.05.00.0A	Mining and Other Underground Activities (Human Intrusion)
1.4.05.00.13	Potash Mining	1.4.05.00.0A	Mining and Other Underground Activities (Human Intrusion)
1.4.05.00.14	Other Resources	1.4.05.00.0A	Mining and Other Underground Activities (Human Intrusion)
1.4.05.00.15	Tunneling	1.4.05.00.0A	Mining and Other Underground Activities (Human Intrusion)
1.4.05.00.16	Construction of Underground Facilities	1.4.05.00.0A	Mining and Other Underground Activities (Human Intrusion)
1.4.05.00.17	Archaeological Excavations	1.4.05.00.0A	Mining and Other Underground Activities (Human Intrusion)
1.4.05.00.18	Deliberate Mining Intrusion	1.4.05.00.0A	Mining and Other Underground Activities (Human Intrusion)
1.4.05.00.19	Heat Storage in Lakes or Underground	1.4.05.00.0A	Mining and Other Underground Activities (Human Intrusion)
1.4.05.00.20	Changes in Groundwater Flow Due to Mining	1.4.05.00.0A	Mining and Other Underground Activities (Human Intrusion)
1.4.05.00.21	Changes in Geochemistry Due to Mining	1.4.05.00.0A	Mining and Other Underground Activities (Human Intrusion)
1.4.06.01.00	Altered Soil or Surface Water Chemistry	1.4.06.01.0A	Altered Soil or Surface Water Chemistry
1.4.06.01.01	Altered Soil or Surface Water Chemistry	1.4.06.01.0A	Altered Soil or Surface Water Chemistry
1.4.06.01.02	Groundwater Pollution	1.4.06.01.0A	Altered Soil or Surface Water Chemistry
1.4.06.01.03	Surface Pollution (Soils, Rivers)	1.4.06.01.0A	Altered Soil or Surface Water Chemistry
1.4.06.01.04	Altered Soil or Surface Water Chemistry by Human Activities	1.4.06.01.0A	Altered Soil or Surface Water Chemistry
1.4.06.01.05	Far Field Hydrochemistry – Acids, Oxidants, Nitrate	1.4.06.01.0A	Altered Soil or Surface Water Chemistry
1.4.06.01.06	Arable Farming	1.4.06.01.0A	Altered Soil or Surface Water Chemistry

Table G-2. Cross Reference of TSPA-SR FEPs to TSPA-LA FEPs (Continued)

SR FEP Number	SR FEP Name	LA FEP Number	LA FEP Name
1.4.07.01.00	Water Management Activities	1.4.07.01.0A	Water Management Activities
		1.4.07.02.0A	Wells
1.4.07.01.01	Water Collection in Cisterns Over Repository	1.4.07.01.0A	Water Management Activities
1.4.07.01.02	Water Management of Nearby Ground Water Basins	1.4.07.01.0A	Water Management Activities
1.4.07.01.03	Water Table Drawdown by Down Gradient Pumping Increases Hydraulic Gradient	1.4.07.01.0A	Water Management Activities
1.4.07.01.04	Surface Water Impoundment Is Constructed Near the Site, Increasing Percolation	1.4.07.01.0A	Water Management Activities
1.4.07.01.05	Dams	1.4.07.01.0A	Water Management Activities
1.4.07.01.06	Human Induced Actions on Groundwater Recharge	1.4.07.01.0A	Water Management Activities
1.4.07.01.07	Human-Induced Changes in Surface Hydrology	1.4.07.01.0A	Water Management Activities
1.4.07.01.08	Dams and Reservoirs, Built and Drained	1.4.07.01.0A	Water Management Activities
1.4.07.01.09	River Rechannelled	1.4.07.01.0A	Water Management Activities
1.4.07.01.10	Damming of Streams or Rivers	1.4.07.01.0A	Water Management Activities
1.4.07.01.11	Reservoirs	1.4.07.01.0A	Water Management Activities
1.4.07.01.12	Lake Usage	1.4.07.01.0A	Water Management Activities
1.4.07.01.13	Water Management Schemes	1.4.07.01.0A	Water Management Activities
1.4.07.02.00	Wells	1.4.07.02.0A	Wells
		2.3.13.04.0A	Radionuclide Release Outside the Reference Biosphere
1.4.07.02.01	Irrigation Wells in Midway Valley Increase Moisture Flux Through Repository	1.4.07.02.0A	Wells
1.4.07.02.02	Irrigation Wells in Midway Valley Reduce Distance to Accessible Environment	1.4.07.02.0A	Wells
1.4.07.02.03	Irrigation Wells in Crater Flats or Jackass Flats Increase Hydraulic Gradient Under Repository	1.4.07.02.0A	Wells
1.4.07.02.04	Wells (High Demand)	1.4.07.02.0A	Wells
1.4.07.02.05	Groundwater Abstraction	1.4.07.02.0A	Wells
1.4.07.02.06	Water Resource Exploitation	1.4.07.02.0A	Wells
1.4.07.02.07	Deep Groundwater Abstraction	1.4.07.02.0A	Wells
1.4.07.02.08	Water Producing Well	1.4.07.02.0A	Wells
1.4.07.02.09	Groundwater Extraction	1.4.07.02.0A	Wells
1.4.08.00.00	Social and Institutional Developments	1.4.08.00.0A	Social and Institutional Developments
1.4.08.00.01	Demographic Change and Urban Development	1.4.08.00.0A	Social and Institutional Developments
1.4.08.00.02	City On the Site	1.4.08.00.0A	Social and Institutional Developments

Table G-2. Cross Reference of TSPA-SR FEPs to TSPA-LA FEPs (Continued)

SR FEP Number	SR FEP Name	LA FEP Number	LA FEP Name
1.4.08.00.03	Urbanization On the Discharge Site	1.4.08.00.0A	Social and Institutional Developments
1.4.08.00.04	Demographic Change, Urban Development	1.4.08.00.0A	Social and Institutional Developments
1.4.09.00.00	Technological Developments	1.4.09.00.0A	Technological Developments
1.4.09.00.01	Cure For Cancer	1.4.09.00.0A	Technological Developments
1.4.09.00.02	Technological Advances in Food Production	1.4.09.00.0A	Technological Developments
1.4.11.00.00	Explosions and Crashes (Human Activities)	1.4.11.00.0A	Explosions and Crashes (Human Activities)
1.4.11.00.01	Bomb Blast	1.4.11.00.0A	Explosions and Crashes (Human Activities)
1.4.11.00.02	Collisions, Explosions and Impacts	1.4.11.00.0A	Explosions and Crashes (Human Activities)
1.4.11.00.03	Underground Test of Nuclear Devices	1.4.11.00.0A	Explosions and Crashes (Human Activities)
1.4.11.00.04	Explosions	1.4.11.00.0A	Explosions and Crashes (Human Activities)
1.4.11.00.05	Nuclear War	1.4.11.00.0a	Explosions and Crashes (Human Activities)
1.4.11.00.06	Underground Nuclear Testing	1.4.11.00.0A	Explosions and Crashes (Human Activities)
1.4.11.00.07	Explosions For Resource Recovery	1.4.11.00.0A	Explosions and Crashes (Human Activities)
1.4.11.00.08	Underground Nuclear Device Testing	1.4.11.00.0A	Explosions and Crashes (Human Activities)
1.4.11.00.09	Changes in Groundwater Flow Due to Explosions	1.4.11.00.0A	Explosions and Crashes (Human Activities)
1.5.01.01.00	Meteorite Impact	1.5.01.01.0A	Meteorite Impact
1.5.01.01.01	Meteorite Impact	1.5.01.01.0A	Meteorite Impact
1.5.01.01.02	Meteorite	1.5.01.01.0A	Meteorite Impact
1.5.01.01.03	Meteorite Impact	1.5.01.01.0a	Meteorite Impact
1.5.01.01.04	Impact of a Large Meteorite	1.5.01.01.0A	Meteorite Impact
1.5.01.02.00	Extraterrestrial Events	1.5.01.02.0A	Extraterrestrial Events
1.5.01.02.01	Extraterrestrial (Events)	1.5.01.02.0A	Extraterrestrial Events
1.5.02.00.00	Species Evolution	1.5.02.00.0A	Species Evolution
1.5.02.00.01	Biological Evolution	1.5.02.00.0A	Species Evolution
1.5.02.00.02	Critical Group - Evolution	1.5.02.00.0A	Species Evolution
1.5.02.00.03	Plant and Animal Evolution	1.5.02.00.0A	Species Evolution
1.5.03.01.00	Changes in the Earth's Magnetic Field	1.5.03.01.0A	Changes in the Earth's Magnetic Field
1.5.03.01.01	Flipping of the Earth's Magnetic Poles	1.5.03.01.0A	Changes in the Earth's Magnetic Field
1.5.03.01.02	Changes of the Magnetic Field	1.5.03.01.0A	Changes in the Earth's Magnetic Field
1.5.03.01.03	Magnetic Pole Reversal	1.5.03.01.0A	Changes in the Earth's Magnetic Field
1.5.03.02.00	Earth Tides	1.5.03.02.0A	Earth Tides
2.1.01.01.00	Waste Inventory	2.1.01.01.0A	Waste Inventory

Table G-2. Cross Reference of TSPA-SR FEPs to TSPA-LA FEPs (Continued)

SR FEP Number	SR FEP Name	LA FEP Number	LA FEP Name
2.1.01.01.01	Inventory	2.1.01.01.0A	Waste Inventory
2.1.01.01.02	Inventory	2.1.01.01.0A	Waste Inventory
2.1.01.01.03	Changes in Radionuclide Inventory (In Waste Form)	2.1.01.01.0A	Waste Inventory
2.1.01.01.04	Waste Product (Glass)	2.1.01.01.0A	Waste Inventory
2.1.01.01.05	Exotic Fuels	2.1.01.01.0a	Waste Inventory
2.1.01.01.06	DOE SNF Gap Radionuclide Inventory	2.1.01.01.0A	Waste Inventory
2.1.01.01.07	DOE SNF Initial Radionuclide Inventory	2.1.01.01.0A	Waste Inventory
2.1.01.01.08	DOE SNF Structure	2.1.01.01.0A	Waste Inventory
2.1.01.01.09	DOE SNF Initial Radionuclide Inventory	2.1.01.01.0A	Waste Inventory
2.1.01.01.10	DOE SNF Hazardous Chemical Inventory	2.1.01.01.0A	Waste Inventory
2.1.01.02.00	Co-Disposal/Co-Location of Waste	2.1.01.02.0A	Interactions Between Co-Located Waste
		2.1.01.02.0B	Interactions Between Co-Disposed Waste
2.1.01.02.01	Other Waste	2.1.01.02.0A	Interactions Between Co-Located Waste
2.1.01.02.02	Co-Disposal of Reactive Wastes	2.1.01.02.0A	Interactions Between Co-Located Waste
2.1.01.02.03	Near Storage of Other Waste	2.1.01.02.0A	Interactions Between Co-Located Waste
2.1.01.02.04	Doe SNF/HLW Glass Interactions	2.1.01.02.0b	Interactions Between Co-Disposed Waste
2.1.01.02.05	DOE SNF Waste Package Placement	2.1.01.02.0A	Interactions Between Co-Located Waste
2.1.01.02.06	DOE SNF Canister Arrangement Within Waste Package	2.1.01.02.0A	Interactions Between Co-Located Waste
2.1.01.02.07	DOE SNF Colocation With HLW	2.1.01.02.0B	Interactions Between Co-Disposed Waste
2.1.01.02.08	DOE SNF Geometry	2.1.01.02.0B	Interactions Between Co-Disposed Waste
		2.1.02.28.0A	Grouping of DSNF Waste Types Into Categories
2.1.01.02.09	DOE SNF Waste Package Placement	2.1.01.02.0A	Interactions Between Co-Located Waste
2.1.01.02.10	DOE SNF Colocation With HLW (Waste Form Degradation Impact)	2.1.01.02.0B	Interactions Between Co-Disposed Waste
2.1.01.02.11	DOE SNF Colocation With HLW (Radionuclide Mobilization Impact)	2.1.01.02.0B	Interactions Between Co-Disposed Waste
2.1.01.02.12	DOE SNF Colocation With HLW (Cladding Degradation Impact)	2.1.01.02.0B	Interactions Between Co-Disposed Waste
2.1.01.03.00	Heterogeneity of Waste Forms	2.1.01.03.0A	Heterogeneity of Waste Inventory
2.1.01.03.01	Damaged or Deviating Fuel	2.1.01.03.0A	Heterogeneity of Waste Inventory
2.1.01.03.02	Heterogeneity of Waste Form	2.1.01.03.0A	Heterogeneity of Waste Inventory
2.1.01.03.03	Deviant Inventory Flask	2.1.01.03.0A	Heterogeneity of Waste Inventory

Table G-2. Cross Reference of TSPA-SR FEPs to TSPA-LA FEPs (Continued)

SR FEP Number	SR FEP Name	LA FEP Number	LA FEP Name
2.1.01.03.04	DOE SNF Canister Atmosphere	2.1.01.03.0A	Heterogeneity of Waste Inventory
2.1.01.04.00	Spatial Heterogeneity of Emplaced Waste	2.1.01.04.0A	Repository-Scale Spatial Heterogeneity of Emplaced Waste
2.1.02.01.00	DSNF Degradation, Alteration, and Dissolution	2.1.02.01.0A	DSNF Degradation (Alteration, Dissolution, and Radionuclide Release)
2.1.02.01.01	DOE SNF Dissolution	2.1.02.01.0A	DSNF Degradation (Alteration, Dissolution, and Radionuclide Release)
2.1.02.01.02	Alteration/Dissolution of DOE SNF	2.1.02.01.0A	DSNF Degradation (Alteration, Dissolution, and Radionuclide Release)
2.1.02.01.03	Oxidation of DOE SNF	2.1.02.01.0A	DSNF Degradation (Alteration, Dissolution, and Radionuclide Release)
2.1.02.01.04	Alteration/Dissolution of Pu Ceramic Waste	2.1.02.01.0A	DSNF Degradation (Alteration, Dissolution, and Radionuclide Release)
2.1.02.01.05	High Integrity Canisters For DOE SNF	2.1.01.02.0B	Interactions Between Co-Disposed Waste
		2.1.02.01.0A	DSNF Degradation (Alteration, Dissolution, and Radionuclide Release)
2.1.02.02.00	CSNF Alteration, Dissolution, and Radionuclide Release	2.1.02.02.0A	CSNF Degradation (Alteration, Dissolution, and Radionuclide Release)
2.1.02.02.01	Source Terms (Expected)	2.1.02.02.0A	CSNF Degradation (Alteration, Dissolution, and Radionuclide Release)
		2.1.02.07.0A	Radionuclide Release from Gap and Grain Boundaries
2.1.02.02.02	Source Terms (Other) (In Waste Form)	2.1.02.02.0A	CSNF Degradation (Alteration, Dissolution, and Radionuclide Release)
2.1.02.02.03	Stability of UO2 (In Waste Form)	2.1.02.02.0A	CSNF Degradation (Alteration, Dissolution, and Radionuclide Release)
2.1.02.02.04	Degradation of Fuel Elements	2.1.02.02.0A	CSNF Degradation (Alteration, Dissolution, and Radionuclide Release)
2.1.02.02.05	Corrosion of Metal Parts (In Waste Form)	2.1.02.02.0A	CSNF Degradation (Alteration, Dissolution, and Radionuclide Release)
		2.1.02.16.0A	Localized (Pitting) Corrosion of Cladding
2.1.02.02.06	Corrosion Prior to Wetting	2.1.02.02.0A	CSNF Degradation (Alteration, Dissolution, and Radionuclide Release)
2.1.02.02.07	Radionuclide Release (Diffusion) Through Failed Cladding	2.1.09.08.0a	Diffusion of Dissolved Radionuclides in Ebs
		2.1.09.24.0A	Diffusion of Colloids in EBS
2.1.02.02.08	Water Turnover, Steel Vessel	2.1.02.02.0A	CSNF Degradation (Alteration, Dissolution, and Radionuclide Release)
		2.1.08.07.0A	Unsaturated Flow in the EBS
		2.1.08.09.0A	Saturated Flow in the EBS
2.1.02.02.09	Dissolution Chemistry (In Waste and EBS)	2.1.02.02.0A	CSNF Degradation (Alteration, Dissolution, and Radionuclide Release)
2.1.02.02.10	Release from Fuel Matrix (Release/Migration Factors)	2.1.02.02.0A	CSNF Degradation (Alteration, Dissolution, and Radionuclide Release)
2.1.02.02.11	Release from Metal Parts	2.1.02.02.0A	CSNF Degradation (Alteration, Dissolution, and Radionuclide Release)

Table G-2. Cross Reference of TSPA-SR FEPs to TSPA-LA FEPs (Continued)

SR FEP Number	SR FEP Name	LA FEP Number	LA FEP Name
2.1.02.02.12	Total Release from Fuel Elements	2.1.02.02.0A	CSNF Degradation (Alteration, Dissolution, and Radionuclide Release)
		2.1.02.07.0A	Radionuclide Release from Gap and Grain Boundaries
2.1.02.02.13	Dissolution of Waste (Release/Migration Factors)	2.1.02.02.0A	CSNF Degradation (Alteration, Dissolution, and Radionuclide Release)
2.1.02.02.14	Release of Radionuclides from the Failed Canister	2.1.02.02.0A	CSNF Degradation (Alteration, Dissolution, and Radionuclide Release)
2.1.02.02.15	Transport and Release of Nuclides, Failed Canister	2.1.09.08.0A	Diffusion of Dissolved Radionuclides in EBS
		2.1.09.08.0B	Advection of Dissolved Radionuclides in EBS
		2.1.09.19.0B	Advection of Colloids in EBS
		2.1.09.24.0A	Diffusion of Colloids in EBS
2.1.02.03.00	Glass Degradation, Alteration, and Dissolution	2.1.02.03.0A	HLW Glass Degradation (Alteration, Dissolution, and Radionuclide Release)
2.1.02.03.01	Degradation and Alteration of Glass Waste Form	2.1.02.03.0A	HLW Glass Degradation (Alteration, Dissolution, and Radionuclide Release)
2.1.02.03.02	Phase Separation (In Waste Form)	2.1.02.03.0A	HLW Glass Degradation (Alteration, Dissolution, and Radionuclide Release)
2.1.02.03.03	Congruent Dissolution (In Waste Form)	2.1.02.03.0A	HLW Glass Degradation (Alteration, Dissolution, and Radionuclide Release)
2.1.02.03.04	Rate of Glass Dissolution	2.1.02.03.0A	HLW Glass Degradation (Alteration, Dissolution, and Radionuclide Release)
2.1.02.03.05	Selective Leaching (In Waste Form)	2.1.02.03.0A	HLW Glass Degradation (Alteration, Dissolution, and Radionuclide Release)
2.1.02.03.06	Coprecipitates/Solid Solutions (In Waste Form)	2.1.02.03.0A	HLW Glass Degradation (Alteration, Dissolution, and Radionuclide Release)
		2.1.09.25.0A	Formation of Colloids (Waste-Form) by Co-Precipitation in EBS
2.1.02.03.07	Precipitation of Silicates /Silica Gel (In Waste Form)	2.1.02.03.0A	HLW Glass Degradation (Alteration, Dissolution, and Radionuclide Release)
2.1.02.03.08	Iron Corrosion Products	2.1.02.03.0A	HLW Glass Degradation (Alteration, Dissolution, and Radionuclide Release)
2.1.02.03.09	Radionuclide Release from Glass	2.1.02.03.0A	HLW Glass Degradation (Alteration, Dissolution, and Radionuclide Release)
2.1.02.03.10	Composition of DHLW Glass	2.1.02.03.0A	HLW Glass Degradation (Alteration, Dissolution, and Radionuclide Release)
2.1.02.04.00	Alpha Recoil Enhances Dissolution	2.1.02.04.0A	Alpha Recoil Enhances Dissolution
2.1.02.04.01	Recoil of Alpha-Decay	2.1.02.04.0A	Alpha Recoil Enhances Dissolution
		2.1.13.02.0A	Radiation Damage in EBS
2.1.02.05.00	Glass Cracking and Surface Area	2.1.02.05.0A	HLW Glass Cracking
2.1.02.05.01	Solute Transport Resistance (In Waste Form)	2.1.02.05.0A	HLW Glass Cracking
		2.1.09.08.0A	Diffusion of Dissolved Radionuclides in EBS
		2.1.09.24.0A	Diffusion of Colloids in EBS
2.1.02.06.00	Glass Recrystallization	2.1.02.06.0A	HLW Glass Recrystallization

Table G-2. Cross Reference of TSPA-SR FEPs to TSPA-LA FEPs (Continued)

SR FEP Number	SR FEP Name	LA FEP Number	LA FEP Name
2.1.02.07.00	Gap and Grain Release of Cs, I	2.1.02.07.0A	Radionuclide Release from Gap and Grain Boundaries
2.1.02.07.01	Gap and Grain Release	2.1.02.07.0A	Radionuclide Release from Gap and Grain Boundaries
2.1.02.07.02	Pb-I Reactions (In Waste Form)	2.1.02.07.0A	Radionuclide Release from Gap and Grain Boundaries
2.1.02.07.03	I, Cs-Migration to Fuel Surface	2.1.02.07.0A	Radionuclide Release from Gap and Grain Boundaries
2.1.02.08.00	Pyrophoricity	2.1.02.08.0A	Pyrophoricity from DSNF
2.1.02.08.01	DOE SNF Pyrophoricity	2.1.02.08.0A	Pyrophoricity from DSNF
2.1.02.08.02	DOE SNF Pyrophoric Event (Waste Heat Impact)	2.1.02.08.0A	Pyrophoricity from DSNF
2.1.02.08.03	DOE SNF Pyrophoric Event (Waste Package Degradation Impact)	2.1.02.08.0A	Pyrophoricity from DSNF
2.1.02.08.04	Acetylene Generation from DSNF Wfmisc—Flammable Gases Generation from DSNF - YMP	2.1.02.29.0A	Flammable Gas Generation from DSNF
		2.1.12.08.0A	Gas Explosions in EBS
2.1.02.08.05	DOE SNF Pyrophoric Event (Waste Form Degradation Impact)	2.1.02.08.0A	Pyrophoricity from DSNF
2.1.02.08.06	DOE SNF Pyrophoric Event (Cladding Degradation Impact)	2.1.02.08.0A	Pyrophoricity from DSNF
2.1.02.09.00	Void Space (In Glass Container)	2.1.01.02.0B	Interactions Between Co-Disposed Waste
		2.1.02.03.0A	HLW Glass Degradation (Alteration, Dissolution, and Radionuclide Release)
		2.1.02.09.0A	Chemical Effects of Void Space in Waste Package
2.1.02.10.00	Cellulosic Degradation	2.1.02.10.0A	Organic/Cellulosic Materials in Waste
		2.1.12.04.0A	Gas Generation (CO2, CH4, H2S) from Microbial Degradation
2.1.02.11.00	Waterlogged Rods	2.1.02.11.0a	Degradation of Cladding from Waterlogged Rods
2.1.02.12.00	Cladding Degradation Before YMP Receives It	2.1.02.12.0A	Degradation of Cladding Prior to Disposal
2.1.02.12.01	Pin Degradation During Reactor Operation	2.1.02.12.0a	Degradation of Cladding Prior to Disposal
2.1.02.12.02	Pin Degradation During Spent Fuel Pool Storage	2.1.02.12.0a	Degradation of Cladding Prior to Disposal
2.1.02.12.03	Pin Degradation During Dry Storage	2.1.02.12.0a	Degradation of Cladding Prior to Disposal
2.1.02.12.04	Pin Degradation During Fuel Shipment and Handling	2.1.02.12.0A	Degradation of Cladding Prior to Disposal
2.1.02.13.00	General Corrosion of Cladding	2.1.02.13.0A	General Corrosion of Cladding
2.1.02.13.01	Cladding Degradation Mechanisms at YMP, Pre-Pin Failure	2.1.02.12.0A	Degradation of Cladding Prior to Disposal
2.1.02.13.02	Corrosion (Of Cladding)	2.1.02.13.0A	General Corrosion of Cladding

Table G-2. Cross Reference of TSPA-SR FEPs to TSPA-LA FEPs (Continued)

SR FEP Number	SR FEP Name	LA FEP Number	LA FEP Name
2.1.02.14.00	Microbial Corrosion (MIC) of Cladding Wfclad—Microbiologically Influenced Corrosion (MIC) of Cladding	2.1.02.14.0A	Microbially Influenced Corrosion (MIC) of Cladding
2.1.02.15.00	Acid Corrosion of Cladding from Radiolysis	2.1.02.15.0A	Localized (Radiolysis Enhanced) Corrosion of Cladding
2.1.02.16.00	Localized Corrosion (Pitting) of Cladding	2.1.02.16.0A	Localized (Pitting) Corrosion of Cladding
2.1.02.17.00	Localized Corrosion (Crevice Corrosion) of Cladding	2.1.02.17.0A	Localized (Crevice) Corrosion of Cladding
2.1.02.18.00	High Dissolved Silica Content of Waters Enhances Corrosion of Cladding	2.1.02.18.0A	Enhanced Corrosion of Cladding from Dissolved Silica
2.1.02.19.00	Creep Rupture of Cladding	2.1.02.19.0A	Creep Rupture of Cladding
2.1.02.19.01	Thermal Cracking (In Waste and EBS)	2.1.02.19.0A	Creep Rupture of Cladding
		2.1.07.05.0A	Creep of Metallic Materials in the Waste Package
		2.1.07.05.0B	Creep of Metallic Materials in the Drip Shield
2.1.02.20.00	Pressurization from He Production Causes Cladding Failure	2.1.02.20.0A	Internal Pressurization of Cladding
2.1.02.21.00	Stress Corrosion Cracking (SCC) of Cladding	2.1.02.21.0A	Stress Corrosion Cracking (SCC) of Cladding
2.1.02.21.01	Inside Out from Fission Products (Iodine) (Failure of Cladding)	2.1.02.21.0A	Stress Corrosion Cracking (SCC) of Cladding
		2.1.13.01.0A	Radiolysis
2.1.02.21.02	Outside in from Salts or WP Chemicals (Failure of Cladding)	2.1.02.21.0A	Stress Corrosion Cracking (SCC) of Cladding
2.1.02.21.03	Stress-Corrosion Cracking of Zircaloy Cladding	2.1.02.21.0A	Stress Corrosion Cracking (SCC) of Cladding
2.1.02.22.00	Hydride Embrittlement of Cladding	2.1.02.22.0A	Hydride Cracking of Cladding
2.1.02.22.01	Hydride Embrittlement from Zirconium Corrosion (Of Cladding)	2.1.02.22.0A	Hydride Cracking of Cladding
2.1.02.22.02	Hydride Embrittlement from WP Corrosion & H2 Absorption (Of Cladding)	2.1.02.22.0A	Hydride Cracking of Cladding
2.1.02.22.03	Hydride Embrittlement from Galvanic Corrosion of WP Contacting Cladding	2.1.02.22.0A	Hydride Cracking of Cladding
2.1.02.22.04	Delayed Hydride Cracking (Of Cladding) Wfclad—Delayed Hydride Cracking (DHC) of Cladding	2.1.02.22.0A	Hydride Cracking of Cladding
2.1.02.22.05	Hydride Reorientation (Of Cladding)	2.1.02.22.0A	Hydride Cracking of Cladding

Table G-2. Cross Reference of TSPA-SR FEPs to TSPA-LA FEPs (Continued)

SR FEP Number	SR FEP Name	LA FEP Number	LA FEP Name
2.1.02.22.06	Hydrogen Axial Migration (Of Cladding)	2.1.02.22.0A	Hydride Cracking of Cladding
2.1.02.22.07	Hydride Embrittlement from Fuel Reaction (Causes Failure of Cladding) Wfclad—Hydride Embrittlement from Fuel Reaction	2.1.02.22.0A	Hydride Cracking of Cladding
2.1.02.23.00	Cladding Unzipping	2.1.02.23.0A	Cladding Unzipping
2.1.02.23.01	Cladding Degradation After Initial Cladding Perforation	2.1.02.23.0A	Cladding Unzipping
2.1.02.23.02	Dry Oxidation of Fuel (Causes Failure of Cladding) Wfclad—Dry Oxidation of Fuel	2.1.02.23.0A	Cladding Unzipping
2.1.02.23.03	Wet Oxidation of Fuel (Causes Failure of Cladding) Wfclad—Wet Oxidation of Fuel	2.1.02.23.0A	Cladding Unzipping
2.1.02.24.00	Mechanical Failure of Cladding	2.1.02.24.0A	Mechanical Impact on Cladding
2.1.02.25.00	DSNF Cladding Degradation	2.1.02.25.0A	DSNF Cladding
		2.1.02.25.0B	Naval SNF Cladding
2.1.02.25.01	DOE SNF Cladding Material	2.1.02.25.0A	DSNF Cladding
2.1.02.25.02	DOE SNF Cladding Condition	2.1.02.25.0A	DSNF Cladding
2.1.02.25.03	Internal Canister/Cladding Corrosion Due to DOE SNF	2.1.02.25.0A	DSNF Cladding
		2.1.03.06.0A	Internal Corrosion of Waste Packages Prior to Breach
2.1.02.26.00	Diffusion-Controlled Cavity Growth Wfclad—Diffusion-Controlled Cavity Growth (DCCG)	2.1.02.26.0A	Diffusion-Controlled Cavity Growth in Cladding
2.1.02.27.00	Localized Corrosion Perforation from Fluoride	2.1.02.27.0A	Localized (Fluoride Enhanced) Corrosion of Cladding
2.1.02.28.00	Various Features of the Approximately 250 DSNF Types and Grouping Into Waste Categories	2.1.02.28.0A	Grouping of DSNF Waste Types Into Categories
2.1.02.29.00	Flammable Gas Generation from DSNF	2.1.02.29.0A	Flammable Gas Generation from DSNF
2.1.03.01.00	Corrosion of Waste Containers	2.1.03.01.0A	General Corrosion of Waste Packages
		2.1.03.01.0B	General Corrosion of Drip Shields
		2.1.03.03.0A	Localized Corrosion of Waste Packages
		2.1.09.28.0A	Localized Corrosion on Waste Package Outer Surface Due to Deliquescence
		2.1.09.28.0B	Localized Corrosion on Drip Shield Surfaces Due to Deliquescence
2.1.03.01.01	Metallic Corrosion	2.1.03.01.0A	General Corrosion of Waste Packages
2.1.03.01.02	Corrosion on Wetting (Of Waste Container)	2.1.03.01.0A	General Corrosion of Waste Packages
2.1.03.01.03	Oxic Corrosion (Of Waste Container)	2.1.03.01.0A	General Corrosion of Waste Packages

Table G-2. Cross Reference of TSPA-SR FEPs to TSPA-LA FEPs (Continued)

SR FEP Number	SR FEP Name	LA FEP Number	LA FEP Name
2.1.03.01.04	Anoxic Corrosion (Of Waste Container)	2.1.03.01.0A	General Corrosion of Waste Packages
2.1.03.01.05	Total Corrosion Rate (Of Waste Container)	2.1.03.01.0A	General Corrosion of Waste Packages
2.1.03.01.06	Corrosion of Copper Canister	2.1.03.09.0A	Copper Corrosion in EBS
2.1.03.01.07	Corrosion of Steel Vessel	2.1.03.01.0A	General Corrosion of Waste Packages
2.1.03.01.08	Container Metal Corrosion	2.1.03.01.0A	General Corrosion of Waste Packages
2.1.03.01.09	Corrosion (Of Waste Container)	2.1.03.01.0A	General Corrosion of Waste Packages
2.1.03.01.10	Uniform Corrosion (Of Waste Container)	2.1.03.01.0A	General Corrosion of Waste Packages
2.1.03.01.11	Corrosive Agents, Sulfides, Oxygen, Etc.	2.1.03.01.0A	General Corrosion of Waste Packages
2.1.03.01.12	Water Turnover, Copper Canister	2.1.03.01.0A	General Corrosion of Waste Packages
		2.1.03.06.0A	Internal Corrosion of Waste Packages Prior to Breach
2.1.03.02.00	Stress Corrosion Cracking of Waste Containers and Drip Shields	2.1.03.02.0A	Stress Corrosion Cracking (SCC) of Waste Packages
		2.1.03.02.0B	Stress Corrosion Cracking (SCC) of Drip Shields
		2.1.09.28.0A	Localized Corrosion on Waste Package Outer Surface Due to Deliquescence
		2.1.09.28.0B	Localized Corrosion on Drip Shield Surfaces Due to Deliquescence
2.1.03.02.01	Stress Corrosion Cracking (Of Waste Container)	2.1.03.02.0A	Stress Corrosion Cracking (SCC) of Waste Packages
		2.1.03.02.0B	Stress Corrosion Cracking (SCC) of Drip Shields
2.1.03.02.02	Stress Corrosion Cracking - Dry Waste Container	2.1.03.02.0A	Stress Corrosion Cracking (SCC) of Waste Packages
2.1.03.02.03	Stress Corrosion Cracking Induced by Secondary Stress (Container Failure)	2.1.03.02.0A	Stress Corrosion Cracking (SCC) of Waste Packages
		2.1.11.05.0A	Thermal Expansion/Stress of In-Package EBS Components
		2.1.11.07.0A	Thermal Expansion/Stress of In-Drift EBS Components
2.1.03.02.04	Stress Corrosion Cracking (In Waste and EBS)	2.1.03.02.0A	Stress Corrosion Cracking (SCC) of Waste Packages
2.1.03.03.00	Pitting of Waste Containers and Drip Shields	2.1.03.03.0A	Localized Corrosion of Waste Packages
		2.1.03.03.0B	Localized Corrosion of Drip Shields
		2.1.09.28.0A	Localized Corrosion on Waste Package Outer Surface Due to Deliquescence
		2.1.09.28.0B	Localized Corrosion on Drip Shield Surfaces Due to Deliquescence
2.1.03.03.01	Localized Corrosion (Of Waste Container)	2.1.03.03.0A	Localized Corrosion of Waste Packages
		2.1.03.03.0B	Localized Corrosion of Drip Shields
2.1.03.03.02	Pitting (Of Waste Container)	2.1.03.03.0A	Localized Corrosion of Waste Packages
2.1.03.03.03	Pitting Corrosion Develops on Containers	2.1.03.03.0A	Localized Corrosion of Waste Packages

Table G-2. Cross Reference of TSPA-SR FEPs to TSPA-LA FEPs (Continued)

SR FEP Number	SR FEP Name	LA FEP Number	LA FEP Name
2.1.03.04.00	Hydride Cracking of Waste Containers and Drip Shields	2.1.03.04.0A	Hydride Cracking of Waste Packages
		2.1.03.04.0B	Hydride Cracking of Drip Shields
2.1.03.04.01	Embrittlement and Cracking	2.1.03.04.0A	Hydride Cracking of Waste Packages
2.1.03.05.00	Microbially-Mediated Corrosion of Waste Container and Drip Shield	2.1.03.05.0A	Microbially Influenced Corrosion (MIC) of Waste Packages
		2.1.03.05.0B	Microbially Influenced Corrosion (MIC) of Drip Shields
2.1.03.06.00	Internal Corrosion of Waste Container	2.1.03.06.0A	Internal Corrosion of Waste Packages Prior to Breach
2.1.03.06.01	DOE SNF Waste Package Internal Corrosion	2.1.03.06.0A	Internal Corrosion of Waste Packages Prior to Breach
2.1.03.07.00	Mechanical Impact on Waste Container and Drip Shield	2.1.03.07.0A	Mechanical Impact on Waste Package
		2.1.03.07.0B	Mechanical Impact on Drip Shield
		2.1.09.03.0A	Volume Increase of Corrosion Products Impacts Cladding
		2.1.09.03.0B	Volume Increase of Corrosion Products Impacts Waste Package
2.1.03.07.01	Other Canister Degradation Processes	2.1.03.04.0A	Hydride Cracking of Waste Packages
		2.1.07.05.0A	Creep of Metallic Materials in the Waste Package
		2.1.13.01.0A	Radiolysis
		2.1.13.02.0A	Radiation Damage in EBS
2.1.03.07.02	Failure of Copper Canister	2.1.03.09.0A	Copper Corrosion in EBS
2.1.03.07.03	Failure of Steel Canister	2.1.03.07.0A	Mechanical Impact on Waste Package
2.1.03.07.04	Reduced Mechanical Strength	2.1.03.07.0A	Mechanical Impact on Waste Package
2.1.03.07.05	Container Failure (Mechanical)	2.1.03.07.0A	Mechanical Impact on Waste Package
		2.1.03.07.0B	Mechanical Impact on Drip Shield
		2.1.07.04.0A	Hydrostatic Pressure on Waste Package
2.1.03.07.06	Falling Rock Hits Container, Increased Seepage Occurs, Speeds Corrosion of Container	2.1.03.07.0A	Mechanical Impact on Waste Package
		2.1.03.07.0B	Mechanical Impact on Drip Shield
2.1.03.08.00	Juvenile and Early Failure of Waste Containers and Drip Shields	2.1.03.08.0A	Early Failure of Waste Packages
		2.1.03.08.0B	Early Failure of Drip Shields
2.1.03.08.01	Canister Failure (Alternative Modes)	2.1.03.08.0A	Early Failure of Waste Packages
		2.1.07.04.0A	Hydrostatic Pressure on Waste Package
2.1.03.08.02	Mis-Sealed Canister	2.1.03.08.0A	Early Failure of Waste Packages
2.1.03.08.03	Container Failure (Early)	2.1.03.08.0A	Early Failure of Waste Packages
2.1.03.08.04	Cracking Along Welds (Of Waste Container)	2.1.03.08.0A	Early Failure of Waste Packages
2.1.03.08.05	Random Canister Defects - Quality Control	2.1.03.08.0A	Early Failure of Waste Packages
2.1.03.08.06	Common Cause Canister Defects - Quality Control	2.1.03.08.0A	Early Failure of Waste Packages
2.1.03.09.00	Copper Corrosion	2.1.03.09.0A	Copper Corrosion in EBS
2.1.03.09.01	Role of Chlorides in Copper Corrosion	2.1.03.09.0A	Copper Corrosion in EBS

Table G-2. Cross Reference of TSPA-SR FEPs to TSPA-LA FEPs (Continued)

SR FEP Number	SR FEP Name	LA FEP Number	LA FEP Name
2.1.03.10.00	Container Healing	2.1.03.10.0A	Advection of Liquids and Solids Through Cracks in the Waste Package
		2.1.03.10.0B	Advection of Liquids and Solids Through Cracks in the Drip Shield
2.1.03.10.01	Corrosion Products (Physical Effects)	2.1.03.10.0A	Advection of Liquids and Solids Through Cracks in the Waste Package
2.1.03.11.00	Container Form	2.1.03.11.0A	Physical Form of Waste Package and Drip Shield
2.1.03.11.01	Stainless Steel Fabrication Flask	2.1.01.02.0B	Interactions Between Co-Disposed Waste
		2.1.02.03.0A	HLW Glass Degradation (Alteration, Dissolution, and Radionuclide Release)
		2.1.03.11.0A	Physical Form of Waste Package and Drip Shield
2.1.03.11.02	Cast Steel Canister	2.1.03.11.0A	Physical Form of Waste Package and Drip Shield
2.1.03.11.03	Canister Thickness	2.1.03.11.0A	Physical Form of Waste Package and Drip Shield
2.1.03.11.04	Container Integrity	2.1.03.11.0A	Physical Form of Waste Package and Drip Shield
2.1.03.11.05	DOE SNF Waste Package Design	2.1.03.11.0A	Physical Form of Waste Package and Drip Shield
2.1.03.11.06	DOE SNF Canister Design	2.1.03.11.0A	Physical Form of Waste Package and Drip Shield
2.1.03.11.07	DOE SNF Waste Package Design	2.1.03.11.0A	Physical Form of Waste Package and Drip Shield
2.1.03.12.00	Container Failure (Long-Term)	2.1.03.01.0A	General Corrosion of Waste Packages
		2.1.03.02.0A	Stress Corrosion Cracking (SCC) of Waste Packages
		2.1.03.03.0A	Localized Corrosion of Waste Packages
		2.1.03.04.0A	Hydride Cracking of Waste Packages
		2.1.03.05.0A	Microbially Influenced Corrosion (MIC) of Waste Packages
		2.1.03.11.0A	Physical Form of Waste Package and Drip Shield
2.1.03.12.01	Canister Failure (Reference)	2.1.03.01.0A	General Corrosion of Waste Packages
		2.1.03.11.0A	Physical Form of Waste Package and Drip Shield
2.1.03.12.02	Long-Term Physical Stability (In Waste and EBS)	2.1.03.01.0A	General Corrosion of Waste Packages
		2.1.03.11.0A	Physical Form of Waste Package and Drip Shield
2.1.04.01.00	Preferential Pathways in the Backfill	2.1.04.01.0A	Flow in the Backfill
2.1.04.01.01	Interaction and Diffusion Between Canisters (And Buffer/Backfill)	2.1.04.05.0A	Thermal-Mechanical Properties and Evolution of Backfill
		2.1.04.09.0A	Radionuclide Transport in Backfill
2.1.04.01.02	Flow Through Buffer/Backfill	2.1.04.01.0A	Flow in the Backfill
2.1.04.01.03	Flow Through Buffer/Backfill	2.1.04.01.0A	Flow in the Backfill

Table G-2. Cross Reference of TSPA-SR FEPs to TSPA-LA FEPs (Continued)

SR FEP Number	SR FEP Name	LA FEP Number	LA FEP Name
2.1.04.02.00	Physical and Chemical Properties of Backfill	2.1.04.02.0A	Chemical Properties and Evolution of Backfill
		2.1.04.04.0A	Thermal-Mechanical Effects of Backfill
		2.1.04.05.0A	Thermal-Mechanical Properties and Evolution of Backfill
2.1.04.02.01	Backfill Characteristics	2.1.04.05.0A	Thermal-Mechanical Properties and Evolution of Backfill
2.1.04.02.02	Inhomogeneities (Properties and Evolution) (In Buffer/Backfill)	1.1.03.01.0B	Error in Backfill Emplacement
		2.1.04.02.0A	Chemical Properties and Evolution of Backfill
2.1.04.02.03	Chemical Alteration of Buffer/Backfill	2.1.04.02.0A	Chemical Properties and Evolution of Backfill
2.1.04.02.04	Backfill Physical Composition	2.1.04.05.0A	Thermal-Mechanical Properties and Evolution of Backfill
2.1.04.02.05	Backfill Chemical Composition	2.1.04.02.0A	Chemical Properties and Evolution of Backfill
2.1.04.02.06	Chemical Degradation of Backfill	2.1.04.02.0A	Chemical Properties and Evolution of Backfill
2.1.04.02.07	Backfill Materials Deficiencies	1.1.03.01.0B	Error in Backfill Emplacement
		2.1.04.01.0A	Flow in the Backfill
		2.1.04.02.0A	Chemical Properties and Evolution of Backfill
2.1.04.02.08	Near-Field Buffer Chemistry	2.1.04.02.0A	Chemical Properties and Evolution of Backfill
2.1.04.02.09	Water Chemistry, Tunnel Backfill	2.1.04.02.0A	Chemical Properties and Evolution of Backfill
2.1.04.02.10	Backfill Effects on Cu Corrosion	2.1.04.02.0A	Chemical Properties and Evolution of Backfill
2.1.04.03.00	Erosion or Dissolution of Backfill	2.1.04.03.0A	Erosion or Dissolution of Backfill
2.1.04.03.01	Erosion of Buffer/Backfill	2.1.04.03.0A	Erosion or Dissolution of Backfill
2.1.04.04.00	Mechanical Effects of Backfill	2.1.04.04.0A	Thermal-Mechanical Effects of Backfill
2.1.04.04.01	Mechanical Failure of Buffer/Backfill	2.1.04.04.0A	Thermal-Mechanical Effects of Backfill
2.1.04.04.02	Mechanical Impact/Failure, Buffer/Backfill	2.1.04.04.0A	Thermal-Mechanical Effects of Backfill
2.1.04.05.00	Backfill Evolution	2.1.04.02.0A	Chemical Properties and Evolution of Backfill
		2.1.04.05.0A	Thermal-Mechanical Properties and Evolution of Backfill
2.1.04.05.01	Hydrothermal Alteration (In Buffer/Backfill)	2.1.04.02.0A	Chemical Properties and Evolution of Backfill
2.1.04.05.02	Small Pieces of Backfill Under Go Phase Changes When Heated and Weld Together	2.1.04.05.0A	Thermal-Mechanical Properties and Evolution of Backfill
2.1.04.05.03	Thermal Degradation of Buffer/Backfill	2.1.04.02.0A	Chemical Properties and Evolution of Backfill

Table G-2. Cross Reference of TSPA-SR FEPs to TSPA-LA FEPs (Continued)

SR FEP Number	SR FEP Name	LA FEP Number	LA FEP Name
2.1.04.06.00	Properties of Bentonite	2.1.04.01.0A	Flow in the Backfill
		2.1.04.02.0A	Chemical Properties and Evolution of Backfill
		2.1.04.03.0A	Erosion or Dissolution of Backfill
		2.1.04.04.0A	Thermal-Mechanical Effects of Backfill
		2.1.04.05.0A	Thermal-Mechanical Properties and Evolution of Backfill
		2.1.04.09.0A	Radionuclide Transport in Backfill
		2.2.01.02.0B	Chemical Changes in the Near-Field from Backfill
2.1.04.06.01	Bentonite Swelling Pressure	2.1.04.04.0A	Thermal-Mechanical Effects of Backfill
2.1.04.06.02	Bentonite Erosion	2.1.04.03.0A	Erosion or Dissolution of Backfill
2.1.04.06.03	Bentonite Plasticity	2.1.04.05.0A	Thermal-Mechanical Properties and Evolution of Backfill
2.1.04.06.04	Bentonite Porewater Chemistry	2.1.04.02.0A	Chemical Properties and Evolution of Backfill
2.1.04.06.05	Mineralogical Alteration - Short Term (In Buffer/Backfill)	2.1.04.02.0A	Chemical Properties and Evolution of Backfill
2.1.04.06.06	Mineralogical Alteration - Long Term (In Buffer/Backfill)	2.1.04.02.0A	Chemical Properties and Evolution of Backfill
2.1.04.06.07	Bentonite Cementation	2.1.04.05.0A	Thermal-Mechanical Properties and Evolution of Backfill
2.1.04.06.08	Quality Control (In Buffer/Backfill)	1.1.03.01.0B	Error in Backfill Emplacement
2.1.04.06.09	Poor Emplacement of Buffer	1.1.03.01.0B	Error in Backfill Emplacement
2.1.04.06.10	Organics/Contamination of Bentonite	1.1.02.03.0A	Undesirable Materials Left
		1.1.03.01.0B	Error in Backfill Emplacement
2.1.04.06.11	Coagulation of Bentonite	2.1.04.05.0A	Thermal-Mechanical Properties and Evolution of Backfill
2.1.04.06.12	Dilution of Buffer/Backfill	2.1.04.02.0A	Chemical Properties and Evolution of Backfill
2.1.04.06.13	Sedimentation of Bentonite	2.1.04.05.0A	Thermal-Mechanical Properties and Evolution of Backfill
2.1.04.06.14	Swelling of Tunnel Backfill	2.1.04.04.0A	Thermal-Mechanical Effects of Backfill
2.1.04.06.15	Swelling Pressure (In Buffer/Backfill)	2.1.04.04.0A	Thermal-Mechanical Effects of Backfill
2.1.04.06.16	Degradation of Bentonite by Chemical Reactions	2.1.04.02.0A	Chemical Properties and Evolution of Backfill
2.1.04.06.17	Colloid Generation (In Buffer/Backfill)	2.1.04.09.0A	Radionuclide Transport in Backfill
2.1.04.06.18	Coagulation of Bentonite	2.1.04.05.0A	Thermal-Mechanical Properties and Evolution of Backfill
2.1.04.06.19	Sedimentation of Bentonite	2.1.04.05.0A	Thermal-Mechanical Properties and Evolution of Backfill
2.1.04.06.20	Swelling of Bentonite Into Tunnels and Cracks	2.1.04.04.0A	Thermal-Mechanical Effects of Backfill
2.1.04.06.21	Uneven Swelling of Bentonite	2.1.04.04.0A	Thermal-Mechanical Effects of Backfill

Table G-2. Cross Reference of TSPA-SR FEPs to TSPA-LA FEPs (Continued)

SR FEP Number	SR FEP Name	LA FEP Number	LA FEP Name
2.1.04.06.22	Thermal Effects On the Buffer Material	2.1.04.05.0A	Thermal-Mechanical Properties and Evolution of Backfill
2.1.04.06.23	Bentonite Emplacement and Composition	1.1.03.01.0B	Error in Backfill Emplacement
2.1.04.06.24	Thermal Evolution (In Buffer/Backfill)	2.1.04.05.0A	Thermal-Mechanical Properties and Evolution of Backfill
2.1.04.06.25	Bentonite Saturation	2.1.04.05.0A	Thermal-Mechanical Properties and Evolution of Backfill
2.1.04.06.26	Buffer Impermeability	2.1.04.05.0A	Thermal-Mechanical Properties and Evolution of Backfill
2.1.04.06.27	Bentonite Swelling	2.1.04.04.0A	Thermal-Mechanical Effects of Backfill
2.1.04.06.28	Resaturation of Bentonite Buffer	2.1.04.01.0A	Flow in the Backfill
2.1.04.06.29	Resaturation of Tunnel Backfill	2.1.04.01.0A	Flow in the Backfill
2.1.04.06.30	Effects of Bentonite on Groundwater Chemistry	2.1.04.02.0A	Chemical Properties and Evolution of Backfill
2.1.04.06.31	Canister/Bentonite Interaction	2.1.04.02.0A	Chemical Properties and Evolution of Backfill
2.1.04.06.32	Interaction With Cement Components	2.1.04.02.0A	Chemical Properties and Evolution of Backfill
2.1.04.06.33	Water Chemistry, Bentonite Buffer	2.1.04.02.0A	Chemical Properties and Evolution of Backfill
2.1.04.06.34	Gas Transport in Bentonite	2.1.04.09.0A	Radionuclide Transport in Backfill
2.1.04.06.35	Effect of Bentonite Swelling on EDZ	2.1.04.04.0A	Thermal-Mechanical Effects of Backfill
2.1.04.07.00	Buffer Characteristics	2.1.04.02.0A	Chemical Properties and Evolution of Backfill
		2.1.04.09.0A	Radionuclide Transport in Backfill
2.1.04.07.01	Buffer Additives	2.1.04.02.0A	Chemical Properties and Evolution of Backfill
2.1.04.07.02	Buffer Evolution	2.1.04.05.0A	Thermal-Mechanical Properties and Evolution of Backfill
2.1.04.07.03	Faulty Buffer Emplacement	1.1.03.01.0B	Error in Backfill Emplacement
2.1.04.07.04	Saturation of Sorption Sites	2.1.04.02.0A	Chemical Properties and Evolution of Backfill
		2.1.09.02.0A	Chemical Interaction With Corrosion Products
2.1.04.07.05	Perturbed Buffer Material Chemistry	2.1.04.02.0A	Chemical Properties and Evolution of Backfill
2.1.04.08.00	Diffusion in Backfill	2.1.04.09.0A	Radionuclide Transport in Backfill
2.1.04.09.00	Radionuclide Transport Through Backfill	2.1.04.09.0A	Radionuclide Transport in Backfill
2.1.04.09.01	Transport and Release of Nuclides, Bentonite Buffer	2.1.04.09.0A	Radionuclide Transport in Backfill
2.1.04.09.02	Transport and Release of Nuclides, Tunnel Backfill	2.1.04.09.0A	Radionuclide Transport in Backfill
2.1.05.01.00	Seal Physical Properties	2.1.05.01.0A	Flow Through Seals (Access Ramps and Ventilation Shafts)

Table G-2. Cross Reference of TSPA-SR FEPs to TSPA-LA FEPs (Continued)

SR FEP Number	SR FEP Name	LA FEP Number	LA FEP Name
2.1.05.01.01	Seal Geometry	2.1.05.01.0A	Flow Through Seals (Access Ramps and Ventilation Shafts)
2.1.05.01.02	Consolidation of Seals	2.1.05.03.0A	Degradation of Seals
2.1.05.01.03	Shaft and Tunnel Seals	2.1.05.01.0A	Flow Through Seals (Access Ramps and Ventilation Shafts)
2.1.05.02.00	Groundwater Flow and Radionuclide Transport in Seals	2.1.05.01.0A	Flow Through Seals (Access Ramps and Ventilation Shafts)
		2.1.05.02.0A	Radionuclide Transport Through Seals
		2.1.05.03.0A	Degradation of Seals
2.1.05.03.00	Seal Degradation	2.1.05.03.0A	Degradation of Seals
2.1.05.03.01	Seal Evolution	2.1.05.03.0A	Degradation of Seals
2.1.05.03.02	Seal Failure	2.1.05.03.0A	Degradation of Seals
2.1.05.03.03	Degradation of Hole and Shaft Seals	2.1.05.03.0A	Degradation of Seals
2.1.05.03.04	Shaft or Access Tunnel Seal Failure and Degradation	2.1.05.03.0A	Degradation of Seals
2.1.05.03.05	Degradation of Hole and Shaft Seals	2.1.05.03.0A	Degradation of Seals
2.1.05.03.06	Loss of Integrity of Shaft or Access Tunnel Seals	2.1.05.03.0A	Degradation of Seals
2.1.05.03.07	Mechanical Degradation of Seals	2.1.05.03.0A	Degradation of Seals
2.1.05.03.08	Chemical Degradation of Seals	2.1.05.03.0A	Degradation of Seals
2.1.06.01.00	Degradation of Cementitious Materials in Drift	2.1.06.01.0A	Chemical Effects of Rock Reinforcement and Cementitious Materials in EBS
2.1.06.01.01	Physio-Chemical Degradation of Concrete	2.1.06.01.0A	Chemical Effects of Rock Reinforcement and Cementitious Materials in EBS
		2.1.06.02.0A	Mechanical Effects of Rock Reinforcement Materials in EBS
2.1.06.01.02	Seal Chemical Composition	2.1.05.03.0A	Degradation of Seals
		2.1.06.01.0A	Chemical Effects of Rock Reinforcement and Cementitious Materials in EBS
2.1.06.01.03	Microbial Growth on Concrete	2.1.06.01.0A	Chemical Effects of Rock Reinforcement and Cementitious Materials in EBS
		2.1.10.01.0A	Microbial Activity in EBS
		2.1.12.04.0A	Gas Generation (CO2, CH4, H2S) from Microbial Degradation
2.1.06.02.00	Effects of Rock Reinforcement Materials	2.1.06.01.0A	Chemical Effects of Rock Reinforcement and Cementitious Materials in EBS
		2.1.06.02.0A	Mechanical Effects of Rock Reinforcement Materials in EBS
2.1.06.02.01	Degradation of Rock Reinforcement and Grout	2.1.06.01.0A	Chemical Effects of Rock Reinforcement and Cementitious Materials in EBS
		2.1.06.02.0A	Mechanical Effects of Rock Reinforcement Materials in EBS

Table G-2. Cross Reference of TSPA-SR FEPs to TSPA-LA FEPs (Continued)

SR FEP Number	SR FEP Name	LA FEP Number	LA FEP Name
2.1.06.03.00	Degradation of the Liner	2.1.06.04.0A	Flow Through Rock Reinforcement Materials in EBS
		2.1.06.05.0B	Mechanical Degradation of Invert
		2.1.06.05.0D	Chemical Degradation of Invert
2.1.06.04.00	Flow Through the Liner	2.1.06.04.0A	Flow Through Rock Reinforcement Materials in EBS
2.1.06.04.01	Fracture Flow Through the Liner	2.1.06.04.0A	Flow Through Rock Reinforcement Materials in EBS
2.1.06.05.00	Degradation of Invert and Pedestal	2.1.06.05.0A	Mechanical Degradation of Emplacement Pallet
		2.1.06.05.0B	Mechanical Degradation of Invert
		2.1.06.05.0C	Chemical Degradation of Emplacement Pallet
		2.1.06.05.0D	Chemical Degradation of Invert
2.1.06.05.01	Cementitious Invert	2.1.06.05.0D	Chemical Degradation of Invert
2.1.06.06.00	Effects and Degradation of Drip Shield	2.1.03.01.0B	General Corrosion of Drip Shields
		2.1.03.07.0B	Mechanical Impact on Drip Shield
		2.1.06.06.0A	Effects of Drip Shield on Flow
		2.1.06.06.0B	Oxygen Embrittlement of Drip Shields
2.1.06.06.01	Oxygen Embrittlement of Ti Drip Shield	2.1.03.03.0B	Localized Corrosion of Drip Shields
		2.1.03.04.0B	Hydride Cracking of Drip Shields
2.1.06.07.00	Effects at Material Interfaces	2.1.06.07.0A	Chemical Effects at EBS Component Interfaces
		2.1.06.07.0B	Mechanical Effects at EBS Component Interfaces
		2.1.09.09.0A	Electrochemical Effects in EBS
2.1.07.01.00	Rockfall (Large Block) Wfclad--Rockfall	1.2.03.02.0B	Seismic-Induced Rockfall Damages EBS Components
		2.1.07.01.0A	Rockfall
2.1.07.01.01	Rockbursts in Container Holes	2.1.07.01.0A	Rockfall
2.1.07.01.02	Cave Ins	2.1.07.01.0A	Rockfall
2.1.07.01.03	Cave in (In Waste and EBS)	2.1.07.01.0A	Rockfall
		2.1.07.02.0A	Drift Collapse
2.1.07.01.04	Roof Falls	2.1.07.01.0A	Rockfall
2.1.07.02.00	Mechanical Degradation or Collapse of Drift	1.2.03.02.0C	Seismic-Induced Drift Collapse Damages EBS Components
		1.2.03.02.0D	Seismic-Induced Drift Collapse Alters In-Drift Thermohydrology
		1.2.03.02.0E	Seismic-Induced Drift Collapse Alters In-Drift Chemistry
		2.1.07.02.0A	Drift Collapse
2.1.07.02.01	Stability (In Waste and EBS)	2.1.07.02.0A	Drift Collapse
2.1.07.02.02	Mechanical (Events and Processes in the Waste and EBS)	1.2.03.02.0C	Seismic-Induced Drift Collapse Damages EBS Components
		1.2.03.02.0D	Seismic-Induced Drift Collapse Alters In-Drift Thermohydrology

Table G-2. Cross Reference of TSPA-SR FEPs to TSPA-LA FEPs (Continued)

SR FEP Number	SR FEP Name	LA FEP Number	LA FEP Name
2.1.07.02.02	Mechanical (Events and Processes in the Waste and EBS) (continued)	1.2.03.02.0E	Seismic-Induced Drift Collapse Alters In-Drift Chemistry
		2.1.07.01.0A	Rockfall
		2.1.07.02.0A	Drift Collapse
2.1.07.02.03	Rockfall Slopes Up Fault	2.1.07.02.0A	Drift Collapse
2.1.07.02.04	Rockfall (Rubble) (In Waste and EBS)	1.2.03.02.0C	Seismic-Induced Drift Collapse Damages EBS Components
		1.2.03.02.0D	Seismic-Induced Drift Collapse Alters In-Drift Thermohydrology
		1.2.03.02.0E	Seismic-Induced Drift Collapse Alters In-Drift Chemistry
		2.1.07.02.0A	Drift Collapse
2.1.07.02.05	Mechanical Failure of Repository	2.1.07.02.0A	Drift Collapse
2.1.07.02.06	Subsidence/Collapse	2.1.07.02.0A	Drift Collapse
2.1.07.02.07	Vault Collapse	2.1.07.02.0A	Drift Collapse
2.1.07.02.08	Creeping of Rock Mass	2.1.07.02.0A	Drift Collapse
2.1.07.03.00	Movement of Containers	2.1.03.07.0A	Mechanical Impact on Waste Package
		2.1.03.07.0B	Mechanical Impact on Drip Shield
		2.1.06.05.0A	Mechanical Degradation of Emplacement Pallet
		2.1.06.05.0B	Mechanical Degradation of Invert
		2.1.08.15.0A	Consolidation of EBS Components
2.1.07.03.01	Movement of Canister in Buffer/Backfill	2.1.06.05.0A	Mechanical Degradation of Emplacement Pallet
2.1.07.03.02	Canister or Container Movement	2.1.06.05.0A	Mechanical Degradation of Emplacement Pallet
2.1.07.03.03	Movement of Canister in Buffer/Backfill	2.1.06.05.0A	Mechanical Degradation of Emplacement Pallet
2.1.07.03.04	Canister Sinking	2.1.06.05.0A	Mechanical Degradation of Emplacement Pallet
2.1.07.04.00	Hydrostatic Pressure on Container	2.1.07.04.0A	Hydrostatic Pressure on Waste Package
		2.1.07.04.0B	Hydrostatic Pressure on Drip Shield
2.1.07.04.01	Excessive Hydrostatic Pressures (In Waste and EBS)	2.1.07.04.0A	Hydrostatic Pressure on Waste Package
2.1.07.04.02	Changed Hydrostatic Pressure on Canister	2.1.07.04.0A	Hydrostatic Pressure on Waste Package
2.1.07.05.00	Creeping of Metallic Materials in the EBS	2.1.07.05.0A	Creep of Metallic Materials in the Waste Package
		2.1.07.05.0B	Creep of Metallic Materials in the Drip Shield
2.1.07.05.01	Creeping of Copper	2.1.03.09.0A	Copper Corrosion in EBS
		2.1.07.05.0A	Creep of Metallic Materials in the Waste Package
2.1.07.05.02	External Stress (In Waste and EBS)	2.1.07.05.0B	Creep of Metallic Materials in the Drip Shield
2.1.07.05.03	Voids in the Lead Filling	2.1.07.05.0A	Creep of Metallic Materials in the Waste Package

Table G-2. Cross Reference of TSPA-SR FEPs to TSPA-LA FEPs (Continued)

SR FEP Number	SR FEP Name	LA FEP Number	LA FEP Name
2.1.07.05.04	Loss of Ductility (Of Waste Container)	2.1.07.05.0A	Creep of Metallic Materials in the Waste Package
2.1.07.05.05	Incomplete Filling of Containers	2.1.07.05.0A	Creep of Metallic Materials in the Waste Package
2.1.07.06.00	Floor Buckling	2.1.07.06.0A	Floor Buckling
2.1.07.06.01	Basin Formation (In Waste and EBS)	2.1.07.06.0A	Floor Buckling
2.1.08.01.00	Increased Unsaturated Water Flux At the Repository	2.1.08.01.0A	Water Influx At the Repository
		2.1.08.01.0B	Effects of Rapid Influx Into the Repository
2.1.08.01.01	Waste Container Is Thermally Quenched by Rapid Influx of Water	2.1.08.01.0B	Effects of Rapid Influx Into the Repository
2.1.08.02.00	Enhanced Influx (Philip's Drip)	2.1.08.02.0A	Enhanced Influx At the Repository
2.1.08.03.00	Repository Dry-Out Due to Waste Heat	2.1.08.03.0A	Repository Dry-Out Due to Waste Heat
		2.2.07.21.0A	Drift Shadow Forms Below Repository
2.1.08.04.00	Cold Traps	2.1.08.04.0A	Condensation Forms on Roofs of Drifts (Drift-Scale Cold Traps)
		2.1.08.04.0B	Condensation Forms at Repository Edges (Repository-Scale Cold Traps)
2.1.08.04.01	Condensation Forms on Backs of Drifts	2.1.08.04.0A	Condensation Forms on Roofs of Drifts (Drift-Scale Cold Traps)
2.1.08.05.00	Flow Through Invert	2.1.08.05.0A	Flow Through Invert
2.1.08.05.01	Fracture Flow Through the Invert	2.1.08.05.0A	Flow Through Invert
2.1.08.05.02	UZ Flow Through/Around the Collapsed Invert	2.1.08.05.0A	Flow Through Invert
		2.2.07.20.0A	Flow Diversion Around Repository Drifts
2.1.08.06.00	Wicking in Waste and EBS	2.1.08.06.0A	Capillary Effects (Wicking) in EBS
2.1.08.07.00	Pathways For Unsaturated Flow and Transport in the Waste and EBS	2.1.08.07.0A	Unsaturated Flow in the EBS
2.1.08.07.01	Residual Canister (Crack/Holes Effects)	2.1.08.07.0A	Unsaturated Flow in the EBS
		2.1.09.08.0A	Diffusion of Dissolved Radionuclides in EBS
		2.1.09.08.0B	Advection of Dissolved Radionuclides in EBS
2.1.08.07.02	Properties of Failed Canister	2.1.09.05.0A	Sorption of Dissolved Radionuclides in EBS
		2.1.09.08.0A	Diffusion of Dissolved Radionuclides in EBS
		2.1.09.08.0B	Advection of Dissolved Radionuclides in EBS
2.1.08.07.03	Container-Partial Corrosion	2.1.08.07.0A	Unsaturated Flow in the EBS
		2.1.09.08.0A	Diffusion of Dissolved Radionuclides in EBS
		2.1.09.08.0B	Advection of Dissolved Radionuclides in EBS
2.1.08.07.04	Hydraulic Conductivity (In Waste and EBS)	2.1.08.07.0A	Unsaturated Flow in the EBS

Table G-2. Cross Reference of TSPA-SR FEPs to TSPA-LA FEPs (Continued)

SR FEP Number	SR FEP Name	LA FEP Number	LA FEP Name
2.1.08.07.05	Consolidation of Waste	2.1.08.15.0A	Consolidation of EBS Components
2.1.08.07.06	Channeling Within the Waste	2.1.08.07.0A	Unsaturated Flow in the EBS
2.1.08.07.07	Unsaturated Transport (Water Transport)	2.1.09.08.0A	Diffusion of Dissolved Radionuclides in EBS
		2.1.09.08.0B	Advection of Dissolved Radionuclides in EBS
2.1.08.07.08	Radionuclide Transport (Water Transport)	2.1.09.05.0A	Sorption of Dissolved Radionuclides in EBS
		2.1.09.08.0A	Diffusion of Dissolved Radionuclides in EBS
		2.1.09.08.0B	Advection of Dissolved Radionuclides in EBS
2.1.08.08.00	Induced Hydrological Changes in the Waste and EBS	1.1.02.00.0A	Chemical Effects of Excavation and Construction in EBS
		1.1.02.00.0B	Mechanical Effects of Excavation and Construction in EBS
		1.2.10.01.0A	Hydrologic Response to Seismic Activity
		1.2.10.02.0A	Hydrologic Response to Igneous Activity
		2.1.08.01.0A	Water Influx At the Repository
		2.1.08.12.0A	Induced Hydrologic Changes in Invert
		2.1.08.14.0A	Condensation on Underside of Drip Shield
		2.1.09.12.0A	Rind (Chemically Altered Zone) Forms in the Near-Field
		2.1.11.01.0A	Heat Generation in EBS
		2.2.01.01.0A	Mechanical Effects of Excavation and Construction in the Near-Field
		2.2.01.01.0B	Chemical Effects of Excavation and Construction in the Near-Field
2.1.08.09.00	Saturated Groundwater Flow in Waste and EBS	2.1.08.09.0A	Saturated Flow in the EBS
2.1.08.09.01	Hydraulic Head (In Waste and EBS)	2.1.08.09.0A	Saturated Flow in the EBS
2.1.08.09.02	Cavitation	2.1.08.01.0B	Effects of Rapid Influx Into the Repository
		2.1.08.09.0A	Saturated Flow in the EBS
2.1.08.10.00	Desaturation/Dewatering of the Repository	2.1.08.03.0A	Repository Dry-Out Due to Waste Heat
2.1.08.10.01	Dewatering of Host Rock (In Waste and EBS)	2.1.08.03.0A	Repository Dry-Out Due to Waste Heat
2.1.08.10.02	Dewatering	2.1.08.03.0A	Repository Dry-Out Due to Waste Heat
2.1.08.11.00	Resaturation of Repository	2.1.08.11.0A	Repository Resaturation Due to Waste Cooling
2.1.08.11.01	Reflooding (In Waste and EBS)	2.1.08.11.0A	Repository Resaturation Due to Waste Cooling
2.1.08.11.02	Brine Inflow (In Waste and EBS)	2.1.08.11.0A	Repository Resaturation Due to Waste Cooling
2.1.08.12.00	Drainage With Transport - Sealing and Plugging	2.1.08.12.0A	Induced Hydrologic Changes in Invert
2.1.08.13.00	Drains	2.1.08.12.0A	Induced Hydrologic Changes in Invert

Table G-2. Cross Reference of TSPA-SR FEPs to TSPA-LA FEPs (Continued)

SR FEP Number	SR FEP Name	LA FEP Number	LA FEP Name
2.1.08.14.00	Condensation on Underside of Drip Shield	2.1.08.14.0A	Condensation on Underside of Drip Shield
2.1.08.15.00	Waste-Form and Backfill Consolidation	2.1.08.15.0A	Consolidation of EBS Components
2.1.09.01.00	Properties of the Potential Carrier Plume in the Waste and EBS	2.1.09.01.0A	Chemical Characteristics of Water in Drifts
2.1.09.01.01	Reactions With Cement Pore Water	2.1.09.01.0A	Chemical Characteristics of Water in Drifts
2.1.09.01.02	Reactions With Cement Pore Water	2.1.09.01.0A	Chemical Characteristics of Water in Drifts
2.1.09.01.03	Induced Chemical Changes (In Waste and EBS)	2.1.09.01.0A	Chemical Characteristics of Water in Drifts
2.1.09.01.04	Interactions of Host Materials and Ground Water With Repository Material	2.1.09.01.0A	Chemical Characteristics of Water in Drifts
		2.1.09.01.0B	Chemical Characteristics of Water in Waste Package
2.1.09.01.05	TRU Silos Cementitious Plume	2.1.09.01.0A	Chemical Characteristics of Water in Drifts
2.1.09.01.06	Water Chemistry, Canister	2.1.09.01.0B	Chemical Characteristics of Water in Waste Package
2.1.09.01.07	Transport of Chemically-Active Substances Into the Near-Field	2.1.09.01.0A	Chemical Characteristics of Water in Drifts
		2.1.09.01.0B	Chemical Characteristics of Water in Waste Package
		2.1.09.08.0A	Diffusion of Dissolved Radionuclides in EBS
		2.1.09.27.0A	Coupled Effects on Radionuclide Transport in EBS
2.1.09.01.08	Incomplete Near-Field Chemical Conditioning	2.1.09.01.0A	Chemical Characteristics of Water in Drifts
2.1.09.01.09	Chemical Processes (In Waste and EBS)	2.1.09.01.0A	Chemical Characteristics of Water in Drifts
2.1.09.01.10	Hyperalkaline Carrier Plume Forms	2.1.06.01.0A	Chemical Effects of Rock Reinforcement and Cementitious Materials in EBS
		2.1.09.01.0A	Chemical Characteristics of Water in Drifts
2.1.09.01.11	Chemical Interactions (In Waste and EBS)	2.1.09.01.0B	Chemical Characteristics of Water in Waste Package
2.1.09.01.12	TRU Alkaline or Organic Plume	2.1.09.01.0A	Chemical Characteristics of Water in Drifts
2.1.09.01.13	Interactions of Waste and Repository Materials With Host Materials	2.1.09.01.0A	Chemical Characteristics of Water in Drifts
		2.1.09.01.0B	Chemical Characteristics of Water in Waste Package
2.1.09.01.14	TRU Alkaline or Organic Plume	2.1.09.01.0A	Chemical Characteristics of Water in Drifts
2.1.09.02.00	Interaction With Corrosion Products	2.1.09.02.0A	Chemical Interaction With Corrosion Products
2.1.09.02.01	Interactions With Corrosion Products and Waste	2.1.09.02.0A	Chemical Interaction With Corrosion Products
2.1.09.02.02	Effects of Metal Corrosion (In Waste and EBS)	2.1.09.02.0A	Chemical Interaction With Corrosion Products

Table G-2. Cross Reference of TSPA-SR FEPs to TSPA-LA FEPs (Continued)

SR FEP Number	SR FEP Name	LA FEP Number	LA FEP Name
2.1.09.02.03	Container Corrosion Products	2.1.09.02.0A	Chemical Interaction With Corrosion Products
		2.1.09.27.0A	Coupled Effects on Radionuclide Transport in EBS
2.1.09.02.04	Chemical Buffering (Canister Corrosion Products)	2.1.09.02.0A	Chemical Interaction With Corrosion Products
		2.1.09.06.0A	Reduction-Oxidation Potential in Waste Package
2.1.09.02.05	Radionuclide Sorption and Co-Precipitation (In EBS)	2.1.09.27.0A	Coupled Effects on Radionuclide Transport in EBS
2.1.09.03.00	Volume Increase of Corrosion Products	2.1.09.03.0A	Volume Increase of Corrosion Products Impacts Cladding
		2.1.09.03.0B	Volume Increase of Corrosion Products Impacts Waste Package
		2.1.09.03.0C	Volume Increase of Corrosion Products Impacts Other EBS Components
2.1.09.03.01	Swelling of Corrosion Products (In Waste and EBS)	2.1.09.03.0A	Volume Increase of Corrosion Products Impacts Cladding
2.1.09.04.00	Radionuclide Solubility, Solubility Limits, and Speciation in the Waste Form and EBS	2.1.09.04.0A	Radionuclide Solubility, Solubility Limits, and Speciation in the Waste Form and EBS
2.1.09.04.01	Elemental Solubility (In Waste and EBS)	2.1.09.04.0A	Radionuclide Solubility, Solubility Limits, and Speciation in the Waste Form and EBS
		2.1.09.10.0A	Secondary Phase Effects on Dissolved Radionuclide Concentrations
2.1.09.04.02	Speciation (In Waste and EBS)	2.1.09.04.0A	Radionuclide Solubility, Solubility Limits, and Speciation in the Waste Form and EBS
2.1.09.04.03	Geochemical Pump (In Waste and EBS)	2.1.09.04.0A	Radionuclide Solubility, Solubility Limits, and Speciation in the Waste Form and EBS
		2.1.09.27.0A	Coupled Effects on Radionuclide Transport in EBS
2.1.09.04.04	Precipitation and Dissolution (In Waste and EBS)	2.1.09.04.0A	Radionuclide Solubility, Solubility Limits, and Speciation in the Waste Form and EBS
2.1.09.04.05	Selective Dissolution of Contaminants Contained in SNF	2.1.02.02.0A	CSNF Degradation (Alteration, Dissolution, and Radionuclide Release)
		2.1.09.04.0A	Radionuclide Solubility, Solubility Limits, and Speciation in the Waste Form and EBS
2.1.09.04.06	Precipitation (Release/Migration Factors)	2.1.09.04.0A	Radionuclide Solubility, Solubility Limits, and Speciation in the Waste Form and EBS
		2.1.09.10.0A	Secondary Phase Effects on Dissolved Radionuclide Concentrations

Table G-2. Cross Reference of TSPA-SR FEPs to TSPA-LA FEPs (Continued)

SR FEP Number	SR FEP Name	LA FEP Number	LA FEP Name
2.1.09.04.07	Speciation Control of Contaminants by Hyperalkaline Plume Formed in the EBS	2.1.09.04.0A	Radionuclide Solubility, Solubility Limits, and Speciation in the Waste Form and EBS
2.1.09.04.08	Solubility Within Fuel Matrix	2.1.09.04.0A	Radionuclide Solubility, Solubility Limits, and Speciation in the Waste Form and EBS
2.1.09.04.09	Solubility and Precipitation (Contaminant Speciation and Solubility)	2.1.09.04.0A	Radionuclide Solubility, Solubility Limits, and Speciation in the Waste Form and EBS
2.1.09.04.10	Solubility Limit (Contaminant Speciation and Solubility)	2.1.09.04.0A	Radionuclide Solubility, Solubility Limits, and Speciation in the Waste Form and EBS
2.1.09.04.11	Radionuclide Source Term (Contaminant Speciation and Solubility)	2.1.09.04.0A	Radionuclide Solubility, Solubility Limits, and Speciation in the Waste Form and EBS
2.1.09.04.12	Elemental Solubility/Precipitation (Contaminant Speciation and Solubility)	2.1.09.04.0A	Radionuclide Solubility, Solubility Limits, and Speciation in the Waste Form and EBS
2.1.09.04.13	Speciation (Contaminant Speciation and Solubility)	2.1.09.04.0A	Radionuclide Solubility, Solubility Limits, and Speciation in the Waste Form and EBS
2.1.09.05.00	In-Drift Sorption Wfmisc—In-Package Sorption	2.1.09.05.0A	Sorption of Dissolved Radionuclides in EBS
2.1.09.05.01	Selective Sorption of Pu from Solution	2.1.09.05.0A	Sorption of Dissolved Radionuclides in EBS
2.1.09.05.02	Sorption	2.1.09.05.0A	Sorption of Dissolved Radionuclides in EBS
2.1.09.05.03	Radionuclide Retardation	2.1.09.05.0A	Sorption of Dissolved Radionuclides in EBS
2.1.09.05.04	Sorption on Filling Material	2.1.09.05.0A	Sorption of Dissolved Radionuclides in EBS
2.1.09.06.00	Reduction-Oxidation Potential in Waste and EBS	2.1.09.06.0A	Reduction-Oxidation Potential in Waste Package
		2.1.09.06.0B	Reduction-Oxidation Potential in Drifts
		2.1.13.01.0A	Radiolysis
2.1.09.06.01	Redox Front (In Waste and EBS)	2.1.09.06.0A	Reduction-Oxidation Potential in Waste Package
		2.1.13.01.0A	Radiolysis
2.1.09.06.02	Reduction-Oxidation Fronts (In Waste and EBS)	2.1.09.06.0A	Reduction-Oxidation Potential in Waste Package
2.1.09.06.03	Localized Reducing Zones (In Waste and EBS)	2.1.09.06.0A	Reduction-Oxidation Potential in Waste Package
2.1.09.06.04	Redox Front (In Buffer/Backfill)	2.1.09.06.0A	Reduction-Oxidation Potential in Waste Package
		2.1.09.06.0B	Reduction-Oxidation Potential in Drifts
		2.1.13.01.0A	Radiolysis

Table G-2. Cross Reference of TSPA-SR FEPs to TSPA-LA FEPs (Continued)

SR FEP Number	SR FEP Name	LA FEP Number	LA FEP Name
2.1.09.06.05	Fe Control of Oxidation State of Contaminants	2.1.09.02.0A	Chemical Interaction With Corrosion Products
		2.1.09.06.0A	Reduction-Oxidation Potential in Waste Package
		2.1.09.27.0A	Coupled Effects on Radionuclide Transport in EBS
2.1.09.07.00	Reaction Kinetics in Waste and EBS	2.1.09.07.0A	Reaction Kinetics in Waste Package
		2.1.09.07.0B	Reaction Kinetics in Drifts
2.1.09.07.01	Chemical Kinetics (In Waste and EBS)	2.1.09.07.0A	Reaction Kinetics in Waste Package
2.1.09.08.00	Chemical Gradients/Enhanced Diffusion in Waste and EBS	2.1.09.08.0A	Diffusion of Dissolved Radionuclides in EBS
		2.1.09.08.0B	Advection of Dissolved Radionuclides in EBS
		2.1.09.27.0A	Coupled Effects on Radionuclide Transport in EBS
2.1.09.08.01	Enhanced Diffusion (In Waste and EBS)	2.1.09.27.0A	Coupled Effects on Radionuclide Transport in EBS
2.1.09.08.02	Chemical Gradients (In Waste and EBS)	2.1.09.27.0A	Coupled Effects on Radionuclide Transport in EBS
2.1.09.08.03	Diffusion in and Through Failed Canister	2.1.09.08.0A	Diffusion of Dissolved Radionuclides in EBS
2.1.09.09.00	Electrochemical Effects (Electrophoresis, Galvanic Coupling) in Waste and EBS WP—Electrochemical Effects in Waste and EBS	2.1.09.09.0A	Electrochemical Effects in EBS
		2.1.09.27.0A	Coupled Effects on Radionuclide Transport in EBS
2.1.09.09.01	Repository Induced Pb/Cu Electrochemical Reactions	2.1.09.09.0A	Electrochemical Effects in EBS
2.1.09.09.02	Natural Telluric Electrochemical Reactions (In Waste and EBS)	2.1.09.09.0A	Electrochemical Effects in EBS
2.1.09.09.03	Electro-Chemical Cracking (In Waste and EBS)	2.1.09.09.0A	Electrochemical Effects in EBS
2.1.09.09.04	Electrochemical Effects/Gradients (In Waste and EBS)	2.1.09.09.0A	Electrochemical Effects in EBS
2.1.09.09.05	Electrochemical Effects of Metal Corrosion	2.1.09.09.0A	Electrochemical Effects in EBS
2.1.09.09.06	Electrochemical Effects (In Waste and EBS)	2.1.09.09.0A	Electrochemical Effects in EBS
2.1.09.09.07	Galvanic Coupling (In Waste and EBS)	2.1.09.09.0A	Electrochemical Effects in EBS
2.1.09.09.08	Electrophoresis (In Waste and EBS)	2.1.09.09.0A	Electrochemical Effects in EBS
2.1.09.09.09	Electrochemical Gradients (In Waste and EBS)	2.1.09.09.0A	Electrochemical Effects in EBS
2.1.09.09.10	Galvanic Coupling (In Waste and EBS)	2.1.09.09.0A	Electrochemical Effects in EBS

Table G-2. Cross Reference of TSPA-SR FEPs to TSPA-LA FEPs (Continued)

SR FEP Number	SR FEP Name	LA FEP Number	LA FEP Name
2.1.09.09.11	Galvanic Coupling (In Waste and EBS)	2.1.09.09.0A	Electrochemical Effects in EBS
2.1.09.10.00	Secondary Phase Effects on Dissolved Radionuclide Concentrations At the Waste Form	2.1.09.10.0A	Secondary Phase Effects on Dissolved Radionuclide Concentrations
2.1.09.11.00	Waste-Rock Contact	2.1.09.11.0A	Chemical Effects of Waste-Rock Contact
2.1.09.12.00	Rind (Altered Zone) Formation in Waste, EBS, and Adjacent Rock	2.1.09.01.0A	Chemical Characteristics of Water in Drifts
		2.1.09.01.0B	Chemical Characteristics of Water in Waste Package
		2.1.09.12.0A	Rind (Chemically Altered Zone) Forms in the Near-Field
2.1.09.12.01	Deep Alteration of the Porosity of Drift Walls	2.1.09.12.0A	Rind (Chemically Altered Zone) Forms in the Near-Field
2.1.09.13.00	Complexation by Organics in Waste and EBS	2.1.09.13.0A	Complexation in EBS
2.1.09.13.01	Methylation (In Waste and EBS)	2.1.09.13.0A	Complexation in EBS
2.1.09.13.02	Humic and Fulvic Acids	2.1.09.13.0A	Complexation in EBS
2.1.09.13.03	Complexation by Organics	2.1.09.13.0A	Complexation in EBS
2.1.09.13.04	Fulvic Acid	2.1.09.13.0A	Complexation in EBS
2.1.09.13.05	Humic Acid	2.1.09.13.0A	Complexation in EBS
2.1.09.13.06	Complexing Agents	2.1.09.13.0A	Complexation in EBS
2.1.09.13.07	Organics (Complexing Agents)	2.1.09.13.0A	Complexation in EBS
2.1.09.13.08	Organics (Complexing Agents)	2.1.09.13.0A	Complexation in EBS
2.1.09.13.09	Organic Complexation	2.1.09.13.0A	Complexation in EBS
2.1.09.13.10	Organic Ligands	2.1.09.13.0A	Complexation in EBS
2.1.09.13.11	Kinetics of Organic Complexation	2.1.09.13.0A	Complexation in EBS
2.1.09.13.12	Introduced Complexing Agents	2.1.09.13.0A	Complexation in EBS
2.1.09.14.00	Colloid Formation in Waste and EBS	2.1.09.02.0A	Chemical Interaction With Corrosion Products
		2.1.09.15.0A	Formation of True (Intrinsic) Colloids in EBS
		2.1.09.16.0A	Formation of Pseudo-Colloids (Natural) in EBS
		2.1.09.17.0A	Formation of Pseudo-Colloids (Corrosion Product) in EBS
		2.1.09.18.0A	Formation of Microbial Colloids in EBS
		2.1.09.25.0A	Formation of Colloids (Waste-Form) by Co-Precipitation in EBS
2.1.09.14.01	Colloid Generation-Source (In Waste and EBS)	2.1.09.16.0A	Formation of Pseudo-Colloids (Natural) in EBS

Table G-2. Cross Reference of TSPA-SR FEPs to TSPA-LA FEPs (Continued)

SR FEP Number	SR FEP Name	LA FEP Number	LA FEP Name
2.1.09.14.02	Agglomeration of Pu Colloids	2.1.09.15.0A	Formation of True (Intrinsic) Colloids in EBS
		2.1.09.16.0A	Formation of Pseudo-Colloids (Natural) in EBS
		2.1.09.17.0A	Formation of Pseudo-Colloids (Corrosion Product) in EBS
2.1.09.14.03	Colloids (In Waste and EBS)	2.1.09.16.0A	Formation of Pseudo-Colloids (Natural) in EBS
		2.1.09.17.0A	Formation of Pseudo-Colloids (Corrosion Product) in EBS
		2.1.09.18.0A	Formation of Microbial Colloids in EBS
2.1.09.14.04	Colloids/Particles in Canister	2.1.09.17.0A	Formation of Pseudo-Colloids (Corrosion Product) in EBS
		2.1.09.18.0A	Formation of Microbial Colloids in EBS
		2.1.09.25.0A	Formation of Colloids (Waste-Form) by Co-Precipitation in EBS
2.1.09.14.05	Colloid Formation	2.1.09.16.0A	Formation of Pseudo-Colloids (Natural) in EBS
		2.1.09.17.0A	Formation of Pseudo-Colloids (Corrosion Product) in EBS
2.1.09.14.06	Colloids	2.1.09.15.0A	Formation of True (Intrinsic) Colloids in EBS
		2.1.09.16.0A	Formation of Pseudo-Colloids (Natural) in EBS
		2.1.09.17.0A	Formation of Pseudo-Colloids (Corrosion Product) in EBS
2.1.09.14.07	Colloids, Complexing Agents	2.1.09.13.0A	Complexation in EBS
		2.1.09.15.0A	Formation of True (Intrinsic) Colloids in EBS
		2.1.09.16.0A	Formation of Pseudo-Colloids (Natural) in EBS
		2.1.09.17.0A	Formation of Pseudo-Colloids (Corrosion Product) in EBS
2.1.09.14.08	Colloid Generation and Transport	2.1.09.15.0A	Formation of True (Intrinsic) Colloids in EBS
		2.1.09.16.0A	Formation of Pseudo-Colloids (Natural) in EBS
		2.1.09.17.0A	Formation of Pseudo-Colloids (Corrosion Product) in EBS
		2.1.09.19.0B	Advection of Colloids in EBS
2.1.09.14.09	Colloid Formation, Dissolution and Transport	2.1.09.15.0A	Formation of True (Intrinsic) Colloids in EBS
		2.1.09.16.0A	Formation of Pseudo-Colloids (Natural) in EBS
		2.1.09.17.0A	Formation of Pseudo-Colloids (Corrosion Product) in EBS
		2.1.09.19.0B	Advection of Colloids in EBS

Table G-2. Cross Reference of TSPA-SR FEPs to TSPA-LA FEPs (Continued)

SR FEP Number	SR FEP Name	LA FEP Number	LA FEP Name
2.1.09.14.10	Colloid Generation and Transport	2.1.09.15.0A	Formation of True (Intrinsic) Colloids in EBS
		2.1.09.16.0A	Formation of Pseudo-Colloids (Natural) in EBS
		2.1.09.17.0A	Formation of Pseudo-Colloids (Corrosion Product) in EBS
		2.1.09.19.0B	Advection of Colloids in EBS
2.1.09.14.11	Colloid Formation and Stability	2.1.09.15.0A	Formation of True (Intrinsic) Colloids in EBS
		2.1.09.16.0A	Formation of Pseudo-Colloids (Natural) in EBS
		2.1.09.17.0A	Formation of Pseudo-Colloids (Corrosion Product) in EBS
		2.1.09.23.0A	Stability of Colloids in EBS
2.1.09.15.00	Formation of True Colloids in Waste and EBS	2.1.09.15.0A	Formation of True (Intrinsic) Colloids in EBS
2.1.09.16.00	Formation of Pseudo-Colloids (Natural) in Waste and EBS	2.1.09.16.0A	Formation of Pseudo-Colloids (Natural) in EBS
2.1.09.16.01	Pseudo-Colloids	2.1.09.16.0A	Formation of Pseudo-Colloids (Natural) in EBS
2.1.09.16.02	Pseudo-Colloids	2.1.09.16.0A	Formation of Pseudo-Colloids (Natural) in EBS
2.1.09.16.03	Natural Colloids	2.1.09.16.0A	Formation of Pseudo-Colloids (Natural) in EBS
2.1.09.16.04	Natural Colloids	2.1.09.16.0A	Formation of Pseudo-Colloids (Natural) in EBS
2.1.09.17.00	Formation of Pseudo-Colloids (Corrosion Products) in Waste and EBS	2.1.09.17.0A	Formation of Pseudo-Colloids (Corrosion Product) in EBS
2.1.09.17.01	Colloid Formation Is Associated With Container Hydrolysis Products	2.1.09.17.0A	Formation of Pseudo-Colloids (Corrosion Product) in EBS
2.1.09.18.00	Microbial Colloid Transport in the Waste and EBS.	2.1.09.18.0A	Formation of Microbial Colloids in EBS
2.1.09.19.00	Colloid Transport and Sorption in the Waste and EBS.	2.1.09.19.0A	Sorption of Colloids in EBS
2.1.09.19.01	Colloid Transport	2.1.09.19.0A	Sorption of Colloids in EBS
		2.1.09.19.0B	Advection of Colloids in EBS
2.1.09.20.00	Colloid Filtration in the Waste and EBS Wfcol—Colloid Filtration	2.1.09.20.0A	Filtration of Colloids in EBS
2.1.09.20.01	Colloid Filtration By the Invert	2.1.09.20.0A	Filtration of Colloids in EBS
2.1.09.20.02	Colloid Filtration (In Pores and Fractures)	2.1.09.20.0A	Filtration of Colloids in EBS
2.1.09.20.03	Colloid Filtration	2.1.09.20.0A	Filtration of Colloids in EBS

Table G-2. Cross Reference of TSPA-SR FEPs to TSPA-LA FEPs (Continued)

SR FEP Number	SR FEP Name	LA FEP Number	LA FEP Name
2.1.09.21.00	Suspensions of Particles Larger Than Colloids	2.1.09.21.0A	Transport of Particles Larger Than Colloids in EBS
		2.1.09.21.0B	Transport of Particles Larger Than Colloids in the SZ
		2.1.09.21.0C	Transport of Particles Larger Than Colloids in the UZ
2.1.09.21.01	Suspended Sediment Transport	2.1.09.21.0A	Transport of Particles Larger Than Colloids in EBS
		2.1.09.21.0B	Transport of Particles Larger Than Colloids in the SZ
		2.1.09.21.0C	Transport of Particles Larger Than Colloids in the UZ
2.1.09.21.02	Rinse	2.1.09.21.0A	Transport of Particles Larger Than Colloids in EBS
		2.1.09.21.0B	Transport of Particles Larger Than Colloids in the SZ
2.1.09.22.00	Colloid Sorption At the Air-Water Interface	2.1.09.22.0A	Sorption of Colloids at Air-Water Interface
2.1.09.23.00	Colloidal Stability and Concentration Dependence on Aqueous Chemistry	2.1.09.23.0A	Stability of Colloids in EBS
2.1.09.24.00	Colloidal Diffusion	2.1.09.24.0A	Diffusion of Colloids in EBS
2.1.09.25.00	Colloidal Phases Are Produced by Coprecipitation (In Waste and EBS)	2.1.09.25.0A	Formation of Colloids (Waste-Form) by Co-Precipitation in EBS
2.1.09.26.00	Colloid Gravitational Settling	2.1.09.26.0A	Gravitational Settling of Colloids in EBS
2.1.10.01.00	Biological Activity in Waste and EBS	2.1.10.01.0A	Microbial Activity in EBS
2.1.10.01.01	Microbial Activity Accelerates Corrosion of Containers	2.1.10.01.0A	Microbial Activity in EBS
2.1.10.01.02	Microbial Activity Accelerates Corrosion of Cladding	2.1.10.01.0A	Microbial Activity in EBS
2.1.10.01.03	Microbial Activity Accelerates Corrosion of Contaminants	2.1.10.01.0A	Microbial Activity in EBS
2.1.10.01.04	Microbes (In Waste and EBS)	2.1.10.01.0A	Microbial Activity in EBS
2.1.10.01.05	Microorganisms (In Waste and EBS)	2.1.10.01.0A	Microbial Activity in EBS
2.1.10.01.06	Microbiological Effects (In Waste and EBS)	2.1.10.01.0A	Microbial Activity in EBS
2.1.10.01.07	Microbial Activity (In Waste and EBS)	2.1.10.01.0A	Microbial Activity in EBS
2.1.10.01.08	Microbial Activity (In Waste and EBS)	2.1.09.13.0A	Complexation in EBS
		2.1.10.01.0A	Microbial Activity in EBS
2.1.10.01.09	Microbial Activity (In Waste and EBS)	2.1.10.01.0A	Microbial Activity in EBS
2.1.10.01.10	Microbial Interactions	2.1.10.01.0A	Microbial Activity in EBS
2.1.10.01.11	Biofilms	2.1.10.01.0A	Microbial Activity in EBS
2.1.11.01.00	Heat Output / Temperature in Waste and EBS	2.1.11.01.0A	Heat Generation in EBS

Table G-2. Cross Reference of TSPA-SR FEPs to TSPA-LA FEPs (Continued)

SR FEP Number	SR FEP Name	LA FEP Number	LA FEP Name
2.1.11.01.01	Glass Temperature (In Waste and EBS)	2.1.11.01.0A	Heat Generation in EBS
2.1.11.01.02	Canister Temperature	2.1.11.01.0A	Heat Generation in EBS
2.1.11.01.03	Temperature, Bentonite Buffer	2.1.11.01.0A	Heat Generation in EBS
2.1.11.01.04	Temperature, Canister	2.1.11.01.0A	Heat Generation in EBS
2.1.11.01.05	Temperature, Tunnel Backfill	2.1.11.01.0A	Heat Generation in EBS
2.1.11.01.06	Heat Generation from Waste Containers	2.1.11.01.0A	Heat Generation in EBS
2.1.11.01.07	Radioactive Decay Heat	2.1.11.01.0A	Heat Generation in EBS
2.1.11.01.08	DOE SNF Expected Waste Heat Generation	2.1.11.01.0A	Heat Generation in EBS
2.1.11.01.09	DOE SNF Expected Waste Heat Generation	2.1.11.01.0A	Heat Generation in EBS
2.1.11.02.00	Nonuniform Heat Distribution / Edge Effects in Repository	2.1.11.02.0A	Non-Uniform Heat Distribution in EBS
		2.1.11.09.0A	Thermal Effects on Flow in the EBS
		2.2.10.01.0A	Repository-Induced Thermal Effects on Flow in the UZ
2.1.11.02.01	Panel/Repository Edge Effects - Thermal	2.1.11.02.0A	Non-Uniform Heat Distribution in EBS
		2.1.11.07.0A	Thermal Expansion/Stress of In-Drift EBS Components
2.1.11.02.02	Panel/Repository Edge Effects - Post-Thermal	2.1.11.02.0A	Non-Uniform Heat Distribution in EBS
		2.1.11.07.0A	Thermal Expansion/Stress of In-Drift EBS Components
2.1.11.02.03	Vault Heating Effects	2.1.11.01.0A	Heat Generation in EBS
		2.1.11.07.0A	Thermal Expansion/Stress of In-Drift EBS Components
		2.1.11.09.0B	Thermally-Driven Flow (Convection) in Waste Packages
		2.1.11.09.0C	Thermally Driven Flow (Convection) in Drifts
2.1.11.03.00	Exothermic Reactions in Waste and EBS Wfmisc—Exothermic Reactions and Other Thermal Effects in Waste and EBS	2.1.11.03.0A	Exothermic Reactions in the EBS
2.1.11.03.01	Concrete Hydration	2.1.11.03.0A	Exothermic Reactions in the EBS
2.1.11.04.00	Temperature Effects / Coupled Processes in Waste and EBS	2.1.11.01.0A	Heat Generation in EBS
2.1.11.04.01	Thermal (Processes)	2.1.11.01.0A	Heat Generation in EBS
2.1.11.04.02	Temperature Effects (Unexpected Effects) (In Waste and EBS)	1.2.04.04.0A	Igneous Intrusion Interacts With EBS Components
		2.1.12.08.0A	Gas Explosions in EBS
2.1.11.04.03	Heat from Radioactive Decay (In Waste and EBS)	2.1.11.01.0A	Heat Generation in EBS
2.1.11.04.04	Long-Term Transients (In Waste and EBS)	2.1.11.01.0A	Heat Generation in EBS
2.1.11.04.05	Time Dependence (In Waste and EBS)	2.1.11.01.0A	Heat Generation in EBS

Table G-2. Cross Reference of TSPA-SR FEPs to TSPA-LA FEPs (Continued)

SR FEP Number	SR FEP Name	LA FEP Number	LA FEP Name
2.1.11.04.06	Coupled Processes (In Waste and EBS)	2.1.09.27.0A	Coupled Effects on Radionuclide Transport in EBS
		2.1.11.09.0A	Thermal Effects on Flow in the EBS
2.1.11.05.00	Differing Thermal Expansion of Repository Components	2.1.11.05.0A	Thermal Expansion/Stress of In-Package EBS Components
		2.1.11.07.0A	Thermal Expansion/Stress of In-Drift EBS Components
2.1.11.05.01	Differential Thermal Expansion of Near-Field Barriers	2.1.11.07.0A	Thermal Expansion/Stress of In-Drift EBS Components
2.1.11.05.02	Shearing of Waste Containers by Secondary Stresses from Thermal Expansion of the Rock	2.1.11.07.0A	Thermal Expansion/Stress of In-Drift EBS Components
2.1.11.05.03	Differential Elastic Response (In Waste and EBS)	2.1.11.07.0A	Thermal Expansion/Stress of In-Drift EBS Components
2.1.11.05.04	Non-Elastic Response (In Waste and EBS)	2.1.11.07.0A	Thermal Expansion/Stress of In-Drift EBS Components
2.1.11.06.00	Thermal Sensitization of Waste Containers and Drip Shields Increases Their Fragility	2.1.11.06.0A	Thermal Sensitization of Waste Packages
		2.1.11.06.0B	Thermal Sensitization of Drip Shields
2.1.11.07.00	Thermally-Induced Stress Changes in Waste and EBS	1.2.04.02.0A	Igneous Activity Changes Rock Properties
		1.2.06.00.0A	Hydrothermal Activity
		2.1.02.08.0A	Pyrophoricity from DSNF
		2.1.03.02.0A	Stress Corrosion Cracking (SCC) of Waste Packages
		2.1.03.02.0B	Stress Corrosion Cracking (SCC) of Drip Shields
		2.1.05.03.0A	Degradation of Seals
		2.1.11.01.0A	Heat Generation in EBS
		2.1.11.03.0A	Exothermic Reactions in the EBS
		2.1.11.05.0A	Thermal Expansion/Stress of In-Package EBS Components
		2.1.11.07.0A	Thermal Expansion/Stress of In-Drift EBS Components
		2.2.01.02.0A	Thermally-Induced Stress Changes in the Near-Field
		2.2.10.04.0A	Thermo-Mechanical Stresses Alter Characteristics of Fractures Near Repository
		2.2.10.04.0B	Thermo-Mechanical Stresses Alter Characteristics of Faults Near Repository
		2.2.10.05.0A	Thermo-Mechanical Stresses Alter Characteristics of Rocks Above and Below the Repository
2.1.11.07.01	Changes in In-Situ Stress Field (In Waste and EBS)	2.1.11.07.0A	Thermal Expansion/Stress of In-Drift EBS Components

Table G-2. Cross Reference of TSPA-SR FEPs to TSPA-LA FEPs (Continued)

SR FEP Number	SR FEP Name	LA FEP Number	LA FEP Name
2.1.11.07.02	Stress Field Changes, Settling, Subsidence or Caving	2.2.06.04.0A	Effects of Subsidence
		2.2.10.04.0A	Thermo-Mechanical Stresses Alter Characteristics of Fractures Near Repository
		2.2.10.04.0B	Thermo-Mechanical Stresses Alter Characteristics of Faults Near Repository
2.1.11.08.00	Thermal Effects: Chemical and Microbiological Changes in the Waste and EBS	2.1.11.08.0A	Thermal Effects on Chemistry and Microbial Activity in the EBS
2.1.11.09.00	Thermal Effects on Liquid or Two-Phase Fluid Flow in the Waste and EBS	2.1.11.09.0A	Thermal Effects on Flow in the EBS
		2.1.11.09.0B	Thermally-Driven Flow (Convection) in Waste Packages
		2.1.11.09.0C	Thermally Driven Flow (Convection) in Drifts
2.1.11.09.01	Convection Effects on Transport (Enhanced Vapor Diffusion)	2.1.11.09.0B	Thermally-Driven Flow (Convection) in Waste Packages
		2.1.11.09.0C	Thermally Driven Flow (Convection) in Drifts
		2.1.11.10.0A	Thermal Effects on Transport in EBS
2.1.11.09.02	Multiphase Flow and Gas-Driven Transport (Water Transport)	2.1.11.09.0A	Thermal Effects on Flow in the EBS
2.1.11.10.00	Thermal Effects on Diffusion (Soret Effect) in Waste and EBS	2.1.11.10.0A	Thermal Effects on Transport in EBS
2.1.11.10.01	Soret Effect (In Waste and EBS)	2.1.11.10.0A	Thermal Effects on Transport in EBS
2.1.11.10.02	Thermal Effects: Transport(Diffusion) Effects (In Waste and EBS)	2.1.11.10.0A	Thermal Effects on Transport in EBS
2.1.11.10.03	Soret Effect (Water Transport)	2.1.11.10.0A	Thermal Effects on Transport in EBS
2.1.12.01.00	Gas Generation	2.1.12.01.0A	Gas Generation (Repository Pressurization)
		2.1.12.02.0A	Gas Generation (He) from Waste Form Decay
		2.1.12.03.0A	Gas Generation (H2) from Waste Package Corrosion
		2.1.12.04.0A	Gas Generation (CO2, CH4, H2S) from Microbial Degradation
		2.1.13.01.0A	Radiolysis
2.1.12.01.01	Formation of Gases (In Wastes and EBS)	2.1.12.01.0A	Gas Generation (Repository Pressurization)
		2.1.12.03.0A	Gas Generation (H2) from Waste Package Corrosion
		2.1.13.01.0A	Radiolysis

Table G-2. Cross Reference of TSPA-SR FEPs to TSPA-LA FEPs (Continued)

SR FEP Number	SR FEP Name	LA FEP Number	LA FEP Name
2.1.12.01.02	Gas Generation	2.1.12.02.0A	Gas Generation (He) from Waste Form Decay
		2.1.12.03.0A	Gas Generation (H2) from Waste Package Corrosion
		2.1.12.04.0A	Gas Generation (CO2, CH4, H2S) from Microbial Degradation
		2.1.13.01.0A	Radiolysis
2.1.12.01.03	Gas Generation, Buffer/Backfill	2.1.12.04.0A	Gas Generation (CO2, CH4, H2S) from Microbial Degradation
		2.1.13.01.0A	Radiolysis
2.1.12.01.04	Chemotoxic Gases (In Waste and EBS)	2.1.12.02.0A	Gas Generation (He) from Waste Form Decay
		2.1.12.03.0A	Gas Generation (H2) from Waste Package Corrosion
		2.1.12.04.0A	Gas Generation (CO2, CH4, H2S) from Microbial Degradation
		2.1.13.01.0A	Radiolysis
2.1.12.01.05	Pressurization (In Waste and EBS)	2.1.12.01.0A	Gas Generation (Repository Pressurization)
2.1.12.02.00	Gas Generation (He) from Fuel Decay	2.1.12.02.0A	Gas Generation (He) from Waste Form Decay
2.1.12.02.01	Helium Gas Production	2.1.12.02.0A	Gas Generation (He) from Waste Form Decay
2.1.12.02.02	Internal Pressure (In Waste and EBS)	2.1.12.02.0A	Gas Generation (He) from Waste Form Decay
2.1.12.02.03	Gas Generation, Canister	2.1.12.02.0A	Gas Generation (He) from Waste Form Decay
2.1.12.02.04	Internal Pressure (In Waste and EBS)	2.1.12.02.0A	Gas Generation (He) from Waste Form Decay
2.1.12.02.05	He Gas Production (In Waste and EBS)	2.1.12.02.0A	Gas Generation (He) from Waste Form Decay
2.1.12.03.00	Gas Generation (H2) from Metal Corrosion	2.1.12.03.0A	Gas Generation (H2) from Waste Package Corrosion
2.1.12.03.01	Chemical Effects of Corrosion	2.1.12.03.0A	Gas Generation (H2) from Waste Package Corrosion
2.1.12.03.02	Effect of Hydrogen on Corrosion	2.1.12.03.0A	Gas Generation (H2) from Waste Package Corrosion
2.1.12.03.03	Hydrogen Production (In Waste and EBS)	2.1.12.03.0A	Gas Generation (H2) from Waste Package Corrosion
2.1.12.03.04	Hydrogen Production by Metal Corrosion	2.1.12.03.0A	Gas Generation (H2) from Waste Package Corrosion
		2.1.12.04.0A	Gas Generation (CO2, CH4, H2S) from Microbial Degradation
2.1.12.03.05	Container Material Inventory	2.1.12.03.0A	Gas Generation (H2) from Waste Package Corrosion
2.1.12.04.00	Gas Generation (CO2, CH4, H2S) from Microbial Degradation	2.1.12.04.0A	Gas Generation (CO2, CH4, H2S) from Microbial Degradation

Table G-2. Cross Reference of TSPA-SR FEPs to TSPA-LA FEPs (Continued)

SR FEP Number	SR FEP Name	LA FEP Number	LA FEP Name
2.1.12.04.01	Effect of Temperature on Microbial Gas Generation	2.1.10.01.0A	Microbial Activity in EBS
		2.1.12.04.0A	Gas Generation (CO2, CH4, H2S) from Microbial Degradation
2.1.12.04.02	Effect of Pressure on Microbial Gas Generation	2.1.12.04.0A	Gas Generation (CO2, CH4, H2S) from Microbial Degradation
2.1.12.04.03	Effect of Radiation on Microbial Gas Generation	2.1.12.04.0A	Gas Generation (CO2, CH4, H2S) from Microbial Degradation
		2.1.13.03.0A	Radiological Mutation of Microbes
2.1.12.04.04	Effect of Biofilms on Microbial Gas Generation	2.1.12.04.0A	Gas Generation (CO2, CH4, H2S) from Microbial Degradation
2.1.12.04.05	Methane and Carbon Dioxide by Microbial Degradation	2.1.12.04.0A	Gas Generation (CO2, CH4, H2S) from Microbial Degradation
2.1.12.05.00	Gas Generation from Concrete	2.1.12.04.0A	Gas Generation (CO2, CH4, H2S) from Microbial Degradation
		2.1.13.01.0A	Radiolysis
2.1.12.06.00	Gas Transport in Waste and EBS	2.1.12.06.0A	Gas Transport in EBS
2.1.12.06.01	Thermo-Chemical Effects (Related to Gas in Waste and EBS)	2.1.12.01.0A	Gas Generation (Repository Pressurization)
		2.1.12.03.0A	Gas Generation (H2) from Waste Package Corrosion
		2.1.12.06.0A	Gas Transport in EBS
		2.1.12.07.0A	Effects of Radioactive Gases in EBS
2.1.12.06.02	Gas Transport	2.1.12.06.0A	Gas Transport in EBS
		2.1.12.07.0A	Effects of Radioactive Gases in EBS
2.1.12.06.03	Gas Effects (In Waste and EBS)	2.1.12.01.0A	Gas Generation (Repository Pressurization)
		2.1.12.06.0A	Gas Transport in EBS
		2.1.12.07.0A	Effects of Radioactive Gases in EBS
2.1.12.06.04	Gas Escape from Canister	2.1.12.06.0A	Gas Transport in EBS
2.1.12.06.05	Gas Flow and Transport, Buffer/Backfill	2.1.12.06.0A	Gas Transport in EBS
2.1.12.06.06	Gas Transport	2.1.12.01.0A	Gas Generation (Repository Pressurization)
		2.1.12.06.0A	Gas Transport in EBS
		2.1.12.07.0A	Effects of Radioactive Gases in EBS
2.1.12.06.07	Unsaturated Flow Due to Gas Production (In Waste and EBS)	2.1.08.07.0A	Unsaturated Flow in the EBS
		2.1.12.01.0A	Gas Generation (Repository Pressurization)
		2.1.12.06.0A	Gas Transport in EBS
		2.1.12.07.0A	Effects of Radioactive Gases in EBS
2.1.12.06.08	Gas Permeability (In Buffer/Backfill)	2.1.12.06.0A	Gas Transport in EBS
2.1.12.07.00	Radioactive Gases in Waste and EBS	2.1.12.07.0A	Effects of Radioactive Gases in EBS
2.1.12.07.01	Radioactive Gas (In Waste and EBS)	2.1.12.07.0A	Effects of Radioactive Gases in EBS

Table G-2. Cross Reference of TSPA-SR FEPs to TSPA-LA FEPs (Continued)

SR FEP Number	SR FEP Name	LA FEP Number	LA FEP Name
2.1.12.07.02	Gaseous and Volatile Isotopes	2.1.12.07.0A	Effects of Radioactive Gases in EBS
		2.1.12.08.0A	Gas Explosions in EBS
2.1.12.08.00	Gas Explosions	2.1.12.08.0A	Gas Explosions in EBS
2.1.12.08.01	H2/O2 Explosions (In Waste and EBS)	2.1.12.08.0A	Gas Explosions in EBS
2.1.12.08.02	Flammability (In Waste and EBS)	2.1.12.08.0A	Gas Explosions in EBS
2.1.12.08.03	Explosions	2.1.12.08.0A	Gas Explosions in EBS
2.1.12.08.04	Explosion	2.1.12.08.0A	Gas Explosions in EBS
2.1.13.01.00	Radiolysis	2.1.13.01.0A	Radiolysis
2.1.13.01.01	Radiolysis (In Waste and EBS)	2.1.13.01.0A	Radiolysis
2.1.13.01.02	Radiolysis	2.1.13.01.0A	Radiolysis
2.1.13.01.03	Radiolysis (In Waste and EBS)	2.1.13.01.0A	Radiolysis
2.1.13.01.04	Radiolysis (In Waste and EBS)	2.1.13.01.0A	Radiolysis
2.1.13.01.05	Radiolysis Prior to Wetting (In Waste and EBS)	2.1.13.01.0A	Radiolysis
2.1.13.01.06	Radiolysis of Brine	2.1.13.01.0A	Radiolysis
2.1.13.01.07	Radiolysis of Cellulose (In Waste and EBS)	2.1.02.10.0A	Organic/Cellulosic Materials in Waste
		2.1.12.04.0A	Gas Generation (CO2, CH4, H2S) from Microbial Degradation
		2.1.13.01.0A	Radiolysis
2.1.13.01.08	Radiolysis	2.1.13.01.0A	Radiolysis
2.1.13.01.09	Radiolysis	2.1.13.01.0A	Radiolysis
2.1.13.02.00	Radiation Damage in Waste and EBS	2.1.13.02.0A	Radiation Damage in EBS
2.1.13.02.01	Radiation Effects (In Waste and EBS)	2.1.13.01.0A	Radiolysis
		2.1.13.02.0A	Radiation Damage in EBS
2.1.13.02.02	Radiation Effects on Bentonite	2.1.13.02.0A	Radiation Damage in EBS
2.1.13.02.03	Material Property Changes (Due to Radiation in Waste and EBS)	2.1.13.02.0A	Radiation Damage in EBS
2.1.13.02.04	Radiation Damage (In Waste and EBS)	2.1.13.02.0A	Radiation Damage in EBS
2.1.13.02.05	Radiation Shielding (In Waste and EBS)	2.1.13.01.0A	Radiolysis
		2.1.13.02.0A	Radiation Damage in EBS
2.1.13.02.06	Radiation Effects on Buffer/Backfill	2.1.13.02.0A	Radiation Damage in EBS
2.1.13.02.07	Radiation Effects on Canister	2.1.13.02.0A	Radiation Damage in EBS
2.1.13.02.08	Radiological Effects on Waste	2.1.13.02.0A	Radiation Damage in EBS
2.1.13.02.09	Radiological Effects on Containers	2.1.13.02.0A	Radiation Damage in EBS
2.1.13.02.10	Radiological Effects on Seals	2.1.13.02.0A	Radiation Damage in EBS
2.1.13.02.11	Radiation Effects on Canister	2.1.13.02.0A	Radiation Damage in EBS
2.1.13.03.00	Mutation	2.1.13.03.0A	Radiological Mutation of Microbes

Table G-2. Cross Reference of TSPA-SR FEPs to TSPA-LA FEPs (Continued)

SR FEP Number	SR FEP Name	LA FEP Number	LA FEP Name
2.1.14.01.00	Criticality in Waste and EBS	2.1.14.15.0A	In-Package Criticality (Intact Configuration)
		2.1.14.16.0A	In-Package Criticality (Degraded Configurations)
		2.1.14.17.0A	Near-Field Criticality
		2.1.14.18.0A	In-Package Criticality Resulting from a Seismic Event (Intact Configuration)
		2.1.14.19.0A	In-Package Criticality Resulting from a Seismic Event (Degraded Configurations)
		2.1.14.20.0A	Near-Field Criticality Resulting from a Seismic Event
		2.1.14.21.0A	In-Package Criticality Resulting from Rockfall (Intact Configuration)
		2.1.14.22.0A	In-Package Criticality Resulting from Rockfall (Degraded Configurations)
		2.1.14.23.0A	Near-Field Criticality Resulting from Rockfall
		2.1.14.24.0A	In-Package Criticality Resulting from an Igneous Event (Intact Configuration)
		2.1.14.25.0A	In-Package Criticality Resulting from an Igneous Event (Degraded Configurations)
		2.1.14.26.0A	Near-Field Criticality Resulting from an Igneous Event
2.1.14.01.01	Criticality (In Waste and EBS)	2.1.14.16.0A	In-Package Criticality (Degraded Configurations)
2.1.14.01.02	Criticality (In Waste and EBS)	2.1.14.16.0A	In-Package Criticality (Degraded Configurations)
2.1.14.01.03	Nuclear Criticality (In Waste and EBS)	2.1.14.16.0A	In-Package Criticality (Degraded Configurations)
2.1.14.01.04	Nuclear Criticality (In Waste and EBS)	2.1.14.16.0A	In-Package Criticality (Degraded Configurations)
2.1.14.01.05	Nuclear Criticality (In Waste and EBS)	2.1.14.16.0A	In-Package Criticality (Degraded Configurations)
2.1.14.01.06	Nuclear Criticality: Heat (In Waste and EBS)	2.1.14.16.0A	In-Package Criticality (Degraded Configurations)
2.1.14.01.07	Nuclear Explosions (In Waste and EBS)	2.1.14.16.0A	In-Package Criticality (Degraded Configurations)
2.1.14.01.08	DOE SNF Criticality In-Situ	2.1.14.16.0A	In-Package Criticality (Degraded Configurations)
2.1.14.01.09	DOE SNF Criticality In-Situ (Radionuclide Inventory Impact)	2.1.14.17.0A	Near-Field Criticality
2.1.14.01.10	DOE SNF Criticality Near-Field (Radionuclide Inventory Impact)	2.1.14.16.0A	In-Package Criticality (Degraded Configurations)
2.1.14.01.11	DOE SNF Criticality In-Situ (Waste Heat Impact)	2.1.14.16.0A	In-Package Criticality (Degraded Configurations)
2.1.14.01.12	DOE SNF Criticality In-Situ (Waste Package Degradation Impact)	2.1.14.16.0A	In-Package Criticality (Degraded Configurations)

Table G-2. Cross Reference of TSPA-SR FEPs to TSPA-LA FEPs (Continued)

SR FEP Number	SR FEP Name	LA FEP Number	LA FEP Name
2.1.14.01.13	DOE SNF Criticality In-Situ (Waste Form Degradation Impact)	2.1.14.16.0A	In-Package Criticality (Degraded Configurations)
2.1.14.01.14	DOE SNF Criticality In-Situ (Cladding Degradation Impact)	2.1.14.16.0A	In-Package Criticality (Degraded Configurations)
2.1.14.01.15	Differential Solubility of Neutron Poisons	2.1.14.16.0A	In-Package Criticality (Degraded Configurations)
2.1.14.01.16	Selective Leaching of Fissile Materials	2.1.14.16.0A	In-Package Criticality (Degraded Configurations)
2.1.14.01.17	Differential Solubility of Fissile Isotopes	2.1.14.16.0A	In-Package Criticality (Degraded Configurations)
2.1.14.02.00	Criticality In-Situ, Nominal Configuration, Top Breach	2.1.14.15.0A	In-Package Criticality (Intact Configuration)
2.1.14.02.01	Criticality - MPC Flooded	2.1.14.15.0A	In-Package Criticality (Intact Configuration)
2.1.14.02.02	Criticality - Nominal Configuration, Partially Flooded, Otherwise Intact	2.1.14.15.0A	In-Package Criticality (Intact Configuration)
2.1.14.03.00	Criticality In-Situ, WP Internal Structures Degrade Faster Than Waste Form, Top Breach	2.1.14.16.0A	In-Package Criticality (Degraded Configurations)
2.1.14.03.01	Waste Package Internal Structures Degrade Faster Than Waste Form	2.1.14.16.0A	In-Package Criticality (Degraded Configurations)
2.1.14.03.02	Waste Package Internal Structures Collapse	2.1.14.16.0A	In-Package Criticality (Degraded Configurations)
2.1.14.03.03	Criticality - Container Partially Gone, Optimal Rod Configuration, Flooded	2.1.14.16.0A	In-Package Criticality (Degraded Configurations)
2.1.14.04.00	Criticality In-Situ, WP Internal Structures Degrade at Same Rate As Waste Form, Top Breach	2.1.14.16.0A	In-Package Criticality (Degraded Configurations)
2.1.14.04.01	Waste Package Internal Structures and the Waste Form Degrade At the Same Rate	2.1.14.16.0A	In-Package Criticality (Degraded Configurations)
2.1.14.04.02	Criticality - Clad and Disintegrated Pellets, Optimally Mixed, Flooded	2.1.14.16.0A	In-Package Criticality (Degraded Configurations)
2.1.14.05.00	Criticality In-Situ, WP Internal Structures Degrade Slower Than Waste Form, Top Breach	2.1.14.16.0A	In-Package Criticality (Degraded Configurations)
2.1.14.05.01	Waste Package Internal Structures Degrade Slower Than Waste Form	2.1.14.16.0A	In-Package Criticality (Degraded Configurations)
2.1.14.06.00	Criticality In-Situ, Waste Form Degrades in Place and Swells, Top Breach	2.1.14.16.0A	In-Package Criticality (Degraded Configurations)

Table G-2. Cross Reference of TSPA-SR FEPs to TSPA-LA FEPs (Continued)

SR FEP Number	SR FEP Name	LA FEP Number	LA FEP Name
2.1.14.07.00	Criticality In-Situ, Bottom Breach Allows Flow Through WP, Fissile Material Collects at Bottom of WP	2.1.14.16.0A	In-Package Criticality (Degraded Configurations)
2.1.14.08.00	Criticality In-Situ, Bottom Breach Allows Flow Through WP, Waste Form Degrades in Place	2.1.14.16.0A	In-Package Criticality (Degraded Configurations)
2.1.14.08.01	Neutron Absorber System Selectively Degrades	2.1.14.16.0A	In-Package Criticality (Degraded Configurations)
2.1.14.08.02	Neutron Sorbers Selectively Flushed from Containers	2.1.14.16.0A	In-Package Criticality (Degraded Configurations)
2.1.14.08.03	Selective Leaching of Neutron Sorbers	2.1.14.16.0A	In-Package Criticality (Degraded Configurations)
2.1.14.09.00	Near-Field Criticality, Fissile Material Deposited in Near-Field Pond	2.1.14.17.0A	Near-Field Criticality
2.1.14.09.01	Criticality - Container Gone, Intact Rods, Flooded	2.1.14.17.0A	Near-Field Criticality
2.1.14.09.02	Criticality - Container Gone, Intact Rods, Dry	2.1.14.17.0A	Near-Field Criticality
2.1.14.09.03	Criticality - Container Gone, Pile of Fuel Pellets, Dry	2.1.14.17.0A	Near-Field Criticality
2.1.14.09.04	Criticality - Container Gone, Pile of Fuel Pellets, Flooded	2.1.14.17.0A	Near-Field Criticality
2.1.14.09.05	Criticality - Container and Cladding Gone, Fuel Powder, Flooded	2.1.14.17.0A	Near-Field Criticality
2.1.14.09.06	Criticality - Container and Cladding Gone, Fuel Powder, Dry	2.1.14.17.0A	Near-Field Criticality
2.1.14.09.07	Formation of a Critical Assembly in a Pool (In Waste and EBS)	2.1.14.17.0A	Near-Field Criticality
2.1.14.09.08	Pu Accumulates in Basin Pool (In Waste and EBS)	2.1.14.17.0A	Near-Field Criticality
2.1.14.09.09	Accumulated 239Pu Decays to 235U in Basin Pool (In Waste and EBS)	2.1.14.17.0A	Near-Field Criticality
2.1.14.10.00	Near-Field Criticality, Fissile Solution Flows Into Drift Lowpoint	2.1.14.17.0A	Near-Field Criticality
2.1.14.10.01	Accumulation of Clays and Sediments in Basin (In EBS)	2.1.14.17.0A	Near-Field Criticality
2.1.14.11.00	Near-Field Criticality, Fissile Solution Is Adsorbed or Reduced in Invert	2.1.14.17.0A	Near-Field Criticality
2.1.14.12.00	Near-Field Criticality, Filtered Slurry or Colloidal Stream Collects on Invert Surface	2.1.14.17.0A	Near-Field Criticality

Table G-2. Cross Reference of TSPA-SR FEPs to TSPA-LA FEPs (Continued)

SR FEP Number	SR FEP Name	LA FEP Number	LA FEP Name
2.1.14.13.00	Near-Field Criticality Associated With Colloidal Deposits	2.1.14.17.0A	Near-Field Criticality
2.1.14.14.00	Out-of-Package Criticality, Fuel/Magma Mixture	2.1.14.18.0A	In-Package Criticality Resulting from a Seismic Event (Intact Configuration)
		2.1.14.19.0A	In-Package Criticality Resulting from a Seismic Event (Degraded Configurations)
		2.1.14.20.0A	Near-Field Criticality Resulting from a Seismic Event
		2.1.14.21.0A	In-Package Criticality Resulting from Rockfall (Intact Configuration)
		2.1.14.22.0A	In-Package Criticality Resulting from Rockfall (Degraded Configurations)
		2.1.14.23.0A	Near-Field Criticality Resulting from Rockfall
		2.1.14.24.0A	In-Package Criticality Resulting from an Igneous Event (Intact Configuration)
		2.1.14.25.0A	In-Package Criticality Resulting from an Igneous Event (Degraded Configurations)
		2.1.14.26.0A	Near-Field Criticality Resulting from an Igneous Event
		2.2.14.10.0A	Far-Field Criticality Resulting from a Seismic Event
		2.2.14.11.0A	Far-Field Criticality Resulting from Rockfall
		2.2.14.12.0A	Far-Field Criticality Resulting from an Igneous Event
2.2.01.01.00	Excavation and Construction-Related Changes in the Adjacent Host Rock	2.2.01.01.0A	Mechanical Effects of Excavation and Construction in the Near-Field
		2.2.01.01.0B	Chemical Effects of Excavation and Construction in the Near-Field
2.2.01.01.01	Disturbed Rock Zone	2.2.01.01.0A	Mechanical Effects of Excavation and Construction in the Near-Field
2.2.01.01.02	Mechanical Effects - Excavation/Backfilling Effects	2.2.01.01.0A	Mechanical Effects of Excavation and Construction in the Near-Field
2.2.01.01.03	Formation of Cracks (Host Rock Disturbed Zone)	2.2.01.01.0A	Mechanical Effects of Excavation and Construction in the Near-Field
		2.2.01.01.0B	Chemical Effects of Excavation and Construction in the Near-Field
2.2.01.01.04	Damaged Zone (Host Rock Disturbed Zone)	2.2.01.01.0A	Mechanical Effects of Excavation and Construction in the Near-Field
		2.2.01.03.0A	Changes in Fluid Saturations in the Excavation Disturbed Zone
		2.2.01.05.0A	Radionuclide Transport in the Excavation Disturbed Zone
2.2.01.01.05	Excavation/Backfilling Effects on Nearby Rock	2.2.01.01.0A	Mechanical Effects of Excavation and Construction in the Near-Field
2.2.01.01.06	Mechanical Effects - Excavation/Backfilling Effects	2.2.01.01.0A	Mechanical Effects of Excavation and Construction in the Near-Field

Table G-2. Cross Reference of TSPA-SR FEPs to TSPA-LA FEPs (Continued)

SR FEP Number	SR FEP Name	LA FEP Number	LA FEP Name
2.2.01.01.07	Enhanced Rock Fracturing	2.2.01.01.0A	Mechanical Effects of Excavation and Construction in the Near-Field
2.2.01.01.08	Creeping of Rock Mass, Near-Field	1.1.02.00.0B	Mechanical Effects of Excavation and Construction in EBS
2.2.01.01.09	Excavation Effects on Nearby Rock	2.2.01.01.0A	Mechanical Effects of Excavation and Construction in the Near-Field
2.2.01.01.10	Disturbed Zone (Hydromechanical) Effects	2.2.01.01.0A	Mechanical Effects of Excavation and Construction in the Near-Field
2.2.01.01.11	Excavation-Induced Changes in Stress	1.1.02.00.0B	Mechanical Effects of Excavation and Construction in EBS
		2.2.01.01.0A	Mechanical Effects of Excavation and Construction in the Near-Field
2.2.01.02.00	Thermal and Other Waste and EBS-Related Changes in the Adjacent Host Rock	2.2.01.02.0A	Thermally-Induced Stress Changes in the Near-Field
2.2.01.02.01	Hydraulic Conductivity Change (Host Rock Disturbed Zone)	2.2.01.01.0A	Mechanical Effects of Excavation and Construction in the Near-Field
		2.2.01.02.0A	Thermally-Induced Stress Changes in the Near-Field
2.2.01.02.02	Water Flow At the Bentonite-Host Rock Interface	2.2.01.02.0B	Chemical Changes in the Near-Field from Backfill
		2.2.01.03.0A	Changes in Fluid Saturations in the Excavation Disturbed Zone
2.2.01.02.03	Properties of Near-Field Rock (Host Rock Disturbed Zone)	2.2.01.02.0A	Thermally-Induced Stress Changes in the Near-Field
2.2.01.02.04	Stress Changes of Conductivity	2.2.01.02.0A	Thermally-Induced Stress Changes in the Near-Field
2.2.01.03.00	Changes in Fluid Saturations in the Excavation Disturbed Zone	2.2.01.03.0A	Changes in Fluid Saturations in the Excavation Disturbed Zone
2.2.01.03.01	Gas Transport/Dissolution (In the EDZ)	2.1.12.06.0A	Gas Transport in EBS
		2.2.01.05.0A	Radionuclide Transport in the Excavation Disturbed Zone
2.2.01.04.00	Elemental Solubility in Excavation Disturbed Zone	2.2.01.04.0A	Radionuclide Solubility in the Excavation Disturbed Zone
2.2.01.05.00	Radionuclide Transport in Excavation Disturbed Zone	2.2.01.05.0A	Radionuclide Transport in the Excavation Disturbed Zone
2.2.01.05.01	Radionuclide Retardation (Excavation-Disturbed Zone)	2.2.01.05.0A	Radionuclide Transport in the Excavation Disturbed Zone
2.2.01.05.02	Radionuclide Release from EDZ	2.2.01.05.0A	Radionuclide Transport in the Excavation Disturbed Zone
2.2.03.01.00	Stratigraphy	2.2.03.01.0A	Stratigraphy
2.2.03.01.01	Mesozoic Sedimentary Cover	2.2.03.01.0A	Stratigraphy
2.2.03.01.02	Permo-Carboniferous Trough	2.2.03.01.0a	Stratigraphy
2.2.03.01.03	Brine Reservoirs	2.2.03.01.0A	Stratigraphy
2.2.03.02.00	Rock Properties of Host Rock and Other Units	2.2.03.02.0A	Rock Properties of Host Rock and Other Units
2.2.03.02.01	Rock Heterogeneity (Host Rock)	2.2.03.02.0A	Rock Properties of Host Rock and Other Units

Table G-2. Cross Reference of TSPA-SR FEPs to TSPA-LA FEPs (Continued)

SR FEP Number	SR FEP Name	LA FEP Number	LA FEP Name
2.2.03.02.02	LPD Effective Hydraulic Properties	2.2.03.02.0A	Rock Properties of Host Rock and Other Units
2.2.03.02.03	MWCF Effective Hydraulic Properties	2.2.03.02.0A	Rock Properties of Host Rock and Other Units
2.2.03.02.04	HPD Effective Hydraulic Properties	2.2.03.02.0A	Rock Properties of Host Rock and Other Units
2.2.03.02.05	Properties of Far-Field Rock	2.2.03.02.0A	Rock Properties of Host Rock and Other Units
2.2.06.01.00	Changes in Stress (Due to Thermal, Seismic, or Tectonic Effects) Change Porosity and Permeability of Rock	2.2.06.01.0A	Seismic Activity Changes Porosity and Permeability of Rock
		2.2.10.05.0A	Thermo-Mechanical Stresses Alter Characteristics of Rocks Above and Below the Repository
2.2.06.01.01	Stress-Produced Porosity Changes	2.2.06.01.0A	Seismic Activity Changes Porosity and Permeability of Rock
2.2.06.01.02	Stress-Produced Permeability Changes	2.2.06.01.0A	Seismic Activity Changes Porosity and Permeability of Rock
2.2.06.01.03	Stress-Produced Permeability Changes	2.2.06.01.0A	Seismic Activity Changes Porosity and Permeability of Rock
2.2.06.01.04	Regional Stress Regime	2.2.06.01.0A	Seismic Activity Changes Porosity and Permeability of Rock
2.2.06.01.05	Regional Stress Regime	2.2.06.01.0A	Seismic Activity Changes Porosity and Permeability of Rock
2.2.06.01.06	Regional Stress Regime	2.2.06.01.0A	Seismic Activity Changes Porosity and Permeability of Rock
2.2.06.01.07	Stress Field (In Geosphere)	2.2.06.01.0A	Seismic Activity Changes Porosity and Permeability of Rock
2.2.06.01.08	Changes in the Stress Field	2.2.06.01.0A	Seismic Activity Changes Porosity and Permeability of Rock
2.2.06.01.09	Changes in Regional Stress	2.2.06.01.0A	Seismic Activity Changes Porosity and Permeability of Rock
2.2.06.01.10	Stress Changes - Hydrogeological Effects	2.2.06.01.0A	Seismic Activity Changes Porosity and Permeability of Rock
2.2.06.02.00	Changes in Stress (Due to Thermal, Seismic, or Tectonic Effects) Produce Change in Permeability of Faults	2.2.06.02.0A	Seismic Activity Changes Porosity and Permeability of Faults
		2.2.06.02.0B	Seismic Activity Changes Porosity and Permeability of Fractures
		2.2.10.04.0A	Thermo-Mechanical Stresses Alter Characteristics of Fractures Near Repository
		2.2.10.04.0B	Thermo-Mechanical Stresses Alter Characteristics of Faults Near Repository
2.2.06.02.01	Aseismic Alteration of Permeability Along and Across Faults	2.2.06.02.0A	Seismic Activity Changes Porosity and Permeability of Faults
2.2.06.02.02	Fracture Dilation Along Faults Creates Zones of Enhanced Permeability	2.2.06.02.0A	Seismic Activity Changes Porosity and Permeability of Faults
		2.2.06.02.0B	Seismic Activity Changes Porosity and Permeability of Fractures

Table G-2. Cross Reference of TSPA-SR FEPs to TSPA-LA FEPs (Continued)

SR FEP Number	SR FEP Name	LA FEP Number	LA FEP Name
2.2.06.02.03	Relaxation of Thermal Stresses by Fault Movement	2.2.06.02.0A	Seismic Activity Changes Porosity and Permeability of Faults
2.2.06.02.04	Seismically-Stimulated Release of Thermo-Mechanical Stress on Bounding Faults	2.2.06.02.0A	Seismic Activity Changes Porosity and Permeability of Faults
2.2.06.02.05	Relaxation of Thermal Stresses by Fault Movement	2.2.06.02.0A	Seismic Activity Changes Porosity and Permeability of Faults
2.2.06.03.00	Changes in Stress (Due to Seismic or Tectonic Effects) Alter Perched Water Zones	2.2.06.03.0A	Seismic Activity Alters Perched Water Zones
2.2.06.03.01	Perched Zones Develop As a Result of Stress Changes	2.2.06.03.0A	Seismic Activity Alters Perched Water Zones
2.2.06.04.00	Effects of Subsidence	2.2.06.04.0A	Effects of Subsidence
2.2.06.04.01	Subsidence	2.2.06.04.0A	Effects of Subsidence
2.2.06.04.02	Large-Scale Rock Fracturing	2.2.06.04.0A	Effects of Subsidence
2.2.06.04.03	Borehole-Induced Solution and Subsidence	2.2.06.04.0A	Effects of Subsidence
2.2.06.05.00	Salt Creep	2.2.06.05.0A	Salt Creep
2.2.07.01.00	Locally Saturated Flow at Bedrock/Alluvium Contact	2.2.07.01.0A	Locally Saturated Flow at Bedrock/Alluvium Contact
2.2.07.02.00	Unsaturated Groundwater Flow in Geosphere	2.2.07.02.0A	Unsaturated Groundwater Flow in the Geosphere
2.2.07.02.01	Unsaturated Rock	2.2.07.02.0A	Unsaturated Groundwater Flow in the Geosphere
		2.2.07.15.0B	Advection and Dispersion in the UZ
2.2.07.02.02	Soil Depth	2.2.07.03.0A	Capillary Rise in the UZ
		2.3.02.02.0A	Radionuclide Accumulation in Soils
2.2.07.03.00	Capillary Rise	1.3.07.02.0B	Water Table Rise Affects UZ
		2.1.04.01.0A	Flow in the Backfill
		2.1.08.06.0A	Capillary Effects (Wicking) in EBS
		2.2.07.03.0A	Capillary Rise in the UZ
		2.2.08.11.0A	Groundwater Discharge to Surface Within the Reference Biosphere
		2.3.11.04.0A	Groundwater Discharge to Surface Outside the Reference Biosphere
2.2.07.03.01	Capillary Rise (Near Surface Hydrology)	2.2.07.03.0A	Capillary Rise in the UZ
2.2.07.04.00	Focusing of Unsaturated Flow (Fingers, Weeps)	2.2.07.04.0A	Focusing of Unsaturated Flow (Fingers, Weeps)
		2.2.07.07.0A	Perched Water Develops
2.2.07.04.01	Effects of Preferential Flow Paths	2.2.07.01.0A	Locally Saturated Flow at Bedrock/Alluvium Contact
		2.2.07.04.0A	Focusing of Unsaturated Flow (Fingers, Weeps)
		2.2.07.19.0A	Lateral Flow from Solitario Canyon Fault Enters Drifts
2.2.07.04.02	Seeps and Weeps Form As a Locally Saturated Flow System	2.2.07.04.0A	Focusing of Unsaturated Flow (Fingers, Weeps)

Table G-2. Cross Reference of TSPA-SR FEPs to TSPA-LA FEPs (Continued)

SR FEP Number	SR FEP Name	LA FEP Number	LA FEP Name
2.2.07.04.03	Fault Control of Fluid Entrance To and Movement Away from the Repository	2.2.07.04.0A	Focusing of Unsaturated Flow (Fingers, Weeps)
		2.2.07.19.0A	Lateral Flow from Solitario Canyon Fault Enters Drifts
2.2.07.04.04	Fingering - Contaminant Transport in Fingers in UZ	2.2.07.04.0A	Focusing of Unsaturated Flow (Fingers, Weeps)
		2.2.07.15.0B	Advection and Dispersion in the UZ
2.2.07.05.00	Flow and Transport in the UZ from Episodic Infiltration	2.2.07.05.0A	Flow in the UZ from Episodic Infiltration
2.2.07.05.01	Episodic Infiltration Enhances Colloid Transport	2.2.07.06.0A	Episodic or Pulse Release from Repository
		2.2.08.10.0B	Colloidal Transport in the UZ
2.2.07.06.00	Episodic / Pulse Release from Repository	2.2.07.06.0A	Episodic or Pulse Release from Repository
		2.2.07.06.0B	Long-Term Release of Radionuclides from the Repository
2.2.07.07.00	Perched Water Develops	2.2.07.07.0A	Perched Water Develops
2.2.07.07.01	Perched Water Develops at Base of Topopah Spring Welded Unit	2.2.07.07.0A	Perched Water Develops
2.2.07.08.00	Fracture Flow in the Unsaturated Zone	2.2.07.08.0A	Fracture Flow in the UZ
2.2.07.08.01	Fracture Flow (In Geosphere)	2.2.07.08.0A	Fracture Flow in the UZ
2.2.07.08.02	Extreme Channel Flow of Oxidants and Nuclides (In Geosphere)	2.2.07.08.0A	Fracture Flow in the UZ
		2.2.07.15.0B	Advection and Dispersion in the UZ
2.2.07.09.00	Matrix Imbibition in the Unsaturated Zone	2.2.07.09.0A	Matrix Imbibition in the UZ
2.2.07.09.01	Resaturation Due to Matrix Imbibition of Episodic Fracture Flow	2.2.07.09.0A	Matrix Imbibition in the UZ
2.2.07.10.00	Condensation Zone Forms Around Drifts	2.1.08.04.0B	Condensation Forms at Repository Edges (Repository-Scale Cold Traps)
		2.2.07.10.0A	Condensation Zone Forms Around Drifts
2.2.07.10.01	Condensation Cap Forms Above Repository	2.2.07.10.0A	Condensation Zone Forms Around Drifts
2.2.07.10.02	Formation of Condensate Over Individual Containers	2.2.07.10.0A	Condensation Zone Forms Around Drifts
2.2.07.10.03	Formation of Condensate Over Individual Panels	2.2.07.10.0A	Condensation Zone Forms Around Drifts
2.2.07.10.04	Formation of Condensate Over the Entire Repository	2.2.07.10.0A	Condensation Zone Forms Around Drifts
2.2.07.10.05	Shedding of Condensation Cap Over One Drift to Another Drift	2.2.07.10.0A	Condensation Zone Forms Around Drifts
2.2.07.10.06	Vault Geometry	2.1.08.04.0A	Condensation Forms on Roofs of Drifts (Drift-Scale Cold Traps)
		2.1.08.04.0B	Condensation Forms at Repository Edges (Repository-Scale Cold Traps)
		2.2.07.10.0A	Condensation Zone Forms Around Drifts

Table G-2. Cross Reference of TSPA-SR FEPs to TSPA-LA FEPs (Continued)

SR FEP Number	SR FEP Name	LA FEP Number	LA FEP Name
2.2.07.11.00	Return Flow from Condensation Cap / Resaturation of Dry-Out Zone	2.1.08.04.0B	Condensation Forms at Repository Edges (Repository-Scale Cold Traps)
		2.2.07.11.0A	Resaturation of Geosphere Dry-Out Zone
2.2.07.11.01	Auto-Catalytic Drainage of Locally Saturated Flow Thru Condensation Cap	2.2.07.11.0A	Resaturation of Geosphere Dry-Out Zone
2.2.07.11.02	Resaturation, Near-Field Rock	2.1.08.01.0B	Effects of Rapid Influx Into the Repository
		2.2.07.11.0A	Resaturation of Geosphere Dry-Out Zone
2.2.07.11.03	Return of Condensate to Same Panel	2.2.07.11.0A	Resaturation of Geosphere Dry-Out Zone
2.2.07.11.04	Resaturation of Dry-Out Zone Is Affected by Vapor Flow	2.2.07.11.0A	Resaturation of Geosphere Dry-Out Zone
		2.2.10.10.0A	Two-Phase Buoyant Flow/Heat Pipes
2.2.07.11.05	Resaturation of Dry-Out Zone Is Effected by Liquid Under Capillary Forces	2.2.07.03.0A	Capillary Rise in the UZ
		2.2.07.11.0A	Resaturation of Geosphere Dry-Out Zone
2.2.07.11.06	Unsaturated Flow Plume Returns Flow from the Condensation Cap	2.2.07.11.0A	Resaturation of Geosphere Dry-Out Zone
2.2.07.12.00	Saturated Groundwater Flow	2.2.07.12.0A	Saturated Groundwater Flow in the Geosphere
2.2.07.12.01	Groundwater Flow (In Geosphere)	2.2.07.12.0A	Saturated Groundwater Flow in the Geosphere
2.2.07.12.02	Groundwater Flow in LPD	2.2.07.12.0A	Saturated Groundwater Flow in the Geosphere
2.2.07.12.03	Groundwater Flow Path	2.2.07.12.0A	Saturated Groundwater Flow in the Geosphere
2.2.07.12.04	Groundwater Flow in MWCF	2.2.07.12.0A	Saturated Groundwater Flow in the Geosphere
2.2.07.12.05	Groundwater Flow Path (In Geosphere)	2.2.07.12.0A	Saturated Groundwater Flow in the Geosphere
2.2.07.12.06	Groundwater Flow (In Geosphere)	2.2.07.12.0A	Saturated Groundwater Flow in the Geosphere
2.2.07.12.07	Boundary Conditions For Flow	2.2.07.12.0A	Saturated Groundwater Flow in the Geosphere
2.2.07.12.08	Groundwater Flow Path (In Geosphere)	2.2.07.12.0A	Saturated Groundwater Flow in the Geosphere
2.2.07.12.09	Hydraulic Gradient Changes (Magnitude, Regional Direction)	2.2.07.12.0A	Saturated Groundwater Flow in the Geosphere
2.2.07.12.10	Groundwater Flow (In Geosphere)	2.2.07.12.0A	Saturated Groundwater Flow in the Geosphere
2.2.07.12.11	Groundwater Flow (In Geosphere)	2.2.07.12.0A	Saturated Groundwater Flow in the Geosphere
2.2.07.12.12	Hydrological (Processes)	2.2.07.12.0A	Saturated Groundwater Flow in the Geosphere
2.2.07.12.13	Turbulence (In Groundwater)	2.2.07.12.0A	Saturated Groundwater Flow in the Geosphere
2.2.07.12.14	Changes in Groundwater Flow	2.2.07.12.0A	Saturated Groundwater Flow in the Geosphere

Table G-2. Cross Reference of TSPA-SR FEPs to TSPA-LA FEPs (Continued)

SR FEP Number	SR FEP Name	LA FEP Number	LA FEP Name
2.2.07.12.15	Enhanced Groundwater Flow	2.2.07.12.0A	Saturated Groundwater Flow in the Geosphere
2.2.07.13.00	Water-Conducting Features in the Saturated Zone SZ—Water Conducting Features	2.2.07.13.0A	Water-Conducting Features in the SZ
2.2.07.13.01	Water-Conducting Features (Types) (In Geosphere)	2.2.07.13.0A	Water-Conducting Features in the SZ
2.2.07.14.00	Density Effects on Groundwater Flow	2.2.07.14.0A	Chemically-Induced Density Effects on Groundwater Flow
2.2.07.14.01	Saline Intrusion (In Geosphere)	2.2.07.14.0A	Chemically-Induced Density Effects on Groundwater Flow
2.2.07.14.02	Salinity Effects on Flow	2.2.07.14.0A	Chemically-Induced Density Effects on Groundwater Flow
2.2.07.14.03	Intrusion of Saline Groundwater	2.2.07.14.0A	Chemically-Induced Density Effects on Groundwater Flow
2.2.07.15.00	Advection and Dispersion	2.2.07.15.0A	Advection and Dispersion in the SZ
		2.2.07.15.0B	Advection and Dispersion in the UZ
2.2.07.15.01	Far-Field Transport: Advection	2.2.07.15.0A	Advection and Dispersion in the SZ
2.2.07.15.02	Far-Field Transport: Hydrodynamic Dispersion	2.2.07.15.0A	Advection and Dispersion in the SZ
2.2.07.15.03	Dispersion (Water Transport)	2.2.07.15.0A	Advection and Dispersion in the SZ
2.2.07.15.04	Solute Transport (Water Transport)	2.2.07.15.0A	Advection and Dispersion in the SZ
		2.2.07.17.0A	Diffusion in the SZ
2.2.07.15.05	Advection (Water Transport)	2.2.07.15.0A	Advection and Dispersion in the SZ
2.2.07.15.06	Convection (Water Transport)	2.1.04.09.0A	Radionuclide Transport in Backfill
2.2.07.15.07	Dispersion (Water Transport)	2.2.07.15.0A	Advection and Dispersion in the SZ
2.2.07.15.08	Convection (Water Transport)	2.2.07.15.0A	Advection and Dispersion in the SZ
2.2.07.15.09	Dispersion (Water Transport)	2.2.07.15.0A	Advection and Dispersion in the SZ
2.2.07.15.10	Dispersion (Water Transport)	2.2.07.15.0A	Advection and Dispersion in the SZ
2.2.07.15.11	Dispersion (Water Transport)	2.2.07.15.0A	Advection and Dispersion in the SZ
2.2.07.15.12	Transport and Release of Nuclides, Near-Field Rock	2.2.07.15.0A	Advection and Dispersion in the SZ
		2.2.07.17.0A	Diffusion in the SZ
		2.2.08.10.0A	Colloidal Transport in the SZ
		2.2.11.03.0A	Gas Transport in Geosphere
2.2.07.15.13	Groundwater Flow (Alluvium of Rhine Valley)	2.2.07.15.0A	Advection and Dispersion in the SZ
2.2.07.15.14	Exfiltration to a Local Aquifer	2.2.07.16.0A	Dilution of Radionuclides in Groundwater
2.2.07.16.00	Dilution of Radionuclides in Groundwater	2.2.07.16.0A	Dilution of Radionuclides in Groundwater
2.2.07.16.01	Dilution (Water Transport)	2.2.07.16.0A	Dilution of Radionuclides in Groundwater
2.2.07.16.02	Dilution of Radionuclides in Groundwater (Water Transport)	2.2.07.16.0A	Dilution of Radionuclides in Groundwater
2.2.07.16.03	Dilution of Radionuclides in HPD	2.2.07.16.0A	Dilution of Radionuclides in Groundwater
2.2.07.17.00	Diffusion in the Saturated Zone	2.2.07.17.0A	Diffusion in the SZ

Table G-2. Cross Reference of TSPA-SR FEPs to TSPA-LA FEPs (Continued)

SR FEP Number	SR FEP Name	LA FEP Number	LA FEP Name
2.2.07.17.01	Far-Field Transport: Diffusion	2.2.07.17.0A	Diffusion in the SZ
		2.2.08.08.0A	Matrix Diffusion in the SZ
2.2.07.17.02	Diffusion (Water Transport)	2.2.07.17.0A	Diffusion in the SZ
2.2.07.17.03	Diffusion (Water Transport)	2.2.07.17.0A	Diffusion in the SZ
2.2.07.17.04	Diffusion (Water Transport)	2.2.07.17.0A	Diffusion in the SZ
2.2.07.17.05	Diffusion (Water Transport)	2.2.07.17.0A	Diffusion in the SZ
2.2.07.18.00	Film Flow Into Drifts	2.2.07.18.0A	Film Flow Into the Repository
		2.2.08.12.0A	Chemistry of Water Flowing Into the Drift
2.2.07.19.00	Lateral Flow from Solitario Canyon Fault Enters Potential Waste Emplacement Drifts	2.2.07.19.0A	Lateral Flow from Solitario Canyon Fault Enters Drifts
2.2.08.01.00	Groundwater Chemistry / Composition in UZ and SZ	2.2.08.01.0A	Chemical Characteristics of Groundwater in the SZ
	SZ—Groundwater Chemistry FEPs	2.2.08.03.0A	Geochemical Interactions and Evolution in the SZ
2.2.08.01.01	Groundwater Chemistry (In Geosphere)	2.2.08.01.0A	Chemical Characteristics of Groundwater in the SZ
		2.2.08.01.0B	Chemical Characteristics of Groundwater in the UZ
		2.2.08.03.0A	Geochemical Interactions and Evolution in the SZ
		2.2.08.03.0B	Geochemical Interactions and Evolution in the UZ
2.2.08.01.02	Deep Saline Water Intrusion	2.2.08.03.0A	Geochemical Interactions and Evolution in the SZ
2.2.08.01.03	Interface Different Waters (In Geosphere)	2.2.08.01.0A	Chemical Characteristics of Groundwater in the SZ
		2.2.08.01.0B	Chemical Characteristics of Groundwater in the UZ
2.2.08.01.04	Water Chemistry in Near-Field Rock	2.2.08.01.0B	Chemical Characteristics of Groundwater in the UZ
		2.2.08.03.0B	Geochemical Interactions and Evolution in the UZ
2.2.08.01.05	Groundwater Geochemistry (In Geosphere)	2.2.08.01.0A	Chemical Characteristics of Groundwater in the SZ
2.2.08.01.06	Saline Intrusion (In Geosphere)	2.2.08.03.0A	Geochemical Interactions and Evolution in the SZ
2.2.08.01.07	Freshwater Intrusion (In Geosphere)	2.2.08.03.0A	Geochemical Interactions and Evolution in the SZ
2.2.08.01.08	Changes in Groundwater Eh	2.2.08.03.0A	Geochemical Interactions and Evolution in the SZ
		2.2.08.09.0A	Sorption in the SZ
		2.2.08.10.0A	Colloidal Transport in the SZ
2.2.08.01.09	Changes in Groundwater Ph	2.2.08.03.0A	Geochemical Interactions and Evolution in the SZ
		2.2.08.09.0A	Sorption in the SZ
		2.2.08.10.0A	Colloidal Transport in the SZ

Table G-2. Cross Reference of TSPA-SR FEPs to TSPA-LA FEPs (Continued)

SR FEP Number	SR FEP Name	LA FEP Number	LA FEP Name
2.2.08.01.10	Oxidizing Conditions	2.2.08.03.0A	Geochemical Interactions and Evolution in the SZ
		2.2.08.03.0B	Geochemical Interactions and Evolution in the UZ
2.2.08.01.11	Groundwater Composition	2.2.08.03.0A	Geochemical Interactions and Evolution in the SZ
		2.2.08.03.0B	Geochemical Interactions and Evolution in the UZ
		2.2.08.06.0A	Complexation in the SZ
		2.2.08.06.0B	Complexation in the UZ
2.2.08.01.12	Ph-Deviations	2.2.08.03.0A	Geochemical Interactions and Evolution in the SZ
2.2.08.01.13	Change of Groundwater Chemistry in Nearby Rock	1.1.02.00.0A	Chemical Effects of Excavation and Construction in EBS
		2.1.13.01.0A	Radiolysis
		2.2.08.03.0B	Geochemical Interactions and Evolution in the UZ
2.2.08.01.14	Saline (Or Fresh) Groundwater Intrusion	2.2.08.03.0A	Geochemical Interactions and Evolution in the SZ
2.2.08.01.15	Saline or Freshwater Intrusion	2.2.08.03.0A	Geochemical Interactions and Evolution in the SZ
2.2.08.01.16	Effects at Saline-Freshwater Interface	2.2.08.03.0A	Geochemical Interactions and Evolution in the SZ
2.2.08.01.17	Chemical Gradients	2.2.08.01.0A	Chemical Characteristics of Groundwater in the SZ
		2.2.08.01.0B	Chemical Characteristics of Groundwater in the UZ
2.2.08.01.18	Non-Radioactive Solute Plume in Geosphere	2.2.08.03.0A	Geochemical Interactions and Evolution in the SZ
		2.2.08.03.0B	Geochemical Interactions and Evolution in the UZ
2.2.08.01.19	Groundwater Chemistry (In Geosphere)	2.2.08.01.0A	Chemical Characteristics of Groundwater in the SZ
		2.2.08.01.0B	Chemical Characteristics of Groundwater in the UZ
		2.2.08.03.0A	Geochemical Interactions and Evolution in the SZ
		2.2.08.03.0B	Geochemical Interactions and Evolution in the UZ
2.2.08.01.20	Intrusion of Saline Groundwater	2.2.08.03.0A	Geochemical Interactions and Evolution in the SZ
2.2.08.01.21	Groundwater Conditions	2.2.08.01.0A	Chemical Characteristics of Groundwater in the SZ
		2.2.08.01.0B	Chemical Characteristics of Groundwater in the UZ
2.2.08.01.22	Mineralogy (Host Rock)	2.2.08.01.0A	Chemical Characteristics of Groundwater in the SZ
		2.2.08.01.0B	Chemical Characteristics of Groundwater in the UZ

Table G-2. Cross Reference of TSPA-SR FEPs to TSPA-LA FEPs (Continued)

SR FEP Number	SR FEP Name	LA FEP Number	LA FEP Name
2.2.08.01.23	Mineralogy (Host Rock)	2.2.08.01.0A	Chemical Characteristics of Groundwater in the SZ
		2.2.08.01.0B	Chemical Characteristics of Groundwater in the UZ
2.2.08.02.00	Radionuclide Transport Occurs in a Carrier Plume in Geosphere SZ—Radionuclide Transport in a Carrier Plume	2.2.08.01.0A	Chemical Characteristics of Groundwater in the SZ
		2.2.08.01.0B	Chemical Characteristics of Groundwater in the UZ
		2.2.08.03.0A	Geochemical Interactions and Evolution in the SZ
		2.2.08.03.0B	Geochemical Interactions and Evolution in the UZ
2.2.08.02.01	Locally-Saturated Carrier Plume Forms (In Geosphere)	2.1.09.12.0A	Rind (Chemically Altered Zone) Forms in the Near-Field
		2.2.07.11.0A	Resaturation of Geosphere Dry-Out Zone
		2.2.08.03.0B	Geochemical Interactions and Evolution in the UZ
2.2.08.02.02	Unsaturated Carrier Plume Forms (In Geosphere)	2.1.09.12.0A	Rind (Chemically Altered Zone) Forms in the Near-Field
		2.2.07.11.0A	Resaturation of Geosphere Dry-Out Zone
		2.2.08.03.0B	Geochemical Interactions and Evolution in the UZ
2.2.08.02.03	Precipitation/Dissolution (Release/Migration Factors)	2.2.08.03.0A	Geochemical Interactions and Evolution in the SZ
		2.2.08.03.0B	Geochemical Interactions and Evolution in the UZ
2.2.08.03.00	Geochemical Interactions in Geosphere (Dissolution, Precipitation, Weathering) and Effects on Radionuclide Transport SZ—Groundwater Chemistry FEPs	2.2.08.01.0B	Chemical Characteristics of Groundwater in the UZ
		2.2.08.03.0A	Geochemical Interactions and Evolution in the SZ
		2.2.08.03.0B	Geochemical Interactions and Evolution in the UZ
2.2.08.03.01	Far-Field Transport: Changes in Groundwater Chemistry and Flow Direction	2.2.08.03.0A	Geochemical Interactions and Evolution in the SZ
		2.2.08.09.0A	Sorption in the SZ
2.2.08.03.02	Effects of Dissolution (In Geosphere)	2.2.08.03.0A	Geochemical Interactions and Evolution in the SZ
		2.2.08.10.0A	Colloidal Transport in the SZ
2.2.08.03.03	Rock Property Changes (In Geosphere)	2.2.08.03.0A	Geochemical Interactions and Evolution in the SZ
		2.2.08.03.0B	Geochemical Interactions and Evolution in the UZ
2.2.08.03.04	Hydraulic Properties-Evolution	2.2.08.03.0A	Geochemical Interactions and Evolution in the SZ
		2.2.08.03.0B	Geochemical Interactions and Evolution in the UZ

Table G-2. Cross Reference of TSPA-SR FEPs to TSPA-LA FEPs (Continued)

SR FEP Number	SR FEP Name	LA FEP Number	LA FEP Name
2.2.08.03.05	Dissolution of Fracture Fillings/Precipitations (In Geosphere)	2.2.08.03.0A	Geochemical Interactions and Evolution in the SZ
		2.2.08.03.0B	Geochemical Interactions and Evolution in the UZ
2.2.08.03.06	Weathering of Flow Paths (In Geosphere)	2.2.08.03.0A	Geochemical Interactions and Evolution in the SZ
		2.2.08.03.0B	Geochemical Interactions and Evolution in the UZ
2.2.08.03.07	Fracture Mineralization and Weathering (In Geosphere)	2.2.08.03.0A	Geochemical Interactions and Evolution in the SZ
		2.2.08.03.0B	Geochemical Interactions and Evolution in the UZ
2.2.08.03.08	Alteration/Weathering of Flow Paths	2.2.08.03.0A	Geochemical Interactions and Evolution in the SZ
		2.2.08.03.0B	Geochemical Interactions and Evolution in the UZ
2.2.08.03.09	Precipitation and Dissolution (Release/Migration Factors)	2.2.08.03.0A	Geochemical Interactions and Evolution in the SZ
		2.2.08.03.0B	Geochemical Interactions and Evolution in the UZ
		2.2.09.01.0A	Microbial Activity in the SZ
		2.2.09.01.0B	Microbial Activity in the UZ
2.2.08.03.10	Chemical Precipitation (Release/Migration Factors)	2.2.08.03.0A	Geochemical Interactions and Evolution in the SZ
		2.2.08.03.0B	Geochemical Interactions and Evolution in the UZ
2.2.08.03.11	Dissolution, Precipitation and Crystallization (Release/Migration Factors)	2.2.08.03.0A	Geochemical Interactions and Evolution in the SZ
		2.2.08.03.0B	Geochemical Interactions and Evolution in the UZ
2.2.08.03.12	Kinetics of Precipitation and Dissolution (Release/Migration Factors)	2.2.08.03.0A	Geochemical Interactions and Evolution in the SZ
		2.2.08.03.0B	Geochemical Interactions and Evolution in the UZ
2.2.08.03.13	Speciation (Contaminant Speciation and Solubility)	2.2.08.03.0A	Geochemical Interactions and Evolution in the SZ
		2.2.08.03.0B	Geochemical Interactions and Evolution in the UZ
		2.2.08.07.0A	Radionuclide Solubility Limits in the SZ
		2.2.08.07.0B	Radionuclide Solubility Limits in the UZ
2.2.08.03.14	Speciation (Geosphere) (Contaminant Speciation and Solubility)	2.2.08.03.0A	Geochemical Interactions and Evolution in the SZ
		2.2.08.03.0B	Geochemical Interactions and Evolution in the UZ
		2.2.08.07.0A	Radionuclide Solubility Limits in the SZ
		2.2.08.07.0B	Radionuclide Solubility Limits in the UZ

Table G-2. Cross Reference of TSPA-SR FEPs to TSPA-LA FEPs (Continued)

SR FEP Number	SR FEP Name	LA FEP Number	LA FEP Name
2.2.08.03.15	Recrystallization (Contaminant Speciation and Solubility)	2.2.08.03.0A	Geochemical Interactions and Evolution in the SZ
		2.2.08.03.0B	Geochemical Interactions and Evolution in the UZ
		2.2.08.07.0A	Radionuclide Solubility Limits in the SZ
		2.2.08.07.0B	Radionuclide Solubility Limits in the UZ
2.2.08.03.16	Speciation (Contaminant Speciation and Solubility)	2.2.08.03.0A	Geochemical Interactions and Evolution in the SZ
		2.2.08.03.0B	Geochemical Interactions and Evolution in the UZ
		2.2.08.07.0A	Radionuclide Solubility Limits in the SZ
		2.2.08.07.0B	Radionuclide Solubility Limits in the UZ
2.2.08.03.17	Kinetics of Speciation (Contaminant Speciation and Solubility)	2.2.08.03.0A	Geochemical Interactions and Evolution in the SZ
		2.2.08.03.0B	Geochemical Interactions and Evolution in the UZ
		2.2.08.07.0A	Radionuclide Solubility Limits in the SZ
		2.2.08.07.0B	Radionuclide Solubility Limits in the UZ
2.2.08.03.18	Groundwater Chemistry (Sorption/Desorption Processes)	2.2.08.03.0A	Geochemical Interactions and Evolution in the SZ
		2.2.08.03.0B	Geochemical Interactions and Evolution in the UZ
2.2.08.04.00	Redissolution of Precipitates Directs More Corrosive Fluids to Containers	2.2.08.04.0A	Re-Dissolution of Precipitates Directs More Corrosive Fluids to Waste Packages
2.2.08.05.00	Osmotic Processes	2.2.08.05.0A	Diffusion in the UZ
2.2.08.06.00	Complexation in Geosphere	2.2.08.06.0A	Complexation in the SZ
		2.2.08.06.0B	Complexation in the UZ
2.2.08.07.00	Radionuclide Solubility Limits in the Geosphere	2.2.08.07.0A	Radionuclide Solubility Limits in the SZ
		2.2.08.07.0B	Radionuclide Solubility Limits in the UZ
		2.2.08.07.0C	Radionuclide Solubility Limits in the Biosphere
2.2.08.07.01	Radionuclide Transport Through LPD (Water Transport)	2.2.08.07.0A	Radionuclide Solubility Limits in the SZ
		2.2.08.07.0B	Radionuclide Solubility Limits in the UZ
2.2.08.07.02	Radionuclide Transport Through MWCF (Water Transport)	2.2.08.07.0A	Radionuclide Solubility Limits in the SZ
		2.2.08.07.0B	Radionuclide Solubility Limits in the UZ
2.2.08.07.03	Solubility Limits/Colloid Formation	2.2.08.07.0A	Radionuclide Solubility Limits in the SZ
		2.2.08.10.0A	Colloidal Transport in the SZ
		3.2.07.01.0A	Isotopic Dilution
2.2.08.07.04	Solubility Limits/Colloid Formation	2.2.08.07.0A	Radionuclide Solubility Limits in the SZ
		2.2.08.10.0A	Colloidal Transport in the SZ
		3.2.07.01.0A	Isotopic Dilution
2.2.08.08.00	Matrix Diffusion in Geosphere SZ—Matrix Diffusion	2.2.08.08.0A	Matrix Diffusion in the SZ
		2.2.08.08.0B	Matrix Diffusion in the UZ
2.2.08.08.01	Matrix Diffusion (Water Transport)	2.2.08.08.0A	Matrix Diffusion in the SZ

Table G-2. Cross Reference of TSPA-SR FEPs to TSPA-LA FEPs (Continued)

SR FEP Number	SR FEP Name	LA FEP Number	LA FEP Name
2.2.08.08.02	Matrix Diffusion (Water Transport)	2.2.08.08.0A	Matrix Diffusion in the SZ
2.2.08.08.03	Matrix Diffusion (Water Transport)	2.2.08.08.0A	Matrix Diffusion in the SZ
		2.2.08.08.0B	Matrix Diffusion in the UZ
2.2.08.08.04	Matrix Diffusion (Water Transport)	2.2.08.08.0A	Matrix Diffusion in the SZ
2.2.08.08.05	Matrix Diffusion (Water Transport)	2.2.08.08.0A	Matrix Diffusion in the SZ
2.2.08.08.06	Matrix Diffusion (Water Transport)	2.2.08.08.0A	Matrix Diffusion in the SZ
2.2.08.08.07	Matrix Diffusion (Water Transport)	2.2.08.08.0A	Matrix Diffusion in the SZ
2.2.08.08.08	Matrix Diffusion	2.2.08.08.0A	Matrix Diffusion in the SZ
2.2.08.09.00	Sorption in UZ and SZ	2.2.08.09.0A	Sorption in the SZ
		2.2.08.09.0B	Sorption in the UZ
2.2.08.09.01	Far-Field Transport: Sorption Including Ion-Exchange	2.2.08.09.0A	Sorption in the SZ
2.2.08.09.02	Far-Field Transport: Changes in Sorptive Surfaces	2.2.08.09.0A	Sorption in the SZ
2.2.08.09.03	Anion-Exclusion General: (In Geosphere)	2.2.08.09.0A	Sorption in the SZ
2.2.08.09.04	Soil Pore Water Ph	2.2.08.09.0A	Sorption in the SZ
2.2.08.09.05	Soil Sorption	2.2.08.09.0A	Sorption in the SZ
2.2.08.09.06	Ion Exchange in Soil	2.2.08.09.0A	Sorption in the SZ
2.2.08.09.07	Sorption (Reversible and Irreversible)	2.2.08.09.0A	Sorption in the SZ
		2.2.08.09.0B	Sorption in the UZ
2.2.08.09.08	Sorption - Nonlinear	2.2.08.09.0A	Sorption in the SZ
2.2.08.09.09	Saturation (Of Sorption Sites)	2.2.08.09.0A	Sorption in the SZ
2.2.08.09.10	Sorption (Geosphere)	2.2.08.09.0A	Sorption in the SZ
2.2.08.09.11	Sorption	2.2.08.09.0A	Sorption in the SZ
2.2.08.09.12	Sorption	2.2.08.08.0A	Matrix Diffusion in the SZ
		2.2.08.09.0A	Sorption in the SZ
2.2.08.09.13	Nonlinear Sorption	2.2.08.09.0A	Sorption in the SZ
2.2.08.09.14	Sorption	2.2.08.09.0A	Sorption in the SZ
		2.2.08.09.0B	Sorption in the UZ
2.2.08.09.15	Nonlinear Sorption	2.2.08.09.0A	Sorption in the SZ
2.2.08.09.16	Sorption	2.2.08.09.0A	Sorption in the SZ
2.2.08.09.17	Radionuclide Sorption	2.2.08.09.0A	Sorption in the SZ
2.2.08.09.18	Sorption	2.2.08.09.0A	Sorption in the SZ
2.2.08.09.19	Actinide Sorption	2.2.08.09.0A	Sorption in the SZ
2.2.08.09.20	Kinetics of Sorption	2.2.08.09.0A	Sorption in the SZ
2.2.08.09.21	Changes in Sorptive Surfaces	2.2.08.09.0A	Sorption in the SZ
2.2.08.09.22	Sorption - Nonlinear (Geosphere)	2.2.08.09.0A	Sorption in the SZ
2.2.08.10.00	Colloidal Transport in Geosphere	2.2.08.10.0A	Colloidal Transport in the SZ
		2.2.08.10.0B	Colloidal Transport in the UZ

Table G-2. Cross Reference of TSPA-SR FEPs to TSPA-LA FEPs (Continued)

SR FEP Number	SR FEP Name	LA FEP Number	LA FEP Name
2.2.08.10.01	Far-Field Transport: Transport of Radionuclides Bound to Microbes	2.2.08.10.0A	Colloidal Transport in the SZ
		2.2.09.01.0A	Microbial Activity in the SZ
2.2.08.10.02	Colloid Transport Occurs in a Carrier Plume (In Geosphere)	2.2.08.01.0A	Chemical Characteristics of Groundwater in the SZ
		2.2.08.03.0A	Geochemical Interactions and Evolution in the SZ
		2.2.08.10.0B	Colloidal Transport in the UZ
2.2.08.10.03	Colloids (In Geosphere)	2.1.09.16.0A	Formation of Pseudo-Colloids (Natural) in EBS
		2.2.08.10.0B	Colloidal Transport in the UZ
2.2.08.11.00	Distribution and Release of Nuclides from the Geosphere SZ—Distribution and Release of Nuclides	2.2.08.11.0A	Groundwater Discharge to Surface Within the Reference Biosphere
2.2.08.11.01	Transport and Geochemical (Processes)	2.2.08.11.0A	Groundwater Discharge to Surface Within the Reference Biosphere
2.2.08.12.00	Use of J-13 Well Water As a Surrogate For Water Flowing Into the EBS and Waste	2.2.08.12.0A	Chemistry of Water Flowing Into the Drift
		2.2.08.12.0B	Chemistry of Water Flowing Into the Waste Package
2.2.09.01.00	Microbial Activity in Geosphere SZ—Groundwater Chemistry FEPs	2.2.09.01.0A	Microbial Activity in the SZ
		2.2.09.01.0B	Microbial Activity in the UZ
2.2.09.01.01	Microbes (In Geosphere)	2.2.09.01.0A	Microbial Activity in the SZ
		2.2.09.01.0B	Microbial Activity in the UZ
2.2.09.01.02	Microbes (In Geosphere)	2.2.08.06.0A	Complexation in the SZ
		2.2.09.01.0A	Microbial Activity in the SZ
		2.2.09.01.0B	Microbial Activity in the UZ
2.2.09.01.03	Microbial Activity (In Geosphere)	2.2.09.01.0A	Microbial Activity in the SZ
		2.2.09.01.0B	Microbial Activity in the UZ
2.2.09.01.04	Far-Field Transport: Biogeochemical Changes	2.2.09.01.0A	Microbial Activity in the SZ
		2.2.09.01.0B	Microbial Activity in the UZ
2.2.09.01.05	Bacteria and Microbes in Soil	2.2.09.01.0A	Microbial Activity in the SZ
		2.2.09.01.0B	Microbial Activity in the UZ
2.2.09.01.06	Chemical Transformations (Biological Processes)	2.2.09.01.0A	Microbial Activity in the SZ
		2.2.09.01.0B	Microbial Activity in the UZ
2.2.10.01.00	Repository-Induced Thermal Effects in Geosphere	2.2.10.01.0A	Repository-Induced Thermal Effects on Flow in the UZ
2.2.10.01.01	Temperature, Far-Field	2.2.10.03.0A	Natural Geothermal Effects on Flow in the SZ
		2.2.10.13.0A	Repository-Induced Thermal Effects on Flow in the SZ
2.2.10.01.02	Temperature, Near-Field Rock	1.1.02.02.0A	Preclosure Ventilation
		2.2.10.01.0A	Repository-Induced Thermal Effects on Flow in the UZ
2.2.10.01.03	Thermal Effects on Groundwater Flow	2.2.10.03.0A	Natural Geothermal Effects on Flow in the SZ

Table G-2. Cross Reference of TSPA-SR FEPs to TSPA-LA FEPs (Continued)

SR FEP Number	SR FEP Name	LA FEP Number	LA FEP Name
2.2.10.01.04	Groundwater - Evolution	2.2.10.01.0A	Repository-Induced Thermal Effects on Flow in the UZ
2.2.10.01.05	Thermal Effects on Material Properties (In Waste and EBS)	2.2.10.01.0A	Repository-Induced Thermal Effects on Flow in the UZ
		2.2.10.13.0A	Repository-Induced Thermal Effects on Flow in the SZ
2.2.10.01.06	Thermal Effects: Rock-Mass Changes	2.2.10.01.0A	Repository-Induced Thermal Effects on Flow in the UZ
2.2.10.01.07	Thermal Effects: Hydrogeological Changes	2.2.10.01.0A	Repository-Induced Thermal Effects on Flow in the UZ
		2.2.10.10.0A	Two-Phase Buoyant Flow/Heat Pipes
		2.2.10.13.0A	Repository-Induced Thermal Effects on Flow in the SZ
2.2.10.02.00	Thermal Convection Cell Develops in SZ	2.1.11.09.0A	Thermal Effects on Flow in the EBS
		2.2.10.02.0A	Thermal Convection Cell Develops in SZ
2.2.10.03.00	Natural Geothermal Effects SZ—Geothermal Effects	2.2.10.03.0A	Natural Geothermal Effects on Flow in the SZ
		2.2.10.03.0B	Natural Geothermal Effects on Flow in the UZ
		2.2.10.13.0A	Repository-Induced Thermal Effects on Flow in the SZ
2.2.10.03.01	Natural Thermal Effects (In Geosphere)	2.2.10.03.0A	Natural Geothermal Effects on Flow in the SZ
		2.2.10.03.0B	Natural Geothermal Effects on Flow in the UZ
2.2.10.03.02	Geothermal Regime	2.2.10.03.0A	Natural Geothermal Effects on Flow in the SZ
2.2.10.03.03	Geothermal Regime	2.2.10.03.0A	Natural Geothermal Effects on Flow in the SZ
2.2.10.03.04	Geothermal Gradient Effects	2.2.10.02.0A	Thermal Convection Cell Develops in SZ
		2.2.10.03.0A	Natural Geothermal Effects on Flow in the SZ
2.2.10.04.00	Thermo-Mechanical Alteration of Fractures Near Repository	2.2.10.04.0A	Thermo-Mechanical Stresses Alter Characteristics of Fractures Near Repository
2.2.10.04.01	Thermal Expansion Closes Most Fractures Close to Repository	2.2.10.04.0A	Thermo-Mechanical Stresses Alter Characteristics of Fractures Near Repository
2.2.10.04.02	Thermally-Induced Fracturing Around Containers Creates a Capillary Barrier	2.2.10.04.0A	Thermo-Mechanical Stresses Alter Characteristics of Fractures Near Repository
2.2.10.04.03	Host Rock Fracture Aperture Changes	2.2.10.06.0A	Thermo-Chemical Alteration in the UZ (Solubility, Speciation, Phase Changes, Precipitation/Dissolution)
2.2.10.05.00	Thermo-Mechanical Alteration of Rocks Above and Below the Repository	2.2.10.05.0A	Thermo-Mechanical Stresses Alter Characteristics of Rocks Above and Below the Repository

Table G-2. Cross Reference of TSPA-SR FEPs to TSPA-LA FEPs (Continued)

SR FEP Number	SR FEP Name	LA FEP Number	LA FEP Name
2.2.10.05.01	Thermal Expansion of Rocks Below Repository Opens Fractures in Paint Brush Unwelded	2.2.10.05.0A	Thermo-Mechanical Stresses Alter Characteristics of Rocks Above and Below the Repository
2.2.10.05.02	Thermo-Mechanical Alteration of Surface Infiltration	2.2.10.05.0A	Thermo-Mechanical Stresses Alter Characteristics of Rocks Above and Below the Repository
2.2.10.06.00	Thermo-Chemical Alteration (Solubility Speciation, Phase Changes, Precipitation/Dissolution)	2.2.10.06.0a	Thermo-Chemical Alteration in the Uz (Solubility, Speciation, Phase Changes, Precipitation/Dissolution)
		2.2.10.08.0A	Thermo-Chemical Alteration in the SZ (Solubility, Speciation, Phase Changes, Precipitation/Dissolution)
2.2.10.06.01	Silica Phase Changes (Accompanied by Volume Change) Occur Due to Elevated Temperature	2.2.10.06.0A	Thermo-Chemical Alteration in the UZ (Solubility, Speciation, Phase Changes, Precipitation/Dissolution)
2.2.10.06.02	Thermochemical Change	2.2.10.06.0A	Thermo-Chemical Alteration in the UZ (Solubility, Speciation, Phase Changes, Precipitation/Dissolution)
2.2.10.06.03	Alteration of Rock Properties Because of 2-Phase Flow	2.2.10.06.0A	Thermo-Chemical Alteration in the UZ (Solubility, Speciation, Phase Changes, Precipitation/Dissolution)
2.2.10.06.04	Heat-Induced Chemical Reactions Plug Small Fractures; Flow Is Preferentially Redirected to Large Fractures	2.2.10.06.0A	Thermo-Chemical Alteration in the UZ (Solubility, Speciation, Phase Changes, Precipitation/Dissolution)
2.2.10.06.05	Alteration of Minerals to Clays (In Geosphere)	2.2.10.06.0A	Thermo-Chemical Alteration in the UZ (Solubility, Speciation, Phase Changes, Precipitation/Dissolution)
2.2.10.06.06	Calcite Precipitation in Hot Region Produces Fluids Depleted in Calcite Which Dissolve Calcite Below the Repository	2.2.10.06.0A	Thermo-Chemical Alteration in the UZ (Solubility, Speciation, Phase Changes, Precipitation/Dissolution)
2.2.10.06.07	Precipitates from Dissolved Constituents of Tuff and Repository Materials Form by Evaporation During Thermal Period	2.2.10.06.0A	Thermo-Chemical Alteration in the UZ (Solubility, Speciation, Phase Changes, Precipitation/Dissolution)
2.2.10.07.00	Thermo-Chemical Alteration of the Calico Hills Unit SZ—Repository Induced Thermal Effects	2.2.10.07.0A	Thermo-Chemical Alteration of the Calico Hills Unit
2.2.10.08.00	Thermo-Chemical Alteration of the Saturated Zone SZ—Repository Induced Thermal Effects	2.2.10.08.0A	Thermo-Chemical Alteration in the SZ (Solubility, Speciation, Phase Changes, Precipitation/Dissolution)
2.2.10.08.01	Precipitation of Zeolites in the Saturated Zone Plugs Pores	2.2.10.08.0A	Thermo-Chemical Alteration in the SZ (Solubility, Speciation, Phase Changes, Precipitation/Dissolution)

Table G-2. Cross Reference of TSPA-SR FEPs to TSPA-LA FEPs (Continued)

SR FEP Number	SR FEP Name	LA FEP Number	LA FEP Name
2.2.10.09.00	Thermo-Chemical Alteration of the Topopah Spring Basal Vitrophyre	2.2.10.09.0A	Thermo-Chemical Alteration of the Topopah Spring Basal Vitrophyre
2.2.10.09.01	Formation of Perched Water On the Altered Topopah Spring Basal Vitrophyre	2.2.10.09.0A	Thermo-Chemical Alteration of the Topopah Spring Basal Vitrophyre
2.2.10.09.02	Sorption of Contaminants By the Altered Topopah Spring Basal Vitrophyre	2.2.10.09.0A	Thermo-Chemical Alteration of the Topopah Spring Basal Vitrophyre
2.2.10.09.03	Redirection of Transport Paths By the Altered Topopah Spring Basal Vitrophyre	2.2.10.09.0A	Thermo-Chemical Alteration of the Topopah Spring Basal Vitrophyre
2.2.10.09.04	Sorption of Actinides on Altered Topopah Spring Basal Vitrophyre	2.2.10.09.0A	Thermo-Chemical Alteration of the Topopah Spring Basal Vitrophyre
2.2.10.09.05	Alteration of the Topopah Spring Basal Vitrophyre	2.2.10.09.0A	Thermo-Chemical Alteration of the Topopah Spring Basal Vitrophyre
2.2.10.10.00	Two-Phase Buoyant Flow / Heat Pipes	2.2.10.10.0A	Two-Phase Buoyant Flow/Heat Pipes
2.2.10.10.01	Heat Pipe -Evolving	2.2.10.10.0A	Two-Phase Buoyant Flow/Heat Pipes
2.2.10.10.02	Heat Pipe -Continuing	2.2.10.10.0A	Two-Phase Buoyant Flow/Heat Pipes
2.2.10.10.03	Heat Pipe Formation, 2-Phase System	2.2.10.10.0A	Two-Phase Buoyant Flow/Heat Pipes
2.2.10.11.00	Natural Air Flow in Unsaturated Zone	2.2.10.11.0A	Natural Air Flow in the UZ
2.2.10.12.00	Geosphere Dry-Out Due to Waste Heat	2.2.10.12.0A	Geosphere Dry-Out Due to Waste Heat
2.2.10.13.00	Density-Driven Groundwater Flow (Thermal)	2.2.10.03.0A	Natural Geothermal Effects on Flow in the SZ
	SZ—Repository Induced Thermal Effects	2.2.10.13.0A	Repository-Induced Thermal Effects on Flow in the SZ
2.2.10.13.01	Density-Driven Groundwater Flow (Thermal)	2.2.10.03.0A	Natural Geothermal Effects on Flow in the SZ
2.2.10.13.02	Density-Driven Groundwater Flows (Temperature/Salinity Differences)	2.2.10.03.0A	Natural Geothermal Effects on Flow in the SZ
2.2.10.13.03	Thermal Buoyancy	2.2.10.03.0A	Natural Geothermal Effects on Flow in the SZ
		2.2.10.13.0A	Repository-Induced Thermal Effects on Flow in the SZ
2.2.10.14.00	Mineralogic Dehydration Reactions	2.2.10.14.0A	Mineralogic Dehydration Reactions
2.2.11.01.00	Naturally-Occurring Gases in Geosphere	2.2.11.01.0A	Gas Effects in the SZ
		2.2.11.02.0A	Gas Effects in the UZ
2.2.11.01.01	Methane Intrusion (In Geosphere)	2.2.11.01.0A	Gas Effects in the SZ
2.2.11.01.02	Natural Gas Intrusion	2.2.11.01.0A	Gas Effects in the SZ
2.2.11.01.03	Geogas	2.2.11.01.0A	Gas Effects in the SZ
2.2.11.01.04	Geogas	2.2.11.01.0A	Gas Effects in the SZ

Table G-2. Cross Reference of TSPA-SR FEPs to TSPA-LA FEPs (Continued)

SR FEP Number	SR FEP Name	LA FEP Number	LA FEP Name
2.2.11.01.05	Gas Generation and Gas Sources, Far-Field	2.2.11.01.0A	Gas Effects in the SZ
		2.2.11.02.0A	Gas Effects in the UZ
2.2.11.01.06	Natural Gas Intrusion	2.2.11.01.0A	Gas Effects in the SZ
2.2.11.01.07	Methane	2.2.11.01.0A	Gas Effects in the SZ
2.2.11.02.00	Gas Pressure Effects	2.2.11.02.0A	Gas Effects in the UZ
2.2.11.02.01	Gas Pressure Effects	2.2.11.02.0A	Gas Effects in the UZ
2.2.11.02.02	Fluid Flow Due to Gas Pressurization (In Waste and EBS)	2.2.11.02.0A	Gas Effects in the UZ
2.2.11.02.03	Disruption Due to Gas Effects	2.2.11.02.0A	Gas Effects in the UZ
2.2.11.03.00	Gas Transport in Geosphere	2.1.04.09.0A	Radionuclide Transport in Backfill
		2.1.12.06.0A	Gas Transport in EBS
		2.1.12.07.0A	Effects of Radioactive Gases in EBS
		2.2.11.01.0A	Gas Effects in the SZ
		2.2.11.02.0A	Gas Effects in the UZ
		2.2.11.03.0A	Gas Transport in Geosphere
2.2.11.03.01	Gases and Gas Transport (In Geosphere)	2.2.11.02.0A	Gas Effects in the UZ
		2.2.11.03.0A	Gas Transport in Geosphere
2.2.11.03.02	Far-Field Transport: Gas Induced Groundwater Transport	2.2.10.10.0A	Two-Phase Buoyant Flow/Heat Pipes
		2.2.11.01.0A	Gas Effects in the SZ
		2.2.11.03.0A	Gas Transport in Geosphere
2.2.11.03.03	Gas Mediated Transport	2.2.11.02.0a	Gas Effects in the Uz
		2.2.11.03.0A	Gas Transport in Geosphere
2.2.11.03.04	Far-Field Transport: Transport of Radioactive Gases	2.2.11.03.0A	Gas Transport in Geosphere
2.2.11.03.05	Gas Discharge	2.2.11.03.0A	Gas Transport in Geosphere
2.2.11.03.06	Transport of Radioactive Gases	2.2.11.03.0A	Gas Transport in Geosphere
2.2.12.00.00	Undetected Features (In Geosphere) SZ—Undetected Features	2.2.12.00.0A	Undetected Features in the UZ
		2.2.12.00.0B	Undetected Features in the SZ
2.2.12.00.01	Undetected Dike Beneath the Repository Passing Thru the Calico Hills Provides a Highly Permeable Flow Path	2.2.12.00.0A	Undetected Features in the UZ
2.2.12.00.02	Undetected Fault Dips Below the Repository Providing a Highly Permeable Flow Path	2.2.12.00.0A	Undetected Features in the UZ
2.2.12.00.03	Undetected Fault Beneath the Repository Acts As a Flow Barrier Altering the Flow System	2.2.12.00.0A	Undetected Features in the UZ
2.2.12.00.04	Undetected Fault Connects Tuff Aquifers to Carbonate Aquifers; Providing a Fast Path	2.2.12.00.0A	Undetected Features in the UZ
2.2.12.00.05	Perched Water Escapes Detection and Waste Is Put in It	2.2.12.00.0A	Undetected Features in the UZ

Table G-2. Cross Reference of TSPA-SR FEPs to TSPA-LA FEPs (Continued)

SR FEP Number	SR FEP Name	LA FEP Number	LA FEP Name
2.2.12.00.06	Undiscovered Mine Shaft (An Old Prospect Hole) in a Wash Acts As a Source For Increased Local Infiltration	2.2.12.00.0A	Undetected Features in the UZ
2.2.12.00.07	Rock Properties-Undetected Features	2.2.12.00.0A	Undetected Features in the UZ
2.2.12.00.08	Undetected Fracture Zone	2.2.12.00.0A	Undetected Features in the UZ
2.2.12.00.09	Undetected Features	2.2.12.00.0A	Undetected Features in the UZ
2.2.12.00.10	Undetected Past Intrusions	2.2.12.00.0A	Undetected Features in the UZ
2.2.12.00.11	Undetected Discontinuities (In Geosphere)	2.2.12.00.0A	Undetected Features in the UZ
2.2.14.01.00	Critical Assembly Forms Away from Repository	2.2.14.09.0A	Far-Field Criticality
2.2.14.01.01	Reconcentration (Release/Migration Factors)	2.2.14.09.0A	Far-Field Criticality
2.2.14.01.02	Reconcentration (Release/Migration Factors)	2.2.14.09.0A	Far-Field Criticality
2.2.14.01.03	DOE SNF Criticality Far-Field (Radionuclide Inventory Impact)	2.2.14.09.0A	Far-Field Criticality
2.2.14.01.04	DOE SNF Criticality Far-Field (Waste Heat Impact)	2.2.14.09.0A	Far-Field Criticality
2.2.14.02.00	Far-Field Criticality, Precipitation in Organic Reducing Zone in or Near Water Table	2.2.14.09.0A	Far-Field Criticality
2.2.14.02.01	Precipitation of U at Reducing Zone Associated W/Organics in Alluvial Aquifer	2.2.14.09.0A	Far-Field Criticality
2.2.14.02.02	Precipitation of U at Reducing Zone Associated W/Organics in Franklin Lake Playa	2.2.14.09.0A	Far-Field Criticality
2.2.14.03.00	Far-Field Criticality, Sorption on Clay/Zeolite in Tsbv	2.2.14.09.0A	Far-Field Criticality
2.2.14.04.00	Far-Field Criticality, Precipitation Caused by Hydrothermal Upwell or Redox Front in the SZ	2.2.14.09.0A	Far-Field Criticality
2.2.14.04.01	Precipitation of U in the Upwelling Zone Along Some Faults	2.2.14.09.0A	Far-Field Criticality
2.2.14.04.02	Precipitation of U Below the Redox Front in the SZ	2.2.14.09.0A	Far-Field Criticality
2.2.14.05.00	Far-Field Criticality, Precipitation in Perched Water Above Tsbv	2.2.14.09.0A	Far-Field Criticality
2.2.14.05.01	Accumulation of Solute in Topographic Lows of the Altered Tsbv	2.2.14.09.0A	Far-Field Criticality

Table G-2. Cross Reference of TSPA-SR FEPs to TSPA-LA FEPs (Continued)

SR FEP Number	SR FEP Name	LA FEP Number	LA FEP Name
2.2.14.06.00	Far-Field Criticality, Precipitation in Fractures of Tsw Rock	2.2.14.09.0A	Far-Field Criticality
2.2.14.07.00	Far-Field Criticality, Dryout Produces Fissile Salt in a Perched Water Basin	2.2.14.09.0A	Far-Field Criticality
2.2.14.08.00	Far-Field Criticality Associated With Colloidal Deposits	2.2.14.09.0A	Far-Field Criticality
2.3.01.00.00	Topography and Morphology	2.3.01.00.0A	Topography and Morphology
2.3.01.00.01	Topography (Current)	2.3.01.00.0A	Topography and Morphology
2.3.01.00.02	Topography (Future)	2.3.01.00.0A	Topography and Morphology
2.3.01.00.03	Terrestrial Surface	2.3.01.00.0A	Topography and Morphology
2.3.01.00.04	Physiography	2.3.01.00.0A	Topography and Morphology
2.3.01.00.05	Geomorphological (Processes)	2.3.01.00.0A	Topography and Morphology
2.3.01.00.06	External Flow Boundaries (Surface Environment)	2.3.01.00.0A	Topography and Morphology
2.3.01.00.07	Changes in Geometry and Driving Forces of the Flow System	2.3.01.00.0A	Topography and Morphology
2.3.02.01.00	Soil Type	2.3.02.01.0A	Soil Type
2.3.02.01.01	Pedogenesis	2.3.02.01.0A	Soil Type
2.3.02.01.02	Soil Formation	2.3.02.01.0A	Soil Type
2.3.02.01.03	Soil Development	2.3.02.01.0A	Soil Type
2.3.02.01.04	Soil	2.3.02.01.0A	Soil Type
2.3.02.02.00	Radionuclide Accumulation in Soils	2.3.02.02.0A	Radionuclide Accumulation in Soils
2.3.02.02.01	Soil Moisture and Evaporation (Water Transport)	2.3.02.02.0A	Radionuclide Accumulation in Soils
2.3.02.02.02	Radionuclide Accumulation in Sediments at Franklin Lake Playa (Water Transport)	2.3.02.02.0A	Radionuclide Accumulation in Soils
		2.3.13.04.0A	Radionuclide Release Outside the Reference Biosphere
2.3.02.02.03	Accumulation in Sediments (Sorption/Desorption Processes)	2.3.02.02.0A	Radionuclide Accumulation in Soils
2.3.02.02.04	Accumulation in Soils and Organic Debris (Sorption/Desorption Processes)	2.3.02.02.0A	Radionuclide Accumulation in Soils
2.3.02.02.05	Soil	2.3.02.02.0A	Radionuclide Accumulation in Soils
2.3.02.02.06	Soil Leaching	2.3.02.02.0A	Radionuclide Accumulation in Soils
2.3.02.02.07	Accumulation in Peat	2.3.02.02.0A	Radionuclide Accumulation in Soils
2.3.02.02.08	Alkali Flats (And Other Playa Deposits)	2.3.02.02.0A	Radionuclide Accumulation in Soils
2.3.02.02.09	Accumulation in Soil (Exposure Factors)	2.3.02.02.0A	Radionuclide Accumulation in Soils
2.3.02.02.10	Soil Leaching to Groundwater	2.3.02.02.0A	Radionuclide Accumulation in Soils
2.3.02.03.00	Soil and Sediment Transport	2.3.02.03.0A	Soil and Sediment Transport in the Biosphere

Table G-2. Cross Reference of TSPA-SR FEPs to TSPA-LA FEPs (Continued)

SR FEP Number	SR FEP Name	LA FEP Number	LA FEP Name
2.3.02.03.01	Soil and Sediment Bioturbation	2.3.02.03.0A	Soil and Sediment Transport in the Biosphere
2.3.02.03.02	Bioturbation	2.3.02.03.0A	Soil and Sediment Transport in the Biosphere
2.3.02.03.03	Sediment Transport Including Bioturbation	2.3.02.03.0A	Soil and Sediment Transport in the Biosphere
2.3.04.01.00	Surface Water Transport and Mixing	1.4.01.03.0A	Acid Rain
		1.4.06.01.0A	Altered Soil or Surface Water Chemistry
		2.2.08.11.0A	Groundwater Discharge to Surface Within the Reference Biosphere
		2.3.04.01.0A	Surface Water Transport and Mixing
		2.3.11.04.0A	Groundwater Discharge to Surface Outside the Reference Biosphere
		2.3.13.04.0A	Radionuclide Release Outside the Reference Biosphere
2.3.04.01.00	Surface Water Transport and Mixing	3.2.10.00.0A	Atmospheric Transport of Contaminants
2.3.04.01.01	Flushing of Water Bodies	2.3.04.01.0A	Surface Water Transport and Mixing
2.3.04.01.02	Lake Mixing (Artificial)	2.3.04.01.0A	Surface Water Transport and Mixing
2.3.04.01.03	Sediment Resuspension in Water Bodies	2.3.04.01.0A	Surface Water Transport and Mixing
2.3.04.01.04	Sedimentation in Water Bodies	2.3.04.01.0A	Surface Water Transport and Mixing
2.3.04.01.05	River Meandering	2.3.04.01.0A	Surface Water Transport and Mixing
2.3.04.01.06	River Meander	2.3.04.01.0A	Surface Water Transport and Mixing
2.3.04.01.07	Freshwater Sediment Transport and Deposition	2.3.04.01.0A	Surface Water Transport and Mixing
2.3.04.01.08	River Flow and Lake Level Changes	2.3.04.01.0A	Surface Water Transport and Mixing
2.3.04.01.09	Surface Water Flow (River Rhine)	2.3.04.01.0A	Surface Water Transport and Mixing
2.3.04.01.10	Sedimentation	2.3.04.01.0A	Surface Water Transport and Mixing
2.3.04.01.11	River Course Meander	2.3.04.01.0A	Surface Water Transport and Mixing
2.3.04.01.12	Surface Water Bodies	2.3.04.01.0A	Surface Water Transport and Mixing
2.3.04.01.13	Surface Water Mixing	2.3.04.01.0A	Surface Water Transport and Mixing
2.3.04.01.14	Stream and River Flow	2.3.04.01.0A	Surface Water Transport and Mixing
2.3.04.01.15	Surface Water Bodies	2.3.04.01.0A	Surface Water Transport and Mixing
2.3.04.01.16	Exfiltration to Surface Waters	2.3.04.01.0A	Surface Water Transport and Mixing
2.3.04.01.17	Lake Formation	2.3.04.01.0A	Surface Water Transport and Mixing
2.3.04.01.18	Dilution of Radionuclides in Surface Water (Aquifer, River, Lake, Etc.)	2.3.04.01.0A	Surface Water Transport and Mixing
2.3.04.01.19	Radionuclide Accumulation in Sediments (Water Transport)	2.3.04.01.0A	Surface Water Transport and Mixing
2.3.06.00.00	Marine Features	2.3.06.00.0A	Marine Features
2.3.06.00.01	Marine Sediment Transport and Deposition	2.3.06.00.0A	Marine Features
2.3.06.00.02	Seas and Oceans	2.3.06.00.0A	Marine Features

Table G-2. Cross Reference of TSPA-SR FEPs to TSPA-LA FEPs (Continued)

SR FEP Number	SR FEP Name	LA FEP Number	LA FEP Name
2.3.06.00.03	Marine Sediment Transport and Deposition	2.3.06.00.0A	Marine Features
2.3.06.00.04	Coastal Surge, Storms and Hurricanes	2.3.06.00.0A	Marine Features
2.3.06.00.05	Coastal Erosion and Estuarine Development	2.3.06.00.0A	Marine Features
2.3.06.00.06	Estuaries	2.3.06.00.0A	Marine Features
2.3.06.00.07	Coastal Erosion	2.3.06.00.0A	Marine Features
2.3.06.00.08	Sea Level Change	2.3.06.00.0A	Marine Features
2.3.06.00.09	Change in Sea Level	2.3.06.00.0A	Marine Features
2.3.06.00.10	Sea-Level Rise/Fall	2.3.06.00.0A	Marine Features
2.3.06.00.11	Sea Level Changes	2.3.06.00.0A	Marine Features
2.3.06.00.12	Sea Level Changes	2.3.06.00.0A	Marine Features
2.3.09.01.00	Animal Burrowing/Intrusion	2.3.02.03.0A	Soil and Sediment Transport in the Biosphere
		2.3.09.01.0A	Animal Burrowing/Intrusion
2.3.09.01.01	Intrusion (Animal)	2.3.09.01.0A	Animal Burrowing/Intrusion
2.3.11.01.00	Precipitation	2.3.11.01.0A	Precipitation
2.3.11.01.01	Precipitation, Temperature and Soil Water Balance	2.3.11.01.0A	Precipitation
2.3.11.01.02	Flood (Meteorology)	2.3.11.01.0A	Precipitation
2.3.11.01.03	Extremes of Precipitation, Snow Melt and Associated Flooding (Meteorology)	2.3.11.01.0A	Precipitation
2.3.11.01.04	Precipitation (Meteorology)	2.3.11.01.0A	Precipitation
2.3.11.02.00	Surface Runoff and Flooding	2.3.02.03.0A	Soil and Sediment Transport in the Biosphere
		2.3.11.02.0A	Surface Runoff and Evapotranspiration
2.3.11.02.01	Runoff (Near Surface Hydrology)	2.3.02.03.0A	Soil and Sediment Transport in the Biosphere
		2.3.11.02.0A	Surface Runoff and Evapotranspiration
2.3.11.02.02	Flooding (Near Surface Hydrology)	2.3.02.03.0A	Soil and Sediment Transport in the Biosphere
		2.3.11.02.0A	Surface Runoff and Evapotranspiration
2.3.11.02.03	Evapotranspiration (Near Surface Hydrology)	2.3.11.02.0A	Surface Runoff and Evapotranspiration
2.3.11.02.04	Flooding Occurs in Drill Hole Wash and Increases Percolation Below the Wash	2.3.11.02.0A	Surface Runoff and Evapotranspiration
2.3.11.02.05	Faulting At the Surface Produces a Scarp Causing an Impoundment	2.3.11.02.0A	Surface Runoff and Evapotranspiration
2.3.11.02.06	River Flooding	2.3.11.02.0A	Surface Runoff and Evapotranspiration
2.3.11.03.00	Infiltration and Recharge (Hydrologic and Chemical Effects)	2.3.11.03.0A	Infiltration and Recharge
2.3.11.03.01	Freshwater Intrusion (In Geosphere)	1.3.07.02.0A	Water Table Rise Affects SZ
		2.3.11.03.0A	Infiltration and Recharge

Table G-2. Cross Reference of TSPA-SR FEPs to TSPA-LA FEPs (Continued)

SR FEP Number	SR FEP Name	LA FEP Number	LA FEP Name
2.3.11.03.02	Groundwater Recharge/Discharge	2.3.11.03.0A	Infiltration and Recharge
2.3.11.03.03	Equilibrated Flow System	2.3.11.02.0A	Surface Runoff and Evapotranspiration
		2.3.11.03.0A	Infiltration and Recharge
2.3.11.03.04	Draining Flow System	2.3.11.03.0A	Infiltration and Recharge
2.3.11.03.05	Recharge Groundwater	2.2.08.01.0B	Chemical Characteristics of Groundwater in the UZ
		2.3.11.03.0A	Infiltration and Recharge
2.3.11.03.06	Surface Water Chemistry	2.2.08.01.0B	Chemical Characteristics of Groundwater in the UZ
		2.3.11.03.0A	Infiltration and Recharge
2.3.11.03.07	Runoff Is Intercepted by Wash Terraces	2.3.11.02.0A	Surface Runoff and Evapotranspiration
		2.3.11.03.0A	Infiltration and Recharge
2.3.11.03.08	Runoff to Washes Infiltrates and Maintains a Zone of Higher Flux to the UZ	2.3.11.02.0A	Surface Runoff and Evapotranspiration
		2.3.11.03.0A	Infiltration and Recharge
2.3.11.03.09	Flow in Ephemeral Streams Tends to Be in Channels and Is a Source of Recharge	2.3.11.02.0A	Surface Runoff and Evapotranspiration
		2.3.11.03.0A	Infiltration and Recharge
2.3.11.03.10	Percolation (Near Surface Hydrology)	2.3.11.03.0A	Infiltration and Recharge
2.3.11.03.11	Groundwater Recharge	2.2.07.15.0B	Advection and Dispersion in the UZ
		2.2.08.05.0A	Diffusion in the UZ
		2.2.08.09.0A	Sorption in the SZ
		2.2.08.10.0A	Colloidal Transport in the SZ
		2.3.11.03.0A	Infiltration and Recharge
2.3.11.03.12	Infiltration (Near Surface Hydrology)	2.3.11.03.0A	Infiltration and Recharge
2.3.11.03.13	Recharge Groundwater (Affects Waste and EBS)	2.2.08.01.0B	Chemical Characteristics of Groundwater in the UZ
		2.3.11.03.0A	Infiltration and Recharge
2.3.11.03.14	Effective Moisture (Recharge)	1.3.01.00.0A	Climate Change
		2.3.11.03.0A	Infiltration and Recharge
2.3.11.03.15	Changes in Groundwater Recharge and Discharge	2.3.11.03.0A	Infiltration and Recharge
2.3.11.03.16	Coupling of Surface Water Flow to Climate/Hydrologic Modeling System	2.3.11.03.0A	Infiltration and Recharge
2.3.11.04.00	Groundwater Discharge to Surface	2.3.02.02.0A	Radionuclide Accumulation in Soils
		2.3.11.04.0A	Groundwater Discharge to Surface Outside the Reference Biosphere
2.3.11.04.01	Discharge Zones	2.3.11.04.0A	Groundwater Discharge to Surface Outside the Reference Biosphere
2.3.11.04.02	Groundwater Discharge	2.3.11.04.0A	Groundwater Discharge to Surface Outside the Reference Biosphere
2.3.11.04.03	Groundwater Discharge	2.3.11.04.0A	Groundwater Discharge to Surface Outside the Reference Biosphere
2.3.13.01.00	Biosphere Characteristics	2.3.13.01.0A	Biosphere Characteristics

Table G-2. Cross Reference of TSPA-SR FEPs to TSPA-LA FEPs (Continued)

SR FEP Number	SR FEP Name	LA FEP Number	LA FEP Name
2.3.13.01.01	Fires (Forest and Grass)	2.3.13.01.0A	Biosphere Characteristics
		2.3.13.04.0A	Radionuclide Release Outside the Reference Biosphere
2.3.13.01.02	Wetlands	2.3.13.01.0A	Biosphere Characteristics
		2.3.13.04.0A	Radionuclide Release Outside the Reference Biosphere
2.3.13.01.03	Ecological Change	2.3.13.01.0A	Biosphere Characteristics
2.3.13.01.04	Microbes (Ecological Systems)	2.3.13.01.0A	Biosphere Characteristics
2.3.13.01.05	Ecological (Processes)	2.3.13.01.0A	Biosphere Characteristics
2.3.13.01.06	Lake Infilling	2.3.13.01.0A	Biosphere Characteristics
2.3.13.01.07	Plants	2.3.13.01.0A	Biosphere Characteristics
2.3.13.01.08	Future Biosphere Conditions	2.3.13.01.0A	Biosphere Characteristics
2.3.13.01.09	Ecological Response to Climate (E.G. Desert Formation)	2.3.13.01.0A	Biosphere Characteristics
2.3.13.01.10	Natural Ecological Development	2.3.13.01.0A	Biosphere Characteristics
2.3.13.02.00	Biosphere Transport	2.3.02.03.0A	Soil and Sediment Transport in the Biosphere
		2.3.04.01.0A	Surface Water Transport and Mixing
		2.3.09.01.0A	Animal Burrowing/Intrusion
		2.3.13.02.0A	Radionuclide Alteration During Biosphere Transport
		2.4.09.01.0B	Agricultural Land Use and Irrigation
		3.2.10.00.0A	Atmospheric Transport of Contaminants
2.3.13.02.01	Sediment/Water/Gas Interaction With the Atmosphere	2.3.13.02.0A	Radionuclide Alteration During Biosphere Transport
2.3.13.02.02	Biogeochemical Processes	2.3.13.02.0A	Radionuclide Alteration During Biosphere Transport
2.3.13.03.00	Effects of Repository Heat on Biosphere	2.3.13.03.0A	Effects of Repository Heat On the Biosphere
2.4.01.00.00	Human Characteristics (Physiology, Metabolism)	2.4.01.00.0A	Human Characteristics (Physiology, Metabolism)
2.4.01.00.01	Critical Group - Individuality	2.4.01.00.0A	Human Characteristics (Physiology, Metabolism)
2.4.03.00.00	Diet and Fluid Intake	3.3.01.00.0A	Contaminated Drinking Water, Foodstuffs and Drugs
2.4.03.00.01	Intake of Drugs	3.3.01.00.0A	Contaminated Drinking Water, Foodstuffs and Drugs
2.4.03.00.02	Human Diet	3.3.01.00.0A	Contaminated Drinking Water, Foodstuffs and Drugs
2.4.03.00.03	Human Soil Ingestion	3.3.01.00.0A	Contaminated Drinking Water, Foodstuffs and Drugs
2.4.03.00.04	Consumption of Uncontaminated Products	3.3.01.00.0A	Contaminated Drinking Water, Foodstuffs and Drugs
2.4.03.00.05	Filtration (Water Processing)	3.3.01.00.0A	Contaminated Drinking Water, Foodstuffs and Drugs

Table G-2. Cross Reference of TSPA-SR FEPs to TSPA-LA FEPs (Continued)

SR FEP Number	SR FEP Name	LA FEP Number	LA FEP Name
2.4.03.00.06	Food Preparation	3.3.01.00.0A	Contaminated Drinking Water, Foodstuffs and Drugs
2.4.04.01.00	Human Lifestyle	2.4.04.01.0A	Human Lifestyle
2.4.04.01.01	Hunter/Gathering Lifestyle	2.4.04.01.0A	Human Lifestyle
2.4.04.01.02	Critical Group - Leisure Pursuits	2.4.04.01.0A	Human Lifestyle
2.4.07.00.00	Dwellings	2.4.04.01.0A	Human Lifestyle
		2.4.07.00.0A	Dwellings
2.4.07.00.01	Building Materials	2.4.07.00.0A	Dwellings
2.4.07.00.02	Critical Group - House Location	2.4.07.00.0A	Dwellings
2.4.07.00.03	Gas Leakage Into Basements	2.4.07.00.0A	Dwellings
2.4.07.00.04	Household Dust and Fumes	2.4.07.00.0A	Dwellings
2.4.07.00.05	Houseplants	2.4.07.00.0A	Dwellings
2.4.07.00.06	Showers and Humidifiers	2.4.07.00.0A	Dwellings
2.4.07.00.07	Space Heating	2.4.07.00.0A	Dwellings
2.4.07.00.08	Water Leaking Into Basements	2.4.07.00.0A	Dwellings
2.4.07.00.09	Outdoor Spraying of Water	2.4.07.00.0A	Dwellings
2.4.07.00.10	Evaporative Coolers	2.4.07.00.0A	Dwellings
2.4.08.00.00	Wild and Natural Land and Water Use	2.4.08.00.0A	Wild and Natural Land and Water Use
2.4.08.00.01	Natural and Semi-Natural Environments	2.4.08.00.0A	Wild and Natural Land and Water Use
2.4.08.00.02	Land and Surface Water Use: Terrestrial	2.4.08.00.0A	Wild and Natural Land and Water Use
2.4.08.00.03	Coastal Water Use	2.4.08.00.0A	Wild and Natural Land and Water Use
2.4.08.00.04	Sea Water Use	2.4.08.00.0A	Wild and Natural Land and Water Use
2.4.08.00.05	Estuarine Water Use	2.4.08.00.0A	Wild and Natural Land and Water Use
2.4.08.00.06	Land and Surface Water Use: Estuarine	2.4.08.00.0A	Wild and Natural Land and Water Use
2.4.08.00.07	Land and Surface Water Use: Coastal Waters	2.4.08.00.0A	Wild and Natural Land and Water Use
2.4.08.00.08	Land and Surface Water Use: Seas	2.4.08.00.0A	Wild and Natural Land and Water Use
2.4.09.01.00	Agricultural Land Use and Irrigation	2.4.09.01.0A	Implementation of New Agricultural Practices or Land Use
		2.4.09.01.0B	Agricultural Land Use and Irrigation
2.4.09.01.01	Crop Fertilizers and Soil Conditioners	2.4.09.01.0A	Implementation of New Agricultural Practices or Land Use
2.4.09.01.02	Crop Storage	2.4.09.01.0A	Implementation of New Agricultural Practices or Land Use
2.4.09.01.03	Fires (Agricultural)	2.4.09.01.0A	Implementation of New Agricultural Practices or Land Use
2.4.09.01.04	Greenhouse Food Production	2.4.09.01.0A	Implementation of New Agricultural Practices or Land Use
2.4.09.01.05	Hydroponics	2.4.09.01.0A	Implementation of New Agricultural Practices or Land Use

Table G-2. Cross Reference of TSPA-SR FEPs to TSPA-LA FEPs (Continued)

SR FEP Number	SR FEP Name	LA FEP Number	LA FEP Name
2.4.09.01.06	Peat and Leaf Harvesting	2.4.09.01.0A	Implementation of New Agricultural Practices or Land Use
2.4.09.01.07	Irrigation	2.4.09.01.0A	Implementation of New Agricultural Practices or Land Use
2.4.09.01.08	Agricultural and Fisheries Practice Changes	2.4.09.01.0A	Implementation of New Agricultural Practices or Land Use
2.4.09.01.09	Irrigation	2.4.09.01.0A	Implementation of New Agricultural Practices or Land Use
2.4.09.01.10	Ploughing	2.4.09.01.0A	Implementation of New Agricultural Practices or Land Use
2.4.09.01.11	Irrigation	2.4.09.01.0A	Implementation of New Agricultural Practices or Land Use
2.4.09.01.12	Critical Group - Agricultural Labor	2.4.09.01.0A	Implementation of New Agricultural Practices or Land Use
2.4.09.01.13	Ashes and Sewage Sludge Fertilizer	2.4.09.01.0A	Implementation of New Agricultural Practices or Land Use
2.4.09.01.14	Irrigation	2.4.09.01.0A	Implementation of New Agricultural Practices or Land Use
2.4.09.01.15	Herbicides, Pesticides and Fungicides	2.4.09.01.0A	Implementation of New Agricultural Practices or Land Use
2.4.09.02.00	Animal Farms and Fisheries	2.4.09.02.0A	Animal Farms and Fisheries
2.4.09.02.01	Fish Farming	2.4.09.02.0A	Animal Farms and Fisheries
2.4.09.02.02	Ranching	2.4.09.02.0A	Animal Farms and Fisheries
2.4.09.02.03	Fish Farming	2.4.09.02.0A	Animal Farms and Fisheries
2.4.10.00.00	Urban and Industrial Land and Water Use	2.4.10.00.0A	Urban and Industrial Land and Water Use
2.4.10.00.01	Industrial Water Use	2.4.10.00.0A	Urban and Industrial Land and Water Use
2.4.10.00.02	Earthmoving	2.4.10.00.0A	Urban and Industrial Land and Water Use
2.4.10.00.03	Earthmoving Projects	2.4.10.00.0A	Urban and Industrial Land and Water Use
2.4.10.00.04	Earthworks	2.4.10.00.0A	Urban and Industrial Land and Water Use
2.4.10.00.05	Land Use Changes	2.4.10.00.0A	Urban and Industrial Land and Water Use
2.4.10.00.06	Land Use Changes	2.4.10.00.0A	Urban and Industrial Land and Water Use
2.4.10.00.07	Post-Closure Surface Activities	2.4.10.00.0A	Urban and Industrial Land and Water Use
2.4.10.00.08	Surface Disruptions	2.4.10.00.0A	Urban and Industrial Land and Water Use
2.4.10.00.09	Biogas Production	2.4.10.00.0A	Urban and Industrial Land and Water Use
3.1.01.01.00	Radioactive Decay and Ingrowth	3.1.01.01.0A	Radioactive Decay and Ingrowth
3.1.01.01.01	Radioactive Decay	3.1.01.01.0A	Radioactive Decay and Ingrowth
3.1.01.01.02	Radioactive Decay	3.1.01.01.0A	Radioactive Decay and Ingrowth
3.1.01.01.03	Radioactive Decay	3.1.01.01.0A	Radioactive Decay and Ingrowth
		3.3.05.01.0A	Radiation Doses
3.1.01.01.04	Radioactive Decay and Ingrowth	3.1.01.01.0A	Radioactive Decay and Ingrowth
3.1.01.01.05	Radioactive Decay	3.1.01.01.0A	Radioactive Decay and Ingrowth
3.1.01.01.06	Radioactive Decay	2.1.13.01.0A	Radiolysis
		2.1.13.02.0A	Radiation Damage in EBS
		3.1.01.01.0A	Radioactive Decay and Ingrowth

Table G-2. Cross Reference of TSPA-SR FEPs to TSPA-LA FEPs (Continued)

SR FEP Number	SR FEP Name	LA FEP Number	LA FEP Name
3.1.01.01.07	Radioactive Decay of Mobile Nuclides	3.1.01.01.0A	Radioactive Decay and Ingrowth
3.1.01.01.08	Radionuclide Decay and Ingrowth	3.1.01.01.0A	Radioactive Decay and Ingrowth
3.1.01.01.09	Radiological Events and Processes	2.1.13.01.0A	Radiolysis
		2.1.13.02.0A	Radiation Damage in EBS
		3.1.01.01.0A	Radioactive Decay and Ingrowth
3.2.07.01.00	Isotopic Dilution	3.2.07.01.0A	Isotopic Dilution
3.2.07.01.01	Mass, Isotopic and Species Dilution	3.2.07.01.0A	Isotopic Dilution
3.2.07.01.02	Natural Radionuclides/Elements (In Host Rock Disturbed Zone)	3.2.07.01.0A	Isotopic Dilution
3.2.10.00.00	Atmospheric Transport of Contaminants	1.2.04.07.0A	Ashfall
		1.2.04.07.0B	Ash Redistribution in Groundwater
		1.2.04.07.0C	Ash Redistribution via Soil and Sediment Transport
3.2.10.00.01	Suspension in Air	3.2.10.00.0A	Atmospheric Transport of Contaminants
3.2.10.00.02	Wind	3.2.10.00.0A	Atmospheric Transport of Contaminants
3.2.10.00.03	Radionuclide Volatilization/Aerosol/Dust Production	3.2.10.00.0A	Atmospheric Transport of Contaminants
3.2.10.00.04	Convection, Turbulence and Diffusion (Atmospheric)	3.2.10.00.0A	Atmospheric Transport of Contaminants
3.2.10.00.05	Deposition (Atmospheric)	3.2.10.00.0A	Atmospheric Transport of Contaminants
3.2.10.00.06	Saltation	3.2.10.00.0A	Atmospheric Transport of Contaminants
3.2.10.00.07	Atmosphere	3.2.10.00.0A	Atmospheric Transport of Contaminants
3.2.10.00.08	Precipitation (Meteoric)	3.2.10.00.0A	Atmospheric Transport of Contaminants
3.3.01.00.00	Drinking Water, Foodstuffs and Drugs, Contaminant Concentrations in	3.3.01.00.0A	Contaminated Drinking Water, Foodstuffs and Drugs
3.3.01.00.01	Water Source (Exposure Factors)	3.3.01.00.0A	Contaminated Drinking Water, Foodstuffs and Drugs
3.3.02.01.00	Plant Uptake	3.3.02.01.0A	Plant Uptake
3.3.02.01.01	Plant Roots (Foodchains)	3.3.02.01.0A	Plant Uptake
3.3.02.01.02	Uptake by Crops (Foodchains)	3.3.02.01.0A	Plant Uptake
3.3.02.01.03	Plant Uptake	3.3.02.01.0A	Plant Uptake
3.3.02.01.04	Uptake by Deep Rooting Species	3.3.02.01.0A	Plant Uptake
3.3.02.02.00	Animal Uptake	3.3.02.02.0A	Animal Uptake
3.3.02.02.01	Carcasses	3.3.02.02.0A	Animal Uptake
3.3.02.02.02	Uptake by Livestock (Foodchains)	3.3.02.02.0A	Animal Uptake
3.3.02.02.03	Uptake in Fish (Foodchains)	3.3.02.03.0A	Fish Uptake
3.3.02.02.04	Animal Diets	3.3.02.02.0A	Animal Uptake
3.3.02.02.05	Animal Grooming and Fighting	3.3.02.02.0A	Animal Uptake
3.3.02.02.06	Scavengers and Predators	3.3.02.02.0A	Animal Uptake

Table G-2. Cross Reference of TSPA-SR FEPs to TSPA-LA FEPs (Continued)

SR FEP Number	SR FEP Name	LA FEP Number	LA FEP Name
3.3.02.02.07	Animal Uptake	3.3.02.02.0A	Animal Uptake
3.3.02.02.08	Animals	3.3.02.02.0A	Animal Uptake
3.3.02.02.09	Animal Soil Ingestion	3.3.02.02.0A	Animal Uptake
3.3.02.03.00	Bioaccumulation	3.3.04.01.0A	Ingestion
		3.3.05.01.0A	Radiation Doses
3.3.02.03.01	Bioconcentration (Foodchains)	3.3.02.01.0A	Plant Uptake
		3.3.02.02.0A	Animal Uptake
		3.3.04.01.0A	Ingestion
3.3.02.03.02	Foodchain Equilibrium	3.3.02.01.0A	Plant Uptake
		3.3.02.02.0A	Animal Uptake
3.3.02.03.03	Biomagnification (Foodchains)	3.3.02.02.0A	Animal Uptake
3.3.02.03.04	Recycling (Exposure Factors)	1.4.07.03.0A	Recycling of Accumulated Radionuclides from Soils to Groundwater
		3.3.02.01.0A	Plant Uptake
3.3.02.03.05	Removal Mechanisms (Exposure Factors)	3.3.02.01.0A	Plant Uptake
		3.3.02.02.0A	Animal Uptake
3.3.02.03.06	Bioaccumulation and Translocation	3.3.02.01.0A	Plant Uptake
		3.3.02.02.0A	Animal Uptake
		3.3.04.01.0A	Ingestion
3.3.03.01.00	Contaminated Non-Food Products and Exposure	3.3.03.01.0A	Contaminated Non-Food Products and Exposure
3.3.03.01.01	Charcoal Production (Exposure Factors)	3.3.03.01.0A	Contaminated Non-Food Products and Exposure
3.3.03.01.02	Critical Group - Clothing and Home Furnishings (Exposure Factors)	3.3.03.01.0A	Contaminated Non-Food Products and Exposure
3.3.03.01.03	Tree Sap (Exposure Factors)	3.3.03.01.0A	Contaminated Non-Food Products and Exposure
3.3.03.01.04	Critical Group - Pets	3.3.03.01.0A	Contaminated Non-Food Products and Exposure
3.3.03.01.05	Smoking	3.3.03.01.0A	Contaminated Non-Food Products and Exposure
3.3.04.01.00	Ingestion	3.3.04.01.0A	Ingestion
3.3.04.01.01	Ingestion	3.3.04.01.0A	Ingestion
3.3.04.02.00	Inhalation	3.3.04.02.0A	Inhalation
3.3.04.02.01	Inhalation	3.3.04.02.0A	Inhalation
3.3.04.03.00	External Exposure	3.3.04.03.0A	External Exposure
3.3.04.03.01	Dermal Sorption (Except Tritium)	3.3.04.03.0A	External Exposure
3.3.04.03.02	Dermal Sorption (Tritium)	3.3.04.03.0A	External Exposure
3.3.04.03.03	Groundshine	3.3.04.03.0A	External Exposure
3.3.04.03.04	Exposure Pathways	3.3.04.03.0A	External Exposure
3.3.04.03.05	Irradiation	3.3.04.03.0A	External Exposure
3.3.04.03.06	Dermal Sorption	3.3.04.03.0A	External Exposure
3.3.04.03.07	Injection	3.3.04.03.0A	External Exposure
3.3.05.01.00	Radiation Doses	3.3.05.01.0A	Radiation Doses

Table G-2. Cross Reference of TSPA-SR FEPs to TSPA-LA FEPs (Continued)

SR FEP Number	SR FEP Name	LA FEP Number	LA FEP Name
3.3.05.01.01	Secular Equilibrium of Radionuclide Chains	3.3.05.01.0A	Radiation Doses
3.3.05.01.02	Radionuclide Uptake and Dosimetry FEPs	3.3.05.01.0A	Radiation Doses
3.3.05.01.03	Radionuclide Uptake and Dosimetry FEPs	3.3.05.01.0A	Radiation Doses
3.3.05.01.04	Radionuclide Uptake and Dosimetry FEPs (Exposure Factors)	3.3.05.01.0A	Radiation Doses
3.3.06.00.00	Radiological Toxicity /Effects	3.3.06.00.0A	Radiological Toxicity and Effects
3.3.06.00.01	Mutagenic Contaminants	3.3.06.00.0A	Radiological Toxicity and Effects
3.3.06.00.02	Biotoxicity	3.3.06.00.0A	Radiological Toxicity and Effects
3.3.06.00.03	Carcinogenic Contaminants	3.3.06.00.0A	Radiological Toxicity and Effects
3.3.06.00.04	Radiotoxic Contaminants	3.3.06.00.0A	Radiological Toxicity and Effects
3.3.06.00.05	Teratogenic Contaminants	3.3.06.00.0A	Radiological Toxicity and Effects
3.3.06.01.00	Toxicity of Mined Rock	1.4.02.01.0A	Deliberate Human Intrusion
		1.4.02.02.0A	Inadvertent Human Intrusion
		1.4.04.00.0A	Drilling Activities (Human Intrusion)
		1.4.04.01.0A	Effects of Drilling Intrusion
		1.4.05.00.0A	Mining and Other Underground Activities (Human Intrusion)
		3.3.06.01.0A	Repository Excavation
3.3.06.02.00	Sensitization to Radiation	3.3.06.02.0A	Sensitization to Radiation
3.3.07.00.00	Non-Radiological Toxicity/Effects	3.3.07.00.0A	Non-Radiological Toxicity and Effects
3.3.07.00.01	Chemical Toxicity of Wastes	3.3.07.00.0A	Non-Radiological Toxicity and Effects
3.3.07.00.02	Chemical Toxicity	3.3.07.00.0A	Non-Radiological Toxicity and Effects
3.3.07.00.03	Non-Radiological Toxicity FEPs	3.3.07.00.0A	Non-Radiological Toxicity and Effects
3.3.08.00.00	Radon and Radon Daughter Exposure	3.3.08.00.0A	Radon and Radon Decay Product Exposure
3.3.08.00.01	Radon Emission	3.3.08.00.0A	Radon and Radon Decay Product Exposure
3.3.08.00.02	Radon Pathways and Doses	3.3.08.00.0A	Radon and Radon Decay Product Exposure

Source: Technical Product Output DTN: MO0706SPAFEPLA.001, Tables FEPS, FEPS_REV00_ICN02, FEPMappingSRtoLA.

Table G-3. Indirect Inputs for Appendix G

Citation	Title	DIRS
BSC 2005	*Development of the Total System Performance Assessment-License Application Features, Events, and Processes*	173800
Freeze et al. 2001	*The Development of Information Catalogued in REV00 of the YMP FEP Database*	154365
SAM 1997	*Safety Assessment of Radioactive Waste Repositories, An International Database of Features, Events and Processes*	139333

APPENDIX H

DESCRIPTION OF FEPS DATABASE

DESCRIPTION OF FEPS DATABASE

The 19 tables that comprise the FEPs database and the fields contained therein are described below.

Columns: This table contains the name of the columns for the FEPs matrix form.

- Counter: Primary key to keep the columns in the desired order.
- Column Number: Column number as specified in the Matrix_Column field of the FEPS Table or MatrixSecondaries Table. They are not necessarily ordered or sequential.
- Column: Name of the column to be displayed on the FEPs matrix.
- ColumnAbbr: Abbreviation of the column name for the printed report.

DeletedFEPInfo: This table contains a list of those TSPA-SR FEPs that were deleted for TSPA-LA. No scope was actually eliminated unless there was a specific design change that caused the elimination of the FEP; however, combining and splitting of FEPs caused some FEPs to be deleted.

- YMP FEP Database Number: The number of the deleted FEP.
- Notes: Information about why the FEP was deleted.

DIRS_Descriptions: This table contains the DIRS descriptions that are used to produce the lists of direct and indirect inputs in the analysis report and the detail report. These descriptions include author, year of publication, and title.

- DIRS_No: The 6 character DIRS number.
- Description: A Memo field that contains the DIRS descriptions for the reference.
- Code: This is a single digit code (1, 2, 3, or 4) that assigns the reference to one of the four areas of the list of inputs and references (documents = 1; codes and standards = 2; input data = 3; and software = 4).
- Title: This field contains the DIRS description shortened to citation style (e.g., author, year, title).

FEP History File: This table contains the changes made to the FEPs database from the preliminary TSPA-LA FEP list (DTN: MO0301SEPFEPS1.000 [DIRS 161496]) through the final qualified TSPA-LA FEP data set (Technical Output DTN: MO0706SPAFEPLA.001). Whenever a change is made to any field in the FEPS Table, the pre-change information in all of the fields of the FEPS table (even unchanged fields) is automatically copied verbatim to the corresponding fields of the FEP History File (listed below). Descriptive information about each change must be entered manually in the Notes field (the update routine will not allow the changes to be saved until something is entered in the Notes field). The FEP History File can,

therefore, be used to examine all changes made to the FEP information in the FEPS table. For example, if the Notes field indicates, "Description edited," then the existing YMP Description in the FEP table can be compared to the previous YMP Description in the FEP History File to see the differences.

- YMP FEP Database Number: The FEP number.
- FEP Name: The FEP name prior to the modification.
- Source Identifier: The source identifier of the FEP prior to the modification.
- YMP Description: The FEP description prior to the modification.
- Screening Decision: The screening decision of the FEP prior to the modification.
- Screening Justification: (Previously called Screening Argument.) The screening justification of the FEP prior to the modification. Screening justifications are only used for excluded FEPs; if the FEP was excluded prior to the modification, there would be an entry in this field regardless of the screening decision after the modification.
- TSPA Disposition: The TSPA disposition of the FEP prior to the modification. TSPA dispositions are only used for included FEPs; if the FEP was included prior to the modification, there would be an entry in this field regardless of the screening decision after the modification.
- Supplemental Discussion: The supplemental discussion related to the FEP prior to the modification.
- AMR: The input FEP AMR prior to the modification. With the publication of this analysis report, there are no more input FEP AMRs. However, the categorization is still useful for viewing and reviewing FEPs, therefore, the field was retained.
- Barrier: This is the barrier to which the FEP is assigned based upon its primary row in the FEP Matrix prior to modification.
- Modified By: The last person to modify the FEP prior to this modification.
- Mod Date: The date the FEP was last modified prior to this modification.
- Mod Time: The time the FEP was last modified prior to this modification.
- Notes: Descriptive information about this modification. This information is also prepended to the Notes (Historical Notes) field of the FEPs table.
- Matrix_Row: The matrix row of the FEP prior to the modification.
- Matrix_Column: The matrix column of the FEP prior to the modification.

- EntryDate: The date this modification was accomplished.

- Keyword History: The former descriptor phrases associated with the FEP. Descriptor phrases were developed during interim screening to capture finer conceptual or modeling details, generally associated with the source FEPs that were not explicitly identified in the FEP name or description. Descriptor phrases were eliminated in May of 2004 but the field was maintained because of the descriptor phrases in the FEP table prior to that date. Descriptor phrases were a predecessor to the TSPA-LA keywords.

FEPMappingNEAtoLA: This table contains the source FEP (NEA and YMP-specific) identifiers and the corresponding TSPA-LA FEP numbers that address the source FEPs. Source FEPs are listed in the SourceFEPs table and source FEP identifiers are listed in Table F-1.

- Unique No: Source FEP number/identifier.

- LA FEP Number: TSPA-LA FEP number.

FEPMappingSRtoLA: This table contains the TSPA-SR FEP numbers and the related TSPA-LA FEP numbers.

- SR FEP Number: TSPA-SR FEP number.

- LA FEP Number: TSPA-LA FEP number.

FEPS: This is the main TSPA-LA FEP table and contains most of the data describing a specific FEP.

- YMP FEP Database Number: Primary key used for identifying the FEP within the database. The number was derived from the TSPA-SR FEP number. In general, the last numeric character of the TSPA-SR number was replaced with an alpha character for the TSPA-LA.

- FEP Name: Short, descriptive title for the FEP.

- Source Identifier: This field once contained the link to the source FEP number/identifier. However, this field is not used for TSPA-LA and is maintained merely to preserve the historical traceability of the FEP.

- YMP Description: Description of each FEP and its potential relevance to YMP.

- Screening Decision: A statement of whether the FEP is included in the quantitative TSPA-LA models or excluded from TSPA-LA on specific criteria (viz. Low Probability, Low Consequence, and/or By Regulation).

- Screening Justification: (Formerly labeled Screening Argument) A summary discussion of the technical basis for exclusion, with citations to appropriate TSPA-LA AMRs and other documents (for excluded FEPs, this is the key text).

- TSPA Disposition: A summary discussion of the implementation of the FEP in TSPA-LA, with citations to appropriate supporting technical AMRs (for included FEPs, this is the key text).

- AMR: Identifies the input FEP AMR. With the publication of this analysis report, there are no more input FEP AMRs. This field was retained because it provides a convenient way to categorize FEPs for viewing and reviewing.

- Barrier: This is the barrier to which the FEP is assigned based upon its primary row in the FEP Matrix.

- Modified By: Name of the last person to modify the FEP record and the computer on which the modification was made.

- Mod Date: Date the FEP record was last modified.

- Mod Time: Time the FEP record was last modified.

- Historical Notes: The entire history of miscellaneous notes and comments related to a FEP. All changes made subsequent to the preliminary TSPA-LA FEP list (DTN: MO0301SEPFEPS1.000 [DIRS 161496]) are automatically captured in the FEP History File Table and the associated Notes are prepended to this field separated from previous notes by a line of asterisks. Prior to the development of data set DTN: MO0501SEPFEPLA.001 [DIRS 172601], the name of this field was "Notes".

- Matrix_Row: Row number of the FEP's home row on the matrix (see Rows Table for row names corresponding to row numbers).

- Matrix_Column: Column number of the FEP's home row on the matrix (see Columns Table for column names corresponding to column numbers).

- Included: A placeholder for the included/excluded status of the FEP. It is completed each time the FEPs database program is initiated. If the Screening Decision is "Included", the word "Included" is written in this field. If the screening decision contains the word "Excluded" regardless of the reason, the word "Excluded" is written in this field. A FEP cannot be both included and excluded. This column with the single word in it makes the coding to do the transform query for building the matrices easier.

- Notes: This field was added during the development of data set DTN: MO0501SEPFEPLA.001 [DIRS 172601], and is different from the "Historical Notes" field. It provides additional information, as appropriate, regarding the traceability of FEPs and the suite of analyses reports.

FEPS_REV00_ICN02: This is the TSPA-SR FEPs table (BSC 2002 [DIRS 159684]) in its entirety. The table is retained for historical purposes. A mapping of these TSPA-SR FEPs to the appropriate TSPA-LA FEPs is provided in FEPMappingSRtoLA Table.

- YMP FEP Database Number: Numeric identifier that places the FEP in the proper location within the database structure. The numbering scheme follows a hierarchical structure classifying FEPs into layers (x…), categories (x.x…), headings (x.x.xx…), primary FEPs (x.x.xx.xx…), and secondary FEPs (x.x.xx.xx.xx).

- FEP Name: Short, descriptive title of the FEP.

- FEP Class: Identification of primary, secondary, and classification (layer, category, heading) entries. Primary FEPs are those FEPs for which the YMP has developed and documented screening discussions. Secondary FEPs are mapped to primary FEPs either because they are redundant with the associated primary FEP or because they represent a subcase of the primary FEP that is more effectively addressed at a higher level. Secondary FEPs are retained in the database for completeness, but users of the database are referred to the related Primary FEPs for the screening discussions.

- NEA Category: Alphanumeric identifier used for the preliminary mapping of the FEPs relative to the NEA database headings. This field is based on preliminary mapping and has been superseded by the YMP FEP Database Number field. It is retained only for traceability to earlier versions of the database. Note that for new FEPs that were identified during and subsequent to the December 1998 to April 1999 workshops, the Source Identifier is repeated in this field.

- Related Primary FEP(s): Identification of entries containing related information. For primary FEPs, other related primary FEPs (if any) are listed. For secondary FEPs and classification entries, this field is blank. Related secondary and classification FEPs can instead be determined through the hierarchical numbering scheme.

- Source Identifier: Alphanumeric identifier that provides traceability to the originator (e.g., NEA contributing program, YMP-specific workshop, AMR, etc.). Source identifier information is in Table F-1. Note that the Source Identifier is not related to the NEA Category or YMP FEP Database Number.

- YMP Primary Description: Description of each primary FEP and its potential relevance to YMP, typically edited from the Originator FEP Description. Where secondary FEPs are associated with a primary FEP, the description also includes all of the features, events and processes described by the secondary FEPs. For shared FEPs, descriptions from each input FEP AMR are listed but are not integrated.

- Originator Description: Verbatim text of the FEP description from originator documentation. The originator is noted in parentheses where possible.

- Screening Decision: A statement of whether the FEP was included in the quantitative TSPA-SR models or excluded from the TSPA-SR on specific criteria provided by the regulations.

- Screening Argument: A summary discussion of the technical basis for the TSPA-SR Screening Decision, with citations to appropriate AMRs (for excluded FEPs, this is the key text).

- TSPA Disposition: A summary discussion of the treatment of the FEP in the TSPA-SR, with citations and cross-references to the appropriate AMRs (for included FEPs, this is the key text).

- Supplemental Discussion: Provides additional information supporting the TSPA-SR Screening Decision beyond what is summarized in the Screening Argument and TSPA Disposition fields.

- AMR: Identifies the TSPA-SR FEP AMR where the screening discussion was documented. Verbatim text for several fields including the Screening Decision, Screening Argument, TSPA Disposition, Supplemental Discussion, and Treatment of Secondary FEPs was taken from the input FEP AMR. The input FEP AMR identifier also indicates the technical subject area in which the FEP was grouped. For shared FEPs, all of the input AMRs are listed.

- IRSR: Identifies NRC IRSR subissues related to the FEP.

- Modified By: Name of the last person to modify the FEP record.

- Mod_Date: Date of last modification to the FEP record.

- Mod_Time: Time of last modification to the FEP record.

- Notes: Miscellaneous notes and comments related to the FEP.

- F Keyword: Placeholder for an identifier feature keyword from a specified list that is used for keyword searches. This field was never implemented for TSPA-SR and is blank.

- E Keyword: Placeholder for an identifier event keyword from a specified list that is used for keyword searches. This field was never implemented for TSPA-SR and is blank.

- P Keyword: Placeholder for an identifier process keyword from a specified list that is used for keyword searches. This field was never implemented for TSPA-SR and is blank.

- Treatment of Secondary FEP(s): For primary FEPs, a list of the underlying secondary FEPs is provided with a short description of the relationship of each secondary FEP to the primary FEP and a summary of how the secondary FEP is addressed in the Screening Argument or TSPA Disposition.

FEPtoRef: This table relates references to individual FEPs. Unlike the Inputs Table it merely ties the DIRS number to the FEP number.

- FEP_No: FEP number.
- DIRS_No: DIRS number of the reference associated with this FEP.

Inputs: This table is a replica of the check copy DIRS database identified by FEP.

- FEP_No: FEP number for the input.
- DIRS_No: DIRS number of the reference. (This input is linked to the DIRS_Descriptions Table to obtain the rest of the citation.)
- Source: Where in the reference the information comes from.
- Input Description: How the information is used in the FEP.
- In_Dir: Indirect or Direct Input?
- Input_Category: Type of input.
- Q Status: Qualified or Not Qualified?
- TBV_TBD_Status: TBV/TBD status from the DIRS database.

KeywordsSource: This table contains a list of TSPA-LA keywords and the associated TSPA-LA FEP. Keywords capture the key aspects of the FEP name, FEP description, and relevant source FEPs. The set of keywords for a single FEP represents the basic scope of the FEP (as defined in the FEP name and FEP description) as well as any finer conceptual or modeling details identified only in relevant source FEPs. TSPA-LA keywords derived from descriptor phrases (see the "FEP History File" Table). They were created by parsing the individual descriptor phrases into individual keywords.

- Keyword: Keywords used for the keyword search function.
- FEP No: Associated TSPA-LA FEP.

MatrixSecondaries: This table contains the matrix rows and columns that a FEP is related to in addition to the home matrix rows and columns identified in the FEPS Table. It is appended to the FEP table to build the FEP matrix. There is no limit to the number of additional matrix boxes that a FEP can relate to.

- YMP FEP Database Number: The TSPA-LA FEP number.
- FEP Name: The name of the FEP.

- Matrix_Row: A secondary matrix row that the FEP "resides" in. (Note: a FEP can reside in multiple secondary matrix rows as appropriate.)

- Matrix_Column: A secondary matrix column that the FEP "resides" in. (Note: a FEP can reside in multiple secondary matrix columns as appropriate.)

- Included: This field is a placeholder that is updated each time the FEP Database is opened. It contains either the word "Included" or "Excluded". Its only purpose is to facilitate the query that fills the grid squares.

Potential FEP Log: This table contains information about the tracking and resolution of all potential FEPs identified between the preliminary TSPA-LA FEP list (DTN: MO0301SEPFEPS1.000 [DIRS 161496]) and the final TSPA-LA FEP data set.

- Log #: A key to track the order of FEP configuration management entries.

- Date Submitted: The date the potential FEP was entered into FEP configuration management.

- Submitted By: The name of the person (or organization) who entered the potential FEP into configuration management.

- Issue Title: A short title/description of the potential FEP.

- Source: The name of the person (or organization) that identified the potential FEP issue. Where appropriate, a source document or e-mail may be identified.

- Discussion of Issue: A discussion of the potential FEP and the reason it might be considered in TSPA-LA.

- Resolution: How the potential FEP was dispositioned (i.e., new FEP, change to existing FEP, or no change).

- Date of Resolution: The date the final disposition of the potential FEP was accomplished.

- Supplemental Information: Additional information to support the resolution of the issue.

Rev Data: This table stores the revision identifier of the data file (e.g., DTN) and of the AMR. The data file revision information is displayed throughout the FEPs database to allow users to ensure that they are using the version of the data that is desired. (Note: There is no software requirement to use the most up-to-date data.) The analysis report revision information is printed in the footer of the analysis report.

- RevNumber: The data file identifier of this revision of the data file. Normally the DTN is included in this field.

- RevDate: The date of the data file revision.

- AMR_Rev: The revision number of the analysis report.
- AMR_Date: The date of the AMR revision (month and year).

RIT_Status: This table contains the include/exclude status of each FEP as of August 2005. It is maintained to produce a status report showing changes to the data since that date.

- YMP FEP Database Number: The FEP number.
- Included: Status, included or excluded.

Rows: This table contains the name of the rows for the FEPs matrix form:

- Counter: Primary key to keep the rows in the desired order.
- Row Number: Row number as specified in the Matrix_Row field of the FEPS Table or MatrixSecondaries Table. They are not necessarily ordered or sequential.
- Row: Name of the row to be displayed on the FEPs matrix.
- RowAbbr: Abbreviation of the row name for the printed report.

Source FEP Categories: This table contains the identifiers for the specific categories of source (NEA and YMP-specific) FEPs. These specific categories are listed in Table F-1.

- SourceCode: Abbreviation used in the source identifier category.
- SourceCategory: The name of the source identifier category.

SourceFEPs: This table contains a list of source FEPs and their descriptions. Source FEPs are NEA and YMP-specific FEPs that provide the basis for the TSPA-LA FEP list. NEA source FEPs and descriptions are taken directly from Version 1.1 of the NEA International FEP database (OECD 2000 [DIRS 152952], Appendix D). Applicable (Section F1) source FEPs are explicitly mapped to one or more TSPA-LA FEPs (see Table "FEPMappingNEAtoLA" or Appendix F) that capture (sometimes explicitly and sometimes implicitly) the subject of the source FEP. In some cases, the source FEPs identify finer conceptual or modeling details that are not otherwise identified explicitly (although they are captured implicitly) in the FEP name and/or FEP description. A list of source FEP categories can be found in Table F-1.

- FEP name: The name of the source FEP.
- FEP description: The description of the source FEP, verbatim from the source.
- Unique No: The source FEP number/identifier assigned to the source FEP.
- Class Code: Numeric identifier for the source identifier category used to group source FEPs in database pull-down menus (corresponds to different source identifiers in Table F-1).

SRFEPTree: This table defines the hierarchical structure of the TSPA-SR FEPs. This table is used to build the TSPA-SR FEPs Tree.

- YMP FEP Database Number: The TSPA-SR FEP number.
- FEP Name: The name of the TSPA-SR FEP.
- ParentFEP: The FEP one level above this FEP.
- Description: The FEP description.

Table H-1. Indirect Inputs for Appendix H

Citation	Title	DIRS
DTN: MO0301SEPFEPS1.000	LA FEP List	161496
DTN: MO0501SEPFEPLA.001	LA FEP List and Screening	172601
FEPS Database Software Program V.2	STN: 10418-.2-00	159684
OECD 2000	*Features, Events, and Processes (FEPs) for Geologic Disposal of Radioactive Waste: An International Database*	152952

APPENDIX I

ANALYSIS OF SENSITIVITY OF TRANSPORT TO CHANGES IN FRACTURE APERTURE

This appendix is referenced in FEPs 1.2.10.01.0A (Hydrologic Response to Seismic Activity); 2.2.01.05.0A (Radionuclide Transport in the Excavation Disturbed Zone); 2.2.06.02.0A (Seismic Activity Changes Porosity and Permeability of Faults); 2.2.06.02.0B (Seismic Activity Changes Porosity and Permeability of Fractures); 2.2.10.05.0A (Thermo-Mechanical Stresses Alter Characteristics of Rocks above and below the Repository); 2.2.10.14.0A (Mineralogic Dehydration Reactions); and 2.2.12.00.0A (Undetected Features in the UZ).

I1. INTRODUCTION

This appendix evaluates the potential for changes to the hydrogeologic system caused by fault displacement to affect radionuclide transport in the unsaturated zone at Yucca Mountain. The repository is bounded on the west by the Solitario Canyon fault and on the east by the Bow Ridge Fault. The northern boundary of this structural block is bounded by the Drill Hole Wash Fault. Intrablock faults include the Ghost Dance, Sundance, and Dune Wash Faults (BSC 2004 [DIRS 169855], Figure C3-1). For the purposes of this analysis, the focus is on two possible effects of fault displacement along the bounding faults: (1) uniform change in fracture properties throughout the UZ flow model domain and (2) change in fracture properties within the faults only. These two hypothetical end-member cases model the bounding cases of mechanical strain being either uniformly distributed throughout the strata bounded by the faults or localized to the individual fault zones. In the physical system, the strain would be spatially distributed in some manner that lies between these end-member cases. This evaluation used the bounding case estimates to determine whether FEPs 2.2.06.02.0A (Seismic Activity Changes Porosity and Permeability of Faults) and 2.2.06.02.0B (Seismic Activity Changes Porosity and Permeability of Fractures) can be excluded.

These two end-member cases were evaluated by simulating the flow and transport in the unsaturated zone for a pulse input tracer at the repository location. For a specific cross-section, computer simulations were performed assuming (1) a change in fracture properties throughout the UZ models (which assumes all fracture apertures are uniformly altered), and (2) a change in fracture properties in the fault zones only. Simulations were performed for the present-day climate and a wetter, glacial-transition climate case. These climates were chosen to span a representative range of climates for future conditions at Yucca Mountain (Section I2.1.4). Tracer breakthrough curves computed at the water table were used to examine the potential impact induced on transport in the unsaturated zone.

The approach for the analysis of fault displacement effects on transport in the unsaturated zone is divided into two distinct components: (1) a review of site description information which provides a basis for defining bounding conditions and for understanding the physical significance of the results (Section I2); and (2) a modeling component to provide quantitative analysis of the sensitivity of the unsaturated zone flow system to changes in hydrologic parameters (Section I3).

I2. SENSITIVITY ANALYSES

I2.1 SITE DESCRIPTION INFORMATION

The spatial and temporal patterns of faulting and fracturing of the volcanic bedrock are the fundamental elements of the structural geology of the repository for high-level radioactive

wastes at Yucca Mountain. To document and discuss these patterns, a comprehensive program of geologic mapping and fractured rock mass studies has been conducted as an integral part of the site characterization. Of particular importance to this analysis are geologic observations related to displacement in fault zones and observations of the characteristics of the fault zones made during the excavation of the ESF and in the ECRB Cross Drift. The observations are briefly described in Section I2.1.1. These observations provide a basis for determining the reasonableness and appropriateness of the range of inputs used in the modeling analysis in Section I3 and for interpreting the level of conservatism represented by the models.

However, the primary controlling factor for amount of flux through the unsaturated zone is the amount of precipitation available to infiltrate and percolate through the unsaturated zone. This variable is highly dependent on climate conditions. To address this variable, present-day average and glacial-transition climate conditions (BSC 2004 [DIRS 170002], Table 6-1) were used as a representative range of climate conditions. The differences in these climate states are briefly explained in Section I2.1.4.

I2.1.1 Geologic Setting

The Yucca Mountain area is cut by steeply dipping, north-south-striking normal faults which separate the Tertiary volcanics into blocks one to four kilometers wide (Scott 1990 [DIRS 106751]). The repository lies in the central block of the central Yucca Mountain structural domain. The central block is bounded on the west by the Solitario Canyon Fault, on the east by the Bow Ridge Fault, and on the north by the northwest-striking Drill Hole Wash Fault. The Bow Ridge and Solitario Canyon Faults dip steeply toward the west, and displacement, amount of brecciation, and number of associated splays varies considerably along their trace (Scott and Bonk 1984 [DIRS 104181]; Day et al. 1998 [DIRS 101557]). The southern boundary is marked by a transition to structural styles that accompany greater magnitudes of extension and continue south. Intrablock faults include the Ghost Dance, Sundance, and Dune Wash Faults.

Surface geologic mapping (Scott and Bonk 1984 [DIRS 104181]; Day et al. 1998 [DIRS 101557]), underground mapping of the ESF, geophysical surveys, and borehole studies show that the Yucca Crest subblock is little deformed, and cut only by widely spaced intrablock faults (Ghost Dance and Dune Wash). Within structural blocks, small amounts of strain are accommodated along intrablock faults. In many cases, intrablock faults appear to represent local structural adjustments in response to displacements on the block-bounding faults. Many of the intrablock faults within this part of Yucca Mountain are short, discontinuous, have minor cumulative displacement (1 to 10 m), and represent the localization of slip along pervasive preexisting weaknesses in the rock mass (Potter et al. 1996 [DIRS 106582]; 1996 [DIRS 106583]). In some cases, intrablock faults are expressions of hanging wall or footwall deformation that affect the block within a few hundred meters of the block-bounding faults. The eastern and southern edges of the central block, however, are cut by numerous faults associated with block margin deformation (Solitario Canyon and Bow Ridge Faults).

I2.1.2 Significance of Geologic Setting to the Analysis

The description in Section I2.1.1 suggests that an analysis of fault displacement effects needs to be considered from two perspectives: the impact on fractures throughout the repository as a whole, and the effect on fractures in the immediate vicinity of the faults only. Furthermore, the range of fault characteristics that was described supports the idea that movement on the Solitario Canyon Fault may be considered the bounding scenario.

The fracture network at Yucca Mountain acts as a significant preexisting weakness in the rock mass that can accommodate extensional strain through distributed slip along many reactivated joints. Evidence for reactivation of joints includes the presence of thin breccia zones along cooling joints and observable slip lineations along joint surfaces (Sweetkind et al. 1996 [DIRS 106957]). There are a number of primary limitations to fracture characteristics within the Paintbrush Group that are related to stratigraphy, upon which any later tectonic signature (such as fault displacement) is superimposed. The existence of distributed slip suggests that changes in strain (such as would be associated with a significant fault displacement) are likely to be propagated throughout the repository area. Also, some fault zones (such as the Ghost Dance and Solitario Canyon) may be on the order of 100 to 400 m wide. Although strain is expected to diminish with distance from the fault, these observations suggest that the effect of strain distributed in the fractures throughout the repository should be considered (Section I3.3.2).

The presence of gouge and brecciated zones only in limited proximity to the fault planes, however, suggests that much of the strain will be mechanically dissipated within or near the fault plane itself. For instance, in the Solitario Canyon Fault zone in the ECRB Cross Drift, the total displacement is approximately 260 m, but the gouge and brecciated zones are limited to less than 20 m. Similarly, the Dune Wash Fault as exposed in the ESF exhibits a cumulative offset of 65 m (Sweetkind et al. 1997 [DIRS 177047], Table 21), but the zone of increased fracture frequency in the vicinity of the fault is only 6 to 7 m wide. A third example is the observation of the Sundance Fault in the ECRB Cross Drift, where the footwall rock is intact, even within the 10 cm of the fault plane. The hanging wall is slightly more fractured, with an intensely fractured zone about 1 m thick. Consequently, an analysis of fault displacement should also consider a case where the effects of strain are limited to the immediate vicinity of the fault zone (Section I3.3.1).

I2.1.3 Fault Displacement Hazards

Fault displacement hazards at Yucca Mountain have been investigated in detail in *Probabilistic Seismic Hazard Analyses for Fault Displacement and Vibratory Ground Motion at Yucca Mountain, Nevada* (CRWMS M&O 1998 [DIRS 103731]). Several original approaches to characterizing the fault displacement potential were developed by the seismic source expert teams. The approaches were based primarily on empirical observations of the pattern of faulting at the site during past earthquakes (determined from data collected during fault studies at Yucca Mountain). Empirical data were fit by statistical models to allow use by the experts. The results of this analysis were curves representing probabilistic predictions of fault displacements.

Nine locations within the preclosure controlled area were identified to demonstrate the fault displacement methodology. The term “preclosure controlled area” is defined in DOE Interim

Guidance (Dyer 1999 [DIRS 105655]). These locations were chosen to represent the range of potential faulting conditions. Two of the nine sites each had four identified faulting conditions. Some of these locations lie on faults that may experience both principal faulting and distributed faulting. The other points are sites only of potential distributed faulting.

With the exception of the block-bounding Bow Ridge and Solitario Canyon Faults (sites 1 and 2, respectively), the mean displacements are 0.1 cm or less at a 10^{-5} annual exceedance probability, and on the order of 1 m or less at 10^{-8} annual exceedance probability (CRWMS M&O 1998 [DIRS 103731], Figures 8-4 through 8-14). For the Ghost Dance Fault, the range of displacements per event is 0.6 m to about 1.5 m at 10^{-8} mean annual exceedance probability (CRWMS M&O 1998 [DIRS 103731], Figure 8-5). Thus, sites not located on a block-bounding fault, such as sites on the intrablock faults, other small faults, shear fractures, and intact rock, are estimated to have displacements significantly less than 0.1 cm for mean annual exceedance probabilities of 10^{-5}.

For Solitario Canyon Fault and Bow Ridge Fault (CRWMS M&O 1998 [DIRS 103731], Figures 8-2 and 8-3), the mean displacements are 7.8 and 32 cm, respectively, for these two faults at a 10^{-5} annual exceedance probability. At lower annual exceedance probabilities, the fault displacement hazard results are driven by the upper tails of uncertainty distributions and are close to 10 m.

For purposes of determining the appropriateness of the chosen bounding conditions based on the Probabilistic Seismic Hazard Assessment, per-event displacements can be used as a comparison. As described in Section I2.1.1, the largest estimate of per event displacement for the faults intersected by the two-dimensional cross section used for the analysis is 1.4 m along the Solitario Canyon Fault. A displacement of 1.2 m corresponds to the 15th percentile curve at a 10^{-8} annual exceedance probability (CRWMS M&O 1998 [DIRS 103731], Figure 8-3). As described in Section I3.2.6, strains associated with a displacement of 10 m are used as bounding conditions. Given that the assumed bounding condition is about a factor of 10 greater than measured displacement and the probabilistic displacement event suggested by the 15th percentile curve, the values used in this analysis are judged to be extremely conservative.

I2.1.4 Climate Data

The primary controlling factor for flow through the unsaturated zone is the amount of infiltration through the system. This variable is highly dependent on precipitation and climate conditions. To address this constraint, present-day average and long-term average conditions were used as a representative range of future climate conditions.

Present-day climate conditions represent relatively dry, interglacial conditions, while the glacial-transition conditions represent typical conditions at Yucca Mountain between the wet and dry extremes based on available paleoclimate data (BSC 2004 [DIRS 170002], Table 6-1). Because these two sets of conditions represent relatively stable (that is, long-term conditions) rather than extreme conditions (that is, short-duration climatic states such as superpluvial periods), they were chosen as representative conditions for this analysis.

I3. EFFECTS OF FAULT DISPLACEMENTS ON UNSATURATED ZONE FLOW AND TRANSPORT

As discussed in Section I2, fault displacements are expected to occur along existing faults in the vicinity of Yucca Mountain. The movement produced by a fault displacement will result in changes in the rock stress in the vicinity of the fault. The change in rock stress will decrease with distance from any given fault that does move. However, the magnitude of the changes in rock stress as a function of distance from the fault depends on the specific details of the fault displacement (e.g., magnitude of fault motion, direction of fault movement, extent of the fault that participates in the movement) and the mechanical properties of the surrounding rock (e.g., fracture spacing, fracture stiffness, geomechanical properties of the rock matrix). Given some change in rock stress, the fractured rock mass will respond to the change in stress through deformation, or strain, in the rock. Of particular importance is the fact that this induced strain can affect the geometry of fractures in the rock. The effects of changes in properties of the rock matrix (as opposed to the fractures) are assumed to have a negligible effect on unsaturated zone flow and transport. Several fracture properties (permeability, capillary pressure, porosity) are a function of fracture aperture, which can be changed significantly by small strains if these strains are allocated entirely to the fracture apertures. The sensitivity of fracture aperture to mechanical strain is due to the small porosity of the fracture continuum. The matrix, on the other hand, has much greater porosity than the fractures in general, and its properties are not expected to be as sensitive to mechanical strain. This approximation is reasonable given the fact that fracture porosity is much less than matrix porosity at Yucca Mountain.

Some of the effects of previous fault displacements at Yucca Mountain can be examined directly. Previous fault displacements have resulted in observable changes to the structure of the surrounding rock (Section I2.1.1). However, geologic observations are not adequate to assess the effects of some of the changes caused by fault displacements that could be important to unsaturated zone flow and transport. In fact, it is difficult to determine the effective hydraulic apertures of the present-day fractures at Yucca Mountain by direct observation (Sonnenthal et al. 1997 [DIRS 101296], Section 7.5.4). Fracture apertures at Yucca Mountain are determined through pneumatic flow tests (giving the fracture permeability) and a theoretical model relating fracture frequency (determined by observation of fractures), fracture permeability, and fracture aperture (Sonnenthal et al. 1997 [DIRS 101296], Section 7.5.4).

I3.1 ANALYSIS APPROACH

A bounding approach is used to assess the potential effects of fault displacement on repository performance. The problem is bounded if large enough changes in fracture aperture are evaluated. Here, "large enough changes" are defined to be changes that can be justified as larger than any expected changes resulting from any fault displacements (near Yucca Mountain) that have an annual exceedance probability greater than 10^{-8} (SNL 2008 [DIRS 179476], Section 6.2, *Low Probability Criteria*). Given an assumed change in aperture, it is possible to estimate the change in fracture hydraulic properties using theoretical models that relate the changes in fracture properties to the changes in fracture aperture (Section I3.2.3). Effects of the modified fracture properties on transport behavior between the repository and the water table can be evaluated using the UZ site-scale flow and transport models. Changes in transport are identified through the use of breakthrough curves for a simulated nonsorbing tracer. Transport of a

nonsorbing tracer is used because this is expected to be more sensitive to changes in fracture aperture, because the effects of fracture aperture dominate fracture-matrix interaction for such a tracer (given fixed matrix properties).

In theory, the effects of a given fault displacement could be evaluated using process-level calculations for the effects of the induced stress and strain on fracture geometry. Then the effects of this change in fracture geometry on the fluid-flow properties of the fracture network could be evaluated. However, this method was not used in this analysis due to the large uncertainty in rock mechanical properties and models relating fault displacement induced changes in stress to changes in fracture apertures on the scale of unsaturated zone model domain.

If the identified changes in transport are small, then it can be concluded that the effects of fault displacement on potential radionuclide transport are negligible and can be excluded from further consideration in TSPA.

The spatial distribution of changes to fracture aperture within the modeling domain is treated using two end-member scenarios:

1. All fracture apertures are altered uniformly throughout the unsaturated zone model domain (fault zones and fractured rock).

2. Only fracture apertures in the fault zones are altered.

Isolating the effects of fault displacement to the fault zones provides the most reasonable expected case, which emphasizes the effects of property contrasts between the fault zones and the fractured rock. A large change in fracture properties over the entire unsaturated zone domain (fault zones and fractured rock) is an extreme bound for the possible effects of fault displacement. These cases bound the expected extremes for the spatial distribution of changes to fracture properties as a result of fault displacement.

Sensitivity calculations are performed for both the present-day (dry) climate and the long-term, glacial-transition (wetter) climate. The average infiltration rates used in the TSPA-SR UZ flow model for the present-day mean climate is about 4.6 mm/yr and for the glacial-transition mean climate is about 18 mm/yr (BSC 2004 [DIRS 169861], Table 6.1-2). The water table elevation remains unchanged in this analysis as a result of fault displacement or climate change. Maintaining a fixed water table provides a reference point for comparisons of the effects of fault displacements on radionuclide transport. This is reasonable as a basis for comparison of the effects of fault displacement.

Fault displacements may result in changes to perched water. However, the effects of these changes in perched water on potential radionuclide transport are assumed to be negligible. The sensitivity of radionuclide transport to different perched water models has been shown to be small (CRWMS M&O 2001 [DIRS 158726], Section 6.7.3). Furthermore, the potential release of the perched water (and associated radionuclides) due to some disruptive event is expected to have a negligible effect on radionuclide releases at the water table (FEP 2.2.06.03.0A (Seismic Activity Alters Perched Water Zones)). Therefore, any additional changes in perched water, except for those changes caused by changes in fracture properties, are not expected to have significant consequences.

Thermal-hydrologic processes due to waste heat from the repository will affect unsaturated zone flow and transport. However, the effects of thermal-hydrologic processes are expected to be negligible with respect to this sensitivity study on the effects of fault displacements on mountain-scale unsaturated zone transport (FEP 2.2.12.00.0A (Undetected Features in the UZ)).

I3.2 USE OF SITE RECOMMENDATION MODEL

In this work, steady-state flow fields with fracture apertures undisturbed or changed (to represent the effects of seismic activity) were first calculated, and then used to run transport simulations. A steady-state flow field had previously been calculated for the site recommendation model (BSC 2004 [DIRS 169861], Section 6.2.3), and this result provided a flow field that could be used as an initial condition to determine the steady state flow fields for these calculations. For this reason these calculations were done using the site recommendation model. The site recommendation and license application models are similar enough that use of the site recommendation model instead of the license application model is appropriate for the purpose of determining the sensitivity of transport to fracture aperture, as will be shown below. The site recommendation and license application flow and transport models are based on the same dual-permeability/active fracture conceptual model and numerical implementation. A significant difference between the models is the shift in repository footprint to the north for the license application case compared with the site recommendation design and some limited changes in parameterization based on new calibrations for the license application case.

Transport results for present-day and glacial-transition climate scenarios are compared in Figures I-1 and I-2. The transport results are for a uniform, instantaneous release of tracer mass from all repository locations at time zero. The tracer is nonsorbing, but can diffuse into the matrix. The present-day scenarios are shown in Figures I-1a and I-1b, which present the fractional cumulative breakthrough curves and average curves, respectively. The average curves are the weighted averages of the site recommendation and license application scenarios. For site recommendation, the weighting factors are 0.24, 0.41, and 0.35 for lower, mean, and upper cases, respectively (BSC 2003 [DIRS 165991], Table 7-1). Note that the "mean" case is not a statistical mean, but is an intermediate case between the upper and lower cases. For license application, the weighting factors are 0.62, 0.16, 0.16, and 0.06 for the 10th percentile map, 30th percentile map, 50th percentile map, and 90th percentile map cases, respectively (SNL 2007 [DIRS 184614], Table 6.8-1). For a unit tracer released at the repository at time zero, the fractional breakthrough curve represents the tracer cumulative arrival at the water table as a function of time. The glacial-transition scenarios are shown in Figures I-2a and I-2b, which present the fractional cumulative breakthrough curves and average curves, respectively. The weighting factors are the same as used for the present-day, both for site recommendation and license application. These curves show that differences between site recommendation and LA are small in comparison with the uncertainty for each climate. The goal of the present analysis is to compare the relative effects of changes in fracture aperture on unsaturated zone transport behavior. Because the conceptual and numerical models for the site recommendation and license application models are nearly the same, and the responses for unsaturated zone transport are similar, the site recommendation model is suitable for its intended use of assessing transport sensitivity to seismic-induced changes in fracture properties.

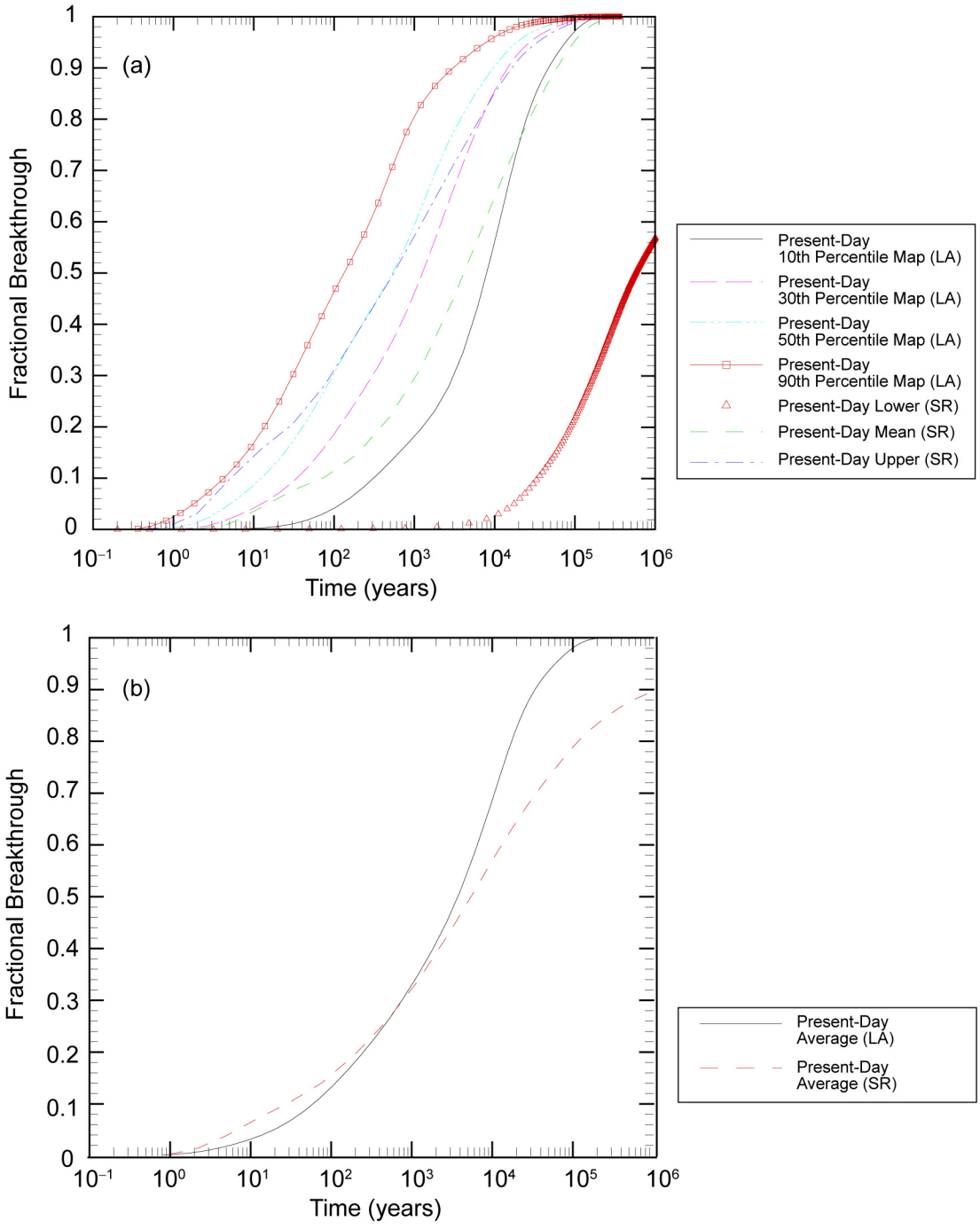

Source: DTN: LB0705TRAVTIME.001 [DIRS 181300], file: *tc_bt_cumu_mass_flux.xls* (license application transport breakthrough curves); DTN: LB9908T1233129.001 [DIRS 147115], files: *pchl1_tr1.out*, *pchm1_tr1.out*, and *pchu1_tr1.out* (site recommendation transport breakthrough curves).

Figure I-1. Comparison of Site Recommendation and License Application Transport Results for an Instantaneous Release of (Nonsorbing) Tracer Mass at the Repository Horizon at Time Zero under Present-Day Climate: (a) Individual Fractional Breakthrough Curves, (b) Average Fractional Breakthrough Curves

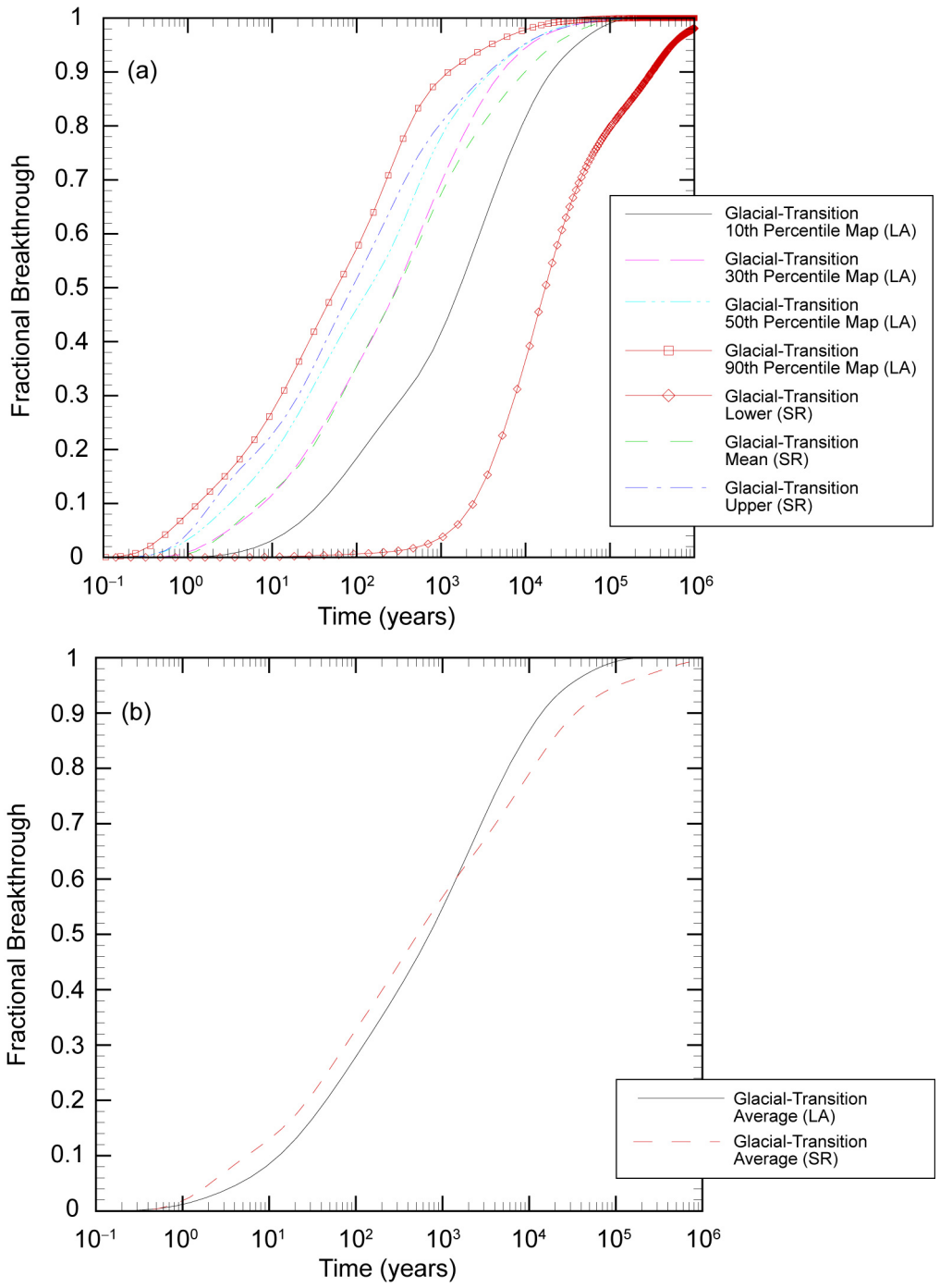

Source: DTN: LB0705TRAVTIME.001 [DIRS 181300], file: *tc_bt_cumu_mass_flux.xls* (license application transport breakthrough curves); DTN: LB9908T1233129.001 [DIRS 147115], files: *glal1_tr1.out*, *glam1_tr1.out*, and g*lau1_tr1.out* (site recommendation transport breakthrough curves).

Figure I-2. Comparison of Site Recommendation and License Application Transport Results for an Instantaneous Release of (Nonsorbing) Tracer Mass at the Repository Horizon at Time Zero under Glacial-Transition Climate: (a) Individual Fractional Breakthrough Curves, (b) Average Fractional Breakthrough Curves

I3.2.1 Problem Domain and Site-Scale Flow and Transport Models

The three-dimensional, site-scale UZ flow and transport model domains are shown in plan view in Figures I-3a and I-3b for the site recommendation and license application models, respectively (BSC 2001 [DIRS 158726], Figure 6-2; SNL 2007 [DIRS 184614], Figure 6.1-1). These figures indicate the differences in gridding and repository locations. Despite these differences, calculation results shown in Section I.3.3 indicate that transport behavior is similar for the two models. In both model grids, faults are represented by vertical or inclined 30-m-wide zones. Although major faults, such as Solitario Canyon Fault, can be wider than 30 m, transport behavior is not sensitive to the width of the fault because of the larger capacity of the faults for conducting water flow.

The site-scale UZ flow model computes unsaturated flow over the model domain. In this model, fractured rock is represented using an active-fracture dual-permeability conceptual model. Transport simulations in this appendix use conservative tracers. The dual-permeability modeling approach using the same three-dimensional TSPA-SR grid is used in the transport simulations. The fracture-continuum permeability and van Genuchten α values for these simulations were obtained from DTNs: LB990801233129.009 [DIRS 118717] and LB990801233129.003 [DIRS 122757]; the grid was obtained from DTN: LB990701233129.001 [DIRS 106785]. The use of these site recommendation rock properties and grid is justified for their intended use in Section I3.1. A discussion of the software used and more details concerning the flow and transport calculations are presented in DTN: LB0408U0170FEP.002 [DIRS 171596].

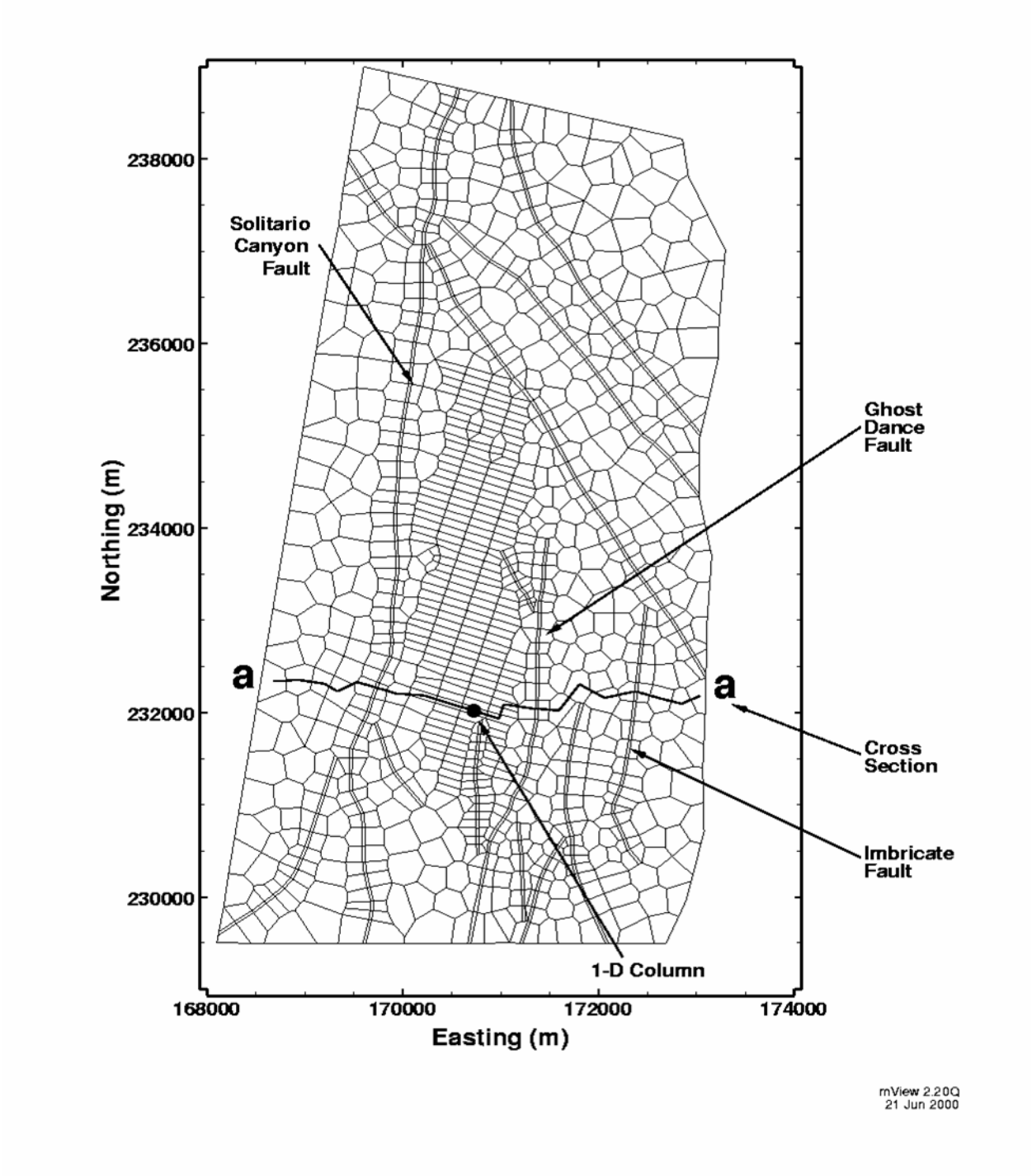

Source: BSC 2001 [DIRS 158726], Figure 6-2.

NOTE: Repository location is the relatively uniformly gridded section in the central part of the domain.

Figure I-3a. Plan View of the UZ Flow Model Domain for Site Recommendation Showing Nearby Faults and Boreholes

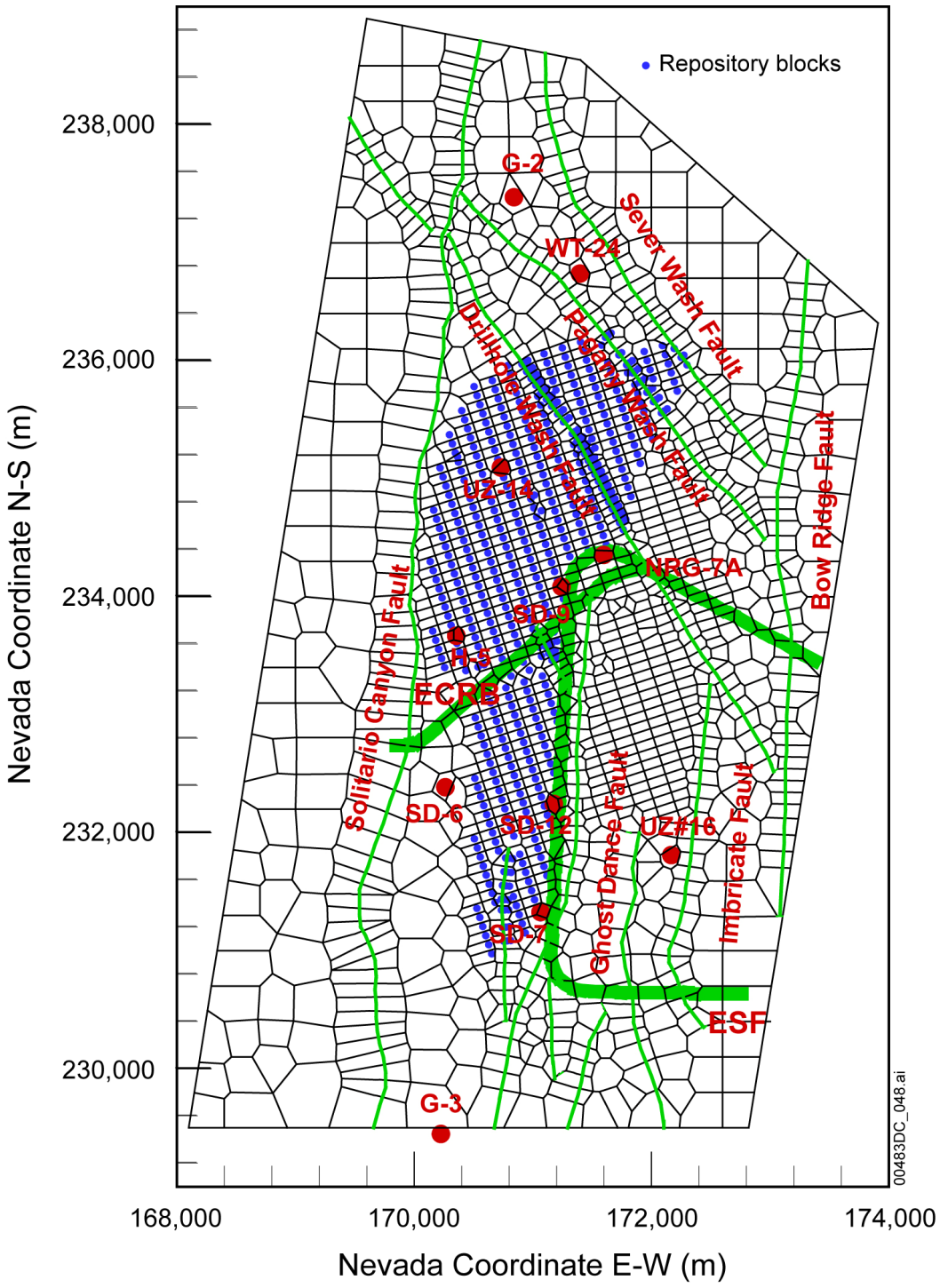

Source: SNL 2007 [DIRS 184614], Figure 6.1-1.

NOTE: Blue dots denote repository location.

Figure I-3b. Plan View of the UZ Flow Model Domain for License Application Showing Nearby Faults and Boreholes

I3.2.2 Bounds on the Change in Fracture Aperture

The approach used to investigate the effects of fault displacements is to evaluate the sensitivity of radionuclide transport in the unsaturated zone to changes in fracture apertures. This is investigated over a wide enough range to bound the potential changes in fracture aperture that could result from any fault displacement at Yucca Mountain with an annual exceedance probability of greater than 10^{-8}. The largest fault movement close to the repository is likely to be along Solitario Canyon Fault. The general topic of seismic hazard at Yucca Mountain has been investigated in detail in *Probabilistic Seismic Hazard Analyses for Fault Displacement and Vibratory Ground Motion at Yucca Mountain, Nevada* (CRWMS M&O 1998 [DIRS 103731]). For Solitario Canyon Fault, the hazard analysis shows fault displacement of about 10 m (CRWMS M&O 1998 [DIRS 103731], Figure 8-3) at an annual exceedance probability of 10^{-8}.

Geomechanical models used to investigate the amount of strain induced by fault movements in the rock at Yucca Mountain show that changes in strain extend several kilometers from a fault movement (Gauthier et al. 1995 [DIRS 103258]; National Research Council 1992 [DIRS 105162], Appendix D). Using a three-dimensional elastic boundary element model of Yucca Mountain, Gauthier et al. (1995 [DIRS 103258]) investigated the effects of a right-lateral, strike-slip fault displacement on a fault dipping 60° E. The fault movement was 1 m along a 30 km section of the fault. The results show strains of 10 microns per meter (10 micro-strain, or 10 μs) up to 8 km from the fault. Geomechanics calculations were also performed in the report by the National Research Council (1992 [DIRS 105162], Appendix D). This calculation was for a normal displacement along a fault dipping 60° E to the vertical. The simulated fault movement was 1 meter along 30 km section from the surface to a depth of 10 km. The results of this calculation show 50 μs two kilometers from the fault plane and 10 μs about 6 km from the fault plane. If these models were used for a 10-m fault movement instead of 1 m, the strains would be amplified proportionally because of the linearity of the elastic model. Therefore, for a bounding fault movement of 10 m along Solitario Canyon Fault, an elastic model would predict strains up to 500 μs two kilometers from the fault and 100 μs six kilometers from the fault. If the conservative approach is taken that all the strain accumulates in the fractures, then an estimate of the change in aperture can be made. First, assume a lower bound aperture of 100 μm in the present-day system (Sonnenthal et al. 1997 [DIRS 101296], Table 7.12) and a fracture spacing of approximately 1 m (Sonnenthal et al. 1997 [DIRS 101296], Table 7.7). Then a tensile strain of 500 μs would result in a new fracture aperture of about 600 μm. For a compressive strain of 500 μs, then the fractures would essentially be closed and the rock matrix would necessarily be compressed.

Changes in fracture properties are related to dilation or compression of existing fractures rather than the generation of new fractures. This approximation relies on the fact that the rock at Yucca Mountain is highly fractured and that fractured rock is mechanically weaker along existing fractures than intact rock. This assumption is supported by the results of the Probabilistic Seismic Hazard Analysis, which show that the probability for fault displacement to occur along existing fractures is more likely than for intact rock (CRWMS M&O 1998 [DIRS 103731], Section 8.2.1). Therefore, strain due to fault displacement is likely to occur along existing fractures rather than initiate new fractures.

I3.2.3 Affected Parameters

Given a change in aperture, theoretical models are available to quantitatively model the associated changes in fracture permeability, fracture capillary pressure, and fracture porosity. Fracture aperture enters flow and transport modeling in different ways. Aperture affects the permeability and capillary pressure used for steady-state unsaturated flow calculations. For radionuclide transport calculations, the fracture aperture affects the fracture porosity. Fracture aperture also affects matrix diffusion for radionuclide transport, but for these simulations the matrix diffusion coefficient was set to zero. The fracture apertures used in these different parameters are not necessarily the same because the theoretical models strictly apply to idealized "parallel plate" fractures. Therefore, the aperture for permeability, capillary pressure, and porosity are generally different values. However, it is assumed that an increase or decrease in aperture will affect these physical characteristics in proportion to the functional dependence on aperture in the theoretical models.

The relationship for permeability, known as the cubic law (Freeze and Cherry 1979 [DIRS 101173], Section 2.12; Sonnenthal et al. 1997 [DIRS 101296], Section 7.5.4), is the following:

$$k = \overline{f}\,\frac{b^3}{12} \qquad \text{(Eq. I-1)}$$

where $\overline{f}$ is the average fracture spatial frequency, k is the permeability, and b is the fracture aperture. As can be seen, the permeability is proportional to the cube of the fracture aperture.

The relationship between capillary pressure and saturation is derived from van Genuchten (1980 [DIRS 100610]), noting that $S_e = \Theta$ in van Genuchten's notation:

$$P_c = \frac{2\tau\cos\theta}{b\rho g}\left[S_e^{-1/m} - 1\right]^{(1-m)} \qquad \text{(Eq. I-2)}$$

where P_c is the capillary pressure (expressed as elevation above the water table by inclusion of ρ and g terms), τ is the surface tension of an air–water interface, θ is the contact angle between the air–water interface and the mineral surface, ρ is the density of water, g is the acceleration of gravity, S_e is the effective water saturation (normalized for the residual and maximum saturations), and m is a parameter describing the variation in capillary pressure with water saturation.

The collection of terms, $\frac{b\rho g}{2\tau\cos\theta}$, is known as the van Genuchten α parameter. The van Genuchten α parameter scales the overall capillary pressure in the system. The parameter m accounts for the distribution of fracture apertures that the air–water interface encounters as a function of water saturation. The van Genuchten α parameter is directly proportional to fracture aperture.

The relationship for porosity, ϕ_f, is the following:

$$\phi_f = \overline{f} b \quad \text{(Eq. I-3)}$$

The porosity is also found to be proportional to the fracture aperture.

Now, let b be changed to b^* ; then correspondingly k, α, and ϕ_f, are changed to k^*, α^*, and ϕ_f^*. These variables can be used to express the following relationships:

$$k^* = (b^* / b)^3 k \quad \text{(Eq. I-4)}$$

$$\alpha^* = (b^* / b)\alpha \quad \text{(Eq. I-5)}$$

$$\phi_f^* = (b^* / b)\phi_f \quad \text{(Eq. I-6)}$$

The factor of change in fracture aperture (b^*/b) is then used to directly assign the new values of permeability, capillary pressure (α), and porosity.

In addition, the volumes for fracture and matrix elements should also be varied to reflect changes in fracture porosity . Assume V_f and V_m as the original fracture and matrix element volumes, then the fracture and matrix element volumes varied due to fracture aperture change can be calculated as:

$$V_f^* = V_f(\phi_f^* / \phi_f) \quad \text{(Eq. I-7)}$$

$$V_m^* = V_m(1 - \phi_f^*)/(1 - \phi_f) \quad \text{(Eq. I-8)}$$

Such variation in fracture and matrix element volumes only changes the partition of the bulk grid-cell volume (into either V_f and V_m or V_f* and V_m*), which itself remains as a constant.

I3.2.4 Calculation Procedures

Steady-state flow fields for single-phase, unsaturated flow are obtained through transient flow simulations to steady-state conditions. Transport calculations are then performed using the steady-state flow fields.

The matrix and fracture parameter values both for the hydrogeologic units and the faults are taken from the TSPA-SR base-case UZ flow model (BSC 2004 [DIRS 169861]) and treated as the base case for this study. Sensitivity cases are conducted using fracture apertures modified as discussed in Section I3.2.3. Flow and transport modeling calculations are performed for present-day and glacial-transition climates. The unsaturated zone flow results from the base-case unsaturated zone flow calculation are processed to obtain the initial condition for calculations involving cases affected by fault displacement.

Based on the cubic law for fracture permeability (Section I3.2.3), a change of a factor of 10 in aperture leads to a change of a factor of 1,000 in permeability. Fracture permeabilities reduced

by a factor of 1,000 were found to be inconsistent with the infiltration rates imposed on the model, because the bulk permeability was insufficient to accommodate the flow conditions. So, either reduced infiltration rates or a smaller reduction factor for the aperture would need to be used. Because the reduced apertures lead to reduced transport rates, this sensitivity does not show a potential adverse impact on performance. A lower-bound reduction in aperture of a factor of 0.2 is considered sufficient. Therefore, a change in fracture aperture by a factor of 0.2 to 10 was used in this sensitivity analysis.

The input and output files for the calculations presented in Section I3.3 are documented under DTNs: LB0408U0170FEP.001 [DIRS 171595] and LB0408U0170FEP.002 [DIRS 171596].

Unsaturated zone flow properties affected by fracture aperture were varied for the sensitivity study reported in this analysis. For the unsaturated zone transport calculations, diffusivity was given a nominal value of 3.2×10^{-11} m^2/s, with a tortuosity of 0.7, for an effective diffusivity of 2.24×10^{-11} m^2/s, as discussed in *UZ Flow Models and Submodels* (BSC 2004 [DIRS 169861], Sections 6.5.2 and 6.7.1). Only nonsorbing transport is investigated here. Dispersion has been shown to have little effect on transport results in the unsaturated zone over a wide range of dispersivities investigated (BSC 2004 [DIRS 169861], Section 6.8.2.1). Therefore, a dispersivity of zero was assigned because ignoring the process of dispersion is not expected to influence the comparison of results.

I3.3 RESULTS

The next two sections describe the effects of fracture aperture changes on unsaturated zone flow and transport between the repository and the water table. Results for cases in which the fracture apertures are varied are compared with the corresponding base cases. Section I3.3.1 considers a three-dimensional model when fracture apertures are only changed in the fault zones. Section I3.3.2 describes the results for transport in a three-dimensional model with fracture apertures changed both in the fault zones and in the fractured rock (uniformly across the entire repository block). These three-dimensional calculations are performed for present-day and the glacial-transition climates. Mass transport calculations correspond to the instantaneous release of tracer mass at the repository at time zero.

I3.3.1 Fracture Apertures Altered in Fault Zones Only; Three-Dimensional Calculations for Present-Day and Glacial-Transition Climates

In this set of calculations, only the fracture apertures for the fault zones are changed by given factors. The flow and transport calculations results shown in this section were performed as described in Section I3.2.4.

As shown in Figures I-4 and I-5, respectively, for the present-day climate and the glacial-transition climate, the breakthroughs for the altered cases remain essentially unchanged from the base case. This indicates that if only the fault fracture apertures are affected by factors of 0.2 to 10, there would be virtually no impact to unsaturated zone flow and transport. The normalized mass arrival rate in these figures is the time-derivative of the breakthrough curve.

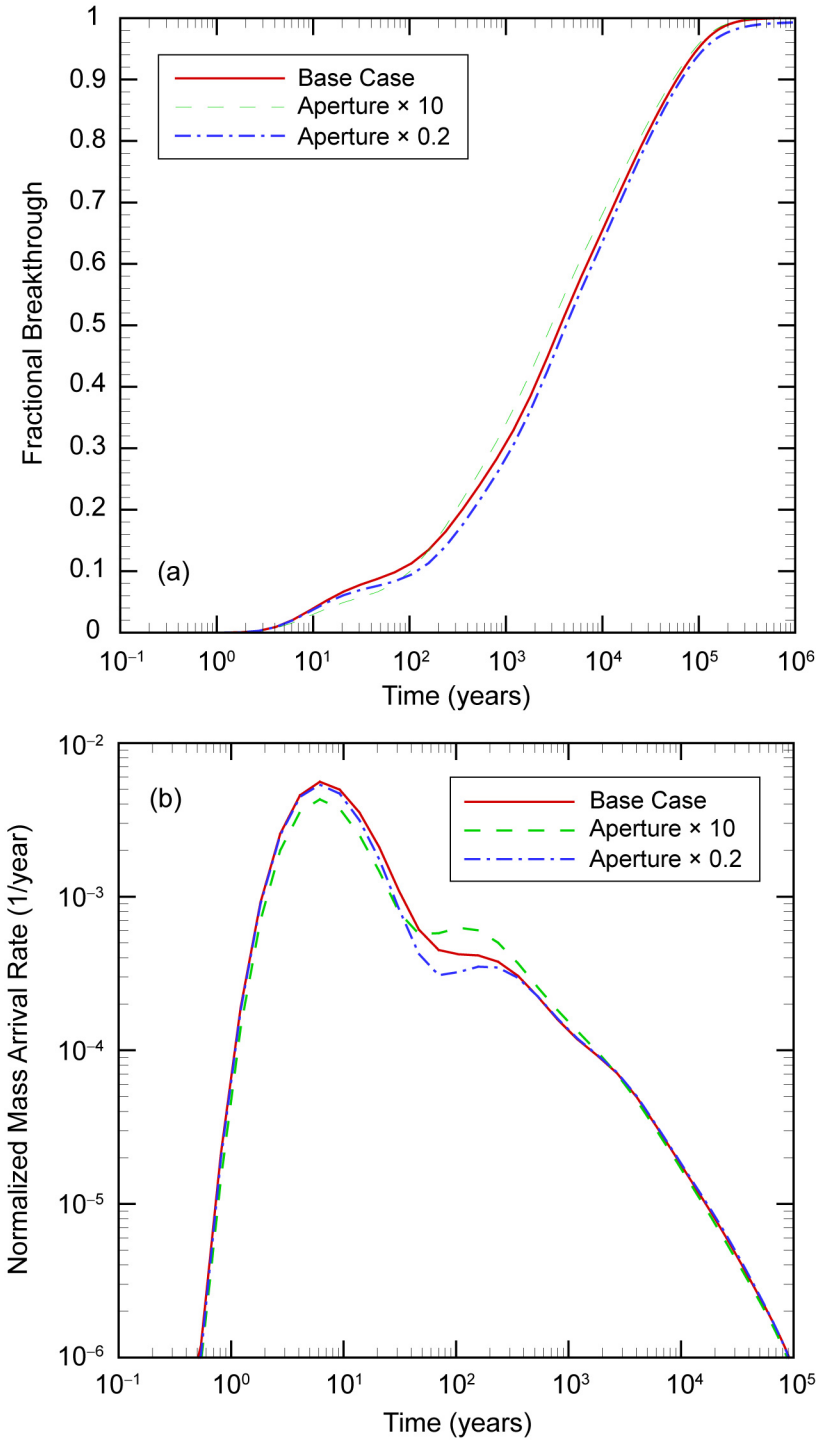

Source: DTN: LB0408U0170FEP.002 [DIRS 171596], file: *PRESENTN.xls*.

Figure I-4. Breakthrough Curves under Present-Day Infiltration When Fracture Property Changes Are Limited to the Fault Fractures

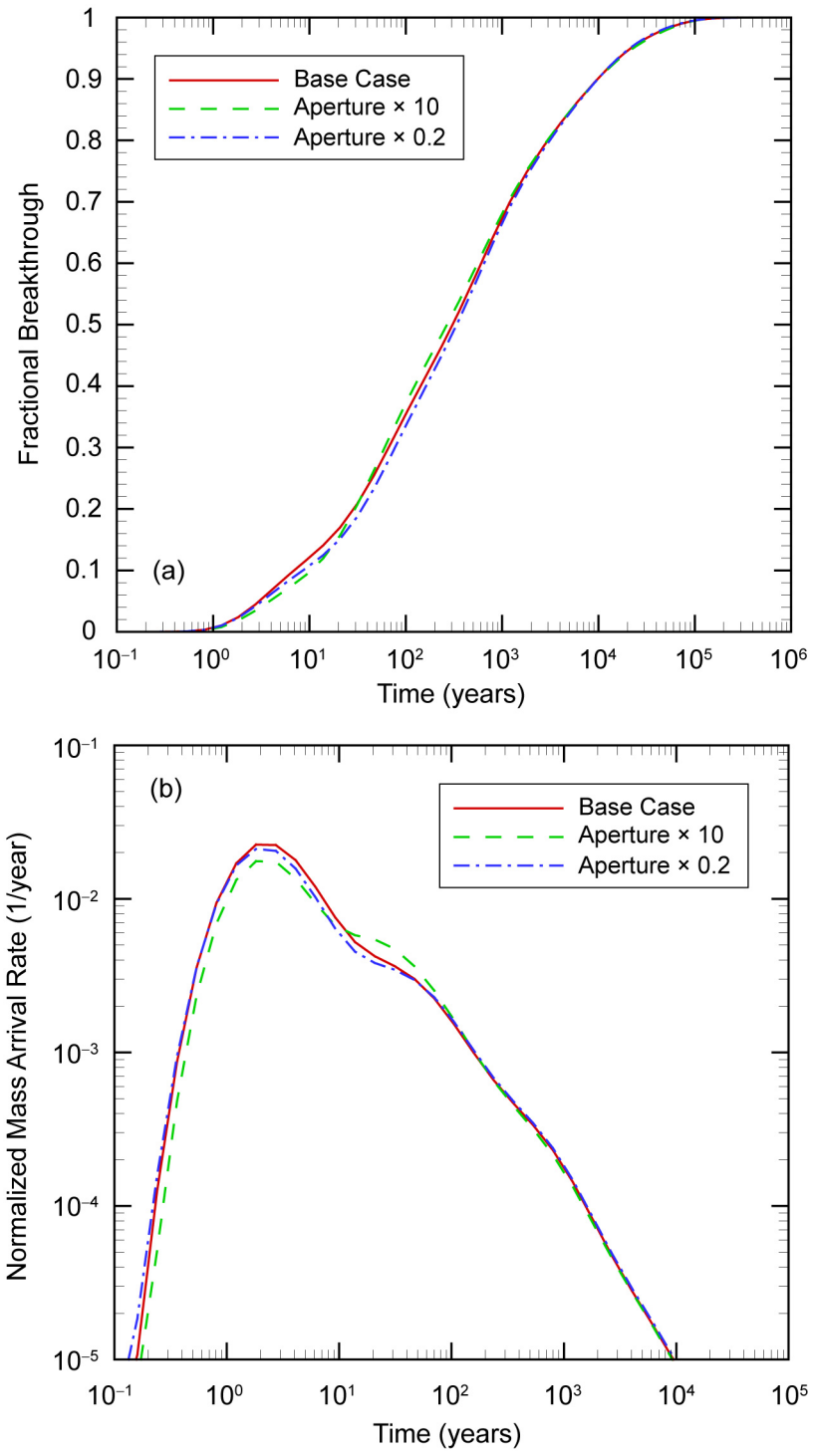

Source: DTN: LB0408U0170FEP.002 [DIRS 171596], file: *GLACIALN.xls*.

Figure I-5. Breakthrough Curves under Glacial-Transition Infiltration When Fracture Property Changes Are Limited to the Fault Fractures

I3.3.2 Fracture Apertures Altered Uniformly Across the Repository Block; Three-dimensional Calculations for Present-Day and Glacial-Transition Climates

The three-dimensional flow and transport calculations described in this section were performed as described in Section I3.2.4. The breakthrough curves for the present-day and the glacial-transition climates are shown in Figures I-6 and I-7, respectively. The results exhibit much greater influence compared with the case in which fracture property changes are confined to the fault zones. For the factor-of-10 case, travel time (for 0.5 fractional breakthrough) is found to decrease by about a factor of 25 for the present-day case and a factor of 11 for the glacial-transition climate. On the other hand, the normalized mass arrival rates are likely to be more significant for dose because the rate of radionuclide mass arrival at the accessible environment is what controls dose rates. Comparisons between peak (maximum) mass arrival rates for present-day and glacial-transition show that the effects of fault displacement are about a factor of 1.4 and 1.3, respectively. Furthermore, the peak doses occur slightly later for the $\times 10$ aperture case. For the $\times 0.2$ aperture case, the breakthrough curves are significantly delayed relative to the base case and the peak mass arrival rate is reduced by substantially more than one order of magnitude.

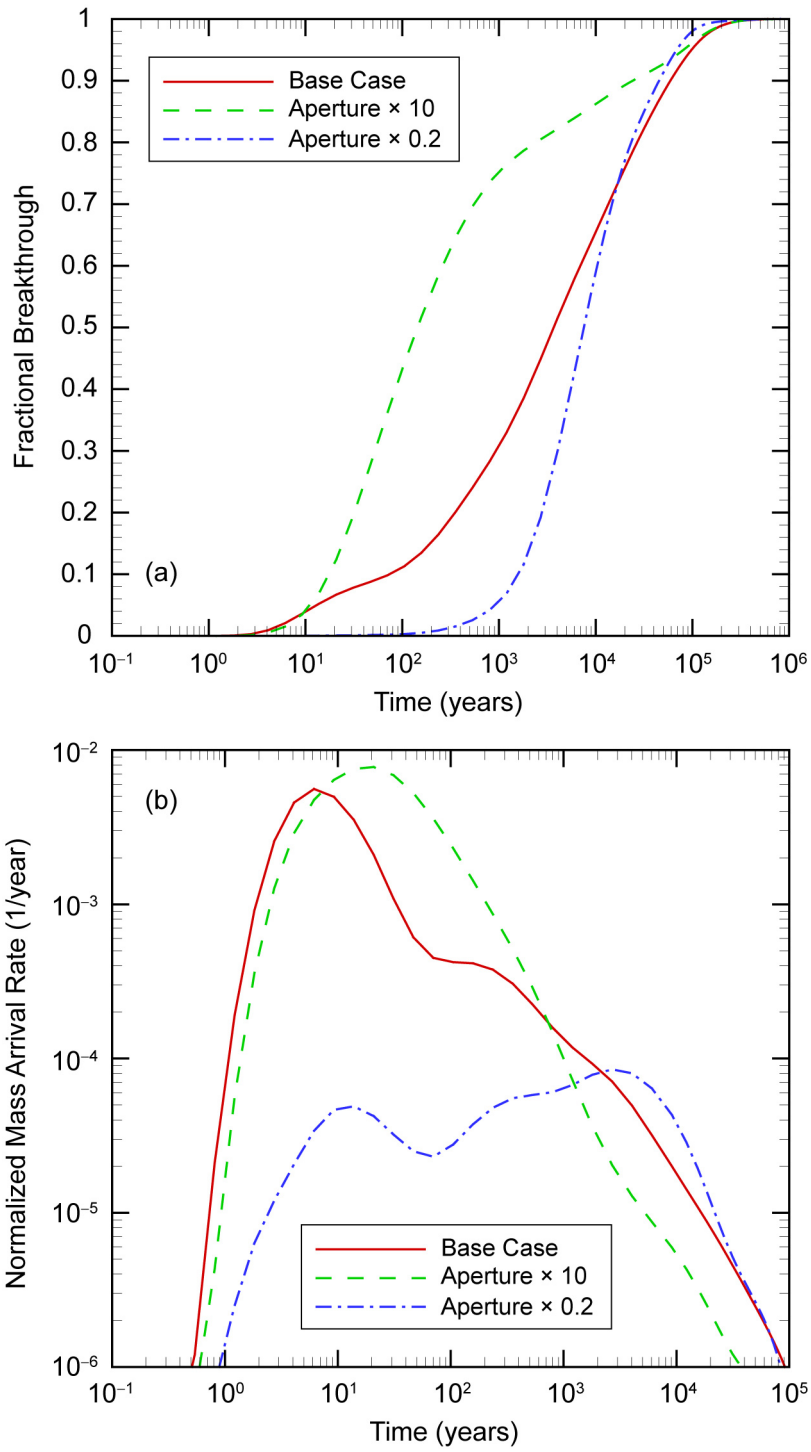

Source: DTN: LB0408U0170FEP.002 [DIRS 171596], file: *PRESENTN.xls*.

Figure I-6. Breakthrough Curves under Present-Day Infiltration with Change in Fracture Properties Throughout the Entire Model Domain

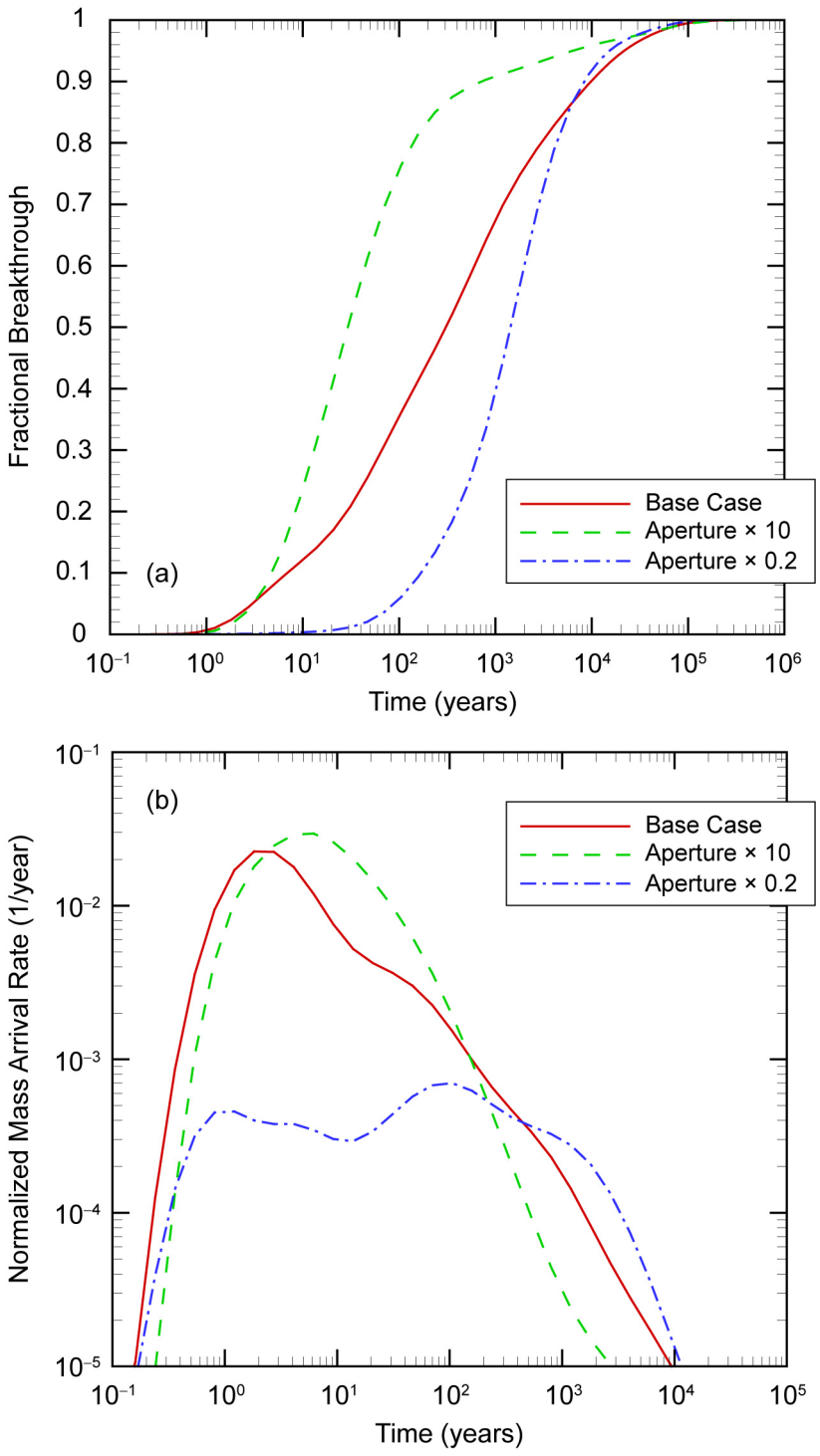

Source: DTN: LB0408U0170FEP.002 [DIRS 171596], file: *GLACIALN.xls*.

Figure I-7. Breakthrough Curves under Glacial-Transition Infiltration with Change in Fracture Properties Throughout the Entire Model Domain

I3.4 Discussion

The effect of changing fracture apertures on mass transport reflects the trend observed in the effect on flow; increased aperture leads to greater transport in fractures and shorter travel time to the water table. This leads to a consistent trend for simulated tracer breakthrough profiles at the water table. If the fracture apertures are decreased, the travel times of the majority of the particles are increased, causing delayed breakthrough. Similarly, if the fracture apertures are increased, the travel times of the majority of the particles are decreased, causing earlier breakthrough. In particular, when fracture apertures are increased, the travel times of some particles are decreased due to enhanced transport in the fractures.

Capillary and gravity forces in the fractures of the dual-permeability model tend to work against fracture-matrix inter-flow and keep water flowing in the fractures. Note that fracture-matrix inter-flow is driven by the matrix-fracture capillary pressure difference. Assuming the inter-flow is from the fractures to the matrix, larger fracture apertures tend to promote fracture-to-matrix flow due to decreased fracture capillary pressure (that is, increased matrix-fracture capillary pressure differential). On the other hand, as fracture aperture is increased, gravity exerts more effect to keep flow within the fractures. The decreased capillary pressure in the fractures is roughly inversely proportional to the fracture aperture. In addition, due to the use of upstream weighting of the relative permeability in the numerical scheme, the fracture relative permeability is used with the matrix absolute permeability to estimate the effective permeability of the fracture-matrix interface for fracture to matrix flow. The fracture relative permeability is the effective permeability for the fracture system at the given flow rate divided by the absolute permeability of the fracture system (i.e., a saturated fracture system). Thus, when the fracture apertures are increased, the fracture relative permeability (for about the same amount of fracture flow) decreases roughly in proportion to the cube of the aperture ratio. This is because the effective permeability is roughly set by the amount of flow and the saturated permeability is proportional to the cube of the fracture aperture (Equation I-1). Therefore, the fracture-matrix interface effective permeability is also reduced by this ratio. This reduction of the fracture-matrix interface effective permeability leads toward greater flow and transport in the fractures when fracture apertures are increased. The above mechanism for enhanced fracture transport when fracture aperture is increased is further promoted by the use of active-fracture dual permeability model. This is because under the active fracture model, liquid flow occurs only over a fraction of fracture-matrix interface area, thus resulting in reduced fracture-matrix transport and increased transport through the fractures.

I4. CONCLUSIONS

This study addresses the potential effects of fault displacement on transport in the unsaturated zone using sensitivity analysis that is conducted by perturbing fracture parameters. The degree of such perturbations is conservatively based on assessment of the geological information of the site.

The sensitivity studies for unsaturated zone flow and transport presented in this analysis suggest that changes in fracture aperture confined to the fault zones show virtually no effect on transport behavior. For an extremely conservative ten-fold increase in fracture aperture applied over the entire unsaturated zone domain, breakthrough is found to be about 25 times earlier for

present-day infiltration and about 11 times earlier for glacial-transition infiltration. Nevertheless, changes in the peak mass arrival rate at the water table are much smaller, factors of 1.4 and 1.3 for present-day and glacial-transition climates, respectively. Effects of such magnitude on travel time and mass arrival rates are no more significant than those caused by uncertainties in infiltration (Figures I-1 and I-2). In addition to infiltration uncertainty, the unsaturated zone radionuclide transport model used for TSPA samples uncertain transport parameters (SNL 2008 [DIRS 184748], Addendum Sections 6.5.5 and 6.5.6, and Section 6.5.7). Therefore, the uncertainty in unsaturated zone radionuclide transport incorporated in the TSPA is greater than the uncertainty in transport that results from infiltration uncertainty. Given the relatively limited changes found for the extremely conservative change in properties over the entire domain, the effects of fault displacement on unsaturated zone transport are expected to be negligible. Therefore, models for TSPA-LA may exclude the effects of fault displacement on unsaturated zone transport as discussed in FEPs 2.2.06.02.0A (Seismic Activity Changes Porosity and Permeability of Faults) and 2.2.06.02.0B (Seismic Activity Changes Porosity and Permeability of Fractures).

Table I-1. Indirect Inputs for Appendix I

Citation	Title	DIRS
BSC 2001	*UZ Flow Models and Submodels*	158726
BSC 2003	*Analysis of Infiltration Uncertainty*	165991
BSC 2004	*Development of Numerical Grids for UZ Flow and Transport Modeling*	169855
BSC 2004	*Future Climate Analysis*	170002
BSC 2004	*UZ Flow Models and Submodels*	169861
CRWMS M&O 1998	*Probabilistic Seismic Hazard Analyses for Fault Displacement and Vibratory Ground Motion at Yucca Mountain, Nevada*	103731
Day et al. 1998	*Bedrock Geologic Map of the Central Block Area, Yucca Mountain, Nye County, Nevada*	101557
DTN: LB990701233129.001	3-D UZ Model Grids for Calculation of Flow Fields for PA for AMR U0000, "Development of Numerical Grids for UZ Flow and Transport Modeling"	106785
DTN: LB990801233129.003	TSPA Grid Flow Simulations for AMR U0050, "UZ Flow Models and Submodels" (Flow Field #3)	122757
DTN: LB990801233129.009	TSPA Grid Flow Simulations for AMR U0050, "UZ Flow Models and Submodels" (Flow Field #9)	118717
Dyer 1999	"Revised Interim Guidance Pending Issuance of New U.S. Nuclear Regulatory Commission (NRC) Regulations (Revision 01, July 22, 1999), for Yucca Mountain, Nevada"	105655
Freeze and Cherry 1979	*Groundwater*	101173
Gauthier et al. 1995	*Impacts of Seismic Activity on Long-Term Repository Performance at Yucca Mountain*	103258
National Research Council 1992	*Ground Water at Yucca Mountain, How High Can It Rise? Final Report of the Panel on Coupled Hydrologic/Tectonic/Hydrothermal Systems at Yucca Mountain*	105162

Table I-1. Indirect Inputs for Appendix I (Continued)

Citation	Title	DIRS
DTN: LB0408U0170FEP.001	Sensitivity Study of Fracture Width Influence on UZ Flow and Transport: Simulations.	171595
DTN: LB9908T1233129.001	"Transport Simulations for the Low, Mean, and Upper Infiltration Scenarios of the Present-Day, Monsoon, and Glacial Transition Climates for AMR U0050, "UZ Flow Models and Submodels"	147115
DTN: LB0408U0170FEP.002	Sensitivity Study of Fracture Width Influence on UZ Flow and Transport: Summaries	171596
Potter et al. 1996	"Fault Styles and Strain Accommodation in the Tiva Canyon Tuff, Yucca Mountain, Nevada"	106583
Potter et al. 1996	"Structural Evolution of the Potential High-Level Nuclear Waste Repository Site at Yucca Mountain, Nevada"	106582
Scott 1990	"Tectonic Setting of Yucca Mountain, Southwest Nevada." Chapter 12 of *Basin and Range Extensional Tectonics Near the Latitude of Las Vegas, Nevada*	106751
Scott and Bonk 1984	*Preliminary Geologic Map of Yucca Mountain, Nye County, Nevada, with Geologic Sections*	104181
SNL 2007	*UZ Flow Models and Submodels*	184614
SNL 2008	*Features, Events, and Processes for the Total System Performance Assessment: Methods*	179476
SNL 2008	*Particle Tracking Model and Abstraction of Transport Processes*	184748
Sonnenthal et al. 1997	"Modeling the Strontium Geochemistry and Isotopic Ratio in the Unsaturated Zone." Chapter 17 of *The Site-Scale Unsaturated Zone Model of Yucca Mountain, Nevada, for the Viability Assessment*	101296
Sweetkind et al. 1996	"Interaction Between Faults and the Fracture Network at Yucca Mountain, Nevada"	106957
Sweetkind et al. 1997	*Administrative Report: Integrated Fracture Data in Support of Process Models, Yucca Mountain, Nevada*	177047
van Genuchten 1980	"A Closed-Form Equation for Predicting the Hydraulic Conductivity of Unsaturated Soils"	100610

APPENDIX J

QUALIFICATION OF DATA AND JUSTIFICATION OF EQUATIONS

This appendix presents the qualification of project and external data for intended use as direct input as well as the justification of equations used in excluded FEPs.

J1. DATA TO BE QUALIFIED

SCI-PRO-004, *Managing Technical Product Inputs*, categorizes technical product input usage as either direct input or indirect input. Direct input is used to develop the results or conclusions in a technical product. Indirect input is used to provide additional information that is not used in the development of results or conclusions. If not classified as established fact, unqualified data acquired or developed by Yucca Mountain Project (YMP) participants (project data) used as direct input to excluded FEPs must be qualified; external source data may be qualified for intended use within a given FEP's screening justification. Equations are justified for intended use in accordance with Attachment 2 Item 4 of SCI-PRO-005, *Scientific Analyses and Calculations*. Data (project and external source) are qualified for intended use in accordance with SCI-PRO-005, Section 6.2.1.M.3. Table J-1 lists the sources of the data to be qualified. A copy of the data qualification plan for project data and external source data can be found at the end of this appendix as Figure J-1. The summary of data to be qualified for intended use, that is part of the data qualification plan, is shown in Table J-2.

The data presented in this appendix were qualified by considering one or more of the data qualification methods provided in Attachment 3 of SCI-PRO-001, *Qualification of Unqualified Data*. The data qualification process included an initial evaluation of the data quality and correctness. The data qualification team evaluated the data by comparing the methods used to plan, collect, and analyze the data against generally accepted scientific or engineering practices. It was determined that the data were adequate and the method was implemented and documented within this appendix. The members of the qualification team are independent of the data set to be qualified. The qualification process attribute(s) that were appropriate for the data under consideration are listed for each data being qualified; data evaluation criteria were based on qualitatively or quantitatively meeting process attributes by the data under consideration.

In this appendix, data are examined on a FEP-by-FEP basis. Data are qualified for intended use for the FEP in which the data are used as direct input. This appendix is organized in subsections listed sequentially by FEP number.

Table J-1. List of Sources by Section and FEP Number

Section	FEP Number	Source	Project or External
J2	1.1.02.00.0B	Craig 2001 [DIRS 171411]	P
J3	1.2.01.01.0A	Fridrich et al. 1998 [DIRS 164051]	P
J4	1.2.04.02.0A	CRWMS M&O 1998 [DIRS 105347]	P
J5	1.2.05.00.0A	Ehlers and Blatt 1982 [DIRS 167802]	E
		Valentine and Krogh 2006 [DIRS 177282]	E
J6	1.2.06.00.0A	Blackwell et al. 2000 [DIRS 183582]	P
		Rousseau et al. 1997 [DIRS 100178]	P
		Wilson et al. 2003 [DIRS 163589]	E
J7	1.2.07.01.0A	Stuckless and Levich 2007 [DIRS 181507]	P
J8	1.2.08.00.0A	Krystinik 1990 [DIRS 135295]	E
		Reeves 1976 [DIRS 104303]	E
		Taylor 1986 [DIRS 102864]	E
		Kieft et al. 1997 [DIRS 100767]	E
		Whelan 2004 [DIRS 170697]	P
J9	1.2.09.02.0A	Freeze and Cherry 1979 [DIRS 101173]	E
J10	1.2.10.01.0A	National Research Council 1992 [DIRS 105162]	E
J11	1.2.10.02.0A	Valentine et al. 1998 [DIRS 119132]	P
J12	1.3.04.00.0A	Thompson et al. 1999 [DIRS 109470]	E
J13	1.3.05.00.0A	Thompson et al. 1999 [DIRS 109470]	E
J14 Appendix D	1.5.01.01.0A	Grieve and Robertson 1984 [DIRS 185030]	E
		Grieve 1987 [DIRS 135254]	E
		Grieve et al. 1995 [DIRS 135260]	E
		Grieve 1998 [DIRS 163385]	E
		Hills and Goda 1993 [DIRS 135281]	E
		Wuschke et al. 1995 [DIRS 129326]	E
J15	1.5.01.02.0A	Karam 2002 [DIRS 167872]	E
		Brakenridge 1981 [DIRS 167873]	E
J16	1.5.03.01.00	Biggins and Thomas 2003 [DIRS 167876]	E
J17	1.5.03.02.0A	Bredehoeft 1997 [DIRS 100007]	E
J18	2.1.02.08.0A	Garvin 2002 [DIRS 169141]	E
J19	2.1.03.07.0A	Garvin 2002 [DIRS 169141]	E
		Piron and Pelletier 2001 [DIRS 165318]	E
		Wachs 2004 [DIRS 184624]	E
J20	2.1.03.10.0B	Siriwardane and Wightman 1983 [DIRS 183688]	E
J21	2.1.06.01.0A	Ziegler 2004 [DIRS 171694]	P
J22	2.1.06.06.0B	Rogers et al. 1988 [DIRS 184108]	E
J23	2.1.09.13.0A	Means et al. 1983 [DIRS 100797]	P
J24	2.1.09.15.0A	Choppin and Stout 1989 [DIRS 168379]	E
		Rai and Swanson 1981 [DIRS 144599]	E
		Wronkiewicz et al. 1996 [DIRS 102047]	P
		Finch and Ewing 1992 [DIRS 113030]	E

Table J-1. List of Sources by Section and FEP Number (Continued)

Section	FEP Number	Source	Project or External
J25	2.1.09.21.0A	Reimus 1995 [DIRS 144604]	P
J26	2.1.09.21.0B	Reimus 1995 [DIRS 144604]	P
J27	2.1.09.21.0C	Reimus 1995 [DIRS 144604]	P
J28	2.1.11.03.0A	Garvin 2002 [DIRS 169141]	E
J29	2.1.11.10.0A	Platten 2006 [DIRS 183864]	E
		Duhr and Braun 2006 [DIRS 183865] [a]	E
		Bird et al. 1960 [DIRS 103524]	E
J30	2.1.12.02.0A	Piron and Pelletier 2001 [DIRS 165318]	E
J31	2.1.13.01.0A	Plys and Duncan 1999 [DIRS 184687]	E
		Garvin 2002 [DIRS 169141]	E
		Morgenstern and Choppin 1999 [DIRS 184023]	E
		Sexton 2007 [DIRS 184742]	E
		Shoesmith and King 1998 [DIRS 112178]	P
J32	2.2.06.01.0A	National Research Council 1992 [DIRS 105162]	E
J33	2.2.06.02.0A	National Research Council 1992 [DIRS 105162]	E
J34	2.2.06.03.0A	Broxton et al. 1987 [DIRS 102004]	P
		Wilson et al. 2003 [DIRS 163589]	E
J35	2.2.07.14.0A	Zhang and Schwartz 1995 [DIRS 183479]	E
J36	2.2.08.07.0C	Doorenbos and Pruitt 1977 [DIRS 103062]	E
J37	2.2.08.11.0A	Paces et al. 1997 [DIRS 109148]	P
J38	2.2.10.11.0A	Martinez and Nilson 1999 [DIRS 174095]	E
J39	2.2.10.14.0A	Smyth and Caporuscio 1981 [DIRS 174060]	P
		Colella et al. 2001 [DIRS 184454]	E
J40	2.2.11.03.0A	DOE 2002 [DIRS 155970]	P
J41	2.2.12.00.0A	Zhou et al. 2003 [DIRS 162133]	E
J42	2.3.13.03.0A	CRWMS M&O 1999 [DIRS 105031]	P
		Jury et al. 1991 [DIRS 102010]	E
		Carslaw and Jaeger 1959 [DIRS 100968] [a]	E

[a] Reference is a source of equation used in excluded FEP.

J2. FEP 1.1.02.00.0B – MECHANICAL EFFECTS OF EXCAVATION AND CONSTRUCTION IN EBS

This FEP uses data from the following report as direct input:

Craig, R.W. 2001. "Transmittal of Level 5 Deliverable SPW205M5, 'Excavation-Induced Fracture Study'." Letter from R.W. Craig (USGS) to T.C. Gunter (DOE/YMSCO), September 26, 2001, with enclosure. ACC: MOL.20011114.0003. [DIRS 171411]

The data to be qualified for intended use within this FEP include:

> Energy is focused on the rock to be removed, so that excess energy is not dispersed into the surrounding rock, as from blasting (Craig 2001 [DIRS 171411], pp. 1, 3, and 8).
>
> Examination of the tunnel walls and associated alcoves, niches, and drillholes has been used to define the character and extent of mechanical damage induced by tunnel boring (Craig 2001 [DIRS 171411], pp. 3 to 11, and 16).
>
> In rock with few fractures, the tunnel boring machine-induced fracturing of the tunnel periphery is confined to a depth of influence of less than 5 centimeters (Craig 2001 [DIRS 171411], p. 16).

J2.1 QUALIFICATION METHOD

The method of qualification of the data from Craig (2001 [DIRS 171411]) listed above is the Technical Assessment method (SCI-PRO-001, Attachment 3, Method 5). The rationale for using this method is that it was the most suitable considering the data and their existing documentation. The technical assessment included determination that the employed methodology was acceptable, determination that confidence in the data acquisition or development was warranted, and confirmation that the data had been used in similar applications. Qualification process attributes used in the technical assessment of these data are selected from the list provided in Attachment 4 of SCI-PRO-001. Attributes specifically applicable to these data are:

- Qualification of personnel or organizations generating the data are comparable to qualification requirements of personnel generating similar data under an approved program that supports the YMP license application process or postclosure science (#1).
- The technical adequacy of equipment and procedures used to collect and analyze the data (#2).
- The extent to which the data demonstrate the properties of interest (e.g., physical, chemical, geological, mechanical) (#3).
- Extent and reliability of the documentation associated with the data (#9).

J2.2 TECHNICAL ASSESSMENT

Qualifications of Personnel or Organizations Generating the Data—The excavation-induced fracture study was conducted by members of the U.S. Bureau of Reclamation Underground Geologic Mapping team, for which Steve Beason was the principal investigator. The U.S. Bureau of Reclamation is one of the government agencies responsible for geologic mapping of federal projects, particularly dam sites and tunnels, and has provided engineering geologic services to the DOE and USGS for characterization of the Yucca Mountain site since the mid-1980s. The YMP geologists from the U.S. Bureau of Reclamation mapped approximately 10 km of underground tunnels at Yucca Mountain, including the ESF and the Enhanced Characterization of the Repository Block (ECRB) Cross-Drift, between 1994 and 1997. The team subsequently compiled their findings in completion reports for the various excavations (e.g., Albin et al. 1997 [DIRS 101367]; Eatman et al. 1997 [DIRS 157677]).

Technical Adequacy of Equipment and Procedures Used—The data collection method consists of recording visual observations made by the mapping geologists in a scientific notebook, which in turn is technically reviewed. This method is typical of geologic investigations; it is prescribed through the procedure that governed the underground mapping, U.S. Geological Survey Procedure YMP-USGS-GP-32, *Underground Geologic Mapping*.

Extent and Reliability of the Documentation Associated with the Data—The underground excavation observations were made and recorded in a scientific notebook (Beason 2003 [DIRS 171953], pp. 77 to 80), following the then-current YMP procedure AP-SIII.1Q, *Scientific Notebooks*, which incorporated the quality assurance requirements of *Quality Assurance Requirements and Description* (DOE 2004 [DIRS 171539], Supplement III), and, by extension, the requirements of 10 CFR 60, Subpart G [DIRS 100015]. A scientific notebook procedure has been used on the YMP since 1996. The Beason notebook (2003 [DIRS 171953], pp. 77 to 81) documents the scientific observations, the person who entered the data in the notebook and the technical review of the notebook entry.

Extent to Which the Data Demonstrate the Properties of Interest—The data were collected to compare the relative excavation effects of different mining techniques, including use of the tunnel boring machine, alpine miner, and drill and blast techniques. This FEP specifically uses the observations derived from the tunnel boring machine excavations. The observations directly relate to concerns regarding ability to maintain the circular cross-section of a tunnel-boring machine tunnel, depth of damage, and significance of the damage to modeling studies.

Data Have Been Used in Similar Applications—The underground tunnel data collected by the U.S. Bureau of Reclamation mapping team has been used extensively for YMP performance assessment and facility layout. The geologic and fracture data provide input into the hydrologic models for the unsaturated zone, and the information obtained regarding the mechanical stability of the rock has been used to determine the extent and orientation of the underground facilities.

J2.3 DATA QUALIFIED FOR INTENDED USE

The data from Craig (2001 [DIRS 171411]) cited above are appropriate for the intended use within FEP 1.1.02.00.0B (Mechanical Effects of Excavation and Construction in EBS). The technical assessment of these data provides sufficient confidence that the data meet qualification criteria outlined above and can be considered qualified for intended use within this FEP.

J3. FEP 1.2.01.01.0A – TECTONIC ACTIVITY – LARGE SCALE

This FEP uses data from the following report as direct input:

Fridrich, C.J.; Whitney, J.W.; Hudson, M.R.; and Crowe, B.M. 1998. *Space-Time Patterns of Late Cenozoic Extension, Vertical-Axis Rotation, and Volcanism in the Crater Flat Basin, Southwest Nevada.* Open-File Report 98-461. Denver, Colorado: U.S. Geological Survey. ACC: MOL.19981014.0299. [DIRS 164051]

The data to be qualified for intended use within this FEP include:

> During the period of peak tectonism (approximately 11.6 million years ago (Ma) to 12.7 Ma), the western part of Crater Flat basin subsided due to the basin extending from 18% to 40% in 1.1 million years or less (Fridrich et al. 1998 [DIRS 164051], p. 1).
>
> After 11.6 Ma, the rate of extension in the basin declined in a roughly exponential manner. The late Quaternary rate of extension is less than 1% of the initial rate (Fridrich et al. 1998 [DIRS 164051], pp. 1 and 13) and may be as low as 0.1% to 0.2% per million years (Fridrich et al. 1998 [DIRS 164051], pp. 19 and 20).
>
> The pattern of Quaternary deformation mimics the pattern of middle Miocene activity, but at substantially lower rates (Fridrich et al. 1998 [DIRS 164051], pp. 1 and 2).

J3.1 QUALIFICATION METHOD

Method 5, Technical Assessment, from Attachment 3 of SCI-PRO-001 is used for qualification of the data identified above. The rationale for using this method is that it was the most suitable considering the data and their existing documentation. The technical assessment included determination that the employed methodology was acceptable and determination that confidence in the data acquisition or development was warranted. Qualification process attributes used in the technical assessment of these data are selected from the list provided in Attachment 4 of SCI-PRO-001. Attributes specifically applicable to these data are:

- The technical adequacy of equipment and procedures used to collect and analyze the data (#2).
- The extent to which the data demonstrate the properties of interest (e.g., physical, chemical, geologic, mechanical) (#3).
- Prior peer or other professional reviews of the data and their results (#8).

J3.2 TECHNICAL ASSESSMENT

The methodology to estimate extension rates are (1) extension in the Miocene bedrock estimated by using the measure of stratal tilting and assuming a tilting domino model, (2) where data permitted the estimates were checked by use of reconstructed cross sections drawn perpendicular to the average strike of extensional faults, and (3) late Quaternary extension was estimated by summing the horizontal components of Quaternary fault displacements along transects

perpendicular to the strikes of major extensional faults (Fridrich et al. 1998 [DIRS 164051], p. 8). Quaternary fault displacement data were from mapping, trenching, and geochronologic studies (Fridrich et al. 1998 [DIRS 164051], p. 7). These methods are typical and well known in structural geologic studies and are used with assumptions appropriately employed for geologic studies of this type.

Standard geologic field methods and measurements were employed by individuals trained to these methods. Stratal tilt measurements (strike and dip) of compaction foliation in ash-flow tuffs were used to estimate the extension rate (Fridrich et al. 1998 [DIRS 164051], p. 6). These data were taken from geologic maps produced by Scott and Bonk (1984 [DIRS 104181]) and Faulds et al. (1994 [DIRS 105126]), supplemented by additional mapping completed by USGS geologist R. B. Scott as well as by Fridrich et al. (1998 [DIRS 164051]). To evaluate the reliability of stratal tilt data taken from compaction foliations, these data were compared against stratal tilt data taken from bedding in the same stratigraphic sections where possible (Fridrich et al. 1998 [DIRS 164051], pp. 6 to 7).

This study and the data it produced were part of an earlier publication (Fridrich et al. 1996 [DIRS 105086]). This earlier version was technically reviewed by two USGS geologists who are regarded as experts in the field of mapping pyroclastic deposits and tectonics of the southern Great Basin and Death Valley region (Fridrich et al. 2003 [DIRS 184915]). All technical comments were satisfactorily resolved.

J3.3 DATA QUALIFIED FOR INTENDED USE

The data from the report by Fridrich et al. (1998 [DIRS 164051]) concerning the rate of extensional tectonics and patterns of deformation since Miocene time (late Quaternary) are appropriate for intended use within FEP 1.2.01.01.0A (Tectonic Activity – Large Scale). The technical assessment presented above provides sufficient confidence that these data meet qualification criteria outlined above and can be considered qualified for intended use within this FEP.

J4. FEP 1.2.04.02.0A – IGNEOUS ACTIVITY CHANGES ROCK PROPERTIES

This FEP uses data from the following synthesis report as direct input:

CRWMS M&O 1998. *Synthesis of Volcanism Studies for the Yucca Mountain Site Characterization Project.* Deliverable 3781MR1. Las Vegas, Nevada: CRWMS M&O. ACC: MOL.19990511.0400. [DIRS 105347]

The data to be qualified for intended use within this FEP include:

> Laboratory analytical data and field observations of mineral alterations around igneous intrusions at natural analogue sites show that alteration extends less than 10 m away from the intrusion–host rock contact. Natural analogue studies in similar host rocks at the Nevada Test Site show that alteration is limited to a zone less than 10 m away from the intrusion/host rock contact (CRWMS M&O 1998 [DIRS 105347], pp. 5-41 through 5-71).

The CRWMS M&O (1998 [DIRS 105347]) report summarizes the Yucca Mountain site characterization data that include the results of natural analogue studies of basaltic intrusions and related alteration of surrounding host rock.

The data of interest are within Chapter 5 of the synthesis report, as indicated from the page numbers cited above. Because this is a synthesis report, the qualification of the data will be based on the source of the data, which is from Valentine et al. (1998 [DIRS 119132]). Valentine et al. (1998 [DIRS 119132]) studied two natural analogue sites: Paiute Ridge, Nevada, and Grants Ridge, New Mexico, and concluded that contact metamorphism from intrusive dikes is generally confined to distances of a few meters around the dike.

Valentine, G.A.; WoldeGabriel, G.; Rosenberg, N.D.; Carter Krogh, K.E.; Crowe, B.M.; Stauffer, P.; Auer, L.H.; Gable, C.W.; Goff, F.; Warren, R.; and Perry, F.V. 1998. "Physical Processes of Magmatism and Effects on the Potential Repository: Synthesis of Technical Work Through Fiscal Year 1995." Chapter 5 of *Volcanism Studies: Final Report for the Yucca Mountain Project.* Perry, F.V.; Crowe, B.M.; Valentine, G.A.; and Bowker, L.M., eds. LA-13478. Los Alamos, New Mexico: Los Alamos National Laboratory. TIC: 247225. [DIRS 119132]

In support of the data described above, the following data will be qualified for intended use:

> Mineral alterations around igneous intrusions at natural analogue sites show that alteration is limited to a zone that extends less than 10 m away from the intrusion/host rock contact (Valentine et al. 1998 [DIRS 119132], p. 5-74).

J4.1 QUALIFICATION METHOD

The method of qualification of the data listed above from Chapter 5 of the synthesis report (CRWMS M&O 1998 [DIRS 105347]) is the Technical Assessment method (SCI-PRO-001, Attachment 3, Method 5). The rationale for using this method is that it was the most suitable considering the data and their existing documentation. The technical assessment included

determination that the employed methodology was acceptable and determination that confidence in the data acquisition or development was warranted. Qualification process attributes used in the assessment of these data are selected from the list provided in Attachment 4 of SCI-PRO-001. Attributes specifically applicable to these data are:

- Qualification of personnel or organizations generating the data are comparable to qualification requirements of personnel generating similar data under an approved program that supports the YMP license application process or postclosure science (#1).
- The technical adequacy of equipment and procedures used to collect and analyze the data (#2).
- The extent to which the data demonstrate the properties of interest (e.g., physical, chemical, geological, mechanical) (#3).
- Extent and quality of corroborating data or confirmatory testing results (#10).

J4.2 TECHNICAL ASSESSMENT

Qualifications of Personnel or Organizations Generating the Data—Dr. Greg A. Valentine led the Hydrology, Geochemistry, and Geology Group at Los Alamos National Laboratory from 2001 until 2008, at which time he accepted a faculty position at SUNY Buffalo in the Department of Geology. He served for five years as the technical lead for igneous consequences at the YMP. His fields of research include numerical simulation of flow in porous media, explosive volcanic eruptions, and magma chamber dynamics. His field studies are related to volcanic hazards assessment, large-volume pyroclastic eruptions, fossil hydrothermal systems, and intrusion mechanisms and dynamics. Dr. Valentine received his Ph.D. in Geological Sciences (1988) from the University of California, Santa Barbara, and B.S. in Geological Engineering and Geology (1984) from the New Mexico Institute of Mining and Technology.

Technical Adequacy of Equipment and Procedures Used—The authors of the study (CRWMS M&O 1998 [DIRS 105347], Chapter 5; Valentine et al. 1998 [DIRS 119132]) used mineral analysis by x-ray diffraction and elemental analysis by neutron activation analysis to determine the extent of contact metamorphism. These are standard analytical techniques and generally accepted scientific practice for these analyses. Depletion of volatile elements near the contact was taken as evidence of metamorphism.

Data Demonstrate the Properties of Interest—The data from Valentine et al. (1998 [DIRS 119132]) show that the hydrologic effect of an igneous intrusion into unsaturated tuff is limited in extent. The theoretical basis for this is provided by the corroborating data.

Extent and Quality of Corroborating Data—The conclusions regarding the extent of rock property changes around igneous intrusions were based on two analogue studies. One of these two studies was subsequently reported by WoldeGabriel et al. (1999 [DIRS 110071]), who studied the effects of a basaltic intrusion at Grants Ridge, New Mexico, on the country rock, consisting of silicic tuffs and volcaniclastic sediments. The field and laboratory data were the

same as those reported by Valentine et al. (1998 [DIRS 119132]) and indicated that the physical changes due to the thermal effects of the intruded plug were confined to within 10 m of the plug.

WoldeGabriel et al. (1999 [DIRS 110071]) provide experimental evidence of limited extent of contact metamorphism and a theoretical explanation, supported by results of numerical simulation, of why the effects of igneous intrusion into unsaturated tuff are localized. A one-dimensional (radial) conductive model was verified against analytical solution and the code FEHM. Results of the numerical simulations are presented in WoldeGabriel et al. (1999 [DIRS 110071], Figures 9 and 13). These results show that 10 m away from the intrusion, the maximum temperature reached was 500°C; 600°C was only reached within 4 m of the intrusion. This localized effect is explained by the fact that the rock was unsaturated at the time of the intrusion. The lack of sufficient water prevents fluid-driven convective heat transfer, hydrothermal circulation, and extensive alteration of the country rock.

The numerical simulation of an analogue site corroborates the evidence that contact metamorphism from an intrusive dike is limited to within 10 m from the dike.

J4.3 DATA QUALIFIED FOR INTENDED USE

The data on rock alteration in the vicinity of igneous intrusions obtained from *Synthesis of Volcanism Studies for the Yucca Mountain Site Characterization Project* (CRWMS M&O 1998 [DIRS 105347], pp. 5-41 through 5-71) are adequate for intended use within FEP 1.2.04.02.0A (Igneous Activity Changes Rock Properties). The data from Valentine et al. (1998 [DIRS 119132], p. 5-74) describing the extent of rock alteration are the same data; they are used as direct input in FEP 1.2.10.01.0A (Hydrologic Response to Igneous Activity) (see FEP 1.2.10.01.0A in this appendix). The technical assessment of these data provides sufficient confidence that these data meet qualification criteria outlined above and can be considered qualified.

J5. FEP 1.2.05.00.0A – METAMORPHISM

This FEP uses data from the following references:

Petrology, Igneous, Sedimentary, and Metamorphic (Ehlers and Blatt 1982 [DIRS 167802])

Emplacement of Shallow Dikes and Sills Beneath a Small Basaltic Volcanic Center – The Role of Pre-Existing Structure (Paiute Ridge, Southern Nevada, USA) (Valentine and Krogh 2006 [DIRS 177282]).

J5.1 QUALIFICATION OF DATA FROM EHLERS AND BLATT 1982

Ehlers, E.G. and Blatt, H. 1982. *Petrology, Igneous, Sedimentary, and Metamorphic.* New York, New York: W.H. Freeman and Company. TIC: 255657. [DIRS 167802]

The data being qualified are stated in the form of boundary conditions required for the onset of regional metamorphism.

> Conditions conducive to the onset of regional metamorphism correspond to temperature of 150 to 200ºC and pressures of 0.5 to 1 kilobars, which occur at depths of 4 to 5 km (Ehlers and Blatt 1972 [DIRS 167802], p. 566).
>
> The geothermal gradient at convergent plate boundaries may range from less than 10°C per km to greater than 25°C per km (Ehlers and Blatt 1982 [DIRS 167802], pp. 684 and 685).

These data are used in this FEP to define the lowest temperature and pressure required for the onset of metamorphism, for comparison against the temperature and pressure increases associated with existing burial rates and geothermal gradients at the Yucca Mountain site.

J5.1.1 Qualification Method

The method of qualification for intended use of the data from the publication by Ehlers and Blatt (1982 [DIRS 167802]) is the Corroborating Data method (SCI-PRO-001, Attachment 3, Method 2). The rationale for using this method is that corroborating data are available for comparison with the unqualified data set and any inferences drawn to corroborate the unqualified data can be clearly identified, justified and documented. Qualification process attributes used in the qualification were selected from the list provided in Attachment 4 of SCI-PRO-001. Attributes specifically applicable to these data are:

- Extent to which the data demonstrate the properties of interest (#3).
- Extent and quality of corroborating data or confirmatory testing results (#10).

J5.1.2 Corroborating Data

The direct input for this FEP is taken from the publication by Ehlers and Blatt (1982 [DIRS 167802]), largely because the values these authors present suggest the least temperature,

pressure, and depth of burial needed for the onset of regional metamorphism (i.e., conservative bounding conditions for onset). Using these conditions as the basis of the FEPs screening is, therefore, conservative. The data from this publication are corroborated by the data presented by other authors (Hyndman 1972 [DIRS 150295], pp. 270 and 272; Press and Siever 1978 [DIRS 167965], pp. 303; Retallack 1991 [DIRS 167870], p. 200).

Ehlers and Blatt (1982 [DIRS 167802], p. 566) indicate that 0.5 to 1 kbar is necessary for the onset of metamorphism, which is clearly conservative compared to the data published by Hyndman (1972 [DIRS 150295], p. 272), who indicates that 2 to 3 kbars of pressure are required. The onset temperature, 150°C to 200°C, given by Ehlers and Blatt (1982 [DIRS 167802], p. 566), is also clearly conservative and as much as one-half of that cited by the corroborating sources. Given the respective pressure gradients, Ehlers and Blatt (1982 [DIRS 167802], p. 566) would suggest metamorphic onset at depths as little as 1 to 2 km, but also indicate that a burial depth of 4 to 5 km is needed. In any case, these conditions are clearly conservative compared to the temperature and pressures, and to the depth of 10 km, based on Hyndman's information. They are also conservative compared to the 9-km depth based on the average thermal gradient, and they are conservative with respect to the onset temperatures presented by Press and Siever (1978 [DIRS 167965], p. 303). They are also more restrictive than the conditions indicated by Retallack (1991 [DIRS 167870], p. 200) of temperatures greater than 200°C and/or burial greater than 7 km.

For the FEPs analysis, all that is needed is to show that existing burial rates and geothermal gradients are insufficient to result in significant temperature and pressure increases. Therefore, a qualitative comparison of existing corroborating data is sufficient to support the intended use of the data as a conservative approach within this FEP.

J5.1.3 Data Qualified for Intended Use

The above literature review and corroboration of the direct input provides an acceptable level of confidence that the data are suitable for their intended use within FEP 1.2.05.00.0A (Metamorphism). The data identified above are qualified for use in the screening justification for this FEP.

J5.2 QUALIFICATION OF DATA FROM VALENTINE AND KROGH 2006

Valentine, G.A. and Krogh, K.E.C. 2006. "Emplacement of Shallow Dikes and Sills Beneath a Small Basaltic Volcanic Center – The Role of Pre-Existing Structure (Paiute Ridge, Southern Nevada, USA)." *Earth and Planetary Science Letters, 246,* 217-230. New York, New York: Elsevier. TIC: 258400. [DIRS 177282].

The data from this report to be qualified for intended use within this FEP include:

> In places the tuff is densely welded and forms black vitrophyre that grades rapidly away from the contact, over a distance of ~20 to 100 cm, into non-welded tuff that is apparently unaffected by the dike (Valentine and Krogh 2006 [DIRS 177282], p. 221).

J5.2.1 Qualification Method

The method of qualification of the data listed above from the journal article by Valentine and Krogh (2006 [DIRS 177282]) is the Technical Assessment method (SCI-PRO-001, Attachment 3, Method 5). The rationale for using this method is that it was the most suitable considering the data and their existing documentation. The technical assessment included determination that confidence in the data acquisition or development was warranted. Qualification process attributes used in the assessment of these data are selected from the list provided in Attachment 4 of SCI-PRO-001. Attributes specifically applicable to these data are:

- Qualification of personnel or organizations generating the data are comparable to qualification requirements of personnel generating similar data under an approved program that supports the YMP license application process or postclosure science (# 1).

- The extent to which the data demonstrate the properties of interest (e.g., physical, chemical, geological, mechanical) (# 3).

- Prior peer or other professional reviews (# 8).

J5.2.2 Technical assessment

Qualifications of Personnel or Organizations Generating the Data—Dr. Greg A. Valentine led the Hydrology, Geochemistry, and Geology Group at Los Alamos National Laboratory from 2001 until 2008, at which time he accepted a faculty position at SUNY Buffalo in the Department of Geology. He served for five years as the technical lead for igneous consequences at the YMP. His fields of research include numerical simulation of flow in porous media, explosive volcanic eruptions, and magma chamber dynamics. His field studies are related to volcanic hazards assessment, large-volume pyroclastic eruptions, fossil hydrothermal systems, and intrusion mechanisms and dynamics. Dr. Valentine received his Ph.D. in Geological Sciences (1988) from the University of California, Santa Barbara, and B.S. in Geological Engineering and Geology (1984) from the New Mexico Institute of Mining and Technology.

Data Demonstrate the Properties of Interest—The data from Valentine and Krogh et al. (1998 [DIRS 177282]) show that the hydrologic effect of an igneous intrusion into unsaturated tuff is limited in extent, which is the property under consideration. The intended use of the data is to support the position that the scale at which permeabilities would change is limited to a few meters around the dike.

Prior Peer or Other Professional Reviews—The article under consideration was published in the professional, peer reviewed journal *Earth and Planetary Science Letters*. This journal publishes high-quality research articles in the area of geoscience, including lunar studies, plate tectonics, ocean floor spreading, and continental drift, as well as basic studies of the physical, chemical, and mechanical properties of the earth's crust and mantle, the atmosphere, and the hydrosphere.

J5.2.3 Data Qualified for Intended Use

The data related to spatial extent of changes in rock properties caused by the dike intrusion were also qualified for intended use in FEP 1.2.04.02.0A (Igneous Activity Changes Rock Properties). The list of authors of source references for those data includes Valentine and Krogh, the authors of the journal article that is the source of data for FEP 1.2.05.00.0A. The intended use of these data is the same for this FEP and for FEP 1.2.04.02.0A. See FEP 1.2.04.02.0A (Igneous Activity Changes Rock Properties) in this appendix for additional information regarding these data.

The technical assessment of the data on changes in permeability in the vicinity of igneous intrusions provides sufficient confidence that the relevant data (Valentine and Krogh 2006 [DIRS 177282], p. 221) are adequate for the intended use within FEP 1.2.05.00.0A (Metamorphism). The data identified above are qualified for use in screening justification for this FEP.

J6. FEP 1.2.06.00.0A – HYDROTHERMAL ACTIVITY

This FEP uses data from the following reports:

Geothermal Resource/Reservoir Investigations Based on Heat Flow and Thermal Gradient Data for the United States (Blackwell et al. 2000 [DIRS 183582])

Results of Borehole Monitoring in the Unsaturated Zone Within the Main Drift Area of the Exploratory Studies Facility, Yucca Mountain, Nevada (Rousseau et al. 1997 [DIRS 100178])

Origin, Timing, and Temperature of Secondary Calcite–Silica Mineral Formation at Yucca Mountain, Nevada (Wilson et al. 2003 [DIRS 163589]).

J6.1 QUALIFICATION OF DATA FROM BLACKWELL ET AL. 2000

Blackwell, D.D.; Wisian, K.W.; Richards, M.C.; and Steele, J.L. 2000. *Geothermal Resource/Reservoir Investigations Based on Heat Flow and Thermal Gradient Data for the United States.* DOE/ID/13504. Washington, D.C.: U.S. Department of Energy. ACC: LLR.20070919.0006. [DIRS 183582]

The data from this report to be qualified for intended use within this FEP include:

> In the Basin and Range province, hydrothermal activity with temperatures exceeding 150°C have been found to be highly correlated to regional heat flow when that flow is in excess of 80 mW/m^2 (Blackwell et al. 2000 [DIRS 183582], Section 2.3).
>
> Most extensional geothermal systems in the U.S. appear to circulate to minimum depths of 4 to 6 km (Blackwell et al. 2000 [DIRS 183582], Section 3.5).

J6.1.1 Qualification Method

The methods of qualification for intended use of the data from the report by Blackwell et al. (2000 [DIRS 183582]) are the Technical Assessment method (SCI-PRO-001, Attachment 3, Method 5) and the Corroborating Data method (SCI-PRO-001, Attachment 3, Method 2). The rationale for using these methods is that they were the most suitable considering the data, their existing documentation, and intended use. The technical assessment was based on the determination that confidence in the data acquisition or development was warranted. Qualification process attributes used in the evaluation of the data corroboration and technical assessment were selected from the list provided in Attachment 4 of SCI-PRO-001. Attributes specifically relevant to these data are:

- Qualification of personnel or organizations generating the data are comparable to qualification requirements of personnel generating similar data under an approved program that supports the YMP license application process or postclosure science (#1).

- The extent to which the data demonstrate the properties of interest (e.g., physical, chemical, geological, mechanical) (#3).

- Extent and reliability of corroborating data or confirmatory results (#10).

J6.1.2 Technical Assessment

Extent to Which the Data Demonstrate the Properties of Interest—The publication describes a project focused on geothermal site-specific heat flow and thermal gradient data in the western United States. It included constructing a database of geothermal site-specific thermal gradient, heat flow, and thermal conductivity results from over 5,300 individual exploration wells. The database was assembled over a period of three years by compiling extensive temperature gradient and heat flow exploration data from the active geothermal system exploration of the 1970s and 1980s. The publication includes synthesis of the data, description of the database, as well as examples of the database applications. The data used for FEP 1.2.06.00.0A (Hydrothermal Activity) were obtained from Section 2.3 of the source (Blackwell et al. 2000 [DIRS 183582]), which discusses a modeling study that used heat flow and gradient from the database and then applied fault data to model an idealized, generic Basin and Range geothermal system as an example of extensional geothermal systems.

Qualification of Personnel or Organizations Generating the Data—The project described in the publication extended the earlier geothermal resource evaluations, which were documented in several publications presented in the peer-reviewed scientific journals. The primary author, D.D. Blackwell, is Hamilton Professor in the Earth Sciences Department of Southern Methodist University, specializing in the thermal state of the lithosphere and the geothermal resources in the United States. He has authored many scientific publications on this subject.

J6.1.3 Corroborating Data

The areas that are not geothermally active are the areas where the heat flow is low. From a regional perspective, the Yucca Mountain area is located adjacent to a large area of anomalously low heat flow (Flynn et al. 1996 [DIRS 112530], p. 92). Evaluation of geothermal characteristics within the Yucca Mountain area indicates that only low-temperature waters occur in and adjacent to Yucca Mountain and that the temperature gradient, and thus the heat flow, is low and below average. This information corroborates the data obtained from the report by Blackwell et al. (2000 [DIRS 183582]) that hydrothermal systems in the Basin and Range Province are found only in the areas where heat fluxes are high.

The hydrothermal water circulation depth is cited to be 4 to 5 km for the Whirlwind Valley hydrothermal system in Northern Nevada, in a region of high geothermal gradient (40°C/km to 60°C/km) (Wollenberg et al. 1975 [DIRS 107327], p. 7). This observation corroborates the minimum 4 to 6 km circulation depth for extensional hydrothermal systems given by Blackwell et al. (2000 [DIRS 183582], Section 3.5).

J6.1.4 Data Qualified for Intended Use

The technical assessment provides sufficient confidence that the data from Blackwell et al. (2000 [DIRS 183582]) presented above are adequate for intended use within FEP 1.2.06.00.0A

(Hydrothermal Activity). These data are qualified for intended use in the screening justification for this FEP.

J6.2 QUALIFICATION OF DATA FROM ROUSSEAU ET AL. 1997

Rousseau, J.P.; Loskot, C.L.; Thamir, F.; and Lu, N. 1997. *Results of Borehole Monitoring in the Unsaturated Zone Within the Main Drift Area of the Exploratory Studies Facility, Yucca Mountain, Nevada*. Milestone SPH22M3. Denver, Colorado: U.S. Geological Survey. ACC: MOL.19970626.0351. [DIRS 100178]

The data from this report to be qualified for intended use within this FEP include:

> In the Yucca Mountain area, the calculated heat flux within the TSw at boreholes NRG-7a, UZ-7a, and SD-12 is 37, 39, and 32 mW/m^2, respectively (Rousseau et al. 1997 [DIRS 100178], Section 5.2).

J6.2.1 Qualification Method

The method of qualification of the data listed above obtained from the report by Rousseau et al. (1997 [DIRS 100178]) is the Corroborating Data method (SCI-PRO-001, Attachment 3, Method 2). The rationale for using this method is that the data under consideration were evaluated previously and compared with the other relevant results. The data corroboration method was the most suitable considering the data, their existing documentation, and their intended use. Qualification process attributes used in the evaluation of the data corroboration and in technical assessment were selected from the list provided in Attachment 4 of SCI-PRO-001. Attributes specifically relevant to these data are:

- The extent to which the data demonstrate the properties of interest (e.g., physical, chemical, geological, mechanical) (#3).

- Extent and quality of corroborating data or confirmatory testing results (#10).

J6.2.2 Corroborating Data

The average of the data under consideration is 36 mW/m^2, with a standard deviation of 3.6 mW/m^2. The calculated heat flow data from Rousseau et al. (1997 [DIRS 100178]) are relevant to evaluating the potential for non-magmatic hydrothermal activity in the Yucca Mountain region and demonstrate the property of interest.

The report by Sass et al. (1988 [DIRS 100644]) provides data that are comparable with the heat flux data presented by Rousseau et al. (1997 [DIRS 100178]). Heat flux measurements are reported in Tables 5 and 6 of Sass et al. (1988 [DIRS 100644]). Of the measurements presented in these tables, the values from boreholes USW G-1, USW G-2, USW G-4, USW H-1, USW H-3, USW-H-4, USW H-5, UE25a4, UE25a5, UE25a6, UE25a7, UE25a1b1H, UZ-1, WT-2, WT-4, WT-6, WT-16, and WT-18 are in the vicinity of the boreholes (BSC 2007 [DIRS 182926]) used by Rousseau et al. (1997 [DIRS 100178]) to estimate heat flux. Note that in *IED Subsurface Facilities Geological Data* (BSC 2007 [DIRS 182926]), borehole designations beginning with "USW" and "UE25" have been abbreviated (e.g., "USW G-1" is

"G-1" and "UE25a4" is "A-4"). Borehole "UE25a1b1H" is shown as two adjacent boreholes, "A-1" and "B-1." Finally, borehole "WT-16" is not shown in the subsurface facilities document (BSC 2007 [DIRS 182926]), but can be seen to be in the general area presented in Figure 2 of Sass et al. (1988 [DIRS 100644]). The average and standard deviation of the UZ heat flux measurements from these boreholes given in Tables 5 and 6 of Sass et al. (1988 [DIRS 100644]) are 38 and 6.1 mW/m^2, respectively. Note that for boreholes with multiple heat flux measurements, the average value was used to determine the average and standard deviation over these boreholes. Thus, the mean of the Sass et al. (1988 [DIRS 100644]) heat fluxes lies within one standard deviation of the mean of the Rousseau et al. (1997 [DIRS 100178]) values (average of 36 mW/m^2 and a standard deviation of 3.6 mW/m^2). The heat flow data from Sass et al. (1988 [DIRS 100644]) have also been presented in the peer-reviewed journal article by Fridrich et al. (1994 [DIRS 100575], Section 9.2 and Figure 7). This favorable comparison indicates the reliability of the heat flux data from Rousseau et al. (1997 [DIRS 100178]).

J6.2.3 Data Qualified for Intended Use

Based on the extent to which the data demonstrate the properties of interest and the existence of corroborating data, the data from Rousseau et al. (1997 [DIRS 100178]) are adequate for intended use within FEP 1.2.06.00.0A (Hydrothermal Activity). Based on the evaluation of corroborating data, the data meet qualification criteria outlined above and can be considered qualified for intended use within this FEP.

J6.3 QUALIFICATION OF DATA FROM WILSON ET AL. 2003

Wilson, N.S.F.; Cline, J.S.; and Amelin, Y.V. 2003. "Origin, Timing, and Temperature of Secondary Calcite–Silica Mineral Formation at Yucca Mountain, Nevada." *Geochimica et Cosmochimica Acta, 67,* (6), 1145-1176. New York, New York: Pergamon. [DIRS 163589].

The data from this journal article to be qualified for intended use within this FEP include:

> Studies of secondary minerals at Yucca Mountain using petrography, fluid-inclusion thermometry, and uranium-lead dating indicate that unsaturated-zone temperatures have remained close to the current ambient values over the past 2 to 5 Ma (Wilson et al. 2003 [DIRS 163589], Section 8).
>
> The unsaturated-zone secondary minerals were interpreted to have been deposited from downward percolating meteoric water and not the result of upwelling groundwaters (Wilson et al. 2003 [DIRS 163589], Sections 7.3 and 8).

J6.3.1 Qualification Method

The methods of qualification for intended use of the data obtained from the scientific paper by Wilson et al. (2003 [DIRS 163589]) listed above are the Corroborating Data method (SCI-PRO-001, Attachment 3, Method 2) and the Technical Assessment method (SCI-PRO-001, Attachment 3, Method 5). The rationale for using these methods is that they were the most suitable considering the data, their existing documentation, their intended use, and availability of corroborating data. The technical assessment was based on the determination that confidence in the data acquisition or development was warranted. Qualification process attributes used in the

qualification of these data were selected from the list provided in Attachment 4 of SCI-PRO-001. Attributes specifically relevant to these data are:

- The extent to which the data demonstrate the properties of interest (e.g., physical, chemical, geological, mechanical) (#3).
- Prior peer or other professional reviews of the data and their results (#8).
- Extent and quality of corroborating data or confirmatory testing results (#10).

J6.3.2 Corroborating Data

These data are corroborated by an independent study by Bish and Aronson (1993 [DIRS 100006]). They correlated temperatures of formation of illite–smectite (from the saturated zone) and ages from K/Ar dating to conclude that no significant hydrothermal alteration has occurred since 10.7 Ma. These are independent data supporting the conclusion of Wilson et al. (2003 [DIRS 163589]). Additional corroborating data are presented by Whelan et al. (2002 [DIRS 160442]). The evaluation criterion is that the corroborating data set confirms that no significant hydrothermal alteration has occurred since 10.7 Ma. The independent study by Bish and Aronson (1993 [DIRS 100006]) supports an even longer period of constant temperature in the UZ at Yucca Mountain; thus the data from Wilson et al. (2003 [DIRS 163589]) are further corroborated.

J6.3.3 Technical Assessment

Extent to Which the Data Demonstrate the Properties of Interest—The property of interest is the long-term stability of the temperature regime at Yucca Mountain. Studies of secondary minerals at Yucca Mountain using petrography, fluid–inclusion microthermometry, and U–Pb dating indicate that temperatures have remained close to the current ambient values over the past two to five million years (Wilson et al. 2003 [DIRS 163589], Section 8). This is demonstrated by the relation between the temperatures (inferred from the composition of fluid inclusions) and the age of the inclusions, inferred from the U–Pb isotope dating. The study reported in the publication by Wilson et al. (2003 [DIRS 163589]) included the temperature regime for the formation of the secondary calcite–silica minerals in primary and secondary porosity of the host Miocene tuffs at Yucca Mountain and is, therefore, relevant to the properties of interest.

Prior Peer or Other Professional Reviews of the Data and their Results—Wilson et al. (2003 [DIRS 163589]) published their experimental results in the scientific journal *Geochimica et Cosmochimica Acta*. Published for over 100 years, *Geochimica et Cosmochimica Acta* is a professional scientific research journal for geochemistry and cosmochemistry. It is sponsored by The Geochemical Society and The Meteoritical Society and is published by Elsevier Science Ltd. Contributions to the journal are evaluated for scientific merit by thorough professional review. Peer review is an essential and integral aspect of *Geochimica et Cosmochimica Acta*. The fundamental role of the reviewer is to advise the Associate Editor and the Executive Editor on the technical merit, or lack thereof, of a manuscript submitted for publication. The Associate Editor writes a report summarizing reviewer opinion, presenting his/her overall evaluation based on his/her own reading of the manuscript and the advice of the reviewers. The peer review

process and the reputation of the journal ensure that the paper received adequate peer review. The journal typically requires three external reviews; Wilson et al. (2003 [DIRS 163589], p. 1,171) acknowledge input from seven reviewers.

J6.3.4 Data Qualified for Intended Use

Based on the extent to which the data demonstrate the properties of interest, the existence of corroborating data, and the data review, the data from Wilson et al. (2003 [DIRS 163589]) are adequate for the intended use within FEP 1.2.06.00.0A (Hydrothermal Activity). These data are qualified for intended use in the screening justification for this FEP.

J7. FEP 1.2.07.01.0A – EROSION/DENUDATION

This FEP uses data from the following report as direct input:

Stuckless, J.S. and Levich, R.A., eds. 2007. *The Geology and Climatology of Yucca Mountain and Vicinity, Southern Nevada and California.* Memoir 199. Boulder, Colorado: Geological Society of America. TIC: 259378. [DIRS 181507]

This FEP uses data from the following report as direct input:

> Using a ^{10}Be cosmogenic dating technique, the calculated maximum possible erosion rates for bedrock outcrops at Yucca Mountain range from 0.4 to 2.7 cm/10,000 years (Stuckless and Levich 2007 [DIRS 181507], p. 83).
>
> The long-term rates of erosion of unconsolidated material from Yucca Mountain hillslopes were calculated to be 0.2 to 6 cm/10,000 years using the rock varnish cation ratio and the in situ cosmogenic ^{36}Cl dating methods (Stuckless and Levich 2007 [DIRS 181507], p. 84).

J7.1. QUALIFICATION METHOD

The methods of qualification of the data from Stuckless and Levich (2007 [DIRS 181507]) are the Corroborating Data and Technical Assessment methods (SCI-PRO-001, Attachment 3, Methods 2 and 5). The rationale for using both methods is that the conditions for the use of corroborating data are met, and the approaches for technical assessment also are applicable. The technical assessment included determination that confidence in the data acquisition or development was warranted and confirmation that the data had been used in similar applications. Qualification process attributes used in the qualification are selected from the list provided in Attachment 4 of SCI-PRO-001. Attributes specifically applicable to these data are:

- The extent to which the data demonstrate the properties of interest (e.g., physical, chemical, geological, mechanical) (#3).
- Prior uses of the data and associated verification processes (# 7).
- Extent and reliability of the documentation associated with the data (#9).

J7.2. CORROBORATING DATA

The estimated maximum rate of erosion on ridge crests, outcrops, and hillslopes over 10,000 years was used in an order-of-magnitude manner to evaluate the potential for erosional processes to breach the geologic repository. The chapter cited within the reference, *Geology of the Yucca Mountain Site Area, Southwestern Nevada*, was authored by W. R. Keefer, J. W. Whitney, and D. C. Buesch (Stuckless and Levich (2007 [DIRS 181507], pp. 53 to 103). *Yucca Mountain Site Description* (BSC 2004 [DIRS 169734], Section 3.4.6) provides a summary description of the erosion processes occurring at Yucca Mountain during Quaternary time. Some of the data reported in that reference are the same as those in the publication by Stuckless and Levich (2007

[DIRS 181507]). Erosion rates were examined on hillslopes and bedrock outcrops on ridge crests in the Yucca Mountain site area. Initially, the surface exposure age of hillslope boulder deposits was calculated using the rock-varnish, cation-ratio dating method (Harrington and Whitney 1987 [DIRS 106095], pp. 967 to 970). Subsequently, cosmogenic ^{10}Be was also used to determine vertical erosion rates on bedrock outcrops on ridge crests of Yucca Mountain. From ^{10}Be measurements, tuff bedrock erosion rates were less than 4 cm per 10,000 years, while rates of erosion for hillslope coluvium were approximately 5 cm per 10,000 years (Gosse et al. 1996 [DIRS 170725]).

Analyses of ^{10}Be concentrations in quartz separates from tuffaceous bedrock exposed on Antler Ridge and the adjacent ridge to the south, on the east flank of Yucca Mountain, indicate a maximum possible erosion rate of bedrock to range from 0.4 to 2.7 cm per 10,000 years (Stuckless and Levich 2007 [DIRS 181507], p. 83). These values are compared in the report with the rock erosion rates measured in Australia and on granite landforms in Alabama Hills in California (Stuckless and Levich 2007 [DIRS 181507], p. 83) and the measured values agree well with the results of those other studies. The long-term erosion rates for Yucca Mountain hillslopes were found to be on the order of 2 cm per 10,000 years and are comparable with the high end of bedrock erosion rates (Stuckless and Levich 2007 [DIRS 181507], p. 84).

J7.3. TECHNICAL ASSESSMENT

Data Demonstrate the Properties of Interest—This report provides a detailed summary of bedrock and hillslope erosion rates for Yucca Mountain using a variety of methods.

Extent and Reliability of Documentation—This report thoroughly documents the ranges of bedrock and hillslope erosion rates for Yucca Mountain using a variety of methods. The report was published as a special Memoir (#199) by United States Geological Survey (USGS), representing one of the world's leading organizations in geological research.

Data Have Been Used in Similar Applications—Some of these data were previously used (YMP 1993 [DIRS 100520], Section 3.4) in other analyses and models supporting performance assessment for the Yucca Mountain repository (BSC 2004 [DIRS 169734], Section 3.4.6.2).

J7.4. DATA QUALIFIED FOR INTENDED USE

The data from Stuckless and Levich (2007 [DIRS 181507]) are appropriate for the intended use within FEP 1.2.07.01.0A (Erosion/Denudation). Based on the existence of corroborating data, the extent to which the data demonstrate the properties of interest, the extent and reliability of the documentation, and previous uses of similar data in similar applications, the erosion rate data can be considered qualified for intended use within this FEP.

J8. FEP 1.2.08.00.0A – DIAGENESIS

Diagenesis is an ongoing process of chemical and physical changes to sediments undergoing compaction, cementation, and burial. This FEP uses data from the following sources as direct input:

"Early Diagenesis in Continental Eolian Deposits" (Krystinik 1990 [DIRS 135295])

Caliche: Origin, Classification, Morphology and Uses (Reeves 1976 [DIRS 104303])

Impact of Time and Climate on Quaternary Soils in the Yucca Mountain Area of the Nevada Test Site (Taylor 1986 [DIRS 102864])

Factors Limiting Microbial Growth and Activity at a Proposed High-Level Nuclear Repository, Yucca Mountain, Nevada (Kieft et al. 1997 [DIRS 100767])

Secondary Mineral Deposits and Evidence of Past Seismicity and Heating of the Proposed Repository Horizon at Yucca Mountain, Nevada (Whelan 2004 [DIRS 170697]).

J8.1 QUALIFICATION OF DATA FROM KRYSTINIK 1990

Krystinik, L.F. 1990. "Early Diagenesis in Continental Eolian Deposits." Chapter 8 of *Modern and Ancient Eolian Deposits: Petroleum Exploration and Production*. Fryberger, S.G.; Krystinik, L.F.; and Schenk, C.J., eds. Denver, Colorado: Society of Economic Paleontologists and Mineralogists, Rocky Mountain Section. TIC: 247781. [DIRS 135295]

The data to be qualified within this FEP include:

> Compaction may reduce eolian sediments by as much as 20% to 30% (Krystinik 1990 [DIRS 135295], p. 8-2), but after this initial stage, compaction does not become an important factor in diagenesis until the onset of grain deformation and pressure solution during deeper burial diagenesis (Krystinik 1990 [DIRS 135295], p. 8-3).

J8.1.1 Qualification Method

The method of qualification for intended use of the data obtained from the scientific paper by Krystinik (1990 [DIRS 135295]) listed above is the Corroborating Data method (SCI-PRO-001, Attachment 3, Method 2). The rationale for using this method is that it was the most suitable considering the data, availability of corroborating data, their existing documentation, and their intended use. Qualification process attributes used in the qualification of these data were selected from the list provided in Attachment 4 of SCI-PRO-001. Attributes specifically relevant to these data are:

- The extent to which the data demonstrate the properties of interest (e.g., physical, chemical, geological, mechanical) (#3).
- Extent and quality of corroborating data or confirmatory testing results (#10).

J8.1.2 Corroborating Data

The two primary mechanisms for early and shallow diagenetic changes are related to compactions and cementation. Krystinik (1990 [DIRS 135295], pp. 8-3 and 8-4) indicates that early diagenesis "begins at or near the depositional interface and entails weathering, compaction, cementation and numerous allied physical, chemical and biochemical processes, at temperature below 50°C." Krystinik notes that "wind-laid sand can be deposited with up to 25% to 40% porosity and that early compaction reduces porosity by as much as 20% to 30%, depending upon sorting." Krystinik further states that "[b]eyond increasing capillarity, compaction does not generally become an important factor in diagenesis until the onset of grain deformation and pressure solution during deeper burial diagenesis." By minimizing compaction, then, the primary means of diagenesis becomes cementation processes.

By way of corroborating the role of compaction in early diagenesis, Palmer and Barton (1987 [DIRS 118483], pp. 32 and 39) compare similar, uncemented sands of increasing ages and burial depth with porosities. In the first 169 meters of burial, the porosity of the sand decreases from 47.2% to 35.6%, but from 169 m to 780 m, the compaction only decreased the porosity an additional 2%, for a total decrease of 13.6%. This corroborates Krystinik's assertion of an initial reduction of no more than a few percent, followed by minimal effects. The lack of compaction during initial burial is also corroborated by the Sclater-Christie compaction curve given by Baldwin and Butler (1985 [DIRS 167871], Figure 3). The curve shows that change in porosity during the first 300 m of burial is insignificant, but becomes increasingly more important at greater depths, with changes of up to 50% porosity relative to the initial porosities occurring at depths approaching 10 km. However, Baldwin and Butler also caution that sandstones show considerable scatter in solidity-depth values and indicate that ranges in values of 25% are common. As a "case-in-point," the work by Salem et al. (1998 [DIRS 167869], pp. 319 to 331) on cratonic sandstones indicates that sandstones undergoing burial between 1.5 and 2.5 km exhibited only a 19% total porosity loss due to compaction. The results of this work match well with the compaction curves of Baldwin and Butler for a 1 to 2 km burial depth, and further corroborates Krystinik's assertion that compaction plays only a minor role during the early stages of shallow burial and diagenesis.

J8.1.3 Data Qualified for Intended Use

Based on the extent to which the data demonstrate the properties of interest and the existence of corroborating data, the data from Krystinik (1990 [DIRS 135295]) are adequate for intended use within FEP 1.2.08.00.0A (Diagenesis). These data are qualified for intended use in the screening justification for this FEP.

J8.2 QUALIFICATION OF DATA FROM REEVES 1976

Reeves, C.C. 1976. *Caliche: Origin, Classification, Morphology and Uses*. Lubbock, Texas: Estacado Books. TIC: 245928. [DIRS 104303]

The data to be qualified within this FEP include:

> The net effects of shallow diagenesis and associated cementation on infiltration in an arid environment are to stabilize the surface environment, and decrease the net vertical infiltration rate (Reeves 1976 [DIRS 104303], p. 110).

J8.2.1 Qualification Method

The method of qualification for intended use of the data obtained from the book by Reeves (1976 [DIRS 104303]) listed above is the Corroborating Data method (SCI-PRO-001, Attachment 3, Method 2). The rationale for using this method is that it was the most suitable considering the data, their existing documentation, and their intended use, as well as availability of corroborating data. Qualification process attributes used in the qualification of these data were selected from the list provided in Attachment 4 of SCI-PRO-001. Attributes specifically relevant to these data are:

- The extent to which the data demonstrate the properties of interest (e.g., physical, chemical, geological, mechanical) (#3).
- Extent and quality of corroborating data or confirmatory testing results (#10).

J8.2.2 Corroborating Data

With regard to the role of cementation in diagenesis and its effects, Reeves (1976 [DIRS 104303], p. 110) indicates that the net effects of shallow diagenesis and associated cementation is to decrease the net vertical infiltration rate and cites multiple studies to support that assertion. This net reduction in infiltration is corroborated by Lattman (1983 [DIRS 167815], pp. 107 to 108) who states, "[t]he formation of caliche inhibits infiltration into a topographic surface. The degree of this inhibition is a function of density and induration of the caliche. Petrocalcic horizons, laminar layers, and case-hardened layers cause the greatest inhibition." It is also corroborated by Arakel (1996 [DIRS 167623], p. 223), who refers to progressive plugging of initial porosity/permeability zones. It should be pointed out that while this holds true for the carbonates, Taylor (1986 [DIRS 102864]) indicates that in the YMP soils studied, in the absence of effective precipitation or drainage to remove newly dissolved silica, it is precipitated elsewhere within the calcrete horizon, or $CaCO_3$ preferentially precipitates after opaline silica bonds adjacent soil grains. Taylor notes that this process may occur without necessarily plugging intervening pores spaces.

J8.2.3 Data Qualified for Intended Use

Based on the extent to which the data demonstrate the properties of interest and the existence of corroborating data, the data from the book by Reeves (1976 [DIRS 104303]) are appropriate for

intended use within FEP 1.2.08.00.0A (Diagenesis). These data are qualified for use in the screening justification for this FEP.

J8.3 QUALIFICATION OF DATA FROM TAYLOR 1986

Taylor, E.M. 1986. *Impact of Time and Climate on Quaternary Soils in the Yucca Mountain Area of the Nevada Test Site*. Master's thesis. Boulder, Colorado: University of Colorado. TIC: 218287. [DIRS 102864]

The technical information to be justified within this FEP include:

> SiO_2 cementation is not dependent on climatic conditions, but cementation does exhibit distinctive trends that correspond with the ages of the surficial deposits (Taylor 1986 [DIRS 102864], Chapter 5).
>
> Accumulation rates are attributable to several climatic scenarios, but climate change was insufficient to significantly decrease the rate of accumulations (Taylor 1986 [DIRS 102864], Chapter 5).
>
> Cementation by opaline SiO_2 is common in the Yucca Mountain study area, and opaline SiO_2 accumulation in the soils is favored over that of $CaCO_3$ (Taylor 1986 [DIRS 102864], Figure 9 and pp. 31 to 33).

J8.3.1 Qualification Method

The method of qualification for intended use of the data obtained from the thesis by Taylor (1986 [DIRS 102864]) listed above is the Corroborating Data method (SCI-PRO-001, Attachment 3, Method 2). The rationale for using this method is that it was the most suitable considering the data, their existing documentation, and their intended use. Qualification process attributes used in the qualification of these data were selected from the list provided in Attachment 4 of SCI-PRO-001. Attributes specifically relevant to these data are:

- The extent to which the data demonstrate the properties of interest (e.g., physical, chemical, geological, mechanical) (#3).
- Extent and quality of corroborating data or confirmatory testing results (#10).

Data evaluation criteria were based on consideration of these attributes and arriving at an affirmative conclusion that a given attribute is met by the data under consideration.

J8.3.2 Corroborating Data

Taylor (1986 [DIRS 102864], Chapter 5) indicates silts that formed in alluvium and eolian fines of Holocene to early Pleistocene or late Pliocene age near Yucca Mountain are characterized by distinctive trends in the accumulation of secondary clay, $CaCO_3$, and opaline SiO_2 that correspond with the ages of the surficial deposits, although there is no macro- or micromorphological evidence that suggests that silica cementation occurred under climatic conditions cooler and wetter than those of the present climate. Taylor also states that

accumulation rates of these materials during the Holocene can be attributed to several possible climatic scenarios associated with the Holocene-Pleistocene climate change, but suggests that precipitation has not been a limiting factor, and that climatic change was not sufficient to significantly decrease rate of accumulation. Taylor also suggests that the climatic change was the result of decreases in temperature rather than precipitation. Modeling results discussed by Taylor suggest that increased precipitation in the future may translocate $CaCO_3$ accumulations to greater depths, where precipitation is greater. Taylor also suggests that the cementation process, particularly for $CaCO_3$, is reversible, and that the material can be redissolved and moved deeper into the soil profile.

The dependence of the accumulation depth of $CaCO_3$, and the dependence of other diagenetic effects related to chemical changes, is corroborated by several sources. Eghbal and Southard (1993 [DIRS 167625], p. 1049) suggest that, in the Mojave Desert, development of carbonate-free argillic horizons probably occurred during pluvial periods, whereas calcification occurred during drier periods. Silicification appears to have been contemporaneous with both clay illuviation and calcification and, thus, may be related to pedochemical conditions rather than to climate. This corroborates the results by Taylor (1986 [DIRS 102864], Chapter 5) discussed above, and for a similar arid setting. Eghbal and Southard further unequivocally state that soils in arid regions are often polygenetically related to climatic variations. This trend for calcification is also corroborated in the abstract by Lattman (1972 [DIRS 167813]) in the statement "[i]t is suggested that extensive calcrete layers in southern Nevada formed during and immediately following the onset of pluvial periods which were times of fan aggradation. They were generally destroyed during the interpluvial, which were times of fan stability or degradation." This statement also tends to suggest that calcification effects may be reversible, whereas silicification may be ongoing regardless of the climate state.

Further corroboration is gained from Chadwick et al. (1995 [DIRS 167626]), who document changes in soil profiles along a transect that reflect cooler and wetter conditions due to elevation changes. However, these serve as a surrogate for change in climate conditions. In particular, they observed that climatic extremes drive pedogenic processes that leave polygenetic imprints on soils of Pleistocene age. In particular, soils that are now dominated by opaline silica, carbonate, and smectite contain evidence of earlier, more acidic, chemical environments conducive to dissolution of primary carbonate and formation of kaolinite. During interglacial times (i.e., drier and warmer), Chadwick et al. attribute the changes to more eolian activity and less effective moisture combining to decrease the depth of leaching, increase base cations, and modify the soil chemical environment in relict paleosols. This trend toward increased calcification during pluvial times is corroborated in the accumulation rates noted in the abstract by Machette (1982 [DIRS 167814]), who indicates that soils <25,000 years old have accumulation rates 2 to 3 times higher than older soils. This observation is attributed to "less effective precipitation and vegetation cover in Holocene time," which is due in large part to a drier climate state. The increased accumulation rates of $CaCO_3$ are also noted by Eghbal and Southard (1993 [DIRS 167624], pp.170 to 171).

Taylor (1986 [DIRS 102864], Figure 9) indicates that the accumulation rate of $CaCO_3$, while occurring, is significantly less than that for SiO_2. This is reflected in statements indicating that carbonate is primarily derived from airborne dust and the opaline SiO_2 from in-place weathering of the parent material and that the cementation by opaline SiO_2 is common in the study area and

that opaline SiO_2 accumulation in the soils is favored over that of $CaCO_3$. Taylor also indicates that SiO_2 cementation is common in the study area, with $CaCO_3$ as an accessory cement. The direct input from Taylor indicating the predominance of SiO_2 over carbonate in the soil cements is corroborated by Lattman (1973 [DIRS 129305], p. 3015). In studies near Las Vegas, Lattman observed that calcium carbonate cementation is not necessarily a significant cementation process in rhyolitic tuffs due to the lack of carbonate source materials. The above statements by Lattman and Taylor's observations of the predominance of SiO_2 cements mentioned above, is mutually corroborative with statements from Krystinik (1990 [DIRS 135295], p. 8-4) that cements other than carbonate may develop, particularly iron, silica, and aluminum. Yaalon (1967 [DIRS 167622], p. 1189) corroborates this by indicating that one of the controlling factors in diagenesis of eolian sands is the original content of $CaCO_3$. As a corroborative example from indirect input, the presence of cements other than carbonate in arid environments is proposed in a study by Salem et al. (1998 [DIRS 167869], pp. 319 to 331). In that particular study, the predominant cements stemming from the generally arid environment were iron and silica.

J8.3.3 Data Qualified for Intended Use

Based on the extent to which the data demonstrate the properties of interest and the existence of corroborating data, the data from the thesis by Taylor (1986 [DIRS 102864]) are considered qualified for intended use within FEP 1.2.08.00.0A (Diagenesis).

J8.4 QUALIFICATION OF DATA FROM KIEFT ET AL. 1997

Kieft, T.L.; Kovacik, W.P., Jr.; Ringelberg, D.B.; White, D.C.; Haldeman, D.L.; Amy, P.S.; and Hersman, L.E. 1997. "Factors Limiting Microbial Growth and Activity at a Proposed High-Level Nuclear Repository, Yucca Mountain, Nevada." *Applied and Environmental Microbiology, 63,* (8), 3128-3133. Washington, D.C.: American Society for Microbiology. TIC: 236444. [DIRS 100767]

The data to be qualified for intended use within this FEP include the following statements:

> Total counts (microscopic direct and plate) ranged from below limit of detection (3.2×10^4 cells per gram) to 2.3×10^5 cells per gram (Kieft et al. 1997 [DIRS 100767], p. 3,130).
>
> Phospholipid fatty acid (PLFA) concentrations were generally low, ranging from 0.1 to 3.7 pmol per gram (Kieft et al. 1997 [DIRS 100767], p. 3,130).

J8.4.1 Qualification Method

The method of qualification for intended use of the external data from Kieft et al. (1997 [DIRS 100767]) is the Corroborating Data method (SCI-PRO-001, Attachment 3, Method 2). The rationale for using this method is that it was the most suitable considering the data, their intended use, as well as availability of corroborating data. Qualification process attributes used in the qualification are selected from the list provided in Attachment 4 of SCI-PRO-001.

Attributes specifically applicable to these data are:

- Extent and quality of corroborating data or confirmatory testing results (#10).
- The extent to which the data demonstrate the properties of interest (e.g., physical, chemical, geologic, mechanical) (#3).

J8.4.2 Corroborating Data

The intended use of the data is to support the statement "Plate count, direct count, and phospholipid fatty acid (PLFA) data indicate a low abundance of microorganisms in Yucca Mountain tuff" (Kieft et al. 1997 [DIRS 100767], p. 3,130) for use in FEP 1.2.08.00.0A. The conclusion statement by Kieft et al. (1997 [DIRS 100767]), "[p]late count, direct count, and PLFA data indicate a low abundance of microorganisms in Yucca Mountain tuff", is supported by data represented in Figures 2 and 3 within the reference. Using a variety of methods, plate count, direct count, and PLFA, the results reported within this source mutually corroborate the statement the microorganisms are in low abundance in Yucca Mountain tuff. Furthermore, these results are consistent with findings from additional studies by Haldeman and Amy (1993 [DIRS 145228]) and Horn (2004 [DIRS 171058]). Kieft et al. report that the range of microorganisms found is on the order of 10^4 to 10^5 cells per gram tuff. Horn et al. (2004 [DIRS 171058]) report values of values of 4×10^4 and 6×10^4 cells per gram of dry rock from an ESF rock core. These results are consistent with previous findings of $<1 \times 10^1$ to 2.4×10^5 colony forming units per gram of dry rock for unsaturated tuff from Rainier Mesa tunnel systems on the Nevada Test Site (Haldeman and Amy 1993 [DIRS 145228]). These data represent an overall low microorganism total count and are adequate and accurate for the intended use within this FEP.

J8.4.3 Data Qualified for Intended Use

Based upon the discussion provided above and the strong corroborative results from additional studies, the data described above support the statement of low abundance of microorganism in Yucca Mountain tuff and are adequate for use within FEP 1.2.08.00.0A (Diagenesis). The data are qualified for use in the screening justification for this FEP.

J8.5 QUALIFICATION OF DATA FROM WHELAN 2004

Whelan, J.F. 2004. *Secondary Mineral Deposits and Evidence of Past Seismicity and Heating of the Proposed Repository Horizon at Yucca Mountain, Nevada.* Water-Resources Investigations Report 03-4321. Reston, Virginia: U.S. Geological Survey. ACC: MOL.20040902.0236. [DIRS 170697]

The data to be qualified for intended use within this FEP include the following statements:

> Calcite and silica (quartz, chalcedony, and opal) are found in some open fractures and lithophysal cavities in the Topopah Spring and Tiva Canyon Tuffs in the UZ. Studies indicate that secondary minerals form in the UZ from meteoric waters percolating along fractures to the water table. Therefore, there is a link between pedogenic deposition on

the overlying soil, infiltration of meteoric water, and secondary mineral deposition in the UZ. Deposits of secondary minerals are sparsely and heterogeneously distributed on less than 10% of potential fracture and cavity depositional sites (Whelan 2004 [DIRS 170697], p. 3).

J8.5.1 Qualification Method

The method of qualification for the data from Whelan (2004 [DIRS 170697]) listed above is the Technical Assessment method (SCI-PRO-001, Attachment 3, Method 5). The rationale for using this method is that it is the most appropriate considering the extent of available documentation. The technical assessment was based on the determination that confidence in the data acquisition or development was warranted. Process attributes used in the qualification of these data are selected from the list provided in Attachment 4 of SCI-PRO-001. Attributes specifically applicable to these data are:

- The extent to which the data demonstrate the properties of interest (e.g., physical, chemical, geologic, mechanical) (#3).

- The extent and reliability of the documentation associated with the data (#9).

J8.5.2 Technical Assessment

The statement under consideration concerns the observation and characterization of secondary mineral deposits in lithophysal cavities along some fracture surfaces within the ESF and ECRB Cross Drift. Secondary mineral studies have been conducted by the USGS since 1995 using a variety of visual and isotopic techniques. The characterization of the secondary calcite and silica deposits from ESF and ECRB tunnel samples is documented in numerous publications (e.g., Whelan et al. 1994 [DIRS 100091]; Whelan and Moscati 1998 [DIRS 109179]; Paces et al. 2001 [DIRS 156507]; Whelan et al. 2002 [DIRS 160442]), in detailed labeled photomicrographs of petrographic thin sections (see, for example, Figure 8 of Whelan 2004 [DIRS 170697]), and by an extensive database of $\delta^{18}O$ and $\delta^{13}C$ analyses (e.g., DTN: GS020908315215.004 [DIRS 164847]), U-series age-dates (e.g., DTN: GS021208315215.009 [DIRS 164750]), and fluid-inclusion homogenization temperatures (e.g., DTN: GS020908315215.003 [DIRS 164846]). The isotopic analyses in particular support the pedogenic origin of the calcite, and its deposition under temperatures generally less than 60°C over at least the past ten million years. The intended use of the data is to support the statement "A principal effect of deeper diagenesis at Yucca Mountain is the infilling and coating of open fractures and lithophysal cavities by calcite and silica (Whelan 2004 [DIRS 170697], p. 3)" within FEP 1.2.08.00.0A (Diagenesis). In this manner the data demonstrates the properties of interest that calcite and silica are present in the unsaturated zone at Yucca Mountain as diagenetic features that have been established over millions of years.

J8.5.3 Data Qualified for Intended Use

The technical assessment of these data provides sufficient confidence that these data are adequate and are considered qualified for intended use within FEP 1.2.08.00.0A (Diagenesis).

J9. FEP 1.2.09.02.0A – LARGE SCALE DISSOLUTION

This FEP uses data and technical information from the following publication as direct input:

Freeze, R.A. and Cherry, J.A. 1979. *Groundwater.* Englewood Cliffs, New Jersey: Prentice-Hall. TIC: 217571. [DIRS 101173]

The data and technical information to be qualified for use within this FEP include:

> In water at 1 atm pressure, 25°C, and pH 7, mineral solubilities are 12 mg/L for quartz, 90 to 500 mg/L for carbonates (depending on CO_2 partial pressure), and 360,000 mg/L for halite (Freeze and Cherry 1979 [DIRS 101173], p. 106).
>
> Extensive carbonate dissolution cavities are not expected to develop because such dissolution is not typically observed in carbonates at great depths below the water table (Freeze and Cherry 1979 [DIRS 101173], pp. 514 to 515).

J9.1 QUALIFICATION METHOD

The method of qualification for the data from Freeze and Cherry (1979 [DIRS 101173]) listed above is the Technical Assessment method (SCI-PRO-001, Attachment 3, Method 5). The rationale for using this method is that it was the most suitable considering the data, their existing documentation, and their intended use. The technical assessment included determination that confidence in the data acquisition or development was warranted. Process attributes used in the qualification of these data are selected from the list provided in Attachment 4 of SCI-PRO-001. Attributes specifically applicable to these data are:

- The extent to which the data demonstrate the properties of interest (e.g., physical, chemical, geologic, mechanical) (#3).
- Qualification of personnel generating the data (#1).

J9.2 TECHNICAL ASSESSMENT

The Extent to Which the Data Demonstrate the Properties of Interest—The specific solubility values used in the FEP are those for carbonate, halite, and quartz. The solubility values were used in a qualitative sense to demonstrate that the predominate Yucca Mountain rock units are relatively insoluble; solubility values were not used quantitatively in a model or calculation. Therefore, use of solubility data from Freeze and Cherry (1979 [DIRS 101173]) in the FEP to support arguments concerning the large-scale dissolution of YMP rock units is technically adequate and appropriate.

Qualification of Personnel or Organizations Generating the Data—R. Allan Freeze is former Professor and Director in the Geological Engineering Program at the University of British Columbia in Vancouver, Canada. He is the coauthor of *Groundwater* (1979) and *Groundwater Contamination: Optimal Capture and Containment* (1993), and the coeditor of *Physical Hydrogeology* (1983). John A. Cherry has been a professor at the University of Waterloo since 1971. He has a Ph.D. in Hydrogeology and is coauthor of the highly acclaimed textbook on

hydrogeology, *Groundwater*, published by Prentice-Hall. The textbook (Freeze and Cherry 1979 [DIRS 101173]) underwent extensive reviews from professional peers and was trial tested by many graduate and undergraduate students before publication.

The publication was designed as a text in introductory groundwater courses normally taught in undergraduate geology, geological engineering, or civil engineering curricula and has been used extensively by university students for almost thirty years. The authors recognized the need to include material beyond the normal geologic and hydraulic aspects of groundwater studies, so they included three major chapters primarily chemical in emphasis. Data used to support FEP 1.2.09.02.0A are from one of the three Freeze and Cherry (1979 [DIRS 101173]) chapters, "Chemical Properties and Principles."

J9.3 DATA QUALIFIED FOR INTENDED USE

Based on the assessment made above, solubility data and information on formation of cavities from Freeze and Cherry (1979 [DIRS 101173]) are appropriate for intended use within FEP 1.2.09.02.0A (Large Scale Dissolution). These data are qualified for use in the screening justification for this FEP.

J10. FEP 1.2.10.01.0A – HYDROLOGIC RESPONSE TO SEISMIC ACTIVITY

This FEP uses data from the following report as direct input:

Ground Water at Yucca Mountain, How High Can It Rise? Final Report of the Panel on Coupled Hydrologic/Tectonic/Hydrothermal Systems at Yucca Mountain (National Research Council 1992 [DIRS 105162]).

J10.1 QUALIFICATION OF DATA FROM NATIONAL RESEARCH COUNCIL 1992

National Research Council 1992. *Ground Water at Yucca Mountain, How High Can It Rise? Final Report of the Panel on Coupled Hydrologic/Tectonic/Hydrothermal Systems at Yucca Mountain.* Washington, D.C.: National Academy Press. TIC: 204931. [DIRS 105162]

The data from the National Research Council report to be qualified for intended use within this FEP concern the predicted changes in the water table elevation in response to seismic activity. The intended use of the data overlaps with FEPs 2.2.06.01.0A (Seismic Activity Changes Porosity and Permeability of Rock) and 2.2.06.02.0A (Seismic Activity Changes Porosity and Permeability of Faults) and includes the following statement:

> Results from the regional stress model approach indicated a maximum water table rise of 50 m (National Research Council 1992 [DIRS 105162], Chapter 5, p. 116).

J10.2 Qualification Method

The same data obtained from the same reference and used in an analogous context were qualified for intended use in FEP 2.2.06.01.0A (Seismic Activity Changes Porosity and Permeability of Rock). The data were qualified for intended use using the Technical Assessment method (SCI-PRO-001, Attachment 3, Method 5) with the consideration of the qualifications of personnel or organizations generating the data and the extent to which the data demonstrate the properties of interest. The rationale for selecting the technical assessment data qualification method and the attributes of the data qualification process used for FEP 2.2.06.01.0A (Seismic Activity Changes Porosity and Permeability of Rock) are also applicable to qualifying the data from the National Research Council report (National Research Council 1992 [DIRS 105162]) for the intended use in FEP 1.2.10.01.0A (Hydrologic Response to Seismic Activity).

J10.3 Data Qualified for Intended Use

Based on the evidence provided for FEP 2.2.06.01.0A (Seismic Activity Changes Porosity and Permeability of Rock) and the intended use of the data in FEP 1.2.10.01.0A (Hydrologic Response to Seismic Activity), the data from the National Research Council (1992 [DIRS 105162]) are appropriate and are qualified for intended use in the screening justification for FEP 1.2.10.01.0A (Hydrologic Response to Seismic Activity).

J11. FEP 1.2.10.02.0A – HYDROLOGIC RESPONSE TO IGNEOUS ACTIVITY

This FEP uses data from the following report as direct input:

Valentine, G.A.; WoldeGabriel, G.; Rosenberg, N.D.; Carter Krogh, K.E.; Crowe, B.M.; Stauffer, P.; Auer, L.H.; Gable, C.W.; Goff, F.; Warren, R.; and Perry, F.V. 1998. "Physical Processes of Magmatism and Effects on the Potential Repository: Synthesis of Technical Work Through Fiscal Year 1995." Chapter 5 of *Volcanism Studies: Final Report for the Yucca Mountain Project.* Perry, F.V.; Crowe, B.M.; Valentine, G.A.; and Bowker, L.M., eds. LA-13478. Los Alamos, New Mexico: Los Alamos National Laboratory. TIC: 247225. [DIRS 119132]

The data to be qualified for intended use within this FEP include:

> Mineral alterations around igneous intrusions at natural analogue sites show that alteration is limited to a zone that extends less than 10 m away from the intrusion/host rock contact (Valentine et al. 1998 [DIRS 119132], p. 5-74).

These data are identical to the data used in FEP 1.2.04.02.0A (Igneous Activity Changes Rock Properties) and the intended use of these data is the same. Therefore, these data are appropriate for intended use within FEP 1.2.10.02.0A (Hydrologic Response to Igneous Activity). Based on the discussion and the qualification presented in this appendix for FEP 1.2.04.02.0A (Igneous Activity Changes Rock Properties), the data can be considered qualified.

J12. FEP 1.3.04.00.0A – PERIGLACIAL EFFECTS

This FEP uses data from the following report as direct input:

Thompson, R.S.; Anderson, K.H.; and Bartlein, P.J. 1999. *Quantitative Paleoclimatic Reconstructions from Late Pleistocene Plant Macrofossils of the Yucca Mountain Region.* Open-File Report 99-338. Denver, Colorado: U.S. Geological Survey. ACC: MOL.19991015.0296. [DIRS 109470]

The data to be qualified for intended use within this FEP include:

> During the last glacial maximum, the mean annual temperature at Yucca Mountain exceeded 0°C (Thompson et al. 1999 [DIRS 109470], Figures 17 and 18).

J12.1. QUALIFICATION METHOD

The methods of qualification for intended use of the data from Thompson et al. (1999 [DIRS 109470]) are the Corroborating Data and Technical Assessment methods (SCI-PRO-001, Attachment 3, Methods 2 and 5). The rationale for using both methods is that the conditions for the use of corroborating data are met, and the approaches for technical assessment also are applicable. The technical assessment included determination that confidence in the data acquisition or development was warranted and confirmation that the data had been used in similar applications. Qualification process attributes used in the qualification are selected from the list provided in Attachment 4 of SCI-PRO-001. Attributes specifically applicable to these data are:

- Qualifications of personnel or organization generating the data are comparable to qualification requirements of personnel generating similar data under an approved program that supports the YMP license application process or postclosure science (# 1).
- The extent to which the data demonstrate the properties of interest (e.g., physical, chemical, geological, mechanical) (#3).
- Prior uses of the data and associated verification processes (# 7).
- Extent and quality of corroborating data or confirmatory testing results (# 10).

J12.2. CORROBORATING DATA

The data on temperature during the last full glacial period in the report by Thompson et al. (1999 [DIRS 109470]) are corroborated by the data from the USGS Open-File Report 83-535 titled *Vegetation and Climates of the Last 45,000 Years in the Vicinity of the Nevada Test Site, South-Central Nevada* (Spaulding 1983 [DIRS 101623], p. 2, Tables 4 and 10), which also indicate the above-freezing annual average temperatures during the last full glaciation period.

J12.3. TECHNICAL ASSESSMENT

Data Were Collected by Qualified Individuals—Robert S. Thompson has been a research geologist at the USGS for over twenty years. Dr. Thompson's research focuses on the interactions between environmental and climatic changes through time, from the Pliocene to the present day and into the future. He leads the Climate Change, Land Use, and Environmental Sensitivity (CLUES) Project, which investigates modern relations between plant distributions and climate, provides quantitative paleoclimatic reconstructions from paleobotanical data, and employs arrays of paleoenvironmental data to assess the ability of climate models to simulate climates different from that of today. He has served in several leadership positions within the USGS, including: Team Chief Scientist for the Global Change and Climate History Team, Team Chief Scientist for the Central Region Earth Surface Process Team, acting Coordinator for the Earth Surface Dynamics program, and acting Regional Geologist in the Central Region.

Data Demonstrate the Properties of Interest—Based on data from modern analogues, the report shows that the estimated mean annual temperature was between 7.9°C and 8.5°C at Yucca Mountain (for an elevation of 5,000 ft. (1,524 m)) during the last glacial maximum (Thompson et al. 1999 [DIRS 109470], Table 4). These data are used to predict that the annual average temperature during the coolest climate state over the next 10,000 years will be above freezing. These data are relevant with respect to the property of interest.

Data Have Been Used in Similar Applications—The data were used in other analyses and models supporting performance assessment for the Yucca Mountain repository (BSC 2004 [DIRS 170002], pp. 6-34 and 6-47; BSC 2004 [DIRS 169734], Sections 6, 6.4.2.1, and 6.5.4, Tables 6-27 and 6-29).

J12.4. DATA QUALIFIED FOR INTENDED USE

The above discussion provides confidence that the data from the report by Thompson et al. (1999 [DIRS 109470]) are appropriate for intended use and are qualified for use in the screening argument for FEP 1.3.04.00.0A (Periglacial Effects).

J13. FEP 1.3.05.00.0A – GLACIAL AND ICE SHEET EFFECT

This FEP uses data from the following report as indirect input:

Thompson, R.S.; Anderson, K.H.; and Bartlein, P.J. 1999. *Quantitative Paleoclimatic Reconstructions from Late Pleistocene Plant Macrofossils of the Yucca Mountain Region.* Open-File Report 99-338. Denver, Colorado: U.S. Geological Survey. ACC: MOL.19991015.0296. [DIRS 109470]

The data to be qualified for intended use within this FEP include:

> During the last glacial maximum, the mean annual temperature at Yucca Mountain exceeded 0°C (Thompson et al. 1999 [DIRS 109470], Figures 17 and 18).

These data are identical to the data used in FEP 1.3.04.00.0A (Periglacial Effects) and are qualified for intended use within FEP 1.3.05.00.0A (Glacial and Ice Sheet Effect). See the section in this appendix that addresses qualification of data for FEP 1.3.04.00.0A (Periglacial Effects) for a complete discussion of the qualification.

J14. FEP 1.5.01.01.0A – METEORITE IMPACT

Data qualification for FEP 1.5.01.01.0A (Meteorite Impact) is presented in Appendix D.

This FEP uses data from the following publications and the report as direct inputs:

Grieve, R.A.F. and Robertson, P.B. 1984. "The Potential for the Disturbance of a Buried Nuclear Waste Vault by a Large-Scale Meteorite Impact." *Workshop on Transitional Processes Proceedings, held in Ottawa, 1982 November 4 and 5. AECL-7822,* 231-269. Pinawa, Manitoba, Canada: Whiteshell Nuclear Research Establishment. TIC: 227319. [DIRS 185030]

Grieve, R.F. 1987. "Terrestrial Impact Structures." *Annual Review of Earth and Planetary Sciences*, 15, 245-269. Palo Alto, California: Annual Reviews. TIC: 246788. [DIRS 135254]

Grieve, R.; Rupert, J.; and Therriault, A. 1995. "The Record of Terrestrial Impact Cratering." *GSA Today*, 5, (10), 194-196. Boulder, Colorado: Geological Society of America. TIC: 246688. [DIRS 135260]

Grieve, R.A.F. 1998. "Extraterrestrial Impacts on Earth: The Evidence and the Consequences." *Meteorites: Flux with Time and Impact Effects.* Grady, M.M.; Hutchinson, R.; McCall, G.J.H.; and Rothery, D.A., eds. Geological Society Special Publication No. 140. Pages 105-131. London, England: Geological Society. TIC: 254143. [DIRS 163385]

Hills, J.G. and Goda, P.M. 1993. "Fragmentation of Small Asteroids in the Atmosphere." *The Astronomical Journal, 105*, (3), 1114-1144. Woodbury, New York: American Institute of Physics. TIC: 246798. [DIRS 135281]

Wuschke, D.M.; Whitaker, H.H.; Goodwin, B.W.; and Rasmussen, L.R. 1995. *Assessment of the Long-Term Risk of a Meteorite Impact on Hypothetical Canadian Nuclear Fuel Waste Disposal Vault Deep in Plutonic Rock*. AECL-11014. Pinawa, Manitoba, Canada: Atomic Energy of Canada Limited, Whiteshell Laboratories. TIC: 221413. [DIRS 129326]

The publications listed above are sources of direct input data and technical information. The justification for the use of technical information as well as the methods of qualification, qualification process attributes, and criteria for the data are presented in Appendix D.

J15. FEP 1.5.01.02.0A – EXTRATERRESTRIAL EVENTS

This FEP uses data from the following journal article and the report as direct inputs:

Gamma and Neutrino Radiation Dose from Gamma Ray Bursts and Nearby Supernovae (Karam 2002 [DIRS 167872])

Terrestrial Paleoenvironmental Effects of a Late Quaternary-Age Supernova (Brakenridge 1981 [DIRS 167873]).

J15. QUALIFICATION OF DATA FROM KARAM 2002

Karam, P.A. 2002. "Gamma and Neutrino Radiation Dose from Gamma Ray Bursts and Nearby Supernovae." *Health Physics, 82,* (4), 491-499. Philadelphia, Pennsylvania: Lippincott Williams & Wilkins. TIC: 255918. [DIRS 167872]

The data to be qualified for intended use within this FEP include:

> 20 mm of rock thickness provides at least seven orders of magnitude reduction in the photon energy absorbed by the rocks (i.e., the absorbed dose) for the incident 20 keV photon radiation (Karam 2002 [DIRS 167872], Table 2).

J15.1.1 Qualification Method

The method of qualification for intended use of the data from Karam (2002 [DIRS 167872]) is the Technical Assessment method (SCI-PRO-001, Attachment 3, Method 5). The rationale for using this method is that it was the most suitable considering the data, their existing documentation, and their intended use. The technical assessment was based on the determination that confidence in the data acquisition or development was warranted. Qualification process attributes used in the qualification are selected from the list provided in Attachment 4 of SCI-PRO-001. Attributes specifically applicable to these data are:

- Qualifications of personnel or organizations generating the data are comparable to qualification requirements of personnel generating similar data under an approved program that supports the YMP license application process or postclosure science (#1).
- The extent to which the data demonstrate the properties of interest (e.g., physical, chemical, geological, mechanical) (#3).
- Extent and reliability of the documentation associated with the data (#9).

J15.1.2 Technical Assessment

Qualifications of Personnel or Organizations Generating the Data—Dr. P. Andrew Karam is currently a Senior Health Physicist for MJW Corporation, Inc., a professional consulting firm specializing in radiological and health physics services for private industry and government agencies. He has also served as a faculty member for Rochester Institute of Technology and the University of Rochester in the departments of Applied Science and Technology, Biological

Sciences, Environmental Health, and Earth and Environmental Sciences. His experiences also include work as a Health Physicist at Ohio State University and as a Radiation Safety Officer at the University of Rochester. His military experience includes eight years in the U.S. Navy's Nuclear Power Program, including three years on an attack submarine as supervisor of the Reactor Laboratories Division.

Dr. P. Andrew Karam has over a quarter century of experience that spans the breadth of radiation safety in the workplace, in the environment, and in the military. An internationally recognized authority, Dr. Karam served on the Health Physics Society's Board of Directors, a National Academy of Sciences subcommittee on the effects of battlefield use of depleted uranium, and on a committee for the National Council of Radiation Protection and Measurements. He provides consulting services to the International Atomic Energy Agency on matters pertaining to radioactive materials security and national radiation safety regulation programs.

Dr. Karam has taught and published extensively on the effects of radiation exposure. He is the author of over 20 peer-reviewed papers (including the reference discussed here), three book chapters, and over 200 non-peer-reviewed technical presentations and publications. *Health Physics*, the journal in which this paper was published, is the premier supplier of cutting edge information about radiation safety for all radiation safety professionals, including health physicists, nuclear chemists, nuclear engineers, biomedical researchers and physicians. *Health Physics* reports on the latest findings in theoretical, applied, and practical disciplines of epidemiology and radiation effects, radiation biology, radioactive material transport, radiation medicine, and good radiation safety practice.

Extent to Which the Data Demonstrate the Properties of Interest—This paper provides a discussion of the frequency of supernovae and gamma ray bursts and quantifies the expected dose in the surface and subsurface. The paper clearly indicates that there is at least seven orders of magnitude reduction in dose within the top 20 mm of rock, suggesting that dose at the repository depth from such events would be negligible.

Extent and Reliability of the Documentation Associated with the Data—Base equations and assumed values are given. The discussions and conclusions are adequately documented and supporting citations are provided.

J15.1.3 Data Qualified for Intended Use

Based on the extensive experience and qualifications of the personnel generating the data, and the extent to which the data demonstrate the properties of interest, these data are considered both adequate and reliable. Therefore, based on the discussions above, these data are qualified for intended use within FEP 1.5.01.02.0A (Extraterrestrial Effects).

J15.2 QUALIFICATION OF DATA FROM BRAKENRIDGE 1981

Brakenridge, G.R. 1981. "Terrestrial Paleoenvironmental Effects of a Late Quaternary-Age Supernova." *Icarus, 46,* (1), 81-93. New York, New York: Academic Press. TIC: 255707. [DIRS 167873]

The data to be qualified for intended use within this FEP include:

> The postulated climatic and environmental effects of supernovae include ozone depletion for between two and six years, small but significant global cooling (from 0.4 K to 2 K), and an increased transfer of stratospheric nitrogen into tropospheric and fixed nitrogen on the Earth's surface (Brakenridge 1981 [DIRS 167873], p. 85).
>
> The estimated time of occurrence of Vela supernova occurred about 11,300 to 8,400 years ago (Brakenridge 1981 [DIRS 167873], p. 85).

J15.2.1 Qualification Method

The method of qualification for intended use of the data from the scientific journal article by Brakenridge (1981 [DIRS 167873]) is the Technical Assessment method (SCI-PRO-001, Attachment 3, Method 5). The rationale for using this method is that it was the most suitable considering the data, their existing documentation, and their intended use. The technical assessment was based on the determination that confidence in the data acquisition or development was warranted. Qualification process attributes used in the qualification are selected from the list provided in Attachment 4 of SCI-PRO-001. Attributes specifically applicable to these data are:

- The extent to which the data demonstrate the properties of interest (e.g., physical, chemical, geological, mechanical) (#3).
- Extent and Quality of Corroborating Data (#10).

J15.2.2 Technical Assessment

Extent to Which the Data Demonstrate the Properties of Interest—The properties of interest demonstrated in the paper by Brackenridge (1981 [DIRS 167873]) are the ways in which a supernova comparable to the Vela event could affect the terrestrial environment, including global climate. The paper by Brakenridge discusses the potential effects of a late Quaternary-Age supernova on the terrestrial paleoenvironment. It discusses the frequency of gamma and X radiation incident upon the earth and discusses potential climate forcing mechanisms and proposes evidence that such events are recorded in paleosoil horizons. The paper indicates that over 120 radio-emitting galactic supernova remnants have been catalogued. Figure 1 of the paper provides a plot of the energy fluence (called the peak flux in the paper) and the timing of the initiating supernova event. At least 24 significant (i.e., greater than 500 erg/cm^2 = 0.5 J/m^2) peaks were observed for events occurring within the 15,000 years before present. Using a value of 120 events in the past 15,000 years suggests a rate of approximately one event per 100 years. The most significant of these peak fluxes was for the Vela supernova, which was calculated to have an energy fluence of about 40,000 ergs/cm^2 (40 J/m^2). The paper indicates (p. 83) that

supernova events release on the scale of 10^{49} to 10^{50} ergs (10^{42} to 10^{43} J) of gamma radiation. The paper asserts (pp. 85 to 86) that such an event has the potential to cause ozone depletion in earth's atmosphere for a period of two to six years and created nitrogen-rich environments at the earth's surface.

Observable effects are suggested to include kerogen-rich sediments at 11 sites worldwide. The effects are also stated to include short-term terrestrial global cooling. The paper also asserts that such events could precipitate increased ultraviolet-light penetration by ozone layer depletion. The increased intensity could be as much as 2 to 10 times the present level. Aside from the potential impact on ^{14}C dating, no other effects are discussed.

Extent and Quality of Corroborating Data—Ruderman (1976 [DIRS 167875]) corroborates that ozone depletion in the atmosphere could occur and that nitrogen-enriched surface conditions could result. Ruderman also cites the work of others and corroborates that supernova explosions result in energy release of 10^{48} to 10^{50} ergs (10^{41} to 10^{43} J). Ruderman briefly mentions that increased ultraviolet influx could have altered life through mutations or suppression. The paper mentions that there is no compelling fossil evidence for past biological cataclysms related to supernova events. Arnold (2003 [DIRS 167638], p. 127) also corroborates the assertions of Brakenridge. Arnold notes that considerable attention has been focused on "the possibility that climate change may be attributable to variations in galactic cosmic-ray fluxes that are modulated by the heliospheric magnetic field." Arnold further discusses the interaction between cosmic rays and the role of ionization trails in cloud formation. This interaction suggests a possible mechanism by which cosmic rays could modify climates. Similarly, Novotna and Vitek (1991 [DIRS 167634], p. 35) also discuss external forcing mechanisms and specifically mention galactic cosmic rays, solar cosmic rays, and equivalent particles from other sources, with galactic cosmic rays being the best candidate for both short-term and long-range forcing via the generation of additional cirrus clouds and subsequent temperature changes in the upper troposphere.

Further corroboration comes from Karam (2002 [DIRS 167872]), who calculates the potential gamma and neutrino radiation dose at and beneath the earth's surface resulting from supernovae and gamma ray bursts. The paper corroborates further the data included in the paper by Brakenridge by indicating that supernovae are noted as occurring at a frequency of about 1 to 2 per century.

J15.2.3 Data Qualified for Intended Use

Based on the extent to which the data demonstrate the property of interest and the existence of corroborating data, the data from Brakenridge (1981 [DIRS 167873]) are appropriate for intended use and are qualified for use in the screening justification for FEP 1.5.01.02.0A (Extraterrestrial Events).

J16. FEP 1.5.03.01.0A – CHANGES IN THE EARTH'S MAGNETIC FIELD

This FEP uses data from the following journal article as direct input:

Biggin, A.J. and Thomas, D.N. 2003. "Analysis of Long-Term Variations in the Geomagnetic Polodial Field Intensity and Evaluation of Their Relationship with Global Geodynamics." *Geophysical Journal International, 152,* ([2]), 392-415. TIC: 255680. [DIRS 167876]

The data to be qualified for intended use within this FEP include:

> During the last 160 million years the number of pole reversals varies from 0 to 50 (Biggin and Thomas 2003 [DIRS 167876], Figure 11).

J16.1 QUALIFICATION METHOD

The method of qualification for intended use of the data from Biggin and Thomas (2003 [DIRS 167876]) is the Corroborating Data method (SCI-PRO-001, Attachment 3, Method 2). The rationale for using this method is that it was the most suitable considering the data, their existing documentation, and their intended use, as well as availability of corroborating data. Qualification process attributes used in the assessment of these data are selected from the list provided in Attachment 4 of SCI-PRO-001. Attributes specifically applicable to these data are:

- The extent to which the data demonstrate the properties of interest (e.g., physical, chemical, geological, mechanical) (# 3).
- Extent and quality of corroborating data or confirmatory testing results (# 10).

J16.2 CORROBORATING DATA

Data Demonstrates Properties of Interest—The property of interest is that pole reversals do occur and that they have been occurring. The last pole reversal occurred approximately 750,000 years ago and is known as the Matuyama-Brunhes Chron Boundary (Sarna-Wojcicki et al. 1997 [DIRS 109161]). It is not possible to predict the next occurrence of a pole reversal; however, any possible past influences are inherent to the geology of Yucca Mountain and would thus be included in analyses. No contradictory information exists indicating significant change to regional or smaller scale geologic or hydrologic systems due to variations in the earth's magnetic field, with the possible exception of a climate change relationship.

Extent and Quality of Corroborating Data—The direct input is from Figure 11 of Biggin and Thomas (2003 [DIRS 167876]). This information is corroborated in the paper by Johnson et al. (1995 [DIRS 185111], Figure 3), in which the timeframe of interest (160 My) is characterized by the highest relative reversal rate of ~60. The information can also be corroborated by data from Odenwald (2003 [DIRS 160892]), which was taken from a National Aeronautics and Space Administration-sponsored site.

J16.3 DATA QUALIFIED FOR INTENDED USE

The above discussion of the direct input provides an acceptable level of confidence that the data are suitable for their intended use, which is for FEP screening. The data described above are qualified for use within FEP 1.5.03.01.0A (Changes in Earth's Magnetic Field).

J17. FEP 1.5.03.02.0A – EARTH TIDES

This FEP uses data from the following journal article as direct input:

Bredehoeft, J.D. 1997. "Fault Permeability Near Yucca Mountain." *Water Resources Research, 33,* (11), 2459-2463. Washington, D.C.: American Geophysical Union. TIC: 236570. [DIRS 100007]

The data to be qualified for intended use within this FEP include:

> Earth tide effects in borehole UE-25 p#1 are cited in (Bredehoeft 1997 [DIRS 100007], p. 2,460), with measured fluctuations in groundwater levels of 2.05 cm.

These data are used to establish that water-level fluctuations in response to earth tides are minimally small (e.g., on the scale of a few centimeters or less), relative to their fluctuations in response to other processes.

J17.1 QUALIFICATION METHOD

The method of qualification for intended use of the data from Bredehoeft (1997 [DIRS 100007]) is the Corroborating Data method (SCI-PRO-001, Attachment 3, Method 2). The rationale for using this method is that it was the most suitable considering the data, their intended use, and availability of corroborating data. Qualification process attributes used in the assessment of these data are selected from the list provided in Attachment 4 of SCI-PRO-001. Attributes specifically applicable to these data are:

- The extent to which the data demonstrate the properties of interest (e.g., physical, chemical, geological, mechanical) (# 3).
- Extent and quality of corroborating data or confirmatory testing results (# 10).

J17.2 CORROBORATING DATA TO BREDEHOEFT 1997

The paper by Bredehoeft (1997 [DIRS 100007]) is focused on the effects of fault permeability at Yucca Mountain. However, earth tides and other water-level fluctuations are specifically analyzed and the magnitude of the fluctuations is stated, which is the property of interest. The referenced information used from Bredehoeft (1997 [DIRS 100007]) is the fluctuation in groundwater levels of 2.05 cm in the deep carbonate aquifer penetrated by borehole UE-25p1. The author cites Galloway and Rojstaczer (1988 [DIRS 156826]) as a source of these data. Information on water-level fluctuations is corroborated by Fenelon (2000 [DIRS 160881]) and Luckey et al. (1996 [DIRS 100465]) as discussed below.

The fluctuation in groundwater level is explained by Kies et al. (1999 [DIRS 160882]) who state: "tidal forces deform the earth; effects induced on fluids near the surface of the earth are documented by the observations of water level changes in wells. These changes are driven by alterations of the pore pressure induced by tidal deformation of porous and fluid-saturated crustal material." These pressure changes can result in related effects such as fluctuations in underground gas concentrations (Kies et al. 1999 [DIRS 160882]) and water-level fluctuation in

wells (Fenelon 2000 [DIRS 160881], p. 14). Kies et al. (1999 [DIRS 160882]) indicate that strain variations induced by earth tides are very small (less than on the order of 10^{-8} strain per year), which would translate to minimal fluctuations in water levels. Corroboration that individual fluctuations are of low magnitude is provided by two studies. Water levels in boreholes at Paiute Mesa (on the Nevada Test Site) were analyzed for earth tide effects and the fluctuation due to earth tides was on the order of several hundredths of a foot (Fenelon 2000 [DIRS 160881], p. 14). Further corroboration is found in the paper by Luckey et al. (1996 [DIRS 100465], pp. 29 to 32), where the lack of consistent, large-magnitude variations in water levels observed in wells near Yucca Mountain is documented.

J17.3 DATA QUALIFIED FOR INTENDED USE

The above corroboration provides a suitable level of confidence that the data from Bredehoeft (1997 [DIRS 100007]) described above are appropriate for intended use; these data are qualified for use in the screening justification for FEP 1.5.03.02.0A (Earth Tides).

J18. FEP 2.1.02.08.0A – PYROPHORICITY FROM DSNF

This FEP uses data from the following report as direct input:

Garvin, L.J. 2002. *Multi-Canister Overpack Topical Report.* HNF-SD-SNF-SARR-005, Rev. 3. Richland, Washington: Fluor Hanford. ACC: MOL.20040510.0106. [DIRS 169141]

The data to be qualified for intended use within this FEP are:

> The maximum water in a sealed multi-canister overpack (MCO) is 4.64 kg (bound in particulate), with less than 200 g being present as free water (Garvin 2002 [DIRS 169141], Table 4-4).
>
> 1.1×10^7 g uranium metal per waste package, assuming that the waste package contains two MCOs and each MCO contains Mark IV fuel (3,804 kg U) and scrap (1,832 kg U) for a total of 5,636 kg U (Garvin 2002 [DIRS 169141], Table 4-4).
>
> The N Reactor SNF contained within MCOs emplaced inside the codisposal waste packages are dried and filled with helium (Garvin 2002 [DIRS 169141], Section 4.1.3.2).

J18.1 Qualification Method

The method of qualification for intended use of data from the report by Garvin (2002 [DIRS 169141]) is the Technical Assessment method (SCI-PRO-001, Attachment 3, Method 5). The applicable elements of the Spent Nuclear Fuel Project QA program, documented in the source reference (Garvin 2002 [DIRS 169141], Section 13.0), and in the references cited therein, were also considered. The rationale for using these methods is that they were appropriate considering the extent of available documentation that allowed the evaluation of the methodology, data acquisition, and data review. The technical assessment was based on the determination that confidence in the data acquisition or development was warranted. Qualification process attributes used in the qualification were selected from the list provided in Attachment 4 of SCI-PRO-001. Attributes specifically applicable to these data are:

- Qualifications of personnel or organizations generating the data (#1).
- The quality and reliability of the measurement control program under which the data were generated (#5).
- The extent to which conditions under which the data were generated may partially meet the QA program that supports the YMP license application process or postclosure science (#6).
- The degree to which independent audits of the process that generated the data were conducted (#11).

J18.2 Technical Assessment

The maximum acceptable MCO water mass data are used to estimate the amount of oxygen that may be available inside a sealed 2-MCO/2-DHLW waste package to support pyrophoric reactions, and thus the presence of scrap baskets are an important aspect.

The evaluation of the qualification of personnel generating the data, quality and reliability of the measurement control program, adequacy of the QA program, and the evidence of independent audits is presented in the documentation of qualification of data from the same report for FEP 2.1.13.01.0A (Radiolysis). It was concluded that the acceptance criteria for these attributes were met. Additional considerations are presented below.

Confidence in the Data Acquisition or Developmental Results is Warranted—The methods used to obtain the MCO fuel loading and water content data are described in footnotes "b," "g," and "h" and associated references in the cited data source (Garvin 2002 [DIRS 169141], Table 4-4). The estimate of the uranium-metal fuel mass loading was appropriately based on the design basis input description and the MCO design description. Estimates of the amount of bound water in the MCOs were based on estimates of the mass of the various particulates that contain bound water and detailed evaluation of the water content of these particulates. These methods are appropriate.

J18.3 Data Qualified for Intended Use

The results of the technical assessment presented above confirm that the specific data on mass of uranium (with scrap baskets), water amount in a sealed MCO, and conditions the N Reactor SNF is sealed under (Garvin 2002 [DIRS 169141], Section 2.2.6.2) are adequate and are qualified for their use in the screening justification for excluded FEP 2.1.02.08.0A (Pyrophoricity from DSNF).

J19. FEP 2.1.03.07.0A – MECHANICAL IMPACT ON WASTE PACKAGE

This FEP uses data from the following reports as direct input:

Multi-Canister Overpack Topical Report (Garvin 2002. [DIRS 169141])

State of the Art on the Helium Issues (Piron and Pelletier 2001 [DIRS 165318])

Calculation of Amount of Free Water Required to Overpressurize DOE SNF Standardized Canister and RW Waste Package (Wachs 2004 [DIRS 184624]).

J19.1 QUALIFICATION OF DATA FROM GARVIN 2002

Garvin, L.J. 2002. *Multi-Canister Overpack Topical Report.* HNF-SD-SNF-SARR-005, Rev. 3. Richland, Washington: Fluor Hanford. ACC: MOL.20040510.0106. [DIRS 169141]

The data to be qualified for intended use within this FEP include the following:

> The design pressure for the multi-canister overpack (MCO) is 450 psi (gauge) at 132°C (Garvin 2002 [DIRS 169141], Section 2.2.6.2).

J19.1.1 Qualification Method

The method of qualification for intended use of data from the report by Garvin (2002 [DIRS 169141]) is the Technical Assessment method (SCI-PRO-001, Attachment 3, Method 5). The applicable elements of the Spent Nuclear Fuel Project QA program, documented in the source reference (Garvin 2002 [DIRS 169141], Section 13.0) and in the references cited therein, were also considered. The rationale for using these methods is that they were appropriate considering the extent of available documentation that allowed the evaluation of the methodology, data acquisition, and data review. The technical assessment was based on the determination that confidence in the data acquisition or development was warranted. Qualification process attributes used in the qualification were selected from the list provided in Attachment 4 of SCI-PRO-001. Attributes specifically applicable to these data are:

- Qualifications of personnel or organizations generating the data (#1).
- The quality and reliability of the measurement control program under which the data were generated (#5).
- The extent to which conditions under which the data were generated may partially meet the QA program that supports the YMP license application process or postclosure science (#6).
- The degree to which independent audits of the process that generated the data were conducted (#11).

J19.1.2 Technical Assessment

The evaluation of the qualification of personnel generating the data, quality and reliability of the measurement control program, adequacy of the QA program, and the evidence of independent audits is presented in the documentation of qualification of data from the same report for FEP 2.1.13.01.0A (Radiolysis). It was concluded that the acceptance criteria for these attributes were met. The design pressure and temperature are used to evaluate the potential for MCO failure from internal pressurization due to gas generation and temperature changes during the first 10,000 years after repository closure. Additional considerations are presented below.

Confidence in the Data Acquisition or Developmental Results is Warranted—The MCO provides confinement of SNF and maintains the SNF in a critically safe configuration. The MCO's structural design has been developed in accordance with the ASME Boiler and Pressure Vessel Code (ASME 1998 [DIRS 155708], Section III, "Rules for Construction of Nuclear Power Plant Components," Subsection NB), consistent with NRC requirements for a 10 CFR Part 72 licensed facility (Garvin 2002 [DIRS 169141], Section 1.2). In addition, the design of the MCO has been reviewed to identify any additional actions, beyond existing DOE requirements, that were necessary to demonstrate nuclear safety equivalence to comparable NRC-licensed facilities (Garvin 2002 [DIRS 169141], Section 1.6).

The design of the MCO has been prepared in accordance with the NRC's design and quality assurance requirements for nuclear power plant components. The stringent nuclear safety requirements provide a level of confidence that the QA program under which the report was generated at least partially meets the QA program that supports the YMP license application process or postclosure science.

J19.1.3 Data Qualified for Intended Use

The results of the technical assessment presented above confirm that the design pressure and temperature for the MCO (Garvin 2002 [DIRS 169141], Section 2.2.6.2) are adequate and are qualified for their use in the screening justification for excluded FEP 2.1.03.07.0A (Mechanical Impact on Waste Package).

J19.2 QUALIFICATION OF DATA FROM PIRON AND PELLETIER 2001

Piron, J.P. and Pelletier, M. 2001. "State of the Art on the Helium Issues." Section 5.3 of *Synthesis on the Long Term Behavior of the Spent Nuclear Fuel.* Poinssot, C., ed. CEA-R-5958(E). Volume 1. Paris, France: Commissariat à l'Énergie Atomique. TIC: 253976. [DIRS 165318]

The data to be qualified for intended use within this FEP are the following:

> The decay helium gas pressure is 90 bars at 20°C in commercial spent nuclear fuel rods with a gap volume of 13 cm^3 and a burnup of 47.5 GWd/MTU after 10,000 years (Piron and Pelletier 2001 [DIRS 165318], Section 5.3.2.4.1).

J19.2.1 Qualification Method

The method of qualification for intended use of the data from the report by Piron and Pelletier (2001 [DIRS 165318]) is the Corroborating Data method (SCI-PRO-001, Attachment 3, Method 2) in accordance with SCI-PRO-005, Section 3. The rationale for using this method is that it was the most suitable considering the data, their intended use, and availability of corroborating data. Qualification process attributes used in the data qualification were selected from the list provided in Attachment 4 of SCI-PRO-001.

> Attribute specifically applicable to these data is extent and quality of corroborating data (#10).

J19.2.2 Corroborating Data

The corroborating data used are decay helium inventory and actinide radionuclide inventory data at 1,000 years for spent nuclear fuel rods with a burnup of 45 GWd/MTU (Guenther et al. 1991 [DIRS 109207], p. D.78).

Description of Qualification Approach and Results—The approach is to use the corroborating data to independently calculate the gap pressure that would occur from the He gas generated as a result of alpha particle decay after 10,000 years.

The steps involved in this calculation are:

- Listing the inventories of decay helium and principal alpha-emitting radionuclides (^{241}Am, ^{240}Pu, ^{239}Pu, and ^{243}Am) in commercial SNF at 1,000 years (Guenther et al. 1991 [DIRS 109207], p. D.78).

- Estimating the change in the helium inventory that will result from alpha decay during the period between 1,000 years and 10,000 years and adding this change to the 1,000-year helium inventory.

- Calculating the pressure at 20°C in the void volume of a fuel rod from the helium gas generated as a result of alpha particle decay at 10,000 years.

The calculations are analogous to those performed for qualifying the data from the same reference for FEP 2.1.12.02.0A (Gas Generation (He) from Waste Form Decay), except that the calculations for this FEP concern the helium gas pressure increase at 20°C (293 K) within the void volume of a fuel rod (13 cm^3), whereas the calculations for FEP 2.1.12.02.0A concern the pressure increase at 50°C (323 K) in the void volume of a commercial SNF waste package (4,737 L).

The amount of helium in a commercial SNF waste package with average burnup of 45 GWd/MTU was 7.3E2 g (1.83E2 gmol He) from the section on corroborating data in FEP 2.1.12.02.0A (Gas Generation (He) From Waste Form Decay). For 21 PWR fuel assemblies with 208 rods per assembly, the amount of helium gas per fuel rod is 4.19×10^{-2} gmol He (1.83E2 gmol He ÷ 21 assemblies ÷ 208 rods per assembly). From the ideal gas law, pV = nRT, where n = 4.19E-2 gmol He; R = 8.3143 N-m/mol/K; T = 293 K, V = 0.000013 m^3;

the resulting pressure is p = 7.86 × 10^6 N/m^2 = 7.86 × 10^6 Pa = 78.5 bars (R, gas constant, rounded and unit conversion from Weast 1985 [DIRS 111561]). The resulting pressure values of 78.5 bar compared to 90 bar (Piron and Pelletier 2001 [DIRS 165318]) is close (within 15%), such that the corroboration is sufficient to meet the needs for the intended use within the FEP.

The calculated pressure that would result from release of the decay helium into the fuel rod gap is 78.5 bars at 20°C after 10,000 years. This value compares favorably with the gap pressure of 90 bars at 20°C after 10,000 years from Piron and Pelletier 2001 ([DIRS 165318], Section 5.3.2.4.1). This result confirms that the gap pressure at 10,000 years from Piron and Pelletier (2001 [DIRS 165318], Section 5.3.2.4.1) is adequate and slightly conservative for its use in excluded FEP 2.1.03.07.0A (Mechanical Impact on Waste Package). The pressure and temperature in the fuel rod gap are used to estimate the pressure change in a waste package if all of the He gas generated as a result of alpha particle decay over 10,000 years was released from the fuel rods into the void volume of a TAD-bearing waste package with commercial SNF.

J19.2.3 Data Qualified for Intended Use

The results of the data evaluation provides a sufficient level of confidence that the data from the publication by Piron and Pelletier (2001 [DIRS 165318]) are appropriate for intended use. The data are qualified use in the screening justification for excluded FEP 2.1.03.07.0A (Mechanical Impact on Waste Package).

J19.3 QUALIFICATION OF DATA FROM WACHS 2004

Wachs, G. 2004. *Calculation of Amount of Free Water Required to Overpressurize DOE SNF Standardized Canister and RW Waste Package.* EDF-NSNF-017, Rev. 1. Washington, D.C.: U.S. Department of Energy, National Spent Nuclear Fuel Program. ACC: LLR.20080109.0001. [DIRS 184624]

The data to be qualified for intended use within this FEP are the following:

> The volume of free (unbound) water is approximately 0.0005 liters in a 15-foot-long DOE SNF Standardized Canister after cold vacuum drying (Wachs 2004 [DIRS 184624], Section 6).

J19.3.1 Qualification Method

The method of qualification for intended use of the data from the report by Wachs (2004 [DIRS 184624]) is the Technical Assessment method (SCI-PRO-001, Attachment 3, Method 5) in accordance with SCI-PRO-005, Section 3. The rationale for using this method is that it was the most suitable considering the data, their existing documentation, and their intended use. The technical assessment was based on the determination that confidence in the data acquisition or development was warranted. Qualification process attributes used in the data qualification were selected from the list provided in Attachment 4 of SCI-PRO-001.

Attributes specifically applicable to these data are:

- Qualifications of personnel or organizations generating the data (#1).

- The extent to which the data demonstrate the properties of interest (e.g., physical, chemical, geologic, mechanical) (#3).

- The quality and reliability of the measurement control program under which the data were generated (#5).

- The extent to which conditions under which the data were generated may partially meet the QA program that supports the YMP license application process or postclosure science (#6).

J19.3.2 Technical Assessment

This report originates from the National Spent Nuclear Fuel Program (NSNFP) with the specific purpose to calculate the minimum amount of free water and physically adsorbed water that if completely dissociated could approach the pressure limits within a DOE SNF Standardized canister. This program works under NSNFP Quality Assurance, which implements *Quality Assurance Requirements and Description* (Wachs 2004 [DIRS 184624], p. 9, Quality Assurance). An external reviewer approving the document (Wachs 2004 [DIRS 184624], p. 1), added confidence that the data are reliable.

This QA program is the same as that evaluated for Garvin (2002 [DIRS 169141]) in FEP 2.1.13.01.0A (Radiolysis). The evaluation of the qualification of personnel generating the data, quality and reliability of the measurement control program, adequacy of the QA program, and the evidence of independent audits is presented in the documentation of qualification of data from the same report for FEP 2.1.13.01.0A (Radiolysis). It was concluded that the acceptance criteria for these attributes were met. Additional considerations are presented below.

Extent to Which the Data Demonstrate the Properties of Interest—The volume of free water is used to estimate the pressure of water vapor in a codisposal waste package at its peak temperature of 191.0°C, shortly after repository closure. Considering the dimensions of a waste package are much larger than the dimensions of a MCO or SNF Standard canister, the relative amount of free water per canister is relatively small compared to the void volume of the waste package. Additionally, high-level waste such as that under consideration for the intended use of this data should not contain sufficient amounts of water to appreciably add to the water contained in the waste package (Wachs 2004 [DIRS 184624], p. 5).

The source document *Calculation of amount of free water required to overpressurize DOE SNF Standardized Canister and RW Waste Package* (Wachs 2004 [DIRS 184624]) was prepared for the National Spent Nuclear Fuel Project similar to the needs of YMP.

J19.3.3 Data Qualified for Intended Use

Based on this technical assessment, and consideration of the qualification process attributes listed above, the data from the report by Wachs (2004 [DIRS 184624]) are appropriate and qualified for their use in the screening justification for excluded FEP 2.1.03.07.0A (Mechanical Impact on Waste Package).

J20. FEP 2.1.03.10.0B – ADVECTION OF LIQUIDS AND SOLIDS THROUGH CRACKS IN THE DRIP SHIELD

This FEP uses data from the following journal article as direct input:

Siriwardane, R.V. and Wightman, J.P. 1983. "Interaction of Hydrogen Chloride and Water with Oxide Surfaces. III. Titanium Dioxide." *Journal of Colloid and Interface Science, 94,* (2), 502-513. New York, New York: Academic Press. TIC: 259837. [DIRS 183688]

The data to be qualified for intended use within this FEP and Appendix C include:

> Specific surface area (6 to 50 m^2/g) of commercial-grade crystalline rutile and anatase (Siriwardane and Wightman 1983 [DIRS 183688], p. 504).

These data are to be used as a conservative estimate of specific surface area for the corrosion product within cracks of the drip shield. Specific surface area is one of the parameters in the equation for estimating saturated hydraulic conductivity of corrosion products in Appendix C. The corrosion product particles are expected to be a few tens of nanometers in size (He et al. 2007 [DIRS 183687], p. 789 and Figure 14-b), and particles of this description are estimated to have specific surface area on the order of 100 m^2/g (Yao and Zhang 1999 [DIRS 184766], Tables I and II). Because the data range is smaller than what is anticipated, the use of the data is a conservative approach within the FEP and associated calculations in Appendix C.

J20.1 QUALIFICATION METHOD

The method of qualification for intended use of the data from Siriwardane and Wightman (1983 [DIRS 183688]) is the Corroborating Data method (SCI-PRO-001, Attachment 3, Method 2). The rationale for using this method is that it was the most suitable considering the data, their intended use, and availability of corroborating data. Qualification process attributes used in the qualification were selected from the list provided in Attachment 4 of SCI-PRO-001. Attributes specifically applicable to these data are:

- The extent to which the data demonstrate the properties of interest (e.g., physical, chemical, geologic, mechanical) (#3).
- Extent and quality of corroborating data or confirmatory testing results (#10).

J20.2 CORROBORATING DATA FOR SIRIWARDANE AND WIGHTMAN 1983

The data described above represent a range of specific surface area values from these commercial sources. The article Siriwardane and Wightman (1983 [DIRS 183688]) uses multiple commercial sources of rutile and anatase. Depending on the synthetic method employed, rutile and anatase can have a wide range in specific surface areas. For example, the method of preparation and resulting specific surface area found in the study by Yao and Zhang (1999 [DIRS 184766], Table I) is on the order of 100 m^2/g. The specific surface area of another commercial source of rutile, found in the journal article by Nag et al. (2007 [DIRS 184817], Table 2), similar in particle size to that under discussion, is on the order of 3 m^2/g. These additional sources corroborate the available range of commercially available rutile and anatase in

the article by Siriwardane and Wightman (1983 [DIRS 183688]) as adequate for the intended use within this FEP. The data range used in the FEP represents a conservative approach and is adequate and accurate for the intended use of the data.

J20.3 DATA QUALIFIED FOR INTENDED USE

The assessment presented above provides sufficient confidence that the data from the article by Siriwardane and Wightman (1983 [DIRS 183688]) are adequate for intended use and are qualified for use in the screening justification for FEP 2.1.03.10.0B (Advection of Liquids and Solids through Cracks in the Drip Shield).

J21. FEP 2.1.06.01.0A – CHEMICAL EFFECTS OF ROCK REINFORCEMENT AND CEMENTITIOUS MATERIALS IN EBS

This FEP uses data from the following reference as direct input:

Ziegler, J.D. 2004. "Transmittal of Appendix D of the Technical Basis Document No. 10: Unsaturated Zone Transport Addressing Key Technical Issue (KTI) Agreement Evolution of Near-Field Environment (ENFE) 1.04." Letter from J.D. Ziegler (DOE/ORD) to the NRC, August 31, 2004, 0902043035, OLA&S:JCP-1434 with enclosure. ACC: MOL.20041027.0242. [DIRS 171694]

The data are taken from the enclosure to the letter. The data to be qualified for intended use within this FEP include:

> Water in equilibrium with portlandite-hillebrandite contains 625 mg total Ca/kg water (Ziegler 2004 [DIRS 171694], Table D-12), which is equivalent to approximately 1.56×10^{-2} mol Ca/kg water.

J21.1 QUALIFICATION METHOD

The qualification method of the data from Ziegler (2004 [DIRS 171694]) is the Corroborating Data method (SCI-PRO-001, Attachment 3, Method 2). Corroborating data are available for comparison with the unqualified data set and any inferences drawn to corroborate the unqualified data can be clearly identified, justified, and documented. Qualification process attributes used in the qualification were selected from the list provided in Attachment 4 of SCI-PRO-001. Attributes specifically applicable to these data are:

- Extent to which the data demonstrate the properties of interest (#3).
- Extent and quality of corroborating data or confirmatory testing results (#10).

J21.2 CORROBORATING DATA

The strategy taken to corroborate the data from Ziegler (2004 [DIRS 171694]) was to determine the calcium concentration independently. These calculations were carried out using the qualified computer code EQ3/6 V.8.1 (STN: 10813-8.1-00 [DIRS 176889]); direct input data were obtained from thermodynamic database (DTN: SN0612T0502404.014 [DIRS 178850], file: *data0.ymp.R5*). The objective of these calculations was to predict the concentration of calcium in solution in the presence of hillebrandite at 25°C and 1 bar. The results of calculations are included in DTN: SN0712CEMENTEQ.001. Caveats and limitations of the calculations are also documented within the same DTN and are appropriate for the intended use of the data.

To corroborate the data from the report by Ziegler (2004 [DIRS 171694]), comparison of the calcium concentrations was made between the results of the calculations described above (included in the output file *portland-hws.3o* in the output DTN: SN0712CEMENTEQ.001) and those from Ziegler (2004 [DIRS 171694]) (as found in the file output file *output.portlandite* in the unqualified DTN: LB0408CMATUZFT.004 [DIRS 171706]). Summary of the main results is provided in Table J21-1. These results indicate that the differences between the two

simulations are small (within 1%; see Table J21-1). It is noted that a comparison of predicted SiO_2(aq) concentration between the two code run outputs shows differences by a factor of approximately 2. This discrepancy is due to differences in the thermodynamic data used for SiO_2(aq) in the EQ3/6 calculations by Ziegler (2004 [DIRS 171694]), (presented in *output.portlandite*) and the data used in the present calculations. This difference in SiO_2 (aq) concentration does not affect the prediction of portlandite solubility given by the total Ca concentration, and the solubility of this phase is the focus of the current comparison. In fact, differences in the predicted total Ca concentrations given in the files *output.portlandite* and *portland-hws.3o* are less than 1%, and are negligible for the intended use of the data. In addition, the differences in predicted pH values are also less than 1%. Table J21-1 below summarizes the main results of the equilibrium solubility calculations given by the output files *output.portlandite* and *portland-hws.3o*. Given the close agreement in the prediction of Ca concentrations for portlandite- hillebrandite solubility, this result confirms the validity of the used for portlandite solubility in Ziegler (2004 [DIRS 171694]).

Within the scope of this criterion, added confidence in the data is given by their qualification process attributes as discussed below and outlined in Attachment 4 of SCI-PRO-001.

Extent to Which the Data Demonstrate the Properties of Interest—The data presented by Ziegler (2004 [DIRS 171694]) provide solubility values for portlandite- hillebrandite. The solubility of portlandite is used in the assessment of the alkaline cement leachate stability. Exposure of the cement leachate to CO_2 leads to plume carbonation and thus its neutralization. It is assumed that the leachate is saturated with respect to portlandite-hillebrandite and the total Ca concentration in solution is sufficient to allow for calcite precipitation as a result of the plume neutralization.

Extent and Quality of Corroborating Data or Confirmatory Testing Results—Table J21-1 below shows a comparison of EQ3/6 code outputs from the code runs performed in this analysis (output DTN: SN0712CEMENTEQ.001) and the data by Ziegler (2004 [DIRS 171694]) (DTN: LB0408CMATUZFT.004 ([DIRS 171706]). Notice the strong agreement (difference less than 1%) between the two outputs for total Ca concentration and pH. These two parameters define portlandite in the presence of hillebrandite solubility.

Table J21-1. Summary of Main Results of EQ3/6 Equilibrium Solubility Calculations

Phase Assemblage	Total SiO_2(aq)[1] (mg/kg H_2O)	Total SiO_2(aq)[2] (mg/kg H_2O)	Total Ca[1] (mg/kg H_2O)	Total Ca[2] (mg/kg H_2O)	pH[1]	pH[2]
Portlandite-hillebrandite	0.14	0.27	625	630	12.37	12.375

[1] Ziegler 2004 [DIRS 171694], Table D-12.
[2] Ouput DTN: SN0712CEMENTEQ.001 (rounded).

J21.3 DATA QUALIFIED FOR INTENDED USE

The data specified above from Ziegler (2004 [DIRS 171694]) are appropriate for intended use within FEP 2.1.06.01.0A (Chemical Effects of Rock Reinforcement and Cementitious Materials in EBS). Based on the extent to which the data demonstrate the properties of interest and the existence of corroborating data by using the qualified code and the thermodynamic database, the data can be considered qualified for use in the screening justification for this FEP.

J22. FEP 2.1.06.06.0B – OXYGEN EMBRITTLEMENT OF DRIP SHIELDS

This FEP uses data from the following journal article as a direct input:

Rogers, J.W., Jr.; Erickson, K.L.; Belton, D.N.; Springer, R.W.; Taylor, T.N.; and Beery, J.G. 1988. "Low Temperature Diffusion of Oxygen in Titanium and Titanium Oxide Films." *Applied Surface Science, 35,* 137-152. Amsterdam, The Netherlands: North-Holland. TIC: 259889. [DIRS 184108]

The data to be qualified for intended use within this FEP include:

> The value of the diffusion coefficient of oxygen in titanium at 300°C is 8.8×10^{-18} cm^2 s^{-1} and has an uncertainty of 70% (Rogers et al. 1988 [DIRS 184108], Table 1 and p. 146).

J22.1 QUALIFICATION METHOD

The method of qualification for intended use of the data from Rogers et al. (1988 [DIRS 184108]) is the Technical Assessment method (SCI-PRO-001, Attachment 3, Method 5). The rationale for using this method is that it was the most suitable considering the data, their existing documentation, and their intended use. The technical assessment was based on the determination that confidence in the data acquisition or development was warranted. Qualification process attributes used in the technical assessment of these data are selected from the list provided in Attachment 4 of SCI-PRO-001. Attributes considered to assess the appropriateness of this external data for the intended use are:

- Qualification of personnel or organizations generating the data are comparable to qualification requirements of personnel generating similar data under an approved program that supports the YMP license application process or postclosure science (#1).

- The extent to which the data demonstrate the properties of interest (e.g., physical, chemical, geological, mechanical) (#3).

J22.2 TECHNICAL ASSESSMENT

The journal article by Rogers et al. (1988 [DIRS 184108]) contains values of oxygen diffusion coefficients in titanium metal and titanium oxide films at various elevated temperatures. These values are based on results of experiments conducted by researchers at Sandia and Los Alamos National Laboratories, both of which are top-level research organizations in the United States of America. These results were published in 1988 in *Applied Surface Science*, a peer-reviewed scientific journal published from The Netherlands. The datum with its associated uncertainty of 70% is used in this FEP screening qualification to represent the oxygen diffusion coefficient in titanium metal at 300°C (573 K). The article by Rogers et al. (1988 [DIRS 184108]) contains measured values of oxygen diffusion coefficients in titanium metal at 300°C (573 K) and above. Thus, this datum (i.e., 8.8×10^{-18} cm^2 s^{-1}) belongs to a data set that represents the material property of interest to a significant extent.

J22.3 DATA QUALIFIED FOR INTENDED USE

Based on the qualifications of the researchers, the reputations of the organizations generating data, and the extent to which the data demonstrate the properties of interest, the data from the journal article by Rogers et al. (1988 [DIRS 184108]) are appropriate for intended use and are qualified for use in the screening justification for FEP 2.1.06.06.0B (Oxygen Embrittlement of Drip Shields).

J23. FEP 2.1.09.13.0A – COMPLEXATION IN EBS

This FEP uses data from the following article:

Means, J.L.; Maest, A.S.; and Crerar, D.A. 1983. *The Organic Geochemistry of Deep Ground Waters and Radionuclide Partitioning Experiments under Hydrothermal Conditions.* ONWI-448. Columbus, Ohio: Battelle Memorial Institute, Office of Nuclear Waste Isolation. TIC: 209098. [DIRS 100797]

The data to be qualified for intended use within this FEP include:

> Total organic carbon is 0.58 mg/L for well UE25b-1 (Means et al. 1983 [DIRS 100797], Table 1), 33% (0.19 mg/L) of which has a molecular weight greater than 1,000 (Means et al. 1983 [DIRS 100797], Table 3).

J23.1 QUALIFICATION METHOD

The method of qualification for intended use of the data from Means et al. (1983 [DIRS 100797]) is the Technical Assessment method (SCI-PRO-001, Attachment 3, Method 5). The rationale for using this method is that it was the most suitable considering the data, their existing documentation, and their intended use. The technical assessment was based on the determination that confidence in the data acquisition or development was warranted. Qualification process attributes used in the technical assessment of these data are selected from the list provided in Attachment 4 of SCI-PRO-001. Attributes considered to assess the appropriateness of this project data for the intended use are:

- Qualification of personnel or organizations generating the data are comparable to qualification requirements of personnel generating similar data under an approved program that supports the YMP license application process or postclosure science (#1).

- The technical adequacy of equipment and procedures used to collect and analyze the data (#2)

J23.2 TECHNICAL ASSESSMENT

The data under consideration is from the technical report by Means et al. (1983 [DIRS 100797]) prepared as a summary of research activities from several potential repository sites in the United States. Samples from the Nevada Test Site were collected and stored at room temperature in polyethylene-lined 55-gallon drums, and were provided to the authors by A.E. Ogard of Los Alamos National Laboratory (Means et al. 1983 [DIRS 100797], p. 1). The methods of analysis are well documented within the report by Means et al. (1983 [DIRS 100797], pp. 4, 5, 7) and consist of standard technical methods for the analysis of total organic carbon. The equipment used is an organic carbon analyzer, specific to this type of assay. It has sufficient resolution to warrant confidence in the results. Gel filtration chromatography (based on size exclusion) was used to obtain semi-quantitative estimates of the molecular weight distributions of natural organic compounds present (Means et al. 1983 [DIRS 100797], p. 12). Further confidence in the results is obtained as the mean value is reported from nine analyses. The results of these

analyses are documented within the report by Means et al. (1983 [DIRS 100797], pp. 7, 17, 18, Tables 1 and 3). The methods outlined by Means et al. (1983 [DIRS 100797]) were used as a comparison in a separate determination by Minai et al. (1992 [DIRS 100801]), adding to the level of confidence that these methods are suitable for the intended use.

Jeffrey L. Means has published multiple articles on the topic of organic geochemistry specifically from groundwaters and the relationship between adsorption with actinides over the last ~30 years as demonstrated by the references within the report by Means et al. (1983 [DIRS 100797]). Based upon his publication record, he is considered an expert in his field.

J23.3 DATA QUALIFIED FOR INTENDED USE

The data specified above from Means et al. (1983 [DIRS 100797]) are appropriate for intended use within FEP 2.1.09.13.0A (Complexation in EBS). Based on the qualifications of the personnel and the technical adequacy of the equipment and procedures used to collect and analyze the data, the data can be considered qualified for use in the screening justification for this FEP.

J24. FEP 2.1.09.15.0A – FORMATION OF TRUE (INTRINSIC) COLLOIDS IN EBS

This FEP uses data from the following journal articles:

"Actinide Behavior in Natural Waters" (Choppin and Stout 1989 [DIRS 168379])

"Properties of Plutonium (IV) Polymer of Environmental Importance" (Rai and Swanson 1981 [DIRS 144599])

"Ten-Year Results from Unsaturated Drip Tests with UO_2 at 90°C: Implications for the Corrosion of Spent Nuclear Fuel" (Wronkiewicz et al., 1996 [DIRS 102047])

"The Corrosion of Uraninite Under Oxidizing Conditions" (Finch and Ewing 1992 [DIRS 113030]).

J24.1 QUALIFICATION OF DATA FROM CHOPPIN AND STOUT 1989

Choppin, G.R. and Stout, B.E. 1989. "Actinide Behavior in Natural Waters." *Science of the Total Environment, 83,* ([3]), 203-216. Amsterdam, The Netherlands: Elsevier. TIC: 255706. [DIRS 168379]

The information to be qualified for intended use within this FEP include:

> For the higher charged actinides, hydrolysis can lead to formation of oligomers and polymers. At the low environmental concentrations of actinides, these are usually a problem only for Pu(IV), whose hydrolytic polymers are rather intractable (Choppin and Stout 1989 [DIRS 168379], p. 209).

J24.1.1 Qualification Method

The method of qualification for intended use of the data from the article by Choppin and Stout (1989 [DIRS 168379]) is the Technical Assessment method (SCI-PRO-001, Attachment 3, Method 5). The rationale for using this method is that it was the most suitable considering the data, their existing documentation, and their intended use. The technical assessment was based on the determination that confidence in the data acquisition or developmental results was warranted. Qualification process attributes used in the technical assessment of these data are selected from the list provided in Attachment 4 of SCI-PRO-001. Attributes specifically relevant to these data are:

- Qualification of personnel or organizations generating the data are comparable to qualification requirements of personnel generating similar data under an approved program that supports the YMP license application process or postclosure science (#1).
- The extent to which the data demonstrate the properties of interest (e.g., physical, chemical, geological, mechanical) (#3).
- Prior peer or other professional reviewers of the data and their results (#8).

J24.1.2 Technical Assessment

Qualifications of Personnel—G. R. Choppin is a well known and respected professional in the technical area of radionuclide chemistry and reactivity. Choppin was contributor and editor to symposium series 216 *Plutonium Chemistry* (Choppin 1983 [DIRS 168395]), has written multiple journal articles (e.g., Choppin 1992 [DIRS 100717]; Choppin 2003 [DIRS 168308]; Choppin 1986 [DIRS 168377]) on the topic of plutonium chemistry, and is regarded as an expert in the field. Choppin's work is published in well-respected journals, which adds confidence in the qualifications of personnel.

Extent to Which the Data Demonstrate the Properties of Interest—The information under consideration reflects a convergent result that polymerization of actinides can take place and that Pu(IV) is the most important. This information demonstrates a well-studied set of observations culminating in a technical statement that becomes a well-accepted position within the scientific field. This statement is corroborated by several other references studied to date on plutonium chemistry by these authors and others (e.g., Rai and Swanson 1981 [DIRS 144599]; Toth et al. 1983 [DIRS 168394]).

Prior Peer and Other Professional Reviews—The paper on actinide behavior in natural waters was published in *Science of the Total Environment*, a well-known, international, peer-reviewed journal for scientific research into the environment and its relationship with humans. The reviewers of the articles submitted for publication in *Science of the Total Environment* are matched to the paper according to their expertise. They are requested to evaluate not only the technical content and organization of the article but also documentation of quality assurance and control, the data presented, and the quality of interpretation and conclusions.

The journal, published by Elsevier, is an international medium for publication of original research on the environment with emphasis on changes caused by human activities. It is concerned with changes in the natural levels and distribution of chemical elements and their compounds that may affect the well-being of the living world, or represent a threat to human health. The scope is multidisciplinary and international and the subjects covered include: (a) all aspects of the contamination or pollution of air, water, soil, and the human food chain; (b) natural and human-induced environmental changes at the global, regional, and local levels; (c) environmental risk management, remediation and treatment, and environmental policy appraisal; (d) effects on human and ecosystem health related to abnormalities in the level and distribution of chemical elements and their compounds in the environment; (e) novel techniques and methods of chemistry and biochemistry applicable to environmental problems and environmental health; (f) gene-environment interactions. The impact factor for this journal in 2006 was 2.359.

J24.1.3 Data Qualified for Intended Use

The information specified above from Choppin and Stout (1989 [DIRS 168379]) are appropriate for intended use within FEP 2.1.09.15.0A (Formation of True (Intrinsic) Colloids in EBS). Based on satisfactorily meeting the combined attributes specified, the information is be considered qualified for use in the screening justification for this FEP.

J24.2 QUALIFICATION OF DATA RAI AND SWANSON 1981

Rai, D. and Swanson, J.L. 1981. "Properties of Plutonium(IV) Polymer of Environmental Importance." *Nuclear Technology, 54,* (1), 107-112. La Grange Park, Illinois: American Nuclear Society. TIC: 221390. [DIRS 144599]

The data to be qualified for intended use within this FEP include:

> Pu(IV) polymer does not make stable suspensions at pH values above 5 and hence would not be expected to be mobile as polymer in the lithosphere (Rai and Swanson 1981 [DIRS 144599]. p. 111).

J24.2.1 Qualification Method

The method of qualification for intended use of the data from the article by Rai and Swanson (1981 [DIRS 144599]) is the Technical Assessment method (SCI-PRO-001, Attachment 3, Method 5). The rationale for using this method is that it was the most suitable considering the data, their existing documentation, and their intended use. The technical assessment was based on the determination that confidence in the data acquisition or developmental results was warranted. Qualification process attributes used in the technical assessment of these data are selected from the list provided in Attachment 4 of SCI-PRO-001. Attributes specifically relevant to these data are:

- Qualification of personnel or organizations generating the data are comparable to qualification requirements of personnel generating similar data under an approved program that supports the YMP license application process or postclosure science (#1).
- The extent to which the data demonstrate the properties of interest (e.g., physical, chemical, geological, mechanical) (#3).
- Prior peer or other professional reviewers of the data and their results (#8).

J24.2.2 Technical Assessment

Qualifications of Personnel—D. Rai and J.L. Swanson are well known experts in the technical area of radionuclide solubility chemistry and speciation (see for example the number of entries in the Technical Information Center). Their work is published in well-respected journals, which adds confidence in the qualifications of personnel.

Extent to Which the Data Demonstrate the Properties of Interest—The information under consideration reflects a convergent result that polymerization of actinides can take place and that Pu(IV) is the most important. This information demonstrates a well studied set of observations culminating in a technical statement that becomes a well-accepted position within the scientific field. Furthermore, the methods used in the determination of Pu(IV) polymer properties are appropriate for the type of data obtained. These methods include fundamental chemical redox assays and standard separation techniques.

Prior Peer and Other Professional Reviews—These data were subjected to professional reviews for inclusion in the IUPAC-NIST Solubility Data Series in the review article by Hala and Miyamoto 2007 [DIRS 185095], p. 1692 and 1703). The lead author, Dhanpat Rai, has authored or co-authored at least 13 peer-reviewed journal articles on plutonium chemistry over the past 30 years, and has provided expertise on actinide chemistry and expected behavior in the nuclear waste environment to the DOE since the late 1970s.

J24.2.3 Data Qualified for Intended Use

The data specified above from Rai and Swanson (1981 [DIRS 144599], p. 111) are appropriate for intended use within FEP 2.1.09.15.0A (Formation of True (Intrinsic) Colloids in EBS). Based on satisfactorily meeting the combined attributes specified, the information is considered qualified for intended use within this FEP.

J24.3 QUALIFICATION OF DATA FROM WRONKIEWICZ ET AL., 1996

Wronkiewicz, D.J.; Bates, J.K.; Wolf, S.F.; and Buck, E.C. 1996. "Ten-Year Results from Unsaturated Drip Tests with UO_2 at 90°C: Implications for the Corrosion of Spent Nuclear Fuel." *Journal of Nuclear Materials, 238,* (1), 78-95. Amsterdam, The Netherlands: North-Holland. TIC: 243361. [DIRS 102047]

The data to be qualified for intended use within this FEP include:

> Size-fractioned analyses revealed that between 1% and 12% of the total amount of uranium was present as a >5 nm size-fraction (the suspended fraction trapped by the filter) (Wronkiewicz et al. 1996 [DIRS 102047], p. 86).

J24.3.1 Qualification Method

The method of qualification for intended use of the data from the article by Wronkiewicz et al. (1996 [DIRS 102047]) is the Technical Assessment method (SCI-PRO-001, Attachment 3, Method 5). The rationale for using this method is that it was the most suitable considering the data, their existing documentation, and their intended use. The technical assessment was based on the determination that confidence in the data acquisition or developmental results was warranted. Qualification process attributes used in the technical assessment of these data are selected from the list provided in Attachment 4 of SCI-PRO-001. Attributes specifically relevant to these data are:

- The technical adequacy of equipment and procedures used to collect and analyze the data (#2).
- The extent to which the data demonstrate the properties of interest (e.g., physical, chemical, geological, mechanical) (#3).
- Prior peer or other professional reviewers of the data and their results (#8).

J24.3.2 Technical Assessment

Technical Adequacy of Equipment and Procedures Used—The experimental apparatus and materials, summarized within the article, are adequate and appropriate for the data collected. Additional documentation of the equipment, methods, and procedures used can be found in sources referenced by Wronkiewicz et al. (1991 [DIRS 176891]) and published by Wronkiewicz et al. (1992 [DIRS 100493]).

Extent to Which the Data Demonstrate the Properties of Interest—The original intended use of the information and data collected within this paper was for the Yucca Mountain Site Characterization Project, as part of its spent fuel scientific investigations. The data under consideration is from the latter years of testing; total testing was performed for 8 to 10 years. Because this data originates from the latter time period, there is sufficient confidence in the data collected and analyzed due to the fact that there were larger volumes of leachate available for sampling. Thus, the determination of uranium release by size fraction was able to be performed, which is the specific property of interest.

Prior Peer and Other Professional Reviews—The paper by Wronkiewicz et al. (1996 [DIRS 102047]) was published in *Journal of Nuclear Materials*. This publication is a peer-reviewed scientific journal that publishes high-quality papers in materials research relevant to nuclear fission and fusion reactors and high power accelerator technologies, and in closely related aspects of materials science and engineering. Both original research and critical review papers covering experimental, theoretical, and computational aspects of either fundamental or applied nature are welcome. The breadth of the field is such that a wide range of processes and properties is of interest to the readership, spanning atomic lattice defects, microstructures, thermodynamics, corrosion, and mechanical and physical properties, for example. The journal is published by Elsevier. The reviewers of the articles submitted for publication in *Journal of Nuclear Materials* are requested to evaluate not only the technical content and organization of the article but also documentation of quality assurance and control, the data presented, and the quality of interpretation and conclusions. The impact factor of this journal in 2006 was 1.261. Furthermore, this report was reviewed by YMP personnel prior to submission and acceptance by *Journal of Nuclear Materials* (see records package for DTN: LL960905751021.019 [DIRS 185101]).

J24.3.3 Data Qualified for Intended Use

The data specified above from Wronkiewicz et al. (1996 [DIRS 102047], p. 86) are appropriate for intended use within FEP 2.1.09.15.0A (Formation of True (Intrinsic) Colloids in EBS). Based on satisfactorily meeting the combined attributes specified, the information is considered qualified for intended use in this FEP.

J24.4 QUALIFICATION OF DATA FROM FINCH AND EWING 1992

Finch, R.J. and Ewing, R.C. 1992. "The Corrosion of Uraninite Under Oxidizing Conditions." *Journal of Nuclear Materials, 190,* 133-156. Amsterdam, The Netherlands: Elsevier. TIC: 246369. [DIRS 113030]

The information to be qualified for intended use within this FEP includes:

> The effect of dissolved silica on the alteration of the UOHs (uranyl oxide hydrates) is profound; the alteration of schoepite can result in the formation of uranyl silicates such as uranophane and soddyite (Finch and Ewing 1992 [DIRS 113030], Section 4.2.2).

J24.4.1 Qualification Method

The method of qualification for intended use of the data from the article by Finch and Ewing (1992 [DIRS 113030]) is the Corroborating Data method (SCI-PRO-001, Attachment 3, Method 2). The rationale for using this method is that corroborating data are available and inferences drawn to corroborate can be clearly identified, justified, and documented. The technical assessment was based on the determination that confidence in the data acquisition or developmental results was warranted. Qualification process attributes used in the technical assessment of these data are selected from the list provided in Attachment 4 of SCI-PRO-001. Attributes specifically relevant to these data are:

- The extent to which the data demonstrate the properties of interest (e.g., physical, chemical, geological, mechanical) (#3).
- Prior peer or other professional reviewers of the data and their results (#8).
- Extent and quality of corroborating data or confirmatory testing results (#10).

J24.4.2 Technical Assessment

Extent to Which Data Demonstrate the Properties of Interest—The information under consideration reflects a convergent result that dissolved silica alters uranyl oxide hydrates by the formation of uranyl silicates. This information demonstrates a well-studied set of observations culminating in a technical statement that becomes a well-accepted position within the scientific field. The statement is further substantiated within the article by the phase diagram (Finch and Ewing 1992 [DIRS 113030], Figure 9). The relevance and quality of the data in this article may be inferred from the observation that, according to SearchPlus, it has been cited 129 times since its publication in 1992, and has averaged 11 citations per year over the past 10 years.

Prior Peer and Other Professional Reviews—The paper by Finch and Ewing was published in *Journal of Nuclear Materials*, a peer-reviewed scientific journal in the field of material research relevant to nuclear installations. This journal and its review requirements were discussed in the section describing the previous data being qualified for intended use in this FEP.

Extent and Quality of Corroborating Data—The statement that, in the presence of silica, uranyl oxide hydrates form uranyl silicates is corroborated by the work done by others. For

example, Wronkiewicz (1992 [DIRS 100493]) demonstrates that UOHs formed early and were subsequently altered to soddyite, followed by uranophane and boltwoodite. Frondel (1958 [DIRS 113267]) characterizes the complete replacement of uraninite by uranophane as a common occurrence, substantiating the technical information that uranyl silicates can form.

J24.4.3 Data Qualified for Intended Use

The data specified above from Finch and Ewing (1992 [DIRS 113030], Section 4.2.2) are appropriate for intended use within FEP 2.1.09.15.0A (Formation of True (Intrinsic) Colloids in EBS). Based on satisfactorily meeting the combined attributes specified, the information is be considered qualified for intended use in the screening justification for this FEP.

J25. FEP 2.1.09.21.0A – TRANSPORT OF PARTICLES LARGER THAN COLLOIDS IN EBS

This FEP uses information from the following reference as direct input:

Reimus, P.W. 1995. *Transport of Synthetic Colloids Through Single Saturated Fractures: A Literature Review.* LA-12707-MS. Los Alamos, New Mexico: Los Alamos National Laboratory. ACC: MOL.19950302.0063. [DIRS 144604]

> The data to be qualified for intended use, obtained from the report by Reimus (1995 [DIRS 144604], Sections 3.2 and 3.3), supports the statement that inorganic particles larger than 1 μm will settle much more rapidly than they diffuse.

Description, justification of the equations and qualification of the data pertaining to the behavior of small particles transported through fractures in the saturated zone is presented in this appendix under the discussion for FEP 2.1.09.21.0B (Transport of Particles Larger than Colloids in the SZ). The use of the information is analogous in FEP 2.1.09.21.0A (Transport of Particles Larger than Colloids in EBS), with the exception that the process occurs in an unsaturated environment in this FEP and in a saturated environment in FEP 2.1.09.21.0B. This difference does not affect the evaluation outcome that the above information is appropriate for intended use. The description and qualification used for this data in FEP 2.1.09.21.0B are identically applicable to this FEP. Therefore, the use of the data and information from the report by Reimus (1995 [DIRS 144604], Section 3.2) is qualified for the intended use within this FEP.

J26. FEP 2.1.09.21.0B – TRANSPORT OF PARTICLES LARGER THAN COLLOIDS IN THE SZ

This FEP uses data from the following reference as direct input:

Reimus, P.W. 1995. *Transport of Synthetic Colloids Through Single Saturated Fractures: A Literature Review.* LA-12707-MS. Los Alamos, New Mexico: Los Alamos National Laboratory. ACC: MOL.19950302.0063. [DIRS 144604]

The data from this reference to be qualified for intended use within this FEP support the statement that:

> Inorganic particles larger than 1 μm will settle much more rapidly than they diffuse (Reimus 1995 [DIRS 144604], Section 3.2).

Specifically, the data concern the equations and related discussion on the forces and velocities that dictate particle movement in a viscous fluid. These data are presented in Sections 3.2 and 3.3 of the report by Reimus (1995 [DIRS 144604]), including the subsections. Supporting equations and justification for use include:

- Gravity Force (F_g) and Velocity (V_g) – acting toward surface (Reimus 1995 [DIRS 144604], Section 3.2.1).
- Hydrodynamic Drag Force (F_H) and Velocity (V_H) – acting away from surface (Reimus 1995 [DIRS 144604], Section 3.3.6).
- Diffusion Force (F_d) and Characteristic Diffusion Velocity (V_d) – can act in both directions, but assumed to act away from surface (Reimus 1995 [DIRS 144604], Section 3.2.1).

J26.1 QUALIFICATION METHOD

The method of qualification for the data from Reimus (1995 [DIRS 144604]) is the Technical Assessment method (SCI-PRO-001, Attachment 3, Method 5). The rationale for using this method is that it is appropriate considering the extent of documentation present for evaluation of methods. The technical assessment was based on the determination that confidence in the data acquisition or developmental results was warranted. Process attributes used in the qualification of these data are selected from the list provided in Attachment 4 of SCI-PRO-001. Attributes specifically applicable to these data are:

- The extent to which the data/information demonstrate the properties of interest (e.g., physical, chemical, geologic, mechanical) (#3).
- Prior uses of the data/information and associated verification processes (#7).

J26.2 TECHNICAL ASSESSMENT

To demonstrate that the particles larger than colloids will not be transported over long distances, forces acting upon particles moving in viscous fluid in fractures were evaluated as part of the exclusion justification for FEP 2.1.09.21.0B (Transport of Particles Larger than Colloids in the SZ). The primary forces considered are the gravitational force, hydrodynamic drag force, and the diffusion force. The equations describing these forces, as well as the associated velocities of particles acted upon by these forces, were obtained from the following literature review by Reimus (1995 [DIRS 144604]).

The report listed above presents a review of the literature pertaining to colloid transport in single saturated fractures. The arguments are supported with references to physical laws and fundamental science compiled from numerous external publications. The literature review revealed that the dominant forces acting upon particles larger than colloids are body forces such as gravity and fluid drag. These body forces greatly influence a large particle's fluid transport behavior, rather than forces generally associated with molecules (e.g., Van der Waals forces). The equations describing particle transport and associated phenomena were obtained primarily from Section 3.2 of the reference (Colloid Transport by Convection, Diffusion and Force Fields) and Section 3.3 (Colloid Interactions with Surfaces)

The derivation of these equations is appropriately described with adequate references to external literature. Technical reviews of the report by Reimus (1995 [DIRS 144604]) were conducted in 1993 by scientific peers (LANL 1994 [DIRS 185000]; LANL 1993 [DIRS 185002]). The reviews offered confidence that information presented in the report was technically correct and adequate for use. In addition to review records, all of the external references used in the report by Reimus (1995 [DIRS 144604]) are available.

J26.3 DATA QUALIFIED FOR INTENDED USE

Based on the assessment made above, equation and related technical information pertaining to the transport of particles larger than colloids in the saturated zone, from the report by Reimus (1995 [DIRS 144604]), is qualified and appropriate for intended use within FEP 2.1.09.21.0B (Transport of Particles Larger than Colloids in the SZ).

J27. FEP 2.1.09.21.0C – TRANSPORT OF PARTICLES LARGER THAN COLLOIDS IN THE UZ

This FEP uses information from the following reference as direct input:

Reimus, P.W. 1995. *Transport of Synthetic Colloids Through Single Saturated Fractures: A Literature Review.* LA-12707-MS. Los Alamos, New Mexico: Los Alamos National Laboratory. ACC: MOL.19950302.0063. [DIRS 144604]

> The data to be qualified for intended use, obtained from the report by Reimus (1995 [DIRS 144604], Sections 3.2 and 3.3), supports the statement that inorganic particles larger than 1 μm will settle much more rapidly than they diffuse.

Description, justification of the equations, and qualification of the data pertaining to the behavior of small particles transported through fractures in the saturated zone is presented in this appendix under the discussion for FEP 2.1.09.21.0B (Transport of Particles Larger than Colloids in the SZ). The use of the information is analogous in FEP 2.1.09.21.0C (Transport of Particles Larger than Colloids in UZ), with the exception that the process occurs in an unsaturated environment in this FEP and in a saturated environment in FEP 2.1.09.21.0B. This difference does not affect the evaluation outcome that the above information is appropriate for intended use. The description and qualification of these data in FEP 2.1.09.21.0B are identically applicable to this FEP. Therefore, the use of the data and information from the report by Reimus (1995 [DIRS 144604], Section 3.2) is appropriate for FEP 2.1.09.21.0C.

J28. FEP 2.1.11.03.0A – EXOTHERMIC REACTIONS IN THE EBS

This FEP uses input from the following report as direct input:

Garvin, L.J. 2002. *Multi-Canister Overpack Topical Report.* HNF-SD-SNF-SARR-005, Rev. 3. Richland, Washington: Fluor Hanford. ACC: MOL.20040510.0106. [DIRS 169141]

The data to be qualified for intended use within this FEP include:

> The maximum water in a sealed MCO is 4.64 kg (bound in particulate), with less than 200 g being present as free water (Garvin 2002 [DIRS 169141], Table 4-4).
>
> 1.1×10^7 g U-metal per waste package, assuming that the waste package contains two MCOs and each MCO contains Mark IV fuel (3,804 kg U) and scrap (1,832 kg U) for a total of 5,636 kg U (Garvin 2002 [DIRS 169141], Table 4-4).

These data are used to support the calculation showing that only a very small fraction (0.5%) of the fuel in the waste package would be oxidized even if both MCOs in a co-disposal package are each assumed to contain 4.64 kg water, and it is also assumed that all the oxygen in this water is available as free oxygen to convert uranium metal to UO_2 in a rapid exothermic reaction.

The data used in FEP 2.1.11.03.0A (Exothermic Reactions in the EBS) obtained from the report by Garvin (2002 [DIRS 169141]) are the same as the data qualified for the intended use in FEP 2.1.02.08.0A (Pyrophoricity from DSNF). These data were qualified for the use within FEP 2.1.02.08.0A by using the Technical Assessment method (SCI-PRO-001, Attachment 3, Method 5), with consideration of the applicable elements of the Spent Nuclear Fuel Project QA program at the organization generating the data (Garvin 2002 [DIRS 169141], Section 13.0). The technical assessment included determination that the employed methodology was acceptable, determination that confidence in the data acquisition or development was warranted, and confirmation that the data had been used in similar applications. The evaluation of the qualification of personnel generating the data, quality and reliability of the measurement control program, adequacy of the QA program, and the evidence of independent audits is presented in the documentation of qualification of data from the same report for FEP 2.1.13.01.0A (Radiolysis). It was concluded that the acceptance criteria for these attributes were met. Meeting of these criteria is also adequate for qualification of these data for their intended use in excluded FEP 2.1.11.03.0A (Exothermic Reactions in the EBS).

J29. FEP 2.1.11.10.0A – THERMAL EFFECTS ON TRANSPORT IN EBS

This FEP uses direct input data from the following journal articles and text book:

The Soret Effect: A Review of Recent Experimental Results (Platten 2006 [DIRS 183864])

Why Molecules Move Along a Temperature Gradient (Duhr and Braun 2006 [DIRS 183865])

Transport Phenomena (Bird et al. 1960 [DIRS 103524]).

J29.1 QUALIFICATION OF DATA FROM PLATTEN 2006

Platten, J.K. 2006. "The Soret Effect: A Review of Recent Experimental Results." *Journal of Applied Mechanics, 73,* 5-15. New York, New York: American Society of Mechanical Engineers. TIC: 259838. [DIRS 183864]

The following data from the above reference are used in FEP 2.1.11.10.0A:

> Typical Soret coefficients for aqueous solutions are on the order of 0.001 to 0.01 K^{-1} (Platen 2006 [DIRS 183864], p. 5).

These data are used in calculations that compare the relative contribution of thermally-driven solute transport to the overall diffusive solute transport mechanism in the EBS.

J29.1.1 Qualification Method

The method of qualification for intended use of the data from Platten (2006 [DIRS 183864]) is the Corroborating Data method (SCI-PRO-001, Attachment 3, Method 2). Corroborating data are available for comparison with the unqualified data set and any inferences drawn to corroborate the unqualified data can be clearly identified, justified, and documented. Qualification process attributes used in the qualification were selected from the list provided in Attachment 4 of SCI-PRO-001. Attributes specifically applicable to these data are:

- Extent to which the data demonstrate the properties of interest (#3).
- Extent and quality of corroborating data or confirmatory testing results (#10).

J29.1.2 Corroborating Data

To qualify the data from Platten (2006 [DIRS 183864]), Soret coefficient data from other sources are compared to those given by this author in order to establish the magnitude of variation of this parameter for solute transport in various types of liquids. The work by Platten (2006 [DIRS 183864]) focuses on binary liquid mixtures, but it provides comparisons of Soret coefficients obtained from other studies for the same type of liquids, indicating good agreement between values. The range of values for Soret coefficient data given by Platten (2006 [DIRS 183864], Tables 2 through 5) are corroborated with those given by Snowdon and Turner (1960 [DIRS 183867], Table 1), Thornton and Seyfried (1983 [DIRS 183866], Table 1), and Petit et al. (1986 [DIRS 183863], Table II). Although these studies were conducted on various

types of liquids (i.e., electrolytes and binary solutions), the obtained Soret coefficients at steady-state are in the order of 10^{-3} to 10^{-2} 1/K depending on the type of solution. This range in Soret coefficients is also in reasonable agreement with that given by de Groot and Mazur (1962 [DIRS 118615], p. 279) in the order of 10^{-5} to 10^{-3} 1/K encompassing mixed liquids and gases; the lower end of the range in Soret coefficients from this reference is attributed to the gases. Sufficient confidence exists due to the overlap in the range specific to aqueous solutions from the various corroborating sources. Thus, the range specified on the order of 0.001 to 0.01 K^{-1} from Platen (2006 [DIRS 183864], p. 5) is adequate for the intended use within this FEP.

Within the scope of this criterion, added confidence in the data is given by their qualification process attributes, as discussed below and outlined in Attachment 4 of SCI-PRO-001.

Extent to Which the Data Demonstrate the Properties of Interest—The range of values for Soret coefficients given by Platten (2006 [DIRS 183864]) provides a general baseline to evaluate the effects of thermal diffusion, for example, in the invert region. Given the temperature gradient (~5°C) for this domain, this translates into a relatively small contribution to the overall diffusive transport mechanism considering the adopted uncertainty for the invert diffusion coefficient (SNL 2007 [DIRS 177407], Figure 6.3-4).

Extent and Quality of Corroborating Data or Confirmatory Testing Results—The large majority of Soret coefficient data given by Snowdon and Turner (1960 [DIRS 183867], Table 1), Thornton and Seyfried (1983 [DIRS 183866], Table 1), and Petit et al. (1986 [DIRS 183863], Table II) are within the range used in the FEP evaluation, therefore validating their intended use.

J29.1.3 Data Qualified for Intended Use

Based on the extent to which the Soret coefficient data demonstrate the properties of interest and the existence of corroborating data for the range used in the evaluation of thermal diffusion in the FEP, the Soret coefficient data from Platten (2006 [DIRS 183864]) are appropriate and are qualified for use in the screening justification for FEP 2.1.11.10.0A (Thermal Effects on Transport in EBS).

J29.2 JUSTIFICATION OF EQUATION FROM DUHR AND BRAUN 2006

Duhr, S. and Braun, D. 2006. "Why Molecules Move Along a Temperature Gradient." *Proceedings of the National Academy of Sciences of the United States of America, 103,* (52), 19678-19682. Washington, D.C.: National Academy of Sciences. TIC: 259839. [DIRS 183865]

The following technical information and equations are used in FEP 2.1.11.10.0A:

- The Soret effect refers to the development of a concentration gradient in response to a temperature gradient. The magnitude of the effect is described by the Soret coefficient (S_T) (Duhr and Braun 2006 [DIRS 183865], p. 19678): $S_T\ (K^{-1}) = D_T/D$, where D_T is the thermodiffusion coefficient, and D is the diffusion coefficient.

- Because of thermodiffusion, a concentration gradient will develop in response to the temperature gradient, as described by (Duhr and Braun 2006 [DIRS 183865], p. 19,678): $c / c_o = \exp\left[- S_T \left(T - T_o\right)\right]$, where the concentration c is normalized to the concentration c_o at temperature T_o.

These relationships are used in calculations that compare the relative contribution of thermally driven solute transport to the overall diffusive solute transport mechanism in the EBS.

The equation given by Duhr and Braun (2006 [DIRS 183865]) provides the fundamental theoretical representation of the Soret effect. In most aqueous solutions, ions diffuse preferentially in the direction of the thermal gradient; that is, from hot to cold regions. This effect depends mainly on the magnitude of the Soret coefficient (S_T) and the temperature gradient. This formulation is widely used in the theoretical description of thermodiffusion in gases and liquids.

To demonstrate that the equation described above is appropriate for intended use, it was corroborated with the one used by Thornton and Seyfried (1983 [DIRS 183866]) to quantify transport by thermal diffusion in pelagic clay. The equation for the Soret effect has also been rigorously described in the classic text by de Groot and Mazur (1962 [DIRS 118615]) on non-equilibrium thermodynamics.

The equation presented by Duhr and Braun (2006 [DIRS 183865]) for thermal diffusion is corroborated here by direct comparison to representations in slightly different form by other authors. The equation given by Duhr and Braun (2006 [DIRS 183865]) for transport of a unary phase by thermal diffusion at steady-state conditions is expressed as:

$$c / c_o = \exp\left[- S_T \left(T - T_o\right)\right] \qquad \text{(Eq. J29-1)}$$

where c is the concentration of the solute at a temperature T (in degrees Kelvin) and c_o refers to the solute concentration at a some reference temperature T_o. S_T denotes the Soret coefficient and is conventionally defined in the classic text on irreversible thermodynamics by de Groot and Mazur (1962 [DIRS 118615]) as $\frac{D_T}{D}$ where D_T stands for the thermal diffusion coefficient and D corresponds to the chemical diffusion coefficient related to Fickian transport. The Soret effect is used to describe thermal diffusion which relates to the transport of molecules in response to temperature gradients (de Groot and Mazur 1962 [DIRS 118615]; Duhr and Braun 2006 [DIRS 183865]). For many liquids and gases, the Soret coefficient (S_T) is a positive quantity expressed in units of 1/T where T is temperature. Equation J29-1 can be corroborated with that given by other authors for transport by thermal diffusion. Thornton and Seyfried (1983 [DIRS 183866]) describe transport of chemical species by thermal diffusion in experiments where fluids are exposed to a thermal gradient. Their paper use the following formulation to defined the total flux as a result of chemical and thermal diffusion (Thornton and Seyfried 1983 [DIRS 183866]):

$$F = -D\left(\frac{dC}{dz} + S_T c \frac{dT}{dz}\right) + R \qquad \text{(Eq. J29-2)}$$

In the above equation, F stands for the total flux, D refers to the chemical diffusion coefficient, c corresponds to the solute concentration, T denotes temperature, z delineates distance, and R represents the flux component resulting from water–rock interactions. Assuming a steady state condition ($F = 0; R = 0$), Equation J29-2 can be rearranged and recasted as:

$$\frac{dc}{c} = -S_T dT \qquad \text{(Eq. J29-3)}$$

Integrating both sides of Equation J29-3 in the limits of c and c_o for the solute concentration, and similarly T and T_o for temperature, one obtains:

$$\ln(c / c_o) = -S_T (T - T_o) \qquad \text{(Eq. J29-4a)}$$

or

$$c / c_o = \exp\left[-S_T (T - T_o)\right] \qquad \text{(Eq. J29-4b)}$$

Corroboration is confirmed by comparing the identical forms of Equations J29-1 and J29-4b. The same result is obtained for a single component by using Equation 237 of de Groot and Mazur (1962 [DIRS 118615], p. 278) along with the rearrangements and manipulations used in Equations J29-3 through J29-4b. The source reference by de Groot and Mazur (1962 [DIRS 118615]) is considered a classic textbook on non-equilibrium thermodynamics and many subsequent studies on Soret coefficients and transport by thermal diffusion makes reference to this treatise.

Based on the evaluation presented above, the formulation of Soret effect presented by Duhr and Braun (2006 [DIRS 183865]) is justified for intended use within FEP 2.1.11.10.0A (Thermal Effects on Transport in EBS).

J29.3 QUALIFICATION OF DATA FROM BIRD 1960

Bird, R.B.; Stewart, W.E.; and Lightfoot, E.N. 1960. *Transport Phenomena.* New York, New York: John Wiley & Sons. TIC: 208957. [DIRS 103524]

The information to be qualified for intended use within this FEP include:

> According to Bird et al. (1960 [DIRS 103524], pp. 565 to 567), "The thermal diffusion term (Soret effect) describes the tendency for species to diffuse under the influence of a temperature gradient; this effect is quite small."

J29.3.1 Qualification Method

The method of qualification for intended use of the data from the report by Bird et al. (1960 [DIRS 103524]) is the Corroborating Data method (SCI-PRO-001, Attachment 3, Method 2) in accordance with SCI-PRO-005, Section 3. The rationale for using this method is that it was the most suitable considering the data and their intended use, and availability of corroborating data. Qualification process attributes used in the data qualification were selected from the list provided in Attachment 4 of SCI-PRO-001. Attributes specifically applicable to these data are:

- Qualifications of personnel or organizations generating the data (#1).
- Extent and quality of corroborating data or confirmatory testing results (#10).

J29.3.2 Technical Assessment

The technical information on the small effect of thermal diffusion are corroborated by Hirschfelder et al. (1964 [DIRS 171800], p. 8), who state: "Diffusion may also result from a temperature gradient (thermal diffusion or the Soret effect), and the transfer of energy may also result from a concentration gradient (diffusion thermo or Dufour effect). These are small effects." The Soret effect (a coupled Onsager process) is negligible when compared to direct Onsager processes, as discussed in report by Hardin and Chesnut (1997 [DIRS 100534], Section 5, p. 5-1). This report, the authors state: "Many of the Onsager-type coupled processes are probably not significant to repository performance because the required potential gradients are nonexistent or the effects are overwhelmed by direct processes such as Darcy flow, Fickian diffusion, and electrical conduction."

The principal author of the textbook, R. Byron Bird, is a Professor Emeritus of Chemical and Biological Engineering at the University of Wisconsin-Madison. He is a member of the National Academy of Engineering and holds numerous awards and honors for his technical work. He has published numerous books and articles on the topics of transport phenomena, polymer fluid dynamics, polymer kinetic theory, and rheology. *Transport Phenomena* by Bird et al. (1960 [DIRS 103524]), with a second edition released in 2002, has been in print for nearly 50 years and is used widely by the scientific and engineering community. His co-authors, Warren E. Stewart (deceased) and Edwin N. Lightfoot, are also members of the NAE and Professors Emeritus at the University of Wisconsin-Madison. The qualifications of the authors of the publication (Bird et al. 1960 [DIRS 103524]) are considered excellent and the resulting information, specifically the magnitude of the Soret effect for thermal diffusion, is therefore considered adequate.

This source is referenced by multiple handbooks, specifically those by Cho et al. (1998 [DIRS 160802]) and Perry et al. (1984 [DIRS 125806]). These are handbooks in the subject areas of heat transfer and chemical engineering, and thus are widely used in the standard work practices on these topics. The extent to which this source of information addresses the Soret effect for thermal diffusion is adequate and accurate for the intended use within this FEP.

J29.3.3 Data Qualified for Intended Use

Based on the discussion above, the data obtained from the textbook by Bird et al. (1960 [DIRS 103524]) regarding the magnitude of Soret effect are appropriate and considered qualified for intended use within FEP 2.1.11.10.0A (Thermal Effects on Transport in EBS).

J30. FEP 2.1.12.02.0A – GAS GENERATION (HE) FROM WASTE FORM DECAY

This FEP uses data from the following report as direct input:

Piron, J.P. and Pelletier, M. 2001. "State of the Art on the Helium Issues." Section 5.3 of *Synthesis on the Long Term Behavior of the Spent Nuclear Fuel.* Poinssot, C., ed. CEA-R-5958(E). Volume 1. Paris, France: Commissariat à l'Énergie Atomique. TIC: 253976. [DIRS 165318]

The data to be qualified for intended use within this FEP include:

> The decay helium gas pressure is 90 bars at 20°C for a commercial SNF rod with a gap volume of 13 cm^3 and a burnup of 47.5 GWd/MTU after 10,000 years (Piron and Pelletier 2001 [DIRS 165318], Section 5.3.2.4.1).

These data are used to estimate the pressure increase at 50°C in the void volume of a commercial SNF waste package that would occur if all of the He gas generated as a result of alpha particle decay were to be released after 10,000 years.

J30.1 QUALIFICATION METHOD

The method of qualification for intended use of the data from the report by Piron and Pelletier (2001 [DIRS 165318]) is the Corroborating Data method (SCI-PRO-001, Attachment 3, Method 2), in accordance with SCI-PRO-005, Section 3. The rationale for using this method is that it was the most suitable considering the data, and their intended use, and availability of corroborating data. Qualification process attributes used in the data qualification were selected from the list provided in Attachment 4 of SCI-PRO-001.

The attribute specifically applicable to these data is the extent and quality of corroborating data (#10).

J30.2 CORROBORATING DATA

The corroborating data used are decay helium inventory and actinide radionuclide inventory data at 1,000 years for spent nuclear fuel rods with a burnup of 45 GWd/MTU (Guenther et al. 1991 [DIRS 109207], p. D.78).

Description of Qualification Approach and Results—The approach is to use the corroborating data to independently calculate the pressure increase at 50°C in the void volume of a commercial SNF waste package that would occur if the He gas generated as a result of alpha particle decay were to be released after 10,000 years.

The steps involved in this calculation are:

- Listing the inventories of decay helium and principal alpha-emitting radionuclides (^{241}Am, ^{240}Pu, ^{239}Pu, and ^{243}Am) in commercial SNF at 1,000 years (Guenther et al. 1991 [DIRS 109207], p. D.78).

- Estimating the change in the helium inventory that will result from alpha decay during the period between 1,000 years and 10,000 years and adding this change to the 1,000 year helium inventory.

- Calculating the pressure increase at 50°C in the void volume of a commercial SNF waste package that would be associated with release of the He gas generated as a result of alpha particle decay at 10,000 years.

The results of data comparison are shown in Table J30-1.

Table J30-1. Nuclide Inventories at 1,000 years and Calculated Helium Inventory Change Due to Decay between 1,000 and 10,000 years

Nuclide	Half Life (years)	Inventory at 1,000 years (g/gU)	Decay Product	Decay Product's Half-Life	Helium Inventory Change (g/gU)
^{4}He		3.89×10^{-5}			
^{241}Am	432.7	3.49×10^{-5}	^{237}Np	2.16×10^{6} years	5.79×10^{-6}
^{240}Pu	6.56×10^{3}	2.58×10^{-3}	^{236}U	2.342×10^{7} years	2.65×10^{-5}
^{239}Pu	2.410×10^{4}	4.99×10^{-3}	^{235}U	7.04×10^{8} years	1.90×10^{-5}
^{243}Am	7.37×10^{3}	2.26×10^{-5}	^{239}Np	2.355 days	2.12×10^{-6}

The third column in Table J30-1 lists the inventories of decay helium and the principal alpha-emitting radionuclides at 1,000 years in commercial SNF with a burnup of 45 GWd/MTU (Guenther et al. 1991 [DIRS 109207], p. D.78). As shown by the decay data summarized in columns 2, 4, and 5 of Table J30-1 (SNL 2007 [DIRS 177424], Tables 4-3 and 4-4), ^{241}Am, ^{240}Pu, and ^{239}Pu decay by alpha particle emission to produce long-lived decay products. The half-lives of these decay products are sufficiently long that decay of the decay product inventory produced from decay of the parent in the interval between 1,000 and 10,000 years does not contribute significantly to the total helium inventory at 10,000 years. The number of helium atoms generated by decay of these radionuclides between 1,000 and 10,000 years is therefore given by the number of decays of the parent nuclide, which is given by: $N_{1000}(1\text{-}e^{-\lambda t})$, where N_{1000} is the number of parent atoms at 1,000 years, λ is the decay constant of the parent atom, and t is the decay time (9,000 years in this case). Because ^{243}Am decays to short-lived ^{239}Np (2.355 days), which then decays by beta particle emission to ^{239}Pu, the helium produced by both the decay of ^{243}Am and ^{239}Pu needs to be considered.

Using the approach described above, the last column in Table J30-1 shows the calculated changes in the helium inventory due to decay of ^{241}Am, ^{240}Pu, ^{239}Pu, and ^{243}Am between 1,000 and 10,000 years (note: because ^{243}Am decay contributes less than 4% of this inventory, the additional contribution from the ^{239}Pu produced in its decay is small and has not been included here). When this helium is added to the 1,000-year helium inventory (Table J30-1, column 3 ^{4}He), the decay helium inventory at 10,000 years is 9.2×10^{-5} g He/g U. Because the average uranium metal content of a commercial SNF waste package is 7.92E6 g (SNL 2007 [DIRS 180472], Table 7-1[a]), the total decay helium in a commercial SNF waste package with average burnup of 45 GWd/MTU is given by: 9.2×10^{-5} g He/g U $\times$ 7.92×10^{6} g U = 7.3×10^{2} g helium, which corresponds to 4.1×10^{3} liters at standard temperature and pressure (7.3×10^{2} g

He / 4 g He/mol × 22.4 liters/mol at STP (rounded and unit conversion from Weast 1985 [DIRS 111561], B-99 and p. F-195). If this helium were released into the 4,737 liter void space of the waste package (SNL 2007 [DIRS 180506], Table 6-3[a]), the resulting pressure increase at 50°C is calculated to be about 1.02 atm using the ideal gas law. (From Boyle's law, $p_1V_1 = p_2V_2$, release of 4.1E3 liters of gas into 4,737 liters of void space of a waste package would cause a pressure increase of $p_2 = 1$ atm × 4.1 × 10^3 L/4,737 L = 0.865 atm at 0°C (273 K). From Gay-Lussac's law, $p_1T_2 = p_2T_1$, the pressure at 50°C (323 K) would be $p_2 = 0.865$ atm × 323 K/273 K = 1.02 atm.)

The results show that the estimated 50°C pressure increase in the waste package void volume that would result from release of the decay helium at 10,000 years is 1.02 atm (~1.03 bar). This result corroborates the conclusion in FEP 2.1.2.12.02.0A (Gas Generation (He) From Waste Form Decay) reached using the data being qualified that the pressure increase at 50°C "would be less than 1.2 bar."

J30.3 DATA QUALIFIED FOR INTENDED USE

The evaluation of the data presented above provides sufficient confidence that data from Piron and Pelletier (2001 [DIRS 165318], Section 5.3.2.4.1) are adequate and are qualified for intended use in the screening justification for FEP 2.1.12.02.0A (Gas Generation (He) From Waste Form Decay).

J31. FEP 2.1.13.01.0A – RADIOLYSIS

This FEP uses direct input data from the following references:

FAI/99-14, Rev. 1, Hydrogen Combustion in an MCO During Interim Storage (Plys and Duncan 1999 [DIRS 184687])

Multi-Canister Overpack Topical Report (Garvin 2002 [DIRS 169141])

Kinetics of the Reduction of $Pu(V)O_2^+$ by Hydrogen Peroxide (Morgenstern and Choppin 1999 [DIRS 184023])

Particulate and Water in Multi-Canister Overpacks (Sexton 2007 [DIRS 184742])

The Effects of Gamma Radiation on the Corrosion of Candidate Materials for the Fabrication of Nuclear Waste Packages (Shoesmith and King 1998 [DIRS 112178]).

J31.1 QUALIFICATION OF DATA FROM PLYS AND DUNCAN 1999

Plys, M.G. and Duncan, D.R. 1999. *FAI/99-14, Rev. 1, Hydrogen Combustion in an MCO During Interim Storage.* SNF-3951, Rev. 0. Richland, Washington: Duke Engineering & Services Hanford. ACC: LLR.20080115.0173. [DIRS 184687]

The data to be qualified for intended use within this FEP include:

> The maximum achievable temperatures and pressures (11 times the initial pressure) for a hydrogen fire in a mixture of oxygen (21%) and helium (79%) inside an MCO is given by Plys and Duncan (1999 [DIRS 184687], Figure 5-1, pp. 6 and 7).

Data Use—The maximum achievable pressure as a result of a hydrogen fire in an MCO is used in excluded FEP 2.1.13.01.0A (Radiolysis) to show that a hydrogen fire involving radiolytic hydrogen is not expected to rupture the waste package.

J31.1.1 Qualification Method

The method of qualification for intended use of the data from the report by Plys and Duncan (1999 [DIRS 184687]) specified above is the Technical Assessment method (SCI-PRO-001, Attachment 3, Method 5). The rationale for using this method is that it was appropriate considering the data to be qualified, the extent of available information on the data, and the personnel that developed the data. The technical assessment was based on the determination that confidence in the data acquisition or developmental results was warranted. Qualification process attributes used in the qualification were selected from the list provided in Attachment 4 of SCI-PRO-001. Attributes specifically applicable to these data are:

- Qualifications of personnel or organizations generating the data (#1).
- The extent to which the data demonstrate the properties of interest (#3).

- The degree to which independent audits of the process that generated the data were conducted (#11).

J31.1.2 Technical Assessment

The confidence in the data acquisition or developmental results was achieved by considering the following attributes:

Qualifications of Personnel or Organizations Generating the Data—Dr. Martin G. Plys, who developed these data, is a recognized expert in modeling the behavior of flammable gas mixtures. He holds a Sc.D. in Nuclear Engineering from the Massachusetts Institute of Technology. He participated in a Hanford flammable gas elicitation study for, and authorship of, the SCOPE analysis tool. He has experience in chemical reaction, flammability, and heat transfer modeling for several Hanford facilities. He has extensive experience in the analysis of hydrogen combustion in severe reactor accidents and has contributed to development and validation of the Modular Accident Analysis Program (MAAP) nuclear reactor accident analysis models that are used worldwide.

The Extent to Which the Data Demonstrate the Properties of Interest—The adiabatic, isochoric, complete combustion model that was used to calculate the temperatures and pressures that would be associated with hypothetical hydrogen combustion events is described by Plys and Duncan 1999 ([DIRS 184687], Section 5.0 and Appendix A). The approach involves calculating the heat of combustion of an oxygen and helium gas mixture (21% oxygen and 79% helium) with different hydrogen concentrations and then calculating the constant volume temperature and pressure increases assuming that all of the heat of combustion is used to heat up the product gas mixture. The post-event temperatures are calculated using appropriate constant volume heat capacity data for the product gas mixtures and the associated pressures are calculated using the ideal gas law. This approach is appropriate for the intended use of the calculated pressures in FEP 2.1.13.01.0A.

Document Reviews—The source document was reviewed internally by the author's company (Fauke & Associates, Inc.) and also by the Hanford Spent Nuclear Fuel Project (Plys and Duncan 1999 [DIRS 184687], Section 1.0). The calculations were verified by independent review or alternate calculations (Plys and Duncan 1999 [DIRS 184687], Appendix D).

J31.1.3 Data Qualified for Intended Use

The technical assessment presented above provides sufficient confidence that data discussed above, obtained from the report by Plys and Duncan (1999 ([DIRS 184687]), are adequate for intended use and are qualified for use in the screening justification for FEP 2.1.13.01.0A (Radiolysis).

J31.2 QUALIFICATION OF DATA FROM GARVIN 2002

Garvin, L.J. 2002. *Multi-Canister Overpack Topical Report.* HNF-SD-SNF-SARR-005, Rev. 3. Richland, Washington: Fluor Hanford. ACC: MOL.20040510.0106. [DIRS 169141]

The data to be qualified for intended use within this FEP include:

- 6,340 kg uranium metal per MCO (Mark IV maximum fuel load without scrap basket (Garvin 2002 [DIRS 169141], Table 4-4).

- 443 kg zirconium cladding per MCO (Mark IV maximum fuel load without scrap basket (Garvin 2002 [DIRS 169141], Table 4-4).

J31.2.1 Qualification Method

The method of qualification for intended use of the data from the report by Garvin (2002 [DIRS 169141]) is the Technical Assessment method (SCI-PRO-001, Attachment 3, Method 5). The applicable elements of the Spent Nuclear Fuel Project QA program, documented in the source reference (Garvin 2002 [DIRS 169141], Section 13.0) and in the references cited therein were also considered. The rationale for using these methods is that they were appropriate considering the extent of available documentation that allowed the evaluation of the methodology, data acquisition, and data review. The technical assessment included determination that the employed methodology was acceptable, determination that confidence in the data acquisition or development was warranted, and confirmation that the data had been used in similar applications. Qualification process attributes used in the qualification were selected from the list provided in Attachment 4 of SCI-PRO-001. Attributes specifically applicable to these data are:

- Qualifications of personnel or organizations generating the data (#1).

- The quality and reliability of the measurement control program under which the data were generated (#5).

- The extent to which conditions under which the data were generated may partially meet the QA program that supports the YMP license application process or postclosure science (#6).

- The degree to which independent audits of the process that generated the data were conducted (#11).

J31.2.2 Technical Assessment

The MCO uranium metal mass data and MCO mass of zirconium cladding are used in excluded FEP 2.1.13.01.0A (Radiolysis) to estimate the pressure increase in the void volumes of an MCO and a 2-MCO/2-DHLW waste package that would occur if radiolysis were to convert all of the available water into hydrogen and oxygen.

J31.2.2.1 Data Acquisition Methodology Is Acceptable

The methods used to obtain the MCO fuel materials are described in footnotes “b” and “c” and associated references in the cited data source (Garvin 2002 [DIRS 169141], Table 4-4). The estimates of the U-metal fuel mass loading and cladding were appropriately based on the design basis feed description and the MCO design description. These methods are appropriate.

J31.2.2.2 Confidence in the Data Acquisition or Developmental Results

Confidence in these data is warranted because:

These data and the supporting documents were reviewed and accepted by an independent team of experts (Garvin 2002 [DIRS 169141], Appendix 4C.1 and Attachment 4C-A).

The QA controls under which the work was performed warrant confidence in the results.

The independent review team noted above includes well-recognized experts; their names, together with abridged versions of their qualifications, are provided in the source document (Garvin 2002 [DIRS 169141], Attachment 4C-A). These reviewers examined the consistency and accuracy of the data, appropriateness of the assumptions, the mathematical derivations used, and the consistency with the underlying analytical results and supporting documents and found them to be technically acceptable (Garvin 2002 [DIRS 169141], Appendix 4C.1).

The Spent Nuclear Fuel Project QA program as implemented through *Quality Assurance Program Plan for Implementation of the OCRWM QARD for the Spent Nuclear Fuel Project* (QAPP-OCRWM-001) was designed to satisfy quality assurance requirements "for federal repository acceptance of SNF and satisfy U.S. Nuclear Regulatory Commission equivalency requirements" (Garvin 2002 [DIRS 169141], Section 13.2). This QA program (Garvin 2002 [DIRS 169141], Section 13) was examined using qualification attributes in SCI-PRO-001, Attachment 4:

Qualifications of Personnel or Organizations Generating the Data—The documentation of the Fluor Hanford organization and personnel training and qualifications (Garvin 2002 [DIRS 169141], Sections 13.6.6 and 13.3.2) was reviewed. This review indicates that the requirements for qualifications and training of the personnel who performed this work are comparable to those that would apply to similar work under the YMP.

Quality and Reliability of the Measurement Control Program—The documentation of work process controls (Garvin 2002 [DIRS 169141], Section 13.6.1) was reviewed. This review showed that calibration and maintenance of equipment for data collection were conducted in accordance with approved procedures indicating that appropriate controls were implemented to ensure data quality and reliability.

Conditions under Which the Data Were Generated—As indicated above, the data were generated under *Quality Assurance Program Plan for Implementation of the OCRWM QARD for the Spent Nuclear Fuel Project* (QAPP-OCRWM-001). Because this program implemented the OCRWM QARD requirements, the data were generated under conditions that meet the YMP requirements.

Independent Audits of the Process That Generated the Data—The documentation of independent assessments (including independent audits) of the QA program under which this work was performed (Garvin 2002 [DIRS 169141], Section 13.6.5) was reviewed. This review indicates that the program for independent audits and assessments under which this work was performed was comparable to the YMP program at that time.

In summary, independent review and evaluation of the QA program under which the work was performed warrant confidence in the data.

J31.2.2.3 Data Have Been Used in Similar Applications

The source document *Multi-Canister Overpack Topical Report* (Garvin 2002 [DIRS 169141]) was prepared for the express purpose of describing the MCO design and project-approved parameter values for use in safety analyses for the K Basins Spent Nuclear Fuel Project. These safety analyses were performed under a DOE requirement to achieve "nuclear safety equivalency" to NRC-licensed facilities (Garvin 2002 [DIRS 169141], Section 1.6).

J31.2.3 Data Qualified for Intended Use

The technical assessment presented above provides sufficient confidence that data in the topical report by Garvin (2002 [DIRS 169141]) are adequate and are qualified for intended use in the screening justification for FEP 2.1.13.01.0A (Radiolysis).

J31.3 QUALIFICATION OF DATA FROM MORGENSTERN AND CHOPPIN 1999

Morgenstern, A. and Choppin, G.R. 1999. "Kinetics of the Reduction of $Pu(V)O_2^+$ by Hydrogen Peroxide." *Radiochimica Acta, 36,* 109-113. München, Germany: Oldenbourg Wissenschaftsverlag. TIC: 259871. [DIRS 184023]

The data to be qualified for intended use within this FEP include:

> Reduction of Pu(V) to Pu(IV) in basic solutions having hydrogen peroxide (H_2O_2) concentrations on the order of 0.04 to 0.00001 moles per liter and pH 7.9 to 10.8. (Morgenstern and Choppin 1999 [DIRS 184023], pp. 109 to 111, Table 1).

J31.3.1 Qualification Method

The method of qualification for intended use of the data from the journal article by Morgenstern and Choppin (1999 [DIRS 184023]) is the Corroborating Data method (SCI-PRO-001, Attachment 3, Method 2) in accordance with SCI-PRO-005, Section 3. Corroborating data are available for comparison with the unqualified data set and any inferences drawn to corroborate the unqualified data can be clearly identified, justified, and documented. Qualification process attributes used in the qualification were selected from the list provided in Attachment 4 of SCI-PRO-001. Attributes specifically applicable to these data are:

- Extent to which the data demonstrate the properties of interest (#3)
- Extent and quality of corroborating data or confirmatory testing results (#10).

J31.3.2 Corroborating Data

The data by Morgenstern and Choppin (1999 [DIRS 184023]) are unique because most of the existing data on the stability of Pu(IV) in peroxide-rich conditions is for very acidic systems. However, there is corroborative evidence on the reduction of Pu(V) and Pu(VI) and the stability

of Pu(IV) peroxide solids in H_2O_2-rich solutions. One method for precipitating Pu from solution is through the formation of a Pu(IV) peroxide solid (Katz et al. 1986 [DIRS 106312], p. 570). Highly charged Pu(IV)-peroxy complexes forms in relatively dilute acid solutions of H_2O_2 and a precipitate forms with more additions of H_2O_2 (Katz et al. 1986 [DIRS 106312], pp. 704 to 705). This demonstrates that Pu(IV) can be stabilized in the presence of H_2O_2 and is consistent with the reduction kinetics of Pu(V) with respect to H_2O_2 concentration in the experiments by Morgenstern and Choppin (1999 [DIRS 184023]). Given the close behavior in the reduction of Pu(V) and the stability of Pu(IV) in the presence of H_2O_2, this confirms the validity of the observations presented by Morgenstern and Choppin (1999 [DIRS 184023]) for Pu(V) reduction kinetics.

Within the scope of this criterion, added confidence in the data is given by their qualification process attributes as discussed below and outlined in Attachment 4 of SCI-PRO-001:

Extent to Which the Data Demonstrate the Properties of Interest—The data presented by Morgenstern and Choppin (1999 [DIRS 184023]) provide evidence for the reduction of Pu(V) to Pu(IV) in H_2O_2 solutions in the basic pH range. These conditions are more relevant to YMP repository environments where alpha radiolysis can result in the generation of H_2O_2.

Extent and Quality of Corroborating Data or Confirmatory Testing Results—The information presented by Katz et al. (1986 [DIRS 106312]) provides ample evidence for the reduction of Pu(V) and stability of Pu(IV) in H_2O_2-bearing acid solutions. Moreover, it presents details on the formation of Pu(IV)-peroxide solids and their solubilities. The study by Katz et al. (1986 [DIRS 106312]) is considered a reference source of actinide chemistry.

J31.3.3 Data Qualified for Intended Use

Based on the extent to which the data demonstrate the properties of interest and the existence of corroborating data, there is sufficient confidence that the data from Morgenstern and Choppin (1999 [DIRS 184023]) are appropriate and are qualified for intended use in the screening justification for FEP 2.1.13.01.0A (Radiolysis).

J31.4 QUALIFICATION OF DATA FROM SEXTON 2007

Sexton, R.A. 2007. *Particulate and Water in Multi-Canister Overpacks (OCRWM)*. KBC-33403, Rev. 0. Richland, Washington: Fluor Hanford. ACC: LLR.20080116.0003. [DIRS 184742]

The data to be qualified for intended use within this FEP include:

> Maximum amount of free and bound water in an MCO is 4.3 kg (Sexton 2007 [DIRS 184742], Table 2-1).
>
> The average value of free and bound water in an MCO is 1.03 kg (Sexton 2007 [DIRS 184742], Table 2-1).

J31.4.1 Qualification Method

The method of qualification for intended use of data from the report by Sexton (2007 [DIRS 184742]) is the Technical Assessment method (SCI-PRO-001, Attachment 3, Method 5). The rationale for using this method is that that it was appropriate considering the extent of available documentation that allowed the evaluation of the methodology, data acquisition, and data review. The technical assessment included the determination that the employed methodology was acceptable and the determination that confidence in the data acquisition or development was warranted. Qualification process attributes used in the qualification were selected from the list provided in Attachment 4 of SCI-PRO-001. Attributes specifically applicable to these data are:

- The technical adequacy of equipment and procedures used to collect and analyze the data (#2).

- The extent to which conditions under which the data were generated may partially meet the QA program that supports the YMP license application process or postclosure science (#6).

J31.4.2 Technical Assessment

The purpose of this document is to establish a conservative estimate for particulate and bound water in each MCO produced by the NSNFP. Known values along with conservative bounding assumptions were used to determine the estimates for each MCO. The calculated values rely on a number of factors such as adhering particulate, void volume, decay heat, minimum fuel temperature, actual rebound rate and drying conditions. All related sources to the document are clearly identified. A sample calculation is provided to aid in transparency.

The Technical Adequacy of Equipment and Procedures—The methodology is standard practice and generally accepted in the field of science and engineering. The calculations, assumptions and bounding conditions are all well described and provide a level of confidence in the reliability of the data generated. Measurements were well described with a margin of uncertainty to allow a conservative estimate in data to be discerned.

Quality Assurance Program—Although the report does not clearly identify the quality assurance program under which the report was originated, personal communication with NSNFP Manager indicated that the report was generated under the NSNFP QA program. Upon reviewing the NSNFP QA procedure (NSNFP 3.04 Rev. 6) it is permissible not to specify a QA section within certain reports. The report was peer reviewed and approved by NSNFP QA for formal public release as indicated on the engineering document change form. The NSNFP QA program at least partially meets a QA program that supports the YMP license application process or postclosure science.

J31.4.3 Data Qualified for Intended Use

The technical assessment presented above provides sufficient confidence that the data from the report by Sexton (2007 [DIRS 184742]) are appropriate for intended use and are qualified for use in the screening justification for FEP 2.1.13.01.0A (Radiolysis).

J31.5 QUALIFICATION OF DATA FROM SHOESMITH AND KING 1998

Shoesmith, D.W. and King, F. 1998. *The Effects of Gamma Radiation on the Corrosion of Candidate Materials for the Fabrication of Nuclear Waste Packages.* AECL-11999. Pinawa, Manitoba, Canada: Atomic Energy of Canada Limited. ACC: MOL.19990311.0212. [DIRS 112178]

The data to be qualified for intended use within this FEP include:

> At 90°C in Q-Brine (Mg-Cl containing brine), Alloy C-4 corrosion rates are about 0.1 μm/y and 0.05 μm/yr in the absence and presence of about 100 rad/hr gamma radiation, respectively (Shoesmith and King 1998 [DIRS 112178], Table 4). For alloy C-4 tested no enhancement of general corrosion rates and no pitting or crevice corrosion was observed in this dose region (Shoesmith and King 1998 [DIRS 112178], p. 29).
>
> In the dose region 100 rad/hr to 1,000 rad/hr and at 90°C, for Alloy C-4 in Q-Brine (Mg-Cl containing brine) pitting and crevice corrosion is observed (Shoesmith and King 1998 [DIRS 112178], p. 30, Table 4). At higher dose rates (1,000 rad/hr to 100,000 rad/hr) extensive pitting and crevice corrosion is present (Shoesmith and King 1998 [DIRS 112178], p. 30, Table 4).
>
> At 90°C in Q-Brine, Titanium Grade 7 (Ti-7, titanium 99.8-paladium) corrosion rates are about 0.1 μm/yr and 0.7 μm/yr in the absence and presence of 10,000 rad/h gamma radiation, respectively (Shoesmith and King 1998 [DIRS 112178], Table 4). For titanium (Ti-7), passivity is maintained within the dose region, 1,000 rad/hr to 10,000 rad/hr, and at 100,000 rad/hr, although the rate of passive film growth could be an order of magnitude higher than at 1,000 rad/hr (but still only 0.4 μm/yr) (Shoesmith and King 1998 [DIRS 112178], pp. 30 to 31).

J31.5.1 Qualification Method

The method of qualification for intended use of the data from the article by Shoesmith and King (1998 [DIRS 112178]) is the Technical Assessment method (SCI-PRO-001, Attachment 3, Method 5). The rationale for using this method is that it was the most suitable considering the data, their existing documentation, and their intended use. The technical assessment was based on the determination that confidence in the data acquisition or development was warranted. Qualification process attributes used in the technical assessment of these data are selected from the list provided in Attachment 4 of SCI-PRO-001. Attributes specifically relevant to these data are:

- Qualification of personnel or organizations generating the data are comparable to qualification requirements of personnel generating similar data under an approved program that supports the YMP license application process or postclosure science (#1).
- The extent to which the data demonstrate the properties of interest (e.g., physical, chemical, geological, mechanical) (#3).

J31.5.2 Technical Assessment

The information under consideration reported by Shoesmith and King (1998 [DIRS 112178]) is a summary of the original work done by Smailos and Köster (1987 [DIRS 159774]) entitled "Corrosion Studies on Selected Packaging Materials for Disposal of High Level Wastes" presented as part of the *Materials Reliability in the Back End of the Nuclear Fuel Cycle* proceeding organized by the International Atomic Energy Agency. In some cases, Shoesmith and King (1998 [DIRS 112178]) rely on a summary paper by Smailos et al. (1990 [DIRS 154820]) where the data is in tabular form. Therefore, the focus of the technical assessment will be primarily on the work by Smailos and Köster (1987 [DIRS 159774]). The data collected are appropriately described with test conditions and standard techniques that described corrosion rates and characterization of corrosion pits by Smailos and Köster (1987 [DIRS 159774]) and Smailos et al. (1990 [DIRS 154820]).

The qualifications of personnel generating the data, Smailos and Köster, as well as Shoesmith, are comparable to the qualification of personnel supporting the YMP license application process. Furthermore, the organizations for the authors have programs specifically for the determination of radioactive waste management. For example, Smailos and Köster are from the Institut fur Nukleare Entsorgungstechnik, and Shoesmith from the Department of Chemistry at The University of Western Ontario is relied upon as an expert in corrosion science. King was associated with the Atomic Energy of Canada, Whiteshell Laboratories at the time of the publication.

Q-Brine is a Mg-Cl containing brine ($NaCl$-KCl-$MgCl_2$-$MgSO_4$-H_2O) with the composition of the brine at 55°C containing by weight per cent 1.4% NaCl, 4.7% KCl, 26.8% $MgCl_2$, 1.4% $MgSO_4$, 65.7% H_2O at 55°C (pH = 4.9 at 25°C) (Smailos and Köster 1987 [DIRS 159774], p. 10). Although this brine containing high Mg-Cl content is not relevant at Yucca Mountain, it offers a bounding chemical environment to assess the influence of gamma radiation on relevant material corrosion. The materials studies include Alloy C-4 (similar to Alloy C-22) and Titanium 99.8 Pd (Titanium Grade 7). For comparison to materials that are susceptible to corrosion induced enhancement by radiation, Table 2 of Shoesmith and King (1998 [DIRS 112178]) shows irons, carbon steels, and low alloy steels with corrosion rates ranging from about 20 to 800 μm/y in Q-Brine at 90°C. The corrosion rate for Titanium Grade 7 (Titanium 99.8 Pd ASTM Grade 7) and Alloy C-4 in the absence of gamma radiation is low, and thus these materials are classified as passive materials in Table 4. Even at dose rates as high as about 10,000 rad/hr the corrosion rates for these materials are low, although Alloy C-4 at the higher dose rates has a higher corrosion rate, which may be attributed to localized corrosion.

The corrosion rate for Titanium 99.8-Pd (Titanium Grade 7) over a test period of about 4 years in Q-brine is on the order of 0.1 to 0.2 mm/yr and was not influenced noticeably by test temperatures up to 200°C (Smailos and Köster 1987 [DIRS 159774], Figure 1, p. 13). The influence of gamma radiation (100,000 rad/hr) on Titanium 99.8-Pd corrosion rate in Q-brine was measured as 0.7 μm/yr (Smailos and Köster 1987 [DIRS 159774], p. 18). The assumption that the oxide layer covering the titanium 99.8-Pd sample is TiO_2 is valid, as any contribution by MgO would be small as their densities are very close and the thickness of the oxide layer is relatively small.

Alloy C-4 data are summarized from Smailos et al. 1990 [DIRS 154820], Table 4, where 1 Gy = 100 rad). The data are supported in the study by Smailos and Köster 1987 [DIRS 159774], Sections 3.1 and 3.2, Figures 1 and 8) demonstrating low corrosion rates for alloy C-4 in the absence of gamma radiation and moderate corrosion rates in the presence of gamma radiation. The micrograph in Figure 10 of the report by Smailos and Köster (1987 [DIRS 159774]) shows an example of pitting for Alloy C-4 in Q-Brine at 90°C with gamma radiation 100,000 rad/hr (1,000 Gy/hr).

J31.5.3 Data Qualified for Intended Use

The data from Shoesmith and King (1998 [DIRS 112178], pp. 29 to 31 and Table 4) are appropriate for intended use in the screening justification for FEP 2.1.13.01.0A (Radiolysis). The technical assessment presented above, along with the qualifications of the personnel generating the data, provides sufficient confidence that these data can be considered qualified for intended use within this FEP.

J32. FEP 2.2.06.01.0A – SEISMIC ACTIVITY CHANGES POROSITY AND PERMEABILITY OF ROCK

This FEP uses data from the following report as direct input:

National Research Council 1992. *Ground Water at Yucca Mountain, How High Can It Rise? Final Report of the Panel on Coupled Hydrologic/Tectonic/Hydrothermal Systems at Yucca Mountain*. Washington, D.C.: National Academy Press. TIC: 204931. [DIRS 105162]

The data to be qualified for intended use within this FEP include:

> Extension rates declined to 5 to 10 mm/yr at 5 Ma; extension rates are still in a declining state (National Research Council 1992 [DIRS 105162], Chapter 2, p. 24).
>
> Plate tectonic activity has imparted crustal extension stresses within the Basin and Range Province (which includes the Yucca Mountain region) during the past 12 million years. Extension rates between 10 and 12 million years ago ranged between 10 and 30 mm/yr (National Research Council 1992 [DIRS 105162], Chapter 2, p. 22).
>
> Predicted seismic events within the Yucca Mountain region over the next 10,000 years will not alter the large and globally extensive stresses imposed in the rock and in effect over the past 10 to 12 million years (National Research Council 1992 [DIRS 105162], Chapter 5, p. 116).

The intended use of extension rate data and predicted seismic events overlaps with FEP 2.2.06.02.0A (Seismic Activity Changes Porosity and Permeability of Faults). The effects of seismic activity on hydrologic properties of rocks overlap with FEP 1.2.10.01.0A (Hydrologic Response to Seismic Activity). The data used in FEP 1.2.10.01.0A concern water table fluctuation data and are qualified for intended use as a part of data qualification for FEP 2.2.06.01.0A. Specifically, the data used in FEP 1.2.10.01.0A (Hydrologic Response to Seismic Activity) are the following:

- Results from the regional stress model approach indicated a maximum water table rise of 50 m (National Research Council 1992 [DIRS 105162], Chapter 5, p. 116).

J32.1 QUALIFICATION METHOD

The method of qualification for intended use of the data from the National Research Council (1992 [DIRS 105162]) is the Technical Assessment method (SCI-PRO-001, Attachment 3, Method 5). The rationale for using this method is that it was the most suitable considering the data, their existing documentation, and their intended use. The technical assessment was based on the determination that confidence in the data acquisition or development was warranted. Qualification process attributes used in the qualification are selected from the list provided in Attachment 4 of SCI-PRO-001. Attributes specifically applicable to these data are:

- Qualifications of personnel or organizations generating the data are comparable to qualification requirements of personnel generating similar data under an approved program that supports the YMP license application process or postclosure science (#1).

- The extent to which the data demonstrate the properties of interest (e.g., physical, chemical, geological, mechanical) (#3).

J32.2 TECHNICAL ASSESSMENT

Qualifications of Personnel or Organizations Generating Data—The project that is the subject of this report was approved by the governing board of the National Research Council, whose members are drawn from the councils of the National Academy of Sciences (NAS), the National Academy of Engineering (NAE), and the Institute of Medicine (IOM). The members of the committee responsible for the report were chosen for their special competencies and with regard for appropriate balance. This report has been reviewed by a group other than the authors according to procedures approved by a Report Review Committee consisting of members of the NAS, NAE, and IOM.

The report was published by the National Academies Press (NAP). The NAP was created by the National Academies to publish the reports issued by the NAS, NAE, and IOM, and the Council, all operating under a charter granted by the Congress of the United States. NAP publishes over 200 books a year on a wide range of topics in science, engineering, and health, capturing the most authoritative views on important issues in science and health policy. The institutions represented by NAP are unique in that they attract the nation's leading experts in every field to serve on their blue ribbon panels and committees. The NAS is a private, nonprofit, self-perpetuating society of distinguished scholars engaged in scientific and engineering research and dedicated to the furtherance of science and technology and to their use for the general welfare. Upon the authority of the charter granted to it by the Congress in 1863, the Academy has a mandate that requires it to advise the federal government on scientific and technical matters. The Council was organized by the NAS in 1916 to associate the broad community of science and technology with the Academy's purposes of furthering knowledge and of advising the federal government. Functioning in accordance with general policies determined by the Academy, the Council has become the principal operating agency of both the NAS and the NAE in providing services to the government, the public, and the scientific and engineering communities. The Council is administered jointly by both academies and the IOM.

Data Demonstrate the Properties of Interest— The National Research Council (1992 [DIRS 105162]) reference provides the basis for regional extensional rates declining from a peak of 10 to 30 mm/yr (10-12 Ma) to 5 to 10 mm/yr (5 Ma) and are in a declining state today. The reference also provides a basis for bounding the extent to which the water table may rise or fluctuate in response to future seismic events. Seismic dislocation and water-level changes are discussed in a report prepared by the Panel on Coupled Hydrologic/Tectonic/Hydrothermal Systems at Yucca Mountain, commissioned by the National Research Council. The panel reviewed an alternative conceptual model that predicted large changes in groundwater level, and concluded that the model was infeasible. The panel stated that seismic dislocation would at most elevate the water levels a few tens of meters (National Research Council 1992 [DIRS 105162]), p. 7). Alternative perspectives on seismic pumping and water-level changes are discussed in the *Final Environmental Impact Statement* (DOE 2002 [DIRS 155970], p. 3-59), which cites the work by the National Research Council. The panel reviewed the alternative conceptual model and concluded that it was infeasible.

J32.3 DATA QUALIFIED FOR INTENDED USE

Based on the evidence provided above, the data and technical information obtained from the report by the National Research Council (1992 [DIRS 105162]) are appropriate for intended use and are qualified and justified for use in the screening justification for FEP 2.2.06.01.0A (Seismic Activity Changes Porosity and Permeability of Rock).

J33. FEP 2.2.06.02.0A – SEISMIC ACTIVITY CHANGES POROSITY AND PERMEABILITY OF FAULTS

This FEP uses data from the following report as direct input:

National Research Council 1992. *Ground Water at Yucca Mountain, How High Can It Rise? Final Report of the Panel on Coupled Hydrologic/Tectonic/Hydrothermal Systems at Yucca Mountain.* Washington, D.C.: National Academy Press. TIC: 204931. [DIRS 105162]

The data to be qualified for intended use within this FEP include:

> Extension rates declined to 5 to 10 mm/yr at 5 Ma; extension rates are still in a declining state (National Research Council 1992 [DIRS 105162], Chapter 2, p. 24).
>
> Plate tectonic activity has imparted crustal extension stresses within the Basin and Range Province (which includes the Yucca Mountain region) during the past 12 million years. Extension rates between 10 and 12 million years ago ranged between 10 and 30 mm/yr (National Research Council 1992 [DIRS 105162], Chapter 2, p. 22).
>
> Predicted seismic events within the Yucca Mountain region over the next 10,000 years will not alter the large and globally extensive stresses imposed in the rock and in effect over the past 10 to 12 million years (National Research Council 1992 [DIRS 105162], Chapter 5, p. 116).

The intended use of extension rate data and predicted seismic events overlaps with FEP 2.2.06.01.0A (Seismic Activity Changes Porosity and Permeability of Rock).

J33.1 QUALIFICATION METHOD

The same data obtained from the same reference and used in an analogous context were qualified for intended use in FEP 2.2.06.01.0A (Seismic Activity Changes Porosity and Permeability of Rock). The data were qualified for intended use using the Technical Assessment method (SCI-PRO-001, Attachment 3, and Method 5). The rationale for using this method is that it was the most suitable considering the data, the data originator, and their intended use. The technical assessment was based on the determination that confidence in the data acquisition or development was warranted and included the consideration of the qualifications of personnel or organizations generating the data and the extent to which the data demonstrate the properties of interest. The same attributes of the data qualification process are applicable to qualifying the data from the National Research Council report (National Research Council 1992 [DIRS 105162]) for the intended use in FEP 2.2.06.01.0A.

J33.2 DATA QUALIFIED FOR INTENDED USE

Based on the evidence provided in this appendix for FEP 2.2.06.01.0A (Seismic Activity Changes Porosity and Permeability of Rock) and the intended use of the data in FEP 2.2.06.02.0A (Seismic Activity Changes Porosity and Permeability of Faults), the data from the National Research Council (1992 [DIRS 105162]) are appropriate and are qualified for intended use in the screening justification for FEP 2.2.06.02.0A (Seismic Activity Changes Porosity and Permeability of Faults).

J34. FEP 2.2.06.03.0A – SEISMIC ACTIVITY ALTERS PERCHED WATER ZONES

This FEP uses data from the following report as direct input:

Distribution and Chemistry of Diagenetic Minerals at Yucca Mountain, Nye County, Nevada (Broxton et al. 1987 [DIRS 102004])

Origin, Timing, and Temperature of Secondary Calcite–Silica Mineral Formation at Yucca Mountain, Nevada (Wilson et al. 2003 [DIRS 163589]).

J34.1 QUALIFICATION OF DATA FROM BROXTON 1987

Broxton, D.E.; Bish, D.L.; and Warren, R.G. 1987. "Distribution and Chemistry of Diagenetic Minerals at Yucca Mountain, Nye County, Nevada." *Clays and Clay Minerals, 35,* (2), 89-110. Long Island City, New York: Pergamon Press. TIC: 203900. [DIRS 102004]

The data to be qualified for intended use within this FEP include:

> Most of the zeolitic deposits at Yucca Mountain formed between 11.3 and 13.9 million years ago, and were largely contemporaneous with the most active period of silicic volcanism within the southwest Nevada volcanic field (Broxton et al. 1987 [DIRS 102004], p. 101).

J34.1.1 Data Qualification Method

The method of qualification for intended use of the data from Broxton et al. (1987 [DIRS 102004]) is the Corroborating Data method (SCI-PRO-001, Attachment 3, Method 2). The rationale for using this method is that it was the most suitable considering the data, their existing documentation, their intended use, and the availability of corroborating data. Qualification process attributes used in the qualification are selected from the list provided in Attachment 4 of SCI-PRO-001. Attributes specifically applicable to these data are:

- The extent to which the data demonstrate the properties of interest (e.g., physical, chemical, geologic, mechanical) (#3).
- Extent and quality of corroborating data (#10).

J34.1.2 Technical Assessment and Corroborating Data

The property of interest is related to the intended use of the data where these data are used to support the statement that most of the zeolitic alteration at Yucca Mountain occurred prior to 11.3 million years ago The important feature is that zeolitic alteration occurred millions of years ago. In this regard, corroborating information from additional studies is discussed.

Corroborating information can be found in the report by Bish et al. (1984 [DIRS 106336], p. 72), which states that "[t]extural relations in the samples examined for the present study indicate that substantial zeolitization had already occurred before the geopetal fillings were deposited. This means that zeolitization even in the youngest affected tuff, which corresponds to approximately

12.5 to 13 Myr (Kistler 1968 [DIRS 133347]), was well advanced within about 1.2 to 1.7 Myr after the tuff was deposited." This reference provides confidence that the information from Broxton et al. (1987 [DIRS 102004]) is reliable.

J34.1.3 Data Qualified for Intended Use

Based on the available corroborating data, the information from Broxton et al. (1987 [DIRS 102004], p. 101) is adequate for intended use FEP 2.2.06.03.0A (Seismic activity alters perched water zones) and is considered qualified for intended use within this FEP.

J34.2 QUALIFICATION OF DATA FROM WILSON ET AL. 2003

Wilson, N.S.F.; Cline, J.S.; and Amelin, Y.V. 2003. "Origin, Timing, and Temperature of Secondary Calcite–Silica Mineral Formation at Yucca Mountain, Nevada." *Geochimica et Cosmochimica Acta, 67,* (6), 1145-1176. New York, New York: Pergamon. [DIRS 163589]

The data from this journal article to be qualified for intended use include:

> Studies of secondary minerals at Yucca Mountain using petrography, fluid-inclusion thermometry, and uranium-lead dating indicate that unsaturated-zone temperatures have remained close to the current ambient values over the past 2 to 5 Ma (Wilson et al. 2003 [DIRS 163589], Section 8).

Qualification of the data from Wilson et al. (2003 [DIRS 163589, Section 8) is presented in this appendix under the discussion for FEP 1.2.06.00.0A (Hydrothermal Activity). The intended use of the data is the same as that presented in FEP 1.2.06.00.0A (Hydrothermal Activity) and the qualification used for this data in FEP 1.2.06.00.0A is identically applicable to this FEP. Therefore, the use of the data and information from the report by Wilson (2003 [DIRS 163589], Section 8) is qualified for the intended use within this FEP.

J35. FEP 2.2.07.14.0A – CHEMICALLY-INDUCED DENSITY EFFECTS ON GROUNDWATER FLOW

This FEP uses data from the following report as direct input:

Zhang, H. and Schwartz, F.W. 1995. "Multispecies Contaminant Plumes in Variable Density Flow Systems." *Water Resources Research, 31,* (4), 837-847. Washington, D.C.: American Geophysical Union. TIC: 252318. [DIRS 183479]

The data to be qualified for intended use within this FEP include:

> In order for density effects to be present in the model simulations, the concentration of the leachate (or contaminant plume) had to be at least 2,000 mg/L (which corresponded to a solution density of 999.7 kg/m^3 at 20°C, in a native groundwater with a density of 998.2 kg/m^3 at 20°C; i.e., a density contrast of ~0.15%) in a very dilute native groundwater at 20°C for a specific discharge of ~30 m/yr through a homogeneous isotropic porous medium with a flow porosity of 0.25, yielding a horizontal seepage velocity of ~120 m/yr (Zhang and Schwartz 1995 [DIRS 183479], pp. 839, 840, 843, and 844).

The intended use of the data is to support the expectation that the density contrast between unsaturated zone water entering the saturated zone and saturated zone water is not large enough to cause significant density-driven flow except for possibly during the relatively short pulse associated with the repository thermal pulse.

J35.1 QUALIFICATION METHOD

The method of qualification for intended use of the data from the report by Zhang and Schwartz (1995 [DIRS 183479]) is the Technical Assessment method (SCI-PRO-001, Attachment 3, Method 5). The rationale for using this method is that it was the most suitable considering the data, their existing documentation, and their intended use. The technical assessment was based on the determination that confidence in the data acquisition or development was warranted. Qualification process attributes used in the technical assessment of these data are selected from the list provided in Attachment 4 of SCI-PRO-001. Attributes specifically relevant to these data are:

- Qualification of personnel or organizations generating the data are comparable to qualification requirements of personnel generating similar data under an approved program that supports the YMP license application process or postclosure science (#1).
- The extent to which the data demonstrate the properties of interest (e.g., physical, chemical, geological, mechanical) (#3).
- Prior peer or other professional reviewers of the data and their results (#8).

J35.2 TECHNICAL ASSESSMENT OF THE DATA

Qualification of Personnel or Organizations Generating the Data—Hubao Zhang and Franklin Schwartz were both at Ohio State University at the time the article was written. The second author, Dr. Schwartz, is a professor in the School of Earth Sciences at Ohio State University and is an Ohio Eminent Scholar. Drs. Zhang and Schwartz are co-authors of the textbook *Fundamentals of Groundwater* released in 2002. Additionally, Dr. Schwartz is co-author of the textbook *Physical and Chemical Hydrogeology* published in 1990. He has numerous awards, including the E.O. Meinzer Award and the Excellence in Science and Engineering Award. In 1992 he was named as a Fellow of the American Geophysical Union.

Extent to Which the Data Demonstrate the Properties of Interest—The simulations presented by Zhang and Schwartz are for the case of a contaminant added to a water table of a flowing groundwater system. They examined several cases to assess the concentration of the contaminant plume required for density-driven sinking to occur. Simulations were conducted with leachate concentrations of 5,000 mg/L, 3,000 mg/L, and 1,000 mg/L. Sinking occurred in the first two cases, and the authors surmise that the cutoff for a sinking plume would occur for concentrations above 2,000 mg/L. These simulations were performed assuming a groundwater density of 998.2 kg/m^3. Regarding the density contrast, the authors state on p. 844 that "As $[Co]_1$ becomes less than about 2,000 mg/L, the density effects become minimal." In Table 1 on p. 838, the density of 2,000 mg/L NaCl is listed as 999.7 kg/m^3. At the bottom of p. 839 it is stated that the density of the ambient groundwater is chosen as 998.2 kg/m^3. Thus, the density contrast is (999.7 – 998.2)/998.2 = 0.0015, or 0.15%. The work of Zhang and Schwartz provides the basis for estimating the concentration of a radionuclide plume necessary to cause density effects on groundwater flow. Thus the data are demonstrated to provide properties of interest.

Peer Review of the Data and Their Results—The data and analysis from Zhang and Schwartz were published in the journal Water Resources Research. Water Resources Research is an interdisciplinary journal integrating research in the social and natural sciences of water. Articles published in Water Resources Research are evaluated through a peer-review process before publication. Therefore, this work has received prior peer review.

J35.3 DATA QUALIFIED FOR INTENDED USE

The above technical evaluation indicates that there is sufficient confidence that the data obtained from the report by Zhang and Schwartz (1995 [DIRS 183479]) are appropriate and are qualified use in the screening justification for FEP 2.2.07.14.0A (Chemically-Induced Density Effects on Groundwater Flow).

J36. FEP 2.2.08.07.0C – RADIONUCLIDE SOLUBILITY LIMITS IN THE BIOSPHERE

This FEP uses direct input from the following report:

Doorenbos, J. and Pruitt, W.O. 1977. *Crop Water Requirements.* FAO Irrigation and Drainage Paper 24. Rome, Italy: Food and Agriculture Organization of the United Nations. TIC: 245199. [DIRS 103062]

> The data from this reference that are being used as direct input are the salinity tolerances for crops (Doorenbos and Pruitt 1977 [DIRS 103062], Table 36, p. 78).

The intended use of these data in FEP 2.2.08.07.0C is to compare the concentration of salts in groundwater with the range of water salinity tolerated by crops without the yield reduction.

J36.1 QUALIFICATION METHOD

The method of qualification for intended use of data from the report by Doorenbos and Pruitt (1977 [DIRS 103062]) is the Technical Assessment method (SCI-PRO-001, Attachment 3, Method 5). The rationale for using this method is that it was appropriate considering the available information on the data and the originating agency. The technical assessment was based on the determination that confidence in the data acquisition or development was warranted. Qualification process attributes used in the qualification were selected from the list provided in Attachment 4 of SCI-PRO-001. Attributes specifically applicable to these data are:

- Qualifications of personnel or organizations generating the data (#1).
- The extent to which the data demonstrate the properties of interest (#3).

J36.2 TECHNICAL ASSESSMENT

Qualifications of Personnel or Organizations Generating the Data—The data on crop salt tolerance were obtained from the publication by the Food and Agriculture Organization of the United Nations. The methods for calculating net irrigation and seasonal irrigation requirements in the report by Doorenbos and Pruitt (1977 ([DIRS 103062]) and the supporting data are widely accepted.

The Food and Agriculture Organization (FAO) is a specialized agency of the United Nations that leads international efforts to defeat hunger. The FAO not only acts as a neutral forum where all nations meet as equals to negotiate agreements and debate policy, but also is also a source of knowledge and information. The Food and Agriculture Organization serves as a network for sharing knowledge related to sustainable food production. It uses the expertise of its staff and other professionals to collect, analyze, and disseminate data that help development of good agricultural practices. FAO Internet publishes technical documents, hundreds of newsletters, reports and books; distributes several magazines; and creates numerous CD-ROMs. The FAO publication and data can be considered reliable and representative of the current state of knowledge.

The Extent to Which the Data Demonstrate the Properties of Interest—The salt tolerance of individual crops is expressed in terms of electrical conductivity. The data from Doorenbos and Pruitt (1977 [DIRS 103062], Table 36, p. 78) are for crop salt tolerance values with no reduction in yield. The data were available for many common crops that can be grown in Amargosa Valley, including the most common crop, alfalfa, and thus were representative of the local conditions.

J36.3 DATA QUALIFIED FOR INTENDED USE

The above technical evaluation indicates that the qualification attributes were met and there is sufficient confidence that the data from the report by Doorenbos and Pruitt (1977 [DIRS 103062]) are appropriate and are qualified for use in the screening justification for FEP 2.2.08.07.0C (Radionuclide Solubility Limits in the Biosphere).

J37. FEP 2.2.08.11.0A – GROUNDWATER DISCHARGE TO SURFACE WITHIN THE REFERENCE BIOSPHERE

This FEP uses data from the following report as direct input:

Paces, J.B.; Whelan, J.F.; Forester, R.M.; Bradbury, J.P.; Marshall, B.D.; and Mahan, S.A. 1997. *Summary of Discharge Deposits in the Amargosa Valley.* Milestone SPC333M4. Denver, Colorado: U.S. Geological Survey. ACC: MOL.19981104.0151. [DIRS 109148]

The general information to be qualified for intended use within this FEP describes the paleospring deposits located in Crater Flat, Crater Flat Wash, Amargosa Valley Diatomite, Indian Pass, Scranton Well, Mesquite Wash, and the Amargosa River Snail Site (Paces et al. 1997 [DIRS 109148], Figure 18).

The specific data, inclusive to the general information above, that are part of the qualification are the following:

> With the exception of the Amargosa River Snail Site, geochemical dating indicates that the last episode of paleospring activity for the majority of paleosprings occurred between 14,000 to 20,000 years ago, or longer (Paces et al. 1997 [DIRS 109148], Figure 18).
>
> Scranton Wells was active 40,000 to 60,000 years ago Mesquite Wash was active 30,000 years ago, and the Amargosa River Snail Site between 9,000 to 12,000 years ago (Paces et al. 1997 [DIRS 109148], Figure 18).

J37.1 QUALIFICATION METHOD

The method of qualification for intended use of the data from Paces et al. (1997 [DIRS 109148]) listed above is the Equivalent QA Program approach (SCI-PRO-001, Attachment 3, Method 1). The rationale for using this method is that it was the most suitable considering the data and available documentation of the QA program. The YMP branch of the USGS had worked in cooperation with the YMP Management and Operating Contractor for many years, and USGS Milestone SPC333M4 (USGS 1997 [DIRS 171970]) activities underwent a DOE Office of Quality Assurance (OQA) surveillance in late 1997. The objective of the surveillance was to verify compliance with USGS technical and implementing procedures in the production of the milestone.

The evaluation criteria are based on the requirements in Attachment 3 and the applicable qualification attributes listed in Attachment 4 of SCI-PRO-001. Use of qualification Method 1, Equivalent QA Program, requires that an initial evaluation of the data quality and correctness be made by comparing the methods used to plan, collect, and analyze the data against generally accepted scientific or engineering practices. If this comparison is adequate, then the acquisition, development, or processing of data must be demonstrated to be functionally equivalent (i.e., similar in scope and implementation) to the general process requirements of *Quality Assurance Requirements and Description* (QARD) (DOE 2007 [DIRS 182051]). A condition of this method is the demonstration of the functional equivalence of the data-gathering process to applicable QARD concepts, as identified by the attributes in SCI-PRO-001, Attachment 4 (e.g., Attributes 1, 2, 5, 6, 8, and/or 11). The attributes specifically applicable to these data are:

- Qualifications of personnel or organizations generating the data are comparable to qualification requirements of personnel generating similar data under an approved program that supports the YMP license application process or postclosure science (#1).

- The technical adequacy of equipment and procedures used to collect and analyze the data (#2).

- The quality and reliability of the measurement control program under which the data were generated (#5).

- The extent to which conditions under which the data were generated may partially meet the QA program that supports the YMP license application process or postclosure science (#6).

- Prior peer or other professional reviews of the data and their results (#8).

J37.2 DEMONSTRATION OF EQUIVALENT QA PROGRAM

The report by Paces et al. (1997 [DIRS 109148]) was prepared by the Environmental Science Team, Earth Science Investigations Program, YMP Branch, Water Resources Division of USGS regarding activities conducted in association with Milestone SPC333M4, "Evaluation of Paleo Ground-Water Discharge" (DOE 1997 [DIRS 171970]). This USGS report analyzes age, isotope, and paleontological data and summarizes the current understanding and implications of paleospring deposits located in the Amargosa Valley area.

In the initial evaluation of data quality and correctness, Paces et al. (1997 [DIRS 109148]) analyze the new age, isotope, and paleontological data and present an interpretive evaluation on past discharge activity in the northern Amargosa Valley. Thermoluminescence data, stable isotope data (O and C), other isotope data (strontium and uranium-series disequilibrium), as well as diatom and ostracode (paleontological) data, are generally accepted by the scientific (geologic and hydrologic) community for use in determining age, temperature, climatic, and environmental conditions of paleo flowing springs. Standard geologic field practices were used for sampling from trench wall and natural outcrops, mass spectrometry was used in collecting isotopic data, and thermoluminescence data were collected by a commonly accepted technique. A list of all procedures used for this activity is found in OQA surveillance record No. USGS-SR-97-061 (DOE 1997 [DIRS 171970], Item 8). These technical procedures are all USGS approved. The data quality and correctness are determined to be adequate for the implementation of the Equivalent QA Program qualification method. OQA Surveillance No. USGS-SR-97-061 (DOE 1997 [DIRS 171970]) was conducted to verify compliance with USGS procedures in the preparation of memorandum report Milestone SPC333M4, "Evaluation of Paleo Ground-Water Discharge," September 23 through October 3, 1997. The conclusion of the surveillance was that the USGS has adequately implemented the QA program as it applied to the activities conducted in association with Milestone SPC333M4. No deficiency documents were issued as a result of this surveillance.

The results of assessment of the functional equivalence of the data-gathering process to applicable QARD concepts, as identified by the attributes in Attachment 4 of SCI-PRO-001, are the following:

Qualifications of Personnel or Organizations Generating the Data—Items 1 and 2, and Attachment 1 of Surveillance Record No. USGS-SR-97-061 (DOE 1997 [DIRS 171970]) indicate that the qualifications of personnel generating the data are comparable to those qualifications approved by the 10 CFR 60, Subpart G [DIRS 100015] program.

Technical Adequacy of Equipment and Procedures Used to Collect Data—Items 3, 4, 8, and 10 of the surveillance record (DOE 1997 [DIRS 171970]) demonstrate the technical adequacy of equipment and procedures used to collect and analyze the data.

Quality and Reliability of the Measurement Control Program—Items 3, 4, 5, 6, 7, 8, and 10 of the surveillance record (DOE 1997 [DIRS 171970]) demonstrate the quality and reliability of the measurement control program under which the data were generated.

Conditions under Which the Data Were Generated May Meet QA Program—The surveillance record determined that the USGS has adequately implemented a QA program as it applies to activities associated with Milestone SPC333M4 (DOE 1997 [DIRS 171970]). This conclusion was based on objective evidence and discussions with USGS personnel. There were no deficiency documents issued as a result of the surveillance. The conditions under which the data were generated partially meet 10 CFR 60, Subpart G [DIRS 100015].

Prior Peer or Other Professional Reviews—Item 11 of the surveillance record (DOE 1997 [DIRS 171970]) demonstrates that technical reviews were done before the data packages were sent to the YMP. Dr. Zell Peterman, Chief of the USGS YMP Environmental Science Team, conducted a management review. The evaluation found that supporting information for the data in the USGS report (Paces et al. 1997 [DIRS 109148]) was suitable for the implementation of the Equivalent QA Program qualification method.

The Equivalent QA Program method was used to determine that qualification Attributes 1, 2, 5, 6, and 8 (Attachment 4, SCI-PRO-001) were satisfied by the USGS QA program. The USGS QA program was found to be the functional equivalent to the general processes required by the QARD (DOE 2007 [DIRS 182051]).

J37.3 DATA QUALIFIED FOR INTENDED USE

The data described above were determined to be appropriate for intended use. Based on the result of evaluation of the Qualify Assurance Program, it was concluded that the data from the report by Paces et al. can be considered qualified for intended use within FEP 2.2.08.11.0A (Groundwater Discharge to Surface within the Reference Biosphere).

J38. FEP 2.2.10.11.0A – NATURAL AIR FLOW IN THE UZ

This FEP uses data from the following report as direct input:

Martinez M.J. and Nilson, R.H. 1999. "Estimates of Barometric Pumping of Moisture through Unsaturated Fractured Rock." *Transport in Porous Media, 36,* (1), 85-119. Dordrecht, The Netherlands: Kluwer Academic Publishers. TIC: 257394. [DIRS 174095]

The data to be qualified for intended use within this FEP include:

> Estimates of the rate of water removal from Yucca Mountain through vapor transport range from 0.001 mm/yr to 0.3 mm/yr (Martinez and Nilson 1999 [DIRS 174095], p. 106).

J38.1 QUALIFICATION METHOD

The methods of qualification for intended use of the data from Martinez and Nilson (1999 [DIRS 174095]) are the Corroborating Data and Technical Assessment methods (SCI-PRO-001, Attachment 3, Methods 2 and 5). The rationale for using these methods is that they were the most suitable considering the data, their existing documentation, their intended use, and the availability of corroborating data. The technical assessment was based on the determination that that confidence in the data acquisition or development was warranted. Qualification process attributes used in the qualification are selected from the list provided in Attachment 4 of SCI-PRO-001. Attributes specifically applicable to these data are:

- Qualifications of personnel or organizations generating the data are comparable to qualification requirements of personnel generating similar data under an approved program that supports the YMP license application process or postclosure science (#1).
- The technical adequacy of equipment and procedures used to collect and analyze the data (#2).
- The extent to which the data demonstrate the properties of interest (#3).
- Extent and quality of corroborating data (#10).

The qualifications of the personnel generating the above data will be presented and demonstrated to be comparable to qualification requirements for personnel supporting the YMP license application process or postclosure science. Corroborating data will also be presented to show that the data are consistent with data in other published reports.

J38.2 TECHNICAL ASSESSMENT

Qualifications of Personnel Generating the Data—Dr. Mario Martinez was the lead author and developer of the data being qualified. Dr. Martinez received a Ph.D. in Engineering from the University of California at Berkeley (1987) with an emphasis in fluid dynamics. Dr. Martinez has extensive experience in developing and applying multicomponent, multiphase models for flow in heterogeneous porous media, including thermally driven two-phase flows for

heterogeneous fractured geologic media. Dr. Martinez has published over 30 papers in refereed journals and proceedings on multiphase flows, fluid dynamics, porous media, and numerical methods. Dr. Martinez's contribution to the YMP began in 1982 and has continued at various part-time levels to the present. Early work included developing finite element simulations tools for flow and transport modeling, resulting in a number of codes (e.g., FEMTRAN, NORIA and SAGUARO). Dr. Martinez was an early researcher in the relatively new subsurface area of fractured media, resulting in one of the first models describing flow into unsaturated fractures and its dependence on fracture and formation characteristics. Martinez also contributed to research into the effects of barometric pumping at Yucca Mountain. During the mid-1990s Martinez led the development of parallel processing codes for multiphase thermal flows in porous materials, resulting in the code PorSalsa, which has also been used on the YMP.

Technical Adequacy and Extent to Which the Data Demonstrate Properties of Interest—Martinez and Nilson (1999 [DIRS 174095], p. 106) present estimates for the annual net outflow of moisture from depth to the surface in the repository vicinity. In their paper, they develop a rigorous model for moisture transport in the fractures and matrix using first principles. These data are used in this FEP to support the statement that estimated rates of water removed as vapor by natural air flow in Yucca Mountain are negligible in comparison with the estimates for average infiltration at this site, which range from 3 to 73 mm/yr (SNL 2007 [DIRS 184614], Table 6.1-2).

J38.3 CORROBORATING DATA

The control volume model used to predict the theoretical maximum outflow was also presented in the report by Tsang and Pruess (1989 [DIRS 184794]). They present a solution that is consistent with Martinez and Nilson (1999 [DIRS 174095]), yielding a result of 0.3 mm/yr. In addition, Tsang and Pruess (1990 [DIRS 172018]) present gas-phase flow and diffusion studies that estimate the upper limit of gas-phase vapor outflow to be 0.1 mm/yr. Both Drs. Tsang and Pruess are senior scientists at Lawrence Berkeley National Laboratory and have worked on the YMP for over 20 years each. These corroborating data indicate that a theoretical upper limit of 0.3 mm/yr is consistent among multiple researchers on the project.

J38.4 DATA QUALIFIED FOR INTENDED USE

The technical assessment and corroborating data methods presented above, along with the qualifications of the personnel generating the data, provide sufficient confidence that the data from Martinez and Nilson (1999 [DIRS 174095], p. 106) are appropriate and qualified for use in the screening justification for FEP 2.2.10.11.0A (Natural Air Flow in the UZ).

J39. FEP 2.2.10.14.0A – MINERALOGIC DEHYDRATION REACTIONS

This FEP uses data from the following reports as direct input:

Review of the Thermal Stability and Cation Exchange Properties of the Zeolite Minerals Clinoptilolite, Mordenite, and Analcime: Applications to Radioactive Waste Isolation in Silicic Tuff (Smyth and Caporuscio 1981 [DIRS 174060])

Use of Zeolitic Tuff in the Building Industry (Colella et al. 2001 [DIRS 184454]).

J39.1 QUALIFICATION OF DATA FROM SMYTH AND CAPORUSCIO 1981

Smyth, J.R. and Caporuscio, F.A. 1981. *Review of the Thermal Stability and Cation Exchange Properties of the Zeolite Minerals Clinoptilolite, Mordenite, and Analcime: Applications to Radioactive Waste Isolation in Silicic Tuff*. LA-8841-MS. Los Alamos, New Mexico: Los Alamos Scientific Laboratory. ACC: HQS.19880517.2065. [DIRS 184454]

The data from that report to be qualified include:

> Volume and weight changes observed upon heating were recorded for a rock sample from the zeolitized Calico Hills Formation. The tuff was soaked in water at 91°C for 48 hours and then kept at approximately 95°C in a drying oven. The core was weighed and measured at the beginning of the experiment and periodically throughout the 32 hour dry-heating period. The amount of water lost between the highest measured volume (hour 1) and the next measurement (hour 2), relative to the total water lost during heating, was 70.6 wt % calculated as 100 × (19.77033 g – 18.5134 g)/(19.7703 g – 17.9906 g) (Smyth and Caporuscio 1981 [DIRS 174060], Tables A-1 and B-1, sample YM-40).
>
> The selected upper bounding value for volume reduction of initially saturated zeolitic tuff heated in air at 95°C was 0.76 vol % (Smyth and Caporuscio 1981 [DIRS 174060], Table A-1, sample YM-38).

J39.1.1 Qualification Method

The method of qualification of the data obtained from the scientific paper by Smyth and Caporuscio (1981 [DIRS 174060]) is the Technical Assessment method (SCI-PRO-001, Attachment 3, Method 5). The rationale for using this method is that it was the most suitable considering the data, their existing documentation, and their intended use. The technical assessment was based on the determination that confidence in the data acquisition or development was warranted. Qualification process attributes used in the technical assessment of these data are selected from the list provided in Attachment 4 of SCI-PRO-001. Attributes specifically relevant to these data are:

- Qualifications of personnel or organizations generating the data are comparable to qualification requirements or personnel generating similar data under an approved program that supports the YMP license application process or postclosure science (#1).

- The extent to which the data demonstrate the properties of interest (e.g., physical, chemical, geological, mechanical) (#3).

J39.1.2 Technical Assessment

Qualification of Personnel or Organizations Generating the Data—Joseph R. Smyth is a professor in the Geological Sciences Department of the University of Colorado at Boulder, where his expertise includes mineral physics. Dr. Smyth has authored or co-authored more than 100 journal articles and refereed reports on the physical properties of minerals. Florie A. Caporuscio is a technical staff member at the Los Alamos National Laboratory with expertise in mineralogy and geochemistry. He earned his B.S. in geology from the University of Massachusetts, his M.S. in geology from Arizona State University, and Ph.D. in geology from the University of Colorado. He served as section chief of the U.S. Environmental Protection Agency's Waste Isolation Pilot Plant (WIPP) Project Technical Review Program.

Extent to Which the Data Demonstrate the Properties of Interest—One of the properties of interest to assess mineralogic dehydration reactions (FEP 2.2.10.14.0A) is the change to the volume and density of the zeolitized tuffs below the repository as the tuffs are heated due to emplacement of radioactive waste in the tunnels and the subsequent cooling as the heat generated by the waste decreases with time. The measurements presented in Appendix A of Smyth and Caporuscio (1981 [DIRS 174060]) are the change in weight and volume of a clinoptilolite-rich core sample of Calico Hills Formation tuff upon hydration, followed by heating at constant temperature. The measurements were performed at temperatures just below 100°C to represent elevated, but non-boiling temperatures to show that weight and volume changes can occur. The measurements presented in Appendix B of Smyth and Caporuscio (1981 [DIRS 174060]) are of density changes in four tuff samples upon heating beginning at 25°C and extending up to 500°C. Except for the first temperature, the temperatures were all above boiling and represent possible conditions near the repository drifts. The data under consideration are used in FEP 2.2.10.14.0A (Mineralogic Dehydration Reactions) to estimate a bounding value for the amount of rock shrinkage due to zeolite hydration that would occur under predicted repository conditions.

J39.1.3 Data Qualified for Intended Use

The data obtained from the report by Smyth and Caporuscio (1981 [DIRS 174060], Appendices A and B) are appropriate for intended use. The above discussion presents adequate confidence that these data can be considered qualified for use in the screening justification for FEP 2.2.10.14.0A (Mineralogic Dehydration Reactions).

J39.2 QUALIFICATION OF DATA FROM COLELLA ET AL. 2001

Colella, C.; de' Gennaro, M.; and Aiello, R. 2001. "Use of Zeolitic Tuff in the Building Industry." *Reviews in Mineralogy and Geochemistry, 45,* 551-587. Washington, D.C.: Mineralogical Society of America. TIC: 259937. [DIRS 184454]

The data to be qualified for intended use within this FEP include:

> Physical changes in zeolitic tuff lead to the possible formation of microcracks. A scanning electron image of such a weathered zeolitic tuff shows microcracks with apertures of about one to two micrometers (Colella et al. 2001 [DIRS 184454], Figure 24).

J39.2.1 Qualification Method

The methods of qualification for intended use of the data obtained from the scientific paper by (Colella et al. 2001 [DIRS 184454]) is the Technical Assessment method (SCI-PRO-001, Attachment 3, Method 5). The rationale for using this method is that it was the most suitable considering the data, their existing documentation, and their intended use. The technical assessment was based on the determination that confidence in the data acquisition or development was warranted. Qualification process attributes used in the technical assessment of these data are selected from the list provided in Attachment 4 of SCI-PRO-001. Attributes specifically relevant to these data are:

- The extent to which the data demonstrate the properties of interest (e.g., physical, chemical, geological, mechanical) (#3).
- Prior peer or other professional reviews of the data and their results (#8).

J39.2.2 Technical Assessment of Data

Extent to which the Data Demonstrate the Properties of Interest—The work of Colella et al. (2001 [DIRS 184454]) documents the uses of zeolitized tuff as a building material. More importantly, they also present the mechanical and physical properties of zeolitic tuff which include physical decay phenomena. Of particular interest to Yucca Mountain studies are the effects of water sorption and desorption into zeolitic tuff.

One observation (Colella et al. 2001 [DIRS 184454], p. 573, Figure 24) is the important role of water in the decay of zeolitic tuff building materials. The evaporation of water from tuff, particularly water with dissolved salts that crystallize during evaporation, may generate internal stresses resulting in the formation of microcracks. These data in the study by Colella et al. (2001 [DIRS 184454]) demonstrate properties of interest to Yucca Mountain.

Prior Peer or Other Professional Reviews of the Data and their Results—The article by Colella et al. (2001 [DIRS 184454]) was published in the Reviews in Minerology and Geochemistry series, submissions to which are technically reviewed and approved. For example, in the Style Guide for the Reviews in Minerology and Geochemistry series, the role of the volume editor is defined: "[t]he volume editor is responsible for the scientific content of the book and its organization. He/she will edit the authors' contributions to assure high quality of the technical content, clarity and succinctness of presentation of the subject matter, cross-referencing from one chapter to another, quality of figures and tables, indexes, etc." Thus, the work of Colella et al. (2001 [DIRS 184454]) was peer-reviewed by the volume editor prior to publication.

J39.2.3 Data Qualified for Intended Use

The above discussion shows that the data demonstrate the properties of interest and are appropriate for intended use. Based on the results of technical assessment, the data obtained from the scientific journal article by Colella et al. (2001 [DIRS 184454]) are also qualified for use in the screening justification for FEP 2.2.10.14.0A (Mineralogic Dehydration Reactions).

J40. FEP 2.2.11.03.0A – GAS TRANSPORT IN GEOSPHERE

This FEP uses data from the following report as direct input:

DOE 2002. *Final Environmental Impact Statement for a Geologic Repository for the Disposal of Spent Nuclear Fuel and High-Level Radioactive Waste at Yucca Mountain, Nye County, Nevada.* DOE/EIS-0250. Washington, D.C.: U.S. Department of Energy, Office of Civilian Radioactive Waste Management. ACC: MOL.20020524.0314; MOL.20020524.0315; MOL.20020524.0316; MOL.20020524.0317; MOL.20020524.0318; MOL.20020524.0319; MOL.20020524.0320. [DIRS 155970]

The data to be qualified include:

> Modeling of potential annual doses from gas-phase geosphere transport of ^{14}C shows that the individual maximum radiological dose is 1.8×10^{-10} mrem/yr, which corresponds to a maximum gas-phase release rate that occurs at 1,700 years following repository closure (DOE 2002 [DIRS 155970], Section I.7).
>
> Based on gas flow studies, radon released from the repository in the gas phase is expected to radioactively decay before reaching the ground surface (DOE 2002 [DIRS 155970], Section I.7.3).

J40.1 QUALIFICATION METHOD

The method of qualification of the data from the DOE report (DOE 2002 [DIRS 155970]) is the Technical Assessment method (SCI-PRO-001, Attachment 3, and Method 5). The rationale for using this method is that it was the most suitable considering the data and the existing documentation regarding the data and the data originator. The technical assessment was based on the determination that that confidence in the data acquisition or development was warranted. Qualification process attributes used in the qualification are selected from the list provided in Attachment 4 of SCI-PRO-001. Attributes specifically applicable to these data are:

- Qualifications of personnel or organizations generating the data are comparable to qualification requirements of personnel generating similar data under an approved program that supports the YMP license application process or postclosure science (#1).
- The technical adequacy of equipment and procedures used to collect and analyze the data (#2).
- The extent to which the data demonstrate the properties of interest (#3).

In this technical assessment, the qualifications of the personnel generating the above data will be presented and demonstrated to be comparable to qualification requirements for personnel supporting the YMP license application process or postclosure science. In addition, the methods used to obtain the data above will be reviewed and evaluated, and a check of the calculations will be performed, where applicable.

J40.2 TECHNICAL ASSESSMENT

Qualifications of Personnel Generating the Data—Dr. Paul Eslinger performed the atmospheric release calculations reported in Appendix I.7 of the source report (DOE 2002 [DIRS 155970]. Dr. Eslinger is a Staff Scientist in the Risk and Decision Sciences Group at Pacific Northwest National Laboratory. He received his Ph.D. in Statistics in 1983 from Southern Methodist University and his M.A. and B.S. in Mathematics. His technical expertise is in statistics, performance estimation for nuclear waste disposal concepts, and risk analysis. Dr. Eslinger led the performance assessment modeling activities for the Environmental Impact Statement for the YMP from 1996 through 2001. The Environmental Impact Statement, prepared for the U.S. Department of Energy and published in 2002, addressed the disposal of commercial spent nuclear fuel and defense high-level radioactive wastes. Dr. Eslinger also led the inventory and performance assessment modeling activities for the second supplemental Environmental Impact Statement for the Waste Isolation Pilot Plant (WIPP) located near Carlsbad, New Mexico. This Environmental Impact Statement, published by the U.S. Department of Energy in 1997, addressed the disposal phase of development of the facility for the long-term disposal of transuranic wastes. Dr. Eslinger was also involved in the Systems Assessment Capability project (1998 through 2006), in which he calculated human, ecological, and economic risk estimates for proposed end-states of the cleanup of the Hanford nuclear reservation. Dr. Eslinger serves as an ad-hoc member of an EPA Federal Insecticide, Fungicide, and Rodenticide Act (FIFRA) Scientific Advisory Panel that is examining stochastic risk assessment approaches for investigating ecological effects of pesticides. Dr. Eslinger also served on a validation review team for the U.S. Department of Energy that examined the long-term performance models for a high-level radioactive waste repository.

Technical Adequacy and Extent to Which the Data Demonstrate Properties of Interest—Sections I.7.1 and I.7.2 of the source report (DOE 2002 [DIRS 155970]) provide calculations of ^{14}C release rates and the resulting individual maximum radiological dose rate. The maximum release rate is based on the amount of ^{14}C available for transport (accounting for decay and perforated cladding) as a function of time. The equations are presented clearly in Section I.7.1, and a hand-check of the calculation for the maximum release rate of 3.3 μCi per year at 1,700 years after repository closure was performed.

As presented in Section I.7.1 (DOE 2002 [DIRS 155970]), the activity (in curies) of ^{14}C available for transport, A_T, from the waste package as a function of time is calculated based on a time interval of every 100 years as follows:

$$A_T = D_F \times F_{FC} \times 0.122 \text{ Ci per package} \qquad \text{(Eq. J40-1)}$$

where:

D_F = time-dependent factor that accounts for radioactive decay (unitless)

F_{FC} = fraction of perforated cladding (unitless).

About 2% of the ^{14}C in commercial spent nuclear fuel exists as a gas in the gap space (Oversby 1987 [DIRS 103446], p. 92). Therefore, the activity of 0.122 Ci per package is determined from the specific activity of ^{14}C (4.46 Ci/g ^{14}C) (Shleien 1992 [DIRS 127299], Table 8.4.1; ^{14}C half-

life is 5,730 years with a specific activity of 0.165 TBq/g; TBq = 27.03 Ci) and the estimated mass of ^{14}C per commercial spent nuclear fuel waste package (1.37 g ^{14}C per package) (DTN: SN0310T0505503.004 [DIRS 168761]).

The time-dependent factor, D_F, is the fraction of ^{14}C remaining, given by the following equation:

$$D_F = \frac{C(t)}{C(t=0)} = e^{-\beta t} \quad \text{(Eq. J40-2)}$$

The half-life of ^{14}C is 5,730 years, so the decay constant, β, is 1.2×10^{-4} yr^{-1}. Assuming the first package fails at a time of 1,700 years after repository closure (the reported time for maximum release of 3.3 μCi per year), D_F is equal to 0.82. The fraction of perforated cladding at 1,700 years, F_{FC}, is estimated to be approximately 0.003 from the results in Figure I-28, which shows a linear increase in perforated cladding for the first 80,000 years (2% of the cladding was reported to fail in the first 10,000 years). The activity of ^{14}C available in a 100-year interval after the waste package failure at 1,700 years is then equal to $0.82 \times 0.003 \times 0.122 = 3 \times 10^{-4}$ Ci. The release rate to the surface is calculated as the available activity of ^{14}C divided by the 100-year interval, or 3 μCi/yr. This is consistent with the reported value of 3.3 μCi per year in Section I.7.1 the source report (DOE 2002 [DIRS 155970]).

Section I.7.2 presents the individual maximum radiological dose rate using a dose conversion factor of 5.6×10^{-14} rem per μCi, as calculated using the GENII code (qualified software on the YMP). For a maximum release rate of 3.3 μCi per year, the maximum dose is calculated as $5.6 \times 10^{-14} \times 3.3 = 1.8 \times 10^{-13}$ rem/yr or 1.8×10^{-10} mrem/yr, which is the value being qualified. This hand-check provides confidence that the development of these data was technically adequate and that it represents the desired property of interest (maximum dose from gaseous ^{14}C).

Section I.7.3 of the source report (DOE 2002 [DIRS 155970]) presents a screening argument for ^{222}Rn. The data to be qualified is the statement that gas-phase ^{222}Rn will decay before reaching the surface, 200 m above the repository horizon. The analysis in Section I.7.3 can also be checked by hand. The analysis calculates the time it would take for gas to reach the surface, assuming a maximum gas flow induced by repository-induced heating. The maximum gas flow, 2×10^{-7} $kg/s/m^2$ was taken from a report by Wu et al. (1995 [DIRS 103690]). The pore velocity is calculated as the maximum gas flow divided by the product of the gas density (approximately 1.2 kg/m^3 at 20ºC) and the effective rock porosity (on the order of 0.1 per SNL 2008 [DIRS 184748], Sections 6.5.3.and 6.5.7), which yields a pore velocity of $\sim 2 \times 10^{-6}$ m/s. For a distance of 200 meters between the repository horizon and the surface, the travel time is calculated as $200/2 \times 10^{-6} = 1 \times 10^{8}$ s, which is consistent with the reported 1,140 days in Section I.7.3. As a result, the estimated amount of ^{222}Rn remaining during this travel time is calculated as follows:

$$\frac{C(t)}{C(t=0)} = e^{-\beta t} \quad \text{(Eq. J40-3)}$$

where the decay constant, β, is 0.18145 $days^{-1}$. The fraction of ^{222}Rn remaining after 1,140 days is calculated to be 1×10^{-90}, as reported in Section I.7.3. Thus, the amount of ^{222}Rn remaining

by the time it reaches the surface is negligible. This hand-check and evaluation of the analysis documented in Section I.7.3 gives confidence that the development of these data was technically adequate and that it represents the desired property of interest (amount of ^{222}Rn that can reach the surface).

J40.3 DATA QUALIFIED FOR INTENDED USE

The data in DOE report (2002 [DIRS 155970], Section I.7) are appropriate for intended use. The technical assessment presented above, along with the qualifications of the personnel generating the data, provides sufficient confidence that these data can be considered qualified for intended use within FEP 2.2.11.03.0A (Gas Transport in Geosphere).

J41. FEP 2.2.12.00.0A – UNDETECTED FEATURES IN THE UZ

This FEP uses data from the following report as direct input:

Zhou, Q.; Liu, H-H.; Bodvarsson, G.S.; and Oldenburg, C.M. 2003. "Flow and Transport in Unsaturated Fractured Rock: Effects of Multiscale Heterogeneity of Hydrogeologic Properties." *Journal of Contaminant Hydrology, 60,* (1-2), 1-30. New York, New York: Elsevier. TIC: 253978. [DIRS 162133]

The data to be qualified for intended use within this FEP include:

> The results of an analysis of smaller-scale heterogeneity indicate that UZ flow and transport are governed primarily by large-scale stratigraphy, structure, and associated hydrological properties rather than by smaller-scale heterogeneity (Zhou et al. 2003 [DIRS 162133], Section 6).

The study by Zhou et al. (2003 [DIRS 162133]) implies that flow and transport in the Yucca Mountain unsaturated zone are mainly determined by large-scale heterogeneity, characterized by property differences between different geological units rather than by property variability within a geological unit.

J41.1 QUALIFICATION METHOD

The method of qualification for intended use of the data from Zhou et al. (2003 [DIRS 162133]) is the Technical Assessment method (SCI-PRO-001, Attachment 3, Method 5). The rationale for using this method is that it was the most suitable considering the data, their existing documentation, and their intended use. The technical assessment was based on the determination that confidence in the data acquisition or development was warranted. Qualification process attributes used in the technical assessment of these data are selected from the list provided in Attachment 4 of SCI-PRO-001. Attributes specifically applicable to these data are:

- Qualification of personnel or organizations generating the data are comparable to qualification requirements of personnel generating similar data under an approved program that supports the YMP license application process or postclosure science (#1).
- The technical adequacy of equipment and procedures used to collect and analyze the data (#2).
- The extent to which the data demonstrate the properties of interest (e.g., physical, chemical, geological, mechanical) (#3).
- Extent and reliability of the documentation associated with the data (#9).

J41.2 TECHNICAL ASSESSMENT

Qualifications of Personnel or Organizations Generating the Data—Dr. Quanlin Zhou has B. Eng. and M. Eng. degrees in Hydrology and Water Resources from Hohai University, Nanjing, P.R. China, and a Ph.D. in Groundwater Hydrology from Technion-Israel Institute of Technology, Haifa, Israel. While at Technion, he was awarded the Miriam and Aaron Gutwirth Prize (1999) and the Irmay Prize (1998). Lawrence Berkeley National Laboratory has been responsible for simulations of UZ flow and transport since the inception of the YMP.

Data Demonstrate the Properties of Interest—The property of interest is the effect of local heterogeneity on flow. Zhou et al. (2003 [DIRS 162133]) used a two-dimensional mesh, with layer heights the same as in the UZ model, and used the same calibrated layer-scale values for the fracture and matrix hydrologic properties. Case A used uniform fracture permeability; in case B the fracture permeability was varied stochastically. The breakthrough curves for nonsorbing tracers were not significantly different in these two cases. The data is used to show that the hydrologic effect of an igneous intrusion would be insignificant because it would be limited in extent. The data from Zhou et al. (2003 [DIRS 162133]) show that a heterogeneity of fracture permeability at this scale would have a negligible effect on flow.

Confidence in the Data Acquisition or Developmental Results Is Warranted—The study by Zhou et al. (2003 [DIRS 162133]) is a sensitivity study, in which flow and transport were evaluated for a base case and for sensitivity cases with the hydrologic properties of rock layers varied on different scales. The base case used layer-uniform hydrologic properties taken from the reports by CRWMS M&O (2000 [DIRS 144426]) and Flint (1998 [DIRS 100033]). The two-dimensional grid used for this study (Zhou et al. (2003 [DIRS 162133], Figure 1) was essentially identical to that used for the site recommendation model. Thus, the site recommendation model is sufficiently similar to the current model to justify its use for sensitivity studies. The software used for the simulations was TOUGH2 V. 1.4 (Pruess et al. 1999 [DIRS 160778]) and T2R3D V.1.4 (Wu and Pruess 2000 [DIRS 153972]). This software has been qualified for the Yucca Mountain project (although for this use the software was not obtained from Software Configuration Management). Therefore both the software and input data are essentially equivalent to qualified software and data, and the use of the results of a sensitivity study to support the conclusion that heterogeneity at a scale of 10 m does not have a significant effect on tracer transport to the water table is qualified.

The software and input data are found to be essentially equivalent to qualified software and qualified data, and the results demonstrate that small scale heterogeneity would have a negligible effect on transport in the UZ.

J41.3 DATA QUALIFIED FOR INTENDED USE

The technical assessment presented above provides sufficient confidence that data from Zhou et al. (2003 [DIRS 162133]) are appropriate and are qualified for intended use in the screening justification for FEP 2.2.12.00.0A (Undetected Features in the UZ).

J42. FEP 2.3.13.03.0A – EFFECT OF REPOSITORY HEAT ON THE BIOSPHERE

This FEP uses data from the following report and textbook as direct input:

Final Report: Plant and Soil Related Processes Along a Natural Thermal Gradient at Yucca Mountain, Nevada (CRWMS M&O 1999 [DIRS 105031])

Soil Physics (Jury et al. 1991 [DIRS 102010]).

J42.1 QUALIFICATION OF DATA FROM CRWMS M&O 1999

CRWMS M&O 1999. *Final Report: Plant and Soil Related Processes Along a Natural Thermal Gradient at Yucca Mountain, Nevada.* B00000000-01717-5705-00109 REV 00. Las Vegas, Nevada: CRWMS M&O. ACC: MOL.19990513.0037. [DIRS 105031]

The following data from this report are used in FEP 2.3.13.03.0A as direct inputs:

> Shrubs removed about 31% (12% to 54%) of the total precipitation that fell during the period studied (CRWMS M&O 1999 [DIRS 105031], Executive Summary).
>
> An analysis of the percentage of shrub cover and of soil temperature at a depth of 45 cm suggests that for each 1°C increase in temperature, the shrub cover decreases by 1.2% and that of annual grasses increases by 5.5% (CRWMS M&O 1999 [DIRS 105031], Section 3.3).

J42.1.1 Qualification Method

The method of qualification of the data from the plant and soil report (CRWMS M&O 1999 [DIRS 105031]) listed above is the Technical Assessment method (SCI-PRO-001, Attachment 3, Method 5). The rationale for using this method is that it was the most suitable considering the data, their existing documentation, and their intended use. The technical assessment included determination that the employed methodology was acceptable and determination that confidence in the data acquisition or development was warranted. Qualification process attributes used in the technical assessment of these data are selected from the list provided in Attachment 4 of SCI-PRO-001. Attributes specifically applicable to these data are:

- The technical adequacy of equipment and procedures used to collect and analyze data (#2).
- The extent to which the data demonstrate the properties of interest (#3).
- Conditions under which the data were generated may partially meet the QA program that supports the YMP license application process or postclosure science (#6).

J42.1.2 Technical Assessment

The Extent to Which the Data Demonstrate the Properties of Interest—The report presents the finding of field studies conducted during 1997 and 1998 by the YMP field biologists examining the relationship between soil temperature, soil moisture, and various aspects of the biotic community at Yucca Mountain. These studies were designed to assess the effects of potential thermal loading on biological communities. The study examined the relationship between the soil temperature and the abundance and percent cover of the species of plants. The study also evaluated the fractional removal of precipitation by shrubs. The data are used to evaluate the reduction in evapotranspiration due to repository heating for sites corresponding to the lower, mean, and upper bounds of shrub cover within FEP 2.3.13.03.0A (Effect of Repository Heat on the Biosphere). The data obtained are site-specific and appropriately demonstrate the properties of interest.

Technical Adequacy of Equipment and Procedures Used to Collect and Analyze Data—The methods used to carry out field studies are adequately described, including the location and representativeness of the study sites, sampling methods, and statistics (CRWMS M&O 1999 [DIRS 105031], Section 2). The data collection spanned a period of over one year, and therefore the values can be used to represent annual average conditions.

QA Conditions under Which the Data Were Generated—The records package for the report includes documentation of the data and data review, which was performed in accordance with quality administrative procedure, QAP-SIII-2, Rev 1. The document was prepared in accordance with the approved Technical Document Preparation Plan and was reviewed by three qualified scientists and a compliance reviewer in accordance with PRO-TS-003, Rev. 1, and with consideration of additional review criteria. The data were submitted to the Technical Data Management System database.

J42.1.3 Data Qualified for Intended Use

The data described above, obtained from the plant and soil report (CRWMS M&O 1999 [DIRS 105031]), are appropriate for intended use. The technical evaluation of the report, the associated data, and the existing documentation and records provides sufficient confidence that these data can be considered qualified for use within FEP 2.3.13.03.0A (Effect of the Repository Heat on the Biosphere).

J42.2 QUALIFICATION OF DATA FROM JURY ET AL. 1991

Jury, W.A.; Gardner, W.R.; and Gardner, W.H. 1991. *Soil Physics.* 5th Edition. New York, New York: John Wiley & Sons. TIC: 241000. [DIRS 102010]

> The datum from this report used in FEP 2.3.13.03.0A as direct input is the thermal conductivity for dry sand (Jury et al. 1991 [DIRS 102010], Table 5.5).

This parameter is used together with the data from the plant and soil report (CRWMS M&O 1999 [DIRS 105031]) to evaluate the response of plant communities to repository heat.

J42.2.1 Qualification Method

The method of qualification for intended use of the data from the textbook by Jury et al. (1991 [DIRS 102010]) is the Technical Assessment method (SCI-PRO-001, Attachment 3, Method 5). The rationale for using this method is that it was the most suitable considering the data, their existing documentation, and their intended use. The technical assessment was based on the determination that confidence in the data acquisition or development was warranted. Qualification process attributes used in the technical assessment of these data are selected from the list provided in Attachment 4 of SCI-PRO-001. Attributes specifically applicable to these data are:

- Qualification of personnel or organizations generating the data are comparable to qualification requirements of personnel generating similar data under an approved program that supports the YMP license application process or postclosure science (#1).

- The extent to which the data demonstrate the properties of interest (e.g., physical, chemical, geological, mechanical) (#3).

J42.2.2 Technical Assessment

Extent to Which the Data Demonstrate the Properties of Interest—The average value of thermal conductivity of dry sand obtained from this reference (0.42 cal cm^{-1} s^{-1} $°C^{-1}$) (Jury et al. 1991 [DIRS 102010], Table 5-5) is equal to 1.81 W/m-K. Thermal conductivity can be considered a basic property of a given material.

Qualification of Personnel or Organizations Generating the Data—The primary author of the text, Dr. William Jury, is a Distinguished Professor of Soil Physics at the University of California, Riverside, and the authority in the field of soil physics. *Soil Physics* by Jury et al. (1991 [DIRS 102010]) is the classic guide to soil physics used as a principal text in many advanced soil physics university courses.

J42.1.3 Data Qualified for Intended Use

Considering the use of the data and the results of the technical evaluation of the data and their source, there is sufficient confidence that the data obtained form the textbook by Jury et al. (1991 [DIRS 102010]) are appropriate for intended use and are qualified for the use in the screening justification for FEP 2.3.13.03.0A (Effect of the Repository Heat on the Biosphere).

J42.3 DESCRIPTION AND JUSTIFICATION OF EQUATION FROM CARSLAW AND JAEGER 1959

The approach to predicting temperature changes near the surface is to determine the flux of repository-generated heat, multiply by depth, and divide by the thermal conductivity (Carslaw and Jaegar 1959 [DIRS 100968], Equation 2):

$$\Delta T = \frac{Q \Delta z}{AK} \qquad \text{(Eq. J42-1)}$$

where Q/A is the heat flux (W/m^2), Δz is depth (m), and K is thermal conductivity of the near-surface (W/m-K).

The equation presented above is the one-dimensional representation of the law of heat conduction (Fourier's law) solved for ΔT. This equation represents fundamentals of the process of heat conduction through matter and was appropriate for intended use in FEP 2.3.13.03.0A (Effect of the Repository Heat on the Biosphere).

Data Qualification Plan

QA: QA

Page 1 of 13

Complete only applicable items.

Section I. Organizational Information

Qualification Title

Data Qualification Report: Project and External Source Data to be Qualified for Intended Use in Document ANL-WIS-MD-000027

Requesting Organization

PA/TSPA/FEPs

Section II. Process Planning Requirements

1. List of Unqualified Data to be Evaluated

Please see attached Table

2. Type of Data Qualification Method(s) [Including rationale for selection of method(s) (Attachment 3) and qualification attributes (Attachment 4)]

Methods, rationales and attributes associated with each data are listed in the attached Table.

3. Data Qualification Team and Additional Support Staff Required

Qualification Chairperson—Susan Boggs
Data Qualification Team Members—Alicia Aragon; Maryla Wasiolek; Robert Jones
The data qualification team members are independent from the data collected or data reduction process.

4. Data Evaluation Criteria

Data evaluation criteria are based on consideration of the attributes identified above and arriving at an affirmative conclusion that a given attribute is met by the data under consideration.

5. Identification of Procedures Used

SCI-PRO-005, Section 6.2.1.M.3

6. Plan coordinated with the following known organizations providing input to or using the results of the data qualification

Performance Assessment sub-organization/disciplines, as applicable.
All PA sub-organizations/disciplines

Section III. Approval

Qualification Chairperson Printed Name	Qualification Chairperson Signature	Date
Susan Boggs		2/28/08
Responsible Manager Printed Name	**Responsible Manager Signature**	**Date**
M. Kathryn Knowles		2/28/08

SCI-PRO-001.1-R1

Figure J-1. A Copy of Data Qualification Plan for Project Data

Table J-2. Data Qualification Plan for Project Data, Project and External Source Data to be Qualified for Intended Use in Document ANL-WIS-MD-000027

Input	Source	Description	FEP	Project or External	Method[1] (Rationale)[2]	Attribute[3]
Bird et al. 1960. *Transport Phenomena*. [DIRS 103524]	pp. 565 to 567	The thermal diffusion term [Soret effect] describes the tendency for species to diffuse under the influence of a temperature gradient; this effect is quite small	2.1.11.10.0A	E	2 (a)	1, 10
Biggin and Thomas 2003. "Analysis of Long-Term Variations in the Geomagnetic Polodial Field Intensity and Evaluation of Their Relationship with Global Geodynamics." [DIRS 167876]	Figure 11	During the last 160 million years the number of pole reversals varied from 0 to 50	1.5.03.01A	E	2 (b)	3, 10
Blackwell et al. 2000. *Geothermal Resource/Reservoir Investigations Based on Heat Flow and Thermal Gradient Data for the United States*. [DIRS 183582]	Section 2.3	Hydrothermal systems have been found to be highly correlated to regional heat flow in excess of 80 mW/m^2	1.2.06.00.0A	P	2, 5 (b)	1, 3, 10
	Section 3.5	Hydrothermal systems have been found to circulate at least 4 km below the surface	1.2.06.00.0A	P	2, 5 (b)	1, 3, 10
Brakenridge 1981. "Terrestrial Paleoenvironmental Effects of a Late Quaternary-Age Supernova." [DIRS 167873]	p. 85	The postulated climatic and environmental effects of the supernovae, including the decrease in average temperature	1.5.01.02.0A	E	5 (b)	3, 10
	p. 85	The estimated time of occurrence of Vela supernova	1.5.01.02.0A	E	5 (b)	3, 10
Bredehoeft, J.D. 1997. "Fault Permeability Near Yucca Mountain." [DIRS 100007]	p. 2460	Earth tide water level fluctuations in borehole UE-25 p#1	1.5.03.02.0A	E	2 (a)	3, 10
Broxton et al. 1987. "Distribution and Chemistry of Diagenetic Minerals at Yucca Mountain, Nye County, Nevada." [DIRS 102004]	p. 101	Most of the zeolitic deposits at Yucca Mountain formed between 11.3 and 13.9 million years ago, and were largely contemporaneous with the most active period of silicic volcanism within the southwest Nevada volcanic field	2.2.06.03.0A	P	2 (a)	3, 10

Table J-2. Data Qualification Plan for Project Data, Project and External Source Data to Be Qualified for Intended Use in Document ANL-WIS-MD-000027 (Continued)

Input	Source	Description	FEP	Project or External	Method[1] (Rationale)[2]	Attribute[3]
Choppin and Stout 1989. "Actinide Behavior in Natural Waters." [DIRS 168379]	p. 209	For the higher charged actinides, hydrolysis can lead to formation of oligomers and polymers. At the low environmental concentrations of actinides, these are usually a problem only for Pu(IV), whose hydrolytic polymers are rather intractable	2.1.09.15.0A	E	5 (b)	1, 3, 8
Colella et al. 2001. "Use of Zeolitic Tuff in the Building Industry." [DIRS 184454]	Figure 24	The SEM image of zeolitic tuff shows microcracks with apertures of about one to two micrometers	2.2.10.14.0A	E	5 (b)	3, 8
Craig 2001. "Transmittal of Level 5 Deliverable SPW205M5, 'Excavation-Induced Fracture Study'." [DIRS 171411]	p. 16	In rock with few fractures, the tunnel-boring machine-induced fracturing of the tunnel periphery is confined to a depth of influence of less than 5 cm	1.1.02.00.0B	P	5 (b)	1, 2, 3, 9
	pp. 1, 3, 8	Energy is focused on the rock to be removed, so that excess energy is not dispersed into the surrounding rock, as from blasting	1.1.02.00.0B	P	5 (b)	1, 2, 3, 9
	pp. 3 to 11, 16	Examination of the tunnel walls and associated alcoves, niches, and drillholes has been used to define the character and extent of mechanical damage induced by tunnel boring	1.1.02.00.0B	P	5 (b)	1, 2, 3, 9
CRWMS M&O 1998. *Synthesis of Volcanism Studies for the Yucca Mountain Site Characterization Project*. [DIRS 105347]	pp. 5-41 through 5-57	Laboratory analytical data and field observations of mineral alterations around igneous intrusions at natural analogue sites show that alteration extends less than 10 m away from the intrusion/host rock contact. Natural analogue studies in similar host rocks at the Nevada Test Site show that alteration is limited to a zone less than 10 m away from the intrusion/host rock contact	1.2.04.02.0A	P	5 (b)	1, 2, 3, 10

Table J-2. Data Qualification Plan for Project Data, Project and External Source Data to Be Qualified for Intended Use in Document ANL-WIS-MD-000027 (Continued)

Input	Source	Description	FEP	Project or External	Method[1] (Rationale)[2]	Attribute[3]
CRWMS M&O 1999. *Final Report: Plant and Soil Related Processes Along a Natural Thermal Gradient at Yucca Mountain, Nevada*. [DIRS 105031]	Executive Summary	Shrubs removed about 31% (12% to 54%) of the total precipitation that fell during the period studied	2.3.13.03.0A	P	5 (b)	2, 3, 6
	Section 3.3	An analysis of the percentage of shrub cover and of soil temperature at a depth of 45 cm suggests that for each 1°C increase in temperature, the shrub cover decreases by 1.2% and that of annual grasses increases by 5.5%	2.3.13.03.0A	P	5 (b)	2, 3, 6
DOE 2002. *Final Environmental Impact Statement for a Geologic Repository for the Disposal of Spent Nuclear Fuel and High-Level Radioactive Waste at Yucca Mountain, Nye County, Nevada*. [DIRS 155970]	Section I.7	Modeling of potential annual doses from gas-phase geosphere transport of ^{14}C shows that the individual maximum radiological dose is 1.8×10^{-10} mrem/yr, which corresponds to a maximum gas-phase release rate that occurs at 1,700 years following repository closure	2.2.11.03.0A	P	5 (c)	1, 2, 3
	Section I.7.3	Based on gas flow studies, radon released from the repository in the gas phase is expected to radioactively decay before reaching the ground surface	2.2.11.03.0A	P	5 (c)	1, 2, 3
Doorenbos and Pruitt 1977. *Crop Water Requirements*. [DIRS 103062]	Table 36, p. 78	The data from this reference that are being used as direct input are the salinity tolerances for crop	2.2.08.07.0C	E	5 (d)	1, 3
Ehlers and Blatt 1982. *Petrology, Igneous, Sedimentary, and Metamorphic*. [DIRS 167802]	pp. 684 to 685	The geothermal gradient at convergent plate boundaries may range from less than 10°C per km to greater than 25°C per km	1.2.05.00.0A	E	2 (e)	3, 10
	p. 566	Conditions conducive to the onset of regional metamorphism correspond to temperature of 150°C to 200°C and pressures of 0.5 to 1 kilobars, which occur at depths of 4 to 5 km	1.2.05.00.0A	E	2 (e)	3, 10

Table J-2. Data Qualification Plan for Project Data, Project and External Source Data to Be Qualified for Intended Use in Document ANL-WIS-MD-000027 (Continued)

Input	Source	Description	FEP	Project or External	Method[1] (Rationale)[2]	Attribute[3]
Finch and Ewing 1992. "The Corrosion of Uraninite Under Oxidizing Conditions." [DIRS 113030]	Section 4.2.2	The effect of dissolved silica on the alteration of the UOHs (uranyl oxide hydrates) is profound; the alteration of schoepite can result in the formation of uranyl silicates such as uranophane and soddyite	2.1.09.15.0A	E	2 (e)	3, 8, 10
Freeze and Cherry 1979. *Groundwater*. [DIRS 101173]	pp. 514 to 515	Extensive carbonate dissolution cavities are not expected to develop because such dissolution is not typically observed in carbonates at great depths below the water table	1.2.09.02.0A	E	5 (b)	1, 3
	p. 106	Carbonate, quartz, and halite solubilities	1.2.09.02.0A	E	5 (b)	1, 3
Fridrich et al. 1998. *Space-Time Patterns of Late Cenozoic Extension, Vertical-Axis Rotation, and Volcanism in the Crater Flat Basin, Southwest Nevada*. [DIRS 164051]	pp. 1	During the period of peak tectonism (approximately 11.6 Ma to 12.7 Ma), the western part of Crater Flat basin subsided due to the basin extending from 18% to 40% in 1.1 million years or less	1.2.01.01.0A	P	5 (b)	2, 3, 8
	pp. 1, 13, 19 and 20	After 11.6 Ma, the rate of extension in the basin declined in a roughly exponential manner. The late Quaternary rate of extension is less than 1% of the initial rate (Fridrich et al. 1998 [DIRS 164051], pp. 1 and 13) and may be as low as 0.1% to 0.2% per million years (Fridrich et al. 1998 [DIRS 164051], pp. 19 and 20).	1.2.01.01.0A	P	5 (b)	2, 3, 8
	pp. 1 and 2	The pattern of Quaternary deformation mimics the pattern of middle Miocene activity, but at substantially lower rates (Fridrich et al. 1998 [DIRS 164051], pp. 1 and 2).	1.2.01.01.0A	P	5 (b)	2, 3, 8

Table J-2. Data Qualification Plan for Project Data, Project and External Source Data to Be Qualified for Intended Use in Document ANL-WIS-MD-000027 (Continued)

Input	Source	Description	FEP	Project or External	Method[1] (Rationale)[2]	Attribute[3]
Garvin 2002. *Multi-Canister Overpack Topical Report*. [DIRS 169141]	Section 2.2.6.2	The design pressure for the MCO is 450 psi (gauge) at 132°C	2.1.03.07.0A	E	5 (f)	1, 5, 6, 11
	Table 4-4	1.1×10^7 g uranium metal per waste package, assuming that the waste package contains two MCOs and each MCO contain Mark IV fuel (3,804 kg uranium) and scrap (1,832 kg uranium) for a total of 5,636 kg uranium	2.1.02.08.0A 2.1.11.03.0A	E	5 (f)	1, 5, 6,11
	Table 4-4	443 kg zirconium cladding per MCO (Mark IV maximum fuel load without scrap basket)	2.1.13.01.0A	E	5 (f)	1, 5, 6,11
	Table 4-4	6,340 kg uranium metal per MCO (Mark IV maximum fuel load without scrap basket)	2.1.13.01.0A	E	5 (f)	1, 5, 6,11
	Table 4-4	The maximum water in a sealed MCO is 4.64 kg (bound in particulate), with less than 200 g being present as free water	2.1.02.08.0A 2.1.11.03.0A	E	5 (f)	1, 5, 6,11
	Section 4.1.3.2	The N Reactor SNF contained within MCOs emplaced inside the codisposal waste packages are dried and filled with helium	2.1.02.08.0A	E	5 (f)	1, 5, 6,11
Grieve and Robertson 1984. "The Potential for the Disturbance of a Buried Nuclear Waste Vault by a Large-Scale Meteorite Impact." [DIRS 185030]	p. 231	Power law for distribution for terrestrial craters	1.5.01.01.0A	E	5 (h)	1, 3
Grieve 1987. "Terrestrial Impact Structures." [DIRS 135254]	pp. 248 and 257, Figure 8	Use of a power law for cratering rate distribution based on observed earth cratering and threshold size for onset of complex cratering	1.5.01.01.0A	E	5 (h)	1, 3
Grieve et al. 1995. "The Record of Terrestrial Impact Cratering." [DIRS 135260]	pp. 194 to 196	Crater rate distribution based on observed earth cratering	1.5.01.01.0A	E	5 (h)	1, 3

Table J-2. Data Qualification Plan for Project Data, Project and External Source Data to Be Qualified for Intended Use in Document ANL-WIS-MD-000027 (Continued)

Input	Source	Description	FEP	Project or External	Method[1] (Rationale)[2]	Attribute[3]
Grieve 1998. "Extraterrestrial Impacts on Earth: The Evidence and the Consequences." [DIRS 163385]	p. 113, Figure 8	Crater diameter to depth of effect relationships. Depth of exhumation is approximately 0.28 times the crater diameter	1.5.01.01.0A	E	5 (h)	1, 3
Hills and Goda 1993. "Fragmentation of Small Asteroids in the Atmosphere." [DIRS 135281]	Figure 18	Earthquake magnitudes due to a meteoroid impact range from Magnitude 5 to slightly less than Magnitude 7 on the Richter scale	1.5.01.01.0A	E	5 (h)	1, 3
Jury et al. 1991. *Soil Physics*. [DIRS 102010]	Table 5.5	Soil conductivity for unsaturated sand	2.3.13.03.0A	E	5 (b)	1, 3
Karam 2002. "Gamma and Neutrino Radiation Dose from Gamma Ray Bursts and Nearby Supernovae." [DIRS 167872]	Table 2	Dose reduction in top 20 mm of rock	1.5.01.02.0A	E	5 (b)	1, 3, 9
Kieft et al. 1997. "Factors Limiting Microbial Growth and Activity at a Proposed High-Level Nuclear Repository, Yucca Mountain, Nevada." [DIRS 100767]	p. 3130	Total counts (microscopic direct and plate) ranged from below limit of detection (3.2 × 104 cells per gram) to 2.3 × 105 cells per gram; Phospholipid fatty acid (PLFA) concentrations were generally low, ranging from 0.1 to 3.7 pmol per gram.	1.2.08.00.0A	E	2 (a)	3, 10
Krystinik 1990. "Early Diagenesis in Continental Eolian Deposits." [DIRS 135295]	pp. 8-2 to 8-3	Compaction may reduce eolian sediments by as much as 20% to 30% but after this initial stage, compaction does not become an important factor in diagenesis until the onset of grain deformation and pressure solution during deeper burial diagenesis	1.2.08.00.0A	E	2 (a) and (b)	3, 10
Martinez and Nilson 1999. "Estimates of Barometric Pumping of Moisture through Unsaturated Fractured Rock." [DIRS 174095]	p. 106	Estimated rate of water removal from Yucca Mountain through vapor transport under isothermal conditions	2.2.10.11.0A	E	2, 5 (a) and (b)	1, 2, 3, 10

Table J-2. Data Qualification Plan for Project Data, Project and External Source Data to Be Qualified for Intended Use in Document ANL-WIS-MD-000027 (Continued)

Input	Source	Description	FEP	Project or External	Method[1] (Rationale)[2]	Attribute[3]
Means et al. 1983. *The Organic Geochemistry of Deep Ground Waters and Radionuclide Partitioning Experiments under Hydrothermal Conditions*. [DIRS 100797]	Tables 1 and 3	Total organic carbon is 0.58 mg/L for well UE25b-1, 33% (0.19 mg/L) of which has a molecular weight greater than 1,000	2.1.09.13.0A	P	5 (b)	1, 2
Morgenstern and Choppin 1999. "Kinetics of the Reduction of $Pu(V)O_2^+$ by Hydrogen Peroxide." [DIRS 184023]	pp. 109 to 111; Table 1	Reduction of Pu(V) to Pu(IV) in basic solutions having hydrogen peroxide (H_2O_2) concentrations on the order of 0.04 to 0.00001 moles per liter and pH 7.9 to 10.8.	2.1.13.01.0A	E	2 (e)	3, 10
National Research Council 1992. *Ground Water at Yucca Mountain, How High Can It Rise? Final Report of the Panel on Coupled Hydrologic/Tectonic/Hydrothermal Systems at Yucca Mountain*. [DIRS 105162]	Chapter 2, p. 24	Extension rates declined to 5 to 10 mm/yr at 5 Ma; extension rates are still in a declining state	2.2.06.01.0A 2.2.06.02.0A	E	5 (b)	1, 3
National Research Council 1992. *Ground Water at Yucca Mountain, How High Can It Rise? Final Report of the Panel on Coupled Hydrologic/Tectonic/Hydrothermal Systems at Yucca Mountain*. [DIRS 105162] (continued)	Chapter 5, p. 116	Results from the regional stress model approach indicated a maximum water table rise of 50 m	1.2.10.01.0A	E	5 (b)	1, 3
	Chapter 5, p. 116	Predicted seismic events within the Yucca Mountain region over the next 10,000 years will not alter the large and globally extensive stresses imposed in the rock and in effect over the past 10 to 15 million years	2.2.06.01.0A 2.2.06.02.0A	E	5 (b)	1, 3
	Chapter 2, p. 22	Plate tectonic activity has imparted crustal extension stresses within the Basin and Range Province (which includes the Yucca Mountain region) during the past 12 million years. Extension rates between 10 and 12 million years ago ranged between 10 and 30 mm/yr	2.2.06.01.0A 2.2.06.02.0A	E	5 (b)	1, 3

Table J-2. Data Qualification Plan for Project Data, Project and External Source Data to Be Qualified for Intended Use in Document ANL-WIS-MD-000027 (Continued)

Input	Source	Description	FEP	Project or External	Method[1] (Rationale)[2]	Attribute[3]
Paces et al. 1997. *Summary of Discharge Deposits in the Amargosa Valley*. [DIRS 109148]	Figure 18	With the exception of the Amargosa River Snail Site, geochemical dating indicates the last episode of paleospring activity for the majority of paleosprings occurred between 14,000 to 20,000 years ago, or longer	2.2.08.11.0A	P	1 (g)	1, 2, 5, 6, 8
	Figure 18	Scranton Wells was active 40,000 to 60,000 years ago, Mesquite Wash active 30,000 years ago, and the Amargosa River Snail Site between 9,000 to 12,000 years ago	2.2.08.11.0A	P	1 (g)	1, 2, 5, 6, 8
Piron and Pelletier 2001. "State of the Art on the Helium Issues." [DIRS 165318]	Section 5.3.2.4.1	The decay helium gas pressure is 90 bars at 20°C in commercial SNF rods with a gap volume of 13 cm^3 and a burnup of 47.5 GWd/MTU after 10,000 years	2.1.03.07.0A 2.1.12.02.0A	E	2 (a)	10
Platten 2006. "The Soret Effect: A Review of Recent Experimental Results." [DIRS 183864]	p. 5	Typical range for Soret coefficients (0.01 to 0.001 K^{-1})	2.1.11.10.0A	E	2 (e)	3, 10
Plys and Duncan 1999. *FAI/99-14, Rev. 1, Hydrogen Combustion in an MCO During Interim Storage*. [DIRS 184687]	Figure 5-1, pp. 6 and 7	The maximum achievable temperatures and pressures (11 times the initial pressure) for a hydrogen fire in a mixture of oxygen (21%) and helium (79%) inside an MCO	2.1.13.01.0A	E	5 (c)	1, 3, 11
Rai and Swanson 1981. "Properties of Plutonium(IV) Polymer of Environmental Importance." [DIRS 144599]	p. 111	Pu(IV) polymer does not make stable suspensions at pH values above 5 and hence would not be expected to be mobile as polyer in the lithosphere	2.1.09.15.0A	E	5 (b)	1, 3, 8
Reeves 1976. *Caliche: Origin, Classification, Morphology and Uses*. [DIRS 104303]	p. 110	Net effects of shallow diagenesis and associated cementation are to stabilize the surface environment and decrease the net vertical infiltration rate	1.2.08.00.A	E	2 (a)	3, 10

Table J-2. Data Qualification Plan for Project Data, Project and External Source Data to Be Qualified for Intended Use in Document ANL-WIS-MD-000027 (Continued)

Input	Source	Description	FEP	Project or External	Method[1] (Rationale)[2]	Attribute[3]
Reimus 1995. *Transport of Synthetic Colloids Through Single Saturated Fractures: A Literature Review*. [DIRS 144604]	Section 3.2	Inorganic particles larger than 1 µm will settle much more rapidly than they diffuse	2.1.09.21.0A 2.1.09.21.0B 2.1.09.21.0C	P	5 (b)	3, 7
	Section 3.2.1	Equations and associated discussion related to: Gravity Force (F_g) and Velocity (V_g) – acting toward surface	2.1.09.21.0A 2.1.09.21.0B 2.1.09.21.0C	P	5 (b)	3, 7
	Section 3.3.6	Equations and associated discussion related to: Hydrodynamic Drag Force (F_H) and Velocity (V_H) – acting away from surface	2.1.09.21.0A 2.1.09.21.0B 2.1.09.21.0C	P	5 (b)	3, 7
	Section 3.2.1	Equations and associated discussion related to: Diffusion Force (F_d) and Characteristic Diffusion Velocity (V_d) – can act in both directions, but assumed to act away from surface	2.1.09.21.0A 2.1.09.21.0B 2.1.09.21.0C	P	5 (b)	3, 7
Rogers et al. 1988. "Low Temperature Diffusion of Oxygen in Titanium and Titanium Oxide Films." [DIRS 184108]	Table 1 and p. 146	The value of the oxygen diffusion coefficient in titanium at 300°C	2.1.06.06.0B	E	5 (b)	1, 3
Rousseau, J.P.; Loskot, C.L.; Thamir, F.; and Lu, N. 1997. Results of Borehole Monitoring in the Unsaturated Zone Within the Main Drift Area of the Exploratory Studies Facility, Yucca Mountain, Nevada. [DIRS 100178]	Section 5.2	The measured heat flux in the Yucca Mountain area at boreholes NRG-7a, UZ-7a, and SD-12 have heat fluxes within the TSw of 37, 39, and 32 mW/m^2, respectively. This gives an average of 36 mW/m^2, and a standard deviation of 3.6 mW/m^2	1.2.06.00.0A	P	2 (e)	3, 10
Sexton 2007. *Particulate and Water in Multi-Canister Overpacks* (OCRWM). [DIRS 184742]	Table 2-1	Maximum amount of free and bound water in an MCO is 4.3 kg	2.1.13.01.0A	E	5 (f)	2, 6
	Table 2-1	The average value of free and bound water in an MCO is 1.03 kg	2.1.13.01.0A	E	5 (f)	2, 6

Table J-2. Data Qualification Plan for Project Data, Project and External Source Data to Be Qualified for Intended Use in Document ANL-WIS-MD-000027 (Continued)

Input	Source	Description	FEP	Project or External	Method[1] (Rationale)[2]	Attribute[3]
Shoesmith and King 1998. *The Effects of Gamma Radiation on the Corrosion of Candidate Materials for the Fabrication of Nuclear Waste Packages*. [DIRS 112178]	Table 4	At 90°C in Q-Brine (Mg-Cl containing brine), Alloy C-4 corrosion rates are about 0.1 μm/yr and 0.05μm/yr in the absence and presence of about 100 rad/hr gamma radiation	2.1.13.01.0A	P	5 (b)	1, 3
	p. 29	For Alloy C-4 tested, no enhancement of general corrosion rates and no pitting or crevice corrosion was observed in this dose region	2.1.13.01.0A	P	5 (b)	1, 3
	p. 30 and Table 4	In the dose region 100 rad/hr to 1,000 rad/hr and at 90°C, Alloy C-4 in Q-Brine (Mg-Cl containing brine) pitting and crevice corrosion is observed	2.1.13.01.0A	P	5 (b)	1, 3
	p. 30 and Table 4	At higher dose rates (1,000 rad/h to 100,000 rad/hr), extensive pitting and crevice corrosion is present	2.1.13.01.0A	P	5 (b)	1, 3
	Table 4	At 90°C in Q-Brine, Titanium Grade 7 (titanium 99.8-paladium) corrosion rates are about 0.1 μm/y and 0.7 μm/y in the absence and presence of 10,000 rad/h gamma radiation, respectively	2.1.13.01.0A	P	5 (b)	1, 3
	pp. 30 to 31	For titanium (Titanium Grade 7) passivity is maintained within the dose region, 1,000 rad/h to 10,000 rad/h, and at 100,000 rad/hr, although the rate of passive film growth could be an order of magnitude higher than at 1,000 rad/hr (but still only 0.4 μm/yr)	2.1.13.01.0A	P	5 (b)	1, 3
Siriwardane and Wightman 1983. "Interaction of Hydrogen Chloride and Water with Oxide Surfaces. III. Titanium Dioxide." [DIRS 183688]	p. 504	Specific surface area (6 to 50 m^2/g) of commercial-grade crystalline rutile and anatase	2.1.03.10.0B	E	2 (a)	3, 10

Table J-2. Data Qualification Plan for Project Data, Project and External Source Data to Be Qualified for Intended Use in Document ANL-WIS-MD-000027 (Continued)

Input	Source	Description	FEP	Project or External	Method[1] (Rationale)[2]	Attribute[3]
Smyth and Caporuscio 1981. *Review of the Thermal Stability and Cation Exchange Properties of the Zeolite Minerals Clinoptilolite, Mordenite, and Analcime: Applications to Radioactive Waste Isolation in Silicic Tuff*. [DIRS 174060]	Tables A-1 and B-1, sample YM-40	Volume and weight changes observed upon heating were recorded for a rock sample from the zeolitized Calico Hills Formation. The tuff was soaked in water at 91°C for 48 hours and then kept at approximately 95°C in a drying oven. The core was weighed and measured at the beginning of the experiment and periodically throughout the 32-hour dry-heating period. The amount of water lost between the highest measured volume (hour 1) and the next measurement (hour 2), relative to the total water lost during heating, was 70.6 wt % calculated as 100 × (19.77033 g – 18.5134 g)/ (19.7703 g – 17.9906 g)	2.2.10.14.0A	P	5 (b)	1, 3
	Table A-1, sample YM-38	The selected upper bounding value for volume reduction of initially saturated zeolitic tuff heated in air at 95°C was 0.76 vol %	2.2.10.14.0A	P	5 (b)	1, 3
Stuckless and Levich 2007. *The Geology and Climatology of Yucca Mountain and Vicinity, Southern Nevada and California*. [DIRS 181507]	p. 83	Using a ^{10}Be cosmogenic dating technique, the calculated maximum possible erosion rates for bedrock outcrops at Yucca Mountain range from 0.4 to 2.7 cm/10,000 years	1.2.07.01.0A	P	2, 5 (a) and (b)	3, 7, 9
	p. 84	The long-term rates of erosion of unconsolidated material from Yucca Mountain hillslopes were calculated to be 0.2 to 6 cm/10,000 years using the rock varnish cation ratio and the in situ cosmogenic ^{36}Cl dating methods	1.2.07.01.0A	P	2, 5 (a) and (b)	3, 7, 9

Table J-2. Data Qualification Plan for Project Data, Project and External Source Data to Be Qualified for Intended Use in Document ANL-WIS-MD-000027 (Continued)

Input	Source	Description	FEP	Project or External	Method[1] (Rationale)[2]	Attribute[3]
Taylor 1986. *Impact of Time and Climate on Quaternary Soils in the Yucca Mountain Area of the Nevada Test Site*. [DIRS 102864]	Chapter 5	SiO_2 cementation is not dependent on climatic conditions, but cementation does exhibit distinctive trends that correspond with the ages of the surficial deposits	1.2.08.00.0A	E	2 (b)	3, 10
	Figure 9 and pp. 31 to 33	Cementation by opaline SiO_2 is common in the Yucca Mountain study area, and opaline SiO_2 accumulation in the soils is favored over that of $CaCO_3$	1.2.08.00.0A	E	2 (b)	3, 10
	Chapter 5	Accumulation rates are attributable to several climatic scenarios, but climate change was insufficient to significantly decrease the rate of accumulations	1.2.08.00.0A	E	2 (b)	3, 10
Thompson et al. 1999. *Quantitative Paleoclimatic Reconstructions from Late Pleistocene Plant Macrofossils of the Yucca Mountain Region*. [DIRS 109470]	Figures 17, 18	During the last glacial maximum, the mean annual temperature at Yucca Mountain exceeded 0°C	1.3.04.00.0A 1.3.05.00.0A	E	2, 5 (a) and (b)	1, 3, 7, 10
Valentine and Krogh 2006. "Emplacement of Shallow Dikes and Sills Beneath a Small Basaltic Volcanic Center – The Role of Pre-Existing Structure (Paiute Ridge, Southern Nevada, USA)." [DIRS 177282]	p. 221	In places the tuff is densely welded and forms black vitrophyre that grades rapidly away from the contact, over a distance of ~20 to 100 cm, into nonwelded tuff that is apparently unaffected by the dike	1.2.05.00.0A	E	5 (b)	1, 3, 8
Valentine et al. 1998. "Physical Processes of Magmatism and Effects on the Potential Repository: Synthesis of Technical Work Through Fiscal Year 1995." [DIRS 119132]	p. 5-74	Mineral alterations around igneous intrusions at natural analogue sites show that alteration is limited to a zone that extends less than 10 m away from the intrusion/host rock contact	1.2.04.02.0a 1.2.10.02.0A	P	5 (b)	1, 2, 3, 10
Wachs 2004. *Calculation of Amount of Free Water Required to Overpressurize DOE SNF Standardized Canister and RW Waste Package*. [DIRS 184624]	Section 6	The volume of free (unbound) water is approximately 0.0005 liters in a 15-foot-long DOE SNF Standardized Canister after cold vacuum drying	2.1.03.07.0A	E	5 (b)	1, 3, 5, 6

Table J-2. Data Qualification Plan for Project Data, Project and External Source Data to Be Qualified for Intended Use in Document ANL-WIS-MD-000027 (Continued)

Input	Source	Description	FEP	Project or External	Method[1] (Rationale)[2]	Attribute[3]
Whelan 2004. *Secondary Mineral Deposits and Evidence of Past Seismicity and Heating of the Proposed Repository Horizon at Yucca Mountain, Nevada*. [DIRS 170697]	p. 3	Calcite and silica (quarts, chalcedony, and opal) are found in some open fractures and lithophysal cavities in the Topopah Spring and Tiva Canyon Tuffs in the unsaturated zone. Studies indicate that secondary minerals form in the unsaturated zone from meteoric waters percolating along fractures to the water table. Therefore, there is a link between pedogenic deposition on the overlying soil, infiltration of meteoric water, and secondary mineral deposition in the unsaturated zone. Deposits of secondary minerals are sparsely and heterogeneously distributed on less than 10% of potential fracture and cavity depositional sites	1.2.08.00.0A	P	5 (b)	3, 9
Wilson et al. 2003. "Origin, Timing, and Temperature of Secondary Calcite—Silica Mineral Formation at Yucca Mountain, Nevada." [DIRS 163589]	Section 8	Studies of secondary minerals at Yucca Mountain using petrography, fluid-inclusion thermometry, and uranium-lead dating indicate that unsaturated-zone temperatures have remained close to the current ambient values over the past 2 to 5 Ma	1.2.06.00.0A 2.2.06.03.0A	E	2,5 (a) and (b)	3, 8, 10
	Sections 7.3, 8	The unsaturated-zone secondary minerals were interpreted to have been deposited from downward percolating meteoric water and not the result of upwelling groundwaters	1.2.06.00.0A	E	2, 5 (a) and (b)	3, 8, 10
Wronkiewicz et al. 1996. "Ten-Year Results from Unsaturated Drip Tests with UO_2 at 90°C: Implications for the Corrosion of Spent Nuclear Fuel." [DIRS 102047]	p. 86	Size-fractioned analyses revealed that between 1% and 12% of the total amount of uranium was present as a >5 nm size-fraction (the suspended fraction trapped by the filter)	2.1.09.15.0A	P	5 (b)	2, 3, 8

Table J-2. Data Qualification Plan for Project Data, Project and External Source Data to Be Qualified for Intended Use in Document ANL-WIS-MD-000027 (Continued)

Input	Source	Description	FEP	Project or External	Method[1] (Rationale)[2]	Attribute[3]
Wuschke et al. 1995. *Assessment of the Long-Term Risk of a Meteorite Impact on a Hypothetical Canadian Nuclear Fuel Waste Disposal Vault Deep in Plutonic Rock*. [DIRS 129326]	p. 3	Spatial relationships of crater diameter to extents and depth of fracturing and exhumation	1.5.01.01.0A	E	5 (h)	1, 3
	Figure 1	Spatial extent of fracturing is assumed to be spherical	1.5.01.01.0A	E	5 (h)	1, 3
	pp. 4 and 26	Cratering rate data for the Canadian shield and application to a hypothetical Canadian repository	1.5.01.01.0A	E	5 (h)	1, 3
Zhang and Schwartz 1995. "Multispecies contaminant plumes in variable density flow systems." [DIRS 183479]	pp. 839, 840, 843, and 844	In order for density effects to be present in the model simulations, the concentration of the leachate (or contaminant plume) had to be at least 2,000 mg/L (which corresponded to a solution density of 999.7 kg/m^3 at 20°C, in a native groundwater with a density of 998.2 kg/m^3 at 20°C; i.e., a density contrast of ~0.15%) in a very dilute native groundwater at 20°C for a specific discharge of ~30 m/yr through a homogeneous isotropic porous medium with a flow porosity of 0.25, yielding a horizontal seepage velocity of ~120 m/yr	2.2.07.14.0A	E	5 (b)	1, 3, 8
Zhou et al. 2003. "Flow and Transport in Unsaturated Fractured Rock: Effects of Multiscale Heterogeneity of Hydrogeologic Properties." [DIRS 162133]	Section 6	The results of an analysis of smaller-scale heterogeneity indicate that UZ flow and transport are governed primarily by large-scale stratigraphy, structure, and associated hydrological properties rather than by smaller-scale heterogeneity	2.2.12.00.0A	E	5 (b)	1, 2, 3, 9

Table J-2. Data Qualification Plan for Project Data, Project and External Source Data to Be Qualified for Intended Use in Document ANL-WIS-MD-000027 (Continued)

Input	Source	Description	FEP	Project or External	Method[1] (Rationale)[2]	Attribute[3]
Ziegler 2004. "Transmittal of Appendix D of the Technical Basis Document No. 10: Unsaturated Zone Transport Addressing Key Technical Issue (KTI) Agreement Evolution of Near-Field Environment (ENFE) 1.04." [DIRS 171694]	Table D-12	Water in equilibrium with portlandite-hillebrandite contains 625 mg total Ca/kg water (which is equivalent to approximately 1.56×10^{-2} mol Ca/kg water)	2.1.06.01.0A	P	2 (e)	3, 10

[1] Method from SCI-PRO-001, Attachment 3.

[2] The rationale is that it (a) is the most suitable considering the information/data, and their intended use, and availability of corroborating data; (b) is the most suitable considering the data, their existing documentation, and intended use; (c) is the most suitable considering the data and the existing documentation regarding the data and the data originator; (d) is appropriate considering the available information on the data and the originating agency; (e) is that corroborating data are available for comparison with the unqualified data set and any inferences drawn to corroborate the unqualified data can be clearly identified, justified and documented; (f) is appropriate considering the extent of available documentation that allowed the evaluation of the methodology, data acquisition, and data review; (g) is that it was the most suitable considering the data and available documentation of the QA program; (h) it is the most suitable considering the methodology, data acquisition or development results, and use in similar applications are applicable.

[3] Attributes from SCI-PRO-001, Attachment 4.

Table J-3. Direct Inputs for Appendix J

Input	Source	Description
Biggin and Thomas 2003. "Analysis of Long-Term Variations in the Geomagnetic Polodial Field Intensity and Evaluation of Their Relationship with Global Geodynamics." [DIRS 167876]	Figure 11	Frequency of earth's magnetic pole reversals
Bird et al. 1960. *Transport Phenomena*. [DIRS 103524]	pp. 565 to 567	The thermal diffusion term [Soret effect] describes the tendency for species to diffuse under the influence of a temperature gradient; this effect is quite small.
Blackwell et al. 2000. *Geothermal Resource/Reservoir Investigations Based on Heat Flow and Thermal Gradient Data for the United States*. [DIRS 183582]	Section 2.3	Hydrothermal systems have been found to be highly correlated to regional heat flow in excess of 80 mW/m^2
	Section 3.5	Most extensional geothermal systems in the U.S. appear to circulate to minimum depths of 4 to 6 km based on a common extrapolation
Brakenridge 1981. "Terrestrial Paleoenvironmental Effects of a Late Quaternary-Age Supernova." [DIRS 167873]	p. 85	The postulated climatic and environmental effects of the supernovae, including the decrease in average temperature
	p. 85	The estimated time of occurence of Vela supernova
Bredehoeft 1997. "Fault Permeability Near Yucca Mountain." [DIRS 100007]	p. 2460	Earth tide water level fluctuations in borehole UE-25 p#1
Broxton and Warren 1987. "Distribution and Chemistry of Diagenetic Minerals at Yucca Mountain, Nye County, Nevada." [DIRS 102004]	p. 101	Most of the zeolitic deposits at Yucca Mountain formed between 11.3 and 13.9 million years ago, and were largely contemporaneous with the most active period of silicic volcanism within the southwest Nevada volcanic field
Choppin and Stout 1989. "Actinide Behavior in Natural Waters." [DIRS 168379]	p. 209	For the higher charged actinides, hydrolysis can lead to formation of oligomers and polymers. At the low environmental concentrations of actinides, these are usually a problem only for Pu(IV) whose hydrolytic polymers are rather intractable.
Colella et al. 2001. "Use of Zeolitic Tuff in the Building Industry." [DIRS 184454]	Figure 24	The SEM image of zeolitic tuff shows microcracks with apertures of about one to two micrometers
Craig 2001. "Transmittal of Level 5 Deliverable SPW205M5, 'Excavation-Induced Fracture Study'." [DIRS 171411]	p. 16	In rock with few fractures, the tunnel boring machine-induced fracturing of the tunnel periphery is confined to a depth of influence of less than 5 cm
	pp. 1, 3, 8	Energy is focused on the rock to be removed, so that excess energy is not dispersed into the surrounding rock, as from blasting

Table J-3. Direct Inputs for Appendix J

Input	Source	Description
Craig 2001. "Transmittal of Level 5 Deliverable SPW205M5, 'Excavation-Induced Fracture Study'." [DIRS 171411] (continued)	pp. 3 to 11, 16	Examination of the tunnel walls and associated alcoves, niches, and drillholes has been used to define the character and extent of mechanical damage induced by tunnel boring
CRWMS M&O 1998. *Synthesis of Volcanism Studies for the Yucca Mountain Site Characterization Project*. [DIRS 105347]	pp. 5-41 through 5-57	Laboratory analytical data and field observations of mineral alterations around igneous intrusions at natural analogue sites show that alteration extends less than 10 m away from the intrusion host rock contact. Natural analogue studies in similar host rocks at the Nevada Test Site show that alteration is limited to a zone less than 10 m away from the intrusion/host rock contact
CRWMS M&O 1999. *Final Report: Plant and Soil Related Processes Along a Natural Thermal Gradient at Yucca Mountain, Nevada*. [DIRS 105031]	Executive Summary	Fractional change in total evapotranspiration due to thermally induced decrease in shrub coverage
	Section 3.3	Relationship between transpiration, percent shrub coverage, and temperature
DOE 2002. *Final Environmental Impact Statement for a Geologic Repository for the Disposal of Spent Nuclear Fuel and High-Level Radioactive Waste at Yucca Mountain, Nye County, Nevada*. [DIRS 155970]	Section I.7	Modeling of potential annual doses from gas-phase geosphere transport of Carbon-14 shows that the individual maximum radiological dose is 1.8×10^{10}
	Section I.7.3	Radon released from the repository in the gas phase is expected to radioactively decay before reaching the ground surface
Doorenbos and Pruitt 1977. *Crop Water Requirements*. [DIRS 103062]	Table 36, p. 78	Salinity tolerance for crops
DTN: SN0612T0502404.014. Thermodynamic Database Input File for EQ3/6 - DATA0.YMP.R5 [DIRS 178850]	*data0.ymp.R5*	Thermodynamic database (used for corroborative calculations in Appendix J)
Ehlers and Blatt 1982. *Petrology, Igneous, Sedimentary, and Metamorphic*. [DIRS 167802]	pp. 684 to 685	The geothermal gradient at convergent plate boundaries may range from less than 10°C per km to greater than 25°C per km
	p. 566	Conditions conducive to the onset of regional metamorphism correspond to temperature of 150°C to 200°C and pressures of 0.5 to 1 kilobars, which occur at depths of 4 to 5 km
EQ3/6 V. 8.1. 2005. WINDOWS 2000. STN: 10813-8.1-00 [DIRS 176889]	Entire	Software used in data comparison
Finch and Ewing 1992. "The Corrosion of Uraninite Under Oxidizing Conditions." [DIRS 113030]	Section 4.2.2	The effect of dissolved silica on the alteration of the uranyl (VI) hydroxides is profound; the alteration of schoepite can result in the formation of uranyl silicates such as uranophane and sodyite
Freeze and Cherry 1979. *Groundwater*. [DIRS 101173]	pp. 514 to 515	Extensive carbonate dissolution cavities are not expected to develop because such dissolution is not typically observed in carbonates at great depths below the water table
	p. 106	Carbonate, quartz, and halite solubilities

Table J-3. Direct Inputs for Appendix J (Continued)

Input	Source	Description
Fridrich et al. 1998. *Space-Time Patterns of Late Cenozoic Extension, Vertical-Axis Rotation, and Volcanism in the Crater Flat Basin, Southwest Nevada*. [DIRS 164051]	p. 1	During the period of peak tectonism (approximately 11.6 Ma to 12.7 Ma), the western part of Crater Flat basin subsided due to the basin extending from 18% to 40% in 1.1 million years or less
	pp. 1, 13, 19, and 20	After 11.6 Ma, the rate of extension in the basin declined in a roughly exponential manner. The late Quaternary rate of extension is less than 1% of the initial rate and may be as low as 0.1% to 0.2% per million years
	pp. 1 and 2	The pattern of Quaternary deformation mimics the pattern of middle Miocene activity, but at substantially lower rates
Garvin 2002. *Multi-Canister Overpack Topical Report*. [DIRS 169141]	Section 2.2.6.2	The design pressure for the MCO is 450 psi at 132°C
	Table 4-4	443 kg zirconium cladding per MCO (Mark IV maximum fuel load without scrap basket)
	Table 4-4	6,340 kg uranium metal per MCO (Mark IV maximum fuel load without scrap basket)
	Table 4-4	1.1×10^7 g U-metal per waste package, assuming that the waste package contains two MCOs and each MCO contains Mark IV fuel (3,804 kg U) and scrap (1,832 kg U) for a total of 5,636 kg U
	Table 4-4	The maximum water in a sealed MCO is 4.64 kg (bound in particulate), with less than 200 g being present as free water
	Section 4.1.3.2	MCOs will be dried and filled with helium
Jury et al. 1991. *Soil Physics*. [DIRS 102010]	Table 5.5	Soil conductivity for unsaturated sand
Karam 2002. "Gamma and Neutrino Radiation Dose from Gamma Ray Bursts and Nearby Supernovae." [DIRS 167872]	Table 2	Dose reduction in top 20 mm of rock
Kieft et al. 1997. "Factors Limiting Microbial Growth and Activity at a Proposed High-Level Nuclear Repository, Yucca Mountain, Nevada." [DIRS 100767]	p. 3130	Total counts (microscopic direct and plate) ranged from below limit of detection (3.2 × 104 cells per gram) to 2.3 × 105 cells per gram; Phospholipid fatty acid (PLFA) concentrations were generally low, ranging from 0.1 to 3.7 pmol per gram.
Krystinik 1990. "Early Diagenesis in Continental Eolian Deposits." [DIRS 135295]	pp. 8-2 to 8-3	Compaction may reduce eolian sediments by as much as 20% to 30% but after this initial stage, compaction does not become an important factor in diagenesis until the onset of grain deformation and pressure solution during deeper burial diagenesis
Martinez and Nilson 1999. "Estimates of Barometric Pumping of Moisture through Unsaturated Fractured Rock." [DIRS 174095]	p. 106	Estimated rate of water removal from Yucca Mountain through vapor transport under isothermal conditions

Table J-3. Direct Inputs for Appendix J (Continued)

Input	Source	Description
Means et al. 1983. *The Organic Geochemistry of Deep Ground Waters and Radionuclide Partitioning Experiments under Hydrothermal Conditions*. [DIRS 100797]	Tables 1 and 3	Total organic carbon is 0.58 mg/L for well UE25b-1, 33% (0.19 mg/L) of which has a molecular weight greater than 1,000
Morgenstern and Choppin 1999. "Kinetics of the Reduction of $Pu(V)O_2^+$ by Hydrogen Peroxide." [DIRS 184023]	pp. 109 to 111; Table 1	Reduction of Pu(V) to Pu(IV) in basic solutions having hydrogen peroxide (H_2O_2) concentrations on the order of 0.04 to 0.00001 moles per liter and pH 7.9 to 10.8
National Research Council 1992. *Ground Water at Yucca Mountain, How High Can It Rise? Final Report of the Panel on Coupled Hydrologic/Tectonic/Hydrothermal Systems at Yucca Mountain*. [DIRS 105162]	Chapter 2	Extension rates declined to 5 to 10 mm/yr at 5 Ma; extension rates are still in a declining state
	Chapter 5, p. 116	Results from the regional stress model approach indicated a maximum water table rise of 50 m
	Chapter 5	Predicted seismic events within the Yucca Mountain region over the next 10,000 years will not alter the large and globally extensive stresses imposed in the rock and in effect over the past 10 to 15 million years
	Chapter 2	Plate tectonic activity imparted crustal extension stresses within the Yucca Mountain region) during the past 12 million years which includes the 5 million years where the extension rates have declined to 5 to 10 mm/yr
Paces et al. 1997. *Summary of Discharge Deposits in the Amargosa Valley*. [DIRS 109148]	Figure 18	With the exception of the Amargosa River Snail Site, geochemical dating indicates the last episode of paleospring activity for the majority of paleosprings occurred between 14,000 to 20,000 years ago, or longer
	Figure 18	Scranton Wells was active 40,000 to 60,000 years ago, Mesquite Wash active 30,000 years ago, and the Amargosa River Snail Site between 9,000 to 12,000 years ago
Piron and Pelletier 2001. "State of the Art on the Helium Issues." [DIRS 165318]	Section 5.3.2.4.1	The decay helium gas pressure is 90 bars at 20°C in commercial SNF rods with a gap volume of 13 cm^3 and a burnup of 47.5 GWd/MTU after 10,000 years
Platten 2006. "The Soret Effect: A Review of Recent Experimental Results." [DIRS 183864]	p. 5	Typical range for Soret coefficients (0.01 to 0.001 K^{-1})
Plys and Duncan 1999. *FAI/99-14, Rev. 1, Hydrogen Combustion in an MCO During Interim Storage*. [DIRS 184687]	Figure 5-1, pp. 6 and 7	The maximum achievable temperatures and pressures (11 times the initial pressure) for a hydrogen fire in a mixture of oxygen (21%) and helium (79%) inside an MCO
Rai and Swanson 1981. "Properties of Plutonium(IV) Polymer of Environmental Importance." [DIRS 144599]	p. 111	Pu(IV) polymer does not make stable suspensions at pH values above 5 and hence would not be expected to be mobile as polyer in the lithosphere

Table J-3. Direct Inputs for Appendix J (Continued)

Input	Source	Description
Reeves 1976. *Caliche: Origin, Classification, Morphology and Uses*. [DIRS 104303]	p. 110	Net effects of shallow diagenesis and associated cementation are to stabilize the surface environment and decrease the net vertical infiltration rate
Reimus 1995. *Transport of Synthetic Colloids Through Single Saturated Fractures: A Literature Review*. [DIRS 144604]	Sections 3.2 and 3.3, including subsections	Equations and associated discussion describing normal and short-range forces and associated velocities affecting particles moving in a viscous fluid
Rogers et al. 1988. "Low Temperature Diffusion of Oxygen in Titanium and Titanium Oxide Films." [DIRS 184108]	Table 1 and p. 146	The value of the oxygen diffusion coefficient in titanium at 300°C
Rousseau et al. 1997. *Results of Borehole Monitoring in the Unsaturated Zone Within the Main Drift Area of the Exploratory Studies Facility, Yucca Mountain, Nevada*. [DIRS 100178]	Section 5.2	The measured heat flux in the Yucca Mountain area at boreholes NRG-7a, UZ-7a, and SD-12 have heat fluxes within the TSw of 37, 39, and 32 mW/m^2, respectively. This gives an average of 36 mW/m^2, and a standard deviation of 3.6 mW/m^2
Sexton 2007. *Particulate and Water in Multi-Canister Overpacks (OCRWM)*. [DIRS 184742]	Table 2-1	Maximum amount of free and bound water in an MCO is 4.3 kg
	Table 2-1	The average value of free and bound water in an MCO is 1.03 kg
Shoesmith and King 1998. *The Effects of Gamma Radiation on the Corrosion of Candidate Materials for the Fabrication of Nuclear Waste Packages*. [DIRS 112178]	pp. 29 to 31; Table 4	Effects of gamma radiolysis on waste package materials when in contact with Mg-Cl brines
Siriwardane and Wightman 1983. "Interaction of Hydrogen Chloride and Water with Oxide Surfaces. III. Titanium Dioxide." [DIRS 183688]	p. 504	Range of specific surface area of commercial grade crystalline rutile
Smyth and Caporuscio 1981. *Review of the Thermal Stability and Cation Exchange Properties of the Zeolite Minerals Clinoptilolite, Mordenite, and Analcime: Applications to Radioactive Waste Isolation in Silicic Tuff*. [DIRS 174060]	Tables A-1 and B-1 (sample YM-40)	Dehydration and shrinkage of zeolitic tuff under experimental heating conditions
	Table A-1, sample YM-38	Upper bounding value for volume reduction of initially saturated zeolitic tuff under experimental heating conditions
Stuckless and Levich 2007. *The Geology and Climatology of Yucca Mountain and Vicinity, Southern Nevada and California*. [DIRS 181507]	p. 83	The calculated maximum possible erosion rates for bedrock outcrops using a ^{10}Be cosmogenic dating technique is 0.4 to 2.7 cm/10,000 years
	p. 84	The long-term erosion rates of stripping of unconsolidated material from Yucca Mountain hillslopes were calculated to be 0.2 to 6 cm/10,000 years using both the rock-varnish carion ratio and the in situ, ^{36}Cl cosmogenic dating methods
Taylor 1986. *Impact of Time and Climate on Quaternary Soils in the Yucca Mountain Area of the Nevada Test Site*. [DIRS 102864]	Chapter 5	SiO_2 cementation is not dependent on climatic conditions, but cementation does exhibit distinctive trends that correspond with the ages of the surficial deposits
	Figure 9 and pp. 31 to 33	Cementation by opaline SiO_2 is common in the study area, and that opaline SiO_2 accumulation in the soils is favored over that of pedogenic calcite $CaCO_3$

Table J-3. Direct Inputs for Appendix J (Continued)

Input	Source	Description
Taylor 1986. *Impact of Time and Climate on Quaternary Soils in the Yucca Mountain Area of the Nevada Test Site*. [DIRS 102864] (continued)	Chapter 5	Accumulation rates are attributable to several climatic scenarios, but climate change was insufficient to significantly decrease the rate of accumulations
Thompson et al. 1999. *Quantitative Paleoclimatic Reconstructions from Late Pleistocene Plant Macrofossils of the Yucca Mountain Region*. [DIRS 109470]	Figures 17, 18	During the last glacial maximum, the mean annual temperature at Yucca Mountain exceeded 0°C
Valentine and Krogh 2006. "Emplacement of Shallow Dikes and Sills Beneath a Small Basaltic Volcanic Center – The Role of Pre-Existing Structure (Paiute Ridge, Southern Nevada, USA)." [DIRS 177282]	p. 221	The resulting effects of dike intrusion may be to increase, decrease or not change permeabilities as compared to the host (unaffected) rock. The scale at which permeabilities would change is limited to a few meters around the dike
Valentine et al. 1998. "Physical Processes of Magmatism and Effects on the Potential Repository: Synthesis of Technical Work Through Fiscal Year 1995." [DIRS 119132]	p. 5-74	Mineral alterations around igneous intrusions at natural analogue sites show that alteration is limited to a zone that extends less than 10 m away from the intrusion/host rock contact around igneous intrusions at natural analogue sites
Wachs, G. 2004. *Calculation of Amount of Free Water Required to Overpressurize DOE SNF Standardized Canister and RW Waste Package*. [DIRS 184624]	Section 6	The volume of free (unbound) water is approximately 0.0005 liters in a 15-foot-long DOE SNF Standardized Canister after cold vacuum drying
Whelan 2004. *Secondary Mineral Deposits and Evidence of Past Seismicity and Heating of the Proposed Repository Horizon at Yucca Mountain, Nevada*. [DIRS 170697]	p. 3	Description of the process of infilling and coating of open fractures and lithophysal cavities by calcite and silica at Yucca Mountin.
Wilson et al. 2003. "Origin, Timing, and Temperature of Secondary Calcite—Silica Mineral Formation at Yucca Mountain, Nevada." [DIRS 163589]	Section 8	Studies of secondary minerals at Yucca Mountain using petrography, fluid inclusion thermometry, and uranium-lead dating indicate that unsaturated-zone temperatures have remained close to the current ambient values over the past 2 to 5 Ma
	Sections 7.3, 8	The unsaturated-zone secondary minerals were interpreted to have been deposited from downward percolating meteoric water and not the result of upwelling groundwaters
Wronkiewicz et al. 1996. "Ten-Year Results from Unsaturated Drip Tests with UO_2 at 90°C: Implications for the Corrosion of Spent Nuclear Fuel." [DIRS 102047]	p. 86	Between 1% and 12% of the total amount of uranium released was present as a >5 nm size-fraction
Zhang and Schwartz 1995. "Multispecies contaminant plumes in variable density flow systems." [DIRS 183479]	pp. 839, 840, 843, and 844	The chemical and physical properties of the leachate for a specified discharge and the medium
Zhou et al. 2003. "Flow and Transport in Unsaturated Fractured Rock: Effects of Multiscale Heterogeneity of Hydrogeologic Properties." [DIRS 162133]	Section 6	An analysis of smaller-scale heterogeneity indicates that UZ flow and transport are governed primarily by large-scale stratigraphy, structure, and associated hydrological properties rather than by smaller-scale heterogeneity

Table J-3. Direct Inputs for Appendix J (Continued)

Input	Source	Description
Ziegler 2004. "Transmittal of Appendix D of the Technical Basis Document No. 10: Unsaturated Zone Transport Addressing Key Technical Issue (KTI) Agreement Evolution of Near-Field Environment (ENFE) 1.04." [DIRS 171694]	Table D-12	Solubility values for portlandite

Table J-4. Indirect Inputs for Appendix J

Citation	Title	DIRS
10 CFR 60 Subpart G 1998	Energy: Quality Assurance	100015
Albin et al. 1997	*Geology of the Main Drift - Station 28+00 to 55+00, Exploratory Studies Facility, Yucca Mountain Project, Yucca Mountain, Nevada*	101367
Arakel 1996	"Quaternary Vadose Calcretes Revisited"	167623
Arnold 2003	"Space Plasma Influences on the Earth's Atmosphere"	167638
ASME 1998	"Rules for Construction of Nuclear Power Plant Components, Division 1, Subsection NB"	155708
Baldwin and Butler 1985	"Compaction Curve"	167871
Beason 2003	Collection of Underground Site Characterization Data [final submittal]. Scientific Notebook SN-USGS-SCI-084-V1	171953
Biggin and Thomas 2003	"Analysis of Long-Term Variations in the Geomagnetic Polodial Field Intensity and Evaluation of Their Relationship with Global Geodynamics"	167876
Bird et al. 1960	*Transport Phenomena*	103524
Bish and Aronson 1993	"Paleogeothermal and Paleohydrologic Conditions in Silicic Tuff from Yucca Mountain, Nevada"	100006
Bish et al. 1984	"Petrofabric Constraints of the Age of Zeolitization at Yucca Mountain"	106336
Blackwell et al. 2000	*Geothermal Resource/Reservoir Investigations Based on Heat Flow and Thermal Gradient Data for the United States*	183582
Brakenridge 1981	"Terrestrial Paleoenvironmental Effects of a Late Quaternary-Age Supernova"	167873
Bredehoeft 1997	"Fault Permeability Near Yucca Mountain"	100007
BSC 2004	*Future Climate Analysis*	170002
BSC 2004	*Yucca Mountain Site Description*	169734
BSC 2007	*IED Subsurface Facilities Geological Data*	182926
Carslaw and Jaeger 1959	*Conduction of Heat in Solids*	100968
Chadwick et al. 1995	"Soil Polygenesis as a Function of Quaternary Climate Change, Northern Great Basin, USA"	167626
Cho et al. 1998	"Basic Concepts of Heat Transfer"	160802
Choppin and Stout 1989	"Actinide Behavior in Natural Waters"	168379
Choppin 1983	"Aspects of Plutonium Solution Chemistry"	168395
Choppin 1992	"The Role of Natural Organics in Radionuclide Migration in Natural Aquifer Systems"	100717
Choppin 2003	"Actinide Speciation in the Environment"	168308

Table J-4. Indirect Inputs for Appendix J (Continued)

Citation	Title	DIRS
Choppin et al. 1986	"Effects of Humic Substances on Plutonium Speciation in Marine Systems"	168377
Colella et al. 2001	"Use of Zeolitic Tuff in the Building Industry"	184454
Craig 2001	"Transmittal of Level 5 Deliverable SPW205M5, 'Excavation-Induced Fracture Study'"	171411
CRWMS M&O 1998	*Synthesis of Volcanism Studies for the Yucca Mountain Site Characterization Project*	105347
CRWMS M&O 1999	*Final Report: Plant and Soil Related Processes Along a Natural Thermal Gradient at Yucca Mountain, Nevada*	105031
CRWMS M&O 2000	*Calibrated Properties Model*	144426
de Groot and Mazur 1962	*Non-Equilibrium Thermodynamics*	118615
DOE 2004	*Quality Assurance Requirements and Description*	171539
DOE 1997	*Quality Assurance Surveillance Record, Verify Compliance with USGS Procedures in the Preparation of "Memorandum Report"*	171970
DOE 2002	*Final Environmental Impact Statement for a Geologic Repository for the Disposal of Spent Nuclear Fuel and High-Level Radioactive Waste at Yucca Mountain, Nye County, Nevada*	155970
DOE 2007	*Quality Assurance Requirements and Description*	182051
Doorenbos and Pruit 1977	*Crop Water Requirements*	103062
DTN: GS020908315215.003	Fluid Inclusion Homogenization Temperatures from the ESF and ECRB, 10/01 to 5/02	164846
DTN: GS020908315215.004	Stable Carbon and Oxygen Isotope Analyses of ESF/ECRB Calcite and USW SD-6 and USW WT-24 Whole Rock; 1/1999-6/2002	164847
DTN: GS021208315215.009	U Abundances, 238U-234U-230TH-232TH Activity Ratios, and Calculated 230TH/U Ages, and Initial 234U/238U Activity Ratios	164750
DTN: LB0408CMATUZFT.004	Leaching of Altered Cementitious Materials - EQ3/6 Simulations for Cementitious Material Transport	171706
DTN: LL960905751021.019	Ten Year Results from Unsaturated Drip Tests with UO2 at 90C: Implications for the Geologic Disposal of Spent Nuclear Fuel	185101
DTN: SN0310T0505503.004	Initial Radionuclide Inventories for TSPA-LA	168761
DTN: SN0612T0502404.014	Thermodynamic Database Input File for EQ3/6 - DATA0	178850
Duhr and Braun 2006	"Why Molecules Move Along a Temperature Gradient"	183865
Eatman et al. 1997	*Geology of the South Ramp - Station 55+00 to 78+77, Exploratory Studies Facility, Yucca Mountain Project, Yucca Mountain, Nevada*	157677
Eghbal and Southard 1993	"Micromorphological Evidence of Polygenesis of Three Aridisols, Western Mohave Desert, California"	167625
Eghbal and Southard 1993	"Stratigraphy and Genesis of Durorthids and Haplargids on Dissected Alluvial Fans, Western Mojave Desert, California"	167624
Ehlers and Blatt 1982	*Petrology, Igneous, Sedimentary, and Metamorphic*	167802
Faulds et al. 1994	*Geologic Map of the Crater Flat Area, Nevada*	105126
Fenelon 2000	*Quality Assurance and Analysis of Water Levels in Wells on Pahute Mesa and Vicinity, Nevada Test Site, Nye County, Nevada*	160881
Finch and Ewing 1992	"The Corrosion of Uraninite Under Oxidizing Conditions"	113030
Flint 1998	*Characterization of Hydrogeologic Units Using Matrix Properties, Yucca Mountain, Nevada*	100033
Flynn et al. 1996	*Geothermal Resource Assessment of the Yucca Mountain Area, Nye County, Nevada*	112530

Table J-4. Indirect Inputs for Appendix J (Continued)

Citation	Title	DIRS
Freeze and Cherry 1979	*Groundwater*	101173
Fridrich et al. 1994	"Hydrogeologic Analysis of the Saturated-Zone Ground-Water System, Under Yucca Mountain, Nevada"	100575
Fridrich et al. 1998	*Space-Time Patterns of Late Cenozoic Extension, Vertical-Axis Rotation, and Volcanism in the Crater Flat Basin, Southwest Nevada*	164051
Fridrich et al. 2003	*Documentation for USGS Review of Chapter 2, Section 2 of the Seismotectonic Framework Report Entitled "Space-Time Patterns of Extension, Vertical-Axis Rotation, and Volcanism in the Crater Flat Basin, Southern Nevada"*	184915
Fridrich et al. 1996	"Space-Time Patterns of Extension, Vertical-Axis Rotation, and Volcanism in the Crater Flat Basin"	105086
Frondel 1958	*Systematic Mineralogy of Uranium and Thorium*	113267
Galloway and Rojstaczer 1988	"Analysis of the Frequency Response of Water Levels in Wells to Earth Tides and Atmospheric Loading"	156826
Garvin 2002	*Multi-Canister Overpack Topical Report*	169141
Gosse et al. 1996	"Applications of In Situ Cosmogenic Nuclides in the Geologic Site Characterization of Yucca Mountain, Nevada"	170725
Grieve 1987	"Terrestrial Impact Structures"	135254
Grieve 1998	"Extraterrestrial Impacts on Earth: The Evidence and the Consequences"	163385
Grieve and Robertson 1984	"The Potential for the Disturbance of a Buried Nuclear Waste Vault by a Large-Scale Meteorite Impact"	185030
Grieve et al. 1995	"The Record of Terrestrial Impact Cratering"	135260
Guenther et al. 1991	*Characterization of Spent Fuel Approved Testing Material—ATM-104*	109207
Hala and Miyamoto 2007	"IUPAC-NIST Solubility Data Series. 84. Solubility of Inorganic Actinide Compounds"	185095
Haldeman and Am 1993	"Bacterial Heterogeneity in Deep Subsurface Tunnels at Rainier Mesa, Nevada Test Site"	145228
Hardin and Chesnut 1997	Synthesis Report on Thermally Driven Coupled Processes	100534
Harrington and Whitney 1987	"Scanning Electron Microscope Method for Rock-Varnish Dating"	106095
He et al. 2007	"Temperature Effects on Oxide Film Properties of Grade-7 Titanium"	183687
Hills and Goda 1993	"Fragmentation of Small Asteroids in the Atmosphere"	135281
Hirschfelder et al. 1964	*Molecular Theory of Gases and Liquids*	171800
Horn et al. 2004	"Bacterial Growth Dynamics, Limiting Factors, and Community Diversity in a Proposed Geological Nuclear Waste Repository Environment"	171058
Hyndman 1972	*Petrology of Igneous and Metamorphic Rocks*	150295
Johnson et al. 1995	"Geomagnetic Polarity Reversal Rate for the Phanerozoic"	185111
Jury et al. 1991	*Soil Physics*	102010
Karam 2002	"Gamma and Neutrino Radiation Dose from Gamma Ray Bursts and Nearby Supernovae"	167872
Kieft et al. 1997	"Factors Limiting Microbial Growth and Activity at a Proposed High-Level Nuclear Repository, Yucca Mountain, Nevada"	100767
Kistler 1968	"Potassium-Argon Ages of Volcanic Rocks in Nye and Esmeralda Counties, Nevada"	133347
Krystinik 1990	"Early Diagenesis in Continental Eolian Deposits"	135295

Table J-4. Indirect Inputs for Appendix J (Continued)

Citation	Title	DIRS
LANL 1993	*Review Sheets, Transport of Synthetic Colloids through Single Saturated Fractures: A Literature Review*	185002
LANL 1994	*Publication Traveler, Transport of Synthetic Colloids through Single Saturated Fractures: A Literature Review*	185000
Lattman 1972	"Relation of Caliche (Calcrete) Horizons to Alluvial Fan Processes in Southern Nevada"	167813
Lattman 1973	"Calcium Carbonate Cementation of Alluvial Fans in Southern Nevada"	129305
Lattman 1983	"Effect of Caliche on Desert Processes"	167815
Luckey et al. 1996	*Status of Understanding of the Saturated-Zone Ground-Water Flow System at Yucca Mountain, Nevada, as of 1995*	100465
Machette 1982	"Morphology, Age, and Rate of Accumulation of Pedogenic $CaCO_3$ in Some Calcareous Soils and Pedogenic Calcretes of Southwestern United States"	167814
Martinez and Nilson 1999	"Estimates of Barometric Pumping of Moisture through Unsaturated Fractured Rock"	174095
Means et al. 1983	*The Organic Geochemistry of Deep Ground Waters and Radionuclide Partitioning Experiments under Hydrothermal Conditions*	100797
Minai et al. 1992	"Humic Material in Well Water from the Nevada Test Site"	100801
Morgenstern and Choppin 1999	"Kinetics of the Reduction of $Pu(V)O_2^+$ by Hydrogen Peroxide"	184023
Nag et al. 2007	"Low-Temperature Hydrothermal Synthesis of Phase-Pure Rutile Titania Nanocrystals: Time Temperature Tuning of Morphology and Photocatalytic Activity"	184817
National Research Council 1992	*Ground Water at Yucca Mountain, How High Can It Rise? Final Report of the Panel on Coupled Hydrologic/Tectonic/Hydrothermal Systems at Yucca Mountain*	105162
Novotna and Vitek 1991	"The Atmospheric Mean Energetic Level and External Forcing"	167634
Odenwald 2003	"Earth – Magnetic Field"	160892
Oversby 1987	"Spent Fuel as a Waste Form – Data Needs to Allow Long Term Performance Assessment under Repository Disposal Conditions"	103446
Paces et al. 1997	*Summary of Discharge Deposits in the Amargosa Valley*	109148
Paces et al. 2001	*Ages and Origins of Calcite and Opal in the Exploratory Studies Facility Tunnel, Yucca Mountain, Nevada*	156507
Palmer and Barton 1987	"Porosity Reduction, Microfabric and Resultant Lithification in UK Uncemented Sands"	118483
Pechala 1985	"The Effect of Extraterrestrial Interactions on Change of Tropospheric Circulation in the Polar Regions of the Earth"	167633
Perry et al. 1984	*Perry's Chemical Engineers' Handbook*	125806
Petit et al. 1986	"The Soret Effect in Dilute Aqueous Alkaline Earth and Nickel Chloride Solutions at 25°C"	183863
Piron and Pelletier 2001	"State of the Art on the Helium Issues"	165318
Platten 2006	"The Soret Effect: A Review of Recent Experimental Results"	183864
Plys and Duncan 1999	*FAI/99-14, Rev. 1, Hydrogen Combustion in an MCO During Interim Storage*	184687
Press and Siever 1978	*Earth*	167965
Pruess et al. 1999	TOUGH2 User's Guide, Version 2.0	160778
Rai and Swanson 1981	"Properties of Plutonium(IV) Polymer of Environmental Importance"	144599

Table J-4. Indirect Inputs for Appendix J (Continued)

Citation	Title	DIRS
Reeves 1976	*Caliche: Origin, Classification, Morphology and Uses*	104303
Reimus 1995	*Transport of Synthetic Colloids Through Single Saturated Fractures: A Literature Review*	144604
Retallack 1991	"Untangling the Effects of Burial Alteration and Ancient Soil Formation"	167870
Rogers et al. 1988	"Low Temperature Diffusion of Oxygen in Titanium and Titanium Oxide Films"	184108
Rousseau et al. 1997	*Results of Borehole Monitoring in the Unsaturated Zone Within the Main Drift Area of the Exploratory Studies Facility, Yucca Mountain, Nevada*	100178
Ruderman 1974	"Possible Consequences of Nearby Supernova Explosions for Atmospheric Ozone and Terrestrial Life"	167875
Salem et al. 1998	"Diagenesis of Shallowly Buried Cratonic Sandstones, Southwest Sinai, Egypt"	167869
Sarna-Wojcicki et al. 1997	"Age and Correlation of Tephra Layers, Position of the Matuyama-Brunhes Chron Boundary, and Effects of Bishop Ash Eruption on Owens Lake, as Determined from Drill Hole OL-92, Southeast California"	109161
Sass et al. 1988	*Temperature, Thermal Conductivity, and Heat Flow Near Yucca Mountain, Nevada: Some Tectonic and Hydrologic Implications*	100644
Sexton 2007	*Particulate and Water in Multi-Canister Overpacks (OCRWM)*	184742
Shleien 1992	*The Health Physics and Radiological Health Handbook*	127299
Shoesmith and King 1998	*The Effects of Gamma Radiation on the Corrosion of Candidate Materials for the Fabrication of Nuclear Waste Packages*	112178
Siriwardane and Wightman 1983	"Interaction of Hydrogen Chloride and Water with Oxide Surfaces. III. Titanium Dioxide"	183688
Smailos and Köster 1987	"Corrosion Studies on Selected Packaging Materials for Disposal of High Level Wastes"	159774
Smailoset al. 1990	*Corrosion Testing of Selected Packaging Materials for Disposal of High-Level Waste Glass in Rock Salt Formations*	154820
Smyth and Caporuscio 1981	*Review of the Thermal Stability and Cation Exchange Properties of the Zeolite Minerals Clinoptilolite, Mordenite, and Analcime: Applications to Radioactive Waste Isolation in Silicic Tuff*	174060
SNL 2007	*EBS Radionuclide Transport Abstraction*	177407
SNL 2007	*Initial Radionuclides Inventory*	180472
SNL 2007	*In-Package Chemistry Abstraction*	180506
SNL 2007	*Radionuclide Screening*	177424
SNL 2007	*UZ Flow Models and Submodels*	184614
SNL 2008	*Particle Tracking Model and Abstraction of Transport Processes*	184748
Snowdon and Turner 1960	"The Soret Effect in Some 0·01 Normal Aqueous Electrolytes"	183867
Spaulding 1983	*Vegetation and Climates of the Last 45,000 Years in the Vicinity of the Nevada Test Site, South-Central Nevada*	101623
Stuckless and Levich 2007	*The Geology and Climatology of Yucca Mountain and Vicinity, Southern Nevada and California*	181507
Taylor 1986	*Impact of Time and Climate on Quaternary Soils in the Yucca Mountain Area of the Nevada Test Site*	102864
Thompson et al. 1999	*Quantitative Paleoclimatic Reconstructions from Late Pleistocene Plant Macrofossils of the Yucca Mountain Region*	109470

Table J-4. Indirect Inputs for Appendix J (Continued)

Citation	Title	DIRS
Thornton and Seyfried 1983	"Thermodiffusional Transport in Pelagic Clay: Implications for Nuclear Waste Disposal in Geological Media"	183866
Toth et al. 1983	"Aspects of Plutonium(IV) Hydrous Polymer Chemistry"	168394
Tsang and Pruess 1990	*Further Modeling Studies of Gas Movement and Moisture Migration at Yucca Mountain, Nevada*	172018
Tsang and Pruess [n.d.]	*Preliminary Studies of Gas Phase Flow Effects and Moisture Migration at Yucca Mountain, Nevada*	184794
Valentine and Krogh 2006	"Emplacement of Shallow Dikes and Sills Beneath a Small Basaltic Volcanic Center – The Role of Pre-Existing Structure (Paiute Ridge, Southern Nevada, USA)"	177282
Valentine et al. 1998	"Physical Processes of Magmatism and Effects on the Potential Repository: Synthesis of Technical Work Through Fiscal Year 1995"	119132
Wachs 2004	*Calculation of Amount of Free Water Required to Overpressurize DOE SNF Standardized Canister and RW Waste Package*	184624
Weast 1985	*CRC Handbook of Chemistry and Physics*	111561
Whelan 2004	*Secondary Mineral Deposits and Evidence of Past Seismicity and Heating of the Proposed Repository Horizon at Yucca Mountain, Nevada*	170697
Whelan et al. 1994	"Paleoclimatic and Paleohydrologic Records from Secondary Calcite: Yucca Mountain, Nevada"	100091
Whelan and Moscati 1998	"9 M.Y. Record of Southern Nevada Climate from Yucca Mountain Secondary Minerals"	109179
Whelan et al. 2002	"Physical and Stable-Isotope Evidence for Formation of Secondary Calcite and Silica in the Unsaturated Zone, Yucca Mountain, Nevada"	160442
Wilson 2003	"Origin, Timing, and Temperature of Secondary Calcite--Silica Mineral Formation at Yucca Mountain, Nevada"	163589
WoldeGabriel et al. 1999	"Effects of Shallow Basaltic Intrusion into Pyroclastic Deposits, Grants Ridge, New Mexico, USA"	110071
Wollenberg et al. 1975	*Geothermal Energy Resource Assessment*	107327
Wronkiewicz et al. 1991	*Leaching Action of EJ-13 Water on Unirradiated UO{subscript 2} Surfaces Under Unsaturated Conditions at 90°C*	176891
Wronkiewicz et al. 1992	"Uranium Release and Secondary Phase Formation During Unsaturated Testing of UO2 at 90°C"	100493
Wronkiewicz et al. 1996	"Ten-Year Results from Unsaturated Drip Tests with UO_2 at 90°C: Implications for the Corrosion of Spent Nuclear Fuel"	102047
Wu et al. 1995	*Preliminary Analysis of Effects of Thermal Loading on Gas and Heat Flow Within the Framework of the LBNL/USGS Site-Scale Model*	103690
Wu and Pruess 2000	"Numerical Simulation of Non-Isothermal Multiphase Tracer Transport in Heterogeneous Fractured Porous Media"	153972
Wuschke et al. 1995	*Assessment of the Long-Term Risk of a Meteorite Impact on Hypothetical Canadian Nuclear Fuel Waste Disposal Vault Deep in Plutonic Rock*	129326
Yaalon 1967	"Factors Affecting the Lithification of Eolianite and Interpretation of Its Environmental Significance in the Coastal Plain of Israel"	167622
Yao and Zhang 1999	"Preparation and Characterization of Mesoporous Titania Gel-Monolith"	184766

Table J-4. Indirect Inputs for Appendix J (Continued)

Citation	Title	DIRS
YMP 1993	*Evaluation of the Potentially Adverse Condition "Evidence of Extreme Erosion During the Quaternary Period" at Yucca Mountain, Nevada*	100520
Zhang and Schwartz 1995	"Multispecies contaminant plumes in variable density flow systems"	183479
Zhou et al. 2003	"Flow and Transport in Unsaturated Fractured Rock: Effects of Multiscale Heterogeneity of Hydrogeologic Properties"	162133
Ziegler 2004	"Transmittal of Appendix D of the Technical Basis Document No. 10: Unsaturated Zone Transport Addressing Key Technical Issue (KTI) Agreement Evolution of Near-Field Environment (ENFE) 1.04"	171694

INTENTIONALLY LEFT BLANK

Addendum Cover Page

Complete only applicable items.

QA: QA

LF - 4/12/2010

1. Total Pages: 440 116

2. Addendum to (Title):
Features, Events, and Processes for the Total System Performance Assessment: Analyses

3. ID (including Revision and Addendum No.):
ANL-WIS-MD-000027 REV00 ADD1

	Printed Name	Signature	Date
4. Originator	Richard Quittmeyer	R.C. Quittmeyer	04/06/2010
5. Checker	Ronald Price	Ronald H. Price	4/6/2010
6. QCS / QA Reviewer	Sourian Kassabian-Darnell	Sourian K. Darnell	04/06/10
7. Responsible Manager / Lead	Clifford Howard	Clifford Howard	04/07/10
8. Responsible Manager	Clifford Howard	Clifford Howard	04/07/10

9. Remarks

Note that this addendum includes an electronic attachment consisting of two Microsoft © Excel © 2003 files named *PDFA Static Stress Drops R1.xls* and *Stress Drops R1.xls*. The files support the screening justification for FEP 1.2.10.01.0A, *Hydrologic Response to Seismic Activity* and Appendix K[a].

INTENTIONALLY LEFT BLANK

Change History	
10. Revision and Addendum No.	11. Description of Change
REV 00, ADDENDUM 01	The screening justifications for FEPs 1.2.03.02.0B, *Seismic Induced Rockfall Damages EBS Components*; 1.2.03.02.0E, *Seismic-Induced Drift Collapse Alters In-Drift Chemistry;* 1.2.10.01.0A, *Hydrologic Response to Seismic Activity*; 2.2.06.01.0A, *Seismic Activity Changes Porosity and Permeability of Rock*; 2.2.06.02.0A, *Seismic Activity Changes Porosity and Permeability of Faults*; 2.2.06.02.0B, *Seismic Activity Changes Porosity and Permeability of Fractures*; and 2.2.06.03.0A, *Seismic Activity Alters Perched Water Zones* are updated to reflect additional analyses. Appendix K[a] is added to the report to document bounding water table rise calculations consistent with the probabilistic seismic hazard analysis for Yucca Mountain. These changes address Condition Reports 13736 and 13839. Also, the screening justification for FEP 2.1.03.04.0B, *Hydride Cracking of Drip Shields*, is modified to add consideration of the initial hydrogen content of the titanium alloys discussed and to refer to "calculated hydrogen content" as "calculated hydrogen pick-up." These changes address Condition Report 13386. For FEPs 2.1.09.02.0A, *Chemical Interaction with Corrosion Products* and 2.1.09.17.0A, *Formation of Pseudo-Colloids (Corrosion Product) in EBS*, the total system performance assessment disposition is changed to clarify the sorption of plutonium and americium onto oxyhydroxide colloids is a kinetic process in the engineered barrier system. The changes result from resolution of Condition Report 13644. In addition, impacts to tables for FEPs 2.1.14.26.0A (Near-Field Criticality Resulting from an Igneous Event), and 2.2.14.12.0A (Far-Field Criticality Resulting from an Igneous Event), resulting from an update to SNL 2007 [DIRS 181395] are implemented. The changes result from resolution of Condition Reports 14019 and 14087. Finally, screening justifications for FEPs 1.2.07.01.0A, *Erosion/Denudation*, and 2.3.01.00.0A, *Topography and Morphology*, are modified to update the citation to *Reclamation Implementation Plan* (YMP/91-14) (DOE 2009 [DIRS 185964]). This addresses an issue associated with Condition Report 13388.

INTENTIONALLY LEFT BLANK

CONTENTS

Page

1[a]. PURPOSE ..... 1-1[a]

2[a]. QUALITY ASSURANCE ..... 2-1[a]

3[a]. USE OF SOFTWARE ..... 3-1[a]

4[a]. INPUTS ..... 4-1[a]
4.1[a] DIRECT INPUTS ..... 4-1[a]
4.2[a] CRITERIA ..... 4-1[a]
4.3[a] CODES, STANDARDS, AND REGULATIONS ..... 4-1[a]

5[a]. ASSUMPTIONS ..... 5-1[a]

6[a]. SCIENTIFIC ANALYSIS DISCUSSION ..... 6-1[a]
6.1[a] METHODS AND APPROACH ..... 6-1[a]
6.2[a] FEATURE, EVENT, AND PROCESS SCREENING ANALYSES ..... 6-1[a]

7[a]. CONCLUSIONS ..... 7-1[a]

8[a]. INPUTS AND REFERENCES ..... 8-1[a]
8.1[a] DOCUMENTS CITED ..... 8-1[a]
8.2[a] CODES, STANDARDS, AND REGULATIONS ..... 8-8[a]
8.3[a] DATA, LISTED BY DATA TRACKING NUMBER ..... 8-9[a]
8.4[a] PRODUCT OUTPUT DATA ..... 8-9[a]
8.5[a] SOFTWARE CODES ..... 8-9[a]

APPENDIX J[a] QUALIFICATION OF DATA AND JUSTIFICATION OF EQUATIONS ..... J-1[a]

APPENDIX K[a] IMPLICATIONS OF THE YUCCA MOUNTAIN PROBABILISTIC SEISMIC HAZARD ANALYSIS FOR EARTHQUAKE-INDUCED WATER TABLE RISE ..... K-1[a]

INTENTIONALLY LEFT BLANK

FIGURES

Page

[No modification to the parent report.]

INTENTIONALLY LEFT BLANK

TABLES

Page

[No modification to the parent report, except for the tables listed below.]

1.2.03.02.0B-2[a].	Indirect Inputs	6-2[a]
1.2.10.01.0A-1[a].	Earthquake-Induced Water Table Rise as a Function of Moment Magnitude and Vertical Extent of Faulting	6-11[a]
1.2.10.01.0A-2[a].	Direct Inputs	6-20[a]
1.2.10.01.0A-3[a].	Indirect Inputs	6-22[a]
2.1.03.04.0B-1[a].	Direct Inputs	6-27[a]
2.1.03.04.0B-2[a].	Indirect Inputs	6-27[a]
2.1.14.26.0A-1[a].	Summary of Igneous Scenario External Criticality Results	6-30[a]
2.2.06.01.0A-1[a].	Direct Inputs	6-34[a]
2.2.06.01.0A-2[a].	Indirect Inputs	6-35[a]
2.2.06.02.0A-1[a].	Direct Inputs	6-37[a]
2.2.06.02.0A-2[a].	Indirect Inputs	6-38[a]
2.2.14.12.0A-1[a].	Summary of Igneous Scenario External Criticality Results	6-43[a]
J-3[a].	Additional Direct Inputs for Appendix J[a]	J-18[a]
J-4[a].	Additional Indirect Inputs for Appendix J[a]	J-19[a]
K-1[a].	Summary of Bounding Water Table Rise Values Consistent with Seismic Source Characterization for the PSHA	K-8[a]
K-2[a].	Probabilities Associated with Source Characterization Cases Giving Bounding Water Table Rise Greater than 175 m	K-9[a]
K-3[a].	Bounding Water Table Rise for an Earthquake Displacement with a 10^{-8} Mean Annual Probability of Being Exceeded	K-11[a]

INTENTIONALLY LEFT BLANK

ACRONYMS

DIRS	Document Input Reference System
DTN	data tracking number (within the Technical Data Management System)
EBS	engineered barrier system
FEP	feature, event, or process
PSHA	probabilistic seismic hazard analysis
TSPA	total system performance assessment

INTENTIONALLY LEFT BLANK

1[a]. PURPOSE

This addendum supplements the discussion of seismically related features, events, and processes (FEPs) in *Features, Events, and Processes for the Total System Performance Assessment: Analyses* (ANL-WIS-MD-000027 REV00) ("the parent report"). The supplemental discussion establishes the consistency between exclusion screening justifications and levels of ground motion used in postclosure analyses. It also examines the consistency of seismic source characterization data and fault displacement hazard results from the probabilistic seismic hazard analysis (PSHA) for Yucca Mountain with bounding estimates of earthquake-related water table rise used in the exclusion screening justification for FEP 1.2.10.01.0A, *Hydrologic Response to Seismic Activity*. These supplemental discussions address the issue identified in Condition Report 13736.

In addition, this addendum supplements the screening justification for FEP 1.2.10.01.0A, *Hydrologic Response to Seismic Activity*, to discuss relevant literature on earthquake-related hydrologic effects that was not previously cited. This supplemental discussion, in combination with the supplemental discussions mentioned in the previous paragraph, address the issue identified in Condition Report 13839.

Supplemental discussions are provided for seismically related FEPs that are excluded from the total system performance assessment (TSPA):

- 1.2.03.02.0B, *Seismic Induced Rockfall Damages EBS Components*
- 1.2.03.02.0E, *Seismic-Induced Drift Collapse Alters In-Drift Chemistry*
- 1.2.10.01.0A, *Hydrologic Response to Seismic Activity*
- 2.2.06.01.0A, *Seismic Activity Changes Porosity and Permeability of Rock*
- 2.2.06.02.0A, *Seismic Activity Changes Porosity and Permeability of Faults*
- 2.2.06.02.0B, *Seismic Activity Changes Porosity and Permeability of Fractures*
- 2.2.06.03.0A, *Seismic Activity Alters Perched Water Zones*

Also, the screening justification for FEP 2.1.03.04.0B, *Hydride Cracking of Drip Shields*, is modified to add consideration of the initial hydrogen content of the titanium alloys discussed and to refer to "calculated hydrogen content" as "calculated hydrogen pick-up." This change is an impact resulting from resolution of the issue identified in Condition Report 13386. Justification of the change and analysis of impacted documents is found in SNL (2007 [DIRS 181339]).

For FEP 2.1.09.02.0A, *Chemical Interaction with Corrosion Products* and FEP 2.1.09.17.0A, *Formation of Pseudo-Colloids (Corrosion Product) in EBS*, the TSPA disposition is changed to clarify the sorption of plutonium and americium onto oxyhydroxide colloids is a kinetic process in the engineered barrier system (EBS). This change is an impact resulting from resolution of the issue identified in Condition Report 13644. Justification of the change and analysis of impacted documents is found in *EBS Radionuclide Transport Abstraction* (SNL 2007 [DIRS 177407]).

In addition, the screening justifications for FEP 2.1.14.26.0A, *Near-Field Criticality Resulting from an Igneous Event* and FEP 2.2.14.12.0A, *Far-Field Criticality Resulting from an Igneous Event*, are modified to update Table 2.1.14.26.0A-1 and Table 2.2.14.12.0A-1, respectively.

These changes represent an impact resulting from the resolution of the issues identified in Condition Reports 14019 and 14087. Errors were corrected in two cases in which the external accumulation model was executed. Justification of the change and analysis of impacted documents is found in SNL (2007 [DIRS 181395].

Finally, screening justifications for FEPs 1.2.07.01.0A, *Erosion/Denudation* and 2.3.01.00.0A, *Topography and Morphology*, are modified to update the citation to the *Reclamation Implementation Plan* (YMP/91-14) (DOE 2009 [DIRS 185964]). This addresses an issue associated with Condition Report 13388.

The supplemental discussions and modifications do not alter any screening decisions.

The following Condition Reports are currently open and affect the parent report, but will not be addressed in this addendum because work to resolve the related issues has not yet been completed:

- Condition Report 14133, *Incomplete descriptions of radioactive volatile components during volcanic eruption in FEP evaluations*
- Condition Report 14112, *Inconsistencies in use of control parameters in ANL-WIS-MD-000024, ANl-WIS-MD-000027, and TDR-BGR-MD-000037*
- Condition Report 14016, *Water-rock interactions not considered in the assumption of secular equilibrium for the transport of Ac-227, Ra-228, and Pb-210*

2[a]. QUALITY ASSURANCE

Development of this addendum and the supporting activities are subject to the Office of Civilian Radioactive Waste Management Quality Assurance Program *Quality Assurance Requirements and Description* (DOE 2009 [DIRS 185965]).

Preparation of this addendum is controlled by SCI-PRO-005, *Scientific Analyses and Calculations*, and other Lead Lab procedures referenced therein. Electronic management of information is controlled as described in *Technical Work Plan for the Performance Assessment Features, Events, and Processes* (TWP-WIS-MD-000036 REV03) (SNL 2007 [DIRS 184327]) and in accordance with IM-PRO-002, *Control of the Electronic Management of Information*.

INTENTIONALLY LEFT BLANK

3[a]. USE OF SOFTWARE

No qualified software was used in carrying out analyses documented in Addendum 01. Controlled unqualified software, which is exempt from software qualification in accordance with IM-PRO-003 Section 2, was used for data organization and simple calculations as documented in Appendix K[a], which includes the electronic file, *PSHA Static Stress Drops R1.xls*. All calculations were carried out using Microsoft® Excel® 2003.

INTENTIONALLY LEFT BLANK

4[a]. INPUTS

[*No modification to the parent report.*]

4.1[a] DIRECT INPUTS

For this addendum, each FEP in Section 6.2[a] and each appendix have their own table of direct inputs and indirect inputs. Direct inputs are appropriately selected and qualified for use in this report. Direct input from external data sources that are qualified for their intended use in this report are provided in Appendix J.4.2[a] CRITERIA

[*No modification to the parent report.*]

4.3[a] CODES, STANDARDS, AND REGULATIONS

[*No modification to the parent report.*]

INTENTIONALLY LEFT BLANK

5[a]. ASSUMPTIONS

[*No modification to the parent report.*]

INTENTIONALLY LEFT BLANK

6[a]. SCIENTIFIC ANALYSIS DISCUSSION

[*No modification to the parent report.*]

6.1[a] METHODS AND APPROACH

[*No modification to the parent report.*]

6.2[a] FEATURE, EVENT, AND PROCESS SCREENING ANALYSES

[*No modification to the parent report, except as indicated for the listed FEPs.*]

FEP: 1.2.03.02.0B

FEP NAME:

Seismic-Induced Rockfall Damages EBS Components

FEP DESCRIPTION:

[*No modification to the parent report.*]

SCREENING DECISION:

[*No modification to the parent report.*]

SCREENING JUSTIFICATION:

[*The following unnumbered section is added to the discussion.*]

Vibratory Ground Motion–Rockfall in the nonlithophysal lithostratigraphic units is evaluated for ground motion with a horizontal (H1) peak ground velocity (PGV) of about 40, 105, 244, and 535 cm/sec (BSC 2004 [DIRS 166107], Table 6-5). This set of PGV values is based on results of the probabilistic seismic hazard analysis (PSHA) for Yucca Mountain and ground motion site-response modeling (BSC 2004 [DIRS 170027], Table E-1). The set corresponds to ground motion hazard with mean annual probabilities of exceedance of 10^{-4}, 10^{-5}, 10^{-6}, and 10^{-7}, respectively, based on the PSHA results.

For PGV values of 105, 244, and 535 cm/sec, 17 three-component sets of time histories are developed for use in rockfall analyses (BSC 2004 [DIRS 170027], Section 6.3.2.3). Recorded strong motion records with appropriate magnitude and distance characteristics form the basis for the developed time histories. The H1 component of each set is scaled to the target PGV level (i.e., 105, 244, or 535 cm/sec) and the other components (H2, V) are scaled to maintain the inter-component variability of the original seismograms.

For a PGV value of 40 cm/sec, one set of three-component time histories was developed. As this set was primarily for preclosure analyses, a different scaling approach was implemented. A recorded strong motion record with appropriate magnitude and distance characteristics was

adjusted such that its response spectra matched the target design response spectra with a mean annual probability of exceedance of 10^{-4}.

Subsequent to the development of time histories, new findings indicated that, at low probabilities, the PSHA hazard curves are inconsistent with the geologic setting at Yucca Mountain (BSC 2005 [DIRS 170137], Section 6; SNL 2009 [DIRS 185977], Section 6.1). That is, the mean annual probability of exceedance for a given level of ground motion is too high. When the hazard curves are conditioned to take the new findings into account, a horizontal (H1) PGV of 4.07 m/sec is found to have a mean annual probability of exceedance of 10^{-8} (BSC 2005 [DIRS 170137], Section 6.8; SNL 2007 [DIRS 176828], Section 6.4.3). The mean annual probabilities of exceedance for the PGV levels associated with the time history suites used in the nonlithophysal rockfall modeling become 10^{-4}, 10^{-5}, 4.5×10^{-7}, and significantly lower than 10^{-9}. Thus, rockfall results for a horizontal PGV of 535 cm/sec are so unlikely that they need not be considered in the screening evaluation for the performance assessment. This result is taken into account in assessing the consequences of seismically induced rockfall in nonlithophysal rock units.

INPUTS:

[*Table 1.2.03.02.0B-2. is replaced with the following:*]

Table 1.2.03.02.0B-2[a]. Indirect Inputs

Citation	Title	DIRS
10 CFR 63	Energy: Disposal of High-Level Radioactive Wastes in a Geologic Repository at Yucca Mountain, Nevada	186479
70 FR 53313	Implementation of a Dose Standard After 10,000 Years	178394
BSC 2004	*Drift Degradation Analysis*	166107
BSC 2004	*Development of Earthquake Ground Motion Input for Preclosure Seismic Design and Postclosure Performance Assessment of a Geologic Repository at Yucca Mountain, NV*	170027
BSC 2005	*Peak Ground Velocities for Seismic Events at Yucca Mountain, Nevada*	170137
BSC 2004	*Creep Deformation of the Drip Shield*	174715
SNL 2007	*Seismic Consequence Abstraction*	176828
SNL 2007	*Mechanical Assessment of Degraded Waste Packages and Drip Shields Subject to Vibratory Ground Motion*	178851

FEP: 1.2.03.02.0E

FEP NAME:

Seismic-Induced Drift Collapse Alters In-Drift Chemistry

FEP DESCRIPTION:

[*No modification to the parent report.*]

SCREENING DECISION:

[*No modification to the parent report.*]

SCREENING JUSTIFICATION:

[*The second paragraph is modified as follows:*]

Although limited rockfall may occur in nonlithophysal host rock units, drift collapse is expected to occur in the lithophysal host rock units, which are characterized by lithophysal voids interconnected by intense fracturing as discussed in *Drift Degradation Analysis* (BSC 2004 [DIRS 166107], Section 6.4.1.1). Postclosure ground motion in lithophysal rock could result in substantial or complete drift collapse (SNL 2007 [DIRS 176828], Section 6.7.1). This justification assumes that seismically induced drift collapse has occurred and thus is not dependent on the level of ground motion that collapses the drift or its mean annual probability of exceedance. The seismically induced drift collapse affects the hydrologic and thermal environment in the EBS. Seepage could increase because the greater span and irregular shape of collapsed drift openings will reduce the effectiveness of the drift wall due to the capillary barrier effect (SNL 2007 [DIRS 181244], Section 6.3). The temperature of the drip shields and waste packages will increase relative to uncollapsed drifts because the drift rubble acts as an insulating blanket over the drip shield (SNL 2008 [DIRS 184433], Section 6.3.17[a]).

INPUTS:

[*No change to the parent document.*]

FEP: 1.2.07.01.0A

FEP NAME:

Erosion/Denudation

FEP DESCRIPTION:

[*No modification to the parent report.*]

SCREENING DECISION:

[*No modification to the parent report.*]

SCREENING JUSTIFICATION:

[*No modification to the parent report, except the reference citation in the first sentence of the second- to-last paragraph is changed as follows:*]

The effects of surface construction and characterization activities at the ground surface on future erosion will also be negligible because of the planned reclamation of the site ground surface. As stated in *Reclamation Implementation Plan* (DOE 2009 [DIRS 185964]), "Recontouring and erosion control practices include backfilling spoil material and grading disturbed sites, so that a stable land form is created that blends with the surrounding topography. Following site decommissioning, disturbed areas will be graded such that the natural drainage pattern (predisturbance drainage) is restored. The sites will be stabilized and recontoured to blend into the natural topography of the area."

INPUTS:

[*No modification to the parent report, except the last row of Table 1.2.07.01.0A-2 is changed as follows:*]

DOE 2009	*Reclamation Implementation Plan*	185964

FEP: 1.2.10.01.0A

FEP NAME:

Hydrologic Response to Seismic Activity

FEP DESCRIPTION:

[*No modification to the parent report.*]

SCREENING DECISION:

[*No modification to the parent report.*]

SCREENING JUSTIFICATION:

[*The Screening Justification is replaced by the following paragraphs:*]

The potential effects of seismic activity on the geology and hydrology of Yucca Mountain are considered under a series of FEPs. This FEP addresses potential effects of seismic activity on the elevation of the water table, on the large hydraulic gradient that exists to the north of the repository, and on ground water chemistry. Potential effects of seismic activity on flow and transport caused by changes in the properties of the rock matrix, faults, and fractures are considered separately under FEPs 2.2.06.01.0A, *Seismic Activity Changes Porosity and Permeability of Rock*, 2.2.06.02.0A, *Seismic Activity Changes Porosity and Permeability of Faults*, and 2.2.06.02.0B, *Seismic Activity Changes Porosity and Permeability of Fractures*, respectively. Potential effects of earthquake-induced drift collapse on flow and transport through emplacement drifts are assessed under FEP 1.2.03.02.0D, *Seismic-Induced Drift Collapse Alters In-Drift Thermohydrology*.

Seismic Effects on Water Table Elevation

Seismic effects on water table elevation fall into two categories (e.g., Montgomery and Manga 2003 [DIRS 186262]): transient and sustained. The transient response is due to the passage of seismic waves and has a duration of minutes. Sustained responses can arise from volumetric strain in the rock, changes in permeability, or compaction of unconsolidated deposits. These responses typically have durations of months and dissipate primarily by the lateral flow of groundwater from areas with a higher water table elevation to the surrounding areas with a lower water table elevation. Both of these responses are short-lived in comparison to the 10,000- and 1,000,000-year compliance periods relevant to the performance assessment of the Yucca Mountain repository.

The significance of a rise in the water table is that it reduces the contribution to the barrier capability of the unsaturated zone by shortening the flow path from the repository to the saturated zone. Conceptually, an earthquake-induced water table rise could eliminate the gap between the water table and emplacement drifts and thereby alter the in-drift environment.

Within the repository footprint, the present-day water table varies from around 730 m above mean sea level in the south to less than 850 m above mean sea level in the north (BSC 2004 [DIRS 169855], Figure 6-2). The repository elevation for emplacement drifts ranges between 1,037 m above mean sea level in the north (BSC 2007 [DIRS 179640], Table 14) and 1,105 m above mean sea level in the south (BSC 2007 [DIRS 179640], Table 12), indicating that the present-day water table depth below the repository horizon ranges from 187 m in the north, based on a repository elevation of 1,037 m and water table elevation of 850 m, to 375 m in the south, based on a repository elevation of 1,105 m and water table elevation of 730 m. For future, wetter climates, the elevation of the water table is taken to have a uniform value of 850 m. Thus, if earthquake-induced water table rise is less the minimum 187 m distance between the elevation of the water table and the lowest elevation of a waste emplacement drift, this effect can be excluded from the TSPA.

Szymanski (1989 [DIRS 106963]) proposed that earthquake-related changes in stress could affect fracture apertures, restricting the ability of water to drain from the Yucca Mountain site and causing a change in the heat-flow regime. He hypothesized that the combined effect of these changes would lead to a rise in the elevation of the water table. Veins of calcium carbonate and silica observed in local faults were interpreted as evidence of past elevated water tables supporting the hypothesis.

To obtain an independent assessment of the hypothesis, DOE asked the National Academy of Sciences' National Research Council to evaluate if the water table at Yucca Mountain had been raised in the geologically recent past to the level of the proposed repository and if such a water table rise was likely to occur within the next 10,000 years. To this end, the National Research Council established the Panel on Coupled Hydrologic/Tectonic/Hydrothermal Systems at Yucca Mountain, Nevada ("the Panel").

The Panel considered two models of earthquake-related water table rise: a dislocation model and a regional stress change model (National Research Council 1992 [DIRS 105162], Chapter 5). Analyses using the dislocation model approach were carried out by Carrigan et al. (1991 [DIRS 100967]) and Bredehoeft (1992 [DIRS 101122]). For typical Basin and Range earthquakes (normal faulting with 1-m slip), Carrigan et al. (1991 [DIRS 100967]) used a two-dimensional model and found the increase in water table elevation was 2 to 3 m for different combinations of elastic properties and aquifer thickness. Extrapolating their results to larger slip values, they found that for a 4-m slip earthquake a water table rise of 17 m was predicted. For a fault-patch model that produced greater strains and stresses, water table rise ranged from 6 to 12 m for different permeability assumptions. Bredehoeft (1992 [DIRS 101122]) used a three-dimensional model to analyze a normal faulting earthquake with 1 m slip whose rupture was 30-km long and extended at a 60-degree dip to a depth of 10 km. For this case, Bredehoeft found that the head change produced by the earthquake was quickly dissipated by local flow. The impact on the water table elevation was a rise on the order of 1 m.

The Panel focused its attention on the regional stress change model because it resulted in a larger earthquake-induced water table rise. The Panel expanded on work by Kemeny and Cook (1990 [DIRS 129658], 1992 [DIRS 100989]) who developed a simple representation of the poroelastic response of the earth's crust to a regional change in stress caused by a normal-faulting earthquake and the consequent effect on the elevation of the water table. In the Kemeny and

Cook representation, the earthquake causes a regional increase in volumetric strain that reduces the pore volume, increasing pore pressure, and resulting in water moving upward to fill pore space above the elevation of the preexisting water table. To create a simple representation that bounds the amount of water table rise, conservative assumptions are made. These assumptions include (Kemeny and Cook 1990 [DIRS 129658], Section 5.3.2):

- All water displaced from the volume due to coseismic stress change goes up the stratigraphic column instantaneously.

- The coseismic volumetric stress change following a normal-faulting earthquake is compressional, uniform with depth, and extends over the vertical extent of faulting.

The first assumption results in immediately propagating the fluid volume displaced from the rock by compression to the water table. It thus gives an upper bound on the water level change. Factors that will reduce the amplitude of the change include time-dependent flow, flow directions other than upward, and impermeable beds. While water level changes can occur rapidly in open boreholes intersecting areas of compressed or dilated rock following poroelastic deformation due to an earthquake, the propagation of these changes to the water table is much less pronounced. Essentially, the excess pore pressure would be dissipated in the more permeable rock units and is not propagated vertically through aquitards and low permeability stratigraphic units to the water table surface.

The second assumption results in displacement of water throughout the volume of rock in the vicinity of the fault. This is conservative because evidence now shows that observed deformations associated with earthquake fault displacements are not uniformly compressive, but rather include areas that undergo dilation (thus potentially lowering the observed water level for any wells intersecting these zones) and others that undergo compression (thus potentially raising the observed water level for any wells intersecting these zones). That is, coseismic poroelastic strains are not uniformly compressive and do not appear to be constant with depth, but instead have a three-dimensional pattern consistent with a dislocation model of fault displacement.

Using the regional stress change approach and conservative assumptions, Kemeny and Cook obtain a simple mechanical model relating water table rise to the static stress drop associated with an earthquake and the vertical extent of faulting:

$$\Delta w = (1.2 \times 10^{-5}) \times \Delta\sigma_{static} \times h$$

in which Δw is water table rise in meters, $\Delta\sigma_{static}$ is static stress drop in bars, and h is depth of faulting in meters. For a static stress drop of 100 bars and a 10 km vertical extent of faulting, the Kemeny and Cook model gives a bounding water table rise of about 10 m (National Research Council 1992 [DIRS 105162], p. 114). The National Research Council used a similar model and looked at the sensitivity to alternate rock and hydrologic properties. Based on their results and the other information available to them (e.g., results from the dislocation models), the Panel concluded that "only a modest rise in the water table of less than 50 m is likely to occur as the result of a nearby earthquake."

The Panel considered a static stress drop of 100 bars as a reasonable upper value to assess the potential for water table rise during a 10,000-year performance period. Other seismic work for Yucca Mountain implies that larger static stress drops are possible for earthquakes near the site. Seismic source characterization and fault displacement hazard results from the probabilistic seismic hazard analysis (PSHA) for Yucca Mountain can be interpreted in terms of static stress drop. In addition, the stress parameter associated with the point-source stochastic ground motion model that is used in one approach to characterize extreme ground motions at Yucca Mountain can be related to static stress drop in a general sense.

Implications of PSHA Results. Seismic source characterization carried out by six expert teams as part of the PSHA for Yucca Mountain (DTN: MO0401MWDRPSHA.000 [DIRS 185267]) contains information on the geometry and maximum magnitudes of fault sources contributing to the ground motion hazard at the site. This information can be used to infer a static stress drop for the maximum magnitude earthquake and the consequent bounding water table rise determined using the Kemeny and Cook model (Appendix K[a]). For 3139 out of the 3150 fault characterization cases developed as part of the PSHA, the calculated water table rise is less than the 187 m distance between the elevation of the water table and the lowest waste emplacement drift. This observation is independent of the probability that a given case represents the actual geologic conditions at Yucca Mountain. When seismic source characterization probabilities are taken into account along with the rate of occurrence of M_{max} events, it is determined that 7 of the 11 cases for which calculated water table rise exceeds 187 m have probabilities more than an order of magnitude less than 10^{-8}. Thus, for the Kemeny and Cook model only four cases resulting in a calculated water table rise exceeding 187 m have probabilities greater than 10^{-8}. Taking into account the intentional bounding nature of the Kemeny and Cook model (e.g., conservative assumptions that poroelastic deformation is everywhere compressional and that all displaced water instantaneously moves vertically), the results support exclusion of seismically induced water table rise from the TSPA.

Fault displacement hazard results from the PSHA (DTN: MO0401MWDRPSHA.000 [DIRS 185267]) also demonstrate that seismically induced water table rise can be excluded from the TSPA (Appendix K[a]). For the fault sites and conditions evaluated in the PSHA, the Solitario Canyon fault has the greatest displacement hazard. For a mean annual probability of exceedance of 10^{-8}, the fault displacement hazard is about 1300 cm. Using this value as the average displacement on the Solitario Canyon and Paintbrush Canyon faults, static stress drop can be calculated using the fault geometry data from the PSHA seismic source characterization. Cases for the Solitario Canyon and Paintbrush Canyon faults alone, and in combination with other faults, give a maximum bounding water table rise of 122 m. Thus, calculated earthquake-induced water table rise using this approach maintains a gap of 65 m or more between the elevation of the water table and the lowest waste emplacement drift.

Implications of Extreme Ground Motion Conditioning. The point-source ground motion model is used to characterize extreme ground at Yucca Mountain, given a probability distribution for extreme stress parameter (point-source stress drop) (SNL 2009 [DIRS 185977], Section 6, Appendix A). To examine the implications of this analysis for potential earthquake-induced water table rise, the relation between stress parameter and static stress drop is required.

Static stress drop for a circular rupture is given by (Kanamori and Anderson 1975 [DIRS 182963]):

$$\Delta\sigma_{static} = \frac{7}{16}\frac{M_0}{a^3} \quad \text{(Eq. 1[a])}$$

in which M_0 is the earthquake moment and a the radius of the circular rupture. For a rectangular rupture expressed in terms of length (L) and width (W), an equivalent radius can be expressed as:

$$a^2 = \frac{L \times W}{\pi} \quad \text{(Eq. 2[a])}$$

The linkage between the static stress drop and the stress parameter is through the effects of source finiteness. The omega-squared (frequency-squared) source model is a widely accepted way to describe the frequency dependence of earthquake ground motion (Aki and Richards 1980 [DIRS 150723], Section 14.1). For a rectangular rupture, the frequency-squared dependence of the far field source model is due to the combination of a finite rupture length and associated duration of rupture, as well as a finite time for the slip to attain its maximum value along the rupture (rise time). For the circular rupture model of Brune, the frequency-squared dependence is due to the rupture finiteness alone; slip being theoretically instantaneous at all points on the rupture surface (Brune 1970 [DIRS 103315], 1971 [DIRS 131516]). Since the rise time is much shorter than the rupture duration (Heaton 1990 [DIRS 186296]), it is neglected in this model and the characteristic source duration (τ) is simply the time required to propagate from the center of the circular rupture to the edge:

$$\tau = \frac{a}{V_R} \quad \text{(Eq. 3[a])}$$

in which V_R is the rupture velocity and a the source radius, which can be replaced by L for length in a rectangular rupture. The characteristic duration gives rise to the corner frequency (f_C) in the omega-squared model:

$$f_C \propto \frac{1}{\tau} \propto \frac{V_R}{L} \quad \text{(Eq. 4[a])}$$

The static stress drop for a general source is given by:

$$\Delta\sigma_{static} = C\,\mu\,\frac{\bar{u}}{L} \quad \text{(Eq. 5[a])}$$

in which C is a geometric constant (7/16 for a circular rupture), μ is the shear modulus, and $\left(\frac{\bar{u}}{L}\right)$ is the strain drop (average slip ($\bar{u}$) over the characteristic dimension of the rupture (L)). Substituting the definition of moment:

$$M_0 = \mu\,\bar{u}L^2 \quad \text{(Eq. 6[a])}$$

in which (L^2) is a characteristic rupture area, into Equation 5[a] results in:

$$\Delta\sigma_{static} = C\,\frac{M_0}{L^3} \quad \text{(Eq. 7[a])}$$

and from Equation 4[a]:

$$\Delta\sigma_{static} = C\ M_0\ \left(\frac{f_C}{V_R}\right)^3 \quad \text{(Eq. 8[a])}$$

Static stress drop, therefore, shows the same functional dependence on M_0 and f_C as does stress parameter ($\Delta\sigma_{SP}$) (Silva et al. 1996 [DIRS 110474], Section 2.2):

$$\Delta\sigma_{SP} = 8.44\ M_0\ \left(\frac{f_C}{\beta}\right)^3 \quad \text{(Eq. 9[a])}$$

Although theoretically linked, static stress drop and stress parameter show a lack of correlation on an individual earthquake basis. Also, they differ in their relation to strong ground motion. Strong ground motion is correlated to stress parameter, which is related to the dynamics of fault rupture. Static stress drop shows a poor correlation to strong ground motion. For this FEP evaluation, the value of static stress drop is taken as equal to the value of stress parameter.

In the point-source modeling to characterize extreme ground motion at Yucca Mountain, a probability distribution was defined for an extreme stress parameter. The extreme stress parameter is the largest stress parameter consistent with the geologic and tectonic setting of Yucca Mountain. In considering the extreme-stress-drop distribution in this screening evaluation, first its probability of exceedance must be addressed. The likelihood of an extreme-stress-drop earthquake can be evaluated in terms of two components: (1) the earthquake recurrence frequency for local faults at Yucca Mountain and (2) the observed distribution of earthquake stress parameters.

As part of the PSHA for Yucca Mountain, a recurrence relation was developed for aggregated local fault sources for the combined interpretations of all the seismic source characterization teams (CRWMS M&O 1998 [DIRS 103731], Figure 4-74). In characterizing local fault sources, each team addressed faults within about 20 km of Yucca Mountain (CRWMS M&O 1998 [DIRS 103731], Appendix E). Thus, this recurrence relation includes contributions from the Solitario Canyon, Windy Wash, Bow Ridge, Paintbrush Canyon, Stagecoach Road, Bare Mountain, and other local faults. For moment magnitudes of 6.0 and 6.5, consistent with events considered in the extreme-stress-drop approach to ground motion conditioning, the mean annual frequencies from this aggregate recurrence relation are approximately 1.3×10^{-4} and 5.0×10^{-5}, respectively.

For the observed distribution of earthquake stress parameters, a lognormal distribution with a median value of 30 bars and a lognormal standard deviation of 0.6 is used. The median value of 30 bars for point-source stress parameter is consistent with a static stress drop of about 30 bars that, for a circular fault rupture, is implied by the moment magnitude-rupture area relations of Wells and Coppersmith (1994 [DIRS 107201], Table 2A). Taking static stress drop as lognormally distributed, a median value of about 30 bars for static stress drop is also obtained using the database of earthquake information developed for the Next Generation of Ground-Motion Attenuation Models (NGA) project (public version 7.3, 02-14-06, http://peer.berkeley.edu/nga/flatfile.html) (Chiou et al. 2008 [DIRS 186319]).

Considering a median stress parameter of 30 bars with a lognormal standard deviation of 0.6, the values used to represent the probability distribution for extreme stress parameter (i.e., 150, 400, and 1100 bars; SNL 2009 [DIRS 185977], Section 5.4) have probabilities of exceedance of about 4×10^{-3}, 8×10^{-6}, and 10^{-9}, respectively. As an extreme-stress-parameter earthquake is conditional on an earthquake occurring, using the recurrence data for an M 6.5 earthquake on a local fault ($5.0 \times 10^{-5)}$ gives combined annual probabilities of exceedance of about 2×10^{-7}, 4×10^{-10}, and 5×10^{-14}, respectively. Thus, the median (400 bars) and high (1100 bars) values used to represent the extreme-stress-parameter distribution have probabilities of exceedance lower than need to be considered for FEP evaluation. Using the same distribution parameters (30 bars, lognormal standard deviation of 0.6), a stress parameter of about 250 bars, conditional on an earthquake occurring on a local fault, has a probability of exceedance of about 10^{-8}. Adopting an equivalency between the value of stress parameter and static stress drop, 250 bars is the static stress drop that needs to be considered in evaluating earthquake-induced water table rise. For the Kemeny and Cook model, using a value of 250 bars for static stress drop and 12 km for the vertical extent of faulting gives a bounding water table rise of 36 m.

In addition to maximum magnitude events, smaller, more frequent earthquakes may also affect the water table elevation. Assuming the smaller **M** earthquakes on local faults in the vicinity of Yucca Mountain affect the water table at the site, point-source stress parameters are determined based on a lognormal distribution with a median of 30 bars and a lognormal standard deviation of 0.6, such that, when combined with the aggregate recurrence rate for a given **M** for local faults, the combined probability of exceedance is about equal to or less than 10^{-8}. For this evaluation, the vertical extent of rupture is computed from an empirical relation between the logarithm of rupture width and moment magnitude (Wells and Coppersmith 1994 [DIRS 107201], Table 2A). The Wells and Coppersmith regression based on normal faulting events is used. A fault dip of 60 degrees is assumed to convert down-dip rupture width to vertical extent of rupture. Results are summarized in Table 1.2.10.01.0A-1[a].

Table 1.2.10.01.0A-1[a]. Earthquake-Induced Water Table Rise as a Function of Moment Magnitude and Vertical Extent of Faulting

Moment Magnitude	Annual Frequency[a]	Point-Source Stress Parameter with a Probability of Exceedance of 10^{-8} (bars)[b]	Static Stress Drop with a Probability of Exceedance of 10^{-8} (bars)[c]	Vertical Extent of Faulting (km)[d]	Water Table Rise (m)
5.50	4.0×10^{-4}	350	350	5	21
6.00	1.3×10^{-4}	290	290	8	28
6.50	5.0×10^{-5}	250	250	12	36
6.75	2.0×10^{-5}	220	220	14	37
7.00	5.0×10^{-6}	170	170	15	31

[a] Annual Frequency is for local faults in the vicinity of Yucca Mountain and is determined from CRWMS M&O 1998 [DIRS 103731], Figure 4-74.

[b] Point-source stress parameter with a probability of exceedance of 10^{-8} is determined using a lognormal distribution with a median of 30 bars and a lognormal standard deviation of 0.6.

[c] Static Stress Drop is taken as equal to the value of point-source stress parameter that has about an 10^{-8} mean annual probability of exceedance.

[d] Vertical Extent of Faulting is computed using the Wells and Coppersmith 1994 [DIRS 107201], Table 2A empirical relation between the logarithm of rupture width (RW) in kilometers and moment magnitude (**M**). The relation based on normal faulting events is used: log (RW) = −1.14 + 0.35 **M**. A fault dip of 60 degrees is used to compute vertical extent of faulting from down-dip rupture width.

Based on the above evaluation, earthquake-induced water table rise consistent with stress parameters having a mean annual probability of exceedance greater than 10^{-8} is about 40 m or less. A rise of the water table by this amount leaves a distance of about 147 m between the water table and the emplacement drift with the lowest elevation. This result supports exclusion of earthquake-induced water table rise from the TSPA.

Observations of Hydrologic Response to Seismic Activity Since the National Research Council Evaluation. A review of literature since 1992 indicates that dislocation model predictions of strain caused by fault displacement during earthquakes can reasonably explain observations of zones of bulk rock compression and dilation. In addition, this same research indicates that water levels in wells within the zones of compression tend to rise while water levels in wells within zones of dilation tend to fall, as expected given the poroelastic theory, although exceptions to this observation are known and reflect the many competing factors that affect the direction of water level change at any particular well in an area. Literature evaluating coseismic poroelastic deformation and associated water level changes are summarized by Roeloffs (1996 [DIRS 186290]) and Manga and Wang (2007 [DIRS 186289]). Representative cases are briefly described below.

Earthquakes in June 2000 along two right-lateral strike-slip faults in southern Iceland exhibit coseismic deformation consistent with a dislocation model, with upward ground movement associated with coseismic extension zones northeast and southwest of the fault and downward ground movement associated with coseismic compression zones northwest and southeast of the fault (Jonsson et al 2003 [DIRS 186291], Figure 2). In addition, predicted coseismic pore-pressure response was shown to reasonably reproduce the observed water level changes in nearby geothermal wells, with areas of water level rise being associated with zones of compression and water level decline being associated with zones of dilation (Jonsson et al. 2003 [DIRS 186291], Figure 3).

A fault model of coseismic strain associated with fault displacement was shown to reasonably correlate to observed groundwater level changes associated with the 2003 Tokachi-oki earthquake. Water level changes in wells in areas of predicted dilation were observed to decrease, while water level changes in wells in areas of predicted contraction were observed to generally increase (Sato et al. 2004 [DIRS 186293], Figure 1).

Observations of step-like coseismic groundwater level changes in confined aquifers were also explained as the poroelastic response to static strains caused by the 1994 earthquake near Parkfield, California (Quilty and Roeloffs 1997 [DIRS 186478]). These authors concluded that the strains predicted by a dislocation model of the rupture were in good agreement with the changes in most of the wells.

Similarly, in an analysis of water level responses following an earthquake at Roermond, Netherlands, it was observed that the water-level response was in general agreement with the expected poroelastic response to volume strains (compression or dilation) predicted by a dislocation model of the event, with 16 of 19 wells with rising water levels corresponding to areas of compression and 7 of 9 wells with water level drops corresponding to areas of dilation,

although the magnitudes and durations were larger than expected (Grecksch et al. 1999 [DIRS 186477]).

The above examples indicate that, since the completion of the National Research Council panel report, scientific evidence supports the conclusion that poroelastic strains induced by faulting are reasonably predicted using a dislocation model. The strains are spatially variable and can be either compression or dilation of the rock mass associated with the event. The strains predicted from a dislocation model are able, in many cases, to explain observed water level responses in confined aquifers.

Earthquake-induced Response of Groundwater Level in Wells versus Response of Water Table Elevation. Observations of water level responses that are interpreted to result from earthquake-induced poroelastic deformation generally are from open boreholes where these water level responses reflect the change in pore pressure associated with the deformation. Groundwater level changes may be associated with changes in hydraulic head when the well is open to a confined aquifer(s) or to water table elevation changes when the well is open to an unconfined aquifer. When wells are open to multiple aquifers, the water level in the well will be controlled by the hydraulic head in the most transmissive unit(s) intersecting the well.

Observed water level responses discussed above are generally for confined aquifers. Although researchers have not focused on water level responses in comparison to water table responses, the available information supports the conclusion that water table responses are generally much less (in several cases an order of magnitude less) than water level responses.

Coseismic water level responses in wells completed in confined aquifers following the 1999 **M** 7.5 Chi-Chi earthquake in Taiwan were observed to range from less than 1 m to more than 5 m, while water level changes in the uppermost unconfined aquifer were shown to be much smaller (ranging from 0 to 0.5 m) (Manga and Wang 2007 [DIRS 186289], p. 302). In addition, most of the observed water level changes in wells completed in confined aquifers following the 2003 Tokachi-oki **M** 8.0 earthquake in Japan could be explained by the poroelastic response and volumetric strain derived from a fault dislocation model, while an earlier earthquake in the same area had responses that could not be explained by poroelastic response because it included responses of unconfined aquifers, which are not highly sensitive to volumetric strain changes (Koizumi et al. 2005 [DIRS 186295]).

The reason for the greater amplitude of response of the water level in confined aquifers is the result of the smaller storativity of confined aquifers. Considering a given poroelastic compression with the resultant volume of water released per unit surface area of the aquifer, the smaller storativity of the confined aquifer will result in a higher water level rise in boreholes that are open to the confined aquifer. In the vicinity of Yucca Mountain, the Death Valley Regional Groundwater Flow Model has estimated the specific storage of confined aquifers of between 10^{-7} and 10^{-4} m^{-1} and a specific yield of unconfined aquifers of about 0.1 (Belcher 2004 [DIRS 173179], Figure F-38). Considering confined aquifer thicknesses of about 10^{2} m implies a storativity of between about 10^{-5} and 10^{-2}, a factor of 10^{4} to 10^{1} less than the specific yield of the unconfined aquifers. Therefore, an earthquake capable of causing a water level rise of 10 m in the confined aquifers at Yucca Mountain would be expected to cause only a 1.0 to 0.001 m rise in the water table.

The distinction between water level rise and water table rise becomes relevant when confining units separate the aquifers. If there are no confining units, the water table response will be equal to the water level response to the poroelastic deformation, although the time it takes to propagate from the deeper zones to shallower water table is a function of the vertical hydraulic diffusivity of the rock mass (Roeloffs 1996 [DIRS 186290], p. 167). Kemeny and Cook (1990 [DIRS 129658], 1992 [DIRS 100989]), in reducing the coupled hydro-mechanical response to a simplified mechanical representation, assumed no confining units and that hydraulic head changes at depth instantaneously propagated to water table elevation changes. In assuming there were no confining units, Kemeny and Cook (1992 [DIRS 100989]) effectively assumed that the water volume released by the compression of the entire saturated thickness of rock (about 10,000 m) became available for raising the water table. While this assumption is consistent with development of a bounding model, observations of water level and water table elevation changes noted above, combined with the known confining units in the saturated zone in the vicinity of Yucca Mountain, indicate this assumption results in an overestimation of realistic water table rise values.

Possible Earthquake-Induced Water Table Fluctuations in the Vicinity of Yucca Mountain. The historical record of water table elevations in the vicinity of Yucca Mountain shows no evidence of past significant rises in the water table associated with seismic events. The observed indicators of previous higher water table elevations and spring discharge elevations are very well correlated with times of previous wetter climates; there is no indication of higher water levels that cannot be reasonably explained by the local effects of a wetter climate. However, water table rises associated with poroelastic deformation due to fault displacement are generally short lived (time periods of months), so observations of such water table rises would not be expected in the geologic record.

Large excursions in the water table resulting from earthquakes in the geologic past could have left evidence of their occurrence in the form of secondary mineral veins. However, multiple lines of evidence from shallow vein minerals and from the deeper unsaturated zone do not indicate that such minerals precipitated from upwelling groundwater from the saturated zone.

There is no evidence from the isotopic geochemistry of shallow calcite veins for large-scale rise in the water table near Yucca Mountain in the geologic past. Stable isotopes of carbon and oxygen from groundwater and calcite veins at Trench 14 and Busted Butte indicate that the calcite could not have precipitated from saturated zone groundwater (National Research Council 1992 [DIRS 105162], Appendix A). Overlap in the carbon and oxygen isotopic compositions of vein calcites and calcite from soils suggest that shallow vein calcites are pedogenic in origin and precipitated from downward percolating infiltration. Differences in the uranium activity ratios in groundwater and shallow calcite veins also preclude upwelling groundwater as the source of these calcite veins. Similarly, discrepancies in the strontium isotopic composition of groundwater and the shallow calcite veins show that this calcite did not precipitate from groundwater in the saturated zone (National Research Council 1992 [DIRS 105162], Appendix A). The National Research Council study concluded (National Research Council 1992 [DIRS 105162], p. 134):

> …the isotopic evidence now available indicates that no prolonged excursion of the water table above its present level has occurred in the last ca. 100 ka.

There is also no evidence of upwelling groundwater from the saturated zone, for at least the last several million years, based on the stable isotopic geochemistry, fluid inclusions, and texture/morphology of secondary calcite and silica from the Exploratory Studies Facility. The carbon and oxygen isotopic compositions of late-stage calcite from the unsaturated zone show little overlap with the range of compositions that could have formed by precipitation from groundwater in the upper saturated zone (National Research Council 1992 [DIRS 105162], Appendix A). Temperatures at the repository horizon have not been impacted by upward flow of warmer groundwater from the saturated zone over the past several million years. Data from fluid inclusion assemblages and integrated uranium-lead age dating from secondary minerals indicate that ambient temperatures have prevailed for approximately the past two to five millions years (Wilson et al. 2003 [DIRS 163589]; Whelan et al. 2008 [DIRS 185452]). Textural and physical evidence indicate that secondary calcite and opal coatings formed under unsaturated flow conditions with slow, uniform growth rates (Paces et al. 2001 [DIRS 156507]).

Observed Earthquake-induced Water Level fluctuations in the Vicinity of Yucca Mountain. Water levels in wells in the vicinity of Yucca Mountain have been observed to change due to coseismic deformation (compression or dilation) associated with nearby earthquakes. Of principal note are the water level responses observed following the June 1992 earthquakes at Landers, California (a **M** 7.6 earthquake that occurred on June 28, 1992, about 300 km southwest of Yucca Mountain), Big Bear Lake, California (a **M** 6.6 earthquake that also occurred on June 28, 1992, about 300 km southwest of Yucca Mountain) and Little Skull Mountain, Nevada (a **M** 5.6 earthquake that occurred on June 29, 1992, about 23 km from Yucca Mountain), and the October 1999 earthquake at Hector Mine, California (a **M** 7.1 about 20 km to the northeast of the Landers earthquake). Short-term fluid pressure oscillations in wells USW H-5 and H-6 associated with the passing seismic waves of the June 1992 earthquakes are illustrated and discussed by O'Brien (1993 [DIRS 101276]; DTN: GS930108312312.003 [DIRS 171974]). In addition, water level offsets, believed to be due to poroelastic deformation of the rock mass, in wells UE-25p#1 and USW H-3 are illustrated in the report by O'Brien (1993 [DIRS 101276]), with a decline of about 50 cm in UE-25p#1 (completed in the confined lower carbonate aquifer) and an increase of 28 cm in USW H-3 (completed in a confined tuff aquifer). The location of these and other observation wells discussed below are identified in *Water-Level Data Analysis for the Saturated Zone Site-Scale Flow and Transport Model* (BSC 2004 [DIRS 170009], Figure 1-2). Similar water level offset observations are observed for well AD-4a (with a water level rise of about 3 ft for the Landers/Little Skull Mountain earthquakes and also about 3 ft for the Hector Mine earthquake). In addition, analyses of water level changes at Devils Hole indicate about a 0.1 to 0.04 m decline following the Landers/Little Skull Mountain and Hector Mine earthquakes, respectively (Cutillo and Ge 2006 [DIRS 186288], Figure 3).

With the exception of the above Devils Hole observations (which indicate a decline in the water table surface following the earthquake), the other observations of water level fluctuations are within confined aquifers. Due to the low storativity of the confined aquifers, it is expected that observation wells, piezometers, or pressure transducers that are measuring water level changes in these confined aquifers would represent a change that is not reflective of the change in the water

table surface, due to the large specific yield of the water table aquifer. To evaluate this, the National Water Information System of the U.S. Geological Survey database of groundwater levels in the vicinity of Yucca Mountain was searched for wells with recorded water levels around the time preceding and immediately following the June 1992 earthquakes. The following observation wells, which are wells that intercept the water table, indicate no discernible change due to these earthquakes: UE-25 WT-17, UE-25 WT-16, USW WT-10, UE-25 WT-14, UE-25 WT-13, USW WT-7, USW WT-1, J-13, and J-12. Well UE-25 WT-4 had about a 1 ft water level increase that quickly dissipated and may even have been an anomalous reading as the data are indicated as being provisional and subject to revision. Well UE-25 WT-6 had about a 3.5 ft increase followed by a decline over about 3 months to a water level that is about 2 ft below the static level before the earthquake. The anomalous behavior at well UE-25 WT-6 may be due to vertical and lateral confinement of this zone which is completed in the low permeability confining unit. Regardless of the explanation of the anomalous behavior at well UE-25 WT-6, the water table response is significantly less than the response in confined aquifers in the area due to the same seismic event. This observation is expected and is consistent with the larger storage in the unconfined aquifers as opposed to the low storativity in the confined aquifers. It reinforces the previously noted general observations that water level responses of the water table are much less than the water level response in wells or piezometers open to confined aquifers.

Implications of Recent Observations of Earthquake-induced Hydrologic Response on the Conclusions of the National Research Council. Based on a review of observed coseismic water level and water table responses, it is concluded that the regional stress change model developed by Kemeny and Cook (1990 [DIRS 129658], 1992 [DIRS 100989]) and adopted by the National Research Council (1992 [DIRS 105162], Chapter 5), while bounding, results in a significant overestimation of the potential rise in the water table associated with earthquakes affecting Yucca Mountain. In particular, there are two principal areas in which the model is unrealistic and inconsistent with the expected water table response following an earthquake:

- The regional stress change model treats strains from normal faulting in an extensional tectonic regime as resulting in a uniform increase in compressive stress throughout the affected volume of rock. Observations since the model was developed and used by Kemeny and Cook and the National Research Council indicate that strains vary spatially and are well predicted by the dislocation model. Predictions of water table rise based on the regional stress change model, therefore, are overestimated, in part because of the unrealistic characterization of earthquake-induced strain.

- Water table response due to the earthquake-induced uniform compressive strain assumed in the regional stress change model is assumed to lead to uniform pore pressure changes that are immediately propagated vertically through the hydrostratigraphic column with a resultant immediate displacement of the water table surface into the available empty pore space above the water table. In addition to ignoring flow in directions other than vertical, which would result from a more realistic characterization of earthquake-induced strains, this assumption also leads to overestimation of water table rise by not taking into account the effect of confining units, which are known to exist in the Yucca Mountain vicinity.

As a result, estimates of potential water table rises based on the Kemeny and Cook regional stress change model, while bounding, significantly overstate the potential and amplitude of a

seismically induced water table rise. In light of this conclusion, the results of the National Research Council Panel, analyses of water-table-rise implications from PSHA results and extreme ground motion conditioning, and observed earthquake-induced hydrologic responses, both in the vicinity of Yucca Mountain and worldwide, support a screening decision to exclude FEP 1.2.10.01.0A (Hydrologic Response to Seismic Activity), from the TSPA.

Additional Modeling since the National Research Council Evaluation. Gauthier et al. (1996 [DIRS 100447], pp. 163 to 164) expanded on the work of Carrigan et al. (1991 [DIRS 100967]) and Bredehoeft (1992 [DIRS 101122]) using the dislocation model. For the flow part of the problem, they used a dual-permeability formulation involving both fracture and matrix flow. They considered three different fault types: normal, listric, and strike-slip. For all three fault types, an earthquake with a 1-m displacement and 30-km rupture length was modeled. For the normal and strike-slip cases, the vertical extent of faulting was 10 km; for the listric case the vertical extent of faulting was 2 km. The greatest response was found for the strike-slip case in which complete saturation of fractures occurs within 1 hour to an elevation of 50 m above the steady-state water table, but drops to 10% saturation after 20 hr. Matrix saturations change little. Smaller rises were obtained for the normal- and listric-faulting cases. The simulated system returned to steady-state conditions within six months.

Seismic Effects on the Large Hydraulic Gradient North of the Repository

Another aspect of the water table rise issue concerns the large hydraulic gradient of up to 0.13 just to the north of the repository (SNL 2007 [DIRS 177391], Section 6.3.1.4). The water table elevation increases from south to north as one moves away from the repository. If this gradient were to migrate southward, the resulting water table below the repository could be much higher than present-day conditions.

Davies and Archambeau (1997 [DIRS 103180], p. 28) hypothesize that the large hydraulic gradient is a result of residual stress effects in the rock induced by the Timber Mountain caldera. Furthermore, the authors suggest that moderate earthquakes in this area could induce a sufficient change in geomechanical strain downstream of the current large hydraulic gradient to induce a similar gradient downstream of the repository. This would result in a large (150 m to 250 m) rise in the water table beneath the repository. However, the hypothesized residual stress effects of the 10-Ma Timber Mountain caldera are inconsistent with stress measurements at Yucca Mountain that show consistency with stress indicators elsewhere at the Nevada Test Site (Stock et al. 1985 [DIRS 101027], Stock and Healy 1988 [DIRS 101022]). Stress indicators for the Nevada Test Site are derived from hydraulic fracturing, overcoring, earthquake focal mechanisms, borehole breakouts, orientations of explosion-produced fractures, and study of Quaternary faults and cinder-cone alignments (Stock et al. 1985 [DIRS 101027], Tables 1 and 3, Figure 11; Stock and Healy 1988 [DIRS 101022], Table 6-1). These studies show a reasonably uniform direction of extension between northwest and west, with a mixed potential-slip regime of normal faulting (mainly for shallow indicators) and strike-slip faulting (mainly for deep indicators). Also, stress measurements in borehole USW G-2, north of the gradient, are within the same (“combined normal and strike-slip”) faulting regime as that indicated by the results from the three holes south of the large gradient (USW G-1, USW G-3, and UE-25 p#1). Based on the stress measurements in the four holes, the tendency for strike-slip faulting is greatest in

the southeastern hole, UE-25 p#1, not in the northern Yucca Mountain area where USW G-2 is located, as Davies and Archambeau (1997 [DIRS 103180]) propose.

Stress measurements are also available from the ESF. Results from hydraulic fracturing experiments in two boreholes in the Thermal Test Facility alcove and one borehole in the Northern Ghost Dance Fault alcove indicate a west-northwest extensional stress regime. The relative magnitudes of the principal stresses are consistent with potential normal faulting (SNL 1996 [DIRS 163645]; DTNs: SN0308F3710195.003 [DIRS 166458] and SNF37100195002.001 [DIRS 131356]).

Principal stress orientations inferred from earthquake focal mechanism studies also indicate a west-northwesterly directed least principal stress. Observed focal mechanisms exhibit a mixture of normal and strike-slip faulting. The overall data suggest a uniform stress regime in the vicinity of Yucca Mountain (von Seggern et al. 2001 [DIRS 156297], Section 9). Available data do not support a residual stress effect from the Timber Mountain caldera, do not support a modern stress field changing from strike-slip in northern Yucca Mountain to normal south of the large hydraulic gradient, and do not support a southward decrease of the least principal stress. Based on these findings, any changes in stress resulting from seismic activity would be expected to have a negligible effect on the location of the large hydraulic gradient. Therefore, migration of the large hydraulic gradient as a result of seismic activity is excluded from TSPA on the basis of low consequence.

Seismic Effects on Saturated Zone Groundwater Chemistry

The effect of a seismically induced hydrologic response on saturated zone groundwater chemistry will be insignificant. Groundwater isotopic and geochemical signatures within the Yucca Mountain region are indicative of groundwater flow directions and flow paths that have existed over the past 10,000 years. Uncorrected groundwater ages determined from ^{14}C (percent modern carbon) data (SNL 2007 [DIRS 177391], Table A6-7 and Section B7) and an exponential decay relationship (SNL 2007 [DIRS 177391], Equation A6-3) range from about 12,000 to 18,000 years old in the vicinity of Yucca Mountain. The analysis of the geochemistry supports the conclusion that the bulk of the groundwater beneath Yucca Mountain is derived from local recharge (SNL 2007 [DIRS 177391], Sections A6.3.6.3 and A6.3.6.4). Therefore, the saturated zone groundwater under the repository and along the saturated zone transport path is primarily paleoclimate recharge water with a small component (2% to 15%) of young water less than 1,000 years old (SNL 2007 [DIRS 177391], Table A6-8). Given that the saturated zone groundwater below the repository comes from local recharge through the unsaturated zone, any saturated zone water that is temporarily forced into the unsaturated zone by seismic activity would be expected to have a negligible effect on chemical composition or temperature relative to natural variations.

For the unsaturated zone, the range of water compositions that is used to define radionuclide sorption coefficients is taken from the range of water compositions found in the unsaturated zone and saturated zone (SNL 2007 [DIRS 177396], Appendix A, Section A4). Therefore, any alteration of composition through mixing of unsaturated zone and saturated zone waters as a result of water table rise is expected to lie within the range of uncertainty for groundwater composition already included in the TSPA. For the unsaturated zone, any effects of water table

rise are expected to have a negligible effect on temperature in comparison with the effects of repository heating, which is excluded in terms of unsaturated zone flow and transport in excluded FEPs 2.2.10.01.0A (Repository-Induced Thermal Effects on Flow in the UZ) and 2.2.10.06.0A (Thermo-Chemical Alteration in the UZ (Solubility, Speciation, Phase Changes, Precipitation/Dissolution)).

Summary

The distance between the elevation of the water table and the lowest waste emplacement drift is about 187 m for both present and future, wetter climates. Multiple lines of evidence indicate that earthquake-induced rises in the water table will be insufficient to eliminate that gap:

- A National Research Council Panel, asked to evaluate the evidence for past earthquake-induced water table rise and the possibility of future earthquake-induced water table rise, concluded that such an effect is unlikely to exceed 50 m over the next 10,000 years.

- Even when a bounding model of water table rise (Kemeny and Cook 1990 [DIRS 129658], 1992 [DIRS 100989]) is used, almost all fault cases defined as part of the PSHA seismic source characterization activity result in calculated water table rise values less than 187 m.

- Even when a bounding model of water table rise (Kemeny and Cook 1990 [DIRS 129658], 1992 [DIRS 100989]) is used, PSHA seismic source characterization and fault displacement hazard results with a 10^{-8} mean annual probability of being exceeded lead to water table rise values of 122 m or less. This leaves a gap between the water table and the lowest waste emplacement drift of at least 65 m.

- Using a bounding model of water table rise (Kemeny and Cook 1990 [DIRS 129658], 1992 [DIRS 100989]), given the recurrence of earthquakes on local faults in the vicinity of Yucca Mountain, point-source stress parameter values yielding a combined probability of exceedance of 10^{-8} lead to water table rise values of less than about 40 m (i.e., a remaining gap of 147 m or more).

- Worldwide observations of sustained hydrologic effects related to earthquakes are generally consistent with a dislocation approach to modeling the poroelastic response of the earth's crust. A regional stress change approach, which Kemeny and Cook (1990 [DIRS 129658], 1992 [DIRS 100989]) combined with conservative assumptions to create a simple bounding model of water table rise, significantly overestimates water table rise because some assumptions, while bounding, are unrealistic.

- Stress measurements in the vicinity of Yucca Mountain are consistent with those for the vicinity of the Nevada Test Site and do not support a residual stress effect from the Timber Mountain caldera that might lead to southward movement of the large hydraulic gradient north of the repository in response to a future earthquake.

Also, the direct effects of seismic activity on the elevation of the water table are short-lived with respect to performance periods of 10,000 and 1,000,000 years.

As a result, groundwater flow and radionuclide transport would not be significantly affected by the hydrologic effects of future seismic activity, and therefore the hydrologic response to seismic activity is excluded from the TSPA on the basis of low consequence.

The effects of seismic activity on groundwater chemistry and temperature are also excluded from the TSPA on the basis of low consequence, because the changes in temperature caused by seismicity will be negligible compared to changes resulting from other natural variations in temperature or through repository heating. Changes in geochemical conditions will also be negligible in terms of the uncertainties in water chemistry already included in the unsaturated zone and saturated zone models used in TSPA.

Based on the previous discussion, omission of FEP 1.2.10.01.0A (Hydrologic Response to Seismic Activity) will not result in a significant adverse change in the magnitude or timing of either radiological exposure to the RMEI or radionuclide releases to the accessible environment. Therefore, this FEP is excluded from the performance assessments conducted to demonstrate compliance with 10 CFR 63.311 and 63.321 and with 10 CFR 63.331 [DIRS 186479], on the basis of low consequence.

INPUTS:

[*Tables 1.2.10.01.0A-1 and 1.2.10.01.0A-2 in the parent report are replaced by Tables 1.2.10.01.0A-2[a] and 1.2.10.01.0A-3[a] as follows:*]

Table 1.2.10.01.0A-2[a]. Direct Inputs

Input	Source	Description
DTN: GS930108312312.003. Earthquake-Induced Water-Level Fluctuations at Yucca Mountain, Nevada, June, 1992. [DIRS 171974]	Files: *S96143_001, S96143_002, and S96143_003*	Data from groundwater monitoring wells describing earthquake-induced water-level fluctuations
DTN: MO0401MWDRPSHA.000 Results of the Yucca Mountain Probabilistic Seismic Hazard Analysis (PSHA). [DIRS 185267]	Seismic source characterization inputs files	PSHA seismic source characterization of fault geometry, maximum magnitude, and recurrence rate
	PSHA fault displacement hazard output file for the Solitario Canyon faults (Site #2)	For the Solitario Canyon fault, fault displacement hazard with a mean annual probability of exceedance of 10^{-8} is about 1300 cm.
DTN: SN0308F3710195.003. Hydraulic Fracturing Stress Measurements in Test Holes: ESF-GDJACK #1, and ESFGDJACK #5, Exploratory Studies Facility at Yucca Mountain, Nevada. [DIRS 166458]	File: *S03305_001*	The relative magnitudes of the principal stresses are consistent with potential normal faulting
Belcher, W.R. 2004. Death Valley Regional Ground-Water Flow System, Nevada and California – Hydrogeologic Framework and Transient Ground-Water Flow Model. [DIRS 173179]	Figure F-38	Specific storage of confined aquifers of between 10^{-7} and 10^{-4} m^{-1} and a specific yield of unconfined aquifers of about 0.1 for the Death Valley Regional Flow System in the vicinity of Yucca Mountain

Table 1.2.10.01.0A-2[a]. Direct Inputs (Continued)

Input	Source	Description
Bredehoeft, J.D. 1992. "Response of Ground-Water System at Yucca Mountain to an Earthquake." [DIRS 101122]	pp. 212 to 222	Prediction of earthquake-induced water table rise on the order of 1 m using three-dimensional dislocation and hydrological models
BSC 2004. Development of Numerical Grids for UZ Flow and Transport Modeling. [DIRS 169855]	Figure 6-2	Elevation of water table beneath the repository footprint
BSC 2007. *Underground Layout Configuration for LA*. [DIRS 179640]	Tables 12 and 14	Elevation of repository emplacement drifts
Carrigan, C.R.; King, G.C.P.; Barr, G.E.; and Bixler, N.E. 1991. "Potential for Water-Table Excursions Induced by Seismic Events at Yucca Mountain, Nevada." [DIRS 100967]	pp. 1,157 to 1,160	Prediction of earthquake-induced water table rise of less than 20 m using two-dimensional dislocation and hydrological models
Chiou et al. 2008. "NGA Project Strong-Motion Database." [DIRS 186319]	Next Generation of Ground-Motion Attenuation Models (NGA) project database (public version 7.3, 02-14-06, http://peer.berkeley.edu/nga/flatfile.html)	Static stress drop data for some earthquakes in the NGA earthquake database
CRWMS M&O 1998. Probabilistic Seismic Hazard Analysis for Fault Displacement and Vibratory Ground Motion at Yucca Mountain, Nevada. [DIRS 103731]	Figure 4-47	Aggregate rate of activity for local faults in the vicinity of Yucca
Grecksch et al. 1999. "Coseismic well-level changes due to the 1992 Roermond Earthquake compared to static deformation of half-space solutions." [DIRS 186477]	Figure 5	General correlation between earthquake-induced water level changes and volumetric strains calculated using a dislocation model approach
Jonsson et al. 2003. Post-Earthquake Ground Movements Correlated to Pore-Pressure Transients." [DIRS 186291]	Figures 2 and 3	General correlation between earthquake-induced water level changes and volumetric strains calculated using a dislocation model approach
Manga and Wang 2007. Earthquake Hydrology [DIRS 186289]	p. 302	Data for water level changes in wells completed in confined and unconfined aquifers for the Chi-chi Taiwan earthquake.
National Research Council 1992. *Ground Water at Yucca Mountain, How High Can It Rise? Final Report of the Panel on Coupled Hydrologic/Tectonic/Hydrothermal Systems at Yucca Mountain*. [DIRS 105162]	Chapter 5, p. 116	An earthquake-induced water table rise over the next 10,000 years is unlikely to exceed 50 m at Yucca Mountain
	Appendix A, p. 134	Isotopic evidence indicates that no prolonged excursion of the water table above its present level has occurred in the last ca. 100 ka.
Quilty, E.G. and Roeloffs, E.A. 1997. "Water-level changes in response to the 20 December 1994 Earthquake near Parkfield, California." [DIRS 186478]	pp. 310 to 317	General correlation between earthquake-induced water level changes and volumetric strains calculated using a dislocation model approach

Table 1.2.10.01.0A-2[a]. Direct Inputs (Continued)

Input	Source	Description
Sato et al. 2004. "Changes in Groundwater Level Associated with the 2003 Tokachi-Oki Earthquake." [DIRS 186293]	Figure 1	General correlation between earthquake-induced water level changes and volumetric strains calculated using a dislocation model approach
SNL 2007. Radionuclide Transport Models Under Ambient Conditions. [DIRS 177396]	Appendix A, Section A4	The range of water compositions that is used to define radionuclide sorption coefficients is taken from the range of water compositions found in the unsaturated zone and saturated zone
SNL 2007. *Saturated Zone Site-Scale Flow Model*. [DIRS 177391]	Table A6-7, Section B7	Uncorrected groundwater ages determined from ^{14}C
	Table A6-8	The SZ groundwater under the repository and along the SZ transport path is primarily paleoclimate recharge water with a small component (2% to 15%) of young water less than 1,000 years old
	Section 6.3.1.4	Hydraulic gradient of up to 0.13 just to the north of the repository
Stock et al. 1985 [DIRS 101027]	Table 1	Hydrofracture stress measurements in boreholes USW G-1 and USW G-2
	Figure 11	Borehole breakout azimuths
	Table 3	Stress indicators for the Nevada Test Site area
Stock, J.M. and Healy, J.H. 1988 [DIRS 101022]	Table 6-1	Hydrofracture stress measurements in boreholes USW G-1, USW G-2, USW G-3, and UE25-p#1
	pp. 90 to 91	Stress directions
Wells and Coppersmith 1994 [DIRS 107201]	Table 2A	Empirical relation between rupture area and moment magnitude Empirical relation between rupture width and moment magnitude

Table 1.2.10.01.0A-3[a]. Indirect Inputs

Citation	Title	DIRS
10 CFR 63	Energy: Disposal of High-Level Radioactive Wastes in a Geologic Repository at Yucca Mountain, Nevada	186479
DTN: SN0308F3710195.003	Hydraulic Fracturing Stress Measurements in Test Holes: ESF-GDJACK #1, and ESF-GDJACK #5, Exploratory Studies Facility at Yucca Mountain, Nevada	166458
DTN: SNF37100195002.001	Hydraulic Fracturing Stress Measurements in Test Hole: ESF-AOD-HDFR1, Thermal Test Facility, Exploratory Studies Facility at Yucca Mountain.	131356

Table 1.2.10.01.0A-3[a]. Indirect Inputs (Continued)

Citation	Title	DIRS
Aki and Richards 1980	Quantitative Seismology, Theory and Methods	150723
Brune 1970	Tectonic Stress and the Spectra of Seismic Shear Waves from Earthquakes.	103315
Brune 1971	Tectonic Stress and the Spectra of Seismic Shear Waves from Earthquakes [Correction]	131516
BSC 2004	Water-Level Data Analysis for the Saturated Zone Site-Scale Flow and Transport Model	170009
Cutillo and Ge 2006	Analysis of Strain-Induced Ground-Water Fluctuations at Devils Hole, Nevada	186288
Davies and Archambeau 1997	Geohydrological Models and Earthquake Effects at Yucca Mountain, Nevada	103180
Gauthier et al. 1996	Impacts of Seismic Activity on Long-Term Repository Performance at Yucca Mountain	100447
Heaton 1990	Evidence for and Implications of Self-Healing Pulses of Slip in Earthquake Rupture	186296
Kemeny and Cook 1990.	Rock Mechanics and Crustal Stress	129658
Koizumi et al. 2005	Evaluation of Groundwater Changes Caused by the 2003 Tokachi-Oki Earthquake (M8.0)	186295
Manga and Wang 2007	Earthquake Hydrology	186289
Montgomery and Manga 2003.	Streamflow and Water Well Responses to Earthquakes	186262
O'Brien 1993	Earthquake-Induced Water-Level Fluctuations at Yucca Mountain, Nevada, June 1992	101276
Paces et al. 2001	Ages and Origins of Calcite and Opal in the Exploratory Studies Facility Tunnel, Yucca Mountain, Nevada	156507
Roeloffs 1996	Poroelastic Techniques in the Study of Earthquake-Related Hydrologic Phenomena	186290
SNL 1996	Hydraulic Fracturing Stress measurements in Test Hole ESF-AOD-HDFR#1, Thermal Test Facility, Exploratory Studies Facility at Yucca Mountain.	163645
SNL 2009	Supplemental Earthquake Ground Motion Input for a Geologic Repository at Yucca Mountain, NV	185977
Szymanski 1989.	Conceptual Considerations of the Yucca Mountain Groundwater System with Special Emphasis on the Adequacy of This System to Accommodate a High-Level Nuclear Waste Repository	106963
USGS National Water Information System	Data for wells UE-25 WT-17, UE-25 WT-16, USW WT-10, UE-25 WT-14, UE-25 WT-13, USW WT-7, USW WT-1, J-13, and J-12	N.A.
von Seggern et al. 2001	Seismicity in the Vicinity of Yucca Mountain, Nevada for the Period October 1, 1997 to September 30, 1999.	156297
Whelan et al. 2008	Thermal History of the Unsaturated Zone at Yucca Mountain, Nevada, USA	185452
Wilson et al. 2003	Origin, Timing, and Temperature of Secondary Calcite-Silica Mineral Formation at Yucca Mountain, Nevada	163589

FEP: 2.1.03.04.0B

FEP NAME:

Hydride Cracking of Drip Shield

FEP DESCRIPTION:

[*No modification to the parent report.*]

SCREENING DECISION:

[*No modification to the parent report.*]

SCREENING JUSTIFICATION:

[*The Screening Justification is replaced by the following paragraphs:*]

The drip shield plates are to be fabricated from Titanium Grade 7, an α-titanium alloy, 15-mm thick (SNL 2007 [DIRS 179354], Table 4-2, Parameter Number 07-04). The drip shields are supported by Titanium Grade 29, an $\alpha + \beta$ titanium alloy, support beams (SNL 2007 [DIRS 179354], Table 4-2, Parameter Number 07-04). The Titanium Grade 29 drip shield support beams, which are external to the drip shield and exposed to seepage water and are more prone to hydrogen absorption than the crossmembers located on the underside of the drip shield (SNL 2007 [DIRS 179354], Table 4-2). Failure of the drip shields due to general corrosion is discussed in included FEP 2.1.03.01.0B (General Corrosion of Drip Shields).

Hydrogen absorption in α-titanium and $\alpha - \beta$ titanium alloys can occur when three general conditions are simultaneously met (Covington 1979 [DIRS 151097], pp. 378 to 381; Schutz and Thomas 1987 [DIRS 144302], p. 673; SNL 2007 [DIRS 181339], Section 6.1.2):

(1) A mechanism exists for generating nascent (atomic) hydrogen on the surface (e.g., the water reduction reaction is a thermodynamically viable cathodic reaction).

(2) The temperature of the drip shield is above approximately 80°C (175°F) such that a surface film of hydride is not formed and the diffusion rate of hydrogen into α-titanium is significant.

(3) Either (a) the solution pH is less than 3 or greater than 12, or (b) impressed potentials are sufficiently cathodic to induce the redox transformation of Ti^{4+} to Ti^{3+}within the passive TiO_2 oxide (approximately −0.7 V versus the saturated calomel reference electrode under near neutral conditions).

By assuming that the only viable cathodic reaction on the titanium surface is the water reduction reaction, condition (1) is always met as long as aqueous corrosion occurs. At certain repository locations, where temperatures are greater than or equal to 80°C (175°F) and concentrated groundwater is present, conditions (2) and (3) may also be satisfied. However, it should be noted that while the aforementioned three conditions are necessary requirements for hydrogen

absorption, they are not sufficient in determining if hydrogen embrittelment will take place. A critical hydrogen concentration within the metal must be achieved in order to reduce the mechanical properties to the extent that hydrogen-induced cracking can occur (SNL 2007 [DIRS 181339], Section 8). It should also be noted that given the oxic conditions that will prevail within any given drift, the assumption that the cathodic current density is solely due to the water reduction reaction will consistently overestimate the hydrogen production rate as the oxygen reduction reaction, the expected cathodic reaction, is assumed not to occur.

The term hydrogen embrittlement is used to refer to the deleterious impact of hydrogen on the mechanical properties of a material. Hydrogen-induced cracking results from the combined action of hydrogen and residual or sustained applied tensile stresses, whereby crack initiation and/or propagation occur at lower stress levels than in the absence of absorbed hydrogen. The critical hydrogen concentration of Titanium Grade 7 is estimated as 1,000 ppm (μg/g) (SNL 2007 [DIRS 181339], Section 5.2). The critical hydrogen concentration of Titanium Grade 29 is estimated at between 400 and 600 ppm (μg/g) (SNL 2007 [DIRS 181339], Section 5.2[a]). The value of f_h, fractional hydrogen absorption efficiency, is conservatively selected as 0.015 (SNL 2007 [DIRS 181339], Sections 8.1 and 8.3.2). By using the 2.5-year general corrosion rates obtained for Titanium Grade 7 obtained at the LTCTF, the 0.999 probability value from the upper 97.5% uncertainty bound general corrosion rate of Titanium Grade 7 in the aggressive environment (90°C SCW) is about 58 nm/yr (SNL 2007 [DIRS 181339], Table 4-1[a]). At 10,000 years, the hydrogen pickup of the Titanium Grade 7 drip shield plate material calculated is 105 μg/g (SNL 2007 [DIRS 181339], Section 8[a] and Table 8-1[a]). Given that the maximum initial hydrogen content in Titanium Grade 7 is 150 μg/g (SNL 2007 [DIRS 181339], Table 4-2[a]), the estimated maximum total hydrogen content in the drip shield plate material at 10,000 years is 255 μg/g, which is well below the critical hydrogen concentration for Titanium Grade 7.

Because no long-term data from the LTCTF are available for general corrosion rate of Titanium Grade 29 in repository-relevant environments, the Titanium Grade 29 general corrosion rate is calculated from conversion factors based upon short-term experiments as discussed in *General and Localized Corrosion of the Drip Shield* (SNL 2007 [DIRS 180778], Section 6.2.2[a]). By using the Titanium Grade 29/Titanium Grade 7 corrosion rate ratio multiplier values, the absorbed hydrogen concentrations in Titanium Grade 29 drip shield support beam material are calculated in *Hydrogen-Induced Cracking of the Drip Shield* (SNL 2007 [DIRS 181339], Section 6.2[a]). Using the 75th percentile multiplier and the 0.999 probability value from the upper 97.5% uncertainty bound of the Titanium Grade 7 general corrosion rate in the specified aggressive environment, at 10,000 years, the hydrogen pickup in the drip shield structural support material (Titanium Grade 29) is 84 μg/g. Given that the maximum initial hydrogen content in Titanium Grade 29 is 150 μg/g (SNL 2007 [DIRS 181339], Table 4-2[a]), the estimated maximum total hydrogen content in the drip shield structural support material at 10,000 years is 234 μg/g. Using the 95th percentile multiplier and the 0.999 probability value from the upper 97.5% uncertainty bound of the Titanium Grade 7 general corrosion rate in the specified aggressive environment, at 10,000 years, the hydrogen pickup in the drip shield structural support material (Titanium Grade 29) is 191 μg/g, yielding an estimated maximum total hydrogen content at 10,000 years of 341 μg/g. These conservatively calculated hydrogen content values are below the critical hydrogen concentrations for Titanium Grade 29 (400 to 600 ppm) (SNL 2007 [DIRS 181339], Section 8.1[a] and Table 8 2[a]).

The locally hydrided regions that may potentially result from galvanic effects (e.g., from failed rock bolts or ground supports contacting the drip shield surface) will not be sufficiently large in magnitude such that they result in hydrogen-induced cracking as illustrated in *Hydrogen-Induced Cracking of the Drip Shield* (SNL 2007 [DIRS 181339], Section 6.3.2). The rationale presented in the reference includes the following points: (1) the contact area is small and has a low anode-to-cathode area ratio, (2) the presence of seepage is anticipated to be intermittent at temperatures greater than or equal to 80°C (175°F), (3) sustaining the water reduction reaction under the repository conditions is unexpected, and (4) the titanium drip shield and the steel component surfaces that may contact it will experience a long period of dry conditions where the temperature is greater than or equal to 85°C (185°F), resulting in the formation of a thermal oxide, in effect passivating both materials, thereby minimizing any potential galvanic interactions and preventing increased hydrogen absorption.

When a titanium alloy containing an appreciable concentration of aluminum (e.g., Titanium Grade 29) is welded with an aluminum-free alloy (e.g., Titanium Grade 7), an abrupt concentration gradient of aluminum is formed at the weld fusion line. This concentration gradient has been found to drive uphill diffusion of hydrogen from the aluminum-rich material to the aluminum-poor material, resulting in the formation of hydride bands along the weld fusion line, increasing the susceptibility of the weld region to hydrogen embrittlement (SNL 2007 [DIRS 181339], Section 6.3[a]). To eliminate the potential for hydride band formation due to hydrogen redistribution, the weld filler metal utilized will be Titanium Grade 28 (SNL 2007 [DIRS 179354], Table 4-2; SNL 2007 [DIRS 181339], Section 6.3[a]). That is, welds made between Titanium Grade 7 plates and Titanium Grade 29 support beams will be conducted utilizing Titanium Grade 28 filler material. Titanium Grade 28 has an aluminum content of 2.5% to 3.5%, providing an intermediate level between the Titanium Grade 7 plates and Titanium Grade 29 support beams. As a result, the abrupt aluminum concentration gradient that has been found to result in hydrogen redistribution and the enhanced hydride formation can take place when high aluminum alloys are welded with a low aluminum filler metal is avoided (SNL 2007 [DIRS 181339], Section 6.3[a]; Kennedy 1993 [DIRS 177388]).

Based on the previous discussion, FEP 2.1.03.04.0B (Hydride Cracking of Drip Shields) is excluded from the performance assessments conducted to demonstrate compliance with 10 CFR 63.311, 63.321, and 63.331 [DIRS 186479], on the basis of low probability.

INPUTS:

Table 2.1.03.04.0B-1[a]. Direct Inputs

Input	Source	Description
SNL 2007. *Hydrogen-Induced Cracking of the Drip Shield*. [DIRS 181339]	Section 8	A critical hydrogen concentration within the metal must be achieved in order to reduce the mechanical properties to the extent that hydrogen-induced cracking Section 6.3.2can occur
	Section 6.3.2	The locally hydrided regions which may potentially result from galvanic effects will not be sufficiently large in magnitude such that they result in hydrogen induced cracking
	Section 8.1[a] and Table 8-2[a]	Calculation of hydrogen content in Titanium Grade 29 support material is below critical concentration
	Section 8[a] and Table 8-1[a]	At 10,000 years, hydrogen content in the Titanium Grade 7 drip shield will be 105 micrograms/gram

Table 2.1.03.04.0B-2[a]. Indirect Inputs

Citation	Title	DIRS
10 CFR 63	Energy: Disposal of High-Level Radioactive Wastes in a Geologic Repository at Yucca Mountain, Nevada	186479
Covington 1979	“The Influence of Surface Condition and Environment on the Hydriding of Titanium”	151097
Kennedy et al. 1993	“Effect of Activity Differences on Hydrogen Migration in Dissimilar Titanium Alloy Welds”	177388
Schutz and Thomas 1987	“Corrosion of Titanium and Titanium Alloys”	144302
SNL 2007	*Total System Performance Assessment Data Input Package for Requirements Analysis for EBS In-Drift Configuration*	179354
SNL 2007	*General Corrosion and Localized Corrosion of the Drip Shield*	180778
SNL 2007	*Hydrogen-Induced Cracking of the Drip Shield*	181339

FEP: 2.1.09.02.0A

FEP NAME:

Chemical Interaction with Corrosion Products

FEP DESCRIPTION:

[*No modification to the parent report.*]

SCREENING DECISION:

[*No modification to the parent report.*]

TSPA DISPOSITION:

[*No modification to the parent report, except the third bullet of the fourth paragraph is changed as follows:*]

- Kinetic sorption of plutonium and americium onto iron oxyhydroxide colloids and fixed corrosion products (Section 6.3.12.2)

FEP: 2.1.09.17.0A

FEP NAME:

Formation of Pseudo-Colloids (Corrosion Product) in EBS

FEP DESCRIPTION:

[*No modification to the parent report.*]

SCREENING DECISION:

[*No modification to the parent report.*]

TSPA DISPOSITION:

[*No modification to the parent report, except the second paragraph is changed as follows:*]

The sorption calculations for iron oxyhydroxide colloids are based on a mechanistic surface complexation-based competitive sorption model, where the sorption coefficients are calculated as a function of dissolved concentration of competing species, pCO_2, and sorption sites (SNL 2007 [DIRS 177407], Sections 6.3.4.2.3 and 6.5.2.4). The results of these calculations are implemented in TSPA by applying reversible sorption of thorium, uranium, and neptunium on iron oxyhydroxide colloids by computing an effective K_d at each timestep. The sorption of plutonium and americium on iron oxyhydroxide colloids is modeled as a kinetic sorption process by applying a forward rate constant as described in *Waste Form and In-Drift Colloids-Associated Radionuclide Concentrations: Abstraction and Summary* (SNL 2007 [DIRS 177423], Section 6.3.12.2).

FEP: 2.1.14.26.0A

FEP NAME:

Near-Field Criticality Resulting from an Igneous Event

FEP DESCRIPTION:

[*No modification to the parent report.*]

SCREENING DECISION:

[*No modification to the parent report.*]

SCREENING JUSTIFICATION:

[*No modification to the parent report, except Table 2.1.14.26.0A-1 is replaced by the following:*]

Table 2.1.14.26.0A-1[a]. Summary of Igneous Scenario External Criticality Results

Scenario	Waste Package Type	Calculated Accumulation or Mass Released from Waste Package (uranium mass, unless otherwise noted (kg))	Mass of Uranium or Plutonium (for FFTF) Required to Achieve Critical Limit of k_{eff} = 0.96 in the Invert (kg)
Igneous	DOE3 (N Reactor)	0.109	Infinite[a]
	DOE9 (TMI II Fuel)	9.24	538
	Commercial SNF	74.8	159
	DOE1 (FFTF) (Plutonium mass)	2.49×10^{-2}	1.66

Source: SNL 2007 [DIRS 181395], Table 6.9-1[a].

[a] "Infinite" means that an infinite amount of fissile waste released in this model will not produce an arrangement that can reach the critical limit.

FEP: 2.2.06.01.0A

FEP NAME:

Seismic Activity Changes Porosity and Permeability of Rock

FEP DESCRIPTION:

[*No modification to the parent report.*]

SCREENING DECISION:

[*No modification to the parent report.*]

SCREENING JUSTIFICATION:

[*The Screening Justification is replaced by the following paragraphs:*]

Plate tectonic activity has imparted crustal extension stresses within the Basin and Range Province (which includes the Yucca Mountain region) during the past 12 million years. The height of this activity occurred between 10 and 12 million years ago, with estimated extension rates ranging between 10 and 30 mm per year (National Research Council 1992 [DIRS 105162], Chapter 2). During this period, major faults and fractures were created in the vicinity of Yucca Mountain. Approximately 5 million years ago, regional extension rates declined to 5 to 10 mm per year. At present, extension rates are still in a declining state (National Research Council 1992 [DIRS 105162], Chapter 2).

Regional extension imparts local extensional, compressional, and/or shear stresses on the crust, depending on location, depth, and the juxtaposition of parent rock units and existing faults and fractures. Release of stress results in seismic activity that creates faults (rupture), and causes fault displacement, vibratory motion, and/or spatial redistribution of stresses not associated with specific faults. Vibratory motion and spatial redistribution of stress in the rock matrix can alter the hydrologic properties of the parent rock by: (1) causing a change in pore pressure, or (2) causing dilation, compression, or breakage of granular structures in the rock, leading to corresponding changes in permeability.

Pore pressure changes associated with seismic events are addressed in detail under excluded FEP 1.2.10.01.0A (Hydrologic Response to Seismic Activity). The discussion is based in part on the results of an assessment conducted by the National Research Council (1992 [DIRS 105162], Chapter 5) that evaluated water table fluctuations for a large normal-faulting seismic event. It was concluded that a future seismic event would not alter the rock hydrologic properties on a regional scale.

Damage of the rock matrix material in lithophysal units due to seismic loading would manifest itself in the form of inter-lithophysal tensile fractures that coalesce to form observable shear fractures with offset. Such damage would indicate that seismically induced cyclic shear stresses had exceeded the shear-strain threshold to cause new fracturing. The shear-strain threshold is an uncertain parameter and thus is characterized as a probability distribution. The exposed

lithophysal rocks in the ESF and the ECRB Cross-Drift show no inter-lithophysal fracturing of this type. Observed fracturing is consistent with a typical cooling-fracture-related history (BSC 2005 [DIRS 170137], Section 6). These findings indicate that the matrix material is largely unaffected by redistribution of strain introduced by seismic activity over the more than 10 million years since the rocks were deposited.

Although there is no evidence that seismically related cyclic shear strains have exceeded the threshold required to produce additional fracturing of the rock at Yucca Mountain in the past about 10 million years, predicted shear strains for conditioned ground motions with mean annual probabilities of exceedance of 10^{-7} and 10^{-8} exceed the lower portion of the shear-strain-threshold distribution. If new fractures are generated by extreme seismic activity, however, their effect is addressed by a fracture sensitivity study (Appendix I) that forms part of the screening exclusion justification for FEPs 2.2.06.02.0A (Seismic Activity Changes Porosity and Permeability of Faults), and 2.2.06.02.0B (Seismic Activity Changes Porosity and Permeability of Fractures).

The generation of new fractures as a result of seismic activity is encompassed within the existing sensitivity analyses for changes in fracture properties. This may be seen through the cubic law used to estimate changes in fracture permeability, k, as a result of changes in the hydraulic fracture aperture, b:

$$k = \frac{f b^3}{12} \qquad \text{(Eq. 10[a])}$$

in which f is the is the fracture frequency. The hydraulic fracture aperture is also given by:

$$B = \frac{\beta \varphi}{f} \qquad \text{(Eq. 11[a])}$$

in which φ is the fracture porosity and β is a scale factor to account for constrictions affecting the hydraulic fracture aperture. For a given seismically-induced strain, ε, which is allocated to fractures, the fracture porosity increases to φ + ε. If the seismically induced strain is taken up entirely by the existing fractures, then the fracture aperture increases to:

$$\frac{\beta(\varphi+\varepsilon)}{f} \qquad \text{(Eq. 12[a])}$$

and the permeability is given by:

$$k = \frac{f\left(\frac{\beta(\varphi+\varepsilon)}{f}\right)^3}{12} = \frac{\beta^3(\varphi+\varepsilon)^3}{12\, f^2} \qquad \text{(Eq. 13[a])}$$

On the other hand, if new fractures are generated to absorb some of the seismically induced strain, then the fracture frequency increases to $\hat{f}$ and the new fracture permeability is given by:

$$k = \frac{\hat{f}\left(\frac{\beta(\varphi+\varepsilon)}{\hat{f}}\right)^3}{12} = \frac{\beta^3(\varphi+\varepsilon)^3}{12\, \hat{f}^2} \qquad \text{(Eq. 14[a])}$$

Because $\hat{f} > f$, the permeability of a system with seismically induced fractures is smaller than the permeability of a system in which the seismic strain is taken up entirely by the existing fractures. Therefore, the possibility of new fractures is included within the range of the existing sensitivity analyses. Other effects pertaining to induced fractures lead to increased fracture-matrix interface area and, therefore, increased fracture-matrix interaction. This results in improved performance with respect to damping of episodic flow and radionuclide transport rates as compared with the system without additional fractures. Thus, low-probability conditioned ground motions are adequately considered in excluding FEP 2.2.06.01.0A (Seismic Activity Changes Porosity and Permeability of Rock), from the TSPA.

Given the relatively high strength of the matrix material and the extensive fracture network in the rock mass, the strain introduced by seismic activity might be accommodated by deformation of, and slip along, existing faults and fractures. The effects of seismic activity on the properties of faults and fractures are discussed under excluded FEP 2.2.06.02.0A (Seismic Activity Changes Porosity and Permeability of Faults), and excluded FEP 2.2.06.02.0B (Seismic Activity Changes Porosity and Permeability of Fractures). However, localized changes in hydrologic properties could occur adjacent to existing faults and fractures due to enhancement of brecciation and gouge zones and possibly due to the creation of new fractures outside of the brecciated zone. Based on data from the ESF, this disturbed rock zone, labeled herein as a "zone of alteration," is correlated with the amount of fault offset (Sweetkind et al. 1997 [DIRS 177047], p. 68). Faults with 1 to 5 m of cumulative offset have a zone of increased fracturing of only 1 to 2 m; faults with tens of meters of offset can have a zone of fracturing up to tens of meters wide (Sweetkind et al. 1997 [DIRS 177047], pp. 68 to 72). The hydrologic properties in the zone of alteration reflect the cumulative response of a dynamic seismic past, demonstrative of rapid extension rates in existence 10 to 12 million years ago and, to a lesser extent, the lower extension rates occurring today. In light of the cumulative nature of seismic processes at Yucca Mountain over more than 10 million years, any changes in hydrologic properties resulting from seismic activity over the 10,000-year to 1,000,000-year postclosure period are expected to be negligible.

The effects of a future seismic event on the hydrologic properties of the host rock are evaluated here based on the fault displacement hazard findings of the PSHA for Yucca Mountain (CRWMS M&O 1998 [DIRS 103731], Sections 4 and 8). The PSHA expert panel assessed the displacement hazard for intact host rock in the vicinity of the repository to be less than 0.1 cm for a 10^{-8} mean annual probability of exceedance (DTN: MO0401MWDRPSHA.000 [DIRS 185267], file: *s7d.frac_mean*; CRWMS M&O 1998 [DIRS 103731], Section 8.2.1). Consequently, the rock matrix is largely unaffected by strain redistribution caused by seismic activity and no significant new faults or fractures are likely to form in the Yucca Mountain vicinity within the next 10,000 to 1,000,000 years.

The small seismic displacement hazard for intact rock, less than 0.1 cm for a 10^{-8} mean annual probability of exceedance, corresponds to the level of displacement that occurred as a result of thermal stress in the Drift Scale Test, as measured in multiple-point borehole extensometers (BSC 2004 [DIRS 169864], Figure 7.4.2-2). The simulations of the displacement response in the Drift Scale Test, based on elastic thermal-hydrological-mechanical (THM) processes, were found to be in agreement with measurements. The dominant mode for stress-induced permeability change for THM processes was found to be elastic fracture opening or closing caused by changes in stress normal to the fractures, as opposed to changes in matrix permeability (BSC 2004

[DIRS 169864], Section 8.2). For seismically induced displacements and stresses, similar in amplitude to those found in the Drift Scale Test, the same conclusions apply to both the unsaturated zone and saturated zone. Therefore, based on the fault displacement hazard for the intact rock matrix, seismically related effects on rock-matrix hydrologic properties will be negligible and may be excluded on the basis of low consequence.

In summary, any changes to hydrologic processes as a result of changes to rock matrix properties caused by seismic activity are expected to be negligible. Based on the previous discussion, omission of FEP 2.2.06.01.0A (Seismic Activity Changes Porosity and Permeability of Rock) will not result in a significant adverse change in the size or timing of either radiological exposures to the RMEI or radionuclide releases to the accessible environment. Therefore, this FEP is excluded from the performance assessments conducted to demonstrate compliance with 10 CFR 63.311 and 63.321 and with 10 CFR 63.331 [DIRS 186479], on the basis of low consequence.

INPUTS:

[*Tables 2.2.06.01.0A-1 and 2.2.06.01.0A-2 in the parent report are replaced by Tables 2.2.06.01.0A-1[a] and 2.2.06.01.0A-2[a] as follows:*]

Table 2.2.06.01.0A-1[a]. Direct Inputs

Input	Source	Description
DTN: MO0401MWDRPSHA.000. Results of the Yucca Mountain Probabilistic Seismic Hazard Analysis (PSHA). [DIRS 185267]	file: *s7d.frac_mean*	Displacement hazard for intact host rock in the vicinity of the repository is less than 0.1 cm for a mean annual probability of exceedance of 10^{-8}.
BSC 2004. Drift Scale THM Model. [DIRS 169864]	Section 8.2	The dominant mode for stress-induced permeability change for THM processes was found to be elastic fracture opening or closing caused by changes in stress normal to the fractures
BSC 2005. Peak Ground Velocities for Seismic Events at Yucca Mountain, Nevada. [DIRS 170137]	Section 6	Observations in the ESF and ECRB Cross-Drift show no evidence that intact rock has been damaged by seismically induced strains in over 10 million years. Most observed fractures are consistent with a cooling-related history.

Table 2.2.06.01.0A-1[a]. Direct Inputs (Continued)

Input	Source	Description
National Research Council 1992. Ground Water at Yucca Mountain, How High Can It Rise? Final Report of the Panel on Coupled Hydrologic/Tectonic/Hydrothermal Systems at Yucca Mountain. [DIRS 105162]	Chapter 2, p. 22	Plate tectonic activity imparted crustal extension stresses within the Yucca Mountain region during the past 12 million years. Extension rates between 10 and 12 million years ago ranged between 10 and 30 mm per year
	Chapter 2, p. 24	Extension rates declined to 5 to 10 mm/yr at 5 Ma; extension rates are still in a declining state
	Chapter 5	Results of assessment by National Research Council of hydrologic responses to seismic events

Table 2.2.06.01.0A-2[a]. Indirect Inputs

Citation	Title	DIRS
10 CFR 63	Energy: Disposal of High-Level Radioactive Wastes in a Geologic Repository at Yucca Mountain, Nevada	186479
BSC 2004	*Drift Scale THM Model*	169864
Sweetkind et al. 1997	*Administrative Report: Integrated Fracture Data in Support of Process Models, Yucca Mountain, Nevada*	177047

FEP: 2.2.06.02.0A

FEP NAME:

Seismic Activity Changes Porosity and Permeability of Faults

FEP DESCRIPTION:

[*No modification to the parent report.*]

SCREENING DECISION:

[*No modification to the parent report.*]

SCREENING JUSTIFICATION:

[*No modification to the parent report, except for the first paragraph of the un-numbered section "Evaluation of Changes in Fault Zone Hydrologic Properties in the UZ," which is replaced by the paragraphs below:*]

Evaluation of Changes in Fault Zone Hydrologic Properties in the UZ—The effects of a given fault displacement on unsaturated zone hydrologic properties could be evaluated using process-level calculations for the effects of the induced stress and strain on fracture geometry. However, this direct approach was not used to specifically evaluate seismic effects because of the large uncertainty in the specification of the seismic event and complexity of translating seismic motion along faults into imposed stresses. An alternative bounding approach that employed two sensitivity studies was used to assess the potential effects of fault displacement on changes in fracture apertures and consequently on fracture hydrologic properties (Appendix I).

Two bounding cases were considered. The first case considered changes in fracture aperture over the entire model domain (including faults). The range of aperture evaluated was selected to accommodate fault displacement hazard for the Solitario Canyon fault with a mean annual probability of exceedance of 10^{-8}. The second case, which considers change in fracture properties within the faults only, is directly applicable to this FEP. The results of the second sensitivity study have shown that fracture aperture changes confined to fault zones resulted in virtually no effect on transport behavior in the unsaturated zone (Appendix I, Section I3.3.1).

Changes in fault properties would also have little effect on flow above the repository because faults carry about 1% of the flow in this region of the unsaturated zone (SNL 2007 [DIRS 184614], Tables 6.6-1 and 6.6-2). Fault permeabilities are high relative to the predicted flux. Changes in fault properties, other than a very substantial reduction in fault permeability, would not be expected to affect this flow percentage. This is because the percentage of flow in the faults above the repository is related to the fault area at the ground surface available for direct infiltration into faults and lateral flow processes in the unsaturated zone. A substantial reduction in fault permeability would result in flow redirection into more permeable zones near faults and would not have a significant effect on water arrival at the repository. A similar conclusion can be reached concerning transient flow between the ground surface and the repository. Any change in transient flow would be limited to the small fraction of flow that moves through faults.

INPUTS:

[*Tables 2.2.06.02.0A-1 and 2.2.06.02.0A-2 in the parent report are replaced by Tables 2.2.06.02.0A-1[a] and 2.2.06.02.0A-2[a] as follows:*]

Table 2.2.06.02.0A-1[a]. Direct Inputs

Input	Source	Description
DTN: MO0401MWDRPSHA.000. Results of the Yucca Mountain Probabilistic Seismic Hazard Analysis (PSHA). [DIRS 185267]	files: *s1.frac_mean* and *s2.frac_mean*	Fault displacement hazard for the Bow Ridge and Solitario Canyon faults
BSC 2004. *Drift Scale THM Model*. [DIRS 169864]	Section 6.8.4	Changes in fracture permeability and capillary strength above a drift as a result of seismic activity are expected to lead to either negligible changes in drift seepage or reduced seepage into drifts
BSC 2005. *Parameter Sensitivity Analysis for Unsaturated Zone Flow*. [DIRS 174116]	Tables 6.2-1, 6.2-4	Sensitivity was evaluated for both an increase and decrease in permeability, with changes to fracture permeability occurring globally over the entire model domain
National Research Council 1992. *Ground Water at Yucca Mountain, How High Can It Rise? Final Report of the Panel on Coupled Hydrologic/Tectonic/Hydrothermal Systems at Yucca Mountain*. [DIRS 105162]	Chapter 2, p. 22	Plate tectonic activity imparted crustal extension stresses within the Yucca Mountain region during the past 12 million years. Extension rates between 10 and 12 million years ago ranged between 10 and 30 mm/yr
	Chapter 2, p. 24	Extension rates declined to 5 to 10 mm/yr at 5 Ma; extension rates are still in a declining state
	Chapter 5	Predicted seismic events within the Yucca Mountain region over the next 10,000 years will not alter the large and globally extensive stresses imposed in the rock and in effect over the past 10 to 12 million years
SNL 2007. *Abstraction of Drift Seepage*. [DIRS 181244]	Sections 6.5.1.1, 6.8.2	Studies on the effects of changes in hydrologic properties of fractures on seepage into repository drifts
	Section 6.4.4.1.2	Changes in fracture permeability and capillary strength above a drift as a result of seismic activity are expected to lead to either negligible changes in drift seepage or reduced seepage into drifts
SNL 2007. *UZ Flow Models and Submodels*. [DIRS 184614]	Tables 6.6-1, 6.6-2	Changes in fault properties would also have little effect on flow above the repository because faults carry about 1% of the flow in this region of the unsaturated zone

Table 2.2.06.02.0A-1[a]. Direct Inputs (Continued)

Input	Source	Description
SNL 2008. *Particle Tracking Model and Abstraction of Transport Processes*. [DIRS 184748]	Figures 6-25, 6-26	Effects of changes in fracture on radionuclide transport
	Section 6.6.3	Effects on radionuclide transport
SNL 2008. *Saturated Zone Flow and Transport Model Abstraction*. [DIRS 183750]	Section 6.5.2.10	Radionuclide breakthrough curves
	Section 6.5.2.3[a]	The saturated zone model uses the flowing interval concept

Table 2.2.06.02.0A-2[a]. Indirect Inputs

Citation	Title	DIRS
10 CFR 63	Energy: Disposal of High-Level Radioactive Wastes in a Geologic Repository at Yucca Mountain, Nevada	186479
Bates and Jackson 1987	*Glossary of Geology*	164050
BSC 2004	*Drift Scale THM Model*	169864
BSC 2004	*Yucca Mountain Site Description*	169734
CRWMS M&O 1998	*Probabilistic Seismic Hazard Analyses for Fault Displacement and Vibratory Ground Motion at Yucca Mountain, Nevada*	103731
Mongano et al. 1999	*Geology of the ECRB Cross Drift - Exploratory Studies Facility, Yucca Mountain Project, Yucca Mountain, Nevada*	149850
SNL 2007	*Saturated Zone Site-Scale Flow Model*	177391
SNL 2008	*Saturated Zone Flow and Transport Model Abstraction*	183750

FEP: 2.2.06.02.0B

FEP NAME:

Seismic Activity Changes Porosity and Permeability of Fractures

FEP DESCRIPTION:

[*No modification to the parent report.*]

SCREENING DECISION:

[*No modification to the parent report.*]

SCREENING JUSTIFICATION:

[*No modification to the parent report, , except for the un-numbered sections "Potential for Fracture Reactivation or the Development of New Fractures" and "Evaluation of Changes in Fracture Hydrologic Properties in the Unsaturated Zone as a Result of Reactivation," which are replaced by the paragraphs below:*]

Potential for Fracture Reactivation or the Development of New Fractures—Redistribution of strain could open new fractures and close some existing fractures, as discussed by Gauthier et al. (1996 [DIRS 100447], p. 163). Much of this redistribution would be expected to occur within the fault zones. Although an analysis of fractures was not the primary purpose of the study, the PSHA (CRWMS M&O 1998 [DIRS 103731], p. 8-7) examines the probability of movement along existing fractures and the development of new fractures. The results lead to the conclusion that the development of new fractures, given current geologic conditions and the existing stress field, is not expected and would be of low consequence.

The PSHA (CRWMS M&O 1998 [DIRS 103731], Section 8.2.1, Points 7 and 8 in Table 8-1) examined displacement hazard for specific locations and conditions, including locations away from mapped faults that were characterized by hypothetical faults with small cumulative offset, shears, fractures, and intact rock. For each location and condition, the PSHA calculated exceedance probabilities for displacement values ranging from 0.1 cm to 500 cm. For intact rock and a mean annual probability of exceedance of 10^{-8}, the PSHA indicates that the displacement hazard is less than 0.1 cm (DTN: MO0401MWDRPSHA.000 [DIRS 185267], file: *s7d.frac_mean*; CRWMS M&O 1998 [DIRS 103731], p. 8-7, Point 7d in Table 8-1). This result is interpreted as the exceedance probability for creating new fractures or faults. Given the existing network of small to large fractures with varying apertures and other characteristics, and the low likelihood of developing new fractures due to seismic activity, the development of new fractures (displacement hazard less than 0.1 cm) in presently intact rock will not noticeably affect groundwater flow or radionuclide transport. Therefore, based on the PSHA, the development of new fractures due to seismic activity is inconsequential, particularly given the existing extensive fracture network.

For existing fractures within the repository area having no measured displacement, the PSHA indicates the displacement hazard with a mean annual probability of exceedance of 10^{-8} is less

than 1 cm (DTN: MO0401MWDRPSHA.000 [DIRS 185267], files: *s7c.frac_mean* and *s8c.frac_mean*; CRWMS M&O 1998 [DIRS 103731], Figures 8-10 and 8-13 for points 7c and 8c). Comparing mean annual exceedance probabilities for a 0.1 cm displacement for a site with intact rock to a site characterized by an existing fracture indicates that movement along existing fractures is more than 10,000 times more likely than the development of new fractures.

The small displacement hazard for intact rock, less than 0.1 cm for a mean annual-exceedance probability of 10^{-8}, corresponds to the level of displacement that occurred as a result of thermal stress in the Drift Scale Test, as measured in multiple-point borehole extensometers (BSC 2004 [DIRS 169864], Figure 7.4.2-2). The simulations of the displacement response in the Drift Scale Test, based on elastic THM processes, were found to be in agreement with measurements. The dominant mode for stress-induced permeability change for THM processes was found to be elastic fracture opening or closing caused by changes in stress normal to the fractures, as opposed to changes in matrix permeability (BSC 2004 [DIRS 169864], Section 8.2). For similar displacements and stresses (as found in the DST) associated with seismic motion, the same conclusions apply to both the unsaturated zone and saturated zone. Therefore, the small seismic displacements in the intact rock matrix will have a negligible effect on rock-matrix hydrologic properties and may be excluded on the basis of low consequence.

Field observations also suggest that creation of new fractures is not currently a dominant process at Yucca Mountain. Field observations indicate that the rock at Yucca Mountain is highly fractured (BSC 2004 [DIRS 166107], Section 6.1.4.1) and that some existing fractures and joints have been subject to reactivation. Evidence for reactivation of joints includes the presence of thin brecciated zones along some cooling joints and observable slip lineations along some joint surfaces (Sweetkind et al. 1996 [DIRS 106957]). Cooling joints, formed originally as tensional openings, have only normal displacement, not shear. However, thin selvages of tectonic breccia are locally present along the trace of some cooling joints, indicating later slip. Formation of brecciated/gouge zones is discussed in excluded FEPs 2.2.06.01.0A (Seismic Activity Changes Porosity and Permeability of Rock) and 2.2.06.02.0A (Seismic Activity Changes Porosity and Permeability of Faults). Based on these field observations, the fracture and fault network appears to act as a significant preexisting weakness in the rock mass that can accommodate extensional strain through distributed slip along some reactivated joints and faults. Coupled with the results of the PSHA for displacement of intact rock, the field observations lead to an expectation that seismically related changes in strain are to be accommodated through reactivation of existing some fractures and faults, rather than through the initiation of new fractures.

Evaluation of Changes in Fracture Hydrologic Properties in the Unsaturated Zone as a Result of Reactivation—The reactivation of fractures can result in a change in fracture properties. The effects of changes in fracture system properties due to seismic activity on mountain-scale flow and radionuclide transport in the unsaturated zone have been investigated using a sensitivity approach (Appendix I). Changes in fracture hydrologic properties were considered in terms of variation in fracture aperture induced by fault displacement. The effects of fracture aperture changes are examined because several fracture hydrologic properties (permeability, capillary pressure, and porosity) are functions of fracture aperture. The sensitivity study was performed (Appendix I) with the nominal UZ three-dimensional flow model using several approaches that together provided bounding cases for determining whether changes in fractures will significantly

impact repository performance. The analysis was performed using a dual-permeability active-fracture flow model and was based on fracture aperture changes that could result from changes in strain conditions or other factors. Given a change in fracture aperture, other fracture hydrologic properties (permeability, capillary pressure, and porosity) were estimated using theoretical models (Appendix I). Calculations were then performed for unsaturated flow and transport using the modified fracture properties and the results were compared to the corresponding base case (Section I3.3). The sensitivity study (Appendix I) included two bounding cases: (1) uniform change in fracture properties throughout the UZ flow model domain and (2) change in fracture properties within the faults only. The first bounding case is particularly applicable to this FEP; the latter case is directly applicable to and is discussed in excluded FEP 2.2.06.02.0A (Seismic Activity Changes Porosity and Permeability of Faults). The two bounding cases were chosen to bound a range of fracture-aperture changes resulting from fault movement. No direct observations for Yucca Mountain relate stress caused by fault displacement to strain and the resultant changes in fracture aperture (Appendix I).

A maximum ten-fold increase in fracture aperture was selected as the model upper-bound value. The justification for this treatment (Appendix I) cites distance-strain relationships derived from models for a 1-m displacement along a strike-slip fault at Yucca Mountain, and for a 1-m displacement on a theoretical normal fault. The changes in fracture apertures for the sensitivity analysis were derived presuming a 10-m fault movement along the Solitario Canyon fault and multiplying the strains cited in the justification for the 1-m faults. The 10-m displacement represents the 85th percentile value for displacement hazard on the Solitario Canyon fault with a 10^{-8} annual probability of exceedance (DTN: MO0401MWDRPSHA.000 [DIRS 185267], files: *s2.frac_mean*; CRWMS M&O 1998 [DIRS 103731], Figure 8-3). For the Solitario Canyon fault, there is a large uncertainty in the displacement hazard with a 10^{-8} annual probability of exceedance. Values range from a median of 3 m to a mean of about 13 m. By contrast, the maximum measured single-event Quaternary displacement on the Solitario Canyon fault over about the last 200,000 years is only 1.3 m (Ramelli et al. 1996 [DIRS 101106], Table 4.7.3). Therefore, the sensitivity analysis parameterization provides a reasonable assessment of potential changes in fracture aperture that could result from seismic activity at Yucca Mountain.

The results of geomechanical models used to investigate the amount of strain induced by fault movements in the rock at Yucca Mountain suggest that a change by a factor of 10 in fracture aperture would bound the effects of tensile strain from such a fault movement (Appendix I, Section I3.2.4). Based on the cubic law for fracture permeability, a change by a factor of 10 in aperture leads to a change by a factor of 1,000 in permeability. Fracture permeabilities reduced by a factor of 1,000 were found to be inconsistent with the infiltration rates imposed on the model, because the bulk permeability was insufficient to accommodate the flow conditions. So, either reduced infiltration rates or a smaller reduction factor for the aperture would need to be used. Because the reduced apertures lead to reduced transport rates, this sensitivity does not show a potential adverse impact on performance. Therefore, a case with a reduction in aperture of a factor of 0.2 is considered sufficient.

The results of the sensitivity study have shown that fracture aperture changes confined to fault zones resulted in virtually no effect on transport behavior in the unsaturated zone (Appendix I, Section I3.3.1) and that increased fracture aperture applied over the entire unsaturated zone

domain results in effects that are no more significant than other uncertainties related to infiltration that are included in the TSPA (Appendix I, Section I4).

This result is also supported by the parameter sensitivity study for unsaturated zone flow (BSC 2005 [DIRS 174116]) and corresponding effects on radionuclide transport (SNL 2008 [DIRS 184748], Section 6.6.3[b]). For this sensitivity, fracture permeability is varied by one standard deviation. The sensitivity was conducted for both an increase and decrease in permeability by this factor, with changes to fracture permeability occurring globally over the entire model domain (BSC 2005 [DIRS 174116], Tables 6.2-1 and 6.2-4). The resulting flow fields were analyzed for effects on radionuclide transport. The transport results show that global variations in fracture permeability have only a small effect on transport relative to other uncertainties (SNL 2008 [DIRS 184748], Section 6.6.3[b]). The effects of fracture permeability in these sensitivities are expected to be overestimated because the effects of changes in capillary strength, which are negatively correlated with permeability (SNL 2007 [DIRS 181244], Section 6.5.1.1), would tend to offset changes in permeability. This is because increased fracture permeability leads to greater flow in fractures, but the associated reduction in capillary strength (represented by an increase in the fracture α), leads to a reduction in fracture flow through enhanced matrix imbibition. This effect may be seen in the response to unsaturated zone flow distributions between fractures, matrix, and faults with changes in fracture α (BSC 2005 [DIRS 174116], Table 6.4-1 (c)) and by the effects of changes in fracture α on radionuclide transport (SNL 2008 [DIRS 184748], Figures 6-25[b] and 6-26[b]).

INPUTS:

[*No modification to the parent report*.]

FEP: 2.2.14.12.0A

FEP NAME:

Far-Field Criticality Resulting from an Igneous Event

FEP DESCRIPTION:

[*No modification to the parent report.*]

SCREENING DECISION:

[*No modification to the parent report.*]

SCREENING JUSTIFICATION:

[*Table 2.2.14.12.0A-1 of the parent report is replaced by the following:*]

Table 2.2.14.12.0A-1[a]. Summary of Igneous Scenario External Criticality Results

Scenario	Waste Package Type	Calculated Accumulation or Mass Released from Waste Package	Mass of Uranium or Plutonium (for FFTF) Required to Achieve Critical Limit of k_{eff} = 0.96		
		Uranium Mass, Unless Otherwise Noted (kg)	Fractured Tuff	Lithophysae Array	Large Lithophysa
Igneous	DOE3 (N Reactor)	0.109	Infinite[a]	Infinite	Infinite
	DOE9 (TMI II Fuel)	9.24	Infinite	Infinite	Infinite
	CSNF	74.8	Infinite	1,390	Infinite
	DOE1 (FFTF) (Plutonium Mass)	2.49×10^{-2}	4.3	4.0	2.2

[a] "Infinite" means that an infinite amount of fissile waste released in this model will not produce an arrangement that can reach the critical limit.

Source: SNL 2007 [DIRS 181395], Table 6.9-1[a].

INPUTS:

[*No modification to the parent report.*]

FEP: 2.3.01.00.0A

FEP NAME:

Topography and Morphology

FEP DESCRIPTION:

[*No modification to the parent report.*]

SCREENING DECISION:

[*No modification to the parent report.*]

TSPA DISPOSITION:

[*No modification to the parent report, except the reference citation in second sentence of the second paragraph is changed as follows:*]

As stated in *Reclamation Implementation Plan* (DOE 2009 [DIRS 185964], Section 5.2.2.1), "Recontouring and erosion control practices include backfilling spoil material and grading disturbed sites, so that a stable land form is created that blends with the surrounding topography.

INPUTS:

[*No modification to the parent report, except the last row of Table 2.3.01.00.0A-1 is changed as follows:*]

DOE 2009	*Reclamation Implementation Plan*	185964

7[a]. CONCLUSIONS

[*No modification to the parent report.*]

INTENTIONALLY LEFT BLANK

8[a]. INPUTS AND REFERENCES

8.1[a] DOCUMENTS CITED

150723 Aki, K. and Richards, P.G. 1980. *Quantitative Seismology*, Theory and Methods. Two volumes. San Francisco, California: W.H. Freeman and Company. TIC: 234297; 243039.

164050 Bates, R.L. and Jackson, J.A., eds. 1987. *Glossary of Geology*. 3rd Edition. Alexandria, Virginia: American Geological Institute. TIC: 8832.

173179 Belcher, W.R. 2004. *Death Valley Regional Ground-Water Flow System, Nevada and California - Hydrogeologic Framework and Transient Ground-Water Flow Model. Scientific Investigations Report 2004-5205*. Reston, Virginia: U.S. Geological Survey. ACC: MOL.20050323.0070.

101122 Bredehoeft, J.D. 1992. "Response of the Ground-Water System at Yucca Mountain to an Earthquake." Appendix D of Ground Water at Yucca Mountain: How High Can It Rise?. Washington, D.C.: National Academy Press. TIC: 233195.

103315 Brune, J.N. 1970. "Tectonic Stress and the Spectra of Seismic Shear Waves from Earthquakes." *Journal of Geophysical Research*, *75*, (26), 4997-5009. Washington, D.C.: American Geophysical Union. TIC: 220215.

131516 Brune, J.N. 1971. "Tectonic Stress and the Spectra of Seismic Shear Waves from Earthquakes [Correction]." *Journal of Geophysical Research*, *76*, (20), 5002. Washington, D.C.: American Geophysical Union. TIC: 220216.

174775 BSC (Bechtel SAIC Company) 2004. *Data Qualification Plan, Qualification of Stress Field at Yucca Mountain as Reported by Stock and Healy 1988 [DIRS 101022] and Stock et al. 1985 [DIRS 101027]*. Las Vegas, Nevada: Bechtel SAIC Company. ACC: MOL.20041214.0117.

174776 BSC 2004. *Data Qualification Plan, Qualification of Water Table Rise Due to Seismic Activity, as Simulated by Carrigan et al. (1991 [DIRS 100967])*. Las Vegas, Nevada: Bechtel SAIC Company. ACC: MOL.20041214.0116.

170027 BSC 2004. *Development of Earthquake Ground Motion Input for Preclosure Seismic Design and Postclosure Performance Assessment of a Geologic Repository at Yucca Mountain, NV*. MDL-MGR-GS-000003 REV 01. Las Vegas, Nevada: Bechtel SAIC Company. ACC: DOC.20041111.0006; DOC.20051130.0003; DOC.20090430.0003.

169855 BSC 2004. *Development of Numerical Grids for UZ Flow and Transport Modeling*. ANL-NBS-HS-000015 REV 02. Las Vegas, Nevada: Bechtel SAIC Company. ACC: DOC.20040901.0001; LLR.20080522.0082; DOC.20090504.0002.

166107 BSC 2004. *Drift Degradation Analysis*. ANL-EBS-MD-000027 REV 03. Las Vegas, Nevada: Bechtel SAIC Company. ACC: DOC.20040915.0010; DOC.20050419.0001; DOC.20051130.0002; DOC.20060731.0005; LLR.20080311.0066; DOC.20090226.0003; DOC.20090331.0006.

169864 BSC 2004. *Drift Scale THM Model*. MDL-NBS-HS-000017 REV 01. Las Vegas, Nevada: Bechtel SAIC Company. ACC: DOC.20041012.0001; DOC.20060103.0002.

170009 BSC 2004. *Water-Level Data Analysis for the Saturated Zone Site-Scale Flow and Transport Model*. ANL-NBS-HS-000034 REV 02. Las Vegas, Nevada: Bechtel SAIC Company. ACC: DOC.20041012.0002; DOC.20050214.0002.

169734 BSC 2004. *Yucca Mountain Site Description*. TDR-CRW-GS-000001 REV 02 ICN 01. Two volumes. Las Vegas, Nevada: Bechtel SAIC Company. ACC: DOC.20040504.0008; LLR.20080423.0019; DOC.20080707.0002.

174715 BSC 2005. *Creep Deformation of the Drip Shield*. CAL-WIS-AC-000004 REV 0A. Las Vegas, Nevada: Bechtel SAIC Company. ACC: DOC.20050830.0007; DOC.20090924.0002.

174116 BSC 2005. *Parameter Sensitivity Analysis for Unsaturated Zone Flow*. ANL-NBS-HS-000049 REV 00. Las Vegas, Nevada: Bechtel SAIC Company. ACC: DOC.20050808.0005; DOC.20060329.0020; LLR.20080522.0105.

170137 BSC 2005. *Peak Ground Velocities for Seismic Events at Yucca Mountain, Nevada*. ANL-MGR-GS-000004 REV 00. Las Vegas, Nevada: Bechtel SAIC Company. ACC: DOC.20050223.0002; DOC.20050725.0002; DOC.20061002.0010.

179640 BSC 2007. *Underground Layout Configuration for LA*. 800-KMC-SS00-00200-000-00B. Las Vegas, Nevada: Bechtel SAIC Company. ACC: ENG.20070727.0004; ENG.20071214.0002; ENG.20080304.0021.

100967 Carrigan, C.R.; King, G.C.P.; Barr, G.E.; and Bixler, N.E. 1991. "Potential for Water-Table Excursions Induced by Seismic Events at Yucca Mountain, Nevada." *Geology*, *19*, (12), 1157-1160. Boulder, Colorado: Geological Society of America. TIC: 242407.

186319 Chiou, B.; Darragh, R.; Gregor, N.; and Silva, W. 2008. "NGA Project Strong-Motion Database." *Earthquake Spectra*, *24*, (1), 23-44. [Oakland, California]: Earthquake Engineering Research Institute. TIC: 260403.

151097 Covington, L.C. 1979. "The Influence of Surface Condition and Environment on the Hydriding of Titanium." *Corrosion*, *35*, (8), 378-382. Houston, Texas: National Association of Corrosion Engineers. TIC: 226671.

103731 CRWMS M&O 1998. Probabilistic Seismic Hazard Analyses for Fault Displacement and Vibratory Ground Motion at Yucca Mountain, Nevada. Milestone SP32IM3, September 23, 1998. Three volumes. Las Vegas, Nevada: CRWMS M&O. ACC: MOL.19981207.0393.

186288 Cutillo, P.A. and Ge, S. 2006. "Analysis of Strain-Induced Ground-Water Fluctuations at Devils Hole, Nevada." *Geofluids*, *6*, 319-333. [Malden, Massachusetts]: Blackwell Publishing. TIC: 260375.

103180 Davies, J.B. and Archambeau, C.B. 1997. "Geohydrological Models and Earthquake Effects at Yucca Mountain, Nevada." *Environmental Geology*, *32*, (1), 23-35. New York, New York: Springer-Verlag. TIC: 237118.

185965 DOE (U.S. Department of Energy) 2009. *Quality Assurance Requirements and Description*. DOE/RW-0333P, Rev. 21. Washington, D.C.: U.S. Department of Energy, Office of Civilian Radioactive Waste Management. ACC: DOC.20090102.0004.

185964 DOE (U.S. Department of Energy) 2009. *Reclamation Implementation Plan*. YMP/91-14, Rev. 3. Las Vegas, Nevada: U.S. Department of Energy, Office of Civilian Radioactive Waste Management. ACC: DOC.20081219.0006.

147175 Dudley, W.W., Jr. 1990. "Multidisciplinary Hydrologic Investigations at Yucca Mountain, Nevada." *High Level Radioactive Waste Management, Proceedings of the International Topical Meeting, Las Vegas, Nevada April 8-12, 1990*. 1, 1-9. La Grange Park, Illinois: American Nuclear Society. TIC: 202058.

100447 Gauthier, J.H.; Wilson, M.L.; Borns, D.J.; and Arnold, B.W. 1996. "Impacts of Seismic Activity on Long-Term Repository Performance at Yucca Mountain." *Proceedings of the Topical Meeting on Methods of Seismic Hazards Evaluation, Focus '95, September 18-20, 1995, Las Vegas, Nevada*. Pages 159-168. La Grange Park, Illinois: American Nuclear Society. TIC: 232628.

186477 Grecksch, G.; Roth, F.; and Kumpel, H.-J. 1999. "Coseismic Well-Level Changes Due to the 1992 Roermond Earthquake Compared to Static Deformation of Half-Space Solutions." *Geophysical Journal International*, *138*, 470-478. Oxford, England: Wiley-Blackwell. TIC: 260449.

106061 Hanks, T.C. and Kanamori, H. 1979. "A Moment Magnitude Scale." *Journal of Geophysical Research*, *84*, (B5), 2348-2350. Washington, D.C.: American Geophysical Union. TIC: 212607.

186296 Heaton, T.H. 1990. "Evidence for and Implications of Self-Healing Pulses of Slip in Earthquake Rupture." *Physics of the Earth and Planetary Interiors*, *64*, 1-20. New York, New York: Elsevier. TIC: 260387.

186291 Jonsson, S.; Segall, P.; Pedersen, R.; and Bjornsson, G. 2003. "Post-Earthquake Ground Movements Correlated to Pore-Pressure Transients." *Nature*, *424*. [London, England]: Nature Publishing Group. TIC: 260376.

182963 Kanamori, H. and Anderson, D.L. 1975. "Theoretical Basis of Some Empirical Relations in Seismology." *Bulletin of the Seismological Society of America*, *65*, (5), 1073-1095. El Cerrito, California: Seismological Society of America. TIC: 259721.

129658 Kemeny, J. and Cook, N. 1990. "Rock Mechanics and Crustal Stress." Section 5 of *Demonstration of a Risk-Based Approach to High-Level Waste Repository Evaluation*. McGuire, R.K., ed. EPRI NP-7057. Palo Alto, California: Electric Power Research Institute. TIC: 216677.

100989 Kemeny, J.M. and Cook, N.G.W. 1992. "Water Table Change Due to a Normal Faulting Earthquake." Section 6 of *Demonstration of a Risk-Based Approach to High-Level Waste Repository Evaluation: Phase 2*. EPRI TR-100384. Palo Alto, California: Electric Power Research Institute. TIC: 206109.

177388 Kennedy, J.R.; Adler, P.N.; and Margolin, H. 1993. "Effect of Activity Differences on Hydrogen Migration in Dissimilar Titanium Alloy Welds." Metallurgical Transactions A, 24A, (12), 2763-2771. New York, New York: Metallurgical Society of AIME. TIC: 258524.

186295 Koizumi, N.; Matsumoto, N.; Fujita, A.; Sato, T.; and Kitagawa, Y. 2005. "Evaluation of Groundwater Changes Caused by the 2003 Tokachi-Oki Earthquake (M8.0)." *Eos*, *Transactions (Supplement)*, *86*, (52), H41 F-0464. Washington, D.C.: American Geophysical Union. TIC: 258374.

186289 Manga, M. and Wang, C.-Y. 2007. Earthquake Hydrology. Treatise on Geophysics. Volume 4. 293-320. New York, New York: Elsevier. TIC: 260373.

149850 Mongano, G.S.; Singleton, W.L.; Moyer, T.C.; Beason, S.C.; Eatman, G.L.W.; Albin, A.L.; and Lung, R.C. 1999. *Geology of the ECRB Cross Drift - Exploratory Studies Facility, Yucca Mountain Project, Yucca Mountain, Nevada*. Deliverable SPG42GM3. Denver, Colorado: U.S. Geological Survey. ACC: MOL.20000324.0614.

186262 Montgomery, D.R. and Manga M. 2003. "Streamflow and Water Well Responses to Earthquakes." *Science*, *300*, 2047- 2049. Washington, D.C.: American Association for the Advancement of Science. TIC: 260364.

101276 O'Brien, G.M. 1993. *Earthquake-Induced Water-Level Fluctuations at Yucca Mountain, Nevada, June 1992*. Open-File Report 93-73. Denver, Colorado: U.S. Geological Survey. ACC: NNA.19930326.0022.

156507 Paces, J.B.; Neymark, L.A.; Marshall, B.D.; Whelan, J.F.; and Peterman, Z.E. 2001. *Ages and Origins of Calcite and Opal in the Exploratory Studies Facility Tunnel, Yucca Mountain, Nevada*. Water-Resources Investigations Report 01-4049. Denver, Colorado: U.S. Geological Survey. TIC: 251284.

186478 Quilty, E.G. and Roeloffs, E.A. 1997. "Water-Level Changes in Response to the 20 December 1994 Earthquake near Parkfield, California." *Bulletin of the Seismological Society of America*, *87*, (2), 310-317. El Cerrito, California: Seismological Society American. TIC: 260450.

101106 Ramelli, A.R.; Oswald, J.A.; Vadurro, G.; Menges, C.M.; and Paces, J.B. 1996. "Quaternary Faulting on the Solitario Canyon Fault." Chapter 4.7 of *Seismotectonic Framework and Characterization of Faulting at Yucca Mountain, Nevada*. Whitney, J.W., ed. Milestone 3GSH100M. Denver, Colorado: U.S. Geological Survey. TIC: 237980.

147173 Raney, R.G. 1988. *Reported Effects of Selected Earthquakes in the Western North America Intermontane Region, 1852-1983, on Underground Workings and Local and Regional Hydrology: A Summary*. NRC FIN D1018. Spokane, Washington: U.S. Department of the Interior, Bureau of Mines. TIC: 217278.

186290 Roeloffs, E. 1996. "Poroelastic Techniques in the Study of Earthquake-Related Hydrologic Phenomena." *Advances in Geophysics*, *37*, 135-195. New York, New York: Academic Press. TIC: 260374.

186293 Sato, T.; Matsumoto, N.; Kitagawa, Y.; Koizumi, N.; Takahashi, M.; Kuwahara, Y.; Ito, H.; Cho, A.; Satoh, T; and Tasaka, S. 2004. "Changes in Groundwater Level Associated with the 2003 Tokachi-Oki Earthquake*." Earth Planets and Space*, *56*, 395-400. Tokyo, Japan: TERRA-PUB. TIC: 260410.

186465 Schramm, K. and Stein, S. 2009. "Apparent Slow Oceanic Transform Earthquakes Due to Source Mechanism Bias." *Seismological Research Letters*, *80*, (1), 102-107. El Cerrito, California: Seismological Society of America. TIC: 260441.

144302 Schutz, R.W. and Thomas, D.E. 1987. "Corrosion of Titanium and Titanium Alloys." In *Corrosion*, Volume *13*, Pages 669-706 of Metals Handbook. 9th Edition. Metals Park, Ohio: ASM International. TIC: 209807.

110474 Silva, W.J.; Abrahamson, N.; Toro, G.; and Costantino, C. 1996. *Description and Validation of the Stochastic Ground Motion Model*. PE&A 94PJ20. El Cerrito, California: Pacific Engineering and Analysis. TIC: 245288.

163645 SNL (Sandia National Laboratories) 1996. *Hydraulic Fracturing Stress Measurements in Test Hole ESF-AOD-HDFR#1, Thermal Test Facility, Exploratory Studies Facility at Yucca Mountain*. WA-0065. Albuquerque, New Mexico: Sandia National Laboratories. ACC: MOL.19970717.0008.

181244 SNL 2007. *Abstraction of Drift Seepage*. MDL-NBS-HS-000019 REV 01 AD 01. Las Vegas, Nevada: Sandia National Laboratories. ACC: DOC.20070807.0001; DOC.20080813.0004; DOC.20081118.0049; DOC.20090330.0027; DOC.20090925.0001.

177407 SNL 2007. *EBS Radionuclide Transport Abstraction*. ANL-WIS-PA-000001 REV 03. Las Vegas, Nevada: Sandia National Laboratories. ACC: DOC.20071004.0001; LLR.20080414.0023; DOC.20090623.0001, DOC.20100331.0001.

180778 SNL 2007. *General Corrosion and Localized Corrosion of the Drip Shield*. ANL-EBS-MD-000004 REV 02 ADD 01. Las Vegas, Nevada: Sandia National Laboratories. ACC: DOC.20060427.0002; DOC.20070807.0004; LLR.20080423.0006; DOC.20071003.0019; DOC.20081209.0001; DOC.20091112.0001.

181395 SNL 2007. *Geochemistry Model Validation Report: External Accumulation Model*. ANL-EBS-GS-000002 REV 01 AD 01. Las Vegas, Nevada: Sandia National Laboratories. ACC: DOC.20071106.0015, DOC.20100205.0001.

181339 SNL 2007. *Hydrogen-Induced Cracking of the Drip Shield*. ANL-EBS-MD-000006 REV 02 ADD 01. Las Vegas, Nevada: Sandia National Laboratories. ACC: DOC.20060306.0007; DOC.20070807.0005; DOC.20081209.0003, DOC.20100210.0002.

178851 SNL 2007. *Mechanical Assessment of Degraded Waste Packages and Drip Shields Subject to Vibratory Ground Motion*. MDL-WIS-AC-000001 REV 00. Las Vegas, Nevada: Sandia National Laboratories. ACC: DOC.20070917.0006; DOC.20080623.0002; DOC.20081021.0001; DOC.20090917.0002.

177396 SNL 2007. *Radionuclide Transport Models Under Ambient Conditions*. MDL-NBS-HS-000008 REV 02 ADD 01. Las Vegas, Nevada: Sandia National Laboratories. ACC: DOC.20050823.0003; DOC.20070718.0003; DOC.20070830.0005; LLR.20080324.0002; DOC.20090114.0005; DOC.20090827.0003.

177391 SNL 2007. *Saturated Zone Site-Scale Flow Model.* MDL-NBS-HS-000011 REV 03. Las Vegas, Nevada: Sandia National Laboratories. ACC: DOC.20070626.0004; DOC.20071001.0013; LLR.20080408.0261; LLR.20080512.0162; DOC.20080623.0001; DOC.20090227.0001; DOC.20090917.0001.

176828 SNL 2007. *Seismic Consequence Abstraction*. MDL-WIS-PA-000003 REV 03. Las Vegas, Nevada: Sandia National Laboratories. ACC: DOC.20070928.0011; LLR.20080414.0012; DOC.20090219.0003; DOC.20090612.0001.

184327 SNL 2007. *Technical Work Plan for the Performance Assessment Features, Events, and Processes*. TWP-MGR-MD-000036 REV 03. Las Vegas, Nevada: Sandia National Laboratories. ACC: DOC.20071207.0001.

179354 SNL 2007. *Total System Performance Assessment Data Input Package for Requirements Analysis for Engineered Barrier System In-Drift Configuration*. TDR-TDIP-ES-000010 REV 00. Las Vegas, Nevada: Sandia National Laboratories. ACC: DOC.20070921.0008; LLR.20080328.0017.

184614 SNL 2007. *UZ Flow Models and Submodels*. MDL-NBS-HS-000006 REV 03 AD 01. Las Vegas, Nevada: Sandia National Laboratories. ACC: DOC.20080108.0003; DOC.20080114.0001; LLR.20080414.0007; LLR.20080414.0033; LLR.20080522.0086; DOC.20090330.0026.

184433 SNL 2008. *Multiscale Thermohydrologic Model*. ANL-EBS-MD-000049 REV 03 AD 02. Las Vegas, Nevada: Sandia National Laboratories. ACC: DOC.20080201.0003; LLR.20080403.0162; LLR.20080617.0077; DOC.20090225.0002.

184748 SNL 2008. *Particle Tracking Model and Abstraction of Transport Processes*. MDL-NBS-HS-000020 REV 02 AD 02. Las Vegas, Nevada: Sandia National Laboratories. ACC: DOC.20080129.0008; DOC.20070920.0003; LLR.20080325.0287; LLR.20080522.0170; LLR.20080603.0082; DOC.20090113.0002.

185746 SNL 2008. *Probabilistic Volcanic Hazard Analysis Update (PVHA-U) for Yucca Mountain, Nevada*. TDR-MGR-PO-000001 REV 01. Las Vegas, Nevada: Sandia National Laboratories. ACC: DOC.20080905.0006.

183750 SNL 2008. *Saturated Zone Flow and Transport Model Abstraction*. MDL-NBS-HS-000021 REV 03 AD 02. Las Vegas, Nevada: Sandia National Laboratories. ACC: DOC.20080107.0006; LLR.20080408.0256.

185977 SNL 2009. *Supplemental Earthquake Ground Motion Input for a Geologic Repository at Yucca Mountain, NV*. MDL-MGR-GS-000007 REV 00 AD 01. Las Vegas, Nevada: Sandia National Laboratories. ACC: DOC.20090108.0015; DOC.20080314.0001; DOC.20090430.0002; DOC.20080328.0001.

101027 Stock, J.M.; Healy, J.H.; Hickman, S.H.; and Zoback, M.D. 1985. "Hydraulic Fracturing Stress Measurements at Yucca Mountain, Nevada, and Relationship to the Regional Stress Field." *Journal of Geophysical Research*, *90*, (B10), 8691-8706. Washington, D.C.: American Geophysical Union. TIC: 219009.

101022 Stock, J.M. and Healy, J.H. 1988. "Stress Field at Yucca Mountain, Nevada." Chapter 6 of *Geologic and Hydrologic Investigations of a Potential Nuclear Waste Disposal Site at Yucca Mountain, Southern Nevada*. Carr, M.D. and Yount, J.C., eds. Bulletin 1790. Denver, Colorado: U.S. Geological Survey. TIC: 203085.

106957 Sweetkind, D.S.; Potter, C.J.; and Verbeek, E.R. 1996. "Interaction Between Faults and the Fracture Network at Yucca Mountain, Nevada." *Eos Transactions, S266*. Washington, D.C.: American Geophysical Union. TIC: 236789.

177047 Sweetkind, D.S.; Barr, D.L.; Polacsek, D.K.; and Anna, L.O. 1997. *Administrative Report: Integrated Fracture Data in Support of Process Models, Yucca Mountain, Nevada*. Milestone SPG32M3. Denver, Colorado: U.S. Geological Survey. ACC: MOL.19990825.0109.

106963 Szymanski, J.S. 1989. *Conceptual Considerations of the Yucca Mountain Groundwater System with Special Emphasis on the Adequacy of This System to Accommodate a High-Level Nuclear Waste Repository*. Three volumes. Las Vegas, Nevada: U.S. Department of Energy, Nevada Operations Office. ACC: NNA.19890831.0152.

156297 von Seggern, D.H.; Smith, K.D.; and Biasi, G.P. 2001. *Seismicity in the Vicinity of Yucca Mountain, Nevada for the Period October 1, 1997, to September 30, 1999*. Reno, Nevada: University of Nevada, Reno, Nevada Seismological Laboratory. ACC: MOL.20010731.0293.

107201 Wells, D.L. and Coppersmith, K.J. 1994. "New Empirical Relationships Among Magnitude, Rupture Length, Rupture Width, Rupture Area, and Surface Displacement." Bulletin of the Seismological Society of America, 84, (4), 974-1002. El Cerrito, California: Seismological Society of America. TIC: 226273.

185452 Whelan, J.F.; Neymark, L.A.; Moscati, R.J.; Marshall, B.D.; and Roedder, E. 2008. "Thermal History of the Unsaturated Zone at Yucca Mountain, Nevada, USA." Applied Geochemistry, 23, 1041-1075. New York, New York: Elsevier. TIC: 260109.

163589 Wilson, N.S.F.; Cline, J.S.; and Amelin, Y.V. 2003. "Origin, Timing, and Temperature of Secondary Calcite–Silica Mineral Formation at Yucca Mountain, Nevada." *Geochimica et Cosmochimica Acta*, *67*, (6), 1145-1176. New York, New York: Pergamon. TIC: 254369.

8.2[a] CODES, STANDARDS, AND REGULATIONS

186479 10 CFR 63. 2009. Energy: Disposal of High-Level Radioactive Wastes in a Geologic Repository at Yucca Mountain, Nevada. Internet Accessible.

185836 40 CFR 197. 2008. Protection of Environment: Public Health and Environmental Radiation Protection Standards for Yucca Mountain, Nevada. Internet Accessible.

178394 70 FR 53313. Implementation of a Dose Standard After 10,000 Years. Internet Accessible.

8.3[a] DATA, LISTED BY DATA TRACKING NUMBER

171974 GS930108312312.003. Earthquake-Induced Water-Level Fluctuations at Yucca Mountain, Nevada, June, 1992. Submittal date: 01/21/1993.

185267 MO0401MWDRPSHA.000. Results of the Yucca Mountain Probabilistic Seismic Hazard Analysis (PSHA). Submittal date: 03/13/2008.

166458 SN0308F3710195.003. Hydraulic Fracturing Stress Measurements in Test Holes: ESF-GDJACK #1, and ESF-GDJACK #5, Exploratory Studies Facility at Yucca Mountain, Nevada. Submittal date: 08/29/2003.

131356 SNF37100195002.001. Hydraulic Fracturing Stress Measurements in Test Hole: ESF-AOD-HDFR1, Thermal Test Facility, Exploratory Studies Facility at Yucca Mountain. Submittal date: 12/18/1996.

8.4[a] PRODUCT OUTPUT DATA

[None developed in the Addendum.]

8.5[a] SOFTWARE CODES

[None cited in the Addendum.]

INTENTIONALLY LEFT BLANK

APPENDIX J
QUALIFICATION OF DATA AND JUSTIFICATION OF EQUATIONS

INTENTIONALLY LEFT BLANK

[*No modification to the parent report, except as noted below.*]

J10[a]. FEP 1.2.10.01.0A – HYDROLOGIC RESPONSE TO SEISMIC ACTIVITY

[This section is by the following:]

This FEP uses data from the following reports as direct input:

National Research Council. 1992. *Ground Water at Yucca Mountain, How High Can It Rise? Final Report of the Panel on Coupled Hydrologic/Tectonic/Hydrothermal Systems at Yucca Mountain*. Washington, D.C.: National Academy Press. TIC: 204931. [DIRS 105162]

Belcher, W.R. 2004. *Death Valley Regional Ground-Water Flow System, Nevada and California - Hydrogeologic Framework and Transient Ground-Water Flow Model*. Scientific Investigations Report 2004-5205. Reston, Virginia: U.S. Geological Survey. ACC: MOL.20050323.0070. [DIRS 173179]

Bredehoeft, J.D. 1992. "Response of the Ground-Water System at Yucca Mountain to an Earthquake." *Appendix D of Ground Water at Yucca Mountain: How High Can It Rise?*. Washington, D.C.: National Academy Press. TIC: 233195. [DIRS 101122]

Carrigan, C.R.; King, G.C.P.; Barr, G.E.; and Bixler, N.E. 1991. "Potential for Water-Table Excursions Induced by Seismic Events at Yucca Mountain, Nevada." *Geology*, *19*, (12), 1157-1160. Boulder, Colorado: Geological Society of America. TIC: 242407. [DIRS 100967]

Chiou, B.; Darragh, R.; Gregor, N.; and Silva, W. 2008. "NGA Project Strong-Motion Database." *Earthquake Spectra*, *24*, (1), 23-44. Oakland, California: Earthquake Engineering Research Institute. TIC: 260403.

Grecksch, G.; Roth, F.; and Kumpel, H.-J. 1999. "Coseismic Well-Level Changes Due to the 1992 Roermond Earthquake Compared to Static Deformation of Half-Space Solutions." *Geophysical Journal International*, *138*, 470-478. Oxford, England: Wiley-Blackwell. TIC: 260449. [DIRS 186477]

Jonsson, S.; Segall, P.; Pedersen, R.; and Bjornsson, G. 2003. "Post-Earthquake Ground Movements Correlated to Pore-Pressure Transients." Nature, 424, . London, England: Nature Publishing Group. TIC: 260376. [DIRS 186291]

Manga, M. and Wang, C.-Y. 2007. *Earthquake Hydrology*. Treatise on Geophysics. Volume 4. 293-320. New York, New York: Elsevier. TIC: 260373. [DIRS 186289]

Quilty, E.G. and Roeloffs, E.A. 1997. "Water-Level Changes in Response to the 20 December 1994 Earthquake near Parkfield, California." *Bulletin of the Seismological Society of America, 87,* (2), 310-317. El Cerrito, California: Seismological Society American. TIC: 260450. [DIRS 186478]

Sato, T.; Matsumoto, N.; Kitagawa, Y.; Koizumi, N.; Takahashi, M.; Kuwahara, Y.; Ito, H.; Cho, A.; Satoh, T; and Tasaka, S. 2004. "Changes in Groundwater Level Associated with the 2003

Tokachi-Oki Earthquake." *Earth Planets and Space, 56,* 395-400. Tokyo, Japan: TERRA-PUB. TIC: 260410. [DIRS 186293]

Stock, J.M.; Healy, J.H.; Hickman, S.H.; and Zoback, M.D. 1985. "Hydraulic Fracturing Stress Measurements at Yucca Mountain, Nevada, and Relationship to the Regional Stress Field." *Journal of Geophysical Research, 90,* (B10), 8691-8706. Washington, D.C.: American Geophysical Union. TIC: 219009. [DIRS 101027]

Stock, J.M. and Healy, J.H. 1988. "Stress Field at Yucca Mountain, Nevada." Chapter 6 of *Geologic and Hydrologic Investigations of a Potential Nuclear Waste Disposal Site at Yucca Mountain, Southern Nevada.* Carr, M.D. and Yount, J.C., eds. Bulletin 1790. Denver, Colorado: U.S. Geological Survey. TIC: 203085. [DIRS 101022]

Wells, D.L. and Coppersmith, K.J. 1994. "New Empirical Relationships Among Magnitude, Rupture Length, Rupture Width, Rupture Area, and Surface Displacement." *Bulletin of the Seismological Society of America, 84,* (4), 974-1002. El Cerrito, California: Seismological Society of America. TIC: 226273. [DIRS 107201]

J10.1[a] QUALIFICATION OF DATA FROM NATIONAL RESEARCH COUNCIL 1992

Data Set for Qualification: The data from the National Research Council report (National Research Council 1992) to be qualified for intended use within this FEP concern the predicted changes in the water table elevation in response to seismic activity. The intended use of the data overlaps with FEPs 2.2.06.01.0A (Seismic Activity Changes Porosity and Permeability of Rock) and 2.2.06.02.0A (Seismic Activity Changes Porosity and Permeability of Faults) and includes the following statements:

- Results from the regional stress model approach indicated a maximum water table rise of 50 m (National Research Council 1992 [DIRS 105162], Chapter 5, p. 116).

- Nonetheless, the isotopic evidence now available indicates that no prolonged excursion of the water table above its present level has occurred in the last ca. 100 ka (National Research Council 1992 [DIRS 105162], Chapter 6, p. 134)

Qualification Method: The same data obtained from the same reference and used in an analogous context were qualified for intended use in FEP 2.2.06.01.0A (Seismic Activity Changes Porosity and Permeability of Rock). The data were qualified for intended use using the Technical Assessment method (SCI-PRO-001, Attachment 3, Method 5) with the consideration of the qualifications of personnel or organizations generating the data and the extent to which the data demonstrate the properties of interest. The rationale for selecting the technical assessment data qualification method and the attributes of the data qualification process used for FEP 2.2.06.01.0A (Seismic Activity Changes Porosity and Permeability of Rock) are also applicable to qualifying the data from the National Research Council report (National Research Council 1992 [DIRS 105162]) for the intended use in FEP 1.2.10.01.0A (Hydrologic Response to Seismic Activity).

Data Qualified for Intended Use: Based on the evidence provided for FEP 2.2.06.01.0A (Seismic Activity Changes Porosity and Permeability of Rock) and the intended use of the data in FEP 1.2.10.01.0A (Hydrologic Response to Seismic Activity), the data from the National Research Council (1992 [DIRS 105162]) are appropriate and are qualified for intended use in the screening justification for FEP 1.2.10.01.0A (Hydrologic Response to Seismic Activity).

J10.2[a] QUALIFICATION OF DATA FROM BELCHER 2004

Data set for qualification:

Belcher, W.R. 2004. *Death Valley Regional Ground-Water Flow System, Nevada and California - Hydrogeologic Framework and Transient Ground-Water Flow Model*. Scientific Investigations Report 2004-5205. Reston, Virginia: U.S. Geological Survey. ACC: MOL.20050323.0070. [DIRS 173179].

Description of Use: In the vicinity of Yucca Mountain, the Death Valley Regional Groundwater Flow Model has estimated the specific storage of confined aquifers of between 10^{-7} and 10^{-4} m^{-1} and a specific yield of unconfined aquifers of about 0.2 (Belcher 2004 [DIRS 173179], Table F-14 and Figure F-38). Considering confined aquifer thicknesses of about 10^{2} m implies a storativity of between about 10^{-5} and 10^{-2}, a factor of 10^{4} to 10^{1} less than the specific yield of the unconfined aquifers. These data are used as typical examples to exclude FEP 1.2.10.01.0A (Hydrologic Response to Seismic Activity).

Method of qualification: Data are qualified by the equivalent QA Program approach.

Evaluation Criteria: The Equivalent QA Program approach is used for the qualification of these data to show the acquisition, development, or processing of data can be demonstrated to be functionally equivalent (i.e., similar in scope and implementation) to the general process requirements of the QARD. The employed practices or procedures must demonstrate industry acceptable scientific, engineering, or administrative practices or processes with appropriate documentation.

Evaluation of the technical correctness of the data to be qualified: Observations of water level responses that are interpreted to result from earthquake-induced poroelastic deformation generally are from open boreholes where these water level responses reflect the change in pore pressure associated with the deformation. Earthquake-induced response groundwater level changes may be associated with changes in hydraulic head when the well is open to a confined aquifer(s) or to water table elevation changes when the well is open to an unconfined aquifer. The reason for the greater amplitude of response of the water level in confined aquifers is the result of the smaller storativity of confined aquifers. Considering a given poroelastic compression with the resultant volume of water released per unit surface area of the aquifer, the smaller storativity of the confined aquifer will result in a higher water level rise in boreholes that are open to the confined aquifer.

Evaluation results: All U.S. Geological Survey (USGS) scientific investigation reports have Bureau Approval (previously referred to as "Director's Approval"), which validates the scientific excellence of the information product. Bureau Approval ensures that all appropriate technical reviews have been conducted and that the product is consistent with all pertinent USGS and

departmental policies. This publication was thoroughly reviewed by technical experts outside the USGS as well.

Limitations on the use of the data: This qualification is limited to use in this report, as described above.

Qualifications of Personnel or Organizations Generating the Data: Claudia Faunt, the first author of Chapter F, *Transient Numerical Model* in Belcher (2004 [DIRS 173179]), earned a Ph.D. in Geological Engineering from the Colorado School of Mines and is currently a hydrologist at the USGS in San Diego, California. She is an expert in the development of hydrogeologic models for groundwater model development using advanced three-dimensional database and visualization methods.

J10.3[a] QUALIFICATION OF DATA FROM BREDEHOEFT 1992

Data set for qualification:

Bredehoeft, J.D. 1992. "Response of the Ground-Water System at Yucca Mountain to an Earthquake." Appendix D of *Ground Water at Yucca Mountain: How High Can It Rise?* Washington, D.C.: National Academy Press. TIC: 233195. [DIRS 101122].

Description of Use: Bredehoeft (1992 [DIRS 101122]) presents a three-dimensional, dislocation model of earthquake-related water table rise used in the analyses to exclude FEP 1.2.10.01.0A (Hydrologic Response to Seismic Activity). A normal faulting earthquake with 1-m slip whose rupture was 30-km long and extended at a 60-degree dip to a depth of 10 km was used in the analysis. For this case, Bredehoeft (1992 [DIRS 101122]) found that the head change produced by the earthquake was quickly dissipated by local flow. The impact on the water table elevation was a rise on the order of 1 m.

Method of qualification: Data are qualified by corroboration with independent data and independent simulations of seismically induced water table rise.

Evaluation Criteria: Data are qualified by corroboration with independent data and independent simulations of seismically induced water table rise.

Evaluation of the technical correctness of the data to be qualified: The Panel on Coupled Hydrologic/Tectonic/Hydrothermal Systems at Yucca Mountain, Nevada established by the National Research Council considered two models of earthquake-related water table rise: a dislocation model and a regional stress change model (National Research Council 1992 [DIRS 105162], Chapter 5). Analyses using the dislocation model approach were carried out by Carrigan et al. (1991 [DIRS 100967]) and Bredehoeft (1992 [DIRS 101122]). For typical Basin and Range earthquakes (normal faulting with 1-m slip), Carrigan et al. (1991 [DIRS 100967]) used a two-dimensional model and found the increase in water table elevation was 2 to 3 m for different combinations of elastic properties and aquifer thickness. Extrapolating their results to larger slip values, they found that for a 4-m slip earthquake a water table rise of 17 m was predicted. For a fault-patch model that produced greater strains and stresses, water table rise ranged from 6 to 12 m for different permeability assumptions. Bredehoeft (1992 [DIRS 101122]) used a three-dimensional model to analyze a normal faulting earthquake with 1

m slip whose rupture was 30-km long and extended at a 60-degree dip to a depth of 10 km. For this case, he found that the head change produced by the earthquake was quickly dissipated by local flow. The impact on the water table elevation was a rise on the order of 1 m.

Evaluation results: These simulated water-table rises are qualified by corroboration with observations cited by Carrigan et al. (1991 [DIRS 100967]). The Dixie Valley – Fairview Peak, Nevada, earthquake, magnitude approximately 7, produced water table excursions of 1 to 3 m, as well as long-term changes in the regional hydrology (Raney 1988 [DIRS 147173], p. 44). The 1983 Borah Peak, Idaho earthquake, magnitude approximately 7.3, caused increases of about 4 m, with water levels returning to normal within two weeks to two months (Dudley 1990 [DIRS 147175]).

Gauthier et al. (1996 [DIRS 100447], pp. 163 to 164) expanded on the work of Carrigan et al. (1991 [DIRS 100967]) and Bredehoeft (1992 [DIRS 101122]) using the dislocation model. For the flow part of the problem, they used a dual-permeability formulation involving both fracture and matrix flow. They considered three different fault types: normal, listric, and strike-slip. For all three fault types, an earthquake with a 1-m displacement and 30-km rupture length was modeled. For the normal and strike-slip cases, the vertical extent of faulting was 10 km; for the listric case the vertical extent of faulting was 2 km. The greatest response was found for the strike-slip case in which complete saturation of fractures occurs within 1 hour to an elevation of 50 m above the steady-state water table, but drops to 10% saturation after 20 hours. Matrix saturations change little. Smaller rises were obtained for the normal- and listric-faulting cases. The simulated system returned to steady-state conditions within six months.

These data serve to qualify the simulation results.

Limitations on the use of the data: This qualification is limited to use in this report, as described above.

Supporting information used in the qualification: Carrigan et al. (1991 [DIRS 100967]), Dudley (1990 [DIRS 147175]), Gauthier et al. (1996 [DIRS 100447]), Raney (1988 [DIRS 147173]).

Qualifications of Personnel or Organizations Generating the Data: John D. Bredehoeft earned a BSE degree in Geological Engineering with honors from Princeton University, and MS and PhD degrees in Geology with a minor in Civil Engineering – Soil Mechanics from The University of Illinois. He worked at the U.S. Geological Survey for 32 years. At the USGS he engaged in both research and high-level management. He is the author of more than 100 research papers in the refereed scientific literature. While at the USGS, Bredehoeft testified before Congress on such diverse topics as the USGS study of the Potomac Estuary, National Policy on the geologic disposal of nuclear wastes, water in the western United States, and the use of numerical models in management decisions. He was a member of the National Academy of Sciences/National Research Council (NAS/NRC) Committee on the Waste Isolation Pilot Plant (WIPP), and a member of the NAS/NRC Panel that reviewed groundwater concerns for the Yucca Mountain Nuclear Repository. He received numerous awards: member of the U.S. National Academy of Engineering; Editor of the scientific journal, Ground Water (1991-95); received both the Horton Medal of the American Geophysical Union (the highest award given to

a hydrologist), the Penrose Medal of the Geological Society of America (the highest award given to a geologist), and made a life-member of the National Ground Water Association (their highest award).

J10.4[a] QUALIFICATION OF DATA FROM CARRIGAN ET AL. 1991

Data set for qualification:

Carrigan, C.R.; King, G.C.P.; Barr, G.E.; and Bixler, N.E. 1991. "Potential for Water Table Excursions Induced by Seismic Events at Yucca Mountain, Nevada." *Geology*, 19, (12), 1157-1160. Boulder, Colorado: Geological Society of America. TIC: 242407 [DIRS 100967].

Description of Use: Numerical simulations by Carrigan et al. (1991 [DIRS 100967]) of tectonohydrological coupling involving earthquakes typical of the Basin and Range Province (approximately 1 m slip) produced 2 to 3 m excursions of a water table 500 m below the ground surface. Extrapolation to an event of about 4 m slip would result in a transient rise of 17 m near the fault (Carrigan et al. 1991 [DIRS 100967], p. 1,159). These data are used as typical examples to exclude FEP 1.2.10.01.0A (Hydrologic Response to Seismic Activity).

Method of qualification: Data are qualified by corroboration with independent data and independent simulations of seismically induced water table rise. No planned method of qualification was abandoned.

Evaluation Criteria: The evaluation criteria, as stated in the data qualification plan (BSC 2004 [DIRS 174776]), are that none of the corroborating data or simulations indicate a water table rise greater than 12 m.

Evaluation of the technical correctness of the data to be qualified: Changes in water level due to seismic activity are identified in the FEP description as being possibly of consequence. Numerical simulations by Carrigan et al. (1991 [DIRS 100967]) of tectonohydrological coupling involving earthquakes typical of the Basin and Range Province (approximately 1 m slip) produced 2 to 3 m excursions of a water table 500 m below the ground surface. Extrapolation to an event of about 4 m slip would result in a transient rise of 17 m near the fault (Carrigan et al. 1991 [DIRS 100967], p. 1,159). Carrigan et al. (1991 [DIRS 100967]) modeled a 100 m wide fracture zone centered on a vertical fault, with vertical permeability increased by a factor of 10^3. Water level excursions in the fracture zone were twice as great as in the adjacent block. For a fault-fracture zone with 1 m slip, transient excursions of about 12 m can occur.

Evaluation results: These simulated water-table rises are qualified by corroboration with observations cited by Carrigan et al. (1991 [DIRS 100967]). The Dixie Valley – Fairview Peak, Nevada, earthquake, magnitude approximately 7, produced water table excursions of 1 to 3 m, as well as long-term changes in the regional hydrology (Raney 1988 [DIRS 147173], p. 44). The 1983 Borah Peak, Idaho earthquake, magnitude approximately 7.3, caused increases of about 4 m, with water levels returning to normal within two weeks to two months (Dudley 1990 [DIRS 147175]). These data serve to qualify the simulation results.

An independent model by Bredehoeft (1992 [DIRS 101122]) calculated a 1-m water table rise due to a magnitude 6 earthquake; this is consistent with the data cited above and the results of Carrigan et al. (1991 [DIRS 100967]).

Limitations on the use of the data: This qualification is limited to use in this report, as described above.

Supporting information used in the qualification: Raney (1988 [DIRS 147173], p. 44); Dudley (1990 [DIRS 147175]), Bredehoeft (1992 [DIRS 101122]).

Reference to data qualification plan: *Data Qualification Plan, Qualification of Water Table Rise Due to Seismic Activity, as Simulated by Carrigan et al. (1991 [DIRS 100967])* BSC 2004 [DIRS 174776].

J10.5[a] QUALIFICATION OF DATA FROM CHIOU ET AL. 2008

Data set for qualification:

Chiou, B.; Darragh, R.; Gregor, N.; and Silva, W. 2008. "NGA Project Strong-Motion Database." *Earthquake Spectra*, 24, (1), 23-44. Oakland, California: Earthquake Engineering Research Institute. TIC: 260403. [DIRS 186319].

Description of Use: For the observed distribution of earthquake stress parameters, a lognormal distribution with a median value of 30 bars and a lognormal standard deviation of 0.6 is used. The median value of 30 bars for point-source stress parameter is consistent with a static stress drop of about 30 bars that, for a circular fault rupture, is implied by the moment magnitude-rupture area relations of Wells and Coppersmith (1994 [DIRS 107201], Table 2A). Taking static stress drop as lognormally distributed, a median value of about 30 bars for static stress drop is also obtained using the database of earthquake information developed for the Next Generation of Ground-Motion Attenuation Models (NGA) project (public version 7.3, 02-14-06, http://peer.berkeley.edu/nga/flatfile.html) (Chiou et al. 2008 [DIRS 186319]).

Method of qualification: The method used is technical assessment.

Evaluation Criteria: The PEER NGA database is an update and extension to the PEER Strong Motion Database, first published in 1999. The latest PEER Strong Motion Database brings together over 10,000 strong ground motion records from 173 different earthquakes in a web-accessible format. The NGA database includes a larger set of records, more extensive meta-data, and some corrections to information in the original database.

Evaluation of the technical correctness of the data to be qualified: The "Next Generation of Ground-Motion Attenuation Models" (NGA) project is a multidisciplinary research program coordinated by the Lifelines Program of the Pacific Earthquake Engineering Research Center (PEER), in partnership with the U.S. Geological Survey and the Southern California Earthquake Center.

The objective of the project is to develop new ground-motion prediction relations through a comprehensive and highly interactive research program. Five sets of ground-motion attenuation

models were developed by teams working independently but interacting with one another throughout the development process. The main technical issues being addressed by the NGA teams include magnitude scaling at close-in distances, directivity effects, polarization of near-field motion (fault-strike-normal component vs. fault-strike-parallel component), nonlinear amplification by shallow soil, and sedimentary basin amplification. The attenuation relationships development is also facilitated by the development of an updated and expanded database of recorded ground motions; conduct of supporting research projects to provide constraints on the selected functional forms of the attenuation relationships; and a program of interactions throughout the development process to provide input and reviews from both the scientific research community and the engineering user community.

Evaluation results: Confidence in the empirical correlations developed in this database is therefore warranted, and the data are qualified for the purpose of screening FEP 1.2.10.01.0A.

Limitations on the use of the data: This qualification is limited to use in this report, as described above.

J10.6[a] QUALIFICATION OF DATA FROM GRECKSCH ET AL. 1999

Data set for qualification:

Grecksch, G.; Roth, F.; and Kumpel, H.-J. 1999. "Coseismic Well-Level Changes Due to the 1992 Roermond Earthquake Compared to Static Deformation of Half-Space Solutions." *Geophysical Journal International*, 138, 470-478. [Oxford, England: Wiley-Blackwell]. TIC: 260449. [DIRS 186477].

Description of Use: A review of literature since 1992 indicates that dislocation model predictions of strain caused by fault displacement during earthquakes can reasonably explain observations of zones of bulk rock compression and dilation. In addition, this same research indicates that water levels in wells within the zones of compression tend to rise while water levels in wells within zones of dilation tend to fall, as expected given the poroelastic theory, although exceptions to this observation are known and reflect the many competing factors that affect the direction of water level change at any particular well in an area. One of the representative cases from literature is Grecksch et al. (1999 [DIRS 186477]), which is briefly described below. This paper is cited in the discussion to exclude FEP 1.2.10.01.0A (Hydrologic Response to Seismic Activity).

Similarly, in an analysis of water level responses following an earthquake at Roermond, Netherlands, it was observed that the water-level response was in general agreement with the expected poroelastic response to volume strains (compression or dilation) predicted by a dislocation model of the event, with 16 of 19 wells with rising water levels corresponding to areas of compression and 7 of 9 wells with water level drops corresponding to areas of dilation, although the magnitudes and durations were larger than expected (Grecksch et al. 1999 [DIRS 186477]).

Method of qualification: The method used is technical assessment.

Evaluation Criteria: The methodology is acceptable. The methodology is comparison between measured water level changes in 81wells that penetrate unconfined or poorly confined aquifers, and calculated surface static volume strain.

Evaluation of the technical correctness of the data to be qualified: Although there are no direct corroborating data for this specific earthquake, the theory advanced by this paper, that water levels in wells within the zones of compression tend to rise while water levels in wells within zones of dilation tend to fall, as expected from poroelastic theory, is also supported by other inputs qualified in this appendix (Jonsson et al. 2003 [DIRS 186291], Quilty and Roeloffs 1997 [DIRS 186478]), Sato et al. 2004 [DIRS 186293]). Therefore these publications corroborate each other.

Evaluation results: Confidence in the data for the purposes of supporting the poroelastic model of co-seismic water level changes is therefore warranted.

Limitations on the use of the data: This qualification is limited to use in this report, as described above.

Supporting information used in the qualification: Jonsson et al. (2003 [DIRS 186291]), Quilty and Roeloffs (1997 [DIRS 186478]), Sato et al. (2004 [DIRS 186293]).

Qualifications of Personnel or Organizations Generating the Data: The qualifications of personnel and organizations generating the data are comparable to the qualification requirements for generating similar data in support of the Yucca Mountain license application: This paper summarizes the Ph.D. dissertation of Gunnar Grecksch at the University of Bonn. It was peer reviewed before publication; Geophysical Journal International is published for the Royal Astronomical Society.

J10.7[a] QUALIFICATION OF DATA FROM JONSSON ET AL. 2003

Data set for qualification:

Jonsson, S.; Segall, P.; Pedersen, R.; and Bjornsson, G. 2003. "Post-Earthquake Ground Movements Correlated to Pore-Pressure Transients." *Nature*, 424. London, England: Nature Publishing Group. TIC: 260376. [DIRS 186291].

Description of Use: A review of literature since 1992 indicates that dislocation model predictions of strain caused by fault displacement during earthquakes can reasonably explain observations of zones of bulk rock compression and dilation. In addition, this same research indicates that water levels in wells within the zones of compression tend to rise while water levels in wells within zones of dilation tend to fall, as expected given the poroelastic theory, although exceptions to this observation are known and reflect the many competing factors that affect the direction of water level change at any particular well in an area. One of the representative cases from literature is Jonsson et al (2003 [DIRS 186291]), which is briefly described below. This paper is cited in the discussion to exclude FEP 1.2.10.01.0A (Hydrologic Response to Seismic Activity).

Earthquakes in June 2000 along two right-lateral strike-slip faults in southern Iceland exhibit coseismic deformation consistent with a dislocation model, with upward ground movement associated with coseismic extension zones northeast and southwest of the fault and downward ground movement associated with coseismic compression zones northwest and southeast of the fault (Jonsson et al 2003 [DIRS 186291], Figure 2). In addition, predicted coseismic pore-pressure response was shown to reasonably reproduce the observed water level changes in nearby geothermal wells, with areas of water level rise being associated with zones of compression and water level decline being associated with zones of dilation (Jonsson et al. 2003 [DIRS 186291], Figure 3).

Method of qualification: The method used is technical assessment.

Evaluation Criteria: The methodology is acceptable. The methodology is development of a correlation between measured water level changes and ground motion, developed by the combination of satellite radar interferograms and water-level changes in geothermal wells following two magnitude-6.5 earthquakes in the south Iceland seismic zone. The deformation is consistent with rebound of a porous elastic material in the first 1–2 months following the earthquakes. This interpretation is confirmed by direct measurements which show rapid (1–2-month) recovery of the earthquake-induced water-level changes. The data collected from these measurements are therefore appropriate for testing the hypothesis that changes in groundwater levels in wells that tap confined aquifers should be approximately proportional to volumetric strain.

Evaluation of the technical correctness of the data to be qualified: Although there are no direct corroborating data for this specific earthquake, the theory advanced by this paper, that water levels in wells within the zones of compression tend to rise while water levels in wells within zones of dilation tend to fall, as expected from poroelastic theory, is also supported by Grecksch et al. (1999 [DIRS 186477]), Sato et al. (2004 [DIRS 186293]) and Quilty and Roeloffs (1997 [DIRS 186478]). Therefore these publications corroborate each other.

Evaluation results: Confidence in the data for the purposes of supporting the poroelastic model of co-seismic water level changes is therefore warranted.

Limitations on the use of the data: This qualification is limited to use in this report, as described above.

Supporting information used in the qualification: Grecksch et al. (1999 [DIRS 186477]), Sato et al. (2004 [DIRS 186293]), Quilty and Roeloffs (1997 [DIRS 186478]).

Qualifications of Personnel or Organizations Generating the Data: The qualifications of personnel and organizations generating the data are comparable to the qualification requirements for generating similar data in support of the Yucca Mountain license application: Sigurjón Jónsson received a Ph.D. in 2002 from the Stanford University, Department of Geophysics, was a post-doctoral fellow at Harvard University during this work, and now is a senior researcher at ETH Zurich. Paul Segall received a Ph.D. in Geology from Stanford University and is now a professor in the department of Geophysics at Stanford.

J10.8[a] QUALIFICATION OF DATA FROM MANGA AND WANG 2007

Data set for qualification:

Manga, M. and Wang, C.-Y. 2007. *Earthquake Hydrology*. Treatise on Geophysics. Volume 4. 293-320. New York, New York: Elsevier. TIC: 260373. [DIRS 186289].

Description of Use: Earthquake-induced Response of Groundwater Level in Wells versus Response of Water Table Elevation. Observed water level responses discussed are generally for confined aquifers. Although researchers have not focused on water level responses in comparison to water table responses, the available information supports the conclusion that water table responses are generally much less (in several cases an order of magnitude less) than water level responses.

Coseismic water level responses in wells completed in confined aquifers following the 1999 M 7.5 Chi-Chi earthquake in Taiwan were observed to range from less than 1 m to more than 5 m, while water level changes in the uppermost unconfined aquifer were shown to be much smaller (ranging from 0 to 0.5 m) (Manga and Wang 2007 [DIRS 186289], p. 302).

Method of qualification: The method used is corroboration with independent data and independent observations.

Evaluation Criteria: The methodology is acceptable. Data are qualified by corroboration with independent data and independent observations of earthquake-induced response of groundwater level compared to the response of water table elevations.

Evaluation of the technical correctness of the data to be qualified: Manga and Wang (2007 [DIRS 186289]) describe the processes by which fluid pressure and hydrologic properties can change following an earthquake. Observations of water level responses that are interpreted to result from earthquake-induced poroelastic deformation generally are from open boreholes where these water level responses reflect the change in pore pressure associated with the deformation. Groundwater level changes may be associated with changes in hydraulic head when the well is open to a confined aquifer(s) or to water table elevation changes when the well is open to an unconfined aquifer. When wells are open to multiple aquifers, the water level in the well will be controlled by the hydraulic head in the most transmissive unit(s) intersecting the well.

Most of the observed water level changes in wells completed in confined aquifers following the 2003 Tokachi-oki M 8.0 earthquake in Japan could be explained by the poroelastic response and volumetric strain derived from a fault dislocation model, while an earlier earthquake in the same area had responses that could not be explained by poroelastic response because it included responses of unconfined aquifers, which are not highly sensitive to volumetric strain changes (Koizumi et al. 2005 [DIRS 186295]).

The reason for the greater amplitude of response of the water level in confined aquifers is the result of the smaller storativity of confined aquifers. Considering a given poroelastic compression with the resultant volume of water released per unit surface area of the aquifer, the smaller storativity of the confined aquifer will result in a higher water level rise in boreholes that are open to the confined aquifer. In the vicinity of Yucca Mountain, the Death Valley Regional

Groundwater Flow Model has estimated the specific storage of confined aquifers of between 10^{-7} and 10^{-4} m^{-1} and a specific yield of unconfined aquifers of about 0.1 (Belcher 2004 [DIRS 173179], Figure F-38). Considering confined aquifer thicknesses of about 10^{2} m implies a storativity of between about 10^{-5} and 10^{-2}, a factor of 10^{4} to 10^{1} less than the specific yield of the unconfined aquifers. Therefore, an earthquake capable of causing a water level rise of 10 m in the confined aquifers at Yucca Mountain would be expected to cause only a 1.0 to 0.001 m rise in the water table.

Evaluation results: Confidence in the data and observations for the purposes of supporting the earthquake-induced response of water level responses in comparison to water table responses is therefore warranted.

Limitations on the use of the data: This qualification is limited to use in this report, as described above.

Supporting information used in the qualification: Belcher (2004 [DIRS 173179]), Koizumi et al. (2005 [DIRS 186295]).

Qualifications of Personnel or Organizations Generating the Data: Michael Manga is a professor of Earth and Planetary Science at the University of California, Berkeley where he has been on the faculty since 2001. His research interest is geological processes involving fluids, including problems in physical volcanology, geodynamics, hydrogeology, and geomorphology. He received a B.S. degree in geophysics from McGill University in 1990, a S.M. degree in Engineering Sciences in 1992 and a Ph.D. in Earth and Planetary Sciences in 1994 both from Harvard University. He was a Miller Fellow at the University of California, Berkeley from 1994 to 1996 and an assistance professor at the University of Oregon from 1996 to 2001.

Chi-Yuen Wang is a faculty member of the Earth and Planetary Science department at the University of California, Berkeley. He has been a professor since 1982 and taught at the university since 1967. His research interests are the interaction of water with earthquakes and active tectonics. He received his B.S. degree in Geology from Taiwan National University in 1954 and his Ph.D. in Geological Sciences from Harvard University in 1964. From 1964 to 1967 he was a geophysicist at the Smithsonian Astrophysical Observatory.

J10.9[a] QUALIFICATION OF DATA FROM QUILTY AND ROELOFFS 1997

Data set for qualification:

Quilty, E.G. and Roeloffs, E.A. 1997. "Water-Level Changes in Response to the 20 December 1994 Earthquake near Parkfield, California." *Bulletin of the Seismological Society of America*, 87, (2), 310-317. El Cerrito, California: Seismological Society of America. TIC: 260450. [DIRS 186478].

Description of Use: A review of literature since 1992 indicates that dislocation model predictions of strain caused by fault displacement during earthquakes can reasonably explain observations of zones of bulk rock compression and dilation. In addition, this same research indicates that water levels in wells within the zones of compression tend to rise while water levels in wells within zones of dilation tend to fall, as expected given the poroelastic theory,

although exceptions to this observation are known and reflect the many competing factors that affect the direction of water level change at any particular well in an area. One of the representative cases from literature is Quilty and Roeloffs (1997 [DIRS 186478]), which is briefly described below. This paper is cited in the discussion to exclude FEP 1.2.10.01.0A (Hydrologic Response to Seismic Activity).

Observations of step-like coseismic groundwater level changes in confined aquifers were also explained as the poroelastic response to static strains caused by the 1994 earthquake near Parkfield, California (Quilty and Roeloffs 1997 [DIRS 186478]). These authors concluded that the strains predicted by a dislocation model of the rupture were in good agreement with the changes in most of the wells.

Method of qualification: The method used is technical assessment.

Evaluation Criteria: The methodology is acceptable. The methodology is development of a correlation between measured water level changes and measured seismic strain. The Parkfield, California area is located on the San Andreas Fault about halfway between San Francisco and Los Angeles and has been intensively monitored with measurements of water level, creep, and borehole volumetric strain. The data collected from these measurements are therefore appropriate for testing the hypothesis that changes in groundwater levels in wells that tap confined aquifers should be approximately proportional to volumetric strain. Water level in eight wells was recorded by pressure transducers with a precision of about 1 mm, at intervals of 15 minutes or less, and were corrected for barometric pressure excursions and verified by manual observations.

Evaluation of the technical correctness of the data to be qualified: This paper has been peer reviewed prior to publication and has since been cited in 19 other peer-reviewed publications. The report was published in the *Bulletin of the Seismological Society of America*, which is the premier journal of advanced research in earthquake seismology and has been published continuously since 1911.

Although there are no direct corroborating data for this specific earthquake, the theory advanced by this paper, that that water levels in wells within the zones of compression tend to rise while water levels in wells within zones of dilation tend to fall, as expected from poroelastic theory, is also supported by Grecksch et al. (1999 [DIRS 186477]), Jonsson et al. (2003 [DIRS 186291]), and Sato et al. (2004 [DIRS 186293]). Therefore these publications corroborate each other.

Evaluation results: Confidence in the data for the purposes of supporting the poroelastic model of co-seismic water level changes is therefore warranted.

Limitations on the use of the data: This qualification is limited to use in this report, as described above.

Supporting information used in the qualification: Grecksch et al. (1999 [DIRS 186477]), Jonnson et al. (2003 [DIRS 186291]), Sato et al. (2004 [DIRS 186293]).

Qualifications of Personnel or Organizations Generating the Data: The qualifications of personnel and organizations generating the data are comparable to the qualification requirements

for generating similar data in support of the Yucca Mountain license application: Evelyn Roeloffs received a Ph.D. in 1982 from the University of Wisconsin, Department of Geology and Geophysics, and led the USGS Parkfield earthquake prediction experiment during 1990-1991.

J10.10[a] QUALIFICATION OF DATA FROM SATO ET AL. 2004

Data set for qualification:

Sato, T.; Matsumoto, N.; Kitagawa, Y.; Koizumi, N.; Takahashi, M.; Kuwahara, Y.; Ito, H.; Cho, A.; Satoh, T; and Tasaka, S. 2004. "Changes in Groundwater Level Associated with the 2003 Tokachi-Oki Earthquake." *Earth Planets and Space*, 56, 395-400. Tokyo, Japan: TERRA-PUB. TIC: 260410. [DIRS 186293]

Description of Use: A review of literature since 1992 indicates that dislocation model predictions of strain caused by fault displacement during earthquakes can reasonably explain observations of zones of bulk rock compression and dilation. In addition, this same research indicates that water levels in wells within the zones of compression tend to rise while water levels in wells within zones of dilation tend to fall, as expected given the poroelastic theory, although exceptions to this observation are known and reflect the many competing factors that affect the direction of water level change at any particular well in an area. One of the representative cases from literature is Sato et al. (2004 [DIRS 186293]), which is briefly described below. This paper is cited in the discussion to exclude FEP 1.2.10.01.0A (Hydrologic Response to Seismic Activity).

A fault model of coseismic strain associated with fault displacement was shown to reasonably correlate to observed groundwater level changes associated with the 2003 Tokachi-oki earthquake. Water level changes in wells in areas of predicted dilation were observed to decrease, while water level changes in wells in areas of predicted contraction were observed to generally increase (Sato et al. 2004 [DIRS 186293], Figure 1).

Method of qualification: The method used is technical assessment.

Evaluation Criteria: The methodology is acceptable. The methodology is development of a correlation between measured water level changes and measured seismic strain. The data collected from 44 wells are therefore appropriate for testing the hypothesis that changes in groundwater levels in wells that tap confined aquifers should be approximately proportional to volumetric strain.

Evaluation of the technical correctness of the data to be qualified: This paper has been peer reviewed prior to publication. The report was published in the Earth Planets Space, which is published for the Seismological Society of Japan. Although there are no direct corroborating data for this specific earthquake, the theory advanced by this paper, that that water levels in wells within the zones of compression tend to rise while water levels in wells within zones of dilation tend to fall, as expected from poroelastic theory, is also supported by Grecksch et al. (1999 [DIRS 186477]), Jonsson et al. (2003 [DIRS 186291]), and Quilty and Roeloffs (1997 [DIRS 186478]). Therefore these publications corroborate each other.

Evaluation results: Confidence in the data for the purposes of supporting the poroelastic model of co-seismic water level changes is therefore warranted.

Limitations on the use of the data: This qualification is limited to use in this report, as described above.

Supporting information used in the qualification: Grecksch et al. (1999 [DIRS 186477]), Jonsson et al. (2003 [DIRS 186291]), Quilty and Roeloffs (1997 [DIRS 186478]).

J10.11[a] QUALIFICATION OF DATA FROM STOCK ET AL. 1985 AND STOCK AND HEALY 1988

Data sets for qualification:

Stock, J.M. and Healy, J.H. 1988. "Stress Field at Yucca Mountain, Nevada." Chapter 6 of *Geologic and Hydrologic Investigations of a Potential Nuclear Waste Disposal Site at Yucca Mountain, Southern Nevada*. Carr, M.D. and Yount, J.C., eds. Bulletin 1790. Denver, Colorado: U.S. Geological Survey. TIC: 203085 [DIRS 101022].

Stock, J.M.; Healy, J.H.; Hickman, S.H.; and Zoback, M.D. 1985. "Hydraulic Fracturing Stress Measurements at Yucca Mountain, Nevada, and Relationship to the Regional Stress Field." *Journal of Geophysical Research, 90*, (B10), 8691-8706. Washington, D.C.: American Geophysical Union. TIC: 219009 [DIRS 101027].

Description of Use: Stock and Healy (1988 [DIRS 101022]) measured in-situ stresses in four boreholes (USW G-1, USW G-2, USW G-3, and UE-25 p#1) and found that in all four boreholes $S_v > S_H > S_h$, where subscripts v, H, and h represent the vertical, greatest horizontal, and least horizontal stress, respectively. This corresponds to a normal faulting regime. The direction of least horizontal stress was N 60° W to N 65° W. Stock et al. (1985 [DIRS 101027]) report the same data. These data are used in FEP 1.2.10.01.0A (Hydrologic Response to Seismic Activity) to show that USW G-2, north of the repository, is in the same normal-faulting regime as the other boreholes.

Method of qualification: Data are qualified by corroboration with qualified data. No planned method of qualification was abandoned.

Evaluation Criteria: The evaluation criteria, as stated in the data qualification plan (BSC 2004 [DIRS 174775]), are that the corroborating data set confirm the relationship $S_v > S_H > S_h$ and that the direction of least horizontal stress reported in the data to be qualified agree within 30° of the direction reported in the corroborating data.

Evaluation of the technical correctness of the data to be qualified: In-situ stresses were measured by the hydraulic fracturing method. This method directly measures S_h by measuring the pressure of injected water needed to open a fracture, and observes the direction of S_h by acoustic televiewer logging. These are standard methods for measuring S_h. The data are therefore judged to be technically correct.

Evaluation results: These data are qualified by comparison with DTN: SNF37100195002.001 [DIRS 131356], which reports the mean of five hydraulic fracturing in situ stress measurements in a 30 m borehole drilled from the thermal test facility alcove in the ESF. The values reported there also show $S_v > S_H > S_h$, with S_h acting in N 75° W (±14°). DTN: SNF37100195002.001 [DIRS 131356] is qualified, and the values reported therein agree with those reported in Stock and Healy (1988 [DIRS 101022]) and Stock et al. (1985 [DIRS 101027]). Therefore both evaluation criteria specified in the qualification plan have been satisfied and the data of Stock and Healy (1988 [DIRS 101022]) and Stock et al. (1985 [DIRS 101027]) are qualified by corroboration.

Limitations on the use of the data: This qualification is limited to use in this report, as described above.

Supporting information used in the qualification: DTN: SNF37100195002.001 [DIRS 131356]

Reference to data qualification plan:

Data Qualification Plan, Qualification of Stress Field at Yucca Mountain as Reported by Stock and Healy 1988 [DIRS 101022] and Stock et al. 1985 [DIRS 101027] (BSC 2004 [DIRS 174775]).

Qualifications of Personnel or Organizations Generating the Data: Joann M. Stock is Professor of Geology and Geophysics at California Institute of Technology. Her research interests involve a wide range of tectonic problems, including global and regional plate tectonic questions, including Tectonic Evolution of the Gulf of California and Stress Field variations around the Los Angeles region. She holds B.S., M.S., and Ph.D. from Massachusetts Institute of Technology.

J10.13[a] QUALIFICATION OF DATA FROM WELLS AND COPPERSMITH 1994

Data set for qualification:

Wells, D.L. and Coppersmith, K.J. 1994. "New Empirical Relationships Among Magnitude, Rupture Length, Rupture Width, Rupture Area, and Surface Displacement." *Bulletin of the Seismological Society of America*, 84, (4), 974-1002. El Cerrito, California: Seismological Society of America. TIC: 226273. [DIRS 107201].

Description of Use: For the observed distribution of earthquake stress parameters, a lognormal distribution with a median value of 30 bars and a lognormal standard deviation of 0.6 is used. The median value of 30 bars for point-source stress parameter is consistent with a static stress drop of about 30 bars that, for a circular fault rupture, is implied by the moment magnitude-rupture area relations of Wells and Coppersmith (1994 [DIRS 107201], Table 2A).

The vertical extent of rupture is computed using trigonometry and an empirical relation between the logarithm of rupture width and moment magnitude (Wells and Coppersmith 1994 [DIRS 107201], Table 2A). The probabilistic fault displacement hazard analysis assessed displacement hazard at the surface whereas the displacement value used in seismic moment

calculations is the average displacement over the entire fault rupture. Wells and Coppersmith (1994 [DIRS 107201], Figures 6 and 7) examined the relation between average surface displacement and average subsurface displacement. They estimated average subsurface displacement from seismic moment and assessments of earthquake rupture area. Based on data from 32 earthquakes, for the ratio of average surface displacement to average subsurface displacement, they found a range of 0.25 to 6.0 with a mode of 1.32.

Method of qualification: The method used is technical assessment.

Evaluation Criteria: The methodology is acceptable. Source parameters for 421 historical earthquakes worldwide were critically evaluated and compiled to develop a series of empirical relationships among moment magnitude (M), surface rupture length, subsurface rupture length, downdip rupture width, rupture area, and maximum and average displacement per event.

Evaluation of the technical correctness of the data to be qualified: This paper was peer reviewed prior to publication and has since been cited in over 1000 other publications. The report was published in *Bulletin of the Seismological Society of America*, which is the premier journal of advanced research in earthquake seismology and has been published continuously since 1911. The completeness of the database used to develop these relationships, and the extensive citation of this article make it, in effect, a source of accepted data.

Evaluation results: Confidence in the empirical correlations developed in this paper is therefore warranted, and the data are qualified for the purpose of screening FEP 1.2.10.01.0A.

Limitations on the use of the data: This qualification is limited to use in this report, as described above.

Qualifications of Personnel or Organizations Generating the Data: The qualifications of personnel generating the data are comparable to the qualifications of personnel developing similar data for the YMP License Application process: Donald Wells received the M.S. degree from San Diego State University, Department of Geology, in 1987, and has managed and participated in several studies to evaluate geologic and seismologic hazards around the world. Kevin Coppersmith convened the expert elicitation panel for *Probabilistic Volcanic Hazard Analysis Update (PVHA-U) for Yucca Mountain, Nevada* (SNL 2008 [DIRS 185746]); he received a Ph.D. from the University of California at Santa Cruz, Department of Earth Sciences, in 1979.

[*Additional rows are added to Table J-3 of the parent report, as follows:*]

Table J-3[a]. Additional Direct Inputs for Appendix J[a]

Input	Source	Description
Belcher, W.R. 2004. Death Valley Regional Ground-Water Flow System, Nevada and California – Hydrogeologic Framework and Transient Ground-Water Flow Model. [DIRS 173179]	Figure F-38	Specific storage of confined aquifers of between 10^{-7} and 10^{-4} m^{-1} and a specific yield of unconfined aquifers of about 0.1 for the Death Valley Regional Flow System in the vicinity of Yucca Mountain
Bredehoeft, J.D. 1992. "Response of Ground-Water System at Yucca Mountain to an Earthquake." [DIRS 101122]	pp. 212 to 222	Prediction of earthquake-induced water table rise on the order of 1 m using three-dimensional dislocation and hydrological models
Carrigan, C.R.; King, G.C.P.; Barr, G.E.; and Bixler, N.E. 1991. "Potential for Water-Table Excursions Induced by Seismic Events at Yucca Mountain, Nevada." [DIRS 100967]	pp. 1,157 to 1,160	Prediction of earthquake-induced water table rise of less than 20 m using two-dimensional dislocation and hydrological models
Chiou et al. 2008. "NGA Project Strong-Motion Database." [DIRS 186319]	Next Generation of Ground-Motion Attenuation Models (NGA) project database (public version 7.3, 02-14-06, http://peer.berkeley.edu/nga/flatfile.html)	Static stress drop data for some earthquakes in the NGA earthquake database
Grecksch et al. 1999. "Coseismic well-level changes due to the 1992 Roermond Earthquake compared to static deformation of half-space solutions." [DIRS 186477]	Figure 5	General correlation between earthquake-induced water level changes and volumetric strains calculated using a dislocation model approach
Jonsson et al. 2003. Post-Earthquake Ground Movements Correlated to Pore-Pressure Transients." [DIRS 186291]	Figures 2 and 3	General correlation between earthquake-induced water level changes and volumetric strains calculated using a dislocation model approach
Manga and Wang 2007. Earthquake Hydrology [DIRS 186289]	p. 302	Data for water level changes in wells completed in confined and unconfined aquifers for the Chi-chi Taiwan earthquake.
National Research Council 1992. *Ground Water at Yucca Mountain, How High Can It Rise? Final Report of the Panel on Coupled Hydrologic/Tectonic/Hydrothermal Systems at Yucca Mountain*. [DIRS 105162]	Chapter 6, p. 134; Appendix A	Isotopic evidence indicates that no prolonged excursion of the water table above its present level has occurred in the last ca. 100 ka.
Quilty, E.G. and Roeloffs, E.A. 1997. "Water-level changes in response to the 20 December 1994 Earthquake near Parkfield, California." [DIRS 186478]	pp. 310 to 317	General correlation between earthquake-induced water level changes and volumetric strains calculated using a dislocation model approach

Table J-3[a]. Additional Direct Inputs for Appendix J[a] (continued)

Input	Source	Description
Sato et al. 2004. "Changes in Groundwater Level Associated with the 2003 Tokachi-Oki Earthquake." [DIRS 186293]	Figure 1	General correlation between earthquake-induced water level changes and volumetric strains calculated using a dislocation model approach
Stock et al. 1985 [DIRS 101027]	Table 1	Hydrofracture stress measurements in boreholes USW G-1 and USW G-2
	Figure 11	Borehole breakout azimuths
	Table 3	Stress indicators for the Nevada Test Site area
Stock, J.M. and Healy, J.H. 1988 [DIRS 101022]	Table 6-1	Hydrofracture stress measurements in boreholes USW G-1, USW G-2, USW G-3, and UE25-p#1
	pp. 90 to 91	Stress directions
Wells and Coppersmith 1994 [DIRS 107201]	Table 2A	Empirical relation between rupture area and moment magnitude
	Table 2A	Empirical relation between fault rupture width and moment magnitude
	Figures 6 and 7	Relation between average surface displacement and average subsurface displacement

[*Additional rows are added to Table J-4 of the parent report, as follows:*]

Table J-4[a]. Additional Indirect Inputs for Appendix J[a]

Citation	Title	DIRS
Belcher 2004	*Death Valley Regional Ground-Water Flow System, Nevada and California - Hydrogeologic Framework and Transient Ground-Water Flow Model*	
Bredehoeft 1992	"Response of the Ground-Water System at Yucca Mountain to an Earthquake"	101122
Carrigan et al. 1991	"Potential for Water-Table Excursions Induced by Seismic Events at Yucca Mountain, Nevada"	100967
Dudley 1990	"Multidisciplinary Hydrologic Investigations at Yucca Mountain, Nevada"	147175
Gauthier et al. 1996	"Impacts of Seismic Activity on Long-Term Repository Performance at Yucca Mountain"	100447
Grecksch et al. 1999	"Coseismic Well-Level Changes Due to the 1992 Roermond Earthquake Compared to Static Deformation of Half-Space Solutions"	186477
Jonsson et al. 2003	"Post-Earthquake Ground Movements Correlated to Pore-Pressure Transients"	186291
Koizumi et al. 2005	"Evaluation of Groundwater Changes Caused by the 2003 Tokachi-Oki Earthquake (M8.0)"	186295
Quilty and Roeloffs 1997	"Water-Level Changes in Response to the 20 December 1994 Earthquake near Parkfield, California"	186478

Table J-4[a]. Additional Indirect Inputs for Appendix J[a] (continued)

Citation	Title	DIRS
Raney 1998	*Reported Effects of Selected Earthquakes in the Western North America Intermontane Region, 1852-1983, on Underground Workings and Local and Regional Hydrology: A Summary*	147173
Sato et al. 2004	"Changes in Groundwater Level Associated with the 2003 Tokachi-Oki Earthquake"	186293
SNF37100195002.001	Hydraulic Fracturing Stress Measurements in Test Hole: ESF-AOD-HDFR1, Thermal Test Facility, Exploratory Studies Facility at Yucca Mountain	131356

APPENDIX K[a]
IMPLICATIONS OF THE YUCCA MOUNTAIN PROBABILISTIC SEISMIC HAZARD ANALYSIS FOR EARTHQUAKE-INDUCED WATER TABLE RISE

INTENTIONALLY LEFT BLANK

[*Appendix K[a] is a new appendix that was not contained in the parent report.*]

APPENDIX K[a]
IMPLICATIONS OF THE YUCCA MOUNTAIN PROBABILISTIC SEISMIC HAZARD ANALYSIS FOR EARTHQUAKE-INDUCED WATER TABLE RISE

K1[a]. INTRODUCTION

A key issue in screening FEP 1.2.10.01.0A (Hydrologic Response to Seismic Activity), is the potential at Yucca Mountain for earthquake-induced water table rise. A Panel established by the National Academy of Sciences' National Research Council "assessed the likelihood that the ground water level could rise to the height of the repository by *any* plausible geological process" during the 10,000 years following its closure (National Research Council 1992 [DIRS 105162], pp. 2 to 3). The Panel concluded that "only a modest rise in water table of less than 50 m is likely to occur as the result of a nearby earthquake" (National Research Council 1992 [DIRS 105162], p. 116). This conclusion was based on consideration of earthquake-related hydrologic responses observed worldwide, predictions of the poroelastic response of the earth's crust to earthquake-related strains made using dislocation and regional stress change models, and the likelihood of earthquakes occurring in the vicinity of Yucca Mountain.

In considering model predictions of earthquake-induced water table rise, the Panel focused on the regional stress change model because it yielded higher values of water table rise. The Panel carried out analyses using a model similar to the one developed by Kemeny and Cook (1990 [DIRS 129658], 1992 [DIRS 100989]). The Kemeny and Cook approach reduces the coupled thermo-hydro-mechanical problem to a simple mechanical model through the use of conservative assumptions. The result is a model that "should represent an upper bound on the rise in the water table due to an earthquake of a specified size" (Kemeny and Cook 1990 [DIRS 129658], p. 5-14). In the regional stress change model, the change in shear stress across the fault during an earthquake (static stress drop) leads to a compressive volumetric strain in the affected rock volume that reduces pore space. The reduced pore space causes water residing in the pores to be expelled and migrate vertically. The expelled water fills unsaturated pore space just above the water table, thereby raising its elevation. Key assumptions are:

- The stress/strain change caused by an earthquake uniformly affects a cuboid of rock that is related to the length of the fault (L) and the vertical extent of faulting (h). The lateral extent of the affected rock volume is assumed to extend perpendicular to the fault strike in both directions for a distance equivalent to the vertical extent of faulting. Thus, the affected volume of rock (V) is given by:

$$V = L \times h \times 2h \qquad \text{(Eq. K1[a])}$$

  All pore water displaced from the affected volume of rock instantaneously moves vertically up the stratigraphic column and occupies unsaturated pore space just above the water table.

Based on these and other assumptions, the Kemeny and Cook model relates water table rise (Δw, meters) to static stress drop ($\Delta\sigma$, bars) and vertical extent of faulting (h, meters) (Kemeny and Cook 1992 [DIRS 100989], Equation 6-1):

$$\Delta w = (1.2 \times 10^{-5}) \cdot \Delta\sigma_{static} \cdot h \qquad \text{(Eq. K2[a])}$$

Subsequent to the Panel assessment, promulgation of specific regulations for a repository at Yucca Mountain (10 CFR 63 [DIRS 186479], 40 CFR 197 [DIRS 185836]) changed the postclosure performance objectives such that water table rise now must be considered past 10,000 years through the period of geologic stability. In addition, a probabilistic seismic hazard analysis (PSHA) was carried out for Yucca Mountain (CRWMS M&O 1998 [DIRS 103731]). As part of the PSHA, six teams of experts characterized seismic sources in the vicinity of Yucca Mountain in terms of their geometry, rate of activity as a function of moment magnitude, and uncertainties in those parameters. The teams also characterized the potential for fault displacement at the earth's surface.

In this appendix, implications of the PSHA for water table rise are evaluated using the bounding model of Kemeny and Cook. Two approaches are used. First, seismic source characterization data for maximum moment magnitude and fault rupture dimension are used to determine static stress drop and the vertical extent of faulting. Equation K2[a] is then used to calculate a bounding water table rise for the given seismic source characterization. These results do not take into account the probability that the given seismic source characterization represents the actual state of nature. For those seismic source characterizations that give large predicted values of water table rise, a second phase of this approach takes into account the likelihood of such an earthquake occurring.

Second, fault displacement hazard results from the PSHA are used to determine the fault displacement on a block-bounding fault that has a mean annual probability of exceedance of 10^{-8}. This fault displacement value is used along with fault rupture dimensions for block-bounding faults from the PSHA to determine static stress drop and vertical extent of faulting. As in the first approach, Equation K2[a] is then used to calculate bounding water table rise. The calculated values of water table rise represent those that are consistent with the maximum fault displacement hazard that is required to be considered in the total system performance assessment.

The results of these analyses provide information supporting the screening evaluation for FEP 1.2.10.01.0A (Hydrologic Response to Seismic Activity). They show that the exclusion screening decision is consistent with the results of the PSHA.

K2[a]. INPUTS

Direct input to the analysis described in this appendix consists of results from the PSHA for Yucca Mountain (CRWMS M&O 1998 [DIRS 103731], Data Tracking Number [DTN] MO0401MWDRPSHA.000 Revision 3 [DIRS 185267]). For one analysis approach, input data consist of interpretations of maximum moment magnitude, subsurface geometry (i.e., vertical extent of faulting and fault dip), fault length, recurrence rate, and logic tree branch probability. Maximum moment magnitude, subsurface geometry, recurrence rate, and branch probability are

taken directly from PSHA input files (DTN: MO0401MWDRPSHA.000 Revision 3 [DIRS 185267]). Fault length data are implicitly contained in input fault geometry files that list coordinates of points defining a given fault interpretation. However, the fault length values used in the calculations are taken from summaries prepared by the PSHA seismic source characterization expert teams (CRWMS M&O 1998 [DIRS 103731], Appendix E), in which fault length interpretations are provided in tabular form.

For a second analysis approach, fault geometry interpretations and fault displacement hazard results for a site on the Solitario Canyon fault form the input. The fault displacement hazard for a site on the Solitario Canyon fault is used because the Solitario Canyon fault is a typical block-bounding fault and has the highest fault displacement hazard of the sites evaluated.

K3[a]. ASSUMPTIONS

Two assumptions are used in carrying out the analyses described in this appendix.

K3.1[a] CIRCULAR FAULT RUPTURE

Assumption: The value of static stress drop determined from fault rupture geometry and maximum moment magnitude or displacement is adequately determined using a relation for a circular fault rupture.

Discussion: Determination of static stress drop from seismic moment and rupture dimension depends on the fault mechanism (e.g., strike-slip, dip-slip) and geometric rupture model (e.g., circular, rectangular) (Schramm and Stein 2009 [DIRS 186465], Table 1, Figure 3). For a fault rupture with a given seismic moment, if rupture area is held constant, static stress drop determined for a circular fault yields a value that is equal to or greater than the one determined assuming a strike-slip or dip-slip rectangular fault rupture, for rupture aspect ratios (length:width) up to 8.

Seismic source characterization carried out during the PSHA results in only a few cases in which the nominal aspect ratio is greater than 8. These cases represent linked or simultaneously rupturing faults for which the length of individual fault segments has been summed to determine the overall tabulated length. This approach is taken because length is used in some approaches to estimate maximum moment magnitude. However, the geometry of fault segments making up these sources generally is characterized by considerable overlap normal to the strike direction, rather than an end-to-end arrangement. Thus the aspect ratio of the source is actually smaller than inferred from the tabulated length.

Use of a circular fault rupture model with an area equal to that for a rectangular source, therefore provides an adequate basis for calculating static stress drops consistent with the PSHA seismic source characterization.

Confirmation Status: This assumption does not need to be confirmed.

K3.2[a] BOUNDING FAULT DISPLACEMENT

Assumption: The fault displacement hazard value for the Solitario Canyon fault with a mean annual probability of exceedance of 10^{-8} is an appropriate bounding value for use in assessing seismically related water table rise.

Discussion: For a circular fault, static stress drop ($\Delta\sigma$) is related to average displacement ($\overline{D}$) over the fault rupture area through the relation (Kanamori and Anderson 1975 [DIRS 182963], Figure 1):

$$\Delta\sigma = \frac{7\pi}{16}\mu\frac{\overline{D}}{a}$$

in which μ is shear modulus and a is fault radius. One approach to evaluate the potential for water table rise using the bounding model of Kemeny and Cook (1990 [DIRS 129658], 1992 [DIRS 100989] is to use the results of the probabilistic fault displacement hazard analysis for Yucca Mountain. The value of fault displacement used in the evaluation is taken as the fault displacement hazard for the Solitario Canyon fault (CRWMS M&O 1998 [DIRS 103731], Site 2 in Figure 4-9) with a mean annual probability of exceedance of 10^{-8}. Linearly extrapolating the logarithms of displacement and mean annual probability of exceedance from the probabilistic fault displacement hazard analysis (DTN: MO0401MWDRPSHA.000 [DIRS 185267]), this value is determined to be 1,300 cm. This value includes contributions from both primary faulting on the Solitario Canyon fault and secondary faulting on the Solitario Canyon fault in response to primary faulting on other faults in the vicinity of the site.

The probabilistic fault displacement hazard analysis assessed displacement hazard at the surface whereas the displacement value used in seismic moment calculations is the average displacement over the entire fault rupture. Wells and Coppersmith (1994 [DIRS 107201], Figures 6 and 7) examined the relation between average surface displacement and average subsurface displacement. They estimated average subsurface displacement from seismic moment and assessments of earthquake rupture area. Based on data from 32 earthquakes, for the ratio of average surface displacement to average subsurface displacement, they found a range of 0.25 to 6.0 with a mode of 1.32.

Results of the probabilistic fault displacement hazard analysis for surface displacement are used without adjustment in the evaluation of seismically related water table rise. This approach is justified because:

- Fault surface displacement hazard includes contributions from both primary and secondary faulting, whereas for water table rise calculations an average subsurface displacement from primary faulting is needed. Surface displacement hazard gives somewhat larger values than would be obtained for primary faulting alone. At larger values of displacement, this effect is small.

- Estimates of average subsurface displacement are uncertain. In particular, assessment of the fault rupture area is not determined directly, but usually estimated from the distribution of aftershocks.

- The Kemeny and Cook model is developed to provide bounding values of seismically related water table rise and thus is conservative.

Confirmation Status: This assumption does not require confirmation.

K4[a]. ANALYSIS

As described in Section K1[a], Kemeny and Cook (1990 [DIRS 129658], 1992 [DIRS 100989]) related earthquake-induced water table rise to the static stress drop and vertical extent of faulting associated with an earthquake (Equation K2[a]). They used a regional stress change model to determine the earthquake-induced change in volumetric strain, and reduced the coupled hydro-thermal-mechanical response of a poroelastic medium to a simple mechanical model through the use of assumptions. By making assumptions that would tend to lead to greater water table rise, they provide a simple model that yields a bounding estimate.

Because the Kemeny and Cook model relates earthquake-induced water table rise to static stress drop and vertical extent of faulting, and results from the PSHA for Yucca Mountain can be used to calculate values for those parameters, bounding water table rise that is consistent with the PSHA characterization of fault sources can be determined. The results of such analyses can then be evaluated with respect to the screening discussion for FEP 1.2.10.01.0A (Hydrologic Response to Seismic Activity).

Two approaches are used to examine the implications of the Yucca Mountain PSHA with respect to earthquake-induced water table rise. One approach uses seismic source characterization data developed as part of the PSHA to calculate static stress drop. The static stress drop is then used along with the associated vertical extent of faulting to estimate earthquake-induced water table rise. Water table rise is calculated using the regional stress change model of Kemeny and Cook (1990 [DIRS 129658], 1992 [DIRS 100989]). The Kemeny and Cook implementation was developed as a bounding representation of the hydrologic response of the crust, modeled as a poroelastic medium, to an earthquake.

A second approach calculates static stress drop using fault displacement hazard determined in the PSHA for a site on the Solitario Canyon fault. As in the first approach, the calculated static stress drop is then used along with the associated vertical extent of faulting to estimate water table rise.

As part of the PSHA, one seismic source characterization expert team (SBK) developed a discrete probability distribution for static stress drop as part of their approach to estimating maximum magnitude (M_{max}) (CRWMS M&O 1998 [DIRS 103731], Appendix E, p. SBK-34). The distribution consisted of static stress drop values of 30, 35, 50, and 100 bars with respective weights of 0.2, 0.5, 0.25, and 0.05. Using the largest value from the static stress drop distribution (100 bars) and the largest value for the thickness of the seismogenic crust from the SBK characterization (17 km) (CRWMS M&O 1998 [DIRS 103731], Table 4-1) in Equation K2[a] gives a calculated bounding water table rise of 20 m.

K4.1[a] BOUNDING WATER TABLE RISE FROM SOURCE CHARACTERIZATION DATA DEVELOPED IN THE PROBABILISTIC SEISMIC HAZARD ANALYSIS

Kanamori and Anderson (1975 [DIRS 182963], Figure 1) summarize the relation between seismic moment and static stress drop and fault dimension. For a circular fault:

$$M_0 = \frac{16}{7}\,\Delta\sigma_{static}\,a^3 \qquad \text{(Eq. K3[a])}$$

in which M_0 is seismic moment, $\Delta\sigma$ is static stress drop, and a is fault radius. Seismic moment is also related to moment magnitude (**M**) by (Hanks and Kanamori 1979 [DIRS 106061]):

$$M = \frac{2}{3}\log M_0 - 10.7 \qquad \text{(Eq. K4[a])}$$

Solving Equation K4[a] for M_0:

$$M_0 = 10^{1.5\,M+16.05} \qquad \text{(Eq. K5[a])}$$

Substituting Equation K5[a] on the left-hand side of Equation K3[a] and solving for static stress drop:

$$\Delta\sigma_{static} = \frac{7}{16}(10^{1.5M+16.05})\,a^{-3} \qquad \text{(Eq. K6[a])}$$

Thus, if the moment magnitude and fault radius for an earthquake are known, the static stress drop can be determined.

As part of the PSHA for Yucca Mountain, six seismic source characterization teams used available data to interpret, for fault sources, the probability of activity, fault geometry, and rate of future earthquakes as a function of magnitude (CRWMS M&O 1998 [DIRS 103731], Section 4, Appendix E). Fault geometry was characterized by fault length (L), fault dip (θ), and the vertical extent of faulting (h). Using fault dip and the vertical extent of faulting, down-dip fault width (W) can be calculated as:

$$W = h/\sin(\theta) \qquad \text{(Eq. K7[a])}$$

As part of the characterization of earthquake occurrence rate, a maximum moment magnitude ($\mathbf{M_{max}}$) was assessed for each source.

For both fault geometry and earthquake occurrence rate, epistemic uncertainty was also assessed by the PSHA expert teams. Uncertainty was represented using discrete probability distributions typically consisting of three to six values for a given parameter. For fault geometry, factors contributing to uncertainty included alternative interpretations of field geologic mapping, uncertainty in the configuration of faults at depth, alternate tectonic models with differing implications for the vertical extent of the seismogenic crust or the depth at which detachment surfaces existed, and limited data on the extent of a fault that had experienced rupture during the Quaternary Period. For $\mathbf{M_{max}}$, uncertainty derived primarily from alternative empirical relations between moment magnitude and fault characteristics such as rupture length, rupture area,

maximum displacement, and slip rate. Because the probability distribution for $\mathbf{M_{max}}$ is dependent on fault geometry, the distribution varies for a given source depending on the combination of fault rupture length, dip, and vertical extent of faulting being considered.

Fault source characterization data used in the PSHA are part of the data with DTN: MO0401MWDRPSHA.000 Rev 3 [DIRS 185267]. For each seismic source characterization expert team, "src_input" files contain the various combinations of $\mathbf{M_{max}}$, fault dip, vertical extent of faulting, fault occurrence rate, and logic tree branch probability for each fault source. Fault length data are implicitly contained in "src.GEOM" files that contain geographic coordinates defining a source. However, rather than compute length from the src.GEOM files, rupture length data are taken from CRWMS M&O (1998 [DIRS 103731], Appendix E) in which the length data are tabulated for each PSHA team. It is assumed that for an $\mathbf{M_{max}}$ earthquake, the entire potential rupture area is involved. This is consistent with the way in which fault geometry data were used in estimating $\mathbf{M_{max}}$ using empirical relations. Only characterization data for "local" faults, as identified by each PSHA team, were analyzed. One exception to this rule was the inclusion of data from the SDO team for the Bare Mountain fault, even though they considered that fault as "regional." All other teams considered the Bare Mountain fault as a "local" fault.

To calculate static stress drop based on PSHA fault source characterization data, fault rupture area for an $\boldsymbol{M_{max}}$ earthquake is taken as the fault rupture length times the down-dip width. The radius (a) of an equivalent circular source with the same rupture area is then computed as:

$$a = \sqrt{\frac{L \times W}{\pi}} \qquad \text{(Eq. K8[a])}$$

Static stress drop is then determined from Equation K6[a]. Static stress drop is calculated for each $\boldsymbol{M_{max}}$ in a given $\boldsymbol{M_{max}}$ uncertainty distribution for each interpreted combination of rupture length and down-dip width (rupture area) for each local fault source for each PSHA team resulting in 3150 estimates of static stress drop from the PSHA seismic source characterization.

This treatment of the fault source characterization data differs somewhat from its use in calculating ground motion hazard. For calculation of ground motion hazard, for a given $\boldsymbol{M}$, a fault rupture length is determined from the Wells and Coppersmith (1994 [DIRS 107201], Table 2A, RDL, All) regression relation between $\boldsymbol{M}$ and subsurface rupture length (L). This value for L is used unless it exceeds the maximum rupture length interpreted for the source, in which case the maximum rupture length value is used. Down-dip rupture width is taken as equal to rupture length (i.e., an aspect ratio of 1.0), unless that value exceeds the maximum down-dip rupture width, in which case the maximum down-dip rupture width is used. The rupture area corresponding to the given value of $\boldsymbol{M}$ is then stochastically located on the fault and used to compute the distance (R) between the fault and the reference site for ground motion hazard. The PSHA ground motion prediction equations are then used to calculate ground motion at the reference site for the given source geometry and $\boldsymbol{M}$. Thus, for a given $\boldsymbol{M_{max}}$, the rupture area used to determine (R) may be less than the maximum rupture area associated with $\boldsymbol{M_{max}}$ that is used to calculate static stress drop and bounding water table rise. However, for combinations leading to larger static stress drops (i.e., relatively high $\boldsymbol{M_{max}}$ and relatively small rupture area),

the ground motion calculations will tend to use the full interpreted rupture area, consistent with the static stress drop calculations.

To estimate the range of hydrologic response associated with the PSHA seismic source characterization, each static stress drop was taken with its associated vertical extent of faulting and used to calculate an earthquake-induced bounding water table rise using Equation K2[a]. Results are summarized in Table K-1[a] in terms of 25-m water-table-rise bins. Of the 3150 values, 13 are greater than 175 m. The nominal distance between the water table elevation, both current and for future, wetter climates, and the elevation of the lowest waste emplacement drift is 187 m. Thus, a small number of calculated values for bounding water table rise exceed the distance between the water table and the lowest emplacement drift.

Table K-1[a]. Summary of Bounding Water Table Rise Values Consistent with Seismic Source Characterization for the PSHA

Water Table Rise Bins (m)	Water Table Rise Value Counts						
	AAR	ASM	DFS	RYA	SBK	SDO	Combined
0 - 25	693	144	278	291	219	750	2,375
25 - 50	35	45	0	120	72	95	367
50 - 75	55	12	0	6	14	98	185
75 - 100	27	12	0	0	9	75	123
100 - 125	24	4	0	0	8	11	47
125 - 150	18	3	0	0	1	1	23
150 - 175	12	0	0	0	0	5	17
175 - 200	5	0	0	0	0	0	5
200 - 225	2	0	0	0	0	1	3
225 - 250	1	0	0	0	0	1	2
> 250	1	1	0	0	0	1	3
	873	221	278	417	323	1,038	3,150

NOTE: The columns under "Water Table Rise Value Counts" give the results for each of the six seismic source and fault displacement characterization teams that participated in the PSHA along with the combined results. The team acronyms correspond to the following teams: AAR=W.J. Arabasz, R.E. Anderson, A.R. Ramelli; ASM=J.P. Ake, D. B. Slemmons, J. McCalpin; DFS=D.I. Doser, C.J. Fridrich, F.H. Swan; RYA=A.M. Rogers, J.C. Yount, L.W. Anderson; SBK=K.D. Smith, R. Bruhn, P.L.K. Knuepfer; SDO=R.B. Smith, C. dePolo, D.W. O'Leary (CRWMS M&O 1998 [DIRS], Table ES-1)

Source: Appendix K[a], Electronic Supplement, file: *PSHA Static Stress Drops R1.xlsm*, worksheet: *Summary 1*.

The above results are independent of the interpreted probabilities a given fault source is active, and that, if active, a given source geometry and M_{max} represent the conditions at Yucca Mountain. The results are also independent of the rate of occurrence of an M_{max} event. Considering these probabilities and M_{max} occurrence rates for the 13 cases with a bounding water table rise greater than 175 m (including two cases with a bounding water table rise between 175 and 187 m), it is determined that for nine of those cases the annual combined probability of occurrence is significantly less than 10^{-8} (Table K-2[a]). For the remaining four cases, the occurrence probabilities are between about 10^{-6} and 10^{-8}. Taking into account the bounding

nature of the Kemeny and Cook model used to calculate water table rise, these results provide support for the conclusion that seismically induced water table rise exceeding the gap between the elevation of the static water table and the lowest waste emplacement drift (about 187 m) has a low probability and can be excluded from the TSPA model.

Table K-2[a]. Probabilities Associated with Source Characterization Cases Giving Bounding Water Table Rise Greater than 175 m

PSHA Expert Team	Fault Source	Probability of Activity	Branch Probability	Annual Occurrence Rate	M_{max} Probability (M_{max})	Interpretation Probability	Annual Combined Probability	Bounding Water Table Rise (m)
AAR	Ghost Dance with L=2 km	0.1	7.61×10^{-4}	3.24×10^{-8}	0.1011 (6.4)	1.0	3.94×10^{-13}	198
			3.26×10^{-4}	4.38×10^{-8}				
AAR	Ghost Dance with L=2.5 km	0.1	1.02×10^{-3}	1.81×10^{-8}	0.1011 (6.5)	1.0	3.59×10^{-13}	200
			4.35×10^{-4}	3.95×10^{-8}				
AAR	Iron Ridge	1.0	2.54×10^{-3}	9.19×10^{-8}	0.1011 (6.9)	1.0	1.69×10^{-10}	190
			1.09×10^{-3}	1.33×10^{-6}				
AAR	Midway Valley	0.1	2.54×10^{-3}	5.77×10^{-8}	0.1011 (6.7)	1.0	5.06×10^{-12}	198
			1.09×10^{-3}	3.26×10^{-7}				
AAR	West Dune Wash #1 with W=4.6	0.1	2.54×10^{-3}	8.58×10^{-9}	0.1011 (7.0)	1.0	2.39×10^{-12}	258
			1.09×10^{-3}	1.97×10^{-7}				
AAR	West Dune Wash #1 with W=7.1	0.1	8.64×10^{-3}	1.34×10^{-8}	0.1011 (7.0)	1.0	1.27×10^{-11}	207
			3.70×10^{-3}	3.07×10^{-7}				
AAR	West Dune Wash #1 with W=9.1	0.1	2.54×10^{-3}	1.72×10^{-8}	0.1011 (7.0)	1.0	4.78×10^{-12}	182
			1.09×10^{-3}	3.95×10^{-7}				
AAR	West Dune Wash #2 with W=4.6	0.1	2.49×10^{-2}	9.24×10^{-8}	0.1011 (6.6)	1.0	5.83×10^{-11}	231
			1.07×10^{-2}	3.25×10^{-7}				
AAR	West Dune Wash #2 with W=7.1	0.1	8.64×10^{-3}	1.44×10^{-7}	0.1011 (6.6)	1.0	3.15×10^{-11}	185
			3.70×10^{-3}	5.06×10^{-7}				
ASM	Iron Ridge	0.9	3.50×10^{-1}	2.15×10^{-8}	0.1011 (7.2)	1.0	6.48×10^{-7}	330
			1.00×10^{-1}	1.27×10^{-6}				
			3.50×10^{-1}	1.38×10^{-5}				
			1.00×10^{-1}	1.38×10^{-5}				
			1.44×10^{-2}	1.84×10^{-8}				
			3.56×10^{-2}	6.62×10^{-8}				
			1.44×10^{-2}	1.11×10^{-5}				
			3.56×10^{-2}	1.66×10^{-5}				
SDO	Stagecoach Road with h=9.1 km	1.0	5.40×10^{-2}	1.78×10^{-5}	0.1011 (7.0)	0.5	5.41×10^{-8}	267
			6.00×10^{-3}	1.80×10^{-5}				

Table K-2[a]. Probabilities Associated with Source Characterization Cases Giving Bounding Water Table Rise Greater than 175 m (Continued)

PSHA Expert Team	Fault Source	Probability of Activity	Branch Probability	Annual Occurrence Rate	M_{max} Probability (M_{max})	Interpretation Probability	Annual Combined Probability	Bounding Water Table Rise (m)
SDO	Stagecoach Road with h=10.9 km	1.0	1.62×10^{-1}	1.78×10^{-5}	0.1011 (7.0)	0.5	1.62×10^{-7}	244
			1.80×10^{-2}	1.80×10^{-5}				
SDO	Stagecoach Road with h=14.4 km	1.0	5.40×10^{-2}	1.78×10^{-5}	0.1011 (7.0)	0.5	5.41×10^{-8}	212
			6.00×10^{-3}	1.80×10^{-5}				

Source: Appendix K[a], Electronic Supplement, file: *PSHA Static Stress Drops R1.xlsm*, worksheet: *Combined Probability* and Worksheet *Summary 2*.

NOTES: 1. Branch probability is for the logic tree branch reflecting a given combination of source geometry, Mmax probability distribution, and occurrence rate determination approach.
2. Annual occurrence rate is for M_{max}. Different values reflect alternative interpretations of occurrence rate for the given source geometry.
3. M_{max} probability is the probability that M_{max} is represented by the value given.
4. Interpretation Probability: The SDO team interpreted that there is a 0.5 probability that the Stagecoach Road fault acts as an independent seismic source and not in combination with other faults.

K4.2[a] BOUNDING WATER TABLE RISE CONSISTENT WITH PROBABILISTIC FAULT DISPLACEMENT HAZARD RESULTS

A second approach to assessing seismically related water table rise in light of the PSHA combines the fault displacement hazard results with the fault source geometry characterizations. Kanamori and Anderson (1975 [DIRS 182963], Figure 1) summarize the relation between static stress drop ($\Delta\sigma$), average displacement across the fault rupture ($\overline{D}$), and fault dimension. For a circular fault:

$$\Delta\sigma_{static} = \frac{7\pi}{16}\mu\frac{\overline{D}}{a} \qquad \text{(Eq. K9[a])}$$

in which μ is shear modulus (taken as 3×10^{11} dyne-cm) and a is fault radius.

In the PSHA for Yucca Mountain, fault displacement hazard was determined for a suite of demonstration points covering the range of fault conditions expected to be encountered at the site (CRWMS M&O 1998 [DIRS 103731], Section 4.3.2). The hazard at sites on faults displaying evidence of activity during the Quaternary Period included contributions from both primary faulting and from secondary displacement associated with primary faulting on other active faults. Sites on pre-Quaternary faults, fractures with no displacement, and intact rock were assessed to be subject to hazard from only secondary displacements. Two of the demonstration sites were on block-bounding Quaternary faults: the Bow Ridge fault and the Solitario Canyon fault. Fault displacement hazard for the Solitario Canyon fault was the highest of all the demonstration sites. Extrapolation of the logarithms of displacement and probability of exceedance indicate that a fault displacement of about 1,300 cm has a mean annual probability of exceedance 10^{-8}. This value bounds fault displacement that need be considered in the TSPA (Assumption K5.2).

To evaluate the implications of the PSHA displacement hazard results, static stress drop was calculated using Equation K9[a] and an average fault displacement value of 1,300 cm. Fault radius was calculated using Equation K8[a] as described in Section K4.1[a]. The calculation was

carried out for PSHA fault source characterizations of the Solitario Canyon fault, the Paintbrush Canyon fault, or fault combinations including one or both of those faults. For each fault source, alternative fault geometries representing epistemic uncertainty were evaluated to give a range of bounding water table rise. A weighted average water table rise was calculated using the logic tree branch probabilities associated with the alternative interpretations of fault geometry. Results are summarized in Table K-3[a].

Table K-3[a]. Bounding Water Table Rise for an Earthquake Displacement with a 10^{-8} Mean Annual Probability of Being Exceeded

PSHA SSC Team	Fault	Average Weighted Static Stress Drop (bars)	Range of Water Table Rise (m)	Average Weighted Water Table Rise (m)[1]	Interpretation Weight[2]
AAR	Solitario Canyon	609	56 to 109	98	0.222
AAR	Stagecoach Road – Paintbrush Canyon	573	50 to 101	91	0.155
AAR	Paintbrush Canyon	688	62 to 114	107	0.067
AAR	Single (Coalesced, Pattern 1)	373	25 to 35	30	0.009
AAR	Single West Side (Coalesced, Pattern 3)	429	36 to 70	58	0.171
AAR	Single Yucca Mountain System (Coalesced, Pattern 2)	431	28 to 40	35	0.015
AAR	West Side 1 (Coalesced, Pattern 4)	643	56 to 103	93	0.583
ASM	Solitario Canyon	616	70 to 102	75	0.95
ASM	Stagecoach Road – Paintbrush Canyon	494	65 to 92	75	0.95
DFS	Solitario Canyon	646	50 to 83	74	0.950
DFS	Stagecoach Road – Paintbrush Canyon	521	31 to 87	73	0.950
DFS	Distributed Faulting Scenario A	317	32 to 42	39	0.010
DFS	Distributed Faulting Scenario B	285	29 to 38	35	0.030
DFS	Distributed Faulting Scenario C	263	26 to 35	32	0.010
RYA	Paintbrush Canyon – Stagecoach Road – Bow Ridge (Coalescing, 2 and 3 faults)	567	62 to 189	100	0.880
RYA	Solitario Canyon – Iron Ridge	596	80 to 205	105	0.390
RYA	Single Coalescing	463	74 to 100	86	0.120
RYA	West Side (Coalescing, 2 faults)	543	72 to 177	96	0.490
SBK	Paintbrush Canyon	677	94 to 131	114	0.500
SBK	Paintbrush Canyon – Stagecoach Road	489	68 to 95	82	0.400
SBK	Solitario Canyon	613	65 to 107	85	0.500

Table K-3[a]. Bounding Water Table Rise for an Earthquake Displacement with a 10^{-8} Mean Annual Probability of Being Exceeded (Continued)

PSHA SSC Team	Fault	Average Weighted Static Stress Drop (bars)	Range of Water Table Rise (m)	Average Weighted Water Table Rise (m)[1]	Interpretation Weight[2]
SBK	Solitario Canyon – Iron Ridge	613	65 to 107	85	0.400
SBK	Coalesced	501	53 to 87	69	0.090
SBK	Detachment	422	29 to 58	46	0.010
SDO	North Paintbrush Canyon	692	82 to 185	115	0.407
SDO	North Paintbrush Canyon – Bow Ridge	654	80 to 173	109	0.009
SDO	Paintbrush Canyon	557	70 to 130	93	0.096
SDO	Paintbrush Canyon – Bow Ridge	557	70 to 130	93	0.009
SDO	Paintbrush Canyon – Stagecoach Road	452	61 to 104	75	0.096
SDO	Paintbrush Canyon – Stagecoach Road – Bow Ridge	452	61 to 104	75	0.009
SDO	Solitario Canyon	586	67 to 98	83	0.575
SDO	Solitario Canyon – South Windy Wash	514	62 to 83	73	0.125
SDO	South Paintbrush Canyon	720	107 to 150	120	0.236
SDO	South Paintbrush Canyon – Bow Ridge	644	90 to 136	107	0.074
SDO	South Paintbrush Canyon – Stagecoach Road	542	80 to 115	90	0.042
SDO	Stagecoach Road	917	90 to 185	122	0.500
SDO	Stagecoach Road – Solitario Canyon	478	62 to 100	79	0.125

Source: Calculations based on the PSHA seismic source characterization and fault displacement hazard results: Appendix K[a], Electronic Supplement, file: *PSHA Static Stress Drops R1.xlsm*, worksheet: *Summary 1*, which includes links to Worksheets *AAR*, *ASM*, *DFS*, *RYA*, *SBK*, and *SDO* for "Range of Water Table Rise."

NOTES:
1. To compute the average water table rise, values are weighted according to their logic tree branch probabilities times the maximum magnitude probability and normalized to the total weight that the given interpretation is active.
2. Interpretation weight is the probability that a given fault configuration (i.e., acting independently, linked with other faults) represents the tectonic conditions at Yucca Mountain. The interpretation weight is the sum of the underlying logic tree branch probabilities when the fault configuration is active.

Calculated values of average weighted water table rise, based on a fault displacement of 1,300 cm and using the fault source characterization results from the PSHA expert teams, are 122 m or less. Thus, for a displacement with a nominal 10^{-8} mean annual probability of being exceeded, a bounding estimate of water table rise still leaves a distance of 65 m or more between the elevation of the water table and the elevation of the lowest waste emplacement drift (an approximately 187-m distance in the absence of seismically induced water table rise). Note also that for most fault interpretations evaluated, the logic tree branch probability is significantly less than 1. Consequently, exclusion of FEP 1.2.10.01.0A (Hydrologic Response to Seismic

Activity), from the TSPA is consistent with the seismic source characterization interpretations and the fault displacement hazard results of the PSHA.

K5[a]. CONCLUSIONS

FEP 1.2.10.01.0A (Hydrologic Response to Seismic Activity), describes some earthquake-related hydrologic effects, including seismically induced water table rise. The low elevation of the water table at Yucca Mountain is a key attribute of the site. Within the repository footprint, the present-day water table varies from around 730 m above mean sea level in the south to less than 850 m above mean sea level in the north (BSC 2004 [DIRS 169855], Figure 6-2). The repository elevation for emplacement drifts ranges between 1,037 m above mean sea level in the north (BSC 2007 [DIRS 179640], Table 14) and 1,105 m above mean sea level in the south (BSC 2007 [DIRS 179640], Table 12), indicating that the present-day water table depth below the repository horizon ranges from 187 m in the north, based on a repository elevation of 1,037 m and water table elevation of 850 m, to 375 m in the south, based on a repository elevation of 1,105 m and water table elevation of 730 m. For future, wetter climates, the elevation of the water table is taken to have a uniform value of 850 m. This appendix examines the potential for seismically induced water table rise to reduce the minimum 187-m distance between the elevation of the water table and the lowest elevation of a waste emplacement drift.

In a simple model, Kemeny and Cook (1990 [DIRS 129658], 1992 [DIRS 100989]) relate seismically induced water table rise to earthquake static stress drop and the vertical extent of faulting. The Kemeny and Cook model is developed to bound seismically induced water table rise.

Although, in general, static stress drop was not explicitly assessed during the PSHA for Yucca Mountain, characterizations of fault length, dip, vertical extent of faulting, and M_{max} carried out by the expert teams can be used to infer a static stress drop. Using these data as input to the Kemeny and Cook model demonstrates that, for 3139 out of 3150 cases, the calculated water table rise is less than the 187 m distance between the elevation of the water table and the lowest waste emplacement drift. This observation is independent of the probability that a given case represents the actual geologic conditions at Yucca Mountain. When seismic source characterization probabilities are taken into account along with the rate of occurrence of M_{max} events, it is determined that 7 of the 11 cases for which calculated water table rise exceeds 187 m have probabilities more than an order of magnitude less than 10^{-8}. Taking into account the intentional bounding nature of the Kemeny and Cook model, the results support exclusion of seismically induced water table rise from the TSPA.

Fault displacement hazard results from the PSHA also demonstrate that seismically induced water table rise can be excluded from the TSPA. For the fault sites and conditions evaluated in the PSHA, the Solitario Canyon fault has the greatest displacement hazard. For a mean annual probability of exceedance of 10^{-8}, the fault displacement hazard is about 1,300 cm. Using this value as the average displacement on the Solitario Canyon and Paintbrush Canyon faults, static stress drop can be calculated using the fault geometry data from the PSHA seismic source characterization. Cases for the Solitario Canyon and Paintbrush Canyon faults alone, and in combination with other faults, give a maximum bounding water table rise of 122 m. Thus,

calculated seismically induced water table rise using this approach maintains a gap of 65 m or more between the elevation of the water table and the lowest waste emplacement drift.

These analyses support exclusion of FEP 1.2.10.01.0A (Hydrologic Response to Seismic Activity), from the TSPA.

OFFICE OF CIVILIAN RADIOACTIVE WASTE MANAGEMENT
SPECIAL INSTRUCTION SHEET

1. QA: QA

This is a placeholder page for records that cannot be scanned.

2. Record Date	3. Accession Number
4/12/2010	

4. Author Name(s)	5. Authorization Organization
Richard Quittmeyer	Lead Lab / Disruptive Events

6. Title/Description

Features, Events, and Processes for the Total System Performance Assessment: Analyses

7. Document Number(s)	8. Version Designator
ANL-WIS-MD-000027 REV 00 AD 01	0 AD 01

9. Document Type	10. Medium
Analyses - Addendum	CD

11. Access Control Code

12. Traceability Designator

13. Comments

THIS IS AN ELECTRONIC ATTACHMENT

Submitter attests to the completeness and accuracy of the data contained on the enclosed CD.

Software used: CH 4-12-10

Microsoft Excel

PSHA Static Stress Drops R1.xls
Stress Drops R1.xls

14. RPC Electronic Media Verification